

# ACUUS

## BELGRADE 2025



19<sup>th</sup> WORLD CONFERENCE OF THE ASSOCIATED  
RESEARCH CENTRES FOR THE URBAN UNDERGROUND SPACE

November 4-7, Belgrade, Serbia

Underground mobility and elevated thinking.  
New opportunities and challenges in the use of underground urban space.

# PROCEEDINGS

**Edited by:**

Prof. Vladan Djokic, PhD  
Prof. Nebojsa Bojovic, PhD  
Prof. Danilo Furundzic, PhD  
Nemanja Sipetic

Image de wirestock sur Freepik



## Organisers



UNIVERSITY OF BELGRADE  
FACULTY OF TRANSPORT AND TRAFFIC ENGINEERING



Институт за архитектуру и урбанизам Србије  
Institute of Architecture and Urban & Spatial Planning of Serbia

## Endorsement



University of Belgrade



Ministry of Science, Technological Development and Innovation  
Republic of Serbia



SERBIAN  
CHAMBER OF  
ENGINEERS



SERBIA  
CONVENTION  
BUREAU



NATIONAL TOURISM  
ORGANISATION  
OF SERBIA

## Golden Sponsor

**STADLER**

## Silver Sponsor



汕頭大學  
SHANTOU UNIVERSITY



## Supported by

**ALVECO**  
CONSTRUCTION



**ENERGORAZVOJ**



**ESENERGOSERVIS**

**HNTB**

**INTERFRIGO**



**INŽENJERING**  
ZRENJANIN

**MULTITEK elektronik®**

**NOVKOL**

**ŠIPING**  
smart technologies

**ŠIDPROJEKT** DOO ŠID  
22240 ŠID, KNEZA MILOŠA 2, REPUBLIKA SRBIJA



**19<sup>th</sup> WORLD CONFERENCE OF THE ASSOCIATED  
RESEARCH CENTRES FOR THE URBAN  
UNDERGROUND SPACE**

Underground mobility and elevated thinking.  
New opportunities and challenges in the use of  
underground urban space.

**CONFERENCE  
PROCEEDINGS**

November 4-7, Belgrade, Serbia

**CONFERENCE PROCEEDINGS OF THE  
19<sup>th</sup> WORLD CONFERENCE OF THE ASSOCIATED RESEARCH CENTRES FOR THE  
URBAN UNDERGROUND SPACE – ACUUS 2025**

November 4-7, Belgrade, Serbia

**The International Conference ACUUS 2025 Proceedings are co-financed by the Ministry of Science,  
Technological Development and Innovation of the Republic of Serbia.**

**All the papers included within the Proceedings are reviewed and regarded as scientific papers.**

Publisher: BBN Congress Management d.o.o.  
Deligradska 9, 11000 Beograd, Srbija  
E-mail: bbn@bbn.co.rs | Web: www.bbn.co.rs

Editors in Chief: Prof. Vladan Djokic, PhD, University of Belgrade, Faculty of Architecture, University of  
Belgrade Rectorate  
Prof. Nebojsa Bojovic, PhD, University of Belgrade, Faculty of Transport and Traffic  
Engineering, Serbia  
Prof. Danilo Furundzic, PhD, University of Belgrade, Faculty of Architecture, Serbia  
Nemanja Sipetic, Associated Research Centres for the Urban Underground Space, Serbia

Prepress: BBN Congress Management d.o.o.  
Deligradska 9, 11000 Beograd, Srbija  
E-mail: bbn@bbn.co.rs | Web: www.bbn.co.rs

Cover design: Marija Marković

Production: BBN Congress Management d.o.o.

Copies: 200

Place of issue: Belgrade

Year of issue: 2025

CIP - Каталогизacija y публикацији  
Народна библиотека Србије, Београд

711(24)(082)(0.034.2)

**ASSOCIATED Research Centres for the Urban Underground Space. World Conference (19 ; 2025 ;  
Beograd)**

Underground mobility and elevated thinking [Elektronski izvor] : new opportunities and challenges in the use  
of underground urban space : proceedings / 19th World Conference of the Associated Research Centres for the  
Urban Underground Space, ACUUS 2025, November 4-7, Belgrade, Serbia ; edited Vladan Djokic ... [et al.] ;  
[organisers University of Belgrade, Faculty of Transport and Traffic Engineering [and] Institute for Architecture  
and Urban & Spatial Planning of Serbia]. - Beograd : BBN Congress Management, 2025 (Beograd : BBN  
Congress Management). - 1 USB fleš memorija ; 1 x 2 x 7 cm

Sistemska zahtevi: Nisu navedeni. - Nasl. sa naslovne strane dokumenta. - Tiraž 200

ISBN 978-86-901646-7-7

a) Урбано планирање -- Подземни објекти -- Зборници

COBISS.SR-ID 178866441



## Scientific committee

1. Prof. Zoran Gligorić, PhD, president, University of Belgrade, Faculty of Mining and Geology, Belgrade, Republic of Serbia
2. Prof. Ray Sterling, PhD, Vice-Chair, Louisiana Tech University, USA
3. Prof. Bruno Barocca, PhD, Gustave Eiffel University in Paris, France
4. Prof. Andreas Benardos, PhD, School of Mining and Metallurgical Engineering at the National Technical University of Athens, Greece
5. Prof. Wout Broere, PhD, Technische Universiteit Delft, Netherlands
6. Prof. Dimitris Kaliampakos, PhD, National Technical University of Athens, School of Mining and Metallurgical Engineering, Greece
7. Prof. Monika Mitew Czajewska, PhD, Politechnika Warszawska, Poland
8. Prof. Filippo Lambertucci, PhD, Sapienza Università di Roma, Italy
9. Prof. Jamal Rostami, PhD, Colorado School of Mines, USA
10. Prof. Priscilla P. Nelson, PhD, Colorado School of Mines, USA
11. Prof. Pavlos Nomikos, PhD, National Technical University of Athens, School of Mining and Metallurgical Engineering, Greece
12. Prof. Fang-Le Peng, PhD, Tongji University, China
13. Prof. Zhi-Guo Yan, PhD, Tongji University, China
14. Prof. Farah Zaini, PhD, University Malaysia Sarawak, Malaysia
15. Prof. Chris Rogers, PhD, University of Birmingham, United Kingdom
16. Nikolai Bobylev, PhD, Institute of Earth Sciences, Saint Petersburg State University, Russia
17. Isabelle Chan, PhD, University of Hong Kong, Faculty of Architecture, China
18. Nataša Danilović Hristić, PhD, Institute for Architecture and Urban & Spatial Planning of Serbia, Serbia
19. Yun-Hao Dong, PhD, Tongji University, China
20. Michael Doyle, PhD, Université Laval School of Architecture in Quebec City, Canada
21. Dexter Hunt, PhD, School of Civil Engineering University of Birmingham, United Kingdom
22. Marija Lalošević, PhD, Institute for Architecture and Urban & Spatial Planning of Serbia, Serbia
23. Božidar Manić, PhD, Institute for Architecture and Urban & Spatial Planning of Serbia, Serbia
24. Michael Mooney, PhD, Colorado School of Mines, USA
25. Jelena Ninić, PhD, School of Civil Engineering University of Birmingham, United Kingdom
26. Yong-Kang Qiao, PhD, Tongji University, China
27. Yingxin Zhou, Knights Synergy (S) Pte Ltd, Singapore
28. Jacques Besner, PhD, Associated Research Centres for the Urban Underground Space, France
29. Giuseppe Gaspari, AECOM, Canada
30. Nemanja Šipetić, Associated Research Centres for the Urban Underground Space, Serbia
31. Sanja Zlatinić, Associated Research Centres for the Urban Underground Space, USA
32. Ilkka Vähäaho, City of Helsinki, Finland
33. Mark Wallace, ARUP, USA
34. Prof. Xiao-Jun Li, PhD, Tongji University, China
35. Behnam Atazadeh, PhD, University of Melbourne, Centre for Spatial Data Infrastructures and Land Administration (CSDILA), Australia
36. Prof. Vojkan Jovičić, PhD, University of Ljubljana, Faculty of Civil and Geodetic Engineering, Slovenia
37. Prof. Dietmar Adam, PhD, Technical University Wien, Institute of Geotechnics, Austria
38. Ikram Loukili, PhD, Moroccan Researcher in Urban Planning and Sustainable Infrastructure, Collège Boréal in Canada, Morocco / Canada
39. Prof. Milorad Jovanovski, PhD, Faculty of Civil Engineering, University "Ss. Cyril and Methodius", Makedonija
40. Giuseppe Pace, National Research Council's Institute for Research on Innovation and Services for Development Member, Italy
41. Prof. Oussama Hamal, PhD, University of Rabat, National School of Architecture (ENAM), Morocco
42. Prof. Vladimir Lojanica, PhD, University of Belgrade – Faculty of Architecture, Serbia
43. Prof. Chu Jian, PhD, Nanyang Technological University (NTU), Singapore
44. Doc. Filip Filipović, University of Belgrade – Faculty of Transport and Traffic Engineering, Serbia

## Organizing Committee

1. Prof. Nebojsa Bojovic, PhD, Chair of Organizing Committee, ACUUS Board Member, University of Belgrade – Faculty of Transport and Traffic Engineering, Serbia
2. Nemanja Sipetic, Vice-Chair of the Conference, Associated Research Centres for the Urban Underground Space, Serbia
3. Marko Popovic, Secretary, BBN Congress Management, Belgrade, Serbia
4. Prof. Danilo Furundzic, PhD, Treasury, University of Belgrade – the Faculty of Architecture, Serbia

### Members:

5. Borko Draskovic, Republic Geodetic Authority, Serbia
6. Prof. Dejan Filipovic, PhD, University of Belgrade – Faculty of Geography, Serbia
7. Sasa Milijic, PhD, Institute of Architecture and Urban & Spatial Planning of Serbia, Serbia
8. Marko Stojcic, City Architect of the City of Belgrade, Serbia
9. Prof. Shuilong Shen, PhD, College of Engineering, Shantou University, China
10. Assoc. Prof. Wu Wei, PhD, School of Civil and Environmental Engineering at NTU, Singapore
11. Asst. Prof. Shi Chao, PhD, School of Civil and Environmental Engineering at NTU, Singapore
12. Dragan Veljovic, Lawyer, Serbia

## REVIEWERS

1. Nemanja Šipetić, Associated Research Centres for the Urban Underground Space, Serbia
2. Doc. Filip Filipović, University of Belgrade – Faculty of Transport and Traffic Engineering, Serbia
3. Prof. Ray Sterling, PhD, Vice-Chair, Louisiana Tech University, USA
4. Prof. Bruno Barocca, PhD, Gustave Eiffel University in Paris, France
5. Prof. Takayuki Kishii, PhD Nihon University, Japan
6. Prof. Monika Mitew Czajewska, PhD, Politechnika Warszawska, Poland
7. Prof. Filippo Lambertucci, PhD, Sapienza Università di Roma, Italy
8. Prof. Chris Rogers, PhD, University of Birmingham, United Kingdom
9. Prof. Vojkan Jovičić, PhD, University of Ljubljana, Faculty of Civil and Geodetic Engineering, Slovenia
10. Prof. Oussama Hamal, PhD, University of Rabat, National School of Architecture (ENAM), Morocco
11. Prof. Pavlos Nomikos, PhD, National Technical University of Athens, School of Mining and Metallurgical Engineering, Greece
12. Prof. Andreas Benardos, PhD, School of Mining and Metallurgical Engineering at the National Technical University of Athens, Greece
13. Prof. Wout Broere, PhD, Technische Universiteit Delft, Netherlands
14. Prof. Priscilla P. Nelson, PhD, Colorado School of Mines, USA
15. Prof. Fang-Le Peng, PhD, Tongji University, China
16. Prof. Farah Zaini, PhD, University Malaysia Sarawak, Malaysia
17. Prof. Xiao-Jun Li, PhD, Tongji University, China
18. Prof. Milorad Jovanovski, PhD, Faculty of Civil Engineering, University “Ss. Cyril and Methodius”, Makedonija
19. Božidar Manić, PhD, Institute for Architecture and Urban & Spatial Planning of Serbia, Serbia
20. Michael Mooney, PhD, Colorado School of Mines, USA
21. Yong-Kang Qiao, PhD, Tongji University, China
22. Behnam Atazadeh, PhD, University of Melbourne, Centre for Spatial Data Infrastructures and Land Administration (CSDILA), Australia
23. Giuseppe Pace, National Research Council’s Institute for Research on Innovation and Services for Development Member, Italia
24. Nataša Danilović Hristić, PhD, Institute for Architecture and Urban & Spatial Planning of Serbia, Serbia
25. Ikram Loukili, PhD, Moroccan Researcher in Urban Planning and Sustainable Infrastructure, Collège Boréal in Canada, Morocco / Canada
26. Michael Doyle, PhD, Université Laval School of Architecture in Quebec City, Canada
27. Dexter Hunt, PhD, School of Civil Engineering University of Birmingham, United Kingdom
28. Marija Lalošević, PhD, Institute for Architecture and Urban & Spatial Planning of Serbia, Serbia
29. Yingxin Zhou, Knights Synergy (S) Pte Ltd, Singapore
30. Ilkka Vähäaho, City of Helsinki, Finland
31. Nikolai Bobylev, PhD, Institute of Earth Sciences, Saint Petersburg State University, Russia
32. Yun-Hao Dong, PhD, Tongji University, China
33. Jelena Ninić, PhD, School of Civil Engineering University of Birmingham, United Kingdom
34. Jacques Besner, PhD, Associated Research Centres for the Urban Underground Space, France
35. Sanja Zlatinić, Associated Research Centres for the Urban Underground Space, USA
36. Mark Wallace, ARUP, USA



# CONTENTS

## ARCHITECTURE AND PLANNING - UNDERGROUND

1.1.153.....	16
<b>BRINGING URBAN TRANSPORTATION INFRASTRUCTURE UNDERGROUND</b>	
Petr Pospisil, Bernd Hagenah	
1.2.122.....	26
<b>EXPLORATION FOR UPGRADING OF URBAN UNDERGROUND SPACE PLAN IN CHINA: UNDERGROUND PLAN</b>	
Haoyu Wang, Dongjun Guo, Xingxing Zhao, Jun Huang, Yanhua Wu, Yulu Chen	
1.3.135.....	39
<b>UNIVERSALITY IN DESIGN: USER-CENTRIC METHODOLOGY FOR INFRASTRUCTURE PROJECTS - BRUSSELS EXPERIENCE</b>	
Gordana Micic	
1.4.181.....	48
<b>RESEARCH ON THE DISTRIBUTION, DEVELOPMENT QUALITY AND DRIVING FORCES FOR THE DEVELOPMENT QUALITY OF URBAN UNDERGROUND SPACE IN CHINA</b>	
Jingwei Zhao, Yu Sun, Haoqi Li, Yingge Zhu	
1.5.126.....	63
<b>RESEARCH ON THE IDEAS AND CHALLENGES OF CREATING A WALKABLE PEDESTRIAN NETWORK BY UTILIZING UNDERGROUND SPACE</b>	
Daisuke Fukumoto, Sadayasu Aono, Kentaro Hayashi, Takeshi Hirose, Kazuya Masuyama	
1.6.214.....	69
<b>RESERVOIRS OF ENERGY: A JOURNEY TOWARDS ENERGY AUTONOMY FOR NINE UK EARTH-SHELTERED HOMES</b>	
JERRY HARRALL, Daniel Kastner, Alvaro Garcia, Max Lee	
1.7.223.....	78
<b>BUILDING BELOW: ARCHITECTURE BETWEEN FINANCE AND SUBTERRANEAN FUTURES</b>	
Danilo Furundžić, Dejan Filipović, Nebojša Bojović	
1.8.48.....	92
<b>DEVELOPING A DATA-DRIVEN BAYESIAN NETWORK MODEL FOR LAYOUT PLANNING OF URBAN UNDERGROUND COMMERCIAL FACILITIES</b>	
Yong-Kang Qiao, Ji-Shuai Xiao, Nikolai Bobylev, Fang-Le Peng	
1.9.85.....	104
<b>EXPLORATION OF IMPLEMENTATION PATHWAYS FOR UNDERGROUND SPACE PLANNING IN KEY URBAN AREAS</b>	
Jian Sun, Min Wang	
1.10.186.....	112
<b>PLANNING PUBLIC URBAN UNDERGROUND SPACES: CULTURAL AMENITIES IN BELGRADE'S RIVERFRONT PARK</b>	
Marija Lalošević, PhD, Milica Hadži Arsenović, Ana Jovović	
1.11.203.....	121
<b>EVALUATION AND PLANNING OF UNDERGROUND SPACE RESOURCES IN COMPLEX BUILT -UP ENVIRONMENT FROM THE PERSPECTIVE OF MULTI-DIMENSIONAL VALUES-- TAKING THE CORE AREA OF THE CAPITAL IN BEIJING AS AN EXAMPLE</b>	
Yiting Zhao, Keijie Wu, Xiaodong Shi, Longqin Lin	

1.12.77.....	133
<b>INTEGRATED UNDERGROUND SPACE PLANNING IN BELGRADE: A SMART CITY PERSPECTIVE</b>	
Milena Grbić, Olivera Stanković, Ksenija Lalović	
1.13.6.....	143
<b>SENSITIVE INTEGRATION OF UNDERGROUND SPACES IN HELSINKI'S URBAN FABRIC: FROM GEOLOGY TO ARCHITECTURE</b>	
Laure Bertrand, Cyrielle Rozé	
1.14.191.....	155
<b>ADVANCING UNDERGROUND URBAN SPACE PLANNING: THE POTENTIAL OF FORESIGHT METHODS IN SYSTEMIC PLANNING AND TRANSITION MANAGEMENT</b>	
Nemanja Sipetic, Vladan Djokic	
1.15.128.....	165
<b>INTEGRATED URBAN REGENERATION OF SUBWAY STATIONS AND URBAN DEVELOPMENT IN CENTRAL TOKYO - THE CASE STUDY OF TORANOMON HILLS STATION TOWER</b>	
Maski Kato	
1.16.78.....	175
<b>EXPLORATION OF URBAN DESIGN CONCEPTS FOR UNDERGROUND PUBLIC SPACES IN RENEWAL AREAS: A CASE STUDY OF BEIJING'S UNDERGROUND SPACE CONSTRUCTION</b>	
Lingjun Meng, Yiting Zhao, Kejie Wu, Jing Guo	
1.17.97.....	182
<b>RESEARCH ON UNDERGROUND SPACE IMAGE AND PRACTICE OF THREE-DIMENSIONAL URBAN DESIGN</b>	
Zhou Fang, Huang Zhang, Yifeng Lin	
1.18.177.....	191
<b>OLD MINES AND INDUSTRIAL TOURISM: THE CASE OF AN ANCIENT MINING GALLERY IN LAVRION, GREECE</b>	
Dimitris Kaliampakos, Athanassios Mavrikos, Dimitris Lamprakis	
1.19.100.....	201
<b>CREATING UNDERGROUND SPACE TO IMPROVE THE APPEAL OF THE NIHONBASHI AREA. (THE CASE STUDY ON THE URBAN REDEVELOPMENT PROJECT OF THE NIHONBASHI 1-CHOME CENTRAL DISTRICT)</b>	
Kazuo Kiyama, Katsuya Amemiya	
1.20.41.....	207
<b>MANAGEMENT OF URBAN UNDERGROUND SPACE DEVELOPMENT IN SHANGHAI: EXPERIENCE AND CHALLENGES</b>	
Chen-Xiao Ma, Zi-Jian Li, Fang-Le Peng	
1.21.211.....	219
<b>UNDERGROUND NETWORK IN TOKYO TORCH PROJECT</b>	
Hayato Tsubota, Mokichi Kuribayashi, Hiroshi Ueda, Hiromi Ban	
1.22.112.....	224
<b>STRENGTHENING UNDERGROUND SPACE CONNECTIVITY TO ENHANCE THE EFFICIENCY OF UNDERGROUND SPACE UTILIZATION: A CASE STUDY OF BEIJING PRACTICES</b>	
Qin Chen	
1.23.121.....	232
<b>REGRESSION ANALYSIS OF THE DEVELOPMENT AREA OF UNDERGROUND SPACE IN SHANGHAI</b>	
De-Xin Liu, Lei Zhu, Yuan-Qin Liao	



1.24.113.....	244
<b>INFRASTRUCTURING HERITAGE. NEW PARADIGMS FOR SUBWAY STATIONS IN THE ARCHAEOLOGICAL CENTER OF ROME</b>	
Filippo Lambertucci	

1.25.180.....	255
<b>HISTORICAL UNDERGROUND STRUCTURES OF BELGRADE: IDENTIFICATION, CLASSIFICATION, AND URBAN POTENTIAL FOR SUSTAINABLE CITY DEVELOPMENT</b>	
Nemanja Sipetic, Saša Milijić	

## OVERCOMING CHALLENGES IN TUNNELING AND UNDERGROUND DESIGN AND CONSTRUCTION

2.1.109.....	269
<b>STUDY ON THE INFLUENCE OF MECHANICAL PROPERTIES OF FRC ON THE MECHANICAL PERFORMANCE OF SHIELD TUNNEL SEGMENTS</b>	
Fan Zhang, Wouter De Corte, Xian Liu, Yihai Bao, Luc Taerwe	

2.2.216.....	281
<b>EXPERIMENTAL CHARACTERIZATION OF JET GROUT USING DIGITAL IMAGE CORRELATION TECHNIQUE</b>	
Ksenija Kavarić, Marko Popović, Aleksandar Savić, Sanja Jocković, Milena Raković	

2.3.99.....	288
<b>TOWARDS AN ADVANCED GEOTECHNICAL MODELLING OF BLOCK-IN-MATRIX ROCK FOR ROBUST TUNNEL DESIGN AND CONSTRUCTION</b>	
Ksenija Micić, Novak Joksimović, Miloš Marjanović, Vojkan Jovičić, Jelena Ninić	

2.4.38.....	299
<b>RESEARCH ON THE HIGH-TEMPERATURE MECHANICAL PROPERTIES OF CORRUGATED STEEL-CONCRETE COMPOSITE STRUCTURES IN TUNNEL ENGINEERING UNDER FIRE</b>	
Bo Lei, Wenqi Ding, Qingzhao Zhang	

2.5.32.....	309
<b>CONQUERING CHALLENGES IN THE DESIGN AND CONSTRUCTION OF AN INTEGRATED UNDERGROUND SINGAPORE METRO STATION</b>	
Hooi Leng Phua, Maznah Mohd Ali, Michelle Wu, Anand Kumar Pochambavi Pochambavi, Si Thu Aung	

2.6.50.....	318
<b>UNDERGROUND URBANIZATION AND GEOTHERMAL POTENTIAL IN MODERN INFRASTRUCTURE: THE CASE OF THE MARIBOR CITY TUNNEL</b>	
Vojkan Jovičić, Mitja Pečovnik, Samo Medved, Željko Vukelić, Elvir Muhić, Marko Kosovel	

2.7.146.....	330
<b>EVALUATION OF SEGMENT UPLIFT RISK DURING SHIELD TUNNELLING BASED ON CLOUD MODEL</b>	
Haoze Wu, Shuilong Shen, Annan Zhou	

2.8.105.....	337
<b>EXTRACTION OF INDIVIDUAL ROCK DISCONTINUITIES BASED ON THREE-LAYER CLUSTERING ALGORITHM FROM 3D POINT CLOUDS</b>	
Bingyi Pan, Wei Wu, Yong Huang, Baolin Chen, Hehua Zhu	

2.9.98.....	345
<b>NORWEGIAN METHOD OF TUNNELLING (NMT) FOR SUSTAINABLE USE OF UNDERGROUND SPACE IN URBAN AREAS</b>	
Krishna Kanta Panthi	

2.10.150.....	355
<b>IDENTIFICATION OF KARST CAVES BASED ON MULTI-SOURCES DATA FUSION DURING SHIELD TUNNELLING</b>	
Xin-Hao Min, Yan-Ning Wang, Shuilong Shen	
2.11.31.....	361
<b>HYBRID EARTH RETAINING SYSTEM FOR THE CONSTRUCTION OF AN UNDERGROUND METRO STATION IN VARIED GROUND</b>	
Hooi Leng Phua, Shi Hui Tan, Teck Siew Chin, Seng Hou Lim, Edward Lim	
2.12.114.....	369
<b>CHALLENGES ASSOCIATED WITH PLANNING AND CONSTRUCTION OF A ROAD TUNNEL THROUGH LESSER HIMALAYAN ROCK MASS – A CASE STUDY</b>	
Bimala Piya Shrestha, Krishna Kanta Panthi	
2.13.40.....	380
<b>UNDERGROUND SPACE OPPORTUNITIES AND TUNNELING IN THE PHILIPPINES</b>	
Mark Wallace	
2.14.68.....	397
<b>ENGINEERING GEOLOGICAL ASSESSMENT AND GROUND BEHAVIOR OF TECTONICALLY DISTURBED ROCKS IN NORTHERN THAILAND. A CASE STUDY OF THE PHAYAO RAILWAY TUNNELS</b>	
Supawit Prarom, Pornkasem Jongpradist, Thanet Thongdetsri, Noppadol Phien-wej, Daniel Dias, Sirisin Janrungautai, Damrong Amorndechaphon, Anat Hasap	
2.15.161.....	408
<b>LABORATORY LOADING TEST OF TUNNEL SUPPORT WITH YIELDING ELEMENTS IN ISOTROPIC STRESS FIELD</b>	
Yota Togashi, Takumi Umetsu, Kentaro Nakai, Fumitaka Mizuno, Kazuo Sakai	
2.16.196.....	416
<b>PRELIMINARY NUMERICAL EVALUATION OF RE-USING OIL STORAGE CAVERNS FOR HYDROGEN STORAGE BY USING LINED ROCK CAVERN TECHNOLOGY</b>	
Wenjun Luo, Ping Zhang, Charlie Chunlin Li, Yang Zou, Zongze Li	
2.17.75.....	425
<b>SIMULATION OF THE SOIL BASE OF A BUILDING FOUNDATION NEAR A DEEP PIT</b>	
Ilizar Mirsayapov, Niyaz Aysin	
2.18.120.....	432
<b>GEOPHYSICAL IMAGING OF STOCKHOLM’S SUBSURFACE AT A MUNICIPAL SCALE— IMPLICATION FOR USE AND PLANNING OF ITS UNDERGROUND URBAN SPACE</b>	
Emmanuel Alofe, Mehrdad Bastani, Ari Tryggvason	
2.19.140.....	441
<b>RESEARCH ON SAFE THICKNESS OF ROCK MASS IN NON-COAL STRATUM TUNNEL WITH HIGH-PRESSURE GAS BLAST BASED ON ENERGY METHOD</b>	
Peidong Su, Xingling An, Yuben Du, Peng Qiu, Yougui Li	
2.20.87.....	452
<b>TRIAXIAL STUDIES OF GRAY CLAYS IN DIFFERENT LOADING MODES AS A FOUNDATION FOR UNDERGROUND CONSTRUCTION.</b>	
Irina V. Koroleva	



## UNDERGROUND AND CLIMATE CHANGE: RESILIENCE, SUSTAINABILITY AND URBAN TRANSFORMATION

3.1.147.....	459
<b>CLIMATIC CHANGE INDUCED VULNERABILITY EVALUATION OF URBAN UNDERGROUND SPACES</b>	
Shuilong Shen <sup>1</sup> , Qian Zheng <sup>2</sup> , Annan Zhou <sup>3</sup>	
3.2.158.....	467
<b>LIFE-CYCLE CARBON FOOTPRINT OF UNDERGROUND INFRASTRUCTURE</b>	
Luyuan Long, Wout Broere, Xuehui Zhang	
3.3.16.....	476
<b>THE EVOLVING RESILIENCE OF GLOBAL METRO NETWORKS</b>	
Yun-Hao Dong, Xiao-Wei Luo, Fang-Le Peng, Wout Broere	
3.4.7.....	488
<b>COMBATTING MODERN CITY PROBLEMS WITH THE USAGE OF UNDERGROUND SPACE: THE CASE STUDY OF GREECE</b>	
Dimitrios Papadomarkakis	
3.5.179.....	496
<b>INFLUENCING FACTORS ANALYSIS OF BEARING CAPACITY OF DEEP UNDERGROUND SPACE AND EVALUATION METHODS IN A COASTAL SOFT SOIL MEGA CITY: A CASE STUDY OF SHANGHAI</b>	
Jianxiu Wang, Yanxia Long, Tongzhen Cui, Hanmei Wang, Xinlei Huang, Yuanbo Gao, Jianzhong Wu, Weiqiang Pan	
3.6.213.....	507
<b>HEAT STORAGE UNDERGROUND: A FEASIBILITY STUDY IN ZURICH'S URBAN CORE</b>	
Antonia Cornaro, Jimi Dellenbag	
3.7.58.....	515
<b>LOW CARBON OPERATION AND MAINTENANCE TECHNOLOGIES AND APPLICATIONS FOR UNDERGROUND WASTEWATER TREATMENT PLANTS</b>	
Jun Huang, Hongling Ji, Ao Li, Fan Gao, Wei Gu	
3.8.96.....	533
<b>FLOOD RISK ASSESSMENT AND RESILIENCE STRATEGIES FOR URBAN METROS UNDER EXTREME RAINFALL</b>	
Shuguang Liu, Weiqiang Zheng, Guihui Zhong, Zhengzheng Zhou	
3.9.29.....	543
<b>UNDERGROUND SMALL MODULAR REACTORS FOR DISTRICT HEATING</b>	
Ilkka Vähäaho, Matti Pentti	
3.10.178.....	551
<b>THE ROLE OF UNDERGROUND MINES IN ENERGY TRANSITION: A REVIEW</b>	
Dimitris Kaliampakos, Athanassios Mavrikos	
3.11.162.....	560
<b>HYDROGEOLOGICAL INVESTIGATION AND MONITORING ANALYSIS OF WATER-RELATED HAZARDS IN OPERATIONAL HIGHWAY TUNNELS IN WATER-RICH REGIONS</b>	
Yubo Luo, Junsheng Yang, Qi He, Zhiheng Zhu, Youcai Tan	

3.12.79.....	573
<b>TRANSFORMATIVE APPROACHES TO UNDERGROUND INFRASTRUCTURE: ROAD TO NET ZERO AND BEYOND</b>	
Kelwalee Jutipanya, Lewis Makana, Aryan Hojjati, Nicole Metje, Dexter VL Hunt, Emma JS Ferranti, Anthony J Hargreaves, Joanne M Leach, Christopher DF Rogers	
3.13.160.....	580
<b>BENEATH THE SURFACE: UNLOCKING URBAN GEOTHERMAL POTENTIAL FROM LEGACY SUBSURFACE ASSETS</b>	
Chrysothemis Paraskevopoulou, Antonia Cornaro	
3.14.138.....	589
<b>SUBTERRANEAN URBANISM FOR WILDFIRE RESILIENCE: POST-DISASTER PLANNING AND GIS-BASED DESIGN IN TOPANGA–PALISADES, LOS ANGELES (2025)</b>	
Mohammad Mahdi Safaee, Hoda Hashemi	
3.15.127.....	602
<b>CARBON EMISSION OPTIMIZATION METHOD FOR OPERATING TUNNELS: AN EVOLUTIONARY GAME-BASED ANALYSIS STUDY</b>	
Yumeng Song, Hehua Zhu, Yi Shen, Panfeng Guan, Shouzhong Feng	
3.16.80.....	613
<b>TOWARDS LOW-CARBON TUNNEL ENGINEERING: A COMPREHENSIVE REVIEW OF EMISSION ESTIMATION AND FORECASTING TECHNIQUES</b>	
Caiwei Wang, Mengqi Zhu, Hehua Zhu, Shiqi Dou	
3.17.151.....	628
<b>VULNERABILITY OF METRO SYSTEM DUE FLOODING IN LARGE ASIAN CITIES</b>	
Ya-Jie Wang, Shui-Long Shen, Annan Zhou	
3.18.27.....	635
<b>UNDERGROUND CIRCULATION OF LOGISTICS AS A STRATEGY FOR LAND OPTIMIZATION AND LOGISTICS EFFICIENCY: A CASE STUDY OF DISTRICT LOGISTICS NETWORK IN JURONG INNOVATION DISTRICT, SINGAPORE</b>	
Wang Chung Ngu, Ek Whye Poon, Wang Wei Yang	
3.19.35.....	650
<b>ANALYSIS OF CARBON EMISSION CHARACTERISTICS AND REDUCTION POTENTIAL ON TUNNEL LIGHTING</b>	
Tao Liu, Hehua Zhu, Yi Shen, Weifeng WU, Liankun Xu, Shouzhong Feng	
<b>SAFETY, SECURITY AND HUMAN FACTORS</b>	
4.1.13.....	659
<b>IMPLEMENTATION OF SMART SITE SAFETY SYSTEM AND 5G/IOT IN TUNNEL CONSTRUCTION IN HONG KONG – SOLUTION FOR SAFETY CONSTRUCTION</b>	
Yifeng LI, Zhikai Wei, Joseph Hong, Chao Guan	
4.2.21.....	671
<b>EXPERIMENTAL STUDY ON THE SMOKE SPREADING CHARACTERISTICS OF FIRE IN THE MERGING SECTION OF THE ARCH BIFURCATION TUNNEL</b>	
Yunxiao Xin, Yaqiong Wang	
4.3.36.....	679
<b>EFFECTS OF GUIDANCE FACILITIES ON DRIVING SAFETY IN ROAD TUNNELS DURING FOGGY WEATHER</b>	
Liankun Xu, Hehua Zhu, Ruoquan Fang, Yi Shen, Tao Liu, Shouzhong Feng	

4.4.63.....	687
<b>QUANTIFYING THE RESILIENCE CONTRIBUTION OF UNDERGROUND PEDESTRIAN SYSTEMS FOR SOLAR EXPOSURE RISK REDUCTION IN URBAN HEATWAVES</b>	
Zongchao Gu, Toshihiro Osaragi, Haipeng Zhu, Jiawei Leng	
4.5.33.....	697
<b>THE DYNAMICS OF TRAVELLATORS FOR MOVING PEOPLE IN UNDERGROUND SPACE</b>	
John Zacharias	
4.6.69.....	705
<b>OPTIMIZATION OF TUNNEL VENTILATION SYSTEMS IN FIRE EMERGENCIES</b>	
Andrei Danilov, Vladimir Chizhikov	
4.7.110.....	713
<b>EVACUATION BEHAVIOR AND SAFETY EGRESS ANALYSIS IN TUNNEL FIRES: A VIRTUAL REALITY SIMULATION STUDY</b>	
Vasilis Kotsakis, Christos Froudakis, Anastasios Kallianiotis, Maria Menegaki, Dimitrios Labrakis	
4.8.137.....	728
<b>LIGHT AND HEALTH IN UNDERGROUND PUBLIC SPACES FOR THE WELL-BEING OF ALL</b>	
Marija Jevtic, Gordana Micic	
4.9.119.....	740
<b>ENHANCING PSYCHOLOGICAL HEALTH THROUGH BIOPHILIC DESIGN: THE INFLUENCE OF SEA VIEWS ON UNDERGROUND OCCUPANTS.</b>	
Isabelle Chan, Samuel Twum-Ampofo	
4.10.154.....	749
<b>ADAPTABLE SAFETY CONCEPTS FOR UNDERGROUND RAIL, TRANSIT, AND ROADWAY APPLICATIONS</b>	
Bernd Hagenah, Petr Pospisil	
4.11.83.....	756
<b>AN EXPERIMENTAL STUDY ON VISUAL COMFORT OF TUNNEL PORTALS IN VIRTUAL REALITY ENVIRONMENTS</b>	
Weihao Zhao, Fang Liu, Weijun Kong	
4.12.94.....	765
<b>INFLUENCE OF GEOMETRIC PARAMETERS AND VELOCITY OF VENT ON HEAVY GAS EXHAUST EFFICIENCY IN TUNNELS</b>	
Yuanqing Ma, Tianqi Wang, Ying Zhang, Angui Li	
4.13.65.....	777
<b>HUMAN PERCEPTION EXPERIMENT IN UNDERGROUND SPACE ENHANCED WITH MIXED REALITY</b>	
Mingyi Lin, Fang Liu	
4.14.206.....	784
<b>ROAD TUNNEL SAFETY EVALUATION AND CRASH ANALYSIS: EXPERIENCES FROM SERBIA</b>	
Dalibor Pešić, Krsto Lipovac, Boris Antić, Emir Smailović, Filip Filipović, Nenad Marković, Jelica Šćekić	

## DIGITALIZATION AND AI TOWARD UNDERGROUND SPACE SOLUTIONS

5.1.136.....	794
<b>GEOLOGICAL ASPECTS OF URBAN PERSONAS: A COMPUTATIONAL AI PIPELINE FOR THE MULTIDIMENSIONAL CHARACTERIZATION OF CITY STREETS IN THE PROVINCE OF QUÉBEC.</b>	
Michael Doyle	
5.2.115.....	796
<b>LESSONS FROM BIM AND AI FOR INDOOR ENVIRONMENTAL QUALITY MANAGEMENT: APPLICATIONS TO UNDERGROUND SPACE ENVIRONMENTAL QUALITY RESEARCH</b>	
Samuel Twum-Ampofo, Isabelle Chan, Hao Chen	
5.3.73.....	808
<b>DIGITAL INTELLIGENCE EMPOWERS THE DEVELOPMENT AND UTILIZATION OF UNDERGROUND SPACE IN MEGACITIES</b>	
Fan Yiqun, Zhang Li	
5.4.51.....	820
<b>MODELING OF PUBLIC PERCEPTION IN METRO-LED UNDERGROUND PUBLIC SPACE FOR PLANNING OPTIMIZATION: A CASE STUDY OF HONG KONG</b>	
Qi Pan, Yun-Hao Dong, Fang-Le Peng, Shiu-Tong Thomas NG	
5.5.184.....	831
<b>INTEGRATION OF GEOGRAPHIC INFORMATION SYSTEMS (GIS) FOR UNDERGROUND SPACE MAPPING ON THE EXAMPLE OF BELGRADE</b>	
Luka Krznarić, Staša Milošević, Hristina Jovanović	
5.6.54.....	838
<b>BUILDING A NAVIGATION SYSTEM USING DIGITAL TWINS OF INFORMATION FROM ABOVE AND BELOW GROUND</b>	
Soichiro Takamine, Suguru Miyazaki	
5.7.76.....	844
<b>APPLICATION OF IMPROVED MACHINE LEARNING METHODS TOWARD BETTER ACCURACIES IN PREDICTING TBM PERFORMANCE</b>	
Dansheng Yao, Mengqi Zhu, Hehua Zhu	
5.8.44.....	853
<b>RESEARCH ON DIGITAL MODELING PATH BASED ON IFC EXTENSION AND BIM LIGHTWEIGHT</b>	
Zhaofeng Yang	

## LEGAL, ENTREPRENEURIAL, AND REAL ESTATE ASPECTS OF UNDERGROUND SPACE

6.1.175.....	860
<b>CLASSIFICATION, CONFLICT MAPPING AND CRITICALITY ASSESSMENT OF UNDERGROUND ASSETS: A HOLISTIC APPROACH FOR INFORMED DECISION MAKERS</b>	
Mária Hámor-Vidó, Tamás Hámor, János Kovács	
6.2.3.....	871
<b>A CRITICAL REVIEW OF THE EXISTING METHODOLOGIES FOR THE ESTIMATION OF THE VALUE OF UNDERGROUND SPACE</b>	
Dimitrios Papadomarkakis	



6.3.131.....	882
<b>RESEARCH ON COMPOSITION OF SHOPS IN UNDERGROUND MALL</b>	
Yuto Nakamura, Masaharu Oosawa	
6.4.157.....	890
<b>ANALYZING CONTRACTUAL PRACTICES IN MAJOR UNDERGROUND INFRASTRUCTURE PROJECTS.</b>	
Doris Skenderas, Chrysothemis Paraskevopoulou, Andreas Benardos	
6.5.95.....	901
<b>SUSTAINABLE URBAN REGENERATION THROUGH “BOUNDARYLESS” UNDERGROUND DEVELOPMENT: INTEGRATION OF UNDERGROUND AND ABOVEGROUND, PUBLIC-PRIVATE PARTNERSHIP, AND CONTINUITY FROM PLANNING TO OPERATION - A CASE STUDY OF SHIBUYA, TOKYO</b>	
Taro Fukuda, Kento Yoshino	
6.6.72.....	910
<b>ENHANCING THE DEVELOPMENT OF UNDERGROUND LAND: ISSUES ON LEGAL, SOCIAL AND ECONOMIC ASPECTS</b>	
Ahmad Hamidi Mohamed, Noorfajri Ismail, Kamilah Wati Mohd, Saiful Aman Haji Sulaiman, Noorasiah Sulaiman	

## ADVANCED TECHNOLOGIES AND INNOVATIVE SOLUTIONS

7.1.104.....	923
<b>FORECASTING THE TBM PERFORMANCE USING GREY-STOCHASTIC SIMULATIONS</b>	
Vladimir Krivošić, Luka Crnogorac, Rade Tokalić, Zoran Gligorić, Branko Glušćević	
7.2.123.....	933
<b>MULTI-RISK MANAGEMENT FOR UNDERSEA TUNNEL CONSTRUCTION BASED ON NSGA-III ALGORITHM</b>	
Sihan Liu, Hongwei Huang	
7.3.149.....	942
<b>FLOOD RISK ASSESSMENT USING A LITERATURE-BASED APPROACH</b>	
Wei-Wei Zhao, Shuilong Shen, Annan Zhou, Yanning Wang	
7.4.197.....	948
<b>A MULTI-FIDELITY DEEP OPERATOR FRAMEWORK WITH GENERATIVE ADVERSARIAL NETWORK FOR LOAD PREDICTION AND DISPLACEMENT RECONSTRUCTION OF TUNNEL STRUCTURES</b>	
Chen Xu, Zhen Liu, Ba Trung Cao, Günther Meschke, Yong Yuan, Xian Liu	
7.5.219.....	956
<b>COMPRESSED AIR ENERGY STORAGE (CAES) SYSTEM IN ARTIFICIAL UNDERGROUND CAVERNS WITHIN THE ROCK SALT FORMATION OF MONOLITHI, IOANNINA, GREECE</b>	
Konstantinos Bampousis, Ioannis Vlachogiannis, Andreas Benardos	

## TECHNICAL TRACK (TECHNICAL SESSION)

8.1.9.....	971
<b>APPLICATION OF EMBEDDED FIBER OPTIC IN THE WHOLE PROCESS MONITORING OF CAVERN DEVELOPMENT PROJECT</b>	
Yifeng Li, Zhikai Wei, Joseph Hong, Xuefeng Li	

8.2.39.....	973
<b>RESEARCH ON CARBON ACCOUNTING AND LOW-CARBON CONSTRUCTION PATH FOR A SUPER LARGE CAVERN PROJECT IN HONG KONG</b>	
Yifeng Li, Juntao Yuan, Wei Li, Zhengqiang Hong, Yingxu Huo	
8.3.59.....	992
<b>DEVELOPING A STANDARD FOR GEOLOGICAL SUITABILITY EVALUATION OF URBAN UNDERGROUND SPACE: A CASE STUDY IN BEIJING</b>	
Hanhan He, Jing He, Tongming Fang, Fangzhen Li, Yiting Zhao	
8.4.207.....	994
<b>INTEGRATING “SCAN TO BIM” TECHNOLOGY INTO THE CONSTRUCTION OF A CAVERN PROJECT</b>	
Hing Shing Lok, Yifeng Li, Zhikai Wei, Joseph zhengqiang Hong	
8.5.124.....	997
<b>TRI-DIMENSIONAL SUSTAINABILITY IN URBAN UNDERGROUND TRANSPORT (INTEGRATING ENVIRONMENTAL, GOVERNANCE, AND RESILIENCE IMPERATIVES)</b>	
Ghada Abdulbaqi Al-Ssadah, Mohammed Mokhtar Ali, Yuan Hong, Zoran Đukanović	
8.6.74.....	1008
<b>RESEARCH ON THE PERFORMANCE-DRIVEN SPATIAL INTERFACE DESIGN FOR CLIMATE-ADAPTIVE URBAN UNDERGROUND SPACE</b>	
Kai Zhou, Jia-Wei Leng	
8.7.210.....	1010
<b>RESEARCH OF DRILLING AND BLASTING METHOD BASED ON A SUPER-LARGE CROSS-SECTION CAVERN IN HONG KONG</b>	
Yifeng Li, Juntao Yuan, Zhengqiang Hong, Wei Li	
8.8.57.....	1021
<b>INNOVATIVE PRACTICES AND SUSTAINABLE DEVELOPMENT FOR CAVERN DESIGN AND CONSTRUCTION BASED ON THE Q-SYSTEM AND ROCK REINFORCED APPROACH</b>	
Joseph Z. Hong, Yifeng Li, Zhikai WEI, Xuefeng Li	

## **ARCHITECTURE AND PLANNING - UNDERGROUND**

## BRINGING URBAN TRANSPORTATION INFRASTRUCTURE UNDERGROUND '

Petr Pospisil<sup>1</sup>, Bernd Hagenah<sup>2</sup>

**Abstract:** Bringing urban transportation infrastructure underground brings many benefits, such as creating space for urban development, the reduction of noise and pollution and, thus, a significant increase in the quality of life, but also improving traffic safety and reducing deterioration of roads and rail by harsh environmental conditions. The high investment costs of building new tunnels or covering existing highways and rail lines with lids pay off on the long term, considering e.g., increasing real estate prices in the adjacent neighborhoods, increased productivity and reduced healthcare costs. The main aspects to be considered during the planning process are (1) total investment and operational costs, (2) impact of construction works, (3) safety, and (4) socio-environmental issues. The paper presents some basic planning principles, and experiences from a few projects in Europe and in the US are shared.

**Keywords:** Transportation, Tunnels, Lids, Safety, Environment

### 1. INTRODUCTION

Urban environments, defined by a web of infrastructure, buildings, and bustling activity, grapple with the challenge of harmonizing rapid development and the expectation of streamlined regional mobility with localized quality-of-life concerns, such as multi-modal mobility, access to open space, and public health.

Mass transit projects in many cities worldwide have been built underground and have been operating for more than 100 years, beginning with London underground in 1863, Boston 1898, New York 1904, or Tokyo 1927. The first road tunnels have been built in the US in Pittsburgh (Stowe tunnel, 1909 and Liberty tunnels 1924) and in New York under the Hudson river (Holland tunnel 1927).



*Figure 1. Construction of New York subway in 1900*

<sup>1</sup> Petr Pospisil, M.Sc., EUR ING, HNTB corp., Bellevue WA, USA, [ppospisil@hntb.com](mailto:ppospisil@hntb.com)

<sup>2</sup> Bernd Hagenah, PhD, HNTB corp., New York, USA, [bhagenah@hntb.com](mailto:bhagenah@hntb.com)

With the development of highway systems in the U.S. and other countries after the 1950s, once deemed essential for social and economic progress, urban highways have been built through cities. Unfortunately, that lead to divided urban centers, fragmented or even eradicated communities, and altered historic, cultural, and natural landscapes worldwide. Urban highways often stand as barriers not only in the physical sense but socially and environmentally as well, and lead to elevated noise and poor air quality. The revitalization and reconnection of urban landscapes brings local socio-economic benefits, fosters community cohesion, facilitates accessibility, improves public health, and provides more equitable access to opportunity.

## 2. NOISE

Environmental noise from highways and railways is a widespread yet often underestimated public health issue. Beyond being a nuisance, chronic exposure to elevated noise levels is associated with increased stress, sleep disturbances, and elevated risks of hypertension, stroke, and cardiovascular disease. These effects contribute to both a decline in quality of life and measurable economic impacts through lost productivity and increased healthcare costs.

According to a preliminary analysis based on models of road, rail and aircraft noise in 2020 from the U.S. Department of Transportation, nearly a third of the U.S. population lives in areas exposed to noise levels of above 45 dB which are associated with adverse health effects (USDOT 2023).

Economists who analyzed health care spending and productivity loss because of heart disease and hypertension have argued that a 5 dB reduction in noise could result in an annual benefit of \$3.9 billion in the US (Swinburn et al., 2015).

Studies also show that noise interferes with learning. In the Bronx, NY a classroom facing an elevated railroad he impact of noise extends to cognitive performance. A study in the Bronx, NY found that classrooms adjacent to elevated rail tracks—exposed to noise levels up to 89 dB – experienced lower student achievement compared to quieter classrooms on the opposite side of the building. After installing effective noise control measures that reduced exposure by 8 dB, test performance between the two groups equalized (Bronzaft et al., 1975).

Bringing transportation infrastructure underground, through tunneling or highway lidding, directly reduces ambient noise levels in adjacent communities. These reductions contribute to lower healthcare expenditures, improved learning environments, and enhanced overall urban well-being. In many European countries, noise mitigation requirements serve as a primary justification—and funding mechanism—for such infrastructure, with the responsible authority (often the state) covering costs under environmental compliance frameworks.

## 3. TUNNELING VS. COVERING EXISTING ROADS AND RAIL LINES

Urban planners strive to bring road and rail traffic underground. Many new urban highways and rail lines are built preferably as tunnels, and many existing urban highways have been covered in various countries worldwide. Tunnels are also the most expensive type of transportation infrastructure in terms of investment. Boring new tunnels has usually the lowest impact on the existing structure, except at the portals and shafts, but can be very challenging in an urban area with existing underground infrastructure.

An economically more feasible approach is lower existing roads and railway lines by excavating and covering, or by simply building a lid over existing depressed infrastructure. This reflects the evolving needs of urban societies, prioritizing human-centric design, environmental consciousness, and holistic urban planning.



**Figure 2.** Building a Highway lid (A7 Stellingen, Hamburg, Germany)



When considering existing highways, the existing physical conditions and length of coverage needed can dictate whether a tunnel or lid may be most feasible or cost-effective. The driving force behind both lidding and tunneling is to address the often-divisive impact of highways and reintegrate disjointed urban spaces, striving for cohesion and unity. Lids can bear a diverse range of loads, e.g., lush green parks, dynamic recreational zones, or foundational supports for buildings, residential housing or vital public infrastructure.

#### 4. BENEFITS FOR THE CITY

Bringing transportation underground has many benefits:

- **Connecting Divided Areas:** Lidding projects reunite neighborhoods and areas previously separated by motorways or rail lines, fostering greater community cohesion.
- **Maximized Land Use:** In densely populated urban settings, where land is at a premium, lids provide additional space, effectively turning air rights into usable real estate. This can pave the way for diverse developmental projects without further land acquisition.
- **Recreational and Green Spaces:** Parks, playgrounds, and open spaces on lids offer residents accessible open space and green infrastructure in otherwise densely developed urban environments, promoting physical health and mental well-being.
- **Diverse Infrastructural Opportunities:** The strength and versatility of these lids allow for a range of structures to be built atop them. The possibilities are expansive, from parks and recreational spaces to commercial establishments, residential buildings, parking lots and public amenities.
- **Economic Boost and Investment Opportunities,** leading to public-private partnerships that can offset some of the costs of lidding projects.
- **Job Creation:** Construction, maintenance, and the businesses that emerge on these lids generate employment opportunities, contributing positively to the local economy.
- **Increased Property Values:** Adjacent areas often see a surge in property values due to reduced noise emissions and increased quality of life.
- **Multi-Modal Corridors:** With regional through-traffic tucked below the lid, there is ample space for multi-modal corridors to accommodate safe and equitable mobility options such as pedestrian pathways, protected bike lanes and dedicated transit-ways, in addition to the potential for low-speed vehicular traffic.



*Figure 3. Klyde Warren Park (Dallas, TX, USA)*

- **Reduction of Noise Pollution:** The lid shields the highway or rail noise effectively from the environment. This results in quieter neighborhoods, reduced healthcare costs, higher productivity and improved overall well-being for residents. Modern lid designs often incorporate materials that reduce noise in the portal areas and in open stretches.

- **Improved Air Quality:** A lid improves the air quality by shielding the neighborhood from road emissions. Natural ventilation induced by the moving traffic is sufficient for diluting pollutants below admissible threshold levels inside the tunnel and in portal areas. Only for very long highway tunnels, adequate ventilation measures such as portal exhaust and filters may be evaluated to improve air quality in the portal regions (Pospisil, 2020).
- **Urban Heat Island Effect Mitigation:** Plants and trees on the lids can reduce the urban heat island effect, a phenomenon where urban areas experience higher temperatures than their rural surroundings. Vegetation provides shade and releases moisture, naturally cooling the surrounding area.
- **Urban Ecosystems:** Lids landscaped with diverse flora can attract and sustain various fauna, essentially becoming urban biodiversity hotspots. Strategically placed green lids can act as corridors or bridges for urban wildlife, reducing the risk of road deaths and promoting ecological connectivity.
- **Managing Flash Storms:** Incorporating green infrastructure elements, such as permeable surfaces and bioswales, plays a vital role in managing the challenges of flash storms. Flash storms can overwhelm conventional drainage systems, leading to urban flooding. However, highway lids designed with permeable surfaces allow rainwater to infiltrate naturally, reducing rapid runoff. Bioswales, in turn, aid in the filtration and absorption of rainwater, enhancing water quality while lessening the burden on stormwater systems.

## 5. BENEFITS FOR MOTORISTS AND ROAD OWNERS

Focusing on roads and highways, bringing transportation infrastructure underground also brings substantial benefits for the road users and owners. Road tunnels and lids provide a safer and more sustainable route than open roads. According to statistical data, the accident rate in tunnels is lower than on open roads. Drivers are shielded from distraction and unfavorable environmental conditions, for instance, sun glare, rain, and ice. Moreover, tunnels prevent collisions by eliminating conflicts with pedestrians and animals crossing.

Shielding from harsh environmental conditions also protects the roadway structure. The lifetime of tunnels is usually longer than that of other infrastructure, such as bridges, and roadway surfaces need to be renewed less frequently than on open roads.



*Figure 4. Inside a highway tunnel*

## 6. KEY CONSIDERATIONS

While offering substantial advantages, highway lidding is complex and demands meticulous planning and foresight. Ensuring the success and longevity of such projects requires addressing a range of technical, financial, environmental, and social considerations (Theis et al., 2024).

The main purpose of the highway, to provide a safe road connection, must not be impaired by the lid construction. Lane and shoulder widths should be maintained.

During the planning stage, it is critical to determine the planned use of the lid, both in terms of initial intended use and any longer-term anticipated use. One of the foremost considerations is ensuring the lid can support the intended structures or greenery above while allowing safe passage for vehicles below. The use of the tunnel is a driving factor in establishing the appropriate dead loads and superimposed loads for which the lid and supporting structure must be designed for. Careful selection of the loading criteria in the planning stage allows for eventual flexibility where it may be needed in the future.

Managing rainwater drainage, snow loads, and other weather-related challenges is pivotal to the lid's longevity and functionality. Structural durability and minimizing future maintenance are core concerns of all transportation authorities. Urban lid projects provide new challenges with regard to structural detailing to maximize service life. With lids more prone to freeze-thaw cycles than deeper tunnels, proper drainage design becomes paramount. In addition to sloping a lid to maintain a minimum pitch to drain, a lid cross-section should include well-draining fill materials, drainage layers, and waterproofing membranes.

Lidding projects demand significant upfront investment. Determining sources of funding – public, private, or a combination – is crucial. Beyond the initial construction, regular inspection, testing and maintenance, energy consumption mainly for tunnel lighting, and occasional repair works and replacement of equipment, needs to be considered for Life Cycle Costs. To justify those costs, assessing the potential return on investment through increased property values, business opportunities, reduced healthcare costs, and other economic boosts need to be considered.

Regulatory and Legal Hurdles can be cumbersome. Especially in densely populated urban centers, navigating the intricacies of land ownership, air rights, and zoning regulations is a fundamental step. Large-scale projects typically require a plethora of permits and approvals from various municipal and state agencies, necessitating careful coordination.

Understanding the potential environmental impacts, including on local ecosystems and water tables, is essential. Soliciting feedback and buy-in from local communities ensures that the resultant development aligns with their needs and aspirations. In areas with historical or cultural significance, the design and execution of lidding projects must be approached with sensitivity.

The very nature of highway lidding means working over or near active traffic lanes. This necessitates understanding and managing the potential disruptions. While some disruptions might last just a few hours or days, others could span weeks or even months. An understanding of the timeframes is essential for planning. To minimize disruptions, significant construction activities might be scheduled during off-peak hours or weekends when traffic volumes are lower. Temporary ramps, bridges, or lanes might need to be constructed to manage traffic flow during the lidding process. Traffic might need to be rerouted. Effective communication to the public is crucial to prevent confusion and congestion.



*Figure 5. Residential development over highway (A3 Altendorf, Switzerland)*



## 7. SAFETY

Collisions impose the most significant risk to drivers on roads. Fires in road tunnels happen less often than collisions but may impose a serious hazard to road users when they get trapped in the smoke inside the enclosed underlying structure. A fire with an extraordinary heat release rate, e.g., burning Flammable Liquid Cargo (FLC), is highly unlikely, but might result in substantial damage and even partial collapse of the lid structure.

The probability of a collision or fire hazard on a defined road section directly correlates to its length and traffic load. Usually, the collision risk in tunnels is lower than on open roads, and the probability of collisions is a magnitude higher than that of vehicle fires. To a large part, the operational risk is related to driver behavior and vehicle conditions, which can only partly be influenced by safety measures on the road infrastructure.

Preventive safety measures are most effective and need to be prioritized (Pospisil, 2011). For road tunnels, such safety measures are:

- Road alignment, considering traffic density, line of sight, lane and shoulder width.
- Most urban highway lids provide unidirectional traffic, with a separation wall between roadways.
- Enforced speed limit adequate to sight distance and traffic conditions.
- Traffic management with signals and barriers for lane or tunnel closures.
- Traffic management in the adjacent road network.
- Tunnel lighting, which is directly related to the allowed speed and sight distance

Since the atmosphere in the tunnel can be wet and corrosive, and adequate protection of the tunnel structure and equipment from corrosion and regular inspections are essential.



*Figure 6. Lane control signs and variable message signs at tunnel portal*

Fire Life Safety measures in road tunnels may include:

- Emergency exits in short distances
- Smoke and fire detection
- Public Addressing System
- Structural fire protection and/or active fire suppression systems, depending on a risk assessment and expected costs for tunnel closure and refurbishment after a large fire.
- Standpipes with fire department connections and fire fighting water supply.
- Longitudinal tunnel ventilation with flow control for smoke management (Pospisil, 2020)
- For very long tunnels with high probability of congestions and rear-end accidents, additional point smoke exhaust by controllable dampers in short intervals may be adequate.

All tunnel systems must be maintained and regularly tested, to ensure reliable function when required.

A critical planning factor is ensuring that emergency services can quickly reach any point on or beneath the lid. Designing clear, accessible egress and ingress routes for scenarios like vehicle breakdowns, accidents, or fires beneath the lid is paramount.

For rail tunnels, the risk resulting from collisions or fires is much lower than on roads. Focus is on preventive measures, train control systems, and facilitating safe evacuation of large numbers of passengers in case of a stalled train or any other emergency, with or without fire. Unlike mountain tunnels in stable geological conditions, lids may collapse due to an explosion or a catastrophic fire incident. Very large fires resulting from freight trains are highly unlikely, but may be considered for potential fire protection measures.

Big data are used to determine quantitative indicators for operational risks, using primarily statistics about accidents and fires on roads and rails. Such statistical data provide input for the event tree development for quantitative risk analysis (QRA). Big data analysis is also applied to evaluate reliabilities and failure rates of specific equipment, which needs to be considered in the QRA event trees. QRA is an important tool for decision making on effective safety systems.

## 8. SUSTAINABILITY

Transportation lidding projects present a unique opportunity to champion sustainable construction methodologies that prioritize the environment, which in turn benefits the local community.

A key component of this eco-friendly approach is material selection. Projects can substantially reduce their environmental footprint by prioritizing recycled construction materials or locally sourced ones.

The primary construction material is concrete, the production of which requires a high energy demand. Therefore, reducing the amount of concrete by optimizing the lid concept directly reduces the ecological footprint. An example of such a measure is to provide longitudinal ventilation instead of transversal ventilation, which would require ventilation ducts and fan buildings, as in older tunnels. With longitudinal ventilation, the fans rarely need to be in operation. Transversal ventilation would bring about massive energy consumption because it slows down the natural ventilation induced by the piston effect of moving vehicles.

Energy efficiency extends beyond the completed project; it begins during construction. Using green machinery powered by electricity or more energy-efficient ones can dramatically curb emissions during the construction phase. Moreover, by optimizing transportation and logistics, materials can be moved more efficiently, reducing fuel consumption and the associated environmental impact.

Waste management is another crucial facet. Emphasizing the reduction of waste at its source and facilitating the recycling of construction debris might reduce landfill contributions. Moreover, ensuring the responsible disposal of hazardous waste in adherence to environmental guidelines safeguards both the environment and the community.

The integration of nature into highway lidding projects serves multiple purposes. Green roofs and vertical gardens enhance aesthetic appeal and offer functional benefits like improved insulation, stormwater management, and air quality enhancement. Considering the global push towards renewable energy, including solar panels or photovoltaic cells in the lid's design can transform these structures into hubs of clean energy generation.

Water, a resource growing scarcer in many regions, must be used judiciously. Employing sustainable water use practices during construction, such as rainwater harvesting, can ensure this vital resource is conserved. Furthermore, designing sections of the lid with permeable surfaces can play a pivotal role in groundwater recharge and effective stormwater management.



**FIGURE 7.** Railway lid with train station (Opfikon, Switzerland)

## 9. EXAMPLES

Examples for new tunnels that successfully replace existing urban highways:

- Madrid M30 ring road tunnels, Spain
- Boston Central Artery, US
- Munich middle ring road tunnels, Germany
- Nordtangente Basel, Switzerland
- Seattle SR99 Alaskan Highway tunnel, US
- Tunnel Blanka, Czech republic
- Stockholm West Bypass, Sweden (under construction)



*Figure 8. Glazed portal section of Petueltunnel, Munich, Germany*

Examples of urban highway lid projects:

- Klyde Warren Park, Dallas, US
- Ueberdeckung Schwamendingen, Switzerland
- A7 lids, Hamburg, Germany



*Figure 9. Einhausung Schwamendingen, Zürich, Switzerland*



A prominent example of covering a railway yard is the Hudson Yards projects in New York City.



**Figure 10.** Hudson Yards, New York, USA

## 10. CONCLUSION

Highway lidding and tunneling are a component of the larger urban fabric and should integrate seamlessly with other urban revitalization efforts. This may include connecting lidded areas with pedestrian-friendly zones, creating green corridors that link parks, or designing multi-modal transport hubs that enhance mobility. Integrating these progressive highway projects with initiatives like urban farming, community gathering spaces, or cultural hubs can create vibrant, multifunctional spaces that truly revitalize urban landscapes.

The most significant challenge for highway lidding projects is securing adequate financing. While the initial capital costs are substantial, the long-term economic and societal benefits provide multiple return of investment.

In Europe, the owner of the highway or railway line is responsible to comply with environmental requirements, in particular noise protection. This obligation can be used to finance tunnel and lid projects. In contrast, in the US, highway owners, which are the state DOTs, mostly refuse any contribution to such projects, and the affected cities lack of adequate funds. A solution may be to involve private funding, for instance in the form of public-private partnerships. The generated revenue can offset a significant portion of the construction costs by offering commercial development rights atop or around the lidded sections. Another avenue is leveraging land value capture mechanisms, where the increase in land and property values resulting from the project can be channeled back into financing the project itself.

With improved air quality and reduced noise pollution, there's potential for significant savings in public healthcare costs. Reduced respiratory issues, mental health benefits and lower stress levels can lead to substantial taxpayer savings. An argument can be made for redirecting a portion of these savings back into the project. A model where future healthcare savings are projected, and a fraction is earmarked for lidding projects can be explored.

Construction disruptions represent another challenge. Building a lid over an active highway significantly affects traffic operations and generates noise and dust from the construction, affecting neighboring areas. A staggered construction schedule can minimize traffic disruptions. Many highway lids were built even over ongoing traffic as far as possible. On the other side, the longer the construction period, the greater the inconvenience to the public and potential economic losses due to traffic delays. Implementing night-time construction, offering alternative routes, or providing incentives for off-peak travel can minimize disruptions. Advanced construction techniques, like prefabricated sections or off-site construction, can speed up the on-site assembly process. Tunnel systems should be pre-assembled and tested as far as possible before being installed in the tunnel to minimize commissioning and testing time. Effective communication with the public, perhaps through digital platforms providing real-time updates, can help manage expectations and reduce frustrations.

## 11. BIBLIOGRAPHY

- [1] Bronzaft, A. L., & McCarthy, D. P., The Effect of Elevated Train Noise On Reading Ability. *Environment and Behavior*, 7(4), 517-528, 1975
- [2] PIARC 2008R15, Urban Road Tunnels, Recommendations to Managers and Operating Bodies for Design, Management, Operation and Maintenance.
- [3] PIARC 2023R26, Improving Road Tunnel Resilience, considering Safety and Availability.
- [4] Pospisil P, Reducing Costs and Improving Safety of Road Tunnels, 2011
- [5] Pospisil P., Road Tunnel Ventilation, Compendium and Practical Guidelines, 2<sup>nd</sup> ed., 2020
- [6] Swinburn TK, Hammer MS, Neitzel RL. Valuing Quiet: An Economic Assessment of U.S. Environmental Noise as a Cardiovascular Health Hazard. *Am J Prev Med*. Sep; 49(3):345-53, 2015
- [7] Theis K., Hagenah B., Pospisil P., Lauzon C., Reconnecting Urban Landscapes through Highway Lidding and Tunneling: A Comprehensive Study on Methodologies, Benefits, and Safety Considerations, North American Tunnel Conference, Nashville TN, 2024
- [8] USDOT. Reconnecting Communities Pilot (RCP) Grant Program Fact Sheet, access 2023

## EXPLORATION FOR UPGRADING OF URBAN UNDERGROUND SPACE PLANNING IN CHINA: UNDERGROUND PLAN

Haoyu Wang<sup>1</sup>, Dongjun Guo<sup>2</sup>, Xingxing Zhao<sup>3</sup>, Jun Huang<sup>4</sup>, Yanhua Wu<sup>5</sup>, Yulu Chen<sup>6</sup>

**Abstract:** Multiple major resources exist below the ground: space, water, geothermal energy, geomaterials and so on. While the necessity of using multiple underground resources (MURs) has been extensively studied. However, most Chinese cities develop the underground space plan lacking examinations assessing the interaction relationship of MURs, which hinders the policy making and planning formulation of MURs synergistic utilization. It is proposed that the urban underground space plan should be upgraded to plan MURs, that is to say underground plan. The need for the transformation and upgrading of underground space plan in China is discussed, and the types and systems of underground space plan and its related plan are analyzed. Finally, the orientation and the major components of future underground plan are put forward. This research work provides a sound understanding of MURs synergistic utilization mechanism, which is supposed to be conducive to the sustainable utilization of MURs and the formulation of MURs plan.

**Keywords:** Urban underground space plan, Underground plan, Upgrading, Multiple underground resources

### 1. INTRODUCTION

Underground space, recognized as the 'Fourth Territory' beyond a nation's land, airspace, and territorial waters, represents an emerging natural resource for urban development and a crucial strategic national asset. With contemporary urban growth constrained by existing ground-level environments, pre-existing structures (buildings and infrastructures), and finite spatial resources, the utilization of urban underground space is garnering increasing attention [1-3]. However, the academic community has gradually realized that multiple resources exist below the ground: space, water, geothermal energy, and geomaterials [4-6], as shown in Table 1. Conceptually, these resources are intrinsically interconnected within a unified underground environment. Singular resource utilization often adversely impacts the exploitation potential of others, creating conflicts, such as underground constructions forming groundwater cut-off walls that obstruct natural aquifer flow paths [7], and challenges in managing spoil from underground excavations [8]. Current underground space planning frameworks predominantly emphasize functional service domains—such as urban transportation, municipal infrastructure, and commercial facilities—while insufficiently integrating the utilization of groundwater, geothermal energy, and geomaterial resources [9,10]. China's 'Dual Carbon' goals and urban renewal initiatives now mandate transformative approaches to underground development, explicitly requiring rational groundwater utilization, geothermal resource exploitation, and construction spoil recycling. Consequently, China's urban underground space development must transition from

<sup>1</sup> PhD, Wang Haoyu, Underground Space, Research Center for Underground Space, Army Engineering University of PLA, Nanjing, 210007, China, [wangh2000yu@qq.com](mailto:wangh2000yu@qq.com)

<sup>2</sup> Prof., Guo Dongjun, Underground Space, Research Center for Underground Space, Army Engineering University of PLA, Nanjing, 210007, China, [guo\\_dongjun@163.com](mailto:guo_dongjun@163.com)

<sup>3</sup> Dr, Zhao Xingxing, Underground Space, Research Center for Underground Space, Army Engineering University of PLA, Nanjing, 210007, China, [zxx\\_hqu@163.com](mailto:zxx_hqu@163.com)

<sup>4</sup> Prof., Huang Jun, Underground Space, JSTI GROUP, Nanjing, 210094, China, [hj130@jsti.com](mailto:hj130@jsti.com)

<sup>5</sup> Lect., Wu Yanhua, Underground Space, Research Center for Underground Space, Army Engineering University of PLA, Nanjing, 210007, China, [yanhua\\_wu@foxmail.com](mailto:yanhua_wu@foxmail.com)

<sup>6</sup> Lect., Chen Yulu, Underground Space, College of Civil Engineering and Architecture, Huanghuai University, Zhumadian 463000, PR China, [yulu2167@163.com](mailto:yulu2167@163.com)

high-speed growth to quality-driven advancement—shifting from the utilization of single resource toward the synergistic utilization of MURs. To achieve this aim, underground space planning should be upgraded to the MURs planning, that is, underground planning.

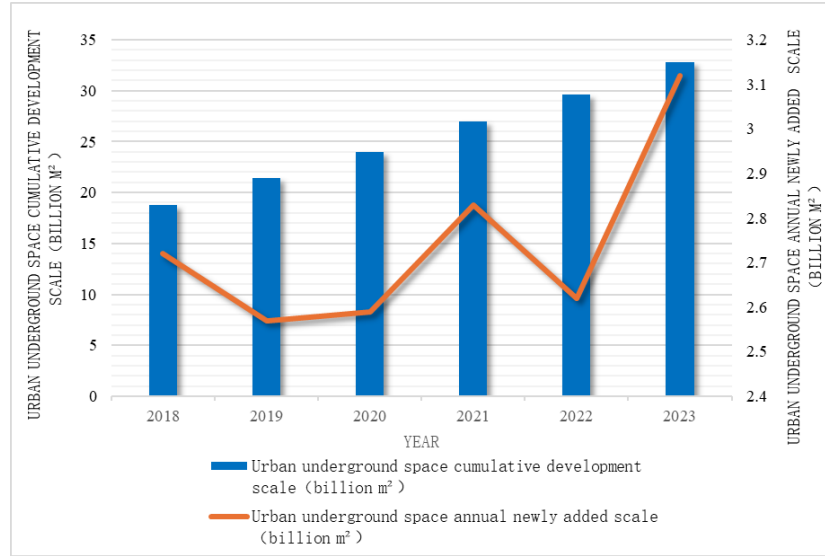
**Table 1.** Descriptions and Value of multiple major resources that existed below the ground <sup>[11-15]</sup>.

Type	Descriptions	Value
Underground space	The underground space is naturally or artificially excavated, remains unexploited, and has the potential to be developed under existing technological conditions.	The use of underground space could alleviate traffic jams and land shortages.
Geothermal energy	Geothermal energy refers to the thermal energy contained in rock-soil mass below the ground.	Geothermal energy is a crucial renewable energy source for constructing energy systems and reducing carbon emissions.
Groundwater	Groundwater is the water reserved in rock and earth mass fractures or holes below the ground.	Important part of water, constitutes half of the world's residential water and approximately 25% of agricultural irrigation water, and used for 38% of the world's irrigated land.
Geomaterials	Geomaterials refer to the useful materials excavated from below ground such as rock, soil, etc.	Effectively using geomaterials helps improve the environment and reduce waste.

## 2. MOTIVATIONS FOR PLANNING MURS IN CHINA

### 2.1. Intensive utilization of MURs

Driven by China's rapid urbanization and technological advancements in underground resource utilization, including ground-source heat pumps (GSHP), tunneling shields, and spoil recycling, urban underground resource exploitation has undergone accelerated development, exhibiting distinct scalability. For underground spatial resources, China's annual growth rate averaged nearly 20% from 2018 to 2023, with cumulative construction reaching 3.276 billion m<sup>2</sup> by end-2023; newly added underground space in 2023 alone approximated 312 million m<sup>2</sup>, accounting for 21.8% of total urban construction completions (see Figure 1 for cumulative and annual development) <sup>[16-20]</sup>. Regarding geothermal resources, China possesses abundant shallow geothermal reserves with utilization leading globally—by 2021, its geothermal heating/cooling capacity hit 1.33 billion m<sup>2</sup>, maintaining the world's largest direct-use scale for years <sup>[21]</sup>. For groundwater, despite stringent controls reducing supply from a 2012 peak of 113.2 billion m<sup>3</sup> to 81.95 billion m<sup>3</sup> in 2023, it still constituted 13.9% of national water supply <sup>[22-24]</sup>, alongside enhanced regulatory frameworks. In geomaterials, Shenzhen exemplifies scale: engineering spoil and slurry reached 81.08 million tonnes in 2023 (≈90% of construction waste, with its Construction Waste Management Plan mandating 40.7 million m<sup>3</sup>/year silt-separation capacity and 52.83 million m<sup>3</sup>/year eco-sintering capability <sup>[25]</sup>. This large-scale utilization establishes the foundation for planning MURs.



**Figure 1.** Schematic diagram of cumulative development scale and annual newly added floor scale of urban underground space in China (2018-2023)

## 2.2. Interactions among MURs

### 2.2.1. Underground space and water

Numerous studies and engineering practices have demonstrated interactions between underground space and groundwater [6,7,26-28]. The impact of underground space on groundwater primarily arises when underground engineering penetrates or traverses aquifers, forming cutoff walls that obstruct groundwater flow paths while contacting groundwater. This leads to structural corrosion, alterations in groundwater levels, and contamination [6,10,26]. Conversely, the impact of groundwater on underground space mainly stems from rising water levels due to groundwater protection or reduced groundwater extraction, thereby modifying the operational environment of underground structures originally constructed above the water table [6,28]. This compromises engineering performance and induces incidents such as sand boiling and structural failures. Specific cases and related research are detailed in Table 2.

**Table 2.** The cases and studies of the interactions between underground space and groundwater.

Type	Description of case and study	Site
Underground space to groundwater	underground space development in the Xiong'an New Area will result in the expansion and deepening of depression cones within aquifers. Groundwater levels on the upstream side of underground structures will rise, while those on the downstream side will decline, with the maximum observed water table increase reaching 7.17 m [26].	Baoding, Hebei.
Underground space to groundwater	The Chengdu University of TCM & Sichuan Provincial People's Hospital Station documented groundwater level alterations over five years post-construction, with the hydraulically upstream side exhibiting approximately 0.8 m of backwater elevation and the downstream side registering circa 0.5 m of drawdown [27].	Chengdu, Sichuan
Groundwater to underground space	The inter-tunnel section of Beijing's Jianguomen Station Metro experienced sand boiling phenomena in its foundation due to groundwater level rebound [28].	Dongcheng District, Beijing.

### 2.2.2. Underground space and geothermal energy

The interactions between underground space and geothermal energy primarily depends on the type of geothermal utilization facility. For ground source heat pump (GSHP) systems, their interplay manifests predominantly as spatial interference between underground structures and ground heat exchangers [15]. For groundwater source heat pump (GWHP) systems, the interaction chiefly arises from aquifer disruption caused by underground space development, which alters groundwater levels and consequently impacts GWHP operational

efficiency <sup>[29]</sup>. Regarding energy geostructures, their synergy is characterized by direct integration within underground engineering frameworks, enabling geothermal harnessing without occupying additional space <sup>[30]</sup>. Specific case studies are detailed in Table 3.

**Table 3.** *The cases of the interactions between underground space and geothermal energy.*

Type	Description of case	Site
Underground space to GSHP	During the construction of Xuzhou Metro Line 1, the project encountered interference from pre-existing GSHP systems. This resulted in the demolition and reconstruction of the affected geothermal systems <sup>[31]</sup> .	Xuzhou city, Jiangsu
Underground space to energy geostructure	In the Shanghai Foxconn Tower project, GSHP pipes were installed within the diaphragm walls forming the foundation pit support structure, creating integrated "Energy Walls." The pipes were embedded at depths of approximately 37 meters, with a pair of U-tubes installed at 1.5-meter intervals, totaling 204 loops <sup>[30]</sup> .	Pudong new area. Shanghai

### 2.2.3. Underground space and geomaterials

The advancement of spoil valorization technology has revolutionized underground construction by enabling the recycling of excavated rock and soil materials for reuse in subgrade formation, landfill site stabilization, and ceramics manufacturing <sup>[29]</sup>, while simultaneously facilitating the repurposing of subterranean voids created during material extraction into functional underground spaces <sup>[10]</sup>. Representative cases are detailed in Table 4.

**Table 4.** *The cases of the interactions between underground space and geomaterials.*

Type	Description of case and study	Site
Underground space to geomaterials	The Haishu District Duantangzhong Road Project in Ningbo utilized dredged sludge and silty clay soils from engineering spoil as primary raw materials for roadbed filler, with the recycled spoil constituting approximately 92% of the final product's composition by weight and supplementary additives accounting for the remaining 8% <sup>[32]</sup> .	Ningbo, zhejiang
Geomaterials to underground space	three underground reservoirs were constructed with a total storage capacity of 7.105 million m <sup>3</sup> , achieving a daily reinjection rate of approximately 9,790 m <sup>3</sup> of treated mine water in the Daliuta Coal Mine within Shendong Mining Area <sup>[33]</sup> .	Yulin, shanxi

### 2.2.4. Geothermal energy, groundwater and geomaterials

Conceptually, the interactions between geothermal energy and groundwater utilization primarily stems from the fact that both resource exploitation activities require water resources. Different types of geothermal energy utilization facilities are subject to distinct impact mechanisms. For ground-source heat pump systems, groundwater extraction leads to a decline in the utilization efficiency of GSHP but does not render them inoperable, whereas for GWHP, groundwater extraction causes a drop in the water table, thereby resulting in an inability to extract groundwater for heat extraction and ultimately rendering them inoperable.

Conceptually, the existence of both geothermal energy and groundwater is intimately linked to underground rock and soil formations. Geothermal energy utilization requires heat extraction from geological media such as rocks, soil, and water, while groundwater resides within underground sediments and rock matrices. Excavation of underground rocks or soils fundamentally alters the geological substrate, causing both geothermal resources and groundwater to cease to be recoverable due to the destruction of their natural hosting environments.

In summary, both the scaled-up utilization of China's underground resources and the interactions among these resources will lead to increasingly pronounced conflicts in engineering practices while simultaneously amplifying the demand for coordinated resource management. Consequently, an integrated planning framework for the MURs becomes imperative.



### 3. PROJECTS FOR USING MURS

#### 3.1. Underground space use and geothermal energy

China has now implemented multiple projects demonstrating synergistic utilization of underground space and geothermal energy. A flagship example is the Beijing Daxing International Airport, completed in 2019, which features two underground levels accommodating high-speed rail, metro, and intercity railway transfers alongside commercial and dining services. For geothermal exploitation, the airport hosts China's largest GSHP system, enabling it to achieve 10% renewable energy utilization—a key sustainability target. This system serves 2.57 million m<sup>2</sup> of space through two energy stations and 10,497 borehole heat exchangers (BHEs), with their layout illustrated in Figure 2. Annually, it extracts 303.2 terajoules (TJ) of shallow geothermal energy, saving 12.25 million m<sup>3</sup> of natural gas—equivalent to 14,873 tonnes of coal—while reducing carbon emissions by over 24,900 metric tonnes [34-37].

Similarly in Beijing, the Dongliuhuan (Jingha Expressway-Luyuan North Street) Renovation Project completed in April 2025 transformed conventional shield tunnels into energy tunnels by integrating heat exchange pipes within the invert segments (Figure 3). This dual-functional infrastructure simultaneously bears surrounding rock loads and extracts geothermal energy. The 800-meter energy tunnel section meets heating/cooling demands for 1,226.3 m<sup>2</sup> of buildings in the South Administration Zone while providing winter de-icing for approximately 40 meters of the F6 ramp roadway [38,39].

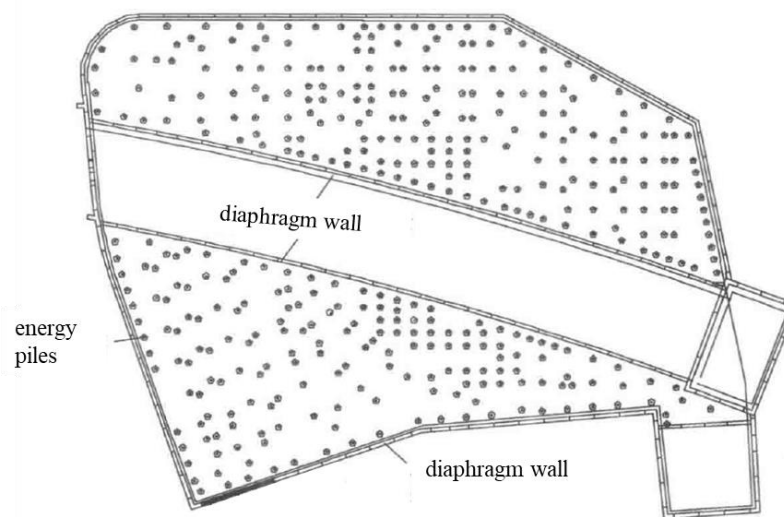
In Shanghai, the Natural History Museum (New Wing) opened in 2015 occupies a 12,000 m<sup>2</sup> site with a total floor area of 45,275 m<sup>2</sup>. The 18-meter-tall structure comprises three above-ground levels and two basement levels. This project employs energy geostructures through heat exchange pipes embedded in bored piles and diaphragm walls (Figure 4). The ground-source heat exchanger system delivers peak cooling and heating capacities of 1,639 kW and 1,178 kW respectively. Although the initial investment for this geothermal system exceeded that of a conventional chiller-boiler setup by ¥2.102 million, it achieves annual operational savings of ¥223,000 with a dynamic payback period of 11.98 years. The system reduces coal consumption by 117.7 tonnes of standard coal equivalent annually while cutting CO<sub>2</sub> emissions by 195.5 tonnes [31,40].



**Figure 2.** Schematic Diagram of Geothermal Borehole Layout at Beijing Daxing International Airport [35]



**Figure 3.** Construction Site of the Snow-Melting and De-Icing Section in the Energy Tunnel <sup>[39]</sup>



**Figure 4.** Schematic Diagram of Geothermal Pipe Embedding in Cast-in-Situ Piles at Shanghai Natural History Museum <sup>[31]</sup>

### 3.2. Underground space use and geomaterials

Nanjing's Southern New District, situated south of the old city beyond Zhonghuamen Gate, spans the tri-junction of Qinhuai, Jiangning, and Yuhuatai districts adjacent to Nanjing South Railway Station. This Tier-1 priority development zone—one of Nanjing's four core urban hubs—covers a planned area of 19.8 km<sup>2</sup> with a 9.94 km<sup>2</sup> central nucleus. Its underground space development totals approximately 4.8 million m<sup>2</sup>, with subterranean construction accounting for ~35% of above-ground floor area <sup>[41,42]</sup>. The district pioneer's construction waste resource recovery in municipal projects, targeting 2.2 million m<sup>3</sup> of spoil recycling. This initiative reduces diesel consumption by source, cutting CO<sub>2</sub> emissions by approximately 19,000 tonnes <sup>[43]</sup>. Figure 5 shows China's first large-scale stationary spoil recycling plant operational in the Southern New District.

On Shenzhen Metro Line 13, the 2.1-km tunnel segment between Yingrenshi and Luozi stations yielded approximately 206,000 m<sup>3</sup> of excavated material, comprising 21,000 m<sup>3</sup> of hard rock and 185,000 m<sup>3</sup> of slurry-type soft soil. To facilitate differentiated treatment and recycling, the Line 13 Spoil Processing Center was established with a peak daily throughput of 4,000 m<sup>3</sup>. Operating at a continuous processing rate of 200 m<sup>3</sup>/h for over 20 hours daily, the center had reclaimed 27,300 m<sup>3</sup> of reusable sand and aggregate resources by 2022 <sup>[44]</sup>. Figure 6 details its slurry separation phase within the treatment workflow.

In Kansas City, Missouri, limestone mining since the late 19th century left extensive abandoned mine workings. By the mid-20th century, mining operators transitioned from solely extracting limestone to strategically converting mined-out voids into available space resource during active excavation <sup>[29]</sup>.



*Figure 5. China's First Large-Scale Stationary Construction Waste Resource Utilization Plant (Self-photographed)*



*Figure 6. Slurry Separation during Construction Waste Processing for Shenzhen Metro Line 13 <sup>[45]</sup>*

### 3.3. Underground space use and water

Xiong'an New Area, strategically positioned within the Beijing-Tianjin-Baoding regional triangle, encompasses a planned 1,770 km<sup>2</sup> as a national-level development zone where the Hebei Xiong'an New Area Planning Outline (hereafter 'Outline') mandate comprehensive utilization of underground space and groundwater <sup>[46]</sup>. The Outline specifically requires orderly underground space utilization, prioritized infrastructure deployment in subsurface areas, and establishment of integrated coordination mechanisms. Concurrently, Xiong'an New Area Master Plan (2018-2035) construction of a groundwater monitoring network featuring 41 well clusters (109 individual wells) across the entire 1,770 km<sup>2</sup> zone, enforcing strict extraction controls to monitor and prevent land subsidence, with primary focus on shallow aquifers  $\leq 50\text{m}$  depth <sup>[47]</sup>.

As the pioneering development sector, the 38-km<sup>2</sup> Start-up Area—under the Hebei Xiong'an New Area Start-up Zone Regulatory Detailed Plan—limits above-ground construction to 28 million m<sup>2</sup> while capping underground space utilization below 10 million m<sup>2</sup>. This zone designates groundwater as the emergency backup supply <sup>[48]</sup>.

## 4. ANALYSIS OF CHINA'S UNDERGROUND SPACE PLANS AND ITS RELATED PLANS GROWTH TREND AND CHARACTERISTICS OF CARBON EMISSIONS

### 4.1. Prevailing typology and characteristics of underground space plans

Underground space plan serves as a specialized sub-system within China's territorial spatial plan framework, providing critical regulatory foundations for the utilization of urban underground space resources. Current multi-tiered underground space plans comprise: (1) underground space development plans, (2) underground components within territorial spatial master plans, (3) specialized underground utilization plans, and (4) detailed underground plans <sup>[49,50]</sup>.

(1) Underground Space Development Plan

These represent the strategic blueprint guiding scientific utilization, orderly construction, and efficient management of urban underground resources over defined periods. Functioning as overarching policy documents, they establish development objectives, guiding principles, implementation strategies, key tasks, and safeguard measures - forming the fundamental basis for subsequent plan and governance.

(2) Underground Space Components in Territorial Spatial Master Plans

Derived from development plans, these components define underground plan frameworks and content requirements within comprehensive territorial plans. They provide directives for specialized underground space utilization plans and detailed underground space plans, articulating development priorities, plan philosophies, formulation depths, and compilation strategies. Crucially, they establish interfaces between underground space plan subsystems and broader territorial plan systems.

(3) Specialized Underground Space Utilization Plans

Operating under master plan guidance, these core instruments coordinate underground space development across entire urban areas. They facilitate vertical integration of plan indicators from master to detailed plans, identify regulatory priorities, and address control requirements. Key elements include spatial configurations, development phasing, objectives/strategies, 3D control mechanisms, facility classification guidance, disaster resilience measures, and implementation safeguards.

(4) Detailed Underground Space Plans

As direct implementation tools, these plans operationalize mandatory requirements from development and master plans while interfacing with specialized plans. They provide statutory bases for underground space allocation and management, offering integrated aboveground-underground development guidelines for design and construction. Content encompasses functional specifications, interconnectivity requirements, quantitative development controls, environmental/cultural provisions, facility siting, and integrated spatial design.

Multi-tiered underground space plan necessitates coordinated utilization of diverse underground space resources according to each tier's positioning, functions, and content. This chapter analyzes existing urban underground space plans to demonstrate their multi-level responses to synergistic resource utilization, as systematized in Table 5.

**Table 5.** *Responsiveness of multi-tiered underground space plans to the synergy utilization of MURs*

Multi-tiered underground space plans	Underground space	Groundwater	Geomaterials	Geothermal energy	Synergy utilization
Underground space Development Plans	√	√	√	–	√
Underground Space Components in Territorial Spatial Master Plans	√	–	√	√	√
Specialized Underground Space Utilization Plans	√	–	–	–	–
Detailed Underground Space Plans	√	–	–	–	–

√ refers to involve; – refers to not involve.

#### 4.2. Interfacing specialized plans with underground space plans

Underground space plans exhibit comprehensive nature, involving multiple specialized plans for underground development. Relevant plans such as civil defense, rail transit, municipal utilities, public services, disaster prevention, and sponge city initiatives all entail underground demands. This paper systematically reviews 16 types of urban specialized plans with underground requirements. By analyzing conflicts in underground space utilization across these plans, it proposes synergistic relationships with MURs. Conflicts between other specialized plans and underground space utilization can be categorized into [51]: ① Conflicts with underground space constraints; ②

Conflicts between specialized plans themselves; ③ Conflicts arising when feedback from underground space plan outcomes is integrated into other specialized plans. Specific details are presented in Table 6.

**Table 6.** Conflicts in underground space utilization among specialized plans and their synergistic relationships with MURs

Specialized Plan	Existing Conflicts	Involved Major Underground Resources				
		Underground space	Groundwater	Geomatics	Geothermal energy	Synergy utilization
Urban Renewal Specialized Plan	①	●	○	○	○	○
Sponge City Specialized Plan	①	●	○	—	—	○
Rail Transit Specialized Plan	②	●	●	○	—	●
Integrated Transportation Specialized Plan	②	●	—	—	—	—
Parking Facilities Specialized Plan	②	●	○	○	○	○
Logistics & Warehousing Specialized Plan	③	●	—	—	○	○
Utility Tunnel Specialized Plan	③	●	○	○	○	○
Municipal Facilities Specialized Plan	③	●	●	—	●	●
Civil Defense Facilities Specialized Plan	②	●	●	●	○	●
Seismic Disaster Prevention Specialized Plan	③	●	○	○	○	○
Mineral Resources Specialized Plan	③	○	●	●	●	●
Cultural Tourism Specialized Plan	③	●	—	—	—	—

New Digital Infrastructure Plan	②	●	—	—	—	—
Smart Infrastructure Plan	②	●	—	—	—	—
Geothermal Resource Specialized Plan	③	○	●	—	●	○
Groundwater Protection & Utilization Plan	③	○	●	—	●	○

● indicates mandatory consideration of synergy, ○ indicates recommended consideration of synergy, — indicates no current need for consideration.

### 4.3. Issues in underground space plans and interfacing plans

Existing underground space plans and interfacing plans exhibit a multi-tiered and highly comprehensive nature, encompassing development plans, territorial spatial master plans, specialized plans, and detailed plans. By analyzing the responsiveness of underground space plans to synergistic utilization of MURs, the conflicts between specialized plans and underground space utilization, and their coordinate relationships with MURs, this study identifies the following issues in China's current underground space plan framework:

#### (1) Inadequate plan transmission mechanisms

While China's underground space development plans and territorial spatial master plans address MURs, their specialized and detailed plans remain predominantly focused on underground space exploitation. Insufficient vertical integration exists between plans (master plans to specialized plans), reflecting incomplete transmission mechanisms.

#### (2) Absence of resource synergy principles

Across all plan tiers, content prioritizes underground space resource development—covering objectives, plan concepts, facility categorization, and spatial arrangement. Synergistic utilization of other underground resources (geothermal, groundwater, geomaterials) receives insufficient attention.

#### (3) Fragmentation of specialized plans interfacing underground space plans

Specialized plans interfacing underground space plans encompass numerous types, functionally spanning multiple levels including transportation, warehousing, civil defense, information technology, cultural tourism, and seismic safety; resource-wise involving diverse underground resources such as space itself, minerals (geothermal inclusive), and water resources; and administratively engaging multiple departments including transportation, water resources, and geology. This cross-sectoral fragmentation characteristic within both specialized underground space utilization plans and related specialized plans thereby substantially increases the complexity of achieving synergistic utilization of MURs.

### 4.4. Some suggestions for upgrading of urban underground space plans

Building upon the analysis of multiple underground resource utilization projects and China's underground space plan framework, this study proposes the following recommendations for upgrading urban underground space plan in China:

(1) Positioning specialized underground space utilization plans as the core vehicle, this approach integrates the synergistic utilization of MURs. Current analysis reveals that development plans and territorial spatial master plans have initiated the incorporation of MURs. Functioning as the primary transmission driver for plan indicators from master plans to detailed plans, specialized underground space utilization plans must transition from singular space resource plan toward multi-resource plan. Thematic coverage includes spatial layout, construction phasing, objectives and strategies, horizontal and vertical control mechanisms, development guidance, facility classification, disaster resilience, and implementation safeguards. Incorporating resources such as groundwater, geothermal energy, and geomaterials into specialized plans would significantly enhance practical engineering



guidance. Consequently, given both operational demands and engineering applicability requirements, specialized underground space utilization plans constitute the fundamental platform for future upgrades.

(2) Refining underground space plan transmission mechanisms. The transmission within underground space plan is multifaceted. It manifests not only between the master plan and specialized plan, but also between development plan and the master plan, between the master plan and detailed plan, and between specialized plans and detailed plans. Establishing a robust coordination mechanism is essential to form a coherent underground space plan system.

(3) Leveraging the coordinating and guiding function of specialized underground space utilization plans. China's current underground development involves numerous specialized plans, with most underground utilization content from interfacing specialized plans with underground space plan already addressed within specialized underground space utilization plans. This framework should activate its coordinating and guiding function to proactively mitigate inter-plan conflicts in underground space utilization while establishing explicit synergistic relationships with MURs, thereby progressively integrating multi-resource synergistic utilization principles into all interfacing specialized plans.

## 5. CONCLUSION

This study briefly outlined motivations for planning MURs in China, and further analyzed the current deficiencies in underground space plans and its related plans for the synergistic utilization of MURs. Recommendations are proposed, including "Positioning specialized underground space utilization plans as the core vehicle," "Refining underground space plan transmission mechanisms," and "Leveraging the coordinating and guiding function of specialized underground space utilization plans." It should be noted that China's underground space plan is characterized by its strong comprehensive nature. This characteristic becomes even more pronounced in the underground plans. Compared to conventional underground space plans, underground plans required richer geological data and greater coordination of departments. This study provides only a preliminary exploration of the framework for underground plans. More in-depth research is warranted regarding its formulation, implementation, and management.

## 6. ACKNOWLEDGMENTS

The authors wish to acknowledge the sponsorship from the National Natural Science Foundation of China (NNSFC) [grant numbers 52378083] and the Natural Science Foundation of Jiangsu Province [grant number BK20231488].

## 7. REFERENCES

- [1] Yi, R. (2023). *The fourth national land: Underground space and future cities*, Beijing, National Administration Press.
- [2] Wu, L. X., Liu, D. X., Yang, Y., et al. (2022). Urban underground space resource assessment: Current status and future prospects. *Chinese Journal of Underground Space and Engineering*, 18(1), 35–49.
- [3] Rönkä, K., Ritola, J., & Rauhala, K. (1998). Underground space in land-use planning. *Tunnelling and Underground Space Technology*, 13(1), 39–49. [https://doi.org/10.1016/S0886-7798\(98\)00029-7](https://doi.org/10.1016/S0886-7798(98)00029-7).
- [4] Parriaux, A., Tacher, L., & Joliquin, P. (2004). The hidden side of cities – towards three-dimensional land planning. *Energy and Buildings*, 36, 335–341. <https://doi.org/10.1016/j.enbuild.2004.01.026>.
- [5] Parriaux, A., Blunier, P., Maire, P., & Tacher, L. (2007). The DEEP CITY project: A global concept for sustainable urban underground management. *Proceedings of the 11th ACUUS International Conference - Underground Space: Expanding the Frontiers*, 255–260.
- [6] Qu, J. J., Gong, X. L., Mei, Q. Q., et al. (2023). Collaborative development and utilization of multiple underground geological resources in Suzhou urban area. *Geological Review*, 69(5), 1859–1868.
- [7] Guo, H. D., Wei, L. S., Zheng, W., et al. (2020). Impact analysis of subway engineering on groundwater environment in Lanzhou fault basin. *Water Resources and Hydropower Engineering*, 51(8), 119–128.
- [8] Chen, G. Y. (2011). Rational utilization of construction waste for building a resource-saving society. *Transport Energy Conservation & Environmental Protection*, (2), 28–32.
- [9] Peng, F. L., Qiao, Y. K., Cheng, G. H., & Zhu, H. H. (2019). Current status, problems and countermeasures of urban underground space planning in China. *Earth Science Frontiers*, 26(3), 57–68.
- [10] Ministry of Housing and Urban-Rural Development of China. (2019). Standard for urban underground space planning: GB/T51358-2019. Standard for urban underground space planning. [https://www.mohurd.gov.cn/gongkai/zhengce/zhengcefilelib/201905/20190530\\_247240.html](https://www.mohurd.gov.cn/gongkai/zhengce/zhengcefilelib/201905/20190530_247240.html). (accessed 8 May 2025)



- [11] Bobylev, N. (2010). Underground space in the Alexander Platz area, Berlin: Research into the quantification of urban underground space use. *Tunnelling and Underground Space Technology*, 25(5), 495–507. <https://doi.org/10.1016/j.tust.2010.02.013>
- [12] Bobylev, N. (2016). Underground space as an urban indicator: Measuring use of subsurface. *Tunnelling and Underground Space Technology*, 55, 40–51. <https://doi.org/10.1016/j.tust.2015.10.024>
- [13] Li, X. Z., Li, C. C., Parriaux, A., Wu, W. B., Li, H. Q., Sun, L. P., & Liu, C. (2016). Multiple resources and their sustainable development in urban underground space. *Tunnelling and Underground Space Technology*, 55, 59–66. <https://doi.org/10.1016/j.tust.2016.02.003>
- [14] Umer, S., Nicolas, S., & Mehdi, B. J. (2021). How coal and geothermal energies interact with industrial development and carbon emissions? An autoregressive distributed lags approach to the Philippines. *Resources Policy*, 74, 102342. <https://doi.org/10.1016/j.resourpol.2021.102342>
- [15] Wang, H. Y., Guo, D. J., Wei, L. X., Su, J. W., Zhao, H. X., & Zhao, X. X. (2025). Synergistic priority utilization of multiple underground resources: Concept, methods, and application. *Tunnelling and Underground Space Technology*, 162, 106642. <https://doi.org/10.1016/j.tust.2025.106642>
- [16] Chinese Society for Rock Mechanics & Engineering. (2018). 2018 Blue Book of China's urban underground space development. <http://www.csrme.com/Academic/Content/index/cateid/274.do>. (accessed 8 May 2025)
- [17] Chinese Society for Rock Mechanics & Engineering. (2019). 2019 Blue Book of China's urban underground space development. <http://www.csrme.com/Academic/Content/index/cateid/274.do>. (accessed 8 May 2025)
- [18] Chinese Society for Rock Mechanics & Engineering. (2020). 2020 Blue Book of China's urban underground space development. <http://www.csrme.com/Academic/Content/index/cateid/274.do>. (accessed 8 May 2025)
- [19] Chinese Society for Rock Mechanics & Engineering. (2022). 2022 Blue Book of China's urban underground space development. <http://www.csrme.com/Academic/Content/index/cateid/274.do>. (accessed 8 May 2025)
- [20] Chinese Society for Rock Mechanics & Engineering. (2023). 2023 Blue Book of China's urban underground space development. <http://www.csrme.com/Academic/Content/index/cateid/274.do>. (accessed 8 May 2025)
- [21] Central People's Government of China. (2023). China ranks first globally in direct utilization scale of geothermal energy. [https://www.gov.cn/yaowen/liebiao/202309/content\\_6904270.htm](https://www.gov.cn/yaowen/liebiao/202309/content_6904270.htm). (accessed 10 May 2025)
- [22] Guan, J. J., Zheng, Y. J., & Cao, X. H. (2024). Challenges and countermeasures for groundwater resources in China. *East China Geology*, 45(3), 255–263.
- [23] Shao, J. L., Bai, G. Y., Liu, C. Z., et al. (2023). Issues and strategies in groundwater management: With discussion on "dual-control" management. *Hydrogeology & Engineering Geology*, 50(5), 1–9.
- [24] Central People's Government of China. (2024). Release of the 2023 China water resources bulletin. Retrieved [https://www.gov.cn/lianbo/bumen/202406/content\\_6957291.htm](https://www.gov.cn/lianbo/bumen/202406/content_6957291.htm). (accessed 10 May 2025)
- [25] Shenzhen Housing and Construction Bureau. (n.d.). Special plan for construction waste management in Shenzhen (2020–2035). <https://zjj.sz.gov.cn/attachment/0/774/774411/8739065.pdf>. (accessed 10 May 2025)
- [26] Gao, Y., Shen, J., Chen, L., Li, X., Jin, S., Ma, Z., & Meng, Q. (2023). Influence of underground space development mode on the groundwater flow field in Xiong'an new area. *Journal of Groundwater Science and Engineering*, 11(1): 68–80. <http://dx.doi.org/10.26599/JGSE.2023.9280007>.
- [27] Hu, Y. Z., & Zhang, X. W. (2023). Impact of underground space development on groundwater cycle in Chengdu. *Ground Water*, 45(4), 94–98. <https://doi.org/10.19807/j.cnki.DXS.2023-04-030>.
- [28] Li, X. S., Sun, B. W., & Yao, X. C. (2007). Impact of groundwater environment changes on safety of underground transportation facilities in Beijing. *Urban Transport of China*, (2), 81–85.
- [29] Zhou, D. K., Li, X. Z., Ma, Y., & Ge, W. Y. (2020). Study on the impact patterns of multiple geological resources during urban underground development. *Geological Journal of China Universities*, 26, 231–240. <https://doi.org/10.16108/j.issn1006-7493.2019034>.
- [30] Li, X. Z. (2022). Efficient and synergistic development of energy underground structure and shallow geothermal energy. The 15th Jiangsu Green Building Development Conference. Nanjing.
- [31] Xia, C. C., Zhang, G. Z., & Sun, M. (2015). Theory and application of energy underground structures: Ground source heat pump systems with buried pipes in subsurface structures, Shanghai, Tongji University Press.
- [32] Shi, X. C. (2022). Research progress and prospect of underground mines in coal mines. *Coal Science and Technology*, 50(10), 216–225.
- [33] Zhejiang Provincial Department of Housing and Urban-Rural Development. (2023). Cases of construction waste resource utilization – Vote now, [https://jst.zj.gov.cn/art/2023/12/7/art\\_1569971\\_58934520.html](https://jst.zj.gov.cn/art/2023/12/7/art_1569971_58934520.html). (accessed 11 May 2025)
- [34] Wu, T. W. (2021). Research on space design of rail transit connection in hub airports based on wayfinding theory. Beijing Jiaotong University. Beijing.
- [35] He, J. C., Bie, S., Yi, W., et al. (2022). Application of ground source heat pump system in Beijing Daxing International Airport. *Heating Ventilating & Air Conditioning*, 52(5), 90–95.
- [36] China Southern Airlines. (2025). Beijing Daxing International Airport. [https://www.csair.com/cn/tourguide/airport\\_service/domestic/domestic/1dpdb182j8mei.shtml](https://www.csair.com/cn/tourguide/airport_service/domestic/domestic/1dpdb182j8mei.shtml). (accessed 11 May 2025)
- [37] Ren, Y. Q., Kong, Y. L., Huang, Y. H., et al. (2023). Operational strategies to alleviate thermal impacts of the large-scale borehole heat exchanger array in Beijing Daxing Airport. *Geothermal Energy*, 11(1).
- [38] Beijing General Municipal Engineering Design & Research Institute Co., Ltd. (2025). Innovation escorts underground passage: Completion of Beijing East Sixth Ring Road reconstruction project. <https://www.bmedi.cn/news/8658.html>. (accessed 13 May 2025)

- [39] Department of Civil Engineering, Tsinghua University. (n.d.). Tsinghua "energy tunnel" technology supports green innovation in East Sixth Ring Road project. <https://mp.weixin.qq.com/s/tKsiK7M5DN366u6v19D42A>. (accessed 14 May 2025)
- [40] Zhou, W. J. (2016). Application of ground source heat pump technology in Shanghai Natural History Museum. *China Engineering Consulting*, (9), 55–57.
- [41] Standing Committee of Qinhuai District People's Congress, Nanjing. (2025). Report on planning and construction of underground space and rail transit in Southern New City. [www.njqhrd.gov.cn/newsDetail.asp?id=5805](http://www.njqhrd.gov.cn/newsDetail.asp?id=5805). (accessed 16 May 2025)
- [42] Nanjing Southern New City Development Strategy and Master Urban Design. (2023). *World Architecture*, (10), 83–85.
- [43] Qi, W. Y., & Wang, Z. J. (2024). Low-carbon practice in urban road construction: Case study on construction waste recycling in Nanjing Southern New City. *Transport & Port Shipping*, 11(5), 65–69+81.
- [44] Yu, Z. H., Yang, D. Y., Zhang, D. W., et al. (2022). Green recycling technology for shield muck in Shenzhen Metro Line 13. *Hazard Control in Tunnelling and Underground Engineering*, 4(4), 100–106.
- [45] Yang, F., Cao, T., Zhang, T., Hu, J., Wang, X., Ding, Z., & Wu, Z. (2023). An implementation framework for on-site shield spoil utilization—A case study of a metro project. *Sustainability*, 15(12), 9304. <https://doi.org/10.3390/su15129304>.
- [46] China Xiong'an. (n.d.). Hebei Xiong'an New Area master plan. [https://www.xiongan.gov.cn/2018-04/21/c\\_129855813.htm](https://www.xiongan.gov.cn/2018-04/21/c_129855813.htm). (accessed 17 May 2025)
- [47] Zhang, X., Han, B., Du, Y. N., Gong, X., Li, H. E., & Zhen, Z. (2025). Construction achievements of shallow groundwater monitoring network in Xiong'an New Area. *North China Geology*, 48(1), 78–86.
- [48] China Xiong'an. (n.d.). Detailed regulatory plan for Xiong'an New Area start-up zone. <https://www.xiongan.gov.cn/download/xaxqqdq.pdf>. (accessed 17 May 2025)
- [49] Zhao, Y., & Yuan, X. G. (2024). Underground space planning in the new era: System, content and methodology. *Shanghai Urban Planning Review*, (4), 102–108.
- [50] Lü, C., Liu, J., Zou, L., et al. (2024). Underground space planning for beautiful China: Key elements in territorial spatial planning system. *Proceedings of 2024 China Urban Planning Annual Conference*. 2–14. <https://doi.org/10.26914/c.cnkihy.2024.037825>.
- [51] Zhao, Y. (2015). Research on underground space planning content at regulatory detailed planning level. *Shanghai Urban Planning Review*, (3), 110–115.

## UNIVERSALITY IN DESIGN: USER-CENTRIC METHODOLOGY FOR INFRASTRUCTURE PROJECTS – BRUSSELS EXPERIENCE

Dr. Eng. Arch. Gordana Micic<sup>1</sup>

**Abstract:** Many urban studies highlight the issue of discontinuities between public spaces, particularly in underground mobility infrastructure. These spaces often suffer from poor connections to the surface, rendering them almost invisible to passers-by and further isolating them from the public realm. This research focuses on a user-centric approach as a key condition for achieving continuity and coherence in metro station design within the broader urban fabric. It aims to establish a comprehensive, 360-degree design methodology, drawing on insights from Brussels' metro station projects.

Through the integration of multimodality principles with sustainability, urban planning, aesthetics, technique and maintenance, the proposed methodology prioritises universal accessibility to create welcoming and inclusive underground public spaces. From a forward-looking perspective, the study examines the intersection of urban temporal and spatial dynamics with aesthetic, functional, and technical elements, translating these into project management mechanisms. It is conducted alongside research on the interface between mobility and urban planning, ensuring that transportation hubs are not just functional nodes but also integrated, accessible, and liveable spaces for all.

**Keywords:** Design, station, multidisciplinary, urban planning, public transport

### 1. INTRODUCTION

City life revolves around public spaces. It is a place for movement, encounter, and civic life, a 'common space' that exists at the intersection of individual and collective spatial experience (Lévy & Lussault, 2013). Public space takes many forms: open or enclosed, freely accessible or regulated, inherited or newly created. Those 'in between' spaces, whether stops, stations or multimodal hubs, are crucial interfaces for facilitating connections between cities and transportation networks.

However, while certain cities, such as Montreal and Toronto (Besner, 2017; Boisvert, 2011), have a well-developed underground pedestrian network, this is not the case in many other cities around the world. The poor connection between subway stations and urban space results in them being invisible or barely perceptible to passers-by. (Bertolini, 2008; Labbé, 2014; Sander, 1996). This physical detachment gives rise to various types of discontinuities and boundaries<sup>2</sup>, imposed<sup>3</sup>, spontaneous<sup>4</sup>, or even imagined<sup>5</sup> (Escallier, 2006; Piermay, 2002). Historically, the design of such infrastructure has been driven by the logic of networks, prioritising speed, efficiency, capacity, and operational functionality (Dupuy, 1987; Kaufmann, 1998). This highlights the need for

<sup>1</sup> Head of Art & Architecture office at STIB-MIVB & Brussels Mobility, Chair of UITP Design & Culture Committee, UCLouvain lecturer

<sup>2</sup> A border is a barrier or boundary that separates two different territories or systems.

<sup>3</sup> Imposed boundaries are often the result of administrative or legal constraints linked to land rights, which define the limits of an area. They may be the result of strategy, planning, development or operating methods.

<sup>4</sup> Spontaneous boundaries emerge naturally in response to marked social, economic or geographical contrasts. They may be the result of inequalities, urban discontinuities (such as wasteland or infrastructure), or physical obstacles (gradients, slopes, slippery ground), creating a break between the city and the network, particularly stations.

<sup>5</sup> Imaginary boundaries are mental barriers created by negative perceptions of a place (cold, dark, dilapidated) or traumatic experiences (theft, harassment). They influence the way people feel and can limit the use of certain urban spaces or services.

coordinated strategies that ensure continuity between surface and underground spaces while supporting sustainable urban infrastructure.

Numerous studies have highlighted a recurring issue: the failure to incorporate users' needs and expectations into the design of transport infrastructure. Public transport operators are still hesitant to embrace user-centric approaches, which they view as abstract and difficult to apply, especially given the diversity of user profiles. For decades, they have based their designs on the notion of a 'standard user', leading to a high degree of standardisation. This model excludes many users whose needs fall outside the norm.

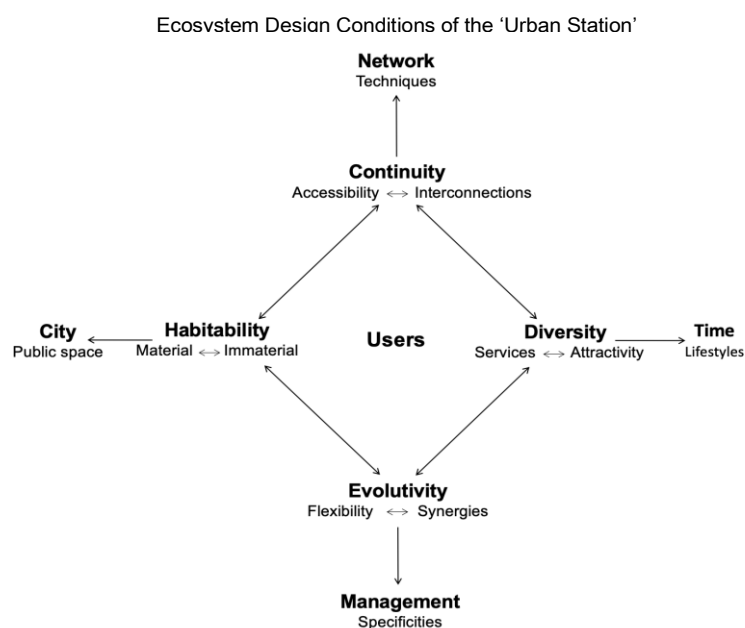
To understand and evaluate alternatives, this article first outlines the defining features of a user-centric model in urban development projects, along with the elementary principles of commonly practised project management. It helps to contextualise the relevance of the Brussels experience, where a user-oriented methodology has been applied to the design of metro stations. The goal here is not to construct a new science of management, but rather to identify, through a pragmatic lens, some key levers and distinctive features that may enhance project quality compared to traditional models. Ultimately, the aim is to bring stations closer to their users and improve their integration with the urban environment.

By interpreting the project process through specific case studies, this research positions itself as an exploratory inquiry. It is rooted in applied work carried out in a professional framework, forming what might be called an empirical laboratory. The scientific research conducted in parallel has directly fed into the development and implementation of these practical experiments.

## 2. LOOKING AT THE PROJECT PROCESS

More than ever, the project process is being called upon to integrate the collective dimension (Boutinet, 1990). The traditional expert model, based on a strict hierarchy, is being called upon to give way to co-production, where users become active partners in the design process. In this way, the project becomes a tool for dialogue between users and project managers. This participatory process makes it easier to identify users' needs and expectations and encourages them to take ownership of the spaces (Declève, Forray, & Michialino, 2002). In this context, architectural and engineering skills need to be enhanced by interpersonal skills and an ability to reconcile often complex requirements, while ensuring the coherence of the project.

Refocusing on the user-centric approach calls for examining traditional design methods, including underground infrastructure, in favour of greater openness, transparency, cross-functionality and innovation (Admiraal & Cornaro, 2018; Toussaint & Zimmermann, 2001). By meeting daily needs and saving time for other activities, the concept of the 'urban station' (Micic, 2021) transforms the journey into a stroll through an environment that is safe, welcoming, aesthetically appealing, and restorative. The ecosystemic design conditions underpinning this transformation are illustrated in Figure 1. The quality of its design determines the quality of its use, and vice versa.

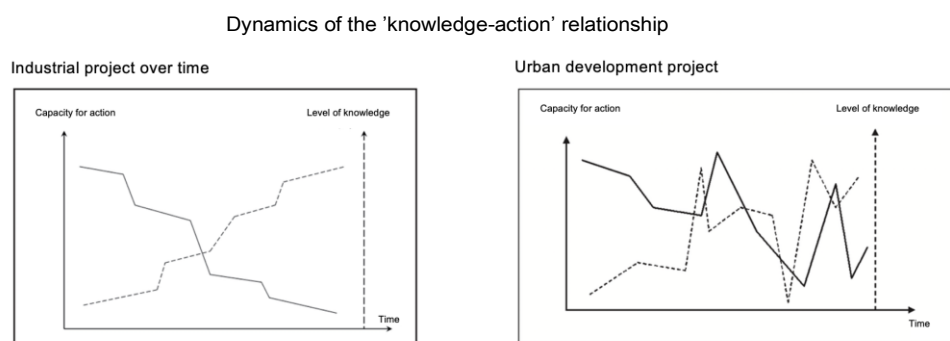


**Figure 1.** Schematisation of the Ecosystem Design Conditions of the 'Urban Station'. Source : (Micic, 2021)

Given the implication of this development on the project process, many project managers are wondering about the ‘what’ and the ‘how to do it’. To grasp the complexity of the project-based approach, it is helpful to revisit three fundamental dimensions: the irreversibility of the process, the dialectical relationship between knowledge and action, and the shifting nature of challenges and management strategies (Arab, 2007; Midler, 1996).

The *knowledge* phase represents the exploratory stage that precedes any concrete action. It involves analysing the context, evaluating the potential of the site, drawing on specialised expertise, and identifying constraints and technical opportunities. This analytical groundwork is essential to developing innovative and context-sensitive responses (Boutinet, 2010). Ultimately, the goal is to transform an initial idea or concept into a tangible, multifaceted reality, rooted in both time and place.

Unlike industrial projects, which typically follow a relatively linear trajectory (Figure 2a), urban design projects are marked by fluctuating and less predictable dynamics (Figure 2b). These projects are primarily engaged during the initial phases: reflection, debate, feasibility studies, preliminary design, and design development. Once this phase is completed, the project tends to solidify and the production phase gradually becomes irreversible (Arab, 2007; Midler, 1996). This inherent instability can be attributed to several factors: the significant heterogeneity and complexity of the elements involved, the often-prolonged duration of such projects, and the persistent tension between the urgency to act and the need for thoughtful reflection. Moreover, it reflects a deeper dialectic between the reversibility and irreversibility of decisions made throughout the process.



**Figure 2.** Dynamics of the activity of the ‘knowledge-action’ project: a) Industrial project over time. Source : (Midler, 1996). b) Urban development project. Source : (Arab, 2007).

From a project management standpoint, the steering process aims to provide structure and guidance for all stakeholders involved, while ensuring coherent and effective governance. Depending on the project's scale and nature, this process mobilises a broad spectrum of actors: public and private authorities, operators, politics, technical experts, institutional partners, various associations, etc. Its role is to coordinate these contributions, anticipate potential risks, whether administrative, political, or technical, evaluate key parameters, and uphold a consistent and unified project vision.

Rooted in the principles of management science, this process is activated from the earliest stages of the project (Gilles, 2011). A central tool in this approach is the ‘golden triangle’ model, which seeks to balance three interdependent dimensions: quality, cost, and schedule (Figure 2). Maintaining this equilibrium throughout the project lifecycle is a core challenge in ensuring its success (Dobson, 2004; Gilles, 2011).

Design and the ‘Golden Triangle’ principle



**Figure 3.** Design and the ‘Golden Triangle’ principle. Source: personal achievement, according to several authors.

In the realm of public projects, political and media pressures often lead to time and financial constraints becoming the primary focus, with quality taking a back seat. While network operators are generally able to define requirements from a technical and operational standpoint, the diverse and heterogeneous expectations of users are often insufficiently addressed. This oversight underscores the importance of clarifying and reinforcing the concept

of ‘quality’ in its broadest sense. Only by doing so can a sustainable and equitable balance be re-established in project development and delivery.

### 3. USER-CENTRIC METHODOLOGY : BRUSSELS EXPERIENCE

The transition toward an accessible city for all gained momentum in the early 21st century, spurred by a growing movement advocating walking as a legitimate and active mode of transport. Committed to enhancing the quality of public space, Brussels Mobility<sup>6</sup>, alongside STIB-MIVB<sup>7</sup> and partners including municipalities, institutions, and civil society, launched a series of initiatives to promote a more accessible, inclusive and sustainable urban environment. Institutional support was solidified with the adoption of the Iris II Regional Mobility Plan in 2010 and further strengthened by the launch of the Strategic Pedestrian Plan<sup>8</sup> in 2012, both foundational to fostering a more pedestrian, walkable and people- friendly city. This vision was formalised through key strategic documents such as the Regional Sustainable Development Plan<sup>9</sup> and the Regional Mobility Plan<sup>10</sup>, which together framed a coherent approach to integrated urban and mobility planning.

#### 3.1. Universal accessibility as a strategic lever in the design of metro stations

Brussels Mobility and the STIB-MIVB have undertaken a systematic accessibility program aimed at upgrading existing metro infrastructure. A key element of this program is the installation of elevators<sup>11</sup> to ensure step-free access. While elevators represent an essential improvement, they are not, in themselves, sufficient to address the full spectrum of needs encountered by people with reduced mobility<sup>12</sup> or special needs.

Recognising these limitations, in 2018, the Collectif Accessibilité Wallonie Bruxelles (CAWaB) initiated a collaboration with Brussels Mobility and STIB-MIVB to develop a dedicated design reference framework for the underground public spaces of metro and pre-metro stations, an equivalent to the vade-mecums already applied to ground public space. To find synergy between all stakeholders, a multidisciplinary committee was established. This committee comprises representatives from regional authorities, all internal departments of the STIB-MIVB, and the association Atingo. As a specialist on universal accessibility and appointed by CAWaB’s members to act as a ‘user expert’<sup>13</sup>, Atingo is crucial in expressing the intricate, sometimes conflicting<sup>14</sup>, realities and requirements of people with reduced mobility.

The decision to incorporate a ‘user expert’(Kerroumi & Forgeron, 2021) into the design process was a pragmatic and strategic alternative to a full-scale participatory approach, which was deemed unfeasible due to time constraints and the technical complexity of the project. Acting as a mediator, the user expert voiced user needs while allowing the process to stay focused and technically manageable. This choice was supported by a wealth of pre-existing empirical data from earlier regional surveys, such as the Regional Mobility Plan, the mobility barometer, and STIB-MIVB’s customer satisfaction survey. While broader participatory methods remain valuable, particularly in large-scale urban planning, they must not compromise the specific and often rigorous needs of people with reduced mobility (PRM).

The overarching objective is to achieve universal accessibility (Mace, Hardie & Place, 1996) across all metro stations in Brussels. Ensuring access to PRM, regarded as one of the most vulnerable user groups, not only fulfils a fundamental equity imperative, but also enhances usability for all categories of users. In this context, findings from the 2008 Health Survey conducted by the Access and Go association (formerly ANLH) reveal that more than 30% of individuals over the age of 15 experience either permanent or temporary physical or psychological limitations. These figures underscore the broader societal relevance of accessibility, positioning it as a cornerstone of inclusive urban mobility.

---

<sup>6</sup> Administration of the Bruxelles-Capitale Regional Public Service.

<sup>7</sup> Acronym for Société des Transports Intercommunaux de Bruxelles – trad.: Brussels Intercommunal Transport Company

<sup>8</sup> The following dimensions are determined by the ten quality criteria, GO10, outlined in the *Strategic Pedestrian Plan*: Network, Itinerary, Intermodality, Experience, Space, Physical Comfort, Autonomy, Mobility hubs, Safety, and Health.

<sup>9</sup> <https://perspective.brussels/fr/outils-de-planification/plans-strategiques/plan-regional-de-developpement-prd/prdd>

<sup>10</sup> <https://be.brussels/fr/transport-mobilite/enjeux-de-la-mobilite/plan-regional-de-mobilite>

<sup>11</sup> Currently, elevators are installed in 57 of the 69 stations. Source : SSE/DITP – RBC & STIB-MIVB.

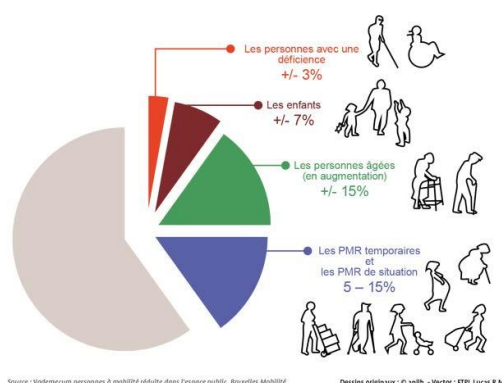
<sup>12</sup> Abrev. PRM

<sup>13</sup> <https://humancentereddesign.org/user-expert-lab>

<sup>14</sup> Findings indicate that interventions effective for one type of disability may not be suitable or appropriate for others.



The proportion of people with reduced mobility by type of disability



**Figure 4.** The proportion of people with reduced mobility by type of disability and permanent or temporary - people aged over 15. Findings from the 2008 Health Survey conducted by the Access and Go association (formerly ANLH). Source: Vademecum for people with reduced mobility in public spaces. Brussels Mobility.

Drawing on the foundational principles of universal design, the committee quickly acknowledged that the subterranean environment of metro stations constitutes a complex, three-dimensional spatial system with distinct operational and functional characteristics. Within this context, the needs of people with reduced mobility (PRM) cannot be addressed in isolation from the technical and logistical constraints traditionally associated with the operation of transit networks.

Beyond accessibility, other important considerations should be made, such as multimodality, urban planning, safety, the integration of diverse urban services (e.g. retail, food services, public services, cultural venues), all framed within principles of sustainability and environmental responsibility. Given this plural complexity, the multidisciplinary committee determined that the scope of action needed to extend beyond the principles of universal design alone. Instead, a more comprehensive ‘global design’ approach was adopted, one that is transversal, systemic, and capable of integrating a wide range of perspectives, requirements and constraints.

To achieve this, the Regional Mobility Commission (CRM) and its specialised subsections (such as those pertaining to active modes and PRM), Beliris, SNCB, equal.brussels, gender associations, academic institutions, and others were among the important institutional actors that contributed to this cooperative effort. The inclusive methodology helped ensure that the resulting standard would be robust, context-sensitive, and broadly applicable.

### 3.2. A Global Design Framework

At the end of 2022, the official reference framework ‘*Directives relatives à la conception des stations de métro de Bruxelles : Stations nouvelles – Projets de rénovation*’<sup>15</sup> was approved. The name of the ‘*Directives*’ was to set them apart from other standards and emphasise their practical application. By applying an integrated and inclusive vision for public mobility spaces, this document consolidates a set of design requirements and operational constraints anchored in core principles: equality of use, flexibility, intuitive simplicity, comfort, well-being, and safety for all users, including the staff. The overarching aim is to ensure that everyone, regardless of gender, age, or (dis)ability, can navigate the metro and pre-metro environment freely, autonomously, and with ease, across the full range of services provided.

More specifically, the *Directives* aim to:

- Enhance the overall quality of the station as a public space.
- Contribute to urban and ecological development.
- Preserve and valorise the architectural and artistic heritage of existing stations.
- Ensure universal accessibility and inclusivity for all.
- Guarantee the safety and security of users, staff, and infrastructure.
- Improve intermodality and encourage multimodal travel, including micro-mobility solutions.
- Anticipate future developments in public transportation networks.
- Reduce the psychological barriers associated with underground environments.
- Make public transit systems safer, more comfortable, and more welcoming for all.
- Facilitate effective maintenance and long-term infrastructure management.

<sup>15</sup> Translation in English: ‘*Brussels Metro and Pre-Metro Station Design Directives: New stations – Renovation projects*’



While adhering to current standards and relevant regulatory frameworks, it offers a holistic approach to the spatial organisation of metro stations, the selection of materials and equipment, and the integration of user-centric design principles. Grounded on detailed knowledge of public behaviour and user needs, the document formulates recommendations aimed at intuitively guiding and orienting individuals within the station environment. For instance, signage should be designed to reinforce users' natural orientation, serving as a complementary element to a thoughtfully conceived spatial layout that is inherently legible and user-friendly.

To distinguish itself from purely technical standards, the *Directives* adopts a structured methodology inspired by the pedestrian user's journey (Figure 5a). Its modular layout is organised into thematic sections containing individual sheets, allowing for flexible consultation and targeted updates. Each component can evolve independently without compromising the coherence of the whole. The document has been supplemented by updated metro standard plans, which provide more technical translations of specific recommendations.

One of the central challenges in developing this design framework was ensuring consistency across the multitude of technical and functional disciplines engaged throughout the design process. Considering the wide range of demands, restrictions, and contextual factors, it was frequently essential to engage in negotiations and identify harmonious solutions to disparate expectations. Those could arise from the unique characteristics of different mobility limitations or from other technical, functional, cultural, architectural, heritage-related, environmental, or social considerations.

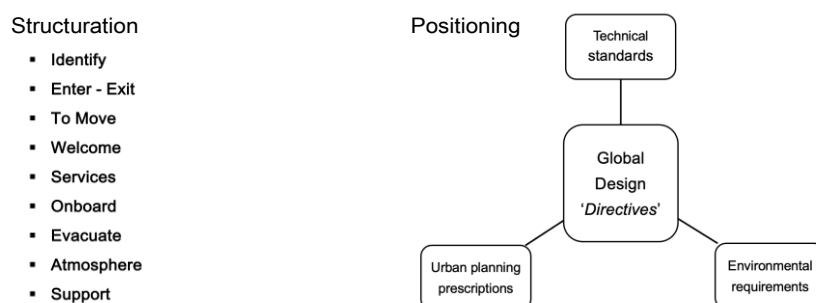


Figure 5. a) Structuring of the 'Directives' for the design of metro and pre-metro stations in Brussels. b) Positioning of the 'Directives' in relation to other reference requirements. Source: Brussels Mobility et la STIB-MIVB.

Crucially, the *Directives* was conceived with the intent to preserve a margin for creativity, an element considered fundamental to sustaining architectural and urban innovation within metro station projects. It does not replace existing documents but rather complements and integrates them, aligning with broader frameworks related to the city, transport networks, and the environment (Figure 5b). Intended for all stakeholders involved in the design, development, or redevelopment of metro stations and their surroundings, whether for comprehensive or targeted interventions, the document provides a clear and structured framework to support project designers throughout the process.

### 3.3. Implementation of *Directives*

Approved at the end of 2022, the *Directives* have entered a two-year implementation phase, allowing project managers to gradually familiarise themselves with the content and test its application across a range of contexts. This experimental period is intended to facilitate final refinements prior to the release of the definitive version of the document.

In practice, however, the implementation of new reference framework, particularly those not immediately perceived as *technically essential*, can present significant challenges. On the one hand, project managers may find it difficult to alter long-standing professional routines. On the other, designers, whether due to a strong attachment to their own creative vision or a limited understanding of accessibility concerns, may underestimate the needs of people with reduced mobility.

Implementation tends to be more straightforward in the context of new projects, where compliance with the reference can be integrated from the outset into the contractual framework binding design teams. In contrast, applying the guidelines to existing metro stations, or to projects already underway or in execution, proves more complex. Any modification of previously "validated" components must contend with various constraints, especially in terms of budget and schedule.

The issue of scope is essential, as all projects have specific intervention limits, often confined to only part of a station. At present, the design framework applies exclusively to the modified sections, while the rest remains unchanged, pending future opportunities for improvement.

Projects are assessed against the reference standards at various stages of their development. To support this process, training sessions are organised for project managers and other key stakeholders, facilitating consistent and informed implementation.

In this context, the design standards also serve as the foundation for a cross-functional audit, designed to produce a comprehensive inventory of publicly accessible infrastructure. This audit aims to create a form of station 'identity card', offering a systemic overview of renovation or transformation needs. This approach supports the development of a strategic renovation plan and helps schedule targeted interventions.

It is self-evident that aligning all stations within the Brussels network with the new standards will require both time and substantial financial investment, particularly for projects dedicated to comprehensive accessibility upgrades. As such, a strategic, phased approach is being adopted, capitalising on ongoing and future projects to limit additional costs. Some recommendations will be implemented in the short term, while others will follow in the medium or long term.

Moreover, it is important to note that certain parts of metro stations fall within the scope of partner-led developments, such as retail, residential, or office projects, and the design guidelines must also be applied in these contexts. The same principle extends to urban development initiatives in the neighbourhoods surrounding stations, whether directly adjacent or in the broader vicinity. This is based on the understanding that a station's boundary does not end at its entrance: the surrounding public space must also facilitate safe, comfortable, and intuitive access for all users.

#### 4. THE RESULTS OF PRACTICE

The two-year implementation phase that followed the guide's approval in late 2022 provided an opportunity not only to test the standard's requirements and constraints but also to evaluate the practical methods of its application. Interestingly, among the many directives it contains, only a few were found to be especially difficult to implement. Ongoing consultation within the multidisciplinary committee helped to clarify these issues and fine-tune the framework where needed.

Nevertheless, its practical implementation turned out to be even more complex. Directives that were easily measurable, such as the precise dimensions or specifications, were generally more easily comprehended and applied. By contrast, technically unmeasurable aspects, like those related to spatial legibility, sensory perception, or architectural expression, required additional support. Exemptions, too, proved challenging. Due to the variety of contextual conditions, deviations from the standard had to be addressed with customised, empirically grounded solutions that followed the same principles used to develop the framework itself.

One persistent challenge lies in the entrenchment of conventional design practices, which often resist change. While inclusive and user-centric approaches are gaining traction, they are not yet fully established. This makes the early, cross-functional integration of the framework into new projects critical. For projects already underway, however, a transition period is necessary as adjustments are constrained by existing contracts, schedules, and budgets.

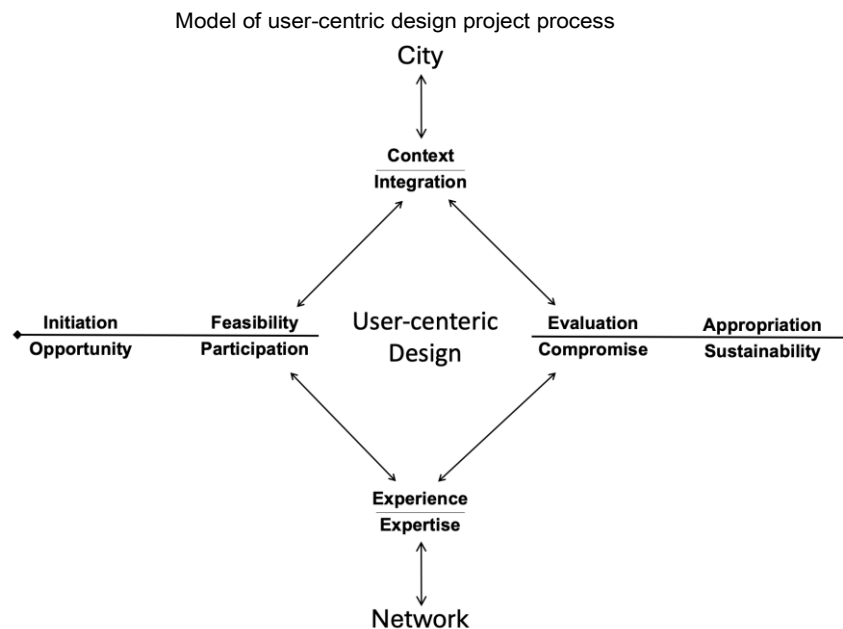
To support both the transition and future planning, the framework serves as the foundation for a systematic audit process of existing stations. These audits produce a detailed inventory of public spaces and allow for the creation of "identity cards" for each station, outlining strengths, weaknesses, and levels of compliance. This facilitates the strategic planning of renovations in short-, medium-, and long-term phases, which are tailored to the available resources and in accordance with broader urban developments.

Training proved essential throughout this process. Many professionals involved in metro development held personal and sometimes narrow views on accessibility, rather than a shared, well-informed understanding. Raising awareness among project managers and stakeholders helped foster a more unified approach to applying the framework and addressing the needs of people with reduced mobility. Support from upper management staff played a crucial role, particularly during the transitional phase when existing projects were already constrained by budget and time.

As the design reference framework, *Directives* not only consolidate technical, aesthetic, and functional best practices, but also help clarify the quality dimension within the traditional quality-cost-deadline (Q-C-D) triangle.

By reducing the risk of overlooking critical user needs, it improves project outcomes and supports smoother execution by aligning design decisions with scheduling and budgetary realities.

Moreover, the data gathered from audits feeds into 3D digital models of station infrastructure, enabling better coordination among stakeholders across the station's lifecycle. These tools also enhance transparency and public communication, offering clear insights for political and civic discussions. It's also a useful tool for outlining requirements for different partners, especially those involved in projects that are adjacent or within the surroundings of metro stations.



**Figure 6.** The project process based on user-centred design. Source : personal achievement from different sources.

Evermore, this methodology provides the basis for a strategic and comprehensive and overview of the metro network. It facilitates the efficient coordination of maintenance operations, assists in the prioritisation of projects, and coordinates future development, all while reducing the likelihood of misalignment or oversight.

## 5. CONCLUSION

The design of underground public spaces, often regarded as inherently complex and opaque, continues to pose significant challenges within urban development. These environments demand a holistic, ecosystemic and integrated design approach that fully incorporates the human dimension. In this regard, a universal design perspective serves as a lever in the global conceptualisation of urban metro stations.

The transition away from traditional methodologies marks a progressive shift toward a more collaborative, user-centric model of urban project development. This kind of framework makes it possible to meet different, and sometimes conflicting, requirements and needs, such as technical, functional, aesthetic, and experiential ones, by promoting coherence and mutual understanding. It underscores the necessity of a multidimensional and interdisciplinary approach to planning, ensuring that the complexity of urban infrastructure is addressed through *fitting* design solutions that meet the expectations of all parties.

The strategic governance of infrastructure projects must commit to the principle of universality, not simply as a technical objective, but as a fundamental right and a cornerstone of urban transformation. While contextual variability necessitates tailored responses, the overarching objective remains consistent: to integrate people's interests into a long-term strategic vision that integrates above- and belowground public spaces into a coherent urban fabric. Cultivating synergies among all stakeholders, with a user-centric approach embedded in the earliest stages of project development, fosters the creation of public spaces that are not only sustainable and legible but also equitable and responsive to actual and future demands for mobility, inclusion, and urban quality of life.

## 6. BIBLIOGRAPHY

- [1] Admiraal, H., & Cornaro, A. (2018). *Underground Spaces Unveiled: Planning and creating the cities of the future* (ICE Publishing ed.). Westminster.
- [2] Arab, N. (2007). *Activité de projet et aménagement urbain : les sciences de gestion à l'épreuve de l'urbanisme*. at *Management & Avenir*, 147-164. Retrieved from <https://www.cairn.info/revue-management-et-avenir-2007-2-page-147.htm>
- [3] Bertolini, L. (2008). *Noeuds et lieux : éléments de méthode pour une analyse comparée des quartiers des gares en réaménagement*. In *Gares et quartiers de gares: signes et marges*. Lille, Rennes et expériences internationales (Italie, Japon, Pays-Bas). Direction and coordination: P. Menerault et A. Barré. Arcueil: INRETS, 2001
- [4] Besner, J. (2017). *Cities Think Underground – Underground Space (also) for People*. Procedia Engineering. Retrieved from <https://www.sciencedirect.com/science/article/pii/S1877705817361325?via%3Dihub>
- [5] Boisvert, M. (2011). *Montréal et Toronto, villes intérieures*. Les Presses de l'Université de Montréal ed. Canada.
- [6] Boutinet, J.-P. (1990). *Anthropologie du projet*. PUF ed.
- [7] Boutinet, J.-P. (2010). *Grammaires des conduites à projet*. Presses Universitaires de France ed.
- [8] Declève, B., Forray, R., & Michialino, P. (2002). *Coproduire nos espaces publics. Formation-action-recherche*. UCL, Presses universitaires de Louvain ed., Vol. Territoires et développements durables, pp. 197.
- [9] Dobson, S. M. (2004). *The Triple Constraints in Project Management*. United States of America: Management Concepts - Vienna, VA.
- [10] Dupuy, G. (1987). *Les réseaux techniques sont-ils des réseaux territoriaux ?* L'Espace géographique 16(3), 175-184. Retrieved from <https://www.jstor.org/stable/44380968>
- [11] Escallier, R. (2006). *Les frontières dans la ville, entre pratiques et représentations*. In *Cahiers de la Méditerranée*. doi:10.4000/cdlm.1473
- [12] Gilles, G. (2011). *Qu'est-ce que le management de projet ?* In *Informations sociales*, 5, 72-80.
- [13] Kaufmann, V. (1998). *Réseaux et territoires - Significations croisées* (sous la direction de Jean-Marc Offner et Denise Pumain). *Flux*, 34, 56-58. Retrieved from [http://www.persee.fr/web/revues/home/prescript/article/flux\\_1154-2721\\_1998\\_num\\_14\\_34\\_1725](http://www.persee.fr/web/revues/home/prescript/article/flux_1154-2721_1998_num_14_34_1725)
- [14] Kerroumi, B., & Forgeron, S. (2021). *L'approche stratégique de la conception universelle*. In Dunod (Ed.), *Handicap : l'amnésie collective. La France est-elle encore le pays des droits de l'homme ?* (pp. 201-216). Retrieved from <https://shs.cairn.info/handicap-l-amnesie-collective--9782100829293-page-201?lang=fr>
- [15] Labbé, M. (2014). *Faut-il passer par le sous-sol pour mieux concevoir la ville ?* In B. Barroca, D. Serre, & Y. Diab (Eds.), *Penser la ville et agir par le souterrain* (pp. 37-66). Presses des Ponts ed. Paris.
- [16] Mace, R., Hardie, G., & Place, J. (1996). *Accessible Environments: Toward Universal Design*. The Center for Universal Design ed.
- [17] Micic, G. (2021). *Infrastructures de mobilité et projet urbain. Évolutivité du design des stations de métro et de pré-métro à Bruxelles*. (PhD). UCLouvain, Presses universitaires de Louvain - PUL. Retrieved from <https://pul.uclouvain.be/book/?gcoi=29303100241030#h2tabFormats>
- [18] Midler, C. (1996). *Modèles gestionnaires et régulations économiques de la conception?* In G. Dir. De Terssac & F. Erhart (Eds.), *Coopération et conception* (pp. 63-85): Octares.
- [19] Piermay, J.-L. (2002). *Les frontières dans la ville un objet incongru ? Le cas des villes sud-sahariennes*. In B. Reitel, P. Zander, J.-L. Piermay, & J.-P. Renard (Eds.), *Villes et frontières* (Economica ed., pp. 275).
- [20] Sander, A. (1996). *Des lieux-mouvements bien singuliers*. In *Les Annales de la recherche urbaine, Gares en mouvements*(71), 45-53. doi:<https://doi.org/10.3406/aru.1996.1953>
- [21] Toussaint, J.-Y., & Zimmermann, M. (2001). *User, observer, programmer et fabriquer l'espace public*. P. p. e. u. romandes ed. CH-Lausanne.

\*Rem.: Personal translation from French to English with the assistance of AI tools.

## RESEARCH ON THE DISTRIBUTION, DEVELOPMENT QUALITY AND DRIVING FORCES FOR THE DEVELOPMENT QUALITY OF URBAN UNDERGROUND SPACE IN CHINA

Jingwei Zhao<sup>1</sup>, Yu Sun<sup>\*2</sup>, Haoqi Li<sup>3</sup>, Yingge Zhu<sup>4</sup>

**Abstract:** As a critical spatial resource for expanding urban land use dimensions, the overall scale of urban underground space has been steadily increasing. Its development quality is influenced by various factors. Based on multi-source data, this study evaluates the development quality of urban underground space in 22 representative Chinese cities using the entropy method across four dimensions: Rari Transit (RT), Underground Space Construction (USC), Underground Space Resilience (USR), and Society Development (SD). Additionally, the PLS-SEM model is employed to analyze the driving forces and their action paths. The findings indicate that: 1) Shenzhen demonstrates the highest development quality in underground space, with underground space resilience (USR) being the most significant dimension affecting its development quality. Economic resilience emerges as the most crucial single indicator; 2) According to the PLS-SEM model, USR exhibits the strongest direct effect and serves as a key mediator. The path "society development(SD) → underground space resilience(USR) → urban underground space development quality(UUSDQ)" shows the most pronounced indirect effect; 3) Based on these results, two strategies are proposed: guiding spatial supply-side reform through social development and enhancing government decision-making efficiency by improving the management mechanism for underground space development. Specific development strategies are also suggested for cities with medium and low-quality underground spaces.

**Keywords:** Urban underground space, Development quality assessment, Entropy weight method, Driving factors, PLS-SEM modeling

### 1. INTRODUCTION

The development and utilization of underground space in Chinese cities encompasses a range of functions, including underground parking, commercial facilities, recreational spaces, and metro stations. Over the past 70 years, the construction approach has transitioned from an initial focus on civil air defense projects to one led by rail transit systems, and more recently, to a model guided by pedestrian activity demands. As a critical component of the so-called "fourth territory," urban underground space offers diverse services such as retail, dining, and entertainment(Tang & Tang, 2024). Its forward-looking spatial characteristics have elevated its development to a national strategic priority, positioning it as a key trend in future urban planning(The website of the Chinese government, 2024).

According to the \*2024 China Urban Underground Space Development Blue Book\*, by the end of 2023, the total built area of urban underground space in China had reached 3,276 billion square meters. The per capita underground construction area increased from 3,49 m<sup>2</sup> in 2022 to 3,6 m<sup>2</sup> in 2023, indicating the vast scale of underground development( Beijing: Strategic Consultation Center et al., 2024). However, with rapid urbanization and the continuous expansion of existing underground infrastructure, available underground space resources are

<sup>1</sup> PhD, Zhao Jingwei, Ph.D. in Geotechnical Engineering, professor, College of Civil Engineering and Architecture, Shandong University of Science and Technology, 579 Qianwan Port Road, Qingdao, China, skd991560@sdust.edu.cn.

<sup>2</sup> MSc, Sun Yu, MSc in Architecture Eng., College of Civil Engineering and Architecture, Shandong University of Science and Technology, 579 Qianwan Port Road, Qingdao, China, skdsunyu@sdust.edu.cn.

<sup>3</sup> MSc, Li Haoqi, MSc in Architecture Eng., College of Civil Engineering and Architecture, Shandong University of Science and Technology, 579 Qianwan Port Road, Qingdao, China, 202482040002@sdust.edu.cn.

<sup>4</sup> PhD, Zhu Yingge, Ph.D. in Geotechnical Engineering, lecturer, College of Civil Engineering and Architecture, Shandong University of Science and Technology, 579 Qianwan Port Road, Qingdao, China, zhuyg0221@sdust.edu.cn.

being rapidly depleted(Wang et al., 2025). Consequently, the quality of underground space development has become increasingly significant. Scholars have conducted extensive empirical studies to identify the driving factors behind urban underground space development from multiple perspectives. For example, Zhao et al. (Zhao et al., 2025)applied a geographical detector method and identified three core indicators — above-ground commercial facility density, underground facility density, and population heat value—that significantly influence the spatial layout of underground commercial areas. Zeng & Chen (Zeng & Chen, 2018) used the length of operational metro lines as a proxy for underground space development intensity and found that cities with high population density and high GDP per unit area tend to develop underground infrastructure more rapidly. Sun et al. (Sun et al., 2018)measured underground development intensity using per-unit-area metrics and employed OLS regression to confirm that development scale is strongly correlated with social indicators such as resident population density, GDP per unit area, and vehicle ownership per hundred residents. Furthermore, Chen et al.(Chen et al., 2021), based on heat map data, demonstrated that population density not only exhibits a strong positive correlation with the morphological distribution and development intensity of underground space but also serves as a predictive factor for future development intensity. These findings collectively indicate that the configuration, form, and evolution of urban underground space are shaped by a multitude of interrelated factors.

Current research on the quality of underground space development primarily focuses on geological environmental conditions(Xiong et al., 2025; Zhang et al., 2023), subsurface resource quality(Guo et al., 2024; Yan et al., 2021), and macro-level governance frameworks(Wang et al., 2019; Yi, 2025). However, during the rapid development of urban underground infrastructure, other multidimensional factors — including policy interventions(Qiao & Peng, 2023), economic drivers(Chen et al., 2018; Yu et al., 2025; Zhao et al., 2025), rail transit expansion(Yu et al., 2025; Zhao et al., 2025), and underground resilience(Li & Wang, 2025; Luo et al., 2023)—also exert significant influence on development quality. Therefore, from a practical application standpoint, there is an urgent need to quantitatively assess the development quality of urban underground space. Additionally, understanding the driving forces across different dimensions and the causal relationships among them remains a critical research gap. To address this, this study employs spatial analysis techniques such as kernel density estimation and spatial autocorrelation to characterize the spatial distribution patterns of urban underground space in China. Subsequently, the entropy method is applied to evaluate the development quality of underground space in 22 selected cities. Finally, the PLS-SEM model is utilized to explore the underlying driving mechanisms and their paths, aiming to provide theoretical insights and practical references for the sustainable development of urban underground space.

## 2. MATERIAL AND METHODS

### 2.1. Spatial analysis

This paper visualizes the distribution and characteristics of underground space in Chinese cities using kernel density estimation and spatial autocorrelation methods. Kernel density estimation is a non-parametric statistical method in spatial analysis (Yang & Li, 2021) that describes the distribution pattern of random variables through density functions. The non-discrete continuous density surface generated by this method can simulate the continuity of density(Huang et al., 2023; Yang et al., 2019). In this study, streets are used as the minimum geographical spatial units to aggregate the kernel density values of underground space POIs (Points of Interest) and treat them as observations. Spatial autocorrelation includes global spatial autocorrelation and local spatial autocorrelation. Global spatial autocorrelation measures the clustering or dispersion of attribute values across spatial units within the entire study area, reflecting systematic spatial associations. Local spatial autocorrelation measures the spatial association between the attribute value of a specific spatial unit and its neighboring units(Fan & Myint, 2014; Meng et al., 2005). The calculation formula is as follows:

$$\text{Global Moran's I} = \frac{\sum_{i=1}^m \sum_{j=1}^m (x_i - \bar{x})(x_j - \bar{x}) W_{ij}}{S^2 \sum_{i=1}^m \sum_{j=1}^m W_{ij}} \quad (1)$$

$$\text{Local Moran's I} = \frac{(x_i - \bar{x}) \sum_{j=1}^m W_{ij} (x_j - \bar{x})}{S^2} \quad (2)$$

In the formula,  $m$  represents the number of geographical units involved in the calculation,  $\bar{x}$  represents the mean of the observed values (expressed as kernel density),  $S^2$  represents the variance of the observed values,  $W_{ij}$  represents the spatial weight between the  $i$ -th element and the  $j$ -th element, and  $x_i$  and  $x_j$  respectively represent the observed values of geographical units  $i$  and  $j$ .

## 2.2. Entropy method

The entropy method is an objective weighting approach that calculates the information entropy of indicators to reflect the magnitude of their information content. Its core principle is to determine the weight values of each evaluation indicator based on their respective information entropy. The calculation process is as follows:

### (1) Standardization processing

Range standardization is applied to render the 15 indicators dimensionless. The calculation formula is as follows:

When the indicator is a positive indicator, positive normalization processing is performed:

$$x_{ij} = \frac{x'_{ij} - \min(x'_{ij})}{\max(x'_{ij}) - \min(x'_{ij})} \quad (3)$$

When the indicator is a negative indicator, reverse normalization processing is applied:

$$x_{ij} = \frac{\max(x'_{ij}) - x'_{ij}}{\max(x'_{ij}) - \min(x'_{ij})} \quad (4)$$

In the formula,  $x'_{ij}$  represents the original data of the  $j$ -th indicator for the  $i$ -th city, and  $x_{ij}$  represents the data after standardization processing.

### (2) Weight computation

$$P_{ij} = \frac{x_{ij}^*}{\sum_{i=1}^n x_{ij}^*} \quad (5)$$

$$d_j = 1 - \left( -K \sum_{i=1}^n (P_{ij} \ln(P_{ij})) \right) \quad (6)$$

$$W_j = \frac{d_j}{\sum_{j=1}^m d_j} \quad (7)$$

In the formula,  $n$  denotes the number of cities,  $m$  denotes the number of evaluation indicators,  $P_{ij}$  denotes the proportion of the  $j$ -th indicator for the  $i$ -th city in the corresponding indicator,  $x_{ij}^*$  denotes the non-negatively shifted data,  $d_j$  denotes the information utility value (i.e., redundancy) of the  $j$ -th indicator, and  $W_j$  denotes the weight coefficient of the  $j$ -th indicator.

## 2.3. Partial Least Squares Structural Equation Modeling (PLS-SEM)

Partial least squares structural equation modeling (PLS-SEM) is a multivariate statistical technique that integrates principal component analysis, canonical correlation analysis, and ordinary least squares regression (Cepeda-Carrion et al., 2019). Unlike traditional methods, PLS-SEM does not require strict assumptions of multivariate normality, enabling researchers to simultaneously examine latent and observed variables. Additionally, it effectively uncovers latent relationships among variables even in the presence of multicollinearity, yielding more robust and reliable results. The PLS-SEM framework comprises two key components: the structural model (inner model), which specifies the relationships among latent variables, and the measurement model (outer model), which assesses the relationships between observed variables and their corresponding latent constructs. The calculation formulas are presented as follows:

$$X = \Lambda_x \xi + \delta \quad (8)$$

$$Y = \Lambda_y \eta + \varepsilon \quad (9)$$

$$\eta = C\eta + \Gamma\xi + \zeta \quad (10)$$

In the equation,  $X$  and  $Y$  represent exogenous and endogenous indicators, respectively.  $\Lambda$  denotes the relationship between observed variables and latent variables, while  $\delta$  and  $\varepsilon$  represent measurement errors.  $\eta$



refers to an endogenous latent variable,  $\xi$  represents an exogenous latent variable,  $C$  indicates the influence of exogenous latent variables on endogenous latent variables,  $\Gamma$  reflects the effect of some endogenous latent variables on other endogenous latent variables, and  $\zeta$  signifies the regression residual (Wang et al., 2022).

### 3. RESEARCH AREA AND DATA SOURCES

#### 3.1. Research Area and Assessment Framework

To analyze the spatial layout characteristics of urban underground space, this study defines the administrative regions of China as the research scope and employs kernel density estimation to visualize the distribution patterns of underground space points of interest (POIs). When assessing the development quality of urban underground space, it is essential to consider its multidimensional nature, which encompasses rail transit infrastructure, administrative governance, and underground space resilience. Given the current strong reliance on rail transit in underground space development and construction, the selected cities must possess comprehensive datasets for all required evaluation indicators. Considering both data integrity and accessibility, this study selects 22 cities from the 58 Chinese cities that have operational rail transit systems. The selected sample includes 9 super-large cities, 10 large cities, and 3 Type-I medium-sized cities (Table 1), representing three distinct levels of urban scale. These cities were chosen due to their early initiation of underground space development, the existence of formal underground space-related laws and regulations, and the overall suitability of their development contexts for quality evaluation.

*Table 1. Basic information of 22 sample cities.*

The underground space cluster to which it belongs	City	City classification	Rail transit mileage (km)	Permanent resident population density (persons/km <sup>2</sup> )	Per capita GDP (ten thousand yuan)
Beijing-Tianjin-Hebei Urban Agglomeration	Beijing	Hyper-city	897	1332	20,02
	Tianjin	Hyper-city	334,92	1140	12,27
	Hebei	Type-I large city	74,28	710	7,29
Shandong Peninsula Urban Agglomeration	Jinan	Megacity	96,7	921	13,52
	Qingdao	Megacity	352,1	918	15,2
Central Plains Urban Agglomeration	Zhengzhou	Megacity	415,55	1719	10,47
	Xian	Megacity	422,21	1295	9,18
Yangtze River Mid-Reach Urban Agglomeration	Wuhan	Hyper-city	518	1622	14,53
	Changsha	Megacity	236,35	898	14,38
Yangtze River Delta Urban Agglomeration	Shanghai	Hyper-city	896	3923	18,98
	Suzhou	Megacity	350	1479	19,03
	Wuxi	Type-I large city	143,93	1619	20,62
	Nanjing	Megacity	484	1449	18,24
	Hangzhou	Hyper-city	516	743	16,02
Chengdu-Chongqing Dual-city Economic Circle	Chengdu	Hyper-city	633,3	1493	10,31
	Chongqing	Hyper-city	575	387	10,09
Guangdong-Hong Kong-Macao Greater Bay Area	Shenzhen	Hyper-city	595,1	8906	19,45
	Guangzhou	Hyper-city	705,1	2532	16,12
	Foshan	Megacity	150	2532	13,81
Guangdong-Fujian-Zhejiang Coastal Urban Agglomeration	Xiamen	Type-I large city	98,4	3135	15,14
Liaozhongnan Urban Agglomeration	Dalian	Megacity	237	599	11,61
	Shenyang	Megacity	188	1799	8,82

Based on existing literature and prior research on urban underground space development, this paper establishes four first-level indicator dimensions: rail transit, underground space construction, underground space resilience, and social development. Rail transit (RT) reflects a city's capacity to integrate rail lines within its underground space, the proportion of public transportation borne by rail transit, and the degree of alignment between rail transit networks and job-residence spatial patterns. Underground space construction (USC) indicates the level of underground development through indicators such as functional diversity, the rate of infrastructure

undergroundization, and facility clustering. Underground space resilience (USR) measures the system's adaptability in policy, economic, and institutional dimensions, using indicators including the number of relevant laws and regulations, GDP per unit area of underground space, and the proportion of investment in science, technology, and education relative to GDP. Social development (SD) captures foundational driving factors for high-quality underground space development, including demand for underground space utilization, economic feasibility, and overall societal development levels. A total of 15 indicators were selected to construct the evaluation framework for urban underground space development quality (Table 2).

**Table 2.** Evaluation Framework for Urban Underground Space Development Quality.

Overall Goal	First-Level Indicators	Second-Level Indicators	Indicator Description	Weight (%)	Indicator Attribute
Urban Underground Space Development Quality (UUSDQ)	Rail Transit (RT)	Integration degree	Average Integration Degree of Rail Transit Lines	3,75	+
		Orbital coverage	Proportion of 800-Meter Rail Transit Coverage for Commuting	4,37	+
		Rail transit passenger share	Rail Transit Passenger Volume as a Share of Total Public Transport Volume	3,66	+
		Commuting accessibility	Proportion of Rail Transit Service Capacity within a 45-Minute Travel Time	2,66	+
	Underground Space Construction (USC)	Static transportation infrastructure	Underground Parking Lot Ratio (Share of Total Parking Lots)	5,48	+
		Underground facility utilization rate	Urban Underground Space POI Density Ratio (Share of Total POIs)	8,09	+
		Functional diversity index	Functional Diversity Index of Underground Facilities in Urban Built-Up Areas	3,06	+
		Underground facility agglomeration level	Optimal Agglomeration Scale from Multi-Distance Spatial Clustering Analysis	6,53	+
	Underground Space Resilience (USR)	Policy resilience	Number of Enacted Laws and Regulations on Underground Space	7,19	+
		Economic resilience	GDP per Unit Administrative Area	17,00	+
		Institutional and organizational resilience	Scientific Research and Education Investment as a Share of Regional GDP	9,48	+
	Society Development (SD)	Population density	Population Density Based on Permanent Residents and Urban Administrative Area	13,48	+
		Nighttime light intensity	Annual Average Nighttime Light Intensity	5,04	+
		Economic development level	Per Capita Regional GDP (Regional GDP Divided by Permanent Resident Population)	5,26	+
		Urbanization rate	Urban Population Proportion in Total Population	4,95	+

### 3.2. Data Source

The vector map of urban administrative districts was obtained from Tianditu ([www.tianditu.gov.cn](http://www.tianditu.gov.cn)); road network data were sourced from OpenStreetMap ([www.openstreetmap.org](http://www.openstreetmap.org)); rail transit commuting proportions and related data were derived from the Commuting Monitoring Report of Major Chinese Cities; per capita GDP, legal regulations, and other relevant data were collected from municipal statistical yearbooks and official government websites; nighttime light data were provided by the Earth Observation Group

(<https://payneinstitute.mines.edu/eog/>); POI (Point of Interest) and additional datasets were extracted from Amaps ([www.amap.com](http://www.amap.com)). All data are valid as of April 2025.

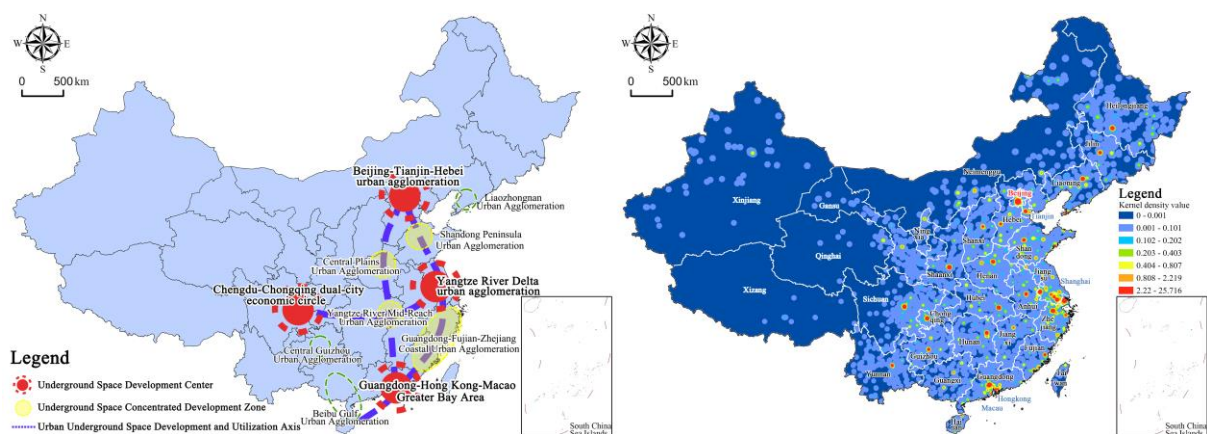
## 4. RESULTS

### 4.1. Spatial Analysis Results

#### 4.1.1. Urban underground space development in China exhibits a spatial pattern characterized by "four centers, four clusters, three axes, and multiple points".

Currently, the development pattern of urban underground space in China exhibits a structure characterized as "four centers, four clusters, three axes, and multiple points." Along the three major urban development axes—coastal regions, the Yangtze River corridor, and the Beijing-Guangzhou line—four key underground space development centers have emerged: the Beijing-Tianjin-Hebei urban agglomeration, the Yangtze River Delta urban agglomeration, the Guangdong-Hong Kong-Macao Greater Bay Area, and the Chengdu-Chongqing dual-city urban agglomeration. These regions represent critical zones for realizing compact and intensive development through functional integration and three-dimensional urban planning in the new era. Moreover, they constitute the leading force driving high-quality underground space development nationwide. In addition, various underground space development clusters have formed around central cities of different scales, including the coastal urban agglomerations of Guangdong-Fujian-Zhejiang, the Shandong Peninsula urban agglomeration, the Central Plains urban agglomeration, and the Yangtze River Mid-reach urban agglomeration. In these areas, underground space development is notably more advanced in the core cities of each urban cluster. Furthermore, in provinces such as Liaoning, Guizhou, and Guangxi, as underground space utilization expands in both scale and sophistication, distinct regional nodes with significant development have gradually taken shape.

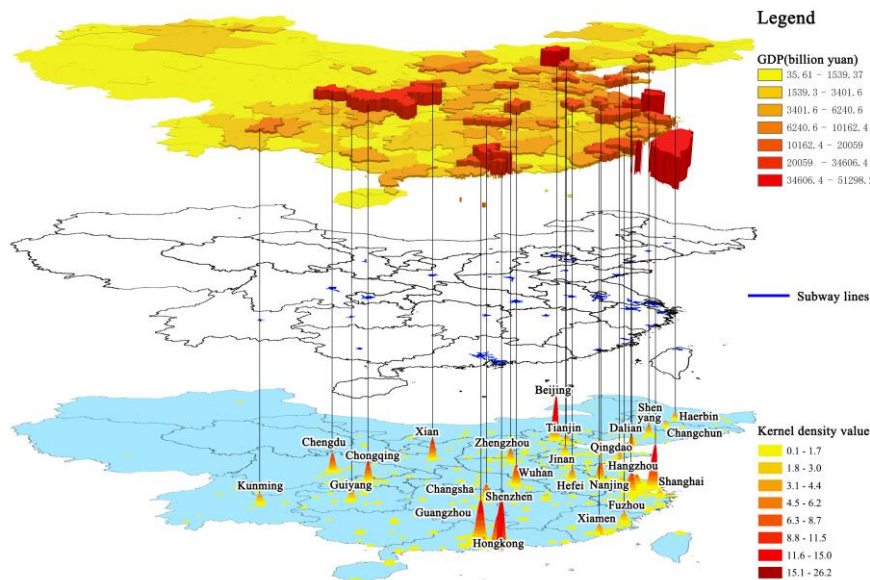
Kernel density analysis of underground facility POIs at a clustering scale of 28 km reveals that most regions exhibit relatively low kernel density values, generally below 0.101. The range of high-density areas falls between 2,22 and 25,716, highlighting substantial disparities in the extent of underground space development and utilization across cities. Spatially, the concentration of underground facilities declines progressively from the eastern coastal regions toward the central and western parts of the country. Provincial capitals and administrative centers demonstrate higher levels of clustering compared to other cities. Moreover, cities with well-developed underground infrastructure exert a radiating influence on surrounding areas. For example, large-scale underground space development centers have formed in metropolitan regions such as the Yangtze River Delta and the Beijing-Tianjin-Hebei urban agglomeration. In contrast, regions in western and northern China—including Xinjiang, Tibet, Qinghai, and Inner Mongolia—show relatively limited underground space development, with facilities remaining spatially fragmented and dispersed (Figure 1).



**Figure 1.** Development Patterns and Spatial Layout Characteristics of Urban Underground Space in China.

The development and construction costs of urban underground space are approximately two to three times higher than those of surface buildings, necessitating substantial financial investment and advanced technological support. Among various underground facilities, the underground rail transit system occupies a central position due to its strong capacity for alleviating urban traffic congestion, efficient use of land resources, and critical role in

advancing sustainable urban development. A superimposed analysis of nuclear density, metro lines, and GDP data for underground space facilities in major Chinese cities reveals a high degree of spatial consistency between underground infrastructure distribution and metro line layouts. This indicates that the planning and layout of underground rail transit systems significantly influence the spatial distribution of underground facilities. Furthermore, the spatial pattern of underground space facilities demonstrates a concentric decline from the city center outward, closely reflecting the agglomeration characteristics of urban economic activities and the spatial structure of urban development. There is also a clear positive correlation between urban GDP levels and the density of underground space facilities—cities with stronger economies can afford higher development costs and adopt more advanced technologies, resulting in a more concentrated and extensive underground facility network (Figure 2).

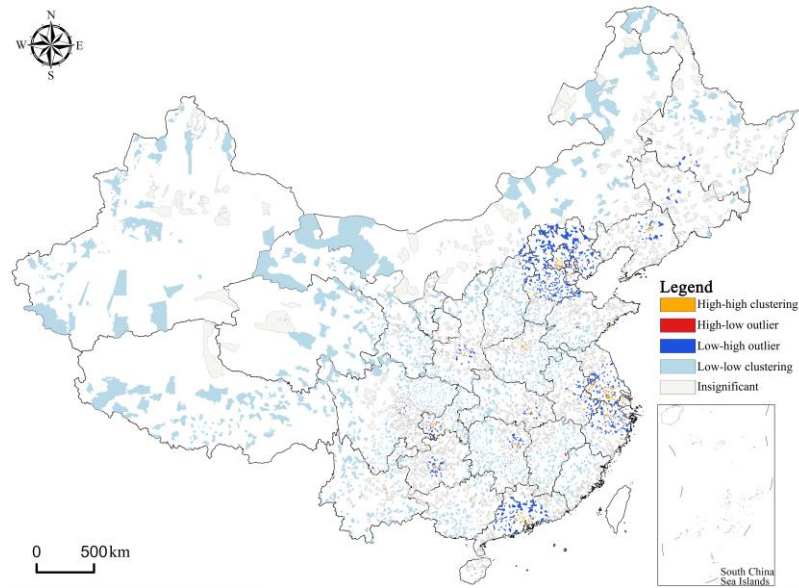


**Figure 2.** Overlay Analysis of Underground Space Agglomeration, Subway Networks, and GDP.

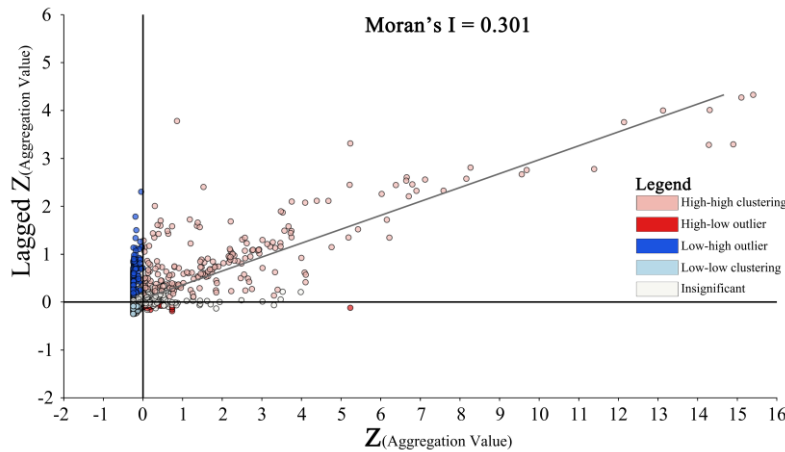
#### 4.1.2. The development centers of urban underground space exhibit significant agglomeration characteristics.

Urban underground facilities were aggregated at the street level as the basic spatial unit for nuclear density calculation, followed by spatial autocorrelation analysis. The global Moran's Index ranges from -1 to 1, where an absolute value closer to 1 indicates stronger spatial correlation within the system. A positive value reflects positive spatial autocorrelation, while a negative value suggests negative autocorrelation. The results show that the global Moran's Index for urban underground space in China is 0,301, with a Z-score of 176,645 and a statistically significant p-value of 0,000. This confirms the presence of significant positive spatial agglomeration in the distribution of underground space across Chinese cities.

According to the local Moran's Index (Figure 3), high - high clustering types are relatively rare, whereas low - low clustering dominates the spatial pattern. However, small-scale high - high clusters have formed around each "underground space development center," surrounded by larger low - high clustering zones. As shown in the local Moran's scatter plot (Figure 4), although the number of low - low clusters (3,384) far exceeds that of high - high clusters (635), the low - low clusters in the third quadrant are distributed closer to the origin, indicating both the cluster and its neighboring areas exhibit nuclear density values significantly below the average. This implies weak spatial autocorrelation among low-density regions—despite their wide distribution, these areas remain scattered and do not form strong spatial agglomeration. In contrast, high - high clusters in the first quadrant are more widely dispersed with higher local Moran's Index values. These clusters, concentrated around the "underground space development centers," not only exhibit higher internal density but also effectively stimulate the development of surrounding underground infrastructure, leading to the formation of multiple low - high clustering development belts. This further demonstrates stronger spatial autocorrelation among high - high clustering areas.



**Figure 3.** The results of the local Moran's I.



**Figure 4.** Scatter plot of local Moran's I.

## 4.2. Assessment of Development Quality

### 4.2.1. Classification of Evaluation Outcomes

The UUSDQ was assessed across 22 cities (Figure 5). Among them, Shenzhen achieved the highest score of 0,748, while Shijiazhuang scored the lowest at 0,143. The average development quality index was 0,334, with a difference of more than 0,605 between the highest and lowest scores, indicating substantial inter-city disparities in underground space development quality. To better reflect these differences, the comprehensive evaluation scores were categorized using one standard deviation as the classification criterion. Accordingly, the UUSDQ was classified into four levels: high (0,469–0,748), relatively high (0,334–0,469), medium (0,197–0,334), and relatively low (0–0,197). Analysis reveals that Shenzhen and Shanghai fall into the high-quality category; seven cities, including Beijing and Guangzhou, are classified as relatively high quality; eleven cities, such as Xi'an and Wuxi, fall into the medium-quality group; and Dalian and Jinan are categorized as having relatively low development quality.



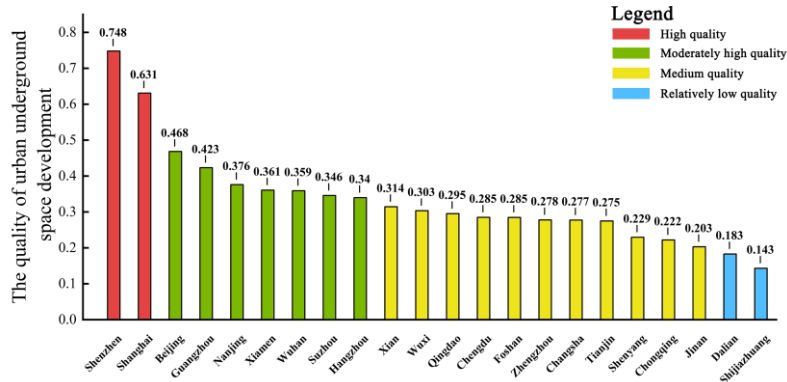


Figure 5. Assessment Results of Urban Underground Space Development Quality.

#### 4.2.2. Analysis of Weighting Factors

As illustrated by the index weights and evaluation scores across each dimension (Figure 6), among the first-level indicators, USR (33,67%) and SD (28,73%) carry the highest weights, and their respective scores contribute significantly to the overall evaluation score. These two dimensions thus represent the most influential factors in determining the quality of urban underground space development. Within the SD dimension, permanent resident population density and urbanization rate reflect the actual demand for underground space development, whereas per capita GDP and nighttime light intensity directly indicate a city's investment capacity and economic strength in this domain. Consequently, the SD dimension holds a substantial weight in the overall assessment. In the USR dimension, laws and regulations, GDP per unit area, and the proportion of investment in scientific research and education exert significant influence across multiple stages, including planning approaches, construction scope, and developmental direction.

Among the second-level indicators, economic resilience within the USR dimension and population density within the social development dimension exhibit the highest individual weights, at 17,00% and 13,48%, respectively.

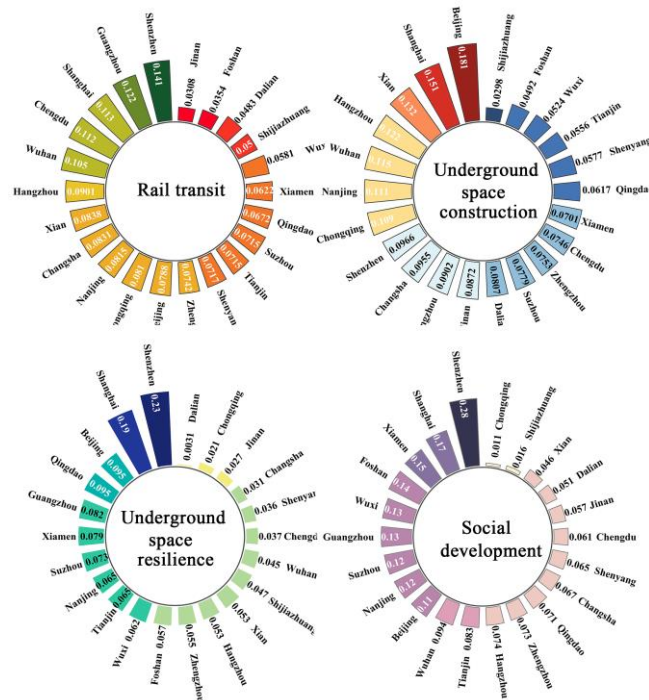


Figure 6. First-Level Indicator Scores for Urban Underground Space Development Quality.

### 4.3. Driving Force Analysis Using the PLS-SEM Model

#### 4.3.1. PLS-SEM Model Development

Although the comprehensive evaluation based on the entropy method revealed differences in UUSDQ scores among cities and highlighted the contribution of key indicators, the use of static weights limited the ability to interpret the dynamic interactions among dimensions. Therefore, this study further employed PLS-SEM to investigate the mechanisms and internal influence paths of each indicator on urban underground space development quality. Data were imported into SmartPLS 4 software, with RT, USC, USR, and SD defined as latent variables and the 15 second-level indicators serving as observed variables. After processing through the PLS-SEM algorithm, the observed variable "policy resilience," which exhibited a negative outer loading, was removed, leading to the construction of the final PLS-SEM model for underground space development quality.

The significance of the model paths and potential multicollinearity were assessed using the bootstrap method (5,000 resamples) and variance inflation factor (VIF) values, respectively. The results indicated that the highest VIF value across all observed variables was 3,445, suggesting no significant multicollinearity issues within the dataset. In the structural model, all path coefficients between latent variables showed p-values less than 0,05, confirming statistical significance (Table 3).

*Table 3. Path Analysis of the PLS-SEM Model.*

Path	Original sample	Standard deviation	T statistics	P value
USC→UUSDQ	0,221	0,109	2,020	0,043*
USR→UUSDQ	0,431	0,128	3,358	0,001***
SD→UUSDQ	0,362	0,112	3,222	0,001***
RT→UUSDQ	0,190	0,087	2,186	0,029*
SD→USR	0,818	0,039	21,011	0,000***
RT→USC	0,555	0,096	5,791	0,000***

Note: \*p<0,05, \*\*\*p<0,001

#### 4.3.2. Results and Analysis of Model Operation

In the PLS-SEM model results, the path values between observed variables and latent variables represent the factor loadings of the observed variables, where the magnitude indicates their explanatory power on the corresponding latent variables. The path values between latent variables are referred to as path coefficients ( $\beta$ ), which reflect the strength of the causal relationships among latent variables. The values within the circles associated with each latent variable represent the coefficient of determination ( $R^2$ ), indicating the proportion of variance in a given latent variable explained by other latent variables in the model. A higher  $R^2$  value suggests stronger explanatory and predictive power of the model (Figure 7). Specifically, the  $R^2$  value for the latent variable "UUSDQ" is 0,984, meaning that RT, USC, USR, and SD collectively explain 98,4% of its variance, demonstrating that the model has strong explanatory capability.

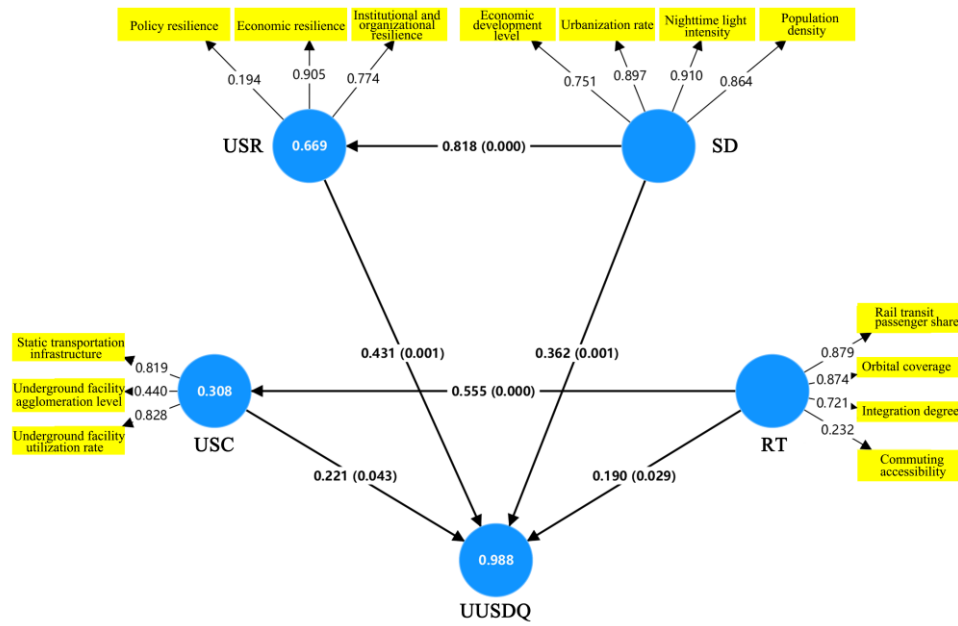


Figure 7. Results of the PLS-SEM Model Operation.

All four dimensions exert a significant positive driving effect on the UUSDQ. Among the direct effect paths influencing this development quality, USR demonstrates the strongest impact ( $\beta = 0.431$ ). The legal framework governing underground space, per capita GDP, and the proportion of investment in science, technology, and education directly enhance the stability of underground resilience from policy, economic, and institutional perspectives, thereby influencing the overall development quality of urban underground space. Thus, USR serves as the key driving force. Additionally, SD also exerts a relatively strong influence ( $\beta = 0.329$ ). Indicators such as per capita GDP, urbanization rate, nighttime light intensity, and permanent resident population density are closely associated with the economic capacity for investment and the demand for underground space, making them important determinants of UUSDQ.

Among all direct effect paths, the path coefficient between SD and USR is the highest ( $\beta = 0.818$ ), indicating a highly significant positive relationship. The comprehensive development level of cities or regions significantly enhances the risk response capability of underground space systems—such as their ability to cope with disasters and resource shortages. In other words, the accumulation of social resources strongly supports the systematic construction of underground space. Infrastructure investment and facility undergroundization driven by SD directly reinforce the resilience of underground space, highlighting its role as a critical driver. Moreover, the path coefficient for “RT → USC” is also substantial ( $\beta = 0.555$ ), suggesting a significant positive correlation. The completeness and operational efficiency of urban rail transit systems strongly promote the efficiency of underground space development, reflecting a high degree of synergy between transportation infrastructure and underground space utilization.

Among the indirect effect paths, only the path “SD → USR → UUSDQ” has a statistically significant P value (0.002), with an indirect effect of 0.352. Notably, the direct effect of SD on USR ( $\beta = 0.818$ ) is significantly stronger than that of USR on UUSDQ ( $\beta = 0.431$ ), indicating that SD constitutes a more fundamental driving factor. According to the mediation effect test method (Wen et al., 2004), USR functions as a mediator within this path. This implies that SD not only directly influences the UUSDQ but also indirectly affects it through the mediating variable of USR.

## 5. DISCUSSION

### 5.1. Discussion on Spatial Analysis

The overall density of underground space in Chinese cities remains relatively low, and its spatial distribution exhibits a clear “core-periphery” pattern. In major development centers such as the Beijing-Tianjin-Hebei region and the Yangtze River Delta, underground space density is significantly higher, displaying a high-high clustering pattern. These regions not only serve as China's key economic growth poles but also feature high GDP levels and

population densities, which provide a solid economic foundation and strong market demand for underground space development. In concentrated development zones and key nodes—such as the Shandong Peninsula urban agglomeration (Jinan, Qingdao), the Central Yangtze River urban agglomeration (Wuhan, Changsha), and the Liaozhongnan urban agglomeration (Shenyang)—underground space development primarily depends on provincial capitals, administrative centers, and prefectural-level cities, leading to the formation of smaller-scale underground clusters. Collectively, these areas constitute the "core areas" of urban underground space in China.

In contrast, the "peripheral areas" surrounding the core regions exhibit lower underground space density, predominantly characterized by low-low clustering. Moreover, the development cost of underground space is relatively high, and its utilization heavily relies on surface infrastructure and urban development. Consequently, despite the large number of low-low clustered zones in these peripheral regions, systematic underground clusters and interconnected networks have yet to emerge due to limitations in development maturity and regional economic capacity. At present, China's macro-level policies on underground space prioritize the advancement of regions with existing advantages in this domain. The focus of underground facility construction lies in comprehensive utility tunnels (The State Council of the People's Republic of China, 2024) and consumption-oriented facilities (The State Council of the People's Republic of China, 2025), further enhancing the development level and spatial concentration of underground space in the core areas.

## 5.2. Discussion on Development Quality Assessment

The evaluation system assesses the quality of urban underground space development by integrating the actual usage efficiency of underground facilities with the level of social development. For example, the indicator "railway coverage" is defined as the proportion of commuting population in central urban areas whose residences and workplaces are both located within 800 meters of a rail transit station. Similarly, the "institutional and organizational resilience" indicator under the underground space resilience dimension is measured by the proportion of investment in science, technology, and education relative to regional GDP. These indicators strictly follow the established criteria for constructing the urban underground space development quality index. Within each of the four quality tiers, spatial disparities among cities are relatively small; however, the gap between the high-quality tier and the relatively high-quality tier is substantial.

Among high-quality cities, Shenzhen demonstrates outstanding performance across RT, USR, and SD dimensions, while Shanghai also ranks highly across all indicators. As a result, both cities are classified as high-quality and significantly outperform other megacities and large cities such as Shijiazhuang and Jinan. In the relatively high-quality group, the overall development quality is constrained by low scores in specific dimensions. For instance, Suzhou ranks 13th in USR, and Xiamen ranks 17th in RT performance. In medium- and lower-quality cities, most indicators score at or below average levels, resulting in an overall lower development quality. Nevertheless, some cities exhibit strengths in certain dimensions—for example, Qingdao ranks 4th in USR, and Suzhou ranks 5th in SD.

According to the entropy method, higher indicator weights indicate greater informational content (Luo et al., 2023), which reflects larger inter-city differences in underground space development quality. USR and SD carry the highest weights at 33.67% and 28.73%, respectively. Economic resilience and population factors rank first and second among individual indicators, with weights of 17.00% and 13.48%. Considering the meanings of these two factors, Shenzhen and Shanghai had population densities of 8.906 people/km<sup>2</sup> and 3.923 people/km<sup>2</sup>, respectively, and economic resilience values of 17.32 billion yuan/km<sup>2</sup> and 7.44 billion yuan/km<sup>2</sup> by the end of 2024. These figures highlight the significantly higher demand for underground space and stronger regional economic support capabilities in these two cities compared to others, contributing to their superior performance on key indicators.

## 5.3. Discussion on Driving Forces and Mechanisms

The PLS-SEM model reveals that underground space resilience exerts the strongest direct positive influence on the quality of underground space development among all latent variables. This finding aligns with its corresponding maximum weight value in the evaluation system. As reflected by its observed indicators, underground space resilience primarily captures the system's capacity to respond to risks and the ability of local governments to provide administrative guidance and intervention in the planning, construction, and management of underground space. Given the highly irreversible nature of underground development, enhanced resilience, forward-looking planning, and supportive legal frameworks are essential for promoting sustainable and healthy development. Therefore, underground space resilience influences development quality through multiple dimensions, including risk mitigation, technological advancement, and strategic planning.

In terms of direct effects, SD demonstrates the most substantial impact on underground space resilience, with a path coefficient of 0.818. This indicates a strong positive relationship between SD and USR. The observed variables associated with this latent construct reflect fundamental factors such as underground space demand,

urban supply capacity, and the extent of infrastructure undergroundization. These factors not only directly shape the overall quality of underground space development from a supply-demand perspective but also rely on underground space resilience as a mediating mechanism to amplify their positive influence. Specifically, the indirect effect path—SD → USR → UUSDQ—demonstrates that SD can drive improvements in underground space quality at a foundational level. The resulting demand and construction activities necessitate both proactive and effective governance from local authorities, as well as the mediating role of underground space resilience.

## 6. CONCLUSION

This study selected 15 evaluation indicators and applied a combined weighting method to assess the quality of underground space development across 22 Chinese cities. The assessment was conducted from four dimensions: RT, USC, USR, and SD. Furthermore, the PLS-SEM model was employed to explore the driving forces and their underlying paths influencing urban underground space development quality. The following conclusions were drawn:

(1) The spatial distribution of underground space in Chinese cities exhibits an overall pattern characterized as "four centers, four clusters, three axes, and multiple points." The degree of agglomeration is higher in eastern coastal regions compared to central and western regions, and provincial capitals and municipalities show greater facility concentration than other cities. A significant positive spatial autocorrelation exists in the distribution of underground space. While low-low clustering areas are more widespread, high-high clustering areas are concentrated around key development centers and clustered zones.

(2) Shenzhen achieves the highest score (0,748) for UUSDQ and outperforms other cities in RT, USR, and SD. Although inter-city differences within each quality tier are relatively small, substantial gaps exist between tiers. In the evaluation system, USR is identified as the most influential dimension, with a weight of 33,67%. Economic resilience ranks as the most impactful single indicator, carrying a weight of 17,00%.

(3) RT, USC, USR, and SD all exert positive driving effects on underground space quality. Among these, USR demonstrates the strongest direct effect, with a path coefficient of 0.431. Moreover, it plays a mediating role in the indirect path "SD → USR → UUSDQ," which has an indirect effect coefficient of 0.352. This provides a novel causal explanation for the determinants of underground space quality.

(4) To enhance underground space development, it is essential to improve management mechanisms and increase government decision-making efficiency, guided by social development-led supply-side reforms. Coordination among planning, administrative approval, and regulatory departments should be strengthened to optimize a government-led, multi-stakeholder public service delivery model that integrates market and social resources. Increasing investment in science, technology, and education can facilitate the transformation of research outcomes into improvements in underground space quality. Additionally, development strategies should prioritize people's needs, allocating underground functions based on population density gradients. In highly urbanized cities, integrating underground space into 15-minute living circle standards or broader regional frameworks can promote the equitable expansion of underground infrastructure.

(5) Cities with high-quality underground space development should consolidate existing strengths while addressing weaker dimensions to achieve comprehensive improvement. For instance, Suzhou and Xiamen exhibit relatively low integration and commuting coverage levels within their tier and should focus on enhancing rail transit efficiency and strengthening its support for residential and employment spaces. Xi'an and Hangzhou could establish dedicated underground space R&D funds to accelerate the industrialization of patented technologies, thereby transforming regional economic innovation into enhanced underground resilience.

(6) For cities with medium- and low-quality development, it is crucial to identify both advantages and weaknesses and implement targeted interventions. Qingdao, despite having a robust legal framework for underground space, suffers from low rail line integration and limited underground facilities. Therefore, constructing commercial and cultural complexes centered on transportation hubs, linking fragmented rail lines, and developing integrated mountain-sea-city transfer systems are recommended. Tianjin demonstrates strong scientific investment (3.33%) and high urbanization rates (>85%), but lags in underground parking and facility penetration. Enhancing vertical development in high-density zones and establishing functional coupling mechanisms across vertical layers can help address this imbalance. Chongqing shows moderate rail transit coverage (20% for commuting populations) but lacks sufficient legal frameworks and economic strength. Strengthening its economic foundation and configuring underground facilities according to population density and development intensity gradients, along with incorporating underground planning into general urban plans, would support sustainable growth.

All 22 cities analyzed in this study have rail transit coverage. During indicator selection and PLS-SEM model construction, rail transit factors were adequately considered. When applying this model to cities without rail transit or expanding the scope of analysis, alternative data sources such as bus card swiping records or ride-hailing GPS



density within underground facility coverage areas can be used to maintain model applicability across diverse regions.

## 7. FUNDING

This research was funded by the Qingdao Philosophy and Social Sciences Planning Project (QDSKL2401105), and the Qingdao Double Hundred Research Project (2024-B-136).

## 8. REFERENCES

- [1] Cepeda-Carrion, G., Cegarra-Navarro, J.-G., & Cillo, V. (2019). Tips to use partial least squares structural equation modelling (PLS-SEM) in knowledge management. *Journal of Knowledge Management*, 23(1), 67–89. <https://doi.org/10.1108/JKM-05-2018-0322>.
- [2] Chen, Y., Zhao, Z., Guo, D., Zou, D., & Chen, Z. (2021). Research on the Correlation between Urban Underground Space and Population Distribution. *Chinese Journal of Underground Space and Engineering*, 17(3), 637–648(in Chinese).
- [3] Chen, Z.-L., Chen, J.-Y., Liu, H., & Zhang, Z.-F. (2018). Present status and development trends of underground space in chinese cities: Evaluation and analysis. *Tunnelling and Underground Space Technology*, 71, 253–270. <https://doi.org/10.1016/j.tust.2017.08.027>.
- [4] Fan, C., & Myint, S. (2014). A comparison of spatial autocorrelation indices and landscape metrics in measuring urban landscape fragmentation. *Landscape and Urban Planning*, 121, 117–128. <https://doi.org/10.1016/j.landurbplan.2013.10.002>.
- [5] Guo, J., Liu, K., & Ma, Y. (2024). A methodology for comprehensive quality evaluation of underground space. *Acta Geologica Sinica - English Edition*, 98(6), 1637–1648. <https://doi.org/10.1111/1755-6724.15147>.
- [6] Huang, J., Lu, H., Jin, H., & Zhang, L. (2023). Urban resilience in China's eight urban agglomerations: Evolution trends and driving factors. *Environmental Science and Pollution Research*, 32(6), 3072–3098. <https://doi.org/10.1007/s11356-023-30971-1>.
- [7] Li, C., & Wang, Y. (2025). Evaluation of the underground space safety resilience of chinese urban agglomerations based on the “stress-state-response”:a case study of underground rail transit in 26 cities. *Journal of Safety Science and Resilience*, S266644962500026X. <https://doi.org/10.1016/j.jnlssr.2025.02.001>.
- [8] Luo, B., Peng, F., Liu, S., & Dong, Y. (2023). Evaluation indicators and models of urban underground space resilience. *Journal of Railway Science and Engineering*, 20(9), 3570–3578. [https://doi.org/10.19713/j.cnki.43-1423/u.t20221866\(in Chinese\)](https://doi.org/10.19713/j.cnki.43-1423/u.t20221866(in Chinese)).
- [9] Meng, B., Wang, J., Zhang, W., & Liu, X. (2005). Evaluation of Regional Disparity in China Based on Spatial Analysis. *SCIENTIA GEOGRAPHICA SINICA*, 25(4). [https://kns.cnki.net/KCMS/detail/detail.aspx?dbcode=CJFQ&dbname=CJFD2005&filename=DLKX200504001\(in Chinese\)](https://kns.cnki.net/KCMS/detail/detail.aspx?dbcode=CJFQ&dbname=CJFD2005&filename=DLKX200504001(in Chinese)).
- [10] Qian Qihu, Chen Xiangsheng, Chen Zhilong, et al. 2024 Blue Book on the Development of Urban Underground Space in China [R]. Beijing: Strategic Consultation Center, Chinese Academy of Engineering; Underground Space Branch, Chinese Society for Rock Mechanics and Engineering; Urban Planning Society of China, 2024. (in Chinese).
- [11] Qiao, Y., & Peng, F. (2023). Advances and Development Thoughts on Three-Dimensional Urban Underground Cadastre. *Chinese Journal of Underground Space and Engineering*, 19(2), 359–367, 409(in Chinese).
- [12] Sun, L., Li, X., Zhou, D., Wang, W., & Liu, C. (2018). Study on the Correlation between Underground Space Development and Socio-economic Factors. *Chinese Journal of Underground Space and Engineering*, 14(4), 859–868, 880(in Chinese).
- [13] Tang, Y., & Tang, Y. (2024). Analysis of the spatial characteristics and driving forces of underground consumer service space in chinese megacities based on multi-source data. *Sustainable Cities and Society*, 116, 105924. <https://doi.org/10.1016/j.scs.2024.105924>.
- [14] The State Council of the People's Republic of China. Guidance on Exploring and Promoting the Development and Utilization of Urban Underground Space (No. 146 of 2024 issued by the Ministry of Natural Resources) [EB/OL]. (2024-07-31) [2025-06-01]. [https://www.gov.cn/zhengce/zhengceku/202409/content\\_6974170.htm\(in Chinese\)](https://www.gov.cn/zhengce/zhengceku/202409/content_6974170.htm(in Chinese)).
- [15] The State Council of the People's Republic of China. Notice on Carrying out the 2025 Central Government Financial Support for Urban Renewal Actions (Cai Ban Jian [2025] No. 11) [EB/OL]. (2025-04-03) [2025-06-01]. [https://www.gov.cn/zhengce/zhengceku/202504/content\\_7017720.htm\(in Chinese\)](https://www.gov.cn/zhengce/zhengceku/202504/content_7017720.htm(in Chinese)).
- [16] The website of the Chinese government. Opinions on Promoting the Innovative Development of Future Industries by Seven Departments Including the Ministry of Industry and Information Technology (MIIT Joint Science and Technology [2024] No. 12) [EB/OL]. (2024-01-18) [2025-01-25]. [https://www.gov.cn/zhengcezhengceku/202401/content\\_6929021.htm\(in Chinese\)](https://www.gov.cn/zhengcezhengceku/202401/content_6929021.htm(in Chinese)).
- [17] Wang, C., Ma, L., Zhang, Y., Chen, N., & Wang, W. (2022). Spatiotemporal dynamics of wetlands and their driving factors based on PLS-SEM: a case study in wuhan. *Science of the Total Environment*, 806, 151310. <https://doi.org/10.1016/j.scitotenv.2021.151310>.

- [18] Wang, C., Zhou, C., Peng, J., Fan, J., Zhu, H., Li, X., Cheng, G., Dai, C., & Xu, N. (2019). A discussion on high-quality development and sustainable utilization of China's urban underground space in the new era. *Earth Science Frontiers*, 26(3), 1–8. <https://doi.org/10.13745/j.esf.sf.2018.9.2>(in Chinese).
- [19] Wang, H., Guo, D., Wei, L., Su, J., Zhao, H., & Zhao, X. (2025). Synergistic priority utilization of multiple underground resources: Concept, methods, and application. *Tunnelling and Underground Space Technology*, 162, 106642. <https://doi.org/10.1016/j.tust.2025.106642>.
- [20] Wen, Z., Zhang, L., Hou, T., & Liu, H. (2004). TESTING AND APPLICATION OF THE MEDIATING EFFECTS. *Acta Psychologica Sinica*, 36(5), 614–620(in Chinese).
- [21] Xiong, Y., Li, X., Yuan, F., Lu, Z., Wu, S., & Dou, F. (2025). 3D evaluation of geological environment quality in underground space based on clustering ensemble. *JOURNAL OF HEFEI UNIVERSITY OF TECHNOLOGY (NATURAL SCIENCE)*, 48(1), 78–84, 91(in Chinese).
- [22] Yan, J., Zhao, Y., Wang, Z., Wang, Liu, K., Ren, T., & Xu, B. (2021). Comprehensive quality evaluation of underground space resources in Yinchuan City. *GEOLOGICAL BULLETIN OF CHINA*, 40(10), 1636–1643(in Chinese).
- [23] Yang, Y., & Li, Q. (2021). Distribution Pattern and Its Formation Mechanism of Public Recreational Space Based on POI Data: A Case Study of the Main Urban Area of Changsha City. *Modern Urban Research*, 3, 91–97. <https://doi.org/10.3969/j.issn.1009-6000.2021.03.013>(in Chinese).
- [24] Yang, Z., He, X., Sui, X., & Zhang, J. (2019). Analysis of the Evolution of Urban Center Space Based on POI: A Case Study of Main Area in Kunming. *URBAN DEVELOPMENT STUDIES*, 26(2), 31–35(in Chinese).
- [25] Yi, R. (2025). Scientific development and utilization of underground space resources to stimulate high-quality urban economic development. *Bulletin of Chinese Academy of Sciences*, 40(4), 725–729. <https://doi.org/10.16418/j.issn.1000-3045.20250108001>(in Chinese).
- [26] Yu, H., Chen, Z., Hu, W., Zhang, J., Xu, C., & Hu, B. (2025). Urban underground space value assessment and regeneration strategies in symbiosis with the urban block: A case study of large residential areas in Beijing. *Tunnelling and Underground Space Technology*, 163, 106728. <https://doi.org/10.1016/j.tust.2025.106728>.
- [27] Zeng, C., & Chen, W. (2018). A Forecasting Model of Urban Underground Space Development Intensity. *Chinese Journal of Underground Space and Engineering*, 14(5), 1154–1160(in Chinese).
- [28] Zhang, P., Zhao, Q., Zhao, L., Liu, J., & Bai, Z. (2023). Evaluation of Geological Environment Quality of Underground Space in Different Layers in Western Zhengzhou. *Chinese Journal of Underground Space and Engineering*, 19(S2), 510–518(in Chinese).
- [29] Zhao, J., Wang, H., Sun, Y., Li, H., & Zhu, Y. (2025). Investigation into the distribution features and determinants of underground commercial spaces in Qingdao city. *Buildings*, 15(10), 1743. <https://doi.org/10.3390/buildings15101743>.

## RESEARCH ON THE IDEAS AND CHALLENGES OF CREATING A WALKABLE PEDESTRIAN NETWORK BY UTILIZING UNDERGROUND SPACE

Daisuke FUKUMOTO<sup>1</sup>, Sadayasu AONO<sup>2</sup>, Kentaro HAYASHI<sup>3</sup>, Takeshi HIROSE<sup>4</sup>, Kazuya  
MASUYAMA<sup>5</sup>

**Abstract:** In recent years, urban development plans have been underway around the world to make it easier for pedestrians to get around by creating and networking walkable spaces that prioritize pedestrians. In such plans, there are many cases where underground space is effectively utilized. There are two types of underground utilization methods. The first method is to relocate functions for non-pedestrian transportation such as cars and trains underground and reorganize the above-ground area as a safe, secure, and comfortable walking space. The second method is to create an attractive underground walking space by taking advantage of the advantage of underground space, which is not easily affected by weather and temperature, and by addressing the problems of underground spaces where it is dark and where it is difficult to distinguish between locations. In this study, we focus on examples of effective use of underground space in forming walkable spatial networks, classify and analyze the characteristics of usage methods, and consider ideas and issues in urban development planning.

**Keywords:** walkable pedestrian network, urban development

### 1. INTRODUCTION

In Japan, the population is decreasing, and the population is aging, making it difficult to maintain and manage social infrastructure. On the other hand, values such as emphasis on work-life balance are diversifying, and there is a need to improve the attractiveness of cities. Considering this situation, the Ministry of Land, Infrastructure, Transport and Tourism is considering urban development that promotes urban, economic, and social diversity and creates added value. At that time, "WEDO" (Walkable, Eyelevel, Diversity, Open) was proposed as a keyword to describe the new urban image.

Therefore, in collaboration with private investment, we aim to realize a rich, human-centered lifestyle, create new value through innovation, and resolve regional issues. We are transforming public and private spaces into human-centered, easy-to-walk spaces, and promoting initiatives to create cities that are "comfortable and inviting to walk" where diverse human resources can gather and interact. To further promote these efforts, there are an increasing number of cases in which underground space is being effectively utilized.

This research focuses on the concept and issues of an easy-to-walk pedestrian network that utilizes underground space and aims to obtain suggestions for future urban development based on its characteristics and effects.

<sup>1</sup> Director, Daisuke FUKUMOTO, Urban Transportation Planner, Director, The institute of Behavioral Sciences, Koraku Mori Bldg. 12F, 1-4-14 Koraku, Bunkyo-ku, Tokyo 112-004 JAPAN, [dfukumoto@ibs.or.jp](mailto:dfukumoto@ibs.or.jp)

<sup>2</sup> Dr, Sadayasu AONO, Urban Transportation Planner, Researcher, The institute of Behavioral Sciences, Koraku Mori Bldg. 12F, 1-4-14 Koraku, Bunkyo-ku, Tokyo 112-004 JAPAN, [saono@ibs.or.jp](mailto:saono@ibs.or.jp)

<sup>3</sup> Researcher, Kentaro HAYASHI, Urban Transportation Planner, Researcher, The institute of Behavioral Sciences, Koraku Mori Bldg. 12F, 1-4-14 Koraku, Bunkyo-ku, Tokyo 112-004 JAPAN, [kentarohayashi@ibs.or.jp](mailto:kentarohayashi@ibs.or.jp)

<sup>4</sup> Researcher, Takeshi HIROSE, Urban Transportation Planner, Researcher, The institute of Behavioral Sciences, Koraku Mori Bldg. 12F, 1-4-14 Koraku, Bunkyo-ku, Tokyo 112-004 JAPAN, [thirose@ibs.or.jp](mailto:thirose@ibs.or.jp)

<sup>5</sup> Researcher, Kazuya MASUYAMA, Urban Transportation Planner, Researcher, The institute of Behavioral Sciences, Koraku Mori Bldg. 12F, 1-4-14 Koraku, Bunkyo-ku, Tokyo 112-004 JAPAN, [kmasuyama@ibs.or.jp](mailto:kmasuyama@ibs.or.jp)

## 2. CASE STUDY

There are many examples of creating easy-to-walk spaces that prioritize pedestrians and making effective use of underground spaces. There are two types of underground usage methods. The first method is to relocate functions that were previously above ground underground, making it possible to walk on the ground safely, securely, and comfortably. The second method is to create a pedestrian network that is less affected by weather and temperature by making the underground space itself easier to walk through.

### 2.1. Relocation of functions from aboveground to underground

First, we focus on the functions that are transferred from aboveground to underground and classify them into three types. It is expected that these will solve the problems that existed on the ground and make it possible to walk on the ground safely, securely, and comfortably. Table 1 shows the correspondence between each case.

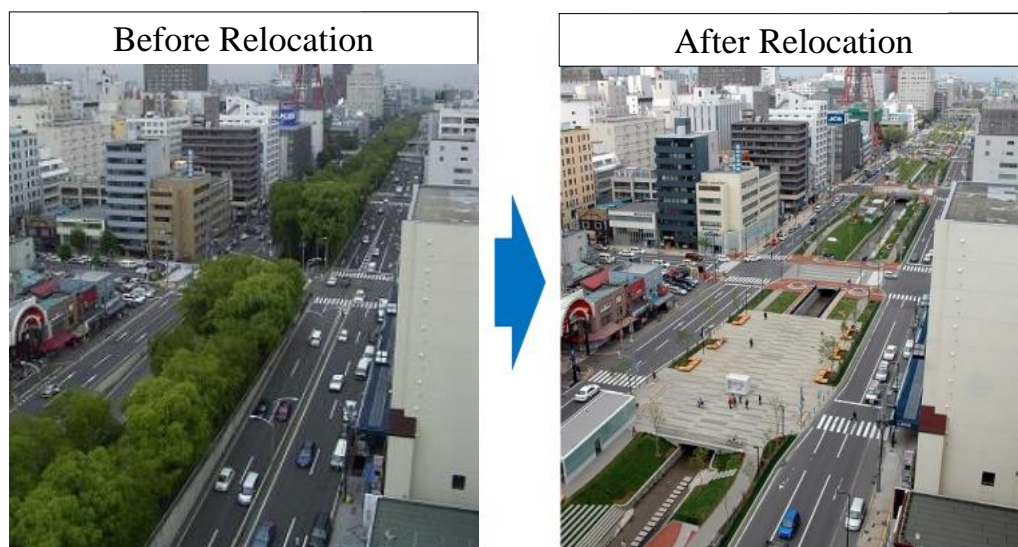
*Table 1. Classification focusing on the type of functions that go underground*

Functions relocated from above ground to underground	Effect on the ground	case study
Car Route	Creation of water-friendly green space	Soseigawa Avenue (Sapporo City)
Railway	Eliminating traffic congestion and urban division caused by railroad crossings	Keio Line (Chofu Station)
Bus Terminal	Reducing congestion on the ground by buses and passengers	Bus Terminal Tokyo Yaesu (Tokyo Station)

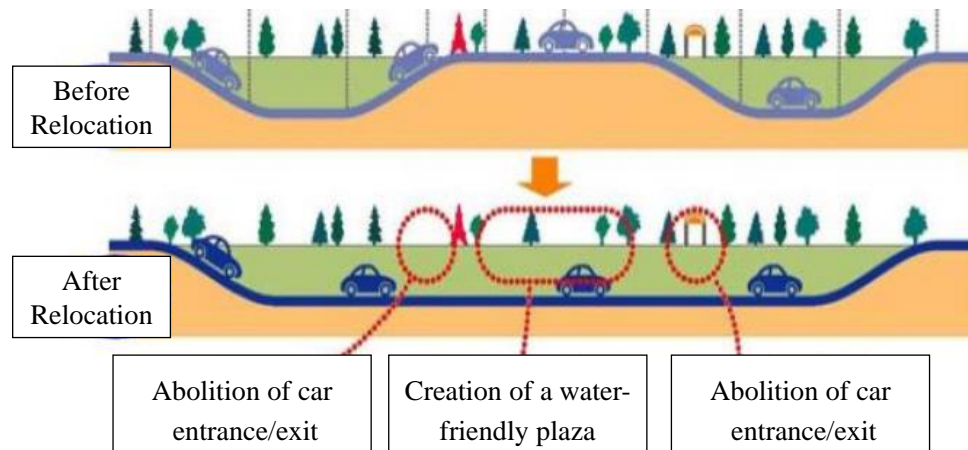
#### 2.1.1. Example of relocating a car route underground (Sapporo City)

Soseigawa Avenue in Sapporo City used to be an eight-lane road, but four of those lanes have been moved underground, and there are several underground passages. At this time, a water-friendly green space was created above the newly relocated underground vehicle running space. This created a plaza space that served as a place for local activities and interaction and was used by a diverse range of people. In addition, by creating a space where people can walk comfortably, it has become possible to create a lively town.

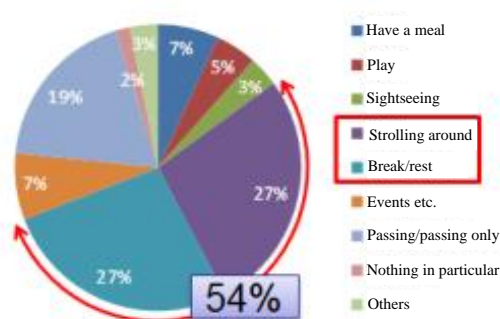
Looking at the activities in the ground area after the relocation, the most frequent visits were for purposes such as walking and resting, and nearly half of the people stayed for more than 30 minutes. This is thought to be because more people spend time in the well-maintained plaza rather than using the surrounding facilities as their destination, and it is believed that this has the effect of creating a lively atmosphere.



*Figure 1. Before and after relocating car routes underground*



*Figure 2. Areas that changed before and after relocation*

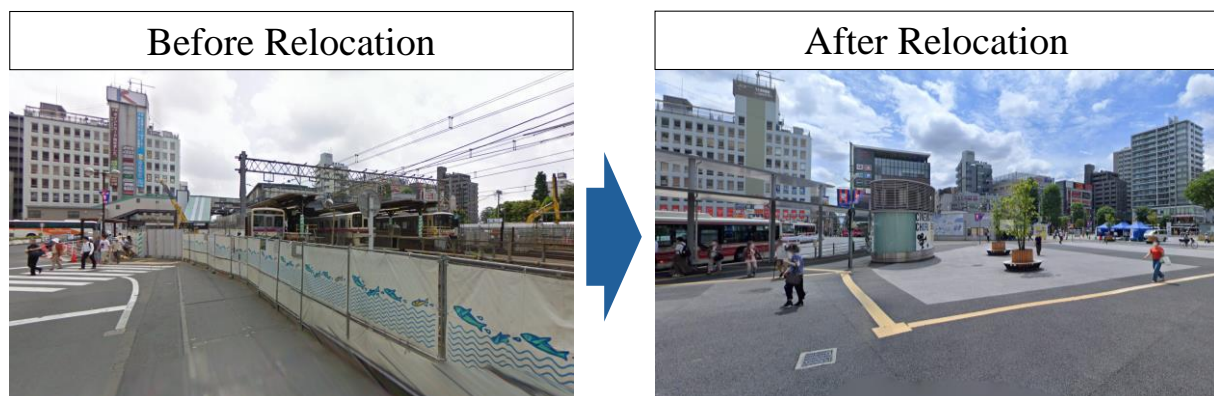


**Purpose of visit**

*Figure 3. Status of above-ground activities after relocation*

### 2.1.2. Example of relocating a railway underground (Keio Line, Chofu Station)

The railway (Keio Line) that ran above ground caused traffic jams at railroad crossings and divided the city. This is an example of how moving underground railways can alleviate traffic congestion and make cities more continuous. As a result, the plaza in front of Chofu Station has been upgraded above ground, and its function as a transportation hub has been strengthened by connecting multiple transportation systems. In addition, a plaza that can be used for multiple purposes has been developed, and events are held here, making the town more lively.



*Figure 4. Before and after relocating a railway underground*



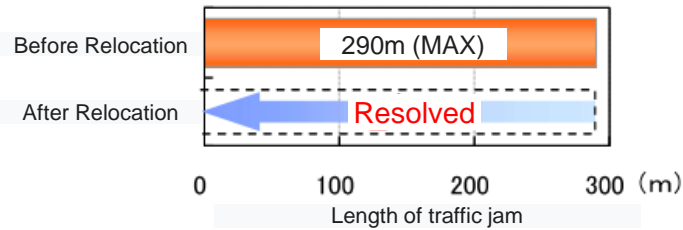


Figure 5. Comparison of maximum length of traffic jams

### 2.1.3. Example of relocating a bus terminal underground (Bus Terminal Tokyo Yaesu, Tokyo Station)

In the Yaesu area near Tokyo Station, bus stops are scattered over a wide area, and the surrounding roads were crowded with buses and passengers. In response to this, an underground bus terminal was constructed in conjunction with large-scale redevelopment to improve convenience for buses and passengers. This eased congestion on the ground and created a comfortable and safe space for pedestrians.

The functions of the bus terminal include a ticketing counter and information desk on the first basement floor, and bus stops on the second basement floor. The above-ground area has become a comfortable space for pedestrians, allowing access to the adjacent underground mall.

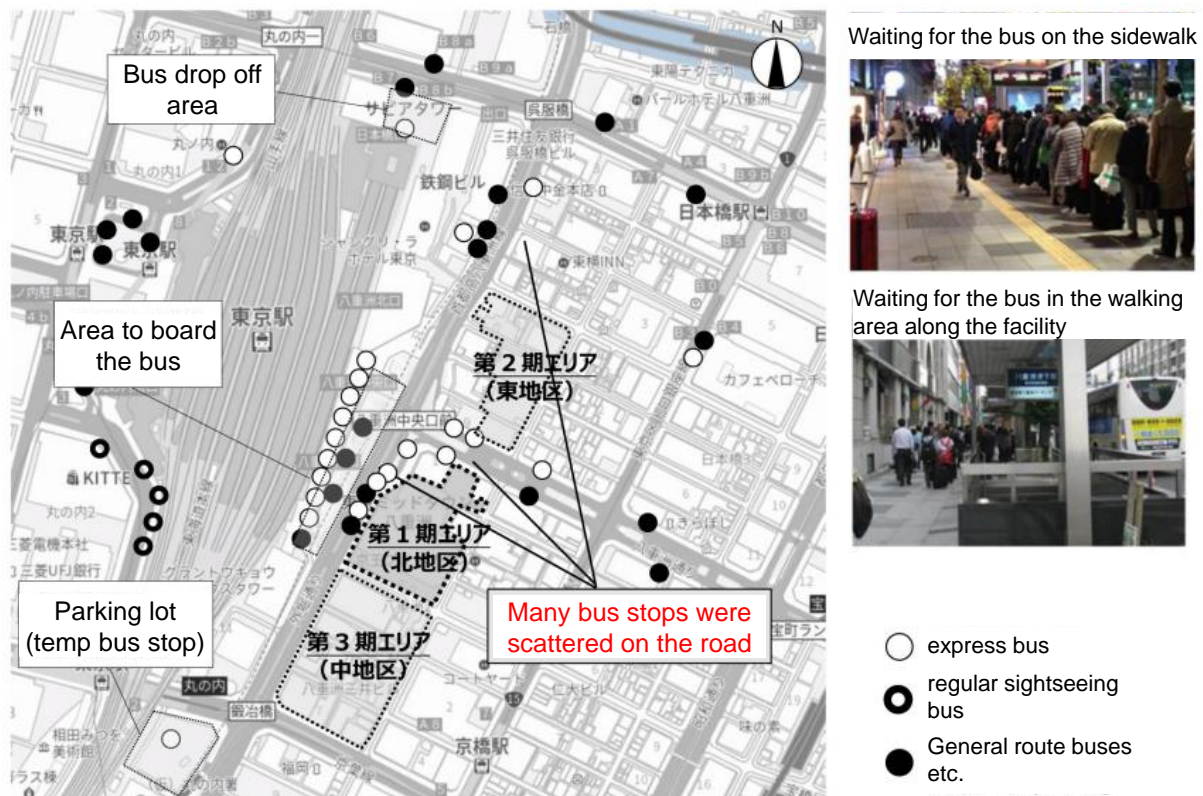


Figure 6. Location and appearance of the bus stop before relocation

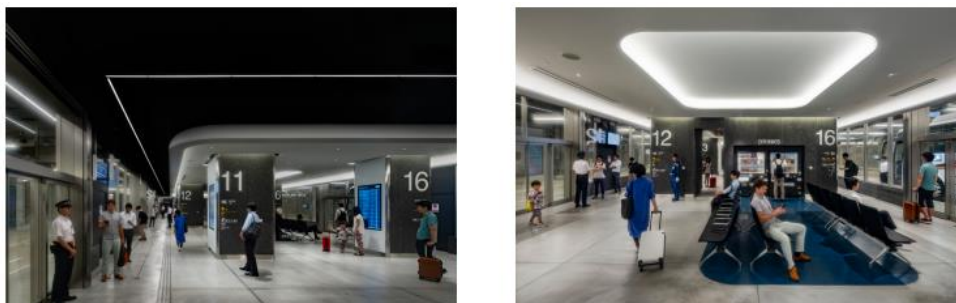


Figure 7. Flow lines and stay space at the underground bus terminal



## 2.2. Ideas for making underground spaces a comfortable walking space

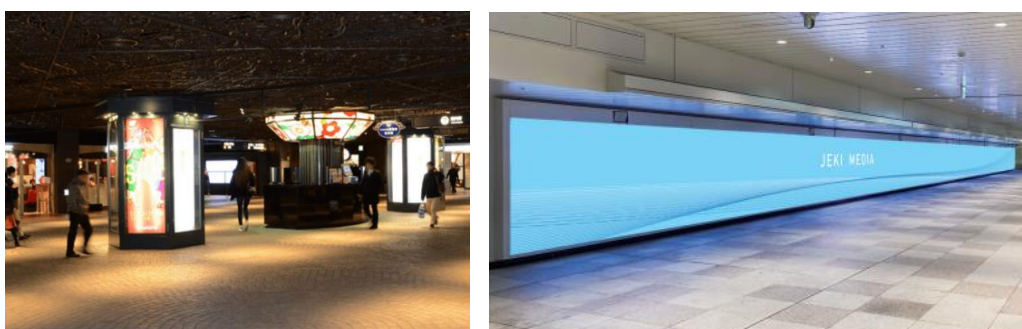
We have summarized the possibilities of making underground walking more enjoyable and comfortable by creating a device that serves as a sign so that people walking underground do not lose their direction or location, a device that allows them to grasp their positional relationship with the above-ground space, and a device that encourages various activities such as not only walking but also staying.

*Table 2. Ideas and expected effects for underground walking space*

Ideas for underground walking space	Expected effects in underground space
Design at eye level	● Signs to prevent people walking underground from losing their direction or location
Lighting from above ground	● Understand the positional relationship with the ground
Utilization at events etc.	● Encourage various activities such as staying in addition to walking.

### 2.2.1. Design at eye level

When walking underground, it can be difficult to locate where you are because the scenery remains the same and there are few facilities or information that can serve as landmarks, so there are examples of creating spaces that are easy to walk by creating landmark designs and placing facilities at eye level. For example, Fukuoka City's Tenjin Underground Mall has been made easy to understand by installing unique lighting and designs, and at Shinjuku Station, huge digital signage has been installed to create a space that can be used for meetings.



*Figure 8. Unique lighting design (left figure) and huge digital signage (right figure)*

### 2.2.2. Lighting from above ground

The disadvantage of underground pedestrian spaces is that they tend to be dark, and it is difficult to determine their position in relation to above-ground areas. Therefore, when creating an underground pedestrian space, in addition to letting in light from above ground to make it brighter, there are also cases where large openings are installed so that landmarks on the ground can be seen, the direction of sunlight can be seen, and pedestrians can see their location on a map. For example, in Sapporo City, where there is a lot of snow, the underground area of Ekimae-dori Avenue has been developed as a long linear walking space, with large openings arranged in succession to make it easy to see the positional relationships. Furthermore, in Fukuoka City's Tenjin Underground Mall, unique lighting and designs have been placed around the openings, making the space easier to locate.



*Figure 9. Continuous arrangement of multiple openings (left figure) and uniquely designed openings (right figure)*

### 2.2.3. Utilization at events etc.

Underground spaces have the disadvantage that because they are closed spaces, few people stay there for long periods of time, and they are often just spaces for walking. Therefore, by relaxing restrictions on the use of underground spaces for events, etc., and clarifying the organization responsible for management, including licensing, there are examples of creating diverse spaces that vary depending on the season, day of the week, and time of day. For example, Sapporo City has established a specialized town development company, and Shizuoka City is encouraging active use of its underground event space by renting it out free of charge. Through such innovations, the basement is not just a space to walk through, but a space where you can stay and engage in a variety of activities, leading to the creation of a fun and comfortable town.



*Figure 10. Underground marche (left figure) and underground performance (right figure)*

## 3. CONCLUSION

In this study, we confirmed that there are a wide variety of examples of creating walkable spaces that give priority to pedestrians, and that there are especially many examples of effective use of underground spaces. Therefore, we analyzed the usage of underground space by dividing it into two types: making the above ground a walkable space and making the underground a walkable space. To make above-ground areas walkable, there is a perspective of relocating functions that are not related to pedestrians, or functions that sometimes hinder safe and comfortable walking underground, and we confirmed the effectiveness and development potential of this approach. On the other hand, when creating an underground pedestrian space, it has the advantage of being less affected by weather and temperature, but it also has the disadvantage of making it difficult to create an attractive space because it gets dark and makes it difficult to understand the positional relationship, so it was confirmed that there are various ways to maximize the function as a network for pedestrians.

In future urban development, we believe it will be important to create spaces that support a variety of activities, such as not only walking, but staying, relaxing, and enjoying, by incorporating ways to proactively utilize underground spaces, while sharing the functions of the entire region. To this end, it will be necessary to clarify the concept of division of functions and the effects obtained by effectively utilizing underground space in the "Guidelines for Underground Space Utilization in Cooperation with Urban Development", which we are currently aiming to introduce. For example, we should aim to be able to quantitatively evaluate the benefits of underground projects, such as not only smoother roads by relieving traffic congestion, but also economic effects from promoting a variety of activities and creating hustle and bustle. In the future, I would like to consider and propose indicators for evaluating these and their calculation methods.

## 4. ACKNOWLEDGMENTS

This research is a representative summary of the research results of the "Urban Development and Collaboration Subcommittee", a research organization of the Urban Underground Space Center of Japan (USJ). We would like to express our gratitude to the members of our research organization.

## RESERVOIRS OF ENERGY: A JOURNEY TOWARDS ENERGY AUTONOMY FOR NINE UK EARTH-SHELTERED HOMES

Dr Jeremy Harrall<sup>1</sup>, Daniel Kastner<sup>2</sup>, Alvaro Garcia<sup>3</sup>, Max Lee<sup>4</sup>

**Abstract:** This paper is a sequel publication to ACUUS 2023<sup>i</sup>, ‘Reservoirs of Heat: A defining characteristic of high thermal mass earth-sheltered buildings.’

Featured below is an advanced analysis of the second case study of the former paper, the nine earth-sheltered homes known as Howgate Close<sup>ii</sup>, in the Nottinghamshire village of Eakring.

Reviewed in this paper is the hypothesis, ‘*to what extent can energy autonomy be achieved in one of the naturally heated Howgate earth-sheltered homes?*’. This evidence-based enquiry is essential in optimising built-in energy security for the future building performance for the balance of eight Howgate homes.

Emerging from Howgate is the advent of a new building paradigm in the UK. One where the level of energy autonomy at Howgate is delivering a net daily cash surplus for the home with a battery installed. As a consequence, there are no more energy bills, relegating the threat fuel-poverty to a distant memory. This is a continuous process of ‘*marginal gains*’<sup>iii</sup>.

What difference a battery makes?

Batteries in buildings, facilitate energy storage and can be thought of as ‘*reservoirs of energy*’.

This paper introduces in-use building performance data from a 1bedroom earth-sheltered dwelling, pre-and-post battery installation. Also discussed, are the wider-ranging impact batteries have in reducing the burden of energy bills.

After the first three years of occupation, the selected 1bed home has exceptionally low average daily total energy costs that are less than 45pence/day (inclusive of Standing Charge). Before the battery install, the home consumed 7KWhrs/day imported energy from the grid and exported 13.5KWhrs/day to the grid.

The next stage of Howgate Close’s development is the inclusion of energy storage facilities to all nine homes. However, the first phase has been to install an 11KWhr BYD battery and a Fronius hybrid inverter to one of the 1bed dwellings. At the time of submitting the full paper, sixteen weeks of in-use building performance data has been gathered. Results from 16.04.2025 to 13.08.2025 record in excess of 50% reduction in daily energy consumption from the grid compared to the same period in 2024.

This paper will add to the accumulating, independent, evidence-based research from the nine earth-sheltered homes of Howgate Close. Additional empirical data is provided in support of the premise that, ‘*high thermal mass buildings should be the building form of choice in reducing heating/cooling loads together with concomitant energy costs.*’

**Keywords:** residual heat reservoir, reservoir of energy, earth-sheltered building, energy storage facility, battery, zero heating, thermal mass, passive solar design.

<sup>1</sup> 23 Reservoir Road, Surfleet, Lincolnshire, PE11 4DH, UK, [jerry@drharrall.com](mailto:jerry@drharrall.com)

<sup>2</sup> Managing Director, Fronius U.K. Ltd., Milton Keynes, MK10 0BD, UK, [kastner.daniel@fronius.com](mailto:kastner.daniel@fronius.com)

<sup>3</sup> Commercial Director, EFT Systems, Bruchtannenstr. 28, 63801 Kleinostheim, [a.garcia@eft-systems.de](mailto:a.garcia@eft-systems.de)

<sup>4</sup> Sales Manager |BYD Energy Storage| Residential, BYD Road, Pingshan, Shenzhen, China, [max.li1@fdbatt.com](mailto:max.li1@fdbatt.com)

## 1. INTRODUCTION

This is a sequel paper to ACUUS 2023<sup>iv</sup>, *'Reservoirs of Heat: A defining characteristic of high thermal mass earth-sheltered buildings.'*

Explored in this 2025 paper is the hypothesis:

*'To what extent can energy autonomy be achieved in one of the naturally heated Howgate earth-sheltered homes, using an energy storage facility?'*

An evidential enquiry will inform future design decisions in the sizing of batteries and inverters to the balance of the eight Howgate homes.

During the first three years of occupation prior to the installation of the first battery, all nine homes experienced low to no heating load requirements. The building characteristic at Howgate responsible for stabilising internal air temperatures was introduced in ACUUS 2023 by this author and is referred to as a *'residual heat reservoir'*. At Howgate, it is this phenomenon, the presence of a body of heat energy retained within the superstructure, that has been sufficient to sustain habitable internal air temperatures of 21C without resort to primary heating equipment. A good starting point for the installation of an energy storage system.



*Figure 1. 2023. Harrall Dr. J.: Southeast View, Howgate Close*

## 2. BUILDING SPECIFICATION OF HOWGATE CLOSE (HC) [SEE FIG1.]

Howgate Close (HC) is a post-hydrocarbon ready residential dwelling, conceived by Dr Chris Parsons, a second generation Eaking Farmer and retired GP. Dr Parsons cited<sup>v</sup>,

*"Howgate Close was an opportunity to address some of society's most pressing issues: rural housing shortages, climate change, soil restoration, carbon sequestration, biodiversity, water management and community cohesiveness."*

Howgate comprises, nine single storey earth-sheltered homes, 5no. 2beds (63m<sup>2</sup>) and 4no.1beds (41m<sup>2</sup>) with a gross development floor area of 479m<sup>2</sup>.

### Location

Howgate Close is located at latitude 53<sup>0</sup> North, centrally located in the British Isles which straddles between the mid-latitudes of 49<sup>0</sup> and 61<sup>0</sup>. The climatic conditions of these Isles are largely related to the influence of the Atlantic Ocean, as such, experiences a temperate maritime climate. Encyclopaedia Britannica<sup>vi</sup> report, nowhere in the UK is located more than 70miles from the coast.



Score	Energy rating	Current	Potential
92+	A	143 1A	145 1A
81-91	B		
69-80	C		

Figure 2. 2023. Extract of Howgate Close Energy Performance Certificate (EPC)

### ‘One-In-A-Million’

The selected building’s As-Built SAP (Standards Assessment Procedure) Rating is 143A<sup>vii</sup>. Of the 15million registered EPC’s (Energy Performance Certificate) <sup>[See Fig2.]</sup> in the UK, Howgate’s’ SAP Ratings are ranked in the top 0.01% of the country’s most energy efficient dwellings, better than one in a million.

### Design Principles

The original project design was undertaken by the Hockerton Housing Project (HHP)<sup>viii</sup> using the design principles applied at HHP by its Architects, Professors Brenda and Robert Vale (The Vale’s).

These design principles were first published in The Vale’s, 1975 book, ‘The Autonomous House’, and implemented at their former Southwell home, featured in their book ‘The New Autonomous House’. In 1991, this was the first UK dwelling to export photovoltaic-generated renewable energy to the National Grid.

Dr Chris Parsons advanced the original construction specification engaging Dr J. Harrall elevating the 87A Design SAP Rating to an As-Built 143A.

Intrinsic to Howgate’s performance is the utilisation of Passive Solar Design (PSD) principles; *southerly orientation, high thermal mass superstructure and a super-insulated building envelope*, allied and enhanced with triple glazing and roof mounted photovoltaics. Other differentiating construction specifications include; solid external walls (no cavities) floating slab (no foundations) contiguous external insulated envelope (no cold bridging) externally located window and door jambs (exceptional Psi values).

### Post-Hydrocarbon Ready

The authors interpretation of a post-hydrocarbon era, is a time when societies primary fuel for heat and power is not derived from oil, gas or coal. The authors concur with the opinion that, *“The post-hydrocarbon era will not appear suddenly. Gradual change and individual decisions will aggregate into wide structures beyond the scope of the individual decisions.”*<sup>ix</sup>

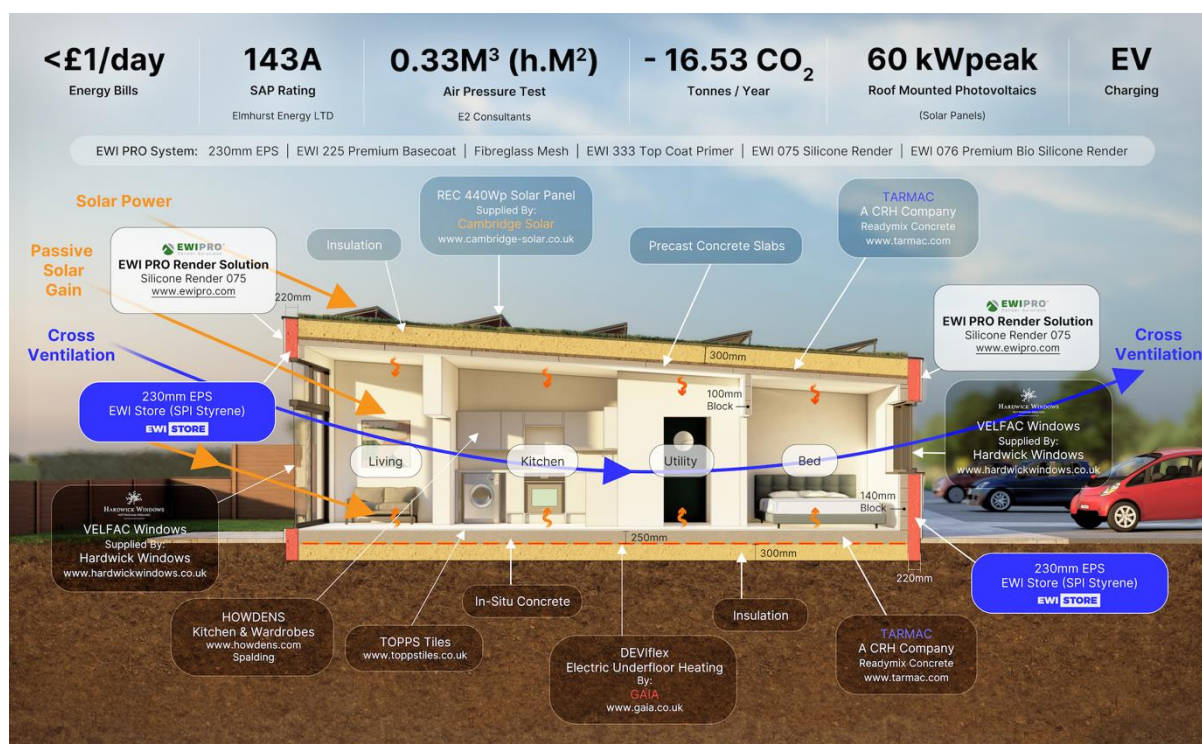
Howgate Close demonstrates the traits of what a post-hydrocarbon neighbourhood could look like: *energy independence, autonomy over essential resources, on-site waste management, transitioning towards fossil-fuel-free lifestyles and a strong community spirit*. These homes are fossil-fuel-free in operation, generating a surplus of energy, managing their own waste water on site with most homes experiencing low to no heating bills.

### Building Performance Specification <sup>[ See Fig 3]</sup>

At Howgate, stable internal air temperatures of 21°C (+/- 2°C) have been recorded over the first 30months of occupation with little to no active heating.

Howgate’s building element specification, significantly out performs the UK Building Regulations ‘Notional Building’ (See Table 1) Improvements in fabric heat transmittance (U-Values) are 28% for its walls (0.13W/m<sup>2</sup>K) 38% for its floors (0.08W/m<sup>2</sup>K) and 36% for the roofs (0.07W/m<sup>2</sup>K) The most significant improvement against the Compliance Standards is Howgate’s Air Pressure Tests (APT) (0.67m<sup>3</sup>@50Pascals) 87% reduced fabric air infiltration.

As-Built SAP calculations produced 143A(2bed) and 129A(1Bed) At HC, exceptionally low Air Pressure Tests were achieved at HW, 0.33m<sup>3</sup>(h.m<sup>2</sup>) @50Pascals, lower than HW by 0.61m<sup>3</sup>.



**Figure 3.** 2025. Howgate Close Typical Cross Section

### Residual Heat Reservoir

At Howgate, it is the combined elements of low thermal bridge junctions, contiguous insulated envelope and high thermal mass superstructure, that optimise the buildings' residual heat reservoir its retained body of heat energy within the building fabric. At Howgate, an uninterrupted layer of 220mm (XPS, walls) to 300mm (EPS, roof and floor) envelopes the building externally. Subsequently, sufficient heat is retained within the thermal mass to sustain elevated internal air temperatures of circa 21°C.

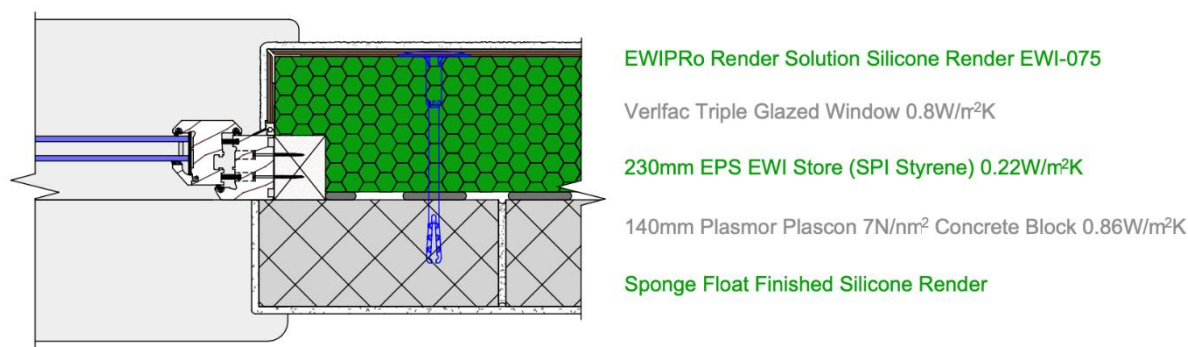
**Table 1.** Howgate Close Fabric Performance Comparison With Notional Building

HOWGATE CLOSE VS UK BUILDING REGULATIONS NOTIONAL BUILDING					
Minimum Standards for Fabric Performance			Notional Building	HOWGATE CLOSE	% Difference
	Part L 2013	Part L 2021	Part L 2021		
External walls	0.3 w/m <sup>2</sup> k	0.26 w/m <sup>2</sup> k	0.18 w/m <sup>2</sup> k	0.13 w/m <sup>2</sup> k	+28
Floors	0.25 w/m <sup>2</sup> k	0.18 w/m <sup>2</sup> k	0.13 w/m <sup>2</sup> k	0.08 w/m <sup>2</sup> k	+38
Roofs	0.2 w/m <sup>2</sup> k	0.16 w/m <sup>2</sup> k	0.11 w/m <sup>2</sup> k	0.07 w/m <sup>2</sup> k	+36
Windows	2 w/m <sup>2</sup> k	2.2 w/m <sup>2</sup> k	1.2 w/m <sup>2</sup> k	0.78 w/m <sup>2</sup> k	+35
Doors	2 w/m <sup>2</sup> k	1.6 w/m <sup>2</sup> k	1.0 w/m <sup>2</sup> k	0.9 w/m <sup>2</sup> k	+10
Air Permeability	10 m <sup>3</sup> /m <sup>2</sup> /hr @ 50Pa	8.0 m <sup>3</sup> /m <sup>2</sup> /hr @ 50Pa	5.0 m <sup>3</sup> /m <sup>2</sup> /hr @ 50Pa	0.67m <sup>3</sup> /m <sup>2</sup> /hr @50Pa	+87



### Thermal Bridges [ See Fig 4 ]

Thermal bridges (aka cold bridges) are thermally weak junctions with significantly higher heat transfer than surrounding materials. These junctions form a bridge between inner and outer surfaces e.g. window jamb, where paths of least resistance for heat transference, can result in up to 30% of total building heat loss. As a consequence, thermal bridges are at risk of internal surface condensation formation, potentially leading to mould growth, presenting a health risk.



**Figure 4.** Window Jamb Detail At Howgate Close

Four principal categories of thermal bridge;

- 1) **Repeating thermal bridges** –regular interruptions in the building fabric e.g. brick mortar joints, wall ties and studs;- *U-Values*
- 2) **Linear (non-repeating) thermal bridges** –gaps in the insulation layer e.g. windows and doors – *Psi-Values*
- 3) **Geometrical thermal bridges** –meeting junctions different building elements e.g. external corners, where the heat loss area is greater than the internal surface – *Psi-Values*
- 4) **Point thermal bridges** –single penetrations in the thermal envelope flues, fastenings, brackets, stanchions – *Chi-Values*

### Linear Thermal Transmittance

For the purposes of this paper, only linear and geometrical thermal bridges are calculated. The heat loss associated with these thermal bridges is expressed as Linear Thermal Transmittance ( $\Psi$ -value) – referred to as *psi-value*. At Howgate Close, there are no repeating thermal bridges and negligible point thermal bridges. A lower Psi-value indicates lower heat loss through a junction.

Calculated Psi-Values<sup>x</sup> for Howgate Close are compared to the UK Building Regulation 'Notional Building' (see Table 1)<sup>xi</sup>. The 'notional building specification' is a recipe approach that will ensure minimum compliance if all standards are met.

Calculated perimeter heat loss from Howgate window and door frames, their average Linear Heat Transference (Psi-Value) is 0.024W/m.K.<sup>xii</sup> Heat transfer through Howgate's bespoke window/door junction is half that of the Notional Building compliance standard. Conversely, a building built to minimum Building Regulation standards, loses twice as much heat from its window/door junctions compared to Howgate Close.

**Table 2:** Comparison Table of Linear Heat Transference

COMPARISON TABLE OF LINEAR HEAT TRANSFERENCE 2D PSI CALCULATION Howgate Close & Notional Building (UK Building Regulations 2023)			
	Notional Building * (Psi-Value W/m.K)	Howgate Close (Psi-Value) W/m.K	Condensation Risk** (f-value) 1 = Zero Risk
Window Jamb	0.05	0.023	0.935
Window Lintel	0.05	0.027	0.956
Window Cill	0.05	0.023	0.927
Roof/Wall	0.08	0.067	0.965
**f-Value: risk of condensation forming on internal surface when external temperature is 0°C and internal room temperature is 20°C			
*Psi-Value: minimum building specification to ensure compliance with UK Building Regulation Standards			
Calculation undertaken by MES <a href="http://www.mesbuildingsolutions.co.uk">www.mesbuildingsolutions.co.uk</a> and commissioned by EWIPRO <a href="http://www.ewipro.com">www.ewipro.com</a>			

### Surface Temperature, Mould growth and Health

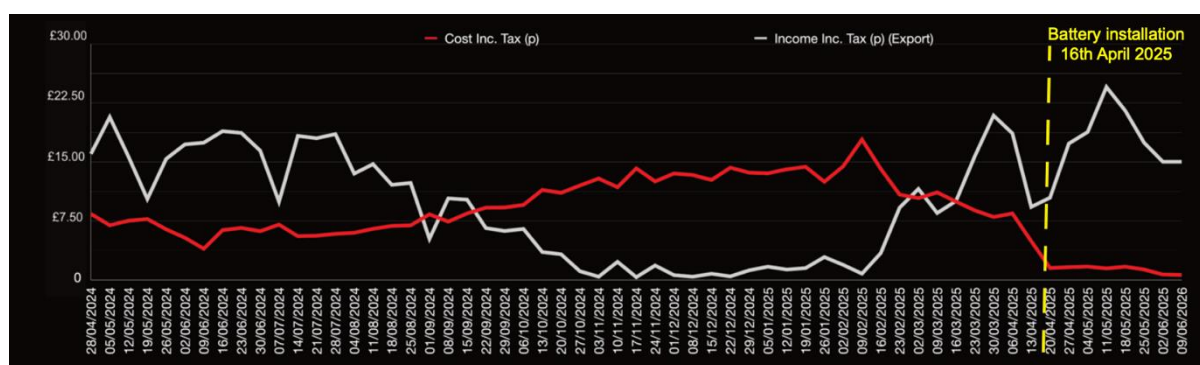
Calculated as part of the Psi-Value calculation is the *f-value*. The *f-value* estimates the risk of surface mould formation in a building. As the *f-value* approaches '1', the calculated incident of internal surface condensation formation at junctions reduces and with it, the risk of mould growth. For comparison, the Notional Building *f-value* compliance threshold is 0.75. At Howgate, its window/door junction average *f-value* is 0.94. The risk of internal surface condensation occurring on window/door junction detail at Howgate is reduced by 19% compared to the compliance standards for Building Regulations.

### Interstitial Condensation

Interstitial condensation can occur between building construction interface layers of roofs, walls and floors. Persistent interstitial condensation within the building fabric can lead to degradation of materials, increased risk of mould formation and a reduction in air quality.

At Howgate, its modified solid externally insulated wall, designs out the cavity wall and locates the insulation on the external face of the solid block wall. A Condensation Risk Analysis<sup>xiii</sup> has evaluated the likelihood of interstitial condensation in Howgate's wall construction. These calculations demonstrate compliance with 'UK Building Regulation Part C'.

The analysis concluded that Howgate's external wall detail, avoided critical surface moisture, with no danger of mould growth. On the incidence of interstitial condensation, it concluded there was no risk of condensation forming at any interface in any month.



**Figure 5.** 2025. 14months of Octopus Bills at Howgate Close 1bed with a battery installed

### 3. WHAT A DIFFERENCE A BATTERY MAKES [SEE FIG 5]

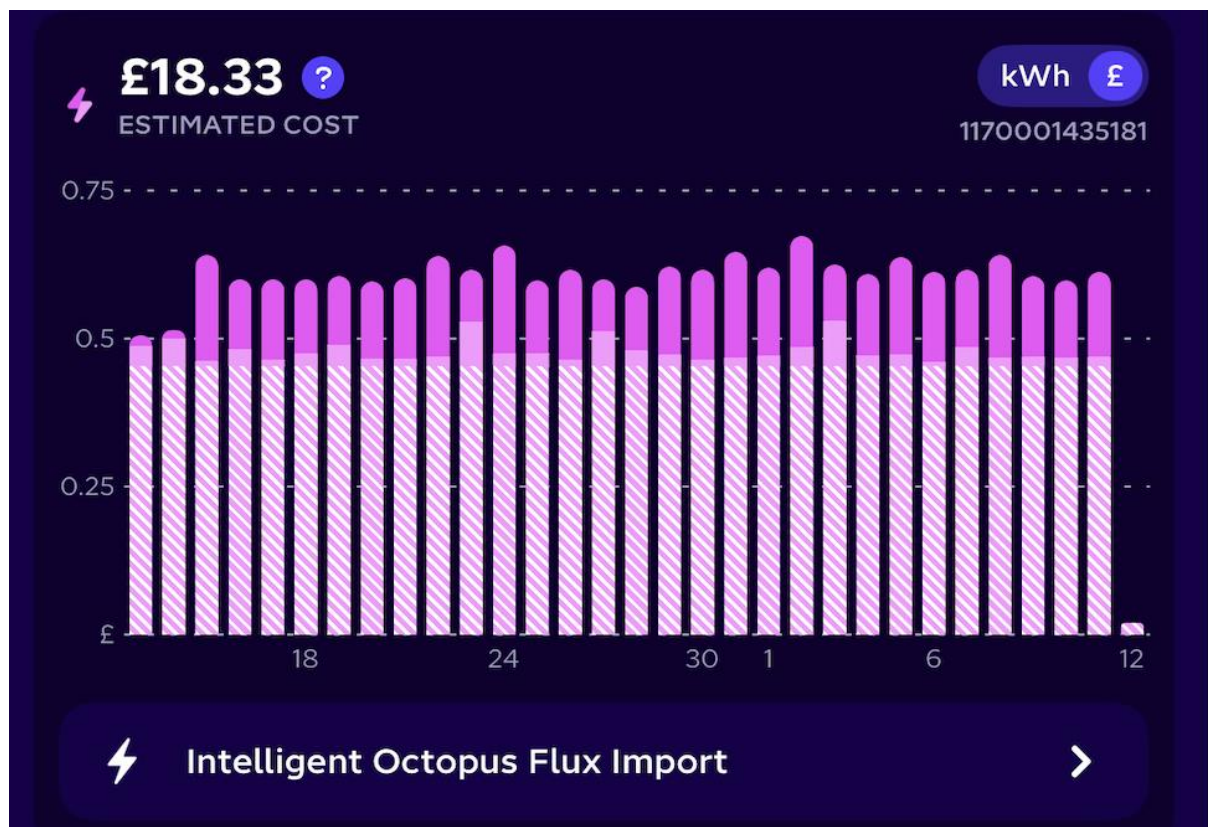
Over the first three years of occupation, the selected 1bed home has recorded exceptionally low average daily total energy costs that are less than 45pence/day (inclusive of Standing Charge)<sup>xiv</sup>. Before the battery install, the home's average daily consumption was 7KWhrs/day imported energy from the grid while exporting 13.5KWhrs/day to the grid.

The next stage of Howgate Close's development is the inclusion of energy storage facilities to all nine homes. However, the first phase has been to install an 11kWhr BYD battery and a Fronius hybrid inverter to one of the 1bed dwellings. At the time of submitting this paper, eight weeks of in-use building performance data has been gathered. Results from 16.04.2025 to 15.06.2025 record in excess of 50% reduction in daily energy consumption from the grid compared to the same period in 2024.

For the period from 12<sup>th</sup> July to 13<sup>th</sup> August 2025, 18kWhrs electricity were imported from the grid<sup>[ See Fig6]</sup> (2.5kWhrs/day) and 298kWhrs (42kWhrs/day) were exported to the grid in the same period of time<sup>[ See Fig7 ]</sup>. Comparing the data from the same period in 2024, 117kWhrs were imported from the grid and 480kWhrs exported to the grid.

99kWhrs less imported, an 85% reduction in energy consumed from the grid and 190kwhrs less exported, a 38% reduction in exported energy.

Despite the presence of the 11kWhr battery, the 1bed still imports energy from the grid on a daily basis. Peak demand for energy occurs regular pattern from 7am for approximately an hour and again around 6pm for another hour. These spikes in energy demand are understood to derive from the combined uses of the following electrical appliances, a 9kW shower, 5kW oven, 3kW kettle and 2kW air fryer in addition to other devices e.g. computers, TV, Smart Metre, router.



**Figure 6.** 12<sup>th</sup> July to 13<sup>th</sup> August 2025 Octopus Bill at Howgate Close 1bed with a battery installed



**Figure 7.** 12<sup>th</sup> July to 13<sup>th</sup> August 2025. Octopus Export Income at Howgate Close for a 1bed with a battery installed

#### Energy Storage Installation [ See Fig 5]

On 16<sup>th</sup> April 2025, at a 1bed Howgate home, the existing Fronius Primo 4.6kW inverter was replaced with Gen24 Primo 4.5kW inverter and BYD HVM 11kWh battery.

From 16<sup>th</sup> April to 13<sup>th</sup> August 2025, the property has been 93% self-sufficient with 434kWh additional benefit from battery storage and 72kWhrs drawn from the grid due to short periods of high loads.



**Figure 8.** 2025. 14months of Octopus Energy imported and exported at Howgate Close 1bed with a battery installed

Over the first 120days of installation, over 1.58MWhrs of renewable energy generated from the roof mounted pv's was exported. 59% of the renewable energy generated was still exported despite the presence of the battery.

Data from July 2024 and 2025 shows higher generation in 2025, probably due to better insolation.

### Some Observations And Feedback

While the Howgate home is demonstrating an encouraging level of self-sufficiency over the first four months since the battery installation, it is recognised the time line is 8 weeks either side of the Summer Solstice, perhaps the months of lowest heating load demand.

Peak energy demand, ‘spiking’, occurs from a few seconds to a couple of minutes. Recommendations to the tenants are to consider higher efficiency appliances to reduce peak loading.

A full year of data in the current working mode would allow for an optimisation of PV, inverter and battery sizing. This would be applicable to any country with similar insolation levels.

## 4. SUMMARY

What difference has the 11kWh battery installed at a 1bed earth-sheltered home at Howgate Close?

In the first four months of the battery installation there has been an 85% reduction in energy consumed from the grid compared to the same period in 2024. Despite a 38% reduction in exporting energy, the revenue from Exported Energy has increased due to the new Tariff in the presence of a battery.

This paper articulates how Howgate Close’s exceptional energy efficiency standards have delivered a low energy demand that compares favourably to the UK Building Regulations ‘Notional Building’. In part due to the consequential low daily energy demand, the installation of a 11kWhr battery has been transformational in reducing reliance on the National Grid.

A further 8 months of in-use building performance data will enable accurate sizing of inverters and batteries for the balance of eight buildings at Howgate Close.

---

<sup>i</sup> Harrall. J. (2023). *Reservoirs of Heat: A defining characteristic of high thermal mass earth-sheltered buildings*. 18<sup>th</sup> World Conference of ACUUS: Advances in Underground Space Development. Singapore

<sup>ii</sup> Harrall. J. (2025) *Howgate Close Case Study*. <https://www.drharrall.com/blog/> last accessed 2025/08/12.

<sup>iii</sup> Brailsford. D. (2012) *21 Days To Glory*. Book. ISBN 9780007506637

<sup>iv</sup> Harrall. J. (2023). *Reservoirs of Heat: A defining characteristic of high thermal mass earth-sheltered buildings*. 18<sup>th</sup> World Conference of ACUUS: Advances in Underground Space Development. Singapore

<sup>v</sup> <https://www.cla.org.uk/cla-east-news/fossil-fuel-free-rural-housing/> Last visited 2025/06/15

<sup>vi</sup> Encyclopaedia Britannica. <https://www.britannica.com/place/England> Last accessed August 12<sup>th</sup> 2025

<sup>vii</sup> HM Government. (2022) Energy Performance Certificate (EPC) No. 0370-3412-0030-2322-6481, 1 Howgate Close. June.

<sup>viii</sup> Hockerton Housing Project. 2016. Eakring Eco Housing Planning Drawings: [www.hockertonhousingproject.org.uk](http://www.hockertonhousingproject.org.uk)

<sup>ix</sup> Cerri. A. (2024) [Post Hydrocarbon People](#) Last visited 2025/06/15

<sup>x</sup> BRE. (2024) [BRE Linear Thermal Transmittance](#) Last visited 2024/02/01

<sup>xi</sup> HM Government (2023) UK Building Regulations 2010: Approved Documents. March

<sup>xii</sup> MES. (2024) MES Building Solutions: Psi Calculations. BuildDesk 3.4.6. 31<sup>st</sup> January

<sup>xiii</sup> MES. (2024) MES Building Solutions: Condensation Calculations. BuildDesk 3.4.6. 31<sup>st</sup> January

<sup>xiv</sup> Octopus Energy Ltd. (2025) Energy Export (13<sup>th</sup> July - 12<sup>th</sup> August 2025) 1bed, Howgate Close, NG22 0FW



## BUILDING BELOW: ARCHITECTURE BETWEEN FINANCE AND SUBTERRANEAN FUTURES

Danilo Furundžić<sup>1</sup>, Dejan Filipović<sup>2</sup>, Nebojša Bojović<sup>3</sup>

### Abstract:

This paper investigates how financialization reshapes the city by transforming architecture and urbanism into instruments of financial capital. Building on the concept of asset urbanism, it argues that urban space increasingly operates as an investment vehicle rather than a collective good. The central question is straightforward: when buildings are treated primarily as financial assets, what becomes of their capacity to provide housing, foster public life, and support environmental resilience? The paper pursues three objectives.

First, it traces the financialization of urban space, showing how architecture is reconfigured into a financial asset. This means examining the mechanisms that convert inherently illiquid real estate into liquid capital, giving rise to new morphological types that act as spatial avatars of finance—most notably luxury mega-basements, commonly known as “iceberg homes.” From these subterranean expansions to super-slender towers, this paper situates architectural form within the logics of finance capitalism. It further considers the development of subterranean public spaces through the economic lens of housing market financialization, shaped by capital flows, speculative investment, and liquidity tools.

Second, it documents the social outcomes of asset urbanism: increasing vacancy rates, the normalization of “zombie urbanism,” and the growing disconnect between statistical density and actual habitation. Within this framework, subterranean megaprojects are analyzed through the same logic as the iceberg phenomenon in luxury mansions. The contribution lies in reframing iceberg urbanism not as an isolated curiosity, but as part of a broader urban condition in which civic facades conceal hidden financial infrastructures. This perspective foregrounds the ethical dilemmas faced by architects, who must navigate between the market imperatives of liquidity and their professional commitments to sustainability and social inclusion.

Third, the paper examines the opportunities and challenges posed by the iceberg phenomenon across global cities, situating it within broader debates on urban inequality, speculative development, and the contested role of architecture in shaping contemporary urban life. In doing so, it incorporates media accounts, regulatory conflicts, and sustainability frameworks to demonstrate how underground expansion simultaneously generates spatial inequalities and ecological risks. Ultimately, it calls for a renewed assertion of architecture’s public role against the universalizing pressures of finance.

### Keywords:

finance capitalism, asset urbanism, zombie urbanism, subterranean megaprojects, iceberg homes, sustainable architecture, the iceberg phenomenon

### INTRODUCTION

The contemporary city is increasingly shaped by financial capitalism, where the built environment circulates as an asset class rather than a setting for everyday life. Financialization has aligned architecture with the logics of liquidity and speculation, displacing use value with exchange value. Within this regime, typologies such as super-slender towers, ex-urban investment mats, and “iceberg homes” operate as spatial avatars of finance, optimized for tradability and abstraction rather than habitation. At the same time, a counter-current persists: sustainability frameworks reposition architecture as an ethical and ecological endeavor grounded in orientation, insulation, material efficiency, and public accessibility.

<sup>1</sup> Phd Danilo S. Furundžić, architect, associated professor, Faculty of Architecture, University of Belgrade.  
<https://orcid.org/0000-0002-6829-520X>

<sup>2</sup> Phd Dejan Filipović, spatial planner, full professor, Faculty of Geography, University of Belgrade.

<sup>3</sup> Phd Nebojša Bojović, traffic engineer, full professor, Faculty of Transport and Traffic Engineering, University of Belgrade.  
<https://orcid.org/0000-0001-5600-3807>



Asset urbanism increasingly pushes cities to expand below ground, turning subterranean infrastructures into hidden containers of value in which civic surface signatures mask capital-intensive bases. The subterranean domain has emerged as a critical frontier of contemporary urban development. As cities grapple with spatial limitations, ecological pressures, and intensified demands for urban amenities, the underground is increasingly mobilized as both a private and public resource. On one side, privatized subterranean expansions exemplify an “iceberg logic”, where planned and civic-oriented subterranean infrastructures—metros, underground highways, parking structures, and logistical networks—illustrate how the underground serves collective needs, reshaping circulation, resilience, and technological integration at the scale of the city. This research situates iceberg urbanism at the intersection of these two tendencies: the private appropriation of subterranean space as a form of wealth securitization, and the public deployment of the underground as infrastructural commons. It examines how subterranean expansion embodies the architectural expression of capital’s financialization, while also revealing the paradoxes of equity, sustainability, and resilience in contemporary urbanism.

Methodologically, this research mobilizes case studies across distinct regulatory and market contexts, tracing how, when surface land and planning regimes constrain growth, functions migrate underground—metros, concourses, utilities, parking, logistics—while minimalist canopies, pavilions, and slim bridges advertise public benefit above. Together these examples show how speculative value can be created, traded, and stored independently of everyday use, producing districts dense on paper yet thin in social life. The paper makes both an empirical and normative contribution: it maps the techniques, actors, and spatial consequences involved in treating the city as an asset class, while testing whether socially and ecologically oriented design can survive within this regime—and under which forms of governance. The conclusion highlights potential policy levers, including decommodified tenure, community land trusts, public and non-profit ownership, and value-capture mechanisms linked to non-market housing. It further proposes criteria to distinguish genuinely civic infrastructure from architectures that primarily serve speculative enclosure.

## 1. ARCHITECTURE AS ASSET: THE FINANCIALIZATION OF URBAN SPACE

Capitalism can be understood as a continuous cycle with three phases: the accumulation of money through trade, its investment in agriculture and manufacturing, and a final stage in which we live today, marked by speculation—where late-stage dominance corresponds to financial expansion [1]. Lapavistas describes this as a “second great financial ascendancy” beginning around 1980 [2], while Jameson emphasizes the persistent triadic rhythm of trade, production, and speculation, noting that our present is defined by the intensification of speculative dynamics [1].

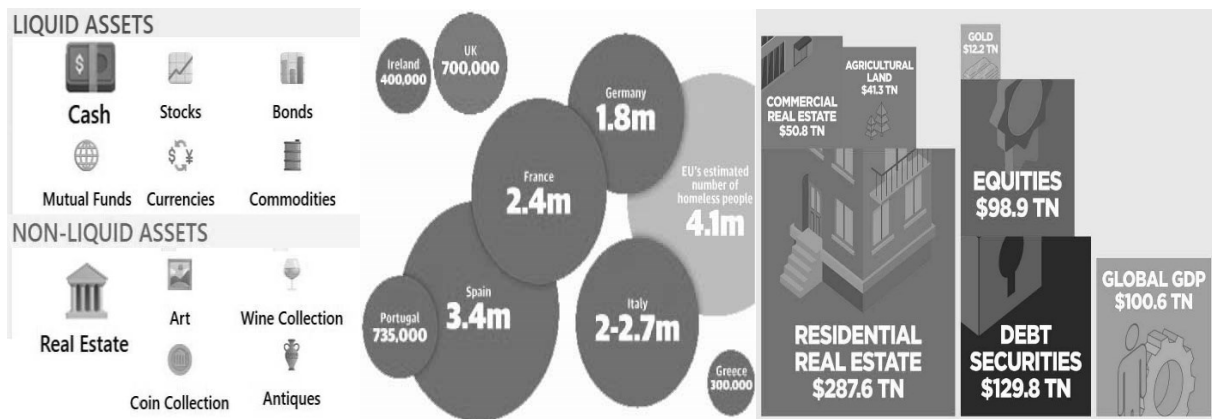
In recent decades, the form, function, and scale of urban environments have undergone profound transformations. Traditionally, the economic understanding of cities rested on the dynamics of supply and demand that shaped the production and consumption of goods and services. Since the 1980s, however, a new mode of capitalism has risen to unprecedented prominence: *finance capitalism*. This system, in which profit is derived less from producing goods than from the exchange of abstract financial instruments, challenges earlier conceptualizations of the city. The urban landscape is now increasingly shaped by financial logics that treat space primarily as an asset. The concept of *asset urbanism* captures this transformation. It denotes the socio-spatial avatar of finance capitalism, emerging when urban spaces function predominantly as investment vehicles, eclipsing their many other possible roles. This condition is captured by the concept of financialization, in which profits arise “primarily through financial channels rather than through trade and commodity production” [3]. Arrighi situates the current era, centered on New York (1870–present), as the successor to three prior hegemonic cycles: Genoa (1340–1630), Amsterdam (1560–1780), and London (1740–1830). These perspectives converge on a decisive turning point in the early 1980s, when two indicators aligned: the rapid growth of global equity capitalization and the explosion of assets under management—the so-called “giant pool of money.” From 1980 to 2018, global stock market capitalization rose from \$1.7 trillion to \$68 trillion, while assets under management expanded from \$12 trillion to about \$101 trillion today. This marked the rise of financial instruments as a “preferred medium of finance and speculation” [4,28].

The sheer scale of this capital has made architecture central to financial circulation. As in earlier hegemonies, significant portions of wealth flow into speculation and conspicuous consumption [4], with real estate historically serving as a privileged medium for both. Today, the housing market illustrates how architecture functions simultaneously as spatial form and financial instrument. Buildings are transformed into vehicles for storing and multiplying capital, increasingly detached from their social or functional use [3]. (Figure 1)

Although real estate has long been defined as illiquid—the opposite of cash in standard finance knowledge—contemporary practice seeks to push it toward liquidity [5]. This occurs through legal frameworks such as condominium statutes that enable fractional ownership, global brokerage networks that ease cross-border transactions, prop-tech platforms that normalize comparability, marketing logics such as rendering-driven pre-sales, and forms that minimize social entanglement [5]. Pre-construction assignment markets in London, Toronto,

and Belgrade allow contracts to be traded years before completion, effectively creating an architectural futures market where floor plans and digital renderings circulate as financial assets. In such cases, the building itself becomes secondary to its virtual representation, which operates as a tradable promise of future value. What circulates, then, are not simply material structures but virtual buildings, functioning primarily as financial rather than architectural objects. In this sense, architectural form itself becomes a financial form: shaped less by physical or urban laws than by the economic logics of liquidity, speculation, and global capital flows.

Historically, architecture and urbanism were evaluated primarily in terms of use value: how spaces supported human activity, habitation, and social life. Today, however, as space becomes financialized, exchange value dominates. The results are evident worldwide: High vacancy rates in global cities as units sit empty, held as speculative investments. The emergence of entire neighborhoods with density on paper but little social life in practice. Distortions in the planning and provision of public services, undermined by speculative vacancy.



**Figure 1.** Liquid vs. Non-Liquid Assets. Empty vacant houses in cities. Total Value of Global Real Estate.  
[Western & Southern Financial Group, 2024]

All listed may be distributed across cities, with varying degrees of prevalence, but a recurring characteristic is the widespread abandonment of units. The vacancy has become systemic, leaving vast portions of urban housing stock unused for much of the year. Concentrated in clusters, these empty properties generate what scholars call “zombie urbanism”—units owned but largely uninhabited, serving as second, third, or fifth homes for wealthy individuals. In extreme cases, entire “ghost cities” emerge, where speculation dominates but social life is absent [1].

Case studies of asset urbanism reveal how speculative logics reshape entire landscapes. In Ireland, the property boom enabled ordinary households to own multiple homes, but the crash left 300,000 vacant units—so-called ghost estates—and countless tax-driven zombie hotels designed more as financial devices than accommodations. Along Spain’s Mediterranean coast, vast stretches were transformed into a linear city serving northern European investors, while projects like Seseña near Madrid prioritized marketable units over livable communities, producing what has been described as “inhumane urbanism”. China offers perhaps the most extreme example, with an estimated 50 million sold but empty apartments, many acquired explicitly as substitutes for stock equities, making housing an overt financial instrument [6]. Taken together, these examples point to a global “zombie urbanism” [7] in which growth and decay coexist, vacancy is normalized, and speculation destabilizes local communities. Overbuilding and under-occupation emerge not as exceptions but as systemic outcomes of treating the city as an asset class. This undermines conventional planning assumptions that link housing supply to demographic growth and density, showing instead that entire districts may function less as places for living than as circulating investment products within global financial flows.

Zombie urbanism, marked by owned but largely uninhabited housing, has become a global phenomenon, though its intensity varies across regions. Governments have responded with fiscal and regulatory measures, including unoccupied penalties and second-home taxes, while political leaders stress the need to restore housing’s social function—as Xi Jinping declared in 2017, “houses are built to be inhabited, not for speculation.” Paris introduced a second-home tax in 2015, and Toronto later adopted similar instruments. These cases illustrate how finance capitalism reconfigures architecture, eroding its primary role as shelter for human habitation

## 2. ICEBERG HOMES: THE HIDDEN ARCHITECTURE OF SPECULATIVE WEALTH

Finance capitalist architecture is inherently unstable, functioning simultaneously as a symbolic spectacle and fungible commodity, and generating recurrent spaces of crisis that mirror the volatility of global markets. By facilitating liquidity and transforming real estate from an illiquid asset into a stock-like financial instrument, these

financial dynamics crystallize into distinct morphological configurations—what may be described as *architectural forms of finance* [1].

On the level of morphology, Soules [5] identifies them as iceberg homes, ex-urban investment mats, super-podiums, super-slender towers, and financial icons. Each of these forms acts as a spatial avatar of finance capitalism, designed to absorb, store, and circulate global investment flows. (Figure 2)

Iceberg homes are residential buildings with disproportionately large subterranean extensions relative to their above-grade, and shall be further elaborated in the subsequent sections of this paper. Ex-urban investment mats take the form of vast horizontal fields of repetitive single-family units, often so self-similar as to be interchangeable. Operating less as communities than as aggregations of investment units, these mats expand asset counts, deepen markets through sheer numerosity, and reduce locality. Super-podiums are towers rising from massive plinth-like bases, where universalized roof podiums detach housing from the street's contingencies, standardize access, ease interchangeability, and provide heightened privacy and urban gardens [8, 9]. While podium-and-tower combinations have historical precedent, their post-1980s proliferation reflects finance capitalism's fixation on maximizing returns through morphological standardization. Super-slender towers are radically thin high-rise forms functioning as spatial "safety deposit boxes in the sky." These structures host simplified high-altitude vault units with minimal shared horizontals, enabling remote global ownership rather than fostering local habitation. Finally, financial icons, exemplified by Frank Gehry's Guggenheim Museum in Bilbao, embody the so-called "Bilbao effect." Here, iconic architecture becomes a vehicle for real estate appreciation, tax growth, and city branding—embedding cultural capital directly into financial circuits.



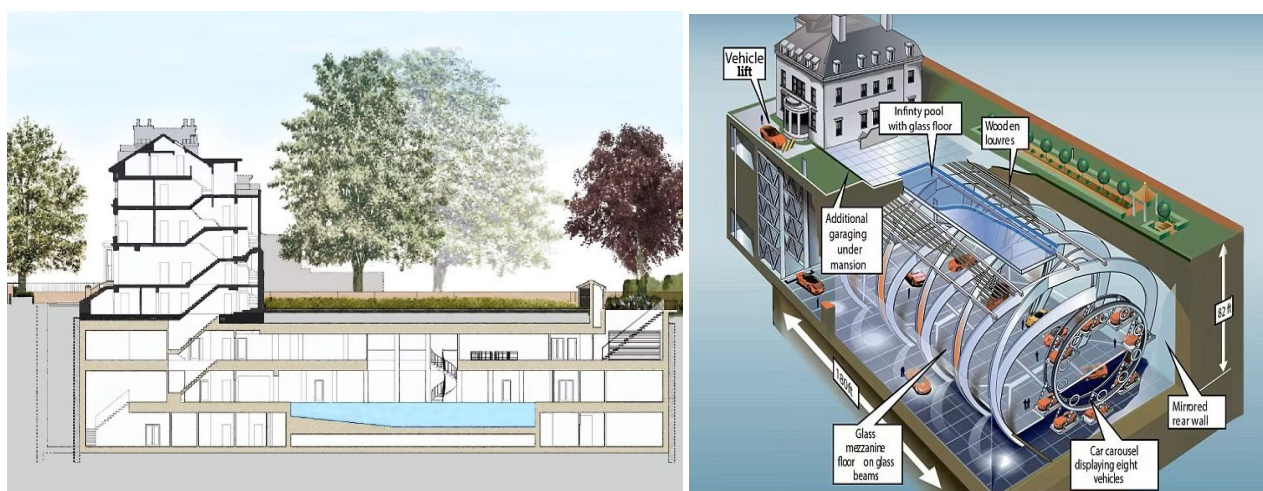
*Figure 2. Architectural forms of finance [author]*

The built environment increasingly serves as speculative wealth storage, turning real estate into an asset class detached from social use. Through pre-sale and assignment practices, housing itself is transformed into a tradable instrument, often exchanged multiple times before completion. In this process, architecture functions less as lived environment and more as financial asset [1]. London's "iceberg homes" or Manhattan's empty luxury towers exemplify this logic, deepening inequality as some areas are overvalued while others remain marginalized [1]. The paradox is further exposed in projects like Vancouver House's one-to-one gifting scheme linking luxury condos with minimal housing in Phnom Penh [Soules 2020]. At the same time, the iceberg house typology exemplifies how architecture can explicitly facilitate speculation. By extending downward rather than upward, these subterranean expansions allow the ultra-wealthy to circumvent planning restrictions, heritage protections, and urban land scarcity [8]. Initially notorious in London's Royal Borough of Kensington and Chelsea, the form has since spread to Aspen, Beverly Hills, Vancouver, Toronto, and Moscow. Despite locally distinct narratives—heritage control, land scarcity, lifestyle branding—the underlying logic remains the same: speculative wealth storage below ground. Such developments demonstrate how architecture becomes increasingly bound to the circuits of global finance [1].

"Iceberg homes" represent a distinctive contemporary urban phenomenon, emerging primarily in cities characterized by land scarcity, restrictive zoning regulations, and stringent conservation requirements. The visible, above-ground structures are designed to comply with local heritage guidelines, while concealing extensive multi-

level underground extensions that frequently surpass the scale of the surface construction. The term “iceberg” highlights the analogy to natural icebergs, the majority of whose mass remains hidden beneath the surface: above-ground envelopes comply with heritage controls while concealing multi-level subterranean spaces that often surpass the scale of the visible house [8]. (Figure 3)

The subterranean facilities typically include additional amenities such as private theaters, gyms, spas, wine cellars, and swimming pools, in more extravagant cases: theaters, art galleries, collection vaults, game rooms, car depots, and even bowling alleys, reinforcing the association of these spaces with exclusivity and concentrated wealth. Iceberg homes often extend up to 18 meters deep and stretch beneath gardens, making them larger than the homes above. The rise of iceberg housing is closely linked to global capital flows and the role of centralized cities that are magnets for international investment. As Arrighi and Lapavistas argue, financialization has transformed real estate into a primary vehicle for speculative capital accumulation [4, 2]. Desirable neighborhoods are marked by stringent zoning regulations and heritage protections that limit above-grade construction, while leaving subterranean expansion largely unregulated. This loophole allowed architects and investors to materialize wealth below ground, producing vast, privately enclosed environments invisible at street level. The continuing rise in real estate values, combined with declining costs of underground construction and advancements in air-conditioning and artificial lighting systems, have encouraged architects and developers to intensify the exploitation of subterranean space. Real estate agents rebrand them as “lower ground” levels to avoid the stigma of basements, yet their impacts are anything but hidden [8].



**Figure 3.** Edmund and Carol Lazarus' Leisure Center and Jon Hunt's Car Museum  
[<https://architizer.com/blog/inspiration/collections/londons-basement-extensions/>]

From a financial perspective, iceberg homes embody both asset security and speculative promise. On one hand, they stabilize property value by creating hidden square meters in highly constrained markets, effectively converting regulatory restrictions into opportunities for capital appreciation. On the other hand, they also amplify speculative pressures by inflating prices in already overheated real estate markets, further detaching housing from social use and reinforcing its role as a financial instrument.

In social terms, the iceberg form exemplifies the privatization of urban life. These houses provide security and privacy but intensify socio-spatial segregation, reinforcing the secessionary aspirations of elites who insulate themselves from the diversity of the city [8, 10]. While the wealthy gain access to customized, subterranean leisure spaces, neighbors and the broader public are excluded from their benefits and must cope with construction disruptions, increased property prices, and the erosion of urban inclusivity. Ecologically, the typology raises concerns over groundwater disruption, soil stability, and localized flooding risks, while also depending heavily on artificial climate control and energy-intensive systems of ventilation, illumination, and drainage [8, 9]. Critics highlight that these forms not only increase ecological vulnerability but also undermine broader urban sustainability goals. At the same time, proponents emphasize that technological innovation in excavation, structural reinforcement, and lighting design has made such projects feasible, pushing architecture to develop new expertise in subterranean living environments [11, 12].

Ultimately, iceberg homes epitomize hidden luxury, inequality, and urban unsustainability. Architecturally, they demand complex solutions for illumination, ventilation, and atmosphere. The reliance on cove lighting and spa-like design highlights how subterranean luxury requires the staging of desire and exclusivity. Detailing of light and finishes in these spaces demonstrates how architecture has been reprogrammed around privacy, securitization, and non-publicness. These interiors are often described as “luxury caves,” underscoring the paradox of private

abundance concealed beneath modest above-ground shells. In this sense, iceberg houses illustrate both the capacity of finance capitalism to invent hidden architectures of desire and the risks it poses for social equity and ecological resilience.

### 3. DIGGING FOR PROFIT: SUBTERRANEAN MANSIONS AND MEGAPROJECTS

London's "iceberg houses" emerged in the late 2000s as ultra-wealthy homeowners, constrained by conservation laws and plot restrictions, maximized living space through subterranean expansion [13]. Between 2008 and 2019, Greater London approved 7,328 basement developments. While most were modest, 18.3% were classified as "large" and 2.3% as "mega-basements," often extending three levels deep or beneath gardens. Collectively, these projects displaced over 1.78 million cubic meters of soil—twelve times the volume of St. Paul's Cathedral—transforming the geology beneath Georgian and Victorian housing stock [8]. Luxury basement development is concentrated in the so-called "basement belt" of Kensington & Chelsea, Westminster, Camden, and Hammersmith & Fulham, where high property values and restrictive planning render subterranean expansion both viable and profitable. Clustering is intense: on some Chelsea streets, six of eight semi-detached houses were retrofitted with deep basements containing pools or cinemas. At the market's 2015 peak, every \$1,000 invested in excavation could yield \$2,000 in added property value, epitomizing housing's transformation into an asset class. [13, 25, 27].

The cultural meaning of basements has inverted. Once associated with poverty, disease, and marginality, they now signify exclusivity and wealth [9, 14]. Graham terms this "luxified troglodytism," where underground space becomes an elite retreat. Whereas skyscrapers make wealth visible, iceberg homes extend it invisibly downward, producing what Rasmussen describes as "private arks of the underworld." London's case is distinctive yet influential: a Manhattan townhouse with an 11.5-meter-deep basement caused years of disruption [7]. Engineering challenges are immense, with projects encountering underground rivers, chalk mines, unexploded World War II bombs, and even hundreds of diggers abandoned beneath completed basements because extraction was too costly [14]. High-profile disputes—such as Robbie Williams versus Jimmy Page—illustrate how such developments fracture neighborhoods [14].

Here the paradox of sustainable design emerges. Contemporary architecture advances along two divergent trajectories: one emphasizing sustainability and equity, championed by Sir Norman Foster, and another exemplified by luxury mega-basements [11, 14]. Foster's "pyramid of sustainable design" stresses fundamentals—orientation, insulation, and form—linking sustainability with democracy and equity [15]. By contrast, iceberg basements operate as "value containers" for offshore wealth, frequently unoccupied, and deepen socio-spatial segregation [16]. Iceberg houses reveal how finance capitalism reconfigures both skylines and underground geographies. They epitomize housing's paradox as both shelter and speculative asset, consolidating resources for the few while externalizing noise, geological risks, and social exclusion [16]. This aligns with Atkinson's concept of the "minimum city," where development serves the 1% alone.

Thus, iceberg homes embody the paradox of architecture in the age of financialization: while sustainability discourse emphasizes ecological responsibility and social equity, subterranean mansions symbolize excess, speculation, and exclusion. They show how finance capitalism appropriates architectural form, not to serve urban resilience, but to anchor private wealth in the depths of the city. Asset urbanism foregrounds the tension between the social purpose of cities and the financial imperatives that increasingly govern their production. When buildings are treated first and foremost as financial devices, their capacity to serve as homes, workplaces, and civic spaces diminishes. As we consider the next fifty years of urbanization, it becomes crucial to address these dynamics: the ghosts of vacant homes, the zombies of speculative estates, and the surreal landscapes of overbuilt yet uninhabited cities all demand new discourses and new tools. To ignore them is to risk surrendering the city entirely to the logic of finance.

The phenomenon of the "iceberg home" should be understood as part of a larger iceberg urbanism: a process in which cities, like houses, are compelled by both social aspirations and financial logics to extend underground, producing new forms of architecture and infrastructure that stimulate economies, diversify social experiences, and innovate spatially, yet simultaneously impose ecological pressures, fiscal risks, and deepening contradictions of financialized urbanism. The subterranean domain is increasingly treated as a resource through which individuals and societies accommodate demands that cannot be met above ground. Homeowners, particularly within the context of London's "iceberg houses," place additional amenities underground, where regulatory frameworks are less restrictive, thereby enhancing property value and accommodating functions otherwise constrained by the built fabric [8, 13]. This practice resonates with a broader phenomenon of iceberg urbanism, whereby urban programs and infrastructures are shifted below ground as the surface of the city, much like historic housing stock, is spatially finite, while social demands for services and amenities continue to expand.

In earlier periods, the Georgian townhouse sufficed for the elite families of London, whose spatial and cultural needs were adequately contained within the existing domestic typology. Today, however, a new global elite has



emerged, characterized by expanded requirements—luxury leisure spaces, private gyms, art storage, and extensive infrastructures—that exceed the limits of traditional houses. As a result, architecture extends downward, producing multi-level basements that embody both the pressures of demand and the dynamics of financial accumulation [12, 17].

This tendency parallels broader social dynamics. As Maslow’s hierarchy of needs illustrates, once basic material requirements are met, individuals and societies develop higher-order needs that include cultural amenities, infrastructures, and enhanced urban services [25]. Contemporary cities, having satisfied fundamental conditions of shelter and survival, now seek to provide complex forms of infrastructural and programmatic support.

Yet the city itself remains spatially finite and governed by historically entrenched regulations. The response, much like in the domestic sphere, has been to move downward into the subterranean. Importantly, the forces driving this shift are not merely the satisfaction of social or cultural needs, but also powerful financial imperatives. Subterranean expansion enhances property values, generates new revenue streams, and positions urban space as an attractive site for global capital [1,3]. Public projects of subterranean urbanism—metros, underground cultural venues, or infrastructural complexes—have similarly been motivated not solely by philanthropic or civic aspirations, but by economic rationalities: the enhancement of land values, the intensification of urban centralities, and the pursuit of profitability through new forms of spatial commodification [15, 9].

At a smaller urban scale, iceberg megaprojects bring into focus the broader consequences of subterranean development. Economically, these ventures frequently rely on massive state investment or complex public–private partnerships, with uncertain prospects for return. As Flyvbjerg and colleagues observe, megaprojects often suffer from cost overruns and benefit shortfalls, creating fiscal strain even as they are justified as engines of growth. Yet paradoxically, they also function as countercyclical stimuli, revitalizing national construction industries and absorbing surplus capital during downturns.

Ecologically, prolonged excavation and the removal of millions of cubic meters of soil alter hydrological systems, destabilize surrounding structures, and embed long-term energy costs into urban metabolism. Extended building phases generate dust, noise, and traffic congestion, while completed infrastructures require continuous energy for ventilation, drainage, and climate regulation, thereby locking cities into higher carbon trajectories. Socially, iceberg megaprojects reshape the collective experience of the city. They introduce new subterranean spaces—transport nodes, cultural complexes, retail corridors—that expand the repertoire of urban life. Multinational design and construction teams contribute to social diversity, while users encounter novel forms of connectivity and cultural exchange. At the same time, however, these spaces often reproduce inequalities of access, embedding new hierarchies of consumption and security within the city’s fabric.

#### **4. OPPORTUNITIES AND CHALLENGES OF THE ICEBERG PHENOMENON**

At the level of public policy, contemporary urbanism reveals a structural paradox in the planning profession. Planners are tasked with two seemingly irreconcilable goals: inflating real-estate values to stabilize tax bases and satisfy property interests, and safeguarding residents’ welfare [15]. Within regimes of predominantly private landownership and hyper-mobile capital, this dual mandate is contradictory, especially in renter-majority cities. Regulation alone rarely shifts outcomes, and we get financial urbanism at its worst. Downzoning often triggers subterranean expansions, as-of-right regimes facilitate the mass production of under-occupied luxury space, and sophisticated “value capture” instruments—bonuses, transferable development rights, inclusionary housing—typically entrench reliance on commodified markets to finance a marginal quantum of “affordable” units [5, 15].

The Hudson Yards megaproject exemplifies this logic: massive public subsidies yielded a mall-anchored district of empty luxury condos with deferred, off-site “affordability,” demonstrating that technical fixes reproduce rather than resolve the problem [15]. By contrast, the Viennese model illustrates a different path. Requiring two-thirds social housing in rezoning, capping land resale prices, and maintaining long-term public or non-profit tenure, Vienna demonstrates that housing can be governed as social infrastructure rather than speculative commodity. Yet these achievements are not technocratic quick wins, they rest on decades of political hegemony in favor of social housing and robust public capacity [15]. Nor has pandemic-era migration to smaller cities provided relief. Out-migration from global centers pushed prices upward both in receiving locales and in origin metros, while disinvested cities—desperate for growth—offered ever larger concessions to real-estate interests, echoing the “race to the bottom” of the Amazon HQ2 spectacle [15,28].

Underground urbanism is not merely about creating spaces beneath the earth: it is about reimagining the fabric of city life. Extending cities into the underground can reduce urban sprawl, preserve green areas, and enhance livability. Subterranean transportation networks—including metro systems and highways—facilitate efficient movement, while large-scale underground warehouses and industrial zones minimize land usage and ecological disruption. Centralizing logistics in confined underground areas can simplify waste management and emergency response, echoing the “walled city” model of resilient infrastructures [8, 16]. A new approach to city planning is



emerging in the face of escalating environmental concerns and burgeoning urban populations. This paradigm harnesses the potential of the vertical dimension, delving into underground and aerial development realms.

By integrating advanced technologies in botany, transportation engineering, logistics, and sustainable practices, urban landscapes can transform into more efficient, self-sustaining ecosystems. The shift towards three-dimensional planning marks a milestone in urban development, addressing urban sprawl, land scarcity, and environmental degradation [18]. One of the most transformative aspects of this model is the integration of vertical farming. Hydroponic farms, operating in vertically stacked layers, allow for continuous food production, supported by robotic maintenance and AI-driven systems. [19] These farms recycle organic waste and CO<sub>2</sub> emissions, reducing dependence on large-scale GMO agriculture. Moreover, aquaculture—such as tilapia or krill farming—can be combined with plant cultivation, simultaneously purifying water and providing food resources. Such closed-loop systems align with circular economy principles and reinforce urban resilience [20, 21].

Climate control remains a pressing challenge in dense urban areas. Geothermal heating and cooling systems, utilizing stable underground temperatures, offer sustainable alternatives to conventional HVAC systems, significantly lowering the urban carbon footprint. Moving industries below ground helps mitigate heat plumes while preserving surface environments. At the same time, rethinking urban spaces emphasizes pedestrian-friendly centers, community gardens, and shared recreational zones. These measures foster social cohesion, promote healthier lifestyles, and reduce reliance on automobiles, aligning with sustainable mobility.

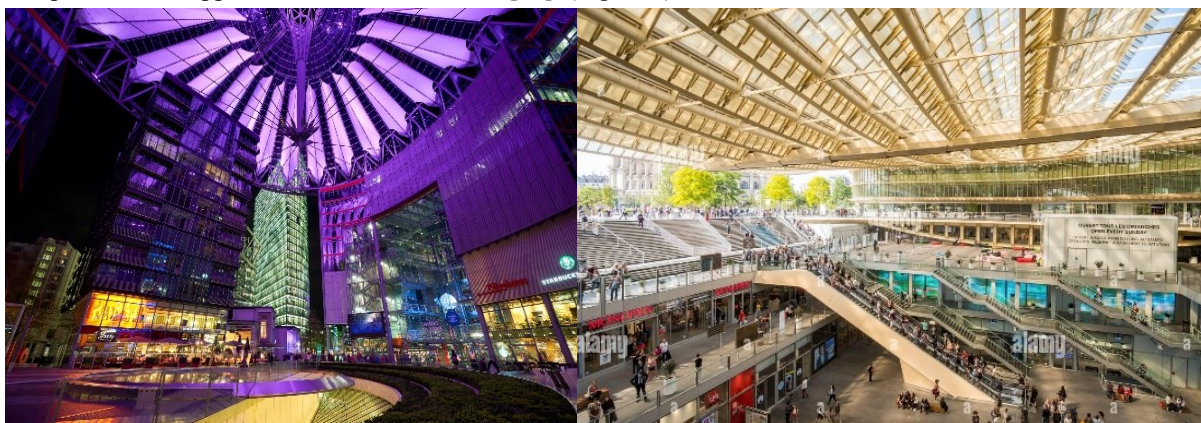
These dynamics foreground the analogy of the iceberg phenomenon. At the scale of private housing, iceberg mansions conceal multi-story subterranean amenities beneath modest above-ground envelopes. At the scale of the city, mega-projects and civil projects reproduce the same effect: the visible, civic-oriented surface structures mask vast, often hidden substructures that concentrate value and extend usable space where surface land is scarce. In this sense, the analogy is obvious: just as wealthy homeowners dig down when constrained by conservation laws or plot restrictions, cities themselves “go underground” to accommodate functions that cannot be placed above ground [22].



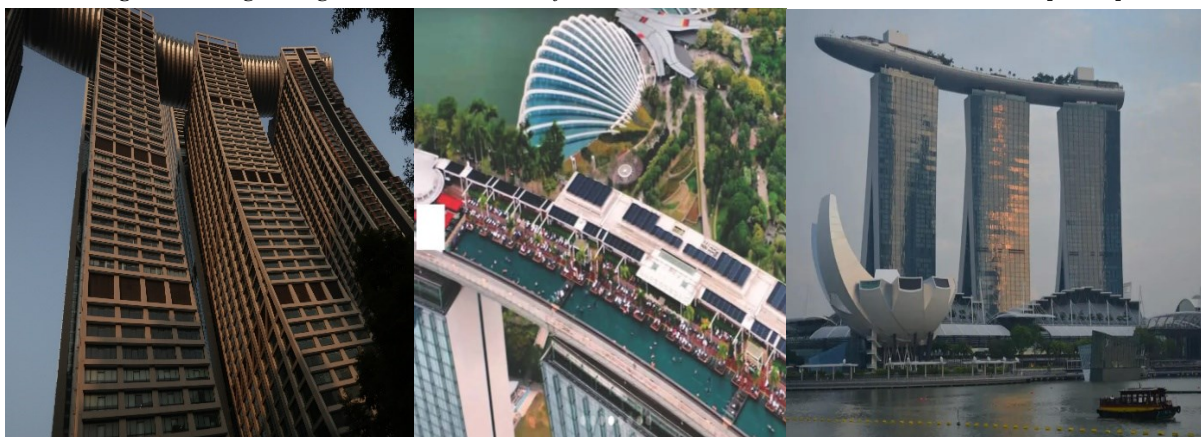
**Figure 4.** *Montreal underground spaces*  
[<https://www.mtl.org/en/experience/guide-underground-city-shopping>]

While Foster declined to design private iceberg houses, he nevertheless translated subterranean lessons into large-scale public projects, underscoring the divergence between exclusive elite expansion and inclusive civic infrastructure. The Bilbao Metro exemplifies this shift: its modest glass fosteritos entrances above ground symbolize urban clarity, while the true financial and functional investment lies in the vast subterranean system of tunnels and stations below [23]. Similarly, the Millennium Bridge in London conveys a minimalist, almost immaterial line over the Thames, yet its structural stability depends on substantial anchoring and engineering concealed beneath the surface [24]. The Great Court of the British Museum dramatizes openness through its glass canopy, though this visibility is underpinned by major underground interventions that reconfigured circulation and services [29]. More recently, the Apple Park campus in Cupertino demonstrates the iceberg logic on a corporate scale: the visible ring building is iconic and symbolic, but the campus relies on massive underground infrastructure, including parking for thousands of cars and extensive servicing systems [30]. Across these cases, the iceberg principle—minimalist or symbolic presence above, substantive weight below—illustrates how subterranean strategies migrated from elite private dwellings to public transport, cultural, and commercial infrastructures.

Montreal's underground network exemplifies this transformation. Originating in the early 1960s with the Place Ville-Marie office tower, the system expanded into a sprawling indoor network linking metro stations, offices, malls, and cultural institutions [31]. (Figure 4) El-Geneidy and colleagues describe how the "Indoor City" evolved through deliberate integration of air rights, underground corridors, and real estate development, reshaping civic space into a tool for private capital deployment. The iceberg phenomenon here is unmistakable: a surface narrative of mobility and public accessibility masking subterranean corridors of profit. However, in some manifestations of iceberg urbanism, the dynamic is reversed: content and financial potency are deliberately elevated above ground to maximize attraction, while functional bases remain buried. Paris's Châtelet–Les Halles illustrates this inversion. Once dominated by a subterranean retail and transit complex, the redevelopment culminated with La Canopée [32] a light-filled canopy sheltering cultural and commercial activity above the buried mall. Similarly, Berlin's Potsdamer Platz employed elevated plazas, sky-bridges, and terraces to lift amenity and social spaces upward while layering commercial infrastructure below [33]. (Figure 5) Singapore's Marina Bay Sands represents an even more dramatic "inverse iceberg." Limited by high groundwater levels and reclaimed land, the development elevated a vast SkyPark—a one-hectare public garden and pool—atop three towers, while retail and convention components were embedded below [34, 35]. In Chongqing, steep topography generates hybrid iceberg forms: public plazas and pedestrian routes unfold on rooftops, while the same structures present as subterranean complexes when approached from other levels [36]. (Figure 6)



*Figure 5. Going underground to accommodate functions: Potsdamer Platz and Forum des Halles [author]*



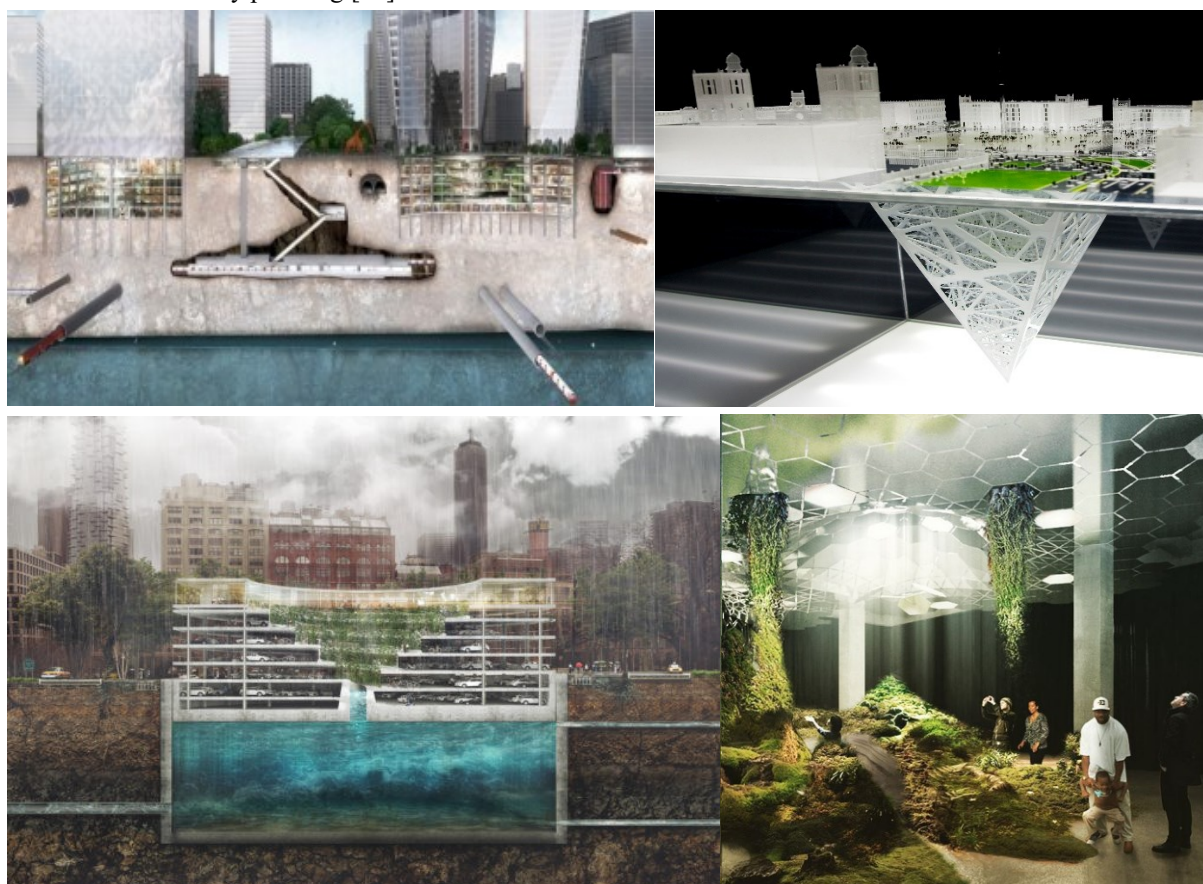
*Figure 6. Inverse iceberg development in Singapore and Chongqing, rooftop public space [author]*

Other initiatives reveal how iceberg logics combine philanthropic justifications with commercial imperatives. New York's Lowline sought to convert an obsolete trolley terminal into the world's first subterranean public park. It was framed as a civic amenity but relied on speculative and hybrid funding: a Kickstarter campaign raised USD 223,000, and the Lowline Lab drew 75,000 visitors, demonstrating both imaginative potential and dependence on corporate sponsorship. Similarly, the Nature Structure exhibition [37, 38] highlighted ecological interventions such as the Netherlands' Sand Motor and Denmark's pop-up rainwater-absorbing garage. Though framed in philanthropic terms—"playing on the same team as nature"—these projects also blurred into speculative circuits of innovation and urban branding. In parallel, Mexico City's BNKR Arquitectura proposed the radical "earthscraper," a 65-story inverted pyramid descending 300 meters below ground. Conceived as a response to historic preservation rules that limit vertical growth around the Zócalo, the project dramatizes the iceberg



phenomenon by envisioning an immense civic and commercial complex entirely hidden beneath the surface. [39] (Figure 7)

To elucidate these structural dynamics, the subsequent comparative overview examines a series of international case studies. By situating underground urban spaces within diverse regulatory, socio-economic, and morphological contexts, these examples illustrate how distinct planning paradigms operationalize subterranean infrastructures to reconcile pressures of mobility, environmental resilience, and capital accumulation. Montreal exemplifies comprehensive integration: underground networks have been woven into long-term strategies to relieve surface congestion, enhance multimodal mobility, and protect cultural heritage, combining metro systems with pedestrian passages, utilities, parking, and retail [40]. Hong Kong demonstrates how extreme density can be leveraged through an efficient mass transit railway coupled with pedestrian subways, cavern uses, and commercial facilities that optimize scarce land while maintaining high standards of service and safety [41]. Chicago's underground trajectory reflects historical reconstruction and technological innovation, translating nineteenth-century imperatives and climate resilience into today's palette of subways, utility corridors, and commercial concourses embedded in statutory planning [42].



**Figure 7.** Iceberg effect at the level of future urban mega-projects: Think Deep UK Social Value proposal, Mexico City's BNKR Arquitectura earthscraper, Danish Third Nature pop/up space-car park, the Lowlane subterranean park

In Tianjin, a major port city, underground transport, logistics, and retail mitigate surface bottlenecks, while strong state and private investment and strict codes support large-scale implementation [40]. Beijing elevates urban underground spaces to a strategic planning instrument, using long-range regulation and coordinated phasing to integrate extensive metro lines, intermodal hubs, and underground commerce while managing environmental impacts [43]. Oslo deploys underground parking, waste and utility tunnels, and selected retail to preserve surface landscapes in a terrain- and cost-constrained context, rigorous environmental permitting and circular-economy practices frame delivery [42]. Seoul, among the world's densest capitals, concentrates underground development in transport and commercial corridors, using deep platforms and expansive shopping passages to absorb flows and activate economic frontages [41].

Zurich blends functionality and culture: high-tech engineering underpins utility tunnels, parking, and rail nodes alongside cultural installations, all governed by exacting safety and environmental rules [40]. Tokyo relies on deep, highly connected rail interchanges and extensive weather-protected pedestrian passages that bind districts together and reduce surface externalities, while carefully managing groundwater and settlement risks [42].



Singapore treats underground space as a national-scale asset, integrating metro interchanges, commercial complexes, service corridors, and innovative water-management infrastructure with park systems to enhance resilience and spatial efficiency. (Figure 8)

Across these cases, urban underground spaces serves transportation, utilities, commerce, recreation, storage, and public-realm functions at typical depths of roughly 10–30 meters [deeper for specialized facilities], with governance ranging from corridor reservation in master plans to public-private partnerships and rail-property models [40]. The common success factors are strategic management, technological and organizational innovation, clear regulatory frameworks, and consistent environmental safeguards, the common pitfalls are fragmented excavation, unclear volumetric rights, and erosion of publicness in over-commercialized tunnels [41].



**Figure 8.** Underground concert cathedrals Tokyo, Zurich and Tianjin  
[Study on the Development of Urban Planning in the Underground Space of the City of Belgrade, URBEL]

Beyond systemwide planning, international practice also illustrates typologies by use. Transport systems are the most prevalent and fastest-growing underground function globally, acting as the backbone that unlocks co-located utilities, retail, and public amenities [40]. Two reference projects illustrate these dynamics: the RIO project as a strategic intervention that returns greenery and public space to the city while reorganizing traffic underground, and Montreal's RESO, where the metro catalyzed a broader lattice of underground pedestrian networks and commercial programs, demonstrating how transit infrastructure can generate durable, multi-functional value below the surface while preserving and enhancing the urban fabric above.

The listed cases show a recurring iceberg phenomenon at the level of urban mega-projects and civil infrastructures: the visible layer emphasizes public goods—mobility, green space, cultural amenities—while hidden layers generate rents, embed revenue streams, and anchor private capital. What appears philanthropic or civic-oriented ultimately participates in the commodifying logic of contemporary capitalism. This is the essence of iceberg phenomenon. Above ground, architecture enacts transparency and civic accessibility, below, it functions as financial apparatus. What presents as sustainable, philanthropic, or citizen-oriented design is simultaneously reconfigured into an extractive infrastructure, privileging liquidity and capital flows over social equity and ecological resilience. The contradiction is stark: even where the motivations appear philanthropic, they are folded back into commercial rationalities. Effective responses must therefore be structural.

Cities face a strategic fork: extract marginal benefits from intensified commodification, or pursue decommodification through public and non-profit tenure, social rent regimes, and collective landholding models that detach land from speculative circuits. Without such a shift, iceberg logics—whether buried, elevated, or hybrid—will continue to structure both private housing and public mega-projects, reshaping the city less as a civic infrastructure of dwelling than as an apparatus for capital circulation.

## CONCLUSIONS: THE ROLE AND RESPONSIBILITY OF ARCHITECTS

In contemporary cities shaped by financialized capitalism, the housing market increasingly operates as a mechanism for rent extraction and capital circulation rather than as an institution oriented to the social function of dwelling—secure, affordable, and stable shelter. The transcript foregrounds several intertwined dynamics: a widening disjunction between wages and housing costs, the accelerated acquisition of large swaths of the housing stock by institutional investors (banks, hedge funds, private equity) who have become major landlords, and the reorientation of urban planning [1]. In the United States, an acceleration of home sales has coincided with declining homeownership rates and record shares of purchases by absentee buyers and large funds. Move-in rents on vacant units have more than doubled over the past two decades, while wages have largely stagnated, producing mounting rent burdens—especially acute in segregated Black and Latino neighborhoods [15]. As an ever-larger share of paychecks is transferred to landlords, Dickensian forms of precarious dwelling reemerge, including “shift-bed” arrangements in which tenants rent a bed for hours rather than a room. This signals a broader transformation: housing increasingly functions as a lucrative business. Urban practice shifts from a public-interest vocation toward “managing land value” to sustain municipal budgets and property owners. Producing spaces deliberately kept under-occupied or empty -as a kind of safety deposit box for wealth preservation rather than as livable space [12, 1].

Public debate framed narrowly as “supply versus demand” misses the object of exchange. What is traded is not generic “units” but specific land positions bundled with cheap credit, construction inputs, and the invisibility of the asset. Demand is also for housing as an investment vehicle, where liquidity, price appreciation, and portability dominate. Under these conditions, the problem is not only an absolute deficit of units but also a surplus of capital seeking asset classes with the properties of safe, transferable, appreciating stores of value [1].

The morphologies identified: ultra-thin pencil towers on Manhattan's Billionaires' Row, “iceberg homes” with disproportionate subterranean extensions, and ex-urban “investment mats” of standardized units—are not stylistic curiosities. They are spatial devices for increasing liquidity: multiplying tradable units, standardizing typologies, minimizing shared horizontal space, and producing “safety-box” apartments optimized for remote, global ownership rather than everyday life. Even emblematic cases such as 432 Park Avenue reveal a double truth: radical aesthetics can coexist with technical effect and litigation, yet when one vehicle loses favor, capital rapidly identifies fresh regulatory gaps and spawns' new spatial mutations [12]. Which are appearing even in Serbia in the BWF Belgrade project.

Bringing together two seemingly opposed narratives—sustainable architecture and financial capitalism—highlights the divergent trajectories of contemporary urban development, where design functions either as an instrument of the public good or as a mechanism of socio-spatial segregation. The iceberg phenomenon in public urbanism, articulated as a collective strategy for climate resilience and social equity, stands in stark contrast to its manifestation in private residences, where it materializes as an expression of privatized wealth, exclusivity, and subterranean expansion. Despite their opposing orientations, both forms are underpinned by a shared architectural



logic and embedded within the same capital-oriented logics of value construction and financialization. Their simultaneous presence within identical urban contexts—most visibly in London—illustrates the contested and ambivalent role of architecture in mediating inequality, resilience, and the circulation of speculative capital in the city.

These two trajectories highlight fundamentally different futures of urbanism. Sustainable design—framed by systems like LEED and championed by Norman Foster—presents architecture as a survival strategy rooted in ecology, equity, and democratic access. In contrast, the spread of iceberg homes, first in London and now in other global cities, highlights architecture's role in speculative wealth storage and privatized underground domains.

Architects today operate within complex multi-actor matrices in which their agency is frequently subordinated to the priorities of marketers, brokers, lenders, lawyers, and platform operators. In many markets, marketers are involved from the earliest stages of design and are even paid more than architects, which radically shifts influence over form toward salability rather than inhabitation. The result, as Soules notes, is a built environment increasingly optimized for liquidity, isolation, and abstraction rather than for “rich domestic life.” Indeed, Soules underscores the paradox of contemporary practice: “charity is part of the game, a humanitarian mask hiding the underlying economic exploitation of people and land” [5]. This formulation resonates with the critique voiced in the discussion, where participants emphasized how marketing prerogatives diminish architecture's capacity to cultivate meaningful social spaces.

Yet, design choices still matter. If financialization rewards programmable emptiness and view-fetish, architects can counter-program through shared horizontals, porous circulation, multi-scalar commons, and mixed-tenure stacks that re-embed housing in social life [1]. Beyond design, professional levers exist: selective refusal of hyper-financialized commissions [7], reforming award criteria to redirect prestige toward socially equitable projects, engaging in policy advocacy to reform condominium laws and assignment-market transparency [18], and pushing for digital ethics in rendering-driven assignment markets. The debate further raises unresolved questions: Do we still need the building if its value trades primarily on renderings? Should we include a tree in the project if it does not generate profit? What constitutes “use” when units are largely uninhabited? Where should the ethical line of practice be drawn? And how might architecture reassert locality against the universalizing pressures of liquidity?

Soules argues that contemporary architecture “oscillates between being a dwelling and being a derivative,” and stresses that the responsibility of architects is to tip the balance back toward the former. More broadly, the translation of architecture into finance-compatible forms—iceberg basements, ex-urban mats, podium megastructures, and super-slender towers—signals the transformation of housing into an asset class optimized for liquidity [5]. Yet these forms are not destiny. By embedding design within social entanglements, architects and planners can resist the reduction of architecture to a purely financial instrument. Ethical refusal of hyper-financialized commissions, reforming award criteria to valorize equity, and advocating for legal and digital transparency provide meaningful avenues for reorienting practice. The task ahead is to reclaim architecture's civic and ecological roles, ensuring that the subterranean futures of cities are shaped not only by capital but also by commitments to justice and sustainability.

## BIBLIOGRAFY

- [1] Aalbers, M. B. (2012). *Subprime cities: The political economy of mortgage markets*. Wiley-Blackwell.
- [2] Jameson, F. (1998). The brick and the balloon: Architecture, idealism, and land speculation. *New Left Review*, 228, 25–46.
- [3] Krippner, G. R. (2005). The financialization of the American economy. *Socio-Economic Review*, 3(2), 173–208. <https://doi.org/10.1093/ser/mwi008>
- [4] Arrighi, G. (1983). *The geometry of imperialism: The limits of Hobson's paradigm* (New ed.). Verso.
- [5] Soules, M. (2021). *Icebergs, zombies, and the ultra-thin: Architecture and capitalism in the twenty-first century*. Princeton Architectural Press.
- [6] Wu, F. (2018). Planning centrality, market instruments: Governing Chinese urban transformation under state entrepreneurialism. *Urban Studies*, 55(7), 1383–1399. <https://doi.org/10.1177/0042098017721828>
- [7] Atkinson, R. (2020). *Alpha city: How London was captured by the super-rich*. Verso.
- [8] Burrows, R. (2019). Living on icebergs: The rise of mega-basements in London. *Urban Studies*, 56(12), 2530–2548. <https://doi.org/10.1177/0042098018795796>
- [9] Graham, S. (2016). *Vertical: The city from satellites to bunkers*. Verso.
- [10] Lapavistas, C. (2013). *Profiting without producing: How finance exploits us all*. Verso.
- [11] Daniel, M. (2022). *Subterranean London: The cultural politics of underground space*. Routledge.
- [12] Atkinson, R. (2016). Limited exposure: Social concealment, mobility and engagement with public space by the super-rich in London. *Environment and Planning A*, 48(7), 1302–1317. <https://doi.org/10.1177/0308518X15598320>
- [13] Burrows, R., Graham, S., & Wilson, A. (2022). Bunkering down? The geography of elite residential basement development in London. *Urban Geography*, 43(9), 1372–1393. <https://doi.org/10.1080/02723638.2021.1934628>
- [14] Garrett, B. (2020). *Subterranean London: Cracking the capital's hidden geographies*. Reaktion Books.
- [15] Stein, S. (2019). *Capital city: Gentrification and the real estate state*. Verso.

- [16] Burrows, R., Webber, R., & Atkinson, R. (2017). Welcome to “Pikettyville”? Mapping London’s alpha territories. *The Sociological Review*, 65(1), 184–201. <https://doi.org/10.1111/1467-954X.12375>
- [17] Baldwin, S., Burrows, R., & Knowles, C. (2019). Troglydism and urban transformation: London basements as elite spaces. *Architectural Research Quarterly*, 23(2), 115–130. <https://doi.org/10.1017/S1359135519000225>
- [18] Arrighi, G. (2010). *The long twentieth century: Money, power, and the origins of our times* (Updated ed.). Verso.
- [19] Đokić, V., Ristić Trajković, J., Furundžić, D., Krstić, V., & Stojiljković, D. (2018). Urban garden as lived space: Informal gardening practices and dwelling culture in socialist and post-socialist Belgrade. *Urban Forestry & Urban Greening*, 30, 247–259. <https://doi.org/10.1016/j.ufug.2017.05.014>
- [20] Despommier, D. (2010). *The vertical farm: Feeding the world in the 21st century*. Thomas Dunne Books.
- [21] Eigenbrod, C., & Gruda, N. (2015). Urban vegetable for food security in cities? A review. *Agronomy for Sustainable Development*, 35(2), 483–498. <https://doi.org/10.1007/s13593-014-0273-y>
- [22] Furundžić, D. S., & Bojović, N. (2023). The potential of underground spaces around metro stations as special urban forms. In *Proceedings of the 18th Conference of the Associated Research Centers for the Urban Underground Space (ACUUS 2023)* (pp. 25–31). Springer. <https://doi.org/10.1007/978-981-97-1257-1>
- [23] Foster + Partners. (1995). *Bilbao Metro* [Architectural firm report]. Retrieved from <https://www.fosterandpartners.com>
- [24] Foster + Partners. (2017). *Apple Park, Cupertino* [Architectural firm report]. Retrieved from <https://www.fosterandpartners.com>
- [25] Maslow, A. H. (1943). A theory of human motivation. *Psychological Review*, 50(4), 370–396. <https://doi.org/10.1037/h0054346>
- [26] Greater London Authority. (2016). *Basement development in London: Policy guidance* [Policy guidance]. Greater London Authority.
- [27] Greater London Authority. (2008). *The London plan: Spatial development strategy for Greater London* [Policy guidance]. Greater London Authority.
- [28] Gotham, K. F. (2009). Creating liquidity out of spatial fixity: The secondary circuit of capital and the subprime mortgage crisis. *International Journal of Urban and Regional Research*, 33(2), 355–371. <https://doi.org/10.1111/j.1468-2427.2009.00874.x>
- [29] Wilson, D. M. (2002). *The British Museum: A history*. British Museum Press.
- [30] Sudjic, D. (2010). *Norman Foster: A life in architecture*. Weidenfeld & Nicolson.
- [31] El-Geneidy, A., Kastelberger, L., & Abdelhamid, H. T. (2011). Montréal’s roots: Exploring the growth of Montréal’s Indoor City. *Journal of Transport and Land Use*, 4(2), 33–46. <https://doi.org/10.5198/jtlu.v4i2.176>
- [32] Berger, P., & Anziutti, J. (2016). LA CANOPEE in Paris — An innovative architecture, a challenge for engineering. *Structural Engineering International*, 26(3), 235–241. <https://doi.org/10.2749/101686616X14636714865383>
- [33] Colomb, C. (2012). *Staging the new Berlin: Place marketing and the politics of urban reinvention post-1989*. Routledge.
- [34] Safdie, M. (2011). Marina Bay Sands: Integrating resort, city, and public space. *Architectural Design*, 81(4), 68–73. <https://doi.org/10.1002/ad.1271>
- [35] Chang, T. C., & Huang, S. (2011). Recreating place, replacing memory: Creative destruction at the Singapore River. *Asia Pacific Viewpoint*, 52(2), 144–158. <https://doi.org/10.1111/j.1467-8373.2011.01445.x>
- [36] Leaf, M. (2018). Subterranean urbanism in Chongqing: Topography, circulation, and hybrid space. *Journal of Urban Design*, 23(4), 567–583. <https://doi.org/10.1080/13574809.2018.1425501>
- [37] Moss, J. (2016). The Lowline: A case study in speculative urbanism and the politics of subterranean public space. *Journal of Urban Design*, 21(5), 617–635. <https://doi.org/10.1080/13574809.2016.1184567>
- [38] Boston Society of Architects. (2018). *NatureStructure: Design for resilient communities* [Exhibition catalog]. BSA Space.
- [39] BNKR Arquitectura. (2011). *Earthscraper: A subterranean alternative to urban growth in Mexico City* [Architectural concept]. BNKR Arquitectura.
- [40] Admiraal, H., & Cornaro, A. (Eds.). (2016). *Think Deep: Planning, development and use of underground space in cities*. ISOCARP/ITACUS.
- [41] Bobylev, N. (2016). Underground space as an urban indicator: Measuring use of subsurface. *Tunnelling and Underground Space Technology*, 55, 40–51. <https://doi.org/10.1016/j.tust.2016.01.010>
- [42] Broere, W. (2016). Urban underground space: Solving the problems of today’s cities. *Tunnelling and Underground Space Technology*, 55, 245–248. <https://doi.org/10.1016/j.tust.2015.11.014>
- [43] Gao, C., Wang, Y., Zhang, X., & Xu, Y. (2021). The main characteristics of urban underground space regulatory plan from the perspective of China’s spatial planning: A practice in Beijing Sub-Center. *IOP Conference Series: Earth and Environmental Science*, 703, 012009. <https://doi.org/10.1088/1755-1315/703/1/012009>

## DEVELOPING A DATA-DRIVEN BAYESIAN NETWORK MODEL FOR LAYOUT PLANNING OF URBAN UNDERGROUND COMMERCIAL FACILITIES

Yong-Kang QIAO<sup>1</sup>, Ji-Shuai XIAO<sup>2</sup>, Nikolai BOBYLEV<sup>3</sup>, Fang-Le PENG<sup>4</sup>

**Abstract:** Underground commercial facilities are intricately linked to urban public life, representing the most impactful use of underground space within urban spatial systems. However, existing planning approaches for these facilities largely depend on the subjective judgments of urban planners, resulting in considerable uncertainties in their development. To address these limitations, this study developed a Bayesian Network model to extract valuable information embedded in a diverse array of multi-source datasets of underground space and urban development. The modeling process combined machine learning techniques and expert knowledge integrating the correlations among influencing factors such as population, commercial vibrancy, transportation accessibility, GDP, land price and strategic locations. The average prediction error rates for the number of floors and total development area of underground commercial facilities were 16.67% and 22.22%, respectively. Case studies in Shanghai and Zhengzhou demonstrated the effectiveness and applicability of the proposed model for master planning of urban underground commercial facilities. It is anticipated that the findings of this study will provide valuable guidance for the sustainable use of urban underground space.

**Keywords:** Urban underground commercial space, Bayesian network, machine learning, expert knowledge, master planning

### 1. INTRODUCTION

In the urban underground space system, underground commercial facilities, such as catering, retail, entertainment, leisure, and sports facilities, are closely integrated with urban public life and represent types of underground infrastructure that have a profound impact on the urban spatial system. However, current planning methods for the development and utilization of underground commercial spaces remain insufficient. The validity of qualitative analyses is often subjective and challenging to verify. Meanwhile, existing quantitative analyses generally rely on easily measurable data collected at the macro city level, making them less suitable for application to land parcel-scale master planning.

Artificial intelligence technology facilitates efficient cleaning, structuring, and knowledge extraction from massive urban multi-source data, offering new approaches for underground commercial space planning. Among such methods, the Bayesian Network model is an effective tool for expressing and reasoning uncertain knowledge (Meng et al., 2023), featuring an intuitive topological structure. This model has been applied in diverse domains, including environmental studies (Ren et al., 2023; Liber et al., 2020), land use (Celio et al., 2014; Sahin et al., 2019), and urban planning (Li., 2020; Xu et al., 2023). Therefore, the Bayesian Network model can extract valuable information from urban development history and provide decision support for planning underground commercial spaces.

<sup>1</sup> PhD, QIAO Yong-Kang, Ph.D. Civil Eng., assistant professor, Research Center for Underground Space & Department of Geotechnical Engineering, Tongji University, Shanghai, PR China, qiaoyongkang@tongji.edu.cn

<sup>2</sup> MSc, XIAO Ji-Shuai, M.Sc. Civil Eng., Research Center for Underground Space & Department of Geotechnical Engineering, Tongji University, Shanghai, PR China, 1256106789@qq.com

<sup>3</sup> PhD, BOBYLEV Nikolai, Ph.D. Geoecology, associate professor, Russian State Hydrometeorological University, Saint Petersburg, Russia, n.bobylev@rshu.ru.

<sup>4</sup> PhD, PENG Fang-Le, Ph.D. Civil Eng., professor, Research Center for Underground Space & Department of Geotechnical Engineering, Tongji University, Shanghai, PR China, pengfangle@tongji.edu.cn

It is noteworthy that within the field of underground space planning, the application of Bayesian networks has primarily focused on data aggregation and suitability analysis. The modeling approaches employed are generally expert knowledge-based, meaning that the network topology and conditional probability tables are mostly derived from expert experience, with limited integration of actual multi-source urban data. The validity and rationality of expert knowledge cannot be disputed, particularly when tackling the complex challenges of urban underground space planning, as experts in relevant fields generally consider multiple intricate factors to generate reasonable planning recommendations. However, models built solely on expert experience may be more subjective and susceptible to errors when applied to real-world complex problems. With the advent of the big data era, cities have accumulated vast amounts of multi-source data, the potential value of which has often been overlooked in previous research.

To address the limitations of subjective planning approaches, this paper leverages a rich array of urban multi-source data, including underground space development data such as the number of floors and the total development area, and ten influencing factors, such as population, commercial vibrancy, transportation accessibility, GDP, land price, etc., to develop a Bayesian Network model to uncover valuable information embedded within underground commercial space datasets. Case studies from two representative Chinese cities, Shanghai and Zhengzhou, demonstrate the effectiveness and applicability of the developed model in the master planning of underground commercial facilities. The objective of this study is to explore and develop a novel master planning method for underground commercial space and to promote the sustainable use of urban underground space.

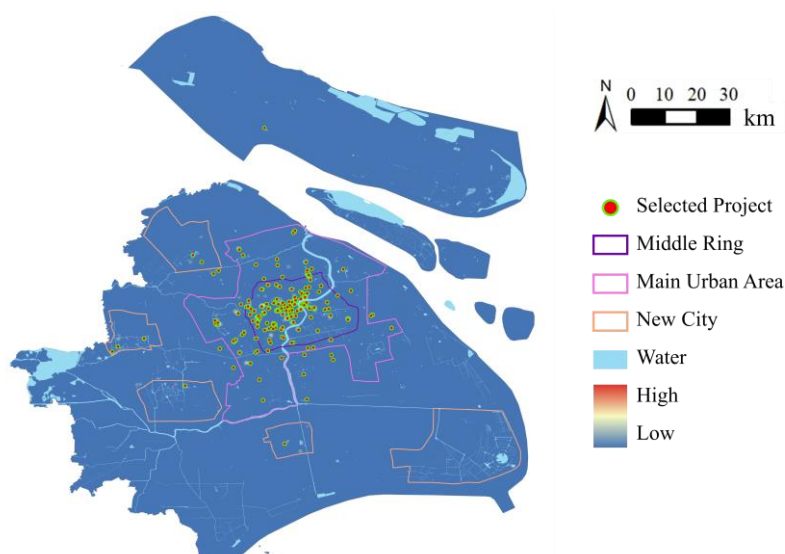
## 2. BRIEF OVERVIEW OF THE CASE STUDY AREAS

### (1) Shanghai

This study focuses on Shanghai as a case study to construct and optimize a Bayesian Network model for the master planning of underground commercial facilities, with the aim of providing useful guidance for other Chinese cities, such as Zhengzhou, by leveraging Shanghai's advanced underground space development experience.

Covering an area of 6,833 km<sup>2</sup> and home to over 24 million residents, Shanghai serves as China's international center for economy, finance, trade, shipping, and scientific and technological innovation. Shanghai has played a pioneering role in the development and utilization of urban underground space in China. To date, the utilization of urban underground space in Shanghai has exceeded 155 million m<sup>2</sup> and includes the world's largest underground rail transit network, intricate underground motorways, and prominent underground complexes with interconnected commercial facilities.

Underground commercial projects (e.g. underground shopping malls) were selected based on actual performance metrics calculated using social media data on Dazhong Dianping platform (Yang et al., 2022), integrating visitation rates and average per capita consumption. Following the calculation of performance for each project and the subsequent exclusion of low-scoring projects, 180 projects with higher performance were selected as the analysis cohort for this study. The spatial distribution of the selected projects is depicted in Figure 1.



**Figure 1.** Spatial distribution map of selected underground commercial projects in Shanghai



## (2) Zhengzhou

The city of Zhengzhou has been developing an underground space master plan since approximately 2020, with a primary focus on underground commercial facilities. This study aims to leverage the established practices of Shanghai, utilizing Bayesian Network modeling, to inform the long-term planning of underground commercial facilities in Zhengzhou. Furthermore, the case of Zhengzhou will be employed to evaluate the transferability of the prediction model, which is based on development experience of Shanghai, to other urban contexts.

Zhengzhou City, the capital of Henan Province, encompasses an area of approximately 7,567 km<sup>2</sup> and has a resident population of 12.8 million. The development of underground space in Zhengzhou has experienced a substantial expansion. By the end of 2020, the total underground space developed in the main urban area of Zhengzhou reached approximately 43.8 million m<sup>2</sup>.

The master plan for underground space utilization in Zhengzhou outlines 45 underground commercial projects, as depicted in Figure 2. The detailed planning parameters will be determined using a Bayesian Network model.

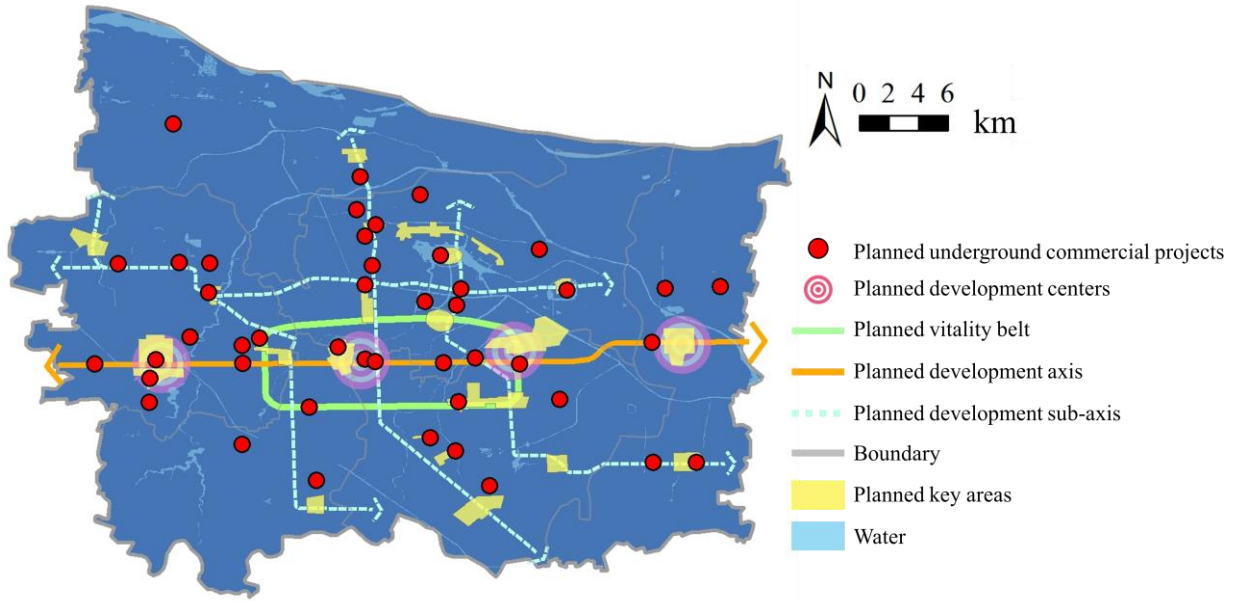


Figure 2. Distribution of planned underground commercial projects in the main urban area of Zhengzhou

## 3. METHODS

### 3.1. Bayesian Network modeling

The construction of the Bayesian Network model is divided into two key components: the topology  $G$  and the probability distribution  $\Theta$ . The topology  $G$  of a Bayesian Network model is a directed acyclic graph, where "directed" signifies that the network structure has a logical, irreversible order, and "acyclic" indicates the absence of loops within the network structure. Nodes in the topology are classified into parent nodes (influencing factors) and child nodes (target variables). These nodes are connected such that parent nodes direct influence towards child nodes. Each node represents a variable and can exist in a finite number of mutually exclusive states. The probability distribution  $\Theta$  of the Bayesian Network model represents the conditional probability table (CPT) for each node  $X_i$  given its parent set  $pa(X_i)$ . The CPT reflects the strength of the relationship between the state  $X_i$  and states of  $pa(X_i)$ . With the topology and probability distribution of the Bayesian network specified, the joint probability for a subset of nodes  $X_i$  conforming to the Markov independence criterion is representable as shown in Equation (1).

$$P(X_1, X_2, \dots, X_n) = \prod_{i=1}^n P(X_i | pa(X_i)) \quad (1)$$

Generally, three main approaches are commonly used to construct Bayesian Network models (Ren et al., 2023; Meng et al., 2023; Chen et al., 2024; Zhao et al., 2024): expert knowledge-based modeling, data-driven (machine learning) modeling, and hybrid modeling combining expert knowledge with machine learning. Each approach presents inherent advantages and disadvantages. Expert knowledge-based modeling is inherently subjective and prone to inaccuracies when dealing with complex systems. Machine learning modeling is free from subjective biases, as the network topology and CTPs are entirely determined by the data. Characterized by strong objectivity and ease of implementation, this approach may yield inaccurate models when data are limited, which is a common



challenge in urban planning scenarios. Hybrid modeling, incorporating expert knowledge with machine learning, introduce some subjectivity and require a clearly defined relationship between parent and child nodes. For this data-driven study, machine learning-based modeling and hybrid modeling were explored, and evaluated based on resulting prediction accuracies. Netica was selected as the Bayesian Network modeling and analysis software.

### **(1) Machine learning modeling**

This study utilized the Tree Augmented Naive Bayes (TAN) algorithm for machine learning-based modeling. Compared to the Naive Bayes algorithm, TAN effectively manages dependencies without fully abandoning the independence assumption, thus enhancing classification performance. TAN is recognized for its performance in practical applications, particularly in scenarios with feature dependencies.

In this study, the TAN algorithm was employed to account for interdependencies among influencing factor nodes. The core principle of TAN involves incorporating interdependence information between attributes in a moderated manner, thereby mitigating complex joint probability calculations without completely disregarding significant interdependencies. Specifically, TAN adopts the "One-Dependence Estimator" strategy, where each attribute depends on at most one other non-class attribute. In the context of this study, this implies that each influencing factor node can have, at most, one other influencing factor node as a parent, in addition to the target variable node.

### **(2) Hybrid modeling combining expert knowledge with machine learning**

This approach comprised two principal steps: network structure determination and CPT learning. Network structure determination relied on expert judgment, whereas CPT learning was primarily data-driven.

#### **a). Network structure optimization**

In the network structure determination stage, directly connecting each of the ten influencing factor nodes to the target variable node, as in a Naive Bayes network, would have resulted in an impractically large state space for the target variable node (e.g., as will be stated in Section 3.3, it would be  $2^7 \times 3^3 = 3456$  states for this study). This state space could not be adequately populated by the available dataset less than 180 cases. Equalizing CPT values for uncovered states would have substantially compromised the model's accuracy and validity. To address this, this study systematically categorized the influencing factors based on their impact on development effectiveness, the strength of logical association between factors, and inter-factor correlation. Based on this classification, four intermediate nodes ( $T_1$ – $T_4$ ) were introduced to connect the influencing factor nodes to the prediction target variables, creating a more scientifically sound analytical framework. The states of these intermediate nodes were determined by logical inference based on the states of their parent nodes. Furthermore, Spearman's rank correlation coefficient analysis was performed to quantitatively assess the correlation between influencing factors. Influencing factors exhibiting a Spearman's rho greater than 0.7 (indicating strong correlation) were connected within the network structure, ensuring that the model topology reflected intrinsic relationships among variables.

#### **b). CPT optimization**

In addition to leveraging expert knowledge during the network structure establishment, the extent of expert input was also adjustable during the CPT determination stage for intermediate and target variable nodes. This strategy aimed to further improve the model's reliability and performance. The approach sought to maximize the complementary strengths of expert experience and machine learning techniques, thereby enhancing the overall modeling effectiveness. Three optimization attempts were conducted in this study, varying the degree of expert knowledge integration during the optimization of the hybrid model.

**Optimization Test I: Maximum Expert Knowledge Integration.** The CPTs for both intermediate and target variable nodes were derived entirely from the sequential analysis method (G1 method). Weight calculations for each node were based on expert knowledge in underground space planning, independent of the case study data. Only the CPTs of the influencing factor nodes were based on the actual case study. Under this configuration, the intermediate and target variable nodes were limited to two states (0 and 1).

**Optimization Test II: Moderate Expert Knowledge Integration.** The state values of the intermediate nodes were calculated using the node weights of the influencing factors, as determined by the sequential analysis method (G1 method). These intermediate nodes were then reclassified based on the calculated state values. Finally, sample statistics for each node were learned using the Incorp Case File function in Netica.

**Optimization Test III: Minimum Expert Knowledge Integration.** A four-classification natural breakpoint method was applied to classify the intermediate nodes, with state judgments based on the parent node states. This optimization model resembled the initially established combined model, but with a greater number of intermediate node classifications to accommodate different combinations of parent node states. Consequently, merging different parent node states based on subjective expert opinion was unnecessary. The CPTs of the intermediate nodes were obtained using the Incorp Case File function, without the incorporation of expert knowledge.

### (3) Determination of prediction model

The prediction models for the three selected target variables were determined in two steps. First, for each target variable, the model type exhibiting the lowest average error rate among the five model types was selected. Second, within this selected model type, the model group with the lowest prediction error rate among the ten model case groups partitioned using K-fold Cross Validation was chosen as the final prediction model.

## 3.2. Nodal indicator selection for Bayesian Network modeling

### (1) Target variables: Key planning parameters for underground commercial space

The purpose of this study is to explore and develop a novel master planning methodology for underground commercial spaces, in which the number of floors and the development area serve as the key planning indicators (Peng et al., 2019; Qiao et al., 2022). In this study, we initially considered six target variables related to these aspects. However, due to length constraints, this paper presents only the two most significant and predictable variables (as demonstrated by the research results) including the number of floors ( $Y_1$ ) and the total development area ( $Y_2$ ). These two variables were modeled as target variables in the proposed framework.

### (2) Influencing factors of underground commercial space development

Existing research on the development and utilization of underground commercial facilities has investigated various factors affecting its scale, development form, and functions (Kaliampakos et al., 2006; Ma et al., 2022; Li., 2020; Peng et al., 2023; Qiao et al., 2024). It can be concluded that factors influencing the development of underground commercial facilities include population size, transportation infrastructure, location, economic conditions, as well as planning policies. Since the actual performance was used as a key case selection criterion in this study, the parent nodal indicators identified as those with direct visitation and price-setting impacts on the performance of underground commercial projects. A system of influencing factors was established based on the general factors affecting underground space development and utilization, as summarized in Table 1.

Table 1. Influencing factors of Bayesian Network modeling for underground commercial facilities

Categories	Influencing factors	Notations	units
Visitation-related	Population density	$X_1$	persons/km <sup>2</sup>
	Commercial density	$X_2$	POIs/km <sup>2</sup>
	Connectivity to underground rail transit stations	$X_3$	/
	Shortest distance to rail transit stations	$X_4$	km
	Density of bus stops	$X_5$	stops/km <sup>2</sup>
	Road network accessibility	$X_6$	/
Pricing-related	Benchmark land price	$X_7$	yuan/m <sup>2</sup>
	Gross Domestic Product (GDP)	$X_8$	yuan/km <sup>2</sup>
	Floor area ratio (FAR)	$X_9$	/
	Public activity central system	$X_{10}$	/

## 3.3. Data collection and pre-processing

### (1) Data collection

Data representing the influencing factors were collected through multiple sources. "Population density ( $X_1$ )" was derived from an online open-access dataset. "Commercial density ( $X_2$ )" was derived from a kernel density map of points of interest (POIs) for shopping services. "Connectivity to underground rail transit stations ( $X_3$ )" and "Shortest distance to rail transit stations ( $X_4$ )" were derived from Amap and online surveys. "Density of bus stops ( $X_5$ )" was derived from kernel density maps of POIs for bus stops. "Road network accessibility ( $X_6$ )" was derived from segmentation analysis of Shanghai's major road networks using the spatial syntax platform Depthmap. "Benchmark land price ( $X_7$ )" was derived from official land price documents issued by the Shanghai Municipal Government. "GDP ( $X_8$ )" was obtained from an online open-access dataset. "FAR ( $X_9$ )" was obtained from online measurements or open-access datasets on Amap. "Public activity central system ( $X_{10}$ )" was sourced from city planning documents issued by the Shanghai Municipal Government.

The data used for target variables were collected from project-specific on-site measurements utilizing the Amap Online Measurement Tool and web searches.

## (2) Data pre-processing

### a). Data discretization

In Bayesian Network models, a greater number of states per node necessitates a larger number of training cases to adequately cover all states. Given that this paper's analysis was based on a subset of underground commercial projects in Shanghai, and the final dataset comprised only 180 cases, data discretization was performed to reduce the number of states per node. This method ensured effective model outcomes.

The categorization of each parent and child node data is shown in Table 2. Initial cutoff values were derived using the natural breakpoint method and subsequently refined through the incorporation of expert knowledge. Spearman's rank correlation analysis and spatial stratified heterogeneity analysis were conducted on the project performance data. The results indicate strong connections between the actual performance of selected cases and three influencing factors: Population density ( $X_1$ ), Shortest distance to rail transit stations ( $X_4$ ), and Benchmark land price ( $X_7$ ). Consequently, these three factors were categorized into three classes, whereas the remaining influencing factors and target variables were categorized into two classes.

*Table 2. Data discretization for influencing factors and target variables*

Factor notations	Units	Number of classes	Classification range and representative values		
			0	1	2
$X_1$	persons/km <sup>2</sup>	3	[972,10000]	[10000,25000)	[25000,51816]
$X_2$	POIs/km <sup>2</sup>	2	[198.8,800]	[800,1562]	
$X_3$	/	2	disconnection	connectivity	
$X_4$	km	3	(0.3,24.2]	(0.1,0.3]	[0,0.1]
$X_5$	stops/km <sup>2</sup>	2	[0,10)	[10, 24.1]	
$X_6$	/	2	[1.04,1.25]	[1.25,1.52)	
$X_7$	yuan/m <sup>2</sup>	3	[192, 2000]	[2000,4000]	[4000, 6701]
$X_8$	yuan/km <sup>2</sup>	2	[538,40000]	[40000,89509]	
$X_9$	/	2	[0,5.5)	[5.5, 38.29]	
$X_{10}$	/	2	(3,10]	[1,3]	
$Y_1$	/	2	1	≥2	
$Y_2$	m <sup>2</sup>	2	[1680,15000]	[15000,113419]	

### b). Grouping of cases using K-fold cross validation

To evaluate the overall performance of the Bayesian Network model and to identify a model with a low prediction error rate, this study employed the cross-validation method for model training. The core principle of cross-validation involves assessing model performance through a judicious partitioning of the available data. Specifically, the dataset is divided into two subsets: a training set, used to train the model, and a validation set, used to evaluate the trained model's performance. By alternating the roles of the training and validation sets, this process enables an objective and accurate assessment of the model's strengths and weaknesses. Considering the accuracy of the validation method and the computational demands of modeling, this study employed K-fold cross-validation to train the Bayesian Network model. This involved partitioning the original dataset into  $K$  groups, using each subset as a validation set in turn, and the remaining  $K-1$  subsets as a training set. The cross-validation procedure was repeated  $K$  times, with each subsample validated once.

In this study, the selected 180 cases were randomly partitioned into ten groups of 18 cases each. In each iteration, one group was designated as the validation set ("validation group  $X$ "), and the remaining nine groups (162 cases) were used as the training set ("training group  $X$ "). This cross-validation process was repeated ten times, resulting in ten Bayesian Network models with differing parameters. The average error rate of each model was used to evaluate its overall performance, and the model exhibiting the lowest error rate was selected as the final prediction model.

## 4. RESULTS

### 4.1. Model building results

#### (1) Modelling results using TAN algorithm

Due to the large number of model iterations and repetitive operations, we present "the number of development layers ( $Y_1$ )" as the target variable node and utilize the training and validation data from the first group for subsequent demonstration purposes.

In Netica, the model shown in Figure 3 was directly constructed using the "Learn TAN Structure" function. With "Number of underground floors ( $Y_1$ )" selected as the target variable, the data from the 18 validation cases in "Validation Group 1" were input using the "Test With Cases" function provided by Netica, resulting in a model prediction error rate of 38.89%.

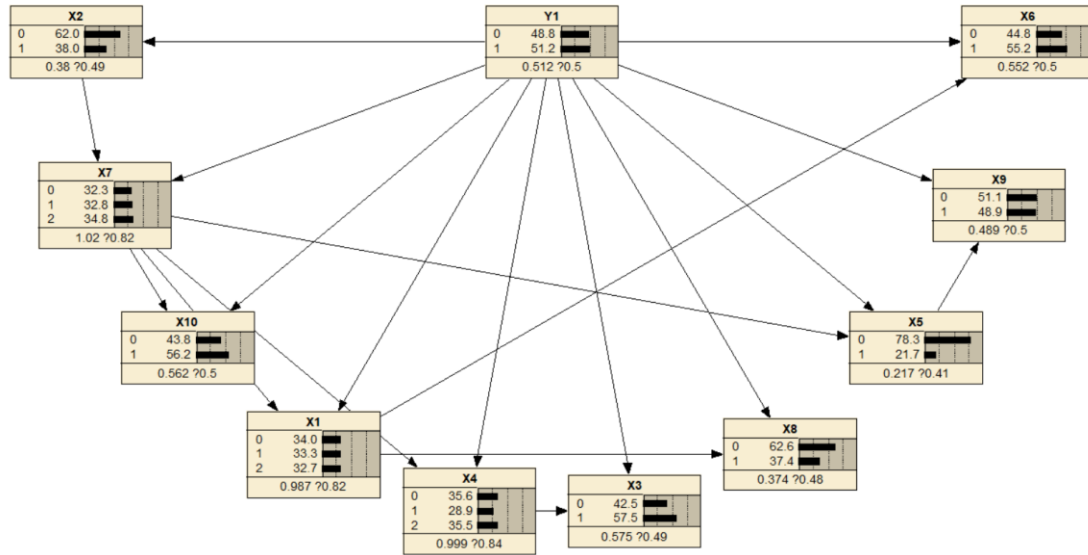


Figure 3. Demonstration of Tree augmented Naive Bayesian Network (TAN) structure

The modeling operation was repeated for the remaining nine datasets, and the average error rate of the TAN model for the target variable "Number of floors ( $Y_1$ )" was calculated after obtaining the error rate for each group. By replacing the target variable nodes and following the same procedure, the model error rate and average error rate for each group of target variable "Total development area"  $Y_2$  were obtained (see Table 3).

## (2) Hybrid modeling results: network structure optimization

This optimization strategy of introducing four intermediate nodes ( $T_1$ – $T_4$ ) enabled the model to maintain a better training effect under the limited sample condition ( $N = 162$ ). The final model structure constructed based on this strategy is shown in Figure 4. This network structure not only ensured the integrity of the correlation relationships between variables but also enhanced the computational efficiency and stability of the model.

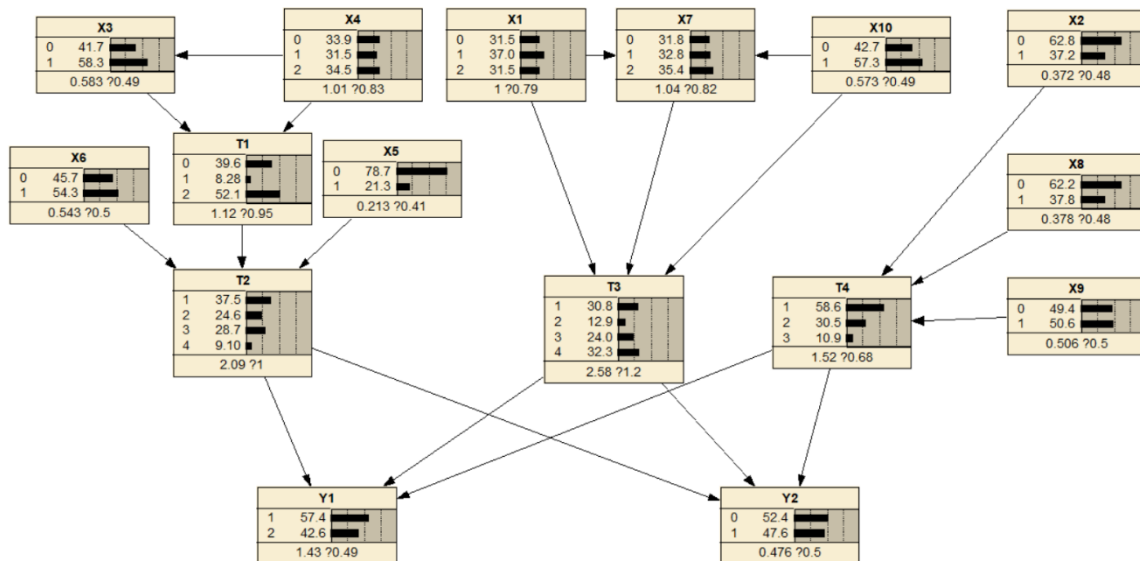


Figure 4. Hybrid modeling results: network structure optimization

Following the same method of CPT learning described in the previous section, ten groups of training data were input into the model to train the respective node CPTs. The corresponding validation cases for each group were then input for validation using the "Test With Cases" function, and the error rates and average error rates for each group of models were obtained, as shown in Table 3.

By comparing the results of TAN modeling and hybrid modeling in Table 3, it was observed that, overall, the two approaches possess distinct advantages and limitations. Their prediction error rates for different target variable datasets exhibited some variability, suggesting the potential for further optimization through parameter tuning.

### (3) Hybrid modeling results: CPT optimization

A comparison of the average error rates for the predictions of the TAN model, and the hybrid model, and the three optimization test models developed in Section 3.1 for each target variable node is presented in Table 3. The optimization attempts involving adjusting the degree of expert experience to incorporate CPT yielded improved prediction results for target variables  $Y_1$ , and  $Y_2$ .

Ultimately, the prediction models identified for target variables  $Y_1$ , and  $Y_2$  are presented in Table 4.

Table 3. Bayesian Network models and average error rates (%)

Groups	Target variables									
	TAN modeling		Hybrid modeling		Optimization test I		Optimization test II		Optimization test III	
	$Y_1$	$Y_2$	$Y_1$	$Y_2$	$Y_1$	$Y_2$	$Y_1$	$Y_2$	$Y_1$	$Y_2$
1	38.89	38.89	33.33	38.89	33.33	44.44	33.33	38.89	38.89	38.89
2	33.33	33.33	50	33.33	27.78	66.67	50	33.33	50	22.22
3	38.89	55.56	16.67	55.56	22.22	44.44	16.67	55.56	16.67	44.44
4	50	27.78	38.89	33.33	33.33	66.67	38.89	33.33	27.78	33.33
5	37.78	38.89	38.89	33.33	33.33	61.11	38.89	33.33	27.78	38.89
6	38.89	38.89	55.56	44.44	44.44	55.56	55.56	44.44	44.44	44.44
7	16.67	33.33	38.89	50	44.44	38.89	38.89	50	33.33	44.44
8	44.44	44.44	27.78	27.78	50	72.22	27.78	27.78	44.44	38.89
9	22.22	38.89	33.33	33.33	33.33	72.22	33.33	33.33	38.89	22.22
10	44.44	66.67	38.89	50	38.89	61.11	38.89	50	27.78	44.44
Average	36.56	41.67	37.22	39.99	36.11	58.33	37.22	39.99	35.00	37.22

Table 4. Determined prediction models

node	Predicted target variables	
	$Y_1$	$Y_2$
Selected model	Optimization Test III Group 3	Optimization Test III Group 9
Prediction error rate	16.67%	22.22%

## 4.2. Application results to the main city of Zhengzhou

### (1) Modeling results with Zhengzhou data

The same method as in the previous section was employed to collect representative data for the ten influencing factors of the two types of predicted objects. However, the data for "FAR ( $X_9$ )" could not be collected because some of the predicted objects had not yet completed construction; thus, this value was left vacant and replaced by the CPT inherent in the Shanghai model. Additionally, a model for Zhengzhou City was established to compare with the Shanghai model identified in Table 4. The results are shown in Table 5.

In Table 5, "Zhengzhou TAN model" and "Zhengzhou hybrid model" were trained using data collected and screened from 60 case studies of underground commercial projects in Zhengzhou. The "Shanghai model (Zhengzhou standard)" and "Shanghai model (Shanghai standard)" were trained by applying data from the same 60 Zhengzhou underground commercial projects to the Shanghai model selected in Table 4. However, given the differences in development status between Shanghai and Zhengzhou, the classification criteria for nodes were



categorized using two standards: "Shanghai standard" and "Zhengzhou standard." Furthermore, because the collected underground commercial projects in Zhengzhou are primarily developed with only one underground floor, and the few projects with two underground floors are concentrated in the core of the main urban area, the prediction error rate for the "number of floors ( $Y_1$ )" was 3.33% across all models, rendering these prediction results of limited comparative significance.

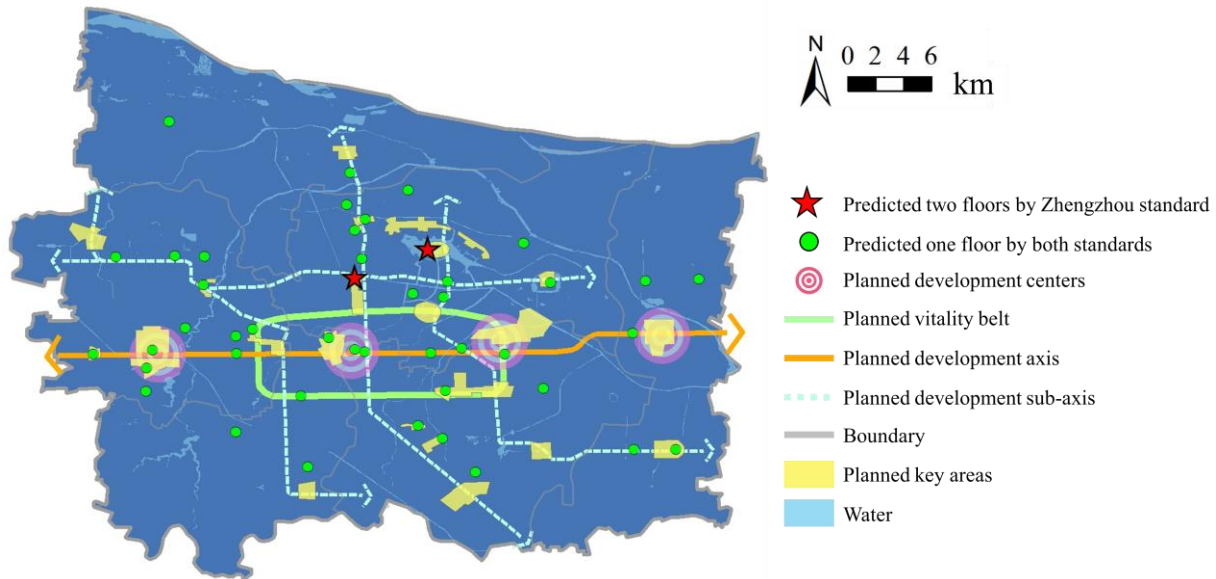
**Table 5.** Comparison of average error rates of various Bayesian Network models (%)

Models	Target variables	
	$Y_1$	$Y_2$
Zhengzhou TAN model	3.33	48.33
Zhengzhou hybrid model	3.33	53.33
Shanghai model (Zhengzhou standard)	3.33	38.33
Shanghai model (Shanghai Standard)	3.33	28.33

Comparison of the models reveals that the error rate of the Shanghai model using Zhengzhou data is lower than that of the TAN model and the hybrid model employing Zhengzhou data. This suggests that the Shanghai model is suitable for predicting key indicators of underground commercial space allocation in Zhengzhou.

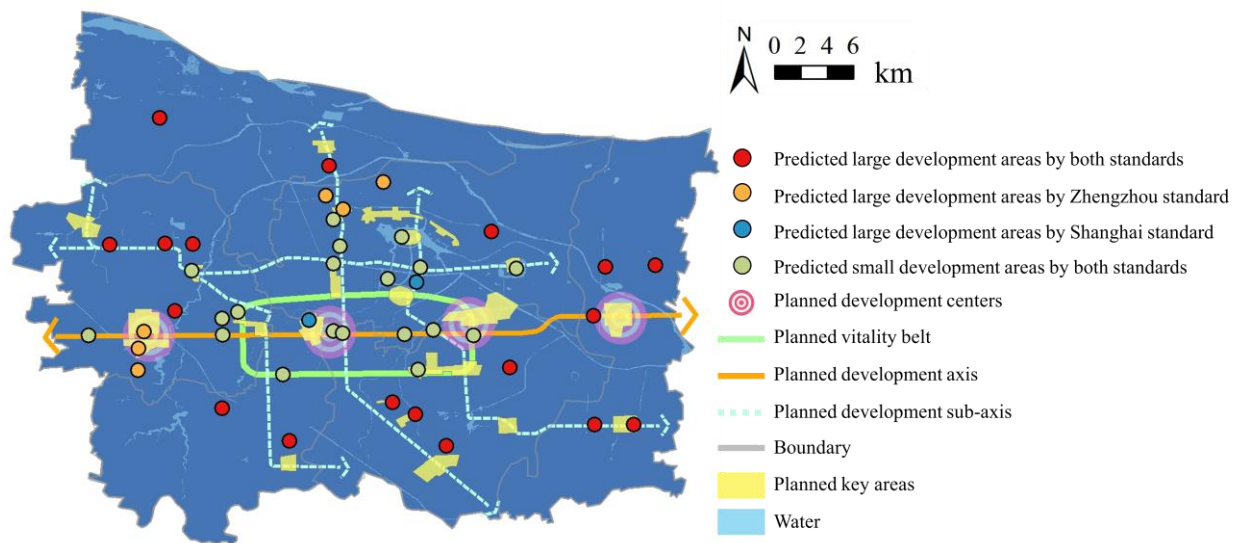
## (2) Modeling results of key planning parameters

Processed data for the influencing factor nodes were substituted into the "Optimization Test III Group 3" model, as identified in Table 4, to predict the target variables. The prediction results for the underground commercial projects in Zhengzhou are shown in Figure 5. Overall, the prediction of the "number of floors ( $Y_1$ )" indicates that, in the development of underground commercial space in the main urban area of Zhengzhou, nearly all underground spaces are suitable for the development of the first underground floor. Only certain plots in the core area, such as the Garden Road Commercial Center and the North Longhu Financial Center, are suitable for the development of a second underground floor.



**Figure 5.** Distribution of predicted "Number of floors ( $Y_1$ )" for planned underground commercial projects

Processed data for the influencing factor nodes were substituted into the "Optimization Test III Group 9" model to predict the target variable "Total development area ( $Y_2$ )".  $Y_2$  is a binary classification variable, with a development area of 15,000 m<sup>2</sup> serving as the cutoff point. A predicted area larger than 15,000 m<sup>2</sup> was classified as "large development area," whereas a smaller area was classified as "small development area." The prediction results for the underground commercial projects are presented in Figure 6. According to the Shanghai standard, projects with an underground commercial space development area exceeding 15,000 m<sup>2</sup> were all located in the periphery of the main city. The predicted underground commercial space development area for projects in the core area of the main city was less than 15,000 m<sup>2</sup>.



*Figure 6. Distribution of predicted "Total development area ( $Y_2$ )" for planned underground commercial projects*

## 5. DISCUSSIONS

This study explored the application of machine learning and expert knowledge-based machine learning models for predicting underground commercial space development in Shanghai and Zhengzhou. The results reveal several key insights regarding model accuracy, influential factors, and implications for future development strategies.

### (1) Model accuracy and limitations

The machine learning-based approach exhibited limited accuracy, potentially due to two primary factors. First, the relatively small dataset ( $N = 162$ ) may have hindered the model's ability to generalize and extract a robust, representative model. Second, the selection of influencing factors might not have been sufficiently comprehensive. Variables affecting the target variables beyond the scope of the master plan were potentially excluded from model consideration.

The hybrid model demonstrated similarly limited accuracy, with challenges arising not only from the dataset size and factor selection, but also from aspects of the expert elicitation process. Specifically, the subjective nature of expert judgments, the number of classifications for intermediate node states, the definition of classification criteria, and the method of CPT generation likely influenced overall model performance.

Further analysis of the Zhengzhou model revealed an error rate higher than observed in the Shanghai model. This discrepancy may primarily stem from differences in sample size. The Zhengzhou dataset contained only 60 available cases. Given the determined prediction model structure, which included three intermediate nodes with four-classified states each, the resulting state space for the target variables comprised 64 ( $4^3$ ) possibilities. The limited sample size (60) likely resulted in sparse data, preventing adequate coverage of all possible state combinations. Consequently, the state CPTs corresponding to some less-realistic cases may have been characterized by an average distribution. This data sparsity can lead to model training converging towards a homogeneous distribution of conditional probabilities, impeding accurate parameter estimation through Bayesian Network learning. Therefore, the limited sample size directly impacts the generalization capabilities of the model, potentially explaining the relatively high error rate observed in the Zhengzhou model.

### (2) Implications for urban planning and future development

Across the analysis, projects suitable for two-floor underground development largely coincided with areas where influencing factors exhibited a "high status" favoring such development. Even in instances where one factor was not at its highest level, the corresponding project area typically demonstrated high values across other influencing factors. This finding underscores that the predicted number of development floors is not primarily determined by a single factor, but rather by a combination of influential variables. This multi-faceted approach coincides with established underground space development in Zhengzhou.

In the forecast results of the Zhengzhou standard, the forecast results of the development area of the projects predicted to develop two floors in the previous section were all lower than 15,000  $m^2$ , and the areas with large development areas of underground commercial space were all the projects previously predicted to develop only one underground floor. The results revealed that projects with underground commercial space exceeding 15,000  $m^2$  were primarily located in the periphery of the main city center. Conversely, predicted underground commercial

space in the core area remained below 15,000 m<sup>2</sup>, less than that of the periphery. Several factors might contribute to these observations:

**a). Historical development.** Sites closer to the city center underwent development earlier with less emphasis on integrated underground commercial space planning. This resulted in smaller development areas. Projects located in the periphery, developed later, benefited from greater consideration of the potential role of underground spaces in addressing urban challenges.

**b). Density and functional integration.** The prediction results suggested a compact and integrated layout in city center and a spacious single-floor layout in the city's periphery. This analysis revealed that underground space planning should be conducted differently with focus on high-density connections in city center and space abundance in city's outskirt. Aligned with this rationale, Zhengzhou might further explore the development of two-layer underground public service spaces in the identified core areas.

## 6. CONCLUSIONS

This study developed a Bayesian Network model to predict the allocation of underground commercial space resources using multi-source underground space and urban development data. The model was empirically applied to Zhengzhou City's planning context, drawing insights from existing studies and case data. The main findings and conclusions are summarized as follows:

(1) Utilizing data from 180 underground commercial projects in Shanghai, multiple Bayesian Network models were constructed through K-fold cross-validation. The optimal model was selected based on the average prediction error rates, which were 16.67% for the number of floors and 22.22% for total development area. These key parameters served as the primary target variables for the modeling process.

(2) In the modeling process, strongly correlated nodes were connected to reflect their inter-relationships. Hybrid modeling combining machine learning with expert knowledge yielded more accurate and efficient models, especially when data were limited, outperforming models built solely on machine learning methods.

(3) Representative data from existing underground commercial projects in Zhengzhou were collected following the same approach used for Shanghai. A Bayesian Network model was established based on these local cases. Comparative analysis revealed that the Shanghai model effectively predicts key indices of underground commercial space allocation in Zhengzhou's main urban area, indicating its suitability for underground commercial space planning applications in other cities.

(4) The prediction results from the Bayesian Network model align well with the actual development trends in Zhengzhou's main urban area. Planning simulations of underground commercial projects suggest that underground commercial space in the core urban area tends to be relatively small (less than 15,000 m<sup>2</sup>), whereas peripheral areas tend to feature larger developments.

Finally, it should be noted that this research faces certain limitations, including constraints related to the data availability, dataset size and the coverage of influencing factors. Future work should aim to incorporate a broader range of influencing factors, enhance the accuracy of the underlying data, and expand the scope of analysis. Such efforts will provide more reliable decision-support tools for underground commercial space planning and the sustainable use of urban underground space resources.

## 7. ACKNOWLEDGMENTS

This work was supported by the National Natural Science Foundation of China (NSFC) [grant numbers 42201284, 42071251].

## 8. BIBLIOGRAPHY

- [1] Celio, E., Koellner, T., Grêt-Regamey, A. (2014). Modeling land use decisions with Bayesian networks: Spatially explicit analysis of driving forces on land use change. *Environmental Modelling & Software*, 52, 222-233.
- [2] Chen, Y., Wang, Y.J., Zheng, X.Z., Tian, D., Jin, L.H. (2024). Risk analysis of dam break accident combining case mining and Bayesian network. *Journal of Hohai University (Natural Sciences)*, 52(4), 12-21. (in Chinese)
- [3] Kaliampakos, D., Benardos, A., Mavrikos, A. (2016). A review on the economics of underground space utilization. *Tunnelling and Underground Space Technology*, 55, 236-244.
- [4] Li, C.Y. (2022). Urban planning design and evaluation based on GIS information and Bayesian Network. *Mathematical Problems in Engineering*, 5, 1-10.
- [5] Liang, H., Zhang, Q. (2022). Do social media data indicate visits to tourist attractions? A case study of Shanghai, China. *Open House International*, 1, 47.

- [6] Liber, Y., Cornet, D., Tournebize, T., Feidt, C., Bedell, J.P. (2020). A Bayesian network approach for the identification of relationships between drivers of chlordecone bioaccumulation in plants. *Environmental Science and Pollution Research*, 27, 41046-41051.
- [7] Ma, C.X., Peng, F.L., Qiao, Y.K., Li, H. (2022). Influential factors of spatial performance in metro-led urban underground public space: A case study in Shanghai. *Underground Space*, 8, 229-251.
- [8] Meng, G.L., Cong, Z.L., Song, B., Li, T.T., Wang, C.G., Zhou, M.Z. (2023). Review of Bayesian network structure learning. *Journal of Beijing University of Aeronautics and Astronautics*. Online. (in Chinese)
- [9] Peng, J., Peng, F.L., Yabuki, N., Fukuda, T. (2019). Factors in the development of urban underground space surrounding metro stations: A case study of Osaka, Japan. *Tunnelling and Underground Space Technology*, 91, 103009.
- [10] Peng, F.L., Dong, Y.H., Wang, W.X., Ma, C.X. (2023). The next frontier: data-driven urban underground space planning orienting multiple development concepts. *Smart Construction and Sustainable Cities*, 1, 3.
- [11] Qiao, Y.K., Peng, F.L., Dong, Y.H., Lu, C.F. (2024). Planning an adaptive reuse development of underutilized urban underground infrastructures: A case study of Qingdao, China. *Underground Space*, 14, 18–33.
- [12] Ren, Y.C., Zhang, R., Zhang, Y.S., et al. (2023). Scenario analysis and simulation deduction of the "Zhengzhou Rainstorm Subway Disaster Event" based on Bayesian network. *Trans Atmos Sci*, 46(6), 904-916. (in Chinese)
- [13] Sahin, O., Stewart, R.A., Faivre, G., Ware, D., Tomlinson, R., Mackey, B. (2019). Spatial Bayesian Network for predicting sea level rise induced coastal erosion in a small Pacific Island. *Journal of Environmental Management*, 238, 341-351.
- [14] Xu, Z.W., Zhou, H., Zhang, C., Yang, M.H., Jiang, M.Y. (2023). A Bayesian Network model for suitability evaluation of underground space development in urban areas: The case of Changsha, China. *Journal of Cleaner Production*, 415, 138135.
- [15] Zhao, R.G., Yang, J.C., Li, J., Zhou, S.H. (2024). Bayesian network evaluation of road network resilience in the Guangdong-Hong Kong-Macao Greater Bay Area city cluster. *Journal of Safety and Environment*, 24(3), 825-835. (in Chinese)

## EXPLORATION OF IMPLEMENTATION PATHWAYS FOR UNDERGROUND SPACE PLANNING IN KEY URBAN AREAS

Jian SUN<sup>1</sup>, Min WANG<sup>2</sup>

**Abstract:** The rational development and utilization of urban underground space is a crucial approach to optimizing spatial resource allocation. This study focuses on key urban districts, drawing on the characteristics of underground space development in internationally exemplary regions. Combining practical insights from China, it summarizes existing issues encountered during the planning and implementation process of underground space projects. Four key influencing factors—regulatory systems, organizational management, spatial information, and technical methods—are identified. An integrated pathway for enhancing urban underground space planning is proposed, comprising top-level design, organizational management, information coordination, and technical execution. The analysis of international case studies broadens research perspectives, and the proposed implementation strategies offer valuable insights for the planning and management of similar urban key district development projects.

**Keywords:** urban underground space planning, regulatory systems, organizational management, spatial information, technical methods

### 1. INTRODUCTION

Under the era of high-quality development, China's urban planning and construction are transitioning from incremental expansion to the enhancement of existing stock. In recent years, China has successively issued several policy documents, including the "Opinions of the Central Committee of the Communist Party of China and the State Council on Establishing a Land and Space Planning System and Supervising Its Implementation," the "Opinions of the General Office of the Central Committee of the Communist Party of China and the General Office of the State Council on Comprehensively Strengthening Resource Conservation," and the "Guiding Opinions of the Ministry of Natural Resources on Exploring and Promoting the Development and Utilization of Urban Underground Space." These documents set higher standards for underground space development, planning, and implementation.

Globally, the development of underground space originated in 18th-century Britain with the construction of subways. Countries and regions such as Japan and Canada have accumulated extensive experience in policies, regulations, planning systems, and practical applications related to underground space development. In mainland China, underground space development began in the 1950s with the construction of bomb shelters and underground storage facilities for wartime preparedness. This evolved from the opening of Beijing's subway in 1969 to large-scale development driven by rail transit during the "Twelfth Five-Year Plan" period, and further into networked development during the "Thirteenth Five-Year Plan." Currently, the utilization of urban underground space in China exhibits multi-layered spatial characteristics and diversified functional features [1].

Numerous scholars have built a substantial research foundation around urban planning implementation. However, most existing studies focus on traditional urban planning aspects, with limited in-depth exploration from the perspective of underground space. This paper concentrates on the planning and implementation of underground space in key urban districts. Based on an international perspective and the analysis of typical cases, it identifies

<sup>1</sup> Engineer, Sun Jian, research direction in urban transportation systems and subterranean space planning and design, Shanghai Municipal Engineering Design and Research Institute (Group) Co., Ltd., Shanghai 200092, China. Email: sunjian2@smedi.com.

<sup>2</sup> Professor level Senior Engineer, Wang Min, research direction in urban transportation systems and subterranean space planning and design, Shanghai Municipal Engineering Design and Research Institute (Group) Co., Ltd., Shanghai 200092, China.



the complex characteristics and implementation challenges of underground space development. A planning and implementation pathway is proposed, encompassing "top-level design, organizational management, information coordination, and technological support," aiming to provide a reference for similar district development projects..

## **2. CHARACTERISTICS OF UNDERGROUND SPACE DEVELOPMENT IN KEY URBAN DISTRICTS**

### **2.1. Attributes of Major Engineering Projects**

The concept of key urban zones originates from the "Central Place Theory" proposed by German geographer W. Christaller in 1933, emphasizing the significance of transportation location and influence on surrounding areas. Projects within these zones exert extensive impacts on regional economic development, environmental sustainability, and social progress, classifying them as significant local infrastructure projects [2].

Given that underground urban space is formed through artificial development of structures within subsurface rock or soil layers beneath the surface, its development possesses inherent engineering attributes [3]. In Chinese provincial and municipal regulations concerning underground space planning and management—exemplified by the "Shenzhen Underground Space Development and Utilization Management Measures"—the definition of key urban zones refers to areas designated as city centers, comprehensive transportation hubs, and similar regions. Projects for underground space development in these zones are characterized by strategic importance, advantageous transportation location, substantial land development potential, rapid progress requirements, and high-quality integrated presentation. Such development constitutes a vital approach to expanding urban spatial capacity.

### **2.2. Project Complexity**

The concept of project complexity was first introduced by Baccarini, who defined it as the heterogeneity and interdependence among interacting components [4]. Qing hua He and colleagues developed a multidimensional model of complexity for major Chinese engineering projects based on grounded theory qualitative research, encompassing six aspects: institutional, environmental, organizational, technical, task-related, and social complexity [5]. Due to their large scale, numerous subcomponents, multifunctionality, open spatial design, and shared facilities, underground space development projects in key urban zones exhibit significant complexity in planning, design, construction, and operational management.

#### **1) Spatial Facility Complexity**

The functional facilities within urban underground spaces are diverse, including underground transportation, municipal utilities, public services, storage, and disaster prevention facilities. These encompass rail transit systems, tunnels, underground garages, municipal pipelines, pedestrian passages, and commercial spaces. The necessity to arrange multiple functions within confined environments requires precise assessment of construction conditions and spatial layout—both horizontal and vertical—resulting in elevated safety risks and technical challenges.

#### **2) Complexity of Stakeholders**

The multifaceted nature of underground space facilities in key urban zones leads to numerous involved parties. Stakeholders include government agencies, developers, design firms, construction enterprises, consulting agencies, and suppliers. Different phases of project development involve varying stakeholders, and the complexity is further compounded by issues of property rights, investment, and operational responsibilities related to underground facilities, thereby increasing planning and implementation difficulties.

### **2.3. Irreversibility**

Subterranean space constitutes an irreversible spatial resource, underscoring the critical importance of scientific planning and sustainable development [7]. Compared to surface development, underground space exploitation exerts long-term impacts on adjacent terrestrial and subterranean infrastructure and environmental conditions. Unsystematic development of underground space may result in irrevocable losses to urban future growth. Therefore, proactive planning of underground space layout and moderate development are of paramount significance.

### **2.4. Economic Correlation**

#### **1) High Development Costs**

Relative to conventional above-ground construction, underground engineering presents increased complexity in hydrological, geological, and environmental conditions, introducing significant uncertainties into design and implementation processes. Typically, underground space development incurs substantial costs. Recent trends favor compact neighborhood configurations characterized by small blocks and dense street networks [8]. However, such small parcel divisions, intricate architectural structures, and deep excavations lead to large-scale foundation pits and support difficulties, indirectly elevating development costs. Additionally, underground construction is constrained by the sequence of land transfer on the surface, complicating the synchronization of foundation pit excavations [9].

In key urban districts with high surface building development intensity, the corresponding underground space development scale is proportionally larger. Large-scale, complex foundation pit groups exhibit varied excavation depths and shapes, with interwoven interfaces forming complex load-bearing support systems and numerous shared enclosures. These projects pose substantial engineering risks, present numerous construction challenges, and demand extensive management and coordination efforts from project stakeholders, with high requirements for technical expertise.

#### 2) Influence of Regional Economic Development

The development of underground space is significantly correlated with regional economic levels. Market research indicates that, geographically, regions such as East China and South China—areas with higher economic development—exhibit larger scales of underground space utilization and more mature development experience, exemplified by cities like Shanghai, Beijing, and Shenzhen. These regions also demonstrate a strong association with urban rail transit infrastructure. Cities with robust economic growth generally achieve higher standards in underground space development, characterized by integrated utilization, combined civil and military functions, and multifunctionality.

### 3. CHALLENGES IN THE PLANNING AND IMPLEMENTATION OF UNDERGROUND SPACE IN KEY URBAN DISTRICTS

#### 3.1. Institutional Framework

The management mechanisms require further refinement, and the planning system necessitates enhancement [10,11]. The primary issues within the underground space regulatory framework include ambiguities in legal definitions concerning operational rights and ownership, unclear legal entities, and inconsistent management standards. Although many major Chinese cities have established foundational plans for underground space utilization, their planning systems and content remain underdeveloped. The hierarchical clarity of underground space planning is insufficient, particularly at the level of control detailed planning that serves as the basis for administrative permits, where relevant provisions are notably lacking. Furthermore, the implementation of planning faces challenges due to inadequate safeguard mechanisms, incomplete supporting policies and regulations, disjointed planning, construction, and management processes, and a tendency to prioritize plan formulation over execution and evaluation.

#### 3.2. Organizational Management

Issues of fragmented authority and management gaps are prevalent, necessitating further research into property rights. Currently, there is a consensus among Chinese cities that urban underground space planning and management fall under the jurisdiction of municipal urban and rural planning authorities. However, in practice, issues such as sectoral segmentation, multiple management entities, and unclear responsibilities are prominent. Effective utilization of underground space requires standardized regulation and coordination of various underground facilities, including construction requirements, sequencing, and interrelations. The complexity of planning, management, and implementation underscores the need for clear delineation of responsibilities among supervisory agencies to ensure integrated oversight across departments.

#### 3.3. Spatial Information

Given the unique nature of urban underground spaces as enclosed environments beneath the surface, limitations of traditional surveying technologies, and the historical lack of unified planning and coordination for development zones and surrounding underground areas, there are notable deficiencies in early-stage statistical standards and fundamental survey data. Challenges include inadequate integration and application of foundational underground space data. The primary difficulty in managing underground space development information lies in acquiring reliable baseline data, compounded by the underground environment's inaccessibility to direct observation,

incomplete urban underground information archives, and multi-agency management. Currently, only a few Chinese cities maintain comprehensive and accurate databases on underground space utilization. Some cities have incorporated underground space information management into local regulations to support refined urban governance. For example, Chengdu and Kunming's "Urban Underground Space Development and Utilization Management Measures" explicitly assign responsibility for underground space information management to urban planning administrative departments.

### 3.4. Technical Methods

Standardization of technical norms remains urgent, alongside the enhancement of management and technical personnel capabilities. For most Chinese cities, underground space utilization remains a relatively unfamiliar domain, requiring multidisciplinary expertise for effective management. Urban underground space planning is characterized by spatial coordination and comprehensive integration. Due to the absence of unified methodologies and technical standards, current practices are primarily exploratory at the local level, resulting in significant disparities in planning outcomes. The lack of relevant policies, regulations, and detailed management guidelines further complicates implementation. It is essential to strengthen legal guidance, supervision, and training for urban planning authorities to familiarize them with emerging trends in underground space development, recognize the importance of standardized planning and management under new conditions, and clarify departmental responsibilities. Additionally, targeted professional training for administrative and planning personnel across regions remains an urgent need.

## 4. EXPLORATION OF IMPLEMENTATION STRATEGIES FOR UNDERGROUND SPACE PLANNING BASED ON CASE STUDY ANALYSIS

### 4.1. Top-Level Design Pathway

By analyzing typical international case studies focusing on the development of distinctive features and management mechanisms for underground space development, it is evident that the integrated utilization of underground space underpins the high-precision development orientation of the district. The management mechanisms require support from relevant policies and regulations, as outlined in Table 1.

*Table 1. Top-Level Design of International Typical Cases in Subterranean Space.*

Representative project	Area	Develop distinctive features	Underground space management mechanism
Tokyo Shinjuku	Japan	Highly intensive integrated development of stations and cities	Mature management regulations system, complete underground space planning system
Montreal	Canada	The world's largest underground pedestrian network	The integrated management system and operational mechanism jointly established by the government and private enterprises; Integrating underground pedestrian network into statutory planning
Canary Wharf	Britain	One of the most important financial regions in the world	Funding from higher-level governments and policy incentives for special development zones; Developer prepares development plan
Chicago Pedway	America	An underground colorful dungeon unaffected by weather and motor vehicles	Land spatial rights, spatial laws, and incentives for building public passages with plot ratio; Regional regulations provide construction guidelines
Paris La Défense	France	The world's first urban complex that combines underground transportation with underground space	Government functional departments have no overlapping powers or superior subordinate relationships; Mature planning system

CityLink Mall	Singapore	Singapore's first air-conditioned underground shopping mall, subway commercial	Land spatial rights, spatial laws, and incentives for building public passages with plot ratio; Draft plan for underground space connectivity in the central urban area and overall blueprint for urban development
---------------	-----------	--	---

After years of exploration and practice, China has essentially established a legal and policy framework for underground space development. Most cities have enacted regulations for the management and utilization of underground spaces, providing detailed provisions for each specific issue. However, comparative analysis of legal policies related to underground space in representative regions reveals that cities with relatively mature experience in underground space development, such as Beijing and Shanghai, lack dedicated management regulations, such as Beijing's relevant administrative measures and Shanghai's Planning and Construction Regulations, as shown in Tables 2 and 3.

**Table 2.** Chinese laws and regulations concerning the development and utilization of underground space.

Classification	Name
national laws	Civil Air Defense Law of the People's Republic of China (October 1996), Land Administration Law of the People's Republic of China (1998/2004), Property Law of the People's Republic of China (October 2007), Urban Real Estate Administration Law of the People's Republic of China (Revised) (August 2007), Urban and Rural Planning Law of the People's Republic of China (January 2008)
National regulations	Regulations on the Management of Urban Underground Space Development and Utilization (Ministry of Housing and Urban Rural Development 1997/2001/2011), Urban Planning Compilation Measures (Ministry of Housing and Urban Rural Development 2006.04), Land Registration Measures (Ministry of Land and Resources 2007.12), Housing Registration Measures (2008.02), Guiding Opinions on Promoting the Construction of Urban Underground Comprehensive Pipe Corridors (General Office of the State Council, November 2015), 13th Five Year Plan for Urban Underground Space Development and Utilization (Ministry of Housing and Urban Rural Development, June 2016), Guiding Opinions on Strengthening Urban Geological Work (Ministry of Land and Resources, September 2017)

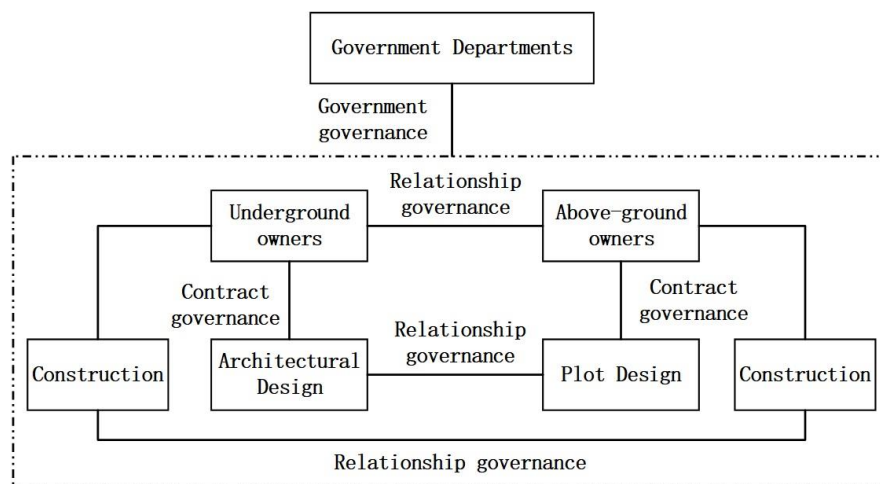
**Table 3.** Regulations on the Management of Underground Space in Typical Regions of China.

Region	Management Measures for Underground Space	Representative project
Beijing	Management Measures for the Safe Use of Civil Air Defense Projects and Ordinary Basements in Beijing	Xiong'an Station Hub Area
Shanghai	Regulations on the Planning and Construction of Underground Spaces in Shanghai	Shanghai Hongqiao, Expo Zone B, West Bund Media Port
Shenzhen	Shenzhen Underground Space Management Measures	Qianhai, Baishizhou, Chao-zong
Nanjing	Management Measures for the Utilization of Underground Space in Nanjing City	Jiangbei New City
Suzhou	Management Measures for the Utilization of Underground Space in Suzhou City	Suzhou Center
Jinan	Management Measures for the Utilization of Underground Space in Jinan City	Hanyu Golden Valley
Fuzhou	Management Measures for the Development and Utilization of Urban Underground Space in Fuzhou City (Trial)	new coastal city

In summary, China has initially established a comprehensive institutional and regulatory management framework for urban underground space development at both national and local levels. However, standards for urban underground space development and management remain inconsistent. Compared to the policy support mechanisms in developed countries and regions internationally, there is still a notable gap. It is therefore necessary to further refine and systematically improve the urban underground space legal and regulatory system.

#### 4.2. Organizational Management Pathways

The development of urban underground spaces involves numerous stakeholders, necessitating a robust leading authority to coordinate regional development and construction. Taking the Shanghai West Coast Media Port underground space development project as an example, the government's political characteristics, social influence, and its discourse power in major construction projects—particularly those driven by government investment—render governmental administrative governance as equally vital as market regulation. This results in a governance framework that synergistically integrates “government plus market” mechanisms, which effectively promotes the planning and implementation of construction projects, as illustrated in Figure 1 [12].



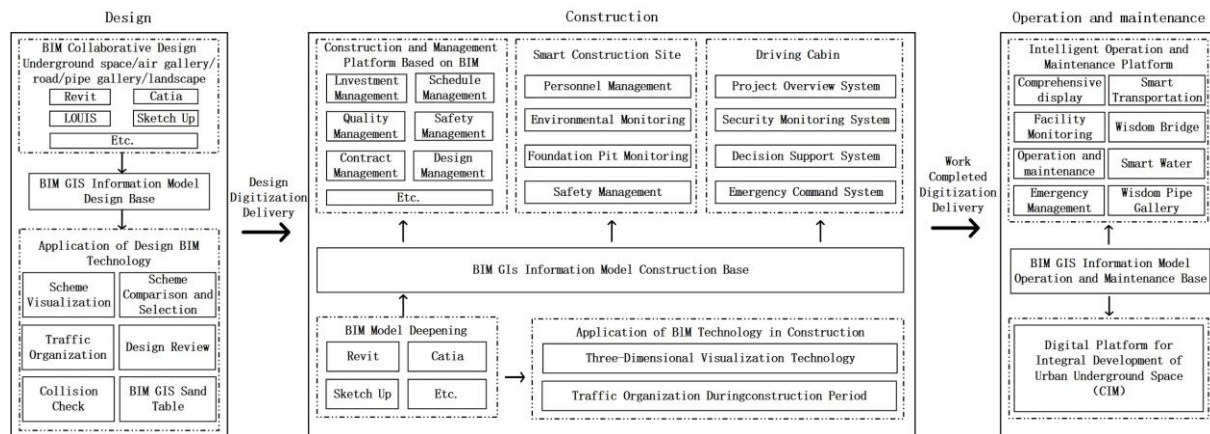
**Figure 1.** Governance Mechanism of the Shanghai West Bank Media Port Project[12].

Underground space development projects in key urban districts typically exhibit a dual collaborative structure involving government and enterprise entities, with coordinated participation from planning agencies, master design units, consulting firms, and overall control organizations. Regarding project stakeholders, the principal can be the government, a platform company, or a land parcel developer. Taking the Shenzhen Bay Super Headquarters Base as a case study, the project initiates development and construction mechanisms during the decision-making phase by establishing a command center and designating a comprehensive development and operation entity—namely, a municipal state-owned enterprise—and forming a strategic implementation platform company for the district. The process involves identifying appropriate construction models to balance the interests of government, investors, builders, operators, and users, thereby establishing an efficient decision-making framework.

#### 4.3. Information Integration Pathways

In the context of the digital economy era, to thoroughly implement the Chinese government's strategic directives for building a "Cyber power," "Digital China," and "Smart Society," most Chinese cities have introduced strategic plans to advance digital and smart city development. The most representative achievement is the application of underground space information management through BIM, GIS, and CIM digital platforms during project design, construction, and operational maintenance phases, as illustrated in Figure 2.





**Figure 2.** Comprehensive digital management of the entire process of urban underground space design, construction, and operation and maintenance.

In addition to ensuring the effective utilization within the industry sector by government agencies and related operational maintenance units, there is also significant potential to leverage underground space information in other domains such as project development, design, construction, safety, and disaster prevention. Under the premise of safeguarding data security and confidentiality, it is recommended to maximize public access to information regarding underground spaces that impact people's livelihoods. Collaborative research with relevant scientific and educational institutions on underground space information management, along with the development of new systems and the adoption of innovative technologies, represents the future direction of underground space information management.

#### 4.4. Technical Support Pathway

For design entities with strong comprehensive capabilities, the introduction of centralized control, along with adherence to guiding principles and regulatory frameworks, is essential. Taking the Guangzhou Mingzhu Science Park project as a case study, a detailed underground space planning approach was employed. The approved "Textual and Graphical Regulations" serve as the legal basis for underground space planning approval and land transfer. Additionally, relying on the detailed underground space plan as a preliminary negotiation platform facilitates horizontal coordination among government departments, landowners, and project implementers, while vertically integrating various professional design teams to ensure consistency of objectives and synchronization of technical standards.

### 5. RECOMMENDATIONS FOR IMPLEMENTATION PLANNING

#### 5.1. Enhancement of Policy Mechanisms for Subterranean Space Development and Utilization

Firstly, streamline and integrate existing operational procedures for development and utilization, establishing a comprehensive workflow encompassing planning, project initiation, approval, construction, acceptance, operation, and maintenance of underground space projects. Secondly, for development models lacking clearly defined procedures, conduct innovative research on mechanisms related to property rights attribution, investment and financing modes, and operational maintenance frameworks.

#### 5.2. Strengthening Organizational Management of Underground Space Development

From planning formulation and approval to the selection of design entities, project development, and post-construction operational management, reinforce the guidance of government authorities and foster market-oriented collaboration, thereby forming context-specific organizational management models. Conduct in-depth studies on interface delineation, rights management, and cost allocation among organizational elements.

### 5.3. Establishment of a Three-Dimensional Underground Space Information Management System

Utilize multi-modal digital technologies such as BIM, GIS, and CIM to develop information databases and system platforms, enabling comprehensive mapping of urban underground space development status. Effective information recording and data management are crucial for collecting, organizing, storing, and sharing underground space information. Additionally, address issues related to data ownership and sharing, clarifying the responsibilities and rights of data custodians.

### 5.4. Enhancement of Technical and Management Training Programs

Implement specialized training mechanisms targeting government agencies, project owners, developers, design firms, construction entities, and operational management units. Use benchmark demonstration projects as case studies to systematically analyze and disseminate key challenges and focal points in underground space development and management processes, thereby elevating the technical and managerial competencies of relevant personnel.

## 6. CONCLUSION

Currently, in the era of stock renewal and digital economy, large-scale district-based development projects are gradually declining. How to optimize and efficiently utilize urban three-dimensional space resources has become a critical issue for urban planning, construction, and management authorities. This paper examines urban underground space development projects from an international perspective, integrating practical project development experiences. Using case study methodology, a strategic framework comprising "top-level design, organizational management, information coordination, and technological support" is proposed. The development and construction of underground spaces in key urban districts constitute a complex systemic engineering task. Effective implementation of planning requires policy support and the concerted efforts of developers and project stakeholders. The adaptability of organizational management models for underground space development remains a subject warranting further in-depth research.

## 7. REFERENCES

- [1] Sun Jun. Development and Challenges in the Utilization of Urban Underground Space Resources Domestically and Internationally [J]. Tunnel Construction (Chinese and English), 2019, 39(5): 699-709.
- [2] Sun Jide, Liu Jing. Study on Organizational Models for Airport Expansion Projects—A Case Study of the Expansion of Airport A [J]. Construction Economics, 2022, 43(z2): 143-147.
- [3] Tong Linxu. Underground Architecture [M]. Beijing: China Architecture & Building Press, 2012.
- [4] Baccarini D. The Concept of Project Complexity—A Review [J]. International Journal of Project Management, 1996, 14(4): 201-204.
- [5] He Qinghua, Tian Zidan, Luo Lan. Construction of a Dimensional Model of Project Complexity in Major Chinese Engineering Projects Based on Grounded Theory [J]. China Science & Technology Forum, 2021(8): 126-134.
- [6] Yu Wengui, Gu Xin. Organizational and Planning Challenges in Underground Space Planning Under the Dilemma of Planning Permits [J]. Urban Planning, 2015, 39(5): 62-67.
- [7] China Urban Underground Space Development Blue Book 2019 [R]. 2020.
- [8] Lu Xiaowei, Luo Meifang. Exploration of Integrated Planning Methods for Underground Space in the Context of Land Intensive Use—A Case Study of the Expo Site B in Shanghai [J]. China Building Decoration and Renovation, 2022(2): 27-28.
- [9] Wang Wanli. Analysis of the Impact and Solutions for Continuous Development of Regional Cluster Projects—A Case Study of the West Coast Media Port Project [J]. Urban Construction, 2021, (11): 249-251.
- [10] Wang Min, Zhang Mengxia, He Lei. Methods for Detailed Planning and Control Pathways for Underground Space Implementation [J]. Journal of Underground Space and Engineering, 2024, 20(3): 710-720.
- [11] Yang Huayong, Jiang Yuan, Li Zhe, et al. Strategic Research on the Development of Comprehensive Governance for Underground Space Development [J]. China Engineering Science, 2021, 23(4): 126-136.
- [12] Xie Jianxun, Wen Bintao, Xu Shiquan, et al. Governance Study of Major Engineering Projects with Regional Integrated Development—A Case Study of Shanghai West Coast Media Port [J]. Journal of Engineering Management, 2018, 32(2): 85-90.

## PLANNING PUBLIC URBAN UNDERGROUND SPACES: CULTURAL AMENITIES IN BELGRADE'S RIVERFRONT PARK

Marija Lalošević<sup>1</sup>, Milica Hadži Arsenović<sup>2</sup>, Ana Jovović<sup>3</sup>

**Abstract:** The increasing demand for urban space in dense city environments calls for innovative solutions to integrate public amenities within limited areas. Underground space can serve not only for utility and transportation systems but also for public facilities that blend uses that are suitable with underground space and those which are not. These innovative solutions create a unique connection between above and below-ground spaces. This paper explores the planning and design of underground spaces, focusing on their use for cultural amenities in city center green areas, placed in Belgrade, Serbia, along the banks of the Sava and Danube rivers. One of the main questions is also how underground spaces can be strategically utilized to enhance urban landscapes while preserving and enhancing green spaces above ground. The paper discusses how the planning of underground urban spaces must consider human needs, creating a balanced relationship between subterranean uses and public accessibility. Case study is used to explore how the integration of underground cultural spaces can enrich public urban life, foster cultural engagement, preserve valuable green areas in city center and contribute to sustainable urban development. Through this exploration, the aim is to define the human measure for planning such spaces, considering factors like comfort, light, ventilation, and connectivity with the urban environment.

**Keywords:** cultural amenities, underground urbanism, public underground spaces, urban sustainability, public use

### 1. INTRODUCTION

The challenge of limited urban space in rapidly growing cities demands innovative approaches to spatial planning, especially for public amenities that support cultural engagement. The governance of spatial development and construction land use in urban areas, characterized by territorial, economic and demographic expansion, has become an exceptionally complex challenge, especially considering the market economy that prevails in all spheres of society. Within such a system, construction land becomes an increasingly valuable commodity on the market, which significantly influences the governance of its development. The greatest pressure in spatial terms is concentrated in city centers, while in terms of land use functions, those most affected are public amenities that do not generate profit but are of great importance to the community, such as green spaces and cultural facilities. The challenge lies in the fact that these amenities are most needed precisely in central urban areas, where market pressure on construction land is at its highest. Although this issue requires broader reflection and a reconsideration of adapting the market functioning model, specifically, finding ways to restrain it in certain segments, it is inevitable that we face the necessity for increasingly rational use of construction land in central urban areas. Underground urbanism offers an opportunity to optimize the use of city space by developing subterranean areas not only for technical infrastructure but also for cultural and public uses. Integrating underground spaces into urban parks presents a dual benefit: preserving above-ground green areas while enriching urban life below ground.

However, it is important to acknowledge that activating underground spaces and modifying it to accommodate human presence brings several challenges that need to be addressed, considering that such spaces are not a natural

<sup>1</sup> PhD, Lalošević Marija, M.Sc.Arch., Institute of Architecture and Urban & Spatial Planning of Serbia, Bulevar kralja Aleksandra 73/II, Belgrade, Serbia, [marija@iaus.ac.rs](mailto:marija@iaus.ac.rs), [ORCID: 0000-0002-4984-9924](https://orcid.org/0000-0002-4984-9924)

<sup>2</sup> Hadži Arsenović Milica, M.Sc.Urb., Urban Planning Institute of Belgrade, Despota Stefana 56, Belgrade, Serbia, [milica.hadziarsenovic@urbel.com](mailto:milica.hadziarsenovic@urbel.com), [ORCID: 0009-0004-9037-1899](https://orcid.org/0009-0004-9037-1899)

<sup>3</sup> Jovović Ana, M.Sc.Urb., Urban Planning Institute of Belgrade, Despota Stefana 56, Belgrade, Serbia, [ana.jovovic@urbel.com](mailto:ana.jovovic@urbel.com), [ORCID: 0009-0009-0097-3842](https://orcid.org/0009-0009-0097-3842)

human habitat and do not provide all the essential needs necessary for human life and health. When it comes to specific functions, however, the situation differs, as certain conditions that may be unsuitable for human occupancy can, conversely, prove highly suitable for particular uses. This is often the case with factors such as limited or absent natural light, air humidity levels, temperature, and similar environmental conditions. Museological and other cultural programs, as well as certain attraction-based functions, represent examples of public amenities that may be appropriately accommodated within underground or semi-subterranean spaces.

Recent global examples demonstrate the successful integration of underground museum spaces within urban parks, blending cultural experiences with green landscapes. The use of underground spaces responds to increasing urban densification, providing an alternative layer for public and cultural activities without compromising the city's ecological and recreational values.

Besides international precedents, understanding the local urban planning and decision-making processes is essential. Effective integration of underground cultural spaces requires careful coordination of strategic urban development and consideration of the quality of planning proposals (Danilović Hristić & Lalošević, 2019). The planning process must balance technical, environmental, and social aspects to achieve sustainable outcomes (Lalošević & Hadži Arsenović, 2025). Recent studies highlight that participatory planning and multi-stakeholder engagement significantly improve the adaptability and resilience of underground urban spaces, ensuring they meet both current and future urban demands (Costa et al., 2024).

## 2. MATERIAL AND METHODS

This research employs a qualitative case study approach, analyzing the urban concept and architectural plans of Park Ušće in Belgrade, with a focus on the Natural History Museum's and the City Aquarium underground facilities. The study is supported by a review of international examples of museums integrated with parks and waterfronts, as well as scientific literature addressing underground cultural spaces and urban public use.

Data sources include urban planning documents, architectural competition submissions, and technical project descriptions from 2024. Secondary sources comprise scholarly articles on underground urbanism, cultural space design, and urban park development.

The methodology combines spatial analysis, architectural critique, and literature synthesis to evaluate how underground cultural spaces can enhance public use and urban sustainability.

## 3. EXAMPLES

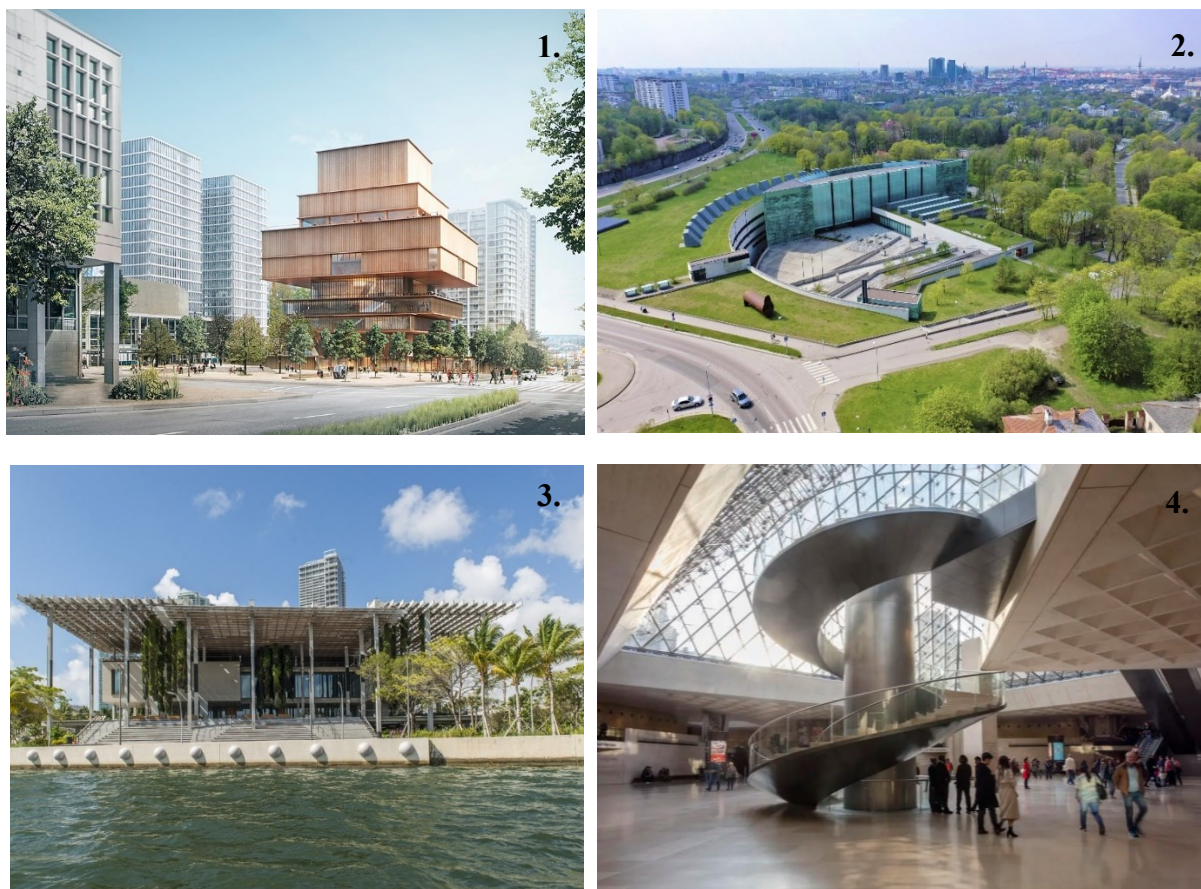
International examples provide valuable insights into how underground spaces can be effectively utilized for cultural facilities within park environments. These cases demonstrate innovative approaches to integrating built structures with the natural landscape. At the same time, they preserve open public space above ground and enhance both the cultural and experiential value of the site.

Several international projects exemplify innovative approaches to integrating cultural facilities within park landscapes using underground or hybrid spatial strategies. **The Vancouver Art Gallery Expansion** plans extensive underground galleries beneath a central public park, preserving the surface-level green space. This integration enables a significant increase in exhibition capacity without compromising urban greenery and park usability. Similarly, **the Kumu Art Museum in Tallinn** combines underground exhibition spaces with a landscaped park environment. The design minimizes visual impact and protects surrounding parkland, exemplifying the harmonious coexistence of cultural use and nature. **The Pérez Art Museum Miami (PAMM)**, situated in a waterfront park, blends outdoor public spaces and terraces with interior galleries, fostering strong connections between art, landscape, and community. Its design enhances access to green space while offering panoramic views of Biscayne Bay, reinforcing the museum's role as an active and inclusive element of the public realm.

Although the use of underground space for cultural purposes has become an increasingly widespread strategy in contemporary urban design, historical examples demonstrate that this approach is not entirely new. A notable case is **the Louvre Museum in Paris**, which represents a major cultural institution situated within a park-like setting along the Seine River. The museum complex exemplifies a layered spatial relationship between above ground and underground space. While the original palace structure defines the surface, a significant part of the museum's modern functions—including its main entrance, circulation areas, and exhibition spaces are located below ground. The addition of the iconic glass pyramid in the late 20<sup>th</sup> century plays an essential role in articulating this relationship: it physically and symbolically connects the subterranean spaces with the historic architecture above, serving as a central point of access and orientation. In this way, it demonstrates how carefully integrated design can reconcile heritage preservation with contemporary spatial demands, activating underground space without



compromising the integrity of the existing urban fabric. This pivotal intervention was the result of an international design competition, underlining the importance of open architectural processes in shaping culturally and historically sensitive urban transformations.



**Figure 1.** Vancouver Art Gallery (source: Vancouver Art Gallery, Vancouver - Herzog & de Meuron | Arquitectura Viva)

**Figure 2.** Kumu Art Museum, Tallinn (source: Kumu Art Museum - Estonian art from the 18<sup>th</sup> century until today)

**Figure 3.** Pérez Art Museum Miami (PAMM) (source: <https://www.jm-a.com/portfolio/perez-art-museum-miami/>)

**Figure 4.** The Louvre Museum in Paris (source: <https://www.louvre.fr/en/explore/the-palace/a-pyramid-for-a-symbol>)

#### 4. RESULTS - PARK UŠĆE URBAN CONCEPT AND UNDERGROUND SPACES

In the city of Belgrade, an outstanding example of valuable public space within the central urban zone is the "Ušće" Park. The area, also known as the "Friendship Park" - Ušće, located on the New Belgrade side of the confluence of the Sava and Danube rivers, represents one of the most significant urban-riverfront contact zones and constitutes an exceptional environmental, functional, and spatial asset of the highest level for the City of Belgrade. Through its spatial organization and function, this area serves as an urban oasis with a prominent role in the city's urban fabric, which contributes to the formation of Belgrade's urban landscape. The area is dominated by the public green areas and the riverfront green zones along the Danube and Sava riverbanks, which together form part of the core structure of Belgrade's green space system (Lalošević & Hadži Arsenović, 2025).

In 2019, a Detailed Regulation Plan was adopted for the area in question, by which the entire space was defined as a public green area - a park. However, within the park, the Plan envisions the construction of institutions of the highest importance for the development of culture in the City of Belgrade and the Republic of Serbia - the Museum of 21st Century Art and the Natural History Museum, an aquarium, as well as the introduction of new attraction-oriented contents. The adopted planning solution did not determine the precise locations of the proposed facilities, but instead outlines their projected capacities, leaving the spatial positioning to be defined in subsequent stages of planning and design elaboration. Given the great importance of the site, the Plan mandates the organization of an international urban-architectural competition aimed at developing a unified urban design solution for the park. The competition is intended to determine the optimal positioning of the aforementioned significant cultural institutions,



an aquarium, a panoramic wheel, and a viewing platform, as well as to identify the best architectural solutions for these facilities. The Plan outlines the basic parameters of the competition brief and prescribes the obligation to develop an Urban Project based on the first prize winning proposal.

The need for the construction of a new building for the Natural History Museum, as one of the planned facilities within the “Ušće” Park, initiated the launch of the design competition in 2024. The competition proposition had two tasks: the first was to develop a site plan for the entire park, proposing locations for all facilities as defined by the Plan; the second task focused specifically on the conceptual architectural design proposal for the Natural History Museum. The first prize winning design was developed within the architectural studio “Mitarh”, and one of its key qualities was the articulation of the buildings as semi-subterranean or underground structures, featuring green roofs that are integrated as an essential part of the park’s landscape. In this way, a substantial portion of the program was incorporated into the park with the aim of minimizing any impact on the integrity of one of the city’s most significant green spaces.



**Figure 5.** First prize winning competition solution – Areal overview of the “Ušće” park (source: Architectural studio Mitarh)



**Figure 6.** First prize winning competition solution – Disposition of facilities within the park (source: Architectural studio Mitarh / author)



A distinctive axis runs throughout the area, connecting the zones from the Museum of Contemporary Art to Hotel Jugoslavija, passing through Friendship Park along the existing wide promenade. This new “Main Alley,” parallel to Nikola Tesla Boulevard and the orthogonal grid of New Belgrade’s Central Zone, serves as the focal point for all movement within the park. In its central section, the Main Alley merges with the riverbank and extends into the river, creating pedestrian access and direct contact with the water. All planned buildings are positioned directly along this axis, forming a cohesive sequence of spatial experiences that unfold continuously along the path from Branko’s Bridge to Hotel Jugoslavija (Lalošević & Hadži Arsenović, 2025).

Technical challenges related to the utilization of underground space, particularly those close to the riverbank, emerged from the very beginning. The competition design proposed that the Natural History Museum and the Aquarium should be housed within a single multi-level subterranean structure, sharing a common repository on the second underground level. However, during the jury review, it was determined that “to improve the proposed solution and enhance its sustainability during both the construction and operational phases, it is necessary to relocate the aquarium space out of the building and accommodate the Natural History Museum’s storage facility in that wing.” This adjustment resulted in the elimination of the second underground level, thereby reducing the risks associated with groundwater and lowering the operational costs of the facility (source: Report on the work of the jury for the competition).

After the competition was completed, work began on developing the first-prize design according to the jury’s inputs and the project brief from the investor, the Natural History Museum. The conceptual design produced through this process became the basis for creating the Urban Project for Ušće Park. As a result of the changes made during the further development of the competition design, the Aquarium building was relocated to the site initially planned for the panoramic wheel, as an additional semi-subterranean building with a walkable green roof integrated into the park space, intended to accommodate an experimental garden. It can be said that these solutions sought to find a balance in activating the underground space-making it suitable not only for human use but also justifiable in terms of investment costs associated with its development.

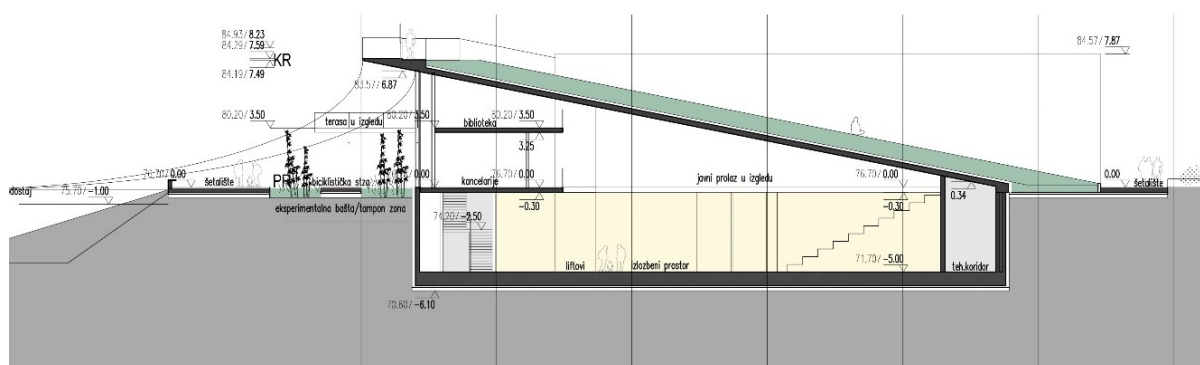
Additionally, in the initial design of the Natural History Museum building, the exhibition space was located along the glass façade on the ground floor, thereby engaging directly with the outdoor area, the promenade, and the main alley. However, during the development process and in collaboration with the investor, a requirement emerged to relocate the exhibition space to the underground level, while offices would be oriented towards the open façade. This request was justified both by the needs of employees regarding the quality of the working environment and by the necessity to protect exhibits from direct sunlight, using the building’s subterranean placement as a natural means to ensure optimal conditions for display. This process can also be characterized as seeking a balanced approach to the use of underground space, considering both human needs and the requirements of the functions, as well as a process of transforming limitations into advantages.



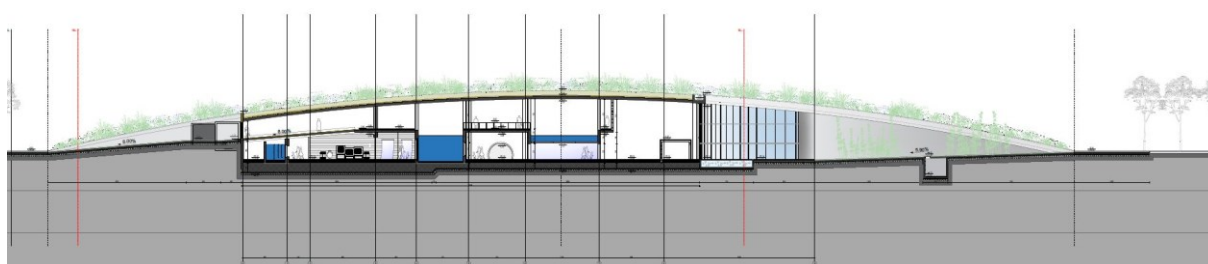
**Figure 7.** Concept Design of the Natural Museum building (source: Architectural studio Mitarh)



**Figure 8.** Concept Design of the Aquarium building (source: Architectural studio Mitarh)



**Figure 9.** Concept Design of the Natural Museum building - Cross-sectional drawing (source: Architectural studio Mitarh)



**Figure 10.** Concept Design of the Aquarium building - Cross-sectional drawing (source: Architectural studio Mitarh)



**Figure 11.** Concept Design of the Natural Museum building – Detaild 3D view (source: Architectural studio Mitarh)



**Figure 12.** Concept Design of the Aquarium building – Detaild 3D view (source: Architectural studio Mitarh)

As a result, the Urban Project for “Ušće” Park was prepared, aiming to preserve all the qualities of the first-prize competition design, while incorporating the aforementioned modifications.

It envisages retaining existing park features while introducing new public amenities aligned with verified urban plans and architectural competitions. The park’s layout reconciles the orthogonal grid of New Belgrade’s Central Zone with the natural flow of the Danube riverbank, creating a hybrid spatial structure.

A key axis, the Main Alley, which remained focal point, connects significant urban nodes from the Museum of Contemporary Art towards the Hotel “Jugoslavija”, running through the Friendship Park, and interfacing with the river’s edge, forming pedestrian access points to the water.

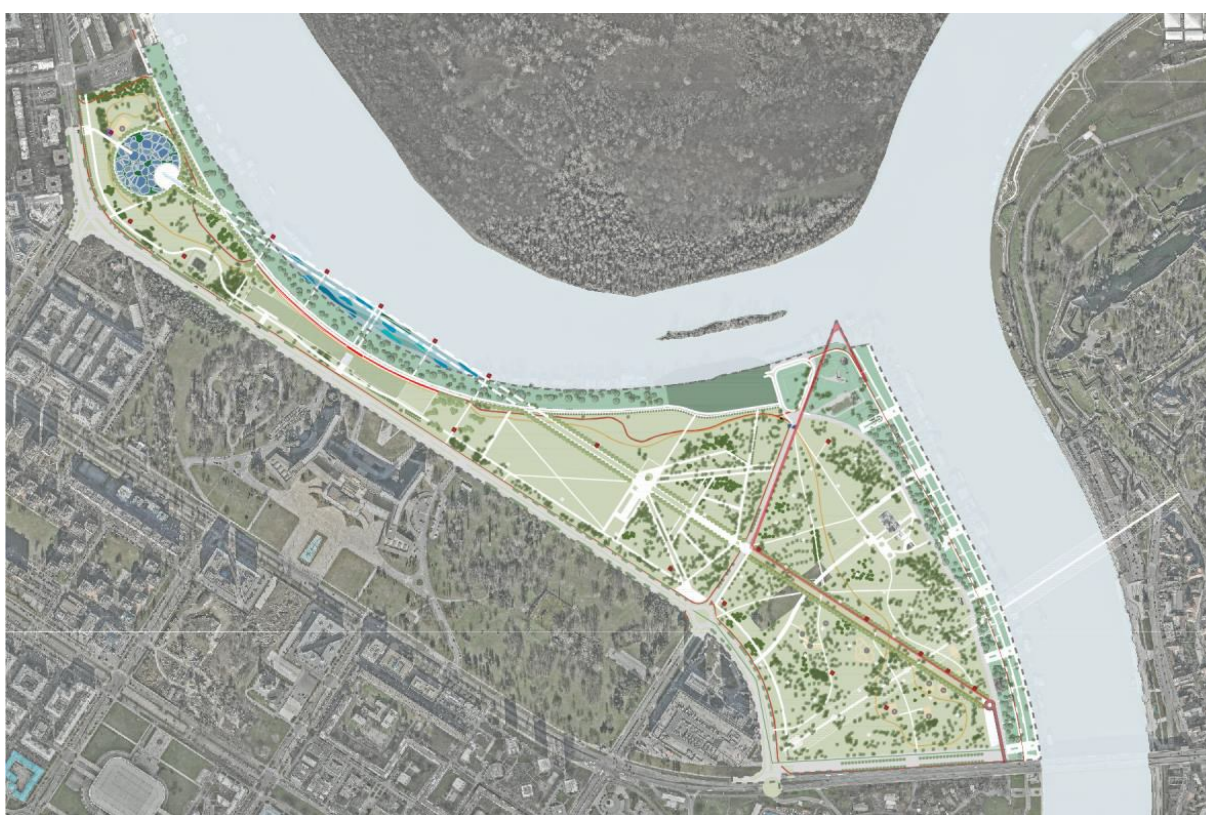
The Natural History Museum is located in the park’s narrowest section, adjacent to Nikola Tesla Boulevard and close to the river, integrating visually with the natural surroundings of the Great War Island while minimizing impact on existing greenery.



The museum building is planned as a partially underground, free-standing structure with two levels: one at -5.00 m and one at ground level ( $\pm 0.00$  m). The roof is designed as a green, accessible public space, gradually rising and blending into the park's landscape. The entrance is positioned centrally at ground level, connected to a plaza linking Nikola Tesla Boulevard with the riverside promenade.

The building is functionally divided into two wings, connected on underground level by exhibition and gallery spaces. The northwest wing houses exhibition areas on two levels, while the southeast wing contains workspaces and museum depots. Administrative offices and public amenities such as a library, reading room, and café/restaurant are oriented towards the river on the ground and gallery levels. An underground garage is accessible via Nikola Tesla Boulevard.

The Aquarium building is designed as a freestanding, circular structure with a green roof that rises in a stepped manner from the edge of the circle toward the center, reaching a height of 8.30 meters. Like the Natural History Museum, it is integrated as an essential part of the park's landscape. The building is partially underground at an elevation of -1.50 meters, featuring a main floor at -1.50 meters and a gallery space at +3.00 meters. The main entrance is located on the southeast side, where a circular entrance square with a fountain connects directly to the Main Alley, serving as its end point.



**Figure 13.** Urban Project of "Ušće" Park – Graphic attachment No. 4: "Composition Plan" (source: Urban planning institute of Belgrade)

## 5. DISCUSSION AND TECHNICAL CHALLENGES

Integrating underground cultural spaces within urban parks requires addressing several technical challenges, including structural design to withstand soil and water pressures, ensuring natural light and ventilation to enhance visitor comfort, and managing hydrological conditions typical for riverfront locations. Advances in green roof technologies and sustainable building materials support the dual function of underground cultural spaces topped by accessible green areas, promoting ecological continuity and public enjoyment.

Moreover, designing underground spaces that foster strong connections with their above-ground contexts enhances public accessibility and social use. Creating visual and physical links to the riverfront, such as transparent facades or accessible green roofs, contributes to a seamless urban experience.

From a planning perspective, collaboration among urban planners, architects, engineers, and stakeholders is crucial to resolve technical constraints while aligning with broader urban development goals. The case of Park

Ušće demonstrates the importance of integrating cultural infrastructure in a way that respects the natural and social fabric of the city.

Integrating underground cultural spaces within urban parks requires addressing several technical challenges:

- Technical-Engineering & Hydrology: Structural integrity under soil and hydrostatic pressure, particularly near riverfronts, demands advanced geotechnical solutions. Post-occupancy evaluations of similar complexes (e.g. Chengdu Tianfu Square) highlight the importance of environmental quality, comfort, orientation, and durable materials;
- Light & Ventilation: Achieving natural light and healthy indoor environments underground is crucial. Studies of subterranean heritage (Costa et al., 2021) emphasize integrating ventilation and daylighting strategies to enhance visitor comfort and sustainability;
- Green Roof & Ecology: Green roof technologies not only mask structures but contribute to biodiversity, stormwater retention, and visual continuity, reinforcing the public park's ecological function;
- Participatory & Multidisciplinary Planning: Effective outcomes rely on early inclusion of stakeholders-citizens, specialists, decision-makers-through participatory GIS and consensus-building to align design with community needs.

Advances in digital planning and whole-lifecycle sustainability frameworks further support the integrated management of underground cultural infrastructure.

## 6. CONCLUSION

The case study of the Natural History Museum and Aquarium within Park Ušće exemplifies the potential of utilizing underground spaces for cultural infrastructure while preserving and enhancing valuable urban green areas. This approach aligns with contemporary urban planning trends that emphasize multifunctionality, environmental sustainability, and public accessibility. By integrating museum functions below ground, the design minimizes surface disruption, maximizes green continuity, and strengthens the park's role as a vital social and cultural destination.

Comparisons with international examples such as the Pérez Art Museum Miami, Vancouver Art Gallery expansion, and Kumu Art Museum in Tallinn highlight a global movement towards blending culture and nature through innovative underground architecture. These examples showcase how underground spaces can accommodate significant cultural programs without sacrificing parkland, promoting greater community engagement and urban vitality. A parallel can be drawn with the Museum of Louvre as a historical example of a major cultural institution set within a park landscape, positioned along the riverbank and integrated into the historical urban setting. The integration of above-ground and below-ground spaces, along with the implementation of an international architectural competition, highlights the importance of expert participation in shaping such significant urban interventions and ensuring context-sensitive, high-quality outcomes.

The technical challenges inherent in such projects-ranging from hydrological issues to structural design-require sophisticated engineering and collaborative planning efforts. However, the long-term benefits in terms of spatial efficiency, cultural enrichment, and environmental stewardship justify these investments.

In summary, underground cultural spaces in parks offer a promising model for contemporary urban development, combining architectural innovation with public benefit. The Park Ušće project, with its thoughtful integration of green roof concepts and seamless urban connections, contributes valuable insights to this evolving field.

In any case, it is essential to continuously seek a refined balance between the benefits of rational land use, transforming constraints into potential, and the extent of human presence in underground spaces, while maintaining ongoing analysis which includes interaction with future users.



## 7. BIBLIOGRAPHY

- [1] Besner, J. (2017). Cities think underground – Underground space (also) for people. *Procedia Engineering*, 209, 49–55.
- [2] Broere, W. (2016). Urban underground space: Solving the problems of today's cities. *Tunnelling and Underground Space Technology*, 55, 245–248.
- [3] Competition Jury. (2024). Report on the work of the jury for the open, single-stage, anonymous urban-architectural competition for the "Friendship Park" – Ušće and the conceptual design of the Natural History Museum in Belgrade. City of Belgrade.
- [4] Danilović Hristić, N., & Lalošević, M. (2019). Relationship of urban planning and decision making and the impact on the quality of proposals. In *Challenges in Architecture, Urban Design and Art, STRAND*, University of Belgrade – Faculty of Architecture (pp. 176–186). Belgrade: Strand – Sustainable Urban Society Association.
- [5] Foroughi, M., Andrade, B., Pereira Roders, A., & Wang, T. (2023). Public participation and consensus building in urban planning from the lens of heritage planning: A systematic literature review. *Cities*, 135, Article 104235.
- [6] Lalošević, M., & Hadži Arsenović, M. (2025). Planning before and after planning. In *Proceedings of the XXI Conference with International Participation: Urbanism and Sustainable Development*, Silver Lake, May 29–31, 2025 (pp. 163–168). Serbian Association of Urban Planners and Republic Geodetic Authority.
- [7] Park, E. J., & Kang, E. (2021). Sublime experience for sustainable underground space: Integration of the artists' works in Chichu Art Museum. *Sustainability*, 13(12), 6653.
- [8] Smaniotto Costa, C., Menezes, M., Ivanova-Radovanova, P., Ruchinskaya, T., Lalenis, K., & Bocci, M. (2021). Planning perspectives and approaches for activating underground built heritage. *Sustainability*, 13(18), 10349.
- [9] Zeng, R., & Shen, Z. (2022). Post-occupancy evaluation of the urban underground complex: A case study of Chengdu Tianfu Square in China. *Journal of Asian Architecture and Building Engineering*, 22(1), 139–154.
- [10] Herzog & de Meuron. (n.d.). Vancouver Art Gallery, Vancouver. *Arquitectura Viva*. Retrieved June 30, 2025, from <https://arquitecturaviva.com/works/galeria-de-arte-de-vancouver-0>
- [11] Art Museum of Estonia. (n.d.). Kumu Art Museum – Estonian art from the 18th century until today. Retrieved June 30, 2025, from <https://kumu.ekm.ee/en/>
- [12] Johnston Marklee. (n.d.). Pérez Art Museum Miami. Retrieved June 30, 2025, from <https://www.jm-a.com/portfolio/perez-art-museum-miami/>
- [13] Pei Cobb Freed & Partners. (n.d.). Grand Louvre Modernization. Retrieved June 30, 2025, from <https://www.pcf-p.com/projects/grand-louvre-modernization/>
- [14] Louvre Museum. (n.d.). A pyramid for a symbol. Retrieved June 30, 2025, from <https://www.louvre.fr/en/explore/the-palace/a-pyramid-for-a-symbol>

## EVALUATION AND PLANNING OF UNDERGROUND SPACE RESOURCES IN COMPLEX BUILT -UP ENVIRONMENT FROM THE PERSPECTIVE OF MULTI-DIMENSIONAL VALUES-- TAKING THE CORE AREA OF THE CAPITAL IN BEIJING AS AN EXAMPLE

Yiting Zhao<sup>1</sup>, Keijie Wu, Xiaodong Shi, Longqin Lin

**Abstract:** In order to effectively support the planning and decision-making of underground space and realize the fine control and guidance of underground space utilization in complex built-up environment, this paper takes the Core Functional Area of the Capital, which has the highest density and the most complex urban environment in Beijing, as an example to explore the resource evaluation methods of underground space in built-up area. Concerning the characteristics of the built-up area, both the stock and incremental resources of underground space are taken into account. The paper establishes a comprehensive evaluation framework for the development potential of underground space resources covering seven value dimensions, including economic value, social demand, ecological environment, historical protection, disaster prevention, spatial layout and functional facilities, and comprehensively sorts out the influencing factors and quantitative indicators in each value dimension, so as to carry out the quantitative evaluation of the underground development potential accurate to plot. The paper hopes to effectively support the zoning and planning of underground space and provide technical support for the fine management and scientific utilization of underground space resources in high-density built-up areas.

**Keywords:** multi-dimensional value; high-density built-up area; underground space; resource evaluation; Planning & control

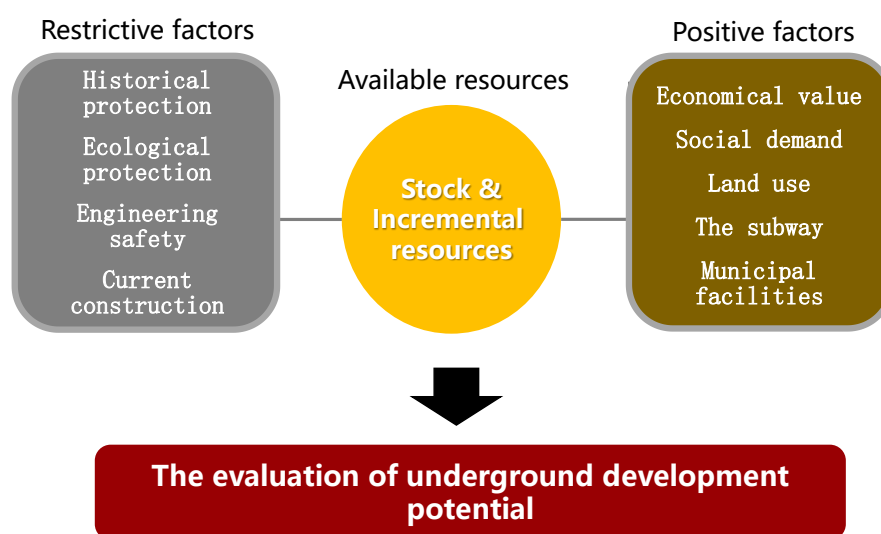
### 1. INTRODUCTION

Urban development is a dynamic and three-dimensional process. With the continuous renewal of land use, the construction space is correspondingly expanded upward and downward. Underground space resources have gradually become an important way to realize urban function and space optimization <sup>[1]</sup>. How to effectively identify underground space resources and scientifically judge the value and potential of underground space development and utilization is an important premise to promote the scientific and orderly utilization of underground space resources. The existing studies on the evaluation of underground space resources mainly focus on the incremental resources of underground space <sup>[2]</sup> from

---

<sup>1</sup> MSc Zhao Yiting, Urban Planner, Beijing Municipal Institute of City Planning & Design, 1437235330@qq.com.

the perspective of eco-geological conditions, which pays less attention to the stock resources of underground space. Meanwhile, the current evaluation of underground resources mainly aims at new areas, which is not suitable for built-up areas with a large number of existing buildings, structures and historical & cultural heritage. In view of the above problems, this paper takes the Core Functional Area of the Capital as an example, to explore the identification and planning decision methods of underground resources in highly built areas, taking into account both the development and renewal needs of underground space. The paper will comprehensively analyze the influencing factors of social, economic, ecological, historical and security conditions to support the fine management and zoning of underground space in complex-built environment.



**Figure 1.** Diagram of underground space resource assessment and planning model in high-density built-up area

## 2. OVERVIEW OF THE CORE FUNCTIONAL AREA OF THE CAPITAL

The Core Functional Area of the Capital has a total area of 92.5 square kilometers and a population of about 1.7 million, which faces multiple needs such as the protection of the old city, the improvement of the living environment, the optimization of the administration environment and the promotion of urban vitality. Meanwhile, the area also has a high degree of underground space development, where more than 70% of the construction land (excluding roads, green space and water) contains underground development. How to effectively identify the available resources of underground space and appropriately guide development of aboveground and underground space is the key to the sustainable development of the built-up area.

## 3. IDENTIFICATION OF UNDERGROUND SPACE RESOURCES

In a broad sense, underground space is a comprehensive concept, which contains not only space resources, but also groundwater, energy, rock & soil and etc. This paper mainly involves space resources, which can be preliminarily divided into stock resources and incremental resources in terms of development status.

### 3.1. Stock resources

Underground stock resources are built spaces that can be used for other purposes after certain transformation. The study considers that the main factors affecting the reutilization of underground stock resources include construction time, building area, underground floors, functional types, etc. A comprehensive analysis was conducted on the underground stock resources within the core area. The study finds that the time of construction is of critical effect as frame structure is widely used in the underground space built after 2000, which has high spatial compatibility. At the same time, the spatial compatibility of the underground space also increases with the building scale, the number of floors and the functional types. By analysis, the stock resources of underground space built after 2000 with an area of more than 5000 square meters have higher potential for reutilization, which account for about 10% of the total amount and 54% of the building area (see Table 1). These stock resources are mostly multifunctional and of concrete frame structure, which makes it more suitable for flexible uses.

*Table 1. Classification and statistics table of underground space stock resources*

Type	amount	building area (10,000m <sup>2</sup> )	Proportion of building area	Proportion of amount	Average building area (m <sup>2</sup> )
General	4467	374.0	0.21	0.67	837.28
Better	1511	456.76	0.25	0.23	3022.91
High quality	663	962.4	0.54	0.10	14515.90
Total	6641	1793.18	1.00	1.00	2700.16

### 3.2. Incremental Resources

From the perspective of urban development conditions and land ownership settings, the incremental resources of underground space in high-density built-up areas are in close combination with the needs of urban renewal. The construction forms mainly include the coordinated construction of the aboveground and underground after demolition of original buildings, the reconstruction and expansion of underground space on the basis of the original buildings & structures, and the new underground projects (see Table 2), which can improve the utilization efficiency of land resources, improve the short board of urban functions, and improve the quality of urban environment on the ground.

*Table 2. Classification and statistics table of underground space incremental resources*

Classification	Resource utilization strategy
Demolish and rebuild	Through the coordinated utilization of ground and underground space, we can improve urban functions and supplement the shortcomings of public facilities.
Reconstruction and expansion	Through the reconstruction and expansion of underground space or adding connectivity on the basis of the original building, to improve the efficiency and functional use of underground space.
New underground projects	By building underground facilities such as parking lot or municipal stations to addressing the issue of insufficient construction space.

#### 4. EVALUATION OF UNDERGROUND SPACE RESOURCES

The development potential of underground space resources is closely linked with the development needs of aboveground. Therefore, the evaluation of underground space resources should take into account various constraints and driving conditions both aboveground and underground, from the economic, social, ecological, historical, security and other dimensions.

##### 4.1. Economic value

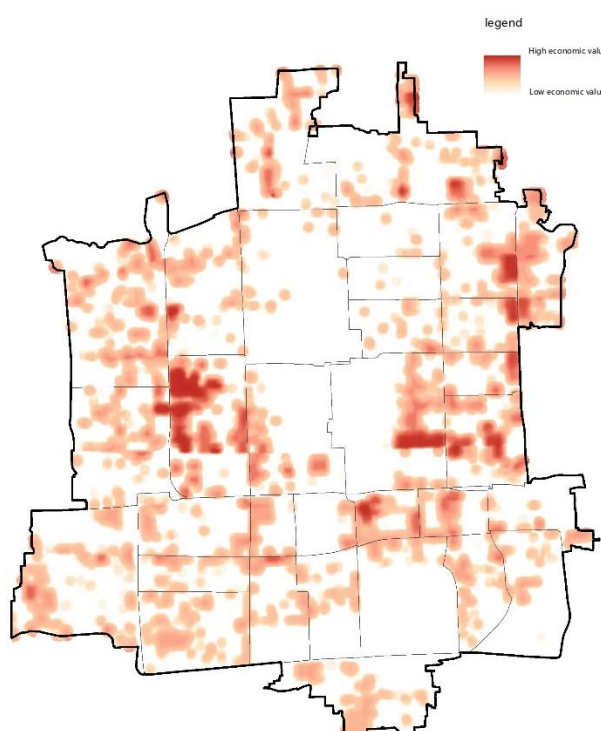
The economic value is an important factor to promote the development and utilization of underground space. The economic value of underground space is often positively correlated with land value, and is also affected by spatial location, functional use, and the number of underground floors <sup>[4]</sup>. Floor utility ratio is widely used to evaluate the three-dimensional value of land. Through the investigation of typical cases in the core area, the study finds that the average floor utility ratio of the underground floor is generally about 60%. In case of direct connection with the subway, the commercial rent price of the underground floor can reach 80% of the aboveground, that is, in addition to the spatial location and land uses, the subway connection also has a significant role in improving the economic value of the underground space. Therefore, in the process of judging the economic value of underground space, the study adopts the floor utility ratio method and takes the first floor of underground space as the evaluation object. Concerning whether it is located in the key functional area or connected with the subway, differentiated floor utility ratio (see Table 3) is adopted to evaluate the commercial rent of the corresponding underground space and form the economic value map (see Figure 2).

**Table 3.** The floor utility ratio of the first underground floor in the Core Area of the Capital

Functional use	Key functional area		General area	
	No subway connection	Connected to the subway	No subway connection	Connected to the subway
Commercial facilities	0.6	0.8	0.5	0.6
offices	0.5	0.6	0.4	0.5
residence	0.3	0.3	0.2	0.2

**Note:** The specific indicators are summarized according to the investigation of typical projects in the core area.





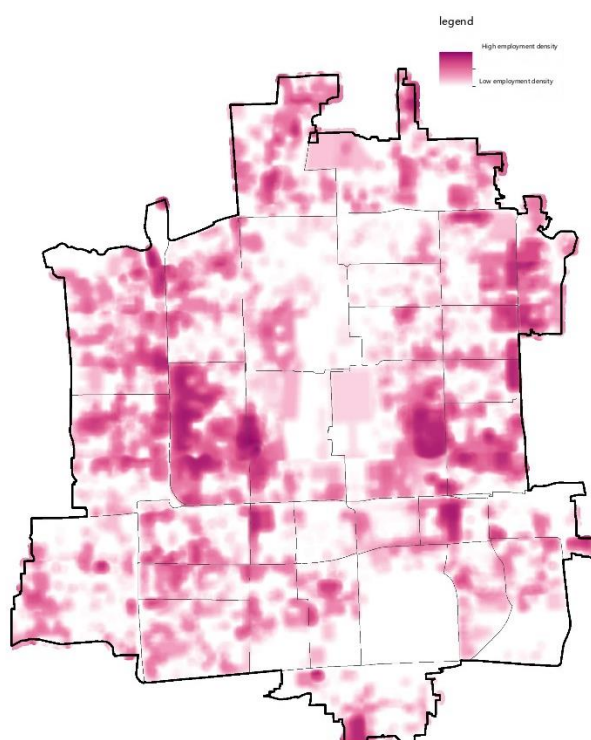
*Figure 2. Economic value assessment of commercial underground space in the Core Area of the Capital*

#### **4.2. Social demand**

High-density built-up areas tend to have a high concentration of people, so the social attributes of the users, their willingness and experiences, are important factors to the social needs of underground space [5] which are also closely related to the crowd concentration and demand. The study focuses on the social demand for underground space of various groups of people including residents, employees, shoppers and etc. A questionnaire survey of about 400 copies is carried out, using the Likert scale to analyze the demand level of different groups. Among them, the demand of shoppers is the highest, with an average of 4.0 (full score of 5.0), which includes shopping, cinema, video games and other entertainment activities. The demand of employees is relatively high, reaching 3.6 on average, mainly involving leisure activities such as exhibition, community activities, dining, fitness, reading in bookstores and etc. The demand of residents is relatively low, about 3.2, mainly involving community activities and convenient service. The social demand of the underground space is comprehensively evaluated in combination with the distribution density of various groups and their demand level (see Table 4), in which the shopping group is set as 1 (the demand score is 4), the employee group is 0.9 (3.6/4), and the residential group is 0.8 (3.2/4). Overall, there is a high correlation between the social demand for underground space and the distribution of economic value (see Figure 3).

**Table 4.** Evaluation of underground space needs of various groups of people

Type of group	Demand level	Distribution density		
		High (person/ha)	Medium (person/ha)	Low (person/ha)
Shopping group	1	150	100	80
Employee group	0.9	200	150	80
Residential group	0.8	120	100	60



**Figure 3.** Distribution of social needs of underground space for employed people in the Core Area of the Capital

### 4.3. Ecological protection

The development and utilization of underground space should coordinate with the ecological environment so as to reduce the cost and safety risk. The ecological factors related to the development and utilization of underground space mainly include green space, farmland, river, groundwater, etc. In areas with important ecological value such as ecological protection area, important river and lake system, underground drinking water resources, the development and utilization of underground space shall not be carried out except for necessary infrastructure construction. Meanwhile, green space, ordinary farmland and water area can be moderately developed and utilized after meeting relevant environmental protection requirements. The impact of groundwater on underground space development involves project cost, groundwater pollution, water infiltration and corrosion, etc. Therefore, a suitable vertical construction scope of underground space should be adopted by referring to the groundwater level and the distribution of confined aquifers, so as to reduce the interference to the hydrogeological environment.

#### **4.4. Historical & Cultural protection**

The development and utilization of underground space should not only respect and protect all kinds of underground historical relics, but also avoid the impact and destruction of ground cultural and historical heritages. The core area has the richest historical and cultural resources in Beijing, where the protection of historical heritages and the control of building height significantly increase the demand for underground space development. On the one hand, the underground development should be moderately controlled according to the requirements of various historical protection areas. On the other hand, the role of underground space in historical preservation and cultural display should be encouraged by putting some functions or facilities underground for better restoration of traditional historical features on the ground. Meanwhile, underground space can also be used as cultural sites such as museums, exhibitions or other cultural display areas.

#### **4.5. Risk protection**

In highly built environment, the risk factors of underground space are very extensive. Among them, geological risks, such as active faults, sand liquefaction, karst collapse and other geological hazard areas should be avoided especially for high-intensity underground development. Current underground buildings, subway, gas pipelines and other infrastructures should be ensured a certain safety distance to avoid the risk of collapse, explosion and other disasters caused by adjacent underground projects. Attention should also be paid to the impact of extreme weathers, such as waterlogging in underground space caused by extreme rainstorms <sup>[6][7]</sup>. Compared with other areas in Beijing, the geological conditions of the core area are relatively suitable. The risks of underground engineering and waterlogging are main factors affecting the development and utilization of underground space. The study comprehensively considers the groundwater level and the burial depth of underground structures to analyze the areas with higher risk of anti-floating and infiltration. By delimiting the protection scope of the subway and underground pipelines, "unforeseen" engineering risks can also be avoided to some extent.

#### **4.6. Spatial layout**

The demand for underground space development is usually affected by spatial factors such as land use, density, space shortage and aggregation of public activities. In general, commercial & business land often has higher demand for underground development than that of residential & public service land, and the higher the intensity or density of above-ground development, the greater the demand for underground space development and utilization <sup>[8][9]</sup>. Meanwhile, central areas with strict the control of above-ground construction often have more demand for underground development <sup>[10]</sup>. The study comprehensively takes into account the spatial factors of central location, development intensity, aboveground control requirements, urban function aggregation (whether it is located in key functional or business areas) to evaluate the spatial demand of underground space development and utilization.

#### **4.7. Functional facilities**

The development and utilization of underground space is also affected by the construction of rail transit and various municipal facilities such as transportation, public service, disaster prevention, safety

facilities and etc. Among them, rail transit has the most prominent impact as the closer to the rail station, the higher the potential demand for the development and utilization of underground space <sup>[11][12]</sup>. For example, the underground commercial facilities and public spaces in Beijing Central Business District are mainly concentrated within 300 meters around the rail station <sup>[13]</sup>, and most of them are directly or indirectly connected with the rail station <sup>[14]</sup>. The areas where large public service facilities concentrated can provide services and transportation space through the overall construction of underground space. Municipal infrastructure, public parking facilities, bus stations and emergency shelters can also improve the improve the level of facility services through the use of underground space and release more open space on the ground <sup>[15]</sup>. The study comprehensively defines the areas where there is a demand for the construction of underground functional facilities, including land within 300 meters around new or renovated rail stations and land for planned facilities which can be integrated developed aboveground and underground to improve the efficiency of land resources.

## 5. COMPREHENSIVE EVALUATION OF DEVELOPMENT AND UTILIZATION POTENTIAL

The study integrates the influencing factors of underground space development and utilization in various dimensions, extracting quantitative indicators from aspects of contributing and restrictive conditions, to comprehensively evaluate the potential of underground space development (see Table 5). The contributing factors include the four dimensions of economy, society, space and facilities, with rent/land price, crowd demand, development intensity, spatial location, rail transit and public facilities as the main indicators. Restrictive factors include the three dimensions of ecological, historical and risk protection. The weighted superposition method is used to comprehensively evaluate the demand and constraint of underground space development and utilization <sup>[16]</sup>.

*Table 5. Dimensions and influencing factors of underground space resource potential assessment*

	Major dimensions	Classification	Main considerations	Evaluation grade	Value
Contributing	Economic dimension	Land value	Land price * floor utility ratio of the first underground floor * coefficient	High, Medium, Low	1、0.5、0.2
		Commercial rent	Shop rent * floor utility ratio of the first floor * coefficient	High, Medium, Low	1、0.5、0.2
	Social dimension	social demand	Population density * demand index	High, Medium, Low	1、0.5、0.2
	Spatial dimension	Land use	Commercial & business, public facilities, residential land	High, Medium, Low	1、0.5、0.2
		Development intensity	Floor area ratio > 2, 1 < Floor area ratio ≤ 2, Floor area ratio ≤ 1	High, Medium, Low	1、0.5、0.2
		Spatial location	Key functional & business areas, commercial centers, public centers, etc.	High, Medium, Low	1、0.5、0.2
		Space scarcity	Central location degree, height control	High, Medium, Low	1、0.5、0.2

	Facility dimension	Rail transit construction	Rail station distance: within 300m, 300-500m, beyond 500m	High, Medium, Low	1、0.5、0.2
			Passenger flow $\geq$ 100,000/day, 50,000-100,000/day, < 50,000/day		
			Connectivity: direct connectivity, combination of entrances and exits, non-connectivity		
		Public service facilities	Large cultural and sports facilities or clusters	Yes, no	1、0.2
		Other functional facilities	Underground municipal facilities, transportation facilities, disaster prevention facilities	Yes, no	1、0.2
Restrictive	Ecological dimension	no construction	ecological protection area, important river and lake system, important farmland, underground drinking water protection area and etc.	The development and utilization of underground space other than necessary infrastructure will not be carried out In principle	
		Restrict construction	Green Park	Yes, no	0.2、1
			Ordinary farmland	Yes, no	0.2、1
			Groundwater reserves or confined aquifers	Yes, no	0.2、1
	Historical dimension	No construction	Protection area and class I control area of cultural relics	The development and utilization of underground space other than historical protection will not be carried out in principle.	
		Restrict construction	Within the core protection scope	The development and utilization of underground space shall not be carried out except for the necessary infrastructure, public service facilities and historical protection.	
			Outside the core protected area	Yes, no	0.2、1
			Underground cultural relics	Necessary archaeological investigation and exploration shall be carried out to encourage the in-situ protection and display of cultural relics.	



Security dimension	No construction	Within 200m on both sides of the active fault zone	The development and utilization of underground space should avoid this area in principle.	
	Restrict construction	Safety protection scope of subway or underground pipeline, old basement/underground pipeline intensive area, other geological risk areas etc.	Yes, no	0.2、 1

## 6. DISCUSSION AND CONCLUSION

The development and utilization of underground space in highly built-up area is in great demand <sup>[17]</sup>. The establishment of a systematic evaluation method of underground space resources is an important way to support the sustainable development of the built-up area. The study explores the identification method of underground space resources and carries out quantitative evaluation of the potential for underground space development and utilization, covering multiple value dimensions such as economy, society, history, ecology, safety, space, and facilities to support refined underground space planning and control zoning. The study hopes to provide technical support for underground space planning decisions in highly built environment. The conclusions of the study are as follows:

The underground space resources in highly built-up areas should include both incremental and stock resources. The latter refers to underground space that has already been built but can carry other functions through renewal and renovation. Generally, underground spaces built with frame structure, relatively large building scale and multiple functions have relatively high compacity and potential for reutilization, and can be prioritized as stock resources of underground space.

The development and utilization of underground space in highly built-up areas are significantly positively correlated with land value, employment population density, rail connectivity, and agglomeration of urban functions. Usually, key functional or business areas, commercial centers, large transportation hubs, and cultural & sports centers are the key areas for underground space development and utilization.

The restrictive factors for the development and utilization of underground space in highly built-up areas mainly include sensitive ecological environment, historical protection requirements, engineering safety, and geological hazard risks. Underground space should be utilized to a limited extent while meeting relevant control requirements. Both horizontal and vertical protection and control range should be considered to ensure the safety.

The comprehensive potential of underground space development in highly built-up areas should be considered in terms of resource conditions, development motivation, and restriction requirements. In the absence of prohibited restrictive factors, the development and utilization of underground space should prioritize areas with high land value/rent, functional clustering, social demand and close connection to the subway, where the integrated development of aboveground and underground should be carried out to effectively improve the efficiency of urban space.

The study mainly summarizes and quantitatively evaluates the influencing factors of underground space in different value dimensions based on case investigation data and practical experience in the core area. It still needs to be verified and calibrated on a larger scale. At the same time, attention should be

paid to different types of underground resources such as groundwater resources, underground rock and soil resources, renewable energy, and their influence on the development and utilization of underground space, in order to effectively coordinate the protection and development needs and achieve sustainable development of underground space in highly built-up areas.

## 7. REFERENCES

- [1] Sterling, R. Admiraal, H. Bobylev, N. et al. (2012). Sustainability issues for underground space in urban areas. *Urban Design Planning*, 2012, 165(4), 241.
- [2] Doyle, R. (2016). From hydro/geology to the streetscape: evaluating urban underground resource potential. *Tunnelling and Underground Space Technology*, 2016, 55, 83.
- [3] Bobylev, N. (2009). Mainstreaming sustainable development into a city's Master plan: a case of urban underground space use. *Land Use Policy*, 2009, 26(4), 1128.
- [4] Shi, Y. Zhou, L. (2017). Land value assessment and spatial variation in underground commercial space in Shanghai. *Acta Geographica Sinica*, 72(10), 1787.
- [5] Tan, Z. Roberts, A C. Christopoulos, G I. et al. (2018). Working in underground spaces: architectural parameters, perceptions and thermal comfort measurements. *Tunnelling and Underground Space Technology*, 71, 428.
- [6] Wang, Y L. Liang, L G. (2010). Subterranean city: the introduction of pedway in Chicago. *Urban Planning Int*, 25 (1), 95.
- [7] Cui, J Q. Allan, A. Taylor, M A P. et al. (2013). Underground pedestrian systems development in cities: Influencing factors and implications. *Tunnelling and Underground Space Technology*, 35, 152.
- [8] Dong, Y H. Peng, F L. Qiao, Y K. et al. (2021). Measuring the monetary value of environmental externalities derived from urban underground facilities: Towards a better understanding of sustainable underground spaces. *Energy Build*, 250, 111.
- [9] Ma, C X. Peng, F L. Qiao, Y K. et al. (2022). Evaluation of spatial performance of metroled urban underground public space: A case study in Shanghai. *Tunnelling and Underground Space Technology*, 124, 104.
- [10] Wang, X. Zhen, F. Huang, X. Zhang, M. et al. (2013). Factors influencing the development potential of urban underground space: Structural equation model approach. *Tunnelling and Underground Space Technology*, 38, 235.
- [11] Monnikhof, R. Edelenbos, J. Vanderkrogt, R. (2018). How to determine the necessity for using underground space: an integral assessment method for strategic decision making. *Tunnelling and Underground Space Technology*, 13(2), 167.
- [12] Peng, J. Peng, F L. Yabukin, N. Fukuda, T. (2019). Factors in the development of urban underground space surrounding metro stations: A case study of Osaka, Japan. *Tunnelling and Underground Space Technology*, 91, 103.
- [13] Zhao, Y T. Wu, K J. (2016). Quantitative evaluation of the potential of underground space resources in urban central areas based on multiple factors: a case study of Xicheng district, Beijing. *Procedia Engineering*, 165, 610.
- [14] Zhao, Y T. (2019). Quantitative Evaluation of Underground Space Development Potential in Urban Center Areas. *Chinese Architecture*, (9), 39.

- [15] Liu, K. Peng, J. Peng F L. (2011) Evaluation Model for the Suitability of Underground Space Resources Exploitation and Utilization. Chinese Journal of Underground Space and Engineering, (7) , 219.
- [16] Wu, X L. Qiao, Y K. Li, Z Y. et al. (2023). Detailed Spatial Control Method for Underground Space in Urban Renewal Areas based on Development Value Monetarization. Urban Development Studies, 30 (5) , 28.
- [17] Wu, K J. Zhao, Y T. Shi X D. (2020). Research on Underground Space Planning Compiling under Territory Spatial Planning System. Tunnel Construction, 40(12), 1683.

## INTEGRATED UNDERGROUND SPACES PLANNING IN BELGRADE: A SMART CITY PERSPECTIVE

Milena Grbić<sup>1</sup>, Olivera Stanković<sup>2</sup>, Ksenija Lalović<sup>3</sup>

**Abstract:** The aim of this paper is to explore the opportunities and challenges of applying underground architecture within the *smart city* concept in Belgrade. The study analyzes the current state of underground space planning, highlighting the prevailing focus on the metro system and the lack of a comprehensive approach. By applying the smart city concept and the *Deep City* model, the research investigates potentials for integrated planning that incorporates technological tools, sustainability, and multidisciplinary collaboration. By comparing domestic practices with international experiences from Helsinki and Singapore, the paper proposes specific guidelines for improving the planning of underground spaces in Belgrade, with the goal of achieving more efficient and sustainable management of this important urban resource. The contribution of this study, supported by strong argumentation, emphasizes the need for a multidisciplinary approach to the planning and design of underground typologies, in order to establish a balance between technological innovation, economic investment, and social benefits. The paper also provides directions for further research on the integration of underground elements in smart cities, with the aim of enhancing the quality of urban life.

**Keywords:** comprehensive analysis, holistic planning, deep city, sustainable development, the indivisibility of urbanism

### 1. INTRODUCTION

Underground spaces have always been a special engineering fascination and a reflection of human ingenuity – from Persian canals (an early example of sustainable engineering) and Roman catacombs (addressing burial constraints as well as urban crowd management and public health), to infrastructure pipes, basement floors of buildings and garages, civil protection facilities, and metro systems that have almost organically evolved over decades in many modern cities, functionally responding to contemporary urban challenges.

Today, as even more efficient ways to expand limited urban space are needed to meet the demands of a growing population, modern underground spaces go beyond traditional models or functions. While earlier underground structures were mostly developed horizontally, there is an increasing number of underground typologies that require spatial development in the vertical dimension. To avoid the “first come, first served” approach seen in many urban areas – including Belgrade – this work highlights the challenge contemporary planners face: how to organize the use of underground space in a way that enables complementary rather than competitive exploitation of resources?

Achieving this requires first understanding and appreciating that underground space encompasses everything between the surface and the Earth’s core, whether biotic or abiotic in origin. In this context, this study treats underground space through the Deep City approach [1], where underground space includes resources classified as physical space, spatial continuity, geocological characteristics, subterranean flora/fauna, excavated materials, cultural heritage, and renewable resources (including groundwater and geothermal energy) [2].

<sup>1</sup> PhD, Grbić Milena, Dipl. Ing. Arch., Associate Professor, University of Novi Sad, Faculty of Civil engineering Subotica, Kozaračka 2a, Subotica, Serbia, [mdelevic@gmail.com](mailto:mdelevic@gmail.com), <https://orcid.org/0000-0001-6485-1478>

<sup>2</sup>MSc, Stanković Olivera, Dipl. Ing. Arch., PhD candidate, University of Belgrade, Faculty of Architecture, Bulevar Kralja Aleksandra 73/II, Belgrade, Serbia, [olivera.arh.urh@gmail.com](mailto:olivera.arh.urh@gmail.com)

<sup>3</sup> PhD, Lalović Ksenija, Dipl. Ing. Arch., Associate Professor, University of Belgrade, Faculty of Architecture, Bulevar Kralja Aleksandra 73/II, Belgrade, Serbia, [ksenija.lalovic@arh.bg.ac.rs](mailto:ksenija.lalovic@arh.bg.ac.rs), <https://orcid.org/0000-0001-7261-7921>

Effective exploitation of underground spatial resources thus requires a multidimensional approach that simultaneously considers functional, transportation, socio-cultural, and landscape-ambient parameters, which in turn indicate the level of complexity and the need for further interdisciplinary concretization ensuring spatial and functional coherence.

Currently, the underground space of Belgrade can be classified into several functional categories: pedestrian underpasses (e.g., beneath Terazije), traffic tunnels (e.g., the Terazije Tunnel), and railway stations (e.g., Vukov Spomenik). At the same time, the underground area holds significant potential related to layers of historical, cultural, and archaeological heritage, as well as to thermal water sources. The development of underground infrastructure is defined by the General Regulation Plan for Rail Systems in Belgrade, which includes elements of detailed elaboration. A key emphasis is placed on the phased implementation of the metro system, which has led to the establishment of the public utility company *Beogradski metro i voz*. Through the official website of this company, information on project status is available. The projects are conceived in phases and encompass the construction of four BG Voz lines and three metro lines.

Belgrade's problem, reflected in the existing planning documentation which practically only considers underground space from the perspective of the metro system, reveals its incoherent approach. The absence of key concepts almost always means their absence in all subsequent elaborations. Planning of underground urban spaces (UUS) in Belgrade still relies on expert and personal experience, cognitive biases, and analog reflections on previous cases, while quantitative research methodologies are minimally used. This means planners mostly depended on subjective knowledge and experience regarding the laws of underground space use, which inevitably leads to sporadic resource exploitation and inconsistencies that sabotage the maximization of efficiency.

In present conditions, as a way to comprehensively utilize resources, this study explores the potentials, challenges, and possibilities of applying integrated underground space planning in Belgrade from a *smart city* perspective. The smart city concept implies holistic management of urban resources through digital technologies, sustainable solutions, and efficient infrastructure, aimed at improving quality of life. The development of new technologies has the potential to revolutionize underground space management. Tools such as Building Information Modeling (BIM) enable precise design and risk assessment, while AI systems optimize traffic flow, climate control, and energy efficiency. Above all, data-driven approaches assist comprehensive planning. By connecting technology, sustainability, and citizen participation, smart cities strive to become more resilient, functional, and better adapted to the real needs of their users, enabling more rational resource use and a higher level of urban comfort. In this context, the primary goal of this work is to identify research trends and key focal points regarding underground space planning currently leading the field, in order to concretely improve Belgrade's planning processes and integrate underground and aboveground planning.

More broadly, the study unequivocally points out the need for greater collaboration among planners, architects, engineers, and decision-makers to fully understand the potentials of this spatial, social, and resource dimension. Integrated planning is essential, requiring coordination and involvement of state and private stakeholders, as well as the entire public. With the help of ICT – Information and Communication Technologies – we can unlock the potential of underground space and make better use of it.

## 2. MATERIAL AND METHODS

From a methodological perspective, this study investigates the potentials, challenges, and possibilities of applying integrated underground space planning in Belgrade from the viewpoint of contemporary smart city concepts. The aim is to improve planning processes by linking underground and aboveground planning into a unified methodological framework.

In a dedicated section, the study analyzes specific problems and the treatment of underground space in Belgrade. Through a general analysis of bibliographic data—primarily General Urban Plans and legislation—a chronological analysis of planning practice was conducted, systematizing the main characteristics, evolutionary trends, and developmental trajectories in planning practice, with particular attention to underground space. Thematic categorization highlights key challenges in the treatment of underground space as an identification of research focal points. A SWOT analysis, employed as a brainstorming tool, was carried out to present Belgrade's underground space as a complex and multilayered segment of the urban fabric that requires thoughtful institutional management and long-term strategic planning.

Simultaneously, by analyzing publicly available planning documents on experiences from leading cities seriously engaged in underground planning, key planning approaches currently shaping this field were identified. Through a comparative analysis of reference international cases (Helsinki and Singapore) – cities and projects leading in the implementation of sustainable and integrated underground infrastructure planning – and by analyzing existing underground urbanism plans, available technologies, and public policies, key factors were



illuminated that have the potential to contribute to sustainable and successful future implementation, thus outlining guidelines for a possible (adequate) planning approach for Belgrade.

Based on all collected data, after identifying key shortcomings in the field (Belgrade) and analyzing successful international examples, the final section proposes appropriate guidelines and recommendations customized for the Belgrade context. These correspond to contemporary planning requirements and have the potential to contribute to more efficient shaping or expansion of the theoretical planning system by adapting it to new developmental approaches.

### 3. RESULTS

#### 3.1. Overview of Underground Planning in Belgrade

The underground infrastructure framework was first mentioned as a concept in the General Urban Plan of Belgrade 1950–70 (1950) [3]. The first comprehensive study on the development of the metro system in Belgrade was conducted in 1968 by the Design Institute of the Yugoslav Railways Community. This study, based on the General Plan, proposed three metro lines; however, only the underground passage at Terazije was implemented, and that on a limited scale compared to the original design, which foresaw its extension toward the railway infrastructure in the deeper layers of the city. The plan also included the introduction of an underground tram system to facilitate passenger movement to other parts of the city center [4].

In the early 1970s, before the preparation of the General Plan of Belgrade 1972–2000 (1972), a Rapid Urban Transport Study was carried out. This study analyzed two metro systems: deep metro and shallow metro (cut and cover), intending to determine the most suitable system for Belgrade [5]. In practice, from 1966, several pedestrian underpasses were built: in New Belgrade at locations identified as favorable for future underground system development, while those at Terazije and Zeleni Venac emerged as necessary solutions due to conflict points and pedestrian safety concerns. These implementations were considered within the concept of underground urbanism, a new planning and design discipline in urban practice at the time [6].

The 1972 General Plan of Belgrade planned two metro lines, and in 1976 a study on the technical and economic feasibility of rapid public urban transport in Belgrade was initiated. The study proposed a transport system supported by a city distribution metro and a regional metro. The intersection of rail systems at three points in the central urban core created opportunities for pedestrian zones, while park-and-ride terminals were planned at city metro termini on the outskirts to reduce pressure from private vehicles on the inner central city zone [4]. In amendments and supplements to this plan until 2000, it was noted that many goals related to transportation set since 1972 had not been realized. Due to the city's different spatial development, it was necessary to reassess and align the planned metro system with the physical changes that had occurred. The BETRAS Study, which accompanied the General Plan 1985–2000 (1985), introduced the term *premetro* in 1989, with the idea that other transport systems would operate on routes planned for the metro until conditions allowed for metro activation [7].

The Strategy for Public Transport Development in Belgrade (1993), part of a broader plan titled Transport Systems of Belgrade – Part II, proposed that the capacity rail system in public transport be principally addressed through the construction of a light metro integrated into other public transport subsystems [8]. The General Plan of Belgrade 2021 (2003) suggested revitalization and rehabilitation of existing public transport forms and gradual introduction of a modern urban rail system such as Light Rail Transit, alongside planned city (and suburban) railways and trams [9]. After adopting the General Plan 2021, numerous activities were undertaken to evaluate necessary transport parameters and to develop detailed planning and project documentation for the light rail system. Simultaneously, experts from other European cities were consulted to form an expert opinion on the metro concept suitable for Belgrade. In mid-2010, the City Assembly adopted the document Belgrade Metro – Basis for Solution Selection. The French consulting company EGIS was commissioned to develop a General Concept and define the metro system in Belgrade, which would serve as a basis for network development.

The most recent overarching planning document, the General Plan of Belgrade until 2041 (currently in early public review since June 2022), is the first plan developed with digital tools. Although its methodology is based on integrated urban development, coordinating spatial, economic, social, and ecological dimensions, the plan's text does not explicitly address underground urbanism. However, it does mention ICT, the Smart City concept, digital twins, and other modern terminology. [10]

The fact that a term is not explicitly defined in the Planning and Construction Act glossary does not mean it cannot be addressed within urban planning documents. When a term is included in the legal glossary, it gains an official, legally binding definition that ensures consistent interpretation across planning stages. However, even in the current 2023 Planning and Construction Act glossary, metro is mentioned as one of the linear infrastructure objects under underground urbanism [11]. More detailed provisions in the Metro and Urban Railway Act (2021) specify concepts linking aboveground and underground segments, such as protective zones of 25m on each side

of the track, 5m below the route, and vertically from the structure to the land surface; infrastructure zones of 5m beside aboveground and 4m from underground metro parts; and that stairs, escalators, halls, platforms, and underpasses represent rare points of integration between aboveground and underground spaces [12].

As this overview has shown, the general characteristics and development of Belgrade's planning documentation have been oriented towards solving current problems while neglecting the city's potential and possible development. Each higher-level planning document had to integrate errors from the city's past development. Specific planning of underground urban spaces is most often associated with transport infrastructure, metro or pedestrian traffic, and sometimes managing stationary traffic beneath larger public areas. In some document sections, planning documentation tends to be closer to analog than digital processing, often lacking topographic bases. According to the Rulebook on Content, Methods, and Procedures for Preparing Spatial and Urban Planning Documents (2019), topography is obtained as needed, although it is a primary element for setting the city's vertical regulation [13].

Overall, Belgrade has evolved from a city with pronounced development potential after the first serious planning document in 1950 – a time when urbanization had not reached a critical threshold – into an urban environment significantly compromised by inconsistent and reactive urban planning approaches. Despite initial ideas and studies, underground Belgrade remains an unexplored urban dimension, with underground transport as a technical challenge and strategic component of sustainable urban mobility that has not achieved functional integration into the broader urban system. This situation points to complex institutional, economic, technical, and spatial barriers and a lack of long-term strategic planning incorporating smart city principles.

Under actual planning conditions, it is almost impossible to fully foresee all potential challenges related to underground space planning. Considering that underground space is a non-renewable resource whose structure cannot be easily altered after construction, it is necessary to highlight Belgrade's potential through objective mapping of its underground space. Additionally, to identify possible management and planning approaches based on good international practices, particular attention will be given to integrated planning emphasizing coordination between underground and aboveground urbanism, as well as an ICT model that could enhance planning processes and urban functionality.

### 3.2. Objective Evaluation of Belgrade's Development Potential

To demonstrate that Belgrade's underground space represents a complex and multilayered segment of the urban fabric requiring thoughtful institutional management and long-term strategic planning, we chose to apply a SWOT analysis as a brainstorming method. We consider SWOT analysis particularly effective in the early stages of strategic reflection, research, and planning, as it enables a systematic examination of internal strengths and weaknesses, as well as external opportunities and threats relevant to the integrated management of underground space.

*Table 1. Strengths*

Strengths	Explanation / Example
Historical and cultural potential	The use of historical underground structures (Roman Well, catacombs, lagums) enables the preservation of Belgrade's cultural identity and the development of unique tourist offers, increasing its international visibility and economic utilization of the space.
Geological suitability	Favorable geological soil structure allows stable construction of underground infrastructure with lower construction costs.
Academic and research support	Laboratories at the Faculty of Mining and Geology and Faculty of Civil engineering, as well as 3D GIS research, support the development and testing of solutions, strengthening the scientific foundation.
Infrastructure potential – transport	Metro, underground garages, tunnels, and pedestrian corridors contribute to reducing traffic congestion, lowering harmful gas emissions, and freeing public spaces for recreation.
Infrastructure potential – energy and logistics	Underground heating plants, storage facilities, and delivery tunnels enable energy efficiency and improve the functionality of the city's network.

**Table 2. Weaknesses**

<b>Weaknesses</b>	<b>Explanation / Example</b>
Regulatory gap	The current Law on Planning and Construction does not recognize the concept of subsurface zoning; the legal status of underground volumes is not clearly defined.
Loss of ecological function of green areas	Installation of underground concrete structures beneath grassy zones reduces soil permeability and degrades the ecosystem of green spaces [14].
Neglected underground structures	Unmaintained and abandoned underground facilities pose safety, sanitary, and aesthetic issues.
High investment costs	Construction of underground infrastructure is on average 3 to 5 times more expensive than above-ground construction [15]
Lack of three-dimensional spatial data	Absence of integrated 3D GIS causes conflicts between existing installations and leads to inefficient planning.

**Table 3. Opportunities**

<b>Opportunities</b>	<b>Explanation / Example</b>
Application of digital twins and 3D GIS technology	Creating integrated three-dimensional underground models allows precise planning, minimizes errors, and enables efficient infrastructure management.
Revitalization of existing underground shelters	Repurposing unused underground spaces into cultural or IT centers can contribute to urban regeneration and content diversification [16]
Utilization of EU funds for sustainable energy	Significant opportunities exist for financing through EU funds, especially for green technologies such as geothermal pumps, energy efficiency, and innovative infrastructure.
Complementarity of underground functions	Data centers, residential spaces, and energy infrastructure can operate synergistically—for example, waste heat from data centers can be used for district heating, sharing installations and optimizing costs.
Application of digital twins and 3D GIS technology	Creating integrated three-dimensional underground models allows precise planning, minimizes errors, and enables efficient infrastructure management.

**Table 4. Threats**

<b>Threats</b>	<b>Explanation / Example</b>
Seismic and hydrogeological risks	High groundwater levels, porous soil, and seismic activity require complex and costly waterproofing and soil stabilization measures.
Uncontrolled construction and urbanization	Unplanned settlements that are later legalized by remediation plans complicate urban planning and slow down the implementation of new planning documentation.
Risk of destruction of cultural-historical layers	Soil vibrations, inadequate archaeological protection, and unregistered sites threaten the preservation of archaeological and historical heritage during underground works.

Negative impacts on end users of space	Factors such as noise, presence of microparticles, increased humidity, and feelings of claustrophobia can negatively affect acceptance and use of underground spaces.
Economic and political instability	Extended timelines, changes in public budget priorities, and unpredictable costs can jeopardize the realization of capital investments in underground infrastructure.

### 3.3. International Practices: Lessons from Helsinki and Singapore

Cities like Helsinki and Singapore were purposefully selected as reference examples in this study because they differ in institutional and planning approaches, each offering valuable insights for defining development directions in the context of Belgrade.

#### 3.3.1. Helsinki

The city of Helsinki represents one of the most advanced examples of macro-level underground space planning in contemporary urbanism. As early as 1986, Helsinki developed the first plan for the allocation of underground space at the city-wide level, which included spatial mapping of underground layers and vertical usage zones [17]. The first General Plan for underground space was adopted in 2010, and since 2017 a revision has been underway, which was adopted in 2021 [18]. This plan holds the legal status of a planning document, making it binding for implementation [19]. Underground spaces are not considered in isolation but are mandatorily integrated into the General Urban Plan and detailed plans. In this regard, vertical integration of aboveground and underground spaces is legally required. The plan specifies reserved areas and coordination relations for key underground transport and utility infrastructure, as well as proposed zones for constructing underground public service facilities and pedestrian systems. Numerous positive effects of urban underground space usage were taken into account, such as contributing to an ecologically sustainable and aesthetically acceptable landscape, expected longevity of constructions, and preservation of potential for urban development for future generations. This attests to the application of sustainable and human-centered development concepts [20]. Among the planning tools for underground space management in Helsinki are:

- **Categorization of underground zones by depth and purpose.** Helsinki plans the underground space in three dimensions, separating functions by vertical layers. Shallower layers are intended for metro and pedestrian zones; middle layers for garages, storage, commercial facilities, while deeper layers are reserved for energy and technical infrastructure.
- **3D Digital Models.** Advanced 3D Geographic Information System (GIS) is used for mapping, linking existing and planned objects, geological conditions, infrastructure, ownership, and usage rights. These models enable simulation of functional conflicts and better strategic decision-making. For example, around 400 functional underground objects are recorded in the plan, while more than 600 locations are designated for future development [21] – from public pools and sports-recreational facilities to data centers. At the same time, the energy aspect is considered: stable underground temperatures enable more efficient cooling of server equipment, while surplus heat will be used for heating residential buildings [16].
- **Centralized Underground Database** integrates data on existing tunnels and underground facilities, permits, usage rights, infrastructure networks, and hazard zones (e.g., groundwater). It is available to investors and designers, speeding up permits and reducing spatial conflicts.
- **Participatory planning and transparency.** Helsinki employs open platforms and digital tools (such as Map Service and Helsinki 3D+) to provide citizens, experts, and decision-makers insight into projects, opportunities for commenting, and better understanding of spatial consequences of underground interventions.

#### 3.3.2. Singapore

Unlike Helsinki, Singapore does not have a separate underground space planning system; instead, it integrates underground planning within its existing two-tier urban planning framework – the legally binding Concept Plan and the non-binding Special and Detailed Control Plans, which serve as guidelines. These plans set long-term strategic directions for the use and development of the entire underground space. Key planning tools for underground space management in Singapore include:

- **Zoning of Underground Areas.** Specific zones for underground development are not explicitly defined. However, an analysis of Singapore’s Master Plan reveals that areas such as Marina Bay, Punggol Digital District, and Jurong Innovation District undergo detailed three-dimensional underground space planning [22,23], which emphasizes the interdependence of layers and functions.
- **Geotechnical 3D Models.** Singapore’s 3D planning primarily focuses on geotechnical aspects and stratification, producing a 3D geological model based on extensive borehole data, enabling efficient planning of urban underground functions.
- **Participatory Planning and Transparency.** Participation efforts in Singapore are more investor-focused. For example, the Urban Redevelopment Authority (URA) developed a Pedestrian Network Strategy aimed at reducing surface congestion. The strategy proposes a 29 km network of underground pedestrian corridors to improve access to central urban zones. Private investors can compete for URA grants to construct underground passages at 20 designated locations. These spaces are exempt from the standard gross floor area limits, incentivizing their implementation. [24].

#### 4. DISCUSSION

Both examples demonstrate a stable legal framework governing the relevant issues: in Singapore, this is the Planning Act [25], while in Finland it is the Maankäyttö- ja rakennuslaki [26]. These laws provide a legal basis that is long-term aligned with the needs of urban development and planning policies. In 2015, Singapore adapted two laws to the requirements of underground urbanism: the State Lands Act, which specifies the depth to which land parcel owners hold property rights – below which the underground space belongs to the state [27] – and the Land Acquisition Act, which enables expropriation of specific underground layers [28].

Serbia, on the other hand, during the same period, underwent multiple amendments to its legal framework, completely changing approaches, terminology, and by-laws. The latest Law on Planning and Construction (2009) has undergone 15 amendments so far, indicating instability and inconsistency in the legal status of spatial and urban planning, or even legislative adjustments influenced by individual interests [29]. A stable and clearly defined legal framework, like those in Singapore and Finland, highlights the importance of the legal system keeping pace with development needs and ensuring predictability and consistency in implementation – an absolute prerequisite for successful urban planning and project execution.

*Table 1. Comparative Overview of Underground Space Governance in Helsinki and Singapore*

Element	Helsinki (Finland)	Singapore
<b>Legal Framework</b>	Land Use and Building Act (1999)	Planning Act (1998); Land Acquisition Act (2015); State Lands Act (2015)
<b>Underground Planning</b>	Underground Master Plan adopted in 2010	Underground development integrated within the overall Master Plan (2019), with concept projections up to 2025
<b>Planning Governance</b>	Collaborative approach involving local and national authorities	Centralized governance under the URA, which oversees planning and implementation
<b>Digital Technology Use</b>	Utilizes 3D modeling and Building Information Modeling (BIM), though not fully integrated into a digital twin	Employs a comprehensive digital twin platform known as Virtual Singapore
<b>Underground Space Usage</b>	Primarily allocated for public infrastructure and community functions	Emphasizes maximizing spatial utilization for a variety of functions
<b>Geological Conditions</b>	Predominantly hard granite bedrock conducive to tunnel construction	Complex mixed soil conditions necessitating advanced geotechnical solutions
<b>Public Participation</b>	Extensive citizen involvement through public consultations, participatory platforms, and urban models	Limited public participation; primarily administrative-led planning with public feedback during master plan development



<b>Role of Underground Space</b>	Focuses on sustainable urban expansion and preservation of public spaces; views underground as a public asset	Addresses urban density challenges and surface space optimization, positioning underground space as a valuable resource
<b>Strategic Orientation</b>	Emphasizes public needs with strong linkages to participatory planning processes	Prioritizes economic development and efficient space use under expert-led centralized management

#### 4.1. Recommendations for Belgrade

The experiences of cities such as Helsinki and Singapore underscore the critical role of institutional coordination, digital infrastructure, comprehensive planning, and legislative frameworks in the development of underground spaces. Belgrade has the opportunity to draw lessons from these examples and create its own model of underground urbanism tailored to local conditions while aligning with global trends. Based on the conducted analyses, the paper recommends several key guidelines for Belgrade:

##### 1. Legal Framework

A new law should be enacted that explicitly defines the legal status of underground space, including usage rights and permits for underground structures, ownership rights in the vertical axis, and the methods for integration into all levels of planning documentation. It is essential to ensure a stable legal and regulatory framework without frequent amendments that destabilize the professional system. Additionally, the establishment of a permanent expert group or institutional system encompassing urban planning, geology, energy, transportation, and communal infrastructure... is recommended to address underground urbanism comprehensively, where the Belgrade metro and rail systems would be one branch within this broader framework.

##### 2. Planning Framework

Belgrade should introduce a strategic framework for underground urbanism, either through a dedicated document following the Helsinki model or via integration into the existing planning system in the manner of Singapore, with mandatory vertical coordination of planning documents. Furthermore, underground space should be explicitly incorporated as a distinct domain within the General Urban Plan of Belgrade 2041, which is currently in draft form. Presently, underground urbanism is not explicitly singled out but is only partially addressed through sections dealing with communal and transport infrastructure.

##### 3. Digitalization and Geographic Information Systems (GIS)

A digital foundation for underground space planning must be established, utilizing a 3D GIS model and a centralized database accessible to all relevant stakeholders. The planning approach should be modernized and aligned with contemporary ICT tools. For example, Helsinki employs a 3D GIS system incorporating data on geology, ownership, and infrastructure, while Singapore utilizes detailed geological models and runs the Digital Underground project, enabling interoperability of data and integration with BIM/GIS standards. Singapore leads in the integration of 3D digital models encompassing all planning layers, including underground space, effectively implementing digital twins.

##### 4. Categorization and Zoning of Underground Space

A zoning system should be developed that combines functional use and depth stratification with predetermined priorities for underground space development.

##### 5. Public Participation and Education

Belgrade requires public digital platforms, educational workshops, and spontaneous information dissemination systems, grounded in the principle that public interest should prevail over individual interests. A combined approach inspired by Helsinki and Singapore could be adopted. Helsinki utilizes digital platforms such as Helsinki 3D+ and Map Service for citizen participation, while Singapore engages the public through consultations during the amendment phases of the Master Plan.

##### 6. Energy Efficiency and Sustainable Use

Planning of underground structures in Belgrade should incorporate options for passive heating and cooling, as well as integration with renewable energy sources, following Helsinki's example of sustainable underground development.

## 5. CONCLUSION

Beograd is at a stage where it can proactively define a model for managing underground space. The experiences of Helsinki and Singapore highlight the importance of a stable institutional framework, digitized infrastructure data, integrated and multi-layered planning, cooperation among all institutions and sectors, and the application of sustainable technological solutions.

Based on all of the above, Belgrade is closer to the Singapore model, as it enables gradual but firmly institutionalized integration of underground space into the existing planning system. A key advantage of the Singaporean approach lies in the consistent application of a hierarchical planning system, strong legislation, and thorough technical-geological grounding. In this light, Belgrade needs to restore the principle of continuity in planning that existed within the Belgrade General Plan 2021, which ceased to be valid upon the adoption of the General Urban Plan 2021. Restoring this type of planning continuity, together with digitalization, interdisciplinarity, and transparent participation, is a fundamental prerequisite for responsible and sustainable development of underground Belgrade.

## 6. BIBLIOGRAPHY

- [1] Joliquen, T., Parriaux, A., Thalmann, P., & Tacher, A. (2007). 3-D cadastre for underground resources: A GIS-based decision tool. In *Proceedings of the 11th FIG International Conference*, Hong Kong.
- [2] Peng, F.-L., Qiao, Y.-K., Sabri, S., Atazadeh, B., & Rajabifard, A. (2021). A collaborative approach for urban underground space development toward sustainable development goals: Critical dimensions and future directions. *Frontiers of Structural and Civil Engineering*, 15(1), 20–45. <https://doi.org/10.1007/s11709-021-0716-x>
- [3] Grad Beograd. (1950). *Generalni urbanistički plan Beograda 1950–1970* [General Urban Plan of Belgrade 1950–1970]. Urbanistički zavod Beograda.
- [4] Predrag Krstić. (2019). Analiza razvoja šinskih sistema u Beogradu [Analysis of the development of rail systems in Belgrade]. *Urbanizam Beograda*, 01/02.
- [5] Grad Beograd. (1972). *Generalni urbanistički plan Beograda 1972–2000* [General Urban Plan of Belgrade 1972–2000]. Urbanistički zavod Beograda.
- [6] Stojanović, B. (1969). Novi aspekti u savremenom urbanističkom planiranju [New Aspects in Contemporary Urban Planning]. *Pogledi i mišljenja*, 1(4), 52–62.
- [7] Grad Beograd. (1985). *Izmene i dopune Generalnog urbanističkog plana Beograda 1972–2000* [Amendments and Supplements to the General Urban Plan of Belgrade 1972–2000]. Urbanistički zavod Beograda.
- [8] Skupština grada Beograda & Srpska akademija nauka i umetnosti. (1993). *Transportni sistemi Beograda – II deo: Strategija razvoja javnog saobraćaja - Laki metro* [Transport systems of Belgrade – Part II: Public transport development strategy – Light metro]. Beograd.
- [9] Grad Beograd. (2003). *Generalni urbanistički plan Beograda do 2021* [General Urban Plan of Belgrade until 2021]. Urbanistički zavod Beograda.
- [10] Grad Beograd. (2023). *Generalni urbanistički plan Beograda do 2041* [General Urban Plan of Belgrade until 2041]. Urbanistički zavod Beograda.
- [11] Skupština Republike Srbije. (2023). *Zakon o izmenama i dopunama Zakona o planiranju i izgradnji* [Law on Amendments and Supplements to the Law on Planning and Construction]. „Službeni glasnik RS“, br. 62/2023.
- [12] Skupština Republike Srbije. (2021). *Zakon o metrou i gradskoj železnici* [Law on the Metro and Urban Railway]. „Službeni glasnik RS“, br. 52/2021.
- [13] Ministarstvo građevinarstva, saobraćaja i infrastrukture Republike Srbije. (2019). *Pravilnik o sadržini, načinu i postupku izrade dokumenata prostornog i urbanističkog planiranja* [Rulebook on the Content, Manner, and Procedure for Drafting Spatial and Urban Planning Documents]. „Službeni glasnik RS“, br. 32/2019.
- [14] Simić, I. (2025). Uticaj podzemnih garaža na gradske zelene površine. *Ecologica Serbica*, 29(1), 13–24.
- [15] Vanhatali, J., & Kallioluoma, M. (2018). Economic evaluation of underground infrastructure projects: Case studies in urban areas. *Tunnelling and Underground Space Technology*, 72, 111–121. <https://doi.org/10.1016/j.tust.2017.12.015>
- [16] Vähäaho, I. (2014). *Urban underground space – Sustainable property development in Helsinki*. City of Helsinki.
- [17] Narvi, S., Vihavainen, U., Korpi, J., et al. (1994). Legal, administrative and planning issues for subsurface development in Helsinki. *Tunnelling and Underground Space Technology*, 9(3), 379–384. [https://doi.org/10.1016/0886-7798\(94\)90035-3](https://doi.org/10.1016/0886-7798(94)90035-3)
- [18] Vahaaho, I. (2016). An introduction to the development for urban underground space in Helsinki. *Tunnelling and Underground Space Technology*, 55, 324–328. <https://doi.org/10.1016/j.tust.2015.09.005>
- [19] City of Helsinki. (2009). *The Helsinki underground master plan: A city growing inside bedrock*. [https://www.appropedia.org/w/images/7/79/Helsinki\\_underground\\_master\\_plan.pdf](https://www.appropedia.org/w/images/7/79/Helsinki_underground_master_plan.pdf)
- [20] Vahaaho, I. (2013). 0-Land\_U Se: underground resources and master plan in Helsinki. In *Advances in Underground Space Development* (pp. 29–42). Society for Rock Mechanics and Engineering Geology.
- [21] Bobylev, N., & Sterling, R. (2017). Underground master planning in Helsinki: Lessons for sustainable urban development. In R. Sterling (Ed.), *Guidelines for the planning and development of underground space* (pp. 45–58). Louisiana Tech University, Underground Space Center.

- [22] Urban Redevelopment Authority. (n.d.-b). *Urban Redevelopment Authority*. Retrieved June 1, 2025, from <https://www.ura.gov.sg/Corporate>
- [23] Urban Redevelopment Authority. (n.d.-a). *Master Plan*. Retrieved April 15, 2025, from <https://www.ura.gov.sg/Corporate/Planning/Master-Plan>
- [24] Urban Redevelopment Authority. (2021). *Urban design guidelines for downtown core planning area (Appendix 4: underground pedestrian network & activity generating use plan)*. <https://www.ura.gov.sg/Corporate/Guidelines/Urban-Design/Downtown-Core>
- [25] Singapore Government. (1998). *Planning Act 1998*. Singapore Statutes Online. <https://sso.agc.gov.sg/Act/PA1998>
- [26] Ministry of the Environment. (1999). *Land Use and Building Act, 132/1999*. Finlex. <https://www.finlex.fi/en/laki/kaannokset/1999/en19990132.pdf>
- [27] Singapore Government. (2015b). *State Lands (Amendment) Act 2015*. Singapore Statutes Online. <https://sso.agc.gov.sg/Acts-Supp/11-2015/Published/20150508?DocDate=20150508>
- [28] Singapore Government. (2015a). *Land Acquisition (Amendment) Act 2015*. Singapore Statutes Online. <https://sso.agc.gov.sg/Acts-Supp/12-2015/Published/20150508?DocDate=20150508>
- [29] Skupština Republike Srbije. (2009). Zakon o planiranju i izgradnji [Law on Planning and Construction]. Službeni glasnik Republike Srbije, br. 72/2009.

## SENSITIVE INTEGRATION OF UNDERGROUND SPACES IN HELSINKI'S URBAN FABRIC: FROM GEOLOGY TO ARCHITECTURE

Laure Bertrand<sup>1</sup>, Cyrielle Rozé<sup>2</sup>

**Abstract:** The increasingly prevalent development of planning underground urban spaces and their application in urban environments raises new questions related to the design of underground structures. Specifically, the challenges in designing underground structures within the geological space and the emergence of new imaginary representations in the world of architecture necessitate a reevaluation of the role of the underground architect in the future and the further advancement of urban environments. This paper explores new approaches to urban design that would help address the current ecological and sociological challenges faced by today's urban environments. As a model, existing underground spaces in Helsinki (Finland) were studied, focusing on how, through architectural and sensory perception, these spaces can evolve into eco-socially acceptable areas, overcoming the current limitations posed by established practices, regulations, and standards. The methodological approach is based on a dialogue between multiple scientific fields: architecture, urbanism, cognitive sciences, geology, and engineering. The aim of the research is to develop specific methodological tools for future underground architects, which would enable a better understanding of underground urban spaces, their sensitivity in pushing the boundaries of design, and their integration into existing urban environments. In addition to revealing that the role of the architect in a highly technical-technological environment is complex, the paper also demonstrates a structural gradation from the geological dimension to architectural space, through human perception, to the graphic and sensory representation of underground structures, thereby illustrating the specific methods used in the study of selected underground spaces. As a result, guidelines and recommendations emerge, intended for project managers seeking tools to mobilize new skills in the field of underground space/structure design. Therefore, this paper should not be interpreted as a list of reproducible solutions for every territory but rather as a sharing of research tools and methodologies applicable in professional practice.

**Keywords:** Eco-social Resilience - Helsinki - Spatial Materiality - Sensory Perception - Underground Architecture

### 1. INTRODUCTION

This study is part of our final-year project at architecture school. It stems from a personal and professional inquiry developed over the years: the role of the underground in the making of the contemporary city. Too often reduced to an abstract line on a plan or confined to purely technical use, the urban ground appeared to us as the hidden side of the city, full of architectural, urban, and sensory potential that remains largely untapped. From this arose a central reflection: how can we recover the memory of these invisible spaces? How can we reveal their sensory and imaginative dimensions?

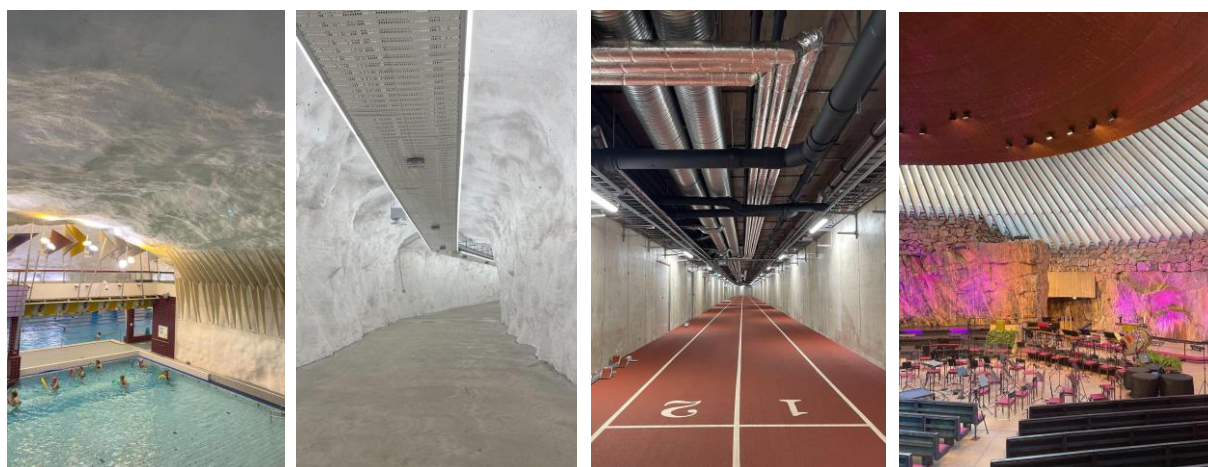
The city of Helsinki emerged as an ideal case study. Known for its exemplary underground planning policy, its favorable granite geology, and a network of underground spaces carefully integrated into urban planning, Helsinki

---

<sup>1</sup> Architect, Bertrand Laure, Urbanism student, École Nationale Supérieure d'Architecture de Lyon, 3 Rue Maurice Audin, 69120 Vaulx-en-Velin, France, laurebetrand2000@hotmail.fr

<sup>2</sup> Architect, Rozé Cyrielle, Civil Engineering student, École Nationale Supérieure d'Architecture de Lyon, 3 Rue Maurice Audin, 69120 Vaulx-en-Velin, France, roze.cyrielle@gmail.com

represents a model still largely unknown to the general public. These spatial configurations—sometimes monumental, often invisible, deeply resonated with us (see Figure 1)



*Set of photographs of the underground spaces in Helsinki, taken during the survey in November 2023.*

As future architects, we felt the need to explore a new way of thinking about the city, one that complements the approaches taught in traditional academic curricula. An approach that addresses environmental, social, and technical challenges while also enhancing the sensory richness of architectural experience. The central question guiding our work is: **In a context of urban densification, environmental crises, and increasing demands for sustainable infrastructure, how can a redefinition of the architect's role contribute to enriching urban underground environments?**

Our approach is based on two complementary axes. The first involves developing specific methodological tools to understand underground spaces, their dynamics and their potential for integration within the city. The second aims to translate these tools into concrete architectural proposals that embody the spatial, constructive, and sensory qualities of the subterranean realm. These experiments were carried out at multiple scales, from urban readings to architectural details, and led us to challenge certain traditional graphic representation methods. Indeed, how can we represent and convey the experience of inherently invisible spaces? What kind of narrative can we develop to legitimize their inclusion in the contemporary urban story?

Our project presents a series of architectural fragments designed as interfaces between the surface and the underground, revealing the richness of Helsinki's subterranean landscape. It is both a critical investigation, questioning the conventional functions of the underground (technical, logistical, hidden), and a sensitive proposal aimed at renewing urban imaginaries. By moving beyond purely technical considerations, we strive to adopt a holistic approach to underground architecture, interweaving geological knowledge, spatial design, and human perception. This exploration highlights the impact of underground materiality on the senses, on usage, and on memory with the goal of designing spaces that are sustainable, sensorially rich, and meaningful. This study is intended for anyone interested in the urban invisible: architects, urban planners, engineers, artists, geologists, or simply the curious. It aims to reinvent our relationship with the ground and to open the way for a new way of imagining and designing the city, one that is conceived simultaneously above and below ground, in response to the challenges of tomorrow.

## **2. MATERIAL AND METHODS: HOW TO GRASP THE INVISIBLE SPACE FROM A METHODOLOGICAL PERSPECTIVE?**

To carry out this research project, we established a structured methodological framework divided into several chronological phases, with the goal of designing architectural proposals presented in the third part of this work. This methodology is organized around three key stages: before our stay in Helsinki (preparation and research), during our time on site in November 2023 (fieldwork, surveys, documentation), and after, through a cartographic production informed by our observations. Our approach thus lies at the intersection of three complementary modes of inquiry: theoretical research (state of the art), action-based research (in situ exploration tools), and research through creation (by translating our analysis into design proposals).



## 2.1. Theoretical Contribution on the Underground: Conceptualization and State of the Art

Initially, we relied on a theoretical framework to familiarize ourselves with certain concepts related to the underground and to conduct a state-of-the-art review of writings on the underground spaces of Helsinki before proceeding with our fieldwork.

The term “urban mangroves”, borrowed from architect David Mangin<sup>3</sup>, is used to describe the dense and branching underground networks of large cities, resembling the roots of a mangrove. It highlights the interplay between transport hubs, destinations, and interfaces in excavated spaces. These spaces, though underground, are highly valued for their commercial profitability and their ability to facilitate urban mobility. However, this raises the question of whether these spaces can accommodate uses beyond commerce. According to Deleuze et Guattari<sup>4</sup>, the root represents a centralized, hierarchical system. In contrast, the rhizome embodies a horizontal, decentralized structure that is in constant expansion. When applied to underground urban networks, it reveals a multitude of connections between independent cores. Unlike the mangrove, the rhizome provides a relevant theoretical framework for thinking about the complex organization of the underground.

Additionally, we drew upon four underground projects that illustrate different contemporary uses of the underground, revealing both its potential and its limitations. The Earthscraper in Mexico city<sup>5</sup> demonstrates that excavation allows for densification without affecting heritage, but it raises social, regulatory, and acceptability issues related to underground living. Data centers and logistical tunnels<sup>6</sup> reveal a strategic use tied to technology, but raise concerns about surveillance, data security, profitability, and energy sustainability. Underground farms<sup>7</sup> respond to the scarcity of urban agricultural land but raise questions about artificiality, energy consumption, and ecological viability. These cases raise a central question: how far can we legitimately dig, and under what conditions?

To frame our approach, we also integrated theoretical references on the concept of the underground, particularly through the idea of the Critical Zone. This concept, developed by researchers such as Bruno Latour, refers to a thin layer of the Earth where rocks, water, life, and humans interact.<sup>8</sup> It allowed us to reposition the underground as a living, dynamic space, constantly interacting with its environment. In parallel, we drew upon the work of architects, artists, and writers on the sensory perceptions of architecture. These references guided our attention toward the materiality of the ground, the atmospheres, and the perceptible clues within underground spaces. As architect Bruno Barroca notes, “The quality of these thick or interior spaces, mostly invisible from the outside, is primarily assessed through the experience of the body in motion, the factors of ambiance (light, heat, sound, smell...), and the clarity of their organization”<sup>9</sup>.

## 2.2. Surveying the City of Helsinki: Between Sensory Mapping and Exchanges

In November 2023, we spent around ten days in Helsinki to conduct an in-depth field survey and further develop our methodological approach. This immersion allowed us to confront our initial hypotheses with on-the-ground realities through meetings with specialists in architecture, urban planning, engineering, and geology. We also employed various observation tools, such as photography during visits to underground spaces, sound recordings to capture the atmosphere of these places, and short street interviews aimed at gathering perceptions, subjective representations, and imaginaries held by Helsinki’s residents regarding the presence of the underground in their city.

---

<sup>3</sup> Mangin, D. & Girodo, M. (2016). *Mangroves urbaines : du métro à la ville* (Paris, Montréal, Singapour), Paris : La Découverte (collection Dominique Carré).

<sup>4</sup> Krtolica, I. (2021). Le rhizome deleuzo-guattarien « Entre » philosophie, science, histoire et anthropologie. *Rue Descartes*, 99, 39-51. <https://doi.org/10.3917/rdes.099.0039>

<sup>5</sup> Tahmasebinia, F., Yu, K., Bao, J., Chammoun, G., Chang, E., Sepasgozar, S., & Alonso Marroquin, F. (2020). *Earthscraper: A Smart Solution for Developing Future Underground Cities*. *IntechOpen*. doi: 10.5772/intechopen.87217

<sup>6</sup> Beqiri, J. (2021). The implications of technological progress in architectural thinking: The future impossibility for an architecture of hiding. *IOP Conf. Series: Earth and Environmental Science* 703 012001, doi:10.1088/1755-1315/703/1/012001

<sup>7</sup> Labbé, M. (2016). *Architecture of underground spaces: From isolated innovations to connected urbanism*. *Tunnelling and Underground Space Technology*.

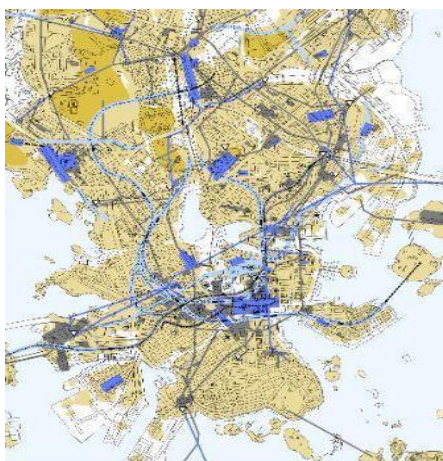
<sup>8</sup> Gaillardet, J., & Boudia, S. (2021). La Zone critique : Vers de nouvelles pratiques scientifiques pour réduire les ignorances dans l’anthropocène. *Revue d’anthropologie des connaissances*, 15(4). <https://journals.openedition.org/rac/25340>

<sup>9</sup> Barroca, B. (2019). Espaces souterrains et synergies spatiales. *Communications*, 105(2), 195–205.

### 2.3. Cartographic Methodology Post-Surveying

Following our field survey, various site recordings, and the documents available to us online, we developed a cartographic analysis method structured around three key aspects: first, underground urban planning, including an understanding of the existing masterplan; second, an analysis of the underground landscape in relation to the geological characteristics of the ground; and finally, a study of the in-between spaces that connect the surface and the underground.

#### 1. Analysis of Underground Urbanism: Overall Concept of Development and Planning of Underground Space in Helsinki



*Master plan of Helsinki's underground spaces, created by the City of Helsinki's Urban Planning Department and approved in December 2010.*

In Helsinki, the planning of underground spaces is governed by a masterplan developed as early as the 2000s, based on a long-term strategic management approach. This guiding plan, which is regularly updated, coordinates current and future uses of the underground in relation to the surface urban fabric. It identifies available bedrock resources, allocates land reserves, and defines planning criteria such as soil quality, accessibility, and potential uses. More than 200 kilometers of tunnels and 400 underground facilities have already been documented.<sup>10</sup>

Based on this masterplan, the method of depth-layer decomposition helped clarify the vertical organization of underground spaces in Helsinki, which is often difficult to interpret in traditional plans. Each stratum serves specific functions: the levels closest to the surface (K1 to K2, up to -5 meters) accommodate cellars, shops, and parking facilities, while intermediate levels (down to -30 meters) house the metro and deeper parking structures. The lower layers (down to -70 meters) are reserved for road tunnels, military, and technical infrastructures. This stratification reveals a lack of direct interconnection between levels, with the few existing links being of a military nature.



*Excerpts of plans showing different depth layers of underground spaces in central Helsinki (1: between -10 and -20m; 2: between -30 and -40m; and 3: between -40 and -70m), personal work, 2024.*

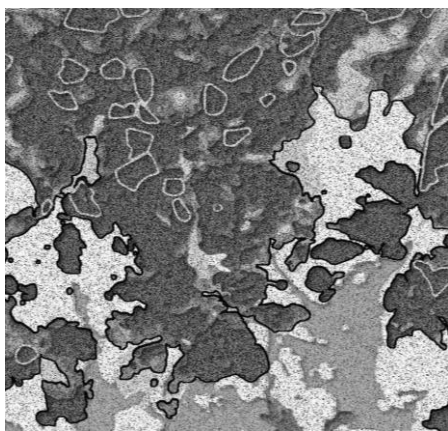
#### 2. The Underground Landscape of Helsinki: Geological Foundation and Architectural Potential

The underground landscape of Helsinki reveals its complexity and geological history through its visible rock stratifications on the map (Figure 5). The predominant presence of plutonic rock, particularly granite, is shown in orange. The geotechnical properties of Helsinki's soil are bimodal, consisting of soft clay and hard bedrock. One-third of the ground is made up of clay with an average thickness of 3 meters. The average depth of the bedrock substrate is 7 meters, but it varies from 0 to 70 meters.<sup>11</sup> This hard and relatively shallow bedrock is ideal for excavation by blasting, requiring minimal support and providing a stable foundation for construction.

<sup>10</sup> Vähäaho, I. (2018). Urban Underground Space - Sustainable Property Development in Helsinki. City of Helsinki, Urban Environment Publications. ISBN 978-952-331-436-8

<sup>11</sup> Ikävalko, O., Satola, I., & Hoivanen, R. (2016). Helsinki TU1206 COST Sub-Urban WG1 Report (22 p.).

The city has strategically reserved vast rocky areas for future developments, recognizing their potential. These favorable geological characteristics, combined with the harshness of the winter climate, have been the main drivers behind the development of this unique underground dimension in Helsinki.



*Map of the bedrock depth  
and designated rocky zones in Helsinki,  
personal photograph, 2024.*



*Guide map of Helsinki's underground spaces overlaid  
on the rock strata, personal work, 2024.*

### **3. Survey of Interfaces Between the Underground World and the Aboveground World**

The survey of interfaces served as a methodological tool to analyze the relationship between underground spaces and the surface. By identifying and mapping visible surface clues, such as staircases, elevators, ventilation shafts, light wells, military doors, and more, we were able to decipher the hidden morphology of buried infrastructures. This work relied on a detailed reading of the urban landscape, combined with an overlay of underground and aerial plans to locate and classify the interfaces into eight major typologies, which we will analyze later.

This survey made the invisible visible, helped us understand the flows (air, light, matter) between the two levels, and questioned their complementarity. It reveals the necessity to conceive surface and underground spaces jointly, within a logic of integrated synergy.

### **3. RESULTS: CONCLUSIONS DRAWN FROM THE METHODOLOGICAL TOOLS**

Returning to the central question concerning the architect's role in designing underground spaces and their use of the methodological tools employed, we now present the conclusions drawn from these analyses. These results shed light on new perspectives for integrating the underground into urban projects, taking into account its spatial, technical, and sensory specificities.

#### **3.1. A “peri-urban” underground space**

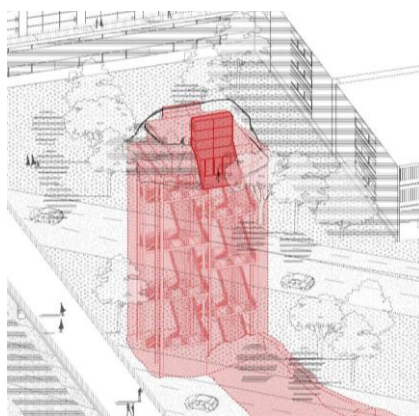
The hypothesis of an underground city in Helsinki is actually invalidated by the way the subsurface is used. It does not form an integrated urban network but acts as a dependent and subordinate space. Like the suburban belt, the underground surrounds the city and serves it, but does not function autonomously. It mainly hosts technical or service functions, similar to those historically relegated to the urban outskirts. This functional and symbolic marginality reinforces its status as a “suburb of the above-ground,” according to Monique Labbé<sup>12</sup>. The underground becomes a receptacle for what the surface rejects, despite strategic planning. This raises questions about the sustainability of its exploitation and the limits needed to avoid depleting the geological resource.

---

<sup>12</sup> Labbé, M. (2004). Offre et demande d'espace souterrain. In *Vingt mille lieux sous les terres: espaces publics souterrains*. Lausanne : PPUR presses polytechnique, p.167



### 3.2. Atlas of interface typologies in Helsinki through redrawing and surveys



*Excerpt from the illustrations of the atlas of interface typologies in Helsinki, personal work, 2024.*

Based on our photographic surveys conducted on-site in Helsinki and a cross-analysis of urban plans, we identified and redrew eight typologies of underground interfaces. The kiosk, a small access structure often located on sidewalks, provides a sheltered transition to the depths. The station, more developed, offers a designed threshold, marking a symbolic pause. The concealed interface, intended for emergencies, remains invisible and inaccessible under normal circumstances. Respiratory structures enable ventilation, though they remain discreet at the surface. The significant device stages a view into the underground, giving public value to the buried space. The fissure in the rocky landscape inserts itself into the granite, evoking depth without explicitly revealing it. Gentle, raw, and expansive slopes accommodate vehicles and sometimes pedestrians leading to deeper spaces. Finally, the emerging shaft, a small discreet element, signals the presence of the underground at the base of façades. Each interface has been graphically reconstructed to reveal the spatial, functional, and symbolic logics of the connection between surface and underground.

### 3.3. The materiality of the subsurface: an organism of flows

In Helsinki, the qualities of the underground are primarily determined by its bedrock. However, the quality of an underground space is not limited to the quality of its rock. The subsurface is a complex domain at the heart of the “Critical Zone,” where interactions occur between the atmospheric, hydric, geological, and biological spheres<sup>13</sup>. Its materiality is a dynamic entity, formed through the progressive transformation of matter<sup>14</sup>, capable of evoking physical sensations and psychological interpretations through its depth, density, and texture. Architect Clotilde Félix-Fromentin describes it as a “giant organism”<sup>15</sup> traversed by flows of materials and information.

Observations in Helsinki reveal this complexity. Uncoated rock walls show tectonic fractures, tool marks, and chemical reactions, such as green, white, and brown stains caused by interactions between living and non-living elements. These phenomena, including efflorescence from water on sprayed concrete and green stains linked to moisture, illustrate constant interactions. Small basins collecting water leaks from ceilings provide a concrete example of managing these material flows and their influence on design.

Therefore, underground architectural design must respond to this changing environment by considering these flows and interactions to ensure the safety and viability of the spaces. Rather than hiding these physical and chemical reactions, which are often perceived as flaws, the challenge is to integrate them in order to affirm the unique identity of the underground landscape. This requires careful planning to address geotechnical risks and ensure the resilience and sustainability of these structures.



*Organic reaction, water collection cups, marks left by drilling tools, efflorescence phenomenon, Formula Center leisure center, personal photographs, november 2023, Helsinki.*

<sup>13</sup> Valentin, C. (2018). Les sols au cœur de la zone critique (Série Les sols). ISTE editions.

<sup>14</sup> His, G. (2015). La matérialité comme récit : d'un récit culturel à la production d'une pensée. Bulletin des bibliothèques de France (BBF), (4), 30-44.

<sup>15</sup> Grout, C., Blain, C., Coulais, J. F., Françoise, C., Sylvie, S., Guillaume, A., et al. (2017). La ville souterraine : représentations et conception. La part de l'invisible (Vol. Les dossiers du Latch). L/E de Lille.

### 3.4. Sensory cues of the underground world: rethinking the design of subterranean architecture

Drawing on observations made in Helsinki and various case studies, we explored the materiality of the underground through human perceptions, focusing on key themes: matter, light, temporality, and vegetation. Underground spaces possess a unique spatiality where sensations are heightened due to their intrinsic characteristics. Their design requires a different approach than surface projects. What are the sensory cues of the underground world? How does the relationship between users and their environment make the underground perceptible? Colonizing the subsurface should not simply be an escape from surface spaces. Burial should not be a way to avoid. To reinvest the imagination in these spaces, they must strive to “create a world.” Underground architecture must therefore consider atmospheres more extensively to offer a pleasant and sensitive experience.

**Matter and surface** constitute the very essence of the underground experience, where perception goes beyond simple geometry to embrace an aesthetic and empathetic dimension. In these spaces, matter predominates and shapes form, directly influencing our comfort and sensations. The choice of robust materials such as stone and concrete, essential to withstand underground constraints, presents the challenge of preserving the intrinsic identity of these places. To achieve this, a technique of partial lining is often favored. This method involves leaving natural rock or the primary structure exposed in places. Far from being a mere artifice, this scenographic revelation of raw material highlights the power and thickness of the surrounding mass, offering a tactile and visual understanding of the environment.

In Helsinki, the underground material, notably granite, is intrinsically linked to architectural design. Its structural robustness is fundamental, of course, but it is through the subtle play of its finishes, the light that sculpts it, and the sensation it produces to the touch that it becomes an essential actor in creating sensory atmospheres.

**Light** plays a direct role in the design of underground spaces, influencing their quality, habitability, and acceptance. Often perceived as dark and oppressive, the underground can instead become a sensitive and attractive place through careful use of natural light, without necessarily relying on artificial lighting.<sup>16</sup> Natural light reveals the carved volumes, structures atmospheres, marks thresholds, and guides the perception of emptiness. Due to its rarity, it enhances contrasts and strengthens the spatial experience. Devices such as light wells, narrow openings, or reflections create subtle connections with the outside. Light can also blur the boundaries between surface and depth, challenging the distinctions between interior and exterior.<sup>17</sup> Finally, it contributes to orientation, thermal comfort, and sensory acclimatization upon descent.



*Projections  
of colored lights on the rock  
wall of the Finlandia parking  
lot, personal photograph,  
november 2023, Helsinki.*

To enrich the experience of underground spaces, artificial lighting remains essential, allowing the creation of a “unity without uniformity.” Architects distinguish five types of lighting atmospheres: base lighting (indirect, diffuse, warm), threshold lighting (such as showers or light gates), pathway lighting (regular punctuations), line lighting (graphic, colored, emphasizing movement), and event lighting (exceptional installations).<sup>18</sup> Depending on the project, light sources may be either prominently visible or skillfully concealed.



*Colored illumination  
of the vaults in the cold water reservoir in  
downtown Helsinki.  
[https://www.researchgate.net/publication/326914950\\_Urban\\_Underground\\_Space\\_Sustainable\\_Property\\_Development\\_in\\_Helsinki](https://www.researchgate.net/publication/326914950_Urban_Underground_Space_Sustainable_Property_Development_in_Helsinki)*



*Tubular structures  
bringing natural light into the  
Potsdamer Platz Berlin metro station.  
<https://www.krapfag.ch/en/reference-projects/metal-construction/light-pipes-berlin-potsdamer-platz/>*

<sup>16</sup> Zunino, G. (2013). Pour une urbanité souterraine de qualité. Urbanités.

<sup>17</sup> Thibaud, J-P. (1996). Mouvement et perception des ambiances souterraines.

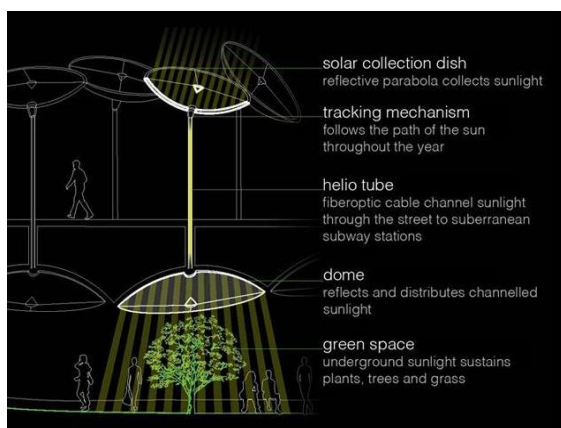
<sup>18</sup> Kohn, B., & Vaysse, J. P. (2004). Stratégies du projet souterrain : charte architecturale du métro du Turin. In P. Von Meiss & F. Radu (Éd.), *Vingt mille lieux sous les terres : espaces publics souterrains* (pp. 136-147). Presses polytechniques et universitaires romandes.



**Temporality** can initially be approached through adaptability and shared use<sup>19</sup>, allowing the underground to be thought of as an evolving space capable of hosting multiple functions depending on the time (day/night, seasons, future uses). In Helsinki, the climatic contrasts emphasize the value of these stable and protected spaces. Their design must anticipate reversible and overlapping uses, integrating sensitive interfaces between surface and underground (light, air, water, sound) from the early design stage. This approach helps to anchor the underground within the urban system as a fully-fledged public space.

Considering temporality in the design of underground architecture also means addressing the impact of the absence of natural temporal cues on users, a challenge especially relevant in climates like Helsinki, where dependence on daylight is reduced. Studies have shown that deprived of sunlight and time indicators, individuals develop “social clocks” to adapt, highlighting human resilience and the need to recreate these temporal references.<sup>20</sup> To counter temporal disorientation, designers incorporate solutions such as lighting that simulates the circadian cycle<sup>21</sup>, reproducing the intensity and color of natural light. Additionally, integrating light wells or windows in semi-buried structures, as seen in the Amos Rex Museum, helps maintain a visual connection with the outside and allows users to perceive the passage of time. Ultimately, the goal is to minimize the disruption between the surface rhythm of life and the underground experience, thereby ensuring user well-being and functionality.

From a certain depth, the temperature of the underground remains stable, independent of daily weather variations such as rain, wind, or sunlight. Often, the physical boundary between the underground space and the outside is airtight and insulated from temperature fluctuations.<sup>22</sup> However, the perception of the climate by users remains a challenge, as elements like air temperature, humidity levels, and air movement serve as important sensory cues.<sup>23</sup> To compensate for this sensory disconnection, architects explore innovative solutions. For example, artistic or structural devices, such as the moving cables at Saint-Maur station or Susumu Shingu’s kinetic sails at Osaka airport, are designed to make the invisible presence of air and its movements perceptible, enriching the underground spatial experience. Water, although a major technical constraint, is also used to connect the underground to the surface: water leaks from groundwater tables can indicate external hydrological and climatic conditions, as demonstrated by Kungsträdgården station and the Tempelpiaukio Church. Rainwater is deliberately allowed to flow along the rock walls, creating a visual and sensory connection to the outside.



*Lowline Project, transmission  
of natural light via fiber optics, designed by James  
Ramsey and Dan Barasch  
<http://thelowline.org/about/project/>*

**Vegetation** positively influences users’ perception and the functionality of spaces, demonstrating that life can thrive underground. It enhances aesthetics and purifies the air, making the environment more acceptable and welcoming. Scientifically proven, exposure to nature, even underground, has therapeutic effects on psychological, cognitive, and physiological health, reducing the fear of confinement.<sup>24</sup> To overcome challenges related to the absence of natural light, innovative solutions such as fiber optic transmission have been developed, enabling photosynthesis and plant growth. Finally, the integration of green walls and the selection of suitable plants improve acoustic comfort and open future possibilities, such as underground agriculture, to optimize space use.

<sup>19</sup> Pradel, B. (2013). Processus de réversibilité et rythmes des transformations urbaines : penser la ville à pile ou face ?. in Scherrer, F. & Vanier, M., Villes, territoires, réversibilité. Paris : Hermann, pp. 237-248

<sup>20</sup> Tafforin, C., Christian, C., & Roumian, J. (2023). Social Clock and Social Sun as Adaptive Strategies of Human Behavior Without Time Cues and Sunlight in an Underground Environment. Journal of Humanities and Social Sciences Studies, 5, 15-26.

<sup>21</sup> Duez, H., & Pourcet, B. (2022, août 1). Récepteurs nucléaires et rythmes circadiens. Med Sci (Paris), 38(8-9), 669-678.

<sup>22</sup> Guide énergie, La région Auvergne-Rhône-Alpes

<sup>23</sup> Von Meiss, P., & Radu, F. (2004). Vingt mille lieux sous les terres : espaces publics souterrains. Presses polytechniques et universitaires romandes..

<sup>24</sup> Santé, environnement et changement climatique. Santé humaine et diversité biologique. Rapport du Directeur général.

### **3.5. Representations of the invisible space: underlying issues**

In Helsinki, the mapping of underground spaces is currently limited. The only existing document, a master plan, reveals a gap between the perception and the reality of these infrastructures. As demonstrated by the method of decomposition by depth layers, Helsinki's underground spaces do not form an interconnected network. Rather, they appear as a series of independent "nodes." These nodes, often isolated and not connected to the metro or to each other, serve specific functions. Movement between them depends entirely on the surface. This disconnection is intentional, notably for security and military reasons, as required by the underground master plan<sup>25</sup>. Thus, the development of an interconnected underground network is secondary to the safety and proper functioning of existing spaces.

As a unique form of architecture shaping void within solid, the underground demands a specific form of representation. It is necessary to reclaim traditional methods such as sections, plans, and elevations and adapt them to this particularity. This reinterpretation involves several approaches: using the negative, extending sections into the subsurface, exploring materiality through models, collages, and decomposition into depth strata. These representational tools are essential to convey the spatiality of the underground, express concepts and atmospheres, develop projects, and clarify the technical aspects of construction and maintenance. Accurate and appropriate representation is an indispensable preliminary step for the effective design and management of underground spaces, thereby facilitating communication among all stakeholders.

### **3.6. Critical reflection on underground programming**

Finally, based on our state of the art and field survey, we can conclude that the programming of underground spaces today remains predominantly functional, technical, or defensive, particularly in Helsinki, where these places are seldom conceived as spaces of urbanity or social interaction.<sup>26</sup> Considered mainly as conduits for flows or shelters, they struggle to be perceived as genuine public spaces. However, a programming approach that integrates human dimensions, light, air, and connections to the surface level could transform these places into high-quality urban environments.<sup>27</sup> It would require moving beyond a purely utilitarian logic to imagine mixed, evolving, and sensitive uses. This implies redefining the relationship between surface and depth by incorporating the underground into an urban strategy of synergy. Finally, energy, climate, and construction challenges (such as the reuse of excavated materials) further strengthen the case for a renewed approach to the subsurface as an active component of the city.

## **4. DISCUSSION: THE INVISIBLE AS A FOUNDATION FOR AN ARCHITECTURAL NARRATIVE**

Building on the conclusions drawn from our methodological tools in the first and second parts, we propose in this final section to envision the underground of Helsinki through architectural experiments called "fragments of the invisible space." These consist of about ten projects exploring the potentials of the underground beyond mere infrastructure. Some of these "fragments" represent symbolic or critical projects, questioning the underground as a consumer of material and involving heavy processes. Other fragments reconnect with the living by highlighting natural elements and underground cycles (water, soil, climate) without obstructing them. Most also aim to take advantage of the environmental qualities of the subsurface (energy, thermal inertia), while carefully managing the interfaces between surface and depth (light, air, water, sound). Finally, they raise the question of possible uses: what role and urban functions can these buried spaces have?

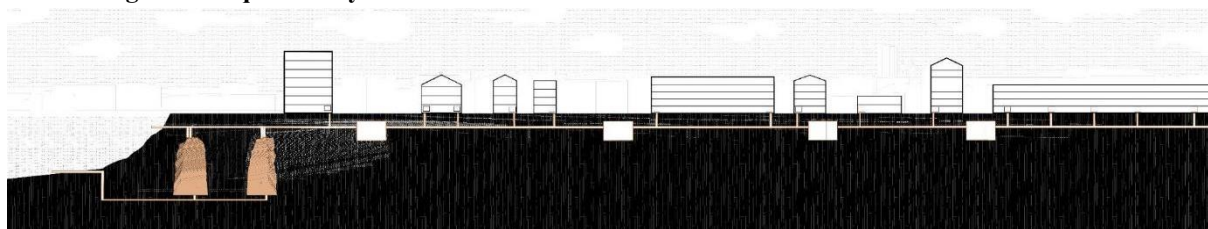
---

<sup>25</sup> Vähäaho, I. (2011). Helsinki Experience with Master Planning for Use of Underground Space, Conference on Planning and Development of Underground Space

<sup>26</sup> Deraëve, S. (2018). Des cartes pour représenter les profondeurs de la ville verticale. *Géographie et cultures*, 107, 67-87.

<sup>27</sup> Zunino, G. (2013). Pour une urbanité souterraine de qualité. *Urbanités*.

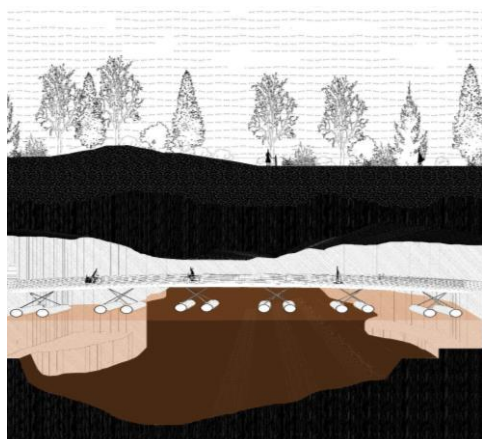
#### 4.1. Fragment “Aquathermy”



*Perspective section illustration of the “Polar Night” fragment in Helsinki, underground market, personal work, 2024.*

The project explores the deep relationship between Helsinki and water, a central element of its urban identity. The route runs along the quays of the Kruununkhaka district, where sounds and architecture engage in a sensitive symbiosis between art and nature. Beneath the surface, a vast aquathermal system exploits the heat stored in water-filled caverns nestled within the granite. This underground network uses heat pumps to capture, transfer, and redistribute thermal energy throughout the year. The system maintains ecological balance by returning the water to the sea at a constant temperature. Thus, water becomes the discreet engine of a sustainable and poetic energy future for the city.

#### 4.2. Fragment “Confined Aquifer”



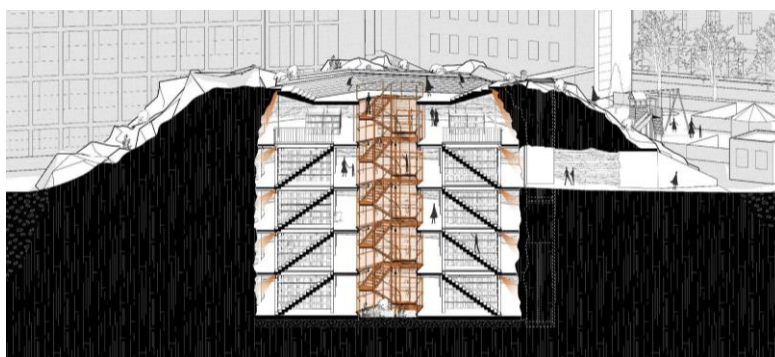
*Perspective section illustration of the “Confined Aquifer” fragment in Helsinki, bike path, personal work, 2024.*

The project offers an immersive cycling experience in the Kluuvi district, where the cyclist traverses the city while engaging in a subtle exploration of the relationship between the underground and the surface. A bike path connects two major axes and transports users through a space where time and climate become almost indefinable. The route symbolically passes above a groundwater table, a living ecosystem that responds to climatic conditions, revealing the constant dynamics between underground waters and surface phenomena. This crossing is made via a floating footbridge that fluctuates with the water levels, offering a tactile experience of the invisible variations below. In this silent cavern, the visitor becomes a witness to the secret vastness of subterranean water, providing a profound awareness of the beauty and fragility of this natural balance. The project invites meditation on the interconnection between earth, water, and climate, while offering a poetic glimpse into the city’s underground world.

#### 4.3. Fragment “Pit”



*Photograph of the model produced for the “Pit” fragment, personal work.*



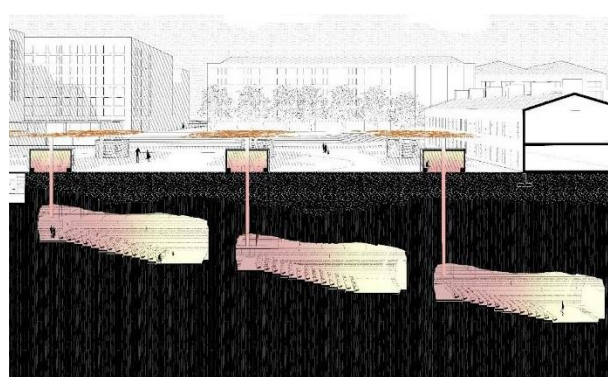
*Perspective section illustration of the “Pit” fragment in Helsinki, underground library, personal work, 2024.*

The Pit project is an underground library carved into a granite hill, where books are protected from direct light and climatic variations. The wooden architecture visually integrates with the rock while standing apart from it, allowing water to flow freely through the fissures, enhancing the atmosphere of the space. Natural ventilation is organized around a central pit, ensuring renewed air. Soft lighting highlights the granite's textures, offering a tactile reading of the space. This fragment demonstrates how an interface can address technical challenges while enriching the project through its design. Here, water is not constrained but integrated, contributing to the poetry of the place. The sequence of thresholds, ascending, crossing, descending, blurs the boundaries between outside and inside.

#### 4.4. Fragment “Cine-thermy”



*Cross perspective section illustration of the “Cine-thermy” fragment in Helsinki, underground cinema, personal work, 2024.*



*Longitudinal perspective section illustration of the “Cine-thermy” fragment in Helsinki, underground cinema, personal work, 2024.*

The project transforms Narinkka Square in Kamppi into a dynamic crossroads where commercial life, culture, and mobility intersect beneath a large canopy. This structure conceals airflow between the ground and the underground, and houses an underground cinema accessible via a central staircase. Inspired by natural caves, the interior architecture blends rock and light to create an immersive atmosphere. Heat generated by spectators and equipment is recovered through a cine-thermal system and redistributed to surface installations. A network of pipes ensures natural ventilation and supports the structure. The project thus combines geology, energy, and architecture into a coherent and sustainable whole.

## 5. CONCLUSION

Exploring Helsinki's underground spaces led us to question the architect's role in relation to these invisible territories, often reduced to technical or utilitarian functions. Despite exemplary planning and a rich geological setting, the underground remains largely compartmentalized, poorly connected to everyday urban uses, and rarely designed as a space for living. It is still conceived mainly as a network of services dominated by logistical, security, or defensive logics.

Our approach, combining theoretical analysis, sensitive surveying, and project-based experiments, aimed to move beyond this fragmented vision. We sought to build a broader understanding of the underground by considering its materiality, light, atmospheres, flows, and its place within contemporary urban narratives. These elements reveal a spatial and sensory potential that remains underexploited, which only a transversal approach can activate.

The architectural fragments developed in this work propose another way to conceive these spaces as extensions of the public realm, places for climatic, social, or cultural experimentation. They show that when designed in synergy with the surface, integrating the soil's unique qualities and working on the interfaces, the underground can accommodate mixed, evolving, and meaningful uses.

This is not about idealizing these spaces or proposing a single model, but rather recognizing them as a legitimate field of intervention that requires specific tools: adapted mapping, rethought modes of representation, and attention to perception and temporality. The underground thus becomes an active component of urban production, both a physical constraint and a resource for the city.



This work does not offer turnkey solutions, but rather a framework and design tools adaptable to other contexts. It calls for an evolution in the architect's role, one able to navigate between surface and depth, between technicality and perception, to fully integrate the underground into contemporary urban thinking.

## 6. BIBLIOGRAPHY

- [1] Barroca, B. (2019). Espaces souterrains et synergies spatiales. *Communications*, 105(2), 195–205.
- [2] Beqiri, J. (2021). The implications of technological progress in architectural thinking: The future impossibility for an architecture of hiding. *IOP Conf. Series: Earth and Environmental Science* 703 012001, doi:10.1088/1755-1315/703/1/012001
- [3] Deraëve, S. (2018). Des cartes pour représenter les profondeurs de la ville verticale. *Géographie et cultures*, 107, 67-87.
- [4] Duez, H., & Pourcet, B. (2022, août 1). Récepteurs nucléaires et rythmes circadiens. *Med Sci (Paris)*, 38(8-9), 669-678.
- [5] Gaillardet, J., & Boudia, S. (2021). La Zone critique : Vers de nouvelles pratiques scientifiques pour réduire les ignorances dans l'anthropocène. *Revue d'anthropologie des connaissances*, 15(4). <https://journals.openedition.org/rac/25340>
- [6] Grout, C., Blain, C., Coulais, J. F., Françoise, C., Sylvie, S., Guillaume, A., et al. (2017). La ville souterraine : représentations et conception. La part de l'invisible (Vol. Les dossiers du Latch). L/E de Lille.
- [7] His, G. (2015). La matérialité comme récit : d'un récit culturel à la production d'une pensée. *Bulletin des bibliothèques de France (BBF)*, (4), 30-44.
- [8] Ikävalko, O., Satola, I., & Hoivanen, R. (2016). Helsinki TU1206 COST Sub-Urban WG1 Report (22 p.).
- [9] Kohn, B., & Vaysse, J. P. (2004). Stratégies du projet souterrain : charte architecturale du métro du Turin. In P. Von Meiss & F. Radu (Éd.), *Vingt mille lieux sous les terres : espaces publics souterrains* (pp. 136-147). Presses polytechniques et universitaires romandes.
- [10] Krtolica, I. (2021). Le rhizome deleuzo-guattarien « Entre » philosophie, science, histoire et anthropologie. *Rue Descartes*, 99, 39-51. <https://doi.org/10.3917/rdes.099.0039>
- [11] Labbé, M. (2004). Offre et demande d'espace souterrain. In *Vingt mille lieux sous les terres: espaces publics souterrains*. Lausanne : PPUR presses polytechnique, p.167
- [12] Labbé, M. (2016). Architecture of underground spaces: From isolated innovations to connected urbanism. *Tunnelling and Underground Space Technology*.
- [13] Mangin, D. & Girodo, M. (2016). *Mangroves urbaines : du métro à la ville* (Paris, Montréal, Singapour), Paris : La Découverte (collection Dominique Carré).
- [14] Pradel, B. (2013). Processus de réversibilité et rythmes des transformations urbaines : penser la ville à pile ou face ?. in Scherrer, F. & Vanier, M., *Villes, territoires, réversibilité*. Paris : Hermann, pp. 237-248
- [15] Tafforin, C., Christian, C., & Roumian, J. (2023). Social Clock and Social Sun as Adaptive Strategies of Human Behavior Without Time Cues and Sunlight in an Underground Environment. *Journal of Humanities and Social Sciences Studies*, 5, 15-26.
- [16] Tahmasebinia, F., Yu, K., Bao, J., Chammoun, G., Chang, E., Sepasgozar, S., & Alonso Marroquin, F. (2020). Earthscraper: A Smart Solution for Developing Future Underground Cities. *IntechOpen*. doi: 10.5772/intechopen.87217
- [17] Thibaud, J-P. (1996). *Mouvement et perception des ambiances souterraines*.
- [18] Vähäaho, I. (2011). Helsinki Experience with Master Planning for Use of Underground Space, Conference on Planning and Development of Underground Space
- [19] Vähäaho, I. (2018). *Urban Underground Space - Sustainable Property Development in Helsinki*. City of Helsinki, Urban Environment Publications. ISBN 978-952-331-436-8
- [20] Valentin, C. (2018). *Les sols au cœur de la zone critique (Série Les sols)*. ISTE editions.
- [21] Von Meiss, P., & Radu, F. (2004). *Vingt mille lieux sous les terres : espaces publics souterrains*. Presses polytechniques et universitaires romandes.
- [22] Zunino, G. (2013). *Pour une urbanité souterraine de qualité*. Urbanités.



## ADVANCING UNDERGROUND URBAN SPACE PLANNING: THE POTENTIAL OF FORESIGHT METHODS IN SYSTEMIC PLANNING AND TRANSITION MANAGEMENT

Nemanja Šipetić<sup>1</sup> and Vladan Đokić<sup>2</sup>

**Abstract:** Underground urban spaces (UUS) are becoming a crucial resource in modern cities due to the increasing limitations of surface space, necessitating the application of specific foresight methods that integrate urban planning, infrastructural, environmental, and technological factors. The historical development of UUS planning represents a dynamic process marked by alternating periods of innovation and stagnation, with the past decade witnessing a slowdown in the development of new approaches. This stagnation is reflected in the frequent repetition of existing guidelines, recommendations, and conclusions, while institutional frameworks demonstrate a limited capacity to absorb new concepts. Within contemporary theoretical and methodological frameworks, the systemic approach to urban underground spaces and Transition Management for UUS emerges as potentially transformative factors in overcoming these challenges. These approaches define the frameworks for the application of foresight methods, provide tools for improving the management process, and enable the inclusion of all relevant stakeholders in decision-making processes, relying on a multidisciplinary and integrated approach. This raises the question: Which foresight methods provide the most adequate results in the context of systemic approaches and Transition Management in UUS planning? In the context of the increasing application of foresight methods in urban planning, this paper conducts a comparative analysis of different foresight methods through theoretical comparisons of potential transformative factors to determine which methods are most suitable for anticipating the future use of underground urban spaces, taking into account the principles of the systemic approach and Transition Management. The study identifies methodological frameworks that can contribute to the development of new UUS utilization models, capable of overcoming social barriers, fostering the integration of all interested parties, and improving the strategic planning process. The aim of this research is to highlight the additional potential of foresight methods in creating sustainable solutions and fostering innovative urban planning practices in the domain of underground urban spaces. Furthermore, the study analyzes key challenges in the implementation of these methods, identifies possible guidelines for selecting the most reliable foresight methods concerning specific urban planning challenges, and proposes directions for future research and strategic development in this field. The research aims to enhance interdisciplinary dialogue among urban planners, engineers, policymakers, and the wider public, ensuring a holistic, innovative, and sustainable approach to underground urban space planning.

**Keywords:** Foresight Methods, Underground Urban Spaces, Systemic Approach, Transition Management

### 1. INTRODUCTION

In the context of rapid urbanization and limited surface space, underground urban spaces (UUS) are emerging as a key resource for the sustainable development of future cities. Traditional planning approaches, focused primarily on surface-level interventions, have proven insufficient to address complex challenges such as traffic congestion, pollution, and land scarcity. UUS are increasingly taking on multifunctional roles; however, their effective utilization is hindered by fragmented planning, sectoral isolation, and inadequate institutional frameworks (Admiraal and Cornaro, 2016). Contemporary challenges call for integrated, three-dimensional planning that synchronizes above-ground and underground functions, along with anticipatory methods such as foresight approaches. This paper explores how foresight tools and methods can contribute to systemic planning

<sup>1</sup> MSc, Šipetić Nemanja, B.Sc. Architecture Eng., research associate, Institute of Architecture and Urban & Spatial Planning of Serbia, Bulevar kralja Aleksandra 73 / II, 11000 Belgrade, e-mail address: [sipetic.nemanja@gmail.com](mailto:sipetic.nemanja@gmail.com), <https://orcid.org/0000-0002-9965-1457>

<sup>2</sup> Prof. Đokić Vladan, rector of the University of Belgrade, University of Belgrade, Studentski trg 1, 11000 Belgrade. E-mail address: [vdjokic@arh.bg.ac.rs](mailto:vdjokic@arh.bg.ac.rs), <https://orcid.org/0000-0002-8655-0964>

and transition management in the development of UUS, offering strategic recommendations for urban planners, policymakers, and researchers to foster more resilient and sustainable cities (Delmastro et al, 2016).

Planning underground urban spaces represents a complex socio-technical challenge requiring interdisciplinarity, long-term strategic thinking, and adaptive governance approaches. To overcome fragmentation and inefficiency in current practices, this study is grounded in three interrelated theoretical pillars: systems planning, transition management, and foresight methodologies. Systems planning enables a holistic understanding of UUS as adaptive systems whose components—ranging from geology and infrastructure to social and regulatory factors—interact dynamically. Rather than pursuing isolated solutions, this approach emphasizes functional integration and conflict anticipation through tools such as 3D GIS modeling and multidisciplinary analyses (v. d. Tann et al.,2020; Bobylev, 2009).

Transition management offers a process-oriented framework for guiding long-term change through participation, experimentation, and social learning, while foresight methods (such as scenario planning, backcasting, Delphi, etc.) support anticipation of uncertain futures and the formulation of desirable development pathways (Slaughter, 1993; Lambert et al., 2024). Together, these concepts enable the design of flexible and inclusive strategies suited to the complexity of UUS, while reinforcing institutional coordination and stakeholder engagement. By integrating these approaches, the paper proposes a theoretical framework for sustainable and anticipatory governance of subsurface resources, aligned with global objectives for urban resilience and sustainability.

## 2. METHODOLOGICAL VISION

The methodology of this research is based on an integrative theoretical framework that combines foresight methods, transition management (TM), and systemic planning, with the aim of enhancing future-oriented planning and governance of Urban Underground Spaces (UUS). Building upon existing literature (Slaughter, 1993; v. d. Tann et al.,2020; Debrock and Coppens, 2023), the approach comprises three core process phases: (1) system analysis and mapping, (2) visioning and scenario development using foresight tools, and (3) development and implementation of transition strategies. A particular emphasis is placed on the social implications of these processes, recognizing the importance of ethics, inclusivity, and participation, as the challenges of UUS planning often lie less in technical limitations and more in the lack of social legitimacy and coordination among stakeholders.

While technology is indispensable, the research acknowledges that its advancement often surpasses the capacity of social and institutional systems to apply it responsibly (Admiraal and Cornaro, 2020). Therefore, special attention is given to social foresight and collective responsibility, in line with the principles of critical futures thinking [9], to encourage more just, sustainable, and long-term legitimate strategies for UUS. The proposed methodological framework rests on participatory and iterative learning processes, enabling the integration of social values across all phases of planning and implementation.

### 2.1. System Analysis and Mapping

This process entails a holistic understanding of the urban underground as a complex adaptive system, as defined by von der Tann et al. (v. d. Tann et al.,2020). Key steps include:

- **System element identification:** Mapping geological, infrastructural, regulatory, and social components of UUS, and defining functional, territorial, and institutional boundaries (v. d. Tann et al.,2020).
- **Interdependency analysis:** Applying systems thinking to explore interactions between underground functions (e.g., metro systems, utility networks, groundwater) and their impacts on aboveground systems.
- **Data collection:** Using GIS tools and 3D geological models to integrate data on geology, infrastructure, and property, enabling spatial and sectoral integration (Delmastro et al, 2016).
- **Stakeholder involvement:** Establishing interdisciplinary teams (engineers, urban planners, ecologists, citizens) to identify priorities and potential conflicts, in accordance with Slaughter's emphasis on participation (Riedy, 2021).

## 2.2. Visioning and Scenario Development through Foresight Methods

The application of foresight methods facilitates the anticipation of future needs and challenges by generating multiple scenarios for UUS use. This process builds on Slaughter's integrative approach (Slaughter, 1993; Riedy, 2021). and the concept of "futures empathy" (Lambert et al., 2024). The process includes, but is not limited to, the following foresight methods:

- **Scenario planning:** Developing alternative futures (e.g., underground cities as transport hubs, green zones, or shelters) based on key uncertainties such as climate change, demographic pressures, and technological innovation (Sliuzas et. al., 2015).
- **Backcasting:** Defining desirable futures (e.g., sustainable, multifunctional UUS) and mapping backward from these goals to identify steps for realization, considering legal and institutional constraints (Debrock and Coppens, 2023).
- **Delphi method:** Structured expert and stakeholder consultation to build consensus on priorities and strategies for UUS (Slaughter, 1993).
- **Causal Layered Analysis (CLA):** Exploring deeper layers of meaning, including social values, worldviews, and myths shaping the perception of underground space, to promote ethical and inclusive visions (Riedy, 2021).
- **Future Design:** A method that fosters "futures empathy" by having participants imagine themselves as future generations, enhancing sensitivity to long-term societal and environmental needs (Lambert et al., 2024).
- **Fuzzy Cognitive Maps (FCM):** Constructing graphical models that represent causal relationships between key UUS factors (e.g., infrastructure, ecology, social acceptability), with fuzzy weights ranging from -1 to 1, enabling scenario simulations and identification of leverage points under uncertainty (Jetter and Kok, 2014).

## 2.3. Development and implementation of transition strategies

The integration of transition management (TM) principles and practices ensures that visions and scenarios are translated into actionable strategies. Key elements include:

- **Transition arena:** Establishing a platform for collaboration among pioneers (e.g., innovators in underground architecture), urban planners, regulators, and citizens to co-develop a shared vision and strategy (Debrock and Coppens, 2023).
- **Transition agenda:** Setting long-term goals and intermediate milestones for the transformation of UUS, including legal reforms, institutional coordination, and pilot projects (Voß et. al., 2009).
- **Experimental niches:** Launching pilot initiatives (e.g., smart underground hubs, green subterranean zones) to test innovations and enable learning-by-doing (Debrock and Coppens, 2023).
- **Monitoring and evaluation:** Continuously tracking and adjusting strategies based on feedback, using indicators of resilience, inclusivity, and sustainability (v. d. Tann et al., 2020).

**Social participation:** Empowering communities through workshops and public consultations, thereby promoting collective responsibility, in line with Slaughter's concept of social foresight (Riedy, 2021).

## 3. APPLICATIONS AND CONTRIBUTIONS OF FORESIGHT METHODS TO SYSTEMIC PLANNING AND TRANSITION MANAGEMENT

This section, drawing on the social implications of Slaughter's critical futures thinking, summarizes the key foresight methods, their applications in systemic planning and transition management, and their contributions to both methodologies in the context of Urban Underground Spaces (UUS). The presented tables are structured

according to Slaughter's layers of futures work (pragmatic, critical, epistemological), in order to highlight their integrative potential.<sup>3</sup>

*Table 1. Pragmatic Level*

Method	Social implications (Slaughter)	Application in systemic planning of Urban Underground Spaces (UUS)	Contribution to systemic planning	Application in transition management (TM)	Contribution to transition management
<b>Scenario planning</b>	It promotes social resilience by exploring multiple futures, enabling communities to prepare for uncertainty (Riedy, 2021).	Scenario development for UUS (e.g., underground transport, green zones, shelters) to anticipate climate and demographic challenges (Sliuzas et. al., 2015).	Enables the identification of key uncertainties and interactions between underground and surface systems, supporting spatial and sectoral integration (v. d. Tann et al., 2020).	Developing diverse scenarios for UUS within the transition arena, enabling pioneers and stakeholders to identify strategic pathways (Debrock and Coppens, 2023).	Supports the development of a transition agenda by identifying alternative pathways and strategies for the transformation of UUS (Debrock and Coppens, 2023).
<b>Delphi method</b>	Fosters collective responsibility by incorporating expert and societal perspectives, ensuring consensus on priorities (Slaughter, 1993).	Consultation with experts and citizens on UUS priorities (e.g., safety, ecology, accessibility) (Debrock and Coppens, 2023).	Enhances coordination among stakeholders and reduces sectoral conflicts, contributing to process integration (v. d. Tann et al., 2020).	Structured engagement of experts and stakeholders within the transition arena to define shared goals and strategies for UUS (Voß et. al., 2009).	Facilitates the formation of a transition arena, enabling interdisciplinary collaboration and consensus on shared goals (Voß et. al., 2009).
<b>GIS and 3D modeling</b>	Increases transparency and accessibility of information, enabling communities to gain insight into the planning process (Sliuzas et. al., 2015).	Visualization of underground resources and infrastructure to improve spatial and resource management (Delmastro et al, 2016).	Supports data integration and spatial analysis, enabling precise mapping of interdependencies (Bobylev, 2009).	Use of GIS tools in pilot projects and experimental niches to test innovations under real-world UUS conditions (Debrock and Coppens, 2023).	Provides a technical foundation for experimental niches, enabling the testing of innovations in real-world conditions (Debrock and Coppens, 2023).
<b>Fuzzy Cognitive Maps (FCM)</b>	Encourages participation and collective responsibility through co-creation of models, enabling the integration of subjective	Development of FCM models to map causal relationships between UUS factors (e.g., infrastructure, costs, social acceptability) and	Enables the modeling of complex interdependencies and uncertainties, supporting systemic integration and risk anticipation (v. d. Tann et al., 2020).	Use of FCM within the transition arena to identify key intervention points and simulate policy impacts on UUS	Enables reflexive governance through the simulation of systemic effects and identification of strategic levers for transition (Debrock and Coppens, 2023).

<sup>3</sup> Slaughter's layers of futures work—pragmatic, critical, and epistemological—provide an integrative framework for exploring futures in complex systems such as urban planning (Riedy, 2021). The *pragmatic level* focuses on practical, short-term aspects, using scenario analysis and the Delphi method to address challenges such as UUS infrastructure planning. The *critical level* investigates underlying social and value assumptions, employing Causal Layered Analysis (CLA) to deconstruct dominant narratives and promote equity in the use of UUS. The *epistemological level* reflects on knowledge systems and worldviews, applying Future Design to develop long-term, ethically grounded strategies that consider the interests of future generations. The integration of these levels balances practical and societal dimensions, enhancing both the sustainability and fairness of UUS planning (Slaughter, 1993; Riedy, 2021).

perspectives and uncertainties (Jetter and Kok, 2014).	simulate “what-if” scenarios (Jetter and Kok, 2014).	(Jetter and Kok, 2014).
--	--	-------------------------

**Table 2.** *Critical Level – Social Implications, Applications, and Contributions*

Method	Social implications (Slaughter)	Application in systemic planning of Urban Underground Spaces (UUS)	Contribution to systemic planning	Application in transition management (TM)	Contribution to transition management
<b>Causal Layered Analysis (CLA)</b>	Reveals hidden values and power structures, promoting ethical and inclusive visions of the future (Riedy, 2021).	Analysis of social narratives about UUS (e.g., “the underground as a technical layer” vs. “a multifunctional resource”) to reshape planning approaches (Al-shanty, 2019).	Enables the reconsideration of sectoral assumptions and the promotion of inclusive strategies, contributing to conceptual integration (v. d. Tann et al., 2020).	Use of CLA within the transition arena to reassess normative goals and values in UUS planning (Voß et. al., 2009).	Fosters reflexivity in transition processes, enabling the reassessment of normative goals and values (Voß et. al., 2009).
<b>Normative foresight</b>	Encourages the creation of desirable futures based on equity and sustainability, empowering communities (Slaughter, 1993).	Defining visions for UUS that prioritize social justice and ecological sustainability (e.g., underground public spaces) (Lambert et al., 2024).	Supports the development of long-term goals that align social and environmental priorities, enhancing process integration (Debrock and Coppens, 2023).	Formulation of normative visions within the transition agenda to guide change toward sustainable UUS practices (Debrock and Coppens, 2023).	Provides a foundation for the transition agenda, guiding change toward desirable and ethical outcomes (Debrock and Coppens, 2023).
<b>Participatory workshops.</b>	Strengthens social cohesion and collective responsibility by involving communities in decision-making processes (Riedy, 2021).	Organizing workshops with citizens and experts for UUS design, with a focus on inclusivity (Sliuzas et. al., 2015).	Increases the legitimacy and social acceptability of plans, contributing to institutional coordination (Voß et. al., 2009).	Engaging communities within the transition arena to co-develop shared visions and pilot projects (Debrock and Coppens, 2023).	Empowers the transition arena by enabling broad participation and social learning (Debrock and Coppens, 2023).

**Table 3.** *Epistemological Level – Social Implications, Applications, and Contributions*

Method	Social implications (Slaughter)	Application in systemic planning of Urban Underground Spaces (UUS)	Contribution to systemic planning	Application in transition management (TM)	Contribution to transition management
<b>Future Design</b>	Promotes “futures empathy,” enabling an understanding of the needs of future generations and fostering	Envisioning UUS from the perspective of future generations (e.g., 2050) to develop sustainable	Encourages long-term thinking and ethical responsibility, enhancing both conceptual and process integration	Use of “futures empathy” within the transition arena to develop visions that consider the interests of future	Supports the development of long-term visions and experimental niches, focusing on sustainability and future



	long-term responsibility (Lambert et al., 2024).	strategies (Lambert et al., 2024).	(v. d. Tann et al., 2020).	generations (Lambert et al., 2024).	generations (Debrock and Coppens, 2023).
<b>Systems thinking</b>	Enables the understanding of complex social and cultural dynamics, supporting holistic strategies (Riedy, 2021).	Analysis of UUS as part of a broader urban system, taking into account ecological, social, and technical interactions (v. d. Tann et al., 2020).	Enables holistic management of interdependencies, contributing to sectoral and spatial integration (Bobylov, 2009).	Applied within the transition agenda to understand the complexity of UUS and to guide change through reflexive processes (Voß et al., 2009).	Provides a framework for reflexive governance, enabling the adaptation of strategies within complex systems (Voß et al., 2009).
<b>Backcasting</b>	Promotes social responsibility by focusing on desirable futures and the strategic steps needed to achieve them (Slaughter, 1993).	Defining ideal states for UUS (e.g., multifunctional underground cities) and mapping the steps for implementation (Debrock and Coppens, 2023).	Supports the development of transition strategies and long-term plans, enhancing process integration (Voß et al., 2009).	Use of backcasting to define intermediate steps within the transition agenda, guiding pilot projects toward sustainable outcomes (Debrock and Coppens, 2023).	Enables a structured process for achieving long-term goals by defining intermediate steps and pilot projects (Debrock and Coppens, 2023).

**Note:** Some foresight methods, such as backcasting, systems thinking, and Fuzzy Cognitive Maps (FCM), can be applied across multiple levels—pragmatic, critical, and epistemological. However, in the table, they are presented under the level where they are most adaptable and effective, based on their relevance and efficiency in specific UUS planning contexts.

#### 4. EVALUATION AND ITERATIVE LEARNING

To ensure the reliability, credibility, and social relevance of strategies for Urban Underground Space (UUS) planning, it is essential to carry out evaluation and enable iterative learning after the foresight process. This process should integrate quantitative, qualitative, and ethical approaches, supported by advanced digital technologies (Zhu et al., 2016). The evaluation is based on the principles of a systemic framework, providing a structured and transparent approach to assessing the validity, utility, and ethical grounding of proposed strategies (Pirainen, et al., 2012). Particular attention is given to participatory and ethical dimensions, in line with the tradition of critical futures thinking advocated by Slaughter and further developed by (Riedy, 2021).

Furthermore, bibliometric analyses (Ko and Yang, 2024) contribute to understanding broader trends and identifying gaps in existing research, which further enhances the reflexive potential of the strategies. This type of comprehensive evaluation framework not only increases the credibility and practical value of planning interventions but also promotes social learning and adaptation to the complex challenges of Urban Underground Spaces (UUS), thereby ensuring fairness and long-term sustainability. Evaluation is carried out as an iterative process across three interrelated levels - functional (usefulness and implementation), technical (feasibility and accuracy), and ethical (fairness and inclusivity) - employing combined methods and digital technologies to enable precise and multidimensional analysis.

**Table 4.** *Elements of Evaluation and Iterative Learning for UUS.*

<b>Evaluation element</b>	<b>Methods and tools</b>	<b>Application in the context of UUS</b>	<b>References</b>
<b>Quantitative indicators</b>	Measurement of metrics (e.g., reduction of CO <sub>2</sub> emissions, accessibility of public spaces, reduction of geological risks). Use of 3D GIS and digital layering. Multi-level grey approach and fuzzy synthesis evaluation methods. Software: SPSS, R, GIS tools.	Assessment of the impact depth of underground structures (e.g., metro lines) and their ecological consequences.  Quantitative analysis of geological and urban planning data for the categorization of underground space suitability (Level I–IV).	von der Tann et al. (2020),  Zhu et al. (2016)
	Causal Layered Analysis (CLA) for narratives.  Critical Systems Heuristics (CSH) by Werner Ulrich. Interviews, workshops, focus groups.  Tools: NVivo, evaluation matrices.	Analysis of social and cultural narratives about UUS (e.g., “the underground as a technical layer” vs. “a multifunctional resource”). CSH questionnaire for assessing stakeholder inclusion (citizens, urban planners, regulators) and ethical implications.	Riedy (2023),  Piirainen et al. (2012)
<b>Statistical methods and bibliometric analyses</b>	Data analysis (SPSS, R).		
	Silhouette coefficients for cluster validation.	Measuring changes in participants’ perceptions of “futures empathy.”	Lambert et al. (2024),
	Latent Dirichlet Allocation (LDA) for topic modeling.  Tools: VOSviewer, Python libraries for NLP.	Identifying thematic gaps in UUS research (e.g., lack of social aspects compared to technical ones).	Ko and Yang (2024)
<b>Iterative processes</b>	Continuous evaluation (a priori, during the process, and a posteriori).	Regular workshops and data analysis to adapt UUS strategies.	Voß et al. (2009), Piirainen et al. (2012),
	Expert reviews, feedback loops. 3D visualization and virtual reality.  Tools: Trello, Confluence, simulation software.	Simulation of different scenarios (e.g., underground transport hubs) to test resilience and alignment with objectives.	Zhu et al. (2016),  Ko and Yang (2024)
<b>Participatory evaluation</b>	Workshops, focus groups, surveys.	Assessing participant satisfaction and trust in UUS strategies.	Piirainen et al. (2012),
	Evaluation matrices for goal alignment.  Tools: Zoom, Microsoft Teams, questionnaires (e.g., Likert scales).	Involving citizens and experts to evaluate the usefulness and inspirational value of outcomes (e.g., plans for underground public spaces).	Riedy (2021)
<b>Ethical reflection</b>	CSH questionnaire for assessing motivation, power, knowledge, and legitimacy.	Identifying power dynamics in UUS planning.	Piirainen et al. (2012),
	Stakeholder discussions.  Tools: Miro, MURAL, Google Docs for documentation.	Ensuring the inclusion of marginalized groups and the interests of future generations through “futures empathy.”	Lambert et al. (2024),  Riedy (2021)

## 5. BRIEF DISCUSSION

The integration of foresight methods into Urban Underground Space (UUS) planning represents a transformative approach that enhances systemic planning (v. d. Tann et al., 2020) and transition management (Voß et al., 2009; Debrock and Coppens, 2023), enabling the anticipation of future challenges, the engagement of diverse stakeholders, and the development of sustainable strategies within complex urban systems. Unlike traditional approaches, which are often reactive and linear (Shin, 2013; Wiranegara, 2017), foresight methods such as scenario planning, backcasting, Delphi, and Causal Layered Analysis (CLA) (Slaughter, 1993; Inayatullah, 2011; Quista and Vergragt, 2006) allow for the creation of alternative futures and the structuring of strategic thinking.

Their value lies in the ability to connect technical expertise with societal values, fostering inclusivity, ethical responsibility, and long-term resilience (Lambert et al., 2024; Tonn, 2003). Foresight also contributes to enhancing the social legitimacy of planning efforts through participatory processes (Renn, 2022; Pace, 2025), while flexible methods such as backcasting and scenario planning enable the adaptation of strategies under conditions of uncertainty (Sliuzas et al., 2015; Oliveira et al., 2018).

However, their application faces numerous challenges. Implementation complexity, resource demands, lack of reliable data, and institutional fragmentation hinder the widespread adoption of foresight approaches (Mahmud, 2011; Admiraal and Cornaro, 2016; Wang et al., 2013). Cognitive biases and actors' limited temporal perspectives further reduce anticipatory effectiveness (Faiella and G. E. Corazza, 2025; Lalot et al., 2019), while institutional and cultural barriers—such as short-term political focus and resistance to change—require systemic reforms and increased awareness (Tonn, 2003; MacDonald, 2012; Zegras and L. Rayle, 2012).

Additionally, the lack of standardization within foresight practice complicates comparative evaluation and institutionalization of methods (Roya et al., 2016; Deng et al., 2023), raising the question of whether a method that inherently demands contextual flexibility can or should be standardized (Krawczyk and Slaughter, 2010).

In the context of systemic planning, foresight enables the integration of geological, infrastructural, ecological, and social aspects into a unified planning framework (Bobylev, 2009; Vähäaho, 2016; Dufvaa and Ahlqvist, 2015). At the same time, within the domain of transition management, foresight contributes to the formation of visions and strategies through participatory and deliberative processes (Debrock and Coppens, 2023; Zhang and Li, 2018; Rijkens-Klompa et al., 2017).

Furthermore, metamodern and human-centered approaches (Fergnani and B. Cooper, 2023; Slaughter, 2002; Daffara, 2011) introduce ethical and cultural dimensions into foresight methods, promoting the concept of a “culture of anticipation” (Slaughter, 2002) and the integration of underground spaces into visions of collective intelligence, solidarity, and sustainability. Models such as UPUS (Wang et al., 2023) and Futures Consciousness (Lalot et al., 2019) further illuminate the psychological and perceptual aspects of planning, while also pointing to the limitations of existing approaches in addressing cultural complexity and inclusivity.

In conclusion, foresight methods constitute a vital resource for UUS planning, but their effective application depends on integration with systemic approaches, institutional support, and the development of methodological frameworks that balance technical precision with social responsibility and cultural reflexivity.

## 6. CONCLUSION

Foresight methods represent a crucial potential for transforming the planning of Urban Underground Spaces (UUS), particularly through their integration with systemic planning (v. d. Tann et al., 2020) and transition management (Voß et al., 2009; Debrock and Coppens, 2023). They enable the anticipation of long-term challenges, the development of alternative visions, and the creation of flexible strategies within the context of complexity, uncertainty, and the imperative for sustainability. Compared to traditional approaches, foresight methods achieve greater anticipatory capacity, a higher degree of social inclusivity, and stronger orientation toward sustainability (Slaughter, 1993; Lambert et al., 2024).

Their strength lies in the combination of technical precision and social responsibility, as well as in fostering participatory processes and collective learning. Through methods such as scenario planning, backcasting, CLA, and the Delphi technique, foresight facilitates a deeper understanding of possible futures and the proactive shaping of desirable development pathways. However, their implementation requires overcoming several challenges, including data scarcity, institutional barriers, cognitive biases, and the lack of methodological standardization (Mahmud, 2011; Faiella and Corazza, 2025; Krawczyk and Slaughter, 2010).

To enhance the practical applicability of foresight methods, their operationalization through locally adapted protocols and guidelines is essential, supported by digital tools such as 3D GIS, AHP-cloud models, and simulation platforms (Deng et al., 2023). In addition, strong institutional support is needed to integrate foresight approaches into legal, planning, and strategic documents (Admiraal and Cornaro, 2016), along with the development of appropriate indicators for monitoring the resilience and sustainability of UUS (Roya et al., 2015; Ko and Yang).

In conclusion, integrating foresight methods into UUS planning should not be viewed as an option but as an imperative for building more resilient, inclusive, and sustainable cities of the future. Their application must be supported through interdisciplinary collaboration, institutional reform, and broad stakeholder education to ensure that urban planning can adequately respond to 21st-century challenges in alignment with the Sustainable Development Goals (SDGs).

## 7. REFERENCES

- [1] [H. Admiraal and A. Cornaro, „Why underground space should be included in urban planning policy – And how this will enhance an urban underground future,” *Tunnelling and Underground Space Technology*, t. 55, pp. 214-220, 2016.
- [2] C. Delmastro, E. Lavagno and L. Schranz, „Underground urbanism: Master Plans and Sectorial Plans,” *Tunnelling and Underground Space Technology*, t. 55, pp. 103-111, 2016.
- [3] L. v. d. Tann, R. Sterling, Y. Zhou and N. Metje, „Systems approaches to urban underground space planning and management – A review,” *Underground Space*, t. 5, pp. 144-166, 2020.
- [4] N. Bobylev, „Mainstreaming sustainable development into a city’s Master plan: A case of Urban Underground Space use,” *Land Use Policy*, t. 26, pp. 1128-1137, 2009.
- [5] R. A. Slaughter, „Futures concepts,” *Futures*, t. 25, br. 3, pp. 289-314, 1993.
- [6] L. M. Lambert, C. Selin and T. Chermack, „Futures empathy for foresight research and practice,” *Futures*, t. 163, p. Article 103441, 2024.
- [7] S. Debrock and T. Coppens, „Transition Management as a Policy Model to Reach Sustainable Use of Urban Underground Space,” *u Proceedings of the 18th Conference of the Associated Research Centers for the Urban Underground Space - ACUUS*, Singapore, 2023; 1–4 November.
- [8] H. Admiraal and A. Cornaro, „Future cities, resilient cities – The role of underground space in achieving urban resilience,” *Underground Space*, t. 5, pp. 223-228, 2020.
- [9] C. Riedy, „The critical futurist: Richard Slaughter’s foresight practice,” *Futures*, t. 132, p. Article 102789, 2021.
- [10] R. Sliuzas, J. Martinez and R. Bennett, „Urban futures: Multiple visions, paths and construction?,” *Habitat International*, t. 46, pp. 223-224, 2015.
- [11] A. J. Jetter and K. Kok, „Fuzzy Cognitive Maps for futures studies—A methodological assessment of concepts and methods,” *Futures*, t. 61, pp. 45-57, 2014.
- [12] J.-P. Voß, A. Smith and J. Grin, „Designing long-term policy: rethinking transition management,” *Policy Sciences*, t. 42, pp. 275-302, 2009.
- [13] Z. a. Al-shanty, „TOWARDS A FUTURISTIC UNDERGROUND CITIES,” *International Journal of Civil Engineering and Technology (IJCIET)*, t. 10, br. 4, pp. 1136-1148, 2019.
- [14] H. Zhu, X. Huang, X. Li, L. Zhang i X. Liu, „Evaluation of urban underground space resources using digitalization technologies,” *Underground Space*, t. 1, pp. 124-136, 2016.
- [15] K. A. Piirainen, R. A. Gonzalez and J. Bragge, „A systemic evaluation framework for futures research,” *Futures*, t. 44, pp. 464-474, 2012.
- [16] B. K. Ko and J.-S. Yang, „Developments and challenges of foresight evaluation: Review of the past 30 years of research,” *Futures*, t. 155, p. Article 103291, 2024.
- [17] H.-s. Shin, „Underground Space Development and Strategy in Korea,” *TUNNEL & UNDERGROUND SPACE*, t. 23, br. 5, pp. 327-336, 2013.
- [18] H. W. Wiranegara, „PROBLEMATIC ASPECTS OF THE USE OF URBAN UNDERGROUND SPACE IN INDONESIA,” *LivaS - International Journal on Livable Space*, t. 2, br. 2, p. 1 – 10, 2017.
- [19] S. Inayatullah, „City futures in transformation: Emerging issues and case studies,” *Futures*, t. 43, pp. 654-661, 2011.
- [20] J. Quista and P. Vergragt, „Past and future of backcasting: The shift to stakeholder participation and a proposal for a methodological framework,” *Futures*, t. 38, pp. 1027-1045, 2006.
- [21] B. Tonn, „The future of futures decision making,” *Futures*, t. 35, pp. 673-688, 2003.
- [22] O. Renn, „Transdisciplinarity: Synthesis towards a modular approach,” *Futures*, t. 130, p. Article 102744, 2021.
- [23] L. A. Pace, C. Bruno and J. O. Schwarz, „Personas in scenario building: Integrating human-centred design methods in foresight,” *Futures*, t. 166, p. Article 103539, 2025.
- [24] A. S. Oliveira, M. D. d. Barros, F. d. C. Pereira, C. F. S. Gomes and H. G. d. Costa, „Prospective scenarios: A literature review on the Scopus database,” *Futures*, t. 100, pp. 20-33, 2018.
- [25] J. Mahmud, „City foresight and development planning case study: Implementation of scenario planning in formulation of the Bulungan development plan,” *Futures*, t. 43, pp. 697-706, 2011.
- [26] X. Wang, F. Zhen, X. Huang, M. Zhang and Z. Liu, „Factors influencing the development potential of urban underground space: Structural equation model approach,” *Tunnelling and Underground Space Technology*, t. 38, p. 235–243, 2013.
- [27] A. Faiella and G. E. Corazza, „Cognitive mechanisms in foresight: A bridge between psychology and futures studies,” *Futures*, t. 166, p. Article 103547, 2025.
- [28] F. Lalot, S. Ahvenharju, M. Minkinen and E. Wensing, „Aware of the future? Development and validation of the Futures Consciousness Scale,” *European Journal of Psychological Assessment*, t. 36, br. 5, pp. 874-888, 2019.
- [29] N. MacDonald, „Futures and culture,” *Futures*, t. 44, p. 277–291, 2012.
- [30] C. Zegras and L. Rayle, „Testing the rhetoric: An approach to assess scenario planning’s role as a catalyst for urban policy integration,” *Futures*, t. 44, p. 303–318, 2012.

- [31] Z. Roya, H. Dexter, B. Peter, B. Nikolay i R. Christopher, „A new sustainability framework for urban underground space,“ *Engineering Sustainability*, p. Article 1500013, 2016.
- [32] F. Deng, J. Pu, Y. Huang and Q. Han, „3D geological suitability evaluation for underground space based on the AHP-cloud model,“ *Underground Space* 8 (2023) 109–122, t. 8, p. 109–122, 2023.
- [33] E. Krawczyk and R. Slaughter, „New generations of futures methods,“ *Futures*, t. 42, p. 75–82, 2010.
- [34] I. Vähäaho, „An introduction to the development for urban underground space in Helsinki,“ *Tunnelling and Underground Space Technology*, t. 55, p. 324–328, 2016.
- [35] M. Dufvaa and T. Ahlqvist, „Elements in the construction of future-orientation: A systems view of foresight,“ *Futures* 73, t. 73, pp. 112–125, 2015.
- [36] X. Zhang and H. Li, „Urban resilience and urban sustainability: What we know and what do not know?,“ *Cities*, t. 72, pp. 141–148, 2018.
- [37] N. Rijkens-Klompa, N. Baerten and D. Rossi, „Foresight for debate: Reflections on an experience in conceptual design,“ *Futures*, t. 86, p. 154–165, 2017.
- [38] A. Fergnani and B. Cooper, „Metamodern futures: Prescriptions for metamodern foresight,“ *Futures*, t. 149, p. Article 103135, 2023.
- [39] R. A. Slaughter, „Futures studies as a civilizational catalyst,“ *Futures*, t. 34, p. 349–363, 2002.
- [40] P. Daffara, „Rethinking tomorrow's cities: Emerging issues on city foresight,“ *Futures*, t. 43, p. 680–689, 2011.
- [41] X. Wang, L. Shen and S. Shi, „Evaluation of underground space perception: A user-perspective investigation,“ *Tunnelling and Underground Space Technology*, t. 131, p. Article 104822, 2023.



## INTEGRATED URBAN REGENERATION OF SUBWAY STATIONS AND URBAN DEVELOPMENT IN CENTRAL TOKYO

### - The Case Study of Toranomom Hills Station Tower –

Masaki Kato  
Mori Building Co.,Ltd.

**Abstract:** Tokyo is one of the world's leading subway cities in the world, with approximately 10 million people using the subway each day. New York City has about 5 million subway passengers per day. In central Tokyo, automobiles account for less than 10% of transportation sharing in the city center, while subways and other railroads account for more than 50%. These are the results of urban development linked to public transport (Transit Oriented Development: TOD), which is one of the sustainable urban models.

This paper addresses the significance the case of Toranomom Hills Station and Toranomom Hills Station Tower in Toranomom, Minato-ku, Tokyo, where embassies and offices are concentrated, where transportation operators and urban developers have worked together to integrate subway station construction and urban development.

Subway stations are built underground in the road, and therefore have many spatial constraints. In addition, urban developers and transportation operators are often separate, and project periods do not coincide, making it very difficult to promote urban development in conjunction with transportation infrastructure. In the Toranomom Hills Station project, the transportation operator and urban developer worked together from planning to disaster prevention to solve these problems, and were able to develop a transportation node that will become a landmark in Toranomom, including a large, atrium station plaza from the second basement floor to the first floor that incorporates natural light.

**Keywords:** Tokyo, subway, urban development, TOD, Toranomom Hills

## 1. INTRODUCTION

Tokyo is one of the world's leading subway cities, with approximately 10 million people using the subway every day (2018). This number is far greater than New York's 5.6 million people (2014) and Paris' 4.2 million people (2011). In central Tokyo, rail transportation's share is very high at 50%, and in recent years, the importance of subway stations has further increased, with an increase in the number of direct trains. In addition, the Ministry of Land, Infrastructure, Transport and Tourism and the Tokyo Metropolitan Government have set policies such as TOD (Transit Oriented Development) and station-city integration, making urban development linked to transportation infrastructure such as stations and bus terminals increasingly important. However, urban developers and transportation operators are often separate entities, and their development periods do not necessarily coincide, so there are many challenges to promoting urban development linked to transportation infrastructure.

Due to the nature of subways, subway stations are often necessarily developed in road areas, and due to the difficulty of acquiring additional land, there are very few examples of subway stations in central Tokyo having station plazas in front of them.

In this paper, the Toranomom Hills Station and Toranomom Hills Station Tower Urban Redevelopment Project made the most of the opportunity to proceed with the construction of a new station and the redevelopment project at the same time. From the project planning stage, multiple stakeholders, including not only urban developers and

railway operators but also academics and government officials, sought station-city integration and held detailed discussions, ultimately finding a solution that allowed the creation of a plaza space that goes beyond the connection between the station and the city, and is in a real sense, one with the station.

In this paper, written with the cooperation of the Urban Renaissance Agency (hereinafter "UR"), the project owner of the new station, and Tokyo Metro Co., Ltd. (hereinafter "Tokyo Metro"), which is responsible for the design, construction, and management of the new station, the author, from the perspective of the coordinator of this redevelopment project, introduces the overall process by which a railway project and an urban development project were linked to create an integrated space between the subway station and the city, with the hope that the paper will be useful for future urban development projects linked to transportation infrastructure.

## 2. TORANOMON HILLS INTEGRATED WITH TRANSPORTATION INFRASTRUCTURE

Toranomon was designated as an urban regeneration emergency development area under the Urban Renewal Special Measures Act of 2002 and became a specific urban regeneration emergency development area in 2012. Its development plan stipulates the basic policies of developing an international business and exchange hub with a living environment and strengthening transportation hub functions.

In the Toranomon Hills area (Figures 1 and 2), urban infrastructure development and urban development have been advanced in a step-by-step and integrated manner through several different redevelopment projects, including Loop Road No. 2, Toranomon Hills Station, and a multi-layered pedestrian network at ground, underground, and elevated deck levels.

Mori Tower, completed in 2014, utilizes the multi-level road system that allows buildings to be built above roads to develop both Loop Road No. 2 and the super-high-rise tower in an integrated manner. With the full opening of Loop Road No. 2 in December 2022, access to central Tokyo, the waterfront, and Haneda Airport has been dramatically improved. Business Tower, completed in 2020, has a bus terminal of approximately 1,000 m<sup>2</sup> for the airport limousine bus and the Tokyo BRT, which connects the city center and the waterfront via Loop Road No. 2, as well as an underground passage connecting the bus terminal to both Toranomon Station on the Ginza Line and Toranomon Hills Station on the Hibiya Line. In addition to creating the open subway station plaza described in this paper, Station Tower, completed in July 2023, features a large-scale 20 m wide pedestrian deck (T-deck) above Sakurada-dori Ave. that connects to the surrounding blocks.

In addition, the reconstruction of Toranomon Hospital and Hotel Okura in the vicinity of Toranomon Hills, and various urban functions and transportation infrastructure such as subway stations and bus terminals are connected by underground passages, pedestrian decks, and lush walkways, and there is a clear focus on urban regeneration centered on public transportation.

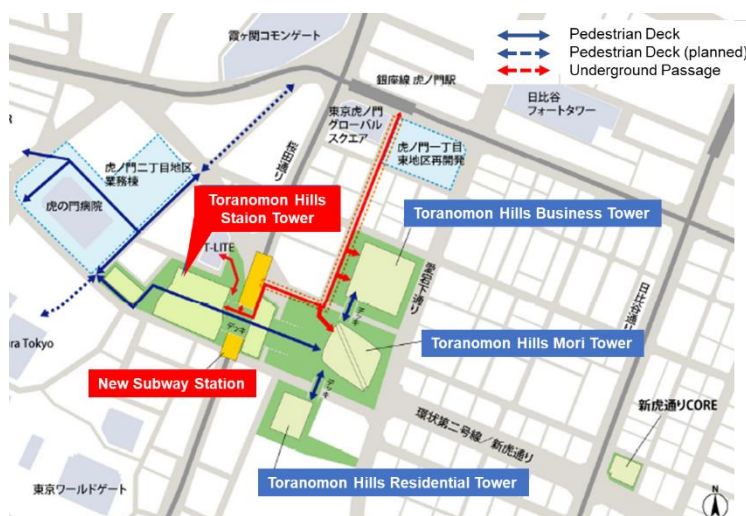


Figure 1. Location map



*Figure 2. Panoramic view of Toranomon Hills*

### 3. PROJECT IMPLEMENTATION STRUCTURE

This project was made possible through close cooperation between two different business entities: the construction of Toranomon Hills Station (hereafter "the new station") and Toranomon Hills Station Tower Urban Redevelopment Project (hereafter "the redevelopment project").

UR was the project owner for the new station, with Tokyo Metro responsible for design, construction and operation and management of the new station after opening, and a joint venture between Kajima Corporation and Obayashi Corporation in charge of construction.

The construction of Toranomon Hills Station Tower, including the underground station plaza, was carried out as a redevelopment project by the Toranomon 1-2-chome District Urban Redevelopment Association (hereafter "the redevelopment association"), which is composed of approximately 30 landowners including Mori Building Co., Ltd (hereinafter "Company M"), who acted as a participating member, designated builder, secretariat manager, coordinator, and design and construction supervision, while Kajima Corporation was responsible for construction.

#### 4. TORANOMON HILLS STATION TOWER URBAN REDEVELOPMENT PROJECT

This redevelopment project was carried out by approximately 30 landowners, including Company M, and involved the construction of Toranomon Hills Station Tower, Edomizaka Terrace, and Glass Rock (hereinafter referred to as "redeveloped buildings"), as well as public facilities such as Minato Ward parks, roads, and pedestrian decks.



*Figure 3. Panoramic view of Toranomon Hills Station Tower*

In 2014, a study group was started by landowners, including Company M. At the same time, the urban planning for the new station was decided, and discussions were held from the beginning with the aim of creating a development integrated with the new station. A preparatory association was established in February 2016, and construction of the new station began at the same time. With the possibility of creating a more convenient and rich space increasing, discussions and considerations in the preparatory association also accelerated with the aim of creating a development integrated with the new station. A development planning proposal was formulated based on the following: 1) Development of a subway station plaza that would contribute to strengthening the transport hub function; 2) Development of a wide pedestrian deck on Sakurada-dori Ave. (National Route 1) that would be the key to forming a pedestrian network connecting Shimbashi and Akasaka; and 3) Development of the Akasaka-Toranomon Greenway on the southern side of the district along Ward Road 1014 in conjunction with the surrounding redevelopment. The development plan was approved in March 2018, the redevelopment association was established in November 2018, the rights conversion plan was approved in March 2019, and new construction began in November of the same year. Toranomon Hills Station Tower (Block A-1) and Toranomon Hills Edomizaka Terrace (Block A-3) were completed in July 2023. Glass Rock (Block A-2) and Minato Ward Park (Block A-4) were completed in August 2024. Although there were various difficulties in carrying out the new station construction and redevelopment project in this area as a whole, thanks to the focused efforts of the association members to promote the local development and the cooperation of all concerned parties, construction was completed in the exceptionally short period of about 10 years since the study sessions began and about 7 and a half years since the preparatory association was established.

#### 5. TORANOMON HILLS STATION DEVELOPMENT

##### 5.1. Committee Recommendations

Since 2000, with the enactment of the Urban Renewal Special Measures Act (2002), large-scale redevelopment buildings have been built one after another in central Tokyo, and congestion inside some train stations has become



a major problem. On the other hand, it has been pointed out that there may be areas in central Tokyo that are unable to realize their potential growth potential due to poor access to train stations. Therefore, in 2010, UR commissioned the Japan Transport Policy Research Institute to conduct a survey, and the Research Committee on Public Transportation Service Levels for Promoting Urban Renewal in Central Tokyo (hereinafter referred to as the "Committee") was formed, consisting of academics with knowledge of urban and railway development, railway operators, related local governments, related organizations, and the Ministry of Land, Infrastructure, Transport and Tourism, and conducted the survey.

The Committee conducted the following activities: 1) Survey of urban development trends and actual use of public transportation, 2) Evaluation of public transportation and identification of key issues, 3) Consideration of improvement measures and case studies, and 4) Consideration of systems for strengthening cooperation between urban development and railway development.

During the study, it was found that there are urban railway inconvenient areas (such as around Harumi and along Loop Road No. 2 around Shimbashi and Toranomon) in specific urban regeneration emergency development areas with poor access to the nearest station and main terminals. It was found that it is important to improve railway station congestion and inconvenient areas in urban areas where the railway share is high in central Tokyo, and that it is important to consider improving railway services in parallel with the promotion of urban regeneration.

Regarding financial resources, it was found that since the effects of railway facility development spread widely among many parties, it is necessary to consider the beneficiary burden, which requires a proportionate burden for the benefits enjoyed, taking into account the ability to bear (ability-based burden). It was found that it is desirable for the national and local governments to continue supporting urban development and railway development in the future, since railway development increases the attractiveness of cities and absorbs development profits in the form of increased tax revenues such as property taxes, and therefore they are one of the beneficiaries and are in a position to be responsible for city development.

As a result of this study, it was determined that the area around Toranomon faced issues related to both congestion within stations and the distance from train stations (an urban area that is inconvenient for railways), and it was recommended that effective improvement measures include constructing new entrances and exits at existing stations, establishing a new Hibiya Line station, developing underground passageways, and developing new access services such as LRT/BRT.

## **5.2. Positioning in administrative plans**

In March 2014, the Tokyo Governor announced the proposal for the National Strategic Special Zone, proposing strengthening Toranomon's transport hub function and indicated the policy of developing a new Hibiya Line station and bus terminal, improving Toranomon Station on the Ginza Line, developing a pedestrian network connecting them, and promoting the development of the surrounding area in an integrated manner. In October of the same year, the Development Plan for the Tokyo Metropolitan Center and Waterfront Area (Loop Road No. 2 Shimbashi/Toranomon District) was formulated as a specific urban regeneration urgent development area, and UR was positioned as the developer of 14 urban development projects necessary to improve the city's international competitiveness, public facilities such as development of a new station, improvement of Toranomon Station and Kamiyacho Station, and development of underground passages to strengthen transport hubs, and the new station. In the Tokyo Metropolitan Long-Term Vision announced in December of the same year, the target year for the development of new stations, bus terminals, and underground passages was set as 2020.

After that, the area was designated as a National Strategic Special Zone by the Prime Minister in June 2015, construction began in February 2016, the name of the station was decided as Toranomon Hills Station in December 2018, and it opened in June 2020. In July 2023, it was connected to the adjacent redeveloped building, creating an integrated station-town space. In this paper, the state in July 2023 will be referred to as the official opening of the new station.



## 6. SPACE DEVELOPMENT OF STATION AND THE DEVELOPMENT

### 6.1. Development classification, property classification, and maintenance classification

The development classification of this project is as shown in Figures 4. The new station was developed within the road area of National Route 1 after widening it as part of this redevelopment project, and the redevelopment project implementation area were developed by this redevelopment project. The property classification and maintenance classification are also the same.



*Figure 4. Cross-section of the new station and subway station plaza (construction division, property division, maintenance division)*

### 6.2. Process toward realization

UR, promoted the new station development, Tokyo Metro, the redevelopment association, and M Company, promoted urban development, conducted study sessions and coordination meetings from the project concept stage to planning, design, construction, and management, respectively, and promoted this project by linking the intention of the planning stage to design, construction, and management.

#### 6.2.1. Planning and design stage

In order to make the most of the opportunity to simultaneously proceed with the new station construction and redevelopment projects on both sides, and to coordinate urban development and railway construction as one of the committee's recommendations, we held a series of study sessions with academic experts to realize a project that integrated subway stations and urban development, and which could not be realized with subway construction alone.

In addition to the participants mentioned above, administrative officials and consultants with specialized knowledge also participated in this study session, and lively discussions were held on multiple fronts, such as understanding each other's projects, including not only the construction plan but also the methods and systems for railway and urban development projects. It was because of the discussions at that time that we were able to proceed with this project with the same feeling, even in the midst of various difficulties, to make it an unprecedented project that integrated the station and the town.

During the study session, it was recognized that while subway stations are becoming increasingly important, due to their nature as underground stations and the conditions of occupying road areas, there are several issues: 1) it is difficult to know where the station is; 2) it is difficult to develop barrier-free facilities such as station plazas and elevators; and 3) it is difficult to understand the flow of people. Therefore, in order to solve these issues, the new station is not only be located within the road area but was developed in an integrated manner with the redevelopment projects being carried out on both sides of the road area. In both the new station and this

redevelopment project, the basic concept for the low-rise areas was set as creating a space that will be the face of the development, connecting the station and the development in an easy-to-understand way without relying on signs, etc., and connecting the development on a broad scale, and the design of the station and redevelopment buildings was thus advanced.

From the perspective of business feasibility, this redevelopment project sought to develop floors that generate as much revenue as possible, but based on the discussions at the study group, an underground station plaza that is integrated with the station was developed on the site of this redevelopment adjacent to the station (Figure 5), with a three-story atrium from the ticket gate floor on the second basement floor to the first floor above ground, allowing natural light to pour into the underground space, and escalators and elevators were installed. This allows for intuitive movement from underground to above ground.

At the platform level on the first basement floor, the platform wall is made of glass screens (Figures 6 and 7), visually connecting the platform and the station plaza, allowing rail users and people moving throughout the development to feel each other's presence.



*Figure 5. Underground Station Plaza*



*Figure 6. Station concourse (second basement floor) and platform (first basement floor) as seen from the underground station plaza*

Stores have been placed around the underground station plaza to better integrate the station with the development. Normally, this space serves as a symbolic plaza that connects the station and the development, but in emergencies it also serves as a temporary shelter (for approximately 340 people) for people unable to return home in an emergency who gather at the station. This underground station plaza has been designated a major public facility in urban planning (district planning that defines redevelopment promotion zones), and will be maintained as a highly public space into the future.

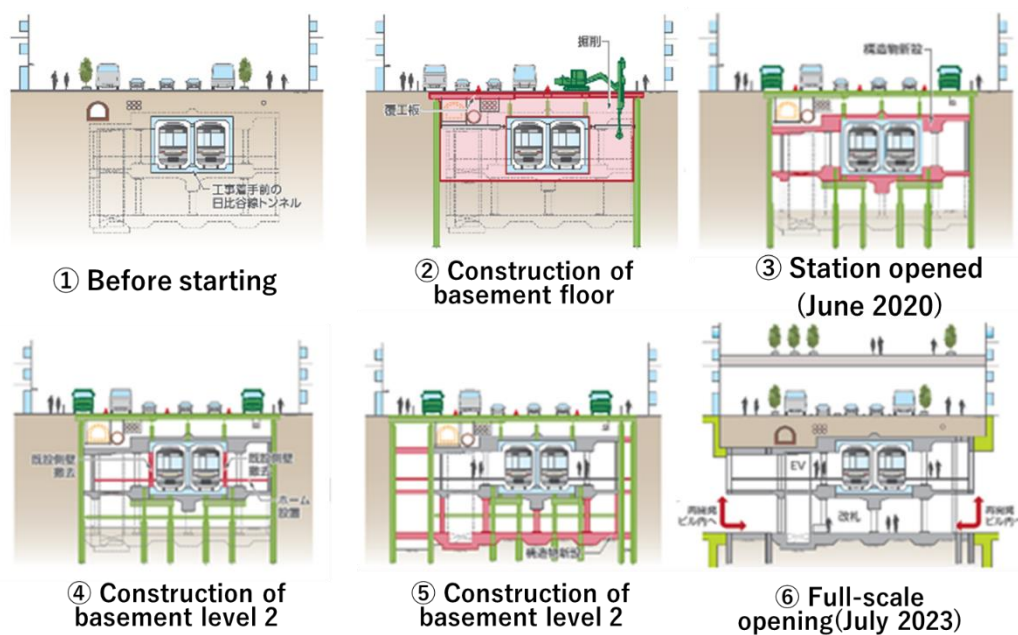


*Figure 7. View of the underground station plaza from the platform*

### 6.2.2. Construction stage

The construction of the new station and this redevelopment project were carried out at the same time while National Route 1 and the Hibiya Line were in service, and the construction site area was limited, so the schedule and construction site area adjustments were posed some problems.

The construction of the new station was set to begin service before the 2020 Tokyo Olympics under the extremely difficult construction conditions of widening and excavating both sides and the underside of the Hibiya Line structure (Figure 8) while National Route 1 and the Hibiya Subway Line were in service. The new station was planned to open in 2023 when the redevelopment buildings were completed, but when it began service in 2020, it was decided to strictly adhere to the June 2020 start of service date by providing the minimum necessary facilities for the station and establishing an entrance and exit for materials and waste soil within the redevelopment project site, as well as an entrance and exit for the start of service in June 2020 (hereinafter the "provisional entrance and exit"). The temporary entrance was relocated in accordance with the progress of the construction of the redeveloped building and was removed when the new station opened in July 2023. After that, the redeveloped building and the ward park were developed as part of this redevelopment project.



*Figure 8. New station construction steps*

The scope of the redevelopment work and the new station construction overlapped, such as the construction of a 20m-wide deck above National Route 1 during the construction of the new station, and the construction period



was limited. Therefore, the Tokyo Metropolitan Government Bureau of Urban Development acted as the secretariat, and a regular liaison and coordination meeting was established as a place for information sharing and cooperation between related parties such as road managers, traffic managers, buried construction companies, UR, Tokyo Metro, and the redevelopment association. This liaison and coordination meeting was very helpful in smoothly coordinating the project.

In addition to the liaison and coordination meeting, coordination meetings between the businesses and construction companies and monthly meetings were held to closely coordinate the two projects. In particular, establishing loading/unloading entrances and temporary entrances within the redevelopment project site had a significant impact on the redevelopment work, and in this way, the schedule was carefully coordinated. Additionally, for construction at the borders of construction zones, an agreement was signed between the projects and the use of retaining walls and temporary structures was shared to reduce costs and construction time. Nevertheless, many unforeseen situations occurred, and adjustments were made between the businesses on each occasion. Road restoration work on National Route 1 is still ongoing.

### 6.2.3. Maintenance and operation

This redevelopment project and the new station are classified as assets and under maintenance management as shown in Figure 7. For the redevelopment buildings, including the part designated as a redevelopment project in the property and maintenance classifications, a management association was formed by the landowners, and a manager based on Article 25 of the Condominium Act (hereinafter the "Article 25 Manager"). Company M was selected as the Article 25 Manager. The Article 25 Manager's duties include not only building management, but also town management, branding the redeveloped buildings, creating a lively atmosphere, and area management in cooperation with surrounding buildings. The subway station plaza is a common area of the redeveloped buildings and is managed and operated by the Article 25 Manager, who holds concerts (Figure 9) and events linked to the information center (TOKYO NODE) at the top of Station Tower (Figure 10). Income from the event is used to cover the operating costs of the event, as well as part of the town management costs of the Article 25 Administrator.



*Figure 9. Event at the subway station plaza ①*

*Figure 10. Event at the subway station plaza ②*

The new station will be the first for Tokyo Metro to not have a dedicated passenger entrance/exit for Tokyo Metro but will instead pass through the underground station plaza that will be developed as part of this redevelopment project, with the entrance to the redeveloped building serving as the subway entrance/exit. The passenger flow from the new station within the redeveloped building to ground level is entirely common to the redeveloped building, and no sectional surface rights have been established for Tokyo Metro. A management agreement has been concluded between Tokyo Metro and the redevelopment building management association, satisfying the requirements of both parties. Furthermore, the necessary evacuation routes (also used for subway work) have been developed within the redeveloped building and are for the exclusive use of Tokyo Metro.

#### **6.2.4. Disaster prevention plan**

The redeveloped building and the new station were treated as a single fire prevention object (hereinafter "this fire prevention object"), because it would have been difficult to create a space that integrated the subway station and the development by dividing each facility into sections according to Article 8 of the Fire Service Act Enforcement Order, and using buffer zones, etc.

The Fire Service Act does not allow multiple managers for a single fire prevention object, so either the building manager or the station manager must be responsible for overall management. However, in this project, the redeveloped building and the new station, which have different management and operation formats, are able to cooperate with each other while separately installing, maintaining, managing, and operating firefighting equipment. An advanced fire and disaster prevention system, including the integrated control panel described below, was built based on the special firefighting equipment, etc. stipulated in Article 17, Paragraph 3 of the Fire Service Act, and has been certified by the Minister of Internal Affairs and Communications.

In addition to organizing a self-defense fire brigade for each of the redeveloped buildings and the new station, the redeveloped buildings and the new station created an overall fire prevention plan, appointed a general fire and disaster prevention manager, and work together to manage daily fire prevention, maintain firefighting equipment, and hold regular meetings. In addition, there are plans to conduct comprehensive fire drills so that initial firefighting activities and evacuation guidance can be carried out quickly and accurately in the event of a fire. The underground station square will also serve as a temporary shelter for approximately 340 people who are unable to return home in the event of a disaster.

## **7. IN CONCLUSION**

A station-development integration project cannot proceed without the cooperation of many stakeholders, including the high technical skills and coordination abilities of urban development companies, railway operators, designers and constructors, as well as the government, buried utility companies for communications, electricity and water, and local residents. Coordination between the station and the development was complicated from the planning and design stages, but at the construction stage, the process and costs become intertwined, making the coordination even more complicated. I once again felt that while systems such as conferences are important for carefully unraveling these issues one by one, the human relationships and trust between the stakeholders played a major role. I believe that an unprecedented space was realized by the strong desire of the stakeholders to realize an unprecedented project that integrates the station and the development, by understanding each other's circumstances and cultures of the railway business and the urban development business, and by considering the optimal solution for station-development integration.

It is extremely difficult to proceed with the development and renewal of transportation infrastructure on its own, due to factors such as the surrounding environment and the difficulty of acquiring land. I feel that in the future, it will be important to advance urban development and the development of transportation infrastructure in an integrated manner in order to advance the renewal of urban functions in the region. Furthermore, I believe that the role of redevelopment coordinator will be expected to go beyond the redevelopment area and coordinate the entire region, including transportation infrastructure, more than ever before.

This project was made possible thanks to the guidance and cooperation of many people involved, including local residents. I would like to express my sincere respect and gratitude here to all involved.



## EXPLORATION OF URBAN DESIGN CONCEPTS FOR UNDERGROUND PUBLIC SPACES IN RENEWAL AREAS

### — A CASE STUDY OF BEIJING' S UNDERGROUND SPACE CONSTRUCTION

Meng Lingjun<sup>1</sup>, Zhao Yiting<sup>1</sup>, Guo jing<sup>1</sup>, Wu Kejie<sup>1</sup>

**Abstract:** Beijing has entered an era of stock planning, facing dual demands: tight spatial resource constraints and high-quality development needs. As a vital "fourth national land resource," the development of underground space is key to urban expansion, functional optimization, and quality enhancement. With growing public demand for better underground public space environments and experiences, exploring systematic and human-centered urban design approaches is crucial. This paper clarifies the practical needs, core challenges, and fundamental principles for designing underground public spaces in urban renewal areas, establishing a theoretical foundation. Building upon urban design theory within the urban renewal context, it focuses on balancing historical preservation, community needs, and underground development. The study develops an integrated design framework addressing both spatial structure and micro-place construction. Using Beijing as a case study, the paper analyzes practical experiences and challenges in underground development during urban RENEWAL. It validates and refines the proposed design approach through case studies, extracting transferable insight.

**Keywords:** Urban renewal; Underground public space; Urban design; Spatial quality; High-quality development; People-oriented

## 1. INTRODUCTION

Urban development in Beijing, China has entered a stage of urban RENEWAL, shifting from large-scale expansion to optimizing existing stock and enhancing quality. Under these constraints, cities face the challenge of achieving high-quality development within limited spatial resources. As the "fourth national spatial resource" beyond terrestrial, aquatic, and aerial spaces, underground space demonstrates growing strategic value in this renewal area. Significant progress has been made in utilizing underground space to alleviate urban traffic, enhance comprehensive carrying capacity, and improve urban resilience, establishing systematic research foundations and practical outcomes. Future development will transition from infrastructure support to accommodating daily human needs. However, a systematic urban design methodology for improving underground space quality remains underdeveloped—particularly regarding how refined design approaches can effectively enhance overall quality and comprehensive value of underground public spaces amid complex renewal constraints. This represents a critical gap requiring urgent resolution.

Therefore, in-depth exploration of underground space development within the urban RENEWAL context—particularly the planning and design of underground public spaces—holds significant practical and strategic significance. This study aims to establish a scientific and systematic urban design framework for underground public spaces. It seeks to offer both theoretical foundations and practical guidelines for Enhancing environmental quality of underground spaces、optimizing functional organization and strengthening spatial attractiveness. Ultimately, this approach advances sustainable urban development and meets the growing public demand for high-quality living environments.

<sup>1</sup> Beijing Municipal Institute of City Planning & Design, China

## 2. CHARACTERISTICS OF UNDERGROUND PUBLIC SPACES AND DEVELOPMENT NEEDS IN URBAN RENEWAL AREAS

### 2.1. Characteristics of Underground Public Spaces

The unique physical environment and functional requirements of underground public spaces present distinct challenges for urban design: **First**, regarding physical and environmental attributes: The notable absence of natural light and ventilation frequently results in dim lighting and poor air quality, adversely affecting occupants' physical and psychological well-being<sup>[1]</sup>. **Second**, the lack of spatial references and natural orientation cues complicates navigation. As extensions of above-ground functions, underground spaces demand tight coordination with surface-level elements—including access points, transportation links, and complementary commercial activities—to ensure functional integration. **Third**, confined environments often induce psychological discomfort, manifesting as sensations of confinement and oppression. **Fourth**, implementation is strictly constrained by geological factors (e.g., geological formations, groundwater levels, soil properties), significantly complicating design processes and introducing uncertainties<sup>[2]</sup>.

### 2.2. Core Challenges in Underground Space Development Under Urban RENEWAL

Underground space development within urban renewal contexts faces multiple core challenges: First, significant difficulties exist in coordinating with existing built environments. In historic urban areas, issues like building foundation stability, intricate subsurface utility networks, heritage conservation requirements, and fragmented property rights—compounded by historically fragmented development patterns—have resulted in scattered, isolated underground spaces lacking integrated network planning. This undermines systemic efficiency and connectivity benefits. Concurrently, substantial barriers impede aboveground-underground integration. Development fragmented by property boundaries creates functional conflicts, compromised pedestrian flows, and disjointed landscapes, hindering synergistic spatial development. Furthermore, the sequential "aboveground-first, underground-later" approach exacerbates planning delays and uncertainties, necessitating refined coordination mechanisms and advance provisioning strategies. Lastly, the multi-ownership, mixed-use nature of complex underground spaces substantially increases operational complexity in maintenance, safety management, and emergency response.

Addressing these challenges constitutes a critical pathway toward high-quality underground space development and sustainable urban renewal—urgently requiring in-depth exploration by academia and industry.

### 2.3. Practical Demands for Underground Public Space Development Driven by Urban RENEWAL

As cities transition into urban renewal phases, the strategic value of underground public spaces intensifies, positioning them as critical pathways to meet multifaceted urban development needs:

- **Enhancing Public Space Quality and Vitality.** Urban renewal prioritizes human-centered environments. Underground public spaces—as integral components of urban spatial systems—require thoughtful design to create **pleasant, safe, and attractive social venues**. Integrating cultural, recreational, and experiential functions can revitalize historic districts.
- **Augmenting Urban Functions and Infilling Gaps.** Historic urban areas often suffer from **inadequate and unevenly distributed** public services, municipal infrastructure (e.g., parking, utility tunnels, substations), and civil defense facilities. Underground spaces effectively address these gaps through functional diversification, strengthening public service capabilities<sup>[3]</sup>.
- **Optimizing Transportation and Pedestrian Networks.** Integrated with transit systems, continuous, accessible, and comfortable underground pedestrian networks improve mobility experiences, connect key nodes, and enable pedestrian-vehicle separation.
- **Preserving Cultural Heritage and Identity.** Through measured and context-sensitive interventions, underground spaces can address community needs while accommodating museums or galleries that activate cultural heritage, fostering regionally distinctive underground environments.
- **Advancing Urban Resilience and Sustainability.** Eco-design and low-impact development models promote sustainable underground space utilization, directly contributing to urban resilience goals.

### **3. URBAN DESIGN FRAMEWORK FOR UNDERGROUND PUBLIC SPACES IN RENEWAL AREAS**

#### **3.1. Theoretical Foundations**

Urban design is a discipline examining the interplay between physical urban forms and human activities/perceptions—provides fundamental theoretical underpinnings for underground public space design. Kevin Lynch's *Image of the City* emphasizes five key elements (paths, edges, districts, nodes, landmarks) crucial for spatial cognition<sup>[4]</sup>. Jan Gehl advocates human-centered approaches, prioritizing behavioral needs and public life while stressing how the quality of streets, squares, and other public spaces determines urban vitality<sup>[5]</sup>. Gordon Cullen's *Townscape* theory reveals methods for crafting engaging urban experiences through spatial sequencing and placemaking. Collectively, these theories highlight the dynamic relationship between activity, space, and perception, underscoring the imperative to create meaningful places that foster social interaction. This is particularly critical in underground environments lacking spatial references, where clear spatial organization and distinctive nodal design are essential for establishing user orientation and spatial comprehension.

#### **3.2. Design Objectives**

The urban design of underground public spaces in stock renewal areas fundamentally prioritizes human activities, experiences, and perceptions—transcending traditional engineering-centric mindsets to achieve human-centered multi-scale integration and systematic development. This approach aims to create multifunctional, interconnected, pleasant, vibrant, and sustainably resilient underground public space systems that organically extend and complement above-ground urban life. Focusing on internal structural organization, functional layouts, and pedestrian circulation systems within underground networks, this study establishes a spatial framework through nodal design and network design to advance urban design theory for underground environments.

#### **3.3. Structural Dimension: Organizational Framework and Circulation System Design**

##### **3.3.1. Shallow Underground Spaces**

In renewal areas, fragmented development of underground spaces has resulted in isolated "underground pods." Priority should be given to establishing integrated shallow underground pedestrian networks through optimizing hierarchical connectivity, enhancing wayfinding systems, and improving spatial sequencing, rhythm, and legibility.

A multi-tiered pedestrian network must be structured according to pedestrian flow volumes and destination significance, comprising primary pathways (connecting major nodes and zones), secondary pathways (linking minor nodes or plots), and connector pathways (accessing individual buildings or facilities). Path alignment should align with natural movement patterns, key functional distributions, and nodal attractions to effectively guide pedestrian flow while avoiding excessively long, monotonous, or disorienting corridors.

Spatial experience should be enhanced through deliberate variations in passage width, clear height, and spatial transitions (e.g., from confined passages to open atria), coupled with sequential organization of flooring materials, wall finishes, ceiling configurations, lighting schemes, and color applications. This approach creates rhythmic, engaging, and intuitively navigable spatial sequences that reinforce environmental legibility.

Implementation requires incentive policies and technical guidelines promoting underground interconnectivity between adjacent plots and new/renovated developments. Specific measures include mandating interface locations, standardizing cross-section dimensions, and specifying elevation requirements to integrate fragmented point-based and linear spaces into cohesive networks.

##### **3.3.2. Integrated Design of Underground Spatial Nodes**

Key nodal integration requires coordinated design across three typologies: transportation hubs, commercial centers, and cultural venues.

At transportation hubs (subway stations, bus terminals), traditional corridor-style transfers should be transformed into living-room-style or street-style interchange spaces to eliminate monotonous underground walking experiences. This facilitates seamless transfers between transportation modes while establishing direct underground connections between hubs and adjacent commercial, office, and residential areas, enabling gradual transitions from public to private realms.

For commercial centers, underground spaces should extend and complement above-ground retail through compelling commercial atmospheres, featured atriums or sunken plazas, and diverse commercial formats that attract pedestrian flow and enhance commercial vitality.

Cultural and sports facilities should incorporate semi-underground designs, incorporating sunken plazas, lightwell atriums, and underground squares at strategic nodes. These open/semi-open public spaces not only

improve natural lighting and ventilation but also provide venues for recreation, social interaction, and small-scale exhibitions—strengthening the public character of underground environments while reinforcing visual and spatial connections with surface-level urban fabric.

### 3.4. Micro-Level Dimension : Placemaking and Environmental Quality Enhancement

Micro-scale design critically shapes user experiences and environmental quality in underground spaces. Key strategies include spatial proportioning, natural element integration, and artificial environment optimization to enhance comfort.

- **Spatial Proportioning and Interface Design:** Space dimensions (width, height, length) must align with functional typologies, pedestrian flows, and activity characteristics to prevent oppressive or excessively vast sensations. Critical interfaces—walls, floors, and ceilings—require deliberate material selection, color schemes, textural qualities, and lighting treatments that support functional objectives and atmospheric goals while ensuring navigational clarity, durability, maintainability, and aesthetic coherence.
- **Integration and Simulation of Natural Elements:** Natural light introduction via skylights and light tube systems reduces reliance on artificial lighting in deep underground areas. Natural ventilation leverages wind/thermal pressure effects through optimized vent placement to supplement mechanical systems, ensuring air freshness. In illuminated zones, shade-tolerant vegetation and ecological water features enhance aesthetics and microclimates.
- **Artificial Environment Refinement:** Comprehensive improvements encompass advanced lighting and acoustic design, systematic wayfinding and information systems, public art reflecting regional cultural identity, user-oriented amenities addressing behavioral need.

## 4. DESIGN MODELS AND BEIJING PRACTICES

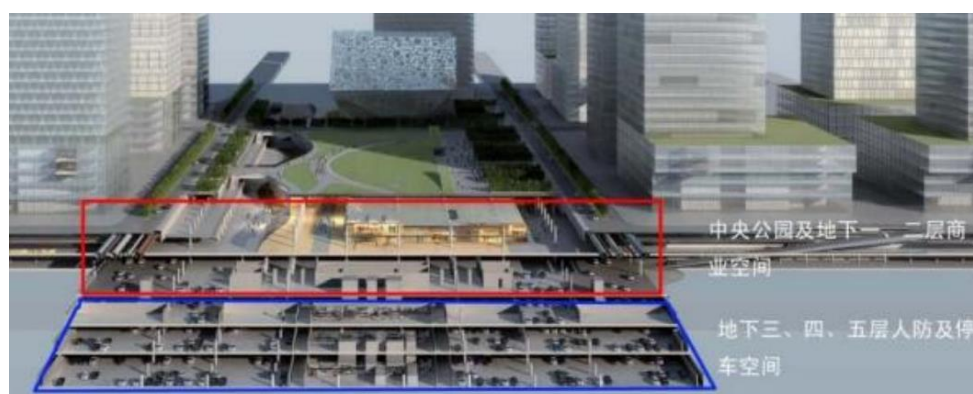
Beijing has pioneered diverse approaches to underground public space utilization amid stock renewal. Representative case studies illustrate practical applications of the proposed urban design framework.

### 4.1. Networked Underground Spaces and Vitality Enhancement in Urban Cores: Cases of Wangfujing/Financial District Renewal

Urban cores (e.g., Wangfujing, Financial Street, CBD) feature high-density built environments with persistent traffic congestion and commercial competition, necessitating enhanced public space quality and economic vitality. Early underground developments suffered from poor connectivity, outdated facilities, and obsolete commercial formats.

Regionally, unified underground planning aligned with transit integration establishes district-wide pedestrian networks and comprehensive service systems. Locally, new or renovated underground passages connect disparate commercial buildings, offices, hotels, and cultural facilities into networked retail complexes. Strategic placement of sunken plazas and atriums creates attractive public nodes that channel pedestrian flow and intensify commercial vibrancy.

At the micro-scale, high-quality commercial environments are achieved through unified wayfinding systems, optimized lighting and HVAC controls, premium finishes, and culturally resonant art installations. These high-investment projects demand intensive coordination; success hinges on unified planning, phased implementation, and refined operational management — particularly regarding property rights delineation and centralized administration to enable effective shallow-space interconnectivity.



**Figure 1.** Beijing CBD Core Area Vertical Design Schematic  
(B1-B2: Commercial Space; B3-B5: Civil Defense & Parking)

#### 4.2. Transforming Existing Transit Stations into Compact Urban Lounges: Ping'anli Metro Station Integration Project in Xicheng District, Beijing

Located within Beijing's core functional area adjacent to the historic Xijiekou district, Ping'anli Station serves as a quadruple-line interchange (M4, M6, M19, planned M3). The renovation project replaces traditional corridor-style transfers with a concourse-style interchange hall. A triple-height atrium channels natural light deep underground, enhancing spatial comfort while strengthening navigational clarity.

The newly added underground integration zone features pre-embedded interfaces for future connections to eastern and northern developments. This "satellite concourse" optimizes multimodal transitions, catalyzing a symbiotic "transit-community" development model. Crucially, courtyard-inspired dispersed volumes mitigate the visual impact of large-scale infrastructure on the surrounding low-rise historical fabric, preserving neighborhood character through sensitive massing articulation.



**Figure 2.** Design of Public Reception Space at Ping'anli Station Underground Hub

#### 4.3. Semi-Underground Cultural Facility: Beijing's Three Hills and Five Gardens Art Center

Located in the northwest corner of Haidian Park, Haidian District, the Three Hills and Five Gardens Art Center is Beijing's first non-heritage-site art museum developed underground. Spanning 21,000 m<sup>2</sup> with 19,000 m<sup>2</sup> situated below grade, its four subterranean levels extend over 30 meters deep. A 14-meter clear height integrated with lightwells floods exhibition spaces with natural light, ensuring visual transparency and comfort.

As a custodial, research, and interpretive hub for Haidian's cultural legacy across eras, the center advances community cultural development through diverse public programs. It fulfills a dual mandate: safeguarding regional heritage while fostering artistic exchange within a modern cultural complex harmonizing conservation, exhibition, and natural landscape integration.



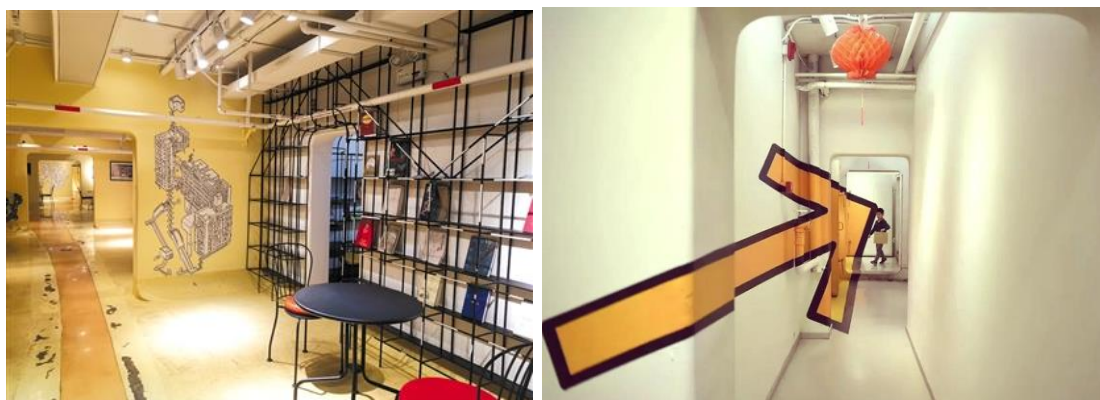


**Figure 3.** Above-Ground & Semi-Submerged Structures of Haidian San Shan Wu Yuan Arts Center

#### **4.4. Community-Driven Underground Micro-Space Activation: Ganluxiyuan Digua Community in Chaoyang District**

Digua Community exemplifies Beijing's innovative repurposing of derelict underground spaces—abandoned basements and civil defense shelters—into neighborhood hubs through *spatial reconfiguration* + *community co-creation*. The Ganluxiyuan project transformed 1,500 m<sup>2</sup> of basement into a "Shared Living Room" featuring free-access zones (book café, "Digua University") and fee-based amenities (board game rooms, table tennis).

Similarly, Anyuan Beili's 560 m<sup>2</sup> Digua Community integrates "Task-Lit Reading Nooks" and "Community Fitness Corners," hosting elder Peking opera clubs and student gatherings. This model pioneers a *multi-stakeholder governance framework* with government oversight, resident-led operations, and cross-sector partnerships.



**Figure 4.** Underground Public Space Renewal: DiGua Community  
(Left: Ganluxiyuan, Chaoyang / Right: Anyuan Beili Community)

## 5. CONCLUSION AND FUTURE RESEARCH DIRECTIONS

High-quality underground public spaces transcend mere transportation nodes or commercial extensions, emerging as vital venues for civic interaction, cultural engagement, and recreational activities that constitute modern urban vitality. Within stock renewal contexts, further research should advance:

**Intelligent Systems:** Implementing digital twins and IoT technologies across underground space lifecycles to establish smart management frameworks.

**Resilience Enhancement:** Optimizing disaster response capabilities through risk-informed design that strengthens mitigation and recovery functions.

**Eco-Innovation:** Developing energy-efficient systems and ecological materials for low-carbon operations.

**Adaptive Reuse:** Innovating retrofitting techniques and reprogramming strategies for civil defense structures and obsolete facilities.

**Governance Reform:** Revising property rights regimes and planning approvals to enable integrated administration.

Coordinated advancement in these domains will catalyze high-quality underground space development, promoting sustainable spatial utilization and enhanced human habitats.

## 6. REFERENCES

- [1] Urban Design. (2024). Green Lighting Design for Underground Spaces from Health Perspectives [Unpublished manuscript]. Retrieved June 3, 2025 from [https://news.sohu.com/a/765001123\\_121123910](https://news.sohu.com/a/765001123_121123910)
- [2] Shi, X., Zhao, Y., & Wu, K. (2020). Scientific planning of megacity underground space in ecological civilization era. *Tunnel Construction (Chinese & English)*, \*40\*(5), 623–630. <https://doi.org/10.3973/j.issn.2096-4498.2020.05.001>
- [3] [Zhuang, Y., & Zhou, L. (2019). Bottom-up structuralism: "Form follows flow" in urban underground space. *Urbanism and Architecture*, (26), 41–48. Retrieved June 3, 2025 from [https://www.sohu.com/a/343665958\\_681890](https://www.sohu.com/a/343665958_681890)
- [4] Lynch, K. (2017). *The Image of the City* (H. FuXiang, Z. Qi, & W. XiaoYa, Trans.). China Architecture & Building Press. (Original work published 1960)
- [5] Zhao, C. (2011). Research on Jan Gehl's people-oriented urban public space design theory [Doctoral dissertation, Northeast Forestry University].

## RESEARCH ON UNDERGROUND SPACE IMAGE AND PRACTICE OF THREE-DIMENSIONAL URBAN DESIGN

Fang Zhou<sup>1</sup>, Zhang Huang<sup>2</sup>, Lin Yifeng<sup>3</sup>

**Abstract:** Underground spaces exhibit distinct spatial and organizational characteristics compared to above-ground environments, leading to significant differences in human perception, cognition, and urban image elements. Building upon Kevin Lynch's foundational theory on urban image, which highlights subway stations as key examples of urban separation with conceptual connections to the surface, this research investigates the urban image of underground spaces. The study employs a mixed-methodology approach, utilizing structured interviews and cognitive map drawing exercises within two established underground complexes in Guangzhou: Huacheng Square and Tianhe business district. This primary data collection is further informed by emerging techniques in 3D reconstruction of underground structures, which aid in characterizing the unique elements of the underground urban image. The research comprehensively summarizes the defining features of these elements and delves into their organizational principles. Furthermore, it explores the integrated spatial image organization between above-ground and underground spaces. Based on this analysis, the study proposes formative principles for organizing underground spatial forms and for three-dimensional urban spatial organization that synthesizes above-ground and underground image elements. These principles are intended to serve as fundamental methods for underground space planning and city design. The practical application and validity of these proposed principles have been tested and demonstrated through implementation in the Xi'an Port District urban design project.

**Keywords:** Underground space, Image, Three-dimensional Urban Design, Spatial form

### 1. INTRODUCTION

Underground spaces are characterized by relative enclosure, artificial interior architecture, and vertically layered structures. The separation between above-ground and underground spaces, insufficient indoor lighting, and visual obstruction from building structures all limit human field of vision, making the perceptible elements in underground spaces far fewer than those above ground, lacking abundant image-supporting elements.

At the same time, the various functions of underground space must be organized on different vertical levels. Coupled with modern cities that coordinate above-ground and underground spaces connected to urban rail transit stations, people's cognition of space must shift from the two-dimensional characteristics of ground space to a more complex and less readily understood three-dimensional space that combines horizontal and vertical features<sup>[4]</sup>.

Kevin Lynch's "The Image of the City" already noted that underground spaces such as subway stations are a significant case of city separation, and they have intangible, conceptual connections with the surface (Kevin Lynch, 2001). However, because of the particular spatial characteristics of underground spaces, they are quite different from the above-ground spaces in spatial perception and cognition and possess unique image characteristics.

This research on urban underground space image builds on Kevin Lynch's pioneering studies and uses the method of interviews plus drawing cognitive maps on actual, constructed underground space cases, to summarize in depth the characteristics of each image element in the urban underground space, to study the organization of these elements and their above-below three-dimensional spatial image organization, and to propose certain principles for underground spatial form and three-dimensional city spatial organization. These can serve as basic

1 Fang Zhou, Underground Space and Planning, Professor Engineer, Guangzhou Transport Planning Research Institute co.,ltd.

2 Zhang Huang, Underground Space and Planning, Senior Engineer, Guangzhou Transport Planning Research Institute co.,ltd.

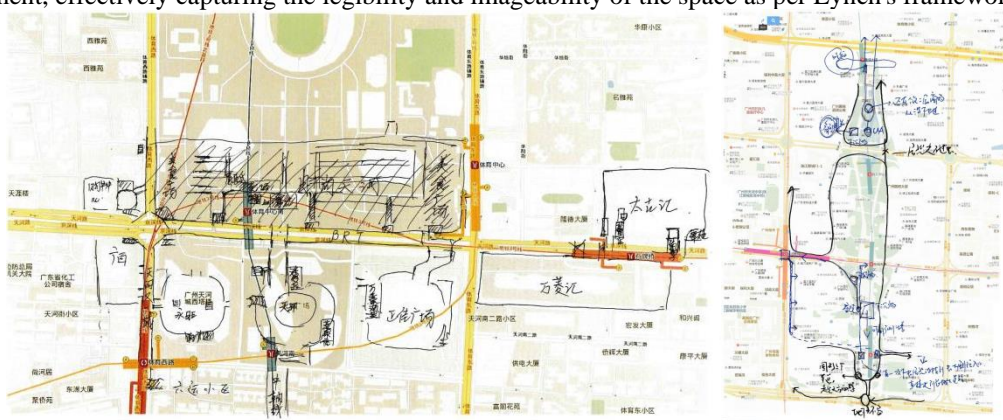
3 Lin Yifeng, Underground Space and Planning, Engineer, Guangzhou Transport Planning Research Institute co.,ltd.

methods and theories for underground space planning and three-dimensional city design, and have been further applied in the urban designs of Xi'an Port Area and the southern area of Guangzhou Pazhou.

## 2. METHODS

### 2.1. The cognitive mapping approach

The study was conducted through in-depth, semi-structured interviews where participants were actively engaged in drawing their mental maps of the underground spaces. This method directly draws inspiration from Kevin Lynch's technique in *The Image of the City*, where residents were asked to sketch their mental images of the urban environment to identify key elements like paths, edges, districts, nodes, and landmarks. In this study, each combined interview and mapping session lasted approximately 30 minutes, resulting in a collection of 40 cognitive maps. This qualitative technique allowed researchers to gain a deep, nuanced understanding of how different user groups perceive, navigate, and remember the spatial layout and defining features of the underground environment, effectively capturing the legibility and imageability of the space as per Lynch's framework.



*Figure 1. Cognitive Map Drawings from the Research*

### 2.2. Questionnaire Survey

The questionnaire survey was developed and deployed as a complementary quantitative tool to validate and generalize the findings from the in-depth cognitive mapping exercises. Following Lynch's principle of gathering diverse public perceptions, the survey, distributed to 302 respondents, was specifically designed based on preliminary insights from the interviews. It aimed to systematically investigate public attitudes, usage patterns, and behavioral characteristics within the underground space. The questions ranged from eliciting first impressions and usage scenarios to probing wayfinding strategies and the recall of memorable spatial elements, effectively translating Lynch's qualitative focus into a structured format to quantify the presence and strength of imageability elements and spatial experiences on a broader scale.

## 3. CASE ANALYSIS

### 3.1. Case Selection and Investigation

This case study selects two cases: Huacheng Square, and the Tianhe business district. Huacheng Square is located in the central area of the Zhujiang New Town CBD in Guangzhou. It was completed and put into use in 2010. The ground level consists of a plaza and park, while the underground area is an integrated complex featuring commercial, transportation, municipal, and parking functions. It connects multiple land parcels around the square as well as the metro station, forming a relatively complex underground space network system. The underground space in the Tianhe business district is a network system gradually formed by multiple projects constructed at different times over the past two decades.

Both cases are of a certain scale, with comparable overall size, and have formed sizable urban underground space systems, making them highly representative for research on urban underground space image.

### 3.2. Roads and Nodes: The Framework of Underground Imagery

The cognitive maps were classified by the main shape elements into three types: point + line, surface, and composite (Table 1). It can be seen that the number of "point + line" elements is much higher; these mainly depict frequently traveled routes, enabling certain descriptions along the way, which to a certain extent is related to the dominant function of underground space for transportation. Respondents who drew "surface" maps are more familiar with the underground space and generally understand its spatial structure. Respondents who drew "composite" maps are extremely familiar with the underground space, clearly comprehending the overall structure, not only the framework of underground paths and nodes but also descriptions of areas and rich memories of various landmarks, and can even accurately correspond them to the surface spaces above.

*Table 1. Statistics on Types of Cognitive Map Shapes*

Case	Point + line type	Surface type	Composite type
Huacheng Square	14	4	2
Tianhe Business District	10	6	4

### 3.3. From Local to Global: Cognitive Formation of Imagery

By analyzing the integrity of the underground space depicted on the cognitive maps, three levels were identified (Table 2): overall completeness, many local parts, and few local parts. The two cases displayed different features. In Huacheng Square, underground space is divided into three weakly connected zones, resulting in cognitive maps characterized mainly by many local areas; whereas in the Tianhe Business District underground space, the presence of many nodal spaces and a simple vertical correspondence led to more overall cognitive maps.

*Table 2. Analysis of Cognitive Map Integrity*

Case	Few local parts	Many local parts	Overall completeness
Huacheng Square	12	7	2
Tianhe Business District	3	8	9

### 3.4. Underground Image Tied to Above-ground Elements

Almost all respondents marked a number of above-ground spatial elements, indicating that ground space image elements play a key role in the cognition of underground spaces (Table 3). Most respondents habitually correspond underground space image elements to surface space, and use the ground image as reference and coordinate to organize underground space imagery, with only a few cases where underground space is used as the base for organizing the above-ground spatial image.

*Table 3. Number of Surface Spatial Elements*

Case	Few (<3)	Moderate (4-8)	Many (>8)
Huacheng Square Underground Space	2	12	6
Tianhe Business District Underground Space	2	7	11

## 4. DISCUSSION

### 4.1. Distinct Characteristics of Underground Space Image Elements Compared to Above-Ground

Compared to Kevin Lynch's established elements of above-ground urban imagery (paths, edges, districts, nodes, landmarks), underground space imagery exhibits distinct characteristics due to its enclosed, interior nature. Paths are the dominant skeletal element in underground cognition, requiring exceptionally high clarity and



continuity in both plan and vertical connections to compensate for the loss of natural orientation cues. Nodes, such as subway stations and sunken plazas, become critically strategic focal points, often possessing landmark qualities and serving as vital integration points connecting the underground with the above-ground world. Districts are primarily perceived through internal thematic differentiation rather than clear physical boundaries. Edges are often virtual or perceived rather than physically distinct, and their permeation is crucial for wayfinding. Landmarks are rare in a traditional, monumental sense; instead, their function is fulfilled by memorable nodes or relies heavily on intensified artistic and cultural elements and signage systems to aid navigation in the homogeneous environment. This underscores that underground space imagery is more dependent on intentional design for legibility compared to the above-ground.

#### **4.2. Paths: The Skeletal Framework with Heightened Continuity Requirements**

Paths serve as the dominant element in structuring underground space imagery, forming the fundamental framework for cognitive maps. Unlike above-ground networks, these paths demand heightened continuity—both planar and vertical—to compensate for limited orientation cues. Breaks in vertical connectivity significantly impair wayfinding, as observed in complex underground transitions where disorientation frequently occurs.

Underground paths are cognitively simplified into straight-line connections between clearly defined origins and destinations, such as subway stations. (He Ye, 2015) This mental compression mirrors schematic subway maps, where complex routes are reduced to direct lines. The necessity of unambiguous start and end points further distinguishes underground path perception from the more networked understanding of surface roads.

#### **4.3. Nodes: Strategic Focal Points and Integration Hubs**

Nodes function as strategic focal points and integration hubs within underground space imagery, serving as the second most dominant element after paths. Typical nodes—such as subway stations, sunken plazas, and atriums—play a more prominent role underground than above ground due to the limited visual references. At the macro level, metro stations often structure the city's image for passengers and act as catalysts for urban development through concepts like TOD. At the micro level, key nodes help users organize mental maps and form the structural framework of complex underground areas.

Underground nodes frequently exhibit landmark qualities by offering volumetric contrast or functional significance within homogeneous environments. They also act as critical interfaces connecting above-ground and underground imagery, enabling vertical spatial integration. When a node is recognizable both above and below ground, it significantly enhances overall spatial continuity and supports cohesive wayfinding across levels.

#### **4.4. Region: Thematic Zones with Weak Physical Boundaries**

Regions in underground spaces are primarily defined by thematic features—such as architectural style, commercial character, or visual themes—rather than physical boundaries. Perceived from within, these areas rely on strong internal uniformity and repetitive spatial characteristics to enhance recognizability and provide a sense of direction (Li Wei et al, 2011). Examples include zoning in underground shopping malls or parking areas where different sections are distinguished by thematic elements rather than structural divisions.

Vertical stratification plays a critical role in organizing underground regions, both in relation to above-ground spaces and within multi-level underground structures (Liang Yu, 2013). Functional differentiation across levels necessitates intentional visual or nodal connections—such as atriums, elevators, or consistent signage—to maintain spatial continuity and prevent cognitive fragmentation between layers.

#### **4.5. Boundaries: Thematic Zones with Weak Physical Boundaries**

Boundaries in underground spaces are predominantly perceptual rather than physical, emerging as transitions in materials, lighting, or spatial scale rather than as tangible linear or surface-like separators. These boundaries are often inconsistent with structural or engineering limits and are sensed more subtly compared to above-ground contexts, where edges tend to be visually explicit and geographically defined.

To form a coherent and imageable spatial system, underground boundaries must be visually or functionally dissolved. Physical or visual continuity—achieved through shared elements like atriums, aligned pathways, or natural lighting—can integrate adjacent areas, weaken the perception of separation, and enhance wayfinding. Successful boundary treatments thus prioritize permeability and interconnection, transforming conventional divisions into opportunities for spatial fluency and place-making.

#### **4.6. Landmarks: Rarely Physical, Often Cultural or Nodal**

Landmarks in underground spaces demand intentional reinforcement due to the lack of natural visual cues and spatial homogeneity. It is difficult to establish large-scale physical landmarks; instead, distinctive nodes with volumetric contrast or those enhanced through cultural, artistic, or architectural treatments often assume landmark roles. These elements provide crucial visual anchors and support spatial identity in an otherwise uniform environment.

Signage systems serve as essential artificial landmarks, especially for new users who rely on them for primary navigation (Guo Mei, 2012). As users become familiar with the space, they depend more on path-based features and internal imagery, using signage mainly for ambiguity resolution or confirmation. Thus, an effective landmark system combines clear signage with designed spatial features to strengthen overall imageability.

### **5. RESULT**

#### **5.1. Organizing Imageability and Spatial Framework through "Path" Elements**

Design and organization of underground paths are fundamental for spatial form in underground spaces. Underground roads, while serving their traffic function, should also have clear directionality, continuity, starting, and ending points. For urban underground space networks, a simple underground road structure and spatial form will help simplify imageability elements in the mind, enabling clearer mental images. This is particularly vital in underground spaces with almost no external references; the comparison between the readability of the Huacheng Square and Tianhe underground spaces serves as a clear example.

#### **5.2. Strengthening the Imageability of "Node" Elements**

First, further emphasizing the start and endpoints of underground roads as imageable spatial nodes will enhance the overall imageability of underground space. Second, reinforcing nodes that connect to the above-ground space—often realized with sunken plazas or skylights—can create a strong sense of place. Third, strategically creating spatial node elements with landmark features, particularly those with significant changes in spatial scale, often form the core of underground spatial organization, with key underground roads connecting to them, resulting in a clearly imageable radial underground network spreading out from the center.

#### **5.3. Organizing Other Imageability Elements Based on "Path + Node"**

Underground roads can use themed boundary features to create underground regions with different themes, which further enhances the sense of orientation, scale, and measurability in the space.

The connection between two underground regions can further break the constraints of underground boundaries; the joining surfaces can enhance interpenetration between the two regions and even form underground spatial nodes, further improving the imageability of underground road connections.

For underground landmarks, in addition to improved signage systems, commercial and service facilities can further enrich boundary element features. Moreover, since underground landmarks have distinctive scale characteristics, aspects of culture, art, and creativity should also be considered and synergistically enhanced with spatial node elements.

### **6. PRACTICAL IMPLEMENTATION**

The research findings on underground space planning theories have been applied in the urban design of the Xi'an Port District urban design project. The Project is situated in the Xi'an International Trade & Logistics Park (Xi'an Port Area), a nationally significant modern logistics and international trade hub in western China. Located in the northeastern part of Xi'an,

#### **6.1. Creating a Vertically Integrated Urban Vitality Corridor along the Central Axis:**

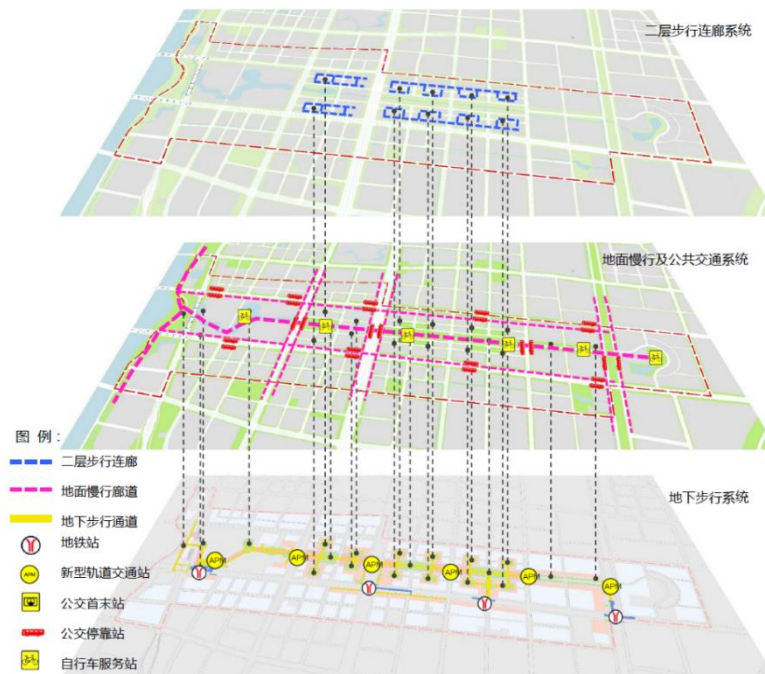
Along the central axis, create a three-dimensional urban park vitality zone consisting of a ground waterfront slow-moving lane, a slow-moving lane on the first underground floor, and an underground rail transit on the second underground floor, with transportation, recreation, and comprehensive service functions as the main features.

The design centers on three major public transport hub cores: Tiyu Zhongxin Station, Shuangzhai Station, and Gangwu Avenue Station. Additionally, a hierarchical node system is implemented: larger three-dimensional park nodes are formed at the center of each 800m×800m block, while smaller internal spatial nodes are created within every 300m×400m block. These nodes are interconnected through the central axis and a public underground space system, forming a cohesive and continuous urban public spatial network.

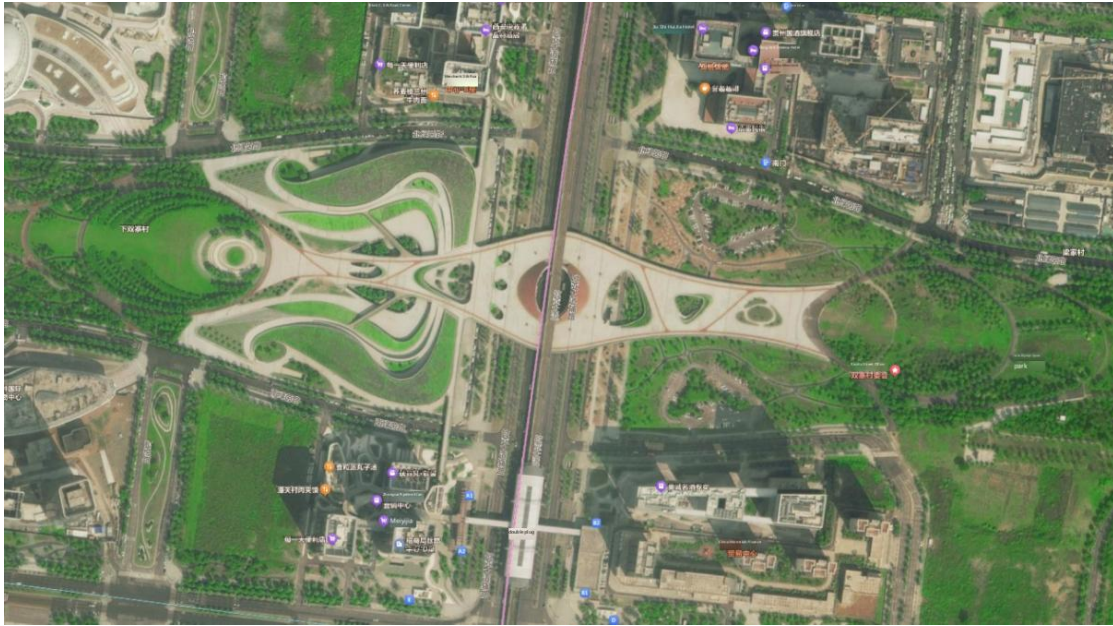


**Figure 2.** Connections between blocks. (Drawn by the author)

Through the sunken square, sunken courtyard, evacuation stairs and vertical transportation facilities, convenient connection between the ground and underground is achieved. The second-floor platform is connected with the central square, the overhead subway station and the surrounding buildings to form a whole. Provide convenient and fast walking space for pedestrians. The ground pedestrian system combines the road's slow lane and the waterfront slow lane as the main slow lane, focusing on creating a landscape environment and creating a relaxed and casual walking atmosphere. The public underground pedestrian passage is straightened as much as possible, with a single main passage forming the skeleton and secondary passages to complete the network, and at the same time connect with the subway and development plots.



**Figure 3.** Diagram of the connection between the underground pedestrian system and the ground level (Drawn by the author)



*Figure 4. Satellite imagery (<https://map.baidu.com/>)*

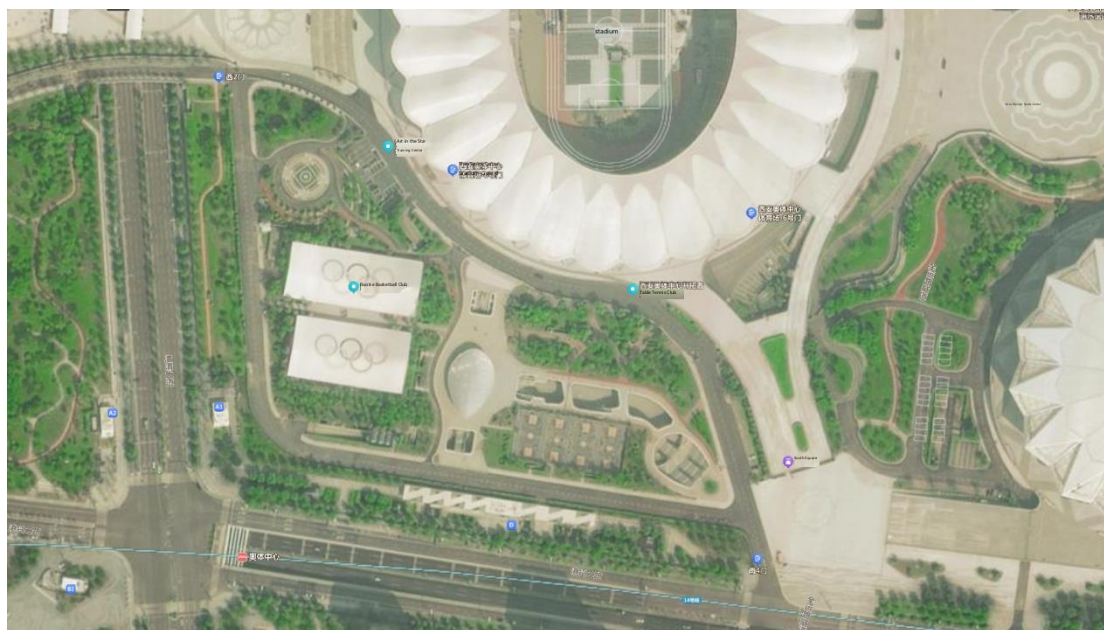
## 6.2. Create nodes and landmarks with distinctive regional characteristics.

At important nodes, the integration of above-ground and underground public spaces is achieved through the organization of two image elements, landmarks and nodes, in three-dimensional space. For example, at the Olympic Sports Center Station in the Port Authority District, based on the principle of three-dimensional urban image organization, an underground distribution hall is set up at the location of the underground passage from the subway station to the Olympic Sports Center, and the hall is treated with a glass roof that can be illuminated. Citizens can see the Olympic Sports Center building through the lighting roof on the first floor below, which can quickly identify the space and effectively integrate the above-ground and underground spaces. This principle has been fully implemented in the subsequent engineering design and implementation, and has now been completed, as shown in the satellite image.



*Figure 5. Renderings of the sunken square (Drawn by the author)*





**Figure 6.** Figure7. Satellite imagery (<https://map.baidu.com/>)

## 7. CONCLUSION

Influenced by the special underground space environment and cognitive mode, the image elements of underground space have their own unique characteristics compared with the image elements on the ground, and there are also certain particularities in the relationship and organization of the image elements. Organizing the image of underground space in combination with the characteristics and relationship of the image elements of underground space is an important principle of underground space morphology organization.

At the same time, the ground space image is an integral part of the city image, and the ground space is also an important reference for the underground space image. There are many connections between the underground space image elements and the ground image. How to deal with the connection between the ground and underground image elements is an important design principle for achieving the integration of urban space.

With the rapid growth of urban underground space construction, the connection between underground space construction and urban ground construction is expanding and strengthening, showing a trend of mutual penetration and mutual influence. It is necessary to change the current situation that urban design only focuses on ground space form. The results of this study can be used as an important principle and method for the organization of urban underground space form and the organization of the overall urban space form, further guiding the development of urban underground space and three-dimensional cities.

## 8. REFERENCES

- [1] Fang Zhou. Research on the intention of urban underground space. Master's thesis. Sun Yat-sen University. 2016
- [2] Kevin Lynch, translated by Fang Yiping and He Xiaojun. Image of the City. Beijing: Huaxia Publishing House, 2001
- [3] Shu Yu, ed. Urban Underground Space Environment Art Design. Shanghai: Tongji University Press, 2015
- [4] Li Xun, Xu Xueqiang. Spatial analysis of urban image of Guangzhou. Human Geography. 1993, 8(3): 27-35
- [5] Xu Leiqing. Themes, paradigms and reflections of urban image research: a review of urban image research in China. New Architecture. 2012, 1: 114-117
- [6] Shao Jizhong. Research on the Image of Urban Underground Space. Architecture and Culture, 2015, 10: 140-141
- [7] Wang Yuan. A critique of Kevin Lynch's "The Image of the City". New Architecture, 2003, 3: 70-73
- [8] Yang Jian, Dai Zhizhong. Analysis of Kevin Lynch's research methods on urban image. Journal of Chongqing Jianzhu University. 2007, 29(2): 19-22
- [9] Li Wei, Yin Feng, Chen Zhilong, Zhang Ping. Study on the sequence design of large underground commercial space. Chinese Journal of Underground Space and Engineering, 2011, 7(4): 637-641,648
- [10] Written by Gideon S. Grani (USA) and Toshio Ojima (Japan), translated by Fang Xu and Haiyi Yu. Urban Underground Space Design, Beijing: China Architecture & Building Press, 2011
- [11] (Japanese) Koizumi Jun, ed., Hu Lianrong, translator. Development and Utilization of Underground Space. Beijing: China Architecture & Building Press, 2012



- [12] Chen Zhilong, Zhu Min. Discussion on the layout model of urban underground pedestrian system. *Chinese Journal of Underground Space and Engineering*, 2007, 3(3): 392-396,401
- [13] Li Wei, Yin Feng, Chen Zhilong, Zhang Ping. Study on the sequence design of large underground commercial space. *Chinese Journal of Underground Space and Engineering*, 2011, 7(4): 637-641,648
- [14] Yang Jian, Dai Zhizhong. Analysis of Kevin Lynch's research methods on urban image. *Journal of Chongqing Jianzhu University*. 2007, 29(2): 19-22
- [15] Gu Chaolin, Song Guochen. Research on urban image and its application in urban planning. *Urban Planning*. 2001, 25(3): 70-73, 77
- [16] Guo Mei. Research on the Identifiable Design of Urban Underground Commercial Streets. Master's thesis. Qingdao University of Technology. 2012
- [17] Xue Gang. Integration of above-ground and underground space. Master's thesis. Xi'an University of Architecture and Technology. 2007
- [18] Qiang Weiyi. Research on the Design of Urban Underground Space Guidance Signage System. Master's thesis. East China Normal University. 2014
- [19] He Ye. Design, implementation and evaluation of underground integrated transportation system in the core area of Zhujiang New Town. Master's thesis. South China University of Technology. 2015
- [20] Liang Yu. Research on the three-dimensional development and design of underground streets in Guangzhou subway stations. Master's thesis. South China University of Technology. 2013
- [21] Lynch, K. *The Image of the City* Cambridge, Mass.: MIT Press. 1960.
- [22] Lynch, K. *Reconsidering the Image of the City*. In: R. M. Hollister and L. Rodwin, (eds.). *Cities of the Mind*. New York: Plenum. 1984.
- [23] Julia Robinson. Architectural Research: Incorporating Myth and Science[J]. *Journal of Architectural Education* 44,1990,(1):20.
- [24] Golledge, R. And G Zannaras. Cognitive approaches to the analysis of human spatial behavior. In: W. H. Ittelson, (ed.). *Environment Cognition*. New York: Seminar Press, 1973.

## OLD MINES AND INDUSTRIAL TOURISM: THE CASE OF AN ANCIENT MINING GALLERY IN LAVRION, GREECE

Dimitris Kaliampakos<sup>1</sup>, Athanassios Mavrikos<sup>2</sup>, Dimitris Lamprakis<sup>3</sup>

**Abstract:** The mining sector is one of the most important economic sectors in the world. Metals, fossil fuel and industrial minerals are essential to every country's economy supporting its growth and development. However, when mines close due to mineral resources exhaustion, environmental concerns, economic or political reasons the impact on the local economies and communities is very hard. Reusing old mine sites and turning them into tourist attractions can help revitalize these communities and boost their economies. Mining tourism is part of industrial tourism, a trend that has been growing significantly in the last three or four decades. Old mines are recognized as having significant potential for industrial tourism as they offer visitors a chance to see and get to know mining tools, equipment and technologies, minerals and rocks, etc. This has resulted in former mine sites being used as museums/educational centers (Britannia Mine Museum, British Columbia), visitor attractions (e.g. Wieliczka Salt Mine, Poland), recreational areas (Zip World, Wales) and even underground theme parks (Salina Turda, Romania). The paper describes the undergoing project of restoring and repurposing of an ancient mining gallery in Lavrion, Greece. The underground mining gallery has evidence of mining activities that span over more than 5,000 years as it was used both by ancient Greeks and contemporary miners in the 19th century to mine the silver ores in the area. The mining gallery will attract visitors and will provide both informative and educational material and activities related to the mining methods, the geology and history of the area.

**Keywords:** closed mines, mining tourism, ancient mine gallery restoration

### 1. INTRODUCTION

The global mining industry is a crucial component of modern society, supplying the raw materials that are indispensable for infrastructure, technology, digital transformation and energy transition. Global mining production is driven by the escalating demand for "critical minerals" – notably lithium, cobalt, and rare earth elements – which are vital for electric vehicle batteries, renewable energy technologies (solar panels, wind turbines), and advanced electronics. While traditional commodities like coal face a declining trajectory in some regions due to decarbonization efforts, overall demand for mined resources is projected to continue its upward trend, particularly for those essential to the green economy (OECD, 2019).

The mining industry is also very important for the economy. Its value is estimated at approximately \$2.26 trillion in 2024, expecting to experience further growth, with projections suggesting it could reach around \$3.0 trillion by 2029. Furthermore, the mining sector contributes to direct and indirect employment worldwide. The coal industry accounts for approximately 8.4 million jobs globally. Within the European Union, the mining and quarrying sector employed around 371,000 individuals in 2022. The future prospects of the mining industry are dependent on both significant opportunities and challenges, such as the demand in critical minerals and energy transition, the digitization and automation of mining operations, sustainability and Environmental, Social, and Governance (ESG) targets as well as geopolitical factors (Herrera Herbert, 2022).

<sup>1</sup>Professor, Kaliampakos Dimitris, Mining Engineer Ph.D., National Technical University of Athens, School of Mining and Metallurgical Engineering, 9 Iroon Polytechniou Str., GR15772, Zografou, Athens, Greece, [dkal@central.ntua.gr](mailto:dkal@central.ntua.gr)

<sup>2</sup>Mavrikos Athanassios, Mining Engineer Ph.D., National Technical University of Athens, School of Mining and Metallurgical Engineering, 9 Iroon Polytechniou Str., GR15772, Zografou, Athens, Greece, [mavrikos@metal.ntua.gr](mailto:mavrikos@metal.ntua.gr)

<sup>3</sup>Lamprakis Dimitris, Mining Engineer Ph.D., National Technical University of Athens, School of Mining and Metallurgical Engineering, 9 Iroon Polytechniou Str., GR15772, Zografou, Athens, Greece, [dlamprakis@metal.ntua.gr](mailto:dlamprakis@metal.ntua.gr)

Without doubt, the mining sector is very important, nevertheless, mining activity usually expands in a rather short period of time. After a mine is closed either because the ore deposit has exhausted or for various economic, technological and even political reasons there remains a significant industrial infrastructure. It may not be able to serve its original purpose but it bears a significant potential that could be exploited. Many mining sites are valuable as industrial monuments, carrying an important legacy and are seen as a testament for miners and mining communities. In this context the concept of industrial tourism has emerged in the last decades (Edwards and Coi, 1996). Industrial tourism is a growing trend that focuses on the adaptive reuse of unused industrial sites, with closed mines emerging as particularly popular attractions. Mining tourism highlights the historical, geological, and cultural significance of former mining sites and creates immersive visitor experiences. Closed underground mines offer a unique window into the industrial heritage of a region, allowing tourists to explore adits, shafts, and machinery that once powered local economies. By transforming disused tunnels and facilities into safe, engaging attractions, regions can both preserve mining heritage and stimulate post-industrial economic regeneration. Sites of former mining activity offer a blend of historical authenticity, technological heritage and socio-economic narratives, transforming places of past labor and resource extraction into spaces for public engagement and education (Guo et al., 2024; Xie et al., 2020; Chazi et al., 2021). One key parameter lies in providing visitors with an immersive, "behind-the-scenes" experience that transcends traditional museum exhibits, allowing for a tangible connection to industrial processes, the challenging lives of miners, and the profound impact of industry on local communities and landscapes. Furthermore, the conversion of closed mines into tourist destinations often serves as a vital strategy for post-industrial regeneration, offering new economic opportunities and helping regions overcome the socio-economic repercussions of mine closures by creating new jobs, supporting local businesses and improving vital infrastructure in these areas. Moreover, mining tourism can have positive effects regarding the protection of historic structures, the preservation of mining culture and history and the establishment of partnerships with schools and universities developing educational material and creating research opportunities (Morea et al., 2016). Among the many successful examples of transforming abandoned mines into thriving tourist operations are the Wieliczka salt mine in Poland (Fig. 1), the Salina Turda salt mine in Romania (Fig. 2) and the Zollverein Coal Mine Industrial Complex in Germany (Fig. 3).



**Figure 1.** The St. Kinga's Chapel in the Wieliczka salt mine, Poland (source: <https://whc.unesco.org/en/list/32> Accessed 05/07/2025)





**Figure 2.** View of the Rudolf Mine in Salina Turda underground theme park (source: <https://www.salinatorda.eu/en/locatie/rudolf-mine/> Accessed 05/07/2025)



**Figure 3.** Aerial view of the Zollverein XII Coal Mine Industrial Complex, which has been inscribed on the UNESCO World Heritage List (source: <https://whc.unesco.org/en/list/975/> Accessed 05/07/2025)

These examples illustrate the diverse approaches to mine repurposing, ranging from historical preservation and educational tours to extreme sports venues and cultural centers. Their success lies in their ability to offer compelling narratives, unique experiences, and often, significant economic contributions to their respective regions.

The paper presents the steps in order to repurpose an ancient mining gallery in the Lavrion Technological Park in Greece. The underground mining works span across almost 5,000 years of mining history in the area as parts of the mining gallery are the remains of the mining works of ancient Greece, while the most recent sections represent the last phase of mining activity in the area across the 19<sup>th</sup> and 20<sup>th</sup> centuries. The paper analyzes the main methodological approach, the questions that need to be answered, the challenges, the risks and the future plans.

## **2. METHODOLOGICAL APPROACH FOR RESTORING OLD MINE GALLERIES**

The process of turning former mining sites into safe facilities that attract tourists involves many challenges and requires careful design. Mines are designed to serve a heavy industrial activity and not to welcome visitors or the general public. The lifespan of underground mining works is short as they are not indent to and the safety factors are kept at a minimum to boost economic output. There are many risks associated with closed mines such as aged and deteriorating infrastructure, roof instability, rock collapse oxidation of metal support elements, etc. In addition, one cannot exclude that the underground space has its own unique characteristics, like lack of lighting, poor ventilation, confined spaces, orientation difficulties and usually water inflow or even flooding. In some underground mines it is possible for pollutants or hazardous material to be present, a condition that further complicates restoration and reuse plans (Guo et al., 2024).

The key actions for the successful repurposing of old underground mine facilities are linked to safety, environmental concerns, authenticity and history, exhibition/educational material and visitor accommodation infrastructure:

- Control and safety requirements: Stability of galleries, ventilation, lighting, fire safety, access - emergency exits and compliance with legislation
- Environmental Concerns Risk: Acid mine drainage, heavy metal leaching. Mitigation: Water treatment systems, sealed waste piles, ongoing environmental monitoring
- Respect for authenticity and history: preserving the historical and aesthetic identity of the site while enhancing it. Risk: Over-theming can undermine historical authenticity. Mitigation: Engage heritage experts, maintain original structures, interpret rather than alter
- Adaptation to the modern visitor experience: interactivity, digital applications (e.g. VR/AR), thematic guided tours.
- Development of educational/exhibition material: Creation of signage, multimedia, mock-ups and guides explaining the operation of the mine.
- Visitor accommodation infrastructures: Installation of parking, toilets, refreshment facilities, ticket offices, etc.

## **3. THE CASE OF THE ANCIENT MINING GALLERY AT LAVRION TECHNOLOGICAL AND CUTLURAL PARK**

### **3.1. Mining activity in Lavrion through history**

The Lavrion area has a very long history in mining activity. There is evidence from archaeological data that mining started in the area as early as 3200 BC (Morin and Delpech, 2018). Research has brought to light ancient ore washing facilities, ancient smelting installations and ancient underground mining works (Conofagos, 1980; Voudouris et al., 2021). The ancient Greeks used slaves to mine the silver ores in the area, contributing to the wealth and strength of the city of Athens. The discovery of higher grade, third contact mineralization around Kamariza area, dated at 483 BC, marked a change in the mining history of Lavrion. It favored more continuous and large scale mining and processing operations (Ross et al., 2023).

Modern metallurgy and mining at Lavrion started at 1864 with the exploitation and the resmelting of the ancient slag heaps (Morin and Delpech, 2018; Markouli, 2019). There were two mining companies, “The Metallurgical Company of Lavrio” (1873–1927) and the “French Mining Company of Lavrio” (1875–1981, FMCL) in the area. Both the Hellenic and French companies have been the essential supporting factors of Lavrio area's development in that new period of the industrialization of Greece. The 1867 workers' settlement was finally developed into a 10.000 inhabitants' town in the beginning of this century. The two companies constructed urban infrastructures, such as schools, churches, a small hospital and port facilities, in order to facilitate their operations and attract



working population. The Hellenic Company is associated with the use, for the first time in Greece, of electricity, the telephone and other technological innovations. Those included the construction of the Attikos railway (1882-1885), thus connecting Lavrion to Athens. Operations ceased permanently in 1989 as a result of the broader de-industrialization all over Greece (<https://en.ltcp.ntua.gr/history/>).

### **3.2. The Lavrion Technological and Cultural Park**

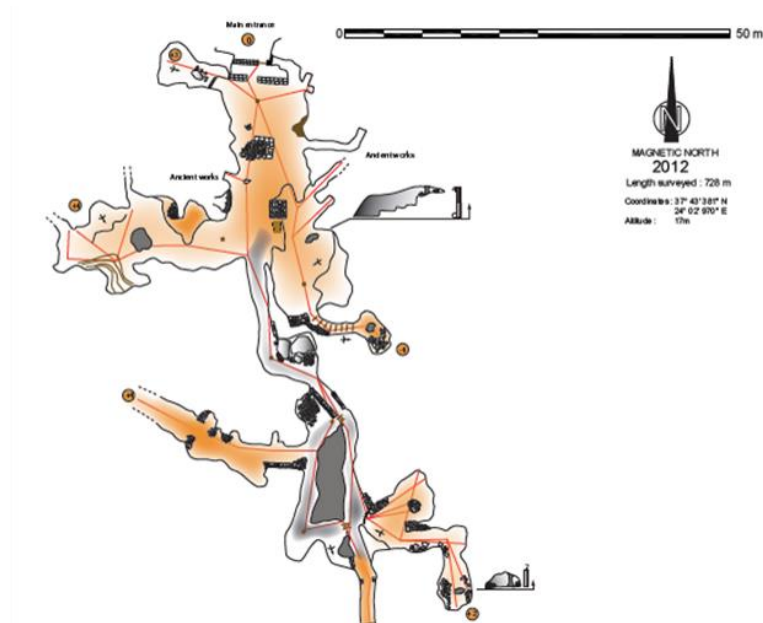
The Lavrion Technological and Cultural Park (LTCP) was founded in 1992 in the facilities of the old French Mining Company of Lavrion (Compagnie Française des Mines du Laurium), at the initiative of the National Technical University of Athens (NTUA), aiming to host and promote research and business activities. In the following years after the closure, NTUA set out an ambitious project to transform the former industrial site into a Technological Cultural Park and Museum of Technology (<https://en.ltcp.ntua.gr/history/>).

Today, the Park occupies a space of 60,78 acres, which includes 41 building units of a total area of 25,000 m<sup>2</sup>, and constitutes a protected national monument by the Ministry of Culture. The LTCP's facilities include industrial, laboratory and professional premises of high aesthetic and architectural value, most of which were built during the period 1875-1940. The site used to host industrial activity until 1988. During the 120 years of the industrial complex operation, it has been subjected to various transformations, renovations and additions, in order to line up with the demands of each technological evolution. Until now, 19,76 acres of facilities and several buildings have been restored, highlighting the LTCP as a unique monument of industrial archaeology and architecture. The industrial buildings have been reconstructed, combining the evaluation of the historical forms with contemporary functionality and house a variety of new and innovative businesses, NTUA's laboratories, as well as cultural and educational institutions. With the support of the local community, the LTCP contributed to the rebirth of the industrial facilities and their operation as a cradle for the development and the implementation of innovative products and activities of technological, educational and cultural content (<https://en.ltcp.ntua.gr/history/>).

### **3.3. The restoration of LTCP's ancient mining gallery into a tourist attraction**

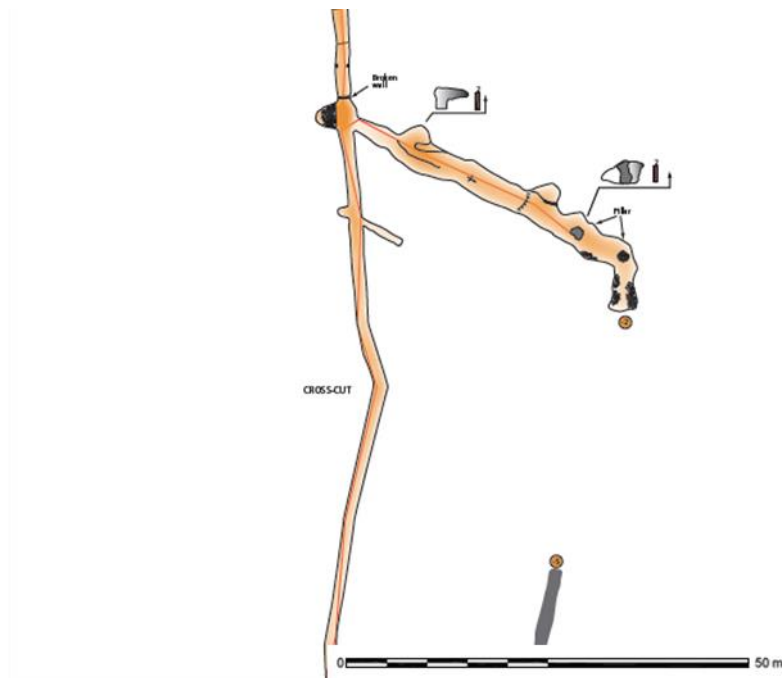
The ancient mining gallery is located on the southern edge of the LTCP. Miners around 1875 followed the ancient galleries that existed in the area in search of mineralization and orebody. There was therefore the excavation of the main original chamber and, subsequently, the extension of the adit further south towards the area of the Kyprianos settlement. After the ore deposit was exhausted, the underground space was used as a storage area for explosives (Fig. 4).





**Figure 5.** Section 1 of the ancient gallery. The entrance to the underground space, the artificial stone pillar and ancient mining works are depicted.

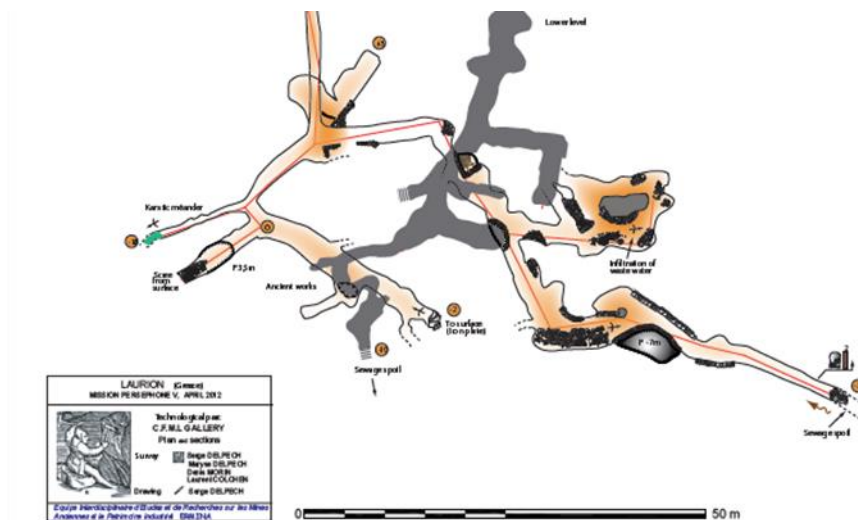
- Section 2. Gallery area (Fig. 6): The gallery area is the central part of the site and consists of the gallery (rectangular/petal-shaped cross-section, 1.5-2.0x2.0m in size), approximately 75-80 m long, extending south of the entrance area. In this area there is a local widening to the east, for ore exploitation, 4-5 m wide. The adit has been drilled mainly within the upper marble and does not show any stability problems.



**Figure 6.** Section 2 of the ancient gallery. The central part consists of an adit of rectangular cross-section, roughly 1.5-2.0x2.0m in size and around 80 m long.

- Section 3. Kyprianos area (Fig. 7): This section concerns the terminal part of the gallery that runs below the Kyprianos area. There are older adits or mining stopes and access is difficult. In addition,

the area is underneath houses and roads and as a result there is inflow of rainwater and sewage. This section is not considered to be of interest for development.



**Figure 7.** Section 3 of the ancient gallery. Most of this part is developed beneath the Kyprianos urban settlement.

In the past there have been some attempts to restore this ancient mining gallery. In 1998, the effort was mainly aimed at improving the safety conditions. To this end, the roof and rock wedges were reinforced using wooden supports. Timber sets were installed along the main gallery and the artificial stone pillar was restored. In addition, access to the edges of the underground rooms (mainly the eastern side) was prohibited for safety reasons.

For the design of the restoration of the ancient mining gallery in the LTCP, the following objectives were considered:

- Ensure the stability of the central area
- Ensure a second access/safety exit
- Ensure appropriate air quality (air supply, humidity control)

There are some challenges or restrictions in this direction. There are mainly linked with the physical limitations of equipment access, the preservation of site form/image using “historic methods/materials”, the limitation in finding, nowadays, skilled personnel familiar with old mining or support techniques and certain legal restrictions on use of areas outside the premises of the LTCP.

As far as the stability of the underground space is concerned, the required work includes conducting extensive and detailed geological mapping and geotechnical measurements of the underground rock mass. Additionally, installation of monitoring instrumentation is deemed necessary in order to examine the behavior of critical underground areas. Another critical component of the design is the analysis of key failure mechanisms of roof, wedges and pillars. Moreover, the development of a calibrated geotechnical simulation that can evaluate the behavior of the underground space and finally the installation of specific support elements that will enhance the stability and safety of the underground space.

With regards to the improvements in the underground gallery and improving public safety, the focus is on improving the entrance area by increasing the cross-section. Furthermore, the excavation of a second access tunnel would vastly improve ventilation and safety and is considered a priority. Finally, the repurposing of this ancient mining gallery into a tourism attraction requires the installation of an appropriate flooring system for easy public movement and appropriate signage, safety lighting, etc.

Regarding the support measures, the underground area of the ancient mining gallery is generally characterized as stable, with only local instability issues at the roof. It is expected that the main stability problems would be related to gravitational failures. Therefore, we suggest using passive support (timber and artificial stone pillars) that are in line with the techniques of the past and respect the historic character of the site. The possibility of using modern materials such as steel or concrete can also be considered, granted that these materials would be used as e.g. the core for artificial pillars and then broken stone material will be used to shape them in an aged form. The use of roof bolts is considered necessary for certain cases.

The excavation of a second access/exit tunnel is of critical importance for the project. It is proposed to develop the second access tunnel at the south-western boundary of the entrance area, inside the LTCP premises. The access tunnel would be approximately 30-35 m long and would facilitate the ventilation of the underground space, thus

improving air quality for visitors and also meet the safety requirements for having two exits in any underground mine.

#### 4. CONCLUSIONS

In recent decades, industrial tourism has emerged as a significant cultural and economic trend. It has gained momentum as a tool for cultural preservation and regional revitalization, particularly in areas marked by industrial decline. This form of tourism, particularly in post-industrial and post-mining regions, transforms inactive industrial and mining facilities into cultural landmarks, thus creating both educational and recreational value. The Lavrion area in Attica, Greece, with its rich mining legacy dating back to antiquity, serves as a compelling case study in this evolving trend. The Lavrion Technological and Cultural Park has been creating remarkable actions and synergies, hence steadily and decisively contributing to the promotion of the distinctive history of the wider region of Lavreotiki. Furthermore, LTCP is an important hub of innovation in the region of Attica, a milestone for the development and evolution of the area of Lavrio. The various scientific, research and educational activities that are hosted in the Lavrion TCP coupled with the multitude of cultural events and happenings have been an important pillar for the revitalization and economic development of the area in the post-mining era.

The restoration of the ancient mining gallery of the Lavrion TCP is an integral reference point of the history of the French Company of Lavrion Mines complex and of Lavrion in general. The necessary studies and the corresponding works for the restoration of its structural stability, safety and functionality should be carried out immediately so that it can find a new use as an emblematic tourist landmark of the area. The restoration can serve as a pilot project that can be used as a tourist attraction in the region. The restoration and transformation of the LTCP's ancient mining gallery into a tourist attraction exemplifies this shift, demonstrating how heritage conservation can coexist with sustainable economic regeneration. By repurposing mining infrastructure for public engagement, can contribute to the revitalization of communities that have historically depended on extractive industries. The introduction of guided tours, interpretive exhibitions, and interactive experiences not only preserves local identity and memory but also generates employment and supports the diversification of the regional economy. Moreover, the integration of mining tourism within broader heritage and eco-tourism networks opens new directions for sustainable development, building upon the area's historical significance and natural beauty. The future prospects of industrial tourism in Lavrion present opportunities towards interdisciplinary collaboration, community engagement and increased international visibility making the Lavrion area a model for innovative heritage-driven development.

#### 5. BIBLIOGRAPHY

- [1] OECD (2019). Global Material Resources Outlook to 2060: Economic Drivers and Environmental Consequences, OECD Publishing, Paris, <https://doi.org/10.1787/9789264307452-en>
- [2] Herrera Herbert, J. (2022). Prospects and trends in the supply of raw materials (Presentation) [Otros]. Universidad Politécnica de Madrid. <https://oa.upm.es/71677/>
- [3] Edwards, J. A., & Coit, J. C. L. i. (1996). Mines and quarries: Industrial heritage tourism. *Annals of Tourism Research*, 23(2), 341–363. [https://doi.org/10.1016/0160-7383\(95\)00067-4](https://doi.org/10.1016/0160-7383(95)00067-4)
- [4] Guo, S., Yang, S., & Liu, C. (2024). Mining Heritage Reuse Risks: A Systematic Review. *Sustainability*, 16(10). <https://doi.org/10.3390/su16104048>
- [5] Xie, H., Zhao, J. W., Zhou, H. W., Ren, S. H., & Zhang, R. X. (2020). Secondary utilizations and perspectives of mined underground space. *Tunnelling and Underground Space Technology*, 96, 103129. <https://doi.org/10.1016/j.tust.2019.103129>
- [6] Ghazi, J. M., Hamdollahi, M., & Moazzen, M. (2021). Geotourism of mining sites in Iran: An opportunity for sustainable rural development. *International Journal of Geoheritage and Parks*, 9(1), 129–142. <https://doi.org/10.1016/j.ijgeop.2021.02.004>
- [7] Morea, A., Vidican, R., Rotar, I., Păcurar, F., Stoian, V., & Hirișcău, A. (2016). Dynamics and Fluctuations of Tourists in Turda Salt Mine – A Case Study. *Agriculture and Agricultural Science Procedia*, 10, 155–159. <https://doi.org/10.1016/j.aaspro.2016.09.046>
- [8] Morin, D., & Delpech, S. (2018). Mines and mining. *The Section of Mediterranean Archaeology*, Department of Archaeology, Ghent University: Ghent, Belgium, 41–43.
- [9] Conophagos, C. E. (1980). The Lavrion and the ancient Greek techniques for silver production (p. 458). *Ekdotiki Athinon*, Athens, Greece (in Greek)
- [10] Voudouris, P., Melfos, V., Mavrogonatos, C., Photiades, A., Moraiti, E., Rieck, B., Kolitsch, U., Tarantola, A., Scheffer, C., Morin, D., Vanderhaeghe, O., Spry, P. G., Ross, J., Soukis, K., Vaxevanopoulos, M., Pekov, I. V., Chukanov, N. V., Magganas, A., Kati, M., ... Zaimis, S. (2021). The Lavrion Mines: A Unique Site of Geological and Mineralogical Heritage. *Minerals*, 11(1). <https://doi.org/10.3390/min11010076>



- [11] Ross, J., Voudouris, P., Melfos, V., Vaxevanopoulos, M., Soukis, K., & Merigot, K. (2023). What did the ancient Greeks mine at Laurion, and when did they mine it? In *Laurion: Interdisciplinary Approaches to an Ancient Greek mining Landscape, Including Selected Papers* (pp. 27–46). *Der Anschnitt Beiheft*.
- [12] Markouli, A. (2019). 19th / 20th Cent. Mining and Metallurgy in Lavrion. In Hulek, F., & Lohmann, H. (Eds.). *Proceedings of the International Conference “Ari and the Laurion from Prehistoric to Modern Times.”* <https://kups.ub.uni-koeln.de/10380/>
- [13] <https://en.ltcp.ntua.gr/history/> (Accessed 05/07/2025)
- [14] Delpech, S., Delpech, M., Morin, D. and Colchen, L. (2012). *Mission Persephone V. C.F.M.L gallery: plan and sections* (April 2012).

**CREATING UNDERGROUND SPACE TO ENHANCE THE APPEAL OF THE  
NIHONBASHI AREA:  
A CASE STUDY OF THE NIHONBASHI 1-CHOME CENTRAL DISTRICT URBAN  
REDEVELOPMENT PROJECT**

**Kazuo Kiyama<sup>1</sup>, Katsuya Amemiya<sup>1</sup>**

**Abstract:** Nihonbashi Bridge is renowned as one of Japan's most iconic and historically significant bridges, and the surrounding area has served as a center of commerce, finance, and culture for approximately 400 years. In recent years, the area has been expected to develop further as a tourist destination, with multiple urban redevelopment projects underway to enhance the appeal of the riverside environment. In addition, construction is progressing to relocate the Metropolitan Expressway—currently built above Nihonbashi Bridge—underground.

Among these initiatives, the Nihonbashi 1-Chome Central District Urban Redevelopment Project (hereafter referred to as “the N1-C”) is scheduled to be the first of the ongoing projects in the area to be completed. The Nihonbashi riverside area currently faces serious challenges for pedestrian circulation, including complicated and multi-level transfer routes between subway stations on different lines, which hinder smooth movement.

To address these issues, the redevelopment association for the N1-C, in which Mitsui Fudosan is also participating, has put forth four key policies: (1) Development of smooth, barrier-free underground routes, (2) Enhancement of transportation connectivity through the installation of new subway ticket gates, (3) Development of seamless connection spaces enabling smooth movement from underground to deck level, and (4) Establishment of an area-wide pedestrian network in coordination with surrounding redevelopment projects.

This paper presents the N1-C as a case study, highlighting its efforts to create underground space in collaboration with various surrounding redevelopment projects while respecting the location and historical context of the Nihonbashi riverside area.

**Keywords:** urban redevelopment project, barrier-free route, transport connectivity, connection space, collaboration

---

<sup>1</sup> Mitsui Fudosan Engineering Advisors Inc.

## 1. BACKGROUND AND EMERGING CHALLENGES IN THE NIHONBASHI AREA

### 1.1. Characteristics and Challenges of the Nihonbashi Area

The Nihonbashi area, with the iconic Nihonbashi Bridge, has played a central role in Japan for several centuries. Since the Edo period (approximately 400 years ago), the area developed as a hub where people, goods, and culture intersected, functioning as the starting point of several historical roads and a base for water transportation. Furthermore, from the Meiji period (approximately 150 years ago), many companies, including financial institutions, established their offices in this area, making it an important driving force behind Japan's economic activity. In this way, the Nihonbashi area, which has long developed as a center of transportation, commerce, and culture, still possesses significant advantages today, such as its proximity to Tokyo Station—the hub of the railway network—and convenient access to the two international airports that serve as gateways to Japan. In recent years, in addition to its growing functions as an international financial and business center, the area is also expected to develop further as a globally recognized tourist destination.

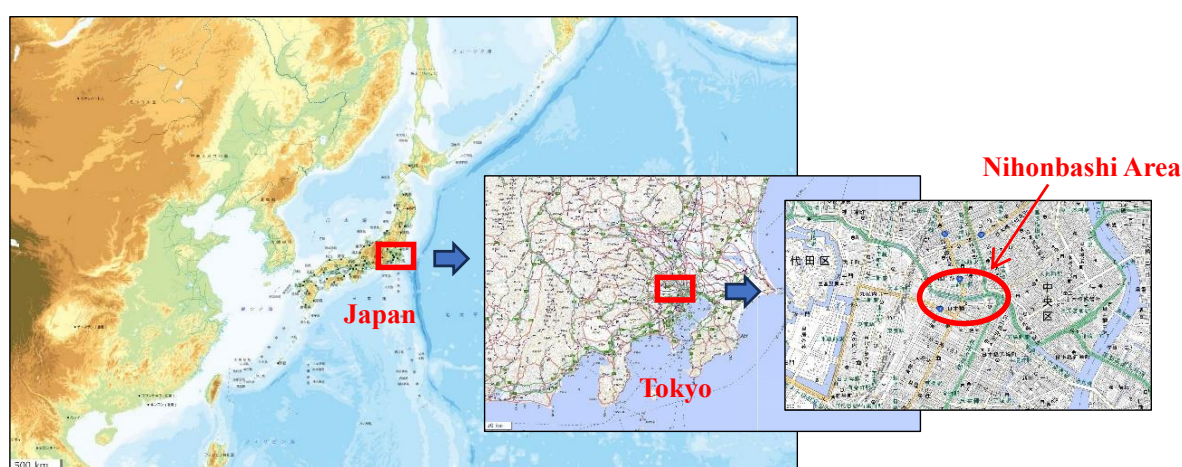


Figure 1. Location of Nihonbashi Area (source: Geospatial Information Authority of Japan)

### 1.2. Undergrounding of the Metropolitan Expressway

In the Nihonbashi area, plans are underway to relocate the Metropolitan Expressway, a large-scale transportation infrastructure, underground. Under the vision of "Restoring the Sky to Nihonbashi," this national project aims to promote urban development that leverages the appeal of the riverside environment.[1]

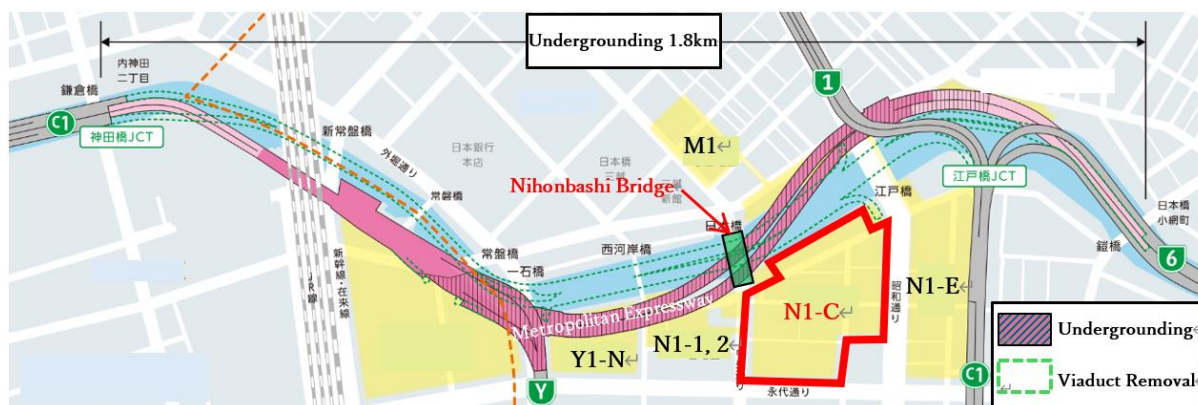


Figure 2. Illustration of the undergrounding of the Metropolitan Expressway (source: Press release by Metropolitan Expressway Co., Ltd.)



**Figure 3.** *Present-day Nihonbashi Bridge with the Metropolitan Expressway overhead (source: Press release by Metropolitan Expressway Co., Ltd.)*



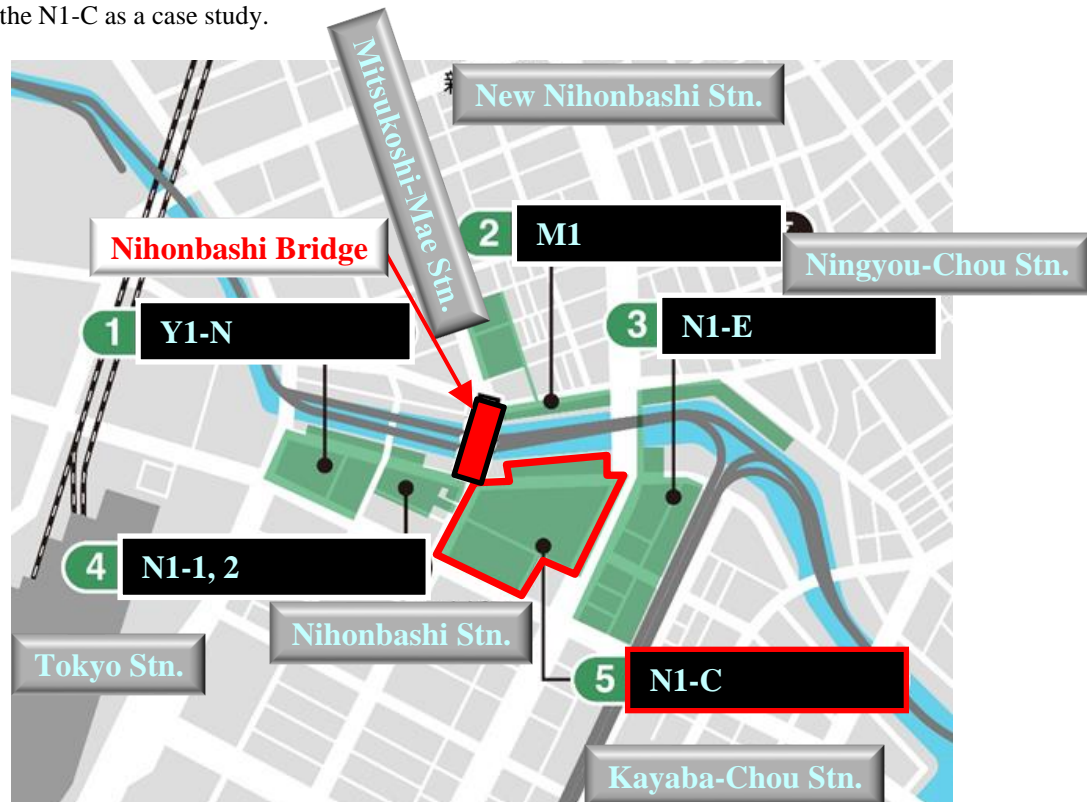
**Figure 4.** *Perspective view of Nihonbashi after the undergrounding of the Metropolitan Expressway (source: Press release by Mitsui Fudosan Co., Ltd.)*

In advancing such a large-scale project, not only the public sector entities such as the national government and the Tokyo Metropolitan Government, but also the private sector entities are cooperating. In the Nihonbashi area, multiple redevelopment projects are underway along the riverside. Each redevelopment project is collaborating under a shared vision and in coordination with the undergrounding of the Metropolitan Expressway, resulting in an integrated approach to urban development throughout the entire Nihonbashi area.



## 2. INITIATIVES IN THE NIHONBASHI 1-CHOME CENTRAL DISTRICT URBAN REDEVELOPMENT PROJECT

The Nihonbashi 1-Chome Central District Urban Redevelopment Project (hereafter referred to as “the N1-C”) is scheduled to be the first among the ongoing redevelopment projects in the Nihonbashi area to be completed. This paper introduces the creation of underground spaces aimed at enhancing the attractiveness of the Nihonbashi area, using the N1-C as a case study.



**Figure 5.** Locations of the five major redevelopment projects along the riverside in the Nihonbashi area (source: Press release by Mitsui Fudosan Co., Ltd.)

The N1-C is adjacent to the iconic Nihonbashi Bridge and is centrally located among the surrounding redevelopment projects, making it the most representative district in the Nihonbashi area. This district has also been designated as an Emergency Development Area, as well as an Urban Regeneration Project, under the relevant law. Furthermore, the redevelopment association for the N1-C, in which Mitsui Fudosan is also participating, has set forth the following four development policies to address issues related to the pedestrian network in the Nihonbashi area.[2]

- (1) Development of smooth, barrier-free underground routes
- (2) Enhancement of transportation connectivity through the installation of new subway ticket gates
- (3) Development of seamless connection spaces enabling smooth movement from underground to deck level
- (4) Establishment of an area-wide pedestrian network in coordination with surrounding redevelopment projects.

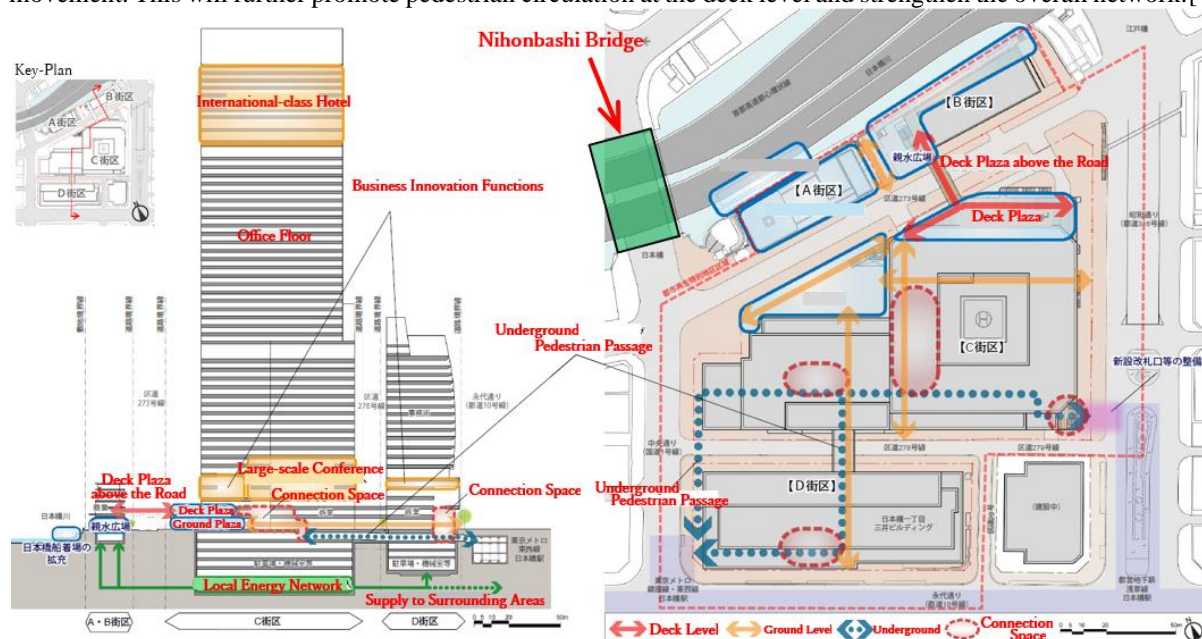
Based on these development policies, various initiatives have been implemented, some of which are described below.

First, with regard to development policies (1) and (2), there are subway stations located underground on both the east and west sides of the N1-C. On the west side, a new underground passage will be constructed to connect with the existing ticket gates, while on the east side, not only a new underground passage but also new ticket gates will be installed at the subway station. In this way, a smooth and barrier-free route will be ensured between the eastern and western subway stations. This will further enhance the district's function as a transportation hub connecting Tokyo Station with the international airports.

Next, with regard to development policies (3) and (4), pedestrian passages, open spaces for walkways, and through-passages that connect to the surrounding roads and plazas of the N1-C will be constructed, establishing an area-wide pedestrian network in coordination with neighboring redevelopment areas. In addition, new



connection spaces will be created to link the underground level with the deck level, enabling smooth vertical movement. This will further promote pedestrian circulation at the deck level and strengthen the overall network. [4]



**Figure 6.** Overview diagram of the pedestrian network (source: Outline of City Planning, Mitsui Fudosan Co., Ltd. and Nomura Real Estate Development Co., Ltd.)

Furthermore, promenades, including waterside plazas, will be constructed along the riverside. These developments will contribute to the creation of a new waterfront pedestrian network that maximizes the appeal of the river space. [3]



**Figure 7.** Perspective view of an urban space integrating people, the river, and the city (source: Press release by Mitsui Fudosan Co., Ltd.)

In order to carry out such large-scale developments, collaboration and coordination with a wide range of stakeholders are essential. Although managing and executing these efforts under the leadership of the N1-C, as a private sector entity, presents significant challenges, they have been successfully implemented.

### 3. IMPLICATIONS OF UNDERGROUND SPACE CREATION FOR THE URBAN REDEVELOPMENT OF NIHONBASHI

Urban development in the Nihonbashi area has entered a new phase by promoting redevelopment projects aimed at overcoming existing challenges. Through the collaboration of multiple redevelopment projects, including the N1-C, a multilayered pedestrian network is being created, linking underground, ground, and deck levels. Furthermore, the plan to relocate the Metropolitan Expressway underground to “restore the sky to Nihonbashi” will not only improve the landscape, but also create spaces that rediscover and utilize the appeal of the waterfront environment. These initiatives will enhance convenience and comfort, promote barrier-free access, and strengthen transportation connectivity, resulting in significant advances in the urban functions of the entire area. The Nihonbashi area is thus expected to evolve into a world-class center for international exchange, where history and innovation are seamlessly integrated.



*Figure 8. Perspective view of the five redevelopment districts centered on the Nihonbashi River and the surrounding Nihonbashi Riverwalk area (source: Press release by Mitsui Fudosan Co., Ltd.)*

### 4. REFERENCES

- [1] Metropolitan Expressway Co., Ltd. (2024, September). Pamphlet for the undergrounding project of the Nihonbashi section of the Metropolitan Expressway. [https://www.shutoko.jp/ss/nihonbashi-tikaka/gallery/nihonbashi\\_pamphlet.pdf](https://www.shutoko.jp/ss/nihonbashi-tikaka/gallery/nihonbashi_pamphlet.pdf)
- [2] Chuo City, Tokyo. (2021, June). Vision for urban development along the Nihonbashi River area 2021. <https://www.city.chuo.lg.jp/documents/5126/kawazoivis2021.pdf>
- [3] Mitsui Fudosan Co., Ltd. (2025, June). Press release: Nihonbashi community development promoted by Mitsui Fudosan. <https://www.mitsui-fudosan.co.jp/corporate/news/2025/0611/>
- [4] Mitsui Fudosan Co., Ltd., & Nomura Real Estate Development Co., Ltd. (2016, May). Outline of Special Urban Regeneration District (Nihonbashi 1-Chome Central District): City planning (draft). <https://www.chisou.go.jp/tiiki/kokusentoc/tokyoken/tokyotoshisaiei/dai12/shiryou1.pdf>



## MANAGEMENT OF URBAN UNDERGROUND SPACE DEVELOPMENT IN SHANGHAI: EXPERIENCE AND CHALLENGES

Chen-Xiao Ma<sup>1</sup>, Zi-Jian Li<sup>2</sup>, Fang-Le Peng<sup>3</sup>

**Abstract:** Since the concept of urban underground space (UUS) utilization was first written into the Shanghai Master Plan (1999-2020), there has been a significant surge in UUS development, with the total area reaching 155 million m<sup>2</sup> by the end of 2023. Establishing a robust management system to promote cooperation between public and private sectors and to achieve interdepartmental collaboration is crucial for ensuring high efficiency of UUS development. This paper systematically analyzed the evolution of UUS management in Shanghai over the past three decades through expert consultations, field investigations and government document analysis. The results indicated that the legislation pathway of 'specialized first, comprehensive later' and 'policies first, regulations later' has shaped the current '1+N+N' regulation framework in Shanghai, providing full coverage of UUS scopes and utilization processes. Furthermore, clarifying municipal and district-level competent authorities for UUS utilization was crucial during the rapid development phase of UUS. Another feature of UUS management in Shanghai was the flexible adjustment of competent authorities in response to urban development demands. Empowering UUS planning with statutory effectiveness standardized UUS development by private sectors. The government-dominated and market-driven mode of UUS construction achieved a win-win situation for the government, the public and developers. As Shanghai has entered a new urbanization phase characterized by urban renewal, the existing UUS management faces new challenges. How to improve the local comprehensive statute for UUS utilization, how to optimize incentive policies, how to construct an effective interdepartmental coordination platform based on the new competent authority, how to establish UUS management mechanisms applicable to urban renewal and how to supplement unit level plans to bridge the gap between UUS master plans and detailed plans, remained critical issues to be addressed. This paper aims to provide insights into UUS management for other high-density metropolitan cities.

**Keywords:** urban underground space, legal system, management mechanism, planning system, Shanghai

### 1. INTRODUCTION

Development of urban underground space (UUS) is a critical strategy to promote urban sustainability and resilience in metropolis (Bobylov et al., 2023; Zhang et al., 2024). Although it has become a consensus in Chinese cities, a top-down management system covering the entire process of UUS utilization has not yet been established at the national level (Xu & Zhu, 2013). A robust management system established by the government is essential for sustainable and highly efficient UUS utilization. Over the past 30 years, many Chinese cities have conducted legislative and management practices for UUS management in accordance with their urban development demands. Among them, Shanghai is a representative city, renowned for its high performance of UUS development and its systematic UUS management framework (Ma & Peng, 2023). Research on UUS management in Shanghai can provide valuable insights for establishment of top-down management systems at the national level and in other Chinese cities.

<sup>1</sup> Postdoc Fellow, Ma Chen-Xiao, Ph.D. in Engineering, Research Center for Underground Space and Department of Geotechnical Engineering, Tongji University, No.1239 Siping Road, Shanghai, P.R. China, zenshiau@163.com.

<sup>2</sup> Mr, Li Zi-Jian, MSc in Engineering, Research Center for Underground Space and Department of Geotechnical Engineering, Tongji University, No.1239 Siping Road, Shanghai, P.R. China, lzjylqs@163.com.

<sup>3</sup> Professor, Director, Peng Fang-Le, Ph.D. in Civil Engineering, Research Center for Underground Space and Department of Geotechnical Engineering, Tongji University, No.1239 Siping Road, Shanghai, P.R. China, pengfangle@tongji.edu.cn (Corresponding author).

Prior studies usually focused on the legislation of UUS property rights. [Zaini et al. \(2017\)](#) analyzed the content related to UUS ownership and the bundle of rights and depth in current laws of Malaysia and compared these with Japan, Finland, and Hong Kong to propose optimization suggestions. [Mária et al. \(2021\)](#) explored UUS governance in the European Union from a space resource perspective. [Zhang et al \(2017\)](#) highlighted that property rights played a crucial role in improving UUS legislative systems and proposed legislative suggestions based on public goods theory. Other scholars also argued for the urgent need to construct a top-down unified UUS legal framework to achieve comprehensive control over UUS development in China ([Zhang et al., 2020](#); [Peng et al., 2024](#)). On the other hand, construction of planning systems is equally important to sustainable UUS utilization. [Yuan et al. \(2019\)](#) proposed the importance of strengthening the coordination mechanism for detailed planning based on the comparison between UUS planning systems in China and Japan. [Von der Tann et al. \(2020\)](#) discussed the principles of systems thinking and presented a perspective on what elements should be included in systemic approaches for planning and management of UUS. [Zhao and Yuan \(2024\)](#) suggested that China should integrate UUS planning into the territorial space planning system to protect UUS resources during its development. Additionally, [Gui \(2018\)](#) analyzed the UUS administrative management system in Beijing and pointed out that it lacked a unified competent authority and interdepartmental coordination mechanisms. In summary, scholars have researched UUS management issues from the following three aspects: legal systems, management mechanisms and planning systems. National level studies were conducted with many valuable suggestions. However, Chinese cities vary significantly in their demands and levels of UUS development. National level studies are usually too macroscopic to directly guide the construction of UUS management systems in specific cities. Therefore, it is still necessary to select specific cities or regions for in-depth and comprehensive studies.

This paper aims to thoroughly analyze the evolution of UUS development management in Shanghai over the past 30 years and summarize the experience and challenges of management systems from the perspective of legal systems, management mechanisms and planning systems. In terms of the methodology, we conducted two expert consultations (including 16 experts from universities, government departments, planning and design institutes, construction enterprises in Shanghai) and 13 field investigations (in 13 UUS management related public sectors) from November 2023 to August 2024. Government policies and planning documents related to UUS utilization were also collected and analyzed. The remainder of this paper is structured as follows. In [Section 2](#), we briefly review the current situation of UUS utilization in Shanghai. [Section 3](#) summarizes the experience of UUS management from three aspects. [Section 4](#) proposes five challenges faced by the government in improving its management performance in the new urbanization stage of urban renewal. Concluding remarks on this research are finally provided in [Section 5](#).

## 2. CURRENT SITUATION OF UUS UTILIZATION IN SHANGHAI

Utilization of UUS in Shanghai dates back to the 19th century, when the buried pipelines (1862) and underground prisons of Louza Police Station (1888) were constructed in the International Settlement ([Huang, 2015](#)). The early development was closely related to the beginning of modern urbanization. [Figure 1](#) illustrates the development trend of UUS from 1862 to the present ([Shanghai Municipal Commission of Housing and Urban-Rural Development, 2023](#)). Owing to the geological conditions, construction technology, economic development and UUS cognition, the utilization of UUS in Shanghai has experienced a long period of slow development in the 20th century, followed by the explosive growth thereafter. Its dominant ideology has also evolved through several stages: high-rise building and buried pipelines (before 1949), civil air defense projects (1949–1978), hybrid mixing of peacetime and wartime functions (1978–1999) and comprehensive functions (from 1999 to the present) ([Qiao & Peng, 2016](#)). In 2002, Shanghai was awarded the hosting rights for the 2010 World Expo, marking the beginning of a period of rapid urbanization in the city. UUS amount surged alongside the construction of the municipality-wide metro system and numerous land development projects in the main city. The total UUS area reached 155 million m<sup>2</sup> in 2023. However, with the gradual transition of urbanization development modes into the urban renewal stage, the annual growth area of UUS exhibited a fluctuating downward trend since 2017, decreasing to below 10 million m<sup>2</sup> in 2023. Newly added UUS was mainly located in urban renewal areas of the city center, peripheral sub-centers and the five developing new towns in the suburbs.

Average UUS intensity for the municipality-wide area of Shanghai reached 24.400 m<sup>2</sup>/km<sup>2</sup> in 2023. [Figure 2\(a\)](#) reveals the intensity distribution across the 16 districts of the city in 2023, showing a gradual decrease from the city center to the suburbs. Huangpu District had the highest development intensity, while Chongming District had the lowest. [Figure 2\(b\)](#) shows the comparison of UUS per capita and UUS intensity of UUS in Shanghai. Huangpu District achieved both the highest UUS per capita and intensity, indicating its highest efficiency of UUS utilization, compared with other areas. Qingpu, Songjiang, Chongming and Jinshan were located in the outer suburbs, where UUS demands were lower than that in other districts, resulting in low values for both indicators. Furthermore, districts of Yangpu, Pudong and Baoshan had relatively high UUS intensity, but their indicators of

UUS per capita were low. It indicated a possible undersupply of UUS, especially in Yangpu, which was the only one located in central urban area among the three districts. On the other hand, Fengxian obtained a high values of UUS per capita with low UUS intensity. Rapid construction of Fengxian New City increased its total UUS area. However, the discrepancy between the two indicators also suggested the possibility of an oversupply of UUS.

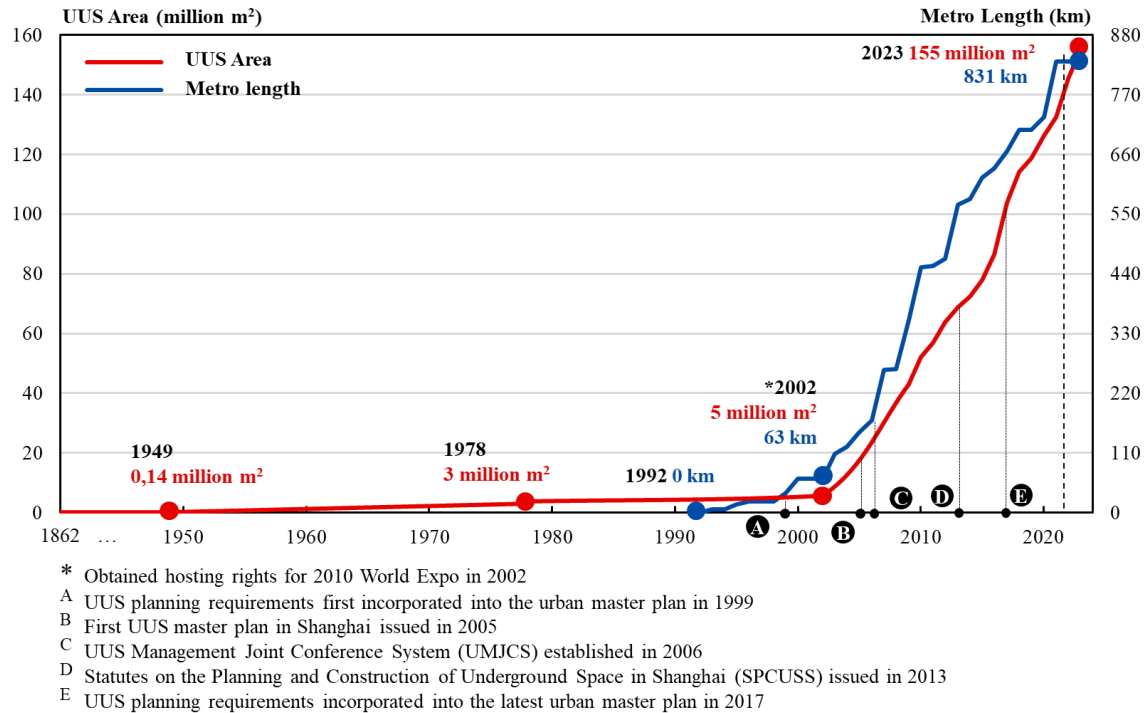


Figure 1. UUS and urban rail transit development in Shanghai (Data source: *Shanghai Municipal Commission of Housing and Urban-Rural Development, 2023*)

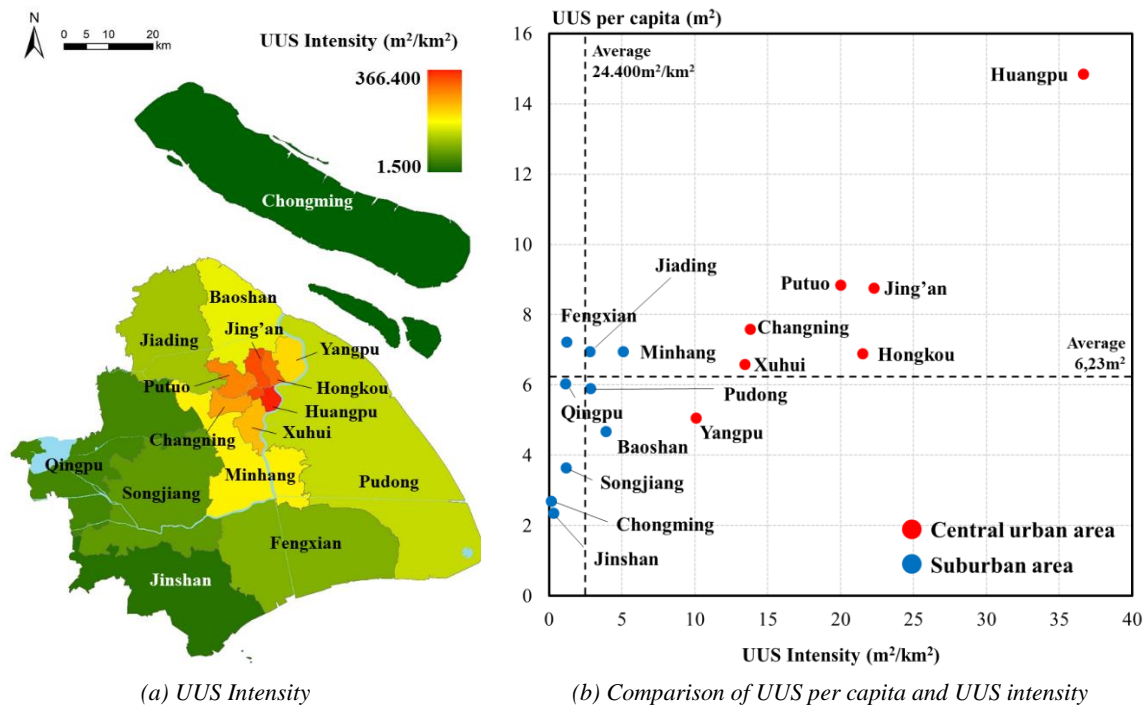
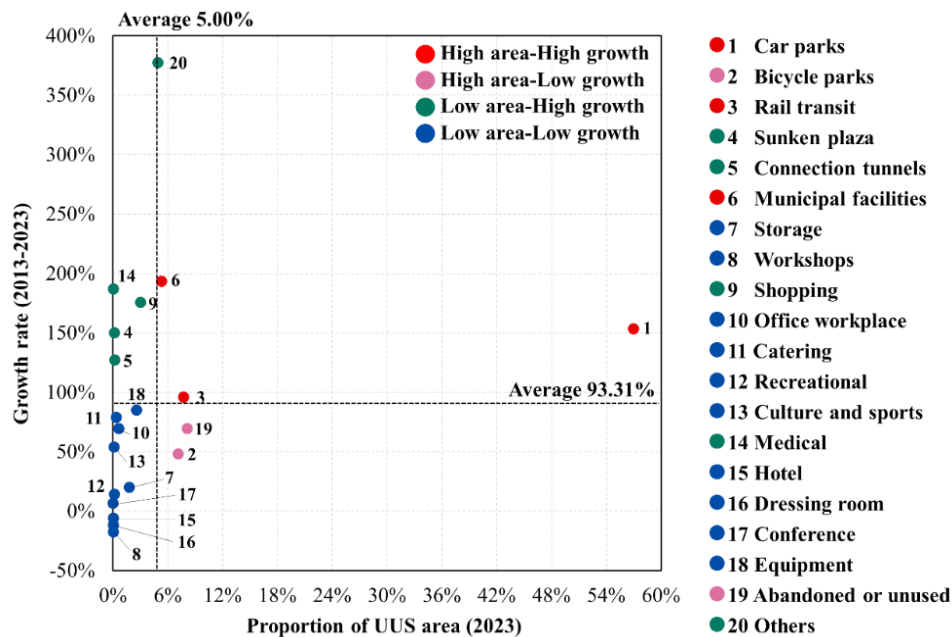


Figure 2. UUS development status of 16 districts in Shanghai in 2023 (Data source: *Shanghai Municipal Commission of Housing and Urban-Rural Development, 2023*)



**Figure 3** compares the growth rates (2013–2023) and area proportions of different UUS functions in Shanghai in 2023. There is an unbalanced distribution of UUS functions. Underground transportation (No. 1-5) and municipal infrastructure (No.6), particularly car parks, accounted for 77,78% of the total UUS area and obtained high growth rates. This was consistent with the analysis results from 2013 (Qiao & Peng, 2016) and indicated that UUS development in Shanghai still primarily focused on addressing urban traffic problems and serving as municipal facilities in Shanghai. Underground service facilities (No. 9-17) accounted for 4,64% of the total UUS area, of which shopping was the dominant function with an extremely high growth rate of 175,42%. Land developers increasingly focused on the economic value of UUS development, especially in metro-led areas, to achieve excess profit returns (Shi & Zhou, 2017; Ma et al., 2024). On the other hand, abandoned or unused space (No.19) obtained a high proportion of 8,15%. Although its growth rate was lower than the average, the phenomenon of low-efficiency utilization of UUS resources still existed.



**Figure 3.** Comparison of growth rate (2013-2023) and area proportion of different UUS functions in Shanghai (Data source: Shanghai Municipal Commission of Housing and Urban-Rural Development, 2023)

### 3. EXPERIENCE OF UUS MANAGEMENT

#### 3.1. Legal system

Shanghai began integrating UUS management requirements into existing regulations and established UUS a legal system in the 1990s. By 2025, Shanghai has developed a systematic '1+N+N' UUS legal framework, with a local comprehensive statute on UUS serving as the core, supplemented and supported by several local specialized statutes on specific underground facilities and a range of related regulations and policies (e.g., regulations, provisions, measures, opinions, rules), as illustrated in Figure 4.

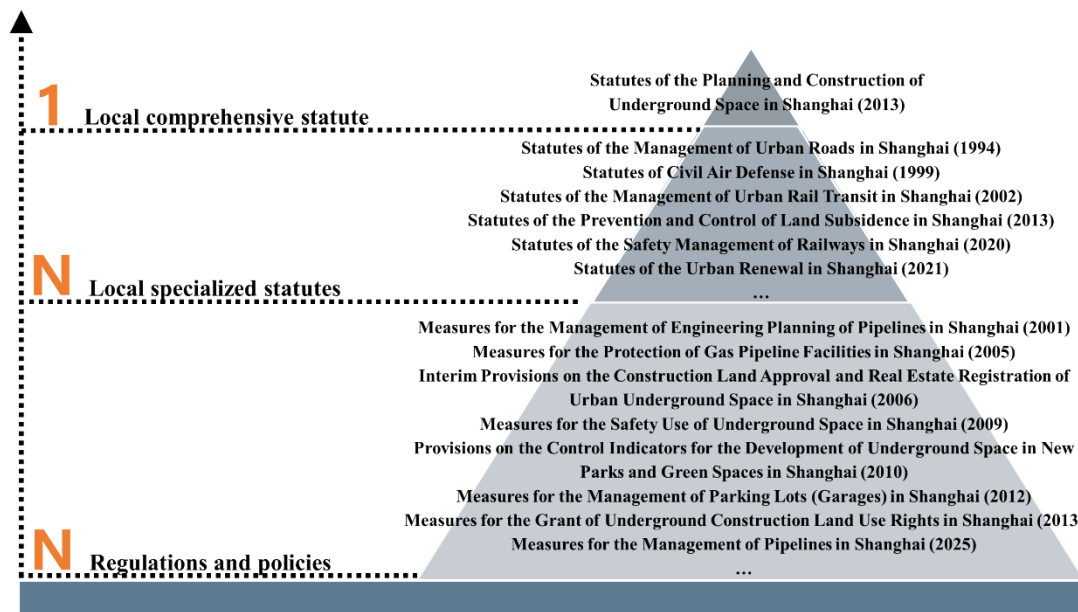


Figure 4. UUS Legal systems in Shanghai

#### (1) Successful legislation pathway of 'Specialized first, Comprehensive later' and 'Policies first, Statutes later'

Similar to the UUS legislation process of Japan (Liu & Shen, 2007), construction of Shanghai's UUS legal system also followed a pathway of 'Specialized first, Comprehensive later' and 'Policies first, Statutes later'. In the 1990s, underground roads, metro systems, civil air defense projects, underground pipelines and underground parking space were among the earliest constructed underground facilities. Public sectors accumulated extensive experience in managing these specialized UUS. Subsequently, before 2013, the government successively promulgated regulations and management measures for urban roads (1994), civil air defense projects (1999), urban pipelines (2001), metro systems (2002), gas pipelines (2005) and parking lots (2012). These measures standardized the space management of urban transportation and municipal infrastructure, including their underground components. On the other hand, local statutes usually have higher legal effects compared with regulations and policies issued by local governments (Zhang et al., 2020). To test the rationality of management requirements and accumulate experience for local legislation, the Shanghai Government formulated several measures on planning and safety use of UUS and its property ownership registration from 2006 to 2010. Establishment and revision of the above-mentioned specialized regulations and diverse UUS-related regulations and policies provided the basis for the legislation of the local comprehensive statute on UUS, namely the Statutes on the Planning and Construction of Underground Space in Shanghai (SPCUSS) in 2013. It was enacted by the Standing Committees of Shanghai People's Congress, representing a legal force second only to the Constitution and national laws.

#### (2) Full coverage of UUS scopes and utilization process in the municipality-wide area

Taking SPCUSS as an example, the definition of UUS was 'the space below the surface within the administrative boundary of this city'. It encompassed both artificially constructed space and undeveloped UUS resources. The full coverage of UUS scopes reflected the principle that the Shanghai Government constructed the UUS legal system from the perspective of natural resource protection and orderly utilization. Therefore, in addition to management regulations on specific underground facilities, the UUS legal system in Shanghai also included policies related to ground subsidence and geothermal resource development. Moreover, the management systems also covered the entire process of UUS planning, construction and operation. They provided detailed regulations or descriptions for land use, real estate registration and development incentives for private sectors related to UUS. This holistic approach ensured that all aspects of UUS utilization were governed by clear and comprehensive legal frameworks, promoting sustainable and efficient development.

### 3.2. Management mechanisms

Shanghai was one of the earliest cities in China to initiate the construction of a comprehensive UUS management model, clarifying the competent authorities for the entire process of UUS utilization and establishing systematic management mechanisms. In July 2006, the Shanghai Government established the UUS Management Joint Conference System (UMJCS), a coordination mechanism involving UUS-related public departments and one

state-owned enterprise (Shanghai Metro Company) responsible for comprehensive management of the major issues of entire process of UUS development, including planning, construction and operation. The Shanghai Municipal Bureau of Civil Affairs (SMBCA) was in charge of the UMJCS, which was actually appointed as the municipal competent authority for UUS development in the city. From 2006 to 2009, the 16 districts of Shanghai also established district-level UMJCSs, with the district civil affairs offices taking charge of UUS development. In September 2014, following a functional adjustment in public departments, the current Shanghai Municipal Bureau of Planning and Natural Resources (SMBPNR) was appointed as the competent authority for UUS development according to the SPCUSS. Furthermore, since 2006, Shanghai has successively established several specialized management platforms or systems targeting UUS utilization, including the Shanghai UUS Information Infrastructure Platform (2006), UUS Expert Consultation Group (2007), UUS Safety Management Mechanism (2009) and Professional Grid-based Management Mechanism for UUS (2010).

#### (1) Clarifying municipal and district-level competent authorities for UUS utilization

Given the multiple functions of UUS, its administrative and approval management in Shanghai involved as many as 20 municipal departments currently as shown in [Table 1](#). Among them, the SMBPNR, Shanghai Municipal Commission of Housing and Urban-Rural Development (SMCHURD) and SMBCA were the three most important departments. They were respectively responsible for the planning and land use approval of UUS, construction management, and the entire process of approval and management of civil air defense projects. Clarifying UUS competent authorities has established a mature top-down management system ([Gui, 2018](#)). Combined with the UMJCS, the mechanism has effectively addressed issues that required interdepartmental coordination in UUS utilization (e.g., compilation of UUS plans, major underground public space or complex projects development management), unmanaged issues under the traditional framework (e.g., safety inspections of existing UUS), and new challenges faced in urban construction regarding UUS development (e.g., establishment of underground land use rights).

**Table 1.** Current UUS-related municipal government departments in Shanghai

Municipal departments	In UMJCS?		Management stages*			
	Yes	No	CA	P	C	O
Shanghai Municipal Bureau of Planning and Natural Resources	•		•	•	•	•
Shanghai Municipal Commission of Housing and Urban-Rural Development	•				•	•
Shanghai Municipal Bureau of Civil Affairs	•			•	•	•
Shanghai Municipal Development & Reform Commission	•			•		•
Shanghai State-owned Assets Supervision and Administration Commission		•				•
Shanghai Municipal Commission of Economy and Informatization	•			•		•
Shanghai Municipal Bureau of Public Security	•					•
Shanghai Municipal Bureau of Finance		•			•	•
Shanghai Municipal Bureau of Ecology and Environment		•		•		•
Shanghai Municipal Commission of Transport	•			•	•	•
Shanghai Municipal Bureau of Water Resources	•			•	•	•
Shanghai Municipal Administration of Culture and Tourism		•			•	•
Shanghai Municipal Commission of Health	•					•
Shanghai Municipal Bureau of Emergency Management	•			•	•	•
Shanghai Municipal Bureau of Fire and Rescue	•				•	•
Shanghai Municipal Administration for Market Regulation	•					•
Shanghai Landscaping & City Appearance Administrative Bureau	•			•	•	
Shanghai Urban Management and Law Enforcement Bureau		•				•
Shanghai Municipal Bureau of Housing Administration	•					•
Shanghai Municipal Bureau of Data		•				•

\* Note: CA, competent authority of UUS management; P, planning; C, construction; O, operation.

#### (2) Flexibly adjusted competent authorities based on to urban development demands

Shanghai's UUS management mechanism was not constructed overnight. The mechanism evolution was highly related to UUS development demands, ensuring that the management could continuously meet the requirements of urban development. Before 2006, UUS development management was characterized by a parallel management mode, in which each department performed its own duties independently. During this period, UUS was mainly composed of civil air defense projects (managed by the SMBCA) with few comprehensive functions, making the traditional mode still effective ([Qiao & Peng, 2016](#)). From 2002 to 2006, Shanghai's urbanization rate jumped from 76,4% to 85,8%, with an average annual population increase of 3,3%. Urban space resources were in short supply. Meanwhile, to host the 2010 World Expo, a series of urban renewal and new city construction projects were conducted. UUS scale increased rapidly and the demand for comprehensive UUS development in the core areas gradually emerged. Then the parallel mode was no longer capable of coping with the increasing

complexity and interconnectivity of UUS development. Due to the inertia of traditional UUS cognition and the established jurisdiction of government departments, the SMBCA was appointed as the competent authority for UUS utilization in 2006. Over the following eight years, UUS functions became increasingly comprehensive and the proportion of civil air defense space gradually decreased. Limited by its departmental functions, the SMBCA was no longer suitable as the chief authority. Since spatial planning has become the primary link in land transfer and development and the city was still in the stage of rapid urbanization. 'Planning-led' has become a common consensus for UUS utilization and protection. Then the UUS management system led by the SMBPNR was ultimately established in 2014.

### 3.3. Planning system

Construction of a comprehensive planning system is fundamental to regulating sustainable utilization of UUS resources (Yuan et al., 2019; Zhang et al., 2022). After multiple changes, Figure 5 reveals the current UUS planning system. It comprised two planning levels, correlating with the top-down territorial space planning system of Shanghai (Zhao & Yuan, 2024). The master level of UUS planning focused on the protection of UUS resources and control of space utilization. In contrast, the detailed level was oriented towards land development, emphasizing the functional positioning, space layout of different underground facilities and UUS interconnectivity requirements. It served as the basis for planning management and land leasing of UUS development.

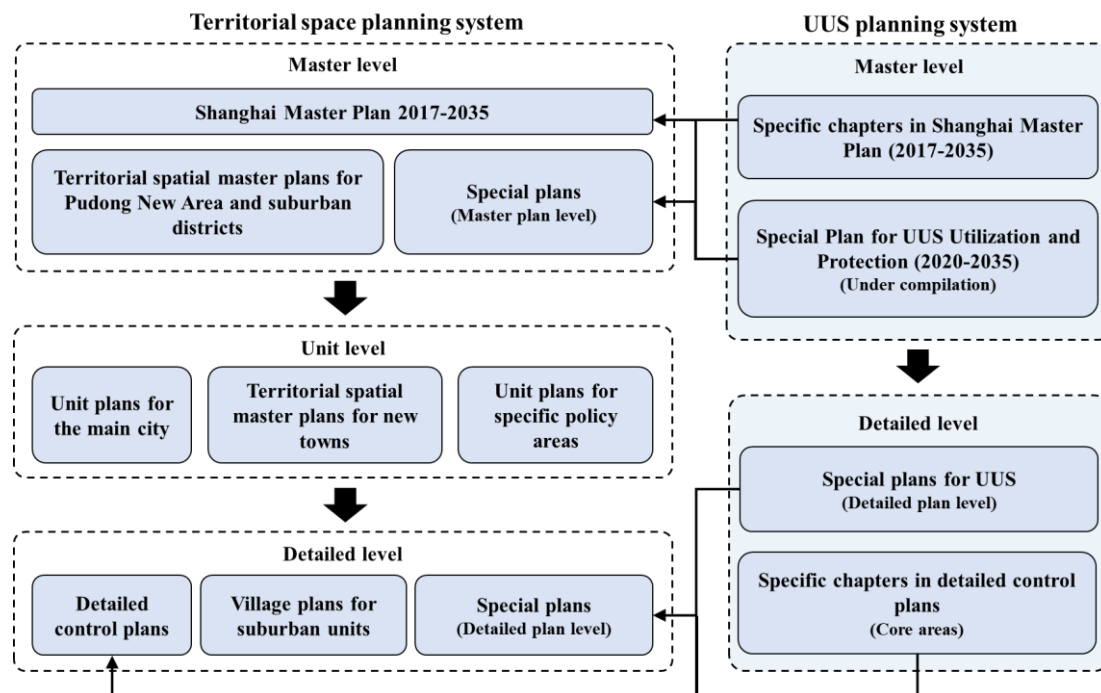


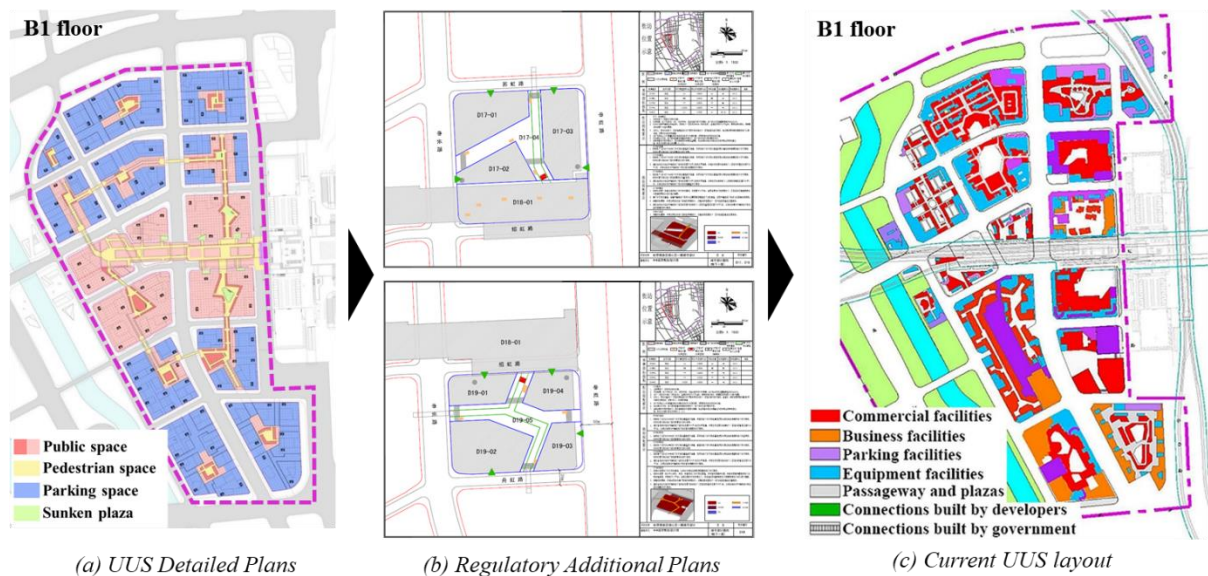
Figure 5. Current UUS planning system and territorial space planning system in Shanghai

#### (1) UUS planning empowering statutory planning effectiveness

Unlike Helsinki's Underground Master Plan (Vähäaho, 2016), UUS master plans and detailed plans were merely special plans with no statutory planning effectiveness according to the Urban and Rural Planning Law in China. Previous studies also indicated that UUS planning failed to regulate UUS utilization due to the lack of legal force (Peng et al., 2019). To address the problem within the existing national legal framework, UUS plans have been consistently integrated into statutory planning systems for aboveground space in Shanghai. At the master level, planning requirements for UUS were incorporated as specific chapters into the Shanghai Master Plan (1999-2020) and the Shanghai Master Plan (2017-2035). Although the two UUS master plans were separately compiled in 2005 and 2020 under the guidance of the two urban master plans, SPCUSS (Article 9) required that the planning outcomes should be integrated into the urban master plan, thereby empowering them the statutory planning effectiveness. At the detailed level, traditional urban detailed plans only involved Regulatory Universal Plans (RUPs) to propose basic requirements such as land use, floor area ratios and density before 2010. An innovative approach was adopted to incorporate the separately compiled UUS detailed plans into traditional detailed plans in the form of Regulatory Additional Plans (RAPs) during the planning compilation of Hongqiao Central Business



District (CBD) in 2010 as shown in **Figure 6**. This effectively imposed the statutory planning effectiveness on UUS detailed plans to standard land development by private sectors (Shanghai Planning and Land Resources Management Bureau et al., 2020; Peng et al., 2020). This approach was retained and normalized as a planning technical requirement in the Shanghai Technical Guidelines for Control Detailed Planning (STGCDP) in 2011: Regardless of whether a separate UUS detailed plan is compiled, it is mandatory to compile RAPs with UUS planning indicators (e.g., construction area of UUS, depth and floors, main functions, UUS scale, connecting passages and sunken plazas) for detailed plans of public activity centers, historical and cultural districts, important waterfront areas, scenic areas and transportation hub areas (Shanghai Planning and Land Resources Management Bureau et al., 2020).



**Figure 6.** Planning and current development layout for UUS in Shanghai Hongqiao CBD (Data source: Peng et al., 2020)

## (2) Government-dominated and market-driven UUS development mode

Based on public land ownership, detailed plans served as the basis for public sectors to regulate land development. According to the data from SMCHURD (Shanghai Municipal Commission of Housing and Urban-Rural Development, 2023), 85.8% of UUS consisted of building basements, which were essentially constructed through land development driven by private sectors. Relying on the UUS planning system with statutory planning effectiveness, municipal departments could exercise macroscopical control over state-owned three-dimensional land resources, obtaining revenue from land leasing to serve for other public service and ensuring public interests. Meanwhile, private sectors flexibly engaged in land development within the requirements of the detailed plans to achieve excess profits. Ultimately, this government-dominated and market-driven UUS development mode enabled a win-win situation for the government, the public and developers.

## 4. CHALLENGES OF UUS MANAGEMENT

Currently, urbanization development stages in Shanghai have shifted from rapid urban expansion to urban renewal. Although the well-developed legal system, management mechanisms and planning system have supported the rapid construction of UUS over the past 25 years, several challenges still remain.

### 4.1. Incomplete local comprehensive statute of SPCUSS

The SPCUSS is regarded as the local comprehensive statute with the highest legal force for UUS utilization in Shanghai. It has undergone two revisions in 2018 and 2020 after its initial release in 2013. However, the current SPCUSS only covers the management and penalty provisions of UUS planning, construction, land use and property rights, lacking provisions for UUS usage and operation. Relevant management requirements are scattered across various specialized management statutes or government regulations. Compared with other 68 Chinese cities that have already issued their local comprehensive statutes, only 10 cities do not include provisions for UUS usage



management. As Shanghai has entered a new urbanization stage of urban renewal, safety use and sustainable operation of existing UUS become more and more important to public administration of the government. With the accumulation of management experiences over the past 12 years, it is high time to supplement the corresponding provisions so as to make the SPCUSS a truly comprehensive local statute covering the entire process of UUS utilization.

#### 4.2. Lack of attractive and implementable incentive policies for UUS development

Incentive policies for UUS development in Shanghai include floor area ratio (FAR) bonuses and reductions in grant fees of UUS land use rights targeting the construction of underground public facilities or public space as tabulated in [Table 2](#). However, these provisions are scattered across different government documents compiled at various times, without a clear definition of the UUS eligible for the incentives. Furthermore, attractiveness of the incentive policies is not as high as that of other metropolis. For example, the Provisions on the Grant of Underground Construction Land Use Rights in Shanghai (2023) did not clearly define the eligible underground public passages for reductions of grant fees. In contrast, the similar provisions also occurred in the Several Opinions on Improving the Management of State-owned Land Supply by Several Opinions on Improving the Management of State-owned Land Supply (2018) issued by the Shenzhen government, by which the eligible passage should be open to the public for 24 hours per day with the main function of interconnection between two buildings. Additionally, an additional area bonus of up to 20% of the passage area was offered for commercial uses, effectively stimulating developers' enthusiasm. Similarly, the Urban Redevelopment Authority of Singapore also proposed that the construction of underground public passages could be excluded from FAR calculations, increase activity-generating use space, and provide cash grants ([Urban Redevelopment Authority, 2021](#)).

*Table 2. Currently effective incentive policies for UUS development in Shanghai*

Types*	Incentive policies	Contents
FB	Technical Provisions on Urban Planning Management in Shanghai (Land Use and Building Management)-Article 20 (2010)	Provision of open space for the public can be rewarded with an area bonus of 1,0 or 1,5 times of the area in the main city
FB	Shanghai Technical Guidelines for Control Detailed Planning-Article 13.4 (2016)	An increase in building area of up to 15% is allowed due to the addition of community public welfare facilities, public parking space, public space on the ground or in the buildings
FB	Provisions on Planning Management of Building Area Calculation in Shanghai-Article 5 (2021)	Basements meeting requirements not included in floor area ratio calculation
FB	Implementation Details of Land Use for Urban Renewal Planning in Shanghai-Article 7 (2022)	Provision of new public space or public facilities can be rewarded with an additional commercial space area ranging from 0,5 to 2,0 times of the area
LE	Provisions on the Grant of Underground Construction Land Use Rights in Shanghai-Article 9 (2023)	No setting UUS land use rights and exemption the grant fees for underground public passages and municipal facilities for regional service developed by planning

\* Note: FB, FAR bonuses; LE, exemption for grant fees of UUS land use rights.

#### 4.3. Readjustment of the UUS competent authority and reconstruction of an interdepartmental coordination platform for UUS utilization

Although the SPCUSS has nominally appointed the planning department as the competent authority for UUS development, there is no dedicated or explicitly designated sector in the department responsible for this task. Furthermore, while the management mechanism based on planning-led principles is quite applicable to the stage of explosive growth of UUS, it may be less suitable for the urban renewal phase. In this stage, it is more important for high-quality usage management of existing UUS to promote higher efficiency of UUS utilization. Therefore, the department in charge of urban construction and operation management may be more appropriate to be appointed as the UUS competent authority.

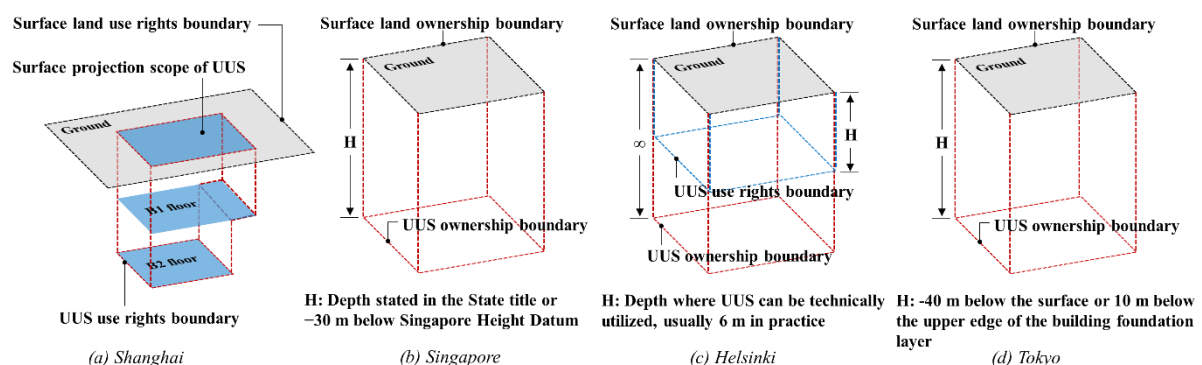
On the other hand, the main scope of the UMJCS has been restricted to UUS safety management since 2014, operated by the SMCHURD. It implies that Shanghai has no longer an interdepartmental coordination and management mechanism for UUS development since 2014. In terms of UUS statistical data, both the planning and construction authorities have established databases within their respective jurisdictions. However, there is a lack of data-sharing mechanism between them and exists an extremely large difference in data volume. Moreover, issues related to the reuse of idle UUS may involve different government departments with ownership change

approval, commercial operation approval, fire safety approval and other administrative management procedures. The absence of an interdepartmental coordination platform makes it difficult to establish a systematic mechanism to promote the high efficiency utilization of existing underground facilities. A new interdepartmental coordination platform is still necessary for UUS utilization during the urban renewal stage. Moreover, even the initially established UMJCS in 2006 still lacked some UUS-related public sectors and state-owned companies (e.g., underground pipeline companies), which should be incorporated in the construction of the new platform.

#### 4.4. No specific management mechanisms for UUS utilization during urban renewal

UUS utilization during urban renewal encompasses both the renovation of existing UUS and newly-built UUS in existing built-up areas (Cui et al., 2021). For the renovation of existing UUS, the Provisions on the Grant of Underground Construction Land Use Rights in Shanghai (2023) proposed that grant fees of UUS land use rights should be determined based on the actual UUS functions and scale. The provisions also regulated the procedures for ownership registration of both existing and newly-added UUS. However, they fail to address the problems of the changes in ownership due to the adjustments of inner space functions in the ownership registered UUS, especially when commercial space is repurposed for public functions. There are no clear procedures or mechanisms for refunding UUS land use rights and their grant fees in such situations. Moreover, no policies have been introduced for the reuse of idle UUS. In contrast, Beijing has established an interdepartmental coordination mechanism to promote this issue, as stipulated in the Guiding Opinions on Using Underground Space to Supplement and Improve Convenient Commercial Service Facilities (2018).

On the other hand, to increase space resources for allocation of parking facilities and other public facilities, additional basements are newly built under existing surface buildings, especially in historical and cultural districts and old residential areas. However, so far there has been no systematic management system and regulatory standard to regulate such UUS construction. Additionally, since the promulgation of the Property Law in 2007, land use rights have been extended to three-dimensional space (Zhang et al., 2017). The Provisions on the Grant of Underground Construction Land Use Rights in Shanghai (2023) also proposed an explicit vertical range of UUS land use rights, defining it as the outer periphery of the underground buildings and structures as shown in Figure 7. It is quite different from the definitions in Singapore, Helsinki and Tokyo, which are all based on surface land ownership boundaries (Vähäaho, 2016; Zhou & Zhao, 2016; Zaini et al., 2017). Therefore, the remaining underground space within the land use scope that has not established UUS land use rights can theoretically still be granted. Nevertheless, the current policies have not proposed the principles and requirements that should be followed. Moreover, the potential demands for such UUS also pose challenges to the traditional two-dimensional cadastral management system, calling for the establishment of three-dimensional cadaster systems (Qiao & Peng, 2023).



**Figure 7.** Comparison of UUS land use rights or ownership boundaries in Shanghai, Singapore, Helsinki and Tokyo

#### 4.5. Absence of unit level UUS planning

Shanghai's two-level UUS planning system creates a disconnection between the planning requirements at the master level and detailed level. On one hand, some of the UUS requirements at master level plans are not implementable (Wu & Zhao, 2021). For example, the Shanghai Master Plan (2017-2035) proposed that the underground proportion of newly built rail transit and municipal facilities (including substations, drainage pump stations and waste transfer stations) in the main city and five new towns should reach 100% by 2035. However, due to the lack of unit level plans to refine the specific areas and feasibility conditions for implementation of the requirement, this requirement is often neglected during the compilation of detailed plans. Meanwhile, the absence of unit level UUS planning also violates Article 9 of the SPCUSS. On the other hand, UUS planning requirements

at master levels do not provide detailed regulations on UUS connectivity, UUS development in public lands and layout of underground public facilities, which are the most important planning contents in RAPs at detailed levels. Due to the absence of unit level UUS planning, except for the five new towns (as they are regulated by Shanghai New Town Planning and Implementation Guideline issued in 2021), there is no explicit planning basis for UUS development while compiling detailed plans in Shanghai. Furthermore, in urban areas outside the five key areas specified in the STGCDP, RAPs with UUS development regulations are not mandatorily required, implying a lack of effectively government control over UUS utilization in these areas.

## 5. CONCLUSION

Shanghai is a representative city of UUS utilization in China, not only due to its large development scale and diverse functions but also because of its systematic management framework. This paper reviewed the evolution of Shanghai's UUS legal system, management mechanisms and planning system over the past 30 years. Considering the current urban renewal demands in Shanghai, this paper also identified the challenges faced by the existing UUS management systems. The findings can provide insights for optimization of UUS management systems in other Chinese cities and establishment of a top-down management system at the national level. The main contributions of this study can be summarized as follows.

(1) The successful legislative pathway of 'Specialized first, Comprehensive later' and 'Policies first, Statutes later' has shaped the '1+N+N' legal system for UUS management in Shanghai. Various government regulations and policies have achieved effective control over all UUS fields (including underground structures and unused space resources) and the entire process of UUS development. However, as the foundation and core of the regulatory system, the SPCUSS has not yet involved provisions for UUS usage management, failing to become a truly comprehensive local statute. Moreover, the incentive policies for UUS development lack sufficient attractiveness and feasibility, making it difficult to motivate private sectors to actively engage in UUS development.

(2) The case study in Shanghai indicates that clarifying municipal and district-level competent authorities for UUS utilization is key to addressing comprehensive UUS development issues. Flexibly adjusting competent authorities in response to urban development demands can effectively improve governance efficiency of public sectors. However, the current planning department-led management system is insufficient to meet UUS utilization demands under the context of urban renewal. The government function adjustment in 2014 also led to the disappearance of the interdepartmental coordination platform for the entire process of UUS utilization. Additionally, the current system still lacks mature management mechanisms for UUS land use rights grant, reuse of idle UUS and three-dimensional cadastral management systems during urban renewal.

(3) Shanghai has established a two-level UUS planning system integrated with the territorial space planning system. By legislation and establishing RAPs, statutory planning effectiveness has been granted to UUS plans at all levels. A government-dominated and market-driven UUS development mode has been constructed to achieve a win-win situation among the government, the public and private sectors in land development. However, the current system lacks unit level plans of UUS, making it difficult to implement the planning requirements of master level plans. Simultaneously, the compilation of UUS detailed plans also lacks a basis of upper level planning.

## 6. ACKNOWLEDGEMENTS

The authors express gratitude to Shanghai Green Building Council, Shanghai Tongji Engineering Consulting Co., Ltd. and SGIDI Engineering Consulting (Group) Co., Ltd. for their help in expert consultations and field investigations. This work was supported by the China Postdoctoral Science Foundation [Grant number: 2024M762417] and National Natural Science Foundation of China (NSFC) [Grant number: 42071251].

## 7. REFERENCES

- [1] Bobylev, N., Guo, D. J. & Benardos, A. (2023). Urban Underground Space Use in a Climate Neutral City. (Eds.). Proceedings of the ITA-AITES World Tunnel Congress 2023, WTC 2023: Expanding Underground-knowledge and Passion to Make a Positive Impact on the World. 9-13. <https://doi.org/10.1201/9781003348030-2>.
- [2] Zhang, Y., Zheng L., He, L. L., Jiao, Y. Y., Peng, H. F. & Ranjith P. G. (2024). Bibliometric Analysis of Research Challenges and Trends in Urban Underground Space. *Deep Underground Science and Engineering*, 3(2), 207-215. <https://doi.org/10.1002/dug2.12086>.
- [3] Xu, S. Y. & Zhu, X. C. (2013). Research on Current Legislation for Urban Underground Space in China. (Eds.). *Advances in Underground Space Development*. 663-671. [https://doi.org/10.3850/978-981-07-3757-3\\_RP-136-P080](https://doi.org/10.3850/978-981-07-3757-3_RP-136-P080).

- [4] Ma, C. X. & Peng, F. L. (2023). Evaluation of Spatial Performance and Supply-demand Ratios of Urban Underground Space Based on POI Data: A Case Study of Shanghai. *Tunnelling and Underground Space Technology*, 131, 104775. <https://doi.org/10.1016/j.tust.2022.104775>.
- [5] Zaini, F. Hussin, K. & Raid, M. M. (2017). Legal Considerations for Urban Underground Space Development in Malaysia. *Underground Space*, 2(4), 234-245. <https://doi.org/10.1016/j.undsp.2017.11.001>.
- [6] Mária, H., Tamás, H. & Lili, C. (2021). Underground Space, the Legal Governance of a Critical Resource in Circular Economy. *Resources Policy*, 73, 102171. <https://doi.org/10.1016/j.resourpol.2021.102171>.
- [7] Zhang, Z., Tang, W. W., Gong, J. & Huan, J. E. (2017). Property Rights of Urban Underground Space in China: A Public Good Perspective. *Land Use Policy*, 65, 224-237. <https://doi.org/10.1016/j.landusepol.2017.03.035>.
- [8] Zhang, Z., Paulsson, J., Gong, J. & Huan, J. (2020). Legal Framework of Urban Underground Space in China. *Sustainability*, 12(20). 10.3390/su12208297.
- [9] Peng, F. L., Qiao, Y. K., Dong, Y. H., Yan, Z. G. & Zhu, H. H. (2024). Development Strategy for Urban Underground Space in the New Development Stage. *Strategic Study of CAE*, 26(3), 176-185. (in Chinese)
- [10] Yuan, H., He, Y. & Wu, Y. Y. (2019). A Comparative Study on Urban Underground Space Planning System Between China and Japan. *Sustainable Cities and Society*, 48, 101541. <https://doi.org/10.1016/j.scs.2019.101541>.
- [11] von der Tann, L., Sterling, R., Zhou, Y. X. & Metje, N. (2020). Systems Approaches to Urban Underground Space Planning and Management - A Review. *Underground Space*, 5(2), 144-166. <https://doi.org/10.1016/j.undsp.2019.03.003>.
- [12] Zhao, Y. & Yuan, X. G. (2024). Underground Spatial Planning in the New Era: System, Contents, and Methods. *Shanghai Urban Planning Review*, 4(4), 102-108. 10.11982/j.supr.20240414. (in Chinese)
- [13] Gui, Y. L. (2018). Reform and Innovation of Urban Underground Management System: A Case Study of Beijing. *Journal of Urban and Regional Planning*, 10(3), 226-242. (in Chinese)
- [14] Huang, L. (2015). Development of the First Underground Space in Shanghai. *Life & Disaster*, (01), 24-27. (in Chinese)
- [15] Shanghai Municipal Commission of Housing and Urban-Rural Development. (2023). Annual Report of Shanghai Underground Space Management Coordination Office in 2023. <https://zjw.sh.gov.cn/>. (in Chinese)
- [16] Qiao, Y. K. & Peng, F. L. (2016). Lessons Learnt From Urban Underground Space Use in Shanghai—from Lujiazui Business District to Hongqiao Central Business District. *Tunnelling and Underground Space Technology*, 55, 308-319. <https://doi.org/10.1016/j.tust.2015.12.001>.
- [17] Shi, Y. S. & Zhou, L. (2017). Land Value Assessment and Spatial Variation in Underground Commercial Space in Shanghai. *Acta Geographica Sinica*, 72(10), 1787-1799. 10.11821/dlxb201710005. (in Chinese)
- [18] Ma, C. X., Dong Y. H. & Peng, F. L. (2024). Development Rules of Metro-led Underground Public Space: A Case Study of Shanghai City. *Geology and Exploration*, 60(1), 9-19. 10.12134/j.dzykt.2024.01.002. (in Chinese)
- [19] Liu, C. Y. & Shen, Y. H. (2007). Study on Laws on Exploration and Utilization of City Underground Space in Japan. *Chinese Journal of Underground Space and Engineering*, 3(4), 587-591. (in Chinese)
- [20] Zhang, M. D., Xie, Z. & He, L. (2022). Does the Scarcity of Urban Space Resources Make the Quality of Underground Space Planning More Sustainable? A Case Study of 40 Urban Underground Space Master Plans in China. *Frontiers in Environmental Science*, 10. 966157. 10.3389/fenvs.2022.966157.
- [21] Vähäaho, I. (2016). An Introduction to the Development for Urban Underground Space in Helsinki. *Tunnelling and Underground Space Technology*, 55, 324-328. <https://doi.org/10.1016/j.tust.2015.10.001>.
- [22] Peng, F. L., Qiao, Y. K., Cheng, G. H. & Zhu, H. H. (2019). Current Situation and Existing Problems of and Coping Strategies for Urban Underground Space Planning in China. *Earth Science Frontiers*, 26(3), 57-68. (in Chinese)
- [23] Shanghai Planning and Land Resources Management Bureau, Shanghai Urban Planning Compilation and Review Center & Shanghai Urban Planning & Design Research Institute. (2020). Framework of Shanghai Urban Design Management. Tongji University Press. (in Chinese)
- [24] Peng, F. L., Qiao, Y. K., Zhao, J. W., Liu, K. & Li, J. C. (2020). Planning and Implementation of Underground Space in Chinese Central Business District (CBD): A Case of Shanghai Hongqiao CBD. *Tunnelling and Underground Space Technology*, 95, 103176. <https://doi.org/10.1016/j.tust.2019.103176>.
- [25] Urban Redevelopment Authority. (2021). Central area underground pedestrian network - Revisions to the cash grant incentive scheme (URA/PB/2021/02-CUDG). [www.ura.gov.sg/Corporate/Guidelines/Circulars/dc21-02](http://www.ura.gov.sg/Corporate/Guidelines/Circulars/dc21-02).
- [26] Cui, J. Q., Broere, W. & Lin, D. (2021). Underground Space Utilisation for Urban Renewal. *Tunnelling and Underground Space Technology*, 108, 103726. <https://doi.org/10.1016/j.tust.2020.103726>.
- [27] Zhou, Y. X. & Zhao, J. (2016). Assessment and Planning of Underground Space Use in Singapore. *Tunnelling and Underground Space Technology*, 55, 249-256. <https://doi.org/10.1016/j.tust.2015.12.018>.
- [28] Qiao, Y. K. & Peng, F. L. (2023). Advances and Development Thoughts on Three-dimensional Urban Underground Cadastre. *Chinese Journal of Underground Space and Engineering*, 19(2), 35-367. (in Chinese)
- [29] Wu, K. J. & Zhao, Y. T. (2021). Comparison of Development and Utilization of Underground Space Between Beijing and Shanghai. *Chinese & Overseas Architecture*, (5), 24-29. 10.19940/j.cnki.1008-0422.2021.05.005. (in Chinese)

## UNDERGROUND NETWORK IN TOKYO TORCH PROJECT

Hayato Tsubota, Mokichi Kuribayashi, Hiroshi Ueda, and Hiromi Ban

**Abstract:** TOKYO TORCH Project (Tokiwa-bashi Project) is a large-scale mixed-use redevelopment project located in front of Tokyo station, where more than one million people use the station each day. As the first phase of the project, two buildings were constructed and operational in 2021 and 2022. Currently, a 390-meter skyscraper, which will be the tallest building in Japan when completed, is under construction. A large-scale underground pedestrian network linking Tokyo station, subway stations, and many buildings is already in place around Tokyo station. The underground space to be developed in the project will complete an underground pedestrian network with a total length of approximately 15 km, which is unparalleled globally. This paper introduces our efforts to create a bustling underground network where everyone can enjoy moving around.

**Keywords:** Studying session, First basement level network, 15km underground network

### 1. INTRODUCTION

Mitsubishi Estate Group is promoting urban development in Otemachi, Marunouchi, and Yurakucho areas, where people and businesses gather and interact to generate innovative value. By viewing the entire area as a platform, the group aims to create a town where people want to work, have offices, and visit, by offering initiatives throughout the area that would be difficult for individual tenants to realize on their own.

This paper introduces the TOKYO TORCH Project (hereinafter referred to as "**TTP**"), the latest project of the group, from the perspective of how the underground space should be utilized.

### 2. OUTLINE OF TTP

**TTP** is a large-scale urban development project located in front of Tokyo station, where more than 1 million passengers get on and off every day. The main uses of **TTP** include offices, stores, a hotel, a hall, an observation deck, rental housing, an electrical substation, a sewage pumping station, and a parking lot, with a total floor area of approximately 740,000 m<sup>2</sup>. (Fig. 1).

The **TTP** site is located in front of National Route 1, which lies between the site and Tokyo station, and is connected to Otemachi station (Fig. 2). Otemachi station, with approximately 240,000 passengers in 2021, has many subway lines including Tozai line, Marunouchi line, Chiyoda line, Hanzomon line, and Mita line. In the planning process of **TTP**, connecting **TTP** with Tokyo station and Otemachi station was recognized as a critical priority for creating a comfortable and bustling underground pedestrian network.





Figure 1. Perspective view of TTP

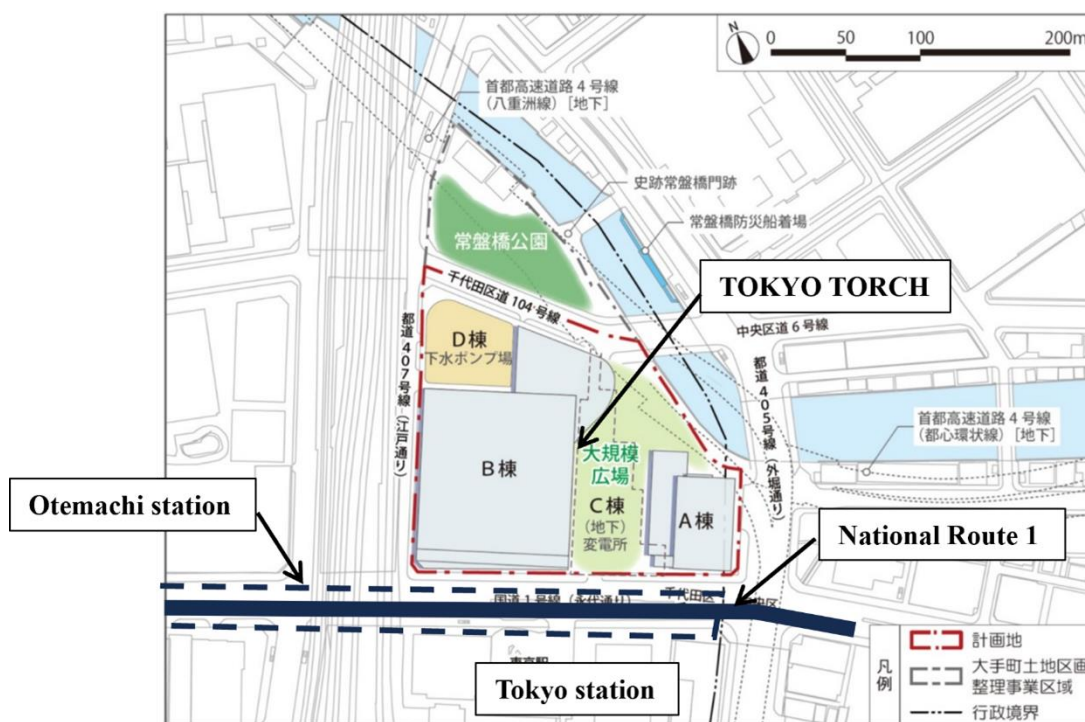


Figure 2. TTP site location



### 3.3. Basement Level of Underground Passages

When studying the network of underground passageways, it is important to consider not only the horizontal but also the vertical flow lines. In the next step of the study session, a discussion was held on the depth at which the underground passageways should be developed. The alternatives were to connect at the second basement level or at the first basement level. A survey of the surrounding underground structures revealed that connecting at the second basement level was difficult due to the presence of highway structures, railroad equipment rooms, parking lots, and other structures at the level. As for the first basement level, infrastructure pipes such as sewage pipes, water pipes, gas pipes, and communication pipes are often buried at the depth of the level, and in many cases, the possibility of relocating these buried objects is critical. Thanks to the underpass plan developed in 1960s, there were few buried objects at the first basement level. In addition, by selecting the first basement level for the pedestrian passageway, the session confirmed the following benefits: strengthening the connection with the first basement level network formed around Tokyo Station, creating a bustling atmosphere in cooperation with the commercial facilities located on the first basement level of the building, and easing traffic congestion on the ground level by promptly guiding pedestrians on the ground level to the first basement level. Thus, the policy of forming a network at the first basement level was settled.

There were some legal restrictions on the use of underground passageways at the first basement level. In Japan, the law requires that the distance between the top of an underground passageway and the road surface (hereinafter referred to as "earth coverage") exceed 3.5 meters. Under unavoidable circumstances, the restriction was to be loosened to 2.5 meters. However, if the underground passageway is at the first basement level, the minimum earth coverage is around 1.6 meters, which does not satisfy the restriction. Through the study sessions, both the public and private sectors recognized the high public benefit of this passageways. This led to a revision of the law in 2022, allowing a lower earth coverage than 2.5 meters provided the circumstances are unavoidable.

## 4. FUTURE OF THE UNDERGROUND NETWORK

The underground passage network proposed in the study session is divided into four areas: west side, center, east side, and under the intersection (Fig. 4). The west and east areas were proposed to be located on the first and second basement levels, the central area on the second basement level, and the area under the intersection on the first basement level, creating a seamless network connecting **TTP** to the train station. Based on the study session's proposal, the team conducted quantitative analysis to study the width and ceiling height of the corridors, which greatly affect pedestrian safety and comfort.

The current status of **TTP** is as follows: the east side area was completed in 2022, the west side and center area are under construction for completion in 2028, and the area below the intersection is to begin construction in 2025. When all these areas are completed, Nihonbashi Station on Tozai line will be connected to Otemachi, Marunouchi, and Yurakucho area via underground passage, forming a vast 15-kilometer underground network around Tokyo Station (Fig. 5).

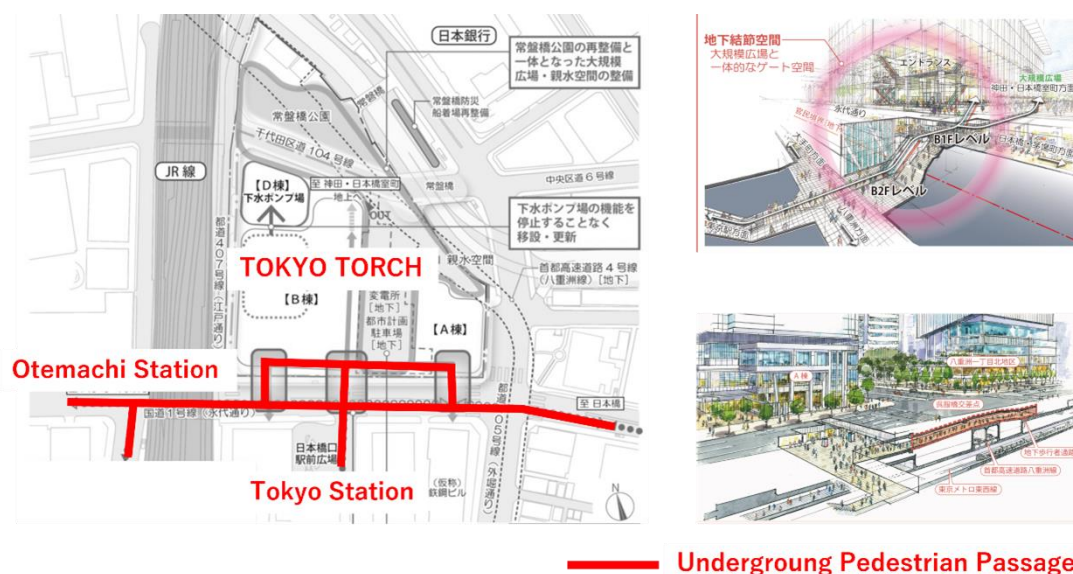


Figure 4. Underground network plan of TTP





*Figure 5. Underground network around Tokyo station*

## 5. SUMMARY

By utilizing underground space for pedestrians, an attractive pedestrian network can be formed, ensuring safety through the separation of pedestrians and cars, comfort regardless of weather conditions, and liveliness ensured by the integration of underground commercial facilities. In order to realize such initiatives, it is essential that road administrators, developers, and railroad operators work together to develop underground facilities for roads, private land, and railroads in an integrated manner.

Mitsubishi Estate Group will continue to promote urban development that provides new value to the entire area through the development of attractive underground spaces.

## 6. BIBLIOGRAPHY

- [1] Kuribayashi et al (2020) Cases of utilizing underground space around Tokyo station, The Foundation Engineering & Equipment, monthly 2020.5, pp72-75
- [2] Matsuda et al (2020) Tokiwabashi Project in front of Tokyo Station, The Foundation Engineering & Equipment, monthly 2020.7, pp79-82

## STRENGTHENING UNDERGROUND SPACE CONNECTIVITY TO ENHANCE THE EFFICIENCY OF UNDERGROUND SPACE UTILIZATION: A CASE STUDY OF BEIJING PRACTICES

Chen Qin<sup>1</sup>

**Abstract:** In the context of rapid urban development and increasingly scarce land resources, the efficient development of underground space has become a crucial strategy for enhancing a city's sustainable development capabilities. In particular, strengthening underground space connectivity has a significant impact on reducing surface traffic pressure, optimizing urban spatial layout, and improving the quality of life for citizens. As the capital of China, Beijing's underground space development and utilization have formed a large scale. How to strengthen underground space connectivity and enhance the overall utilization efficiency of underground space is an important issue facing Beijing's underground space development in the new era. This paper discusses Beijing's practical to promote connectivity within underground spaces, focusing on the establishment of an underground vehicular connectivity system, the facilitation of underground connections between subway stations and surrounding areas, and the enhancement of systemic connectivity in urban key functional areas. It proposes the necessity of strengthening underground space connectivity and its role in promoting urban development.

**Keywords:** Underground Space Connectivity, Utilization Efficiency of Underground Space, Beijing Practices

### 1. INTRODUCTION

With the rapid urban development, megacities generally face severe challenges such as increasingly scarce land resources, worsening traffic congestion, and an urgent need to expand public spaces. Against this backdrop, seeking space underground and pursuing benefits through depth has become a critical pathway to enhance urban carrying capacity and sustainable development. Meanwhile, based on the growth of demand and the advancement of science and technology, underground space development has shifted from a single function to comprehensive and networked. Among them, connectivity has become a key strategy to improve the efficiency of underground space utilization. Beijing, the capital of China, has formed a large scale of underground space with decades of rapid urban construction. In the new development phase, how to strengthen underground space connectivity and create integrated aboveground-underground urban spaces has become an important issue for the city's development. This paper focus on Beijing's practical exploration in strengthening underground space connectivity. By analyzing the experiences and challenges of typical cases in planning, design and construction models, it evaluates the multi-dimensional benefits of underground space connectivity. These findings aim to provide valuable insights for advancing underground space connectivity in other megacities like Beijing.

### 2. NECESSITY AND MULTIFACETED BENEFITS

The underground space connectivity is an inevitable requirement for modern urban development at a certain stage. By establishing an efficient and convenient underground connectivity network, cities can not only effectively alleviate surface traffic pressure and optimize urban functional layouts, but also significantly improve

---

<sup>1</sup> Senior Engineer, Chen Qin, Beijing Municipal Institute of City Planning & Design, Beijing, China, happy\_cq@sina.com.



commuting experiences and quality of life for urban residents, thereby injecting new vitality into urban development.

The underground space connectivity, far more than simple physical passage linkages; it represents a multidimensional and systematic conceptual connotation. At the physical level, the underground space connectivity primarily refers to the direct spatial linkage and convenient transition between different underground spaces, as well as between underground spaces and above-ground buildings, achieved through various forms such as underground pedestrian walkways, vehicular tunnels, and underground public spaces. On a deeper level, the underground space connectivity also have multi-dimensional and systematic core value. Through physical connectivity, it achieves functional synergy, promoting the complementary and organic integration of different underground space functions such as commercial, office, cultural, entertainment, and transportation, forming a multifunctional underground zone and elevating the overall service level.

The benefits and positive impacts of underground space connectivity can be summarized as follows:

## 2.1. Enhancing Spatial Efficiency

The scattered underground space can be integrated by connectivity. This not only revitalizes existing underground assets but also provides broader systemic access possibilities for the development of new underground spaces. As a result, it significantly enhances the comprehensive utilization efficiency of urban land and spatial resources.

## 2.2. Enhancing Urban Resilience

An interconnected underground space network can serve as critical pathways, shelters for evacuation, material transport, and emergency refuge in urban emergency situations, thereby improving the city's capacity to respond to natural disasters and emergencies.

## 2.3. Stimulating Economic Vitality

The connectivity can create new economic benefits for underground space. In particular, strengthening the seamless connection between underground space and the surrounding subway systems can significantly attract passenger flow, enhance commercial value, and drive regional economic development.

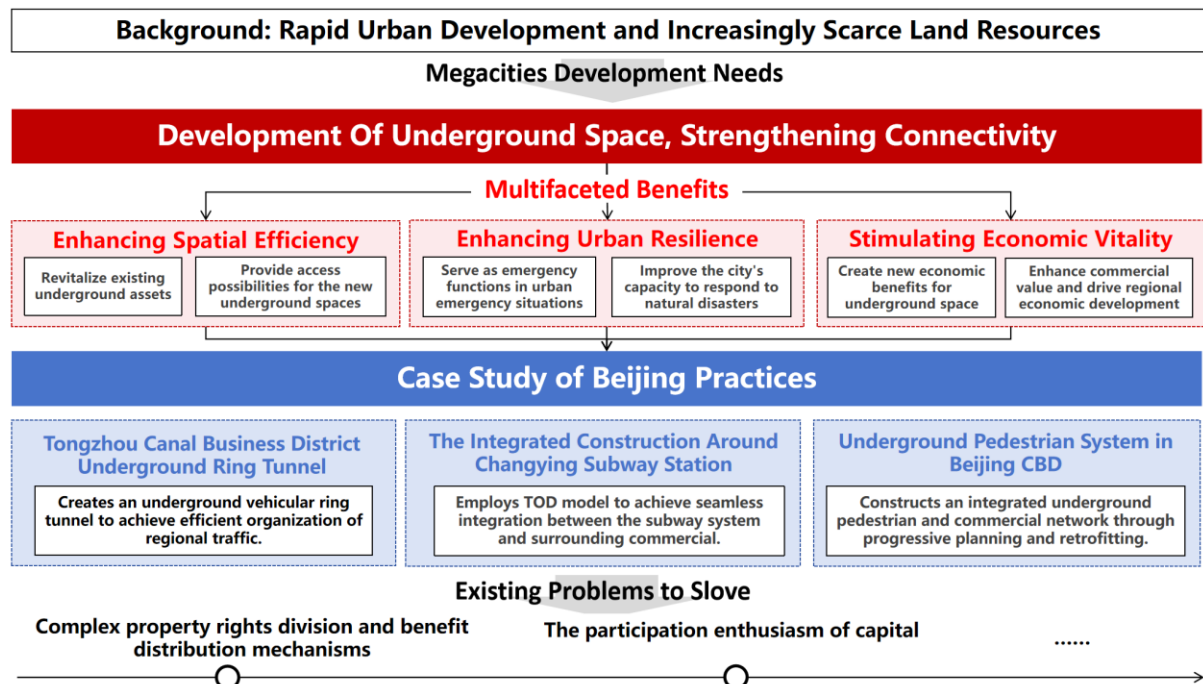
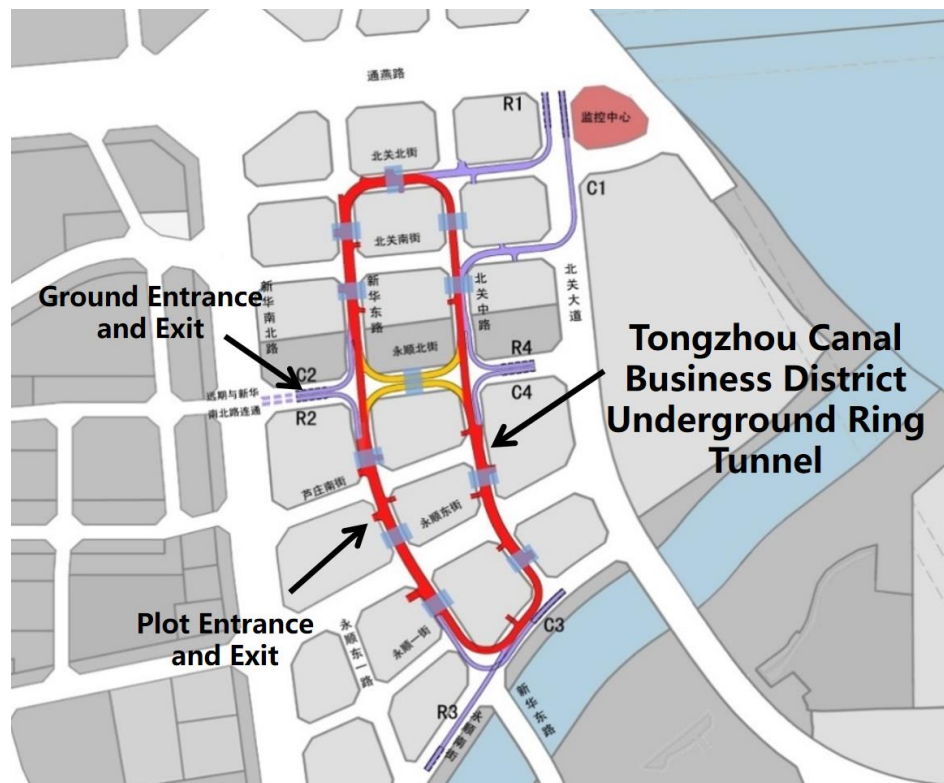


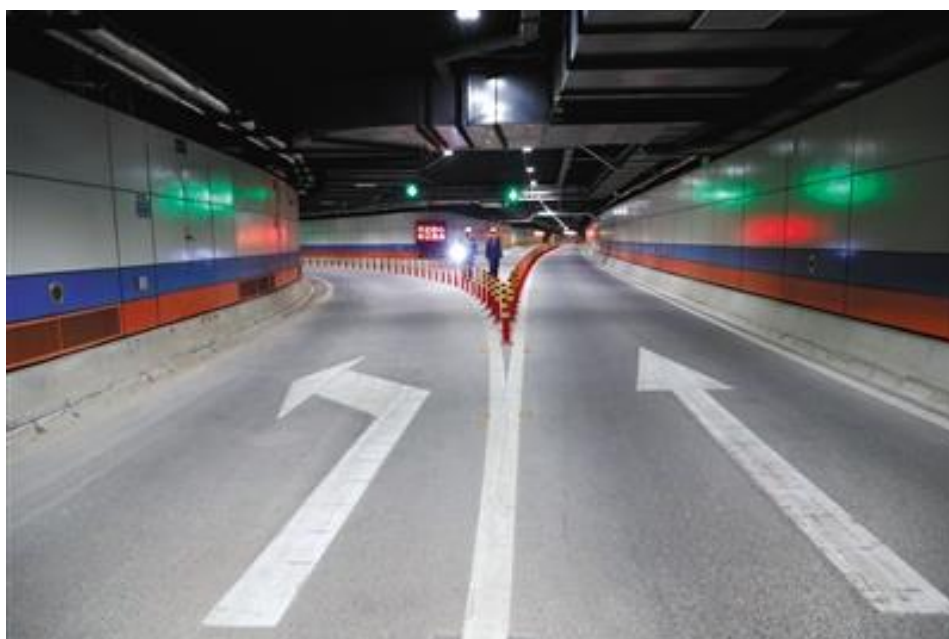
Figure 1. Technical Framework Diagram

### 3. TONGZHOU CANAL BUSINESS DISTRICT UNDERGROUND RING TUNNEL

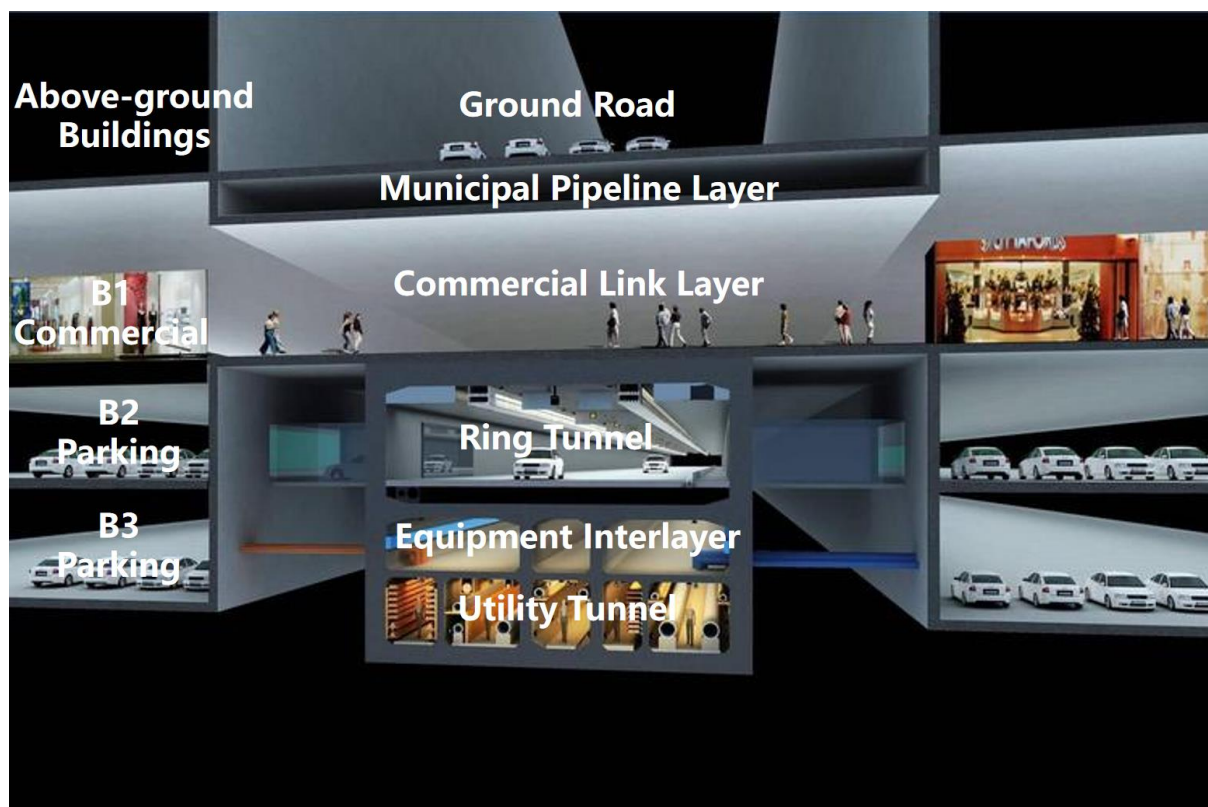
The Tongzhou Canal Business District is located within the sub-center of Beijing's Tongzhou District. The area has a high building density, heavy pedestrian and vehicular traffic, and likely to cause surface traffic congestion. To improve the ground traffic environment and achieve interconnection among plots, a 1.5-kilometer underground ring tunnel was constructed approximately 10 meters below the surface, with a width of 14 meters and a height of 4 meters. This tunnel interconnects all 22 plots within the district. It guides vehicular traffic underground and leaves the road surface for pedestrians and bicycles to use. This design forms an efficient dual-layer transportation system, effectively separating fast and slow traffic system.



*Figure 2. Schematic Diagram of Tongzhou Canal Business District Underground Ring Tunnel*



*Figure 3. Interior Scene of Tongzhou Canal Business District Underground Ring Tunnel*



*Figure 4. Schematic Cross-section of Tongzhou Canal Business District Underground Ring Tunnel*

### **3.1. Underground ring Tunnel Enhances Regional Vehicular Connectivity and Shared Parking Resources to Optimize Surface Traffic Conditions.**

The tunnel has built 22 entrances and exits, connecting the underground parking lots of surrounding commercial buildings, office buildings and residential apartments, achieving complete underground connection within the area and sharing underground parking resources. The tunnel is equipped with traffic monitoring devices, electronic display screens, and intelligent traffic signals to dynamically optimize traffic flow efficiency in real time.

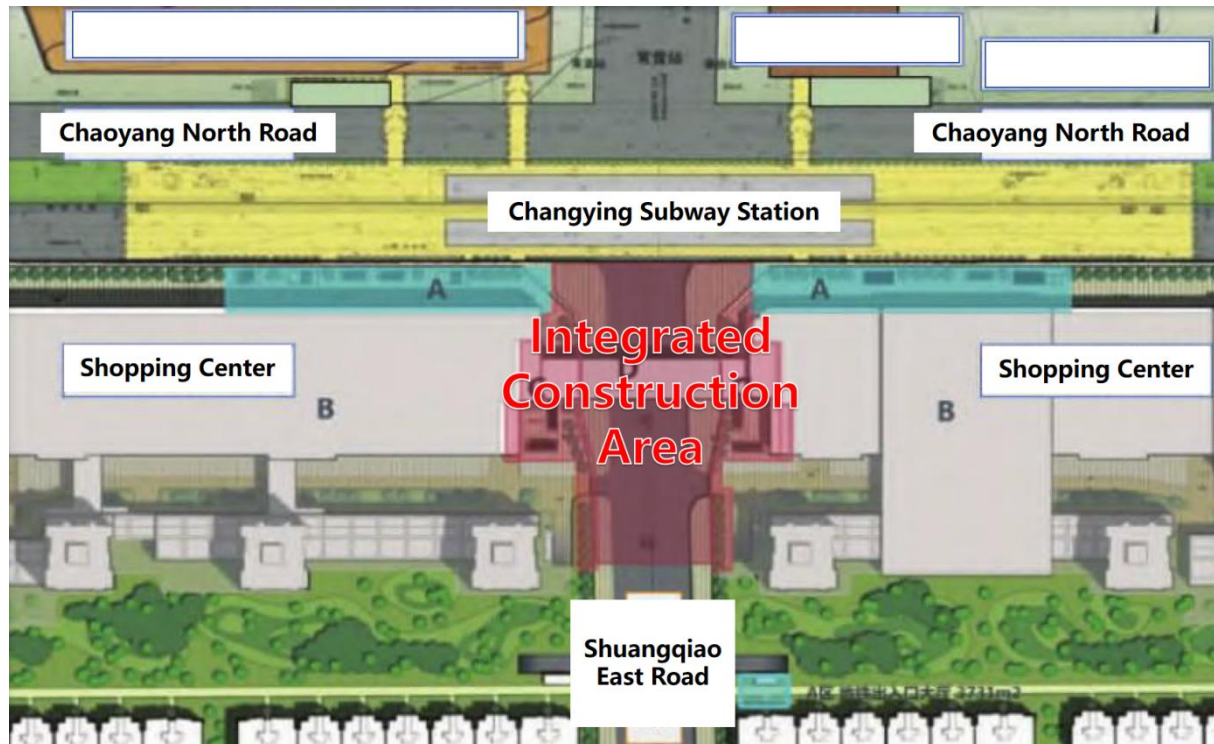
### **3.2. The B1 Level is Designed as an Integrated Underground Walkway System Enhancing Area Accessibility.**

The tunnel designed a pedestrian level (B1) above the vehicular traffic layer, which is connected to the surrounding office buildings, commercial complexes and subway stations, and also has commercial spaces. People can move between subways and different buildings without going to the ground, unaffected by the weather, and carry out activities such as commuting, dining and social activities. The system establishes a safe, comfortable, and efficient underground pedestrian circulation network.

## **4. THE INTEGRATED CONSTRUCTION AROUND CHANGYING SUBWAY STATION**

The Changying Station of Beijing Subway Line 6 is located in Chaoyang District, Beijing. The station is close to the shopping center on the south side. To effectively disperse passenger flow and organic integrate with surrounding commercial areas, the station adopted an integrated development model during construction. This design seamlessly connects the station concourse with the underground levels of the commercial complex, providing a comfortable and convenient shopping experience for subway passengers and shoppers.





*Figure 5. Schematic Diagram of Underground Connectivity Construction Mode at Changying Subway Station*



*Figure 6. Rendering of Underground Connectivity at Changying Subway Station*

#### **4.1. Connect the Subway Systems with Commercial Spaces and Utilize the Flow of Traffic to Enhance the Value of Commercial Spaces.**

The integrated design model fully opens the southern space of the subway station concourse, connecting it with the underground commercial area. At the same time, the underground space of the road is integrated to form a "T"-shaped structure. The total underground construction area of the integrated development is 7,477 square meters, including 4,000 square meters of commercial facilities, effectively converting subway passenger flow into commercial customer flow.

#### 4.2. Clarify the Construction Funds and Settlement Methods to Ensure that the Integrated Construction is Implemented Simultaneously.

In the integrated construction of subway, funding sources is often a significant challenges. The Changying Station project stipulates that construction funds for the integrated area will be advanced by the subway company first, and then paid by the property management unit after settlement. This operational model not only solves construction financing issues, but also provides a strong guarantee for the simultaneous planning, design and construction of subway facilities, underground passageways, and commercial spaces.

### 5. UNDERGROUND PEDESTRIAN SYSTEM IN BEIJING CBD

Beijing Central Business District (CBD), located in the central part of Chaoyang District, is a strategically planned zone that integrates commercial, financial, technological, office, entertainment, and residential functions. As a pivotal gateway for Beijing's international engagement and a nationally significant business district. The CBD is currently the area with the largest development scope, utilization depth and construction scale of underground space in Beijing. Through the comprehensive underground integration, the underground space serves as a shared platform, achieving resource sharing in the high-density built environment.



*Figure 7. Schematic Planning Diagram of Underground Space System at B1 Level in CBD*



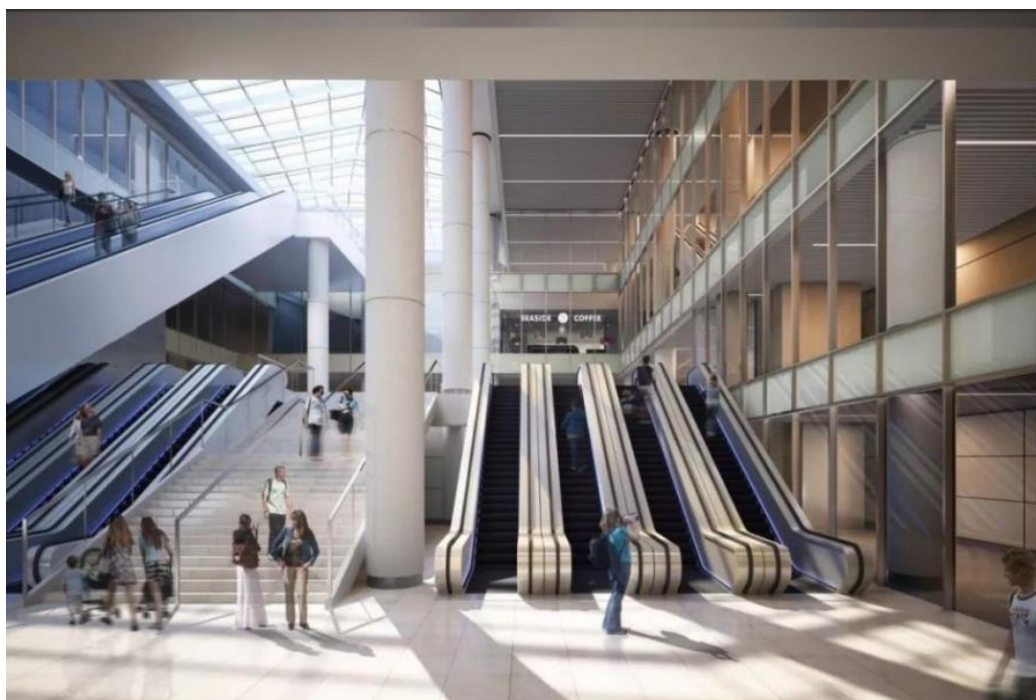


Figure 8. Rendering of CBD Subway Transfer Hall

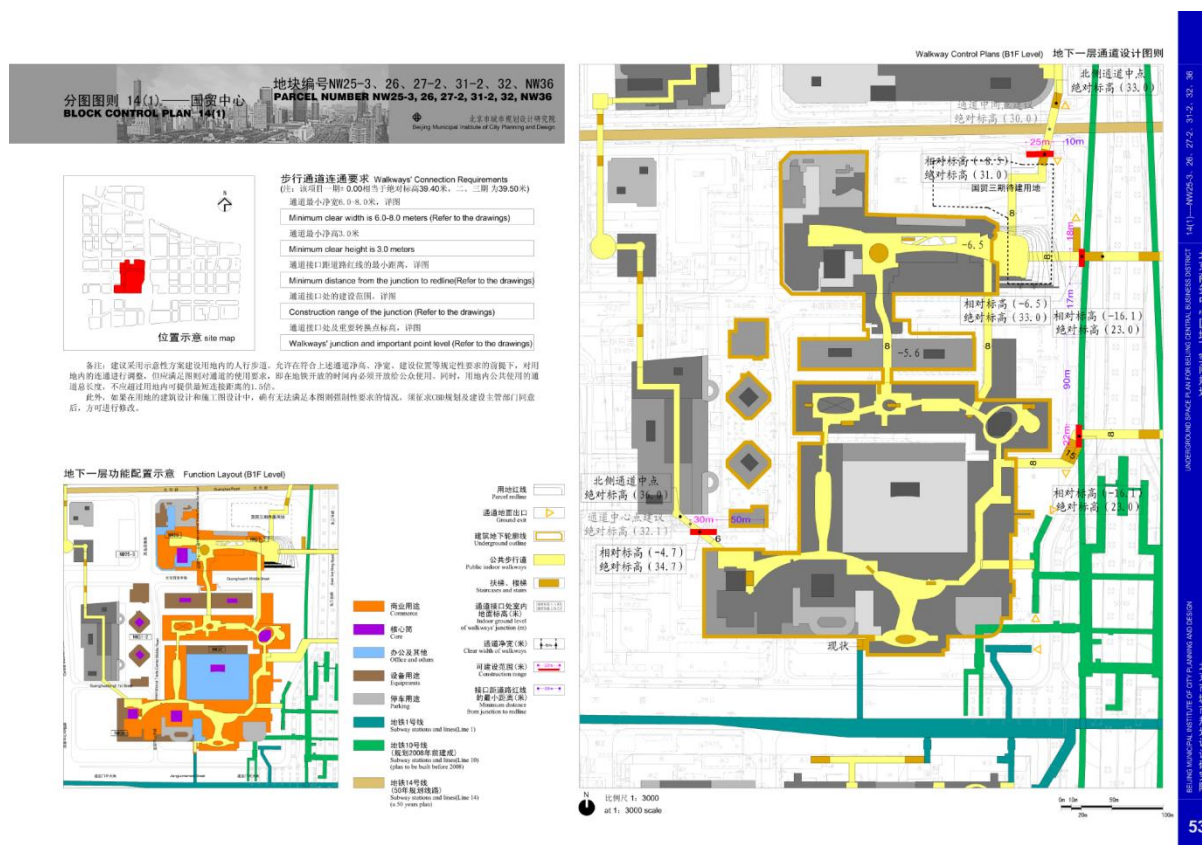


Figure 9. Block Control Plan in Underground Plan For Beijing Central Business District

### **5.1. Developing an Underground Pedestrian System to Establish a Networked Public Space Framework Below Ground.**

The CBD has developed an approximately 10-kilometer underground pedestrian system at the B1 level, connecting commercial facilities, public spaces, and subway stations. This network links 6 subway stations and 5 bus terminals, covering about 221 hectares in the most densely developed business area with the highest pedestrian flow of CBD. The pedestrian walkways are lined with commercial, cultural and recreational amenities, creating comfortable all-weather environments for walking, shopping and entertainment.

### **5.2. Formulated Master Planning and Coordinated Implementation of Underground Space Development.**

In 2005, the CBD formulated the Underground Plan For Beijing Central Business District, which specified technical parameters such as connectivity locations, vertical, widths, and heights for both project sites and public areas. The plan established detailed zoning regulations that effectively guided the specific design and implementation of each project, and also provided predictive guidance for future development.

## **6. EXPERIENCE AND SUMMARY**

These three cases exemplify the critical role of underground connectivity from different perspectives. Taking the new district development as an opportunity, Tongzhou Canal Business District creates an underground vehicular ring tunnel to achieve efficient organization of regional traffic and optimization of above-ground space. Changying subway station employs a Transit-Oriented Development (TOD) model to achieve seamless integration between the subway system and surrounding commercial and residential functions, enhancing district vitality and resident accessibility. As a high-density urban core, Beijing CBD constructs an integrated underground pedestrian and commercial network through progressive planning and retrofitting, seamlessly linking transportation hubs with major buildings.

From the three cases, we can also summarize valuable practical experience from Beijing in underground space connectivity. First, tailored approaches should be adopted based on local conditions and project categories. Different planning concepts, construction models and technical solutions should be applied to new urban districts, built-up area redevelopment, and subway stations to enhance the relevance and effectiveness of underground connectivity. Second, it is essential to strengthen planning guidance and policy support, as scientific top-level design and consistent policy frameworks form the critical foundation for promoting orderly development of underground spaces connectivity.

However, Beijing's current underground space connectivity work still face many challenges. For instance, cross-parcel and cross-ownership underground connections involve complex property rights division and benefit distribution mechanisms. Additionally, the high construction costs and long return periods of underground projects have dampened the participation enthusiasm of social capital. Therefore, subsequent efforts should focus on improving legal frameworks and establishing long-term mechanisms to promote the connectivity and efficient utilization of underground spaces.

## **REFERENCES**

- [1] Design Documentation of Tongzhou Canal Business District underground ring tunnel
- [2] Design Documentation for the integrated construction scheme of Changying subway station
- [3] Design Documentation for underground space in Beijing Central Business District
- [4] Underground Plan For Beijing Central Business District (2025)
- [5] Beijing Underground Space Planning (2023-2035)

## REGRESSION ANALYSIS OF THE DEVELOPMENT AREA OF UNDERGROUND SPACE IN SHANGHAI

LIU De-xin<sup>1</sup>, ZHU Lei<sup>2\*</sup>, LIAO Yuan-qin<sup>3</sup>

**Abstract:** This article is based on the development history and current status of underground space in Shanghai. Using the annual development area of underground space in Shanghai as the dependent variable, SPSS analysis methods were employed to select data from 2016 to 2022. Independent variables such as population density, gross regional domestic product, average sales price of residential housing, and metro passenger volume were analyzed using linear regression. The main conclusions indicate that while population density, GRDP, and metro passenger volume jointly influence the development area of urban underground space, there is basically no interaction between them. However, GRDP and the average sales price of residential housing can significantly affect the development area of urban underground space.

**Keywords:** regression analysis; development area of underground Space; Shanghai

### 1. INTRODUCTION

Underground space is part of land resources, and its development and utilization strategies are related to urbanization processes, industrial structures, population policies, regional economies, and more. In September 2024, the Ministry of Natural Resources issued the Guiding Opinions on Exploring and Promoting the Rational Development and Utilization of Urban Underground Space, which mentions the need to "coordinate efforts to promote the reasonable development and utilization of urban underground space and fully tap into the potential of underground resources."

For many years, demand forecasting in quantitative methods for the development and use of urban underground space has been a challenge and focal point in both urban planning and underground space utilization WU Li-xin, JIANG Yun, LIANG Yue, XU Lei, CHEN Xue-xi, ZHU Wen-jun. (2004). Fundamental Research on Capacity Assessment of Development and Utilization of Urban Underground Space. Geography and Geo-Information Science, (04) , 44-47., especially with difficulties in data collection Nikolai Bobylev.(2010).Underground space in the Alexanderplatz area, Berlin: Research into the quantification of urban underground space use. Tunnelling and Underground Space Technology incorporating Trenchless Technology Research,25(5),495-507.. Therefore, analyzing relevant factors to predict the demands and trends in urban underground space development can aid in accurate planning and provide spatial support for high-quality economic and social development.

As China's economic and financial center, a global first-tier City and an international metropolis, Shanghai began the utilization of urban underground space resources in the mid-19th century, having gone through three stages: the germinal stage, a focus on civil defense, and a combination of peace and war considerations. Currently, it is transitioning from a high-speed development phase to a slower one.

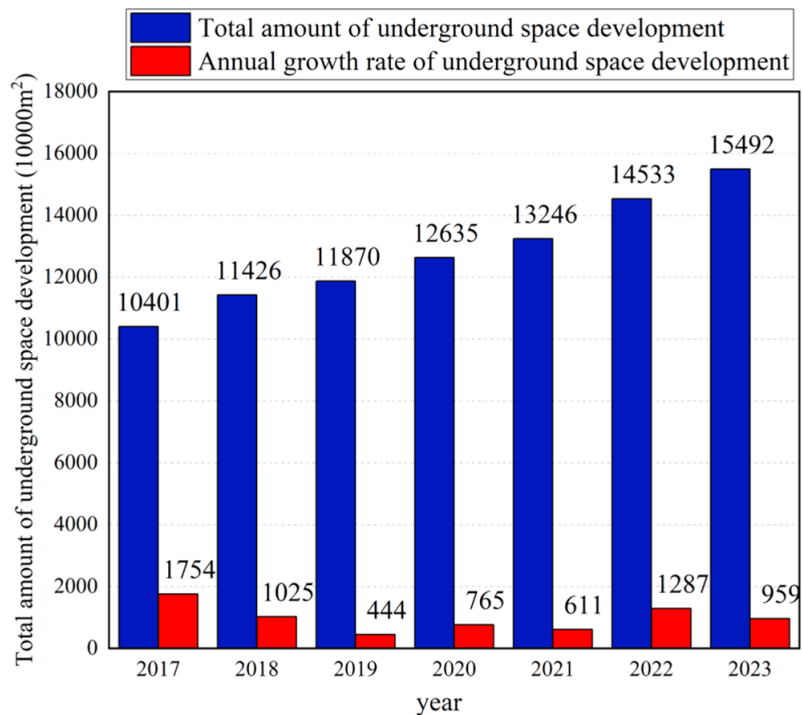
By the end of 2023, there were a total of 43,639 underground projects completed citywide, with a total construction area reaching 155 million m<sup>2</sup>, an average development intensity of 24,400 m<sup>2</sup> per km<sup>2</sup>, and a per capita

<sup>1</sup> Master of Engineering, Liu Dexin, Shanghai Shentong Rail Transit Research & Consulting Co., Ltd., Email: ldx58557@163.com

<sup>2</sup> Doctor of Engineering, Zhu Lei, Professor of Engineering, Shanghai Shentong Rail Transit Research & Consulting Co., Ltd., Email: 2364661025@qq.com (\*Corresponding author)

<sup>3</sup> Director of the Investigation Department, Liao Yuan-qin, Registered Surveyor/Master of Surveying and Mapping, Shanghai Institute of Natural Resources Survey and Utilization, Email: liaoyuanqin@163.com

scale of 6.23 m<sup>2</sup>. Since 2017, the annual newly added development scale of Shanghai's underground space has fluctuated between 4.44 million and 10.24 million m<sup>2</sup>.



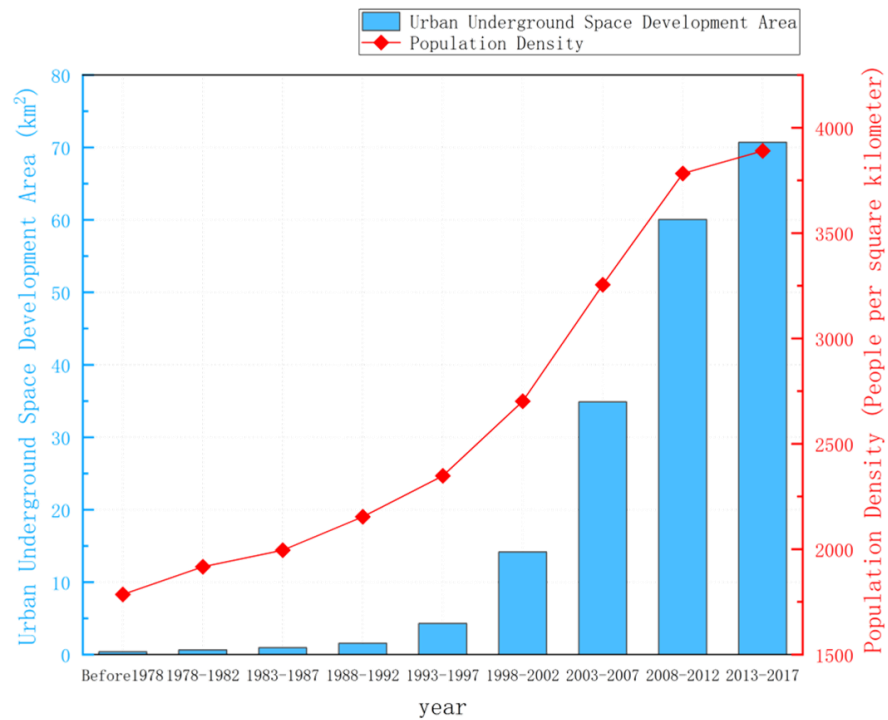
**Figure 1.** Annual Development Volume and Yearly Growth of Shanghai's Underground Space from 2017 to Present

In recent years, Shanghai has faced numerous changes in its urban planning and construction domains: urbanization development has shifted toward optimizing existing stock, the city has continued to grapple with severe imbalances in population age structure, macroeconomic growth has slowed down, and fluctuations persisted in the real estate market. Furthermore, the proportion of underground space used for rail transit has reached 7.8%, while the overall connectivity rate of underground spaces with surrounding areas stands at 36.7% MA Chen-xiao. (2023). Evaluation methods of spatial performance and planning optimization of urban underground space in the context of inventory land redevelopment. [Doctoral dissertation, Tongji University].. In terms of layout demands for underground space, based on the requirements outlined in the Shanghai Urban Master Plan (2017–2035), the city aims to further refine its overall underground space framework by leveraging rail transit networks and various public centers, with a focus on main urban districts, new towns, transfer hubs, and public activity centers ZHANG De-ying, LIAO Yuan-qin, ZHENG Geng-he. (2025). Analysis of population import status of five new towns in Shanghai from the spatio-temporal behavior perspective. *Shanghai Land & Resources*, 46(01):1113-1120..

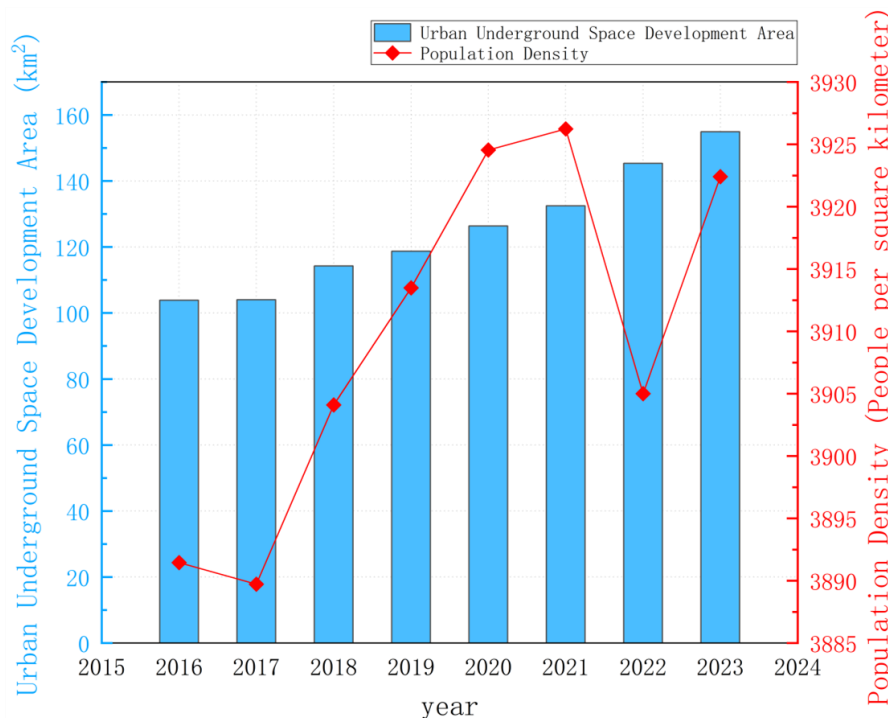
## 2. RESEARCH METHODS

By reviewing related literatures HE Lei, DAI Shen-zhi, WANG Dai-xia, et al. (2018). Empirical study on forecasting the demand for the scale of urban underground space in Shanghai. *Urban Planning*, 42(03),30-40+58., it is concluded that a socioeconomic system generally includes three elements: gross domestic product, population, and real estate prices. In this analysis, Shanghai serves as the research subject, with the development area of urban underground space acting as the dependent variable. Factors such as population density, regional gross domestic product (GRDP), and average sales price of residential commodity housing are considered for selection as independent variables. Data analysis will identify appropriate independent variables using SPSS software to perform single-factor and multiple-factor linear regression based on the least squares method. This approach analyzes the relationships between the dependent variable and each independent variable. The conclusions drawn from these analyses will be used to predict future demands for urban underground spaces, thereby guiding their development and utilization.

## 2.1. Population density



**Figure 2.** Relationship Curve between Shanghai's Population Density and Urban Underground Space Development Area (1978–2017)



**Figure 3.** Relationship Curve between Shanghai's Population Density and Urban Underground Space Development Area (2016–2023)

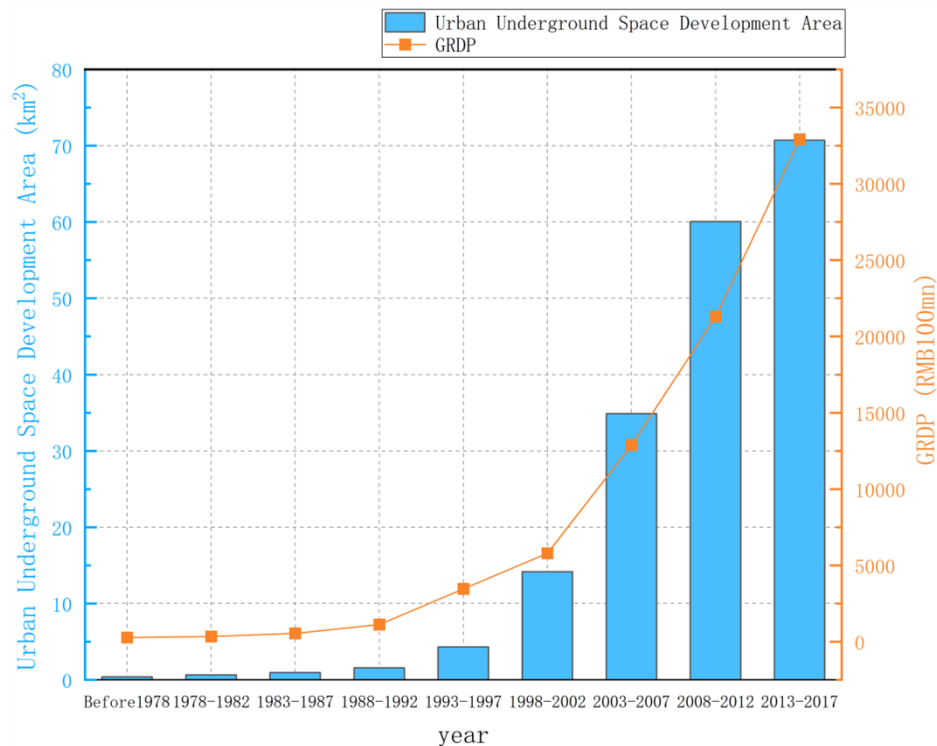
Based on the above chart, it is evident that between 1978 and 2017, both the population density of Shanghai City and the development area of underground spaces were in a phase of rapid growth. Additionally, their growth trends are quite similar, suggesting there exists a certain influential relationship between them, which is relatively close to being linearly correlated.



Between 2016 and 2023, the development of underground spaces in Shanghai also experienced a growth phase. However, unlike previous periods, the rate of increase was relatively slow. While population density continued to grow, it showed some fluctuations in certain years, which preliminary analysis suggests may be due to factors like the pandemic. These anomalies could significantly impact subsequent regression analyses.

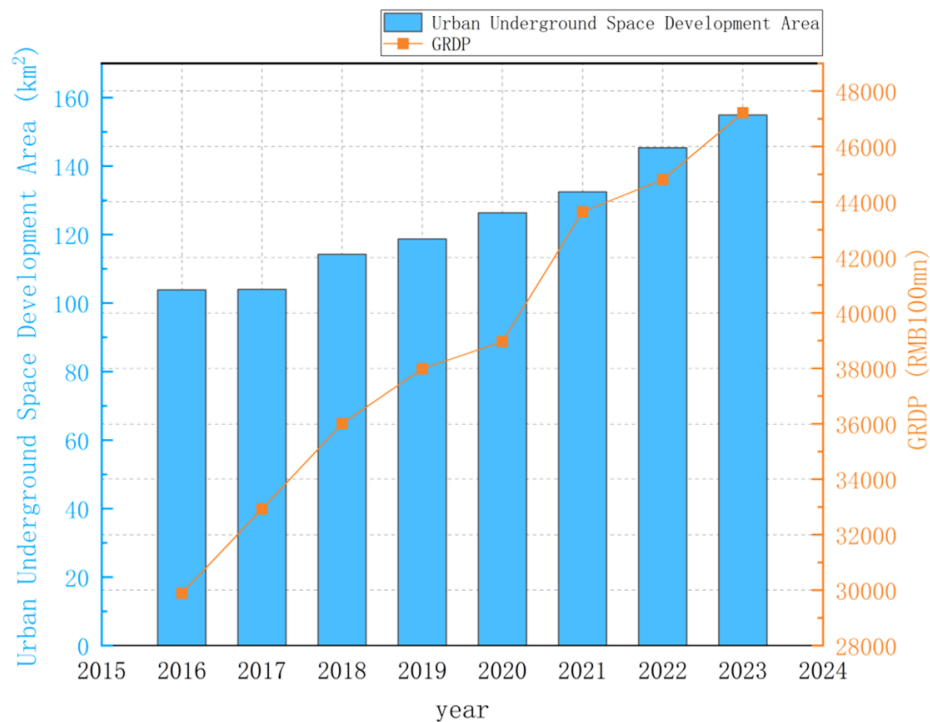
## 2.2. Regional gross domestic product

In light of the need to conduct a multivariate regression analysis on the development area of Shanghai's urban underground space and its various influencing factors, measures should be taken to avoid issues of multicollinearity that could lead to inaccurate results. Therefore, for economic factors, it selects Shanghai's GRDP rather than per capita GDP.



**Figure 4.** Relationship Curve between Shanghai's GRDP and Urban Underground Space Development Area (1978–2017)

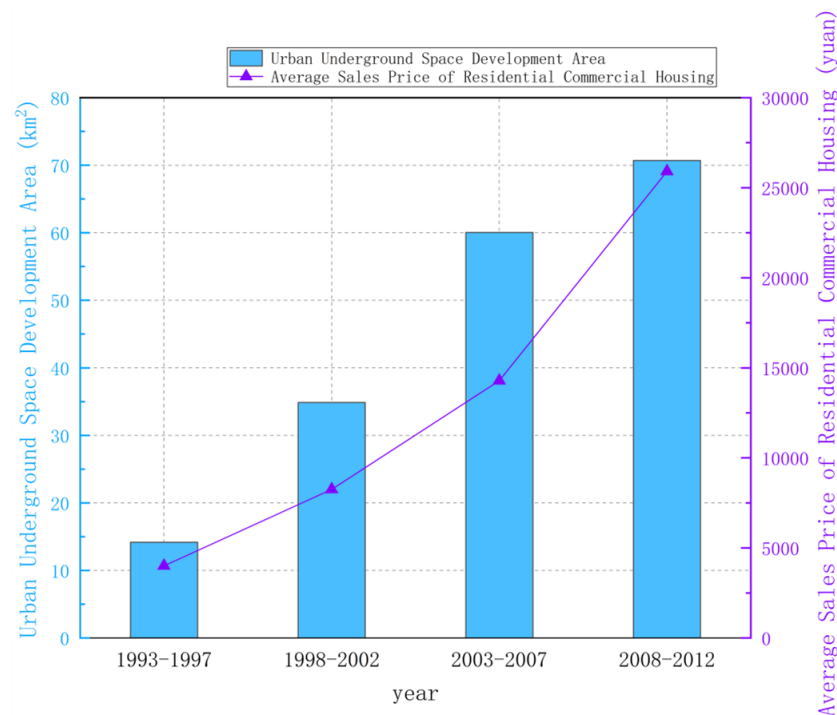
Based on the above chart, it is evident that from 1978 to 2017, Shanghai's GRDP was also in a phase of rapid growth, similar to its population density. It can be preliminarily judged that there exists a relationship akin to linear correlation between the region's gross domestic product and the development area of underground space.



**Figure 5.** Relationship Curve between Shanghai's GRDP and Urban Underground Space Development Area (2016–2023)

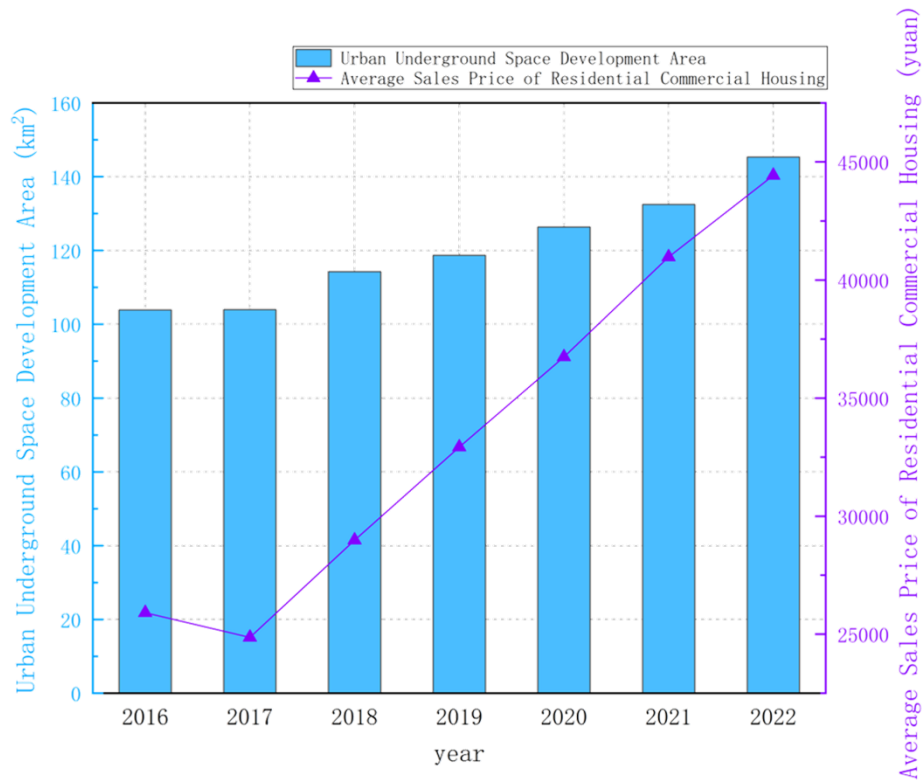
Between 2016 and 2023, both the GRDP of Shanghai and the development area of underground spaces experienced growth phase. However, the trend for the expansion of underground space development gradually slowed down.

### 2.3. Average sales price of residential commodity housing



**Figure 6.** Relationship Curve between the Average Sales Price of Residential Commodity Housing in Shanghai and Urban Underground Space Development Area (1993–2012)

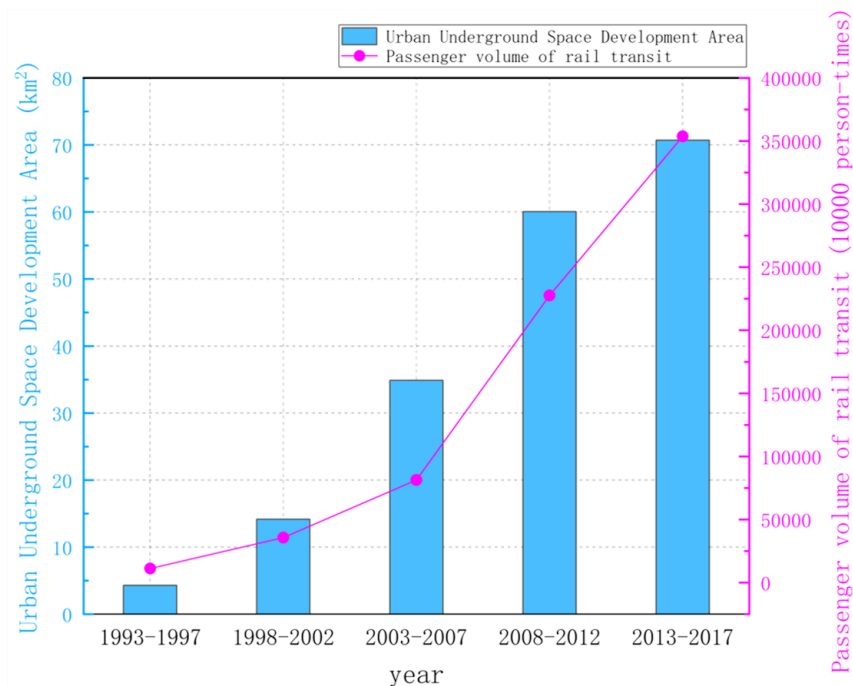
Based on the above chart, it can be observed that from 1978 to 2012, the average sales price of residential commodity housing in Shanghai was also in a rapid growth phase. It is preliminarily judged that the average sales price of residential commodity housing is one of the factors influencing the development area of underground spaces.



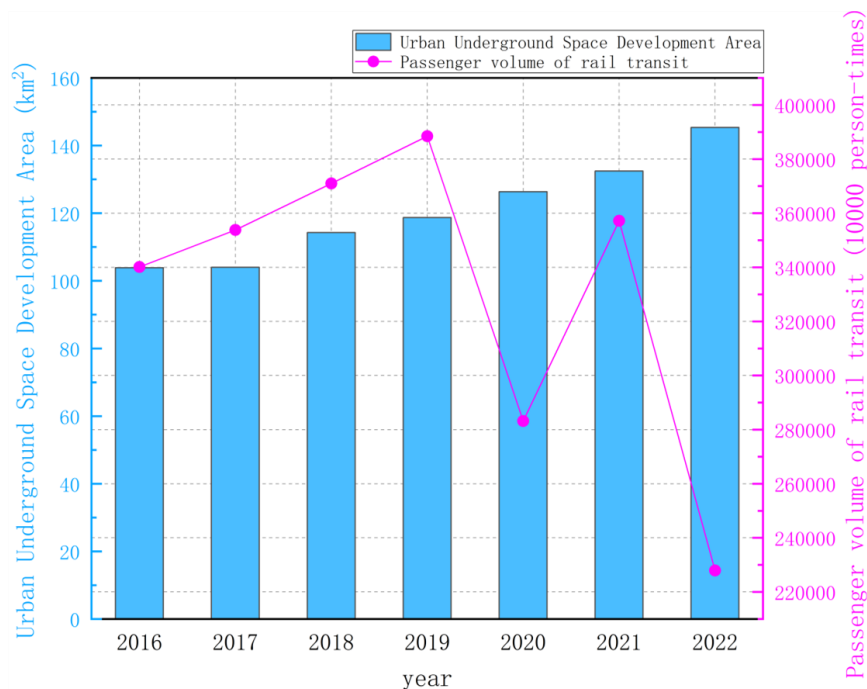
**Figure 7.** Relationship Curve between the Average Sales Price of Residential Commodity Housing in Shanghai and Urban Underground Space Development Area (2016–2022)

From 2016 to 2022, with the exception of a few years that saw slight declines, the overall average sales price for residential commodity housing in Shanghai remained in a phase of rapid growth.

## 2.4. Rail transit passenger volume



**Figure 8.** Relationship Curve between Subway Passenger Volume in Shanghai and Urban Underground Space Development Area (1993–2017)

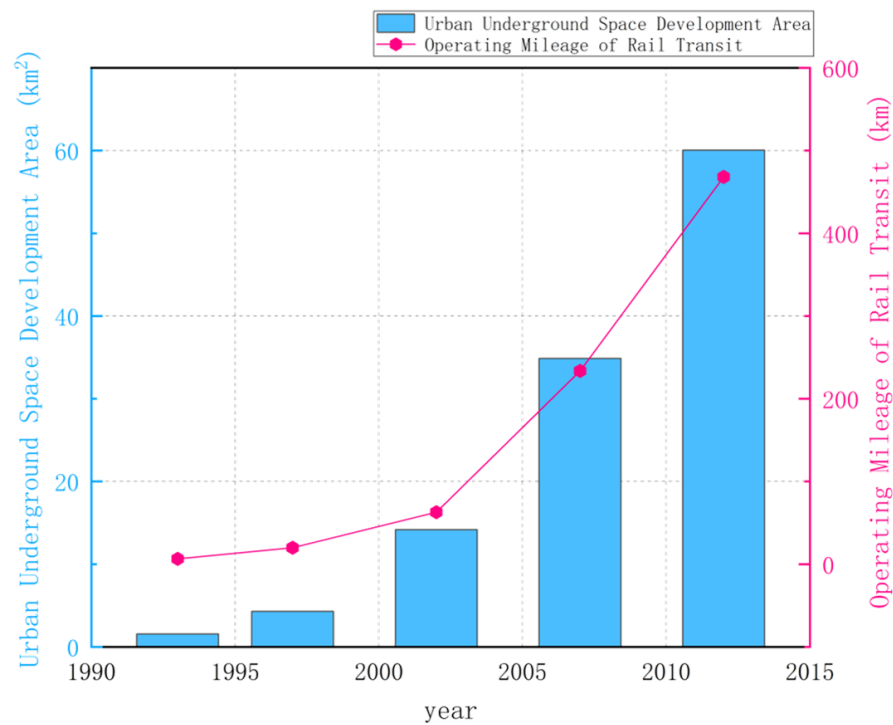


**Figure 9.** Relationship Curve between Subway Passenger Volume in Shanghai and Urban Underground Space Development Area (2016–2022)

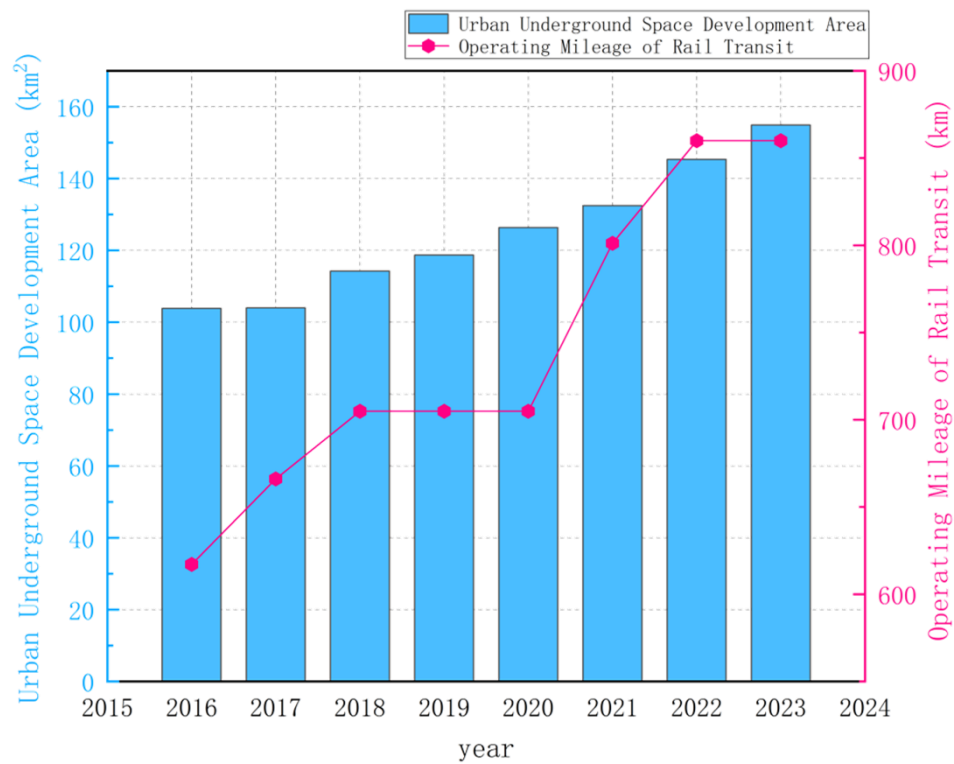
According to the above two pictures, it can be seen that from 1993 to 2017, passenger volume of Shanghai's rail transit also experienced rapid growth. Similarly, passenger volume of rail transit should be considered as one of the factors influencing the development area of underground spaces.

Between 2016 and 2022, the passenger volume of Shanghai's rail transit system exhibited trends similar to those of population density. During certain years, there was noticeable volatility, with an overall decline observed. This volatility primarily occurred between 2019 and 2022, suggesting that factors such as the pandemic likely played a significant role in these fluctuations.

## 2.5. Operating mileage of rail transit

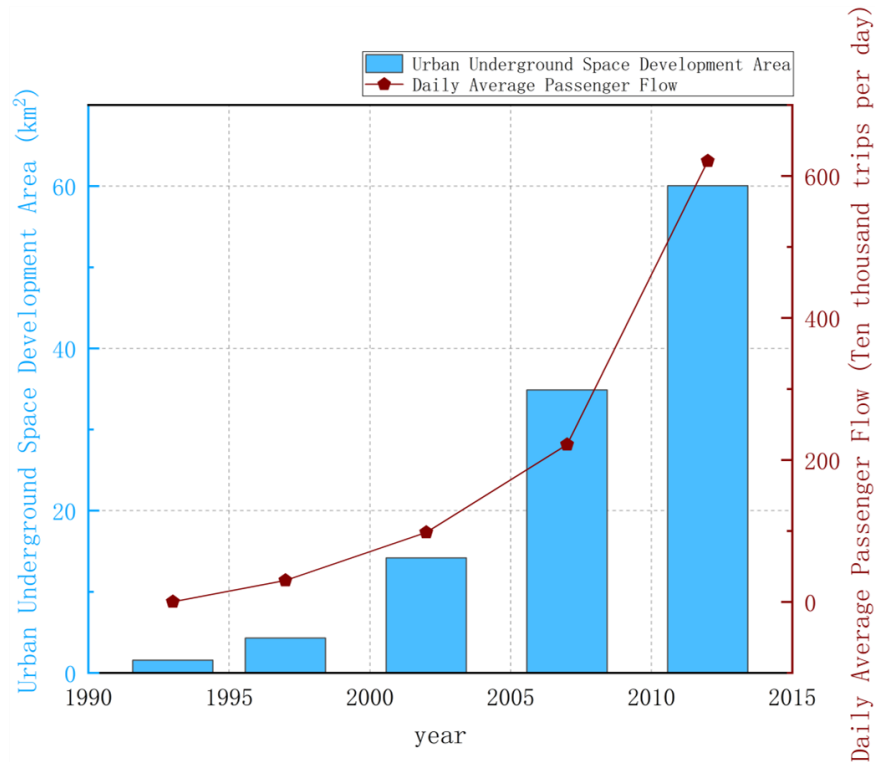


**Figure 10.** Relationship Curve between Operating mileage of rail transit in Shanghai and Urban Underground Space Development Area (1993–2012)

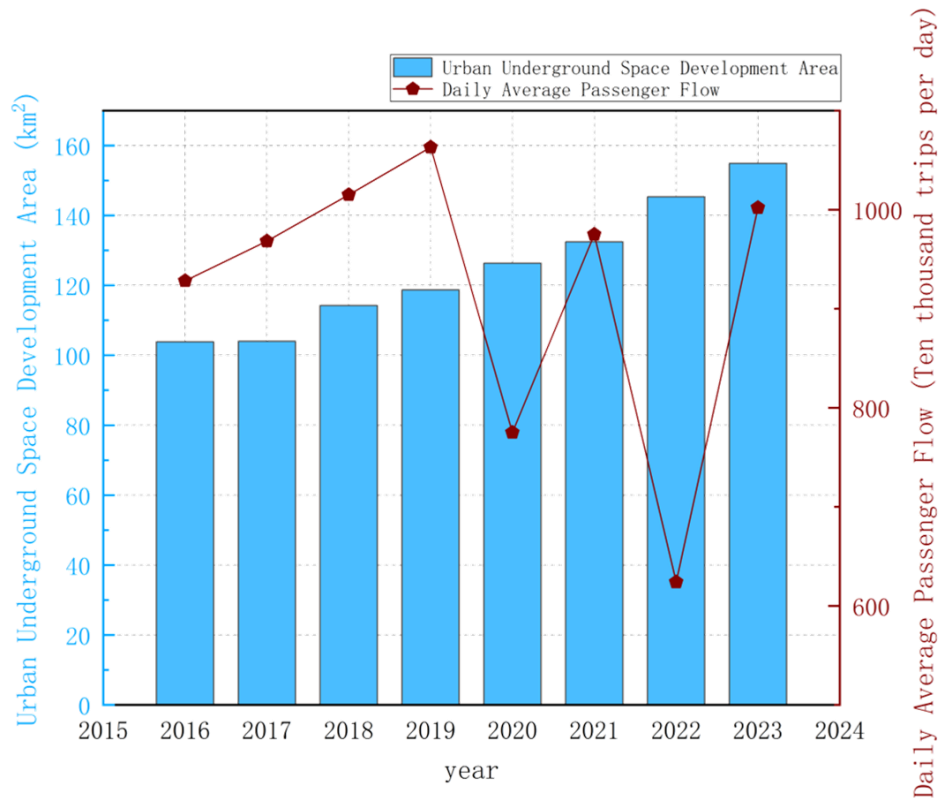


**Figure 11.** Relationship Curve between Operating mileage of rail transit in Shanghai and Urban Underground Space Development Area (2016–2023)





**Figure 12.** Relationship Curve between Daily Average Subway Ridership in Shanghai and Urban Underground Space Development Area (1993–2012)



**Figure 13.** Relationship Curve between Daily Average Subway Ridership in Shanghai and Urban Underground Space Development Area (2016–2023)

After analysis, it is determined that there is a significant correlation between the total length of Shanghai's subway lines, average daily subway ridership, and overall railway passenger volume. Therefore, one variable was chosen among them; "railway passenger volume" was selected due to its broader scope and encompassing nature

as an independent variable. Meanwhile, "subway line mileage" and "average daily subway ridership" are used for auxiliary analysis and supplementary explanation.

Based on the data analysis results, it is found that there exists a certain correlation between these independent variables and the scale of urban underground space development. Consequently, four independent variables were preliminarily selected: population density, GRDP, average sales price of residential commodity housing, and railway passenger volume. The sample data range from 2016 to 2022 for linear regression analysis.

### 3. RESEARCH RESULTS

#### 3.1. Single factor regression

Firstly, the population density, GRDP, rail transit passenger volume and the average sales price of residential commodity housing are analyzed by single factor regression analysis with urban underground space development area, according to the results, the degree of influence is analyzed, and the significant factors are combined with the development area of urban underground space for multi-factor analysis.

*Table 1. Summary of Single Factor Regression Analysis Results*

Influence factor	Significance	Coefficient	Constant	Linear relationship
Population Density ( $x_1$ )	0.131	655815.246	-2442075035	$y = 655815.246x_1 - 2442075035$
GRDP ( $x_2$ )	<0.001	2717.238	18142557.27	$y = 2717.238x_2 + 18142557.27$
Rail Transit Passenger Volume ( $x_3$ )	0.105	-178.423	179889435.7	$y = -178.423x_3 + 179889435.7$
Average Sales Price of Residential Commodity Housing ( $x_4$ )	<0.001	2000.216	53612237.42	$y = 2000.216x_4 + 53612237.42$

The table shows that while population density and railway passenger volume have some impact on the development area of urban underground spaces, this influence is not significant. In contrast, GRDP and the average sales price of residential commodity housing significantly affect the development area of urban underground spaces.

#### 3.2. Multiple factor regression

The analysis was conducted using four independent variables: population density, GRDP, railway passenger volume, and the average sales price of residential commodity housing. The model summary is shown in the table below.

*Table 2. Multiple Regression Analysis Model Summary*

Overview	Adjusted R <sup>2</sup>	Durbin-Watson value
Variable : Population Density、GRDP、Rail Transit Passenger Volume、Average Sales Price of Residential Commodity Housing Dependent variable : Urban Underground Space Development Area	0.981	2.491

According to the table, 98.1% of the variation in urban underground space development area can be explained by the combined influence of population density, GRDP, railway passenger volume, and the average sales price of residential commodity housing. Additionally, the Durbin-Watson statistic is around 2, indicating that the samples for these four independent variables are mutually independent and there is no mutual influence among them.

**Table 3.** Summary of Multiple Regression Analysis Results

Influence factor	Significance	Coefficient	VIF
Population Density ( $x_1$ )	0.623	-61184.526	3.194
GRDP ( $x_2$ )	0.275	1108.445	21.619
Rail Transit Passenger Volume ( $x_3$ )	0.363	-34.548	3.727
Average Sales Price of Residential Commodity Housing ( $x_4$ )	0.228	1156.133	34.171
Constant		290641379.2	

From the analysis results, it is evident that the VIF values for GRDP and average residential commodity housing sales prices are excessively large. This suggests a mutual influence between GRDP and the average residential commodity housing sales price. Consequently, only one variable should be retained. Here, we choose to retain the GRDP and eliminate the average residential commodity housing sales price before conducting the regression analysis again. The results are as follows:

**Table 4.** Summary of Multiple Regression Analysis Results

Influence factor	Significance	Coefficient	VIF
Population Density ( $x_1$ )	0.819	29528.021	2.406
GRDP ( $x_2$ )	0.008	2295.177	3.089
Rail Transit Passenger Volume ( $x_3$ )	0.058	-73.409	1.551
Constant		-56967866.1	

After multiple regression calculations, the results indicate that the significance level P-value for GRDP is  $0.008 < 0.05$ , and for rail transit passenger volume, it is 0.058, approaching 0.05, suggesting statistical significance at this level. We reject the null hypothesis that the regression coefficient is zero, indicating that the model essentially meets the requirements. Furthermore, all VIF (Variance Inflation Factor) values are below 10, with strict VIF values being less than 5, confirming there is no issue of multicollinearity. Therefore, the model construction is sound.

Based on the calculated coefficients for population density ( $x_1$ ), GRDP ( $x_2$ ), and railway passenger volume ( $x_3$ ), the linear relationship between these three independent variables and urban underground space development area can be expressed as:

$$y = 29528.021x_1 + 2295.177x_2 - 73.409x_3 - 56967866.1$$

#### 4. CONCLUSION

1. Single factor regression analysis shows that population density and rail transit passenger volume have some impact on the development area of urban underground spaces, but these effects are not statistically significant. In contrast, GRDP and the average sales price of residential commodity housing significantly influence the development area.

2. The results of the multiple regression analysis indicate that GRDP and rail transit passenger volume have a significant impact on the development area of urban underground spaces. In comparison, population density has a relatively smaller influence. Together, these three factors can explain 98.1% of the variation in the development area of urban underground spaces, with a small remaining portion possibly influenced by other minor factors.

3. Under certain conditions, based on the linear relationship between the three independent variables and the development area of urban underground spaces, it is possible to preliminarily predict the demand and developmental trends for urban underground space. This provides some reference for rationally planning the development of such spaces.

## ACKNOWLEDGMENTS

First and foremost, I would like to extend my most sincere gratitude to Professor Zhu Lei, the corresponding author of this thesis. Throughout the research process of the thesis, Dr. Zhu provided systematic guidance and constructive suggestions on the precise positioning of the research topic, the scientific control of the research direction, the in-depth guidance on data analysis, and the key links of thesis revision and improvement. Her professional competence and rigorous attitude laid a core foundation for the successful completion of the thesis and made outstanding contributions. At the same time, I sincerely thank the Shanghai Natural Resources Research Center for providing research funding for this study. The funding support has provided an important guarantee for the orderly conduct of the research work, data acquisition, analysis and verification, ensuring the smooth progress of this study.

## REFERENCES

- [1] WU Li-xin, JIANG Yun, LIANG Yue, XU Lei, CHEN Xue-xi, ZHU Wen-jun. (2004). Fundamental Research on Capacity Assessment of Development and Utilization of Urban Underground Space. *Geography and Geo-Information Science*, (04) , 44-47.
- [2] Nikolai Bobylev.(2010).Underground space in the Alexanderplatz area, Berlin: Research into the quantification of urban underground space use. *Tunnelling and Underground Space Technology incorporating Trenchless Technology Research*,25(5),495-507.
- [3] MA Chen-xiao. (2023). Evaluation methods of spatial performance and planning optimization of urban underground space in the context of inventory land redevelopment. [Doctoral dissertation, Tongji University].
- [4] ZHANG De-ying, LIAO Yuan-qin, ZHENG Geng-he. (2025). Analysis of population import status of five new towns in Shanghai from the spatio-temporal behavior perspective. *Shanghai Land & Resources*, 46(01):1113-1120.
- [5] HE Lei, DAI Shen-zhi, WANG Dai-xia, et al. (2018). Empirical study on forecasting the demand for the scale of urban underground space in Shanghai. *Urban Planning*, 42(03),30-40+58.

## INFRASTRUCTURING HERITAGE. NEW PARADIGMS FOR SUBWAY STATIONS IN THE ARCHAEOLOGICAL CENTER OF ROME

Filippo Lambertucci<sup>1</sup>

**Abstract:** With the design of the San Giovanni station in a museological and archaeological key, a new design paradigm has been defined for the new stations of Line C, currently under construction in Rome.

After a long and consolidated accustom to considering the confrontation between infrastructural modernization and the protection of historical and archaeological heritage as a battle, the stratification of the city of Rome is finally recognized as a value to be integrated into the design of the infrastructure. As of 2018, after the success of the San Giovanni station, other important stations are being built at exceptional archaeological sites, in the historic center, such as under the Colosseum itself, or even in areas marginal to it, such as the Amba Aradam station, where the unexpected discovery of an entire building from the imperial age has led to the construction of a literal underground museum.

The paper aims to analyze the methodological characteristics, the artistic resources involved and the design solutions adopted in relation to both the construction aspects and the urban insertion and integration; the new stations are designed to take on a central role in the appreciation and understanding of the historical stratification and the surrounding urban space, bringing the simple traveler, through an involuntary museum, to an aesthetic and cultural experience in the very same moment of his journey.

The aim is to demonstrate how the design synergy between archaeology, architecture and engineering can constitute a unique resource for urban contexts rich in history, and how the recognition of this potential in the planning phase can lead to significant results in terms of overall urban quality, as in the case of the future Venezia station, in the very center of the touristic and administrative heart of Rome, which will be able to involve numerous adjacent archaeological and cultural sites in a large urban node.

**Keywords:** Underground space design; Archaeology; Mobility; Involuntary museum; Interior Architecture;

### 1. INTRODUCTION

Rome is unique in the modern world for the sheer volume and density of archaeological remains that lie beneath its streets. The city's layers of history present both a challenge and an opportunity for modern infrastructure development, especially transportation. Among the most ambitious and complex projects in this domain is the construction of Line C of the Rome Metro. Unlike most cities, where subway tunnels can be bored with relative ease, any underground work in central Rome quickly becomes an archaeological expedition. Line C represents a monumental effort not only in engineering but in heritage preservation and public archaeology.

As Line C traverses some of the most archaeologically sensitive areas of the city, from San Giovanni to Venezia, it has become as much a cultural project as a transportation one. The stations along this route—San Giovanni, Porta Metronia, Colosseo/Fori Imperiali, and Venezia—are becoming exemplary for their integration of archaeological discoveries into their design. These stations are not just transit hubs; they are museum-like spaces that invite commuters to experience the city's past in a deeply immersive way. This paper explores the intricate relationship between underground transportation and archaeology in Rome, examining how these new metro stations serve as innovative examples of urban archaeology, public education, and the dialogue between ancient heritage and contemporary life.

<sup>1</sup> PhD, Lambertucci Filippo, architect, associate professor and head of Re\_Lab at DIAP – Dipartimento di Architettura e Progetto, Sapienza Università di Roma, via Flaminia 359, 00196 Roma, Italy, [filippo.lambertucci@uniroma1.it](mailto:filippo.lambertucci@uniroma1.it).



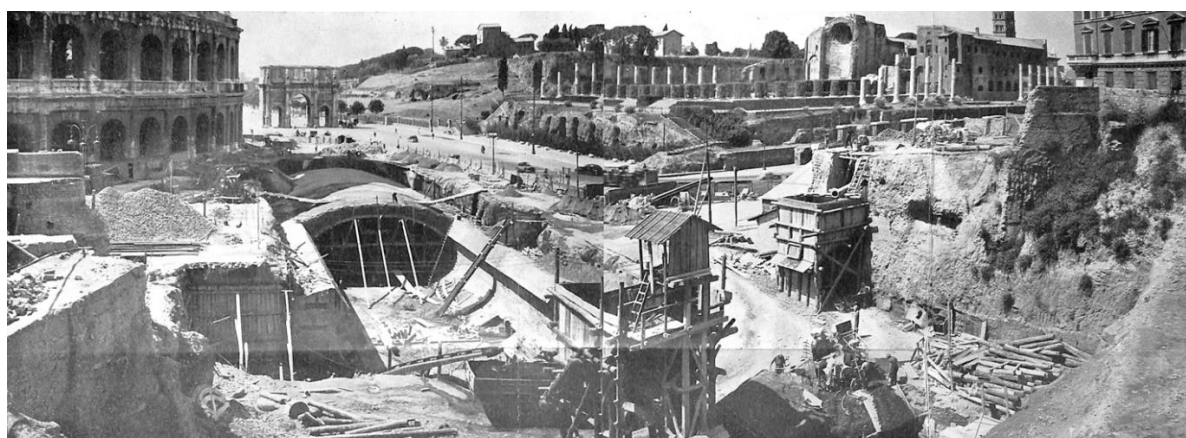
## 2. THE CHALLENGE OF BUILDING UNDERGROUND IN ROME

Constructing a subway line in any major city is a complex task, but in Rome, the stakes are exceptionally high due to the city's historical stratigraphy. Excavations reveal as many as 25 distinct historical layers in certain locations, ranging from prehistoric settlements to 20th-century constructions. This accumulation poses formidable obstacles to modern construction projects. Italian heritage law mandates archaeological oversight for any construction that disturbs the ground, particularly in historically sensitive zones such as the historical centre. Accordingly, any extension of underground infrastructure must be coordinated with comprehensive archaeological surveys and preservation efforts, as outlined, among others, by Cecchi[1].

For a long time, the relationship between infrastructure and archaeology was perceived as an irreconcilable conflict: archaeology was primarily viewed as an obstacle to the regular progress of construction work. Conversely, infrastructure projects were regarded by heritage protection and conservation authorities as potentially hazardous and destructive events.

This antagonistic perspective characterized the development of Rome's first two metro lines. The first, Line B, completed in the 1950s, and the second, Line A, completed in the 1980s, both reflect this legacy. Archaeology was not yet seen as an asset, but rather simply as a hindrance, incapable of informing or influencing the design of either the route or the stations. Construction on Line B began in the late 1930s, during a period marked by enthusiastic but indiscriminate urban demolitions. The line cuts through the historic centre with extensive open-cut excavations, passing adjacent to monuments such as the Colosseum and the Arch of Constantine, effectively plowing through the ground and removing all archaeological remains without distinction, as reported by Perrone [2]. In this context, the Superintendency was unable to provide proactive guidance, managing only—with great difficulty—to partially document the results of the excavations, as in Bucci et alii [3].

Some years later, the construction of Line A followed similar principles, demonstrating comparable disregard for the design potential presented by significant archaeological discoveries, such as those at Termini station or Piazza della Repubblica [4]. Only a few remnants were isolated and incorporated into the station projects, which showed little to no concern for acknowledging archaeological traces, let alone valorising them—often relegating these remains to small, ineffective display cases.



*Figure 1. The dig for the B Line in the late '30's. In the background, from the left, the Colosseum the Arch of Constantine and the Palatine Hill*

## 3. METRO LINE C: A HYBRID INFRASTRUCTURE PROJECT

Line C is the third metro line in Rome and aims to connect the eastern suburbs to the Vatican area via the historical center. The project has faced repeated delays, primarily due to archaeological finds, and the legal and cultural framework of Italian cultural heritage laws has progressively transformed the Line C construction process into a hybrid between an infrastructure project and a large-scale archaeological dig.

The archaeological dimension finally assumes a more proactive and design-oriented role, rather than merely serving as a form of documentation. A method has been developed that encompasses an extensive campaign of preventive investigations, alongside excavation and site management techniques that simultaneously allow for accelerated construction timelines while ensuring archaeological documentation and design outcomes that are both more sensitive and detailed [5]. Notably, as the line, originating from the distant periphery, crosses the Aurelian

Walls and enters the historic center, the stations are fundamentally excavated using stratigraphic methods aligned with archaeological best practices.

These excavation processes are complemented by timely surveying techniques, employing advanced three-dimensional digital recording technologies. At the same time, there is a growing awareness and sensitivity toward the opportunities that archaeological discoveries can offer. However, it is important to acknowledge that the entire Line C has been conceived with a coordinated and consistent architectural identity across all stations.

Thus, while sensitivity to archaeology as a discovery grows, there has yet to emerge a fully mature design approach oriented toward deeper integration with the urban and, more broadly, the public realm. Throughout the line, stations are engineered to optimize construction efficiency and technical-distributive solutions, leaving limited flexibility to adapt to unforeseen archaeological findings. Consequently, stations in the historic center possess predetermined forms driven by requirements largely independent of the historical layering and potential revealed beneath the city.

As a result, accommodating the increasing public demand for higher-quality spaces attentive to archaeological heritage necessitates the adoption of contract amendments—variations to previously approved projects. This inevitably entails increased costs, bureaucratic complexity, and extended timelines, which could be mitigated through more open and integrated planning processes from the earliest design phases [6].

Nonetheless, Line C inaugurates a new phase that is charting a path toward heightened awareness, initiated with the San Giovanni station, and is setting new standards for infrastructure interventions within the historic fabric of the city. Despite the many challenges of an experimental beginning and uncertainties among political and economic decision-makers, four new stations are redefining the state of the art in the dialectic between protecting the heritage of the historic city and meeting the technical demands of contemporary urban life.

### **3.1. San Giovanni: The First “Archaeological Station”**

San Giovanni, opened in 2018, is the first station of the Line C within the Aurelian Walls and the first to adopt the “archaeological station” format. Its design represents a groundbreaking approach -born thanks to a lucky coincidence- to integrating ancient history with modern infrastructure.

The construction site of the station was initially intended to proceed according to the original plan — namely, a unified design applicable to the entire length of the metro line. Simultaneously, however, an independent study conducted by Sapienza University of Rome was theoretically exploring the design potential of a paradigm shift in the relationship between infrastructure and heritage. It was only thanks to the intervention of the Special Superintendency for Archaeology, Fine Arts, and Landscape of Rome — the heritage protection authority responsible for overseeing the construction — that the potential of this research was recognized and the proposed approach adopted by the general contractor for Line C.

Yet, the central thesis of the research was quite simple, and perhaps even obvious for a city like Rome: to consider the opportunities arising from the intersection of infrastructure and archaeology. Although new procedures for preliminary investigations and archaeological excavation methods had already been in place for some time, adequate design measures in response to archaeological findings had not yet been implemented.

The research thesis, therefore, emerged at a particularly opportune moment to be adopted and tested as an experimental case. Naturally, by 2013, the structural elements and all technical spaces had already been finalized and were practically impossible to modify; as such, the proposals had to be limited to interior arrangements alone. Meanwhile, the excavations uncovered an extraordinary number of artifacts — approximately 40,000 — as well as several particularly significant discoveries, such as an imperial-era farmhouse. These findings sparked enthusiasm and interest not only among archaeologists but also within the broader public, providing crucial support and initiating a shift in cultural perception. This shift challenged the longstanding practice of simply removing such materials and relegating them to storage in distant, closed warehouses.

Conservation, all too frequently, results in the sequestration and subsequent disappearance of archaeological finds. Italian museum storage facilities are filled with artworks and artifacts; yet can a heritage that is largely inaccessible and forgotten truly be considered well-preserved? Is technical and physical preservation alone sufficient, or does a significant part of cultural value reside in its accessibility and interpretation by a broader audience beyond specialized scholars?

The interior design project for the San Giovanni station seeks to address these questions by foregrounding access to information as a foundational principle of meaningful and holistic conservation [7].

The absence of the artifacts themselves undoubtedly complicates the interpretive process; however, it simultaneously clarifies the importance of the conceptual dimension. In this approach, interpretive frameworks are developed to render the significance of the archaeological materials intelligible to the public. The exhibition is constructed as a narrative—one that emerges from the very absence of the removed artifacts. Through this narrative, the design aims to reconstruct both the historical context and the layered stories to which these objects

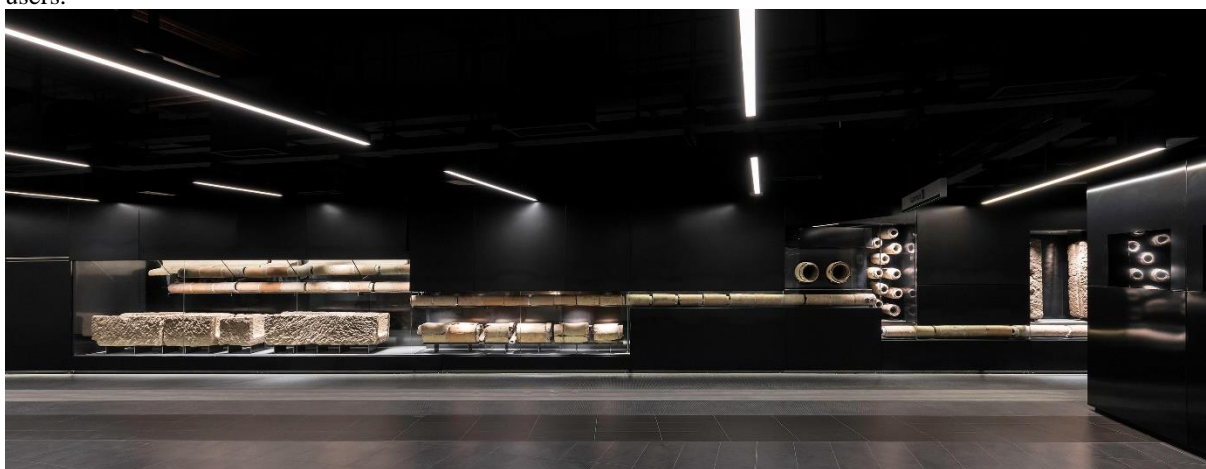
silently attest. Since the excavation has effectively erased the site's physical context, the display becomes the primary medium through which meaning can be reconstituted and conveyed [8].

“The challenge was therefore to elaborate a museographical concept that instead of competing with the conditions typical of a normal museum exhibition, [...] must rather deal with the conditions of a real physical impact with a mass of passengers who must take a train as their first concern [9]”.

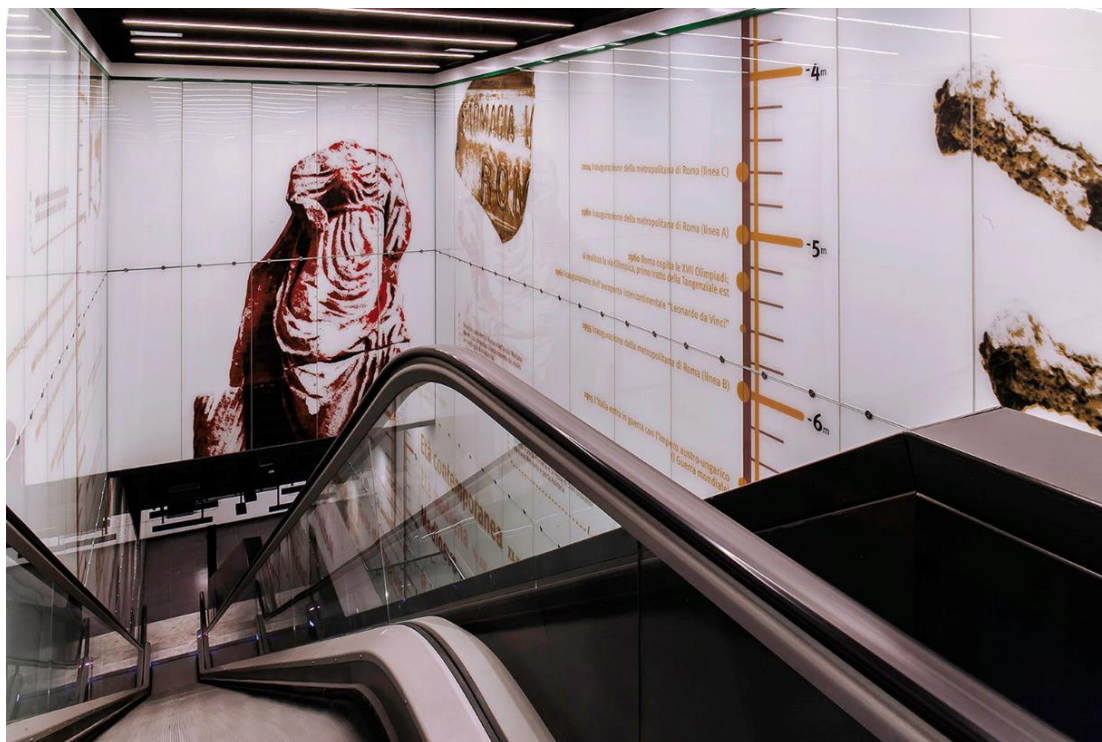
So, the station was designed to display a sort of "time tunnel" concept that immerses passengers in a journey through history as they descend from street level to the train platforms.

The strategy, therefore, was to emphasize a strong narrative approach—prioritizing the communicative and educational dimensions of the passenger experience rather than focusing solely on architectural themes. At the same time, it was essential to remain aware that a metro station is not a museum; it cannot be designed with the same delicacy and refinement characteristic of exhibition spaces, particularly given that its users have different priorities, such as receiving accurate information and feeling secure.

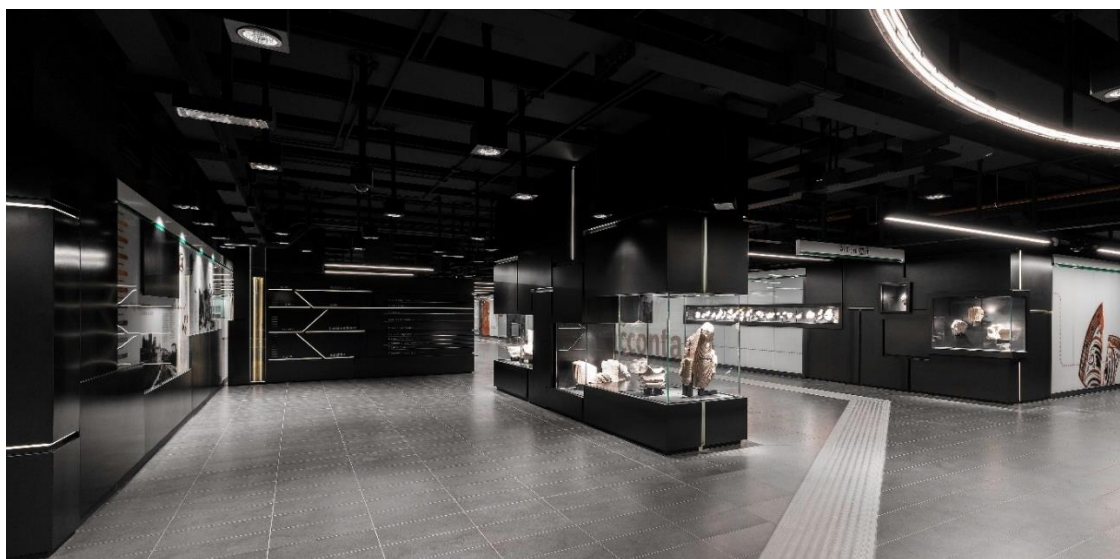
These parameters thus prompted the development of a design strategy capable of balancing the needs of both the commuter and the visitor, thereby contributing to the cultural experience of both regular and occasional city users.



**Figure 2.** San Giovanni station, the mezzanine floor with late-imperial roman plumbing and sewage artifacts



**Figure 3.** San Giovanni station, the narrating walls with the strata-meter indicating depth and cronology



*San Giovanni station, the entrance hall with the archaeological displays*

### **3.2. Porta Metronia: A Gateway to the Subterranean Past**

To be opened in 2025, Porta Metronia station, designed by the roman office ABDR studio, continues the vision laid out at San Giovanni. Located near the ancient gate of the same name, the station sits at a pivotal point in the city's archaeological topography.

The excavation works carried out at the Porta Metronia station enabled the analysis of approximately 50,000 cubic meters of archaeological stratigraphy, encompassing a surface area of 3,300 square meters and reaching an average depth of 15 meters below the current ground level.

Between 2015 and 2018, the archaeological investigations at the Amba Aradam/Ipponio station brought to light an extensive and remarkably well-preserved architectural complex. Characterized by its formal coherence, architectural articulation, and exceptional state of conservation, the site is now recognized as one of the most significant archaeological discoveries in recent Roman history. In response to its cultural value, the Special Superintendency for Archaeology, Fine Arts, and Landscape of Rome mandated the dismantling, conservation, and reinstallation in situ of the remains. This directive required a fundamental reconfiguration of the station's architectural layout, compelling a reconciliation between infrastructural performance and heritage preservation.

The excavated area—measuring approximately 1,750 square meters—revealed a substantial Roman military compound dating to the 2nd century CE, including more than thirty rooms, many featuring finely preserved frescoed walls and mosaic pavements, as well as a two-story domestic structure, likely the residence of a commanding officer, which spatially integrates with the broader barracks system.

These exceptional findings necessitated a comprehensive reconsideration of the spatial and functional organization of the station's public realm.

In alignment with the Superintendency's conservation guidelines, the architectural remains will be reassembled at their original locations and elevations. This approach maintains the spatial legibility of the site, offering an interpretive framework that supports both experiential immersion and historical understanding.

Rather than merely documenting the archaeological finds and subsequently concealing them, the design team opted to integrate the remains directly into the spatial configuration of the station, effectively transforming the transit space into an archaeological exhibition.

Unfortunately, the ambitious vision of creating a unified public circulation system—linking the station, the archaeological display, and the redevelopment of the surface area to restore visibility to the Aurelian Walls—underwent significant reductions. Most notably, the decision to convert the archaeological zone into a dedicated museum resulted in the loss of one of the project's most meaningful attributes: the full spatial and experiential integration of infrastructure, heritage, and public space within a cohesive urban framework.





**Figure 4.** *Porta Metronia station, Left, the discovery of the large barracks, before its removal and repositioning; Right, impression of the barracks museum, with the lowered pedestrian square on the right.*

### 3.3. Colosseo/Fori Imperiali: At the Heart of Ancient Rome

The Fori Imperiali station is embedded within an archaeological and urban context of extraordinary value, which demands from the infrastructure a design coherence commensurate with the significance and quality of its surroundings.

Although located in an area already subject to extensive urban transformation, the excavations have led to unexpected and significant discoveries, further enriching the historical interpretation of the site. This underscores, once again, the strategic role of such infrastructure—not merely as a site of archaeological inquiry, but as a vehicle for enhancing and understanding an area of exceptional cultural value.

The station is nestled among inestimable and universally iconic vestiges, which alone would warrant a high architectural standard. However, it is also the site of important new findings—most notably, a system of wells from various periods and with diverse functions. These wells offer a valuable spatial and chronological cross-section that virtually intersects the station's environment.

The design concept seeks to respond directly to the compelling characteristics of the context, particularly the evocative power of these new discoveries, which contribute a new chapter to the area's history. The overarching design strategy defines two complementary and dialectical elements: a background space and a series of eloquent, precious presences that serve to narrate archaeology:

the cavity of the station is a space of dim light, with a neutral yet materially expressive character, evoking the density and darkness of the excavated earth;

within this penumbra, the archaeological elements stand out like treasured artifacts at the bottom of a well, serving as a prelude to the visitor's encounter with what is arguably the most significant archaeological area in the world, just above the surface.

Once again, a station is not a museum; it retains characteristics and requirements that necessitate spatial management focused on safety and the efficient movement of large crowds. For this reason, the archaeological narrative is articulated through discrete points that enliven and distinguish the sequence of station environments with their exceptional significance.

The design of the space and the archaeological narrative are two sides of the same coin. Together, they synthesize spatial qualities and communicative elements to ensure clarity in both functional trajectories and narrative episodes. Their interaction is designed to offer an integrated, multi-layered experience for a diverse public.

The spatial composition of the station is defined through three fundamental elements:

- An opaque, "raw" material to form the general backdrop, conceived as a materially dense and virtually dark enclosure;
- A luminous, "precious" material to highlight the spaces of archaeological narrative and spatial experience;
- Light, as an immaterial but decisive orchestrator of the overall scenography.

These three components underpin the narrative structure, with historical and archaeological moments conceived as luminous gems embedded in the dark mass of the underground space. According to this framework, the different levels of the station are designed not as isolated episodes, but as parts of a continuous sequence shaped by the travellers' perceptual experience as they move through the station.

The concourse level, just below the street, is most influenced by its proximity to the monumental landscape, sharing the ancient elevation of the nearby Temple of Peace. This unusually large space evokes a basilica-like environment, emphasized in the design through accentuation of the two ends—facing the Imperial Forums and the Colosseum—where two key exhibit areas are located. At the center, a grand staircase shaft opens—a unique feature in Roman stations—which, due to its scale and depth, is envisioned as a luminous gem and a spatial element reminiscent of the architectural order and measured proportions of a Forum: a "Station Forum," so to speak.



The mezzanine level is more compact but follows a similar layout: the central area is dominated by stair groups inhabiting the void of the Station Forum; the two ends are conceived as refined backdrops housing archaeological exhibits. On one side, reconstructions of the spaces unearthed during excavation are displayed: on the other, an arrangement of some of the wells discovered in this zone. As elsewhere, the remaining space serves as a neutral interlude between these events.

Based on a scientific plan developed with the Parco Archeologico del Colosseo, the station spaces are organized into thematic areas, each with a distinct spatial character tailored to its topic, consistent with station functionality and service requirements, and capable of narrating and communicating effectively to the public.

The atmospheric staging relies on a highly restricted palette of materials and colours, chosen to express with maximum clarity the duality inherent in the narrative:

The raw, cavernous underground space is evoked—almost as if hewn from a quarry—through the continuity of floor and cladding.

The key archaeological and architectural elements are highlighted by golden-finished metal cladding, which glows in contrast with the background, emphasizing their precious character—not only in terms of content, but also as navigational markers.

Finally, light assumes a central role in creating an atmospheric dimension that favours penumbra, transforming what is usually a purely technical space into an unexpected site of cultural experience.



**Figure 5.** Colosseo station, the imperial forums interpretation point, a free access area before entering the fare zone



**Figure 6.** Colosseo station, archaeological display in a calm corner of the passenger flow at the mezzanine



*Figure 7. Colosseo station, the grand stairway hall, a forum among the imperial forums*

### **3.4. Venezia: The Potential of Archaeological Integration**

Venezia station, whose construction began in 2024 and is expected to end in 2032, is located in the middle of Piazza Venezia, at the nexus of ancient and modern Rome, lying beneath the Altare della Patria and within sight of Trajan's Column and the Capitoline Hill.

Preliminary excavations have already revealed an astonishing range of archaeological materials, including several layers of the ancient Via Lata (now via del Corso) and parts of the Hadrian's Auditoria and structures dating to the early Imperial period. Due to the site's sensitivity and the density of finds, the construction timeline has been extended repeatedly.

The functional needs mainly arise from the nature of being a traffic junction in the area. Pedestrian and vehicular flows, as well as underground utilities, are elements that define the project's configuration.

The ground-level entrances to the station have been designed by CREW office to serve the different areas of the square and to connect the station with the surroundings, rich of monuments and cultural institutions. Once users have reached the first underground level of the station through the ground-level access points, they will have the option to safely access the museum complexes, such as Palazzo Venezia, Hadrian's Atheneum, the Archaeological Park of the Fori Imperiali, museum area of the Vittoriano, without dealing with street traffic.

The directive, issued by the Soprintendenza di Roma, to incorporate a dedicated museum level within the station, profoundly influenced the design of the atrium level, fostering direct spatial and thematic links to the adjacent museums and archaeological findings and informing the overall aesthetic language of the station's interiors, even where such references are primarily expressed through decorative means.

Piazza Venezia represents a highly complex urban node, characterized by persistent challenges in managing surface traffic that have yet to be resolved. At the same time, it is surrounded by a high concentration of monumental and archaeological sites, positioning it as a potentially significant pivot for pedestrian connectivity.

To date, the project appears to emphasize the grandeur and technical complexity of the intervention, while leaving many of its potentialities partially unrealized—particularly regarding the urban integration of heritage assets, tourist circulation paths, and mobility needs. These aspects seem to constitute the true value that the station could embody by fully developing and advancing the conceptual model initiated with the San Giovanni project.





**Figure 8.** Venezia station, Left, the atrium level with the links to the surrounding museums and archaeological sites; Right, construction site in the core of traffic flows of the historic center



**Figure 9.** Venezia station, impression of the atrium floor with archaeological displays

#### 4. NARRATIVE AS A FRAMEWORK FOR THE DISLOCATED MUSEUM

As Laudato points out, "the archaeological heritage, bringing its authority to the Metro, also confers its potential of cultural significance, in some way enhancing the Metro space as an integral part of the historical narrative emphasizing the local sense of place"[10].

When works of art are situated within architectural settings, their presence inevitably occupies an ambiguous space—one defined by the tension between the artwork and the environment that contains it. This ambiguity becomes particularly significant in the context of heritage and its sites, as it activates more intricate layers of meaning and interpretation.

The continued and active presence of heritage within its original or intended location evokes notions of authenticity and a sense of place, both conceptually and experientially. In doing so, according to Merrill, it transfers to infrastructural spaces certain attributes traditionally associated with the museum—namely, its role as both a product and producer of socio-cultural meaning and urban identity [11]. At the same time, this process endows infrastructure with the responsibility of evolving hybridized frameworks that transcend the conventional, distinct typologies of both the museum and the subway.

A new vision of transit spaces—centred not only on informational but explicitly narrative dimensions—is beginning to establish new standards for mobility environments. This approach promotes a more mature understanding of such spaces as public realms, capable of delivering broader and often unexpected experiences that respond to the evolving expectations of their users. Narration, in this case, is not mere description but activation of an intangible context through the symbolic domain of language as defined by Knappett [12].

This dimension seems to be appreciated, to the point that the San Giovanni station also has reviews on Trip Advisor, while among the aspects that most capture travellers' attention is the clear reference to methods of engagement typical of museum spaces, as Campetella report in his research: "I move quickly and sometimes find myself among a group of tourists focused on viewing different points of the station. It makes me smile to think of foreign tourists who, among all the things they can visit in Rome, choose to go down into the metro." [13]

So, if we can assume the infrastructure as a materialized consensus, as a product of a complex and continuously in progress dialogue among not only the carriers of the expert language of technology, planning and politics, but also among end users, who are not only passive consumers but active agents of a consensus response, we must recognize the centrality of beauty and significance of the spaces of mobility, as discussed by Smith[14].

It must be recognized in fact that a new way of conceiving the stations was even formalized by the Campania Region with Resolution N. 637/2006 which defines the guidelines for the design and construction of the regional metro stations, with which it explicitly sets for new standard stations of pleasantness, comfort of use and safety, explicitly referring to a need to arouse emotions above all through elements without codified functions [15].

This represents a paradigmatic shift that finally acknowledges the economic value of aesthetic quality, challenging the reductive notion of technology as the sole determinant of cost-efficiency in public infrastructure projects. Recent studies have substantiated and quantified the economic impact of design excellence and beauty. The strategic approach adopted in the design of the new Naples Metro stations has not only fostered virtuous urban behaviour and catalyzed processes of regeneration but has also generated an autonomous form of cultural and touristic appeal. These interventions have enhanced public perception of the transit system, expanding both its usage and its catchment area through an increased sense of value and civic engagement [16].

## 5. CONCLUSION: TOWARD A NEW PARADIGM OF URBAN ARCHAEOLOGY

The construction of Metro Line C in Rome exemplifies a new paradigm in the intersection of urban development and cultural heritage. Rather than viewing archaeology as an obstacle to infrastructure, the city has embraced it as a central element of design and function. The stations at San Giovanni, Porta Metronia, Colosseo/Fori Imperiali, and the forthcoming Venezia station each illustrate how archaeological discoveries can be transformed into cultural assets.

This integration has wide-reaching implications—not only for Rome but for other ancient cities grappling with similar challenges. It demonstrates that with the right investment, interdisciplinary collaboration, and public vision, it is possible to harmonize modern urban needs with the preservation and celebration of the past.

Moreover, the museum-like qualities of these stations contribute to a broader cultural shift. They help foster a public appreciation for archaeology and history, making these disciplines part of everyday urban life. As passengers descend into the depths of Rome, they do not leave the city's story behind, they descend into it, becoming part of its ongoing narrative.

In this regard, Marc Augé says that the subway gives the opportunity to brush against the history of others: by extension we can then say that it offers very concretely also the opportunity to brush against the history of the city itself [17].

Line C is more than a transportation project; it is a statement about what it means to live in a city where the ancient and the modern are in constant dialogue.

One could go in a natural way through archaeology by making the banal utilitarian act of taking a train or, on the contrary, offering the tourist who arrives there an experience of great effect by the immersion in the living fabric of history that suddenly appears descending from train.

If put in a system, even on modest Rome's underground network, an approach that engages the archaeological layers and underground and surface spaces of the city around the subway stations, existing and future, could produce an extraordinary result. Around the stations, and not only the central ones, it is in fact possible to reconnect a vast and articulated system of historical, archaeological, urban spaces, which can recompose a lost and yet fundamental dimension in a city like Rome.

The result is an accretive structure similar to a rhizome, and like this, as outlined by Deleuze, impossible to plan in conventional terms, but essential to be foreseen as an act of reconquering one side of the lost and precious city [18].

## 6. ACKNOWLEDGMENTS

The project for the San Giovanni station was born from an independent research program on the relationship between infrastructure and heritage funded by Sapienza University of Rome and carried out by the Re\_Lab team. The project is the result of intense teamwork that involved architects, engineers, graphic designers, archaeologists and heads of the Superintendency. Special thanks goes to the architect Sonia Martone, Director of the Palazzo Venezia Museum.

Museography and interior design: Sapienza, Università di Roma - Diap Department - Re-Lab, Regeneration Laboratory

Team leaders: prof. arch. Filippo Lambertucci, prof. arch. Andrea Grimaldi.

Design team: arch. Livio Carriero, arch. Amanzio Farris, arch. Valerio Ottavino, arch. Samuel Quagliotto, arch. Leo Viola.

Graphic design: prof. arch. Carlo Martino with Sara Palumbo, Delia Emmulo

General design: Metro C spa, coordinator eng. Eliano Romani

Scientific supervision: Soprintendenza Speciale per il Colosseo e l'Area archeologica centrale di Roma: Rossella Rea, with Irene Baroni, Anna De Santis, Francesca Montella, Simona Morretta;

Archaeological excavation, display and reconstruction of the archaeological finds: Cooperativa Archeologia, Anna Giulia Fabiani, Agostina Audino, Anna Giulia Fabiani, Adone Pelly, Savino Sbarra, Michele Zaccardo, Fabiana Moro, Adone Pelly, Laura Rivaroli, Angelica Pujia, Francesca Montozzi

Restoration of the archaeological finds: Istituto Superiore per la Conservazione e il Restauro (wood and organic finds)

The project for the Fori Imperiali/Colosseo station originated from the success of the San Giovanni station; the management of the Colosseum Archaeological Park commissioned Filippo Lambertucci and the Sapienza Re\_Lab team for the preliminary design while the General Contractor MetroC commissioned the same subjects for the executive design. Museography and interior design: Sapienza, Università di Roma - Diap Department - Re-Lab, Regeneration Laboratory

Team leaders: prof. arch. Filippo Lambertucci, prof. arch. Andrea Grimaldi,.

Design team: arch. Livio Carriero, arch. Amanzio Farris, arch. Edoardo Marchese, arch. Valerio Ottavino, arch. Leo Viola. Graphic design: Chiara Raho

General design: Metro C spa, coordinator eng. Eliano Romani

Scientific supervision: Parco Archeologico del Colosseo, Alfonsina Russo director, Elisa Cella, Federica Rinaldi. Display and reconstruction of the archaeological finds: Cooperativa Archeologia: Anna Giulia Fabiani

## 7. BIBLIOGRAPHY

- [1] Cecchi, R. (Ed.) (2010). *Roma archaeologia. Interventi per la tutela e la fruizione del patrimonio archeologico. Secondo rapporto*. Milano, Italy: Mondadori Electa spa.
- [2] Perrone, V. (1955). *La metropolitana di Roma*. Roma, Italy: Istituto Poligrafico dello Stato
- [3] Buzzetti, C., Pisani Sartorio, G. (Ed.), (2015). *Le scoperte archeologiche sul tracciato della Metropolitana B di Roma (1939-1953) dall'Archivio Gatti*. Roma, Italy: «L'ERMA» di BRETSCHNEIDER
- [4] Paris, R. (Ed.) (1996). *Antiche stanze: un quartiere di Roma imperiale nella zona di Termini*. Milano, Italy: Giorgio Mondadori.
- [5] Egidio R., Filippi F., Martone S. (Ed.) (2010). *"Archeologia e infrastrutture. Il tracciato fondamentale della Linea C della metropolitana di Roma", Bollettino d'Arte, Volume Speciale 2010*, Roma, Italy: Ministero per i beni e le attività culturali.
- [6] Rea, R. (Ed.) 2011. *Cantieristica archeologica e opere pubbliche. La linea C della metropolitana di Roma*, Milano, Italy: Mondadori Electa spa.
- [7] Lambertucci, F., (2019), *Archeologia per chi va in metro. La nuova stazione di San Giovanni a Roma*. Con A. Grimaldi, Macerata, Italy: Quodlibet
- [8] Lambertucci, F., (2019), Attraversare per rammemorare. L'infrastruttura come museo dislocato. In *FESTIVAL DELL'ARCHITETTURA MAGAZINE* pp.26-34. - ISSN:2039-0491 (N.50)
- [9] Lambertucci, F., (2018), Archaeology for commuters. The San Giovanni archaeo-station on the new metro Line C in Rome. In *Tunnelling and Underground Space Technology* pp.95-105. - ISSN:0886-7798 vol. 78, Elsevier
- [10] Laudato M. (2019), Mobilizing cultural resources: The functional role of heritage in metro projects. In: *Tunnels and Underground Cities. Engineering and Innovation Meet Archaeology, Architecture and Art: Proceedings of the WTC 2019 ITA-AITES World Tunnel Congress*, Naples, CRC Press/Balkema, Leiden.
- [11] Merrill S. (2015), Identities in transit: the (re)connections and (re)brandings of Berlin's municipal railway infrastructure after 1989. *Journal of Historical Geography*, 50, Elsevier, 76-91.
- [12] Knappett C. (2005), *Thinking Through Material Culture, An Interdisciplinary Perspective*, Philadelphia, University of Pennsylvania Press
- [13] Campetella, P. (2018), Viaggiatori e visitatori. Studio preliminare sulla fruizione della stazione San Giovanni della metropolitana di Roma, in: *CADMO*, n.2/2018, pp.47-64, Milano: Franco Angeli.
- [14] Smith M. L. (2016): *Urban infrastructure as materialized consensus*, in: *World Archaeology*, vol 48. Pages: 164-178
- [15] Regione Campania: *Linee Guida per la progettazione e realizzazione degli interventi nelle stazioni della Metropolitana Regionale*, Napoli, Italy: Delibera Regionale n. 637/2006
- [16] Cascetta E., Carteni, A., Henke I. (2014), Stations quality, aesthetics and attractiveness of rail transport: empirical evidence and mathematical models (pp. 307-32) in: *Ingegneria Ferroviaria* 69
- [17] Augé, M., (2002). *In the Metro*. Minneapolis, MN: University of Minnesota Press. Originally published as *Un ethnologue dans le métro*, Paris, France: Hachette, 1986.
- [18] Deleuze G., Guattari F., (1976), *Rhizome. Introduction*, Paris, Éditions de Minuit.



## HISTORICAL UNDERGROUND STRUCTURES OF BELGRADE: IDENTIFICATION, CLASSIFICATION, AND URBAN POTENTIAL FOR SUSTAINABLE CITY DEVELOPMENT

Nemanja Šipetić<sup>1</sup> and Saša Milijić<sup>2</sup>

**Abstract:** The rapid growth of the global population has intensified the imbalance between urban expansion and sustainable resource management, including water, materials, energy, air, and space. In response, contemporary urban planning increasingly explores the integration of underground spaces to enhance sustainability, functionality, and spatial efficiency. Historically, underground spaces have served military, religious, infrastructural, economic, and residential purposes, often emerging from necessity rather than systematic planning. Today, their identification, analysis, and classification are crucial for strategic urban planning, particularly in cities with significant historical and cultural contexts. This study examines Belgrade's underground structures, developed over its urban history, with the aim of inventorying, categorizing, and establishing typologies to inform future interdisciplinary planning. Notably, Serbia's legal framework does not recognize underground urbanism, emphasizing the need for scientific research and policy development in this field. The research methodology includes direct and indirect observation, institutional and field data analysis, and classification based on four key criteria: construction material, spatial dimension, current function, and historical origin. The study examines over 160 documented underground structures, excluding those under the jurisdiction of the Ministry of Defense. Institutional control and restricted access have historically limited documentation efforts, yet public interest in Belgrade's underground heritage has grown in recent decades. This research contributes to the development of scientifically grounded criteria for evaluating and integrating underground spaces into urban sustainability frameworks. The findings offer insights into the socio-historical significance of these spaces and provide recommendations for their future use and conservation.

**Keywords:** Underground Structures of Belgrade, Urban Underground Heritage, Valorization<sup>3</sup>, Identification and Classification

### 1. INTRODUCTION

Increasing urbanization and the scarcity of surface resources are increasingly emphasizing the need for strategic utilization of underground spaces as a spatial-functional asset in contemporary urban development. Confronted with global challenges such as climate change, overpopulation, and spatial crises regarding infrastructure and public services, cities are progressively incorporating underground space into urban policies—not merely as a technical solution, but as an integral component of resilience, circular economy, and cultural identity preservation [1] [2]. Unlike the historical, predominantly reactive development of underground structures—driven by wartime

<sup>1</sup> MSc, Šipetić Nemanja, B.Sc. Architecture Eng., research associate, Institute of Architecture and Urban & Spatial Planning of Serbia, Bulevar kralja Aleksandra 73 / II, 11000 Belgrade, e-mail address: [sipetic.nemanja@gmail.com](mailto:sipetic.nemanja@gmail.com), <https://orcid.org/0000-0002-9965-1457>

<sup>2</sup> Dr. Saša Milijić, director of the Institute of Architecture and Urban & Spatial Planning of Serbia, Bulevar kralja Aleksandra 73 / II, 11000 Belgrade, e-mail address: [sasam@iaus.ac.rs](mailto:sasam@iaus.ac.rs), <https://orcid.org/0000-0002-9235-2841>

<sup>3</sup> In this paper, the term valorization is used in the sense commonly applied in European heritage studies, meaning not only the evaluation and recognition of the cultural and historical significance of underground heritage, but also the process of its activation, adaptive reuse, and integration into contemporary urban development.

conditions, climate extremes, or technical necessities—contemporary trends emphasize proactive and holistic planning, supported by digital tools such as 3D modeling and geographic information systems (GIS) [3] [4] [5].

At the same time, growing attention is being directed toward historical underground spaces, which often remain outside the scope of official urban planning documentation despite their cultural, spatial, and social potential. As Heyns et al. [6] emphasize, underground spaces are not merely physical volumes, but carriers of cultural memory and symbolic meaning, and should be integrated into future urban scenarios as active resources. In this context, Belgrade—with its multilayered urban history and over 160 identified underground structures (excluding military and police facilities)—represents a significant yet underutilized potential. Despite increasing public interest and the cultural value of these spaces, there is a lack of systematic planning and regulatory support necessary to enable their functional and cultural reintegration into the modern city [7] [8]. The absence of a legal framework and the fragmented nature of existing knowledge further complicate decision-making processes related to their protection, transformation, or adaptive reuse [9] [10].

This paper aims to lay the foundation for a strategic and scientifically grounded understanding of Belgrade's underground heritage through (1) a systematic inventory and categorization of subsurface structures; (2) analysis of key parameters such as material, dimensions, function, and historical origin; (3) development of guidelines for interdisciplinary planning and integration into urban policies; and (4) recommendations for preservation and future use in accordance with principles of sustainable development and cultural valorization. Drawing from global best practices and contemporary theoretical approaches, the study highlights the importance of underground heritage as an active urban asset and a catalyst for new models of planning and cultural governance.

#### *Documenting Subsurface Structures: Between Historical Legacy and Contemporary Planning*

Subsurface structures have a long and diverse history dating back thousands of years, serving as shelters, water reservoirs, religious sanctuaries, infrastructure conduits, and defense systems. From the tunnels of Petra and the Eupalinian aqueduct on Samos, to the Roman catacombs and the underground cities of Cappadocia, these spaces attest to the capacity of ancient societies to respond to spatial, climatic, and security challenges with a high degree of technical sophistication [11] [12] [13] [14]. These historical underground forms are not merely remnants of the past—they embody collective memory, technological innovation, and spatial survival strategies. Contemporary authors such as Varriale [10] and Sandford [15] emphasize that underground heritage must be viewed as a dynamic resource, not a passive relic. As Sandford notes, “heritage is not what we inherit, but what we choose to carry into the future.” Documenting underground spaces, therefore, is not only an academic imperative—it is a strategic step toward planning more sustainable cities. At the same time, Heyns et al. [6] warn that subsurface planning must also account for intangible dimensions—collective memory, local narratives, and cultural significance. This is particularly relevant in historically layered cities, where ignoring symbolic meanings can lead to spatial injustice. Belgrade is a prime example, with its multi-layered urban development comprising Roman corridors, medieval lagums (subterranean cellars), and modern underground infrastructures. More than 160 documented structures (excluding military and police-controlled underground facilities) testify to an informal yet functional development of the subsurface—most often as a response to war, climate stress, or infrastructural needs. Despite growing public interest, institutional barriers and the legal invisibility of underground space in Serbia continue to hinder its systemic valorization and integration.

The study by Qiao et al. [16] highlights the spatial dilemma facing historic cities: the tension between preserving cultural heritage and accommodating the demands of contemporary urban development. They propose underground solutions as a viable compromise—allowing the physical separation of new functions from heritage assets, but only under conditions of meticulous planning that considers the depth of intervention, cultural appropriateness, and anticipation of future needs. For this reason, Costa and colleagues [9] advocate for the planning-based classification of “Urban Underground Heritage” (UUH), which encompasses both the physical and symbolic values of subterranean spaces. Their recommendations emphasize proactive mapping, digital documentation, and early involvement of heritage professionals in the urban planning process. The *Underground4value* handbook [17] goes a step further, calling for participatory methodologies and anticipatory tools—such as scenario planning and the “Living Labs” approach—to co-create the future of underground spaces with local communities. In this spirit, valorization is not a static act, but rather a dialogical and adaptive process grounded in continuous learning, testing, and redefinition of spatial values over time [10]. Ultimately, historical records of underground structures—including material typologies, dimensions, functions, and origins—not only preserve memory but also form the foundation for responsible urban planning. In a cityscape striving for resilience, functionality, and cultural sustainability, subsurface spaces must be integrated into the urban vision—not as invisible remnants of the past, but as visible assets for the future.

## 2. METHODOLOGY

The aim of the research was to systematize and classify Belgrade's underground structures in order to better understand, protect, and incorporate them into future urban development strategies. The methodological framework of the study included the following outlined steps.

### 2.1. Data Collection

The following methods were used:

- **Direct observation:** Field visits to accessible locations, conducted in collaboration with local institutions and guides.
- **Indirect observation:** Analysis of existing archives, publications, digital sources, and visual materials.
- **Institutional data analysis:** Incorporating information from urban planning institutes, heritage conservation bodies, and municipal administrations.
- **Field research:** On-site data collection and comparative verification of available information.

### 2.2. Classification criteria

The classification of subsurface structures was based on a set of interdisciplinary parameters designed to reflect both their physical characteristics and historical-functional relevance. Key criteria included:

- **Construction material** (e.g., loess, limestone, clay, brick, concrete),
- **Size and surface area**, distinguishing small (up to 200 m<sup>2</sup>), medium (200–500 m<sup>2</sup>), and large structures (over 500 m<sup>2</sup>),
- **Historical period** of construction (e.g., pre-17th century, Ottoman period, Austro-Hungarian period, WWII, SFRY, post-socialist period),
- **Original and current function** (e.g., wine cellar, warehouse, shelter, tunnel, tomb, etc.),
- **Current state** (e.g., active, abandoned, collapsed, conserved, repurposed), and
- **Geological context**, such as the type of substrate in which the structure was built.

These classification criteria provided the basis for statistical analysis and the development of planning recommendations (Figures 1).

Угринавацка 12	Земун	Loess	Brick, Concrete	24,64	small	Lagum		Collapsed		Austro-Hungarian (18th–19th century)
Угринавацка 17	Земун	Loess	Brick, Concrete, Loess	Око 50	small	Lagum		Collapsed		Austro-Hungarian (18th–19th century)
Угринавацка 23	Земун	Loess	Loess, Brick	35,07	small	Lagum		Collapsed		Austro-Hungarian (18th–19th century)
Угринавацка 24	Земун	Loess	Brick, Concrete, Loess	Око 50	small	Lagum		Collapsed		Austro-Hungarian (18th–19th century)
Гаџаха Приштина 45	Савски венац	Limestone	Brick, Concrete	41,1	small	Hospitality facility		Active		Ottoman period (19th century)
Угринавацка 17	Савски венац	Sarmatian sediments	Brick, Concrete	17,55	small	Shelter		Active		World War II period
Омичева 17	Савски венац	Senonian sediments	Brick, Concrete	61,25	small	Depot		Active		World War II period
Прокон	Савски венац	Sarmatian sediments	Brick, Clay	219,2	medium	Depot		Collapsed		World War II period
Бул. војводе Мишића 83	Савски венац	Limestone	Concrete	221	medium	Depot		Collapsed		Ottoman period (18th–19th century)
Савски венац 1	Савски венац	Limestone	Concrete	417,6	medium	Shelter		Active		Socialist Federal Republic of Yugoslavia

Figure 1. Section of database collected through fieldwork, sorted in Excel spreadsheet

### **2.3. Scope of research**

The research encompasses an analysis of more than 160 documented subsurface structures within the territory of the City of Belgrade, excluding facilities under the jurisdiction of the Ministry of Defense and Ministry of Interior due to access restrictions and security protocols. The data have been systematically organized by city municipalities (11 out of 17 Belgrade municipalities, as no underground structures were identified in the remaining ones), including precise addresses, ownership status, functional designation, and current physical condition of each structure. All data were entered into a tabular database using Microsoft Excel, enabling further processing, classification, and graphical presentation through a series of simple and comparative analyses.

#### **Simple Analyses**

The simple statistical analyses were conducted to provide an initial identification of the spatial and structural distribution of urban built heritage (UBH). These included the following parameters:

1. Distribution of structures by municipality;
2. Proportional presence of structures across different geological environments;
3. Prevalence of building material types;
4. Total floor area (in m<sup>2</sup>) of all structures;
5. Size categorization: small (<200 m<sup>2</sup>), medium (200–500 m<sup>2</sup>), and large structures (>500 m<sup>2</sup>);
6. Functional range of use;
7. Assessment of current physical condition;
8. Chronological distribution of construction periods.

#### **Comparative Analyses**

The comparative analyses use the same criteria as the simple ones but enable deeper insights into intersections among various parameters, such as:

1. Structure size in relation to historical periods of construction;
2. Functional typologies contextualized by historical eras;
3. Current condition of structures in relation to geological environments;
4. Condition of structures based on current or original use;
5. Geological characteristics per municipality in relation to the prevalence of structures;
6. Distribution of materials in specific construction periods;
7. Functional distribution of structures across city municipalities.

This data structure and set of derived analyses provide the basis for establishing evaluation criteria, as well as guidelines for the preservation, revitalization, and strategic inclusion of UBH in sustainable urban development models. The author considers the chosen analytical framework to offer a reliable foundation for future interdisciplinary spatial interventions.

### **2.4. Ethical and Safety Considerations**

The research was conducted in accordance with established ethical principles and safety protocols. No underground structure was physically altered or forcibly accessed; all site visits were carried out only with the consent of property owners or relevant institutions. Special attention was given to safety risks, including damaged structures, unstable soil conditions, and insufficient ventilation.

## **3. RESULTS OF THE STUDY**

### **3.1. Results of Basic Statistical Analyses**

Based on data derived from the accompanying diagrams, a statistical analysis was conducted on the underground structures in Belgrade, focusing on their function, physical condition, construction period, surface area, municipal distribution, and building materials used. The following are key findings:

1. The highest concentration of underground structures is located in the municipality of Zemun (45.73%), followed by Stari Grad (17.07%), Čukarica (7.93%), Rakovica (6.71%), and Novi Beograd (6.10%). Other municipalities such as Palilula (4.27%), Vračar and Savski Venac (each 3.66%), Zvezdara (2.44%), Voždovac (1.83%), and Grocka (0.61%) show significantly lower representation.
2. Regarding presence of structures across different geological environments, loess is dominant (51.22%), followed by limestone (32.93%) and clay (8.54%). Sandstone (3.05%), sarmat (1.83%), and sand (0.61%) are minimally used (Figures 2). When material combinations are considered, the most prevalent are loess and brick (25.00%), brick, concrete and loess (23.17%), and brick and concrete (16.46%). Limestone alone accounts for 12.80%, while other material combinations such as concrete, brick, and clay occur in less than 8% of the structures.
3. The most common functions of these spaces include wine cellars and storage vaults (lagums) (48.17%), followed by warehouses (13.41%), shelters and bunkers (each 10.37%). Transportation tunnels make up 6.10%, mines 4.27%, while tombs (1.83%), garages, depots, and gas plants (each 1.22%) are much less represented. Fishponds, Roman baths, and hospitality venues hold a marginal share (each 0.61%).
4. In terms of current condition, the majority of structures are partially collapsed (39.63%), followed by abandoned (25.61%), conserved (17.68%), and active (9.15%). Renovated structures account for 7.32%, while demolished ones are very rare (0.61%) (Figures 3).
5. As for the period of construction, most structures date back to the Austro-Hungarian era (18th–19th century, 51.83%), followed by the World War II period (19.51%) and the Ottoman period (18th–19th century, 12.80%). Other historical phases—pre-17th century, Socialist Federal Republic of Yugoslavia, and post-socialist period—each account for 3.05–3.66%, while early 20th century, the second half of the 18th century, and the 19th-century Ottoman era are represented at only 0.61%.
6. The total estimated floor area of underground structures is 344,676 m<sup>2</sup>. Large structures dominate in size with 338,400 m<sup>2</sup>, while medium-sized (2,952 m<sup>2</sup>) and small ones (3,324 m<sup>2</sup>) occupy significantly less space. Small structures represent the majority in number (70.73%), followed by medium-sized (16.46%) and large ones (12.80%).

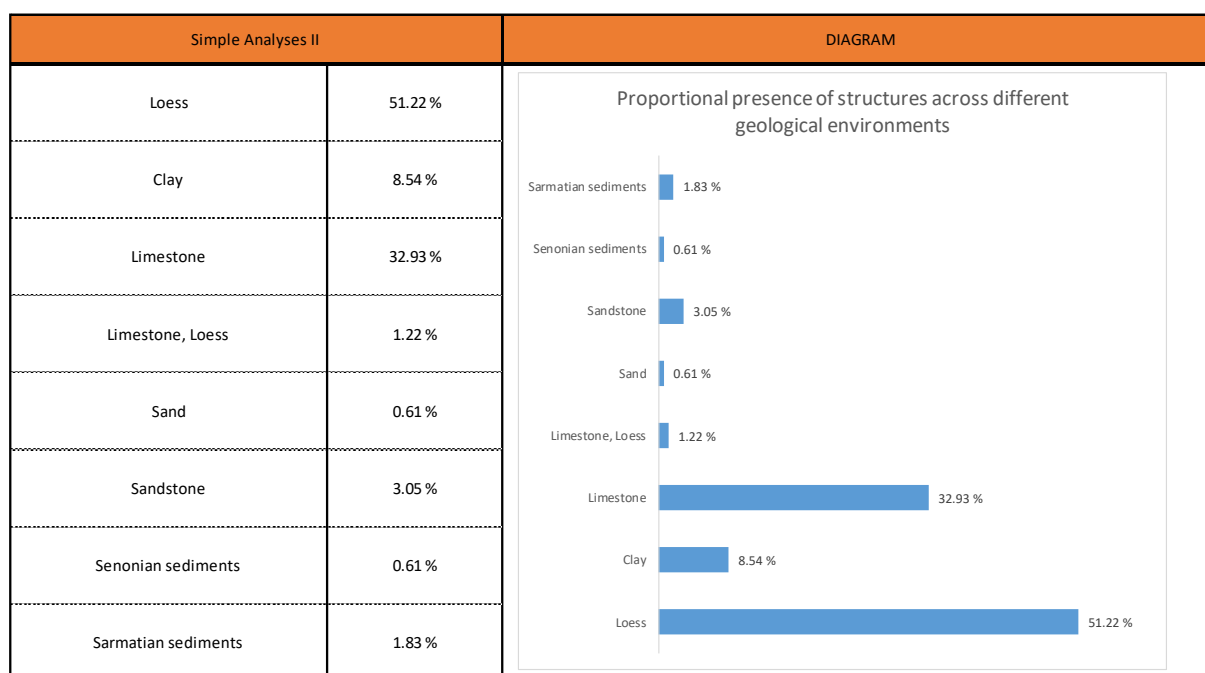


Figure 2. Results of basic analysis of proportional presence of structures across different geological environments.



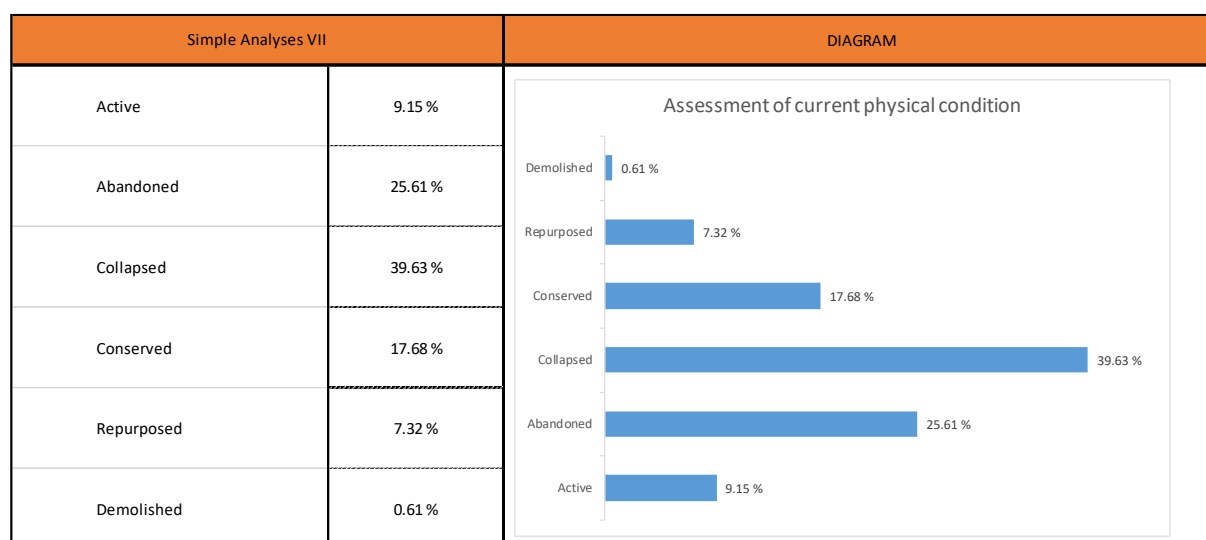


Figure 3. Results of basic analysis of current physical condition of structures.

The analysis reveals that underground structures in Belgrade are primarily lagums and warehouses constructed in loess and limestone, with the highest concentrations found in Zemun and Stari Grad. While most structures originate from the Austro-Hungarian era, a significant portion is either collapsed or abandoned, highlighting the urgent need for conservation or adaptive reuse. Although fewer in number, large underground structures account for most of the total floor area, pointing to their considerable potential for future urban development initiatives.

### 3.2. Results of Comparative Analyses

Comparative analyses of underground structures in Belgrade, conducted using various criteria (function, geological context, construction materials, historical period, and current condition), reveal a significant degree of spatial and historical diversity.

The distribution of functions by municipality highlights a strong dominance of certain structure types in specific areas. In Zemun, wine cellars and vaults (lagums) dominate (94.67%), while shelters are most represented in Voždovac (100%) and Palilula (71.43%). In Stari Grad and Savski Venac, storage facilities prevail (53.57% and 50% respectively), while bunkers are predominant in Čukarica (76.92%). Rakovica shows a balanced representation of mines and bunkers (36.36% each), whereas Vračar and Grocka include more specialized structures such as tombs.

The geological base across municipalities also reflects territorial specificity. Loess soils are prevalent in Zemun and New Belgrade, while older urban cores like Stari Grad and Palilula are predominantly founded on limestone. Clay is the dominant substrate in Voždovac and Grocka, and mixed formations (limestone, clay, sandstone, sarmatian sediments, and senonian sediments) are registered in Rakovica, Čukarica, and Savski Venac. These geological conditions directly influence the stability, durability, and preservation of the structures.

Construction materials, in a historical context, indicate that loess and brick were dominant during the Austro-Hungarian period (95.12%). In the Ottoman era, concrete, brick, and limestone were more commonly used. During the Socialist and post-Socialist periods, concrete became the prevailing material, signaling a shift in construction technologies and material availability. Brick remained a consistently used material across nearly all periods, while limestone was crucial during the Ottoman and Royal (Kingdom of Yugoslavia) periods (Figures 4).

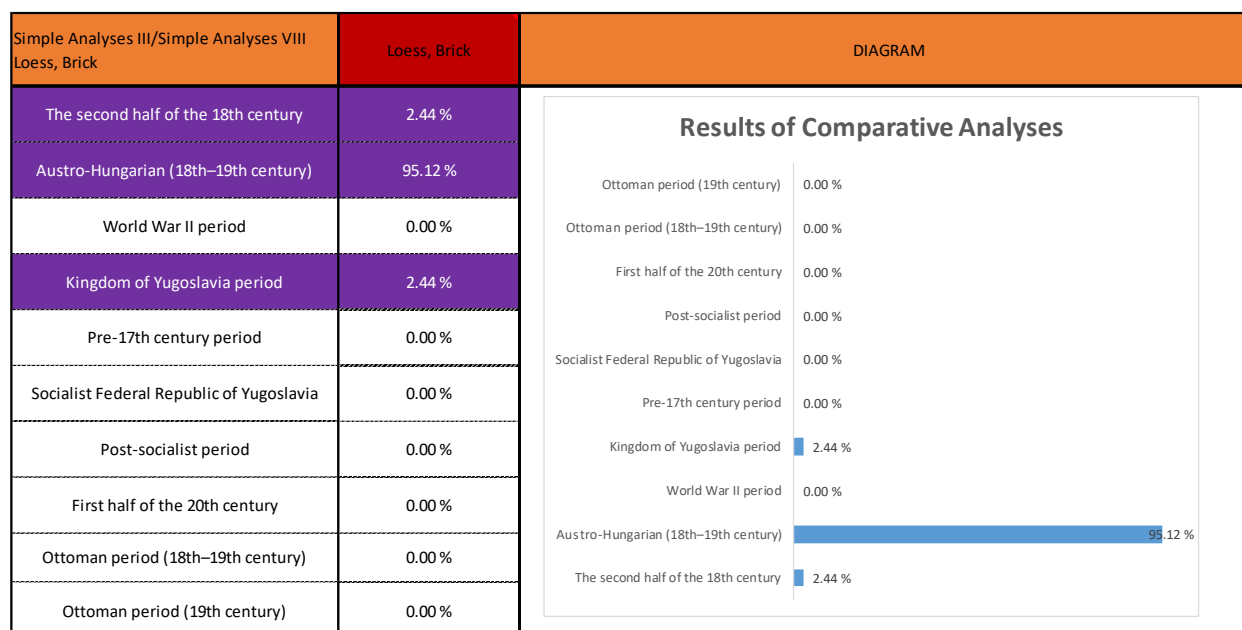


Figure 4. Results of comparative analysis of material distribution across construction periods, with brick- and loess-built structures as evaluation criteria.

When analyzing the size of structures in relation to their construction period, smaller structures were typical of earlier times (Austro-Hungarian – 68.97%; pre-17th century – 19.05%), while large structures became dominant in the post-Socialist period (28.57%). Medium-sized structures peaked during World War II (25.93%) and in the 18th–19th centuries.

Functional distribution across time periods reflects the evolution of urban and security needs. Lagums prevailed during the Austro-Hungarian era (90.59%), while shelters and bunkers were characteristic of the WWII period. In the SFRY and post-socialist periods, traffic-related structures and garages became dominant, signaling a new functional direction for underground urban space.

Preservation status relative to geological environment indicates that structures built in loess are generally partially collapsed or abandoned, while those in limestone are often preserved or still functional. Clay-based structures show moderate preservation, whereas those built in alluvial and senonian sediments-dominant soils are in the best condition, likely due to advanced construction techniques. Structures in sandstone are fully abandoned, while those in sarmatian sediments environments show a balanced condition profile.

Finally, preservation by function shows that traffic tunnels and shelters are most often active, while lagums and bunkers are largely abandoned or collapsed. Conserved structures are mostly warehouses and shelters, while repurposed ones are typically former bunkers and shelters. Demolished structures were exclusively former shelters, often due to human factors.

These results provide a complex picture of Belgrade's underground heritage in terms of historical, geological, and functional heterogeneity. They serve as a foundation for setting priorities in preservation, further research, and potential adaptation of these spaces within the framework of modern urban development.

### 3.3. Socio-Historical Analysis

In recent decades, there has been a noticeable rise in public interest in Belgrade's underground heritage, driven by a combination of interconnected socio-historical factors. Firstly, urban expansion and renewed interest in alternative spaces within the city fabric have created a demand for the revitalization of neglected or forgotten underground structures. This is particularly evident in municipalities such as Zemun<sup>4</sup> and Stari Grad<sup>5</sup>, where the

<sup>4</sup> Zemun is today a municipality of Belgrade, historically a separate town situated on the right bank of the Danube River, with a strong Austro-Hungarian architectural and cultural influence, distinct from Belgrade's Ottoman and later Serbian urban layers.

<sup>5</sup> Stari Grad (Old Town) is the historic core of Belgrade, located at the confluence of the Sava and Danube rivers, characterized by its layered urban fabric that includes Roman, Ottoman, and Serbian heritage.

concentration of historical wine cellars and storage facilities is the highest. At the same time, increasing ecological and cultural awareness among citizens and professionals has led to a new valorization of these spaces as potential cultural, touristic, and communal assets. A trend has emerged toward transforming former military and industrial facilities into public and commercial venues such as museums, galleries, wine cellars, and cultural centers. From a historical perspective, most of these underground structures originate from the Austro-Hungarian and Ottoman periods, which further enhances their cultural and historical value and their potential integration into collective memory narratives. On the other hand, a significant number of structures are in a state of collapse or neglect, indicating uneven preservation policies but also highlighting opportunities for intervention and investment. Technological advancements and the growing popularity of urban exploration, along with the development of new mapping and evaluation methodologies—such as the concept of Underground Built Heritage (UBH)—are contributing to the institutionalization of this topic within urban planning, conservation strategies, and cultural policy.

In summary, underground structures have evolved beyond their original, often forgotten functions to become subjects of growing social, professional, and political interest. This shift opens up new possibilities for their protection, adaptive reuse, and integration into the contemporary urban life of Belgrade.

#### 4. DISCUSSION

It should first be noted that the implementation of this research was constrained by specific factors that influenced the scope, accessibility, and depth of the analysis of Belgrade's underground architectural heritage in the following ways:

- **Institutional barriers and restricted access:** Entry to certain structures was either impossible or severely limited due to their classification as closed, secured, or military-controlled zones, particularly those managed by the Ministry of Defense and the Ministry of Internal Affairs.
- **Incomplete historical documentation:** A significant portion of structures built before the 20th century is inadequately documented, complicating precise reconstruction of their original functions, configurations, and transformations over time.
- **Limited digitalization of archives:** The lack of access to digital archival resources further complicated the consolidation of data, especially concerning legal status, functional use, and ownership of underground structures.
- **Temporal limitation of data:** The study included only structures documented up to the year 2018, meaning that more recent underground interventions and constructions were not part of the analysis.
- **Undocumented sites and oral traditions:** There is a likelihood that additional underground structures exist, yet remain undiscovered and are passed down only through oral history and local narratives. Although not included in the formal research scope, these elements represent a valuable basis for future investigations.
- **Presentation constraints:** Due to the volume of material and spatial constraints of this work, it was not possible to present the entire database or the full results of the graphical analyses. Nevertheless, key findings and conclusions are discussed in the "Discussion" section, accompanied by a critical review of the results.

These limitations do not undermine the relevance or validity of the research, but they must be considered when interpreting the results and planning subsequent research or intervention phases.

The integration of Belgrade's underground structures into sustainable urban development requires a clearly defined balance between the preservation of cultural heritage and the fulfillment of the city's contemporary needs. Research findings indicate that underground facilities—particularly the lagums in Zemun and storage spaces in Stari Grad—hold significant potential for revitalization. However, their current condition (39.63% collapsed and 25.61% neglected) highlights an urgent need for systematic mapping and digital documentation, as proposed by Costa et al. [9]. These findings also confirm the challenges outlined in the "Study on the Development of Urban Underground Spaces" [18], which notes that underground structures remain largely excluded from Belgrade's strategic spatial planning frameworks.

UNESCO's Historic Urban Landscape (HUL) approach [8] advocates a holistic view of integrating subsurface spaces into the broader urban context, relieving pressure on surface infrastructure while contributing to the

preservation of spatial identity. In this sense, Belgrade could alleviate the strain on its above-ground assets by incorporating and functionally rehabilitating segments of its underground infrastructure—particularly those structures with cultural, historical, or touristic value. However, the current legal framework in Serbia remains fragmented and only partially addresses this domain. The Law on Cultural Heritage [19] recognizes underground structures as part of immovable cultural assets but lacks clear guidelines for their adaptive reuse. Similarly, the Law on Planning and Construction [20] does not provide concrete tools for incorporating underground spaces into spatial planning documents, while the Law on Emergency Situations [21] addresses shelters purely from a safety perspective, overlooking their historical and cultural significance. The Rulebook on Specific Conditions for Establishing Institutions for the Protection of Cultural Heritage [22] and the Rulebook on the Content, Manner, and Procedure of Developing Spatial and Urban Planning Documents [23] leave room for interpretation but are seldom directly applied to underground structures.

International authors such as Peng [24], Li [25] and Bobylev [26] emphasize the importance of underground spaces as assets for sustainable development—not only for transport and utility infrastructure, but also as spatial reserves for new cultural, educational, and commercial functions. Belgrade's underground structures, particularly those in Zemun, Stari Grad, and Čukarica, could be strategically repurposed to support local economic development and tourism. The 2024 study [18] further highlights the absence of mechanisms for categorizing underground spaces based on usability and infrastructural capacity. It critically notes the lack of a centralized database and standardized criteria for identifying potential, risks, and degrees of endangerment. Despite the formally stated need for underground integration, actual implementation remains limited by institutional barriers, fragmented jurisdiction, and the absence of a coherent financial framework.

However, as Zhang et al. [27], emphasize, the creation of plans alone is insufficient without clear implementation mechanisms, institutional coordination, and public engagement. To date, Belgrade has not developed a comprehensive database of underground structures, nor does it possess a strategy for their valorization and activation. An analysis of international case studies—such as Lisbon, Paris, and Tokyo—demonstrates that the successful integration of underground heritage depends on the existence of a regulatory framework that fosters collaboration among urban planners, archaeologists, ecologists, and technological innovators. In Belgrade, such a multidisciplinary approach has yet to be systematized. The authors of the 2024 study [18] suggest that the most urgent step is the development of pilot projects in municipalities with the highest concentration of underground structures (Zemun, Stari Grad), aligning with recommendations from international literature [28] [24].

An additional challenge lies in the unresolved issue of jurisdiction. The study emphasizes the need to clearly define whether the management of underground spaces falls under the authority of local governments, the Institute for the Protection of Cultural Monuments, or a dedicated agency. The absence of an integrated management system leads to institutional passivity, leaving many significant underground structures outside the scope of urban development processes.

The geological characteristics of Belgrade—comprising layers of loess, limestone, clay, and sandstone—present both a challenge and an opportunity for the further understanding and classification of underground structures. Materials such as loess exhibit a higher tendency toward collapse, while structures built in limestone are generally well-preserved and stable. In this context, the digitalization and 3D mapping of the subsurface emerge as crucial steps toward improved planning and utilization of these spaces.

In addition to technical and legal aspects, attention must also be given to intangible values—collective memory, legends, and urban myths associated with these structures. Authors such as Heyns [6] and Pace [17] emphasize the importance of involving the local community in planning and decision-making processes. In Belgrade, this could be implemented through pilot projects or initiatives such as "living labs," particularly in areas of the city with a pronounced historical memory.

Also, Belgrade possesses a rich and diverse stock of underground structures that—if properly valorized—could contribute to relieving surface-level urban pressure, enhancing the city's cultural offer, and increasing its functional resilience, as illustrated by international examples from Lisbon, Madrid, or Kyoto. However, without reform of the legal framework, the creation of a functional registry, financial support, and pilot adaptation programs, this potential remains marginalized. To unlock it, clear management strategies, adequate financial backing, and, crucially, strong socio-political will are essential. In this context, the "Urban Underground Space Development Study" represents an important step toward institutional awareness, but it must be followed by concrete regulatory, budgetary, and urban planning measures [18].

Finally, to move from descriptive mapping to concrete planning, an evaluation framework was developed and presented (Table 1). This framework operationalizes the reuse potential of historical underground structures through explicit criteria, enabling planners to establish priorities for interventions in future planning. Such a methodology aims to achieve comprehensive and systemic urban planning.

*Table 1. Evaluation Framework for Reuse Potential of Underground Structures*

Criterion	Description	Indicators / Parameters	Possible Values
<b>Physical condition</b>	Degree of preservation of the structure	Conserved / Active / Neglected / Collapsed	Active / Neglected / Collapsed
<b>Geological stability</b>	Subsoil type and construction material	Loess / Limestone / Clay / Sandstone	Stable / Unstable
<b>Historical-cultural value</b>	Cultural and symbolic importance of the structure	Heritage status / Local significance / None	High / Medium / Low
<b>Location and accessibility</b>	Position within the city and accessibility to users/visitors	Central / Peripheral / Easily accessible / Remote	Easily accessible / Limited access
<b>Reuse potential</b>	Suitability for adaptive reuse in a contemporary context	Tourism / Cultural / Commercial / Civic functions	High / Limited
<b>Regulatory framework</b>	Legal status and planning documentation	Cultural heritage site / No status / Planning act	Protected / Unprotected

This model can be applied to a comparative analysis between two or more types of structures. For example, Zemun's wine cellars (lagumi), despite their deteriorated condition and unstable loess geology, demonstrate exceptional cultural and touristic reuse potential. Conversely, storage facilities in Stari Grad, built in limestone and partially conserved, represent a more immediate and feasible opportunity for adaptive reuse into museums or cultural centers. This comparison can be visualized in Table 2.

*Table 2. Evaluation Framework for Two Comparative Case Studies*

Criterion	Description	Indicators / Parameters	Example (Zemun – Wine Cellars)	Example (Stari Grad – Storage Facilities)
<b>Physical condition</b>	Degree of preservation and usability without major interventions	Active / Conserved / Neglected / Collapsed	Mostly neglected or collapsed, approx. 65%	Partially conserved, some repurposed
<b>Geological stability</b>	Stability of subsoil and construction material	Loess / Limestone / Clay / Sandstone	Loess – prone to collapse, requiring remediation	Limestone – more stable, suitable for reuse
<b>Historical-cultural value</b>	Cultural and symbolic significance for the local and wider community	Monument status / Local significance / None	High historical and touristic value	High cultural value (trade, urban heritage)
<b>Location and accessibility</b>	Position within the urban fabric and accessibility for visitors/services	Central / Peripheral / Easily accessible	Good accessibility within Zemun urban core	Central location – Old Town
<b>Reuse potential</b>	Suitability for new functions in a contemporary context	Cultural / Touristic / Commercial / Civic	High potential for tourism and wine-related uses	High potential for museums and galleries
<b>Regulatory framework</b>	Legal status and planning instruments for protection/adaptation	Cultural heritage site / No status / Planned	Partial protection, lacking clear planning tools	Protected sites, but no reuse guidelines



Based on the evaluation framework (Table 1), a priority ranking of reuse potential was established (Table 3). This ranking allows planners to distinguish between high-priority structures that can immediately contribute to cultural and touristic development (e.g., wine cellars in Zemun, storage facilities in Stari Grad) and those with medium or low potential requiring long-term strategies (e.g., bunkers in Čukarica, mines in Rakovica, shelters in Palilula and Voždovac).

*Table 3. Priority Ranking of Reuse Potential for Belgrade's Underground Structures*

Location / Type	Physical Condition	Cultural Significance	Geological Stability	Reuse Potential	Priority
<b>Zemun – Wine Cellars (Lagumi)</b>	Neglected / Collapsed	High	Loess – unstable	Tourism, wine routes, cultural functions	<b>High</b> (with remediation)
<b>Stari Grad – Storage Facilities</b>	Conserved / Partially active	High	Limestone – stable	Museums, galleries, cultural centers	<b>High</b>
<b>Čukarica – Bunkers</b>	Partially preserved	Medium	Mixed substrate	Educational and memorial centers	<b>Medium</b>
<b>Rakovica – Mines</b>	Partially collapsed	Medium	Clay / Limestone	Industrial heritage, thematic parks	<b>Medium</b>
<b>Voždovac – Shelters</b>	Active / Conserved	Low	Clay – moderately stable	Civic / Safety functions	<b>Low</b>
<b>Palilula – Shelters</b>	Neglected	Low	Limestone	Limited technical potential	<b>Low</b>

## 5. CONCLUSION

Belgrade possesses a layered heritage of underground structures—lagums, bunkers, shelters, mines, and storage spaces—that represent a significant yet overlooked asset within the city's urban fabric. Analysis shows that the largest concentration and surface area of these structures are found in Zemun and Stari Grad, primarily built during the Austro-Hungarian period within loess and limestone formations. Unfortunately, more than 65% of them are currently in a state of neglect or collapse, highlighting a lack of systematic care and a clearly defined institutional framework. At the same time, the Study on the Development of Urban Underground Spaces in Belgrade emphasizes the urgent need to recognize these spaces not as infrastructural burdens, but as urban resources.

A key challenge in the revitalization of underground spaces lies in the legal and planning vacuum: although the Law on Cultural Heritage recognizes certain structures as cultural monuments, there are no guidelines for their adaptive reuse or integration into contemporary urban planning. In practice, current spatial plans almost entirely overlook the existence of these structures, preventing their contribution to relieving public surface space or fostering tourism and cultural development. Moreover, the lack of coordination between the heritage protection sector and infrastructure management further delays any concrete interventions.

The solution lies in initiating institutional and operational mechanisms that place the underground realm at the forefront of spatial and cultural development. It is essential to establish specialized teams for mapping, evaluation, and management of subterranean structures, alongside the implementation of digital databases and the active involvement of local communities through participatory models. Adaptive reuse pilot projects—such as the transformation of lagums into museum spaces—can serve as replicable models for broader application. Ultimately, Belgrade's underground spaces have the potential not only to contribute to the preservation of the city's identity, but also to become catalysts for its sustainable development—provided they are properly integrated into urban planning strategies and public policies.

Belgrade's underground cannot be fully understood without considering its deeply rooted socio-historical context. Over the centuries, the city's subterranean structures have been shaped by complex interactions among military, political, economic, and cultural forces. The lagums in Zemun date back to the Austro-Hungarian period, originally serving as wine and goods storage facilities, while bunkers, shelters, and mines across other municipalities

emerged during turbulent eras such as World War II, socialist industrialization, and the Cold War. These structures are not merely technical installations—they are physical embodiments of collective memory, reflecting the shifts in Belgrade's urban identity, from a commercial crossroads to a city continuously shaped by political and security pressures.

For this reason, the revitalization of these spaces should not be viewed solely as a functional or aesthetic task, but rather as a socio-cultural project. Shaped by wars, political regimes, trade routes, and everyday life, Belgrade's underground structures hold the potential to become educational and symbolic spaces of memory and identity. Their adaptive reuse—as museums, galleries, public spaces, or even climate-resilient infrastructure—can bridge the city's past and present, adding meaningful value for the local community. The preservation and activation of these sites must therefore be guided by an awareness of their cultural and historical significance, fostering a balance between urban development and respect for the city's layered heritage.

As a synthesis of the findings and a step toward practical applicability, Tables 1 and 2 present an evaluation framework and a priority ranking for the reuse potential of Belgrade's underground structures. These tools are not only intended to guide immediate planning interventions but also to serve as a methodological reference for future research.

## 6. ACKNOWLEDGMENTS

The authors extend their sincere gratitude to Mr. Zoran Lj. Nikolić and Mr. Vidoje D. Golubović, authors of the book *Belgrade Beneath Belgrade*, for their outstanding fieldwork, enthusiasm, and perseverance in documenting Belgrade's underground structures. Their research and publishing efforts represent not only a valuable source for academic and professional analysis, but also a significant step toward the popularization of underground urban heritage for cultural and tourism purposes. Their book, conceived as a journey through the historical layers beneath the city, inspires the broader public to perceive Belgrade as a multilayered historical organism—both above and below ground.

## 7. REFERENCES

- [1] W. Broere, „Urban underground space: Solving the problems of today's cities,” *Tunnelling and Underground Space Technology*, t. 55, pp. 245-248, 2016.
- [2] C. Delmastro, E. Lavagno i L. Schranz, „Underground urbanism: Master Plans and Sectorial Plans,” *Tunnelling and Underground Space Technology*, t. 55, pp. 103-111, 2016.
- [3] P. Maire, P. Blunier, A. Parriaux i L. Tacher, „Underground Planning and Optimisation of The Underground Resources' Combination Looking For Sustainable Development in Urban Areas,” u *Going Underground: Excavating the Subterranean City*, Manchester, Salford University and Centre for the Study of Cities and Regions, 2007, pp. 1-15.
- [4] H.-Q. Li, A. Parriaux, P. Thalmann i X.-Z. Li, „An integrated planning concept for the emerging underground urbanism: Deep City Method Part 1 concept, process and application,” *Tunnelling and Underground Space Technology*, t. 38, p. 559-568, 2013.
- [5] S. Mielbya, I. Eriksson, S. D. Campbell i D. Lawrence, „Opening up the subsurface for the cities of tomorrow - The subsurface in the planning process,” *Procedia Engineering* 209 (2017) 12-25, t. 209, pp. 12-25, 2017.
- [6] A. C. L. Heyns, L. Harper i N. Bertram, „The undergrounds' underground: strategies for mapping what is both covered and invisible,” u *Proceedings of the Annual Design Research Conference 2019: Real/Material/Ethereal*, Melbourne: Monash University, 2020, 2020.
- [7] H. Admiraal i A. Cornaro, „Why underground space should be included in urban planning policy – And how this will enhance an urban underground future,” *Tunnelling and Underground Space Technology*, t. 55, pp. 214-220, 2016.
- [8] UNESCO, „RECOMMENDATION ON THE HISTORIC URBAN LANDSCAPE,” u *General Conference of UNESCO at its 36th session*, Paris, 2011.
- [9] C. S. Costa, M. Menezes, P. I. Radovanova, T. Ruchinskaya, K. Lalenis i M. Bocci, „Planning Perspectives and Approaches for Activating Underground Built Heritage,” *Sustainability*, t. 13, p. Article No 10349, 2021.
- [10] R. Varriale, „Underground Built Heritage: A Theoretical Approach for the Definition of an International Class,” *Heritage*, t. 4, p. 1092-1118, 2021.
- [11] C. R. Ortloff, „Water engineering at Petra (Jordan): recreating the decision process underlying hydraulic engineering of the Wadi Mataha pipeline system,” *Journal of Archaeological Science*, t. 44, pp. 91-97, 2014.
- [12] E. D. Chiotis, „Tunnel and ventilation design of the Eupalinos' aqueduct in Samos, Greece,” *The International Journal for the History of Engineering & Technology*, t. 94, br. 2, pp. 108-128, 2024.

- [13] O. Aydana i R. Ulusay, „Geotechnical and geoenvironmental characteristics of man-made underground structures in Cappadocia, Turkey,“ *Engineering Geology*, t. 69, br. 3-4, pp. 245-272, 2003.
- [14] S. M. Strenacikova i J. M. Strenacikova, „Mysterious Roman catacombs: The study of early Christian burials and faith symbols,“ *Theory and history of Culture and Art*, t. 17, br. 4, pp. 619-634, 2024.
- [15] R. Sandford, „Thinking with heritage: Past and present in lived futures,“ *Futures*, t. 111, pp. 71-80, 2019.
- [16] Y.-K. Qiao, F.-L. Peng, Y. Liu i Y.-C. Zhang, „Balancing conservation and development in historic cities by underground solutions,“ u 4th Annual International Conference on Urban Planning and Property Development (UPPD 2018), Singapore, 2018.
- [17] G. Pace i R. Salvarani, *Underground Built Heritage Valorisation - A Handbook*, Roma: Cnr Edizioni, 2021.
- [18] URBEL, *Study of Urban Planning Development in the Underground Space of the City of Belgrade*, Belgrade: Urban Planning Institute of Belgrade, 2024.
- [19] R. o. S. Official Gazette, „Law on Cultural Heritage, No. 71/1994, 52/2011 (other laws), 99/2011 (other law), 6/2020 (other law), 35/2021 (other law), 129/2021 (other law), and 76/2023 (other law).,“ Republic of Serbia, Belgrade, 1994.
- [20] R. o. S. Official Gazette, „Law on Planning and Construction, No. 72/2009, 81/2009 (corr.), 64/2010 (CC decision), 24/2011, 121/2012, 42/2013 (CC decision), 50/2013 (CC decision), 98/2013 (CC decision), 132/2014, 145/2014, 83/2018, 31/2019, 37/2019 (other law), 9/2020, 52/2021, and,“ Republic of Serbia, Belgrade, 2009.
- [21] R. o. S. Official Gazette, „Law on Emergency Situations, No. 111/2009, 92/2011, and 93/2012,“ Republic of Serbia, Belgrade, 2009.
- [22] R. o. S. Official Gazette, „Rulebook on Detailed Conditions for Commencing Work and Performing Activities of Cultural Heritage Protection Institutions, No. 21/1995 and 67/2022 – other rulebook,“ Republic of Serbia, Belgrade, 1995.
- [23] R. o. S. Official Gazette, „Rulebook on the Content, Manner, and Procedure for the Preparation of Spatial and Urban Planning Documents, No. 32/2019 and 47/2025,“ Republic of Serbia, Belgrade, 2019.
- [24] F.-L. Peng, Y.-K. Qiao, S. Sabri, B. Atazadeh i A. Rajabifard, „A collaborative approach for urban underground space development toward sustainable development goals: Critical dimensions and future directions,“ *Frontiers of Structural and Civil Engineering*, t. 15, br. 1, pp. 20-45, 2021.
- [25] X. Li, H. Xu, C. Li, L. Sun i R. Wang, „Study on the demand and driving factors of urban underground space use,“ *Tunnelling and Underground Space Technology*, t. 55, pp. 52-59, 2016.
- [26] N. Bobylev, „Mainstreaming sustainable development into a city’s Master plan: A case of Urban Underground Space use,“ *Land Use Policy*, t. 26, pp. 1128-1137, 2009.
- [27] M. Zhang, Z. Xie i L. He, „Does the scarcity of urban space resources make the quality of underground space planning more sustainable? A case study of 40 urban underground space master plans in China,“ *Frontiers in Environmental Science*, p. 10:966157, 2022.
- [28] C. Paraskevopoulou, A. Cornaro, H. Admiraal i A. Paraskevopoulou, „Underground space and urban sustainability: an integrated approach to the city of the future,“ u *Changing Cities IV Spatial Design, Landscape and socioeconomic dimensions*, June 2019, Crete, Greece, Iraklion, 2021.

## **OVERCOMING CHALLENGES IN TUNNELING AND UNDERGROUND DESIGN AND CONSTRUCTION**

## STUDY ON THE INFLUENCE OF MECHANICAL PROPERTIES OF FIBER REINFORCED CONCRETE ON PERFORMANCE OF PRECAST TUNNEL SEGMENTS

Fan Zhang<sup>1</sup>, Wouter De Corte<sup>2</sup>, Xian Liu<sup>3</sup>, Yihai Bao<sup>4</sup>, Luc Taerwe<sup>5</sup>

**Abstract:** Reinforced concrete (RC) segments rebars partially replaced by fibers have attempted to prove superior performance in some studies, but the research on how the mechanical parameters of fiber reinforced concrete (FRC) ( $f_{R1}$  and  $f_{R3}$  according to the fib Model Code) and remaining rebars affect the segment properties is still limited. Moreover, when considering both the serviceability and ultimate states of the segments, multiple factors need to be studied to ensure that the FRC segments with rebars (RC-FRC segments) can be truly superior to the RC segments. For this purpose, based on numerical models verified by four-point bending tests on RC-FRC segments, this paper uses numerical simulations to explore the influence of FRC mechanical parameters and the amount of reinforcement on various segment properties such as stiffness, crack width, yield load, ultimate load, ductility, and safety reserve. A total of 92 simulations were conducted, combining different parameters: two RC segments with rebar areas 1.006 mm<sup>2</sup> and 2.454 mm<sup>2</sup>, and ninety RC-FRC segments with rebars partially replaced by FRC (3MPa, 5MPa, 7MPa of  $f_{R1}$ , and 0.5, 0.9, 1.3 of  $f_{R3}/f_{R1}$ , combining with five levels of remained rebar areas for each RC segment). Additionally, a modified FRC constitutive model was used to make the simulation more accurate when the crack width is small. The simulation results indicate that, the more of the rebars remained, the larger are the segment stiffness, yield load and ultimate load, but in all cases the ductility and safety reserve are negligibly influenced. As for FRC, the larger of the  $f_{R1}$ , the larger are the segment stiffness, yield load, ultimate load and safety reserve, and the smaller the crack width, but it has a negligible effect on the ductility. The larger of the  $f_{R3}/f_{R1}$  ratio, especially when it is larger than 0.9, the larger are the ultimate load, safety reserve and ductility, but it does not affect the stiffness and yield load of the segment. The study indicates that to ensure the performance of RC-FRC segments, the mechanical properties of the FRC and the replaced rebars should be carefully determined. Furthermore, it is recommended to replace the rebars with FRC that has a high  $f_{R1}$  value and a  $f_{R3}/f_{R1}$  ratio larger than 0.9, to enhance the toughness of the segment.

**Keywords:** FRC segment, residual strength, stiffness, bearing capacity, ductility

### 1. INTRODUCTION

With the wide implementation of the tunnel boring machine for the construction of subway and other tunnels, the shield tunnel method has been used very often. As the main load-bearing component of shield tunnel lining<sup>6</sup>, the mechanical performance of the segment directly affects the safety and durability of the tunnel lining. In recent years, fiber-reinforced concrete (FRC) has been increasingly used in shield tunnel segments, such as São Paulo Metro Line 5 (de Andrade et al., 2024) [1], Barcelona Line 9 subway (de la Fuente et al., 2012) [3], Brenner Base

<sup>1</sup> MSc, Fan Zhang, PhD student, College of Civil Engineering, Tongji University, 1239 Siping Road, Shanghai 200092, China, Department of Structural Engineering and Building Materials, Ghent University, Technologiepark Zwijnaarde 60, 9052 Ghent, Belgium, FanZhang@tongji.edu.cn

<sup>2</sup> PhD, Wouter De Corte, Professor, Department of Structural Engineering and Building Materials, Ghent University, Technologiepark Zwijnaarde 60, 9052 Ghent, Belgium, wouter.decorte@ugent.be

<sup>3</sup> PhD, Xian Liu, Professor, College of Civil Engineering, State Key Laboratory for Hazard Reduction in Civil Engineering, Tongji University, 1239 Siping Road, Shanghai 200092, China, xian.liu@tongji.edu.cn

<sup>4</sup> PhD, Yihai Bao, Professor, Department of Civil and Systems Engineering, Johns Hopkins University, Baltimore, MD 21218, USA, ybao11@jh.edu

<sup>5</sup> PhD, Luc Taerwe, Professor, College of Civil Engineering, Tongji University, 1239 Siping Road, Shanghai 200092, China, Department of Structural Engineering and Building Materials, Ghent University, Technologiepark Zwijnaarde 60, 9052 Ghent, Belgium, luc.taerwe@ugent.be

<sup>6</sup> Shield tunnel lining: it means “the precast concrete segmental liner” installed in the back of the tunnel boring machine as ground support as the machine advances.



Tunnel (Caratelli et al., 2011) [18], the thermal tunnels in Copenhagen (Kasper et al., 2008) [4] and Shenzhen, China (Cui et al., 2022) [5], because it allegedly performs better in terms of crack resistance, ductility, and ability to improve the whole lifecycle performance of tunnel lining while reducing cost (de la Fuente et al., 2017) [2].

FRC is made by mixing steel fibers, polypropylene fibers, basalt fibers, etc., and plain concrete (PC). There are various methods to evaluate the performance of FRC. For example, ASTM C1609/C1609M (2024) [6] and ASTM C1550-20 (2020) [7] evaluate performance based on post-crack energy absorption, while EN14651 (2007) [8] and RILEM TC 162 TDF (2003) [9] use post-crack residual strength. Regardless of the evaluation methods, they are all based on post-crack performance, since fibers influence crack initialization and development due to their ability to bridge cracks. The fib Model Code for concrete structures 2020 (MC2020) [10] further classifies FRC according to its residual strengths  $f_{R1}$  (when the crack mouth opening displacement (CMOD) is 0.5 mm) and  $f_{R3}$  (when CMOD is 2.5 mm), obtained by the three-point bending test of the notched beam (EN14651 (2007) [8])(Table 1). This classification makes it possible to select FRC by strength grade, which is similar to selecting rebar and bolts in structural design, making it more convenient to design an FRC structure. Moreover, MC2020 stipulates that for structure,  $f_{R1}$  must be greater than  $0.4f_{ct}$  (tensile strength), and  $f_{R3}/f_{R1}$  must be greater than 0.5. The Chinese standard for FRC segments (GB/T 38901-2020) [11] further specifies that when the rebar in the reinforced concrete segments (RC segments) is partially replaced by FRC (RC-FRC segments), the FRC classification must be greater than or equal to 3a, and when the rebar is fully replaced, the classification must be greater than or equal to 3c (refer to Table 1 for specific mechanical properties). These standards have further promoted the application of FRC in tunnel segments. However, there are still difficulties in engineering applications, mainly due to three issues: how to select suitable FRC, how many rebars can be replaced by FRC, and whether the mechanical performance of the RC-FRC segment with the rebar partially replaced meets the requirements and technical and performance specifications.

**Table 1.** Classification of FRC according to MC2020

Classification index 1	$f_{R1}$	Classification index 2	$f_{R3}/f_{R1}$
1	$1 \text{ MPa} \leq f_{R1} < 1,5 \text{ MPa}$	a	$0,5 \leq f_{R3}/f_{R1} < 0,7$
1,5	$1,5 \text{ MPa} \leq f_{R1} < 2 \text{ MPa}$	b	$0,7 \leq f_{R3}/f_{R1} < 0,9$
2	$2 \text{ MPa} \leq f_{R1} < 2,5 \text{ MPa}$	c	$0,9 \leq f_{R3}/f_{R1} < 1,1$
2,5	$2,5 \text{ MPa} \leq f_{R1} < 3 \text{ MPa}$	d	$1,1 \leq f_{R3}/f_{R1} < 1,3$
3	$3 \text{ MPa} \leq f_{R1} < 3,5 \text{ MPa}$	e	$1,3 \leq f_{R3}/f_{R1}$
N	...		

\*Example: 4c means  $4 \text{ MPa} \leq f_{R1} < 4,5 \text{ MPa}$ , and  $0,9 \leq f_{R3}/f_{R1} < 1,1$ .

Although there has already been some research on the FRC subject matter, most studies have predominantly focused on the crack width and bearing capacity, and these studies were made on segments with specific rebars replaced by a specific FRC. There was a lack of systematic parametric analysis on different FRC and replaced rebars, and analysis on stiffness, ductility and bearing strength reserve. de Andrade et al. (2024) [1] demonstrated the feasibility of partially replacing steel reinforcement with FRC through experimental and numerical methods, by evaluating parameters such as crack spacing and width, as well as ultimate load capacity. Liu et al. (2020) [12] employed FRC with fiber grades 3,5c and 4c to partially replace steel reinforcement. The results showed that the load-bearing capacity at a crack width of 0,2 mm and the ultimate load capacity were comparable to those of conventional RC segments, while the stiffness of the FRC segments was significantly improved. Zheng et al. (2020) [13] used FRC with a fiber content of 0,45 % to replace 55 % of the steel reinforcement, resulting in an enhanced load-bearing capacity compared to RC segments. Similarly, Conforti et al. (2017, 2019) [14][15] reported improved segment performance when using FRC of grade 2e to partially replace steel reinforcement. However, Tengilimoglu & Akyuz (2020) [16] observed a significant reduction in flexural performance when 60 % of the steel reinforcement was replaced with FRC of classification 1c.

Segments made with steel reinforcement entirely replaced by FRC can be considered a special case. Although FRC segments without rebars have been successfully applied in certain engineering projects, such as the water conveyance tunnel inner lining reported by Zhou et al. (2025) [17], which demonstrated superior performance compared to RC inner linings, the load bearing capacity has been found insufficient when used as primary load bearing components (Caratelli et al., 2011, Abbas et al., 2014) [18][19]. These studies, while valuable, often emphasize specific aspects and lack a comprehensive systematic analysis, making it difficult for engineers to determine whether FRC segments can meet the full range of engineering requirements.

To address these limitations, this study conducts an extensive parametric analysis by using numerical simulations to investigate the influence of varying residual strengths of FRC and different reinforcement areas on the mechanical performance of RC-FRC segments with reinforcement partially replaced. The parameters examined include stiffness, crack width, yield load, ultimate load, safety reserve, and ductility. The numerical model is validated against experimental results and incorporates an improved post-cracking trilinear constitutive model for FRC to more accurately reflect its performance at the serviceability limit state (SLS). The findings aim

to provide designers with a comprehensive understanding of the mechanical performance of RC-FRC segments under both SLS and ultimate limit states (ULS), and suggest how to select suitable FRC according to the residual strength.

## 2. RC-FRC SEGMENT NUMERICAL MODEL

### 2.1. Simulation sets

To investigate the influence of residual strength parameters of FRC and the amount of replaced reinforcement on various mechanical properties of RC-FRC segments—including stiffness, load-bearing capacity, and ductility—this study developed a series of simulation sets.

Preliminary analyses indicated that the effect of FRC becomes more obvious when the reinforcement ratio of the segment is relatively low. Therefore, this study is based on segments designed corresponding to tunnel depths of 15 m and 25 m in a certain city, with longitudinal reinforcement diameters of 16 mm and 25 mm, respectively. To reduce computational time, a half-segment model was adopted in the simulations. Each segment model includes five longitudinal rebars on both intrados and extrados. The reinforcement areas of the reference RC segments are  $1.006 \text{ mm}^2$  and  $2.454 \text{ mm}^2$ , respectively. For the RC-FRC segments, the reinforcement area was reduced incrementally by  $200 \text{ mm}^2$  in each simulation case.

With respect to the residual strengths of FRC, according to the classification in MC2020 and the requirement in [GB/T 38901-2020](#) [11], FRC should at least be 3a. On the other hand, based on experimental experience, FRC with a fiber content of  $55 \text{ kg/m}^3$  typically achieves an  $f_{R1}$  value of approximately 7 MPa, while the ratio  $f_{R3}/f_{R1}$  rarely exceeds 1.3. In practical engineering applications, it is also challenging to increase the fiber content beyond this level for structural fiber. In light of these considerations, the simulations in this study adopt FRC with  $f_{R1}$  values of 3 MPa, 5 MPa, and 7 MPa, and  $f_{R3}/f_{R1}$  ratios of 0.5, 0.9, and 1.3.

The simulation sets for RC-FRC segments are presented in Table 2. In this table, each RC-FRC segment scenario is defined by a unique combination of reinforcement area and FRC residual strengths, resulting in a total of 90 simulation cases. Including the two reference cases of RC segments, a total of 92 simulation sets were analysed. The RC-FRC segments with a reinforcement area smaller than  $1000 \text{ mm}^2$  will be compared with the RC segment with a reinforcement area of  $1006 \text{ mm}^2$ , set as group 1, and the other RC-FRC segments will be compared with the RC segment with a reinforcement area of  $2454 \text{ mm}^2$ , set as group 2. Additionally, a simulation according to the test in [Zhang et al. \(2025a\)](#) [20] was made, to verify if the simulation model is correct.

**Table 2.** Simulation sets

	RC segments	RC-FRC segments with the rebar partially replaced				
Rebar area ( $\text{mm}^2$ )	1.006	806	606	406	206	6
	2.454	2.254	2.054	1.854	1.654	1.454
$f_{R1}$ (MPa)	0	3MPa	5MPa	7MPa		
$f_{R3}/f_{R1}$ (MPa)	0	0,5	0,9	1,3		

### 2.2. Simulation model

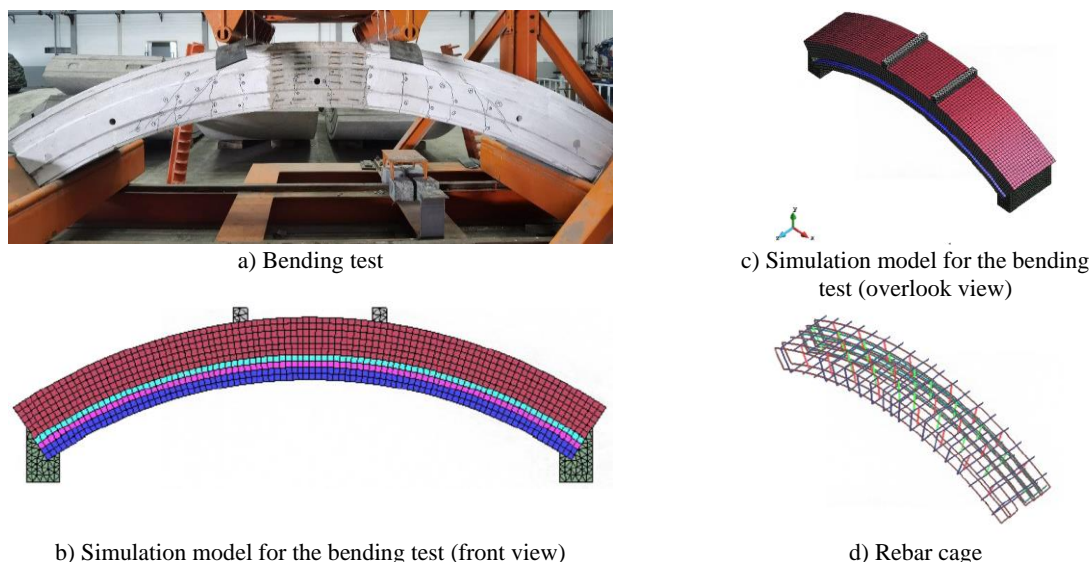
#### 2.2.1. Model information

All the models were developed based on the experimental segment tested by [Zhang et al. \(2025a\)](#) [20]. The segment has a width of 750 mm, a thickness of 400 mm, an outer diameter of 6.900 mm, and an angle of  $67,5^\circ$ . Four-point bending test was adopted. The distance between the loading beams is 900 mm, and the span between the rotational centers of the supports is 3.389 mm.

In the numerical model, the concrete was modelled using hexahedral solid elements with an element size of 40 mm. The supports and loading beams were modelled using tetrahedral solid elements, also with an element size of 40 mm. Reinforcement was modelled by embedded linear elements. In the verification model, the number and the location of reinforcement rebars were consistent with the experimental setup. In the parametric analysis models, five longitudinal rebars were uniformly distributed, with stirrups spaced at 180 mm intervals.

Both the loading beams and supports were connected to the segment using fixed contacts. The left support was constrained in all translational degrees of freedom, while the right support was constrained in all translational degrees of freedom except for the X-axis. All rotational degrees of freedom were left unconstrained. The load was applied to the top surface of the loading beam to simulate the experimental loading process, continuing until the segment failure occurred.

Additionally, in the experiment conducted by [Zhang et al. \(2025a\)](#) [20], a concrete weak region was observed at a position 80-120 mm from the intrados due to the bundled two rebars. This led to the development of circumferential cracking in that region during testing. To replicate this behavior in the validation model, a weak region was set there, with the concrete strength set to 42 % of the other regions. In contrast, for the parametric analysis models, the concrete strength was assumed to be uniform throughout the entire segment.



**Figure 1.** The bending test and the simulation model

### 2.2.2. Constitutive model

In the numerical model, both the rigid supports and loading beams were modelled as linearly elastic materials with an elastic modulus of 200 GPa.

The reinforcement was modelled using a bilinear constitutive model. Before yielding, the steel exhibited an elastic modulus of 200 GPa. The yield strength was set to 400 MPa, and after yielding, the ultimate tensile strain was defined as 0,025, corresponding to a post-yield strength of 420 MPa.

To more accurately capture the tensile behavior of FRC under SLS, characterized by small crack widths, this study adopts an improved post-cracking trilinear tensile constitutive model proposed by [Zhang et al. \(2025b\)](#) [21]. As illustrated in Figure 2, this model is a modification of the constitutive curve defined in the MC2020, where the original curve OABCDE is refined to OABC'DE. The parameters of each point in the improved model are calculated using the formulas provided in Table 3. In these formulas,  $f_{ct}$  denotes the tensile strength of concrete, and  $E_c$  is the elastic modulus of concrete. In the verification model, due to the use of C60 concrete,  $f_{ct}$  is taken as 2,85 MPa and  $E_c$  as 36.000 MPa. In the parametric analysis models, C50 concrete is assumed, with the value of  $f_{ct}$  2,64 MPa and the value of  $E_c$  34.500 MPa. The compressive strength of concrete,  $f_{cm}$ , is set to 48 MPa in the verification model based on experimental results, and 32,4 MPa in the parametric analysis models according to [GB 50010-2010](#) [23]. The residual strengths  $f_{R1}$  and  $f_{R3}$  are 4,73 MPa and 5,29 MPa in the verification model, while in the parametric analysis models, they are assigned according to the values listed in Table 2. The characteristic length  $l_{cs}$ , which corresponds to the element size, is set to 40 mm.

The addition of fibers enhances the post-peak ductility of concrete under compression. Therefore, the constitutive model for FRC in compression must be capable of capturing this ductile behavior. However, current codes do not provide a standardized compressive constitutive model specifically for FRC. Some researchers have proposed compressive models for steel fiber reinforced concrete based on parameters such as fiber length, diameter, and content. In this study, the compressive constitutive model of FRC is proposed by [Lu et al. \(2017\)](#) [22], which was developed through fitting experimental data. The details of the constitutive model can be found in [Lu et al. \(2017\)](#) [22].

However, there is no research has established a clear relationship between the residual tensile strength and the compressive ductility of FRC. As a result, once the residual tensile strength is defined, a corresponding compressive constitutive model cannot be directly determined. Nevertheless, based on the constitutive model proposed by [Lu et al. \(2017\)](#) [22] and the steel fiber properties reported in the experiment by [Zhang et al. \(2025a\)](#) [20], it can be calculated that when the fiber content increases from 15 kg/m<sup>3</sup> to 55 kg/m<sup>3</sup>, the strain corresponding to post-peak compressive stress when it is half of the compressive strength increases only slightly—from 0,01 to 0,012 (Figure 3). This variation is relatively small and is approximately three times the strain observed in plain concrete when its strength drops to half of its compressive strength.

Therefore, a unified post-peak compressive constitutive model is adopted for all FRC with different residual strengths. Specifically, after reaching the peak compressive strength, the concrete strength is assumed to decrease linearly to 50 % of the peak value, with the corresponding strain set to three times that of plain concrete at the same strength reduction level. At this point, the concrete is considered to have completely failed, and the structure is assumed to be incapable of sustaining further load. The detailed constitutive parameters are provided in Table 4.

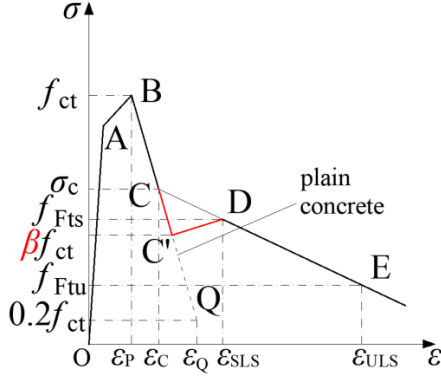


Figure 2. Diagram of the concrete constitutive model in tension

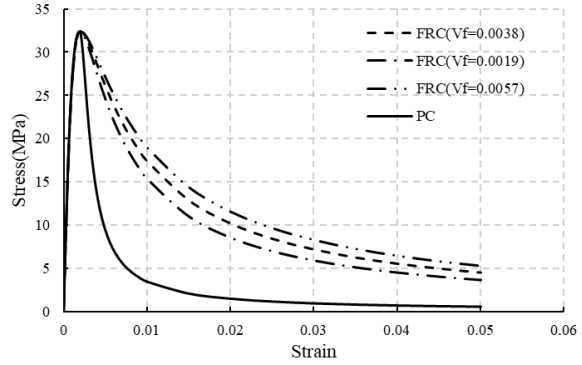


Figure 3. Diagram of the concrete constitutive model in compression

Table 3. Calculation equations for the concrete constitutive model in tension

Points	Stress	Strain
Point A	$\sigma_A = 0.9f_{ct}$	$\varepsilon_A = \sigma_A/E$
Point B	$\sigma_B = f_{ct}$	$\varepsilon_B = 0.00015$
Point C'	$\sigma_{C'} = 0.8f_{Fts}$	$\varepsilon_{C'} = \frac{\varepsilon_Q - \varepsilon_B}{\sigma_Q - \sigma_B} \cdot (\sigma_{C'} - \sigma_B) + \varepsilon_B$
Point D	$\sigma_D = f_{Fts} = 0.37f_{R1}$	$\varepsilon_D = \varepsilon_{SLS} = CMOD_1/l_{cs}$
Point E	$f_{Ftu} = f_{Fts} - \frac{2.5}{CMOD_3} (f_{Fts} - 0.57f_{R3} + 0.26f_{R1})$	$\varepsilon_D = \varepsilon_{ULT} = 2.5/l_{cs}$
Point Q	$\sigma_Q = 0.2f_{ct}$	$\varepsilon_Q = 0.085f_{cm}^{0.18}/f_{ct}l_{cs} + \varepsilon_B - 0.8f_{ct}/E_c$

Table 4. Constitutive parameters for concrete

	Verification model	PA model
$f_{ct}$	2.85 MPa	2.64 MPa
$f_{cm}$	48 MPa	32.4 MPa
$E_c$	36000 MPa	34500 MPa
$f_{R1}$	4.73 MPa	Table 2
$f_{R3}$	5.29 MPa	Table 2
$\varepsilon_{cu} (PC)$	0.0046	0.0036
$\varepsilon_{cu} (FRC)$	0.0135	0.0112

### 3. SIMULATION RESULTS

#### 3.1. Verification of numerical model

##### 3.1.1. Verification of constitutive model

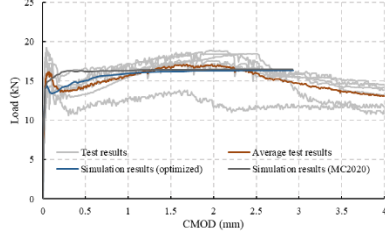
To simulate the tensile behavior of FRC, an optimized post crack trilinear constitutive model was employed. To validate this model, a notched FRC beam was simulated under a three-point bending test, following the experimental setup of Zhang (2025a) [20]. The modelling approach is consistent with that described by Zhang et al. (2025b) [21], and the material parameters were assigned according to Table 4. The simulation results are presented in Figure 4.

The simulation result is compared with the test results (Zhang et al., 2025a) [20] and the simulation result by using the post crack bilinear constitutive model in MC2020. As shown in the figure, the optimized trilinear model provides a more accurate response to FRC behavior under small crack openings. In contrast, the bilinear model proposed in MC2020 tends to overestimate the tensile performance of FRC. Therefore, the use of the optimized constitutive model enables a more reliable assessment of the structural performance of FRC segments under SLS.

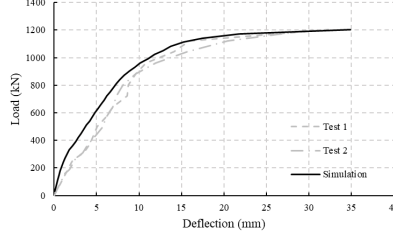


### 3.1.2. Verification of the segment under bending

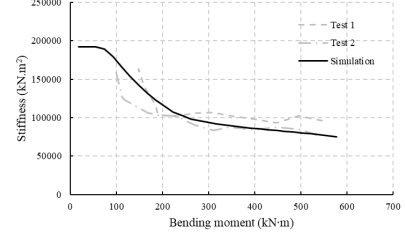
Following the experimental loading steps, the load–mid-span deflection curve is presented in Figure 5. Additionally, the average concrete strain within a region of approximately 558 mm around mid-span was extracted to calculate the flexural stiffness of the segment. The resulting stiffness–bending moment curve is shown in Figure 6. As shown in the two figures, both the simulated deflection and the stiffness evolution closely match the experimental results, confirming the accuracy of the simulation model.



**Figure 4.** Simulation results for the notched beam with optimised post-cracking trilinear model



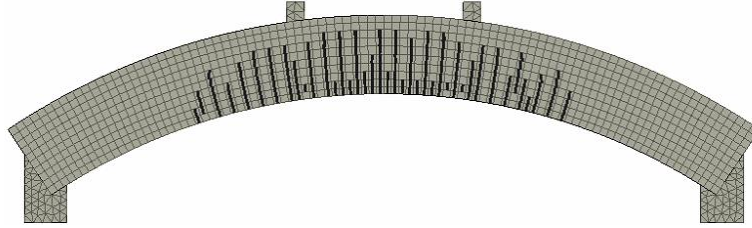
**Figure 5.** Comparison of simulation and test deflection curves



**Figure 6.** Comparison of simulation and test stiffnesses

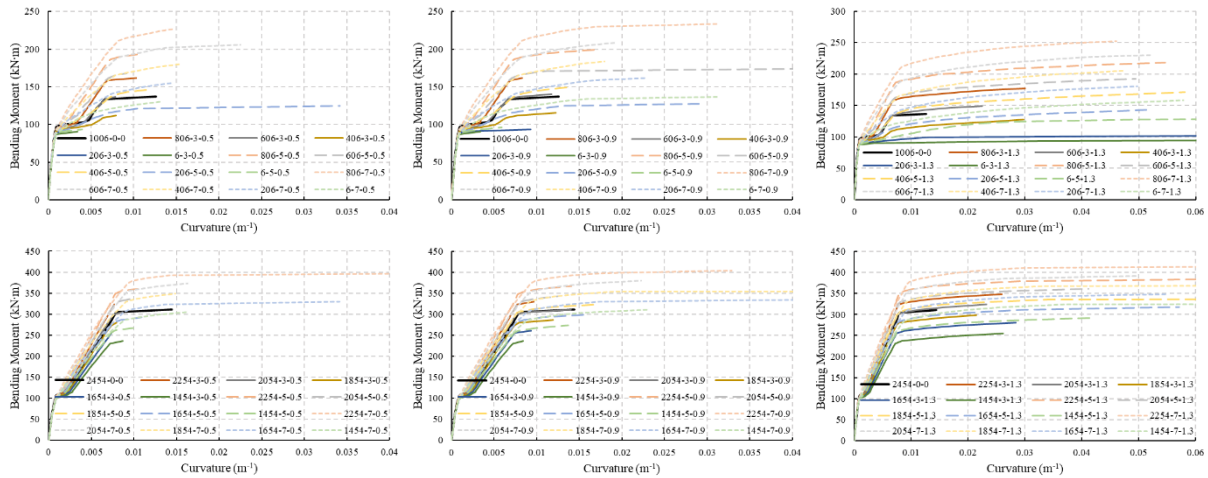
### 3.2. Simulation results of RC-FRC segments

The RC-FRC segments failed because of the bending cracks (Figure 7), which were the same for each simulation set.



**Figure 7.** Crack pattern of segments

Using the same method as aforementioned, the average strain within the pure bending region at the middle span was extracted to calculate the curvature of the segment. The resulting bending moment–curvature curves for RC-FRC segments with different FRC residual strengths and rebar areas are shown in Figure 8. In the figure, each simulation case is labelled as  $a-b-c$ , where  $a$  represents the reinforcement area,  $b$  denotes the value of  $f_{R1}$ , and  $c$  indicates the ratio  $f_{R3}/f_{R1}$ .



**Figure 8.** Bending moment – curvature curves of different simulation groups

As shown in Figure 8, depending on the combination of the remained reinforcement area and FRC residual strengths, the load-bearing capacity of RC-FRC segments may perform better or worse than that of RC segments. However, the segment response under bending can generally be divided into four stages: (1) elastic stage before



cracking, (2) post-cracking stage until the load can be borne stably, (3) stable load-bearing stage until the rebar yields, and (4) yield stage until reaching the ultimate load.

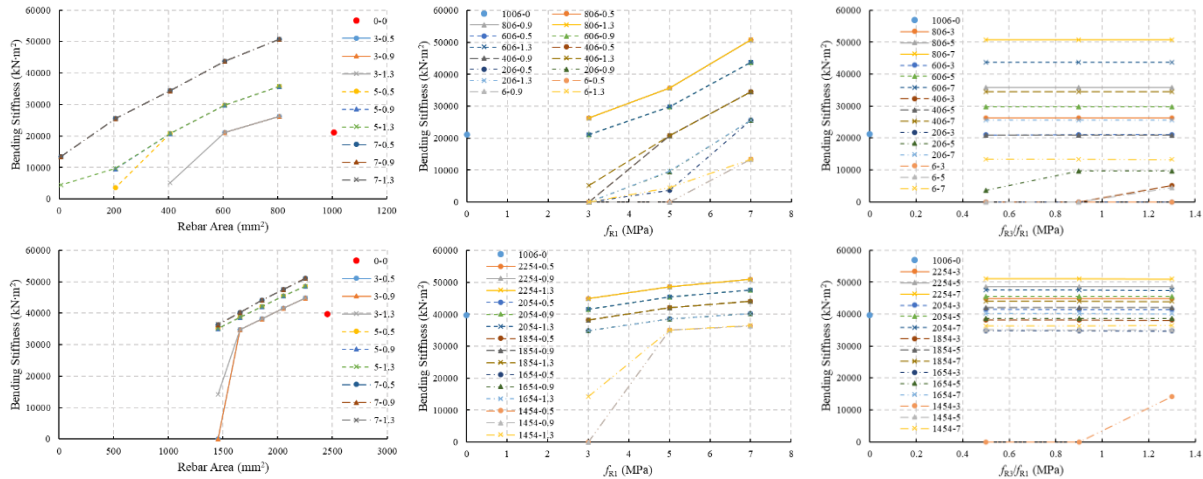
In the elastic stage, curvature increases linearly with load. Due to the reduced reinforcement in RC-FRC segments, the concrete carries more tensile force. Since fibers do not increase the tensile strength of concrete, the cracking load of RC-FRC segments is slightly lower than that of RC segments. In the second stage, curvature increases rapidly under relatively small loads because of crack initiation; however, this effect diminishes as  $f_{R1}$  and  $f_{R3}$  values increase. During the third stage, curvature again increases approximately linearly with load. After reinforcement yields, curvature grows rapidly with increasing load until the ultimate load is reached.

## 4. ANALYSIS AND DISCUSSION

### 4.1. Analysis of the bending stiffness

The bending stiffness of the segment is defined as the bending moment divided by the curvature.

Since tunnel segments typically service with cracks, the bending stiffness at 124 kN·m and 249 kN·m before the rebars yielding was extracted and compared with RC segments having reinforcement areas of 1.006 mm<sup>2</sup> and 2.454 mm<sup>2</sup>, respectively. Using a controlled variable method, where only one parameter (reinforcement area,  $f_{R1}$  or  $f_{R3}/f_{R1}$ ) is varied at a time, the influence of each parameter on the bending stiffness of RC-FRC segments was analyzed. The bending stiffness of RC-FRC segments under different reinforcement areas and FRC residual strengths is shown in Figure 9.



a) The curves of segment stiffness versus reinforcement area (for the legend a-b, a represents the value of  $f_{R1}$ , and b represents the ratio  $f_{R3}/f_{R1}$ ; 0 denotes the RC segment)  
b) The curves of segment stiffness versus  $f_{R1}$  (for the legend a-b, a represents the reinforcement area, and b represents the ratio  $f_{R3}/f_{R1}$ ; 0 denotes the RC segment)  
c) The curves of segment stiffness versus  $f_{R3}/f_{R1}$  (for the legend a-b, a represents the reinforcement area, and b represents  $f_{R1}$ ; 0 denotes the RC segment)

**Figure 9.** The curves of the segment stiffness versus different parameters

As shown in Figure 9, the bending stiffness increases approximately linearly with both the reinforcement area and the value of  $f_{R1}$ , while is negligibly influenced by the ratio of  $f_{R3}/f_{R1}$ . When the FRC residual strengths are the same, increasing the reinforcement area reduces the strain in each rebar under the same load, consequently, resulting in a reduction in segment curvature and an increase in bending stiffness.

Regarding the residual strength of FRC,  $f_{R1}$  represents the mechanical performance of FRC at a crack width of 0.5 mm. Since the behavior of FRC at crack widths below 0.5 mm is primarily governed by  $f_{R1}$ , a higher  $f_{R1}$  indicates better crack control and smaller deformation under the same load. As cracks in the segment are typically smaller than 0.5 mm before yielding, increasing  $f_{R1}$  leads to an enhancement in bending stiffness.

In contrast, the ratio  $f_{R3}/f_{R1}$  primarily determines the value of  $f_{R3}$ , which reflects the mechanical performance of FRC at a crack width of 2.5 mm. Since cracks in the segment generally do not reach this width before rebar yielding, the value of  $f_{R3}/f_{R1}$  has a negligible effect on the segment's bending stiffness.

## 4.2. Analysis of the crack width

Taking group 2 with the RC segment with the reinforcement area of 2.454 mm<sup>2</sup> as an example, the crack width at a bending moment of 249 kN·m was extracted for comparison. Using the same controlled variable method, the influence of different parameters on the crack width of RC-FRC segments was analyzed, as shown in Figure 10.

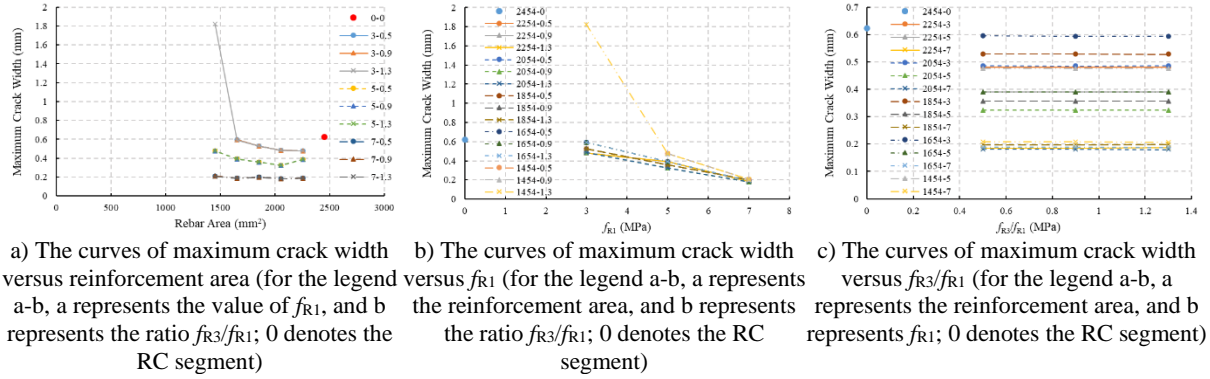


Figure 10. The curves of the maximum crack width versus different parameters

As shown in Figure 10, the maximum crack width of the segment decreases approximately linearly with increasing reinforcement area and the value of  $f_{R1}$ , while it is negligibly influenced by the ratio of  $f_{R3}/f_{R1}$ . When the FRC residual strengths are the same, increasing the reinforcement area reduces the stress carried by each rebar under the same load, thereby resulting in narrower cracks.

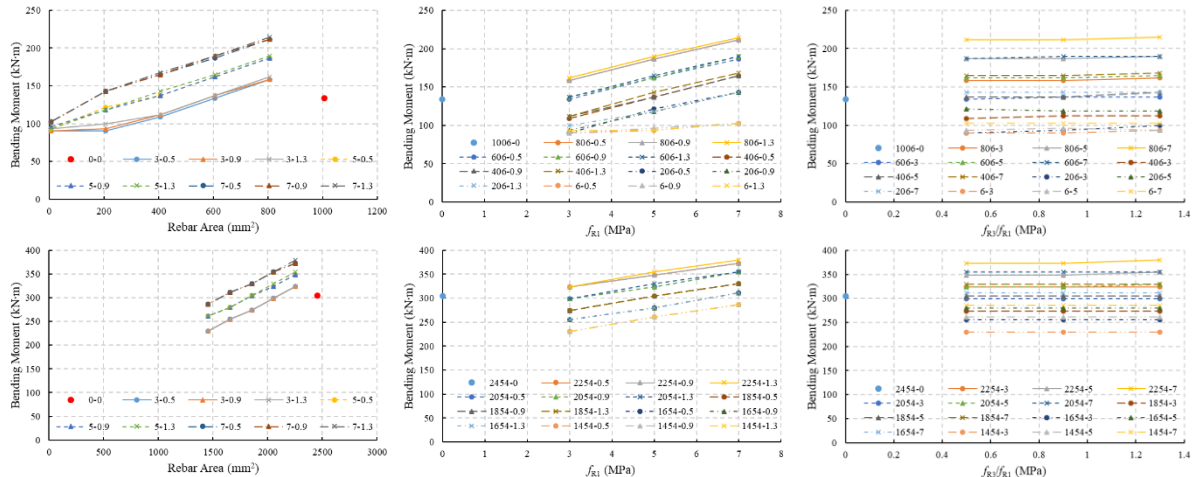
Regarding the residual strengths of FRC, a higher  $f_{R1}$  means a better crack control ability when the crack width is smaller than 0,5mm, leading to smaller cracks under the same load. As shown in Figure 10, under a bending moment of 249 kN·m, the maximum crack width in most cases remains smaller than 0,5 mm. Therefore, increasing  $f_{R1}$  effectively reduces the maximum crack width.

In contrast, the ratio of  $f_{R3}/f_{R1}$  primarily determines the mechanical performance of FRC when the crack width is larger than 2,5 mm. Since the crack width in the segment typically remains smaller than 0,5 mm before yielding, the value of  $f_{R3}/f_{R1}$  has a negligible effect on the maximum crack width.

## 4.3. Analysis of the yield load

The yield load of the RC-FRC segments was extracted and analyzed using the same controlled variable method, as shown in Figure 11. The yield load of the segment increases approximately linearly with both the reinforcement area and the value of  $f_{R1}$ , while is negligibly influenced by the ratio of  $f_{R3}/f_{R1}$ . When the FRC residual strengths are the same, increasing the reinforcement area means the rebar can bear more load. As a result, a higher yield load can be obtained.

Regarding the FRC residual strengths, a higher  $f_{R1}$  means the FRC can bear more load before the crack reaches 0,5mm. Since crack widths typically remain smaller than 0,5 mm before reinforcement yielding, the increase of  $f_{R1}$  results in a larger yield load. In contrast, the ratio of  $f_{R3}/f_{R1}$  primarily determines the mechanical performance of FRC when the crack width is larger than 2,5 mm, thus it has a negligible effect on the yield load.

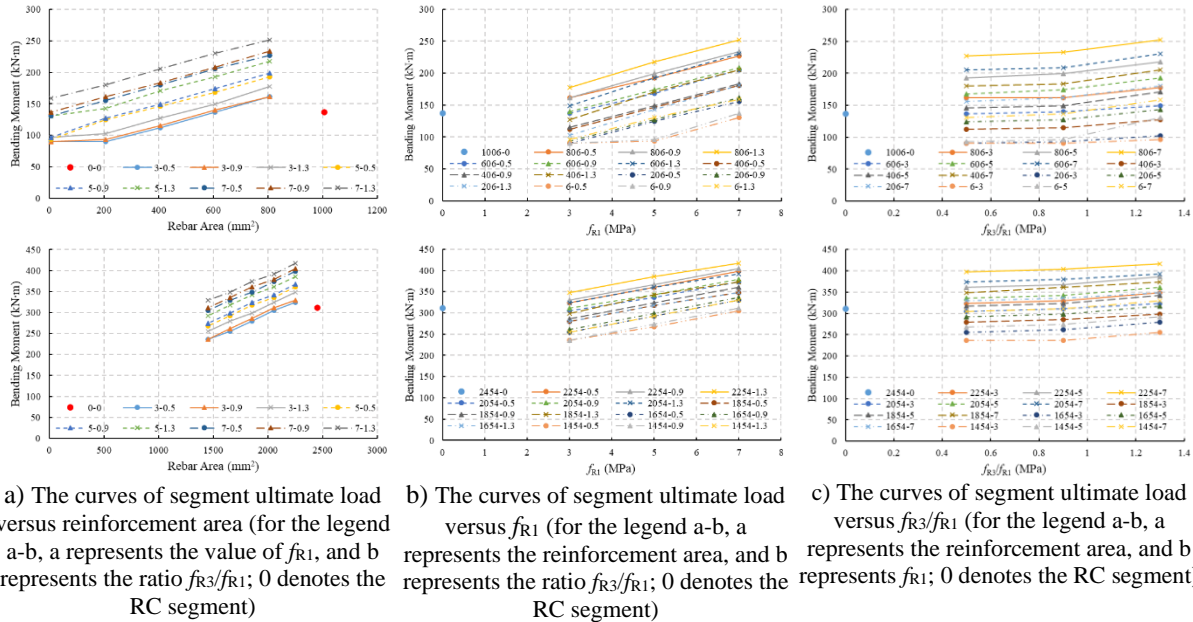


- a) The curves of segment yield load versus reinforcement area (for the legend a-b, a represents the value of  $f_{R1}$ , and b represents the ratio  $f_{R3}/f_{R1}$ ; 0 denotes the RC segment)
- b) The curves of segment yield load versus  $f_{R1}$  (for the legend a-b, a represents the reinforcement area, and b represents the ratio  $f_{R3}/f_{R1}$ ; 0 denotes the RC segment)
- c) The curves of segment yield load versus  $f_{R3}/f_{R1}$  (for the legend a-b, a represents the reinforcement area, and b represents  $f_{R1}$ ; 0 denotes the RC segment)

**Figure 11.** The curve of the segment yield load versus different parameters

#### 4.4. Analysis of the ultimate load

The ultimate load of the RC-FRC segments was extracted and analysed using the same controlled variable method, as shown in Figure 12. The ultimate load increases approximately linearly with both the reinforcement area and the value of  $f_{R1}$ , following the same trend observed for the yield load. In addition, an increase in the ratio of  $f_{R3}/f_{R1}$  also leads to an increase in the ultimate load, particularly when  $f_{R3}/f_{R1}$  exceeds 0.9. This is because, before failure, the crack width typically exceeds 0.5 mm, and the FRC enters the residual strength range governed by  $f_{R3}/f_{R1}$ . Therefore, a larger  $f_{R3}/f_{R1}$  enhances the segment's ultimate load. Moreover, when  $f_{R3}/f_{R1}$  exceeds 0.9, the FRC exhibits noticeable strain hardening behavior, which further contributes to the increase in ultimate load. Nevertheless, the influence of the reinforcement area and  $f_{R1}$  remains more significant in terms of the magnitude of improvement.



**Figure 12.** The curves of the segment ultimate load versus different parameters

#### 4.5. Analysis of the safety reserve

If a structure can bear more load after yielding (which may be caused by some accidents), this structure can be safer in engineering. Therefore, the safety reserve is defined as the difference between the ultimate load and the yield load, to reflect the safety of the structure under accidents. The safety reserve of the RC-FRC segment under different reinforcement areas and FRC residual strengths is shown in Figure 13. The safety reserve increases approximately linearly with increasing of  $f_{R1}$ , and also with increasing of  $f_{R3}/f_{R1}$ , particularly when  $f_{R3}/f_{R1}$  is larger than 0.9. In contrast, the reinforcement area has a negligible effect on the safety reserve.

Before reinforcement yielding, crack widths typically remain smaller than 0.5 mm. Therefore, with the increase of  $f_{R1}$ , the ultimate load can be increased. Besides, the values of  $f_{R1}$  and  $f_{R3}/f_{R1}$  both determine the strength of FRC when the crack is larger than 0.5mm, thus both the larger values of  $f_{R1}$  and  $f_{R3}/f_{R1}$  can enhance the ultimate load, resulting in an increase of safety reserve. Additionally, when  $f_{R3}/f_{R1}$  is larger than 0.9, the FRC exhibits noticeable stress hardening, which significantly contributes to the increase in safety reserve.

Since the reinforcement has a limited stress increase after yielding, but with large strain increasing, increasing the reinforcement area has a limited effect on the ultimate load, thus the reinforcement area has a negligible effect on the safety reserve. This also results in the safety reserve of RC-FRC segments being significantly higher than that of RC segments.

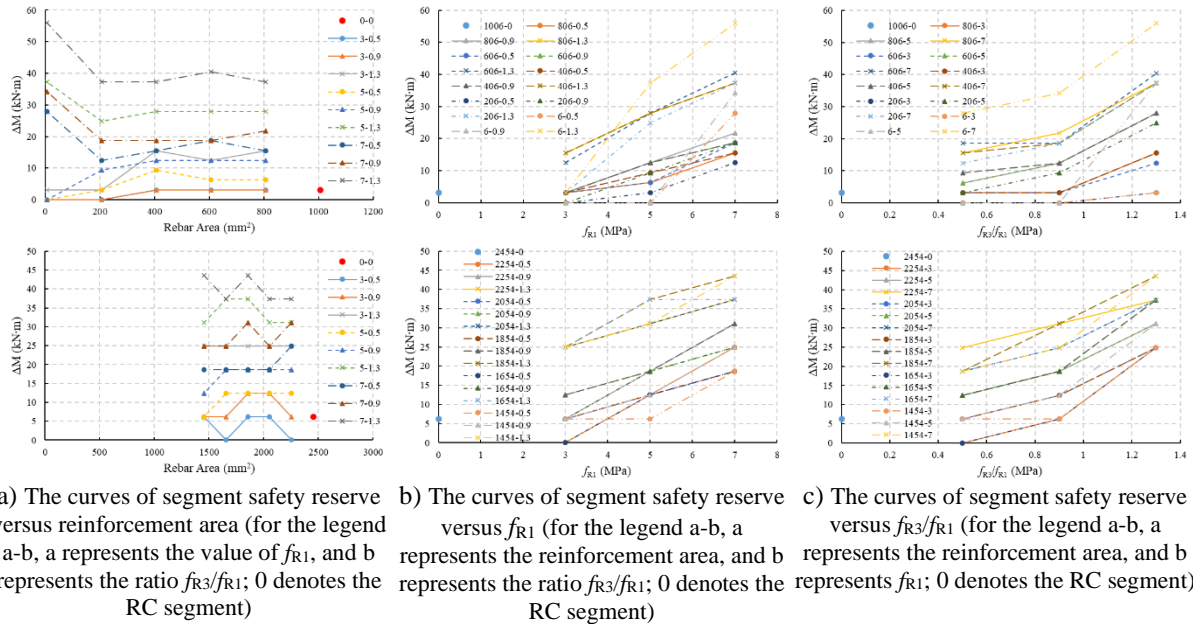


Figure 13. The curves of the segment safety reserve versus different parameters

#### 4.6. Analysis of the ductility

While safety reserve reflects structural safety from a load-bearing perspective, structural safety is also closely related to the deformation capacity after yielding—i.e., ductility. In this study, ductility is defined as the ratio of curvature at ultimate load to curvature at yield load. The ductility of RC-FRC segments under different reinforcement areas and FRC residual strengths is shown in Figure 14.

Small increments in load may result in large increases in deformation when the load is close to the ultimate load. This can lead to noticeable variation in the calculated ultimate curvature, resulting in slight fluctuations in the ductility curves.

As shown in Figure 14, reinforcement area and  $f_{R1}$  have limited influence on segment ductility, while the value of  $f_{R3}/f_{R1}$  has a significant effect when it exceeds 0.9. As discussed above, reinforcement area and  $f_{R1}$  primarily affect the yield point. Although the  $f_{R1}$  has some effect on the segment after yielding, the value of  $f_{R3}/f_{R1}$  is the most important parameter that improves the performance at the ultimate state, especially when it is larger than 0.9, a stress-hardening behavior will be exhibited, which means the material has good ductility, consequently, improves the ductility of RC-FRC segment.

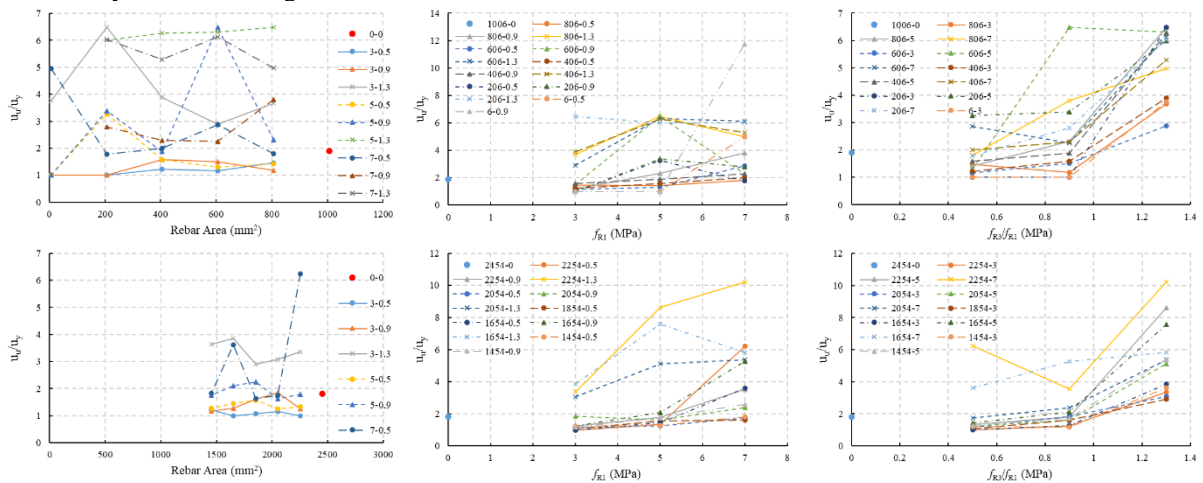


Figure 14. The curves of the segment ductility versus different parameters

The influence of different parameters on the mechanical performance of RC-FRC segments is summarized in Table 5. Both the reinforcement area and the value of  $f_{R1}$  have a noticeable impact on bending stiffness, crack width, yield load, and ultimate load, but a negligible effect on ductility. The reinforcement area has negligible influence on the safety reserve, whereas the value of  $f_{R1}$  has a considerable effect. The ratio of  $f_{R3}/f_{R1}$  has negligible influence on bending stiffness, crack width, and yield load; however, when it exceeds 0,9, it has a noticeable impact on ultimate load, safety reserve, and ductility.

**Table 5.** The degree of influence of different parameters on the mechanical performances of segments with rebars partially replaced by FRC

	Stiffness	Crack width	Yield strength	Ultimate strength	Strength reserve	Ductility
Rebar area	Noticeable	Noticeable	Noticeable	Noticeable	Negligible	Negligible
$f_{R1}$	Noticeable	Noticeable	Noticeable	Noticeable	Noticeable	Negligible
$f_{R3}/f_{R1}$	Negligible	Negligible	Negligible	Noticeable when it is larger than 0,9	Noticeable when it is larger than 0,9	Noticeable when it is larger than 0,9

In addition, the safety reserve of RC-FRC segments is consistently no lower than that of RC segments. However, for bending stiffness, yield load, ultimate load, and ductility, both higher and lower situations appear. This indicates that there exists an optimal combination of reinforcement area and residual strengths for RC-FRC segments, under which all mechanical properties can meet or exceed those of RC segments.

Considering the influence of FRC residual strengths on segment performance, it is recommended to select FRC with a relatively high  $f_{R1}$  and a  $f_{R3}/f_{R1}$  ratio larger than 0,9. This combination can effectively enhance the overall mechanical performance of the structure. The larger the  $f_{R1}$ , the more rebars can be replaced, and the more fibers are needed. However, since the costs of rebars and fibers differ, designers should consider both the improvements in mechanical properties and the associated cost. By weighing these factors, they can determine the optimal  $f_{R1}$  value.

## 5. CONCLUSION

Based on the verification of the numerical model against experimental results, a parametric analysis of the mechanical performance of RC-FRC segments was conducted using an optimized trilinear tensile constitutive model for FRC. The following conclusions can be drawn:

1) The optimized post-cracking trilinear constitutive model for FRC more accurately captures the mechanical behavior of structural FRC under small crack widths and is, therefore, more suitable for evaluating the performance of FRC structures at the serviceability limit state.

2) With increasing reinforcement area, the bending stiffness, yield load and ultimate load of RC-FRC segments with rebar partially replaced increase approximately linearly, while the maximum crack width decreases. However, the safety reserve and ductility are negligibly affected.

3) With increasing  $f_{R1}$ , the bending stiffness, yield load, ultimate load and safety reserve of RC-FRC segments with rebar partially replaced increase approximately linearly, and the maximum crack width decreases. The ductility is negligibly affected.

4) The ratio of  $f_{R3}/f_{R1}$  has a negligible effect on bending stiffness, maximum crack width, and yield load. However, when it is larger than 0,9, the ultimate load, safety reserve, and ductility of the RC-FRC segment are significantly improved due to the stress-hardening behavior of FRC.

5) It is recommended to use FRC with a relatively high  $f_{R1}$  and a  $f_{R3}/f_{R1}$  ratio larger than 0,9 in structural applications to maximize the mechanical performance of the RC-FRC segment with rebar partially replaced.

There is an optimal combination between the remained reinforcement area and the residual strengths of FRC in RC-FRC segments. Further research is needed to determine this optimal combination.

## 6. ACKNOWLEDGEMENTS

The first author would like to express his appreciation for the scholarship from the China Scholarship Council (No. 202306260206) for his study at Ghent University.



## 7. REFERENCES

- [1] de Andrade, G. G., de Figueiredo, A. D., Galobardes, I., da Silva, M. A. A. P., de la Fuente, A., & Bitencourt, L. A. G. (2024). Experimental and numerical investigation of flexural behavior of precast tunnel segments with hybrid reinforcement. *Tunnelling and Underground Space Technology*, 154, 106094. <https://doi.org/10.1016/j.tust.2024.106094>
- [2] de la Fuente, A., Blanco, A., Armengou, J., & Aguado, A. (2017). Sustainability-based approach to determine the concrete type and reinforcement configuration of TBM tunnels linings: Case study of extension line to Barcelona Airport T1. *Tunnelling and Underground Space Technology*, 61, 179-188. <https://doi.org/10.1016/j.tust.2016.10.008>
- [3] de la Fuente, A., Pujadas, P., Blanco, A., & Aguado, A. (2012). Experiences in Barcelona with the use of fibres in segmental linings. *Tunnelling and Underground Space Technology*, 27(1), 60-71. <https://doi.org/10.1016/j.tust.2011.07.001>
- [4] Kasper, T., Edvardsen, C., Wittneben, G., & Neumann, D. (2008). Lining design for the district heating tunnel in Copenhagen with steel fibre reinforced concrete segments. *Tunnelling and Underground Space Technology*, 23(5), 574-587. <https://doi.org/10.1016/j.tust.2007.11.001>
- [5] Cui, H., Li, Y., Bao, X., Tang, W., Wang, S., & Chen, X. (2022). Thermal performance and parameter study of steel fiber-reinforced concrete segment lining in energy subway tunnels. *Tunnelling and Underground Space Technology*, 128, 104647. <https://doi.org/10.1016/j.tust.2022.104647>
- [6] American Society for Testing and Materials. (2024). Standard test method for flexural performance of fiber-reinforced concrete (using beam with third-point loading (ASTM C1609/C1609M-24). ASTM International.
- [7] American Society for Testing and Materials. (2020). Standard test method for flexural toughness of fiber reinforced concrete (using centrally loaded round panel) (ASTM C1550-20). ASTM International.
- [8] European Committee for Standardization. (2007). Test method for metallic fibre concrete—Measuring the flexural tensile strength (limit of proportionality (LOP), residual) (EN 14651:2005+A1:2007).
- [9] RILEM TC 162-TDF. (2003). Test and design methods of steel fiber reinforced concrete. *Materials and Structures*, 36, 560-567.
- [10] International Federation for Structural Concrete. (2024). fib Model Code for concrete structures 2020.
- [11] Standardization Administration of China. (2020). Fiber reinforced concrete shield segments (GB/T 38901-2020).
- [12] Liu, X., Sun, Q., Yuan, Y., & Taerwe, L. (2020). Comparison of the structural behavior of reinforced concrete tunnel segments with steel fiber and synthetic fiber addition. *Tunnelling and Underground Space Technology*, 103, 103506. <https://doi.org/10.1016/j.tust.2020.103506>
- [13] Zheng, A., Xu, B., & Chen, X. (2020). Study on reliability of steel fiber reinforced concrete segments of metro in marine strata. *Modern Tunnelling Technology*, 57(4), 52-58.
- [14] Conforti, A., Tiberti, G., Plizzari, G. A., Caratelli, A., & Meda, A. (2017). Precast tunnel segments reinforced by macro-synthetic fibers. *Tunnelling and Underground Space Technology*, 63, 1-11. <https://doi.org/10.1016/j.tust.2016.12.005>
- [15] Conforti, A., Trabucchi, I., Tiberti, G., Plizzari, G. A., Caratelli, A., & Meda, A. (2019). Precast tunnel segments for metro tunnel lining: A hybrid reinforcement solution using macro-synthetic fibers. *Engineering Structures*, 199, 109628. <https://doi.org/10.1016/j.engstruct.2019.109628>
- [16] Tengilimoglu, O., & Akyuz, U. (2020). Experimental study on hybrid precast tunnel segments reinforced by macro-synthetic fibres and glass fibre reinforced polymer bars. *Tunnelling and Underground Space Technology*, 106, 103612. <https://doi.org/10.1016/j.tust.2020.103612>
- [17] Zhou, W.-D., Zhang, D.-M., Bu, X.-H., & Wang, X.-H. (2025). Mechanical behaviour of double lining with outer segmental lining and inner fibre reinforced concrete lining under internal water pressure. *Tunnelling and Underground Space Technology*, 155(1), 106151. <https://doi.org/10.1016/j.tust.2024.106151>
- [18] Caratelli, A., Meda, A., Rinaldi, Z., & Romualdi, P. (2011). Structural behaviour of precast tunnel segments in fiber reinforced concrete. *Tunnelling and Underground Space Technology*, 26(2), 284-291. <https://doi.org/10.1016/j.tust.2010.10.003>
- [19] Abbas, S., Soliman, A. M., & Nehdi, M. L. (2014). Experimental study on settlement and punching behavior of full-scale RC and SFRC precast tunnel lining segments. *Engineering Structures*, 72, 1-10. <https://doi.org/10.1016/j.engstruct.2014.04.024>
- [20] Zhang, F., De Corte, W., Taerwe, L., Cao, W., & Liu, X. (2025a). A Study on the Bending Stiffness of Reinforced Concrete Tunnel Segments with Added Steel Fibers. *Materials*, 18(1), 48. <https://doi.org/10.3390/ma18010048>
- [21] Zhang, F., De Corte, W., Liu, X., Bao, Y., & Taerwe, L. (2025b). A Modified Trilinear Post-Cracking Model for Fiber-Reinforced Concrete to Improve the Evaluation of the Serviceability Limit State Performance. *Materials*, 18(7), 1395. <https://doi.org/10.3390/ma18071395>
- [22] Lu, X., Zhang, Y., & Nian, X. (2017). Experimental study on stress-strain curves for high-strength steel fiber reinforced concrete under monotonic and repeated compressive loadings. *Journal of Building Structures*, 38(1), 135-143. <https://doi.org/10.14006/j.jzjgxb.2017.01.015>
- [23] Ministry of Housing and Urban-Rural Development of the People's Republic of China, & General Administration of Quality Supervision, Inspection and Quarantine of the People's Republic of China. (2015). *Code for design of concrete structures* (GB 50010-2010).

## EXPERIMENTAL CHARACTERIZATION OF JET GROUT USING DIGITAL IMAGE CORRELATION TECHNIQUE

Ksenija Kavarić<sup>1</sup>, Marko Popović<sup>2</sup>, Aleksandar Savić<sup>3</sup>, Sanja Jocković<sup>4</sup>, Milena Raković<sup>5</sup>

**Abstract:** Jet grouting is a well-established and versatile ground improvement technique widely used to enhance the mechanical performance of weak or heterogeneous soils. It has proven effective across diverse soil conditions, motivating further experimental and parametric characterization. While sustainability goals have encouraged the use of eco-friendly additives, cement-based mixtures remain predominant due to their adaptability and reliable performance. Despite its widespread application, the mechanical behavior and failure mechanisms of in-situ jet grout columns have received limited experimental investigation, especially under uniaxial loading. This study explores the potential of Digital Image Correlation (DIC) as an advanced, non-contact optical technique for measurement of full-field displacements and strains on the surface of an object and fracture behavior during mechanical testing. Although DIC is more or less regularly used for concrete, natural rock, and composites, its application to jet grouting materials is rarely reported. Core samples were obtained from an active construction site, specifically from a coarse-grained soil layer, and were subjected to laboratory testing to evaluate key mechanical parameters such as: compressive strength, stiffness, and stiffness-to-strength ratios. The experimental approach aims to assess material variability and evaluate the relevance of standard modulus-based design parameters. The findings contribute to a deeper understanding of jet grout behavior and demonstrate the value of DIC as a complementary method for the performance assessment and design verification of jet grouted systems in coarse-grained soils.

**Keywords:** jet grout, digital image correlation, uniaxial strength, modulus

### 1. INTRODUCTION

Soil improvement techniques have become an essential component of modern geotechnical engineering, particularly in the construction of foundations, excavation support systems, and seepage control barriers in challenging ground conditions (Croce et al., 2014; Nicholson, 2015). Among these techniques, jet grouting has emerged as one of the most versatile and widely applied methods, thanks to its capacity to improve soil properties and address a broad range of geotechnical challenges (Croce et al., 2014; Tinoco et al., 2011). Despite its extensive use, the technology's complex behavior and associated uncertainties often remain poorly understood by many practitioners, leading to both underutilization and misapplication (Toraldó et al., 2018).

Jet grouting is an in-situ mixing process in which a cement-based grout is injected into the soil at high pressure (300–600 bars) through small-diameter nozzles located at the end of a drill string (Croce et al., 2014; Nicholson, 2015; Wang et al., 2013; Tinoco et al., 2011; Akin, 2016). The high-velocity jet cuts and erodes the soil, simultaneously mixing it with grout to create soil-cement columns with improved mechanical and hydraulic

<sup>1</sup> MSc, Kavarić Ksenija, M.Sc. Structural Eng., PhD Student, University of Belgrade Faculty of Civil Engineering, Bulevar kralja Aleksandra 73, Belgrade, Serbia, [ksenija.kavaric@novkol.co.rs](mailto:ksenija.kavaric@novkol.co.rs)

<sup>2</sup> MSc, Popović Marko, M.Sc. Structural Eng., PhD Student, University of Belgrade Faculty of Civil Engineering, Bulevar kralja Aleksandra 73, Belgrade, Serbia, [mpopovic@grf.bg.ac.rs](mailto:mpopovic@grf.bg.ac.rs), <https://orcid.org/0000-0002-3304-5438>

<sup>3</sup> Professor, Savić Aleksandar, PhD. Structural Eng., University of Belgrade Faculty of Civil Engineering, Bulevar kralja Aleksandra 73, Belgrade, Serbia, [sasha@grf.bg.ac.rs](mailto:sasha@grf.bg.ac.rs), <https://orcid.org/0000-0002-1777-6775>

<sup>4</sup> Professor, Jocković Sanja, PhD. Structural Eng., University of Belgrade Faculty of Civil Engineering, Bulevar kralja Aleksandra 73, Belgrade, Serbia, [borovina@grf.bg.ac.rs](mailto:borovina@grf.bg.ac.rs), <https://orcid.org/0000-0002-3896-4791>

<sup>5</sup> MSc, Milena Raković, M.Sc. Structural Eng., PhD Student, University of Belgrade Faculty of Civil Engineering, Bulevar kralja Aleksandra 73, Belgrade, Serbia, [mrakovic@grf.bg.ac.rs](mailto:mrakovic@grf.bg.ac.rs), <https://orcid.org/0000-0001-9670-1677>

properties (Wang et al., 2013; Nicholson, 2015; Croce et al., 2014). Depending on the system used, jet grouting is generally classified into single-fluid, double-fluid, and triple-fluid systems, each varying in terms of erosion efficiency and mixing capabilities (Croce & Flora, 2000; Croce et al., 2014; Tinoco et al., 2011).

Despite its extensive application in practice, the mechanical behavior and failure mechanisms of jet-grouted columns have been the subject of limited experimental investigation. The behavior of jet-grouted soilcrete is highly dependent on numerous variables, including soil type, operational parameters (e.g., injection pressure, nozzle diameter, grout composition), and environmental conditions (Correia et al., 2009; Toraldo et al., 2018; Akin, 2016). Previous studies have demonstrated that the physical and mechanical properties of jet-grouted columns, such as: uniaxial compressive strength, unit weight, porosity, and stiffness, are significantly affected by both the granulometric characteristics of the treated soil and the jet grouting process parameters (Croce & Flora, 2000; Akin, 2016). A particularly important aspect of jet grouting is the variability in the strength and stiffness of the produced columns, which often requires site-specific testing and empirical correlations for design purposes (Tinoco et al., 2011; Toraldo et al., 2018).

In recent years, increasing attention has been given to the use of non-destructive techniques as reliable indicators for assessing the quality and mechanical properties of soilcrete. Among these, Digital Image Correlation (DIC) has emerged as a valuable tool, offering full-field strain measurements with high spatial resolution and providing detailed insight into localized deformation and fracture behavior that are difficult to capture with conventional instrumentation such as LVDTs (Linear Variable Differential Transformer) or strain gauges.

With the aid of DIC static modulus of elasticity of compressed concrete can be accurately obtained, in reasonable comparison to the LVDT method (Loh et al. 2022). This method enables additional observations, such as characterization of the cracking patterns, impossible to be performed using only LVDT method. The stress field obtained by the DIC test showed that the cracking modes of the mortar and concrete specimens were different (Zhang et al. 2022): concrete specimens cracked from the center, and mortar specimens cracked from the edge, which could affect the reliability of the tensile strength calculation of mortar specimens. There have been also reported data acquisition based on the StereoDIC in uniaxial compression testing of rock cores. The authors point out the positive effects of such approach, including: full field shape, deformation and strain fields on the surface of the specimen, almost no need for specimen preparation (other than applying the group of dots on the surface), possibility to avoid areas of local disturbances and failures, acquisition of a larger amount of data compared to conventional methods, enabling proper statistical analysis in estimating the desired properties (Abdulqader et al., 2020). Another study (Lingga et al., 2019) has shown relatively small mean differences of 5.1% and 14.5% in lateral and axial strain measurements of concrete samples, in comparison to conventional LVDT and string potentiometer methods. The authors reported that the placement of point of interest is greatly influencing the 3D-DIC's generated elastic properties, and strongly recommended a comprehensive analysis what to examine on the specimen, prior to the experiment. Although widely applied in materials science, the application of DIC to jet grouting materials remains limited.

The objective of this study is to investigate the mechanical behavior of jet-grouted material formed in a gravelly sand stratum through uniaxial compression testing combined with DIC strain monitoring. Core samples were extracted from an active construction site. The experimental program focuses on evaluating key mechanical parameters such as uniaxial compressive strength (UCS), Young's modulus, and stiffness-to-strength ratios ( $\beta$ ). Special attention is given to capturing the stress-strain response and characterizing potential variability in stiffness and strength. The outcomes are discussed in the context of existing literature to assess the applicability of standard modulus-based design approaches and to explore the advantages of using DIC in the evaluation of jet grout performance under field conditions.

## 2. MATERIALS AND METHODS

The samples analyzed in this study were collected from the construction site of the National Football Stadium located in Surčin, Serbia. During the installation of bored piles, localized soil collapse of the surrounding ground was observed, which indicated inadequate stability of the soil mass. As a remedial measure, jet grouting was applied as a ground improvement technique to enhance both the strength and stiffness of the weak and heterogeneous subsurface layers and to ensure the safe continuation of piling works.

According to the geotechnical report prepared by Geomehanika DOO (2023), the geological profile at the site consists of the following layers:

- Humus (h) - humus and humified dust, with plant root remnants and organic matter. The layer thickness is approximately 0.70m locally and up to 1.10m. This layer was removed during the construction of the facilities.
- Silty - sandy clay (pr) - yellow-brown silty (loess-like) material with the presence of sandyclayey material.

- Silty Sand (p-pr) - sandy material, yellow-brown in color, limonitic, fine-grained, watersaturated. With increasing depth, a change to gray-brown color, well-cemented, well-granulated.
- Silty Clay (pr-gl) - silty clayey material, yellow to brown in color, moderately plastic, moderately compressible. With increasing depth, the percentage of sandy fraction in the mass increases.
- Gravelly Sand (p\*) - sandy-silty material with the presence of fine-grained gravel in the matrix. Gravel clasts up to 5 cm, well-compacted layer, gray to brown in color, fine to medium-grained sand.
- Silty Clay (gl-pr) - brown to brownish material, hard consistency, slightly compressible. The material exhibits moderate to high plasticity.

Although jet grouting was carried out in both silty sand and gravelly sand, this paper focuses only on the investigation of columns formed in the gravelly sand layer. The same report indicates that the gravelly sand layer is found at depths between 20 and 26 meters. This layer is characterized by an internal friction angle of 35–40°, cohesion of 0–2 kPa, bulk density of 18.8–19.0 kN/m<sup>3</sup>, and natural moisture content ranging from 6.6% to 30.8%.

To assess the uniaxial compression performance of jet-grouted material, the Digital Image Correlation technique was performed. Digital Image Correlation (DIC) is a non-contact optical measurement technique used for measuring full-field displacements and strains on the surface of an object. The DIC method is based on analysing the changes in the pattern of a specimen's surface between sequential images by using correlation algorithms. By comparing subsets of pixels from the undeformed and deformed images, DIC can determine how points on the surface have moved, enabling precise calculations of displacement and strain.

Digital Image Correlation is the leading optical measurement method. This method is widely used in various materials and structural testing within most industry segments, in research and development at universities and research facilities, due to its accuracy, versatility, and ability to capture complex deformation behaviour in real-time. The DIC has several advantages over traditional measurement techniques such as strain gauges, extensometers and displacement transducers. It provides a full-field strain map, enabling detection of strain heterogeneity and localised effects. As a non-contact measurement technique, it eliminates a mechanical interaction with the specimen under testing, reducing the potential measurement errors or damage to the specimen surface. Modern DIC systems are robust and handle rough or uneven concrete surfaces more effectively than traditional sensors. A significant advantage of DIC is post-processing capability. It allows reprocessing the same data and refining the analysis without repeating the physical test, flexible and advanced data extraction, enhanced visualisation of deformation of the specimen under test and integration with other data sources data such as force data, thermography or acoustic emissions, as shown in Figure 1.



*Figure 1. Testing experimental setup and one of the cracking patterns of the specimen*

### 3. LABORATORY TESTING AND RESULTS

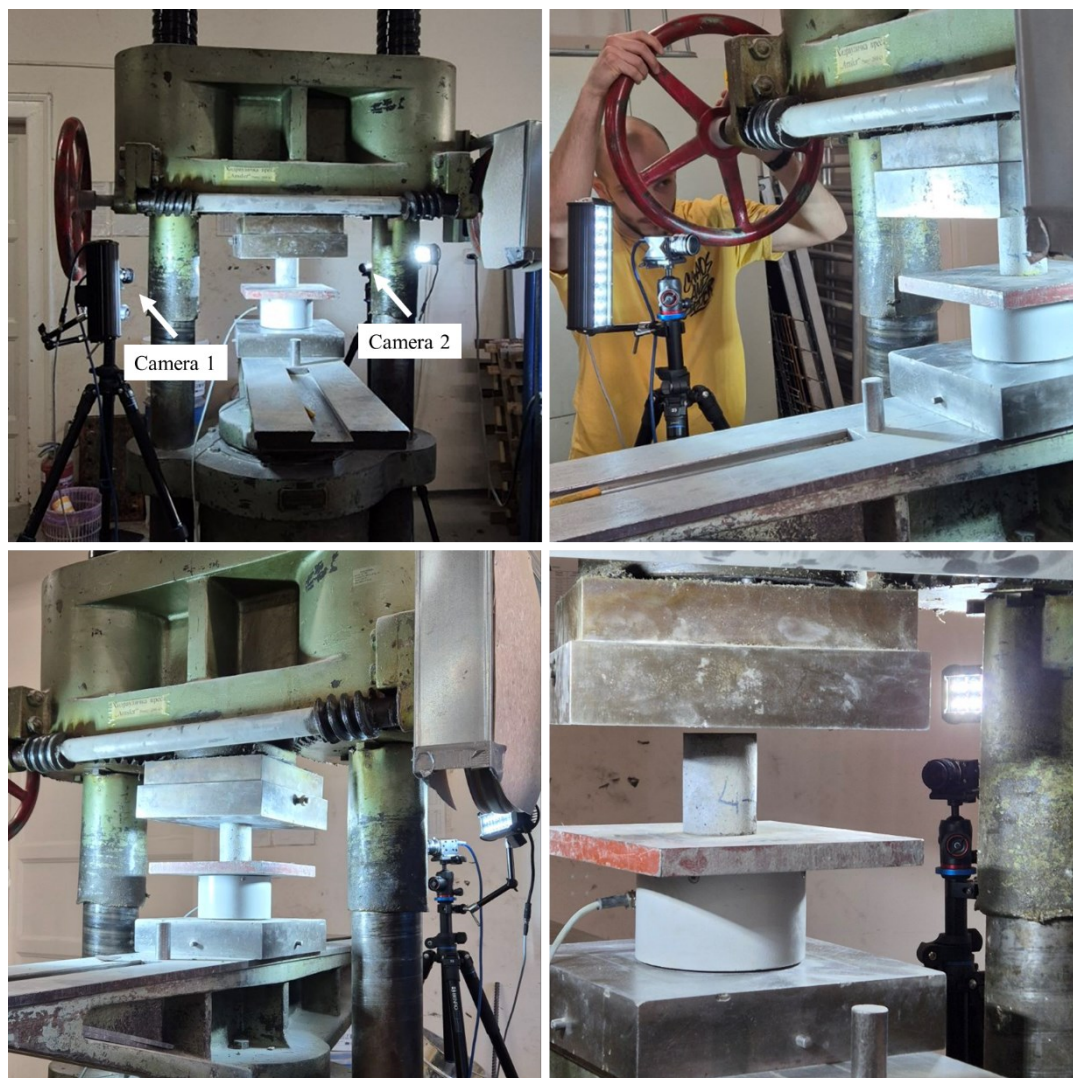
Eight core Ø70/H70 samples of the jet grouting columns were taken by core drilling of the jet columns at the depth of 20 m to 26 m, and prepared in the laboratory for uniaxial compressive strength testing. The columns were formed using the double-fluid system, with a diameter of 1500 mm and a water–cement ratio of 1.0. The specimens had an age ranging from 28 to 84 days at the time of testing.

The Amsler and Sohn compressive testing device was used for loading the specimens. The acquisition of load values was conducted by the load cell placed under the tested specimen. Between the load cell and the specimen was thick steel plate, intended to eliminate deformations of the lower surface of the specimen. For strain measurement of cores subjected to uniaxial compression testing, the X-Sight M16 DIC system was used. Two 2D DIC sets were installed, allowing the recording of specimen surfaces and measurements from two sides. The DIC



setup consists of 16 megapixel cameras and LED lights. The appropriate speckle pattern was applied to the specimen surface by spray paint.

Figure 2 shows the testing experimental setup for uniaxial compression testing combined with DIC strain monitoring.



**Figure 2.** Experimental setup for uniaxial compression testing combined with DIC strain monitoring

The results of uniaxial compression testing with strain monitoring by DIC are presented in Figures 3 and 4. A total of eight samples were analyzed, all extracted from a jet-grouted layer composed predominantly of gravelly sand. The detailed results, including uniaxial compressive strength (UCS), calculated Young's moduli, and stiffness-to-strength ratios:

$$\beta = \frac{E}{q_u} \quad (1)$$

are summarized in Table 1.

Figure 3 shows the initial portion of the stress-strain curves, up to 0.2% axial strain, which was used for the determination of the Young's modulus ( $E$ ) as the tangent modulus. This part of the curve reflects the elastic response of the material and is critical for assessing deformation behavior under service loads. Figure 4 shows the full stress-strain curve for one representative sample, illustrating the characteristic mechanical behavior of jet grout under uniaxial loading. A nearly linear pre-peak segment is followed by brittle failure. The curves exhibit an almost linear trend up to peak stress, indicating that the modulus remains practically constant throughout the loading phase until failure. This confirms the quasi-elastic behavior of the jet-grouted material under uniaxial compression.



The complete dataset in Table 1 includes not only the mechanical parameters but also the corresponding depth intervals from which the core samples were obtained.

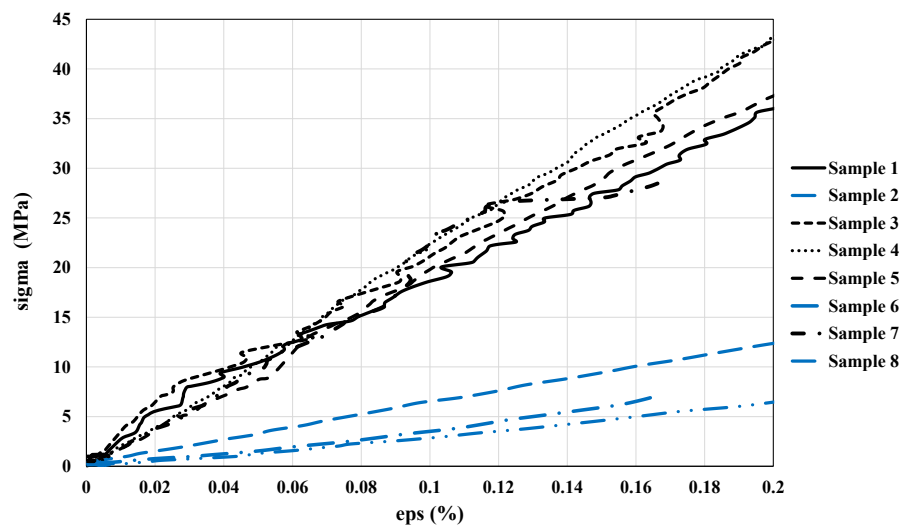


Figure 3. Initial portions of stress–strain curves used to determine Young’s moduli

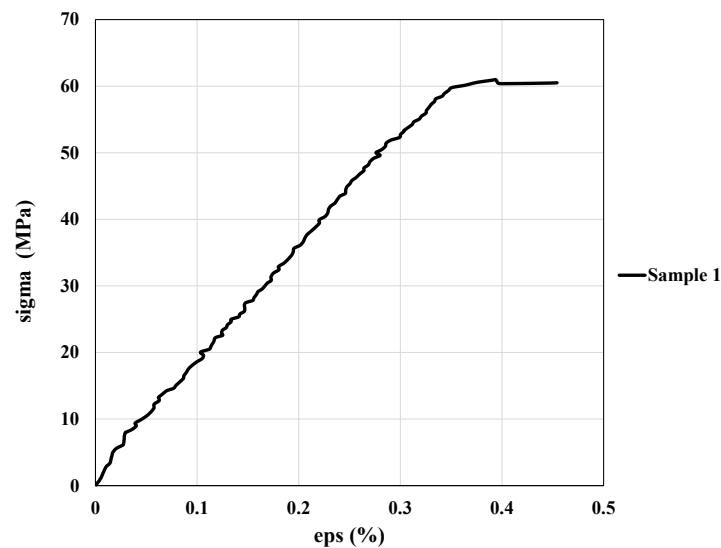


Figure 4. Representative stress–strain curve from uniaxial compression test

Table 1. Full dataset from laboratory testing of jet grout specimens

Sample No.	Depth (m)	UCS $q_u$ (MPa)	Young moduli $E$ (GPa)	$\beta$
1	20.0-21.0	61.0	16.8	275
2	21.0-23.0	25.0	6.2	248
3	22.0-23.0	69.7	17.6	252
4	23.3-23.8	67.4	20.0	296
5	23.3-23.8	41.1	17.7	430
6	24.0-25.0	17.9	4.4	245
7	25.0-26.0	30.0	17.5	583
8	25.0-26.0	23.0	3.9	169

#### 4. DISCUSSION

The uniaxial compression tests conducted on eight core samples of jet grout extracted from a gravelly sand layer indicated two clearly performance groups, as evident from the stress-strain diagrams. The first group of high-performance samples (1, 3, 4, 5, 7) exhibit UCS values between 30 and 69.7 MPa and Young's moduli ranging from 16.8 to 20.0 GPa. The calculated  $\beta$  ratios vary from 252 to 583. This group reflects behavior typical for well-executed jet grouting in coarse soils, where cement infiltration is efficient and uniform. The results are closely aligned with the values reported by Croce et al. (1994) and Mongiovì et al. (1991), where jet grout formed in gravelly sand exhibits UCS in the range of 10-70 MPa and  $\beta$  values between 210 and 670. In particular, the high modulus of Sample 7 (17.5 GPa) despite moderate UCS (30 MPa) suggests a dense internal structure with potentially high cement content in a localized region, possibly caused by non-uniform jet dispersion or grout migration.

The second group of the low-performance samples (2, 6, 8) are characterized by significantly lower UCS values (17.9-25 MPa) and elastic moduli between 3.9 and 6.2 GPa. The  $\beta$  values range from 169 to 248. These values fall below the expected mechanical thresholds for gravelly sand and instead resemble jet grout performance in finer soils such as silty sands (Croce et al., 2014). This can likely be attributed to local soil heterogeneity, inefficient mixing, or grout dilution by groundwater.

Although the number of tests performed in the gravelly sand layer was relatively limited, the computed coefficient of variation (CV) of 49.3% indicates a high degree of variability in stiffness. This value is consistent with findings reported by Croce et al. (2014), where CV values for sandy and gravelly soils typically range between 15% and 47%, and are generally lower than those found in finer soils (CV = 48–75%).

The  $\beta$  ratio is commonly used to estimate stiffness from strength in cases where direct modulus measurements are unavailable. In the literature, this parameter is typically defined using the secant modulus at 50% of peak stress ( $E_{50}$ ), due to slight nonlinearities observed before failure. However, in this study, the stress-strain response was approximately linear up to peak stress, as confirmed by DIC strain analysis. As a result, the measured modulus effectively corresponds to  $E_{50}$ , eliminating the need for further distinction between tangent and secant stiffness.  $\beta$  values range from 169 to 583, with most falling between 250 and 450, which matches the lower-to-mid spectrum reported for gravelly sand soils (typically 210-1200, Croce et al., 2014). The relatively low  $\beta$  values may be attributed to a combination of factors, such as material inhomogeneity, extraction from field conditions rather than controlled laboratory settings, and minor degradation associated with coring operations.

The disparity between these two groups highlights the critical importance of quality control, particularly in field conditions where local changes in soil texture or grouting parameters can cause substantial differences in mechanical properties. Literature confirms that core samples from field-executed jet grout columns show greater scatter compared to laboratory-prepared samples, due to extraction-induced damage and spatial inhomogeneity (Correia et al, 2009). Overall, the consistency between the experimental data and published literature supports the validity of the applied methodology and highlights the potential of DIC as a reliable tool for assessing the mechanical behavior of jet-grouted materials.

#### 5. CONCLUSIONS

The conducted investigation highlights both the potential and the challenges of applying jet grouting in coarse-grained soils under real field conditions. The results reveal considerable variability in the mechanical performance of the tested samples, with two clearly defined performance groups identified. While the majority of samples exhibit strength and stiffness consistent with expected values for gravelly sand, lower-performing samples confirm the strong influence of local soil heterogeneity and grout distribution on the final properties. The good agreement between experimental results and published data supports the reliability of the applied methodology, while the use of Digital Image Correlation (DIC) proved to be a valuable tool for precise stiffness evaluation.

Based on the analysis of the cracking pattern of the specimens, jet grouts were found to be closer to the mortar behavior under load, showing cracking from the edge. It should be noted that the specimens reached the compressive strength values correspondent to the higher concrete strength classes, with large ultimate strains reaching more than 0.4%, which is much higher ductility than for concrete.

Overall, the findings emphasize the need for strict quality control and continuous monitoring during construction to ensure consistent performance of jet-grouted elements. Further research based on a larger dataset is recommended to better understand the influence of soil composition and grouting parameters on the mechanical behavior of treated soils.

## 6. ACKNOWLEDGEMENTS

This investigation is financially supported by the Ministry of Science, Technological Development and Innovation of the Republic of Serbia under Contract No.: 200092.

## 7. BIBLIOGRAPHY

- [1] Croce, P., Flora, A., & Modoni, G. (2014). Jet grouting. Technology, Design and Control. NW: SRS Press Taylor & Francis Group, 9.
- [2] Nicholson, P. G. (2015). Soil improvement and ground modification methods. Butterworth-Heinemann.
- [3] Tinoco, J., Correia, A. G., & Cortez, P. (2011). Application of data mining techniques in the estimation of the uniaxial compressive strength of jet grouting columns over time. *Construction and Building Materials*, 25(3), 1257-1262.
- [4] Toraldo, C., Modoni, G., Ochmański, M., & Croce, P. (2018). The characteristic strength of jet-grouted material. *Geotechnique*, 68(3), 262-279.
- [5] Wang, Z. F., Shen, S. L., Ho, C. E., & Kim, Y. H. (2013). Jet grouting practice: an overview. *Geotechnical Engineering Journal of the SEAGS & AGSSEA*, 44(4), 88-96.
- [6] Akin, M. K. (2016). Experimental studies on the physico-mechanical properties of jet-grout columns in sandy and silty soils. *Journal of African Earth Sciences*, 116, 190-197.
- [7] Croce, P., & Flora, A. (2000). Analysis of single-fluid jet grouting. *Géotechnique*, 50(6), 739-748.
- [8] Correia, A. G., Valente, T., Tinoco, J., Falcão, J., Barata, J., Cebola, D., & Coelho, S. (2009). Evaluation of mechanical properties of jet-grouting columns using different test methods. In *Proceedings of the 17th International Conference on Soil Mechanics and Geotechnical Engineering (Volumes 1, 2, 3 and 4)* (pp. 2169-2171). IOS Press.
- [9] Loh, T.B., Yutong Wu, Goh S.H., Kong K.H., Goh K.L., Chong J.J. (2022), Determination of Static Modulus of Elasticity of Concrete in Compression using Digital Image Correlation (DIC) Method, 16th International Conference on Advances in Experimental Mechanics, 213-215.
- [10] Zhang H., Pan Q., Zheng K., Jin C., Pan L. (2022) Mesoscale Study on Splitting Tensile Damage Characteristics of Concrete Based on X-ray Computed Tomography and Digital Image Correlation Technology, *Materials* 2022, 15(13), 4416;
- [11] Abdulqader A., Rizos D.C. (2020) Advantages of using digital image correlation techniques in uniaxial compression tests, *Results in Engineering* 6, June 2020, 100109
- [12] Lingga B.A., Derek B.A., Sepehri M., Yuanvuan P. (2019) Assessment of digital image correlation method in determining large scale cemented rockfill strains, *International Journal of Mining Science and Technology* 29 (5) (2019) 771-776.
- [13] Geomehanika DOO (2023), Geotechnical study for the realization of the International specialized exhibition EXPO Belgrade 2027, with accompanying contents - the entire National Football Stadium (NFS) - Phase 1. 23-09/67.
- [14] Croce, P., Gajo, A., Mongiovì, L., & Zaninetti, A. (1994). Una verifica sperimentale degli effetti della gettiniezione. *Rivista Italiana di Geotecnica*, 28(2), 91-101.
- [15] Mongiovì, L., Croce, P., & Zaninetti, A. (1991). Analisi sperimentale di un intervento di consolidamento mediante gettiniezione. *II Convegno Nazionale dei Ricercatori del Gruppo di Coordinamento degli Studi di Ingegneria Geotecnica del CNR*, 101-118.

## TOWARDS AN ADVANCED GEOTECHNICAL MODELLING OF BLOCK-IN-MATRIX ROCK FOR ROBUST TUNNEL DESIGN AND CONSTRUCTION

Ksenija Micić<sup>1</sup>, Novak Joksimović<sup>2</sup>, Miloš Marjanović<sup>3</sup>, Vojkan Jovičić<sup>4</sup>, Jelena Ninić<sup>5</sup>

**Abstract:** Block-in-matrix rock assemblages, also known as 'bimrocks', represent structurally complex units consisting of hard rock blocks embedded in a soft matrix, with both components differing in geological origin, lithology, rheology and geometry. Considered geotechnically complex formations and being characterized by internal heterogeneity and multi-level spatial variability, such formations are extremely demanding to model using conventional geotechnical approaches. Underground construction, including urban tunnelling in such heterogeneous environments poses numerous challenges, with the most significant ones being high stratal disruptions, stress concentrations at the interface between blocks and matrix, and the inability to accurately predict the behaviour of the rock mass. Besides geological formation, structural analysis and geomechanical characterization, previous studies have only explored methods for probabilistic generation of various block configurations within the rock mass. To tackle the bimrock as an underexplored issue, we present a methodology for up-to-date bimrock ground modelling including lithological and mechanical parameter spatial variability assessment, paired with numerical simulations for the underground construction. Employing the three main modelling components – voxel based geological model, conditional random field parameter model and FEM numerical model, this study aims at introducing a novel, automated and reliable approach for block-in-matrix modelling. It presents an innovative framework for geotechnical modelling of bimrocks, with significant potential for further improvement in accuracy and functionality of the modelling components, as well as the identification of the most sensitive modelling parameters.

**Keywords:** block-in-matrix, ground model, numerical simulation, conditional random field, tunnelling

### 1. INTRODUCTION

Block-in-matrix (BiM) materials are heterogeneous geological formations composed of strong rock blocks embedded within a weaker matrix, frequently encountered in fault zones, mélanges, landslide masses, and foundation formations. Their mechanical behaviour, particularly shear strength and deformation characteristics, is strongly governed by the Volumetric Block Proportion (VBP), which quantifies the fraction of the domain occupied by blocks. Accurate estimation of VBP is therefore essential for reliable geotechnical modelling and design.

In the extensive literature on the influence of VBP on slope stability, tunnel deformation, and material strength (Napoli et al, 2018; Napoli et al, 2021; Guo et al, 2024), it is generally concluded that higher VBP leads to an increase in shear strength and reduced deformation. However, the challenge lies in estimating the true 3D VBP from limited field measurements, usually 1D boreholes (yielding Linear Block Proportions - LBP), 2D outcrop images (Areal Block Proportions - ABP), or point sampling (Point Block Proportions - PBP). These lower-dimensional measurements often underestimate the actual VBP, particularly for small-scale samples or in domains

<sup>1</sup> MSc Micić Ksenija, Geological Engineer, Teaching assistant, University of Belgrade, Faculty of Civil Engineering, Bulevar kralja Aleksandra 73, Belgrade, Serbia, e-mail address: [kmicic@grf.bg.ac.rs](mailto:kmicic@grf.bg.ac.rs), <https://orcid.org/0000-0002-4101-4412>

<sup>2</sup> MSc Joksimović Novak, Civil Engineer, Teaching assistant, University of Belgrade, Faculty of Civil Engineering, Bulevar kralja Aleksandra 73, Belgrade, Serbia, e-mail address: [njoksimovic@grf.bg.ac.rs](mailto:njoksimovic@grf.bg.ac.rs), <https://orcid.org/0009-0001-2627-8874>

<sup>3</sup> PhD Marjanović Miloš, Civil Engineer, Assistant professor, University of Belgrade, Faculty of Civil Engineering, Bulevar kralja Aleksandra 73, Belgrade, Serbia, e-mail address: [mimarjanovic@grf.bg.ac.rs](mailto:mimarjanovic@grf.bg.ac.rs), <https://orcid.org/0000-0002-7968-3873>

<sup>4</sup> PhD Jovičić Vojkan, Civil Engineer, Associate professor, University of Ljubljana, Faculty of Civil Engineering and Geodesy, Jamova 2, 1000 Ljubljana, Slovenia, e-mail address: [vojkan.jovicic@fgg.uni-lj.si](mailto:vojkan.jovicic@fgg.uni-lj.si)

<sup>5</sup> PhD Ninić Jelena, Civil Engineer, Associate professor, University of Birmingham, School of Engineering, Edgbaston, Birmingham, United Kingdom, e-mail address: [j.ninic@bham.ac.uk](mailto:j.ninic@bham.ac.uk)

with high heterogeneity (Medley, 1994; Napoli et al, 2020; Napoli et al, 2023). To bridge this gap, several researchers introduced the concept of Uncertainty Factors (UF) and Coefficient of Variation (COV), providing correction factors to estimate 3D VBP from LBP or ABP, with the main assumption that sufficient sampling reduces uncertainty (Medley, 1994; Napoli et al, 2020; Zhang et al, 2025).

Most of the existing studies on BiM materials employ 3D modelling procedures, varying the block volumes, shapes, orientations, and focusing on VBP estimation error assessment. However, building geometry models in a fully stochastic manner and introducing virtual drilling only at later stages disrupts the authentic workflow of investigation and modelling within an actual project. This leads to neglecting the role of site investigations as the sole source of ground truth and failing to construct primary models based on that knowledge.

Furthermore, despite the significant progress in understanding the mechanical behaviour of BiM formations, direct implementation of such complex geological structures in numerical analyses remains highly challenging. Traditional approaches often rely on simplified deterministic models or homogenization techniques that neglect the inherent heterogeneity of BiM materials, particularly the influence of discrete block configurations. More advanced strategies have been recently investigated (Napoli et al, 2018; Napoli et al, 2021; Guo et al, 2024). However, they predominantly focus on VBP estimation or conceptual modelling, without fully integrating realistic ground models into FEM simulations in a manner consistent with the actual site investigation data.

The limitations elaborated above are the primary motivation for the present research, which proposes a hybrid concept for forming voxel-based BiM ground models, combining the inevitable stochastic nature of BiM material modelling with the fundamental role of investigation data, and directly importing them to FEM for data-driven numerical simulations that account for both block configurations and spatial variability of matrix properties.

## 2. BLOCK IN MATRIX GROUND MODEL

### 2.1. Borehole-constrained model reconstruction

In this study, we introduce a BiM model reconstruction strategy that involves constraining the stochastic nature of BiM materials with the only subsurface knowledge one can obtain during a project – field investigation works. Since the whole workflow we present herein is built on synthetic data, great attention has been put into maintaining the realism of physical, geological and geotechnical characteristics of different modelling features.

The 3D BiM model reconstruction is executed in several steps, interconnected within an original, fully automated Python-based modelling system, as follows: (i) borehole placement in the domain of interest; (ii) LBP calculation from the borehole block intercepts; (iii) borehole block intercept to block sphere reconstruction; (iv) VBP estimation using UF; (v) 3D BiM model reconstruction for the defined VBP span, respecting the blocks produced from the existing boreholes.

The domain of interest is defined as 50x200x50 m in X, Y and Z, respectively. Within this space, 10 boreholes are placed, with 7 of them distributed along the domain centreline, following the tunnel alignment in Y direction, and the other 3 randomly placed in the rest of the domain, all respecting the rule of minimum distance in between. Each borehole contains randomly produced block and matrix intercepts, such that for the 50 m total borehole depth, there are maximum 8 block intercepts. The global LBP (for all boreholes) is obtained as a ratio of total length of block intercepts and total length of boreholes (Medley, 1994).

Reconstructing block spheres from block linear intercepts includes introducing multiple assumptions, constraints and rules, all in accordance with the existing literature. To estimate the most probable block diameter  $D$  based on a measured chord length  $L$  (the block intercept in the borehole) probability theory is employed, where the probability density function (PDF) for observing a chord of length  $L$  in a sphere of known diameter  $D$  is expressed as (Medley, 1994):

$$f(L) = \frac{4L}{D^2} \quad (1)$$

However, in practice, the true diameter is unknown and only the chord is observed, so the goal is to estimate the most probable diameter  $D$  based on this observation, taking into account prior knowledge of block size distribution in bimrock. This inverse problem is ideally suited for Bayesian inference, where a prior distribution (block size probability) is paired with the likelihood, to obtain the posterior probability:

$$P(D|L) = \frac{P(L|D) \cdot P(D)}{P(L)} \quad (2)$$

In this expression,  $P(D|L)$  represents the posterior: probability of diameter  $D$  given measured chord  $L$ ,  $P(L|D)$  is the likelihood: PDF of observing chord  $L$  in a sphere of diameter  $D$ ,  $P(D)$  is the prior: the known distribution of



block sizes, commonly modeled by a truncated power-law or negative exponential distribution (Medley and Lindquist, 1995):

$$f(d) = \frac{(D-1)}{a^{1-D} - b^{1-D}} d^{-D} \quad (3)$$

where  $f(d)$  represents the probability density function of the cumulative distribution function from which diameters are sampled,  $D$  is the fractal dimension,  $a$  is the minimum block diameter and  $b$  is the maximum block diameter.

Combining the expressions yields the probability density function of the sphere's diameter, based on the measured chord and the known distribution of block diameters, as follows:

$$P(D|L) \propto \frac{(D-1)}{a^{1-D} - b^{1-D}} d^{-D} \cdot \frac{4L}{d^2} \quad (4)$$

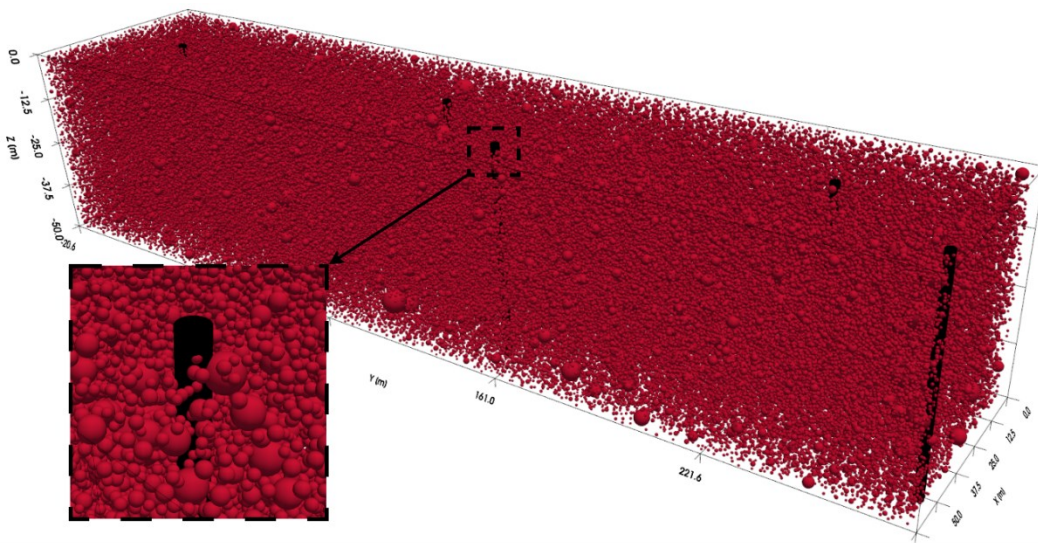
To generate a 3D BiM model, it is essential to define the VBP as the governing parameter for block generation within the matrix. As established in previous studies, LBP derived from boreholes does not directly equal the true VBP and requires a correction through the uncertainty factors (Medley, 1994, Napoli et al, 2020). This adjustment procedure is applied here following the method proposed by Napoli et al. (2022).

Based on the assumed global LBP of 30% from the borehole data and applying the appropriate uncertainty factor from the relevant fitting equation ( $UF = 0.075$ ), the corresponding estimated VBP falls within the range of 27.75 – 32.25%. This range then guides the target VBP input domain used for BiM model generation.

The procedure for populating the model with stochastic spheres (for a given VBP) begins by analytically calculating the actual baseline block volume in the domain, using only the volume of spheres identified from the borehole intercepts. This initial block volume is treated as known input, and any additional block volume needed to reach the desired VBP is added afterwards. The model-filling rules and constraints follow the established approaches in the literature (Medley, 1994, Napoli et al, 2020). Sphere diameters are sampled from a truncated power-law distribution (Equation 3) with a fractal dimension of 2.5, ensuring that the generated spheres do not overlap with each other or with borehole-derived spheres.

The characteristic length  $L_c$  is set to the tunnel diameter of 10 meters (Napoli et al, 2022). Accordingly, the minimum and maximum sphere diameters are equal to  $0.05L_c$  and  $0.75L_c$ , respectively, in line with widely accepted criteria for block scale limits in bimrocks (Medley, 1994).

Finally, to explore multiple plausible scenarios of the ground model under the proposed hybrid methodology, three distinct BiM models are generated, corresponding to VBP=27.5%, VBP=30%, and VBP=32.5%, respectively, all developed in accordance with the procedure described above. Figure 1 presents a 3D portion of the 27.5% BiM model, along with the enlarged block distribution around a borehole in the domain of interest.



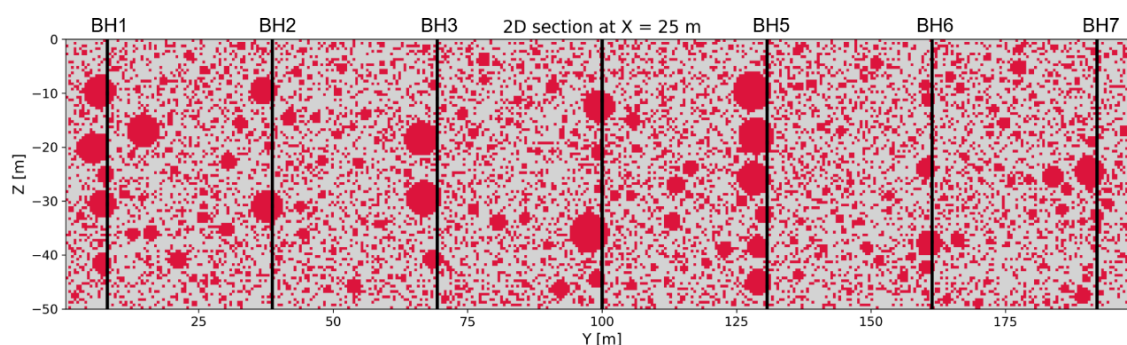
**Figure 1.** A portion (cut in Y) of the VBP=27.5% 3D BiM model (elongated 3x in Y for the representation sake) with a close-up excerpt from the volume showing sphere block distribution around a borehole

## 2.2. Voxelization

Voxelization represents a spatial discretization technique that converts 3D space into a grid of volume elements – voxels, that can either be of uniform or varying dimensions. Applying this method to create a structured cell grid allows for utilization and linking of various simulation and modelling tools. To achieve full interoperability between multiple sequences in the proposed modelling system, while providing simple and efficient data exchange within different platforms, the voxelization method is adopted to discretize the BiM ground model domain.

3D BiM model is transformed into binary cell-based spatial domain following a simple two-step algorithm. First, the entire model is discretized into a structured 3D voxel grid of uniform size, configured based on the smallest sphere diameter and set to 0.5 m. Each voxel is then evaluated for whether its centre lies within any of the generated spheres: if inside a block sphere, it is marked as block (code=1), otherwise it is considered matrix (code=0). The voxel grid is constructed along the Cartesian axes X, Y and Z (negative downward for depth). For each sphere, a local voxel neighbourhood is searched based on its radius. Euclidean distance from each candidate voxel centre to the sphere centre determines the voxel inclusion. Figure 2 shows a voxelized 2D longitudinal section consisting of centreline (along the possible tunnel direction, at half X distance) boreholes and blocks in matrix represented with 2D rectangles. Larger blocks are, in general, distributed around boreholes due to fully synthetic and random block intercept positioning and dimensioning.

In this particular case, voxelization is recognized as an adequate way of representing the distinct heterogeneity of the BiM material through discretization into cell-based elements. In addition, it enables direct simulation of parameter spatial variability on the BiM grid, as well as numerical modelling in the same framework, both of which constitute the subsequent phases in the execution of the proposed workflow.



**Figure 2.** 2D voxelized section of the VBP=27.5% BiM model. Matrix is represented in gray, while blocks are visualized in red

## 2.3. Spatial variability of strength and deformation parameters

Soil and rock properties across a site typically exhibit spatial correlation, meaning that values measured at nearby locations tend to be similar. This spatial dependence occurs in both horizontal and vertical directions and gradually decreases with the increasing separation distance. Such behaviour can be captured and quantified using the interdependence-analysis statistical tools such as covariance models. These models enable the realistic simulation of subsurface variability by incorporating both the magnitude and the structure of spatial correlations. Subsequently, they make up the basis for generating Conditional Random Fields (CRFs), a geostatistical tool from the Random Field Theory, that can effectively be employed to simulate the soil or rock properties' distribution across the domain of interest.

CRFs can be regarded as a structured set of simulated parameter values over a defined grid, which inherently preserves its stochastic nature while simultaneously incorporating constraints based on known values at observed locations. To construct a conditional realization of a random field, it is first necessary to generate an unconditional realization and then apply a kriging interpolation technique to condition it to the observed data. Although various methods exist for generating each of the components of the final model, the following briefly outlines the procedure used in this work, which is considered simple yet powerful, and computationally efficient.

Herein, the focus is directed toward assessing the spatial variability of strength and deformation parameters of the matrix, while the blocks are treated as homogeneous, with constant mechanical properties. This is justified by the fact that blocks are defined as geotechnically significant bodies within a bonded matrix of finer texture, emphasizing the mechanical contrast between the block bodies and the matrix infill (Medley, 1994; Medley & Lindquist, 1995). Moreover, given the considerably higher strength and stiffness of the blocks, their failure is

unlikely to govern the overall system behaviour. Therefore, the variability of block properties is excluded from the analysis.

To derive the unconditional realizations of cohesion, friction angle and Young's modulus values, we employ the Randomization method that uses the spectral density of the covariance function to simulate a field in the Fourier domain (Heße et al, 2014; Müller et al, 2021). To that end, a Gaussian random field can be characterized by the corresponding expectation value and covariance (or semivariogram) model as:

$$u(x) = \sqrt{\frac{\sigma^2}{N}} \sum_{i=1}^N (a_i \cos(k_i \cdot x) + b_i \sin(k_i \cdot x)) \quad (5)$$

where  $N$  represents the number of Fourier modes,  $a_i$ ,  $b_i$  are the independent random variables that follow a standard normal distribution, and vectors  $k_i$  represent independent random vectors, sampled from the spectral density of the variogram model.

To constrain the simulation with the known measurement data, in this case represented by the samples taken from the boreholes, ordinary kriging is utilized. Kriging is an interpolation routine that derives the best linear unbiased estimate of a value at an unsampled point by leveraging known measurements and a predefined spatial covariance model (Wackernagel, 2003). This procedure is performed with the aid of weighting factors determined for the minimum value of the variance of the kriging error, as follows:

$$k(x_0) = \sum_{i=1}^N \lambda_i Z_i = \sum_{i=1}^N \lambda_i(x_0) Z(x_i) \quad (6)$$

where  $x_i$  represents the spatial points with measurement values  $Z_i$ , and  $\lambda_i$  are the weighting factors. Ordinary kriging considers the global mean unknown, and estimates the local mean for each prediction location, while using the spatial correlation among data points to make predictions.

For the matrix CRF modelling a total of 98 conditioning points (samples from boreholes) is taken into account, with cohesion  $c$  (kPa), internal friction angle  $\phi$  (°) and Young's modulus  $E$  (GPa) values configured as per literature presented in Table 1. Block parameter values used for numerical analyses are set up as the constant mean value of the values determined from the samples, also shown in Table 1. CRFs are generated as full domain 3D realizations, but to accommodate the numerical analyses needs in Plaxis 2D, the ground model CRFs are also incorporated within 2D cross-sections, as detailed in Section 3.1. To that end, Figure 3 presents 2D sliced CRF datasets for previously listed matrix parameters, all corresponding to one 2D slice utilized in numerical modelling.

**Table 1.** Block and matrix geomechanical parameter values used for CRF and numerical modelling

Parameter		Matrix	Blocks	Reference
$c$ (kPa)	$min$	5.06	905.08	modified after:  Napoli et al, 2018; Xue and Nag, 2011; Kezdi, 1974; Obrzud and Truty, 2012; Koloski et al, 1989
	$max$	14.98	1093.54	
	$\mu$	9.61	1008.16	
$\phi$ (°)	$min$	24.02	49.06	
	$max$	31.93	50.99	
	$\mu$	27.94	50.02	
$E$ (GPa)	$min$	1.53	7.01	
	$max$	3.49	7.39	
	$\mu$	2.58	7.21	

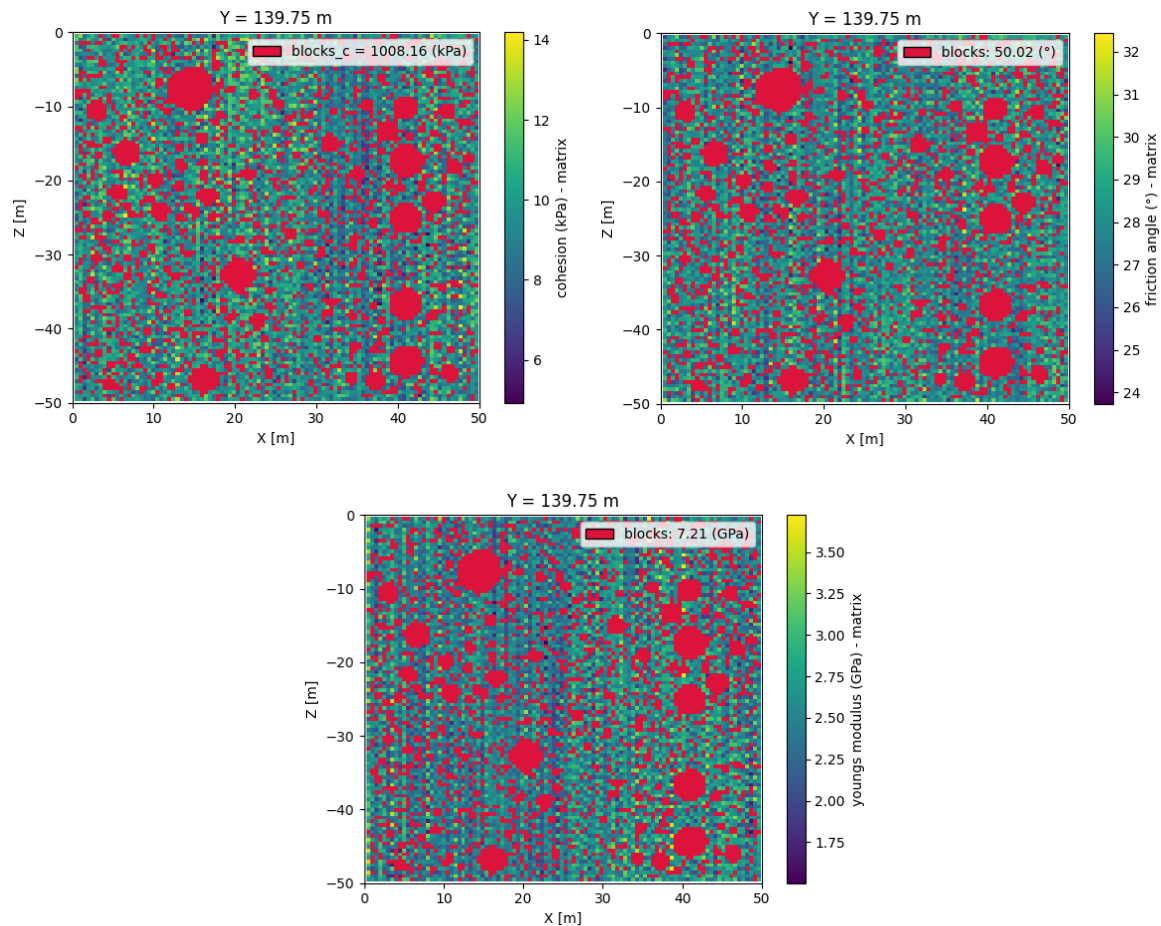
### 3. FINITE ELEMENT ANALYSIS

The proposed methodology is illustrated through a representative case study involving the excavation of a circular tunnel with a diameter of 10 m. In order to ensure the reproducibility of results and facilitate meaningful comparisons with prior research, the overall tunnel excavation scenario is conceptually aligned with the framework presented by Napoli et al. (2021). Nonetheless, the present study introduces modifications: the incorporation of spatial variability in the geomechanical properties of the matrix (CRFs), and the application of domain voxelization to discretize the heterogeneous ground conditions (Figure 4).

The excavation process is modelled using the convergence–confinement method (Rabcewicz, 1964), a widely adopted approach that effectively captures the progressive stress redistribution in the surrounding rock mass as tunnel advance proceeds.

The mechanical behaviour of both matrix and block components of the bimrock is represented using the Mohr-Coulomb elastic-perfectly plastic constitutive model. The material parameters for the blocks are assumed constant, while those of the matrix are spatially randomized using CRFs to reflect inherent geological variability. This

approach allows for a more realistic simulation of the heterogeneous response of the rock mass under excavation-induced stress changes.



**Figure 3.** CRF realizations of matrix parameters, sliced in 2D for FEM numerical analysis

As the focus of this research is to explore the influence of rock mass heterogeneity on tunnel behaviour rather than to design a structural support system, the tunnel is modelled without any lining. This simplification enables a clearer assessment of the stress-strain response of the surrounding bimrock material during excavation.

To minimize boundary effects and avoid artificial constraints on deformation, each numerical model includes an external zone consisting of homogeneous continuum material, extending a distance of 5 times the tunnel diameter ( $5L_c$ ) in all directions from the excavation boundary (Figure 4). This outer zone is modelled with coarser resolution of voxels and with average matrix properties in order to reduce the computational cost while maintaining physical accuracy near the tunnel. The displacements are restrained at the edges of the model.

The model boundaries are fully fixed, meaning that both translational displacements are restrained along all external edges. The initial stress state is simulated as an isotropic stress field with a value of vertical and horizontal stress of 1.74 MPa throughout the domain. This approach corresponds to an overburden depth of approximately 80–85 m, consistent with previous studies (Napoli et al, 2021).

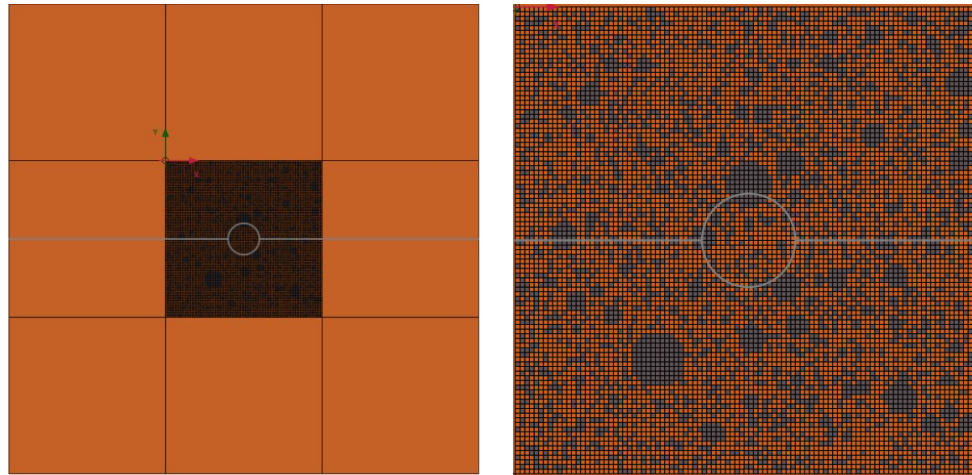
The analysis is performed under drained conditions, without consideration of groundwater effects. Tunnel excavation is simulated in ten incremental steps, each corresponding to a 10% stress relief around the excavation boundary, following the principles of the convergence–confinement method.

For each 3D realization of the ground domain, ten 2D cross sections are extracted and analysed. In total, thirty finite element simulations are conducted using the PLAXIS 2D software package (version 2024.3, Bentley Systems). The simulated tunnel response is evaluated based on the excavation perimeter radial displacement, radial displacements in a horizontal cross section through the excavation centre and the extent and geometry of plastic zones developing around the tunnel excavation. The results are compared with a fully deterministic model, that utilizes a fully homogeneous material matrix (without blocks) and constant (mean) values of material parameters.



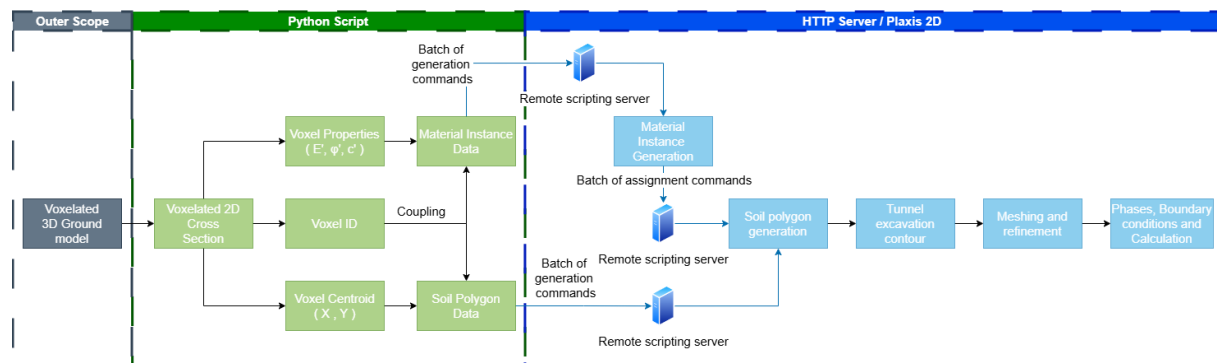
### 3.1. Integration of ground model

The integration of the BiM ground model into the numerical simulation workflow is performed by slicing the 3D model at predefined intervals along the tunnel alignment. These slices generate a series of cross-sectional datasets in use as inputs for corresponding 2D numerical models. Each resulting cross section preserves voxel-level information, explicitly indicating whether the intersected voxel corresponds to a matrix or block domain. Based on this classification, each voxel is assigned a specific set of material properties (Figure 5).



**Figure 4.** Generated model in Plaxis 2D (left) and close-up of the interior voxelized section from the 3D ground model slice (right)

Due to the high resolution of the voxelized ground model, each 2D cross section typically contains many distinct soil polygons (ten thousand to be exact). As a result, it is necessary to automate the entire preprocessing and modelling procedure. This includes the generation of 2D geometry, definition of material properties, assignment of materials to corresponding polygons, specification of calculation phases, progressive tunnel excavation deconfinement, initialization of in-situ stress conditions, and post-processing of simulation results. Manual handling of such volume of data would be infeasible and error-prone.



**Figure 5.** Flowchart of ground model slice to FEM integration

To facilitate automation, PLAXIS 2D HTTP API is utilized in conjunction with its Python wrapper (Figure 5). This allows programmatic access to the modelling environment. In the first stage, cross-sectional data derived from the 3D ground model is decomposed into separate datasets: one describing the geometry and the other containing the material property assignments. These datasets are processed in batches to optimize the performance. Specifically, groups of 200 soil polygons are handled at a time, for which Python scripts generate raw PLAXIS commands for geometry creation, material definition, and assignment.

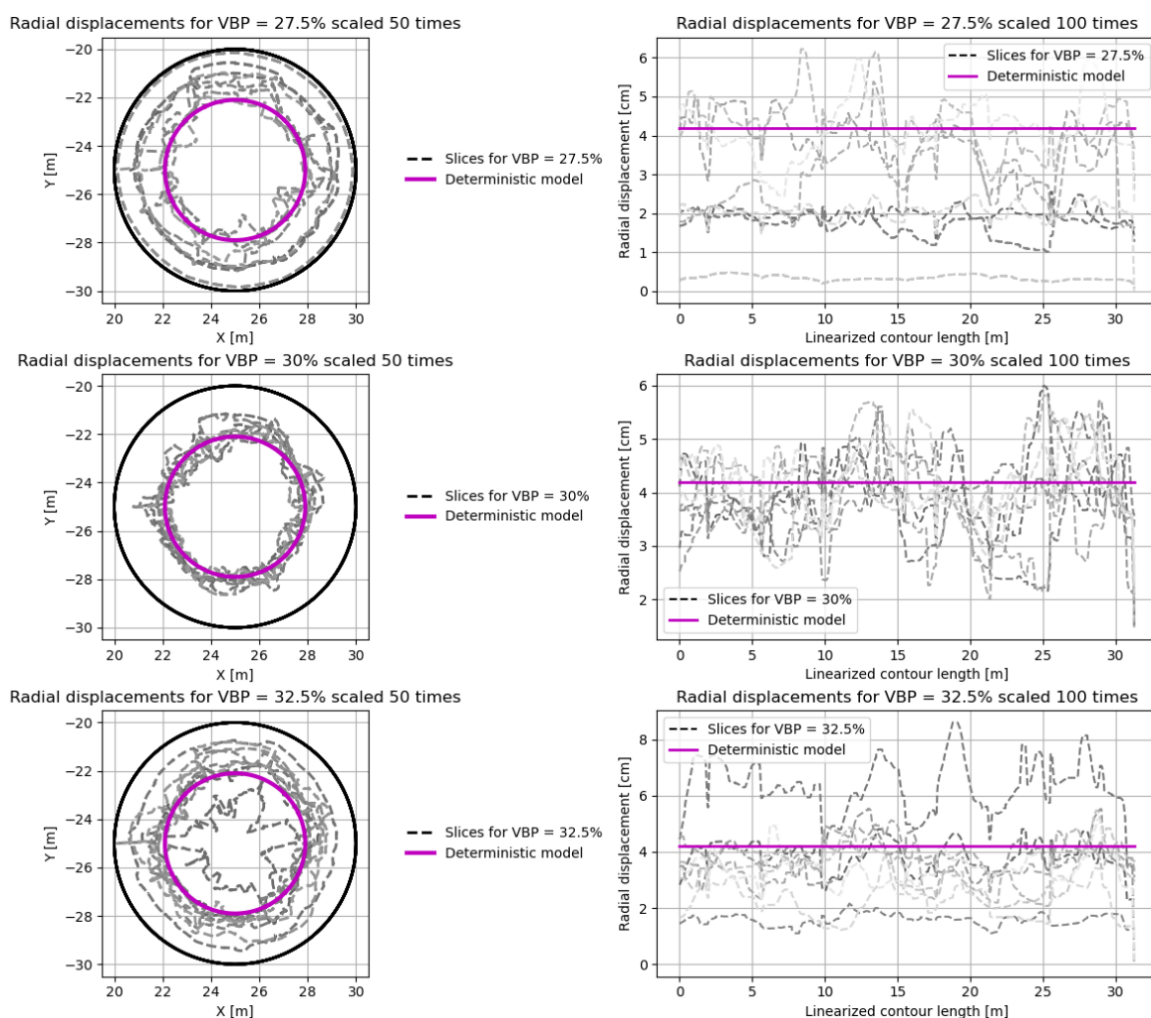
Rather than executing each command individually, which would lead to substantial overhead due to GUI refresh operations and potential congestion of the HTTP API server, all commands for each batch are assembled into a single request and transmitted at once. This batching strategy proves to be essential in maintaining the responsiveness of the PLAXIS 2D interface and avoiding performance degradation on the server side. By reducing the frequency of API calls, the approach significantly improves computational efficiency, allowing for rapid and reliable generation of all simulation-ready models.



#### 4. RESULTS AND DISCUSSION

The simulation results (see Figure 6) clearly highlight the considerable variability present within the analysed ground configurations. Given the relatively small differences between the considered volumetric block proportions of 27.5%, 30%, and 32.5%, the extracted 2D cross sections from the 3D ground model often exhibit comparable block configurations. As a result, each of these sections can realistically represent any of the analysed VBP scenarios. This demonstrates that, within the inherent stochastic framework of the model, multiple realizations of block distributions can exist for the same target VBP, contributing to the diversity of mechanical responses observed.

A consistent trend identified across the majority of simulations is that the application of the bimrock model, as opposed to a fully deterministic ground model, generally results in a reduction of radial displacements along the tunnel boundary (Figure 6). Consequently, tunnel convergence is effectively reduced in most analysed cases. This behaviour is primarily attributed to the reinforcing effect of rigid blocks embedded within the weaker matrix, which is consistent with previous findings in the literature (Napoli et al, 2021). Nevertheless, a substantial degree of result dispersion is evident, which is characteristic for ground conditions corresponding to low VBP values, situated near the lower threshold of geotechnical significance.

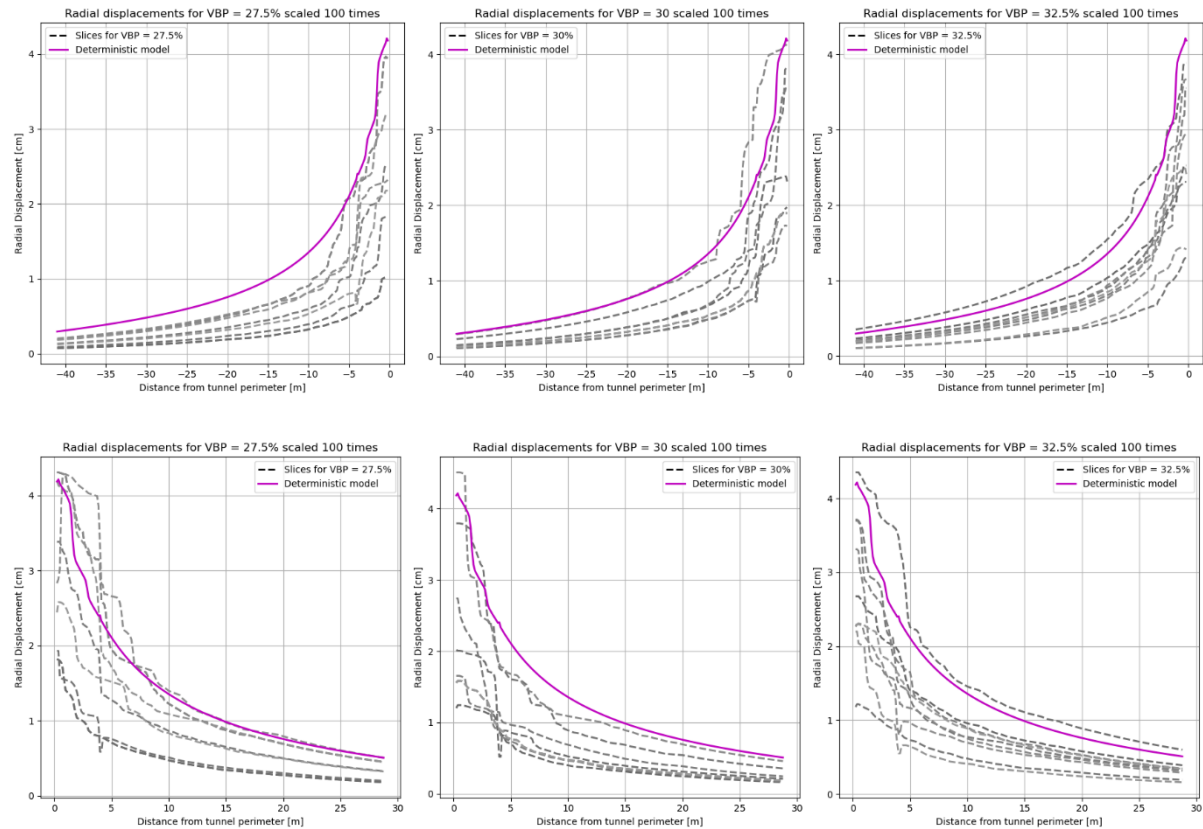


**Figure 6.** Radial displacement in tunnel cross section (left) and radial displacement vs linearized contour length (right)

Such low VBP values inherently imply a wide spectrum of possible ground configurations, whereby the spatial distribution and orientation of blocks relative to the tunnel excavation can vary significantly. In certain configurations, blocks positioned favourably around the excavation contribute to enhanced stability and reduced deformations. Conversely, unfavourably positioned blocks can lead to stress concentrations and localized deformation amplification.

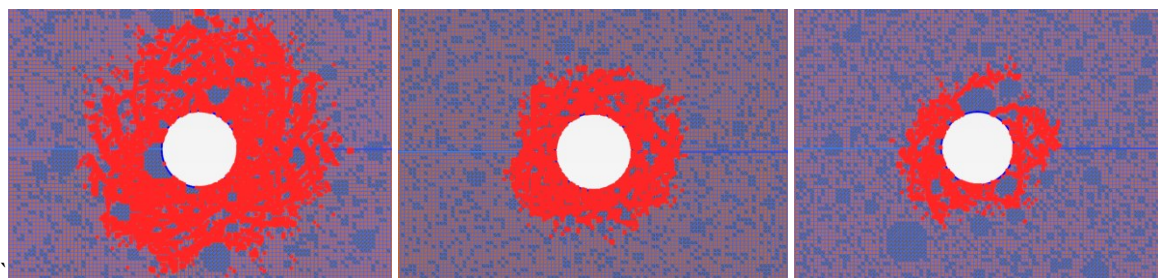
The analysis of radial displacements along the tunnel perimeter clearly reveals a highly non-uniform deformation pattern when compared to the idealized, homogeneous response predicted by deterministic models.

This outcome is a direct consequence of the diverse block arrangements generated within each cross section, and has direct implications on the design of tunnel linings. Specifically, the presence of non-uniform and non-symmetric deformations results in uneven loading on the tunnel lining, which must be carefully considered during structural design, as it may lead to an unfavourable distribution of bending moments and compromise the lining's structural performance.



**Figure 7.** Radial displacements vs. distance from tunnel perimeter for horizontal cross section, measured from left (top) and right sidewall (bottom) and different VBPs

The occurrence of ground model cross sections exhibiting larger radial displacements (compared to the deterministic baseline) is attributed to weaker matrix zones located at critical positions along the tunnel boundary, as given in Figure 7, which shows displacement profiles along the left and right sidewalls as a function of distance from the tunnel perimeter. These zones, resulting from the CRF-based parameter assignment, introduce less favourable excavation conditions compared to a homogeneous matrix assumption. In contrast, in the majority of other analysed cases, the results align well with literature expectations, with a general reduction in radial displacements due to the presence of blocks which is accompanied by significant scatter, characteristic of low-VBP bimrock conditions.



**Figure 8.** Plastic material zones for slices of 27.5%, 30% and 32.5% VBP, respectively

The effects of ground heterogeneity are also reflected in the stress distribution and the development of plastic zones within the rock mass. Particularly critical are the zones located in the immediate vicinity of the tunnel excavation, where both the stress patterns and the deformation response differ significantly from those predicted

by a deterministic model assuming homogeneous ground conditions. As shown in Figure 8, plastic yielding primarily occurs within the weaker matrix material, while the embedded blocks generally remain in the elastic state. The extent of the plastic zone varies for each analysed VBP configuration, depending on the specific block arrangement. Nevertheless, in most cases, the overall plastic zone is smaller compared to that obtained with the homogeneous deterministic model.

Based on all the above, it is evident that the proposed framework, even though it is presented on simulated data, exhibits implications directly relevant for real-world tunneling projects. In practical settings, its applicability depends on collaboration between geotechnical engineers, tunnel designers, and project managers. Performing field and laboratory investigations early in the project lifecycle comes essential to capturing block content, orientation, and representative geomechanical parameters of both matrix and blocks. These inputs determine the reliability of the subsequent stochastic block generation and CRF-based property assignment. Regarding the project management, the key impact lies in integrating presented models into risk assessment and decision-making processes, especially when addressing the excavation methods, support systems, and monitoring strategies. By explicitly acknowledging the uncertainty associated with block-in-matrix formations, project teams can better anticipate variability in ground behaviour, allocate contingencies, and establish more adaptive design and management frameworks.

## 5. CONCLUSIONS AND FUTURE PERSPECTIVE

This study presents a comprehensive modelling framework for reliable representation of block-in-matrix formations in tunnelling projects. By combining borehole-constrained stochastic block generation, voxel-based ground model discretization, and conditional random field simulation of matrix property variability, the methodology enables realistic generation of 3D BiM ground models for numerical analyses. A notable advancement of this study is the introduction of spatial variability in the geomechanical properties of the matrix, implemented through CRFs constrained by synthetic borehole data. This modelling approach introduces zones with locally enhanced or reduced geomechanical strength within the voxelized domain, thereby providing a more realistic representation of subsurface heterogeneity.

The case study of tunnel excavation within such a heterogeneous rock mass highlights several key findings. The results demonstrate that, even within the same target volumetric block proportion, a wide range of ground configurations can be generated, significantly influencing tunnel response. Compared to deterministic homogeneous models, BiM models generally exhibited reduced radial displacements and convergence due to the stiffening effect of rigid blocks embedded in the weaker matrix. However, considerable variability and scatter in displacements were observed, particularly for low VBP values, consistent with literature findings.

The matrix spatially variable properties yield a more realistic representation of ground heterogeneity; however, the presented results are primarily focused on the influence of VBP and block configuration on the tunnel behaviour. Plastic deformation zones develop mainly within the weaker matrix, with their extent and distribution strongly dependent on the specific block arrangement and local property variations. In general, plastic zones were smaller compared to those predicted by deterministic models, highlighting the combined influence of block positioning and matrix variability on tunnel stability.

Overall, the proposed modelling workflow represents an advancement in the realistic simulation of BiM formations for tunnelling applications. From a practical standpoint, its successful application to preliminary design stages requires careful consideration of the data available from field investigations. For BiM model construction, borehole logs should ideally include lithological descriptions, block frequency estimates, groundwater conditions, and depth-resolved laboratory measurements, as these inputs provide the basis for calibrating the model and generating realistic stochastic realizations. This capability to produce multiple realizations of block distributions enables designers to examine a spectrum of plausible ground conditions, thereby supporting probabilistic design approaches and more robust decision-making.

One of the main challenges encountered in the proposed workflow is establishing an effective link between the matrix material CRFs, the voxel-based ground model, and the subsequent finite element (FEM) simulations. A promising direction for future development lies in enhancing interoperability with the existing Building Information Modelling (BIM) platforms, such as Autodesk Revit, which could serve as an intermediate environment for management, visualization, and data exchange between CRF-based ground models and FEM software. Such integration would significantly streamline the workflow and improve data consistency across modelling stages.

In addition, further research would focus on incorporating real-world data obtained from tunnel face mapping to improve the estimation of VBP based on surface scans, as well. Implementing a workflow for continuous ground model updates using this type of observational data during excavation would provide an important step towards adaptive and more reliable tunnelling design in heterogeneous ground conditions.

## 6. ACKNOWLEDGMENTS

This research is supported by the Science Fund of the Republic of Serbia, Project No. 345 - Digital and Numerical Model Integration for Optimization in Geotechnics – DiNum-GEO. Authors are partially supported by Serbian Ministry of Science, Technological Development and Innovation via Project 200092.

## 7. BIBLIOGRAPHY

- [1] Guo, S., Wei, Q., Qi, S., Xue, L., Zheng, B., Wang, H., Li, J., Song, S., Liang, N., Zou, Y. & Huang, Z. (2024). Research progress on the geomechanical properties of block-in-matrix rocks. *Materials*, 17(5), 1167. <https://doi.org/10.3390/ma17051167>.
- [2] Heße, F., Prykhodko, V., Schlüter, S., & Attinger, S. (2014). Generating random fields with a truncated power-law variogram: A comparison of several numerical methods. *Environmental Modelling & Software*, 55, 32–48. <https://doi.org/10.1016/j.envsoft.2014.01.013>.
- [3] Kezdi, A. (1974). *Handbook of Soil Mechanics*. Elsevier.
- [4] Koloski, J., Schwarz, S., & Tubbs, D. (1989). Geotechnical properties of geologic materials. *Engineering Geology in Washington, Bulletin 78(1)*. Washington Division of Geology and Earth Resources.
- [5] Medley, E. W. (1994). The engineering characterization of melanges and similar block-in-matrix rocks (bimrocks). Doctoral dissertation. University of California, Berkeley.
- [6] Medley, E. & Lindquist, E. (1995). The engineering significance of the scale-independence of some Franciscan melanges in California, USA, The 35th U.S. Symposium on Rock Mechanics (USRMS), Reno, Nevada.
- [7] Müller, S., Schüler, L., Zech, A., & Heße, F. (2022). GSTools v1.3: A toolbox for geostatistical modelling in Python. *Geoscientific Model Development*, 15, 3161–3182. <https://doi.org/10.5194/gmd-15-3161-2022>.
- [8] Napoli, M. L., Barbero, M., Ravera, E., & Scavia, C. (2018). A stochastic approach to slope stability analysis in bimrocks. *International Journal of Rock Mechanics and Mining Sciences*, 101, 41–49. <https://doi.org/10.1016/j.ijrmms.2017.11.009>.
- [9] Napoli, M. L., Milan, L., Barbero, M., & Scavia, C. (2020). Identifying uncertainty in estimates of bimrocks volumetric proportions from 2D measurements. *Engineering Geology*, 278, 105831. <https://doi.org/10.1016/j.enggeo.2020.105831>.
- [10] Napoli, M. L., Barbero, M., & Scavia, C. (2021). Tunneling in heterogeneous rock masses with a block-in-matrix fabric. *International Journal of Rock Mechanics and Mining Sciences*, 138, 104655. <https://doi.org/10.1016/j.ijrmms.2021.104655>.
- [11] Napoli, M. L., Milan, L., Barbero, M., & Medley, E. (2022). Investigation of virtual bimrocks to estimate 3D volumetric block proportions from 1D boring measurements. *Geosciences*, 12(11), 405. <https://doi.org/10.3390/geosciences12110405>.
- [12] Napoli, M. L., Milan, L., Barbero, M., & Medley, E. (2023). Application of the point counting technique for estimating the VBP of geotechnically complex formations (Bimrocks/Bimsoils). In 15th ISRM Congress, Salzburg, Austria.
- [13] Obrzud, R., & Truty, A. (2012). The Hardening Soil Model – A Practical guidebook. Z Soil.PC 100701 report.
- [14] Rabcewicz, L. (1964). The New Austrian Tunneling Method (NATM). *Water Power*, 16(8), 453–457.
- [15] Wackernagel, H. (2003). *Multivariate geostatistics: An introduction with applications* (3rd ed.). Springer. <https://doi.org/10.1007/978-3-662-05294-5>.
- [16] Xue, J., & Nag, D. (2011). Reliability analysis of shallow foundations subjected to varied inclined loads. *Geotechnical safety and risk: Proceedings of the ISGSR 2011*, 377–384. Bundesanstalt für Wasserbau.
- [17] Zhang, H., Huang, C., Wang, L., Cao, Y., & Boldini, D. (2025). Estimation of volumetric block proportions from 1D boring of bim-materials considering different block forms. *Engineering Geology*, 353, 108094. <https://doi.org/10.1016/j.enggeo.2025.108094>.

## RESEARCH ON THE HIGH-TEMPERATURE MECHANICAL PROPERTIES OF CORRUGATED STEEL-CONCRETE COMPOSITE STRUCTURES IN TUNNEL ENGINEERING UNDER FIRE

Bo Lei<sup>1</sup>, Wenqi Ding<sup>2</sup>, Qingzhao Zhang<sup>3</sup>

**Abstract:** Corrugated steel-concrete (CSC) composite structures have been increasingly applied in tunnel engineering due to their excellent mechanical properties. Due to the frequent occurrence of tunnel fires, accurately evaluating the high-temperature mechanical properties of CSC composite structures is crucial for determining the stability of lining structures under tunnel fires. This paper employs the novel S32001 duplex stainless steel to investigate the thermo-mechanical coupling of CSC composite structures through numerical simulation. The study explores the load-bearing capacity and deformation characteristics of CSC composite structures under various temperature conditions and the ISO 834 standard heating curve, while evaluating structural stability across different operating conditions. Research indicates that CSC composite structures exhibit similar deformation characteristics under temperature conditions ranging from 100 °C to 500 °C, with vertical displacement and stress levels increasing as temperature rises and time progresses. Under the ISO834 heating curve, corrugated steel plates heats up relatively quickly and the trough temperature is higher than the peak temperature. The temperature field distribution of the concrete in the cross-section of the specimen shows the “corrugated” pattern, with the most pronounced corrugation and maximum temperature gradient occurring at the troughs. Significant thermal deformation differences exist at the interface between the rebar cage and concrete, resulting in pronounced internal cracking at this area. No delamination occurred at the interface between the corrugated steel plate and concrete, and the overall deformation of the CSC composite structures remained controllable. This study demonstrates the superior fire resistance of CSC composite structures, aiding in fire protection design for such structures in tunnel engineering and providing guidance for the stability research of tunnel lining structures under fire scenarios.

**Keywords:** Tunnel engineering, Corrugated steel-concrete composite structures, Fire, Numerical simulation, High-temperature mechanical properties

### 1. INTRODUCTION

Corrugated steel prefabricated structures have the advantages of good load-bearing performance, strong cross-sectional bending resistance, light weight and easy assembly, fast construction speed, adaptability to various cross-sections, recyclability for reuse, and environmental friendliness (Che et al, 2021). They are widely used in tunnel sheds, connecting passages, shafts, inclined shafts, water conveyance tunnels, and comprehensive pipe galleries (Figure 1). In recent years, the application of corrugated steel plates in tunnel support structures has gradually increased, and scholars have conducted relevant research on their mechanical properties. Such as the analysis of the monitoring laws of corrugated steel shed tunnel structures, the research on the construction technology of corrugated steel prefabricated initial support structures in tunnels, the study on the influence of corrosion on the

<sup>1</sup> PhD, Lei Bo, Civil Engineering, Department of Geotechnical Engineering, College of Civil Engineering, Tongji University, 1239 Siping Road & Key Laboratory of Geotechnical and Underground Engineering, Ministry of Education, Shanghai, 200092, China, 2111001@tongji.edu.cn

<sup>2</sup> Prof., Ding Wenqi, Civil Engineering, Department of Geotechnical Engineering, College of Civil Engineering, Tongji University, 1239 Siping Road & Key Laboratory of Geotechnical and Underground Engineering, Ministry of Education, Shanghai, 200092, China, dingwq@tongji.edu.cn

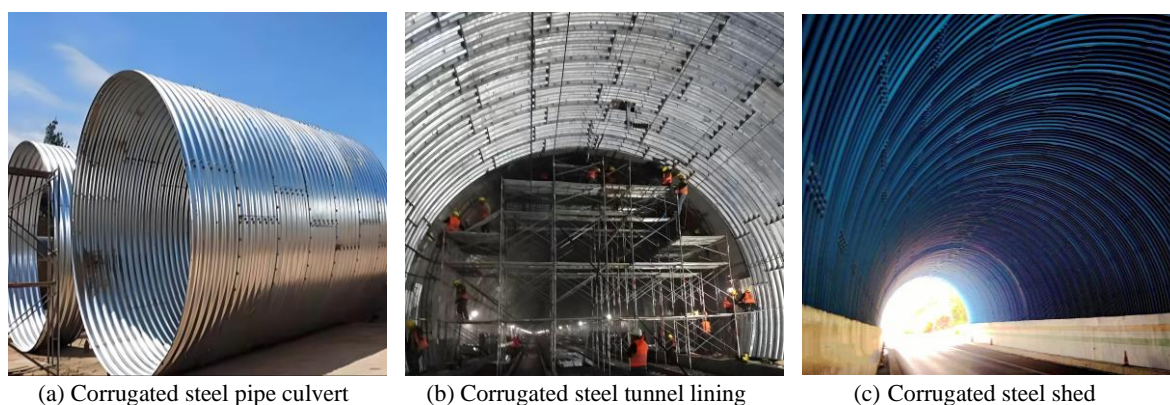
<sup>3</sup> Assoc. Prof., Zhang Qingzhao, Civil Engineering, Department of Geotechnical Engineering, College of Civil Engineering, Tongji University, 1239 Siping Road & Key Laboratory of Geotechnical and Underground Engineering, Ministry of Education, Shanghai, 200092, China, zhangqingzhao@tongji.edu.cn



performance of buried corrugated steel culverts, and the research on the mechanical properties of corrugated steel prefabricated panels used in the repair of shield tunnel segments, etc (Nakhostin et al, 2022; Yu et al, 2020).

In order to enhance the structural bearing capacity, corrugated steel plates are often combined with concrete to form corrugated steel-concrete composite structures, which have been gradually promoted and applied in tunnel engineering. Due to the frequent occurrence of tunnel fires, the study on the high-temperature mechanical properties of tunnel lining structures has gradually increased in recent years ((Morovat Mohammed A. and Engelhardt Michael D., 2020; Shaheen et al, 2020). Many scholars have conducted relevant experimental and theoretical studies on the mechanical properties of steel at high temperatures (Jiang et al, 2020; Sun et al, 2022). For common steel, strength exhibits a significant decline when the ambient temperature reaches 500 °C. At 600 °C, the steel will lose most of its strength and stiffness (Al-Thairy, 2020). Duplex stainless steel has relatively good strength and ductility, and its strength and ductility are superior to those of single-phase austenitic stainless steel or ferritic stainless steel (Jeong et al, 2015). Maraveas and Vrakas (2014) analyzed the temperature field distribution of reinforced concrete sections under different fire temperature rise curves through non-coupled heat transfer transient numerical analysis. Tomar and Khurana (2020) studied the distribution of air in the tunnel and the surface temperature of the tunnel lining under fire conditions with and without fire prevention measures through numerical simulation. Li et al. (2023) investigated the effects of temperature on the shrinkage behavior and hardening slope of steel yield surfaces, establishing a new yield criteria for stainless steel and high-strength alloy steel under temperature influence.

Research findings on the high-temperature thermodynamic behavior of tunnel structures remain relatively scarce at present. Existing studies primarily focus on reinforced concrete lining structures, with limited systematic investigations into the high-temperature fire resistance of steel lining structures. Research on the load-bearing capacity and stability of corrugated steel-concrete composite structures under fire conditions is insufficient, and studies on the high-temperature performance of novel duplex stainless steel corrugated plate structures are even fewer. This paper employs numerical simulation to investigate the load-bearing capacity and deformation characteristics of corrugated steel-concrete composite structures under various temperature conditions and standard heating curve, verifying the excellent fire resistance performance of the composite structures, which has reference significance for engineering design.



**Figure 1.** Applications of corrugated steel structures.

## 2. NUMERICAL ANALYSIS

### 2.1. Finite Element Model

In this study, the sequential coupling method is adopted to calculate the thermodynamic coupling behavior of corrugated steel-concrete composite structures at high temperatures. The specific implementation is divided into two steps: Firstly, the distribution result of the temperature field of the corrugated steel-concrete composite structure is calculated based on the fire scene. Then, the calculation result of the temperature field is applied as a boundary condition to the mechanical model to calculate the force and deformation behavior of the structure.

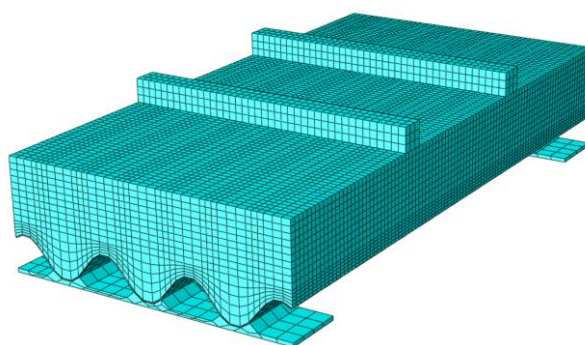
The finite element model is established based on the actual geometric dimensions of the specimen. The wave distance-wave height-thickness of the corrugated steel plate is 380mm-140mm-5mm. The length of the steel plate is 2.40m and the width is 1.24m. The steel grade is the new duplex stainless steel S32001, with a room-temperature elastic modulus  $E_{cs}=258.86\text{GPa}$ . The plain concrete strength grade is C30, with dimensions matching the corrugated steel plate (length and width) and the thickness of 30 cm. The steel bar grades are all HRB400, with an elastic modulus  $E_s=200\text{GPa}$ . Among them, the diameter of the longitudinal force-bearing steel bar is 22mm, and

the diameters of the supporting and transverse distributed steel bars are 12mm. The base plate beneath the corrugated steel plate is made of Q235 grade steel.

The corrugated steel plate, concrete, backing plates and loading frames are simulated using three-dimensional solid elements, and the reinforcing bars are all simulated using truss elements. The grid division of each component is shown in Figure 2. The concrete and the steel cage are embedded constraints, the concrete and the corrugated steel plate are in hard contact, the corrugated steel plate and the steel cage are tie constraints, the corrugated steel plate and the base plates are tie constraints, and the concrete and the loading frame are tie constraints. The vertical force is applied to the specimen by the vertical jack through two distribution beams, and the corresponding vertical load is applied at the corresponding position in the finite element model. The horizontal force acts directly on the specimen through the horizontal jack, so the corresponding horizontal load is applied at the center position of the jack's flexible head.

The calculation of the temperature field adopts the transient heat transfer analysis method, which can describe the real-time changes of the temperature field over time. Under actual fire conditions, complex situations such as evaporation of internal moisture in concrete and concrete cracking may occur, making the calculation difficult to achieve. In this study, certain simplifications have been made: (1) The three-dimensional load structure method is adopted for the thermodynamic sequential coupling calculation, considering the heat transfer effects of corrugated steel plate, steel cages and concrete, and the influence of the stratum is treated according to the boundary conditions of heat dissipation and static load; (2) The temperature changes caused by the evaporation of water inside the concrete are not taken into account. (3) The impact of concrete cracking is not analyzed for the time being.

The number of grids in the model is 61450. In the pure thermal calculation example, the element types of corrugated steel plate, concrete, backing plates and loading frames are DC3D8R, and the element type of the steel cage is DC1D2. In the mechanical calculation example, the unit types of corrugated steel plate, concrete, backing plates and loading frames are C3D8R, and the unit type of the steel cage is T3D2.



*Figure 2. Three-dimensional finite element calculation model.*

## 2.2. Material Parameters

In thermodynamic simulation, it is necessary to determine the thermodynamic parameters of the materials. In the process of taking values for the thermodynamic parameters of the materials, this paper references the “Eurocode 2: Design of concrete structures, EN 1992-1-2” and “Eurocode 3: Design Of Steel Structures-Part 1-2: General Rules-Structural Fire Design”.

### (1) Thermal parameters of steel

Table 1 presents the thermal parameters of steel, including the coefficient of thermal expansion, thermal conductivity, specific heat capacity and density.

*Table 1. Thermal parameters of steel.*

Parameters	Symbol	Value	Unit
Coefficient of thermal expansion	$\alpha_s$	$1.4 \times 10^{-5}$	m/(m·°C)
Thermal conductivity coefficient	$\lambda_s$	45	W/(m·°C)
Specific heat capacity	$c_s$	600	J/(kg·°C)
Density	$\rho_s$	7850	kg/m <sup>3</sup>

### (2) High-temperature mechanical parameters of steel

#### 1) Elastic modulus

The elastic modulus at different temperatures is calculated according to Equations (1) and (2):

$$E_{sT} = \chi_{sT} E_s \quad (1)$$

$$\chi_{sT} = \begin{cases} \frac{7T - 4780}{6T - 4760} & (20^\circ\text{C} \leq T \leq 600^\circ\text{C}) \\ \frac{1000 - T}{6T - 2800} & (600^\circ\text{C} \leq T \leq 1000^\circ\text{C}) \end{cases} \quad (2)$$

In the formula,  $E_{sT}$  is the elastic modulus value of steel at high temperature;  $E_s$  is the elastic modulus value of steel at room temperature, and  $\chi_{sT}$  is the elastic modulus reduction coefficient of steel at high temperature.

## 2) Material strength

The strength at different temperatures is calculated according to Equations (3) and (4):

$$f_{sT} = \eta_{sT} f_s \quad (3)$$

$$\eta_{sT} = \begin{cases} 1.0 & (20^\circ\text{C} \leq T \leq 300^\circ\text{C}) \\ 1.24 \times 10^{-8} T^3 - 2.096 \times 10^{-8} T^2 & (300^\circ\text{C} \leq T \leq 800^\circ\text{C}) \\ +9.228 \times 10^{-3} T - 0.2168 & (800^\circ\text{C} \leq T \leq 1000^\circ\text{C}) \\ 0.5 - T / 2000 & (800^\circ\text{C} \leq T \leq 1000^\circ\text{C}) \end{cases} \quad (4)$$

In the formula,  $f_{sT}$  is the strength value of steel at high temperature, and  $f_s$  is the strength value of steel at room temperature, and  $\eta_{sT}$  is the strength reduction coefficient of steel at high temperature.

## (3) Thermal parameters of concrete

1) Density and coefficient of thermal expansion: The density of concrete is taken as  $2300\text{kg/m}^3$ , and the coefficient of thermal expansion of concrete is taken as  $\alpha_c = 1.8 \times 10^{-5} \text{ m/(m} \cdot ^\circ\text{C)}$ .

2) Thermal conductivity  $\lambda_c$ : The unit of thermal conductivity is  $\text{W/(m} \cdot ^\circ\text{C)}$ , and its value varies with temperature  $T$  as follows:

$$\lambda_c = 1.68 - 0.19 \frac{T}{100} + 0.0082 \left( \frac{T}{100} \right)^2 \quad (5)$$

3) Specific heat capacity: The unit of specific heat capacity is  $\text{J/(kg} \cdot ^\circ\text{C)}$ , and the relationship between specific heat capacity and temperature  $T$  is taken as follows:

$$c_c = 890 + 56.2 \frac{T}{100} - 3.4 \left( \frac{T}{100} \right)^2 \quad (6)$$

## (4) High-temperature mechanical parameters of concrete

The calculation formulas for the elastic modulus and axial compressive strength of ordinary concrete under high-temperature conditions are as follows:

$$E_{cT} = \chi_{cT} E_c \quad (7)$$

$$f_{cT} = \eta_{cT} f_c \quad (8)$$

In the formula,  $E_{cT}$  is the elastic modulus value of concrete at high temperature,  $E_c$  is the elastic modulus value of concrete at room temperature, and  $\chi_{cT}$  is the elastic modulus reduction coefficient of concrete at high temperature.  $f_{cT}$  is the axial compressive strength value of concrete at high temperature, and  $f_c$  is the axial compressive strength value of concrete at room temperature.  $\eta_{cT}$  is the axial compressive strength value reduction coefficient of concrete at high temperature. Table 2 shows axial compressive strength and elastic modulus reduction coefficient of ordinary concrete at high temperature.

**Table 2.** Axial compressive strength and elastic modulus reduction coefficient of ordinary concrete at high temperature.

T/°C	20	100	200	300	400	500	600	700	800	900	1000	1100
$\chi_{cT}$	1.0	0.625	0.432	0.304	0.188	0.1	0.045	0.03	0.015	0.008	0.004	0.001
$\eta_{cT}$	1.0	1.00	0.95	0.85	0.75	0.6	0.45	0.30	0.15	0.08	0.04	0.01

### 2.3. Load Conditions

The load conditions in this paper are mainly divided into two parts. The first part is the high-temperature mechanical analysis of corrugated steel-concrete composite structures at different temperatures. Corresponding overall uniform temperature field boundary conditions are applied to the composite structures under different temperature conditions. The temperature value range under the high-temperature condition is 100 °C to 500 °C, and one condition is calculated at intervals of 100 °C. There are a total of five conditions. Each working condition lasts for 2 hours. The axial force of the composite structure is 600KN and the vertical force is 1000KN.

The second part is that the specimen is heated for 2 hours on the ISO834 heating curve, accompanied by mechanical loading. The axial force of the composite structure is 600KN and the vertical force is 1000KN to explore the high-temperature mechanical properties of the composite structure. Figure 3 shows the typical fire temperature rise curves, where the formula of the ISO834 temperature rise curve is shown as Equation (9) :

$$T = 345 \lg(8t + 1) + 20 \quad (9)$$

In the formula,  $T$  represents the temperature in the fire environment and  $t$  represents the duration of the fire.

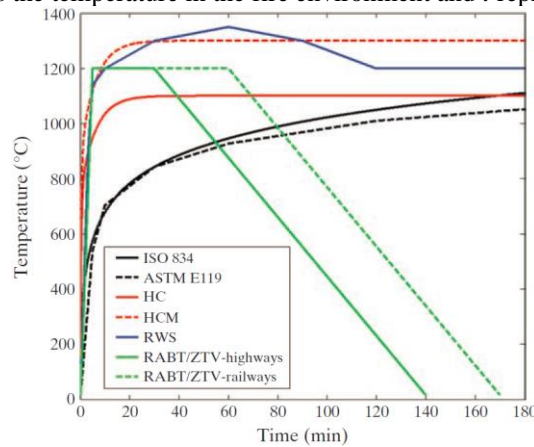
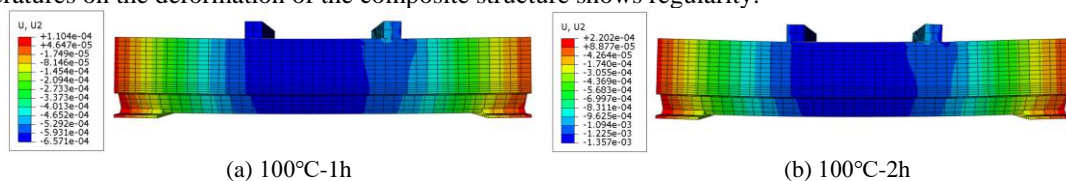


Figure 3. Typical temperature rise curves.

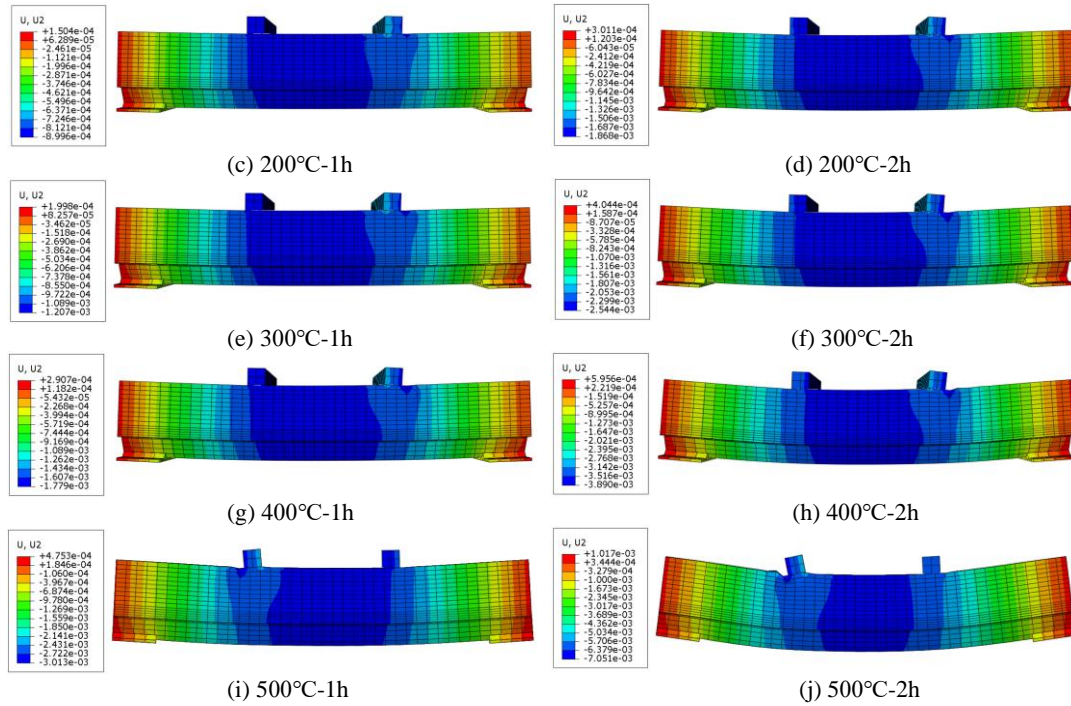
## 3. NUMERICAL SIMULATION RESULTS AT DIFFERENT TEMPERATURES

### 3.1. Displacement varies with time at different temperatures

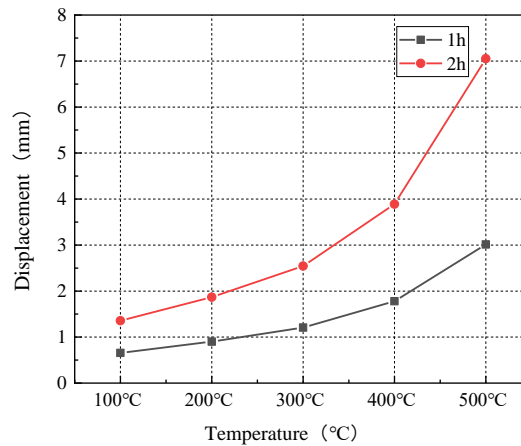
From the numerical simulation results, the vertical displacement cloud maps of each temperature condition lasting for 1 hour and 2 hours are extracted, and the graphs of vertical displacement varying with time under different temperature conditions are drawn, as shown in Figs. 4 and 5. As shown in Figs. 4 and 5, the deformation of the corrugated steel-concrete composite structure under different temperature working conditions is relatively similar. The upper part of the structure is under compression and the lower part is under tension. The overall structure bends upward. At the same time, the vertical displacement increases with the increase of temperature. The maximum mid-span vertical displacements of the composite structure maintained for 1 hour at temperatures of 100 °C, 200 °C, 300 °C, 400 °C and 500 °C are 0.657mm, 0.9mm, 1.207mm, 1.779mm and 3.013mm, respectively. The maximum mid-span vertical displacements of the composite structure maintained for 2 hours at temperatures of 100 °C, 200 °C, 300 °C, 400 °C and 500 °C for 2 hours are 1.357mm, 1.868mm, 2.544mm, 3.890mm and 7.051mm, respectively. The mid-span vertical displacement ratios of the composite structure maintained at temperatures of 100 °C, 200 °C, 300 °C, 400 °C and 500 °C for 2 hours and 1 hour are 2.065, 2.076, 2.108, 2.187 and 2.34, respectively. It can be known that with the increase of time, the influence of different temperatures on the deformation of the composite structure shows regularity.







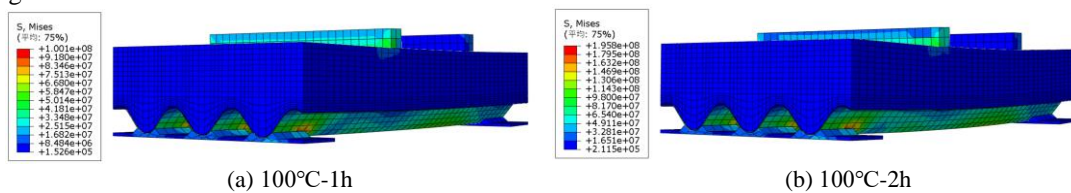
**Figure 4.** Displacement variation with time at different temperatures (Unit: m, deformation magnified 15 times).



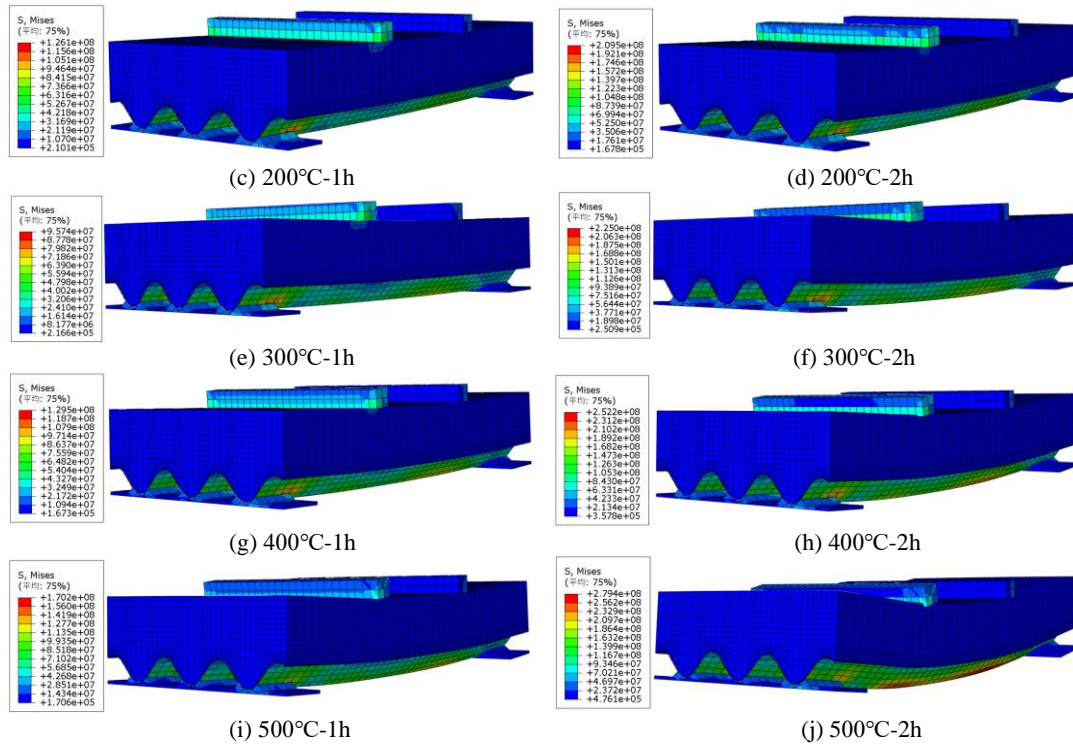
**Figure 5.** Graph of vertical displacement varying with time under different temperature conditions.

### 3.2. Stress variations with time at different temperatures

From the numerical simulation results, the Mises stress cloud diagrams of each temperature condition lasting for 1 hour and 2 hours are extracted (Figure 6). As shown in Figure 6, the maximum Mises stresses for the composite structure maintained at 100 °C, 200 °C, 300 °C, 400 °C, and 500 °C for 2 hours are 195.8 MPa, 209.5 MPa, 225 MPa, 252.2 MPa, and 279.4 MPa, respectively. Stress levels increased with rising temperature and prolonged duration.







**Figure 6.** Stress variation over time at different temperatures (Unit: Pa, deformation amplification 15 times).

## 4. NUMERICAL SIMULATION RESULTS UNDER THE ISO834 TEMPERATURE RISE CURVE

### 4.1. Temperature field distribution varies with time

The temperature field distribution of the whole composite structure, concrete, steel cage and corrugated steel plate with time after heating for 1 hour under the ISO834 heating curve is shown in Figure 7. As shown in Fig. 7(c)~(d), the maximum temperatures of the corrugated steel plate reach 946 °C and 1047 °C after 1 hour and 2 hours of heating, respectively. The trough temperature is higher than the peak temperature, and the temperature field distribution along the longitudinal direction of the specimen is consistent.

As shown in Fig. 7(e)~(f), the temperature field at the bottom of the concrete is similar to that of the corrugated steel plate. Due to the low thermal conductivity and large specific heat capacity of the concrete material, the overall heating rate of the concrete is significantly slower than that of the steel. After 1 hour and 2 hours of heating, the maximum concrete temperatures reach 798 °C and 886 °C, respectively, demonstrating significant thermal inertia. The cross-sectional temperature field distribution along the thickness direction of the concrete shows a "wavy" feature. The closer it is to the trough, the more obvious the wavy feature becomes. From 1 hour to 2 hours, the corrugated cloud pattern of the cross-section gradually expands upwards. The thickness of the concrete affected by fire gradually increases, the overall temperature keeps rising, and the temperature gradient keeps increasing.

As shown in Fig. 7(g)~(h), the temperature difference between the bottom of the stiffening ribs and the adjacent corrugated steel plate is relatively small. After 1 hour and 2 hours of heating, the temperatures at this location reach 852 °C and 946 °C, respectively, exceeding the temperature of the underlying concrete in contact with the corrugated steel plate. The temperature of the stiffening ribs gradually decreases from bottom to top. The upper transverse and longitudinal bars are far away from the heating surface and have a lower temperature. Moreover, as the heating duration increases, the temperature beneath the stiffening ribs rises significantly, while the temperature of the upper ribs shows little change, resulting in a continuously widening temperature gradient within the stiffening ribs. Due to the different thermal parameters of the steel cage and the concrete, the amount of thermal deformation at the contact part between the steel cage and the concrete varies, resulting in deformation misalignment between the two. Moreover, as the temperature rises, the internal damage of the concrete increases, and the concrete at the contact point with the steel cage experiences significant stress, leading to notable internal cracks.

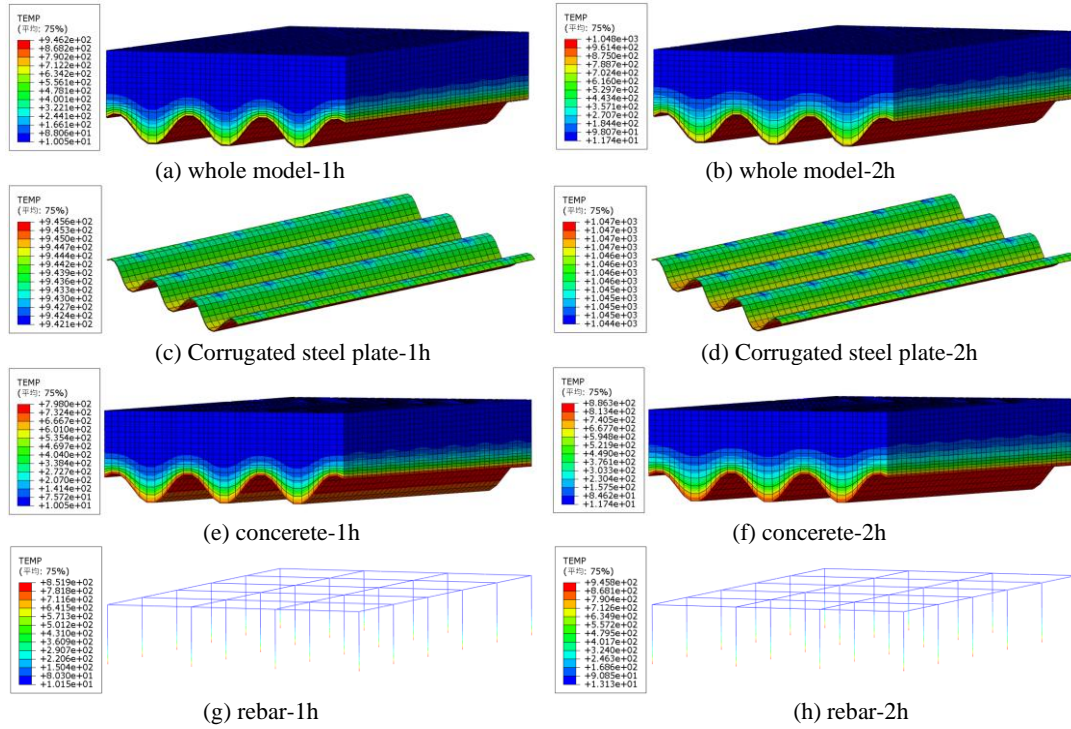


Figure 7. The temperature field distribution of the specimen under ISO834 heating curve

(Unit:  $^{\circ}\text{C}$ , deformation magnified 15 times).

#### 4.2. Displacement varies with time

From the numerical simulation results, the vertical displacement cloud maps of heating for 1 hour and 2 hours under the ISO834 heating curve are extracted, as shown in Figure 8. It can be known from Figure 8 that under the ISO834 heating curve, the upper part of the corrugated steel-concrete composite structure is compressed and the lower part is tensioned, and the overall structure bends upward. The composite structure exhibited maximum mid-span vertical displacements of 4.035 mm and 13.27 mm after 1 hour and 2 hours of heating, respectively. Also, the vertical displacements increased significantly with the increase of heating time.

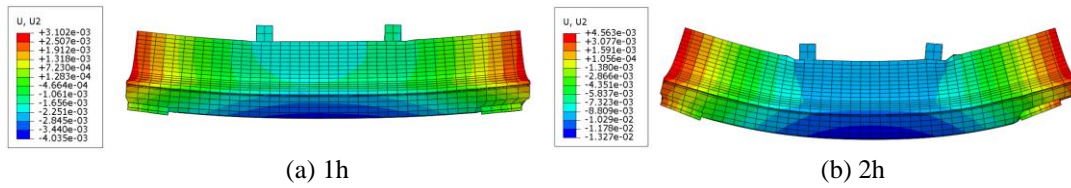


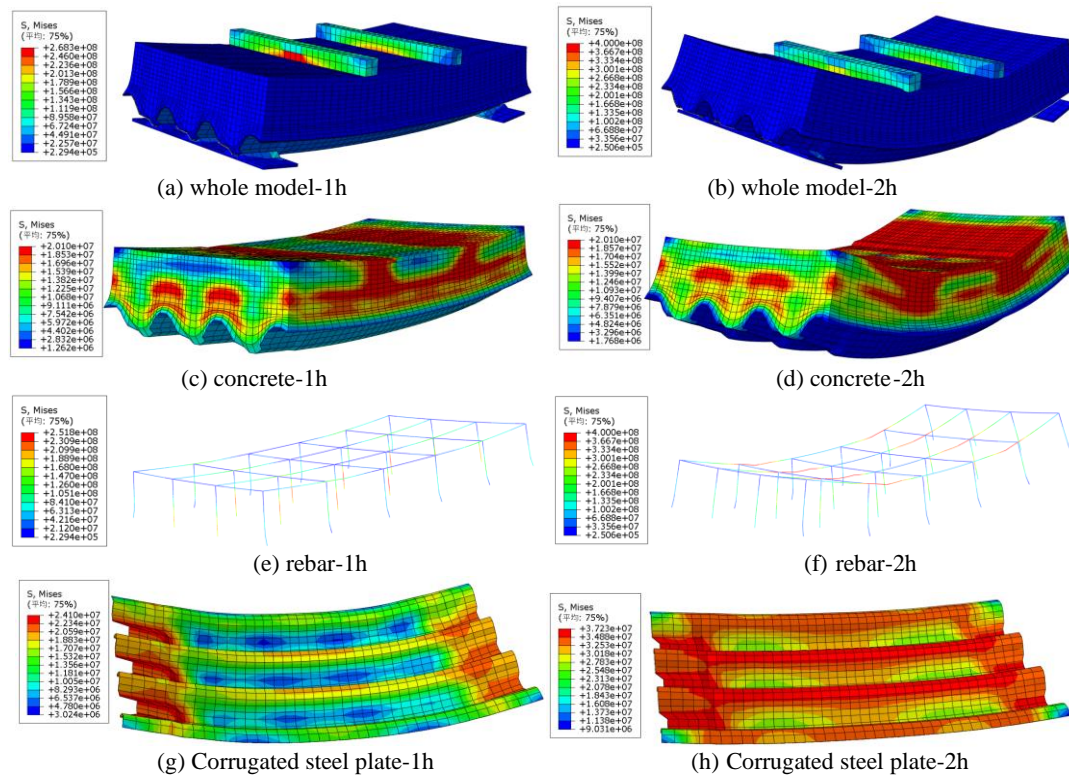
Figure 8. The displacement of the specimen under ISO834 temperature rise curve varies with time

(Unit: m, deformation magnified 15 times).

#### 4.3. Stress varies with time

To observe the stress distribution of the corrugated steel-concrete composite structure during the fire exposure process, the stress cloud diagrams corresponding to the composite structure, concrete, steel cage and corrugated steel plate at 1 hour and 2 hours of fire exposure are extracted respectively, as shown in Figure 9. It can be seen from Figure 9 that the stress on the upper part of the concrete and the upper part of the wave crest is relatively large, and the stress on the longitudinal bars at the upper part of the steel cage and the bars at the upper part of the wave crest is also relatively large, and all the stresses keep increasing over time. As shown in Fig. 9(g)-(h), when the fire exposure time reaches 1 hour and 2 hours, the temperature of the corrugated steel plate has approached  $1000^{\circ}\text{C}$ . At this temperature, the yield strength of the corrugated steel is 18.3MPa. The corrugated steel shows a large area of yield, and the stress at the wave crest is significantly higher than that at the wave trough. A significant stress concentration phenomenon also occurs at the welding area between the bottom corrugated steel plate and backing plates. This is primarily due to the continued use of existing Q235 carbon steel bearing plates in this

calculation example. Differences in thermodynamic parameters between the bearing material and the new duplex stainless steel corrugated steel lead to variations in thermal deformation between the two materials, resulting in stress concentration at their contact areas.



**Figure 9.** The stress of the specimen varies with time under the ISO834 heating curve (Unit: Pa, deformation amplification 15 times).

## 5. CONCLUSIONS

In this study, numerical simulation methods are adopted to analyze the bearing capacity and deformation characteristics of corrugated steel-concrete composite structures under different temperature conditions and ISO heating curves, and the following conclusions are obtained:

(1) The deformation of corrugated steel-concrete composite structures under temperature conditions ranging from 100 °C to 500 °C is relatively similar. The upper part of the structure is under compression, the lower part is under tension, and the overall structure bends upward. The vertical displacement and stress level increase with the rise in temperature and the passage of time.

(2) Under the ISO834 heating curve, the maximum temperature of the corrugated steel plate after 2 hours of heating is 1047 °C, and the trough temperature is higher than the peak temperature. The temperature field distribution of the steel plate is consistent along the longitudinal distribution of the specimen. The temperature field distribution of the specimen cross-section shows a "wavy" feature. The closer it is to the trough, the more obvious the wavy feature becomes. The temperature is the highest and the temperature gradient is the greatest at the trough. There is a significant difference in the amount of thermal deformation at the contact part between the steel cage and the concrete, which can lead to obvious internal cracks at this location.

(3) Under the ISO834 heating curve, both the vertical displacement and stress of the corrugated steel-concrete composite structure keep increasing over time. After being exposed to fire for 2 hours, the corrugated steel plate shows a relatively large area of yield, but the overall deformation of the composite structure is within the allowable range.

Our research group has conducted the full-scale fire test on corrugated steel-concrete composite structures under the ISO 834 heating curve. The corrugated steel-concrete composite structure maintains stability under simultaneous fire heating and mechanical loading, with no delamination observed at the interface between the corrugated steel plate and concrete. This validates the excellent fire resistance of this composite structure. Subsequent work will involve stability verification and fire-resistance design for corrugated steel-lined tunnels under fire scenarios, based on test results, numerical simulations, and theoretical analysis.



## 6. ACKNOWLEDGMENTS

The authors wish to acknowledge the sponsorship from the National Natural Science Foundation of China(NO.52378405), the Major Science and Technology Special Project of Yunnan Provincial Department of Transportation(No.202302AD080007), and “Transportation Science and Technology Demonstration Project of the Ministry of Transport: Intelligent Construction Science and Technology Demonstration Project of Complex Environment Tunnels along the Jinsha River Expressway in Yunnan Province”.

## 7. REFERENCES

- [1] Al-Thairy, H. (2020). A simplified method for steady state and transient state thermal analysis of hybrid steel and FRP RC beams at fire. *Case Studies in Construction Materials*, 13, e00465. <https://doi.org/10.1016/j.cscm.2020.e00465>
- [2] Che, H., Tong, L., Liu, S., Yang, Q. (2021). Field investigation on the mechanical performance of corrugated steel utility tunnel (CSUT). *Journal of Constructional Steel Research*, 183, 106693. <https://doi.org/10.1016/j.jcsr.2021.106693>
- [3] Jeong, C. U., Heo, Y.-U., Choi, J. Y., Woo, W., Choi, S.-H. (2015). A study on the micromechanical behaviors of duplex stainless steel under uniaxial tension using ex-situ experimentation and the crystal plasticity finite element method. *International Journal of Plasticity*, 75, 22–38. <https://doi.org/10.1016/j.ijplas.2015.07.005>
- [4] Jiang, S., Zhu, S., Guo, X., Chen, C., Li, Z. (2020). Safety monitoring system of steel truss structures in fire. *Journal of Constructional Steel Research*, 172, 106216. <https://doi.org/10.1016/j.jcsr.2020.106216>
- [5] Li, S., Ding, W., Zhang, Q. (2023). Development of a new temperature-dependent yield criterion for stainless and high-strength alloy steels in construction engineering. *Case Studies in Construction Materials*, 18, e02149. <https://doi.org/10.1016/j.cscm.2023.e02149>
- [6] Maraveas, C., and Vrakas, A. A. (2014). Design of Concrete Tunnel Linings for Fire Safety. *Structural Engineering International*, 24(3), 319–329. <https://doi.org/10.2749/101686614X13830790993041>
- [7] Morovat Mohammed A. and Engelhardt Michael D. (2020). Critical Review of Test Methods for Mechanical Characterization of Steel for Structural-Fire Engineering Applications. *Journal of Structural Engineering*, 146(11), 04020228. [https://doi.org/10.1061/\(ASCE\)ST.1943-541X.0002787](https://doi.org/10.1061/(ASCE)ST.1943-541X.0002787)
- [8] Nakhostin, E., Kenny, S., Sivathayalan, S. (2022). A numerical study of erosion void and corrosion effects on the performance of buried corrugated steel culverts. *Engineering Structures*, 260, 114217. <https://doi.org/10.1016/j.engstruct.2022.114217>
- [9] Shaheen, M. A., Foster, A. S. J., Cunningham, L. S., Afshan, S. (2020). Behaviour of stainless and high strength steel bolt assemblies at elevated temperatures—A review. *Fire Safety Journal*, 113, 102975. <https://doi.org/10.1016/j.firesaf.2020.102975>
- [10] Sun, G., Li, Z., Wu, J., Ren, J. (2022). Investigation of steel wire mechanical behavior and collaborative mechanism under high temperature. *Journal of Constructional Steel Research*, 188, 107039. <https://doi.org/10.1016/j.jcsr.2021.107039>
- [11] Tomar, M. S., and Khurana, S. (2020). A numerical study on the influence of different tunnel lining insulation materials in a road tunnel fire. *Materials Today: Proceedings*, 28, 665–671. <https://doi.org/10.1016/j.matpr.2019.12.274>
- [12] Yu, C., Ding, W., Wu, T., Zhang, Q. (2020). Study on calculation method of new corrugated steel reinforcement structure of highway tunnel. *IOP Conference Series: Materials Science and Engineering*, 741(1), 012073. <https://doi.org/10.1088/1757-899X/741/1/012073>
- [13] (CEN) European Committee for Standardization. Eurocode 2: Design of concrete structures, EN 1992-1-2 [S]. 2004.
- [14] Standardization European Committee For. Eurocode 3: Design Of Steel Structures - Part 1-2: General Rules - Structural Fire Design [S]. 2005.

## CONQUERING CHALLENGES IN THE DESIGN AND CONSTRUCTION OF AN INTEGRATED UNDERGROUND SINGAPORE METRO STATION

Hooi Leng, Phua<sup>1</sup>, Maznah Mohd Ali<sup>2</sup>, Michelle Wu<sup>3</sup>, Anand Kumar Pochambavi<sup>4</sup>, Si Thu Aung<sup>5</sup>

**Abstract:** Singapore is highly built-up city-state with very limited land for development to meet its very needs. Hence, to optimise the land, majority of Singapore's Metro Lines are underground to free up the above ground spaces, and intensify the development potential and land value capture.

The fully underground Thomson-East Coast Line (TEL) will be Singapore's sixth metro line. Stretching 43 kilometers long with 32 stations, it is progressively being opened in stages from 2020 to 2026. The TEL will connect to all of Singapore existing MRT lines at eight interchange stations. Of these, Woodlands Station is one of the largest stations and will connect to the existing elevated Station. Being at the center of Woodlands Regional Center development in the nexus of Singapore's Northern Region, the new Woodlands Station will also be integrated with existing and future developments to form a seamless multi-modal transport hub, and also house other commercial and civic uses.

The construction of Woodlands Station presented significant engineering challenges, ranging from excavation in soft ground to hard granite, and in very close proximity to the foundations and viaduct piers of the existing operational elevated MRT line. This required innovative construction techniques and close performance monitoring. The work site was overcrowded with many major underground utilities serving the key industries, commercial developments and residential estates which had to be carefully treated. The construction of this station also affected a bus interchange and electrical substations, which had to be relocated in advance as mitigation measures to construction and programme risks. It is also one of the largest stations on TEL which by its scale and geometry posed unique challenge to the design of the temporary earth retaining system.

This paper presents the challenges to the station's design and construction and how it was successfully executed.

**Keywords:** Underground, Challenges, Innovative, Construction, Performance

### 1. INTRODUCTION

Contract T203 comprises the construction and completion of Thomson-East Coast Line Woodlands Station (WDL), crossover tunnels, Addition and Alteration works (A&A) to the existing North South Line (NSL) Woodlands Station and Woodlands Bus Interchange and the associated ancillary works. The Station is located adjacent to the existing North-South Line Woodlands Station (refer to Figure 1 below for the overall site plan).

WDL Station is a two-level station located beneath the green field bounded by three major roads, and an operational metro viaduct. Within its vicinity are residential and commercial buildings. It is also an interchange station to the existing NSL Woodlands Station and is linked via an elevated transfer link bridge. The link will

<sup>1</sup> Director Er. Phua, Hooi Leng, M.SC, Land Transport Authority, Singapore. [phua\\_hooi\\_leng@lta.gov.sg](mailto:phua_hooi_leng@lta.gov.sg)

<sup>2</sup> Deputy Director, Maznah Mohd Ali, Land Transport Authority, Singapore. [maznah\\_mohd\\_ali@lta.gov.sg](mailto:maznah_mohd_ali@lta.gov.sg)

<sup>3</sup> Senior Project Manager, Michelle Wu, Land Transport Authority, Singapore. [michelle\\_wu@lta.gov.sg](mailto:michelle_wu@lta.gov.sg)

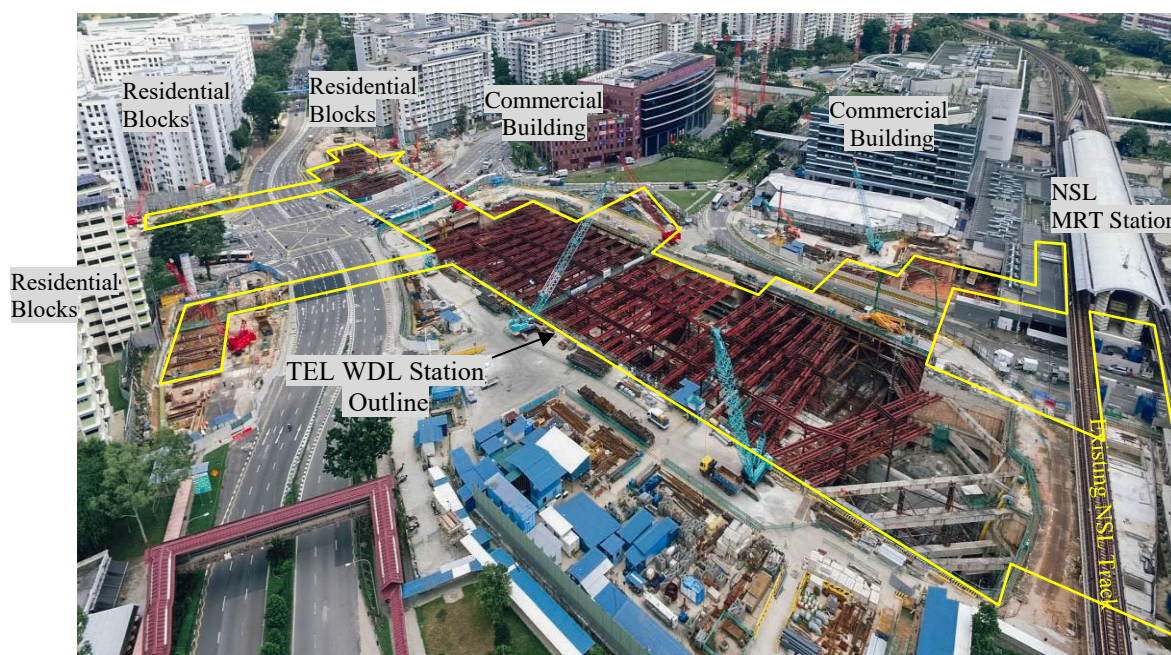
<sup>4</sup> Project Manager, Anand Kumar Pochambavi, Land Transport Authority, Singapore. [anand\\_kumar\\_pochambavi@lta.gov.sg](mailto:anand_kumar_pochambavi@lta.gov.sg)

<sup>5</sup> Executive Project Engineer, Si Thu Aung, Land Transport Authority, Singapore, [si\\_thu\\_aung@lta.gov.sg](mailto:si_thu_aung@lta.gov.sg)



involve A&A works to the connection area and paid platform area of the existing NSL Woodlands Station. The station has 5 entrances and a subway link connecting it to the existing Woodlands Bus Interchange. The crossover tunnel which is approximately 150m long abuts the WDL station at the southern end and is underneath a major road junction.

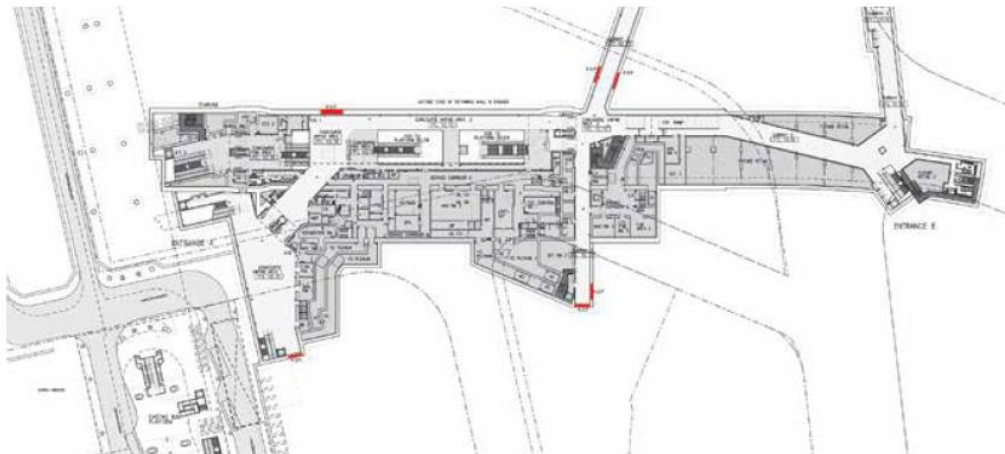
To intensify the usage of the station, WDL was also designed as a civil defence shelter. During national emergencies, the station would be converted into a defence shelter to hold and protect the occupants from aerial, chemical and biological chemical attacks.



*Figure 1. WDL Station Site plan*

## 2. CREATING THE NEXUS OF A NEW PRINCINT

The new Woodlands Station will expand the existing multi-modal transport hub to improve the connection of the precinct to the rest of Singapore. More than just a transport facility, it also serves to catalyst the rejuvenation of Singapore's northern regional hub by being the nexus of the new developments that will surround and be seamlessly connected to the expanded transport hub. Critical to the layout of the station was how it would interface with the development options of the adjacent sites. Potential future commercial development options that sit directly over and those abutting the station were simulated to increase the integration to maximize the land value capture of the area. One such outcome was the conversion of the incidental space above the cut and cover box of the cross over tunnel, to become an underground pedestrian linkway with retail shops, as a lifestyle hub. Aside from better utilizing this incidental space, the uses would also enrich the station experience and journey. Provisions were made for the pedestrian linkway to branch-off to connect to existing and future developments and community nodes. Highlighted in red (Figure 2) are the knock-out panel provisions within the station.



*Figure 2. Provisions of Knock-out panels to expand future station connections*

### 3. GEOLOGICAL STRATA

Soil investigation (SI) works were conducted by the Client prior to the tender, and additional SI done by the Contractor after award, to understand the overall ground conditions for the planning and design of the Earth Retaining Stabilising Structure (ERSS), foundation (piling) and excavation.

#### 3.1. Types of Geological Strata:

- a) General Fill: Comprising of backfilled materials which is highly variable and includes sandy silt, sandy clay, clayey sand, gravelly clay and silt occasionally mixed with stone, decayed wood and roots. These materials are variable in both depth and composition.
- b) Kallang Formation: Kallang Formation was found on the south, north-west and western sections of the station. The thickness is approx. 3 to 4m with the maximum thickness at 7.5m.
- c) Bukit Timah Granite: The Bukit Timah Granite was the predominant stratum, and encountered in various states of weathering, from residual soils (Grade VI) to intact unweathered, unstained rock (Grade I). Boulders with core lengths of no more than 5m were also encountered.

Figures 3 & 4 shows the geological profile for the Station. Proposed ERSS is Secant Bore Pile (SBP) and the toe level of the SBP has to follow the station formation level (FL) which is deeper than the high rock head levels (RHL). Therefore, SBP is socketed into the rock.

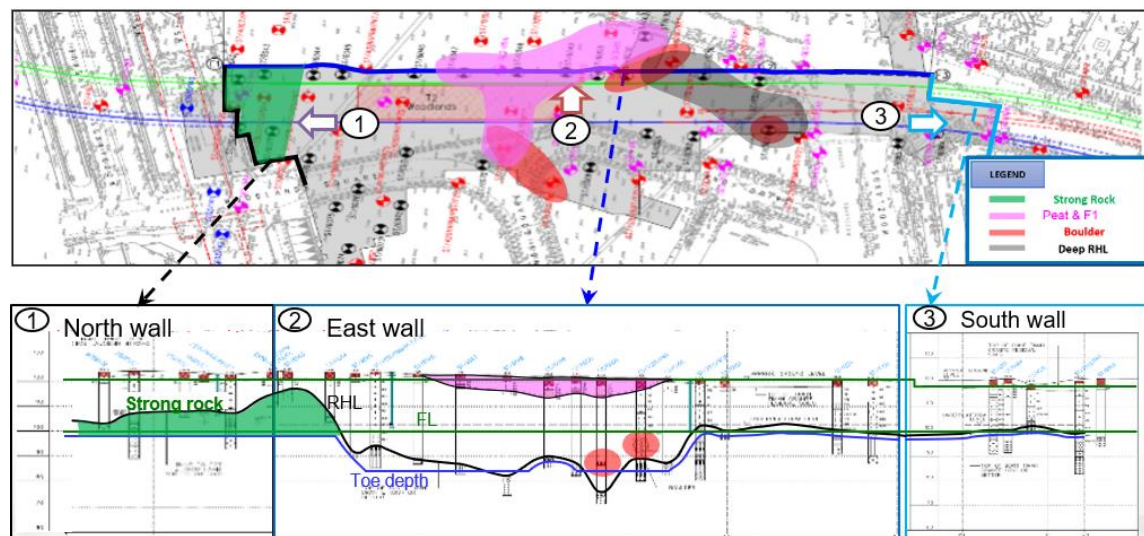


Figure 3. Geological profile at North, East and South Wall

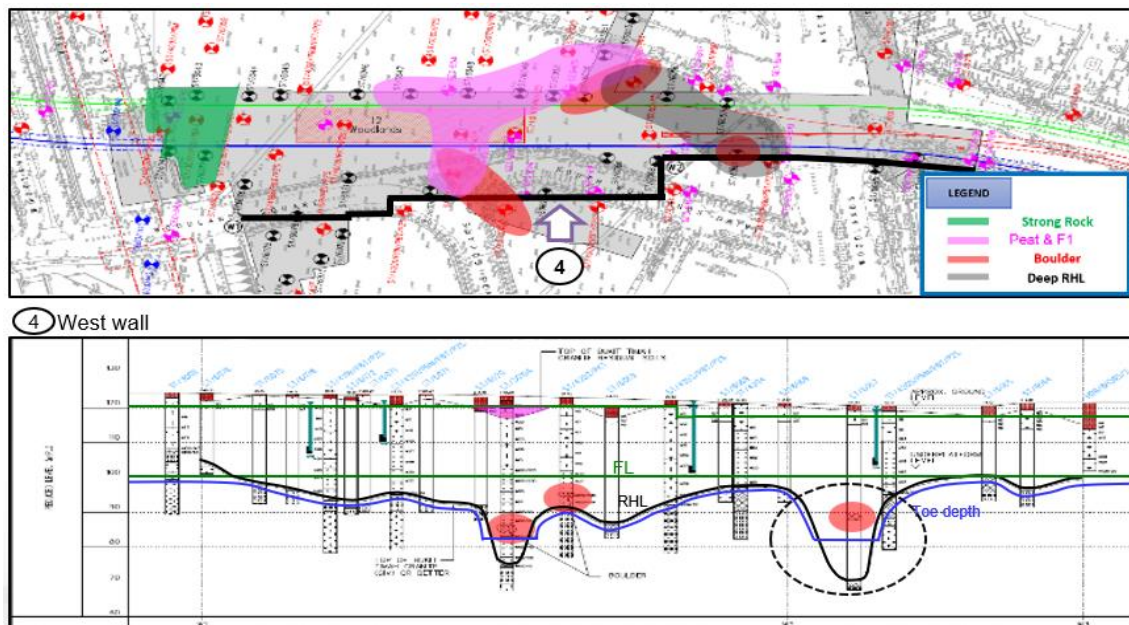


Figure 4. Geological profile at West Wall

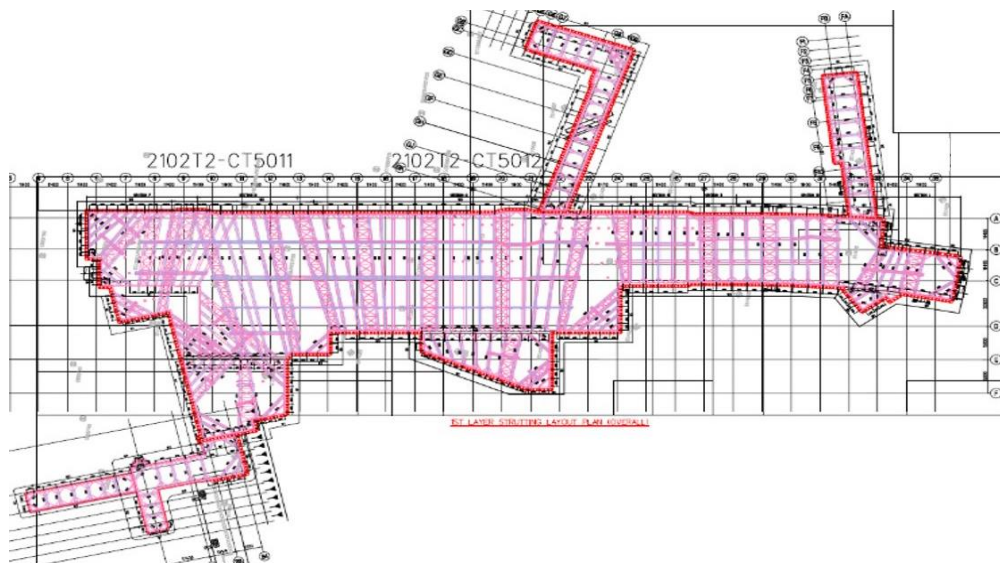
#### 4. ENGINEERING CHALLENGES:

##### 4.1 Challenge 1: Ensuring Dry Excavation in Granite

Ensuring a watertight earth retaining cofferdam for the station excavation was essential to mitigate against the risk of water drawdown that can induce consolidation settlement and affect the buildings, streets and utilities on the peripheral of the excavation. To ensure an effective cut-off, the toe of the Earth Retaining Stabilising Structure (ERSS) had to be socketed in the un-weathered granite to provide an effective cutoff for any potential underdrainage. The earth retaining system also had to have sufficient lateral stiffness to minimise the ground movement of the adjacent structures especially the NSL viaduct.

Secant Bored Pile (SBP) walls consisting of 1300mm diameter & 1600mm diameter (Hard piles) with 1200mm diameter and 1500mm diameter (Soft pile) and supported by 4 layers of steel struts were adopted for the station and cut and cover tunnels (refer to Figure 5 below for the ERSS layout).





*Figure 5. Secant Bore Pile (SBP) layout with struts*

#### **4.2 Challenge 2: Granite Excavation Close to Existing Live Rail Viaduct**

The main construction challenge was undertaking the bulk excavation of the station whilst ensuring the continued operations and safety of the NSL viaduct which was 5m behind and along the entire side of the north end of the station. Compounding this was the ‘fresh to moderate weathered granite’ outcrop at this location, of which the foundations of the NSL viaduct were also founded on, which had to be excavated away.

A combination of rock splitting (Figure 6), and controlled blasting (Figure 7) was adopted to ensure that the vibrations remained within the allowable thresholds for the NSL viaduct. Rock splitting method was initially used to excavate about 15,500 m<sup>3</sup> of the granite. Towards the base, the rock splitting method was unable to split the un-weathered rock, which hampered the progress of the excavation. After careful consideration, controlled blasting was adopted using electronic detonators for the final 1,600 m<sup>3</sup> of rock.

Due to these measures, the vibrations on the NSL viaduct was kept to well within the maximum allowable limit of 15mm/s.



*Figure 6. Rock Splitting Method*



*Figure 7. Controlled Rock Blasting*

#### **4.3 Challenge 3: Underpinning of Existing Rail Station Structure**

To develop an inter-modal transport hub between rail and bus, a direct underground pedestrian subway link was built to connect new Woodlands station with the existing bus interchange. The link was built directly below





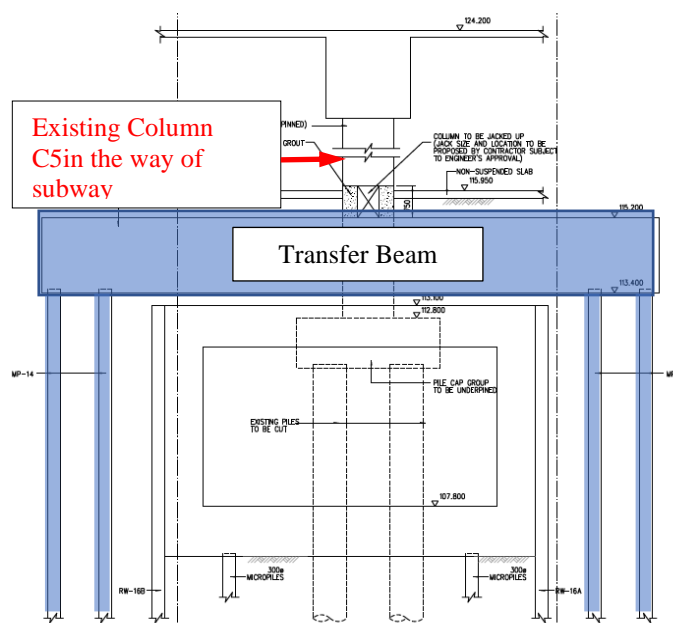


Figure 10. Underpinning of existing station column C5

#### 4.4. Challenge 4: Low Ground Clearance for Traffic Decking

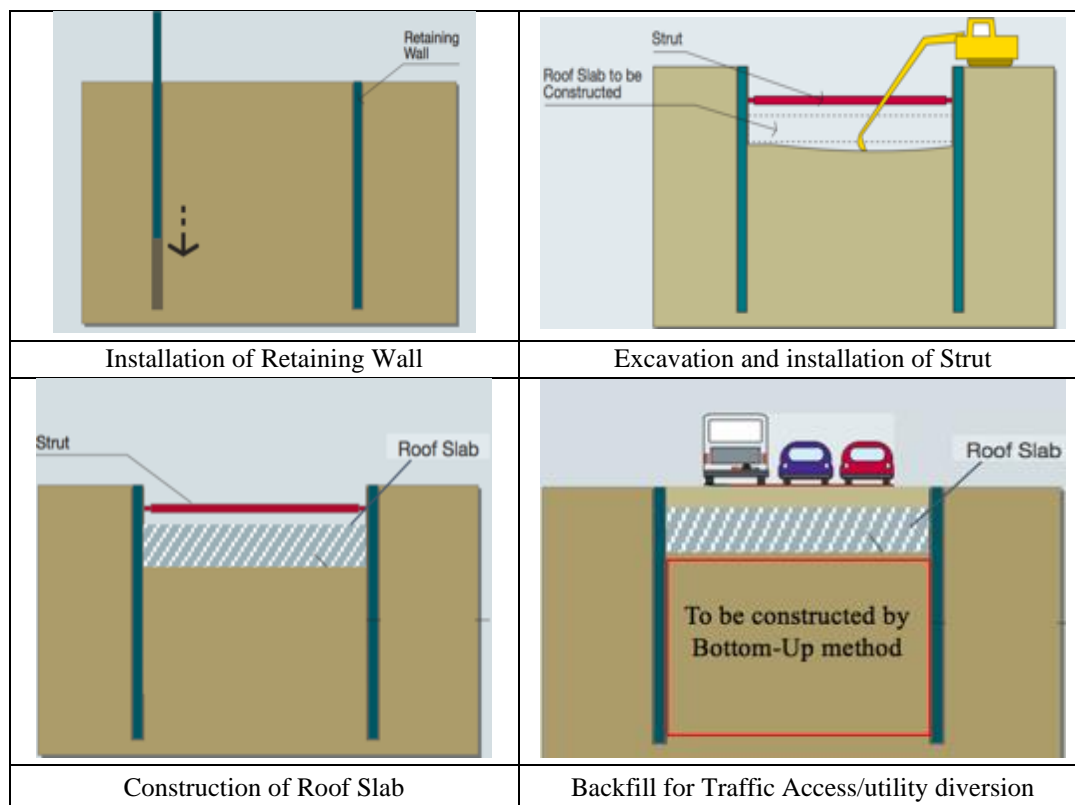
The layout of the station was divided into 16 zones of ERSS design (refer to Figure 11). TEL Woodlands station was envisaged to be bottom-up construction. However, this scheme posed a significant constructability issue for Zone H1 due to low ground clearance of 0.3m to 1.2m between the top of the roof slab and existing ground surface with a major arterial road above. For a bottom-up construction, a traffic deck would have to be installed across the excavation of this zone. To create working space for the installation of the roof slab below the traffic deck, the traffic carriageway would need to be raised by up to 2.5m, to provide the vertical clearance to accommodate the temporary traffic deck above the station roof slab. However, due to the proximity of Zone H1 to the existing junction of Woodlands Avenue 5 and Woodlands Avenue 2, raising the deck will not be feasible as the temporary traffic deck would need to match the surrounding road levels.

A semi-top-down construction was hence adopted at Zone H1, whereby the roof slab was constructed first and backfilled followed by traffic diverted on top of this Zone. This permanent roof slab where semi top-down construction method is adopted, also served as strut to provide lateral support for to the ERSS for the excavation.



**Figure 11.** Zoning plan for ERSS design

Sequence of Semi-Top-Down construction is demonstrated in the below Figure 12.



**Figure 12.** Semi Top-Down Construction

## 5. CONCLUSION

TEL Woodlands Station was a challenging project which had to be planned, designed, and constructed with many factors into consideration like working nearby the existing operational MRT track, residential area, hard soil conditions etc. It was well executed with all the mitigation measures in place, close supervision of works, detailed monitoring programme implementation, and ensuring the safety procedures always comply to Singapore Standards during construction phase. Contributories to the successful completion of the project were attributed to:

- a) Sufficient time be given upfront, during the planning stage by the client to identify all the engineering risks, and design it out as best possible, and only to carry it to the construction stage if it could be tolerably managed.
- b) Early identification of Soil Condition is critical to determine the design of ERSS and excavation. Sufficient soil investigation works to be carried out prior to the tender and design requirements should be clearly specified for contractors;
- c) Construction methods shall be studied in detail and a suitable one adopted as one the most most effective in terms of time including cost for the long run of the project;
- d) Traffic Diversion and the sequence of each activity has to be planned at the start of the project in conjunction with the ERSS layout and concept to ensure a seamless flow and continuity of works; and
- e) Affected utilities shall be diverted prior to the construction of specific work activity, and ideally to be completed at the design stage as a programme risk mitigation so as not to delay the construction phase.

## UNDERGROUND URBANIZATION AND GEOTHERMAL POTENTIAL IN MODERN INFRASTRUCTURE: THE CASE OF THE MARIBOR CITY TUNNEL

Vojkan Jovičić<sup>1</sup>, Mitja Pečovnik<sup>2</sup>, Samo Peter Medved<sup>3</sup>, Željko Vukelić<sup>4</sup>, Elvir Muhić<sup>2</sup>, Marko Kosovel<sup>5</sup>

**Abstract:** Innovative technologies for construction of underground infrastructure can significantly enhance sustainability and contribute to environmental protection in urban areas. This paper illustrates an example of the planned construction of the Maribor City Tunnel, designed to alleviate traffic congestion in the historic city centre. Planned as a single-tube, two-way tunnel approximately 980 meters in length, the project planning required comprehensive research to evaluate its feasibility and potential impacts on the urban environment.

The study presented in the paper examines how the tunnel can be effectively integrated with the existing traffic infrastructure. Attention is given to the architectural design of the tunnel entrances, considering both aesthetic and functional aspects. The research also considers the geological and geomechanical conditions for tunnel construction, as well as the need to protect groundwater. The study further evaluates strategies for safeguarding existing structures in the city centre by selecting appropriate excavation and construction methods. Structural elements foreseen for construction, such as diaphragm walls at the tunnel portal and the tunnel's inner lining, offer significant potential for exploiting geothermal energy. Upgrading structural elements could enable effective heat exchange between the ground and the structure at short distances. Urban underground structures are particularly well-suited for this due to their proximity to buildings, ensuring short and efficient connections between energy producers and consumers.

Six critical conditions were identified as key to the project feasibility: traffic integration, geological and geomechanical factors, groundwater protection, excavation methods, safeguarding of existing structures and utilisation of geothermal potential. Given the central location of the construction site in the city of Maribor, there is a need for comprehensive monitoring of parameters such as groundwater levels, noise, dust, and impacts on natural and cultural heritage. The intricate interplay of technical, environmental, and urban planning factors, required for the successful execution of a large-scale urban infrastructure project, is presented in the paper.

**Keywords:** underground urbanisation, tunnelling, geothermal energy, feasibility, environmental impact

### 1. INTRODUCTION

Underground urbanization has emerged as one of the major challenges of contemporary development. With urban populations on the rise and surface space increasingly constrained, constructing buildings and infrastructure below ground offers a viable solution to accommodate societal needs while preserving valuable land above ground (Mair and Taylor 1999). Despite its promise, underground development involves significantly higher costs than traditional above-ground construction. These elevated costs are driven by the complexities of excavation,

<sup>1</sup> PhD, Jovičić, Vojkan, M.Sc. Civil Eng., Prof., Faculty of Civil and Geodetic engineering, Jamova cesta 2, Ljubljana, Slovenia, Vojkan.Jovicic@irgo.si.

<sup>2</sup> Pečovnik, Mitja, M.Sc. Geotechnical Eng., IRGO Consultling d.o.o., Slovenčeva 93, Ljubljana, Slovenija, Mitja.Pecovnik@irgo.si

<sup>2</sup> Muhić, Elvir, M.Sc. Geotechnical Eng., IRGO Consultling d.o.o., Slovenčeva 93, Ljubljana, Slovenija, Elvir.Muhic@irgo.si

<sup>3</sup> PhD, Medved, Samo Peter, M.Sc. Civil Eng., formerly Municipality of Maribor, Heroja Staneta street 1, Maribor, Slovenia, samopeter.medved@gmail.com

<sup>4</sup> PhD, Vukelić, Željko, M.Sc. Geotechnical Eng., Prof., Faculty of Natural Sciences and Engineering, Aškerčeva cesta 12, Ljubljana, Slovenia, Zeljko.Vukelic@ntf.uni-lj.si

<sup>5</sup> Kosovel, Marko, M.Sc. Architecture Eng., ACMA, Lokarjev drevored 1, Ajdovščina, Slovenia, marko.kosovel@acma.si.

integration of subterranean utilities, and the use of constrained space. Moreover, underground projects demand advanced technical expertise and innovative solutions to address often difficult ground conditions, as well as the requirements for effective ventilation, lighting, and drainage and low environmental impact.

Ongoing maintenance and rigorous safety standards also make underground infrastructure more demanding to operate. Nevertheless, advancements in technology are enabling sustainable approaches that reduce environmental impact. Integrating geothermal energy systems presents a compelling opportunity. These systems leverage thermodynamic and geological principles to model and harness subsurface heat for energy use. Given that modern Western societies allocate nearly 50% of total energy consumption to heating and cooling, geothermal solutions offer both sustainable and economic benefits.

This paper presents a feasibility case study for tunnel construction in Maribor, Slovenia, which is the second largest city in the country with population of 120.000. The study involves constructing a 980-meter tunnel beneath the city's historic centre and addresses several critical technical and environmental considerations for spatial placement of the underground structure: (a) integration with existing traffic infrastructure, (b) urban placement of portal areas, (c) architectural design of tunnel entrances, (d) geological and geomechanical conditions, (e) protection of groundwater and water resources, (f) tunnel safety measures, (g) excavation and construction techniques, (h) protection of existing structures and public infrastructure, and (i) potential for geothermal energy utilization.

If designed with a thermoactivated inner lining and equipped with ground-to-water and water-to-water heat pumps, the tunnel will be able to exploit geothermal energy from underground water sources. This project illustrates how shallow geothermal systems, when integrated with energy-efficient building technologies, can deliver substantial energy savings and environmental advantages in urban contexts. The feasibility and cost-effectiveness of implementing shallow geothermal systems depend on factors such as site-specific geological and hydrological conditions, the scale and energy demand of the infrastructure, and the prevailing regulatory and incentive frameworks. The paper outlines how these challenges can be addressed through comprehensive research and provides practical insights for applying similar approaches in future underground urban development initiatives.

## **2. SPATIAL INTEGRATION OF THE TUNNEL INTO EXISTING URBAN INFRASTRUCTURE**

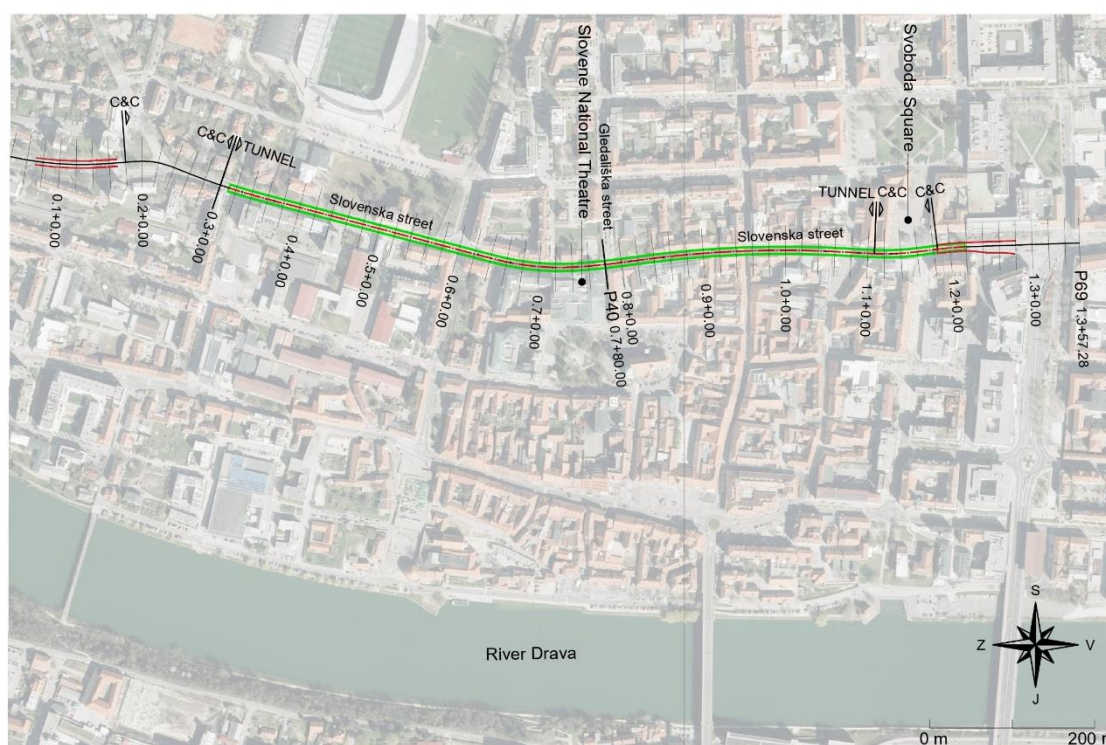
The objective of the research work was to address a central question: whether the construction of the proposed tunnel is viable transport alternative with an acceptable level of impact on the urban environment in which it is intended to be implemented. In terms of traffic conditions, the study defines the technical requirements for the realization of the Maribor city tunnel, focusing on several critical domains. These include the integration of the tunnel into the existing transportation network, the spatial placement of portal areas within the urban fabric, and the architectural design of visible elements at the tunnel entrances. As part of the decision-making process, the client, Municipality of City of Maribor commissioned research to identify the key feasibility constraints and to provide an initial assessment of whether the tunnel could be realized under the most critical conditions considering: the tunnel's integration into the existing road infrastructure, the geological and geomechanical suitability of the site, the safeguarding of groundwater and hydrological resources, the implementation methods for excavation and construction, and the protection of existing structures and public utilities. Each of these critical factors was analysed individually resulting in the key findings that, in addition to the alignment defined by the desired traffic configuration, the depth and location of the groundwater table significantly influenced the tunnel's spatial layout. Specifically, the decision to align the tunnel above the groundwater level and thereby minimizing hydrogeological risks has had considerable implications for other aspects of the design and planning process, as further elaborated in the paper. Consequently, the study considered the geological and geomechanical conditions of the site, to include the protection of groundwater and water resources.

Special attention was devoted to the architectural articulation of the tunnel's entrance and exit elements. Recognizing that the tunnel represents a novel and potentially disruptive intervention within the historical urban landscape, the design aims to integrate the structure in a visually and contextually sensitive manner. The proposed architectural solution adopts a neutral aesthetic with gently curved forms, intended to enhance the visual experience for both pedestrians and motorists. From an urban design perspective, the identity and character of the existing environment at both portal zones were carefully considered. In particular, the eastern portal is deliberately concealed within important Freedom Square (Trg svobode), in order to preserve the square's symbolic and spatial centrality within the historic core of Maribor.

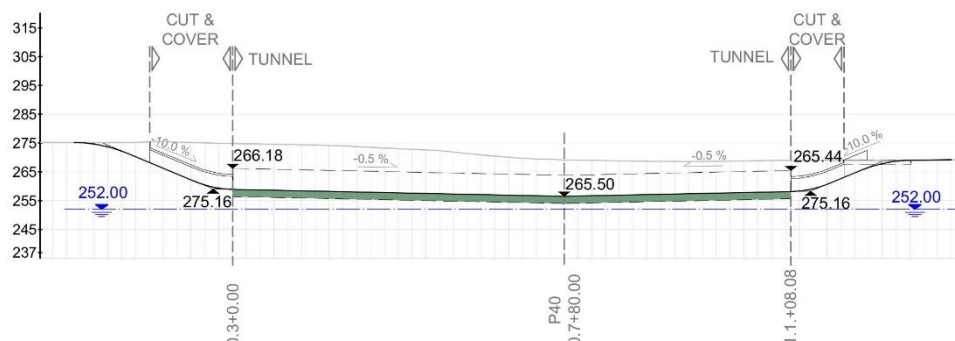


## 2.1. Tunnel route

The horizontal alignment of the tunnel route, which has an approximate length of 980 meters, is presented in Figure 1. The technical and geometric road design elements within the tunnel section are based on a design speed of 50 km/h. However, due to spatial constraints, the entrance and exit ramps of the tunnel are designed for a reduced design speed of 40 km/h. The selection of these technical and geometric elements adheres to the Regulation on Road Design, the Decree on Technical Standards and Conditions for the Design of Road Tunnels in the Republic of Slovenia, and the Directive 2004/54/EC on Minimum Safety Requirements for Tunnels in the Trans-European Road Network, hereinafter referred to as “the Directive”. Transition curves have been applied throughout the tunnel design, and the minimum horizontal radius used has been verified to ensure adequate visibility within the tunnel. The alignment is designed to run beneath existing streets, considering the optimum accessibility to the construction site and low impact of neighbouring buildings. As indicated in the longitudinal profile Figure 2 the lowest point of the tunnel is located at profile section P40 (within the area of the Maribor National Theatre), where the tunnel’s invert is at the lowest point positioned 2.0 meters above the highest groundwater level.



**Figure 1.** Route of Maribor City tunnel



**Figure 2.** Longitudinal profile of Maribor city tunnel

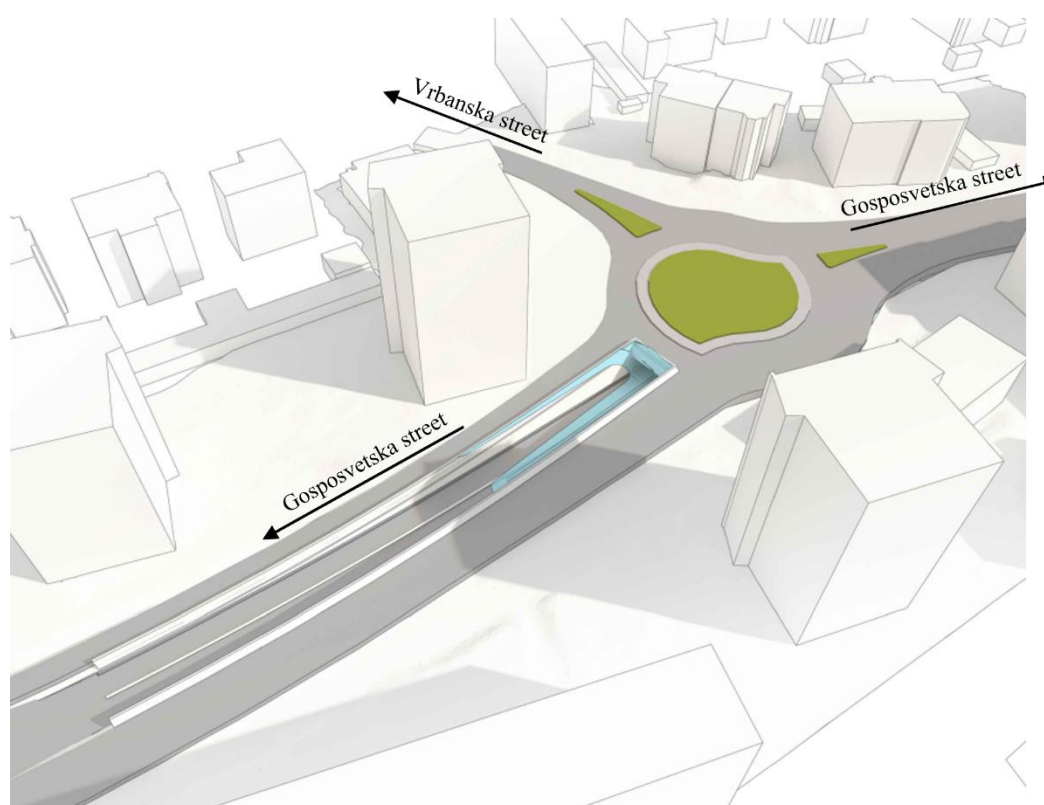
At this lowest point, an emergency shaft leading to the surface is planned, along with a power station and a reservoir intended to collect contaminated water from within the tunnel. From this lowest point, the tunnel gradient extends in both directions at a minimum slope of 0.50%. Given the tunnel type, it is designed as a depression

tunnel, which allows for the application of concave vertical curves. As illustrated in the tunnel's longitudinal profile, the overburden depth along the alignment ranges from 4.0 to 9.5 meters.

## 2.2. Urban Integration of Tunnel Portal Areas

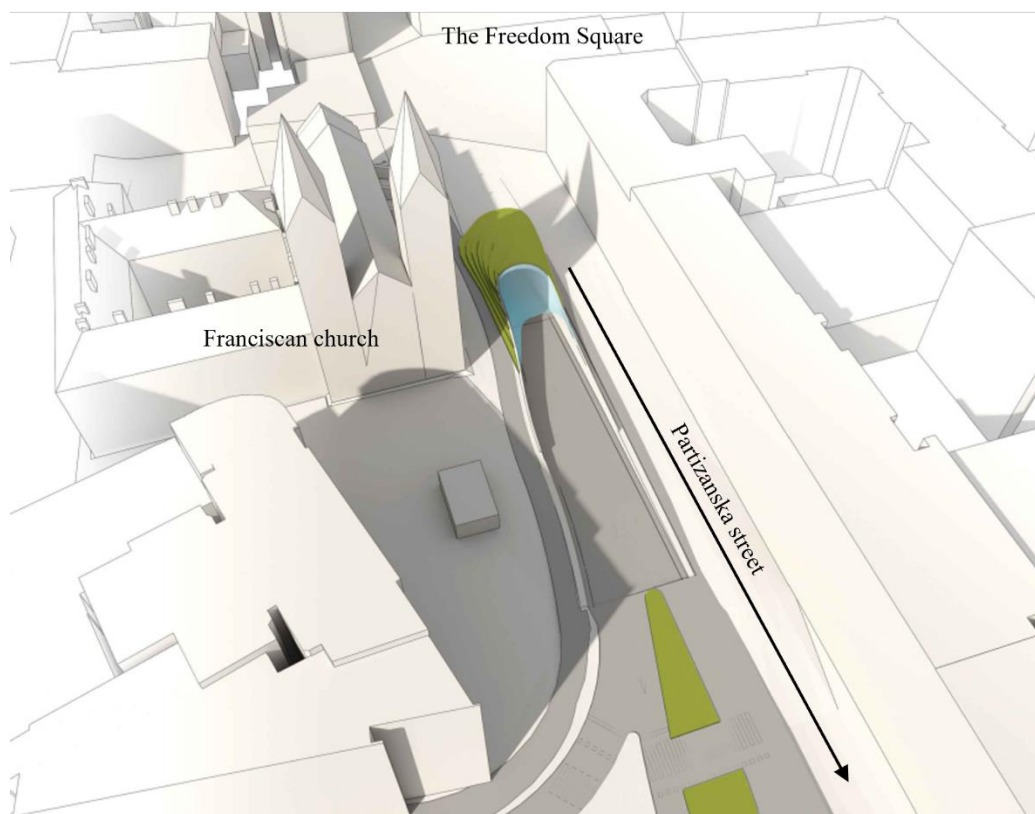
It is essential to ensure that the new tunnel route does not degrade the existing quality of the urban environment, including pedestrian connectivity, accessibility for cyclists and individuals with special needs, the relationship between public spaces and urban buildings, key visual perspectives (vistas), and cultural heritage. In this context, the research study has sought optimal solutions for the placement of the tunnel's entry zones on both the eastern and western portals. This difficult task considered several key criteria: ensuring adequate space around the portal structures to accommodate all forms of traffic; ensuring low impact of the portal structures on adjacent buildings and urban space; preserving cultural heritage; optimizing the location of access ramps in terms of gradient, length, and dimensions; and ensuring low influence of new elements on the existing functionality of public space, the proportionality between built volumes, the visual perspectives, air quality, and noise.

The tunnel access ramps, each approximately 80 to 100 meters in length, represent significant spatial interventions and act as level barriers in the urban fabric. As a result, it is critical to position these ramps in locations where there is no essential need for perpendicular crossings. Grade-separated crossings of the ramp area (e.g., pedestrian underpasses or overpasses) are technically feasible but often problematic in practice. These solutions can be physically challenging due to elevation changes, or aesthetically and psychologically uninviting, leading to avoidance by users. As indicated in Figure 3, for these reasons, the western portal ramp of sufficient length runs along main Gosposvetska Street. Additional room for the portal structure was enabled by roundabout crossing which provide with an elegant and a functional solution.



**Figure 3.** Western portal area with the long ramp running along Gosposvetska street.

The urban integration of the eastern portal, shown in Figure 4, is more demanding in nearly all respects. The entry area has been shifted as far as possible away from Freedom Square to preserve its integrity. The visible, covered portion of the eastern access is situated on the north side of the Franciscan Church, maintaining a minimum clearance of 10 meters. To prevent the spread of noise to the surroundings, the portal will be partially covered by a green embankment, as indicated in the figure.



*Figure 4. Eastern portal area is in the vicinity of historical Freedom Square and Franciscan church.*

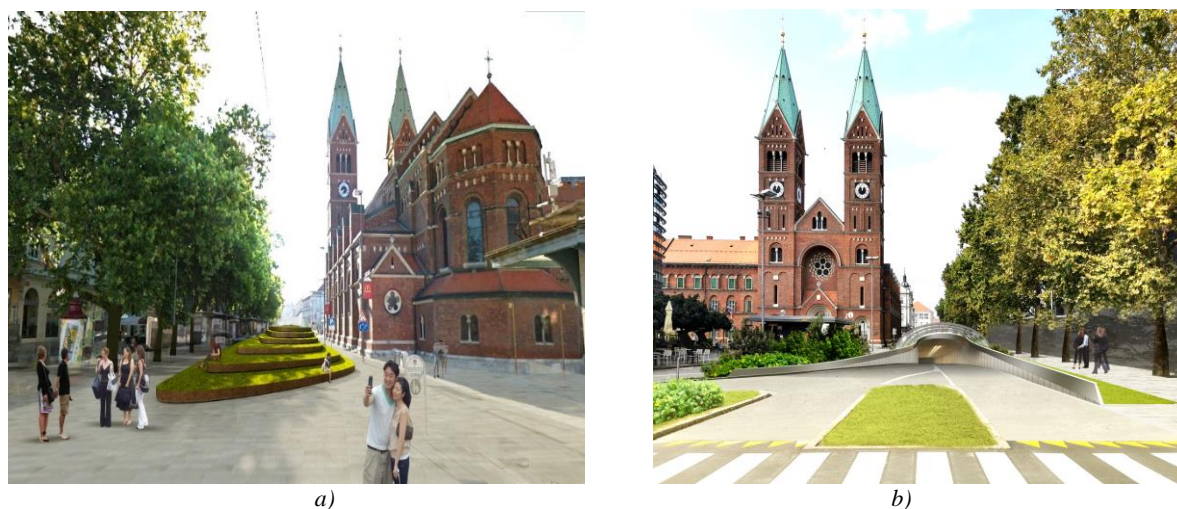
### **2.3. Architectural Design of the Visible Elements at the Tunnel Entrance Area**

The form of the visible tunnel elements at the surface, such as the covered entrance sections, fences, and associated areas, is architecturally highly significant. The tunnel represents a new presence in the urban space and must coexist in relation to the existing buildings within the delicate environment of the old town centre. The existing buildings belong to various historical periods, with some of them protected as cultural heritage. The design of the tunnel entrances is also crucial from the perspective of spatial perception by both pedestrians and drivers. An inappropriate approach to the design or placement of new structures in the environment can quickly result in irreversible damage. In the case of the area under consideration, we considered that the visible elements of the future underground street, where it transitions to the surface as a tunnel, are designed to be subordinate to the existing space and buildings, in such a way that they do not visually dominate or compete architecturally.

Due to spatial limitations, it is not possible to completely conceal the covers over traffic ramps and fences or to place them entirely below the level of the existing ground. Therefore, it is inevitable that some parts of the tunnel structure will emerge as new objects in the public space currently occupied by streets or pedestrian zones. For this reason, it is essential that these visible elements are thoughtfully planned and designed to meet both functional and safety requirements, while also exhibiting an architectural character that harmonizes with the surrounding built environment. The proposed visualisations of architectural solutions for designing the visible elements of the tunnel entrance areas are shown in Figure 5 and Figure 6 for the west and east portal respectively.

Since the tunnel elements appearing in the public space are part of traffic infrastructure, from a design perspective they are best seen as urban architecture or urban landscape, rather than related to high-rise buildings. As such, the design should bring these elements closer to the character of a square or street, taking care not to significantly obstruct or divide the space vertically. Following this concept, the eastern entrance is located in the forecourt of Trg slobode (Liberty Square), which is a pedestrian-only area next to the Franciscan Church, one of the city's most recognizable buildings. From an architectural design perspective, the eastern entrance presents a much greater challenge, as the structure must not only serve a functional role but also enhance the existing life and activities of Liberty Square, while not overly disrupting the space's visual integrity, both from the square itself and from the street view facing the main façade of the Franciscan Church.





**Figure 5.** Visualisation of the East portal: a) view towards the South, b) view towards the North.



**Figure 6.** Visualisation of the West portal: view towards the South

In contrast, the western entrance will be placed along the street axis of Gospodsvetska Street, where a level pathway currently exists and will remain functionally unchanged. In this case, there is only one structure visible near the square, and it will be observable from multiple directions.

#### **2.4. Geological, hydrogeological and geomechanical conditions for tunnel constructions**

The geological and geomechanical investigations showed that the tunnel area is covered by Quaternary alluvial deposits forming a terrace of the Drava River. These deposits consist of sandy and, more rarely, silty gravel with occasional lenses of sand or silty sand (typically less than 1 meter thick). Individual layers of conglomerate also appear as in some places the gravel becomes partially lithified. In terms of mineral composition, the gravel alternates between sections dominated by carbonate clasts and those dominated by quartz clasts. The gravel deposits are typically medium to very dense. In the lower 1–2 meters above the bedrock, there is often an increased presence of silt, i.e., silty gravel or sand, which most likely represents Plio-Quaternary sediments, which is loose and less load bearing. The thickness of the entire sediment package in the wider area ranges from 25 to 35 meters, so that the maximum thickness in the tunnel zone to be at the western end (approximately 35 m) and at the eastern end around 27 m.

The pre-Quaternary bedrock beneath the alluvial sediments consists of Miocene sedimentary rocks, predominantly marlstone, with occasional tuff, sandstone, and conglomerate interbeds. The bedrock slightly dips towards the Drava River (generally south-southwest). According to archival data, it is expected to appear at around 240 m a.s.l. on the western end of the tunnel, and around 242 m a.s.l. on the eastern end. It can be concluded that geological conditions in the tunnel area are predominantly homogeneous, and the tunnel can be fully constructed within the terraced gravel/sand layer.

According to available data from the national monitoring system groundwater occurs along the planned tunnel route at elevations up to 252.0 m above sea level (a.s.l.). However, based on the surrounding hydraulic field, this may represent an anomaly or measurement error and require on-site verification. The critical elevation above which excavation is permitted from the groundwater protection standpoint is 254 m a.s.l. It is highlighted that meeting this requirement results in relatively low tunnel overburden during excavation. Consequently, the impact of tunnel construction on existing residential and commercial buildings, as well as other urban public infrastructure, should be significantly increased.

### **3. BOUNDARY CONDITIONS FOR TUNNEL CONSTRUCTION**

#### **3.1. Geometry, security and functionality**

The tunnel is designed in an oval shape with an invert (bottom arch), with a maximum height of approximately 9.5 meters (measured from the base of the invert to the crown of the primary lining) and approximately the same maximum width, as shown in Figure 7. The roadway width is 7.0 meters (comprising  $2 \times 3.25$  m traffic lanes and a 0.5 m central safety strip), with sidewalks on both sides ( $2 \times 0.7$  m). The clear vertical height is 4.5 meters. In case of further planning, profile optimization should also consider the type of ventilation and rounding of the invert thickness, considering this is a relatively shallow tunnel. Characteristic cross section of the tunnel is shown in Figure 7.

According to Water Protection Regulation Act (Official Gazette of the Republic of Slovenia Nos. 24/07, 32/11, 22/13 2007) the tunnel can be constructed in full compliance with the applicable, provided the tunnel invert remains at least 2 meters above the highest recorded groundwater level, i.e., above elevation 254.0 m a.s.l.

As already explained, hydrogeological conditions dictate that the lowest elevation point for tunnel construction must be fixed at 254 meters above sea level, due to groundwater protection. This means that any reduction in tunnel profile height will directly increase the overburden and thereby reduce the impact of the tunnel on existing surface structures. According to our assessments, the total tunnel height, which is preliminarily estimated at approximately 9.5 meters, could be reduced to around 8.5 meters without significant functional loss. This would result in an overburden thickness (distance between the tunnel crown and surface level) ranging between 5.0 and 10.0 meters, which is manageable in terms of impacts on existing buildings.

The tunnel is designed as a non-drained structure, meaning that no groundwater will be extracted from the surrounding soil. This is the most favourable solution from a maintenance standpoint, as no permanent water pumping will be required. Given that the tunnel is expected to be continuously above the groundwater table, the hydrostatic pressure acting on the tunnel lining will be low, and only intermittent seepage of rainwater may occur.

Safety in tunnel during the function is ensured through proper tunnel design (e.g., clear profile, alignment elements, appropriate spatial placement), as well as safety equipment inside the tunnel and user safety features (emergency exits, fire water supply, traffic control, etc.). In addition to the EU Directive 2004/54/EC (Official Journal reference: OJ L 167, 30.4.2004, n.d.) on minimum safety requirements for tunnels in the trans-European road network, we also considered the Regulation on Technical Norms and Conditions for the Design of Road Tunnels in Slovenia (Official Gazette of RS, Nos. 48/06, n.d.). For technical guidance, the Austrian RVS guidelines (Forschungsgesell and Verkehr 2008) are used, which comprehensively cover road tunnel design from safety aspect.



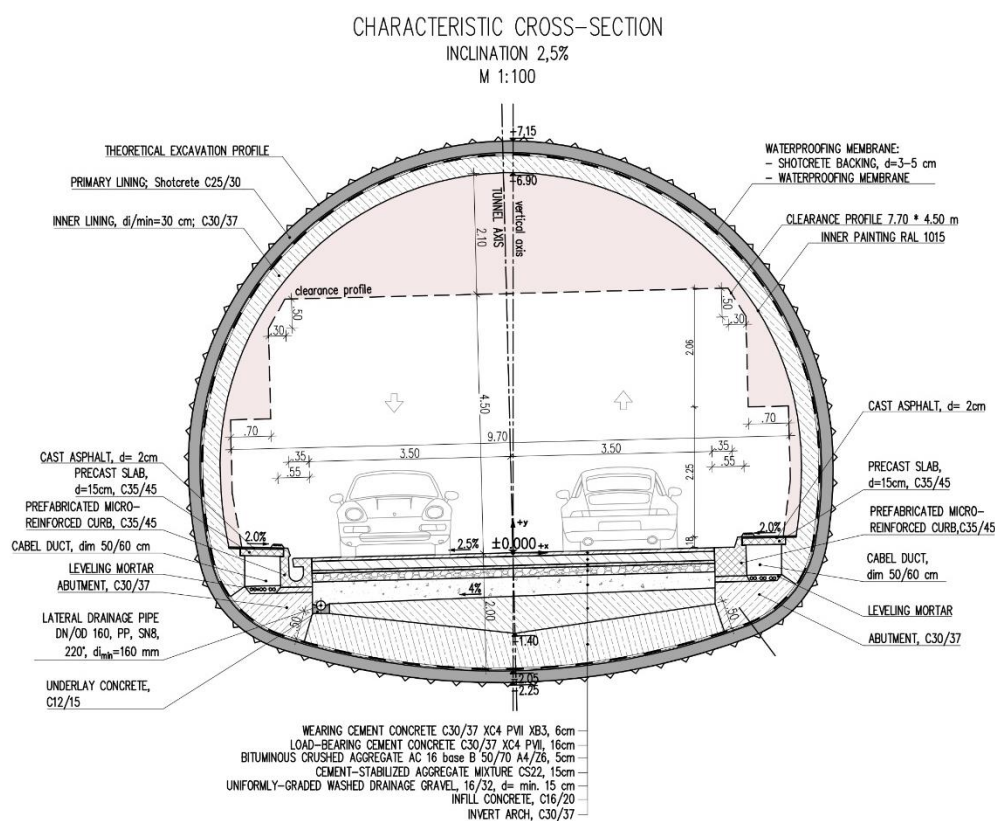


Figure 7. Tunnel characteristic cross section

The tunnel is designed for the speed limit of 50 km/h. The longitudinal slope is 0.5%, sloping toward the centre while the vertical clearance is 4.5 m. For stormwater drainage, hollow curbs with drainage grooves are planned along the entire tunnel and open cut sections, also fire traps (siphons) of appropriate capacity will be placed every 60 m to separate fire sectors. A wastewater collection tank (including wash water) of at least 50 m<sup>3</sup> is required for tunnels longer than 500 m.

Based on tunnel design data and expected traffic volumes (approx. 16,350 vehicles/day, with up to 2% heavy vehicles and 1.5% buses, and no transport of hazardous materials allowed), the expected annual fatality risk, which was calculated using RVS guideline 09.03.11., falls into Risk Class III (out of four). This classification defines the design safety requirements to be met, according to the RVS guidelines so that the tunnel will feature an emergency exit approximately in the middle as escape routes must connect to the public road network, and emergency vehicle access must be ensured. As per RVS 09.01.24, emergency bays are not required for tunnels under 1,000 m while emergency exits must be provided within 250–500 m of the portals. Being a single-tube tunnel in an urban area, emergency exits can be via stairways and elevators (minimum area 1.5 × 2.5 m). The vertical height of the escape route is approximately 16 m, which per the guidelines does not require elevators for emergency services.

The tunnel must be equipped with emergency communication and a wet fire-fighting network. Safety niches will be placed every 120 m while presence of electrical niches will be included during ventilation system planning. The wet fire network must provide 20 l/s water flow at 6–12 bar pressure for 90 minutes, even under worst hydraulic conditions. Fire water supply may be provided by a nearby hydrant network considering that a separate water reservoir (min. 120 m<sup>3</sup>) and pump station must be installed. Based on vehicle volume and tunnel design, longitudinal ventilation is planned per RVS 09.02.22. All necessary support facilities are to be located between profiles, roughly at the midpoint of the tunnel, where undeveloped land is available. These will be combined into a single underground facility housing: a) wastewater tank and pump station, b) drainage tank and pump station, c) emergency stairway and elevator, and d) operations centre including transformer room, low- and medium-voltage rooms, control room and battery room. The operational building has three underground levels and reach ground level, with the possibility of additional floors for non-tunnel-related purposes. Central control system, located in operational building, would allow both remote control from the national motorway operations centre and local control from the on-site control room.

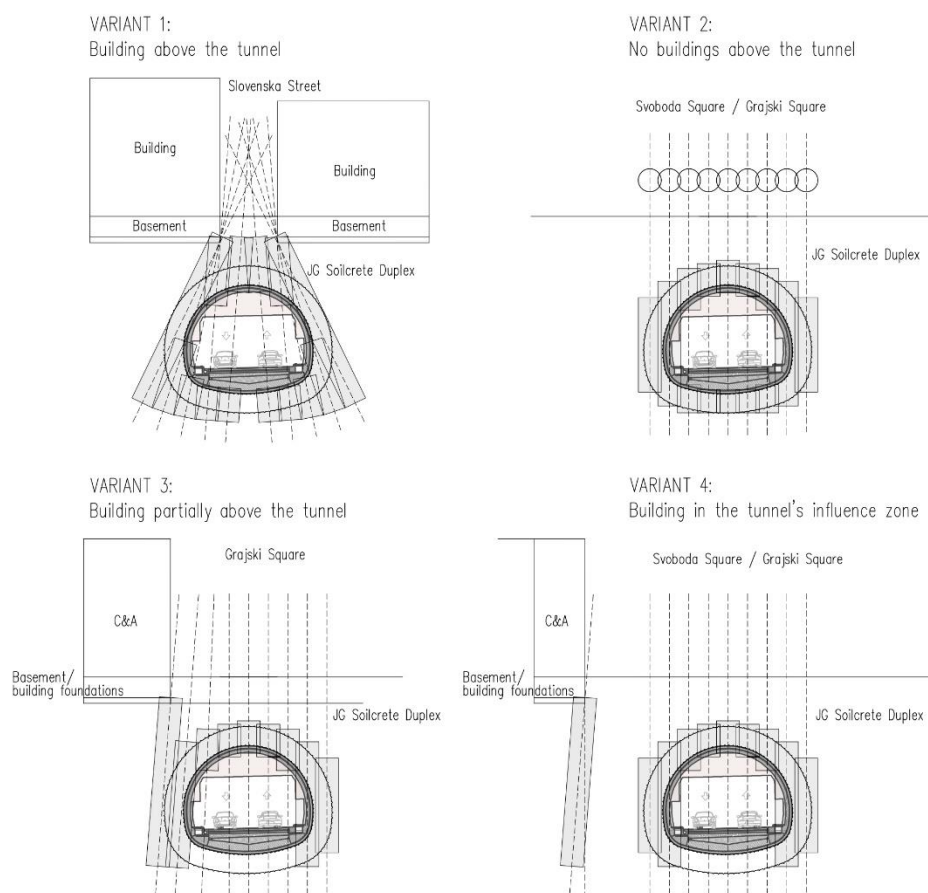
### 3.2. Conditions for tunnel construction

The method of tunnel construction is influenced by several factors, such as tunnel depth, shape, length, presence of groundwater, and the selection of technological methods suited to the given geological and geotechnical conditions. During tunnel excavation, changes in the local stress field are inevitable, which lead to ground displacements and consequently surface settlements. Excessive settlements can damage surrounding roads, underground pipelines, and structures located within the influence zone of the tunnel alignment. The relatively shallow overburden of approximately 5.0 to 10.0 meters in a densely urbanized area represents the most significant challenge for construction. Consequently, the construction method must be tailored to minimize displacements and reduce the impact on sensitive structures in the historic city centre located within the tunnel excavation's influence zone. Characteristic cross-section, shown in Figure 7, shows a tunnel with an invert, reaching a maximum height of approximately 9.5 meters (measured from the bottom of the invert to the crown of the primary lining) and approximately the same maximum width.

The chosen method for tunnel construction NATM (New Austrian Tunnelling Method) is based on utilizing the beneficial interaction between the soil and the tunnel lining (Rabcevicz 1964). During excavation, a self-supporting arch forms in the ground above the tunnel, making use of the soil's self-bearing capacity. The required stability of the excavation is ensured using appropriate support measures such as radial anchors and spread shotcrete lining. A key factor for maintaining stability is a flexible support system that mobilizes the soil's bearing capacity while preventing excessive deformations that could lead to collapse. Geotechnical monitoring, essential in NATM, allows for real-time adaptation and modification of support types and surface displacement control during excavation.

Due to the lack of cohesion in coarse-grained soils such as gravel and sand, necessitates ground improvement to ensure tunnel stability during excavation. In urban environments, such as the historic centre of Maribor, ground improvement is also critical for deformation control to minimize impact on surrounding infrastructure. Ground improvement in terrace gravel and sand can be achieved using various techniques, including jet grouting, injection grouting, micro piling, ground freezing, etc (Xanthakos, Abramson, and Bruce 1994). Jet grouting, which is considered most appropriate for given geological conditions, is a ground stabilization technique that involves the high-pressure injection of cementitious slurry (ranging from 300 to 700 bar) through nozzles mounted on a rotating drill string. This process forms soil-cement columns with significantly enhanced geomechanical properties due to the mixing of native soil with cement slurry. The technique involves erosion of the surrounding soil matrix using high-velocity water or slurry jets, followed by rotational lifting of the drill, allowing the eroded soil to mix with the slurry. This results in the formation of a quasi-cylindrical column that solidifies over a few days into a concrete-like material. Jet grouting can be executed either vertically from the surface or horizontally along the tunnel axis (to reinforce tunnel walls or the excavation face). Longitudinal jet grouting has been shown to be an effective and versatile method in multiple applications. Also, horizontal fan-shaped arrays of jet grout columns, inclined slightly forward in the direction of tunneling, are used to stabilize the tunnel crown and sidewalls (Croce, Modoni, and Russo 2004).

Past experience confirms that jet grouting is particularly suitable for surface settlement control when combined with full-perimeter (360°) column placement and supplemental stabilization walls, especially within the NATM framework. A documented case involving a small-diameter tunnel under an active railway demonstrates successful implementation in similarly composed soils (De Salvo and Silvestri 2014). Given the relatively shallow tunnel cover (5 to 10 m) and the alignment's location beneath an existing roadway in a dense urban environment, ground improvement beneath nearby building foundations will also be necessary. This can be achieved through vertical jet grout columns installed from the ground surface. The advantage of this method is that ground stabilization can occur independently from tunnel advanced injections. This parallel workflow significantly accelerates excavation and construction, as activities do not depend on one another or require phase transitions. Different variants of a combination of semi-vertical jet grouting need for tunnel construction as well as for building protection is given in Figure 8.



**Figure 8.** Different variants of a combination of semi-vertical jet grouting columns (in grey) needed for tunnel construction.

#### 4. USE OF GETHERMAL ENERGY TO COMPLEMENT TUNNEL CONSTRUCTION

Subsurface urbanization represents one of the key contemporary challenges in civil engineering; however, when coupled with innovative technologies, it enables sustainable development and contributes significantly to environmental protection. The construction of the Maribor City tunnel has the potential to embody a modern approach to underground urbanization. Structural elements such as diaphragm walls at the tunnel portals and the tunnel's inner lining offer considerable potential for geothermal energy exploitation. This forms an opportunity that is crucial for the tunnel's sustainability and environmental contribution.

By upgrading selected geotechnical structures, it is possible to achieve efficient thermal exchange between the ground, which serves as a natural heat reservoir. Geotechnical structures in urban areas are particularly suited for this application due to their proximity to consumers, enabling efficient utilization of this renewable energy source through short energy transmission distances (Markiewicz et al. 2005).

These structures, functioning as energy geo-structures in conjunction with a heat pump system, could provide heating and cooling to aboveground buildings or tunnel facilities (e.g., technical facilities located between Slovenska and Gledališka streets) shown in Figure 1, significantly reducing their operational energy costs. From an implementation standpoint, the integration of geothermal systems into the Maribor urban tunnel would not result in a significant increase in capital investment, especially when considering the potential reduction in long-term operational costs for energy consumers. The geothermal potential can be exploited as a closed loop system with the help of heat exchangers, which can be incorporated into any permanently constructed element of the tunnel or as an open loop system that consist of pumping and reinjecting wells. In both scenarios, the technical room's location would be advantageous for placing other hardware components and serve as a distribution point for transferring thermal energy to end-users. Therefore, we can conclude that the tunnel's extensive geothermal potential is positively influenced by its location in the city centre.

Due to the specific geological and hydrological context of the Maribor City tunnel, as well as its proximity to the Drava River, the implementation of a hydrothermal water-to-water system is particularly advantageous. The geothermal source lies directly beneath the tunnel, making it feasible to exploit the aquifer through an open-loop configuration. Such systems typically consist of a pair of geothermal wells; one for water extraction (pumping well) and another for its return (reinjection well). The system's dimensioning is critically dependent on local hydrogeological characteristics and thermal demand. Key factors include the aquifer's permeability, depth, and the velocity and direction of groundwater flow. In this case, the groundwater flows perpendicularly to the tunnel axis, which is favourable for maintaining the thermal integrity of the resource and achieving stable operating temperatures.

From a technical and operational standpoint, three potential well placement configurations have been identified. Two of these are positioned near the tunnel portals, where extracted groundwater can be routed through existing infrastructure (specifically, the kinetic zone) into technical rooms located within the storage niche. The third, and most cost-efficient, option entails installing both wells within the technical area itself in the area of the operational building. However, this solution presents limitations in terms of thermal efficiency, as it restricts the separation between pumping and reinjection zones, which is critical for maintaining the desired temperature gradient. Accurate delineation of the pumping well's influence zone is also essential. This thermal capture area is governed by parameters such as aquifer depth, hydraulic conductivity of the geological medium, and prevailing groundwater flow patterns. Only through a detailed hydrogeological analysis can the optimal well layout and spacing be achieved, ensuring both sustainable resource utilization and system performance.

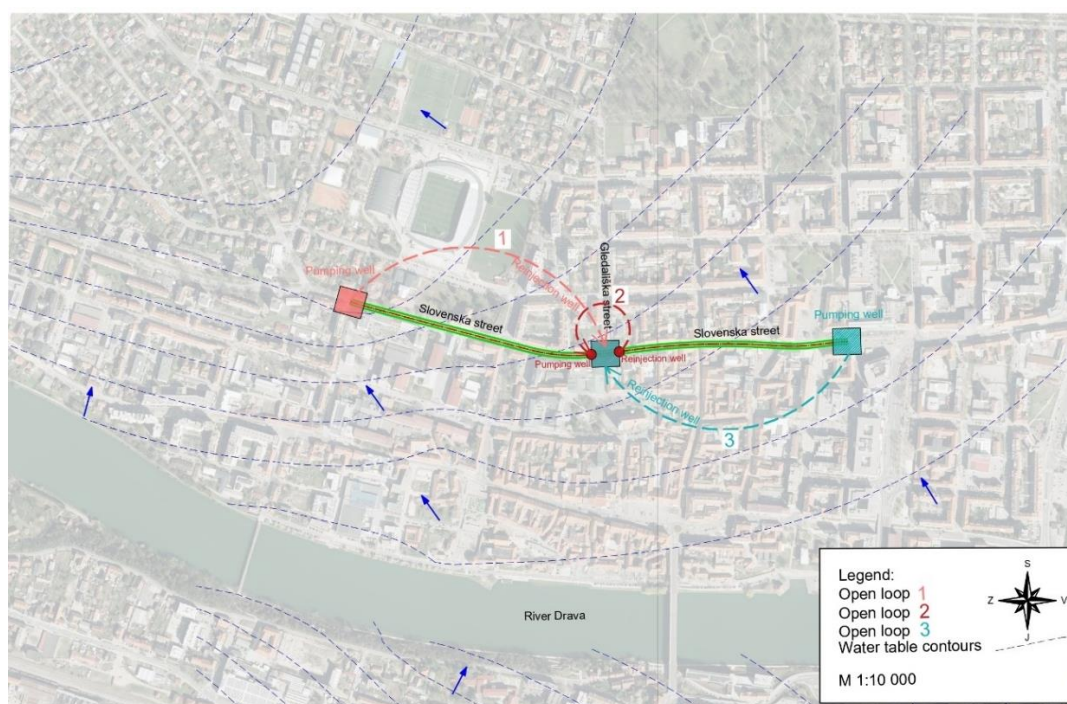


Figure 9. Different variants of implementation of a hydrothermal open-loop water-to-water system.

## 5. CONCLUSIONS

Based on the findings presented in the research study, the construction of the Maribor City tunnel is considered a feasible development within the framework of the acceptable technical and construction criteria. From an urban planning perspective, the Maribor City tunnel can be successfully integrated in a manner that meets the need for an east–west link through the city centre, as defined in Maribor's Comprehensive Transport Strategy (June 2015). With respect to integration into the existing road infrastructure a 980 meters single tune tunnel will alleviate traffic congestion in the centre of the town. The proposed route follows alignment on the existing streets for a minimal impact, following a concave alignment with a longitudinal gradient of 10% at the ramp sections and 0.5% in the central part of the route. The lowest tunnel elevation is at 254.0 m above sea level, located approximately halfway along the alignment, where an emergency exit shaft and operational building is also planned. The tunnel is designed for traffic speeds of up to 50 km/h, with entry/exit ramps limited to 40 km/h. The estimated of 5.0 to 10.0 m can be achieved without compromising tunnel functionality.

The design concept presented in this study respects the identity and functionality of the urban areas at both tunnel portals. The portal areas are designed to harmonize with the surrounding built environment, avoiding visual dominance or stylistic conflict. Visible elements are deliberately conceived to fulfil both functional and safety requirements while contributing architectural value that complements the existing urban fabric. These elements form an integral part of the road infrastructure and are carefully scaled to preserve spatial continuity, avoiding any disruptive separation of the public space.

The geological profile along the tunnel route is assessed as relatively homogeneous, allowing full excavation within the terrace gravel of the Drava River basin. The tunnel can be constructed in full compliance with the applicable Water Protection Regulation Act (Official Gazette of the Republic of Slovenia Nos. 24/07, 32/11, 22/13, 79/15), provided the tunnel invert remains at least 2 meters above the highest recorded groundwater level, i.e., above elevation 254.0 m a.s.l. From a construction standpoint, the New Austrian Tunneling Method (NATM) combined with jet grouting for ground improvement is identified as the optimal approach. NATM, which relies on adapting the primary support and excavation sequence, allows effective stability control and minimization of deformation impacts when paired with jet grouting. Excavation progresses sequentially, synchronized with phased ground improvement. The advantage of pre-excavation vertical jet grouting columns from the surface over horizontal injections during excavation lies in the decoupling of ground improvement from tunnel advance, accelerating the overall construction schedule. However, it must be emphasized that such ground improvement is essential and will significantly increase project costs.

The tunnel structure presents a significant opportunity for geothermal energy utilization. The tunnel lining and associated geostructures could, in combination with heat pumps, be used to heat and cool existing buildings or internal tunnel facilities. This would notably reduce tunnel operational energy costs. Due to the specific geological and hydrological context of the Maribor City tunnel, as well as its proximity to the Drava River, the implementation of a hydrothermal water-to-water system is particularly advantageous. The geothermal source lies directly beneath the tunnel, making it feasible to exploit the aquifer through an open-loop configuration. Further research is needed, including a detailed hydrogeological analysis, to devise the optimal well layout and spacing, ensuring both sustainable resource utilization and system performance.

## 6. REFERENCES

- [1] Croce, Paolo, Giuseppe Modoni, and Giacomo Russo. 2004. "Jet-Grouting Performance in Tunnelling." In *GeoSupport 2004*, 910–22. Reston, VA: American Society of Civil Engineers. [https://doi.org/10.1061/40713\(2004\)78](https://doi.org/10.1061/40713(2004)78).
- [2] Forschungsgesell-, Österreichische, and schaft Straße – Schiene Verkehr. 2008. RVS 09.03.11 Tunnel Safety - Tunnel Risk Model, FSV.
- [3] Mair, R J#, and R N Taylor. 1999. "Bored Tunnelling in the Urban Environments." In *Fourteenth International Conference on Soil Mechanics and Foundation Engineering. Proceedings International Society for Soil Mechanics and Foundation Engineering*. Vol. 4.
- [4] Markiewicz, R, D Adam, J Hofinger, and W Unterberger. 2005. "Extraction of Geothermal Energy from Tunnels." In *Proceedings of the 16th International Conference on Soil Mechanics and Geotechnical Engineering*, 1629–32. IOS Press.
- [5] Official Gazette of RS, Nos. 48/06, 54/09. n.d. Regulation on Technical Norms and Conditions for the Design of Road Tunnels in Slovenia.
- [6] Official Gazette of the Republic of Slovenia Nos. 24/07, 32/11, 22/13, 79/15. 2007. Water Protection Regulation Act.
- [7] Official Journal reference: OJ L 167, 30.4.2004, p. 39-91. n.d. Directive 2004/54/EC of the European Parliament and of the Council of 29 April 2004 on Minimum Safety Requirements for Tunnels in the Trans-European Road Network.
- [8] Rabcevicz, L. V. 1964. "The New Austrian Tunelling Method (Part 1 and Part 2)." *Water Power* November 1: 511-515 and pp. 19-24.
- [9] Salvo, F De, and C. Silvestri. 2014. "Settlements Induced by Jet-Grouting Execution in Tunnel." In *AMITOS - Fourth Mexican Congress on Tunnels and Underground Works 2014 Underground Space, Option of the Future*.
- [10] Xanthakos, Petros P, Lee W Abramson, and Donald A Bruce. 1994. *Ground Control and Improvement*. John Wiley & Sons.



## EVALUATION OF SEGMENT UPLIFT RISK DURING SHIELD TUNNELLING BASED ON CLOUD MODEL

Haoze Wu<sup>1</sup>, Shui-Long Shen<sup>2</sup> Annan Zhou<sup>3</sup>

**Abstract:** Tunnel segment uplift during shield tunneling involves dynamic and uncertain factors, posing significant challenges to accurate risk evaluation. Conventional static assessment methods typically overlook the changing importance of influencing factors as tunnelling progresses. To address this issue, this paper proposes a novel dynamic risk assessment framework combining entropy-based constant weight determination, variable weight theory, and cloud model analysis. Initially, a comprehensive risk evaluation index system is established, encompassing geological, construction, design, material, and management factors. Subsequently, the entropy weight method is employed to objectively determine constant weights, highlighting the inherent variability among factors based on measured data. These constant weights are dynamically adjusted using variable weight theory, thereby capturing real-time changes during tunnel construction. Furthermore, cloud model theory is utilized to quantify uncertainties and translate quantitative assessment data into probabilistic risk levels. A case study from the Guangzhou-Foshan metro line demonstrates that the proposed method yields more accurate and adaptive risk predictions compared to traditional static methods, effectively supporting safer decision-making in shield tunnelling operations.

**Keywords:** Shield tunnel, lining uplift, risk evaluation, cloud model

### 1. INTRODUCTION

Shield tunnelling technology is extensively utilized in constructing urban transit networks and underground utilities, playing an essential role in modern urban infrastructure (Gao et al., 2025). Nonetheless, it introduces significant geotechnical risks, notably the uplift of tunnel segments during the construction phase (Epel et al., 2021). Segment uplift, defined as the vertical displacement of newly placed tunnel segments due to excessive grouting pressures and buoyant forces, can result in alignment deviations, structural deficiencies, and increased maintenance demands, ultimately compromising tunnel safety and operational reliability.

Traditional methods for assessing segment uplift risks rely predominantly on empirical observations, numerical simulations, and analytical models. Empirical methods, although valuable in capturing specific project insights, offer limited predictive capability for general use due to site-specific constraints (Zhao et al., 2023). Numerical simulations, such as finite element analyses (Gong et al., 2018), can accurately represent the complex interactions between soil, grout, and tunnel segments but typically require extensive computational resources, making them less practical for real-time applications (Rashid et al., 2024). Analytical approaches, meanwhile, offer computational efficiency yet frequently depend on simplified assumptions that might overlook critical variations in real-world conditions (Wang et al., 2024). Moreover, these traditional methods cannot fully account for or replace the critical influence and practical judgment provided by experienced machine operating crews. Therefore, an effective risk assessment framework should integrate both computational analyses and practical construction considerations, including operator experience. Shield tunnelling is inherently dynamic; operational parameters such as grouting pressure, advance speed, and thrust force continuously fluctuate, significantly influencing the segment uplift risks (Ye et al., 2023). Current static risk assessment frameworks, characterized by fixed weighting systems, cannot adequately adapt to these changing conditions and thus fail to provide timely and precise evaluations (Lin et al., 2023).

<sup>1</sup> PhD candidate, Wu Haoze, M.Sc. Civil Engineering, Shantou University, Shantou, China; Email: 19hzwu@stu.edu.cn.

<sup>2</sup> Professor, Shen, Shui-Long, PhD Civil Engineering, Shantou University, Shantou, China; Email: shensl@stu.edu.cn.

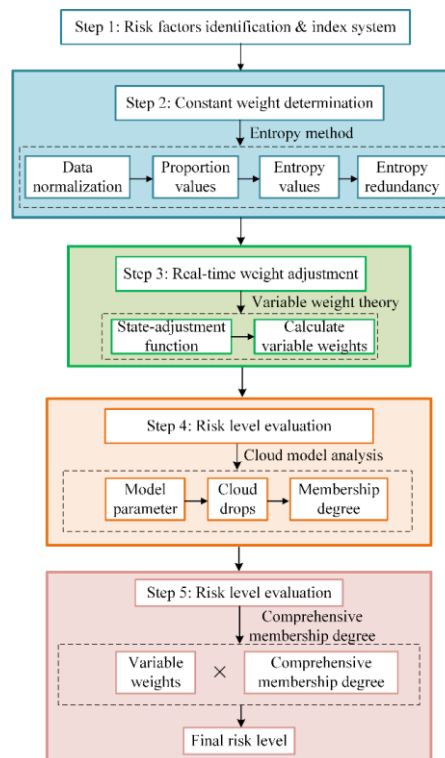
<sup>3</sup> Professor, Zhou, Annan, Ph.D. Civil Engineering, School of Engineering, RMIT University, Melbourne, Australia, annan.zhou@rmit.edu.au.

Addressing these challenges, this study proposes a novel dynamic risk assessment framework that integrates the entropy weight method with variable weight theory and cloud model theory (Guo et al., 2024). Firstly, an extensive risk indicator system is established, systematically identifying critical influencing factors from geological, construction, material, design, and management perspectives. The entropy weight method is then solely employed to objectively determine constant weights for these risk indicators, effectively capturing their intrinsic importance based on data dispersion characteristics. To dynamically adapt to real-time changes during construction, variable weight theory is introduced, enabling the continuous recalibration of indicator weights according to actual tunnelling conditions (Cicek et al., 2025). Furthermore, cloud model theory is utilized to quantify uncertainties and fuzziness inherent in measured data, converting real-time quantitative assessments into probabilistic risk levels with improved reliability and accuracy (Pak et al., 2025). The proposed approach is validated through its application to a real shield tunnelling project at the Pazhou branch of the Sui-Guan-Shen Intercity Line. The results demonstrate significantly enhanced predictive accuracy and responsiveness compared to conventional methods. Consequently, this framework provides robust decision support and substantially improves the safety management and operational reliability of shield tunnelling projects.

## 2. MATERIAL AND METHOD

### 2.1. Model architecture

As illustrated in Fig. 1, the proposed framework for uplift risk assessment in shield tunnelling is composed of five sequential steps. In Step 1, key risk factors are identified and a multi-level evaluation index system is established. Step 2 employs the entropy weight method to compute the constant weights of the indicators based on data dispersion characteristics. This process involves data normalization, calculation of proportion values, entropy values, and entropy redundancy. In Step 3, the variable weight theory is applied to dynamically adjust the indicator weights in real time using a state-adjustment function, thereby enhancing the model's responsiveness to evolving construction conditions. Step 4 introduces cloud model theory to quantify the uncertainty and fuzziness of the measured data. Cloud model parameters are used to generate cloud droplets and determine the membership degree of each indicator with respect to predefined risk levels. Finally, in Step 5, the comprehensive membership degrees are aggregated using the dynamically updated weights to determine the final uplift risk level through the principle of maximum membership. This integrated framework ensures both adaptability and robustness in risk evaluation throughout the shield tunnelling process.



**Figure 1.** Flowchart of this study

## 2.2. Project background

This case study focuses on the shield tunnel segment between Hualong Station and Mingjing Shaft along the Pazhou branch of the Sui-Guan-Shen Intercity Line in Guangzhou, China. The project employs an Earth Pressure Balance (EPB) shield machine, which is designed to maintain soil stability by balancing excavation face pressure with controlled slurry pressure. The EPB shield constructs twin single-track tunnels approximately 2.47 km in length, lined with precast reinforced concrete segments, typically arranged in rings comprising several interlocking segments. The tunnel passes through complex geological strata, including silty clay, completely weathered granite, highly weathered granite, and moderately weathered granite. Due to the variability in geotechnical conditions and the dynamic operational parameters such as grouting pressure (0.4 to 3.9 bar), advancing speed (10 to 60 mm/min), and thrust force (8,000 to 50,000 kN), segment uplift emerged as a significant construction risk, highlighting the need for effective real-time risk evaluation and management strategies.

Considering the unique operational and geological conditions associated with Earth Pressure Balance (EPB) shield tunnelling, critical risk factors contributing to segment uplift are systematically identified and categorized into geological, operational, design, material, and management aspects, as shown in the fishbone diagram (Figure 2). Geological factors primarily include soil properties such as compression modulus, internal friction angle, permeability coefficient, and cohesion. Operational factors cover key shield parameters such as advancing speed, grouting pressure, grouting speed, and total thrust force. Design factors encompass burial depth, drainage effectiveness, and anti-floating design measures. Material factors focus on grout properties including bleeding time, initial setting time, water-cement ratio, and early strength. Management factors relate to aspects of construction oversight such as quality control procedures, personnel management, and equipment maintenance practices. These representative indicators were selected based on comprehensive literature review and current industry standards to ensure relevance specifically tailored to EPB shield tunnelling contexts.

## 2.3. Calculation of constant and variable weights

Segment uplift risk factors in shield tunnelling are classified into five groups: geological, operational, design, material, and management. The constant weights  $W_j$  for each indicator are determined using the entropy method, capturing data variation quantitatively. The calculation is expressed as follows:

$$W_j = \frac{1 - e_j}{\sum_{j=1}^n (1 - e_j)}$$

where entropy is computed by:

$$e_j = -k \sum_{i=1}^m p_{ij} \ln(p_{ij}), k = \frac{1}{\ln(m)}, p_{ij} = \frac{x_{ij}}{\sum_{i=1}^m x_{ij}}$$

where  $x_{ij}$  denotes the value of the  $j$ th indicator for the  $i$ th evaluation object,  $m$  is the number of evaluation objects, and  $n$  is the number of indicators.

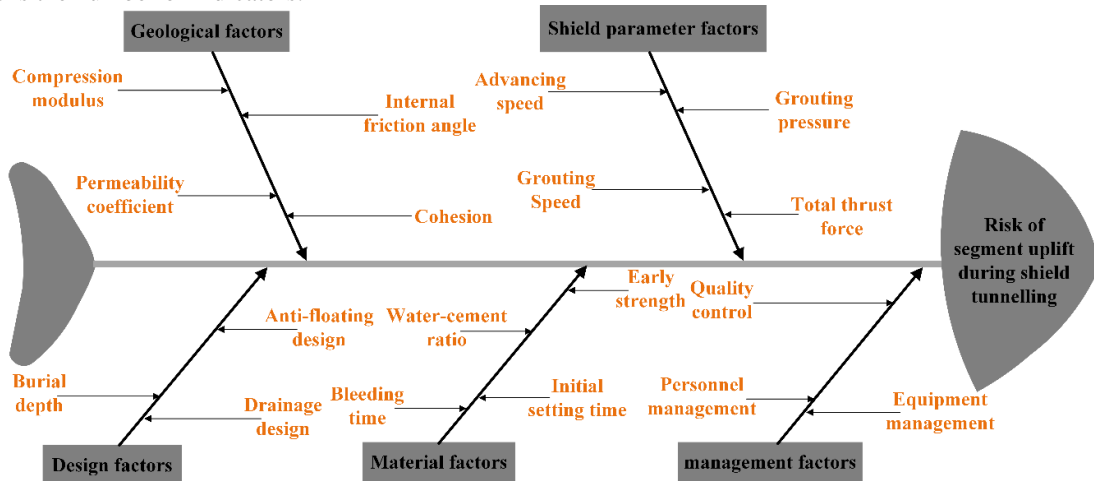


Figure 2. Fishbone diagram of tunnel uplift risk factors.

$$\alpha_j = \begin{cases} \exp [k(c - x_j)], & x_j \leq \beta \\ 1, & x_j > \beta \end{cases}$$

where  $\alpha_j$  is the variable weight coefficient,  $x_j$  is the normalized value of indicator  $j$ ,  $k$  is the penalty coefficient, and  $c$  is the threshold defining sensitivity. The final variable weights are:

$$W'_j = \frac{\alpha_j W_j}{\sum_{j=1}^n \alpha_j W_j}$$

#### 2.4. Cloud model-based risk assessment

Cloud model theory captures both fuzziness and randomness in risk assessment by using three parameters: expectation  $E_x$ , entropy  $E_n$ , and hyper-entropy  $H_e$ . The membership degree  $\mu(x)$  for each indicator value is generated as:

$$\mu(x) = e^{-\frac{(x-E_x)^2}{E_n}}$$

where  $E'_n$  is a normally distributed random value with mean  $E_n$  and variance  $H_e^2$ .

The comprehensive membership  $\mu_p$  at risk level  $p$  combines the cloud-generated membership degrees with variable weights:

$$\mu_p = \sum_{j=1}^n W'_j \mu_{jp}$$

where  $\mu_{jp}$  is the membership degree of indicator  $j$  at risk level  $p$ . The final risk level is determined by the maximum comprehensive membership degree.

### 3. RESULTS

#### 3.1. Brief description of VW method

The proposed variable weight (VW) method begins with constant weights objectively determined through the entropy weight method, effectively capturing the relative importance of risk factors based on data dispersion characteristics. Initially, these constant weights establish a stable and balanced foundation, appropriate for risk assessment under representative or typical tunnelling conditions.

As tunnelling advances, operational and geological conditions inevitably fluctuate, introducing dynamic and evolving risks. To address this variability, the VW method incorporates real-time monitoring data to dynamically recalibrate these constant weights, emphasizing indicators that exhibit significant variations or approach critical risk thresholds. Specifically, the method utilizes a state-adjustment function to systematically enhance the weights of indicators displaying deviations or deteriorations from expected safe operational levels. This approach is mathematically defined through a state-adjustment function, in which a penalty coefficient and a sensitivity threshold regulate the amplification rate of the indicator weights based on their real-time monitored states. Indicators that cross the predefined threshold levels are assigned amplified weights proportionally, effectively highlighting critical changes in risk conditions.

By continuously recalibrating indicator weights, the VW method adeptly responds to emerging risks and evolving geological and operational scenarios, thus significantly improving the sensitivity and adaptability of the risk assessment process. This dynamic adjustment ensures a timely and accurate reflection of actual conditions, enabling decision-makers to quickly identify critical issues and take proactive mitigation measures. Consequently, this method provides a more realistic and responsive risk assessment compared to traditional static methods, enhancing overall safety and operational efficiency during shield tunnelling projects.

#### 3.2. Risk analysis results

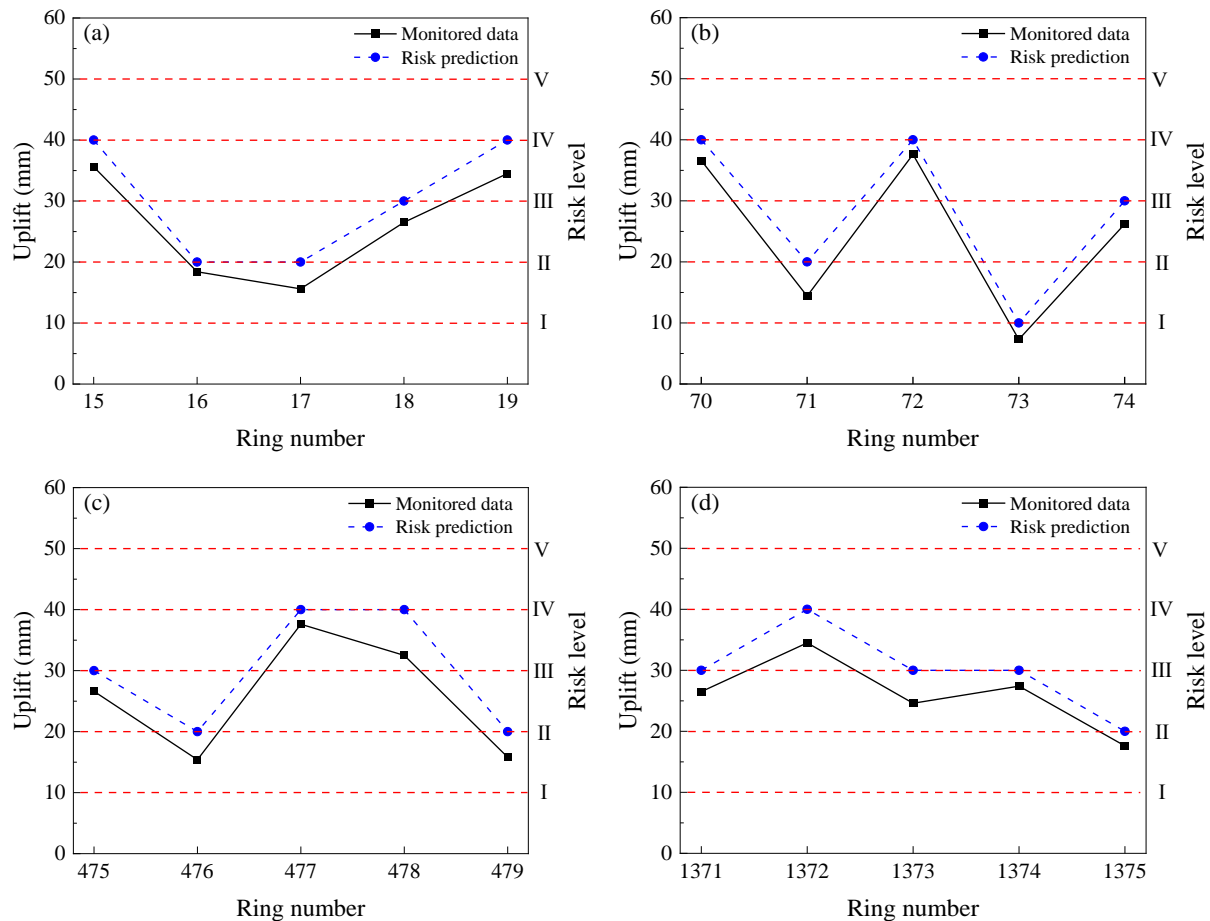
Figure 3 presents the measured segment uplifts and corresponding risk predictions using the proposed variable weight-cloud model across four distinct geological strata. In the silty clay stratum (Figure 3a), the measured uplift values exhibited noticeable fluctuations, closely aligning with the predicted risk levels, particularly from ring 15 to ring 19. This congruence highlights the model's precision in effectively capturing local variations induced by factors such as shallow burial depth, weak soil cohesion, and low internal friction angles, which collectively contribute to heightened vulnerability to uplift. The precise alignment between predicted and actual uplifts further demonstrates the model's capability to adapt rapidly to variations in soil properties, providing critical insights into the operational parameters that require immediate attention.

In the completely weathered granite stratum (Figure 3b), segment uplift exhibited moderate fluctuations, largely influenced by dynamic construction parameters such as grouting pressure, advancing speed, and thrust

force. The model's predictions effectively mirrored these fluctuations, clearly identifying periods of increased risk corresponding to elevated grouting pressures and accelerated advancement rates. This detailed correlation emphasizes the model's capability to dynamically adjust to operational parameter changes, offering real-time guidance on managing segment uplift risks. The model's responsiveness thus allows construction teams to anticipate and proactively mitigate potential uplift issues, significantly reducing the likelihood of adverse events.

For the highly weathered granite stratum (Figure 3c), the measured uplifts demonstrated relatively higher peaks, reflecting the more complex and unstable geological conditions characteristic of this stratum. The proposed model accurately captured these critical intervals, precisely predicting high-risk scenarios driven by intense variations in ground conditions and operational parameters. Notably, the model effectively identified critical thresholds of grouting pressure and advancing speed, enabling timely alerts for operational adjustments. This high accuracy is particularly valuable for ensuring that tunnelling operations can adapt to rapidly evolving geological challenges, thus maintaining overall structural safety and operational efficiency.

Lastly, within the moderately weathered granite stratum (Figure 3d), the observed uplift values showed a strong consistency with the model's predictions. The moderately stable geological conditions in this stratum interacted predictably with varying operational parameters, and the model adeptly reflected these interactions. This consistency underscores the model's robustness in accommodating both predictable and unexpected changes, verifying its versatility across different geological contexts. The clear and continuous correspondence between the measured uplift data and the predicted risk levels across this stratum not only validates the reliability of the proposed framework but also highlights its practical applicability for managing uplift risks in diverse and challenging tunnelling scenarios.



**Figure 3.** Segment uplift measurement and uplift risk predictions: (a) silty clay, (b) completely weathered granite, (c) highly weathered granite, (d) moderately weathered granite.

#### 4. DISCUSSION

To validate the effectiveness of the proposed variable weight-cloud model (VW-CM), a comparative evaluation against the Analytic Hierarchy Process (AHP) method was performed. Table 1 presents a detailed comparison



between these two methodologies for selected tunnel rings located within the highly weathered granite stratum. As demonstrated in Table 1, both the VW-CM and AHP methods yielded consistent predictions for segment uplift risk at rings 475, 477, and 479, indicating a strong agreement under relatively stable geological and operational conditions. Nevertheless, significant differences emerged at rings 466 and 468, clearly highlighting the strengths of the VW-CM approach in addressing dynamic and variable tunneling environments.

Specifically, at ring 476, the AHP method significantly underestimated the uplift risk by assigning a Level I classification, in contrast to the more accurate Level II risk indicated by the VW-CM approach. Conversely, at ring 478, the AHP method predicted a lower risk level (Level V) compared to the VW-CM method's Level IV, underscoring AHP's limitations due to reliance on fixed expert-derived weights. The observed discrepancies are primarily attributable to the fixed weighting structure inherent to AHP, which limits its adaptability to changing operational and geological conditions. In contrast, the VW-CM method dynamically adjusts indicator weights based on real-time construction data, effectively capturing fluctuations in critical factors such as grouting pressure, geological conditions, and operational parameters. Additionally, the embedded cloud model within VW-CM quantitatively accounts for inherent uncertainties, further enhancing the reliability and robustness of risk predictions.

**Table 1.** Comparison of uplift risk between VW-CM and AHP methods.

Strata	Ring number	VW-CM	AHP
Highly weathered granite	475	III	III
	476	II	I
	477	IV	IV
	478	IV	V
	479	II	II

## 5. CONCLUSIONS

This study presents an innovative risk assessment framework for evaluating tunnel segment uplift during shield tunneling, integrating variable weight theory and cloud model analysis. Through systematic identification of risk factors and dynamic adjustments using real-time data, the proposed model significantly enhances risk evaluation precision, offering practical insights and actionable recommendations for tunnel construction management.

A comprehensive risk indicator system was first developed, effectively encompassing geological, operational, and management factors, providing a robust and structured basis for dynamic risk evaluation. This system facilitates clear identification and prioritization of influential factors, significantly streamlining risk management processes. Furthermore, by incorporating variable weight theory, the model enables real-time recalibration of indicator weights, greatly improving the framework's responsiveness and adaptability to dynamically evolving construction conditions. Such dynamic adjustments ensure timely detection and accurate evaluation of emerging risks, thereby allowing for proactive and targeted mitigation measures. Additionally, the introduction of cloud model theory effectively quantifies the inherent uncertainties and randomness associated with tunneling parameters. By capturing both fuzziness and randomness within operational and geological variables, the cloud model significantly enhances the robustness, credibility, and overall predictive accuracy of the risk assessments, thus supporting better-informed and more reliable decision-making in complex tunneling environments.

It must be recognized that despite the high precision and adaptability provided by the proposed risk assessment framework, the practical experience and judgment of tunnel construction personnel remain indispensable. Their skills, acquired through extensive hands-on experience, enable rapid identification of segment uplift risks. Future research could focus on integrating advanced machine learning techniques with this framework, incorporating continuous optimization through the feedback of experienced on-site personnel to automate the risk assessment process further and enhance predictive accuracy. Additionally, extending this approach to other types of underground construction could verify its generalizability and broader applicability.

## 6. ACKNOWLEDGMENTS

The research work was funded by Guangdong Province and Guangdong Provincial Basic and Applied Basic Research Fund Committee (2022A1515240073).

## 7. REFERENCES

- [1] Cicek, K., Demirci, S.M. E., Sengul, D. (2025). A hybrid failure analysis model design for marine engineering systems: A case study on alternative propulsion system. *Engineering Failure Analysis*, 167, 108929. <https://doi.org/10.1016/j.engfailanal.2024.108929>.
- [2] Epel, T., Mooney, M.A., Gutierrez, M. (2021). The influence of face and shield annulus pressure on tunnel liner load development. *Tunnelling and Underground Space Technology*, 117, 104096. <https://doi.org/10.1016/j.tust.2021.104096>.
- [3] Gao, W., Ge, S.S., Cui, S., Chen, X. (2025). Intelligent decision on shield construction parameters based on safety evaluation model and sparrow search algorithm. *Reliability Engineering & System Safety*, 260, 110973. <https://doi.org/10.1016/j.res.2025.110973>.
- [4] Gong, Q.M., Zhao, Y., Zhou, J.H., Zhou, S.H. (2018). Uplift resistance and progressive failure mechanisms of metro shield tunnel in soft clay. *Tunnelling and Underground Space Technology*, 82, 222–234. <https://doi.org/10.1016/j.tust.2018.08.038>.
- [5] Guo, D.S., Meng, F.Y., Wu, H. N., Yang, X. X., Liu, Z. (2024). Risk assessment of shield tunneling crossing building based on variable weight theory and cloud model. *Tunnelling and Underground Space Technology*, 145, 105593. <https://doi.org/10.1016/j.tust.2024.105593>.
- [6] Lin, S.S., Zhou, A.N., Shen, S.L. (2023). Safety assessment of excavation system via TOPSIS-based MCDM modelling in fuzzy environment. *Applied Soft Computing*, 138, 110206. <https://doi.org/10.1016/j.asoc.2023.110206>.
- [7] Pak, U.S., Nam, G.H., Paek, M.R., Kim, Y.S., Won, I.S. (2025). Variable universe triangular cloud model-based controller design for real-time control of rotary parallel inverted pendulum. *International Journal of Dynamics and Control*, 13(3), 116. <https://doi.org/10.1007/s40435-025-01613-w>.
- [8] Rashidell, A., Abedi, M., Dias, D., Ramesh, A. (2024). Seismic analysis of segmental shallow tunnels adjacent to building foundations under soil liquefaction and its mitigation. *Soil Dynamics and Earthquake Engineering*, 178, 108479. <https://doi.org/10.1016/j.soildyn.2024.108479>.
- [9] Wang, B., Li, J.T., Zhao, C.Y., Wang, J. (2024). An improved analytical solution for solving the shield tunnel uplift problem. *Journal of Rock Mechanics and Geotechnical Engineering*, 16, 4570–4585. <https://doi.org/10.1016/j.jrmge.2024.05.011>.
- [10] Ye, X.W., Zhang, X. L., Zhang, H.Q., Ding, Y., Chen, Y.M. (2023). Prediction of lining upward movement during shield tunneling using machine learning algorithms and field monitoring data. *Transportation Geotechnics*, 41, 101002. <https://doi.org/10.1016/j.trgeo.2023.101002>.
- [11] Zhao, Y.R., Chen, X.S., Hu, B., Huang, L.P., Li, W.S., Fan, J.J. (2023). Evolution of tunnel uplift and deformation induced by an upper and collinear excavation: A case study from Shenzhen metro. *Transportation Geotechnics*, 39, 100953. <https://doi.org/10.1016/j.trgeo.2023.100953>.

## EXTRACTION OF INDIVIDUAL ROCK DISCONTINUITIES BASED ON THREE-LAYER CLUSTERING ALGORITHM FROM 3D POINT CLOUDS

Bingyi Pan<sup>1</sup>, Wei Wu<sup>2\*</sup>, Yong Huang<sup>3</sup>, Baolin Chen<sup>4</sup>, Hehua Zhu<sup>5</sup>

**Abstract:** Accurate characterization of rock discontinuities is essential for tunnel stability analysis, as discontinuities play a fundamental role in governing the mechanical behavior and failure mechanisms of the surrounding rock mass. The advancement of remote surveying methods has enabled the rapid identification of discontinuities and extraction of pertinent geometric information from 3D point clouds of the rock mass. Nevertheless, traditional methods that rely on point features are insufficient in their ability to eliminate fragmented non-structural regions during the process of individual discontinuity extraction. This paper presents a novel three-layer clustering approach that aims to extract individual discontinuities from 3D point clouds automatically. To begin with, the rock mass point cloud is filtered to extract core points and remove non-structural regions. Subsequently, an improved density-based spatial clustering of applications with noise (IDBSCAN) is employed to identify planar units within core points. To merge adjacent fragmented planar units, these units are re-clustered based on their spatial relationships, resulting in the identification of individual discontinuities. A weighted modified k-means++ method is then used to cluster individual discontinuities according to their respective normal vectors. Consequently, the orientation, set, and trace of each individual discontinuity can be obtained respectively through geometric analysis. This method is applied to one tunnel case and compared with previous studies. The results suggest that the proposed method has a high level of reliability and accuracy when it comes to automatically extracting individual discontinuities from 3D point clouds, providing a more robust foundation for tunnel design and construction.

**Keywords:** Individual discontinuities, Rock mass, 3D point clouds, Automatic extraction

### 1. INTRODUCTION

The identification of discontinuities is crucial for evaluating the strength, stability, and mechanical behavior of the rock mass. Conventional measurement methods primarily rely on geological engineers manually measuring using geological compasses or scanlines. However, these methods have significant drawbacks as they are time-consuming, pose risks to geological engineers, and cannot measure certain areas (Chen et al., 2016). Recently, rapid advancements in remote surveying technologies have enabled the use of laser scanners or photogrammetry to acquire 3D point clouds of the rock outcrop. This offers safe and highly precise non-contact measurement methods capable of capturing areas that are inaccessible to manual measurement.

In recent times, numerous studies have focused on extracting discontinuities from 3D point clouds of the rock outcrop obtained through photogrammetry or laser scanning methods (Chen et al., 2021; Singh et al., 2023). Certain studies employ a manual point selection method from 3D point clouds, followed by plane fitting to identify discontinuities (Assali et al., 2016; Drews et al., 2018). This approach necessitates operators with professional geological expertise and is time-consuming. Moreover, automatic methods for discontinuity identification have garnered attention, primarily focused on clustering-based and region growing-based approaches (Hu et al., 2020; Kong et al., 2020). Singh et al. (2021, 2022) introduced sinusoidal waves and local point descriptors as supplements to the point features used in clustering methods. Subsequently, researchers performed density

<sup>1</sup> Bingyi Pan, Department of Geotechnical Engineering, Tongji University, Shanghai, China, 2111040@tongji.edu.cn.

<sup>2</sup> Wei Wu, Department of Geotechnical Engineering, Tongji University, Shanghai, China, weiwu@tongji.edu.cn.

<sup>3</sup> Yong Huang, China Railway First Survey and Design Institute Group Co., Ltd., Xi'an, China, 32186254@qq.com.

<sup>4</sup> Baolin Chen, Zhejiang Institute of Communications Co., Ltd., Hangzhou, China, chenbaolin1992@126.com.

<sup>5</sup> Hehua Zhu, Department of Geotechnical Engineering, Tongji University, Shanghai, China, zhuhehua@tongji.edu.cn.

clustering on the grouped points to identify individual discontinuities. However, due to the relatively uniform nature of 3D point clouds in the rock outcrop, this method fails to effectively eliminate non-structural regions. The region growing method utilizes the nearest neighbor relationship among point clouds for direct growth, which is affected by the global threshold and tends to incorporate fragmented non-structural surface regions. Additionally, Ge et al. (2022) suggested using artificial neural networks for automatic grouping of discontinuities. However, data labeling is still necessary for each rock outcrop point cloud.

Given the limitations of traditional discontinuity identification methods in effectively eliminating non-structural regions, this paper employs a three-layer clustering approach to extract individual discontinuities from 3D point clouds of the rock mass and perform grouping. Initially, the point normal vector of each point is acquired as a point feature by conducting principal component analysis (PCA) on the point clouds. Subsequently, the point clouds of the rock mass are filtered to extract the core points and remove non-structural regions. Next, a three-layer clustering method is applied to identify and group the individual discontinuities. Lastly, geometric analysis is employed to determine the orientation, set, and trace information for each individual discontinuity.

## 2. METHODOLOGY

### 2.1. Point normal vector calculation

To efficiently obtain the point normal vector, this paper utilizes a combination of the k-nearest neighbor (KNN) algorithm with a fixed number of nearest neighbor points and the principal component analysis (PCA) method. By specifying the number of nearest neighbor points  $k$ , the KNN algorithm rapidly retrieves the  $k$  nearest neighbor points, including the point itself, from the point clouds of the rock mass. The fundamental concept involves minimizing the sum of squared distances between the nearest neighbor points and the fitting plane to determine the fitting plane, and subsequently utilizing its normal vector as the point normal vector for that specific point. This approach is equivalent to performing PCA on a matrix formed by the 3D coordinates of the nearest neighbor points. The covariance matrix of the 3D coordinate matrix needs to be calculated first using the following equation:

$$C = \frac{1}{k-1} P^* P \quad (1)$$

where  $P$  is the 3D coordinate matrix of the nearest neighbor points in  $k$  rows and three columns (after centralization);  $k$  is the number of the nearest neighbor points (including the query point itself);  $C$  is the covariance matrix of  $P$ , with three rows and three columns. The covariance matrix  $C$  is decomposed into its three eigenvalues  $\lambda_1, \lambda_2, \lambda_3$  ( $\lambda_1 \geq \lambda_2 \geq \lambda_3$ ). The unit eigenvector corresponding to  $\lambda_3$  is considered as the point normal vector of that query point.

### 2.2. Three-layer clustering approach

#### 2.2.1. Core point identification

To eliminate non-structural regions and filter the point clouds of the rock mass, the core points are initially identified as the points to be clustered from the point clouds. Ester et al. (1996) employed the concept of nearest neighbor point density to search for core points, but without fully accounting for the curvature information. In this study, the core points must satisfy two conditions:

Condition 1: the flatness coefficient  $\eta = \frac{\lambda_3}{\lambda_1 + \lambda_2 + \lambda_3}$  must be below the set threshold to roughly identify

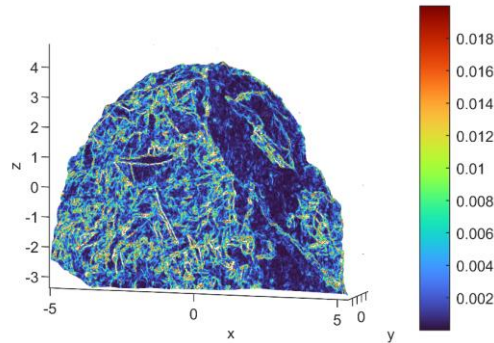
points with lower curvature (figure 1). Only points that meet the flatness threshold condition  $\eta < \eta_{\max}$  ( $\eta_{\max}$  is a predetermined constant) are retained for the density calculation;

Condition 2: the density of all neighbor points meeting condition 1 for the queried point should surpass the density of all points in the point clouds that meet condition 1, which is calculated using the following equation:

$$\frac{k_f}{k} > \frac{N_f}{N} \quad (2)$$

where  $k_f$  is the number of the nearest neighbor points that meet the flatness condition,  $k$  is the number of the nearest neighbor points for each point,  $N_f$  is the number of points among all points that satisfy the flatness condition, and  $N$  is the number of all points in this dataset.

Evaluating these two conditions suggests that local curvature information can effectively eliminate non-structural regions and identify core points.



**Figure 1.** Flatness index of the tunnel face.

### 2.2.2. Core point clustering

After obtaining the core points, it is necessary to cluster them initially to obtain planar units. The traditional DBSCAN algorithm clusters based on the density of the point cloud, which does not consider the coplanar features of the discontinuity point cloud. To take full advantage of the coplanarity of the discontinuity point cloud, the calculation of the angle between the  $k$ -nearest neighboring points is added to perform the density connectivity judgment. The IDBSCAN algorithm is adopted here, with the following steps:

1. Select the core point with the highest flatness coefficient as the initial clustering point and search for core points with density direct connection (using the  $k$ -nearest neighbor relationship) to join the cluster. At the same time, the added points must meet the requirement that the angle between their normal vector and the fitting plane normal vector of the existing points in the cluster is below the threshold;
2. Repeat step 1 until there are no more core points with density direct connection;
3. Choose the core point with the highest flatness coefficient from the remaining core points as another initial clustering point for further clustering;
4. Iteratively perform step 1-3 until all core points have been traversed.

Clustering the core points allows for comprehensive consideration of the nearest neighbor angle relationship, resulting in the acquisition of planar units.

### 2.2.3. Planar unit clustering

Planar units are clusters of core points, which can still exhibit fragmentation. Additionally, there might be multiple planar units associated with a single individual discontinuity. Hence, it is necessary to cluster planar units. The clustering of planar units involves the following steps:

1. Retrieve the  $k$  nearest neighbor points for all the points within each planar unit and determine the connectivity of the planar units based on the intersection relationship among these nearest neighbor points;
2. Utilize the planar unit with the highest flatness coefficient as the initial clustering unit to search for connected planar units and incorporate them into the cluster. The added planar units must also fulfill the condition that the angle between their normal vector and the fitting plane normal vector of the existing points in the cluster is below the threshold;
3. Repeat step 2 until no more connected planar units are found, and conclude the clustering process;
4. Choose the planar unit with the highest flatness coefficient from the remaining planar units as the initial clustering unit for further clustering;
5. Iterate through steps 2-4 until all planar units have been processed.

Following the clustering of planar units, each resulting cluster can be considered as an individual discontinuity. The identification process of individual discontinuities comprehensively considers local point features and local plane features, effectively eliminating fragmented and undulating non-structural regions.

### 2.2.4. Individual discontinuity clustering

The number of sets is an important parameter for discontinuities. The clustering of individual discontinuities considers the structural characteristics of the rock mass in a more comprehensive manner compared to direct point



clustering. This is achieved by removing non-structural regions during clustering, leading to more accurate clustering results. The fast k-means++ algorithm proposed by Wu et al. (2020) is highly efficient and capable of achieving automatic optimal grouping. However, it is based on point clustering. Here, a modified k-means++ algorithm is employed for weighted clustering based on individual discontinuities. The process involves the following steps:

1. Calculate the total number of the point clouds belonging to each individual discontinuity as the clustering weight of each individual discontinuity;
2. Select the individual discontinuity normal vector with the highest weight as the initial clustering center;
3. Choose the normal vector of the individual discontinuity that has the farthest distance from its closest known initial clustering center as an additional initial clustering center, and repeating this step until all  $k'$  initial clustering centers have been determined;
4. Divide the remaining individual discontinuities into clusters according to their nearest initial clustering centers, and k-means algorithm is applied to identify the final clustering center.

The distance  $d$  between different individual discontinuities in the clustering process is defined as follows:

$$d(n_i, n_j) = \arccos(|n_i \cdot n_j|) \quad (3)$$

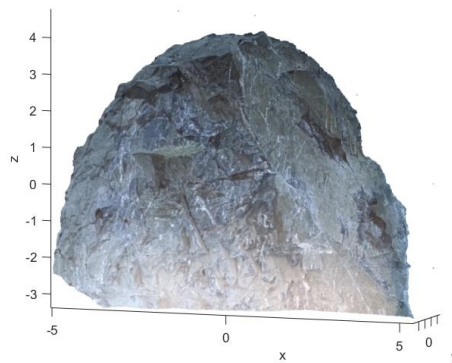
Where,  $n_i$  and  $n_j$  represent the normal vectors of two individual discontinuities, respectively. To obtain the optimal number of sets  $k'_{opt}$ , a fast silhouette algorithm is adopted (Wu et al., 2020), which is efficient for large scale of data. When the silhouette value reaches its maximum, the corresponding number of sets  $k'$  can be considered as the optimal number of sets  $k'_{opt}$ .

### 2.3. Geometric analysis

Geometric analysis of the extracted individual discontinuities allows for obtaining their orientation, set, and trace information. Orientations are determined through a polar projection transformation of the normal vectors of individual discontinuities, resulting in the dip direction and dip angle. The sets are determined through the three-layer clustering process. To accurately represent the intersection between the discontinuities and the rock outcrop, the intersection lines formed by the intersection of the disk models representing the individual discontinuities and the rock outcrop are acquired. These intersection lines are subsequently projected onto a 2D plane to obtain the traces. The proposed trace mapping method extensively utilizes the extracted individual discontinuity information and ensures a one-to-one correspondence between the discontinuities and the exposed traces, preventing the occurrence of one discontinuity corresponding to multiple traces.

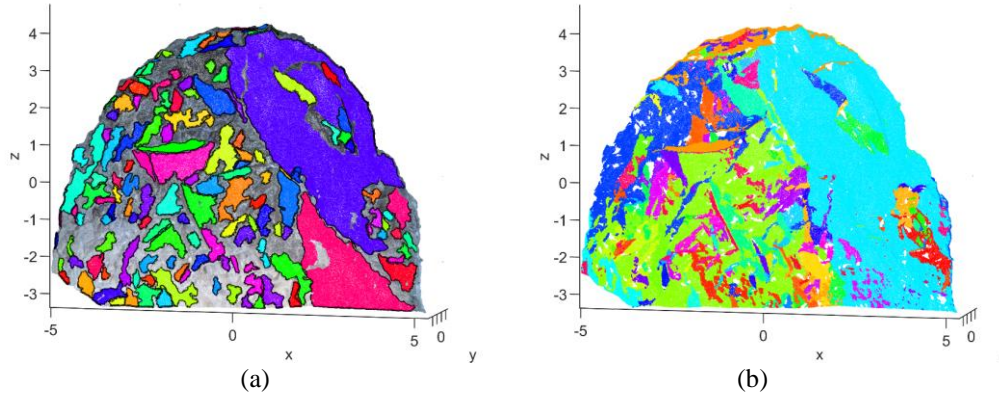
## 3. APPLICATION

This paper adopts point clouds of one tunnel face collected in railway tunnel in Tibet, China. Due to the complicate site conditions, it is very convenient to utilize digital photogrammetry technology combined with structure from motion (SfM) to acquire point clouds. Nine photos were taken in field from different angles, which were then used for 3D reconstruction to obtain point clouds. The CloudCompare software was used to pre-process the raw point clouds. The point clouds, which consist of 235681 points, are shown in figure 2.



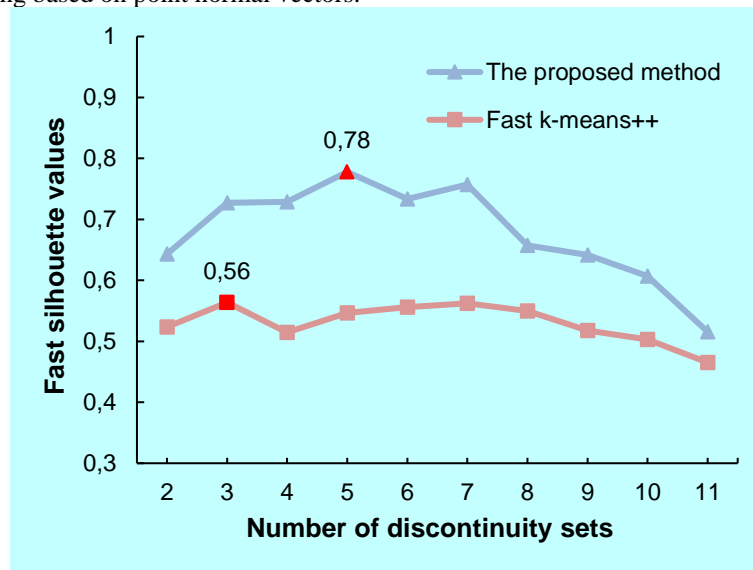
**Figure 2.** Point clouds of the tunnel face.

146 individual discontinuities are identified using the proposed method, while 513 individual discontinuities are identified using the fast k-means++. The discontinuities identified using the proposed method contain an average of 1081 points and a maximum of 48116 points, while the discontinuities identified using the fast k-means method contain an average of 459 points and a maximum of 76102 points. The results are shown in figure 3, where different colors represent distinct individual discontinuities identified by each method. The results demonstrate that the proposed method effectively eliminates a significant number of broken regions, whereas the fast k-means++ preserves these regions and generates numerous small non-structural planes.



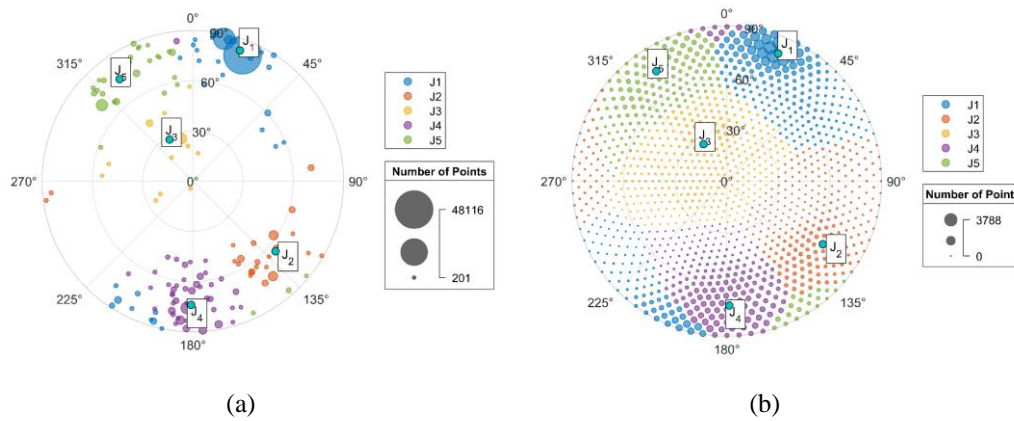
**Figure 3.** Individual discontinuities extracted by (a) the proposed method, and (b) fast k-means++. (Each color represents an individual discontinuity.)

The fast silhouette algorithm is used to calculate the fast silhouette values for different numbers of sets in both this method and the fast k-means++, as presented in figure 4. The results indicate that the optimal number of sets  $k'_{opt}$  for this method is 5, whereas for the fast k-means++, it is 3. Manual discrimination confirms that the tunnel face should possess 5 sets of discontinuities, providing evidence that clustering based on individual discontinuities outperforms clustering based on point normal vectors.



**Figure 4.** Comparison between the proposed method and the fast k-means++.

To facilitate comparison, the optimal number of sets  $k'_{opt}$  is selected as 5 for both the proposed method and fast k-means++ (figure 5). The orientation results of each set are presented in table 1. It is evident that the dip directions and dip angles of each set exhibit no significant differences, with a maximum dip direction deviation of 7 degrees and a maximum dip angle deviation of 3.1 degrees.



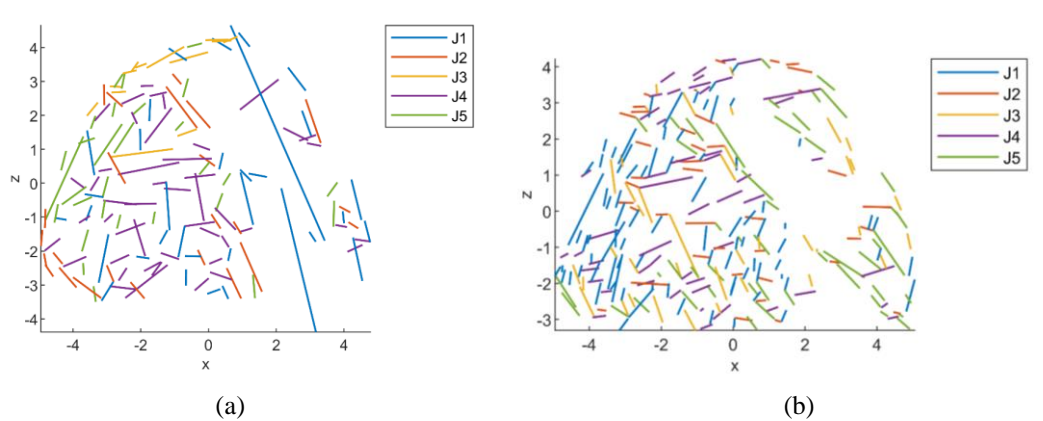
**Figure 5.** Cluster results of the tunnel face using (a) the proposed method, and (b) fast k-means++.

**Table 1.** Comparison of discontinuity orientations using the proposed method with the fast k-means++.

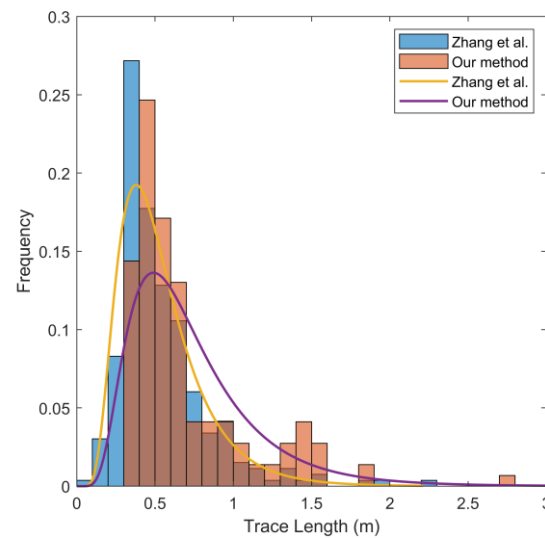
Set	The proposed method		Fast k-means++		$\Delta \delta $	$\Delta \theta $
	$\delta/\theta$ (°)	Number of discontinuities	$\delta/\theta$ (°)	Number of discontinuities		
J <sub>1</sub>	19.8/82.9	33	22.0/79.8	108	2.2	3.1
J <sub>2</sub>	130.3/64.7	24	123.3/66.7	128	7.0	2.0
J <sub>3</sub>	330.7/28.4	13	327.7/25.3	84	3.0	3.1
J <sub>4</sub>	180.8/74.0	47	178.9/72.2	86	1.9	1.8
J <sub>5</sub>	324.3/75.0	29	327.3/75.8	107	3.0	0.8

Note:  $\Delta|\delta|$  and  $\Delta|\theta|$  represent the dip direction and dip angle differences respectively.

This method obtains 146 traces by finding the intersection line formed by the intersection of the disk models representing discontinuities and the exposed tunnel face. According to the method of Zhang et al. (2020), 265 3D traces are obtained based on 3D curvature and projected onto the 2D plane of the tunnel face. The average length of the traces identified by this method is 0.77m and the maximum length is 6.93m, while the results of Zhang et al. (2020) have an average length of 0.54m and a maximum length of 2.22m. A comparison (figure 6 and figure 7) reveals that the intersection method is superior in capturing longer traces that represent discontinuities. Conversely, the method based on 3D curvature yields numerous short traces, many of which are contour segments of the same discontinuity.



**Figure 6.** Trace mapping using (a) the proposed method, and (b) the method of Zhang et al. (2020).



**Figure 7.** The trace length histograms and fitted log-normal distribution using the proposed method and the method of Zhang et al. (2020).

#### 4. DISCUSSION

According to the analyses and comparisons of the results, the proposed method shows excellent accuracy in automatically identifying discontinuities in the rock mass. A major advantage of this method over the fast k-means++ algorithm, which directly clusters discontinuities based on point features, is that it directly identifies individual discontinuities without the need for prior point grouping, thus avoiding errors in identifying individual discontinuities due to incorrect grouping. At the same time, areas of fragmentation due to blasting or weathering are removed and do not affect the identification of individual discontinuities.

For individual discontinuity clustering, the proposed method inherits well the advantages of the fast k-means++ algorithm for the density-based pre-selection of initial clustering centroids. In addition, fast silhouette algorithm employed helps to determine the optimal clustering automatically. Furthermore, the trace generated from the intersection between the disk model and the exposed surface of the rock mass is more consistent with the facts.

It should be noted that this method additionally considers the nearest neighbor curvature information to accurately identify individual discontinuities, but has not yet fully considered structural features, which may lead to the presence of random discontinuities in the results. Regarding computational efficiency, the proposed three-layer clustering method involves more aggregation operations than standard clustering algorithms. For large-scale point clouds (approaching one million points), the computation time increases from tens of seconds to several minutes. While this is a notable increase, the performance still meets the real-time needs of most engineering applications, representing a reasonable trade-off for the higher accuracy achieved.

The proposed algorithm is designed to be robust in complex geological conditions, such as those with significant fragmentation from blasting or weathering. Its core strength lies in the initial filtering of non-structural regions, which allows it to isolate and identify major discontinuities even in a noisy environment. The quality of the input data also plays a role. While the core point identification step provides some resilience to noise and variations in point density, extremely sparse or low-quality data could still affect the reliability of normal vector calculations and, consequently, the accuracy of the final discontinuity extraction.

#### 5. CONCLUSION

A three-layer clustering method for extracting individual discontinuities is presented in this paper. The effectiveness of the proposed method is demonstrated through its application to a tunnel face case and comparison with existing methods. The proposed method efficiently eliminates non-structural regions and identifies individual discontinuities. Furthermore, the results of the optimal grouping calculation based on individual discontinuity align more closely with manual judgment than those based on point normal vectors, underscoring the significance of prioritizing the identification of individual discontinuities. It is worth noting that the extraction process currently

does not utilize point cloud color information. Future research endeavors will enhance the accuracy of individual discontinuity identification by integrating color and texture information.

## 6. ACKNOWLEDGEMENTS

This work was supported by the National Natural Science Foundation of China [42272338, 41827807, 41902275]; Shanghai Sailing Program [18YF1424400]; Joint Fund for Basic Research of High-speed Railway of National Natural Science Foundation of China, China Railway Corporation [U1934212]; China State Railway Group Co., Ltd. [P2019G038]; Department of Transportation of Zhejiang Province [202213]; China Railway First Survey and Design Institute Group Co., Ltd. [19-21-1, 2022KY53ZD(CYH)-10]; China Railway Tunnel Group Co., Ltd. [CZ02-02-08]; PowChina Hebei Transportation Highway Investment Development Co., Ltd. [TH-201908]; Sichuan Railway Investment Group Co., Ltd. [SRIG2019GG0004]; The Science and Technology major program of Guizhou Province [2018]3011.

## 7. REFERENCES

- [1] Assali, P., Grussenmeyer, P., Villemin, T., Pollet, N., & Viguier, F. (2016). Solid images for geostructural mapping and key block modeling of rock discontinuities. *Computers & Geosciences*, 89, 21–31. <https://doi.org/10.1016/j.cageo.2016.01.002>.
- [2] Chen, J., Huang, H., Zhou, M., & Chaiyasarn, K. (2021). Towards semi-automatic discontinuity characterization in rock tunnel faces using 3D point clouds. *Engineering Geology*, 291, 106232. <https://doi.org/10.1016/j.enggeo.2021.106232>.
- [3] Chen, J., Zhu, H., & Li, X. (2016). Automatic extraction of discontinuity orientation from rock mass surface 3D point cloud. *Computers & Geosciences*, 95, 18–31. <https://doi.org/10.1016/j.cageo.2016.06.015>.
- [4] Drews, T., Miernik, G., Anders, K., Höfle, B., Profe, J., Emmerich, A., & Bechstädt, T. (2018). Validation of fracture data recognition in rock masses by automated plane detection in 3D point clouds. *International Journal of Rock Mechanics and Mining Sciences*, 109, 19–31. <https://doi.org/10.1016/j.ijrmms.2018.06.023>.
- [5] Ester, M., Kriegel, H.-P., Sander, J., & Xu, X. (1996). A Density-Based Algorithm for Discovering Clusters in Large Spatial Databases with Noise. *Kdd*, 96(34), 226–231.
- [6] Ge, Y., Cao, B., & Tang, H. (2022). Rock Discontinuities Identification from 3D Point Clouds Using Artificial Neural Network. *Rock Mechanics and Rock Engineering*, 55(3), 1705–1720. <https://doi.org/10.1007/s00603-021-02748-w>.
- [7] Hu, L., Xiao, J., & Wang, Y. (2020). Efficient and automatic plane detection approach for 3-D rock mass point clouds. *Multimedia Tools and Applications*, 79(1), Article 1. <https://doi.org/10.1007/s11042-019-08189-6>.
- [8] Kong, D., Wu, F., & Saroglou, C. (2020). Automatic identification and characterization of discontinuities in rock masses from 3D point clouds. *Engineering Geology*, 265, 105442. <https://doi.org/10.1016/j.enggeo.2019.105442>.
- [9] Singh, S. K., Banerjee, B. P., Lato, M. J., Sammut, C., & Raval, S. (2022). Automated rock mass discontinuity set characterisation using amplitude and phase decomposition of point cloud data. *International Journal of Rock Mechanics and Mining Sciences*, 152, 105072. <https://doi.org/10.1016/j.ijrmms.2022.105072>.
- [10] Singh, S. K., Banerjee, B. P., & Raval, S. (2023). A review of laser scanning for geological and geotechnical applications in underground mining. *International Journal of Mining Science and Technology*, 33(2), 133–154. <https://doi.org/10.1016/j.ijmst.2022.09.022>.
- [11] Singh, S. K., Raval, S., & Banerjee, B. P. (2021). Automated structural discontinuity mapping in a rock face occluded by vegetation using mobile laser scanning. *Engineering Geology*, 285, 106040. <https://doi.org/10.1016/j.enggeo.2021.106040>.
- [12] Wu, W., Zhang, K., & Zhu, H. (2020). A fast automatic extraction method for rock mass discontinuity orientation using fast k-means++ and fast silhouette based on 3D point cloud. *IOP Conference Series: Earth and Environmental Science*, 570(5), 052075. <https://doi.org/10.1088/1755-1315/570/5/052075>.
- [13] Zhang, K., Wu, W., Zhu, H., Zhang, L., Li, X., & Zhang, H. (2020). A modified method of discontinuity trace mapping using three-dimensional point clouds of rock mass surfaces. *Journal of Rock Mechanics and Geotechnical Engineering*, 12(03), Article 03.



## NORWEGIAN METHOD OF TUNNELING (NMT) FOR SUSTAINABLE USE OF UNDERGROUND SPACE

Krishna Kanta Panthi<sup>1</sup>

**Abstract:** The debate for the minimization of carbon emission through minimized / reduced use of fossil energy sources has been ongoing for some decades now. However, carbon emission is not only limited to fossil energy sources, but a substantial amount of carbon is emitted through the production of cement and cementitious products like, for example concrete. On the other hand, the use of underground space for the development of different transport and utility infrastructures is becoming popular due to limited use of surface area, environmental and health friendly solutions. Nonetheless, how to reduce the use of cementitious products while developing underground space is an important issue that needs to be carefully evaluated so that use of underground space is long-term sustainable and environmentally friendly solution. Hence, the aim of this manuscript is to discuss about Norwegian Method of Tunnelling (NMT), which could serve to minimize the use of cementitious product while developing an underground space. The manuscript aims to highlight on the main principals behind the Norwegian Method of Tunnelling (NMT), the optimized and long-term sustainable solutions it offers by substantially reducing time and costs for underground space development.

**Keywords:** Norwegian Method of Tunneling (NMT), Design of Underground Space, Rock Support, Sustainability

### 1. INTRODUCTION

The land in the city area is being used for various purposes such as official, residential and industrial buildings, sports arenas, parks, greenery areas, city transport etc. The surface space in large city areas is always scarce. Populace living in the cities desire to have more open space, greenery areas, parks for external activities. Therefore, it is important that the surface area in the cities should be optimally used. One way to do it is to utilize underground space in a maximum possible way. This can be done through the utilization of underground space for city metro lines, vehicular transportation system, parking arena etc. It is noted here that the use of underground space is not new for mankind. For thousands of years, underground space has been used for various purposes. Most early uses were related to the responses to specific geological events, security concerns and/or climate adaptations (Benser 2017). However, according to Bobylev and Sterling (2016), in the past century or so, the use of underground space has emerged as a broader means of supporting the infrastructure and space needs of the rapidly increasing world population. It is particularly the case in the major cities.

Norway is among the countries that utilizes and will utilize underground space for the transportation network, parking arenas, sports halls in the city areas in a maximum possible way. This is because the use of underground space ascertains availability of freer surface for different social and cultural activities. In addition, the use of underground space helps to reduce pollution and makes city areas environmentally friendly and long-term sustainable. Hence, underground space is prioritized as much as it is viable both with respect to costs and ground conditions. Analyzing the statistics given by Norwegian Tunnelling Society (NFF 2024), a rough estimate indicates that Norway has over 7400 km of tunnels and underground facilities. railway tunnels and caverns built for hydropower roughly cover 4500 km (89.92 million cu.m.), road tunnels cover about 1850 km (101.83 million cu.m.), railway and metro tunnels cover about 650 km (21.76 million cu.m.), water supply tunnels cover almost 350 km (5.85 million cu.m.) and remaining belong to drainage tunnels, sports and storage caverns. All together

<sup>1</sup> Professor Krishna Kanta Panthi, PhD in Rock Engineering, Norwegian University of Science and Technology (NTNU), S. P. Andersen vei 15a, 7491 Trondheim, Norway, e-mail address: [krishna.panthi@ntnu.no](mailto:krishna.panthi@ntnu.no).

almost 250 million solid cubic meters of underground excavation have been made in Norway excluding the underground excavation that has been made for mineral abstractions.

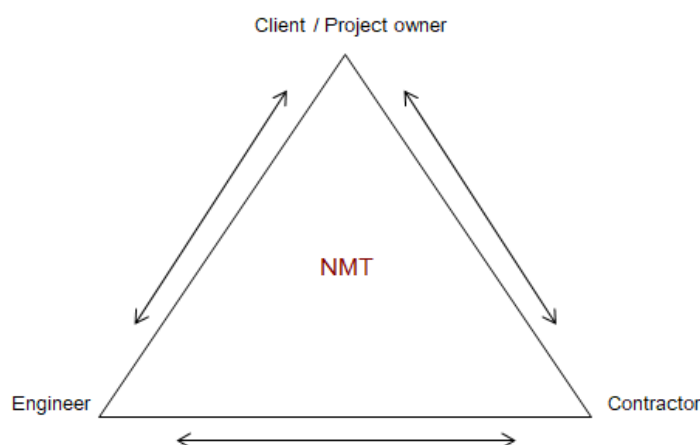
The tunnels and caverns excavation experience gained over many decades for hydropower, water supply, highways, railways and metros, drainage systems, oil and gas storage, sports arenas, parking arenas etc., Norway has developed its own approach to underground design and construction, which can be defined as Norwegian Method of Tunneling (NMT). The manuscript dedicates to highlight on the design and construction approaches used in NMT, which is somewhat different than that practiced by other countries in the world. The aim is to discuss the cost effectiveness and environmental friendliness of the NMT, which is very much needed in the development of underground space to improve transportation networks and other underground space use in the urban areas.

## 2. NORWEGIAN METHOD OF TUNNELING (NMT)

The excavation method in NMT primarily bases on the Drill and Blast and open hard rock TBM (gripper TBM) Methods (Barton et al. 1992). It is emphasized that NMT acknowledges the fact that in-situ stresses within the rock mass increase confinement to the surrounding rock mass in the periphery of an underground excavation (tunnel, shaft or cavern). The homogeneous and intact rock mass is therefore able to withstand the load exerted to it, i.e. rock mass has self-supporting capacity. In case there exist jointed rock mass, the withstand capacity of the rock mass is enhanced by reinforcing its body mass with the use of rock support consisting of application of rock bolts/rock anchors and steel-fiber shotcrete. The applied thickness of steel fiber shotcrete (Srf) is in general vary between 8 to 15 cm thick. In addition, pre-injection grouting is used for groundwater control. If weakness and fault zones containing swelling clay are met in tunnels that are built to convey water (hydropower, irrigation, water supply and sewage tunnels), the cast-in concrete is applied. On the other hand, if weakness and fault zones are met in road and railway tunnels, the applied rock support consists of systematic bolting and application of Ribs of Reinforced Shotcrete (RRS).

In general, Q-system (Barton et al. 1974; Grimstad and Barton 1993) is used for rock mass characterization, documentation of engineering geological information, estimation of rock support requirement during planning and design phases and preliminary rock support decision during construction. In NMT, it is important to emphasize that the preliminary rock support applied in tunnels and caverns is considered as part of final rock support (Barton et al. 2024)

Hence, the key aspects of NMT include use of in-situ stress information, relationships developed utilizing data from previous tunnelling projects (empirical relations) and numerical modelling for design of tunnels and caverns. In addition, well-organized engineering geological investigations during planning, design and construction phases of underground excavations, well planned tunnelling equipment and well-trained tunnel crew and risk searing approach to construction contracts are key elements for the successful use of NMT. Regarding the construction contracts it is important to minimize disputes through mutual understanding in the responsibility of each party and good coordination (Figure 1).



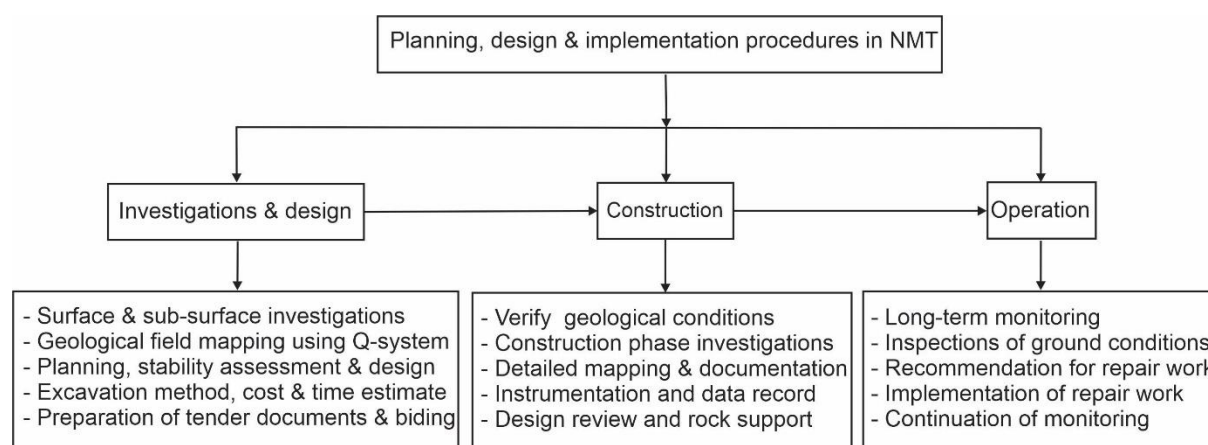
**Figure 1.** Triangular communication that NMT adopts in contract management.

The Client/Project owner is responsible for overall project management. In addition, the client is also responsible for appointing an expert group. The role of an expert group is to make periodic inspections of an underground space under construction, to quality control and to recommend needed design changes by giving

improved solutions. The Engineer is responsible for overall design, construction supervision, engineering geological mapping and documentation and rock support decisions. Similarly, the Contractor is responsible for the implementation of the project according to the contract, for excavation and rock support application according to the design and instruction given by the Engineer, for the execution of health, safety and environmental issues set in the construction contract, for construction management. It is important that there is three-way communication between the parties as indicated in Figure 1.

### 3. PLANNING, DESIGN AND CONSTRUCTION PROCEDURES IN NMT

The main aim of engineering geological design of an underground project is to achieve optimum technical and economic solutions based on engineering geological knowledge gathered during investigation and construction stages. A key requirement for successful planning and design is to ensure that the data and information collected through engineering geological investigations and field mapping are of good quality. In this regard, the description of rock mass quality conditions in both quantitative and qualitative terms is very important. Hence, high quality engineering geological mapping and engineering geological investigations are prerequisites for proper planning, design and construction stages. Furthermore, careful preparation of tender documents explaining clear objectives, bidding process, face mapping and recording of actual ground conditions and follow-ups during construction of underground projects are key essences of NMT. In general, NMT follows the process as given in Figure 2.



**Figure 2.** Steps of planning, design, construction and operation of underground structures in NMT.

Following the steps highlighted in Figure 2 left and center, it is possible to identify the features like rock mass quality condition, rock mass mechanical properties, topographical and in-situ stress conditions, complexity of the underground structures, construction methods, cost and time required for the construction.

### 4. DESIGN CONSIDERATION FOR UNDERGROUND STRUCTURES

Norwegian tunnelling community has gained over 100 years of experience in the construction and operation of underground space, which gave possibility to gather large amount of data, which made it possible to develop several "rules-of thumb" that are being used for planning and design purposes. It is emphasized here that NMT recognizes the value of proper engineering geological documentation using Q-system of rock mass classification (Barton et al. 1974 and Grimstad and Barton 1993) for regulating the description of rock mass conditions and initial support recommendations. In addition, observation of site conditions and numerical modelling approaches are used to verify the stability conditions and final rock support needs.

The design of underground structures should be made in such a way that the design provides cost effective, long-term stable and sustainable solutions. This can be achieved by considering rock mass as the part of a structural element that counteracts any load or pressure exerted by unloaded rock mass after excavation. Therefore, any design considerations should be based on the results from comprehensive engineering geological investigations. The aim of the design should be to achieve stability and long-term functionality of an underground structure in consideration (Panthi and Broch, 2022). This can be achieved through proper consideration regarding placement design, orientation and shape & size of an underground structure under consideration.

#### 4.1. Location design of underground structures

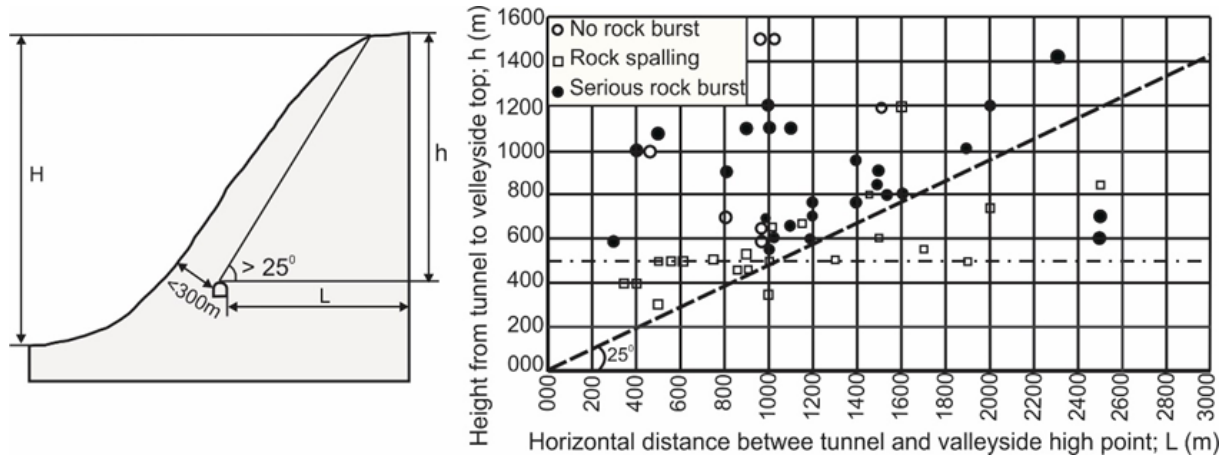
For a successful design, it is important to find out the best location for the underground structure in consideration so that it is placed in a best quality of rock mass available in the given topography. According to Hudson and Harrison (1993), an underground excavation may face mainly two modes of failure. The first one is the block failure when pre-existing blocks in the roof and side walls of an underground opening become free to move after the excavation has been made. The second one is stress failure when induced stress around the excavation exceeds the rock mass strength. In this regard, it is mentioned here that near the surface, in-situ stresses are in general an-isotropic, and discontinuities mainly control stability. On the opposite, deep into the rock mass, the in-situ stress magnitudes are increased, and frequency of discontinuity occurrence are reduced due to enhanced confinement (Panthi 2023; Panthi and Broch 2022). Hence, stability is controlled by induced stresses in deep cited underground structure. Therefore, the stability challenges vary greatly depending upon the way an underground scheme is located.

The underground structures that are located at shallow overburden have low gravitational vertical stress, which may cause higher level of stress anisotropy. Similarly, at low overburden areas (near surface) the rock mass is prone to high degree of weathering. In such a situation, the rock mass may have low level of interlocking effect between the rock blocks that may cause reduction in arching effect leading to potential block falls from the roof and side walls of an underground opening. The stability assessment should therefore be associated with potential block fall (Figure 3).



**Figure 3.** Potential block fall from the roof of an underground structure located at shallow overburden

The underground structures that are located at great depth with high overburden may face stability challenges associated with the high in-situ rock stresses. In one hand, increased in-situ rock stresses increase the confinement in the rock mass and in the other hand, high in-situ rock stresses may cause rock burst/rock spalling or squeezing conditions if rock mass strength is less than the induced stresses (Panthi 1012). Therefore, the placement of the underground structure should be made in such a way that it achieves favorable stress condition. If the topographic condition does not give possibility for such location, in-depth stability assessment should be made using empirical, analytical and numerical modelling approaches. One of the rules of thumbs that is being used in Norway is expressed in Figure 4. In addition, the strength reduction factor (SRF) of Q-system also provides a qualitative assessment for the placement design of the underground structures.

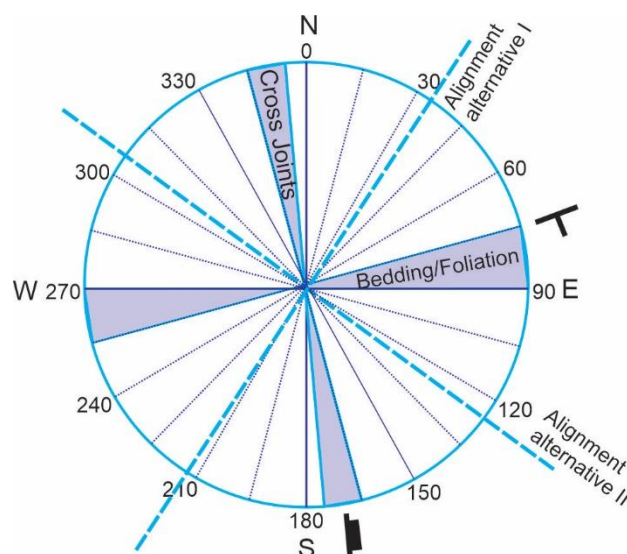


**Figure 4.** Location of underground openings in relation to topographic conditions (left), and plot of rock burst/spalling in relation to height ( $h$ ) from the tunnel roof to the top of valley-side and horizontal distance from an underground opening to the top of valley side ( $L$ ) (Panthi 2018 based on Selmer-Olsen 1965).

Figure 4 shows tunnel cases that were passing through a topography where vertical rock cover directly above the tunnel is relatively small in comparison to the vertical height between the tunnel and the top of the valley-side slope (the plateau). Similarly, these tunnels are relatively short distance (mostly not exceeding 300 m) from the valley surface. This Norwegian rule of thumb is very useful to make placement design of underground structures, which should also be supplemented by numerical modelling.

#### 4.2. Fixing orientation of underground structures

Correct and optimum alignment of an underground structure is very important to minimize instability. In this regard, fixing orientation with respect to mapped data of major and systematic joints and discontinuity systems is a decision-making factor for an underground structure. Therefore, it is vital that detailed discontinuity mapping is made, congregated, and systematized. During planning phase mapping, the major discontinuity systems such as bedding / foliation planes, cross joints, major fault/weakness zones present in the locality should be identified. The basic rule that should be adopted is to orient the length axis of an underground opening along the bisection line of the maximum intersection angle between the two predominant joint systems (Figure 5) and parallelism with other minor joint systems should be avoided as possible (Panthi and Broch 2022). The optimization also includes the prevention of adverse cavern orientation relative to the orientation of weakness zones and major principal stress.



**Figure 5.** Rosette of joint systems and possible orientation alternatives of length axis of an underground opening.



### 4.3. Design of size and shape of underground structures

The shape and size of an underground opening depends on its function. Most of the tunnels in Norway have an inverted D shape in cases if tunnels are excavated using drill and blast method. Similarly, the caverns are also of inverted D shape with deep walls since these have been excavated using drill and blast method. The size of tunnels and caverns are mainly dependent on the purpose of construction and needed space requirement. For example, the road tunnels in Norway are inverted D-shaped and are mainly excavated by fully mechanized drill and blast (D&B) method. The size of road tunnels depends on Annual Average Daily Traffic (AADT) and size vary from T4 (4 m wide) to T14 (14 m wide). Similarly, the railway tunnels are either inverted D shaped or circular depending on the excavation method used, i.e., excavated with drill and blast method or excavated using TBM, however, mostly dominated by inverted D shapes.

## 5. ROCK SUPPORT DECISION FOR UNDERGROUND STRUCTURES IN NMT

Fully mechanized Drill and Blast (D&B) method is the essence of NMT. Norwegian tunneling community believes the principal that the rock mass has its own capacity to self-support, which means substantial load is carried by the rock mass itself. A key requirement for NMT is that it is important to consistently carry out mapping rock mass quality and record the actual ground conditions in both quantitative and qualitative terms. In this regard, Q-system of rock mass classification plays an important role. In addition, the main principle of rock support should be to strengthen existing rock mass surrounding the periphery of an underground opening. Priority is given to the use of flexible support.

### 5.1. Rock support in normal ground conditions

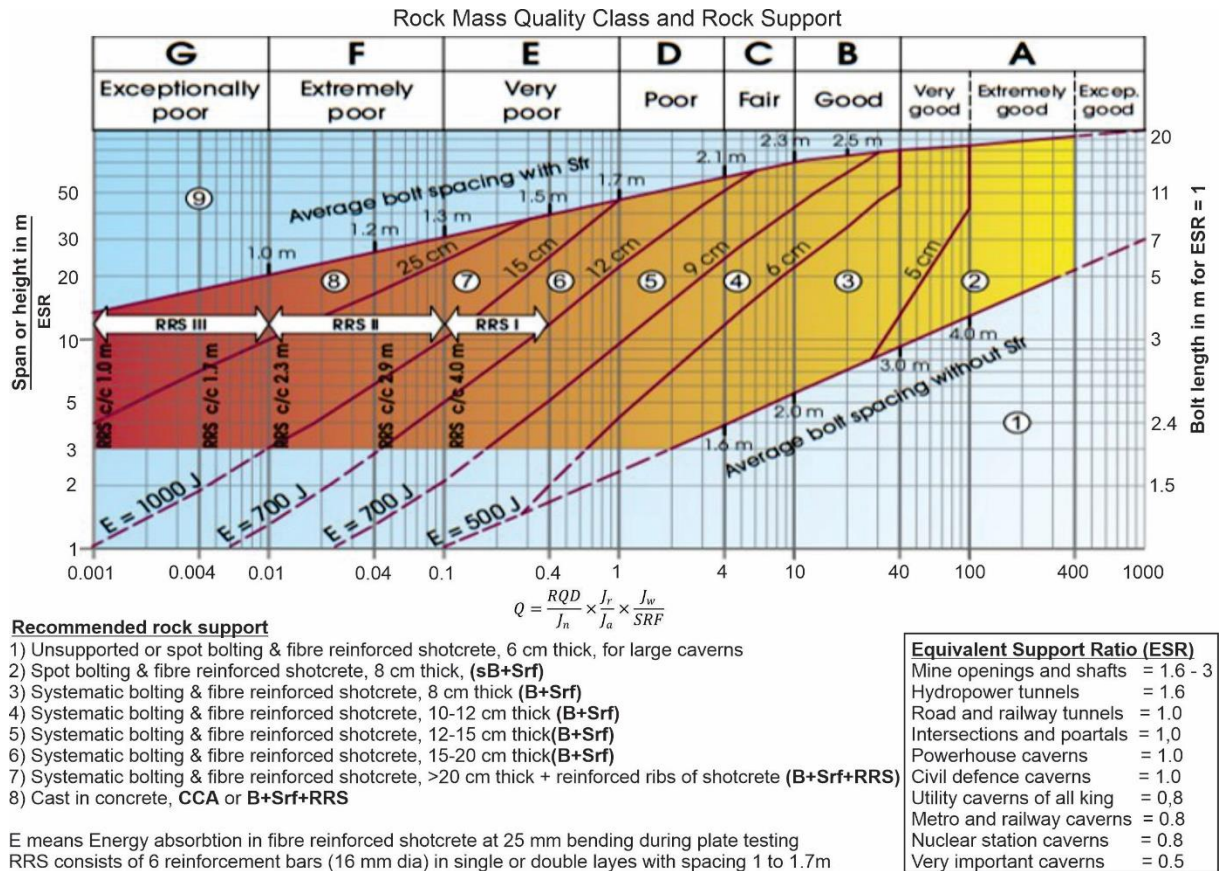
In NMT, the immediate rock support measures right after excavation and mucking include mechanical scaling and immediate application of end-anchored rock bolts, as spot bolts, to strengthen loosened rock blocks. Additional rock support is applied after face mapping and assessment of rock mass quality conditions by detailed observation and application of Q-system of rock mass classification. In general, rock support consisting of a combination of systematic rock bolts (B) and steel fiber shotcrete (Sfr) is a preferred choice in NMT as both temporary and permanent rock support (Figure 6). The rock support chart of Q-system updated in 1993 by Grimstad and Barton (1993) has been further updated by NGI (2015) that helps to recommend preliminary rock support (Figure 7).



**Figure 6.** An under-construction road tunnel supported by systematic bolting and fiber reinforced shotcrete.

In addition, pre-excavation grouting is carried out to control groundwater depletion and water inflow (seepage). The grouting pressure applied varies from 10 to 80 bars depending upon where an underground opening is

constructed. If an underground opening is constructed in the city area, it is important not only to control water inflow but also it is necessary to restrict groundwater depletion from the surface requiring much stricter regulations.

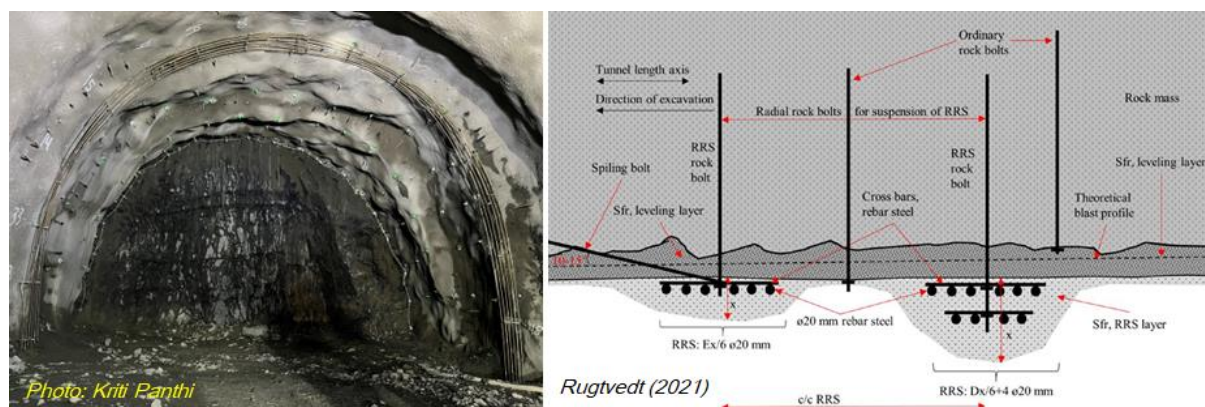


**Figure 7.** Support chart according to rock mass class (NGI 2015), updated to suit urban underground structures.

It is emphasized here that the blocky rock mass where joints and discontinuities are clay-filled, rock support in combination with systematic bolting (B) and steel fiber shotcrete (Sfr), as seen in Figure 6, is used. Barton et al (1992) state with some certainty that B+Sfr are the two most versatile tunnel support methods yet devised, because they can be applied to any profile as temporary or as permanent support, just by changing bolt spacing and thickness of steel fiber shotcrete. Although the high level of experience in the Norwegian tunnelling community has allowed "rules-of thumb" and much "previous experience" to dictate a lot of the support estimates, more and more companies are realizing the value of a documentation method such as the Q-system for regulating the description of rock mass conditions and support recommendations.

## 5.2. Rock support in difficult ground conditions

In general Norway is a hard rock province where intact rock strength is more than 40 MPa, which provides possibility to achieve good underground excavation progress in normal ground conditions. However, these hard rock mass often constitute faults and weakness zones. Underground excavation through faults and weakness zones poses challenges and difficulties since these zones represent very poor to extremely poor rock mass quality, which are unable to self-support. To address this challenge, NMT favors using a thick load bearing ring that constitutes spiling bolts, circumferential bolts and reinforced rib of shotcrete (RRS) (Figure 7 and Figure 8-right). The beauty of the application of RRS is that it can form and match an uneven underground excavation profile (Figure 8-left), which is very difficult to achieve with the application of lattice girder or steel ribs. In addition, installation of spiling bolts, systematic circumferential bolts and reinforced ribs of shotcrete is straight forward and relatively quick, which immediately helps to control difficult ground against collapses.

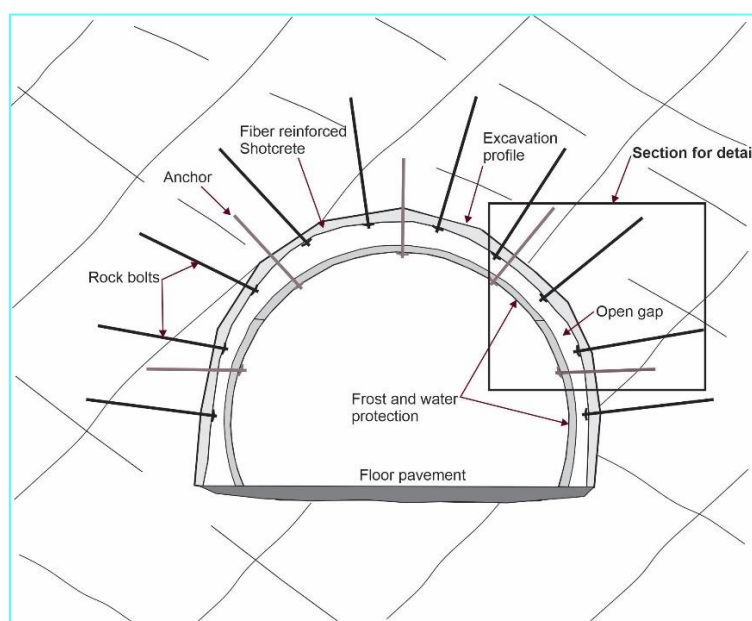


**Figure 8.** Photo showing RRS application in difficult ground (left) and schematic arrangement of RRS with bolts.

As seen in Figure 8-right, RRS can be designed with different configurations. The main parameters influencing the configuration and load bearing capacity depend on the use of single layer or double layers of reinforcement bars (generally 6 numbers 16 mm diameter reinforcement bars are used), spacing between RRS, quality and thickness of steel fiber shotcrete, length & spacing of rock bolts and spiling bolts. Spiling bolts are rock bolts that are mounted at an angle between 5 to 10 degrees from the tunnel face contour towards the direction of excavation.

### 5.3. Groundwater and frost control (water shielding)

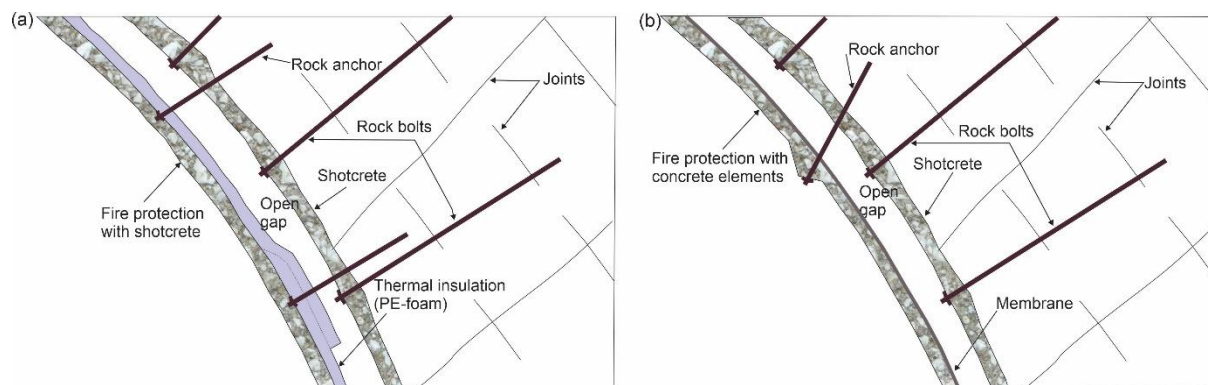
Among the important features of the Norwegian Method of Tunneling (NMT) is the use of rock support in combination of pre-injection grouting, systematic bolting and application of steel fiber shotcrete, which is not fully waterproof. This means, the underground structures are considered as drained structures. Following the Norwegian tunneling experience, pre-injection grouting enables to achieve water tightness down up to 1-2 liters per minute per 100 m tunnel length (Hognestad et al. 2005). The remaining water seepage should drain through the drainage system built in the side walls of tunnel invert, which implies drainage of groundwater from immediate surrounding rock mass of the underground structures. Many under the sea (subsea) road tunnels in rock mass have been successfully designed and constructed according to the drained structures principle since 1982 (Nilsen and Henning 2009). The flexible rock support solutions however require an inner lining structure, which collects and drains seeped groundwater from the rock mass down to the drain structures located side wall of the tunnel invert. In areas where a tunnel is exposed to freezing, thermal insulation is also needed to prevent formation of ice. The principal sketch of water shielding system that is being used for road and railway tunnels is shown in Figure 9.



**Figure 9.** Schematic principal arrangement of water shielding and frost insulation system in use in Norway.



The water shielding systems have main functions consisting of waterproofing, drainage of seeped water and thermal insulation to avoid formation of ice near portal areas. In general, there are mainly two types of shielding that are in use in tunnels in urban areas (Figure 10). The first one is a combination of shotcrete and polyurethan foam (PE-foam) as shown in Figure 10a and the second one is a combination of concrete elements and waterproofing membrane as shown in Figure 10b.



**Figure 10.** Details of water shielding and frost insulation arrangement in Norway. a) Water shielding arrangements with shotcrete and PE-foam; b) Water shielding arrangements with concrete elements and waterproof membrane.

An open gap that is left between water shield and tunnel rock support applied in combination of bolting and shotcrete gives possibility to carry out periodic inspections on the condition of installed rock support, periodic repair work of the rock support without losing any space required for the vehicular and train movements. This flexibility is very important for the long-term sustainability of underground space use. In addition, the solution provides the possibility to reduce unnecessary concrete use.

## 6. ISSUE OF SUSTAINABILITY

The 17 UN Sustainable Development Goals (SDGs) recognize that ending poverty and other deprivations must go together with strategies that improve health and education, reduce inequality, and achieve sustainable economic growth and at the same time addresses climate change issues and preserve earth's oceans and forests. Hence, sustainability is directly linked to the interconnections between social equity, economic growth and environmental issues. This means, the sustainable development of underground space should meet the needs of the present without compromising the environment and need for the future. The Norwegian tunneling industry is proactive in this regard and actively recommends needed changes in regulations regarding construction processes and material use (NFF 2022) to achieve both sustainable and environmentally friendly underground solutions.

The use of life cycle assessment (LCA) in NMT to evaluate tunnel construction projects is an essential part and the contractors, material producers, and the project owners actively use process and results from the LCA. The LCA studies performed have indicated that the construction phase of a tunnel contributes to about 50 to 60 percentages of greenhouse gas (GHG) emissions, which are mainly related to the use of material and energy sources. The emissions are mainly from the use of cement associated to rock support and tunnel lining and to some degree tunnelling process itself (Huang et al 2015). NMT always aims to reduce the quantity of concrete, cement and steel as rock support and rock grouting considering rock mass as self-supporting element. It is important to decrease the use of resources and the most important task of NMT is to become more sustainable tunneling. Small reductions in each material resource can contribute to enhance sustainability.

Sustainable use of materials means using the lowest possible volume of materials with the longest service life and quality. Many different materials are used in the construction of underground space. However, among the most important resource materials are cement and concrete. It is a well-known fact that cement is among the major contributors to GHG emission in the construction of underground space. The production of one ton Portland cement emits 900 kg of CO<sub>2</sub>, which accounts for 88% of the emissions associated with the production of concrete mix. Hence, reduction in the use of cement plays a key role in the reduction of GHG. This is because, following to Khaiyum et al (2023), cement industry is responsible for 5–8% of global GHG emissions.

## 7. CONCLUSION

Sustainable development of underground space should meet the needs of the present without compromising the environment and need for the future. The Norwegian Method of Tunneling (NMT) takes in account the rock mass as self-supporting material. NMT prioritizes the use of rock support consisting of systematic bolting, steel fiber shotcrete and pre-excavation grouting as both preliminary and final support, which contributes to considerably reduce the use of concrete products. The Norwegian tunneling industry is proactive, which collaborates with the government authorities and actively recommends needed changes in regulations regarding construction processes and material use to achieve both sustainable and environmentally friendly underground solutions.

## 8. BIBLIOGRAPHY

- [1] Besner, J. (2017). Cities think underground—Underground space (also) for people. *Procedia engineering*, vol. 209, pp. 49-55.
- [2] Bobylev, N.; Sterling, R. L. (2016). Urban underground space: A growing imperative. *Perspectives and current research in planning and design for underground space use. Tunnelling and Underground Space Technology*, vol. 55, pp. 1-4.
- [3] Barton, N.; Grimstad, E.; Aas, G.; Opsahl, O. A.; Bakken, A.; Johansen E.D. (1992). Norwegian Method of Tunnelling – Part 1. *World Tunnelling*, June 1992, pp. 1-6.
- [4] Barton, N.; Lien, R.; Lunde, J. (1974). Engineering Classification of Rock Mass for the Design of Tunnel Support. *Rock Mechanics*, vol. 6 (4), pp. 189-236.
- [5] Barton, N.; Grimstad, E.; Panthi, K. K. 2024. Viewpoint concerning critique of NMT. *The International Journal on Hydropower & Dams*. October 2024. Available in <https://www.hydropower-dams.com/forum/> [Assessed on Feb 27, 2025].
- [6] Grimstad, E.; Barton, N. (1993). Updating of the Q-system for NMT. *Proceedings of the International Symposium on Sprayed Concrete - Modern Use of Wet Mix Sprayed Concrete for Underground Support*, Fagernes. Norwegian Concrete Association, Oslo, pp. 46-66.
- [7] Hudson, J. A.; Harrison, J. P. (1997). *Engineering rock mechanics an introduction to the principle*. Pergamon Press, New York, 458p.
- [8] Hognestad, H.O.; Frogner, E. (2005). State-of-the-art micro-cement pre-injection for the Jong-Asker rail tunnel, Norway. *Proceedings of 31<sup>st</sup> ITA-AITES World Tunnel Congress, Istanbul. Underground Space Use: Analysis of the Past and Lessons for the Future – Erdem, Solak (eds). A.A Balkema, London. pp 925-930.*
- [9] Holter, K. G.; Buvik, H.; Nermoen, B.; Nilsen, B. (2013). Future trends for tunnel lining design for modern rail and road tunnels in hard rock and cold climate. *Proceedings of World Tunnel Congress WTC1013 - Underground - the way to the future! G. Anagnostou & H. Ehrbar (eds). Geneva, Switzerland. 9p.*
- [10] NFF. (2025). Norwegian Tunneling Society. [www.tunnel.no](http://www.tunnel.no) [Assessed on Feb 07, 2025].
- [11] Nilsen, B.; Henning, J. E. (2009). Thirty years of experience with subsea road tunnels. *Proceedings of International Conference Strait Crossings*. Tapir, Trondheim, Norway, pp 35-44.
- [12] Panthi, K. K.; Broch, E. (2022). Underground Hydropower Plants. In: Letcher, Trevor M. (eds.) *Comprehensive Renewable Energy*, 2nd edition, vol. 6, pp. 126–146. Oxford: Elsevier.
- [13] Panthi, K. K. (2023). Methods applied for the stability assessment in rock engineering. *Journal of Nepal Geological Society*, vol. 65, pp. 29–34. <https://doi.org/10.3126/jngs.v65i01.57741> .
- [14] Panthi, K. K. (2012). Evaluation of rock bursting phenomena in a tunnel in the Himalayas. *Bulletin of Engineering Geology and the Environment*, vol. 71, pp. 761–769.
- [15] Panthi, K. K. (2018). Rock burst prediction methods and their applicability. Chapter 11.2 - Rock burst: Mechanisms, Monitoring, Warning and Mitigation. Elsevier, 10p.
- [16] Selmer-Olsen, R. (1965). Stability in tunnels in valley-side slopes. *IVA rapport 142*, pp. 77-83.
- [17] Rugtvedt, L. (2021). Planning and engineering geological assessments of Prestås and Bjønnås tunnels along E18 between Langangen and Rugtvedt in Porsgrunn. MSc thesis in Geotechnology supervised by Prof. Panthi. Department of Geoscience and Petroleum, Norwegian University of Science and Technology, Norway, 266p.
- [18] NFF (2022). Sustainability in Norwegian Tunneling. Norwegian Tunneling Society (NFF), Publication no. 30, 127p. ISBN 978-82-92641-51-4.
- [19] Huang, L.; Bohne, R. A.; Bruland, A. 2015. Life cycle assessment of Norwegian road tunnel. *International Journal of Life Cycle Assessment*, vol. 20, pp. 174–184.
- [20] Khaiyum, M.Z.; Sarker, S.; Kabir, G. (2023). Evaluation of Carbon Emission Factors in the Cement Industry: An Emerging Economy Context. *Sustainability* 2023, vol. 15, 15407.



## IDENTIFICATION OF KARST CAVES BASED ON MULTI-SOURCES DATA FUSION DURING SHIELD TUNNELLING

Xin-Hao Min<sup>1</sup>, Yan-Ning Wang<sup>2</sup>, Shui-Long Shen<sup>3</sup>

**Abstract:** This study proposes an enhanced method that integrates KCII with the Energy per Revolution Index (EPRI) derived from shield operational parameters. The method fuses operational parameters such as thrust, torque, cutterhead rotational speed, advance rate, soil chamber pressure, and penetration rate. Data are processed based on each cutterhead revolution, which represents dynamic characterization of geological conditions ahead of the tunnel face. A sliding window approach calculates the mean and standard deviation of KCII and EPRI to establish identification thresholds. Four distinct identification logics are developed and evaluated: KCII only, dual conditions of EPRI indicators, a combined approach of all indicators, and any two indicators. Application to two sections of Xuzhou Metro Line 4 validates method effectiveness and demonstrates high accuracy and robust generalization. Results shows that the multi-indicator fusion logic significantly improves accuracy compared to single-indicator methods, and offers real-time geological insights to support safer and more efficient shield tunnelling operations.

**Keywords:** Shield tunnelling, Karst strata, Earth pressure balance, Shield parameters, Identification method

### 1. INTRODUCTION

Shield tunnelling technology has become indispensable in modern urban infrastructure development, particularly when navigating complex geological conditions like karst regions (Peng et al., 2023). Karst caves present significant risks, such as water inrush, collapse, and equipment damage, requiring precise real-time identification and management (Cho et al., 2021). However, conventional geological exploration methods, including borehole drilling and advanced geological forecasting, face critical challenges such as limited resolution, high operational cost, and delayed identification capability (Li, et al., 2017; Ghosh et al., 2018; Chen et al., 2021).

To tackle the energy consumption during shield tunnelling, Teale (1965) proposed an index called Specific Energy (SE) based on energy analysis. Tarkoy and Marconi (1991) proposed another index, FPI, based on stress state analysis. Yamamoto et al. (2003) proposed TPI to evaluate the geological condition ahead of the tunnel face. Yan et al. (2023) proposed a more generalized index, GFII, to identify the geological characteristics when a shield is passing through a mixed soil-rock strata. Among these, the Karst Cave Identification Index (KCII) offered improved geological recognition capabilities. Despite this advancement, KCII remained primarily qualitative, limiting its effectiveness in dynamic operational environments due to insufficient temporal resolution and quantitative characterization capabilities.

To overcome these limitations, this study proposes a novel approach integrating KCII with a newly developed Energy per Revolution Index (EPRI), calculated using real-time shield tunnelling parameters. This integrated method provides high-frequency, quantitative monitoring of geological changes based on the energy consumed per cutterhead revolution, enhancing the detection sensitivity and accuracy of karst cave identification. Furthermore, a sliding window algorithm and multiple logic scenarios are applied to establish robust criteria for distinguishing karst features from intact rock formations.

<sup>1</sup> Ph.D. Candidate, Min, Xin-Hao, B.Eng. Civil Engineering, Shantou University, Shantou, China; 21xhmin@stu.edu.cn.

<sup>2</sup> Assoc. Prof., Wang, Yan-Ning, Ph.D. Civil Engineering, College of Engineering, Shantou University, Shantou, China, wangyn@stu.edu.cn.

<sup>3</sup> Professor, Shen, Shui-Long, Ph.D. Civil Engineering, Dean College of Engineering, Shantou University, Shantou, China, shensl@stu.edu.cn.

The effectiveness of the proposed methodology is demonstrated through extensive field application in the Xuzhou Metro Line 4. Comparative analysis confirms that the multi-indicator approach not only significantly improves detection accuracy but also enhances the method's adaptability and generalization across different geological conditions. This comprehensive, quantitative approach contributes to safer tunnelling practices and provides valuable insights for geological risk management during construction.

## 2. MATERIAL AND METHODS

### 2.1. Data Acquisition and Pre-processing

In this study, the shield machine parameters, including the thrust (F), torque (T), cutterhead rotational speed (CRS), advance rate (AR), soil-chamber pressure (P) and penetration rate (PR), were automatically recorded and saved during construction. For each second, the instantaneous angular increment of the cutterhead is  $\Delta\theta = \text{CRS}/60 \times 360^\circ$ . The cumulative angle  $\Sigma\theta$  is reset whenever it exceeds  $360^\circ$ , and the elapsed seconds define the duration of one complete revolution. All raw measurements within that interval are averaged, yielding a revolution-based dataset that synchronises mechanical response with the excavation face.

### 2.2. Identification indices

Wang et al. (2025) established the mechanical equilibrium conditions required for tunnel face stability based on the earth pressure balance principle and proposed the Karst Cave Identification Index (KCII) as a novel evaluation indicator. The dimensionless KCII is computed as:

$$KCII = \frac{P \cdot CRS \cdot V_e}{F \cdot AR} \quad (1)$$

where F is the thrust of the shield machine (kN), AR is the advance rate (m/s), CRS is the cutterhead rotational speed (r/s), P is the soil pressure in soil chamber (kPa), and  $V_e$  is the volume of the soil chamber ( $\text{m}^3$ ).

Specific Energy (SE) quantifies the energy required to excavate a unit volume of soil/rock. The formula of SE is as follows:

$$SE = \frac{F}{A} + \frac{2\pi \cdot CRS \cdot T}{A \cdot AR} \quad (2)$$

where SE is the Specific Energy (SE) of the shield machine, F is the thrust (N); A is the cutterhead area ( $\text{m}^2$ ); CRS is the cutterhead rotational speed (r/s); T is the cutterhead torque (N.m); AR is the advance rate (m/s).

However, its conventional formulation necessitates the complete excavation of one cubic meter of material to compare energy dissipation across the tunnel face, rendering it incapable of real-time geological assessment via energy fluctuations. Based on the time it takes for the cutterhead to rotate once, the energy consumption per unit volume is converted into an Energy per Revolution Index (EPRI) that is related to time. The formula is as follows:

$$EPRI = F \times AR \times 16.7 + T \times CRS \times 1.05 \quad (3)$$

the rate of change of energy consumption per revolution of the cutter head,  $\Delta EPRI$  is:

$$\Delta EPRI = \frac{\Delta E_{total}}{\Delta t} = \frac{EPRI_2 - EPRI_1}{\Delta t \cdot EPRI_1} \quad (4)$$

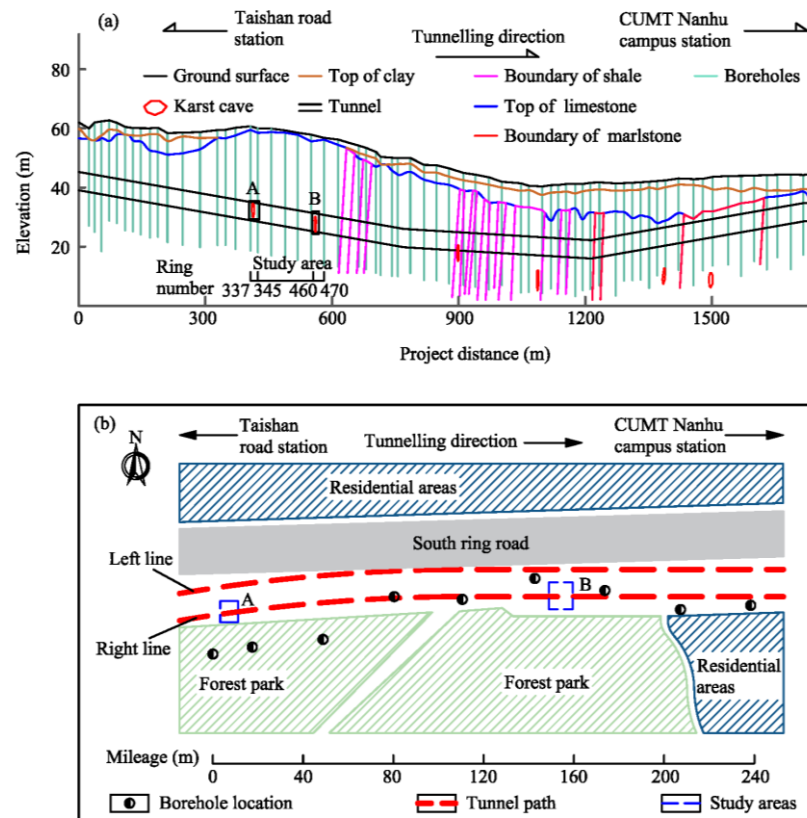
### 2.3. Identification method

A sliding window of three consecutive revolutions traverses the index time series. Within each window, the mean and standard deviation of KCII, EPRI and  $\Delta EPRI$  are computed in real time. Thresholds for the three indices are derived from a benchmark window located entirely within a karst cavity confirmed by borehole evidence, and these thresholds are then used as fixed references for subsequent detection. Each window is classified under four

decision schemes: KCII only; EPRI together with  $\Delta$ EPRI; all three indices jointly; any two indices. Windows that satisfy the selected scheme are labelled as cave; all other windows are labelled as intact rock.

## 2.4. Project background

**Figure 1** shows the locations and geological conditions of the two research sections of the Xuzhou Metro Line 4 where this method was applied. Sections 337-345 constitute Area A, while sections 460-470 constitute Area B. Each of these areas contains a detected cave. The cave in Area A measures: width x height = 4.2 x 6.2 (m), approximately in the range of 340-344; the cave in Area B measures: width \* height = 3.6 x 4.5 (m), approximately in the range of 463-468. Both caves are within the tunnel's influence area.

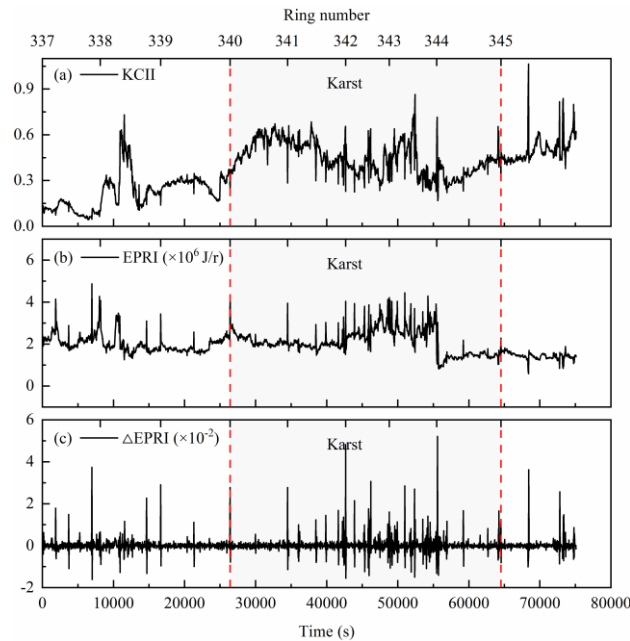


**Figure 1.** Overview of study area: (a) plane position diagram and (b) geological profiles with the area ratio of the cave in the tunnel

## 3. RESULTS

### 3.1. Indices calculation

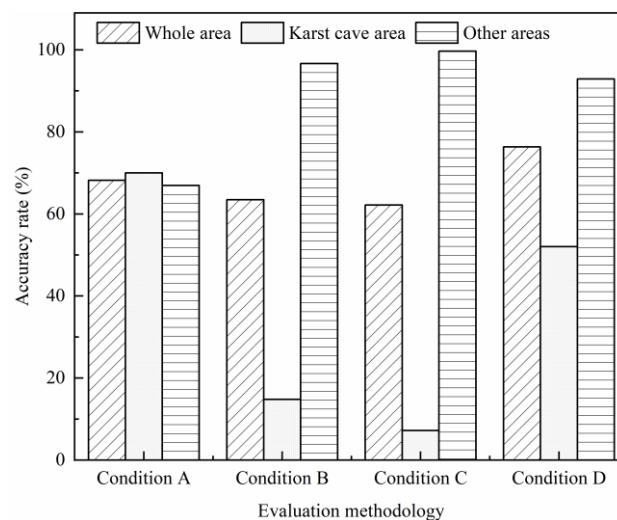
**Figure 2** shows the calculation results of the three indicators, as well as the relationship between these results and time and geological features. In the karst-affected zones of Study Area A, analysis reveals a mean KCII value of 0.04. The EPRI demonstrates substantial volatility with a mean of 2,349,650 kJ/rev and a standard deviation of 488,620. Conversely, the  $\Delta$ EPRI metric exhibits minimal variation, registering a mean of 0.00014 with a standard deviation of 451,909.



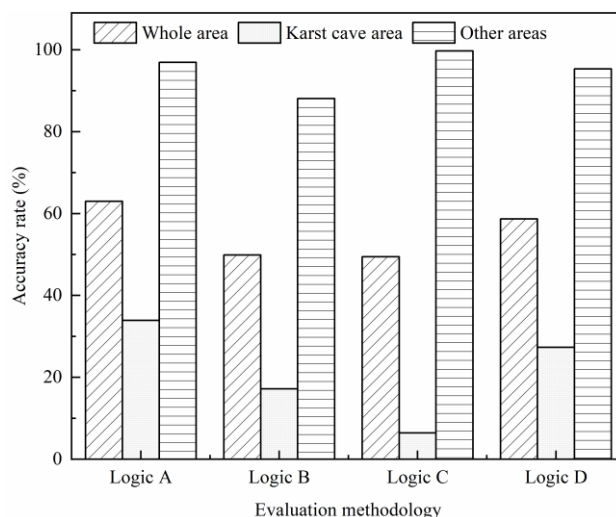
**Figure 2.** Calculation results of indicators in study area A

### 3.2. Accuracy rate of stratum identification

**Figures 3 and 4** summarise the recognition performance of four logical schemes in the calibration zone, rings 337 to 345, and the validation zone, rings 460 to 470, respectively. In **Figure 3**, the highest overall accuracy, 76.3 %, is attained by Logic D, the any two indices scheme, which balances sensitivity in the cavity with specificity outside it, whereas Logic A, the KCII only scheme, captures the cavity most effectively with a hit rate of 70.0 %. **Figure 4** shows that applying the same thresholds to an independent geological segment leads to a decline in overall accuracy; nevertheless, Logic A achieves the best whole section score, 63.0 %, and maintains accuracy outside the cavity above 96 %. These trends indicate that indicator redundancy improves robustness in the learning zone, while KCII alone remains the most portable cue for unseen ground conditions.



**Figure 3.** Accuracy rate of identification in Area A



**Figure 4.** Accuracy rate of identification in Area B

## 4. DISCUSSION

The field application confirms that per-revolution resampling effectively captures the response of the cutterhead. This resampling also removes high-frequency noise that masks geological signals. Within this framework, KCII reflects stress equilibrium at the excavation face. EPRI and its normalized increment ( $\Delta\text{EPRI}$ ) detect rapid energy changes due to lithological differences. These combined indices provide a comprehensive diagnostic capability superior to any single indicator.

In the calibration zone (rings 337–345), Logic D (any two indices) achieves the highest overall accuracy (approximately 76%). This indicates index redundancy enhances robustness when thresholds are set locally. Logic A (KCII-only) shows the highest detection rate within the cavity. Logic C (all three indices) minimizes false positives in intact rock. Therefore, the choice of logic depends on whether higher sensitivity or specificity is required during construction.

Testing thresholds on an independent section (rings 460–470) highlights threshold portability. Overall accuracy declines to approximately 63% under Logic A. However, the false-positive rate outside cavity zones remains below 4% with Logic C. This result shows sliding-window statistics remain robust across intact rock zones. However, reduced sensitivity within cavities suggests thresholds need adaptive adjustment or integration with machine-learning techniques for geological conditions varying significantly in stiffness or fill properties.

The method shows strong karst-cavity discrimination in this project. Subsequent work will investigate its application to other projects to further improve the method's applicability.

## 5. CONCLUSION

This study proposes an real-time karst-cave identification in shield tunnelling by integrating per-revolution resampling with a tri-index diagnostic system (KCII, EPRI,  $\Delta\text{EPRI}$ ) and a sliding-window decision algorithm. Application to two segments of Xuzhou Metro Line 4 shows the reliability and transferability of the proposed method. Per-revolution resampling aligns shield parameters with excavation-face mechanics, which ensures accurate identification indices computations without extra instrumentation. A 3-revolution sliding window is calibrated using data from a known cavity. This window distinguishes anomalous energy signatures. Logic D achieves the highest overall accuracy (76%). Logic C effectively reduces false positives to below 4% in intact rock. Although thresholds derived from one cavity maintain acceptable performance in other sections, detection sensitivity decreases, suggesting adaptive thresholding refinement as necessary for varied geological conditions. The method's adaptability in international contexts will be further investigated in future work.

## 6. ACKNOWLEDGEMENTS

The research work was funded by Guangdong Provincial Basic and Applied Basic Research Fund Committee (2022A1515011200), Science and Technology Planning Project of Guangdong Province of China



(STKJ2021129), Research on intelligent construction technology and key control technology of shield tunnel for protecting environment in karst area (CR17GD-GD-XZ6103-JSFW-2023-001).

## 7. BIBLIOGRAPHY

- [1] Chen, Z., Zhang, Y., Li, J., Li, X., Jing, L. (2021). Diagnosing tunnel collapse sections based on TBM tunnelling big data and deep learning: A case study on the Yinsong Project, China. *Tunnelling and Underground Space Technology*, 108, 103700. <https://doi.org/10.1016/j.tust.2020.103700>.
- [2] Cho, J.W., Jeon, S., Yu, S.H., Chang, S.H. (2010). Optimum spacing of TBM disc cutters: A numerical simulation using the three-dimensional dynamic fracturing method. *Tunnelling and Underground Space Technology*, 25, 230-244. <https://doi.org/10.1016/j.tust.2009.11.007>.
- [3] Ghosh, R., Gustafson, A., Schunnesson, H. (2018). Development of a geological model for chargeability assessment of borehole using drill monitoring technique. *International Journal of Rock Mechanics and Mining Sciences*, 109, 9-18. <https://doi.org/10.1016/j.ijrmms.2018.06.015>
- [4] Li, S.C., Liu, B., Xu, X.J., Nie, L.C., Liu, Z.Y., Song, J., Sun, H.F., Chen, L., Fan, K.R. (2017). An overview of ahead geological prospecting in tunnelling. *Tunnelling and Underground Space Technology*, 63, 69-94. <https://doi.org/10.1016/j.tust.2016.12.011>
- [5] Tarkoy, P.J., Marconi, M. (1991). In: *Difficult Rock Comminution and Associated Geological Conditions*. Institute of Mining and Metallurgy, London, pp. 195–207.
- [6] Teale, R. (1965). The concept of specific energy in rock drilling. *International Journal of Rock Mechanics and Mining Sciences & Geomechanics Abstracts* 2 (1), 57–73. [https://doi.org/10.1016/0148-9062\(65\)90022-7](https://doi.org/10.1016/0148-9062(65)90022-7)
- [7] Yamamoto, T., Shirasagi, S., Yamamoto, S., Mito, Y., Aoki, K. (2003). Evaluation of the geological condition ahead of the tunnel face by geostatistical techniques using TBM driving data. *Tunnelling and Underground Space Technology* 18 (2–3), 213–221. [https://doi.org/10.1016/S0886-7798\(03\)00030-0](https://doi.org/10.1016/S0886-7798(03)00030-0)
- [8] Yan, T., Shen, S.L., Zhou, A. (2023). GFII: A new index to identify geological features during shield tunnelling. *Tunnelling and Underground Space Technology*, 142, 105440. <https://doi.org/10.1016/j.tust.2023.105440>

## HYBRID EARTH RETAINING SYSTEM FOR THE CONSTRUCTION OF AN UNDERGROUND METRO STATION IN VARIED GROUND

Edward, Lim<sup>1</sup>, Seng Hou, Lim<sup>2</sup>, Hooi Leng, Phua<sup>3</sup>, Teck Siew, Chin<sup>4</sup>, Shi Hui, Tan<sup>5</sup>

**Abstract:** The Thomson East-Coast Line Contract T202 Woodlands North Station was constructed beneath a secondary forest in hilly terrain. The 800-metre-long cut-and-cover underground structures comprise three main components: the northern overrun tunnel, the station structure, and southern crossover tunnels. The site's geology features hard granite bedrock overlaid by undulating residual soil of highly weathered granite.

The selection of an appropriate earth retaining support system for deep excavation required careful consideration of multiple factors: site constraints, groundwater movement, economic viability, programme requirements, permanent structure configuration, and the availability and competency of domestic specialist contractors. The implementation complexity was further heightened by the varied ground conditions.

A hybrid system was adopted for the cut-and-cover construction, incorporating, Contiguous Bored Pile Walls, Soldier Pile-Timber lagging and open-cut excavation with perimeter soil drains.

The design complexity was further increased by the need to accommodate future integrated underground development adjacent to Woodlands North station, requiring specific temporary earth retaining systems to protect the constructed station from unbalanced movement during future excavation works.

This paper examines the considerations, experiences and challenges encountered throughout the design and construction phases of this hybrid earth retaining system.

**Keywords:** Hybrid-Earth Retaining System, Contiguous Bored Pie Wall, Soldier pile-timber, open-cut excavation, highly weathered granite

## 1. INTRODUCTION

The 43km Thomson East Coast Line (TEL) is Singapore's sixth MRT line, adding 31 new stations to the existing rail network. It enhances connectivity between the north, central and eastern part of Singapore. Contract T202 is located at the northernmost point of the whole TEL as shown in Figure 1 below.



Figure 1. Contract T202, being the northernmost contract in Thomson East Coast Line

<sup>1</sup> Technical Director, Er. Lim, Edward, Asia Infrastructure Solutions Pte Ltd, [edward.lim@asiainfrasolutions.com](mailto:edward.lim@asiainfrasolutions.com)

<sup>2</sup> Senior Manager, Lim, Seng Hou, Penta-Ocean Construction Co., Ltd, [shlim@mail.penta-ocean.co.jp](mailto:shlim@mail.penta-ocean.co.jp)

<sup>3</sup> Project Director, Er. Phua, Hooi Leng, Land Transport Authority, [phua\\_hooi\\_leng@lta.gov.sg](mailto:phua_hooi_leng@lta.gov.sg)

<sup>4</sup> Principal Project Manager, Chin, Teck Siew, Land Transport Authority, [chin\\_teck\\_siew@lta.gov.sg](mailto:chin_teck_siew@lta.gov.sg)

<sup>5</sup> Senior Project Manager, Tan Shi Hui, Land Transport Authority, [tan\\_shi\\_hui@lta.gov.sg](mailto:tan_shi_hui@lta.gov.sg)

This paper focuses on the cut and cover excavation within this contract and discusses the various types of Earth Retaining and Stabilising Structure (ERSS) system that were adopted. A key aspect of this project was that, due to constraints such as geological conditions, existing hilly terrain, and requirements of construction access, a combination of various ERSS systems was required to facilitate the excavation. Employing a single approach, such as maintaining a consistent open cut slope gradient across the site, was not feasible in certain areas due to site limitations. Likewise, using structural retaining walls throughout the entire project proved impractical. As a result, the ERSS was designed as a hybrid system, with different methods applied to suit specific locations.

## 2. PROJECT SITE

Contract T202 comprised of the construction and completion of Woodlands North Station (WDN), at grade cut and cover overrun tunnels North of WDN, cut and cover for crossover tunnels South of WDN, Tunnel Boring Machine (TBM) launch shaft and 2 mainline bored tunnels. WDN is approximately 270m-long and 48 m-wide and 22m below ground when completed, as shown in **Error! Reference source not found.**

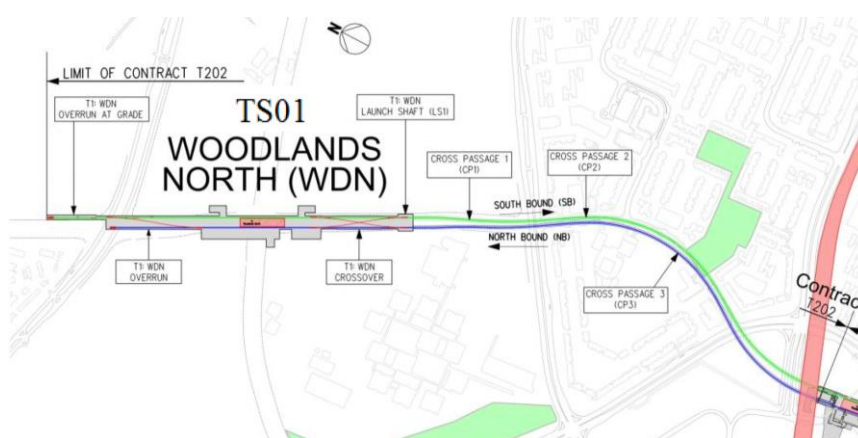


Figure 2. Overall layout plan of Contract T202

### 2.1. Site Topography

The reduced level of the original forest with hilly terrain around the site ranged from RL145m to RL130m (see Figure 3 below). The forest was cleared and excavated to reach the general target formation level at RL102m.

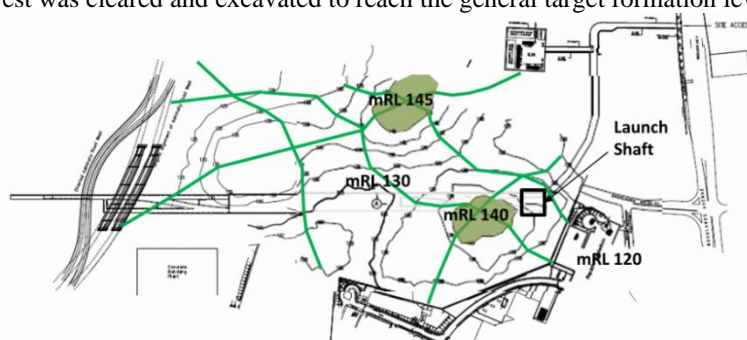


Figure 3. Existing Topography before excavation

### 2.2. Geological Profile

The project site is situated within the Bukit Timah Granite Formation (BTG), which is the predominant rock formation in Singapore. Along T202 WDN, the BTG exists in various weathering states, ranging from residual soils (Grade VI) to intact, unweathered, unstained rock (Grade I). Sharp boundaries are frequently observed between residual soils (GV/GVI) and moderately to slightly weathered granites (GIII/GII). The rockhead level undulates significantly, featuring numerous valleys and considerable depth variations throughout the site. Large boulders are commonly encountered during excavation, with the largest specimens measuring approximately 8

metres. These geological characteristics present substantial challenges for the design of Earth Retention Stabilising Systems (ERSS) and foundations.

Figure 4 below illustrates the elevation view of the permanent structures in relation to the geological profile, specifically at the central portion of the WDN permanent structures. The rock-head exhibits an undulating profile, with some sections rising above the permanent structure level. Rock outcrops that impeded excavation to formation level necessitated removal through controlled blasting techniques followed by excavation. These rock outcrops were also a crucial factor in determining the most suitable Earth Retention Stabilising System (ERSS) for the project.

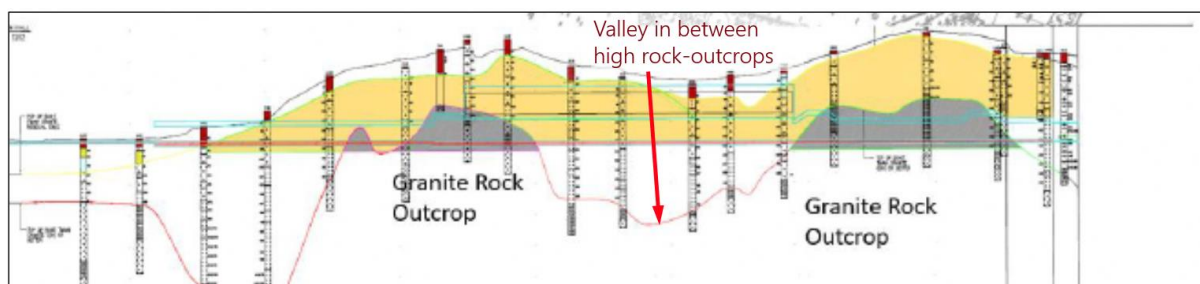


Figure 4. Elevation view of WDN permanent structure levels relative to the Granite Rock-Head Levels

### 3. OVERALL CONSIDERATIONS ON THE GEOMETRY OF EARTH AND RETAINING STABILIZING STRUCTURES (ERSS)

#### 3.1. Considerations During Development of ERSS Scheme Geometry

The site was situated in a relatively green area, where open cut slopes were considered as the Earth Retention Stabilising System (ERSS) for most WDN structures. However, open cut slopes were not feasible throughout the site, necessitating a combination of ERSS schemes. The following factors were considered during the ERSS scheme development:

- Sufficient horizontal space was required to create safe slope gradients. With excavation heights exceeding 30 metres in some areas, the horizontal distance from the edge of the WDN permanent structure to the slope crest would readily exceed 60 metres.
- Even where horizontal space was adequate, assessment was necessary to determine whether existing structures at the slope crest could be affected by potential settlement.
- The impact of groundwater drawdown from open cut slopes required evaluation, as this could adversely affect surrounding buildings, even those situated at considerable distances from the excavation site.
- Due to the extensive width of the slopes, material delivery to the lowest excavation point was not feasible using cranes positioned at the slope crest. Consequently, construction access routes were required to serve the lower areas.
- Interface management with other ERSS types was crucial. Open cut slopes required excavation in nearly all four directions to form a closed excavation. In some instances, these interfaced with other ERSS types, such as rock slopes or structural retaining walls.

#### 3.2. ERSS Scheme

Considering these factors, The ERSS scheme for the overall site resulted in what was reflected Figure 5 below. The stretch of the excavation was approximately 650m length, and the whole excavation open at the same time at one point.

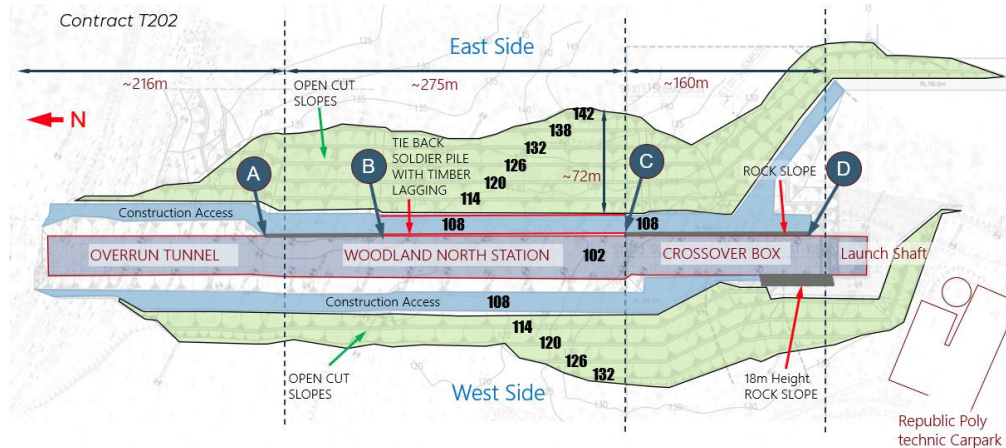


Figure 5. ERSS Overall Layout Plan for WDN

Taking advantage of the good rock properties of the high rock-head outcrops along the East length of the excavation, a steep gradient was formed on the rock slopes between Point A and B, and between Point C and D. Tie-back soldier piles with timber lagging were used between Points B and C, where there was a valley between the rock outcrops.

#### 4. DESIGN AND CONSTRUCTION CONSIDERATION OF THE INDIVIDUAL TYPES OF ERSS

##### 4.1. Open Cut Soil Slopes

The extensive site area for T202 construction permitted the implementation of an open cut excavation method. This involved forming a 1(Vertical):2(Horizontal) soil slope, incorporating turfing and drainage systems as the earth retaining solution for the project.

The open cut slope design utilised both limit equilibrium analysis and finite element analysis through the c'-phi reduction method in Plaxis 2D, ensuring a minimum factor of safety of 1.4. Given the site's hilly terrain, groundwater levels were expected to vary significantly across the location. For design purposes, assuming a full groundwater table would have resulted in an impractically conservative design. Conversely, assuming too low a groundwater level could have compromised safety.

To establish an appropriate initial design groundwater level, a correlation graph was developed, as shown in Figure 6. This graph plots the relationship between existing ground levels and their corresponding water levels, based on data collected from various water standpipes across the site over a minimum monitoring period of six months, as documented in the factual report.

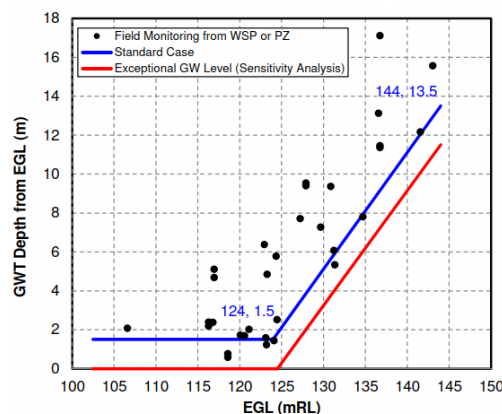


Figure 6. Proposed Initial Groundwater Table obtained from piezometers and water standpipes



The ground water profile for soil slopes had to be kept below the designed ground water drawdown to maintain a high degree of stability. To achieve this, the slopes were turfed to channel surface runoff to a system of surface C7 drains, limiting percolation into the soil, followed by a system of subsoil drains to drain off groundwater to the same system of C7 drains, as shown in Figure 7 below.



Figure 7. Soil Slopes Surface Protection using turfing, subsoil pipes and cut-off drains

#### 4.2. Rock Slope Excavation

In areas where rock was encountered, controlled blasting techniques were employed to create 3.75(Vertical):1(Horizontal) rock slopes, as illustrated in Figure 8.

Rock slope stability was assessed through detailed rock mapping conducted by a competent geologist. The 'Q' system was specified to determine the necessary degree of treatment for the rock slope. Areas with the highest Q-value required only a 50-millimetre thick shotcrete treatment, whilst those with the lowest Q-value necessitated a 120-millimetre thick shotcrete application with rock dowel reinforcement. The rock quality mapped in T202 generally exhibited high Q-values, eliminating the need for rock dowel installation.

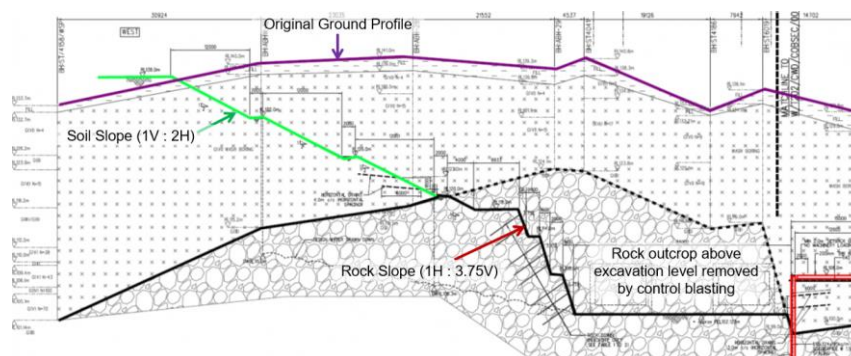


Figure 8. Typical Cross Section View of a Rock Slope below Soil Slope Sections

#### 4.3. Use of Soldier Pile and Timber Lagging Wall with Open Cut Excavation

A line of soldier pile and timber lagging wall with tie backs was introduced along the Eastern open cut excavation section to create a 15m wide construction access as well as to reduce the extent and volume of slope cutting. The wall is depicted in Figure 9 below.



Figure 9. Soldier Pile and Timber Lagging Wall with Open Cut Excavation

#### 4.4. Launch Shaft – Strutted Excavation with CBP Walls and Rock Slopes

The launch shaft cofferdam measured approximately 36.8 metres wide, 48 metres long and 17 metres deep from the pre-excavated working platform. The retaining system, as shown in Figure 10, comprised contiguous bored piles (CBPs) of 1.5-metre diameter spaced at 1.6-metre intervals, supported laterally by multiple levels of steel laced struts. Although initially designed as a four-sided cofferdam, the contractor modified the design to a three-sided configuration. This modification involved removing the retaining wall at the rear of the cofferdam, creating space for the TBM back-up gantry facilities to be installed concurrent with the initial drive operation. This design adaptation enabled the main drive to commence immediately following the completion of the initial drive.



Figure 10. Plan View of the Launch Shaft



#### 4.4.1. Design Considerations

Due to the open-end nature, the design had focused on identifying the load path due to the imbalance load from the South Wall, then taking steps to ensure the load from the South Wall is transferred to the foundation, as shown in Figure 11 below.

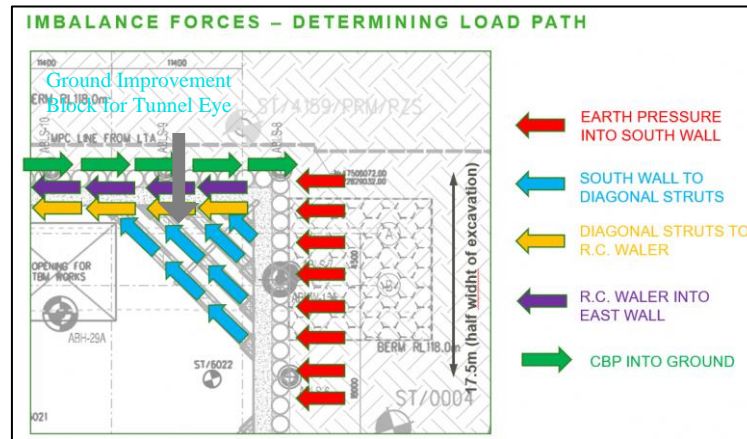


Figure 11. Expected Load Path from South CBP Wall to East CBP Wall

The stability was achieved through geotechnical resistance provided by shaft friction between the soil/rock interface and the contiguous bored pile (CBP) wall. Although the surrounding open cut excavation permitted groundwater drawdown for slope stability, weep holes were installed along the bored pile interface gaps to maintain groundwater flow. The remaining gaps were shotcreted to prevent soil loss whilst preserving the drainage function.

#### 4.4.2. Construction of the CBP-Rock Slope Hybrid System

Figure 12 illustrates the extent of the contiguous bored pile (CBP) system with steel struts and the rock slope with steel struts. Boulders presented significant challenges during both the CBP installation and subsequent excavation work. To navigate through boulder layers during CBP boring operations, drilling speeds were reduced. During the excavation phase, exposed boulders were systematically broken down using hydraulic breakers, as demonstrated in Figure 13.

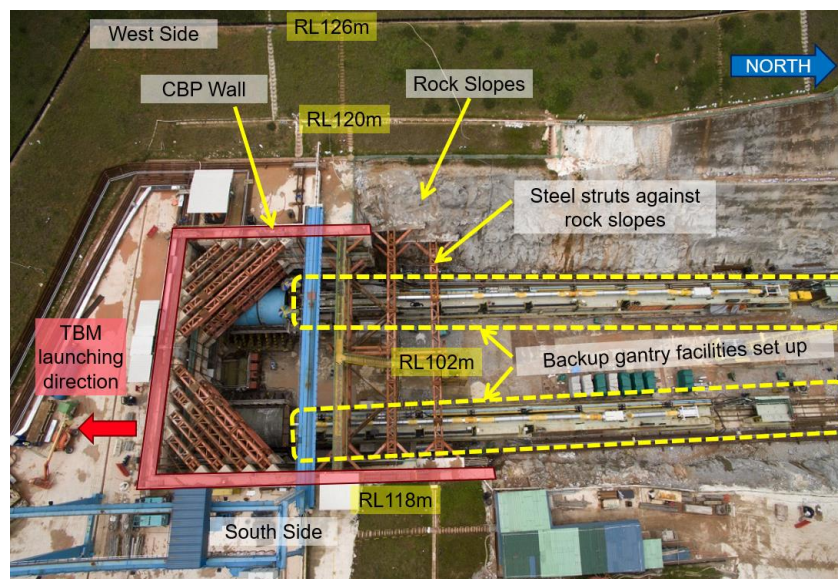


Figure 12. Aerial View of the Launch Shaft – some steel struts were struttged against the rock slopes



Figure 13. Boulders broken by hydraulic breakers

## 5. CONCLUSION

Despite various constraints, including limited space, undulating rock-head profiles, and construction site access requirements, a comprehensive excavation scheme was successfully developed and implemented. This scheme enabled simultaneous exposure of the entire excavation length (as illustrated in Figure 14) without requiring sectional backfilling and re-excavation. This strategic approach proved crucial in completing the extensive excavation works within the prescribed timeline.

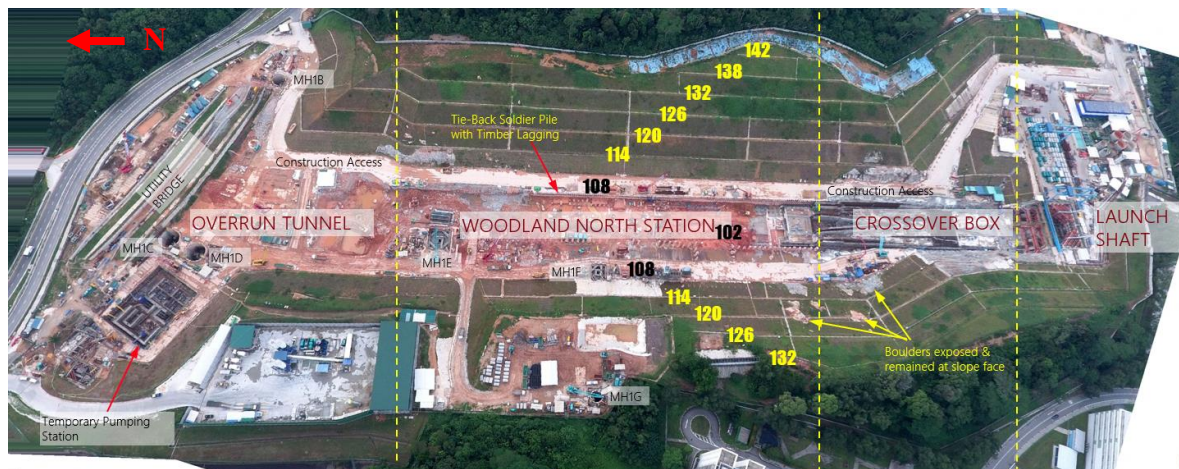


Figure 14. Aerial View of Overall WDN Station Excavation

Close collaboration between the construction and design teams proved essential in understanding the builder's constraints, limitations and operational requirements. Although the construction phase presented various challenges, the Earth Retention Stabilising System (ERSS) scheme proved successful, enabling the achievement of all project objectives.

## 6. BIBLIOGRAPHY

- [1] E.K.H. Lim, I. Yogarajah, T.G. Ng., S.H. Lim, K. Uchida, "Design and Construction of a Three-Sided ERSS Wall for Launch Shaft, Underground Singapore 2018



## CHALLENGES ASSOCIATED WITH PLANNING AND CONSTRUCTION OF A ROAD TUNNEL THROUGH LESSER HIMALAYAN ROCK MASS – A CASE STUDY

Bimala Piya Shrestha<sup>1</sup>, Krishna Kanta Panthi<sup>2</sup>

**Abstract:** Tunneling is crucial in infrastructure development, including hydropower, irrigation, water supply, sewerage, and transportation sectors. However, these underground projects are often accompanied by uncertainty and risk, particularly concerning stability and safety. The Himalayan region, characterized by relatively young tectonics, varying geological conditions, and fractured rock mass, is prone to challenges associated with block falls and stress-induced instabilities. Several factors, including lithology, rock mass conditions, structural geology, in situ stress conditions, groundwater conditions, tectonic activities, and topography, influence the utilization of underground space. This study aims to understand and evaluate the behavior of the surrounding rock mass of a proposed road tunnel intended to connect the second-largest city, Pokhara, with the Kaligandaki Corridor. The proposed road tunnel traverses the Lesser Himalayan geological formation in central Nepal. The ground behavior has been characterized using Rock Mass Rating (RMR) and the Q-system of rock mass classification. In addition, stability conditions have been evaluated using both analytical and numerical approaches for various rock formations where varying rock mass quality and rock cover prevail. The majority of the tunnel stretch is characterized by poor-quality rock mass. The analysis identified wedge failure in the phyllite with intercalation of bands of metasandstone at the eastern portal. These conditions necessitate the implementation of stabilization measures consisting of systematic rock bolting and steel fiber shotcrete. Furthermore, some sections with highly schistose and fractured rock mass exhibited squeezing behavior, with the highest tunnel strain of 15.01%, indicating the need for specialized support measures to accommodate the anticipated ground deformation.

**Keywords:** Tunneling, Lesser Himalaya, Rock mass quality, Ground behavior, Stability, and safety

### 1. INTRODUCTION

According to Panthi (2006), tunneling technology in Nepal has potential applications in multiple domains such as hydropower, transportation, irrigation, water supply, and storage facilities. However, the majority of tunnels constructed to date have been developed in the energy sector, with comparatively limited applications in other domains. Nepal's mountainous terrain, uneven topography, dynamic monsoon, and rock mass influenced by deep weathering conditions necessitate extensive cut slope stabilization and retaining structures for surface construction works, including roads, leading to higher construction and maintenance costs. Thus, it is difficult to establish "sustainable transport with high mobility, safety, and comfort" (JICA, 2019). The challenging topography of steep and unstable mountainous terrain imposes the adoption of tunneling solutions to enable shorter and more efficient transportation routes, while minimizing environmental disturbance (Panthi, 2006). Tunnel construction offers a direct and safer route, significantly reducing travel time and improving regional connectivity, thereby facilitating the efficient movement of goods and services. In recent years, Nepal has made notable progress in the development of its transportation infrastructure with the inclusion of road tunnels such as the Nagdhunga road tunnel, Siddhababa road tunnel, and twin-tube tunnels at the Kathmandu-Terai Fast Track Road projects.

Tectonically, the Himalayan region is characterized by a highly dynamic geological setting. The ongoing compressional tectonic deformation and active reverse faulting mechanism contribute to the accumulation of rock stresses as well as distressing conditions. As a result of active tectonic processes and intense, prolonged monsoon

<sup>1</sup> PhD scholar, Piya Shrestha, Bimala, Rock and Tunnel Engineering, Norwegian University of Science and Technology (NTNU), Trondheim, Norway, bimalap@stud.ntnu.no

<sup>2</sup> Professor, Panthi, Krishna Kanta, Rock and Tunnel Engineering, Norwegian University of Science and Technology (NTNU), Trondheim, Norway, krishna.panthi@ntnu.no



rains, the rock mass in the Himalayas is generally weathered and fractured near the surface, while schistose, deformed, and faulted at depth. Hence, planning, design, and construction of tunnels and caverns in this region have always been challenging. As a result, instability issues such as plastic deformation, rock burst, tunnel collapses, and water ingress are common in tunneling in the Himalayas (Panthi and Nilsen, 2007; Panthi, 2012; Dwivedi et al, 2013; Shrestha, 2014; Basnet et al., 2014).

Stability and safety are fundamental considerations in tunneling, especially in the context of transportation infrastructure. Road tunnels constructed through challenging terrain, such as mountains and urban environments, require careful design to ensure long-term structural integrity and serviceability. Despite careful planning, underground construction is often accompanied by numerous challenges, primarily associated with geological uncertainties and their implications for tunnel stability. To effectively address these issues, it is imperative to acquire detailed geological and geotechnical information during planning, design, and construction of a tunnel project (Panthi and Nilsen, 2007). A comprehensive understanding of the surrounding rock mass behavior, the selection of appropriate construction techniques, and the performance evaluation of support systems are essential for the successful execution of tunneling projects (Zhang et al., 2025). Hence, identifying and assessing potential failure mechanisms based on rock mass characteristics is especially crucial during planning and design phases. Such insights enable the formulation of initiative-taking strategies and mitigation measures that ensure tunnel stability.

To assess deformation at the tunnel periphery during excavation and to design suitable support measures required, various analytical and numerical simulation methods have been developed over the years (Carranza-Torres and Fairhurst, 2000; Vlachopoulos and Diederichs, 2009; Su et al., 2021). In recent decades, the integration of advanced construction and monitoring technologies, as well as numerical modeling techniques, has significantly enhanced the ability to predict and manage tunnel behavior.

This study aims to conduct an overall geological assessment and perform stability analyses of selected sections of the proposed road tunnel alignment along the Baglung-Pokhara highway, which connects the Kaligandaki corridor with the second-largest city, Pokhara. The tunnel alignment traverses through varying rock mass quality and overburden conditions. The analyses employ both analytical and numerical modeling approaches to assess the stability conditions of a 14 km long road tunnel proposed to traverse through Lesser Himalayan rocks. The existing 38 km long stretch of Pokhara Baglung Highway, Hemja (Kaski) to Patichaur (Parbat), traverses through steep topography with challenging Himalayan mountainous terrain. The proposed road tunnel will reduce the road length to 14 km and will serve as a strategic segment that will connect Pokhara with the Kaligandaki corridor, which is under construction, and will help to enhance cross-border trade and mobility between Nepal, India, and China.

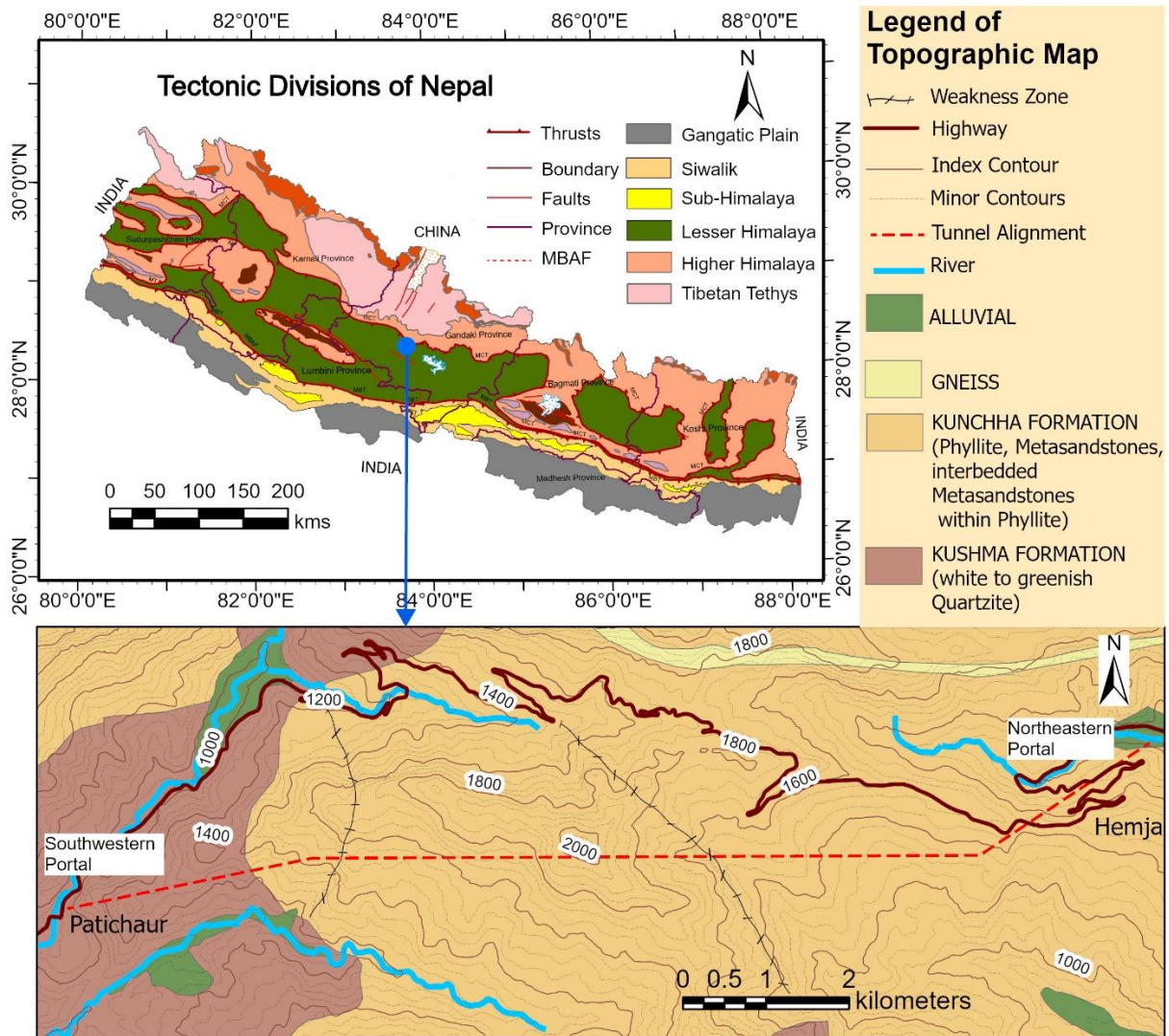
## 2. REGIONAL AND SOCIOECONOMIC SETTING

The Baglung Pokhara Highway connects the Kaligandaki Corridor. The 38 km stretch from Hemja Pokhara (Kaski) to Patichaur (Parbat) passes through steep topography and challenging geological conditions. The proposed 14 km road tunnel will replace a 38 km-long, meandering road. The development of this road tunnel will significantly enhance regional and cross-border trade by shortening the existing road length that traverses steep terrain with several sharp bends. This shortening will reduce travel distance, travel time, and transportation cost. In addition, road alignment will serve as a strategic connection between the city (Pokhara) and the Kaligandaki Road Corridor. The under-construction 445 km long Kaligandaki Road Corridor (Kantipur Post, 2025) will function as a land bridge between China and India by connecting the Korala border at Tibet, China, to the north and the Sunauli border with Northern India to the south. This will enable smoother movement of goods such as agricultural and industrial products, as well as local consumer items. At the same time, it will enable to establish of satellite cities and towns connecting the city, Pokhara, which will enhance domestic trade among the agrarian districts of Kaski, Parbat, Myagdi, and Mustang, allowing farmers to access larger city markets more efficiently. Furthermore, being the Mustang district a tourist destination, the improved (shortened) road will substantially improve connectivity, supporting tourism-driven trade. This is because the faster travel to tourist destinations like Jomsom and Mustang encourages greater flows of visitors, thereby expanding local markets for hospitality, handicrafts, and cultural products.

## 3. PROJECT DESCRIPTION

The proposed road tunnel project is expected to shorten the existing road from 38 km to 14 km. Entry and exit portals of the tunnel are planned to be located at 28°17.434' N, 083°52.568' E and 28°16.489' N, 083°44.607' E, respectively (Figure 1). The eastern entry portal is proposed at an elevation of 1167 m at Hemja, Kaski District, near Ghatte Khola (16 km northwest of Pokhara). The western exit portal is proposed at an elevation of 912 meters.

The tunnel alignment traverses hilly terrain with significant elevation variation, ranging from 900 m to 2050 m above mean sea level (amsl).



**Figure 1.** Regional geological map with tunnel alignment (modified on Geological Map of Nepal, Department of Mines and Geology, 2023)

## 4. ENGINEERING GEOLOGICAL CONDITIONS

### 4.1. Geological formation

The proposed road tunnel alignment traverses the Lesser Himalaya Sequence, which is a geologically complex region situated between the Siwalik zone to the South and the Higher Himalaya zone to the North (Figure 1). Tectonically, this zone is bounded by two major thrust systems: the Main Boundary Thrust (MBT) in the south and the Main Central Thrust (MCT) in the north. Both tectonic faults have played a significant role in the Himalayan orogeny, contributing extensive deformation to the rock mass. Notably, the MBT remains tectonically active, resulting in deformed, faulted, folded, sheared, jointed, and weathered rock mass conditions along the alignment. The area is influenced by numerous major thrust faults located nearby, such as the Phalebas thrust and the Barigad fault in the west, which show signs of lateral movement. The area consists of low to medium-grade metamorphic rocks, which are intruded by higher-grade crystalline nappes and klippen (Upreti, 1999). The tunnel alignment intersects two major lithostratigraphic units consisting of the Kushma Formation (Ku) and the Kunchha Formation (Kn). These formations are predominantly composed of greenish-grey, medium-foliated, moderately weathered phyllite; white to yellow, greenish, fine-grained quartzite; and metasandstone interbedded with phyllite.

rocks. These rocks are famously known in the Lesser Himalayas of Nepal for their variable mechanical behavior under tunneling conditions (Sapkota & Paudel, 2018).

#### 4.2. Rock mass condition

Required observations and measurements of the rock mass were conducted by the authors during multiple field visits to the project area. Various locations were selected based on the rock types, outcrop extent, rock-cut surfaces, and prevailing topography. Field investigations revealed that the exposed rocks predominantly consist of metasandstone to quartzite of a greenish-white color, exhibiting a fine to medium-grained crystalline texture and medium to thick-bedded structures at the southwestern exit portal near Patichaur, which belongs to the Kushma Formation (Figure 1). Joint persistence ranges from 3-10 meters with joint apertures between 1-5 mm commonly filled with silt/sand. The majority of outcrops in this area are slightly to moderately weathered and exhibit features of medium-grade metamorphism. In contrast, the northeastern entry portal (Figure 1), planned to be located within the Kunchha Formation, exposes lithologies composed mainly of deformed, fine to medium-grained, light grey phyllite, frequently intercalated with bands of metasandstone. The zone is characterized by intense fracturing and structural disturbance, which reflects significant tectonic deformation.

A field mapping was conducted during the dry season. The presence of lichens and vegetative growth along joint surfaces suggested seasonal moisture ingress, which is due to water seepage during the monsoon, indicating potential for damp to wet conditions in the rock mass. Furthermore, divergent dip directions of the foliation planes combined with anticline and syncline structures point to the presence of large-scale folding. The area has numerous local faults and folds that indicate intense tectonic activity, which is typical in the Lesser Himalayan region.

A notable tectonic fracture zone between the boundary of metasandstone and graphitic phyllite was encountered near Bhadaure (at 28°17'3.71"N, 83°48'44.06"E) of Kaski district. This fracture zone is projected to intersect the tunnel alignment at an approximate chainage of 5+000 m (Figure 2). The zone comprises crushed and highly fractured rock mass with reduced strength and stiffness, presenting a challenging segment for tunnel construction.

#### 4.3 Rock mass quality characterization

The rock mass quality along the tunnel alignment was assessed using both RMR (Bieniawski, 1973) and Q system (Barton et al, 1974) of rock mass classifications. These classification methods are user-friendly and practical, which are widely used in Nepal and elsewhere. The Q system incorporates the Stress Reduction Factor (SRF) and thus gives a better assessment of the rock mass response to in situ stress conditions. In addition, the Q system directly links the rock mass quality class and allows us to estimate preliminary rock support measures, which is particularly valuable for tunnel design. On the other hand, the RMR system provides correlation to standup time and can be used to cross-check and validate the results obtained from the Q system. The rock mass quality along the tunnel alignment varies from extremely poor to good quality rock mass class (Table 1). All relevant parameters, such as discontinuity conditions, spacing, groundwater conditions, and rock strength, were evaluated through detailed field mapping. The RMR values along the tunnel alignment range from 31 to 77. Similarly, the Q-values varied significantly, ranging from as low as 0.01 (extremely poor rock mass class) to a maximum of 11.56 (good rock mass class). Both classification methods indicate substantial heterogeneity in rock mass quality across the tunnel alignment (Table 1 and Figure 2). Extremely poor-quality rock mass class is associated with highly sheared, folded, and weathered phyllitic zones, while fair to good-quality rock mass corresponds to relatively massive and intact metasandstone and quartzite units.

**Table 1.** Rock mass quality description along the tunnel length

Chainage of the tunnel	RMR values	Q values	Rock class	Quality
From 0+000 to 4+939	53-56	1-4	IV	Poor
From 4+940 to 5+000	31	0.01	VI	Extremely Poor
From 5+001 to 9+749	65-77	10.56-11.56	II	Good
From 9+750 to 9+850	31-35	0.02-0.04	VI	Extremely Poor
From 9+851 to 11+199	52-55	1.21-3.11	IV	Poor
From 11+200 to 13+500	60-65	4.17-10	III	Fair to good

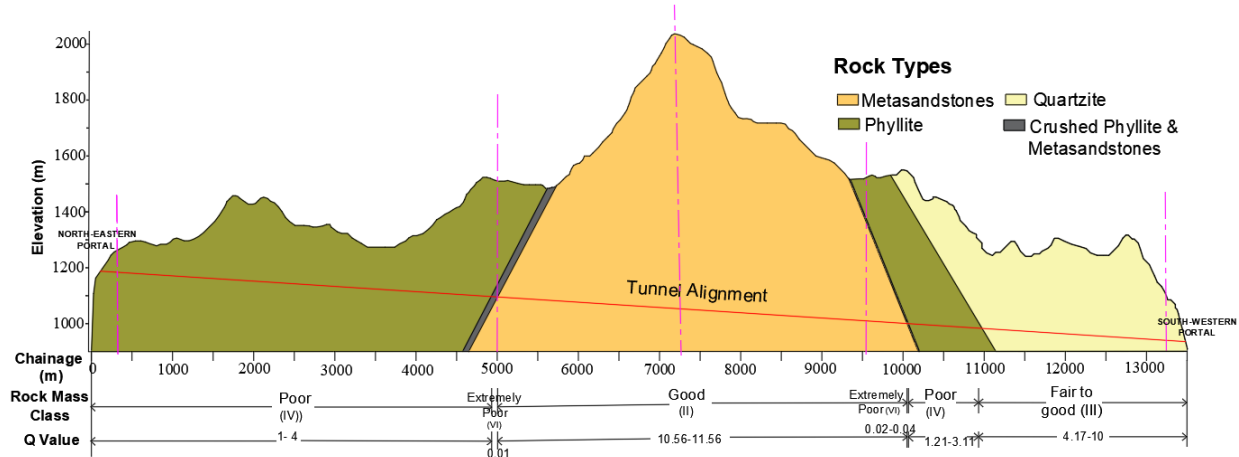


Figure 2. Rock class distribution over tunnel alignment

## 5. TUNNEL SHAPE, SIZE, AND EXCAVATION METHOD

Road tunnels serve as an alternative transportation system to a surface road or bridge, offering reduced travel time and distance, and should have the same traffic capacity as the surface roads they are intended to replace. The shape and dimensions of the tunnel cross-section are primarily determined by serviceability requirements, prevailing ground conditions, and tunnel construction aspects (Ezekiel, 2018). Since the construction is considered to follow the drill and blast or sequential excavation method, a horseshoe-shaped tunnel has been proposed. Traffic volume, being a key factor in road design (number of lanes and road width), is normally assessed using Annual Average Daily Traffic (AADT). According to the Highway Management Information System (HMIS) unit, Department of Roads, Ministry of Physical Infrastructure and Transport, Government of Nepal, the recorded AADT on the Pokhara – Baglung Highway is 9157 in PCUs in 2024/2025. Based on these traffic trends, projected growth, and the planned connection of the Baglung-Pokhara Highway to the Kaligandaki Corridor, the Annual Average Daily Traffic (AADT) is estimated to cross over 10,000 vehicles in the coming years. Since section 17.3 (Road tunnels) of the ‘Nepal Road Standard 2070’ does not provide details of the road tunnel geometry, the Norwegian Standard has been adopted as the reference for defining the detailed geometrical cross-section of the planned road tunnel. Hence, the tunnel cross-section profile selected for this 14 km long road tunnel is type 9.5 (T9.5), following Norwegian Public Roads Administration (2004) as illustrated in Figure 3 and Table 2.

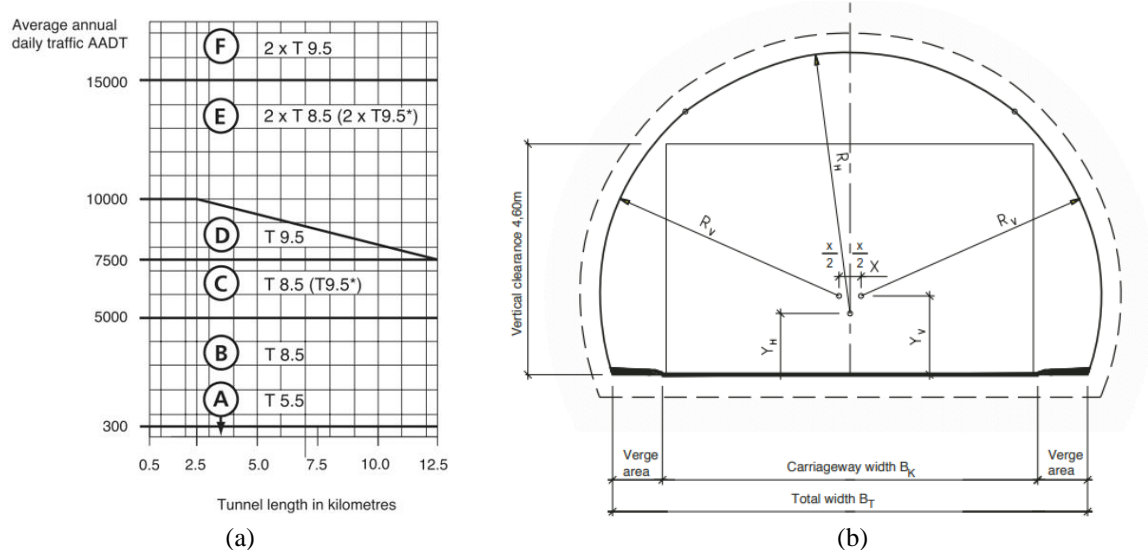


Figure 3. (a) Traffic pattern (b) Cross-sectional geometry of tunnel (Norwegian Public Roads Administration, 2004)

The tunnel system includes all underground structures such as cross passages, adits, shafts, escape routes, and other ancillary components such as ventilation shafts for technical equipment. These elements will be designed based on operational, organizational, and safety considerations. According to DOR (2013), the tunnel will have a



maximum gradient of less than 7%. The selection of a tunnel excavation depends on factors such as the type of ground, tunnel size, the availability of resources, including machinery/equipment, funds, and time. The conventional drill and blast method of tunneling could be well-suited for the construction of this road tunnel. The detailed dimensions of the proposed tunnel profile have been presented in Table 2.

**Table 2.** The cross-section geometry (profile) details of the road tunnel

Description	Details
Length	14 km
Total Effective Width ( $B_T$ )	9.5 m
Carriageway Width ( $B_K$ )	7 m
Theoretical Excavation Area	66.53 m <sup>2</sup>
Theoretical Required Area	53.53 m <sup>2</sup>
Roof Radius ( $R_H$ )	5.2 m
Wall Radius ( $R_V$ )	4.79 m
Centre Distance to Roof Radius( $Y_H$ )	1.22 m
Centre Distance to Wall Radius( $Y_V$ )	1.57 m
Centre Point to Wall Radius( $X$ )	0.44 m
Shape	Horseshoe shape
Construction Method	Drill and blast
Strike of Tunnel	N 75° E

## 6. ESTIMATION OF ROCK MASS PROPERTIES

For analyzing the stability of the tunnel, it is crucial to understand the rock mass characteristics and their interaction with the provided support under loading conditions. Proper estimation of the physical and mechanical properties of the rock mass is essential for understanding the behavior of the surrounding rock mass. Table 3 summarizes the rock mass properties along the tunnel alignment. The physical and mechanical characteristics of intact rocks were obtained either by field mapping or laboratory tests conducted by [Panthi \(2006\)](#) and [Shrestha and Panthi \(2014\)](#).

**Table 3.** Engineering geological, and mechanical properties of rocks at different chainages

Description/Chainage(m)	0+285	5+000	7+300	9+820	13+220
Rock type	Graphitic phyllite	Siliceous phyllite	Meta sandstone	Siliceous phyllite	Quartzite
Uniaxial compressive Strength (UCS), MPa	39	39	73	39	221
Young's modulus (E), GPa	27	14	46	14	83
Poisson's ratio( $\nu$ )	0.1	0.1	0.14	0.1	0.2
Unit weight ( $\gamma$ ), MN/m <sup>3</sup>	0.0278	0.0286	0.0265	0.0286	0.026
GSI	48	26	60	48	55
Vertical stress ( $\sigma_v$ ), MPa	3.48	12.36	26.29	14.24	9.54
Friction angle( $\phi$ )	43 <sup>0</sup>	39 <sup>0</sup>	47 <sup>0</sup>	39 <sup>0</sup>	55 <sup>0</sup>
Cohesion (C) MPa	1.52	0.9	4.2	0.9	12.6

## 7. STABILITY ANALYSIS METHODOLOGY

Stability assessment is a prime task for planning excavation and construction strategies and estimating rock support. The stability of tunnels primarily depends on two factors: rock mass quality (strength of rock mass, deformability properties, strength anisotropy, conditions of discontinuities, and degree of weathering) and mechanical processes (groundwater conditions and influence of in-situ stress) ([Panthi, 2023](#)). Various methods are in practice to assess the stability of the tunnel based on these factors. In this paper, stability conditions were assessed through both analytical and numerical approaches across various sections, as illustrated in Figure 2, characterized by differing rock mass qualities and rock cover conditions.

### 7.1. Analytical/ semi-analytical approaches

When the strength of the rock mass is lower than the induced stress, overstressing can occur around the periphery of the underground opening. Instability, such as rock spalling and rock bursts, is typically observed in relatively unjointed and massive rock masses. In contrast, squeezing-related instabilities are characteristic of low-



quality, highly deformable rock mass (Palmström, 1995). In addition, underground structures at shallow depths with jointed rock mass experience low gravity stresses within the surrounding rock mass, which result in increased stress anisotropy. Rocks are often highly weathered near the surface, which reduces interlocking between the rock blocks (the natural arching effect) and increases the risk of wedge falls (block falls). Potential wedges can be identified with structural, geometrical, and geological data (Hoek, 2001).

Before conducting the analytical and numerical analyses, the squeezing conditions in the selected sections were initially evaluated using empirical criteria proposed by Singh et al. (1992). Although this approach is useful for identifying the occurrence of squeezing, it does not provide a quantitative measure of its severity. In sections classified as non-squeezing, where the rock mass exhibited a distinctly jointed structure, wedge stability analysis was employed to assess potential block failures. At both portal sides of the tunnel, the rock mass is intersected by multiple joint sets, resulting in the formation of wedges that may slide or fall into the tunnel opening. Hence, to investigate these potential modes of instability within the jointed rock mass, the UNWEDGE software was used.

Analytical and semi-analytical approaches serve as valuable tools in assessing tunnel stability, particularly during planning and design phases. These methods provide insight into stress redistribution, deformation patterns, and potential failure mechanisms surrounding tunnel openings. In sections with squeezing ground conditions, the stability analysis was conducted using an analytical Convergent Confinement Method (CCM), which simplifies the 3D rock support interaction into a more practical 2D analysis by integrating Ground Reaction Curve (GRC), Support Characteristic Curve (SCC), and Longitudinal Deformation Profile (LDP). This approach provides a realistic representation of rock mass convergence as confinement decreases around the tunnel, and the results were subsequently verified through numerical modeling to ensure their reliability.

## 7.2. Numerical Modeling

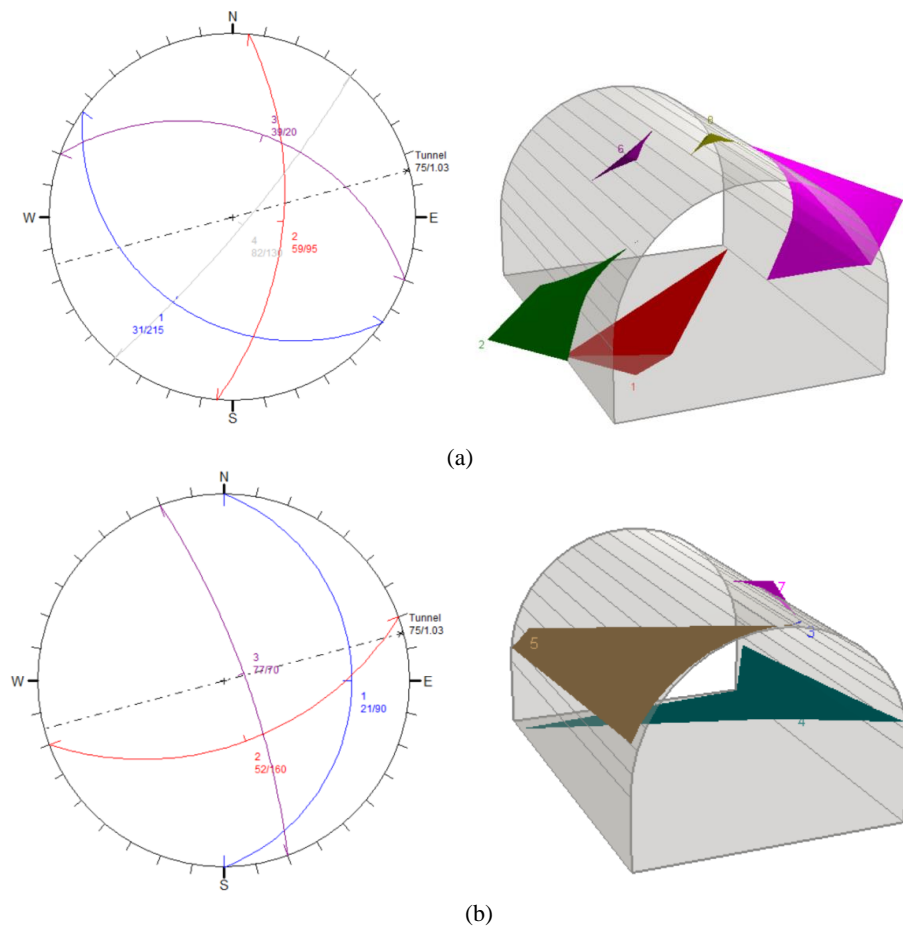
For the present study, wedge analysis was conducted using the UNWEDGE program of Rocscience to identify the potential wedge. The mapped dip direction and dip amount of major discontinuities have been utilized to identify potential wedges that can slip from walls or fall from the roof, and the safety factors of these wedges have been determined. For wedge stability, rock bolts and shotcrete can be installed, depending on the size, shape, and type of wedges (Hoek, 2001).

Numerical simulations of tunnel excavation have been conducted for various sections (Figure 2) with rock masses of varying quality conditions and overburden depths. A two-dimensional finite element software (RS<sup>2</sup>) is used to develop numerical models. The tunnel excavation sequence is simulated by assuming a full-face excavation method. The external boundary of the model domain is defined as five times the diameter of the tunnel to minimize the influence of boundary effects. All boundaries of the box models are subjected to fixed constraints. Mohr and Coulomb failure criterion is used to characterize the elastoplastic behavior of the surrounding rock mass. The simulations have been conducted for a horseshoe-shaped tunnel with a span of 11.35 meters. A graded mesh composed of six-noded triangular elements is generated to ensure sufficient resolution for the tunnel boundary.

The model accounts for both vertical and horizontal stresses resulting from the gravitational effect. In addition, tectonic stresses significantly contribute to the overall magnitude of horizontal stress. In the central region of the Himalayas, tectonic stresses are predominantly oriented in the north-south direction (Panthi, 2012). As the tunnel alignment follows a 75°-255°, orientation, it experiences substantial in-plane tectonic stress (normal to the tunnel alignment). Further, the field observation and assessment concluded that the rock mass at the weakness zone (section 5+000m) will represent weathering grade II, which subsequently will reduce the intact rock strength and elasticity modulus by 40% (Panthi 2006), giving intact rock strength and elasticity modulus of 25 MPa and 10 GPa, respectively. Hence, the rock mass strength and rock mass deformation modulus given in Table 1 have been reduced accordingly to the analysis.

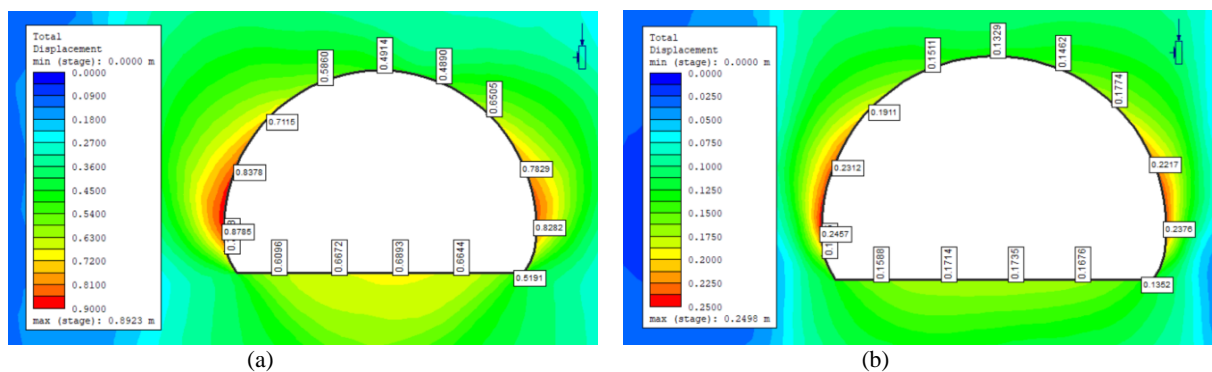
## 8. RESULTS

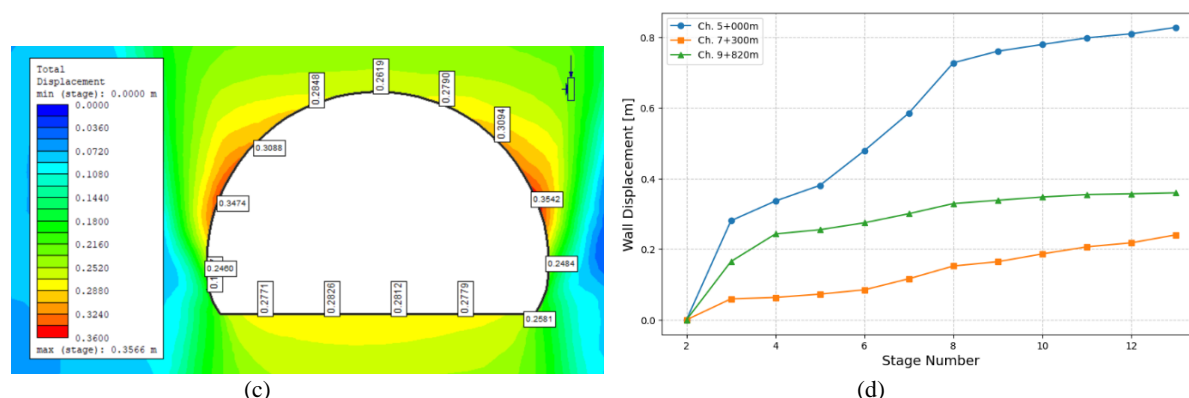
The trend of the tunnel axis is 75° clockwise from the North, and it plunges at 1.03° from the eastern portal, respectively. While analyzing the wedge, the computer program UNWEDGE identified various locations and dimensions of potential wedges, along with safety factors, that formed in the roof and side walls of the tunnel opening. At section 0+285m, where four joint sets were mapped. A total of eight wedges have been formed around the tunnel opening with a different factor of safety, where the roof wedge [8] is found to be unstable (Figure 4a). Similarly, three joint sets were mapped at section 13+220m, where a total of seven wedges may form around the opening of the tunnel. Most of these wedges were found to be stable (Figure 4b).



**Figure 4.** Stereographic projection and 3D wedge view (a) at section 0+285m (b) at section 13+220m

Tunnel excavation results in a reduction of the strength of the surrounding rock mass, which induces plastic deformation (squeezing). This effect is particularly pronounced in fracture zones that are already in a plastic state prior to excavation. This is further evidenced by the significant deformations observed along the tunnel periphery. The analysis presented in this section revealed that a maximum strain of 13.63% is determined using the Convergence Confinement Method and 15.01% by numerical analysis conducted before the installation of tunnel support systems (Figure 5).





**Figure 5.** Deformation around the tunnel periphery (a) at section 5+000m (b) at section 7+300m (c) at section 9+820m, and (d) Horizontal wall displacement along the sections

At sections 7+300m and 9+820m, the calculated tunnel strains using the Convergence Confinement Method are 0.24% and 3.75 %, respectively, while the corresponding values obtained from numerical modeling are 0.32% and 6.6%, respectively. As illustrated in Figure 5(d), the maximum deformation occurs along the tunnel wall at chainages 5+000m and 9+820m, whereas 0.32% of deformation occurs at the tunnel invert in section 7+000m, indicating slight floor heaving.

## 9. DISCUSSION

The stability assessment and deformation analysis of the tunnel have revealed critical insights into the rock mass behavior and strategies for planning support systems. Both the western and eastern portals are situated on a gentle slope, where the rock mass comprises quartzite and phyllite rocks with intercalation of metasandstone, exhibiting three or more joint sets on each side. Construction of the portal requires cutting the gentle slope to some extent. Cut slopes shall be stabilized permanently by shotcrete and rock bolts or other slope protection measures. The wedge stability analysis conducted by UNWEDGE software identified several potential wedges at sections 0+285m (Northeastern portal) and 13+220m (Southwestern portal). The stereographic projection and 3D wedge model, as depicted in Figure 4, revealed the formation of distinct wedges around the tunnel perimeter. These wedges are stable in massive quartzite; however, one roof wedge in section 0+285m is found to be unstable, indicating the need for support in the roof where instability is most pronounced.

The tunnel site is characterized by numerous shear zones, faults, and folds. The stress redistribution in folded, faulted, and fractured rock mass due to the excavation reduces the rock mass strength and contributes to further instability, causing squeezing conditions. Field observations and the deformation analyses exhibit these concerns, particularly at the fracture zones at 5+000m, where the presence of crushed metasandstone and phyllite resulted highest tunnel strain. This result indicates the need for reliable support measures with yielding joints. In contrast, section 7+000m, where fair quality rock mass (metasandstone) and high rock cover prevail, showed minimal deformation, whereas section 9+820m, which is characterized by weathered siliceous phyllite, showed moderate strain levels.

The quality of the rock mass, along with the proposed tunnel alignment, exhibits substantial spatial variation over short distances. This heterogeneity is primarily attributed to active tectonic processes, intense monsoons, and the presence of geological structural features. Such variations in geological conditions pose substantial engineering challenges, as evidenced by the evaluation results obtained for selected specific sections of tunnel alignment. These findings indicate the necessity for section-specific support designs and the implementation of continuous monitoring strategies throughout the construction period.

In some cases, the extent and reliability of subsurface investigations are compromised due to logistical, financial, or topographical constraints, particularly in regions with steep terrain, where conventional investigation methods may not yield accurate or comprehensive data (KC et al., 2022). Therefore, the application of advanced and reliable subsurface investigation techniques is essential to ensure the safe and effective execution of tunneling works.

Beyond the technical considerations, the tunnel project holds considerable socioeconomic and environmental significance. This road tunnel is expected to reduce travel time and transportation costs, thereby promoting local and regional trade, which will significantly boost the economy and tourism in the region. Overall, the integration of analytical and numerical analysis has enabled the development of reliable support measures tailored to the

prevailing rock mass conditions. These engineering solutions, coupled with socio-economic evaluations, highlight the tunnel's transformative potential for remote mountain communities and regional trade.

## 10. CONCLUSIONS

This paper provides an understanding of the stability and deformation analysis of the proposed road tunnel in the Lesser Himalayas, offering valuable insights into the rock engineering behavior of the surrounding rock mass. The UNWEDGE program identified the potential wedges at the sections (0+285m and 13+220m), with various safety factors, emphasizing the potential for instability, especially around the roof and sidewalls. Strain analysis using the Convergence Confinement Method and numerical method indicates substantial plastic deformation, particularly in the weakness zone, with strain observed at 5+000m (up to 15.01%). In contrast, sections like 7+300m showed lower deformation due to stronger rock mass. These findings underline the necessity for section-specific support measures, particularly in fracture zones affected by faulting, folding, and jointing. Beyond technical considerations, the tunnel project presents considerable economic, social, and ecological benefits, improving regional connectivity. Overall, the project development integrating efficient engineering geological measures followed by optimized community benefits could demonstrate the tunnel's transformative role in improving infrastructure resilience and regional development in the challenging Himalayan terrain.

## 11. ACKNOWLEDGMENTS

The authors would like to acknowledge NORAD, which supported this research through NORHED II Project 70141 6: *Capacity Building in Higher Education within Rock and Tunnel Engineering in Nepal*, operated by the Norwegian University of Science and Technology (NTNU), Norway, in collaboration with Pashchimanchal Campus, Institute of Engineering (IoE-WRC), Tribhuvan University (TU), Nepal. The authors are thankful for both financial and moral support in conducting this research.

## 12. REFERENCES

- [1] Aryal, M. (2025). The Kaligandaki corridor road gives new hope to isolated mountain communities. *The Kathmandu Post* (10-05-2025).
- [2] Basnet, C. B., Panthi, K. K., & Shrestha, P. K. (2014). Analysis of Squeezing Phenomenon in the Headrace Tunnel of Chameliya Project, Nepal. *Hydro Nepal: Journal of Water, Energy and Environment*, 13(13), 44–51. <https://doi.org/10.3126/hn.v13i0.10039>
- [3] DOR. (2013). Nepal Road Standard 2070. *Department of Roads*, 55.
- [4] Dwivedi, R. D., Singh, M., Viladkar, M. N., & Goel, R. K. (2013). Prediction of tunnel deformation in squeezing grounds. *Engineering Geology*, 161, 55–64. <https://doi.org/10.1016/j.enggeo.2013.04.005>
- [5] Evert, H. (2001). *Practical\_Rock\_Engineering.pdf*. *Course Notes*, 190.
- [6] [http://ssrn.aviyaan.com/traffic\\_controller/get\\_detail/Pokhara](http://ssrn.aviyaan.com/traffic_controller/get_detail/Pokhara), cited on September 4, 2025
- [7] Ezekiel. (2018). *Design and Construction of Road Tunnels : Part 1 Planning*. 111.
- [8] JICA. (2019). *Federal Democratic Republic of Nepal | Data Collection Survey on Urban Transport in Kathmandu Valley | Final Report*. July 1–24. [https://openjicareport.jica.go.jp/pdf/12326708\\_01.pdf](https://openjicareport.jica.go.jp/pdf/12326708_01.pdf)
- [9] KC, D., Gautam, K., Dangi, H., Kadel, S., & Hu, L. (2022). Challenges in Tunneling in the Himalayas: A Survey of Several Prominent Excavation Projects in the Himalayan Mountain Range of South Asia. *Geotechnics*, 2(4), 802–824. <https://doi.org/10.3390/geotechnics2040039>
- [10] Norwegian Public Roads Administration. (2004). *Road Tunnels 03.04*.
- [11] Palmström, A. (1995). Characterizing Rock Burst and Squeezing by the Rock Mass Index. *Design and Construction of Underground Structures*, c(February), 23–25.
- [12] Panthi, K. (2006). Analysis of engineering geological uncertainties related to tunnelling in Himalayan rock mass conditions. In *the Norwegian University of Science and Technology* (Vol. 5, Issue February).
- [13] Panthi, K. K. (2012). Evaluation of rock bursting phenomena in a tunnel in the Himalayas. *Bulletin of Engineering Geology and the Environment*, 71(4), 761–769. <https://doi.org/10.1007/s10064-012-0444-5>
- [14] Panthi, K. K. (2023). Methods applied for the stability assessment in rock engineering. *Journal of Nepal Geological Society*, 65(September), 29–34. <https://doi.org/10.3126/jngs.v65i01.57741>
- [15] Panthi, K. K., & Nilsen, B. (2007). Uncertainty analysis of tunnel squeezing for two tunnel cases from the Nepal Himalaya. *International Journal of Rock Mechanics and Mining Sciences*, 44(1), 67–76. <https://doi.org/10.1016/j.ijrmms.2006.04.013>
- [16] Sapkota, N., & Paudel, L. P. (2018). Geological Study of the Lesser Himalaya in the Kusma-Baglung Area, Western Nepal. *Bulletin of the Department of Geology*, 20(1980), 29–36. <https://doi.org/10.3126/bdg.v20i0.20721>

- [17] Shrestha, P. K. (2014). *Stability of tunnels subjected to plastic deformation - a contribution based on the cases from the Nepal Himalaya*. 124.
- [18] Shrestha, P. K., & Panthi, K. K. (2014). Groundwater effect on faulted rock mass: An evaluation of Modi Khola pressure tunnel in the Nepal Himalaya. *Rock Mechanics and Rock Engineering*, 47(3), 1021–1035. <https://doi.org/10.1007/s00603-013-0467-7>
- [19] Su, Y., Su, Y., Zhao, M., & Vlachopoulos, N. (2021). Tunnel Stability Analysis in Weak Rocks Using the Convergence Confinement Method. *Rock Mechanics and Rock Engineering*, 54(2), 559–582. <https://doi.org/10.1007/s00603-020-02304-y>
- [20] Upreti, B. N. (1999). An overview of the stratigraphy and tectonics of the Nepal Himalaya. *Journal of Asian Earth Sciences*, 17(5–6), 577–606. [https://doi.org/10.1016/S1367-9120\(99\)00047-4](https://doi.org/10.1016/S1367-9120(99)00047-4)
- [21] Vlachopoulos, N., & Diederichs, M. S. (2009). Improved longitudinal displacement profiles for convergence confinement analysis of deep tunnels. *Rock Mechanics and Rock Engineering*, 42(2), 131–146. <https://doi.org/10.1007/s00603-009-0176-4>
- [22] Zhang, T., Zhao, J., Kuang, R., & Li, C. (2025). Stability Analysis and Support Optimization of Tunnel Surrounding Rock with Weak Interlayer Based on Catastrophe Theory. *Buildings*, 15(3). <https://doi.org/10.3390/buildings15030507>



## PHILIPPINES UNDERGROUND SPACE AND TUNNELS, PAST PRESENT AND POSSIBLE FUTURE

Mark Wallace<sup>1</sup>

**Abstract:** As the Philippines continues to grow and develop the demands of the growing country puts pressure on existing Infrastructure and services to provide much needed water supply, drainage, irrigation and transport to meet those increasing demands. There have been some significant tunnels and underground infrastructure built and this paper will outline the legacy and old networks and how the country is developing and expanding its underground facilities and infrastructure to meet that demand. Metro Manila, Metro Cebu and Metro Davao are some of the major urban areas that are looking at developing underground solutions to provide a balance to new metro lines and road networks to ease significant traffic congestion as well as meet urban growth demand from other sectors such as water, sewage, flood and power. A country with significant challenges in social, environmental and geohazards is continuing to grow rapidly with one of the quickest growing economies in Southeast Asia. This paper explores the past, present, and future of underground spaces and tunnels in the Philippines, examining their historical significance, current applications in transportation, utilities, and potential to be applied to future infrastructure development. As the country continues its economic ascent, the strategic use of underground spaces and tunnel options will be crucial in ensuring sustainable urban growth, ease of movement and resilient infrastructure development.

**Keywords:** Underground Space, Tunnels, Infrastructure, Rail, Road, Water, Transport, History, Philippines

### 1. INTRODUCTION

The Philippines, an archipelago of over 7,600 islands with a rich history shaped by its strategic location in Southeast Asia. From pre-colonial societies and Spanish colonization to American rule and eventual independence, the nation has undergone significant transformations. In recent decades, the Philippines has emerged as one of Asia's fastest-growing economies, driven by a booming services sector, remittances from overseas workers, and increasing foreign investments. Since the Duterte administration from 2016 to 2022 there has been a much-needed focus on improving much needed infrastructure in the Country across all sectors and this has been extended by the current Marcos administration. Much of this development is being partly funded and supported by Japanese International Cooperation Agency (JICA), Asian Development Bank (ADB), and Asia Infrastructure Investment Bank (AIIB). Many local developers and investment organizations are also helping to develop the much-needed infrastructure through PPP projects and the Government has a balance of investing in Government procured projects as well as private sector procured projects.

The country has a generally mountainous geography with around 65% of the country in hill terrain. Many of the growing urban areas lie on flood plains or flood prone areas and the country lies on the ring of fire around the Pacific so it experiences all the issues of a young tectonic country with frequent earthquakes, volcanic activity with numerous associated geohazards. It is also impacted by major cyclones and typhoons in the wet rainy season with associated risks from landslides, flash floods and general flooding on their major rivers.

---

<sup>1</sup> Director of Infrastructure, Arup & President of the Philippine Tunneling Society, [mark.wallace@arup.com](mailto:mark.wallace@arup.com) ; [philtunnelsociety@gmail.com](mailto:philtunnelsociety@gmail.com)

It is a socially conscious country aware of its roots, environment and rich history of its peoples and differing religions. It is well known for its fabulous beaches, marine environment and ecology which are some of the major draws for tourists to the country.

In recent years the country has seen significant growth with the per capita GDP currently at around USD4,350 in 2025 having rapidly grown from around USD1,053 in 2000 and expected to rise to around USD13,300 by 2050 as a 2 trillion economy.

With ever increasing wealth and a growing widespread urban congestion for a population of over 110M people there is demand to improve all the associated supporting infrastructure including transport, water supply, sewage, power. There are 6 recognized metropolitan urban areas in the Philippines with the 3 largest forming Metro Manila and the Greater Capital Region having expanded to over 20 million residents while Metro Cebu and Metro Davao have around 3.5M residents each. All these urban areas continue to expand, putting pressure on the existing infrastructure, transport and services. The situation is further compounded with the need to provide resilient and climate driven solutions but still maintain the environmental and social integrity of the country.

The legal context of the underground in the Philippines was defined by law in 2016 under RA10752, Sec 3&4 where the National Government Projects may acquire the strata below a private property below 50m without the need to provide any compensation and can occupy the subterranean areas for the purposes of the infrastructure project. The infrastructure types listed as subways, tunnels, underpasses, waterways, floodways or utility facilities. Its also applies to projects where a concessionaire or developer may undertake a project on behalf of the Government. The subterranean law is currently being reviewed, and this may be changed to raise the typical level to 40m depth and to allow shallower depths for key critical projects.

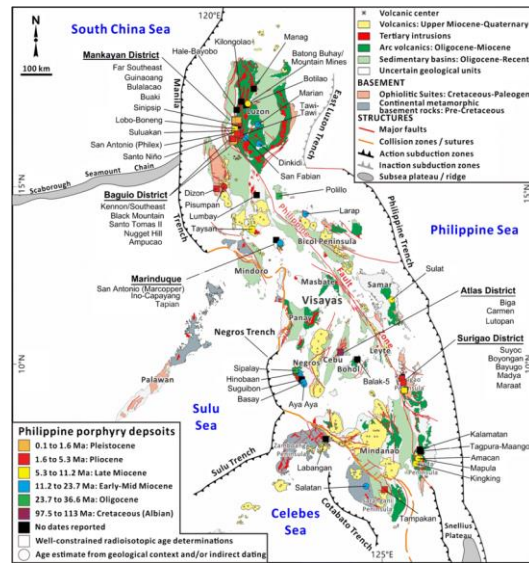
This paper only covers infrastructure related tunnels but there are a quite a few underground tunnels in some of the mining projects in the Philippines especially the underground gold mining operations in the North Luzon region in the Sierra Madre Mountains.

### **1.1. Geology of the Philippines**

The Philippines is an archipelago of island formed by the subduction of the Pacific oceanic plate below the Asian plate and comprises a series of uplifted and volcanic formed islands and landmasses. It is about 1,600km long by an average width of around 400km.

The region is characterized by lithologies and regional structure developed during Cretaceous-Tertiary period. During this period there was an extensive ultramafic intrusion tectonism, andesitic and dacitic volcanism and the sediments are diverse including sandstone, conglomerate, tuffs, siltstone, shale, reef limestone and coal. Diorite, quartzdiorite and andesitic stocks were intruded at various times. The oldest rocks found in the region are Cretaceous spilite, shale, greywacke and cherts. There are various trenches and subduction zones adjacent too and within the country that contribute to an actively seismic terrain with significant earthquakes that can be felt all over the country. Some areas are more seismically active than others. Volcanism due to the island arc nature of the country is widespread with many active volcanoes and some of the largest volcanic eruptions can and have occurred from volcanoes in the country. There are many young rocks formed in sedimentary basins that are generally weakly cemented while there are areas of very hard rock through intrusions on the island arcs and lava flows from the previous volcanic activities. In many places there are uplifted sedimentary rocks including limestones, shales, mudstones, sandstones etc.

Various geohazards can be found such as ground shaking, liquefaction of soils, landslides, tsunami and seiches and there are various dangers from rainfall driven landslides and debris flows over the mountainous areas and flooding in the wet season in low laying areas and major river floodplains.



**Figure 1 – Geological and Tectonic Map of the Philippines.** (source: JICA)

In Metro Manila there are various deposits of weak sedimentary and volcanic rocks underlying the city at shallow depth. These deposits can be cut vertically down to 20 to 30 m depth relatively easily with minimal support to the surrounding rock faces that usually only need soil nail and shotcrete facings to control stability. There are few joints in the rock masses and they are generally massive although due to their weak nature there can be deep cracks and fissure that need to be considered. Groundwater can range from shallow to deep depending on whether there are nearby existing fluvial areas and where there may be deep well pumping for water supply. An example of the type of basement excavation that can be undertaken in Metro Manila are shown below:



**Figure 2 – Deep Basement Excavation for a high rise building in Ortigas Metro Manila.**

## 1.2. Drivers for Tunnel and Underground Solutions

However, rapid urbanization and population growth have placed immense pressure on the country's infrastructure, leading to congestion, water shortages, and inadequate transportation systems. To address these challenges, the Philippines must expand and modernize its infrastructure, including the development of underground spaces and tunnels.

Historically, underground development in the country has been limited, with notable examples such as military tunnels from World War II and small-scale utility passages. However, recent projects like the Metro Manila Subway and underground water drainage systems signal a shift toward utilizing subsurface spaces to alleviate urban strain.

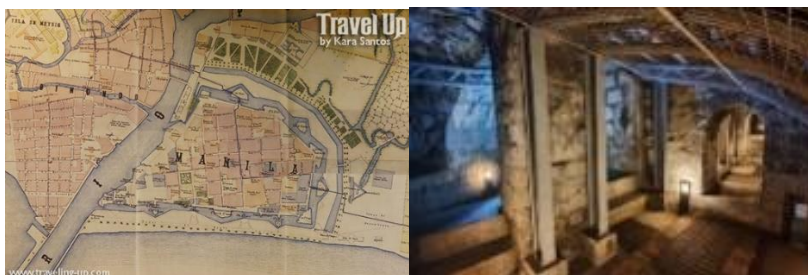
## 2. HISTORIC TUNNELS

### 2.1. Spanish Era Tunnels

The history of underground spaces and tunnels in the Philippines dates back to the Spanish colonial period (1565–1898), when the need for fortifications, water systems, and religious structures led to some of the country's earliest

subterranean constructions. Unlike modern infrastructure tunnels, these early underground passages were primarily built for military, religious, and utilitarian purposes.

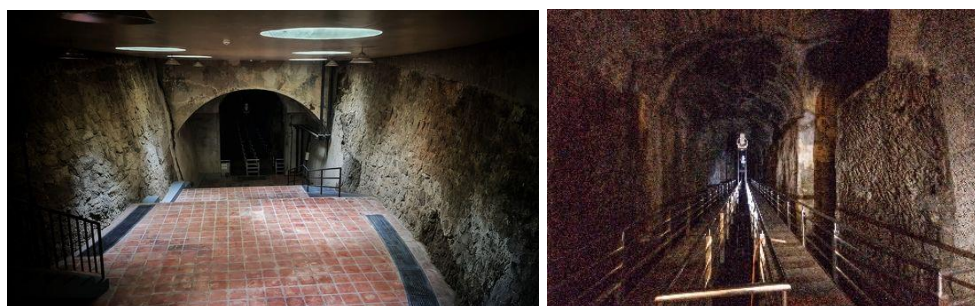
One of the most notable underground structures from the Spanish era is the Fort Santiago Tunnels and Dungeons in Intramuros, Manila. Beneath the historic fortress, a network of tunnels and dungeons was constructed, serving as storage for supplies, secret escape routes, and prison cells. Philippine national hero Jose Rizal was incarcerated in those dungeons before his execution in 1896. These tunnels were further extended and strengthened during World War II when they were used by Japanese forces to imprison Filipino and American soldiers.



**Figure 3** – Old Map of Intramuros Fort Santiago and Inset Photo Dungeons (source: [traveling-up.com](http://traveling-up.com))

Many other Spanish Forts in the country had tunnels and underground chambers for military purposes. Such as at the old Spanish Fort in Puerto Princessa.

The Spanish also identified that the river and water supplies were becoming polluted even in the mid 1800's and this led to them developing some above ground aqueducts and some distribution tunnels that fed clean water from the Marikina River into the Manila City areas. Between 1878 and 1882 the Carriedo Water System Network was built and this incorporated various subterranean systems including an underground storage cavern (15 million gallons) and various brick lined tunnels to supply different parts of the city. The water supply system was named after Francisco Carriedo y Peredo, a Spanish philanthropist who funded Manila's first piped water network



**Figure 4** – Entrance to El Deposito (left) and the Main Storage Chamber (right) (source: [facebook/tourism san juan](https://www.facebook.com/tourism.san.juan))

The Spanish also built underground structures for religious purposes. Some churches and cathedrals, such as San Agustin Church in Intramuros, have crypts and catacombs beneath them, serving as burial sites for Spanish clergy and elite colonizers. Many of these Spanish-era tunnels have deteriorated over time due to neglect, natural disasters, and urban development. However, some, like those in Fort Santiago, have been preserved as historical landmarks. These early underground structures reflect the ingenuity of colonial engineering and set a precedent for later tunnel construction in the Philippines, particularly in military and urban water management applications.

The Spanish colonial tunnels may not compare in scale to modern infrastructure projects, but they represent the Philippines' first steps in underground development—a legacy that continues to influence contemporary underground construction in the country.

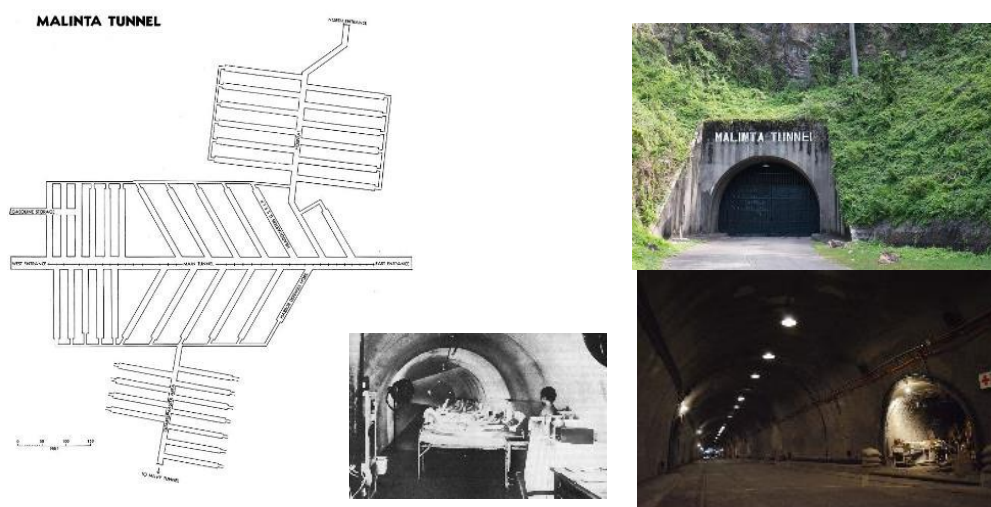
While the Spanish built tunnels for civil defense and water supply, they also extended their reach into the mountainous regions and they were reported to have built some tunnels in Baguio to traverse ridges and steep terrain more easily for road construction. These are discussed later in the road tunnel section.



## 2.2. American and WWII Japanese Tunnels

The early 20th century saw significant underground construction in the Philippines, first under American colonial rule (1898–1946) and later during the Japanese occupation (1942–1945). These tunnels were primarily military in nature, serving as defensive fortifications, supply routes, and secret hideouts. Unlike the Spanish-era tunnels, which were limited in scope, the American and Japanese periods introduced more extensive underground networks, some of which still exist today as historical sites.

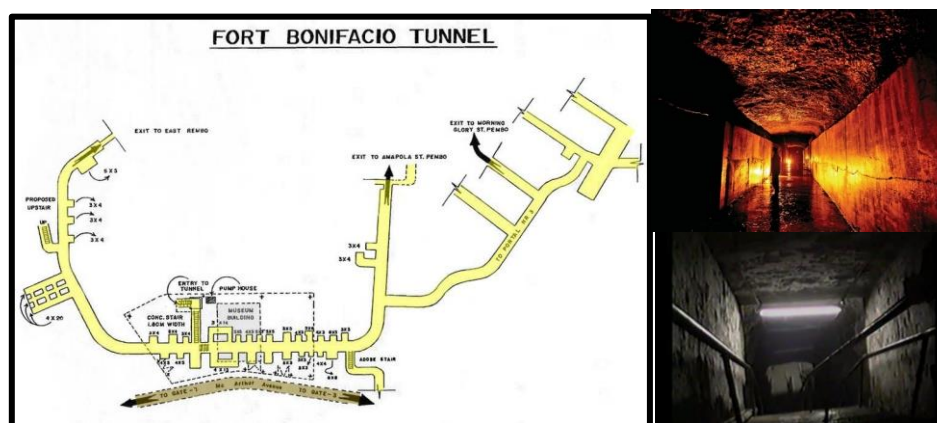
A well-known network was built on Corregidor Island that formed an island defense at the mouth of Manila Bay and was a strategic military stronghold during the war. The Malinta Tunnel network was expanded significantly by the Americans from 1932 to 1934 and had a 253m long main tunnel 7.3m wide by 5.5m high and then had 13 lateral branch tunnels on both sides and 49m long by 4.6m wide that served as a hospital during the second world war.



**Figure 5** – Malinta Tunnel Network, Portal and Underground Tunnels and Chambers. (source:uswarmemorial.org)

The Americans also built an extensive network of tunnels and chambers in Fort Bonifacio in the 1910's ("Fort McKinley") in the middle of Manila. They built a network of over 2.2km of tunnel up to 30m deep up to 4m wide to service many of the buildings and facilities in the former camp. Some mapping of the network has been done and there have been recorded at least 32 chambers and a 6m wide deep well within the system. Many of it remains unmapped and unrecorded in the area.

During World War II, the Japanese Imperial Army expanded and constructed numerous tunnels across the Philippines, using forced labor (including Filipino and Allied POWs). These tunnels served as hideouts, supply depots, weapons and ammunition storage and detention facilities.



**Figure 6** – Fort Bonifacio Tunnel Network and Tunnels / Shafts / Adits, (source:facebook/memoriesoldmanila)

Many of these tunnels are now **\*\*historical landmarks\*\***, serving as reminders of the Philippines' wartime past.



Some, like Malinta Tunnel, have been preserved for tourism, while others remain hidden or collapsed. The Japanese tunnels, in particular, are associated with brutal wartime atrocities, making them significant yet somber historical sites.



**Figure 7** – Typical Japanese Tunnels in Baguio and Davao, now Tourist attractions (source: thebaguiochannel.com & tracesofwar.com)

These underground structures highlight the Philippines' strategic military importance in the 20th century and provided examples of how the ground in many areas could be relatively easily mined and excavated. By the end of the 1950's there was around 5.5km of old historic tunnels but there are likely to be many unrecorded or undocumented war and military tunnels around the country especially in strategic areas and at former engagements.

### 3. WATER TUNNELS

#### 3.1. Early Years to 1990's

Even when the Spanish were occupying the Philippines the seasonal variations in the rainfall meant that there needed to be a reliable clean water supply to their forts and camps and in Manila this started with the Carreido Water Supply system that then was expanded into the Manila Metropolitan Water District water supply network by the Americans. By the 1930's it was obvious that water supply needed to be reliably provided to the growing city and various dams and water supply projects were initiated. The Wawa Dam at Montalban provided the initial aqueducts in pipes and later by 1939 the IPO Dam required the first 6.3km tunnel aqueduct to bring water from the newly constructed dam to Metro Manila area.

By the 1960's and 1970's the Philippine Government already knew that the water supply for drinking water as well as irrigation needed to be secured for the growing Metro Manila and Luzon plain areas and formed the National Irrigation Administration and the Manila Waterworks & Sewerage System to further manage and supply water to the city.

Two further water supply tunnels (1969 & 1992) both approximately 6.3km long were also built from IPO dam to supply expanding water works facilities. By the end of the 1990's there were around 33.1km of water tunnels.

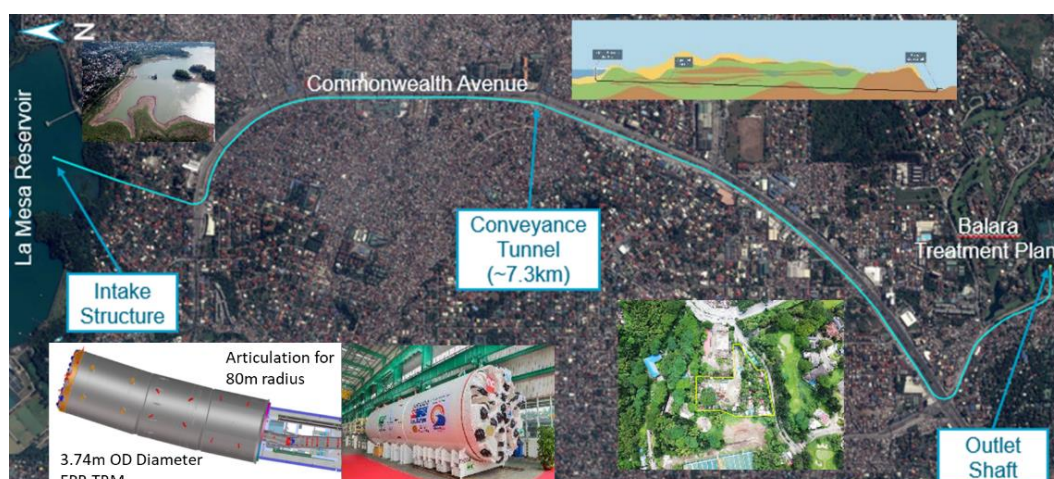
#### 3.2. 1990's to 2025

As the Philippines has expanded and in particular Metro Manila there has been an increased focus on providing water to the Metro Manila and the Greater Capital Region. Various schemes have been formulated and implemented to transfer catchment river water that would have flowed to the east and north back towards the capital. The Umiray Angat Transbasin Project was the first major aqueduct that brought water through a 13km 4.88m diameter hard rock TBM from rivers flow to the north and divert it to the southerly populated areas to the Angat and IPO dam systems. Recently there has been an investment in replacing and updating the water supply aqueducts to secure the water supply for the greater capital region. Angat Tunnel No 4 that was a hard rock double shield TBM was 6.3km long and 4.7m diameter with a design flow of 1600MLD and was completed 2019 and operational by 2020. Another subparallel Tunnel No 5 6.43km and 4m diameter was completed in 2024.



**Figure 8** – Angat AWTIP T5 Tunnel alignment and Photos. (source: Arup)

In addition, projects like the Novaliches-Balara Aqueduct No 4 (NBAQ4) that comprised a 7.3km long, 3.74m diameter EPB TBM had a double articulated shield to provide a tight turning radius of 80m along the alignment to stay underneath existing public roads and land. This system provided a lower water take off from La Mesa dam and a more resilient tunnel scheme for possible future earthquakes.



**Figure 9** – NBAQ4 Tunnel alignment, geology cross section and EPB TBM (source: Novabala & Arup)

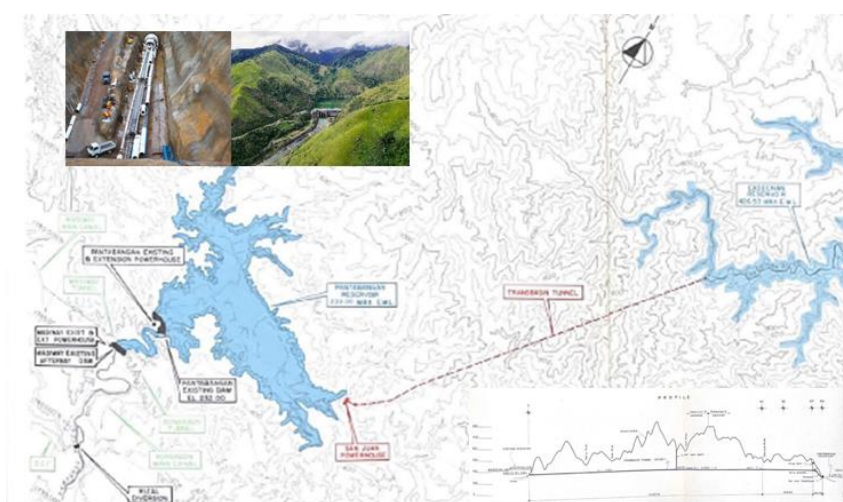
The expansion of the water supply networks is continuing to be replaced and maintained and by 2025 there will be around 60km of dedicated water tunnels in the Philippines mostly in Luzon.

### 3.3. 2030 Onwards

There is no doubt that the Philippines needs to secure its water supply as the Metropolitan Waterworks and Sewerage System (MWSS) office struggles to supply around 20M households and businesses in the Calabarzon region and with the current phase of water tunnels as well as recognition of the existing aging aqueducts there is a need to upgrade, increase capacity and supply to the region. This is ongoing and there are more water supply tunnels underway and being planned. Climate change as well as seasonal changes in rainfall are impacting water security and over the next few decades there should be up to 105km of water tunnels projected to be built, mostly in Luzon but there are significant water demands in other Metropolitan Areas that tunnels may provide viable and secure supply options. Currently WAWA, Kaysakat, LTE, Kaliwa water supply projects will construct more tunnels in the near future. There are even plans for small / short tunnels to improve the low water take-offs from some of the dams to provide more resilient and supply options in the case of drought.

The Philippines has suffered power shortages during the 1990's to the early 2000's and there has been steadily improving power supply and distribution but there is increasing demand in the country for power. The current trend is to promote more renewable energy and there are many hydropower projects in the Philippines. With its mountainous terrain there are many simple run-of-river and dam based hydroelectric schemes that have been built and planned over the last 2 decades. A few of those have been integrated with irrigation and power generation.

One of the longest tunnels in the Philippines is the Casecan Hydro and Irrigation Project that transfers water across watersheds from the Cagayan River basin to the south to the Pantabangan Reservoir. This tunnel was formed by various techniques including drill and blast and by TBM and extends to around 26.6km for the main tunnel aqueduct / headrace tunnels and has around 2.5km of branch tunnels and adits to provide a network of about 29km in the system. It's a pressurized tunnel and produces about 150MW of power into the Philippine NGCP transmission grid.



There are more than 70 existing hydropower projects in the Philippines and typically relatively small as run of river schemes that currently generate 1.2GW of electricity for the country. There is around 75km of existing hydropower tunnels forming supply and headrace sections both gravity and pressurized but reliable information on each of the plants has not been forthcoming and the known hydropower tunnels are likely to exceed 81km in the next few decades. The hydropower tunnels are found throughout the mountainous areas of the Philippines and in steep terrain areas prone to landsliding and flash floods. There is likely though to be competing aspects of water supply as well as uncertainty in seasonal fluctuations due to climate change that may impact sustained future growth of this area of tunnel development. Indeed, many existing facilities may be looking to optimize and expand and there could be further growth in the hydropower tunnels in the Philippines especially as dual-purpose tunnels.

## 5. ROAD TUNNELS

387





**Figure 11** – Asin Road Tunnels Benguet, Baguio (left), Tangadan Tunnel (middle), Gessang Tunnel (right) (source: [Instagram.com/p/DGXfZp9yOXg](https://www.instagram.com/p/DGXfZp9yOXg) & [traveling-up.com](https://traveling-up.com) & Lanz Michael Bautista)



**Figure 12** – Patiking Tunnel, Dupag (left), Bontoc Single Lane Tunnel (middle), Halsema Highway “Half Tunnel” (right) (source: [sean.doctolero.com](https://sean.doctolero.com) & [spiritedthoughts.wordpress.com](https://spiritedthoughts.wordpress.com) & [rusa4.wordpress.com](https://rusa4.wordpress.com) )

There are some tunnels in Mindanao with a notable road tunnel at Malabang “Picong” Tunnel 2 lane road tunnel with walkways and central divider that was built by the Americans in the 1930’s and is around 60m long. A more recent longer highway tunnel was the Kaybiang Tunnel completed in 2013 at 300m long was the longest drill and blast road tunnel in the Philippines until recently.



**Figure 13** – Picong Tunnel, Lanao del Sur, Mindanao (left), Kaybiang Tunnel (middle), Badiwan Viaduct Tunnel (rock protection shed) Marcos Highway (source: [mindanaochronicles.com](https://mindanaochronicles.com) & [outoftownblog.com](https://outoftownblog.com) & [youtube.com/watch?v=gZR9Vx3AVPs](https://youtube.com/watch?v=gZR9Vx3AVPs))

In several of the main highways in the mountains there has been at least 3 protection tunnels or sheds built to protect the road or highway against local landslides and rockfalls. 75m long (Dalton Pass Tunnel, built approx. 1995), 320m long (Marcos Highway, built 2001), 150m long (Kennon Road Tunnel, built 2024).

In the urban areas of the country there have been various cut and cover road tunnels to provide better traffic flow and interchange improvements. There are many in Metro Manila and a recent notable one in Cebu on the South Coastal Road. A notable cut and cover underpass road tunnel that is combined with the MRT3 railway was built in 2000 to provide better access to the Makati District of Manila and to allow traffic to freely navigate the major interchange. Various other underpasses and in the city suffer from flooding problems.



**Figure 14** – Cebu South Coast Road (left), EDSA Ayala Underpass Tunnel (right) (source: [google maps](https://google.com/maps) & [en.wikipedia.org/patrickroque01](https://en.wikipedia.org/patrickroque01))

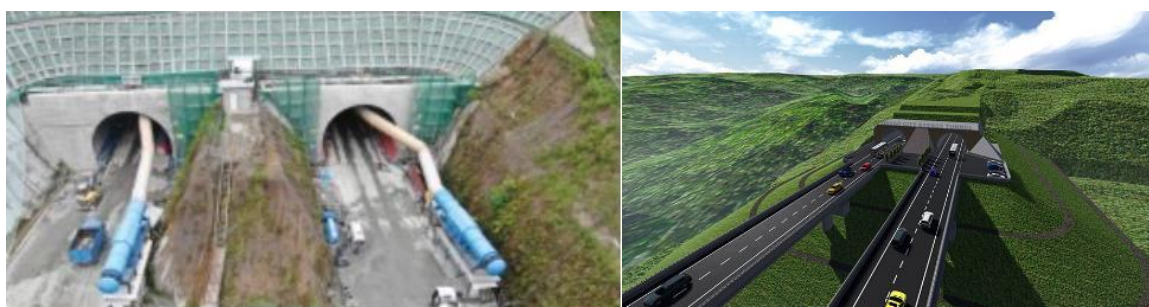
Some of the new expressways that have been built over the last few years are also incorporating some tunnels.

In particular the Subic Freeport Expressway added another tunnel to the existing two-way tunnel built in 1990 and by 2020 the road had been widened and upgraded to a dual carriageway with the construction of another 108m long 12m wide by 9.6m high drill and blast tunnel.



**Figure 15** – Subic Freeport Expressway Tunnels (old 1996 and new 2020) (source *sta clara international corporation*)

One of the recent ongoing highway tunnel projects is the current Davao City Bypass scheme that incorporates the Philippines longest highway tunnel. The Davao Bypass tunnels are approximately 2.3km long and dual carriageway with some cross passages and are due for completion in 2025.



**Figure 16** – Davao City Bypass Twin Tube Dual Carriageway (source: *pna.gov.ph & mindanews.com/DPWH-XI*)

There are various planned and future highways proposed in some of the more mountainous areas of the country to solve traversing the hilly terrain and provide better infrastructure for the country.

## 6. RAIL TUNNELS

### 6.1. Early Years

Towards the end of the 19<sup>th</sup> century the Philippines had many 1000's of kilometers of railway but no operating tunnels. In 1913 there was a short 500m long 7.5m wide about 4m high rail tunnel constructed for a planned spur line to connect through to Baguio for Aringay. The tunnel was never used and the spur line abandoned by the First World War. Later it was used by the Japanese forces as an Army HQ center. It was renamed the Centennial Railway Tunnel in the last few years and is becoming a tourist attraction in the area.





**Figure 17** – “Centennial Railway Tunnel (Abandoned) (source: [en.wikipedia.org/wiki/centennial\\_tunnel](https://en.wikipedia.org/wiki/centennial_tunnel))

## 6.2. Rail Tunnels Now and in the Future

The Philippines has started on a major campaign to regain the previous rail heritage that it had. Currently the country only has several hundred kilometers of railway in the Metro Manila and Calabarzon area. The Philippine Government with JICA funding are building the Metro Manila Subway Project (MMSP) with over 33.1km of underground railway with 15 underground stations with dual tunnel tubes with a typical metro rail diameter of around 7m and up to 25 tunnel boring machines to drive the tunnels between stations.



**Figure 18** – “MMSP alignment and Contracts with DOTr Transport Secretary Visiting CP101 Site, (source: [pna.gov.ph/articles/1220290](https://pna.gov.ph/articles/1220290))

In addition the North South Commuter Rail (NSCR) Project has also a short section of tunnel planned to connect and allow interchange with the MMSP line. Some cut and cover sections of the NSCR can also be found near Clark Airport. MRT 7 a privately financed project by San Miguel also has some cut and cover section in Quezon City where the sensitivity of cultural heritage and a need to prevent future surface disturbance has led to several stations being placed underground as well as their connecting running tunnels. There have been plans for an underground metro line in Makati and this may also be resurrected in the future, to again, further improve connectivity in one of the main CBD areas of the capital.

There are also various other railways being planned and these will undoubtedly include some tunnel and underground solutions to allow the railways to navigate the hilly terrain or to hide the railways underneath the existing busy congested roads of the cities in the Philippines. Indeed, in Cebu there are tentative plans to consider building a Metro Line up to 67.5km long designated as the Urban Mass Rapid Transit (UMRT) in some JICA studies and is planned to be from southwest to northeast through the city. Much of the alignment could be placed underground, especially in the densely populated and land congested parts of the city. This project could significantly ease the overwhelming traffic congestion in the city.

## 7. OTHER TUNNELS AND UNDERGROUND SPACE

There are some interesting other types of tunnels and underground spaces in the Philippines. It is generally relatively easy to excavate in the Guadalupe formation rocks in Metro Manila and hence there are various deep

basements that could be integrated with underground Metro stations in the future. There are also various pedestrian underpasses in downtown parts of the city.

## 7.1. Pedestrian Underpasses

The Philippines has some pedestrian underpasses that cross busy highways and streets. In Makati Ayala have developed a series of eight underpasses that connect across the busy roads and provide a safe means of crossing and allow traffic to flow more freely. They have incorporated murals and advertising in the underpasses that are heavily used and serviced by escalators and lifts. Similarly in Quezon City for the Circle / Elliptical road to connect to the memorial. In Manila City the Lagusnilad pedestrian underpass connects Rizal park to the Manila City Hall and while it was built in the 1960's it has been recently upgraded and improved in the 2020's with the inclusion of better lighting along with murals and advertising to offset the electricity lighting costs.



Figure 19 – Ayala Triangle Underpass Photos / Examples (source:morefunwithjuan.com)

## 7.2. Underground Shopping

There is a small dedicated underground retail area at the famous Quaiipo Church in Metro Manila. An underground underpass was constructed in the 1960's that incorporated various retail booths within the underpass. This underpass was the first pedestrian underpass and opened in 1964 and was reopened in 2014 after an extensive refurbishment. The underpass incorporates 6 entrances up to 200 retail booths.

## 8. COMPLETED TUNNELS UP TO 2025

A full catalogue of the past, present and possible future tunnels are outlined in **Appendix A** to this paper. These tunnels cover a wide range of types of tunnel to service a range of infrastructure sectors. By the end of 2025 there will be around 150km of tunnels in the Philippines and mostly built in the Calabarzon region to supply and provide underground infrastructure to Metro Manila.

For a metropolitan area of around 15 to 20M people the number of tunnels is surprisingly low and appears to be historically focused at water supply with many built in the 1960's to the 1990's to supply Metro Manila. Hydropower projects also contributed a large proportion of the tunnels up to 2025 with many of them servicing both irrigation and water supply as well as hydropower energy generation which is another significant demand for the growing metropolis.

It is clear that many of the old tunnels formed in the 1960's are needing to be refurbished / replaced and are getting to end of life. Indeed, the current driver for better transport options is delivering a significant amount of rail tunnels over the next decade.

Table 1 – Tunnel Type and Length Constructed by 2025

Tunnel Type	Length Constructed By 2025 (km)
Road	7.50
Rail	5.25
Water	53.71
Major Culvert	0.34
Underpass	1.24
Utility	0.00
Historic	5.49
Hydropower	77.63
<b>Total Length (km)</b>	<b>151.15</b>

## 9. FUTURE TUNNELING CHALLENGES AND OPPORTUNITIES

With the ever-increasing growth of the Philippine economy the countries cities will continue to grow and therefore underground solutions will be more attractive to provide solutions that meet public demands and expectations. The driver will be the demand for land and Right of Way issues and the inevitable need to minimize provide solutions that minimize impacts on the existing traffic in the urban areas.

Various railway lines will be extended and there will be further phases of expansion for the Metro Manila Subway and there are potential plans to develop inner circle lines to service Makati and BGC that would provide a easier circulation of people around the city. Some of the potential projects highlighted by DOTr, DPWH, MWSS, DOE, NEDA suggest that there will be over 130km of new tunnels to be built up to 2035. The majority of those tunnels will be in the rail and water sector to service the various major demands that the cities in the Philippines are encountering.

*Table 2 – Tunnel Type and Length to be Constructed 2025 to 2035*

<b>Tunnel Type</b>	<b>Length Planned between 2025 to 2035 (km)</b>
Road	13.00
Rail	67.60
Water	50.89
Hydropower	3.40
<b>Total Length (km)</b>	<b>134.89</b>

With the addition of the current tunnelling projects being constructed just now and in final stages of planning there will be over 280km of tunnels in the Philippines by the end of 2035.

*Table 3 – Tunnel Type and Length Constructed by 2035*

<b>Tunnel Type</b>	<b>Length Constructed By 2035 (km)</b>
Road	19.70
Rail	72.85
Water	104.60
Major Culvert	0.34
Underpass	1.24
Utility	0.00
Historic	5.49
Hydropower	81.03
<b>Total Length (km)</b>	<b>285.24</b>

As tunnels and underground solutions continue to be needed there will be likely demand to organize the underground spaces in the cities in the Philippines in a more coordinated manner with the need for urban planning and underground master plans developed to ensure that future generations can still provide options and solutions in the urban areas through tunnel options. As the Philippines has been growing the pre capita gross domestic product (GDP) has steadily risen up to 2000 where it was around

## 10. CONCLUSIONS

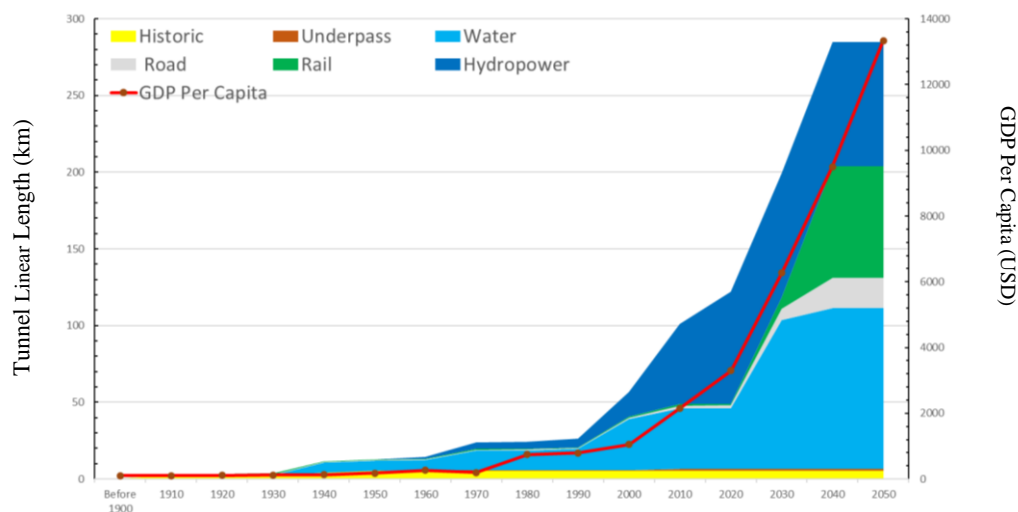
The Philippines is set for a significant development in tunnels and tunnelling in the country. Historically there are many legacy tunnels and underground spaces in the Philippines that are now being developed and used as tourist attractions. Essential infrastructure tunnels to provide water and hydropower have formed the main backbone of the tunnels in the Philippines in the 1960's to the early 2000's. While most of the tunnels are located in the Calabarzon region there will be many other underground solutions needed in the Philippines and other cities are likely to need underground solutions to service and provide infrastructure for their cities.

The growth of tunnelling is likely to continue in the future and the focus is already moving to transport orientated tunneling and underground solutions. The fast-increasing trend in GDP in the Philippines seems to be tracking the initial increase in tunnel projects and this is likely to continue in the near future. It may be that the trend is in line with affordability of the tunnel options as they are usually more expensive than surface or elevated projects. It seems that there is no choice now as the urban congestion has increased to a level demanding urban underground metro systems in many of the cities in the Philippines.

**Table 4 – Tunnel Length Constructed by Key Decades**

Year	Length of Tunnel Completed
1960	14.8 km
1980	24.8 km
2000	57.7 km
2020	122.5 km
2035	285.4 km

The population of the Philippines in 2020 was around 109M people with continued growth up to around 130M by 2040. As the population grows the urban population is growing faster as people migrate to the cities and major urban areas with cities like Metro Manila and Cebu expected to have increased traffic congestion as the populations expand. Metro rail as well as underground metro systems will be essential to meet that demand. Indeed, water supply, deep sewer networks, underground utility including cable tunnels and underground highways etc. will be needed to provide the Philippines with more livable cities.



**Figure 20 – Total Length of Tunnels in the Philippines per Type and Per-Capita GDP Growth**

## 11. ACKNOWLEDGMENTS

The Author would like to sincerely thank Mr Malcolm Lorimer (Executive Director & Head of Major Projects for First Balfour and Treasurer of the Philippine Tunneling Society) for his constructive advice and review of the paper for the various case studies and examples outlined in the paper.

## 12. APPENDICES

### Appendix A – Initial Catalogue of Known Tunnels and Underground Infrastructure in the Philippines

No	Project name / Tunnel name	Approx. Year of Completion	Type of Tunnel	Length (m) (km)
1	Asin Tunnels 1 & 2, Benguet, Baguio.	Built by POW's 1700/1800's refurbished 1850's	Road	95m and 158m Approx
2	Fort Santiago (Intramuros) Tunnels	Pre 1890's	Historic	> 300m of tunnels, not fully known
3	Puerto Princesa City Cuartel / WWII tunnels	1700s	Historic	100m Approx
4	El Desposito Network Underground Reservoir	1878-1882	Water	150m
5	Fort Bonifacio Tunnels	1910	Historic	> 2.24km Approx (many not recorded)

6	"Centennial" Railway Tunnel, Aringay, La Union	1913	Rail	0.5km Approx
7	Gessang & Patiking Tunnels, Dupag, Apayao	1920	Road	60m Approx
8	Malabang Tunnel, Lanao del Sur, Mindanao.	1930	Road	60m Approx
9	Malinta Tunnels, Fort Mills, Corregidor	1932	Historic	1.429km various tunnels and adits
10	Tangadan Tunnel, San Quintin, Ilocos Sur.	1934	Road	40m Approx
11	AWTIP Tunnel No 1	1939	Water	6.3km Approx
12	Ilagan Japanese Tunnel - Sto. Tomas, Ilagan City, Isabela	1942	Historic	40m Approx
13	Japanese Malagos Tunnel - Hillcrest Subdivision, Matina Balusong, Davao City	1942	Historic	300m Approx
14	Digos Tunnel	1942	Historic	150m Approx
15	Albay Town WWII Tunnels	1942	Historic	0.63km Approx
16	Wawa Dam WWII Japanese Tunnel, Rodriguez, Rizal.	1945	Historic	50m Approx
17	Baguio WWII Tunnels	1945	Historic	150m Approx
18	Amlan Mining Drainage Tunnel, Negros Oriental	1950	Major Culvert	340m Approx
19	Ambuklao Hydropower Plant / Dam, Bokod Benguet	1956	Hydropower	500m
20	Angono-Binangonan, Petroglyphs Tunnel	1960	Historic	100m Approx
21	Binga Hydropower Plant	1960	Hydropower	800m
22	Lagusnilad Vehicle Underpass, City of Manila	1960's	Underpass	240m Approx
23	Lagusnilad "Manila City Hall" Pedestrian Underpass, City of Manila	1960's	Underpass	60m Approx
24	Lacson Underpass, Quiapo, Manila.	1964	Underpass	0.15km Approx
25	Angat Dam Power Facilities, Norzagaray Bulacan 3No Tunnels	1967	Hydropower	1.8km, 607m, 597.5m
26	AWTIP Tunnel No 2	1969	Water	6.3km Approx
27	Bontoc Tunnel, Mountain Province.	1980	Road	30m approx
28	Half Tunnel Halsema Highway, Atok, Benguet.	1980	Road	150m approx
29	Magat Hydroelectric Power Plant / Dam, Ramon Isabella	1983	Hydropower	630m & 630m
30	Laiban Dam Tunnel, (Not used)	1984	Water	0.96km (twin tube 480m)
31	AWTIP Tunnel No 3	1992	Water	6.3km Approx
32	Dalton Pass Rockfall Protection Tunnel (Shed)	1995	Road	75m Approx
33	Makati Ayala Pedestrian Underpasses (8No.)	1995 to 2021	Underpass	0.4km Approx
34	Old Subic Expressway Tunnel	1996	Road	90m
35	EDSA Ayala Road Tunnel, Underpass Makati City	2000	Road	650m Approx
36	EDSA Ayala MRT3 Tunnel, Underpass Makati City	2000	Rail	650m Approx



37	EDSA Magallanes Tunnel - Underpass	2000	Underpass	45m Approx
38	Umiray-Angat Transbasin Project (UATP)	2000	Water	13.1km
39	Bakun AC 70 MW Hydropower Plant - HEDCOR Benguet and La Union	2000	Hydropower	10.45km
40	Badiwan Viaduct "Marcos Highway" Tunnel Shed	2001	Road	320m Approx
41	Casacnan Dam Tunnels	2002	Hydropower	Main 26.6km, total length of 29.066km of tunnels and adits
42	Villa Siga Hydropower Plant, Panay Island	2004	Hydropower	4.4km
43	C5 Underpass, Katipunan and Bonny Serrano Interchange Underpass	2007	Underpass	200m Approx
44	Quezon City Circle / Elliptical Pedestrian Underpass	2007	Underpass	60m Approx
45	26.25MW Sibulan A Hydroelectric Plant	2009	Hydropower	3km
46	Cebu South Coastal Road Tunnel Cut&Cover	2010	Road	610m
47	Malamig Tunnel, along Plaridel Bypass Road	2012	Underpass	25m Approx
48	Sipat-Dampol Tunnel along Plaridel Calumpit Road	2012	Underpass	30m Approx
49	Tambubong Tunnel along Plaridel Bypass Road	2012	Underpass	25m Approx
50	Kaybiang Tunnel, Ternate Cavite	2013	Road	300m Approx
51	14MW Sabangan Hydropower Plant - HEDCOR Benguet and La Union	2015	Hydropower	3km
52	8MW Catuiran Hydropower Project – Or Mindoro	2015	Hydropower	3.4km
53	Manolo Fortich 2 Hydropower Plant	2017	Hydropower	6km
54	60 MW run-of-river hydro project, Cordillera Hydro Electric Power Company's (COHECO)	2019	Hydropower	8km
55	Subic Freeport Expressway (SFEX) Tunnel	2020	Road	108m
56	AWTIP Tunnel No 4	2020	Water	6.3km Approx
57	SUMAG River Diversion Tunnel	2023	Water	0.6km
58	NBAQ4 Aquaduct - La Mesa Dam to Balara Water Treatment Works	2023	Water	7.2km
59	AWTIP Tunnel No 5	2024	Water	6.5km
60	Kennon Road Landslide Rockfall Tunnel (Shed)	2024	Road	150m Approx
61	MRT7 North Ave to Quezon Memorial and University Ave, Quezon City. Cut&Cover	Due 2025	Rail	4.1km
62	Siguil River 14.5MW Hydropower Plant, Maasim, Sarangani	Due 2025	Hydropower	786m
63	25MW Lake Mainit Hydropower Project, Jabonga and Magdagooc, Agusan Del Norte	Due 2025	Hydropower	3km
64	225MW AGUS III Hydropower Plant	Due 2030	Hydropower	3km & 400m
65	Paranaque Spillway	Due 2035	Water	7.2km Approx

66	Upper Wawa Pumping Station Main Access Tunnel	Due 2025	Hydropower	1.016km
67	Davao City Bypass Construction Project	Due 2025	Road	2.3 km
68	North South Commuter Rail Phase 2 - Malolos - Clark Segment, Cut&Cover	Due 2026	Rail	2.2km
69	Kaysakat Raw Water Supply Tunnel	Due 2026	Water	6.09km
70	Kaliwa Dam Tunnel	Due 2027	Water	21.9km
71	LTE Raw Water Supply Aquaduct	Due 2028	Water	15km
72	North South Commuter Rail Contract 3B	Due 2030	Rail	4.7km
73	Angat Dam New Low Level Outlet Tunnel	Due 2030	Water	0.7km
74	Metro Manila Subway Project (MMSP)	Due 2030	Rail	33.1km
75	Proposed Dalton Pass Bypass Tunnels	Due 2031	Road	6.5km Approx

Note: Many tunnels and underground infrastructure are not well documented and in some cases the networks are more extensive than declared. The list does not include mining related tunnels of which there are quite a few in the Philippines. Please email ([philtunnelsociety@gmail.com](mailto:philtunnelsociety@gmail.com)) if you have other information on other tunnels, lengths and type of construction to add to the Catalogue or to update the information provided in the above, thank you in advance.

### 13. REFERENCES

- [1] <https://en.wikipedia.org/wiki/Philippines>
- [2] [https://en.wikipedia.org/wiki/List\\_of\\_metropolitan\\_areas\\_in\\_the\\_Philippines](https://en.wikipedia.org/wiki/List_of_metropolitan_areas_in_the_Philippines)
- [3] [https://en.wikipedia.org/wiki/Economy\\_of\\_the\\_Philippines](https://en.wikipedia.org/wiki/Economy_of_the_Philippines)
- [4] Mines and Geosciences Bureau. (2010). Geology of the Philippines, 2<sup>nd</sup> Edition. MGB. <https://doi.org/10.1016/j.proeng.2016.11.792>.
- [5] [https://en.wikipedia.org/wiki/Malinta\\_Tunnel](https://en.wikipedia.org/wiki/Malinta_Tunnel)
- [6] <https://globalnation.inquirer.net/51592/war-tunnel-history-under-ritz-fort-boni>
- [7] <https://thebaguiochannel.com/?p=3876>
- [8] <https://secret-ph.com/exploring-the-hidden-gems-of-davao-city/>
- [9] [https://en.wikipedia.org/wiki/National\\_Irrigation\\_Administration](https://en.wikipedia.org/wiki/National_Irrigation_Administration)
- [10] [https://en.wikipedia.org/wiki/Metropolitan\\_Waterworks\\_and\\_Sewerage\\_System](https://en.wikipedia.org/wiki/Metropolitan_Waterworks_and_Sewerage_System)
- [11] [https://web.archive.org/web/20120704171010/http://www.nscb.gov.ph/secstat/d\\_popn.asp](https://web.archive.org/web/20120704171010/http://www.nscb.gov.ph/secstat/d_popn.asp)
- [12] <https://psa.gov.ph/content/philippine-population-projected-be-around-13867-million-2055-under-scenario-2>

## ENGINEERING GEOLOGICAL ASSESSMENT AND GROUND BEHAVIOR OF TECTONICALLY DISTURBED ROCKS IN NORTHERN THAILAND. A CASE STUDY OF THE PHAYAO RAILWAY TUNNELS

Prarom S<sup>\*1,6</sup>, Jongpradist P<sup>2</sup>, Thongdetsri T<sup>3</sup>, Phienwej N<sup>4</sup>, Dias D<sup>5</sup>, Janrungautai S<sup>6</sup>,  
Amorndechaphon D<sup>7</sup>, Hasap A<sup>8</sup>

**Abstract:** This paper presents a geotechnical analysis of the southern Phayao Tunnels (T3), which are part of the Denchai-Chiang Rai-Chiang Khong Railway Construction Project (Contract 2, Ngao-Chiang Rai section) in the Lampang-Phrae Basin, Thailand. The geological and geotechnical challenges during tunnel construction are highlighted, focusing on analyzing rock mass behavior and events during tunnel excavation. The research has integrated data from three sources, including borehole investigation data, seismic refraction survey data, and actual field observations, to provide a comprehensive overview of the project area's geological conditions for assessing the rock mass's geotechnical properties. In evaluating rock mass properties, the study applied the Rock Mass Rating (RMR) system and Geological Strength Index (GSI), which helped efficiently classify and predict rock mass behavior in the tunnel area. Additionally, the study monitored and analyzed tunnel movements (convergence monitoring) to assess structural stability. Incidents that occurred during construction were analyzed in detail to identify the main causes and contributing factors and present effective and appropriate problem-solving approaches during tunnel excavation operations. The results of this study not only enhance understanding of tunnel construction in complex geological structures but also present recommendations for developing practical guidelines for future tunnel construction projects, especially in the context of challenging geological conditions in Thailand. The knowledge gained from this study can be applied to planning and risk management for large infrastructure projects facing similar geotechnical challenges.

**Keywords:** Tectonically Disturbed Rocks, Complex Geological Structures, Engineering Geological Assessment, Ground Behavior

### 1. INTRODUCTION

Thailand's accelerating infrastructure development has intensified tunnel construction activities to support economic expansion. Excavation through geologically complex and tectonically disturbed formations poses considerable engineering challenges, including complex predicted rock mass characteristics, structural discontinuities, and ground instability concerns. Mae Tang-Mae Ngad water diversion tunnel project, one of the projects that tunneled through a complex geological setting [1], demonstrates the consequences of unpredictable geological complexity, resulting in ground failure, support structure collapse, and project delays with associated cost escalations and safety risks during excavation and support installation phases. The construction project of the Denchai-Chiang Rai-Chiang Khong railway line, the State Railway of Thailand (SRT), covers four twin tunnels. The 2,700-meter-long Phayao Tunnel (T3) is a challenging project due to its complex geological conditions, which require excavation through the contact of unconsolidated sediment and rock geology, as well as through active fault lines as shown in Fig 1.

<sup>1</sup>\*Railway Engineering and Technology, School of Engineering, University of Phayao, E-mail address: [suphawit.pra@gmail.com](mailto:suphawit.pra@gmail.com)

<sup>2</sup> Department of Civil Engineering, Faculty of Engineering, King Mongkut's University of Technology Thonburi

<sup>3</sup> Department of Civil Engineering, School of Engineering, University of Phayao

<sup>4</sup> Department of Civil & Infrastructure Engineering (CIE), Geotechnical and Earth Resources Engineering (GTE), Asian Institute of Technology

<sup>5</sup> Laboratory 3SR, Grenoble Alpes University, Grenoble, France

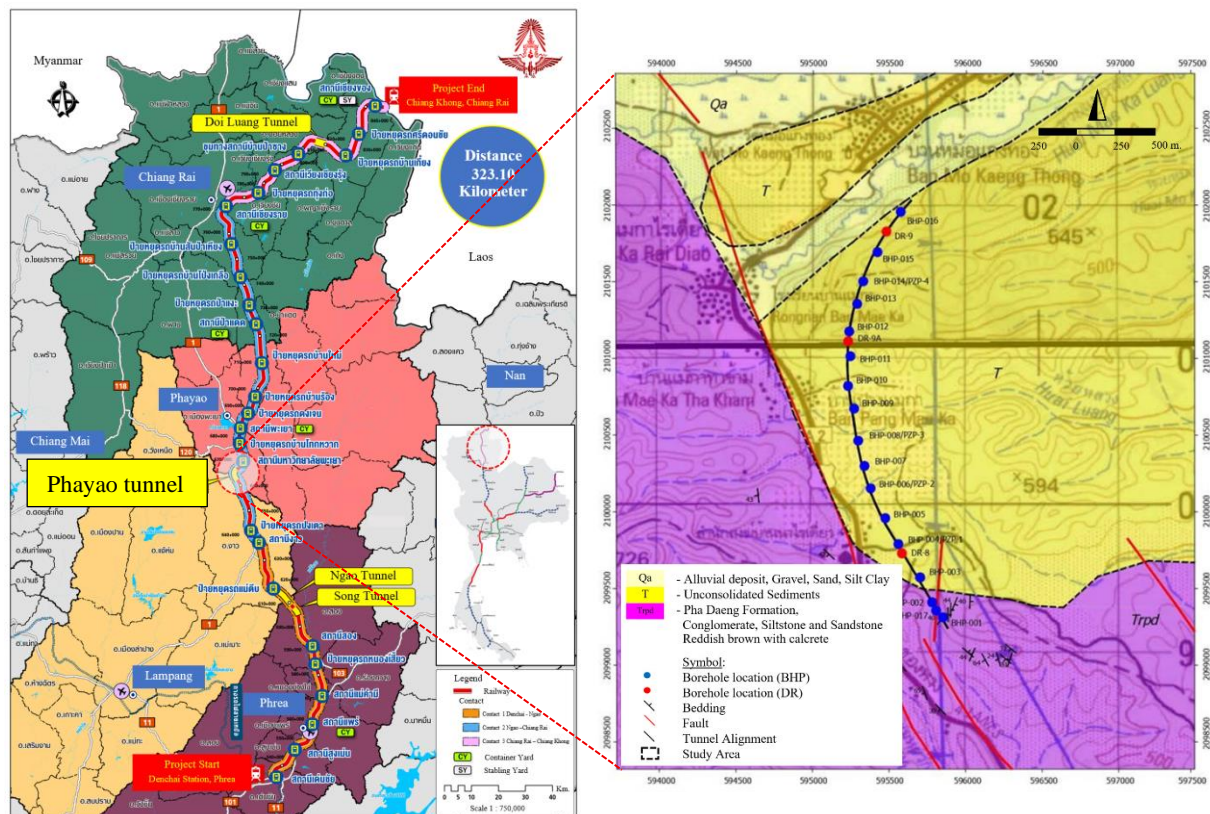
<sup>6</sup> MAA Consultants, Co.Ltd

<sup>7</sup> Automotive and Transportation Technology Center (ATTC), School of Engineering, University of Phayao

<sup>8</sup> Railway Transportation System Testing Centre (RTTC) of TISTR, Thailand Institute of Scientific and Technological Research (TISTR)

The construction of the 500-meter-long southern part of Phayao Tunnel presented complex geotechnical challenges during the excavation that required careful geological data analysis, in-depth understanding of rock mass behavior, and effective management throughout the construction process. These challenges necessitated specialized geotechnical approaches to ensure tunnel access, structural stability, and construction safety while maintaining the project timeline.

The research aims to analyze the geological and geotechnical conditions encountered in the Phayao tunnel, focusing on the direction and impact of rock mass discontinuities, rock mass classification and behavior prediction, tunnel wall convergence analysis and significant incidents during excavation and the impact of geotechnical challenges on construction timelines. The findings from this study provide valuable insights into tunnel engineering in similar geological conditions and contribute to the development of geotechnical knowledge in complex geological environments.



**Figure 1.** Figure 1 Railway route of the Denchai-Chiang Rai-Chiang Khong double railway project (Modified SRT, 2024) and the geological plan of Phayao Tunnel (T3) length is 2,700 meters.

## 2. GEOLOGICAL SETTING

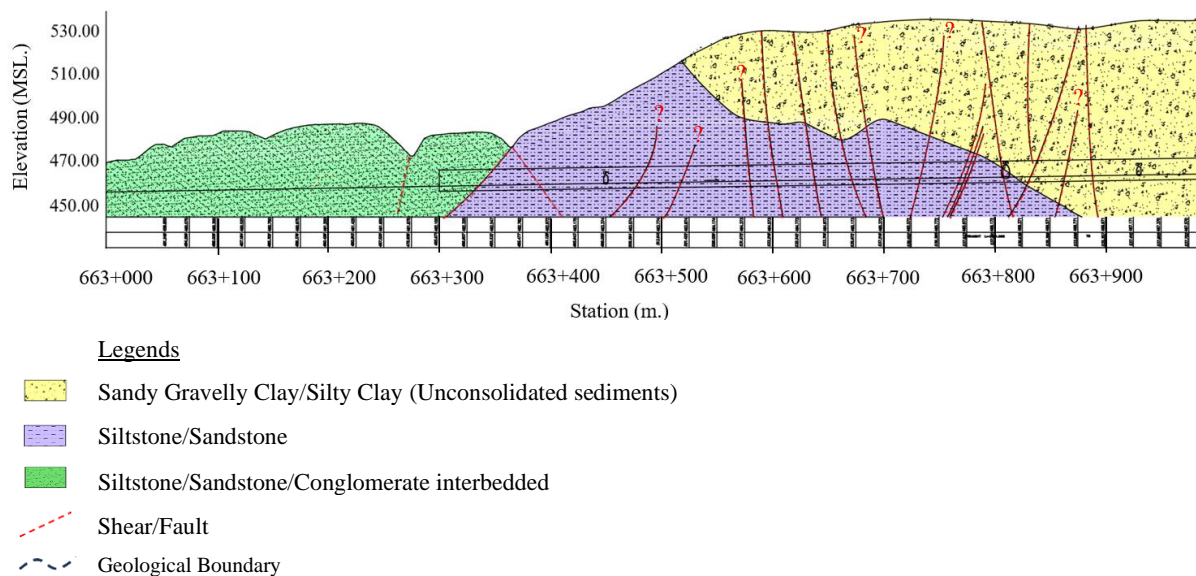
### 2.1. Regional Geology and Local Geology of the Tunnel Alignment

The Lampang Phrae basin is part of a larger structural system in Northern Thailand, characterized by a complex formation of Triassic sedimentary rocks. This basin developed during the Mesozoic era and comprised various siliciclastic sedimentary rocks, including sandstones, mudstones, claystones, and some limestone units. The rock layers are deposited in two interconnected sub-basins: the Lampang sub-basin (located westward) and the Phrae sub-basin. (located eastward) [2] The geological formations in the study area are characterized by Triassic age sedimentary rocks, primarily composed of the Pha Daeng formation within the Lampang group. [3] These sedimentary rocks exhibit a complex lithological composition, featuring interbedded siltstone, sandstone, and conglomerate layers with distinctive brown to reddish-brown coloration. From thin to thick bedding, the rock mass strength is classified as medium to strong rocks according to the International Society for Rock Mechanics [4] standards, representing fresh to slightly weathered [3] geological conditions that present unique challenges for engineering and tunneling projects.

The tunnels are situated within the Pha Daeng Formation and Permo-Triassic volcanic rocks of the Lampang Phrae Basin, part of the Sukhothai Arc. The current geological structure results from tectonic disturbances related to plate movements, including subduction, collision, and fracturing during the Mid-Paleozoic to Late Mesozoic periods.[5] The geological map, as shown in Fig. 1, reveals a complex terrain with the purple-shaded area representing the Pha Daeng formation (Trpd) of the Lampang Group. This section is characterized by significant geological heterogeneity. The blue dots show multiple boreholes strategically positioned along the tunnel alignment. The longitudinal section (Fig. 2) indicates the presence of notable structural features, including faults (red lines) that intersect the tunnel route, suggesting potential geotechnical challenges. The purple geological zone, representing the Pha Daeng formation, appears to dominate the southern portal of the study area. The presence of multiple geological boundaries and the apparent structural complexity underscore the need for detailed geotechnical investigation and adaptive engineering strategies when tunneling through this geologically dynamic zone. The excavation distance of the tunnels on the south portal is approximately 500 meters of rock for each track (totaling nearly 1 kilometer of cumulative excavation).

As shown in Fig. 2, the actual geology during the tunneling, as measured by the tunnel face mapping, seismic refraction survey and borehole investigation data, revealed a complex subsurface structure with different geological units (sedimentary rocks, siltstone interbedded with sandstone) intersected by numerous faults (red lines), that were not observed prior to construction. This inconsistency highlights a significant geotechnical risk in tunnelling projects, where preliminary investigations cannot critical structural features like fault zones and discontinuity that can substantially impact construction methods, assessments, groundwater management, and ultimately project cost and schedule, emphasizing the importance of adaptive design approaches and comprehensive site investigation methods in underground construction.






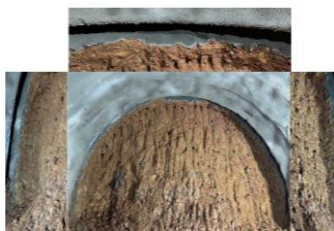
As shown in Table 1, the geological documentation reveals a progressive transformation of sedimentary rock formations encountered during excavating the two double-track tunnels, characterized by siltstone and interbedded sandstone with brown to reddish-brown coloration. In contrast to the regional geology previously prescribed, rock mass along the tunnelling route exhibits complex geological characteristics, with intact rock strength ranging from 0 to 25 MPa, (weak rock) with moderate to low structural integrity. Progressive sections demonstrate increasing tectonic disturbance, transitioning from slightly weathered, medium-thickness beds to highly sheared rock masses with significant structural deformation. The geological profiles show progressively more complex structural conditions, including laminated sandstone, clay-filled joint planes, and nearly chaotic rock layers with broken and deformed sedimentary structures. These observations underscore the critical importance of detailed geotechnical investigation and adaptive engineering strategies when navigating through tectonically complex geological environments, where rock mass characteristics can change dramatically over relatively short distances.



**Figure 2.** The picture shows the rock accumulation along the tunnel excavation of Phayao tunnel (T3) (The actual geology after the tunneling is completed)



Table 1 Shows geological information that appear on the face along the Phayao tunnel excavation route.

STA 663+329.916	STA 663+600.116	STA 663+725.116
		
Siltstone brown to reddish brown, slightly to moderately weathered, medium to thick bed. The strength form field estimation is 25-50 MPa.	Siltstone interacted with laminated sandstone, brown to reddish brown, moderately to highly weathered, medium to thick bed. Highly sheared rock mass of low strength, the strength form field estimation is 5-25 MPa.	Siltstone interacted with laminated sandstone, brown to reddish brown, highly weathered, thin bed. Highly sheared rock mass of low strength is present filled with clay along the joint and bedding planes. Tectonically disturbed sheared siltstone with broken deformed sandstone layers. almost a chaotic structure
STA 663+775.278	STA 663+818.278	STA 663+826.116
		
Slightly disturbed of siltstone, with occasional thin sandstone and breccia bed, slightly weathering and soft to medium hard. The strength form field estimation is 1-5 MPa.	Silty clay, pale brown, silt and clay size particles, low cohesion.  Sandy gravelly clay, pale brow to yellow, angular to subrounded gravel, pebble to boulder size sandstone, silt, and clay matrix with high cohesion.	Gravelly clayey sand, yellowish brown, medium to fine sand, gravel sized grain, angular to rounded particles, silt and clay matrix with moderate to low cohesion.

### 3. TUNNEL CONSTRUCTION

#### 3.1. Cycle Time

The south tunnel excavation, which started in mid-May 2023, there were many problems caused by challenging geological conditions during the tunnel excavation, such as poor to very poor rock materials, roof collapses (occurred 7 times), mostly occurring when drilling through the fault zone and accumulating groundwater, resulting in deviations from the plan. Each roof collapse repair initially took about 1-2 weeks, then as experience increased. The total excavation time of the south portal of both tracks (Up and Down track) in the rock unit was 24 months, and the average daily progress rate was approximately 0.82 meters per day. Tunneling methods refer to the conventional tunnelling method standards by drilling and blasting at the beginning part around 50 meters, which is divided into two levels as Top Heading and Benching, before changing to a mechanical excavator (excavator with hydraulic breaker) when the geological conditions are not suitable. Tunneling with a mechanical excavator is divided into 3 levels: Top Heading, Benching, and Invert.

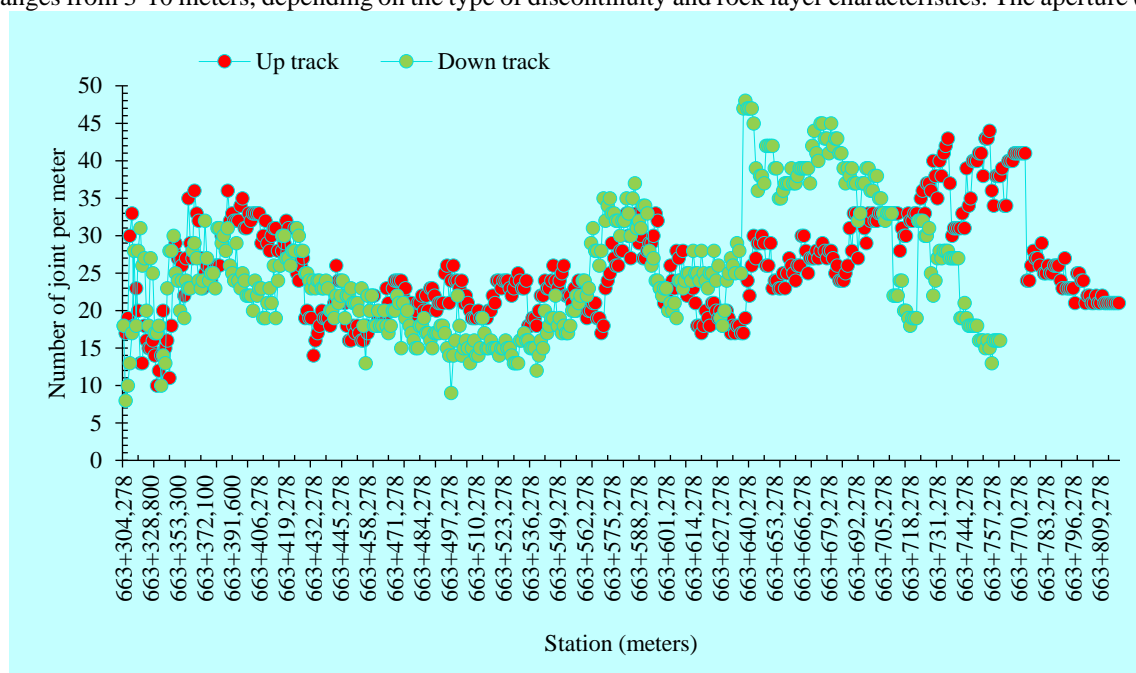
## 4. GEOTECHNICAL ANALYSIS

### 4.1. Rock mass Classification and Ground Behavior type

The Rock Mass Rating (RMR) system is adopted to classify the rock masses in this project. The main rock is siltstone interbedded with sandstone, a sedimentary rock prone to cracking and mechanical changes when exposed to water. The data show that most rocks have uniaxial compressive strength (UCS) values in the range of 0 to 25 MPa, which is considered very weak to medium strength rock, which may affect stability during tunneling.

Rock Quality Designation (RQD) and joint frequency data showed that early in the tunnel, 10-25 joints per meter indicated relatively good rock quality. However, as the excavation progressed (see Fig. 3), the number of joints increased continuously until reaching a peak of more than 47 joints per meter on the down track tunnel, indicating that the rock was fragmented and had a low RQD. This is consistent with the joint frequency curve showing that the joint set increased from the middle to the end of the excavation.

Analysis of discontinuity spacing and groundwater conditions in the tunnel area revealed two main rock units: siltstone interbedded with sandstone, and disturbed siltstone and sandstone. The spacing between discontinuities ranges from 3-10 meters, depending on the type of discontinuity and rock layer characteristics. The aperture (crack



*Figure 3. The number of joints per meter along south tunnel*

width) typically exceeds 5 mm, particularly in faults with a high movement probability. Joint surface roughness is smooth to slickenside, indicating polishing from geological movement. Joint infilling consists of hard and soft materials, with faults specifically containing soft materials that may reduce rock mass strength. Regarding groundwater conditions, most areas exhibit levels ranging from dry to moist, which could affect tunnel stability. Therefore, tunnel structure stability plans should incorporate drainage and reinforcement, especially in areas with faults and highly porous rock masses.

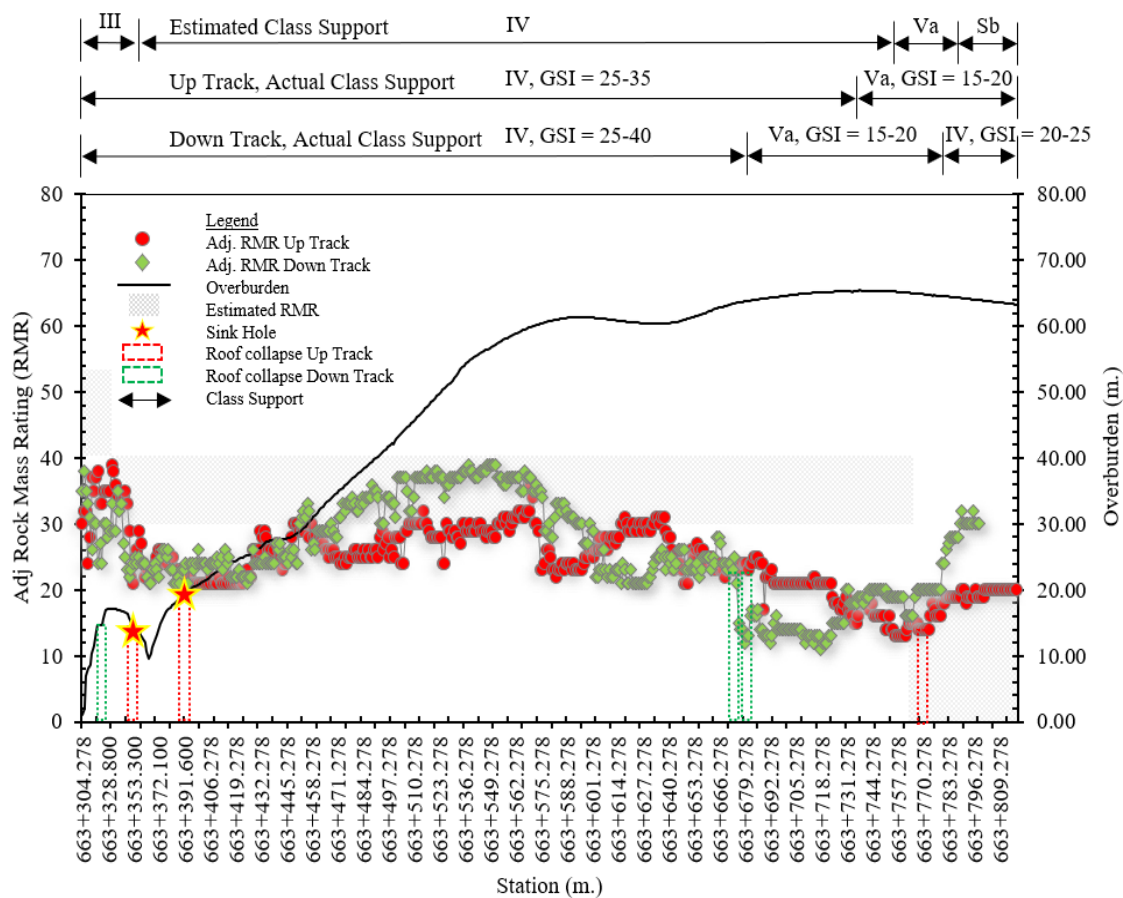
Orientation analysis of discontinuity in Phayao Tunnel found that the discontinuities in the area have dip angle values of 20°-90° with various dip directions. The bedding plane has a dip direction of 60°-100° and 230°-260° depending on the rock type. The joints have a dip angle value of 20°-60° and the faults have a maximum dip angle value of 90°, indicating the geological movement in the past. The various orientations of the fractures may affect the stability of the tunnel, especially in areas where multiple faults and fractures intersect, which can easily cause the collapse of the rock mass.

As shown in Fig. 4, geotechnical data analysis along the entire 500-meter Phayao Tunnel excavated in rock (from south portal) reveals a clear relationship between RMR, GSI values, and geological conditions. The tunnel was excavated through two major rock units characterized by numerous joints, faults, high groundwater infiltration, and highly weathered rock. In these geologically complex areas, RMR and GSI values have significantly decreased. This decrease correlates with seven tunnel roof collapses, particularly at the interfaces between rock units. Rock mass quality fluctuates most dramatically in fault zones, while overburden layer thickness increases progressively along the drilling distance of both up-track and down-track tunnels. This study's

results indicate that changes in geotechnical index values can serve as important indicators for predicting areas at risk of tunnel instability. Areas with extensive faulting and highly weathered rock require special pre-support measures to maintain stability.

The analysis of the evolution of the Rock Mass Rating (RMR) system in the Phayao Tunnel found that the estimated and actual values of the rock mass rating were significantly different, especially in the groups of rock classes III, IV and V. The estimated tunnelling length of class III was 10.31%, but it was not found in the actual excavation. The actual tunnelling length of class V was much higher than the estimation, from 5.15% to 18-21%, indicating that the rock in the area was in a worse condition than expected, resulting in the need for additional support measures. The average actual excavation rate was 0.82 m/day, with several roof collapses, resulting in delays and the need to adjust the stabilization method during tunnel excavation.

Fig. 5 illustrates geotechnical and geological data and a classification of ground behavior types along the tunnel alignment. This analysis demonstrates the relationship between five key parameters: Overburden (thickness of soil above the tunnel), Adjusted RMR (modified rock mass rating index), GSI (geological strength index), groundwater conditions, and fault line occurrences.[6] The area is divided into five distinct categories according to ground behavior, labeled GT1 through GT4, with each type exhibiting unique properties.



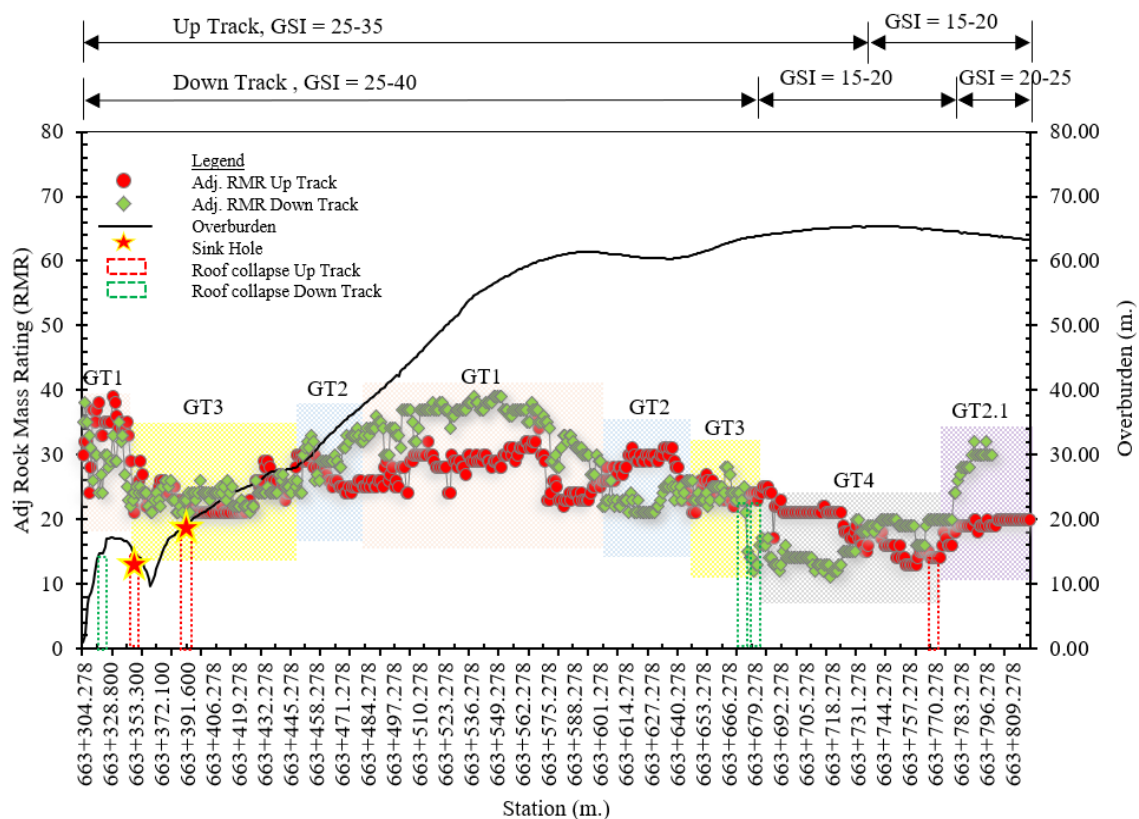
**Figure 4.** Shows the analysis of the evolution of the Rock Mass Rating (RMR) system in the Phayao tunnel.

The analysis reveals complex relationships between rock mass properties and tunnel behavior throughout the excavation distance. The area is classified into five ground types (GT1-GT4 and GT2.1) with distinct characteristics. Zone GT1 has adjusted RMR values of 30-40 and GSI of 35-45, indicating medium-low quality rock mass, yet still prone to Wedge/Chimney/Shearing behavior, especially in the section between stations 663+300 to 663+400 where multiple sink holes were detected. The most concerning zones are GT3 and GT4, with very low RMR values (15-25) and low GSI (20-30), indicating very poor rock quality (Class IV-V), combined with high overburden (60-65 meters) in the section between stations 663+700 to 663+780 where roof collapse incidents occurred. The moist groundwater conditions further increase the collapse risk. Special emphasis should be placed on additional reinforcement planning and support system installation in GT3 and GT4 zones, considering the combined factors of rock mass properties, moisture conditions, and overburden load to prevent future collapse incidents.

## 4.2. Reinforcement Design and Monitoring Analysis

The design of support systems and reinforcement in tunnels is critical for preventing collapse and enhancing structural stability.[7] Support systems help resist pressure from rock mass, groundwater forces, and seismic activities, ensuring tunnel strength and operational safety while reducing ground settlement that could impact the surrounding environment and structures. Based on geotechnical analysis data, excavation methods, support systems, and appropriate reinforcement, as well as predicted rock mass behavior during construction of the Phayao tunnel, excavation methods, support systems, and reinforcement can be modified according to geological conditions encountered during tunneling. Continuous on-site inspection and evaluation by tunnel engineers and geologists is necessary to assess rock mass changes and determine appropriate support measures, especially in cases of poor-quality rock (RMR Class support IV and V) and excavations through fault zones.

Additional measures beyond the specified design to ensure safety during the operation are as follows: From station 663+345.300 (Up track), the length from portal around 40 m. and station 663+323.700 (down track), the length from portal around 22 m, a spray flashcrete with a thickness of approximately 5 cm. is immediately used to cover the full face of the tunnel to ensure safety during the installation of steel ribs and rock bolt of the excavation stage, additional pre-support such as pipe forepoling or pipe roofs to reduce the possibility of tunnel roof collapse. This additional installation continued until the excavation of the southern tunnel was completed, when the excavation through the contact of unconsolidated sediment and rock geology.



**Figure 5.** The classification of ground behavior (Ground Behavior Type) along of Phayao Tunnel.

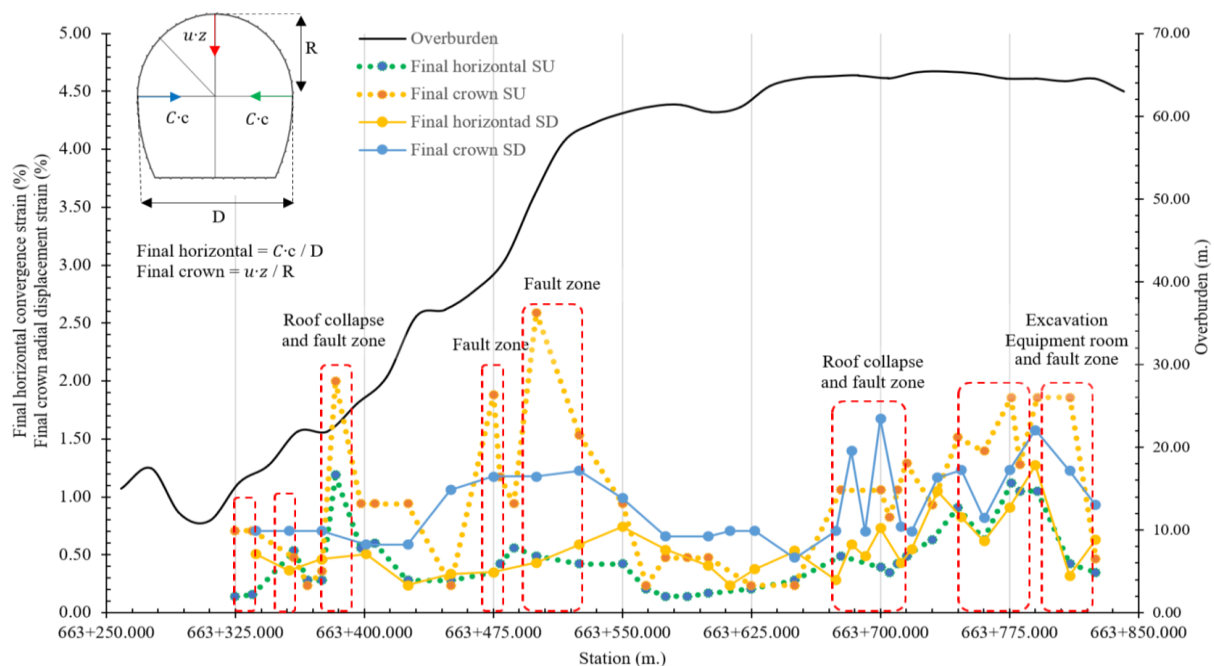
Moreover, from station 663+353.300 (up track) and station 663+375.500 (down track), it was decided to change the excavation method from blasting to mechanized excavation in areas sensitive to vibration. Additionally, from station 663+398.278 (up track) and station 663+391.616 (down track), the excavation cycle length needed to be reduced from 1.5 m. to 1.0 m of class support IV due to the unfavorable geological conditions encountered to enable the installation of the support system quickly and efficiently. This reduction in excavation and change in excavation method continued until the end of the excavation of the south portal tunnel.

As shown in Fig. 6, analysis of tunnel wall deformation in rock from station 663+250 to 663+850 meters, under 15-65 meters of overburden, demonstrates the relationship between horizontal and crown convergence strain at 63 monitoring sections. Critical points with roof collapse and fault zones were identified at seven locations showing abnormally high deformation (1.0-1.5%), particularly at station 663+500, and in the 663+700 to 663+800 region displaying irregular movement near the excavation of equipment room which are directly affected by changes in the contact of unconsolidated sediments and rock geology. The differences between up-track and down-track



tunnel values reflect asymmetric deformation due to rock mass heterogeneity. In contrast, the low deformation values at stations 663+500 to 663+625 indicate improved rock mass quality. The crown-to-horizontal convergence ratio provides insights into joint orientation within the rock mass. This data is very important for tunnel engineers to consider and decide on the appropriate excavation method, with high-convergence-strain areas requiring additional reinforcement to enhance tunnel construction safety.

Analysis of convergence monitoring at STA 663+500 (Monitoring section U8) reveals asymmetric deformation behavior, with maximum crown settlement reaching 110 mm, significantly exceeding the horizontal convergence. This reflects the influence of high vertical stress and the presence of horizontal joints in the rock mass. Time-displacement experienced the greatest settlement of 110 mm within 80 days, with high deformation rates during the first 40 days gradually decreasing until stabilization after 60-70 days. Meanwhile, horizontal displacement demonstrates inward movement toward the tunnel axis from both sides. This behavior corresponds to time-dependent deformation and ground reaction curve theories in low-quality rock mass near the fault zone. Additional reinforcement measures should be considered, such as increasing shotcrete thickness, installing longer rock bolts, or implementing steel ribs in this area to control deformation within acceptable limits and prevent long-term tunnel collapse.



**Figure 6.** Final convergence and crown radial displacement at 63 section monitoring cross-sections in the Phayao tunnel (including Up track and Down track tunnel)

## 5. THE CASE STUDY OF TUNNELLING EXPERIENCE

During the excavation of the southern Phayao Tunnel, along the total distance of both tunnels (up and down tunnel), approximately 1,000 meters, there were seven incidents of tunnel roof collapses. Table 2 lists the collapse patterns and relevant geotechnical and geological parameters. Most tunnel collapse events showed rock mass behavior with a tendency to shear and raveling failure. For example, 1 in 7 incidents at STA 0+770.278 at the up-track tunnel was excavated using the mechanical method. This section encounters extremely challenging geotechnical conditions with severely damaged rock formations and strengths below 1 MPa, having been extensively damaged by tectonic disturbance. The geological profile featured collapse-prone structures with multiple shear zones, faults, and structurally deficient rock formations. The extremely low rock mass rating (RMR) of less than 20 classified the area as very poor rock with critical stability durations of only 24-54 minutes before collapse. The engineering assessment confirms that these severe instability factors, particularly the tectonically compromised structure and extremely brief standup time, were the direct causes of the roof failures experienced during tunneling operations. After the incident, as shown in Fig. 7, the correction was done by spraying flashcrete to cover the pile of rocks that fell in the tunnel. Install the pre-support of pipe roof in sufficient quantity according to the geological conditions. Then, inject cement water through the pipe roof according to the amount specified and wait for the cement to set according to the specified time. Then remove the fallen material and continue



excavating according to the standard tunneling procedure. The work site has made corrections according to the operating procedures, which took 12 days to fix.

## 6. THE CONCLUSION

This research presents the geotechnical solutions for constructing the 1,000-meter-long south part tunnels of the main tunnels of a Railway Project, excavated through the complex geology of the Lampang-Phrae Basin. The study found that the tunnel faced three main challenges: (1) excavation through the siltstone interbedded with sandstone layer with low strength (UCS 0-25 MPa) and five to six main fracture systems, (2) the variable overburden of the tunnel roof and (3) the presence of faults and groundwater infiltration caused the RMR value to be less than 20, which is considered a very poor rock. The research method used the integration of geological data (Detailed Geological Mapping) together with the analysis of geotechnical indexes, including adjusted RMR and GSI along the tunnel. The analysis results revealed the most problematic of the four main rock mass behaviors (GT1-GT4 and GT2.1), especially in the GT3 and 4 zones. Despite experiencing seven roof collapses that caused construction delays, the systematic approach of thorough geological understanding, timely installation of additional reinforcement and pre-support systems, continuous monitoring of tunnel wall movements, and accurate prediction of rock mass behavior significantly improved construction safety and reduced the frequency of tunnel roof failures.

Finally, excavating the south portal tunnel into the rock took approximately 24 months, encountering much more challenging conditions than anticipated. The adaptive engineering approaches will be beneficial for future tunnel construction in similar tectonically complex geological environments.

*Table 2 Summary of the tunnel roof collapse incident of the southern Phayao Tunnel.*

Formation	STA.	Geological Unit	RMR	GSI	Overburden (m.)	Fault lines	Ground water	Ground Behavior
Pha Daeng	663+323.700	Siltstone /Sandstone	24	29	16.80	yes	Damp	Chimney
	663+345.300	Siltstone /Sandstone	33	38	16.30	yes	Damp	Chimney
	663+347.660	Siltstone /Sandstone	29	34	15.74	yes	Damp	Chimney
	663+395.700	Siltstone /Sandstone	15	20	20.30	yes	Damp	Shear/Ravelling
	663+674.116	Siltstone /Sandstone	14	19	25.84*	yes	Moist	Shear/Ravelling
	663+678.116	Siltstone /Sandstone	12	17	28.51*	yes	Moist	Shear/Ravelling
	663+770.278	Siltstone /Sandstone	14	19	12.37*	yes	Moist	Shear/Ravelling

\* The overburden only considers the rock units and does not focus on the unconsolidation sediments cover.





**Figure 7.** Show the incident roof collapse at STA 0+770.278 (Up track)

- a.) Geological characteristics after the collapse of the tunnel.
- b.) Starting to spray flashcrete to cover the pile of rocks.
- c.) Install the pre-support of pipe roof.
- d.) Inject cement water through the pipe roof.
- e.) Remove the fallen material and continue excavating.
- f.) Install the steel rib and proceed to the normal tunneling process.

## 7. ACKNOWLEDGMENTS

This research has received funding support from the NSRF via the Program Management Unit for Human Resources & Institutional Development, Research and Innovation [grant number B13F670082-11]

The compilation of this research data would like to thank the officials and personnel of the State Railway of Thailand, the CSDCC Consulting Group, the CH. Karnchang-Sino-Thai Engineering & Construction Public Company Limited, CKST Joint Venture, the Den Chai-Chiang Rai-Chiang Khong Railway Construction Project, Contract 2, Ngao-Chiang Rai Section, and Right Tunneling Public Company Limited for supporting the data and facilitating the research to achieve the objectives.

## 8. BIBLIOGRAPHY

- [1] Harnpattanapanich, T., Phienwej, N., Rodploy, J., Monthanopparat, N., Tanomtin, C., & Kongdang, K., 2023. Solving problem of encountering a huge cavern in a TBM drive for water diversion tunnel project in Northern Thailand. *Geomechanics and Tunnelling*, 16(3), 304-311.
- [2] Feng, Q., Chonglakmani, C., Helmcke, D., Ingavat-Helmcke, R., and Liu, B., 2005, Correlation of Triassic stratigraphy between Simao and Lampang-Phrae Basins: implications the tectonopaleogeography of Southeast Asia, *Journal of Asian Earth Science*, v. 24, pp. 777-785
- [3] Chonglakmani, C., Grant-Mackie, J.A., 1993. Biostratigraphy and facies variation of the marine Triassic sequences in Thailand. In: Thanasuthipitak, T. (Ed.), *Proceedings of the International Symposium on Biostratigraphy of Mainland Southeast Asia: Facies and Paleontology 1*. Chiang Mai University, Chiang Mai, pp. 97-123
- [4] ISRM (International Society for Rock Mechanics)., 2007. *The complete ISRM suggested methods for rock characterization, testing and monitoring: 1974-2006*. Commission on Testing Methods, ISRM, Lisbon.

- [5] Hara, Y., 2017. Sandstone provenance and U–Pb ages of detrital zircons from Permian–Triassic forearc sediments within the Sukhothai Arc, northern Thailand: record of volcanic-arc evolution in response to Paleo-Tethys subduction *Journal of Asian Earth Sciences* Volume 146, 15 September 2017, Pages 30-55
- [6] Marinos, V., Prountzopoulos, G., Fortsakis, P., Koumoutsakos, D. and Papouli, D., 2012. Tunnel Information and Analysis System: A geotechnical database for tunnels. *Geotechnical and Geological Engineering*. doi: 10.1007/s10706-012-9570.
- [7] The International Tunnelling and Underground Space Association (ITA)., 2019. Guidelines for the Design and Construction of Tunnels.

## LABORATORY LOADING TEST OF TUNNEL SUPPORT WITH YIELDING ELEMENTS IN ISOTROPIC STRESS FIELD

Yota Togashi<sup>1</sup>, Takumi Umetsu<sup>2</sup>, Kentaro Nakai<sup>3</sup>, Fumitaka Mizuno<sup>4</sup>, Kazuo Sakai<sup>5</sup>

**Abstract:** Yielding elements which have a trilinear stress-strain relationship are often used to prevent support deformation in the mountain tunnel construction for a squeezing rock. Yielding elements are usually placed between shotcrete, and it is expected to have the effect of releasing the radial deformation to the circumferential orientation while maintaining the axial force of the support. Although uniaxial compression tests have been conducted on several types of yielding elements and the evaluation of displacement at actual construction sites where this technology is applied, there are few examples of experimental verification of the mechanical behavior of tunnel support with yielding elements. In this study, tunnel support loading tests on a 1/20 scale were conducted to study the mechanical properties of the tunnel model including yield elements. This experiment can be loaded with nine jacks to the tunnel support model with displacement control. The model was prepared using young aged mortar and ordinary use EPS with a foam ratio of 30 times as yielding elements. Note that rock bolts were not modeled here. The yielding elements were placed on each side wall of the support model, and isotropic compressive loads were gradually applied, assuming a squeezing rock. The results demonstrated that the deformation of the yielding elements to circumferential orientation is dominant as a result of loading. It was also confirmed that the axial force of the tunnel support increases and failure occurs at the point when the yielding elements are almost fully compressed (strain level: 80%). Peak loads leading to failure were almost the same for the cases with and without the yielding elements. The effect of the yielding elements in an isotropic stress field was confirmed in the tunnel support model experiment.

**Keywords:** Tunnel support loading test, yielding element, squeezing rock, mountain tunnel, shotcrete

### 1. INTRODUCTION

Yielding elements which have a trilinear stress-strain relationship are often used to prevent tunnel support deformation in the mountain tunnel construction for a squeezing rock [1]. Yielding elements are usually placed between shotcrete, and it is expected to have the effect of releasing the radial deformation to the circumferential orientation while maintaining the axial force of the support. The original idea was to install hard wooden members between concrete linings in the early 1900s [2]. Various types of yielding elements have been developed. For example, hollow or mortar-filled steel pipes are arranged around the circumference of the support [3, 4], hollow steel pipes are laminated to form a honeycomb structure [5], and rectangular concrete mixed with steel fiber or glass beads [6, 7] have been used. In recent years, lightweight yielding element have also been proposed for ease of installation [8]. However, although uniaxial compression tests have been conducted on yielding elements [7, 8]

<sup>1</sup> Ph.D., Togashi, Yota, PE.Jp in construction., Associate Professor, Graduate School of Science and Engineering, Saitama University, 255 Shimo-Okubo Sakura Saitama, Japan, [togashi@mail.saitama-u.ac.jp](mailto:togashi@mail.saitama-u.ac.jp).

<sup>2</sup> Student, Umetsu Takumi, B. Eng. in Civil Engineering, Graduate School of Science and Engineering Saitama University, 255 Shimo-Okubo Sakura Saitama, Japan, [t.umetsu.228@ms.saitama-u.ac.jp](mailto:t.umetsu.228@ms.saitama-u.ac.jp).

<sup>3</sup> Student, Nakai Kentaro, B. Eng. in Civil Engineering, Graduate School of Science and Engineering Saitama University, 255 Shimo-Okubo Sakura Saitama, Japan, [nakai.k.512@ms.saitama-u.ac.jp](mailto:nakai.k.512@ms.saitama-u.ac.jp).

<sup>4</sup> Research Engineer, Mizuno Fumitaka, M. Sc., Taisei Advanced Center of Technology, Taisei Corporation, 344-1 Nase-cho Totsuka, Yokohama, [mznhmt00@pub.taisei.co.jp](mailto:mznhmt00@pub.taisei.co.jp).

<sup>5</sup> Senior Research Engineer, Sakai Kazuo, Dr. Eng., Taisei Advanced Center of Technology, Taisei Corporation, 344-1 Nase-cho Totsuka, Yokohama, [skikzo01@pub.taisei.co.jp](mailto:skikzo01@pub.taisei.co.jp).



and the evaluation of displacement at actual construction sites where this technology is applied [9], there are few examples of experimental verification of the deformation behavior of tunnel support with yielding elements.

On the other hand, in the Japanese railroad industry, tunnel support loading experiments have been conducted since the early 1990s to elucidate the mechanism of tunnel deformation and to confirm the effectiveness of countermeasures [10]. Since the 2000s, large tunnel lining loading test equipment has been developed, and tests have been widely conducted not only in mountain tunnels [11] but also in shielded tunnels [12]. However, we have yet to find a case in which yielding support experiments have been conducted.

In this study, tunnel support loading tests on a 1/20 scale were conducted to study the mechanical properties of the tunnel support model including yield elements. The model was prepared using young aged mortar, assuming shotcrete, and styrene foam of normal use, assuming yielding element. In following chapter, we show the results of loading under isotropic stress assuming a squeezing ground.

## 2. TUNNEL SUPPORT LOADING TEST

In this study, a tunnel support loading test apparatus was developed as shown in Fig. 1. This device is capable of independently loading a 1/20 sized tunnel support model with nine jacks. Loads can be applied to the tunnel model by applying forced displacement to the rigid loading platen with a screw jack. The depth of the loading plates is 110 mm, and each plate can load the model uniformly in the depth direction. Teflon sheets are placed at the boundary between the loading plate and the support model, and the sheets are also placed at the bottom of the model to follow the large radial displacement due to yielding element deformations. A load cell (Sensor and Control Company Limited. SC301A) is installed directly above the loading platen, and the load can be displayed on a digital monitor (Gravity DFR0009) via a Single Board Computer (Arduino Uno) and amplifier (HX711).

Here, the tunnel model is subjected to a gradually increasing isotropic loading that assumes a squeezing rock. The measurement interval was every 0.05 – 0.1 kN. The loading proceeded by controlling the load so that all load cells had the same value while adjusting 9 screw jacks. Loads were measured with nine load cells, and strain gauges were placed at five locations on the inner edge of the yielding support model (red locations in the figure) to measure the circumferential strain of the tunnel. Displacements of the yielding element model were measured at the radial center during each loading phase. It should be noted that this experiment did not use rock bolts assuming that their effect to be only suspending or sewing support to the ground.

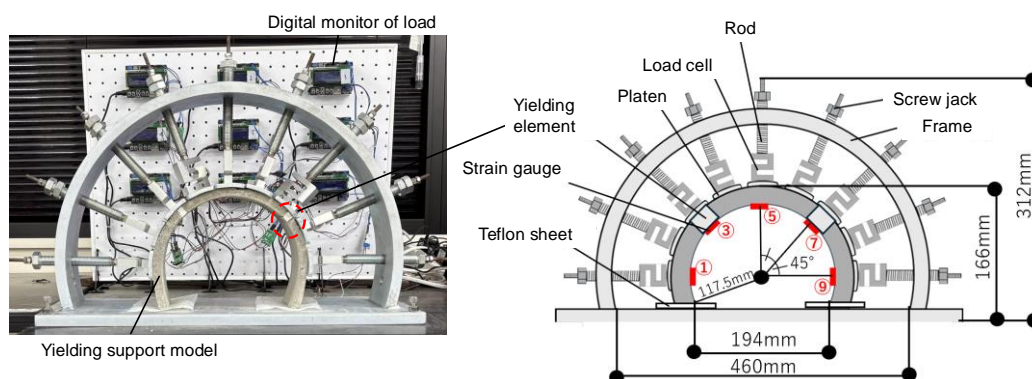


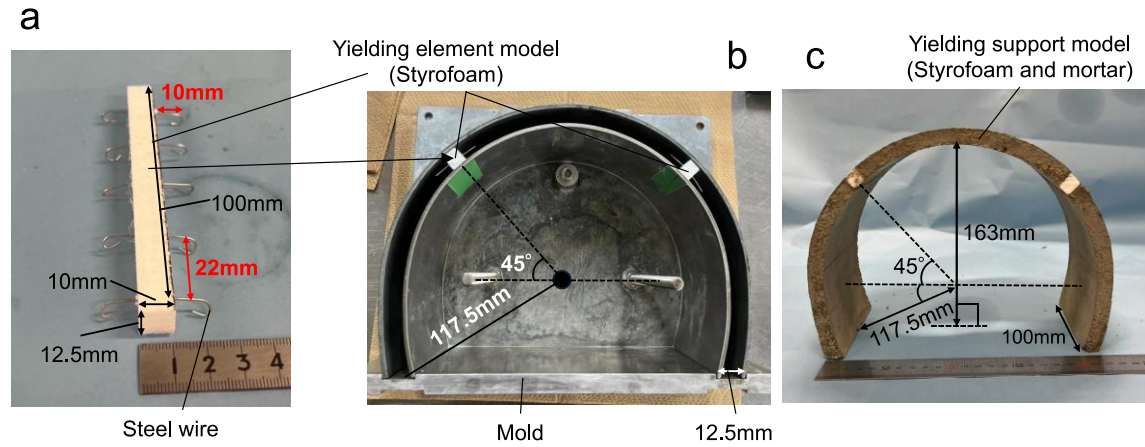
Figure 1. Tunnel support loading test apparatus.

## 3. MATERIAL PROPERTIES FOR YIELDING SUPPORT MODEL

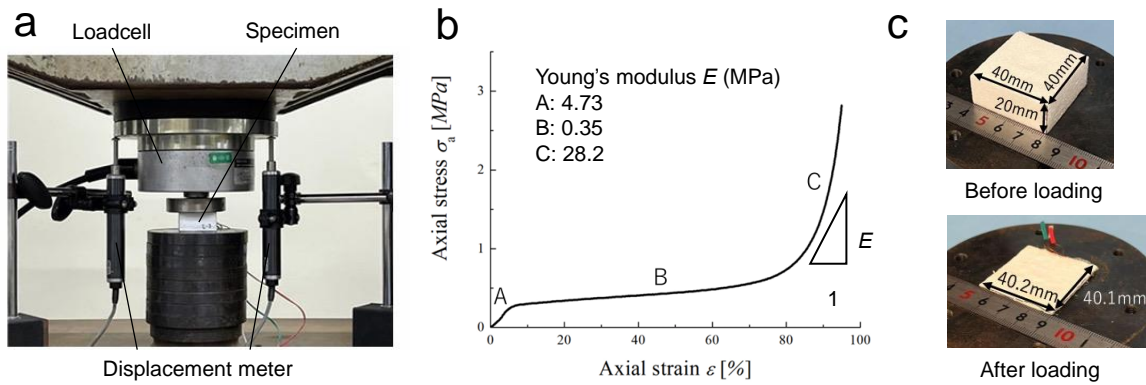
Figure 2 shows the preparation of the yielding support model in this study. The yielding support model is composed of styrofoam for normal use (30 times the foam ratio, density:  $0.0368 \text{ Mg / m}^3$ ) and a young aged (2-day curing) mortar that assumes shotcrete. The styrene foam has been subjected to uniaxial compression tests, as shown in Fig.3 (a). The dimensions of the uniaxial compression specimen are 40 mm wide, 40 mm deep, and 20 mm high. Fig. 3(b) shows the stress-strain relationship. As can be seen, the trilinear stress-strain relationship was confirmed. As shown in Fig. 3(c), there is almost no lateral displacement and almost no Poisson effect. The mortar was made of 40% ordinary Portland cement, 40% silica sand # 4 (dominant grain size: 0.6 mm - 0.85 mm), and 20% deionized water by weight. The mortar was subjected to uniaxial compression and Brazilian tests, and the mechanical properties are shown in Table 1. The authors proposed a method for estimating Mohr-Coulomb failure



criteria by uniaxial compression and Brazilian tests [13], and this method was used to identify the shear resistance angle  $\phi$  and cohesion  $c$  of the mortar. This method has been confirmed to be valid for low stress fields [14].



**Figure 2.** Yielding support model: (a) yielding element model by styrofoam, (b) yield element model setting in the mold, (c) appearance of the model.



**Figure 3.** Uniaxial compression test of yielding element: (a) test setting, (b) stress-strain relationship, (c) specimen size and deformation.

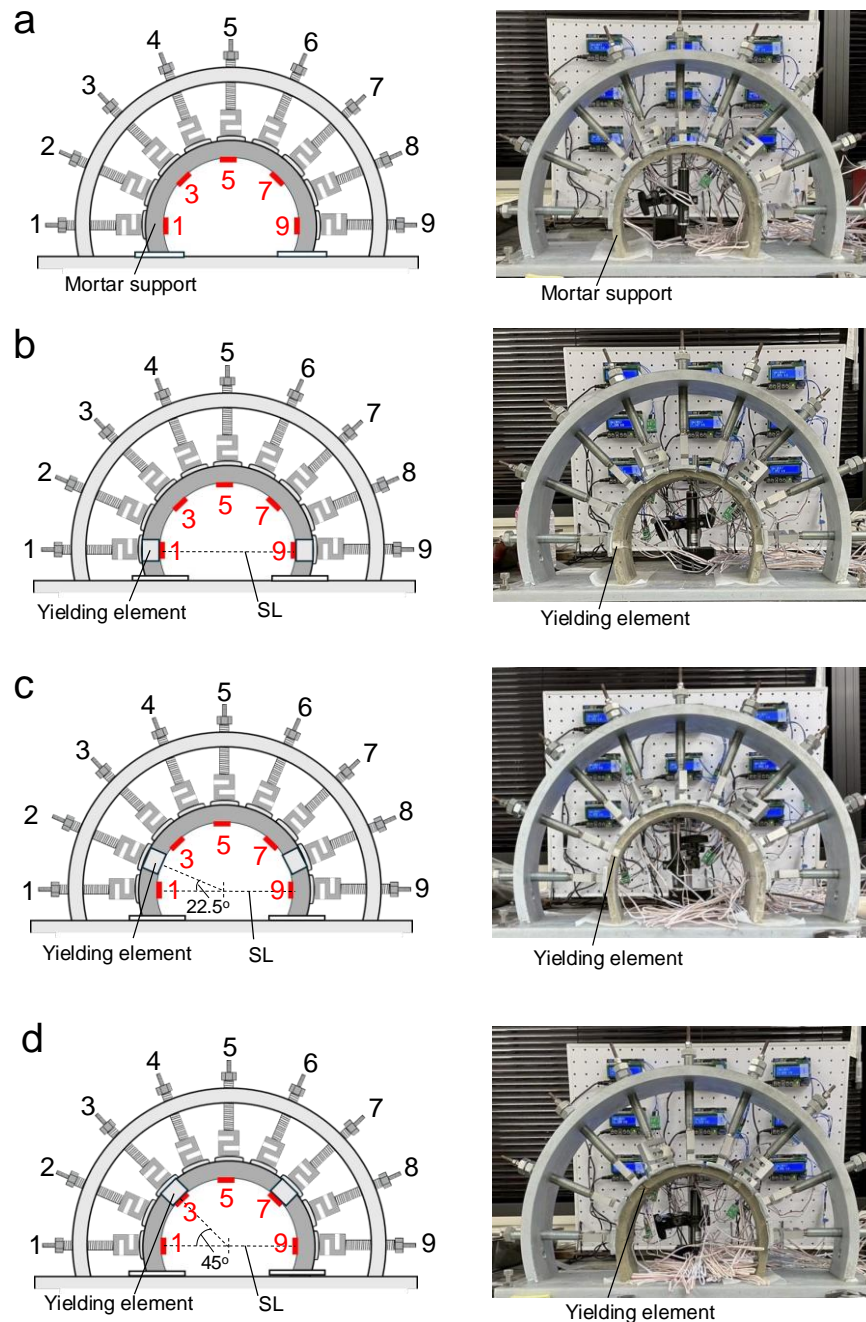
**Table 1.** Mechanical properties of young aged mortar (2-day curing)

Young's Modulus $E$ (MPa)	Uniaxial compressive strength $q_u$ (MPa)	Tensile strength $\sigma_t$ (MPa)	Shear resistance angle $\phi$ ( $^\circ$ )	Cohesion $c$ (MPa)
2333	6.0	0.6	48.8	1.1

Next, the yielding support model is described. As shown in Fig. 2 (a), the yielding element model has a tunnel circumferential length of 10 mm and a radial length of 12.5 mm, the same as the mortar. Steel wires with a hooked end are passed through the yielding element to be fixed after mortar solidification between crown and side wall parts of mortar supports. Two yielding element models are placed symmetrically on the formwork as shown in Fig. 2 (b), and mortar is poured between them. The yielding element was placed on the side of support at 0, 22.5, and 45 degrees inclined from the spring line. After two days of mortar curing, the yielding support model shown in Fig. 2(c) is completed. Note that the inner and outer edges of the mold can be removed separately.

Figure 4 shows test cases studied here. Fig. 4 (a) shows the normal case, a young aged mortar-only specimen. Fig. 4 (b, c, d) shows the experimental cases of yielding support, where yielding elements are placed symmetrically in two tunnel sections at 0°, 22.5°, and 45° from the spring line (SL), respectively, in order to examine the influence of the position of the yielding element. The nine screw jacks are numbered to distinguish loads and radial displacements. Strain gauges were placed at the red points on the inner edges of the tunnel support specimens to measure the circumferential strain. In the case with the red mark on the yielding element, the strain gage was

placed on the mortar at a slightly displaced position. Strain in the yielding element model was calculated from displacements measured at the radial center of the styrofoam.



**Figure 4.** Test cases of tunnel support loading test: (a) normal case (only mortar), (b) case of yielding element on spring line, (c, d) cases with yielding elements at 22.5° and 45° from spring line.

#### 4. TUNNEL SUPPORT LOADING TEST RESULTS

Figure 5 shows the relationship between loading step and isotropic load (loading path) separately for each experimental case. At first, measurements were taken every 0.05 kN or 0.1 kN, and the measurement interval was changed to every 0.2 kN when the loading progressed to a certain degree or when the deformation of the yield element had converged, thus changing the slope of the loading path. The last loading step in this figure represents the load at the end state. Comparing the normal case (a) and the yielding support cases (b,c,d), the ultimate loads are approximately the same or at least 20% smaller in the yielding support case.

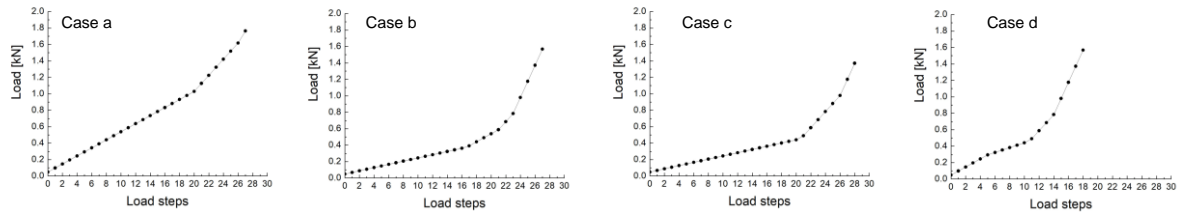


Figure 5. Loading paths for isotropic stress field

Figure 6 (a) shows the relationship between the loading step and the axial displacement of the tunnel crown. In the legend, (A) is the value measured by a contact-type displacement meter, (B) is the value calculated from a screw jack, and (C) is the displacement measured with a ruler for confirmation. Compared to case a without yielding element, the final displacement is about 6.5 times larger in the cases with yielding element. In the yielding support cases (b, c, d), the displacement increases rapidly. As shown later, the deformation of the yielding element increases rapidly at this point (load steps 16 for cases (b, c) and 6 for case (d)). The isotropic load at the point of rapid increase in displacement is about 0.4 kN. Fig. 6 (b) shows the relationship between the displacements of the nine screw jacks and the loading steps. Thus, this figure shows the trend of radial displacement at nine jacking positions. The numbers in the precedents represent the position of the jack in Fig. 4. The displacement is larger in the yielding support case than in the no- countermeasure case (a), and the displacement increases at the points where the yielding support displacement is larger in cases with yielding elements. The characteristic feature here is that the radial displacement above the yielding element is large, and the displacement is smaller toward the bottom end of the tunnel. This is because in Case b, the yielding element is displaced vertically, while in Cases c and d, the yielding element can be displaced horizontally due to these inclined settings. Figure 6(c) shows the relationship between the strain of the yielding element and the loading step. Strain is shown as a positive value in the compression direction. As the displacement of the retractable members increases rapidly as the loading proceeds, the deformation of the tunnel support also increases, as described so far. The isotropic load that causes rapid displacement of the yielding element is about 0.4 kN. Assuming that the same degree of circumferential axial force is applied, the circumferential cross-sectional area of the yielding element is 0.01 m x 0.1 m, which means that normal stress of 0.4 MPa is applied. This corresponds to the stress in the range where Young's modulus is smallest in the stress-strain relationship shown in Fig. 3(b). Since the results are mechanically interpretable, we believe that reasonable experimental results and trends have been obtained.

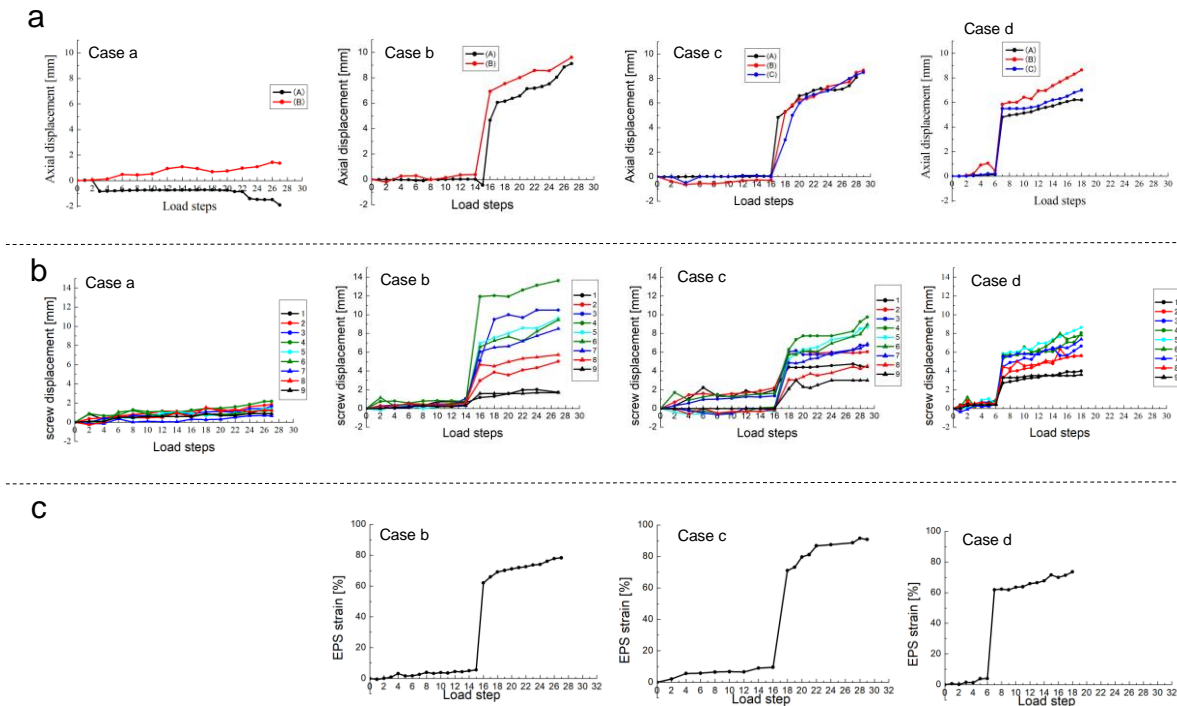
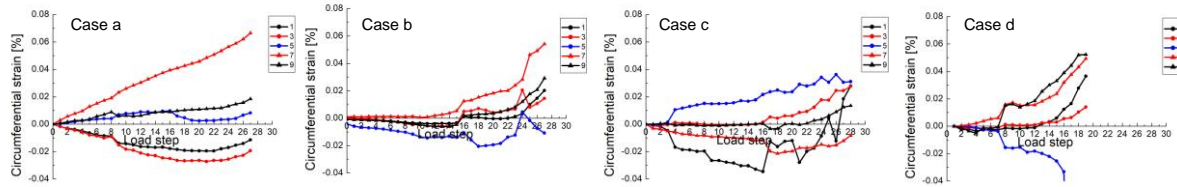


Figure 6. Relationships between load steps, (a) axial, (b) screw jack displacements, and (c) styrene foam strain.



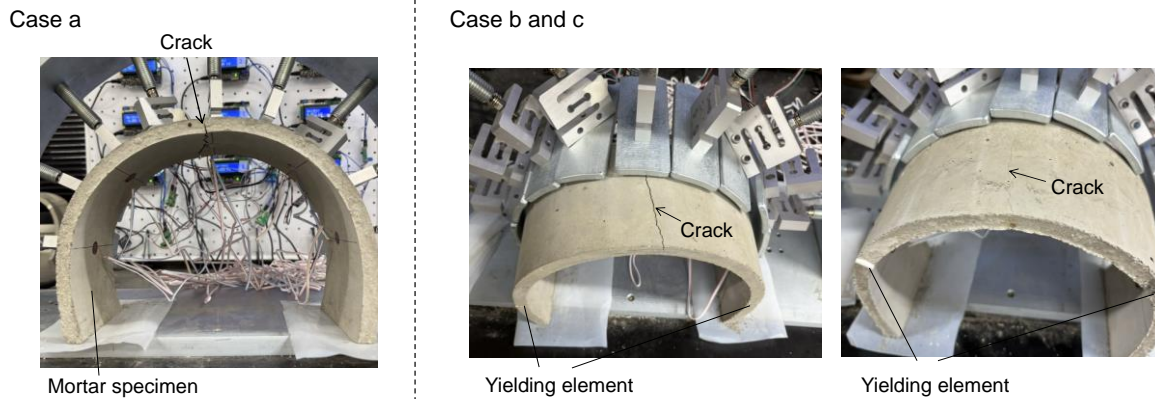
Figure 7 shows the relationship between the loading step and the tunnel circumferential strain measured at several locations on the inner side of the tunnel support. The numbers in the legends correspond to the measurement positions in Fig. 4. These represent strains in the mortar section equivalent to shotcrete, and the differences in the magnitude of the measured values are about the same. Most of the data show values in the compressive direction (positive), which is due to the isotropic loading. On the other hand, there is a large variation, with many data showing strain in the tensile direction (negative). This may be due to the fact that the tunnel shape is not a perfect circle and the inside of the tunnel support is susceptible to bending.



**Figure 7.** Relationships between load steps and circumferential strain

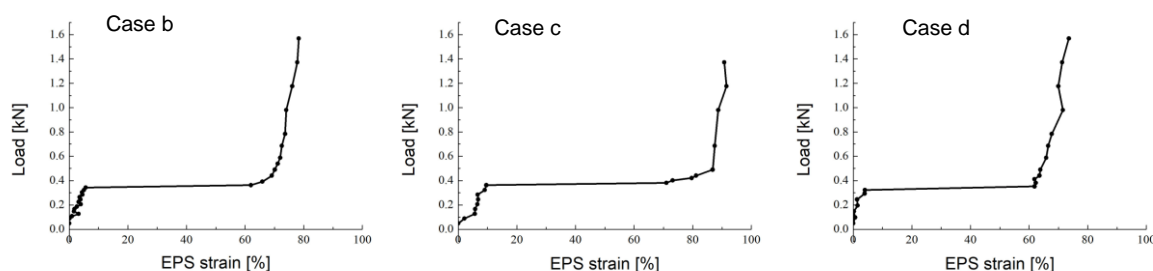
## 5. DISCUSSION

In order to further understand the deformation mechanism of yielding support, we first discuss the properties of the specimen at failure. Figure 8 shows some photographs of the specimens after the loading test. In both the three cases with and without yielding elements, the crown of the tunnel support specimen cracked, leading to failure. Similar failure conditions and ultimate loads were observed in the no-countermeasure and yielding support cases. Therefore, it can be said that the yielding element allows radial displacement in squeezing rock and retains some of the strength of the support even after it is fully compressed. In addition, Fig. 8, together with the radial displacement results in Fig. 6 (b), suggests that this is a flexural-tensile failure, since the deformation at the top of the supported specimen is large in all experimental cases, including normal Case a.



**Figure 8.** Examples of tunnel support specimen after ultimate load condition

To confirm that the yielding element behaves as expected, Fig. 9 shows the relationship between the isotropic load applied to the specimen in the tunnel support loading experiment and the strain in the yielding element model. Thus, a trilinear relationship is obtained in all cases, and the strain levels at which the slope changes in Fig. 3(b) (A, B, and C in Fig. 3(b)) are approximately equal. According to the calculation at the load level where the deformation increases as discussed in Fig. 6, the tunnel circumferential axial force equivalent to the applied isotropic load acts on the yielding element. Since the same deformation behavior of the yielding element is obtained in the three experimental cases of yielding support, the position of the yielding element does not affect the deformation in an isotropic stress field.



*Figure 9. Relationship between isotropic load and yielding element strain in tunnel support loading tests*

## 6. CONCLUSIONS

In this study, tunnel support loading experiments were conducted to experimentally understand the mechanical behavior of tunnel supports including yielding elements. As a result, the following findings were obtained.

- In this study, we employed a tunnel support model with two symmetrically installed yield elements, and conducted experiments with three different positions of the yielding element.
- At strain levels where the displacement of the yielding element increases rapidly, the deformation of the yielding support increases rapidly.
- The yielding support fails after the yielding element has been fully compressed, at a load equivalent to that of a shotcrete equivalent mortar specimen.
- When the yielding element is placed at an angle, the deformation of the yielding element causes horizontal displacement. On the other hand, if the yielding element is placed near vertical, only vertical displacement will occur. The deformation of yielding support depends on the position of the yielding element.
- The mechanical behavior of tunnel supports containing yielding elements was clarified experimentally for the first time in laboratory scale.

## 7. ACKNOWLEDGEMENT

Mr. Oishi K, a fourth-year undergraduate student at the Rock Mechanics Laboratory of Saitama University, assisted in conducting the experiments in this study. We would like to express our gratitude for his cooperation.

## 8. REFERENCES

- [1] Wittke, W. (2014). Rock Mechanics Based on an Anisotropic Jointed Rock Model (AJRM). Wiley, 91-114.
- [2] Kovári, K. (2009). Design methods with yielding support in squeezing and swelling rocks. Proc. World Tunnel Congress 2009, 1-10.
- [3] Schubert, W. (1996). Dealing with squeezing conditions in alpine tunnels. Rock Mech Rock Eng, 29(3), 145-153.
- [4] Sakai, K., Schubert, W. (2019). Study on ductile support system by means of convergence confinement method. Proceedings of ISRM2019 Specialized Conference, YSRM2019 & REIF2019, 1-6.
- [5] Podjadtke, R. (2009). Development and application of stress controllers – system honeycomb – in modern tunnelling. Proceedings of Shotcrete for Underground Support XI, 1-9.
- [6] Thut, A., Steiner, P., Stolz, M. (2006). Tunnelling in Squeezing Rock-Yielding Elements and Face Control. Proc. 8th International Conference on Tunnel Constructions and Underground Structures, 1-7.
- [7] Ohara, N., Kaneko, T., Sakai, K., Tani, T., Ichida, T. (2017). Study of design methodology and applicability of yielding support for tunnelling. Proc. 45<sup>th</sup> Rock mechanics symposium, 103-108. (In Japanese)
- [8] Entfellner, M., Hamdi, P., Wang, X., Wannenmacher, H., Amann, F. (2023). Investigating High-Strength Expanded Polystyrene (HS-EPS) as yielding support elements for tunnelling in squeezing ground conditions. Tunnelling and Underground Space Technology, 140, 105261.
- [9] Entfellner, M., Wannenmacher, H., Schubert, W. (2023). Yielding elements made of high-strength expanded polystyrene (HS-EPS). Proc. Expanding Underground. Knowledge and Passion to Make a Positive Impact on the World, 1864-1871.
- [10] Asakura, T., Kojima, Y., Ando, T., Sato, Y., Matsuura, A. (1994). Fundamental study on static deformation behavior of tunnel lining. Proc. JSCE, 493, 79-88. (In Japanese)



- [11] Yashiro, K., Kojima, Y., Arai, Y., Okano, N., Takemura, J. (2009). A study on numerical simulation method for plain concrete tunnel lining considering softening due to compression failure. *Proc. JSCE*, 65(4), 1024-1038. (In Japanese)
- [12] Tsuno, K., Kinoshita, K., Ushida, T. (2020). Investigation of deformation of shield tunnel based on large-scale model test. *QR of RTRI*, 61(1), 16-21.
- [13] Kotabe, H., Togashi, Y., Osada, M., Hatakeyama, K. (2024). Unsaturated strength of tuff and its water retention drying curve. *J Soc Mater Sci Japan*, 73(3), 212-219.
- [14] Togashi, Y., Kotabe, H., Osada, M., Asamoto, S., Hatakeyama, K. (2025). Strength changes associated with water transport in unsaturated tuff during drying. *Int J Rock Mech Min Sci*, 186, 105984.

## PRELIMINARY NUMERICAL EVALUATION OF RE-USING OIL STORAGE CAVERNS FOR HYDROGEN STORAGE BY USING LINED ROCK CAVERN TECHNOLOGY

Wenjun Luo<sup>1</sup>, Ping Zhang<sup>2</sup>, Charlie Chunlin Li<sup>3</sup>, Yang Zou<sup>4</sup>, Zongze Li<sup>5</sup>

**Abstract:** The growing demand for large-scale geological hydrogen storage has driven the exploration of innovative and cost-effective methods for repurposing existing underground infrastructure. This study aims to assess the feasibility of converting underground oil storage caverns into Lined Rock Caverns (LRCs) for hydrogen storage. Two construction schemes are proposed and analyzed using numerical simulations, with parameters derived from an existing LRC demonstration project. The maximum allowable gas pressure is determined based on the cavern depth and surrounding rock mass properties, and then the structural response under pressurized conditions is evaluated. The results indicate that the proposed design of dividing original cavern into Multi-caverns using concrete pillars demonstrates favorable structural performance, reducing both the tensile stress level and stress concentration on the steel liner. Meanwhile, the proposed Long-cavern design offers higher hydrogen storage capacity and lower construction costs. In both schemes, the tensile stress level on the steel liner remains low, suggesting significant potential for liner optimization in material selection and liner thickness. These findings confirm the technical feasibility of repurposing oil storage caverns for hydrogen storage and present a sustainable and economically viable solution to meet future energy storage demands.

**Keywords:** Lined rock cavern, Oil storage cavern; Hydrogen storage; Numerical simulation

### 1. INTRODUCTION

Against the backdrop of a global transition toward low-carbon energy systems, hydrogen has emerged as a key component of the future clean energy mix due to its high energy density and zero carbon emissions as a secondary energy carrier (Kovač et al., 2021). With the increasing penetration of renewable energy sources, hydrogen is not only regarded as an effective medium for energy storage but also offers a promising solution to seasonal imbalances in energy supply and demand (Evro et al., 2024). Among the various hydrogen storage methods, underground hydrogen storage has attracted growing attention due to its combined advantages in capacity, cost-effectiveness, and safety (Zhang et al., 2024). In particular, Lined Rock Caverns (LRCs)—a type of underground hydrogen storage structure suitable for hard rock geological formations—create a gas-tight environment through the incorporation of a steel liner and concrete liner, demonstrating strong engineering adaptability and excellent sealing performance (Masoudi et al., 2024).

LRCs rely primarily on the surrounding rock mass to withstand internal gas pressure and prevent structural failure, while the primary function of the liner system is to ensure gas-tight sealing. In the Sweden's project 'Hydrogen Breakthrough Ironmaking Technology', this technology has been tested in Luleå with positive feedback (Vattenfall Press Office, 2025). However, the construction of new LRCs is associated with substantial costs (Papadias and Ahluwalia, 2021). Repurposing unused oil storage caverns for hydrogen storage by using LRCs could eliminate the need for new cavern excavation, thereby significantly reducing costs. To explore the potential role of hydrogen derived from non-fossil sources—as well as hydrogen-based fuels such as ammonia and

1. MSc, Wenjun Luo, Mining and Rock Engineering, PhD Candidate, Department of Civil, Environmental and Natural Resources Engineering, LTU, 97187 Lulea, Sweden, [wenjun.luo@ltu.se](mailto:wenjun.luo@ltu.se)

2. PhD, Ping Zhang, Mining and Rock Engineering, Professor, Department of Civil, Environmental and Natural Resources Engineering, LTU, 97187 Lulea, Sweden, [ping.zhang@ltu.se](mailto:ping.zhang@ltu.se)

3. PhD, Charlie Chunlin Li, Mining and Rock Engineering, Professor, Department of Geoscience and Petroleum, NTNU, Postboks 8900, NO-7491, Trondheim, Norway, [charlie.c.li@ntnu.no](mailto:charlie.c.li@ntnu.no)

4. PhD, Yang Zou, Mining and Rock Engineering, Senior Lecturer, Department of Civil, Environmental and Natural Resources Engineering, LTU, 97187 Lulea, Sweden, [yang.zou@ltu.se](mailto:yang.zou@ltu.se)

5. PhD, Zongze Li, Mining and Rock Engineering, Postdoctoral Fellow, Department of Civil, Environmental and Natural Resources Engineering, LTU, 97187 Lulea, Sweden, [zongze.li@associated.ltu.se](mailto:zongze.li@associated.ltu.se)

methanol—across different types of Nordic ports, the project "*Hydrogen, Ammonia, and Methanol in Hydrogen Hubs in the Nordic Region (H2AMN)*" has been proposed. In this context, it is necessary to investigate the feasibility of converting decommissioned oil storage caverns located near ports into LRCs for storing compressed hydrogen gas. Nevertheless, oil storage caverns typically have a much greater length than width, which poses design challenges for LRC retrofitting. Moreover, the shallow depth of these caverns near ports results in relatively weak confinement from the surrounding rock, making it necessary to calculate the allowable maximum gas pressure and investigate their stability.

Lu (1998) conducted three-dimensional numerical modeling and analyses of LRCs, revealing the roles and stability of the surrounding rock, concrete liner, and steel liner. Johansson (2003) analyzed rock mass deformation and steel liner strain, and proposed a design methodology for storing high-pressure gas in LRCs. Glamheden and Curtis (2006) presented in detail the cavern layout, geometry, and excavation process of the LRC demonstration project in Skallen, Sweden. Based on deformation monitoring data collected during excavation, they conducted a preliminary assessment of post-excavation stability. Damasceno (2022) further investigated the response of the LRC at Skallen to high internal pressure and examined the interactions among different LRC components. Masoudi et al. (2024) discussed the unique challenges of using LRC technology for hydrogen storage and pointed out that the experience in storing high-pressure natural gas in lined rock caverns remains at an early stage. Similarly, in the field of compressed air energy storage, Perazzelli and Anagnostou (2016) performed numerical simulations to analyze uplift failure in shallow caverns. Their results demonstrated that the safety against uplift failure largely depends on rock mass strength, overburden depth, horizontal stress, and cavern type (unlined cavern or shaft), highlighting that the assessment of uplift resistance is a critical aspect of cavern stability evaluation. Therefore, when repurposing shallow-buried caverns into LRCs for high-pressure hydrogen storage, further analysis is required to assess the design parameters and determine the maximum allowable gas pressure, especially considering the typically shallow depth and extended length of such caverns.

Based on the construction experience of LRC demo project at Skallen, Sweden, this study conducts numerical simulations to analyze the behavior of LRCs retrofitted from shallow-buried caverns, using reference parameters such as the surrounding rock properties, cavern geometry, and in-situ stress field from the Skallen project. Two retrofitting schemes are proposed. The first is the Multi-caverns scheme (Scheme I), in which the original unlined cavern is divided into several compartments using concrete pillars, and an LRC is constructed within each compartment. The second is the Long-cavern scheme (Scheme II), in which a single long LRC is constructed along the entire unlined cavern length. To avoid ambiguity, the term "unlined cavern" in this paper refers to an unlined rock cavern with exposed rock surfaces, while "Multi-caverns" and "Long-cavern" specifically denote LRC with concrete or similar liners. Accordingly, the dimensions of the retrofitted cavern are slightly smaller than those of the original unlined cavern. A theoretical model is first developed for the Long-cavern scheme to evaluate the overburden rock's resistance to uplift. Based on unlined cavern dimensions, unlined cavern depth, and rock mass parameters, the maximum allowable gas pressure is calculated. The analysis focuses on rock mass displacement, stress distribution, plastic zones, and tensile stress in the steel liner. Various cavern depths are considered to enhance understanding of their influence on LRC behavior. For the Multi-caverns scheme, the effect of different cavern spacings on cavern performance is examined. The study primarily investigates the mechanical behavior of the two retrofitting schemes under varying cavern depths and compares their respective storage capacities, providing valuable insights for future engineering applications.

## 2. CALCULATION OF MAXIMUM GAS PRESSURE

The internal gas pressure within a LRC can induce uplift of the overburden, making it necessary to evaluate the resistance provided by the overburden against such uplift. In Scheme I, where multiple caverns are located in close proximity, the zones of influence on the overburden induced by gas pressure from each individual caverns partially overlap. Therefore, the worst effect can be approximated by modeling the gas pressure acting on the overburden in a single long cavern, as in Scheme II. The resisting overburden rock mass is illustrated in Figure 1. The resistance against uplift is provided by both the self-weight of the overburden and the tensile strength of the rock mass (Damasceno et al., 2020). For a long cavern, the maximum allowable internal gas pressure can be calculated using the following equation:

$$P_{max} = \frac{\frac{1}{2} \rho \cdot g \cdot d \cdot [A_1 + A_2 + \sqrt{A_1 \cdot A_2}]}{A_2} + \frac{T_0 \cdot (A_1 - A_2)}{A_2} \quad (1)$$

where  $P_{max}$  is the maximum gas pressure inside the cavern,  $\rho$  is the rock mass density,  $g$  is the gravitational acceleration,  $d$  is the cavern depth,  $A_1$  is the area of the overburden's top surface,  $A_2$  is the area of the overburden's bottom surface, and  $T_0$  is the tensile strength of the rock mass.  $A_1$  can be calculated based on the unlined cavern's length and width, while  $A_2$  can be determined from the unlined cavern length, width, depth, and the friction angle  $\varphi$  of the rock mass. On the right-hand side of the equation, the first term represents the contribution of the weight

of the overlying rock mass, and the second term accounts for the resistance provided by the tensile strength of the rock.

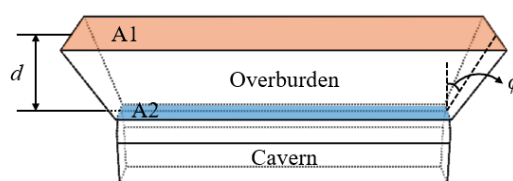


Figure 1. Overburden of a long cavern.

### 3. NUMERICAL SIMULATION

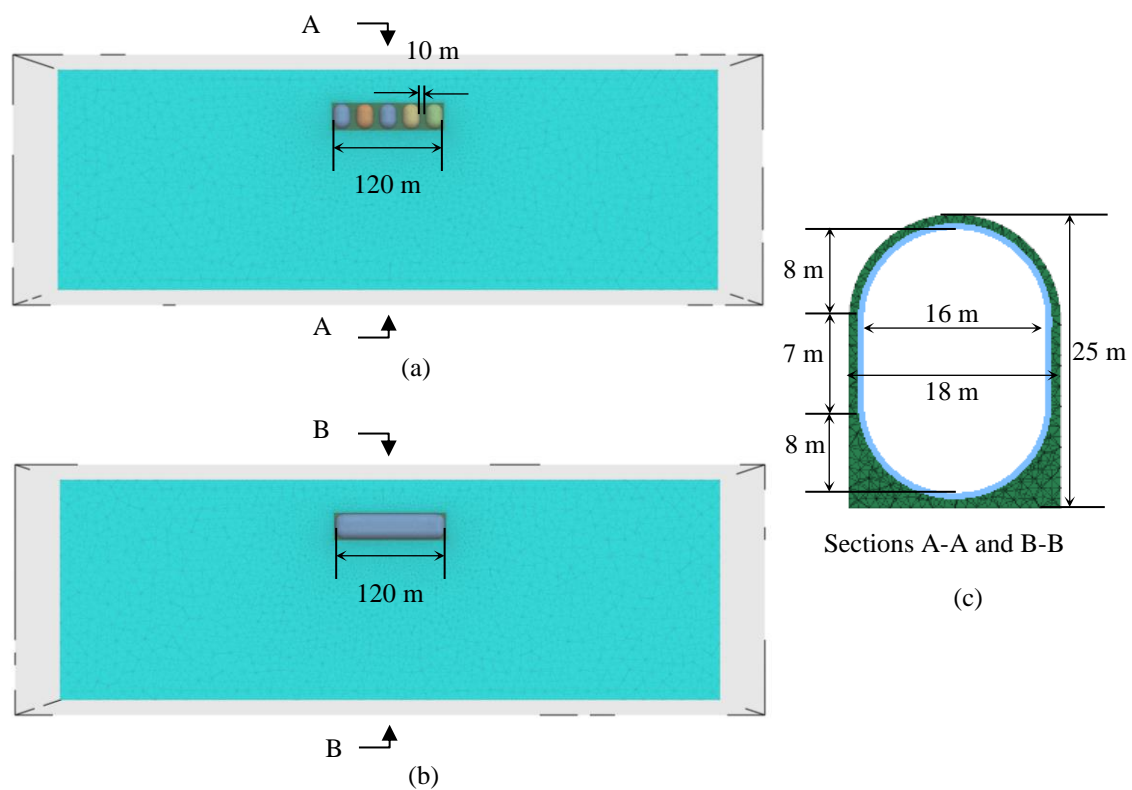
This study utilizes FLAC3D for numerical analysis. Based on the shallow-buried, unlined oil storage caverns investigated in the H2AMN project, two schemes are proposed for establishing a three-dimensional numerical model, drawing from existing LRC designs. In the numerical model, different types of elements are used to simulate various LRC components, including the rock mass, concrete liner, steel liner, and sliding layer. Specifically, solid elements are used to model the surrounding rock and concrete liner, while liner structural elements are used to simulate the steel liner. The sliding layer is treated as the interface between the concrete liner and the steel liner. Two schemes are simulated, considering different unlined cavern depths and varying cavern spacings in Scheme I.

#### 3.1. Model geometry and boundary conditions

According to the Port of Gothenburg and Port of Piteå, the existing oil caverns are unlined and buried at the depth of 20 to 30 m, and they are usually longer than 100 m, around 20 m in width and about 30 m in height. Based on the basic information provided, a conceptual numerical cavern model with slight small dimension was created with the overburden of 30 m. The unlined cavern is 122 m long, 18 m wide and 25 m high, with the cross-section of a semi-circular arch in the top. After installing the concrete and steel liners, the cross-section of the LRC has a semi-circular geometry in both the top and the bottom. The cross-sections of the cavern and the retrofitted LRC are shown in Figure 2c. Due to the difference in shape between the original unlined and the final lined caverns, the concrete liner thickness becomes uneven along the cavern periphery. Based on the LRC design of the Skallen project in Sweden (Damasceno, 2022), the minimum concrete liner thickness in all models is chosen as 1 m, and the steel liner thickness is set as 0,012 m. For the multiple caverns in Scheme I, the top and bottom of each cavern are semi-spherical with a radius of 8 m, and the middle section is a cylindrical shape with a height of 7 m. The concrete between two adjacent caverns is referred to as the pillar, with the reference thickness of 10 m which is also taken as the cavern spacing in this study and is shown in Figure 2a. For the long cavern in Scheme II, no pillars are placed along the cavern length, as illustrated in Figure 2b, resulting in a LRC length of 120 m.

To investigate the sensitivity of the two schemes to the burial depth, both schemes are compared under two additional unlined cavern depths of 20 m and 40 m. Additionally, in Scheme I, to further assess the impact of cavern spacing, analyses are performed for cavern spacings of 5 m and 2,5 m. All of the simulated cases are summarized in Table 1. M-2 and L-2 are the benchmark cases for Scheme I and Scheme II, respectively, with the corresponding numerical models shown in Figures 2a and 2b.

The in-situ stress in the numerical model is applied based on the stress field evaluated by Glamheden and Curtis (2006), as shown in Table 2. The top of the model represents the ground surface with no constraints. Roller boundary conditions are applied to the sides of the model, and fixed constraints are applied to the bottom. The major horizontal principal stress is parallel to the Y-axis of the numerical model, the minor horizontal principal stress is parallel to the X-axis, and the vertical stress is along the Z-axis of the numerical model.



**Figure 2.** Numerical models of lined rock caverns for two benchmark cases in two schemes.

**Table 1.** Numerical simulation cases.

Case	Scheme	Unlined cavern depth (m)	Cavern spacing (m)	Gas pressure (MPa)
M-1	Multi-caverns	20	10	P1
M-2	Multi-caverns	30	10	P1
M-3	Multi-caverns	40	10	P1
L-1	Long-cavern	20	-	P1
L-2	Long-cavern	30	-	P1
L-3	Long-cavern	40	-	P1
M-4	Multi-caverns	30	5	P1
M-5	Multi-caverns	30	2,5	P1

**Table 2.** In-situ stress (Glamheden and Curtis 2006).

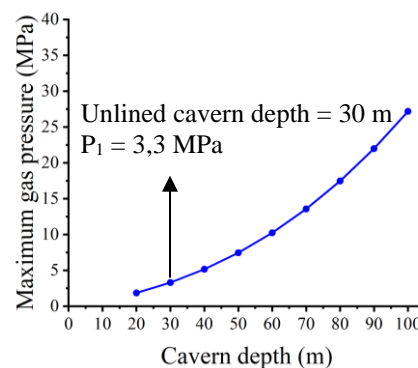
	Value	Unit
Major horizontal stress ( $\sigma_H$ )	0,061z-0,32	MPa
Minor horizontal stress ( $\sigma_h$ )	0,0295z-0,1063	MPa
Vertical stress ( $\sigma_V$ )	0,0265z	MPa

(Note: z means the depth in the numerical model)



**Table 3.** Parameters of rock mass, concrete liner and steel liner (Modified after Glamheden and Curtis (2006); Damjanac et al. (2002)).

	Parameters	Value	Unit
Rock mass	Density	2650	kg/m <sup>3</sup>
	Elastic modulus	36	GPa
	Poisson's ratio	0,25	
	Cohesion	13,4	MPa
	Tensile strength	0,4	MPa
	Friction angle	34	°
	Dilation angle	0	°
Concrete liner	Density	2400	kg/m <sup>3</sup>
	Bulk modulus	16,7	GPa
	Shear modulus	12,5	GPa
	Cohesion	9,6	MPa
	Friction angle	45	°
	Tension strength	2,7	MPa
Steel liner	Elastic modulus	200	GPa
	Poisson's ratio	0,3	
	Density	8000	kg/m <sup>3</sup>



**Figure 3.** Relationship between the maximum gas pressure to avoid uplift of overburden and the depth of cavern.

### 3.2. Constitutive model and parameters

Both the rock mass and concrete use an elasto-plastic constitutive model, while the steel liner is modeled with an elastic constitutive model. The rock mass parameters are set based on the values estimated by Glamheden and Curtis (2006). Since the rock mass may experience tensile failure after the application of gas pressure inside the Lined Rock Cavern, the tensile strength of the rock mass is taken into account. The parameters for concrete and steel liner are referenced from the values provided in the Itasca report (Damjanac et al., 2002). The parameters for the rock mass, concrete, and steel liner are shown in Table 3. Johansson (2003) conducted experimental tests on the bitumen as the sliding layer and monitored the deformation between the steel liner and the concrete in the field. The sliding layer parameters were obtained through calibration, and the shear stiffness is 43 MPa/m and the normal stiffness is 45 GPa/m. The friction coefficient is 0,1.

Based on the input parameters, the maximum gas pressure inside the cavern can be calculated using equation (1). The relationship curve between the cavern depth and maximum gas pressure is shown in Figure 3. As the cavern depth increases, the maximum gas pressure that can be applied inside the lined cavern increases non-linearly. According to the unlined cavern dimensions, depth, rock mass density and friction angle provided above, maximum gas pressure  $P_1$  in Table 1 is calculated to be 3,3 MPa.

The numerical model is first subjected to boundary conditions with in-situ stress and displacement constraints. After the in-situ stress is applied, the cavern is excavated and the model is run into equilibrium. Finally, the concrete liner and steel liner are applied, and the corresponding gas pressure is applied to the inner surface of the steel liner and the model reaches the final equilibrium.

## 4. RESULTS AND ANALYSIS

The lined rock cavern primarily relies on a steel liner to contain the compressed, sealed hydrogen gas. Under internal gas pressure, the steel liner experiences tensile stress. If the tensile stress reaches or exceeds the strength of the steel liner, there is a risk of liner failure, which could result in hydrogen leakage. On the other hand, failure of the rock mass and concrete liner can also cause stress concentration on the steel liner, increasing the risk of failure. Additionally, the rock mass failure zone can reflect the risk of uplift in the overburdens of the cavern. This study mainly uses numerical simulations to compare the tensile stress distribution on the steel liner and the failure zones in the rock mass and concrete liner across different cases. Figure 4 shows the sectional distribution of tensile stress on the steel liner in each case, while Figure 5 shows the sectional view of the failure zones in the rock mass and concrete liner. Importantly, the failure zones in the rock mass during the excavation stage and the operation stage (exclude the failure zones from the excavation stage) are summarized and presented in Table 4 for further analysis of the failure zones. In addition, the failure zones within the concrete liner during the operational stage are separately quantified.

### 4.1. Comparison of two benchmark cases

Cases M-2 and L-2 are selected as benchmark cases, with the maximum internal gas pressure determined based on parameters such as rock mass density, friction angle, tensile strength, unlined cavern depth, and unlined cavern geometry. Under internal gas pressure loading, the steel liner is predominantly subjected to tensile stress, while tensile failure primarily occurs in the concrete liner and the surrounding rock mass.

As shown in Figure 4b, the steel liner in Case M-2 exhibits relatively low stress levels, with a maximum tensile stress of 26,2 MPa. Stress concentration occurs near the mid-height and bottom of each cavern, while the stress concentration at the bottom is less pronounced. In contrast, as depicted in Figure 4e, stress concentrations in Case L-2 are observed at both the top and bottom of the steel liner, with more severe concentration at the top. The maximum tensile stress reaches 33,8 MPa at the top and 32,8 MPa at the bottom.

Figure 5b indicates that in Case M-2, the failure zones are relatively limited and are distributed within both the concrete liner and the surrounding rock mass. The damaged zones of concrete liner are primarily located along the flanks of each cavern in the strike direction, with negligible failure zones of rock mass observed at the cavern crown. In contrast, Figure 5e shows that in Case L-2, the failure zones within the concrete liner are more extensive, predominantly concentrated around the crown, invert, and near the cavern ends. The damage zones at the top and bottom of the rock mass in the cave room is relatively large, and it is worth noting that the rock mass near the ground surface also has a lot of damage zones. Further analysis is required by referring to Table 4, which summarizes the volumes of failure zones generated during both the excavation and operational stages. During excavation, both Case M-2 and Case L-2 exhibit some degree of failure in the rock mass. However, in the operational stage, the volume of failure zones in Case M-2 is significantly smaller than that in Case L-2. Similarly, for the concrete liner, the extent of damage during the operational stage in Case M-2 is also much less compared to Case L-2.

On the other hand, from a design perspective, the total volume of the five caverns in Case M-2 is 17.760 m<sup>3</sup>, with 32.899 m<sup>3</sup> of concrete and a steel liner area of 5.781 m<sup>2</sup>. In contrast, the total volume of the caverns in Case L-2 is 36.110 m<sup>3</sup>, with 14.549 m<sup>3</sup> of concrete and a steel liner area of 7.840 m<sup>2</sup>. Therefore, Case L-2 requires significantly less investment in these key materials than Case M-2, but in terms of the failure zones, Case M-2 offers greater safety.

### 4.2. Effect of cavern depth

A comparative analysis of Cases M-1, M-2, and M-3 is conducted to evaluate the influence of cavern depth on Scheme I, while Cases L-1, L-2, and L-3 are compared to assess the depth effect on Scheme II.

As shown in Figures 4a, 4b, and 4c, the tensile stress on the steel liner in Scheme I is mainly concentrated in the mid-span and invert regions of the cavern, with peak tensile stresses of 26,6 MPa, 26,2 MPa, and 25,9 MPa, respectively. These results indicate that, in Scheme I, variations in burial depth have a limited effect on the distribution and magnitude of tensile stress in the steel liner.

Figures 5a, 5b, and 5c show that the overall extent of the failure zones increases with burial depth. However, the total volume data at different stages in Table 4 for Cases M-1, M-2, and M-3 reveal that, during the excavation stage, the volume of failure zones in the rock mass increases gradually with burial depth. In contrast, during the operational stage, the volumes of failure zones in both the rock mass and concrete liner are relatively small and tend to decrease with increasing burial depth. Therefore, for Scheme I, under a given internal gas pressure and within a certain burial depth range, greater burial depth has an adverse effect on cavern stability during the excavation but benefits the long-term operation of the LRC.

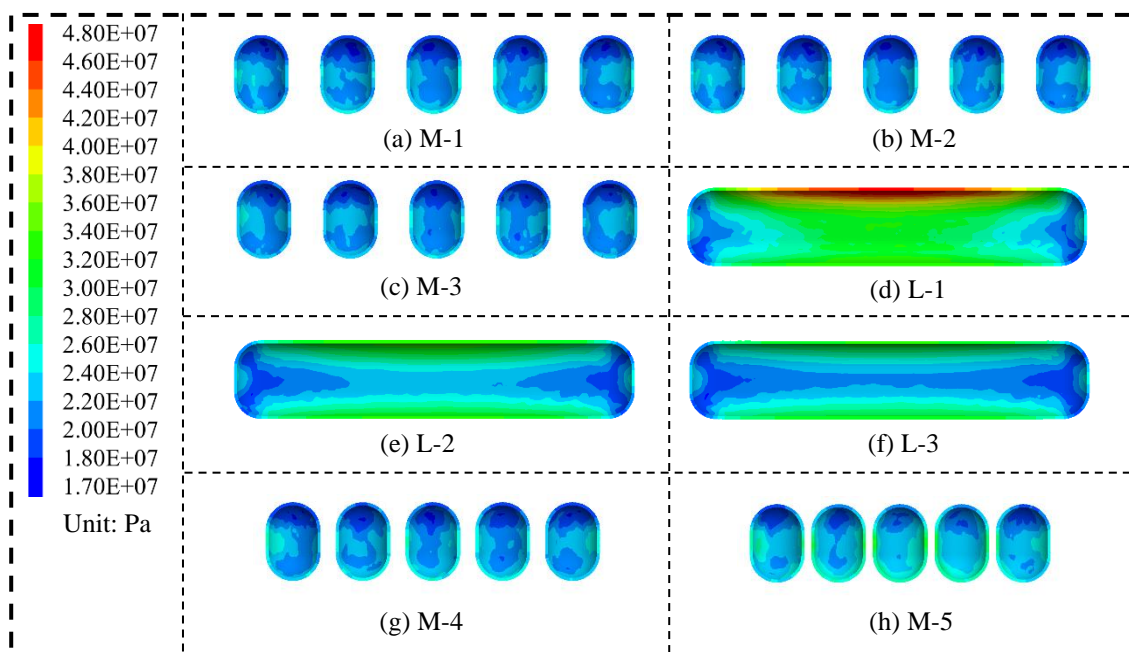


Figure 4. Tensile stress distribution of steel liner in each case.

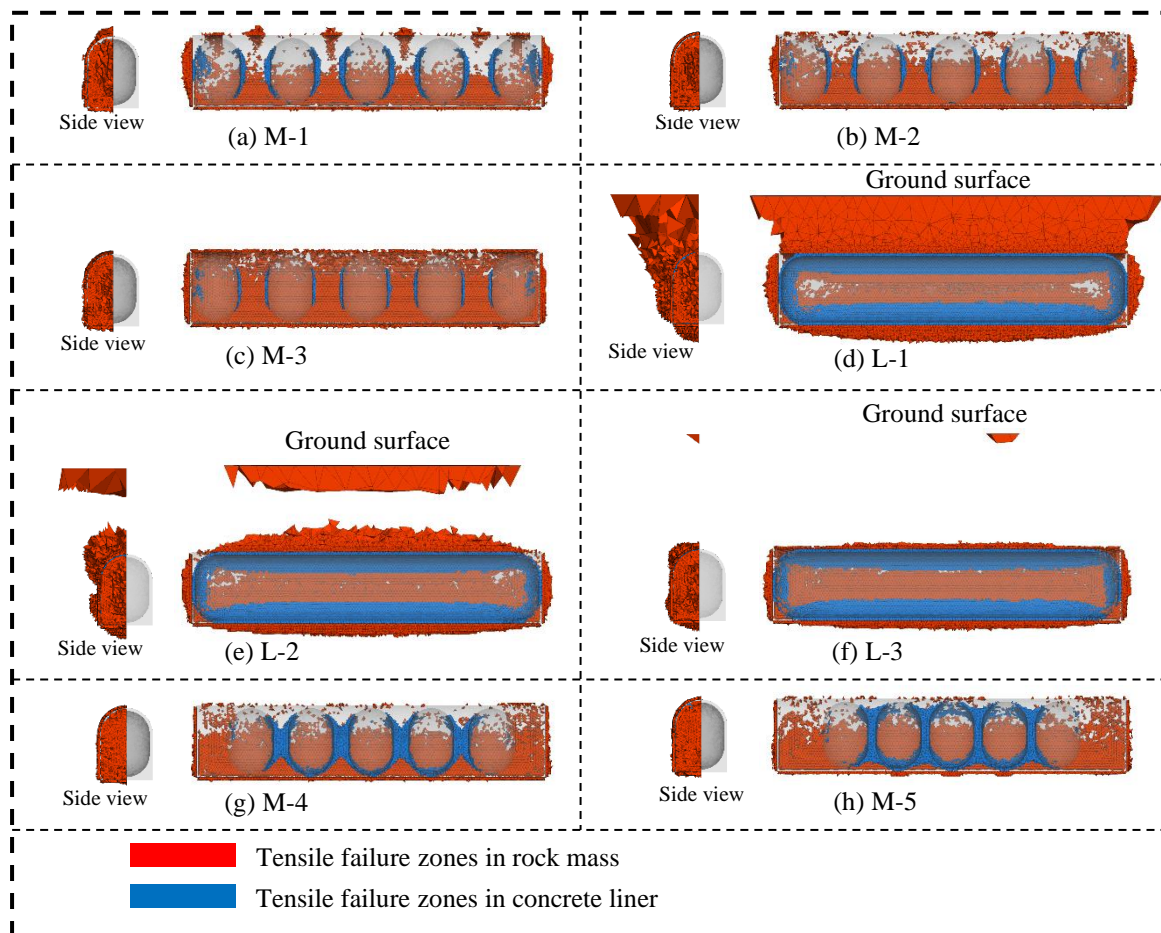


Figure 5. Failure zones in each case.

**Table 4.** Volume of the failure zones in different stages and materials. (Unit: m<sup>3</sup>)

Stage	Case	M-1	M-2	M-3	L-1	L-2	L-3	M-4	M-5
	Material								
Excavation	Rock	3695,0	5427,3	6958,2	3720,9	5398,7	7115,7	5331,3	5411,3
Operation	Rock	1006,9	208,5	82,4	104572,1	35792,9	4890,8	7,5	29,3
	Concrete	596,0	356,7	176,0	5940,1	5449,6	5409,6	1212,2	1777,1

In Figures 4d, 4e, and 4f, the tensile stress in the steel liner for Scheme II is mainly concentrated at the cavern crown and the invert, with peak values of 48,0 MPa, 33,8 MPa, and 32,3 MPa, respectively. Stress concentration at the cavern ends is relatively minor. These results suggest that, although burial depth has a limited influence on the stress distribution within the steel liner, the peak tensile stress in Case L-1 is significantly higher than in Cases L-2 and L-3.

As shown in Figures 5d, 5e, and 5f, the extent of the failure zones near the ground surface decreases significantly with increasing depth, and in Case L-1, the failure zones extends from the cavern crown all the way to the ground surface. This indicates that the internal gas pressure in Case L-1 induces significant tensile failure in the overburden, increasing the uplift of the overburden and thereby elevating the risk of LRC failure. According to Table 4, in Scheme II, the failure zones are predominantly generated during the operational stage and tend to decrease with increasing burial depth. In other aspects, the influence of burial depth under a given internal gas pressure in Scheme II is similar to that observed in Scheme I.

In summary, although the maximum tensile stresses in the steel liner are relatively low across all cases, the relatively high tensile stress observed in Case L-1 of Scheme II—along with the extensive tensile failure in both the rock mass and concrete liner I—raises concerns regarding the long-term stability and integrity of the LRC system. Therefore, Scheme I demonstrates better overall stability under shallow burial conditions. On the other hand, the maximum tensile stress in the steel liner decreases with increasing burial depth, and the extent of failure generated during the operational stage also tends to decrease. These observations suggest that increasing the burial depth contributes positively to the stability of the LRC.

#### 4.3. Effect of cavern spacing in Scheme I

This section focuses on analyzing the influence of cavern spacing on the performance of the steel liner in Scheme I. A comparison is made among Cases M-2 (benchmark case), M-4, and M-5, all with a burial depth of 30 m. As shown in Figures 4a, 4g, and 4h, the tensile stress in the steel liner increases progressively as the cavern spacing decreases, with peak tensile stresses of 26,2 MPa, 27,9 MPa, and 34,2 MPa, respectively. Figures 5a, 5g, and 5h further reveal that the extent of the failure zones between caverns expands with reduced spacing, and in Cases M-4 and M-5, the failure zones merge between adjacent caverns.

These results indicate that, at a burial depth of 30 m, reducing the cavern spacing leads to increases in both the tensile stress within the steel liner and the extent of the failure zones. Although the increase in tensile stress is relatively modest and remains within a low range in comparison with the steel yielding strength, and no significant tensile failure is observed in the overburden, when a reduced cavern spacing is adopted in Scheme I to lower concrete consumption and construction costs, it is essential to ensure sufficient safety margins.

## 5. DISCUSSION AND CONCLUSIONS

Based on the context of repurposing a shallow and large oil storage cavern for hydrogen storage by using LRC system, this study proposes two preliminary construction options: the Multi-caverns and the Long-cavern schemes. Considering the critical design principle of preventing uplift of the overburden in LRC, an equation was developed to estimate the maximum allowable gas pressure at various cavern depths for a long cavern. The performance of the caverns in the two schemes was then compared under different cavern depths, and the influence of cavern spacing in Scheme I was also investigated. The comparative analysis leads to the following conclusions:

1) The modified rigid cone model estimates maximum gas pressure based on rock mass thickness, internal friction angle, and tensile strength. This model has limitations, as it has not been compared with actual overburden failure. Furthermore, the model's applicability to shallow caverns requires further validation.

2) Scheme I, characterized by smaller cavern volumes and higher concrete consumption, demonstrates better control over failure propagation and liner stress, particularly at shallow depths. In contrast, Scheme II, with larger

cavern volumes and reduced concrete usage, introduces a higher risk of extensive tensile failure in the surrounding rock, especially above the cavern crown. Although the stress levels in the steel liner remain low, the widespread rock mass damage in Scheme II may compromise its long-term performance. Furthermore, the cost factors involved in steel liner welding, concrete construction, support, grouting, and maintenance require further consideration.

3) The influence of burial depth on LRC behavior was evaluated through Cases M-1 to M-3 in Scheme I and Cases L-1 to L-3 in Scheme II. In Scheme I, increased depth had little impact on the tensile stress of steel liner but significantly enlarged failure zones during excavation. However, in the operational stage, both rock mass and concrete liner showed reduced damage with greater depth, indicating that deeper placement benefits long-term performance. In Scheme II, the highest tensile stress and most severe failure occurred in the shallowest case (L-1), suggesting increased risk of gas leakage at low depths. Overall, greater depth improves LRC system stability under both schemes.

4) The effect of cavern spacing was studied in Scheme I through Cases M-2, M-4, and M-5, all at a burial depth of 30 m. Results show that reduced spacing leads to moderately increased tensile stresses in the steel liner and enlarged, even connected, failure zones between caverns. Although the tensile stress remains within safe limits and no significant failure occurs in the overburden, the interaction between adjacent caverns becomes more pronounced. Therefore, when using smaller spacing to reduce material usage and costs, adequate structural reinforcement must be ensured to prevent failure at pillar zones and maintain the integrity of the system.

## 6. ACKNOWLEDGEMENTS

The work has been carried out within the project "Hydrogen, ammonia, and methanol in hydrogen hubs in the Nordic region" with the acronym H2AMN to the Council of Ministers, Nordic Energy Research (NER) (project no. 2315912-0611). The authors gratefully acknowledge the funding from this project and the seed project from CH2ESS, Luleå University of Technology, Sweden.

## 7. REFERENCES

- [1] Damasceno D.R. (2022). Modeling aspects of reliability-based design of lined rock caverns. Ph.D. Thesis. Royal Institute of Technology (KTH), Stockholm, Sweden, 85 p.
- [2] Damasceno D.R., Spross J. and Johansson F. (2020). Reliability-based design methodology for lined rock cavern depth using the response surface method. ISRM EUROCK. ISRM, 2020.
- [3] Damjanac B., Carranza-Torres C. and Dexter R. (2002). Technical review of the LRC concept and design methodology - steel liner response. Itasca Consulting Group, Inc.
- [4] Evro S., Oni B.A. and Tomomewo O.S. (2024). Carbon neutrality and hydrogen energy systems. *International Journal of Hydrogen Energy*. 78, 1449–1467. <https://doi.org/10.1016/j.ijhydene.2024.06.407>.
- [5] Glamheden R. and Curtis P. (2006). Excavation of a cavern for high-pressure storage of natural gas. *Tunnelling and Underground Space Technology*. 21, 56–67. <https://doi.org/10.1016/j.tust.2005.06.002>.
- [6] Johansson J. (2003). Cavern wall design principles. Licentiate thesis, Royal Institute of Technology (KTH), Stockholm, Sweden, 139 p.
- [7] Kovač A., Paranos M. and Marciuš D. (2021). Hydrogen in energy transition: A review. *International Journal of Hydrogen Energy*. 46, 10016–10035. <https://doi.org/10.1016/j.ijhydene.2020.11.256>.
- [8] Lu M. (1998). Finite element analysis of a pilot gas storage in rock cavern under high pressure. *Engineering Geology*. 49, 353–361. [https://doi.org/10.1016/S0013-7952\(97\)00067-7](https://doi.org/10.1016/S0013-7952(97)00067-7).
- [9] Masoudi M., Hassanpouryouzband A., Hellevang H. and Haszeldine R.S. (2024). Lined rock caverns: A hydrogen storage solution. *Journal of Energy Storage*. 84, 110927. <https://doi.org/10.1016/j.est.2024.110927>.
- [10] Perazzelli P. and Anagnostou G. (2016). Design issues for compressed air energy storage in sealed underground cavities. *Journal of Rock Mechanics and Geotechnical Engineering*, 8(3), 314–328. <https://doi.org/10.1016/j.jrmge.2015.09.006>.
- [11] Papadias D.D. and Ahluwalia R.K. (2021). Bulk storage of hydrogen. *International Journal of Hydrogen Energy*. 46, 34527–34541. <https://doi.org/10.1016/j.ijhydene.2021.08.028>.
- [12] Vattenfall press office (2025). HYBRIT: Large-scale storage of fossil-free hydrogen gas successfully proven. <https://group.vattenfall.com/press-and-media/pressreleases/2025/hybrit-large-scale-storage-of-fossil-free-hydrogen-gas-successfully-proven>. 27.02.2025.
- [13] Zhang L., Jia C., Bai F., et al. (2024). A comprehensive review of the promising clean energy carrier: Hydrogen production, transportation, storage, and utilization (HPTSU) technologies. *Fuel*. 355, 129455. <https://doi.org/10.1016/j.fuel.2023.129455>.



## SIMULATION OF THE SOIL BASE OF A BUILDING FOUNDATION NEAR A DEEP PIT

Ilizar Mirsayapov<sup>1</sup>, Niyaz Aysin<sup>2</sup>

**Abstract:** The densification of urban development necessitates the construction of buildings with a developed underground volume. In this process, existing building foundations are often located at the edge of deep excavations. The task of assessing the impact of constructing deep foundations on surrounding structures is important and relevant. An analysis has been conducted based on data from foundation settlements near the edges of deep excavations using numerical modeling results and geotechnical monitoring studies by Russian and foreign authors. To evaluate additional settlement of building foundations near deep excavations, research was carried out to study the stress-strain state of the ground near a deep excavation in a laboratory model created in a flat tank with transparent walls. Displacement values were recorded using video recording and electronic sensors, then processed. The experimental results correlate well with those obtained by other researchers. A pattern for distribution of horizontal stresses and displacements beyond the boundaries of the deep excavation model has been established. Based on these findings, a method for calculating foundation settlements near deep excavations considering changes in the stress-strain state of the surrounding soil mass has been proposed. Based on the research results, it has been found that there is an uneven change in the stress-strain state of soils under building foundations along the edges of excavations. Deformation of the soil mass beneath the foundations of buildings located within the collapse prism occurs non-linearly and unevenly. Construction of deep excavations leads to changes in the stress-strain state of the soil mass supporting foundations situated at the edge of the excavation. This causes changes in the ratio between vertical and horizontal stresses, resulting in altered deformation characteristics of the soil and consequently increased settlement.

**Keywords:** Numerical simulation, Geotechnical monitoring, Soil mechanics, Deep pit, Clay soil.

### 1. INTRODUCTION

Urban densification creates a need for constructing buildings with extensive underground volumes. Existing building foundations are frequently located adjacent to the edges of deep excavations. Assessing the influence of deep foundation construction on surrounding developments remains both significant and timely.

The stress-strain condition of soil foundation beneath building foundations close to excavation pits is highly complex. Deformations occur due to influences such as deformation of retaining structures, defects or damage caused during installation of retaining elements, and soil excavation activities (Mirsayapov & Aysin, 2021). Other factors include distance from the building's foundation to the retaining structure, type and rigidity of the foundation itself, overall structural stiffness, and total load exerted by the building onto its subsoil base.

Research by Jiang et al. (Jiang, Lu, Chen, Liu, & Li, 2021) indicates that when excavating a trench 18 meters deep, maximum surface soil settlements occurred at distances of 8 meters and reached 9.5 mm, corresponding to a maximum displacement of the retaining wall by 13.9 mm. Here, the coefficient characterizing maximum subsidence outside the trench  $f_1 = s/H$  equals 0.05%. Studies by Dong et al. (Dong, Burd, & Houlsby, 2018) show that for a 12-meter-deep excavation, maximum settlements measured 7.5 mm at points 10 m away from the edge, while horizontal movements amounted to 5.6 mm with a maximum retaining wall shift of 14 mm, yielding  $f_1 = 0.075\%$ .

Monitoring results presented by Nikiforova N.S. (Nikiforova, 2010) demonstrate that at the “Okhotny Ryad” site in Moscow, maximum settlements approached 13 mm given a depth of 16 meters, accompanied by horizontal

<sup>1</sup> Professor Ilizar Mirsayapov, geotechnical engineer, head of department, Kazan State University of Architecture and Construction, Zelenaya st., Kazan, Russia, [mirsayapov1@mail.ru](mailto:mirsayapov1@mail.ru).

<sup>2</sup> Mr. Niyaz Aysin senior lecturer, Kazan State University of Architecture and Construction, Zelenaya st., Kazan, Russia.

shifts measuring 10 mm, thus leading to  $f_1 = 0.2\%$ . According to Ter-Martirosyan Z.G. et al.'s investigations (Ter-Martirosyan, Ter-Martirosyan, & Vanina, 2022), the greatest foundation settlement next to a rigid-retaining wall reached 44 mm for a 15-meter-deep trench, giving  $f_1 = 0.29\%$ . Meanwhile, research by Zertsalov M.G. et al. (Zertsalov & Kazachenko, 2021) reveals that at depths of 9 meters, maximum soil surface settlements equalled 16 mm just half a meter from the trench's edge, producing  $f_1 = 0.18\%$ . However, generally speaking, the range of  $f_1$  lies between 0.1% and 10.1%, averaging about 1.1% (Mangushev, Ilyichev, Nikiforova, & Sapin, 2016).

According to Nikiforova N.S. et al.'s work (Nikiforova & Vnukov, 2011), simply installing cutoff screens without additional measures proves insufficient to reduce extra settlements below normative levels in Moscow's engineering-geological conditions. Similarly, studies by Ilyichev V.A. et al. (Ilyichev, Mangushev, & Nikiforova, 2012), Nikiforova N.S. et al. (Nikiforova, Konovalov, & Zekhniev, Geotechnical problems in the construction of unique objects, 2010), Shishkin V.Ya. et al. (Shishkin, Pogorelov, & Makeev, 2011) indicate that jet-grouting cutoff screens may not provide adequate protection against excessive settlement of neighboring building foundations in Moscow and St. Petersburg when working in trenches ranging from 10–20 meters deep.

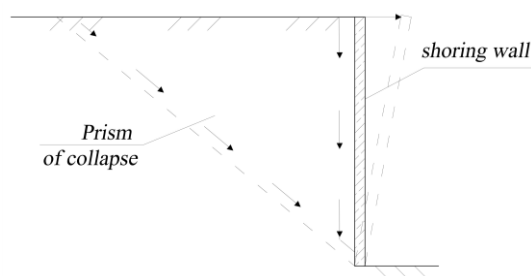
This study focuses on foundation bases adjacent to deep excavations in clayey soils. Specifically, it investigates the stress-strain behavior of clay soils underlying building foundations positioned directly above excavation edges. Its objective is to simulate deformations occurring in such foundation bases to assess additional foundation settlements. Key tasks include:

- Reviewing current literature related to the subject matter,
- Laboratory-scale modeling of stress-strain conditions in clay soils forming part of building foundations situated above excavation rims,
- Processing and analyzing research outcomes,
- Developing a methodology for calculating additional foundation settlements taking into account alterations in the stress-strain condition of soil supporting foundations adjacent to deep excavations.

## 2. MATERIAL AND METHODS

When determining soil deformations (both vertical and horizontal) in the foundations of buildings located at the edge of an excavation, the limit state of the system consisting of "excavation retaining structure - soil foundation - foundation" is studied based on the Coulomb theory. It is based on several assumptions:

1. The system is examined in a state of ultimate equilibrium (Figure 1), i.e., at the moment when the wall begins to move and the failure wedge starts sliding.
2. The failure wedge slides along a straight plane through the soil and the back face of the retaining structure.
3. The failure wedge is assumed to be a perfectly rigid body.
4. In classical Coulomb theory, only fill material is analyzed.



**Figure 1.** Ultimate State According to Coulomb Theory

Field and laboratory experimental studies reveal that soil within the failure wedge undergoes irregular nonlinear deformations, including both horizontal and vertical displacements. Additionally, during deformation processes, vertical and slightly inclined cracks appear. As the failure wedge moves backward away from the excavation, its length increases. Analysis of geotechnical monitoring results for the foundation base of a building near a deep excavation shows uneven distribution of horizontal and vertical soil deformations across the area between the excavation and the building foundation, depending on the rigidity of the retaining structure and the building itself.

Building deformation near the excavation demonstrates that, as the soil base shifts towards the excavation, complex motions occur within the failure wedge – horizontal and vertical displacements, as well as bending within the failure wedge, leading to crack formation. During complicated deformation and crack formation, the failure wedge penetrates further inward toward the building, encompassing a larger portion of the foundation. This

phenomenon is clearly demonstrated by the schematic representation of crack formation in the concrete basement floor of a building located near a deep excavation.

Initially, cracks spread over a distance of 1.5 meters from the wall (from the first foundation). Subsequently, these defects expanded, new cracks appeared, affecting adjoining foundations, indicating ongoing deformation of the building's foundation soil base.

Modeling of the foundation was performed in a flat tank with transparent vertical walls (ACIS 0.7.1 manufactured by NPPC Geotec). The test setup is illustrated in Figure 2.

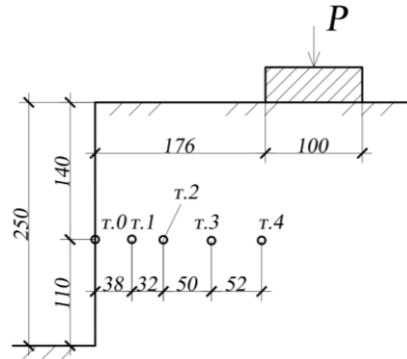


Figure 2. Test Scheme and Location of Points Under Consideration

### 3. RESULTS AND DISCUSSIONS

Experimental and numerical studies of the behavior of soil foundation beneath buildings located at the edge of an excavation demonstrate uneven distribution of horizontal stresses and deformations, as well as vertical deformations (settlements) in the area between the excavation and the building foundation, depending on the rigidity of the retaining structure.

The maximum magnitude of both vertical and horizontal displacements is observed at the retaining structure, and they are approximately equal to each other. Then, as one moves away from the edge of the excavation, both horizontal and vertical displacements decrease.

Figures 4-5 present graphs illustrating the development of vertical displacements (settlements) and horizontal displacements derived from experimental and numerical studies.

Analysis of the obtained results allows us to identify trends in the variation of key parameters describing the stress-strain state of the soil foundation beneath a building located at the edge of an excavation.

Based on the provided charts, we can conclude that horizontal stresses decrease, which subsequently reduces the lateral earth pressure coefficient within the considered soil array. Consequently, within the zone influenced by the excavation, the strength and modulus of soil deformation diminish, while vertical soil deformations increase, ultimately leading to greater overall settlements accounting for shear and vertical deformations.

To determine additional horizontal soil displacements within the active soil pressure prism, proceed as follows. Determine boundary values of horizontal displacements ( $\Delta$ ) at the excavation enclosure (see Figure 3):

$$\Delta = \Delta_1 + \Delta_2 + \Delta_3 \quad (1)$$

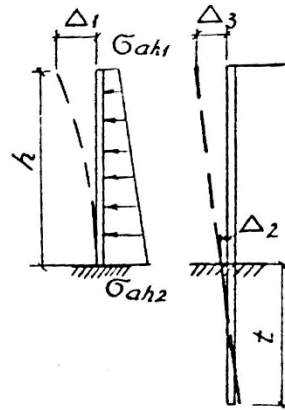
Where:

$\Delta_2$  – wall section displacement at the bottom of the excavation;

$\Delta_3$  – displacement arising from rotation of the wall section at the bottom of the excavation;

$\Delta_1$  – deflection of the wall segment with free length, subjected to trapezoidal loading diagram with top ordinate  $\sigma_{ah1}$  and bottom ordinate  $\sigma_{ah2}$ , at excavation depth  $H$ , with the stiffness of the retaining structure being  $EI$ .

$$\Delta_1 = \frac{H^4}{120EI} (11\sigma_{ah1} + 4\sigma_{ah2}) \quad (2)$$

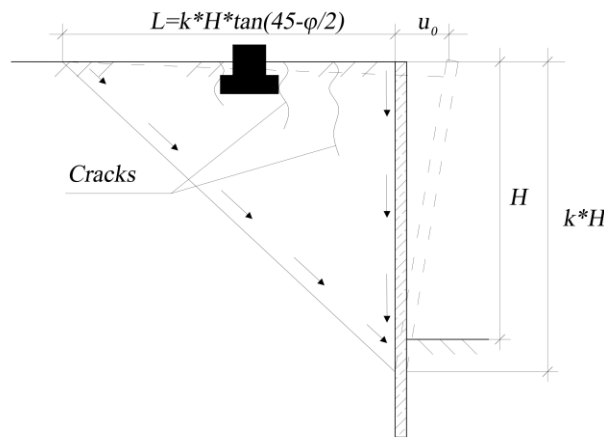


**Figure 3.** Diagram for calculating deformations of cantilever wall.

Based on the graphs presented in Figure 4, additional values of horizontal displacements between the excavation and the foundation are determined.

Using the results of experimental studies, the unevenness of absolute horizontal displacements  $\Delta x_i$  and relative horizontal displacements  $\varepsilon_{xi}$  within the active soil pressure prism  $L$  is assessed (as depicted in Figure 4).

$$L = k \cdot H \cdot \tan\left(45^\circ - \frac{\varphi}{2}\right) \quad (3)$$



**Figure 4.** Scheme for Determining Settlements and Horizontal Displacements of Foundations Near Excavations.

Within the length of the active pressure prism in different zones of compressible strata, the change in horizontal pressure is calculated using the following formula:

$$\Delta\sigma_{xi} = \varepsilon_{xi} \cdot E_0, \quad (4)$$

$$\varepsilon_{xi} = \frac{\Delta x_i}{L}, \quad (5)$$

Then, the total value of horizontal pressure is equal to:

$$\sigma_{xi} = \sigma_{x1} - \Delta\sigma_{xi} \quad (6)$$

$$\xi_{xi} = \frac{\sigma_{xi}}{\sigma_{zi}} = \frac{\sigma_{x1} - \Delta\sigma_{xi}}{\sigma_{zi}}, \quad (7)$$

where  $\sigma_{x1}$  represents the horizontal pressure in the soil after applying the load.

The vertical stress from the self-weight of the clay soil is calculated.

External load  $PP$  acting on the foundation is divided into steps, taking into account time and duration of application. The height of the compressible layer is determined according to SP 22.13330.2016.

$$H_S = Z; \sigma_{zp} = 0,5 \cdot \sigma_{zg} \quad (8)$$

Where:

$H_S$  – thickness of the compressible layer taken at depth  $Z$ .

$\sigma_{zp}$  – vertical normal stress at depth  $Z$  due to additional load on the foundation along the vertical axis of the structure.

$\sigma_{zg}$  – vertical normal stress at depth  $Z$  due to the self-weight of the soil.

The active compression zone is divided into separate layers along the depth of the foundation, taking into account stratifications of the soil.

The natural stress state due to the self-weight of the clay soil is determined. At the level of the foundation sole and midway through each layer below the foundation sole, vertical stresses  $\sigma_{zg}$  and horizontal stresses  $\sigma_{xgi}$ ,  $\sigma_{ygi}$  from the self-weight of the soil are computed. The magnitude of lateral pressure  $\sigma_{xgi}$  and  $\sigma_{ygi}$  constitutes fractions  $\xi_{xg}$  and  $\xi_{yg}$  respectively of the vertical pressure  $\sigma_{zgi}$ . Values of  $\xi_{xg}$  and  $\xi_{yg}$  are accepted as equal to each other and numerically equal to 0.25.

Additional vertical stresses  $\sigma_{zpi}$  are determined using a model of the foundation as a linearly deformable homogeneous isotropic semi-space:  $\sigma_{zpi} = P \cdot \alpha$ , where  $\alpha$  is the stress dissipation factor.

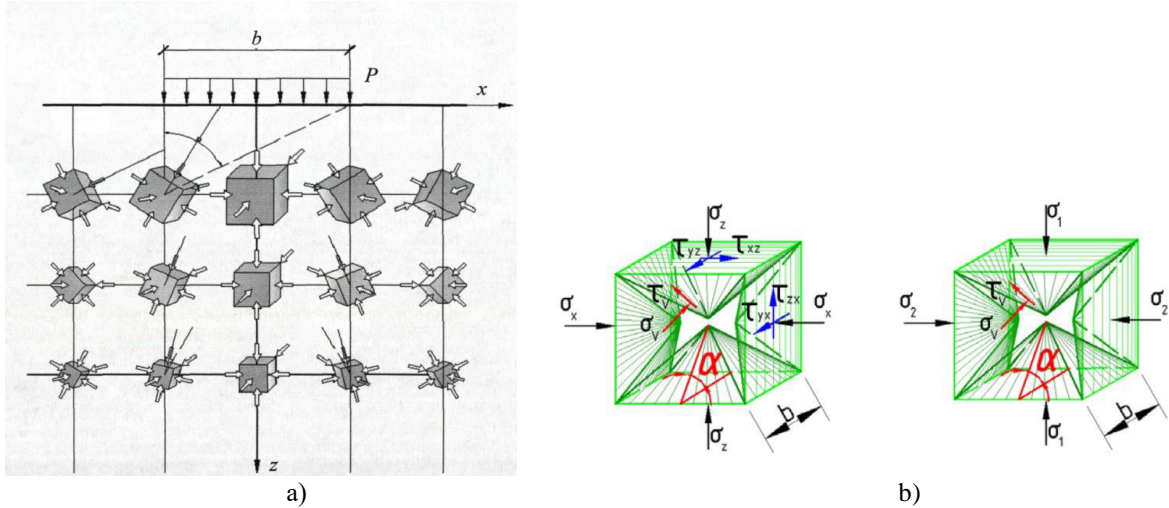
Additional horizontal stresses  $\sigma_{xpi}$  and  $\sigma_{ypi}$  are determined assuming one-dimensional consolidation with a lateral pressure coefficient  $\xi = 0.5$ .

Summated stress values are calculated from the combination of soil self-weight and additional loads on the foundation (Figure 8).

$$\sigma_{zi} = \sigma_{zgi} + \sigma_{zpi} \quad (9)$$

$$\sigma_{xi} = \sigma_{xgi} + \sigma_{xpi} - \Delta\sigma_{xi} \quad (10)$$

$$\sigma_{yi} = \sigma_{ygi} + \sigma_{ypi} - \Delta\sigma_{yi} \quad (11)$$



**Figure 5.** a) Structure of stress-strain state of soil under the foundation footing; b) Structure of stress-strain state in elementary soil volume.

The mean normal stress and stress intensity are calculated as follows:

$$\sigma = \frac{\sigma_{xi} + \sigma_{yi} + \sigma_{zi}}{3} \quad (12)$$

$$\sigma_i = \frac{1}{2} \sqrt{(\sigma_{xi} - \sigma_{yi})^2 + (\sigma_{yi} - \sigma_{zi})^2 + (\sigma_{xi} - \sigma_{zi})^2 + 6(\tau_{xy}^2 + \tau_{yz}^2 + \tau_{zx}^2)} \quad (13)$$

When the axes of principal stresses and strains coincide with the central axis of the foundation, we determine the values of volumetric strain and strain intensity.

$$\varepsilon_v = \varepsilon_1 + \varepsilon_2 + \varepsilon_3 \quad (14)$$

$$\Delta\varepsilon_v(t) = \Delta\varepsilon_1 + \Delta\varepsilon_2 + \Delta\varepsilon_3$$

$$\varepsilon_i = \frac{2}{3}(\varepsilon_3 - \varepsilon_1) \quad (15)$$



$$\Delta\varepsilon_i = \frac{2}{3}(\Delta\varepsilon_3 - \Delta\varepsilon_1)$$

In other cases, we use the condition of coaxiality of tensors of incremental stresses and strains:

$$\Delta\tau = \Delta\sqrt{I_{2\sigma}}$$

$$\frac{\Delta(\varepsilon_x - \varepsilon_y)}{\Delta(\sigma_x - \sigma_y)} = \frac{\Delta(\varepsilon_y - \varepsilon_z)}{\Delta(\sigma_y - \sigma_z)} = \frac{\Delta(\varepsilon_z - \varepsilon_x)}{\Delta(\sigma_z - \sigma_x)} = \frac{\Delta\varepsilon}{\Delta\sigma_i} = \chi$$

Values  $\varepsilon_1, \varepsilon_2, \varepsilon_3$  are adopted based on the results of laboratory tests, which correspond to soil stresses at each point according to the soil profile and creep profile documentation.

Conditional instantaneous moduli are defined:  $K_V$  – bulk modulus, and  $G_V$  – shear modulus, characterizing the transition from the natural state of the foundation to the state after local load application. Instantaneous moduli  $K_V$  and  $G_V$  take into account the transition at the moment of applying additional vertical load.

$$K_V(t) = \frac{\Delta\sigma}{\Delta\varepsilon_V + \Delta\varepsilon_V(t)}, \quad (16)$$

$$G_V(t) = \frac{\Delta\sigma_i}{3(\Delta\varepsilon_i + \Delta\varepsilon_i(t))}. \quad (17)$$

Increment of axial strain in the  $i$ -th layer after horizontal soil displacement within the failure wedge is determined by the formula:

$$\Delta\varepsilon_{zi} = \frac{\Delta\sigma_z(t)}{G_V(t)} - \Delta\sigma \frac{3K_V(t) - G_V(t)}{3K_V(t) \cdot G_V(t)} \quad (18)$$

Settlement of the foundation divided into equal layers up to the conditional depth of the compressible layer at time  $t$  is calculated using the formula:

$$S = \sum_{i=1}^n (\varepsilon_{z0} + \varepsilon_{zpl} + \Delta\varepsilon_{zi}) \cdot h_i \quad (19)$$

where:

$h_i$  – thickness of the  $i$ -th layer;

$\varepsilon_{z0}$  – increment of axial strain at the moment of external load application;

$\varepsilon_{zpl}$  – increment of axial strain due to creep;

$\Delta\varepsilon_{zi}$  – increment of axial strain of the  $i$ -th layer considering horizontal soil displacement within the active pressure soil prism;

$n$  – number of layers.

#### 4. CONCLUSION

The research findings reveal a pattern of uneven change in the stress-strain state of soils in the foundation of buildings located at the edge of excavations. The deformation of the soil mass beneath the foundations of buildings situated within the collapse prism occurs non-linearly and inconsistently. Deep excavation works cause changes in the stress-strain state and induce additional vertical, horizontal, and flexural deformations in the soil mass supporting the foundations located at the rim of the excavation. This leads to variations in the ratios of vertical and horizontal stresses, which affect the deformation and rheological characteristics of the soil, ultimately resulting in increased settlement of the foundation of buildings situated at the edge of deep excavations.

#### 5. BIBLIOGRAPHY

- [1] Dong, Y., Burd, H., & Houlsby, G. (2018). Finite element parametric study of the performance of a deep excavation. *Soils and Foundations*(58), 729-743. doi:10.1016/j.sandf.2018.03.006

- [2] Ilyichev, V. A., Mangushev, R. A., & Nikiforova, N. S. (2012). Experience in the development of underground space in Russian megacities. *Soil Mechanics and Foundation Engineering*, 15-17.
- [3] Jiang, X., Lu, Q., Chen, X., Liu, J., & Li, P. (2021). Numerical Analysis of Deep Foundation Pit Excavation Process. *IOP Conf. Series: Earth and Environmental Science*(719), 032051. doi:10.1088/1755-1315/719/3/032051
- [4] Mangushev, R. A., Ilyichev, V. A., Nikiforova, N. S., & Sapin, D. A. (2016). Construction and design of pits. *Handbook of geotechnics*, 675-758.
- [5] Mirsayapov, I. T., & Aysin, N. N. (2021). Evaluation of Subgrade Vertical Deformations of the Building with the Influence of a Deep Pit. *Lecture Notes in Civil Engineering*(126), 51-58. doi:10.1007/978-3-030-64518-2\_7
- [6] Nikiforova, N. S. (2010). Adjustment of the method for calculating settlements of buildings during underground construction based on experimental studies. *Vestnik MGSU*(4), 293-300.
- [7] Nikiforova, N. S., & Vnukov, D. A. (2011). Protection of buildings near deep pits with geotechnical screens. *Vestnik MGSU*(5), 108–112.
- [8] Nikiforova, N. S., Konovalov, P. A., & Zekhniev, F. F. (2010). Geotechnical problems in the construction of unique objects. *Soil Mechanics and Foundation Engineering*, 2-8.
- [9] Shishkin, V. Y., Pogorelov, A. E., & Makeev, V. A. (2011). Strengthening existing buildings during the construction of a building with a foundation pit of 18–20 m. *Housing Construction*, 32–38.
- [10] Ter-Martirosyan, Z. G., Ter-Martirosyan, A. Z., & Vanina, Y. V. (2022). Settlement and bearing capacity of bases and foundations near a vertical excavation. *Vestnik MGSU*, 17(4), 443-453. doi:10.22227/1997-0935.2022.4.443-453
- [11] Zertsalov, M. G., & Kazachenko, S. A. (2021). Numerical-analytical method for engineering assessment of the influence of pit development on the movements of the adjacent soil mass, taking into account the rigidity of the enclosing structure. *Mechanics of composite materials and structures*(27), 396-409. doi:10.33113/MKMK.RAS.2021.27.03.396\_409.07

## GEOPHYSICAL IMAGING OF STOCKHOLM'S SUBSURFACE AT A MUNICIPAL SCALE— IMPLICATION FOR USE AND PLANNING OF ITS UNDERGROUND URBAN SPACE

Emmanuel Alofe<sup>1</sup>, Mehrdad Bastani<sup>2</sup>, Ari Tryggvason<sup>3</sup>

**Abstract:** The absence of the underground space and its usage in the current Stockholm city plan raises concerns about the urban underground space planning culture of Sweden. This issue becomes even more alarming because it is unclear, both in the literature and among practitioners, whether a map of Stockholm's subsurface exists at a municipal or district scale for planning purposes, despite the extensive use of the subsurface. Therefore, we processed airborne geophysical datasets, namely magnetic and very-low-frequency (VLF) electromagnetic, acquired over Stockholm municipality, to produce municipal-wide geophysical signature maps of the underground infrastructures in Stockholm. Stockholm's underground metro, a significant infrastructure across the city, served as a guide for the geophysical imaging, which included other underground infrastructures with similar geophysical signatures. Two maps were produced: the VLF electrical current density map, which was derived using a transformation from its raw data; and the magnetic anomaly map, which shows the residual between measured and upward continued (UC) fields. Our results show that Stockholm's central area, known as the *innerstaden* in Swedish, has a significantly higher infrastructure density than other areas, necessitating a rethink for further underground development in this area. We also find geophysical signatures, typical of major infrastructures, beneath the development focus areas proposed in the city plan outside the *innerstaden* area, which should be incorporated into the developments in these areas. Although our results are presented as 2D maps and are thus limited in the vertical dimension, the transformation algorithms and filters applied during processing were in 3D. In spite of the results' dimensionality, they provide preliminary insights into the subsurface of Stockholm municipality at a resolution that may be suitable for strategic planning decision at a municipal scale. These results could be further developed into 3D models for a more holistic municipal-scale planning of Stockholm's underground space.

**Keywords:** magnetics, VLF, underground, Stockholm, planning

### 1. INTRODUCTION

The current Stockholm city plan—"Vision 2040 – a Stockholm for everyone." (Stockholms stad, 2018)—has no mention of the underground space nor its usage. This lack of planning for Stockholm's underground space (SUS) is alarming given the city's historic use of its subsurface (BeFo, 2018; Tengborg and Sturk, 2016). The first-come, first-served underground development approach in Sweden is well-known, both in the literature (BeFo, 2020; Bobylev, 2009; Clarke, 2000; Kuchler et al., 2024; Tengborg and Sturk, 2016; Volchko et al., 2020) and among practitioners. Conclusively, these studies have shown an urgent need for a shift towards sustainable practices, particularly if Sweden is to fulfill Goal 11 of the UN's Sustainable Development Goals (SDGs).

Several issues have been identified in the legislation and policies surrounding the planning of the Swedish underground in some of the aforementioned studies, and solutions have been proposed. However, to the best of our knowledge, there has been no published research on providing images of the underground space for planning purposes in Sweden. Meanwhile, it remains a mystery, even to practitioners, whether a 3D or even 2D map of SUS—e.g., for allocating space to new underground infrastructures—exists at a municipal or district-area scale.

<sup>1</sup>Mr. Alofe Emmanuel, MSc. Georesource Exploration (SINReM), doctoral researcher at the department of earth sciences, Uppsala University, Sweden, [emmanuel.alofe@geo.uu.se](mailto:emmanuel.alofe@geo.uu.se).

<sup>2</sup>Dr. Bastani Mehrdad, PhD Geophysics, a senior geophysicist at the Swedish Geological Agency (SGU), Sweden, [mehrdad.bastani@sgu.se](mailto:mehrdad.bastani@sgu.se).

<sup>3</sup>Dr. Tryggvason Ari, PhD Geophysics, associate professor at the department of earth sciences, Uppsala University, Sweden, [ari.tryggvason@geo.uu.se](mailto:ari.tryggvason@geo.uu.se).

Perhaps the mystery or non-existence of such information contributes to why Stockholm's underground planning (SUP) continues to receive scholarly attention without tangible action. Moreover, the invisibility of underground space has been identified as a unique challenge for urban planners and designers, a challenge that imaging capabilities used in geoscience may help solve (Admiraal and Cornaro, 2016).

The geodata national archive at *Sveriges geologiska undersökning* (SGU)—which translates to Swedish Geological Agency in English—holds nationwide geophysical measurements acquired over time at different precisions and resolutions. Airborne magnetic and very low-frequency (VLF) electromagnetic data are examples of datasets from the archive that were considered for imaging subsurface infrastructures, particularly because of their suitable sampling density. It is elementary knowledge in geophysics that air-filled or reinforced cavities in poorly magnetic or resistive bedrock exhibit a significant susceptibility and conductivity contrast, and thus are well-delineated on magnetic and VLF-derived electrical current density maps. However, VLF data, due to its narrow frequency band, have better resolution in the horizontal direction than in the vertical direction (Beamish, 1994; Pedersen et al., 1994). In practice, VLF data have been proven suitable for 2D mapping of conductive and resistive zones in the upper few hundred to tens of meters of the crust (Paal, 1965; Pedersen et al., 2009). Similarly, magnetic methods have also been effective in near-surface investigations. In fact, visual inspection of raw magnetic data, depending on its quality, is often sufficient to reveal subsurface structures (Hansen et al., 2005; Nabighian et al., 2005).

Therefore, our study aims to provide municipal-scale 2D magnetic signatures and electrical current density maps of Stockholm's underground space, which primarily consists of the Stockholm metro (subsequently referred to in its Swedish translation, *tunnelbana*) and similar structures, derived from regional airborne magnetic and VLF datasets. The objectives are to infer anthropogenic substructures from signatures observed on the two maps and analyze them in relation to the Stockholm city plan's development focus areas (DFAs), with the hope that these maps would help guide planning decisions at early developmental stages.

## 2. MATERIAL AND METHODS

This study's airborne magnetic and VLF data were jointly acquired in 1995 using a fixed-wing aircraft flown with 200 m line spacing at 60 m height. There are 128 lines within the study area, and measurements were taken at a frequency of 4 Hz along these lines. Most major underground infrastructures in Stockholm predate the acquisition of data.

### 2.1. Magnetic data

Firstly, the geomagnetic influence was removed, and the resulting magnetic anomaly data were interpolated onto a 50 m rectangular grid covering a total area of 26 x 24 km. Within this grid is a buffer zone around the administrative boundary of Stockholm municipality, which was necessary to avoid edge effects from Fourier-based filters (e.g., upward continuation) applied at a later stage. Interpolation within the grid was done using a multi-trend algorithm developed by Naprstek and Smith (2019), which is particularly suited for interpolating and enhancing thin, linear features at varying angles to the flight direction. As seen in Figure 1a, the main target, the *tunnelbana*, has lines at horizontally varying angles to the North-South flight direction.

Reduction-to-pole (RTP) was the next step in the magnetic data processing. RTP is essential for removing data dependence on the angle of geomagnetic inclination by recomputing the induced magnetic field of the sources as if they lie parallel to the magnetic pole. The structural information of the sources is not lost despite the recomputation of the RTP process (Rajagopalan, 2003).

Regional-residual magnetic fields separation was achieved through upward continuation (UC)—by removing magnetic fields that were continued upwards to 10, 30, and 60 m heights from the magnetic data, respectively. The UC of a magnetic field to a height  $h$  above a measurement plane is a mathematical technique that maps the magnetic sources from a depth of  $h/2$  below the plane downwards (Jacobsen, 1987). This means that UC is essentially a low-pass filter that enhances the signal from magnetic sources at a specific depth and below, while attenuating those above it. It then follows that airborne magnetic data obtained at 60 m height will be theoretically equivalent to ground survey data continued upwards to 60 m. Therefore, by applying the UC filters as previously described, each residual field would contain enhanced signals from magnetic sources at 30 m depth downwards. Subsequently, we refer to the fields as the UC-separated residual fields, and in cases where specificity is required, as UC $x$  residual field, where  $x$  is the appropriate continuation height.

As of the data acquisition date, only one metro station of the *tunnelbana* was at 35 m depth, all other subsurface stations were at an average depth of 20 m and had connections to the surface stations. Given the data flight height, it meant that the magnetic signatures of the stations would form part of the shallower high-frequency components of the UC-separated residual fields. The 2D power spectra (Spector and Grant, 1970) of each UC-separated residual

fields were analyzed to choose the best, from which the depth to magnetic sources was estimated (Equation 1). In this case, the best meant the residual field that had signatures whose form is best correlated to the infrastructural layout of the *tunnelbana*. A high-pass filter with a moderate taper was applied to the chosen UC-separated residual field for enhancement of constituent wavelengths less than 1 km. The high-pass filter parameters used gave the most correlated signal of the trace target after several attempts. The analytic signal amplitude of the filtered residual field was then computed using the 3D analytic signal derivatives in Equation 2, as described by Roest et al. (1992). These authors had successfully shown that the analytic signal amplitude exhibits maxima over magnetization contrasts, thereby properly delineating magnetic sources.

$$D = -\frac{1}{4\pi} \text{slope segment} \xrightarrow{\text{yields}} -\frac{1}{4\pi} \left( \frac{e_2 - e_1}{k_2 - k_1} \right) \quad (1)$$

where  $D$  is the depth to the top of the magnetic source ensemble corresponding to each slope segment on a power spectrum in km,  $e$  is the log of the power amplitude, and  $k$  is the wavenumber in cycle/km.

$$|AS(x, y)| = \sqrt{\left(\frac{\partial M}{\partial x}\right)^2 + \left(\frac{\partial M}{\partial y}\right)^2 + \left(\frac{\partial M}{\partial z}\right)^2} \quad (2)$$

where  $|AS|$  is the analytic signal amplitude in nT/m;  $M$  is the magnetic field in nT; and  $x$ ,  $y$ , and  $z$  are the cartesian coordinate system axes, respectively.

## 2.2. VLF data

The tensor tipper, relating the vertical and the two horizontal magnetic field components of the two transmitters used in the data acquisition was calculated using all the signals within a closely spaced frequency band. Estimation of the tensor tipper from multiple transmitters is well described by Pedersen et al. (1994) and is preferred because it eliminates the direction bias that would be introduced by estimating the tipper from a single transmitter. Therefore, the tensor tipper, as calculated, depends only on the subsurface conductivity structures (Pedersen et al., 2009; Pedersen and Oskooi, 2004). Pedersen and Oskooi (2004) also proved that the possible frequency dependence of tensor tipper, cautioned by Pedersen et al. (1994: 865), was not an issue in a narrow frequency band, such as in the data acquisition (15 – 30 kHz). The tensor tipper was further transformed to an apparent electrical current density map using the Becken and Pedersen (2003) transformation algorithm. The apparent current density map contained the electrical conductivity distribution of the subsurface conductors, a significant part of which is the *tunnelbana*.

## 3. RESULTS

The evolution of the magnetic data processing steps, from residual separation through filtering to power spectrum analysis, is presented in Figure 1. The UC10 residual field was reduced by a factor of 10 from the measured signal amplitude (cf. Figures 1b and 1c labels). This is also true for the filtered UC10 residual field (Figure 1d). However, targeted signals were still visible on the residual. Persistent regional features were further attenuated using a high-pass filter (Figure 1d).

The 2D power spectra of the residual and measured fields exhibit a two-segment slope, differing only in the second segment (Figure 1e). The highest power spectrum belonged to the UC10 residual field, but was slightly lower when compared to its filtered spectrum (Figure 1f). The labels on the power spectra are the calculated depth to the top of magnetic source ensembles for each slope segment using Equation 1.

The overlay of the *tunnelbana* layout on the analytic signal amplitude of the UC10 residual field and the apparent electrical current density are shown in Figures 2a and b, respectively. In both cases, a distinct high-magnitude signal is present along the length of the overlaid layout. The signal is evident along the entire length of the layout in some places (e.g., the green line section from *Hässelby-Vällingby* to *Enskede-Årsta-Vantör* district areas in Figure 2a and b) and partially in others. Whereas, the current density signal was visible along some sections of the layout in Figure 2a (e.g., the green line section within the *Skarpnäck* district area and the red line section within the *Skärholmen* district area), where the magnetic signal was absent.

Some signatures are not associated with the *tunnelbana* layout, e.g., around the airport located east of *Bromma*. Within the central city area—*Södermalm*, *Norrmalm*, *Kungsholmen*, and *Östermalm*—of Stockholm, there is a higher magnetic signature density than in the other city areas. We refer to this observation as a density bias. A similar density bias can also be observed within *Farsta* compared to the neighboring district areas of *Skarpnäck*



and *Enskede-Årsta-Vantör* (Figure 2a). In both cases, the density biases are better observed on the magnetic analytic signal maps than on the current density maps. Figures 2c and 2d show the magnetic and apparent current density maps in relation to Stockholm's DFAs, respectively. A selection of major ongoing development projects within Stockholm was also included. Specifics of the development areas and projects gleaned from official sources (Stockholms stad, n.d., 2018; Trafikverket, 2024) are itemised in Figure 2e. Our results indicate that all of the highlighted development areas have notable magnetic signatures.

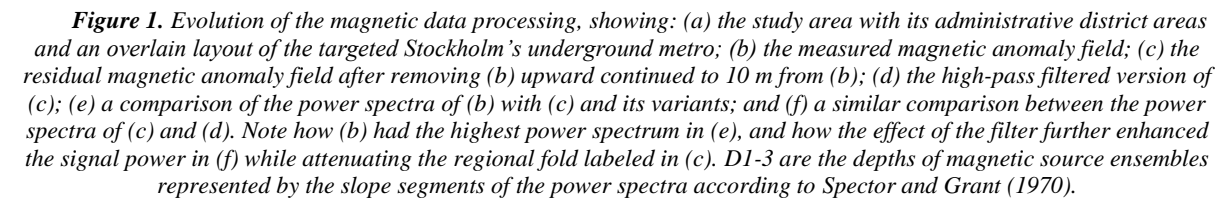
## 4. DISCUSSION

### 4.1. Geophysical imaging

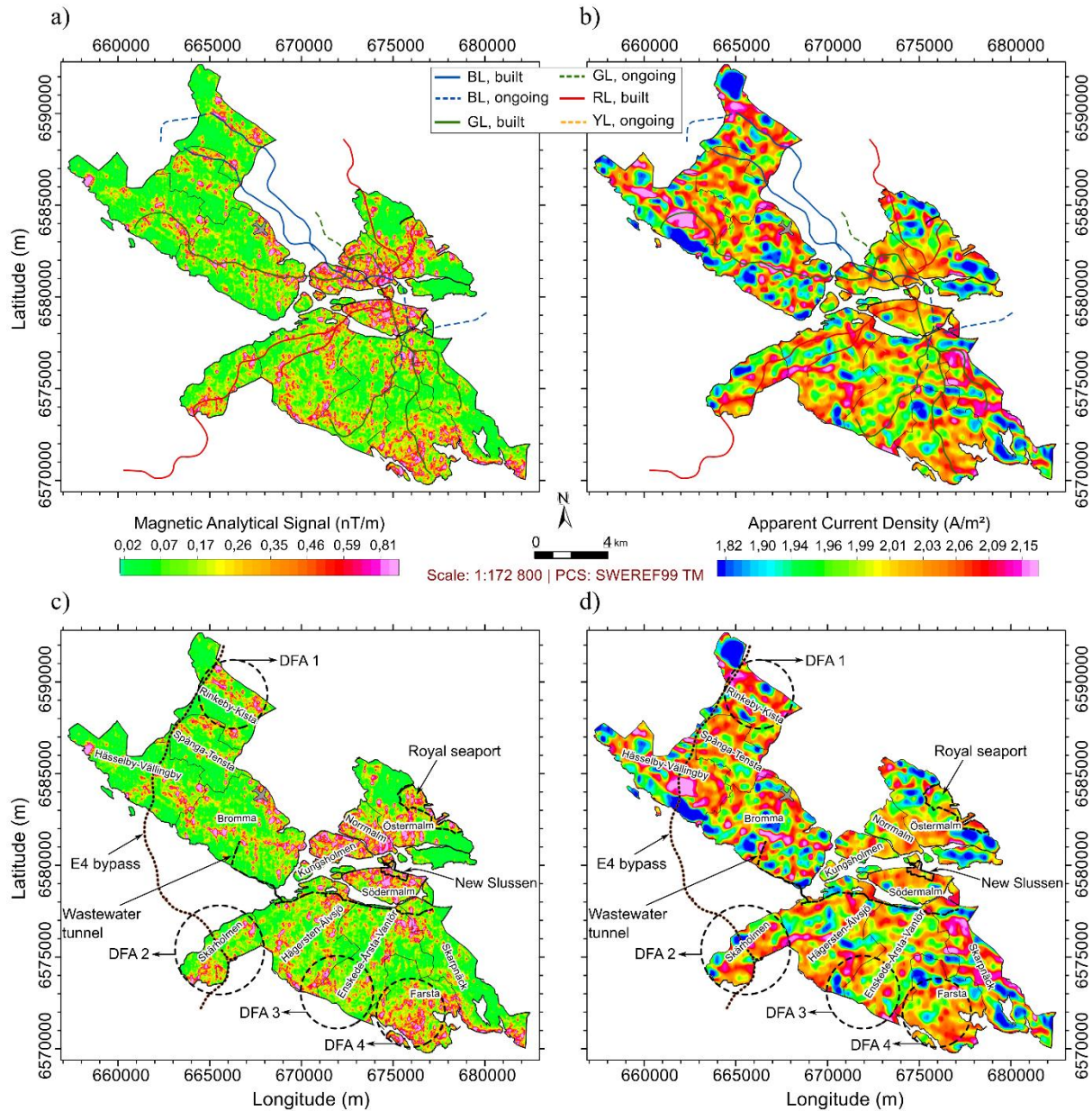
According to Spector and Grant (1970), each slope segment on an average power spectrum of potential field data indicates an independent ensemble of geometrical magnetic bodies that can be characterized by a joint frequency distribution of a set of attributes. One such attribute is the depth of occurrence of the ensemble, which can be estimated from Equation 1. However, there is a condition that applies: all the magnetic bodies must be magnetized parallel to the geomagnetic vector and measured close to the north magnetic pole (Spector and Grant, 1970: 295). This requirement necessitated the reduction of the magnetic data to the magnetic north pole before the power spectrum analysis. Accordingly, all the power spectra in Figures 1e and f suggest the presence of two independent ensembles of magnetic sources. Based on depth of occurrence (2 km) and longer wavelength, the first ensemble from the left is clearly of regional geologic origin, while the other has a mix of local geologic and anthropogenic origins.

The origin of the magnetic sources becomes visually evident on the UC10 residual map (cf. Figure 1b and c). The term "residual" as used here means the magnetic field from predominantly anthropogenic magnetic sources. These residual fields exhibit similar high-frequency characteristics to the full magnetic anomaly fields shown in Figure 1e. Thus, in separating the residual fields, we used a numerically stable filter, such as the UC filter, that retains a physical meaning in the spatial domain (Jacobsen, 1987). This means that the UC30 residual field could be said to contain enhanced magnetic fields from sources between 30 and 45 m depth. This is reasonably close to the approximately 47 m depth to the top of the shallower magnetic source ensemble estimated from the statistical method of Spector and Grant (1970). However, the UC10 residual field, corresponding to 30 – 35 m depth, had a better power spectrum (Figure 1e) and is the closest to the average depth of the trace target, the *tunnelbana*. Therefore, we chose that as the best in this case. Further attenuation of persistent regional features (e.g., the fold shown in Figure 1c) using a high-pass filter enhanced the UC10 residual field, as illustrated in Figures 1d and f.

The regional-residual separation reduced the UC10 residual signal, making it difficult to delineate the outlines of the magnetic sources. The computation of the analytic signal amplitude of its filtered field revealed a high-amplitude outline that aligned with the sections of the *tunnelbana* layout that existed before the data acquisition (Figure 2a)—note the absence along ongoing sections. Computation of the analytic signal amplitude is a widely used derivative-based approach for edge delineation of magnetic structures. It maximizes over the edges of these structures (Nabighian, 1984; Roest et al., 1992). Further indications of the *tunnelbana* can also be seen in the apparent electrical current density map derived from the VLF data (Figure 2b). The correlation between the layout of the *tunnelbana* and the high-amplitude signals on both the magnetic analytic signal amplitude and electrical current density maps provides strong geophysical evidence that these signals indeed originate from the *tunnelbana*.







Excerpts From Stockholm City Plan "Vision 2040 – a Stockholm for everyone"	
<p><b>Development focus areas (DFAs)</b></p> <p><b>DFA 1: Kista-Husby-Akalla</b> → Planned to be a regional hub. → 6000 homes + offices/schools to be built.</p> <p><b>DFA 2: Skärholmen-Vårberg</b> → Planned to be a regional hub. → 4000 homes + 5 recreational facilities to be built.</p> <p><b>DFA 3: Hagsätra-Älvsjö</b> → Planned to be a regional hub. → New homes + 5 schools + 6 recreational facilities to be built.</p> <p><b>DFA 4: Fagersjö-Farsta</b> → Planned to be a strategic hub for southern suburbs development. → New homes + 5 schools + 4 recreational facilities to be built.</p>	<p><b>Ongoing major developments:</b></p> <p><b>inside the inner city</b></p> <ul style="list-style-type: none"> <li>○ Royal Seaport → One of the largest urban developments in Europe. → 12000 homes + 35000 workplaces + schools to be built.</li> <li>○ New Slussen → Major redevelopments in sync with the city's growth and flood management*. → A new lock + 2 water channels + a tunnel + bridges + a park + a bus terminal to be built*.</li> </ul> <p><b>outside the inner city</b></p> <ul style="list-style-type: none"> <li>○ Wastewater tunnel → A 14km connection to the eastern treatment facilities.</li> <li>○ E4 bypass → 86% of the 21km European highway's new route is in tunnels**.</li> </ul>

\*Stockholms Stad, n.d. \*\*Trafikverket, 2024

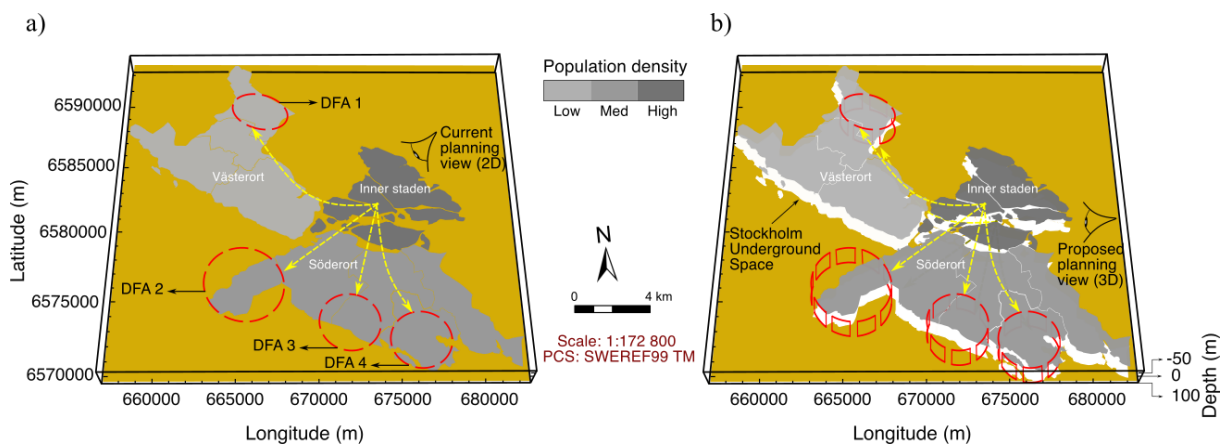
**Figure 2.** Correlation of analytic signal amplitude of the filtered magnetic residual anomaly field and VLF-derived apparent electrical current density with Stockholm's underground metro, (a) and (b), respectively. (c) and (d) are their analyses in relation to the development focus areas (DFAs) of the current Stockholm city plan and a selection of ongoing infrastructural developments summarized in (e). Note how the correlation on both (a) and (b) strongly suggests the metro as the source of the aligned high-magnitude signals and how, by extension, similar signals would indicate the presence of major infrastructures within the DFAs and other development areas in (c) and (d).

It is then logical that other signatures, particularly on the magnetic analytic signal map, may belong to subsurface structures of anthropogenic origin—e.g., the linear magnetic signature within *Hägersten-Älvsjö*, flanked by the red and ongoing yellow line (Figure 2a). Another such signal, observable on both the magnetic and current maps, correlates with the *Bromma* airport location (denoted with an airplane symbol in Figure 2). Furthermore, the aforementioned magnetic analytic signal density biases within the inner-city area of Stockholm and the *Farsta* district area are also supported by ground truths—e.g., the *Farsta* district area has notable underground structures associated with both the *tunnelbana* and the *Nynäs* railway stations.

However, it is essential to note that the magnetic analytic signal amplitude map has been enhanced for magnetic sources within the average depth of occurrence of the trace target (30 – 35 m depth), whereas the current density map shows the conductivity distribution of structures from the surface to a few tens of meters depth. Thus, some missing signals on the magnetic map, particularly along the *tunnelbana* layout, that are visible on the current map, could be argued to belong to shallower sections of the layout. Conversely, the signals on the latter, which are not observed on the former, can also be attributed to deeper conductors of possible geologic origin. Therefore, the magnetic analytic signal amplitude map forms the primary basis of the analysis for Stockholm's DFAs, with the VLF current density map serving in a secondary capacity.

#### 4.2. Analysis of Stockholm city plan in relation to geophysical images

The current Stockholm city plan ("Vision 2040 – a stockholm for everyone") contains strategic areas, i.e., DFAs (Figure 3a), to be developed into regional hubs that will relieve the stress of the disproportionately higher population density in the inner-city area (*Innerstaden*) compared to the southern (*Söderort*) and western (*Västerort*) areas of Stockholm municipality. The aim is to facilitate a radial population spread into the DFAs in the western and southern areas (see yellow arrows in Figure 3). This is particularly strategic given that the city has the Baltic bay on its eastern border. Notwithstanding, it is imperative to integrate the third (vertical) dimension into the development of these DFAs in order to avoid the current underground situation below the inner area of Stockholm (see the magnetic analytic signal image of its subsurface, Figure 2c). Particularly since there is evidence of existing major infrastructures beneath some of these DFAs as well (e.g., within DFAs 2 and 4). Unlike the surface, the underground space is a non-renewable resource (Bobylov, 2009), which should be tapped sustainably because once transformed, it becomes a permanent feature.



**Figure 3.** Comparison between (a) the current model of planning and expansion in Stockholm as evidenced in the city plan and (b) a proposed model based on the geophysical images of Stockholm's underground space.

Our results do not indicate that vertical expansion below the surface is impossible or should not be undertaken within the inner area of Stockholm. But, we emphasize the need to also have a parallel expansion strategy along the third dimension, as illustrated in Figure 3b. We also propose applying planning expertise and priorities used on the surface to the underground. We recommend the definition of development focus volumes (DFVs) rather than areas (DFAs); this could vary for different counties of a country or even for different cities within a municipality. In Stockholm, for instance, we suggest a volume that reaches a depth of 100 m, based on the average depth of occurrence of infrastructural signatures obtained from magnetic results and publicly available depth information about existing and planned infrastructures. Admittedly, our proposal highlights the limitations of two-dimensional imaging and underscores the need for a detailed three-dimensional model of SUS. Nevertheless, our 2D results show, for the first time, preliminary insights into the state of the space below the cityscape of Stockholm at a municipal scale. This implies that 2D and 3D models of the underground space are not mutually exclusive, especially for underground planning purposes.

## 5. CONCLUSION

Geophysical imaging based on multiple physical properties provides an effective way to gain insight into the state of the underground space for city planners and designers in situations where such information is not readily available and accessible. Similarly, 2D geophysical images can provide valuable preliminary information when 3D models of the underground space are not available, indicating that 2D imaging and 3D modeling are not mutually exclusive for underground planning. There needs to be good storage of data at the appropriate scale and resolution for realistic imaging and modeling of the urban underground space. In order to forestall the tendency for skewed underground development in favor of the central urban areas of cities, it is necessary to integrate a data-driven underground development plan early-on into the city plan.

## 6. ACKNOWLEDGMENTS

We express our gratitude for the research grant (grant no: 2021-00106) from the Swedish Research Council Formas, within the National Research Program for Sustainable Spatial Planning (*Nationella forskningsprogrammet för hållbart samhällsbyggande*), which made this study possible. We also thank the Swedish Geological Agency (*Sveriges geologiska undersökning*, SGU) for supplying the geophysical datasets used in this study. We would also like to extend our appreciation to the anonymous reviewers for their valuable feedback.

## 7. REFERENCES

- [1] Admiraal, H., & Cornaro, A. (2016). Why underground space should be included in urban planning policy - And how this will enhance an urban underground future. *Tunnelling and Underground Space Technology*, 55, 214–220. <https://doi.org/10.1016/j.tust.2015.11.013>
- [2] Bastani, M., Persson, L., Mehta, S., & Malehmir, A. (2015). Boat-towed radio-magnetotellurics - A new technique and case study from the city of Stockholm. *Geophysics*, 80(6), B193–B202. <https://doi.org/10.1190/GEO2014-0527.1>
- [3] Bastani, M., Wang, S., Malehmir, A., & Mehta, S. (2022). Radio-magnetotelluric and controlled-source magnetotelluric surveys on a frozen lake: Opportunities for urban applications in Nordic countries. *Near Surface Geophysics*, 20(1), 30–45. <https://doi.org/10.1002/nsg.12180>
- [4] Beamish, D. (1994). Two-dimensional, regularised inversion of VLF data. In *Journal of Applied Geophysics* (Vol. 32).
- [5] BeFo. (2018). *Sweden Underground – Rock Engineering and How it Benefits Society* (U. Lindblom, L. Ericsson, T. Winqvist, P. Tengborg, & U. Håkansson, Eds.). BeFo Rock Engineering Research Foundation. <https://www.befo.se/publikationer/sweden-underground-rock-engineering-and-how-it-benefits-society/>
- [6] BeFo. (2020). Nya dimensioner i svensk planering – en utredning om undermarksplanering och geosystemtjänster / New dimensions in Swedish planning- an investigation on subsurface planning and geosystem services. *BeFo Rock Engineering Research Foundation*, 214. <https://www.befo.se/publikationer/nya-dimensioner-i-svensk-planering-en-utredning-om-undermarksplanering-och-geosystemtjanster/>
- [7] Bobylev, N. (2009). Mainstreaming sustainable development into a city's Master plan: A case of Urban Underground Space use. *Land Use Policy*, 26(4), 1128–1137. <https://doi.org/10.1016/j.landusepol.2009.02.003>
- [8] Brodic, B., Malehmir, A., Bastani, M., Mehta, S., Juhlin, C., Lundberg, E., & Wang, S. (2017). Multi-component digital-based seismic landstreamer and boat-towed radio-magnetotelluric acquisition systems for improved subsurface characterization in the urban environment. *First Break*, 35(8), 41–47. <https://doi.org/10.3997/1365-2397.35.8.89804>
- [9] Clarke, R. J. (2000). Planning and mapping of underground space — an overview. *Tunnelling and Underground Space Technology*, 15(3), 271–286. [https://doi.org/10.1016/S0886-7798\(00\)00056-0](https://doi.org/10.1016/S0886-7798(00)00056-0)
- [10] Dahlin, T., & Wisén, R. (2016). Underwater ERT Surveys for Urban Underground Infrastructure Site Investigation in Central Stockholm. *17th Nordic Geotechnical Meeting Challenges in Nordic Geotechnics 25th – 28th of May*. <https://www.issmge.org/publications/online-library>
- [11] Hansen, R. O., Racic, L., & Grauch, V. J. S. (2005). 6. Magnetic Methods in Near-Surface Geophysics. In *Near-Surface Geophysics* (pp. 151–176). Society of Exploration Geophysicists. <https://doi.org/doi:10.1190/1.9781560801719.ch6>
- [12] Jacobsen, B. H. (1987). CASE FOR UPWARD CONTINUATION AS A STANDARD SEPARATION FILTER FOR POTENTIAL-FIELD MAPS. *Geophysics*, 52(8), 1138–1148. <https://doi.org/10.1190/1.1442378>
- [13] Karous, M., & Hjelt, S. E. (1983). Linear filtering of VLF dip-angle measurements. *Geophysical Prospecting*, 31(5), 782–794. <https://doi.org/https://doi.org/10.1111/j.1365-2478.1983.tb01085.x>
- [14] Kuchler, M., Craig-Thompson, A., Alofe, E., & Tryggvason, A. (2024). SubCity: Planning for a sustainable subsurface in Stockholm. *Tunnelling and Underground Space Technology*, 144. <https://doi.org/10.1016/j.tust.2023.105545>



- [15] Nabighian, M. N. (1984). Toward a three-dimensional automatic interpretation of potential field data via generalized Hilbert transforms: fundamental relations. *Geophysics*, 49(6), 780–786. <https://doi.org/10.1190/1.1441706>
- [16] Nabighian, M. N., Grauch, V. J. S., Hansen, R. O., LaFehr, T. R., Li, Y., Peirce, J. W., Phillips, J. D., & Ruder, M. E. (2005). The historical development of the magnetic method in exploration. *Geophysics*, 70(6). <https://doi.org/10.1190/1.2133784>
- [17] Naprstek, T., & Smith, R. S. (2019). A new method for interpolating linear features in aeromagnetic data. *Geophysics*, 84(3), JM15–JM24. <https://doi.org/10.1190/geo2018-0156.1>
- [18] Paal, G. (1965). Ore prospecting based on VLF-radio signals. *Geoexploration*, 3(3), 139–147. [https://doi.org/10.1016/0016-7142\(65\)90016-5](https://doi.org/10.1016/0016-7142(65)90016-5)
- [19] Pedersen, L. B., & Oskooi, B. (2004). Airborne VLF Measurements and Variations of Ground Conductivity: A Tutorial. *Surveys in Geophysics*, 25(2), 151–181. <https://doi.org/10.1023/B:GEOP.0000028161.90659.4b>
- [20] Pedersen, L. B., Persson, L., Bastani, M., & Byström, S. (2009). Airborne VLF measurements and mapping of ground conductivity in Sweden. *Journal of Applied Geophysics*, 67(3), 250–258. <https://doi.org/10.1016/j.jappgeo.2007.11.002>
- [21] Pedersen, L. B., Qian, W., Dynesius, L., & Zhang, P. (1994). An airborne tensor VLF system. From concept to realization. *Geophysical Prospecting*, 42(8), 863–883. <https://doi.org/10.1111/j.1365-2478.1994.tb00246.x>
- [22] Rajagopalan, S. (2003). Analytic Signal vs. Reduction to Pole: Solutions for Low Magnetic Latitudes. *ASEG Extended Abstracts*, 2003(2), 1–4. <https://doi.org/10.1071/aseg2003ab136>
- [23] Roest, W. R., Verhoef, J., & Pilkington, M. (1992). Magnetic interpretation using the 3-D analytic signal. *GEOPHYSICS*, 57(1), 116–125. <https://doi.org/10.1190/1.1443174>
- [24] Ronczka, M., Wisén, R., & Dahlin, T. (2018). Geophysical pre-investigation for a Stockholm tunnel project: Joint inversion and interpretation of geoelectric and seismic refraction data in an urban environment. *Near Surface Geophysics*, 16(3), 258–268. <https://doi.org/10.3997/1873-0604.2018009>
- [25] Spector, A., & Grant, F. S. (1970). Statistical models for interpreting aeromagnetic data. *Geophysics*, 35(2), 293–302. <https://doi.org/10.1190/1.1440092>
- [26] Stockholms stad. (n.d.). *New Slussen*. Retrieved February 14, 2025, from [https://vaxer.stockholm/siteassets/stockholm-vaxer/projekt/sodermalm-sdo/sodermalm/slussen/webb/dokument/new\\_slussen\\_english.pdf](https://vaxer.stockholm/siteassets/stockholm-vaxer/projekt/sodermalm-sdo/sodermalm/slussen/webb/dokument/new_slussen_english.pdf)
- [27] Stockholms stad. (2018). *Stockholm City Plan*. [https://vaxer.stockholm/siteassets/stockholm-vaxer/tema/oversiktsplan-for-stockholm/english\\_stockholm\\_city\\_plan.pdf](https://vaxer.stockholm/siteassets/stockholm-vaxer/tema/oversiktsplan-for-stockholm/english_stockholm_city_plan.pdf)
- [28] Svensson, M. (2016). GeoBIM for optimal use of geotechnical data. *17th Nordic Geotechnical Meeting Challenges in Nordic Geotechnic 25th – 28th of May*. [www.trust-geoinfra.se](http://www.trust-geoinfra.se)
- [29] Tengborg, P., & Sturk, R. (2016). Development of the use of underground space in Sweden. *Tunnelling and Underground Space Technology*, 55, 339–341. <https://doi.org/10.1016/j.tust.2016.01.002>
- [30] Trafikverket. (2024, January 9). *E4 The Stockholm bypass Project*. <https://bransch.trafikverket.se/en/startpage/projects/Road-construction-projects/the-stockholm-bypass/>
- [31] Volchko, Y., Norrman, J., Ericsson, L. O., Nilsson, K. L., Markstedt, A., Öberg, M., Mossmark, F., Bobylev, N., & Tengborg, P. (2020). Subsurface planning: Towards a common understanding of the subsurface as a multifunctional resource. *Land Use Policy*, 90. <https://doi.org/10.1016/j.landusepol.2019.104316>

## RESEARCH ON SAFE THICKNESS OF ROCK MASS IN NON-COAL STRATUM TUNNEL WITH HIGH-PRESSURE GAS BLAST BASED ON ENERGY METHOD

Su Peidong<sup>1</sup>, Li Yougui<sup>2</sup>, Qiu Peng, An Xingling.

**Abstract:** High-pressure gas outbursts and coal and rock outbursts are common geological disasters in tunnel engineering. Domestic and foreign research results regarding coal and gas outbursts are rich and relatively mature, but there are few discussions on high-pressure gas outbursts in non-coal tunnels. This study focuses on the tunnel gas and rock outburst mechanism in non-coal formations. From the perspective of the energy method, gas and rock outbursts occur when the energy supply exceeds the energy consumption. The energy sources are the elastic potential energy of the rock mass and the gas expansion work, and the energy-consumption part is mainly the rock mass breaking work and the ejection work. The energy model is used to study the mechanism of high-pressure gas and rock eruption, derive the formula of high-pressure gas pressure and minimum safe thickness of rock mass; combined with the Hongdoushan No. 1 slope well engineering case verified the mathematical expression. The critical condition for the outstanding is that the outstanding energy is completely used to break the rock. High-pressure gas blasting safety thickness formula for outburst prevention, high-pressure gas pressure has a significant influence on the minimum safe thickness of the rock mass. The energy method considers the effects of the ground stress, the gas pressure, and the physical and mechanical properties of the surrounding rock on the outburst and comprehensively considers the factors that affect the outburst. The FLAC3D software was used to invert the gas pressure during the high-pressure gas outburst in the Hongdoushan No. 1 inclined well to be 7.5 MPa, which was consistent with the actual situation, and the applicability of the formula was verified. The results of this study can provide ideas for preventing outbursts of high-pressure gas in non-coal formation tunnels and reducing outburst accidents.

**Keywords:** gas and rock outburst; energy method; safe thickness; non-coal tunnel

### 1. INTRODUCTION

Gas and rock outbursts during tunnel construction can cause tunnel face collapse, with fractured rock and gas intruding into the tunnel space, damaging the support structure and construction machinery. Large volumes of released gas may lead to suffocation or even explosion (Zhang, K. et al., 2019). Coal and gas outbursts are common in tunnel construction (Zhao, Z. et al., 2020; Proctor, R.J., 2002). Many studies have examined gas outbursts in coal strata, and specialized technologies for preventing such events during tunnel construction have been developed by drawing on coal-mining experience (Huang, Z. et al., 2017; Wang, X., 2019; Zhou, A. et al., 2017; Li, B. et al., 2021; Li, Q. et al., 2015; Zhu, B., 2012; Lin, B. Zhou, S., 1995; Zhu, C. Cai, S., 2020). Unfortunately, research on high-pressure gas and rock outbursts in tunnels excavated in non-coal strata is limited. The existing research results are mainly related to the geological environments in which outbursts occur and outburst prediction and prevention; research results regarding the outburst mechanism are scarce.

Research on the outburst geological environment is mainly performed through data collection and onsite investigation to obtain relevant data on the outburst's regional tectonic evolution history, oil and gas reservoirs, coal, and other mineral resources, together with onsite sampling and indoor analysis to determine the cause of the gas. Additionally, according to the geological structure and geological history data, patterns of outburst occurrence have been established, and corresponding prevention measures proposed (Huang, M. et al., 2010; Zhou, G., 1992;

<sup>1</sup>PhD, Su Peidong, Geological engineering, professor, School of Earth Science and Technology, Southwest Petroleum University, Xindu Avenue, 610500, Chengdu Sichuan, China, spdong@126.com.

<sup>2</sup>PhD, Li Yougui, Geological engineering, School of Earth Science and Technology, Southwest Petroleum University, Xindu Avenue, 610500, Chengdu Sichuan, China, 2071503124@qq.com.

Lv, C.Cui, Y., 2002; Sun, J., 2009; Zhi, Y., 2007; Tang, S., 2009; Jiang, L. et al., 2010) . Additionally, Polish researchers studied the pressure and volume of residual gas after the outburst of gas and dolomite in Polish copper mines, as well as the porosity changes in the outburst zone, and concluded that the gas and rock outbursts are in close proximity to the cavitation (Wierzbicki, M.Młynarczuk, M., 2013) . Domestic researchers have investigated the geological environment in the early stage of research on gas and rock outbursts, and a few have used mathematical methods, physical experiments, or hypotheses to study the outburst mechanism.

In recent years, owing to the development of deep underground engineering, the engineering problems encountered in the deep environment are different from those of the shallow surface. In particular, the frequency of gas and rock outbursts is increasing. Gas and rock outbursts have attracted the attention of scholars. Mathematical methods such as attribute mathematics, the fuzzy analytic hierarchy process, probability theory, fuzzy logic, and the random forest algorithm are applied to gas and rock outburst prediction. Zhang et al. (Zhang, K. et al., 2019) selected eight factors that affect the outburst of non-coal strata and used attribute mathematics to establish a gas-outburst risk evaluation system in the exploration stage of tunnel excavation in non-coal strata. The analytical method determines the weight of the evaluation index, and the risk level of the evaluation object is determined by the confidence standard. Skoczylas(Hudeček, V. et al., 2013) obtained relevant knowledge and experience by consulting experts engaged in the assessment and prediction of gas and rock outbursts and then established an expert system for estimating the risk of gas and rock outbursts using fuzzy logic. To forecast the cost of rock and gas outbursts from the hard coal deposit “Nowa Ruda Pole Piast Wacaw-Lech,” Bodlak(Maciej, B. et al., 2018) used the random forest algorithm together with the “XGBoost” machine-learning method to establish a degree of gas and rock outburst prediction model, which can predict the rock and gas outburst range. The outburst range prediction is based on the outburst rock mass, gas volume, and outburst cavity length. Tai et al. (Qi, T. et al., 2018) used the solid–liquid–gas coupling method to predict gas eruption in a shield tunnel.

Scholars have made efforts to highlight the outburst mechanism. Huo et al.(Huo, Z. et al., 2021) discussed the mechanism of rock and CO<sub>2</sub> outburst, established a physical model of rock and CO<sub>2</sub> outburst, analyzed the rock and CO<sub>2</sub> outburst process and mechanical environment, and pointed out that the key structural theory and energy method are applicable to non-coal formation gas and rock outburst and that the outburst criterion of rock and CO<sub>2</sub> is established via the energy method. Guo(Guo, C., 2010) studied the mechanism of gas and rock outburst and pointed out that the outburst energy comes from rock elastic deformation energy, gas expansion energy, and rock gravitational potential energy. Wang et al. (Wang, L. et al., 2022) measured the ground stress, rock mechanical parameters, and CO<sub>2</sub> gas pressure and calculated the tunnel stress field using numerical software. They discussed the outburst mechanism from a mechanical viewpoint.

Owing to the low incidence of gas and rock outbursts and the lack of information, universities, scientific research institutions, and enterprises have not regarded gas outbursts as an important research object and often ignore gas and rock outbursts. In early research, the geological environment after the outburst occurred was analyzed, and anti-outburst countermeasures were proposed. In recent years, owing to the development of engineering deep underground, gas and rock outbursts have caused numerous losses and serious accidents. Gas and rock outbursts are among the major disasters occurring deep underground. However, little research has been performed on the outburst mechanism of gas and rock. Few scholars have seen this and conducted related research on the outburst mechanism. The research is not sufficiently deep, and the theory is imperfect.

No experts or scholars have studied the minimum thickness of the rock mass before gas and rock outburst. For this purpose, a comprehensive method for outburst mechanism research—the energy method—is introduced into the tunnel engineering non-coal formation gas and rock outburst mechanism research. The energy method takes into account the physical and mechanical properties of rocks, the gas rock mass, and the in situ stress impact on outburst. First, the relevant assumptions and basic theory of the energy method are introduced. Next, the energy method is used to derive the formula for the gas pressure and the minimum thickness of the rock mass, and the formula is used to calculate the gas pressure before the outburst in an actual outburst case. Finally, the calculation results of the energy method are validated using the FLAC3D software.

## **2. MATERIAL AND METHODS**

### **2.1. Hongdoushan tunnel highlights the background**

#### **2.1.1. Outstanding phenomena**

After the gas and rocks outburst in the Hongdoushan No. 1 inclined shaft, the gas vented back into the tunnel. The dissolved residual CO<sub>2</sub> pressure in the water is 0.2–0.3 MPa; the main gas component is CO<sub>2</sub>, followed by N<sub>2</sub> and O<sub>2</sub>; and the associated gases include H<sub>2</sub>S, NH<sub>3</sub>, SO<sub>2</sub>, CO, and other harmful gases. Through sampling and indoor analysis, it is determined that the gas is a mixed-source gas of mantle and metamorphic origin. The maximum accumulation length of ejected rock in front of the shaft is 15 m, and the total volume is 150 m<sup>3</sup>. The

ejected rock mass is granitic mylonite, which is a loose mixture of silty fine sand, powder, and crushed rock fragments, with rock blocks measuring 10–20 cm in size. The color is dark gray, and water was observed within the outburst deposits (Figure 1). The surrounding rock is strongly weathered granitic mylonite; the rock strength is slightly lower, joints are well developed, with many closed joints, and the integrity of the rock mass is poor. There is a weak interlayer with water seepage.



**Figure 1.** Outburst phenomenon of the Hongdoushan No. 1 inclined shaft

### 2.1.2. Onsite survey data

The physical and mechanical properties of the rock mass in the area are presented in Table 1. Based on field inspection after removal of the outburst deposits, it is found that the outburst deposits were loose, with a large proportion consisting of fine particles and powder. The density of outburst deposits was determined to be  $1.6 \text{ t/m}^3$ . The tunnel site has experienced multiple stages of tectonic activities, and faults are developed in the area. Deep gas in the formation migrates through faults to the shallow rock mass fracture zone for storage; because of the strong tectonic activities, *in situ* stress measurement was performed to prevent rock outbursts (Table 2). The data indicate that the energy required to create a new fracture surface in medium-strength rocks ( $W$ ) is  $0.1\text{--}0.12 \text{ MJ/m}^2$  (Xu, X. Yu, J., 1984). The distribution of specific energy for crushing granite with diamond bits in the granite formation is presented in Table 3 (Tan, Z., 2007).

**Table 1.** Rock mechanics index of the Hongdoushan outburst section (survey data)

Geotechnical type	era Cause	Degree of soil moisture or bedrock weathering	Natural density	Cohesion	Internal friction angle	Substrate friction coefficient	Compression Modulus	Poisson's ratio
			$\rho$	$c$	$\varphi$	$f$	$E_s$	$\mu$
			g/cm <sup>3</sup>	kPa	(°)		MPa	
Biotite Granite	$\gamma 51$	W4	1,95	15	25	0,30	6	0,27
		W3	2,40	/	45	0,45	/	0,25
		W2	2,65	/	65	0,65	/	0,22

**Table 2.** In situ stress measurement results of hydraulic fracturing in the Hongdoushan No. 1 inclined well

Serial number	Measurement section depth (m)	Fracturing parameters (MPa)						Principal stress value (MPa)			Rupture direction (°)
		Pb	Pr	Ps	PH	P0	T	SH	Sh	Sv	
1	290,5–291,1	/	8,01	6,51	2,91	2,01	/	9,51	6,51	7,70	N23°W
2	377,5–378,1	/	9,76	7,82	3,78	2,88	/	10,82	7,82	10,00	
3	492,7–493,3	/	12,10	10,00	4,93	4,03	/	13,86	10,00	13,06	
4	710,7–711,3	/	16,55	14,16	7,11	6,21	/	19,71	14,16	18,83	N36°W
5	791,7–792,3	/	18,38	15,96	7,92	7,02	/	22,49	15,96	20,98	
6	886,9–887,5	/	19,79	17,24	8,87	7,97	/	23,97	17,24	23,50	

## 2.2. Energy law theory

The model takes tunnel excavation as an example and makes the following assumptions.

(1) The tunnel face cross-section is circular. (2) The main energy of outburst comes from the expansion energy of gas and the elastic potential of the ejected rock mass. (3) The failure of the rock mass conforms to the Mohr–Coulomb criterion. (4) The rock mass is assumed to behave elastically. (5) For the convenience of calculation, it is assumed that the outburst pushes out all the rock masses in front of the outburst termination line.

The gas in the tunnel and the rock-mass outburst mainly provide released energy for gas expansion to do work and to release the elastic potential of the rock mass. The energy consumed during the ejection process of the outburst mainly includes the surface energy required for the generation of a new surface and the kinetic energy required to throw the rock mass (Wang, G. et al., 2015; Song, S., 1966). According to the principle of conservation of energy, the following formula is obtained:

$$E_2 + W = E_1 + A_i \quad (1)$$

where  $E_2$ ,  $W$ ,  $E_1$ , and  $A_i$  ( $i = 1, 2$ ) represent the work done by gas expansion, the elastic potential of the rock mass, the surface energy required for the formation of a new surface, and the kinetic energy required for throwing the rock mass, respectively.

The mass-conservation formula of the gas and rock mass during the outburst process is

$$M = \rho_1 V_1 = \rho_2 V_2 \quad (2)$$

where  $M$  represents the rock mass,  $\rho_1$  represents the average density before the rock mass is thrown,  $V_1$  represents the volume before the rock mass is thrown,  $\rho_2$  represents the average density after the rock mass is thrown, and  $V_2$  represents the volume after the rock mass is thrown.

### 2.2.1. Surface energy required for new surface generation

The new surface theory (Xu, X. Yu, J., 1984) is used to solve the breaking work of the protruding rock mass. The rock mass is broken from fragmentation  $D$  to fragmentation  $d$ , and its crushing ratio is expressed by  $i$ .

$$i = D/d \quad (3)$$



From  $D$  to  $d$ , the change in the surface area of the rock per unit volume is proportional to  $1/d - 1/D$ . Therefore, the crushing specific work is expressed as

$$e = K_R(1/d - 1/D) \quad (4)$$

where  $K_R$  is a constant that depends on the properties of the rock and the fragmentation method.

When the crushing ratio is very large,  $1/D$  is smaller than  $1/d$ ,  $1/D$  can be omitted, and Eq. (4) can be written as

$$e = K_R/d \quad (5)$$

If the particles are regarded as spherical, the surface area per unit volume is  $6/d$ . Let  $W$  represent the energy used to establish a new surface area per unit. Then, Eq. (5) can be written as

$$e = 6W\sum(\gamma_i 1/d_i) \quad (6)$$

Combining Eqs. (3)–(6) yields

$$E_1 = eV_1 = 6W\sum(\gamma_i 1/d_i)V_1 \quad (7)$$

where  $V_1$  represents the volume of the rock mass before the outburst, and  $\gamma_i$  represents the percentage of fragmented coal particles that have a particular size.

### 2.2.2. Calculation of gas internal energy

The internal energy of the expanding gas can be calculated according to the adiabatic process (Li, C. et al., 2012). According to the first law of thermodynamics,

$$dQ = dE_2 + PdV \quad (8)$$

In the adiabatic process, there is no heat exchange with the surroundings; i.e.,  $dQ = 0$ . Thus, Eq. (8) can be written as

$$dE_2 + PdV = 0 \quad (9)$$

From thermodynamics, the change in gas energy due to a gas-temperature change can be expressed as follows:

$$dE_2 = MC\gamma dT/U \quad (10)$$

where  $M$  and  $U$  represent the mass and molecular weight of the gas, respectively, and  $C\gamma$  and  $T$  represent the constant-volume molecular heat capacity and absolute temperature of the gas, respectively. Substituting Eq. (10) into Eq. (9) yields

$$W = \int dw = - \int_{T_1} T^2 MC\gamma/U dT = M/UC\gamma(T_1 - T_2). \quad (11)$$

The gas pressure–temperature relationship in the adiabatic process is expressed as follows:

$$\begin{aligned} P_1 V_1^n &= P_2 V_2^n \\ V_1^{n-1} V_1 &= V_2^{n-1} T_2 \\ P_1^{n-1} T_1^{-n} &= P_2^{n-1} T_2^{-n} \end{aligned} \quad (12)$$

where  $n = C_P/C_V$ ;  $P_1$ ,  $V_1$ , and  $T_1$  represent the outburst gas pressure, volume, and temperature, respectively;  $P_2$ ,  $V_2$ , and  $T_2$  represent the atmospheric pressure, volume, and temperature in the roadway, respectively;  $n$  is the adiabatic coefficient of the gas; and  $C_P$  represents the constant-pressure molecular heat capacity of the gas. After a series of derivations, the formula for the work done by gas expansion is obtained:

$$E_2 = w = P_2 V_2 / (n - 1) [((p_1/p_2)^{n-1/n}) - 1]. \quad (13)$$

### 2.2.3. Determination of elastic potential of rock mass

The elastic deformation energy is stored in the rock mass and does external work. According to elastic mechanics, this stored elastic strain energy per unit volume of coal can be mathematically expressed as follows(Xian, X. et al., 2001):

$$E_2 = w = P_2 V_2 / (n - 1) [((\frac{p_1}{p_2})^{\frac{1}{n}}) - 1]. U^e = 1/2 E [(\sigma_1^2 + \sigma_2^2 + \sigma_3^2) - 2\mu(\sigma_1\sigma_2 + \sigma_1\sigma_3 + \sigma_2\sigma_3)]. \quad (14)$$

The energy in a certain area is given as

$$W = \int V_s U^e dV \quad (15)$$

where  $V_s$  represents the volume of the rock mass before the outburst. In Eq. (12),  $\sigma_1$ ,  $\sigma_2$ , and  $\sigma_3$  represent the three principal stresses (in MPa), and  $E$  represents the elastic modulus of the rock mass before the outburst (in MPa);  $\mu$  represents the Poisson's ratio of the rock mass (dimensionless).

### 2.2.4. Rock particle movement

As an outburst propagates, fragmented rock particles move from their original location into the tunnel. Different gas and rock outburst intensities lead to different accumulation patterns of rock particles in the tunnel.

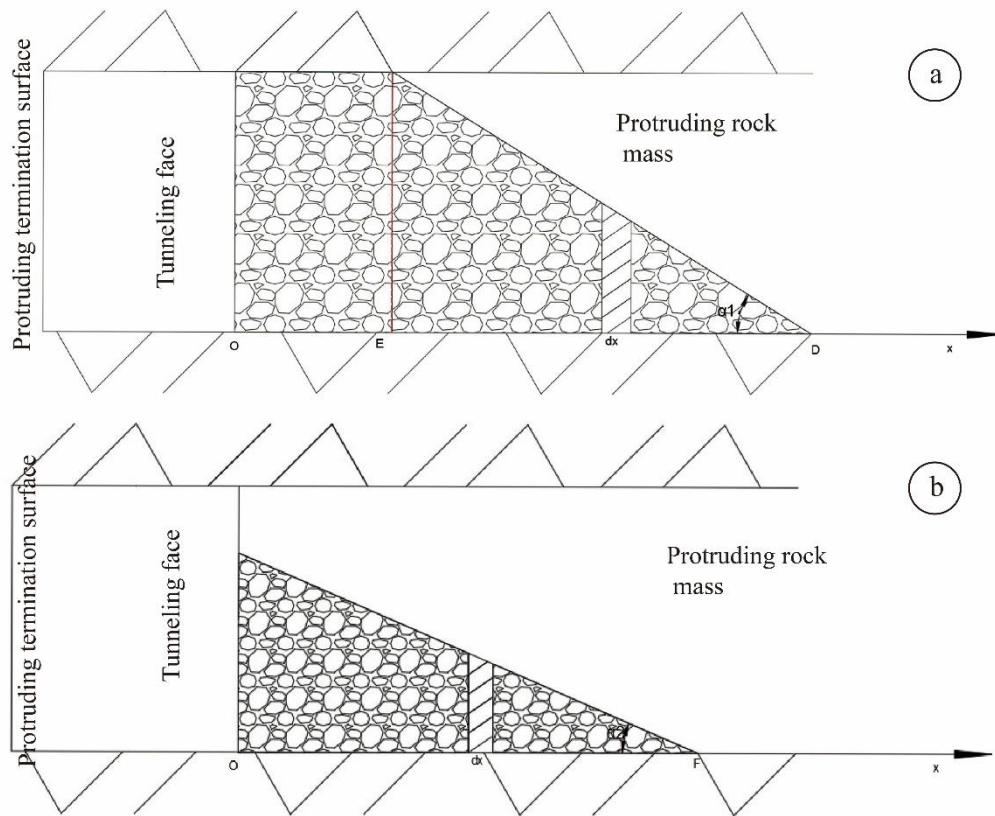


Figure 2. Accumulation of protrusions in the roadway(Xiong, Y. et al., 2015)

According to the calculation method of (Su) B.B. ХОДОТ (translated by Song et al.( 1966) ) combined with the hypothesis of this article, the ejection work of the unit is obtained as follows:

$$dA = x g f_1 dm \quad (16)$$

The coal mass of the slope part for the two types of outbursts can be roughly calculated as  $dm = 2rpf(x)dx$ , which is combined with the calculation formula (16) of the throwing power to obtain the expression for calculating the outburst.

When the outburst intensity is high, as shown in Figure 2(a), the calculation formula is

$$A_1 = \int_0^{OD} dA = \int_0^{OE} xgf_1 p 1/2 \pi r^2 dx + \int_{OE}^{OD} xgf_1 2rpf(x)dx = 1/4 \pi gpf_1 r^2 |OE|^2 + 2rpgf_1 \tan \alpha_1 [1/3 ( \quad ) \quad ] \quad (17)$$

$$1/2 |OD| |OE|^2]$$

When the outburst intensity is low, as shown in Figure 2(b), the calculation formula is

$$A_2 = \int_0^{OF} OF dA = \int_0^{OF} OF xgf_1 2rpf(x)dx = 1/3 rpgf_1 |OF|^3 \tan \alpha_2 \quad (18)$$

Here,  $f_1$  is the friction coefficient (dimensionless),  $\rho$  represents the density of the rock mass after the outburst,  $\alpha_1$  and  $\alpha_2$  represent the angles between the protruding body and the horizontal plane,  $|OF|$  represents the length of the deposit,  $r$  represents the height of the roadway, and  $g$  represents the gravitational acceleration.

Additionally, the equation for the minimum rock thickness based on the energy method is derived:

$$1 = \{6W \sum (\gamma_i 1/d_i) V_i - P_2 V_2 / (n-1) [((p_1/p_2)^{n-1}/n) - 1]\} / (s \times U^e) \quad (19)$$

where  $s$  represents the cross-sectional area of the protruding part of the rock mass.

Takes into account the impact of construction on the depth of the disturbance of the working face is  $L=1+l_1$ , where  $l$  represents the calculated thickness of the rock mass, and  $l_1$  represents the depth of the impact of construction on the working face.

## 2.3. Application of energy-method model

### 2.3.1. FLAC3D model and boundary conditions

To eliminate the boundary effect, according to the theory of elastic mechanics, the surrounding rock within six times the radius of the tunnel is assumed to remain in the *in situ* stress state. When modeling in the FLAC3D software, the thickness of the surrounding rock around the tunnel is six times the tunnel radius. In the physical model, the radial gradient mesh around the cylindrical tunnel and the hexahedral block grid unit are used. The tunnel radius is set as 3 m. The plugging rock mass should be set as a fluid–solid coupling model, because the local rock mass is set as a fluid–solid coupling model. It cannot run in FLAC3D; thus, the gas pressure is modeled as a uniformly distributed stress acting on the surface of the rock mass. The gas pressure is set as 3, 4, 5, 6, 7.5, and 9 MPa, and the rock-mass sealing thickness is 2.6 m. The upper surface of the Z axis is free, and the other surfaces are set as fixed constraints. The physical and mechanical parameters of the rock mass are those of granite (Table 3). The *in situ* stress is applied according to the measured values, and the *in situ* stress is generated by the elastic solution method. Then, the tunnel is excavated to calculate the deformation of the the sealed section of the rock mass under different stress levels.

Table 3. Physical and mechanical parameters of granite

Density (g/cm <sup>3</sup> )	Elastic modulus (GPa)	Poisson's ratio $\mu$	Cohesion (MPa)	Internal friction angle (°)
2,65	60	0,25	30	53

### 2.3.2. Energy calculation for prominent examples

The key parameters are presented in Table 4. According to the data in the table, the thickness of the sealing rock mass is calculated as approximately 2.6 m. When the energy method is used to calculate the potential energy of a rock mass, it is difficult to obtain the stress distribution in the rock mass. Assuming that the aforementioned stress is uniformly distributed in the outburst rock mass, the elastic potential of the outburst rock mass is calculated as 0.55 MJ. The calculations of the crushing work and ejection work are presented in Tables 5 and 6, respectively.

**Table 4. Rock-mass outburst parameters**

Elastic modulus E (GPa)	Poisson's ratio $\mu$	Maximum horizontal stress (MPa)	Vertical stress (MPa)	Minimum horizontal stress (MPa)	Rock-mass density before outburst (g/cm <sup>3</sup> )	Rock-mass density after outburst (g/cm <sup>3</sup> )	Outstanding rock volume (m <sup>3</sup> )	Tunnel section area (m <sup>2</sup> )
60	0,25	23,97	17,24	23,5	2,65	1,6	150	34,6

**Table 5. Crushing-work calculation parameters**

Fine-particle size (m)	Fine-particle content	Stone size (m)	Block-stone content	Breaking specific work (J/m <sup>2</sup> )	Rock mass (m <sup>3</sup> )	Breaking work (MJ)
0,02	0,7	17	0,3	0,039	89,9	736,809

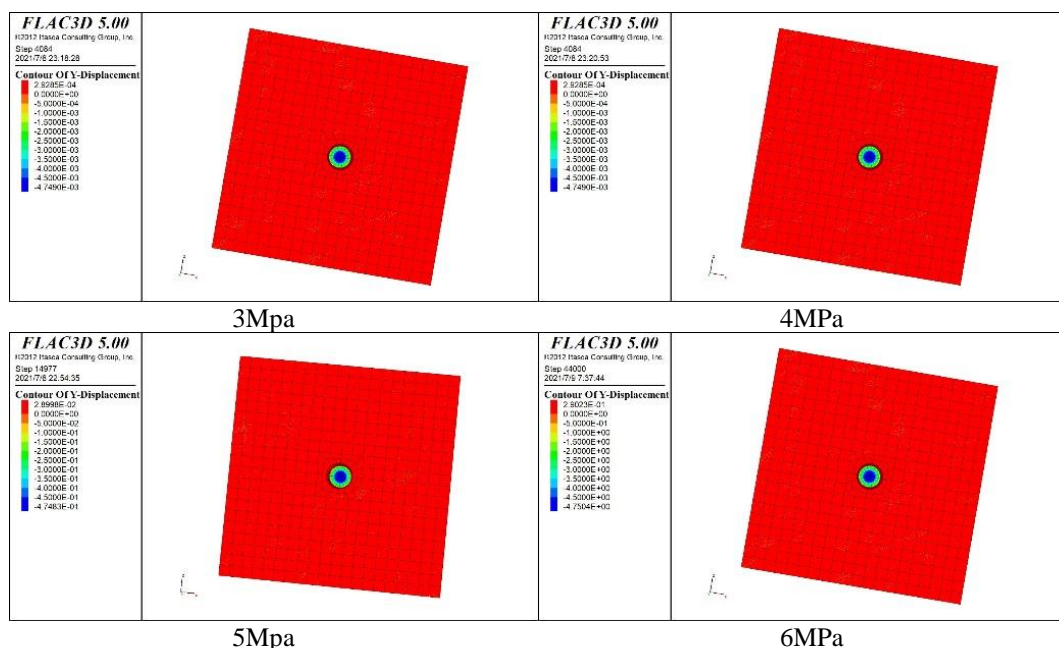
**Table 6. Mobile-power calculation parameters**

Angle of protrusion stacking (°)	Stack length (m)	Coefficient of friction	Mobile work (MJ)
21,8	15	1,33	57,32

Because the gas pressure before the outburst and the gas volume after the outburst could not be determined, by collecting CO<sub>2</sub> and rock-outburst cases, it was found that the gas volume has no correlation with the outburst rock mass. Thus, a trial calculation method was adopted to calculate the gas pressure and gas volume. The polytropic index was 1.25, and the residual gas pressure was 0.25 MPa; after the trial calculation, the final gas pressure was 7.5 MPa, and the gas volume was 814,469 m<sup>3</sup>.

### 3. RESULTS

According to the inversion of the key parameters, the sealing thickness of the granite rock mass is 2.6 m, the gas pressure is 7.5 MPa, and the gas volume is 814,469 m<sup>3</sup>. The numerical simulation results using FLAC3D (Figures 4 and 5) indicate that the deformation of the tunnel face is 4.7 cm when the gas pressure is 3 MPa, the deformation of the tunnel face is 4.7 cm when the pressure is 4 MPa, and the maximum deformation of the tunnel face under the gas pressure of 5 MPa is the maximum deformation of the tunnel face is 4.7 m when the applied pressure is 6 MPa at 47 cm, and the maximum deformation of the tunnel face remains unchanged at 4.7 m when the pressure exceeds 6 MPa. The first inflection point in the deformation curve corresponds to the onset of rock failure (blocks in the tunnel, uplift of the tunnel face, etc.), while the second inflection point represents the subsequent crushing and ejection of fractured rock.



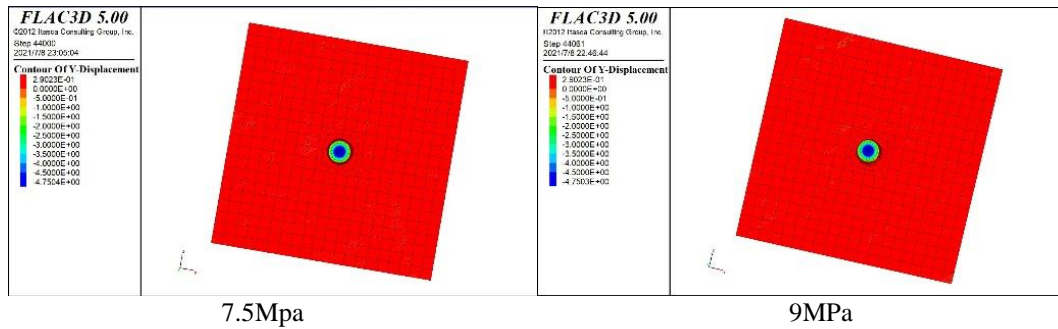


Figure 3. Finite-difference calculation results

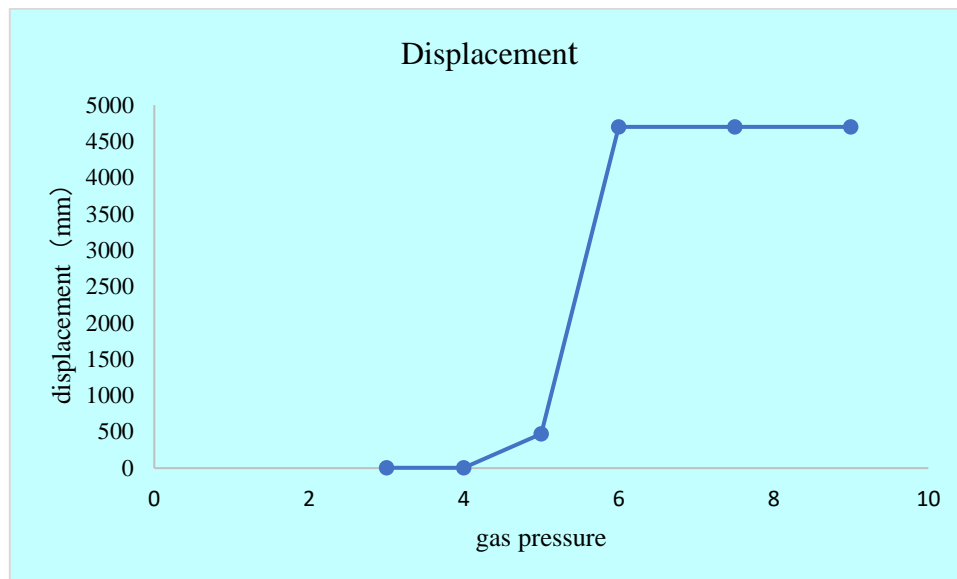


Figure 4. Deformation trend of the tunnel face under different pressures

#### 4. DISCUSSION

The gas pressure obtained via energy-method inversion is 7.5 MPa. The FLAC3D calculation results indicate that the rock outburst occurs when the gas pressure is 6 MPa. The calculation result of the energy method exceeds the outburst critical gas pressure calculated via the numerical software, confirming that the energy method is suitable for non-coal formation gas and rock protrusion. The gas pressures calculated via the numerical method and the energy method differ, and the use of the energy method does not affect it. The energy-method results indicate that the elastic potential of the rock mass is low. The gas expansion energy is four orders of magnitude higher than the elastic potential, and the crushing work of the granite is one order of magnitude larger than the ejection work. The reason for the high breaking power of the rock mass is that the granite is hard, and the broken granite has a large proportion of fine particles. The low elastic potential of the rock mass may be related to the small volume of the protruding rock mass and the elastic modulus of granite, which is several orders of magnitude higher than those of other rocks.

The FLAC3D calculation results indicate that the rock has cracks under the combined action of the 3-MPa air pressure and ground stress. After the gas pressure is increased to the pressure that can destroy the rock, the amount of rock-mass deformation suddenly increases by an order of magnitude. Then, the amount of rock-mass deformation gradually increases with the increase in the gas pressure. Finally, the amount of rock-mass deformation is a constant value. The sudden increase in rock deformation occurs because the expansion energy of the gas is mainly used to break the rock. While the amount of rock deformation remains unchanged, the broken rock mass is thrown out.

The gas and rock outburst positions are changeable, and explosions can occur on both sides of the tunnel, the bottom of the tunnel, and the top of the tunnel. When gas and rock outbursts occur at these locations, the calculated cross-sectional area should be the area of the gas acting surface in the direction of the tunnel facing surface. The



gas pressure can be determined through testing, and the gas volume can be calculated by consulting relevant data. The mechanical parameters of the rock can be obtained through testing. The critical condition for outburst defined in this article is that the outburst energy source is completely used for the surface energy in the outburst process. Therefore, the sizes of the rock particles and the corresponding percentage can be determined according to the relevant outburst records, and the specific work of rock fragmentation can be obtained by referring to "Rock Fragmentation" or other relevant records.

The final safe thickness is the sum of the thickness obtained via the energy method and the excavation disturbance thickness. The disturbance thickness can be calculated using numerical software or determined via geophysical methods.

## 5. CONCLUSION

(1) The energy method was used to derive the formula for the safe thickness when there is no moving work:  $l = \{6W \sum (\gamma_i / d_i) V_1 - P_2 V_2 / (n-1) [((p_1/p_2)n - 1/n) - 1]\} / (s \times U_e)$ ; the final safety thickness is given as  $L = l + l_1$ .

(2) This method takes into account the effects of the *in situ* stress, rock physical and mechanical parameters, and gas pressure on the outburst. The outburst energy source is gas expansion work, which highlights the elastic potential of the rock mass in the range and the gravitational potential energy of the rock mass; the outburst energy consumption The breaking work of the required energy for rock breaking to form a new surface, and the work of moving the rock mass in the roadway.

(3) The energy-method theory was used to calculate the gas pressure before the Hongdoushan No. 1 inclined well outburst accident, and the FLAC3D software was used to verify that the gas pressure obtained via the energy method will cause an outburst in granite under actual conditions.

## 6. REFERENCES

- [1] Guo C, 2010. Study on the conditions and mechanism of rock and gas outburst.,
- [2] Huang M, Shen W, Liu W, 2010. Safety measures for tunnel excavation under conditions of harmful gas and rock outburst. Sichuan Hydropower, 99.
- [3] Huang Z, Liang Y, Guo D, Jiang X, 2017. Prediction model for coal-gas outburst using the genetic projection pursuit method. International Journal of Oil, Gas and Coal Technology: IJOGCT 16, 271-282.
- [4] Hudeček V, Zapletal P, Stonis M, 2013. Results from dealing with rock and gas outburst prevention in the czech republic. Arch. Min. Sci. 58, 2013.
- [5] Huo Z, Xue W, Shu L, 2021. Discussion on coal mine rock and CO<sub>2</sub> outburst mechanism in my country. Coal Science and Technology 49, 155-161.
- [6] Jiang L, Wang J, Li W, 2010. Inorganic source CO<sub>2</sub> outburst prevention technology for steeply inclined and extra-thick coal seams. Coal Mine Safety, 23-26.
- [7] Li B, Wang E, Shang Z, Liu X, Li Z, Li B, Wang H, Niu Y, Song Y, 2021. Optimize the early warning time of coal and gas outburst by Multi-source information fusion method during the tunneling process. Process Saf. Environ. Protect. 149, 839-849.
- [8] Li C, Jie B, Cao J, Wang T, Xueying W, 2012. Coal and gas outburst intensity energy evaluation model. Journal of China Coal Society, 1547-1552.
- [9] Li Q, Lin B, Zhai C, 2015. A new technique for preventing and controlling coal and gas outburst hazard with pulse hydraulic fracturing: a case study in Yuwu coal mine, China. Nat. Hazards 75, 2931-2946.
- [10] Lin B, Zhou S, 1995. Outburst preventive mechanism of stress relaxation groove in coal tunnel. Chinese Journal of Geotechnical Engineering, 32-38.
- [11] Lv C, Cui Y, 2002. Study on mechanism and prevention and cure of CO<sub>2</sub> outburst in Zhangergou Coal Mine. Coal Geology of China, 21-23.
- [12] Maciej B, Jan K, Andrzej Z, 2018. Machine Learning in predicting the extent of gas and rock outburst. E3S Web of Conferences 71, 9.
- [13] Proctor R J, 2002. The San Fernando Tunnel explosion, California. Eng. Geol. 67, 1-3.
- [14] Qi T, Lei B, Wang R, Li Y, Li Z, 2018. Solid-fluid-gas coupling prediction of harmful gas eruption in shield tunneling. Tunneling & Underground Space Technology 71, 126-137.
- [15] Song S, 1966. Coal and Gas Outburst. Beijing: China Industry Press.
- [16] Sun J, 2009. Research on CO<sub>2</sub> outburst prevention technology. Coal Science and Technology, 110-112.
- [17] Tan Z, 2007. Variation characteristics of penetrating energy for diamond drilling in weathered granite formation. Chinese Journal of Geotechnical Engineering 29, 1303-1306.
- [18] Tang S, 2009. Technology for prevention and control of coal and CO<sub>2</sub> outburst in steeply inclined and extra-thick coal seams. Coal Mine Safety, 83-85.
- [19] Wang G, Wu M, Wang H, Huang Q, Yang Z, 2015. Sensitivity analysis of factors affecting coal and gas outburst based on a energy equilibrium model. Chinese Journal of Rock Mechanics and Engineering, 238-248.

- [20] Wang L, Han X, Xia Y, 2022. Study on Diffusion Mechanism and Calculation Method of Environmental Carbon Dioxide in Highway Tunnel. *Refrigeration & Air Conditioning* 36, 909-913.
- [21] Wang X, 2019. Numerical simulation research of coal and gas outburst near tectonic region in Ping ding shan mining area(Article). *Arab. J. Geosci.* 12, 583.
- [22] Wierzbicki M, Młynarczyk M, 2013. Structural aspects of gas and dolomite outburst in Rudna copper mine, Poland. *International Journal of Rock Mechanics & Mining Sciences* 57, 113-118.
- [23] Xian X, Xu J, Wang H, 2001. Prediction of potential dangerous areas (belts) of coal and gas outburst. *Engineering Science in China* 3, 39-47.
- [24] Xiong Y, Huang G, Luo J, Tang X, Honggang D, 2015. Theoretical analysis and experimental study on energy dissipation of coal and gas outburst. *Chinese Journal of Rock Mechanics and Engineering*, 3694-3702.
- [25] Xu X, Yu J, 1984. *Rock Fragmentation*. Beijing: Coal Industry Press.
- [26] Zhang K, Zheng W, Xu C, Chen S, 2019. Risk assessment of gas outburst in tunnels in non-coal formation based on the attribute mathematical theory(Article). *Geomatics, Natural Hazards and Risk* 10, 483-504.
- [27] Zhao Z, Lei Y, Com L, 2020. Mechanism Analysis of Uncovering Coal in Crosscut and Gas Outburst Based on Flac3D. *J. Coast. Res.* 103, 333-338.
- [28] Zhi Y, 2007. Analysis of prevention and control technology for slicing top coal mining in thick coal seam with steep CO<sub>2</sub> outburst. *Gansu Science and Technology*, 144-145.
- [29] Zhou A, Wang K, Kiryaeva T, Oparin V, 2017. Regularities of two-phase gas flow under coal and gas outbursts in mines. *J. Min. Sci.* 53, 533-543.
- [30] Zhou G, 1992. Research on the cause of CO<sub>2</sub> gas outburst in Yingcheng Coal Mine. *Northeast Coal Technology*, 61-63.
- [31] Zhu B, 2012. Study on Mechanism of Migration and Outburst of Natural Gas in Tunnel. *ADVANCES IN CIVIL ENGINEERING AND ARCHITECTURE INNOVATION*, PTS 1-6 368-373, 2736-2739.
- [32] Zhu C, Cai S, 2020. Study on Borehole Arrangement Methods for Gas Extraction by Hydraulic Slotting in Long-Distance Through-Coal Seam Tunnel. *Geofluids* 2020, 1-8.

## TRIAXIAL STUDIES OF GRAY CLAYS IN DIFFERENT LOADING MODES AS A FOUNDATION FOR UNDERGROUND CONSTRUCTION

Irina V. Koroleva<sup>1</sup>

**Abstract:** Statement of the problem. The safety of underground structures depends on the reliability of the foundation. When designing foundations of buildings with a developed underground part and foundations of underground structures, the question of the mechanical characteristics of soils arises. The least studied at the moment are gray clays, since in their natural state they occur at significant depths and have not been studied before. The main objective of this study is to identify the features of deformation of gray clays of a damaged structure under triaxial loading at different values of moisture, holding time in a desiccator and loading conditions. To achieve this goal, the following tasks were solved: identical samples of clays of a damaged structure were created; triaxial experimental studies were carried out; the ultimate strength of the samples and deformation characteristics were determined; graphical dependencies of strength, deformation modulus and shear modulus on moisture and loading conditions were constructed. Results. Experimental triaxial studies were performed on samples made of soil with a disturbed structure. The main results of the studies are new data on the development of vertical deformations and general deformation moduli, as well as shear moduli under triaxial loading depending on different soil moisture values, the time of sample holding in a desiccator before testing, the magnitude of lateral pressure and the presence of the first loading stage. Conclusions. The established influence of the factors under consideration on the deformation of gray clay under triaxial compression should be taken into account when calculating the settlement of building foundations and underground structures.

**Keywords:** clay soil, triaxial compression, mechanical properties of soil, moisture, foundation

### 1. INTRODUCTION

Well-designed foundations are the guarantee of safety of underground structures. Being one of the weakest building materials, soil often plays a decisive role in the destruction of underground structures, uneven soil subsidence, landslides and slope instability, which leads to a number of infrastructure damages and to some extent to human casualties (Sadono, 2017; Houston Sandra L. et al, 2001). Clayey soils of semi-solid consistency, such as clay, are problematic soil types in construction (Mohamad et al, 2016; Ural, 2018), since such soils generally have low shear strength and high compressibility (Ural, 2018; Uge, 2017; Giao et al, 2023). The physical properties and deformability of clayey soils depend on their age and genesis (Sharafutdinov, 2023; Lunev and Katsarskii, 2022). Moisture and the presence of defects are some of the factors affecting the shear strength of the soil, and time affects the stress-strain state, where deformation and strength change depending on the load. In the design process, it is assumed that the physical and mechanical characteristics of the soil base are constant throughout the life cycle of the building. In reality, the mechanical characteristics of foundation soils are unstable (Elhassan A.A. et al, 2023; Malizia and Shakoor, 2018) and continuously change under the influence of man-made (Bian et al, 2016; Cabello-Suarez L.Y. et al, 2017; Chen H., 2018), technological (Mirsayapov and Aysin, 2019; Song et al, 2020) and external force effects (Mirsayapov and Sharaf, 2023; Mirsayapov and Aysin, 2023; Mirsayapov and Koroleva, 2023). The features of deformation of samples at the following values of specified moisture are considered: 38 %, 40 % and 42 %. Some researchers believe that moisture close to the plasticity index is optimal for clays (Musbah et al, 2024; O'Kelly, 2023; Haigh et al, 2013).

<sup>1</sup> PhD Koroleva Irina V., Geotechnical Eng., associate professor, Kazan State University of Architecture and Engineering, Zelenaya st., Kazan, Russia, 79178711218@yandex.ru.

The tests were carried out on a triaxial compression device, which better simulates the behavior of soil in the field (Leong et al, 2013).

The problem of changes in the strength and deformation characteristics of grey clay, arising as a result of the influence of such factors as changes in moisture and time, is practically not discussed in the existing literature.

The aim of this study is to analyze the influence of soil moisture, the presence of the first stage of loading and defects in the structure of the sample caused by this loading, the time of holding the sample in a desiccator before the beginning of the second stage of two-stage loading, the magnitude of lateral pressure at the second stage on the features of deformation of gray clays of a damaged structure under triaxial loading conditions.

Research objectives:

- creation of identical samples from clays with a damaged structure;
- conducting triaxial experimental studies;
- determination of the ultimate strength of samples and their deformation characteristics;
- construction of graphical dependencies of strength, deformation modulus and shear modulus on moisture and loading conditions.

## 2. MATERIAL AND METHODS

Experimental studies are laboratory tests of gray clay with a disturbed structure at different moisture values and loading histories. The soil was crushed, moistened and formed into a monolith by layer-by-layer compaction (Mirsayapov and Koroleva, 2011a, 2019). This technique allowed us to obtain identical twin samples without large pores and inclusions, the presence of which in soils with an undisturbed structure does not allow us to perceive the samples as identical.

To create a two-stage loading, tests were carried out in two triaxial compression devices. For the first stage, a cubic device with a rib height of 100 mm was used, and for the second – a cylindrical one. Cubic triaxial compression was carried out in a device developed in the laboratory of the Department of Foundations, Foundations, Dynamics of Structures and Engineering Geology of the Kazan State University of Architecture and Civil Engineering, which was used in previous studies (Mirsayapov and Koroleva, 2011a) and made it possible to establish the failure mode (Mirsayapov and Koroleva, 2011b) under static deviatoric loading ( $\sigma_1 > \sigma_2 = \sigma_3$ ). This test made it possible to create a shear plane in the sample during deviatoric loading and subsequent failure according to the "crushing" scheme (Mirsayapov and Koroleva, 2011b, 2016). After failure, a cylindrical sample with a diameter of 38 mm and a height of 76 mm was cut out from the cubic soil sample, placed in a sealed desiccator for aging from 0 to 5 days, and then subjected to triaxial loading in a pneumatic stabilometer. Stabilometric tests were conducted at two values of lateral pressure  $\sigma_2 = \sigma_3 = 100$  kPa and  $\sigma_2 = \sigma_3 = 300$  kPa. It should be noted that the vertical stress deviator ( $\sigma_1 - \sigma_3$ ) was applied in steps of 10 % from  $\sigma_2 = \sigma_3$  until the sample was destroyed. The destruction criterion was the achievement of a vertical deformation in the amount of 15 % of the initial height of the sample.

The research program planned 4 series of tests.

The samples of the first and second series were not tested in a cubic triaxial compression device, i.e. they did not have a "plane of failure", while in the first series the sample was subjected to triaxial compression ( $\sigma_1 > \sigma_2 = \sigma_3$ ) in a stabilometer immediately after production, and in the second series it was kept in a desiccator for 5 days after production, and then placed in a cylindrical triaxial compression device for loading.

In the third and fourth series, soil samples with a disturbed structure were tested in a triaxial cubic device and acquired a defect in the form of a "destruction plane", then the cut samples of the third series were tested in a stabilometer, and in the fourth series, the samples were first kept in a desiccator for 5 days and then subjected to triaxial loading in a cylindrical device.

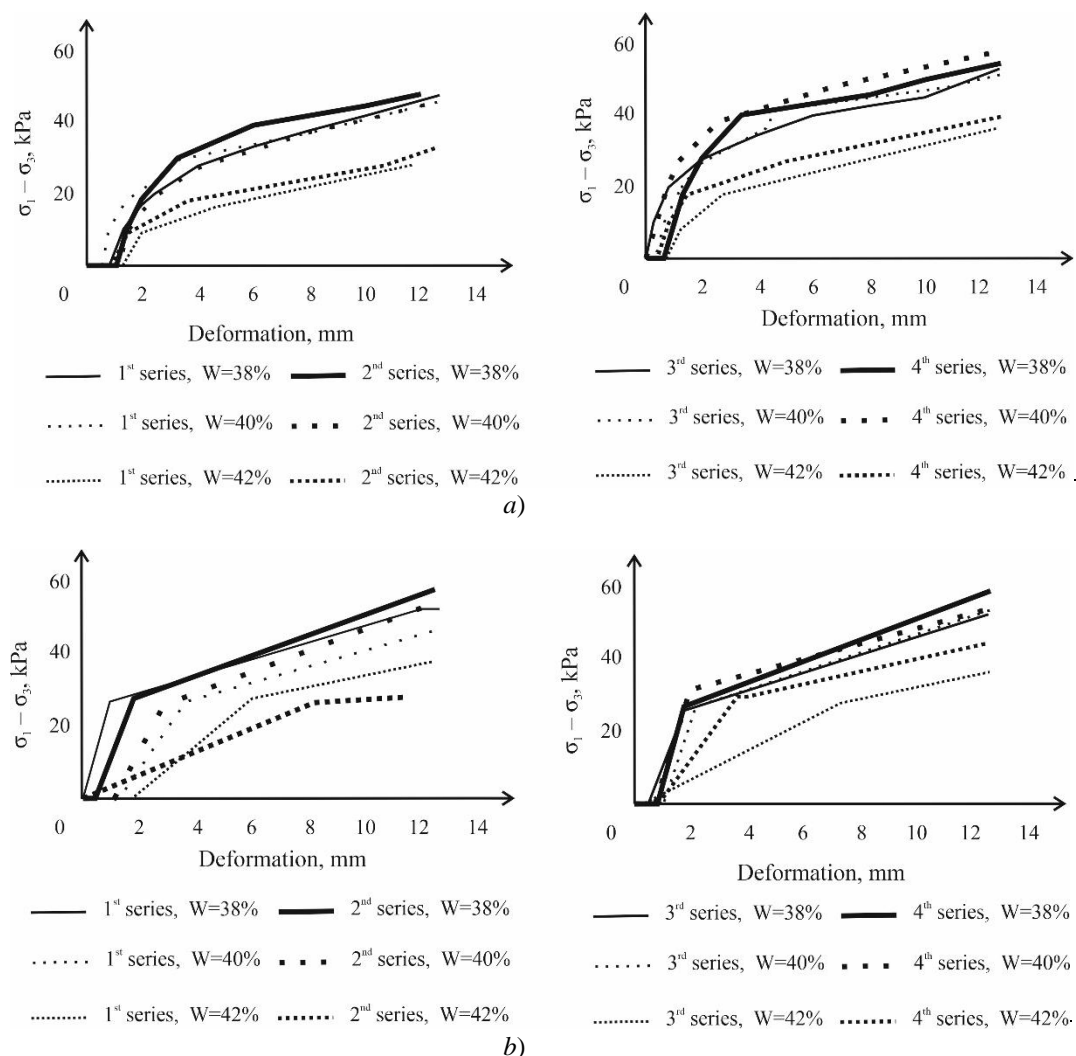
The experiments were carried out with artificially created soil samples of a disturbed structure with the following characteristics: plasticity index  $IP = 50,8$ ; moisture content at the yield point  $WL = 0,924$ ; moisture content at the rolling point  $WP = 0,416$ ; fluidity index  $IL = -0,07$  at moisture content  $W = 38\%$ ;  $IL = -0,03$  at  $W = 40\%$  and  $IL = 0,007$  at  $W = 42\%$  (the fluidity indices characterize natural soil according to GOST 25100 - 2020 "Soils. Classification" as hard and semi-hard clays).

The degree of soil water saturation  $S_r \leq 0,8$ . During the test, the samples were not additionally saturated with water, pore and effective pressures were not measured, and their influence was not assessed.

Thus, the main factors influencing the change in deformations, the modulus of total deformations and the shear modulus of samples under loading in a stabilometer are the magnitude of the lateral pressure, the moisture of the sample and the presence of a "plane of destruction" obtained as a result of the first stage of loading in a cubic device (3<sup>rd</sup> and 4<sup>th</sup> series).

### 3. RESULTS AND DISCUSSIONS

The samples of the first series of loading were taken as "standard" since they lacked the first stage of loading, and therefore the "plane of destruction", and they were not kept in a desiccator and were tested immediately after manufacture. The plotted graphs of deformation development (Fig. 1) allowed us to establish that the samples of second series have smaller deformations at the same value of the vertical stress deviator ( $\sigma_1 - \sigma_3$ ) as the samples of first series. This indirectly confirms the restoration of colloidal bonds in the sample of the damaged structure during its holding in the desiccator.



**Figure 1.** Development of soil sample deformations under different loading conditions: a) at  $\sigma_2 = \sigma_3 = 100$  kPa, b) at  $\sigma_2 = \sigma_3 = 300$  kPa.

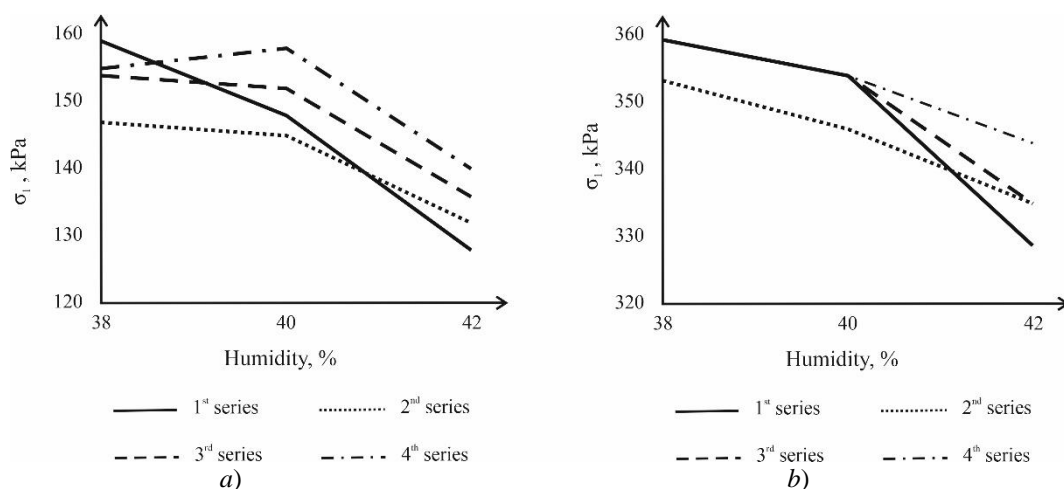
The presence of a destruction plane in the sample (Fig. 1, 3<sup>rd</sup> and 4<sup>th</sup> series) did not increase the rate of deformation development, but slowed it down at the first stages of loading by 1,4–1,8 times, and by 28 % with further loading. This is explained by the occurrence of zones of different density in the sample (Mirsayapov and Koroleva, 2011a, 2011b, 2019), which arose at the first stage of loading, and by the processes of reorientation of solid soil particles under loading. It is noted that in clays of semi-solid consistency, vertical deformations increase at a higher rate, since in this case the film water acts as a "lubricant" and helps to achieve the ultimate relative deformations that record the destruction of the sample. The data on the modulus of general deformations and the shear modulus, given in the article, were calculated automatically by the testing equipment program.

Based on the experimental studies results, the growth of vertical deformations graphs for each series of loading, changes in the modulus of general deformations  $E$  and the shear modulus  $G$  depending on the moisture of the

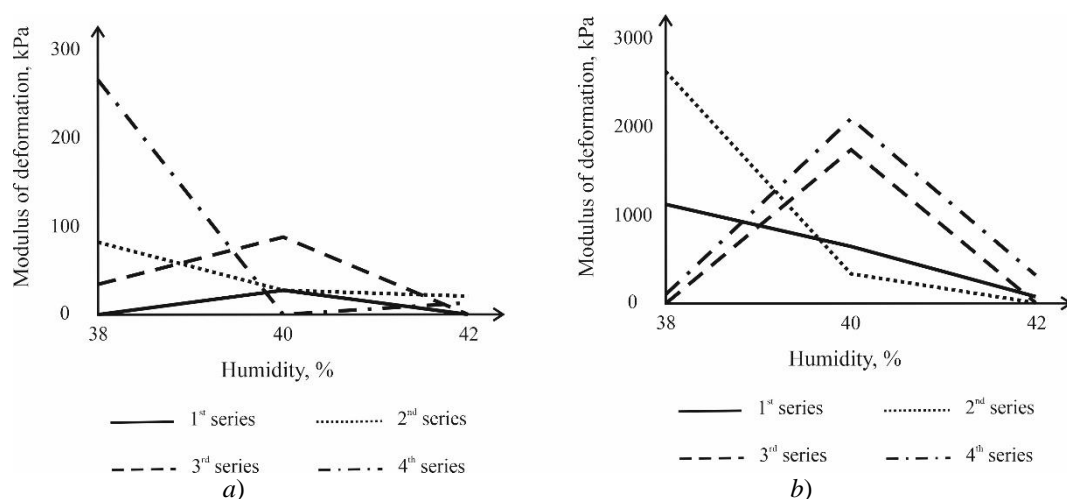


sample and the presence of holding time in the desiccator were constructed; the strength of the sample was also graphically assessed at different values of lateral pressure.

It has been established that soil moisture plays an important role: the higher the moisture content, the lower the vertical stress that the specimen can withstand when tested until failure (Fig. 2). Upon closer examination, it is evident that moisture content close to the rolling limit resulted in an increase in strength for specimens of 4<sup>th</sup> series at  $\sigma_2=\sigma_3=100$  kPa and does not have a significant effect at lower moisture content under conditions of  $\sigma_2=\sigma_3=300$  kPa. A further increase in moisture content results in a decrease in strength by 20 % and 10 % for specimens of first and second series and by 15 % and 5 % for specimens tested at the first loading stage, respectively. It should be noted that the holding time in the desiccator resulted in the expected increase in strength compared to specimens without holding at a moisture content of 42%. The presence of a fracture plane and a loosening zone around it (Mirsayapov and Koroleva, 2011a, 2011b, 2019) did not result in the predicted decrease in specimen strength, but, on the contrary, contributed to its increase. This is caused by additional compaction of the soil when loaded into the stabilometer.



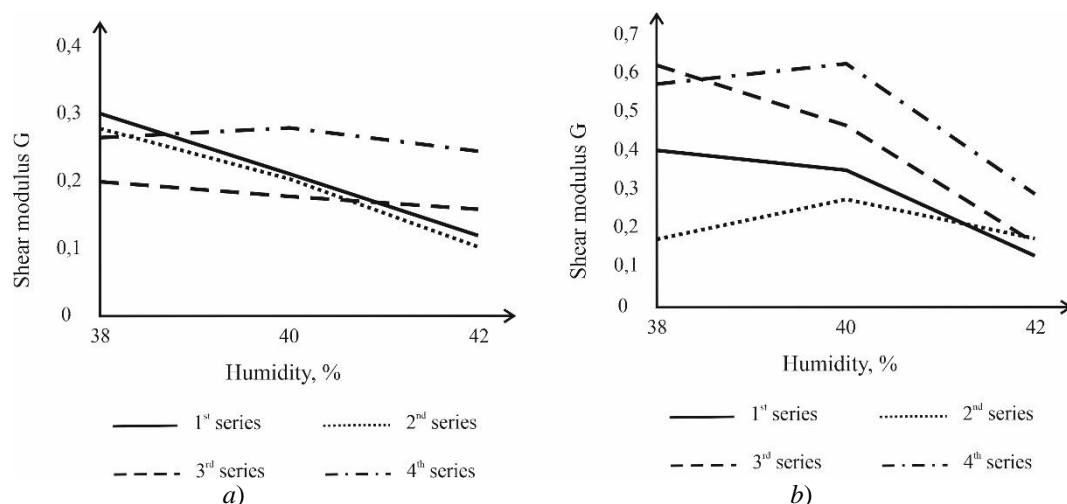
**Figure 2.** Change in the strength of a soil sample depending on moisture under different loading conditions: a) at  $\sigma_2=\sigma_3=100$  kPa, b) at  $\sigma_2=\sigma_3=300$  kPa.



**Figure 3.** Change in the value of the modulus of general soil deformations from moisture under different loading conditions: a) at  $\sigma_2=\sigma_3=100$  kPa, b) at  $\sigma_2=\sigma_3=300$  kPa.

The graph of deformation modulus change under different lateral loads (Fig. 3) shows that deformation modulus increases with moisture increase to 40 % under lateral load of 100 kPa 1<sup>st</sup> and 3<sup>rd</sup> series (Fig. 3a) and under  $\sigma_2=\sigma_3=300$  kPa 3<sup>rd</sup> and 4<sup>th</sup> series (Fig. 3b), but its value decreases significantly with moisture increase to the rolling limit (41,6 %) for all samples except 4th series under  $\sigma_2=\sigma_3=100$  kPa. The holding time in a desiccator

under 38 % moisture allows to reduce soil deformability for all tested samples, which is associated with restoration of structural bonds in soil with damaged structure. It should be noted that under lateral load of 300 kPa (Fig. 3b), deformation modulus in “without destruction” samples decreases with moisture increase from 38 % to 42 %. In another case, for samples “with destruction”, the deformation modulus increases at 40 % moisture, with a further increase in moisture, the deformation modulus decreases. These results allow us to conclude that moisture has a significant effect on the deformation properties of clay soil with a damaged structure.



**Figure 4.** Change in the value of the modulus of general soil deformations from moisture under different loading conditions: a) at  $\sigma_2 = \sigma_3 = 100$  kPa, b) at  $\sigma_2 = \sigma_3 = 300$  kPa.

The shear modulus  $G$  characterizes the ability of the soil to resist shear deformation and is determined based on the results of standard triaxial tests. The value of the shear modulus of the disturbed structure soil depends on the moisture, the presence of the first of the two loading stages and the holding time after it. Analyzing the obtained graphical dependencies (Fig. 4), it can be noted that the value of the shear modulus  $G$  decreases with an increase in moisture from 40 % to 42 % for all tests, which is explained by the formation of a water film that reduces the friction force between clay particles. The shear resistance of the samples is higher in the case of  $\sigma_2 = \sigma_3 = 300$  kPa after two-stage tests. "Rest" in a desiccator made it possible to improve the shear resistance to 35 % (series 4<sup>th</sup>, Fig. 4) due to strengthening caused by the restoration of water-colloidal bonds in the decompaction zone. The samples of the second series did not have a loosening zone acquired during the first stage of loading, so free water played the role of a lubricant and reduced the shear strength.

The issues of clays structural strength were studied in the works (Meng et al, 2020; Aiwu et al, 2023), the results obtained by the authors do not contradict these studies.

## 4. CONCLUSION

1. The deformation characteristics of clays with a damaged structure were studied under two-stage triaxial loading. Graphic dependences of the change in the deformation modulus  $E$ , shear modulus  $G$  and the magnitude of the destructive load were obtained depending on the soil moisture, the presence of the loading first stage and defects in the sample structure caused by this loading, the time of the sample holding in a desiccator before the beginning of the second stage of two-stage loading, the lateral pressure magnitude at the second stage. The deformation development graphs for each series of loading were analyzed.

2. It has been established that moisture is the main factor influencing the deformation characteristics of soil. An increase in the moisture of the disturbed structure soil to 42% almost always leads to a decrease in the deformation modulus  $E$  and the shear modulus  $G$ , as well as to an increase in the rate of increase in vertical deformations.

3. Under two-stage loading conditions, especially in the case of exposure in a desiccator (4<sup>th</sup> series), the soil exhibits higher deformation characteristics.

4. Water in soil with a disturbed structure plays a dual role: in the loosened zone it promotes the restoration of water-colloidal bonds and increases the deformation modulus  $E$  and the shear modulus  $G$ , and in soil without loosening it acts as a “lubricant” and accelerates deformation processes.

## 5. REFERENCES

- [1] Sadono, K.W. et al. (2017). Analisis Geologi Teknik Pada Kegagalan Bendung Cipamingkis, Bogor, Provinsi Jawa Barat. *Seminar Nasional Kebumihan*(10), 190–201.
- [2] Houston, Sandra L. et al. (2001). Geotechnical Engineering Practice for Collapsible Soils. *Geotechnical and Geological Engineering*(19), 333–355.
- [3] Mohamad, N.O., Razali, C.E., Hadi, A.A.A., Som, P.P. (2016). Challenges in Construction over Soft Soil - Case Studies in Malaysia. *IOP Conference Series: Materials Science and Engineering*, 136.
- [4] Ural, N. (2018). The Importance of Clay in Geotechnical Engineering. *InTech*, 83-102.
- [5] Uge, B. U. (2017). Performance, Problems and Remedial Measures for Roads Constructed on Expansive Soil in Ethiopia – A Review. *Civil and Environmental Research*(9), 28-37.
- [6] Giao, P.H. et al. (2023). Geological-geotechnical correlation of a deltaic subsoil profile and characterization of its uppermost soft marine clay deposit with reference to infrastructure development in the Saigon-Dong Nai delta, Vietnam. *Bull Eng Geol Environ*(82), 441. doi:10.1007/s10064-023-03461-4.
- [7] Sharafutdinov, R.F. (2023). Clay soil stiffness under consolidated isotropic drained triaxial tests. *Magazine of Civil Engineering*(121), 12106. doi:10.34910/MCE.121.6.
- [8] Lunev, A.A., Katsarskii, R.S. (2022). Influence of Water Content and Degree of Compaction on the Mechanical Properties of Soils of Various Geneses. *Soil Mechanics and Foundation Engineering*(59), 417-421.
- [9] Elhassan, A.A. et al. (2023). Effect of Clay Mineral Content on Soil Strength Parameters. *Alexand. Eng. J.*(63), 475-485.
- [10] Malizia, J.P., Shakoov, A. (2018). Effect of Water Content and Density on Strength and Deformation Behavior of Clay Soils. *Eng. Geol.*(244), 125-131.
- [11] Bian, H., Liu, S., Cai, G., Chu, Y. (2016). Influence of diesel pollution on the physical properties of soils. *Jpn. Geotech. Soc. Spec. Publ.*(2), 552-555. doi:10.3208/jgssp.CHN-16.
- [12] Cabello-Suarez, L.Y. et al. (2017). Impact of diesel contamination on the compressibility of a clayey soil. *2017 XIII international engineering congress (CONIIN)* (pp. 1-5). Santiago de Queretaro, Mexico: IEEE.
- [13] Chen, H., Shan, W., He, X. (2018). Influence of Diesel Contamination on Engineering Properties of Soil and Its Mechanism. *Proceedings of GeoShanghai 2018 international conference: fundamentals of soil behaviours* (pp. 620–627). Singapore: Springer Singapore.
- [14] Mirsayapov, I.T., Aysin, N.N. (2019). Influence of a deep construction pit on a technical condition of surrounding buildings. *Proceedings of the Geotechnics Fundamentals and Applications in Construction: New Materials, Structures, Technologies and Calculations* (pp. 197–201). St.-Petersburg, Russia: Springer.
- [15] Song, D., Chen, Z., Dong, L. (2020). Monitoring analysis of influence of extra-large complex deep foundation pit on adjacent environment: a case study of Zhengzhou City, China. *Geomatics, Natural Hazards and Risk*(11), 2036–2057.
- [16] Mirsayapov, I., Sharaf, H. M. A. (2023). Studies of Clay Soils Under Triaxial Block Cyclic Loading. *Lecture Notes in Networks and Systems*(574), 2378–2386.
- [17] Mirsayapov, I., Aysin, N. (2023). Clay Soil Deformations Under Regime Long-Term Triaxial Compression Taking into Account Initial Defects. *Lecture Notes in Civil Engineering*(291), 99–108.
- [18] Mirsayapov, I. T., Koroleva, I. V. (2023). Influence of initial defects on the strength of clay soil under triaxial compression. *Smart Geotechnics for Smart Societies*, 417–421. doi:10.1201/9781003299127-45.
- [19] Musbah, A., Mohammed, M. and Alfghia, A. (2024). The Effect of Mineral Composition and Quantity of Fines on the Atterberg Limits and Compaction Characteristics of Soils. *Open Journal of Civil Engineering*, 258-276. doi:10.4236/ojce.2024.142014.
- [20] O’Kelly, B. C. (2023). Theory of liquid and plastic limits for fine soils, methods of determination and outlook. *Geotech. Res.*, 1-9.
- [21] Haigh, S. K.; Vardanega, P. J.; Bolton, M. D. (2013). The plastic limit of clays. *Géotechnique*(63), 435–440..
- [22] Leong, E. C., Nyunt, T. T., Rahardjo, H. (2013). Triaxial Testing of Unsaturated Soils. In: *Laloui, L., Ferrari, A. (eds) Multiphysical Testing of Soils and Shales. Springer Series in Geomechanics and Geoengineering*. (p. 978). Berlin, Heidelberg: Springer. doi:10.1007/978-3-642-32492-5\_3.
- [23] Mirsayapov, I. T., Koroleva, I. V. (2011a). Physicomechanical properties of clay soil in the conditions of a spatial tension. *Bulletin of Civil Engineers*(26), 82-87. (in Russian)
- [24] Mirsayapov, I. T., Koroleva, I. V. (2011b). Prediction of deformations of foundation beds with a consideration of long-term nonlinear soil deformation. *Soil Mechanics and Foundation Engineering*(48), 148–157. doi:10.1007/s11204-011-9142-8.
- [25] Mirsayapov, I. T., Koroleva, I. V. (2016). Strength and Deformability of Clay Soil Under Different Triaxial Load Regimes that Consider Crack Formation. *Soil Mechanics and Foundation Engineering*(53), 5-11. doi:10.1007/s11204-0169356-x.
- [26] Mirsayapov, I. T., Koroleva, I. V. (2019). Studies of the water migration effect on changes in the clay soil physicommechanical characteristics under triaxial loading conditions. *News KSUAE*, 168-174. (in Russian)
- [27] Meng, F. et al. (2020). e-p curve-based structural parameter for assessing clayey soil structure disturbance. *Bull. Eng. Geol. Environ*(79), 4387–4398. doi:10.1007/s10064-020-01833-8.
- [28] Aiwu, Y., Shaopeng, Y., Jing, Z., Xianwei, Z. (2023). Effect of thixotropy on mechanical properties of soft clay with different initial disturbance degrees. *International Journal of Geotechnical Engineering*(17), 1-12. doi:10.1080/19386362.2023.2246231.

**UNDERGROUND AND CLIMATE CHANGE:  
RESILIENCE, SUSTAINABILITY AND URBAN TRANSFORMATION**

## CLIMATIC CHANGE INDUCED VULNERABILITY EVALUATION OF URBAN UNDERGROUND SPACES

Shuilong Shen<sup>1</sup>, Qian Zheng<sup>2</sup>, Annan Zhou<sup>3</sup>

**Abstract:** Urban underground spaces (UUS) are increasingly vulnerable to climatic change-induced disasters, e.g., flooding, subsidence, and extreme heat, necessitating advanced strategies for risk mitigation. This study integrates risk-informed and deterministic models into vulnerability evaluation frameworks to enhance risk assessment and early warning systems for UUS. Multi-source data, e.g., geological, hydrological, and urban infrastructure datasets are integrated into both risk-informed and deterministic models to quantify dynamic risks and spatial-temporal vulnerabilities. In the risk-informed model, a perception-based survey is conducted to evaluate stakeholders' awareness of underground risks to reveal discrepancies between perceived and actual threats. The inundation disaster in Zhengzhou in July 2021 is used as a site case to conduct the analysis. Results demonstrate that risk-informed vulnerability evaluation with participatory perception data significantly improves risk prediction accuracy and public preparedness. The proposed framework offers scalable solutions for cities globally and advocates for smarter integration of technology, infrastructure, and community engagement in climate adaptation strategies.

**Keywords:** Climatic change, urban underground space, risk assessment, risk-formed model, vulnerability evaluation.

### 1. INTRODUCTION

With the intensification of climate change, extreme precipitation events have become more frequent, significantly increasing the risk of urban flooding (IPCC, 2023). Climate change poses a severe challenge to urban hydrological systems. Excessive urbanisation has led to a reduction in natural vegetation and an increase in impervious surfaces. Flood management has become more intricate due to climate change and heavy rainfall, which have also intensified the risk of urban flooding and waterlogging. This highlights the urgency of comprehensively assessing flood risks and formulating proactive flood prevention strategies. Many cities, particularly inland ones, struggle with insufficient drainage systems that cannot cope with these extreme weather events (Liu et al., 2024). Urban flooding and water accumulation are increasingly frequent, particularly in inland cities, due to the fragile drainage systems that struggle to handle heavy rainfall. For example, floods in China during 2021 affected 34.81 million people, resulted in 146 deaths or missing individuals, caused 72,000 houses to collapse, and led to direct economic losses of 123 billion yuan (Chan, 2023). Among the many affected areas, underground space is particularly vulnerable and has become a key risk area in urban flooding (He et al., 2024). Over the years, the cumulative area of underground construction has significantly increased. This growth reflects the rapid expansion of urban underground spaces (UUS), particularly in subway systems, which in turn leads to a notable increase in the number of facilities exposed to flood risks (Yan et al., 2021). Once drainage capacity is restricted, extensive flooding can occur within a very short period of time, causing traffic paralysis, damage to facilities, and even casualties. Such incidents have occurred many times, which caused serious economic losses and posed a major threat to urban operations and public safety. Therefore, strengthening the identification and assessment of flood risks in underground spaces is a key step in improving the overall resilience of cities and optimizing emergency response mechanisms. This fact also highlights the urgency and necessity of conducting urban flood risk assessments and formulating targeted flood control strategies.

<sup>1</sup> Professor, Shen, Shuilong, PhD. Civil Engineering, Dean, College of Engineering, Shantou University, Shantou, China, shensl@stu.edu.cn.

<sup>2</sup> PhD, Zheng, Qian, Civil Engineering, Shantou University, Shantou, China, e-mail: 18zheng3@stu.edu.cn

<sup>3</sup> Professor, Zhou, Annan, Ph.D. Civil Engineering, School of Engineering, RMIT University, Melbourne, Australia, annan.zhou@rmit.edu.au.



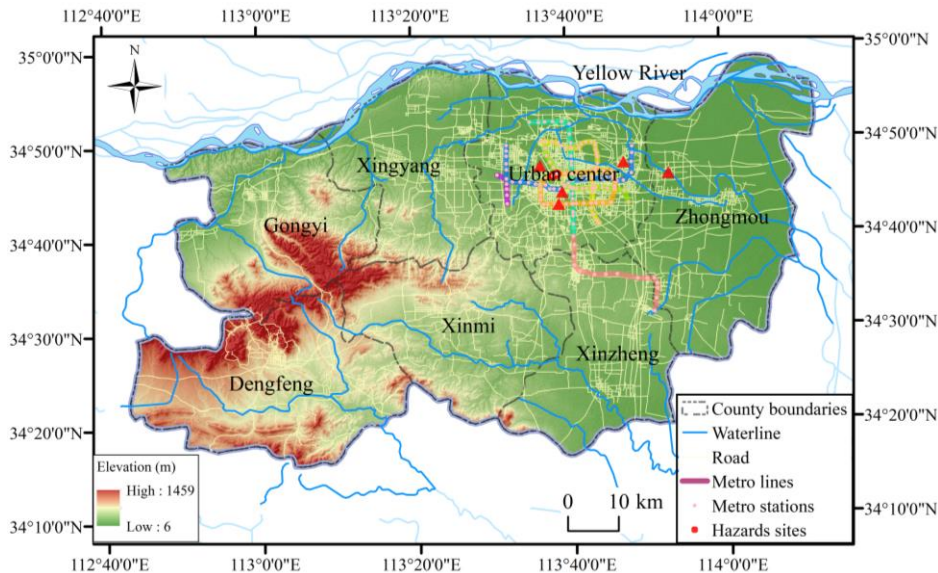
Underground spaces, such as subway systems, underground commercial areas, and parking lots, face substantial risks during such events (Lyu et al., 2020; Yan et al., 2021). This paper presents an integrated approach to assess urban flooding risks, resilience, and evacuation strategies, with a particular focus on underground spaces. The study uses the 2021 Zhengzhou “7.20 Storm” as a case study, providing an in-depth analysis of the vulnerability of underground spaces to flooding.

## 2. MATERIAL AND METHODS

### 2.1. Zhengzhou Disaster

The “7.20 Storm” in Zhengzhou, which occurred in July 2021, resulted in catastrophic flooding across the city. Zhengzhou received 624 mm of rainfall, nearly matching its annual average, with 201.9 mm of rainfall recorded in just one hour, breaking national records. According to the national investigation report (DIT-SC, 2022), approximately 14.79 million people were affected in this severe event, with 380 reported deaths. Among them, Zhengzhou accounted for 95.5% of the total deaths and missing people. The direct economic loss reached 120.06 billion yuan. Zhengzhou alone accounted for 40.9 billion yuan, or 34.1% of the total. The disaster severely impacted underground spaces, particularly the subway system. All stations on Line 5 of the Zhengzhou subway were flooded, and transport services were disrupted for several days. The impact on underground infrastructure underscored the vulnerability of such spaces to extreme weather.

Figure 1 shows the geological and hydrological distribution of the administrative area of Zhengzhou. The city centre is the most developed zone, with seven subway lines and a dense road network by 2022. The entire topography of Zhengzhou is characterised by a high elevation in the southwest and a low elevation in the northeast. This case study highlights the urgency of strengthening flood resilience measures in urban underground spaces. The official report from the national disaster investigation group criticized the event, stating, “The overall cause is a natural disaster, but there are also significant man-made factors involved”. The findings suggest a need for better flood risk assessment tools, enhanced flood management strategies, and the optimization of evacuation planning for these spaces.



**Figure 1.** Distribution of geomorphology, hydrology, and administrative region of Zhengzhou

### 2.2. Methods

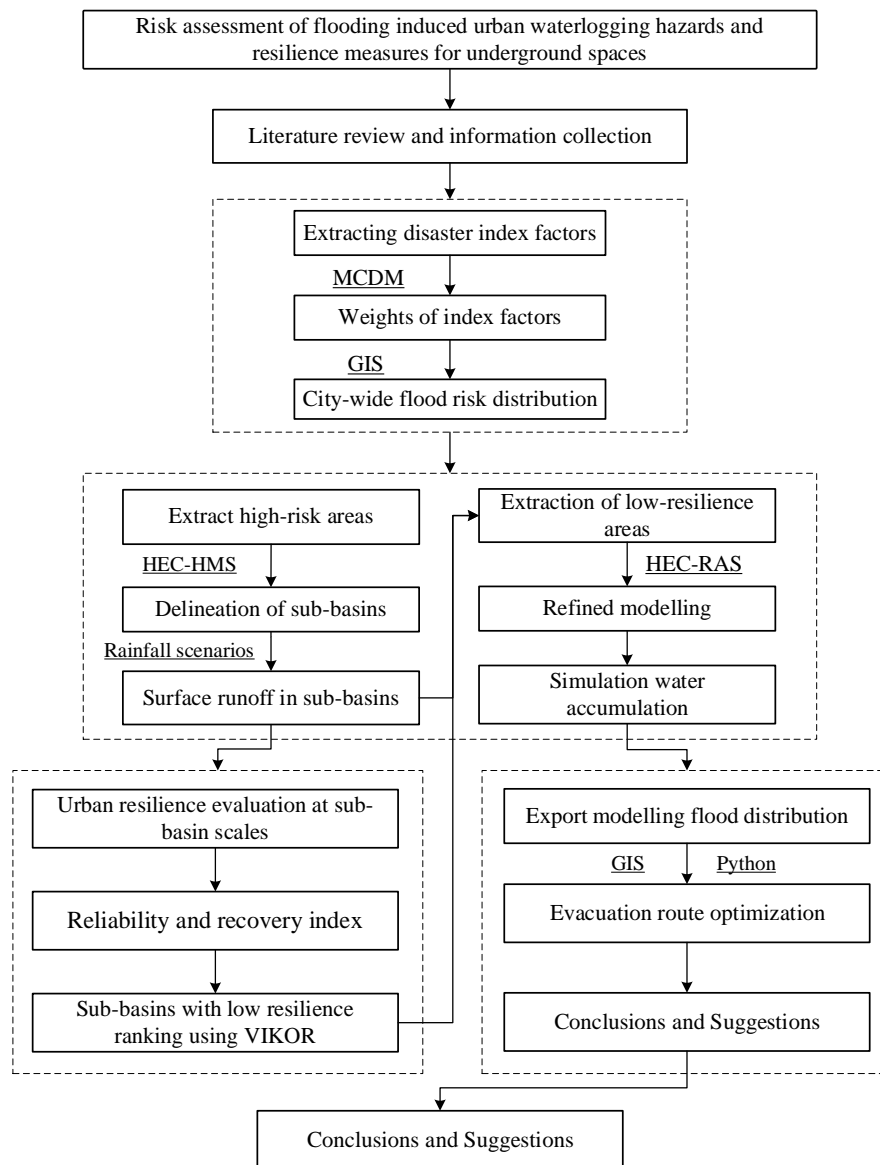
This study adopts a qualitative-to-quantitative and global-to-local analytical approach to comprehensively assess urban flooding and waterlogging hazards and resilience measures. The schematic of the research procedure in this study is illustrated in Figure 2.

First, disaster-related factors are extracted and weighted using Multi-Criteria Decision Making (MCDM) methods. Based on the weighted factors, the risk levels across different areas are assessed and classified. By combining historical rainfall data with hydrological simulations (HEC-HMS), sub-basins in the high-risk area can be delineated and their surface runoff calculated.

Then, Geographic Information Systems (GIS) are used to extract high-risk zones from the city-wide flood risk distribution map. Urban resilience is assessed using methods as CRITIC, VIKOR, focusing on the recovery capacity and reliability of each sub-basin, especially those with dense underground infrastructure. This part of the analysis progresses from the overall flood risk to the resilience of local sub-basins, gradually identifying key problem areas.

To further refine the modelling process, HEC-RAS is employed to simulate the inundation process and predict spatial distribution of water accumulation under different rainfall scenarios. A consistency check is conducted by comparing simulation outputs with observed water accumulation points, ensuring model validity and reliability.

Finally, GIS and Python are used to export modelling flood distribution. Based on these, evacuation routes are optimized by integrating road topology and flood data, focusing on high-risk and low-resilience underground spaces. This approach systematically combines qualitative analysis and quantitative modelling, advancing from overall risk to localized response planning, provides scientific support for enhancing flood resilience in high-risk urban areas.



**Figure 2.** Outline of research methodology used in the study

### 3. RESULTS

The results of the flood risk mapping, resilience assessment, and scenario simulations emphasize the critical need for targeted interventions in high-risk areas, particularly those with underground infrastructure such as

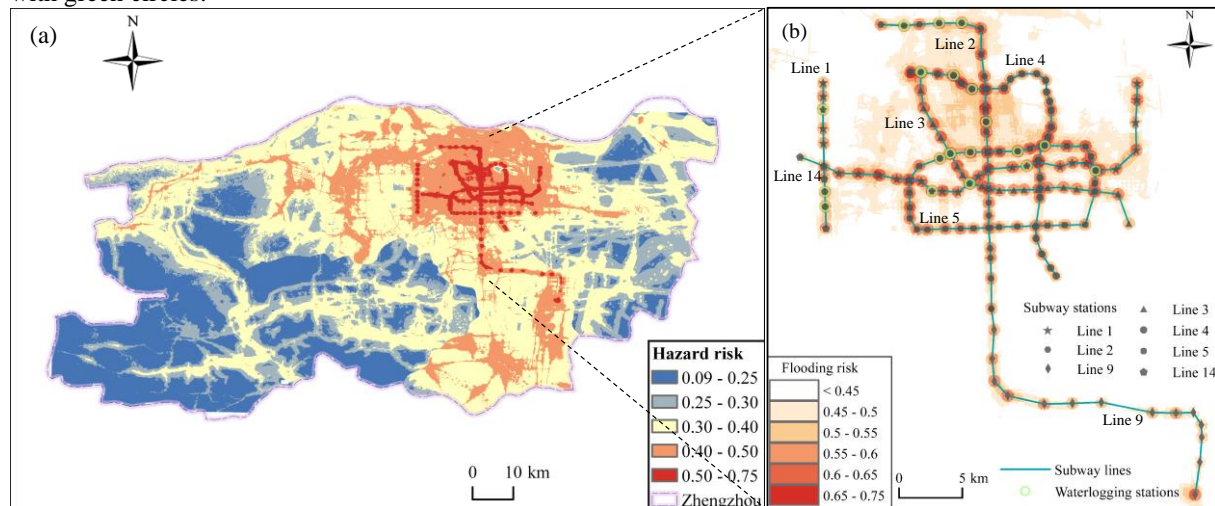
subway systems. The vulnerability of these spaces, especially in the urban center and near subway stations, highlights the need for integrated flood management systems and strategic evacuation planning.

### 3.1 Urban centre resilience

Risk mapping was conducted using the G-DEMATEL-AHP method, integrating grey theory with Decision-Making Trial and Evaluation Laboratory (DEMATEL) and Analytical Hierarchy Process (AHP) to evaluate the urban flood risk (Zheng et al., 2022). The method considered several factors, such as rainfall distribution (“7.20 Storm”), land use type, and the location of underground infrastructure. The integration of these factors allows for a comprehensive evaluation of the flood risk across urban regions, taking both environmental and infrastructural variables into account.

Figure 3 presents the risk distribution results, which includes a city-wide flood risk map and the subway system risk distribution. As shown in Figure 3(a), the results of the risk mapping process identified several high-risk zones (red areas), particularly in the urban centre and near subway stations. In these areas, the flood risk is significantly amplified due to inadequate drainage systems and dense infrastructure. These findings underline the critical need for improved flood management strategies, especially in regions with high concentrations of underground spaces like subway systems, which are particularly vulnerable during extreme weather events.

Figure 3(b) provides a more detailed view of the subway system's flood risk distribution, with flood risk values represented by a gradient of colors. Light orange indicates lower flood risk (<0.45), while dark red shows higher risk (>0.65). Subway stations and lines are marked with distinct symbols, and waterlogging stations are highlighted with green circles.



**Figure 3.** Risk distribution results: (a) city-wide flood risk map and (b) subway system risk distribution.

Beyond validating the model’s accuracy, the results also highlight structural and functional factors contributing to flood vulnerability in underground systems. All lines experienced some degree of damage, but stations that were most severely affected—such as Haitansi Station (Line 5) and Henan Sports Centre Station (Line 3)—also serve as major transfer hubs. Notably, Line 5 is a circular line with numerous intersecting stations, making it a critical component of the subway network. Its structural layout and centrality lead to high passenger flow and system interconnectivity, which in turn increase its vulnerability to flooding. These stations often have more complex layouts, deeper or wider underground volumes, and higher passenger throughput. Such characteristics not only increase exposure to floodwater but also complicate emergency drainage and evacuation operations. This suggests that flood risk in underground spaces is influenced not only by geographic location but also by functional importance and structural design complexity.

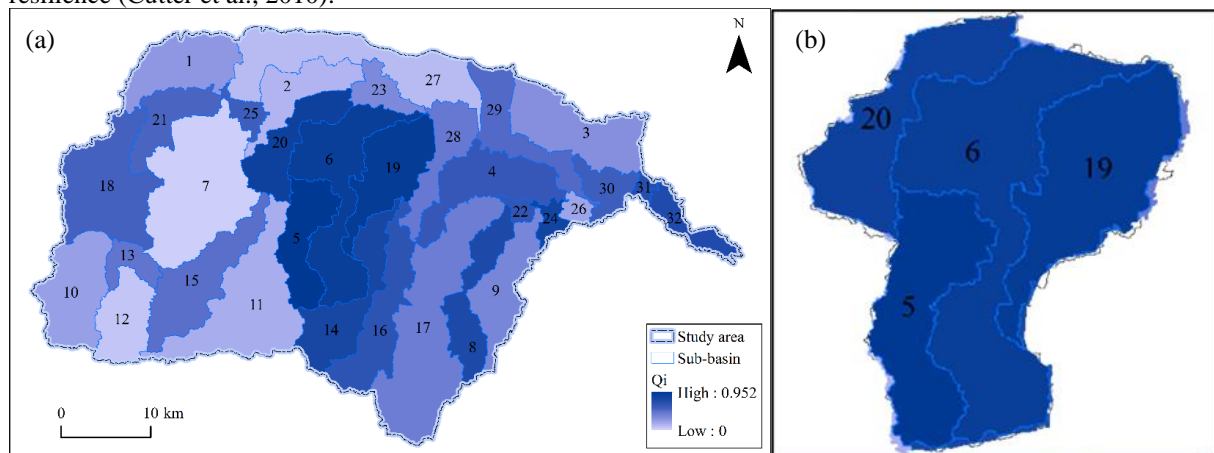
### 3.2 Urban center resilience

To evaluate the resilience of urban spaces to flooding, this study developed a sub-basin-scale resilience assessment framework guided by the Sendai Framework for Disaster Risk Reduction. The framework integrates physical, socio-economic, and infrastructural factors using methods such as CRITIC, GRA, and VIKOR. This multi-criteria decision analysis (MCDM) approach provides a comprehensive resilience index for different sub-basins.

Figure 4 shows the spatial distribution of resilience across the study area, with (a) presenting the overall resilience map by sub-basin and (b) highlighting the resilience index values for each sub-basin. The map in (a) illustrates a gradient of resilience levels, where darker blue indicates higher resilience and lighter shades represent

lower resilience. Notably, sub-basins 5, 6, 19, and 20, located in the urban centre, exhibit the lowest resilience ( $Q_i > 0.7$ ). These areas are characterized by dense underground infrastructure, low shelter accessibility, and complex post-disaster response environments, making them particularly vulnerable to flooding. In contrast, sub-basins in the southeastern region—such as 4, 8, 14, 16, and 24—also show lower resilience ( $Q_i > 0.5$ ), largely due to their downstream location and lower elevation, which make them more susceptible to cumulative runoff. Furthermore, sub-basins 31 and 32, located at the river outlets, are exposed to compound flood risks, including stagnation in low-lying areas, insufficient drainage capacity, and delayed recovery due to limited infrastructure and evacuation access.

The resilience assessment revealed significant spatial disparities in the resilience of different sub-basins. For example, the urban centre, with its dense underground infrastructure and poor shelter accessibility, exhibited the lowest resilience index. This indicates that areas with high underground space density are particularly vulnerable to flooding and should be prioritized for resilience improvements (He et al., 2024). These findings underscore the need for targeted interventions in flood-prone areas, particularly in the urban core, where the integration of flood management systems, infrastructure upgrades, and enhanced shelter access will be crucial for improving overall resilience (Cutter et al., 2010).



**Figure 4.** Spatial distribution of urban resilience: (a) urban resilience index for sub-basins in high-risk area, (b) identified low-resilience and high-risk area.

### 3.3 Waterlogging: Scenario simulation

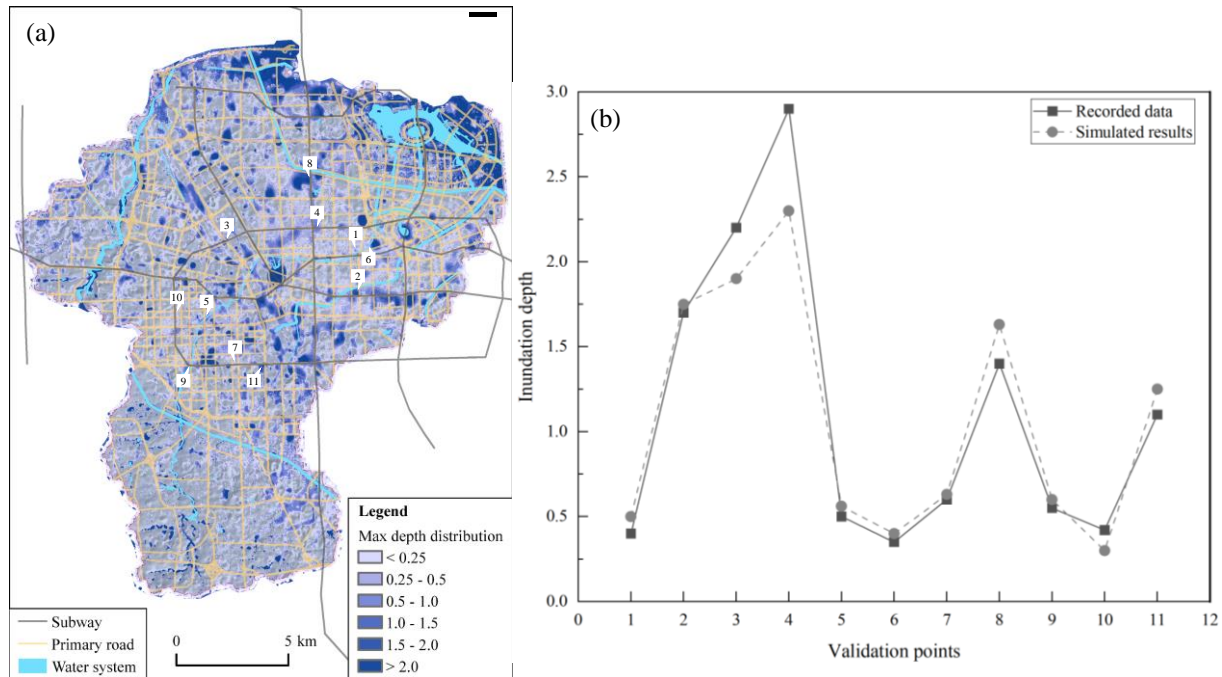
Flood risk simulations were performed using HEC-HMS and HEC-RAS models, focusing on six rainfall scenarios with different return periods (3, 5, 10, 30, 50, and 100 years). HEC-HMS was used to simulate the rainfall-runoff processes, estimating the volume and timing of surface runoff for each scenario. The runoff data generated by HEC-HMS was then used as input for HEC-RAS, which modeled the propagation of floodwaters across the urban landscape. These simulations were conducted specifically within sub-basins previously identified as high flood risk and low resilience, based on earlier risk and resilience assessments. These scenarios simulate the potential flood depths and inundation areas under various rainfall conditions, offering insights into the spatial-temporal evolution of flooding. The simulations were validated with data from the “7.20 Storm,” showing consistent results with actual flood events.

Figure 5 shows the flood inundation simulation and model validation results for the “7.20 Storm” scenario using HEC-RAS model. Figure 5(a) displays the maximum flood depth distribution map, with varying colour scales representing flood depths ranging from less than 0.25 m to more than 2 m. The map highlights critical urban infrastructures such as subways, primary roads, and water systems. Several validation points (1–11) are marked on the map to compare simulated and observed flood depths.

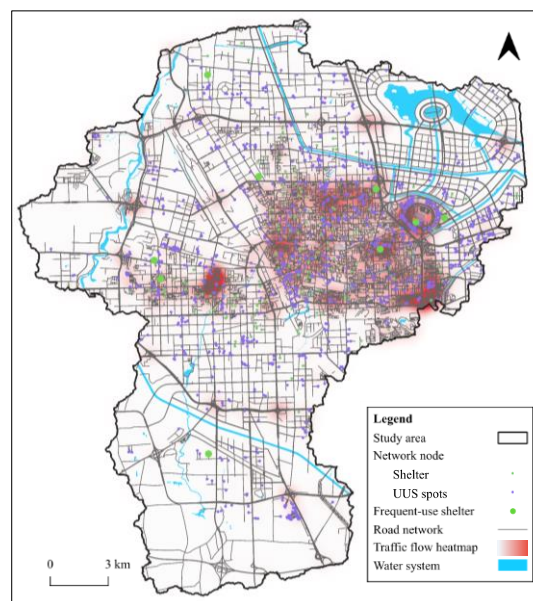
Figure 5(b) compares the flood depths recorded at the validation points with the simulated results. The solid squares represent recorded data, while the dashed circles represent the simulated results. It is evident that the simulated results closely align with the observed data for most validation points, particularly in areas with higher flood depths, such as validation points 4 and 5, indicating the model's good fit for extreme rainfall scenarios. However, some discrepancies are observed at certain validation points (e.g., points 6, 8, and 10), where the simulation slightly deviates from the recorded data. This may be due to localized geographic or infrastructure factors influencing the flood behaviour.

The results indicated that low-lying areas, primary roads, and underground spaces are particularly vulnerable during extreme rainfall events. The flood depth increased significantly under longer return period scenarios, emphasizing the need for adaptive flood management strategies and the optimization of urban drainage systems.





**Figure 5.** Flood inundation simulation and model validation results: (a) Maximum flood depth distribution under extreme rainfall scenario; (b) Validation of simulated depth against observed data.



**Figure 6.** "7.20 Storm" traffic and shelter flow analysis

### 3.4 Evacuation planning

Evacuation planning plays a critical role in enhancing urban resilience during floods. In this study, an evacuation route optimization framework was developed using GIS, road network topology, and flood risk models. The framework aims to optimize evacuation routes from underground spaces to designated emergency shelters, considering flood risk, shelter accessibility, and potential congestion during evacuation. Route calculation was based on the Dijkstra algorithm, which identifies the shortest and safest paths on the weighted road network under flood constraints. Flood inundation depth used in the optimization process was derived from previous HEC-RAS simulation results, ensuring that evacuation routes account for spatial variations in flood severity.

Figure 6 presents a heat map of traffic flow, with red areas indicating heavy traffic and the intensity reflecting congestion levels. The road network is shown as grey lines, and water systems (rivers, lakes) are displayed. Shelters are marked as green points, including both official and planned (Plan) shelters, while UUS spots are represented by purple points. For clarity, road network nodes are omitted in the map. Frequent-use shelters are determined by



identifying shelter locations with evacuation flows greater than 25, marked as large green points. All eight frequent-use shelters are from the proposed planned shelters, highlighting their strategic importance. One of these shelters, located in the southern area, addresses the shortage of shelters in that region, further emphasizing the value of the proposed shelters in evacuation planning.

Simulation results revealed that the number of existing shelters is inadequate to support large-scale evacuation needs, especially in high-risk areas (Shu et al., 2025). To address this, the study proposes the inclusion of non-traditional shelters, such as school playgrounds and public squares, to enhance shelter accessibility. These locations offer good accessibility and sufficient open space, making them effective supplements to official shelters.

#### 4. DISCUSSION

To further enhance urban flood resilience, future efforts could focus on the development of a mobile application that bridges the gap between flood risk evaluation and public awareness. Such an app could integrate real-time AI analytics to deliver localized early warnings, adaptive evacuation routes, and dynamic flood risk communication. By leveraging sensor networks deployed in underground spaces, the system may monitor critical environmental indicators—such as water levels and structural stability—thus enabling timely responses to extreme weather events.

Given the simulation results indicating that low-lying areas, major roads, and underground infrastructure are especially vulnerable, the envisioned system should support dynamic evacuation planning. In particular, it could utilize real-time flood depth data (e.g., derived from HEC-RAS outputs) to continuously update and optimize evacuation routes, aiming to reduce congestion and improve safety during emergencies.

Additionally, resilience assessments have underscored the importance of shelter accessibility. In future iterations, the app could incorporate updated information on official and proposed shelters, especially in high-risk zones with limited coverage. By including non-traditional shelters—such as school playgrounds and public squares—the platform may help enhance the spatial equity of emergency resources.

Ultimately, this app-based system is envisioned as an adaptive, real-time decision-support tool. It could not only improve situational awareness among residents but also assist emergency planners in coordinating effective responses. By linking spatiotemporal flood modeling with public communication strategies, this approach holds promise for strengthening urban resilience in the face of intensifying climate risks.

#### 5. CONCLUSION

This paper presents a comprehensive approach to assessing urban flood risks, focusing on the vulnerability of underground spaces such as subway systems. By combining flood risk mapping, resilience assessments, and scenario simulations, the study identifies high-risk areas and emphasizes the need for targeted flood management strategies. The main findings of this study are as follows:

(1) This study proposed the G-DEMATEL-AHP methodology to improve the efficiency of flood risk assessment and designed a corresponding questionnaire format to enhance the accuracy and reliability of data collection.

(2) A sub-basin-level urban resilience assessment framework was developed based on the Sendai Framework, combining CRITIC, GRA, and VIKOR methods to evaluate both reliability and recovery, with particular attention to the role of underground spaces for localized resilience planning.

(3) It integrated HEC-HMS and HEC-RAS models to simulate surface runoff and flood inundation, and introduced an equivalent rainfall calculation method to better represent the impact of extreme rainfall and urban drainage systems.

(4) The study demonstrated the necessity of supplementing official shelters with additional planned shelters to overcome issues such as limited capacity and poor accessibility, thereby improving overall shelter availability and evacuation effectiveness during flood emergencies.

#### 6. ACKNOWLEDGMENTS

The research work was funded by Guangdong Provincial Basic and Applied Basic Research Fund Committee (2022A1515240073).

## 7. BIBLIOGRAPHY

- [1] Chan, S.C., Kendon, E.J., Fowler, H.J., Youngman, B.D., Dale, M., Short, C. (2023). New extreme rainfall projections for improved climate resilience of urban drainage systems. *Climate Services*, 30, 100375.
- [2] Cutter, S.L., Burton, C.G., Emrich, C.T. (2010). Disaster resilience indicators for benchmarking baseline conditions. *Journal of Homeland Security and Emergency Management*, 7(1).
- [3] Disaster Investigation Team of State Council (DIT-SC) (2022). Investigation Report on July 20, 2021 Torrential Rain Disaster in Zhengzhou, Beijing: Henan Province, Peoples' Republic of China, 2022. (1), p. 46. (in Chinese).
- [4] He, R., Tiong, R.L., Yuan, Y., Zhang, L. (2024). Enhancing resilience of urban underground space under floods: Current status and future directions. *Tunnelling and Underground Space Technology*, 147, 105674.
- [5] IPCC, (2023). Sections. In: Climate Change 2023: Synthesis Report. Contribution of Working Groups I, II and III to the Sixth Assessment Report of the Intergovernmental Panel on Climate Change [Core Writing Team, H. Lee and J. Romero (eds.)]. IPCC, Geneva, Switzerland, 35-115. Available online: <https://doi.org/10.59327/IPCC/AR6-9789291691647> (accessed on October 4, 2024)
- [6] Liu, M.Y., Xu, X.Z., Xiao, P.Q., Cao, Y.Q. (2024). Advocating integration of human responses in the flood resilience framework for inland cities of northern China. *Water Policy*, 26(7), 652-670.
- [7] Lyu, H., Zhou, W., Shen, S., Zhou, A. (2020). Inundation risk assessment of metro system using AHP and TFN-AHP in Shenzhen. *Sustainable Cities and Society*, 56, 102103.
- [8] Shu, X., Ye, C., Xu, Z., Liao, R., Song, P., Zhang, S. (2025). An Enhanced Framework for Assessing Pluvial Flooding Risk with Integrated Dynamic Population Vulnerability at Urban Scale. *Remote Sensing*, 17(4), 654.
- [9] Yan, F., Qiu, W., Sun, K., Jiang, S., Huang, H., Hong, Y., Hou, Z. (2021). Investigation of a large ground collapse, water inrush and mud outburst, and countermeasures during subway excavation in Qingdao: A case study. *Tunnelling and Underground Space Technology*, 117, 104127.
- [10] Zheng, Q., Shen, S., Zhou, A., Lyu, H. (2022). Inundation risk assessment based on G-DEMATEL-AHP and its application to Zhengzhou flooding disaster. *Sustainable Cities and Society*, 86, 104138.

## LIFE-CYCLE CARBON FOOTPRINT OF UNDERGROUND INFRASTRUCTURE

Luyuan Long<sup>1</sup>, Wout Broere<sup>1\*</sup>, Xuehui Zhang<sup>1,2</sup>

**Abstract:** The construction industry is a major source of greenhouse emissions, and underground infrastructure, including tunnels, is responsible for a significant proportion of the overall carbon emissions. Studies on the carbon footprint of tunnels often focus on only part of the full life cycle or on a particular type of tunnels only, and do not consider and compare the carbon emissions of different types of tunnels over the full life cycle. This paper compares the carbon footprint of the four common types of tunnels, namely, shield tunnels, new Austrian tunnelling method (NATM) tunnels, cut-and-cover tunnels, and immersed tunnels, during the design, construction, operation and maintenance (O&M), as well as dismantling phases. A case study of a real-world tunnel project is used to quantify carbon emissions and reveal differences in emission magnitude and distribution across tunnel types and life cycle stages. Finally, this paper suggests several key carbon reduction measures for achieving a low-carbon design.

**Keywords:** Carbon footprint, Life cycle assessment, Tunnels, Low-carbon design

### 1. INTRODUCTION

In recent years, civil infrastructure has experienced rapid growth driven by economic development and urbanization. However, the construction industry has simultaneously emerged as one of the largest contributors to greenhouse gas (GHG) emissions, ranking third among industrial sectors in the United States (EPA, 2009) and accounting for approximately one-third of global carbon emissions (UNEP, 2009; UNEP, 2018; Gan et al., 2019). Among various GHGs, carbon dioxide (CO<sub>2</sub>) is the most prevalent emission resulting from human activities.

Tunnels are a common form of civil infrastructure and have seen rapid development in recent years due to their ability to traverse complex terrain and reduce land use on the surface. However, tunnels account for substantial CO<sub>2</sub> emissions throughout their entire life cycle, including construction, operation, maintenance, and dismantling. Moreover, studies have shown that tunnels are among the most carbon-intensive constructions compared to other types of infrastructure. For instance, Chang and Kendall (2011) reported that although tunnels and elevated structures together accounted for only 15% of the total length of a high-speed rail project, they were responsible for as much as 60% of the CO<sub>2</sub> emissions. Similarly, in a carbon emission assessment of a mountainous highway project in China, Fei et al. (2017) found that on a per-kilometer basis for a four-lane section, tunnels and bridges exhibited the highest energy intensities, contributing 49.83% and 37.57% of total emissions, respectively, while roadbed and pavement works accounted for only 12.60%. These findings highlight the need to conduct carbon emission assessments for high-emission-density infrastructure such as tunnels in the context of global carbon neutrality.

Life cycle carbon emission analysis of tunnels typically focuses on quantifying the distribution and sources of carbon emissions across four main phases: design, construction, operation and maintenance, and dismantling. These insights form the foundation for developing targeted mitigation strategies. The design phase primarily involves planning and technical decision-making. Although this stage generates relatively low emissions directly, the choices made, such as material selection and construction methods, have a profound influence on

<sup>1</sup> Geo-Engineering Section, Department of Geoscience and Engineering, Delft University of Technology, Delft, the Netherlands.  
Corresponding author: Dr. Wout Broere, w.broere@tudelft.nl

<sup>2</sup> Department of Civil and Environmental Engineering, The Hong Kong Polytechnic University, Hung Hom, Kowloon, Hong Kong, China

emissions in subsequent phases. The construction phase tends to dominate the life cycle emissions profile, largely due to the energy-intensive production of key materials such as cement and steel. The operation and maintenance phase also contributes significantly, with emissions arising from material and energy consumption related to maintenance activities, ventilation, and lighting. In contrast, the dismantling phase is less frequently encountered in practice, as tunnels are typically designed for long service lives. Nonetheless, should this phase be required, it is expected to incur substantial carbon costs due to heavy material and equipment demands.

This study aims to examine carbon emissions associated with underground infrastructure, with a particular focus on various types of tunnels. Upon completion of the emission calculations, practical mitigation strategies should be proposed to support the transition toward low-carbon tunnel development in future projects.

This paper is organized into four main sections. The first section is the introduction. The second section is related to current practical and widely adopted methodologies for calculating tunnel-related carbon emissions. The third section is a case study showing the carbon emission distribution of various types of tunnels. Finally, the fourth section draws on the strategies for low-carbon tunnels.

## 2. EXISTING METHODS FOR CARBON EMISSION CALCULATION

Three commonly used methods for carbon emission calculation include the emission factor method, the input–output method, and the inventory analysis method.

The emission factor method calculates carbon emissions based on the average amount of greenhouse gases emitted per unit of product under normal technological, economic, and management conditions. This method is widely accepted and recommended by the Intergovernmental Panel on Climate Change (IPCC) as a standardized approach for carbon accounting. It follows the equation:

$$\text{Emissions} = \text{Activity Data} \times \text{Emission Factor} \quad (1)$$

The input–output method relies on input–output matrices to capture inter-dependencies within the economy. It enables the conversion of monetary values in sectors such as construction into corresponding energy consumption and carbon emissions. This approach is especially suitable for macro-level assessments in commercial and industrial applications.

The inventory analysis method involves breaking down the system into individual processes and summing the emissions across all stages. It also employs the same basic formula but focuses on process-level detail. This makes it more appropriate for micro-level carbon assessments.

In the field of civil engineering, the emission factor method is currently the most widely adopted. However, when applied to different life cycle stages, the calculation scenarios and data requirements may vary. The following sections provide a detailed discussion of these stage-specific approaches. The proposed framework in this paper is illustrated in Figure 1.

### 2.1. Design phase

The design phase mainly involves desktop-based activities, with electricity use for office operations being the main source of emissions. These emissions are typically negligible compared to those from other phases and are often excluded from life cycle assessments (LCA). However, it is important to recognize the far-reaching influence of design decisions on total life cycle carbon emissions. While the direct emissions from this phase are minimal, the choices such as construction materials and tunnel dimension can significantly shape the emissions profile of subsequent stages. Material parameters relevant to carbon emission are often associated with cement, concrete, and steel consumption. Design of dimensions may include tunnel cross-sectional dimensions, tunnel length, and reinforcement ratio. In summary, while the design phase is often excluded from direct LCA calculations due to its minimal emissions, its decisions substantially influence the overall life cycle carbon footprint of a tunnel and therefore need careful attention.

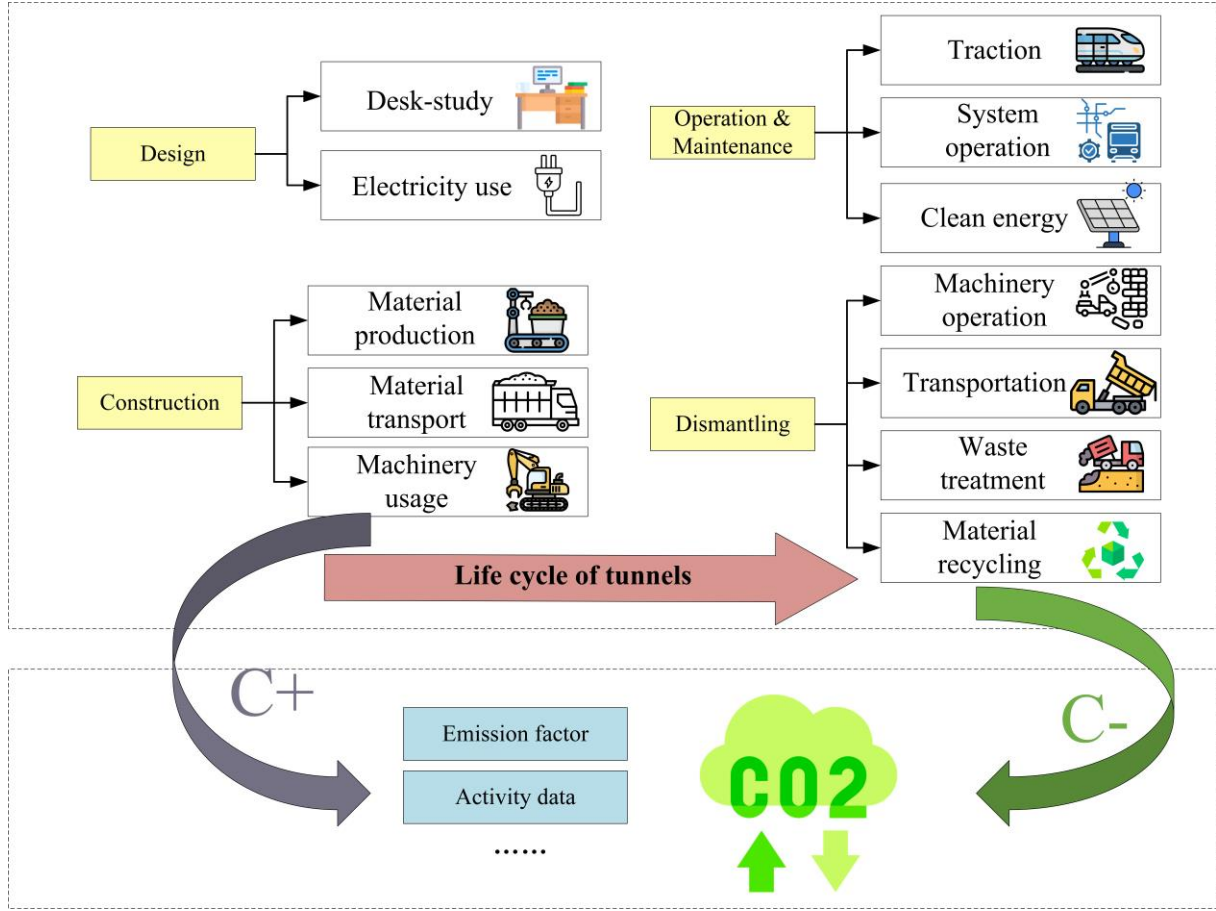


Figure 1. The life cycle of carbon emission assessment of tunnels

## 2.2. Construction phase

Carbon emissions from material production during the construction phase are determined by accounting for both primary and recycled material inputs. These emissions depend on the material quantities, their respective emission factors, and the associated recycling rates, as expressed in the following equation:

$$C_p = \sum_i (M_{p,i} \times (1 - R_i) \times EF_{p,i} + M_{p,i} \times R_i \times EF_{r,i}) \quad (2)$$

where:  $C_p$  denotes the carbon emissions from materials production (tCO<sub>2</sub>),  $M_{p,i}$  represent the consumption of each type of material (t),  $R_i$  is the recycling rate for each type of material,  $EF_{p,i}$  and  $EF_{r,i}$  refer to the carbon emission factors of primary material and recycled material, respectively (tCO<sub>2</sub>/t).

Total carbon emissions from material transportation are estimated based on the quantity of materials transported, the type and amount of energy or fuel consumed, the transport distance, and the corresponding emission factors, as represented in the following equation:

$$C_t = \sum_i (E_{t,i} \times F_{t,i} \times D_{t,i} \times EF_{t,i}) \quad (3)$$

where:  $C_t$  represents the carbon emissions related to transporting (kgCO<sub>2</sub>),  $E_{t,i}$  is the quantity of material  $i$  transported (kg),  $F_{t,i}$  is the fuel or energy consumption per ton per kilometer for transporting material  $i$  (kg/t · km),  $D_{t,i}$  is the transport distance (km).  $EF_{t,i}$  is the carbon emission factor for the fuel or energy used by the transport equipment (tCO<sub>2</sub>/t).

Total carbon emissions caused from construction energy use are calculated by multiplying the amount of energy consumed by the corresponding carbon emission factor for the type of energy used by construction machinery, as expressed in the following equation:

$$C_m = \sum_i (E_{m,i} \times EF_{m,i}) \quad (4)$$



where:  $C_m$  is the carbon emissions energy consumption of machinery,  $E_{m,i}$  is the total energy consumption for each type of construction machinery, determined based on actual consumption,  $EF_{m,i}$  is the carbon emission factor for the energy used by each type of construction machinery.

### 2.3. Operation and maintenance phase

This study includes the energy consumption from train traction as part of the operational phase carbon emissions. In addition, energy use by lighting and ventilation systems constitutes two other major contributors that significantly affect operational emissions. Taken together, the total carbon emissions during the operation phase can be expressed by the following equation:

$$C_{op} = (E_{\text{traction}} + E_{\text{systems}} - S_{\text{clean}}) \cdot T_{\text{life}} + E_{\text{maint}} \quad (5)$$

where:  $C_{op}$  represents the total carbon emissions during the operation and maintenance phase ( $kgCO_2e$ );  $E_{\text{traction}}$  denotes the annual emissions from traction energy consumption ( $kgCO_2e/\text{year}$ );  $E_{\text{systems}}$  corresponds to the annual emissions from tunnel system operations, including lighting and ventilation ( $kgCO_2e/\text{year}$ );  $S_{\text{clean}}$  represents the annual carbon offset from clean energy technologies in auxiliary systems ( $kgCO_2e/\text{year}$ );  $T_{\text{life}}$  denotes the operational lifespan of the tunnel (years); and  $E_{\text{maint}}$  represents the cumulative emissions from maintenance activities ( $kgCO_2e$ ).

### 2.4. Dismantling phase

Tunnels are often classified as control structures and, upon reaching the end of their service life, are typically decommissioned in place rather than dismantled. However, full-scale dismantling may still occur, particularly in the context of infrastructure expansion. For example, the Huangmeishan Tunnel in China was dismantled in 2022 to facilitate the upgrade of a four-lane dual carriageway to an eight-lane configuration. During the operational phase, partial dismantling may also be required when severe localized deterioration arises. In such cases, segments of the tunnel lining and support structure must be removed and subsequently reinforced or re-cast to restore structural integrity.

Current research on tunnel dismantling remains limited. However, the carbon emissions associated with this phase can be estimated using calculation methods developed for the dismantling of buildings. A representative example is the model proposed by Xiao (2021), which provides a basis for adapting emission estimates in the context of tunnels.

$$E_{\text{end}} = Q_c + Q_t + Q_h + Q_m \quad (6)$$

where:  $Q_c$  represents carbon emissions from dismantling machinery operations;  $Q_t$  denotes carbon emissions from the transportation of construction waste;  $Q_h$  indicates carbon emissions from waste treatment activities, including landfill and incineration;  $Q_m$  represents carbon emissions generated during the recovery of recyclable materials.

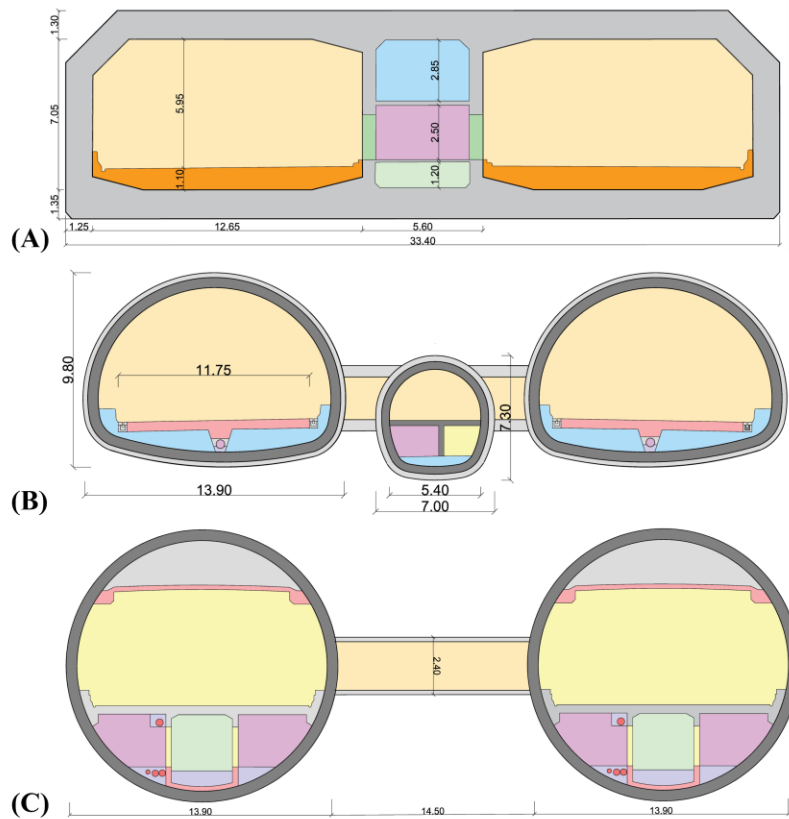
## 3. CASE STUDY

### 3.1. Engineering background

Dalian is a key regional economic center in China. With accelerating urbanization and ongoing industrial restructuring, the city has been expanding steadily northward.. However, north-south traffic connections remain insufficient. Severe and persistent congestion during peak hours continues to hinder mobility, posing a critical constraint on the development of adjacent urban clusters. To address this challenge, the 5.1-kilometer Dalian Bay undersea tunnel project was initiated. The tunnel will directly link the city's northern and southern districts, greatly enhancing overall accessibility and optimizing the regional transportation network.

Three alternative schemes were considered for the undersea tunnel crossing: an immersed tunnel, a drill-and-blast tunnel, and a shield tunnel. The immersed tunnel design comprises a 3,600 m immersed section, a 1,294 m buried section, and a 286 m open-cut section, yielding a total length of 5,430 m. Its structural cross-section is illustrated in Figure 2(A). The drill-and-blast tunnel extends approximately 9,214 m with cross-section shown in Figure 2(B). The shield tunnel alternative has a total length of approximately 4,765 m, comprising a 2,630 m

shield-driven segment, a 1,755 m buried section, and a 380 m open-cut section. Its typical cross-section is depicted in Figure 2(C).



**Figure 2.** Cross-sections of three types of tunnel: (A) Immersed tunnel; (B) Drill-and-blast tunnel; (C) Shield tunnel.

### 3.2. Carbon emission calculation of the construction phase

This study first focuses on carbon emissions during the tunnel construction phase for the three proposed tunnel schemes. The calculations account for the design lengths, cross-sections (considering main tunnel, connection passages, and cross-passages), and steel reinforcement distribution for each tunnel. Since this engineering case is based on detailed project conceptual design documents, material transportation  $C_t$  and machinery energy consumption  $C_m$  are temporarily excluded from consideration. The carbon emissions taken for the calculation in this case are from the regional database, shown in Table 1.

**Table 1.** Primary carbon emission factors used in this case study

Material type	Carbon emission factor	Factor unit	Source
Concrete	385	Kg CO <sub>2</sub> /m <sup>3</sup>	Ministry of Housing and Urban-Rural Development of the People's Republic of China, (2019)
Steel	2340	Kg CO <sub>2</sub> /t	
Electricity	0.5876	Kg CO <sub>2</sub> / kWh	National Power CO <sub>2</sub> Emission Factors, (2021)

The emission calculation process takes into account different sections of the tunnel. For instance, the immersed tunnel in this project is divided into immersed, buried, and open sections, each corresponding to distinct cross-sectional functionalities, resulting in varying cross-sectional areas. The primary quantities for the three types of tunnels are summarized in Table 2.

**Table 2.** Amount of major material use in three types of tunnel

Tunnel type	Concrete (m <sup>3</sup> )	Steel(t)
Immersed tunnel	681917.14	26765.25
Drill-and-blast tunnel	534270.86	20970.13
Shield tunnel	249953.24	9810.66

The final results include the total carbon emissions generated during construction for each scheme, as well as the unit carbon emissions per unit length for each cross-section. The key design parameters and carbon emission calculations for the three tunnels are summarized in Table 3.

**Table 3.** Carbon emission calculations during the construction phase for three types of tunnel

Tunnel type	Length (m)	CO <sub>2</sub> emissions (t CO <sub>2</sub> )	Unit length CO <sub>2</sub> emissions (t CO <sub>2</sub> /m)
Immersed tunnel	4799	329260.92	68.61
Drill-and-blast tunnel	9534	257970.52	27.06
Shield tunnel	4765	120688.90	25.33

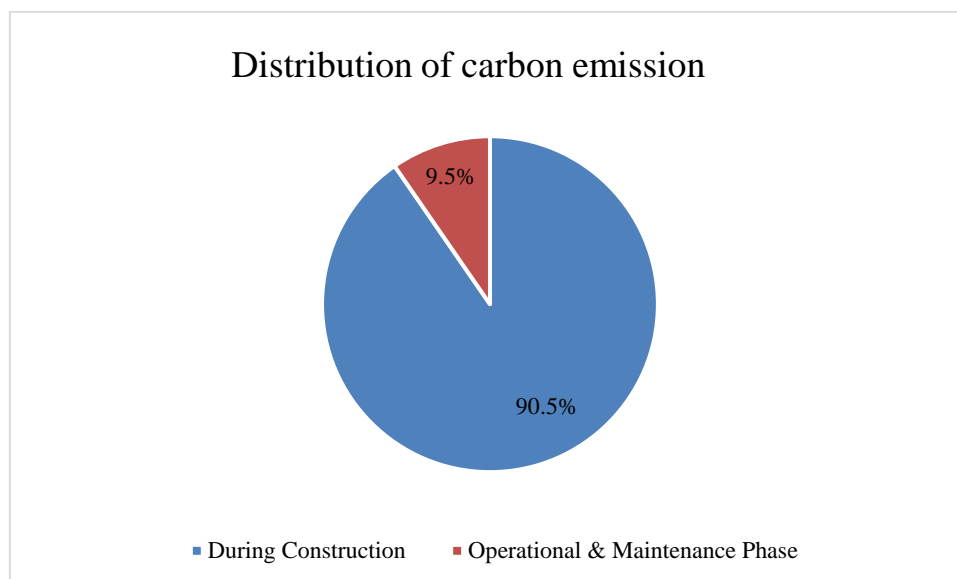
The calculations reveal that the shield tunnel has both the lowest total carbon emissions and unit length carbon emissions compared to the other two options. While the drill-and-blast tunnel demonstrates a lower unit carbon emission than the immersed tunnel, its total carbon emissions are slightly higher due to its length being twice that of the others. This highlights the impact that initial design choices, like the construction method, may have on the emission footprint of the overall project. Further note that for the final determination, the selection also needs to consider construction speed, cost, traffic capacity, alignment, construction risks, and local planning. For example, while the shield tunnel has advantages in terms of shorter length and carbon performance, the site presents complex geological conditions. These include fault zones and hard rock strata, which may lead to challenges such as cutter head jamming. Additionally, the shield method for undersea tunnels faces geological risks, including sudden water inflows. Comparatively, the immersed tunnel offers advantages in terms of alignment, structural reliability and a lower risk during construction, although it performs worst in carbon emission. Due to these advantages, the immersed tunnel was actually chosen as the final scheme.

### 3.3. Carbon emission calculation of the operation & maintenance phase

Based on annual power consumption for operations, including ventilation and lighting, the tunnel's yearly electricity use is estimated at 506.32 MWh, with the regional electricity carbon emission factor at 0.5876 kgCO<sub>2</sub>/kWh. Then assuming a service life of 100 years, the total carbon emissions from electricity consumption for ventilation, lighting, communication, and other electrical equipment are estimated at 29,751.36 tons. Due to the uncertainties involved, maintenance activities are to be estimated. For the immersed tunnel, maintenance activities contribute about 14% of emissions during the operations and maintenance phase, or around 4% of the entire lifecycle (Wu et al., 2024). Therefore, maintenance activities are estimated to result in approximately 4,843 tons of carbon emissions over the 100-year service period. Consequently, the total carbon emissions for the operations and maintenance phase are estimated at 34,594 tons.

### 3.4. Carbon emission distribution in the life cycle

As carbon emissions directly generated during the design phase are minimal, and emissions from the dismantling phase are not considered in this case study, the carbon emission distribution for the immersed tunnel is shown in Figure 3, based on the calculation results from the preceding sections.



**Figure 3.** Percentages of carbon emissions in different phases

As shown in Figure 3, the majority of carbon emissions from the immersed tunnel occur during the construction phase. In contrast, emissions during the operational period are relatively low. This is mainly due to the implementation of several energy-saving strategies, including an optimized power distribution system, energy-efficient transformers, an LED dimming control system, and a highly efficient ventilation system. However, the emissions generated by the traffic using the tunnel during its lifetime are not considered in this study, nor are they compared with the emission reductions obtained by the improved traffic situation that the tunnel will achieve. Therefore, unlike in the case of metro tunnels where the energy consumption of the trains can be relatively straightforward included in the emission calculations, and has been found to significantly contribute to the overall emissions during the operational phase (Long et al., 2025), the scope of this study does exclude the influence of any traction systems. As a result, the carbon emissions calculated are primarily generated concentrated in the construction phase. A wider scope, including the traffic in the tunnel as well as the traffic avoided in the larger urban area would be needed for a full comparison of the impact of the tunnel construction. This is beyond the scope of this study.

#### 4. APPROACHES TO REDUCING THE CARBON FOOTPRINT OF TUNNELS

Achieving low-carbon tunnel infrastructure begins with strategic interventions at the design stage, where decisions have long-term implications for material demand and energy consumption. One of the most effective approaches is to minimize the use of carbon-intensive materials such as cement and steel. This approach can be realized by optimizing tunnel cross-sectional dimensions, reducing reinforcement ratios, and adopting thin lining designs, which have been shown to significantly lower embodied carbon (Spyridis & Bergmeister, 2024). In addition, the use of prefabricated and modular structures helps reduce material waste and on-site energy consumption, particularly when combined with LCA and sensitivity analysis to inform design decisions. The integration of digital tools, such as building information modeling (BIM), machine learning, and LCA platforms, further enhances the potential to refine structural configurations and reduce carbon footprints. On the material side, substituting ordinary Portland cement with low-carbon alternatives such as fly ash or slag-based binders can yield considerable emission savings (Barbhuiya et al., 2025), while the use of recycled steel and high-recycled-content concrete contributes further benefits (Guo et al., 2025). Novel materials such as geopolymers, concrete and foam glass panels are also under exploration for their low-carbon potential. In terms of tunnel structures, innovations like sprayed concrete linings and spray-applied waterproof membranes have demonstrated both technical reliability and carbon reduction advantages (Peñaloza et al., 2024). These material and structural adjustments collectively offer significant opportunities to decarbonize tunnel construction.

Beyond construction, operational emissions, particularly in metro tunnel systems, are largely driven by traction power and electromechanical systems such as lighting, ventilation, and climate control. For instance, traction energy alone may account for up to 84% of operational-phase greenhouse gas emissions (Da Fonseca-Soares et al., 2023). To mitigate these impacts, energy-efficient technologies such as LED lighting, intelligent

control systems, and regenerative braking should be implemented. Moreover, integrating renewable energy sources (such as solar and wind) into tunnel systems can further reduce reliance on fossil-based electricity. Architectural interventions, such as optimizing the vertical profile of stations, particularly through U-shaped or parabolic designs, have been shown to improve energy efficiency by facilitating gravity-assisted acceleration and braking (Xin et al., 2014). During the end-of-life phase, although its contribution to total emissions is relatively low, carbon reduction can still be achieved by increasing the recycling rate of construction waste, shortening transportation distances, and minimizing fuel consumption through improved demolition methods. Establishing a pre-demolition material inventory and tracking system can also enhance the efficiency of resource recovery. Altogether, a comprehensive life-cycle strategy encompassing design, construction, operation, and dismantling is essential to low-carbon tunnel infrastructure.

## 5. CONCLUSION

This study highlights the importance of life cycle assessment of carbon emissions in tunnels. While existing research tends to focus on individual stages, comprehensive full life cycle studies remain limited. To address this gap, this paper presents a synthesis of current low-carbon tunnel practices, including: (1) methodologies for quantifying emissions across all life stages; (2) a case study highlighting differences among various tunnel types and the corresponding carbon emission distribution; and (3) practical strategies for reducing emissions. The aim of this study is to serve as a reference for engineers, planners, and decision-makers, aiming to contribute to the carbon neutrality in underground engineering.

Although the proposed computational framework is applicable at the project level, several important areas remain open for future investigation. First, there is an urgent need to establish standardized and cross-sectoral protocols for setting the calculation boundaries, aiming a consistent and accurate emission accounting across industries. Second, the statistics of engineering activities in the operational and maintenance phase, as well as the dismantling phase, should be further collected to finalize the carbon emission calculation in the full life cycle of tunnels. Finally, the development of digitally integrated, regionally scalable emission accounting systems may further enhance the efficiency and transparency of carbon tracking and decision-making in underground infrastructure projects.

## 6. BIBLIOGRAPHY

- [1] Barbhuiya, S., Das, B. B., Adak, D., Kapoor, K., & Tabish, M. (2025). Low carbon concrete: advancements, challenges and future directions in sustainable construction. *Discover Concrete and Cement*, 1(1), 1-24.
- [2] Chang, B., & Kendall, A. (2011). Life cycle greenhouse gas assessment of infrastructure construction for California's high-speed rail system. *Transportation Research Part D: Transport and Environment*, 16(6), 429-434.
- [3] Da Fonseca-Soares, D., Eliziário, S. A., Galvinicio, J. D., & Ramos-Ridao, A. F. (2023). Life-Cycle Greenhouse Gas (GHG) Emissions Calculation for Urban Rail Transit Systems: The Case of Pernambuco Metro. *Applied Sciences*, 13(15), 8965.
- [4] Fei, L., Zhang, Q., & Xie, Y. (2017, June). Study on energy consumption evaluation of mountainous highway based on LCA. In *IOP Conference Series: Earth and Environmental Science* (Vol. 69, No. 1, p. 012036). IOP Publishing.
- [5] Gan, V. J., Wong, C. L., Tse, K. T., Cheng, J. C., Lo, I. M., & Chan, C. M. (2019). Parametric modelling and evolutionary optimization for cost-optimal and low-carbon design of high-rise reinforced concrete buildings. *Advanced engineering informatics*, 42, 100962.
- [6] Guo, C., Xu, J., Yang, L., Guo, X., Liao, J., Zheng, X., ... & Wang, M. (2019). Life cycle evaluation of greenhouse gas emissions of a highway tunnel: A case study in China. *Journal of Cleaner Production*, 211, 972-980.
- [7] Guo, Y., Dong, C., Chen, Z., Zhao, S., Sun, W., He, W., ... & Guo, C. (2025). Evaluation of greenhouse gas emissions in subway tunnel construction. *Underground Space*.
- [8] IEA, UNEP, 2018 Global Status Report: towards a zero-emission, efficient and resilient buildings and construction sector, International Energy Agency and the United Nations Environment Programme, 2018.
- [9] Long, L., Zhang, X., Broere, W., de Nijs, R., & Xia, T. (2025). Assessing life-cycle carbon footprint of tunnels. In *Tunnelling into a Sustainable Future-Methods and Technologies* (pp. 4574-4581). CRC Press.
- [10] Ministry of Housing and Urban-Rural Development of the People's Republic of China. (2019). Standard for building carbon emission calculation (GB/T 51366-2019). China Architecture & Building Press. (in Chinese).
- [11] National Power CO<sub>2</sub> Emission Factors. (2021). Ministry of Ecology and Environment. [https://www.mee.gov.cn/xxgk2018/xxgk/xxgk01/202404/t20240412\\_1070565.html](https://www.mee.gov.cn/xxgk2018/xxgk/xxgk01/202404/t20240412_1070565.html)
- [12] Peñaloza, G. A., Vignisdottir, H. R., Kristensen, T., & Ramsnes, E. (2024). Greenhouse gas emission reduction potential in road tunnels—Can we reach the European Union goals with existing materials and technologies?. *Tunnelling and Underground Space Technology*, 153, 106011.



- [13] Spyridis, P., & Bergmeister, K. (2024). Sustainable tunnel design: concepts and examples of reducing greenhouse gas emissions through basic engineering assumptions. *Tunnelling and Underground Space Technology*, 152, 105886.
- [14] UNEP-SBCI, Buildings and Climate Change – Summary for Decision Makers, United Nations Environment Programme (UNEP), 2009.
- [15] Wu, H., Zhou, W., Bao, Z., Long, W., Chen, K., & Liu, K. (2024). Life cycle assessment of carbon emissions for cross-sea tunnel: A case study of Shenzhen-Zhongshan Bridge and Tunnel in China. *Case Studies in Construction Materials*, 21, e03502.
- [16] Xiao, X. (2021). Study on life cycle carbon emission and life cycle cost of green buildings (Master's thesis, Beijing Jiaotong University). Beijing Jiaotong University.
- [17] Xin, T., Roberts, C., He, J., Hillmanssen, S., Zhao, N., Chen, L., ... & Su, S. (2014, October). Railway vertical alignment optimisation at stations to minimise energy. In *17th International IEEE Conference on Intelligent Transportation Systems (ITSC)* (pp. 2119-2124). IEEE.

## THE EVOLVING RESILIENCE OF GLOBAL METRO NETWORKS

Yun-Hao Dong<sup>1</sup>, Xiao-Wei Luo<sup>2</sup>, Fang-Le Peng<sup>3</sup>, Wout Broere<sup>4</sup>

**Abstract:** Metro systems are essential for urban functionality worldwide, and their resilience is a growing concern. While network analysis has offered insights into structural resilience, a comprehensive understanding of dynamic resilience, particularly its temporal evolution in expanding networks and response to multifaceted disruptions, remains underdeveloped. Previous research has often focused on large systems in a few megacities, neglecting smaller networks. This study addresses these gaps by introducing a novel framework to evaluate the dynamic resilience of evolving metro networks. We compiled data for twelve global cities, modeling their metro systems as evolving complex networks, incorporating geographic coordinates, station opening dates, and catchment area population data. A key contribution is a comprehensive resilience metric that integrates network serviceability, based on population-weighted global efficiency, and quantifies vulnerability as the rate of efficiency loss per disrupted node. We formulated three universally applicable disruption scenarios, including critical node, critical region, and critical line disruptions. Each disruption was simulated at both light (10% node removal) and heavy (20% node removal) intensities, reflecting diverse real-world disruption scenarios. These strategies leverage a comprehensive node centrality index derived from degree, closeness, and betweenness centralities, with edge weights based on reciprocal Euclidean geodesic distances. Applying this framework, we analyzed the resilience evolution across the 12 case study cities, uncovering distinct and common patterns. Findings indicate that dynamic resilience provides critical insights complementary to static efficiency measures and that resilience trajectories are highly dependent on disruption size, intensity, and city-specific network characteristics. This study offers a robust methodology for assessing metro network resilience evolution, providing data-driven insights to enhance the robustness of critical public transport systems and inform strategies for developing more resilient cities.

**Keywords:** evolving resilience, metro network, serviceability, disruption scenarios

### 1. INTRODUCTION

Over the past century, metro systems have been widely recognized as efficient and environmentally friendly public transportation solutions (Dong et al., 2023; Lin et al., 2021). These systems play a critical role in alleviating transportation pressures in more than 200 large- and medium-sized cities worldwide. The concept of a metro system, however, varies across different contexts. In this study, a metro system is defined as an intra-city (non-intercity) rail transit system operating on a fully grade-separated right of way. With the deepening of global theoretical research and practical applications in transit-oriented development (Singh et al., 2017), the contributions of metro systems extend beyond transportation (Lin et al., 2022). They have become a key driver in the reconfiguration of urban morphology and function through their bidirectional influence on land use along metro corridors (Dong et al., 2022; Zhang, 2020). The morphological characteristics of metro networks play a significant role in shaping this transformative power (Ingvardson & Nielsen, 2018; Lyu et al., 2016). Specifically,

<sup>1</sup> PhD, Dong Yun-Hao, Underground Space, postdoc, Department of Geotechnical Building and Engineering, Tongji University, 1239 Siping Road, P.R. China, Department of Architecture and Civil Engineering, City University of Hong Kong, 83 Tat Chee Avenue, Hong Kong SAR, P.R. China, yunhdong@cityu.edu.hk.

<sup>2</sup> PhD, Luo Xiao-Wei, Construction Management, professor, Department of Architecture and Civil Engineering, City University of Hong Kong, 83 Tat Chee Avenue, Hong Kong SAR, P.R. China, xiaowluo@cityu.edu.hk.

<sup>3</sup> PhD, Peng Fang-Le, Underground Space, professor, head of Tongji University Underground Space Research Center, Department of Geotechnical Building and Engineering, Tongji University, 1239 Siping Road, P.R. China, pengfangle@tongji.edu.cn

<sup>4</sup> PhD, Wout Broere, Underground Space, professor, GeoEngineering Section, Delft University of Technology, Delft, The Netherlands, w.broere@tudelft.nl

a metro network refers to the complex topological configuration formed by the spatial distribution of metro lines and stations as they expand in number and coverage (Gonzalez-Navarro & Turner, 2018).

The continuous evolution of these morphological characteristics not only impacts the operational efficiency and resilience of metro systems but also influences the coupling relationships between metro stations and the surrounding built environment (An et al., 2019; Dong et al., 2021). Among these factors, the resilience of metro networks has garnered increasing attention (Yu et al., 2023). A high-resilience system, capable of withstanding partial failures under specific scenarios, is regarded as essential for reliable public transportation and the development of resilient cities (Derrible & Kennedy, 2010).

While network science's topological analysis has significantly enhanced our understanding of metro network resilience (Pei et al., 2022), a thorough grasp of dynamic resilience in metro systems is still lacking. Despite significant efforts to study metro network growth (Yu et al., 2023), prior research has not sufficiently explored the evolution of resilience in expanding metro networks, particularly their ability to recover from complex and multifaceted disruptions. Additionally, the focus has predominantly been on larger metro systems in a few megacities, overlooking the resilience dynamics of smaller-scale networks. This oversight highlights the need for a more inclusive approach that captures the resilience characteristics of metro networks of varying sizes and complexities.

This gap in understanding prompts two critical research questions: 1) How can we effectively evaluate the dynamic resilience of metro networks? 2) Are there global differences or similarities in the evolution of metro network resilience? To address these questions, we introduced a comprehensive network resilience metric that considers serviceability based on refined network modeling. We also proposed three universally applicable disruption strategies with bi-level disruption intensities. Ultimately, a case study involving 12 global cities was conducted to uncover regular patterns in resilience.

The structure of the remainder of this paper is organized as follows: **Section 2** presents an analytical framework for assessing the resilience of evolving metro networks. **Section 3** delivers analysis results concerning the resilience of metro networks across twelve global cities, highlighting distinct and common patterns. **Section 4** discusses the implications for building more resilient metro systems and outlines the research limitations. Finally, **Section 5** provides the concluding remarks of this study.

## 2. MATERIAL AND METHODS

### 2.1. Overview of the metro networks in case study cities

#### 2.1.1 Selection of case study cities and data collection

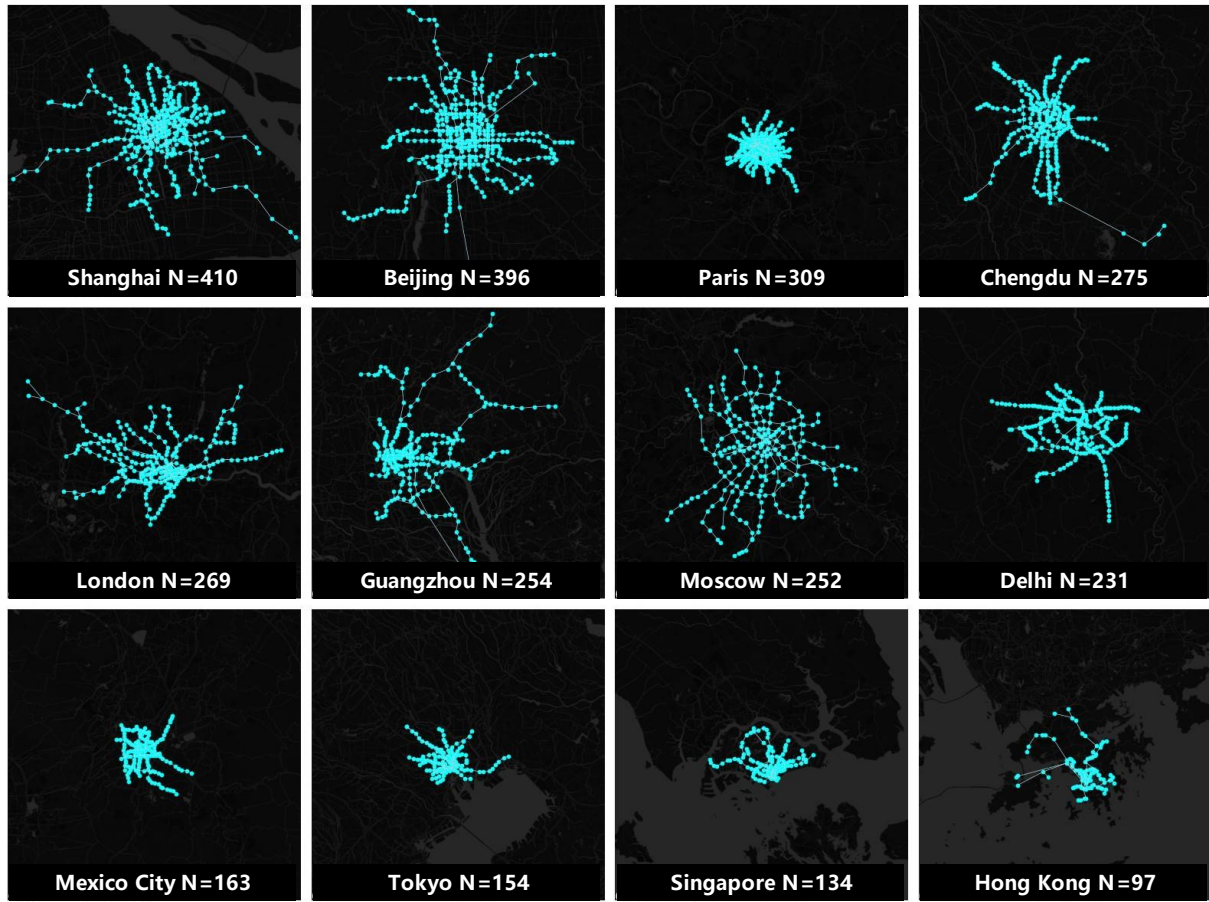
The selection of case study cities is crucial for identifying patterns in the network resilience. Previous studies often focused on large-scale metro networks in global cities. However, many cities have not yet developed large-scale metro systems, and the performance of medium to large-scale metro networks is also significant for cities that are later developers of such infrastructure. Consequently, we implemented a primary selection strategy based on scale diversity to include metro networks ranging from medium to large scales across the globe. In addition to scale, we also considered the representativeness of the cases globally, considering factors such as the speed of network evolution and socioeconomic status. Ultimately, 12 worldwide cities were selected for case studies, including Shanghai, Beijing, Paris, Chengdu, London, Guangzhou, Moscow, Delhi, Mexico City, Tokyo, Singapore, and Hong Kong.

Data collection relevant to metro systems in the selected cities was based strictly on official data from the respective public transit authorities and Google map, with a cutoff at the end of 2024. The metro-relevant data includes station names, opening dates, geographic coordinates, and topological connections within the metro system. Additionally, we collected population data at a 1km resolution (similar to a metro catchment area with a radius of 800m) from WorldPop (Lloyd et al., 2017) to enhance our computation of network resilience. To eliminate the confusion caused by the multiple definitions of metro, we focused solely on rail transit systems with independent rights-of-way and does not include inter-city rail transit.

#### 2.1.2 Characteristics of the metro networks in case study cities

From a general perspective, the metro networks in the case study cities exhibit diverse characteristics in several aspects. Firstly, in terms of size as illustrated in **Figure 1**, the number of operational stations of the twelve metro networks range from medium to high scales, such as Hong Kong (N=97), to large scales like Moscow (N=252), and even to ultra-large scales such as Shanghai (N=410). Secondly, there is diversity in the evolution time of these networks, including the time-honored metro system in London (operational for 162 years), and the rapidly developed metro system in Chengdu (operational for 15 years). Thirdly, the case study cities generally strike a balance between countries in the Global South (China: Beijing, Shanghai, Guangzhou,

Chengdu, Hong Kong; India: Delhi) and the Global North (France: Paris; UK: London; Russia: Moscow; Mexico: Mexico City; Japan: Tokyo; Singapore). Although all selected cities are developed urban areas within their regions, they vary in their socio-economic status.



**Figure 1.** Metro network of case study cities ( $N$  denotes the number of stations)

## 2.2. Assessing the resilience of evolving metro networks

Unlike previous studies that focused on the performance of metro networks under deliberate disruptions, this study introduces a resilience analysis framework that incorporates temporal complex networks, universally applicable network disruption scenarios, and resilience metrics that integrate serviceability. The modeling and computation of the network were primarily conducted using NetworkX library in Python (Hagberg et al., 2008). The assessment model is detailed as follows.

### 2.2.1 Temporal complex networks construction

The network modeling incorporated the metro networks' topological characteristics (Kanwar et al., 2019), real-world geographic position, and temporal development data. Initially, the development progress was quantified by calculating the ratio of the number of metro stations in different years to the number at the end of the period, selecting those years where the development progress exceeded both 5% annually and 30% overall as the temporal cross-sections for analysis. For selected year  $T$ , metro stations are denoted as vertices/nodes  $V_t$ , and the rail transit connections between them as edges/links  $E_t$  (modeled following the L-space approach), thus forming the graph  $G_t(V_t, E_t)$ . Additionally, each station  $i$  records the catchment area population  $P_{Ti}$  and geographical coordinates ( $lon_{Ti}, lat_{Ti}$ ) as necessary attributes in year  $T$ . Given that the available population data spans from 2000 to 2020, this study substituted population data for any post-2020 temporal interfaces with the 2020 figures as the proxy, while pre-2000 cross-sections were excluded from consideration.

### 2.2.2 Targeted disruption strategies formulation

#### (1) Evaluation of comprehensive node centrality

Assessing the importance of nodes within a network is a prerequisite for formulating specific disruption scenarios. This study focused on the refined topological structure of metro networks, emphasizing the evaluation of node centrality as the importance index. Although many classic centrality measures have been applied in transportation network analysis, they often assess one aspect of node importance. Therefore, we adopted a comprehensive node centrality index that integrates multiple classic centrality indicators to effectively identify critical nodes. Moreover, the weights of all edges are based on the reciprocal of Euclidean geodesic distances to more accurately capture the true distances between station nodes.

Firstly, we measured the degree centrality  $C_D(v)$  using expression (1). This metric quantifies the connectivity strength of a metro station by summing the weights of its edges, where  $d(u, v)$  denotes the geodesic distance between station  $u$  and station  $v$ ,  $N(v)$  denotes the neighborhood of station  $v$ .

$$C_D(v) = \sum_{u \in N(v)} \frac{1}{d(u, v)} \quad (1)$$

Secondly, we measured the closeness centrality  $C_C(v)$  using expression (2). This metric evaluates how efficiently a station is connected to all other stations in the graph, where  $N$  represents the total number of stations.

$$C_C(v) = \frac{N-1}{\sum_{u \neq v} d(u, v)} \quad (2)$$

Thirdly, we measured the betweenness centrality  $C_B(v)$  using expression (3). This metric quantifies the extent to which a station acts as a critical junction by computing its occurrence on the shortest paths between other stations. Specifically, it considers the number of these paths that pass through the station in question (station  $v$ )  $\sigma_{st}(v)$ , compared to the total number of shortest paths between all pairs of stations (from station  $s$  to station  $t$ )  $\sigma_{st}$ .

$$C_B(v) = \sum_{s \neq v \neq t} \frac{\sigma_{st}(v)}{\sigma_{st}} \quad (3)$$

Ultimately, we adopted the TOPSIS method (Behzadian et al., 2012; Du et al., 2014) to integrate the aforementioned metrics using expression (4), thus providing a comprehensive indicator to measure the importance of a specific metro station. To capture the importance of network characteristics over time, the weights of the three basic centrality measures in the TOPSIS calculation were determined using the Criteria Importance Through Inter-criteria Correlation (CRITIC) objective weighting method. In other words, the comprehensive centrality index  $C_{CP}(v)$  measures the likelihood that a metro station's failure would severely disrupt the network, based on how many connections it has, how easily passengers can reach other destinations through it, and how much passenger traffic flows through it.

$$C_{CP}(v) = F_{topsis}(C_D(v), C_C(v), C_B(v)) \quad (4)$$

#### (2) Specific disruption scenarios

Specific disruption modelling strategies significantly influence the analysis of metro network resilience. Existing strategies typically involve the sequential removal of nodes based on their importance until the network ceases to function. In contrast, we adopted a single-round disruption approach, where the network is subjected to a single disruption to evaluate its performance before and after the event. This method provides a clearer perspective on the dynamic evolution of network performance across different temporal cross-sections. The disruption scenarios in this study were designed based on network topology configurations, with a focus on disruption scale and scope to approximate various real-world metro incidents and disasters.

For disruption scale, light and heavy disruption were defined in this study to simulate general and severe disturbances in metro networks. Based on metro network performance loss curves, the thresholds for light and heavy disruptions were set at 10% and 20% of the total number of nodes, respectively (Sun et al., 2024).

For disruption scope, three types of specific disruptions are introduced, namely critical node disruptions, critical region disruptions, and critical line disruptions. These strategies were visualized in **Figure 2**, along with pseudocode for selecting affected nodes. Notably, the thresholds for light and heavy disruptions might vary for critical region and line disruptions, particularly for large-scale disruptions such as those on critical metro lines. The proposed specific disruption strategies were further described as follows.

- a) **Critical node disruptions:** This scenario considers the most crucial nodes within the metro network to maximize operational disruption. It reflects real-world scenarios such as local power failures, targeted



cyberattacks, strategic sabotage, or other catastrophic failures affecting key transit hubs or critical metro stations.

- b) **Critical area disruptions:** This scenario simulates disasters or natural events (e.g., flooding, earthquakes) that impact geographically concentrated regions. Stations were selected based on the highest cumulative centrality within a 2 km radius (a general impact zone for disasters regarding metro stations).
- c) **Critical line disruptions:** This scenario disrupts entire metro lines by targeting all stations on a line, prioritizing lines with the highest cumulative centrality. It represents scenarios such as systematic failures, large scale power failures, equipment breakdown or other disruptions that disable entire transit lines.

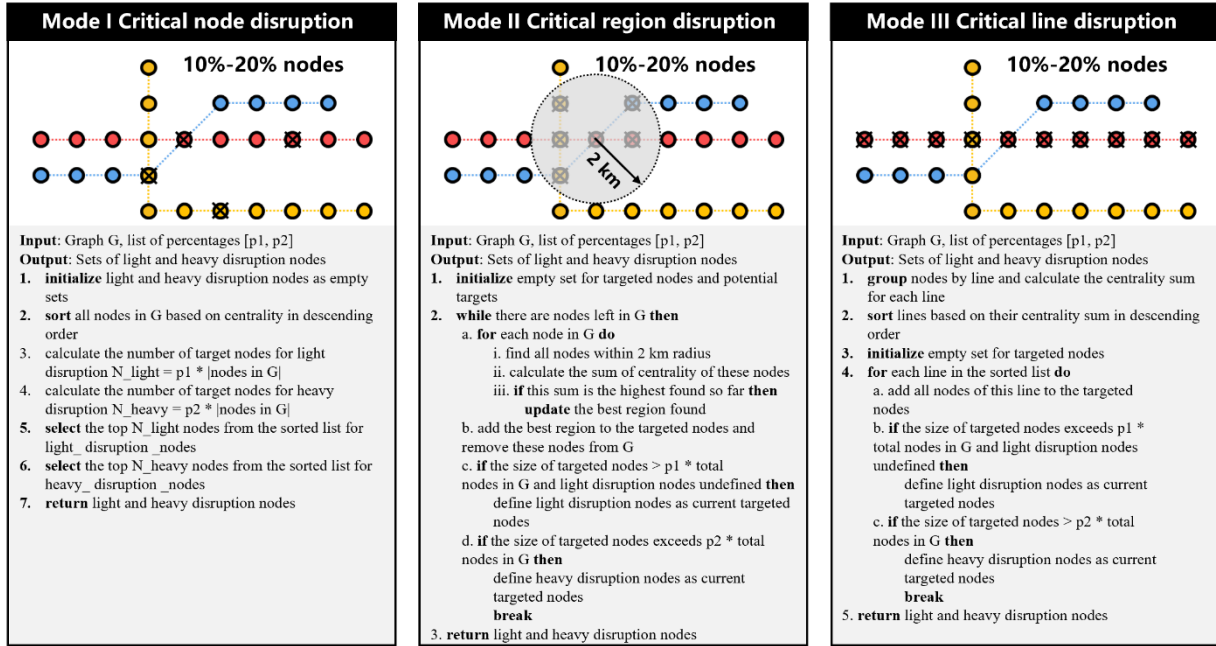


Figure 2. Graphic representation and pseudocode of specific disruption scenarios

### 2.2.3 Evaluation of metro network resilience integrating serviceability

Building on classic network resilience metrics, we introduced the concept of metro serviceability and proposed an improved resilience evaluation metric for metro networks. Global network efficiency is one of the most widely used indicators for resilience assessment of transport and infrastructure networks (Pei et al., 2022). However, global efficiency typically measures distance by considering only topological depth, even when edge weights are adjusted using actual geodesic distances. As a result, it still primarily reflects the topological properties of the network.

Metro networks, as critical components of urban public transportation systems, are deeply embedded within the urban functional systems. The changes in their service capacity under disruptions provide a more accurate reflection of their resilience as transportation networks. To this end, we approximated the service population of a metro station  $p_i$  using the average population within a 1km catchment area. Based on this, we proposed a serviceability-integrated global efficiency metric,  $E_{service}$ , as defined in expression (5).

$$E_{service} = \sum_{i \neq j} \frac{p_i + p_j}{d_{ij}} \quad (5)$$

Furthermore, we introduced a resilience metric for a temporal state  $T$ , denoted as  $R_T$ , as shown in Equation (6).  $P_T$  denotes the total population within metro-led region at time  $T$ . Here,  $T'$  represents the post-disruption state. The proposed indicator portrays the resilience metric as a measure of sensitivity to changes in the network state, reflecting the extent to which each disrupted station impacts the overall network resilience. It measures both efficiency loss per capita per failed station. Given that a higher value of this metric indicates lower resilience, this study refers to it as *network vulnerability*.

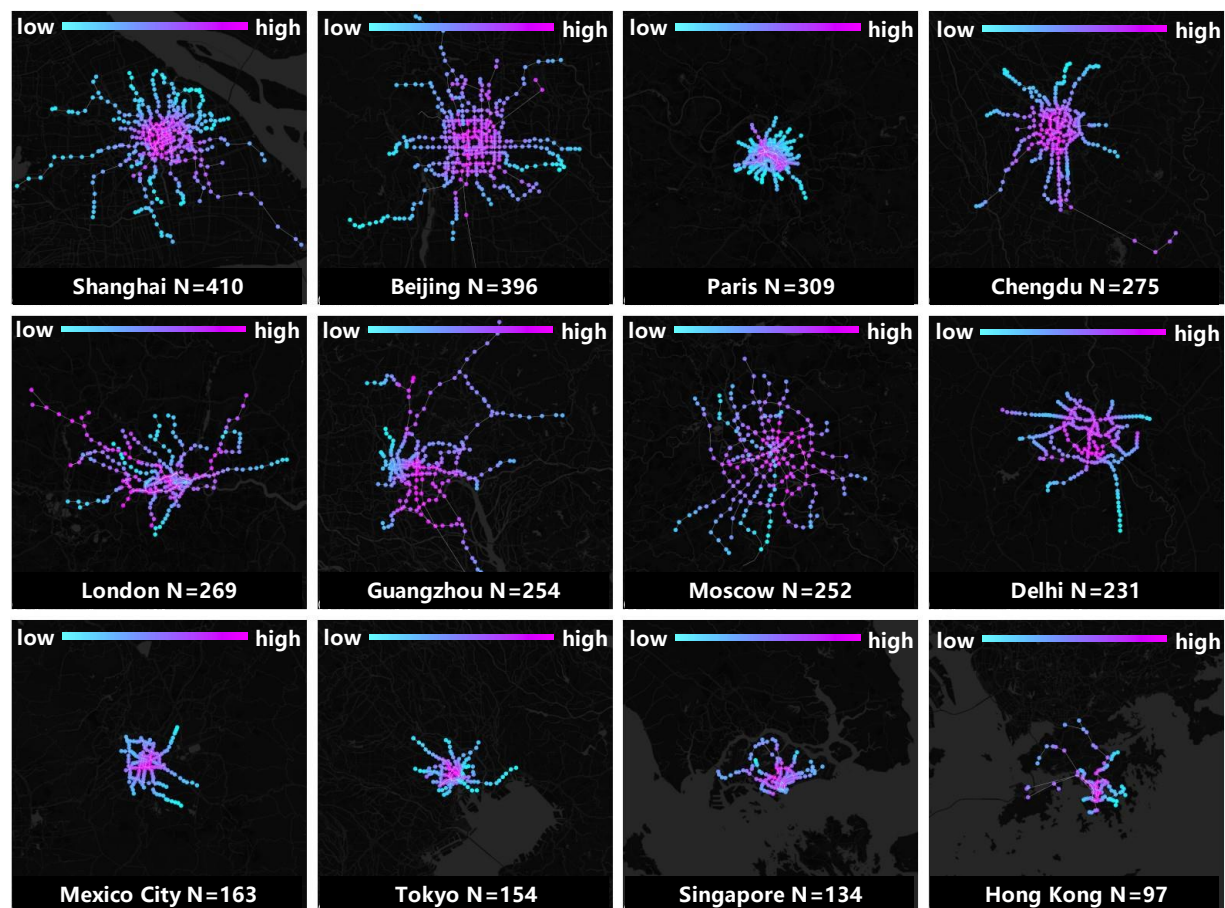
$$R_T = \frac{E_{service,T} - E_{service,T'}}{(N_T - N_{T'}) \cdot P_T} \quad (6)$$

### 3. RESULTS

The comprehensive node centrality is evaluated and visualized (**Figure 3**). Subsequently, the evolution of resilience under three types of critical disruptions across 12 selected cities is depicted in **Figures 4 to 8**. The circles in the figures represent the temporal cross-sectional data analyzed for each city, with the color bars derived from linear interpolation of this cross-sectional data. The color progression from light to dark in the color bars indicates increasing network resilience, aligning with the resilience metric introduced in Section 2.2.3. The variation in color for each city's color bar characterizes the resilience dynamics throughout different stages (the number of stations at a specific cross-section relative to the total number of stations in the final state, which is represented as the *development ratio* on the horizontal axis in the figures). This variation, viewed from the perspective of resilience change rate (network vulnerability), describes the evolutionary process of networks in different cities. Additionally, the size of the circles represents network efficiency combined with serviceability, providing a supplementary portrayal of resilience from the perspective of initial resilience magnitude.

#### 3.1. Comprehensive node centrality evaluation

As shown in **Figure 3**, we could observe the distribution of station importance across 12 selected cities. Overall, the metro networks in these cities generally exhibit a pattern where central areas have higher centrality, while peripheral areas show lower centrality. This primarily reflects the contributions of betweenness centrality and closeness centrality to the comprehensive centrality measure.



*Figure 3. Comprehensive node centrality*

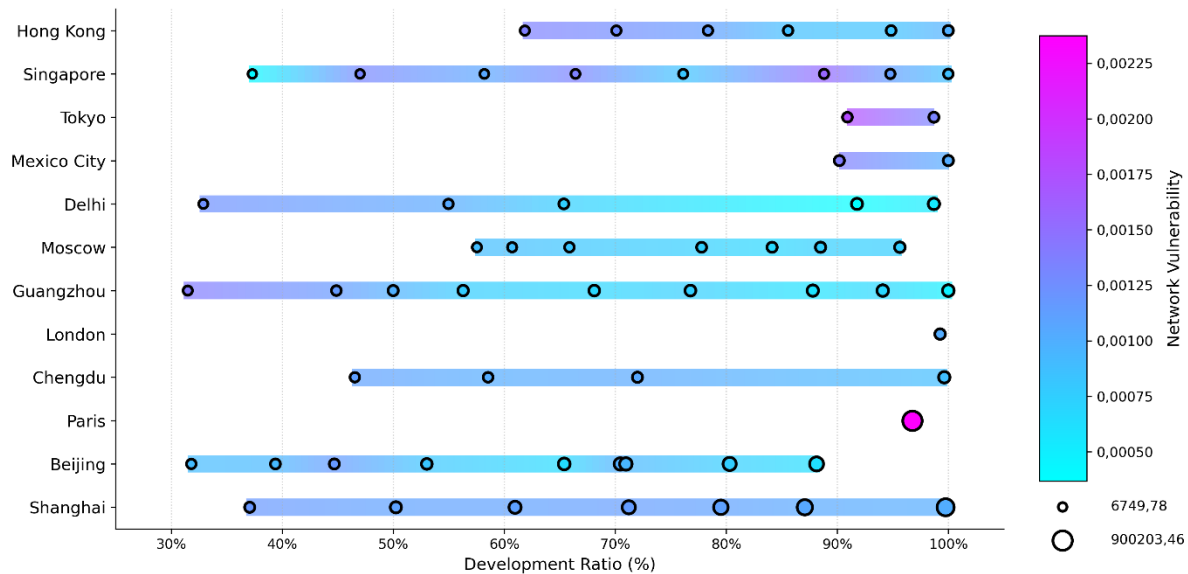
In some cities (e.g., London and Guangzhou), certain stations located on suburban lines also display slightly higher centrality (though still lower compared to central areas). This phenomenon may be attributed to the influence of degree centrality, and the objective weighting method used to calculate the centrality might have amplified this characteristic to some extent. Notably, our measurement approach is entirely based on the topological configuration of the network and real-world geographic distribution. By designing disruption

strategies based on this measure and incorporating the service population reflecting socio-economic development when measuring resilience, our approach aligns with the classic *Natural Movement* concept in Space Syntax studies (Hillier et al., 1993). Essentially, this involves examining how pure topological features influence the composite functionality. In this study, we shifted the focus to the service functionality of metro networks.

### 3.2. Resilience evolution under critical node disruption

As shown in **Figure 4**, the resilience evolution of metro networks in various cities under light node disruptions shows distinct patterns. The y-axis represents the cities, and the x-axis shows the network development ratio (i.e., the ratio of current to final station count). The resilience evolution for each city is visualized as a color band, where warmer colors indicate higher vulnerability. Circles denote network expansion events, and their size corresponds to the serviceability-integrated global efficiency metric (ranging from 6749.78 to 900203.46). The colors between circles are linearly interpolated. Assuming the metro-led region has a population of 1 million, a network vulnerability value of 0,00050 indicates that each attacked station causes a global efficiency loss of  $1000000 \times 0,00050 = 500$  units on average.

Considering light node disruptions, Hong Kong, Tokyo, Mexico City, Delhi, and Guangzhou demonstrate a continual growth in network resilience, with particularly high resilience levels observed in Guangzhou and Delhi. In contrast, Singapore and Beijing exhibit characteristics of fluctuating resilience. Although the metro networks in Moscow, Chengdu, and Shanghai also continue to grow, the changes in their resilience are less pronounced. London and Paris are unique cases; due to their early established metro systems and the analysis only incorporating demographic data after 2000, only one data point was included for each city. London network shows higher resilience, while the Paris network displays the lowest resilience. It is important to note that this resilience is primarily evaluated based on the rate of efficiency change (network vulnerability). Consequently, while the Paris metro network shows lower resilience, it presents the highest initial network efficiency, which aligns with its highly centralized and dense network distribution. Similarly, the metro networks in Shanghai and Beijing also exhibit high initial network efficiencies.



**Figure 4.** Resilience evolution under light node disruption

**Figure 5** illustrates the resilience evolution of metro networks under heavy node disruption. Compared to the patterns observed under light disruption scenarios, the general trends in resilience evolution across the cities remain largely consistent, yet there is a noticeable improvement in resilience levels at various stages. Specifically, the change in high resilience levels is minimal, shifting only slightly from 0,0005 to 0,0004. However, the limit of low resilience levels has significantly decreased by approximately 37% (from 0,00225 to 0,0014).

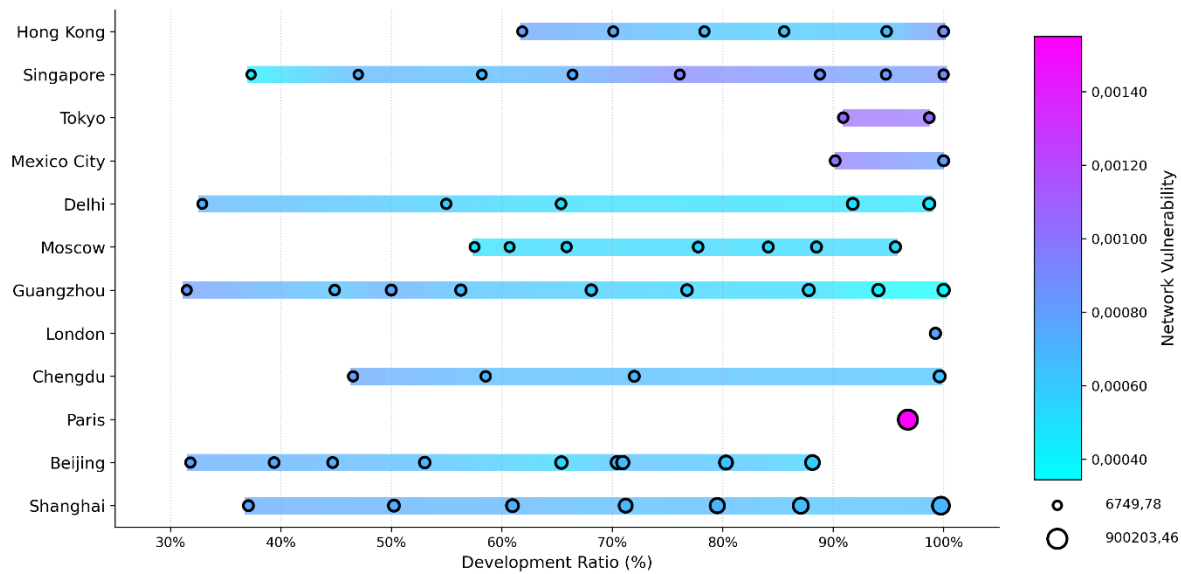


Figure 5. Resilience evolution under heavy node disruption

### 3.3. Resilience evolution under critical region disruption

Figure 6 presents the resilience evolution of metro networks in various cities under a light region disruptions. In this scenario, Hong Kong, Mexico City, Moscow, and Guangzhou exhibit varying degrees of continual resilience improvement. Tokyo and Chengdu show no significant changes in resilience; Singapore, Delhi, Beijing, and Shanghai all demonstrate a pattern where resilience initially decreases and then increases. Paris continues to display the lowest level of resilience, while London's resilience is moderate. Additionally, it is observed that under this disruption mode, the resilience evolution in Singapore, Moscow, and Beijing remains high.

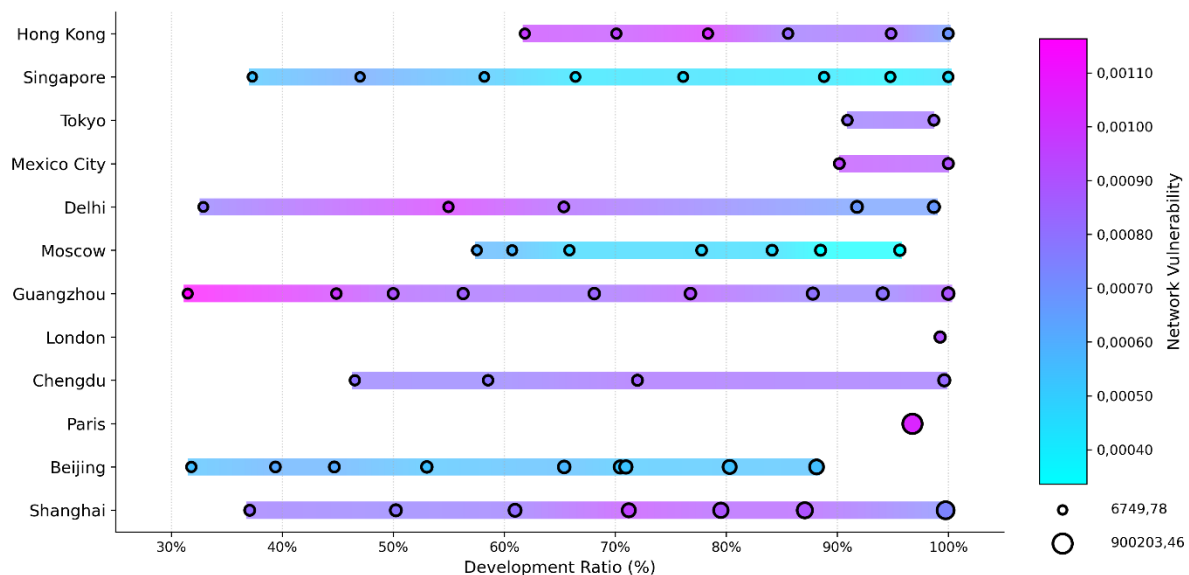
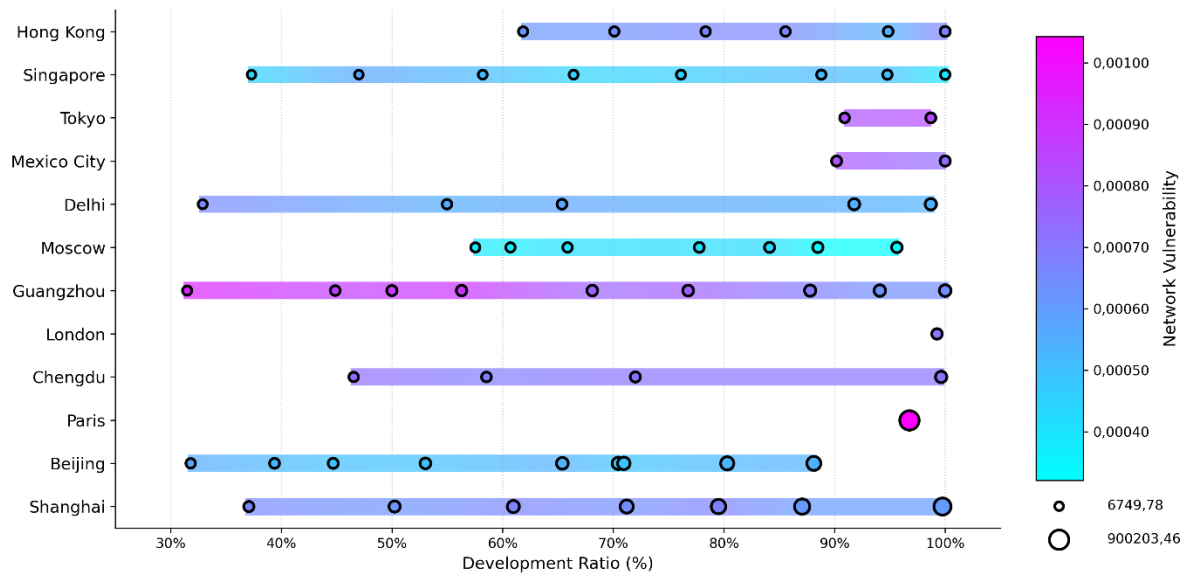


Figure 6. Resilience evolution under light region disruption

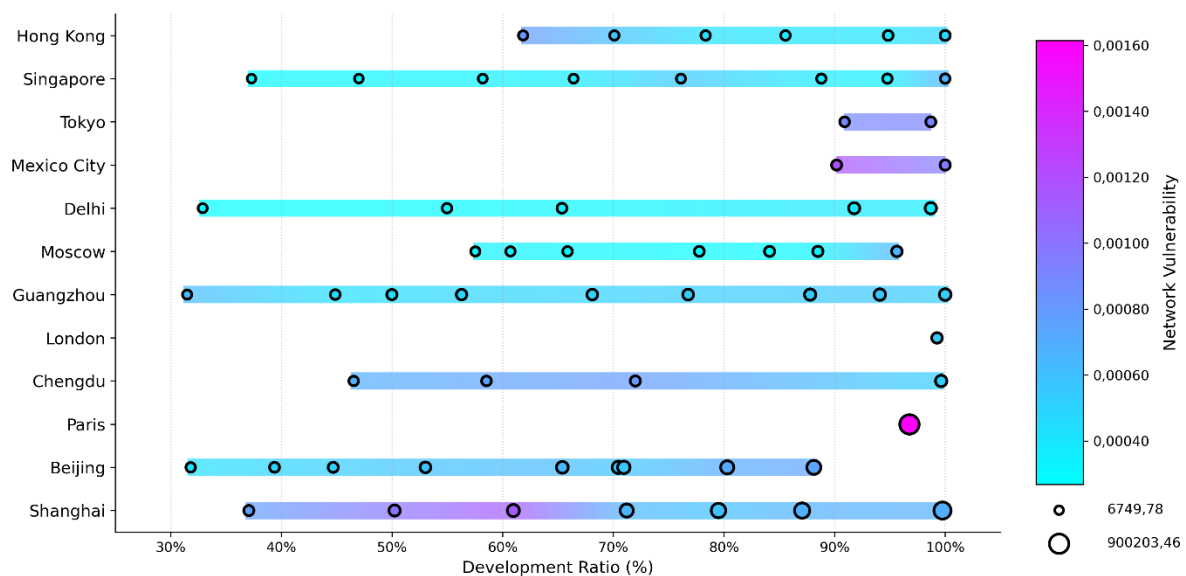


*Figure 7. Resilience evolution under heavy region disruption*

The pattern of metro network resilience evolution under a heavy region disruption differs from that observed under a light region disruption, as depicted in **Figure 7**. Except for Guangzhou, no other cities show significant changes in resilience. Additionally, the range of resilience metrics does not undergo significant alterations (ranging from 0,0004 to 0,0011 in light region disruption versus 0,0004 to 0,0010 in heavy region disruption), suggesting that the scale of the region disruption has a minimal impact on the resilience of metro networks. However, the evolution of resilience in metros appears to be more sensitive to lighter disruptions.

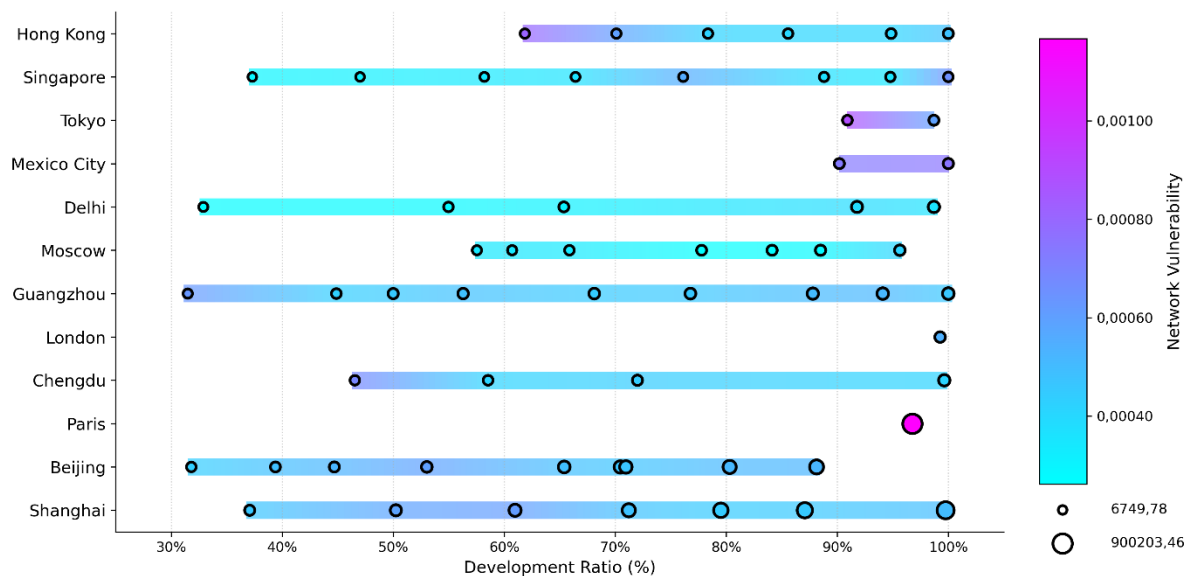
### 3.4. Resilience evolution under critical line disruptions

As shown in **Figure 8**, under a light line disruption, Hong Kong, Chengdu, and Shanghai exhibit a clear trend of continual network resilience improvement, while Beijing experiences slight fluctuations in network resilience. Other cities do not show dramatic changes in their network resilience. From the perspective of resilience levels, Hong Kong, Singapore, Delhi, Moscow, Guangzhou, and Beijing generally maintain a consistently high state, while the resilience evolution of other networks remains confined to moderate to low values.



*Figure 8. Resilience evolution under light line disturbance*





**Figure 9.** Resilience evolution under heavy line disturbance

**Figure 9** further delineates the resilience changes under a heavy line disruption. For cities like Hong Kong, Delhi, and Moscow, the pattern of resilience change is consistent with the light line disruption, primarily because a line disruption is a major form of disturbance that can cause significant node removal in smaller-scale networks, regardless of the disturbance's intensity. Moreover, Shanghai's resilience pattern under a heavy disturbance no longer shows continuous improvement but rather a decrease followed by an increase. Changes in other cities are not significantly different, but the high vulnerability values under a light disturbance have decreased by 37,5% (from 0,0016 to 0,0010, similar to the change under critical node disturbance), while the low vulnerability values remain unchanged at 0,0004.

## 4. DISCUSSION

### 4.1. Implications on the resilient development of metro networks

This study, based on refined metro network topological modeling, we constructed three disturbance scenarios and integrated a resilience metric that incorporates service levels to examine the characteristics of resilience development during the evolution of metro networks. Analyzing results from 12 global cities, we extracted key findings about changes in metro network resilience, providing significant insights for the development of resilient metro networks.

Firstly, the evaluation of metro network resilience should consider both static and dynamic perspectives. Traditional analyses of transport networks often measure resilience using efficiency metrics. However, this study further examined the rate of resilience change (network vulnerability) under specific disturbance scenarios. The Paris metro system serves as a typical example; it has a relatively concentrated and dense spatial distribution, resulting in high network efficiency. Yet, it exhibits very low network vulnerability across various disturbances, indicating room for improvement in its dynamic resilience. Focusing solely on a static or dynamic perspective during network planning might not adequately capture the characteristics of metro network resilience. In practice, urban planners can combine spatiotemporal population projections with metro network planning to investigate dynamic changes in network resilience over the long term, moving beyond a purely static analysis."

Secondly, the resilience of metro networks exhibits strong differentiation across different disturbance scenarios, intensities, and cities. The driving forces behind this phenomenon are complex, possibly due to the direction and speed of network expansion and the overall network configuration during its evolution. The mismatch between the distribution of the service population in the catchment area and the metro network, where metro transportation is not the dominant mode, might also influence this phenomenon. Therefore, it is imprudent to blindly follow the resilience development patterns of a single case city; a comprehensive evaluation combining specific resilience analysis scenarios and spatial growth patterns is necessary.

Thirdly, resilience evolution trends under different disturbance intensities show similar characteristics within the same disturbance strategy. For critical node and line disturbance, high values of network vulnerability change

by about 37% under both light and heavy disturbance intensities. However, critical region disturbances do not significantly affect the distribution of high and low values of network vulnerability. This provides useful insights for planners in designing resilience analysis scenarios.

Finally, despite their vast differences in scale, both the Moscow and Beijing metros demonstrate strong network resilience under various disturbance scenarios, with Beijing's initial network efficiency being higher than Moscow's. These two systems are likely to share similar overall configuration characteristics and expansion patterns, which ensure similar overall resilience evolution. This type of robust metro network system is worth analyzing and emulating by planners. Moreover, the development of graph databases that integrate static network structure with the trajectory and velocity of dynamic growth would enable more effective identification and pattern learning for such resilient networks.

## 4.2. Limitation and prospects

Despite that this study introduced the concept of resilience evolution to explore the patterns of metro network resilience in global cities, there are still three main areas where the research could be further improved.

Firstly, while this study includes twelve diverse metro networks from around the world as case studies, the sample size is still limited and focused on larger, multi-line networks. Future research should extend this methodology to a broader range of cities, or even conduct a full sample of global comprehensive study, to acquire a more complete understanding of the resilience evolution of metro networks, and should include smaller networks to highlight the impact of lower interconnectivity on network vulnerability.

Secondly, the proposed framework is limited by multisource data collection issues and does not fully consider factors such as the actual operating conditions of metro networks, real impact of disasters and disturbances, the age or type of metro stations (elevated or underground), and the distribution of emergency response resources. For more detailed studies on resilience enhancement, improvements in modeling methods are needed.

Lastly, while the evolving resilience of global metro networks has been studied, the interplay between metro systems and other urban systems requires further exploration. On one hand, metro networks should be analyzed in conjunction with public transport and road networks. On the other hand, the integration of urban development and metro expansion should be further examined to provide deeper insights into comprehensive urban resilience.

## 5. CONCLUSION

This study has advanced the understanding of metro network resilience by introducing a dynamic evolutionary perspective, moving beyond traditional static assessments. We developed a comprehensive analytical framework that integrates refined network modeling, considering real-world geographic, serviceability, and temporal development data, with universally applicable specific disruption scenarios (critical node, critical region, and critical line disruptions, each simulated at light and heavy intensities). Through a comparative case study of 12 global metro networks, encompassing diverse network scales, evolutionary timelines, and socio-economic contexts, we have identified distinct and common patterns in resilience evolution. The primary findings of this study are summarized as follows.

(1) Dynamic resilience offers crucial insights beyond static efficiency. The Paris metro, for instance, exhibits high initial network efficiency but demonstrates lower dynamic resilience (higher vulnerability) under various disruptions, highlighting the necessity of considering both perspectives in network planning.

(2) Resilience is highly contextual. It varies significantly across different disturbance scenarios, intensities, and individual cities, likely influenced by network expansion patterns, overall configuration, and the alignment between service population distribution and metro network coverage. This underscores the caution against universally applying resilience development patterns from a single case.

(3) Disruption intensity impacts vulnerability consistently within certain strategies. For critical node and line disruptions, an increase in disruption intensity led to a comparable percentage change (approximately 37%) in high network vulnerability values. However, critical region disruptions showed less sensitivity to changes in disruption scale.

(4) Despite differences in scale, both the Moscow and Beijing metro systems demonstrated strong resilience across various scenarios, suggesting that their overall configuration and expansion patterns contribute significantly to this robustness and are worthy of further study for emulation.

This study contributes a novel methodology for evaluating the evolving resilience of metro networks and provides empirical evidence of diverse resilience trajectories. The insights gained can inform urban planners and policymakers in developing more resilient metro systems capable of withstanding multifaceted disruptions, thereby enhancing the reliability of urban public transportation and contributing to the creation of resilient cities.

Future work should aim to expand the sample of cities for a more globally comprehensive understanding and incorporate a richer set of operational and contextual factors to further refine resilience assessment models

## 6. ACKNOWLEDGMENTS

This work was supported by the National Natural Science Foundation of China (NSFC) [grant number: 42301289], and Hong Kong Scholars Program [grant number: XJ2023059].

## 7. REFERENCES

- [1] An, D. D., Tong, X., Liu, K., & Chan, E. H. W. (2019). Understanding the impact of built environment on metro ridership using open source in Shanghai. *Cities*, 93, 177-187. <https://doi.org/10.1016/j.cities.2019.05.013>
- [2] Behzadian, M., Otaghsara, S. K., Yazdani, M., & Ignatius, J. (2012). A state-of the-art survey of TOPSIS applications. *Expert Systems with Applications*, 39(17), 13051-13069. <https://doi.org/10.1016/j.eswa.2012.05.056>
- [3] Derrible, S., & Kennedy, C. (2010). The complexity and robustness of metro networks. *Physica a-Statistical Mechanics and Its Applications*, 389(17), 3678-3691. <https://doi.org/10.1016/j.physa.2010.04.008>
- [4] Dong, Y. H., Peng, F. L., & Guo, T. F. (2021). Quantitative assessment method on urban vitality of metro-led underground space based on multi-source data: A case study of Shanghai Inner Ring area. *Tunnelling and Underground Space Technology*, 116, 104108. <https://doi.org/10.1016/j.tust.2021.104108>
- [5] Dong, Y. H., Peng, F. L., Li, H., & Men, Y. Q. (2023). Spatiotemporal characteristics of Chinese metro-led underground space development: A multiscale analysis driven by big data. *Tunnelling and Underground Space Technology*, 139, 105209. <https://doi.org/10.1016/j.tust.2023.105209>
- [6] Dong, Y. H., Peng, F. L., Zha, B. H., Qiao, Y. K., & Li, H. (2022). An intelligent layout planning model for underground space surrounding metro stations based on NSGA-II. *Tunnelling and Underground Space Technology*, 128, 104648. <https://doi.org/10.1016/j.tust.2022.104648>
- [7] Du, Y. X., Gao, C., Hu, Y., Mahadevan, S., & Deng, Y. (2014). A new method of identifying influential nodes in complex networks based on TOPSIS. *Physica a-Statistical Mechanics and Its Applications*, 399, 57-69. <https://doi.org/10.1016/j.physa.2013.12.031>
- [8] Gonzalez-Navarro, M., & Turner, M. A. (2018). Subways and urban growth: Evidence from earth. *Journal of Urban Economics*, 108, 85-106. <https://doi.org/10.1016/j.jue.2018.09.002>
- [9] Hagberg, A., Swart, P. J., & Schult, D. A. (2008). Exploring network structure, dynamics, and function using NetworkX.
- [10] Ingvarsson, J. B., & Nielsen, O. A. (2018). How urban density, network topology and socio-economy influence public transport ridership: Empirical evidence from 48 European metropolitan areas. *Journal of Transport Geography*, 72, 50-63. <https://doi.org/10.1016/j.jtrangeo.2018.07.002>
- [11] Kanwar, K., Kumar, H., & Kaushal, S. (2019). Complex network based comparative analysis of Delhi Metro network and its extension. *Physica a-Statistical Mechanics and Its Applications*, 526, 120991. <https://doi.org/10.1016/j.physa.2019.04.227>
- [12] Lin, D., Broere, W., & Cui, J. Q. (2022). Metro systems and urban development: Impacts and implications. *Tunnelling and Underground Space Technology*, 125, 104509. <https://doi.org/10.1016/j.tust.2022.104509>
- [13] Lin, D., Nelson, J. D., Beecroft, M., & Cui, J. Q. (2021). An overview of recent developments in China's metro systems. *Tunnelling and Underground Space Technology*, 111, 103783. <https://doi.org/10.1016/j.tust.2020.103783>
- [14] Lloyd, C. T., Sorichetta, A., & Tatem, A. J. (2017). High resolution global gridded data for use in population studies. *Scientific Data*, 4, 170001. <https://doi.org/10.1038/sdata.2017.1>
- [15] Lyu, G., Bertolini, L., & Pfeffer, K. (2016). Developing a TOD typology for Beijing metro station areas. *Journal of Transport Geography*, 55, 40-50. <https://doi.org/10.1016/j.jtrangeo.2016.07.002>
- [16] Pei, A. H., Xiao, F., Yu, S. B., & Li, L. L. (2022). Efficiency in the evolution of metro networks. *Scientific Reports*, 12(1), 8326. <https://doi.org/10.1038/s41598-022-12053-3>
- [17] Singh, Y. J., Lukman, A., Flacke, J., Zuidgeest, M., & Van Maarseveen, M. F. A. M. (2017). Measuring TOD around transit nodes - Towards TOD policy. *Transport Policy*, 56, 96-111. <https://doi.org/10.1016/j.tranpol.2017.03.013>
- [18] Sun, X. H., Liu, Y., Mi, Y. M., & Lv, K. (2024). Identification of key stations and routes in urban metro and conventional bus networks from a resilience perspective. *Complex Systems and Complexity Science*, 1-9 (in Chinese).
- [19] Yu, X. Y., Chen, Z., Liu, F., & Zhu, H. H. (2023). How urban metro networks grow: From a complex network perspective. *Tunnelling and Underground Space Technology*, 131, 104841. <https://doi.org/10.1016/j.tust.2022.104841>
- [20] Zhang, H. R. (2020). Metro and urban growth: Evidence from China. *Journal of Transport Geography*, 85, 102732. <https://doi.org/10.1016/j.jtrangeo.2020.102732>

## COMBATTING MODERN CITY PROBLEMS WITH THE USAGE OF UNDERGROUND SPACE: THE CASE STUDY OF GREECE

Dimitrios Papadomarkakis<sup>1</sup>

**Abstract:** By the year 2030, the global population is projected to reach 8.6 billion, with further growth expected to 9.8 billion by 2050. Presently, over half of the world's population resides in cities and urban areas. This rapid population increase, coupled with the global trend of urbanization, has precipitated numerous transportation and environmental challenges. Among the proposed solutions to address these issues is the development of Urban Underground Space (UUS). The strategic utilization of subterranean spaces can significantly contribute to meeting the escalating demands of urban areas by providing reliable transportation, harnessing green energy sources, and promoting environmental sustainability. This study investigates the current use of underground space in the region of Attica, Greece, serving as a case study to elucidate how urban underground spaces can alleviate traffic congestion, foster sustainable urban development, support the creation of compact cities, and address various related concerns.

**Keywords:** Urban Underground Space (UUS), Metro Lines, Underground Parking Facilities, Underground Hazardous Waste Repository.

### 1. INTRODUCTION

Many cities worldwide are confronting rapid population growth, leading to a higher concentration of individuals in urban areas (Cui et al., 2021). By 2050, it is projected that 70% of the global population will reside in cities, with the urban population more than doubling since the turn of the century (United Nations, 2007, 2013; Broere, 2016). Cities experiencing uncontrolled population growth will inevitably encounter significant challenges regarding efficient transportation infrastructure. If these infrastructures are not adequately upgraded to meet the demands of future "mega" cities, traffic congestion will increase exponentially, resulting in prolonged travel times. Moreover, the daily number of vehicles in circulation will rise, exacerbating the already critical issue of CO<sub>2</sub> emissions. Additionally, urban expansion to accommodate growing populations will capture valuable farmland, leading to substantial losses. As urban populations augment, the energy demands of cities will escalate dramatically, raising critical questions about the optimal placement of power suppliers to ensure comprehensive coverage. Over the past 40 years, the development of Urban Underground Space (UUS) has significantly contributed to addressing transportation, environmental, and land use challenges that typically arise during urban development (Cui et al., 2021). Generally, the development of the latter in order to combat modern city problems has been studied by various researchers (e.g. Hurtado and Perello, 1999; Bobylev, 2009; Broere, 2016; Li et al., 2016; Qian, 2016; Vahaaho, 2016; Yu et al., 2023).

Prominent examples of underground space utilization include Shanghai's extensive subway system, Tokyo's intricate underground shopping complexes (Cui et al., 2021), Toronto's subterranean parking structure beneath Nathan Phillips Square, and the Wierchowice underground gas storage facility in the Wrocław province of Poland. Since the dawn of the 21st century, Greece, particularly the region of Attica, has witnessed a significant surge in the use of underground spaces. Notably, on January 29, 2000, the first two lines of the Athens metro, Lines 2 and 3, were inaugurated, encompassing a total length of 13 kilometers and 14 stations (Elliniko Metro A.E., 2025). Nearly 24 years later, the Athens metro has expanded to include two operational lines with a combined

<sup>1</sup> Undergraduate Student, Laboratory of Tunnelling, School of Mining and Metallurgical Engineering, National Technical University of Athens, 9 Iroon Polytechniou Str., GR 15780, Zografou Campus, Athens, Greece. E-mail address: [papadomarkakisdimitrios@gmail.com](mailto:papadomarkakisdimitrios@gmail.com)

length of 59,7 kilometers and 40 stations (Elliniko Metro A.E., 2025). Furthermore, a third line, Line 4, is currently under construction, projected to span approximately 12,8 kilometers with 15 new stations, and further expansions of this line are in the preliminary stages of development (Elliniko Metro A.E., 2025). Furthermore, in recent years, numerous underground parking structures have been established, such as the Siggrou-Fix underground parking facility, which provides 640 parking spaces distributed across six underground levels and is directly connected to Line 2 of the Athens metro. Additionally, in 2010, new underground storage facilities were constructed at the Lavrion Technological and Cultural Park (LTCP) for the purpose of storing hazardous toxic wastes, with the repository reaching a depth of 40 meters.

Despite numerous discussions highlighting the potential of underground spaces to address urban challenges, general awareness remains low (Broere, 2016). Consequently, this study aims to analyze the current and prospective utilization of UUS in the region of Attica, Greece, with a focus on the examples previously mentioned. Specifically, the main uses of UUS in the area of interest are the Athens metro, underground parking facilities, and an underground hazardous waste repository. Ultimately, this study intends to elucidate how the development of UUS can deliver sustainable solutions for mitigating traffic congestion and CO<sub>2</sub> emissions, enhancing parking space availability, and safely storing hazardous wastes.

## 2. METHODOLOGY

The study will examine the three major current usages of UUS in the region of Attica, Greece, which are the following:

- The Athens metro,
- Underground parking facilities, and an
- Underground hazardous waste repository.

To accurately assess the positive impact of the Athens metro on the daily lives of citizens, the results from two questionnaires conducted over the past 20 years (e.g. Golias, 2002; Mitoula and Papavasileiou, 2023) were utilized. The first survey of Golias (2002) was conducted during the inaugural year of the Athens metro's operation, while the second survey of Mitoula and Papavasileiou (2023) was carried out nearly 18 years later. This approach allowed for an examination of the metro's initial impact and also investigated its long-term significance after almost two decades of operation.

As for the underground parking stations in Athens, numerous such structures have been constructed over the past two decades to alleviate the scarcity of parking relative to the increasing number of registered vehicles. Details regarding the capacities and number of floors of the largest facilities in Athens were provided. Additionally, due to the complete absence of primary surveys that examine the social impact of underground car parks in the city of Athens, studies that have been conducted on other large urban centers such as Sydney and Boston were utilized. As a result, the positive contribution of such structures was investigated, particularly towards their effectiveness in combatting the growing issue of limited parking spaces.

Finally, a brief historical background of the area currently occupied by the Lavrion Technological and Cultural Park (LTCP) will be provided to elucidate the environmental contamination issues that have plagued the region. Then the study conducted by Benardos and Kaliampakos (2006), in which they proposed the creation of an underground repository to manage the significant amount of waste in the area will then be thoroughly presented. This analysis will highlight the advantages of such facilities compared to other waste management methods, such as landfilling and incineration. Furthermore, the creation of this underground repository showcased how historical industrial sites could be rehabilitated and repurposed to meet modern environmental and technological needs while preserving cultural heritage, through the sustainable utilization of underground space.

## 3. THE ATHENS METRO

### 3.1. Historical background

The urban area of Athens, the capital of Greece, encompasses 1,470 km<sup>2</sup> (Golias, 2002). In 2020, the total number of vehicles in Athens reached 4,4 million, 69% of which were private vehicles (Chaziris and Yannis, 2023). Traffic in Athens has steadily increased since the advent of motorization in the 1960s (Chaziris and Yannis, 2023), culminating in the implementation of restrictions in 1982 to limit the use of private vehicles within the city center. Specifically, on even-numbered days of the month, only vehicles with an even last digit on their license plate are permitted to enter, while those with an odd last digit are prohibited. In the 1980s, the concept of constructing a metro system began to gain traction, but serious efforts did not materialize until the early 1990s. Consequently, the construction of the Athens metro commenced in November 1992 with the deployment of Tunnel



Boring Machines (TBMs). The planned Lines 2 and 3 were gradually delivered, encountering significant delays in certain excavation segments. In 1997, it was announced that the two lines would be operational by December 1999, but last-minute technical issues delayed the opening by one month (Elliniko Metro A.E., 2025). Finally, on January 29, 2000, the initial sections of Lines 2 and 3 were inaugurated. Line 2, connecting Sepolia with Syntagma, and Line 3, connecting Syntagma with Ethniki Amyna, each comprising of seven stations. Additionally, on November 15, 2000, five additional kilometers and five more stations were added to Line 2, completing the originally planned 12-station line. In April 2003, one more station, extending Line 3 by 1,4 kilometers, was added.

Over the past 20 years, Lines 2 and 3 of the Athens metro have continuously expanded, with the latest addition being three new stations on Line 3, delivered on October 10, 2022. Since its inception, the Athens metro has significantly contributed to reducing traffic congestion, thereby decreasing CO<sub>2</sub> emissions and noise levels. The system has a recorded daily ridership of approximately 938.000 passengers (Elliniko Metro A.E., 2025), a figure expected to rise dramatically to around 1,278 million passengers with the completion of Line 4 (Klontza, 2021). Fig. 1 illustrates the routes of the train (green line) and metro Lines 2, 3 (red and blue line respectively), and the planned route of metro Line 4 (yellow line).

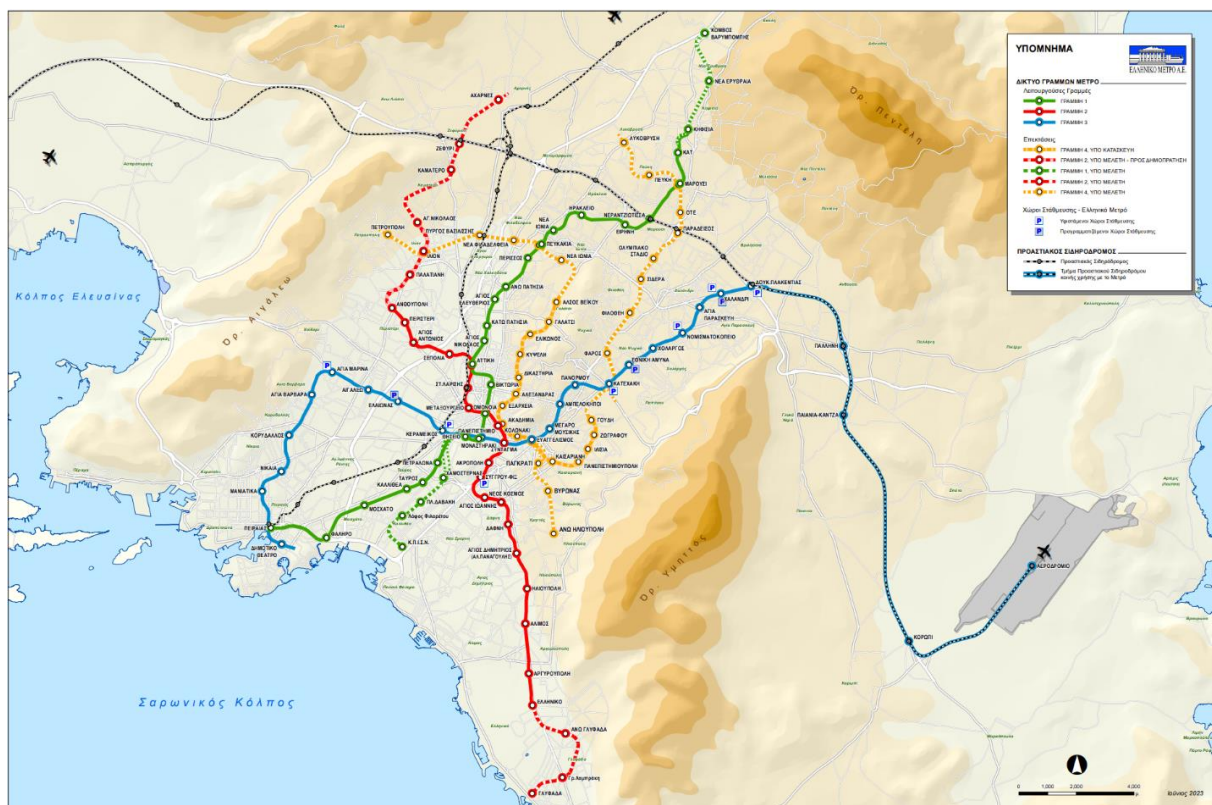


Figure 1. Map of the Athens metro (Elliniko Metro A.E., 2025).

### 3.2. Impact assessment

As it was previously mentioned results of two separate surveys, with the first having been conducted one year after the metro's introduction (Golias, 2002) while the other 18 years later (Mitoula and Papavasileiou, 2023), were utilized in order to showcase both the initial, as well as the long-lasting positive impact of the metro on the daily lives of the citizens of Athens. The 2002 survey by Golias (2002) initially focused on the modes of transportation utilized by the new metro riders before the metro's introduction. Specifically, over 50% of the new metro users transitioned from bus usage, while 24% shifted from private modes of transport (16% from cars, 7% from taxis, and 1% from motorcycles) (Golias, 2002). Another significant finding of the study is that due to the limited network initially offered by the Athens metro in its first year of operation, 57% of its users were forced to use an additional mode of transport to complete their journeys. This issue has gradually diminished due to the extensive expansions and additions made over the past 20 years. As previously mentioned, in 2000 both metro lines had a combined length of 13 km with 14 stations, while today, the network has expanded to a combined length of 59,7 km with 40 stations (Elliniko Metro A.E., 2025).

Furthermore, it was understood that the two primary criteria influencing public transport users' choice of transport mode were travel costs and travel time (Golias, 2002). The ticket cost is uniform across buses, the metro,

and other forms of public transport. Consequently, the travel cost of the metro, or public transport in general, can only be compared with private modes of transport such as cars, motorcycles, and taxis. Undoubtedly, the metro is significantly more economical than private modes, especially given the recent surge in gas and petrol prices due to the ongoing conflicts in the Middle East and Ukraine. Regarding travel time, the Athens metro is by far the fastest mode of transport in Athens, especially during the morning and afternoon rush hours. Particularly, according to reports by Elliniko Metro A.E. (2025) the Athens metro only requires 14 minutes to cover a distance of 10km, while for the same distance in the morning and afternoon rush hours a car requires at least 45 minutes. Ultimately, the metro uniquely combines both low cost and rapid travel time, thus meeting the primary criteria sought by daily users. Almost all other available options, including buses, private vehicles, combinations of modes, and walking, fail to meet both criteria. For instance, while the bus offers low cost, it is prone to traffic congestion. Conversely, private modes of transport neither offer low cost nor quick travel times. The only other option which offers both affordability and swift travel time is the train, also known as Line 1 (see green line in Fig. 1).

Overall, the survey revealed that the two newly established metro lines, unequivocally alleviated a significant portion of the traffic issues in the serviced areas. Undoubtedly, the Athens metro, despite initially offering a limited number of stations, profoundly improved the daily lives of citizens by providing a new, sustainable, rapid, and affordable mode of transport that could directly compete with private cars. However, a critical question remains: has the Athens metro continued to positively impact the daily lives of citizens almost two decades later? The latter question was answered by examining the results of a more recent survey conducted by Mitoula and Papavasileiou (2023).

The latter survey centered its 27 questions around three key "pillars" of sustainable development: the environmental and economic impact, and the societal influence of the Athens metro. Firstly, over 75% of the surveys participants believed that the metro has positively contributed to the environment of Athens (Mitoula and Papavasileiou, 2023). It is worth noting that according to recent statistical reports by Elliniko Metro A.E. (2025) the extension of metro line 3 to Piraeus has reduced the number of vehicles by nearly 11.000 per day, consequently decreasing CO<sub>2</sub> emissions by 60 tonnes daily. Interestingly, more than 93% of participants observed increased trade in the vicinity of metro stations, particularly noting a surge in hotels, restaurants, coffee shops, commercial outlets, and even museums (Mitoula and Papavasileiou, 2023). Citizens have also perceive that the Athens metro has fostered commerce in surrounding districts by facilitating the creation of new businesses, thereby generating ongoing job opportunities (Mitoula and Papavasileiou, 2023). Furthermore, over 90% of participants indicated that the overall quality of life has improved due to the Athens metro, which they attributed to a combination of the aforementioned economic and environmental benefits (Mitoula and Papavasileiou, 2023). Additionally, more than 92% of the participants believed that the metro has contributed significantly to the general development of Athens (Mitoula and Papavasileiou, 2023).

Several general questions were also posed regarding potential improvements to the Athens metro. More than 53% of respondents suggested that the network of stations should be expanded (Mitoula and Papavasileiou, 2023), highlighting the metro's recognized contribution to improving daily life in multiple aspects and the public's desire for further development. Additionally, over 70% and 68% of participants, respectively, indicated that the metro's travel cost is not prohibitive and that ticket prices remain reasonable and affordable for daily users (Mitoula and Papavasileiou, 2023). These findings suggest that the metro continues to offer a cost-effective travel solution nearly 20 years later, consistent with the 2002 survey's indication that users highly value travel cost. Moreover, over 70% of participants believe the metro is well-maintained (Mitoula and Papavasileiou, 2023), reflecting its nearly 25-year longevity without significant issues. Finally, almost 85% expressed satisfaction with the metro's quality, citing clean and accessible stations throughout Athens (Mitoula and Papavasileiou, 2023). Overall, this more recent study not only confirmed the conclusions suggested by the early 2002 survey but also highlighted the Athens metro's significant contribution to the economic growth of the city. The overwhelming majority of respondents expressed strong views that the Athens metro has greatly benefited the environment, economy, and society of Athens, solidifying its status as a sustainable mode of transport that supports the three key pillars of sustainable development. Additionally, when asked about potential improvements, more than 50% of respondents immediately suggested expanding the metro network to increase the number of citizens it can serve daily.

To sum up, the Athens metro stands as the largest and most promising example of underground space utilization in the Attica region. The citizens of Athens have rightfully recognized its significant positive impact on their daily lives. This recognition is supported by two pivotal surveys: one conducted by Golias (2002), only 12 months after the metro's opening, and another by Mitoula and Papavasileiou (2023), when the metro had been in operation for nearly 18 years. By closely examining the results from the two separate surveys, a more definitive conclusion can be drawn about the effectiveness of the metro and its overall impact. The 2002 survey captured the initial positive impressions of the metro's users, who viewed it as the newest and most sustainable mode of transport, capable of directly competing with passenger vehicles. Despite these positive views, there were concerns about its long-term effectiveness due to the initially limited network. However, the 2020 survey, conducted nearly two decades later, addressed these concerns and provided comprehensive answers. It demonstrated that the metro's

positive impact is not only lasting but has also grown over time. The metro has significantly reduced noise pollution, alleviated chronic traffic congestion, and decreased CO<sub>2</sub> emissions. Moreover, citizens reported that the metro has contributed to the economic development of Athens, further enhancing its societal impact. When considering the low travel costs and quick travel times, two key criteria valued by daily users, the Athens metro emerges as the most sustainable mode of transport. Its network, already expanded significantly, continues to grow to better serve the city's population. The Athens metro exemplifies how effective underground space utilization can address and mitigate real-time urban challenges. This is particularly relevant as urbanization continues to rise globally, amplifying the need for sustainable and innovative transportation solutions.

#### 4. UNDERGROUND PARKING FACILITIES

The underground space of Athens has been utilized to create several major underground parking stations in order to combat the persistent problem of parking. As illustrated in Table 1 below, the ten largest underground parking stations for vehicles (particularly cars) in the region of Attica are listed, along with one underground bus depot. It is worth noting that the parking station in Syggrou-Fix is a particularly vital one due to its direct connection to the Athens metro and its strategic location, particularly being less than 3 km away from the city center and under 6 km away from the sea. Another significant facility with direct metro access is the Nomismatokopio underground car park, which offers 630 parking spots distributed over three floors. In Agia Paraskevi, the ninth largest underground parking station provides 360 car spots on a single floor, while also maintaining a convenient link to the metro. Lastly, the Katehaki underground bus depot stands out with its capacity to house 284 buses, all on a single floor. This facility plays a crucial role in accommodating a major part of the city's public transportation fleet, contributing to a more organized and efficient urban transit system.

**Table 1.** The ten largest underground parking stations of Attica for private vehicles are presented, along with one underground bus depot.

Parking Station	Capacity (Parking Spots)	Number of Floors
Piraeus	727	4
Nea Smyrni Square	665	3
Rizari Street	660	4
Paidon Hospital Square	651	5
Syggrou-Fix	640	6
Nomismatokopio	630	3
Kaniggos Square	491	4
Pedion tou Areos	365	5
Agia Paraskevi	360	1
Kerameikos	270	5
Katehaki Bus Depot	284 (for buses)	1

As it was mentioned in the earlier part of the present paper there is a very large gap in the existing literature, as well as statistical data, for the assessment of the social, environmental and economic impact of the various underground parking stations that have been created in the past 25 years in the region Attica, and particularly Athens. As a result, the author will present two case studies from other large urban centers, particularly the city of Sydney in Australia and Boston in the U.S.A., where similar issues of limited parking availability were faced but were subsequently combatted using underground car parks. The Sydney Opera House is undoubtedly one of the most important landmarks of the city of Sydney. The latter monument was opened in October of 1973, and according to reports of the Sydney Opera House (2025) more than 10,9 million people visit the site every year. One disadvantage of this historic building, that was clear from its first decade of operation, was its difficult accessibility due to its lack of parking facilities. However, in the early 1990s it was decided to create a large underground helical shaped car park, in order to meet the growing parking issues. The choice of the underground structure was chosen on the basis that an above-ground facility of the same magnitude would greatly affect the visual beauty of the monument. The facility has 12 different floors and approximately 1.100 parking spaces (ITA WG13, 1995). Additionally, the whole excavation of the cavern was executed without disrupting the surface, and in general the aesthetic appeal of the area, due to it being a very high-profile touristic attraction. Overall, this large underground car park under the Sydney Opera House illuminates the advantages of underground space utilization, and particularly underground parking facilities, in producing realistic solutions that can face the major environmental problems of modern cities, such as covering the basic need of accessible parking spaces.

In the early 1980s a very big concern of urban planners in downtown Boston was the lack of open spaces. Subsequently, in 1983 it was proposed to create a 1,7-acre public park as well as an underground parking facility on Post Office Square, which is located in Boston's downtown financial district. The underground car park was opened to the public in June of 1991, and had a capacity of 1.400 parking spots (ITA WG13, 1995). Generally, with the construction of the aforementioned underground structure the available parking space increased in the area by almost 50% (ITA WG13, 1995) without losing any of the valuable surface space. Moreover, the creation of the underground car park increased the overall revenues of the city of Boston, since more people could easily access its downtown. Finally, the option of placing the parking facility underground paved the way to sustainably utilize the above-ground area, transforming the Post Office Square into a much-needed green park right into the heart of Boston (ITA WG13, 1995).

These two examples of large underground car parks perfectly showcase how such underground structures can help alleviate modern issues that most large urban centers face, especially when surface areas are limited. Consequently, all of these direct and indirect benefits that are yielded from the development of underground car parks can be considered valid for the case study of the present paper, particularly the region of Attica, however no efforts have been made yet to study the extent of their social, environmental, and economic impact.

## 5. UNDERGROUND HAZARDOUS WASTE REPOSITORY

In 2010, Greece opened its first, and to this day, its only underground repository, with a storage capacity of approximately 3.000 m<sup>3</sup> for toxic wastes, in Lavrio, Attica, within the renowned Lavrion Technological and Cultural Park (LTCP). The proposal for its construction was first put forth by Benardos and Kaliampakos (2006), using the room-and-pillar mining technique, with the excavation taking place in a competent marble formation. The room-and-pillar method was chosen for its cost-effectiveness and it essentially exploited the natural structural stability provided by the marble.

Lavrio boasts a rich mining and metallurgical history, dating back to the 5th century BC when ancient Athenians established underground operations to extract silver. These deposits were further metallurgically exploited for their high lead content from the 19th century until the early 1990s. Due to the presence of heavy industries for all almost a whole century, the buildings within the LTCP complex were highly contaminated. Efforts to preserve the area, given its significant cultural heritage, began in the early 1990s. The extent of the environmental contamination became evident when it was found that the land within the park was extensively covered in waste and slag materials, remnants of the old metallurgical processing. This resulted in the soil having excessively high levels of lead, zinc, arsenic, cadmium, copper, and other toxic substances, far exceeding the acceptable environmental standards. The more hazardous wastes, particularly those with the highest arsenic concentrations, were placed in steel drums. These drums were intended to be stored in the innovative underground repository created within the LTCP. This facility represented a significant advancement in hazardous waste management, utilizing UUS to safely contain and isolate toxic materials from the environment.

The establishment of the underground repository in Lavrio not only addressed the immediate environmental hazards but also marked a significant step forward in sustainable waste management practices in Greece. It demonstrated that managing hazardous wastes through the use of underground space offers clear advantages over commonly used remediation techniques. Additionally, this project showcased how historical industrial sites could be rehabilitated and repurposed to meet modern environmental and technological needs while preserving cultural heritage, through the sustainable utilization of underground space. This approach not only mitigated the environmental risks, but also revitalized the historically significant area of Lavrio. To summarize, the underground repository in Lavrio has significantly improved the safe storage of hazardous wastes. However, the development of such facilities has not yet been widely adopted in Greece, as evidenced by the fact that no other such repositories have been established since then. In contrast, other European countries have recognized the sustainability and cost-effectiveness of underground storage solutions and continue to develop them. With studies such as the one conducted by Benardos and Kaliampakos (2006) nearly two decades ago, and studies like the present, the perpetual and invaluable benefits of underground repositories for storing highly toxic wastes, which pose extreme risks to public health, should be emphasized and made clear to the public.

## 6. FUTURE UNDERGROUND PROJECTS

The most prominent future developments for the utilization of UUS in the Attica region primarily involve extensions to the two existing metro lines, particularly Line 2, and the creation of Line 4. Line 4 is expected to be fully operational by 2029 and will connect Petroupoli with Ano-Ilioupoli and Likobrisi (Elliniko Metro A.E., 2025). As illustrated in Fig. 1, this new line will feature 35 new stations. Early estimations suggest that it will serve

more than 340.000 passengers daily and reduce the number of circulating cars by 53.000 (Klontza, 2021). This development will address the increasing demand from citizens to expand the metro network, providing a cheaper and faster transport alternative compared to other modes of travel. Regarding Line 2, there are plans for 9 new stations. Three of these will extend the current terminus at Elliniko towards Glyfada, and six will extend the Anthoupoli terminus towards Axarnes. Additionally, it is under consideration to incorporate underground parking facilities near these new stations to alleviate the persistent parking problems and reduce visual and noise pollution (Elliniko Metro A.E., 2025). Lastly, there have been proposals to expand the underground repository in Lavrio, though these plans have yet to materialize.

## 7. CONCLUSIONS

The constant increase in urbanization has created significant challenges in modern cities. These issues range from extreme traffic congestion and severe environmental pollution in all its forms, resulting in unhealthy living conditions for citizens, to a lack of sufficient parking spaces and difficulties in managing the uncontrollably increasing hazardous wastes. Given the limited availability of surface space, the utilization of subsurface areas has become a necessity in modern urban planning. This study, focusing on the region of Attica, Greece, demonstrated that large underground projects, such as the creation of the metro, have a lasting positive impact on citizens. The benefits of the Athens metro were confirmed by two separate surveys: one conducted during its inaugural year and another almost 18 years later. Both surveys indicated that citizens recognized the environmental, economic, and societal contributions of the metro, with a strong demand for network expansion. Additionally, the utilization of underground space has proven to be a sustainable solution for creating parking stations, offering numerous advantages over surface car parks. However, the extent of the impact of the latter underground structures has not yet been assessed in the region of Attica, and particularly Athens, hence making their overall evaluation difficult. Furthermore, the case of Lavrio decisively demonstrated that the utilization of underground space can effectively manage hazardous waste. Creating underground repositories for various types of waste (toxic, nuclear, etc.) significantly lowers monitoring costs and mitigates the risk of leakage or environmental contamination, thanks to the impenetrable geological formations used in their construction. The room-and-pillar mining technique also reduces construction costs, making these repositories a superior choice over traditional methods like landfilling or incineration. In summary, while the future development of Athens' subsurface looks promising with the ongoing expansion of existing metro lines and the construction of a new Line 4, many opportunities remain to fully exploit the city's underground potential. Initiatives should focus on creating more underground car parks and especially underground repositories to enhance urban sustainability and effectively address the pressing challenges posed by urbanization.

## 8. BIBLIOGRAPHY

- [1] Benardos, A.G., Kaliampakos, D.C. (2006). Design of an Underground Hazardous Waste Repository in Greece. *Tunnelling and Underground Space Technology*, 2006.
- [2] Bobylev, N. (2009). Mainstreaming sustainable development into a city's Master plan: A case of Urban Underground Space. *Land Use Policy*, Vol. 26, pp. 1128-1137. [10.1016/j.landusepol.2009.02.003](https://doi.org/10.1016/j.landusepol.2009.02.003)
- [3] Broere, W. (2016). Urban underground space: Solving the problems of today's cities. *Tunnelling and Underground Space Technology*, Vol. 55, pp. 245-248. <https://doi.org/10.1016/j.tust.2015.11.012>
- [4] Chaziris, A., Yannis, G. (2023). A critical assessment of Athens Traffic Restrictions using multiple data sources. *Transportation Research Procedia*, Vol. 72, pp. 375-382. <https://doi.org/10.1016/j.trpro.2023.11.417>
- [5] Cui, J., Broere, W., Lin, D. (2021). Underground space utilization for urban renewal. *Tunnelling and Underground Space Technology incorporating Trenchless Technology Research*, Vol. 108, 103726. <https://doi.org/10.1016/j.tust.2020.103726>
- [6] Elliniko Metro A.E. (2025). Website link: <https://www.emetro.gr>
- [7] Golias, J.C. (2002). Analysis of traffic corridor impacts from the introduction of the new Athens Metro system. *Journal of Transport Geography*, Vol. 10, pp. 91-97. [https://doi.org/10.1016/S0966-6923\(01\)00033-3](https://doi.org/10.1016/S0966-6923(01)00033-3)
- [8] Cano-Hurtado, J.J., Canto-Perello, J. (1999). Sustainable development of urban underground space for utilities. *Tunnelling and Underground Space Technology*, Vol. 14, pp. 335-340. [https://doi.org/10.1016/S0886-7798\(99\)00048-6](https://doi.org/10.1016/S0886-7798(99)00048-6)
- [9] International Tunnelling Association (1995). Working Group No. 13, Final Report "Underground Car Parks: International Case Studies". *Tunnelling and Underground Space Technology*, Vol. 10, No. 3, pp. 321-342. [https://doi.org/10.1016/0886-7798\(95\)00021-P](https://doi.org/10.1016/0886-7798(95)00021-P)
- [10] Klontza, O. (2021). Metro-How Line 4 changes Athens. *To Vima*, November 21 2021. <https://www.tovima.gr/2021/11/21/society/metro-pos-i-grammi-4-allazei-tin-athina/>



- [11] Li, X.Z., Li, C., Parriaux, A., Wu, W., Li, H.Q., Sun, L., Liu, C. (2016). Multiple resources and their sustainable development in Urban Underground Space. *Tunnelling and Underground Space Technology*, Vol. 55, pp. 59-66. <https://doi.org/10.1016/j.tust.2016.02.003>
- [12] Mitoula, R., Papavasileiou, A. (2023). Mega infrastructure projects and their contribution to sustainable development: the case of the Athens Metro. *Economic Change and Restructuring*, Vol. 56, pp. 1943-1969. <https://doi.org/10.1007/s10644-023-09493-w>
- [13] Qian, Q. (2016). Present state, problems and development trends of urban underground space in China. *Tunnelling and Underground Space Technology*, Vol. 55, pp. 280-289. <https://doi.org/10.1016/j.tust.2015.11.007>
- [14] Sydney Opera House (2025). Interesting facts about the Sydney Opera House. <https://www.sydneyoperahouse.com/building/interesting-facts-about-sydney-opera-house>
- [15] United Nations (2007). World Population Prospects: The 2007 Revision. Technical Report. United Nations, Department of Economic and Social Affairs, Population Division. [https://www.electroluxgroup.com/en/wp-content/uploads/sites/2/2010/07/2007WUP\\_ExecSum\\_web.pdf](https://www.electroluxgroup.com/en/wp-content/uploads/sites/2/2010/07/2007WUP_ExecSum_web.pdf)
- [16] United Nations (2013). World Population Prospects: The 2012 Revision. Technical Report ESA/P/WP.228. United Nations, Department of Economic and Social Affairs, Population Division. <https://www.un.org/en/development/desa/publications/world-population-prospects-the-2012-revision.html>
- [17] Vahaaho, I. (2016). An introduction to the development for urban underground space in Helsinki. *Tunnelling and Underground Space Technology*, Vol. 55, pp. 324-328. <https://doi.org/10.1016/j.tust.2015.10.001>
- [18] Yu, P., Liu, H., Wang, Z., Fu, J., Zhang, H., Wang, J., Yang, Q. (2023). Development for urban underground space in coastal cities in China: A review. *Deep Underground Science and Engineering*, Vol. 2, pp. 148-172. <https://doi.org/10.1002/dug2.12034>

## INFLUENCING FACTORS AND EVALUATION INDEX SYSTEM FRAME FOR THE BEARING CAPACITY OF DEEP UNDERGROUND SPACE IN COASTAL SOFT SOIL CITIES: A CASE STUDY OF SHANGHAI

Jianxiu Wang<sup>1</sup>, Yanxia Long<sup>2</sup>, Hanmei Wang<sup>3</sup>, Tongzhen Cui<sup>4</sup>, Xinlei Huang<sup>5</sup>, Yuanbo Gao<sup>6</sup>, Jianzhong Wu<sup>7</sup>, Weiqiang Pan<sup>8</sup>

**Abstract:** Shanghai, a coastal megacity built on soft deltaic soil, faces growing demand for deep underground space (DUS) development as its shallow and intermediate layers approach saturation. However, the complex interplay of geological, hydrogeological, and environmental factors significantly constrains the carrying capacity of DUS. This study investigates the bearing capacity of DUS in Shanghai as a representative coastal soft soil city. Through systematic analysis of deep stratigraphic conditions, confined aquifer systems, and environmental geological risks (e.g., land subsidence, liquefaction, and gas escape), the key influencing factors are identified. Special attention is given to the coupled effects of thermal–hydraulic–mechanical–chemical (THMC) processes. Based on these insights, a multi-dimensional evaluation index system is proposed, incorporating geotechnical, hydrogeological, environmental, and spatial utilization factors. The framework provides a basis for carrying capacity assessment under current engineering conditions. The findings offer methodological guidance and geological support for the planning and sustainable development of DUS in Shanghai and similar coastal cities.

**Keywords:** Deep Underground Space, Coastal Soft Soil, Bearing Capacity, Evaluation index, Influencing Factors Analysis

### 1. INTRODUCTION

The development of urban underground space (UUS) is an important approach to achieving sustainable urban development. It can effectively alleviate the tension between people and land in modern cities, expand urban space, and improve the urban environment. (Sterling et al., 2012; Bobylev, 2016; Admiraal & Cornaro, 2020; Qiao et al., 2022). However, with the acceleration of urbanization, megacities such as Shanghai, Beijing, Guangzhou, and Tokyo (Kishii, 2016) are facing a series of challenges including continuous population growth, traffic congestion, and resource shortages. The contradiction between the rapidly expanding demand for urban space and the limited availability of spatial resources has become increasingly prominent. Meanwhile, as the development of shallow and middle UUS becomes increasingly saturated, the exploitation of deep underground space (DUS) has become an inevitable trend in addressing the above challenges. (Li et al., 2018; Li et al., 2025).

<sup>1</sup> Professor, Wang Jianxiu, PhD, Geotechnical Engineering, College of Civil Engineering, Tongji University, 1239 Siping Road, Shanghai 200092, China, [wang\\_jianxiu@163.com](mailto:wang_jianxiu@163.com).

<sup>2</sup> PhD student, Long Yanxia, MSc, Civil Engineering, College of Civil Engineering, Tongji University, 1239 Siping Road, Shanghai 200092, China, [2010328@tongji.edu.cn](mailto:2010328@tongji.edu.cn).

<sup>3</sup> Professor, Wang Hanmei, PhD, Shanghai Institute of Natural Resources Survey and Utilization Research, 930 Lingshi Road, Shanghai 200072, China, [whm76@sigs.com.cn](mailto:whm76@sigs.com.cn).

<sup>4</sup> Master's student, Cui Tongzhen, BEng, Urban and Rural Planning, Zhejiang University of Science and Technology, 318 Liuhe Road, Hangzhou 310023, China, [905990760@qq.com](mailto:905990760@qq.com).

<sup>5</sup> Senior Engineer, Huang Xinlei, MSc, Shanghai Institute of Natural Resources Survey and Utilization Research, 930 Lingshi Road, Shanghai 200072, China, [huangxl2009@126.com](mailto:huangxl2009@126.com).

<sup>6</sup> Senior Engineer, Gao Yuanbo, BEng, Sinhydro Bureau No.11 Co. Ltd, 59 Lianhua Street, Zhengzhou 450001, China, [gaoyuanbo0706@outlook.com](mailto:gaoyuanbo0706@outlook.com).

<sup>7</sup> Senior Engineer, Wu Jianzhong, MSc, Shanghai Institute of Natural Resources Survey and Utilization Research, 930 Lingshi Road, Shanghai 200072, China, [wujianzhong@sigs.com.cn](mailto:wujianzhong@sigs.com.cn).

<sup>8</sup> Professor, Pan Weiqiang, PhD, Shanghai Tunnel Engineering Co., Ltd, 118 Dalian Road, Shanghai 200082, China, [pwq21@163.com](mailto:pwq21@163.com).

As a typical coastal megacity built on soft soil, Shanghai has seen the shallow and middle underground space in its central urban areas approach saturation amid the ongoing intensification of urban development. (Qian and He, 2024). The development of DUS has become a strategic choice for enhancing urban carrying capacity and achieving sustainable development. However, the development of deep underground space is not merely an extension of shallow or intermediate layers; it faces more complex challenges related to geological conditions, groundwater, and structural stability, making it significantly more difficult. Although Shanghai has accumulated extensive experience in shallow underground development, deep development still requires further investigation. According to the Shanghai Master Plan (2017–2035) (Liu and Zhu, 2020), areas below 50 meters are designated as deep underground space and are a key focus for future urban expansion (Li et al., 2018). However, UUS carrying capacity is constrained by engineering geological and hydrogeological conditions, the coupled effects of thermal–hydraulic–mechanical–chemical (THMC) processes, and the current level of engineering technology (Li et al., 2016; Price et al., 2018). Therefore, it is essential to systematically identify and evaluate the key factors influencing its carrying capacity.

Existing studies have explored the driving forces, limiting factors, and evaluation methods of urban underground space (UUS) development from multiple perspectives. Bobylev (2009), He et al. (2012), and Chen et al. (2018) identified urban population density and per capita GDP as key drivers of underground space development. Li et al. (2013a) emphasized that land prices and construction costs are primary indicators for assessing the economic viability of UUS. Li et al. (2013b) further proposed the "Deep City Method," which integrates four types of underground resources with three urban indicators to establish a scoring system for identifying cities with development potential. Lu et al. (2016) developed a multi-level engineering geological suitability evaluation framework for UUS using the FAHP-TOPSIS method. Regarding constraints, complex geological conditions are recognized as major factors affecting development difficulty and cost (Mukhtar et al., 2019; Lai et al., 2023), while groundwater can compromise structural stability and increase corrosion risks (Mukhtar et al., 2019; Attard et al., 2017). Other factors, such as topography, economic conditions, and land use, have also been considered in suitability assessments (Zhang et al., 2021). He et al. (2020) established a geological suitability evaluation index system based on fundamental and constraint conditions, applying fuzzy mathematics and AHP to assess UUS development in a region of Beijing. Peng and Peng (2018a, 2018b) combined AHP, MUGM, and EM methods within a GIS platform to evaluate construction suitability, potential value, and volumetric capacity. From a safety perspective, Zhou et al. (2024) integrated geotechnical analysis, urban planning theory, and artificial intelligence to develop an intelligent resilience evaluation model, assessing the impact of UUS development on surrounding buildings and enhancing the scientific basis for safe spatial planning.

Existing studies have made some progress in evaluating underground space development, particularly in assessing geological suitability and development potential. However, research on deep underground space has mostly focused on planning, with limited work on the definition and quantitative analysis of carrying capacity. This paper defines underground space carrying capacity as the maximum development intensity that can be supported while ensuring safety and functionality, considering geological conditions, technical feasibility, and societal needs. Taking Shanghai as a case study, this paper reviews its deep underground space development, analyzes key influencing factors and evaluation methods, and proposes an assessment framework suitable for soft soil areas to support future safe and scientific development.

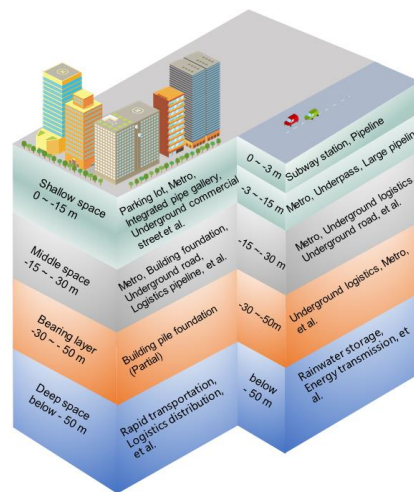
## **2. DUS IN SHANGHAI**

### **2.1. Current Status of Deep Underground Space Development and Utilization in Shanghai**

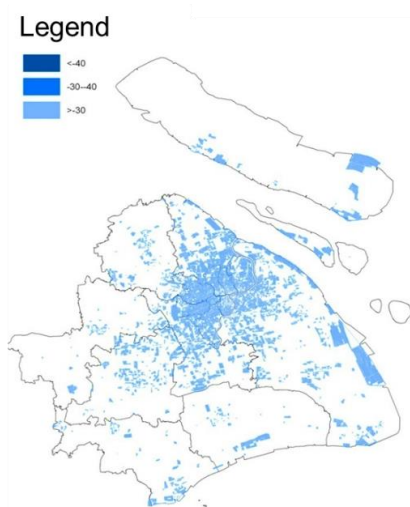
In recent years, with the continuous intensification of urban construction, the development and utilization of underground space in Shanghai has expanded rapidly. By the end of 2022, approximately 43,000 underground engineering projects had been completed, with a total floor area of about  $1.45 \times 10^9$  m<sup>2</sup>, encompassing a wide range of functions including transportation, municipal infrastructure, public services, and warehousing logistics. Among these, facilities for daily life services account for as much as 86% of the total, while rail transit and public infrastructure make up approximately 8% and 6%, respectively. In terms of development depth, the development of UUS in Shanghai shows a more obvious characteristic of stratified use (Figure 1). At present, basement structures are generally buried within 30 m of the surface (Figure 2), tunnel projects are primarily located at depths of 20–40 m, and some building foundations extend to 30–50 m into bearing soil layers (Figure 3). As shown in Figure 2 and Figure 3, the underground space in the central urban area of Shanghai has been developed at a relatively high density. The volumetric distribution of shallow underground space utilization is illustrated in Figure 4. It can be observed that shallow and intermediate underground space development in central Shanghai exhibits a pattern of 'widespread utilization with localized saturation'. Along both sides of the Huangpu River, underground space utilization is particularly intensive, with many land parcels exhibiting development volumes

exceeding 30.000 to 100.000 m<sup>3</sup>, some of which have reached a high level of development intensity. This trend indicates that the potential for further expansion in shallow and intermediate underground space is rapidly diminishing. New development projects are increasingly constrained by structural saturation, functional conflicts, and safety risks. Therefore, it is urgently necessary to extend development into deeper underground layers to achieve a more graded use of underground space resources and an optimized spatial-functional layout.

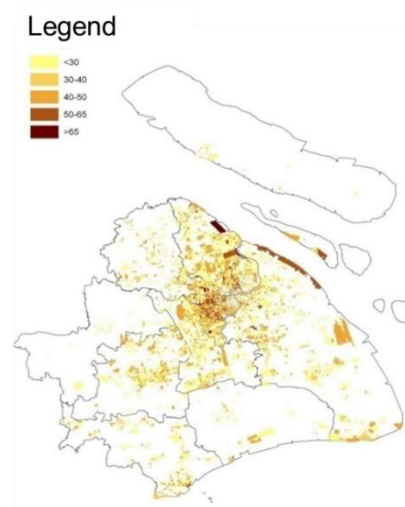
As the mid-shallow underground space becomes increasingly saturated, the construction of new linear infrastructure, such as rail transit lines and utility tunnels, facing growing spatial conflicts and engineering difficulties. Consequently, the demand for deep underground space development is emerging. According to the *Shanghai Master Plan (2017–2035)*, underground space deeper than 50 m is classified as “deep underground space” and is primarily reserved for key functional systems such as high-speed transportation, logistics distribution, stormwater regulation, and energy transmission (Figure 5). Shanghai has entered the initial stage of deep underground space development. Representative projects include the Suzhou Creek deep drainage and storage tunnel (pilot section), where the shield shaft excavation depth reaches nearly 60 m, diaphragm walls extend down to 103m -105 m, and tunnel sections are typically located at depths of 50m - 60 m. The hard X-ray free-electron laser facility features shaft depths of around 50 m and diaphragm walls extending to approximately 100 m. The Shanghai Yangtze River Tunnel and Bridge project reaches a maximum burial depth of 55 m beneath the riverbed. Compared with shallow and intermediate layers, deep underground space offers advantages such as greater integrity, minimal surface interference, strong enclosure, and substantial development potential, making it particularly suitable for accommodating critical infrastructure. For a megacity like Shanghai, the systematic development of deep underground space has become an urgent necessity, and evaluating its bearing capacity is a fundamental prerequisite to ensuring its safe, efficient, and sustainable utilization.



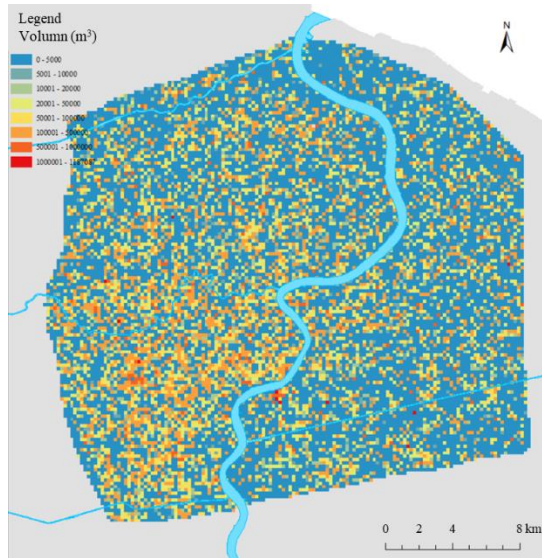
**Figure 1.** Vertical stratified utilization of UUS in Shanghai



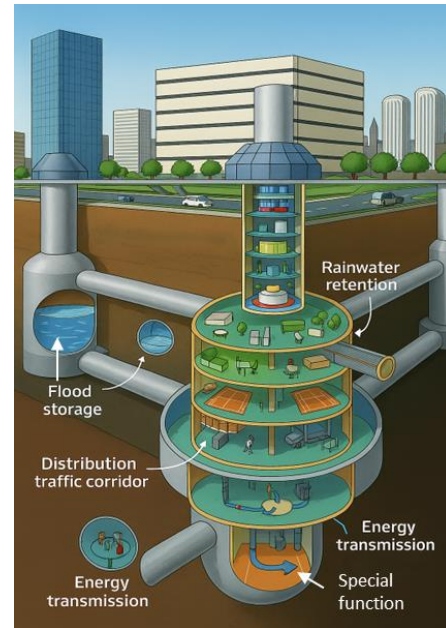
**Figure 2.** Basement depth distribution in Shanghai



**Figure 3.** Length of underground pile foundation in Shanghai



**Figure 4.** Utilization volume of shallow and middle underground space in the central urban area of Shanghai



**Figure 5.** Functional layout of DUS of Shanghai

## 2.2. Characteristics of Deep Soil Strata in Shanghai

Shanghai is located on a deltaic alluvial plain and is representative of regions characterized by natural soft soil. The subsoil profile can be divided into 12 major soil layers, containing one phreatic aquifer, one micro-confined aquifer, and five confined aquifers. These layers are notable for their large cumulative thickness and abundant groundwater. The soil strata within the shallow to intermediate underground space primarily consist of soft clay and sandy soils, while those in the deep underground space are mainly composed of silty fine sand and sandy clay. The geological distribution of deep underground space (50m -100 m) in Shanghai is presented in Table 1.

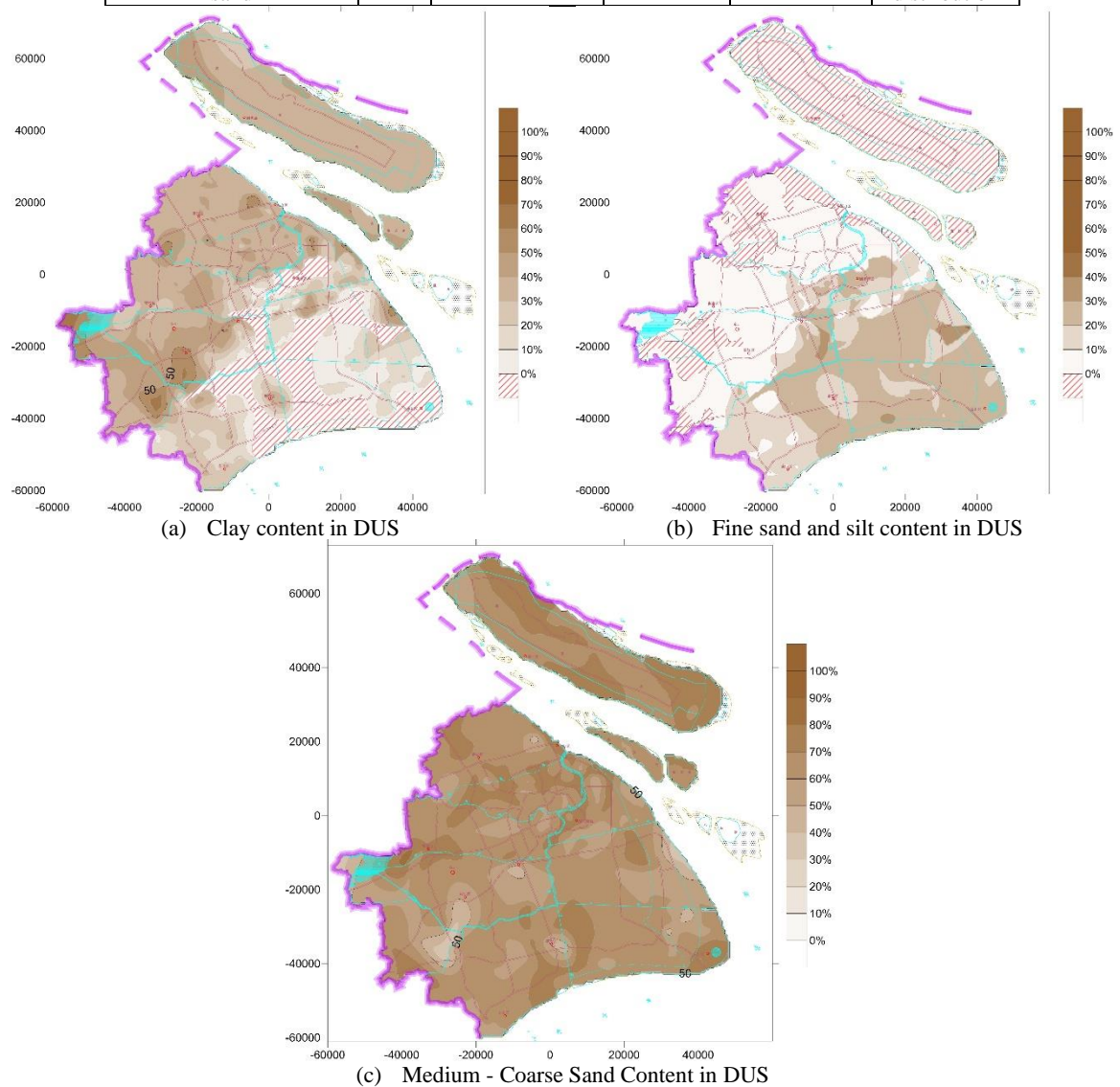
As shown in Table 1 and Figure 6, medium to coarse sand accounts for approximately 64.69% of the deep strata, while clay makes up nearly one-third. The deep sandy layers are generally of low bearing capacity and moderate compressibility, with limited liquefaction potential. In contrast, deep clayey soils are prone to significant plastic deformation and consolidation settlement. The layer ⑧, a relatively thick clay stratum, is considered suitable for construction and may act as an effective barrier to the first and second confined aquifers. Laboratory testing has identified the layer ⑧ as overconsolidated clay, indicating favorable conditions for deep underground space development in areas where it is well developed.

Compared to shallow and intermediate strata, deep soils exhibit lower plasticity indices and liquid limits, fewer silt particles, and a higher proportion of clay particles. Except for layer ⑧<sub>1</sub>, the deep soil layers mainly consist of plastic to stiff clays and medium-dense to dense silty soils and silts, characterized by high strength, good uniformity, relatively low compressibility, and strong bearing capacity. Overall, from the perspective of physical and mechanical soil properties, although deep underground development presents more engineering challenges than shallow development, the deep strata in coastal regions such as Shanghai remain suitable for underground space exploitation.



**Table 1.** Geological conditions of deep underground space in Shanghai

Geological layer	No.	Top burial depth (m)	Thickness (m)	State or compaction	Distribution
Gray clay with silty sand	⑧ <sub>1</sub>	40.0~60.0	6.0~30.0	Soft-Plastic to plastic	Partial absence
Gray silty clay interbedded with silty sand	⑧ <sub>2</sub>	50.0~60.0	10.0~20.0	Plastic or medium dense	Partial absence
Grayish-blue fine sand with clay	⑨ <sub>1</sub>	65.0~77.0	5.0~8.0	Medium dense to dense	Stable distribution
Grayish-blue fine silty sand with medium sand	⑨ <sub>2</sub>	75~81.0	5.0~10.0	Dense	Stable distribution
Blue-gray or brown-gray clay	⑩	86.0~101.0	4.0~10.0	Hard-Plastic	Extensive distribution
Grayish-blue fine silty sand	⑪	88.0~101.0	10.0~30.0	Dense	Extensive distribution



**Figure 6.** Proportions of different soil types in DUS of Shanghai

### 3. ANALYSIS OF INFLUENCING FACTORS OF THE DUS BEARING CAPACITY

Under the current level of engineering technology and safety regulations, the bearing capacity of deep underground space (DUS) is defined as the maximum capacity of deep subsurface strata in a specific area to accommodate various underground space functions. This capacity not only reflects the sustainable development potential of underground space resources but also represents the critical threshold for ensuring urban operational safety and coordinated resource utilization. It is a complex quantitative system influenced by the coupling of multiple factors. The core of DUS bearing capacity evaluation lies in the comprehensive assessment of the quantity, quality, suitability, and limiting factors of deep underground space resources. Urban underground resources include not only underground space itself but also groundwater, geological materials, and underground geothermal energy (Li et al., 2016; Attard et al., 2017; Li et al., 2018). Therefore, this evaluation process must account for multiple dimensions, such as regional geological structure, geotechnical conditions, hydrogeological characteristics, environmental sensitivity, and the existing state of surface and shallow underground space development. Notably, deep underground space interacts significantly with other underground resources. On one hand, deep excavation and construction may lead to changes in groundwater levels, thermal field disturbances, or the destabilization of geotechnical strata. On the other hand, factors such as groundwater abundance, geotechnical strength, and the distribution of geothermal energy may in turn constrain the feasibility of deep space development. Shanghai has a low frequency and low intensity of seismic activity, and the overall stability of the region is favorable. This section will analyze the key influencing factors of DUS bearing capacity in Shanghai and establish a comprehensive evaluation index framework accordingly.

#### 3.1. Engineering geology condition

Engineering geological conditions are a fundamental factor influencing the development and utilization of underground space. For deep underground space, its bearing capacity primarily depends on the depth to bedrock, the thickness of clay layers, soil uniformity, and the composition of stratigraphic sequences.

Shanghai is covered by a thick Quaternary layer, with the bedrock surface overlain by deposits ranging from 150 to 350 meters in thickness. Bedrock outcrops are found in the western and southwestern regions. In the central urban area, the bedrock is generally buried deeper than 160 meters, though exceptions exist—such as in parts of Xuhui District, where the bedrock rises significantly and can be as shallow as 60 meters below ground surface. Therefore, particular attention must be paid to bedrock depth during deep underground development.

In the main regions targeted for deep underground space development in Shanghai, the strata are primarily composed of silty fine sand and sandy clay. Due to the low permeability of clay, compressive deformation under long-term loading continues to accumulate. In addition, heterogeneity in regional geological conditions can lead to differential settlement of soil layers. Excessive differential settlement may result in longitudinal deformation or excessive curvature of deep tunnels, leading to segmental damage of the tunnel lining. Furthermore, the absence of the ⑧ layer in some areas significantly increases soil non-uniformity, which may adversely affect the overall stability of underground structures.

Therefore, in the context of Shanghai, stratigraphic composition, soft soil thickness, and soil uniformity are critical factors affecting the bearing capacity of deep underground space. A comprehensive evaluation and proper mitigation of these factors must be conducted prior to development.

#### 3.2. Geotechnical characteristics

Geotechnical characteristics have a direct influence on the ease of excavation and the stability of the surrounding rock. Therefore, geotechnical stability is one of the important influencing factors for the carrying capacity of underground spaces. The geotechnical properties that influence the bearing capacity of underground space primarily include strength characteristics, deformation behavior, unloading response, and permeability. Under otherwise identical conditions, stronger soil or rock masses generally correspond to greater usable underground space capacity within a given area. Strength indicators such as cohesion, internal friction angle, and the standard value of bearing capacity are key parameters for evaluating geotechnical stability. The compression modulus is an important parameter reflecting the soil's resistance to deformation—higher values indicate greater resistance to external disturbance.

Deep underground space development typically causes significant disturbance to the surrounding soil, substantially altering the in-situ stress state. The coefficient of earth pressure at rest ( $K_0$ ) helps characterize the unloading behavior of deep soils and plays a critical role in understanding their deformation mechanisms. In deep strata, stress paths are dominated by unloading or unloading followed by reloading, with mechanical behavior differing significantly from shallow layers. For example, under consolidation pressures ranging from 6 to 10 MPa,

increased stress leads to enhanced microstructural anisotropy in clay, which is macroscopically reflected by large variations in the K value.

In addition, the permeability coefficient is a key parameter for evaluating the waterproofing capacity of geotechnical layers. Higher permeability indicates weaker water resistance. Severe groundwater seepage can destabilize surrounding rock masses and soil structures, compromising excavation safety and ultimately reducing the bearing capacity of the underground space.

### 3.3. Hydrogeology

Shanghai has abundant groundwater with a high water table. The groundwater aquifers within the range of 0 to 100 meters below the surface are sequentially classified as phreatic, micro-confined, and confined aquifers, with the first and second confined aquifers (I and II) being closely related to the development and utilization of deep underground space, as shown in Figure 7. The first confined aquifer corresponds to Layer ⑦ and lies above Layer ⑧. It is widely distributed and, influenced by sedimentary environments and ancient river channel cutting, shows significant variation in depth, thickness, and water yield. The second confined aquifer corresponds to Layer ⑨, and is widely distributed and stable. It is one of the most permeable and water-rich aquifers in the Shanghai area, with high artesian pressure.

There is a close hydraulic connection between the various confined aquifers in the region. The first and second confined aquifers are connected in areas where Layer ⑧ is absent; the second confined aquifer is locally connected with the third confined aquifer (at depths of 110–120 meters); in some areas of the central urban district, such as the Lujiazui area, all three confined aquifers are interconnected.

Artesian water poses significant challenges to the development and utilization of deep underground space in Shanghai. First, the first and second confined aquifers are deep sand layers, resulting in high shield tunneling resistance. Second, the artesian pressure in these aquifers is high, which can easily lead to blowouts and sand flows during excavation. Finally, in areas where confined aquifers are interconnected, improper dewatering during construction can cause widespread ground subsidence.

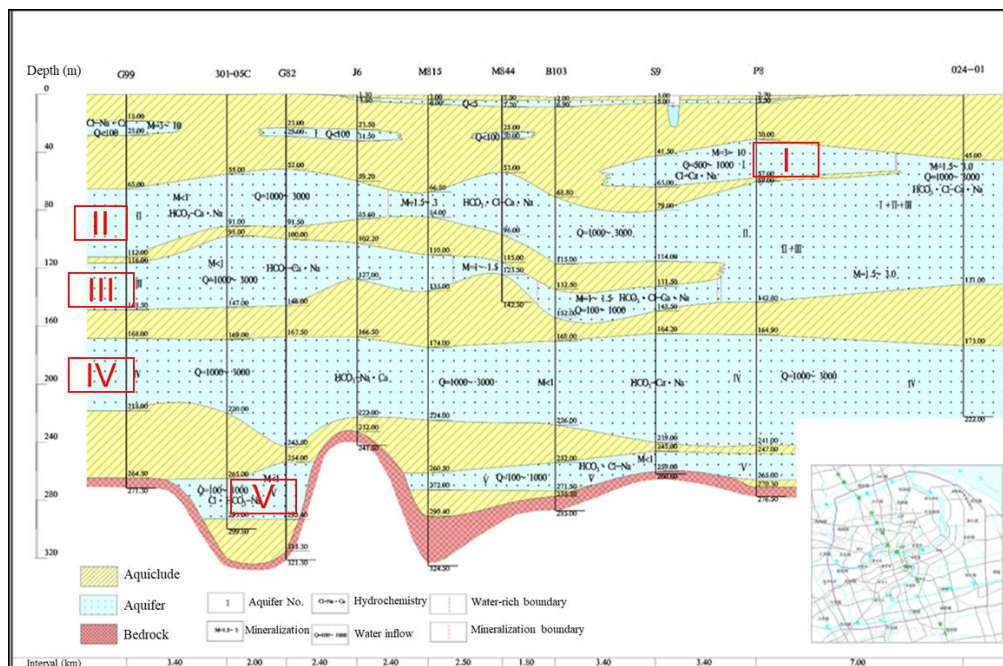


Figure 7. Typical Hydrogeological Profile of Shanghai

### 3.4. Environmental geology

According to the unique geological and environmental conditions of Shanghai, the main environmental and geological problems that occur during the development and utilisation of underground space are the following: ground subsidence, sand liquefaction, and gas escape. However, the impact of thermal-hydrological mechanical-chemical (THMC) coupling on the development and utilisation of underground space has been less considered.

### **3.4.1. Ground subsidence**

Ground subsidence caused by the environmental effects of underground space development has become one of the major environmental geological challenges in Shanghai. Although long-term control measures such as zoning management and stratified regulation have yielded positive results of keeping the overall subsidence trend relatively stable, significant localized uneven settlement remains. This is particularly relevant to the construction of deep underground space (DUS), which induces more complex and extensive disturbance to the subsurface strata.

During DUS construction, large-scale excavation and the associated engineering activities often disturb deep soil layers, causing consolidation deformation. To facilitate safe excavation, it is usually necessary to perform deep dewatering operations to lower the artesian water pressure around the foundation pit. However, such depressurization can lead to a significant drawdown of the confined groundwater levels outside the excavation zone. When the target aquifer cannot be fully isolated, the resulting hydraulic imbalance may trigger widespread ground settlement, especially differential settlement within the dewatering-induced subsidence funnel. This not only threatens the structural safety of deep underground projects but also poses risks to existing surface structures and shallow to intermediate underground spaces. Therefore, ground subsidence, particularly that induced by groundwater drawdown and soil disturbance, must be considered a critical factor in the evaluation of DUS bearing capacity.

### **3.4.2. Sand Liquefaction**

Shanghai has a high water level, and the chalk and sandy chalk layers within the influence of underground space development generally have the characteristics of sandy soil seepage liquefaction. There have been many engineering accidents due to sand liquefaction problems during the construction of underground projects in the Shanghai area.

### **3.4.3. Deep natural gas escape**

Natural gas is widely developed within the Quaternary strata in the Shanghai area and can be categorized into three gas-bearing reservoir systems. The development of deep underground space is mainly affected by the second and third gas-bearing layers, typically buried at depths of 30 – 50 m and 50 – 70 m, respectively. Although these layers have a relatively limited distribution, they are characterized by high pressure and large gas flow rates. If encountered during excavation, the sudden release of gas may pose serious safety risks to personnel, cause instability in the surrounding soil, and even lead to the danger of explosion.

### **3.4.4. Coupling of multiphysical fields in the deep underground Environment**

In deep underground space environments, the geological system is composed not only of rock, soil, and groundwater, but also of interrelated thermal, hydraulic, mechanical, and chemical (THMC) fields. In Shanghai, the deep subsurface (typically below 50 m) features water-rich, low-permeability soils such as silty sand and sandy clay, where confined aquifers are widely distributed. These strata are subject to elevated geostress, temperature gradients, and mineralized groundwater with active geochemical interactions.

The development and utilization of deep underground space inevitably disturb the original equilibrium of the subsurface system. Excavation and dewatering lead to stress redistribution, which in turn induces changes in pore water pressure, groundwater seepage, and geochemical reactions. The confined groundwater exhibits higher pressure and deeper flow paths, making its hydromechanical coupling effects more pronounced than in shallow layers. Temperature gradients at greater depths also intensify thermally induced deformation, especially under long-term loading or structural heat emissions.

The THMC coupling effect in deep strata is thus characterized by enhanced mechanical sensitivity, delayed consolidation behavior, and complex water – rock – heat – stress interactions. These interdependencies alter the displacement and strength responses of the geotechnical body, influencing not only construction safety but also the long-term bearing capacity of the surrounding formations. Therefore, it is essential to incorporate THMC coupling mechanisms into the assessment and planning of deep underground space development, particularly in soft-soil megacities like Shanghai.

## **3.5. Ground and underground space status**

In the development of deep underground space (typically below 50 m), the current utilization of both surface and underground space constitutes a key factor influencing its bearing capacity. Unlike shallow and intermediate underground spaces, deep space is less directly affected by surface usage conditions, yet certain constraints still exist.

### **(1) Influence of ground space utilization**

The surface space in urban areas consists of high-rise buildings, heritage sites, historical landmarks, public squares, green spaces, and roads. In densely built-up zones, the vertical load transferred by high-rise structures may affect the stability of underlying strata, necessitating stability assessments for any deep-level excavation. Areas with high floor area ratios (FAR) also tend to have dense underground infrastructure, which limits construction access. Moreover, cultural heritage sites, conservation zones, and critical infrastructure are often associated with protection layers that restrict vertical development. Although deep underground space lies below most of these influence zones, the potential for indirect disturbance—such as vibration, groundwater changes, or settlement, must still be evaluated. Thus, surface utilization impacts deep underground space development primarily through protection requirements and structural load effects.

#### (2) Influence of underground space utilization

By contrast, the bearing capacity of deep underground space is more directly constrained by the existing use of shallow and intermediate underground layers. Structures such as metro tunnels, underground commercial facilities, utility corridors, and pipelines present physical barriers to deeper development. Their structural extents, buffer zones, and operational safety requirements must all be accounted for. In addition, some areas have been designated as underground restricted development zones, such as heritage tunnels, key pipeline protection corridors, and groundwater source protection zones, where new deep excavation is prohibited or strictly controlled.

Given these conditions, the assessment of deep underground space bearing capacity requires careful delineation of developable zones, interference zones, and reserved protection layers based on existing surface and subsurface usage. Compared with shallow space development—which is more sensitive to surface occupation—deep underground development places greater emphasis on compatibility with existing subsurface systems and hierarchical space utilization. This reflects the need for integrated vertical planning and coordinated management of underground resources.

## 4. FRAMEWORK OF AN EVALUATION INDEX SYSTEM FOR THE DUS BEARING CAPACITY

Taking into account the complexity of deep underground space development and the characteristics of multi-source coupling, this study establishes a comprehensive evaluation system for bearing capacity based on five primary categories of indicators: engineering geology, geotechnical characteristics, hydrogeology, environmental geology, and current space utilization (including ground space and underground space), as shown in Figure 8. The system aims to comprehensively reflect the physical and mechanical properties of strata, environmental sensitivity, and engineering suitability, serving as a fundamental basis for assessing regional development suitability and conducting quantitative evaluations.

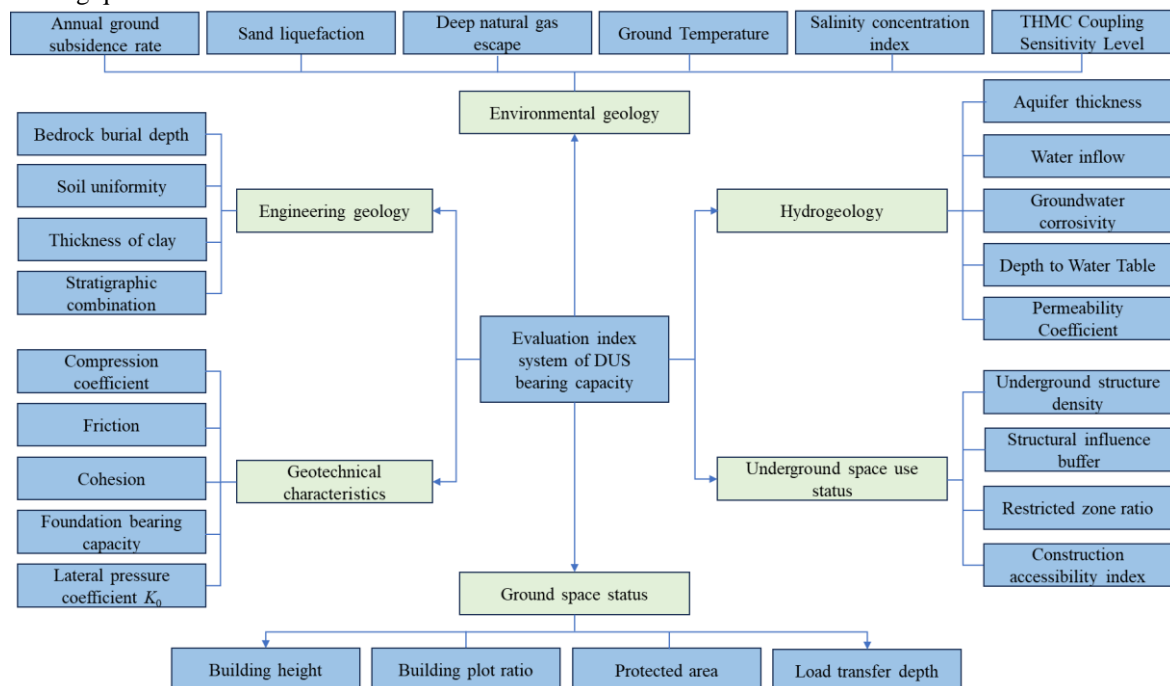


Figure 8. Evaluation index system framework of the DUS bearing capacity



## 5. CONCLUSIONS

This study addresses the critical need for evaluating the carrying capacity of deep underground space (DUS) in megacities, focusing on Shanghai as a representative case. The city's unique coastal soft soil conditions, thick Quaternary strata, and multi-aquifer system present both challenges and opportunities for DUS development. Through detailed analysis of geological, hydrogeological, and environmental factors, key constraints such as bedrock depth, soft soil thickness, confined aquifer pressure, and THMC coupling effects were identified. In addition, the spatial utilization status, both above and below ground was incorporated to reflect realistic development limitations. A comprehensive evaluation index system was constructed, integrating five dimensions: engineering geology, geotechnical characteristics, hydrogeology, environmental geology, and current space utilization. The system allows for structured, multi-factor assessment of DUS carrying capacity. The study confirms that deep development is becoming an inevitable direction for megacities like Shanghai as shallow resources near saturation. A scientific assessment of DUS carrying capacity is therefore essential for safe, efficient, and sustainable underground development. The findings lay the foundation for future quantitative modeling of DUS bearing capacity.

Moving forward, the proposed index system can be further refined through quantitative modeling, spatial data integration, and multi-criteria decision analysis (MCDA), enabling region-specific evaluation of deep underground space carrying capacity under varying geological and urban conditions.

## 6. ACKNOWLEDGMENTS

This research was funded by the Shanghai Municipal Science and Technology Project (18DZ1201301; 19DZ1200900); Shanghai Institute of Geological Survey (2023(D)-003(F)-02); Key Laboratory of Land Subsidence Monitoring and Prevention, Ministry of Natural Resources of the People's Republic of China (No. KLLSMP202101; KLLSMP202201); Shanghai Municipal Science and Technology Major Project (2021SHZDZX0100) and the Fundamental Research Funds for the Central Universities.

## 7. REFERENCES

- [1] Admiraal, H., & Cornaro, A. (2020). Future cities, resilient cities – The role of underground space in achieving urban resilience. *Underground Space*, 5(3), 223–228. <https://doi.org/10.1016/j.undsp.2019.02.001>
- [2] Attard, G., Rossier, Y., Winiarski, T., & Eisenlohr, L. (2017). Urban underground development confronted by the challenges of groundwater resources: Guidelines dedicated to the construction of underground structures in urban aquifers. *Land Use Policy*, 64, 461–469. <https://doi.org/10.1016/j.landusepol.2017.03.015>
- [3] Bobylev, N. (2009). Mainstreaming sustainable development into a city's Master plan: A case of Urban Underground Space use. *Land Use Policy*, 26(4), 1128–1137. <https://doi.org/10.1016/j.landusepol.2009.02.003>
- [4] Bobylev, N. (2016). Underground space as an urban indicator: Measuring use of subsurface. *Tunnelling and Underground Space Technology*, 55, 40–51. <https://doi.org/10.1016/j.tust.2015.10.024>
- [5] Chen, Z.L., Chen, J.Y., Liu, H., Zhang, Z.F. (2018). Present status and development trends of underground space in Chinese cities: Evaluation and analysis. *Tunnelling and Underground Space Technology*, 71, 253–270. <https://doi.org/10.1016/j.tust.2017.08.027>
- [6] He, J., Zhou, Y.X., Zheng, G.S., Wang, J.M., Liu, Y. (2020). Research on the Geological Suitability Evaluation System of Underground Space Resource Utilization in Beijing. *Chinese Journal of Underground Space and Engineering*, 16(4), 955-966.
- [7] He, L., Song, Y., Dai, S., & Durbak, K. (2012). Quantitative research on the capacity of urban underground space – The case of Shanghai, China. *Tunnelling and Underground Space Technology*, 32, 168–179. <https://doi.org/10.1016/j.tust.2012.06.008>
- [8] Kishii, T. (2016). Utilization of underground space in Japan. *Tunnelling and Underground Space Technology*, 55, 320–323. <https://doi.org/10.1016/j.tust.2015.12.007>
- [9] Lai, Y., Wang, Y., Cheng, J., Chen, X., & Liu, Q. (2023). Review of constraints and critical success factors of developing urban underground space. *Underground Space*, 12, 137–155. <https://doi.org/10.1016/j.undsp.2023.03.001>
- [10] Li, H. Q., Fan, Y. Q., & Yu, M. J. (2018). Deep Shanghai project – A strategy of infrastructure integration for megacities. *Tunnelling and Underground Space Technology*, 81, 547–567. <https://doi.org/10.1016/j.tust.2018.08.008>
- [11] Li, X., Li, C., Parriaux, A., Wu, W., Li, H., Sun, L., & Liu, C. (2016). Multiple resources and their sustainable development in Urban Underground Space. *Tunnelling and Underground Space Technology*, 55, 59–66. <https://doi.org/10.1016/j.tust.2016.02.003>
- [12] Li, Y.Y., Cai, X.K., Wang, Y.H. (2025). Challenges and Strategies of Urban Deep Underground Space Development in China. *Chinese Journal of Underground Space and Engineering*, 21(1), 1-15, 69.

- [13] Liu, Y., Zhu, L.C. (2020). Current Status and Future Perspectives of Urban Underground Space Development in Shanghai, *Chinese Journal of Underground Space and Engineering*, 40(7), 941-952. <https://doi.org/10.20174/j.JUSE.2025.01.01>
- [14] Lu, Z., Wu, L., Zhuang, X., & Rabczuk, T. (2016). Quantitative assessment of engineering geological suitability for multilayer Urban Underground Space. *Tunnelling and Underground Space Technology*, 59, 65–76. <https://doi.org/10.1016/j.tust.2016.06.003>
- [15] Mukhtar, A., Yusoff, M. Z., & Ng, K. C. (2019). The potential influence of building optimization and passive design strategies on natural ventilation systems in underground buildings: The state of the art. *Tunnelling and Underground Space Technology*, 92, 103065. <https://doi.org/10.1016/j.tust.2019.103065>
- [16] Peng, J., & Peng, F.L. (2018a). A GIS-based evaluation method of underground space resources for urban spatial planning: Part 1 methodology. *Tunnelling and Underground Space Technology*, 74, 82–95. <https://doi.org/10.1016/j.tust.2018.01.002>
- [17] Peng, J., & Peng, F.L. (2018b). A GIS-based evaluation method of underground space resources for urban spatial planning: Part 2 application. *Tunnelling and Underground Space Technology*, 77, 142–165. <https://doi.org/10.1016/j.tust.2018.03.013>
- [18] Price, S. J., Terrington, R. L., Busby, J., Bricker, S., & Berry, T. (2018). 3D ground-use optimisation for sustainable urban development planning: A case-study from Earls Court, London, UK. *Tunnelling and Underground Space Technology*, 81, 144–164. <https://doi.org/10.1016/j.tust.2018.06.025>
- [19] Qiao, Y.K., Peng, F.L., Wu, X.L., & Luan, Y.P. (2022). Visualization and spatial analysis of socio-environmental externalities of urban underground space use: Part 1 positive externalities. *Tunnelling and Underground Space Technology*, 121, 104325. <https://doi.org/10.1016/j.tust.2021.104325>
- [20] Sterling, R., Admiraal, H., Bobylev, N., Parker, H., Godard, J.P., Vähäaho, I., Rogers, C. D. F., Shi, X., & Hanamura, T. (2012). Sustainability issues for underground space in urban areas. *Proceedings of the Institution of Civil Engineers - Urban Design and Planning*, 165(4), 241–254. <https://doi.org/10.1680/udap.10.00020>
- [21] Zhang, Y., Zhu, J., Liao, Z., Guo, J., Xie, H., & Peng, Q. (2021). An intelligent planning model for the development and utilization of urban underground space with an application to the Luohu District in Shenzhen. *Tunnelling and Underground Space Technology*, 112, 103933. <https://doi.org/10.1016/j.tust.2021.103933>
- [22] Zhou, C., Su, Y., He, L., Peng, L., Zhang, Y., Wu, G., & Kiong Soh, C. (2024). An intelligent resilience evaluation model for the development of urban underground space with safety concern of surrounding existing built environment. *Tunnelling and Underground Space Technology*, 149, 105783. <https://doi.org/10.1016/j.tust.2024.105783>

## HEAT STORAGE UNDERGROUND: A FEASIBILITY STUDY IN ZURICH'S URBAN CORE

Antonia Cornaro, Jimi Dellenbag, Amberg Engineering AG

**Abstract:** This feasibility study investigates the potential of underground heat storage as a key component of sustainable energy infrastructure in Zurich's urban core. It focuses on leveraging subsurface spaces to support the expansion of district heating networks, with particular emphasis on seasonal thermal energy storage (STES). Central to the study is the proposed shift from a surface substation (*Kraftwerk Selnau*) to multifunctional underground sites that enable efficient and resilient thermal storage solutions. Key proposals include a centralised cavern concept in the University District and the adaptive reuse of existing structures such as the decommissioned former railway tunnel, *Letten Tunnel* for seasonal heat storage. The evaluation highlights how underground heat storage can enhance energy system resilience, reduce surface space use, and contribute significantly to Zurich's climate goals. The findings advocate for further exploration of cavern-based thermal energy storage systems as a future-proof strategy for urban energy supply.

**Keywords:** Seasonal Thermal Energy Storage, District heating networks, Heating and cooling, Planning of underground space, City planning

### 1. INTRODUCTION

#### 1.1. District heating Zurich – Substation Selnau

The Selnau electricity substation, which has been out of use for its original purpose for nearly three decades, has since been reimagined as and evolved into a dynamic cultural and social hub. Today, it contributes to the vitality of the Selnau neighbourhood, serving as a landmark at the gateway between Selnaustrasse, Gessnerallee, and Zurich's main station. With its diverse offerings for the public, Selnau fosters community engagement, entrepreneurial innovation, and sustainable urban development (see Figure 1).



Figure 1. Kraftwerk Selnau in its current use as a business startup and cultural meeting hub (Pictures by Authors, 2023)

In parallel, the city of Zurich is pursuing the expansion of its district heating network *Coolcity*, considering the conversion of the former Selnau substation into a heat generation site for this network within the city center. To explore alternatives, the independent association IG SELNAU—comprising professionals from various disciplines in the built environment—commissioned a feasibility study to explore alternative solutions. This was carried out by SCAUT, Amberg Engineering and Rapp. The objective was to assess whether equivalent energy and urban development goals could be achieved by locating the planned energy center(s) in other underground sites within Zurich's central area, thereby preserving Selnau's current public and cultural use.

## **1.2. Underground space utilisation and urban development**

Various aspects highlighted in this study play an important role from an urban development perspective. The evaluated underground concepts consider energy infrastructure for a district heating and cooling network in a dense urban setting. Whilst evaluating the possibilities of shifting the preferred location of the heat production plant, a strong focus on sustainability is incorporated into the final concepts. Our proposed solution integrates a large seasonal heat storage system into an already existing underground structure.

## **1.3. District heating network from an urban development perspective**

A well-planned and efficiently operated district heating (and cooling) network makes a significant contribution to sustainable urban development by:

- Promoting energy efficiency and resource efficiency as well as energy independence.
- Improving quality of life in urban areas due to higher air quality and a reduction of the urban heat island effect.
- Increasing energy security and affordability for inhabitants.
- Strengthening the local economy.

It is therefore an important part of the multitude of efforts to pave the way forward in creating more sustainable cities.

## **1.4. Aqua thermal energy utilisation - water as a source for district energy systems**

The use of lake water as a source for district energy systems is an increasingly established approach in cities aiming to reduce the environmental impact of heating and cooling. Aqua thermal energy harnesses the relatively stable temperatures of large water bodies—such as seas, lakes, or rivers—to provide both heating in winter and cooling in summer, typically through heat pumps and heat exchangers. This method allows for efficient, low-emission thermal energy production.

Several cities have already implemented seawater-based district heating and cooling systems on a significant scale, including Stockholm and Växjö in Sweden, Helsinki in Finland, Oslo in Norway, Vancouver in Canada, and Copenhagen in Denmark. These cities use aqua thermal energy as a cornerstone of their sustainable energy strategies, demonstrating its potential to reduce reliance on fossil fuels while supporting the decarbonization of urban heating and cooling networks. Beyond these examples, interest in aqua thermal energy is growing globally, with many municipalities exploring its integration into future-proof energy infrastructure.

To enhance the efficiency of aqua thermal systems, Seasonal Thermal Energy Storage (STES) is often used. STES allows excess heat collected during warmer months to be stored—typically in underground caverns, boreholes, or water tanks—and retrieved in colder periods when demand is higher. This enables a balanced, year-round supply of renewable thermal energy.

# **2. CLIMATE RESILIENCY OF CITIES**

To ensure long-term sustainability, cities must adapt to the mounting challenges posed by climate change—among them, increasingly frequent heatwaves, storms, and flooding. These shifts not only stress urban infrastructure but also intensify energy demands for heating and cooling. At the same time, technological advancements and growing urban populations are reshaping how energy systems must operate: more flexibly, more efficiently, and with far lower emissions.

In this evolving context, energy resilience has become a critical aspect of urban resilience. It refers to the ability of heating and cooling systems to reliably operate during disruptions, adapt to changing conditions, and support cities in recovering quickly from both climate-related and human-made crises. Resilient energy infrastructure must

be low-carbon, decentralized, and future-proof—especially in the face of volatile temperatures and increasing demand for indoor climate regulation.

Seasonal Thermal Energy Storage (STES) systems offer a promising solution. By capturing and storing thermal energy—such as heat from renewable sources or excess summer warmth—these systems allow cities to meet heating needs in winter and cooling needs in summer with minimal environmental impact. Underground spaces play a vital role here, enabling large-scale storage of thermal energy in subsurface aquifers, boreholes, or cavern systems, while freeing up valuable surface space for other uses.

Incorporating these systems into risk-informed urban planning is essential for preventing future disruptions and ensuring equitable access to thermal comfort. Inclusive planning, especially with a focus on vulnerable populations, not only reduces risk but also supports sustainable and just urban development.

As Brown (2014) argues, transitioning from traditional, single-purpose infrastructure to multifunctional, closed-loop systems—like those found in nature—can increase overall system resilience. In this "post-industrial paradigm," infrastructure must be versatile, interconnected, and synergistic. Thermal energy systems that combine surface and subsurface components are a prime example of this approach, integrating renewable energy, storage, and efficient distribution.

As Admiraal and Cornaro (2018) emphasize, harmonizing development above and below ground can offer strategic advantages in meeting urban resilience goals. With the majority of the global population projected to live in urban areas, using the "third dimension"—not just building upwards, but also downwards—will be crucial (SCAUT, 2019).

Our feasibility study embraces these principles by exploring how underground thermal energy storage and district heating and cooling infrastructure can contribute to a climate-resilient, sustainable future for Zurich's inner city.

### 3. SUBSTATION SELNAU

The Selnau substation has served as a cultural, event, and meeting space for nearly 30 years, breathing new life into the Selnau district. Located at the gateway of the Selnaustrasse / Gessnerallee axis leading to Zurich's main railway station, it attracts a wide and diverse audience with its variety of offerings. As a key destination in the area, the substation plays a significant role in Zurich's urban development, fostering sustainability, innovation, and the growth of a vibrant urban community.

Today, the substation hosts co-working spaces popular among startups and entrepreneurs—particularly those focused on sustainability—alongside a contemporary art museum, a café, and a restaurant.

Prof. Dr. David Kaufmann, head of the City and Landscape Network and urban development expert at ETH Zurich, shared the following with IG Selnau:

"Places like the Selnau power station, where many people come together without major commercial intent, are vital for successful and dynamic urban development. It is becoming increasingly difficult for such organisations and their non-commercial uses to secure space in central urban areas. The energy transition is adding pressure on these venues. The Selnau power station is a prime example. Cities need holistic strategies that drive the energy transition while also preserving the livability of the urban environment."

- Impact Hub Zurich, which manages a portion of the building, reports the following activities in the substation:
- Annual visitors of between 100,000 and 120,000 for work, socialising, and events
- Over 100 cultural events per year, including exhibitions, music, and dance events
- Civic and policy engagement events
- Regular programmes focused on climate protection, sustainability, and innovation
- Daily use of facilities and catering services by freelancers and small businesses from the fields of business, culture, and science

The transformation of the Selnau substation from industrial infrastructure into a community-oriented space stands as a notable success for both the city of Zurich and the local Selnau neighbourhood. While this study does not quantify the social value or estimate the capitalised value of such public uses, these aspects merit further investigation in a dedicated analysis. What is clear is that transforming this lively community and business hub into an energy infrastructure would leave an unwanted void in this part of the city.

### 4. SWISS FEDERAL STRATEGY FOR UNDERGROUND SPACE UTILISATION

In the context of this study, it is highly relevant to reference the Swiss Underground Strategy, developed in 2022 by the Federal Geological Commission (EGK) on behalf of the Federal Department of Defence.



This strategy outlines a vision for harnessing the potential of the underground, aiming to strike a balance between utilisation and protection, while aligning with the responsibilities and priorities of both federal and cantonal authorities. A key goal is to improve the coordination of underground spatial planning.

As stated in the foreword to the strategy:

“The future of Switzerland lies largely underground. Climate adaptation, the energy transition, and the national energy supply are driving increased use of subsurface space.”

It further notes:

“There are vast reserves of underground space that can support higher-density land use in response to urbanisation. [...] This positions Switzerland to play a leading role in international innovation.”

Two specific objectives from the strategy are particularly relevant to this feasibility study:

(2) Sustainability: Responsible management of the subsurface contributes to Switzerland’s sustainable development.

(5) Innovation: The innovation potential of underground resources is actively being leveraged.

The concepts and solutions explored in this feasibility study directly support these strategic goals. In contrast, the reference scenario—repurposing the centrally located Selnau substation for surface-level heat production—does not align well with the aims of the national strategy or does so only to a limited extent.

## 5. SUBSTATION SELNAU: PLANNED CONVERSION AND TECHNICAL DIFFICULTIES

Zurich’s municipal energy provider, ewz, is planning to convert the Selnau substation into a district heating and cooling plant. This transformation would bring an end to the site’s current public use, and existing tenants would be relocated outside the city centre. The facility is expected to provide a heating output of 55 MW and a cooling output of 36 MW.

The system will use water from Lake Zurich, extracted from a depth of around 25 metres, where the temperature remains approximately 5°C throughout the year. The thermal energy from the lake water will be transferred to a secondary circuit via heat exchangers located at a lakeside installation. From there, the energy is transported to the Selnau substation through a micro tunnel of about 850 metres in length and 3.6 metres in diameter.

The substation will house heat pumps, a small thermal buffer, and electrical systems. The building will be fully utilised from the start, leaving no space for future expansions or upgrades. To fit all necessary equipment, the demolition of the monumental Control Room (*Kommandoraum*), which is under historic preservation status (see Figure 2), will be required. Securing the necessary permissions for this will likely be time-consuming and complex.

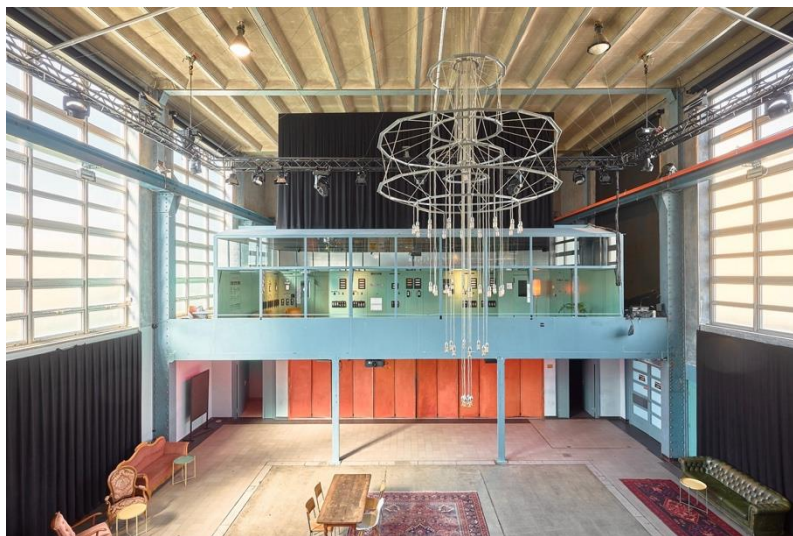


Figure 2. Monumental Control Room in Substation Selnau (IG Selnau, 2023)

The target excavation area for tunnel connection and pipeline integration lies underneath the substation’s main hall and will need to be newly excavated. However, since no construction vehicles can enter the building, all excavation will have to be carried out through the windows. The site’s location next to the Sihl River also presents geological and hydrological challenges, further complicating construction efforts. At this stage, permissions for construction have not yet been granted.

The planned plant's location at the western edge of the inner city's supply area is not ideal in terms of heat distribution. This feasibility study, therefore, explores alternatives that might place heat production facilities closer to key consumers and in locations that allow for simpler construction conditions in the underground.

While the use of lake water as an energy source is both sustainable and innovative, the Selnau site lacks the space for a seasonal or large-scale thermal storage system. As a result, any surplus heat, especially the heat produced from cooling, can only be stored temporarily before being discharged into the Limmat River, and eventually returned to the lake. On particularly cold winter days, when the heat pump capacity is insufficient, gas boilers will need to provide the additional required heat. A larger seasonal thermal storage system could help reduce this dependency on fossil fuels.

Furthermore, the pipeline and tunnel infrastructure being constructed for this project is designed for this specific use only. It will not support any future connections to other energy networks, which limits its adaptability and conflicts with the goal of multi-functional infrastructure in sustainable urban development.

As outlined above, both the site and system configuration of the Selnau facility have several drawbacks. An alternative approach could involve a distributed network, such as an anergy system. In this type of setup, the lake water is delivered at low temperature through a shared piping network directly to buildings. Individual heat pumps located in each building would then provide the necessary heating and cooling. This approach removes the need for a central plant like the one planned at Selnau. A similar model already exists in Geneva and is known as *Genilac*.

## **6. FEASIBILITY STUDY WITH EMPHASIS ON SEASONAL THERMAL ENERGY STORAGE**

To meet the required heating and cooling demands for the Coolcity perimeter, various structurally different system configurations were evaluated. The primary goal was to identify feasible underground sites and assess their suitability for energy generation and long-term storage. Special attention was given to the potential integration of seasonal thermal energy storage (STES) to enhance energy efficiency and reduce environmental impact.

### **6.1. Overview of System Variants**

Three spatial configurations for the heating plant were assessed:

- A decentralised solution using shafts at multiple locations within the Coolcity perimeter
- A combined centralised–decentralised approach, involving a reduced facility at the Selnau substation and an additional nearby site
- A fully centralised solution located just outside the Coolcity perimeter

### **6.2. Underground Location Types**

Three underground construction types were considered:

- Conversion of basements in existing public or private buildings for district heating purposes
- Cut-and-cover underfloor systems, which allow continued use of the surface space above
- Mined underground systems, where heating infrastructure is built below the surface in a cavern system without disrupting above-ground activity

The latter is particularly well-suited for large-scale heat storage integration.

### **6.3. Site Selection Process**

- Step 1: Identification of 17 potential sites in Zurich where underground space is available and construction is viable. Five of these were located outside the Coolcity perimeter to potentially cover a larger area. See sites depicted with their considered type of construction (Figure 3): shaft, cavern or re-used underground space.
- Step 2: Geological evaluation based on existing data. Most sites within the perimeter are situated in loose rock formations, limiting construction methods. The Lindenhof hill was the only site within the perimeter with more favourable conditions (30 meters of moraine). Promising locations outside the perimeter include the Sihlberg and the University district, the latter offering access to molasse layers and existing underground infrastructure.
- Step 3: Hydrogeological assessment. Most locations within the perimeter had unfavourable conditions, except Lindenhof. However, due to archaeological protection regulations, the top 10 meters of Lindenhof cannot be used. Its lower layers, which intersect groundwater, pose additional challenges, limiting the possible cavern size.

- Step 4: Site-specific evaluation of constructability and thermal storage potential.

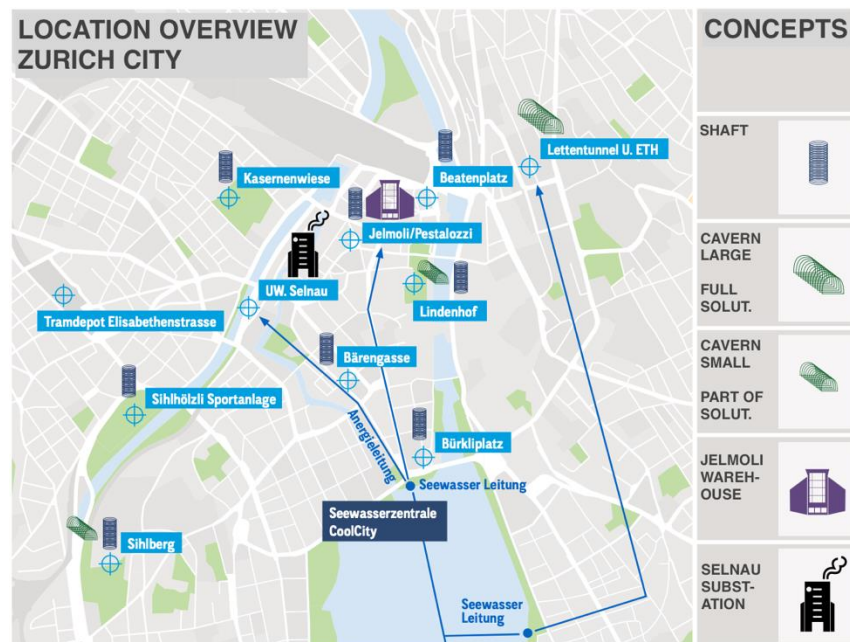


Figure 3. Evaluated locations and their assessed solutions in Zurich city (SCAUT, 2023)

## 6.4. Evaluation of Concepts

### 6.4.1. Shaft Network Concept

This concept involved the construction of seven shafts throughout the Coolcity perimeter. Each shaft would have a 13-meter outer diameter (10 meters internal), allowing minimal environmental disruption. However, due to the area's geology and hydrogeology, construction costs would be relatively high. Splitting a heating plant across seven units increases system complexity and operational inefficiency.

Importantly, this approach does not allow for the integration of large-scale seasonal heat storage, which would reduce long-term fossil fuel use. Based on cost, complexity, and lack of scalable storage, the shaft solution was deemed the least favourable.

### 6.4.2. ETH Cavern Concept

Located in the University district just outside the Coolcity perimeter, this concept combines existing and new underground structures (see Figure 4):

- A former parking garage (Parkhaus Zentral)
- A decommissioned 2 km-long railway tunnel (Letten Tunnel)

- A newly constructed underground cavern (see Figure 4, right)

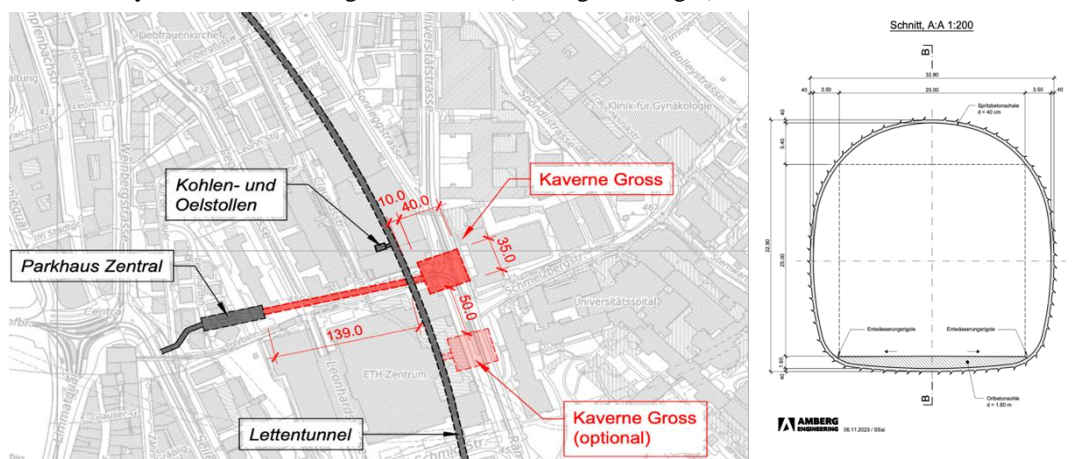


Figure 4. ETH Cavern concept (left), Cavern design (right) (Amberg Engineering, 2023)

The Letten Tunnel offers a unique opportunity for seasonal heat storage, with a total volume of 50,000 cubic meters. Using it as a seasonal thermal storage system allows excess summer heat to be stored and reused during winter, eliminating the need for fossil-fuel peak load systems, as currently planned for Coolcity. This could reduce CO<sub>2</sub> emissions by approximately 3,000 tonnes annually.

Further benefits include:

- Proximity to a planned lake water energy extraction point, enabling synergies with other heating systems
- Reuse of existing infrastructure, lowering costs and environmental impact
- Space for future expansion, with the option to build additional caverns
- Closer location to major heat consumers compared to the current Selnau site
- The ETH concept offers the best combination of geological, hydrogeological, spatial, and technological conditions for integrated energy generation and seasonal thermal energy storage (STES).

#### 6.4.3. Combined Selnau–Lindenhof Concept

This solution splits the heating plant between the existing Selnau substation (for the western perimeter) and a new, smaller cavern at Lindenhof (for the eastern part). While this improves network coverage, it has several drawbacks:

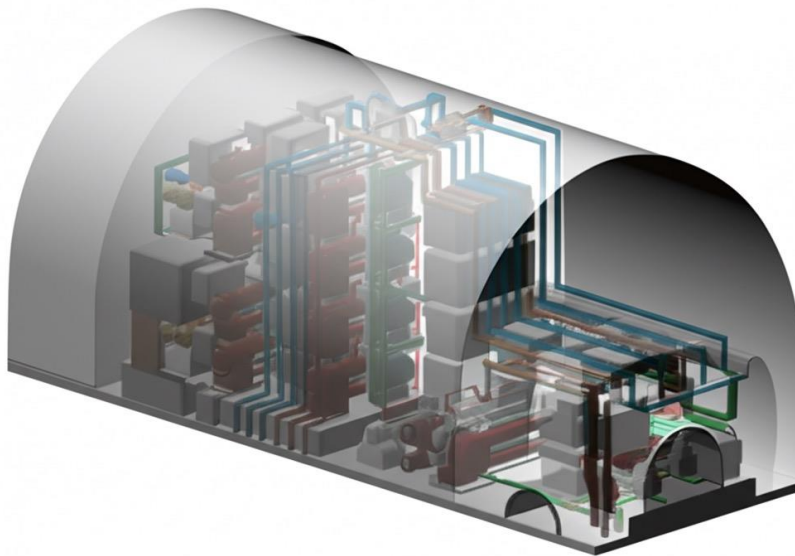
- Higher overall construction and operation costs
- Continued reliance on suboptimal hydrogeological conditions at Selnau
- Limited excavation depth at Lindenhof reduces its suitability for heat storage
- The potential for seasonal thermal storage is minimal in this setup, making it less attractive from a long-term sustainability perspective.

## 7. PROPOSED SOLUTION

Each concept has strengths and drawbacks. The shaft-based solution is flexible but relatively expensive and unsuitable for STES. The combined Selnau–Lindenhof option improves coverage but introduces cost inefficiencies and fails to eliminate fossil fuel reliance effectively. The ETH cavern concept (see Figure 5) offers the best long-term value, due to:

- Integration of a large-scale seasonal thermal energy storage system
- Reuse of existing underground infrastructure
- High geological and hydrogeological suitability
- Proximity to planned energy extraction points and major heat users
- Potential for system expansion through additional caverns

Given its sustainability, technical feasibility, and lower environmental impact, further development of the ETH concept is strongly recommended.



*Figure 5. Proposed solution: Heating and cooling plant in a cavern*

## 8. CONCLUSION

This feasibility study demonstrates that underground heat storage has strong potential to contribute to Zurich's or any city's sustainable energy future. While the planned conversion of the Selnau substation faces significant technical and spatial challenges, alternative underground concepts—particularly the ETH cavern approach—offer more resilient, scalable, and climate-aligned solutions. By reusing existing infrastructure such as the Letten Tunnel and integrating large-scale Seasonal Thermal Energy Storage, Zurich can reduce its reliance on fossil fuels, lower CO<sub>2</sub> emissions, and strengthen urban energy resilience. Advancing the cavern-based concept would not only align with the Swiss Underground Strategy but also safeguard valuable cultural and social spaces at Selnau, making it the most future-proof option for the city's district heating network.

## 9. REFERENCES

- [1] Admiraal, H; Cornaro, A; Future Cities, Resilient Cities, ICE Publishing (2018), <https://www.icevirtuallibrary.com/doi/full/10.1680/usu.61453.115>
- [2] Brown, L. J., & Dixon, D. (2014). Urban design for an urban century: Shaping more livable, equitable, and resilient cities. John Wiley & Sons.
- [3] Studie - IG Selnau. (2024). IG Selnau. <https://www.ig-selnau.ch/studie>
- [4] SCAUT - About us. (2019). <https://www.scaut-association.com/de/General-information-About-SCAUT>



## LOW-CARBON OPERATION AND MAINTENANCE TECHNOLOGIES AND APPLICATIONS FOR UNDERGROUND WASTEWATER TREATMENT PLANTS

Jun Huang<sup>1</sup>, Hongling Ji<sup>2</sup>, Fan Gao<sup>3</sup>, Ao Li<sup>4</sup>, Wei Gu<sup>5</sup>

**Abstract:** As an important part of urban infrastructure, the stable operation and energy saving and emission reduction of underground wastewater treatment plants are of great significance to the sustainable development of cities. This paper discusses in depth the potential and practical path of underground wastewater treatment plants in terms of resilient, energy saving and low-carbon operation and maintenance. Through the investigation of the construction and development history and operation and maintenance of underground wastewater treatment plants at home and abroad, this paper analyzes and summarizes the problems such as operation and maintenance energy consumption, environmental pollution, comprehensive energy utilization, and intelligent monitoring of underground wastewater treatment plants, puts forward the resilience of underground wastewater treatment plants and low-carbon operation and maintenance ideas. Aiming at the problems of high energy consumption in operation and maintenance of underground wastewater treatment plants, difficulties in overhauling and odor treatment, etc., this paper carries out the research on the utilization of thermal energy of wastewater, refined intelligent control, and development and application of high-efficiency energy-saving equipment. Combined with different typical application cases, this paper explores the measures of low-carbon operation and maintenance management and intelligent monitoring system of underground wastewater treatment plants, explores the thermal energy, photovoltaic and reclaimed water utilization of wastewater, puts forward feasible and resilient operation and maintenance strategy and resource utilization scheme to realize cost reduction and efficiency which provide strong support for the sustainable development of the city. The research results of this paper provide an important reference value for guiding the resilient operation and maintenance of underground wastewater treatment plants and the application of low-carbon technologies.

**Keywords:** underground wastewater treatment plant, resilient operation and maintenance, energy saving and low-carbon, heat utilization, odor treatment

### 1. INTRODUCTION

With the acceleration of global urbanization, green ecological development needs and the continuous improvement of residents' environmental requirements, underground wastewater treatment plants with land intensification, high resource utilization and environmental friendliness have become the development trend and direction of urban wastewater treatment plants. Underground wastewater treatment plants in China have entered a stage of rapid development. Cities with a higher level of development and a larger population density have begun to explore the construction of underground wastewater treatment plants to address the contradiction between the shortage of land resources and the improvement of the ecological environment. As the main structure of underground wastewater treatment plant is limited space, the operation process of ventilation, deodorization, lighting, communication, inspection requirements are higher, facing a series of problems such as high energy consumption, maintenance difficulties, odor treatment, etc. These problems not only affect its own stable operation, but also pose a challenge to the sustainable development of the city.

<sup>1</sup> PhD in Civil Engineering, Professor, Chief Engineer of JSTI Group Co., Ltd, Nanjing, China, [hj130@jsti.com](mailto:hj130@jsti.com)

<sup>2</sup> B.Eng. in HVAC, Professor, Standing Director of Jiangsu Underground Space Society, Ltd, Nanjing, China, [1074618720@qq.com](mailto:1074618720@qq.com)

<sup>3</sup> Master of Landscape Architecture, Deputy Secretary-General of Jiangsu Underground Space Society, Nanjing, China, [bjfugf@163.com](mailto:bjfugf@163.com)

<sup>4</sup> PhD in Civil Engineering, Secretary-General of Jiangsu Underground Space Society, Nanjing, China, [15115279@bjtu.edu.cn](mailto:15115279@bjtu.edu.cn)

<sup>5</sup> B.S. in IMIS, Asset Administrator of Nanjing Water Group Co., Ltd, Nanjing, China, [15850686341@163.com](mailto:15850686341@163.com)

In recent years, the concept of resilience and low-carbon has received widespread attention globally, and in the face of increasingly severe environmental challenges and resource constraints, the traditional operation and maintenance mode of wastewater treatment plants has been difficult to meet the needs of cities to realize the coordinated development of economy, society and environment. Therefore, how to realize energy saving, emission reduction and low-carbon development on the basis of ensuring the stable operation of underground wastewater treatment plants has become an urgent problem to be solved.

This paper discusses the current situation, application cases and challenges of low-carbon operation and maintenance technology of underground wastewater treatment plants, and puts forward the development ideas of low-carbon operation and maintenance of underground wastewater treatment plants from the aspects of multi-energy complementary integrated energy utilization, energy saving and consumption reduction, resource recycling, low-carbon operation and maintenance technology research and application.

## **2. DEVELOPMENT HISTORY AND OPERATION AND MAINTENANCE STATUS OF UNDERGROUND WASTEWATER TREATMENT PLANTS**

### **2.1. International development of underground wastewater treatment plants**

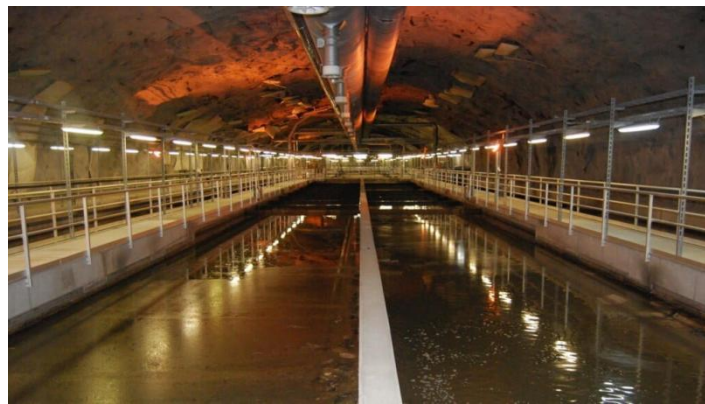
Underground wastewater treatment plant development has been experienced for a long time. In the 1930s because of the cold climate, the Nordic countries built part of the wastewater treatment facilities underground. In 1932 in Helsinki, Finland, built the world's first underground wastewater treatment plant. In 1942, the world's first modern underground wastewater treatment plant was built in Stockholm, Sweden, in response to heavy winter snow and ice. Limited by the engineering technology at that time (such as ventilation, seepage control, construction machinery, etc.), the initial underground wastewater treatment plant is small in scale, the function of the plant focuses on the primary treatment (sedimentation, filtration), and the overall process is still mainly above ground.

Starting from the 1960s, with the acceleration of urbanization, the increasing scarcity of land resources, and the tightening of environmental regulations, coupled with the gradual maturity of underground wastewater treatment technologies (including key technologies such as ventilation, deodorization, and corrosion prevention), the technical support for the construction of underground wastewater treatment plants was established. Developed countries such as European countries, Japan, South Korea, and Canada have successively built multiple underground wastewater treatment plants. In 1994, the Viikinmäki Underground Wastewater Treatment Plant in Helsinki, Finland, was completed and put into operation near the city center, replacing approximately 10 small-scale above-ground wastewater treatment plants. As shown in Figure 1, the plant is primarily constructed within bedrock, making it one of the largest and technologically leading underground wastewater treatment plants in Europe at that time. Its model of deeply integrating underground space with urban functions provides a sustainable solution for wastewater treatment in high-density cities. In 1996, the Ariake Water Reclamation Center in Tokyo, Japan, was commissioned fully underground. The reclaimed water after treatment is used for urban non-potable purposes, landscape environments, and industrial water supply. The above-ground area is equipped with public facilities such as a gymnasium, heated swimming pool, and tennis courts, enhancing the overall regional environment and residents' quality of life, and providing important support for the city's sustainable development.

Since the 21st century, with the rise of concepts such as sustainable development, resource recycling, and ecological integration, underground wastewater treatment plants have entered a stage of diversified development. The Bekkelaget sewerage treatment plant in Oslo, Norway, put into operation in 2000, is constructed in a cave of the Oslo Fjord as shown in Figure 2. Using natural rock masses as structural support and centering on geological space innovation and resource circulation technology, it has achieved a low-carbon paradigm of "zero land expansion, negative energy growth, and complete resource recycling", providing a standardized path for the construction of wastewater plants in highly sensitive areas. The Changi Water Reclamation Plant in Singapore adopted the world's first multi-layer vertical stacking design to achieve maximum compactness and optimize land use, realizing the goals of "minimized land use, maximized production capacity, and near-zero emissions", and becoming a benchmark case for the sustainable development of environmental infrastructure in high-density cities. For underground wastewater treatment plants in selected international cities, please refer to Table 1.



**Figure 1.** Viikinmäki underground wastewater treatment plant, Helsinki, Finland  
(<https://esemag.com/wastewater/wastewater-treatment-plant-monitors-its-ghg-emissions/>)



**Figure 2.** Bekkelaget sewerage treatment plant, Oslo, Norway (<https://pstprojektai.lt/project/bekkelaget-water-treatment-plant/>)

**Table 1.** Typical cases of underground wastewater treatment plant globally

Year of construction	Name	Features	Remarks
Completed in 1942, multiple renovations	Henriksdal Underground Wastewater Treatment Plant, Stockholm, Sweden	Partial underground structure, with main facilities located in rock caverns	The world's first wastewater treatment plant built out of rock
Commissioned in 1987	Dokhaven Underground Wastewater Treatment Plant, the Netherlands	A 50.000 m <sup>2</sup> park is built above ground, with a total land area only 1/4 of that of a above-ground plant	The first underground wastewater treatment plant in the Netherlands
Commissioned in 1987, renovated in 2008	Geolide Underground Wastewater Treatment Plant, France	The famous Stade Vélodrome football stadium is built above the plant, achieving "no visual, no olfactory, no resounding nuisance"	The world's largest underground wastewater treatment plant in terms of land area

Year of construction	Name	Features	Remarks
Commissioned in 1998	Ariake Water Reclamation Center, Tokyo, Japan	Adopts a double-layer underground structure (upper layer for treatment facilities, lower layer for stormwater storage); the ground level is planned as a large sports stadium and commercial complex, creating a paradigm of "underground water management and surface-level empowerment" in high-density urban areas	The Paradigm of "Underground Water Management and Surface-level Empowerment" in High-density Urban Areas
Put into operation in 2001, upgraded and expanded in 2017	Bekkelaget Wastewater Treatment Plant, Oslo, Norway	<input type="checkbox"/> Sewage collected via underground tunnel systems, gravity flow design reduces pumping energy consumption <input type="checkbox"/> Ground transformed into coastal public spaces, including walkways, viewing platforms, and art installations	Provides a standardized path for constructing wastewater treatment plants in highly sensitive areas
Commissioned in 2009	Incheon Wastewater Treatment Plant, South Korea	Semi-underground construction type, with multiple light wells and green spaces set on the top	A representative facility in South Korea
Commissioned in 2008	Changi Water Reclamation Plant, Singapore	<input type="checkbox"/> Operates in conjunction with the Deep Tunnel Sewerage System, using gravity flow for sewage transportation with significant energy savings <input type="checkbox"/> Adopts NEWater technology to achieve circular reuse of sewage to drinking water <input type="checkbox"/> Ground planned as a coastal barrage park	One of the largest underground wastewater treatment plants in Asia

## 2.2. Development of underground wastewater treatment plants in China

With the continuous acceleration of urbanization and the increasing improvement of environmental requirements in China, underground wastewater treatment plants have attracted the attention of the state and various provinces and cities due to their advantages such as green harmony and natural friendliness. Currently, there are more than 200 underground wastewater treatment plants either under construction or in operation, mainly concentrated in areas with relatively developed economies, high population density, and high requirements for land resources and environmental quality, with Guangdong and Zhejiang Province having the largest number <sup>[1]</sup>. The construction sites are mainly located in urban central areas and residential districts, and the construction forms include semi-underground, fully underground, tunnel-type, etc.

Hong Kong Stanley wastewater treatment plant is Asia's first underground wastewater treatment plant built in a cavern, built in 1995, as shown in Figure 3, mainly consists of three large cavernous chambers of about 120m long, 15m wide and 17m high, and is connected by more than 450m of roadway access and ventilation tunnels and shafts. It has a wastewater treatment capacity of 12.000 m<sup>3</sup>/d and serves a population of about 27.000 people.



**Figure 3.** Stanley wastewater treatment plant- tunnel type, Hong Kong, China  
([https://sc.news.gov.hk/TuniS/www.news.gov.hk/tc/record/html/2017/12/20171210\\_121806.lin.shtml](https://sc.news.gov.hk/TuniS/www.news.gov.hk/tc/record/html/2017/12/20171210_121806.lin.shtml))

Shenzhen Buji Wastewater Treatment Plant has the top of its underground structures covered with 1.5m deep soil, planted with deep-rooted large tropical plants. The above-ground space is transformed into a municipal leisure park, equipped with sports facilities such as football fields, basketball courts, and badminton halls.



**Figure 4.** Buji wastewater treatment plant, Shenzhen, China  
(<https://www.163.com/dy/article/FKG6MQV50550AQSU.html>)

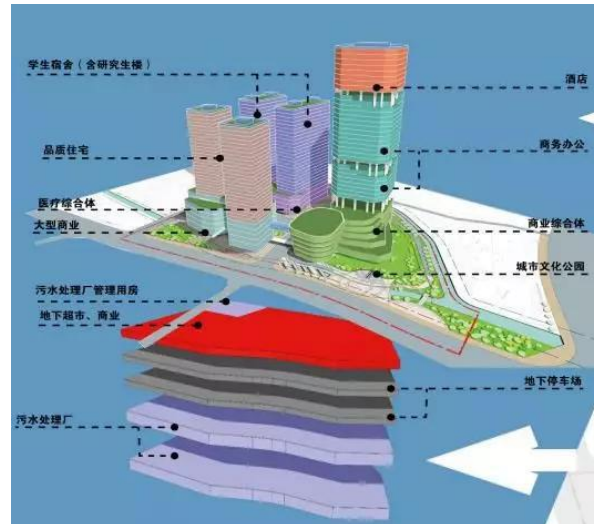
Neijiang Xiejiahe Underground Water Reclamation Plant, where the above-ground area is a sponge park featuring basketball courts, vehicle parking spaces, greenbelts, and pedestrian walkways, reclaimed water used as landscape water supplement for Xiejia River, municipal greening, and road flushing, effectively promoting water resource recycling. Photovoltaic power generation systems are installed above ground, enabling both sewage reclamation and photovoltaic power generation to achieve energy conservation and carbon reduction.



**Figure 5.** Xiejiahe underground water reclamation plant, Neijiang, China  
(<https://local.newssc.org/system/20231125/003465519.htm>)



Figure 6 shows the Guiyang hospital Water Reclamation Plant with dormitories and super high-rise office buildings built above, while Figure 7 depicts the landscape of Guangzhou Jingxi Underground Wastewater Treatment Plant. The undergrounding of municipal infrastructure has unleashed enormous ecological value, achieving a "win-win" situation for the composite development and utilization of urban green parks and underground spaces. Underground wastewater treatment plants in some Chinese cities are shown in Table 2 <sup>[2]</sup>.



**Figure 6.** Guiyang hospital water reclamation plant  
([https://www.sohu.com/a/365193326\\_120157162?scm=1002.44003c.fe0183.PC\\_ARTICLE\\_REC](https://www.sohu.com/a/365193326_120157162?scm=1002.44003c.fe0183.PC_ARTICLE_REC))



**Figure 7.** Jingxi underground wastewater treatment plant, Guangzhou, China  
(<https://news.qq.com/rain/a/20231114A0A58C00>)

**Table 2.** Typical cases of underground municipal infrastructure in China

City	Year of construction	Name	Features	Remarks
Hong Kong	1991	Stanley Wastewater Treatment Plant (Capacity 12.000 m <sup>3</sup> /d)	The main body of the plant is hidden inside the mountain and blends in with the surrounding environment	Asia's first underground wastewater treatment plant built in a cavern

City	Year of construction	Name	Features	Remarks
	2012	Happy Valley Underground Stormwater Storage Scheme (Capacity 60.000 m <sup>3</sup> /d)	<ul style="list-style-type: none"> <li>Collecting and storing rainwater and groundwater for urban water use to conserve water resources;</li> <li>The roof of the cistern incorporates the design concept of “green trees and lawn on the roof of the cave”, where the green elements not only cover the surrounding pump and fan rooms, but also enhance public connectivity by providing a recreational area for public enjoyment.</li> </ul>	/
Beijing	2014	Huai Fang Underground Water Reclamation Plant (Capacity: 600.000 m <sup>3</sup> /d)	<ul style="list-style-type: none"> <li>Utilizes reclaimed water to construct artificial wetlands, with 13 hectares of the 16-hectare wetland park built on the plant's roof.</li> <li>China's first design attempt to integrate roof wetland landscaping with large-scale underground water reclamation infrastructure.</li> <li>Sludge is used for biogas power generation, with the electricity produced applied to all stages of water reclamation, achieving circular energy use.</li> <li>Enables land resource utilization and ecological environment improvement, providing a new green development concept for the construction, development, and intensive land use of gray infrastructure.</li> </ul>	Asia's largest fully underground water reclamation plant and the largest rooftop wetland park in China
Shanghai	2015	Nanxiang Water Reclamation Plant (Capacity 150.000m <sup>3</sup> /d)	Construct a water ecological park and water environment science museum above ground, saving land resources to half of that of traditional water plants.	The first underground water reclamation plant in Eastern China
Guangzhou	2010-2022	Underground wastewater treatment plants (Capacity 2,04 million m <sup>3</sup> /d)	Adopting the concept of “building a plant underground and a park on the ground”, the rain garden, wetland park and other facilities are built on the top of the underground wastewater treatment plant to improve the surrounding environment, to further alleviate the “neighbor avoidance effect”, and to effectively revitalize the land value.	China's largest wastewater treatment plants cluster
Guiyang	2016	Pengjiawan Wastewater Treatment Plant (Capacity 60.000 m <sup>3</sup> /d)	The ground level is a landscape park, with the wastewater treatment plant located on underground floors 3-4 and the underground floors 1-2 serving as a complex.	China's first case of an underground wastewater treatment plant combined with urban renewal.

City	Year of construction	Name	Features	Remarks
Chengdu	2022	Qilong Water Purification Plant (Capacity 100.000 m <sup>3</sup> /d)	<ul style="list-style-type: none"> <li>the construction of ground landscape to enhance the surrounding environment and land development value;</li> <li>compared with conventional above-ground wastewater treatment plant to save at least 30% of the land use;</li> <li>to achieve organic unity of economic benefits and social benefits, ecological benefits.</li> </ul>	/
Hangzhou	2022	Zhijiang Classification and Reduction Complex (Capacity 600 tons/day)	<ul style="list-style-type: none"> <li>A green ecological and environmentally friendly plant centered on people-oriented principles.</li> <li>An "ecological-type" transfer station project that plays a demonstrative and leading role in the construction of underground transfer stations.</li> </ul>	The first large-scale underground garbage transfer station in China

### 2.3. Status of operation and maintenance of underground wastewater treatment plants

The development of underground wastewater treatment plants has gone through an initial exploratory stage of small-scale construction, a development stage centered on capacity expansion, and entered a mature stage marked by the four-dimensional coordination of "water quality, resources, energy, and community". With their unique design and efficient treatment capabilities, underground wastewater treatment plants have effectively solved the problem of urban sewage discharge, improved the living environment of surrounding residents, reduced pollution to natural water bodies, and protected ecological balance. According to statistics, there are currently more than 200 underground wastewater treatment plants successfully constructed and stably operated in over 10 countries worldwide, all of which have achieved good economic, social, and ecological environmental benefits <sup>[3]</sup>. As the demand for intensive land use and environmental friendliness becomes increasingly urgent, and with the continuous maturity and improvement of wastewater treatment technologies, underground wastewater treatment plants will undoubtedly receive more attention from more countries and regions in the future due to their advantages of small land occupation, low environmental impact, and high treatment efficiency.

Based on the special working conditions of underground spaces, such as closure, high humidity, and lack of natural lighting, the configuration standards for lighting engineering, ventilation, and odor removal in underground wastewater treatment plants are significantly higher than those of above-ground counterparts, directly leading to increased operational energy consumption and carbon emissions. External factors such as process complexity and water quality fluctuations further exacerbate the pressure of energy consumption. According to relevant literature statistics, the total life-cycle carbon emissions of underground wastewater treatment plants are approximately 36.5% higher than those of above-ground plants <sup>[4]</sup>. Various countries and regions have already made certain explorations in energy self-sufficiency and carbon neutrality of wastewater treatment plants, but in specific practices, due to differences in water quality, water quantity, policy support, technical maturity, energy supply structure, etc., achieving carbon neutrality in wastewater treatment plants still has a long way to go.

## 3. TYPICAL CASES OF UNDERGROUND WASTEWATER TREATMENT PLANT CONSTRUCTION AND ANALYSIS OF LOW-CARBON OPERATION AND MAINTENANCE APPLICATIONS

### 3.1. Low-carbon operation and maintenance policy for underground wastewater treatment plants

Wastewater treatment plants, as an important part of urban infrastructure, consume large amounts of water, electricity and other energy, and their overall carbon emissions remain high. According to data from the United Nations Framework Convention on Climate Change (UNFCCC), carbon emissions from wastewater treatment in the EU reached 23 million tons in 2019, while the figure for the United States was 45 million tons. Although the greenhouse gas emissions from wastewater treatment plants have been reduced in recent years, wastewater treatment plants are still an important source of greenhouse gas emissions globally, and also one of the faster-growing sources of emissions. In the context of the global active response to climate change and the promotion of low-carbon development, the low-carbon operation and maintenance of underground wastewater treatment plants,

as an important urban infrastructure, not only helps to reduce greenhouse gas emissions and alleviate environmental pressures, but also enhances the economic benefits and sustainable development of wastewater treatment plants themselves. The EU's European Climate Law legislatively defines the goal of achieving climate neutrality by 2050, requiring all types of infrastructure to consider low-carbonization during operation and maintenance, and to reduce carbon emissions through measures such as energy conservation and emission reduction, and improving energy efficiency. The Water Environment Federation (WEF) has proposed that wastewater treatment plants should no longer be waste treatment facilities, but rather water resource recovery plants, an idea that has been widely recognized.

In December 2023, the National Development and Reform Commission (NDRC), the Ministry of Housing and Urban-Rural Development (MOHURD), and the Ministry of Ecology and Environment (MEE) of China jointly issued the Implementation Opinions on Promoting Synergistic Efficiency Improvement in Pollution Reduction and Carbon Emission Control for Sewage Treatment. The document states that sewage treatment is an energy-intensive industry, accounting for over 1% of the total energy consumption in society. Meanwhile, wastewater contains substantial energy resources, presenting enormous potential for energy utilization. The guidelines propose multiple energy-saving and carbon-reducing measures, including promoting high-efficiency energy-saving equipment, optimizing load matching, establishing smart water management systems, and popularizing sewage-source heat pump technology. These measures aim to enhance resource recycling, energy conservation, and carbon reduction in sewage treatment, thereby reducing greenhouse gas emissions.

### **3.2. Typical cases of low-carbon operation and maintenance technologies for underground wastewater treatment plants**

The Kakolanmäki underground wastewater treatment plant in Turku, Finland, was converted from an abandoned underground rock quarry. It has a designed maximum treatment capacity of 144.000 m<sup>3</sup>/day and an average flow rate of 120.000 m<sup>3</sup>/day, commissioned on January 1, 2009. As a typical case integrating energy utilization and thermal energy recovery, the secondary effluent of the plant has an average temperature of 14 °C, serving as a heat source to recover waste thermal energy for heating and cooling the plant and surrounding areas. By 2020, the comprehensive energy consumption of the Kakolanmäki plant was 35 GWh/a, while its self-generated energy reached 225 GWh/a. The total recovered energy (electricity and thermal energy) was 6.4 times higher than its own energy consumption, with nearly 90% recovery efficiency of waste thermal energy for heating/cooling. Achieving a 333% carbon neutrality rate, it has become an underground energy plant<sup>[5]</sup>. The practice of this plant demonstrates that the key to carbon-neutral operation of wastewater treatment lies in emphasizing the recovery of substantial waste thermal energy from effluents.



**Figure 8.** Kakolanmäki wastewater treatment plant, Turku, Finland  
([https://www.filtralite.com/en/case\\_studies/filtralite-clean-kakolanmaki-wastewater-treatment-plant-finland](https://www.filtralite.com/en/case_studies/filtralite-clean-kakolanmaki-wastewater-treatment-plant-finland))

The PANTAI Wastewater Treatment Plant, Malaysia's first underground wastewater treatment facility, is located in the Pantai District of Kuala Lumpur. Originally designed with a capacity of 320.000 tons per day, the plant became an "urban eyesore" due to urban expansion, negatively impacting the cityscape and residents' quality of life while restricting the development potential of surrounding areas. In 2014, the facility was transformed into an underground treatment plant, with its former site converted into a sports park spanning nearly 100.000 m<sup>2</sup> of green space. The project integrates multiple green and low-carbon technologies, including intelligent control systems, water-source heat pumps, fiber-optic daylighting, biogas power generation, rainwater recycling, and photovoltaic power generation. The heat recovered by water-source heat pumps is used for heating and cooling

the administrative complex and equipment buildings. Landscape water bodies serve as underground lighting channels, while fiber-optic systems combined with lighting windows in the green space maximize natural light for illumination in enclosed areas. High-efficiency energy-saving measures include precision aeration systems and intelligent lighting controls. This initiative has successfully created an environmentally friendly model that revitalizes ecosystems and emphasizes green energy conservation. The low-carbon technologies reduce carbon emissions by 21,659.3 to 22,432.0 tons of CO<sub>2</sub> equivalent annually and save operational costs by CNY 9,312 to 9,612 million per year<sup>[6]</sup>.



**Figure 9.** PANTAI Wastewater Treatment Plant ,Kuala Lumpur, Malaysia  
(<https://penetronmalaysia.com/portfolio/pantai-treatment-plant/>)

The Hongqiao Wastewater Treatment Plant in Shanghai adopts an intensive underground layout, with all sewage treatment structures sunken underground. Its design integrates the construction concept of "sponge city", establishing two major systems: an underground reclaimed water system and an above-ground reclaimed water system. During rainy days or when exceeding the design flow, sewage first enters a storage tank for temporary retention, then undergoes treatment on sunny days. With a green coverage rate of over 90%, the plant has created an innovative "garden-on-top, plant-below" environmental model, effectively resolving the contradiction between sewage treatment and surrounding environment. While researching the reuse of urban sewage as a water resource, the Hongqiao Underground Wastewater Treatment Plant has developed its energy attributes by using high-temperature water-source heat pumps to absorb sensible heat from sewage, replacing gas boilers to produce high-temperature hot water (85°C–90°C) for sludge drying. Compared with natural gas boilers, high-temperature water-source heat pumps are more economical, ensuring the thermal demand and efficiency for sludge dewatering and drying while significantly reducing energy consumption in sludge treatment, achieving synergistic effects of pollution reduction and carbon emission mitigation. As of the first half of 2023, the project reduced natural gas consumption by 530,000 m<sup>3</sup> year-on-year, saving CNY 2.37 million in natural gas costs. After deducting electricity consumption, the energy cost for sludge drying decreased by 22%. Under design conditions, the system can recover 51,103 GJ of heat annually, saving 341 tons of standard coal and reducing carbon emissions by 745 tons. In September 2023, the technical transformation project of "low-temperature vacuum sludge drying with high-temperature water-source heat pumps" was awarded the "Top 10 Excellent Cases of Waste Heat Utilization in Shanghai".

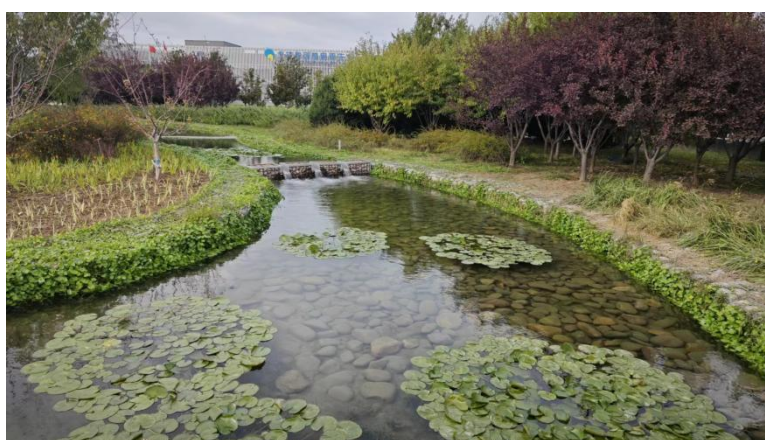


**Figure 10.** Hongqiao Wastewater Treatment Plant, Shanghai, China (<https://www.shanghaiwater.com/Events/3236.html>)

The Huai Fang Water Reclamation Plant in Beijing is Asia's largest fully underground reclaimed water plant and China's first benchmark project to achieve the integration of "above-ground wetland + underground



wastewater treatment" functions. With a designed daily treatment capacity of 600,000 m<sup>3</sup>, all structures are built underground, while the above-ground area features a wetland park nourished by reclaimed water, covering approximately 18 hectares. This urban ecological green lung absorbs about 1,200 tons of carbon dioxide annually. Treated sewage is purified through surface artificial wetlands and replenishes downstream rivers via dedicated pipelines, achieving 100% reuse of reclaimed water and aquatic ecosystem restoration. The plant demonstrates the possibility of symbiosis between wastewater treatment facilities and urban ecology, providing a Chinese solution for high-density cities to address the "neighbor avoidance effect" and achieve green transformation. The plant applies sewage source heat pump technology to extract waste heat from the wastewater treatment process, supplying heating and cooling for the plant's office area and surrounding buildings. Biogas generated from sludge anaerobic digestion powers about 30% of the plant's electricity demand. Dried sludge is converted into nutrient soil or incinerated for power generation, achieving 100% resource utilization. The ground wetland park is equipped with distributed photovoltaic panels with a capacity of 1.2 megawatts, generating approximately 1.5 million kWh of electricity annually to further reduce carbon emissions. Through a series of green and low-carbon measures, the plant has achieved efficient, resource-oriented, and ecological wastewater treatment. Compared with traditional plants, this plant reduces carbon emissions per unit of water treatment by over 40%, being awarded the "Beijing Green Ecological Demonstration Zone" and becoming a model for underground reclaimed water plants in China.



**Figure 11.** Huai Fang Water Reclamation Plant, Beijing, China (<https://sainteco.com/newsinfo/6472923.html>)

### **3.3. Underground wastewater treatment plant low-carbon operation and maintenance technology application analysis**

By analyzing the typical cases of operation and maintenance of underground wastewater treatment plants at home and abroad, it can be seen that the application of toughness and low-carbon operation and maintenance technology is mainly reflected in the following four aspects.

1) Diversified renewable energy application to achieve efficient utilization of energy and comprehensive benefit enhancement. Recycling of wastewater waste heat, wastewater contains a large amount of waste heat resources, through the wastewater source heat pump to implement the transfer and utilization of energy, used in the plant or the surrounding buildings for heating, cooling or sludge drying link. Utilizing the biogas generated in the process of anaerobic digestion of sludge to generate electricity, and at the same time installing solar photovoltaic panels on the roof of the plant, open space and other areas to realize "self-generation and self-consumption + surplus electricity on the Internet". According to the International Water Association (IWA), Denmark's Marselisborg Wastewater Treatment Plant recovered biogas from sludge anaerobic digestion for power generation, achieving 100% energy self-sufficiency in 2016 and a 50% power surplus.

2) Reuse of water and sludge resources to implement resource recycling and sustainable development. The deeply treated reclaimed water is used for urban greening irrigation, road spraying, river and landscape replenishment, etc. The utilization rate of reclaimed water in some of the plants reaches 100%, which saves water resources and at the same time improves the water ecological environment of the city. Through anaerobic digestion, aerobic fermentation and other technologies, sludge is transformed into biogas, organic fertilizer and other resources.

3) Application of intelligent operation and maintenance management technologies. Sensors are used to real-time monitor operation parameters of underground wastewater treatment plants, including water quality, quantity, and equipment status. Real-time data automatically adjusts equipment operation parameters to avoid long-term high-load or low-efficiency operation, achieving optimized control of the wastewater treatment process. This

improves energy consumption management efficiency and precision, enhancing energy efficiency while ensuring the safe and stable operation of underground plants.

4) Construction mode innovation and enhancement of urban resilience. Comprehensive integration of single-function wastewater treatment plant with urban landscape, implementation of wastewater recycling and water ecological restoration, through the addition of storage ponds to cope with extreme weather or sudden loads, to ensure the stability of the system.

#### 4. CHALLENGES OF RESILIENCE AND LOW-CARBON OPERATION AND MAINTENANCE TECHNOLOGIES FOR UNDERGROUND WASTEWATER TREATMENT PLANTS

##### 4.1. High construction and operation and maintenance costs

The construction of underground wastewater treatment plants requires deep foundation pit excavation, support, waterproofing, high-strength building materials, and complex construction technologies. Meanwhile, underground equipment must have characteristics such as corrosion resistance, moisture-proofing, and explosion-proofing, with procurement costs significantly higher than ordinary equipment. During construction, supporting facilities like fire protection, ventilation, and lighting must also be considered, further increasing construction costs. The unit construction investment of underground wastewater treatment plants is 1,5 to 2 times higher than that of traditional above-ground plants.

In terms of energy consumption, the daily operation of underground wastewater treatment plants requires 24-hour artificial lighting and comprehensive mechanical supply-exhaust ventilation systems to meet environmental requirements. Odor collection and treatment cover areas such as tanks, pretreatment sections, and sludge zones, leading to increased odor treatment volume. The enclosed underground environment and discharge outlets located in populated areas raise gas emission standards, while the upgraded process configuration and additional equipment for deodorization systems also contribute to higher energy consumption. Although low-carbon operation and maintenance technologies like renewable energy utilization and energy recovery help reduce energy consumption, the high upfront costs of technical transformation and equipment investment make it difficult to fully offset energy expenses in the short term.

In terms of equipment maintenance, the humid underground environment and limited ventilation make equipment prone to corrosion and damage, resulting in frequent repairs and replacements, which increases maintenance costs. Safety requirements for fire protection, flood control, etc., in underground spaces also add to construction and operation costs. According to relevant literature, the lighting energy consumption of fully underground wastewater treatment plants with the same scale and treatment standards is approximately 4 to 6 times higher than that of above-ground plants, ventilation energy consumption is 4 to 6 times higher, and deodorization energy consumption is 2 to 3 times higher. The unit energy consumption indicators and composition of some underground wastewater treatment plants in China are shown in Table 3<sup>[7]</sup>.

**Table 3.** Unit energy consumption index and composition of an underground wastewater treatment plant

Item	Unit energy consumption kw-h/m <sup>3</sup>	Percentage%
Secondary Sewage Treatment	0,221	43,30
Advanced Sewage Treatment	0,072	14,04
Sludge handling	0,044	8,55
Lighting	0,008	1,58
Ventilation and air conditioning	0,061	11,97
Deodorization	0,079	15,37
Transformer damage	0,027	5,19
Total	0,511	100

##### 4.2. Difficulty in operation and maintenance management

Underground wastewater treatment plants adopt clustered, integrated, and modular layouts for some structures to save land area and make full use of vertical space. This intensive spatial design poses multiple challenges for plant operation and maintenance, including limited operational space, difficult fault diagnosis and repair, complex system coordination, insufficient digital adaptation, and superimposed cost risks. With the increasing demand for urban wastewater treatment, existing facilities may fail to meet processing requirements. However, expansion

requires more underground space, involving complex engineering design and construction, which is costly and difficult to implement, making capacity expansion arduous.

The relatively enclosed underground space of these plants features a complex and changeable environment. Equipment failures, pipeline leaks, or poor ventilation can all lead to the accumulation of hazardous gases. These hidden dangers not only damage the facilities but also threaten the safety of maintenance personnel. Although digital and intelligent technologies have been widely applied in underground wastewater treatment plants, deficiencies remain in data management, such as incomplete data collection and poor data sharing, affecting the scientificity and timeliness of operation and maintenance decisions.

#### **4.3. Lack of synergy between a variety of low-carbon technologies**

Underground wastewater treatment plants have actively introduced renewable energy technologies such as solar and wind power, while also exploring energy reuse methods like wastewater residual heat recovery. However, there is often a lack of effective coordination between these energy supply technologies and in-plant energy consumption technologies—such as the configuration of solar/wind energy and energy cascade utilization—making it difficult to form an organic whole and leading to low energy utilization efficiency.

Resource recovery technologies help improve the resource utilization efficiency and resilience of wastewater treatment plants. However, some wastewater treatment processes fail to fully consider the needs of subsequent resource recovery during design and optimization, making it difficult to effectively extract and utilize resources from treated sewage or sludge.

#### **4.4. Lack of technical standards for low-carbon operation**

The technical standards for low-carbon operation and maintenance of underground wastewater treatment plants are still incomplete. Most existing standards related to wastewater treatment plants are formulated based on above-ground facilities, failing to fully consider the particularities and complexities of underground plants. This includes insufficient technical specifications and operation guidelines for underground plants in aspects such as energy optimization of process schemes, selection of high-efficiency energy-saving equipment, utilization of renewable energy, resource circular use, and operation management. As a result, different regions and enterprises may adopt varying standards and practices during actual construction and operation, prone to issues like inappropriate technology selection and poor operation effects, which hinder the promotion and development of green and low-carbon underground wastewater treatment plants.

### **5. THOUGHTS ON LOW-CARBON OPERATION AND MAINTENANCE TECHNOLOGIES FOR UNDERGROUND WASTEWATER TREATMENT PLANTS**

With the promotion of the "carbon peaking and carbon neutrality" goals of China, the requirements for low-carbon development in the wastewater treatment industry will become increasingly stringent. Carrying out research and application of low-carbon operation and maintenance technologies for underground wastewater treatment plants is an inevitable choice to achieve the sustainable development of the wastewater treatment industry.

#### **5.1. Multi-energy complementary integrated energy application model**

The low-carbon operation and maintenance of underground wastewater treatment plants involve multiple technical fields, including renewable energy, high-efficiency energy-saving equipment, energy recovery, and intelligent control utilization. Effectively integrating these technologies to achieve optimized system operation presents a complex technical challenge. The research on multi-energy complementary integrated energy systems for underground wastewater treatment plants aims to fully leverage various energy forms, realizing efficient energy utilization and diversified supply.

Specifically, it is necessary to explore low-carbon pathways such as sewage thermal energy utilization and sludge energy utilization: converting waste heat into heating and cooling energy through waste heat recovery technology, and transforming organic matter in sewage into biogas for heating and power generation via biogasification technology. Meanwhile, study the application pathways of photovoltaic (PV), energy storage, direct current (DC), and flexible technologies in underground wastewater treatment plants—install PV modules in the overhead areas of above-ground structures, achieve energy storage through energy storage electrical equipment and energy storage devices, and carry out application research on low-voltage DC power supply for existing power distribution system equipment such as lighting, fans, and air conditioners.

Actively explore and promote the construction of "four-in-one" wastewater treatment plants that integrate wastewater treatment, wetland parks, photovoltaic power generation, and integrated energy applications to reduce reliance on traditional energy, lower energy costs, and cut carbon emissions. Establish an energy collaborative management mechanism by building an intelligent integrated energy management platform in accordance with the principles of digital, intelligent, refined, and integrated energy control. Through real-time monitoring and analysis of supply-demand dynamics for various energy sources, this platform enables intelligent monitoring and optimized management of the entire energy system, enhancing energy efficiency and ensuring stable, reliable energy supply. Such measures promote energy conservation and carbon reduction to achieve a win-win situation for economic and environmental benefits, demonstrating the feasibility of integrating ecological protection with industrial development.

*Table 4. Multi-energy complementary pathway table*

Input Energy	Conversion Technology	Output Form	Main Applications	Complementary Logic
Sludge biogas	Biogas combined heat and power (CHP)	Electricity and waste heat	Equipment power supply, digester heating	Substitutes for photovoltaic power during cloudy days/nights; waste heat assists in heating
Solar energy	Photovoltaic power generation	Electricity	Lighting, water pumps, deodorization equipment	Prioritizes power supply on sunny days; surplus power stored or fed into the grid
Sewage thermal energy	Sewage source heat pump	Thermal/cooling energy	Plant heating/cooling	Collaborates with biogas waste heat to meet seasonal demands
Solar thermal energy	Solar water heating system	Thermal energy	Process hot water, domestic hot water	Supplements biogas waste heat to reduce gas consumption
Grid electricity	Intelligent power distribution system	Electricity	Peak regulation or emergency backup	Automatically switches on when renewable energy is insufficient

## 5.2. Development and research of energy efficient equipment

Underground wastewater treatment plants, as major energy consumers, are facing unprecedented pressure for energy conservation and emission reduction. By exploring and applying new technologies, materials, and processes, researching and developing high-efficiency energy-saving equipment, and promoting the industrial application of new technologies, the technical level and competitiveness of the wastewater treatment industry can be improved. This provides strong support for energy conservation, emission reduction, cost reduction, efficiency improvement, and sustainable development of wastewater treatment plants, driving the industry towards intelligence, greening, and low-carbonization.

Improving equipment energy efficiency is crucial for low-carbon operation and maintenance. It is necessary to intensify research and development of water treatment technologies and equipment featuring high efficiency, energy conservation, land saving, integration, and intelligence to achieve compact and efficient equipment. For example, the application of precision aeration systems and intelligent dosing systems can reduce operation costs. The development of high-efficiency energy-saving odor treatment equipment adopts advanced nanosecond pulse plasma technology and intelligent control systems, with the technical core of generating short-pulse plasma through a stable high-voltage power supply. A specially configured reaction chamber enhances removal efficiency, while intelligent control technology real-time monitors the equipment's operation status and automatically adjusts working parameters. This achieves functions such as improving deodorization efficiency, enhancing emission gas quality, increasing automation, and boosting operational stability. According to current research results, this odor

treatment process equipment consumes 30% to 60% less energy than conventional chemical deodorization equipment, saves 40% to 60% of operation and maintenance costs overall, and reduces equipment floor space by over 30% compared with biological treatment processes under the same treatment scale. It effectively addresses the pain points of traditional deodorization equipment, such as large footprint, low efficiency, high energy consumption, and difficult maintenance.

### 5.3. Application of multi-functional integrated robot inspection

Underground wastewater treatment plants feature narrow spaces, crisscross pipes, dense equipment, and hazardous gases. Inspection personnel need to navigate through narrow passages and equipment intervals, which not only restricts mobility but also poses high safety risks. Meanwhile, manual inspection is inefficient, making it difficult to comprehensively and timely cover all corners and equipment of the plant. Aiming at the environmental characteristics of underground wastewater treatment plants, multi-functional integrated inspection robots are developed to real-time monitor environmental parameters such as gas composition, temperature, humidity, and pressure, and conduct condition detection on various equipment. These robots integrate with the intelligent management system of underground wastewater treatment plants to achieve real-time data sharing and interaction.

Based on equipment operation status and historical inspection data, the inspection frequency and key areas are dynamically adjusted, and inspection routes are optimized to improve the pertinence and effectiveness of inspections, providing a basis for process regulation and equipment maintenance. This enhances the overall intelligent management level, operation efficiency, and safety stability of underground wastewater treatment plants, driving the wastewater industry towards intelligence and automation.

### 5.4. Research on fine-grained intelligent control system technology

Conduct research on fine-grained intelligent control system technologies for underground wastewater treatment plants, adopting a multi-parameter control strategy of "feed forward + model + feedback". Utilize deep learning algorithms to model and predict the wastewater treatment process, develop an intelligent process regulation system to achieve full-process intelligent control of underground plants, and explore potential energy-saving, consumption-reduction, and operation optimization strategies through big data analysis. Based on feed forward information such as influent water quality and quantity, combined with wastewater treatment models, predict process operation parameters in advance and automatically adjust control parameters like aeration volume and chemical dosage. Real-time evaluate and adjust the regulation effects through feedback information to ensure the process operates at optimal conditions, reducing energy consumption and carbon emissions while maintaining stable effluent compliance.

Install preventive maintenance devices to real-time monitor the equipment of underground wastewater treatment plants. Establish a full-life cycle management system for equipment to manage the entire process from procurement, installation, operation, maintenance to decommissioning, improving equipment operational safety and reliability while reducing maintenance costs.

### 5.5. Low-carbon operation and maintenance technology application case and carbon reduction analysis

For low-carbon operation and maintenance technology, take a new underground wastewater treatment plant with a design capacity of 100,000 m<sup>3</sup>/d in Jiangsu Province, China, as an example, the project covers an area of about 30,000m<sup>2</sup> and the ground is a park. Through the application of low-carbon technologies such as biogas power generation, photovoltaic power generation, solar thermal collector, wastewater heat source, reclaimed water reuse, energy-efficient equipment, green space, etc., the carbon emission reduction of each technology is estimated to provide a reference for the green and low-carbon operation and maintenance of underground wastewater treatment plants.

#### 1) Biogas power generation

The sludge output of the plant is relatively stable throughout the year, with an average monthly sludge production of about 2,400 tons. The daily biogas production after thermal anaerobic digestion is about 704m<sup>3</sup>/d, and the biogas generator set with combined heat and power supply is used to realize biogas combustion for power generation.

Calculation formula for carbon reduction of electric energy recovery (1)

$$C_d = L_d \cdot EF_d / M_n \quad (1)$$



Where,  $C_d$  is the carbon reduction of electric energy recovery,  $\text{kg CO}_2/\text{m}^3$ ;  $L_d$  is the total electric energy produced in the evaluation year,  $\text{kWh/a}$ ;  $EF_d$  is the electric power emission factor of the area,  $\text{kg CO}_2/\text{kWh}$ ;  $M_n$  is the total amount of domestic wastewater treatment in the evaluation year,  $\text{m}^3/\text{a}$ .

The annual biogas power generation is calculated to be about 514.000kwh, and according to the carbon dioxide emission index of 0,7035kg/kWh for the East China Power Grid, the annual carbon emission reduction is about 361,6t.

#### 2) Photovoltaic (PV) power generation system

The case plant is located in an area with moderate solar resources, where the annual total horizontal irradiance is 1.400–1.500  $\text{kWh/m}^2$ . To fully utilize solar energy, PV modules are installed overhead in the covered areas and green belts of the underground wastewater treatment plant. Fixed or tracking PV systems are selected based on installation positions—tracking systems can increase power generation by approximately 15%–25% compared to fixed systems at the same installed capacity. PV walkways are also set up in some pedestrian passages.

Meanwhile, the PV-storage-direct current-flexible (PVSDCF) technology prioritizes PV power for DC motor systems. For example, DC motors replace some asynchronous motors in lighting and ventilation equipment to reduce voltage conversion losses and improve equipment energy efficiency. The case plant's PV system can generate about 181.000 kWh of electricity annually, reducing carbon dioxide emissions by approximately 127,34 tons per year.

#### 3) Wastewater source heat pump system application

Utilizing heat pump technology to recycle the heat energy contained in wastewater is one of the important means for wastewater treatment plants to realize the synergistic effect of pollution reduction and carbon reduction. In the effective reduction of fuel, electricity and other energy consumption, saving operating costs while significantly reducing greenhouse gas emissions. The normal water temperature of the recycled water source is  $16^\circ\text{C}$ – $17^\circ\text{C}$ , in winter, the heat pump device extracts the heat energy resources contained in the water and transfers them together with the consumed energy to the buildings to achieve the purpose of heating; in summer, the wastewater source heat pump unit can also absorb heat from the high temperature environment and release the heat into the water to achieve the effect of refrigeration; and it can provide a cooling and heating source for the equipment rooms in the plant and the nearby buildings.

According to the theoretical calculation of energy and resource recovery of wastewater treatment plant, the theoretical cold/heat in wastewater can be calculated in equation (2):

$$Q=M \times \Delta T \times C \quad (2)$$

Where:  $Q$  indicates the cold/heat,  $\text{kJ}$ ;  $M$  indicates the mass of wastewater,  $\text{kg}$ ;  $\Delta T$  indicates the temperature difference between the wastewater in and out of the extraction, according to the project to take  $8^\circ\text{C}$ ;  $C$  indicates the specific heat capacity of the wastewater, take  $4,18\text{kJ}/(\text{kg} \cdot ^\circ\text{C})$ ;

According to the definition of the cooling coefficient COP, the actual heat supply/cooling capacity of the heat pump can be calculated in equation (3):

$$Q_{h/c} = Q \pm W = Q \pm Q / \text{COP} \pm I \quad (3)$$

Where,  $Q_{h/c}$  indicates the total heating/cooling capacity of the heat pump (subscript h/c represents the heating/cooling conditions respectively),  $\text{kJ}$ ;  $W$  indicates the contribution of the electrical energy consumed by the heat pump to the output thermal energy; COP is calculated as 3,7.

Carbon reduction can be calculated in equation (4):

$$C_h = Q_{h/c} \times EF_h / M_n \quad (4)$$

Where,  $C_h$  is the amount of carbon reduction by heat energy recovery,  $\text{kg CO}_2/\text{m}^3$ ;  $Q_{h/c}$  is the heat energy that can be exported to the outside of the wastewater treatment system in the evaluation year,  $\text{GJ/a}$ ;  $EF_h$  is the emission factor of fossil fuels,  $\text{kg CO}_2/\text{GJ}$ ;  $M_n$  is the total amount of domestic wastewater treatment in the evaluation year,  $\text{m}^3/\text{a}$ .

In this case, the water source heat pump calculates the heat energy recovery by 75% of the average treated water volume in daily operation, and the amount of wastewater extracted by the water source heat pump is calculated by  $2737,5 \times 104\text{m}^3$  for the whole year, and the actual carbon emission can be reduced by about 1.080t per year.

#### 4) Reclaimed water reuse system

The project site is equipped with a large number of green roofs, which effectively reduce the total roof runoff and runoff pollution load. Meanwhile, decentralized intelligent carbon fiber rainwater collection modules are set in the green belts to carry out source treatment of rainwater runoff. The tail water enters the ecological wetland for

further purification, and the reclaimed water is used for landscape and road watering, reducing the consumption of tap water and realizing the circular utilization of reclaimed water. The reclaimed water reuse volume of this project is 10,22 million tons, and the annual carbon emission reduction is about 3.004,7 tons.

5) Application of energy-efficient equipment and refined intelligent control system

The project adopts a precise aeration control system, which collects corresponding instrument signals to real-time track and evaluate the dissolved oxygen and aeration demand of each aeration control zone according to the changes of pollution load and process operation status in the sewage plant. It automatically controls the blower and air regulating valve, adjusts and distributes the aeration volume on demand, stably and accurately controls the dissolved oxygen in the aerobic zone, and ensures the efficient and stable operation of the sewage treatment process. At the same time, low-carbon strategies are adopted to minimize the aeration volume, reduce the energy consumption and chemical consumption of the sewage treatment plant, and achieve refined operation and management of the sewage treatment plant. The precise aeration system can save about 5,0694 million kWh of electricity annually, reducing carbon dioxide emissions by about 3.566,3 tons.

6) Application of landscape green space carbon sink

The project adopts fully underground construction, and the ground greening ecosystem forms a carbon sink space, which also alleviates the heat island effect and achieves the purpose of regulating microclimate.

The estimation method for carbon sequestration of plants in green spaces follows the Technical Guide for Carbon Accounting and Emission Reduction Pathways in Urban Water Affairs Systems, and the calculation formula is as shown in (5):

$$C_{zb}=EF_{zb} \cdot S_{zb} \quad (5)$$

Where,  $C_{zb}$  is the amount of carbon sequestered by vegetation, kg CO<sub>2</sub>-eq;  $EF_{zb}$  is the carbon sequestration factor of vegetation, kg CO<sub>2</sub>-eq /m<sup>2</sup> ;  $S_{zb}$  is the area covered by plants, m<sup>2</sup> .

The greening area of this project is nearly 20.000m<sup>2</sup>, and the annual carbon sequestration is about 2,9t.

The low-carbon technical scheme of the case underground sewage treatment plant makes full use of multiple energy recycling technologies such as biogas power generation, photovoltaic power generation, sewage thermal energy, and reclaimed water reuse, with obvious carbon reduction effects. It saves 3.331,42 tons of standard coal and reduces carbon dioxide emissions by 8.664,54 tons annually. See Table 5 for details, with remarkable economic and environmental benefits.

**Table 5.** Statistics on the amount of standard coal saved and carbon dioxide emission reduction by the application of low-carbon technologies

Low-carbon technology	Standard coal consumption (tons)	CO <sub>2</sub> emissions (tons)	note
biogas	139,08	361,6	The CO <sub>2</sub> emission index is taken as 0,7035 kg/kWh (with reference to the East China Power Grid)
photovoltaic power generation	48,98	127,34	
wastewater source heat pump	415,38	1.080	
reclaimed water reuse	1.155,65	3.004,7	
energy efficient equipment and fine intelligent control	1.572,71	4.088	
landscape green space carbon sink	/	2,9	
total	3.331,42	8.664,54	

## 6. CONCLUSION

As an important part of urban infrastructure, the resilience and low-carbon operation and maintenance of underground wastewater treatment plant is of great significance for the sustainable development of the city.

1) Sustained technological innovation to achieve the green transformation of underground wastewater treatment plants. With the innovation of underground wastewater treatment process technologies and the application of advanced resource recovery technologies, multi-faceted measures such as process optimization, equipment upgrading, resource recycling, energy consumption optimization, and clean energy utilization can further improve the energy efficiency and resource recovery rate of underground wastewater treatment plants. This promotes their transformation from purely wastewater treatment facilities to "resource factories," achieving a win-win situation for environmental and economic benefits, and providing strong support for urban sustainable development.

2) Deepening integrated development models to promote ecological harmony. Further deepen the integrated development of underground wastewater treatment plants with urban ecological construction, urban planning, and technological innovation. Achieve harmonious coexistence between underground wastewater treatment plants and urban functional areas as well as the urban ecosystem, accelerate the carbon neutrality process of underground wastewater treatment plants, and enhance the overall ecological environment quality of cities and the living standards of residents.

3) Policy guarantee for low-carbon operation and maintenance. Strengthen policy guidance, introduce policy mechanisms and targeted policies to encourage the resilient and low-carbon operation and maintenance of underground wastewater treatment plants, stimulate the enthusiasm and innovation of enterprises, and provide strong support for the implementation of low-carbon operation and maintenance projects. Meanwhile, formulate and improve technical standards for low-carbon operation of underground wastewater treatment, provide a basis for the standardized and healthy development of underground wastewater treatment plants, and promote the development of underground wastewater treatment plants towards a green and low-carbon direction.

## 7. REFERENCES

- [1] CHEN Xiucheng. Analysis of Land Quota and Land Conservation Design Conditions for Underground Wastewater Treatment Plants[J]. China Water & Wastewater, 2023, 39(4): 53-58.
- [2] HUANG Jun, LIU Qilong, ZHAO Guang, JI Hongling, et al. Reflection on Green Development of Municipal Infrastructure Undergroundization under Urban Renewal: A Case Study of Jiangsu Province[J]. Tunnel Construction, 2024, 44(2): 000.
- [3] Sun S, Lin H, Lin J, et al. Underground wastewater treatment plant: a summary and discussion on the current status and development prospects[J]. Water Science and Technology, 2019, 80(9): 1601.
- [4] HAO Xiaodi, YU Wenbo, et al. Comprehensive Benefit Evaluation of the Full Life Cycle of Underground Wastewater Treatment Plants[A]. China Water & Wastewater, 2021(07): 37.
- [5] HAO Xiaodi, ZHAO Zicheng, LI Ji, LI Shuang, JIANG Han. Energy and Resource Recovery Methods and Carbon Emission Accounting for Wastewater Treatment Plants: A Case Study of the Kakolanmäki WWTP in Finland[J]. Chinese Journal of Environmental Engineering, 2021(09).
- [6] DING Yao, WANG Xueyuan, WANG Yin, ZHANG Xuebing. Low-Carbon Technology Assessment for Urban Wastewater Treatment Plants under the "Dual Carbon" Goal: A Case Study of the PANTAI WWTP in Malaysia[J]. China Exploration & Design, 2023(12).
- [7] CHEN Xiucheng. Analysis of Energy Consumption Indicators and Energy-Saving Directions for Underground Wastewater Treatment Plants[A]. Water & Wastewater Engineering, 2022(03): 48.
- [8] CHEN X C. Analysis of land quota and land conservation design direction of underground wastewater treatment plant[J]. China Water & Wastewater, 2023, 39(4): 53-58.

## FLOOD RISK ASSESSMENT AND RESILIENCE STRATEGIES FOR URBAN METROS UNDER EXTREME RAINFALL

Shuguang Liu<sup>1</sup>, Weiqiang Zheng<sup>2</sup>, Guihui Zhong<sup>3</sup>, Zhengzheng Zhou<sup>4</sup>

**Abstract:** Shanghai, located at the Yangtze River estuary, is one of China's fastest-growing cities in underground transportation and also highly vulnerable to flood disasters. With extreme weather events becoming more frequent, the city's metro system faces increasing flood risks. This study selects eight indicators—including rainfall intensity, terrain slope, and passenger volume—and uses the entropy weight method to assign indicator weights. A flood risk assessment framework is developed and applied to 282 metro stations in Shanghai's central urban area. The spatial distributions of hazard, exposure, vulnerability, and defense indices are analyzed, and stations are classified into different risk zones. Based on the assessment, targeted disaster mitigation strategies are proposed to enhance flood resilience. Results indicate that flood risk generally decreases from northeast to southwest, and the spatial pattern of overall risk aligns closely with hazard levels. Stations in the northeastern region show high hazard and require improved responses to extreme rainfall. Central stations, characterized by high exposure and weak mitigation capacity, need enhanced surface and drainage infrastructure. Southwestern and southeastern stations show high vulnerability, highlighting the need for better emergency preparedness. The findings contribute to resilience-oriented urban planning and provide technical support for sustainable development in flood-prone metropolitan areas.

**Keywords:** Flood risk assessment; Indicator system; Metro stations; Shanghai; Resilience-based mitigation

### 1. INTRODUCTION

Flood disasters are among the most severe natural hazards affecting human society. Floods and their cascading impacts have become major obstacles to sustainable urban development and the advancement of urban resilience. According to the *Blue book on urban underground space development in China 2024*, 19 out of 93 underground space disasters and accidents in China in 2023 were caused by water-related events—accounting for nearly one-fifth of all cases [1]. Urban underground spaces are particularly vulnerable due to poor drainage, limited rescue accessibility, and frequent secondary disasters [2]. On July 20, 2021, a severe flood struck Henan Province, China, resulting in extreme urban inundation in Zhengzhou. Water flooded into metro trains in Tunnel Line 5, leading to 14 fatalities. On May 21, 2020, heavy rainfall in Guangzhou caused floodwaters to backflow into metro tunnels, shutting down the entire Metro Line 13. These frequent extreme events pose growing threats to the increasingly developed underground transportation systems in cities and hinder the sustainable development of modern urban environments.

Common flood risk assessment approaches include historical loss analysis, scenario simulation, and indicator-based methods. Historical analysis relies on past disaster records to assess risk levels across different entities. For instance, Rodda (2005) reviewed data from 30 major floods in the Czech Republic to map inundation and water depth [3]. Scenario simulation builds hydrological-hydrodynamic models for specific cases to simulate flood

<sup>1</sup> Professor, Liu, Shuguang, Ph.D. Geography, College of Civil Engineering, Tongji University, Siping Road No.1239, Shanghai, China, liusgliu@tongji.edu.cn.

<sup>2</sup> Ph.D. Student, Zheng, Weiqiang, B.Sc. Harbor, Waterway and Coastal Engineering, College of Civil Engineering, Tongji University, Siping Road No.1239, Shanghai, China, zhengweiqiang@tongji.edu.cn.

<sup>3</sup> Professor, Zhong, Guihui, Ph.D. Civil Engineering, College of Civil Engineering, Tongji University, Siping Road No.1239, Shanghai, China, 04098@tongji.edu.cn.

<sup>4</sup> Associate Professor, Zhou, Zhengzheng, Ph.D. Hydraulic Engineering, College of Civil Engineering, Tongji University, Siping Road No.1239, Shanghai, China, 19058@tongji.edu.cn.

progression and assess risks, widely applied in East Asia—for example, Liu et al. (2022) on building flood zoning [4], Shin et al. (2021) on underground escape routes [5], and Lyu et al. (2019) on submersion in metro systems [6]. Indicator-based methods evaluate risks by selecting multiple factors that represent the characteristics of hazards and the environment. These include studies by Lyu et al. (2018), Wang et al. (2021), and Yuan et al. (2024) on metro flood risk and submersion time [7-9]. Such methods typically incorporate hazard, exposure, vulnerability, and defense indicators.

Each method, however, has limitations. Historical analysis depends heavily on detailed event records, often unavailable for underground spaces. Scenario simulations face challenges in accurately defining boundary conditions and modeling real underground structures, especially for large-scale applications [6]. Indicator-based approaches, while widely used, often suffer from subjectivity in indicator selection and weighting, and are highly region-specific [7]. Additionally, they usually provide only relative, rather than absolute, risk levels [10].

Shanghai, located at the confluence of the Yangtze River and the East China Sea, is the last major city through which the Yangtze flows. Each flood season, the city faces compound threats from storm surges, extreme rainfall, astronomical tides, and upstream discharges. In October 2013, Typhoon Fitow caused severe flooding in central Shanghai, inundating 97 roads and over 900 residential communities, affecting more than 100,000 people and causing economic losses of CNY 890 million. In July 2021, Typhoon In-Fa triggered widespread street and residential flooding. Therefore, Shanghai's underground spaces face severe challenges in flood disaster prevention and control.

Given the limited attention paid to flood risk assessment and resilience planning for urban underground transport systems, and considering that metro stations in central urban area of Shanghai (within the outer-ring road) are mostly underground and located in zones of high population density and economic activity, this study focuses on evaluating the flood risk and resilience of these metro systems. The study targets underground facilities within metro stations, including entrances and subsurface spaces, and proposes resilience-based flood mitigation strategies to support the sustainable development of underground transport infrastructure in Shanghai. The remainder of this paper is organized as follows: Section 2 introduces the methodology; Section 3 describes the study area and data sources; Section 4 presents the risk assessment results; Section 5 offers concluding remarks.

## 2. METHODOLOGY

### 2.1. Pearson type III distribution and its $L$ -moment estimators

This study computes rainfall-related indicators based on rainfall frequency analysis. The Pearson Type III (P-III) distribution is used to fit the annual maximum series of rainfall. The P-III distribution is recommended in China's national flood control standards as a suitable distribution for modeling annual maxima. The probability density function (PDF) and cumulative distribution function (CDF) of the P-III distribution are [11]:

$$f_x(x) = \frac{(x-\xi)^{\alpha-1} e^{-(x-\xi)/\beta}}{\beta^\alpha \Gamma(\alpha)}, \quad F_x(x) = G\left(\alpha, \frac{x-\xi}{\beta}\right) / \Gamma(\alpha), \quad (1)$$

where  $\xi$ ,  $\beta$ , and  $\alpha$  are referred to as the location, scale, and shape parameters, respectively.  $\Gamma(x)$  and  $G(s, x)$  denote the gamma function and the lower incomplete gamma function, respectively, which are defined as:

$$\Gamma(x) = \int_0^\infty p^{x-1} e^{-p} dp, \quad G(s, x) = \int_0^x p^{s-1} e^{-p} dp. \quad (2)$$

The value of the scale parameter  $\beta$  is typically related to the physical characteristics of the studied object. In rainfall frequency analysis,  $\beta$  is usually taken to be positive ( $\beta > 0$ ).

We adopt the  $L$ -moment method to obtain point estimates of the distribution parameters. Hosking and Wallis (1997) recommended using  $L$ -moments as linear combinations of the expectations of order statistics [11]. The  $L$ -moment method estimates the parameters by solving a system of equations that equates the population  $L$ -moments to their corresponding sample  $L$ -moments.

Assume that  $X_1 < X_2 < \dots < X_n$  is an ordered sample of size  $n$  drawn from the P-III distribution defined in Equation (1). The population  $L$ -moments (or  $L$ -moment ratios) are defined as follows:

$$\lambda_1 = \xi + \alpha\beta, \quad \lambda_2 = \pi^{-0.5} \beta \Gamma(\alpha + 0.5) / \Gamma(\alpha), \quad \tau_3 = 6I_{1/3}(\alpha, 2\alpha) - 3, \quad (3)$$

where  $I_x(s, t)$  is the incomplete beta function and defined as:

$$I_x(s, t) = \frac{\Gamma(s+t)}{\Gamma(s)\Gamma(t)} \int_0^x p^{s-1} (1-p)^{t-1} dp. \quad (4)$$

The sample  $L$ -moments (or  $L$ -moment ratios) are defined as:



$$\begin{cases} \lambda_1 = b_1, \lambda_2 = 2b_2 - b_1, \tau_3 = (6b_3 - 6b_2 + b_1)/(2b_2 - b_1) \\ b_t = \frac{1}{n} \sum_{i=t}^n \frac{(i-1)(i-2)\dots(i-t+1)}{(n-1)(n-2)\dots(n-t+1)} X_n, t = 1, 2, 3 \end{cases} \quad (5)$$

## 2.2. Entropy weight method

The entropy weight method is a technique used to determine indicator weights based on the concept of information entropy [12]. The greater the variation in the observed values of an indicator, the more significant it is considered in the evaluation process. Conversely, when the values of a specific indicator show little variation among evaluation objects, its contribution to the assessment is limited. As a mathematical method that assigns weights based on the degree of data dispersion, the entropy weight method ensures that the weighting process remains objective, effective, and scientifically grounded.

An evaluation matrix is constructed based on the selected  $M$  flood-related indicators and  $N$  corresponding evaluation objects. Since different indicators represent various dimensions and scales, their values are not directly comparable. Therefore, normalization must be performed before applying the entropy weight method. Let the weight matrix be:

$$Q = \begin{pmatrix} q_{11} & \dots & q_{1N} \\ \vdots & \ddots & \vdots \\ q_{M1} & \dots & q_{MN} \end{pmatrix}, \quad (6)$$

where  $q_{ij}$  ( $1 \leq i \leq M, 1 \leq j \leq N$ ) is the (normalized) value of the  $i$ -th indicator for the  $j$ -th evaluation object. Then the proportion of  $q_{ij}$  is defined as:

$$w_{ij} = q_{ij} / \sum_{s=1}^N q_{is}. \quad (7)$$

The entropy value of the  $i$ -th indicator is defined as:

$$H_i = - \left( \sum_{s=1}^N w_{is} \ln w_{is} \right) / \ln N. \quad (8)$$

Thus, the entropy weight of the  $i$ -th indicator is:

$$W_i = (1 - H_i) / \sum_{s=1}^M (1 - H_s). \quad (9)$$

## 3. STUDY AREA AND DATA

### 3.1. Study area

Shanghai City, located at the lower reaches of the Yangtze River, spans an area of 6,340.5 km<sup>2</sup> near the East China Sea (Figure 1). It falls within a subtropical monsoon zone, experiencing an average annual precipitation of 1,097 mm. The flood season, lasting from May to September, is marked by frequent cyclonic storms, which are the main contributors to extreme rainfall events. In 2024, Shanghai's Gross Domestic Product (GDP) reached CNY 5.39 trillion, accounting for nearly 39.97% of the national GDP, while occupying less than 0.66% of the country's total land area. The city's high degree of urbanization and population density make it particularly vulnerable to extreme rainfall events.

Considering that metro stations in the central urban area of Shanghai are primarily underground, while suburban stations are mostly above ground, this study focuses on metro stations located within the central urban area (i.e., within the outer-ring road), as shown in Figure 1. In terms of administrative divisions, the study area mainly includes the entire of Yangpu, Hongkou, Jing'an, and Huangpu Districts, the majority of Changning, Xuhui, Putuo, and Pudong (New Area) Districts, as well as parts of Minhang, Jiading, and Baoshan Districts.

### 3.2. Data

**Metro stations.** The study focuses on 282 metro stations located within Shanghai's central urban area that had been completed by the end of 2019, as shown in Figure 1. The spatial distribution of these stations is as follows: 94 in Pudong New Area (for convenience, referred to as "Pudong District" in the following text), 34 in Xuhui

District, 29 in Yangpu District, 27 in Putuo District, 20 in Baoshan District, 19 in Jing'an District, 18 in Huangpu District, 14 in Changning District, 13 in Hongkou District, 11 in Minhang District, and 3 in Jiading District.

**Rainfall data.** Daily rainfall observations from 1961 to 2019 were collected from 15 rain gauges distributed across Shanghai (locations shown in Figure 1). The data were downloaded from the China Meteorological Data Center (<http://data.cma.cn/>).

**Topographic data.** The 2018 Digital Elevation Model (DEM) of Shanghai was used to characterize the city's terrain, as shown in Figure 1.

**Hydrological data.** The spatial distribution of water bodies in Shanghai as of 2019 was incorporated into the analysis (see Figure 1).

**Passenger flow data.** The average daily passenger volume for each metro station was represented by the December 2018 ridership data. These data were sourced from online public (<https://mlzhongguo.com/article/detail-2108.html>).

**Physical attributes of metro stations.** Information on the structural features of each metro station was obtained through a combination of field surveys and satellite imagery from Baidu Maps (<https://map.baidu.com/>).

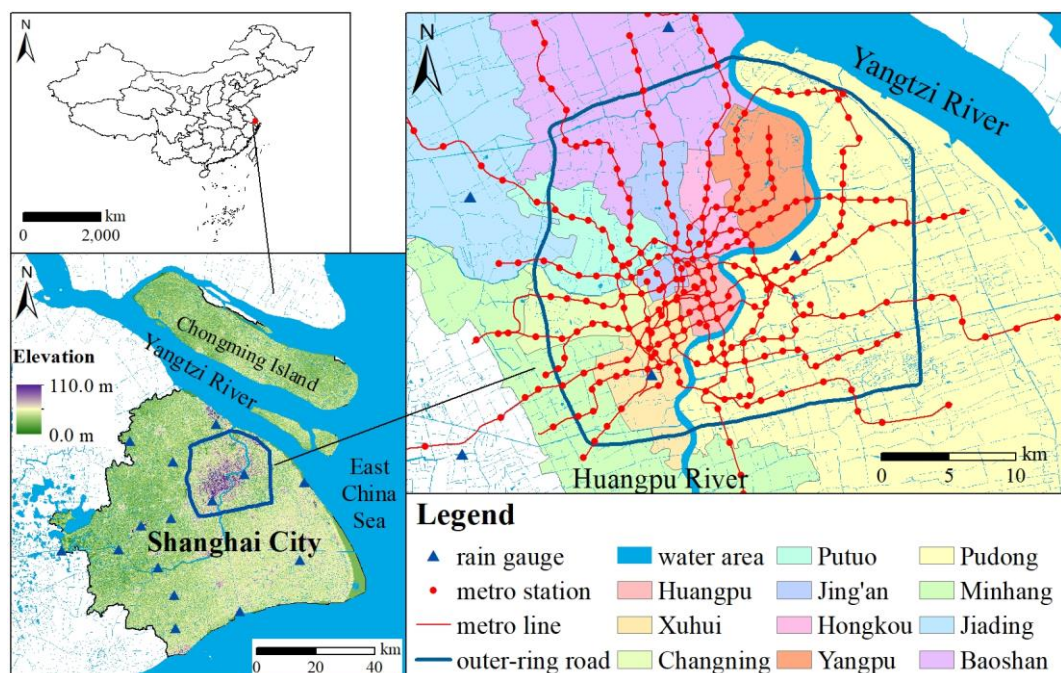


Figure 1. Study area and location of metro stations

## 4. RESULTS

### 4.1. Indicators and their entropy weights

Based on the practice of urban flood management in China, flood risk is generally influenced by four major dimensions: hazard (H), exposure (E), vulnerability (V), and defense (D). This study selects appropriate indicators from each of these dimensions, considering data availability and the actual conditions of Shanghai.

**Hazard.** Rainfall is the most direct flood-inducing factor in Shanghai. The greater the rainfall intensity and the more frequent the extreme precipitation events, the higher the flood risk. Therefore, rainfall intensity and rainfall frequency are selected as hazard indicators. Considering that the flood protection standard for central Shanghai has reached a return period of 50 years, we use the 100-year design rainfall depth (i.e., exceedance probability of 0.01) to represent extreme rainfall intensity. According to the standards issued by the China Meteorological Administration, a 24-hour rainfall of 100.0 mm is classified as "heavy rainstorm". Hence, we use the exceedance probability of 100.0 mm daily rainfall to represent extreme rainfall frequency.

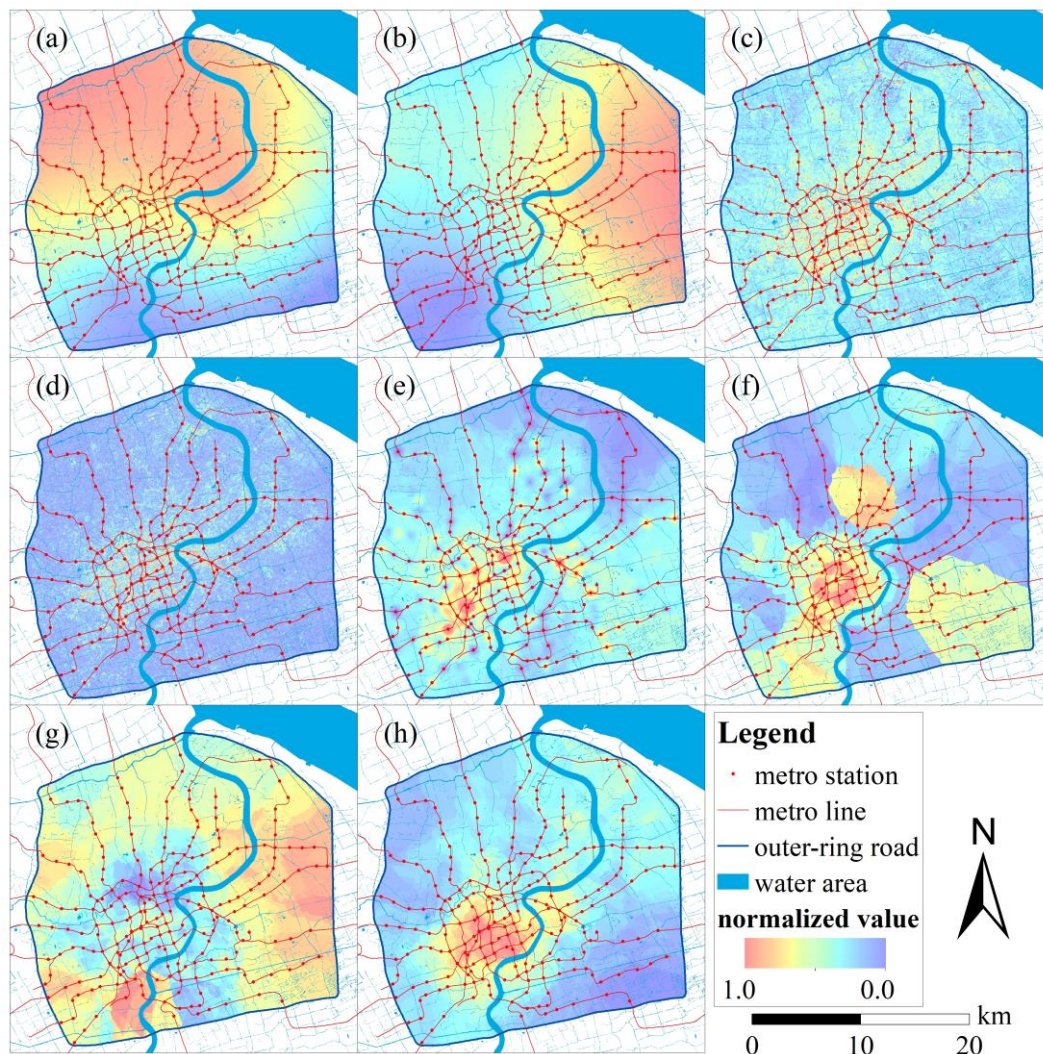
**Exposure.** Urban terrain characteristics are key environmental factors contributing to flood exposure for underground spaces in Shanghai. Metro stations located in lower and flatter terrain are considered more exposed. Therefore, the relative elevation and terrain slope are selected as indicators of exposure.

**Vulnerability.** The metro stations (including concourse and platform levels) serve as the main elements at risk in this study. Their vulnerability depends on both physical and social attributes. Physical vulnerability includes

flood-blocking and water intake conditions, while social vulnerability is represented by the station's passenger volume. Specifically, flood-blocking capacity is measured by hump height (i.e., the stair height at entrances); water intake potential is represented by the number of station entrances; and social importance is represented by average daily passenger volume.

**Defense.** There are currently no explicit design standards for flood protection and drainage capacity in Chinese metro stations. Drainage systems are typically designed only for daily operations. Therefore, the key determinant of a station's flood defense capability is its drainage condition, proxied by the distance to the nearest water body. A longer drainage distance implies weaker drainage capacity and thus lower adaptive capacity.

The spatial distribution of all indicators is shown in Figure 2, where the higher (normalized) values mean the more dangerous situations in flood. The entropy weight method was used to determine the weight of each indicator, with results presented in Table 1. Among hazard indicators, rainfall frequency holds greater weight than rainfall intensity, suggesting that sustained heavy rainfall events pose higher risks to metro stations in Shanghai. For exposure, slope carries significantly higher weight than elevation, indicating that stations located in flatter areas are more prone to flood risks. Among vulnerability indicators, passenger volume has the highest weight, reflecting the increased economic and social vulnerability of highly trafficked stations. In terms of adaptive capacity, drainage distance also holds considerable weight, underscoring its role in mitigating flood impacts. Overall, slope, passenger volume, and drainage distance are the most influential factors in flood risk for Shanghai's metro system.



**Figure 2.** Spatial distribution of the indicators, where the higher values mean the more dangerous situations. (a) rainfall intensity. (b) rainfall frequency. (c) relative elevation. (d) terrain slope. (e) stair height. (f) number of entrances. (g) passenger volume. (h) drainage distance

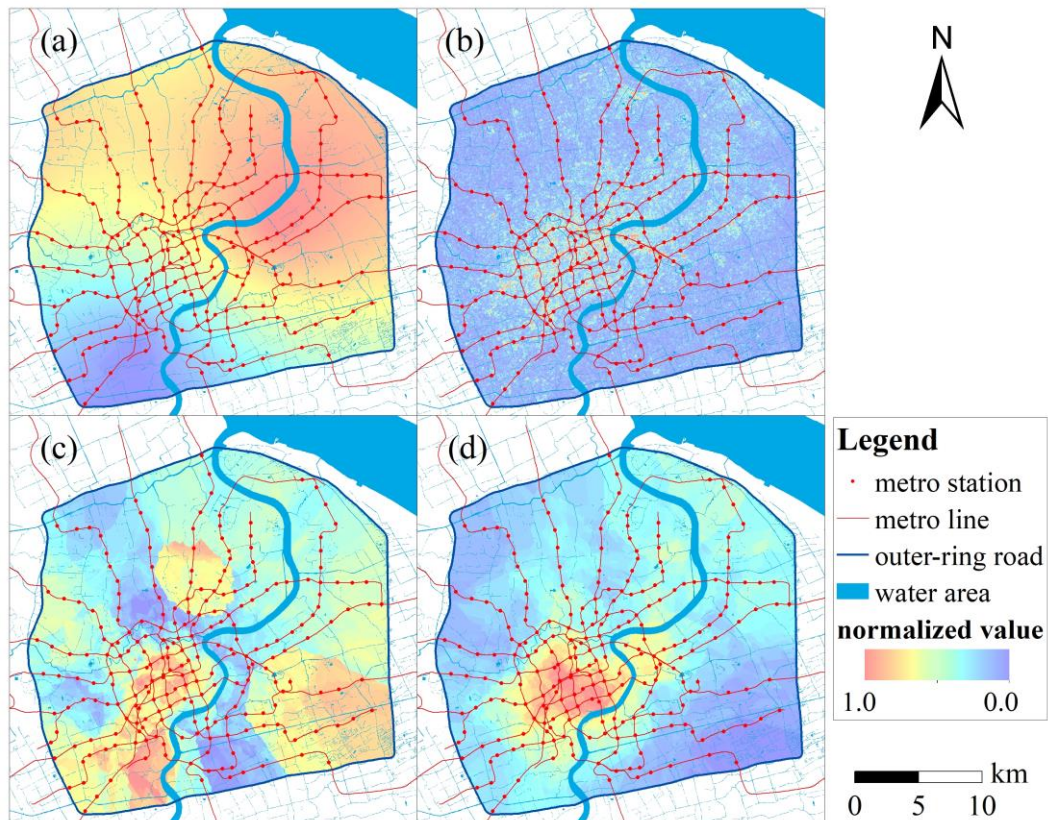


**Table 1.** Selected Indicators and their weights

Dimension	Indicator	Weight	Data Source
H	rainfall intensity	0.102200	rainfall frequency analysis
	rainfall frequency	0.127900	
E	relative elevation	0.007898	DEM of Shanghai
	terrain slope	0.236700	
V	stair height	0.055520	field surveys and satellite imagery
	number of entrances	0.011620	
	passenger volume	0.325500	
D	drainage distance	0.132800	land-use type of Shanghai

#### 4.2. Flood risk assessment for metro stations

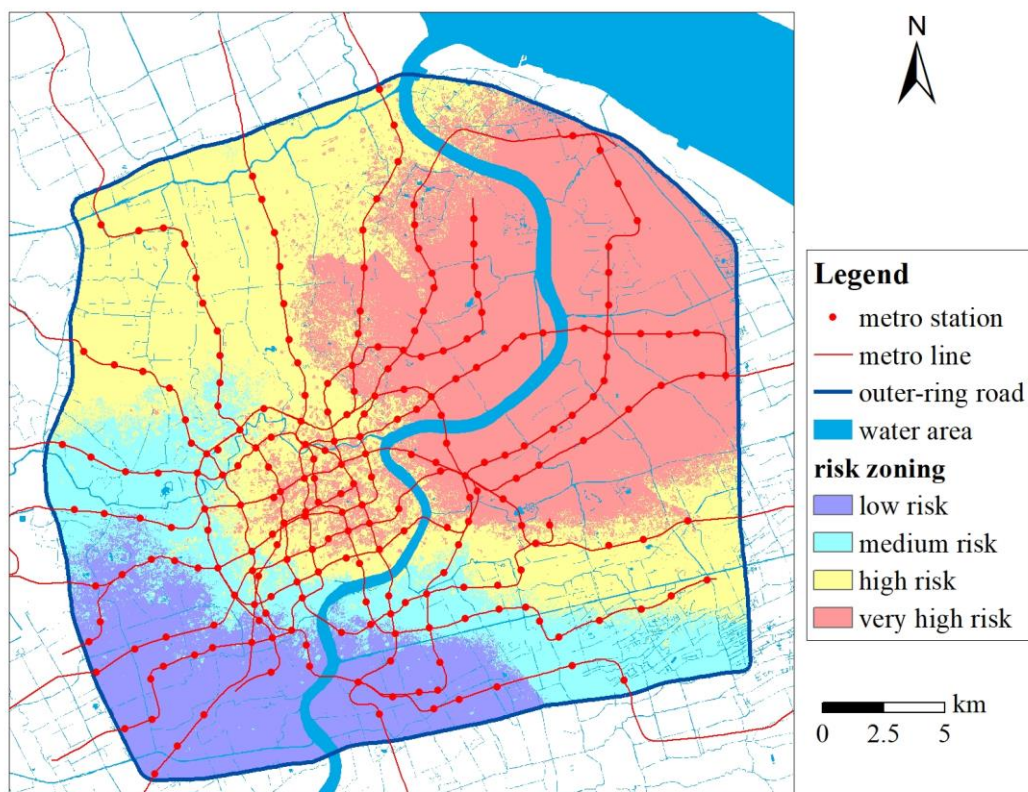
The values of rainfall intensity and rainfall frequency were combined using entropy weights to assess the hazard level, as shown in Figure 3(a). The spatial distribution of hazard levels demonstrates a decreasing trend from northeast to southwest within the study area. Metro stations with higher hazard levels are mainly located in Pudong, Yangpu, and Hongkou Districts. The spatial distribution of exposure, representing the disaster-prone environment, is shown in Figure 3(b). Overall, the exposure of metro stations in Shanghai is relatively low due to the city's generally flat terrain. The central urban area exhibits similar topographic features across different locations, resulting in comparable exposure values among metro stations. Areas with flatter terrain are scattered and mainly concentrated in Huangpu, Xuhui, and Changning Districts. The spatial distribution of vulnerability is illustrated in Figure 3(c). Metro stations with higher vulnerability are primarily located in the southwestern and southeastern corners of the study area, including Huangpu, Xuhui, Pudong, and Hongkou Districts. These stations are situated in bustling commercial areas with high passenger density. Moreover, many of them were constructed earlier, and typically have lower stair heights at entrances, indicating weaker inundation-blocking capability. The spatial distribution of defense is shown in Figure 3(d). Overall, metro stations with weaker adaptive capacity are concentrated in central urban areas such as Huangpu, Xuhui, and Changning Districts. These areas are highly urbanized with low water system coverage, resulting in longer drainage distances for metro stations and therefore weaker disaster mitigation capacity.



**Figure 3.** Spatial distribution of the dimensions. (a) hazard. (b) exposure. (c) vulnerability. (d) defense.

Considering that the defense dimension primarily function after flood events occur, its contribution to the overall flood risk is moderately reduced. According to the *Shanghai Flood and Drought Disaster Risk Assessment and Zoning Project*, the weights for hazard, exposure, vulnerability, and defense are set at 0.3, 0.3, 0.3, and 0.1, respectively. Based on the evaluation results of these four dimensions, flood risk zoning for metro stations within the study area was conducted. The comprehensive flood risk values were first calculated and then classified into four risk levels—low, medium, high, and very high—using the natural breaks method. The results are shown in Figure 4.

Overall, the flood risk zoning of metro stations within the outer-ring road closely resembles the spatial distribution of hazard level. Metro stations identified as very high risk are mainly located in the northeastern and central parts of the study area. In the northeast, both the intensity and frequency of heavy rainfall are high, making the region more prone to extreme rainfall events and thus presenting a high hazard. In the central area, relatively flat and low-lying terrain leads to rapid accumulation of surface water under extreme rainfall, resulting in high exposure levels. High-risk metro stations are primarily distributed in the northwest and southeast. In the northwest, high rainfall intensity leads to increased hazard levels; in the southeast, although the hazard level is relatively low, the stations experience high passenger volume, contributing to greater vulnerability level. Medium-risk metro stations are mainly located in the southwestern-central region, including Xuhui and Changning Districts. Despite higher vulnerability level and weaker defense level, these areas are less affected by intense or frequent rainfall events, resulting in relatively lower overall flood risk. Low-risk metro stations are located in the southwestern part of the study area, primarily in Minhang District. Although the vulnerability level in this region is relatively high, the other indicators suggest lower flood risk, contributing to the overall lower comprehensive risk. The number of metro stations at different risk levels in each district is shown in Table 2.



**Figure 4.** Flood risk zoning for metro stations

**Table 2.** Number of metro stations at different risk levels in each district

District	Low risk	Medium risk	High risk	Very high risk
Pudong	11	18	13	52
Xuhui	17	7	6	4
Yangpu	0	0	4	29
Putuo	0	14	12	1
Baoshan	0	1	18	1



Jing'an	0	1	14	4
Huangpu	0	0	10	8
Changning	4	9	1	0
Hongkou	0	0	7	6
Minhang	7	4	0	0
Jiading	0	1	2	0
Total	39	55	87	101

### 4.3. Flood disaster mitigation strategies

Metro stations with high hazard levels are primarily located in the northeastern part of the study area, where flood control should focus on coping with extreme rainfall events. With the ongoing process of urbanization, the temporal patterns of regional heavy rainfall have become increasingly complex. Overall, rainfall extremes and totals are increasing, while the number of rainy days is decreasing, indicating a growing concentration of precipitation. In areas with high rainfall intensity (northern regions), greater emphasis should be placed on non-structural measures to improve sensitivity to storm forecasts and early warnings, thereby reducing the threat posed by high-intensity rainfall to metro stations. In contrast, for areas with high rainfall frequency (eastern regions), structural measures should be prioritized. These include enhancing flood protection standards at metro stations, such as raising entrance humps and increasing drainage capacity, to effectively manage frequent and intense extreme rainfall.

Metro stations with high exposure level are mainly located in the central area, where the primary concern is the adverse terrain conditions. Due to Shanghai's overall low elevation, altering relative elevation is difficult. Therefore, reducing the flatness of surrounding areas and mitigating the risk of localized inundation becomes critical. Structural measures such as increasing the gradient near metro station entrances can help redirect water away and reduce the risk of water accumulation.

Metro stations with high vulnerability level are mainly distributed in the southwestern and southeastern regions. The focus here is to establish effective on-site flood protection mechanisms. Given a fixed number of entrances, increasing hump heights at station entrances can help reduce the impact of urban flooding. In addition, expanding the station concourse area can facilitate water dispersion, thereby lowering the risk of severe flooding loss. As these metro stations typically have high passenger volumes, non-structural measures are also crucial. These stations should actively conduct emergency flood drills, plan evacuation routes in advance, arrange emergency rescue deployments, and develop scientifically sound contingency plans to ensure timely and effective response and evacuation in the event of a flood.

Metro stations with weak defense level are mainly located in the central area, primarily due to high urban development density and low surface water coverage. For these stations, targeted structural measures can be implemented within the station premises, such as installing dedicated dewatering pump stations or establishing storage and drainage facilities to enhance flood resilience.

### 4.4. Discussion

In this study, the entropy weight method was employed to determine the weights of the selected indicators, thereby avoiding the influence of subjective judgments regarding their relative importance. However, it is important to emphasize that the results obtained reflect only a form of *relative risk*, and may still differ from the actual *absolute risk*. In other engineering fields, risk is often defined in probabilistic terms. However, applying such definitions to flood risk assessment remains particularly challenging.

Although rainfall frequency analysis enables probabilistic estimation of rainfall intensity, many uncertainties still exist in the process of translating rainfall into urban flooding. First, the spatial distribution of rainfall is highly complex. While techniques such as stochastic storm transposition are developing rapidly [13], their application in urban flood management remains limited due to the spatial scale of urban areas [14]. Second, for underground spaces, it is particularly difficult to accurately predict the depth of water accumulation at station entrances during heavy rainfall events. Although hydrological and hydrodynamic models have seen significant advancements, the assumptions made within these models can result in discrepancies between simulation outputs and actual conditions, thus limiting their direct applicability to flood mitigation practices [15].

Given the difficulty in precisely identifying hazard levels and the high cost of altering exposure or vulnerability level, China's flood mitigation practices have increasingly focused on improving defense level [16]. For example, even when water accumulation exceeds the height of entrance humps, authorities may artificially increase water-blocking measures or close stations based on advance warnings, effectively preventing water ingress. Although such emergency measures are difficult to quantify in flood risk assessments, they play a crucial role in disaster prevention and control.

Moreover, flood resilience in underground spaces often relies heavily on the overall urban flood management system. Within this context, our findings gain greater significance. This study identifies the specific vulnerabilities of different regions to flood disasters, providing valuable insights for targeted resource allocation and enhancing the overall flood resilience of the metro system.

## 5. CONCLUSION

This study focuses on metro stations located within the outer-ring road of Shanghai and develops a flood risk assessment framework for the Shanghai metro system using an indicator-based approach. The main conclusions are as follows:

(1) Eight indicators were selected from four dimensions: hazard, exposure, vulnerability, and defense. The entropy weight method was used to determine the weights of each indicator. In terms of hazard, rainfall frequency has a slightly greater influence on metro flood risk than rainfall intensity. For exposure, terrain slope plays a more significant role than relative elevation. Regarding vulnerability, passenger volume has a major impact on flood risk. Among the eight indicators, their relative influence on metro flood risk in descending order is: passenger volume, terrain slope, drainage distance, rainfall frequency, rainfall intensity, stair height, number of entrances, and relative elevation.

(2) Based on the established indicator system, flood risk and its spatial distribution were assessed for metro stations within the outer-ring road. The spatial patterns of hazard, exposure, vulnerability, and defense were analyzed, and metro stations were classified into four flood risk categories: very high, high, medium, and low, based on the integrated risk values. Hazard levels tend to decrease from the northeast to the southwest of the study area. Exposure is generally low, but scattered areas with higher exposure exist in flat city-center zones. Vulnerability is higher in the southwestern and southeastern corners, primarily due to high passenger volumes. Defense is generally strong, but metro stations in Huangpu, Xuhui, and Changning Districts face greater flood drainage pressure. The very high- and high-risk metro stations are mainly located in the central and northeastern parts of the study area, while low-risk stations are mostly found in the southwestern region.

(3) Based on the results of flood risk assessment and zoning, targeted flood mitigation and drainage measures are proposed to enhance the resilience of Shanghai's metro system. For very high- and high-risk areas, priority should be given to strengthening entrance protection facilities, upgrading pumping capacity, and developing emergency passenger evacuation plans. For medium-risk areas, optimizing drainage systems, improving the layout of discharge channels, and ensuring regular maintenance are recommended. For low-risk areas, maintaining the current level of protection while reinforcing routine inspection and early warning systems would be appropriate. The implementation of such differentiated strategies can effectively improve the overall flood prevention and resilience of the metro system.

## 6. ACKNOWLEDGMENTS

This study was supported by the National Natural Science Foundation of China (Grant Nos. 42271031 and 42371030). The authors sincerely appreciate the assistance from Runyao Lin (College of Environmental Science and Engineering, Tongji University), Congju Liu (College of Civil Engineering, Tongji University), and Zhi Li (College of Civil Engineering, Tongji University), for their contributions to data collection from Baidu Maps. The authors sincerely appreciate the valuable feedback provided by the reviewers, whose insightful comments have significantly contributed to enhancing the quality of this paper.

## 7. REFERENCES

- [1] Strategic Consulting Center of Chinese Academy of Engineering, Chinese Society for Rock Mechanics and Engineering (Sub-society for Underground Space), & China Association of City Planning (Sub-association for Underground Space Planning). (2024). Blue book on urban underground space development in China 2024 (in Chinese). Proceedings of the 7th International Academic Conference on Underground Space, Shenzhen, China. <https://www.planning.org.cn/uploads/ueditor/php/upload/file/20241205/1733379580688450.pdf>
- [2] Bi, W., Schooling, J., & Macaskill, K. (2024). Assessing flood resilience of urban rail transit systems: Complex network modelling and stress testing in a case study of London. *Transportation Research Part D: Transport and Environment*, 134, 104263. <https://doi.org/10.1016/j.trd.2024.104263>
- [3] Rodda, H. J. E. (2006). The development and application of a flood risk model for the Czech Republic. *Natural Hazards*, 36(1–2), 207–220. <https://doi.org/10.1007/s11069-004-4549-4>

- [4] Liu, S., Zheng, W., Zhou, Z., Zhong, G., Zhen, Y., & Shi, Z. (2022). Flood risk assessment of buildings based on vulnerability curve: A case study in Anji County. *Water*, 14(21), 3572. <https://doi.org/10.3390/w14213572>
- [5] Shin, E., Kim, H., Rhee, D. S., Eom, T., & Song, C. G. (2021). Spatiotemporal flood risk assessment of underground space considering flood intensity and escape route. *Natural Hazards*, 109(2), 1539–1555. <https://doi.org/10.1007/s11069-021-04888-2>
- [6] Lyu, H., Shen, S., Yang, J., & Yin, Z. (2019). Inundation analysis of metro systems with the storm water management model incorporated into a geographical information system: A case study in Shanghai. *Hydrology and Earth System Sciences*, 23(10), 4293–4307. <https://doi.org/10.5194/hess-23-4293-2019>
- [7] Lyu, H., Sun, W., Shen, S., & Arulrajah, A. (2018). Flood risk assessment in metro systems of mega-cities using a GIS-based modeling approach. *Science of the Total Environment*, 626, 1012–1025. <https://doi.org/10.1016/j.scitotenv.2018.01.138>
- [8] Wang, G., Liu, Y., Hu, Z., Zhang, G., Liu, J., Lyu, Y., Gu, Y., Huang, X., Zhang, Q., & Liu, L. (2021). Flood risk assessment of subway systems in metropolitan areas under land subsidence scenario: A case study of Beijing. *Remote Sensing*, 13(4), 637. <https://doi.org/10.3390/rs13040637>
- [9] Yuan, X., Wu, M., Tian, F., Wang, X., & Wang, R. (2024). Identification of influencing factors and risk assessment of underground space flooding in the mountain city. *International Journal of Disaster Risk Reduction*, 113, 104807. <https://doi.org/10.1016/j.ijdrr.2024.104807>
- [10] Zhen, Y., Liu, S., Zhong, G., Zhou, Z., Liang, J., Zheng, W., & Fang, Q. (2022). Risk assessment of flash flood to buildings using an indicator-based methodology: A case study of mountainous rural settlements in southwest China. *Frontiers in Environmental Science*, 10, 931029. <https://doi.org/10.3389/fenvs.2022.931029>
- [11] Hosking, J. R. M., & Wallis, J. R. (1997). *Regional frequency analysis: An approach based on L-moments*. Cambridge University Press. <https://doi.org/10.1017/CBO9780511529443>
- [12] Liu, H., Li, Z., & He, Q. (2023). Suitability assessment of multilayer urban underground space based on entropy and CRITIC combined weighting method: A case study in Xiong'an New Area, China. *Applied Sciences*, 13(18), 10231. <https://doi.org/10.3390/app131810231>
- [13] Smith, J. A., Baeck, M. L., Villarini, G., Welty, C., Miller, A. J., & Krajewski, W. F. (2015). Analyses of a long-term, high-resolution radar rainfall data set for the Baltimore metropolitan region. *Water Resources Research*, 48, W04504. <https://doi.org/10.1029/2011WR010641>
- [14] Zhuang, Q., Liu, S., & Zhou, Z. (2020). Spatial heterogeneity analysis of short-duration extreme rainfall events in megacities in China. *Water*, 12(12), 3364. <https://doi.org/10.3390/w12123364>
- [15] He, R., Tiong, R. L. K., Yuan, Y., & Zhang, L. (2024). Enhancing resilience of urban underground space under floods: Current status and future directions. *Tunnelling and Underground Space Technology*, 147, 105674. <https://doi.org/10.1016/j.tust.2024.105674>
- [16] He, R., Zhang, L., & Tiong, R. L. K. (2025). Responding of metro stations to upcoming floods: To close or to protect? *Reliability Engineering & System Safety*, 256, 110683. <https://doi.org/10.1016/j.ress.2024.110683>

## UNDERGROUND SMALL MODULAR REACTORS FOR DISTRICT HEATING

Ilkka Vähäaho<sup>1</sup> and Matti Pentti<sup>2</sup>

**Abstract:** Underground space is a resource for those functions that do not need to be on the surface. From the point of sustainability there are several benefits of locating technical maintenance systems underground such as expenses are shared by several users, land is released for other construction purposes, the city's appearance and image are improved.

Electricity and heat differ from each other in terms of energy distribution. Electricity can be transmitted through extensive distribution networks over thousands of kilometres across national borders. Heat, on the other hand, is both produced and consumed in connection with the local or regional district heating network. Centralised heat production is represented by district heating, where heat is distributed to customers through hot water or steam flowing in underground pipes. Distribution networks typically cover individual cities and multiple industrial sites.

District heating is commonly used throughout Europe, with around 3 500 networks serving 60 million people. 75 % of production is covered by fossil fuels, so the need to reduce emissions is considerable. Existing large networks are located in the Nordic and Baltic countries and Eastern and Central Europe.

There are just a few Small Modular Reactor (SMR) projects in the world designed for heat production only. The Low-temperature District heating Reactor (LDR-50) technology by a Finnish technology company is based on well-known light water reactor technology. The goal is to commission the first underground plant based on small nuclear reactor technology to be connected to the district heating network in 2030. So far, several cities in Finland, Poland and Baltic countries have been investigated as possible locations for underground SMR plants.

**Keywords:** Cut and Cover, district heating, Drill and Blast, Small Modular Reactor, sustainability

### 1. INTRODUCTION

Half of the energy we consume is used for heating and cooling and most of that energy still comes from fossil fuels. Heating alone accounts for up to 12 gigatons of CO<sub>2</sub> emissions annually. Transitioning to carbon-free nuclear has enormous potential to make an enormous impact. The Finnish designed Low-temperature District heating Reactor LDR-50, with its small modular design, offers unmatched efficiency, making it ideal for dense urban environments. Each unit generates 50 MW of zero-carbon thermal power. A few units can warm an entire medium sized city, whatever the weather (Steady Energy, 2025).

The LDR-50 is small, in fact so small that, it can be built underground. No need for chimneys, mountains of coal, colossal fuel tanks, or large supporting superstructures. This invisible, yet impactful solution is the answer to urban heating headaches. No polluted air, water, or skylines - just clean, reliable warmth.

Water scarcity is a growing crisis, propelled by climate change and overconsumption. Desalination has the potential to generate theoretically unlimited fresh water but that comes at a high environmental cost due to its current reliance on fossil fuels.

Acceptability for the use of nuclear energy has increased significantly, and it is assumed that acceptability will be even higher when the plant is placed underground. There are also many other advantages of underground solutions over terrestrial alternatives. Table 1 presents some main advantages of underground solutions (Vähäaho, 2016).

---

<sup>1</sup> Alef Geo-Consulting

<sup>2</sup> Steady Energy

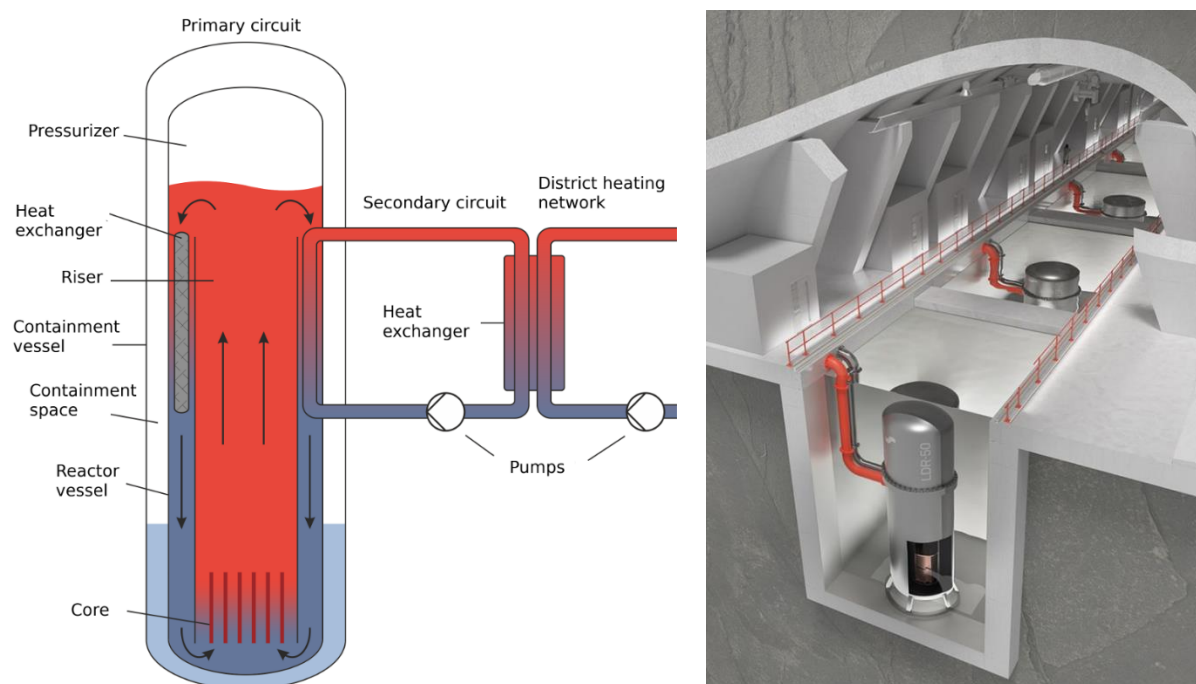
**Table 1. Advantages of underground solutions over terrestrial alternatives.**

1	Reliability of energy distribution through a looped tunnel network
2	Optimisation of energy production in the transmission network
3	Costs are shared between multiple users
4	The land is released for other construction
5	The appearance of the city is improved when technical facilities and wires are placed in tunnels and streets/plots do not need to be opened
6	Tunnel construction works have significantly fewer disadvantages
7	Quarry from tunnel construction can be utilised
8	Equipment in tunnels requires less maintenance and is easier to maintain
9	Failure of technical systems does not pose a great danger to the public
10	Tunnels are a safe option in a crisis

## 2. LOW-TEMPERATURE DISTRICT HEATING REACTOR

The Low-temperature District heating Reactor (LDR-50) is a small-scale nuclear reactor for district heating. LDR-50 operates at a temperature of less than 160 °C. The designation LDR-50 refers to a reactor with a thermal power of up to 50 MW and 300 GWh/reactor/year. There is no external cooling water circulation. Coolant circulates between the core and the main heat exchangers by natural convection. Heat is transferred to the district heating network via the secondary circuit. Spent nuclear fuel can primarily be stored at the plant for several years, at least two years, after which it is safely transferred to dedicated intermediate storage or final repository.

LDR is based on well-known light water reactor technology. Figure 1 shows LDR-50 operating principle and an illustration of an underground LDR-50 heating plant.

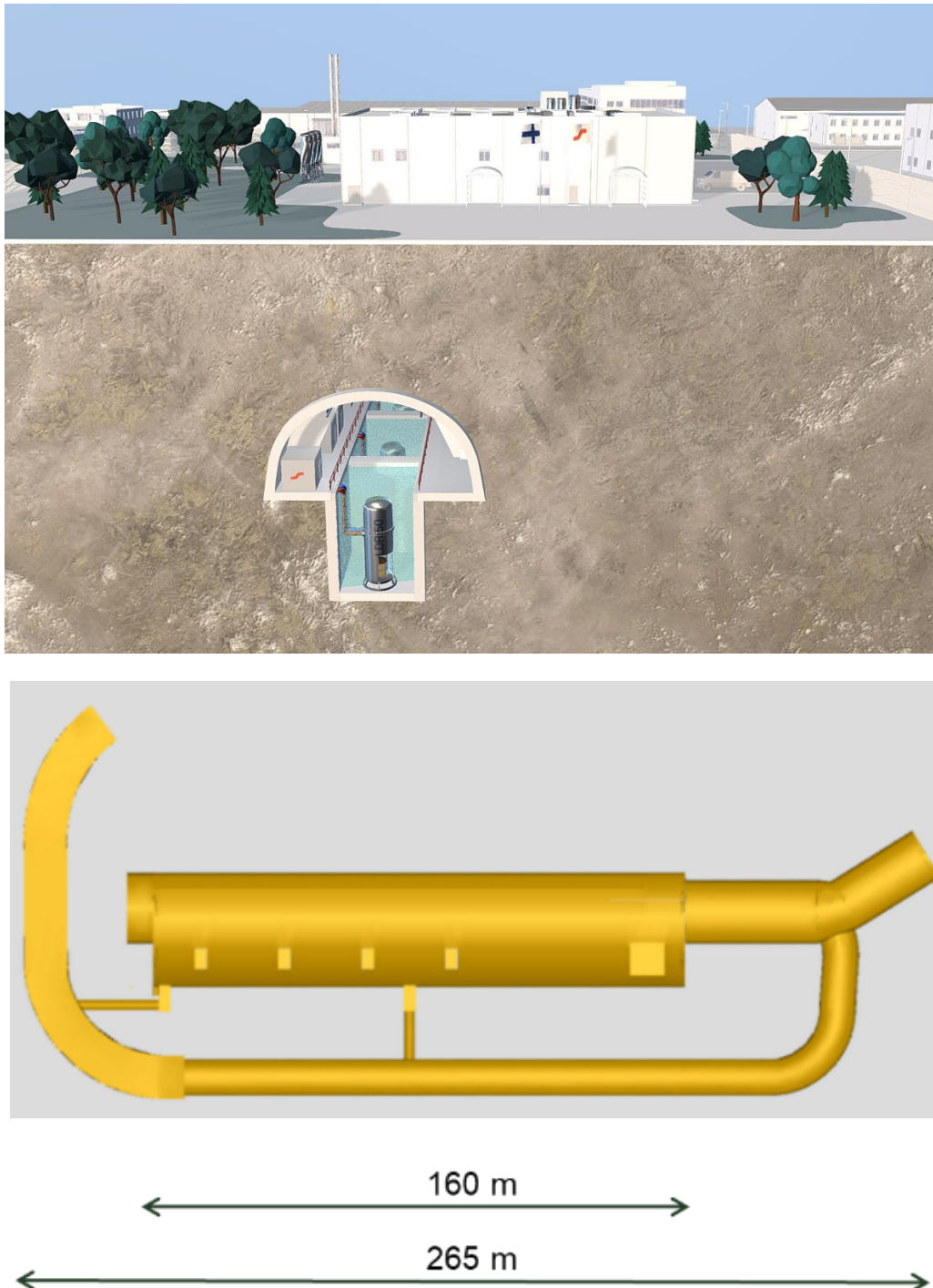


**Figure 1. LDR-50 operating principle and illustration of an underground LDR-50 heating plant.**



### 3. PRELIMINARY SKETCH OF AN UNDERGROUND FOUR-REACTOR LDR-50 HEATING PLANT

The size of the hall of the four reactors is approximately 35 metres wide, 33 metres high and 200 metres long, length depending on the number of reactors (Figure 2). The reactor vessel is about 11 metres high, i.e. about 20 metres from floor to ground.



*Figure 2. Preliminary sketch of an underground four-reactor LDR-50 plant.*

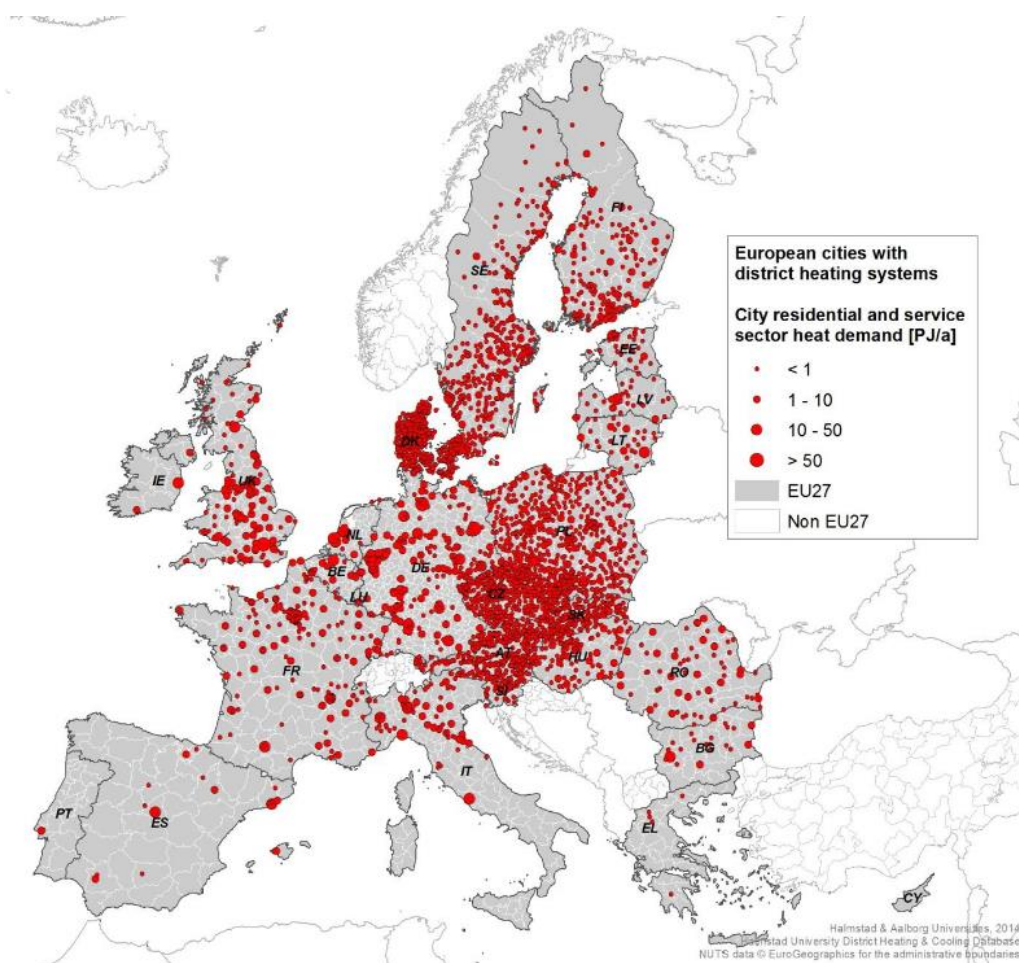
#### 4. WHO IS THIS NEW TECHNOLOGY FOR?

Heating of residential buildings and other premises consumes a lot of energy in countries with cold winter climate. In Europe, the homes of 60 million people are kept warm by 3,500 local district heating networks (VTT, 2025).

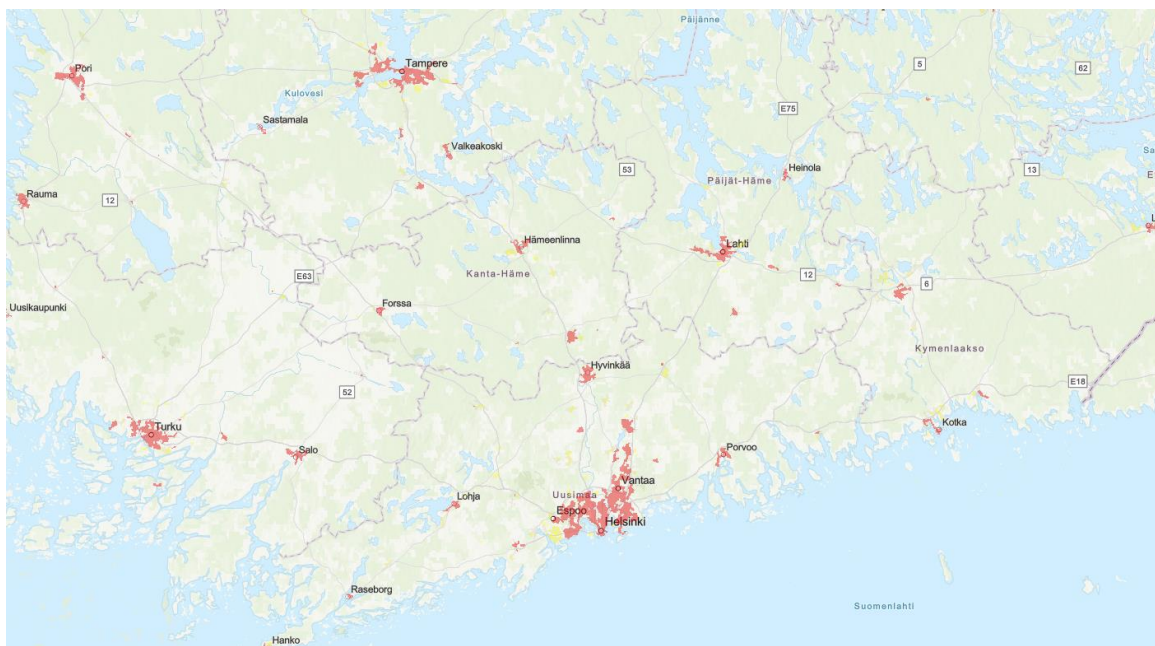
The principle of LDR technology is to provide carbon-free energy to existing energy companies. Our project has started with research and development work. The next step is to build a pilot reactor and then start operations and expand to full-scale heat production at an underground plant by 2030. In addition to Finland, locations have so far been explored in Poland and Baltic countries, Estonia as an example.

Location of existing district heating networks in EU countries can be viewed using the Halmstad University District Heating and Cooling database (Persson et al., 2012). The dataset was created by extracting all hectare grid cells from the Heat Roadmap Europe 4 heat demand density raster with values of 500 GJ/ha and above, converting this raster data subset into a polygon layer, and adding various attributes from other sources, mainly data on current district heating systems from the Halmstad University District Heating and Cooling database.

Figure 3 shows European cities with district heating systems (district heating areas by red colour). Figure 4 shows an example of locations of existing district heating networks in Southern Finland.



*Figure 3. European cities with district heating systems.*



**Figure 4.** An example of locations of existing district heating networks in Southern Finland.

## 5. PLACEMENTS OF UNDERGROUND SMALL MODULAR REACTORS IN POLAND, ESTONIA AND FINLAND

From the point of view of the placement of an underground small modular reactor (SMR) plant, the following are the starting points for each country and region:

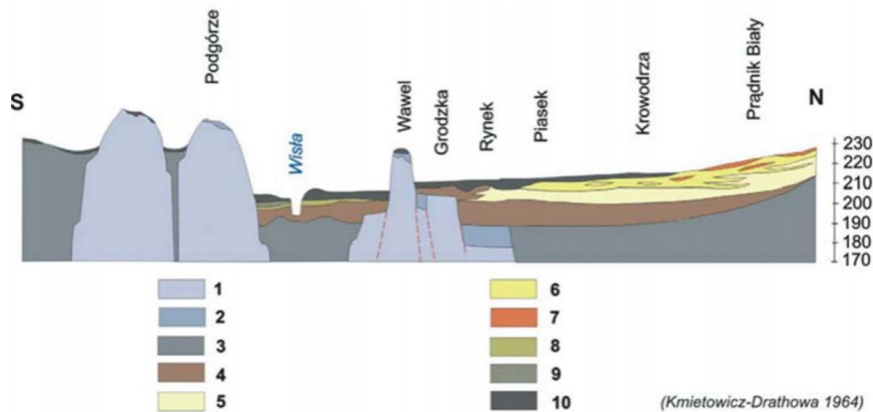
- district heating market
- legislation and regulations
- zoning situation
- earthquake risk
- geology
- groundwater
- soil contamination

Following a preliminary evaluation of the above points, an in-depth analysis of alternative locations is expected to be carried out in accordance with the IAEA (International Atomic Energy Agency) Safety standards. In the following, we will focus only on the effects of geology on the placements of underground SMR plants. The feasibility of the following methods was investigated: Drill and Blast (D&B) Method, New Austrian tunnelling Method (NATM), Tunnel Boring Method (TBM) and Cut and Cover Method.

In **Poland**, four cities were studied in terms of the feasibility of the SMR plant. The recommendation for the basic solution for underground SMR plant in all the cities studied is the Cut and Cover Method and its implementation with Diaphragm Wall Construction. This recommendation is especially meant for tentative economic analyses.

Poland is covered with deposits of different genesis: alluvial, eolian, lacustrine, glacial, fluvioglacial and sea deposits. Most of the rocks found on Poland's area are sedimentary rocks (detrital, chemical, organogenic); in southern area within mountain ranges we can find igneous and metamorphic rocks. For example, near the centre of Warsaw the thickness of quaternary deposits is more than 100 metres. Figure 5 shows an example of the geological conditions of the city of Krakow in southern Poland (Gaszyńska-Freiwald and Truty, 2024).



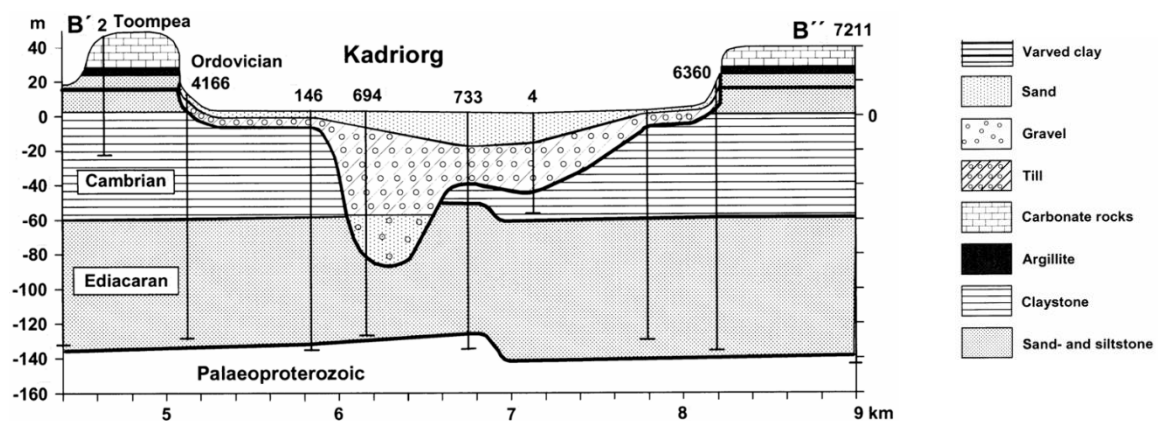


Schematic geological cross section through subsoil of Krakow: 1 – Jurassic limestones, 2 – Cretaceous marls, 3 – Miocene clays, 4 – Carpathian gravels, 5 – limestone gravels of Prądnik Stream, 6 – Pleistocene sands, 7 – less, 8 – Holocene sands, 9 – Holocene loam, 10 – anthropogenic fill

**Figure 5.** Schematical geological cross section through subsoil of Krakow in Poland.

In **Estonia**, three cities were studied in terms of the feasibility of the SMR plant. Cut and Cover method is the most suitable method for all studied cities.

Buried valleys is a speciality in Estonia. Special attention should also be paid to groundwater protection during the construction and operation phase. In terms of the construction of underground spaces and tunnels, buried valleys are the most difficult and expensive sites from a geological point of view, and their location is the most important initial information in the planning and constructing underground. Fortunately, the public register of Estonian underground data (Geological Survey of Estonia, 2025) is the best that has come across in SMR investigations so far. Figure 6 shows an example of a buried valley in Tallinn, Estonia (Vaher et al., 2012).



**Figure 6.** An example of buried valley cross section in Kadriorg branch of the Tallinn incision.

Buried valleys are ancient river or subglacial (beneath a glacier) drainage networks that are now abandoned and have become either partly or completely buried by more recent sediment. As such, buried valleys often exhibit little or no surface expression within the modern landscape. The concealed occurrence of buried valleys can have significant and often unexpected implications for groundwater and hydrocarbon or geothermal resources. Buried valleys can also be significant stores of sand and gravel mineral resources, which can act as traps for contaminants as well as pathways into groundwater aquifers (British Geological Survey, 2025).

In **Finland**, five cities, in a total of 10 different locations, were studied in terms of the feasibility of the SMR plant. In all cases, placement has been sought in hard pre-Cambrian bedrock. In Finland, a self-supporting rock space is an inexpensive alternative by far. The construction method is invariably D&B method.

Helsinki is a forerunner in the utilisation of underground space both in Finland and internationally. Helsinki makes use of the underground opportunities in a variety of ways. As far as is known, Helsinki has the world's only underground master plan that covers the entire city. The underground master plan is the city's strategic land use

plan, which reserves underground spaces for the city's vital functions and traffic in the long term. The underground master plan supports and enables the densification of the urban structure and a pleasant environment above ground. In Helsinki, there is a practice according to which the property above cannot restrict the use of the underground space if it does not cause any harm and the property above does not lose anything. For decades, the City of Helsinki's practice has been that the right of use of an above-ground property extends six metres from the lowest corner point of the plot, even if the right of ownership extends to the centre of the Earth. Helsinki's underground master plan 2021 includes several sites that have already been zoned for underground operations.

Helsinki's landscape is quite flat – the highest natural point is only 60 metres above sea level. One third of Helsinki's ground is clay with an average thickness of three metres and shear strength of around 10 kPa. The average depth of soil material upon bedrock is seven metres but varies from 0 to almost 70 metres. The bedrock quality in Finland is, for the most part, ideal for tunnelling and building underground spaces since the bedrock mainly consists of old pre-Cambrian rocks and there are only a few places where younger sedimentary rocks exist. There are no sedimentary rocks in the Helsinki area; however, there are several fracture zones formed by rock block movements that cross the bedrock in the city centre. It is important to identify the locations and properties of these zones in the planning and excavation of rock constructions. In the early stages of the Svecofennian Orogeny, rock deformations were ductile; later, the rock cooled down and the deformations at the topmost layers became brittle and formed faulted structures. The fault zones were subsequently fractured by weathering, hydrothermal alterations, recrystallisation and later movements. Being more fragmented than surrounding areas, the fractured zones have eroded more rapidly and are seen as depressions in the topography. The fractured zones have had a great impact in defining the shoreline of Helsinki's city centre. The fractured zones are usually under a thick layer of soil and therefore hard to examine. However, there are signs of movements on nearby rock surfaces which help to locate those zones (Vänskä and Raudasmaa, 2005).

Figure 7 gives an example of the public Map Service of the City of Helsinki with information on bedrock, soil and bedrock surveys and fracture zones of bedrock (Helsinki Map Service).



**Figure 7.** An example of the public Map Service of the City of Helsinki with information on bedrock, soil and bedrock surveys and fracture zones of bedrock.



## 6. CONCLUSIONS

Heating of residential buildings and other premises consumes a lot of energy in countries with cold winter climate. In Europe, the homes of 60 million people are kept warm by 3,500 local district heating networks.

Acceptability for the use of nuclear energy has increased significantly, and it is assumed that acceptability will be higher when the plant is placed underground. There are also many other advantages of underground solutions over terrestrial alternatives.

In this research only the effects of geology on the placement of an underground SMR plant have been studied, though the main arguments are district heating market, local legislation and regulations and zoning situation. The feasibility of the following methods was investigated: Drill and Blast (D&B) Method, New Austrian tunnelling Method (NATM), Tunnel Boring Method (TBM) and Cut and Cover Method.

Placements of underground small modular reactors have been studied so far in Poland, Estonia and Finland. Total number of studied cities is 12.

Poland is covered with deposits of different genesis: alluvial, eolian, lacustrine, glacial, fluvioglacial and sea deposits. Most of the rocks found on Poland's area are sedimentary rocks; in southern area within mountain ranges we can find igneous and metamorphic rocks. For example, near the centre of Warsaw the thickness of quaternary deposits is more than 100 metres. In Poland the basic recommendation for underground SMR plants is the Cut and Cover Method and its implementation with Diaphragm Wall Construction.

Buried valleys is speciality in Estonia. In terms of the construction of underground spaces and tunnels, buried valleys are the most difficult and expensive sites from a geological point of view, and their location is the most important initial information in the planning and constructing underground. Fortunately, the public register of Estonian underground data is the best that has come across in SMR investigations so far. Cut and Cover method is the most suitable method for all studied cities in Estonia.

Helsinki is a forerunner in the utilisation of underground space both in Finland and internationally. Helsinki makes use of the underground opportunities in a variety of ways. Underground space is a resource for those functions that do not need to be on the surface. The underground master plan is the city's strategic land use plan, which reserves underground spaces for the city's vital functions in the long term. In Finland, five cities in a total of 10 different locations, were studied in terms of the feasibility of the SMR plant. In all cases, placement has been sought in hard pre-Cambrian bedrock. In Finland, a self-supporting rock space is an inexpensive alternative by far. The construction method is invariably D&B method.

## 7. BIBLIOGRAPHY

- [1] Steady Energy, (2025). <https://www.steadyenergy.com/solution>
- [2] Vähäaho, I. (2016). Development for urban underground space in Helsinki, Energy Procedia 96 (2016) 824–832, SBE16 Tallinn and Helsinki Conference; Build Green and Renovate Deep, 5–7 October, 2016.
- [3] VTT Technical Research Centre of Finland (2025).
- [4] Persson, U., Nilsson, D., Möller, B., Werner, S., (2012), Halmstad University Mapping Local European Heat Resources - a Spatial Approach to Identify Favourable Synergy Regions for District Heating, 13th International Symposium on District Heating and Cooling, Copenhagen 3-4 September, 2012.
- [5] Gaszyńska-Freiwald, G. and Truty, A. (2024), Discussion with the Polish Geotechnical Society, 7 November, 2024.
- [6] Geological Survey of Estonia, (2025), <https://xgis.maaamet.ee/xgis2/page/link/pXS1JSP5>
- [7] Vaher, R., Miidel, A., Raukas, A., Tavast, E., (2010). Ancient buried valleys in the city of Tallinn and adjacent area; pp. 37–48, doi: 10.3176/earth.2010.1.03
- [8] British Geological Survey, 2025.
- [9] Vänskä, P. and Raudasmaa, P. (2005). Helsingin keskustan kallioruhjeet (Fracture zones in the bedrock of Helsinki City Centre), City of Helsinki, Real Estate Department, Geotechnical Division, Publication 89, (in Finnish with English abstract).
- [10] Helsinki Map Service, <https://kartta.hel.fi/>

## THE ROLE OF UNDERGROUND MINES IN ENERGY TRANSITION: A REVIEW

Dimitris Kaliampakos<sup>1</sup>, Athanassios Mavrikos<sup>2</sup>

**Abstract:** Driven by global population growth, demand for energy is constantly rising. The dependence on fossil fuels as energy sources results in ever growing CO<sub>2</sub> emissions, which in turn contributes to climate change. The transition from fossil fuel dependency towards a sustainable, low-carbon energy system is considered as a necessity for the future. A shift to renewable energy sources is associated with several problems due to their stochastic production nature that poses significant challenges for grid reliability and energy security. A solution to this end would be to be able to store excess energy from renewable sources so that it can be available when needed. The main technologies that have been proposed are underground hydrogen storage, pumped hydro storage, compressed air energy storage and gravitational energy storage. Furthermore, nuclear energy has recently come to the foreground due to its zero carbon emissions and contribution to grid stability. A common factor among all the proposed approaches is the use of underground space, underground mines in particular, and the inherent geological and structural characteristics of underground environments. Underground mines offer considerable advantages to this end and the utilization and repurpose of abandoned underground mines presents a significant opportunity. The paper discusses the factors contributing to the need for energy transition and the main obstacles that hinder the wider use of renewable energy sources. Furthermore, the advantages of underground mines and underground space in general are analyzed. The most promising storage technologies are presented through notable cases and reviewed.

**Keywords:** energy transition, climate change, underground space

### 1. INTRODUCTION

World demographics are driving up the demand for electricity, as expanding urbanization, industrial activity, and improvements in living standards require greater energy consumption (Chaurasia, 2020; Ali et al., 2025; Yakymchuk et al., 2025). World energy production continues to rely on the combustion of fossil fuels as a primary source of electricity generation. However, fossil fuels consumption increases carbon emissions thus significantly contributing to global warming, extreme weather events, sea-level rise, and biodiversity loss (World Weather Attribution, 2024). A number of scientific reports, including assessments by the Intergovernmental Panel on Climate Change (IPCC), stress the necessity of halving global emissions by 2030 to avert catastrophic climate impacts (IPCC, 2023). The environmental implications of this dynamic underline a pressing need for a comprehensive energy transition. Shifting towards renewable energy sources such as solar, wind, and hydropower is essential not only to mitigate carbon emissions but also to ensure sustainable and resilient energy systems capable of meeting future demands without further environmental deterioration (Liu and Han, 2024). Without rapid decarbonization of the energy sector, the world is on track to exceed the 1.5°C warming threshold outlined in the Paris Agreement, risking irreversible environmental and societal damage (UNEP, 2023; Foster et al., 2024; Islam and Kieu, 2021).

Despite their critical role in achieving a low-carbon future, renewable energy technologies present several limitations and challenges. Among them, the primary concern is their inherent intermittency. Solar and wind energy production is stochastic and depends on weather conditions that are variable by nature. This results in fluctuations in energy supply, quite the opposite needed for a stable electrical grid. Seemingly, the only efficient

<sup>1</sup>Professor, Kaliampakos Dimitris, Mining Engineer Ph.D., National Technical University of Athens, School of Mining and Metallurgical Engineering, 9 Iroon Polytechniou Str., GR15772, Zografou, Athens, Greece, dkal@central.ntua.gr

<sup>2</sup>Mavrikos Athanassios, Mining Engineer Ph.D., National Technical University of Athens, School of Mining and Metallurgical Engineering, 9 Iroon Polytechniou Str., GR15772, Zografou, Athens, Greece, mavrikos@metal.ntua.gr

way to integrate large-scale deployment of renewable energy systems is by having adequate storage capacity. Currently, many research efforts focus on energy storage technologies such as hydrogen storage, pumped hydro, compressed air and gravitational systems (Molina et al, 2025; Qin et al., 2025; Liu et al., 2025; Li and Deussen, 2025). Furthermore, nuclear energy is also considered as a key enabler due to its zero carbon emissions and ability to act as a baseload supplier in electrical grids (Wang et al., 2023; Imran et al, 2024; Fattahi et al., 2022). Underground space and in particular underground mines offer significant opportunities in this direction. As the demand for large-scale, efficient, and sustainable energy storage grows, the reutilization of underground mines presents many advantages. The geological and structural characteristics of underground space, result in reduced surface land use, the insulation properties of the surround rock mass provide thermal stability and the availability of mine infrastructure can contribute to the success of the solution. As a result, the adaptation of these storage technologies to the underground environment is increasingly studied. Moreover, underground mines can address a critical disadvantage of nuclear energy production, the disposal of nuclear waste. Underground nuclear repositories in former mines have been in operation for many years and are considered the safest option.

The paper analyzes the main storage technologies in the context of reutilization of underground mines. Through the presentation of prominent cases, the paper reviews the advantages, opportunities and challenges of each technology and draws conclusions for the future emphasizing the role of underground space as a key enabler of energy transition.

## 2. THE UTILIZATION OF UNDERGROUND MINES IN ENERGY TRANSITION

Currently energy storage relies mainly on pumped hydro storage, which accounts for approximately 90% of the total capacity and on battery energy storage systems (IEA, 2024; REN21, 2024). However, battery storage systems are expected to grow significantly in the near future representing around 85-90% of new grid scale battery storage capacity (IEA, 2024; REN21, 2024). Energy storage systems are an essential factor in the process of energy transition and underground energy storage presents significant advantages:

- Storage capacity: underground formations offer vast void volumes, enabling energy storage at very large scales.
- Flexibility in terms of duration: underground energy storage can supply energy for days up to seasons, balancing out variations between renewable energy generation and demand.
- High thermal inertia and constant temperatures: the intrinsic insulation properties of the underground space, minimize heat losses and improve round-trip efficiency.
- Reduced surface footprint and environmental impact: by moving energy storage facilities in the underground space surface land is preserved, there is minimal visual impact and the ecosystem is not affected.
- Can accommodate a variety of technologies: underground space can support a range of storage types, like thermal storage, compressed air, gases (natural gas, hydrogen) and even pumped hydro storage.

The utilization of underground mines and underground spaces for energy storage has various strategic advantages with regards to the goals of energy transition (Cornaro and Kompatscher, 2024). One obvious advantage is the availability of existing infrastructure. Abandoned or closed underground mines have extensive tunnel and shafts networks that can be reused and serve other purposes. Around the world there is a large number of inactive underground mines that can be repurposed to meet the needs of energy storage. Underground mines are particularly well-suited for high-capacity storage technologies such as hydrogen storage, pumped hydro storage, compressed air energy storage, and gravitational systems, which require large, stable volumes to operate efficiently.

The range of storage technologies presents different advantages and trade-offs, that make each technology suitable for different roles in the process of energy transition (Fig. 1).

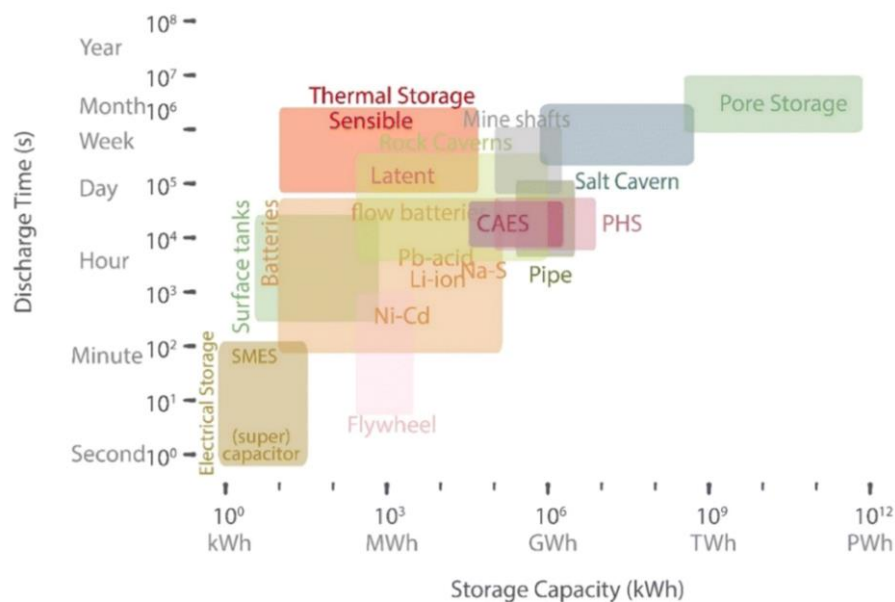
Underground hydrogen storage achieves an efficiency in the range of 30–40%. The main concept of this technology is that hydrogen that is produced by excess energy from renewable sources is stored in mined caverns in salt domes. It is considered appropriate for long-duration and seasonal storage at far larger scale than other technologies. Therefore, it is important for balancing renewable energy over weeks or months. Hydrogen storage can also be integrated in many sectors, such as industry, transportation and heating contributing to the decarbonization targets. However, its main disadvantages are the high capital costs and complex safety and infrastructure requirements (Sambo et al., 2022; Tackie-Otto and Haq, 2024; Ali et al., 2025).

Pumped hydro storage is probably the most mature technology, having been used in surface water reservoirs and hydroelectric power plants for over a century. It requires two reservoirs, an upper and a lower one with an adequate elevation difference and reaches an efficiency of 75-85%. Underground mines have inherent elevation differences that facilitate the deployment of this technology (Xi et al., 2022; Colas et al., 2023; Menendez et al., 2019).

Compressed air energy storage systems utilize underground salt caverns to store pressurized air. Then according to demand, the pressurized air is used to drive generators. The process offers efficiency up to 70% and has relatively rapid deployment times and reduced environmental impact compared to surface-based infrastructure. These systems are especially well-suited for medium-duration applications between 4 and 12 hours (Zhou et al, 2025; Cornaro and Kompatscher, 2024; Bu et al, 2024; Schmidt et al., 2024).

Gravitational energy storage systems capture excess electricity by lifting a heavy mass to store energy as gravitational potential. When energy is needed, the mass is lowered in a controlled manner to drive generators or mechanical linkages that convert the potential energy back into electrical power. The average efficiency of this technology is around 75-85%, depending on friction and mechanical losses. Gravitational energy storage systems have lifespans of over 40 years and low environmental impact. They can be installed in a modular design utilizing existing mine shafts to provide fast-response, long-duration storage with low capital costs and small surface footprint (Hunt et al., 2023; Kulpa et al., 2021; Wang et al., 2025).

Nuclear power plants can supply electricity reliably with zero-carbon emissions. Therefore, as a baseload supplier they strengthen grid resilience and stability and address solar and wind variability. Nuclear power plants require high capital costs, but their main disadvantage is related to the safe disposal of spent nuclear fuel. Underground repositories are generally regarded as the safest long-term solution for radioactive waste. By having engineered barriers coupled with selected properties of the surrounding host rock the isolation of nuclear waste from the biosphere is ensured (Dong et al., 2025; Mauke and Herbert, 2015; Chapman and Hooper, 2012).



**Figure 1.** Storage capacity and discharge time comparison of various energy storage technologies (source: Ali et al., 2025)

### 3. REVIEW OF SELECTED CASES

Among the various underground energy storage technologies being considered only two have a Technology Readiness Level high enough to be regarded as mature and proven in large scale, namely underground hydrogen storage (especially in salt domes) and compressed air energy storage. The other technologies are in a less mature state with laboratory or pilot plant studies being conducted but further research, investments and efforts are required to scale up and prove their competitiveness.

Notable examples of underground hydrogen storage include the Clemens hydrogen storage site, created in 1983 in a salt dome at a depth of 900 m in Texas, USA. The storage volume is in the order of 580,000 m<sup>3</sup>. Furthermore, in the UK, at Teesside, the facility was built in 1972 at a depth of 350 m. Hydrogen is stored in three caverns with each cavern having a storage volume approximately 70,000 m<sup>3</sup> (Matos et al., 2019).

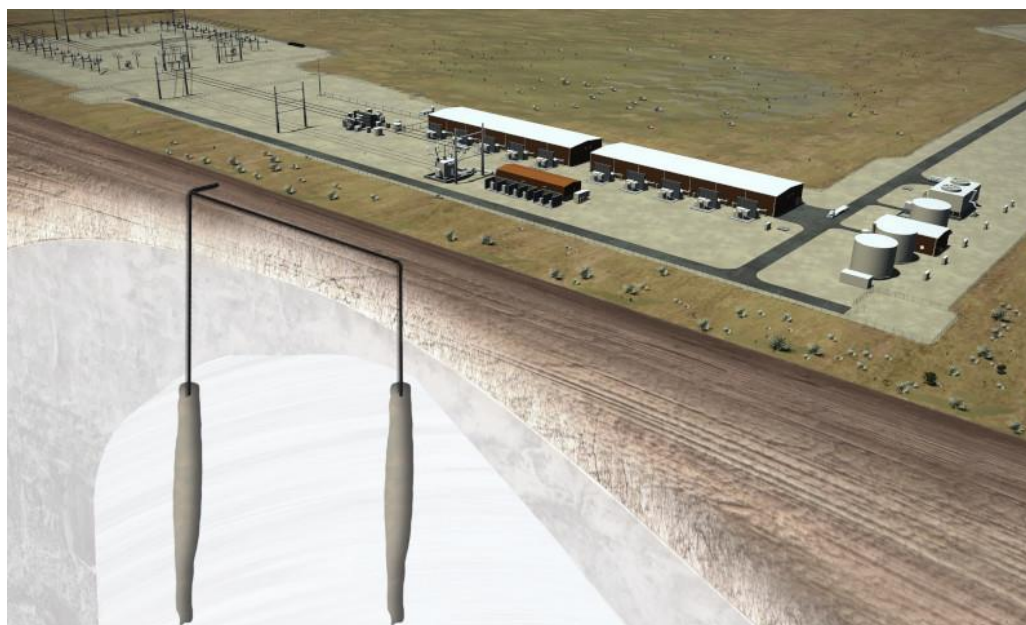
Regarding compressed air energy storage, there are two CAES facilities in operation: the Huntorf plant in Germany and the McIntosh plant in USA (Matos et al., 2019). The former was commissioned in 1978 in two salt caverns having a total volume of 310,000 m<sup>3</sup>, its power capacity is 290 MW having a 2-3-hour discharge period. Recently, its main purpose is to contribute to balancing the quickly growing energy production from wind farms in Northern Germany. The McIntosh CAES facility has been in operation since 1991 in Alabama, USA. It has a

power capacity of 110 MW and a discharge period of about 26 hours. Hydrogen is stored in a 560,000 m<sup>3</sup> salt cavern (Matos et al., 2019).

Despite the differences in maturity level, deployment scale or technological developments among underground energy storage alternatives, there is a growing body of literature covering many aspects of these energy storage technologies. We have selected characteristic examples for each technology to showcase how each of them contributes to energy transition and sustainability goals.

### 3.1. Advanced Clean Energy Storage (ACES) Delta project, Utah, USA

The Advanced Clean Energy Storage (ACES) Delta project, in Utah, USA aims to support the decarbonization of the Western U.S. power grid by storing green hydrogen produced via electrolysis using excess renewable energy, particularly solar and wind (Fig. 2). According to the design, two underground salt caverns, each having a capacity of approximately 5,500 tons of hydrogen, will be constructed in salt domes using the solution mining technique. Their combined capacity is equivalent to 300GWh. The stored hydrogen will be used to fuel the adjacent Intermountain Power Project (IPP), which is undergoing a transition from coal to a combined-cycle gas turbine system designed to operate initially on a 30% hydrogen blend, with plans to increase to 100% hydrogen by 2045. The project has received significant financial support, including a \$504 million loan guarantee from the U.S. Department of Energy, which serves as a strong indicator that government officials consider hydrogen to be a key parameter for energy transition (<https://aces-delta.com/> 24.06.2025).



**Figure 2.** Representation of the ACES Delta project in Utah, USA (source: <https://aces-delta.com/> 24.06.2025)

### 3.2. Compressed Air Energy Storage, Hubei Province, China

A notable example of an underground compressed air energy storage (CAES) system is the “Nengchu-1” project in Yingcheng, Hubei Province in China (Fig. 3). The facility has a power rating of 300 MW and became fully operational in early 2025. The system comprises two underground salt-caverns that are located at approximately 600 m in depth in a repurposed salt mine. The total volume of compressed air is around 700,000 m<sup>3</sup> that translates to a storage capacity of 1,500 MWh. The facility achieves conversion efficiencies nearing 70%, enabling it to store energy for up to eight hours and discharge for five hours daily, generating approximately 500 GWh per year. The project is expected to reduce 411,000 tons of CO<sub>2</sub> emissions annually, contributing significantly to the country’s green energy goals. The project was completed in two years underlining the advantages, in terms of time, logistics and economy, when CAES is deployed in repurposed salt mines (China Energy Engineering Group Co., Ltd., 2025; Li et al., 2023).

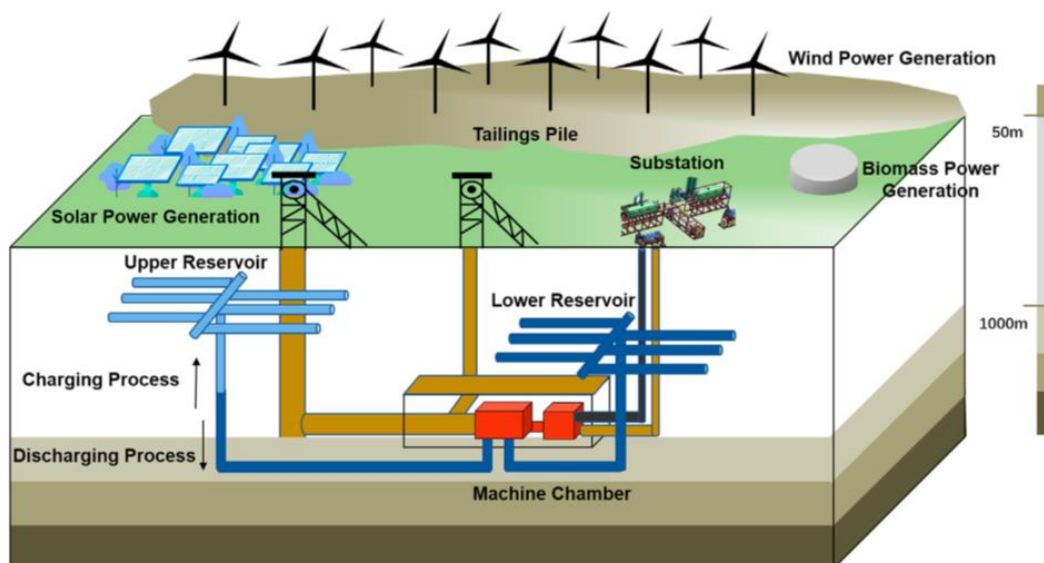




*Figure 3. Surface pressure-bearing spherical tanks at the "Nengchu-1" facilities (source: [http://en.ceec.net.cn/art/2025/1/10/art\\_138\\_2510992.html](http://en.ceec.net.cn/art/2025/1/10/art_138_2510992.html) 24/06/2025)*

### 3.3. Underground pumped hydro storage

Until now, there is no fully underground hydro pump storage facility in operation. There are some power plants that are built underground but the water reservoirs are on the surface. However, the concept has been researched in the past and is coming to the forefront again. A recent study by Xi et al. (2022) evaluates a feasibility framework for Pumped Storage Power Stations using Abandoned Mines (PSPSuM) in China's Yellow River basin, repurposing 91 disused mines to deliver a collective installed capacity of 15,830 MW (Fig. 4). Their multidisciplinary evaluation integrates spatial-structural criteria (reservoir volume, shaft stability, terrain configuration), hydro-mechanical design (optimal head, pump-turbine selection), and environmental-economic assessments, demonstrating that subterranean pumped storage can attain round-trip efficiencies of approximately 80 % while leveraging existing mine infrastructure to minimize land-use impacts. By coupling off-peak renewable generation (primarily wind and solar) with these underground reservoirs, the PSPSuM concept not only mitigates the intermittency of renewables in resource-rich regions (e.g., Inner Mongolia, Gansu, Qinghai) but also enables annual CO<sub>2</sub> reductions on the order of one million tons, aligning large-scale energy storage with ecological restoration and rural revitalization goals under China's dual carbon targets.

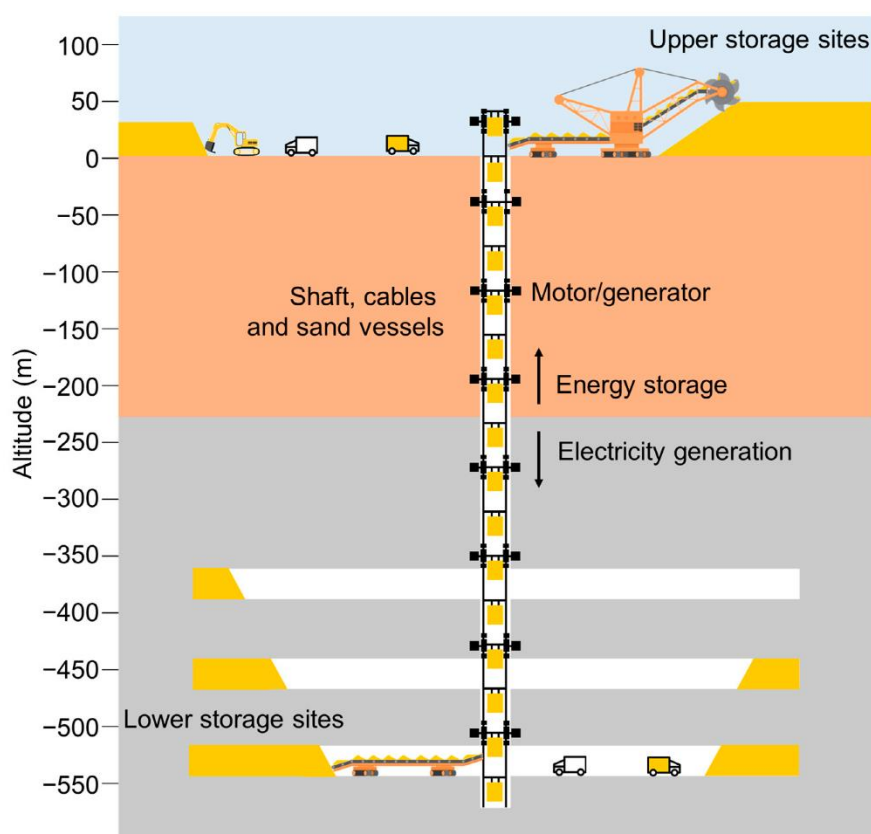


*Figure 4. The engineering concept of underground pumped hydro storage (source: Xi et al, 2022)*

### 3.4. Gravitational energy storage systems

Although currently no full-scale underground gravitational storage facility has yet been constructed, there are some pilot projects and research initiatives that have explored the feasibility and potential of underground gravitational energy storage systems utilizing mine shafts. Gravitricity, based in UK is a company that has developed the “GraviStore” system. It is an underground gravity energy storage system, which raises and lowers heavy weights to store and deliver electrical energy. Excess renewable or cheap electricity is used to lift weights, storing their potential energy until needed. Lowering the weight turns the potential energy into kinetic energy, generating electricity. The system delivers sub-second electricity on demand, with each module capable of providing up to 8MW of electric power or 32MWh of energy. It has been engineered to repurpose existing mining infrastructure, including mine shafts and mine hoists, enabling a fast deployment timeframe and low costs.

A similar concept is described in the work of Hunt et al (2023). The authors investigate Underground Gravity Energy Storage (UGES) using regenerative braking (Fig. 5). The core idea is to exploit decommissioned mine shafts as reversible gravitational reservoirs: during peak-price periods, bulk material (e.g., sand) is released down the shaft, and the descending mass drives motor–generators operating in braking mode to convert potential energy into electricity; conversely, surplus off-peak grid power reverses the machine, elevating sand back to surface storage and thus replenishing stored energy. This bidirectional electromechanical cycle leverages existing vertical shafts and electric motor/generators to achieve high round-trip efficiency, near-zero self-discharge over long durations, and scalable capacity dictated by shaft depth and mine size. Continued advancements in mechanical engineering, materials science, and grid integration will be critical for transitioning gravitational storage from conceptual demonstration to commercial viability, particularly leveraging abandoned mine shafts as strategic energy assets.



**Figure 5.** A schematic representation of the proposed Underground Gravity Energy Storage system (source: Hunt et al., 2023)

### 3.5. Nuclear waste disposal

Deep geological repositories have been used for long-term disposal of radioactive waste for many years, usually in former underground mines such as the Morsleben in Germany, the SFR facility in Sweden and the Waste Isolation Plant and Yucca Mountain in the USA. Two new, ongoing projects in this direction are the Forsmark deep geological repository for spent nuclear fuel in Sweden and the Onkalo repository in Finland.

The Forsmark project was approved by the Swedish government in 2022. The facility is designed to securely store up to 12,000 tons of high-level radioactive waste for up to 100,000 years. The underground repository will consist of 60 kilometers of tunnels excavated 500 meters beneath the surface in ancient 1.9-billion-year-old bedrock. The spent fuel will be encapsulated in corrosion-resistant copper canisters, which will then be surrounded by bentonite clay to prevent groundwater intrusion and ensure long-term containment. Construction is projected to span several decades, with the facility expected to begin accepting waste in the late 2030s and to be fully operational by around 2080. The estimated cost of the project is approximately 12 billion Swedish kronor (about \$1.08 billion) and will be funded by the nuclear industry (SKB, 2008; Johnson, 2025).

The Onkalo repository, located near the Olkiluoto Nuclear Power Plant in Eurajoki, represents the world's first permanent disposal facility for spent nuclear fuel. The facility utilizes the KBS-3 method, involving the encapsulation of spent fuel in copper canisters, which are then placed in boreholes approximately 520 meters underground within stable granite bedrock. The canisters are surrounded by bentonite clay to provide additional isolation. Construction started in 2004, with the first trial placements of empty canisters occurring in 2024. The repository is expected to begin accepting spent fuel in the mid-2020s and is projected to be sealed by the end of the 21st century. The facility is designed to accommodate approximately 6,500 tons of uranium, equating to about 3,250 canisters, and is anticipated to remain operational for approximately 100 years before being sealed permanently (Young et al., 2020; Posiva, 2024).

## 4. CONCLUSIONS

The supply of raw materials to our societies has always been linked with the mining industry. A large part of that is attributed to underground mines. Around the world there is a large number of these underground mining facilities that are not used anymore. It seems that these facilities have an opportunity to be of service to our civilization one more time. This time their primary purpose will not be the extraction of raw materials but to contribute to the transition of energy production to renewable sources. The potential of transforming underground mines for energy storage that can help balance energy production fluctuations, strengthen the resilience of electric grids and ensure stability in the system is increasingly coming into the spotlight. The utilization of the vast voids and existing infrastructure of decommissioned mines can help energy storage projects to achieve quick, cost-effective deployment while minimizing new land disturbance. Legacy mine shafts and tunnels can be repurposed and meet the modern needs of energy production worldwide. From reservoirs for pumped hydro systems, airtight caverns for compressed-air energy storage and large elevation differences for gravity-based energy storage systems, closed mines can play a key role in energy transition and decarbonization.

However, the roadmap to the full integration of underground energy storage systems in energy grids worldwide is filled with many scientific and technological challenges. There are many geological and geomechanical uncertainties when we develop the underground space for energy storage. Deep geological formations exhibit complex heterogeneity in rock type, discontinuities networks and stress fields, resulting in challenges to predict long-term stability and deformation under cyclic loading. Furthermore, the interaction between stored media (gas, brine, thermal fluids, etc.) and the surrounding rock mass can cause chemical reactions, mineral dissolution or precipitation affecting porosity and permeability. Another issue is temperature variations during charging and discharging cycles. These induce thermal stresses in rock and seal materials and thermodynamic losses that can reduce round-trip efficiency. Moreover, there are specific problems associated with gases like hydrogen and CO<sub>2</sub>. In particular, due to hydrogen's small molecular size, often there is increased diffusion and leakage risks, while CO<sub>2</sub>'s acidity can accelerate rock dissolution. In addition, another factor is microbial activity consuming hydrogen or metabolizing CO<sub>2</sub>, that affects storage volumes. Clearly underground energy storage holds considerable potential for the future of energy supply and offers key advantages to electrical grid stability, energy security and can enhance energy transition efforts. Emerging research is already focusing on addressing the challenges and critical issues that will allow the world to utilize the underground space and develop more robust and efficient energy storage systems.

## 5. BIBLIOGRAPHY

- [1] Chaurasia, A. (2020). Population effects of increase in world energy use and CO<sub>2</sub> emissions: 1990–2019. *The Journal of Population and Sustainability*, 5(1), 87–125. <https://doi.org/10.3197/jps.2020.5.1.87>
- [2] Ali, M., Isah, A., Yekeen, N., Hassanpouryouzband, A., Sarmadivaleh, M., Okoroafor, E. R., Al Kobaisi, M., Mahmoud, M., Vahrenkamp, V., & Hoteit, H. (2025). Recent progress in underground hydrogen storage. *Energy Environ. Sci.*, 18(12), 5740–5810. <https://doi.org/10.1039/D4EE04564E>
- [3] Yakymchuk, A., Maxand, S., & Lewandowska, A. (2025). Economic Analysis of Global CO<sub>2</sub> Emissions and Energy Consumption Based on the World Kaya Identity. *Energies*, 18(7), 1661. <https://doi.org/10.3390/en18071661>
- [4] World Weather Attribution 2024 (2024). When Risks Become Reality: Extreme Weather In 2024, available at: <https://www.worldweatherattribution.org/when-risks-become-reality-extreme-weather-in-2024/> (Accessed 25.06.2025)
- [5] IPCC, (2023). Climate Change 2023: Synthesis Report. Contribution of Working Groups I, II and III to the Sixth Assessment Report of the Intergovernmental Panel on Climate Change [Core Writing Team, H. Lee and J. Romero (eds.)]. IPCC, Geneva, Switzerland, pp. 35–115, doi: 10.59327/IPCC/AR6-9789291691647
- [6] Liu, H., & Han, P. (2024). Renewable energy development and carbon emissions: The role of electricity exchange. *Journal of Cleaner Production*, 439, 140807. <https://doi.org/10.1016/j.jclepro.2024.140807>
- [7] United Nations Environment Programme (2023). Emissions Gap Report 2023: Broken Record – Temperatures hit new highs, yet world fails to cut emissions (again). Nairobi. <https://doi.org/10.59117/20.500.11822/43922>
- [8] Forster, P. M., Smith, C., Walsh, T., Lamb, W. F., Lamboll, R., Cassou, C., Hauser, M., Hausfather, Z., Lee, J.-Y., Palmer, M. D., von Schuckmann, K., Slangen, A. B. A., Szopa, S., Trewin, B., Yun, J., Gillett, N. P., Jenkins, S., Matthews, H. D., Raghavan, K., Ribes, A., Rogelj, J., Rosen, D., Zhang, X., Allen, M., Aleluia Reis, L., Andrew, R. M., Betts, R. A., Borge, A., Broersma, J. A., Burgess, S. N., Cheng, L., Friedlingstein, P., Domingues, C. M., Gambarini, M., Gasser, T., Gütschow, J., Ishii, M., Kadow, C., Kennedy, J., Killick, R. E., Krummel, P. B., Liné, A., Monselesan, D. P., Morice, C., Mühle, J., Naik, V., Peters, G. P., Pirani, A., Pongratz, J., Minx, J. C., Rigby, M., Rohde, R., Savita, A., Seneviratne, S. I., Thorne, P., Wells, C., Western, L. M., van der Werf, G. R., Wijffels, S. E., Masson-Delmotte, V., and Zhai, P. (2025). Indicators of Global Climate Change 2024: annual update of key indicators of the state of the climate system and human influence, *Earth Syst. Sci. Data*, 17, 2641–2680, <https://doi.org/10.5194/essd-17-2641-2025>
- [9] Islam, Md and Kieu, E. (2021). Climate Change and Food Security in Asia Pacific: Response and Resilience. 10.1007/978-3-030-70753-8
- [10] Molina, R. A., Barros, J. J. C., López, M. del P. de la C., Coira, M. L., & Gochi, A. del C. (2025). A comparative sustainability assessment of several grid energy storage technologies. *Applied Energy*, 396, 126248. <https://doi.org/10.1016/j.apenergy.2025.126248>
- [11] Qin, Z., Ma, J., Zhu, M., & Khan, T. (2025). Advancements in energy storage technologies: Implications for sustainable energy strategy and electricity supply towards sustainable development goals. *Energy Strategy Reviews*, 59, 101710. <https://doi.org/10.1016/j.esr.2025.101710>
- [12] Liu, J., Pei, J., Wei, J., Yang, J., & Xu, H. (2025). Development status and prospect of salt cavern energy storage technology. *Earth Energy Science*, 1(2), 159–179. <https://doi.org/10.1016/j.ees.2025.01.001>
- [13] Li, Z., & Deusen, D. (2025). Role of energy storage technologies in enhancing grid stability and reducing fossil fuel dependency. *International Journal of Hydrogen Energy*, 102, 1055–1074. <https://doi.org/10.1016/j.ijhydene.2024.12.489>
- [14] Wang, Q., Guo, J., Li, R., & Jiang, X. (2023). Exploring the role of nuclear energy in the energy transition: A comparative perspective of the effects of coal, oil, natural gas, renewable energy, and nuclear power on economic growth and carbon emissions. *Environmental Research*, 221, 115290. <https://doi.org/10.1016/j.envres.2023.115290>
- [15] Imran, M., Zaman, K., Nassani, A. A., Dincă, G., Khan, H. ur R., & Haffar, M. (2024). Does nuclear energy reduce carbon emissions despite using fuels and chemicals? Transition to clean energy and finance for green solutions. *Geoscience Frontiers*, 15(4), 101608. <https://doi.org/10.1016/j.gsf.2023.101608>
- [16] Fattahi, A., Sijm, J., Broek, M. V. den, Gordón, R. M., Dieguez, M. S., & Faaij, A. (2022). Analyzing the techno-economic role of nuclear power in the Dutch net-zero energy system transition. *Advances in Applied Energy*, 7, 100103. <https://doi.org/10.1016/j.adapen.2022.100103>
- [17] International Energy Agency (IEA). (2024). Global installed energy storage capacity by scenario, 2023 and 2030.
- [18] Available at: <https://www.iea.org/data-and-statistics/charts/global-installed-energy-storage-capacity-by-scenario-2023-and-2030> (Accessed 12.09.2025)
- [19] REN21. (2024). Renewables 2024 Global Status Report. REN21 Secretariat, Paris. Available at: <https://www.ren21.net/reports/global-status-report/> (Accessed 12.09.2025)
- [20] Cornaro, A., & Kompatscher, M. (2024). Underground Space Use for Renewable Energy Production and Storage (pp. 259–265). [https://doi.org/10.1007/978-981-97-1257-1\\_33](https://doi.org/10.1007/978-981-97-1257-1_33)
- [21] Sambo, C., Dudun, A., Samuel, S. A., Esenenjor, P., Muhammed, N. S., & Haq, B. (2022). A review on worldwide underground hydrogen storage operating and potential fields. *International Journal of Hydrogen Energy*, 47(54), 22840–22880. <https://doi.org/10.1016/j.ijhydene.2022.05.126>
- [22] Tackie-Otoo, B. N., & Haq, M. B. (2024). A comprehensive review on geo-storage of H<sub>2</sub> in salt caverns: Prospect and research advances. *Fuel*, 356, 129609. <https://doi.org/10.1016/j.fuel.2023.129609>
- [23] Xi, F., Yan, R., Shi, J., Zhang, J., & Wang, R. (2022). Pumped storage power station using abandoned mine in the Yellow River basin: A feasibility analysis under the perspective of carbon neutrality. *Frontiers in Environmental Science*, Volume 10-2022. <https://doi.org/10.3389/fenvs.2022.983319>



- [24] Colas, E., Klopries, E.-M., Tian, D., Kroll, M., Selzner, M., Bruecker, C., Khaledi, K., Kukla, P., Preuße, A., Sabarny, C., Schüttrumpf, H., & Amann, F. (2023). Overview of converting abandoned coal mines to underground pumped storage systems: Focus on the underground reservoir. *Journal of Energy Storage*, 73, 109153. <https://doi.org/10.1016/j.est.2023.109153>
- [25] Menéndez, J., Schmidt, F., Konietzky, H., Fernández-Oro, J. M., Galdo, M., Loredó, J., & Díaz-Aguado, M. B. (2019). Stability analysis of the underground infrastructure for pumped storage hydropower plants in closed coal mines. *Tunnelling and Underground Space Technology*, 94, 103117. <https://doi.org/10.1016/j.tust.2019.103117>
- [26] Zhou, A., Li, P., Fan, L., Yi, Z., Tang, X., & Fei, W. (2025). Influence of drainage system on the stability of underground CAES gas storage under different lateral pressure coefficients. *Tunnelling and Underground Space Technology*, 159, 106444. <https://doi.org/10.1016/j.tust.2025.106444>
- [27] Bu, X., Huang, S., Liu, S., Yang, Y., Shu, J., Tan, X., Chen, H., & Wang, G. (2024). Efficient utilization of abandoned mines for isobaric compressed air energy storage. *Energy*, 311, 133392. <https://doi.org/10.1016/j.energy.2024.133392>
- [28] Schmidt, F., Menéndez, J., Konietzky, H., Jiang, Z., Fernández-Oro, J. M., Álvarez, L., & Bernardo-Sánchez, A. (2024). Technical feasibility of lined mining tunnels in closed coal mines as underground reservoirs of compressed air energy storage systems. *Journal of Energy Storage*, 78, 110055. <https://doi.org/10.1016/j.est.2023.110055>
- [29] Hunt, J. D., Zakeri, B., Jurasz, J., Tong, W., Dąbek, P. B., Brandão, R., Patro, E. R., Durin, B., Filho, W. L., Wada, Y., Ruijven, B. v., & Riahi, K. (2023). Underground Gravity Energy Storage: A Solution for Long-Term Energy Storage. *Energies*, 16(2), 825. <https://doi.org/10.3390/en16020825>
- [30] Kulpa, J., Kamiński, P., Stecula, K., Prostański, D., Matusiak, P., Kowol, D., Kopacz, M., & Olczak, P. (2021). Technical and Economic Aspects of Electric Energy Storage in a Mine Shaft—Budryk Case Study. *Energies*, 14(21). <https://doi.org/10.3390/en14217337>
- [31] Wang, Q., Guo, J., Li, R., & Jiang, X. (2023). Exploring the role of nuclear energy in the energy transition: A comparative perspective of the effects of coal, oil, natural gas, renewable energy, and nuclear power on economic growth and carbon emissions. *Environmental Research*, 221, 115290. <https://doi.org/10.1016/j.envres.2023.115290>
- [32] Dong, D., Wang, Z., Guan, J., & Xiao, Y. (2025). Research on safe disposal technology and progress of radioactive nuclear waste. *Nuclear Engineering and Design*, 435, 113934. <https://doi.org/10.1016/j.nucengdes.2025.113934>
- [33] Mauke, R., & Herbert, H.-J. (2015). Large scale in-situ experiments on sealing constructions in underground disposal facilities for radioactive wastes – Examples of recent BfS- and GRS-activities. *Progress in Nuclear Energy*, 84, 6–17. <https://doi.org/10.1016/j.pnucene.2015.04.010>
- [34] Chapman, N., & Hooper, A. (2012). The disposal of radioactive wastes underground. *Proceedings of the Geologists' Association*, 123(1), 46–63. <https://doi.org/10.1016/j.pgeola.2011.10.001>
- [35] Matos, C. R., Carneiro, J. F., & Silva, P. P. (2019). Overview of Large-Scale Underground Energy Storage Technologies for Integration of Renewable Energies and Criteria for Reservoir Identification. *Journal of Energy Storage*, 21, 241–258. <https://doi.org/10.1016/j.est.2018.11.023>
- [36] Advanced Clean Energy Storage (ACES) Delta project, <https://aces-delta.com/> (Accessed 24.06.2025)
- [37] China Energy Engineering Group Co., Ltd., [http://en.ceec.net.cn/art/2025/1/10/art\\_138\\_2510992.html](http://en.ceec.net.cn/art/2025/1/10/art_138_2510992.html) (Accessed 25.06.2025)
- [38] Li, H., Ma, H., Liu, J., Zhu, S., Zhao, K., Zheng, Z., Zeng, Z., & Yang, C. (2023). Large-scale CAES in bedded rock salt: A case study in Jiangsu Province, China. *Energy*, 281, 128271. <https://doi.org/10.1016/j.energy.2023.128271>
- [39] SKB, 2008. Site description of Forsmark at completion of the site investigation phase. Technical Report TR-08-05, Swedish Nuclear Fuel and Waste Management Co., Stockholm, Sweden (<https://skb.se/publication/1868223/TR-08-05.pdf> Accessed 25/06/2025)
- [40] Johnson, S., (2025, January 15). Sweden starts building 100,000 year storage site for spent nuclear fuel. Reuters. <https://www.reuters.com/business/energy/sweden-starts-building-100000-year-storage-site-spent-nuclear-fuel-2025-01-15/> (Accessed 25.06.2025)
- [41] Young, R. P., Nasser, M. H. B., & Sehzadeh, M. (2020). Mechanical and seismic anisotropy of rocks from the ONKALO underground rock characterization facility. *International Journal of Rock Mechanics and Mining Sciences*, 126, 104190. <https://doi.org/10.1016/j.ijrmms.2019.104190>
- [42] Posiva Oy, (2024). Introducing ONKALO and its principle of operation, <https://www.posiva.fi/en/index/news/pressreleasesstockexchangereleases/2024/thisisonkaloandthishowitworks.html> (Accessed 25.06.2025)



## HYDROGEOLOGICAL INVESTIGATION AND MONITORING ANALYSIS OF WATER-RELATED HAZARDS IN OPERATIONAL HIGHWAY TUNNELS IN WATER-RICH REGIONS

Yubo Luo<sup>1</sup>, Junsheng Yang<sup>2</sup>, Qi He<sup>3</sup>, Zhiheng Zhu<sup>4</sup>, Youcai Tan<sup>5</sup>

**Abstract:** Water-related hazards frequently occur in operational highway tunnels in Guangdong Province, China, posing significant risks to tunnel safety and stability. This study combines hydrogeological investigations with an analysis of 36 documented cases from six tunnels in the region. The key characteristics examined include hazard depth and location within the tunnel, surrounding rock lithology, hazard manifestations, rock mass quality, preferential seepage pathways, and surface topography, all of which were evaluated for their influence on hazard occurrence. In the Dayaoshan No. 1 Tunnel, monitoring instruments were installed to obtain six months of continuous rainfall and water pressure data, which facilitated an investigation of their correlations. The findings indicate that poor rock mass quality, intense rock weathering, concentrated heavy rainfall, runoff-converging topography, and subsurface preferential seepage pathways are critical contributors to water-related hazards in tunnels. The water pressure response to rainfall demonstrates both temporal lag and spatial variability, with a lag time of approximately 3–7 days in this case. Moreover, drainage blockages were found to sustain elevated water pressure levels. Based on the case study, the formation of tunnel water-related hazards can be generalized into three sequential stages: (1) continuous heavy rainfall induces rapid infiltration through preferential pathways; (2) drainage system failure maintains high water pressure; and (3) prolonged high water pressure ultimately leads to structural damage.

**Keywords:** water-related hazards, operational highway tunnels, rainfall–water pressure monitoring, hydrogeological investigation

### 1. INTRODUCTION

Operational highway tunnels in water-rich regions are highly susceptible to water-related hazards, particularly in areas characterized by abundant groundwater resources and karst topography. Intense rainfall often induces abrupt increases in groundwater pressure, seepage, and even sudden water inrush events (Li et al., 2015; Wang et al., 2019), posing substantial challenges to both tunnel safety and long-term maintenance (Wu et al., 2024). These risks are further aggravated during the summer rainy season, when extreme precipitation can raise groundwater pressures by several hundred kilopascals within just a few days (Li et al., 2023; Lin et al., 2019). Under such circumstances, tunnel operations may be disrupted, maintenance costs escalate sharply, and failures can result in not only severe economic losses but also major safety threats (Wang et al., 2022; Zhang et al., 2024).

Previous studies have attempted to classify water-related hazards in tunnels. For example, categorized water and mud inrush disasters into three types: karst-related, fault-related, and others (Li et al., 2018). Karst-related hazards involve dissolution fractures, caves, conduits, and underground rivers. Fault-related hazards include water-rich faults, water-conducting faults, and water-blocking faults. Other causes are associated with intrusion contacts, interlayer fractures, and differential weathering.

<sup>1</sup> PhD student, Yubo Luo, Central South University, No. 932 Lushan South Road, Changsha, China, [luo.yubo@csu.edu.cn](mailto:luo.yubo@csu.edu.cn)

<sup>2</sup> Professor, Junsheng Yang, PhD, Central South University, No. 932 Lushan South Road, Changsha, China, [jsyang@csu.edu.cn](mailto:jsyang@csu.edu.cn)

<sup>3</sup> PhD student, Qi He, Central South University, No. 932 Lushan South Road, Changsha, China, [254801041@csu.edu.cn](mailto:254801041@csu.edu.cn)

<sup>4</sup> Senior Engineer, Zhiheng Zhu, PhD, Guangdong Hualu Transportation Technology Co., Ltd., No. 399 Congyun Road, Guangzhou, China, [zzh8207@163.com](mailto:zzh8207@163.com)

<sup>5</sup> Master student, Youcai Tan, Central South University, No. 932 Lushan South Road, Changsha, China, [1623455719@qq.com](mailto:1623455719@qq.com)

During tunnel operation in karst regions, common issues such as lining cracks and water leakage are frequently observed (Fan et al., 2024). In severe cases, these can escalate into mud inrushes and collapses (Fan et al., 2018). Karst conduits and large faults near tunnel alignments often result in elevated water pressures, sediment accumulation, and large-scale inrushes (Ou et al., 2024).

The direct mechanism underlying such hazards is typically the buildup of external water pressure behind the lining exceeding its load-bearing capacity, ultimately leading to structural damage (Fan et al., 2024). Based on numerical analyses, the internal and external causes of tunnel water-related hazards are identified as the geological conditions of the tunnel zone and extreme weather conditions, respectively (Ma et al., 2022). For instance, when a tunnel intersects a water-rich fault, excavation disturbance substantially increases the probability of water-related hazards during operation (Peng et al., 2020). Lithology, adverse geological conditions, groundwater level, geomorphology, stratal inclination, lithological contacts, and fissure development have been identified as important indices for hazard risk evaluation (Wang et al., 2016). Similarly, rock solubility, geological structures, surface catchment capacity, and hydrogeological conditions have been highlighted as critical factors in the sudden occurrence of water inflows in karst tunnels (Zhao et al., 2024).

In monsoon climate zones such as Guangdong Province, China, rainfall is highly seasonal, with the majority concentrated in summer. Continuous heavy rainfall provides a substantial source of groundwater recharge (Lyu and Yin, 2023). To address the resulting risks, quantitative groundwater monitoring systems within tunnels have been established, allowing for in situ measurement of pore pressure and drainage to identify potential hydraulic instabilities (Čokorilo Ilić et al., 2019). Improved methods for sensor precision and wireless transmission in complex tunnel environments have been developed, enabling real-time monitoring of water pressure, displacement, and stress (Wang et al., 2021). The acceleration of rainfall infiltration through subsurface seepage pathways further complicates tunnel stability. In karst regions, conduit flow demonstrates both laminar and turbulent regimes. While turbulent flow dominates under high-intensity rainfall, significantly affecting the seepage field, laminar flow largely governs the drainage recession process (Chang et al., 2015). Moreover, increases in conduit diameter within certain ranges enhance the overall drainage capacity of tunnels (Gao et al., 2024).

Despite these advances, a comprehensive understanding of the mechanisms underlying water-related hazards in operational highway tunnels remains limited. The concealed nature of the subsurface environment, coupled with variability in lithology, joint development, and groundwater networks, complicates the study of subsurface seepage pathways and their contributions to hazard development (Gouy et al., 2024; Pardo-Igúzquiza et al., 2012). This challenge is especially pronounced in operational tunnels, where seepage pathways may evolve over time, extending into deeper strata.

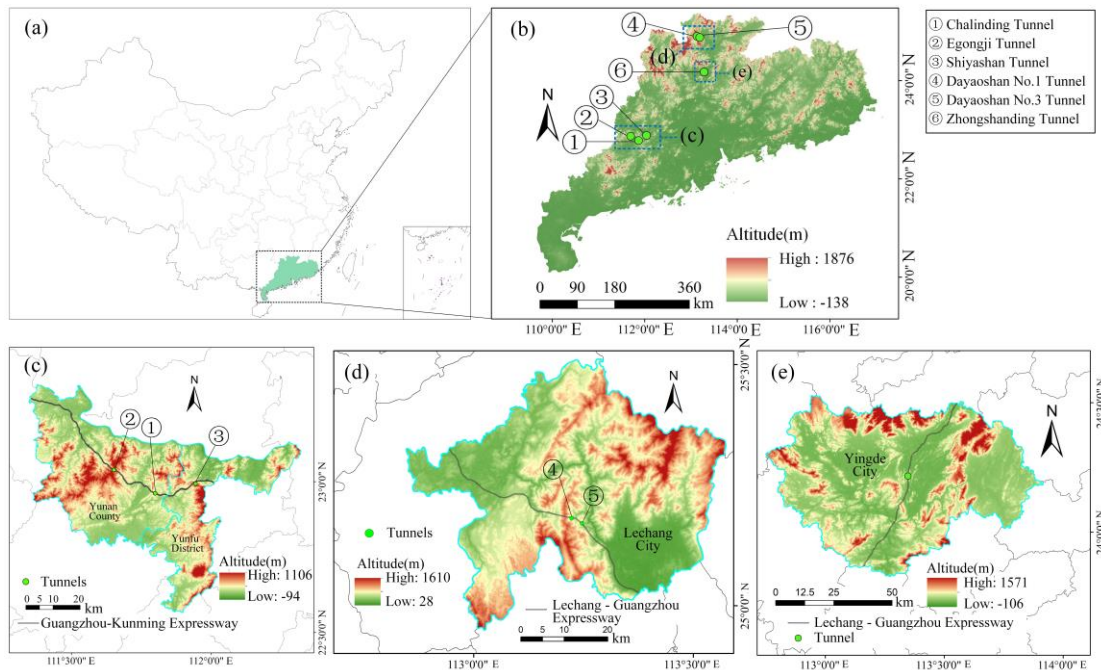
Therefore, long-term field monitoring in operational tunnels—particularly through synchronized measurements of rainfall, pore pressure, and drainage—is essential. Such monitoring not only quantifies the lag between surface precipitation and water pressure response within the tunnel, but also provides a means to assess the performance of drainage and waterproofing systems under real operational conditions.

In this study, hydrogeological investigations were carried out in six operational highway tunnels in Guangdong Province, China, and a six-month continuous monitoring program was implemented in a representative tunnel. By capturing and analyzing the rainfall–water pressure–drainage sequence, this study identifies the temporal delay in water pressure response and evaluates the risks posed by hydraulic loads during drainage system failures. Ultimately, the study aims to clarify the complete process from rainfall to hazard occurrence in operational highway tunnels and to summarize the mechanisms underlying these water-related hazards.

## 2. HYDROGEOLOGICAL INVESTIGATION OF TUNNEL HAZARDS

### 2.1. Overall Location

The geographical locations of the tunnels investigated for hazards are shown in Figure 1. All six surveyed tunnels are located within Guangdong Province, China (Fig. 1(a)), and are twin-tube separated expressway tunnels. Among them, Chalinding Tunnel, Egongji Tunnel, and Shiyashan Tunnel are situated in the mountainous western region of Guangdong Province, while Dayaoshan No. 1 Tunnel, Dayaoshan No. 3 Tunnel, and Zhongshanding Tunnel are located in the mountainous northern region of Guangdong Province, as shown in Fig. 1(b). Fig. 1(c-e) illustrates the specific location of each tunnel within the district-level administrative divisions. Tunnels ①-③ are situated along the Guangzhou-Kunming Expressway, and Tunnels ④-⑥ are located on the Lechang-Guangzhou Expressway.



**Figure 1.** The geographical location of the investigated tunnels

## 2.2. Statistical Characteristics of Hazards

The longitudinal geological profiles of the left tubes of Chalinding Tunnel and Dayaoshan No. 1 Tunnel are presented in Fig. 2, with the locations of identified hazards clearly annotated.

In Chalinding Tunnel, several hazard locations were documented. At LK123+959.5–971.5, the sidewall experienced lining bulging and cracking in 2012. The section LK124+392–433 developed a full-length longitudinal crack with a maximum length of 12 m on the sidewall in 2020, an area adjacent to a geophysical anomaly zone. Within LK125+005–050, the drainage ditch suffered a water and mud inrush in 2014. Seismic imaging at this location revealed 23 karst development zones and one structural fracture zone nearby. At LK125+270, the vehicular cross-passage experienced significant water leakage in 2013, followed by recurring drain-hole blockages in 2019, 2021, and 2022. A nearby solution cavity was also identified.

In Dayaoshan No. 1 Tunnel, key hazard-related features were observed. Near the left tube entrance, a solution cavity developed both laterally and vertically. Approximately 20 m into the cavity from the entrance, the invert elevation decreases by about 8 m, and groundwater is present at the bottom. Within a 500 m radius of the entrance, thirteen surface subsidences were recorded, suggesting a potential link to hazards in this area. Near the tunnel's fault zone, joint fissures are highly developed and contain abundant fissure water. On the surface above the tunnel, five major gullies act as runoff channels, and a small reservoir is situated on a hilltop approximately 650 m from the tunnel exit.

The regional topography and contour maps for all six tunnels are shown in Fig. 3. Hazards were consistently observed near gully lines. In Zhongshanding Tunnel, four of five documented hazards were located within karst collapse zones. Fig. 3 further indicates that hazards were significantly less frequent beneath hilltops compared with foothills, where the majority were concentrated.

Based on the hydrogeological investigation across the tunnel group, the characteristics of 36 hazard points were statistically analyzed. This analysis integrated tunnel inspection records, regional elevation maps, and longitudinal profiles. For each hazard point, information was compiled on tunnel burial depth, surrounding rock grade, lithology, hazard manifestation, position within the tunnel, nearby preferential seepage pathways, and corresponding surface topography. These data are summarized in Table 1.

Fig. 4 presents categorized statistics for all hazard characteristics. Regarding burial depth (Fig. 4a), 88.9% of hazards occurred at depths exceeding 50 m, with 12 buried deeper than 150 m. This indicates that the groundwater pressures causing tunnel damage are generally modest (Luo et al., 2024). This distribution pattern, together with the findings in Fig. 4f, suggests a close association with preferential seepage pathways. The statistical results for hazard location within the tunnel (Fig. 4b) show that the majority occurred at the crown (15 cases) and pavement (11 cases), while others were distributed on sidewalls, construction joints, drainage ditches, and cross-passages.

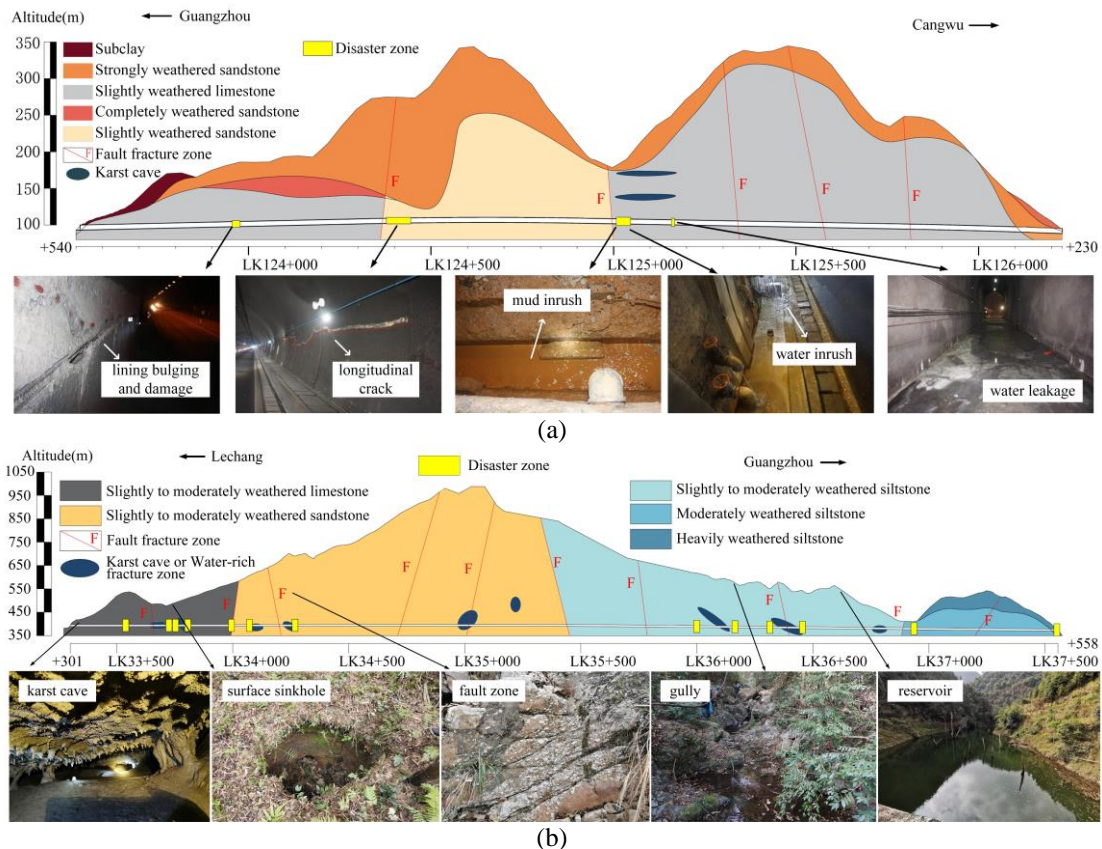
Analysis of lithology and weathering degree (Fig. 4c) revealed sandstone (17 cases) and siltstone (14 cases) as the dominant rock types in hazard zones, while limestone accounted for only 5. Slightly to moderately weathered

rocks were most prevalent. Physical weathering processes such as freeze–thaw cycles, thermal expansion–contraction, excavation unloading, and root wedging fracture the rock and create new fissures, thereby increasing pathways for groundwater flow. Chemical weathering, including carbonate dissolution, increases porosity and generates new pores. Both processes enhance hydraulic conductivity. Although more weathered rocks generally show a higher probability of hazards, the deep burial (>50 m) of most hazard points in this study correlates with less-weathered rock masses compared with near-surface zones (as shown in Fig. 2a). Consequently, hazards in highly weathered rock masses were rare, accounting for only 5.6% of the total.

The statistics for hazard manifestation (Fig. 4d) indicate that crack seepage was the most common phenomenon (50%), followed by water leakage (38.9%). Four severe cases involved structural damage and water/mud inrush. Concerning surrounding rock grade (Fig. 4e), rock masses worse than Grade IV accounted for 80.5% of hazards. Poorer rock quality correlates with fragmentation, porosity, and joint development, all of which increase hazard probability.

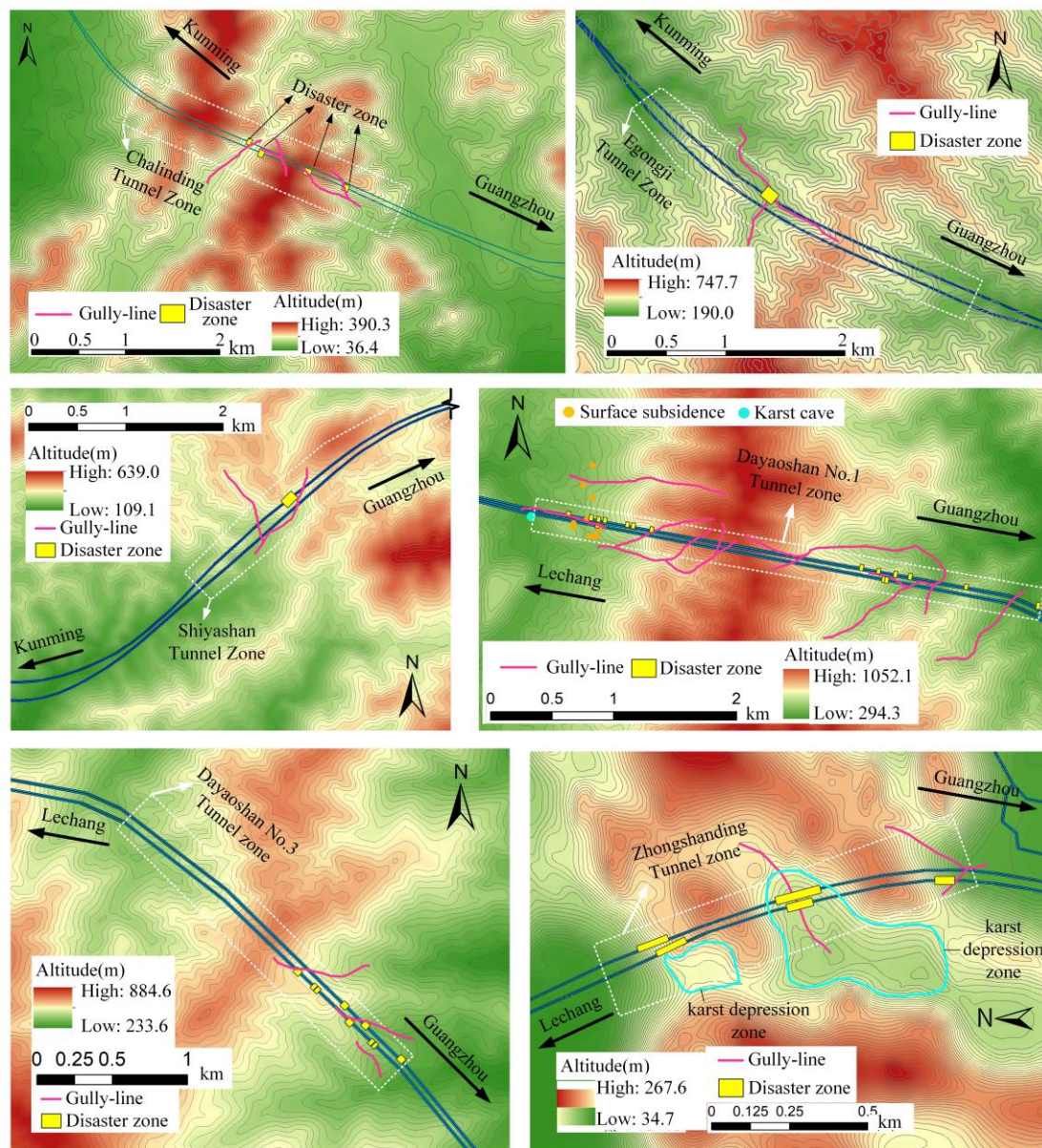
Investigation of preferential seepage pathways near hazard points (Fig. 4f) showed that more than half were associated with such pathways. In areas with well-developed joints or fault belts, fractures provide efficient conduits for surface water infiltration. In water-rich and karst terrains, these pathways accelerate the rise of groundwater levels following rainfall, while storage structures maintain locally elevated water pressures.

Finally, the analysis of surface topography above hazard locations (Fig. 4g) revealed that 75% corresponded to catchment structures. Specifically, 8 hazard sites were located beneath depressions, 21 beneath valleys or ravines, and 8 beneath sinkholes, karst collapse depressions, or funnels. Several sites corresponded to more than one converging topographic feature.



**Figure 2.** Geological profile of tunnels. (a) Chalinding Tunnel (left line). (b) Dayaoshan No.1 Tunnel (left line).





**Figure 3.** Tunnel surface topography and contour lines. (a) Chalinding Tunnel. (b) Egongji Tunnel. (c) Shiyashan Tunnel. (d) Dayaoshan No.1 Tunnel. (e) Zhongshanding Tunnel



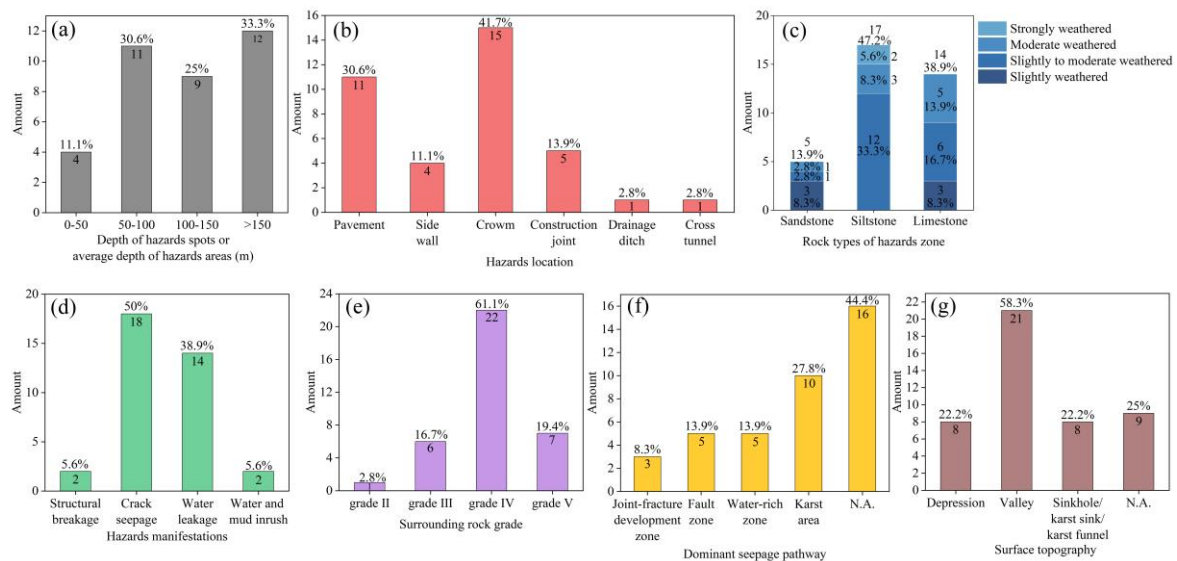


Figure 4. Statistical results of tunnel water-related hazards characteristics

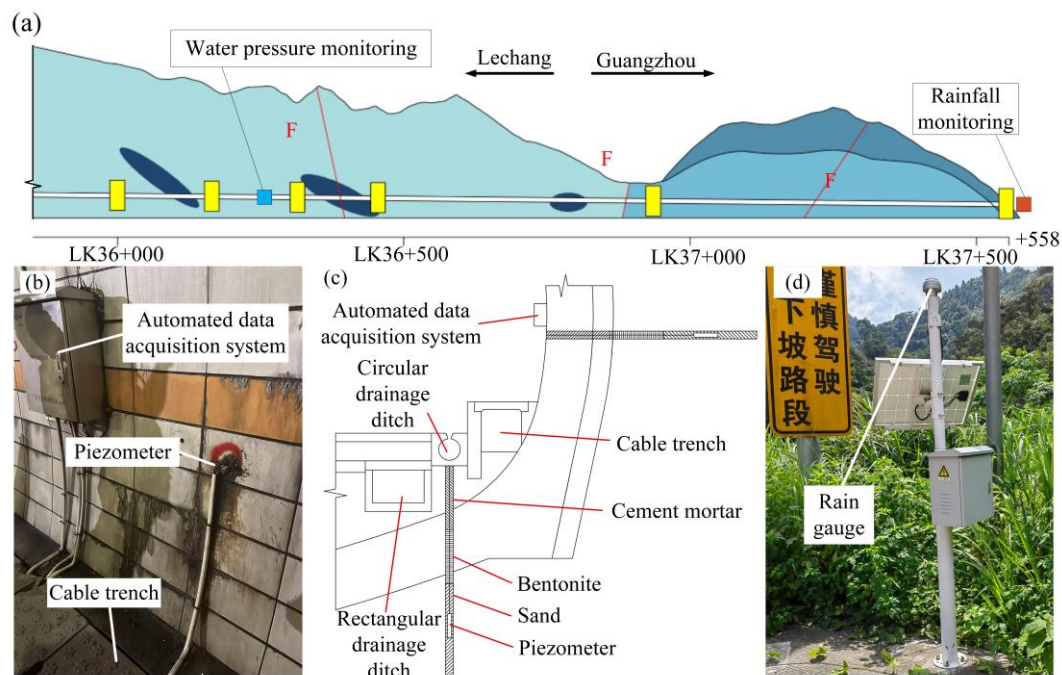
### 3. HYDROLOGICAL MONITORING

#### 3.1. Monitoring Program

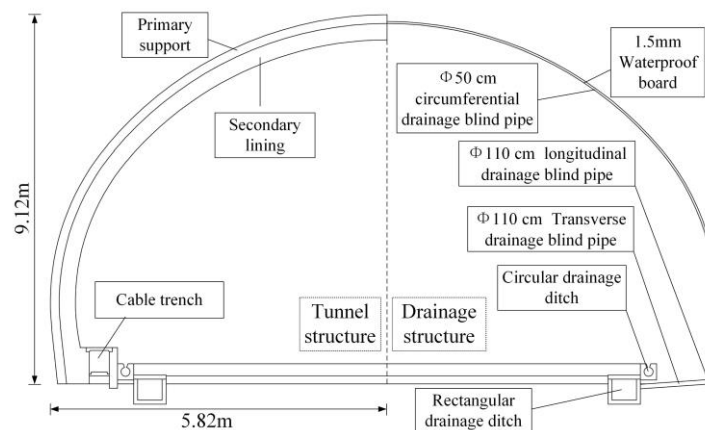
All six tunnels investigated in this study are located within a subtropical monsoon climate zone. Under the influence of this climate, rainfall is highly seasonal and concentrated in the summer months. Investigation results show that most tunnel water-related hazards occur between May and September, coinciding with the peak rainfall period. To further analyze the triggering mechanisms of these hazards, a comprehensive hydrological monitoring system was installed at the Dayaoshan No. 1 Tunnel. At the LK36+265 section of the left tube, four piezometers were installed, and one rain gauge was deployed on the ground surface near the tunnel exit. The instrument layout is illustrated in Fig. 5(a).

The configuration of the piezometers is shown in Fig. 5(b). Four vibrating-wire piezometers were installed at specific positions: the overtaking lane side ditch, the overtaking lane sidewall, the slow lane side ditch, and the slow lane sidewall. An automated data acquisition and wireless transmission system was employed to enable continuous monitoring. The installation procedure is illustrated in Fig. 5(c). A borehole approximately 4 cm in diameter and 2.5 m deep was drilled at each designated location. Sand was first placed at the bottom of the hole, followed by the piezometer. The borehole was then backfilled with sand to a depth of approximately 1.2 m, overlain by a 0.7 m thick bentonite layer, and finally sealed with cement mortar grout.

Dayaoshan No. 1 Tunnel adopts a unidirectional drainage slope. The tunnel cross-section and its waterproofing and drainage system are presented in Fig. 6. Circumferential and longitudinal drainage blind pipes were installed outside the tunnel lining, with circumferential pipes spaced at 20 m intervals. Water collected by these pipes was conveyed through transverse pipes into the side ditches and subsequently discharged from the tunnel. The rain gauge, shown in Fig. 5(e), is equipped with a piezoelectric sensor and powered by a solar panel mounted at the top.



**Figure 5.** Instrumentation Layout in Dayaoshan No.1 Tunnel



**Figure 6.** Tunnel structure and drainage system of Dayaoshan No.1 Tunnel LK36+265

### 3.2. Monitoring Results

The Chinese rainfall intensity classification standard defines seven levels of precipitation based on 24-hour cumulative rainfall: drizzle ( $<0.1$  mm), slight rain (0.1–9.9 mm), moderate rain (10.0–24.9 mm), heavy rainfall (25.0–49.9 mm), rainstorm (50.0–99.9 mm), heavy rainstorm (100.0–249.9 mm), and extremely heavy rainstorm ( $>250$  mm). During the six-month monitoring period, a series of intense rainfall events were recorded, including two extremely heavy rainstorms, ten heavy rainstorms, eleven rainstorm events, and twenty heavy rainfall events, as shown in Fig. 7.

A six-month continuous monitoring campaign of rainfall and water pressure in the Dayao Mountain No. 1 Tunnel was conducted from April 1 to September 30, 2024. Figure 7 presents the rainfall–water pressure monitoring results at section LK36+265 of the tunnel. Among the four piezometers installed within this section, the one located on the sidewall of the passing lane failed to provide valid data due to malfunction. Under frequent heavy rainfall conditions, a total of 21 distinct water pressure rise intervals were identified by the remaining three piezometers, each of which was consistently preceded by consecutive rainfall events. The longest continuous water pressure increase occurred at monitoring point ①, located in the side ditch of the slow lane. Following four

consecutive days of rainfall not less than the *Rainstorm* grade and two additional days reaching the *Extremely Heavy Rainstorm* grade, the water pressure began to rise from the fifth day onward. This increase lasted for eight consecutive days, during which the water pressure rose from approximately 0 to 34.2 kPa, yielding a net increment of 32.2 kPa. The largest water pressure increment was recorded at monitoring point ③, located in the side ditch of the passing lane. After three consecutive days of rainfall not less than the *Rainstorm* grade, the water pressure began to increase on the fourth day, reaching a cumulative increment of 58.6 kPa within five days.

Before July 2024, the overall trend at all three monitoring points showed a gradual rise in water pressure. Following rainfall-induced pressure increases, the water pressure decayed slowly. Inspection revealed that drainage pipes in the tunnel were partially clogged. After cleaning and dredging the drainage pipes and ditches in early July, the water pressure began to decrease progressively. These observations indicate a strong correlation between surface rainfall and water pressure increases in the tunnel, with a noticeable lag effect. During extended dry periods, water pressure gradually declined to nearly zero, suggesting that effective tunnel drainage maintained the groundwater level below the tunnel floor. Conversely, during consecutive rainfall events, infiltration from the ground surface recharged the subsurface, raising the surrounding groundwater level and thereby elevating the water pressure around the tunnel, which in turn increased the risk of water-related hazards.

To further characterize the temporal lag in water-pressure response to rainfall, a statistical analysis was conducted on the daily pressure increment within successive days after rainfall events. Because Spearman's rank correlation coefficient ( $\rho$ ) is a non-parametric measure that captures monotonic (including non-linear) associations between variables (Xue et al., 2023; Yin et al., 2018), it was adopted to quantify the relationship between rainfall and water-pressure changes. For each of the three monitoring locations—slow lane drainage channel, slow lane side wall, and overtaking lane drainage channel—the daily water-pressure change on days 1–7 following rainfall was computed. Rainfall intensity was stratified into four groups:  $\geq 0$  mm day<sup>-1</sup> (all events),  $\geq 10$  mm day<sup>-1</sup> (moderate rain or above),  $\geq 25$  mm day<sup>-1</sup> (heavy rain or above), and  $\geq 50$  mm day<sup>-1</sup> (rainstorm or above). For each rainfall group and each post-event day, Spearman's  $\rho$  between daily rainfall  $h$  (mm) and the daily water pressure change  $\Delta p$  (kPa) was calculated:

$$\rho = \frac{\sum_{i=1}^n (R_{h,i} - \bar{R}_h)(R_{\Delta p,i} - \bar{R}_{\Delta p})}{\sqrt{\sum_{i=1}^n (R_{h,i} - \bar{R}_h)^2} \sqrt{\sum_{i=1}^n (R_{\Delta p,i} - \bar{R}_{\Delta p})^2}} \quad (1)$$

$$\bar{R}_h = \frac{1}{n} \sum_{i=1}^n R_{h,i} \quad (2)$$

$$\bar{R}_{\Delta p} = \frac{1}{n} \sum_{i=1}^n R_{\Delta p,i} \quad (3)$$

On the basis of Fig. 8, the lagged influence of rainfall on water pressure does not extend beyond seven days; accordingly,  $n=7$  was adopted.

The distribution of Spearman's  $\rho$  across lag days is shown in Fig. 9. For all three locations, the peak Spearman correlation occurs within the  $\geq 10$  mm day<sup>-1</sup> subset. Within this subset, the slow lane drainage channel exhibits its largest  $\rho$  on days 6–7; the slow lane side wall peaks on day 3; and the overtaking lane drainage channel peaks on days 3–4. Hence, after rainfall events of at least 10 mm day<sup>-1</sup>, the most pronounced lag in water-pressure response at these three sites is approximately 6–7 days, 3 days, and 3–4 days, respectively.

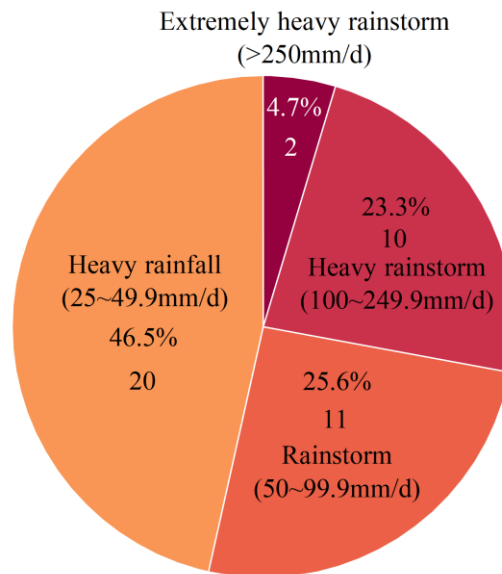
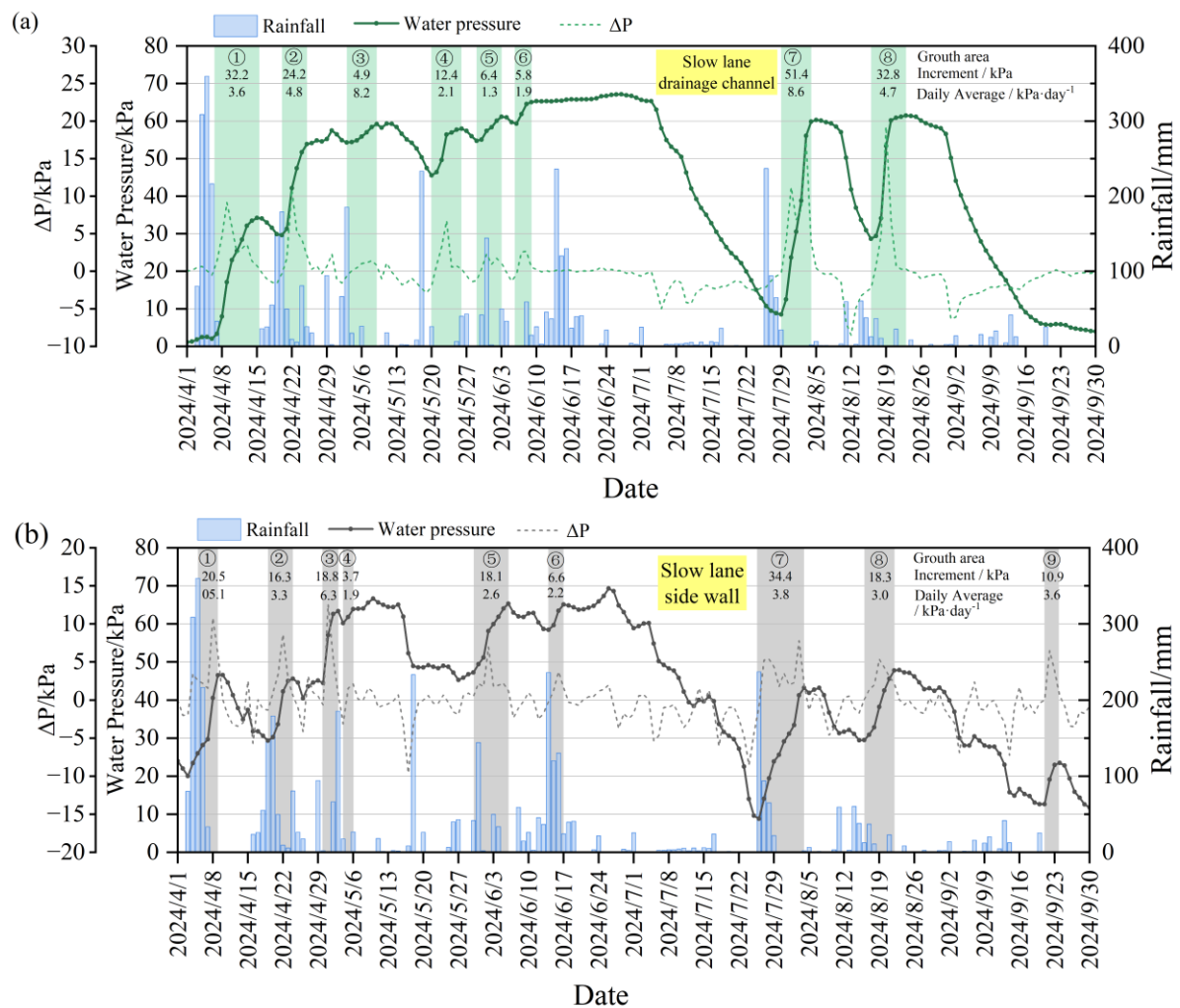
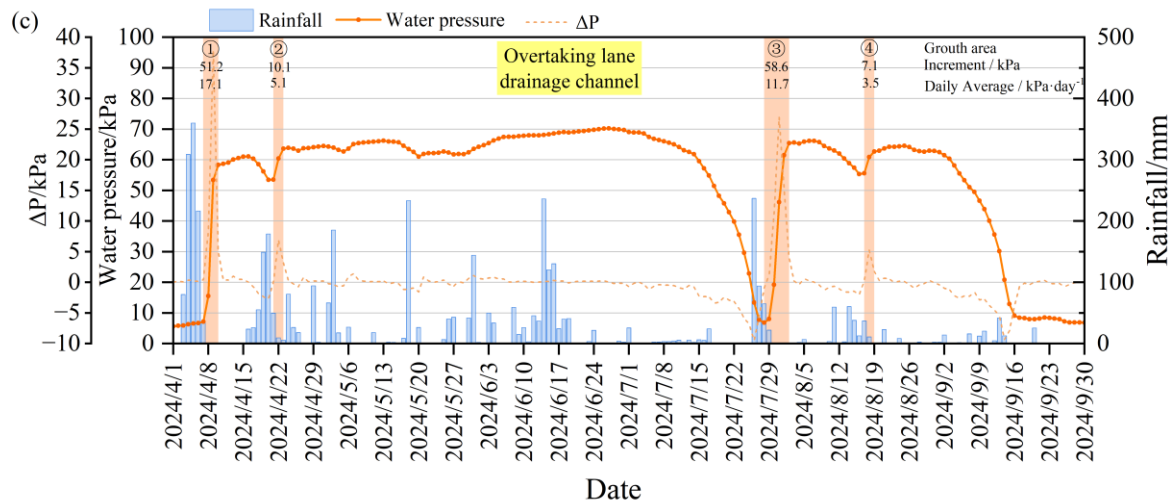
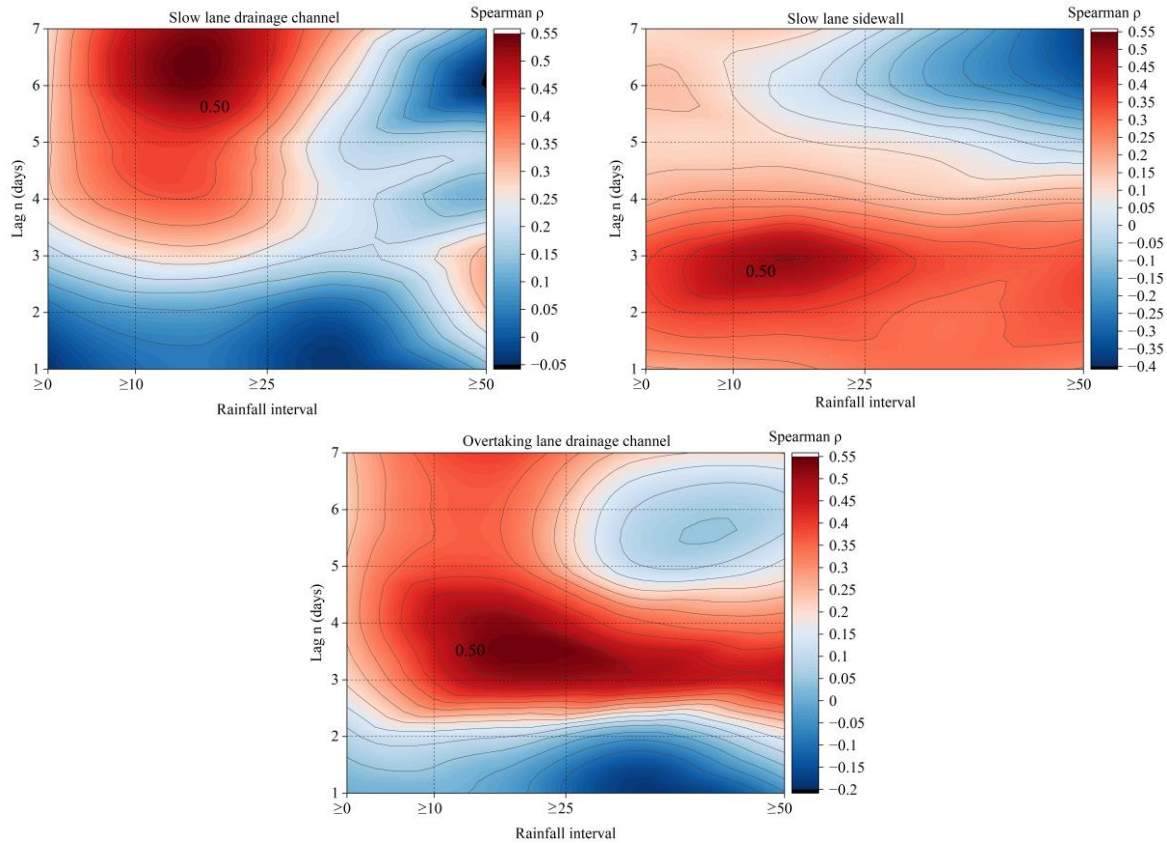


Figure 7. Rainfall Intensity Distribution





**Figure 8.** Rainfall- Water Pressure Monitoring Results. (a) Slow lane drainage channel. (b) Slow lane side wall. (c) Overtaking lane drainage channel.



**Figure 9.** Time lag distribution of water pressure.

#### 4. ANALYSIS OF INFLUENCING FACTORS AND DISCUSSION

Based on hydrogeological investigations and monitoring data, the factors and processes contributing to water-related hazards in operational highway tunnels in water-rich areas are summarized in Fig. 10. Under the combined influence of climatic, geological, and drainage conditions, the development of such hazards can be divided into three main stages:



### (1) Initial stage:

During this phase, continuous heavy rainfall occurs at the surface, and a significant rise in water pressure typically follows three to five days of persistent torrential rain (Fig. 9). Part of the rainfall infiltrates directly through surface soils and rock layers, while the remainder converges into runoff in valleys and gullies (Fig. 2b).

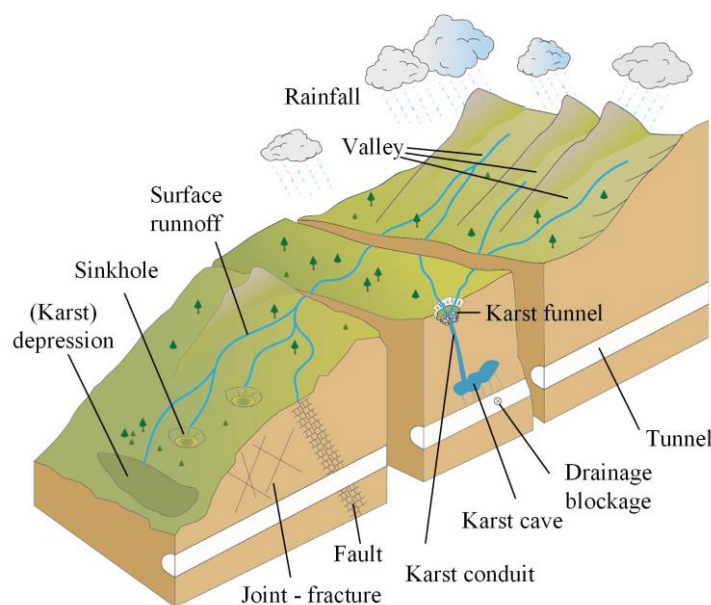
### (2) Infiltration stage:

Rainfall or surface runoff infiltrates through preferential seepage pathways. In karst regions, surface features such as sinkholes or swallow holes may exist. Subsurface carbonate rocks undergo physical and chemical dissolution, forming caves and conduits that connect the surface to the subsurface. These conduits often exceed 10 cm in diameter (Wang et al., 2020), and caves can range from several meters to tens of meters in scale. In non-karst regions with highly weathered rocks (Fig. 4c), strata commonly exhibit well-developed joints and fractures, allowing rainfall to infiltrate as fracture flow into deeper layers. Fault zones function similarly, as tectonic fault planes provide natural underground pathways for surface water infiltration. Surface collapses induced by erosion may also create small depressions or pools, where rainwater either infiltrates or evaporates. Ultimately, surface water accumulates in low-lying areas, forming wetlands or draining into rivers.

### (3) Tunnel Impact stage:

In operational highway tunnels, drainage systems are generally designed to discharge infiltrating water completely, thereby maintaining the natural water table below the tunnel level (Fig. 8). However, due to variable forms and rates of seepage, infiltrated water eventually reaches the tunnel vicinity after different durations, leading to a rapid rise in water pressure. If waterproofing and drainage systems perform effectively and the discharge capacity matches the rate of groundwater rise, the water pressure decreases gradually and returns to a stable level. By contrast, if the waterproofing system fails (e.g., due to damaged waterproof boards or clogged drainage pipes caused by sediment or crystallization), or if extreme short-term rainfall combined with preferential pathways (e.g., karst conduits) causes groundwater levels to rise faster than the designed drainage capacity, water pressure around the tunnel remains elevated for extended periods. This sustained high-pressure environment may induce leakage, water and mud inrush, structural cracking, or even failure within a short timespan.

Given the concealed nature of groundwater seepage, numerous research challenges remain. On one hand, detecting subsurface seepage pathways through field investigation or predicting their behavior using stochastic methods can help clarify groundwater flow mechanisms and guide targeted measures for sealing channels and intercepting surface water. This reduces rapid inflow near tunnels and enhances operational safety. On the other hand, under well-characterized hydrogeological conditions, theoretical calculations and numerical simulations can be employed to analyze the rainfall–groundwater seepage–tunnel response process over large regions. Such analyses enable quantification of the complete sequence from rainfall to water pressure increase and subsequent reduction, and help evaluate the impacts of different seepage pathways on operational tunnels. By leveraging quantitative data, the mechanisms of water-related hazards can be investigated in greater depth.



**Figure 10.** Progress of Tunnel Hazards

## 5. CONCLUSION

(1) Hydrogeological investigations of six operational expressway tunnels revealed that water-related hazards occur most frequently beneath valley lines or topographic depressions. Their occurrence is strongly correlated with surface topography and the presence of subsurface preferential seepage pathways. These hazard-prone locations are typically associated with highly weathered rock, poor surrounding rock conditions, and intensively karstified or water-rich zones.

(2) Monitoring of rainfall and water pressure demonstrated a strong correlation between increases in tunnel water pressure and short-term, continuous heavy rainfall events. The water pressure response to rainfall exhibited a clear time lag, generally exceeding two days, with the lag duration influenced by rainfall intensity, rainfall duration, geological conditions, and drainage capacity. Specifically, for the slow lane drainage channel, slow lane side wall, and vertaking lane drainage channel in this case, the most pronounced lag after rainfall events of  $\geq 10$  mm/day was approximately 6–7 days, 3 days, and 3–4 days, respectively.

(3) The formation of tunnel water-related hazards follows a distinct sequence: rainfall infiltration through preferential pathways, the build-up of sustained high water pressure around the tunnel, and subsequent hazard development. Failures of waterproofing and drainage systems were found to significantly amplify the risk of such hazards.

## 6. ACKNOWLEDGMENTS

This study was supported by the National Natural Science Foundation of China (Grant number 52378422) and Research Project on the Post-Evaluation Methodology System and Key Maintenance Technologies for Highway Tunnel Drainage Systems.

## 7. BIBLIOGRAPHY

- [1] Li, L., Lei, T., Li, S., Zhang, Q., Xu, Z., Shi, S., & Zhou, Z. (2015). Risk assessment of water inrush in karst tunnels and software development. *Arabian Journal of Geosciences*, 8(4), 1843–1854. <https://doi.org/10.1007/s12517-014-1365-3>
- [2] Wang, X., Li, S., Xu, Z., Li, X., Lin, P., & Lin, C. (2019). An interval risk assessment method and management of water inflow and inrush in course of karst tunnel excavation. *Tunnelling and Underground Space Technology*, 92, 103033. <https://doi.org/10.1016/j.tust.2019.103033>
- [3] Wu, X., Feng, Z., Yang, S., Qin, Y., Chen, H., & Liu, Y. (2024). Safety risk perception and control of water inrush during tunnel excavation in karst areas: An improved uncertain information fusion method. *Automation in Construction*, 163, 105421. <https://doi.org/10.1016/j.autcon.2024.105421>
- [4] Li, Z., Chen, Z., He, C., Chen, K., Zhang, H., Ma, C., Li, X., & Liu, M. (2023). Experimental simulation of seepage field distribution for small interval tunnel under varying-head infiltration. *Transportation Geotechnics*, 41, 101029. <https://doi.org/10.1016/j.trgeo.2023.101029>
- [5] Lin, P., Li, S. C., Xu, Z. H., Wang, J., & Huang, X. (2019). Water Inflow Prediction during Heavy Rain While Tunneling through Karst Fissured Zones. *International Journal of Geomechanics*, 19(8), 04019093. [https://doi.org/10.1061/\(ASCE\)GM.1943-5622.0001478](https://doi.org/10.1061/(ASCE)GM.1943-5622.0001478)
- [6] Wang, J., Chen, Y., Nie, J., Yan, Z., Zhai, P., & Feng, J. (2022). On the role of anthropogenic warming and wetting in the July 2021 Henan record-shattering rainfall. *Science Bulletin*, 67(20), 2055–2059. <https://doi.org/10.1016/j.scib.2022.09.011>
- [7] Zhang, S., Song, D., Ye, F., Fu, W., Zhang, B., & Xiao, Q. (2024). Research on flow field characteristics in the karst tunnel face drilling hole (conduit) under the coupling between turbulence and seepage. *Tunnelling and Underground Space Technology*, 143, 105455. <https://doi.org/10.1016/j.tust.2023.105455>
- [8] Li, S., Xu, Z., Huang, X., Lin, P., Zhao, X., Zhang, Q., Yang, L., Zhang, X., Sun, H., & Pan, D. (2018). Classification, geological identification, hazard mode and typical case studies of hazard-causing structures for water and mud inrush in tunnels. *Chinese Journal of Rock Mechanics and Engineering*, 5, 1041–1069. <https://doi.org/10.13722/j.cnki.jrme.2017.1332> (in Chinese)
- [9] Fan, H., Chen, H., Zhao, D., Zhu, Z., Zhao, Z., Zhu, Y., & Gao, X. (2024). Study on lining water pressure distribution and early warning control standard of in-service karst tunnel. *Rock and Soil Mechanics*, 45(7), 2153–2166. <https://doi.org/10.26599/RSM.2024.9436338>
- [10] Fan, H., Zhang, Y., He, S., Wang, X., Wang, X., & Wang, H. (2018). Hazards and treatment of karst tunneling in Qinling-Daba mountainous area: Overview and lessons learnt from Yichang–Wanzhou railway system. *Environmental Earth Sciences*, 77(19), 679. <https://doi.org/10.1007/s12665-018-7860-1>
- [11] Ou, X., Ouyang, L., Zheng, X., & Zhang, X. (2024). Hydrogeological analysis and remediation strategies for water inrush hazards in highway karst tunnels. *Tunnelling and Underground Space Technology*, 152, 105929. <https://doi.org/10.1016/j.tust.2024.105929>

- [12] Ma, Y., Yang, J., Li, L., & Li, Y. (2022). Analysis on ultimate water pressure and treatment measures of tunnels operating in water rich areas based on water hazard investigation. *Alexandria Engineering Journal*, 61(8), 6581–6589. <https://doi.org/10.1016/j.aej.2021.11.040>
- [13] Peng, Y., Wu, L., Zuo, Q., Chen, C., & Hao, Y. (2020). Risk assessment of water inrush in tunnel through water-rich fault based on AHP-Cloud model. *Geomatics, Natural Hazards and Risk*, 11(1), 301–317. <https://doi.org/10.1080/19475705.2020.1722760>
- [14] Wang, Y., Yin, X., Jing, H., Liu, R., & Su, H. (2016). A novel cloud model for risk analysis of water inrush in karst tunnels. *Environmental Earth Sciences*, 75(22), 1450. <https://doi.org/10.1007/s12665-016-6260-7>
- [15] Zhao, R., Zhang, L., Hu, A., Kai, S., & Fan, C. (2024). Risk assessment of karst water inrush in tunnel engineering based on improved game theory and uncertainty measure theory. *Scientific Reports*, 14(1), 20284. <https://doi.org/10.1038/s41598-024-71214-8>
- [16] Lyu, H.-M., & Yin, Z.-Y. (2023). Flood susceptibility prediction using tree-based machine learning models in the GBA. *Sustainable Cities and Society*, 97, 104744. <https://doi.org/10.1016/j.scs.2023.104744>
- [17] Čokorilo Ilić, M., Mladenović, A., Čuk, M., & Jemcov, I. (2019). The Importance of Detailed Groundwater Monitoring for Underground Structure in Karst (Case Study: HPP Pirot, Southeastern Serbia). *Water*, 11(3), 603. <https://doi.org/10.3390/w11030603>
- [18] Wang, S., Li, L., Cheng, S., Yang, J., Jin, H., Gao, S., & Wen, T. (2021). Study on an improved real-time monitoring and fusion prewarning method for water inrush in tunnels. *Tunnelling and Underground Space Technology*, 112, 103884. <https://doi.org/10.1016/j.tust.2021.103884>
- [19] Chang, Y., Wu, J., & Liu, L. (2015). Effects of the conduit network on the spring hydrograph of the karst aquifer. *Journal of Hydrology*, 527, 517–530. <https://doi.org/10.1016/j.jhydrol.2015.05.006>
- [20] Gao, Y., Huang, F., Wang, D. (2024). Evaluating physical controls on conduit flow contribution to spring discharge. *Journal of Hydrology* 630, 130754. <https://doi.org/10.1016/j.jhydrol.2024.130754>
- [21] Gouy, A., Collon, P., Bailly-Comte, V., Galin, E., Antoine, C., Thebault, B., & Landrein, P. (2024). KarstNSim: A graph-based method for 3D geologically-driven simulation of karst networks. *Journal of Hydrology*, 632, 130878. <https://doi.org/10.1016/j.jhydrol.2024.130878>
- [22] Pardo-Igúzquiza, E., Dowd, P. A., Xu, C., & Durán-Valsero, J. J. (2012). Stochastic simulation of karst conduit networks. *Advances in Water Resources*, 35, 141–150. <https://doi.org/10.1016/j.advwatres.2011.09.014>
- [23] Luo, Y., Yang, J., Xie, Y., Fu, J., & Zhang, C. (2024). Investigation on evolution mechanism and treatment of invert damage in operating railway tunnels under heavy rainfall. *Bulletin of Engineering Geology and the Environment*, 83(5), 160. <https://doi.org/10.1007/s10064-024-03655-4>
- [24] Xue, Y., Zhang, W., Wang, Y., Luo, W., Jia, F., Li, S., & Pang, H. (2023). Serviceability evaluation of highway tunnels based on data mining and machine learning: A case study of continental United States. *Tunnelling and Underground Space Technology* 142, 105418. <https://doi.org/10.1016/j.tust.2023.105418>
- [25] Yin, M., Jiang, H., Jiang, Y., Sun, Z., & Wu, Q. (2018). Effect of the excavation clearance of an under-crossing shield tunnel on existing shield tunnels. *Tunnelling and Underground Space Technology* 78, 245–258. <https://doi.org/10.1016/j.tust.2018.04.034>
- [26] Wang, C., Wang, X., Majdalani, S., Guinot, V., & Jourde, H. (2020). Influence of dual conduit structure on solute transport in karst tracer tests: An experimental laboratory study. *Journal of Hydrology*, 590, 125255. <https://doi.org/10.1016/j.jhydrol.2020.125255>

## TRANSFORMATIVE APPROACHES TO UNDERGROUND INFRASTRUCTURE: ROAD TO NET ZERO AND BEYOND

Kelwalee Jutipanya<sup>1</sup>, Lewis O Makana<sup>2</sup>, Aryan Hojjati<sup>3</sup>, Nicole Metje<sup>4</sup>, Dexter VL Hunt<sup>5</sup>,  
Emma JS Ferranti<sup>6</sup>, Anthony Hargreaves<sup>7</sup>, Joanne M Leach<sup>8</sup> and Christopher DF Rogers<sup>9</sup>.

**Abstract:** The urgency to address climate change and achieve net zero targets underscores the critical role of underground infrastructure in considerations of urban resilience and sustainability. This paper leverages insights from the "Road to Net Zero" (RtNZ) initiative in the UK, integrating advanced methodologies such as carbon optioneering tools and autonomous robotics. By addressing the complexities of underground systems, the research presents a cohesive framework for sustainable urban development and infrastructure management.

Drawing on the RtNZ Design Options Framework, the paper explores opportunities to minimize the carbon emissions for four alternative design options for streetworks: trenching, minimum dig techniques, trenchless technologies, and autonomous robotics. Actions in support of carbon reduction form part of a structured pathway to address systemic challenges in subsurface management and highlight the importance of integrating innovative solutions for sustainable infrastructure development.

The integration of data-driven tools, such as the RtNZ Optioneering Tool that accounts for all social, environmental and indirect economic consequences of streetworks, combined with advanced thinking from projects such as Mapping and Assessing the Underworld, offers robust methodologies to quantify impacts, mitigate risks, and optimize design decisions. Pipebots, as a future vision, exemplify transformative solutions to subsurface challenges, combining autonomous capabilities with enhanced ecological stewardship. The overarching threads of sustainability, resilience, and health and safety form part of this 'total value analysis', which takes a whole subsurface perspective.

**Keywords:** Streetworks, Sustainability, Resilience, Optioneering, Decarbonization.

### 1. INTRODUCTION

It is neither possible nor desirable to divorce considerations of the urban subsurface from what exists and happens at the surface. Fundamentally, the subsurface serves as an ecosystem service provider, and what occurs below ground must work in harmony with surface activities. The workspace focused on herein is the street corridor, and because they tend to be much more complicated, urban street corridors provide the most serious challenges. Referring to Figure 1, it is clear that the streets accommodate many different types of flow and serve many purposes – in short, streets have enormous value.

<sup>1</sup>Ms, Jutipanya, Kelwalee (Ken), Civil Eng., School of Eng., University of Birmingham, Birmingham, B15 2TT, [kxj234@student.bham.ac.uk](mailto:kxj234@student.bham.ac.uk)

<sup>2</sup>Dr, Makana, Lewis, Geotechnical Eng., School of Eng., University of Birmingham, Birmingham, B15 2TT, UK, [l.makana@bham.ac.uk](mailto:l.makana@bham.ac.uk)

<sup>3</sup>Dr, Hojjati, Aryan, Infrastructure Eng., National Research Council Canada, Ottawa, K1A 0R6, Canada, [aryan.hojjati@nrc-cnrc.gc.ca](mailto:aryan.hojjati@nrc-cnrc.gc.ca)

<sup>4</sup>Prof, Metje, Nicole, Infrastructure Eng., School of Eng., University of Birmingham, Birmingham, B15 2TT, UK, [n.metje@bham.ac.uk](mailto:n.metje@bham.ac.uk)

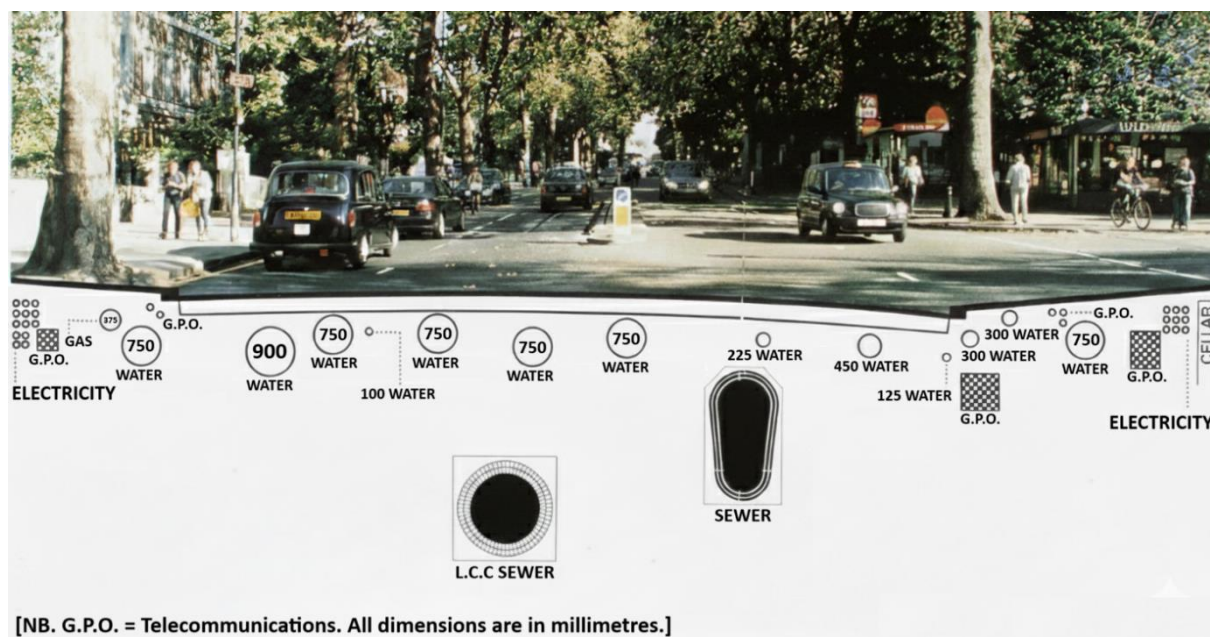
<sup>5</sup>Dr, Hunt, Dexter, Geotechnical Eng., School of Eng., University of Birmingham, Birmingham, B15 2TT, UK, [d.hunt@bham.ac.uk](mailto:d.hunt@bham.ac.uk)

<sup>6</sup>Assoc Prof, Ferranti, Emma, Civil Eng., School of Eng., University of Birmingham, Birmingham, B15 2TT, UK, [e.ferranti@bham.ac.uk](mailto:e.ferranti@bham.ac.uk)

<sup>7</sup>Dr, Hargreaves, Tony, Civil Eng., School of Eng., University of Birmingham, Birmingham, B15 2TT, UK, [a.j.hargreaves@bham.ac.uk](mailto:a.j.hargreaves@bham.ac.uk)

<sup>8</sup>Dr, Leach, Joanne, Civil Eng., School of Eng., University of Birmingham, Birmingham, B15 2TT, UK, [j.leach@bham.ac.uk](mailto:j.leach@bham.ac.uk)

<sup>9</sup>Prof, Rogers, Christopher, Geotechnical Eng., School of Eng., University of Birmingham, Birmingham, B15 2TT, UK, [c.d.f.rogers@bham.ac.uk](mailto:c.d.f.rogers@bham.ac.uk)



**Figure 1.** The urban street corridor – a complex workspace (Image courtesy of Mike Farrimond)

A starting point for the analysis of the value of street corridors is to consider the urban metabolism - that is, all flows into, through and out of these spaces. A typical urban street scene, such as that represented in Figure 1, will show people moving by active travel (walking, cycling, scootering), people traveling in personal vehicles or via public transport, and goods being transported and delivered by vehicles. Natural flows include animals, birds, insects, and what is carried by the wind (e.g., pollen, seeds, leaves). These streets are also places in which we live and work - they host residential frontages, social spaces, businesses, and nature in the form of street trees. All of this has inherent value that should be recognized, appreciated, protected and where possible enhanced.

The subsurface aspect of the urban metabolism includes the flows transmitted by the buried pipes and cables that carry the essential services and resources required for urban living, while the ground also transmits gases, water, chemicals, and microorganisms (Hojjati et al., 2016). The subsurface must also provide physical support to the buried infrastructure and the overlying transport infrastructure, and it must accommodate the roots of the green infrastructure, particularly trees. The subsurface, therefore, also provides many different forms of value, and this should likewise be appreciated, protected, and where possible enhanced (Rogers et al., 2020).

Moreover, this workspace – the urban street corridor – is dynamic: its surface and subsurface infrastructures change with time. While green infrastructure grows, the non-natural infrastructures (the roads and buried infrastructures) age and deteriorate, requiring maintenance and repair, while there is a seemingly progressive need for the installation of new infrastructure. Alongside this developing landscape is the overarching need for the subsurface engineer to introduce considerations of sustainability and resilience to any intervention, and adopt geoethics principles.

This has many implications for the subsurface engineer. The most obvious is that we should occupy subsurface space responsibly, using only what we need and avoiding unnecessarily compromising the use of this space in the future. More generally, we should ensure that the materials, equipment, and site operations involved in streetworks are chosen to minimize the adverse impact on the environment, society, and the economy. The Road to Net Zero project (LCRIG., 2025; RTNZ Project., 2025), on which this paper is focused, started with a premise of the need to decarbonize construction works, but soon evolved into an evaluation of all potential negative outcomes to be balanced against all the positive outcomes of essential streetworks. This evolution has resulted in the development of an optioneering tool that enables a subsurface engineer to appraise the overall value of an intervention and to minimize the environmental and social harms, which usually translate into economic losses due to their climate and health impacts.

The urban street corridor therefore represents a complex landscape, which in turn needs a systemic approach to engineering in this system-of-systems. This approach to working is usually invoked because of the physical interdependencies between engineered systems – activity associated with one buried pipeline has the potential to impact adjacent buried pipelines and cables, and the overlying road structure (Figure 2). This tacitly assumes that the ground, which supports both the buried and surface infrastructures, is a passive medium. However, if it were to be treated as an infrastructure in its own right, then the engineering process would be far more effective. In essence, this means that we must treat the ground with respect – establish its properties in the undisturbed condition



and use engineering judgment to deduce the change of properties according to different types of construction activity. At this point, it becomes immediately evident that open cut excavation will compromise the strength and stiffness of the ground due to lateral stress relief movement (i.e., volume increase), either in the short term or long-term (Torbaghan et al., 2020).



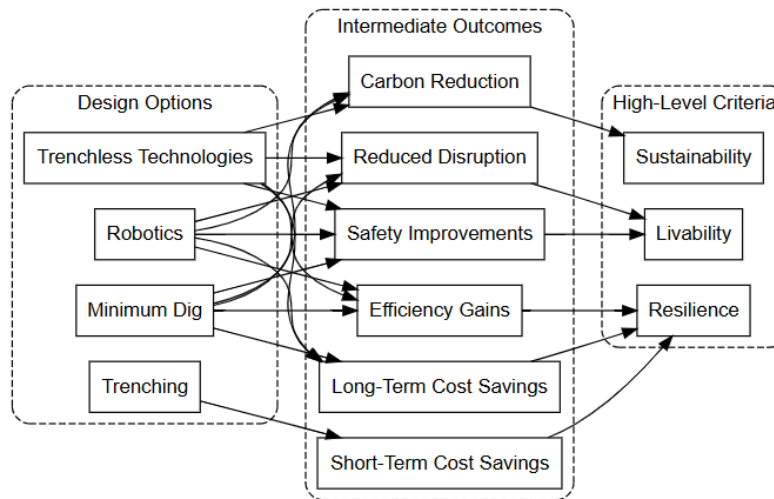
*Figure 2. Complex interdependencies between physical infrastructures, both old and new*

## 2. PERSPECTIVES ON AND DESIGN OPTIONS FOR ENGINEERING IN THE SUBSURFACE

There is an extensive array of experience, guidance, rules and responsibilities on which to draw when carrying out streetworks, whether using techniques that have been used for centuries (trenching) or more recent technological innovations (trenchless technologies, robotics and AI). Interestingly, the rules around governance are explicitly and comprehensively described by Haylen and Butcher (2019), and yet there is no mention of the overarching imperatives of sustainability, resilience, decarbonization or consideration of environmental consequences; indeed ‘society’ is mentioned only once in relation to the congestion costs of overrunning works. The messages on governance, therefore, stop short of explaining the purpose of these rules. It was for this reason that the Road to Net Zero project — ironically funded from Lane Rental Funds to prevent unnecessary overruns — was launched to extend such guidance on how to drastically reduce carbon emissions from streetworks, and more generally to promote delivery of environmental and social good.

Given that subsurface construction contributes substantially to the UK’s emissions (e.g., via use of diesel machinery, material production and consumption, and waste transport), a multi-faceted ‘optioneering’ approach has been adopted (Rogers, 2018). This approach entails evaluating a range of alternative design strategies for underground infrastructure interventions, rather than relying on the conventional, default option of open-cut excavation. Four main categories of design options - Trenching, Minimum Dig, Trenchless Technologies, and Robotics and AI - have been identified to cover the breadth of viable interventions. Each represents a different pathway to decarbonization and reduced disruption in the congested urban subsurface, and together they form a toolkit for progressing towards low-carbon streetworks while also accounting for their different sustainability, resilience, and livability outcomes, which are the key criteria in the total value framework (in which all social, environmental, and economic impacts are assessed together; Rogers et al., 2022). By evaluating options against these criteria - something that has been identified as a need for decades (e.g., Burtwell et al., 2006) but never adequately addressed — the optioneering process identifies solutions that minimize total harm and maximize net benefits, moving subsurface infrastructure projects closer to Net Zero carbon while enhancing urban resilience and quality of life (see Figure 3). The following section outlines these options, discussing their technical rationale (key benefits, drawbacks, and assumptions) with references to the RtNZ design framework (Rogers et al., 2023).

Conventional open-cut trenching remains the default for utilities and highways due to its simplicity and decades of institutional expertise, but it is energy- and carbon-intensive, producing high fuel use, waste, and social disruption. Electrification and automation can improve its fuel efficiency and yield a modest benefit-cost ratio (BCR ~1.6–2.8). In contrast, minimum-dig (or ‘keyhole surgery’) techniques precisely target only the point at which activity is required, using for example narrow slots, coring, robotic mini-excavators, and advanced polymer liners. This second approach dramatically reduces excavation volumes, equipment emissions, materials, and traffic impacts, delivering very high net benefits (BCR ~4.1) provided accurate underground mapping and crew upskilling is used. However, the opportunities to use such techniques are relatively few because of the reliance on accurate prior diagnosis of the problem and targeting of the works. Trenchless methods (e.g., horizontal directional drilling (HDD) and microtunneling for new installation, pipe bursting and pipe splitting for size-for-size replacement, and relining of a defective host pipe using cured-in-place liners or thin-walled plastic insertions) avoid continuous surface excavation by installing or renewing pipes via localized entry and exit pits.



**Figure 3.** Conceptual progression from each design option to a holistic **total value analysis** optioneering model.

Typical scenarios show a reduction in carbon emissions by up to ~68%, and greatly reduced spoil haulage and surface reinstatement. Although they require more specialized planning, potentially higher upfront costs for equipment purchase and additional care in ground-condition assessment, the drastically reduced surface (notably traffic; Goodwin, 2005) disruption can result in greatly lowered carbon, other environmental and social costs. Finally, advanced robotics spanning autonomous excavators, drones, sensor-equipped crawlers, and AI-driven ‘digital workers’ offers a cross-cutting enabler that enhances precision, safety, and efficiency across all approaches. In view of the fact that this technology is emerging, this currently requires significant capital investment, digital skills, regulatory adaptation, and mature integration to realize its transformative potential.

The four generic design options therefore present a spectrum of trade-offs between technological disruptiveness, ease of implementation, and multidimensional value. Table 1 summarizes several key metrics across the options. Robotics and AI stand somewhat apart as an enabling layer: they can amplify the benefits of the other methods (e.g., by automating precision tasks), although on their own they both require further development to realize their full impact. The most appropriate path forward, therefore, is one that invests in innovation adoption (to unlock the high-value options) while managing risks with interim improvements—ultimately steering the sector onto a net-zero trajectory with broad societal gain.

**Table 1.** Key comparative metrics across alternative design options.

(Carbon Reduction values are indicative, based on hypothetical case analyses of site works alone. Disruption Level refers to relative level of surface and community disruption caused by the works. Adoption Readiness reflects current maturity and industry uptake.)

Option	Carbon Reduction Potential of Site Works	Disruption Level	Adoption Readiness
<b>Trenching</b>	<b>Moderate:</b> incremental improvements yield ~20-40% emission cuts by using electrified plant and vehicles	<b>High:</b> requires full excavation (partial or full road closures, high waste volumes)	<b>High:</b> fully mature technique (widely practiced)
<b>Minimum Dig</b>	<b>High:</b> considerable reductions by avoiding large excavations	<b>Low:</b> minimal surface opening; targeted intervention only	<b>Medium:</b> proven in niche uses, but slow uptake so far
<b>Trenchless Technology</b>	<b>High:</b> up to ~68% less CO <sub>2</sub> than open-cut in selected scenarios of different technologies	<b>Low:</b> only entry/exit pits needed; surface largely undisturbed	<b>High:</b> wide range of established methods exist
<b>Robotics and AI</b>	<b>Very High to Medium:</b> includes indirect gains via efficiency and automation	<b>None to Medium:</b> depends on application (can eliminate or reduce time on site)	<b>Low:</b> emerging technology (pilot stage development)

### 3. ACCOUNTING FOR THE CONSEQUENCES OF STREETWORKS

All actions have consequences; the consequences of actions occurring in the urban street corridor extend to all societal and environmental dimensions (Hayes et al., 2012), and therefore also economic consequences – the street corridors house our ‘economic infrastructures’ and potentially disrupt our ‘social infrastructures’. The choice of streetworks design options is therefore a considerable responsibility. Key components of the assessment of these consequences include: (1) Social impact metrics including traffic congestion delays for vehicles and pedestrians (e.g., converted to lost time costs), noise and dust pollution affecting nearby residents, and any public safety risks; (2) Environmental impact metrics including greenhouse gas (GHG) emissions from construction machinery, air quality degradation, waste generation, and damage to green infrastructure (such as harm to street trees or biodiversity); and (3) Indirect economic impacts including business revenue losses due to reduced footfall during road closures, vehicle operating costs from detours, accelerated road wear from works, and other knock-on effects on the local economy. By capturing these factors, an optioneering tool, such as that being created in the RtNZ project, embodies recommendations from recent research: the total impact of utility projects can only be assessed by evaluating all direct and indirect costs alongside social and environmental externalities (Hojjati et al., 2018).

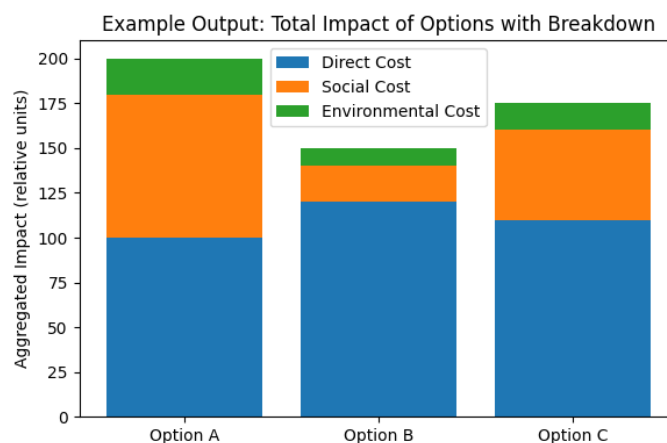
In practice, the optioneering system prompts engineers to input key details of a proposed streetworks operation (such as location, duration, equipment and site operations, affected traffic volumes and facilities and communities affected). These inputs are then processed through a comprehensive consequences calculator that quantifies the reach and magnitude of impacts under each scenario (i.e., design option and context). For example, the tool might estimate the GHG emissions of open-cut trenching versus a trenchless method in terms of the direct works, while simultaneously computing the cumulative expected traffic delays and disruption to local business and integrating them into a monetized cost in each case. Any impacts that cannot be easily quantified (for instance, temporary loss of community amenity or cultural disturbance) are noted qualitatively in the form of an associated narrative so that they are not ignored in the decision-making process. Integrating such multi-dimensional analysis early in the planning stage, engineers can undertake truly holistic design evaluation of subsurface projects. Each candidate solution for utility maintenance or installation is therefore judged not only on engineering feasibility and upfront cost, but also on how well it minimizes total harm and maximizes net benefits across stakeholders and the environment. This broad evaluative perspective would mark a significant shift in subsurface engineering philosophy, from a narrow focus on the asset being buried in the ground, to a system-wide consideration of how the work on that asset reverberates through the urban ecosystem.

### 4. REQUIRED OUTPUTS AND OUTCOMES

The RtNZ optioneering tool is designed to inform and enhance decision-making, not to supplant human judgment. It serves as a sophisticated decision support mechanism that compiles complex data into actionable insights for engineers, project managers, and policymakers. In using the tool, decision-makers are presented with outputs that transparently compare the anticipated consequences of different design choices, thereby enabling evidence-based decisions. It is important to note, however, that the tool itself remains agnostic; it does not “choose” the best option on behalf of the user. Instead, it illuminates the trade-offs inherent in each option, allowing stakeholders to weigh priorities (such as budget constraints versus environmental goals) in light of quantitative evidence – only the decision-maker can fully appreciate the context. This aligns with best practices in infrastructure management, where computational models and multicriteria analyses support the expert’s decision rather than making it autonomously. The ultimate selections still rely on professional judgment, regulatory context, and stakeholder values, but the tool’s comprehensive output ensures those decisions are far better informed than before. In essence, the optioneering tool functions as a catalyst for better decision-making, one that provides a common platform of facts and projections that all parties can discuss, thus depoliticizing debates and focusing attention on holistic outcomes.

The expected outputs of the optioneering tool include quantitative summaries, comparative graphics, and detailed breakdowns for each evaluated scenario. For each candidate solution (e.g., a conventional open-cut repair versus a trenchless repair), the tool can output a suite of metrics: estimated project carbon emissions (in CO<sub>2</sub>-equivalent), total duration of road disruption and associated delay cost to commuters, number of people or businesses directly impacted, projected accident risk or safety incidents, noise levels, excavated material waste volume, and so on. Many of these results are monetized or scored against benchmarks – for example, hours of traffic delay might be converted into monetary cost using standard values of travel time – and carbon emissions might be translated into an equivalent social cost of carbon. By presenting results in common units (e.g. currency or score indices), the tool facilitates an apples-to-apples comparison of alternatives on a single dashboard. In addition, the tool can flag any threshold exceedances or regulatory compliance issues (for example, if an option would produce noise above allowable levels at night, or if expected road disruption exceeds what permit conditions

allow). The outputs are typically delivered both in tabular form (detailed reports) and as visualizations that condense the information, such as bar charts stacking impact categories (Figure 4), radar charts of sustainability criteria, or map-based illustrations of the spatial extent of disruption for each option. These user-friendly outputs empower project planners to identify the dominant impacts of each option at a glance, and to pinpoint where design modifications could yield improvements (e.g., if one option's carbon footprint is high, perhaps alternative machinery or materials could be considered).



**Figure 4.** Conceptual output from optioneering tool.

(Conceptual output from an ‘all consequences’ optioneering analysis, comparing three design alternatives for a hypothetical streetworks project. Each bar represents an option’s aggregated impact (lower is better), subdivided into direct construction cost (blue segment), indirect social costs such as traffic delay and inconvenience (orange segment), and environmental costs such as carbon footprint (green segment). In this illustrative example, Option B has a higher direct expense than Option A but far lower social and environmental costs, resulting in the lowest total impact when all consequences are accounted for. Such output visuals enable stakeholders to immediately grasp the trade-offs and net benefits of more sustainable engineering choices.)

## 5. CONCLUSIONS

That we live in a complex world, made up of a system-of-systems, is universally understood, and this complexity is exemplified in urban street corridors that support civilized life. Not only are they the places in which we live and work, but we rely on them to support the urban metabolism - if they operate efficiently and effectively, then all urban systems have the potential to function as intended. Disrupting these systems to install a new buried utility pipeline, or repair or upgrade an existing pipeline, therefore has potentially serious consequences. It is essential to identify and characterize such consequences so that any proposed streetworks activity can be evaluated in terms of net value. This means balancing the value realized (for example, providing new or protected utility service provision, many of which are essential and make the works unavoidable) against the value compromised to those who live, work, and pass through the affected area. Such an evaluation must consider all forms of movement through the urban street corridor, direct impacts on the local context, and more indirect impacts on the wider environment.

The RtNZ project is addressing this issue of national (and global) importance by developing an optioneering tool that makes transparent the full consequences of adopting different design options for streetworks, and then iterating them - choosing different equipment that might achieve the same result (e.g., electrically powered excavators to replace those using diesel engines), different site routines, alternative materials to use in the works, different material sources (with an eye on transport distances, hence emissions), different transport regimes for staff moving to and from site, the rapidity and timing of the works, the GHG emissions in the street corridor and its impact on traffic management, and so on. While the original motivation for the research described in this paper, as the project title implies, was to make transparent the carbon consequences of alternative approaches to streetworks, it rapidly became evident that the broader scope now adopted in this work is critical if those commissioning and carrying out streetworks are “to do the right thing.” This is to look after the interests of the end user of all the services offered by urban street corridors, and ultimately that is every one of us. One final point here, of course, is that these findings are not limited to urban areas but are relevant wherever buried infrastructure and surface infrastructure coincide.

## 6. ACKNOWLEDGEMENTS

The authors gratefully acknowledge the financial support of the UK Engineering and Physical Sciences Research Council under grant numbers EP/F065965 (Mapping The Underworld), EP/I016133 (Resilience of Critical Local Infrastructures), EP/J017698 (Liveable Cities), EP/K012398 (iBUILD), EP/N010523 (Self-Repairing Cities), EP/K021699 (Assessing The Underworld), EP/P013635 (UKCRIC National Buried Infrastructure Facility) and EP/R017727 (Coordination Node for UKCRIC) and EP/S016813 (Pervasive Sensing of Buried Pipes). More specifically, the authors also gratefully acknowledge the financial support of Transport for London (TfL) under its Lane Rental Funds and the intellectual contributions from Road to Net Zero collaborators at TfL, the Highway Authorities and Utilities Committee (HAUC), GeoPlace and EA Technology.

## 7. REFERENCES

- [1] Torbaghan, M.E., Curioni, G., Hayati, F., Royal, A.C.D., Chapman, D.N., Atkins, P.A. and Rogers C.D.F. (2020). An Investigation into the relationship between Trenching Practice and Road Deterioration through a Field Trial. *Proceedings of the Institution of Civil Engineers – Infrastructure Asset Management*, **7**(4), 282-296.
- [2] Haylen, A. and Butcher, L. (2019). Street Works in England. In *UK Parliament*. House of Commons Library (Roads). <https://commonslibrary.parliament.uk/research-briefings/cbp-8500/> (Accessed 24<sup>th</sup> June 2025)
- [3] LCRIG (2025). *Road to Net Zero: Project Update*. Local Council Roads Innovation Group. (<https://lcrig.org.uk/news/road-to-net-zero-project-update/>) (accessed 11th June 2025)
- [4] Burtwell, M.H., Evans, M., McMahon, W. and Kingdom, U. (2006). *Minimising street works disruption: the real costs of street works to the utility industry and society*. UK Water Industry Research Limited, London, UK.
- [5] Goodwin, P. (2005). Utilities' Street Works and the Cost of Traffic Congestion. (<https://www.uwe.ac.uk/research/centres-and-groups/cts/research-themes/the-travel-environment/street-works-and-congestion> 11/06/2025)
- [6] Hayes, R., Metje, N., Chapman, D.N., and Rogers, C.D.F. (2012). Sustainability Assessment of UK Streetworks. *Proceedings of the Institution of Civil Engineers – Municipal Engineer*, **165**(4), 193–204.
- [7] Hojjati, A., Jefferson, I., Metje, N., & Rogers, C. D. F. (2018). Sustainability assessment for urban underground utility infrastructure projects. *Proceedings of the Institution of Civil Engineers – Engineering Sustainability*, **171**(2), 68–80.
- [8] Rogers, C.D.F., Makana, L.O., Leach, J.M. *et al.* (2022) *The Little Book of Theory of Change for Infrastructure and Cities*. University of Birmingham, UK. ISBN 978-0-70442-981-9.
- [9] Rogers, C.D.F. (2018). Engineering Future Liveable, Resilient, Sustainable Cities using Foresight. In *Proceedings of the Institution of Civil Engineers–Civil Engineering*, **171**(6), 3-9.
- [10] Hojjati, A., Jefferson, I., Metje, N., & Rogers, C. D. F. (2016). Sustainable asset management for utility streetworks. In *Transforming the Future of Infrastructure through Smarter Information: Proceedings of the International Conference on Smart Infrastructure and Construction*, 27–29 June 2016 (pp. 669-674). ICE Publishing.
- [11] RTNZ Project. (2025). *Road to Net Zero Project Website*. Geoplace, <https://www.roadtonetzero.org.uk/> (accessed 1st June 2025).
- [12] Rogers, C. D. F., Hojjati, A., Jefferson, I., & Metje, N. (2020). Novel business models in support of trenchless cities. In *37th International NO-DIG Conference and Exhibition 2019*.



## BENEATH THE SURFACE: UNLOCKING URBAN GEOTHERMAL POTENTIAL FROM LEGACY SUBSURFACE ASSETS

Chrysothemis Paraskevopoulou<sup>1</sup>, Antonia Cornaro<sup>2</sup>

**Abstract:** Urbanisation is accelerating at an unprecedented rate, with an estimated 70% of the global population expected to live in urban areas by 2050. This growth challenges cities to maintain liveability while meeting ambitious sustainability targets. Among the most pressing concerns is the decarbonisation of space heating, which accounts for approximately 18% of the UK's total energy use. This paper explores how legacy underground structures—specifically disused coal mines and shallow aquifers—can be repurposed for sustainable geothermal energy, contributing to low-carbon urban heating systems. Drawing on two case studies in the Leeds region in the UK, the research presents a scalable framework for assessing the geothermal viability of subsurface environments. The first study investigates the feasibility of geothermal heat extraction from aquifers beneath the University of Leeds campus, using legacy hydrogeological data combined with thermal modelling. The second assesses the regional thermal potential of abandoned coal mine workings in the Pennine Coal Measures, leveraging historical mining records and borehole data to evaluate city-scale opportunities for minewater heating networks. The findings demonstrate that legacy data, when systematically integrated, can reveal untapped thermal resources that align with net-zero goals. The proposed methodology is transferable to other urban settings with similar geological and post-industrial contexts, offering a replicable model for sustainable underground energy planning.

**Keywords:** Subsurface sustainability, Urban sustainable heating, Legacy data reuse and analysis Aquifer thermal potential, Minewater heat recovery

### 1. INTRODUCTION

Urbanisation is accelerating worldwide, with the United Nations projecting that 70% of the global population will reside in urban areas by 2050 [1]. This trend exerts enormous pressure on urban infrastructure, resource efficiency, and environmental resilience. Among the most urgent priorities is the decarbonisation of urban heating, which accounts for nearly 18% of the UK's total energy use [2]. As cities attempt to grow sustainably while maintaining green and open spaces, innovative energy strategies are essential to transition from fossil fuels to low-carbon alternatives [3, 4].

One such opportunity lies beneath our feet: the urban subsurface. Across the United Kingdom and many post-industrial nations, historical urban development was accompanied by extensive subsurface interventions—most notably, coal mining and urban aquifer tapping [5]. These features, often viewed as legacies of environmental degradation, are now being reconsidered as assets in the transition to net-zero cities. Abandoned coal mines, with their extensive voids, can serve as reservoirs for low-enthalpy geothermal energy, while shallow aquifers in urban catchments also offer potential as natural heat exchangers [3, 5].

Despite growing interest, the geothermal potential of such legacy structures remains underexplored at the city scale. Much of the existing literature [5] focuses on small-scale mine water heat pump systems or isolated aquifer thermal energy storage (ATES) units. What is missing is a methodical approach to scaling these technologies using

<sup>1</sup> Professor (Associate) and AG2 on Urban Sustainability co-Leader, ITACUS Committee on Underground Space of ITA-AITES, Chrysothemis Paraskevopoulou, Tunnel/Mining/Geotech Engineer, PhD, MBA, MSc, MEng, Associate Professor, University of Leeds, Leeds, United Kingdom, [c.paraskevopoulou@leeds.ac.uk](mailto:c.paraskevopoulou@leeds.ac.uk), [chrys.parask@gmail.com](mailto:chrys.parask@gmail.com).

<sup>2</sup> Lecturer and Expert Underground Space, Chair ITA Committee of Underground Space of ITA-AITES, Antonia Cornaro, MA Urban Planning NYU, BA SocSci, Amberg Engineering, Trockenloostrasse 21, CH-8105 Regensdorf, Switzerland, [acomaro@amberg.ch](mailto:acomaro@amberg.ch)

publicly available historical data. This study addresses that gap by integrating two case studies in the Leeds region: a coalfield geothermal assessment across the Pennine Coal Measures, and a shallow aquifer feasibility study beneath the University of Leeds campus.

Through spatial, thermal, and hydro-geological analysis of legacy datasets—including borehole logs, mining records, and aquifer maps—this paper develops a transferable methodology for evaluating subsurface geothermal resources. This work contributes to urban sustainability by outlining pathways for retrofitting existing urban geologies into functioning components of low-carbon energy systems, reinforcing the role of underground spaces in resilient, future-proof cities.

## 2. BACKGROUND

### 2.1. Underground Space and Urban Sustainability

The underground environment represents a valuable and underutilized resource in the sustainable development of cities [6]. With surface land becoming increasingly constrained, the **subsurface offers critical opportunities** for energy production, storage, transportation, waste management, and climate adaptation [7, 8]. Integrating underground infrastructure into urban design not only frees up surface space for green areas and social functions but also aligns with broader sustainability objectives—particularly climate action, clean energy, and responsible resource use. In the context of the United Nations Sustainable Development Goals (SDGs), subsurface developments can directly or indirectly support more than ten of the 17 goals [6]. [3] presented a histogram that visualises this relationship, underscoring how geothermal energy, waste heat storage, and aquifer (*e.g.*, *SDG 7, 11, 13*) use contribute to global sustainability targets as shown in Figure 1.



**Figure 1.** Top: Histogram illustrating the relevance of subsurface use to the UN Sustainable Development Goals - Longer bars indicate stronger alignment; and, Bottom: Sustainable development goals introduced in the 2030 Agenda for sustainable development proposed by the United Nations members in 2015 (adapted from [3 & 8]).

## 2.2. Urban Heating and Energy Transitions

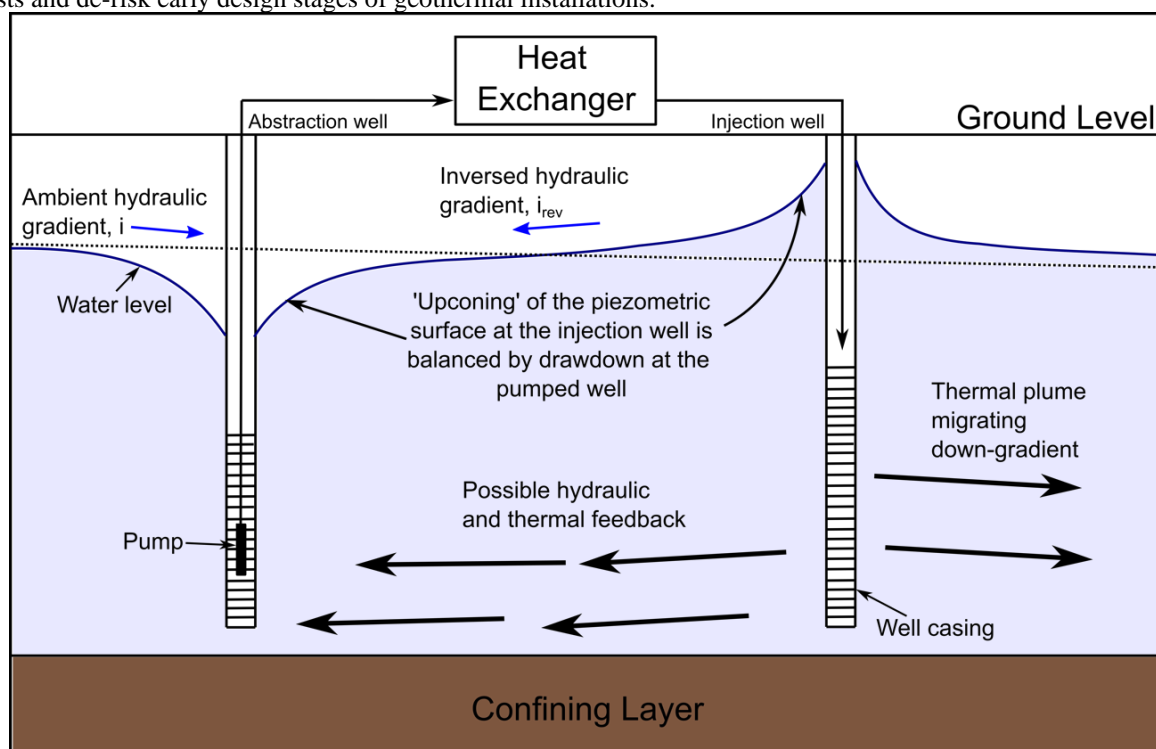
Heating remains one of the most carbon-intensive energy demands in cities. In the UK, around **40% of energy consumption in buildings** is attributed to heating, primarily supplied by fossil fuel-based gas boilers [9]. Transitioning to low-carbon heating systems is essential for meeting net-zero targets and improving energy resilience in urban areas [3, 4, 5].

District heating systems powered by **renewable or residual heat sources**—such as wastewater, ambient heat, or geothermal energy—have gained traction across Europe as a pathway for large-scale decarbonization [9]. Among these, shallow geothermal resources stand out for their reliability, longevity, and minimal environmental footprint [4].

## 2.3. Shallow Geothermal Systems and Subsurface Potential

Shallow geothermal systems encompass a range of technologies designed to harness the thermal capacity of the ground. These include **ground source heat pumps (GSHPs)**, **aquifer thermal energy storage (ATES)**, and **minewater-based systems**, which are well-suited to urban settings due to their scalability and compatibility with building-level or district-scale heating networks [10, 11]. An example is shown in Figure 2 and 3 (right).

[4] assessed the geothermal feasibility of the **University of Leeds campus** using legacy hydro-geological data. Borehole records and groundwater temperature data were modelled to estimate sustainable extraction rates and seasonal recharge potential. This approach showed how previously overlooked data could reduce site investigation costs and de-risk early design stages of geothermal installations.

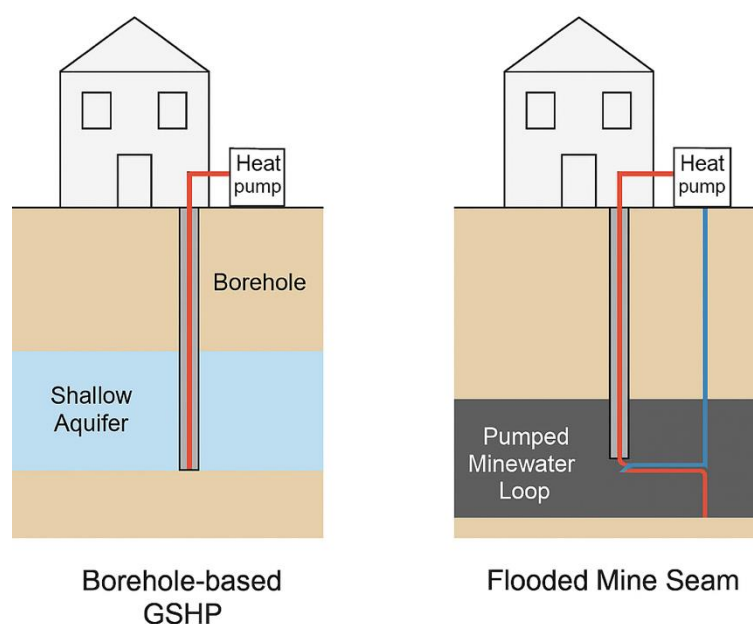


**Figure 2.** Schematic cross section illustrating the possibility of hydraulic and thermal feedback in a well 'doublet' [4].

## 2.4. Minewater Geothermal Energy and Industrial Legacies

Similarly, abandoned coal mines are now seen as **geothermal assets** [4]. Filled with groundwater at moderate depths, they can maintain temperatures of 12–20°C, which can be harvested using minewater heat pumps. [3] mapped coal seams within the **Greater Leeds area** to evaluate regional geothermal potential, using GIS-based analysis of seam depth, continuity, and overburden thickness.

The findings indicate that large-scale minewater heating networks could be deployed using existing shaft infrastructure and district-scale heat exchange systems. Such systems shown in Figure 3 not only reduce emissions but also revalorise post-industrial land as energy-positive environments.



**Figure 3.** Conceptual cross-section of minewater and aquifer-based geothermal systems operating in an urban subsurface context. (left side = borehole-based GSHP in shallow aquifer; right side = flooded mine seam with pumped minewater loop. Integrated with heat pump units and surface buildings.)

## 2.5. Research Gap and Contribution

Despite isolated pilot projects, city-scale geothermal planning remains limited, particularly in legacy urban landscapes. There is a clear need for a **replicable framework** that integrates public domain geological and hydrological data to pre-screen sites and support local energy planning. Your published case studies collectively respond to this need—demonstrating methods for **data-driven geothermal screening** using available legacy datasets and confirming that both aquifers and coalfields hold viable potential for integration into urban heating transitions.

## 3. METHODOLOGY

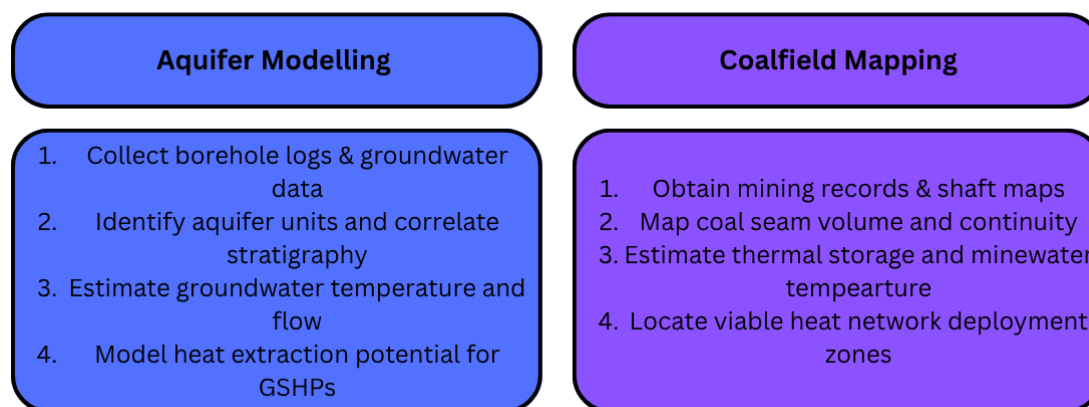
This study draws upon two independent yet thematically linked case studies carried out in the city of Leeds, UK: (1) a shallow aquifer-based geothermal feasibility study at the University of Leeds campus [4], and (2) a regional-scale coalfield geothermal screening across the Greater Leeds area [3]. Both studies rely on publicly available legacy data, demonstrating how historical subsurface information can be used to de-risk early-stage geothermal energy development.

The key datasets used in both studies include (Table 1). These data were pre-processed in GIS environments (ArcGIS Pro, QGIS) and integrated using 3D spatial modelling to estimate geothermal gradients, potential extraction zones, and infrastructure integration potential.

**Table 1.** Key datasets in the two case studies..

Data Type	Source	Application
Borehole logs and lithological data	British Geological Survey (BGS) GeoIndex & OpenGeoscience	Hydrostratigraphy, depth to aquifers
Mining seam maps & shaft data	Coal Authority	Mine depth, seam continuity, void distribution
Groundwater monitoring records	Environment Agency & University archives	Temperature profiling, recharge rates
Building and campus energy use	University estates & planning records	Estimating thermal demand
Surface elevation and geology	Ordnance Survey and BGS 1:50,000 scale maps	Overlay analysis, topographic constraints

The modelling approach used in both cases based on the key datasets obtained is showing in Figure 4.



**Figure 4.** Workflow diagram summarising the geothermal potential screening methodology applied in both case studies: Left: for shallow aquifer modelling and Right: for coalfield geothermal mapping.

### 3.1. Site 1: Shallow Aquifer Assessment (University of Leeds)

This sub-study used 19 borehole logs from within and around the University campus to assess the hydrogeological characteristics of the shallow sandstone aquifer. The key steps involved:

- **Stratigraphic correlation** of borehole logs to identify aquifer units (Millstone Grit, Sherwood Sandstone Group)
- **Groundwater temperature estimation** using proxy data and nearby Environment Agency wells
- **Sustainable yield estimation** using simplified Darcy flow assumptions
- **Thermal potential modelling** to size a potential ground source heat pump system

Energy demand was estimated based on university building typologies (teaching, laboratory, residential), which was then cross-referenced with available heat extraction potential per m<sup>2</sup> of borefield footprint.

### 3.2. Site 2: Coalfield Geothermal Potential (Greater Leeds)

This larger-scale assessment focused on post-industrial coalfields within the Pennine Middle and Lower Coal Measures, encompassing areas such as Middleton, Rothwell, and Garforth. The following workflow was employed:

- Digitisation of historic **coal seam maps** and identification of **seams >1 m thickness**
- 3D spatial modelling to define **accessible depth windows** (100–500 m)
- Identification of **existing mine shafts** and vertical access points
- **Heat capacity estimation** using known volumetrics and temperature gradients (ca. 26–30°C/km)
- GIS-based screening to identify **district heating cluster potential** zones

### 3.3. Analytical Assumptions

To ensure comparability across both case studies, consistent assumptions were applied:

- **Heat extraction rate** for shallow systems: 20–50 W/m<sup>2</sup> [3,4]
- **Thermal conductivity** estimates: 2.0–3.0 W/m·K depending on lithology [3,4]
- **Coefficient of performance (COP)** for GSHP systems: 3.5 (standard for UK retrofits)
- Temporal scope assumed: **20-year project lifespan** with potential extension

All estimates were conservatively framed, with emphasis placed on using only existing data—no new drilling or intrusive ground investigation was required at this stage.



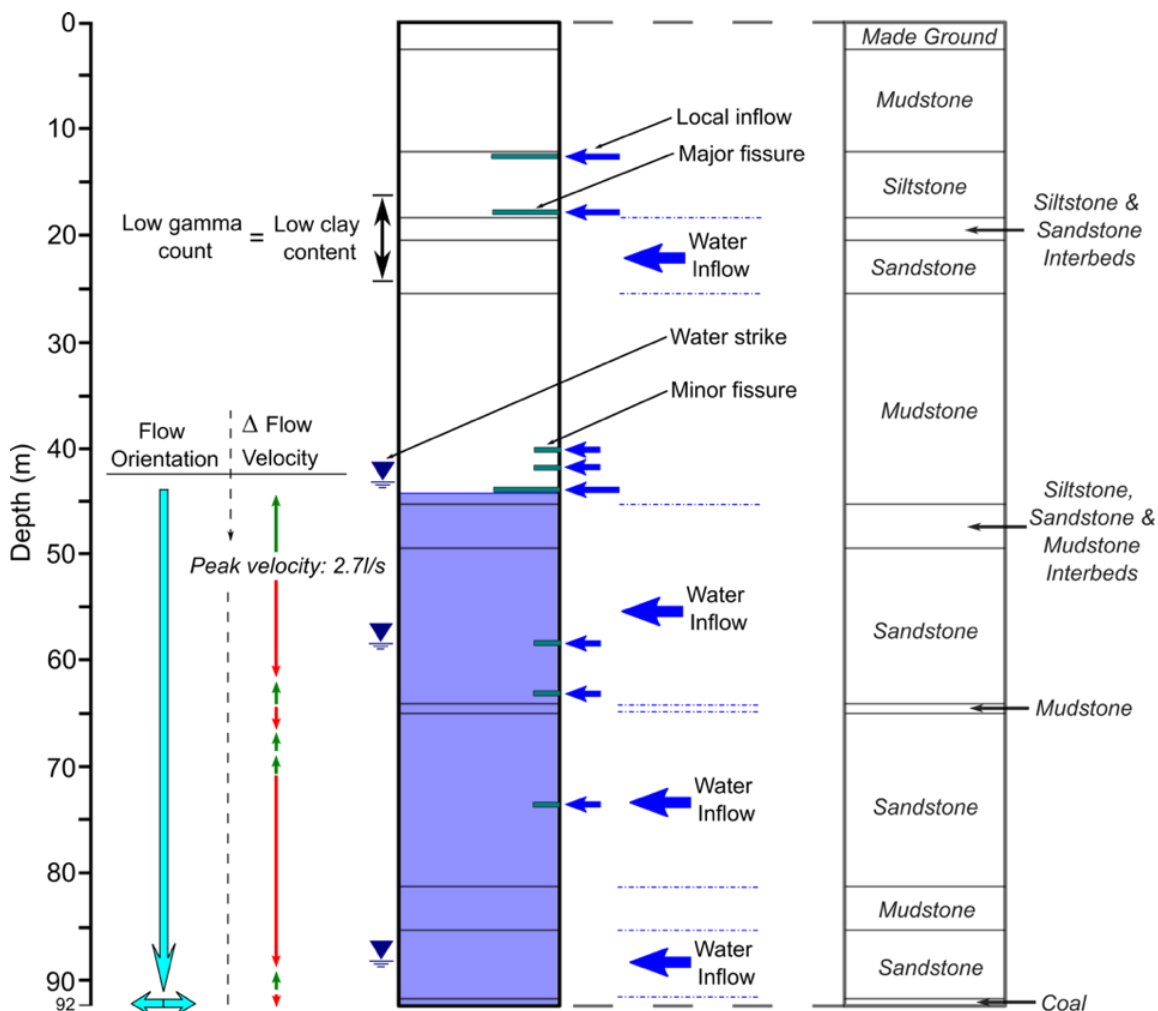
## 4. RESULTS

### 4.1. Shallow Aquifer Case Study: University of Leeds Campus

The hydrogeological assessment of the University of Leeds site confirmed the presence of a shallow fractured sandstone aquifer (Millstone Grit), with depths ranging between 10 m and 45 m and thicknesses exceeding 15 m in certain areas. Groundwater temperatures at depth were inferred to be between 10–11.5°C, based on regional thermal gradient extrapolation and nearby Environment Agency monitoring wells.

- **Extractable thermal energy** was conservatively estimated at **17–28 W/m<sup>2</sup>** of borefield area.
- For a 6,000 m<sup>2</sup> available borefield footprint, this yields a **heat supply of ~120–160 kWth**.
- Over a 20-year period, and accounting for seasonal variations, this equates to a potential **~2.5 GWh/year** of clean thermal energy.
- Demand modelling showed this output could serve up to **6 medium-sized academic buildings**, offsetting approximately **340 tonnes of CO<sub>2</sub> annually**.

An example cross-section of the analysis is shown in Figure 5. Constraints included limited access due to existing buried services and buildings, but adaptive borehole layouts (L-shaped or radial) were found to mitigate surface disruption.



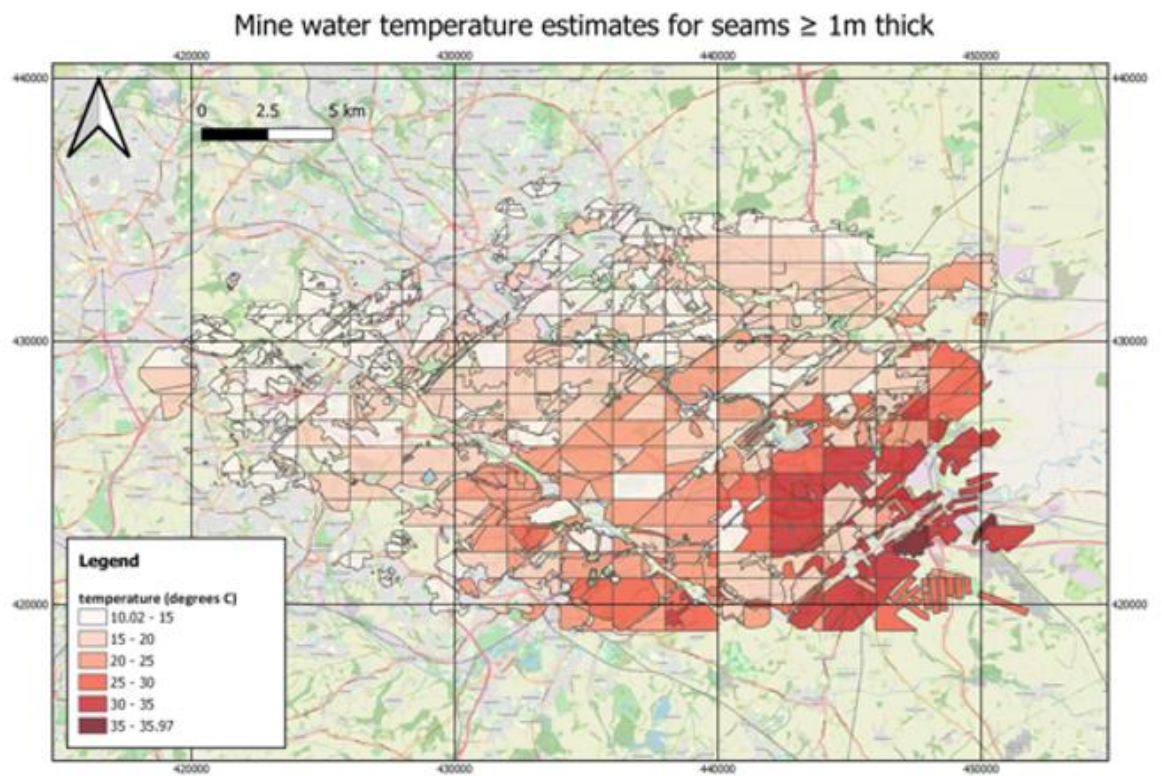
**Figure 5.** One-dimensional schematic cross section through borehole X, summarising the hydrological conditions inferred from geophysical logs [4].

#### 4.2. Coalfield Geothermal Screening: Greater Leeds Area

Analysis of legacy mining datasets identified over 350 km<sup>2</sup> of accessible coal seams, with over 75 seams exceeding 1 m in thickness and occurring at depths of 150–400 m. Seam temperature estimates ranged from 13–20°C, suitable for low-enthalpy heating systems when combined with high-efficiency heat pumps.

- Estimated minewater volumetric capacity suggests extractable thermal power of 3–8 MWth across five high-potential clusters (e.g., Middleton, Rothwell, Garforth).
- A conservative model indicates potential for >40 GWh/year thermal output across the region.
- These areas show strong alignment with residential heat demand zones and existing district energy infrastructure.

Example of a heat map is shown in Figure 6. The mapping tool developed by [3] enables spatial screening of subsurface potential and cross-referencing with socio-technical variables such as fuel poverty indices, network connection density, and land availability.



**Figure 6.** GIS heat map overlaying coal seam depth of 1 m, shaft locations, and local building density to identify candidate heat network zones [3].

#### 4.3. Comparative Potential and Integration Pathways

While the university site supports decentralised, small-scale systems, the coalfield zones present opportunities for regional decarbonisation strategies, especially when integrated with municipal housing or industrial heat users. A summary comparison is shown in Table 2.

**Table 2.** Comparative Potential and Integration Pathways.

Parameter	University Campus (Aquifer)	Greater Leeds (Coalfields)
Depth	10–45 m	150–400 m
Temperature range	10–11.5°C	13–20°C
Estimated output	~2.5 GWh/year	~40 GWh/year (multi-site)
Technology	Vertical GSHPs	Minewater heat pumps
Network scale	Building cluster	District-level
Carbon reduction potential	~340 tonnes CO <sub>2</sub> /yr	>6,000 tonnes CO <sub>2</sub> /yr

## **5. DISCUSSION**

### **5.1. Leveraging the Urban Subsurface for Sustainability**

The re-utilization of subsurface space, including aquifers and abandoned coalfields, represents a strategic opportunity to decarbonize urban heating while advancing sustainability goals. As demonstrated in both Leeds-based case studies, the integration of legacy data with modern spatial modelling can offer a low-cost, non-invasive starting point for planning geothermal infrastructure — aligning directly with SDG 7 (Affordable and Clean Energy) and SDG 11 (Sustainable Cities and Communities) [6, 8].

Shallow geothermal systems, while spatially constrained, are ideal for campus-scale or institutional users with predictable demand and land control. Conversely, minewater geothermal presents a city-scale solution, with heat recovery potential capable of serving thousands of households. The complementary nature of these systems reinforces the need for tiered urban geothermal strategies.

### **5.2. Economic Feasibility**

Initial capital expenditures for shallow ground source heat pump (GSHP) systems are typically higher than conventional gas boilers (ca. £1,000–£1,800 per kW<sub>th</sub> installed), but operational cost savings and government incentives (such as the UK's Boiler Upgrade Scheme or potential carbon credits) can deliver payback within 8–12 years.

For minewater systems, infrastructure costs are higher due to the need for heat exchange equipment, network piping, and water treatment. However, the scale of thermal delivery — particularly in high-density areas — offers greater returns over time. A 3 MW<sub>th</sub> minewater system, for instance, could deliver £150,000–£200,000 in annual energy savings depending on fossil fuel displacement rates.

### **5.3. Policy and Planning Implications**

Urban planning systems must evolve to treat subsurface as a finite, strategic resource, rather than an unregulated void. Integrating geothermal feasibility studies into local development frameworks and city masterplans could significantly streamline adoption.

Furthermore, the availability of digitised borehole, shaft, and geological data presents an opportunity for governments to build open-access geothermal mapping platforms — supporting both public and private sector actors in early decision-making.

Example: The Coal Authority's minewater heat project database, and the BGS's OpenGeoscience portal, already offer strong precedents for replicable national-scale geothermal resource screening.

### **5.4. Data Gaps and Limitations**

Despite promising results, several limitations persist:

- Legacy data coverage is uneven, with gaps in key hydrogeological parameters like transmissivity and water chemistry.
- Temperature profiles are often absent or outdated, requiring inference from regional gradients.
- Subsurface infrastructure conflicts (e.g., sewer lines, tunnelling) can reduce available installation zones, especially in dense urban cores.

Thus, while legacy datasets are powerful, targeted ground validation (e.g., temperature logging or pumping tests) remains essential before full-scale implementation.

### **5.5. Transferability**

The methodology developed through these studies is highly transferable to other post-industrial cities in the UK (e.g., Glasgow, Newcastle, Sheffield) and internationally — particularly where mining legacies or campus-scale aquifers exist. By standardising workflows that integrate GIS, legacy data, and thermal modelling, cities can make evidence-based decisions with minimal upfront investment.

## **6. CONCLUSIONS**

This study has demonstrated the substantial potential of repurposing urban subsurface environments — particularly shallow aquifers and legacy coal mine workings — for sustainable geothermal heating solutions. By

leveraging freely available historical and geological data, both case studies in Leeds illustrate that low-carbon, decentralized or district-scale heating infrastructure can be feasibly assessed without intrusive investigation, reducing project risk at early stages.

The University of Leeds aquifer study showed that even constrained urban campuses can benefit from targeted ground source heat systems, offering significant carbon savings and a pathway to institutional energy autonomy. Meanwhile, the Greater Leeds coalfield screening identified large-scale thermal potential in disused mineworkings, underlining the viability of minewater systems as part of city-scale heating transitions — especially in post-industrial urban contexts.

The findings support four key recommendations:

- Integrate geothermal screening into early-stage masterplanning for new developments and urban retrofits, particularly in areas with known subsurface data.
- Develop national or municipal-level geothermal mapping platforms that combine geological, demand, and infrastructure layers, enabling transparent feasibility assessments.
- Adopt a dual-scale strategy that pairs shallow aquifer heat pumps for localized users (campuses, schools, hospitals) with deeper minewater networks for dense residential zones.
- Incentivise low-carbon heating infrastructure through consistent policy frameworks, building regulations, and financial support — especially for heat network deployment and retrofitting.

By shifting how we understand and value the subsurface, cities can align thermal energy use with broader climate resilience, circular economy principles, and sustainable development objectives.

## 7. REFERENCES

- [1] United Nations (2018). 2018 Revision of World Urbanization Prospects. Retrieved from: <https://www.un.org/uk/desa/68-world-population-projected-live-urban-areas-2050-says-un>
- [2] Ritchie, H., Roser, M., 2021. CO2 and greenhouse gas emissions. Our World in Data [Online]. Retrieved from: <https://ourworldindata.org/emissions-by-sector#energy-electricity-heat-and-transport-73-2>
- [3] Paraskevopoulou, C., Connolly, A., Kearsley, T., Shaw, N. 2025. Utilising the Subsurface for Sustainable Green Energy Solutions. In: Agrawal, M. (eds) Underground Spaces for Climate Resilience and Sustainability. Advances in 21st Century Human Settlements. Springer, Singapore. [https://doi.org/10.1007/978-981-96-0547-7\\_6](https://doi.org/10.1007/978-981-96-0547-7_6)
- [4] Green, N., Paraskevopoulou, C., Bramham, E., Clark, R., Shaw, N., 2025. Using legacy data to investigate the geothermal potential of UK's aquifers: a feasibility study at the University of Leeds, UK, Geoenergy Science and Engineering, Volume 254, 2025, 214025, ISSN 2949-8910, <https://doi.org/10.1016/j.geoen.2025.214025>.
- [5] Cheuklun Ng, Paraskevopoulou, C., Shaw N. Stability Analysis of Mineshafts used for Minewater Heat Recovery in the UK. *Geotechnical & Geological Engineering*, 37, 5245-5268(2019). <https://doi.org/10.1007/s10706-019-00978-y>
- [6] Paraskevopoulou, C., Cornaro, A., Admiraal, H., Paraskevopoulou, A. 2019. Underground space and urban sustainability: an integrated approach to the city of the future. In: Proceedings of the International Conference on Changing Cities IV: Spatial, Design, Landscape & Socio-economic Dimensions. 4th International Conference on “CHANGING CITIES: Spatial, Design, Landscape & Socio-economic Dimensions, 24-29 Jun 2019, Chania, Greece. University of Thessaly. ISBN 978-960-99226-9-2
- [7] Kaliampakos, D. (2016). Underground development: A springboard to make city life better in the 21st century. *Procedia Engineering*, 165, 205-213. <https://doi.org/10.1016/j.proeng.2016.11.792>.
- [8] Paraskevopoulou, A., Cornaro, A., Paraskevopoulou, C., 2022. Underground Space and Street Art towards resilient urban environments. In: Proceedings of the International Conference on Changing Cities IV: “*Making our Cities Resilient in times of Pandemics*”. June 2022, Corfu, Greece.
- [9] Farr, G., Busby, J., Wyatt, L., Crooks, J., Schofield, D., Holden, A., 2020. The temperature of Britain's coalfields. *Q. J. Eng. Geol. Hydrogeol.* 54 (3), 95–109. <https://doi.org/10.1144/qjegh2020-109>.
- [10] Banks, D., Athresh, A., Al-Habaibeh, A., Burnside, N., 2017. Water from Abandoned Mines as a Heat Source: Practical Experiences of open- and closed-loop Strategies, United Kingdom, 5. <https://doi.org/10.1007/s40899-017-0094-7>.
- [11] Fraser-Harris, A., McDermott, C., Receveur, M., Mouli-Castillo, J., Todd, F., Cartwright-Taylor, A., Gunning, A., Parsons, M., 2022. The Geobattery Concept: a Geothermal Circular Heat Network for the Sustainable Development of near Surface Low Enthalpy Geothermal Energy to Decarbonise Heating, 2. <https://doi.org/10.3389/esss.2022.10047>.

## SUBTERRANEAN URBANISM FOR WILDFIRE RESILIENCE: POST-DISASTER PLANNING AND GIS-BASED DESIGN IN TOPANGA–PALISADES, LOS ANGELES (2025)

Mohammad-Mahdi Safaei<sup>1</sup>, Hoda Hashemi<sup>2</sup>

**Abstract:** The increasing frequency and intensity of wildfires, particularly in urban-wildland interface zones, pose serious threats to cities such as Los Angeles. The January (2025) wildfire in the Topanga – Palisades Highlands region revealed systemic vulnerabilities in both urban planning and structural resilience. This research explores the use of underground architecture as a passive defense mechanism against wildfire intrusion. Through geospatial analysis, thermal mapping, and case comparison with international precedents—including projects in Wrocław (Poland), Athens (Greece), and the UBC thermal void pilot in Canada—the study identifies key design strategies for enhancing thermal resistance, minimizing damage, and ensuring emergency survivability. A pilot reconstruction model is proposed, emphasizing clustered earth-sheltered housing, adaptive ventilation, and multi-layered zoning. The findings demonstrate that underground systems, when integrated with local topography and supported by robust regulatory frameworks, can significantly enhance wildfire resilience and long-term sustainability in vulnerable urban zones.

**Keywords:** Underground architecture, wildland-urban interface, wildfire resilience, passive defense, earth-sheltered buildings

### 1. INTRODUCTION

In recent decades, the intensification of wildfires at the urban-wildland interface has emerged as one of the most pressing challenges facing cities situated near forests and dry terrains. According to the National Interagency Fire Center (NIFC, 2024), the United States experienced over 7.6 million acres of wildfire damage in (2023) alone, with California accounting for nearly 28% of all incidents. Climate change has exacerbated this trend by increasing temperature extremes, reducing humidity, and prolonging drought periods—especially in regions such as Southern California, where cities like Los Angeles (LA) face chronic wildfire threats. The January (2025) Los Angeles wildfire stands as a stark reminder of the vulnerability of built environments to fast-moving fires. The incident, which affected the Topanga Canyon and Palisades Highlands areas, spread rapidly due to a combination of steep terrain, dry Santa Ana winds, combustible vegetation, and inadequate spatial buffers. While emergency response systems managed partial containment within 72 hours, structural losses were significant, particularly in hillside neighborhoods with poor defensible space planning and non-resistant building materials. Although current strategies focus heavily on rapid suppression, firefighting aircraft, and public alerts, a critical gap remains in the deployment of fire-resilient urban infrastructure. Traditional surface architecture offers limited protection against heat penetration and smoke, and urban planning often lacks integration with fire behavior modeling. Against this backdrop, underground architecture presents a potentially transformative solution—leveraging the thermal

<sup>1</sup> PhD. Safaei, Mohammad Mahdi, Faculty member of Architecture Department, South Tehran Branch, Islamic Azad University (IAU), Tehran, Iran [mm-safaei@azad.ac.ir](mailto:mm-safaei@azad.ac.ir)

<sup>2</sup> MURP, Hashemi, Hoda, Master degree in Urban Planning, University of Tehran, Iran. [hashemi.hodaa@gmail.com](mailto:hashemi.hodaa@gmail.com)



inertia and shielding capabilities of earth-integrated design to passively resist heat propagation, enhance survivability, and improve long-term sustainability in high-risk zones.

## 2. LITERATURE REVIEW AND COMPARATIVE ANALYSIS OF SUBTERRANEAN ARCHITECTURE RESPONSE TO WILDFIRES

The intensification of wildfires in the past two decades has spurred the growth of specialized literature in the field of resilient design and passive defense infrastructure. Among various urban interventions, underground architecture has emerged as a sustainable, civilian, and cost-effective solution for retrofitting the urban-wildland interface (WUI). The following case studies illustrate validated academic and pilot initiatives that have incorporated subterranean systems for wildfire protection.

### 2.1. Poland – Semi-Subterranean Units in Kraków and Wrocław

Following the (2015) wildfire in the southwestern forests near Wrocław, Poland's National Foundation for Climate Reconstruction (PNRF), along with the Kraków University of Technology (PK) and Wrocław University of Environmental Sciences, launched a pilot to design thermally resilient underground dwellings. These were half-buried residential units constructed with compacted native soil, sub-surface drainage layers, vegetated roofs, and clay-sealed insulation envelopes.

According to a study in the *Journal of Sustainable Urban Forms* (2022), the structures showed no more than a 12°C internal temperature rise during 45-minute direct flame exposure. In a follow-up report from Wrocław's Fire-Resilient Structures Lab (2023), these units reportedly withstood the (2018) Bielany Wrocławskie wildfire unscathed, while 35% of conventional buildings in the same region suffered severe damage.

Over 63% of residents in post-occupancy surveys (2022) reported a higher perception of safety and thermal comfort compared to conventional housing. Key user-reported benefits included passive ventilation, reduced energy costs, and heat camouflage.

**Table 1. SWOT – Poland (Wrocław / Kraków Semi-Subterranean Units)**

<b>Strengths</b>	High thermal resistance, Integration with landscape Soil-based insulation, Community support (63%)
<b>Weaknesses</b>	Initial excavation costs, Limited natural light Complex drainage systems, Cultural reluctance (rural zones)
<b>Opportunities</b>	EU climate adaptation funding, Urban fringe redevelopment
<b>Threats</b>	Legal constraints in dense areas, Groundwater interference risks

### 2.2. Canada – UBC FireSmart Thermal Belt

The *FireSmart* initiative developed by the Climate Risk Lab at the University of British Columbia (UBC) focused on the city fringe of Kelowna. The strategy utilized “subsurface thermal buffer zones” composed of moist soil corridors, passive air tunnels, and gradient-based insulation layers.

Key findings from *UBC-CRL Report* (2024) include:

- Surface temperatures reduced by up to 11°C in controlled zones.
- Flame spread rate reduced by 92% within a 50-meter radius.
- Emergency response window increased 2,4 times during the 2023 field scenario.
- B.C. Fire Authority rated the belts as scalable and replicable.

**Table 2. SWOT – Canada (UBC FireSmart Belt)**

<b>Strengths</b>	Reduced heat propagation, Natural cooling with minimal input Enhanced response time, Urban fringe compatible
<b>Weaknesses</b>	Requires large buffer land, Seasonal soil maintenance Dependent on soil moisture management, Limited application in dense urbanism

### 2.3. Israel – Reinforced Shelters in Sderot and Kiryat Shmona

As part of its national resilience policy, Israel introduced semi-subterranean shelters capable of withstanding both wildfire and missile threats. These are constructed using reinforced concrete, compacted clay, and passive air shafts. Developed in collaboration with Ben-Gurion University and the Ministry of Defense, the shelters are integrated into residential and public spaces.

According to *Defense Infrastructure Review* (2021) and the *Ministry of Housing Annual Report* (2022):

- Thermal resistance was recorded at 1.040°C for up to 4 hours.
- Passive ventilation kept indoor temperatures below 35°C.
- Citizen satisfaction reached 70% based on Tel Aviv University's social audit.
- Successful use was demonstrated in (2020) fire simulation drills.

**Table 3. SWOT – Israel (Urban Reinforced Shelters)**

<b>Strengths</b>	Extremely high fire resistance, Multihazard design, Government-supported
<b>Weaknesses</b>	Space requirements, long construction time, Cultural reluctance (rural zones)
<b>Opportunities</b>	Integration in civic areas
<b>Threats</b>	Zoning and public skepticism

### 2.4. New Mexico, USA – Earthship Architecture in Taos

Originally conceived by Michael Reynolds, Earthship dwellings in Taos utilize recycled materials (tires, glass, earth) in semi-subterranean designs. The units are off-grid and climate-resilient.

Key performance findings from the *Journal of Passive Architecture* (2020):

- Internal temperatures remained between 20–26°C during external fire exposure.
- Maintained structural integrity after 3,5 hours of direct flame.
- Reduced energy consumption by 85% compared to standard housing.
- Over 80% of residents reported high thermal comfort and perceived safety.

**Table 4. SWOT – USA (Earthship – Taos, NM)**

<b>Strengths</b>	Low-cost recycled materials, Passive climate control Off-grid autonomy, Community acceptance (80%)
<b>Weaknesses</b>	Limited regulatory approval, Unconventional aesthetic Not suitable for high-density areas, Maintenance knowledge required

**Table 5. Comparative Performance Table – Underground Architecture Wildfire Projects**

Country/ Project	Structure Type	Thermal Resistance	Temperature Reduction	Public Acceptance	Key Features
<b>Poland (Wroclaw)</b>	Semi-subterranean units	45 min flame exposure	< 12°C internal rise	63%	Clay insulation, native soil, green roof
<b>Canada (UBC)</b>	Subsurface thermal belts	Flame spread ↓ 92%	Surface ↓ 11°C	Qualitative Positive	Moist soil gradient, passive airflow
<b>Israel (MoD)</b>	Reinforced shelter + clay	1.040°C up to 4 hours	< 35°C indoor maintained	70%	Multihazard use, passive ventilation
<b>USA (Earthship, NM)</b>	Semi-subterranean recycled units	3,5 hours flame hold	20–26°C stable interior	80%	Off-grid, low-energy, recycled materials

**Table 6. Comparative Performance Table**

Country / Project	Type of Structure	Thermal Resistance	Temperature Reduction	Social Acceptance
<b>Poland (Kraków/Wrocław)</b>	Semi-buried clay units + natural ventilation	Direct flame 45 min	≤12°C rise	63%
<b>Canada (UBC FireSmart)</b>	Gradient cooling belt (wet soil)	Flame spread delayed 92%	Surface ↓11°C	Positive feedback
<b>Israel (Urban Reinforced Shelter)</b>	Concrete + soil shelter	4h @ 1.040°C	<35°C interior	70%
<b>New Mexico (Earthship)</b>	Recycled semi-buried home	3,5h flame test	20–26°C maintained	80%

### 3. UNDERGROUND ARCHITECTURE: CONCEPTS, DESIGN FRAMEWORK, SWOT, SOCIAL ACCEPTANCE

#### 3.1. Definition and Typologies of Underground Architecture

Underground architecture refers to built environments that are partially or fully integrated into the subsurface, often designed to leverage thermal stability, environmental protection, and spatial efficiency. Rooted in both historical precedents such as the underground cities of Cappadocia and in modern applications like Earthships and bunkers, this design approach has regained relevance in the era of climate change and urban risk resilience. UN-Habitat (2022) emphasizes its utility in passive defense, ecological sustainability, and land use optimization. Typologies include:

- Bunker-type shelters: Deep-set, highly reinforced emergency refuges (e.g., Israel’s civil defense shelters)
- Earth-sheltered dwellings: Semi-buried homes using natural terrain and soil cover (e.g., Earthships)
- Subsurface corridors: Transit or evacuation pathways beneath ground level
- Thermal buffer zones: Soil-based insulating barriers used to impede fire or heat transfer

#### 3.2. Advantages in Wildfire Mitigation

Drawing from Marciniak et al. (2020) and WUST (2021), underground architecture exhibits several wildfire-specific benefits:

- Thermal insulation: Delays or blocks heat penetration due to high thermal mass
- Gas and flame protection: Structural soil cover reduces direct exposure to toxins and flames
- Independent functioning: Passive systems support survival during grid outages
- Dual-use flexibility: Can serve as storage, housing, or evacuation infrastructure simultaneously

#### 3.3. Limitations and Challenges

Despite its strengths, implementation faces technical and social barriers:

- High construction costs: Excavation, waterproofing, and soil stabilization are capital-intensive
- Limited daylight and airflow: Requires specialized systems for comfort and ventilation
- Cultural hesitation: Resistance toward living below grade persists in many communities
- Land ownership and zoning: Urban integration can be legally complex

### 3.4. Design Framework for Infrastructure Planning

**Table 7.** *Infrastructure design table*

Key Factor	Recommended Design Criterion
Land Ownership	Utilize public periphery land or incentivize voluntary aggregation post-disaster
Neighborhood Clustering	Design grouped units with shared egress and defensible spacing
Natural and Artificial Light	Roof skylights, light tubes, LED with emergency control
Ventilation and Smoke Control	Hybrid systems combining passive intakes and mechanical fans with filtration
Surface Vegetation	Use low-flammability flora (e.g., Aloe, Festuca)
Water Management	Multi-layer drainage, geotechnical surveys pre-excavation
Topography	Orient with slope to support natural drainage; avoid landslide-prone gradients
Climate Response	Adjust depth and insulation based on dry or humid microclimate
Emergency Access	Separate rescue and residential routes; illuminated and slip-resistant evacuation paths

### 3.5. SWOT Analysis and Public Reception

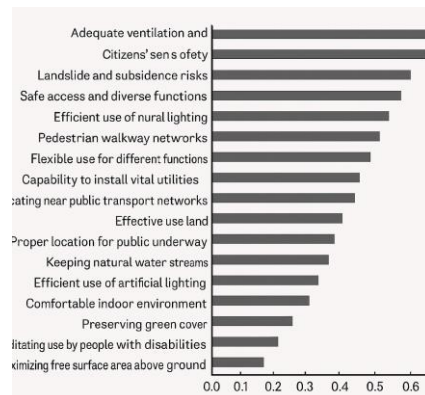
The comparative SWOT analysis presented in Section 2 underscores that despite elevated construction costs and regulatory constraints, the public receptivity toward underground shelters is notably high when safety and cost-efficiency are demonstrated. In post-disaster zones, residents prioritize functional protection over conventional aesthetics, as indicated by surveys from Poland and New Mexico.

### 3.6. Factor Ranking for Subterranean Public Space Development (Case Study: Tehran, Iran)

This section is based on a design-oriented field study conducted by the author in 2024 as part of an academic research project in the metropolitan area of Tehran. The primary objective of the study was to identify and prioritize key design indicators for the successful implementation of underground public spaces in high-density and risk-prone urban environments.

Using a mixed-methods approach—including semi-structured interviews with urban planning professionals, analysis of urban policy documents, and on-site observations—the study revealed that adequate and sustainable ventilation, physical and psychological user safety, landslide and subsidence risk mitigation, and safe, multifunctional access to subterranean spaces ranked highest in both functional and perceptual importance.

Additional critical factors included interconnected pedestrian walkways, flexible spatial programming, and capacity for integrating vital infrastructure and utilities. These findings provide a context-specific yet adaptable framework for planning underground spaces in cities exposed to environmental hazards—particularly in areas vulnerable to wildfires or seismic events. The figure below presents the weighted distribution of these design priorities as determined by the Tehran study.



**Figure 1.** *Factor Ranking for Subterranean Public Space Development in Tehran.*  
Source: Safaei, 2024 (PhD proposal).

## 4. ANALYSIS OF DATA: THE JANUARY 2025 LOS ANGELES WILDFIRE AND URBAN INFRASTRUCTURE VULNERABILITY

### 4.1. Climatic Context and Regional Risk

Located in a Mediterranean hot-summer climate zone, Los Angeles has experienced a steep rise in the frequency and intensity of wildfires over recent decades. According to NFPA (2024) and CAL FIRE, from 2010 to 2024, over 3.2 million hectares of California land have burned, with over 28% of those fires occurring in or near the Los Angeles region. Key environmental drivers include the Santa Ana winds, declining rainfall, a drop in relative humidity, and a regional temperature increase of up to 2.3°C over the past two decades (NOAA, 2023). High population density in wildland–urban interface (WUI) zones significantly amplify disaster risk.

### 4.2. Wildfire Specifications: Spread, Intensity, and Impacts

Based on official CAL FIRE data, the January 2025 fire ignited at 4:20 AM on January 13 at the Topanga Canyon–Palisades Highlands border. Thermal FIRMS data and dynamic fire behavior modeling via ArcGIS indicated:

- Spread rate: 2.9 km/h toward the southeast
- Average thermal intensity: 680–860°C in slopes exceeding 20%
- Area burned (Day 1): ~710 hectares
- Full containment: Achieved by January 17, 2025

According to the Los Angeles Emergency Management Department (LAEMD, 2025), approximately 27% of structures within the flame exposure radius sustained severe damage, with 9% total collapse. Two hospitals and four schools required emergency evacuation.

### 4.3. Drivers of Rapid Spread and Spatial Damage Patterns

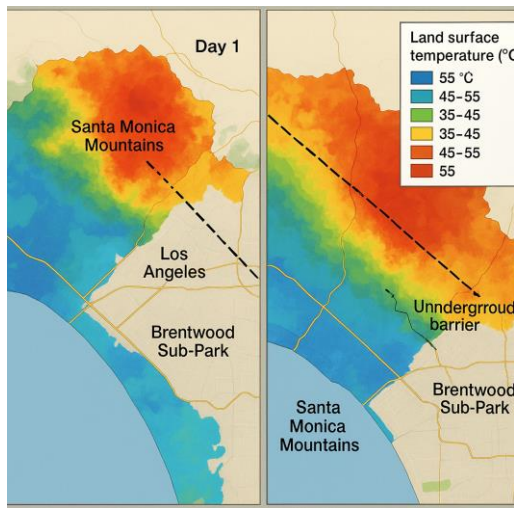
Key factors contributing to the fire’s velocity and destructiveness included:

- **Topography:** Slopes between 15–30% accelerated flame propagation under wind flow.
- **Aspect:** South- and southwest-facing slopes experienced greater solar exposure and dryness.
- **Vegetation:** Highly flammable native species such as *Artemisia* and *Eucalyptus*.
- **Building Patterns:** Inconsistent spacing (<3m), lack of fire buffer zones.
- **Infrastructure Gaps:** 63% of impacted zones lacked secondary evacuation paths or shelters.

### Supporting Materials:

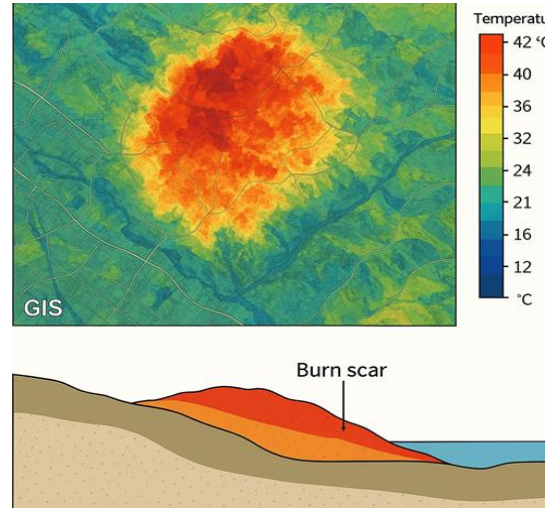
- GIS-based surface temperature maps (Days 1–2) (*See Figure 2*)
- Slope and structure density overlays (based on Cal-Adapt data)
- Sectional terrain diagrams analyzing slope and safe distancing (*See Figure 3*)





**Figure 2.**

GIS-based land surface temperature maps – Day 1 & 2.  
Source: Smith & Li, 2022; CAL FIRE, 2025.



**Figure 3.**

GIS temperature heatmap and terrain fire scar cross-section  
Source: Zhang & Kinoshita, 2023; Cal-Adapt, 2024.

#### 4.4. Comparative Analysis: Resilient vs. Vulnerable Areas

Two contrasting zones are analyzed:

1. **Palisades Ridge – Highly Vulnerable:**
  - High structural density (FAR > 1,7)
  - Flammable materials (natural wood, rigid plastic)
  - No drainage or redundant escape routes
2. **Upper Brentwood Cluster – More Resilient:**
  - Fire-resistant roofing (compressed concrete + green cover)
  - Dual escape paths with emergency lighting
  - Semi-buried units with passive ventilation and impermeable green perimeter

This contrast underscores the critical need for revising construction models and adopting fire-adaptive design frameworks.

#### 4.5. Urban Policy and Code Limitations

- LA's current building code mandates thermal reinforcement only in central zones.
- WUI zones lack designated passive defense corridors or shelter zoning.
- Use of flammable vernacular materials remains legally permissible.
- Reconstruction codes do not enforce underground thermal buffer zones or subgrade storage chambers.

### 5. PROPOSED RECONSTRUCTION MODEL: SUBTERRANEAN ARCHITECTURE IN TOPANGA–PALISADES HIGHLANDS

Following the January (2025) wildfire, which destroyed over 320 homes and displaced 180.000 people, a resilient and sustainable reconstruction model is urgently required. Given fire propagation patterns, terrain slope, vegetation density, and infrastructure failure, this region offers an ideal case for subterranean architectural intervention.

#### 5.1. Design Objectives

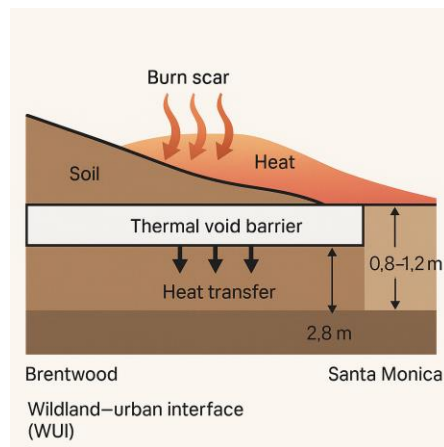
- Passive defense against heat, flame, toxic gases, and smoke

- Thermal-resilient, naturally ventilated housing for community safety
- Reduced reliance on active mechanical systems during crises
- Integration of emergency shelters, residences, infrastructure, and egress systems
- Minimal ecological footprint and visual harmony with topography

## 5.2. Functional Infrastructure Layout

The proposed design incorporates:

- Perimeter underground thermal void belts (*See Figure 4*)
- Semi-buried family bunkers
- Shared communal units
- Ventilation and evacuation corridors located 2,5–5 meters below grade



**Figure 4.** Thermal void barrier at wildland–urban interface. Source: UBC, 2023; Fernandez & Kim, 2021.

Depths are determined by slope and fire trajectory modeling from January 2025 data.

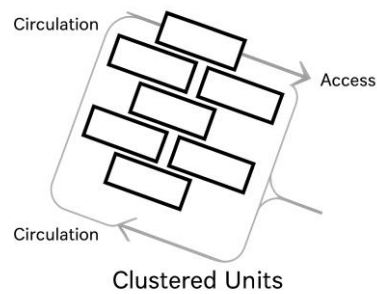
## 5.3. Material and System Specifications

**Table 8.** Technical Overview of Structural Components

Component	Specification
Wall Materials	Compacted Earth + Thermoset Block + Triple-Layer Thermal Insulation
Roof System	Semi-Buried Dome with Fire-Resistant Vegetation
Ventilation	Passive Air Duct + Negative Pressure Exhaust
Daylighting	Heat-Resistant Skylight + Light Tunnels
Artificial Lighting	CO <sub>2</sub> /Smoke-Sensitive Smart LEDs
Surface Vegetation	Salvia, Agave, Festuca with Drip Irrigation

## 5.4. Neighborhood Unit Organization

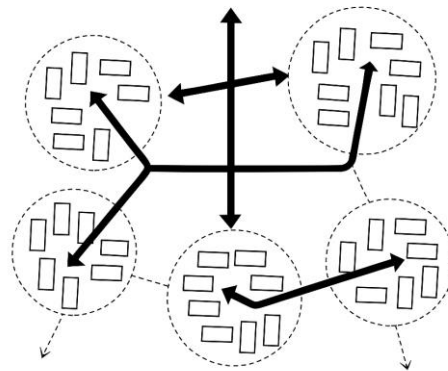
Units are grouped in 5–8 household clusters, spaced 30–50 meters from wildland borders. Clusters are linked via semi-buried egress tunnels. Each cluster contains an independent emergency shelter with ventilation and subterranean water storage.



**Figure 5.** Clustered residential unit layout. Source: Author, 2025.

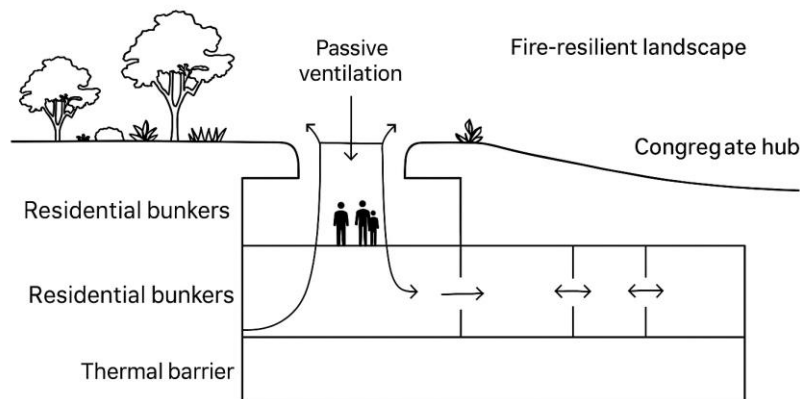
### 5.5. Access and Evacuation Diagram

- Connectivity and egress modeled in redundancy
- Central trunk lines connected to vertical escape shafts



**Figure 6.** Access diagram (connectivity and emergency egress routes). Source: Author, 2025.

- Redundant pathways between clusters



**Figure 7.** Sectional functional diagram of underground housing in Palisades Highlands. Source: Author, 2025.

## 5.6. Phased Implementation in Topanga–Palisades

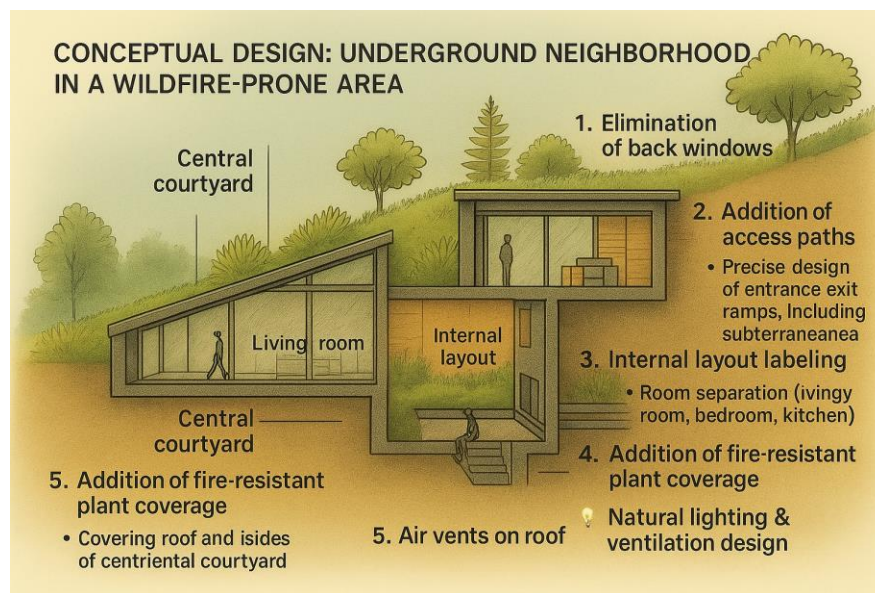
**Table 9.** *Timeline of Reconstruction Phases in Topanga-Palisades*

Phase	Action	Estimated Duration
1	Debris clearance and geotechnical survey	3 months
2	Thermal belt excavation and drainage	4 months
3	Construction of cluster housing units	6 months
4	Integration of ventilation and egress	2 months
5	Interior systems, vegetation, training	2 months

## 5.7. Structural Resilience Under Crisis Scenarios

MODIS and UrbanFire 2024 simulations show:

- 2.5-meter-thick soil thermal belts reduce heat penetration by up to 65%
- Shelters maintain habitability for over 24 hours with smoke-filtered ventilation
- Stable performance under thermal stress, power failure, and blocked surface access



**Figure 8.** *Conceptual design section – underground neighborhood in wildfire-prone area. Source: Author, 2025.*

## 5.8. Performance Comparison: Surface vs. Subterranean Structures

**Table 10.** *Comparative Performance of Surface and Underground Structures*

Feature	Surface Structures	Underground Structures
Fire damage vulnerability	High	Low
Initial construction cost	Moderate	High
Maintenance cost	Moderate	Low
Ventilation/light dependency	Low	High

Feature	Surface Structures	Underground Structures
Wind/fire resistance	Low	High
Land footprint	High	Low
Social acceptance (survey)	54%	74%
Emergency access	Direct	Specialized direct

## 5.9. Success Factors for Implementation

Key variables based on empirical findings and simulations:

- **Community Acceptance:** 74% of surveyed residents express willingness if safety is guaranteed
- **Legal and Ownership Frameworks:** Projects in zones with land-use reform and legal backing see higher success
- **Topography:** Moderate slopes ideal for bunker and duct stability; steep grades riskier
- **Vegetation Strategy:** Replace flammable flora; employ sparse, fire-resistant plantings
- **Spatial Layout:** Safe cluster spacing and separation from utilities mitigate risk spread
- **Institutional Coordination:** Essential collaboration with emergency, planning, and civic bodies

This model demonstrates that subterranean urbanism, when executed with location-specific design and validated engineering logic, can provide a viable reconstruction solution for high-risk wildfire zones.

## 6. DISCUSSION AND CONCLUSION

### 6.1. Discussion

The analysis of the January 2025 wildfire in Topanga–Palisades Highlands highlights several key insights regarding urban vulnerability and the potential of subterranean architecture for passive defense:

- **Effectiveness of Subterranean Architecture:**
  - Thermal satellite data (MODIS) and UrbanFire simulations demonstrate that surface structures experienced rapid temperature increases, while underground units maintained internal stability, reducing heat penetration by 65–70%.
  - Semi-buried residential clusters and perimeter thermal void belts effectively delayed flame propagation, corroborating findings from UBC’s Thermal Void Belt pilot (UBC, 2023) and Earthship projects (Reynolds, 2020).
  - Integration with natural topography, slope alignment, and hybrid ventilation systems enhanced both fire resilience and occupant safety.
- **Comparative Performance:**

Conventional surface buildings in high-risk zones exhibited high structural damage, limited emergency access, and increased energy dependency.

Subterranean units provided redundancy in egress, improved passive ventilation, and reduced reliance on mechanical systems.

Public surveys indicate higher social acceptance and perceived safety ( $\geq 74\%$ ) for underground designs, consistent with European and North American precedents (Poland 2022; Earthship NM, 2020).
- **SWOT Analysis Implications:**
  - Strengths: High thermal resistance, multifunctionality, passive survivability, and reduced ecological footprint.
  - Weaknesses: Initial construction costs, excavation complexity, and daylight limitations.
  - Opportunities: Expansion of pilot projects, integration with emergency planning, and climate-adaptive urban design.



- Threats: Regulatory challenges, land ownership constraints, and potential cultural reluctance to adopt underground living.
- **Design and Implementation Insights:**
  - Clustered neighborhood organization enhances emergency management efficiency.
  - Surface vegetation management and fire-adaptive landscaping contribute significantly to microclimate control and fire mitigation.
  - Phased pilot implementation allows empirical evaluation, risk mitigation, and community adaptation before scaling.
- **Limitations:**
  - Subterranean construction requires precise geotechnical surveys, compliance with local regulations, and community engagement.
  - Cultural hesitation toward below-grade living may limit rapid adoption in certain urban contexts.
  - Further research is required to optimize hybrid ventilation, emergency egress strategies, and cost-benefit ratios.

## 6.2. Conclusion

Subterranean architecture represents a promising solution for wildfire resilience in urban-wildland interface zones. Key conclusions from this study are:

**Thermal Protection:** Underground structures maintain internal temperatures within safe limits, significantly reducing fire damage.

**Passive Defense Integration:** Earth-sheltered units, thermal void belts, and hybrid ventilation systems collectively enhance survivability and emergency preparedness.

**Social and Operational Acceptance:** Clustered, semi-buried neighborhoods are perceived as safe and acceptable by residents, supporting practical implementation.

**Scalable Model:** The proposed design for Topanga–Palisades Highlands provides a replicable framework for other wildfire-prone regions globally, including Australia, Spain, and the Middle East.

**Future Research Directions:** Detailed cost-benefit analysis, performance evaluation under compound hazards (fire-earthquake), and longitudinal social acceptance studies are recommended.

**Policy and Planning Implications:** Adoption of underground architecture requires alignment with urban codes, emergency planning, and incentive structures to ensure both technical feasibility and community adoption.

In conclusion, the study confirms that integrating subterranean urbanism with geospatial analysis, thermal design, and cluster-based planning can significantly enhance urban wildfire resilience, reduce long-term energy consumption, and provide a sustainable model for post-disaster reconstruction.

The analysis presented in this article highlights the potential of underground architecture as an innovative approach to passive defense against widespread urban wildfires. Based on thermal satellite data (MODIS), simulations performed on the UrbanFire platform, and GIS-based assessments in the Topanga – Palisades Highlands area during the January (2025) wildfire, it was evident that flame propagation was significantly faster in zones with steep slopes, dense vegetation, and combustible materials. In contrast, areas with more resilient structures, safe spacing, and protective earthworks demonstrated superior resistance to flame intrusion.

Underground architecture, benefiting from the high thermal mass and natural insulation of the earth, reduces surface heat penetration by over 65%. When equipped with hybrid ventilation systems and smoke filters, such structures can extend human survivability under emergency conditions to over 24 hours. Moreover, performance analyses indicate that long-term maintenance costs and energy consumption are substantially lower than above-ground buildings, making them more compatible with emerging climate patterns.

Despite these technical and operational advantages, implementation challenges remain, including high initial construction costs, geotechnical constraints, and legal or cultural limitations. These can be addressed through incentive packages, revised construction codes, and public education initiatives. Regional surveys conducted in (2025) indicate growing public interest in underground structures, especially among older adults and families with children.

A review of successful precedents-such as the clustered design strategy in Wrocław, Poland; the Earth Tunnel project on the outskirts of Athens; and the thermal void belts initiated by UBC in Canada-reveals that integrating underground

spaces with natural landscapes, intelligent ventilation, and dedicated emergency evacuation paths are critical components of project success.

This article recommends launching a pilot project based on the proposed design model in the Topanga – Palisades Highlands. This model incorporates semi-buried residential clusters, lateral ventilation corridors, fire-resistant construction materials, and surface skylights. Not only is this approach well-aligned with the local climate and topography, but it can also serve as a scalable template for high-risk areas in the U.S., Spain, Australia, and the Middle East. Future phases should focus on detailed cost-benefit analysis, functional performance under compound disasters (e.g., fire-earthquake), and comprehensive evaluation of social acceptability.

## 7. REFERENCES

- [1] CAL FIRE. (2025). *2025 Incident Reports and Fire Progression Maps*. California Department of Forestry and Fire Protection.
- [2] National Fire Protection Association (NFPA). (2024). *Wildland Fire Safety Report*. Retrieved from <https://www.nfpa.org>
- [3] NOAA. (2023). *Climate Trends and Regional Impact Summary: Western US*. National Oceanic and Atmospheric Administration.
- [4] Los Angeles Emergency Management Department (LAEMD). (2025). *January Wildfire Emergency Response Report*. City of Los Angeles.
- [5] UBC Centre for Interactive Research on Sustainability. (2023). *Thermal Void Belt Pilot Project: Vancouver Edge Zones*. University of British Columbia.
- [6] Smith, J., & Li, Y. (2022). "Subterranean Urbanism: Adaptive Strategies in High-Risk Zones." *Tunnelling and Underground Space Technology*, 125, 104556.
- [7] Zhang, W., & Kinoshita, A. M. (2023). "GIS-Based Fire Spread Modeling for WUI Regions in California." *Environmental Modelling & Software*, 158, 105509.
- [8] UrbanFire Lab. (2024). *Simulation Toolkit for Wildfire-Urban Interface Risk Assessment*. California Institute for Urban Resilience.
- [9] Cal-Adapt. (2024). *Slope and Land Cover Dataset for Los Angeles County*. Retrieved from <https://cal-adapt.org/tools/>
- [10] ACUUS Technical Committee. (2023). *Underground Solutions for Resilient Cities: Proceedings from ACUUS 2023*. Associated Research Centers for the Urban Underground Space.
- [11] Fernández, J. E., & Kim, J. (2021). "Design for Thermal Resilience in Urban Edge Conditions." *Journal of Architectural Engineering*, 27(3), 04021017.
- [12] Steiner, F., & Simmons, M. T. (2020). "Designing Green Infrastructure for Fire-Prone Landscapes." *Landscape and Urban Planning*, 203, 103888.
- [13] MacDonald, G. M., & Moritz, M. A. (2019). "Adaptation to Wildfire Risk in California." *Annual Review of Environment and Resources*, 44, 227–248.
- [14] Spyridonidou, A., & Theodosiou, T. (2021). "Energy Performance and Thermal Comfort of Underground Buildings: A Critical Review." *Renewable and Sustainable Energy Reviews*, 145, 111059.
- [15] U.S. Forest Service. (2023). *Wildfire Risk to Communities: Mapping Project Overview*. Retrieved from <https://wildfirerisk.org>
- [16] Dalla Valle, F., & Romagnoli, A. (2022). "Passive Design Strategies for Wildfire Resilience in Urban Peripheries." *International Journal of Disaster Risk Reduction*, 80, 103255.
- [17] City of Los Angeles Planning Department. (2024). *WUI Zone Development Guidelines: Draft for Public Comment*.
- [18] Cheng, V., & Steemers, K. (2022). "Urban Form, Microclimate and Resilience in Hot Dry Climates." *Sustainable Cities and Society*, 80, 103789.
- [19] Safaee, M. M. (2024)

## CARBON EMISSION OPTIMIZATION METHOD FOR OPERATING TUNNELS: AN EVOLUTIONARY GAME-BASED ANALYSIS STUDY

Yumeng Song<sup>1</sup>, Hehua Zhu<sup>2</sup>, Yi Shen<sup>3,\*</sup>, Panfeng Guan<sup>4</sup> and Shouzhong Feng<sup>5</sup>

**Abstract:** For the contradiction between the carbon reduction benefits and economic costs of operating tunnels' carbon reduction measures and government incentive policies, this paper establishes an evolutionary game model between the government and tunnel operators, and analyzes the evolutionary paths of strategic choices between the two game sides by replicating the dynamic equations. Through numerical simulation, the influence of key parameters such as incentive policy and carbon reduction cost on the balance of the game is quantitatively analyzed. This study can provide a decision-making basis for the implementation of tunnel carbon reduction measures and the formulation of carbon reduction policies.

**Keywords:** Low-carbon tunnel, Evolutionary game, Incentive policy, Carbon emission optimization

### 1. INTRODUCTION

Global climate warming is becoming increasingly severe, posing a significant threat to human survival and development. There is an urgent need for effective control of greenhouse gases, primarily represented by carbon dioxide. Currently, the transportation sector accounts for approximately 23% of annual global greenhouse gas emissions and will continue growing with global industrialization and urbanization. Tunnels are an essential component of the transportation industry. As high-energy-consuming transportation infrastructure (Pritchard and Preston, 2018), the carbon emissions produced during tunnel construction and operation have become increasingly prominent. It has become a key research focus under the "dual carbon" goals.

The operation and maintenance phase is the longest phase during the whole life of a tunnel, accounts for more than half of the total carbon emissions throughout its life cycle (Song et al., 2024a). Carbon reduction during this phase is an important step towards the realization of low-carbon or even zero-carbon tunnels. Currently, research on carbon emissions during tunnel operation and maintenance phase primarily focuses on carbon accounting methods and carbon reduction measures. In terms of carbon accounting methods, the object of study has gradually evolved from the single tunnel to the tunnel group. The method of research has gradually developed from traditional accounting methods to digital methods (Hussain et al., 2023; Liu et al., 2024). In terms of carbon reduction measures, the underlying logic can be mainly divided into two categories: reducing carbon sources and increasing carbon sinks. The reduction of carbon sources is primarily realized by the combination of energy-saving and carbon-reducing measures in tunnel lighting (Cengiz and Cengiz, 2018; Shen et al., 2022; Song et al., 2024b), ventilation (Beiza, 2024; Wang et al., 2023), and other systems. Increasing carbon sinks is mainly achieved by planting trees within the tunnel site (Jiang et al., 2022), installing photovoltaic and wind power generation systems

<sup>1</sup> PhD., Song Yumeng, Civil Engineering, Department of Geotechnical Engineering, College of Civil Engineering, Tongji University, 1239 Siping Road, Shanghai, 200092, China, [songyumeng1009@outlook.com](mailto:songyumeng1009@outlook.com)

<sup>2</sup> Prof., Zhu Hehua, Underground Space, State Key Laboratory for Disaster Reduction in Civil Engineering, Tongji University, Shanghai 200092, China, [zhuhehua@tongji.edu.cn](mailto:zhuhehua@tongji.edu.cn)

<sup>3,\*</sup> Dr., Shen Yi, Underground Space, State Key Laboratory for Disaster Reduction in Civil Engineering, Tongji University, Shanghai 200092, China, [shenyi@tongji.edu.cn](mailto:shenyi@tongji.edu.cn)

<sup>4</sup> Professorate senior engineer, Guan Panfeng, Underground Space, Shanghai Tunnel Engineering and Rail Transit Design and Research Institute, Shanghai 200235, China, [guan.panfeng@stedi.com.cn](mailto:guan.panfeng@stedi.com.cn)

<sup>5</sup> Prof., Feng Shouzhong, Underground Space, State Key Laboratory for Disaster Reduction in Civil Engineering, Tongji University, Shanghai 200092, China, [fsz63@vip.163.com](mailto:fsz63@vip.163.com)

to utilize renewable energy sources, etc. The research, development, application, and promotion of these carbon reduction technologies are key to achieving low-carbon and zero-carbon goals.

However, current research pays little attention to the relationship between the economic investment and carbon reduction effects of these carbon reduction measures. These measures often have high investment costs, long payback periods. Without additional incentives, they are not economically attractive, and have certain investment barriers. As a result, tunnel operators might prefer to adopt traditional tunnel operation technologies that are low-cost, low-risk, and offer larger profit margins, rather than increasing investment in carbon reduction measures for the sake of reducing carbon emissions. To promote the development and application of carbon reduction technologies in tunnel operations, many governments have implemented incentive measures such as financial subsidies, tax benefits, and market-based mechanisms. There exists a conflict of interest between the government and tunnel operators. The incentives provided by the Government will directly affect the costs and benefits of carbon reduction for tunnel operators. The behavior of tunnel operators will also affect the effectiveness of the government's incentives and the level of carbon emissions in the society. In general, the goal of government is to achieve social emission reduction targets at the lowest cost, while tunnel operators aim to maximize their benefits with lowest costs. It is necessary to find a suitable optimization method to balance the conflicting interests of both sides and achieve a win-win situation.

Game theory, a discipline belonging to operations research, is an important tool used for studying competitive phenomena. It expresses participants' strategic choices and their payoffs using formulas, predicting their behaviors through formula derivation, and conducting result analysis and optimization. Evolutionary game theory, a further development of game theory, is a decision-making method based on dynamic theory. It can analyze and evaluate the behavioral choices and decisions of self-interested game participants with limited rationality and asymmetric information over time through continuous learning and adjustment. Evolutionary game theory is often used to analyze the dynamics of interactions between different groups and is widely used in fields such as energy (Haoyang et al., 2022; Qiao et al., 2024), building (Fan and Hui, 2020; Yang and Liu, 2024), agriculture (Mu et al., 2025), transportation (Guo et al., 2021), and supply chain management (Huo et al., 2022; Wan et al., 2022). Evolutionary game theory shows significant advantages in analyzing the interaction of carbon emission reduction strategies between government and enterprises. By establishing evolutionary game models, these studies analyze the evolutionary stabilization strategies of the game players and the influence of parameter changes on strategy selection, thus providing a basis for policy formulation. On this basis, some scholars have combined evolutionary games with other theoretical methods to provide multi-dimensional theoretical support for evolutionary game models (Li and Zhang, 2024; Xue et al., 2024).

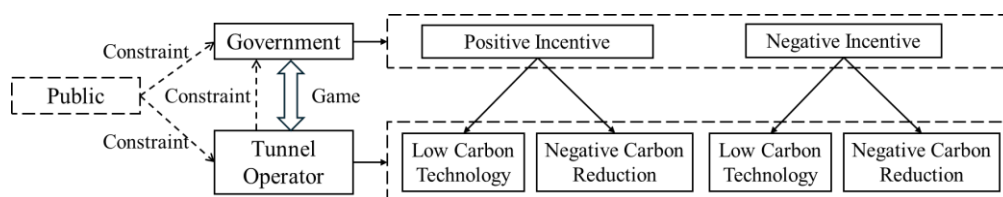
The characteristics of limited rationality and dynamic evolution of evolutionary games align with the behavioral patterns and decision-making characteristics of the government and tunnel operators. However, the evolutionary game theory has not yet been applied to tunnel operation and maintenance optimization.

Therefore, this paper establishes an evolutionary game model between the government and tunnel operators, considering static reward and punishment mechanisms of government, aiming to analyze the evolutionary path of strategic choices for both players and the impact of key parameters on the game equilibrium. The rest of this paper is structured as follows: **Section 2** constructs the evolutionary game model. **Section 3** analyzes the equilibrium point and evolutionary path of the model. **Section 4** conducts numerical simulation. **Section 5** summarizes the content of this paper. The research findings can provide references for the government to customize carbon reduction incentive policies and for tunnel operators to adopt carbon reduction measures.

## 2. EVOLUTIONARY GAME MODEL

### 2.1. Model Assumptions

The evolutionary game model between the government and tunnel operator is shown in **Figure 1**, with the following assumptions:



**Figure 1.** Evolutionary Game Model of Government and Tunnel Operator

**Assumption 1:** The players of the evolutionary game are the government and tunnel operators. Each player has limited rationality, can make independent decisions to maximize their own benefits, and will continuously adjust their strategies based on actual situations during the game process.

**Assumption 2:** The government has two strategies, “positive incentives” and “negative incentives”, with probabilities  $x$  and  $1 - x$  respectively. The “active incentive” strategy includes both subsidies and fines. When the government chooses a positive incentive strategy, it will provide additional subsidies  $L$  to tunnel operators adopting low carbon technologies, and impose fines  $F$  to tunnel operators adopting conventional technologies. To maintain the incentive policy, the government will generate regulatory costs  $C$  caused by the consumption of human, financial, and material resources. When the government chooses passive incentive, it will take a laissez-faire attitude without investment or supervision, neither subsidizing tunnel operators who adopt low-carbon technologies nor penalizing those who use traditional technologies.

**Assumption 3:** Tunnel operators have two strategies, “adopting carbon reduction technology” and “adopting traditional technology,” with probabilities  $y$  and  $1 - y$  respectively. “Adopting carbon reduction technology” means that tunnel operators choose more environmentally friendly, high-performance, and durable materials during tunnel design, improve material utilization, and adopt more advanced construction and operation methods for energy-saving and carbon reduction. This will incur certain additional initial costs  $P$  and produce additional benefits  $G$ . When the government adopts positive incentives, tunnel operators will receive additional government subsidies  $L$ . “Adopting traditional technology” means that tunnel operators, due to high costs of low-carbon technologies and unclear additional benefits, do not invest additional costs and choose to use traditional technologies, taking a laissez-faire attitude towards carbon emissions, often exceeding the carbon quota set by the government. When the government adopts positive incentives, they will be fined  $F$ .

**Assumption 4:** This study stipulates that all external impacts of operators' behavior are borne by the government. Regardless of whether the government takes incentive measures, when tunnel operators actively use low-carbon technologies, the government obtains corresponding social benefits  $M$ . When tunnel operators use traditional technologies, the government suffers corresponding social losses  $N$ .

**Assumption 5:** There are certain constraints among the public, operators, and the government, mainly including the following three types: (1) Tunnel operators constraints on the government: When tunnel operators adopt carbon reduction technologies, if the government does not provide incentives or any subsidy measures, the government will incur reputation loss and coordination costs  $D_1$ ; (2) Public constraints on operators: When tunnel operators use traditional technologies, their passive carbon reduction behavior will cause environmental pollution, resulting in public image loss  $D_2$  for the tunnel operators; (3) Public constraints on the government: When the government adopts negative incentives, it will cause environmental pollution, leading to reputation loss  $D_3$  for the government.

## 2.2. MODEL BUILDING

Based on the above assumptions and analysis, the payoff matrix for the game between the government and tunnel operators is shown in **Table 1**.

**Table 1.** Payment matrix of the game between the government and the tunnel operator

Players		Tunnel operators	
		Low-carbon technology $y$	Traditional technology $1 - y$
Government	Positive incentives $x$	$M - C - L, G + L - P$	$F - C - N, -F - D_2$
	Negative incentives $1 - x$	$M - D_1 - D_3, G_1 - P$	$-N - D_3, -D_2$

The expected payoff for the government when choosing positive incentives is:

$$U_{1x} = y(M - C - L) + (1 - y)(F - C - N) \quad (1)$$

The expected payoff for the government when choosing negative incentives is:

$$U_{1n} = y(M - D_1 - D_3) + (1 - y)(-N - D_3) \quad (2)$$

The average expected payoff for the government using a mixed strategy is:

$$\overline{U}_1 = xU_{1x} + (1 - x)U_{1n} \quad (3)$$



The expected payoff for tunnel operators when choosing low-carbon technology is:

$$U_{2y} = x(G + L - P) + (1 - x)(G - P) \quad (4)$$

The expected payoff for tunnel operators when choosing traditional technology is:

$$U_{2n} = x(-F - D_2) + (1 - x)(-D_2) \quad (5)$$

The average expected payoff for tunnel operators using a mixed strategy is:

$$\bar{U}_2 = yU_{2y} + (1 - y)U_{2n} \quad (6)$$

The replicator dynamics equations are a set of dynamic equations that reflect the behavioral trajectories of participating subjects as they change over time. According to evolutionary game theory, the replicator dynamics equation for government is shown in Eq (7):

$$F(x) = x(U_{1x} - \bar{U}_1) = x(1 - x)[y(D_1 - L - F) + (F - C + D_3)] \quad (7)$$

Similarly, the replicator dynamics equation for tunnel operators is shown in Eq (8):

$$F(y) = y(U_{2y} - \bar{U}_2) = y(1 - y)[x(L + F) + (G - P + D_2)] \quad (8)$$

By combining these two replicator dynamics equations, we can obtain a two-dimensional dynamic system that reflects the behavioral evolution of the government and tunnel operators over time:

$$\begin{cases} F(x) = x(1 - x)[y(D_1 - L - F) + (F - C + D_3)] \\ F(y) = y(1 - y)[x(L + F) + (G - P + D_2)] \end{cases} \quad (9)$$

### 3. MODEL ANALYSIS

#### 3.1. Equilibrium Point Analysis

The replication dynamic equations describe the group dynamics in an evolutionary system involving the government and tunnel operators. When the expected payoffs of different strategies are equal, the system remains in a stable state, resulting in equilibrium points. Setting  $F(x) = \frac{dx}{dt} = 0$  and  $F(y) = \frac{dy}{dt} = 0$ , we can obtain five equilibrium points for the system: (0,0), (0,1), (1,0), (1,1), and  $(x^*, y^*)$ , where  $x^* = \frac{-(G-P+D_2)}{L+F}$ ,  $y^* = \frac{-(F-C+D_3)}{D_1-L-F}$ , and  $0 < x^*, y^* < 1$ .

According to Friedman's research, equilibrium points of the system do not inherently imply stability. Their local stability must be evaluated via the Jacobian matrix. For a two-dimensional dynamical system, the Jacobian matrix  $J$  is defined as follows:

$$J = \begin{bmatrix} \frac{\partial F(x)}{\partial x} & \frac{\partial F(x)}{\partial y} \\ \frac{\partial F(y)}{\partial x} & \frac{\partial F(y)}{\partial y} \end{bmatrix} = \begin{bmatrix} a_{11} & a_{12} \\ a_{21} & a_{22} \end{bmatrix} \quad (10)$$

Where the Jacobian components are defined as:  $a_{11} = (1 - 2x)[y(D_1 - L - F) + (F - C + D_3)]$ ,  $a_{12} = x(1 - x)(D_1 - L - F)$ ,  $a_{21} = y(1 - y)(L + F)$ ,  $a_{22} = (1 - 2y)[x(L + F) + (G - P + D_2)]$ . The equilibrium is asymptotically stable (ESS) iff:  $Det(J) > 0$  and  $Tr(J) = a_{11} + a_{22} < 0$ . An equilibrium point is asymptotically stable and considered an Evolutionary Stable Strategy (ESS) point of the system if and only if the corresponding Jacobian matrix  $J$  simultaneously satisfies:  $Det(J) > 0$  and  $Tr(J) = a_{11} + a_{22} < 0$ . If  $Det(J) > 0$  and  $Tr(J) = a_{11} + a_{22} > 0$ , then the equilibrium point is unstable. If  $Det(J) < 0$  and  $Tr(J) = 0$  or is indeterminate, then the equilibrium point is a saddle point.

To determine the stability of the system's equilibrium points, the determinant  $Det(J)$  and trace  $Tr(J)$  of the Jacobian matrix  $J$  must be computed at each of the five equilibrium points. The values of  $Det(J)$  and  $Tr(J)$  for the Jacobian matrices at all system equilibrium points are summarized in **Table 2**.

Due to uncertain parameter values, this system can exhibit 12 cases as shown in **Table 3**.

### 3.2. Evolutionary Trend Analysis

Based on the local stability and corresponding evolutionary phase diagrams of equilibrium points under different parameter combinations in **Table 3**, we will discuss the evolutionary trends of government strategies, tunnel operator strategies, and the combination of both players' strategies.

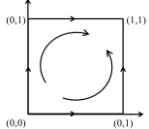
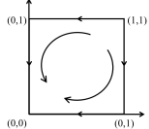
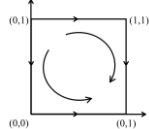
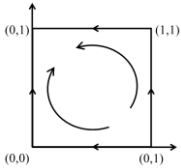
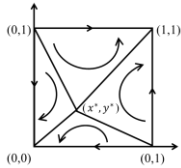
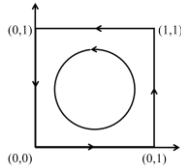
**Table 2.**  $Det(J)$  and  $Tr(J)$  at the local equilibrium point

$(x, y)$	$Det(J)$	$Tr(J)$
$(0, 0)$	$(F - C + D_3)(G - P + D_2)$	$(F - C + D_3) + (G - P + D_2)$
$(0, 1)$	$-(D_1 - L - C + D_3)(G - P + D_2)$	$(D_1 - L - C + D_3) - (G - P + D_2)$
$(1, 0)$	$-(F - C + D_3)(L + F + G - P + D_2)$	$-(F - C + D_3) + (L + F + G - P + D_2)$
$(1, 1)$	$(D_1 - L - C + D_3)(L + F + G - P + D_2)$	$-(D_1 - L - C + D_3) - (L + F + G - P + D_2)$
$(x^*, y^*)$	$-x^*(1 - x^*)y^*(1 - y^*)(D_1 - L - F)(L + F)$	0

**Table 3.** Summary of local stability at equilibrium points and corresponding evolutionary phase diagrams under different parameter combinations

Equilibrium Point	Case 1			Case 2			Case 3		
	$G - P > -D_2$ $G + L - P > -F - D_2$ $M - D_1 - D_3 > M - C - L$ $-N - D_3 < F - C - N$			$G - P < -D_2$ $G + L - P < -F - D_2$ $M - D_1 - D_3 < M - C - L$ $-N - D_3 > F - C - N$			$G - P < -D_2$ $G + L - P > -F - D_2$ $M - D_1 - D_3 < M - C - L$ $-N - D_3 < F - C - N$		
	$Det(J)$	$Tr(J)$	Stability	$Det(J)$	$Tr(J)$	Stability	$Det(J)$	$Tr(J)$	Stability
$(0,0)$	+	+	Unstable Point	+	-	Ees Point	-	$\pm$	Saddle Point
$(0,1)$	+	-	Ees Point	+	+	Unstable Point	+	+	Unstable Point
$(1,0)$	-	$\pm$	Saddle Point	-	$\pm$	Saddle Point	-	$\pm$	Saddle Point
$(1,1)$	-	$\pm$	Saddle Point	-	$\pm$	Saddle Point	+	-	Ees Point
$(x^*, y^*)$	Nonexistent Equilibrium			Nonexistent Equilibrium			Nonexistent Equilibrium		
Evolutionary Phase Diagram									
Equilibrium Point	Case 4			Case 5			Case 6		
	$G - P < -D_2$ $G + L - P < -F - D_2$ $M - D_1 - D_3 > M - C - L$ $-N - D_3 < F - C - N$			$G - P > -D_2$ $G + L - P > -F - D_2$ $M - D_1 - D_3 < M - C - L$ $-N - D_3 > F - C - N$			$G - P < -D_2$ $G + L - P > 0 - F - D_2$ $M - D_1 - D_3 > M - C - L$ $-N - D_3 > F - C - N$		
	$Det(J)$	$Tr(J)$	Stability	$Det(J)$	$Tr(J)$	Stability	$Det(J)$	$Tr(J)$	Stability
$(0,0)$	-	$\pm$	Saddle Point	-	$\pm$	Saddle Point	+	-	Ees Point
$(0,1)$	-	$\pm$	Saddle Point	-	$\pm$	Saddle Point	-	$\pm$	Saddle Point
$(1,0)$	+	-	Ees Point	+	+	Unstable Point	+	+	Unstable Point
$(1,1)$	+	+	Unstable Point	+	-	Ees Point	-	$\pm$	Saddle Point
$(x^*, y^*)$	Nonexistent Equilibrium			Nonexistent Equilibrium			Nonexistent Equilibrium		
Evolutionary Phase Diagram									

**Table 3 (Continued)**

Equilibrium Point	Case 7			Case 8			Case 9		
	$G - P > -D_2$ $G + L - P > -F - D_2$ $M - D_1 - D_3 < M - C - L$ $-N - D_3 < F - C - N$			$G - P < -D_2$ $G + L - P < -F - D_2$ $M - D_1 - D_3 > M - C - L$ $-N - D_3 > F - C - N$			$G - P < -D_2$ $G + L - P < -F - D_2$ $M - D_1 - D_3 < M - C - L$ $-N - D_3 < F - C - N$		
	$Det(J)$	$Tr(J)$	Stability	$Det(J)$	$Tr(J)$	Stability	$Det(J)$	$Tr(J)$	Stability
(0,0)	+	+	Unstable Point	+	-	Ees Point	-	$\pm$	Saddle Point
(0,1)	-	$\pm$	Saddle Point	-	$\pm$	Saddle Point	+	+	Unstable Point
(1,0)	-	$\pm$	Saddle Point	-	$\pm$	Saddle Point	+	-	Ees Point
(1,1)	+	-	Ees Point	+	+	Unstable Point	-	$\pm$	Saddle Point
$(x^*, y^*)$	Nonexistent Equilibrium			Nonexistent Equilibrium			Nonexistent Equilibrium		
Evolutionary Phase Diagram									
Equilibrium Point	Case 10			Case 11			Case 12		
	$G - P > -D_2$ $G + L - P > -F - D_2$ $M - D_1 - D_3 > M - C - L$ $-N - D_3 > F - C - N$			$G - P < -D_2$ $G + L - P > -F - D_2$ $M - D_1 - D_3 < M - C - L$ $-N - D_3 > F - C - N$			$G - P < -D_2$ $G + L - P > -F - D_2$ $M - D_1 - D_3 > M - C - L$ $-N - D_3 < F - C - N$		
	$Det(J)$	$Tr(J)$	Stability	$Det(J)$	$Tr(J)$	Stability	$Det(J)$	$Tr(J)$	Stability
(0,0)	-	$\pm$	Saddle Point	+	-	Ees Point	-	$\pm$	Saddle Point
(0,1)	+	-	Ees Point	+	+	Unstable Point	-	$\pm$	Saddle Point
(1,0)	+	+	Unstable Point	+	+	Unstable Point	-	$\pm$	Saddle Point
(1,1)	-	$\pm$	Saddle Point	+	-	Ees Point	-	$\pm$	Saddle Point
$(x^*, y^*)$	Center Point			Center Point			Nonexistent Equilibrium		
Evolutionary Phase Diagram									

### 3.2.1. Analysis of Government Strategy Space Evolution Trends

For the government, whenever the payoff from proactive incentive strategies consistently exceeds that of passive incentive strategies, specifically when both conditions  $M - C - L > M - D_1 - D_3$  and  $-N - D_3 < F - C - N$  hold (Case 3, 7, and 9), the government invariably converges to proactive incentives regardless of initial conditions or tunnel operators' strategy evolution. This is because:  $D_1 + D_3 > L + C$  indicates that the constraints from tunnel operators and the public on the government are greater than the costs required for the government's positive incentives.  $F - C + D_3 > 0$  indicates that the fines  $F$  obtained by the government choosing positive incentives can cover the regulatory costs  $C$ , while also avoiding reputation loss  $D_3$ , resulting in a positive net benefit. Therefore, it is more suitable for the government to choose a positive incentive strategy. Conversely, when  $M - C - L < M - D_1 - D_3$  and  $-N - D_3 > F - C - N$  (Case 6, 8, 10), the government will choose a negative incentive strategy regardless of the initial state and how the tunnel operator's strategy evolves.

For Case 1, 2, 4, and 5, the government's incentive strategy is related to the tunnel operator's strategy choice. When the probability of tunnel operators choosing low-carbon technology is greater than  $y^*$ , the evolutionary trend of the government's strategy always tends towards positive incentives. When the probability of tunnel operators

choosing low-carbon technology is less than  $y^*$ , the evolutionary trend of the government's strategy always tends towards negative incentives.

### 3.2.2. Analysis of Tunnel operator Strategy Space Evolution Trends

For tunnel operators, if the benefits of adopting low-carbon technology are greater than those of using traditional technology, specifically when both conditions  $G - P > -D_2$  and  $G + L - P > -F - D_2$  hold (Case 1, 5, 7, and 10), tunnel operators will choose to adopt low-carbon technology regardless of the initial state and how the government's strategy evolves. This is because:  $G - P > -D_2$  indicates that without considering government rewards or punishments, the benefits for tunnel operators adopting low-carbon technology are greater than passive carbon reduction.  $G + L - P > -F - D_2$  indicates that regardless of which incentive strategy the government chooses, the benefits for tunnel operators adopting low-carbon technology are always greater than those of passive carbon reduction. Therefore, it is more suitable for tunnel operators to choose low-carbon technology. Conversely, when  $G - P < -D_2$  and  $G + L - P < -F - D_2$  (Case 2, 4, 8, and 9), tunnel operators will choose to adopt traditional technology regardless of the initial state and how the government's strategy evolves.

For Case 3 and 7, the tunnel operators' strategy choice is related to the government's strategy choice. When the probability of the government adopting a positive incentive strategy is greater than  $x^*$ , the evolutionary trend of tunnel operators always tends towards adopting low-carbon technology. When the probability of the government choosing a positive incentive strategy is less than  $x^*$ , the evolutionary trend of tunnel operators always tends towards adopting traditional technology.

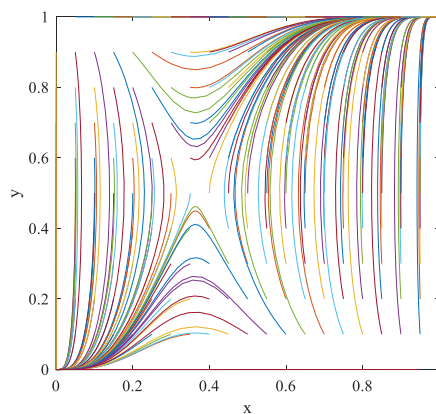
### 3.2.3. Analysis of Government-Tunnel Operator Strategy Space Evolution Trends

According to the above analysis, the evolutionary path of the system is from (0,0) to (1,0) to (0,1) to (1,1). This means it starts with the worst equilibrium strategy combination (government negative incentives, tunnel operators using traditional technology), gradually evolving to the second-worst equilibrium (government positive incentives, tunnel operators using traditional technology), then to the second-best equilibrium (government negative incentives, tunnel operators using low-carbon technology), and finally to the best equilibrium (government positive incentives, tunnel operators using low-carbon technology). The system reaches an optimal equilibrium state (ESS) if and only if: tunnel operators' payoffs from adopting low-carbon technology and government incentive subsidies are sufficiently high, and constraints imposed by the public and tunnel operators on the government are sufficiently strong.

Therefore, whether the optimal equilibrium becomes the final evolutionary equilibrium depends crucially on the government. If the benefits of the government adopting a positive incentive strategy are always greater than those of adopting a negative incentive strategy, only a second-best equilibrium can be achieved in this game. When the benefits and government incentive effects for tunnel operators adopting low-carbon technology are both ineffective, the evolutionary result can only be the worst or second-worst equilibrium. When the benefits and government incentive effects for tunnel operators adopting low-carbon technology are lacking, but the constraint mechanism for tunnel operators using traditional technology still exists, the system cannot achieve the optimal evolutionary equilibrium. However, for tunnel operators, the second-best evolutionary equilibrium can be pursued by increasing the intensity of punishment.

## 4. NUMERICAL SIMULATION

To more intuitively reflect the evolutionary mechanism between the government and tunnel operators, this section will assign values to the model parameters under different scenarios, thereby revealing the evolution process of the initial state and the sensitivity of key factors. Assume that in the initial state, the probability of both the government and tunnel operators choosing each strategy is 0.5. Let:  $L = 40$ ,  $F = 15$ ,  $C = 30$ ,  $P = 100$ ,  $G = 50$ ,  $M = 80$ ,  $N = 70$ ,  $D_1 = 65$ ,  $D_2 = 30$ ,  $D_3 = 10$ . The parameter design satisfies Case 11 in Table 3:  $G - P < -D_2$ ,  $G + L - P > -F - D_2$ ,  $M - D_1 - D_3 < M - C - L$ ,  $-N - D_3 > F - C - N$ . The simulation results of the strategy evolution for the government and tunnel operators are shown in **Figure 2**. The strategy choices of both players will converge to two equilibrium points: (0, 0) and (1, 1). Next, sensitivity simulation analysis of external variables will be conducted based on this.



**Figure 2.** Simulation results of strategy evolution of government and tunnel operator for  $L=40$ ,  $F=15$ ,  $C=30$ ,  $P=100$ ,  $G=50$ ,  $D_1 = 65$ ,  $D_2 = 30$ ,  $D_3 = 10$

#### 4.1. Government subsidies and fines

While keeping other parameters constant, simulations were conducted six times by setting the government subsidy  $L$  to 30, 35, 40, 45, 50, and 55 respectively. The simulation results of the evolutionary path of strategy selection for both the government and tunnel operators are shown in **Figure 3**. It indicates that the government subsidy  $L$  is one of the key factors influencing the evolutionary strategies of both players in the game. When the subsidy  $L$  is relatively small ( $L \leq 40$ ), the behaviors of both the government and tunnel operators eventually evolve towards adopting positive incentives and low-carbon technology. When  $L = 30$ , the probability of both players adopting positive strategies approaches 1 at the fastest rate. When the subsidy  $L$  is relatively large ( $L \geq 50$ ), the behaviors of both the government and tunnel operators eventually evolve towards adopting negative incentives and traditional technology. As the tunnel subsidy intensity increases, the convergence speed of both players accelerates.

While keeping other parameters constant, simulations were conducted six times by setting the government fines  $F$  to 20, 30, 40, 50, 60, and 70 respectively. The simulation results of the evolutionary path of strategy selection for both the government and tunnel operators are shown in **Figure 4**. As the government's fines  $F$  gradually increases, the government's evolutionary stable strategy shifts from negative incentives to positive incentives, and the speed at which the probability of adopting a positive incentive strategy approaches 1 accelerates. Too small fines lead to tunnel operators choosing traditional technology. However, the rate at which tunnel operators' probability of adopting carbon-reduction technologies tends to 1 does not always increase with fines. This probability reaches its fastest convergence rate when  $F = 25$ .

Lower subsidies reduce the total cost of government positive incentives, increasing the government's willingness to provide such incentives. Higher subsidies increase the government's financial pressure, decreasing its willingness to offer positive incentives. A small fine  $F$  cannot provide sufficient driving force for both parties to evolve towards positive carbon reduction strategies. Excessively high fines  $F$  can have a counterproductive effect on the time it takes to reach evolutionary equilibrium. Therefore, it is necessary to formulate appropriate subsidy and fine levels based on actual situations, which may achieve twice the result with half the effort. It should be noted that the convergence rate of tunnel operators is greater than that of the government. This indicates that tunnel operators have a higher parameter sensitivity to these measures. It also suggests that the reward and punishment mechanism is an effective means of incentivizing tunnel operators.

#### 4.2. Carbon Reduction Technology Cost $P$ and Efficiency Gain $G$

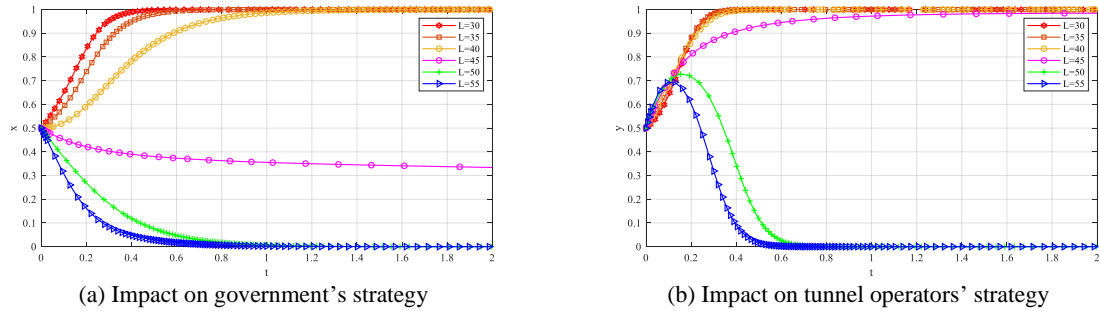
While keeping other parameters constant, simulations were conducted six times by setting the carbon reduction technology cost  $P$  to 80, 90, 100, 110, 120, and 130 respectively. The simulation results of the evolutionary path of strategy selection for both the government and tunnel operators are shown in **Figure 5**. When  $P \leq 100$ , both the government and tunnel operators' strategies are positive, and the system's stabilization speed accelerates as  $P$  decreases. When  $P \geq 110$ , both the government and tunnel operators' strategies are negative, and the system's stabilization speed accelerates as  $P$  increases.

While keeping other parameters constant, simulations were conducted six times by setting the carbon reduction technology efficiency gain  $G$  to 35, 40, 45, 50, 55, and 60 respectively. The simulation results of the evolutionary

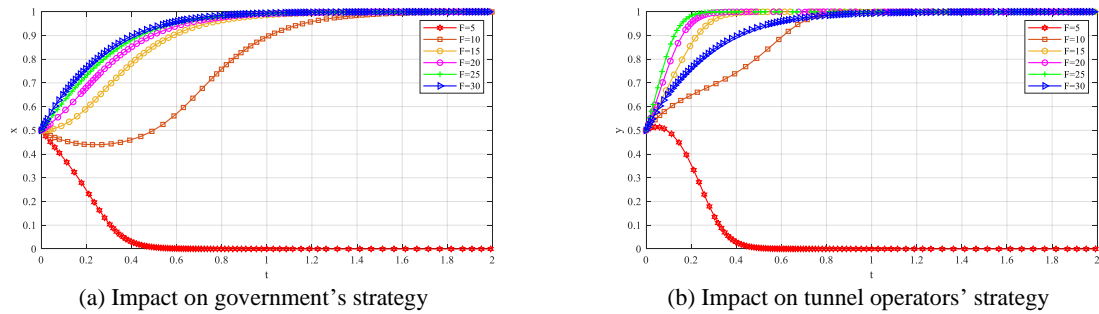


path of strategy selection for both the government and tunnel operators are shown in **Figure 6**. When  $G \geq 45$ , both the government and tunnel operators' strategies are positive, and the system's stabilization speed accelerates as  $G$  increases. When  $G \leq 40$ , both the government and tunnel operators' strategies are negative, and the system's stabilization speed accelerates as  $G$  decreases.

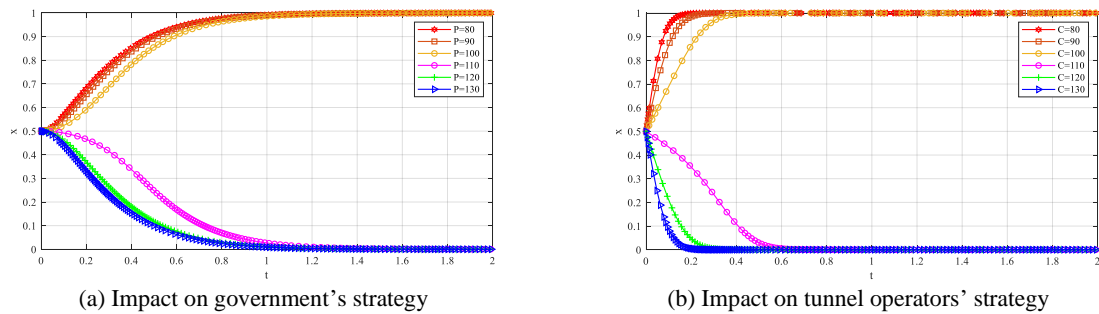
Reducing the cost  $P$  and increasing the efficiency gain  $G$  can enhance their willingness to adopt carbon reduction measures. Additionally, the stabilization rate of tunnel operators is significantly higher than that of the government. Tunnel operators have a higher parameter sensitivity to them.



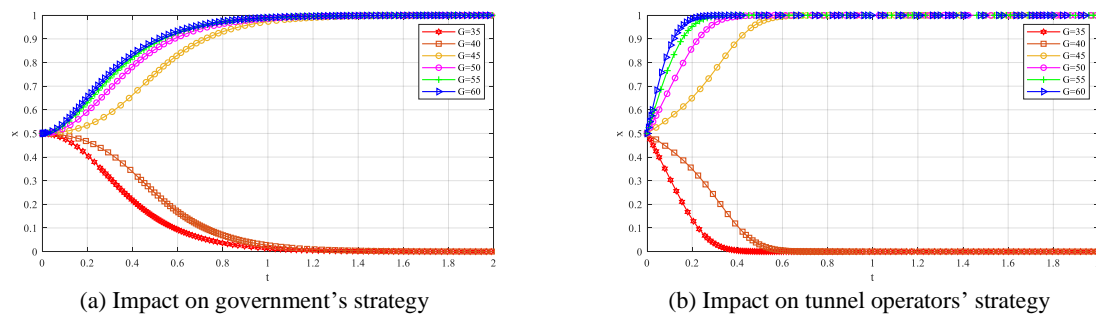
**Figure 3.** Impact of government subsidy  $L$  to tunnel operators adopting low-carbon technologies on the evolutionary strategies of both sides of the game



**Figure 4.** Impact of government fines  $F$  to tunnel operators adopting traditional technologies on the evolutionary strategies of both sides of the game



**Figure 5.** Impact of carbon-reduction technology costs  $P$  on the evolutionary strategies of both sides of the game



**Figure 6.** Impact of carbon-reduction technology efficiency gain  $G$  on the evolutionary strategies of both sides of the game

## 5. CONCLUSION

In summary, this paper establishes an evolutionary game model between the government and tunnel operators. Through replicator dynamic equations, it analyzes the evolutionary path of strategic choices for both players. Through numerical simulation, it analyzes the impact of key parameters on the game equilibrium. The main conclusions are as follows:

- (1) The government's strategy choice is the key factor in determining whether the system can achieve optimal equilibrium. Only when the government adopts a positive incentive strategy can the system possibly converge to the optimal equilibrium of (positive incentive, adopting carbon reduction measures); otherwise, the system will fall into a suboptimal equilibrium state of (negative incentive, adopting carbon reduction measures).
- (2) Tunnel operators typically exhibit faster convergence speeds than governments. At the national level, long-term policy frameworks should be established for governments. For tunnel operators, a "high-frequency, small-step" incentive strategy should be employed.
- (3) Reward and punishment mechanisms are effective tools for incentivizing tunnel operators, and thus governments should design them judiciously. Specifically, government subsidies ( $L$ ) are not the primary factor influencing tunnel operators' decisions, and their value should be kept reasonably. Excessively high subsidies not only diminish the government's willingness to provide positive incentives but also prove counterproductive in encouraging operators to adopt low-carbon technologies. Regarding fines ( $F$ ), a fine that is too low fails to provide sufficient impetus for both players to adopt positive carbon reduction strategies. Conversely, an excessively high fine will prolong the time required to achieve evolutionary equilibrium, also proving counterproductive.
- (4) Lower adoption costs ( $P$ ) and higher efficiency gains ( $G$ ) for low-carbon technologies will incentivize tunnel operators to implement these measures. While pursuing maximum efficiency gains, operators must also prioritize cost control. Furthermore, the development and adoption of these technologies will drive down usage costs, while the increasing benefits of carbon emission reduction will bolster investor confidence. This dynamic can ultimately foster a self-sustaining green development paradigm.

## ACKNOWLEDGMENTS

The authors wish to acknowledge the sponsorship from the Research on Key Technologies for the Planning, Design, and Construction of the S7 Shanghai-Chongming West River-Crossing Tunnel (Y202445) and Research Fund of State Key Laboratory for Disaster Reduction in Civil Engineering (SLDRCE19-A-14). The support from the China Railway 14th Bureau Group Co., Ltd is highly appreciated.

## REFERENCE

- [1] Beiza, J. (2024). A developed tunnel ventilation system modeling for an intelligent transportation system. *JOURNAL OF ADVANCED TRANSPORTATION*, 2024, 1–14. <https://doi.org/10.1155/2024/6417493>
- [2] Cengiz, M. S., and Cengiz, C. (2018). Numerical analysis of tunnel led lighting maintenance factor. *IIUM ENGINEERING JOURNAL*, 19(2), 154–163. <https://doi.org/10.31436/iiumej.v19i2.1007>

- [3] Fan, K., and Hui, E. C. M. (2020). Evolutionary game theory analysis for understanding the decision-making mechanisms of governments and developers on green building incentives. *Building and Environment*, 179, 106972. <https://doi.org/10.1016/j.buildenv.2020.106972>
- [4] Guo, Y., Luo, G., and Hou, G. (2021). Research on the evolution of the express packaging recycling strategy, considering government subsidies and synergy benefits. *International Journal of Environmental Research and Public Health*, 18(3), 1144. <https://doi.org/10.3390/ijerph18031144>
- [5] Haoyang, W., Lei, G., and Ying, J. (2022). The predicament of clean energy technology promotion in China in the carbon neutrality context: Lessons from china's environmental regulation policies from the perspective of the evolutionary game theory. *Energy Reports*, 8, 4706–4723. <https://doi.org/10.1016/j.egyr.2022.03.142>
- [6] Huo, H., Liu, H., Bao, X., and Cui, W. (2022). Game analysis of supply chain enterprises' choice of carbon emission reduction behavior under environmental regulation and consumers' low carbon preference. *DISCRETE DYNAMICS IN NATURE AND SOCIETY*, 2022, 3013289. <https://doi.org/10.1155/2022/3013289>
- [7] Hussain, M., Zheng, B., Chi, H.-L., Hsu, S.-C., and Chen, J.-H. (2023). Automated and continuous BIM-based life cycle carbon assessment for infrastructure design projects. *RESOURCES CONSERVATION AND RECYCLING*, 190, 106848. <https://doi.org/10.1016/j.resconrec.2022.106848>
- [8] Jiang, Z., Jia, C., Zheng, P., Gong, Y., Li, N., Ahmed, A., Zhang, Z., and Luo, D. (2022). A transverse deceleration energy harvester based on a sliding plate for self-powered applications in near-zero energy road tunnels. *Sustainable Cities and Society*, 84, 104014. <https://doi.org/10.1016/j.scs.2022.104014>
- [9] Li, Y., and Zhang, J. (2024). Evolutionary game analysis of low-carbon incentive behaviour of power battery recycling based on prospect theory. *SUSTAINABILITY*, 16(7), 2793. <https://doi.org/10.3390/su16072793>
- [10] Liu, T., Zhu, H., Shen, Y., Li, T., and Liu, A. (2024). Embodied carbon assessment on road tunnels using integrated digital model: Methodology and case-study insights. *TUNNELLING AND UNDERGROUND SPACE TECHNOLOGY*, 143, 105485. <https://doi.org/10.1016/j.tust.2023.105485>
- [11] Mu, H., Chen, P., Wang, H., Li, N., and Xu, N. (2025). Tripartite evolutionary game analysis of fishery carbon sink trading in China based on prospect theory. *POLISH JOURNAL OF ENVIRONMENTAL STUDIES*, 34(1), 245–261. <https://doi.org/10.15244/pjoes/182897>
- [12] Pritchard, J. A., and Preston, J. (2018). Understanding the contribution of tunnels to the overall energy consumption of and carbon emissions from a railway. *Transportation Research Part D-Transport and Environment*, 65, 551–563. <https://doi.org/10.1016/j.trd.2018.09.010>
- [13] Qiao, Y., Qiao, R., and Qiao, Y. (2024). Competitive game model and evolutionary strategy analysis of green power and thermal power generation. *SYMMETRY-BASEL*, 16(8), 959. <https://doi.org/10.3390/sym16080959>
- [14] Shen, Y., Deng, Y., Li, T., Zhou, L., Feng, S., and Zhu, H. (2022). Determining multidimensional diffuse reflection effects in city tunnel lighting environment. *Building and Environment*, 212, 108796. <https://doi.org/10.1016/j.buildenv.2022.108796>
- [15] Song, Y., Zhu, H., Shen, Y., Yan, Z., and Feng, S. (2024a). Zero-carbon tunnel: Concept, methodology and application in the built environment. *JOURNAL OF CLEANER PRODUCTION*, 479, 144031. <https://doi.org/10.1016/j.jclepro.2024.144031>
- [16] Song, Y., Zhu, H., Shen, Y., Deng, Y., and Feng, S. (2024b). Multi-dimensional tunnel lighting environment model: Determining illuminance with regression analysis and parametric study on key factors. *Tunnelling and Underground Space Technology*, 151, 105864. <https://doi.org/10.1016/j.tust.2024.105864>
- [17] Wan, S., Zhang, J., and Cheng, X. (2022). Behavior choice and emission reduction in a dynamic supply chain with a capital-constrained retailer. *DISCRETE DYNAMICS IN NATURE AND SOCIETY*, 2022, 5857852. <https://doi.org/10.1155/2022/5857852>
- [18] Wang, Y., Du, P., Chen, Y., Hua, S., Wang, J., Shi, C., and Liu, K. (2023). Mixed ventilation approach combined with single-shaft complementary system for highway tunnels. *Tunnelling and Underground Space Technology*, 132, 104927. <https://doi.org/10.1016/j.tust.2022.104927>
- [19] Xue, X., Ji, A., Luo, X., Dou, Y., and Fan, H. (2024). INTEGRATING EVOLUTIONARY GAME AND SYSTEM DYNAMICS FOR MULTI-PLAYER SAFETY REGULATION OF MAJOR INFRASTRUCTURE PROJECTS IN CHINA. *JOURNAL OF CIVIL ENGINEERING AND MANAGEMENT*, 30(4), 307–325. <https://doi.org/10.3846/jcem.2024.21175>
- [20] Yang, X., and Liu, K. (2024). Low-carbon construction in China's construction industry from the perspective of evolutionary games. *BUILDINGS*, 14(6), 1593. <https://doi.org/10.3390/buildings14061593>

## TOWARDS LOW-CARBON TUNNEL ENGINEERING: A COMPREHENSIVE REVIEW OF EMISSION ESTIMATION AND FORECASTING TECHNIQUES

Caiwei Wang<sup>1</sup>, Mengqi Zhu<sup>2</sup>, Hehua Zhu<sup>3</sup>, Shiqi Dou<sup>4</sup>

**Abstract:** As global tunnel construction expands in scale, increasing attention is focused on carbon emissions. Life Cycle Assessment (LCA) has emerged as a prominent research focus and is widely applied for carbon accounting across sectors. However, LCA application within tunnel engineering specifically remains exploratory. This study traces the evolution of LCA from general carbon emission research to tunnel-specific carbon accounting. We comprehensively review existing literature on tunnel carbon emission estimation based on LCA principles and further examine relevant emission forecasting research. Finally, recommendations are provided to advance full life-cycle carbon research for tunnels, aiming to refine LCA methodologies and accelerate progress towards zero-carbon tunnels.

**Keywords:** Carbon emission, tunnel engineering, life cycle assessment, carbon emission estimation

### 1. INTRODUCTION

In recent years, the intensification of global warming and the frequent occurrence of extreme weather events have brought greenhouse gas (GHG) emissions to the forefront of international concerns (IPCC, 2021). According to data from the National Oceanic and Atmospheric Administration (NOAA), the global average temperature has risen by 1.1°C since the Industrial Revolution (Aboagye et al., 2023), with carbon dioxide (CO<sub>2</sub>) — the primary anthropogenic GHG — contributing up to 80.1% of total emissions (Wang et al., 2015). Aligned with the Paris Agreement's goal of limiting global warming "well below 2°C" and pursuing efforts to limit it to 1.5°C, 137 countries have committed to carbon neutrality targets through legislative or policy frameworks (Liu et al., 2024). This global imperative necessitates systematic carbon emission research across industries to devise scientifically robust mitigation strategies.

Current academic research has extensively explored carbon emission accounting methods and reduction strategies. In the power sector, Li et al. (2024) comprehensively reviewed direct and indirect emission accounting systems and proposed directions for data integration optimization. Zheng et al. (2024) conducted bibliometric analyses in social sciences, elucidating the evolution and theoretical foundations of carbon accounting models. In urban planning, Chen et al. (2019) compared the strengths and limitations of inventory, modeling, and remote sensing inversion methods for emission estimation. Despite these interdisciplinary advancements, carbon emission research specific to tunnel engineering remains significantly understudied.

As a critical component of modern infrastructure, tunnels play an irreplaceable role in urban spatial expansion and transportation network development (Admiraal & Cornaro, 2016). With accelerating global urbanization,

<sup>1</sup> PhD Candidate, Caiwei Wang, B.Sc. Civil Eng., Department of Geotechnical Engineering, School of Civil Engineering, Tongji University, 1239 Siping Road, Yangpu District, Shanghai, P.R. China, 2431019@tongji.edu.cn

<sup>2</sup> Postdoctoral Researcher, Mengqi Zhu, Ph.D. Civil Eng., Department of Geotechnical Engineering, School of Civil Engineering, Tongji University, 1239 Siping Road, Yangpu District, Shanghai, P.R. China, mqzhu@tongji.edu.cn

<sup>3</sup> Professor, head of National Key Laboratory for disaster prevention and mitigation of Civil Engineering, Hehua Zhu, Ph.D. Civil Eng., Department of Geotechnical Engineering, School of Civil Engineering, Tongji University, 1239 Siping Road, Yangpu District, Shanghai, P.R. China, zhuhehua@tongji.edu.cn

<sup>4</sup> PhD Candidate, Shiqi Dou, B.Sc. Civil Eng., Department of Geotechnical Engineering, School of Civil Engineering, Tongji University, 1239 Siping Road, Yangpu District, Shanghai, P.R. China, 2310059@tongji.edu.cn

tunnel construction has expanded substantially: by the end of 2023, the total lengths of highway and railway tunnels in China exceeded 30,000 km and 20,000 km, respectively (Seo & Kim, 2013). However, environmental impact research in this field lags notably. Seo & Kim (2013) revealed that due to high-energy-consuming materials and complex construction processes, tunnel projects generate approximately four times the carbon emissions per unit area compared to surface roads. Moretti et al. (2016) further demonstrated that each linear meter of tunnel construction entails a full-life-cycle consumption of 2.3 tons of concrete, resulting in 1.8 tons of CO<sub>2</sub> equivalent emissions. These findings underscore the urgent need to explore carbon reduction potential in tunnel engineering.

This study focuses on carbon emissions across the entire life cycle of tunnels, aiming to address three key gaps: first, systematically reviewing the evolution of Life Cycle Assessment (LCA) applications in tunnel carbon accounting; second, developing a predictive model covering construction, operation, and decommissioning phases; third, proposing integrated carbon reduction strategies combining technological innovation and management optimization. The research outcomes will provide theoretical and practical guidance for low-carbon transformation in infrastructure construction in developing countries, facilitating the realization of carbon neutrality in the transportation sector.

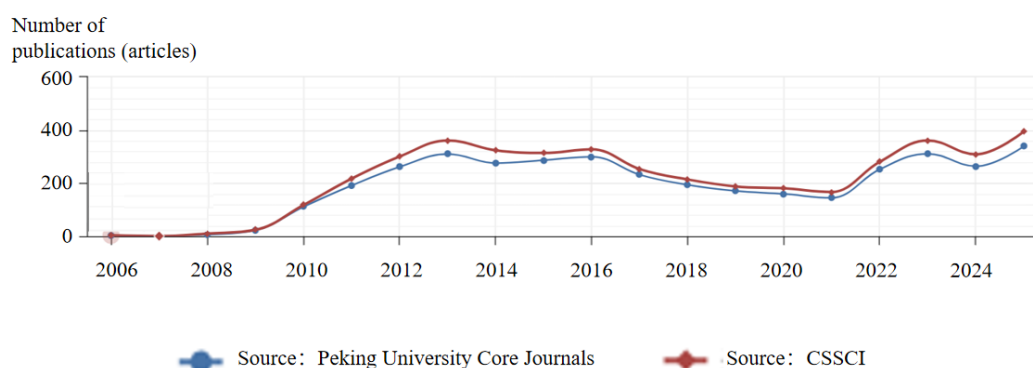
## 2. BIBLIOMETRIC ANALYSIS

This section employs CiteSpace and the built-in bibliometric tools of the China National Knowledge Infrastructure (CNKI) database to analyze the body of literature related to carbon emission research in both China and the broader international context. The analysis focuses on the temporal distribution of carbon emission studies and examines how this body of research has gradually been applied to the field of tunnel engineering.

### 2.1. Carbon emissions

This section analyzes the temporal distribution of carbon emission research in China using the built-in bibliometric tools of the CNKI database, which was selected as the primary regional database for Chinese-language academic publications. The keyword used for the literature search was “carbon emissions” with the source type limited to peer-reviewed academic journals and the publication period restricted to 2005–2025. After an initial screening of the search results, a total of 11,831 relevant research articles were identified. Among these, 7,733 were published in journals indexed by the PKU Core (Peking University Core Journals), and 4,098 appeared in journals indexed by the Chinese Social Sciences Citation Index (CSSCI).

The temporal distribution of the two categories of publications is illustrated in Figure 1. As shown in the figure, carbon emissions began to attract attention in China around 2009. Since then, the annual number of publications has gradually increased. However, research activity declined around 2017 before regaining momentum in 2021, with the number of publications continuing to rise and reaching approximately 400 per year. This trend may be related to the signing of the Paris Agreement. Overall, these changes reflect the growing national emphasis on carbon emissions and the increasing attention the topic has received within the research community.



**Figure 1.** Temporal Distribution of Research Publications on Carbon Emissions in China

To explore the key aspects of carbon emission research, this study utilizes the Web of Science (WOS) Core Collection as the bibliometric database. A precise search was conducted using the keyword “carbon emission,” with the document type restricted to articles and the time span set from 2005 to 2025. The search yielded over 200,000 publications. After relevance screening, 483 representative articles were selected for keyword co-occurrence analysis using the CiteSpace tool. Keywords with a frequency greater than 40 occurrences were identified as key thematic labels. As shown in Figure 2, carbon emission



research spans a wide range of fields, including industry, agriculture, and climate, and covers diverse perspectives such as policy frameworks, environmental impacts, and carbon dioxide equivalent (CO<sub>2</sub>e) calculations. Among these, the keyword “carbon emission calculation” appeared most frequently, over 70 times, highlighting it as a major research hotspot. Therefore, it is essential to conduct a focused review of existing research findings and practical experiences within this specific domain.

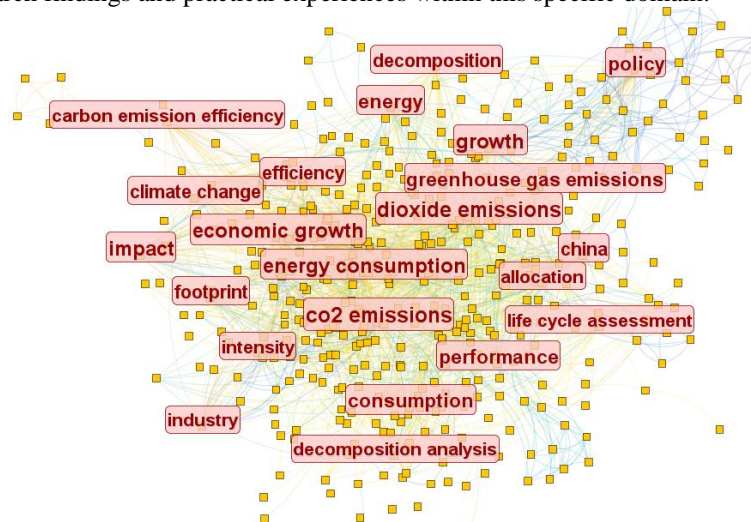


Figure 2. Keyword Co-Occurrence Network of Carbon Emission Research

## 2.2. Carbon emissions in civil engineering

As illustrated in Figure 2, the application of carbon emission research within the field of civil engineering has emerged as a significant hotspot. To further analyze the key research areas of carbon emissions across various branches of civil engineering, an additional thematic search using the term "civil engineering project" was conducted within the previously identified dataset of 200,000 publications. After manual screening, 318 articles directly related to carbon emissions in civil engineering were identified. These selected articles were then subjected to visual analysis using CiteSpace, and the resulting keyword co-occurrence network is presented in Figure 3.

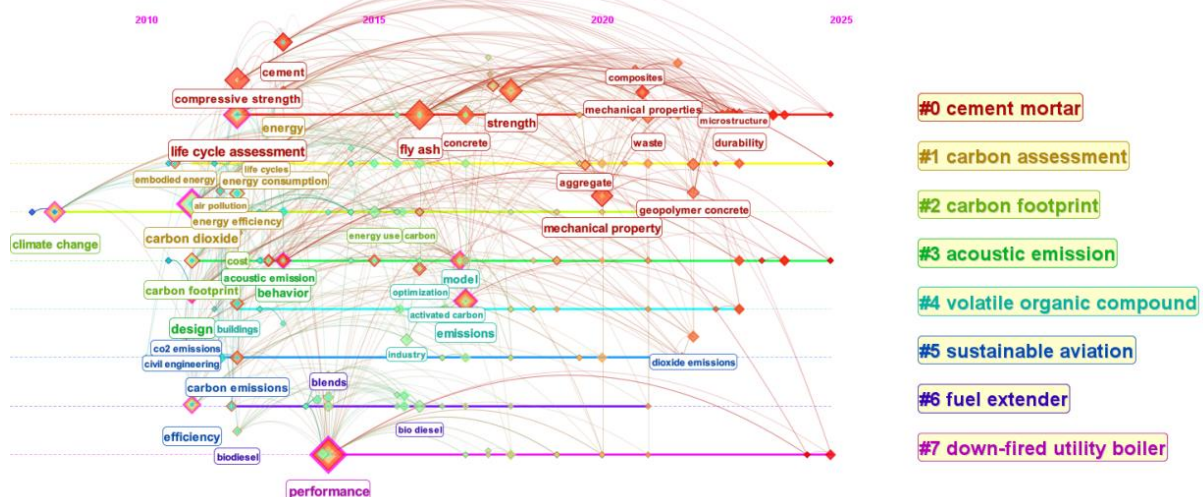
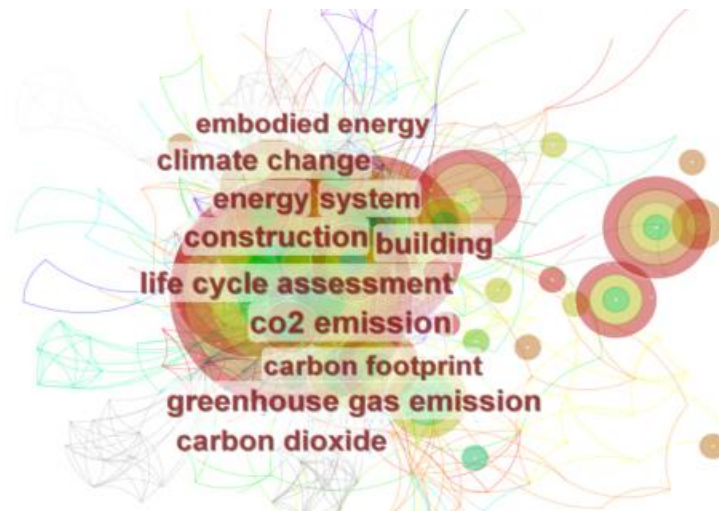


Figure 3. Cluster Timeline Analysis of Keywords in Articles Related to Carbon Emission



**Figure 4.** Keywords Clustering with Frequency More than 30 Times

The keyword visualizations are presented in Figures 3 and 4. As shown in Figure 3, carbon emission calculation is a primary focus within the civil engineering domain. Among material-related terms, “cement mortar” appears with the highest frequency. Over time, the central themes of carbon emission research have shifted—from early focuses on CO<sub>2</sub> quantification and air pollution impacts to broader concerns such as sustainable development, tunnel construction, and micro-scale infrastructure. Figure 4 presents a cluster analysis of keywords with a frequency exceeding 30 occurrences. The analysis reveals a concentration of research on systems, structures, and life cycle assessment (LCA), while studies specifically addressing carbon emission calculations in tunnel engineering remain relatively limited. Dou et al. (2024) pointed out that the life-cycle research on low-carbon tunnels has yet to form a complete and coherent life-cycle framework, with studies at various stages remaining rather general and fragmented.

### 3. TUNNEL CARBON EMISSION CALCULATION BASED ON LCA

To obtain the latest research on carbon emission calculation throughout the entire life cycle of tunnels, this study defined two sets of keywords—“carbon emission” and either “tunnel” or “tunneling”—and combined them into a single search string. The Web of Science Core Collection was selected as the database, with citation indexes limited to SCI and SSCI, resulting in 1,526 publications. After manual screening, 31 articles were identified as highly relevant to the topic of carbon emission calculations across the tunnel life cycle. Currently, the widely accepted tunnel life cycle framework divides carbon emissions into four stages: the survey and design stage, the construction stage, the operation and maintenance stage, and the demolition and recycling stage. Given the relatively limited research focused on the survey and design stage, this paper organizes and reviews the literature based on the remaining three stages—construction, operation and maintenance, and demolition and recycling—as summarized in Tables 1, 2, and 3, along with relevant analysis and discussion.

**Table 1.** Carbon Emission Calculation during the Tunnel Construction Phase

Reference	Method	Metric	Conclusion	Further work
Tabrizikahou & Nowotarski, 2021	VSM JIT technique TPM techniques	CO <sub>2</sub>	This facilitates construction engineers and project managers in acquiring building designs and planning strategies oriented toward minimizing energy consumption.	The outcomes of the proposed approach are subject to the influence of region-specific practices and conditions.
Zhao et al., 2022	emission coefficient	CO <sub>2</sub>	Carbon dioxide emissions were quantified for each phase of slurry shield tunnel construction. Notable disparities were identified among different	

Song, Zhu, Shen, Yan, et al., 2024	Emission-Factor Approach (EFA)	CO <sub>2</sub> -eq	<p>construction rings, with the highest CO<sub>2</sub> emission being more than three times greater than the lowest.</p> <p>The carbon emissions of a highway tunnel in Jiangxi Province were calculated, with the material production phase accounting for the largest proportion at 91.5%.</p> <p>Concrete and steel had the highest carbon emissions, and Concrete in portals, linings, and waterproofing had the highest emissions</p>	<p>Carbon emissions are represented in terms of carbon dioxide (CO<sub>2</sub>) emissions rather than carbon dioxide equivalents (CO<sub>2</sub>e), with a primary focus on CO<sub>2</sub> generated during material production.</p>
Seo & Kim, 2013	Emission-Factor Approach (EFA)	CO <sub>2</sub> -eq	<p>The embodied CO<sub>2</sub> emissions of three tunnels were estimated.</p> <p>The increased embodied energy and emissions from wider tunnels can be offset by reduced operational emissions.</p>	<p>Further research is needed to better quantify the relationship between operational energy emissions and actual tunnel diameter.</p> <p>The calculation method will depend on train type, service type, and expected operational lifespan.</p>
Pritchard & Preston, 2018	Estimation based on existing research data	CO <sub>2</sub> -eq	<p>A carbon emission calculation model for the construction process was established based on the new prefabricated invert technology, incorporating constraints of cyclic advancement on material transportation.</p> <p>The calculation revealed that carbon emissions during prefabricated invert construction were reduced by over 15% compared to cast-in-place construction, with reduced cement and steel consumption contributing the most to emission reduction.</p>	<p>The carbon accounting model can be further optimized by incorporating cycle-induced constraints on material transportation and accounting for on-site transport conditions.</p>
Zou et al., 2024	Emission-Factor Approach (EFA)	CO <sub>2</sub> -eq		

Rafael Dami' & Clara I. Zamorano, 2011	CML-IA baseline	CO <sub>2</sub>	<p>The environmental impact assessment revealed that support structures, linings, and infrastructure works accounted for at least 70% of the total environmental burden across all considered impact categories for the five RMR classes in railway tunnel construction.</p>	<p>Due to limited operational data for railway tunnels and the fact that tunnel maintenance is primarily condition-based, the maintenance and operational phases were not considered in this study.</p> <p>Since tunnel decommissioning rarely occurs, the end-of-life recycling phase was also excluded from consideration.</p>
Wang et al., 2023	Input- output methods and process analysis methods	CO <sub>2</sub> -eq	<p>The modified process analysis method was employed to calculate CO<sub>2</sub> emissions during shield tunnel construction.</p> <p>The results indicate that the reinforced concrete precast segments contribute the most to carbon emissions</p>	<p>The combined use of traditional calculation methods and neural network models enables comprehensive and accurate analysis of carbon emissions in the construction industry.</p>
Liu et al., 2024	process- based project inventory analysis method	CO <sub>2</sub> -eq	<p>The embodied carbon per meter of tunnel varies between 7.97-24.27 t depending on surrounding rock conditions, with significantly increased emissions observed as rock quality deteriorates.</p> <p>In highway tunnels, the material production phase contributes the highest proportion (79%-87%) of embodied carbon, while the transportation phase accounts for the lowest share.</p> <p>In the material production phase, concrete and steel are the primary carbon emission contributors, with concrete accounting for the largest share at approximately 50%-80%.</p>	<p>Digital models can leverage their visual capabilities to compare different design schemes or material types, ultimately reducing project carbon emissions.</p>
Guo et al., 2025	Emission- Factor Approach (EFA)	CO <sub>2</sub> -eq	<p>During the case project's construction phase, building material production was the primary emission source, contributing 78.65% of total emissions, while construction machinery energy consumption and transportation accounted for 18.87% and 2.48% respectively</p>	

			<p>The greenhouse gas emissions from building material production showed a highly significant positive correlation (Pearson's <math>r^* = 0.999</math>, <math>p^* = 0.000 &lt; 0.001</math>) with the total building emissions)</p> <p>The construction of support structures—particularly pipe splicing, initial lining, and secondary lining works—represents the primary emission-intensive activities in metro tunnel construction phases.</p>	
Shi et al., 2024	Process-based hybrid life cycle assessment model		<p>Using the hybrid method, GHG emissions from auxiliary materials were identified.</p> <p>Under severe data gaps, the hybrid method complements missing data and effectively improves data quality.</p>	<p>Due to insufficient upstream material and energy data, emissions related to upstream fuel were not considered.</p> <p>This study focuses on carbon emissions during the construction phase, which represents only a small portion of the life cycle. Future research should consider the impact of upstream fuel emissions.</p>
Mao et al., 2013	Emission-Factor Approach (EFA)	CO <sub>2</sub> -eq	<p>Differences in construction methods affect carbon emissions; semi-prefabricated structures emit slightly less than traditional ones.</p>	<p>Future research will examine more cases to explore the link between prefabrication and emissions.</p>
Chen et al., 2024	BIM and EN 15978 life cycle modules	CO <sub>2</sub> -eq	<p>Summarized embodied carbon calculation methods, considering geotechnical conditions and quantifying emissions from transport and construction stages.</p>	<p>Advocates integrating carbon assessment into geotechnical analysis to evaluate life-cycle economic benefits from a holistic perspective, enriching future research and practice in tunnel construction decarbonization</p>
Kamari et al., 2022	BIM	CO <sub>2</sub> -eq	<p>Concrete-based materials contribute most to the embodied carbon emissions of buildings.</p> <p>Wooden elements can reduce the model's carbon emissions.</p>	<p>Data provided by BIM is insufficient for direct use in LCA.</p>



				LCA-related methods vary significantly, including boundary conditions, calculation methods, and impact categories.
				Supplementary indicators may be added in the future for comprehensive project evaluation.
Wang et al., 2015	Emission-Factor Approach (EFA)	CO <sub>2</sub>	<p>An empirical method for estimating CO<sub>2</sub> emissions was proposed based on four highway construction projects in Southwest China.</p> <p>CO<sub>2</sub> emissions mainly occurred during material production, followed by on-site construction, with transportation contributing the least.</p>	<p>Future work could include developing specific construction guidelines (e.g., equipment selection, green construction technologies).</p>
Guo et al., 2019	Database analysis and calculation (Source: China Life Cycle Database (CLCD))	CO <sub>2</sub>	<p>Considered different rock mass classifications and identified the dependency of LCA on rock mass types.</p>	<p>Future studies will consider the carbon emissions from the demolition and recycling phases.</p>
Yang et al., 2018	BIM	CO <sub>2</sub> -eq	<p>BIM-based life cycle assessment (LCA) models can comprehensively evaluate the environmental performance of buildings throughout their life cycle.</p>	<p>The integration of LCA and BIM is hindered by software compatibility issues.</p>
Han et al., 2012	I-O LCA	CO <sub>2</sub> -eq	<p>A model was proposed to assess carbon emissions during the construction phase.</p>	<p>Analyzing the cost and schedule of construction methods will aid in selecting more environmentally friendly and cost-effective approaches in future studies.</p>
Huang et al., 2020	the ReCiPe Midpoint (E) V1.06 method		<p>Explored the environmental impacts of D&amp;B construction for Norwegian standard highway tunnels.</p> <p>Compared the environmental impacts of D&amp;B construction across tunnels of different sizes and lengths.</p>	<p>Carbon emissions from tunnel operation, maintenance, and demolition phases have not yet been considered.</p>

Huang et al., 2015	ILCD 2011 Midpoint V1.03 method	Explored the environmental impacts of rock support on 24 highway tunnels with varying sizes and rock mass classifications. All environmental impacts showed higher sensitivity to rock mass classification than to tunnel size.	Technical improvements should focus on reducing rebound and optimizing the design of shotcrete additives and binders.
-----------------------	--	---	---

**Table 2.** Carbon Emission Calculation during the Tunnel Operation and Maintenance Phase

Reference	Method	Metric	Conclusion	Further work
Brimblecombe et al., 2015	Sen's slope LSR regression	CO <sub>2</sub> -eq	Integrated hourly traffic volume and derived carbon emission factors for diesel and gasoline/LPG fleets inside the tunnel using bivariate regression.	Variations in road gradient between tunnels and traffic speed may affect the accuracy of multiple regression analysis. Further research can focus on specific tunnels with long-term measurement series, including changes in traffic composition, to minimize uncertainty.
Zou et al., 2024	Emission-Factor Approach (EFA)	CO <sub>2</sub> -eq	Incorporate carbon emissions generated during the early tunnel operation phase into the assessment system, considering the indirect impact of significantly improved construction efficiency on emissions.	Carbon emission calculations for the demolition and recycling phase require further refinement.
Song, Zhu, Shen, & Feng, 2024	Emission-Factor Approach (EFA)	CO <sub>2</sub> -eq	Tunnel lighting carbon emissions are significantly higher than those from ventilation.	High diesel engine emissions prevented the assessment of gasoline engine contributions using statistical models.
Weingartner et al., 1997	Measurement and Calculation Method	CO <sub>2</sub> -eq	During tunnel operation, carbon emission factors for diesel engines were calculated based on aerosol emission measurements, revealing that the majority (63%) of diesel vehicles were heavy-duty.	Energy-saving technologies for tunnel ventilation and lighting will effectively promote carbon
Guo et al., 2025	Database analysis and calculations (Source: China Life Cycle	CO <sub>2</sub> -eq	A 4-km, four-lane highway tunnel in China emits approximately 375,500 tons of CO <sub>2</sub> equivalent. Over half of the greenhouse gas emissions during the	

	Database, CLCD)		operation phase come from tunnel ventilation and lighting.	reduction in Chinese tunnels.
Raposo et al., 2019	BIM	CO <sub>2</sub> -eq	Evaluated the cost and environmental impacts of seismic retrofitting and demolition of prefabricated components using an integrated LCA and BIM approach.	The integration of LCA and BIM is influenced by the databases used.
Audi et al., 2020	CML method EDIP method	CO <sub>2</sub> -eq	Calculated carbon emissions from bus traffic inside the tunnel during operation, power consumption of tunnel ventilation and lighting, and power consumption of roadway lighting.	LCA cannot cover all aspects, mainly socioeconomic factors, but it still provides a robust set of midpoint indicators.

**Table 3.** Carbon Emission Calculation during the Tunnel Deconstruction and Material Recovery Phase

Reference	Method	Conclusion	Further work
Wu et al., 2024	Emission-Factor Approach (EFA)	Carbon emissions from the demolition and recycling phase contribute only 4.9% of the total life cycle emissions, much lower than the operation and maintenance phase.	Life cycle assessment (LCA) of carbon emissions for cross-sea transport infrastructure is still an emerging field, with detailed baseline data for practical analysis difficult to obtain.
Xie et al., 2020	Hybrid analysis method	Embodied carbon accounts for 0.15% of life cycle energy consumption at end-of-use. Recycling and reuse of building materials after use help minimize life cycle emissions (LCE).	
Akbar Nezhad & Nadoushani, 2014	BIM	Assessed the cost, energy consumption, and carbon emission impacts of demolition and recycling phase strategies.	
Yahya et al., 2016	Impact Pathway Approach (IPA)	The ecological impact of metal waste treatment in the construction industry mainly arises from fuel consumption by machinery. The disposal of rebar waste incurs the highest total ecological cost, followed by sorting facilities and recycling strategies, ranked second and third respectively.	Future research should focus on integrating ecological indicators into BIM-based project development strategies.

Based on the number of studies and research content summarized in Tables 1, 2, and 3, it is evident that current research on tunnel carbon emissions using LCA theory remains limited both domestically and internationally, with a notable lack of unified standardized methodologies. Compared to the construction sector, tunnel carbon emission studies still lack comprehensive quantitative analysis methods. Different researchers consider varying indicators and employ diverse approaches when calculating tunnel carbon emissions. The most commonly used methods are the carbon emission factor method and the direct calculation method based on available data. The carbon emission factor method requires defining the calculation boundaries according to the different life cycle stages of the tunnel to accurately quantify carbon emissions. However, limitations arise due to differences in database types and the varying scope of data collected across databases. Consequently, using databases to calculate tunnel carbon emissions often faces issues such as incomplete data and limited coverage of certain tunnel life cycle phases.

A comparison of the number of publications in Tables 1, 2, and 3 indicates that current research on tunnel carbon emissions predominantly focuses on the construction phase. During this stage, emissions are typically

quantified based on factors such as geological conditions, excavation methods, material production, and transportation processes. Tunnels are generally designed for long service lives, and the operation phase accounts for the largest proportion of total life cycle carbon emissions. However, studies addressing emissions during the operation and maintenance phase remain limited compared to those focused on construction. Tunnel lighting, in particular, contributes significantly to carbon emissions during this phase and is commonly assessed using database-driven direct calculation methods. Research on the deconstruction and recovery phase of tunnels is even more scarce, likely because most tunnels are still in operation and have not yet reached the end of their service lives. Existing studies in this area primarily examine the impact of recycling strategies on carbon emissions and their associated economic benefits.

In summary, while continuing to advance research on carbon emissions during the construction phase, future efforts should place greater emphasis on investigating emissions during the operation, maintenance, and decommissioning phases to achieve a more comprehensive understanding of the full life-cycle carbon footprint of tunnels.

#### 4. TUNNEL CARBON EMISSION PREDICTION BASED ON LCA

Carbon emissions during the operation and maintenance phase of tunnels account for more than 80% of the total emissions over the tunnel's life cycle (Opher et al., 2021). Conducting predictive studies is therefore essential for quantifying the full carbon footprint, identifying high-emission components, and enabling timely, dynamic adjustments. Such efforts can effectively support the adoption of low-carbon materials and construction technologies. At present, research on the prediction of tunnel carbon emissions remains relatively limited. A search of the WoS database using the keywords "tunnel" and "prediction" yielded a small number of relevant publications. After performing a relevance-based screening and analysis, the findings are summarized in Table 4.

*Table 4. Research on Carbon Emission Prediction for Tunnels*

Reference	Models/Software	Method	Parameter	Conclusion	Further work
Zhao et al., 2022	SSA-SVR	Random forest (RF) Support vector regression (SVR) sparrow search algorithm (SSA) Grey wolf optimizer and genetic algorithm (GWO)	cohesiveness of the soil, internal friction angle, penetration resistance, earth pressure, buried depth, advancing speed, torque, total thrust force, advancing time, mud inflow rate, mud density	CO <sub>2</sub> emissions during material production, material transportation, and prefabrication of structural components show little variation. Carbon dioxide emissions vary greatly among different stages of shield tunneling. Torque is the most significant factor affecting CO <sub>2</sub> emissions, while slurry inflow has the least impact. Two theoretical models were proposed to predict greenhouse gas emissions from tunnel construction, providing emission references during the design phase.	The prediction model targets CO <sub>2</sub> emissions during different stages of slurry shield tunnel construction, but further consideration is needed for emissions during operation, maintenance, and other construction methods.
Xu et al., 2019	IBM SPSS Statistics 20.0 (IBM)	Linear regression analysis	Rock mass classification, Overburden depth, Rock mass quality, Excavation method for inter-pipe clearance, Tunnel alignment deviation	The influencing factors, ranked from greatest to least, are total material quantity, excavation area, excavation method, rock mass classification, and overburden depth, with a significant correlation between rock mass classification and excavation method.	The prediction accuracy partially depends on local upstream material and energy emission levels as well as geological conditions. The model may not be applicable to other regions.

Wang et al., 2023	neural network models	CNN-LSTM and BPNN	Cohesion Internal friction angle Penetration resistance Earth pressure Overburden depth Advance rate Cutter torque Shield thrust Shield cutter operating time	A relatively accurate estimate of carbon emissions during shield tunnel construction can be obtained, applicable to carbon emission prediction and control in similar tunnel projects.	
Seyfar et al., 2021	Python	BPNN RF and XGBoost	City of Chicago Energy Benchmark Database	Assessed energy consumption of multi-family residential buildings in Chicago and evaluated the impact of various variables on building energy use. Improving transportation efficiency and increasing biofuel blending in regular diesel are potential policies for reducing GWP emissions. Explosives production and blasting are the main contributors to HTP, but truck transportation also plays a significant role in mitigating HTP impacts. The influence of various factors on carbon emissions in the Yellow River Basin varies across different periods. Significant provincial differences exist in total carbon emissions.	Most building energy benchmark data are self-reported, so data accuracy remains a concern in these studies.  Selected six categories as impact indicators: climate change (GWP), human toxicity (HTP), photochemical oxidant formation (POFP), particulate matter formation (PMFP), terrestrial acidification (TAP), terrestrial ecotoxicity (TETP)
Huang et al., 2015	ReCiPe Midpoint (E) V1.06/World ReCiPe E method		Excavation area Cross-sectional area Tunnel length		
Zhao et al., 2022	QAP model	SSA-LSTM	Population Per capita GDP Industrial structure Energy intensity Urbanization rate		Inter-provincial differences should be fully considered when formulating emission reduction policies.

Based on Table 4, current research on tunnel carbon emission prediction still holds substantial potential for development. The primary prediction methods can be broadly categorized into two types: mechanism-driven models and data-driven models. The former is grounded in physical equations and engineering principles, using established calculation formulas in combination with various databases to simulate and predict trends in tunnel carbon emissions. The latter rely on machine learning or statistical techniques—such as linear regression, support vector machines (SVM), and random forests—to analyze existing data and predict carbon emissions.

As indicated in the table, existing predictive algorithms predominantly focus on estimating carbon emissions during tunnel construction. However, a significant research gap exists concerning the temporal nonlinearity of emissions during the operation phase—a critical period due to its dominant contribution to the tunnel's overall life cycle emissions.

Limited research has addressed regional variability, revealing substantial differences in total emissions across regions. These disparities stem from factors like economic structure, energy mix, industrial distribution, climate, and population density. Furthermore, variations in renewable energy adoption, transportation modes, and urbanization levels further exacerbate the spatial heterogeneity of emissions.

Future research on tunnel carbon emission prediction should prioritize developing integrated models that combine mechanism-driven and data-driven approaches to enhance accuracy and robustness. While current efforts concentrate on construction, expanding the scope to encompass operation, maintenance, and end-of-life phases is essential for enabling holistic low-carbon optimization throughout the entire life cycle. Additionally, establishing



localized, spatiotemporally dynamic carbon emission factor databases is recommended. This would reduce reliance on generic or foreign datasets and better reflect local conditions.

## 5. CONCLUSION

This study focuses on the application of LCA in tunnel engineering to carbon emissions in tunnel engineering, systematically reviewing and analyzing the current methodologies for carbon emission calculation, prediction models, and carbon reduction/sequestration measures. The aim is to clarify research progress, identify key challenges, and provide references for future studies. Based on the literature review and problem analysis, the following two main conclusions are drawn:

- (1) Tunnel carbon emission calculations primarily concentrate on the construction phase, with insufficient coverage of the entire life cycle. Existing research largely focuses on accounting for carbon emissions during construction, emphasizing the carbon footprints of materials such as concrete and steel, energy consumption and emissions from construction equipment, and indirect emissions during transportation. Considerations for carbon emissions in the design, operation, maintenance, and decommissioning phases remain inadequate, and a comprehensive full life cycle carbon accounting system has yet to be established.
- (2) Carbon emission prediction models are continuously evolving, but accuracy and adaptability require further enhancement. Current prediction methods include statistical regression, machine learning, and BIM-LCA integration techniques, achieving some progress in improving prediction efficiency and dynamic responsiveness. However, many models still suffer from high dependency on input data, parameter uncertainties, and difficulties in covering complex construction scenarios, limiting their broad practical application in engineering projects.

In summary, although tunnel carbon emission research has made preliminary progress in the construction phase, challenges remain in full life cycle coverage and prediction accuracy. Future efforts should accelerate the systematic development of carbon accounting methods, promote the deep integration of intelligent prediction and carbon reduction technologies, and establish a systematic, sustainable low-carbon tunnel development model aligned with the “dual carbon” goals, thereby supporting the high-quality transformation of green infrastructure.

## 6. REFERENCES

- [1] Aboagye, E. M., Zeng, C., Owusu, G., Mensah, F., Afrane, S., Ampah, J. D., & Brenyah, S. A. (2023). A review contribution to emission trading schemes and low carbon growth. *Environmental Science and Pollution Research*, 30(30), 74575–74597. <https://doi.org/10.1007/s11356-023-27673-z>
- [2] Admiraal, H., & Cornaro, A. (2016). Why underground space should be included in urban planning policy – And how this will enhance an urban underground future. *Tunnelling and Underground Space Technology*, 55, 214–220. <https://doi.org/10.1016/j.tust.2015.11.013>
- [3] Akbar Nezhad, A., & Nadoushani, Z. S. (2014). *Estimating the Costs, Energy Use and Carbon Emissions of Concrete Recycling Using Building Information Modelling*. <https://doi.org/10.22260/ISARC2014/0051>
- [4] Akinade, O. O., Oyedele, L. O., Bilal, M., Ajayi, S. O., Owolabi, H. A., Alaka, H. A., & Bello, S. A. (2015). Waste minimisation through deconstruction: A BIM based Deconstructability Assessment Score (BIM-DAS). *Resources, Conservation and Recycling*, 105, 167–176. <https://doi.org/10.1016/j.resconrec.2015.10.018>
- [5] Audi, Y., Jullien, A., Dauvergne, M., Feraille, A., & D’aloia Schwartzentruber, L. (2020). Methodology and application for the environmental assessment of underground multimodal tunnels. *Transportation Geotechnics*, 24, 100389. <https://doi.org/10.1016/j.trgeo.2020.100389>
- [6] Brimblecombe, P., Townsend, T., Lau, C. F., Rakowska, A., Chan, T. L., Močnik, G., & Ning, Z. (2015). Through-tunnel estimates of vehicle fleet emission factors. *Atmospheric Environment*, 123, 180–189. <https://doi.org/10.1016/j.atmosenv.2015.10.086>
- [7] Chen, G. Q., Chen, H., Chen, Z. M., Zhang, B., Shao, L., Guo, S., Zhou, S. Y., & Jiang, M. M. (2011). Low-carbon building assessment and multi-scale input-output analysis. *Communications in Nonlinear Science and Numerical Simulation*, 16(1), 583–595. <https://doi.org/10.1016/j.cnsns.2010.02.026>
- [8] Chen, G., Shan, Y., Hu, Y., Tong, K., Wiedmann, T., Ramaswami, A., Guan, D., Shi, L., & Wang, Y. (2019). Review on City-Level Carbon Accounting. *Environmental Science & Technology*, 53(10), 5545–5558. <https://doi.org/10.1021/acs.est.8b07071>
- [9] Chen, X., Huang, M., Bai, Y., & Zhang, Q.-B. (2024). Sustainability of underground infrastructure – Part 1: Digitalisation-based carbon assessment and baseline for TBM tunnelling. *Tunnelling and Underground Space Technology*, 148, 105776. <https://doi.org/10.1016/j.tust.2024.105776>
- [10] Dou, S., Zhu, H., Wu, S., & Shen, Y. (2024). A review of information technology application in reducing carbon emission: From buildings to tunnels. *Journal of Cleaner Production*, 452, 142162. <https://doi.org/10.1016/j.jclepro.2024.142162>

- [11] Gil-Martín, L. M., Gómez-Guzmán, A., & Peña-García, A. (2015). Use of diffusers materials to improve the homogeneity of sunlight under pergolas installed in road tunnels portals for energy savings. *Tunnelling and Underground Space Technology*, 48, 123–128. <https://doi.org/10.1016/j.tust.2015.03.001>
- [12] Guo, C., Xu, J., Yang, L., Guo, X., Liao, J., Zheng, X., Zhang, Z., Chen, X., Yang, K., & Wang, M. (2019). Life cycle evaluation of greenhouse gas emissions of a highway tunnel: A case study in China. *Journal of Cleaner Production*, 211, 972–980. <https://doi.org/10.1016/j.jclepro.2018.11.249>
- [13] Guo, Y., Dong, C., Chen, Z., Zhao, S., Sun, W., He, W., Zhang, L., Wang, Y., Hu, N., & Guo, C. (2025). Evaluation of greenhouse gas emissions in subway tunnel construction. *Underground Space*, 22, 263–279. <https://doi.org/10.1016/j.undsp.2024.12.001>
- [14] Han, S., Hyun, C., & Moon, H. (2012). *Evaluation Model for Carbon Dioxide Emissions of Construction Methods*. 1799–1808. <https://doi.org/10.1061/9780784412329.181>
- [15] Huang, L., Bohne, R. A., Bruland, A., Jakobsen, P. D., & Lohne, J. (2015). Environmental impact of drill and blast tunnelling: Life cycle assessment. *Journal of Cleaner Production*, 86, 110–117. <https://doi.org/10.1016/j.jclepro.2014.08.083>
- [16] Huang, L., Jakobsen, P. D., Bohne, R. A., Liu, Y., Bruland, A., & Manquehual, C. J. (2020). The environmental impact of rock support for road tunnels: The experience of Norway. *Science of The Total Environment*, 712, 136421. <https://doi.org/10.1016/j.scitotenv.2019.136421>
- [17] Kamari, A., Kotula, B. M., & Schultz, C. P. L. (2022). A BIM-based LCA tool for sustainable building design during the early design stage. *Smart and Sustainable Built Environment*, 11(2), 217–244. <https://doi.org/10.1108/SASBE-09-2021-0157>
- [18] Koh, T., Hwang, S., Pyo, S., Moon, D., Yoo, H., & Lee, D. (2019). Application of Low-Carbon Ecofriendly Microwave Heat Curing Technology to Concrete Structures Using General and Multicomponent Blended Binder. *Journal of Materials in Civil Engineering*, 31(2), 04018385. [https://doi.org/10.1061/\(ASCE\)MT.1943-5533.0002472](https://doi.org/10.1061/(ASCE)MT.1943-5533.0002472)
- [19] Li, Y., Yang, X., Du, E., Liu, Y., Zhang, S., Yang, C., Zhang, N., & Liu, C. (2024). A review on carbon emission accounting approaches for the electricity power industry. *Applied Energy*, 359, 122681. <https://doi.org/10.1016/j.apenergy.2024.122681>
- [20] Liu, T., Zhu, H., Shen, Y., Li, T., & Liu, A. (2024). Embodied carbon assessment on road tunnels using integrated digital model: Methodology and case-study insights. *Tunnelling and Underground Space Technology*, 143, 105485. <https://doi.org/10.1016/j.tust.2023.105485>
- [21] Mao, C., Shen, Q., Shen, L., & Tang, L. (2013). Comparative study of greenhouse gas emissions between off-site prefabrication and conventional construction methods: Two case studies of residential projects. *Energy and Buildings*, 66, 165–176. <https://doi.org/10.1016/j.enbuild.2013.07.033>
- [22] Moretti, L., Cantisani, G., & Di Mascio, P. (2016). Management of road tunnels: Construction, maintenance and lighting costs. *Tunnelling and Underground Space Technology*, 51, 84–89. <https://doi.org/10.1016/j.tust.2015.10.027>
- [23] Opher, T., Duhamel, M., Posen, I. D., Panesar, D. K., Brugmann, R., Roy, A., Zizzo, R., Sequeira, L., Anvari, A., & MacLean, H. L. (2021). Life cycle GHG assessment of a building restoration: Case study of a heritage industrial building in Toronto, Canada. *Journal of Cleaner Production*, 279, 123819. <https://doi.org/10.1016/j.jclepro.2020.123819>
- [24] Pritchard, J. A., & Preston, J. (2018). Understanding the contribution of tunnels to the overall energy consumption of and carbon emissions from a railway. *Transportation Research Part D: Transport and Environment*, 65, 551–563. <https://doi.org/10.1016/j.trd.2018.09.010>
- [25] Rafael Dami´ & Clara I. Zamorano. (2011). Life cycle greenhouse gas assessment of infrastructure construction for California’s high-speed rail system. *Transp. Res. D Transp. Environ.*, 16(6), 429.
- [26] Raposo, C., Rodrigues, F., & Rodrigues, H. (2019). BIM-based LCA assessment of seismic strengthening solutions for reinforced concrete precast industrial buildings. *Innovative Infrastructure Solutions*, 4(1), 51. <https://doi.org/10.1007/s41062-019-0239-7>
- [27] Seo, Y., & Kim, S.-M. (2013). Estimation of materials-induced CO<sub>2</sub> emission from road construction in Korea. *Renewable and Sustainable Energy Reviews*, 26, 625–631. <https://doi.org/10.1016/j.rser.2013.06.003>
- [28] Seyrfar, A., Ataei, H., Movahedi, A., & Derrible, S. (2021). Data-Driven Approach for Evaluating the Energy Efficiency in Multifamily Residential Buildings. *Practice Periodical on Structural Design and Construction*, 26(2), 04020074. [https://doi.org/10.1061/\(ASCE\)SC.1943-5576.0000555](https://doi.org/10.1061/(ASCE)SC.1943-5576.0000555)
- [29] Shi, X., Kou, L., Liang, H., Wang, Y., & Li, W. (2024). Evaluating Carbon Emissions during Slurry Shield Tunneling for Sustainable Management Utilizing a Hybrid Life-Cycle Assessment Approach. *Sustainability*, 16(7), Article 7. <https://doi.org/10.3390/su16072702>
- [30] Song, Y., Zhu, H., Shen, Y., & Feng, S. (2024). Green tunnel lighting environment: A systematic review on energy saving, visual comfort and low carbon. *Tunnelling and Underground Space Technology*, 144, 105535. <https://doi.org/10.1016/j.tust.2023.105535>
- [31] Song, Y., Zhu, H., Shen, Y., Yan, Z., & Feng, S. (2024). Zero-carbon tunnel: Concept, methodology and application in the built environment. *Journal of Cleaner Production*, 479, 144031. <https://doi.org/10.1016/j.jclepro.2024.144031>
- [32] Tabrizikahou, A., & Nowotarski, P. (2021). Mitigating the Energy Consumption and the Carbon Emission in the Building Structures by Optimization of the Construction Processes. *Energies*, 14(11), Article 11. <https://doi.org/10.3390/en14113287>
- [33] Vitale, P., Arena, N., Di Gregorio, F., & Arena, U. (2017). Life cycle assessment of the end-of-life phase of a residential building. *Waste Management*, 60, 311–321. <https://doi.org/10.1016/j.wasman.2016.10.002>

- [34] Wang, X., Duan, Z., Wu, L., & Yang, D. (2015). Estimation of carbon dioxide emission in highway construction: A case study in southwest region of China. *Journal of Cleaner Production*, 103, 705–714. <https://doi.org/10.1016/j.jclepro.2014.10.030>
- [35] Wang, Y., Kou, L., He, X., Li, W., Liang, H., & Shi, X. (2023). A Modified Process Analysis Method and Neural Network Models for Carbon Emissions Assessment in Shield Tunnel Construction. *Sustainability*, 15(12), Article 12. <https://doi.org/10.3390/su15129604>
- [36] Weingartner, E., Keller, C., Stahel, W. A., Burtscher, H., & Baltensperger, U. (1997). Aerosol emission in a road tunnel. *Atmospheric Environment*, 31(3), 451–462. [https://doi.org/10.1016/S1352-2310\(96\)00193-8](https://doi.org/10.1016/S1352-2310(96)00193-8)
- [37] Wu, H., Zhou, W., Bao, Z., Long, W., Chen, K., & Liu, K. (2024). Life cycle assessment of carbon emissions for cross-sea tunnel: A case study of Shenzhen-Zhongshan Bridge and Tunnel in China. *Case Studies in Construction Materials*, 21, e03502. <https://doi.org/10.1016/j.cscm.2024.e03502>
- [38] Xie, B.-C., Zhai, J.-X., Sun, P.-C., & Ma, J.-J. (2020). Assessment of energy and emission performance of a green scientific research building in Beijing, China. *Energy and Buildings*, 224, 110248. <https://doi.org/10.1016/j.enbuild.2020.110248>
- [39] Xu, J., Guo, C., & Yu, L. (2019). Factors influencing and methods of predicting greenhouse gas emissions from highway tunnel construction in southwestern China. *Journal of Cleaner Production*, 229, 337–349. <https://doi.org/10.1016/j.jclepro.2019.04.260>
- [40] Yahya, K., Boussabaine, H., & Alzaed, A. N. (2016). Using life cycle assessment for estimating environmental impacts and eco-costs from the metal waste in the construction industry. *Management of Environmental Quality: An International Journal*, 27(2), 227–244. <https://doi.org/10.1108/MEQ-09-2014-0137>
- [41] Yang, X., Hu, M., Wu, J., & Zhao, B. (2018). Building-information-modeling enabled life cycle assessment, a case study on carbon footprint accounting for a residential building in China. *Journal of Cleaner Production*, 183, 729–743. <https://doi.org/10.1016/j.jclepro.2018.02.070>
- [42] Yu, S., Shi, L. (Serena), Zhang, L., Liu, Z., & Tu, Y. (2023). A solar optical reflection lighting system for threshold zone of short tunnels: Theory and practice. *Tunnelling and Underground Space Technology*, 131, 104839. <https://doi.org/10.1016/j.tust.2022.104839>
- [43] Yu, Y., Gu, H., Liang, B., Sun, Q., & Zou, J. (2025). Evaluation and Optimization of Adjacent Tunnel Light Environment Scheme to Low Carbon. *Energy Science & Engineering*, 13(4), 1691–1705. <https://doi.org/10.1002/ese3.2085>
- [44] Zhao, J., Kou, L., Jiang, Z., Lu, N., Wang, B., & Li, Q. (2022). A novel evaluation model for carbon dioxide emission in the slurry shield tunnelling. *Tunnelling and Underground Space Technology*, 130, 104757. <https://doi.org/10.1016/j.tust.2022.104757>
- [45] Zheng, S., Xie, X., & Zhou, B. (2024). Accounting Method and Indicators of Multilevel CO2 Emissions Based on Cost During Construction of Shield Tunnels. *Applied Sciences*, 14(20), Article 20. <https://doi.org/10.3390/app14209552>
- [46] Zou, Z., Kong, C., Gu, S., Zhao, X., Yang, L., Zhou, Y., Huang, G., & Gao, X. (2024). Research on carbon emission quantification and evaluation for prefabricated inverted arch construction in drill and blast tunnels. *Journal of Cleaner Production*, 459, 142485. <https://doi.org/10.1016/j.jclepro.2024.142485>

## VULNERABILITY OF METRO SYSTEM DUE FLOODING IN LARGE ASIAN CITIES

Ya-Jie Wang<sup>1</sup>, Shui-Long Shen<sup>2</sup>, Annan Zhou<sup>3</sup>

**Abstract:** Climate change aggravates the frequent occurrence of extreme weather events, and flood disasters show significant characteristics of increasing intensity, expanding scope and worsening urban impacts. As hubs of population and wealth concentration, the vulnerability of cities is exposed in disasters. The hardened surface leads to the decrease of rainwater permeability, and the disorderly expansion makes the newly built urban area occupy the flood channel, forming a vicious circle of chronic waterlogging during rainfall events. We analyze the correlation between urban structural and morphological influencing factors and flood disasters in large asian cities, based on which we obtain the relationship between each influencing factor and flood disasters. We use complementary AHP calculate the flood vulnerability across East, South, and Southeast Asian countries. We also analyse the contribution to the city vulnerability due to existence of metro system. We find that the most vulnerable cities are Pearl River Delta in China, then, the cities from southeastern China, Japan, and major cities in India. The development of underground space in cities has a "double-edged sword" effect. It can improve transportation efficiency but also increases the vulnerability of the urban system. The metro system significantly enhances economic vulnerability, but has a limited impact on casualty vulnerability.

**Keywords:** Climate change, flood, urban structure, metro system, vulnerability.

### 1. INTRODUCTION

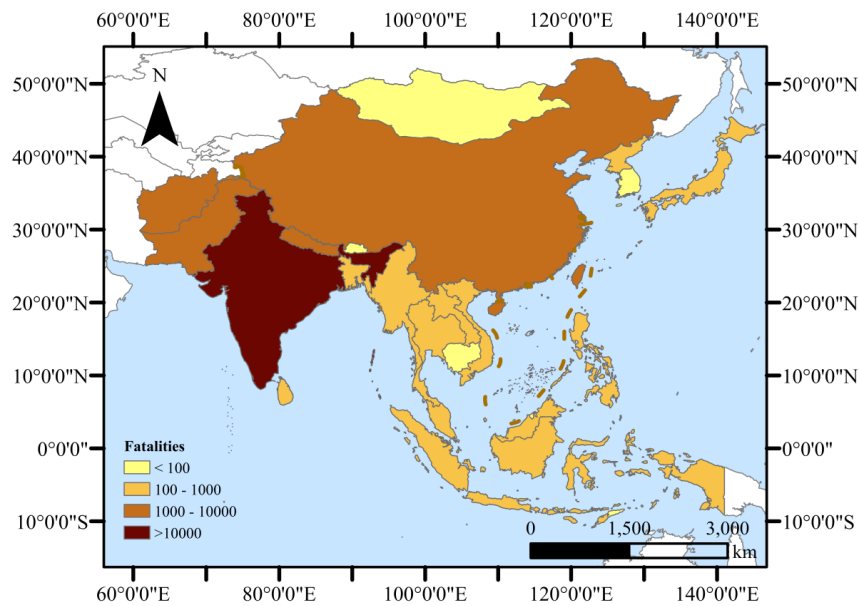
According to the Intergovernmental Panel on Climate Change (IPCC, 2023), global warming persists, driven by both natural factors and human activities, notably carbon emissions (IPCC, 2023). This ongoing global warming is leading to a more uneven distribution of temperatures worldwide, resulting in increased instances of extreme precipitation in various regions (Lyu et al., 2023). These extreme precipitation events often trigger floods and geological disasters, significantly impacting societal well-being and economic stability (Davenport et al., 2021). Flood disaster, characterized by the overflow of rivers or surface water due to heavy rainfall or snowmelt, causes the inundation of urban and rural areas and pose significant threats to lives and property of residents. Particularly in densely populated urban centers, existing drainage systems struggle to cope with the effects of intense rainfall, leading to issues like waterlogging, traffic disruptions, and structural failures. Globally, extreme precipitation events are becoming more intense and frequent, heightening the risk of flooding, especially in urban areas. While some areas may experience an increase in extreme precipitation, others may witness a decrease, highlighting regional variability (Myhre et al., 2019).

IPCC underscores the substantial impact of extreme precipitation on infrastructure and human settlements. Projections for the future indicate a sustained rise in both the frequency and intensity of extreme precipitation events under various climate change scenarios. East, South, and Southeast Asia are frequently subjected to flood disasters. As illustrated in Figure 1, the spatial distribution of flood-induced fatalities across national jurisdictions in these regions from 2014 to 2024 demonstrates that most countries experienced mortality exceeding 100 fatalities. This impact is particularly pronounced in high-population-density nations such as India and China. Concurrent with global economic development, continuous expansion of urban areas has accelerated the growth of built-up environments and road infrastructure. These developments have exacerbated flood-induced economic losses, rendering urban flood vulnerability a critical challenge for all affected nations.

<sup>1</sup> Ph.D. Candidate, Wang, Ya-Jie, M.Sc. Civil Engineering, Shantou University, Shantou, China; 20yjiwang1@stu.edu.cn.

<sup>2</sup> Professor, Shen, Shui-Long, Ph.D. Civil Engineering, Dean College of Engineering, Shantou University, Shantou, China, shensl@stu.edu.cn.

<sup>3</sup> Professor, Zhou, Annan, Ph.D. Civil Engineering, School of Engineering, RMIT University, Melbourne, Australia, annan.zhou@rmit.edu.au.



**Figure 1.** Flood-induced fatalities across southeastern Asia from 2014-2024 (Data from GDDP)

Many studies have showed that socio-economic and demographic factors are influencing urban flood vulnerability. With the uneven development of economy and population, and different degrees of extension to urban infrastructure, the spatial distribution of urban flood vulnerability is also different in the world. Concurrent with rapid economic growth, urban expansion has accelerated built-environment development at an unprecedented scale. Asia's built-up area increased by 58,000 km<sup>2</sup> (2010-2020), while road infrastructure grew by 1.2 million km—predominantly in floodplains (Seto et al., 2017). This uncontrolled spatial development has directly exacerbated flood vulnerability, transforming episodic hazards into systemic crises. Annual flood-induced economic losses in the region now exceed US\$32 billion, with infrastructure damage accounting for 67% of total costs (UNDRR, 2023).

While socioeconomic drivers of vulnerability (e.g., GDP, population density) are established (Hallegatte et al., 2020), critical knowledge gaps persist regarding: (1) The quantifiable role of infrastructure configuration (e.g., metro systems) in modulating vulnerability; (2) Spatially explicit interactions between urban morphology and flood consequences. This study addresses these gaps through a novel analytical framework integrating multi-source geospatial data with historical disaster footprints.

## 2. MATERIAL AND METHODS

### 2.1. Complementary AHP

The Analytic Hierarchy Process (AHP), proposed by Saaty in the 1970s (Saaty, 1977), is a systematic, simple, flexible, and effective decision-making method that combines qualitative and quantitative approaches. Dong (1996) first introduced fuzzy theory into AHP, developing an improved AHP method that eliminates the need for consistency testing—namely, the 0.1–0.9 scale complementary AHP. This approach employs a 0.1–0.9 five-point scale to construct a complementary judgment matrix, which is then transformed into a fuzzy consistent judgment matrix using a conversion formula, ultimately deriving the priority vector. However, the traditional AHP method primarily relies on empirical knowledge or expert judgment during the decision-making process. In this study, we utilize the correlation coefficients between each factor and historical flood disaster consequences as empirical values to determine and quantify the relative importance of pairwise factors, thereby obtaining the weight ranking of each factor. Finally, in ArcGIS, the weights of each factor are integrated with their corresponding numerical values through raster calculation to generate the risk ranking of urban flood vulnerability and its visualized spatial distribution.

In the complementary fuzzy scale, a value of 0.1 indicates that Factor A is more important than Factor B, whereas a value of 0.9 denotes that Factor B is more important than Factor A. Thus, we established a relationship in the difference  $\Delta$  of correlation coefficient between the two factors and the complementary fuzzy scale value.



## 2.2 Data on urban characteristics

To explore the relationship between various factors of urban form and structure and the consequences of flood risks, we conducted a correlation analysis of the data of these factors and historical flood consequences. Based on the boundary vector data of 243 countries, we respectively tallied the flood death toll, economic losses, GDP, population, built-up area of cities, road length and metro length of each corresponding country. This study utilized the geopandas library in Python to handle geospatial data. We transformed the coordinate systems (CRS, Coordinate Reference System) of the national boundary vector data and the built-up area data of cities into EPSG: 3857, that is, Web Mercator projection, to facilitate spatial analysis. We used intersects as the connection condition for spatial linking between datasets, meaning that the geometry of buildings intersects with national boundaries. Then, we used the geometry.area attribute in geopandas to calculate the area of each building, and finally aggregated the area of all buildings by country. The method for calculating the road length of each country was the same.

## 3. RESULTS

### 3.1 Analysis of urban characteristics and flood disasters

Through correlation analysis of 243 countries, we quantified how urban structural factors influence flood consequences, revealing that economic losses are predominantly driven by GDP, metro infrastructure and population, while fatalities correlate most strongly with population and road networks. Utilizing national-scale aggregations of global road networks and built-up areas, we implemented a novel 0.1–0.9 scale complementary AHP method that substitutes empirical correlation coefficients for subjective expert judgments in pairwise comparisons. This approach identified population and GDP as paramount vulnerability determinants (Figure 2), with population exhibiting the greatest consequence-dependent variability, while effectively mitigating scoring biases inherent in traditional AHP frameworks.

We use correlation coefficients to calculate the difference  $\Delta$  between each two factors, and complementary AHP can calculate the weights of each factor in various situations. When we consider the situation of metro system, the impact of the population on economic loss vulnerability is the greatest, and the weights of other factors are the same. The impact of the GDP on casualty vulnerability is the greatest. The impact of the metro system ranks second. When we disregard the influence of the metro, the impact of population on economic vulnerability remains the greatest. With all other factors remaining the same, GDP has the greatest impact on casualty vulnerability, and all other factors are the same. It can be seen that the correlation coefficients between the weak factors and the flood consequences are relatively close, and their influence weights are the same. Population, GDP and metro distribution are the three most crucial factor.

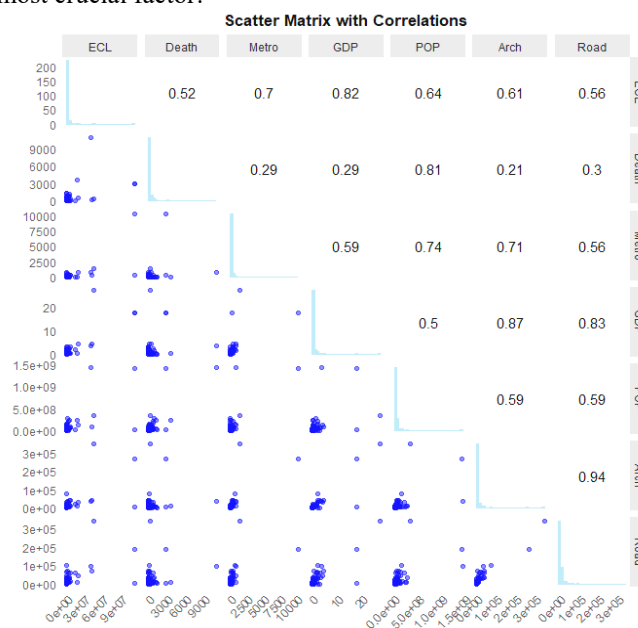
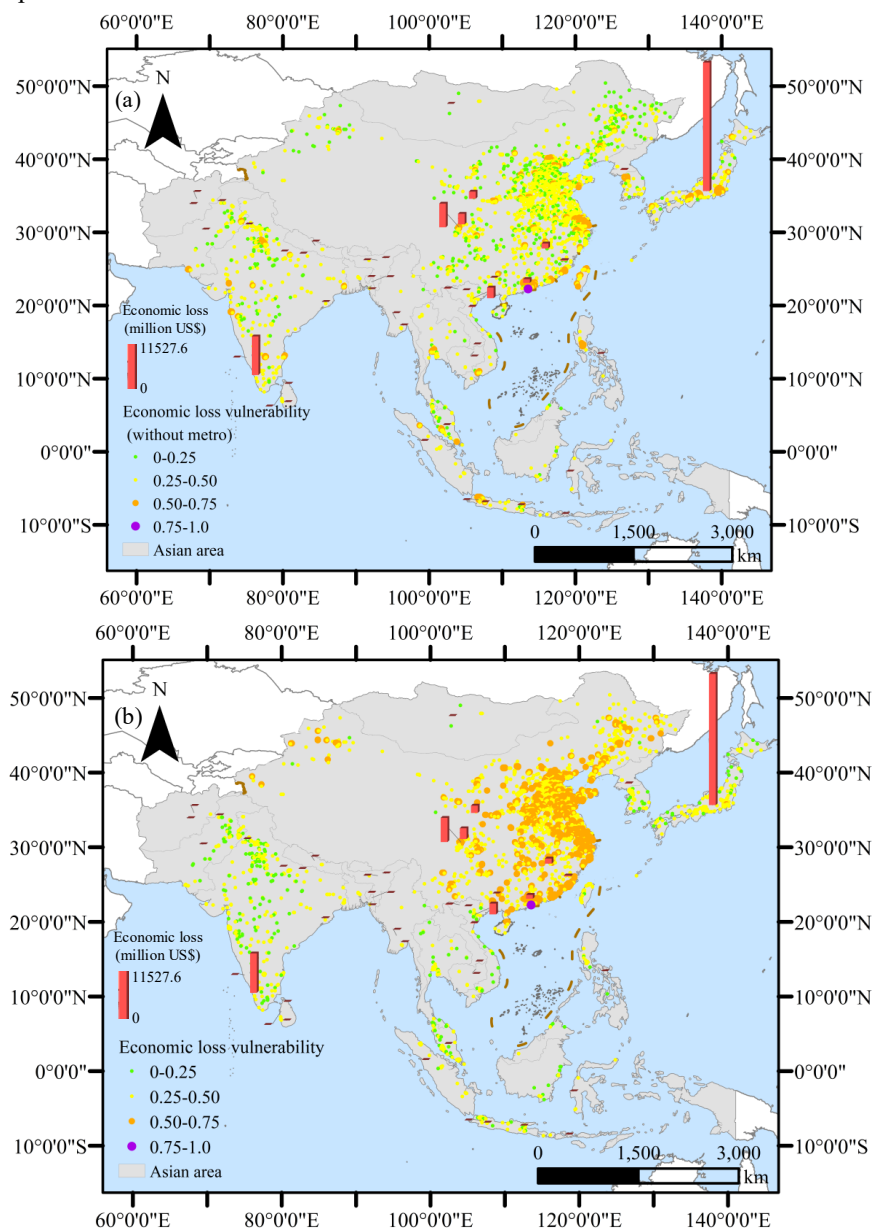


Figure 2. The scatter matrix and correlations of each factor

### 3.2 Intensity distribution of urban vulnerability

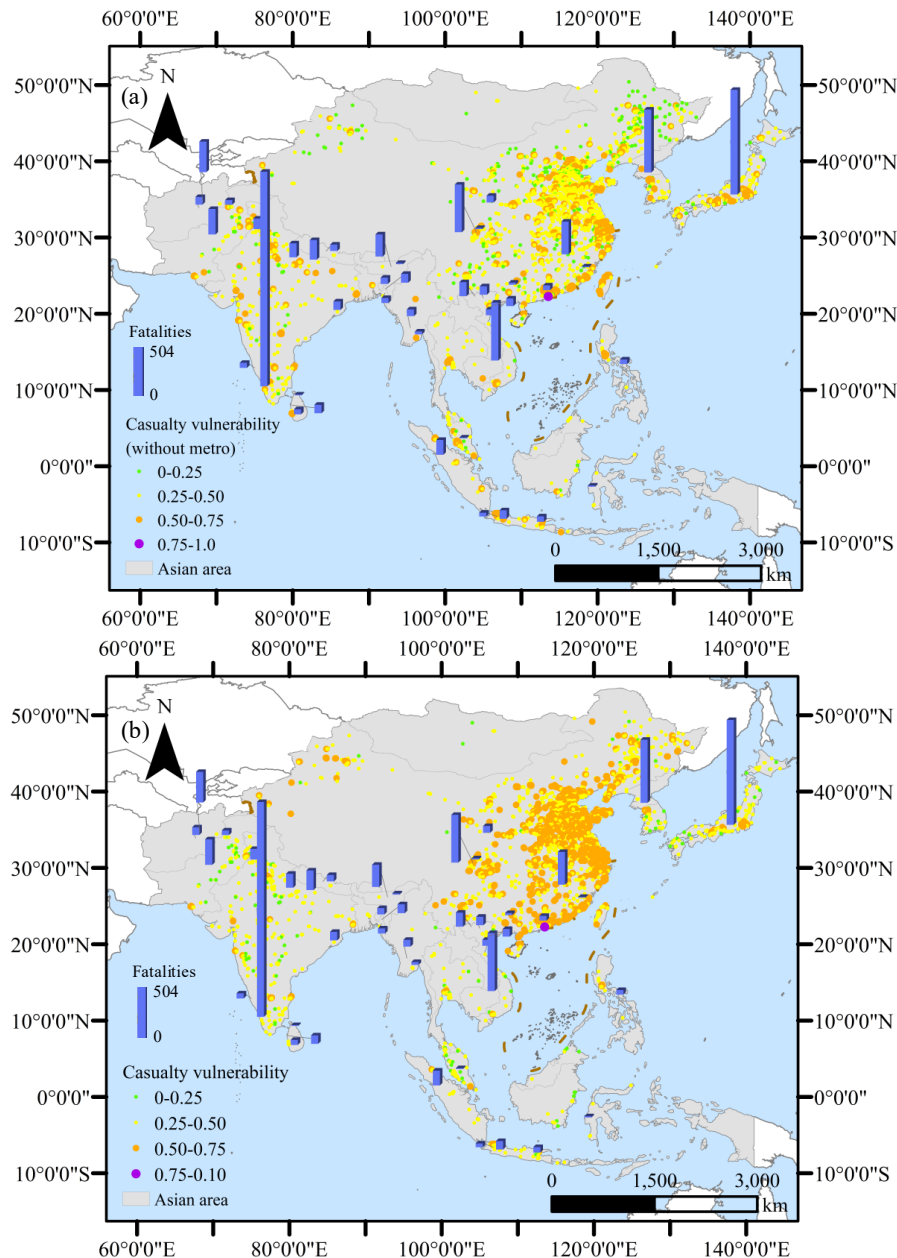
We use the integrated methodology to assess spatial heterogeneity in flood vulnerability across 24 East, South, and Southeast Asian nations. These outputs were benchmarked against 2018 observed economic loss and death patterns. Critically, metro infrastructure was incorporated as a dynamic variable—reflecting both its inevitability in urban development and disproportionate exposure to subsurface flooding—with comparative scenarios presented in Fig. 3 and 4.

Figure 3 presents the spatial distribution of urban flood economic vulnerability contrasted against 2018 observed losses. GDP constitutes the primary determinant, while metro infrastructure demonstrates significant secondary influence, though exclusively applicable to economically advanced, high-density nations. Spatial analysis reveals: absent metro considerations, vulnerability peaks in China's Pearl River Delta, with secondary clusters in Southeast China, Japan, and India; Incorporating metro exposure elevates vulnerability in the Pearl River Delta, followed by Southeast China and the Tokyo metropolitan region. Crucially, 2018 loss epicenters (Japan, South India, Southeast China) align with high-vulnerability zones (orange/purple markers), exemplified by Japan's record 10 billion dollars losses—its most severe event in 45 years—occurring within a core economic vulnerability hotspot.



**Figure 3.** Flooding induced economic loss in 2018: (a) without metro, (b) with the effect of metro

Figure 4 shows the distribution of the intensity of urban vulnerability and makes a comparison with the actual number of deaths in 2018. For vulnerability, population distribution is the most significant factor of correlation. The calculation results indicate that the areas with higher vulnerability include the southeast of China, Delhi, Mumbai, Bangalore in India, North Korea, Tokyo in Japan, Bangkok in Thailand, Manila in the Philippines, Jakarta in Indonesia, and the regions of Nigeria in Africa and China, Japan, India, and Vietnam in Asia. If the influence of metros is considered, the correlation coefficient is 0.29, indicating that compared to the vulnerability of economic losses, the impact of metro construction on vulnerability is relatively small, and the most significant factor is still population.



**Figure 4.** Flooding induced fatalities in 2018: (a) without metro, (b) with the effect of metro

#### 4. DISCUSSION

This study utilized a vast global dataset to explore the degree of correlation between urban structure and flood risk consequences, as well as the evaluation of urban flood property and health vulnerability under different urban structures. Due to the uneven spatial distribution of various urban structures and the varying importance of influencing factors, the economic losses and casualties caused by floods are affected. This understanding is beneficial for providing effective references for future urban planning, mitigating urban flood risks, and for the

government to formulate relevant policies. The urban characteristic factors in our study are based on the data from 2018. However, with the development of society and economy, the indicators of each factor will also change every year. Based on this study, we can predict the future economic vulnerability of urban floods and provide research support for flood risk management.

The results show the distribution of flood-related economic losses and health vulnerability across various cities under the combined factors. At the same time, it also indicates that some developed cities, such as Hong Kong, Shanghai in China, Tokyo in Japan, have higher economic loss vulnerability. Their GDP and population distribution remain high, and the management and renovation of urban buildings and transportation infrastructure should be given more attention to avoid causing more flood-related economic losses. In addition, in places like Delhi in India, Mumbai in India, Manila in the Philippines, etc., the population density is high and the vulnerability of human deaths is high, but the infrastructure development is lagging behind. International rescue, local government urban development planning, and flood prevention awareness publicity should also be given more attention.

We will also consider the development of the metro as a separate factor. This is because, with the advancement of society, many countries are expanding their underground space resources, and the construction of underground rail transit is also developing year by year. Therefore, this study believes that it is necessary to consider the metro as an important factor. However, the study used the total length of metro in each country, that is to assume that the length of the metro in each country and each region is its total length. When calculating using ArcGIS, the point data of metro lengths in the same country were the same. Therefore, the calculation results can be used as a reference. The accuracy of the results still needs to be determined by collecting the actual distribution density of metros in various countries in the future. However, from the calculation results, China is a country with the fastest metro development, and metro transportation is also the most affected by floods globally. The Chinese government should pay attention to the development of urban underground space and take corresponding protective measures.

## 5. CONCLUSIONS

- (1) There is significant spatial heterogeneity in the vulnerability of urban flooding. Regions in East Asia, South Asia, and Southeast Asia have become global hotspots of vulnerability due to high population density and rapid urbanization (such as the Pearl River Delta in China, Delhi in India, and Tokyo in Japan). The dominant factors for different consequences vary. Economic loss vulnerability has a strong positive correlation with GDP, while casualty vulnerability is mainly driven by population density. Meanwhile, metro systems have a "double-edged sword" effect, improving transportation efficiency but increasing system vulnerability. The metro systems significantly enhances economic vulnerability but has a limited impact on casualty vulnerability.
- (2) To enhance flood disaster management, governments should adopt a tiered mitigation strategy tailored to regional vulnerability profiles: For high economic vulnerability zones (GDP exceeding \$1 trillion), such as major metropolitan areas, implementing upgraded metro flood protection standards is critical—exemplified by China's post-Zhengzhou 7.20 incident (DIT-SC,2022) regulations mandating 50-year flood-resilient design benchmarks. In high fatality vulnerability zones (population density surpassing 5,000 inhabitants/km<sup>2</sup>), like densely populated urban corridors, deploying mobile network-based early warning systems modeled after Jakarta's successful implementation should be prioritized.
- (3) Meanwhile, emerging metro cities undergoing rapid urbanization (e.g., Hanoi, Bangkok) must incorporate compulsory underground floodgate installations and vertical evacuation route networks into their infrastructure planning. This comprehensive approach addresses both economic asset protection and life safety considerations through targeted, evidence-based interventions that account for each region's distinct risk characteristics and development stage.

## 6. ACKNOWLEDGMENTS

The research work was funded by Guangdong Provincial Basic and Applied Basic Research Fund Committee (2022A1515240073).

## 7. BIBLIOGRAPHY

- [1] Davenport, F.V., Burke, M., Diffenbaugh NS. (2021). Contribution of historical precipitation change to US flood damages. *Proceedings of the National Academy of Sciences of the United States of America*. 118(4), e2017524118.
- [2] Disaster Investigation Team of State Council (DIT-SC) (2022). Investigation report on July 20, 2021 torrential rain disaster in Zhengzhou, Henan Province, Peoples' Republic of China, Beijing, 2022.1. p.46. Available online: <https://www.mem.gov.cn/gk/sgcc/tbzdsgdcbg/202201/P020220121639049697767.pdf> (in Chinese).
- [3] Dong, D. (1996). Mathematical transformation solution for the consistency problem of ahp judgment matrices. *Annual Conference of the Decision Science Professional Committee, Systems Engineering Society of China*. 99-104.
- [4] Global Disaster Data Platform (GDDP). Available online: <https://www.gddat.cn/newGlobalWeb/#/globalScale>. (in Chinese, accessed on March 3, 2025).
- [5] Hallegatte, S., Rentschler, J., Rozenberg, J. (2020). Lifelines: The resilient infrastructure opportunity. World Bank.
- [6] Intergovernmental Panel on Climate Change (IPCC) (2023). *Climate Change 2023: Synthesis Report (Full Volume) Contribution of Working Groups I, II and III to the Sixth Assessment Report of the Intergovernmental Panel on Climate Change*, [Core Writing Team, H. Lee and J. Romero (eds.)]. IPCC, Geneva, Switzerland, 184 pp. <https://doi.org/10.59327/IPCC/AR6-9789291691647>. (accessed on March 3, 2025).
- [7] Lyu HM, Yin ZY, Zhou AN, Shen SL. (2023). MCDM-based flood risk assessment of metro systems in smart city development: A review. *Environmental Impact Assessment Review*, 101, 107154.
- [8] Myhre G, Alterskjær K, Stjern CW, Hodnebrog O, Marelle L, Samset BH, Sillmann J, Schaller N, Fischer E, Fischer M, Stohl A (2019). Frequency of extreme precipitation increases extensively with event rareness under global warming. *Scientific Reports*. 9:16063.
- [9] Saaty TL. 1977. A scaling method for priorities in hierarchical structures. *Journal of Mathematical Psychology*. 15(3), 234–281. [https://doi.org/10.1016/0022-2496\(77\)90033-5](https://doi.org/10.1016/0022-2496(77)90033-5).
- [10] Seto KC, Golden JS, Alberti M, Turner BL. (2017). Sustainability in an urbanizing planet, *Proceedings of the National Academy of Sciences of the United States of America*. 114 (34), 8935-8938.
- [11] United Nations Office for Disaster Risk Reduction (UNDRR). (2023). *Global assessment report on disaster risk reduction 2023: Mapping resilience for the Sustainable Development Goals*. Available online: <https://www.undrr.org/gar2023>. (accessed on March 3, 2025).



## UNDERGROUND CIRCULATION OF LOGISTICS AS A STRATEGY FOR LAND OPTIMIZATION AND LOGISTICS EFFICIENCY: A CASE STUDY OF DISTRICT LOGISTICS NETWORK IN JURONG INNOVATION DISTRICT, SINGAPORE

Er. Ngu Wang Chung<sup>1</sup>, Wang Wei Yang<sup>2</sup>

**Abstract:** The District Logistics Network (DLN) in Jurong Innovation District (JID) exemplifies an innovative approach to underground logistics that optimizes land use and enhances freight movement efficiency. Situated 15 meters below ground, this 3.5-kilometre-long network, with an average width of 14 meters, accommodates prime movers with 40' containers and is designed for future integration with Automated Guided Vehicles (AGVs) or Autonomous Vehicles (AVs). By relocating prime movers' circulation to the subterranean level, the DLN unlocks surface land for higher-value activities, such as businesses, amenities, and parks, while creating a greener, more liveable urban-industrial environment. DLN significantly improves logistics efficiency by connecting directly to factories and companies' basement loading/unloading bays. This seamless underground system allows goods and cargo to be transported directly from the expressways to businesses without traversing internal surface roads. As a result, the estate experiences less congestion, faster delivery times, and smoother operations.

Safety is also enhanced by reducing heavy vehicles traffic on surface roads, which adjoin residential neighbourhoods in Bulim. The removal of heavy vehicles from surface circulation minimizes the risks to residents and other road users, contributing to a safer and more pedestrian-friendly environment. Additionally, the reduced surface road widths and underground circulation mitigate noise and air pollution, further enhancing the quality of life for the surrounding community. Despite adverse underground conditions, including soil cavities, limestone, and peaty clay, the project overcame these engineering challenges through innovative solutions, ensuring the successful implementation of this ambitious infrastructure. As Singapore's first subterranean district logistics network, the DLN sets a benchmark for integrating logistics and land optimization strategies. It demonstrates how underground circulation can contribute to sustainable urban development, improving both logistics efficiency and the liveability of industrial estates.

**Keywords:** Sustainability, Innovative Design, Logistics Efficiency, Underground Infrastructure, Land Optimization, Geotechnical Engineering, Urban Geology, Sustainable Urban Development

### 1. INTRODUCTION

#### 1.1. Background on Logistics Flow and Handling in Singapore

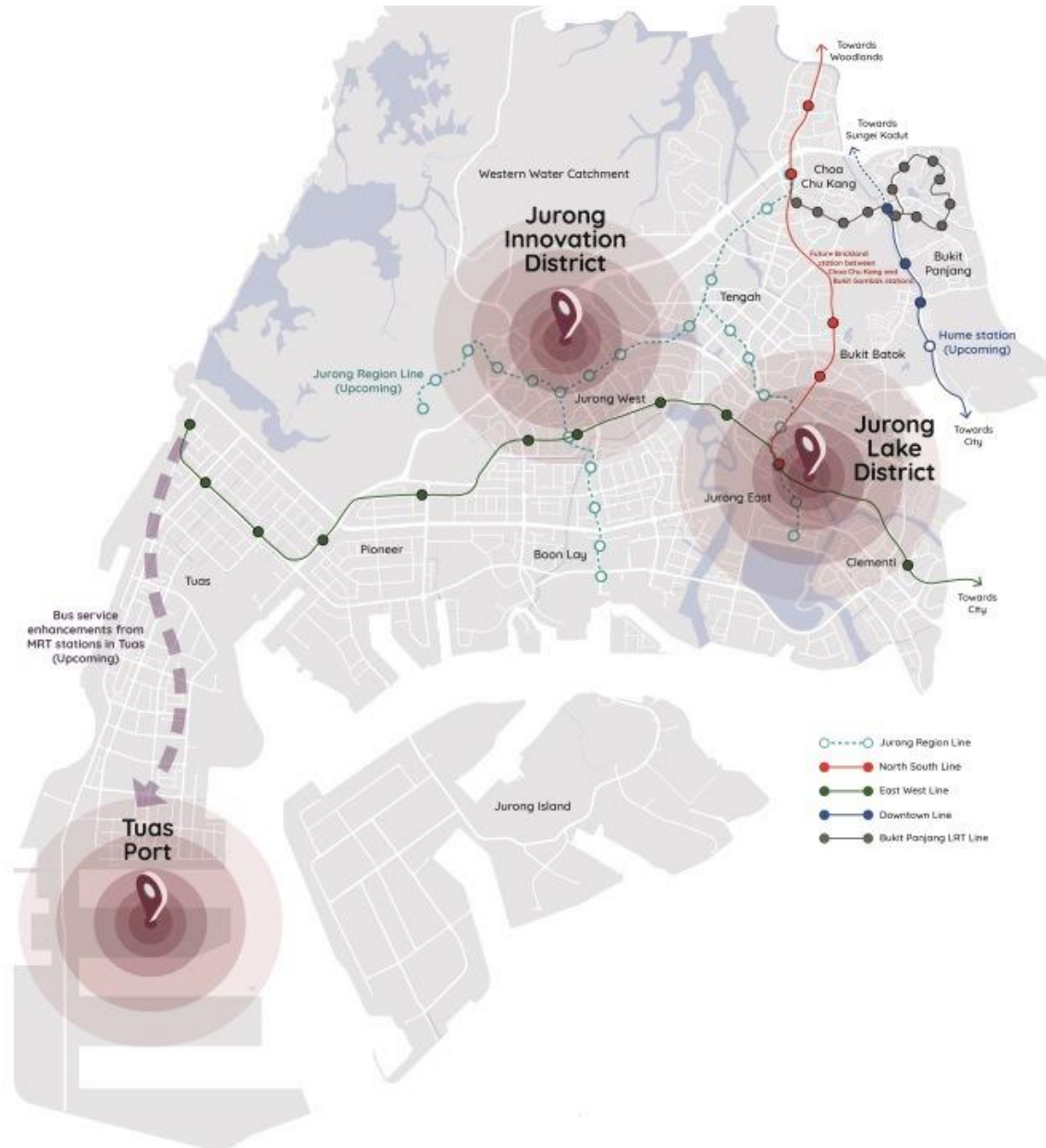
As a land-scarce nation, Singapore relies extensively on underground spaces to optimize land use. In addition to underground train networks, Singapore had developed caverns for hydrocarbon storage (CTRL+SHIFT, 2023) and is in the midst of expanding deep tunnel sewerage system (Public Utilities Board Singapore, 2025) to free up surface land used for sewerage treatment.

Logistics movement in Singapore has thus far relied on Heavy Goods Vehicles (HGVs) that travel on surface roads - the HGVs begin their journeys from seaports or through the Malaysia-Singapore links and carry containers as long as 40' through the internal roads of industrial estates, before delivering them at the loading and unloading bays of each factory unit. However, this conventional process poses several inefficiencies for Singapore from a

<sup>1</sup> Er. Ngu Wang Chung, BSc (Civil), Deputy Director, New Estates Division 1, JTC Corporation, Singapore, [NGU\\_Wang\\_Chung@jtc.gov.sg](mailto:NGU_Wang_Chung@jtc.gov.sg)

<sup>2</sup> Mr. Wang Wei Yang, BSc (Civil), Principal Project Manager, New Estates Division 1, JTC Corporation, Singapore, [WANG\\_Wei\\_Yang@jtc.gov.sg](mailto:WANG_Wei_Yang@jtc.gov.sg)

land intensification perspective. Firstly, HGVs require wider roads with bigger turning radii (Land Transport Authority Singapore, 2019), as well as expansive loading/unloading bays. In addition, each factory requires a warehouse of its own for the storage of raw materials and semi-finished goods for production. Lastly, the decentralised nature of freight traffic is prone to last mile congestion, which exacerbates environmental concerns such as air pollution (Robert de Souza, 2014).



**Figure 1.** Location Map of Jurong Innovation District (JID) (URA, n.d.)

## 1.2. Overview of the District Logistics Network (DLN)

The District Logistics Network (DLN) at Jurong Innovation District (JID) comprises an underground road network, with the aim of alleviating the inefficiencies of conventional freight movement. All HGVs entering the estate will be directed to the underground road network which leads directly to the companies' doorstep via the basement Goods Receiving Area (GRA).

The DLN is designed with a width of 10.4m and a clear height of 5.5m to accommodate different types of AGVs or AVs in the future. At present, JTC is developing a 3.5-kilometre-long network at Bulim industrial

precinct, one of the 5 precincts within JID - the first phase has been completed in January 2025, and the rest of the network by 2030.

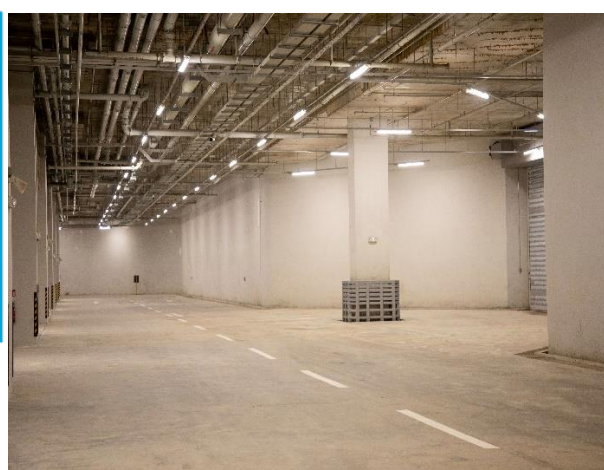
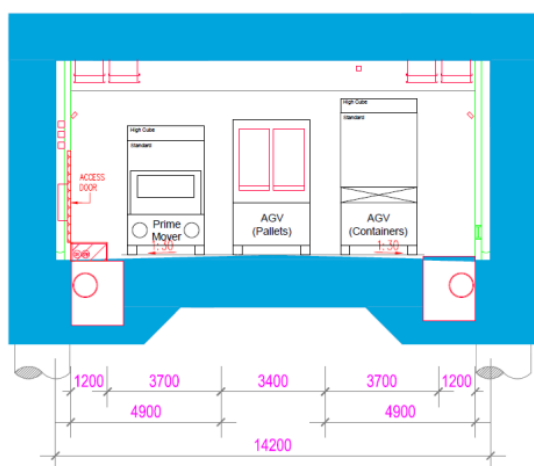
### 1.3. Vision and Purpose of the District Logistics Network

#### 1.3.1. Vision of the DLN

The District Logistics Network (DLN) represents an innovative subterranean logistics infrastructure conceived to greatly improve freight movement efficiency while optimising land utilisation in Singapore's industrial landscape. The network's architectural framework embodies three fundamental design principles: operational versatility to accommodate both conventional manned vehicles and future AGVs or AVs, scalable infrastructure capable of serving varying throughput volumes across multi-tenanted and single-tenant facilities, and systematic redundancy to ensure operational resilience during vehicular incidents or mechanical failures. The infrastructure's 14.2metre width configuration supports dual 40-foot container traffic while incorporating future-ready provisions for AGV integration. This forward-looking design philosophy enables the progressive transition from manual operations to automated systems, ensuring the DLN's long-term viability as a cornerstone of Singapore's next-generation logistics ecosystem.

#### 1.3.2. Width of the DLN

The width of the DLN was designed to accommodate two 40' trucks with enough room to bypass in the event of vehicular breakdown or similar, with futureproofing to support AGVs or AVs. This works out to be 14.2m wide for a 3-lane underground road as seen in Figure 2.



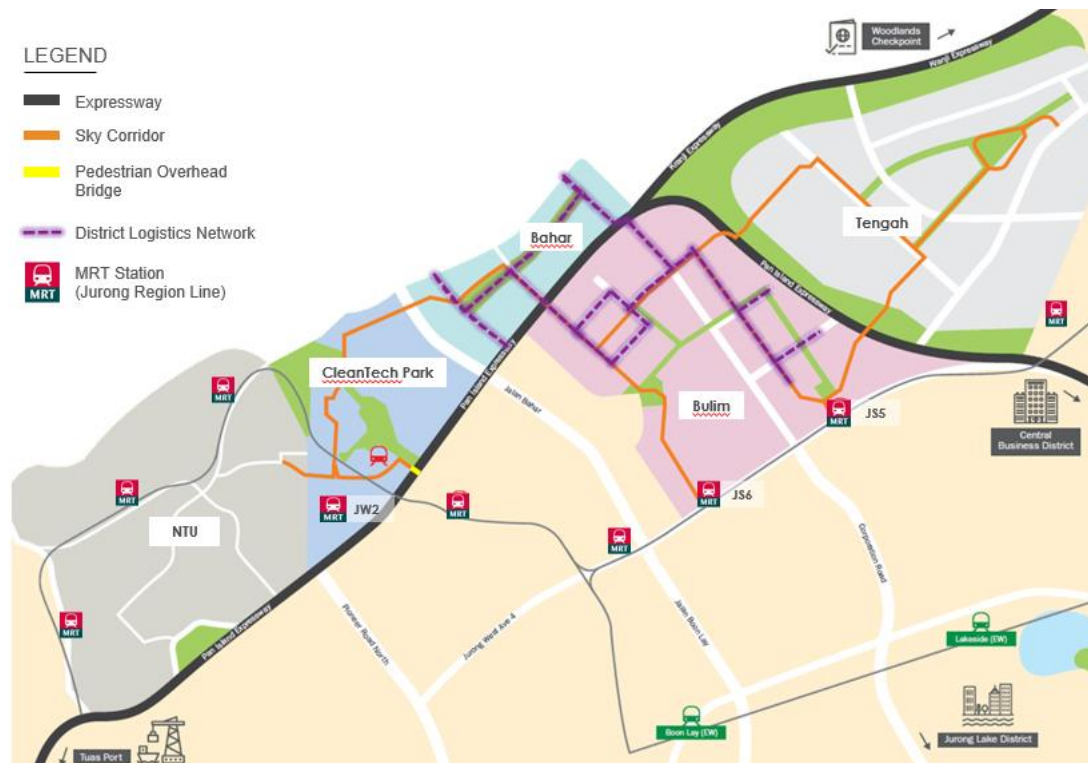
*Figure 2. (Left) Cross section of underground road with 3 lanes*

*Figure 3. (Right) Photo of the completed underground road*

#### 1.3.3. Routing of the DLN

The routing of the DLN underground road would be implemented in two phases – the first phase has been completed in 2025, and the second phase is expected to be completed in 2030. Within the first phase of the DLN (“DLN Phase 1”), a ring-shaped network with one-way traffic flow was adopted to house the underground road at basement 2 level of Bulim Square, a four-tower industrial development with a gross floor area of approximately 160,000 m<sup>2</sup> by JTC. Bulim Square is built and owned by JTC and is specifically designed to accommodate Small and Medium-sized Enterprises (SMEs), with factory units ranging from 120m<sup>2</sup> to 1200m<sup>2</sup>. In doing so, tenants in Bulim Square could be directly served by the DLN.

A ring-shaped network also avoided a single point of failure if a localized section of the underground road had to be closed in Bulim 1. The ring network extended beyond Bulim to its adjacent industrial plots through 6 “finger” connections designed with knock-out panels to allow for future integration with the basement of future industrial buildings.



*Figure 4. General Alignment of District Logistics Network (DLN) in Phase 1*

## 2. PLANNING AND DESIGN OF THE DISTRICT LOGISTICS NETWORK

### 2.1. Key Benefits – Land Optimisation

The District Logistics Network (DLN) facilitates the relocation of logistics circulation and loading/unloading operations from surface level to basement facilities. This subterranean integration yields an estimated land savings of 2.46 hectares (refer to Appendix A.1), through two primary mechanisms: reduction of land required for surface roads, and reduction of loading/unloading bays.

By channeling logistics traffic underground, the DLN enables surface roads to accommodate larger volumes of non-logistics traffic, which in turn increases plot ratios for surrounding buildings. This is particularly significant in the traffic-constrained Bulim area, where the DLN unlocks additional Gross Floor Area (GFA) development potential that would otherwise be limited by surface traffic capacity.

From a cost-benefit perspective, this configuration reduces land acquisition cost by approximately SGD 24.63 million, as developers need only purchase the requisite underground strata. Moreover, given Singapore's geographical constraints as a city-state with limited industrial land availability, the liberated surface area can be allocated to higher-value economic activities.

Furthermore, by relocating logistics traffic underground, the DLN enables a reduction in nuisance buffer (NEA, n.d.) traditionally required between industrial and nearby existing residential areas to mitigate noise and air pollution impacts. These nuisance buffers, which typically constrain industrial development, could potentially be narrowed<sup>3</sup> given the reduced industrial traffic and associated emissions at the surface level. This creates opportunities for more flexible land use planning and allows industrial areas to be situated closer to residential developments without compromising environmental quality standards or resident comfort.

<sup>3</sup> Subject to detailed Industrial Siting Consultation (ISC) with National Environment Agency (NEA)



## 2.2. Key Benefits – Improved Logistics Efficiency

The District Logistics Network (DLN) has been conceptualised with several key objectives and design considerations. Primary among these are the optimisation of infrastructure utilisation through round-the-clock operations, maximising return on investment, and the incorporation of future-ready automation capabilities, particularly in facilitating sophisticated logistics interfaces between Distribution Centres and basement Goods Receiving Area (GRA). The network has been specifically engineered to provide Small and Medium-sized Enterprises (SMEs) with access to economies of scale in logistics operations, whilst ensuring connectivity, scalability, and flexibility for phased implementation. Importantly, the design adheres to Singapore's Land Transport Authority (LTA) regulations, ensuring that the network can be utilised by existing road vehicles immediately in its manual operational phase without any further retrofitting.

In DLN Phase 1, the provision of dedicated underground routes for manual Heavy Goods Vehicles (HGVs) fundamentally transforms logistics operations by separating them from surface traffic patterns in JID. This strategic separation not only minimises rush-hour congestion but also ensures consistent and predictable journey times for freight movement. Enhanced reliability in delivery schedules is particularly crucial for manufacturing operations that depend on precise just-in-time logistics. Furthermore, the optimised traffic flow significantly improves operational efficiency, as HGV operators can maintain consistent delivery schedules without the productivity losses typically associated with surface traffic delays. Singapore motorists lost 52 hours a year to rush hour traffic in 2024, according to technology firm TomTom's traffic index (Xiang, 2025), underscoring the broader benefits of such traffic segregation strategies.

The dedicated infrastructure network enables SMEs to plan for round-the-clock operations, marking a significant departure from conventional industrial estates where goods movements are typically restricted to "office" hours (8am~5pm, approximately 9 hours). With extended operating hours of up to 24 hours, productivity is projected to increase up to 2.5 times through more streamlined operations, significantly reducing human resource requirements for driving, loading, and unloading activities. The system's continuous operation capability allows companies to optimize their resource allocation, particularly in terms of receiving/dispatching docks and transport vehicles. Rather than dimensioning basement Goods Receiving Area (GRA) for peak handling capacity, companies can plan for consistent average volumes throughout the day, leading to more efficient resource utilization.

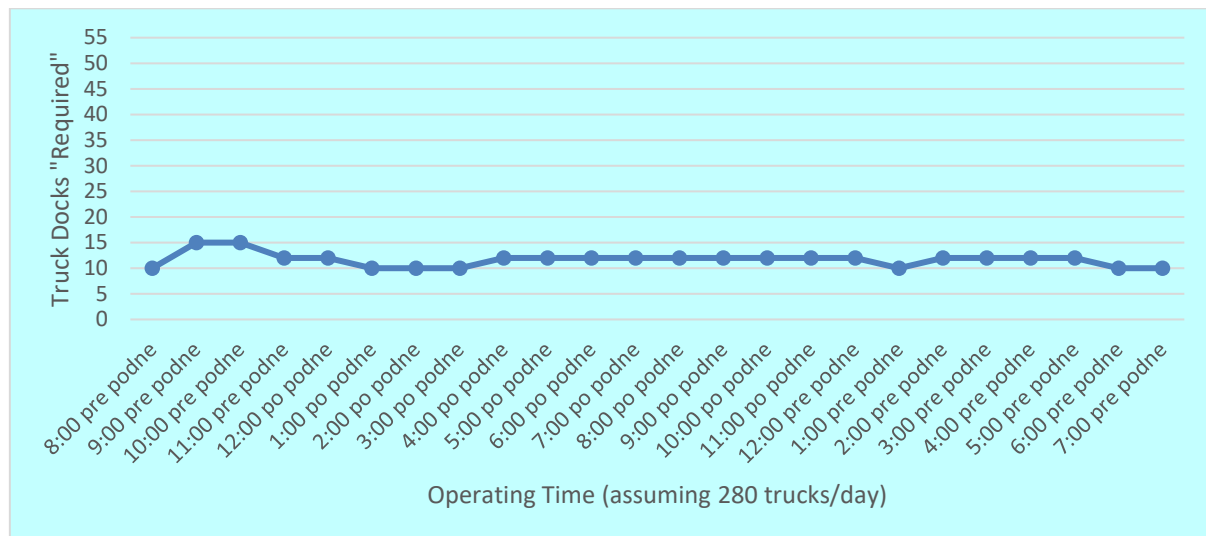
Building upon these productivity enhancements, the DLN has been designed with future automation capabilities in mind, enabling all logistics movements within the network to operate round the clock. This automation-ready infrastructure allows for "lights-out" operations, while the implementation of electrically driven automated vehicles positions the DLN as an environmentally sustainable logistics solution. The system's design enables significant reduction in common resources such as receiving/dispatching Truck docks, as facilities no longer need to be dimensioned for peak handling capacity but can be planned for consistent average volumes throughout the day. This represents a transformative advancement compared to traditional industrial estates, optimizing both operational efficiency and resource utilization while minimizing environmental impact.



**Figure 5.** (Left) Demand for Trunk Docks based on 8am to 5pm (9hrs) operations

**Figure 6.** (Right) Photo of the completed Trunk Docks





**Figure 7.** Demand for Trunk Docks based on 24/7 (24hrs) operations

### 3. ENGINEERING CHALLENGES ENCOUNTERED WITHIN THE DLN UNDERGROUND ROAD

#### 3.1. Site and Existing Infrastructure Constraints

The project presented several engineering challenges due to its location and close proximity with existing residential and industrial developments. The presence of an operational bus depot and arterial road networks demanded traffic management protocols while maintaining operational continuity.



**Figure 8.** (Left) Existing 5.5m wide drain serving surrounding catchment

**Figure 9.** (Right) Existing Bus Depot in close proximity

The subsurface development was significantly constrained by the presence of existing sewers and 5.5m wide drains, alongside a common services space requirement at Basement 1 level. Alternative solutions which involved diversion for the 5.5m wide drains were evaluated but proved economically unfeasible due to the existing drains and sewers' gravitational alignment requirements.

To ensure these “live” services for drainage and sewerage are not affected during construction, the engineering team implemented temporary pile supports and a reinforced concrete (RC) beam to underpin the services, enabling top-down construction methodology in the DLN Core 1 area. This approach required precise engineering coordination, particularly where the Common Services Space (CSS) crosses beneath the existing drain. The solution encompassed:

- Structural assessment of existing H-pile and drain conditions
- Enhanced existing H-pile bracing systems
- Strategic localised drain diversions for soldier pile installation

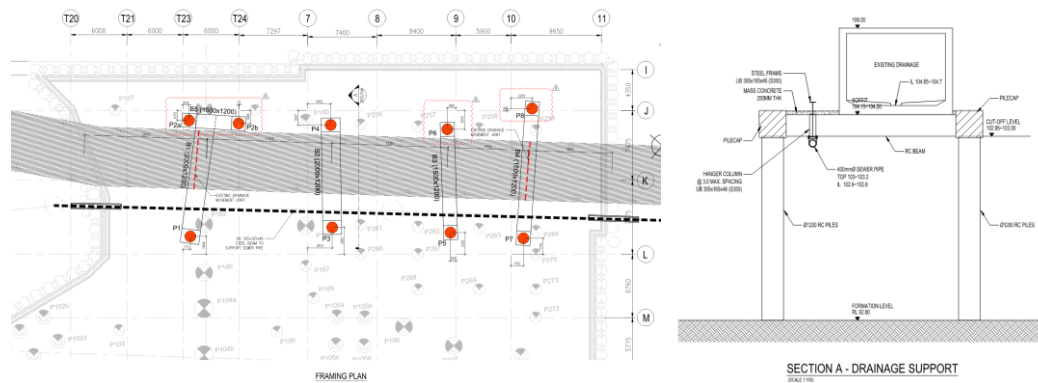


Figure 10. Temporary support layout for 5.5m drain and sewer to facilitate DLN Core 1 Top-Down Construction

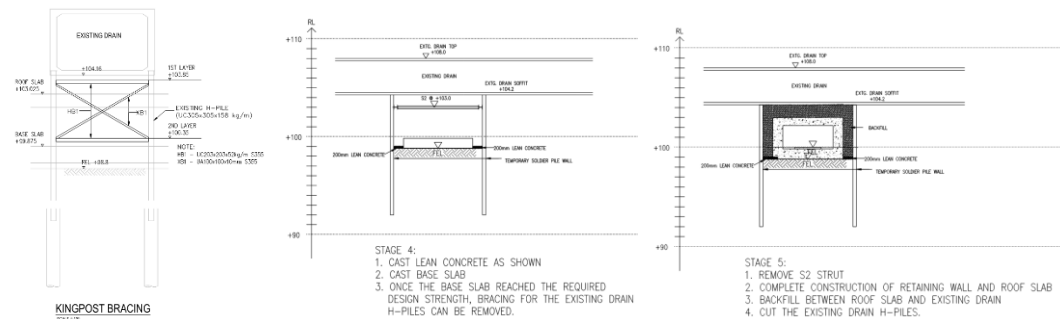


Figure 11. Strengthening localise area of drain existing H-pile to facilitate the construction of under-crossing CSS

### 3.2. Design Integration and Construction Methodology in conjunction with Bulim Square

To ensure an unobstructed transport network, the DLN tunnel was designed as a column-free structure, with some junctions spanning approximately 40 meters in both directions. An efficient structural framing system using waffle slabs and two-way beams was adopted to reduce material usage and allow space for services to pass through.

The structural design incorporated comprehensive loading considerations. The tunnel roof slab, spanning approximately 18-20m with maintenance corridor, was engineered to withstand a permanent load from 6m thick soil layer and an overburden traffic load of 25kN/m<sup>2</sup>. These loading parameters necessitated a reinforced concrete tunnel roof slab depth ranging from 1.0-1.2m. The design additionally accounted for full water pressure conditions, including detailed analysis of tension pile requirements for uplift resistance.

The construction methodology for this project employed a hybrid approach, combining both open cut and top-down methods to optimise construction efficiency whilst minimising disruption to the surrounding infrastructure. In the vicinity of Bulim Square, open cut excavation was implemented due to the absence of immediate surface constraints, matching with Bulim Square bottom-up construction and the need for rapid construction progress with better construction quality control with waterproofing application.

However, for sections further from Bulim Square, a top-down construction sequence using Secant Bored Pile (SBP) with temporary soil nailing was adopted to maintain ground stability, minimum disturbance to existing sewer, drains, existing road networks, nearby bus depot operation and surface activities. Using ground anchors, with proper assessment of ground conditions, frees up space within the DLN footprint for construction activities, unlike the diagonal strut method, which restricts movement due to the struts.

This strategic combination was driven by several key considerations: firstly, the phasing requirements necessitated maintaining access to Bulim Square throughout construction; secondly, the top-down method provided inherent structural support in areas with deeper excavation depths; and thirdly, this arrangement allowed for concurrent surface and subsurface activities, thereby optimising the construction schedule.



*Figure 12. Key Cross Section showing the integration of District Logistics Network and Bulim Square*

### 3.3. Geotechnical Challenges – Adverse Ground conditions

The geotechnical characteristics of the DLN site present significant engineering challenges, predominantly comprising loose to medium gravelly silty sand extending to an average depth of 4 metres, which is subsequently underlain by the Jurong Formation<sup>4</sup>. The presence of karstic limestone formations, identified during comprehensive soil investigation, necessitated extensive subsurface characterisation prior to foundation works.

To mitigate risks associated with potential subsurface cavity voids, a systematic cavity mapping programme was implemented. The investigation methodology incorporated multiple probe drillings utilising 75mm diameter boreholes extending to depths of 65-75 metres. This extensive ground investigation exercise enabled the development of detailed three-dimensional subsurface models, critical for identifying and characterising subsurface features.

The geotechnical data obtained informed the development of specialised Earth Retaining or Stabilizing Structures (ERSS) techniques. The design approach incorporated:

- Detailed cavity risk assessment and classification
- Zone-specific pile installation methodologies
- Modified casting sequences tailored to varying cavity conditions
- Enhanced quality control protocols during foundation work

To address the challenging ground conditions, the engineering team implemented several engineering solutions. These included pre-treatment of identified cavity zones using specialised grouting techniques, along with custom-designed pile reinforcement configurations for zones with varying cavity risks. The team also installed real-time monitoring systems on surrounding existing infrastructure and buildings to detect anomalies during pile installation, whilst implementing adaptive pile design modifications based on encountered ground conditions.

The successful implementation of these measures demonstrated the effectiveness of integrated geotechnical solutions in managing complex subsurface conditions. The approach not only ensured structural integrity but also optimised construction efficiency while maintaining stringent safety standards.

<sup>4</sup>The Jurong Formation is a bedrock formation (primarily mudstone and sandstone, shale, siltstone, conglomerate and fossil-rich limestone) that dates to the Late Triassic (Gang, 2012)

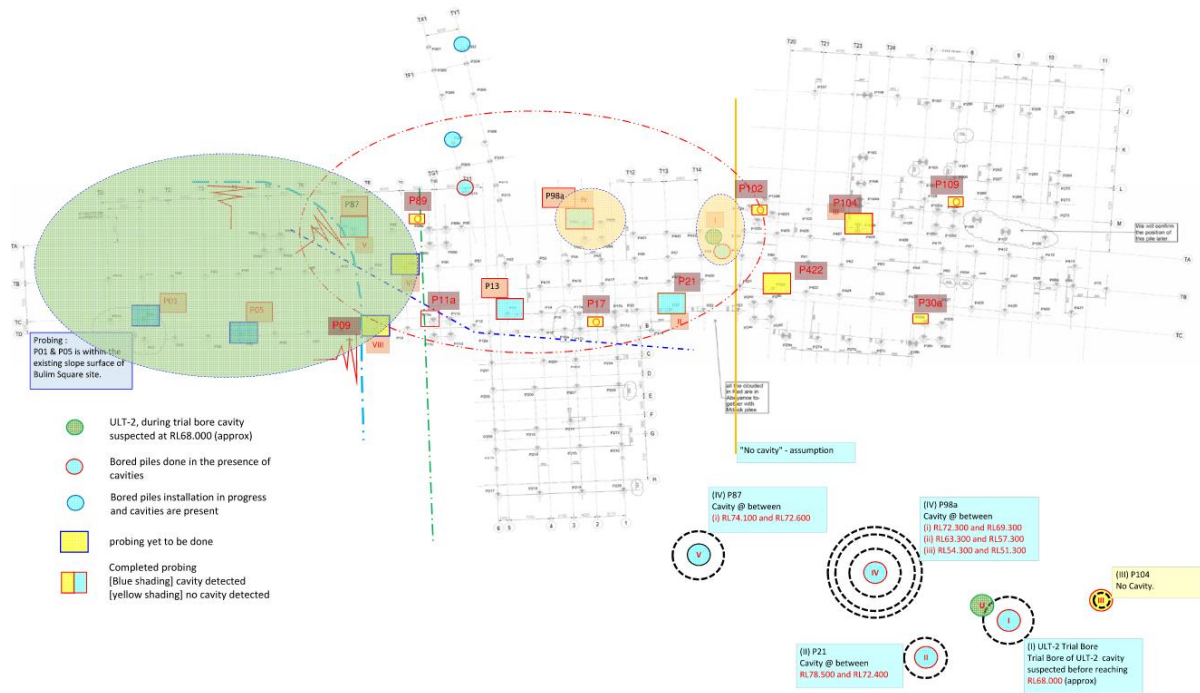


Figure 13. Systematic Cavity Mapping to determine potential subsurface cavity voids

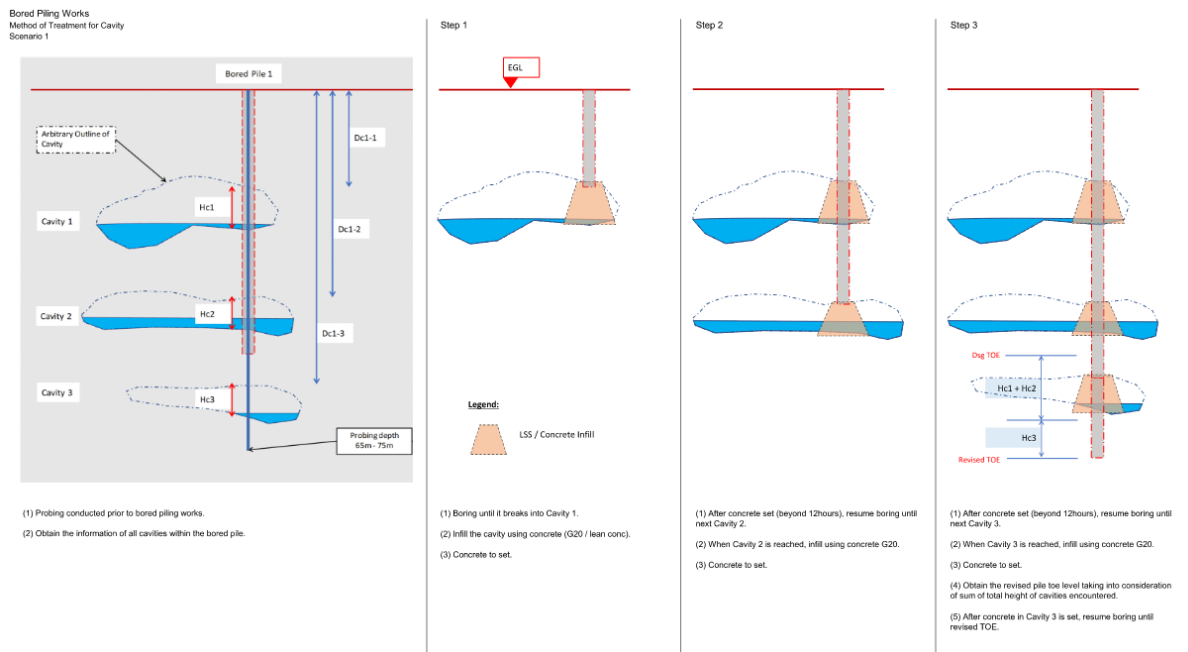


Figure 14. Pre-treatment of identified cavity zones using specialised grouting techniques

### 3.4. Design challenges as Innovative Infrastructure

The District Logistics Network (DLN) represents Singapore's first underground logistics infrastructure of its kind, necessitating innovative approaches to mechanical and electrical (M&E) provisions, particularly in ventilation and fire safety systems. This innovative infrastructure demanded exceptional engineering solutions that transcend conventional infrastructure requirements.

The mechanical ventilation system incorporates dual functionalities: environmental control during normal operations and smoke management during emergencies. During standard operations, the system maintains optimal



air quality and temperature through strategic air exchange, while being prepared for immediate reconfiguration in emergency scenarios.

Classified as a “Building” under Singapore Civil Defence Force (SCDF) regulations, the DLN must comply with Fire Code 2018 requirements. However, this classification presented unique engineering challenges, as traditional building code compliance proved incompatible with the tunnel's operational demands. The primary constraint emerged from the Fire Code's prescribed smoke zone requirements, which traditionally mandate physical barriers, such as smoke curtain or fire shutter - a feature incompatible with the continuous vehicle movement essential to the DLN's operations.

To resolve this technical contradiction, a full Performance-based fire safety design approach was developed instead and approved through regulatory consultation. The smoke ventilation system in the DLN was designed to comply with NFPA 502 – Standard for Road Tunnels, supported by comprehensive Computational Fluid Dynamics (CFD) modelling to validate its effectiveness. This solution successfully demonstrates smoke containment within designated zones without physical barriers.

The DLN is designed to accommodate constant traffic flow throughout its network, where in the event of fire, Heavy Goods Vehicles (HGVs) may be located on both side of fire site. Under this scenario, several objectives regarding smoke control have to be met, such as effective smoke extraction and undisturbed smoke stratifications (Association, 2020). To achieve effective smoke control while considering DLN's traffic layout and design, the smoke management strategy utilises sophisticated zonal control mechanisms which necessitate the implementation of Partial Transverse Ventilation with high-level or ceiling extraction points. This alternative design approach considers that conventional "push-pull" ventilation solutions or jet fans may inadvertently direct smoke towards HGVs in the affected zones. This design choice was validated through extensive simulation studies and risk assessments.

The ventilation system's architecture divides the DLN tunnel into virtual smoke zones, each spanning approximately 200 to 300 metres, which is in accordance with PIARC's recommendation to limit the incident zone where smoke is prevented from propagating further (Operation, 2007). These virtual zones feature high-capacity reversible fans with variable frequency drives, enabling dynamic operational flexibility between supply and exhaust modes. During fire incidents, the system executes a coordinated response: the affected zone transitions to negative pressure exhaust mode, while the two adjacent zones operate in positive pressure supply mode, creating aerodynamic containment of smoke within the fire zone. This sophisticated approach ensures effective smoke management without compromising operational continuity, unlike physical smoke zones where activation of smoke barriers or smoke curtains will affect HGV movement.

The smoke management strategy encompasses multiple operational scenarios, each tailored to specific zones within the DLN. These scenarios have been extensively modelled and validated through computational analysis to ensure robust emergency response capabilities. The implemented solution addresses three critical scenarios, each corresponding to distinct spatial and ventilation characteristics:

Smoke Zone 1 (SZ-1):

- Features three strategically positioned 10m x 10m air wells
- Utilises passive ventilation principles through natural convection
- Demonstrates optimal smoke evacuation without mechanical intervention

Smoke Zone 2 (SZ-2) - Partial Transverse Ventilation:

- During fire incidents, implements a hybrid ventilation strategy
- Receives coordinated support from SZ-3, which provides 100% mechanical supply air
- Achieves complete smoke extraction through Air Well 3 via natural ventilation principles
- System design ensures maintained pressure differentials for effective smoke containment

Smoke Zone 3 (SZ-3) - Partial Transverse Ventilation:

- Employs a sophisticated multi-source air management approach
- Utilises SZ-2 for 50% natural replacement air supply
- Supplements ventilation with 50% mechanical air supply from the northern terminus
- Incorporates 100% mechanical exhaust capabilities through dedicated extraction systems
- Maintains calculated pressure gradients to prevent smoke migration



This zonal strategy exemplifies the integration of passive and active ventilation systems, optimising both energy efficiency and emergency response capabilities. The design's effectiveness has been validated through extensive Computational Fluid Dynamics (CFD) modelling and full-scale testing protocols.

#### **Tunnel Smoke Ventilation Design – Partial Transverse System (PTS)**

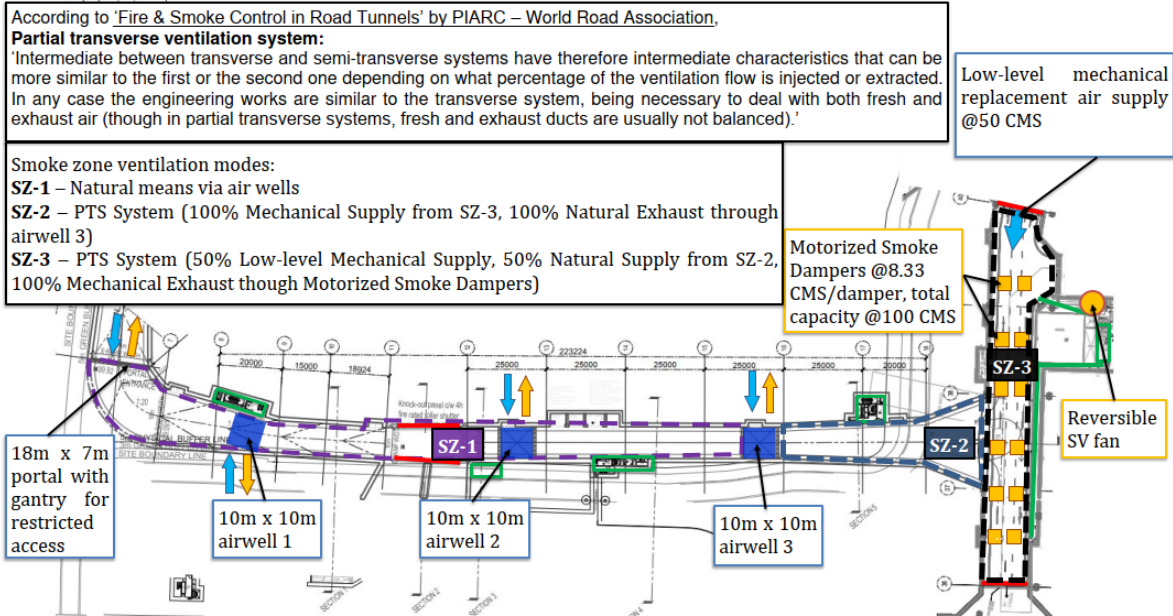


Figure 15. Tunnel Smoke Ventilation Design – Partial Transverse System (PTS)

#### **23) LOCATION OF DESIGN FIRE SCENARIOS**

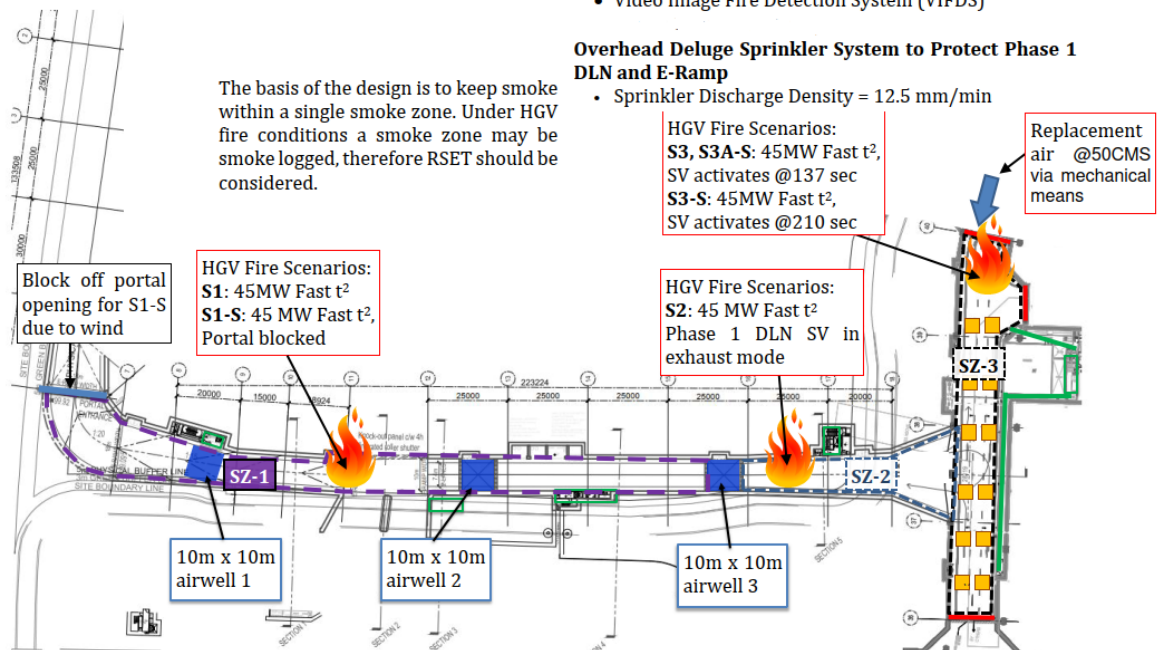


Figure 16. Location of Design Fire Scenarios

## **4. CONCLUSION AND FUTURE DEVELOPMENTS**

### **4.1. The future with Centralised Distribution Centre (CDC)**

The future of the District Logistics Network (DLN) at Jurong Innovation District (JID) would comprise a Centralised Distribution Centre (CDC) operating in tandem with the underground road network, with the aim of alleviating the inefficiencies of conventional freight movement. All HGVs entering the estate will be directed underground to the DLN's distribution centre, where containers of goods will break-bulk and be repacked into pallets and stored until required by companies. Upon companies' requests, the goods will then be loaded onto automated guided vehicles (AGVs) and transported to the companies' doorstep via the basement Goods Receiving Area (GRA).

One key advantage of the CDC in Bulim is that it allows industrial tenants and lessees in Bulim to declutter their production area by operating in a just-in-time (JIT) mode. Given that the CDC is sited within 1.5 km of the factories in Bulim, immediate stocks required for production within the next 2 days can be moved into the Goods Receiving Area (GRA) for temporary storage, below the tenants' production area, within approximately 1 hour of activating the stocks. A dedicated underground road also means that the response time is less vulnerable to adverse traffic conditions. Furthermore, this will reduce the movement of goods from many different 3rd party logistics (3PL) providers or warehouses between Bulim and various locations in Singapore, thus easing the local traffic conditions around JID.

Another benefit of the DLN is the promotion of centralized logistics operations. By sharing logistics resources, the bullwhip effect can be mitigated with improved system efficiency (Dongfei Fu, 2014). Given that the CDC will be able to manage product inventories and allow for JIT delivery, stocks may be delivered at any time and not only during peak hours. This would normalise the traffic level within the underground road throughout the day and allow for the DLN's design to be optimized.

In addition, centralisation would enable a larger throughput volume of goods to be handled, which makes automation more effective. As such, the CDC will feature an automated storage and retrieval system (ASRS) that operates continuously, enabling efficient handling of varying load sizes and types. The system's modular design allows for progressive capacity expansion, accommodating future growth and technological advancements. Furthermore, the network incorporates smart technologies for real-time tracking and monitoring, ensuring optimal route planning and resource allocation for last-mile delivery of palletized stocks to be handled by autonomous goods vehicles (AGVs), which will ply the underground road network between the CDC and the factory GRA.

Lastly, the DLN and CDC will contribute to environmental sustainability by replacing fuel consumption by HGVs for the last-mile delivery of goods with electric-powered AGVs or AVs. Bringing the last-mile transportation of goods underground will also improve surface air quality and allow for surface roads to be reduced in width. The freed-up space can then be used for park spaces and greenery, contributing to JID's 30% estate-wide green cover target.

### **4.2. Conclusion**

The District Logistics Network demonstrates the feasibility of subterranean logistics infrastructure as a transformative solution for land-scarce urban environments. Through innovative engineering solutions addressing complex geotechnical challenges, including karstic limestone formations and adverse ground conditions, the project successfully implemented a 3.5-kilometre underground network capable of accommodating 40-foot containers while meeting stringent safety and operational requirements. The integration of sophisticated ventilation systems compliant with NFPA 502 standards, coupled with the future implementation of a Centralised Distribution Centre (CDC), positions the DLN as a benchmark for sustainable urban logistics.

The infrastructure has demonstrably enhanced logistics efficiency by unlocking approximately 2.46 hectares of surface land while enabling just-in-time operations validates its role in advancing Singapore's vision of integrated underground space utilisation. As industrial estates evolve toward greater automation and environmental sustainability, the DLN's design principles and implementation strategies offer valuable insights for future underground logistics infrastructure development globally.



$$\begin{aligned} \text{Land savings} &= \\ &[\text{Bay area} \times \text{No. bays}] \\ &= [(14.0 \times 3.3) \times (690000 \div 3000)] \\ &= 10,626 \text{sqm} \end{aligned}$$

\*Assumes loading bay provision based on lower bound requirement of 1 bay per 3,000sqm GFA for multi-user industrial developments.

### Conclusion

Based on the overall land savings of approx. 14,000sqm+10,626sqm = 24,626sqm (2.46ha), we can estimate from the Singapore Land Authority's LBC Table (see Table 1) that the prevailing land value in this area as of Mar 2025 is roughly \$1000 per sqm, allowing us to derive a land cost savings of approx. 24,626sqm x \$1000/sqm = SGD \$24.63 million.

Table 1 shows the prevailing land betterment charge rates (SLA, SLA, n.d.) (SLA, <https://www.onemap.gov.sg/#/LBCQueryInfo>, n.d.) for industrial developments in the Bulim area (Group D – \$707psm) which is approximate to 70% of the land value. Hence, land value is approximately \$1000 per sqm.

**BULIM SQUARE**  
1, BULIM LANE 2, SINGAPORE 648110

**Sector 114**

Group	Sep 2024 ▼	Mar 2025 ▼	Change
A	\$10,500	\$10,500	\$0
B1	\$4,830	\$4,970	\$140
B2	\$6,720	\$6,720	\$0
C	\$5,250	\$5,460	\$210
D	\$693	\$707	\$14
E	\$735	\$770	\$35
F	\$10	\$10	\$0
G	\$34	\$34	\$0
H	\$1	\$1	\$0

Table 1 - Prevailing land betterment charge rates (Group D - \$707psm)

## 7. BIBLIOGRAPHY

- [1] Association, N. F. (2020). NFPA 502: Standard for Road Tunnels, Bridges, and Other Limited Access Highways.
- [2] CTRL+SHIFT. (2023). Jurong Rock Caverns. Retrieved from <https://www.ctrlshift.gov.sg/engineering-marvels/jurong-rock-caverns/>
- [3] Dongfei Fu, C. M.-H. (2014). Decentralized and centralized model predictive control to reduce the bullwhip effect in supply chain management. *Computers & Industrial Engineering*, 73, 21-31.
- [4] Gang, C. J. (2012). *Geology of Singapore*. Singapore: IES Academy and GeoSS.
- [5] Land Transport Authority Singapore. (2019). Code of Practice - Street Work Proposals Relating to Development Works. Retrieved from [https://www.lta.gov.sg/content/ltagov/en/industry\\_innovations/industry\\_matters/development\\_construction\\_resources/street\\_works/requirements\\_for\\_street\\_work\\_proposals.html](https://www.lta.gov.sg/content/ltagov/en/industry_innovations/industry_matters/development_construction_resources/street_works/requirements_for_street_work_proposals.html)
- [6] NEA. (n.d.). Retrieved 07 09, 2025, from <https://www.nea.gov.sg/our-services/development-control/guidelines-for-building-plan-submission/industrial-siting-consultation>
- [7] Operation, P. C. (2007). Systems and equipment for fire and smoke control in road tunnels. PIARC. Retrieved from <https://www.piarc.org/en/order-library/5425-en-Systems%20and%20equipment%20for%20fire%20and%20smoke%20control%20in%20road%20tunnels>
- [8] Public Utilities Board Singapore. (2025). Deep Tunnel Sewerage System. Retrieved from <https://www.pub.gov.sg/Professionals/Requirements/Used-Water/DTSS>

- [9] Robert de Souza, M. G.-C.-S.-S. (2014). Collaborative Urban Logistics – Synchronizing the Last Mile (A Singapore Research Perspective). *Procedia - Social and Behavioral Sciences* (125), 422 - 431.
- [10] SLA. (n.d.). <https://www.onemap.gov.sg/#/LBCQueryInfo>. Retrieved 06 25, 2025, from <https://www.onemap.gov.sg/#/LBCQueryInfo>
- [11] SLA. (n.d.). SLA. Retrieved 06 27, 2026, from [www.sla.gov.sg/articles/press-releases/2025/revision-of-land-betterment-charge-rates-from-1-march-2025](http://www.sla.gov.sg/articles/press-releases/2025/revision-of-land-betterment-charge-rates-from-1-march-2025)
- [12] URA. (n.d.). URA. Retrieved Jun 10, 2025, from <https://www.ura.gov.sg/Corporate/Planning/Master-Plan/Master-Plan-2019/Regional-Highlights/West-Region>
- [13] Xiang, T. K. (2025, 03 21). The Straits Times. Retrieved 06 27, 2025, from <https://www.straitstimes.com/life/made-in-singapore-erp-and-the-polarising-traffic-solution-pioneered-by-the-republic>



## ANALYSIS OF CARBON EMISSION CHARACTERISTICS AND REDUCTION POTENTIAL ON TUNNEL LIGHTING

Tao Liu<sup>1</sup>, Hehua Zhu<sup>2</sup>, Yi Shen<sup>3\*</sup>, Weifeng WU<sup>4</sup>, Liankun Xu<sup>5</sup>, Shouzhong Feng<sup>6</sup>

**Abstract:** The problem of global warming caused by excess carbon emission has aroused great concern of all countries in the world. As an important part of underground space, road tunnels produce a large amount of carbon emissions in the operation process. In this study, the carbon emission of the tunnel life cycle was calculated and evaluated, and the role of lighting was analyzed. The eye movement characteristics and carbon emissions ratio of each lighting section were studied for the tunnel graded lighting. The carbon emission uncertainty analysis of tunnel lighting was carried out considering the influence of multiple factors such as traffic volume and design speed, and the carbon reduction potential was studied based on particle swarm optimization algorithm. The results show that the carbon emission of tunnel lighting is closely related to the length of tunnel, and the sum of carbon emission of the entrance section and the middle section exceeded 80%. With the increase of tunnel length, the proportion of lighting carbon emission in the middle section of the tunnel continues to increase. In addition, the carbon reduction potential of tunnel lighting was analyzed.

**Keywords:** Carbon emission, Tunnel lighting, Optimization method, Reduction potential analysis

### 1. INTRODUCTION

Under the backdrop of global warming, low-carbon and sustainable development have become the recognized development trends of the international community (Chen et al, 2016; Yuan et al, 2011). At the Global Climate Change Conference on December 12, 2015, the heads of state of many countries adopted the Paris Agreement, calling on all countries around the world to work together to address climate change. The goal is to keep the global average temperature range within 2°C and strive to limit the temperature rise to within 1.5 °C (Zou et al, 2023).

Infrastructure construction has significant practical significance in expanding domestic demand, improving people's livelihood and promoting industrial development in various regions (Melo et al, 2013). Large-scale transportation infrastructure construction and subsequent operation are believed to generate a large amount of carbon emissions (Wang et al, 2015). Among them, tunnels are regarded as the most energy-intensive part of transportation infrastructure and should be given particular attention (Zhan et al, 2018). At present, there are still relatively few studies on carbon emissions from tunnel engineering. Guo et al. (2019) selected eight highway tunnels in southwest China as the research objects, conducted research on the influencing factors of carbon emissions in each process of tunnel construction, and used statistical analysis methods to identify the key influencing factors of carbon emissions from tunnel construction. However, these studies mainly focus on the

<sup>1</sup> PhD, Liu Tao, Civil Engineering, Department of Geotechnical Engineering, College of Civil Engineering, Tongji University, 1239 Siping Road, Shanghai, 200092, China, lta@tongji.edu.cn

<sup>2</sup> Prof., Zhu Hehua, Underground Space, State Key Laboratory for Disaster Reduction in Civil Engineering, Tongji University, Shanghai, 200092, China, zhuhehua@tongji.edu.cn

<sup>3</sup> Dr, Shen Yi, Underground Space, State Key Laboratory for Disaster Reduction in Civil Engineering, Tongji University, Shanghai, 200092, China, shenyi@tongji.edu.cn

<sup>4</sup> Dr, WU Weifeng, Civil Engineering, Shanghai Tunnel Engineering and Rail Transit Design and Research Institute, Shanghai, 200235, China, wu.weifeng@stedi.com.cn

<sup>5</sup> PhD, Xu Liankun, Civil Engineering, Department of Geotechnical Engineering, College of Civil Engineering, Tongji University, 1239 Siping Road, Shanghai, 200092, China, xuliankun@tongji.edu.cn

<sup>6</sup> Prof., Feng Shouzhong, Underground Space, State Key Laboratory for Disaster Reduction in Civil Engineering, Tongji University, Shanghai, 200092, China, fsz63@vip.163.com

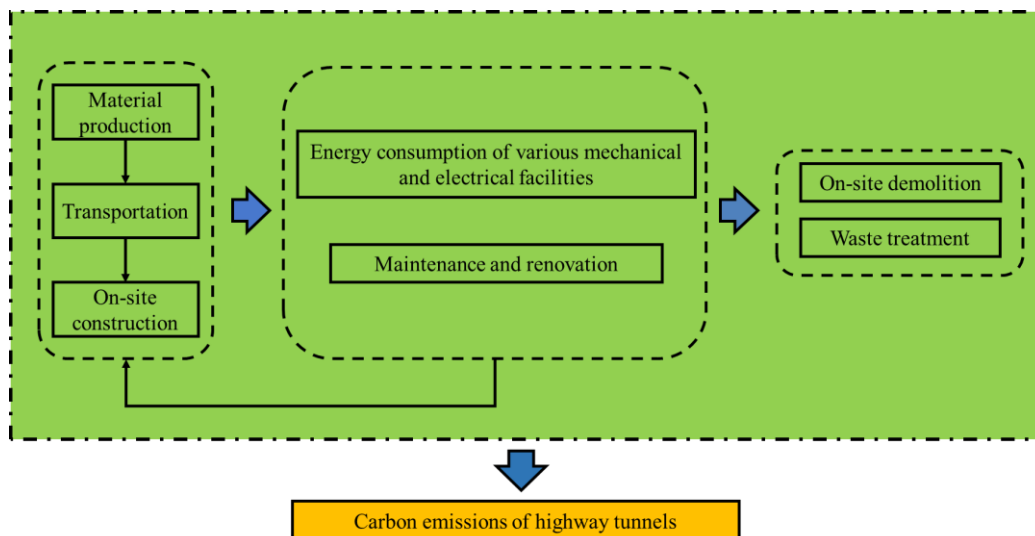
carbon emissions during the construction of tunnels. To ensure the safety and efficient operation of highway tunnels, various electromechanical facilities such as monitoring, ventilation and lighting need to be installed in the tunnels. The carbon emissions during the operation of the tunnels are also very huge (Peeling et al, 2016). In addition, for the same tunnel, different lighting design schemes can lead to significant differences in the carbon emissions from the tunnel's lighting. Therefore, the carbon emissions throughout the entire life cycle of a tunnel should also be carried out in combination with the characteristics of tunnel lighting. In recent years, research on carbon emissions based on the LCA(Life Cycle Assessment) theory has received increasing attention.

Based on tunnel cases, this study conducted a quantitative analysis of tunnel carbon emissions, studied the characteristics of carbon emissions at each stage of the tunnel, and focused on analyzing and evaluating the carbon emissions of tunnel lighting. The research results can provide data support for exploring the emission reduction potential at each stage of the tunnel.

## 2. METHODS

### 2.1. Calculation boundary

When assessing the carbon emissions throughout the entire life cycle of a tunnel, it is necessary to first analyze and classify the CO<sub>2</sub> sources of the tunnel at different stages and define a reasonable calculation boundary. Based on the previous life cycle assessment theories and the division of stages (Dou et al, 2024), this study divides the entire life cycle of the tunnel into the construction stage, the operation stage and the demolition stage. Specifically, the carbon emissions in the construction stage include those generated from the three processes of material production, transportation and on-site construction. For carbon emissions during the operation stage, tunnels consume various types of energy during operation, thereby generating carbon emissions. Additionally, for structures with a relatively short natural lifespan, maintenance and replacement will be carried out during operation, which also leads to carbon emissions. Carbon emissions during the demolition stage refer to the carbon emissions caused by the energy consumed when using equipment to dismantle the tunnel at the end of its service life. The detailed stage division and boundary definition are shown in Figure 1.



*Figure 1. Life cycle carbon emission assessment boundary of highway tunnel.*

### 2.2. Inventory analysis

This study adopts the process-based inventory analysis method. Inventory analysis is the most time-consuming stage in the entire LCA (Life Cycle Assessment) research and is the process by which LCA collects and organizes basic data. The bill of quantities for the tunnel construction stage can be obtained from the survey and design data and construction drawings of the tunnel in the early stage. The energy consumption during the construction process can be obtained from the on-site measured data and the national stipulated quota system for highway engineering. For various energy consumption data during the tunnel operation period, they can be obtained by combining the quantity table of various equipment during the operation period and the operation plan. For the carbon emission factors of various related materials and energy sources, based on previous studies (Li et al, 2018; Shao et al, 2014),

this study established a carbon emission factor database suitable for tunnels. After completing the inventory analysis, calculate the carbon emissions of each stage of the tunnel based on the carbon emission calculation model, and finally obtain the carbon emissions of the entire life cycle of the tunnel.

### 2.3. Tunnel carbon emission calculation model

The IPCC(Intergovernmental Panel on Climate Change) has provided a calculation method for carbon emissions, which indicates that the carbon emissions generated by energy activities can be calculated with the help of carbon emission factors. By combining the data of activities that affect carbon emissions with the emission coefficient per unit activity, the carbon emissions corresponding to energy activities can be obtained.

#### 2.3.1. Construction stage

During the construction stage of the tunnel, the carbon emissions from the material production refer to the carbon emissions generated by the consumption of coal, oil, electricity and other energy sources during the production process of various major building materials such as steel and cement. For the carbon emissions of tunnel material production, the calculation method is as shown in equation (1) :

$$C_m = \sum_i^n mf_i \times m_i \quad (1)$$

where,  $i$  represents the type of material,  $mf_i$  is the carbon emission factor corresponding to the  $i$ -th material, and  $m_i$  is the consumption of the  $i$ -th material.

During the transportation of raw materials for highway tunnels from the production site to the construction site, the transportation equipment will consume fuels such as gasoline and diesel, thereby generating carbon emissions. The calculation method is shown in equation (2) :

$$C_t = \sum_i^n tf_i \times L_i \times m_i \quad (2)$$

where,  $i$  represents the type of material,  $tf_i$  is the carbon emission factor corresponding to the transportation mode of the  $i$ -th material,  $L_i$  is the transportation distance of the  $i$ -th material, and  $m_i$  is the transportation volume of the  $i$ -th material.

For the carbon emissions during the on-site construction stage of highway tunnel, the calculation method is as shown in equation (3) :

$$C_c = \sum_i^n cf_i \times (M_p / M_i) \times c_i \quad (3)$$

where,  $i$  represents the category of construction equipment,  $cf_i$  is the carbon emission factor corresponding to the energy consumption of the  $i$ -th type of construction equipment,  $M_p$  is the amount of work that the  $i$ -th type of construction equipment needs to complete,  $M_i$  is the amount of work completed by the  $i$ -th type of construction equipment within a unit of time, and  $c_i$  is the energy consumption of the  $i$ -th type of construction equipment within a unit of time.

#### 2.3.2. Operation stage

After the tunnel is completed, various types of energy need to be consumed to ensure its normal use and the safety of vehicle operation. The carbon emissions during the operation of the tunnel can be derived from equation (4):

$$C_o = \sum_i^n q_i \times w_i \times t_i \times ff_i \quad (4)$$

where,  $i$  represents the type of operational equipment,  $q_i$  is the quantity of specific operational equipment,  $w_i$  is the power demand of a specific facility in watts,  $t_i$  is the operating time of the equipment, and  $ff_i$  is the carbon emission factor corresponding to the energy consumption of the  $i$ -th type of operational equipment.

For the carbon emissions during the tunnel renovation period, the calculation method of carbon emissions during the tunnel construction stage can be referred to for assessment.

### 2.3.3. Demolition stage

When a highway tunnel is out of use, various types of mechanical equipment need to be used for demolition. Therefore, the carbon emissions during this period mainly came from the energy consumption of dismantling equipment. However, for the demolition stage, there is currently a lack of accurate calculation models, and most of them are mainly estimated (Zhang and Wang, 2015). Based on relevant studies, this study takes the carbon emissions of the demolition stage as 90% of the carbon emissions during the on-site construction process of the tunnel.

$$C_d = 0.9 \times \sum_i^n cf_i \times (M_p / M_i) \times c_i \quad (5)$$

For the treatment of tunnel waste after demolition, the carbon emissions in this study are considered as the carbon emissions caused by the energy consumption of transportation equipment to transport the waste to the landfill, and the calculation method is carried out with reference to equation (2).

### 2.3.4. Total carbon emissions

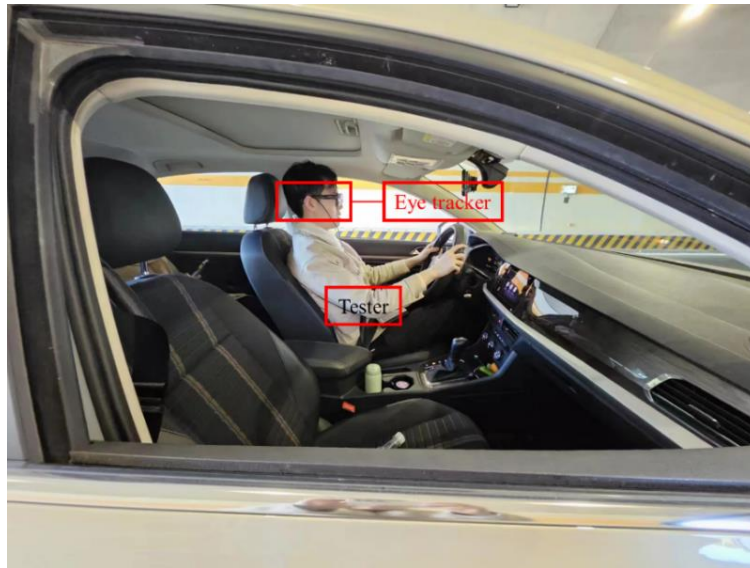
In summary, the calculation method for the total carbon emissions of highway tunnels throughout their life cycle can be derived from equation (6).

$$C_{tot} = C_m + C_t + C_c + C_o + C_d \quad (6)$$

where,  $C_{tot}$  represents the total carbon emissions throughout the entire life cycle of a highway tunnel,  $C_m$  represents the carbon emissions generated during the material production,  $C_t$  represents the carbon emissions generated during the transportation,  $C_c$  represents the carbon emissions generated during the on-site construction,  $C_o$  represents the carbon emissions generated during the operation stage,  $C_d$  represents the carbon emissions generated during the demolition stage.

## 2.4. Tunnel driving eye movement test

While analyzing the carbon emissions of tunnel lighting, it is necessary to analyze the impact of different tunnel lighting sections on drivers from the perspective of engineering safety. This study carried out eye movement tests for tunnel driving. The test vehicle selected was an ordinary small car. During the driving process, the driver wore a wireless eyeglass-type eye tracker to record the eye movement data and psychological parameters of the driver in real time when driving the vehicle through the tunnel. As shown in Figure 2, At the beginning of the test, the driver wore the eye tracker as required for the test and drove the vehicle through the tunnel under normal lighting. The test recorder used the software provided with the instrument to record the physiological parameter data of the driver. Afterwards, the physiological indicators collected under the lighting environment will be analyzed.



**Figure 2.** Driver's eye movement test under tunnel lighting.

### 3. CASE ANALYSIS

#### 3.1. Project overview

Taking four types of tunnels of different lengths in a certain area in southern China as examples, including one extra-long tunnel, one long tunnel, one medium tunnel and one short tunnel, the specific length data are shown in Table 1.

*Table 1. Overview of each highway tunnel.*

Type	Name	Length/m
Extra-long tunnel	Tuochuan tunnel	4650
Long tunnel	Wuyuan tunnel	1670
Medium tunnel	Wangpingtan tunnel	619
Short tunnel	Ziyang tunnel	417

According to the carbon emission calculation model proposed in this study, the carbon emissions throughout the life cycle of these four tunnels were calculated. The design life cycle of the tunnels was considered to be 100 years. For various bill of quantities data, this study gives priority to obtaining them from on-site construction units. For the missing transportation distance and other relevant data, certain assumptions need to be made. This study is supplemented based on China's "GBT 51366-2019 Calculation Standard for Building Carbon Emissions".

#### 3.2. Refined assessment of energy consumption in tunnel operation stage

For highway tunnels, the energy consumption during operation is huge. Existing studies show that the current electricity consumption of highway tunnels mainly occurs in lighting facilities and ventilation facilities (Qiu et al, 2020). Therefore, the carbon emission calculation in this study mainly focuses on the two parts of tunnel lighting and ventilation. The lighting of the tunnel studied in the case is more scientific and reasonable. Dimming strategies as shown in Table 2 are set according to different seasons and weather conditions. In order to accurately assess the lighting energy consumption during the operation of each tunnel in the case, this study obtained the local weather information of the past year and calculated the lighting carbon emissions during the operation period considering the weather. For the ventilation of tunnels, under conditions where the tunnel length, traffic mode and local weather conditions are suitable, fan equipment is not necessary. It is entirely dependent on the combined effect of the movement of car pistons and natural wind to expel harmful gases and smoke from the tunnel. When natural ventilation fails to meet the ventilation requirements, mechanical ventilation is then selected. In this case, mechanical ventilation is provided for the extra-long and long tunnels, while natural ventilation is adopted for the medium and short tunnels. Based on the fan configuration and equipment parameters of each tunnel, combined with equation (4), the ventilation carbon emissions during the operation stage of each tunnel can be calculated.

*Table 2. The standards for dimming classification of case tunnel lighting.*

Lighting type	Season and weather	Brightness outside the tunnel	Explanation
Enhance lighting	Summer sunny day	L20 (S)	Closed at night
	Sunny days in other seasons/Cloudy days in summer	0.5 L20 (S)	
	Cloudy days in other seasons/Cloudy days in summer	0.25 L20 (S)	
	Overcast or heavily overcast days in other seasons	0.125 L20 (S)	
Basic lighting	Day/Night		Brightness 2.5cd/m <sup>2</sup>

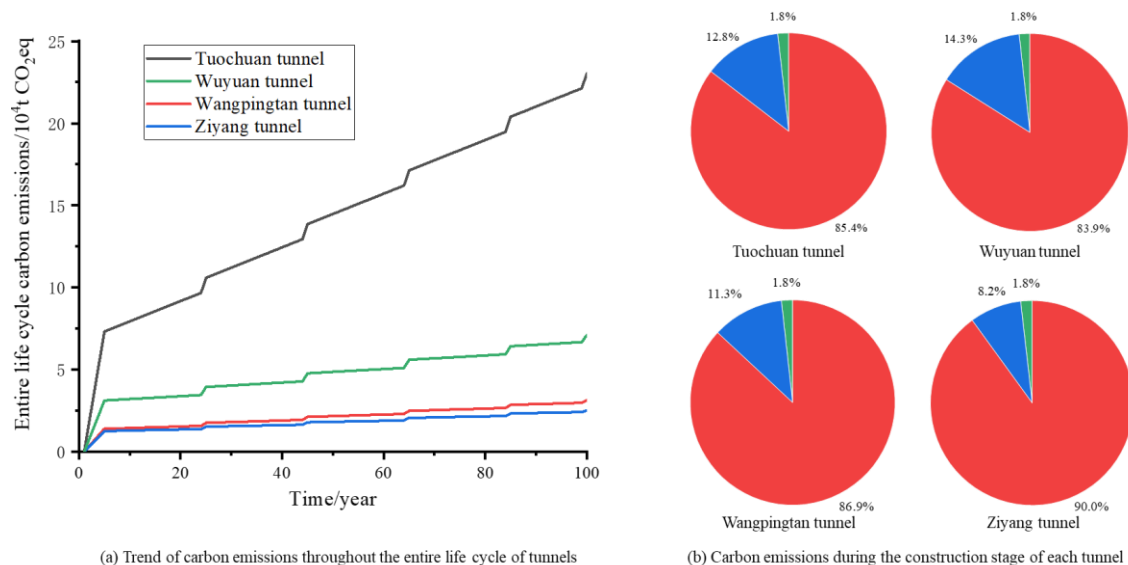
The renovation work during the tunnel operation mainly focuses on the maintenance of the road surface, and the service life of the road surface is considered to be 20 years. The demolition work of the tunnel is considered to be completed within one year, and the transportation distance of the demolition waste is considered to be 20 km.



## 4. RESULTS

### 4.1. Growth trend and characteristics of carbon emissions

Based on the calculation of carbon emissions at each stage of the tunnel, the changes in carbon emissions throughout the entire life cycle of each tunnel are shown in Figure 3. The carbon emission results throughout the entire life cycle of the tunnel show that there is a relatively large carbon emission in the initial stage of the tunnel's construction. After entering the operation stage, the carbon emissions of the tunnel rise steadily. The longer the tunnel, the greater the carbon emission rate during the operation stage. During the operation stage, as the renovation project progresses, the carbon emissions of the tunnel will also experience a short-term increase.



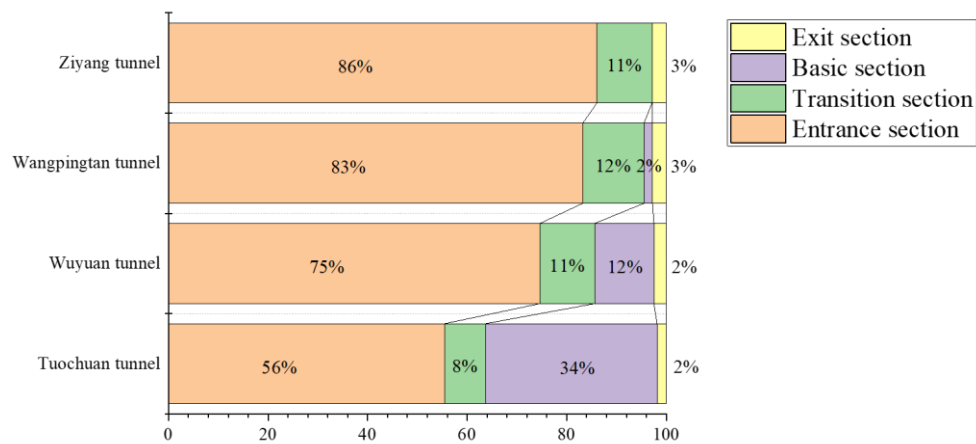
**Figure 3.** The changing trend and characteristics of carbon emissions throughout the life cycle of tunnels.

In addition, as shown in Figure 3, during the tunnel construction period, the carbon emissions of the material production part were the highest, and those of the material transportation part were the lowest. From the perspective of total emissions, as the length of the tunnel increases, the carbon emissions during the tunnel construction stage increase significantly, and the carbon emissions during the construction stage are directly proportional to the length of the tunnel.

### 4.2. Growth trend and characteristics of carbon emissions

According to the carbon emission results throughout the entire life cycle of the tunnel, it can be known that the carbon emissions during the operation stage of the tunnel account for a relatively high proportion. Among them, tunnel lighting has always been regarded as a high-energy-consuming part and has huge potential for emission reduction. Unlike external lighting, as a semi-enclosed space, there is a significant difference in the brightness of the environment inside and outside the tunnel. When drivers pass through the tunnel, they have the problem of adapting to light and dark. To meet the drivers' visual adaptation needs in high and low brightness environments and ensure the safety of tunnel driving, tunnel lighting is generally set up in the entrance section, transition section, middle section and exit section according to different design brightness levels. In tunnels of different lengths, the settings of each lighting section are also not the same. In order to assess the lighting carbon emissions of each section of the tunnel, it is necessary to calculate the energy consumption of each lighting section of tunnels of different lengths.

Based on the lighting fixture settings of each tunnel in the case, the carbon emissions of different lighting sections of the four tunnels in the highway tunnel were analyzed. The proportion of carbon emissions of each section is shown in Figure 4. It can be known from the results that the carbon emission proportion of the entrance sections of these four tunnels is the highest, accounting for approximately 50% to 80%. The proportion of carbon emissions in the middle section increases with the increase of the tunnel length. Therefore, the entrance section of the tunnel has extremely high carbon reduction potential. During the subsequent operation stage, relevant measures can be taken to reduce the carbon emissions caused by lighting in the entrance section of the tunnel.

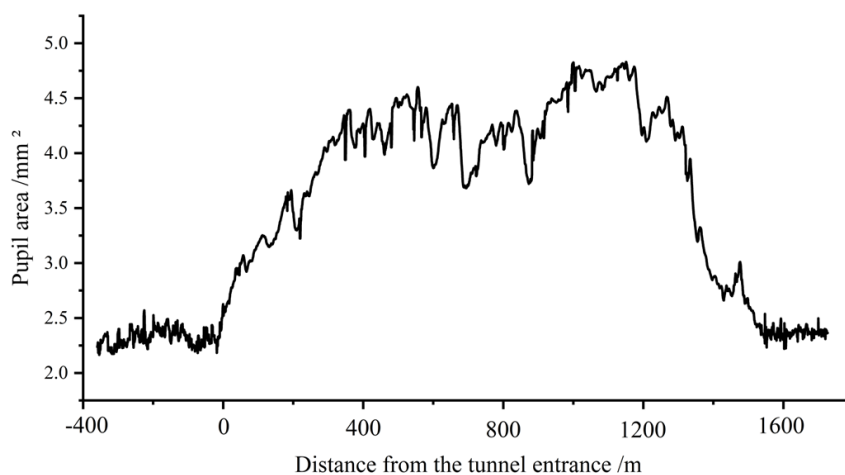


**Figure 4.** The proportion of carbon emissions in each lighting section of the case tunnel.

### 4.3. Driver's eye movement characteristics

As shown in Figure 5, before approaching the tunnel entrance, the pupil area fluctuates between 2.0 and 2.5 mm<sup>2</sup>. At the moment of entering the tunnel (the 0m coordinate point), the pupil area shows a sharp increase and remains at a high level continuously in the middle section of the tunnel, with the peak reaching 4.8 mm<sup>2</sup> and the average value stabilizing above 4.0 mm<sup>2</sup>. This regular feature confirms that the relatively dim environment inside the tunnel prompts the pupil to expand the amount of light intake to enhance the sensitivity of retinal imaging. It is worth noting that the data of this section still shows slight oscillations, which may be due to the periodic distribution of lighting fixtures inside the tunnel or the alternation of light and shadow caused by vehicle movement. When the vehicle approaches the exit, the pupil area shows a gradual downward trend and falls back to about 3.3mm<sup>2</sup> at 1600m. This physiological response reflects the driver's pre-adaptation mechanism to the high-intensity natural light outside the tunnel - iris contraction to reduce glare interference and provide a buffer for the visual function transition after the exit.

The changes in pupil area during tunnel passage reveal the psychological adaptation characteristics related to the driver's cognitive load and emotions. The pupil area shows an accelerating dilation trend when approaching the entrance of the tunnel. This reflects the driver's instinctive vigilance towards the semi-enclosed space and a certain degree of anxiety at the entrance section.



**Figure 5.** The variation characteristics of the pupil area of the driver when passing through the tunnel.

## 5. CONCLUSIONS

This paper analyzes the carbon emissions of highway tunnels throughout their entire life cycle and divides the boundaries, establishing carbon emission calculation models for each period. And based on the case of each tunnel, case calculations were carried out, and the following main conclusions can be obtained:

(1) During the tunnel construction stage, the carbon emissions from the material production section are the highest, accounting for approximately 70%. Therefore, various low-carbon materials have a very promising application prospect. The carbon emissions of the material transportation section are the lowest, while those of the on-site construction section are in the middle.

(2) Regarding the total carbon emissions throughout the entire life cycle of a tunnel, there will be a significant increase in carbon emissions as the tunnel length increases. Moreover, the relative magnitudes of carbon emissions during the construction stage and the operation stage also vary due to the different lengths of the tunnels.

(3) Based on life-cycle assessment, tunnel entrance sections account for 50%-80% of lighting-related carbon emissions due to high-intensity illumination requirements. Meanwhile, pupil area monitoring shows that the driver's pupils dilate faster and anxiety intensifies at the entrance. The research indicates that the design of entrance lighting not only imposes an ecological burden but also a cognitive burden. By optimizing the lighting scheme in the entrance area, there is huge potential for carbon emission reduction.

## 6. ACKNOWLEDGMENTS

The authors wish to acknowledge the sponsorship from the Research on Key Technologies for the Planning, Design, and Construction of the S7 Shanghai-Chongming West River-Crossing Tunnel (Y202445) and Research Fund of State Key Laboratory for Disaster Reduction in Civil Engineering (SLDRCE19-A-14). The support from the China Railway 14th Bureau Group Co., Ltd is highly appreciated.

## 7. REFERENCES

- [1] Chen, W., Yin, X., Zhang, H. (2016). Towards low carbon development in China: A comparison of national and global models. *Climatic Change*, 136(1), 95–108. <https://doi.org/10.1007/s10584-013-0937-7>
- [2] Dou, S., Zhu, H., Wu, S., Shen, Y. (2024). A review of information technology application in reducing carbon emission: From buildings to tunnels. *Journal of Cleaner Production*, 452, 142162. <https://doi.org/10.1016/j.jclepro.2024.142162>
- [3] Guo, C., Xu, J., Yang, L., Guo, X., Liao, J., Zheng, X., Zhang, Z., Chen, X., Yang, K., Wang, M. (2019). Life cycle evaluation of greenhouse gas emissions of a highway tunnel: A case study in China. *Journal of Cleaner Production*, 211, 972–980. <https://doi.org/10.1016/j.jclepro.2018.11.249>
- [4] Li, W., An, C., Lu, C. (2018). The assessment framework of provincial carbon emission driving factors: An empirical analysis of Hebei Province. *Science of The Total Environment*, 637–638, 91–103. <https://doi.org/10.1016/j.scitotenv.2018.04.419>
- [5] Melo, P. C., Graham, D. J., Brage-Ardao, R. (2013). The productivity of transport infrastructure investment: A meta-analysis of empirical evidence. *Regional Science and Urban Economics*, 43(5), 695–706. <https://doi.org/10.1016/j.regsciurbeco.2013.05.002>
- [6] Peeling, J., Wayman, M., Mocanu, I., Nitsche, P., Rands, J., Potter, J. (2016). Energy Efficient Tunnel Solutions. *Transportation Research Procedia*, 14, 1472–1481. <https://doi.org/10.1016/j.trpro.2016.05.221>
- [7] Qiu, W., Liu, Y., Lu, F., Huang, G. (2020). Establishing a sustainable evaluation indicator system for railway tunnel in China. *Journal of Cleaner Production*, 268, 122150. <https://doi.org/10.1016/j.jclepro.2020.122150>
- [8] Shao, L., Chen, G. Q., Chen, Z. M., Guo, S., Han, M. Y., Zhang, B., Hayat, T., Alsaedi, A., Ahmad, B. (2014). Systems accounting for energy consumption and carbon emission by building. *Communications in Nonlinear Science and Numerical Simulation*, 19(6), 1859–1873. <https://doi.org/10.1016/j.cnsns.2013.10.003>
- [9] Wang, X., Duan, Z., Wu, L., Yang, D. (2015). Estimation of carbon dioxide emission in highway construction: A case study in southwest region of China. *Journal of Cleaner Production*, 103, 705–714. <https://doi.org/10.1016/j.jclepro.2014.10.030>
- [10] Yuan, H., Zhou, P., Zhou, D. (2011). What is Low-Carbon Development? A Conceptual Analysis. *Energy Procedia*, 5, 1706–1712. <https://doi.org/10.1016/j.egypro.2011.03.290>
- [11] Zhan, J., Liu, W., Wu, F., Li, Z., Wang, C. (2018). Life cycle energy consumption and greenhouse gas emissions of urban residential buildings in Guangzhou city. *Journal of Cleaner Production*, 194, 318–326. <https://doi.org/10.1016/j.jclepro.2018.05.124>
- [12] Zhang, X., Wang, F. (2015). Life-cycle assessment and control measures for carbon emissions of typical buildings in China. *Building and Environment*, 86, 89–97. <https://doi.org/10.1016/j.buildenv.2015.01.003>
- [13] Zou, C., Wu, S., Yang, Z., Pan, S., Wang, G., Jiang, X., Guan, M., Yu, C., Yu, Z., Shen, Y. (2023). Progress, challenge and significance of building a carbon industry system in the context of carbon neutrality strategy. *Petroleum Exploration and Development*, 50(1), 210–228. [https://doi.org/10.1016/S1876-3804\(22\)60382-3](https://doi.org/10.1016/S1876-3804(22)60382-3)

## **SAFETY, SECURITY AND HUMAN FACTORS**

## IMPLEMENTATION OF SMART SITE SAFETY SYSTEM AND 5G/IOT IN TUNNEL CONSTRUCTION IN HONG KONG – SOLUTION FOR SAFETY CONSTRUCTION

Joseph Z. HONG<sup>1</sup>, Yifeng LI<sup>2</sup>, Zhikai WEI<sup>3</sup> and Chao GUAN<sup>4</sup>

**Abstract:** To enhance safety management, the Hong Kong Government issued a technical circular in 2023, promulgating the adoption of smart site Safety System (4S) in public works projects with a contract sum exceeding \$30 million. Confined space (such as a tunnel, a cavern, etc.) is considered as one of the most dangerous environments for construction, and is therefore specially listed in 4S plan as a separate item. This paper begins by summarizing common risks in tunnel construction and introduces the corresponding elements of 4S in confined space management, including confined space access control, worker health monitoring, equipment management, air quality monitoring, AI CCTV, electronic locking systems, and their integration into a Central Management Platform (CMP). For each functional component, the paper elaborates on targeted problem-solving approaches through 4S implementation, as well as the corresponding actions to be taken by administrators and safety officers in response to various alerts and notifications. Additionally, the paper highlights specific challenges that may arise during the application of 4S in confined space projects and proposes practical solutions. Furthermore, the paper discusses the application of 5G/IoT technologies during tunnel construction, which supports 4S functionalities and internet-based communication. The adoption of smart site systems represents an emerging trend in engineering project practices. It is hoped that the experiences summarized in this study will assist industry peers in strengthening confined space project management and fostering a safer working environment.

**Keywords:** Tunnel Construction; Smart Site Safety System (4S); 5G/IoT implementation; AI Safety Monitoring; Centralized Management Platform

### 1. INTRODUCTION

Tunnel construction is widely recognized as one of the most hazardous activities in the construction industry due to the confined and dynamic nature of the working environment. According to the “Code of Practice for Safety and Health at Work in Confined Spaces” (Labour Department, HKSARG, 2024), the major hazards in a confined space include five main situations, namely: (1) flammable, explosive or oxygen enriched atmosphere; (2) excessive environmental heat; (3) toxic / harmful gases or oxygen deficient atmosphere; (4) in-rush of liquid; or (5) in-rush of free flowing solids.

The risks associated with tunnel construction necessitate the adoption of safety management systems. Thus, in “Guidance Notes on Safety and Health of Hand-dug Tunnelling Work” of Occupation Safety and Health Branch (Labour Department, HKSARG, 2017), project teams should establish safe systems and safety precautions for construction, which mainly includes risk assessment and permit-to-work system, tunnel tag in / out system, air monitoring, electricity management, monitoring devices etc.

<sup>1</sup> Mr. Joseph Z. HONG, M.Eng., B.Eng., Assistant Site Manager, Civil Department, China State Construction Engineering (Hong Kong) Limited, 27/F, China Overseas Building, 139 Hennessey Road, Hong Kong China, e-mail address: zhengqiang.hong@cohl.com.

<sup>2</sup> Mr. Yifeng LI, M.Sc., B.Eng., Assistant General Manager, Civil Department, China State Construction Engineering (Hong Kong) Limited, 27/F, China Overseas Building, 139 Hennessey Road, Hong Kong China, e-mail address: li\_yf@cohl.com.

<sup>3</sup> Mr. Zhikai WEI, M.Eng., B.Eng., Deputy Site Manager, Civil Department, China State Construction Engineering (Hong Kong) Limited, 27/F, China Overseas Building, 139 Hennessey Road, Hong Kong China, e-mail address: weizhikai@cohl.com.

<sup>4</sup> Mr. Chao GUAN, M.Sc., B.Eng., PhD candidate on Smart City, Assistant Director, Transcendence Company Limited, 19/F, Exchange Tower, 33 Wang Chiu Road, Kowloon Bay, Hong Kong China, e-mail address: chris\_guan@cohl.com.



In recent years, the integration of high-tech solutions has revolutionized safety management in tunnel construction. In February 2023, the Hong Kong Government issued a technical circular, promulgating the adoption of smart site Safety System (4S) in public works projects with a contract sum exceeding \$30 million (Development Bureau, HKSARG, 2023), aiming to enhance safety management in construction stage. Projects are divided into 16 categories with different recommendations and options of 4S products. For tunnelling, the recommended items are: centralized management platform (CMP), digitalized permit-to-work system, hazardous areas access control by electronic lock and key system, unsafe acts / dangerous situation alert for mobile plant operation, smart monitoring devices for workers and frontline site personnel and confined space monitoring system. Other optional items are also listed in the circular.

## 2. CURRENT 4S IMPLEMENTATION STATUS IN HONG KONG

A preliminary study (Chan et al., 2024a) after the issuing of the 4S technical circular interviewed four groups of stakeholders, including government engineer, supplier, site safety officer and safety trainer, to figure out the thoughts and doubts about the implementation and training of 4S in projects from different perspectives. As the study was carried out before the actual implementation of 4S, problems such as integration of the system, power supply of products were raised out by stakeholders, which later became true problems for the industry. The following study about the design and implementation of 4S (Chan et al., 2024b) reports two existing sites implementing 4S. It is found that the responsibility of 4S management was unclear, leading to many uncertainties in follow-up of incidents and maintenance of components; Meanwhile, trainings should be provided in different themes for different site personnel from different backgrounds. The method of developing a training course on 4S was also discussed in another study (Chan et al., 2025).

Although the technical circular of 4S has been put into effect for more than three years, there are still a large number of public projects had commenced before the issuing of the circular. Most clients / employers / project managers from these projects issued instructions to contractors for partly / fully implementing 4S. However, the release of tunnel projects is not as expected, only few tunnel projects are currently on the market. As of April 2025, 523 projects with different scales were granted with the 4S Labelling in Hong Kong, of which there are only 6 tunnel construction projects (<https://www.cic.hk/content/4s-labelling/en/project-list>).

Lacking experience and references makes the project / research team encountered a lot of problems, and considering optimization plan for 4S. As a mature contractor who has its own smart construction industry, while had constructed and is constructing major tunnel projects in Hong Kong, this project / research team have carried out on-site researches about the implementation of 4S in tunnel projects for over two years, and has its own understanding of the development and use of 4S components.

## 3. 4S COMPONENTS AND NETWORK SUPPORT FOR TUNNEL CONSTRUCTION

As listed in the 4S Technical Circular (Development Bureau, 2023), 4S components and relevant solutions implemented for tunnel construction can be summarized in Table 1.

**Table 1.** Recommended 4S Products for “Tunnelling” Package in 4S Technical Circular and solutions implemented.

Recommended 4S Products	Solutions
Centralized management platform (CMP)	CMP for website and mobile devices
Digitalized permit-to-work system for high-risk activities (e-permit)	E-permit including confined space, lifting, hot work, ladder use etc.
Hazardous areas access control by electronic lock and key system	E-lock with QR code, can unlock by card or mobile apps
Unsafe acts / dangerous situation alert for mobile plant operation danger zone	Machinery 360-degree AI camera system
Smart monitoring devices for workers and frontline site personnel	Smart watches or smart helmets for locating and health detection
Safety monitoring system using Artificial Intelligence	CCTV with AI implanted or real-time AI post processing

Confined space monitoring system	Tag in / out system for entry counting and control; Air monitoring system for air quality inside tunnel
----------------------------------	--

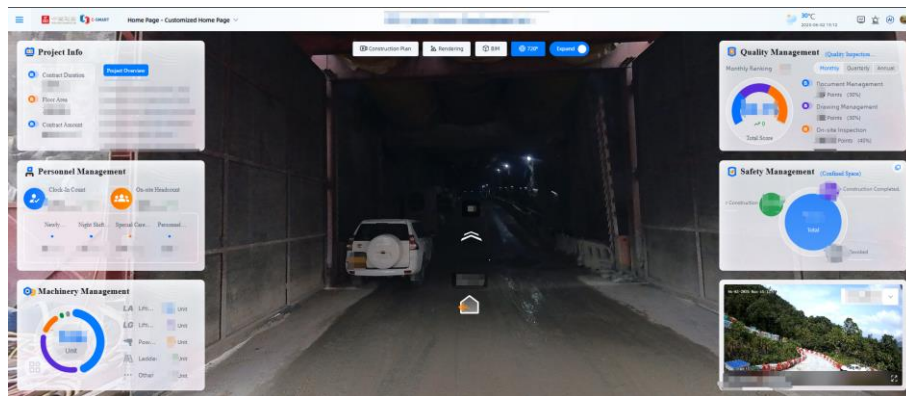
Understandings and optimizations from the project / research team of 4S components related for tunnel construction use are proposed in the following sections.

### 3.1. 4S Components for Tunnel Construction

#### 3.1.1. Centralized Monitoring Platform (CMP)

The Centralized Management Platform (CMP) should be a web-based with access control intelligent and intuitive platform to manage and collect all signals received from 4S. CMP should also centralize construction data, including BIM, site progress, intelligent alerts and early warnings, apps data, IoT sensor data, and weather information, etc. for better demonstration. It should provide the site staff and stakeholders with a more transparent and accurate up-to-date overview anytime, anywhere (Figure 1).

CMP should be placed in the control center, access available through any device with internet access and browser. Details of computer hardware and software and associated furniture refer to contract. The contractor should have its own control center be in its site office.

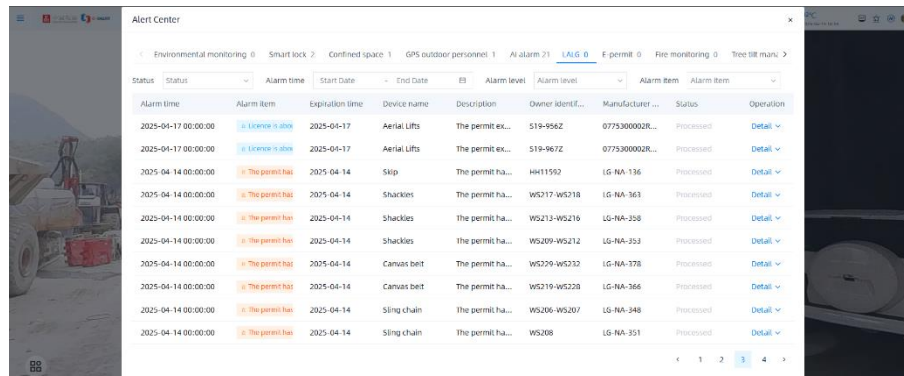


**Figure 1.** Dashboard of CMP.

For a tunnel project, alert center is a necessary part of CMP. The alert center should be able to display notifications from products, especially confined space air monitoring, confined space worker status, AI CCTV, LALG, e-permits, machinery 360-degree AI Cameras, etc. As a confined space always generates important air quality alerts and worker status alerts, it is recommended to divide alerts into different levels (2 to 3 levels) to reduce unnecessary interferences. Details of the levels should be negotiated with the client / employer / project manager, and liaise with supplier for customization.

Taking 3-level alert system customized for the project / research team as an example, notifications are recommended to be marked with different colors such as red, orange and blue separately to reflect different importance. For a red situation, the alert will pop-up in CMP immediately and push to relevant personnel via mobile app simultaneously; for an orange situation, the alert will pop-up in CMP without app notification; for a blue situation, the alert will pop-up in backstage instead of dashboard, avoiding bunches of unnecessary notifications.

Only authorized personnel (e.g. safety officers) can eliminate the alerts after issues are solved and conditions turn back to normal. Frontlines who do not have the accesses to CMP, may call relevant authorized personnel to deal with the alerts after making sure everything working normally (Figure 2).



Alarm time	Alarm item	Expiration time	Device name	Description	Owner Ident...	Manufacturer ...	Status	Operation
2025-04-17 00:00:00	<a href="#">License is due</a>	2025-04-17	Aerial Lifts	The permit ex...	S19-956Z	0775300002R...	Processed	<a href="#">Detail</a>
2025-04-17 00:00:00	<a href="#">License is due</a>	2025-04-17	Aerial Lifts	The permit ex...	S19-967Z	0775300002R...	Processed	<a href="#">Detail</a>
2025-04-14 00:00:00	<a href="#">The permit has</a>	2025-04-14	Skip	The permit ha...	H41159Z	LG-NA-136	Processed	<a href="#">Detail</a>
2025-04-14 00:00:00	<a href="#">The permit has</a>	2025-04-14	Shackles	The permit ha...	W5217-W5218	LG-NA-363	Processed	<a href="#">Detail</a>
2025-04-14 00:00:00	<a href="#">The permit has</a>	2025-04-14	Shackles	The permit ha...	W5213-W5216	LG-NA-358	Processed	<a href="#">Detail</a>
2025-04-14 00:00:00	<a href="#">The permit has</a>	2025-04-14	Shackles	The permit ha...	W5209-W5212	LG-NA-353	Processed	<a href="#">Detail</a>
2025-04-14 00:00:00	<a href="#">The permit has</a>	2025-04-14	Canvas belt	The permit ha...	W5229-W5232	LG-NA-378	Processed	<a href="#">Detail</a>
2025-04-14 00:00:00	<a href="#">The permit has</a>	2025-04-14	Canvas belt	The permit ha...	W5219-W5228	LG-NA-366	Processed	<a href="#">Detail</a>
2025-04-14 00:00:00	<a href="#">The permit has</a>	2025-04-14	Sling chain	The permit ha...	W5206-W5207	LG-NA-348	Processed	<a href="#">Detail</a>
2025-04-14 00:00:00	<a href="#">The permit has</a>	2025-04-14	Sling chain	The permit ha...	W5208	LG-NA-351	Processed	<a href="#">Detail</a>

Figure 2. Different Levels of Alerts.

### 3.1.2. Digitalized Permit-to-Work System for High-Risk Activities (e-permit)

A permit-to-work system is a mean to ensure safety and health of the workers who enter and work in a construction space, enhancing management and control, and encouraging higher transparency for operation.

As stated in the code (Labour Department, 2024), a confined space e-permit is required before entering a tunnel after any change of conditions (Figure 3). The permit should be displayed conspicuously at the entrance of the confined space, and the Labour Department will conduct spot checks. However, according to the present 4S technical circular, e-permit of confined space is required, and this requirement is written in the project contract so that the contractor is to follow.

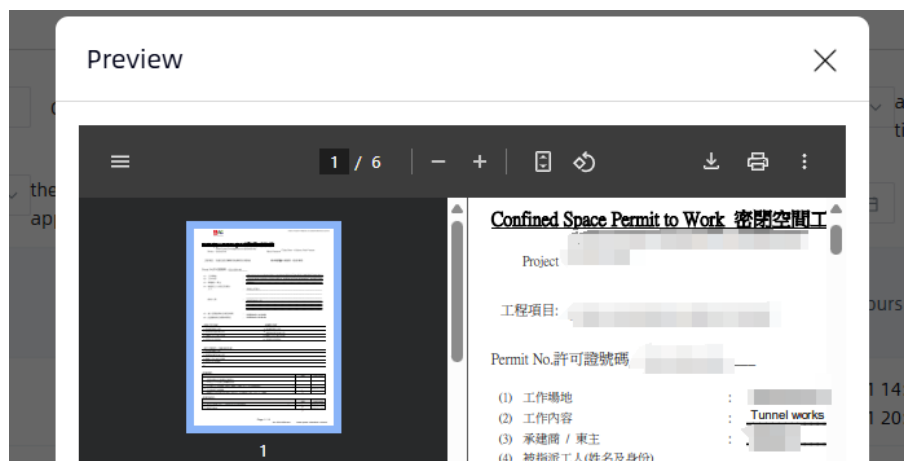
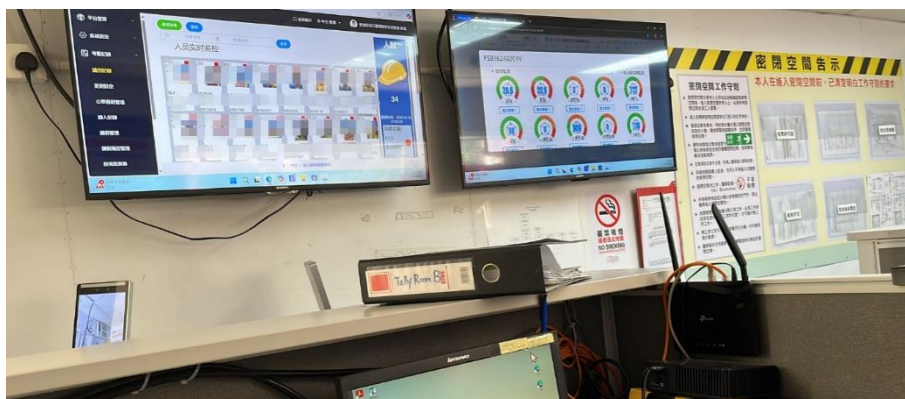


Figure 3. Preview of Confined Space E-permit.

To make sure the safety construction environment and enhance management, it is suggested to set a display system at the tally room (tunnel access control points) for display of confined space e-permit. This system can not only display the e-permit, but also the air monitoring dashboard, entering counting etc. (Figure 4).

In practice, although e-permit is in use, the Labour Department also checks the paper permit. Two regulations should be unified.



*Figure 4. Arrangements in Tally Room.*

### 3.1.3. Smart Monitoring Device for Workers and Frontline Site Personnel

Smart monitoring devices, which detect the location, health conditions (body temperature, heart beat etc.) and standstill, including but not limited to smart wristband and/or smart helmet, should be provided to every worker and frontline site personnel.

As the cost of a monitoring device is relatively high, service life and reusability which may affect the total cost should be taken into consideration. Thus, smart watches are the most recommended gears for tunnel workers as they are easy for collecting back and reuse. Watches are usually distributed to personnel for daily wear and keep; or distributed in the tally room (tunnel access control points) after tag in for registration, and collected back after personnel exiting tunnel.

Watches can be classified by the locating method, including GPS, LoRa, or Bluetooth. Due to the inability to receive GPS signals inside the tunnel, Lora watches were initially used in one of the projects. Zoners needed to be installed inside tunnel for locating watches, which need uninterrupted power supply, making it inconvenient for use.

In the latest practice, GPS watches with Bluetooth were introduced to another tunnel project, which only required installation of Bluetooth beacons. The beacons would be installed every 25-50 meters inside tunnels for locating watches, and are equipped with batteries, which can last over 1 year. Instead of demolishing the whole LoRa zoners for maintenance, users only need to replace Bluetooth beacons by a new one and reconnected to the CMP, saving a lot of time and cost (Figure 5).



*Figure 5. Zoner of LoRa Watches and Beacon of Bluetooth Watches.*

As requested by the Mines Division, Geotechnical Engineering Office of Civil Engineering Development Department of HKSAR, mobile phones and other communication devices are prohibited within 15 m of the explosives. Thus, blast engineers, shotfirers, miners and other staff related to blast works are not allowed to wear watches. This has resulted in a place where the regulations violate each other. In practice, for safety reasons, relevant site staff are not distributed with watches while carrying out blast works.

### 3.1.4. Confined Space Monitoring System – Tag in /out System

The purpose of tag in / out system is to prevent staff from randomly entering or exiting the confined space area, which may affect daily blast works as evacuations with people counting are required.

Site staff with Certificate of Certified Worker under Section 4(1) of the Factories and Industrial Undertakings (Confined Spaces) Regulation (HKSAR Government, 1999) or other regulations such as the Safety Supervision of Work in Confined Space (Drainage Services Department, HKSARG, 2021), are given tunnel tags for punching. In practice, information such as the expiration of certificate and photo of site staff should be input to the card, preventing unqualified staff from entering the tunnel area (Figure 6).

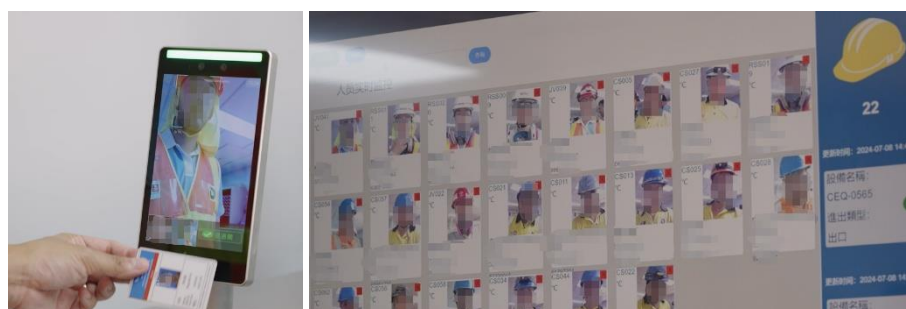


Figure 6. Tag in /out System at Tally Room.

### 3.1.5. Confined Space Monitoring System – Air Monitoring System

Air monitoring system detects oxygen, carbon monoxide, carbon dioxide, hydrogen sulfide, methane, combustible gas, temperature, humidity etc. As this system highly relies on sensors, regular maintenance should be arranged to retain the accuracy. As the sensors are quite expansive and installed in tunnel at fixed locations, protections such as metal cases should be installed to prevent the sensors from being damaged from flying rocks generated by blasting (Figure 7).

In practice, as the air monitoring system are not installed close to blast faces, manual air tests are still vital for the renew of confined space permit. The air monitoring system may only be a reference at current stage.



Figure 7. Air Monitoring System Dashboard.

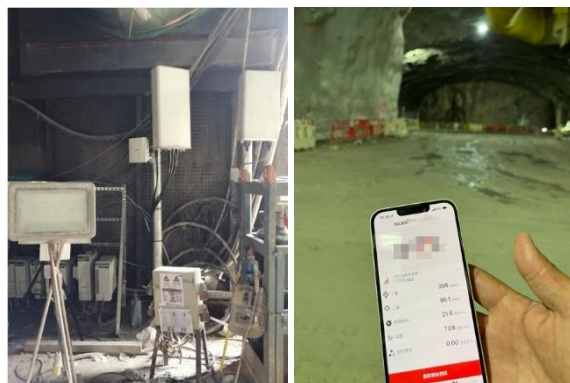
## 3.2. 5G, Wi-Fi and IoT for Tunnel under Construction

As excavation progresses deeper, network connectivity within the underground space deteriorates significantly. Many projects encounter this issue, yet due to cost considerations, dedicated network infrastructure is often not deployed.

To facilitate communication between the tunnel interior and exterior, provide network connectivity for smart devices, and establish an IoT (Internet of Things) system for interconnected equipment, the project / research team progressively installs 5G/Wi-Fi base stations in alignment with tunnel blasting progress in two tunnel projects. This approach aims to achieve near-complete coverage of the under-construction tunnel space. These two tunnel projects are also the first two projects applying 5G/IoT inside tunnel during construction (Figure 8).



Once the base stations are operational, on-site personnel can maintain uninterrupted internet access and communicate with external colleagues via voice calls. Additionally, network-dependent devices within the tunnel (such as e-locks, watches, air monitoring system, etc.) can establish real-time connections to the central control platform and transmit alarm signals when necessary.



*Figure 8. 5G / Wi-Fi Stations and Test.*

#### **4. RESPONSIBILITIES AND ACTIONS BY SITE STAFF**

As mentioned in Section 2 of this paper, former study had found that the responsibility of 4S management tended to be unclear and confusing. To enhance efficiency of 4S management, project / research team develop and assign responsibility to individuals including site top management, site safety team, site engineers, site frontlines, electricians etc. to better fulfill the safety regulations and 4S contract requirements.

##### **4.1. Responsibility**

###### **4.1.1. Site Top Management**

- (1) Assigning competent persons for confined space management and 4S management;
- (2) Ensure and arrange all resources for 4S;
- (3) Liaise with related parties on the implementation of 4S, propose to the client / employer / project manager new 4S products for possible instructions.

###### **4.1.2. Site Safety Team**

- (1) Lead 4S implementation, maintain daily functions and products;
- (2) Supervise 4S operation of other site staff;
- (3) Enhance safety management by organizing unsafe act workshops, regular safety education etc. as per assisted by 4S information;

###### **4.1.3. Site Competent Personnel**

- (1) Supervise 4S operation of subcontractors according to respective sections;
- (2) Report to site safety team for instruction on any issue related to 4S;

###### **4.1.4. Electricians**

- (1) Maintain 4S products including CCTV, e-locks, air monitoring system according to instructions of safety team;
- (2) Only registered electricians assigned by site top management is eligible for opening e-locks.

##### **4.2. Actions to Emergencies detected by 4S in Tunnel**

###### **4.2.1. Alerts from Workers by Watches**

Alerts are automatically generated when exceeding thresholds of worker's health index, or triggered by pressing the button by a worker over 3 seconds for an SOS (Figure 9).

Site safety team receives any alert from watches immediately by notification from CMP or phone message. Site safety team will contact the worker immediately for condition checking, and contact frontline in charge to find and check the condition of the worker according to the location displayed on CMP.



*Figure 9. SOS Sending by Worker.*

#### **4.2.2. Alerts from AI CCTV**

AI CCTV are automatically triggered when personnel are detected not wearing personal protection equipment properly, entering restricted area, or being too close to a vehicle etc.

Site safety team receives any alert from AI immediately by notification from CMP or phone message. If it is a true alert, site safety team will contact the frontline in charge to remind relevant persons, site safety team may also contact the person directly if recognized. No matter which situation, name of the person involved will be recorded for further education (Figure 10). If it is a false alert (usually appears when the helmet is block from the camera by umbrella, or fail to recognize the reflective tape on shirt), site safety team will mark the alert as “false alert” on CMP.



*Figure 10. Unsafe Act Detected by AI CCTV and Further Safety Education.*

#### **4.2.3. Alerts from Air Monitoring System**

Air monitoring systems are automatically triggered when related gas are detected exceeding thresholds.

Site safety team receives any alert from AI immediately by notification from CMP or phone message, and contacts the frontline in charge to remeasure gas inside tunnel using CP/CW handheld gas meter (Figure 11). Frontline in charge will reply to site safety team if the alert is true or false warning. If the alert is true, evacuation is to be conducted until the condition turns back to normal; if false, site safety team will mark the warning as “false alert”.



**Figure 11.** Site Safety Team Reminding Frontline for Manuel Check in Tunnel.

## 5. CHALLENGES ENCOUNTERED DURING TUNNEL 4S IMPLEMENTATION

In the process of promoting the implementation of 4S, challenges arise from various aspects, primarily including human factors, environmental factors, and management factors.

### 5.1. Human Factors

Human factors constitute the most significant influencing elements to implementation, primarily include usage willingness, enforcement compliance, and work convenience.

#### 5.1.1. Usage Willingness

Most site staff (whether from main contractor or sub-contractors) initially experience a period of adaptation when the 4S system is first implemented. Research/project team summarized from two main tunnel projects (one commenced for three years and the other for one and a half years) that it is particularly evident in the use of health monitoring watches—over 70% of the workers fail to develop the habit of wearing watches during work (Figure 12); Meanwhile, while watches can be distributed and collected at tally rooms (tunnel access control points), monitoring workers operating outside the tunnel area remains challenging. This presents a natural disadvantage compared to building projects, where work zones are more easily controlled.



**Figure 12.** Low Wear Rate of Watches.

Additionally, the use of AI Machinery 360° Cameras, equipped with audible-visual alarms (triggering 100-decibel alerts to warn nearby personnel), leads to mental fatigue for operators due to repeated alarm exposure. Consequently, many operators deliberately deactivate the devices (Figure 13).



*Figure 13. Unplugged Devices by Plant Operators.*

### **5.1.2. Enforcement Compliance**

Full implementation can generally be ensured within the main contractor's internal workforce. However, since the mandatory adoption of 4S in Hong Kong is relatively recent, many subcontract contracts lack explicit clauses on 4S compliance, resulting in enforcement difficulties. Currently, this research/project team primarily rely on positive reinforcement, such as monthly "Safety Star" awards for workers with high device usage rates.

### **5.1.3. Work Convenience**

Certain tasks—such as those performed by registered shotfirers and blasting engineers (who handle explosives and must avoid electromagnetic interference)—prohibit the use of wearable devices. Moreover, trades like shotcrete operators, rebar tiers, and form workers require extensive wrist movement, making smartwatch wear highly impractical during operations.

## **5.2. Environmental Factors**

Environmental factors are the most critical determinants affecting product durability and cost control, including operational environments and maintenance environments.

### **5.2.1. Operational Environments**

A representative case involves AI Machinery 360° Camera. Plants (especially excavators) are particularly prone to collisions during rotational movements, often resulting in detached or lost AI cameras and audible-visual alarms (Figure 14). These incidents lead to unpredictable replacement costs, compelling management to develop enhanced protective measures.



*Figure 14. Damage of Cameras Caused by Operation.*

Another case happens with health monitoring watches. The research/project team identified a significantly higher watch damage rate among shotcrete operators compared to other trades, with device lifespans rarely exceeding two months of continuous use. Post-failure analysis revealed that all damaged watches were fully encrusted with concrete slurry, and internal inspection confirmed moisture ingress—a finding consistent with the humid, slurry-intensive working conditions characteristic of applying shot concrete. This phenomenon poses substantial challenges for cost management and equipment sustainability.

### **5.2.2. Maintenance Environments**

Tunnel blasts generate flying debris while producing substantial hazardous gases and dust. This necessitates robust external casing for air monitoring instruments to protect internal electronic components, along with frequent

filter replacements. However, the exact quantities of replacements are difficult to predict due to the unpredictable nature of blasting damage. Consequently, accurately estimating these costs during the bidding phase remains challenging. In practice, this research/project team make close coordination with Clients and Project Managers to optimize equipment placement—ensuring data validity while minimizing damage risks.

### 5.3. Management Factors

Management factors may contribute to false alarms, escalated management costs and damaged devices.

#### 5.3.1. False Alerts

The AI CCTV for restricted area monitoring requires precise demarcation of restricted zones at the post-processing layer. However, as construction progresses, CCTV cameras frequently require realignment or relocation. When restricted zone parameters are not updated timely, false alarms will be tremendously generated, which have a significant increase in security team workload, and deterioration of clients / employers / project managers relations.

#### 5.3.2. Management Cost

The implementation of the 4S system in tunnel construction generates substantial daily alerts across multiple monitoring domains, including gas detection, AI detection, and personnel monitoring, all of which necessitate prompt response and resolution. As the principal oversight entity, the Safety Department is tasked with dual responsibilities: (1) acquiring operational proficiency of 4S, and (2) maintaining continuous system monitoring through dedicated full-time personnel who serve as the primary liaison with Clients and Project Managers. From a cost perspective, the employment of a full-time Assistant Safety Officer (typical monthly remuneration: HKD 18,000 – 22,000) represents a significant long-term financial commitment. For a 5-year tunnel project, this position contributes over HKD 1 million in additional labor expenditures. Contractors must incorporate these anticipated costs during the project planning and budgeting phases to ensure adequate resource allocation.

#### 5.3.3. Damaged Devices

During the use of Smart Locks, regular charging is required to maintain functionality. However, due to the extensive area of the tunnel project, inspection oversights occasionally occur, leading to situations where electronic locks are completely drained and rendered inoperable.

A critical incident arose when a circuit breaker inside tunnel tripped, and the Smart Lock securing the electrical cabinet had depleted its battery, preventing access. This occurred during an urgent situation requiring immediate power restoration for scheduled blasting operations. Without notifying the project / research team, the subcontractor resorted to cutting the electronic lock using hydraulic shears to expedite repairs (Figure 15). This ad-hoc intervention resulted in financial losses and subsequent disputes between the involved parties.



*Figure 15. Damaged E-locks by Workers for Power Repair.*



## 6. CONCLUSION

This paper introduces the implementation of 4S in Hong Kong tunnel engineering based on two major tunnel projects under construction. Requirements for tunnel engineering and 4S in tunnel engineering were firstly summarized according to the government's regulations, and the practices of this project / research team in actual projects were introduced.

This paper then summarizes the corresponding product selection based on the 4S functions that need to be met, combined with the actual situation of two tunnel projects under construction. Understandings of the required implementation functions and related configurations for some tunnel specific functions and products (CMP, worker health monitoring, tag in / out system, and air monitoring device, etc.) are proposed, and elaborate on the ways to cover 5G / Wi-Fi network communication and IoT in the tunnel under construction to ensure the smooth use of 4S products in the tunnel.

To make clear of the responsibility of different staff in the operation of 4S, this paper described the work distribute based on actual project management, and standardizes the measures that different site staff shall take when different alerts occur, in order to improve relevant management efficiency.

At last, the project / research team summarizes the main problems encountered in actual management from three aspects: human factors, environmental factors, and management factors:

(1) For human factors, suitable and effective solutions for enhancing the use rate of 4S products are not yet found and applied, as they are the most complex factors and greatly affect the outcome of implementation. Design of the products may focus more on the experiences of users, and management methods should be negotiated and agreed upon with subcontractors from the beginning for effective management.

(2) For environment and management factors, contractors may focus more on the potential extra cost and make reasonable estimation on the tendering stage, to avoid unexpected situations of insufficient management manpower and budget.

## 7. ACKNOWLEDGMENTS

This paper is sponsored by the Technology Research and Development Project of China State Construction International Holdings Limited (CSCI-2023-Z-17).

## 8. BIBLIOGRAPHY

- [1] Labour Department, HKSARG. (2024). Code of Practice for Safety and Health at Work in Confined Spaces (Second edition). Hong Kong, China.
- [2] Labour Department, HKSARG. (2017). Guidance Notes on Safety and Health of Hand-dug Tunneling Work. Hong King, China.
- [3] Development Bureau, HKSARG. (2023). Development Bureau Technical Circular (Works) No. 3/2023: Smart Site Safety System. Hong Kong, China.
- [4] Chan, Y.W., Cheung, S.K.S., Ng, K.K., et al. (2024). A Preliminary Study on Developing and Training the Smart Site Safety System (SSSS) for Construction Industry in Hong Kong - Technology in Education. Innovative Practices for the New Normal, ICTE 2023. Singapore, 199-207.
- [5] Chan, Y.W., Tsang, Y.F., Cheung, S.K.S., et al. (2024). A Study on the Design and Implementation of the Smart Site Safety System from the Stakeholders' Perspectives – Blended Learning. Intelligent Computing in Education, ICBL 2024. Singapore. 287-299.
- [6] Chan, Y.W., Ng, K.K., & Cheung, S.K.S. (2025). Implementation of smart training on construction site safety: A case study in Hong Kong. Journal of Educational Technology Development and Exchange, 18(1), 30-49.
- [7] Construction Industrial Council, <https://www.cic.hk/content/4s-labelling/en/project-list>.
- [8] HKSAR Government. (1999). Factories and Industrial Undertakings (Confined Spaces) Regulation. Hong Kong, China.
- [9] Drainage Department, HKSARG. (2021). Safety Supervision of Work in Confined Space. Hong Kong, China.

## EXPERIMENTAL STUDY ON THE SMOKE SPREADING CHARACTERISTICS OF FIRE IN THE MERGING SECTION OF THE ARCH BIFURCATION TUNNEL

Yunxiao Xin<sup>1</sup>, Yaqiong Wang<sup>2</sup>

**Abstract:** Branching tunnels are a crucial component of underground transportation networks, and their structural shape results in a more complex distribution of wind flow fields in the bifurcated section compared to normal tunnels. Especially, the arch tunnels have a sudden change of cross-section at the bifurcation point, which makes it more difficult to control the spread of smoke in the tunnel at the bifurcation. This paper takes the Dapeng Tunnel of the Shenzhen Outer Ring Expressway as the research object, and studies the fire smoke spreading rule for the merging section of the arch bifurcation tunnel through model experiments. The results show that when the fire source is located in the normal section, the critical wind speed is higher than that of a normal tunnel, and smoke backflow is more likely to occur upstream of the fire source. When the fire source is located in the transition section of the tunnel, smoke tends to accumulate in this section during the spread process and form a long backflow upstream of the fire source. When the fire source is located in the transition section, the critical wind speed is essentially the same as that of a normal tunnel, and smoke tends to accumulate and flow back into the non-fire source bifurcation section in the tunnel transition section. In the transition section of the tunnel, smoke tends to fluctuations at the tunnel roof and eddies at the side walls of the transition section. By increasing the wind speed at the entrance of the main tunnel and ramp, it is possible to significantly suppress smoke backflow and reduce temperature, thereby effectively controlling the scale of the tunnel fire.

**Keywords:** Bifurcated tunnel, Arched section, Fire ventilation, Smoke spread, Model experiment

### 1. INTRODUCTION

As a closed and narrow underground space, the structural characteristics of tunnels can cause fires to spread quickly and complicate evacuation and rescue, posing serious challenges to tunnel operation safety. With the development of underground transportation networks, the application of bifurcation tunnels in urban tunnels has become increasingly widespread. The merging point formed by the connection between the ramp and the main road in a branching tunnel can cause serious interference to the ventilation and smoke exhaust inside the tunnel. At the same time, vehicles near the branching point are susceptible to collision accidents due to factors such as obstructed visibility and lane changes (Wang et al., 2014). Therefore, it is necessary to study the diffusion law of fire smoke in bifurcation tunnels and develop reasonable smoke emission and control plans.

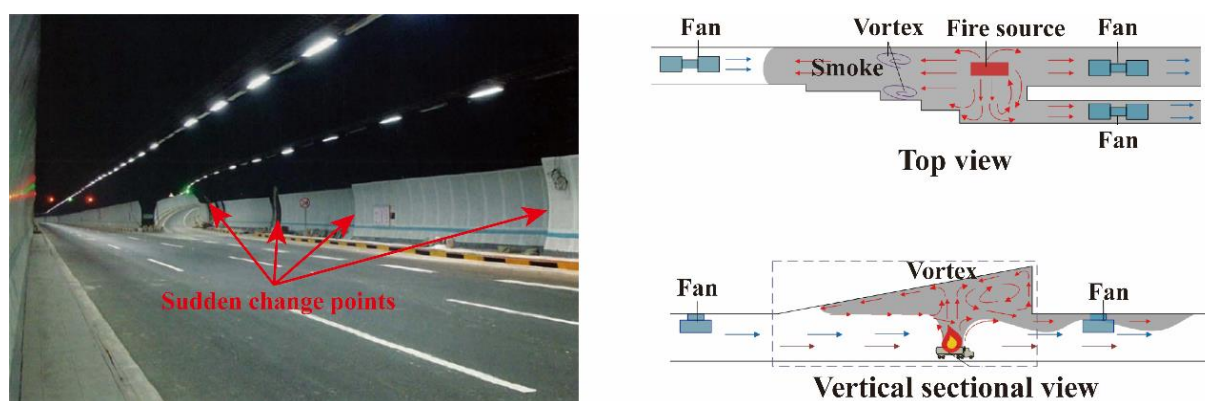
The adverse effects of tunnel fires mainly manifest as temperature and smoke diffusion. Kurioka et al. (2003) constructed a prediction model for the maximum temperature of the roof jet by conducting a series of scale tunnel fire model experiments on the distribution characteristics of fire temperature in tunnels. Through conducting inclined tunnel fire tests, Hu et al. (2013) found that the highest temperature at the top of inclined tunnels was significantly lower than that of horizontal tunnels, and constructed a temperature attenuation prediction model based on slope parameters. Yao et al. (2018) conducted small-scale experimental research on the impact of sealing at both ends of the tunnel on the maximum temperature rise and constructed a prediction model for the maximum temperature rise. Gao et al. (2021) conducted a study on the fire scenario of a comprehensive pipe gallery with one end closed, and systematically analyzed the distribution law of the highest temperature rise on the ceiling and

<sup>1</sup> Lecturer, Xin, Yunxiao, Ph.D. in Geological Engineering, Teacher, School of Highway, Chang'an University, Middle Section of Nan'er huan Road, Xi'an, China, hapoaaa@foxmail.com.

<sup>2</sup> Professor, Wang, Yaqiong, Ph.D. in Tunnel Engineering, Teacher, School of Highway, Chang'an University, Middle Section of Nan'er huan Road, Xi'an, China, ys08@gl.chd.edu.cn.

the characteristics of hot smoke flow. Huang et al. (2019, 2021) conducted fire tests on small-sized bifurcated tunnels under longitudinal ventilation and established segmented function-based maximum temperature prediction models and longitudinal temperature distribution models, respectively. Chen et al. (2020, 2023) conducted small-scale fire tests on bifurcation tunnels, analyzed the effect of ramp slope on the critical wind speed and maximum temperature rise response of the main tunnel, and constructed a roof maximum temperature rise prediction model based on slope parameters. Li et al. (2010) conducted experimental research on the smoke propagation law of tunnel fires in a 12-meter-long horizontal tunnel model, and proposed a calculation formula for the smoke reflux length of tunnel fires. Gao et al. (2022) conducted experimental research on inclined tunnel fires and found that as the slope of the tunnel increases, the highest temperature rise area at the top of the tunnel exhibits a clear downstream migration characteristic, and the increase in the highest smoke temperature demonstrates a decreasing trend. Lu et al. (2022a, 2022b) studied the effects of bifurcation angle and longitudinal position of the fire source on the temperature distribution at the top of a bifurcated tunnel fire through model experiments and numerical simulations, and constructed a prediction formula for the maximum temperature at the top of the tunnel to decay along the longitudinal direction. Li et al. (2021) studied the effect of the longitudinal position of the fire source on the maximum temperature of the ceiling using FDS, and found that under low longitudinal wind speed conditions, the maximum temperature of smoke in bifurcated tunnels was significantly lower than that in single point entry and exit tunnels, and the change in the longitudinal position of the fire source did not show a significant effect on the maximum temperature inside the tunnel. Lei et al. (2021) analyzed the influence of the location of the fire source on the longitudinal distribution characteristics of temperature in a bifurcated tunnel through physical model experiments, and found that when the fire source is located in the bifurcation area, the temperature of the smoke inside the tunnel is slightly lower than that when the fire source is far away from the bifurcation area.

Through a series of related studies on bifurcation tunnel fires, we have gained a certain understanding of the characteristics of smoke propagation in bifurcation tunnels and developed relevant smoke control plans. However, the existing research objects are mostly rectangular cross-section bifurcation tunnels, and the influencing parameters of bifurcation tunnel structures are mostly focused on changes in bifurcation angles and ramp slopes. Unlike rectangular-section bifurcation tunnels, the cross-section of arched-section bifurcation tunnels undergoes a sudden change in the bifurcation transition section. Therefore, smoke tends to generate eddies at structural changes during the spreading process, which makes it easier for smoke to gather at bifurcation points, as shown in Figure 1. Meanwhile, the sudden change at the top makes it difficult for the upstream airflow to fully cover the entire space inside the tunnel, resulting in difficulty in suppressing the backflow of smoke at the top of the bifurcation transition section. Therefore, it is necessary to study the spread characteristics of fire smoke in arched section bifurcation tunnels under different bifurcation forms and fire source positions, and propose reasonable fire smoke exhaust plans.

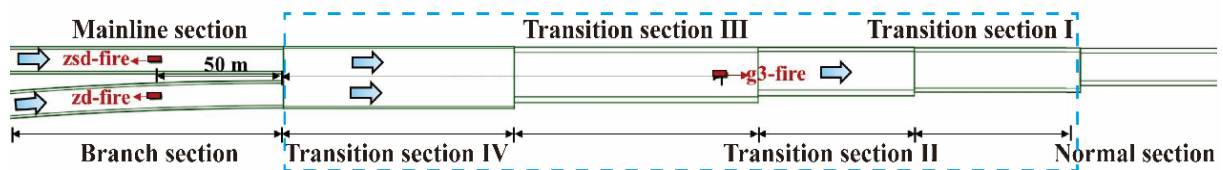


**Figure 1.** The sudden change in cross-section of the arched bifurcation tunnel.

## 2. MATERIAL AND METHODS

This article takes the bifurcation and merging area of the Shenzhen Dapeng Tunnel as the prototype to study the arch-shaped bifurcation tunnel. The direction of wind flow in the tunnel is consistent with the direction of traffic flow, with the main line of the tunnel consisting of 3 lanes and the branching area consisting of 2+2 lanes. According to the structural characteristics of the bifurcation tunnel, it can be divided into the normal section, transition section, main section, and branch section. The transition section is further divided into transition sections I-IV according to the size of the cross-section. The division of tunnel sections is shown in Figure 2. Due to the

different impacts of fires occurring in different locations, this article sets the fire source at the centerline of the main section, branch section, and transition section III.

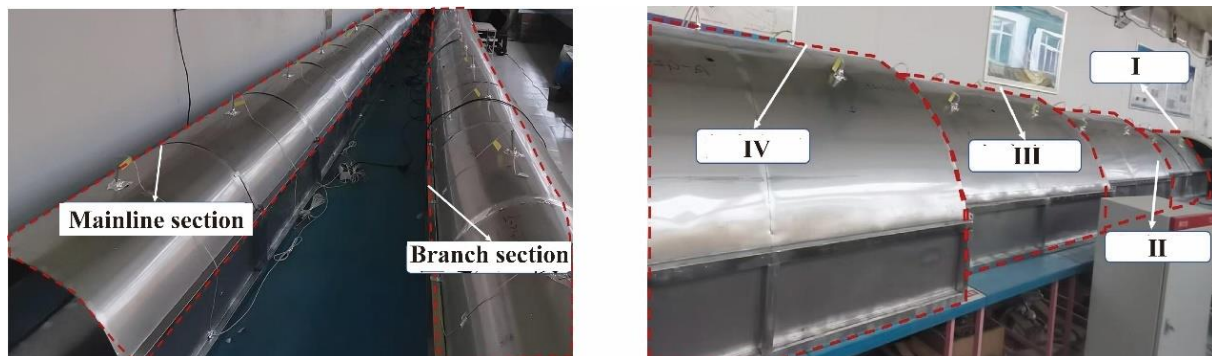


**Figure 2.** Schematic diagram of tunnel physical model segments.

To observe the actual effects of fire temperature and smoke diffusion in bifurcation tunnels, a physical experimental model with a similar scale of 1:12 was built for the merging section of the bifurcation tunnels. The model was simplified according to the principle of similarity and the characteristics of the tunnel prototype. The specific dimensions of the physical model are shown in Table 1. To resist the high temperature generated by fire tests, the main structure of the tunnel model is made of stainless-steel plates, and observation windows are set on the side walls for easy observation. The experimental model adopts a modular design and is assembled from multiple tunnel components. Each joint of the experimental model is sealed, and the layout effect of the model is shown in Figure 3. A set of temperature acquisition modules is installed every 1 meter in the model to collect the temperature inside the tunnel. At the same time, a laser with a power of 200 MW and a wavelength of 532 nm is selected to observe the diffusion pattern of smoke inside the tunnel.

**Table 1.** Dimensional parameters of the tunnel model.

Section	Lane number	Length(m)	Width(m)	Heigh(m)
Mainline	2	15	0.82	0.6
Branch	2	2	0.82	0.6
TransitionI	3	2	1.33	0.73
Transition II	3	2	1.46	0.82
Transition III	3	2	1.67	0.91
Transition IV	4	2	1.86	0.98



**Figure 3.** Tunnel fire experiment model.

Install variable frequency axial flow fans at the upstream center of the entrance section of the tunnel model to provide different wind speeds required for testing. The required wind speeds for the experiment are 0.43, 0.72, and 0.87 m/s, respectively, and their corresponding actual wind speeds are 1.5, 2.5, and 3.0 m/s. The actual heat release rate of the simulated tunnel fire source is 20 MW. According to the similarity criterion, the heat release rate of the model test fire source can be converted to 40.09 kW. The test fire source uses 99% anhydrous ethanol as fuel, supplemented by smoke cake as a smoke tracer substance. According to the heat calculation, when the size of the test tray is determined to be 27 × 35 cm and the height of the ethanol liquid surface is 1 cm, the corresponding heat release rate is 40.31 kW, which can meet the test requirements. The propagation characteristics of smoke generated by fire sources at different locations under different wind speed conditions can be obtained through physical model experiments.



### 3. RESULTS AND DISCUSSION

#### 3.1. Smoke spread characteristics of mainline section fires

Figure 4 shows the flame and smoke propagation patterns at the entrance section of the main tunnel under different wind speed conditions when the fire source is located on the main section of the tunnel. The high-temperature smoke released by the combustion of the fire source rises due to the buoyancy effect of heat, forming vertical smoke. When the wind speed is 0.43 m/s, the inertia force of longitudinal ventilation is small, and the thermal buoyancy force plays a dominant role. The smoke impacts the top and spreads upstream and downstream of the fire source, resulting in smoke backflow. When the wind speed is 0.72 m/s, the inertial force gradually becomes dominant, and the smoke mainly spreads downstream. When the wind speed is 0.87 m/s, the inertial force increases significantly, and there is no obvious reverse flow of smoke, and the concentration of smoke decreases significantly. The above phenomenon indicates that as the longitudinal wind speed increases, the effect of the inertial force of the airflow gradually becomes higher than that of the thermal buoyancy force, and the phenomenon of smoke backflow continues to decrease.



Figure 4. The spread of smoke from a fire in the mainline section.

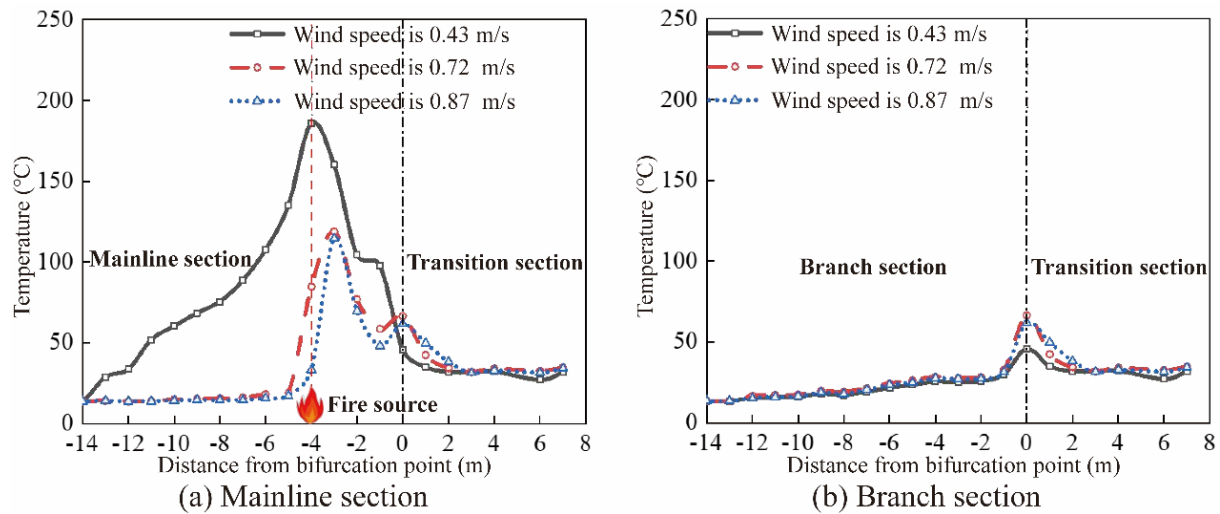


Figure 5. Temperature distribution at the top of the tunnel under the fire in the mainline section.

Figure 5 demonstrates the temperature distribution at the top of the tunnel under different wind speed conditions when the fire source is located on the main section of the tunnel. As the wind speed increases, the temperature near the fire source decreases significantly, and the location of the highest temperature gradually shifts downstream. The highest temperatures corresponding to wind speeds of 0.43, 0.72, and 0.87 m/s are 186.0, 118.9, and 114.5 °C, respectively. When the wind speed is 0.43 m/s, the temperature upstream of the fire source increases significantly, indicating a significant phenomenon of smoke backflow; When the wind speed increases to 0.72 m/s, the phenomenon of smoke backflow upstream of the fire source disappears; When the wind speed further increases to 0.87 m/s, there is no significant change in the temperature upstream of the fire source, and the smoke no longer flows back. When the smoke spreads to the transition section, since the cross-section of the transition section is 2.5 times that of the main section, the smoke disperses within the transition section, resulting in a significant decrease in temperature. As the wind speed increases, smoke can enter the transition section faster. The expansion of the cross-section will lead to a decrease in wind speed in the transition section, leading to smoke accumulating in the transition section. Therefore, the temperature in the transition section will increase slightly with an increase in tunnel wind speed. Under different wind speed conditions, the top temperature of the ramp side reaches its maximum value at the bifurcation point. This is because there is a structural change at the bifurcation



point, with the height of the transition section IV being 0.98 m and the height of the branch section being 0.60 m. Smoke accumulates at the top of the transition section IV, leading to a significant increase in temperature at this point. Due to the low wind speed inside the ramp, the smoke accumulated in the transition section IV gradually flows back into the ramp, leading to the temperature at the top of the ramp to rise. Furthermore, as the wind speed increases, the smoke is brought into the transition section faster, leading to a sudden decrease in airflow velocity within the transition section. This accelerates the accumulation of smoke, leading to more smoke flowing into the ramp and exacerbating the backflow of smoke on the ramp. As a result, the temperature at the top of the ramp demonstrates an upward trend.

### 3.2. Smoke spread characteristics of branch section fires

Figure 6 shows the flame and smoke propagation patterns under different working conditions when the fire is located on the branch section. When the wind speed is 0.43 m/s, the smoke rises and impacts the top, and then spreads upstream and downstream of the fire source, forming a phenomenon of smoke backflow; When the wind speed is 0.72 m/s, the smoke generated by the fire source mainly spreads downstream of the fire source, and a small part of the smoke still shows backflow; When the wind speed further increases to 0.87 m/s, there is no significant backflow of smoke and the smoke concentration decreases significantly. The performance under this condition is similar to the phenomenon when the fire source is located in the main tunnel. As the longitudinal wind speed increases, the inertial force of longitudinal ventilation gradually plays a dominant role in the competition with thermal buoyancy, and the phenomenon of smoke backflow gradually decreases.

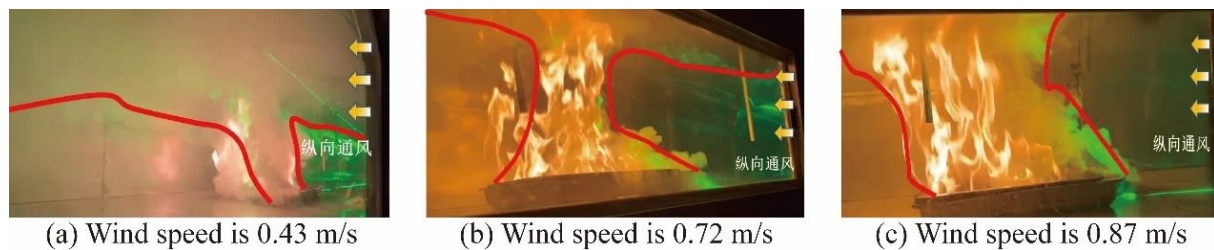


Figure 6. The spread of smoke from a fire in the branch section.

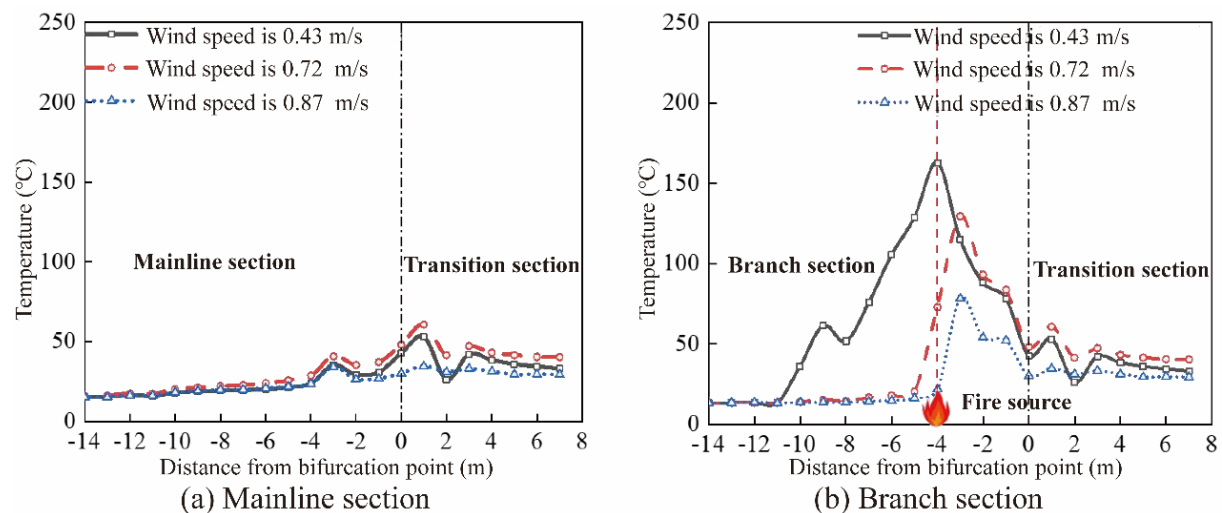


Figure 7. Temperature distribution at the top of the tunnel under the fire in the branch section.

Figure 7 shows the temperature point lines at the top of the tunnel under different wind speed conditions when the fire source is located on the branch section. Under the influence of different wind speeds, the top temperature reaches its maximum near the bifurcation point. Due to the structural mutation at the bifurcation point, smoke will accumulate at the top of the transition section IV. The wind speed inside the main tunnel is low, and the smoke accumulated in the transition section IV gradually flows back into the main section, causing the top temperature to rise. The change in wind speed within the branch section affects the smoke in the transition section IV, indirectly affecting the backflow phenomenon within the branch section. As the wind speed increases, the top temperature near the fire source decreases significantly, and the highest temperature shifts downstream of the fire source. The corresponding highest temperatures at wind speeds of 0.43, 0.72, and 0.87 m/s are 163.0, 129.6, and 78.4 °C, respectively. When the wind speed is 0.43 m/s, the temperature upstream of the fire source increases significantly,

indicating a significant phenomenon of smoke backflow at this time. Due to the curved characteristics of the ramp hindering the backflow of smoke, smoke accumulates 9 meters upstream of the fire source, resulting in a significant increase in temperature. When the wind speed increases to 0.72 m/s, the temperature upstream of the fire source is very low, indicating that only a small portion of the smoke is flowing back. When the wind speed further increases to 0.87 m/s, there is no significant change in the temperature upstream of the fire source, indicating no obvious smoke backflow. After entering the transition section, the flue gas experiences a significant decrease in temperature due to the increased cross-section of the transition section. When the wind speed increases to 0.72 m/s, smoke enters the transition section and accumulates, causing a slight increase in temperature inside the transition section. When the wind speed increases to 0.87 m/s, the smoke enters the transition section faster and is quickly carried away without obvious smoke accumulation, resulting in a decrease in temperature in the transition section.

### 3.3. Smoke spread characteristics of transition section fires

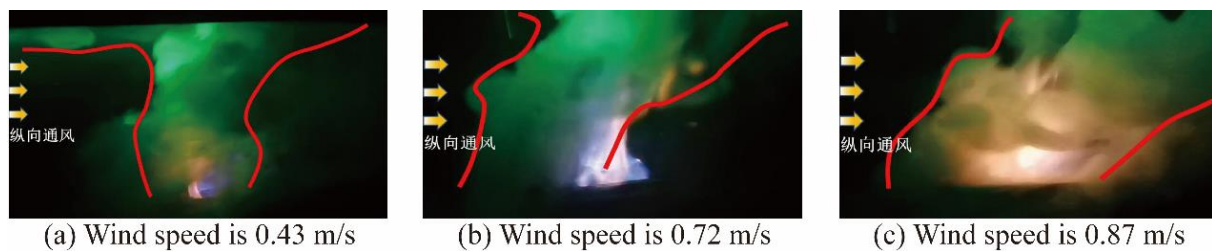


Figure 8. The spread of smoke from a fire in the transition section.

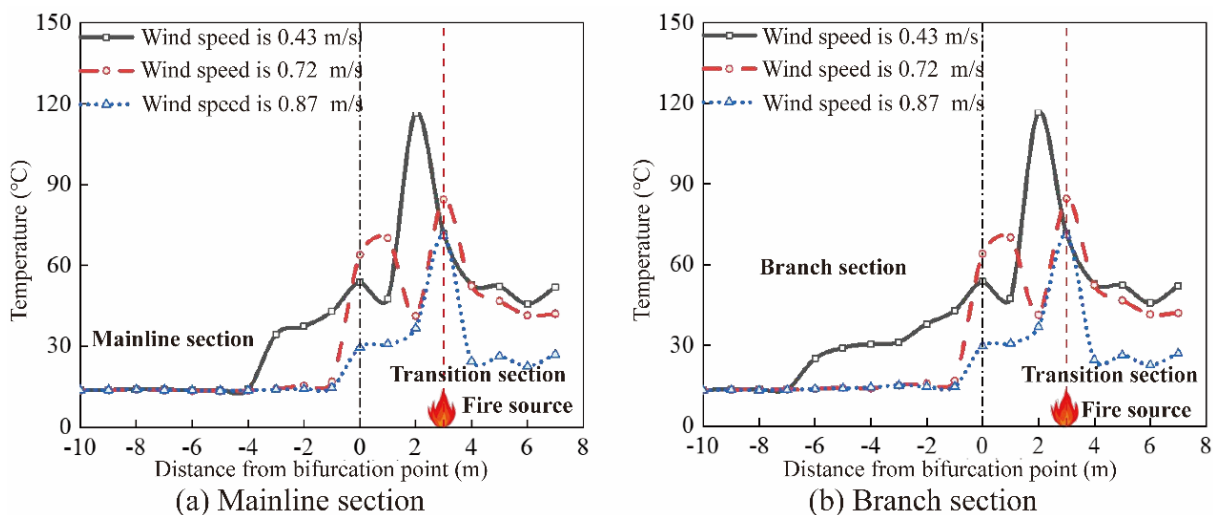


Figure 9. Temperature distribution at the top of the tunnel under the fire in the transition section.

Figure 8 shows the flame and smoke propagation patterns under different wind speed conditions when the fire source is located in the transition section, and Figure 9 shows the temperature point line diagram at the top of the tunnel under different wind speed conditions. When the wind speed is 0.43 m/s, the smoke generated by the fire source impacts the top and spreads upstream and downstream of the fire source, resulting in a significant backflow of smoke. When the wind speed is 0.72 m/s, some smoke flows backwards; When the wind speed further increases to 0.87 m/s, the smoke mainly spreads downstream of the fire source. As the wind speed increases, the distribution of smoke in the transition section undergoes significant changes. When the wind speed is 0.43 m/s, the smoke backflow area is not limited to the transition section, and there is smoke backflow in both the main section and the branch section. When the wind speed increases to 0.72 m/s, the reverse flow of smoke is mainly concentrated in the transition section, and the temperature increases significantly at the bifurcation point. When the wind speed is high, it is difficult for smoke to flow back into the mainline and branch sections, and the sudden contraction of the cross-section causes smoke to accumulate in the transition section. After the wind speed further increases to 0.87 m/s, the reverse flow of smoke is concentrated in the transition section, and the temperature is only higher at the fire source. The further increase in wind speed significantly enhances the longitudinal ventilation inertia force, which can quickly discharge smoke, thereby suppressing smoke backflow and reducing smoke accumulation at the top, resulting in a significant decrease in top temperature. Compared with the fire source located in the main section and the branch section, it is more difficult to control the smoke when the fire source is located in the

transition section. When the wind speed reaches 0.87 m/s, there is still a small amount of smoke flowing backwards in the transition section. This is because the cross-section of the tunnel transition section suddenly expands, causing the high-speed airflow generated by longitudinal ventilation to mainly concentrate in the lower part of the transition section, with lower longitudinal wind speed at the top. The smoke generated by the fire source cannot be quickly carried downstream and accumulates at the top, resulting in smoke backflow.

#### 4. CONCLUSION

(1) When the fire source is located on the mainline or ramp of the tunnel, increasing the longitudinal wind speed effectively eliminates upstream smoke backflow and reduces peak temperatures, thereby controlling fire scale. This highlights the importance of equipping tunnels with variable-frequency axial fans in practice.

(2) When the fire source is located in the transition section, sudden changes in cross-section cause airflow stratification and the formation of local low-speed zones, resulting in smoke accumulation and backflow. To address this, tunnel designs should incorporate smooth geometric transitions or supplementary ceiling-level jet fans in transition sections to minimize stagnant zones.

(3) Structural mutations at bifurcation points intensify turbulence and promote vortex formation, leading to elevated temperatures at junctions and sidewalls. To mitigate these effects, designers should consider rounded structural transitions, smoke barriers, or targeted extraction vents at bifurcation points to interrupt vortex circulation and facilitate smoke removal.

(4) Increasing wind speed at the entrances of both the main tunnel and ramp is an effective strategy to suppress smoke backflow and limit temperature rise. Operationally, tunnel emergency response plans should prioritize synchronized ventilation control across both the mainline and ramps, with automatic detection systems triggering rapid fan speed adjustments.

Overall, the findings suggest that practical fire safety in arched bifurcation tunnels requires a combination of proactive structural design, such as smoother transitions and strategically placed extraction points, and robust dynamic ventilation control systems capable of adapting airflow distribution in real time.

#### 5. ACKNOWLEDGMENTS

This study was financially supported by the Fundamental Research Funds for the Central University, CHD (No. 300102214107), Natural Science Basis Research Plan in Shaanxi Province of China (No. 2024JC-YBQN-0320).

#### 6. REFERENCES

- [1] Wang, X, Song, Y, Huang, H, et al. (2014) Analysis of risk factors for suburban highways using hierarchical negative binomial model. *China Journal of Highway and Transport* 27(1), 100-106.
- [2] Kurioka, H, Oka, Y, Satoh, H, et al. (2003) Fire properties in near field of square fire source with longitudinal ventilation in tunnels. *Fire Safety Journal* 38(4), 319-340.
- [3] Hu, L, Chen, L, Wu, L, et al. (2013) An experimental investigation and correlation on buoyant gas temperature below ceiling in a slopping tunnel fire. *Applied Thermal Engineering* 51(s1-2), 246-254.
- [4] Yao, Y, He, K, Min, P, et al. (2018) Maximum gas temperature rise beneath the ceiling in a portals-sealed tunnel fire. *Tunnelling and Underground Space Technology* 80, 10-15.
- [5] Gao, Z, Li, L, Zhong, W, et al. (2021) Characterization and prediction of ceiling temperature propagation of thermal plume in confined environment of common services tunnel. *Tunnelling and Underground Space Technology* 110, 103714.
- [6] Huang, Y, Li, Y, Li, J, et al. (2019) Experimental investigation on maximum gas temperature beneath the ceiling in a branched tunnel fire. *International Journal of Thermal Sciences* 145, 105997.
- [7] Huang, Y, Li, Y, Li, J, et al. (2021) Experimental study on the temperature longitudinal distribution induced by a branched tunnel fire. *International Journal of Thermal Sciences* 170, 107175.
- [8] Chen, C, Nie, Y, Zhang, Y, et al. (2020) Experimental investigation on the influence of ramp slope on fire behaviors in a bifurcated tunnel. *Tunnelling and Underground Space Technology* 104, 103522.
- [9] Chen, C, Lu, T, Zhang, Y, et al. (2023) Experimental study on temperature profile and critical velocity in bifurcated tunnel fire with inclined transverse cross-passage. *International Journal of Thermal Sciences* 186, 108120.
- [10] Li, Y, Lei, B, Ingason, H. (2010) Study of critical velocity and backlayering length in longitudinally ventilated tunnel fires. *Fire Safety Journal* 45(6-8), 361-370.

- [11] Gao, Z, Li, L, Sun, C, et al. (2022) Effect of longitudinal slope on the smoke propagation and ceiling temperature characterization in sloping tunnel fires under natural ventilation. *Tunnelling and Underground Space Technology* 123, 104396.
- [12] Lu, X, Weng, M, Liu, F, et al. (2022a) Study on smoke temperature profile in bifurcated tunnel fires with various bifurcation angles under natural ventilation. *Journal of Wind Engineering and Industrial Aerodynamics* 225, 105001.
- [13] Lu, X, Weng, M, Liu, F, et al. (2022b) Effect of bifurcation angle and fire location on smoke temperature profile in longitudinal ventilated bifurcated tunnel fires. *Tunnelling and Underground Space Technology* 127, 104610.
- [14] Li, Y, Zhang, X, Sun, X, et al. (2021) Maximum temperature of ceiling jet flow in longitudinal ventilated tunnel fires with various distances between fire source and cross-passage. *Tunnelling and Underground Space Technology* 113, 103953.
- [15] Lei, P, Chen, C, Zhang, Y, et al. (2021) Experimental study on temperature profile in a branched tunnel fire under natural ventilation considering different fire locations. *International Journal of Thermal Sciences* 159, 106631.

## EFFECTS OF GUIDANCE FACILITIES ON DRIVING SAFETY IN ROAD TUNNELS DURING FOGGY WEATHER

Liankun Xu<sup>1</sup>, Hehua Zhu<sup>2</sup>, Ruoquan Fang<sup>3</sup>, Yi Shen<sup>4\*</sup>, Tao Liu<sup>5</sup>, Shouzhong Feng<sup>6</sup>

**Abstract:** The traffic accident rate increases significantly on foggy days. Typically, the light intensity within tunnels is significantly lower than outside, resulting in poorer visibility. The tunnel sidewalls become indistinct, making it challenging to discern the tunnel's alignment. Although the self-luminous visual guidance facilities have been adopted in some tunnels, their effects and setting methods have not been studied in depth. Given this, thirty subjects were invited to conduct a virtual reality driving test to investigate the impact of the location and color of visual guidance facilities on driving safety and comfort. In this process, driving data and physiological data were collected, and subjective evaluation questionnaires were conducted. The results show that the self-luminous visual guidance facilities can make the alignment of tunnel clearer, and can improve the driver's sense of speed in foggy weather. Moreover, the drivers' nervousness is effectively alleviated. The guidance facilities located at the bottom of the sidewall are less disruptive than those located in the middle of the sidewall. Compared with the red guidance facilities, the yellow guidance facilities can relieve the driver's tension more effectively.

**Keywords:** Road tunnel, Guidance facilities, Foggy weather, Driving safety

### 1. INTRODUCTION

During foggy weather, the rates of road departure (Das et al, 2019) and rear-end (Li et al, 2023) accidents increase significantly, and the injury and fatality rates of traffic accidents related to fog are notably higher (Sadeghi & Goli, 2024). To enhance traffic safety in foggy conditions, some scholars have conducted research on the light source characteristics of lamps (Jin et al. 2015; Dong et al, 2020). There are also some studies that have explored the role of advanced driver-assistance systems and intelligent transportation facilities in foggy weather (Guan et al. 2022; Zhai et al. 2023).

The semi-enclosed structure of tunnels makes traffic accidents occurring in them often more severe than those on open roads (Liu et al., 2025). Enhancing the brightness inside tunnels and setting up traffic safety facilities are both important measures to improve tunnel traffic safety. Increasing the brightness inside tunnels can improve visibility, but it requires a high cost of electricity (Zhao et al., 2022). In comparison, traffic safety facilities, due to their low cost and high efficiency, are attracting increasing attention from scholars.

<sup>1</sup> PhD, Xu Liankun, Civil Engineering, Department of Geotechnical Engineering, College of Civil Engineering, Tongji University, 1239 Siping Road, Shanghai, 200092, China, xuliankun@tongji.edu.cn

<sup>2</sup> Prof., Zhu Hehua, Underground Space, State Key Laboratory for Disaster Reduction in Civil Engineering, Tongji University, Shanghai, 200092, China, zhuhehua@tongji.edu.cn

<sup>3</sup> Mr., Ruoquan Fang, Underground Space, Traffic Engineering Construction Bureau of Jiangsu Province, Nanjing 210004, China, 736526263@qq.com

<sup>4</sup> Dr, Shen Yi, Underground Space, State Key Laboratory for Disaster Reduction in Civil Engineering, Tongji University, Shanghai, 200092, China, shenyi@tongji.edu.cn

<sup>5</sup> PhD, Liu Tao, Civil Engineering, Department of Geotechnical Engineering, College of Civil Engineering, Tongji University, 1239 Siping Road, Shanghai, 200092, China, lta@tongji.edu.cn

<sup>6</sup> Prof., Feng Shouzhong, Underground Space, State Key Laboratory for Disaster Reduction in Civil Engineering, Tongji University, Shanghai, 200092, China, fsz63@vip.163.com



During foggy weather, the tunnel sidewalls become blurred, and the effectiveness of non-self-luminous visual guidance facilities such as reflective rings is weakened (He et al, 2024). It is difficult to identify the tunnel alignment, and accidents involving collisions with the sidewalls are more likely to occur. Although visual guidance facilities have been applied in some tunnels, their effects have not been studied in depth. This paper investigates the impact of visual guidance facilities with different installation heights and colors on driving safety in foggy tunnels through virtual reality driving experiments.

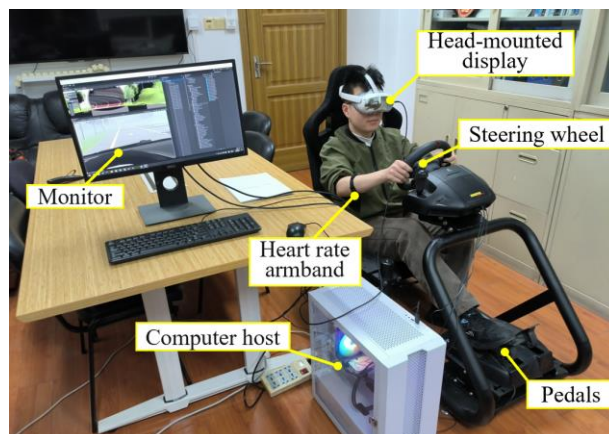
## 2. MATERIAL AND METHODS

### 2.1. Subjects

This experiment recruited a total of 30 participants with driving licenses, including 24 males and 6 females, with ages ranging from 19 to 28 years old (mean = 24.5 years, standard deviation = 2.11 years). Their driving experience ranged from 1 to 8 years (mean = 4.2 years, standard deviation = 1.92 years). To avoid the influence of external factors, participants were not allowed to engage in vigorous exercise within 1 hour before the experiment.

### 2.2. Apparatus and software

The devices utilized in the test are depicted in **Figure 1**, including a head-mounted display, a driving simulator, a computer, and a heart rate armband. The head-mounted display was a Pico 4 Enterprise, which featured a 105° field of view, a 90 Hz refresh rate, and a resolution of 2160×2160 pixels per eye. It was capable of collecting eye movement data, with an acquisition frequency of 100 Hz for eye movement data. The driving simulator employed the “Logitech MOMO Racing Force” steering wheel and pedals, which provided driving data such as speed at a rate of 10 Hz. A CYCPLUS H1 heart rate armband output real-time heart rate at 1 Hz. The VR experimental scene had been modeled using 3ds Max and then imported into the Unity platform for lighting rendering and experimental interaction.



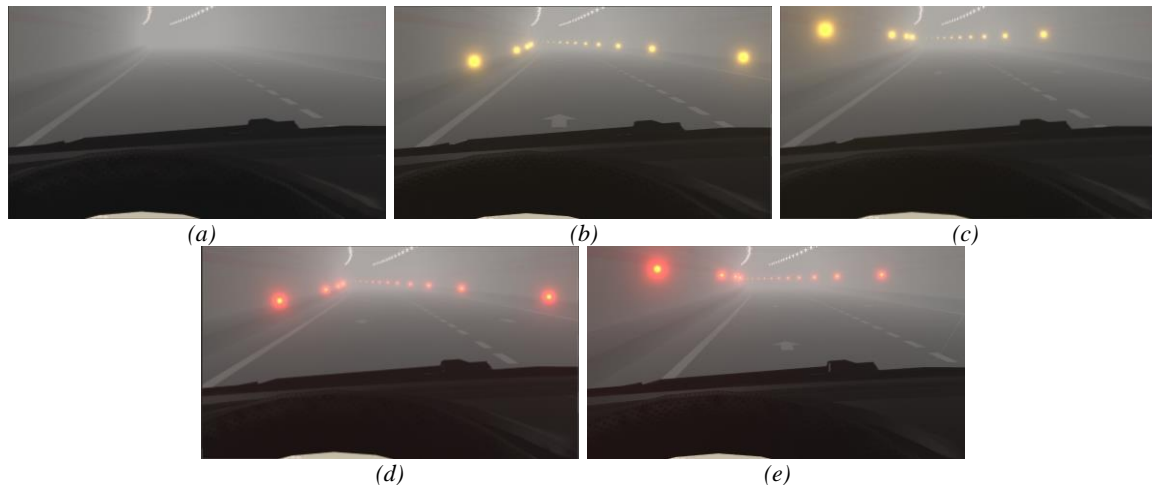
*Figure 1. Test apparatus*

### 2.3. Scenarios

The test scenarios included a 1200-meter tunnel and 500-meter open road sections before and after it. Both had single-direction dual lanes that were 3.75 meters wide.

The fog concentration inside and outside the tunnel was the same. The fog concentration parameter was determined based on the visibility threshold where participants could barely see the outline of a red vehicle parked 250 meters away outside the tunnel.

The modeling results of the interior zone of the tunnel in each scenario are shown in **Figure 2**. Scenario (a) was the control group without guidance facilities (Abbreviated as CG). Scenarios (b) and (c) featured yellow guidance facilities installed at the bottom and middle of the tunnel sidewalls, respectively (Abbreviated as YB and YM). Scenarios (d) and (e) had red guidance facilities installed at the bottom and middle of the tunnel sidewalls, respectively (Abbreviated as RB and RM).



**Figure 2.** The interior zone of the tunnel: (a) Control group (CG); (b) Yellow bottom (YB); (c) Yellow middle (YM); (d) Red bottom (RB) (e) Red middle (RM).

## 2.4. Procedures

Before the formal experiment, a brief five-minute training session was arranged for the participants to enable them to get accustomed to the operation of the head-mounted display and the driving simulator. Subsequently, the participants engaged in a ten-minute free driving session as a pre-experiment, which served the dual purpose of allowing them to become familiar with the simulator's operation and verifying the proper functioning of the equipment.

During the formal experiment, participants initiated their driving 500 meters outside the tunnel in each scenario. They then proceeded into a 1200-meter-long tunnel and halted 200 meters after exiting the tunnel to complete a set of experiments. After completing each set of experiments, participants took a five-minute break. They then moved on to the next set of experiments until all five sets were completed. The order of the experimental scenarios was randomized.

After all experiments were completed, each participant needed to complete a questionnaire, which included subjective evaluations of their driving experience, basic information (such as driving experience, age, and gender) and the degree of realism of the virtual environment (including tunnels, fog, and guiding facilities) on a scale from 1 (not realistic) to 10 (very realistic).

The questions related to driving experience in the questionnaire are as follows:

(1) Level of the clarity of tunnel alignment in scenarios (b) (c) (d) and (e). (-1: More blurred than the control group; 0: Similar to the control group; 1 to 4: Higher numbers correspond to greater clarity relative to the control group.)

(2) The effect of alleviating tension in scenarios (b) (c) (d) and (e). (-1: More nervous than the control group; 0: Similar to the control group; 1 to 4: Higher numbers correspond to more relaxed relative to the control group.)

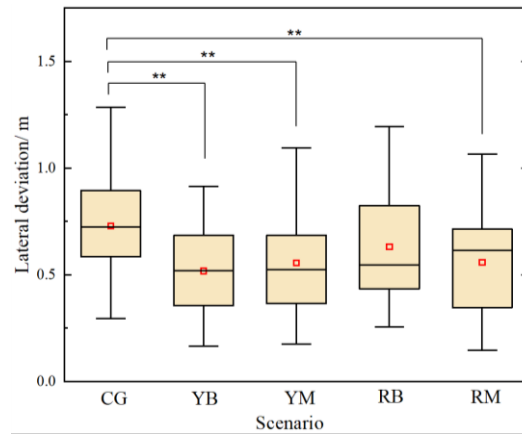
(3) Level of disturbance caused by guiding facilities in scenarios (b) (c) (d) and (e). (0: No interference; 1: Negligible; 2: Minor interference; 3: Major interference; 4: Severe interference; 5: Intolerable).

## 3. RESULTS AND DISCUSSION

### 3.1. Lateral deviation

The maximum lateral offset within the central 600 meters of the tunnel is used to reflect the driver's lane-keeping performance inside the tunnel (Wang et al, 2024). The statistical results are shown in **Figure 3**. The average lateral deviations for the 30 participants across the five scenarios are 0.73m, 0.52m, 0.56m, 0.63m and 0.56m, respectively. The results by the ANOVA method show significant differences among the groups ( $F = 3.397$ ,  $p = 0.011$ ). Subsequent pairwise comparisons reveal significant differences between Scenario CG and each of Scenario YB ( $p = 0.001$ ), Scenario YM ( $p = 0.008$ ) and Scenario RM ( $p = 0.009$ ). No significant differences are found among the remaining groups. Although there is no significant difference between Scenario RB and Scenario CG, the average deviation of Scenario RB is also smaller than that of Scenario CG.

Setting up visual guiding facilities can effectively reduce the maximum lateral deviation. By comparing the mean values of the lateral deviation, it can be seen that the yellow guidance facilities located at the bottom of the sidewall (Scenario YB) have a better effect on improving lane-keeping ability.



**Figure 3.** Maximum lateral deviation inside the tunnel (\*:  $p < 0.05$ ; \*\*:  $p < 0.01$ ; \*\*\*:  $p < 0.001$ )

### 3.2. Gaze point distribution

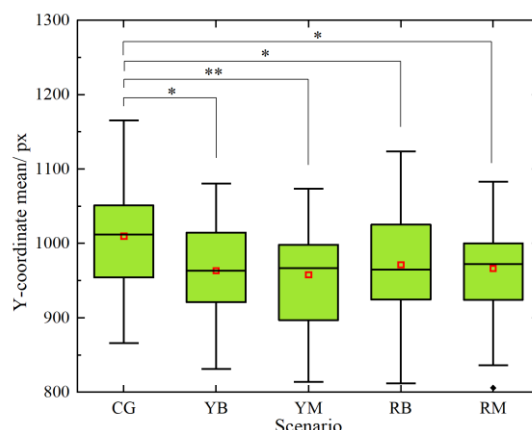
The screenshots used to record eye movements are  $1500\text{px} \times 1500\text{px}$  in size, with the origin located at the top-left corner of the screen. The X-axis extends horizontally to the right, and the Y-axis extends vertically downward. The mean values of gaze point distribution characteristics within the middle 600 meters of the tunnel for the 30 participants are shown in **Table 1**, which reflect the spatial allocation of their attention. For the average values of the X-coordinates, the standard deviations of the X-coordinates and the Y-coordinates, there are no significant differences among the five scenarios. But for the average values of the Y-coordinates, the results by the ANOVA show significant differences among the groups ( $F = 2.443$ ,  $p = 0.049$ ).

**Table 1.** The gaze point distribution characteristics of the experimenters

Indicator	Scenario	Mean (px)	Significance
Average values of the X-coordinates	Scenario CG	924.5	0.909
	Scenario YB	919.7	
	Scenario YM	913.9	
	Scenario RB	917.5	
	Scenario RM	917.9	
Standard deviations of the X-coordinates	Scenario CG	24.94	0.950
	Scenario YB	24.95	
	Scenario YM	22.34	
	Scenario RB	23.82	
	Scenario RM	24.95	
Average values of the Y-coordinates	Scenario CG	1009.8	0.049*
	Scenario YB	963.3	
	Scenario YM	957.8	
	Scenario RB	971.1	
	Scenario RM	966.3	
Standard deviations of the Y-coordinates	Scenario CG	24.30	0.393
	Scenario YB	22.43	
	Scenario YM	22.27	
	Scenario RB	19.07	
	Scenario RM	21.02	

As shown in **Figure 4**, subsequent pairwise comparisons reveal significant differences between Scenario CG and each of Scenario YB ( $p = 0.014$ ), Scenario YM ( $p = 0.006$ ), Scenario RB ( $p = 0.041$ ) and Scenario RM ( $p = 0.022$ ). No significant differences are found among the remaining groups. Compared with Scenario CG, the mean

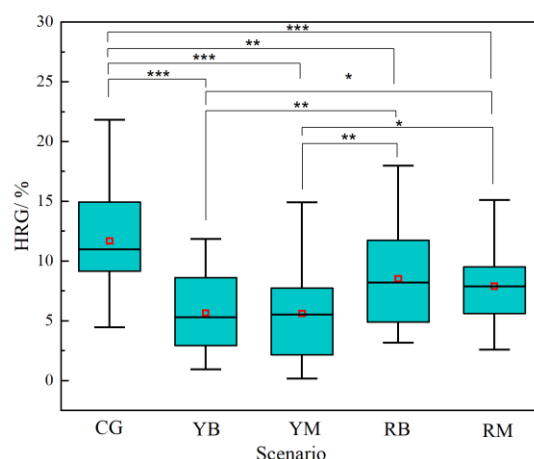
Y-coordinates of the gaze points decrease in the scenarios with guiding facilities. Setting up visual guidance facilities can raise the gaze point positions, making the average gaze points farther away. This might be explained by the fact that the tunnel alignment becomes clearer, reducing driver tension and shifting their focus from the immediate vicinity to a more distant view.



**Figure 4.** Y-coordinate mean of the gaze point for the participants (\*:  $p < 0.05$ ; \*\*:  $p < 0.01$ ; \*\*\*:  $p < 0.001$ )

### 3.3. Heart rate growth

When driving experience increases workload and stress, drivers' heart rate rise significantly (Feng et al, 2018). The average heart rate growth rate (HRG) within the middle 600 meters of the tunnel (i.e., from 300 m to 900 m after entering the tunnel) is adopted as a physiological indicator to assess the level of tension inside the tunnel. The results are shown in **Figure 5**. The average HRG for the 30 participants across the five scenarios are 11.7%, 5.7%, 5.6%, 8.5% and 7.9%, respectively. The results by the ANOVA method show significant differences among the groups ( $F = 13.515$ ,  $p < 0.001$ ).

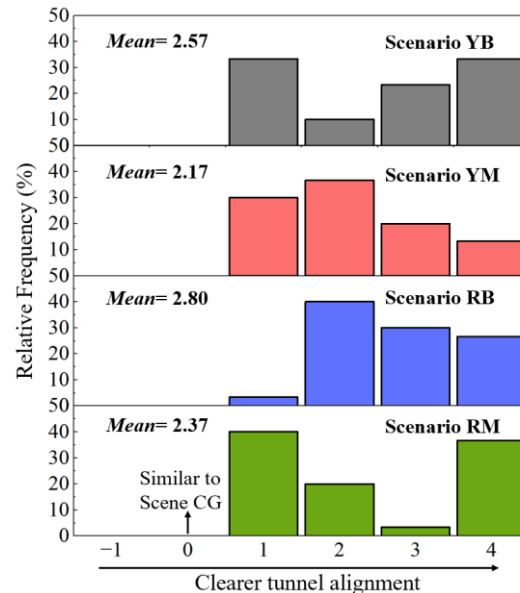


**Figure 5.** HRG inside the tunnel (\*:  $p < 0.05$ ; \*\*:  $p < 0.01$ ; \*\*\*:  $p < 0.001$ )

Subsequent pairwise comparisons reveal significant differences between Scenario CG and each of Scenario YB ( $p < 0.001$ ), Scenario YM ( $p < 0.001$ ), Scenario RB ( $p = 0.001$ ) and Scenario RM ( $p < 0.001$ ). Significant differences are also found between Scenario YB and each of Scenario RB ( $p = 0.003$ ) and Scenario RM ( $p = 0.021$ ), as well as between Scenario YM and each of Scenario RB ( $p = 0.003$ ) and Scenario RM ( $p = 0.020$ ). No significant differences are found among the remaining groups. Setting up visual guidance facilities can reduce the drivers' HRG, and the effect of yellow guiding facilities is better than that of red guiding facilities. The location of the guiding facilities has little influence on HRG.

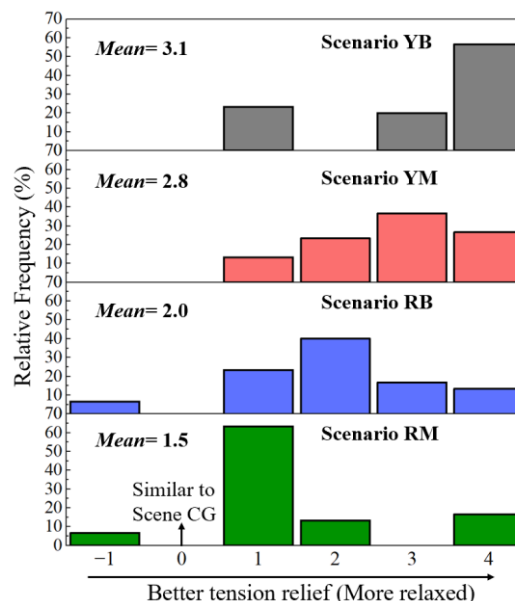
### 3.4. Subjective feeling

Questionnaires are administered to investigate the impact of setting up guiding facilities on the clarity of tunnel alignment, with the results shown in **Figure 6**. All the test subjects believe that the guiding facilities can improve the clarity of the tunnel alignment. Judging from the average value of subjective evaluation, the effects of the four guiding facilities are not much different. The effect of the red guiding facilities in improving the clarity of the tunnel alignment is slightly better than that of the yellow guiding facilities, and the effect of the guiding facilities located at the bottom of the sidewall is slightly better than that in the middle of the sidewall.



**Figure 6.** Subjective evaluation of the clarity of tunnel alignment

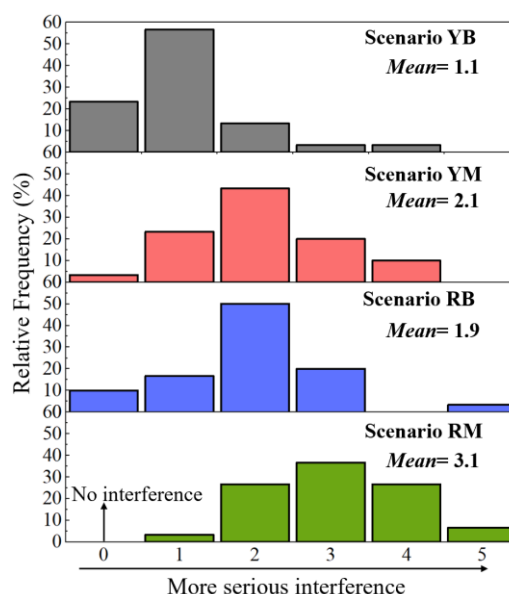
The subjective evaluation of the effect of four guiding facilities in relieving tension is shown in the **Figure 7**. From the average values of subjective evaluation, all four guiding facilities can alleviate the tension of driving in the tunnel on foggy days, but the effects are different. The effect of the yellow guiding facilities in alleviating tension is obviously better than that of the red guiding facilities, with those located at the bottom of the sidewall being the most effective. It is worth noting that some testers believe that the red guiding facilities have intensified the tension because red represents warning and danger.



**Figure 7.** Subjective evaluation of the effect of alleviating tension



The subjective evaluation of degree of visual interference of the four guiding facilities is shown in the **Figure 8**. The degree of visual interference in Scenario RM is the highest, while that in Scenario YB is the lowest. The interference degree of the red guiding facilities is higher than that of the yellow ones. The guiding facilities set in the middle of the sidewall cause more severe interference than those at the bottom of the sidewall. This is because the red guiding facilities are too conspicuous to be ignored. The guiding facility located in the middle of the sidewall is basically at the same level as the driver's line of sight. When the driver passes through this facility, the flickering effect is more obvious.



**Figure 8.** Subjective evaluation of degree of visual interference

## 4. CONCLUSIONS

Setting up visual guiding facilities can effectively enhance the clarity of tunnel alignment and reduce the maximum lateral deviation during vehicle travel. These facilities can also help drivers focus their gaze further ahead, lower the heart rate increase of drivers, and alleviate the tension experienced while driving in tunnels during foggy conditions. Among the four types of guiding facilities tested in this study, the yellow guiding facilities located at the bottom of the sidewall were found to be the most effective in relieving tension and causing the least visual interference.

## 5. ACKNOWLEDGEMENTS

The authors wish to acknowledge the sponsorship from the Research on Key Technologies for the Planning, Design, and Construction of the S7 Shanghai-Chongming West River-Crossing Tunnel (Y202445) and Research Fund of State Key Laboratory for Disaster Reduction in Civil Engineering (SLDRCE19-A-14). The support from the China Railway 14th Bureau Group Co., Ltd is highly appreciated.

## 6. REFERENCES

- [1] Das, A., Ahmed, M. M., & Ghasemzadeh, A. (2019). Using trajectory-level SHRP2 naturalistic driving data for investigating driver lane-keeping ability in fog: An association rules mining approach. *Accident Analysis & Prevention*, 129, 250–262. <https://doi.org/10.1016/j.aap.2019.05.024>
- [2] Dong, L., Zhao, E., Chen, Y., Qin, G., & Xu, W. (2020). Impact of LED Color Temperatures on Perception Luminance in the Interior Zone of a Tunnel considering Fog Transmittance. *Advances in Civil Engineering*, 2020, 3971256. <https://doi.org/10.1155/2020/3971256>

- [3] Feng, Z., Yang, M., Zhang, W., Du, Y., & Bai, H. (2018). Effect of longitudinal slope of urban underpass tunnels on drivers' heart rate and speed: A study based on a real vehicle experiment. *Tunnelling and Underground Space Technology*, 81, 525–533. <https://doi.org/10.1016/j.tust.2018.08.032>
- [4] Guan, W., Chen, H., Li, X., Li, H., & You, X. (2022). Study on the Influence of Connected Vehicle Fog Warning Systems on Driving Behavior and Safety. *Journal of Advanced Transportation*, 2022, 8436388. <https://doi.org/10.1155/2022/8436388>
- [5] He, S., Du, Z., Han, L., Jiang, W., Jiao, F., & Ma, A. (2024). Unraveling the impact of fog on driver behavior in highway tunnel entrances: A field experiment. *Traffic Injury Prevention*, 25(5), 680–687. <https://doi.org/10.1080/15389588.2024.2319333>
- [6] Jin, H., Jin, S., Chen, L., Cen, S., & Yuan, K. (2015). Research on the Lighting Performance of LED Street Lights With Different Color Temperatures. *IEEE Photonics Journal*, 7(6), 1–9. <https://doi.org/10.1109/JPHOT.2015.2497578>
- [7] Li, J., Hao, S., Chi, J., Zhao, N., Liu, R., & Song, M. (2023). An Effect Assessment on Application of the Guiding Device for Highway Traffic Safety in Rain and Fog Weather. 2023 2nd Asia-Pacific Computer Technologies Conference (APCT), 42–47. <https://doi.org/10.1109/APCT58752.2023.00016>
- [8] Liu, T., Zhu, H., Shen, Y., Xu, L., & Feng, S. (2025). Parametric analysis and experimental investigation on lighting quality in tunnel due to invalid luminaires. *Building and Environment*, 273, 112732. <https://doi.org/10.1016/j.buildenv.2025.112732>
- [9] Sadeghi, P., & Goli, A. (2024). Investigating the impact of pavement condition and weather characteristics on road accidents. *International Journal of Crashworthiness*, 0(0), 1–17. <https://doi.org/10.1080/13588265.2024.2348269>
- [10] Wang, S., Du, Z., Zheng, H., Han, L., Xia, X., & He, S. (2024). Improving driving safety in freeway tunnels: A field study of linear visual guiding facilities. *Tunnelling and Underground Space Technology*, 143, 105489. <https://doi.org/10.1016/j.tust.2023.105489>
- [11] Zhai, B., Wang, Y., Wu, B., & Wang, W. (2023). Adaptive Control Strategy of Variable Speed Limit on Freeway Segments under Fog Conditions. *Journal of Transportation Engineering, Part A: Systems*, 149(10), 04023097. <https://doi.org/10.1061/JTEPBS.TEENG-7699>
- [12] Zhao, X., Liu, Q., Li, H., Qi, J., Dong, W., & Ju, Y. (2022). Evaluation of the effect of decorated sidewall in tunnels based on driving behavior characteristics. *Tunnelling and Underground Space Technology*, 127, 104591. <https://doi.org/10.1016/j.tust.2022.104591>

## QUANTIFYING THE RESILIENCE CONTRIBUTION OF UNDERGROUND PEDESTRIAN SYSTEMS FOR SOLAR EXPOSURE RISK REDUCTION IN URBAN HEATWAVES

Gu Zongchao<sup>1</sup>, Osaragi Toshihiro<sup>2</sup>, Zhu Haipeng<sup>3</sup>, Leng Jiawei<sup>4</sup>.

**Abstract:** Urban heatwaves pose significant risks to pedestrian comfort and mobility. This study develops a simulation-based framework to evaluate the climate resilience performance of underground pedestrian systems (UPS) in mitigating solar exposure during extreme heat events. Integrating meteorological data, urban morphology, and pedestrian flows, the model employs multi-agent simulation and a spatiotemporal “path-risk” exposure framework to estimate the potential reduction in surface-level exposure enabled by UPS use. The method is applied to the Tenjin district in Fukuoka, Japan, where hourly UPS effectiveness is quantified under different climatic and demand conditions. A set of spatial resilience indicators is proposed to reveal dynamic patterns of risk avoidance, system contribution, and beneficiary distribution. Results show that resilience benefits are driven by both solar exposure intensity and pedestrian demand, with marked temporal variability and spatial heterogeneity. The findings highlight the role of UPS as a strategic climate adaptation infrastructure and provide a decision-support tool for resilience-informed urban planning and underground space design.

**Keywords:** Underground pedestrian system, Urban heatwave resilience, Solar exposure mitigation, Agent-based simulation, Spatiotemporal risk modeling.

### 1. INTRODUCTION

Urban heatwaves, as one of the most pervasive climate disturbances in recent years, have significantly altered the comfort of pedestrian microenvironments, indirectly affecting residents’ travel behaviors and public health (Hess et al, 2023). During hot summer months, street environments exposed to direct solar radiation increase the risk associated with pedestrian activity (Basu et al, 2024, Melnikov et al, 2022, Azegami et al, 2023, Melnikov et al, 2017). High-temperature exposure reduces the comfort and safety of street-level walking environments, subsequently decreasing the willingness of residents to use public transportation such as subways and buses. This shift in travel behavior may lead to increased carbon emissions, thereby exacerbating urban heat island effects and contributing to global climate warming.

Underground pedestrian systems (UPS) play a vital role in mitigating the impact of urban heatwaves. Characterized by environmental stability, underground spaces provide effective protection against extreme weather. In recent years, UPSs in areas surrounding transit stations have developed towards networked, large-scale, and systematic configurations, allowing pedestrians to directly access services within the station domain (Gu et al, 2018). When surface-level pedestrian systems are impaired by high temperatures or adverse weather, networked UPSs offer alternative routes for regional pedestrian mobility (Cui and Lin, 2016, Zacharias and Wang, 2021). Moreover, pedestrian flow in UPSs contributes potential commercial vitality and social service value, further

<sup>1</sup> Associate Professor, Gu Zongchao, Architecture Planning, Southeast University, Sipailou No.2, Nanjing, China, gzc991001@hotmail.com.

<sup>2</sup> Professor, Osaragi Toshihiro, Architecture Planning, Institute of Science Tokyo, osaragi.t.20f7@m.isct.ac.jp

<sup>3</sup> Lecturer, Zhu Haipeng, Architecture Design, Southeast University, Zhuhaipeng0801@hotmail.com

<sup>4</sup> Professor, Leng Jiawei, Architecture Design, Southeast University, jw\_leng@seu.edu.cn

driving the development of such networks. As such, the planning of UPS has become an essential strategy for reconciling the conflict between urban travel demands and climate disturbances (Zacharias, 2000).

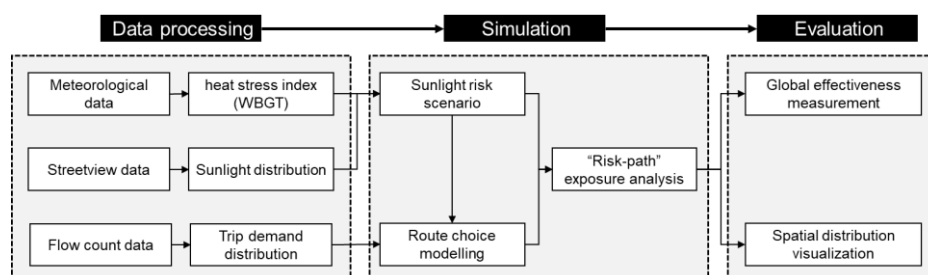
Practical cases in Sapporo, Montreal, and Singapore have demonstrated that connected underground pedestrian networks can effectively mitigate the impact of snow accumulation and solar exposure on transit passenger flows (Hess et al, 2023). However, there is a notable lack of systematic, quantitative assessments regarding the contribution of UPSs to the climate resilience of pedestrian systems. Establishing a measurable framework for evaluating UPS resilience performance is critical—not only to guide decisions in underground spatial development but also to provide a verification tool for urban designers and planners seeking to enhance the adaptive capacity of UPS networks.

Quantitative evaluation of UPS resilience presents several challenges. In the context of summer heat exposure, the efficacy of UPSs in reducing pedestrian exposure risk is influenced by a complex interplay of climatic conditions, street-level environmental factors, three-dimensional network structures, pedestrian demand, and behavioral decisions. As such, the response of UPSs to heat stress represents a complex systems problem. From the perspective of environmental risk, the urban thermal environment is shaped by variables such as temperature, humidity, wind speed, and solar radiation, all of which exhibit significant spatial and temporal heterogeneity. Consequently, heat exposure scenarios dynamically vary with time, date, and weather conditions. In terms of pedestrian behavior, the spatial and temporal distribution of underground pedestrian flows reflects distinct daily rhythms, causing the benefits of UPS interventions to shift over time. Additionally, individual perception of heat risks and corresponding path adjustments introduce further uncertainty into exposure outcomes. Thus, the mitigation capacity of UPSs cannot be accurately captured through static analyses of spatial pedestrian distribution and risk exposure.

To address these challenges, this study proposes a climate resilience performance evaluation model for UPSs based on spatiotemporal exposure simulation using a “path-risk” framework. Applying this model to the Tenjin district of Fukuoka, Japan, the study estimates the spatiotemporal distribution of solar exposure during summer and quantifies the contribution of the Tenjin UPS in reducing pedestrian sun exposure. Furthermore, spatial visualization metrics are established to reveal the dynamic distribution patterns of risk scenarios, beneficiary populations, and system response efficiency, thereby uncovering the mechanisms through which climatic conditions and travel demand affect the resilience performance of UPSs

## 2. METHODS

The basic framework of the model is shown in Figure 1. This model integrates multi-source inputs, including meteorological observations, urban morphology, and pedestrian flow data. It employs multi-agent simulation across various spatiotemporal scenarios to identify the spatial relationship between pedestrian routes and solar exposure risk. Based on the simulation results, the quantitative indicators are defined to evaluate the effectiveness of the UPS in mitigating high-temperature stress. Spatial visualization techniques are then applied to reveal the spatiotemporal dynamics of the systems’ resilience response.



**Figure 1.** Model framework.

## 2.1. Study area and available data

This study chooses the Tenjin district of Fukuoka City, Japan, as the case study location (Figure 2(a)) for the simulation experiment. Fukuoka City is located at 33 degrees north latitude and features a humid subtropical climate with hot summers and mild winters. According to historical meteorological data published by the Japan Meteorological Agency, the highest average monthly temperatures typically occur in August. To capture the temporal extent and representativeness of summer heat exposure, the simulation period is set from July 1st to September 30th.

This study selects the Tenjin underground shopping street and its surrounding connected urban blocks as the study area (Figure 2(b)). The underground shopping street features a linear spatial layout and maintains strong connectivity with adjacent land parcels and transit stations, as illustrated in Figure 3(a). Using open-access urban spatial information models, data on block morphology, building locations, and pedestrian pathways (both surface and underground) were extracted. Based on these data, a three-dimensional pedestrian network connecting facilities within the study area was constructed (Figure 3(b)).

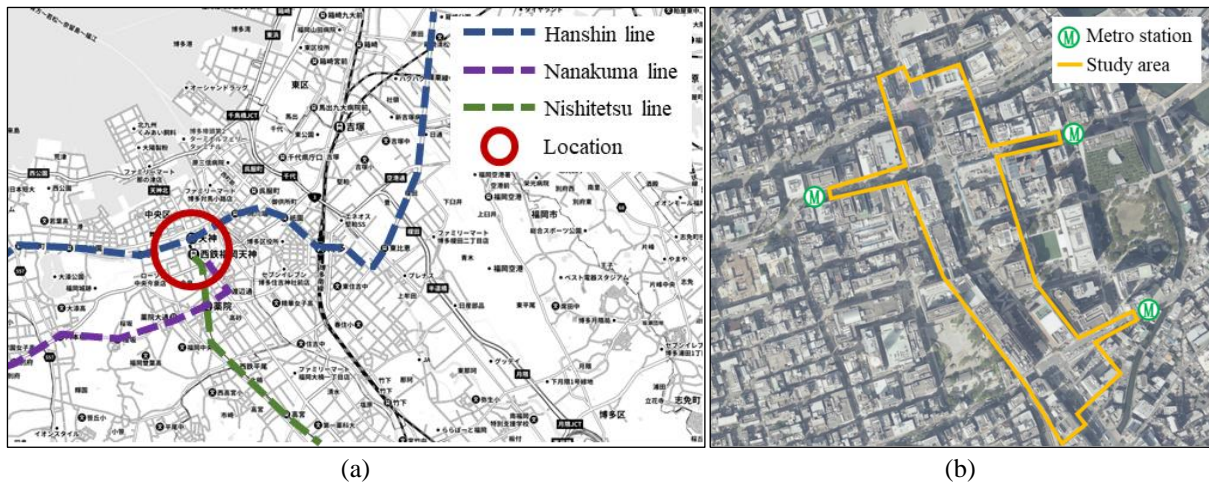


Figure 2. Location and study area.

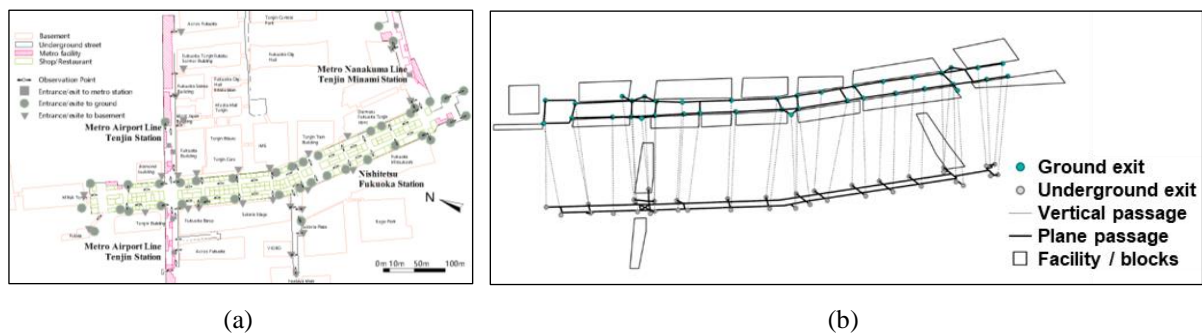


Figure 3. 3-dimensional pedestrian network modelling: (a) area of underground shopping streets; (b) connection between ground and underground pedestrian system.

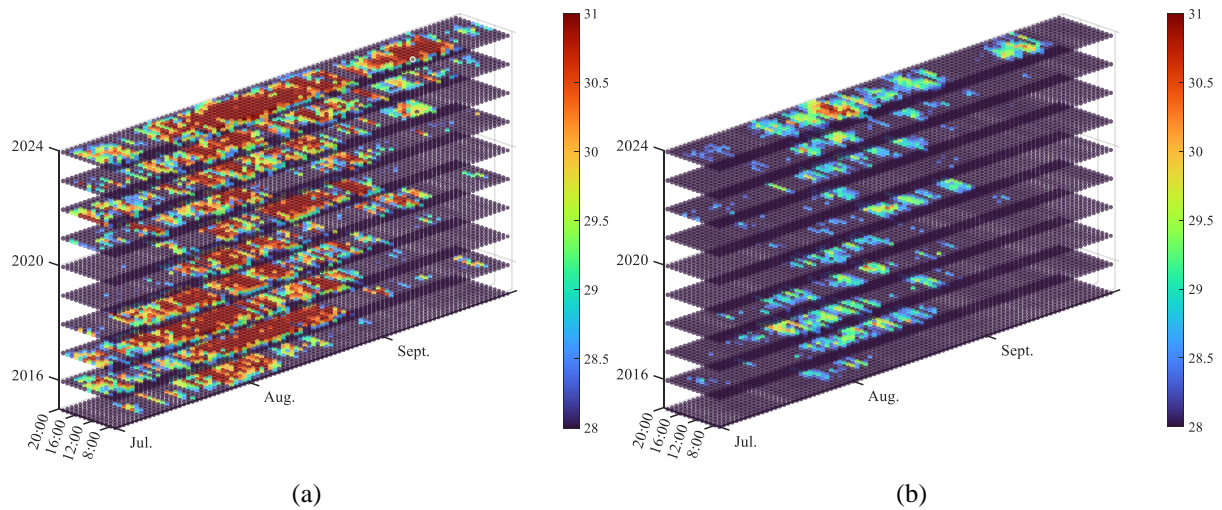
The model utilizes three primary data sources as input: meteorological observations, pedestrian flow counts, and streetview imagery. Meteorological data are derived from publicly available weather station records released by Japan's Ministry of the Environment (JME) and the Japan Meteorological Agency (JMA). These datasets include hourly recordings of temperature, humidity, weather conditions, wind speed, sunshine duration, and Wet-Bulb Globe Temperature (WBGT) index from 2015 to 2024. Pedestrian flow data are provided by the Fukuoka City government and consist of bidirectional pedestrian counts at major links of the Tenjin underground shopping street. This data recorded hourly from 7:00 to 20:00 on both weekdays and weekends. Streetview data were collected via the Google Street View API at 10-meter intervals along the street network, allowing for detailed analysis of shading conditions and visual environmental features.



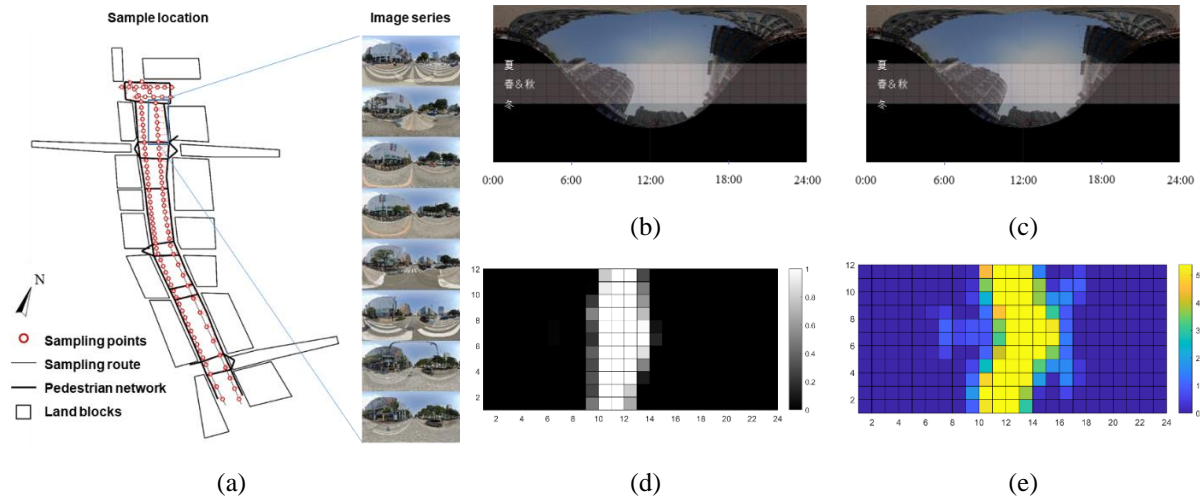
## 2.2. Heat risk scenario identification

A heatwave is typically defined as a weather event during which the maximum daily temperature exceeds 35°C for three days. However, under direct solar radiation, pedestrians may experience equivalent thermal stress at significantly lower ambient temperatures (Hess et al, 2023). To more accurately define heatwave conditions, this study adopts the Wet Bulb Globe Temperature (WBGT) index, recommended by the Japan Ministry of the Environment(JME), as the key climatic parameter for heat risk assessment. According to the JME's heat alert policy, periods when the WBGT exceeds 31 (approximately equivalent to an air temperature of 35°C) are classified as "heatwave periods." In this study, street segments exposed to direct sunlight during these periods are defined as "solar exposure risk scenarios." The spatiotemporal distribution of such heatwave scenarios is therefore jointly determined by the timing of extreme heat and the spatial layout of exposed pedestrian facilities.

To assess whether the UPS can effectively support surface-level streets and mitigate heat exposure risks, this study is to check the WBGT index under shaded condition. Using weather station observations and the heat stress index framework provided by the JME and JMA, the WBGTs for each street link across time periods under both sunlit and shaded scenarios are estimated (Figure 4). It is found that the heat stress can be significantly mitigated if pedestrians move through the underground paths without direct sunlight.



**Figure 4.** Time distribution of WBGT index in the past ten years: (a) WBGT in sunlight; (b) WBGT in shadow.



**Figure 5.** Method of estimating sunlight scenario's spatiotemporal distribution in street networks: (a) streetview image sampling; (b) overlap solar trajectory; (c) projection transformation; (d) sunlight probability matrix; (e) sunlight route length.

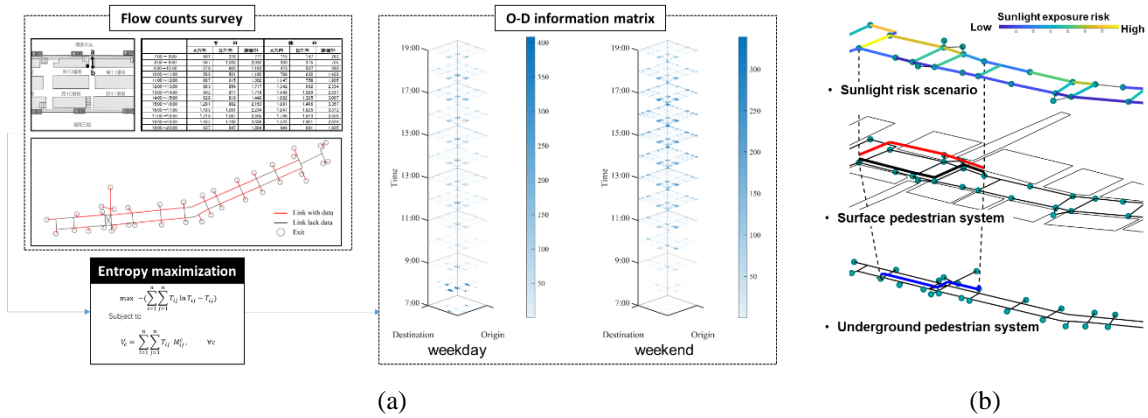
The spatiotemporal distribution of sun-exposed pedestrian links is determined by urban morphology, geographical orientation, and street-level environmental conditions. To capture the dynamics of sunlight risk across the pedestrian network, this study adopts a sequential street view image analysis approach (Zhu and Gu,

2022). As shown in Figure 5, by aggregating the temporal distribution of sunlit conditions at each sampling point (Figure 5(a)), we obtain time-series data on the sunlight and shaded lengths of each surface street. When integrated with WBGT indexes, a time series of sun-exposure risk across pedestrian paths is obtained.

### 2.3. Pedestrians' sunlight exposure estimation

The effectiveness of the UPS in mitigating solar exposure risk can be assessed by evaluating the additional exposure pedestrians would face if underground paths became inaccessible. This exposure level is influenced by pedestrian demand in the underground system, the spatial distribution of heatwave conditions above ground, and pedestrian route choice behavior under thermal stress.

Maximum Entropy model is adopted to estimate the trip demand that would be assigned to the surface network during UPS disruptions. Using observed flow data from underground passages, the module estimated the hourly origin-destination (O-D) matrix  $\{T_{ij}\}_t$  for all entry-exit pairs.



**Figure 6.** Method of recreating pedestrians' trip demand and potential trajectories: (a) OD estimation module; (b) trip assignment in surface street networks.

The Route Choice model considers pedestrian preference for shaded paths during extreme heat events. A utility-based function is constructed for each street link, incorporating factors such as route length, sun exposure length, intersection wait time, and vertical motion. The cost function is formulated as follows:

$$C_{lt} = d_l + \alpha_1 S_l + \alpha_2 W_l + \alpha_3 D_{lt} \quad (1)$$

The values of coefficients  $\alpha_n$  are setting based on previous research. Detailed references and parameter settings are provided in Table 1.

**Table 1.** Transition Efficient between pedestrian facility/environment factors and link distance.

Parameters	Weighting	Unit transfer	Reference
Length ( $d_l$ )	1	-	Hiroyuki Satoh et al, 2002
Stair ( $S_l$ )	1.2(upwards) / 0.6(down)	meter/step	
Traffic signal ( $W_l$ )	30	meter/turn	Nishimura and Osaragi, 2009
Sunlight duration ( $D_{lt}$ )	0.196/ 0.098 (tree shading)	meter/sec	Melnikov et al, 2022

To account for the influence of cloud cover and similar meteorological factors on sun exposure and pedestrian decision-making, this study classifies pedestrian route choice behavior into two categories: distance (or time) priority and utility-based priority.

During periods of significant cloud cover, which mitigates solar radiation, pedestrians are considered to adopt a distance-priority strategy, selecting the route with the shortest travel time (red line in Figure 6(b)). Conversely, under clear sky conditions with direct sunlight, pedestrians are expected to adopt a utility-priority strategy, choosing paths based on a trade-off between sun exposure and physical cost (black line in Figure 6(b)).

For each OD pair ( $i-j$ ), both route types were generated by the Dijkstra algorithm under different solar exposure conditions. The proportion of pedestrian traffic along a surface-level road segment  $l$  at time  $t$  is determined by the following equation:

$$P_{ijlt} = Y_t L_{ijlt} + (1 - Y_t) K_{ijlt}, \quad (2)$$

where  $P_{ijlt}$  denotes the proportion of trips from origin  $i$  to destination  $j$  traversing segment  $l$  at time  $t$ ;  $Y_t$  is the normalized sunlight duration (range: 0–1) at time  $t$ ;  $L_{ijlt}$  and  $K_{ijlt}$  are the frequencies with which link  $l$  is chosen under distance-priority and utility-priority decision-making.

By aggregating sun exposure durations across two types of route choices, the expected heat exposure risk for pedestrians between each OD pair is measured. Accordingly, the expected exposure reduction benefit provided by the UPS system for underground users is calculated as:

$$W_{ijt} = Y_t B_t \sum_l P_{ijlt} D_{lt} \quad (3)$$

where  $B_t$  is boolean indicator of  $WBGT > 31$  (1 if true, 0 otherwise).

## 2.4. Performance indicator definition of UPS's resilience

**Global Resilience Effectiveness:** The total exposure reduction achieved by the UPS system at time  $t$  is calculated as the sum of expected exposure mitigation across all OD pairs:

$$F_t = \sum_i \sum_j T_{ijt} W_{ijt} \quad (4)$$

**Risk Coverage Index:** This index quantifies the contribution of UPS in reducing exposure risks on surface-level street networks, defined as the cumulative added exposure under the absence of the UPS:

$$R_{lt} = \sum_i \sum_j T_{ijt} P_{ijlt} D_{lt} \quad (5)$$

**Resilience Benefit Index:** Taken the street blocks and facilities as spatial unit, this index defines the cumulative risk avoidance of pedestrians between a specific O-D pairs as the spatial variation in exposure risk avoided by users, revealing the spatial distribution of benefit recipients:

$$G_{ijt} = T_{ijt} W_{ijt} \quad (6)$$

**Resilience Contribution Efficiency Index:** This indicator evaluates the efficiency distribution of the UPS network, assigning avoided exposure risk to each network component:

$$E_{klt} = \sum_i \sum_j G_{ijt} U_{ijklt} \quad (7)$$

where  $U_{ijklt}$  represents the frequency that OD path ( $i$ - $j$ ) traverses network element  $k$  (Gu and Osaragi, 2017).

## 3. RESULTS AND DISCUSSION

### 3.1. Results of system indicators

Figure 7 illustrates the relationship between the annual resilience effectiveness of the UPS system in mitigating pedestrian heat exposure and ambient temperature variations. Compared to daily maximum temperature, the consistency between the UPS performance and mean daytime temperature is notably stronger. While the effectiveness of the UPS system showed an increasing trend from 2021 to 2023, the overall contribution remained lower than in 2020, a year with lower average temperatures. This suggests that temperature alone is not the decisive factor driving the system's response.

To further explore the underlying causes of these variations, Figure 8 presents a temporal analysis of the UPS's exposure mitigation effectiveness across different dates and hours over the past decade. Although the total number of responsive days increased during 2021–2023, the effectiveness was fragmented due to frequent rainfall events, which interrupted continuous solar exposure and reduced UPS demand. In contrast, the reduced precipitation in 2024 resulted in prolonged clear-sky conditions, which significantly enhanced the UPS system's mitigation performance.

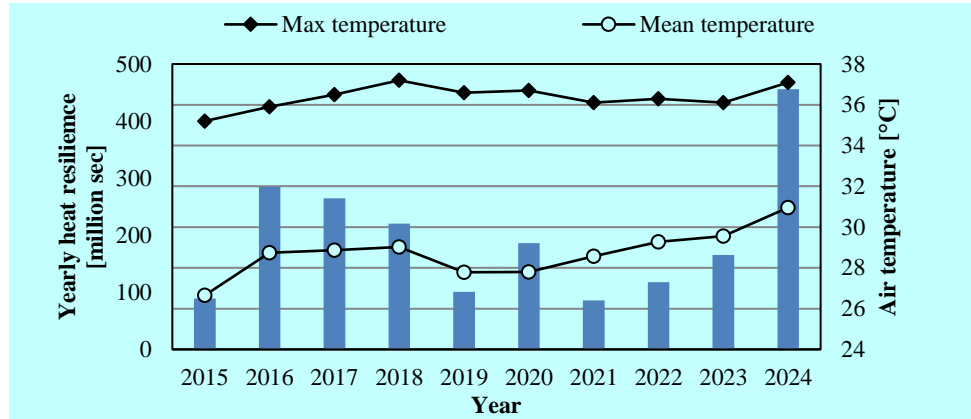


Figure 7. Yearly variation of UPS's resilience effectiveness and air temperatures.

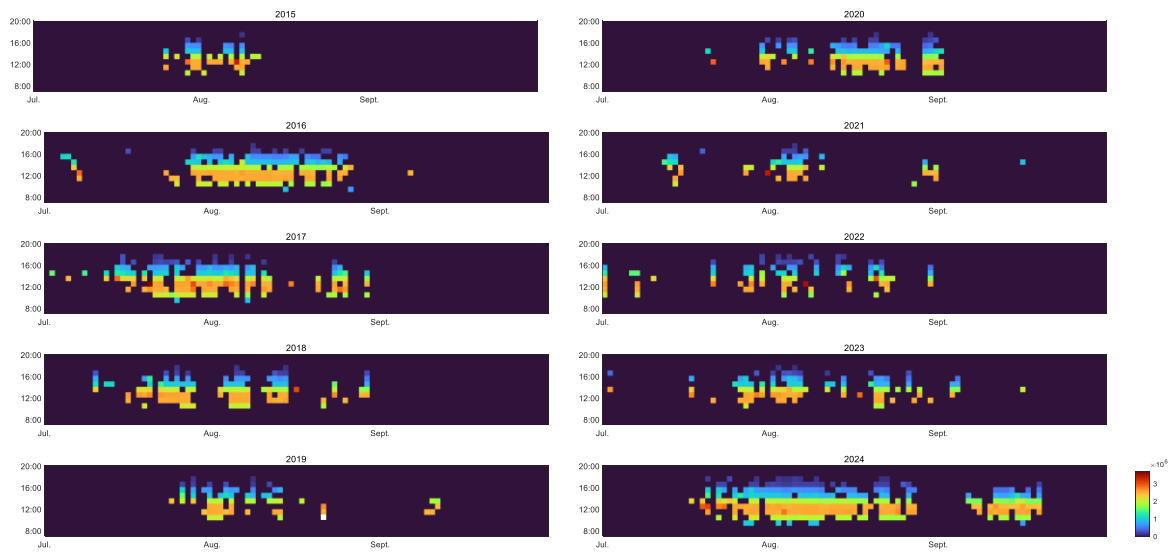


Figure 8. Time-specific performance of UPS in mitigating pedestrians' sunlight exposure during the past 10 years.

### 3.2. Spatial distribution of performance indicators

Figure 9 presents the spatiotemporal variation of three resilience contribution indicators (Risk Coverage Index, Resilience Benefit Index, and Contribution Efficiency Index) across different street elements over the past decade. Each layer in the figure illustrates the longitudinal change of these values from bottom (earlier years) to top (recent years). A strong alignment is observed between the temporal patterns of these indicators and the overall system effectiveness, revealing the UPS network's ability to globally respond to climate fluctuations.

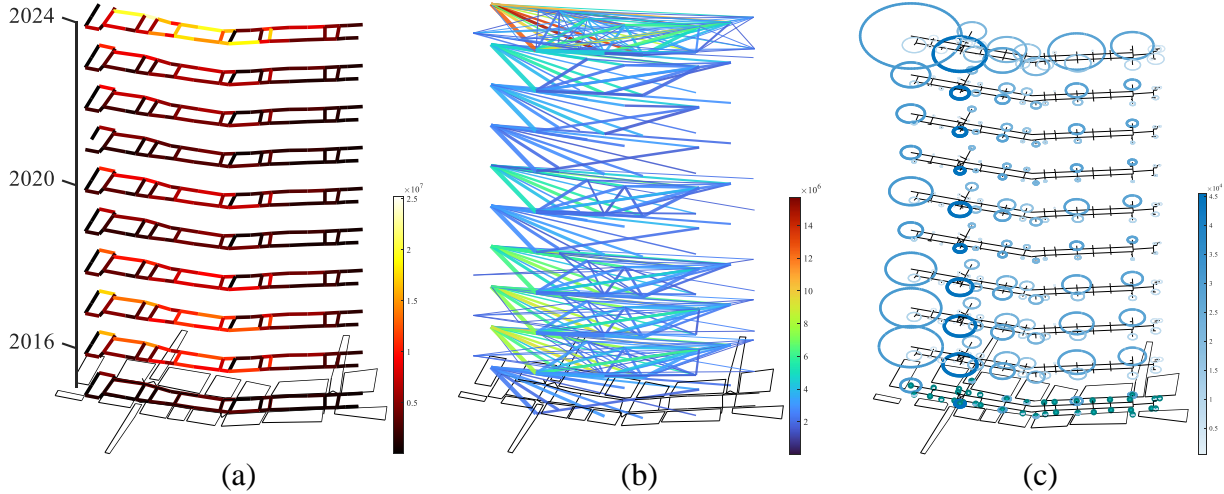
In Figure 9(a), the spatial distribution of the Risk Coverage Index shows a significant north-south gradient, with higher values concentrated in the northeastern parts (left) of the study area. This is attributable to the greater pedestrian demand in the north. Besides that, the orientation of southern streets, which aligned east-west, making them more likely to be shaded by surrounding buildings and thus less prone to intense solar exposure (see Figure 2(b)).

Figure 9(b) visualizes the Resilience Benefit Index between O-D pairs. Line colors reflect the degree of solar exposure avoided due to UPS use, while line width indicates the volume of travelers along each O-D pair. The presence of long, wide paths with low benefit scores (cold-colored lines) suggests that travel volume and distance alone do not account for resilience gains; rather, trips' spatial relation between risk scenarios play critical roles.

In Figure 9(c), the spatial distribution of Contribution Efficiency (represented by the radius of the circular plots) appears discontinuous. Interestingly, entrances directly connected to the surface show lower efficiency values than those integrated into commercial complexes. This is due to the convenient vertical circulation systems (e.g., escalators) within commercial facilities, which facilitate seamless movement between underground systems

and surrounding amenities. The increasing the actual usage intensity leads to high contribution efficiency. Notably, the correlation between entry/exit traffic volume and contribution efficiency is strong,

In summary, the spatial variation of the UPS system's resilience effectiveness is highly heterogeneous, shaped by a combination of climatic dynamics, urban morphology, infrastructure layout, and mobility demand. These interactions cannot be adequately captured using single-variable linear models.

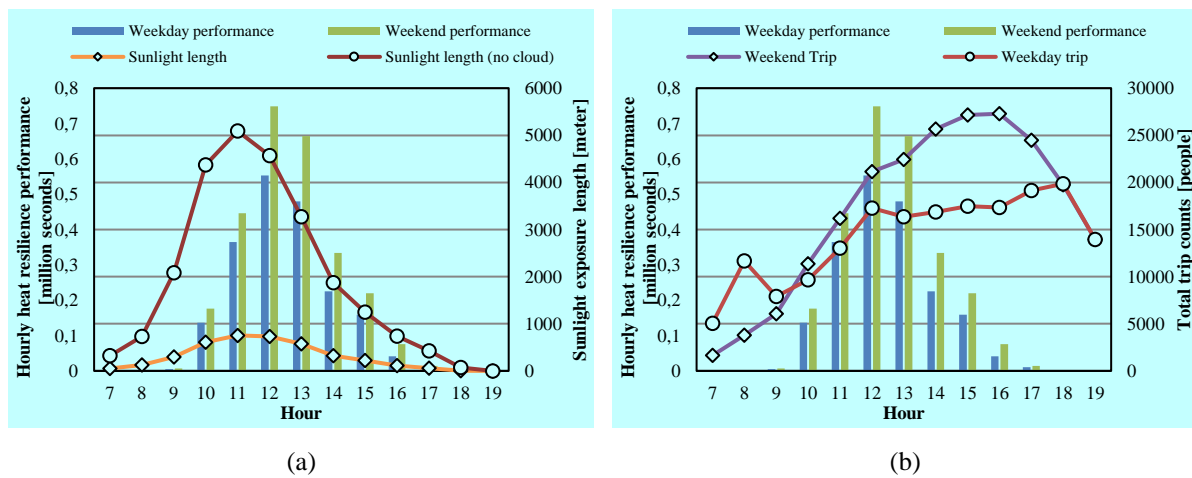


**Figure 9.** Spatiotemporal distribution of resilience response performance indexes: (a) Risk Coverage Index; (b) Resilience Benefit Index; (c) Resilience Contribution Efficiency.

### 3.3. Influence of underground trip demands on UPS's resilience contribution

This study selects 2024, the year with the highest solar exposure risk, to analyze hourly average global resilience effectiveness in the weekdays and the weekends. As shown in **Figure 10(a)**, the UPS system's mitigating effect becomes evident starting at 10:00 AM and disappeared after 4:00 PM. This pattern results from reduced solar exposure in early morning and late afternoon due to building shadows and lower solar altitude angles. Accordingly, the UPS's resilience effects during peak commuting hours are not activated.

The daily contribution index variation follows an approximately normal distribution which peaks around 12:00 PM. It is found that the peak lags behind the temporal peak of surface solar exposure (red curves in Figure 10(a)). This lag is thought to be caused by the increasing pedestrian flow during midday, which sustains high UPS effectiveness even after exposure levels begin to decline. Hence, UPS's global resilience contribution is determined by the coupled effect of trip demand and climate factors.



**Figure 10.** Influencing factors that cause differences in the contribution performance of UPS in the weekdays and weekends.

A comparison between weekdays and weekends reveals that starting at 10:00 AM, the total number of underground travelers on weekends are higher than that of weekdays. It is thought to leading to consistently higher



contribution index values throughout the day. However, after 12:00 PM, even as pedestrian volumes continue to grow, no corresponding rise in the UPS resilience effectiveness is observed. This suggests that the spatial extent of solar exposure plays a dominant influence on UPS resilience performance, rather than the effect of sheer traveler volume.

#### 4. DISCUSSION

The proposed framework presents advances in assessing the climate resilience contribution of UPS. By incorporating solar exposure during walking and waiting phases into pedestrian routing decisions, the model mathematically described how users dynamically navigate in surface street networks. This allows for a more realistic estimation of the respective contributions of each network to overall system resilience under heat stress. Furthermore, the integration of agent-based simulation across multiple temporal and spatial scenarios enables the model to reflect the variability and uncertainty of urban pedestrian responses to environmental conditions. This dynamic structure captures the complex interplay between climate disturbances, built form, and pedestrian decision-making processes, which is essential for understanding resilience as a complex system outcome. In addition, the model jointly considers user-side travel demand and system-side service capacity, providing a comprehensive framework for resilience assessment across different spatial units and time periods. The spatial visualization of resilience indicators facilitates practical application in planning, allowing for evidence-based support in scenario evaluation, stakeholder responsibility allocation, and the optimization of underground spatial design. Overall, the framework not only quantifies the climate resilience benefits of UPS with improved behavioral reliability but also extends its utility to urban design and management contexts where spatial equity and adaptive performance are increasingly central concerns.

Despite the model's demonstrated contributions, several limitations should be acknowledged. At present, solar exposure is the sole environmental variable integrated into the routing decision process, while other relevant climatic factors, such as ambient temperature, wind conditions, and humidity, remain unaccounted for. Incorporating these elements in future work would enhance the model's reliability in representing pedestrian behavioral response to dynamic heat stress. Moreover, the current framework focuses exclusively on UPS users, thereby omitting pedestrians within the broader station area, whose exposure and routing decisions may also be shaped by underground accessibility. The assessment of resilience relies primarily on exposure duration as the outcome metric; future research should consider integrating comprehensive thermal indices, such as the PET and account for heterogeneous comfort preferences across user groups. Additionally, the representation of origins and destinations by entrance-exits may oversimplify actual movement patterns within large facilities, potentially underestimating the spatial granularity of beneficiary distributions.

#### 5. CONCLUSION

To address the challenge of quantifying the climate resilience performance of UPS, this study presents a simulation-based model that evaluates UPS effectiveness in mitigating sun exposure in heat waves. The model integrates spatiotemporally heterogeneous variables, such as climate conditions, urban morphology, pedestrian demand, and street-level thermal environments, and uses scenario-based agent simulations to derive quantitative and spatially explicit resilience indicators. These reveal the dynamic complexity of multi-factor responses within three-dimensional pedestrian networks.

Key findings from the case study include:

- Spatiotemporal heterogeneity in pedestrian flows and sun-exposure risk significantly amplifies both the complexity and unpredictability of resilience responses.
- System efficacy depends on both pedestrian volume and exposure severity, with exposure levels playing a dominant role in temporal variability of resilience benefit.
- Trip demands disparities and temporal shifts (e.g., weekday vs. weekend) shape cumulative exposure and resilience effectiveness, highlighting time-dependent patterns in user benefit.
- UPS resilience potential cannot be inferred solely from surface heat stress indicators, spatial patterns of effectiveness depend strongly on the underground network structure and pedestrians' dynamic response.

Moving forward, the model will be extended using city-scale pedestrian trajectory data to examine response patterns across diverse climatic scenarios. This will support the development of a more comprehensive multi-hazard resilience framework, providing a robust basis for resilience-informed planning, policy formulation, and the adaptive design of underground pedestrian systems.

## 6. ACKNOWLEDGMENTS

This study was supported by the Humanities and Social Sciences Youth Foundation of China (Grant No. 24YJCZH068) and the National Natural Science Foundation of China (Grant No. 51808094). The pedestrian traffic survey data used in this paper were obtained from by Fukuoka City Government.

## 7. REFERENCES

- [1] Hess, J., Meister, A., Melnikov, V. R., Axhausen, K. W. (2023). Geographic information system-based model of outdoor thermal comfort: Case study for Zurich. *Transportation Research Record: Journal of the Transportation Research Board*, 2023, 2677(3): 1465–1480.
- [2] Basu, R., Colaninno, N., Alhassan, A., & Sevtsuk, A. (2024). Hot and bothered: Exploring the effect of heat on pedestrian route choice behavior and accessibility. *Cities*, 159(3), 105000.
- [3] Melnikov, R., Christopoulos, I., Krzhizhanovskaya, V., et al. (2022). Behavioural thermal regulation explains pedestrian path choices in hot urban environments. *Scientific Reports*, 12(1), 2441.
- [4] Azegami, Y., Imanishi, M., Fujiwara, K., & Kusaka, H. (2023) Effects of solar radiation in the streets on pedestrian route choice in a city during the summer season. *Building and Environment*, 235, 110250.
- [5] Melnikov, R., Krzhizhanovskaya, V., Sloot, A. (2017). Models of Pedestrian Adaptive Behaviour in Hot Outdoor Public Spaces. *Procedia Computer Science*, 108, 185-194.
- [6] Gu, Z., Lu, W., Osaragi, T., Wu L. (2018). A Study on Underground Space in Front of Rail Transit Station Based on Pedestrians' Spatio-Temporal Distribution: The Case of Underground Pedestrian System of Large Railway Station in Japan, *New Architecture*, 3, 30-35. (in Chinese)
- [7] Cui, J., Lin, D. (2016). Utilisation of underground pedestrian systems for urban sustainability. *Tunnelling and Underground Space Technology*, 55, 194-204.
- [8] Zacharias, J., Wang B. (2021). 2021 IOP Conf. Ser.: Earth Environ. Sci. 703, 012002.
- [9] Zacharias, J. (2000). Modeling Pedestrian Dynamics in Montreal's Underground City. *Journal of Transportation Engineering, American Society of Civil Engineers*, 126(5), 405-412.
- [10] Zhu, H., Gu, Z. (2022) A method of estimating the spatiotemporal distribution of reflected sunlight from glass curtain walls in high-rise business districts using street-view panoramas. *Sustainable Cities and Society*, 79, 103671.
- [11] Gu Z., Osaragi T. (2016). Estimating Pedestrians' Movement in Underground Space based on Flow Count Data, *Journal of Architecture and Planning*, 2016, 81(730):2625-2634.
- [12] Nishimura, K., Osaragi, T. (2009). Spatio-temporal Distribution of Pedestrians in District around Railroad Terminal Station. *Summaries of Technical Papers of Annual Meeting Architectural Institute of Japan*, 721-722.
- [13] Hiroyuki, S., Yoshitaka, A., Dai, N., et al. (2002). A Study on Factor Analysis of the Transfer Resistance and Estimating the Benefit of Reducing Project at Terminal. *Infrastructure Planning Review*, 19, 803-812.
- [14] Gu, Z., Osaragi, T. (2017). Estimating Pedestrians' Route Choice Probability in Underground Space based on OD Matrix and Flow Count Data, *Journal of Architecture and Planning*, 82(739), 2285-2293.

## THE DYNAMICS OF TRAVELLATORS IN UNDERGROUND SPACE

John Zacharias<sup>1</sup>

**Abstract:** Travellators, also known as moving walkways, are typically installed to move people quickly and over extended distances in large facilities. They are commonly used in airport terminals and in underground corridors between metro stations, and are generally believed to enable moving larger numbers of people more quickly from point to point than can be achieved without the facility. Utility from the user perspective includes perceived time and kinetic energy savings, while management aims to increase throughput where there is heavy demand. An empirical study is necessary to evaluate how such facilities are actually used and to what extent these utility goals are achieved. Variables in resulting throughput, measured as speed, include 1) standees on the moving traveller, 2) moving pedestrians on the traveller, 3) pedestrians walking on the ground, 4) total pedestrian volume 5) incline of the walking surface. The case study is in the MTR system of Hong Kong, which has several examples of travellers. The heavily used corridors between Central Station and Hong Kong Station provided the test case of four travellers and related open floor areas. Counts were extracted from video capture. The traveller improved efficiency by about 17% during non-saturated flow conditions. Those walking on the traveller walked more slowly than those on firm ground but travelled faster overall because of the traveller motion. The traveller serves to organize the traffic streams, offers an alternate experience of displacement and a place for screen-related activities.

**Keywords:** traveller, moving walkway, pedestrians, underground network, Hong Kong

### 1. INTRODUCTION

Travellers or moving walkways, are installed in many underground walking systems to achieve certain desired improvements in the displacement of people from one place to another. A review of the commercial websites of traveller suppliers provides an overview of the presumed benefits of their inclusion in underground facilities. Travellers are said to be needed “where there is a high volume of pedestrian traffic and a need to move people quickly and efficiently over short to medium distances” [1]. In theory, higher pedestrian speed increases throughput in limited channel space. The promised higher speeds for pedestrians is accomplished with their safety in mind [2], in recognition of boarding and exiting difficulties for some passengers [3]. The higher speeds and channelling of movement are seen as the means to reduce congestion in busy transport terminals [4]. Because travellers are unidirectional, they gather pedestrians moving in a single direction from heterogeneous flows that often have conflicting trajectories.

The engineering and behavioural principles constituting the theory of travellers has been elaborated to some extent, as explained in the literature review below. There are, however, very few empirical studies of their operation in practice, in particular to assess the announced benefits in terms of mobility, accessibility and efficiency. Most of the published literature is concerned with traveller applications in airport terminals, the results of which must be taken with caution when considering their implementation in transport facilities and underground walkway systems. Possible reasons for differences in airports is that most pedestrians are managing luggage or luggage carts, and it is more likely that they are not overly familiar with the facility. As a result, they tend to move more slowly than in systems dominated by commuters and shoppers [5]. Nevertheless, some of the findings are of interest for the general application of travellers in underground walkway systems, as discussed

<sup>1</sup> Zacharias, John, PhD, urban planner, Chair Professor, College of Architecture and Landscape, Peking University, Beijing, PRC 1100871.  
johnzacharias@pku.edu.cn

below. The main purpose of the present work, then, is to assess improved efficiency in terms of travel speed in the presence of the traveller facility, and to assess to what extent that improved efficiency is conditioned by pedestrian volume, standing firm behaviour of some users and walking surface incline. Regardless the expected efficiencies delivered by walking on a traveller, the recommended procedure for using a traveller with safety in mind is to board and stand firm. The conditions in which people stand firm and are transported also needs understanding, since standing behaviour has a major effect on the theoretical efficiency of the system, as does a dense pedestrian flow.

The present study is an analysis of observations taken from the travellers installed in the Hong Kong MTR. Mean pedestrian speed is the dependent variable, with simultaneous counts of pedestrians standing on the traveller, walking on the traveller, walking on the bypass route, and degree of incline as independent variables. The numbers were derived from 38 video records on 4 travellers, with a total of 3,322 observations. Details of the field protocols and analysis will be found in the Methods section of this paper that follows consideration of the literature below.

The literature can be considered in three main categories, as follows: The planning and engineering of the traveller facilities, human responses to the operations of the mechanical system, and the range of walking behaviours that interface with the traveller.

Travellers will be implemented typically where there is a perceived long distance between hubs, activity centres and transport stations. They tend to be located where there are no incipient activities along the route that might induce a diversion, and are typically associated with major generators of movement, like metro and rail stations. An exchange space is needed where there is a cross-flow or where there are emergency exits to the ground level. It remains uncertain how length of traveller is related to use rate, but the length is often constrained by the needs of the larger facility. For example, [6] propose an analytical procedure for determining the placement and length of the traveller so as to minimize travel distance to exits and destinations along the route. Their case is the airport terminal with serially placed gates parallel to the moving walkway, although the model could be adapted to underground commercial facilities. A more extensive network of such travellers requires consideration of existing pedestrian flows. For example, in Tokyo at the Shinjuku JR station there are underground travellers taking pedestrians toward the Shinjuku CBD from the JR Station but without return movement, based on the principle that the start of the working day is more time-constrained than the end of the day. The Mid-Levels Escalator in Hong Kong, which is actually a traveller over much of its length, moves downward at the beginning of the working day but upward for the rest of the day. In this way it offers energy saving to users needing to climb to the Mid-Levels, but has also generated renewal and investment in those higher elevation areas [7]. As with all other people movers, the traveller may expand the activity space for individuals. Travellers have been installed in several locations in the Hong Kong MTR system, between Tsim Sha Tsui (TST) and TST East stations, at Sai Ying Pun station, among others.

It is argued that in reducing travel time and energy consumption, that travellers will be induced to travel longer distances. Following this reasoning, patronage of the MTR could be promoted through these labour and time-saving features. It is also argued that the traveller accommodates those with mobility constraints although users must be able to stand and move on their own [8][9]. In close proximity, the movement of all individuals is constrained by the behaviours of others and prompts various coping behaviours [10]. That increased proximity on the traveller may also be a factor in the decision to use it rather than to walk in the less constrained by-pass route. The tendency to use a labour-saving movement device is highly dependent on the location of the device. In the case of escalators in underground space, it was found that 71% of the variance in choice was attributable to the distance between the escalator and stairway [11].

As metro systems expand and greater connectivity is needed between lines, there are more long, undifferentiated corridors to take pedestrians from one station to another. The design of these corridors needs to take into consideration capacity, to account for sudden bursts in the flow of disembarking passengers. As metro systems develop and have more connectivity, there may be shifts in patronage among lines, placing more or less demand on fixed, underground corridors. A single traveller in one direction on such a corridor disturbs the usual right-left self-assignment of flow in conditions of high pedestrian volume. A corridor with travellers in both directions also induces uncertainty: should one walk on the bypass corridor next to the traveller moving in the same direction, regardless of the prevailing left-right bias in the local environment? Many systems, including Hong Kong's MTR, have tried to resolve conflicting flows by providing directional arrows on the floor. Cross-flows are, however, inevitable given all the pre-existing structures.

Travellers have been implemented with different operating speeds. The higher the speed, the more difficulty some pedestrians have in boarding and exiting, such that audible warnings are included in the facility, particularly for the exit condition. Hawkins & Atha (1976) found that 44% of individuals boarding used a half-step to board, which involves slowing slightly. Only 22% of individuals walked onto the traveller without a gait change. Their interpretation of the video record suggests that 31% of boarding individuals had balance problems which might

lead to avoidance in using the facility. Ironically, the mobility aims of the traveller for those individuals with reduced mobility are thus thwarted by the mechanical action of the facility.

Other problems arise in the spaces upon exiting and boarding with the greater likelihood of cross-movements and sudden crowd formation in the exit area, with slow-moving crowds in the boarding area when the flow is very heavy [8]. There are risks involved in a crowded and fast-moving situation with the mechanical accelerator of flow rate and locations where falls are more likely. Underground space planning will aim to ensure adequate exchange space between traveller facilities, access to emergency exits, generous ceiling height, optimized legibility and the avoidance of blind corners. But ultimately, the great majority of passengers will be trapped on the traveller in the case of an emergency necessitating evacuation.

The accelerated traveller, or accelerated moving walkway (AMW) has been implemented in a few facilities such as Schiphol airport, Amsterdam and Lester Pearson airport in Toronto. Boarding speed is the same as for the usual traveller but then accelerates using moving plates to achieve speeds much higher than normal walking speed. In the context of imagining it augmenting local mobility, there remain significant problems in the network [12][13]. Higher mechanical speeds appear to induce slower pedestrian pace, in an apparent desire for a certain level of comfort or familiarity. Such behaviour, if evidenced, would reduce theoretical efficiency. There is limited empirical evidence to support this theory, however, so it is important to collect speeds in all the conditions of the study case.

While this paper is primarily concerned with the efficiency argument for travellers, individuals and their choices remain the core of the question. Individuals are sensitive to instrumental aspects of facility use – usability and usefulness, social-spatial interaction, aesthetics, sense of control and multi-tasking being notable among them [14]. There is no obvious link between these ways of experiencing the traveller and the measured efficiency of the system, although both may inform decisions to build. But the election to use is a gauge of preference [15]. We might not learn the specifics of that response but still it lends insight into the world of transport and comfort. The latter is a fast-emerging field of enquiry into the hedonic and instrumental motivators for choice that appear to explain a significant part of choice behaviour [16]. Thus, it is important to pay attention to the intensity of use of the options.

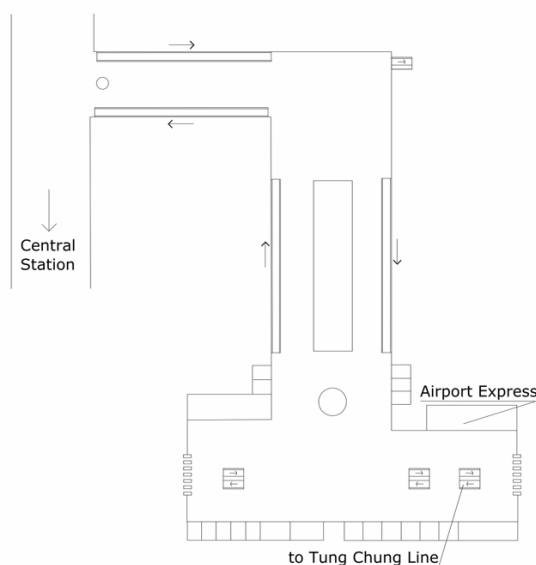
In theory, humans will optimize energy expenditure while moving. However, on a moving walkway, this would mean standing firm. Some do stand firm, others walk. Observations in airports [9] showed that walking speed on travellers is lower than by-pass walking speed. However, airports may be particular situations because passengers are transporting luggage and may or may not be time-constrained. A second theory is that visual flow will result in humans reconciling the movement of their legs with their apparent movement from visual flow [17]. This should result in faster than by-pass walking speed on the traveller but less than the addition of normal walking speed and traveller speed. In addition, the presence of others on the traveller may then influence both the decision to walk and the decision to enter the traveller. It is also observed that perceived higher speed – what one can see of the environment surrounding the traveller facility – results in a shorter gait [18]. These new variables require consideration with an empirical study in a case more typical of movement and exchange networks underground. The goal is to identify the co-factors in the functioning of these systems in their daily use, as a guide to their planning. Also, it is useful to be able to understand the contribution of aids to movement such as this one in relation to other needs in the movement system.

## 2. MATERIAL AND METHODS

A broader introductory study of traveller installations revealed certain salient social features of people-moving devices, which were then validated in the Hong Kong case. The travellers observed in this study are located in the underground concourses between Hong Kong Station and Central MTR station. There are four travellers, one ascending, one descending, and two at level, parallel to a divided or undivided by-pass channel. The flows vary markedly over the day, largely as a result of the concentration of commuting movement within two main peak periods. Samples are taken to cover all but the highest level flows, but still representing sufficient variation on all variables to work in regression analysis.

At the extreme ends of the joined traveller sets are station exchange spaces – Central Station and Hong Kong Station – with complex movement among several lines and corridor commercial space (figure 1). Space allocation for by-pass walks is critical at the point of choice and a requirement for this study was for such by-pass space to exceed requirement. In this case, the corridors were near saturation – slowed speed, shorter steps for the great majority of individuals – only once in our observations. The total travel time between Central Station and Hong Kong Station is as little as 3 minutes while walking on the travellers.





**Figure 1.** The layout of the travelators between Central Station and Hong Kong Station

Group behaviour, including mimicking those surrounding one, may enter into the decisions to stand, walk or by-pass. To examine this issue, standees were considered for their group characteristics. Modest increases in overall pedestrian volume results in greater increases in density on the travelator, which might then induce the decision to by-pass or to stand firm.

Video segments from an oblique angular view of the facility enabled subsequent extraction of traversal time and stance – in our case, the binary standing firm and walking. The vast majority of observed individuals did one or the other exclusively. There were 37 samples from 36 s to 99 s in duration, where 3,342 individuals were coded as walking on the travelator, standing firm on the travelator or walking on the by-pass and the generated walking speed derived from the time taken to go from end to end of the travelator, standing or walking. A database for the coded individuals is created with these data.

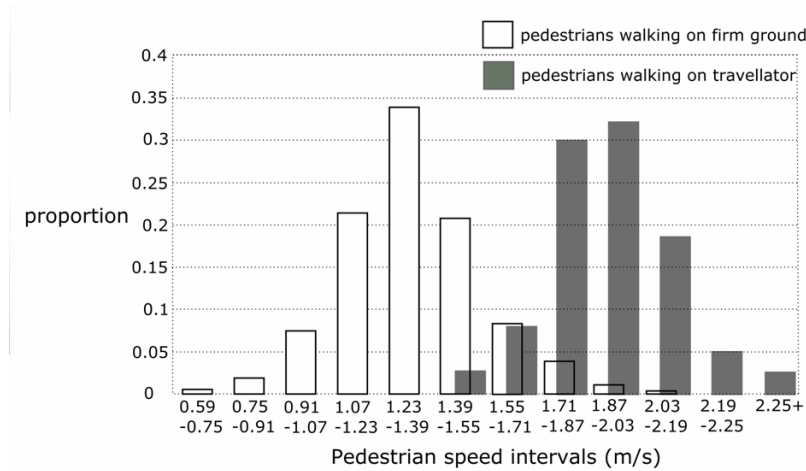
A bivariate analysis seeks out the basic relationships between the variables in the behavioural outcome of the travelators. A regression analysis with the resulting mean speed of individuals passing through the channel will show the extent to which these variables are interacting. Speed is the indicator for efficiency understood as throughput. Inferences from the modelling of movement are drawn to illustrate features that deserve consideration in the design phase for the reasons of the behavioural outcomes. The final analysis is of revealed benefits in relation to the commitments in space and funds for such travelator projects.

### 3. RESULTS

Flow rates varied from 0,33 to 6,02 persons/sec. with a mean of 1,89 (SD = 1,34). While average speed of all pedestrians declined slightly as pedestrian volume rose (-,11), the decline was not significant. This is in keeping with our observation that there were nearly no cases of saturated and impeded flow. The numbers of standees had an expected negative effect on walking speed for those on the travelator (-,29;  $p=0,79$ ), in keeping with the observation that moving pedestrians must pass the standee usually on the left but will tend to do so at slightly reduced speed. The number of standees also had a significant negative effect on overall walking speed (-,61;  $p=,000$ ) but not because they represent an increasing proportion of the total flow. With increasing numbers of walkers on the travelator, average speed of those walking on the facility declined (-,48;  $p=,003$ ), although the number of those walking on the travelator had no significant effect on average speed overall. At the higher volumes of walkers on the travelator, it is seen that reduced spacing also reduces stride length. The number of standees had a strong positive relationship with the number walking on the by-pass route (,64;  $p=,000$ ), in all likelihood indicating that individuals tended to choose walking on the ground when they saw larger numbers of standees on the travelator. They would perhaps anticipate that their progress would be limited by the standees.

Overall, those walking on the travelator move faster on average (1,91m/s; SD=0,19) than those walking on the floor (1,42m/s; SD=0,22), because the travelator is moving at 0.79m/s. Without the mechanical assist, they

would be walking at 1,12m/s. Overall walking speed (1,66m/s) is increased through the use of the traveller over the walking speed on the ground by 17%. This includes those standing on the traveller (figure 2).



**Figure 2.** The frequency distribution of moving speeds on firm ground and on the travellers.

The incline or its absence had no significant impact on speeds or the distribution of standees and those walking. Accordingly, this variable is eliminated from the regression analysis.

At the highest volume flows, there is bunching and stasis at the entrance to the traveller that might persist for several seconds per individual, that is not factored in the flows on the traveller or beside it. This occurs again before the end of the track since disembarking pedestrians slow their pace and often make a half-step to exit the facility. At higher pedestrian flow, i.e. >5 p/s, the stopped queue at the end of the track may persist for several seconds. The exchange spaces adds complexity where some individuals must find their way around others moving across the vector of movement.

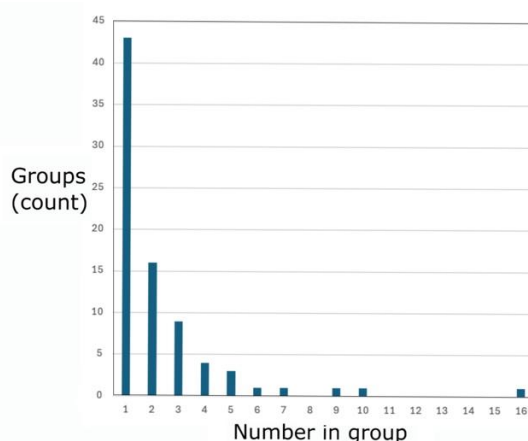
A linear regression model examines the variable effects of each of the movement components on the resulting speed (table 1). The presentation is hierarchical, to enable detection of the contribution of individual variables. Evidently, standing behaviour on the traveller is the biggest factor in transit speed in the corridor, even if this variable is weakly related to the others. In this model, 44% of the variance can be explained by 4 independent variables. Although the direction of this model is clear, with the direction of effect of individual variables fitting with theory, further interpretation is limited by data availability.

**Table 1.** Linear regression for overall transit speed as a function of four predictor variables.

Regression Variable	Regression Coefficient	t-value	SEE	Standard. B	ANOVA R <sup>2</sup>	F-value
Standing	-,011	-4,500***	0,150	-5,872	,37	20,252***
Standing	-,008	-2,55**	0,148	-4,271	,41	11,640***
Walking	-,002	-1,512		-0,498	,41	11,640***
Standing	-,007	-2,240**	0,145	-3,737	,42	7,865***
Walking	-,003	-1,686*		-0,746		
Walking/WW	-,001	0,790		-0,101		
Standing	-,008	-2,314**	0,150	-4,271	,42	5,903***
Walking	-,002	-0,1032		-0,497		
Walking/WW	,001	0,879		0,101		
Flow	-,040	-0,653		-153,610		

\*p<,10; \*\*p<,05; \*\*\*p<,01

Standing behaviour is a result of several factors but is not induced by total flow on the traveller or the total pedestrian volume. Individual standees (n=43), more than 1 m from any other individual, are typically concentrating on their cellphones. Others are in conversation with one or more others. There is also a tendency to fall into the line of standees when the line is already long. Thus, standing behaviour is a result of individual behaviours and response to others' behaviours (figure 2).



*Figure 2. The frequency distribution of grouped standing behaviour.*

#### 4. DISCUSSION

The theoretical and laboratory-based predictions that pedestrians will slow their voluntary walking speed when on a track moving in the direction of their walk [17][18] are borne out in the present empirical study. This is a novel finding because it derives from the real world of actual, unguided human behaviour and also is supportive of the psychological theory from a behavioural perspective. There are many other, uncontrolled factors that could have weighed on the walking pace, including momentary distractions, pauses, anchor points, the space itself and the dynamics of others, footwear, preceding physical activity, etc. While these remain tantalizingly beyond the scope of the present investigation, what remains is the clear identification of the dynamics of movement on and beside the traveller and their relation with the desired aims of efficiency.

Following this result of differential speeds, the faster the track is moving, the slower the pace of the transported pedestrians, as evidenced in the observed behaviours on the AMWs at L.B. Pearson International Airport and Schiphol International Airport. Overall, as the present case demonstrates, average speed of displacement on the traveller is slightly increased over observed walking speed on the parallel way, the effect of which is attenuated by slightly slower walking speed. The point is that behaviour enters into a symbiosis with the infrastructure, using the infrastructure for a variety of purposes. The behaviours themselves appear to seek some kind of balance among a variety of issues including utility, energy consumption, cognitive load, thought. The infrastructure variations on the experience of travel in the underground also offers clear time savings for a small minority of athletic-minded users.

While metro systems continue to develop worldwide and introduce more underground space and movement systems, there is also the opportunity to make corridors that are not purely transport linkages. The TST tunnel that also offers access to the K-11 Art Mall in Hong Kong is a case in point where two major bi-directional travellers also offer faster and more direct routes between the stations. The new underground 430 m-long concourse at Shinjuku, Tokyo, between the Takashimaya department store and the Isetan store is meant to bring these two commercial powerhouses closer together, using an underground, climate-controlled pathway without stops. The wider urban plans for development of traveller systems envisioned by Scarinci et al (2017a) are likely to garner more attention as underground networks develop.

To consider such movement systems as generalized infrastructure introduces the question of how we want to control the channel containing the traveller since the traveller is essentially a closed system without access to the spaces to either side. A possible solution is a multi-scalar approach to the movement system, to retain ground-based movement that is more distributed while longer and dedicated trajectories are handled on travellers, and then even longer trips on underground rail. That was the promise of the earliest urban application of the traveller at the 1900 Exposition Universelle in Paris, where the Rue de L'Avenir consisted of two parallel tracks that carried passengers for up to 3,5 km at 1,17 m/s and 2,36 m/s next to a fixed walkway. The 3,5 km distance with nine intervening stations could be accomplished in 26 minutes. If the passengers on the faster track had been walking at the usual pace, the entire trip could be done in 15 minutes. These distances and times are already optimal among the available other choices. While such an implementation is now more difficult on the ground with so many competing interests, it is much more feasible underground. Not surprisingly, the longest and most heavily used travellers are in underground space.

While speed delivers the desired efficiency, higher entry speeds are related to mishap rates. It may be that experience and training could reduce these events but it remains a novel experience to step onto a moving walkway

for most people [19]. Mishaps on travellers occur and are perhaps less risky than those on escalators but nevertheless may involve falls. More work is needed to solve the entry and exit speed differential problem.

The more general policy issue concerns whether this is a good investment in underground space when larger distances are to be traversed. In the present case, there was a 17% increase in speed and thus in throughput with the traveller, but only in off-peak periods. Whether this efficiency boost alone is sufficient for the infrastructure and its maintenance is a question when considering where else the money could be spent. The results of this study do not support the implementation of travellers for the purposes of increasing throughput at peak travel times.

One could make an argument for the qualitative aspects of the facility. From a practical standpoint, the traveller organizes some proportion of the movement, inducing movement cohorts and reducing movement conflicts. The traveller offers a respite to those wanting to focus on their cellphones while continuing their progress and offering accelerated movement to those wanting to save time. The footprint is relatively small, while contributing to the demarcation of the movement space, something that is traditionally achieved through a colonnades or a line of bollards.

## 5. CONCLUSION

This study evaluated the efficiency claims for travellers by examining a real case of several travellers in a busy underground transport corridor.

The research revealed in quantitative terms the contribution of a traveller in a movement corridor to overall movement efficiency measured in time and throughput. Users walk at lower speed than when they are walking on firm ground, but are moving at overall faster speed than those on the ground. The use of the traveller for sedentary activity is notable, with 12,1% of those transiting the space remaining stationary on the traveller, to stand, rest, engage in a chat or review some feeds on an electronic device. The standing space is consistently on the righthand side of the moving track in the Hong Kong case, allowing a single person to pass. Those who choose to walk on the parallel ground are 20,2% of the total in the present sample, but at peak time this figure rises to over 80%. The traveller notably does not deliver added efficiency at the peak travel times in the morning and early evening. At those points, the wider walking corridor can accommodate a rank of pedestrians if all are travelling in the same direction, while the crowded traveller may be subject to congestion, slow speeds or no personal locomotion around the entry point and on the track nearer the exit. This means that at peak times, movement on the traveller is slower than on the ground. On average and at non-peak times, the traveller delivers efficiencies but not at peak times.

The promise of such systems in underground space is to link two locations more closely than can otherwise be achieved on the surface. In certain applications, the traveller can deliver efficiencies and help organize the movement while in other instances it is likely to be neither necessary nor cost-efficient. From the present study, we can conclude that distance alone is not a good foundation for going ahead with implementation.

The strength of this article is the validation of theory regarding behaviour with empirical observation. It is not known whether such observed behaviours are universals. Ideally, one would have access to a long video record from CCTV cameras, which was not available in this case. This would allow the inclusion of highest volume-flow and variations by time of the day and day of the week.

## 6. REFERENCES

- [1] The Lift Consultancy. Consulted 2025-05-10 <https://theliftconsultancy.co.uk/how-does-a-travelator-moving-walk-work/>
- [2] Fujitec. Consulted 2025-05-10 <https://www.fujitecindia.com/resource/blogs/understanding-travelators-a-comprehensive-guide>
- [3] Hawkins, N.M. & Atha, J. (1976). A study of passenger behaviour on a slow speed traveller system. *Ergonomics* 19, 4, 499-517.
- [4] Dazen. Consulted 2025-05-10 <https://dazenelevator.com/what-is-a-travelator/>
- [5] Rastogi, R., Thaniarasu, I. & Chandra, S. (2011). Design implications of walking speed for pedestrian facilities. *Journal of Transportation Engineering* 137, 10, 687-696. Doi: 10.1061/(ASCE)TE.1943.5436.0000251.
- [6] Boysen, N., Biskorn, D. & Schwerdfeger, S. (2021). Walk the line: optimizing the layout design of moving walkways. *Transportation Science* 55, 4, 908-929. <https://doi.org/10.1287/trse.2021.1051>
- [7] Zacharias, J. (2013) The Central–Mid-levels Escalator as urban regenerator in Hong Kong. *Journal of Urban Design*, 18, 4, 559-570.
- [8] Christensen, C.B. (2023). Congested metro materialities: how platform escalators afford “friction” in the Copenhagen Metro. *Applied Mobilities* 8, 4, 287-304. Doi: 10.100/23800127.2022.2034098

- [9] Young, S.B. (1999). Evaluation of pedestrian walking speeds in airport terminals. *Transportation Research Record: Journal of the Transportation Research Board* 1674, 20-26.
- [10] Kim, K., Hallonquist, L., Settachai, N. & Yamashita, E. (2006). Walking in Waikiki, Hawaii – measuring pedestrian level of service in an urban resort district. *Transportation Research Record: Journal of the Transportation Research Board* 1982, 104-112.
- [11] Zacharias, J. and Ling, R. (2014). Choosing between stairs and escalator in shopping centers—the impact of location, height and pedestrian volume. *Environment & Behavior* 47, 6. DOI: 10.1177/0013916513520418
- [12] Scarinci, R., Markov, I. & Bierlaire, M. (2017). Network design of a transport system based on accelerating moving walkways. *Transportation Research Part C* 80, 310-328. <http://dx.doi.org/10.1016/j.trc.2017.04.016>
- [13] Scarinci, R., Bahrami, F., Ourednik, A. & Bierlaire, M. (2017a). An exploration of moving walkways as a transport system in urban centers. *EJTIR* 17, 2, 191-206.
- [14] Burkhardt, J.M., Cahour, B. & Allinc, A (2024). Exploring user experience of transport modes through the multiple dimensions of psychological comfort. *European Conference on Cognitive Ergonomics 2024, ECCE 2024*.
- [15] Roncoli, C., Chandakas, E. & Kaparias, I. (2023). Estimating on board passenger comfort in public transport vehicles using incomplete automatic passenger counting data. *Transportation Research Part C: Emerging Technologies* 146, 103963. <https://doi.org/10.1016/j.trc.2022.103963>
- [16] Abenoza, R.F., Cats, O., Susilo, Y.O. (2019) How does travel satisfaction sum up? An exploratory analysis in decomposing the door-to-door experience for multimodal trips. *Transportation* 46, 1615–1642.
- [17] Srinivasan, M. (2009). Optimal speeds for walking and running, and walking on a moving walkway. *Chaos: An interdisciplinary journal of nonlinear science* 026112. <https://doi.org/10.1063/1.3141428>
- [18] Mohler, B. J., Thompson, W. B., Creem-Regehr, S. H., Pick, H. L. Jr., & Warren, W. H. Jr. (2007). Visual flow influences gait transition speed and preferred walking speed. *Experimental Brain Research* 181, 221.
- [19] Hawkins, N.M, Atha, J. and Ashford, N. (1974). Behavioural observations of pedestrians boarding a slow speed conveyor. Department of Transport Technology, University of Technology, Loughborough, Report TT7411.



## OPTIMIZATION OF TUNNEL VENTILATION SYSTEMS IN FIRE EMERGENCIES

Andrei Danilov<sup>1</sup>, Vladimir Chizhikov<sup>2</sup>

**Abstract:** The issue of ensuring safe evacuation conditions from underground structures of subways, railway, and road tunnels remains relevant, as evidenced by statistical data on fires at these facilities. One of the key factors determining human safety in emergencies is the high efficiency and reliability of tunnel ventilation systems during fire emergency modes.

The aim of this work is a comparative analysis of the efficiency of smoke exhaust valves with different orientations relative to the tunnel axis (longitudinal and transverse arrangement) and the development of an optimal activation algorithm for tunnel ventilation devices based on the obtained results, considering various tunnel gradients and distances between smoke valves. Given the significant cost and complexity of full-scale experiments, the research was conducted using developed CFD models implemented in the Fire Dynamics Simulator (FDS) program. The tunnel section model used for numerical experiments consists of a computational domain including a 700-meter-long tunnel section of constant cross-section with variable gradient sections, a fire source, and variable-geometry smoke exhaust valves ensuring the required exhaust flow rate of combustion products. To ensure stable ventilation, the computational domain is connected to two tunnel sections of identical cross-section, modeled using a combined scheme with HVAC elements.

The results of the computational experiments demonstrate a significant (over twofold) increase in smoke extraction efficiency, measured by the reduction in the smoke-filled zone length, when using transversely oriented smoke exhaust valves compared to the longitudinal valve arrangement scheme. The simulation results enable the selection of an optimal activation algorithm for the tunnel ventilation system during a tunnel fire, considering the fire source location and the gradient of the emergency tunnel section, using an addressable fire alarm system.

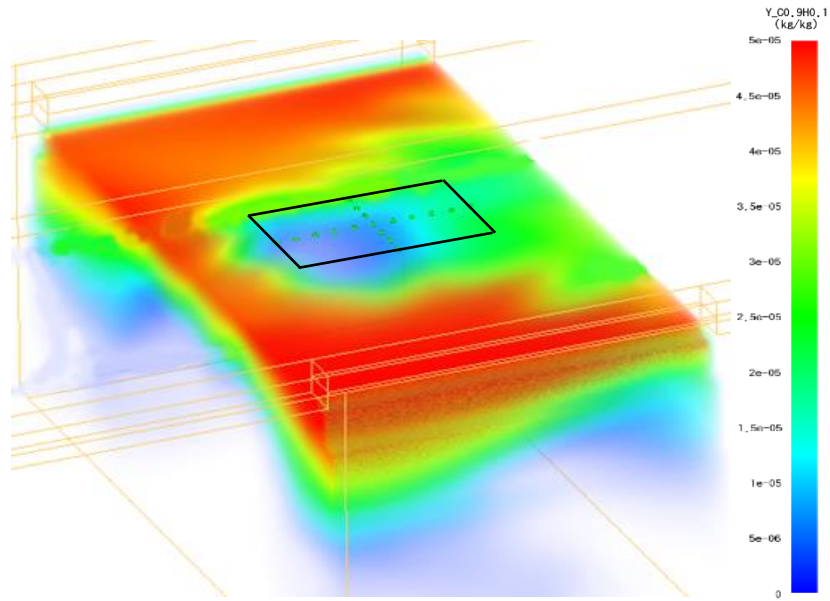
**Keywords:** tunnel fire, tunnel ventilation, smoke exhaust duct, smoke exhaust valve, smoke-filled zone.

### 1. INTRODUCTION

This article, part of a comprehensive analysis of tunnel ventilation organization in double-track subway tunnels, addresses the optimal arrangement and configuration of smoke exhaust valves for tunnel ventilation system ducts, as well as the selection of a smoke exhaust system activation algorithm integrated with the fire detection system. Analysis of smoke exhaust system modeling results showed that with longitudinal valve installation, due to airflow characteristics near the valve, the smoke front can advance beyond the valve, reducing valve efficiency. This is confirmed by analyzing the distribution of ash particle concentrations across the valve cross-section. Figure 1 shows the 3D distribution of soot mass fraction concentrations in the valve area. The distribution reveals that the central zone of the valve (area of maximum airflow velocity) extracts clean, smoke-free air from the lower part of the tunnel's traffic zone. Only a small peripheral area of the valve effectively removes combustion products. Furthermore, on gradients, the smoke layer front spreads unimpeded along the tunnel ceiling slab between the valve boundaries and the tunnel lining, especially with increasing tunnel gradient. This phenomenon (Plug-holing) has been noted by several researchers [1, 2], but no recommendations for mitigating it were proposed. Only in [3] was it concluded that the area of the smoke exhaust valve has little significant effect on extraction efficiency, while increasing the valve width may improve efficiency. Therefore, numerical modeling of transversely arranged valves, installed across almost the entire width of the tunnel ceiling slab, is of significant interest.

1 Head of Center for research of fire hazardous factors LLC, Andrei Danilov, 7, Tallinskaya str., Saint-Peterburg, Russia, 195196, e-mail address – [adanilav@gmail.com](mailto:adanilav@gmail.com)

2 PhD, Vladimir Chizhikov, Fire Eng., Center for research of fire hazardous factors LLC, 7, Tallinskaya str., Saint-Peterburg, Russia, 195196, e-mail address – [vovach1952@gmail.com](mailto:vovach1952@gmail.com).

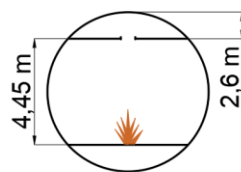
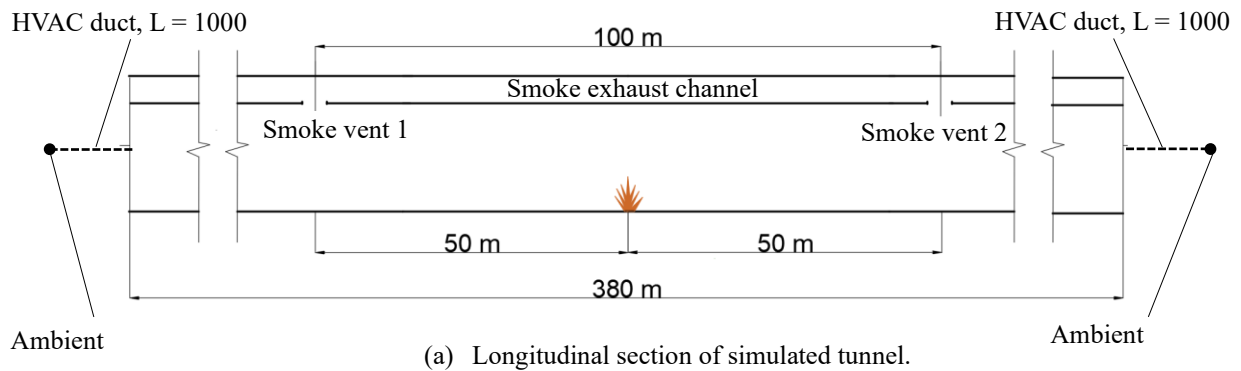


**Figure 1.** 3D distribution of soot mass fraction in the smoke exhaust valve area.

## 2. RESEARCH METHODOLOGY

A double-track subway tunnel with an internal lining diameter of 10.4 m was chosen as the model. Simulations were performed using a combined FDS (version 6.9.1) and HVAC model. The computational domain is 380 m x 10 m x 6.5 m. The grid cell size, following recommendations [4], was set to 0.25 m x 0.25 m x 0.25 m. Two connected tunnels, each 1000 m long, were modeled using HVAC elements to conserve computational resources. The model replicates the configuration of a section between stations. The gradient of the tunnel section within the computational domain can vary from 0 to 40 ‰. Smoke removal flow rate –  $50 \text{ m}^3 \cdot \text{s}^{-1}$ .

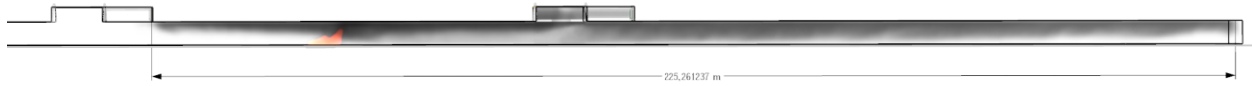
Fire power was set at 6 MW, and the distance between smoke exhaust valves at 100 m. The schematic of the computational model is shown in figure 2. Smoke exhaust valve dimensions were set to 2 m x 4 m for longitudinal arrangement and 1 m x 8 m for transverse arrangement.



(b) Cross-section of simulated tunnel.

**Figure 2.** Arrangement of simulated tunnel.

A preliminary assessment of valve orientation efficiency involved modeling the dynamics of hazardous fire factors propagation under identical initial and boundary conditions (tunnel geometry, fire power, distance between valve axes, exhaust flow rate per valve, valve area, tunnel gradient  $U = 25\%$ ,  $L = 50$  m). The results indicated a significant reduction (over twofold) in the smoke-filled zone length when using transverse valve orientation (Figures 3, 4).



**Figure 3.** Smoke spread in tunnel (longitudinal arrangement of smoke exhaust valves,  $t = 200$  s).



**Figure 4.** Smoke spread in tunnel (transverse arrangement of smoke exhaust valves,  $t = 200$  s).

Based on these preliminary results, additional studies were conducted to evaluate the proposed solution's effectiveness and its impact on the overall smoke exhaust system algorithm. The extent of the smoke-filled zone was chosen as the efficiency criterion. This extent is considered a function of the tunnel section gradient and the distance from the valve axis to the fire source.

The following model was adopted for processing experimental results:

$$y(a, x) = a_0 + a_1 \cdot x_1 \cdot x_1 + a_2 \cdot x_2 \cdot x_2 + a_3 \cdot x_1 + a_4 \cdot x_2 + a_5 \cdot x_1 \cdot x_2 \quad (1)$$

where:

$y(a, x)$  - function value;

$a_i$  - model coefficients;

$x_1$  - dimensionless gradient value;

$x_2$  - dimensionless distance from the smoke exhaust valve axis.

Model coefficient determination, adequacy assessment, and coefficient significance evaluation followed algorithms described in [5]. Numerical experiments also monitored gas flow rate changes at the left and right boundaries of the computational domain and velocities within the grid. Simulations covered the following parameter ranges: tunnel gradient – 0 – 40 ‰, distance from Valve 1 axis to fire source – 10 – 90 m.

### 3. RESULTS

A series of computational experiments yielded the following results:

1. Using:

$$x_{1i} = \frac{U_i - 0.5(U_{max} + U_{min})}{0.5(U_{max} - U_{min})}, \quad x_{2i} = \frac{L_i - 0.5(L_{max} + L_{min})}{0.5(L_{max} - L_{min})}, \quad (2)$$

where:

$U_i$  - current tunnel section gradient value, ‰;

$U_{max} = 40$  ‰ – maximum gradient value;

$U_{min} = 0$  ‰ – minimum gradient value;

$L_i$  - current distance from Valve 1 to fire source, m;

$L_{max} = 90$  m – maximum distance value;

$L_{min} = 10$  m – minimum distance value.

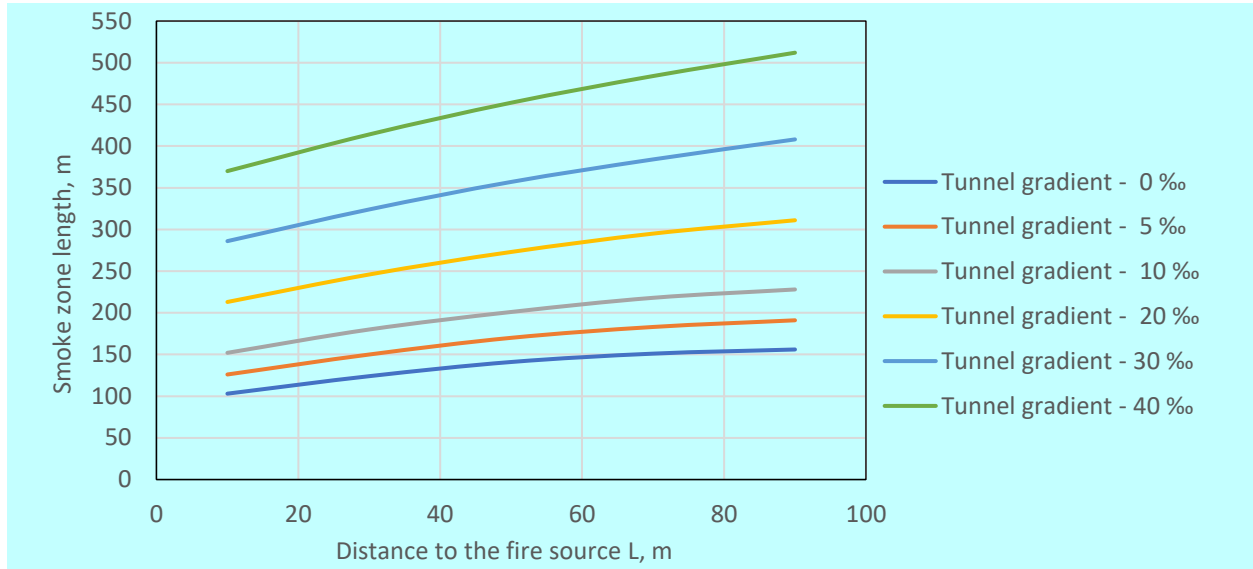
Substituting the experimentally derived coefficients into function (1) yields:

$$L_s = 273,4847 + 22,9572 \cdot x_1 \cdot x_1 - 10,619 \cdot x_2 \cdot x_2 + 155,642 \cdot x_1 + 48,8189 \cdot x_2 + 21,7516 \cdot x_1 \cdot x_2 \quad (3)$$

where:

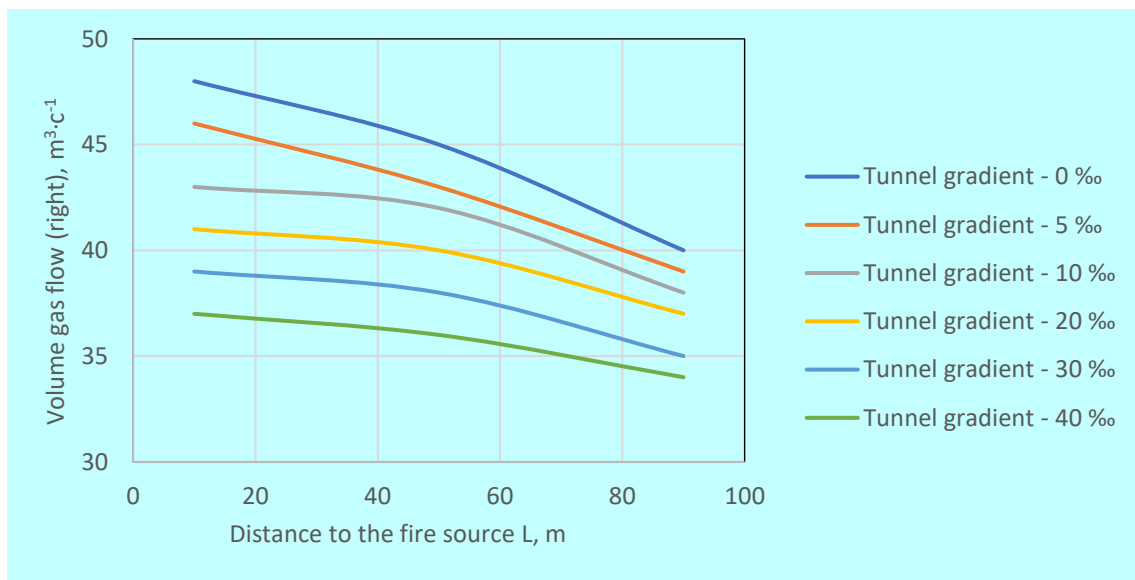
$L_s$  - smoke-filled zone length, m.

Graphical representation is shown in Figure 5. The above results pertain only to longitudinal valve arrangement. For transverse orientation, the smoke-filled zone did not exceed the distance between valves ( $\leq 100$  m).



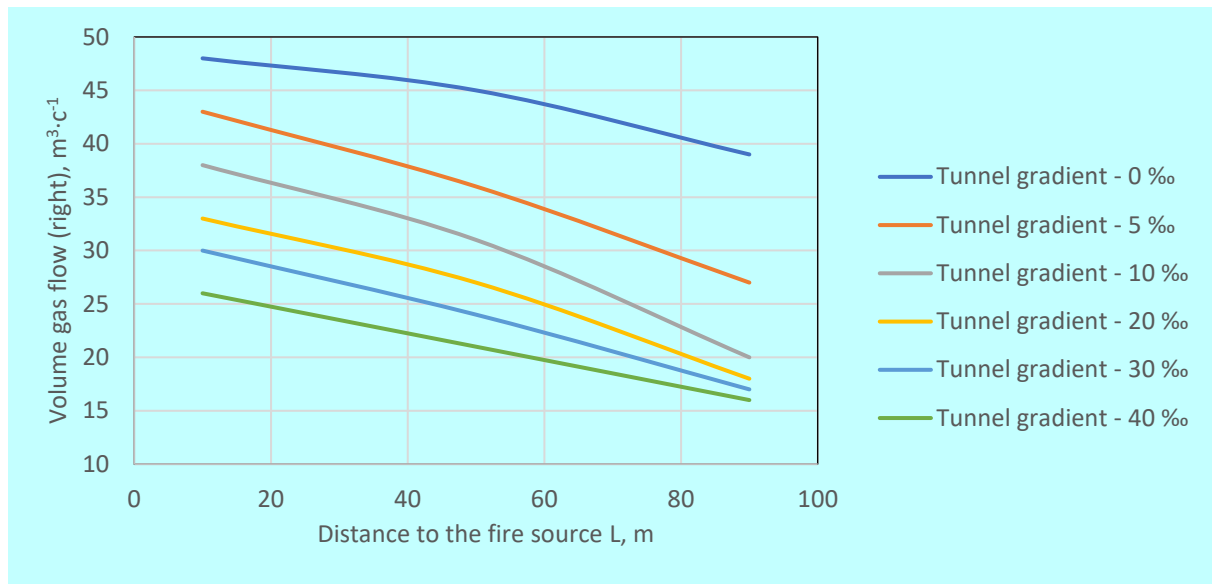
**Figure 5.** Dependence of the smoke zone length on the distance to the fire source

2. Calculations revealed a trend of decreasing gas flow rate in the right branch of the computational domain as the tunnel gradient and distance to the fire source increased. For transversely arranged valves, the average gas flow rate for gradients between 0 and 40‰ was 44.3 -- 35.7  $\text{m}^3 \cdot \text{s}^{-1}$  (Figure 6).



**Figure 6.** Dependence of the volume gas flow on the distance to the fire source (transverse arrangement of valves)

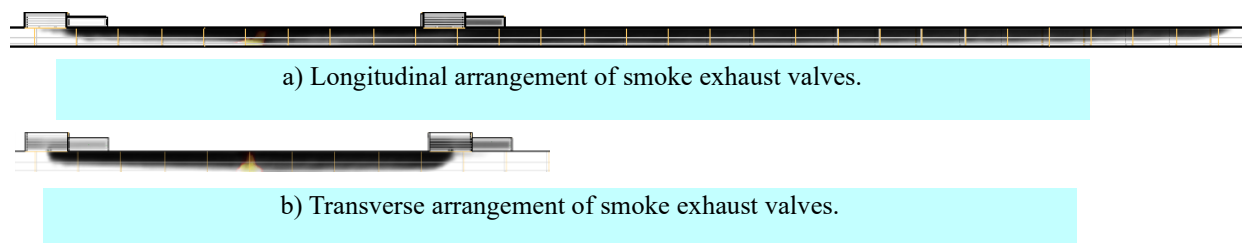
For longitudinally arranged valves, the average flow rate was 44.0 - 21.0  $\text{m}^3 \cdot \text{s}^{-1}$  (Figure 7).



**Figure 7.** Dependence of the volume gas flow on the distance to the fire source (longitudinal arrangement of valves)

Absolute gas flow rates upstream of the fire (against the combustion product flow) were on average 50% higher for transverse valves compared to longitudinal valves.

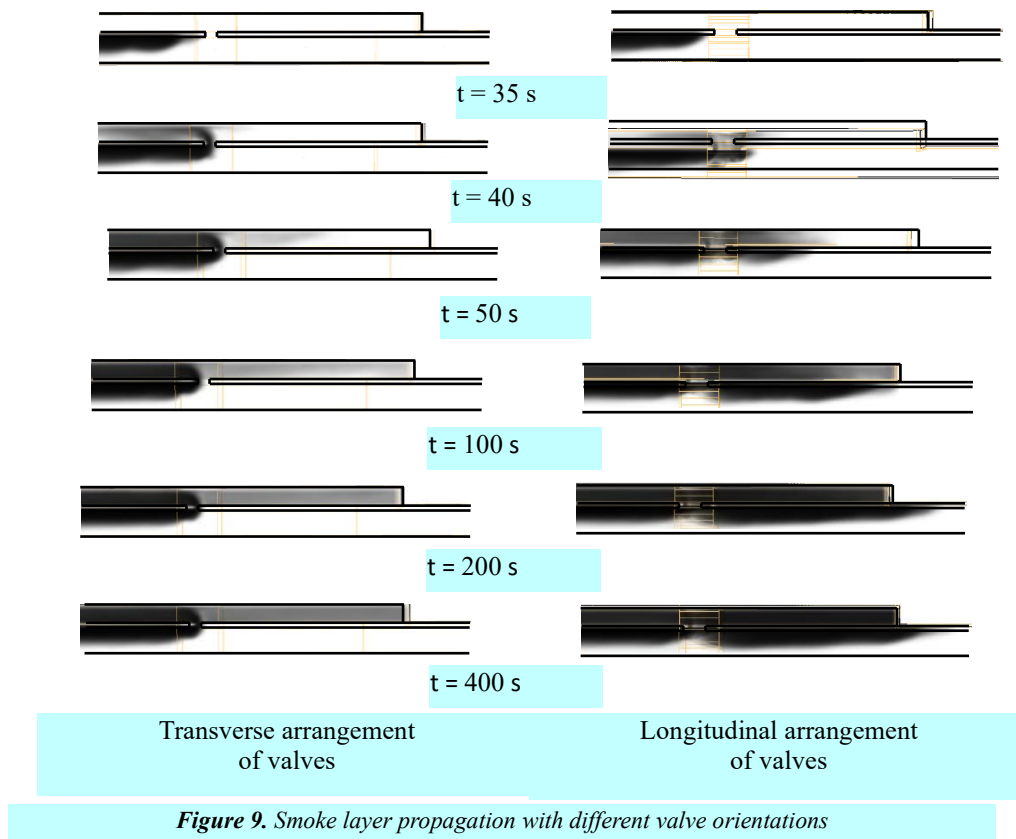
3. For tunnel gradients exceeding 10% with longitudinal valves, activating valves on both sides of the fire source significantly increased (over twofold) the smoke-filled zone and rendered the downstream valve ineffective. For the transverse valve scheme, both valves continued to function effectively, and the smoke-filled zone did not exceed the distance between valves (Figure 8).



**Figure 8.** Smoke spread in tunnel ( $U = 20\%$ ,  $L = 50\text{ m}$ ,  $t = 500\text{ s}$ ).

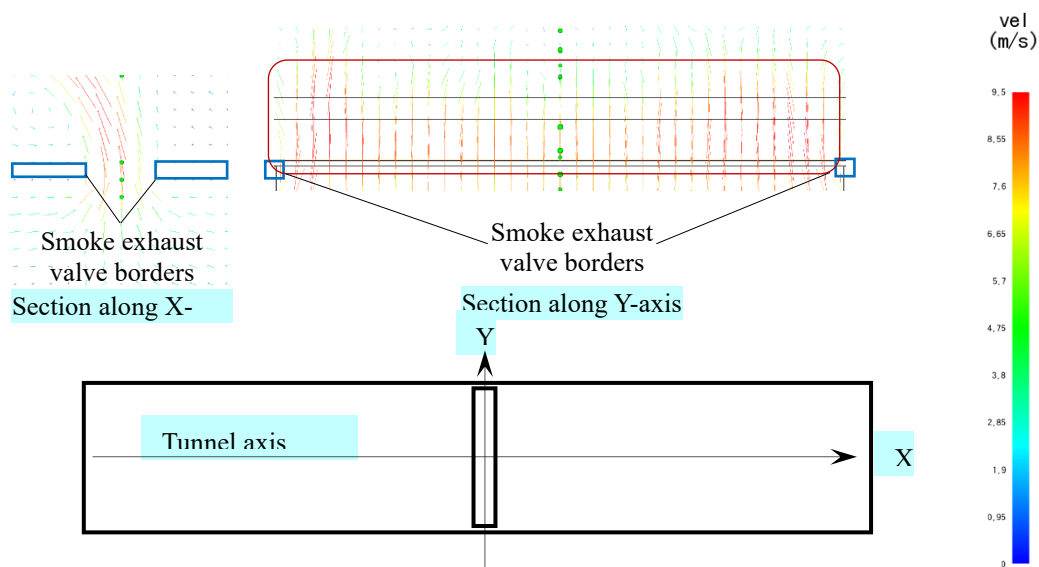
4. Comparative analysis of smoke propagation dynamics under identical conditions showed that with transverse valves, smoke did not propagate along the tunnel but was entirely captured by the valve (Figure 9) and contained throughout the simulation period. With longitudinal valves, smoke propagated along the tunnel axis until a steady-state mode was reached ( $t \approx 280\text{ s}$ ), where further smoke front movement was halted by counter airflow between  $t = 35\text{...}300\text{ s}$ .



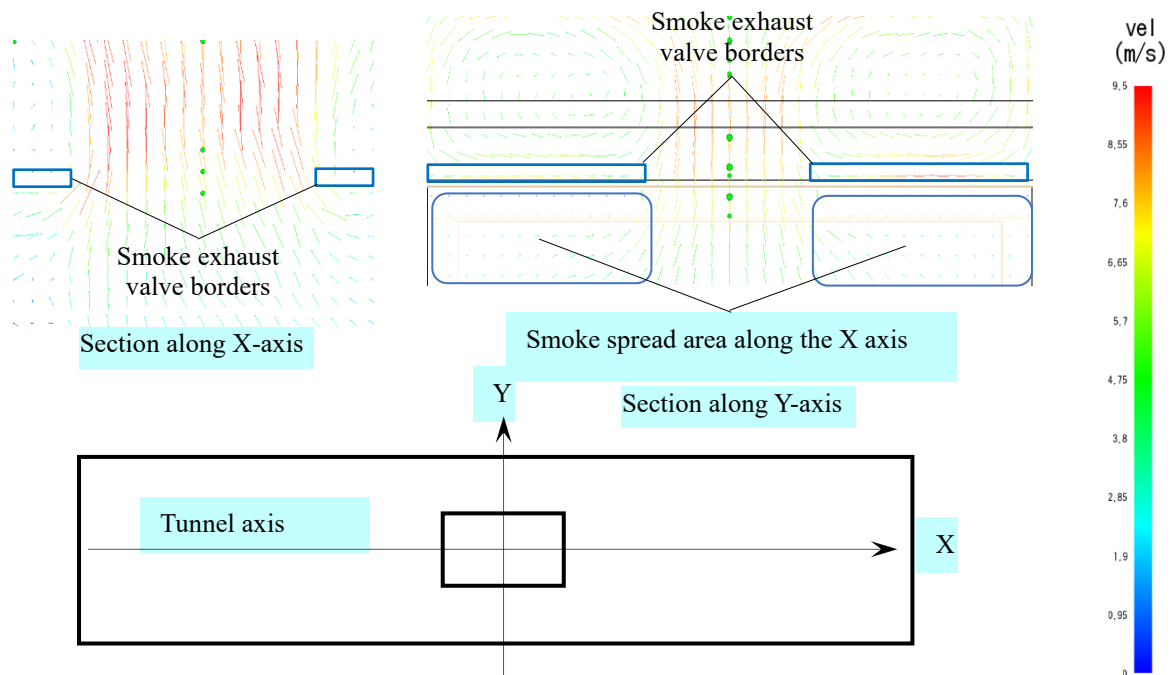


**Figure 9.** Smoke layer propagation with different valve orientations

Velocity fields in valve cross-sections are shown in Figures 10 and 11. For transverse valves (Figure 10), the velocity field in the Y-section shows a nearly uniform distribution of the vertical velocity component across the entire tunnel width (with increased velocities near the lining) -- zone marked by a red line. For longitudinal valves (Figure 11), the zone of stable vertical velocity (red line) constitutes only a small part of the tunnel cross-section (relative to valve width). Areas under the ceiling slab near the tunnel lining (marked blue in Figure 11) allow unimpeded smoke passage along the X-axis.

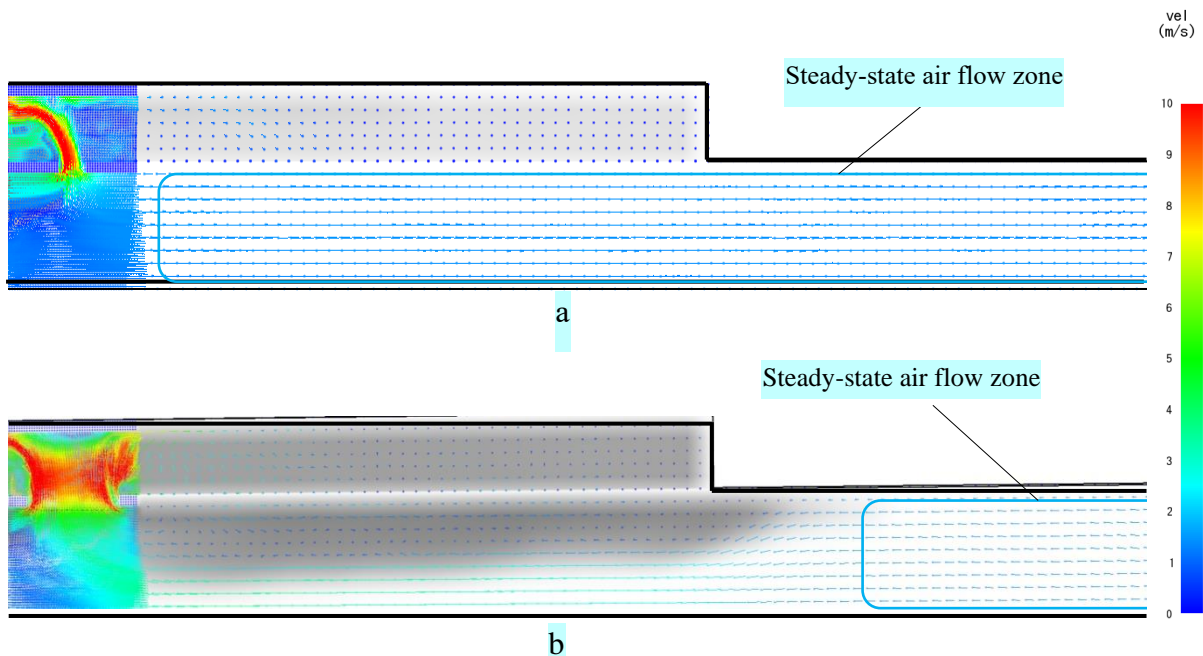


**Figure 10.** Velocity fields in the cross-section of the smoke exhaust valve (transverse arrangement of valves)



**Figure 11.** Velocity fields in the cross-section of the smoke exhaust valve (longitudinal arrangement of valves)

5. For transverse valves, a steady-state airflow mode formed downstream of the valve (blue rectangle, Figure 12a) shortly after activation, creating a barrier preventing smoke front passage beyond the valves. For longitudinal valves (Figure 12b), this steady-state airflow zone formed significantly later (~100s delay) and was located 40...80 m from the valve (depending on exhaust rate), allowing the smoke front to propagate beyond the inter-valve distance



**Figure 12.** The structure of air flow distribution in the area of smoke exhaust valves for transverse (a) and longitudinal (b) arrangement of valves

#### 4. DISCUSSION

The results demonstrate that transverse valve arrangement has significant advantages over the longitudinal scheme for the following reasons:

The gas flow structure near transversely oriented valves exhibits distributed exhaust across the entire tunnel width (Fig. 10), eliminating pathways for combustion products along the ceiling edges (Fig. 11).

The flow structure downstream of the valve and higher upstream gas flow rates indicate that transverse valves maintain higher opposing gas velocities against advancing combustion products and preserve smoke layer stratification.

Modeling confirmed that transverse valves limit the smoke-filled zone to the distance between valves.

Containing the smoke layer within the inter-valve distance for gradients  $>10\%$  was unattainable with longitudinal valves.

For longitudinal valves within a detection zone equal to the valve spacing, reducing the smoke-filled zone length requires activating valves downstream (uphill) of the fire, which is often ineffective and complicates the activation algorithm integrated with fire detection.

The activation algorithm for transversely arranged valves simplifies to activating the valves immediately adjacent to the fire source on both sides.

#### 5. CONCLUSIONS

The analysis of valve performance parameters for both arrangement configurations validates the obtained results.

The presented smoke exhaust system design will ensure confinement of the smoke-filled zone within the chosen valve spacing while optimizing ventilation equipment costs.

The transverse arrangement of smoke valves relative to the tunnel axis is the optimal solution, with the valve width maximized based on the tunnel's structural constraints. An algorithm for activating valves based on signals from an addressable alarm system, using the criterion of minimizing the tunnel's smoke-filled zone length, has been determined. The obtained results can be utilized in designing ventilation systems for subway, railway, and road tunnels.

#### 6. REFERENCES

- [1] Linjie Li, Zihe Gao, Jie Ji, Jianyun Han. Research on the Phenomenon of Plug-holing under Mechanical Smoke Exhaust in Tunnel Fire. *Procedia Eng.* 2015, 62, 1112–1120.
- [2] Xu, Pai and Zhu, Daiqiang and Xing, Rongjun and Wen, Chuanyong and Jiang, Shuping and Li, Linjie, Study on Smoke Exhaust Performance in Tunnel Fires Based on Heat and Smoke Exhaust Efficiency Under the Lateral Centralized Mode. *Case Studies in Thermal Engineering* 34 (2022) 102002.
- [3] 18. Liu, Y.; Yang, D. Experimental study on synergistic effect of exhaust vent layout and exhaust rate on performance of ceiling central smoke extraction in road tunnel fires. *Int. J. Therm. Sci.* 2023, 183, 107886.
- [4] K. McGrattan, S. Hostikka, J.E. Floyd, *Fire Dynamics Simulator (Version 6), User's Guide*, vol. 1019, NIST special publication, 2024, 488 p.
- [5] Hartman K., Letsky V., Schaefer V. Experimental design in process engineering research. «Mir», M., 1977, 522 p.

## EVACUATION BEHAVIOR AND SAFETY EGRESS ANALYSIS IN TUNNEL FIRES: A VIRTUAL REALITY SIMULATION STUDY

Vasilis Kotsakis<sup>1</sup>, Christos Froudakis<sup>2</sup>, Anastasios Kallianiotis<sup>3</sup>, Maria Menegaki<sup>4</sup> and Dimitrios Labrakis<sup>5</sup>

**Abstract:** The rapid development of underground transport tunnels is accompanied by the inevitable risk of road accidents, which can result in major fires. The required safety egress time (RSET) is a critical parameter in designing fire mitigation strategies for tunnels. In these environments, where visibility is severely reduced due to smoke, evacuation behavior—including pre-evacuation time, encompassing alarm response, reaction time, and vehicle abandonment—plays a significant role in overall safety. This study employed a virtual reality (VR) simulation in Unreal Engine of a full-scale road tunnel, paired with computational fluid dynamics (CFD) modeling, to examine occupant behavior during tunnel fires across different scenarios. These scenarios varied based on smoke presence, alarm activation speed, and proximity to the fire source. The key factors analyzed were: (a) evacuation decision-making, (b) pre-evacuation time, and (c) route-finding strategies. The results indicate that pre-evacuation time is influenced by the type of emergency warning signals, smoke spreading, alarms, and occupants' behavior. Most participants relied on exit signs to navigate their way out. However, smoke-filled routes often led some individuals to bypass nearby exits in favor of more distant ones, revealing important implications for tunnel design and safety planning.

**Keywords:** tunnel vehicle accident, virtual reality experiment, evacuation behavior, evacuation time

### 1. INTRODUCTION

The growth and dynamics of underground projects in recent years is driven by the general trend of sustainable development that determines the choices of the modern world at a strategic level. The rapid increase in population, combined with the lack of appropriate land-use planning, has often in the past led to a significant deterioration in the quality of life, particularly in urban areas, where the lack of space and environmental conditions for the development of vital activities has often been observed. The main concept in the design of an underground project is the safety of people during construction and operation. In case of emergency such as toxic release or fire, a core emergency response strategy for the safety of people is the structure evacuation.

Human behavior can highly influence the accident occurrence as well as the development of the event (e.g. fire) and the safe management of the incident. Depending on the situation, human behavior can be classified into several categories: routine behavior before an incident, including preventive measures; actions that may contribute to the occurrence of accidents or fires; responses to the presence of fire; behavior related to rescue and evacuation; and actions associated with firefighting (Thematic Network Fire in Tunnels, 2006). Several studies have been investigated the human behavior during emergency evacuation in road or rail tunnels either using computer software (Qin et al., 2020; Ronchi et al., 2012) or real scale experiments (Carlson et al., 2019; Fridolf et al., 2013; Storm & Celander, 2022). Similar studies have also been conducted to investigate evacuation procedures through real-scale fire drills in other underground facilities (Kallianiotis et al., 2022). It is widely acknowledged across the

<sup>1</sup> MSc., Kotsakis Vasilis, Mining Eng., [billkg13@hotmail.com](mailto:billkg13@hotmail.com)

<sup>2</sup> MSc., Froudakis Christos, Mining Eng., [christosfroudakis123@gmail.com](mailto:christosfroudakis123@gmail.com)

<sup>3</sup> PhD, Kallianiotis Anastasios, Mining Eng., researcher, National Technical University of Athens Zografou Campus 9, Iroon Polytechniou Str., 15780 Zografou Greece, [kallianiotis@metal.ntua.gr](mailto:kallianiotis@metal.ntua.gr)

<sup>4</sup> Professor, Mengaki Maria, Mining Eng., National Technical University of Athens Zografou Campus 9, Iroon Polytechniou Str., 15780 Zografou Greece, [menegaki@metal.ntua.gr](mailto:menegaki@metal.ntua.gr)

<sup>5</sup> PhD, Labrakis Dimitrios, Mining Eng., National Technical University of Athens Zografou Campus 9, Iroon Polytechniou Str., 15780 Zografou Greece, [dlabrakis@metal.ntua.gr](mailto:dlabrakis@metal.ntua.gr)

literature that one of the primary factors influencing human behavior and evacuation procedures during tunnel fire incidents is the reduction of visibility caused by smoke. Visibility refers to the distance at which an observer can discern an object against its background, while obscuration describes the reduction in light intensity as it passes through smoke. In fire safety analysis, calculated visibility is commonly used as a criterion for occupant tenability, whereas obscuration is primarily employed to visually represent smoke in simulations. The intensity of light passing a smoked environment is attenuated based on Beer–Lambert Law (1) in which  $I$  is the light intensity;  $K$  is the extinction coefficient;  $L$  is the distance that light travels in the smoked area; and  $I_0$  is incident intensity.  $K$  is calculated from equation (2) in which  $K_m$  is the mass specific extinction coefficient and in FDS is equal to  $8700\text{m}^2/\text{Kg}$  and  $\rho_s$  is the smoke density. Finally, the visibility  $S$  is calculated from equation (3) in which the constant  $C$  is depending on type of sign and for reflective one is between 2 to 4 and for illuminating is between 5 to 10 (Jin, 1997). The default value in FDS is 3 since the visibility refers to a reflective sign (McGrattan et al., 2023a, 2023b).

$$I = I_0 e^{-KL} \quad (1)$$

$$K = K_m \rho_s \quad (2)$$

$$S = \frac{C}{K} \quad (3)$$

A reduction in visibility does not directly impair occupants but significantly affects their movement speed (Fridolf et al., 2013; Jin, 1997), thereby increasing the time spent in hazardous environments with high concentrations of toxic gases (e.g., CO) and temperatures. The toxicity resulting from fire products is assessed based on the concentration of carbon monoxide (CO) and carbon dioxide (CO<sub>2</sub>) generated during the combustion process, as well as the reduction of oxygen (O<sub>2</sub>) levels, which may lead to hypoxic conditions (SFPE, 2016). The maximum value of the Fractional Effective Dose (FED<sub>tot</sub>) is 1.0, indicating the threshold for incapacitation, and is calculated using Equation (4). The individual FED for carbon monoxide exposure (FED<sub>CO</sub>) is determined according to Equation (5). The physiological effects of elevated CO concentrations on the human body are summarized in Table 1. According to SFPE (SFPE, 2016) and to NFPA (NFPA, 2014) the tenability limits of high temperature are presented in Table 2.

$$FED_{tot} = FED_{CO} \times V_{CO2} \times FED_{O2} \quad (4)$$

$$FED_{CO} = \sum_{t1}^{t2} \frac{[CO]}{35000} \times \Delta t \quad (5)$$

**Table 1.** Consequences to human health after carbon monoxide exposure (Purser & McAllister, 2016)

CO Concentration in ppm	Consequences
<b>35</b>	Headache and dizziness after constant exposure 6 to 8 hours.
<b>100</b>	Slight headache after 2 to 3 hours.
<b>200</b>	Slight headache after 2 to 3 hours. Loss of judgment
<b>400</b>	Frontal headache after 1 to 2 hours.
<b>800</b>	Dizziness, nausea, convulsions within 45 minutes. Unconsciousness within 2 hours.
<b>1600</b>	Headache, tachycardia, dizziness and nausea within 20 minutes. Death in less than 2 hours.
<b>3200</b>	Headache, dizziness and nausea within 5 to 10 minutes. Death within 30 minutes.
<b>6400</b>	Headache and dizziness in 1 to 2 minutes. Convulsions and respiratory arrest, death in less than 20 minutes.
<b>12800</b>	Unconsciousness after 2-3 inhalations. Death in less than 3 minutes.



*Table 2. Maximum exposure time per exposure temperature*

<b>Expose Temperature (°C)</b>	<b>Without Incapacitation (min)</b>
<b>80</b>	3,8
<b>75</b>	4,7
<b>70</b>	6,0
<b>65</b>	7,7
<b>60</b>	10,1
<b>55</b>	13,6
<b>50</b>	18,8
<b>45</b>	26,9
<b>40</b>	40,2

Several studies have been conducted to investigate human behavior during tunnel evacuation procedures through the implementation of Virtual Reality (VR) applications (Moscoso et al., 2024; Ronchi et al., 2015; Skjermo et al., 2024). Nevertheless, the integration of Computational Fluid Dynamics (CFD) results into Virtual Environments has not yet been fully achieved with high precision; only a limited number of studies have attempted to address this gap (Cha et al., 2012; Zhang et al., 2023).

In the current study, the human behavior in a road tunnel accident, both in smoked and clear environment, is assessed. Fire Dynamic Simulator (FDS) a CFD software has been conducted to simulate fire and its products (smoke, toxic gases etc.) propagation inside a typical road tunnel section. The CFD results were converted into three-dimensional visual data and integrated into the virtual 3D environment. To record the human behavior a VR application has been designed and developed in Unreal Engine software to simulate emergency fire scenarios in road tunnel in order to record the user behavior and evacuation time.

In summary, an illustrative full-size road tunnel in virtual reality (VR) environment and CFD simulation were conducted to perform an experiment to study the occupant's behavior in a tunnel fire in 6 different scenarios (smoke presence/absence, alarm activation faster/slower, distance to fire source near/far). The main factors studied in this research are: (a) evacuation time (b) pre-evacuation time and (c) route-finding method.

## 2. METHODOLOGY

To develop a realistic virtual reality environment, all constituent components must be appropriately integrated. Initially, the 3D design of the tunnel structure, along with 3D models of vehicles, safety equipment, exit doors, and other relevant elements, was created to comply with national and international regulations (Greek Government Journal, 2007; NFPA, 2013; OMOE, 2002). Additionally, non-playable characters (NPCs) were incorporated into the Virtual Reality Environment (VRE) and programmed to behave as typical individuals would during an emergency evacuation—specifically, by attempting to locate the nearest exit without engaging in other activities (e.g., firefighting). A critical aspect in the event of a fire in a road tunnel is the significant reduction in visibility caused by smoke propagation within the enclosed space. To simulate this realistically, an initial fire and smoke propagation analysis was conducted using PyroSim software (Thunderhead Engineering, 2024b) which features a user-friendly interface and employs the Fire Dynamics Simulator (FDS) model developed by NIST (McGrattan et al., 2023a, 2023b, 2023c). As there is currently no open-source plugin or application programming interface (API) available to directly integrate FDS results into Unreal Engine (UE), this study manually analyzed the time-dependent visibility data along the tunnel length and replicated the smoke effects in UE using the Niagara Effects system.

The completed virtual reality environment (VRE) is presented to users through the Meta Quest 2 VR headset, where head orientation is managed by the headset itself, and user movement is controlled via hand-held controllers. For each participant, reaction time, position, final exit choice and distance travelled are recorded and stored in a local database on the PC. As the smoke effect implemented in Unreal Engine (UE) includes only the visibility parameter, it does not incorporate data on toxic gas concentrations or smoke temperature, which are necessary for assessing the impact of smoke on tunnel users during evacuation. However, FDS results can be integrated into Pathfinder, an agent-based evacuation simulation software. Therefore, user trajectories obtained from the database

are used to constrain virtual agents in Pathfinder to follow the same paths taken by real users, enabling an estimation of the smoke impact along those trajectories.

The aforementioned workflow methodology is presented in a Figure 1 and are analyzed in the following sections.

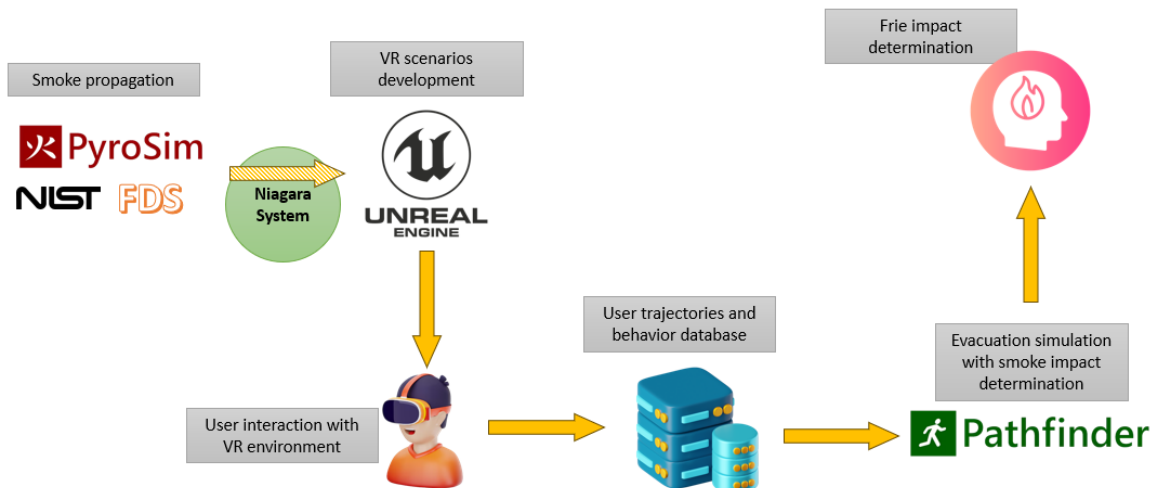


Figure 1. Methodology graphical abstract

## 2.1. Tunnel design

The tunnel model employed in this study is based on a typical single-bore road tunnel with a two-lane and circular cross-section (Figure 2-a,b), measuring 10m in width and 1,200 meters in length, with emergency exits positioned at intervals of 350m (Figure 2-c). The model also includes moving vehicles, human actors representing occupants of other vehicles, as well as dynamic elements such as fire and smoke.

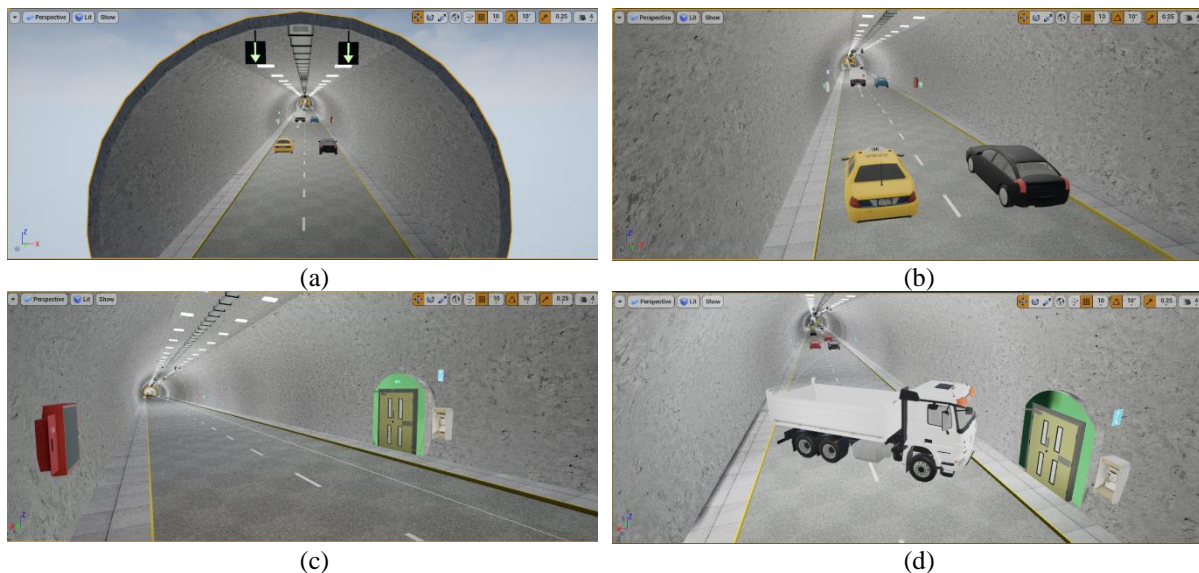
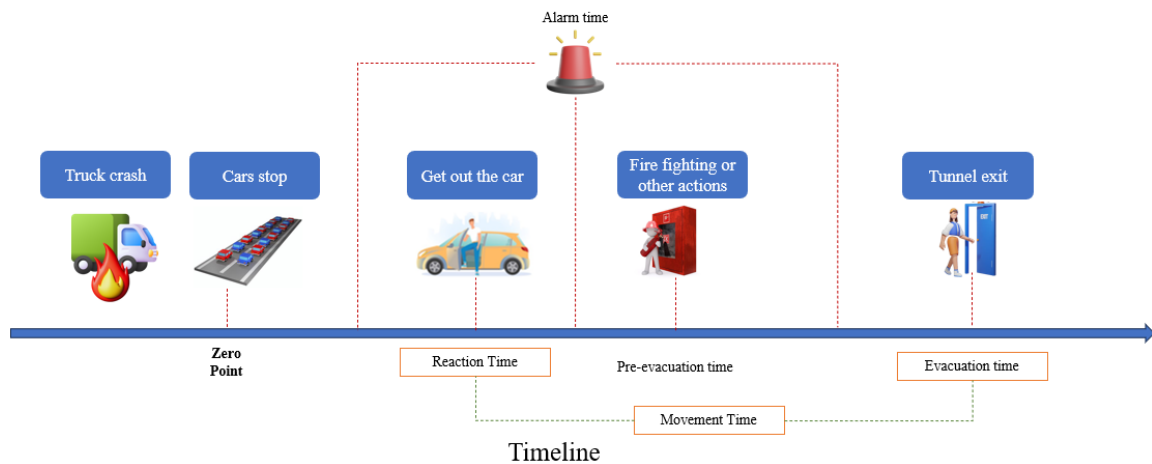


Figure 1. 3D visualization of tunnel model in UE: (a) tunnel model perspective; (b) tunnel indoor traffic; (c) exit door and emergency devices position; (d) truck fire event location.

The background scenario of the simulated incident involves a truck driver losing control of the vehicle, resulting in a collision with the tunnel wall and the subsequent ignition of a fire in the truck's cargo. To represent a worst-case scenario, the crash is assumed to occur adjacent to an emergency exit—specifically, the second exit located 700 meters from the tunnel entrance—thereby rendering it inaccessible to users during the evacuation procedure (Figure 2-d).

## 2.2. Scenario design

The main scenario begins with the user positioned in the driver's seat of a car, simulating a typical tunnel transit. At a randomized point in time, the car comes to a stop due to a truck accident ahead. The stopping distance varies, placing the user either in close proximity to the accident—providing a clear line of sight—or farther away, where visibility of the incident is limited. The moment the truck collision occurs is defined as the "zero point", marking the start of the evacuation time. An emergency alarm is activated following the incident, and the overhead lane control signals change from green arrows to red "X" symbols (Figure 1-a), instructing approaching drivers to stop their vehicles. The alarm activation time varies and is set to either 20 seconds or 60 seconds after the zero point, depending on the simulation scenario. Users must independently decide when to exit their vehicle and how to respond prior to initiating evacuation—this may include actions such as firefighting or investigating the cause of the accident. Ultimately, users must identify and select an available exit to evacuate the tunnel. Evacuation is considered complete once the user exits either through an emergency exit or returns to the tunnel entrance. Figure 2 illustrates the events timeline of the tunnel accident and evacuation.



**Figure 2.** Evacuation actions timeline

In addition, several assumptions were made regarding other parameters:

- Car speed ranges from 50 to 80 km/h
- Air flow is opposite to cars direction, so as the smoke covers faster the area where the cars have been trapped inside the tunnel, with a velocity of 1m/s approximately
- Traffic load 20-30 trapped vehicles inside the tunnel
- Each vehicle transfers 1 or 2 passengers (driver or driver plus one)
- 10% of the NPCs will leave from the tunnel entrance and 90% will leave from the nearest exit (Kinatader et al., 2015)
- Unimpeded occupants' speed (both NPC and user) 1.2m/s (Nelson & Mowrer, 2002)
- NPCs are forced to get out of car and appear in the tunnel 30 sec after the zero point

In addition to the scenario design parameters, the presence of fire and smoke resulting from the accident is incorporated into the simulation to observe and record users' behavioral responses and the timing of their activation. Accordingly, six distinct scenarios were developed, varying the states of three key parameters, as summarized in Table 3.

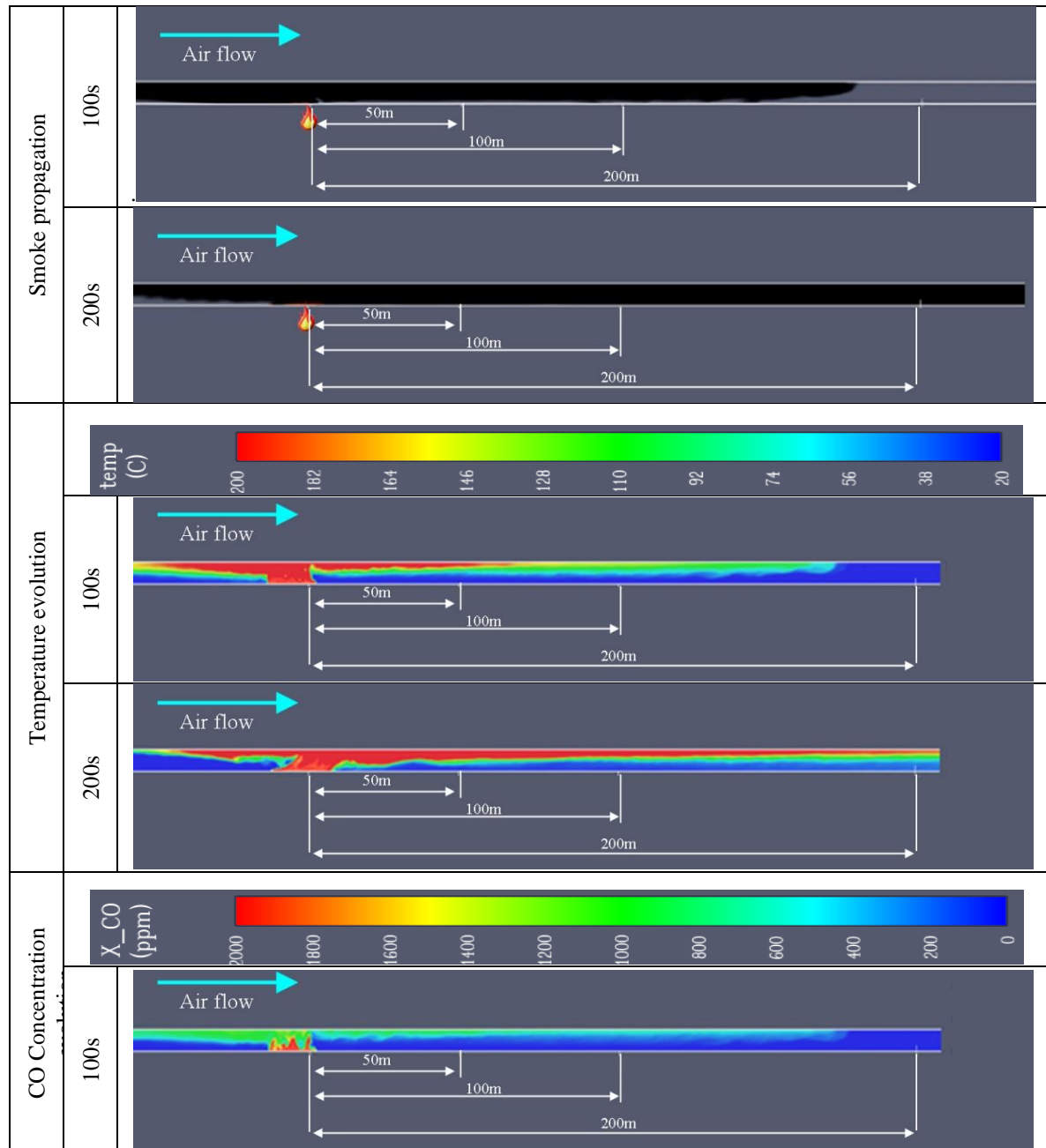
**Table 3.** Simulated scenarios.

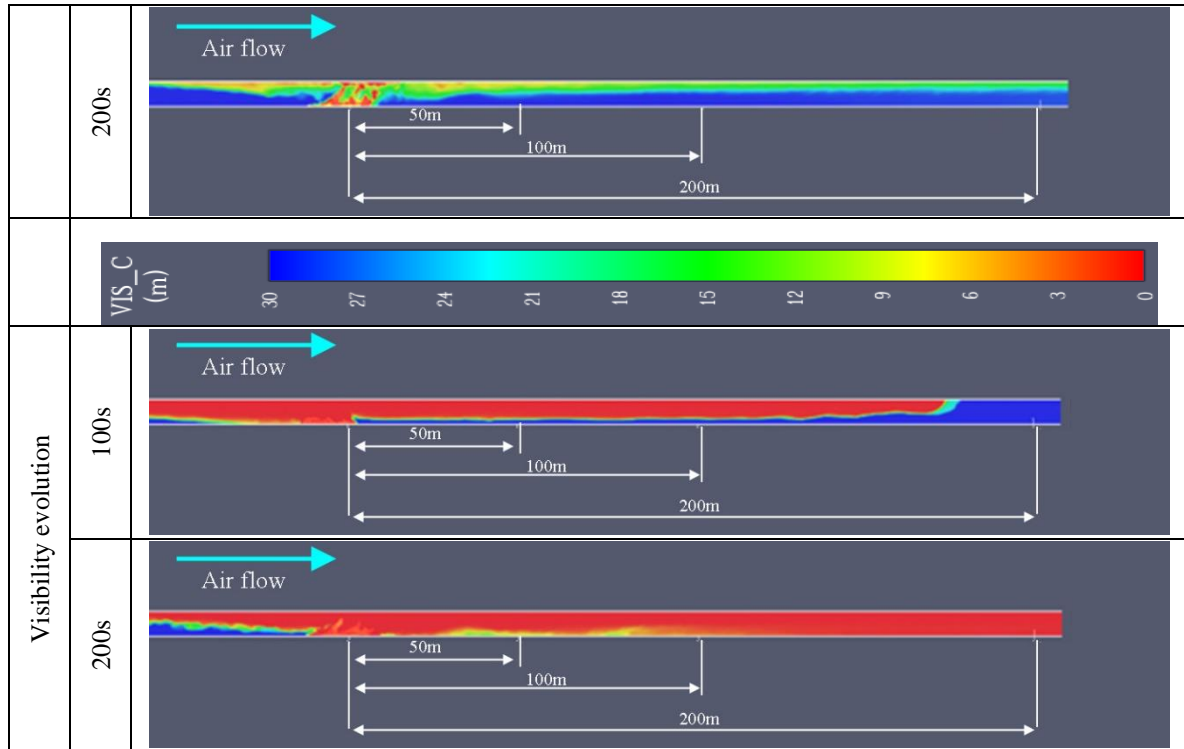
Scenario ID	Fire and smoke	Visibility to fire incident	Alarm activation time (sec)
1	YES	Clear	60
2	NO	Clear	60
3	YES	Clear	20
4	YES	Limited	60
5	NO	Limited	60
6	YES	Limited	20

### 2.3. Fire simulation

The fire used in the analysis is caused by a heavy vehicle resulting a peak Heat Release Rate (HRR) up to 100MW (Greek Tunneling Society, 2011) and polyurethane (GM27) was chosen as the combustible material for simulation purposes, since it is a widely used material worldwide; it is highly flammable (McKenna & Hull, 2016; PIARC, 2004) and is included in a variety of other materials. The natural air flow of 1m/s inside the tunnel is achieved by the pressure differential between the tunnel portals which is 3 Pa.

The fire simulation results, along the tunnel length from the side view, are presented in Figure 3 and shows that the smoke covers the tunnel after 200s from fire ignition; the temperature reaches high values after 100s in the first 100m and more than 200m after 200s from fire ignition; CO concentration does not reach critical high values at the breathing zone; and the visibility drops dramatically even in breathing zone in short time.





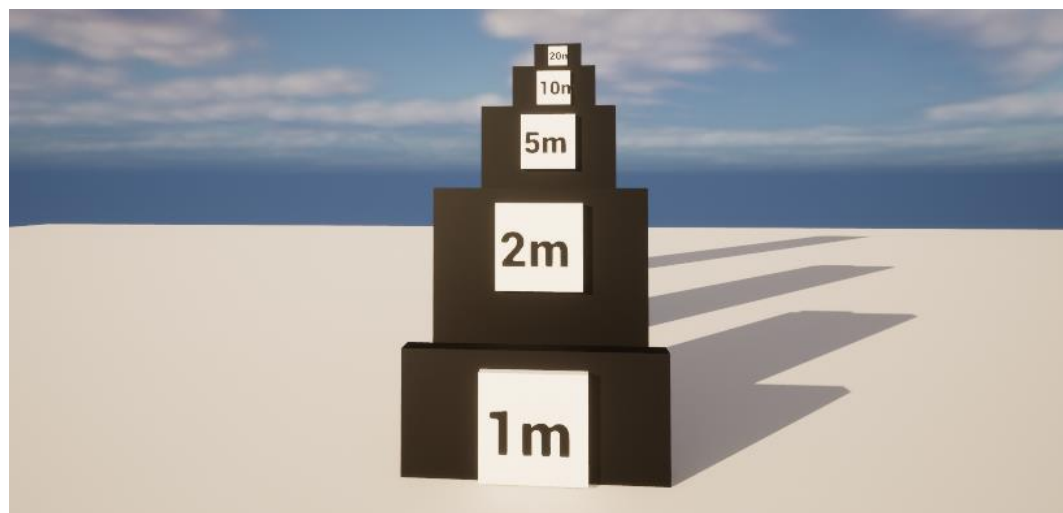
**Figure 3.** Fire simulation results

The results will be used in two ways:

1. The evolution of visibility along the tunnel, specifically within the breathing zone, will be used to define visibility limits in the virtual reality environment through the implementation of the Niagara effect in Unreal Engine (UE).
2. The evolution of carbon monoxide (CO) concentration and temperature will be integrated into the Pathfinder software to assess the impact of smoke and fire on occupants. This is achieved by constraining the movement of computer agents to match the user trajectories recorded during the VR experiment.

The Niagara Fluids effect is a plugin in UE that enables the creation and real-time simulation of dynamic particle effects. In this application, it is used to visually represent smoke generated from the truck fire scenario. To replicate the smoke propagation, the Niagara effect was instantiated multiple times along the tunnel length and activated at specific time intervals to align with the smoke evolution data obtained from the FDS (Figure 3). The properties of each instance were configured using time-based curves to match the visibility levels at corresponding locations, as calculated by FDS. To determine the visibility limitations produced by the Niagara effect settings, simple visibility markers—white squares placed on black backdrops—were positioned at varying distances from a Niagara instance within the UE environment (Figure 4-a). The properties of Niagara instance adjusted accordingly to achieve the desired visibility limit (Figure 4-b,c). A comparison between the FDS-derived visibility and the corresponding UE implementation is presented in Figure 5.





(a)

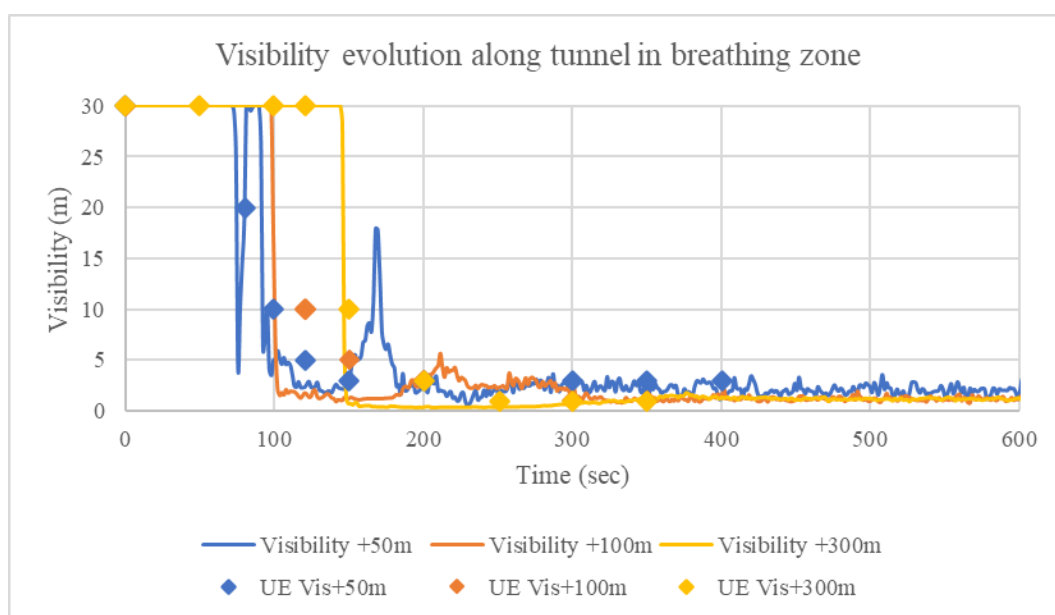


(b)



(c)

**Figure 4.** Niagara system smoke implementation and visibility measurement; (a) reflective sign positioning; (b) low visibility 1-2 m; (c) higher visibility 10 m



**Figure 5.** Visibility evolution in FDS and in UE

### 3. VR EXPERIMENT IMPLEMENTATION AND RESULTS

The VR experimental protocol consisted of four parts: i) information and guidelines concerning the VR headset and controllers operation to avoid self-injury and hardware damage, ii) familiarization with VR application, by offering 2-3 minutes moving freely in a demo level, iii) running the experiment in random level according to scenario ID (Table 1), iv) answering a questionnaire for demographics records and VR application based questions.

Participants (N=112) were recruited on a voluntary basis from the university community. The sample is relatively gender balanced (F(male)=51.8%) but very young (ages between 18-54 but only a few above 40) due to increased student participation. The experiment was conducted in the Laboratory of Mining Engineering and Environmental Mining at the National Technical University of Athens (NTUA), within an enclosed room. Participant movement within the virtual environment was controlled using a hand-held joystick. However, walking speed could not be adjusted and therefore remained fixed (1.2 m/s) across all participants and visibility conditions, which constitutes a limitation of the study. As the study took place during the COVID-19 pandemic, all official health and safety protocols were strictly followed (Figure 6).



*Figure 6. VR experiment implementation*

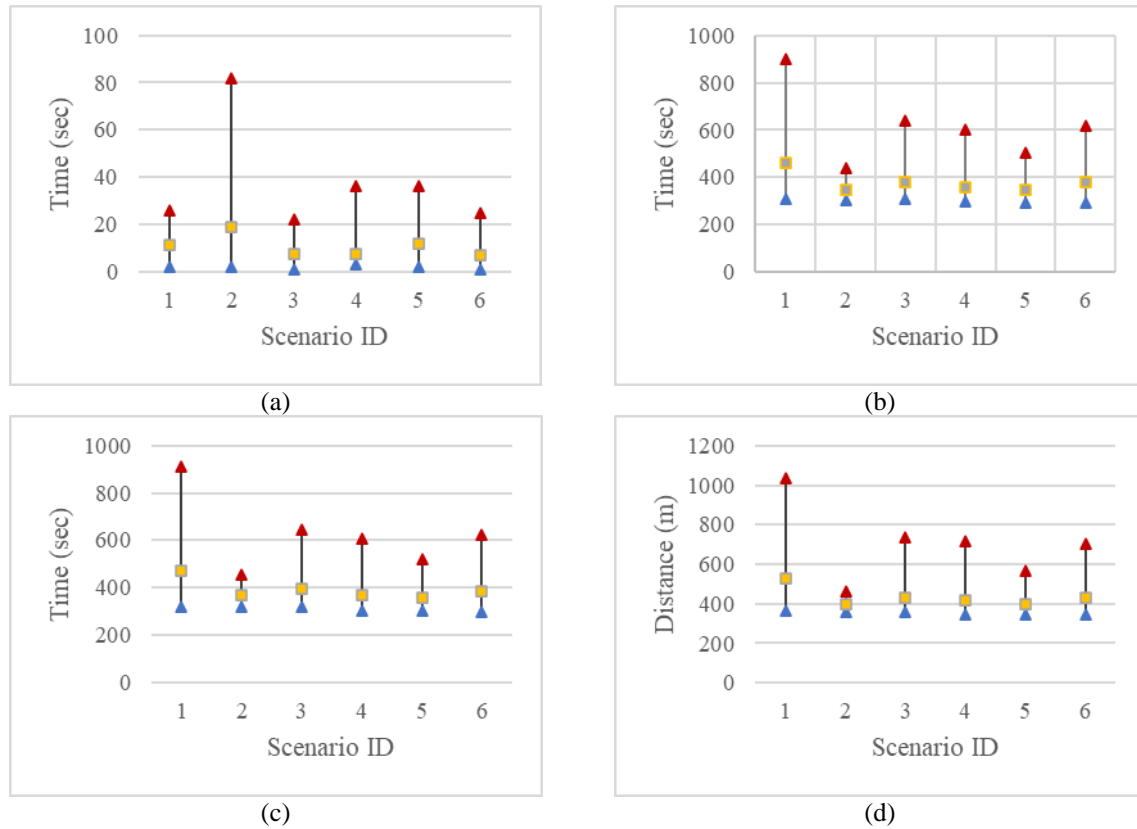
The results related to reaction time indicate that the absence of visible smoke and fire (Scenarios 2 & 5) leads to an increase in reaction time (Figure 7-a)—that is, a delay in the decision to exit the vehicle—since users do not have a clear visual indication of forthcoming danger. Similarly, in the Scenarios 2 & 5 the movement time, the evacuation time and the travelled distance is smaller due to clear visibility (Figure 7-b,c,d).

In addition, Figure 8 indicates that in lack visibility conditions, users did not use emergency exit (56% of them confused and got lost and 44% used the tunnel entrance by their own initiative) or even failed to find a way out of the tunnel, in contrast to scenarios without smoke in which all users exited via the nearest exit (emergency exit). As illustrated in Figure 9, 59% of users across all scenarios relied on exit signage to navigate their way out, while 20% followed other occupants (NPCs), with this behavior being more prevalent in scenarios with a clear environment. The remaining 20% of users either exited through a familiar route (typically the tunnel entrance) or found their way out by chance (random choice). Moreover, the VR experiment revealed that 23% of participants (approximately one in four) moved toward the fire incident, driven by curiosity about the event.

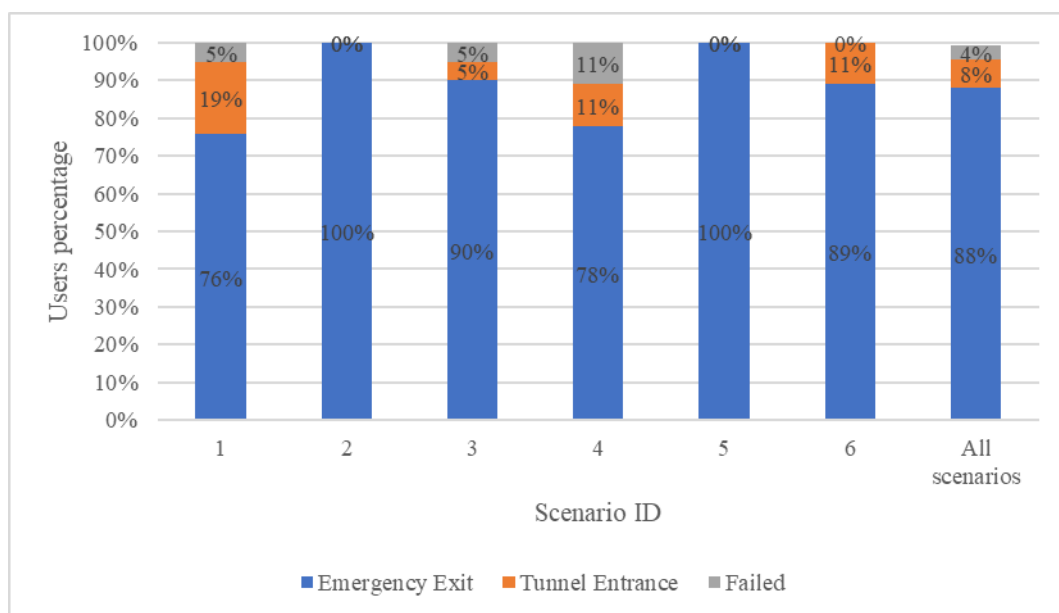
Moreover, Figure 10 presents the reaction times of all participants across all scenarios, using a color-coded representation, in relation to other potential influencing events such as the appearance of NPCs (non-playable characters) within the visible field of the tunnel and the activation of the emergency alarm (in Scenarios 3 and 6 the alarm activated earlier; at 20th second). The results indicate that the majority of participants initiated evacuation

independently and were not influenced by these external events. However, a small subset of participants appeared to be influenced by the visual presence of NPCs, as they became visible in the tunnel environment while participants remained in their vehicles.

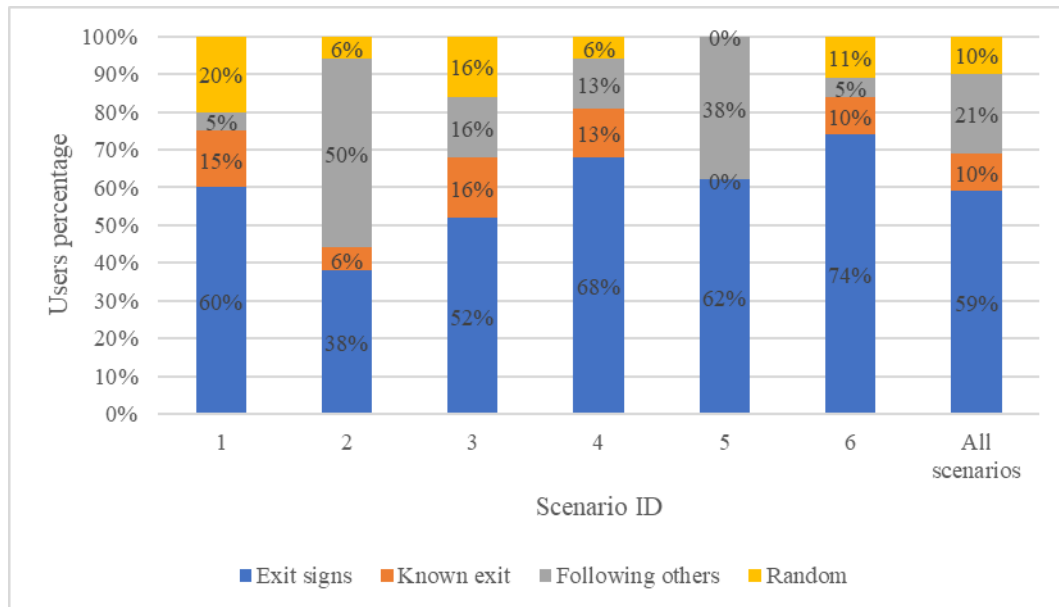
Additionally, both reaction time and total evacuation time were recorded and analyzed based on participants' prior training in fire safety. Only 25% of the participants had received even minimal fire event training. As shown in Figure 11, the group without fire training exhibited slightly longer reaction and evacuation times; however, the increase was relatively small.



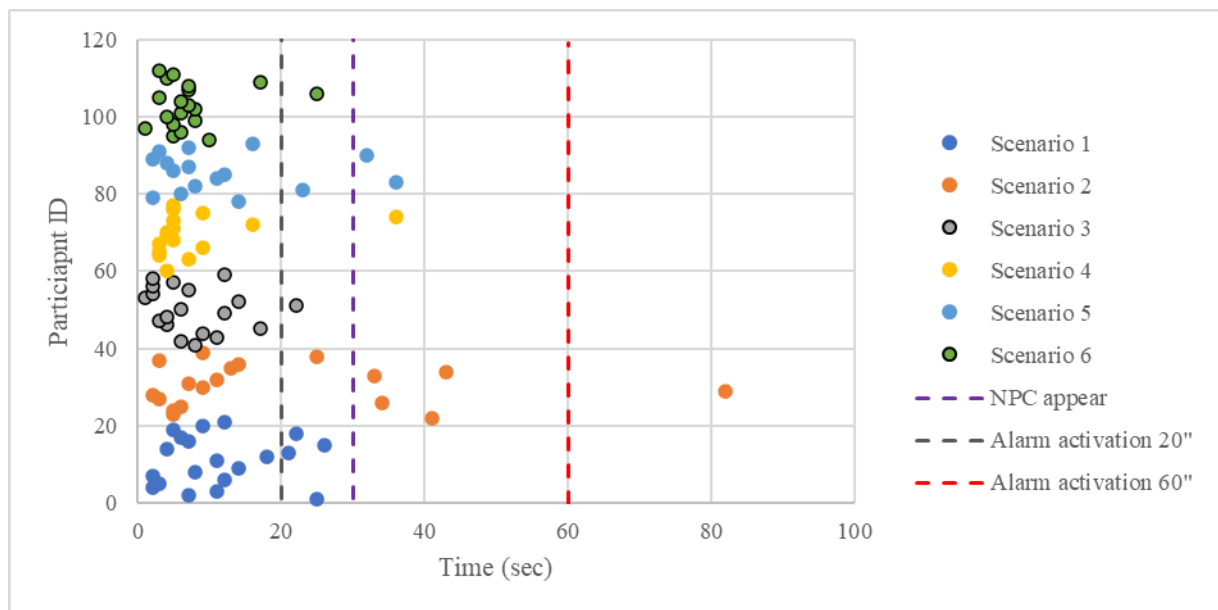
**Figure 7.** VR experiment results for each scenario: (a) Reaction time; (b) Movement time; (c) Evacuation time; (d) Travelled distance



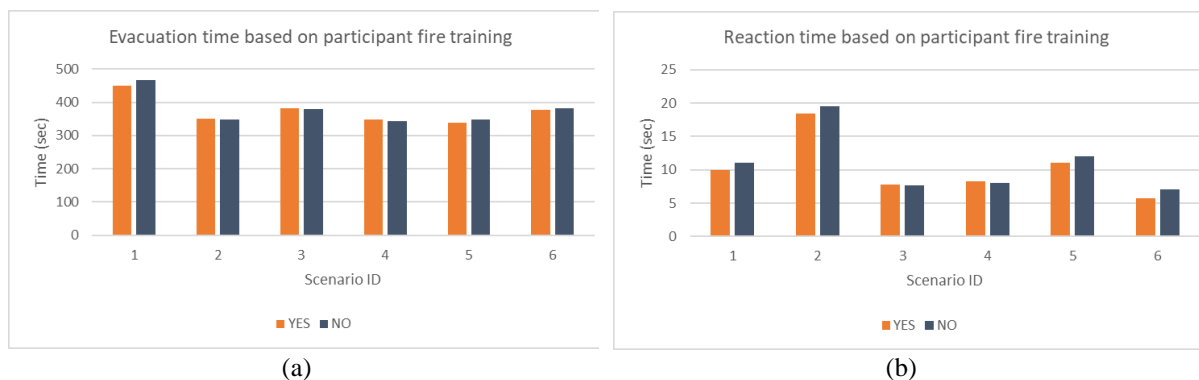
**Figure 8.** Users exit preference results



**Figure 9.** How the users choose their exit



**Figure 10.** Users reaction time in contrast to alarm activation and NPC reaction



**Figure 11.** Participants results based on fire training; (a) evacuation time; (b) reaction time

#### 4. COMPUTER EVACUATION SIMULATION RESULTS

This chapter presents the results of the scenarios executed in the Pathfinder simulation software. During the analysis, several key variables were selected for observation:

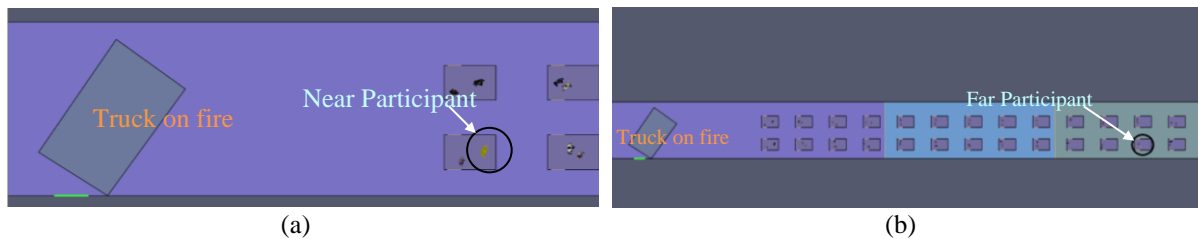
- Temperature
- Carbon monoxide exposure
- Fractional Effective Dose (FED)

The FED is a metric used to assess the cumulative exposure of occupants to atmospheric pollutants. Gases such as carbon monoxide and carbon dioxide can accumulate as an occupant moves through a burning structure. Pathfinder utilizes data derived from the FDS, including gas concentrations, visibility, and temperature, to calculate these variables and evaluate the impact of fire and smoke on evacuees (Thunderhead Engineering, 2024a).

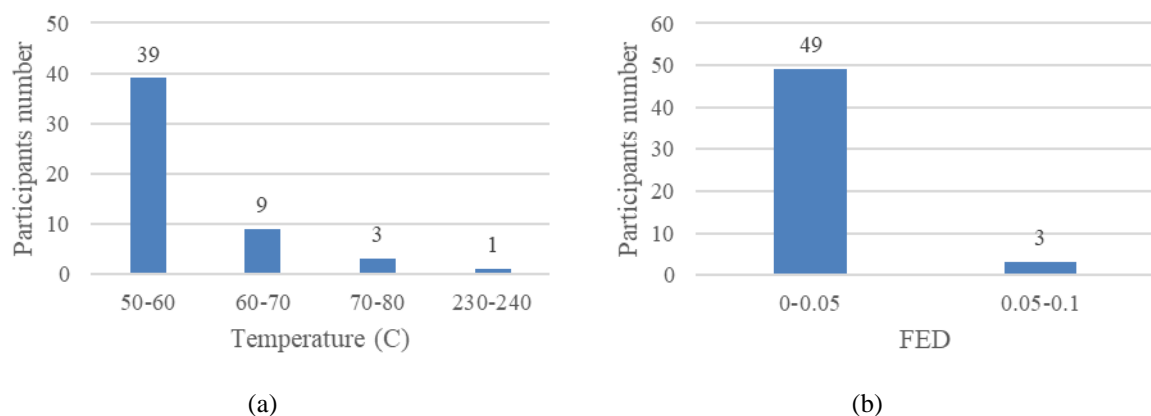
In the pathfinder software 1 scenario was designed so as to cover the different participants behavior concerning four parameters:

- Distance from fire (Figure 12)
- Reaction time
- Move toward to fire incident
- Exit choice

Figures 13-a and 13-b present the maximum exposure temperature and the maximum FED value at the end of the evacuation for all participants, respectively. Only those participants who moved toward the fire incident prior to initiating evacuation exceeded the established tenability limits, as defined in Table 1 & 2. Figure 14 illustrates the temperature exposure of one such participant in relation to their distance from the fire. The data show a rapid increase in temperature as the participant approaches the fire source, with temperatures returning to tenable levels only after moving away from the fire zone.

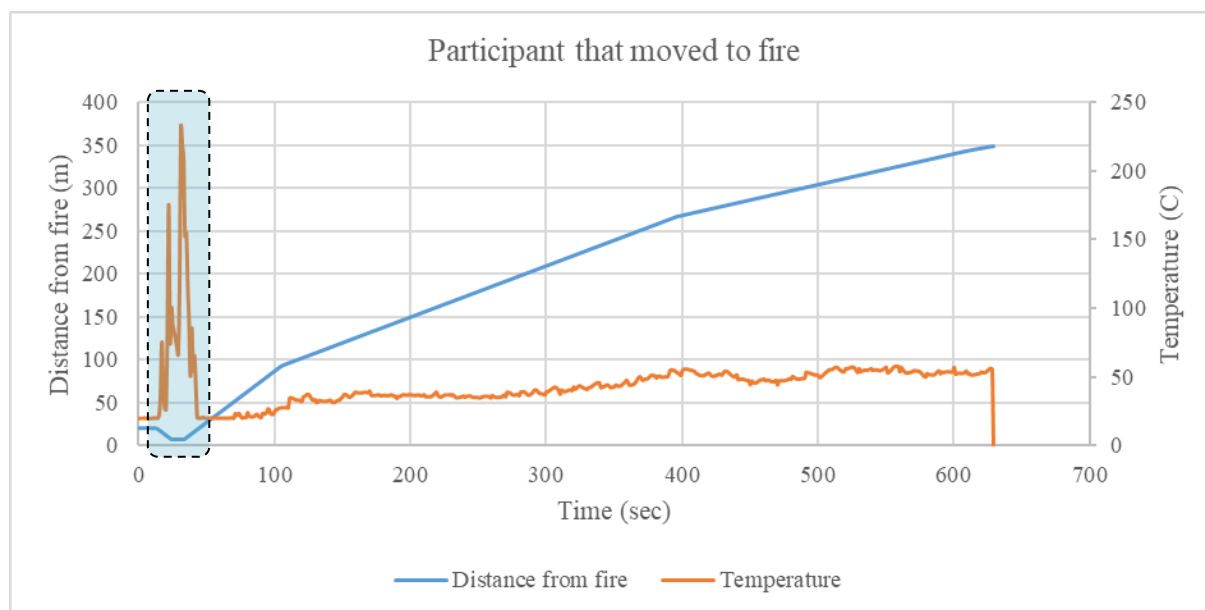


**Figure 12.** Pathfinder fire event design and (a) near to fire participant; (b) far from fire participant



**Figure 13.** Evacuation simulation results: (a) maximum exposure temperature; (b) maximum FED value





*Figure 14. Behaviour and temperature exposure of the participant that moved toward to the fire*

## 5. DISCUSSION-CONCLUSION

A full-scale virtual reality (VR) model of a road tunnel, integrated with CFD-based fire and smoke simulation, was developed to investigate occupant behavior during tunnel fire incidents across six distinct scenarios. These scenarios varied in terms of smoke presence, alarm activation time (early or delayed), and proximity to the fire source (near or far). The primary behavioral factors analyzed in this study include; evacuation decision-making; pre-evacuation time; total evacuation time; and route-finding strategies.

As shown from the experiment results, the shortest travel distances were recorded in Scenarios 2 and 5, where no smoke was present. This is attributed to the unobstructed visibility in these cases. In contrast, in Scenario 1—where smoke is present and the user is positioned closer to the accident—the longer travel distances may be explained by users mistakenly moving toward the incident or becoming disoriented during the evacuation process. The initial movement decisions of the users were examined—specifically, whether they moved toward the accident or not and found that approximately one in four participants initially moved toward the accident. Regarding the exit selection and the decision-making process behind exit choice, in one hand 88% of users evacuated through an emergency exit, 8% exited via the tunnel entrance, and 4% failed to evacuate and on the other hand 59% of participants actively searched for signage to guide their exit, 22% followed other individuals (NPCs), 12% exited from the point of entry, and 7% found their way out by chance. Among the occupants who chose to exit through the tunnel entrance, 56% did so intentionally, while 44% selected this route due to confusion or failure to locate the emergency exit. No significant differences were observed in response times or total evacuation times between participants with prior fire safety training and those without and in the scenarios where no smoke was present, visual and auditory cues did not serve as primary triggers for vehicle abandonment.

Regarding the assessment of participants' exposure to fire and smoke, only those who approached the fire zone exceeded the established temperature tenability limits. All other occupants were able to reach an exit while maintaining a safe margin within acceptable tenability thresholds. These findings highlight the importance of evacuating in the direction away from the fire, as temperatures near the fire source increase rapidly due to both hot smoke gases and radiant heat from the flames.

The results of this study provide valuable insights into human behavior during tunnel fire evacuations under varying conditions of visibility, alarm timing, and proximity to the hazard. These findings can support the scientific community in refining evacuation models, improving safety protocols, and enhancing the design of tunnel emergency systems. Future studies could build upon this work by incorporating physiological monitoring of participants, expanding scenario diversity, improving VR interactivity and immersivity or validating results with real-world drills and observational data.

## 6. ACKNOWLEDGMENTS

The authors would like to all staff members and student of Mining Engineering and Environmental Mining laboratory for supporting the experimental procedure. In addition, they would like to extend a special note of appreciation to Thunderhead Engineering group, for providing educational license to use and work on Pathfinder and Pyrosim platform as well as for the excellent and direct cooperation of its members.

## 7. BIBLIOGRAPHY

- [1] Carlson, E.-S., Kumm, M., Zakirov, A., & Dederichs, A. (2019). Evacuation tests with elevated platforms in railway tunnels. *Fire Safety Journal*, 108, 102840. <https://doi.org/10.1016/j.firesaf.2019.102840>
- [2] Cha, M., Han, S., Lee, J., & Choi, B. (2012). A virtual reality based fire training simulator integrated with fire dynamics data. *Fire Safety Journal*, 50, 12–24. <https://doi.org/10.1016/j.firesaf.2012.01.004>
- [3] Fridolf, K., Ronchi, E., Nilsson, D., & Frantzich, H. (2013). Movement speed and exit choice in smoke-filled rail tunnels. *Fire Safety Journal*, 59, 8–21. <https://doi.org/10.1016/j.firesaf.2013.03.007>
- [4] Greek Government Journal. (2007). *Greek Government Journal* 230/2007. 1.
- [5] Greek Tunneling Society. (2011). *Guidelines of risk analysis without the involvement of vehicles transporting dangerous goods through road tunnels falling within the scope of Decree 230/07 (Scenario Approach)*. GTS.
- [6] Jin, T. (1997). Studies On Human Behavior And Tenability In Fire Smoke. *Fire Safety Science*, 5, 3–21. <https://doi.org/10.3801/IAFSS.FSS.5-3>
- [7] Kallianiotis, A., Papakonstantinou, D., Giouzelis, N., & Kaliampakos, D. (2022). Evacuation in an Underground Space: A Real-Time Investigation of Occupants' Travel Speed in Clear and Smoked Environments. *Infrastructures*, 7(4), 57. <https://doi.org/10.3390/infrastructures7040057>
- [8] Kinateder, M., Gromer, D., Gast, P., Buld, S., Müller, M., Jost, M., Nehfischer, M., Mühlberger, A., & Pauli, P. (2015). The effect of dangerous goods transporters on hazard perception and evacuation behavior – A virtual reality experiment on tunnel emergencies. *Fire Safety Journal*, 78, 24–30. <https://doi.org/10.1016/j.firesaf.2015.07.002>
- [9] McGrattan, K., McDermott, R., Hostikka, S., Floyd, J., & Vanella, M. (2023a). *Fire Dynamics Simulator (6th Edition) Technical Reference Guide, Volume 2: Verification*. U.S. Department of commerce National Institute of Standards and Technology.
- [10] McGrattan, K., McDermott, R., Hostikka, S., Floyd, J., & Vanella, M. (2023b). *Fire Dynamics Simulator (6th Edition) Technical Reference Guide, Volume 3: Validation*. U.S. Department of commerce National Institute of Standards and Technology.
- [11] McGrattan, K., McDermott, R., Hostikka, S., Floyd, J., & Vanella, M. (2023c). *Fire Dynamics Simulator User's Guide*. U.S. Department of commerce National Institute of Standards and Technology.
- [12] McKenna, S. T., & Hull, T. R. (2016). The fire toxicity of polyurethane foams. *Fire Science Reviews*, 5(1), 3. <https://doi.org/10.1186/s40038-016-0012-3>
- [13] Moscoso, C., Skjermo, J., Karlsson, H., Arnesen, P., Södersten, C.-J., Hoem, Å. S., & Jenssen, G. D. (2024). Analysis of spatial and design factors for users' acceptance of rescue rooms in road tunnels: An exploratory study using Virtual Reality. *Fire Safety Journal*, 150, 104272. <https://doi.org/10.1016/j.firesaf.2024.104272>
- [14] Nelson, H. E. "Bud," & Mowrer, F. W. (2002). Emergency Movement. In *SFPE Handbook of Fire Protection Engineering 3rd edition* (pp. 367–380). NFPA.
- [15] NFPA. (2013). *NFPA 502: Standard for road tunnels, bridges, and other limited access highways* (2014 edition). NFPA.
- [16] NFPA. (2014). *NFPA 130, Standard for Fixed Guideway Transit and Passenger Rail Systems*. NFPA.
- [17] OMOE. (2002). *OMOE Road Project Design Guidelines*. OMOE.
- [18] PIARC. (2004). *Fire and Smoke Control in Road Tunnels*.
- [19] Purser, D. A., & McAllister, J. L. (2016). Assessment of Hazards to Occupants from Smoke, Toxic Gases, and Heat—Chapter 63. In *SFPE Handbook of Fire Protection Engineering* (pp. 2308–2428). Springer.
- [20] Qin, J., Liu, C., & Huang, Q. (2020). Simulation on fire emergency evacuation in special subway station based on Pathfinder. *Case Studies in Thermal Engineering*, 21, 100677. <https://doi.org/10.1016/j.csite.2020.100677>
- [21] Ronchi, E., Colonna, P., Capote, J., Alvear, D., Berloco, N., & Cuesta, A. (2012). The evaluation of different evacuation models for assessing road tunnel safety analysis. *Tunnelling and Underground Space Technology*, 30, 74–84. <https://doi.org/10.1016/j.tust.2012.02.008>
- [22] Ronchi, E., Kinateder, M., Müller, M., Jost, M., Nehfischer, M., Pauli, P., & Mühlberger, A. (2015). Evacuation travel paths in virtual reality experiments for tunnel safety analysis. *Fire Safety Journal*, 71, 257–267. <https://doi.org/10.1016/j.firesaf.2014.11.005>
- [23] SFPE. (2016). *SFPE Handbook of Fire Protection Engineering, 5th Edition*. Springer.
- [24] Skjermo, J., Moscoso, C., Nilsson, D., Frantzich, H., Hoem, Å. S., Arnesen, P., & Jenssen, G. D. (2024). Analysis of visual and acoustic measures for self-evacuations in road tunnels using virtual reality. *Fire Safety Journal*, 148, 104224. <https://doi.org/10.1016/j.firesaf.2024.104224>
- [25] Storm, A., & Celander, E.-S. (2022). Field evacuation experiment in a long inclined tunnel. *Fire Safety Journal*, 132, 103640. <https://doi.org/10.1016/j.firesaf.2022.103640>
- [26] Thematic Network Fire in Tunnels. (2006). *Fire in Tunnels* [General Report].

- [27] Thunderhead Engineering. (2024a). *Pathfinder Verification and Validation*.
- [28] Thunderhead Engineering. (2024b). *PyroSim User Manual*.
- [29] Zhang, X., Chen, L., Jiang, J., Ji, Y., Han, S., Zhu, T., Xu, W., & Tang, F. (2023). Risk analysis of people evacuation and its path optimization during tunnel fires using virtual reality experiments. *Tunnelling and Underground Space Technology*, 137, 105133. <https://doi.org/10.1016/j.tust.2023.105133>

## LIGHT AND HEALTH IN UNDERGROUND PUBLIC SPACES FOR THE WELL-BEING OF ALL

Prof. Dr. Marija Jevtic<sup>1</sup>  
Dr. Eng. Arch. Gordana Micic<sup>2</sup>

**Abstract:** Ensuring adequate lighting in underground public spaces is a fundamental prerequisite for their accessibility and their use. Without sufficient illumination, these environments become difficult to navigate, compromising their usability and safety. Artificial lighting must, therefore, meet essential operational criteria, supporting visibility, orientation, and security for both users and personnel, related to comfort and well-being for all.

This article examines the conceptual and experiential quality of lighting in metro stations, adopting a user-centric perspective that integrates spatial, functional, and sensory dimensions. It aims to highlight the essential tools of thoughtful lighting design to enhance the development of universal and inclusive underground public spaces.

**Keywords:** Design, station, lighting, metro, accessibility, art public

### 1. INTRODUCTION

Access to underground spaces remains challenging for many users due to physical, psychological, and sensory barriers. Fear of enclosed environments, feelings of confinement or insecurity, and memories of harassment or aggression are all factors that influence perceptions of safety and comfort. Such ambivalence is historically grounded, as subterranean spaces have long carried symbolic, religious, and defensive connotations (Leclerc, 2010). In this regard, Plato's allegory of the cave acquires renewed significance: it is through light that alternative spatial realities become accessible.

Grounded in the premise that light is a condition for the appropriation and usability of underground spaces. It examines how lighting can sustain urban continuity between surface and subterranean public environments, with particular emphasis on their capacity to meet essential requirements for human health and well-being. Adopting an empirical approach, it investigates the roles and effects of lighting in metro stations by combining theoretical perspectives with practical analysis of spatial components. Drawing on contemporary research, this study delineates best practices in lighting design as a means of user-centric frameworks that improve urban health, inclusivity, and overall well-being.

### 2. WHY LIGHT IS IMPORTANT FOR HUMAN BEINGS IN UNDERGROUND SPACE?

Light is essential not only for vision but also for regulating physiological processes, mood, and behaviour. While natural light serves as the primary biological synchroniser, technological advancements have led to the development of human and circadian lighting systems that replicate natural daylight variations indoors. These

<sup>1</sup> Faculty of Medicine University Novi Sad / ULB - School of Public Health, Brussels, <https://orcid.org/0000-0002-1194-0765>

<sup>2</sup> Head of Art & Architecture office at STIB-MIVB & Brussels Mobility, Chair of UITP Design & Culture Committee, UCLouvain lecturer

systems adjust both intensity and spectral composition throughout the day, enhancing morning alertness and evening relaxation, with documented benefits for mood, cognitive performance, and sleep quality in schools, workplaces, and healthcare settings (Figueiro et al., 2017; Browning et al., 2020).

In urban planning, particularly in underground and metropolitan areas, dynamic biologically effective lighting can improve user comfort, reduce disorientation, and enhance perceived safety. Cities such as Stockholm, Munich, or Seoul have piloted innovative strategies, including daylight-mimicking LED systems based on the Human-Centric Lighting (HCL) approach, artistic light installations, and the integration of greenery in metro stations, to improve spatial experience and psychological well-being (Rossi et al., 2012; Frontiers in Psychology, 2021). The main health risks and benefits of lighting in subway environments are summarised in Table 1.

Incorporating artificial lighting as a determinant of urban health supports the planning of health-promoting infrastructure within the “Health in All Policies” (HiAP) framework and aligns with the United Nations Sustainable Development Goals, particularly SDG 3 (Good Health and Well-Being) and SDG 11 (Sustainable Cities and Communities).

**Table 1.** Summary of the impact of natural and artificial light on human health and well-being, with a focus on different approaches to the design of underground and metro environments.

Topic	Health Effects: Benefits / Risks	References / Examples
Natural Light	Regulates circadian rhythms, improves mood, supports vitamin D synthesis, and enhances cognition. Lack of daylight leads to disorientation, fatigue, and stress.	(CIE, 2019); (Vandewalle et al., 2009)
Artificial Light	Can disrupt circadian rhythm, affect sleep, mental health, and ocular health if poorly managed.	(Lucas et al. 2014); (Figueiro et al. 2017)
Artificial Light (Metro)	Beneficial when appropriately adapted and timed according to the duration and moment of exposure. Insufficient or poorly designed artificial lighting can create a sense of oppression, discomfort, or even anxiety, making the underground space feel unwelcome and off-putting.	(Rossi et al. 2012); (Frontiers in Psychology, 2021; ) (Terrin, 2008),
Simulate daylight, artistic lighting, green design	Reduces stress, evokes emotion, facilitates natural orientation and calming effects, provides a pleasant feeling and improves user experience.	Stockholm Metro, London Underground, STM Montreal
Human-Centric Lighting	Support circadian health, improve alertness and productivity, improve accessibility, and reinforce the feeling of security and comfort	Tunable LEDs in offices, hospitals, metros
Public Health Policy	Support urban design with healthy lighting in transport and public spaces	Urban resilience policies; WHO Healthy Cities; SDGs (3, 11);

Psychological responses to lighting, such as those illustrated by the Kruithof effect<sup>3</sup>, indicate that users generally prefer warm light at lower illumination levels and cooler light at higher intensities. Although this phenomenon remains a subject of debate, it highlights the need to align lighting conditions with users’ perceptual comfort and cultural expectations. Emerging research further suggests that highly correlated colour temperature (CCT) lighting may enhance alertness, offering new directions for the design of lighting in transit environments and beyond (Figure 1).

<sup>3</sup> The Kruithof effect, or Kruithof curve, identifies optimal combinations of colour temperature and illuminance that are perceived as pleasant and natural, offering a valuable framework for comfortable interior lighting design.





**Figure 1.** From left to right: T-Centralen metro station in Stockholm<sup>4</sup>, Elisabeth line in London and Place-d'Armes in Montreal.

However, not all lighting is beneficial. Inappropriate lighting, whether overly intense, poorly directed, or mistimed, can disrupt circadian rhythms, impair sleep, increase stress, and negatively affect mental health. Evening exposure to blue-enriched light, for instance, may suppress melatonin production, delay sleep onset, and contribute to chronic sleep deprivation, which is itself linked to cardiovascular, metabolic, and psychological disorders (Lucas et al., 2014; CIE, 2019).

### 3. LIGHT AND UNDERGROUND SPACE

However, light plays a central role in the design of public spaces, acting as a universal language that conveys orientation, understanding, and emotion (Matic, 2018). It shapes spatial perception and directs visual attention, functions that are particularly critical in underground environments, which are often perceived as disorienting or even hostile.

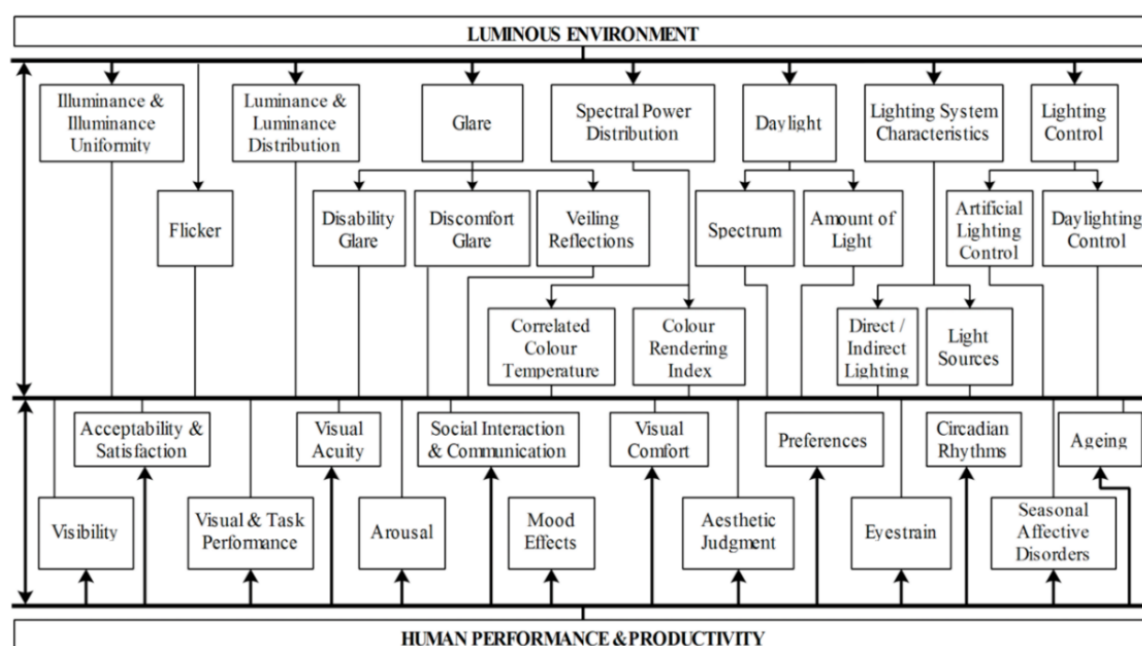
This is why designing lighting for underground spaces requires careful consideration of context-specific constraints, such as geotechnical conditions, humidity, the absence of natural light, safety and accessibility requirements. These factors directly influence architectural and technical decisions. Strategies such as covered trenches, the reuse of existing cavities, and spatial developments around access points are often employed to bring light into user pathways, improve spatial legibility, reveal volumes, and enhance perceived safety (Palisse, 2017).

Beyond functional illumination, the quality of light is a major user-centric concern. Monique Labbé (2014) emphasises the importance of integrating natural light, open views, and visual cues within a sensitive design approach. Louis Kahn similarly advocates for the inclusion of natural light, even in minimal amounts, to reveal materiality and spatial depth, qualities often lost with static artificial lighting (Kahn, 1996). Chelkoff and Thibaud explore how light intensity influences spatial perception: when strong, it reduces the feeling of being underground; when dim, it heightens the sense of enclosure (Chelkoff and Thibaud, 1997). The nature of the light source and its integration are therefore decisive, as shown in the work of Ponizy, who demonstrates how concealed luminaires can enhance the immersive quality of a space (Ponizy, 2016).

In some environments, such as metro stations or underground shopping centres, the absence of natural light has become normalised. However, this practice does not guarantee a satisfactory spatial ambiance. In certain cases, natural light must even be excluded (for reasons of thermal performance, security, or waterproofing), allowing for more precise control of artificial lighting. Yet insufficient lighting can negatively impact perceived safety and diminish the quality of the spatial experience (Cousseau, 2019).

Lighting in underground environments transcends its technical function; it is a complex driver of architectural, sensory, and social quality. As a design component, it calls for an integrated and multidisciplinary approach that considers the full range of technical, perceptual, and sensitive factors shaping user experience (Figure 2). When technical and functional performance, atmosphere, and comfort are brought into alignment, lighting becomes a powerful tool for humanising infrastructure.

<sup>4</sup> All photos in this paper, unless otherwise indicated, are subject to © Gordana Micic.



**Figure 2.** Co-relation between Luminous environment and Human performance & productivity in design. Source: (Gligor, 2004)

Lighting design in underground public spaces, such as metro stations, represents a complex challenge situated at the intersection of technical demands, functional constraints, and sensory aspirations. These enclosed, infrastructure-heavy environments require thoughtful design to ensure safety, guide passenger flows, and create atmospheres conducive to comfort and spatial orientation.

#### 4. DESIGNING LIGHT: TOWARDS A USER-CENTRIC APPROACH

Historically, lighting in such contexts has followed a predominantly technicist approach, governed by strict regulatory standards. This orientation reflects the need for high levels of safety, constant visibility, maintenance efficiency, and energy performance. Lighting was thus primarily considered as a technical system to be optimised. Network operators often impose additional, sometimes overly restrictive requirements, further limiting designers' creative freedom and leading to the homogenisation of atmospheres across different stations. Yet this approach is increasingly being challenged in the face of evolving urban contexts and growing user expectations for more inclusive, experience-oriented environments.

In response, there is a pressing need to move toward more holistic practices that reconcile technical requirements with sensory and emotional dimensions. Lighting becomes not just a means of illumination, but also a tool for ambiance, wayfinding, and the enhancement of spatial qualities, capable of addressing both functional imperatives and users' perceptual and affective needs.

Light accompanies the movement of users, and by mastering variations in colour temperature, intensity, and the interplay of light and shadow, while maintaining coherence with architectural form and spatial volumes, designers can create environments with strong identity and meaning. Human spatial perception is inherently multisensory; thus, animating space through a coordinated scenography, architectural, artistic, and urban ensures that sensory information is harmoniously conveyed, producing a fluid and comfortable spatial experience (Figure 3). In contrast, conflicting sensory cues can cause perceptual dissonance, leading to discomfort or confusion. From this perspective, ensuring sensitive coherence becomes essential to facilitating an intuitive and pleasant reading of the environment.

Lighting can adopt variable tones and colours informed by actual or desired movement patterns, reflecting the diverse mobility habits of users. In some cases, lighting systems are adaptive, responding to user density and time of day, while simultaneously guiding movement and highlighting preferred pathways. By doing so, they not only facilitate navigation but also support intuitive wayfinding.



**Figure 3.** *The Sensual City Journey.* Source : Sensual City Studio in Thresholds.

The transformative properties of light, which enhance and reveal the expressive character of architectural forms, are fundamental to establishing a unique spatial identity. In this sense, lighting becomes an active design element, both functional and symbolic, that contributes to the legibility, atmosphere, and distinctiveness of underground public environments.

#### 4.1. Look at Lighting Quality

Lighting design in underground public spaces is structured around two complementary and inseparable types of light: general lighting and ambient lighting. Together, they shape spatial legibility, sensory quality, and user experience. General lighting ensures overall visibility, visual comfort, and safety. It provides uniform illumination along circulation routes and maintains light levels appropriate to the functional use of the space. In contrast, ambient lighting introduces nuance through contrasts, shadows, rhythms, and highlights. It sculpts volumes, defines pathways, and enhances spatial orientation. By revealing architectural details, it contributes to intuitive navigation, a calming atmosphere, and a stronger sense of place, all of which reinforce the feeling of safety throughout the journey.

When conceived from a user-centric perspective, the articulation between general and ambient lighting must adhere to the principles of universal accessibility to allow everyone to travel in comfortable and pleasant conditions. Working in synergy, these two lighting modes create spaces that are functional, legible, balanced, and adaptable to ensure a high quality of experience throughout the user journey.

Despite this, in practice, lighting design is still introduced too late in the project timeline, typically during the execution phase. This delayed integration limits designers' flexibility and can result in additional costs. To guide decisions and ensure consistency across infrastructure, several transit authorities have developed thematic guidelines that include dedicated lighting chapters. Authored by technical and institutional experts, these documents serve as design frameworks. However, interpretations of these guidelines vary among designers, influencing how lighting is conceptualised and implemented in underground environments.

The case of Brussels illustrates this evolution. The development of the '*Directives relatives à la conception des stations de métro de Bruxelles : Stations nouvelles – Projets de rénovation*'<sup>5</sup> established a collaborative, cross-disciplinary process which included all stakeholders involved with accessibility 'user expert'. This approach demonstrated the value of combining operating user perspectives to develop not only enlightening solutions but also meaningful compromises between technical efficiency and aesthetic ambition, both literally and figuratively.

From this study, while crossing other different research and prescriptions, we propose a synthesis of the key requirements and constraints shaping lighting design in underground public spaces, as outlined in Table 2. These constraints provide a framework that guides design practice, posing a creative challenge for designers, who must balance ambition with feasibility within the limits of infrastructural realities.

---

<sup>5</sup> Translation in English: '*Brussels Metro and Pre-Metro Station Design Directives: New stations – Renovation projects*'

**Table 2.** *A user-centric and cross-disciplinary categorisation of lighting design criteria for underground public spaces: requirements and constraints and insights from diverse sources.*

Category	Requirements	Constraints
Contextual and urban	Take account of the urban situation and the surrounding light levels by enhancing accesses Encourage the contribution of natural light The shape and orientation of the building should encourage the penetration of natural light in a coherent manner Contribute to the creation of an identity for access and buildings as an urban landmark.	Take account of areas protected as cultural heritage, which restricts the possibilities for integration Deal with pre-existing street furniture, which can create obstacles No light pollution of the environment and vice versa.
Basic features	A gradual transition in lighting from the outside to the inside. A level of lighting that is uniform and sufficient for everyone, with the quality of daylight, throughout the dominant pathway: from the outside to boarding. Ensuring the visibility of the area Facilitating orientation and legibility of the route - luminous guide-lines, reinforcement of signage and landmark elements such as works of art and the like. Improve lighting in high-risk areas (staircases, escalators, ramps, lifts, doors, signage, reception, ticket validation machines, platforms, toilets, etc.).	Complexity of traffic flows Eliminate shaded areas on dominant routes Avoid the risk of glare Respect the minimum prescribed lighting level. Avoid excessive light pollution
Atmosphere and comfort	A pleasant and soothing atmosphere with diffused light Prioritise natural light, or a light spectrum close to natural light Reduce the feeling of confinement Ensure smooth light transitions Integrates art works and cultural activities	Risk of monotony or over-stimulation Deep or very large spaces that are difficult to homogenise Avoid permanent light integrated into the floor and/or frontal light in the walls to avoid glare
Structure and materiality	Considering and enhancing the structure and volumes in an integrated way Working with the properties of materials: diffuse reflection, texture, etc. Support and enhance the artistic and architectural heritage. Use materials and colours in an intelligible way to enhance the luminosity of the space	No direct glare - hide the source of light Easy access at all weather Easy maintenance
Safety and security	Limiting shaded areas conducive to insecurity Integrating emergency and lighting systems Integrating stand-alone emergency lighting Ensuring visibility for surveillance cameras Blue lighting for high-risk areas (anti-social behaviour, drug use or similar)	Increased lighting in high-risk areas: staircases, escalators, lifts, access control lines, etc. Emergency conditions (evacuation, breakdown)
Economy and maintenance	Use lighting fixtures that are durable and resistant to moisture, physical damage (depending on location) and easy to maintain.	Installation easily and permanently accessible Budgetary limitations
Sustainability and environment	Optimising performance, comfort and energy efficiency to reduce energy consumption Intelligent lighting management with monitoring: dimming (peak times, presence detection), adjusting lighting according to natural light, etc. Favour energy saving, recyclable or recycled luminaires.	Technical constraints of the subsoil (ventilation, heat, humidity) Use of standardised and interchangeable materials Integration into old or complex structures
Innovation and experimentation	Original visual features Integration of innovative lighting systems	Need for compatibility with current standards

High-quality lighting design therefore relies on a delicate balance between uniformity, controlled contrast, and coherent atmospheres to meet both functional needs and perceptual expectations across diverse user groups. Design prescriptions and guidelines offer shared criteria that should foster consistency in station layout. Some operators, however, add specific qualitative requirements that may appear more restrictive. Yet this dual function, ensuring performance standards and communicating expectations clearly to less experienced designers, can streamline collaboration and save time, particularly in relation to universal accessibility.

It is a fact that such constraints, expressed through design charters, can limit the creative freedom of architects and lighting designers, especially concerning natural light integration, visual openings, or ambience diversity. While architects often view these limits as restrictive, lighting designers may find them intellectually stimulating. Designing within constraints becomes a creative challenge, demanding ingenuity from the design team. The ability to argue and propose variants allows for the mitigation of normative limitations, especially when it comes to enhancing visual comfort and reducing the sense of enclosure.

#### **4.2. Between the Measurable and the Immeasurable**

Evaluating the quality of lighting in underground environments involves a multifaceted approach, at the intersection of photometric performance and subjective perception (Flynn et al, 1992). While certain sources of visual discomfort, such as glare, flicker, or poor colour rendering, can be reliably quantified, the broader notion of visual comfort remains difficult to measure comprehensively. This complexity also arises from the interaction between the three-dimensional boundaries of space and the temporal dimension of movement, both of which shape and transform the spatial perception of the physical environment (Capron, 2021).

In his doctoral research, Jordi Nonne proposes a structured framework for evaluating visual comfort quality, articulated around three core dimensions: performance, ambience, and comfort. His model is interesting because it attempts to go beyond strictly normative approaches by integrating the sensory qualities of light into spatial design. It incorporates six key photometric parameters, which must be assessed holistically:

- Illuminance level (lux): general visibility.
- Uniformity: Providing consistent light distribution to avoid abrupt changes in brightness that disrupt perception.
- Contrast: Essential for spatial legibility, as it shapes depth perception and volumetric reading through transitions between light and shadow.
- Colour Rendering Index (CRI): Accurate colour fidelity supports spatial recognition and aesthetic experience.
- Correlated Colour Temperature (CCT): Influences overall atmosphere; to balance comfort and functionality. Designers must also consider the spatial positioning of light sources and their relation to the black-body locus in the chromatic space.
- Light distribution: Modulates spatial experience and visual hierarchy. Each lighting device produces zones of higher and lower luminance,  $S_a$  and  $S_u$ , respectively. The ratio  $S_a/S_u$  indicates the degree of diffusion: a balanced ratio correlates with enhanced visual comfort (Nonne, 2015).

Although its practicality remains limited, this model paves the way for a more nuanced evaluation of lighting quality, integrating functional performance with subjective perception and artistic and architectural expression. It allows for the generation of multiple lighting scenarios that accommodate individual perceptions, particularly relevant in complex environments such as underground public spaces.

Drawing from several standards and other technical sources, recommended measurable values on the dominant path for metro stations are detailed in Table 3. These measurements must be conducted across multiple sampling fields representative of each spatial zone. While such reference values provide essential design benchmarks, they may be adapted according to station-specific boundaries and characteristics such as spatial configuration and surface materials. The overarching goal remains the same: to ensure sufficient, coherent, and comfortable lighting that enhances the user experience in constrained underground settings.

Achieving balanced lighting uniformity, particularly critical for universal accessibility, requires careful calibration across the entire user journey. Uniformity is necessary because it expels excessive contrasts, which can cause discomfort or distraction. Most indoor lighting designs prioritise appropriate illuminance levels, even though the human eye responds primarily to luminance, or light reflected from surfaces, rather than the direct intensity of the sources.



**Table 3.** Recommended measurable values on the dominant path for metro stations, according to different sources.

Area/Assignment	Illuminance level (Lux)	Uniformity (U <sub>0</sub> )	IRC Max (Ra)	CCT (K)
Access hoppers: External / Interior	200-300	≥ 0,4	≥ 80	3500–4500
Elevator - cabin	150	≥ 0,4	≥ 80	3000–4000
Circulation zones	200	≥ 0,4	≥ 80	3000–4000
Welcoming hall	200-300	≥ 0,6	≥ 80	3500–4000
Ticket machine / ATM	300-500	≥ 0,5	≥ 80	3500–4000
Control zone / gates	200-300	≥ 0,5	≥ 80	3500–4000
Boarding platforms	200	≥ 0,4	≥ 80	3000–4000
Public sanitary facilities	200-300	≥ 0,5	≥ 80	3000–4000
Technical areas	150-200	≥ 0,6	≥ 80	4000–5500
Overnight maintenance	70	≥ 0,6	≥ 80	4000–5500

Despite the value of measurable data, particularly concerning visual discomfort, certain subjective dimensions remain beyond the scope of current instrumentation. These “sensitive” factors, as described by several authors, are rooted in individual experience and perception. While not directly measurable, they play a crucial role in user appropriation of space. Based on various sources, they can be summarised as follows:

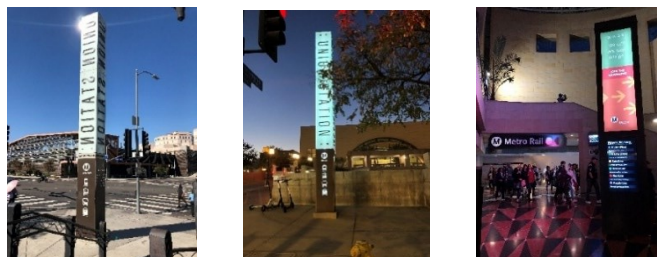
- Overall perceived visual comfort: A product of multiple factors, like uniformity, contrast, colour temperature, and ambience, combined with personal variables such as age, visual fatigue, preferences, and visual impairments - difficult to guarantee universally pleasant ambient conditions.
- Perception of ambience: Contributes to impressions of intimacy, calm, dynamism, or stress. Ambience results from a nuanced combination of intensity, distribution, colour temperature, shadows, and their interaction with structure, materials, and spatial volumes.
- Perception of safety: Lighting may affect users’ feelings of safety independently of measurable illuminance values, particularly in ambiguous, isolated, dark or visually cold environments.
- Aesthetic perception: Lighting that enhances the spatial and material qualities of a space can foster emotional satisfaction and a positive experience. Conversely, inadequate lighting can diminish spatial legibility and reduce user comfort.

However, the challenge lies in reconciling quantifiable criteria with the more subjective dimensions of visual comfort, which engineers may regard as immeasurable. Accordingly, it is essential to test different lighting scenarios using mock-ups and to engage not only technical experts but also users, or even “expert users” with experience in universal accessibility. Depending on the context, broader user consultations should also be conducted to ensure the proposed solutions meet the diverse needs and expectations of all users.

## 5. LOOKING FOR USER-CENTRIC CREATIVE LIGHTING : SOME EXAMPLES

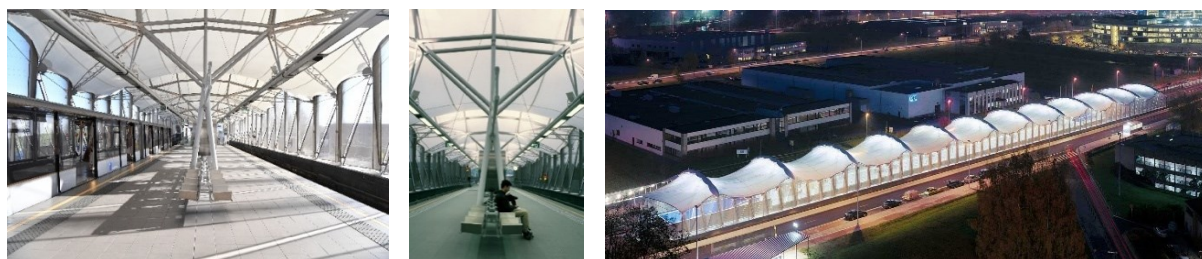
To illustrate our insight, we present a series of atmospheric sequences that accompany users throughout their journey in a metro station. These successive environments are conceived as a visual landscape and as a natural extension of the surrounding urban context. Each sequence serves as a spatial landmark, inviting either contemplation or reorientation, with its own distinct identity in which lightning plays an integral and inseparable role.

1. In the urban landscape, the first step for users is to identify the station entrance. Backlit signage, featuring the metro logo or station name, must stand out clearly as well by night as by day, to ensure visibility and intuitive access for all users (Figure 4, left and centre). Directions, network lines with real-time arrivals, connections, and info services that are available need to be displayed at strategic points and tailored to the requirements of people with reduced mobility (Figure 4, right).



**Figure 4.** Day and night retro-lit station totems (left and centre) and information totems (right) at Union Station in Los Angeles.

2. Another way of enhancing the visibility of a metro station is the creation of a surface-level kiosk. As illustrated in Figure 5, the design emphasises a structure that optimises natural light during the day, while inverting the effect at night to become a luminous beacon. Light and architecture form a whole.



**Figure 5.** Erasme metro station, Brussels. Images © Samyn and Partners & STIB-MIVB.

3. Urban constraints do not always permit straightforward access between underground stations and the surface. In response, a multifunctional solution has been developed, integrating a tree planter, seating, and a skylight into a single urban element, bringing natural light into the station while enhancing the public space above (Figure 6).



**Figure 6.** Trône metro station, Brussels.

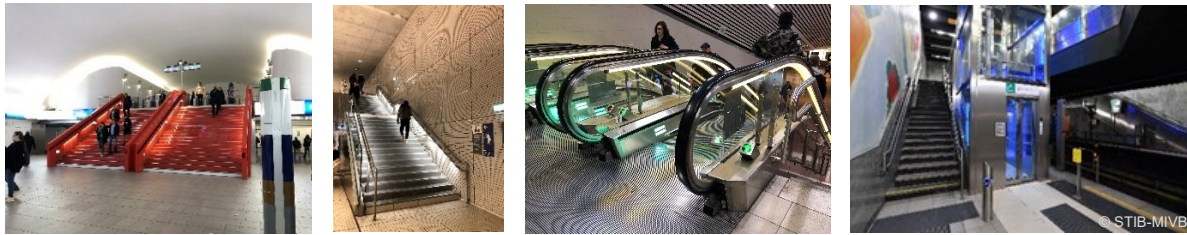
4. In spaces where daylight is absent, designer Barbara Hediger<sup>6</sup> creates the illusion of the sky, offering a sense of time and light variation by intensity and colour. This approach helps reduce the feeling of confinement, a key consideration in enclosed environments like underground stations and workspaces (Figure 7).



**Figure 7.** Space Belgolaise - Dispatching STIB-MIVB, Brussels. Images © Barbara Hediger

<sup>6</sup> According to Barbara Hediger, lighting designers are essential to converting architectural vision and creating unique ambiances. Particularly when it comes to 'orchestrating' light to facilitate seamless transitions between different spaces. Online interview, 10 July 2025, 11 a.m.

5. Enhancing lighting at the ends of stairways improves visibility for individuals with visual impairments. The use of green and red lighting reinforces directional cues and supports intuitive wayfinding (Figure 8, stairs and escalators). Similarly, employing distinctive colours for elevators makes them easier to locate, contributing to a more navigable and accessible environment (Figure 8, right).



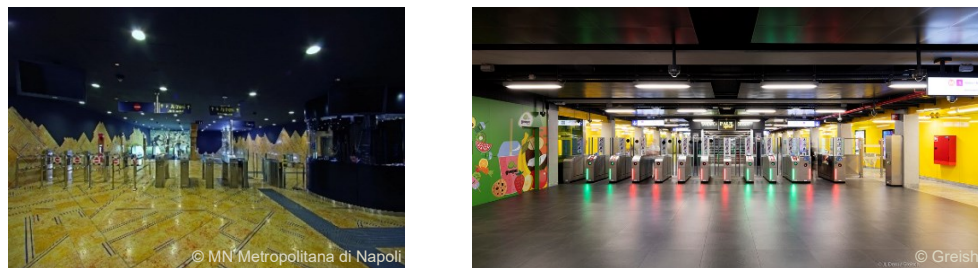
**Figure 8.** From left to right: stairs at Saint-Lazare station in Paris, escalator at Stockholm City station; lifts at Jacques Brel station, Brussels

6. Connecting corridors, can also be the subject of light and sound art that contributes to the creation of identity. An immersive artistic installation by Tine Havelock Stevens and collaborators invites user participation, enriching the overall atmosphere with a sense of fluidity and shared experience (Figure 9).



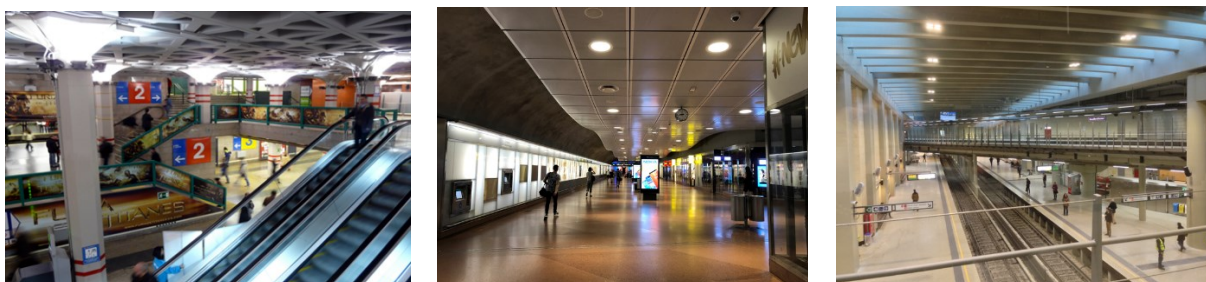
**Figure 9.** Installation by Tine Havelock Stevens and collaborators at a pedestrian tunnel connecting underground transport amenities in a metro station, Sydney

7. The ticket validation area is a critical zone often considered at risk. Although the design of the surrounding area may be exceptional (Figure 10, left), the complete integration of access gates may be confusing for people with cognitive and visual impairments. That is why this area should be clearly marked using contrasting colours to enhance spatial legibility and supported by reinforced lighting that subtly indicates direction, thereby facilitating smoother and more intuitive wayfinding (Figure 10, right).



**Figure 10.** Left: Toledo metro station, Naples. Right: De Brouckère metro station, Brussels.

8. High visibility and spatial legibility through well-designed light provide a sense of reassurance (Figure 11, left and centre). At the Shuman station, top skylights allow daylight to reach platform level, with brightness regulated by sensors that adjust to outdoor light intensity (Figure 11, right).



**Figure 11.** From left to right: Metro station, Madrid; Stockholm City Station; Schuman station, Brussels.

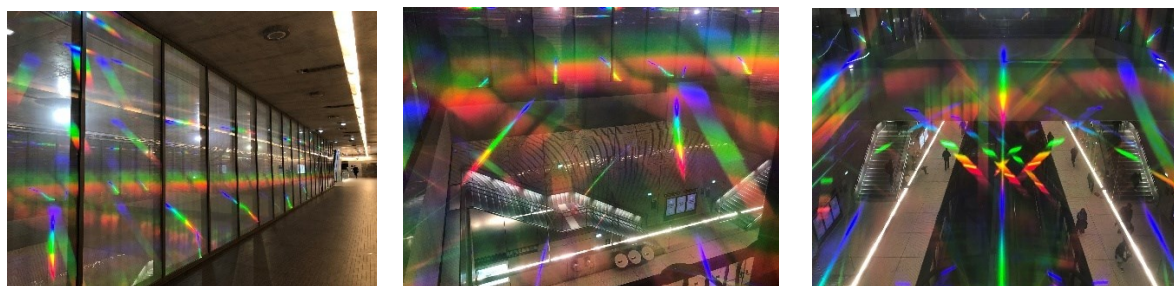


9. Enhancing the visibility and legibility of user information, particularly safety signage, through the strategic use of lighting, geometric forms and adhesive materials is a highly important component of inclusive design. Such approaches ensure that guidance and safety information remain accessible to all users, regardless of their sensory or cognitive abilities (Figure 12).



**Figure 12.** Left: Information point at Stockholm City station. Centre: Stockholm Underground. Right: SOS device, Barcelona.

10. An insightful example of working with light and materiality is found in the work by Kimsooja at the Mairie de Saint-Ouen station in Paris (Figure 13). By integrating light diffraction into the design, the artist creates a sensory and poetic experience. As light interacts with the glass walls, it splits into vibrant colour spectra, transforming the space into a dynamic, ever-changing artwork that offers users a unique immersive experience, with perceptions shifting in relation to their movement.



**Figure 13.** Installation by Kimsooja at Mairie de Saint-Ouen station, Paris.

## 6. CONCLUSION

A lighting charter, when conceived as a structuring rather than a constraining framework, proves instrumental in user-centric design. It encourages interdisciplinary collaboration among architects, engineers, designers, stakeholders, and expert users, while remaining sensitive to context, sustainability, and maintenance. Instead of imposing uniform solutions, it provides coherence and usability while leaving space for creative interpretation and atmospheric expression.

Effective lighting design enhances spatial legibility, facilitates wayfinding, and reinforces the sense of security, particularly in underground environments where the absence of natural light poses significant challenges. Transitions between surface and subterranean spaces are always critical: carefully orchestrated lighting gradients support visual adaptation, facilitate orientation, and mitigate discomfort. Tools such as mock-ups and on-site light mapping, measuring both illuminance and luminance, allow evidence-based decision-making, ensuring that technical performance aligns with perceptual quality. Luminance offers a closer correlation to human perception and feedback, and thus serves as a more reliable measure of user experience.

Beyond functionality, lighting enriches architectural narratives and subtly guides movement through space. Variations are not limited to explicit spatial functions but are used to create sensory depth, stimulate affective engagement, and enhance the immersive qualities of underground environments. In this regard, lighting contributes to the perception of time, spatial and functional hierarchies, and bodily experience, activating both physical and emotional dimensions of inhabiting space. While it does not alone define the atmosphere of a place, it remains a fundamental component in understanding and shaping its overall quality.

Crucially, lighting should complement rather than dominate architectural forms, except where artistic expression intentionally takes precedence. This dual role, technical and aesthetic, positions lighting at the intersection of engineering precision and design creativity.

Designing for underground environments requires a holistic approach that integrates natural and artificial sources in relation to spatial and temporal dynamics. Factors such as placement, intensity, direction, ambient and intended effect must be considered not in isolation but as part of a user-centric design strategy that directly impacts well-being, safety, universal accessibility, and urban inclusion. In this sense, lighting is not a secondary technical component but a strategic lever for healthier and more sustainable urban spaces.

Ultimately, the quality of lighting, together with spatial clarity and architectural legibility, forms the foundation of accessible, fluid, and inclusive underground environments. By enhancing user-centric design, encouraging public space appropriation, and reinforcing attractiveness of public transportation, lighting emerges as a pivotal agent in advancing urban continuity and the quality of human experience.

## 7. BIBLIOGRAPHY

- [1] Browning, W. D., et al. *The Impact of Biophilic Design on Health and Productivity*. Terrapin Bright Green, 2020.
- [2] Capron, Jean-Luc. *Spatio-temporal Factors of Coloured Light Sequences in the Built Environment: the case of a choral concert – Part One*. International Colour Association (AIC) Conference 2021 (Milan, du 30/08/2021 au 03/09/2021). In: Proceedings of the International Colour Association (AIC) Conference 2021, AIC : Milan2021, p. 667-672 <http://hdl.handle.net/2078.1/251994>
- [3] Chlkoff Grégoire, Thibaud Jean-Paul, *Ambiances sous la ville, une approche écologique des espaces publics souterrains*, Ed. CRESSON, Grenoble. 1997.
- [4] CIE (Commission Internationale de l'Éclairage). CIE S 026/E:2018 – *System for Metrology of Optical Radiation for ipRGC-Influenced Responses to Light*, 2019.
- [5] Cousseau Louise, *Illuminez les dessous : une étude de la conception des espaces souterrains par le prisme de la lumière*. Ed. Sciences de l'Homme et Société. 2019. <https://dumas.ccsd.cnrs.fr/dumas-03131669>
- [6] Figueiro, M.G., et al. *Circadian-effective light and its impact on alertness and performance in the workplace*. *Lighting Research & Technology*, 49(4), 2017. 460–475.
- [7] Flynn, E. John, Kremers, A. Jack, Segil, W. Arthur, Steffy, R. Gary. *Architectural Interior Systems. Lighting, Acoustics, Air Conditioning*. Third Edition. Van Nostrand Reinhold, New York. 1992.
- [8] Frontiers in Psychology. *Lighting underground: The role of artificial light on mood and alertness*. 2021
- [9] Gligor, V., *Luminous environment and productivity at workplaces*. Thesis (Licentiate), Helsinki University of Technology, Espoo. 2004.
- [10] Kahn Louis, *Silence et lumière*, Ed. Linteau, Paris. 1996.
- [11] Labbé Monique, *Faut-il passer par le sous-sol pour mieux concevoir la ville*, in BARROCA Bruno, *Penser la ville et agir par le souterrain*, Presses ENPC, Paris. 2014, pp.37-66.
- [12] Leclerc Yann, *Grottes, couloirs et adyta: l'espace souterrain dans les sanctuaires du monde grec antique*. PhD thesis, Art history, Université de Bordeaux 3. 2010.
- [13] Lucas, R.J. et al. *Measuring and using light in the melanopsin age*. *Trends in Neurosciences*, 37(1), 1–9. 2014.
- [14] MATIC Zorica (dir.), *Lumière dans la cité, vecteur de cohésion sociale ?*. Ed. Les Idées Lumières, Paris. 2018.
- [15] Nonne Jordi, *Caractérisation de la qualité des éclairages artificiels (Rendu des couleurs et confort visuel) en particulier pour les sources de lumière à diodes électroluminescentes (DEL)*, PhD Thèse, Laboratoire commun de métrologie LNE-CNAM, Paris. 2015.
- [16] PALISSE Jean-Pierre, *Projet National de Recherche Ville 10D-ville d'idées*, Rapport d'étape, IREX. 2017.
- [17] PONIZY Anna, *Suggestion de la lumière naturelle par des techniques d'éclairage artificiel : État des lieux et prospective*, Mémoire de master de l'ENTPE de Lyon, 2016.
- [18] Rossi, M., et al. *Lighting quality and perception in underground spaces*. *Building and Environment*, 49, 2012. 117–123.
- [19] Terrin Jean-Jacques, *Le monde souterrain*, Ed. Hazan, Paris. 2008
- [20] Vandewalle et al. *Light as a modulator of cognitive brain function*. *Trends in Cognitive Sciences*. 2009.

\*Rem. 1 : All photos in this paper, unless otherwise indicated, are subject to © Gordana Micic.

\*Rem. 2 : Personal translation from French to English with the assistance of AI tools.



## ENHANCING PSYCHOLOGICAL HEALTH THROUGH BIOPHILIC DESIGN: THE INFLUENCE OF SEA VIEWS ON UNDERGROUND OCCUPANTS.

Isabelle Y. S. Chan <sup>1</sup>, Samuel Twum-Ampofo <sup>2</sup>

**Abstract:** Occupying underground spaces can be associated with poor psychological health. This is due to the unique constraints of the environment, which typically include isolation from the outside world, risk of poor ventilation, and anxiety related to potential safety risks within these spaces. While exposure to nature, such as sea views, is associated with positive psychological health outcomes, little is known if similar effects can be achieved by integrating sea view elements as visual stimuli in underground spaces. In this study, we investigated the impact of virtual sea views on psychological health and cognition by exposing participants to a simulated static sea view, a dynamic sea view, and a control room with no sea view. Participants completed cognitive tasks under each condition, and their subjective emotional responses were collected using questionnaires. Wilcoxon signed-rank test was used to compare participants' health state for each virtual scenario before and during the cognitive tests. Kruskal-Wallis tests were applied to conduct inter-group comparisons. The results from the psychological state assessment showed that static and dynamic sea views can protect against negative emotional shifts. For the cognitive tests, the inverse efficiency score assessment revealed superior efficiency across different tests for different environmental conditions. Further analysis using the Mann-Whitney test with Bonferroni correction suggests that both static sea view (IES = 2.22) and non-sea view conditions (IES = 1.06) were effective for the Stroop test (working memory). However, the IES scores favor the non-sea view control group.

**Keywords:** Psychological Health, Biophilia, Sea view, Virtual Reality, Underground Space

### 1. INTRODUCTION

The mounting pressures from rapid urban growth have led to a paradigm shift in urban development, with planners utilizing underground spaces to augment available developmental space. By increasing developable space, governments can better accommodate the growing population, meet their evolving needs, and pursue sustainability goals [1]. However, this paradigm shift in urban development faces a major hurdle in gaining social acceptance. Underground spaces pose unique indoor environmental challenges for human occupancy, which include the risk of suboptimal ventilation, limited daylight, lack of connection to nature, and a sense of isolation from the outside world [2]. Hence, enhancing the health and perception of underground space occupants remains a topical issue in the academic literature.

Human health is a multidimensional construct encompassing physical, psychological, and social dimensions [3]. As the development of underground spaces expands to include workspaces where occupants reside and work for extended periods, the psychological dimension has emerged as a particularly contentious issue to be addressed in underground space design [4]. According to Ringstad [5], occupants of underground spaces tend to face heightened anxiety due to perceived health and safety risks. In some cases, people's cultural values frame the underground as inhospitable [5]. Such barriers highlight the need to mitigate indoor environmental stressors and reshape perceptions of underground spaces.

Beyond this, productivity, a critical business metric, may be adversely affected by declines in the health of underground workers. Thus, it is prudent to examine workers' cognitive functioning when assessing overall health status [6,7]. In this context, stress reduction theory explains how exposure to nature (e.g., greenery, natural waters)

<sup>1</sup> Chan Y.S, Isabelle, The University of Hong Kong, iyschan@hku.hk.

<sup>2</sup> Twum-Ampofo, Samuel, The University of Hong Kong, samtwum@connect.hku.hk.

can lead to the restoration of psychological health following stress or trauma [6]. Similarly, Schertz and Berman [8] posit that exposure to nature-based interventions promotes restorative states, reducing stress and enhancing cognition. In this line of inquiry, researchers have examined the impact of blue spaces on human health, highlighting their potential to support psychological health and cognitive restoration (e.g., [9],[10],[11]).

As defined by Grellier et al. [12], blue spaces are “outdoor environments, either natural or manmade, that prominently feature water and are accessible to humans either proximally (being in, on or near water) or distally/virtually (being able to see, hear, or otherwise sense water)”. To date, evidence from some studies suggests that exposure to sea views offer a promising approach to improving psychological health by alleviating stress [10] and depression [13]. Nevertheless, a previous systematic review of the state of art of research on exposure to blue spaces and psychological health states revealed very limited studies to date [13]. Accordingly, this study aims to contribute to the knowledge base on the impact of blue spaces on human psychological health and cognition by investigating their effect as visual stimuli in the novel, understudied underground space environment. The study aimed to evaluate the psychological effects of integrating sea view elements into underground spaces, informing design strategies that enhance the psychological health and cognition of underground occupants.

## 2. THEORETICAL FRAMEWORK: BLUE SPACES AND POSITIVE AFFECT

Severin et al. [14] characterized sea views as therapeutic landscapes. Therapeutic landscapes have physical and social features that promote physical, psychological, and even spiritual well-being. Growing empirical evidence demonstrates that exposure to blue spaces like the sea views, rivers, and lakes yields significant benefits for human psychological health ([14], [15]). The evidence documented to date spans several mechanisms, including driving physical activity (e.g. swimming, walking), social cohesion (i.e. a place of engagement in social relationships), and emotional regulation due to their therapeutic nature [15]. Using exposure to the sea as a case study, Severin et al. [14] identified several pathways through which emotional regulation may occur via sea views. These include feelings of awe driven by the sea’s vastness and power, a sense of mental freedom by releasing challenging thoughts, feelings, and emotions, a break from the fast-paced urban environment that serves as psychological safe-havens, and allowing individuals to experience emotional vulnerability without judgment. Thus, while the therapeutic benefits of sea view exposure are acknowledged, little is known if the integration of sea views as design elements in underground spaces can similarly mitigate the psychological health concerns associated with occupying underground spaces. Therefore, to fill this gap, a virtual reality experiment was conducted to investigate the impact of two types of sea views (static sea view and dynamic sea view) and a control, non-sea view scenario on the psychological health and cognition of underground occupants. To the best of our knowledge, this study is the first to examine the health impacts of blue spaces on individuals occupying underground environments. It adds to the existing literature by extending the focus beyond psychological health to include cognitive effects, highlighting their relevance in enhancing the quality of underground workspaces. Accordingly, and guided by the theoretical framework and prior empirical findings, the following hypotheses were proposed:

**H1:** Individuals exposed to a sea view will report higher levels of positive psychological well-being compared to those without.

**H2:** Individuals exposed to a sea view will demonstrate better cognitive performance than those without.

## 3. METHOD

### 3.1. Experiment design

Three immersive virtual office environments were developed using 3D Max and Unity software. Fifty-five participants (26 males, 29 females) were recruited via posters and emails. The participants were randomly assigned to three groups to experience three different virtual office environments: static sea view (wallpaper = 19), dynamic sea view (motioned,  $n = 20$ ), or non-sea view control ( $n = 13$ ). The mean body mass index (BMI) of these participants was 21.92 kg/m<sup>2</sup>, which was considered a healthy level [16].

Participants' emotional states were assessed based on six indicators: calmness, tension, upset, relaxation, contentment, and worry. The study required the participants to complete four tasks in the virtual environment. The tasks were the go/no-go visual task, Stroop test, n-back test and calculation test. The tasks served as proxies, providing insight into a person’s response inhibition [17], cognitive flexibility [18], working memory [19], and numerical processing, respectively. First, the participants reviewed and signed a consent form after which they completed a questionnaire survey to record their basic information and how they felt before exposing them to the underground virtual world. We also screened for caffeine consumption, their level of physical activity and

medications prior to the experiment. The participants donned the VIVE Pro 2 headset, and images were enhanced for clarity by adjusting an interpupillary distance (IPD) knob. Virtual reality (VR) is acknowledged to enhance experimental control by enabling systematic manipulation of indoor environments, minimizing confounding variables and allowing for immersive simulations of natural settings [20,21]. In addition, studies leveraging the capability of VR have demonstrated its effectiveness in delivering emotionally impactful visual stimuli, with statistically significant differences observed between treatment and non-treatment groups across various experimental contexts [21,22].

A brief tutorial was conducted to familiarize participants with the controls and interactions in the VR environment. Next, we confirmed that the participants did not experience any motion sickness or discomfort. Using a job interview scenario, participants were required to complete four cognitive tests. Following the completion of the experiment, we confirmed that the participants did not experience any discomfort and provided them with a coupon as a token of appreciation.



*Figure 1. Virtual Office Environment*

### **3.2. Measurements**

The visual reaction time test required participants to promptly click a “press” button when a green dot popped up on a virtual computer monitor, ignoring all other colored dots. In the Stroop test, several colored words with their respective meanings were displayed on a virtual computer monitor. The goal was for participants to recognize the word whose color was inconsistent with its meaning (e.g., the participant was expected to click the yellow-colored word “Blue”). For the n-back test, participants quickly clicked “press” when the current number matched the one presented two trials earlier. Regarding the calculation test, participants completed simple calculations encompassing addition, subtraction, multiplication, and division. To assess participants’ psychological state, the study employed the State-Trait Anxiety Inventory (STAI). Although some researchers argue that individual differences (such as personality type, gender, and prior spatial experiences) combined with the inherent subjectivity of human perception, may introduce bias in environmental perception studies that use questionnaires, the use of subjective evaluations was deemed feasible and valuable. This is because human judgments of spatial environments tend to follow statistically consistent patterns despite such individual variability (e.g., [23,24,25]).

### **3.3. Data analysis**

The Shapiro-Wilk test revealed that the dataset was not normally distributed hence non-parametric tests were employed. The visual distribution of the data was first presented using box plots. Descriptive statistics and the Wilcoxon signed-rank test were used to compare the changes in participants’ psychological health before and during the cognitive tests. The aim was to evaluate whether the visual impression of the space impacted the participants’ psychological health perceptions (emotions). Task performance was analyzed using the inverse efficiency score (IES), and subsequently, the Kruskal-Wallis test was used to compare cognitive performance between different groups of participants. IES was adopted following recommendations by Townsend and Ashby [26] on its ability to provide comprehensive insight by combining both the speed of task completion and the

accuracy involved. In IES analysis, greater efficiency is reflected by a lower IES, reflecting one's ability to combine both speed and accuracy in performing a given task. Following the proposal of Bruyer and Brysbaert [27], IES was calculated using the formula;

$$\text{Inverse efficiency score} = \frac{\text{Task Time}}{\text{Accuracy}} \quad (1)$$

Where;

$$\text{Accuracy} = \frac{N_{\text{true}}}{N_{\text{true}} + N_{\text{false}} + N_{\text{missing}}} \quad (2)$$

## 4. RESULTS AND DISCUSSIONS

### 4.1. Assessment of Emotional States

The analyzed dataset revealed that the three spatial scenarios (static sea view, dynamic sea view, and non-sea view control group) influenced the participants psychological health differently. In determining time reference points, T0 represented the baseline condition prior to exposure to any virtual environment. T1 represented the moment subjects began the cognitive tests, while T2 represented the end of the cognitive tests. Figures. 2-7 show the participants' psychological state in the different scenarios (i.e., T0-1 and T1-2).

The Wilcoxon signed-ranks tests revealed that with the exclusion of two metrics (feeling upset and feeling worried), the remaining emotional metrics reached statistical significance in one or two groups. Hence the analysis focused exclusively on those emotional metrics that showed significant differences. Table 1 presents these directional effects visually, with the following key patterns emerging:

#### Calmness

Wilcoxon signed-ranks tests revealed a statistically significant decrease in self-reported calmness in the control group between timepoints T1 and T2 ( $Z = -2.68$ ,  $*p < 0.01$ ). For the static and dynamic sea view groups, no difference in time points T1 and T2 were observed, although that of the dynamic sea view group reached statistical significance ( $Z = -2.23$ ,  $*p < 0.05$ ). The statistically significant result could be attributed to the Wilcoxon test's sensitivity to consistent subtle shifts in individual responses, rather than a change in the group's overall central tendency. Thus, some individuals perceived their calmness levels differently at the end of the cognitive test thereby influencing the sensitivity to the ranked pairwise changes.

#### Tension

Wilcoxon signed-ranks tests indicated a statistically significant increase in self-reported tension between T1 and T2 for both the control group ( $Z = -2.750$ ,  $*p < 0.01$ ) and the static sea view group ( $Z = -2.448$ ,  $*p < 0.05$ ). No significant change in tension was found in the dynamic sea view group ( $Z = -0.73$ ). A visual inspection of the box plot however indicates a positively skewed distribution of tension scores for the dynamic group between T1 and T2.

#### Relaxation

Whereas relaxation levels in the static sea view group remained unchanged, a decline was noted in the dynamic sea view group. This shift was however not statistically significant. On the other hand, a statistically significant decrease in self-reported relaxation was observed in the control group between T1 and T2 ( $Z = -3.27$ ,  $*p < 0.01$ ).

#### Contentment

For the dynamic and static sea view groups, no statistically significant changes in contentment were found between T1 and T2 (Dynamic:  $Z = -0.63$ ; Static:  $Z = -1.10$ ). However, a statistically significant result was found for the control group ( $Z = -2.26$ ,  $*p < 0.05$ ). Despite this statistical finding, the median contentment score for this group was identical at T1 and T2. Visual analysis of the box plots indicated a wider interquartile range and longer whiskers at T2 compared to T1, suggesting the statistically significant result could be due greater variability in responses of some participants.

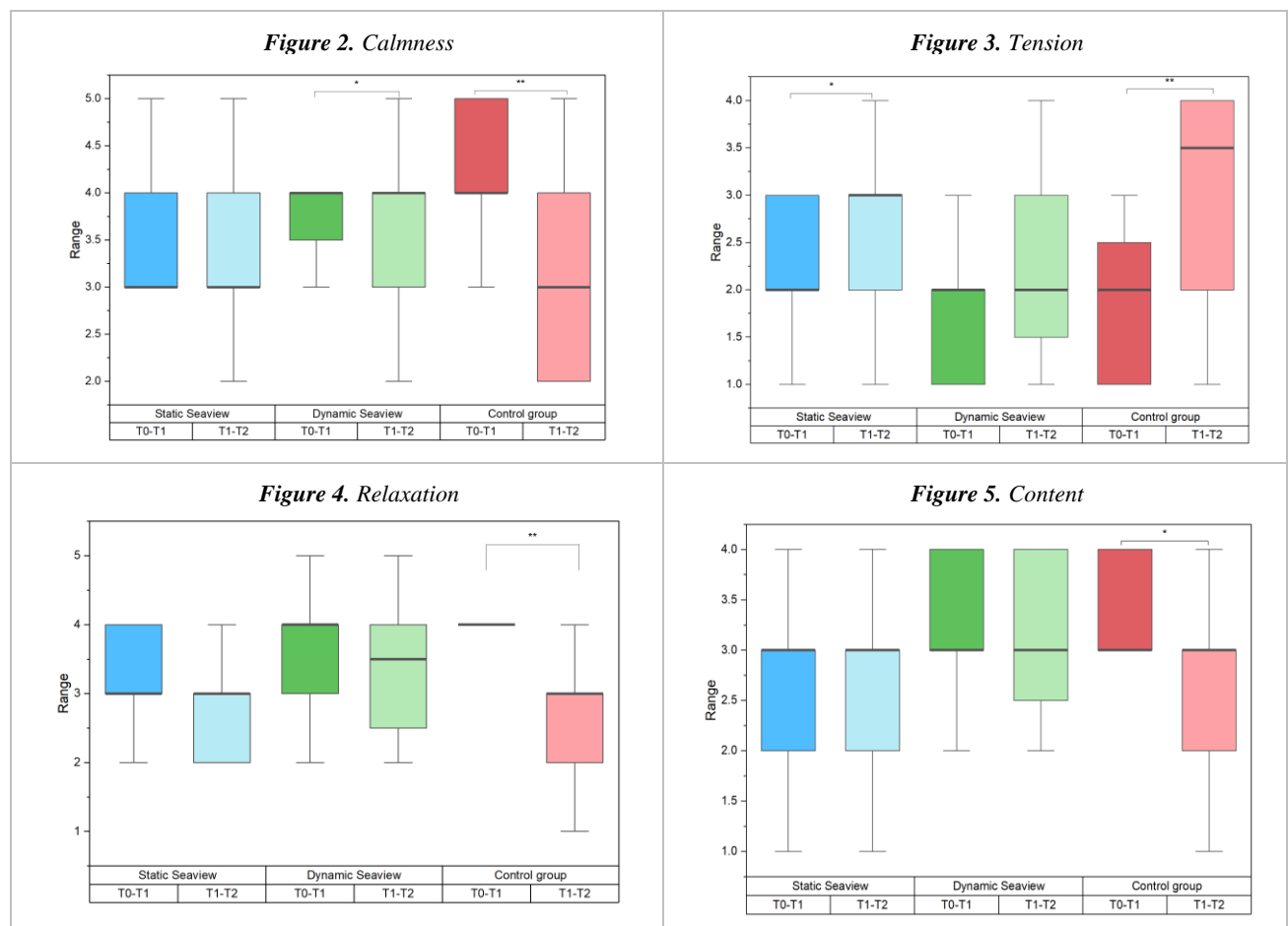
### Discussion of emotional state results

The analyzed dataset revealed that both static and dynamic sea views buffered against psychological decline across various metrics (ref. Fig. 2,3 and 4). This finding provides deeper insight into the protective, and not merely restorative, potential of nature exposure ([7],[28]). Thus, the presence of natural elements like sea views in confined underground spaces may lie in its capacity to prevent a decline rather than promote psychological health. While the treatment groups in most cases maintained baseline levels, the control group exhibited a significant increase in tension and decreased in calmness and relaxation. This pattern aligns well with Stress Reduction Theory ([7],[28]).

Furthermore, the results indicated that the static and dynamic sea view groups exhibited different psychological health effects. While both maintained pre-test calmness, the dynamic view also prevented a significant rise in tension. Although this effect did not reach statistical significance, a larger sample might provide conclusive evidence. On the other hand, the static sea view group exhibited a rise in tension, although, this increase was less pronounced than that observed in the control group. This suggests that static sea view provides a partial buffer compared to the control.

Further analysis, guided by Russell's [29] Circumplex Model of Affect, revealed the mechanics of this protective effect. According to Russell's [29] model, emotions like calmness (pleasant, low-arousal) and tension (unpleasant, high-arousal) are conceptual opposites. Thus, two opposite emotions cannot be felt at the same time. Consistent with this model, the dynamic sea view maintained stable levels of calmness and tension levels, whereas the control group exhibited a decline in calmness and an increase in tension. These patterns validate the effectiveness of dynamic sea views in sustaining calmness and reducing tension.







As summarized in Table 1, the results suggest that static and dynamic sea views offer protective benefits against negative emotional shifts, with dynamic exposure demonstrating marginally stronger effects. This underscores the nuanced role of natural stimuli in emotional regulation. However, due to the inconsistent effects of sea view exposure on restoration and positive emotions, we reject Hypothesis H1.



\* $p < 0.05$ , \*\* $p < 0.01$  Statistically significant



*Descriptive Emotional Impact Matrix*

Emotional state	Static sea view	Dynamic sea view	Control group
 Calmness	—	—	↓ **
 Tension	↑ *	—	↑ **
 Upset	—	—	↑
 Relaxation	—	↓	↓ **
 Contentment	—	—	—
 Worry	—	↓	—

Key: ↑ improvement, — no change, ↓ decrease, \* $p < 0.05$ , \*\* $p < 0.01$  Statistically significant

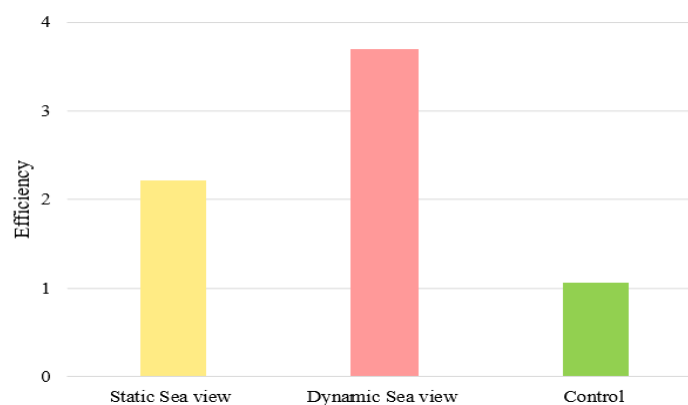
## 4.2. Cognitive Assessment: Task Performance


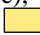
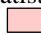
Participants' performance across four cognitive tasks (go/no-go, Stroop, n-back, and calculation) was analyzed using the inverse efficiency score, Kruskal-Wallis results and Mann-Whitney tests.

### 4.2.1. Inverse Efficiency Scores

Inverse Efficiency Scores (IES) were used to assess both accuracy and speed, with lower scores indicating better performance. The inverse efficiency analyses indicated that all scenes yielded distinct advantageous performance alongside some drawbacks. First, participants performed better on the n-back test (cognitive flexibility) under static sea view. For dynamic sea view, the participants performed better in the go/no-go task (response inhibition), n-back test (cognitive flexibility) and the calculation test (numerical processing). In the Control group, the participants performed better in the Stroop test (working memory). However, the Kruskal-Wallis test revealed that amongst all the tasks, only results from the Stroop test (working memory) reached statistical significance ( $p = 0.026$ ).

*Figure 6. Stroop test\**



(Lower IES = Better Performance), \* $p < 0.05$  Statistically significant  
 Best performance  Medium  Least

#### 4.2.2. Mann-Whitney with Bonferroni correction

Following the identification of a significant difference across the groups on the Stroop test, a post-hoc analysis using Mann-Whitney tests with a Bonferroni-adjusted alpha of 0.05/3 (0.0167) was conducted for pairwise comparisons to determine which groups differed. Three analyses were run; Static vs. Dynamic, Static vs. Control and Dynamic vs. Control. The test revealed statistically significant differences in Stroop's tests for static sea view versus dynamic sea view, and dynamic sea view versus the control group. Static sea views (IES= 2.22) were superior to dynamic sea views (IES=3.70) suggesting a suitability of static sea view for tasks requiring working memory. Also, the Stroop test in the non-sea view control environment (IES= 1.06) yielded superior performance compared with that taken in the dynamic sea view environment (IES=3.70). Notably, no significant difference was found between the Stroop test results of the static sea view and the control group. This suggests that both environments are effective although, the control group had a lower IES of 1.06 compared to the static sea view's 2.22. Therefore, Hypothesis 2 is not supported.

*Mann-Whitney tests with Bonferroni correction*

Pairwise Comparison	p-value
Static Sea view vs. Dynamic Sea view	0.011*
Static Sea view vs. Control	0.659
Dynamic Sea view vs. Control	0.012*

Bonferroni threshold ( $p^* < .0167$ ).

## 5. CONCLUSION

This study examined the impact of simulated sea view scenarios (static, dynamic, control) on psychological enhancement and cognition of underground occupants via virtual reality. The results suggest that the presence of sea views (static and dynamic) may overall protect the emotional state of underground occupants compared to the control group, although further studies with larger samples are needed for further validation. Nevertheless, these preliminary results align with existing qualitative research highlighting the positive emotional impact of blue spaces [14,30]. Regarding cognitive performance, the Mann Whitney test with Bonferroni corrections indicated that both static sea view and non-sea view conditions (control group) were conducive for tasks involving working memory. This insight suggests that the integration of sea views in underground space may be dependent on the functional use of the space. Future studies should also examine how the functional use of space may mediate the psychological and cognitive effects of sea view elements. Also, researchers could replicate this study with larger samples and could utilize advanced neuroscience behavioral technologies like eye tracking to unveil the interaction of study participants with the visual elements within a virtual world. Furthermore, a qualitative approach could reveal whether the integration of blue spaces such as the dynamic blue space may inadvertently evoke a longing to be outside or frustration in participants confined to a constrained space. Previous research on coastal blue spaces has highlighted that, in certain cases, individuals with traumatic associations to coastal settings may not experience the intended restorative benefits, suggesting that personal history and context can significantly shape responses to blue space exposure [31].

In conclusion, this study demonstrates that integrating sea views into underground spaces can protect occupants from psychological deterioration, with dynamic exposures offering a marginally superior benefit. For architects and designers, this suggests that dynamic digital displays of nature could be a valuable strategy for windowless or underground spaces. Future research should investigate longer exposure times and incorporate physiological measures to further elucidate the mechanisms behind this protective effect.

## 6. ACKNOWLEDGMENT

This work was supported by the General Research Fund (Grant No.17203920) under the Research Grant Council, HKSAR.

## 7. BIBLIOGRAPHY

- [1] Chan, I. Y., Twum-Ampofo, S., Ababio, B. K., Ghansah, F. A., & Li, S. (2025). Towards a whole process engineering approach for enhancing physical and psychological health in underground environments: A systematic review. *Tunnelling and Underground Space Technology*, 161, 106530.
- [2] Chan, I. Y., Dong, Z., & Chen, H. (2024). Impacts of connections to the outside on underground space occupants' psychophysiological health: A virtual reality-based experimental approach. *Tunnelling and Underground Space Technology*, 147, 105675.
- [3] Huber, M.A., 2014. Towards a new, dynamic concept of health: Its operationalisation and use in public health and healthcare and in evaluating health effects of food.
- [4] Dunleavy, G., Bajpai, R., Tonon, A. C., Cheung, K. L., Thach, T. Q., Rykov, Y., Soh, C. K., de Vries, H., Car, J., & Christopoulos, G. (2020). Prevalence of psychological distress and its association with perceived indoor environmental quality and workplace factors in under and aboveground workplaces. *Building and Environment*, 175, 106799.
- [5] Ringstad, A. J. (1994). Perceived danger and the design of underground facilities for public use. *Tunnelling and Underground Space Technology*, 9(1), 5–7.
- [6] Wang, C., Zhang, F., Wang, J., Doyle, J. K., Hancock, P. A., Mak, C. M., & Liu, S. (2021). How indoor environmental quality affects occupants' cognitive functions: A systematic review. *Building and environment*, 193, 107647.
- [7] Ulrich, R. S., Simons, R. F., Losito, B. D., Fiorito, E., Miles, M. A., & Zelson, M. (1991). Stress recovery during exposure to natural and urban environments. *Journal of environmental psychology*, 11(3), 201-230.
- [8] Schertz, K. E., & Berman, M. G. (2019). Understanding nature and its cognitive benefits. *Current Directions in Psychological Science*, 28(5), 496-502.
- [9] Britton, E., Kindermann, G., Domegan, C., & Carlin, C. (2020). Blue care: A systematic review of blue space interventions for health and wellbeing. *Health promotion international*, 35(1), 50-69.
- [10] Dempsey, S., Devine, M. T., Gillespie, T., Lyons, S., & Nolan, A. (2018). Coastal blue space and depression in older adults. *Health & place*, 54, 110-117.
- [11] Wheeler, B. W., White, M., Stahl-Timmins, W., & Depledge, M. H. (2012). Does living by the coast improve health and wellbeing? *Health & place*, 18(5), 1198-1201.
- [12] Grellier, J., White, M. P., Albin, M., Bell, S., Elliott, L. R., Gascón, M., ... & Fleming, L. E. (2017). BlueHealth: a study programme protocol for mapping and quantifying the potential benefits to public health and well-being from Europe's blue spaces. *BMJ open*, 7(6), e016188.
- [13] Gascon, M., Zijlema, W., Vert, C., White, M. P., & Nieuwenhuijsen, M. J. (2017). Outdoor blue spaces, human health and well-being: A systematic review of quantitative studies. *International journal of hygiene and environmental health*, 220(8), 1207-1221.
- [14] Severin, M. I., Raes, F., Notebaert, E., Lambrecht, L., Everaert, G., & Buysse, A. (2022). A qualitative study on emotions experienced at the coast and their influence on well-being. *Frontiers in Psychology*, 13, 902122.
- [15] Nutsford, D., Pearson, A. L., Kingham, S., & Reitsma, F. (2016). Residential exposure to visible blue space (but not green space) associated with lower psychological distress in a capital city. *Health & place*, 39, 70-78.
- [16] Mainous III, A. G., Tanner, R. J., Rahmanian, K. P., Jo, A., & Carek, P. J. (2019). Effect of sedentary lifestyle on cardiovascular disease risk among healthy adults with body mass indexes 18.5 to 29.9 kg/m<sup>2</sup>. *The American Journal of Cardiology*, 123(5), 764–768.
- [17] Raud, L., Westerhausen, R., Dooley, N., & Huster, R. J. (2020). Differences in unity: The go/no-go and stop signal tasks rely on different mechanisms. *NeuroImage*, 210, 116582.
- [18] Scarpina, F., & Tagini, S. (2017). The stroop color and word test. *Frontiers in psychology*, 8, 557.
- [19] Meule, A. (2017). Reporting and interpreting working memory performance in n-back tasks. *Frontiers in psychology*, 8, 352.
- [20] Roberts, A. C., Christopoulos, G. I., Car, J., Soh, C. K., & Lu, M. (2016). Psycho-biological factors associated with underground spaces: What can the new era of cognitive neuroscience offer to their study?. *Tunnelling and Underground Space Technology*, 55, 118-134.
- [21] Yin, J., Arfaei, N., MacNaughton, P., Catalano, P. J., Allen, J. G., & Spengler, J. D. (2019). Effects of biophilic interventions in office on stress reaction and cognitive function: A randomized crossover study in virtual reality. *Indoor air*, 29(6), 1028-1039.
- [22] Yeom, S., Kim, H., Hong, T., Ji, C., & Lee, D. E. (2022). Emotional impact, task performance and task load of green walls exposure in a virtual environment. *Indoor air*, 32(1), e12936.
- [23] Tan, Z., Roberts, A. C., Lee, E. H., Kwok, K. W., Car, J., Soh, C. K., & Christopoulos, G. (2020). Transitional areas affect perception of workspaces and employee well-being: A study of underground and above-ground workspaces. *Building and Environment*, 179, 106840.

- [24] Higashiyama, A., & Kitano, S. (1991). Perceived size and distance of persons in natural outdoor settings: The effects of familiar size. *Psychologia: An International Journal of Psychology in the Orient*.
- [25] Gilinsky, A. S. (1951). Perceived size and distance in visual space. *Psychological review*, 58(6), 460.
- [26] Townsend, J. T., & Ashby, F. G. (2014). Methods of modeling capacity in simple processing systems. In *Cognitive theory* (pp. 199-239). Psychology Press.
- [27] Bruyer, R., & Brysbaert, M. (2011). Combining speed and accuracy in cognitive psychology: Is the inverse efficiency score (IES) a better dependent variable than the mean reaction time (RT) and the percentage of errors (PE)? *Psychologica Belgica*, 51(1).
- [28] Ulrich, R. S. (1983). Aesthetic and affective response to natural environment. In *Behavior and the natural environment* (pp. 85-125). Boston, MA: Springer US.
- [29] Russell, J. A. (1989). Measures of emotion. In *The measurement of emotions* (pp. 83-111). Academic Press.
- [30] Ting, H. Y., & Bahauddin, A. (2022). The impact of blue space in the interior on mental health. *ARTEKS: Jurnal Teknik Arsitektur*, 7(1), 53-60.
- [31] Tashiro, A., Kogure, M., Nagata, S., Itabashi, F., Tsuchiya, N., Hozawa, A., & Nakaya, T. (2021). Coastal exposure and residents' mental health in the affected areas by the 2011 Great East Japan Earthquake and Tsunami. *Scientific Reports*, 11(1), 16751.

## ADAPTABLE SAFETY CONCEPTS FOR UNDERGROUND RAIL, TRANSIT, AND ROADWAY APPLICATIONS

Bernd Hagenah, Petr Pospisil

**Abstract:** This paper discusses the rapid advancements in rail and transit operation, with a focus on the transition towards driverless systems and automatic train operation. This shift necessitates a close integration between rail systems and tunnel safety systems to mitigate risks and ensure passenger safety. The paper proposes a safety concept that goes beyond the traditional approach of relying solely on specific fire and life safety standards. This concept aims to achieve cost savings and higher safety levels by considering additional elements and human factors. The outlined methodology can be adapted for various underground applications, including safety concepts during construction and for road tunnels.

**Keywords:** Safety Concept, Driverless Systems, Rail Systems, Tunnel Safety Equipment

### 1. INTRODUCTION

The landscape of underground rail and transit is undergoing a significant transformation, driven by rapid technological advancements. However, a concurrent revolution in safety philosophy, driven largely by European standards, provides a critical framework for managing this change. The European Technical Specifications for Interoperability (TSI) have spearheaded a move away from purely prescriptive safety rules towards more dynamic, performance-based approaches. Specifically, the TSI for Safety in Railway Tunnels (TSI-SRT) provides a structure for developing comprehensive safety concepts built on modern principles.

This framework enables the application of Quantitative Risk Assessments (QRA), allowing designers and operators to systematically evaluate scenarios, differentiate between acceptable and unacceptable risks, and implement targeted, effective mitigation measures. The power of this approach was demonstrated in landmark European projects such as the Gotthard Base Tunnel, where for the first time, rail operating systems and tunnel safety infrastructure were deeply interconnected. This integration created a holistic safety environment where the tunnel and the train act as a single, coordinated system during an incident.

This paper addresses current gaps in traditional safety philosophies by explicitly targeting four categories of risks often underrepresented in prescriptive standards:

- Operational risks (loss of train control, derailments, unexpected stops in tunnels).
- Technological risks (failure of automation, inadequate system integration across signaling, ventilation, and communications).
- Human-factor risks (absence of onboard staff, passenger misperception of safety, reliance on centralized operators).
- Emerging risks (cybersecurity vulnerabilities, extreme weather impacts, and resilience against prolonged outages).

To mitigate these risks, the proposed safety concept extends beyond traditional fire-centric approaches. It incorporates non-traditional elements such as:

- System integration of vehicle, signaling, and tunnel equipment into a single safety logic.
- Quantitative Risk Assessment (QRA) as a design driver, replacing prescriptive distances and capacities with proven, project-specific safety targets.



- Defense-in-depth layering (Prevention, Mitigation, Evacuation, Rescue) applied consistently across construction, operation, and maintenance phases.
- Consideration of socio-technical factors like public acceptance, user guidance in unattended operations, and AI-supported incident detection.

The methods adopted in this study include risk analysis frameworks (both qualitative and quantitative), comparative benchmarking against reference projects (e.g., Gotthard and Loetschberg Base Tunnels), and systems engineering approaches that integrate civil, rolling stock, and safety equipment into one coherent operational model.

Validation of this approach is achieved through demonstrated precedents from European base tunnels where risk-based concepts have already been accepted by authorities; simulation studies (fire dynamics, evacuation, system response times) verifying safety targets; and lifecycle feedback, where the concept is iteratively updated based on operational data and emergency training and drills.

This paper argues that these types of integrated safety concepts are no longer just best practice but a fundamental requirement for the next generation of transit: driverless and automatic train operation. As the human operator's role is reduced or eliminated, the seamless interaction between the vehicle and its environment becomes the primary guarantor of safety. An adaptable safety methodology is proposed, built on the principles proven in projects like the Gotthard Base Tunnel, that can be applied to the unique challenges of automated systems to achieve higher safety levels and cost-efficiencies. This framework's flexibility also allows its adaptation for safety planning during construction and for road tunnel applications.

## **2. A PARADIGM SHIFT IN EUROPEAN RAILWAY SAFETY**

Building on the introduction of the TSI framework, which harmonized safety standards across Europe, this section highlights how these principles now underpin cross-border railway design and safety integration. Previously, the continent's rail network was a fragmented landscape of national systems, each developed in relative isolation. This resulted in significant disparities in technology, operating procedures, and underlying safety requirements. A train crossing a border often had to be compatible with entirely different signaling, power, and safety philosophies, creating what were effectively "technical islands."

This lack of harmonization was a major barrier to a truly integrated European rail network. The introduction of the TSIs established a common basis for both technical equipment and safety concepts. For the first time, there was a shared methodology for defining safety targets and a common language for demonstrating compliance. This forced a convergence of national standards towards a unified, higher benchmark, fundamentally changing how cross-border projects were designed and how system-wide safety was managed. It is this revolutionary, integrated approach that now provides the foundation for tackling the next generation of railway challenges.

## **3. THE CHANGING LANDSCAPE OF RAIL AND TRANSIT OPERATION**

The evolution in rail and transit operation is best understood through the internationally recognized framework of Grades of Automation (GoA), outlined in standards like IEC 62290 (see [3]). This scale categorizes systems based on the division of responsibility between human operators and technology. The progression from manual to fully automated systems represent the most significant operational shift in modern railway history.

The transition from GoA1 (manual) to GoA4 (fully unattended) represents a shift in safety responsibility from human operators to integrated systems. While GoA1–GoA2 retain human oversight, GoA3 removes driving duties but maintains onboard staff for emergencies, and GoA4 eliminates all staff presence, relying entirely on system automation.

The global transit industry shows a clear and accelerating trend towards implementing GoA3 and GoA4 systems for new lines and major upgrades. The drivers for this are compelling: increased line capacity through reduced headways, improved service regularity, greater operational flexibility, and lower long-term staffing costs.

However, this transition has profound implications for safety design. In GoA1 and GoA2 systems, the driver serves as the ultimate real-time sensor, capable of identifying and reacting to a vast range of unexpected hazards. In GoA3 and especially GoA4 systems, this human layer of response and mitigation is removed from the vehicle. The responsibility for ensuring safety shifts entirely to the integrated system of the train, the signaling, and the tunnel infrastructure itself.

#### 4. LIMITATIONS OF TRADITIONAL SAFETY CONCEPTS

For decades, safety in underground transit has been guided by robust and well-established prescriptive standards, with North America's NFPA 130 being a prominent example (see [2]). These documents have been instrumental in establishing a strong safety baseline, codifying lessons learned from past incidents and creating a common set of requirements for system designers. However, the foundational philosophy of many of these traditional standards is inherently prescriptive, and they were developed around an operational paradigm that assumes the presence of a human driver. As the industry pivots to driverless (GoA3) and unattended (GoA4) operations, the limitations of this approach become critically apparent. The primary weaknesses of these traditional, prescriptive concepts are:

**Implicit Reliance on Human Intervention:** Prescriptive rules often assume the presence of an onboard operator (driver) to perform crucial functions during an emergency. This includes stopping the train at a designated location, communicating with passengers and the control center, assessing a hazard, and directing an evacuation. In a GoA4 system, these intelligent actions must be fully automated and integrated into the system's logic. A simple prescriptive rule, for example, may not specify how a driverless train should detect a fire and decide whether to proceed to the next station or initiate an immediate stop and evacuation – a decision that is fundamental to a safe outcome.

**Rigid, "One-Size-Fits-All" Requirements:** Prescriptive standards provide clarity but often lack flexibility, such as specifying a maximum distance between emergency exits (e.g., 250 meters or 800 feet). While this "deemed-to-satisfy" approach is easy to enforce, it lacks adaptability. It does not inherently account for project-specific conditions. For instance, a rigid spacing requirement may be insufficient in a very deep tunnel with long evacuation times, or conversely, it may be overly conservative and unnecessarily costly in a shallow tunnel with a highly advanced ventilation system. This rigidity stifles innovation and prevents the implementation of more effective, performance-based solutions where designers can demonstrate an equivalent or higher level of safety through engineering analysis rather than by simply checking a box.

**A Siloed Approach to Safety Subsystems:** Traditional standards often specify requirements for various subsystems – such as ventilation, communications, and signaling – in separate chapters or sections. They are treated as independent domains rather than as components of a single, integrated safety system. This is a significant drawback for automated systems, where the emergency response depends entirely on the seamless, coordinated interaction between these very subsystems. A GoA4 train system must communicate its status to the ventilation system to manage smoke, to the signaling system to protect the area, and to the central control system to coordinate the response. A safety concept that treats these as separate entities fails to address the most critical aspect of automated safety.

Therefore, while these standards provide a valuable foundation, relying on them alone for GoA4 systems is insufficient. The shift to driverless operation demands a corresponding shift from a prescriptive, siloed safety philosophy to a holistic, performance-based, and deeply integrated one, as outlined by the TSI framework.

#### 5. UNDERSTANDING THE THREATS, RISKS, AND PROTECTION GOALS

To create an applicable safety concept, it is essential to identify the threats, analyze the associated risks, and clearly formulate the protection goals. Without this fundamental analysis, the result is not a true safety concept, but merely a loose collection of regulations that will likely fail to achieve the required level of safety.

##### 5.1. Threats and Risks

A systematic identification of threats is required to understand what the system must be protected from. For railway operations, these threats include, for example:

- **Collisions:** These include collisions with objects on the track (e.g., debris lost by preceding trains), other trains, people, or fixed infrastructure elements (e.g., noise barriers, partition walls, tunnel portals, bridge piers, etc.).
- **Derailements:** While derailements can have a probability of occurrence similar to that of vehicle fires, their specific dynamics are often given less consideration in the early stages of tunnel safety planning.
- **Toxic Gas Release and Explosions:** This describes the dangers that originate from freight traffic.
- **Fires:** Train fires (passenger and freight trains), and fires of technical equipment (e.g., in tunnels).

## 5.2. Protection Goals

To understand what and who must be protected, key protection goals must be defined. The frequently encountered protection goals listed here are typical; they are generally refined and supplemented for the specific project during its course. The examples are:

- Protection of life and limb for all persons (passengers, staff).
- Protection of life and limb for rescue forces, as well as providing environmental conditions that allow them to carry out their work.
- Protection of the infrastructure asset against loss (i.e., avoid collapse).
- Ensuring insurability of the asset.
- Preservation of prestige and brand reputation.
- Rapid resumption of revenue service.
- No negative impact on flora and fauna, both during revenue service and in the event of maintenance or an incident.

## 5.3. Risk Evaluation

For the risk evaluation, it is sensible to proceed as simply and transparently as possible. Generally, two different approaches can be found, a Quantitative Risk Assessment and a Qualitative Risk Assessment.

- Qualitative Risk Analysis: The object being investigated (e.g., a rail tunnel) is compared with a typical (average) rail tunnel regarding its risks.
- Quantitative Risk Analysis: The available data on the operation and the object itself are collected and analyzed. It is important to know and be able to assess the accuracy of the data and assumptions, as well as their limits; for example, Which assumptions were made and under which conditions are they valid?

## 6. SAFETY CONCEPT

To manage the complexities of modern underground transit systems, which involve a deep integration of civil, mechanical, electrical, and systems engineering, an overarching safety strategy is essential. The proven approach championed by the European TSI-SRT (see [1]) provides a uniquely flexible and robust framework. Applications for long rail tunnels are outlined in [5] and [6]. The safety philosophy is built upon a "defense in depth" model, structuring safety measures into four distinct layers. If a hazard breaches one layer of defense, the next is there to contain it. This ensures there is no single point of failure and builds system-wide resilience. The four layers are:

**Prevention:** This is the first and most critical layer. It encompasses all measures taken to prevent an incident from occurring in the first place. For underground systems, this includes passive measures like fire-retardant materials and active measures guided by a formal RAMS (Reliability, Availability, Maintainability, and Safety) process, as defined in standards like EN 50126 (see [4]). This process ensures the high reliability of rolling stock, the implementation of robust maintenance regimes, and the integrity of Automatic Train Protection (ATP) systems to prevent incidents.

**Mitigation:** If a hazardous event does occur, this second layer aims to limit its consequences and control its escalation. Key mitigation measures include advanced fire and smoke detection systems that can quickly identify an incident's location and intensity. It also includes active fire suppression systems, like water mist or sprinklers, and – most critically – the tunnel ventilation system, which is used to control smoke flow, maintain tenable conditions, and create a clear path for evacuation.

**Evacuation:** This layer focuses on ensuring passengers and staff can safely perform self-rescue and move to a place of ultimate safety (e.g., an adjacent tunnel or the surface). This is enabled by a combination of passive and active systems, including clear emergency signage, reliable emergency lighting, dedicated walkways, and frequent, easily accessible cross-passages between tunnel bores. The design of the train itself, with wide doors and clear gangways, is also a critical component of this layer.

**Rescue:** The final layer consists of measures that facilitate effective intervention by external emergency services. Beyond access, this layer ensures responders can work safely. It includes the provision of dedicated access shafts and adits for firefighters, secure and reliable communication systems that work deep underground, high-capacity water supplies (hydrants), and well-defined emergency procedures that are coordinated between the transit operator and local first responders.

By structuring a safety concept around these four layers, designers can ensure all aspects of a potential incident are considered, from its initial cause to its final resolution. This holistic approach is fundamental to ensuring safety in driverless systems where technology, not a human operator, must manage the entire chain of events.

## 7. IMPLICATIONS OF THE MODERN SAFETY CONCEPT ON GOA4 SYSTEM DESIGN AND OPERATION

### 7.1. Impact on Safety Planning and Design

In the planning phase, the safety concept forces a fundamental shift away from simply following a checklist of standards toward a holistic, analysis-driven design process.

- **Front-Loaded Safety Analysis:** Unlike traditional projects where safety compliance can be a checkbox exercise, this modern approach requires comprehensive Risk Assessments at the earliest stages of planning. The results of this analysis directly influence fundamental design decisions, such as tunnel alignment, ventilation system capacity, and vehicle specifications.
- **Mandatory System Integration:** The concept invalidates the traditional "siloed" approach to engineering. It is no longer possible for the vehicle designers, signaling engineers, and civil/tunnel engineers to work independently. The safety concept requires them to design the train and the tunnel as a single, coordinated system. For example, the vehicle's on-board fire detection system (Mitigation layer) must be designed from the outset to communicate seamlessly with the tunnel's ventilation control system and evacuation times.
- **From "Deemed-to-Satisfy" to "Proven Safe":** A designer cannot simply state that a fixed egress distance of 250 meters is safe because it's in a rulebook. Instead, they must use the risk analysis to prove that the combination of vehicle fire resistance, smoke control, and evacuation procedures will achieve the defined Protection Goals (e.g., protecting human life ) for that specific project. This allows for—and requires—more innovative and efficient solutions.

### 7.2. Impact on Systems Operation

For a GoA4 system, where there is no driver to manage unforeseen events, the safety concept becomes the operational playbook.

- **Automated, Pre-Defined Emergency Scenarios:** The entire response to an incident (like a fire or derailment) must be pre-engineered and automated. The "human layer of response" is replaced by a technological one. When a GoA4 train detects a fire, the integrated system must automatically execute a pre-defined sequence: report the incident, activate the appropriate ventilation scenario, adjust the operation of other trains, and provide clear evacuation guidance, all without human intervention.
- **Centralized and Enhanced Human Supervision:** The role of the human operator is shifted from the vehicle to a central control room. The safety concept dictates that these operators must have advanced tools to supervise the system's health and manage complex, automated emergency responses. Their role changes from direct intervention to high-level supervision and exception handling.
- **Maintenance Becomes a Core Safety Function:** In this model, the "Prevention" layer is paramount. The reliability of every component underpins the entire safety case. Therefore, the operational phase must include robust, predictive maintenance and continuous system health monitoring to ensure the risk levels calculated during the design phase remain valid throughout the system's life.

## 8. EXAMPLE GENERIC TABLE OF CONTENTS FOR A GENERIC SAFETY CONCEPT

Chapter	Content	Comment
1	Introduction	Short description of the asset/infrastructure for which the safety concept is developed
2	Objectives	Compiling the objectives of the safety concept.
3	Basics	Compile all information about the asset/infrastructure such as: owner, operators, operational concept, geography,

		temporal and geographical delimitations, status of the project/planning phase, standards, etc.
4	Threats, Risks and Protection Goals	Compile all reasonable threats and risks, as well as the protection goals and conduct a safety assessment.
5	Safety Concept	Formulate the safety concept based on the threats, risks, and protection goals,
5.1	First Priority: Prevention	Describe the prevention methods
5.2	Second Priority: Mitigation	Describe Mitigation Methods
5.3	Third Priority: Evacuation	Describe Evacuation Methods
5.4	Fourth Priority: Rescue	Describe Rescue Methods
6	Derived Requirements for Operations and Equipment	Based on the safety concept, recommendations are drawn for the operational concept, technical equipment, safety protocols in case of incidents, and training for staff and responders, etc.
7	Lifecycle Management of the Safety Concept	Based on operational experience, a safety concept must be regularly reviewed and adapted if necessary. Furthermore, training for operations and for responders must also be adapted

## 9. ADAPTABILITY TO OTHER APPLICATIONS

The strength of the risk-based, four-layered safety concept lies in its philosophical approach rather than a rigid set of rules, making its core principles highly adaptable. While this paper has focused on its application to automated rail systems, the framework's flexibility allows it to be effectively applied to other complex underground environments, such as road tunnels and construction sites.

### 9.1. Application to Road Tunnels

When applied to road tunnels, the methodology remains the same, but the specific inputs change. The initial step is to identify the unique threats and risks associated with road traffic, such as the wider variety of vehicle types, potential for hazardous materials from freight traffic, and the behavior of non-professional drivers. The protection goals, such as the protection of life and the infrastructure asset, are then defined for this specific context.

The four layers of defense are subsequently tailored to these risks:

- Prevention: Measures would focus on traffic management, vehicle monitoring, and robust maintenance of tunnel systems to prevent incidents from occurring.
- Mitigation: This layer is critical and would involve advanced fire detection and powerful ventilation systems designed to manage smoke from various fire sources, controlling the incident's escalation.
- Evacuation: The strategy would focus on providing clear guidance and safe passage for drivers and passengers who are unfamiliar with the environment, using systems like emergency lighting and signage.
- Rescue: This involves ensuring efficient and safe access for external emergency services, a principle shared with rail applications.

### 9.2. Applications to Construction Phases

The safety concept is also a valuable tool for managing risk during the construction phase of a tunnel project. The process again begins with identifying the specific threats, which in this context include risks from construction machinery, temporary electrical installations, and fires involving building materials. The primary protection goal is ensuring the safety of all construction personnel and protecting the partially completed structure against catastrophic loss.

The four-layered strategy would be applied as follows:

- Prevention: This is the most critical layer, enforced through strict site safety protocols, worker training, and management procedures to prevent accidents.
- Mitigation: Measures would include fire detection and suppression systems suitable for a construction environment and plans to contain events like water ingress or localized collapse.
- Evacuation: This requires establishing and maintaining clearly marked and unobstructed escape routes that are adapted as the construction progresses.



- **Rescue:** The plan must ensure that emergency responders can access a potentially complex and changing site and requires well-defined emergency procedures coordinated with local first responders.

## 10. FUTURE CHALLENGES AND EMERGING CONSIDERATIONS

As automated transit systems evolve, the safety landscape will continue to face new and complex challenges. One key concern is cybersecurity, which becomes critical as GoA4 systems rely heavily on centralized communication, remote diagnostics, and data-driven control. Protecting safety-critical systems against cyber threats is no longer a purely IT issue – it is integral to operational safety.

Another emerging consideration is artificial intelligence (AI) in incident detection and decision-making. While AI holds potential for faster and more nuanced responses, its deployment raises questions of transparency, reliability, and accountability, especially in life-critical scenarios.

Additionally, public trust and user acceptance of fully unattended systems remain a sociotechnical hurdle. Despite the high safety performance of GoA4 systems, passengers may perceive them as less safe without onboard staff – underscoring the importance of user-centered design, transparent communication, and emergency support systems.

Finally, climate resilience must be addressed in future safety planning. Underground infrastructure is increasingly vulnerable to extreme weather events, including flash flooding and power outages. Safety concepts must evolve to incorporate adaptive strategies that ensure system robustness under changing environmental conditions.

## 11. SUMMARY

As the transit industry transitions toward fully driverless (GoA4) operations, traditional prescriptive safety standards – designed around the presence of a human operator – are no longer sufficient. To address this, this paper advocates for the adoption of an adaptable, performance-based safety concept.

This approach is already proven in practice; and successfully applied to major European infrastructure projects, including high-speed lines and landmark tunnels like the Gotthard and Loetschberg Base Tunnels. Rooted in the European TSI framework, this approach uses risk analysis to structure safety measures into a four-layered "defense in depth" model: Prevention, Mitigation, Evacuation, and Rescue. Adopting this framework fundamentally reshapes projects by requiring:

- Deep system integration, treating the train, tunnel and operation as a single, coordinated system from the start of design.
- A shift from rigid rules to "proven safe" solutions validated by risk analysis.
- Automated emergency responses and centralized human supervision in place of on-board staff.

Beyond these established benefits, the contribution of this paper is to clearly identify four categories of risks (operational, technological, human-factor, and emerging) and demonstrate how they can be mitigated through a non-traditional, layered approach. The study introduces methods such as quantitative and qualitative risk assessment, systems engineering integration, and benchmarking against European base tunnel precedents. Finally, the proposed safety concept is validated through simulation studies, proven precedents, and lifecycle feedback mechanisms, ensuring that the approach is not only innovative but also practical and reliable.

This holistic approach provides a robust path to achieving superior safety and efficiency, with a flexible framework readily adaptable to other underground applications.

## 12. BIBLIOGRAPHY

- [1] The European Technical Specifications for Interoperability for Safety in Railway Tunnels (TSI-SRT)
- [2] NFPA 130, Standard for Fixed Guideway Transit and Passenger Rail Systems.
- [3] IEC 62290, Railway applications – Urban guided transport management and command/control systems
- [4] EN50126, Railway applications – The specification and demonstration of Reliability, Availability, Maintainability and Safety (RAMS)
- [5] Hagenah, B., Cassady, S., Cancia, M., Zlatanovic, S., Vetsch, H-P., Safety Challenges in Long Rail Tunnels, North American Tunneling Conference (NAT), United States, 2021
- [6] Hagenah, B., Cassady, S., Pospisil, P., Vetsch, H.-P., Ockajak, R., Safety in Long Rail Tunnels, UC (ITA - AITES), Prague, 2023

## AN EXPERIMENTAL STUDY ON VISUAL COMFORT OF TUNNEL PORTALS IN VIRTUAL REALITY ENVIRONMENTS

ZHAO Weihao<sup>1</sup>, LIU Fang<sup>2</sup>, KONG Weijun<sup>3</sup>

**Abstract:** An appropriately-designed tunnel portal can provide drivers with a smooth visual transition and enhance driving comfort. However, with the increasing complexity of landscape elements, overly refined designs may distract drivers, potentially compromising driving safety. Despite this concern, research on the impact of different types of tunnel portal landscapes on drivers' visual comfort remains inadequate. It is worth exploring for identifying tunnel portal landscapes which distract drivers' attention and increase accident risk. A virtual experimental system based on VR (Virtual Reality) was configured to examine landscaping portals characterized by different styles. Electrodermal activity data, eye movement data, driving performance and subject data were collected for further analysis. The results showed that i) the distraction of landscaping portals to drivers varied under low and high-speed driving conditions, with distractions caused by refined type landscape being particularly noticeable, and drivers tend to more concentrate on driving with the increase of speed; ii) landscaping the portals will improve driving comfort, but the improving effect is less prominent in high-speed roads than low-speed roads; iii) driving safety and comfort decreased with the increase of speed under all three styles of tunnel portals, landscape design for tunnel portals should adapt to the design speed. The results of this investigation provide new insights into measures for improving the visual comfort of road tunnel portals.

**Keywords:** tunnel portal landscape; virtual reality (VR); visual comfort; safety

### 1. INTRODUCTION

With increasing implementation of human-centered design in infrastructure, tunnel portal design has been expanded beyond conventional safety requirements (Canto-Perello and Curiel-Esparza, 2001). Under the prerequisite of ensuring essential protective functions, the impact of portal environments on drivers' visual perception and psychological experience is now prioritized as a critical design factor (China Journal of Highway and Transport Editorial Department, 2022).

Well-designed tunnel portal landscapes significantly enhance driving comfort, and thus some scholars advocate incorporating substantial artificial elements to create elaborate landscapes (Chen and Yang, 2019; Wen et al., 2024). However, visually-striking landscapes may distract drivers, potentially increasing safety risks (Yuan, 2014). This perspective favors landscape strategies prioritizing natural ecological restoration (Ye et al., 2022). To support decisions on appropriate designs in tunnel portal landscapes, it is vital to develop tools for quantifying drivers' perception in driving environments.

This study developed a VR-based driving platform to investigate drivers' perception on three representative designs of a tunnel portal. The integrated experimental framework synchronizes VR scenarios, high-fidelity driving simulators, and multimodal biosensing to record real-time oculomotor patterns, EDA (electrodermal activity), and operational behaviors. The purpose of this study is quantitatively capture drivers'

<sup>1</sup> Graduate student, ZHAO Weihao, State Key Laboratory of Disaster Reduction in Civil Engineering, Tongji University, Shanghai 200092, China, zhaoweihaol031@163.com

<sup>2</sup> Professor, LIU Fang, State Key Laboratory of Disaster Reduction in Civil Engineering, Tongji University, Shanghai 200092, China, liufang@tongji.edu.cn

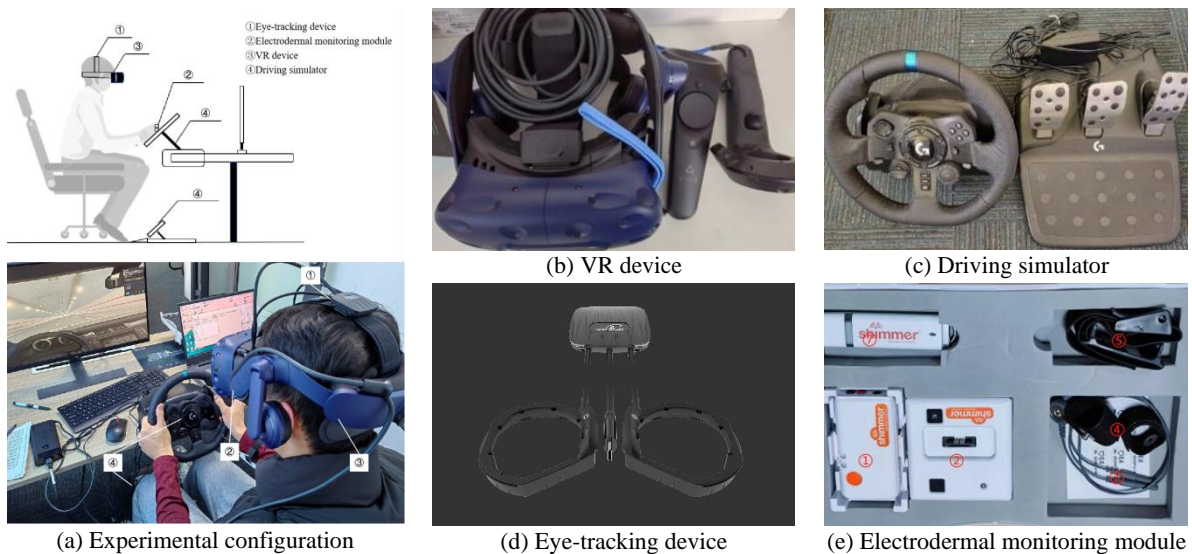
<sup>3</sup> MSc, KONG Weijun, State Key Laboratory of Disaster Reduction in Civil Engineering, Tongji University, Shanghai 200092, China, 2132417@tongji.edu.cn

psychophysiological responses to different designs of tunnel portals under various driving speeds. Findings from this study could support the principle of speed-adaptive design in tunnel portals.

## 2. METHODOLOGY

### 2.1. Experimental Setup

The configuration of the experimental system is illustrated in Figure 1a. To capture drivers' eye movement data in both simulated and real-world driving scenarios, an aSee VR eye tracker was employed, as shown in Figure 1b. The system was integrated with an HTC VIVE PRO virtual reality headset (Figure 1c) to ensure compatibility with the eye-tracking device. A Logitech G923 TRUEFORCE steering wheel (Figure 1d) was utilized to mimic driving feedback within the virtual environment. EDA data was used for a quantitative indicator of emotional responses under varying experimental conditions, and was recorded using ShimmerCapture v0.6 (Figure 1e).

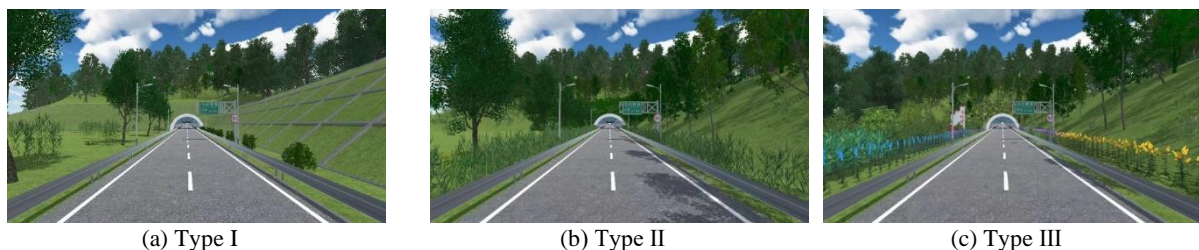


**Figure 1.** Experimental setup

### 2.2. Virtual displays

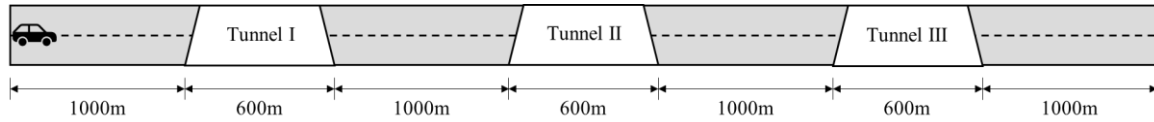
The virtual environment was constructed featuring a 35 m mountain elevation with 9.5 m high roadway slopes. The tunnel structure spans 600 m in length and 9.2 m in width with an external diameter of 12.7 m and internal diameter of 11.3 m, providing 7.5 m vertical clearance. The mountain massif and the tunnel were integrated into the Unity3D-based simulation platform.

Three tunnel portal landscape typologies (Figure 2) were engineered to assess driving safety-comfort relationships: Type I (Artificial Finishing Type), Type II (Natural Restoration Type), and Type III (Refined Landscape Type).



**Figure 2.** Three designs of the tunnel portal

As illustrated in Figure 3, the simulation environment is configured as a mountainous freeway section incorporating three 600-meter-long tunnels spaced at an interval of 1000 m. Each portal interface was programmed with modular switching capability among the three preset landscape typologies.



**Figure 3.** Basic scene

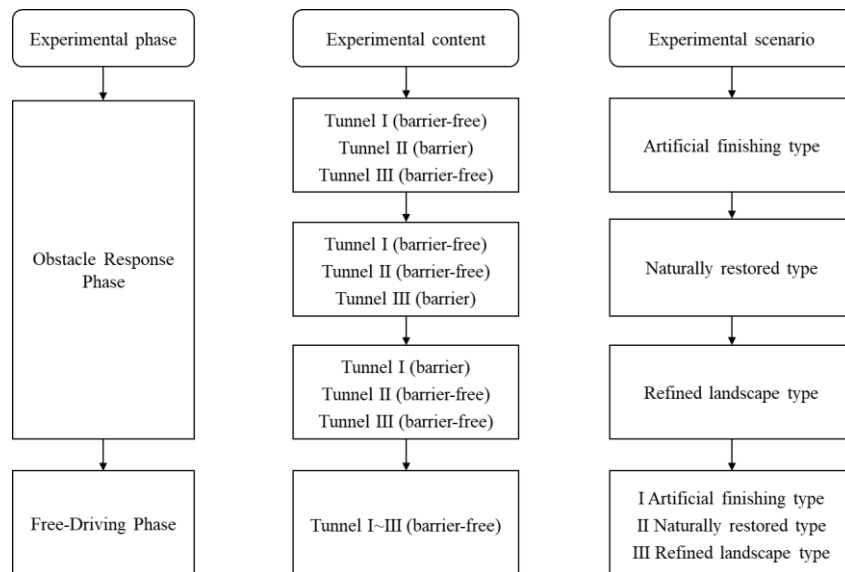
### 2.3. Testers

The experiment recruited 42 testers with driving experience. 男性23名，女性29名。To ensure the accuracy and reliability of the experimental data, testers were required to meet the following criteria: (1) a driving experience of at least one year, including experience driving through tunnel sections; (2) normal auditory, visual, and tactile perception abilities; (3) the capacity to clearly understand technical terms and verbally articulate their subjective experiences; and (4) adherence to a healthy and regular lifestyle for 24 hours prior to the formal trials to maintain physiological stability.

### 2.4. Experimental design

Prior to formal testing, testers completed operational training and signed informed consent forms alongside baseline demographic documentation. All collected information remained strictly confidential per consent agreements, accessible exclusively to research personnel. Then standardized training was administered covering experimental objectives, procedural workflows, VR equipment operation, and simulator controls to minimize cognitive biases. Pre-tests were conducted to enhance experimenters' operational proficiency, reduce procedure-related errors, and establish contingency protocols. The pre-test data were excluded from final analyses.

The formal experiment comprised three batches. Each participant completed four trial sequences as illustrated in Figure 4.



**Figure 4.** Flowchart of experimental design

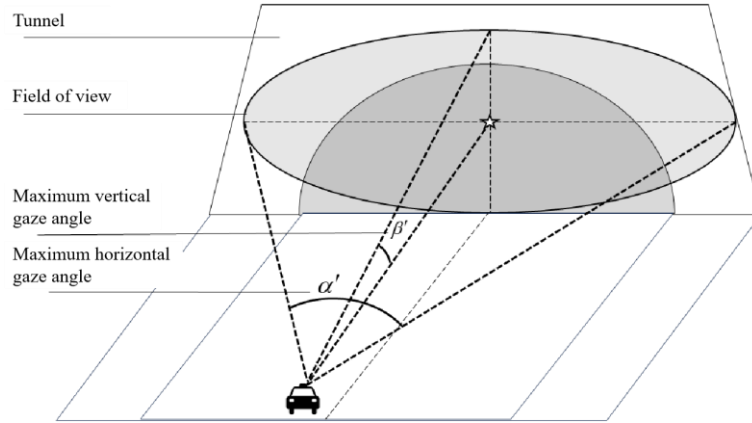
### 2.5. Data collection

Data from 42 testers were collected across three modalities. Eye movement data were recorded using an eye tracker, extracting the number of fixation points during the 8-second period preceding each tunnel portal traversal. Driving behavior data were programmatically logged during both the obstacle-response and free-driving phases, yielding 6 trials per tester. Specifically, the obstacle-response phase dataset contained time stamps, speed, and positional parameters, while the free-driving phase recorded the average transit speed at portal traversals. EDA data were synchronously collected during the free-driving phase for each tunnel landscape type, with a per-recording acquisition duration of 8 seconds. Subjective data were collected using questionnaires administered immediately after participants completed a drive through each of the three tunnel types.

### 3. EVALUATION MODEL

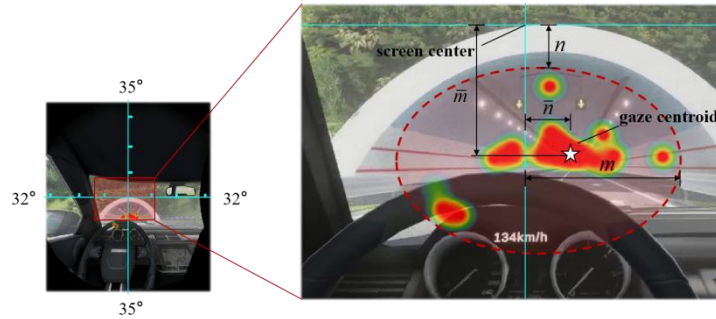
#### 3.1. Delineating driving field of view

Based on cognitive psychology principles, the driving field of vision consists of a set of driver gaze points, with its distribution center defined as the gaze centroid (Lappi, 2016b; Lappi, 2022). As shown in Figure 5, the driving field of vision is characterized by the maximum horizontal gaze angle ( $\alpha'$ ) and maximum vertical gaze angle ( $\beta'$ ).



**Figure 5.** Schematic diagram of driving visual field

Figure 6 shows the driver's eye movement heatmap over a specific time period, where  $n$  and  $m$  represent the maximum horizontal and vertical distances of the gaze points from the screen center, respectively;  $\bar{n}$  and  $\bar{m}$  denote the horizontal and vertical distances of the gaze centroid from the screen center.



**Figure 6.** Calculation schematic of driving visual field range

The position coordinates of gaze points within the screen coordinate system are acquired using a VR eye tracker. Combined with the screen's field-of-view angles ( $32^\circ$  horizontally per side,  $35^\circ$  vertically per side), viewing angle parameters relative to the screen center are calculated. To unify the reference to the gaze centroid, a viewing angle correction is applied via coordinate transformation.

The maximum Horizontal Gaze Angle Correction ( $\alpha'$ ) is computed as:

$$\alpha' = |\alpha - \bar{\alpha}| \times 2 \quad (1)$$

where  $\alpha$  is the maximum horizontal angle of gaze points relative to the screen center,  $\bar{\alpha}$  is the horizontal gaze angle of the gaze centroid relative to the screen center. They are computed as:

$$\alpha = \arctan\left(\frac{n \times \tan 32^\circ}{n_{\max}}\right) \quad (2)$$



$$\bar{\alpha} = \arctan\left(\frac{\bar{n} \times \tan 32^\circ}{n_{\max}}\right) \quad (3)$$

where  $n_{\max}$  is the horizontal distance from the screen center to the left/right edge (normalized to 0.5 for half-width).

Similarly, the maximum Vertical Gaze Angle Correction ( $\beta'$ ) is computed as:

$$\beta' = \beta - \bar{\beta} \quad (4)$$

where  $\beta$  is the maximum vertical angle of gaze points relative to the screen center,  $\bar{\beta}$  is the vertical gaze angle of the gaze centroid relative to the screen center.

$$\beta = \arctan\left(\frac{m \times \tan 35^\circ}{m_{\max}}\right) \quad (5)$$

$$\bar{\beta} = \arctan\left(\frac{\bar{m} \times \tan 35^\circ}{m_{\max}}\right) \quad (6)$$

where  $m_{\max}$  is the vertical distance from the screen center to the left/right edge.

### 3.2. Accessing driving safety

Driving safety is determined by the obstacle-response braking distance defined as the spatial interval between the braking initiation point and the obstacle. A scenario is classified as safe if the obstacle-response braking distance exceeds the safe stopping distance; otherwise, it is deemed hazardous. As illustrated in Figure 7, the obstacle-response braking distance and the driving speed are derived from testers' velocity-distance profiles during obstacle encounters. The inflection point on the curve indicates the braking initiation—corresponds to the obstacle-response speed (plotted on the x-axis) and braking distance (plotted on the y-axis).

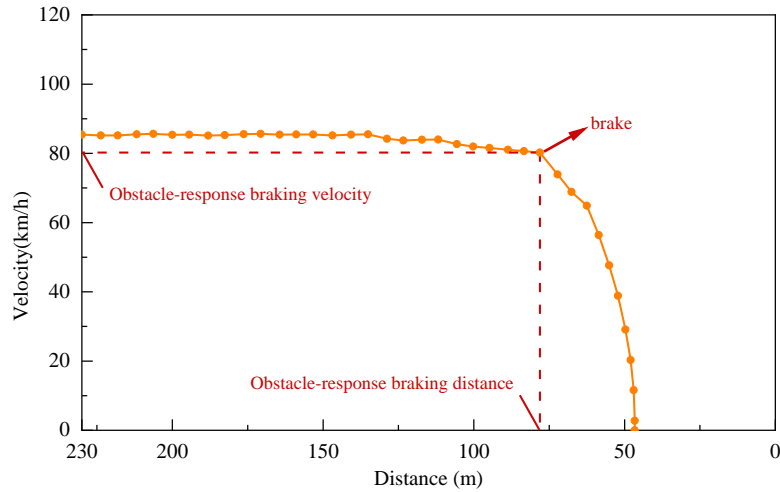


Figure 7. Calculation method of obstacle-response braking distance and speed

The safety stopping distance increases with the driving speed, and it can be calculated as follows :

$$S = v^2 / 2\mu g + S_0 \quad (7)$$

where  $v$  is the obstacle-response speed (m/s),  $\mu$  is the road friction coefficient (e.g., 0.8 for concrete surfaces),  $g$  is gravitational acceleration (9.8 m/s<sup>2</sup>), and  $S_0$  is the reserved safety distance (i.e., 20 m).

The obstacle-safety rate ( $\eta$ ) is defined as the ratio of safe trials to total trials:

$$\eta = \frac{p}{q} \quad (8)$$

where  $p$  is the number of safe scenarios, and  $q$  is the total number of trials.

The fixation frequency ( $k$ ) serves as another key metric for evaluating driving safety, demonstrating how information processing mechanisms affect safety performance. It can be computed as:

$$k = \frac{\sum_{i=1}^z P_i}{z \times t} \quad (9)$$

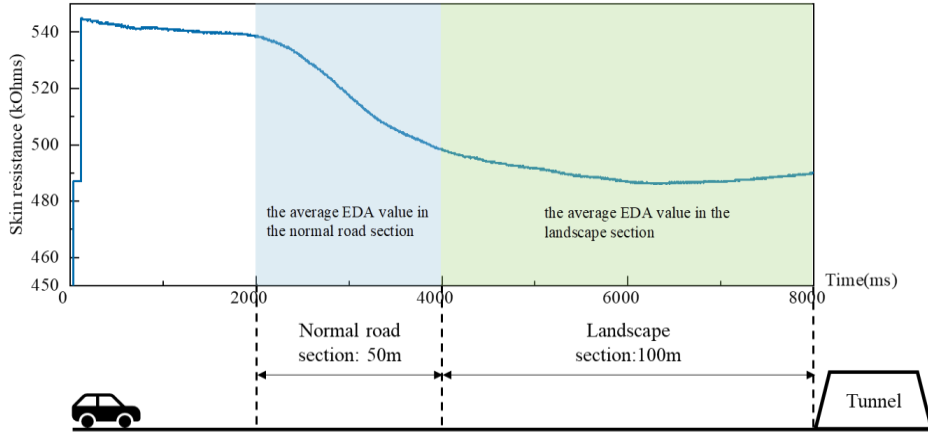
where  $P_i$  is the fixation count for the  $i^{\text{th}}$  tester,  $t$  is the eye-tracking data duration (i.e., 8 seconds in this study), and  $z$  is the total number of testers.

### 3.3. Assessing driving comfort

Driving comfort refers to the psychological state of relaxation and reduced tension experienced by drivers during vehicle operation, a subjective perception requiring integrated psychophysiological evaluation. This study adopts a combined approach of subjective questionnaires and EDA analysis.

Subjective questionnaires assess tunnel satisfaction and driving comfort based on the distribution and mean values of the five-point scale (2, 1, 0, -1, -2).

EDA-based comfort quantification relies on relative changes in skin potential difference. Figure 8 presents a typical EDA curve obtained from the experiment. Here we define a 100 m landscape section immediately before tunnel entry.



**Figure 8.** Schematic diagram of average electrodermal response calculation

The electrodermal response rate ( $\delta$ ) is calculated as:

$$\delta = (P' - P_0) / P_0 \quad (10)$$

where  $P'$  represents the average EDA value in the landscape section, and  $P_0$  denotes the baseline EDA value in the normal road section. Studies indicates (Posada-Quintero and Chon, 2020; Yan and Jia, 2022) that high electrodermal response rates correlate with heightened driver stress, inversely impacting comfort. Therefore, a positive  $\delta$  signifies tension, while a negative  $\delta$  indicates predominant comfort states.

## 4. RESULTS

### 4.1. Gaze Angle

Figure 9 illustrates the comparison of gaze angles as testers approached different tunnel portal types. For the Type III, mean maximum horizontal gaze angles were lower at close range and higher at greater distances. Under low-speed conditions, the Type I showed a significant increase in mean maximum horizontal gaze angles with increasing distance, consistent with the expansion of the visual field during near navigation. This increasing trend was even more pronounced under high-speed conditions.

For the Type III, a distinct inverse relationship between gaze angles and distance was observed during low-speed operation. This effect is attributed to the visual anchoring of composite landscape elements, which suppressed gaze dispersion. However, at high speeds, the stabilizing influence of the Type III was confined to the proximal segments near the portal. This targeted stabilization near the tunnel entrance effectively mitigates acute visual impacts for drivers during high-velocity approach.

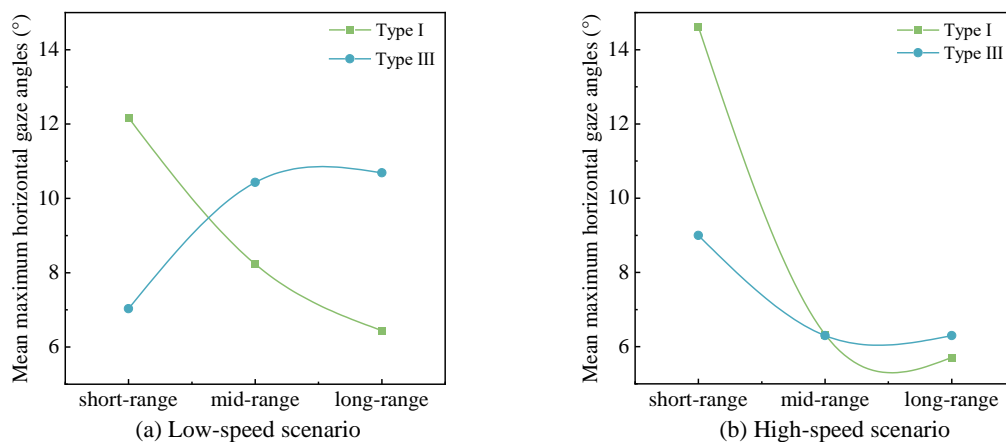


Figure 9. Average gaze angles of testers at different driving speeds

### 4.2. Fixation and Safety

Figure 10 reveals relationships between fixation frequencies and obstacle-safety rates across 3 tunnel portal types under low-speed and high-speed conditions. Under low-speed operations, Type I exhibited the highest obstacle-safety rate concurrently with the lowest fixation frequency; this combination indicates that its visually simplified design effectively reduces cognitive load, thereby enhancing safety margins. In contrast, both Type II and Type III showed progressively lower safety rates and higher fixation frequencies, confirming that increased landscape complexity under low speeds disperses driver attention, thus compromising safety performance. Conversely, under high-speed scenarios, Type II demonstrated optimal safety performance at moderately elevated fixation frequencies, suggesting its balanced visual complexity optimally directs attentional resources for proactive hazard detection. This analysis establishes that simplified landscapes (Type I) excel during low-speed approaches, whereas interfaces with moderated complexity (Type II) provide superior safety resilience in high-speed navigation.

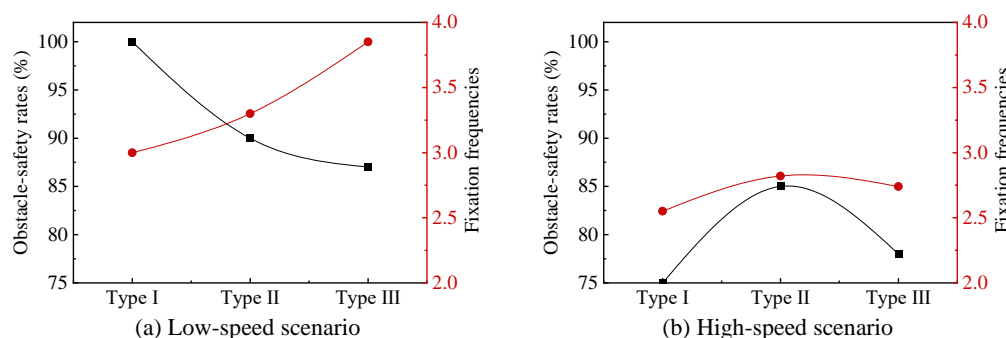


Figure 10. Average fixation frequencies and obstacle-safety rates of participants under different speed conditions

### 4.3. Speed Dependency and Driving comfort

Driving performance exhibited significant interactions between driving speed and portal landscape complexity, primarily affecting safety rates and driver comfort.

As illustrated in Figure 11, tunnels with refined landscape designs received significantly higher ratings in terms of driving comfort compared to those with artificial or natural restoration landscapes. These results suggest that visually enriched environments may have a more positive effect on drivers' perceptual comfort.

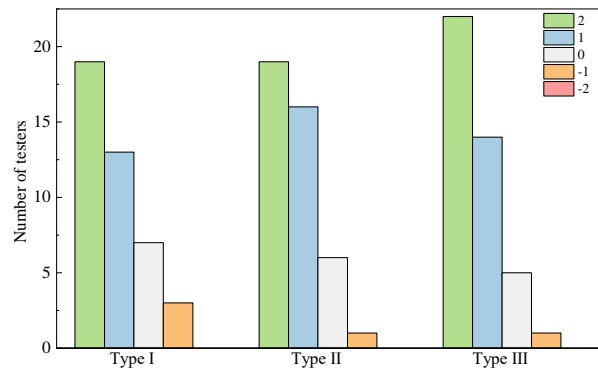


Figure 11. Subjective Ratings Distribution

As shown in Figures 12, under low-speed conditions, obstacle-safety rates decline progressively from Type I to Type III, while electrodermal responses concurrently rise, revealing a fundamental safety-comfort trade-off. Specifically, Type III maximizes driver comfort through optimized visual richness, yet this induces excessive cognitive engagement with environmental details, directly impairing hazard identification capacity and resulting in its lowest safety performance. Conversely, under high-speed operations, both metrics exhibit an inverted U-curve relationship with landscape complexity: Type II peaks at the curve apex with harmonized high safety and comfort, whereas Type I and Type III underperform at the curve troughs. This demonstrates that Type II's moderated visual complexity optimally balances cognitive load, avoiding attentional underload from sparse stimuli (Type I) while preventing overload from hypercomplexity (Type III).

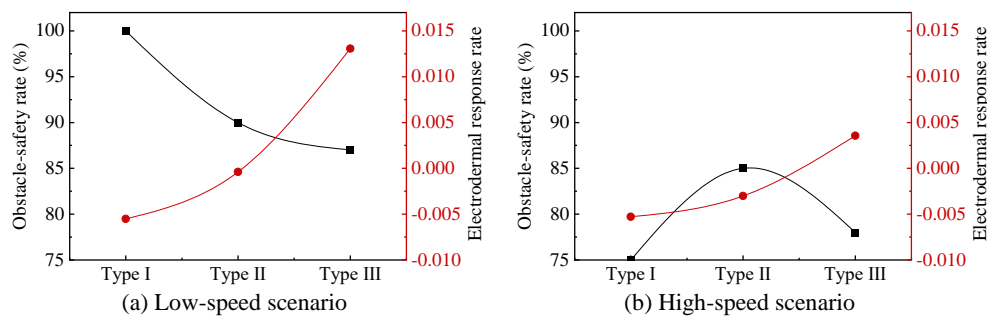


Figure 12. Obstacle-safety rates and electrodermal response rates of participants under different speed conditions

## 5. CONCLUSIONS

This study quantitatively investigated the impact of tunnel portal landscape design on drivers' visual comfort and safety across varying driving speeds using a comprehensive VR-based experimental approach. Through synchronized collection and analysis of eye movement data, EDA, and driving performance metrics from 42 participants navigating three distinct portal landscape typologies under controlled low- and high-speed conditions, we aimed to provide empirical evidence for speed-adaptive design strategies. This study reaches the following conclusions:

(1) The distraction caused by tunnel portal landscapes varies significantly with driving speed. Type III designs, while aesthetically engaging, led to noticeable visual distractions under low-speed conditions. However, drivers exhibited increased concentration at higher speeds, mitigating the adverse effects of complex visual stimuli.

(2) Landscaping tunnel portals generally enhanced driving comfort, particularly in low-speed scenarios. However, this improvement diminished on high-speed roads. Conversely, safety performance deteriorated with increasing speed across all landscape types, emphasizing the need for speed-adaptive design strategies.

(3) Landscape selection for tunnel portals is critically influenced by design speed. Under low-speed conditions, Type III designs significantly enhance driving comfort while preserving safety, as their moderate visual complexity prevents cognitive overload. In contrast, high-speed environments limit the comfort benefits of landscape interventions; here, Type II configurations achieve optimal safety-compatibility through ecological integration, balancing hazard anticipation with fatigue reduction.

## 6. BIBLIOGRAPHY

- [1] Canto-Perello, J., & Curiel-Esparza, J. (2001). Human factors engineering in utility tunnel design. *Tunnelling and Underground Space Technology*, 16(3), 211–215. [https://doi.org/10.1016/s0886-7798\(01\)00041-4](https://doi.org/10.1016/s0886-7798(01)00041-4)
- [2] China Journal of Highway and Transport Editorial Department. (2022). Review on China's traffic tunnel engineering research: 2022. *China Journal of Highway and Transport*, 35(4), 1-40. <https://doi.org/10.19721/j.cnki.1001-7372.2022.04.001>
- [3] Chen, F., & Yang, Y. (2019). Influence of tunnel entrance environment on driver's vision and physiology in mountainous expressway. *IOP Conference Series Earth and Environmental Science*, 295(4), 042138. <https://doi.org/10.1088/1755-1315/295/4/042138>
- [4] Wen, X., Ye, F., Su, E., Zhang, X., Han, X., Liu, J., & Zhu, W. (2024). Color design method for tunnel wall-type portals considering harmonization with time-varying environments: A study of driving simulation. *Tunnelling and Underground Space Technology*, 147, 105671. <https://doi.org/10.1016/j.tust.2024.105671>
- [5] Yuan Y. (2014). On the landscape design of mountain highway tunnel portals considering the psychological and physiological behaviors of a driver. *Modern Tunnelling Technology*, 51(3), 30-34. <https://doi.org/10.13807/j.cnki.mtt.2014.03.005>
- [6] Ye, F., Su, E. J., Liang, X. M., Zhang, X. B., Xia, T. H., & Wei, Y. C. (2022). Review and thinking on landscape design of highway tunnel. *China Journal of Highway and Transport*, 35(1), 23-37. <https://doi.org/10.19721/j.cnki.1001-7372.2022.01.003>
- [7] Lappi, O. (2022). Gaze Strategies in Driving - An Ecological Approach. *Frontiers in Psychology*, 13. <https://doi.org/10.3389/fpsyg.2022.821440>
- [8] Lappi, O. (2016b). Eye movements in the wild: Oculomotor control, gaze behavior & frames of reference. *Neuroscience & Biobehavioral Reviews*, 69, 49–68. <https://doi.org/10.1016/j.neubiorev.2016.06.006>
- [9] Yan, Y., & Jia, Y. (2022). A review on human comfort factors, measurements, and improvements in Human-Robot collaboration. *Sensors*, 22(19), 7431. <https://doi.org/10.3390/s22197431>
- [10] Posada-Quintero, H. F., & Chon, K. H. (2020). Innovations in Electrodermal Activity Data Collection and Signal Processing: A Systematic review. *Sensors*, 20(2), 479. <https://doi.org/10.3390/s20020479>



## INFLUENCE OF GEOMETRIC PARAMETERS AND VELOCITY OF VENT ON HEAVY GAS EXHAUST EFFICIENCY IN TUNNELS

Yuanqing Ma<sup>1</sup>, Tianqi Wang<sup>2</sup>, Ying Zhang<sup>3</sup>, Angui Li<sup>4</sup>

**Abstract:** Underground spaces are relatively enclosed, which imposes stringent requirements on ensuring personnel safety and achieving effective removal of harmful gases. Notably, high-density harmful gases (hereafter referred to as "heavy gases") tend to accumulate in human breathing zones, posing a severe threat of fatalities and injuries. Consequently, research on exhaust strategies to enhance the removal efficiency of heavy gases in tunnels has become an urgent necessity. In this study, a series of computational fluid dynamics (CFD) simulations were conducted to investigate the removal process of heavy gas contaminants in tunnels. Specifically, the effects of three key parameters—namely the aspect ratio ( $w/h$ ), vent area ( $A$ ), and vent height ( $h_v$ )—on the performance of side-mounted exhaust vents for addressing heavy gas leakage in tunnels were systematically analyzed. The results reveal that with the increase in  $w/h$  and  $A$ , both the height of the heavy gas layer downstream of the vent and the heavy gas density exhibit a decreasing trend. However, excessively large  $A$  and  $h_v$  can lead to the discharge of fresh air through the vents when the exhaust velocity is low, which is detrimental to the overall exhaust efficiency. Within the parameter range investigated in this study, an optimal vent height of 0.1 m was identified. Furthermore, the highest exhaust efficiency of 0.18 was achieved when the vent area was 2 m<sup>2</sup> and the exhaust velocity was 6 m/s. The findings of this research provide a theoretical and data-driven basis for the optimal design of ventilation systems tailored to heavy gas control, thereby facilitating the effective removal of heavy gases in underground spaces.

**Keywords:** Heavy gas; Underground Space; Side exhaust; Exhaust efficiency; Gas leakage.

### 1. INTRODUCTION

Due to the development demands of advanced industrial manufacturing and carbon transportation, higher requirements are imposed on the utilization, transportation, and storage of specialty gases (Zeng et al., 2021). Most specialty gases exhibit higher density than air, and once their concentration exceeds a specific threshold, they turn toxic and pose severe hazards to human health (Cai et al., 2020). Under the influence of the negative buoyancy effect, such heavy gases tend to accumulate and spread in the lower regions of enclosed spaces (e.g., industrial workshops, storage warehouses) (Ma et al., 2023). In recent years, improper storage and usage practices have frequently triggered heavy gas leakage accidents, leading to significant casualties and massive economic losses (Hou et al., 2021). Consequently, conducting research on the leakage mechanisms and exhaust characteristics of heavy gases carries substantial theoretical significance. It provides critical support for optimizing personnel evacuation designs, enhancing hazard prediction systems, and developing high-efficiency ventilation systems (Wang et al., 2024). Therefore, investigating the laws governing heavy gas leakage and elimination is of profound theoretical value for improving safety management in related fields.

<sup>1</sup> PhD student, Ma Yuanqing, Heating, Gas Supply, Ventilating and Air Conditioning Engineering, School of Building Services Science and Engineering, Xi'an University of Architecture and Technology, 710055 Xi'an, China, myq\_c@xauat.edu.cn.

<sup>2</sup> PhD student, Wang Tianqi, Heating, Gas Supply, Ventilating and Air Conditioning Engineering, School of Building Services Science and Engineering, Xi'an University of Architecture and Technology, 710055 Xi'an,

<sup>3</sup> Dr., Zhang Ying, Heating, Gas Supply, Ventilating and Air Conditioning Engineering, School of Building Services Science and Engineering, Xi'an University of Architecture and Technology, 710055 Xi'an, China, myq\_c@xauat.edu.cn.

<sup>4</sup> Professor, Li Angui, Heating, Gas Supply, Ventilating and Air Conditioning Engineering, School of Building Services Science and Engineering, Xi'an University of Architecture and Technology, 710055 Xi'an, liangui@xauat.edu.cn

Extensive research has been conducted on the leakage and diffusion characteristics of heavy gases. However, the majority of existing studies focus primarily on leakage scenarios in industrial workshops (Kassomenos et al., 2008) and open atmospheric environments (Blackmore et al., 1982; Hanna et al., 1993). For instance, Li et al. (Li et al., 2023b) employed numerical simulations to investigate how the diameter and shape of leakage sources affect the diffusion characteristics of R290 in an enclosed room following leakage, while further analyzing the explosion risks induced by R290 leakage. Wang et al. (Wang et al., 2013) used computational fluid dynamics (CFD) to study the continuous release and diffusion process of carbon dioxide (CO<sub>2</sub>) in a ventilated industrial workshop, and analyzed the effects of release rate, airflow velocity, and obstacles on CO<sub>2</sub> propagation. Gao et al. (Gao et al., 2023) examined the concentration distribution of heavy gases with different densities and the effectiveness of integrated ventilation systems in a typical office space. Li et al. (Li et al., 2023a) simulated the impact of the speed and size of moving obstacles in a chemical plant on chlorine (Cl<sub>2</sub>) leakage diffusion. Additionally, Fatahian et al. (Fatahian et al., 2020) demonstrated via CFD simulations that the gas mass fraction increases significantly immediately after release. Notably, there remains a paucity of research on heavy gas leakage and diffusion accidents in narrow and long spaces (e.g., tunnels). In particular, the relationship between the emission behavior of hazardous gases and ventilation system performance in such narrow and long spaces has not been clearly elucidated.

Research on ventilation systems specifically tailored to heavy gas control also remains limited. Currently, most ventilation facilities in tunnels are installed at the top of the space, primarily designed for removing flue gases (a type of positively buoyant gas) (Cong et al., 2021; Lei et al., 2023). In contrast, vent positions for scenarios involving potential heavy gas leakage are mostly determined based on empirical experience. This empirical approach not only fails to fully exploit the performance potential of ventilation equipment but also leads to unnecessary resource waste.

Prior studies have suggested that vents should be installed on the lower sides of enclosed spaces; this configuration allows heavy gases to be exhausted via a shorter path, thereby minimizing the scope of their hazardous impact (Han et al., 2020). However, further research is still required to optimize the design parameters (e.g., vent size, airflow rate) and spatial positions of such heavy gas-targeted ventilation systems (Wang et al., 2025).

Against this backdrop, this study designed a total of 55 simulation cases to investigate the heavy gas elimination performance of side-mounted vents in a tunnel. Specifically, the extraction efficiency of vents with different aspect ratios, cross-sectional areas, and heights above the ground was compared. Within the parameter range investigated in this study, the optimal parameters and spatial positions of side-mounted vents for heavy gas elimination were analyzed. The findings of this research provide a theoretical and technical basis for the optimal design of exhaust systems addressing heavy gas leakage in underground spaces (e.g., tunnels).

## 2. NUMERICAL SIMULATION METHOD

### 2.1. Governing equations

The spatial dispersion behavior of heavy gas flows can be efficiently analyzed using the professional computational fluid dynamics (CFD) software FLUENT (Zhang et al., 2020). Turbulent flow effects in such scenarios can be modeled via three primary approaches: the Reynolds-Averaged Navier – Stokes (RANS) method, Large Eddy Simulation (LES), or fully resolved through Direct Numerical Simulation (DNS). A review of existing literature on heavy gas turbulent flow simulation reveals that the RANS method offers an optimal balance between result accuracy and computational efficiency—this compromise makes it well-suited for engineering-scale studies. Given that the primary objective of this research is to analyze the steady-state elimination of heavy gases, the Reynolds time-averaged Navier – Stokes (RANS) equations were selected as the governing equations. All simulations in this study were implemented using FLUENT, where the Navier – Stokes equations were solved by coupling the fundamental equations of continuity, momentum, and species transport. The core governing equations are presented as follows (Inc, 2022):

$$\frac{\partial \rho}{\partial t} + \text{div}(\rho u_i) = 0 \quad (1)$$

$$\frac{\partial u_i}{\partial t} + (u_i \cdot \nabla) u_i = -\frac{1}{\rho} \nabla p + \frac{\mu}{\rho} \Delta u_i + F_{bi} \quad (2)$$

$$\frac{\partial c}{\partial t} + u_j \frac{\partial c}{\partial x_j} = \frac{\partial}{\partial x_j} \left( D \frac{\partial c}{\partial x_j} \right) \quad (3)$$

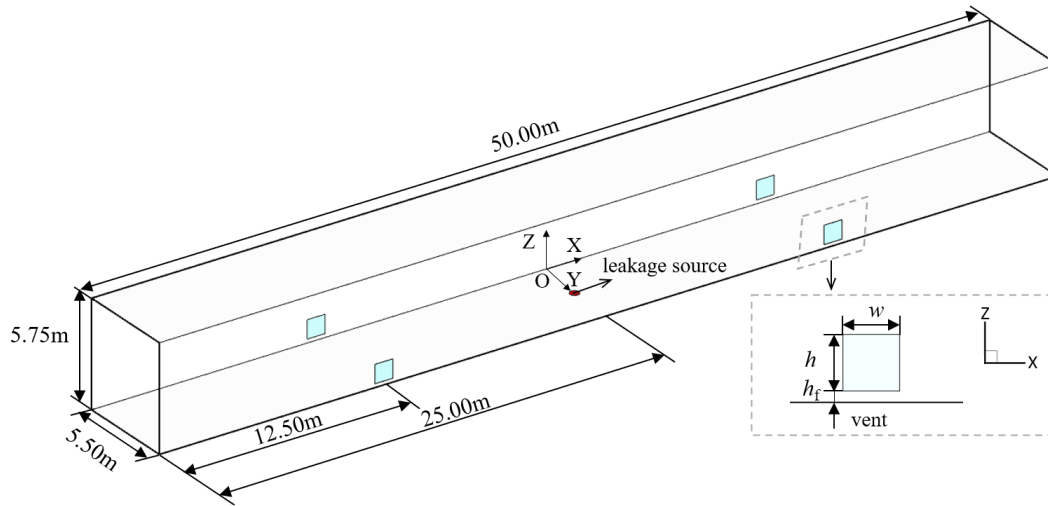
where  $\mu$  is the dynamic viscosity, mPa·s;  $\rho$  is the density of the mixture, kg/m<sup>3</sup>;  $F_{bi}$  is the mass force, N/kg;  $c$  is the concentration of heavy gas;  $D$  is the diffusion coefficient of heavy gas.

**Table 1.** Details of CFD boundary conditions.

Parameter	Value
Cases	Steady, 3-D calculations
Fluid	SF <sub>6</sub>
Far field	Pressure outlet: 0-gauge pressure
Inlet	Velocity: 10 ~ 15 m/s Hydraulic diameter = 0.5 m
Vent	Velocity: 6 ~ 14 m/s
Ground	Wall (no slip)

## 2.2. Geometric model

A typical tunnel was selected as the research object, and the geometric dimensions of the computational domain are illustrated in Figure 1. The heavy gas leakage source was positioned at the center of the tunnel bottom, with a diameter of 0.5 m. Four symmetrically arranged side vents were installed on both sides of the tunnel; their specific geometric dimensions and spatial positions are provided in Figure 1. Sulfur hexafluoride (SF<sub>6</sub>) was chosen as the surrogate for heavy gas in the leakage simulations, and a velocity inlet boundary condition was applied to the leakage source to simulate continuous gas release. All vents were set as velocity outlets, with the exhaust velocity ( $u_e$ ) varied at five levels: 6, 8, 10, 12, and 14 m/s. Additionally, pressure outlet boundary conditions were assigned to both ends of the tunnel, while the tunnel walls were set to a no-slip boundary condition. Detailed specifications of the CFD boundary conditions are summarized in Table 1.



**Figure 1.** Schematic of the computational domain

In this study, four sets of key parameters were designed to investigate their effects on heavy gas elimination performance, with the following variable levels:

- Vent area ( $A$ ): 1.00, 1.30, 1.54, and 2.00 m<sup>2</sup>;
- Vent aspect ratio ( $w/h$ ): 1.00, 1.30, 1.53, and 2.00;
- Vent height above the ground ( $h_f$ ): 0.10, 0.20, 0.30, and 0.50 m;
- Exhaust velocity ( $u_e$ ): 6, 8, 10, 12, and 14 m/s.

A total of 55 experimental conditions were designed in this study, with detailed parameter combinations provided in Table 2. Among these, Cases 53~55 were conducted under the condition of non-functional vents (i.e., vents not in operation). The primary purpose of these three cases was to measure the height of the heavy gas layer  $h_i$  under different leakage intensities, providing a baseline reference for analyzing the effect of vent operation on heavy gas elimination.

**Table 2.** Simulation conditions.

Case	$w$ (m)	$w/h$	$w \times h$ (m <sup>2</sup> )	$h_f$ (m)	$Q_0$ (m <sup>3</sup> /s)	$u_e$ (m/s)
1					1.96	8.00
2					2.36	8.00
3	1.00	1.00	1.00	0.20	2.94	8.00
4					2.36	6.00
5					2.36	10.00

6					2.36	12.00
7					2.36	14.00
8						6.00
9						8.00
10				0.10	2.36	10.00
11						12.00
12						14.00
13						6.00
14						8.00
15				0.30	2.36	10.00
16						12.00
17						14.00
18						6.00
19						8.00
20				0.50	2.36	10.00
21						12.00
22						14.00
23						6.00
24						8.00
25	1.14	1.30	1.00	0.20	2.36	10.00
26						12.00
27						14.00
28						6.00
29						8.00
30	1.24	1.53	1.00	0.20	2.36	10.00
31						12.00
32						14.00
33						6.00
34						8.00
35	1.41	2.00	1.00	0.20	2.36	10.00
36						12.00
37						14.00
38						6.00
39						8.00
40	1.14	1.00	1.30	0.20	2.36	10.00
41						12.00
42						14.00
43						6.00
44						8.00
45	1.24	1.00	1.54	0.20	2.36	10.00
46						12.00
47						14.00
48						6.00
49						8.00
50	1.41	1.00	2.00	0.20	2.36	10.00
51						12.00
52						14.00
53					1.96	\
54	1.00	1.00	1.00	1.00	2.36	\
55					2.94	\

The volume flux of the inlet  $Q_0$  can be expressed as:

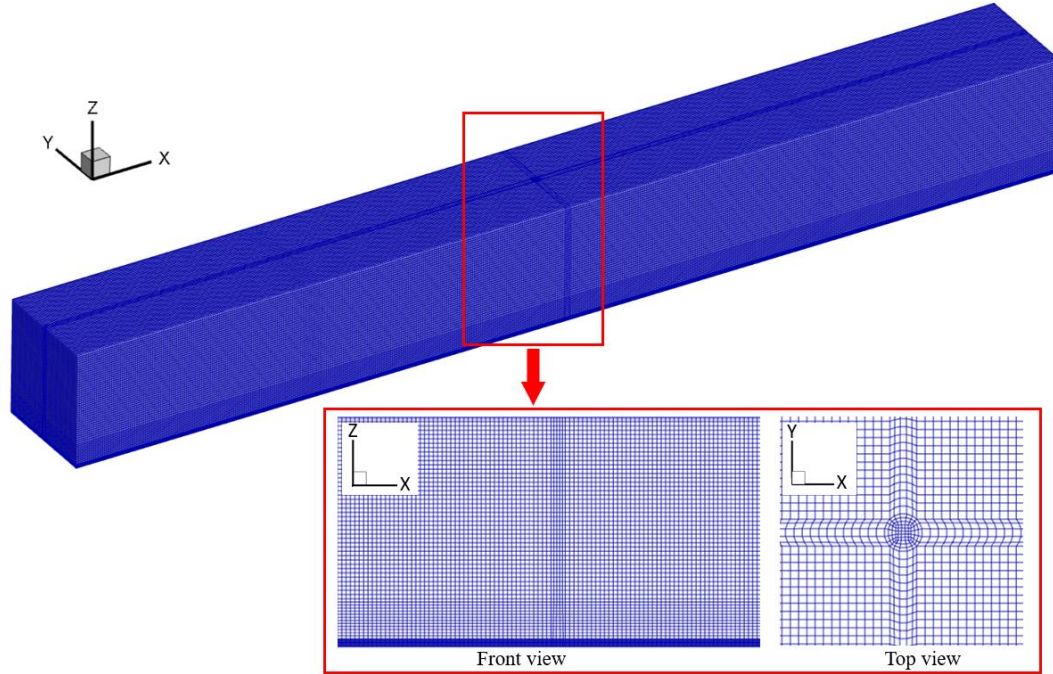
$$Q_0 = \pi \frac{D^2}{4} u_0 \quad (4)$$

where  $D$  is the diameter of the leakage source, m;  $u_0$  is the velocity of the leakage source, m/s.

### 2.3. Grid independence verification and turbulence model validation

Prior studies have indicated that grid resolution is a key factor influencing the prediction accuracy and computational cost-effectiveness of buoyancy-driven flow simulations (Ma et al., 2025). To investigate the impact of grid resolution on simulation results, four structured hexahedral grid systems with different cell counts were

constructed prior to the formal CFD simulations: Grid System A (970,425 cells), Grid System B (1,262,029 cells), Grid System C (1,592,045 cells), and Grid System D (1,982,439 cells). Given the high density gradients and velocity gradients near the leakage inlet (where flow field changes are most significant), local mesh refinement was implemented in this region to capture the detailed flow characteristics. The overall mesh structure of Grid System C and a magnified view of the refined mesh near the leakage inlet are presented in Figure 2.

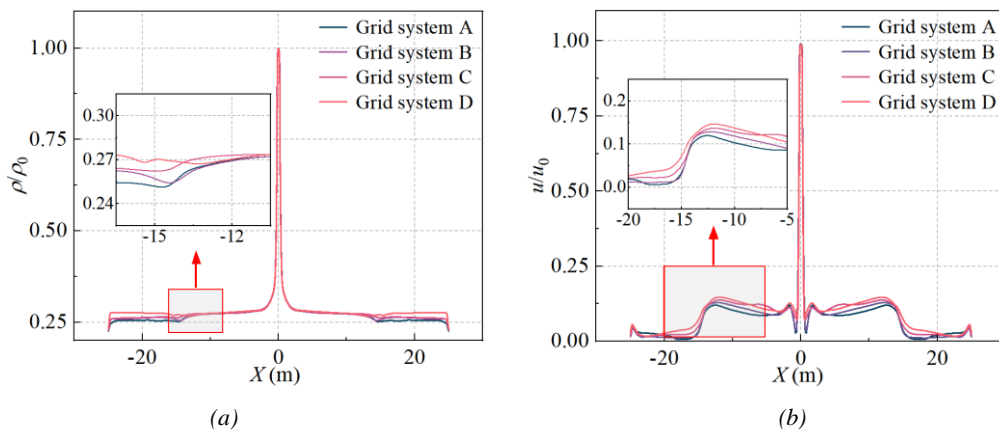


**Figure 2.** Details of grid system C

Figure 3 presents the density and velocity profiles along the centerline at  $Z = 0.7$  m for the four grid systems. It can be observed that the simulation results of Grid System C and Grid System D are relatively consistent, indicating that the solution tends to converge when the grid density reaches the level of Grid System C.

To further quantify the prediction accuracy of each grid system, three commonly used evaluation metrics were adopted: Mean Absolute Error (MAE), Mean Square Error (MSE), and Mean Absolute Percentage Error (MAPE). The simulation results of the four grid systems were compared with the results obtained from Large Eddy Simulation (LES) (serving as a high-fidelity reference) to calculate the prediction errors for each grid. The detailed error calculation results are summarized in Table 3, where it is shown that the MAPE values of both Grid System C and Grid System D are less than 10%—a threshold generally considered acceptable for engineering simulations.

Considering the balance between computational accuracy and computational cost (Grid System D requires significantly higher computational resources than Grid System C while providing negligible accuracy improvement), Grid System C was ultimately selected as the optimal grid configuration for all subsequent simulations in this study.



**Figure 3.** Density and velocity profiles of four grid systems (a) Density; (b) velocity.



**Table 3.** Detailed parameters of the grid system.

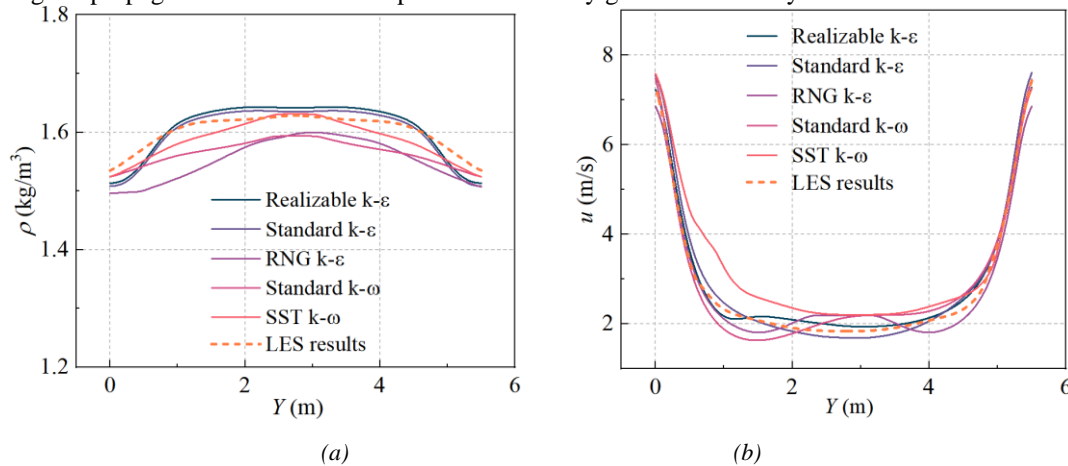
Grid system	Total number of cells	Error with LES					
		$\rho / \rho_0$			$u / u_0$		
		MAE	MSE	MAPE	MAE	MSE	MAPE
A	970,425	0.31	0.81	15.88%	0.10	0.05	23.31%
B	1,262,029	0.29	0.76	14.34%	0.09	0.05	16.40%
C	1,592,045	0.20	0.54	8.26%	0.08	0.04	9.70%
D	1,982,439	0.05	0.05	3.37%	0.03	0.01	5.56%

To identify the most appropriate turbulence model for the present study, five typical turbulence models were selected for verification and comparison: the standard  $k-\varepsilon$  model, SST  $k-\omega$  model, realizable  $k-\varepsilon$  model, RNG  $k-\varepsilon$  model, and standard  $k-\omega$  model.

Figure 4 presents a comparison between the simulation results of these five turbulence models and the Large Eddy Simulation (LES) results (used as the high-fidelity reference) regarding the centerline density decay and centerline velocity decay of the vent. Among the models tested, the standard  $k-\omega$  model exhibited more accurate profile characteristics for the vertical centerline velocity.

Quantitatively, the deviations between the vent centerline density decay predicted by each turbulence model and the LES results are as follows: 12.30% (standard  $k-\varepsilon$  model), 9.10% (SST  $k-\omega$  model), 4.66% (realizable  $k-\varepsilon$  model), 6.67% (RNG  $k-\varepsilon$  model), and 2.86% (standard  $k-\omega$  model). Similarly, the deviations in vent centerline velocity decay from the LES results are: 11.04% (standard  $k-\varepsilon$  model), 14.04% (SST  $k-\omega$  model), 2.30% (realizable  $k-\varepsilon$  model), 10.38% (RNG  $k-\varepsilon$  model), and 2.28% (standard  $k-\omega$  model).

Combined with the above quantitative and qualitative analysis, as well as consistent findings from previous literature (Xing et al., 2013; Zhang et al., 2020), the standard  $k-\omega$  model was determined to be suitable for predicting the propagation and elimination processes of heavy gases in this study.



**Figure 4.** Density and velocity decay of different turbulence models. (a) Density; (b) velocity.

### 3. RESULTS AND DISCUSSIONS

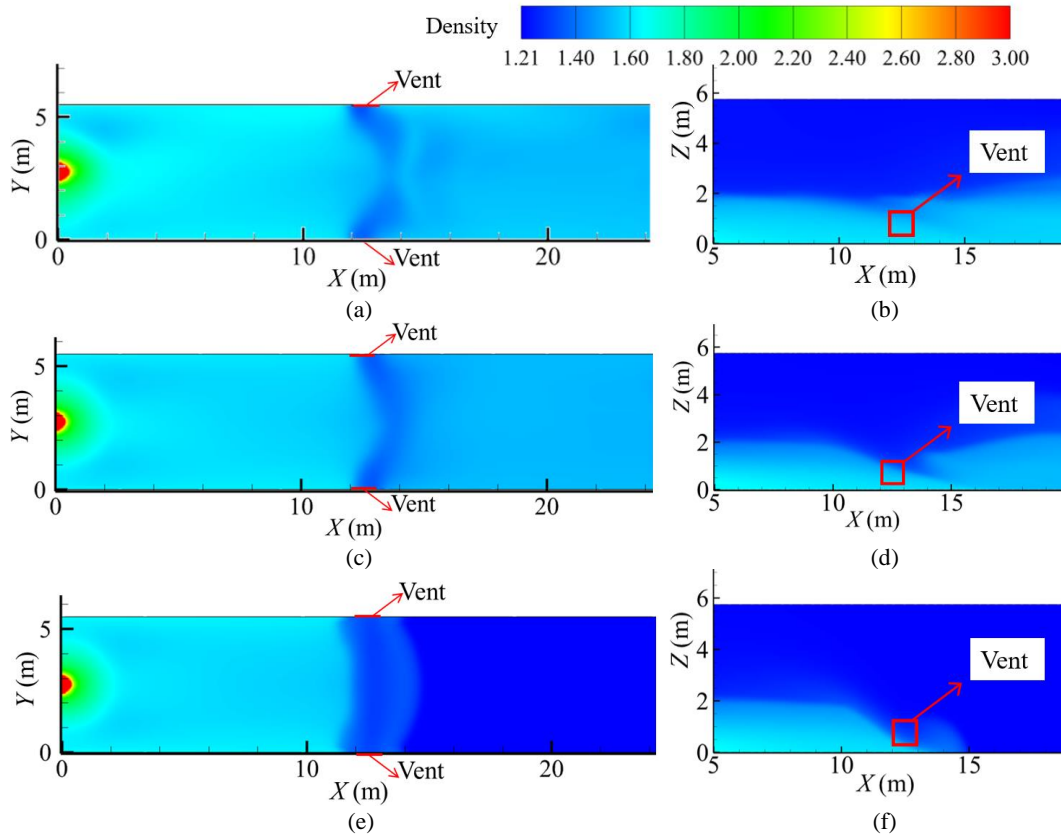
#### 3.1. Heavy gas height of downstream vent

When heavy gas leakage occurs in a tunnel, the contaminant gas exhibits obvious stratification due to the negative buoyancy effect: it tends to accumulate in the lower region of the tunnel and propagate longitudinally along the ground. Once the side vents on both sides of the tunnel are activated, the heavy gas can be rapidly discharged through these side vents via a shorter flow path—this configuration leverages the low-altitude distribution of heavy gas to enhance exhaust efficiency.

As the exhaust velocity increases, the exhaust air volume rises accordingly, which in turn reduces the height of the heavy gas layer ( $h_e$ ). However, when  $h_e$  drops below the upper edge of the side vents, a significant amount of fresh air (from the upper region of the tunnel) is drawn into the vents. This phenomenon dilutes the heavy gas concentration at the vent inlet, ultimately leading to a decline in heavy gas elimination efficiency.

The primary objective of this study is to optimize the design of exhaust systems for high-density gases. From a mechanistic perspective, the key focus is to minimize the occurrence of fresh air entrainment, thereby ensuring

the stable and efficient operation of the exhaust system. The top view and front view of the heavy gas flow pattern under exhaust velocities ranging from 6 m/s to 14 m/s are presented in Figure 5.

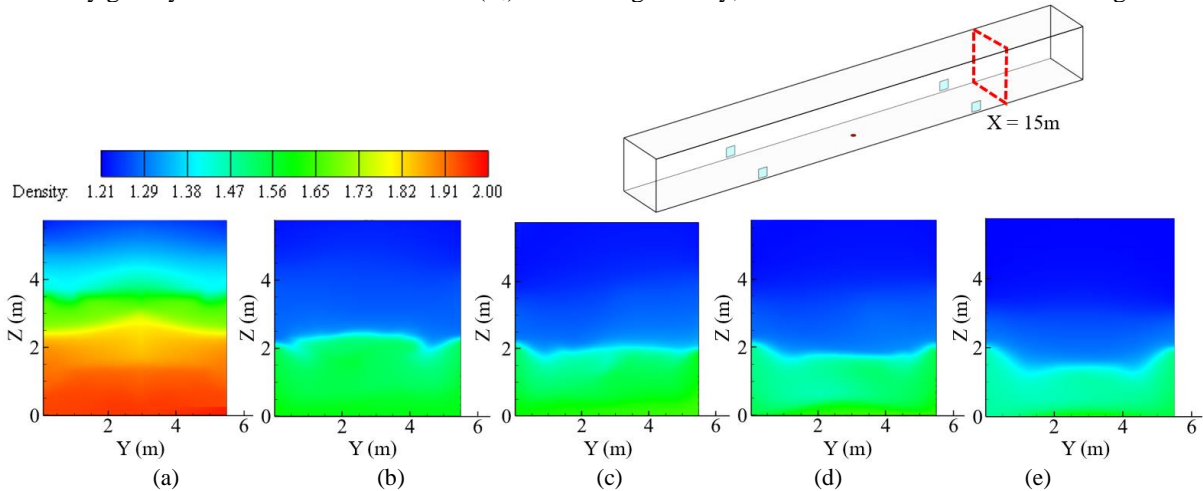


**Figure 5.** Heavy gas flow pattern under different exhaust velocities

(a)  $u_e=6\text{m/s}$ , top view; (b)  $u_e=6\text{m/s}$ , front view; (c)  $u_e=10\text{m/s}$ , top view; (d)  $u_e=10\text{m/s}$ , front view; (e)  $u_e=14\text{m/s}$ , top view; (f)  $u_e=14\text{m/s}$ , front view.

When upper vents (i.e., top-mounted vents) are used, the height of the heavy gas layer is higher compared to the scenario without exhaust. Moreover, upper vents disrupt the stable stratification of heavy gas and expand the scope of heavy gas contamination.

The heavy gas elimination performance is closely associated with the vent layout density (i.e., number of vents per unit tunnel length) and the tunnel's geometric characteristics. As the exhaust velocity increases, the height of the heavy gas layer downstream of the vents ( $h_e$ ) decreases gradually, as illustrated in the side view of Figure 6.

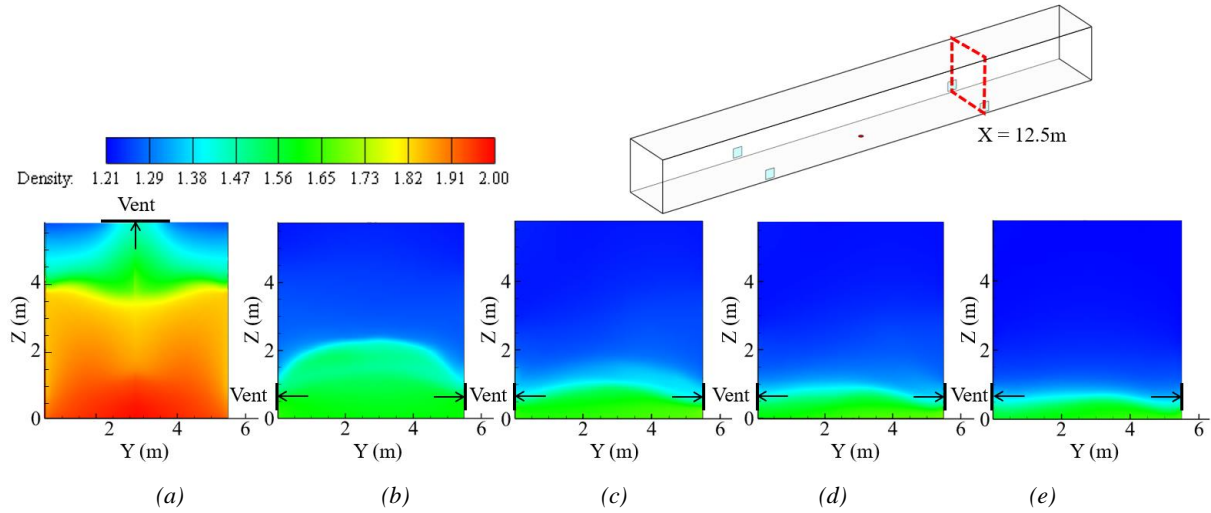


**Figure 6.** Heavy gas height at  $X=15\text{m}$

(a)  $u_e=8\text{m/s}$ , top exhaust; (b)  $u_e=6\text{m/s}$ , Case 4; (c)  $u_e=8\text{m/s}$ , Case 5; (d)  $u_e=10\text{m/s}$ , Case 6; (e)  $u_e=12\text{m/s}$ , Case 7.

When the inlet volume flux  $Q_0$  of the heavy gas leakage source is  $2.36 \text{ m}^3/\text{s}$  and the exhaust volume of a single side vent exceeds  $8 \text{ m}^3/\text{s}$  (see Figure 7(c)), the height of the heavy gas layer drops below the upper edge of the vent. This triggers the formation of a concave region in the heavy gas layer at the vent location, with the corresponding side view presented in Figure 7.

As the exhaust volume continues to increase, the height of the heavy gas layer downstream of the vent decreases gradually. However, when the exhaust volume further rises (e.g., reaching the level corresponding to Figure 7 (e)), the amount of fresh air entrained into the vent increases significantly. When the exhaust volume increases to  $12 \text{ m}^3/\text{s}$ , the entrainment and discharge of fresh air through the vent become particularly prominent—this phenomenon dilutes the heavy gas concentration at the vent inlet and undermines the overall elimination efficiency.



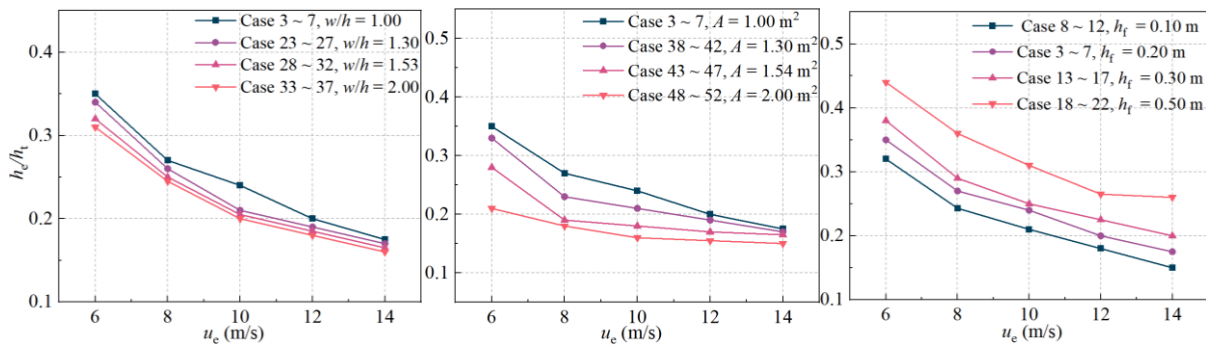
**Figure 7.** Heavy gas height at  $X=12.5\text{m}$

(a)  $u_e=8\text{m/s}$ , top exhaust; (b)  $u_e=6\text{m/s}$ , Case 4; (c)  $u_e=8\text{m/s}$ , Case 5; (d)  $u_e=10\text{m/s}$ , Case 6; (e)  $u_e=12\text{m/s}$ , Case 7.

The suppression effect of the exhaust system on heavy gas propagation can be quantified using the ratio of the heavy gas layer height downstream of the vent ( $h_e$ ) to the heavy gas layer height without exhaust ( $h_t$ , i.e., the baseline height). As shown in Figure 8, the decreasing trend of the  $h_e/h_t$  ratio gradually slows down with the increase in exhaust velocity ( $u_e$ ). This phenomenon is attributed to the entrainment and discharge of fresh air by the vents, which dilutes the heavy gas concentration at the vent inlet and thereby reduces the heavy gas elimination efficiency.

Figure 8(a) illustrates the variation of the  $h_e/h_t$  ratio with increasing  $u_e$ . Within the parameter range of this study, it can be observed that under the same exhaust velocity ( $u_e$ ), the heavy gas layer height downstream of the vent ( $h_e$ ) decreases as the vent aspect ratio ( $w/h$ ) increases. The underlying mechanism is that, for vents with the same cross-sectional area, a higher aspect ratio corresponds to a lower vent height ( $h_e$ ); this lower height makes it easier for fresh air to be entrained into the vents even at relatively low exhaust velocities ( $u_e$ ), thereby enhancing the suppression of heavy gas propagation.

Figures 8(b) and 8(c) depict the variation of the  $h_e/h_t$  ratio under different vent areas ( $A$ ) and vent heights above the ground ( $h_t$ ), respectively. The results indicate that an increase in vent area ( $A$ ) and a decrease in vent height ( $h_t$ ) can effectively enhance the suppression effect on heavy gas propagation while maintaining the stability of the heavy gas stratification—this is because larger vent areas and lower vent heights are more conducive to capturing the low-altitude heavy gas layer without excessive fresh air entrainment.



(a) (b) (c)

**Figure 8.** Variation of  $h/h_i$  under different (a)  $w/h$ ; (b) vent area; (c)  $h_i$ .

### 3.2. Average density of vent and Froude number

Since the density difference between heavy gas and air, the mass flow flux of pollutants discharged from the vent can be expressed as:

$$M_e = u_e w \int_{h_f}^{h_f+h} \rho_e dz \quad (5)$$

where  $u_e$  is exhaust velocity, m/s;  $w$  is the width of the vent, m;  $h$  is the height of the vent, m;  $h_f$  is the vent height above the floor, m;  $\rho_e$  is the density of heavy gas exhaust through the vent, kg/m<sup>3</sup>.

The average density of heavy gas discharged from the vent can be expressed as:

$$\rho = \frac{M_e}{u_e w h} \quad (6)$$

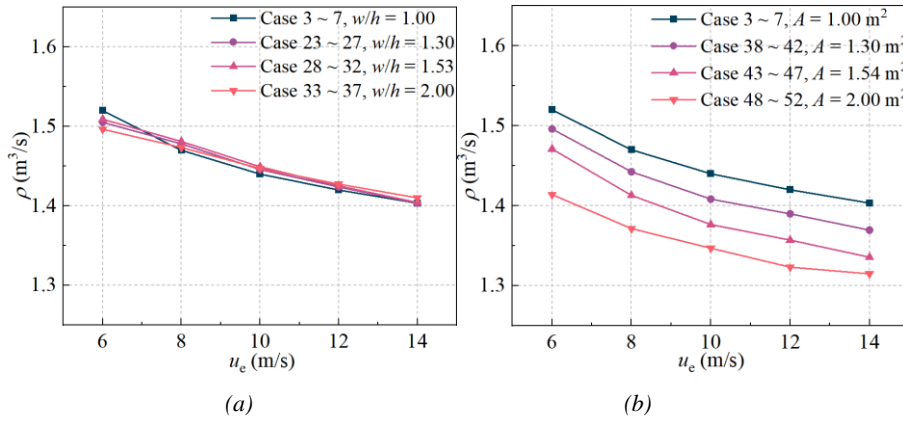
A modified Froude number is introduced, which represents the ratio of inertial force to buoyancy. Froude number  $Fr$  of exhaust outlet can be expressed as:

$$Fr = \frac{u_e}{Lg(\rho - \rho_a)/\rho_a} \quad (7)$$

Where  $\rho_a$  is the ambient density, kg/m<sup>3</sup>;  $L$  is the characteristic length of tuyere, m;  $g$  is the acceleration of gravity, 9.81 kg/m<sup>3</sup>.

From Figures 9 (a)~(c), it can be observed that the effect of  $w/h$  on  $\rho$  is negligible. In contrast, an increase in  $A$  exerts a significant influence on  $\rho$ , while  $h$  only has a certain effect under low exhaust velocities ( $u_e$ ). Additionally, under the same exhaust volume, a higher average heavy gas density at the vent inlet corresponds to a higher  $\rho$ —this is because a denser heavy gas concentration at the vent indicates more effective capture of the target contaminant, rather than excessive entrainment of fresh air.

The Froude number ( $Fr$ ) is defined as the ratio of inertial force to buoyancy force, which characterizes the relative dominance of these two forces in the flow field. As shown in Figure 9(d), increasing  $A$  significantly increases the  $Fr$  value at the vent. A higher  $Fr$  indicates that inertial force becomes more dominant than buoyancy force in the exhaust flow, meaning the momentum consumed for heavy gas elimination is greater—this further explains why a larger vent area enhances the ability to overcome the negative buoyancy of heavy gas and improve elimination efficiency.



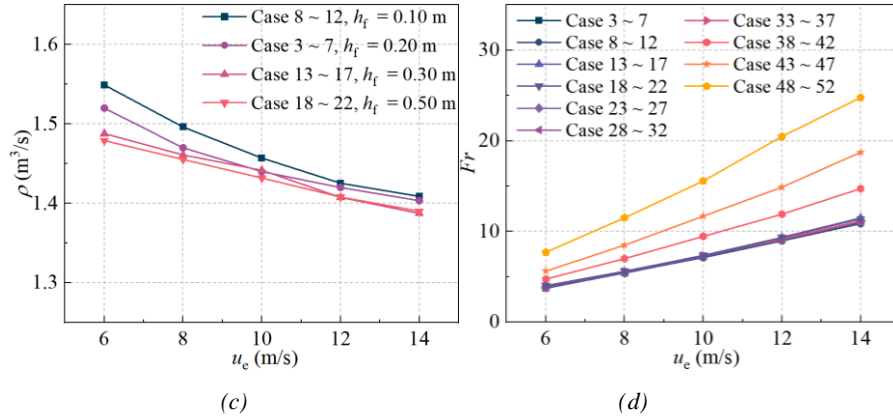


Figure 9. Variation of  $\rho$  and  $Fr$  (a)  $w/h$ ; (b) vent area; (c)  $h_f$ ; (d)  $Fr$ .

### 3.3. Exhaust efficiency

Exhaust efficiency is another critical index for evaluating the performance of ventilation systems in heavy gas elimination scenarios. As defined by (Vauquelin, 2008), exhaust efficiency is quantified as the ratio of two key parameters: the total mass flow rate of heavy gas discharged through the vents and the total mass flow rate of heavy gas present in the tunnel under natural conditions (i.e., without mechanical exhaust). This efficiency metric directly reflects the capability of the ventilation system to capture and remove heavy gas, making it a reliable quantitative indicator for assessing the overall performance of heavy gas elimination systems. The specific mathematical definition of exhaust efficiency is as follows:

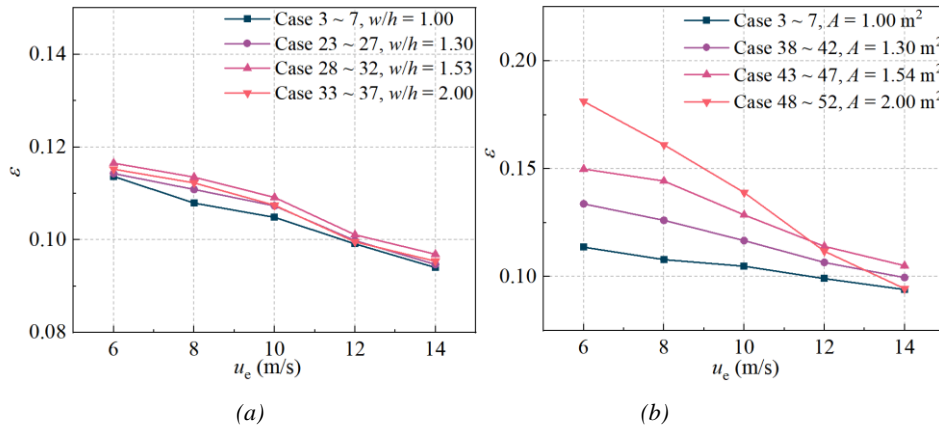
$$\varepsilon = \frac{M_e}{M} \quad (8)$$

where  $M$  is the mass flow flux of heavy gas in the tunnel without mechanical exhaust:

$$M = W \int_0^h \rho u dz \quad (9)$$

where  $W$  is the width of the tunnel, m.

This section compares the effects of  $w/h$ ,  $A$ , and  $h_f$  on exhaust efficiency, with the results presented in Figure 10. As shown in the figure, under the same exhaust volume, the vents achieve the optimal exhaust performance when the  $w/h$  is 1.53. At a fixed  $u_e$ , exhaust efficiency decreases with an increase in  $A$ . For instance: When  $A$  is 2 m², the exhaust efficiency values at  $u_e$  of 6 m/s and 14 m/s are 0.18 and 0.09, respectively—representing a decrease of 47.9%. When  $A$  is 1 m², the exhaust efficiency values at  $u_e$  = 6 m/s and  $u_e$  = 14 m/s are 0.11 and 0.09, respectively—corresponding to a decrease of 17.3%. These results indicate that for a given  $A$ , there exists an optimal  $u_e$  that maximizes exhaust efficiency. Additionally, exhaust efficiency increases as  $h_f$  decreases, and this trend is particularly pronounced at high  $u_e$ . Specifically, when  $u_e$  = 14 m/s, the exhaust efficiency at  $h_f$  = 0.1 m is 14.4% higher than that at  $h_f$  = 0.5 m.





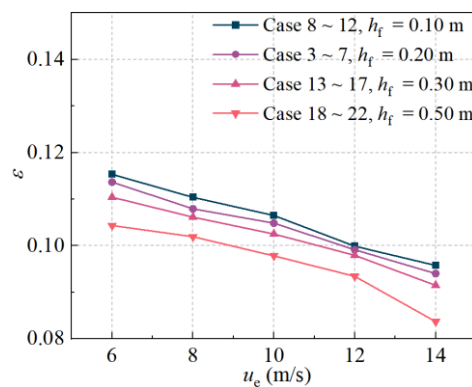


Figure 10. Variation of  $\varepsilon$  under different (a)  $w/h$ ; (b) vent area; (c)  $h_f$ .

#### 4. CONCLUSION

This study investigated the effects of three key parameters—vent aspect ratio  $w/h$ , vent area  $A$ , and vent height above the ground  $h_f$ —on the performance of side-mounted exhaust vents for addressing heavy gas leakage in tunnels. Vent performance was evaluated from three dimensions: the height of the heavy gas layer downstream of the vents, the exhaust Froude number  $Fr$  and exhaust efficiency  $\varepsilon$ . The main conclusions are as follows:

(1) Increasing the  $w/h$  and  $A$  can reduce the height of the heavy gas layer downstream of the vents. Within the parameter range of this study, there exists an optimal vent height  $h_f$  of 0.1 m; under the same exhaust volume, this height results in the lowest heavy gas height downstream the vent.

(2) The average heavy gas density at the vent inlet is inversely proportional to both  $A$  and  $h_f$ . Excessively large  $A$  or  $h_f$  can lead to the entrainment and discharge of fresh air through the vents, even at low  $u_e$ . This fresh air entrainment dilutes the heavy gas concentration at the vent inlet, which is detrimental to efficient heavy gas elimination.

(3) At relatively low  $u_e$ , increasing  $A$  can improve  $\varepsilon$ ; however, at high  $u_e$ , increasing  $A$  significantly reduces  $\varepsilon$ . Within the scope of this study, the maximum  $\varepsilon$  was achieved when the vent area was 2 m<sup>2</sup> and the exhaust velocity was 6 m/s.

It is important to note that when designing ventilation systems for heavy gas elimination,  $\varepsilon$  must be considered in conjunction with the heavy gas mass flow rate discharged through the vents. The core design objective is to maximize the heavy gas mass flow rate while minimizing fresh air entrainment and discharge. Future research will focus on two directions: first, conducting experimental validation of the heavy gas elimination performance simulated in this study; second, explore the design methodology of a ventilation system that balances smoke extraction and heavy gas elimination, aiming to achieve optimal hazard prevention effects.

#### ACKNOWLEDGMENTS

The study was supported by Shaanxi Province Technical Innovation Guidance Special Project (No. 2023GXLH-051), Foundation of International Joint Laboratory on Low Carbon Built Environment, Ministry of Education (Xi'an University of Architecture and Technology). The authors are grateful for the support.

#### REFERENCES

- [1] Blackmore, D.R., Herman, M.N., Woodward, J.L., 1982. Heavy gas dispersion models. *Journal of Hazardous Materials* 6, 107-128. doi:[https://doi.org/10.1016/0304-3894\(82\)80036-8](https://doi.org/10.1016/0304-3894(82)80036-8)
- [2] Cai, J., Chen, J., Ahmad, S., Zhao, J., Cheng, H., Zi, S., Xiao, J., 2020. Investigation into the effect of upstream obstacles and hazardous sources on dispersion in the urban environment with LES model. *Journal of Hazardous Materials* 390, 121953. doi:<https://doi.org/10.1016/j.jhazmat.2019.121953>
- [3] Cong, H., Bi, M., Bi, Y., Li, Y., Jiang, H., Gao, W., 2021. Experimental studies on the smoke extraction performance by different types of ventilation shafts in extra-long road tunnel fires. *Tunnelling and Underground Space Technology* 115, 104029. doi:<https://doi.org/10.1016/j.tust.2021.104029>

- [4] Fatahian, E., Salarian, H., Fatahian, H., 2020. Numerical Investigation of Hazardous Gas Dispersion Over Obstacles and Residential Areas. *International Journal of Engineering* 33, 2087-2094. doi:<https://doi.org/10.5829/ije.2020.33.10a.27>
- [5] Gao, N., Wang, R., Wu, Y., Wu, Z., 2023. Study on impact factors of tracer gas method in investigations of gaseous pollutant transport and building ventilation. *Building Simulation* 16, 413-426. doi:<https://doi.org/10.1007/s12273-022-0947-3>
- [6] Han, O., Zhang, Y., Li, A., Li, J., Li, Y., Liu, H., 2020. Experimental and numerical study on heavy gas contaminant dispersion and ventilation design for industrial buildings. *Sustainable Cities and Society* 55, 102016. doi:<https://doi.org/10.1016/j.scs.2020.102016>
- [7] Hanna, S.R., Chang, J.C., Strimaitis, D.G., 1993. Hazardous gas model evaluation with field observations. *Atmospheric Environment. Part A. General Topics* 27, 2265-2285. doi:[https://doi.org/10.1016/0960-1686\(93\)90397-H](https://doi.org/10.1016/0960-1686(93)90397-H)
- [8] Hou, J., Gai, W.-m., Cheng, W.-y., Deng, Y.-f., 2021. Hazardous chemical leakage accidents and emergency evacuation response from 2009 to 2018 in China: A review. *Safety Science* 135, 105101. doi:<https://doi.org/10.1016/j.ssci.2020.105101>
- [9] Inc, A., 2022. ANSYS Fluent Theory Guide.
- [10] Kassomenos, P., Karayannis, A., Panagopoulos, I., Karakitsios, S., Petrakis, M., 2008. Modelling the dispersion of a toxic substance at a workplace. *Environmental Modelling & Software* 23, 82-89. doi:<https://doi.org/10.1016/j.envsoft.2007.05.003>
- [11] Lei, P., Chen, C., Jiao, W., Shi, C., 2023. Experimental study on collaborative longitudinal ventilation of smoke control for branched tunnel fires considering different branch angles. *Tunnelling and Underground Space Technology* 136, 105097. doi:<https://doi.org/10.1016/j.tust.2023.105097>
- [12] Li, G., Wang, J., Wang, M., Lin, Y., Yu, X., Zong, R., 2023a. Experimental and numerical study of heavy gas dispersion in presence of obstacle motion. *Process Safety and Environmental Protection* 177, 1494-1505. doi:<https://doi.org/10.1016/j.psep.2023.07.092>
- [13] Li, Y., Yang, J., Wu, X., Zhou, P., Liu, Y., Han, X., 2023b. Explosion risk analysis of R290 leakage into a limited external space. *Applied Thermal Engineering* 225, 120122. doi:<https://doi.org/10.1016/j.applthermaleng.2023.120122>
- [14] Ma, Y., Li, A., Che, J., Wang, T., Yang, C., Che, L., Liu, J., 2023. Investigation of heavy gas dispersion characteristics in a static environment: Spatial distribution and volume flux prediction. *Building and Environment* 242, 110501. doi:<https://doi.org/10.1016/j.buildenv.2023.110501>
- [15] Ma, Y., Li, A., Wang, T., Che, J., Yang, C., Zhang, X., Wu, D., 2025. Characteristics of inclined negatively buoyant jet of dense gas leakage. *Physics of Fluids* 37, 025123. doi:<https://doi.org/10.1063/5.0251179>
- [16] Vauquelin, O., 2008. Experimental simulations of fire-induced smoke control in tunnels using an “air–helium reduced scale model”: Principle, limitations, results and future. *Tunnelling and Underground Space Technology* 23, 171-178. doi:<https://doi.org/10.1016/j.tust.2007.04.003>
- [17] Wang, T., Li, A., Ma, Y., Zhang, Y., 2025. Analysis of parameters for top exhaust ventilation to minimize heavy gas dispersion in fixed leakage source spaces. *Journal of Building Engineering* 103, 112091. doi:<https://doi.org/10.1016/j.jobe.2025.112091>
- [18] Wang, T., Li, A., Ma, Y., Zhang, Y., Yin, H., 2024. Enhancing heavy gas capture in confined spaces through ventilation control technology. *Building Simulation* 17, 1161-1182. doi:10.1007/s12273-024-1131-8
- [19] Wang, Z., Hu, Y., Jiang, J., 2013. Numerical investigation of leaking and dispersion of carbon dioxide indoor under ventilation condition. *Energy and Buildings* 66, 461-466. doi:<https://doi.org/10.1016/j.enbuild.2013.06.031>
- [20] Xing, J., Liu, Z., Huang, P., Feng, C., Zhou, Y., Zhang, D., Wang, F., 2013. Experimental and numerical study of the dispersion of carbon dioxide plume. *Journal of Hazardous Materials* 257, 40-48. doi:<https://doi.org/10.1016/j.jhazmat.2013.03.066>
- [21] Zeng, L., Gao, J., Lv, L., Du, B., Zhang, Y., Zhang, R., Ye, W., Zhang, X., 2021. Localization and characterization of intermittent pollutant source in buildings with ventilation systems: Development and validation of an inverse model. *Building Simulation* 14, 841-855. doi:<https://doi.org/10.1007/s12273-020-0706-2>
- [22] Zhang, Y., Wang, L., Li, A., Tao, P., 2020. Performance evaluation by computational fluid dynamics modelling of the heavy gas dispersion with a low Froude number in a built environment. *Indoor Built Environment* 29, 656-670. doi:<https://doi.org/https://doi.org/10.1177/1420326X19856041>

## HUMAN PERCEPTION EXPERIMENT IN UNDERGROUND SPACE ENHANCED WITH MIXED REALITY

Mingyi Lin<sup>1</sup>, Fang Liu<sup>2</sup>

**Abstract:** Underground spaces are rapidly expanding, with their functions increasingly extending to commercial, entertainment, and residential areas. However, the inherent characteristics of closure and complexity in these environments significantly impact user experience and safety. An experimental system was developed to explore human perception in underground spaces.

The system consisted of three main components: a mixed reality (MR) device, a set of wearable biosensors, and a data platform. Typical elements of the underground environment were built by digital tools and overlaid onto real-world physical space using the MR device. Scenarios, such as fire hazards or earthquakes, were simulated based on physical mechanism and introduced into the MR environment. During these simulations, human responses were monitored via wearable biosensors. All data were transmitted to and stored on the data platform, where analysis revealed correlations between human responses and environmental factors, providing insights for the optimization of underground spaces.

A fire drill scenario was studied as the application of this system. Smoke is generated by mixed-reality device according to the data derived from Fire Dynamics Simulator(FDS), after which the participant was asked to find the exit under low visibility. Meanwhile, the response of participants, including electroencephalogram(EEG), electrodermal activity(EDA) and photoplethysmographic(PPG), was collected for further analysis. It was indicated that the system could effectively build a vivid experimental scenario with less modeling work and higher movement freedom than virtual reality(VR) and provided a more immersive experience than augmented reality(AR). The human physiological signal can be recorded and utilized as a supplement for subjective response in the future.

**Keywords:** human factors, underground space, mixed reality, fire drill

### 1. INTRODUCTION

Underground spaces are continuously evolving, taking on increasingly diverse functions beyond basic municipal and civil defense purposes. However, certain characteristics of underground environments, such as confined spaces and monotonous designs, negatively impact user experience. Currently, numerous scholars have conducted research in this field, which can be categorized by methodology into field experiments, indoor model experiments, and indoor extended reality experiments.

Field experiments and indoor model experiments were widely used in early research, where participants performed tasks in actual underground structures or scaled-down simulated spaces. Their feedback was collected and analyzed through physiological monitoring devices or questionnaires.(Chirag Deb, 2010; Yang & Jun, 2018, 2019; Yang & Moon, 2018)

However, perception experiments often require modifying environmental variables to study their impact on human responses—something that is difficult to achieve efficiently with traditional field or indoor experiments. As a result, VR/AR technologies have gradually gained attention among researchers, offering a more flexible and controlled experimental environment.

<sup>1</sup> PhD candidate, Mingyi Lin, Civil Engineering, Tongji University, 1239 Siping Road, Shanghai, P.R. China, 2310085@tongji.edu.cn

<sup>2</sup> Professor, Fang Liu, Civil Engineering, Tongji University, 1239 Siping Road, Shanghai, P.R. China, liufang@tongji.edu.cn

In VR/AR-related research, crowd evacuation has received significant attention. Researchers typically construct virtual scenarios of underground space where hazards such as fire(S. Lu, M. Rodriguez, Z. Feng, D. Paes, A. B. Daemei, R. Vancetti, S. Mander, T. Mandal, 2025) or earthquake(Mitsuhara, 2024) take place. Participants navigate using omnidirectional treadmills or handheld controllers. These experiments investigate factors such as lighting conditions(Cailing, 2018; Mossberg et al., 2021) and guidance signage(S, 2019; Zhuang et al., 2025) on evacuation efficiency. Some studies focus on behavioral patterns in crowds, such as group coordination (60), while also considering influences like spatial familiarity and individual wayfinding habits(C. Wang et al., 2025). Other scholars have conducted VR wayfinding experiments in daily commuting scenarios, using metrics like navigation time and error rates to propose optimizations for signage systems.(S. Wang et al., 2021) Additionally, VR environments enable rapid feedback on spatial design alternatives. For instance, researchers have modified layouts(Yao et al., 2019) and material interfaces(Sun et al., 2022) in underground shopping streets, analyzing participants' dwell time and subjective preferences to derive design recommendations. In contrast, AR technology has seen relatively limited experimental application, primarily serving as a navigation aid(Demirkan, 2020) to test its effectiveness in real-world scenarios.

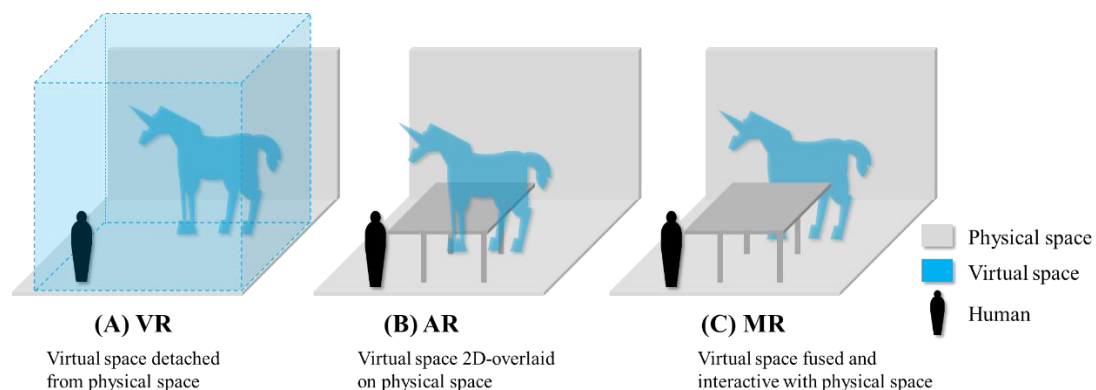
Based on the aforementioned review, current VR/AR technologies can effectively assist in constructing highly immersive human-factor experimental environments and conveniently adjusting environmental elements, proving more economical compared to field experiments. However, these methods exhibit the following limitations: the fidelity of scenarios heavily depends on modeling precision, resulting in high modeling costs; subjects are often confined to the vicinity of equipment with limited freedom of movement; and the incorporation of certain environmental elements lacks scientific mechanisms.

This study leverages mixed reality technology to superimpose virtual elements onto real physical environments, effectively reducing modeling workload while enhancing pedestrian mobility. Furthermore, a lightweight and modular human-factor data lifecycle management system was developed to address issues of inconsistent data formats and collaborative analysis difficulties in existing methods. Finally, to overcome the prevalent lack of scientific mechanisms in current research, the proposed framework supports remote integration of external scientific datasets, thereby establishing evidence-based simulation for key environmental parameters.

## 2. MIXED REALITY

Mixed reality is a technique to deeply combine virtuality and reality in various proportions, making them a continuum(Mann et al., 2018). The concept of mixed reality was firstly put forward by Paul Milgram and Fumio Kishino in 1990s(Milgram & Kishino, 1994), after which is getting increasingly popular, just as virtual reality(VR) and augment reality(AR). However, there are some differences among the three techniques, which means that MR can be considered as a further development of VR and AR.

The distinguishing feature of MR can be demonstrated in the figure below. MR device can perceive depth information in real space, enabling virtual elements to maintain realistic relative positional relationships with real-world objects. In contrast, AR can only overlay two-dimensional virtual "masks" onto real space, where virtual objects merely cover the physical environment without reflecting proper spatial relationships. Meanwhile, in VR technology, the real and virtual worlds are completely disconnected—when users are immersed in the virtual environment, they cannot perceive any information from the real world.



**Figure 1.** Comparison among VR, AR and MR

Based on the above characteristic, MR technique can more effectively utilize existing physical space than AR and VR do. As a result, only limited work is required in virtual modeling to establish highly immersive scenario, which not only reduces modeling cost but also allows users to move freely within the physical space. These advantages have enabled MR to find applications across numerous fields.

In order to reveal the implementation situation of this inspiring technique, 22094 papers are searched from Web of Science by key word MIXED REALITY and divided into 14 major fields. It is illustrated that MR is widely utilized in computer science, medicine, humanities, and arts. However, the technique sees fewer applications in architecture including underground space. What's more, MR is mainly used as an assistance for the design, construction and management of architectures, while the application on human perception experiment is relatively insufficient, resulting in a lack of scientifically quantifiable indicators for environmental evaluation. Therefore, in this research MR is used to set up the experiment system for human perception experiment, mainly contributing to construct the experimental scenario. In addition, associated devices such as data collection and management are also integrated.

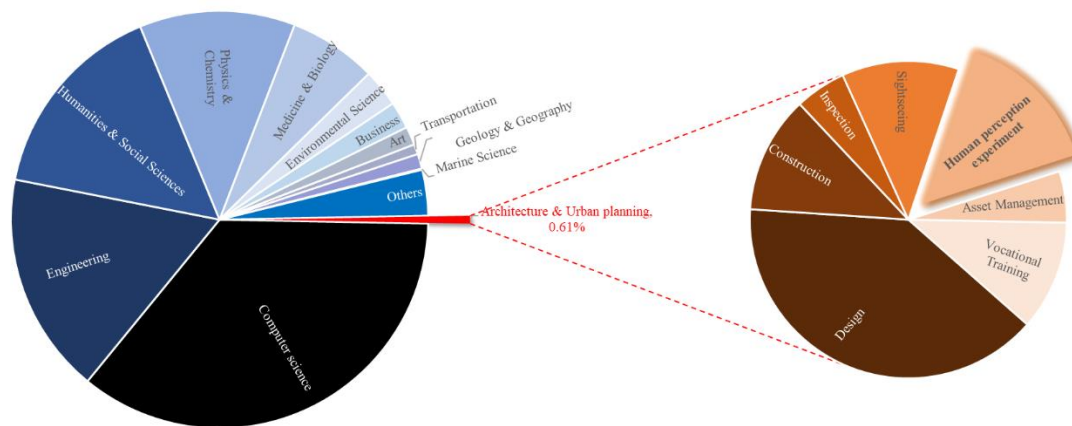


Figure 2. Application of MR in architecture & Urban planning and other fields

### 3. HUMAN PERCEPTION SYSTEM ENHANCED WITH MIXED REALITY

#### 3.1. Framework

The framework consists of MR-based scenario building device, a set of bio-sensors and a data management system. The scenario construction is based on both virtual elements and real-world site to provide an immersive experience, the human response to which will be collected by bio-sensors in the meantime. Acquired data will be transmitted to a management platform for further analysis and real-time display.

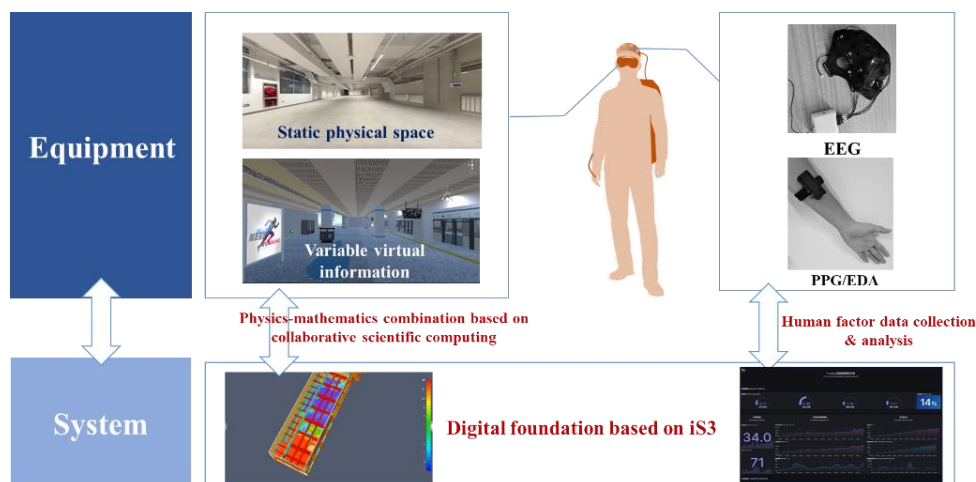


Figure 3. Framework of equipment system of human perception experiment



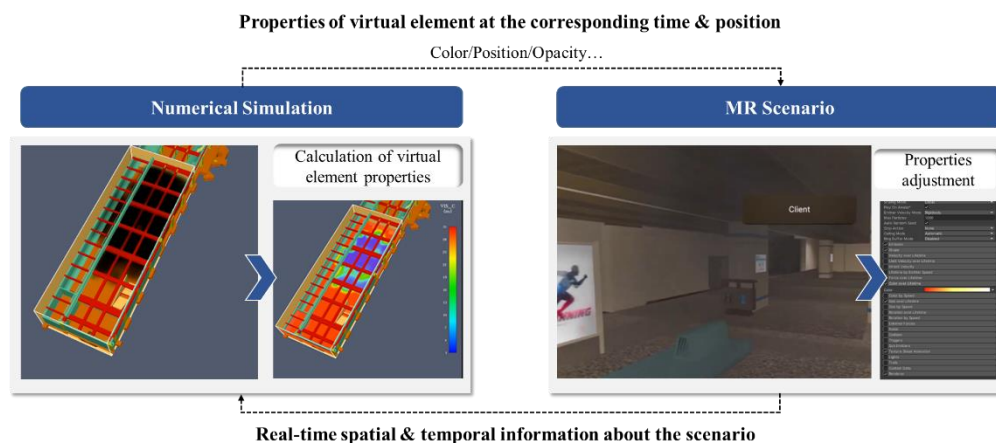
### 3.2. Scenario building based on MR

The scenario is developed using Unity and displayed by Apple Vision Pro. The 3D information of physical space, including the coordinates of surrounding structural surfaces are sensed by radars on MR helmet, after which the virtual elements will be located on the correct positions as according to the scenario design scheme.

What's more the scenario should be dynamically adjustable in order to effectively investigate the impact of specific environmental factors on participant experience. Therefore, the virtual elements can be controlled by both manual operation and numerical simulation.

The manual control of virtual elements is achieved using Mirror plugin used for multi-players game framework. The experimenter operate the server, while the participant can be considered as a client. The order of changing the status of virtual objects is given by server and transmitted to the participant via KCP protocol.

In addition, some objects can be adjusted according to simulation result for the scientific nature of experiment. The simulation is firstly carried out on software such as Abaqus, FDS, and so on, after which online database will make the data stored and exposes an interface for external requests. During the experiment, the simulation result will be invoked in real-time to dynamically adjust relevant virtual element attributes—such as transparency, position, and velocity, ensuring the object's appearance and motion conform to scientific principles.



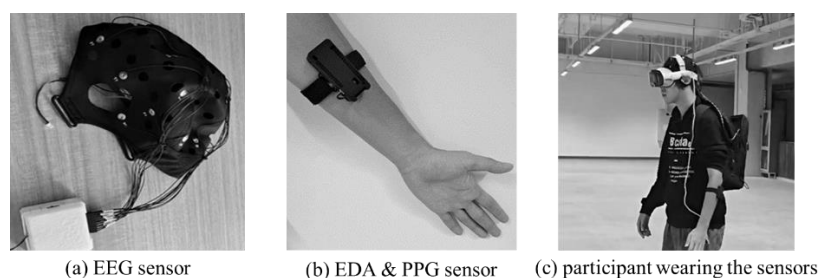
**Figure 4.** The integration of scientific mechanism into scenario

### 3.3. Physiological data collection

The human response to the scenario can be measured for the quantitative analysis on the dimensions of emotion and cognition activities. A set of wearable devices is developed to measure EEG, EDA and PPG.

The EEG signals are acquired via 3D-printed flexible brush electrodes integrated into an elastic fabric cap, enabling 18-channel EEG wave collection. Through time-domain and frequency-domain analysis, the activity levels of different EEG frequency bands can be identified, reflecting cognitive load and arousal states.

The EDA and PPG sensors are integrated into a single chip. Emotional fluctuations trigger vasoconstriction/vasodilation (affecting blood flow) and sweat gland secretion (altering skin conductance). These changes are captured as EDA and PPG signals, which not only derive basic physiological metrics (e.g., heart rate variability, skin temperature) but also reflect emotional responses.



**Figure 5.** Wearable bio-sensors

### 3.4. Full lifecycle data management

The acquired physiological data is managed by an online platform equipped with database, analysis module and display panel. Both structured and unstructured data can be stored and requested via API for further analysis and presentation.

The intelligent analysis module operates as a microservice that processes raw physiological signals through time-domain and frequency analysis to extract key features, enabling the assessment of emotional states and cognitive activity levels. The default analytical capabilities include emotion composition analysis based on skin conductance level (SCL), heart rate and body temperature conversion derived from PPG, as well as waveform separation and extraction across EEG frequency bands. By integrating these multimodal physiological measurements, the module provides comprehensive insights into both affective and cognitive dimensions of human states. In addition, users can also customize new modules and integrate them into the framework due to its modular architecture and high extensibility.

The data control panel is developed on an open-source framework, offering highly customizable settings that allow users to selectively display key information. This enables real-time monitoring of participants' physiological feedback and preliminary analysis results during experiments.

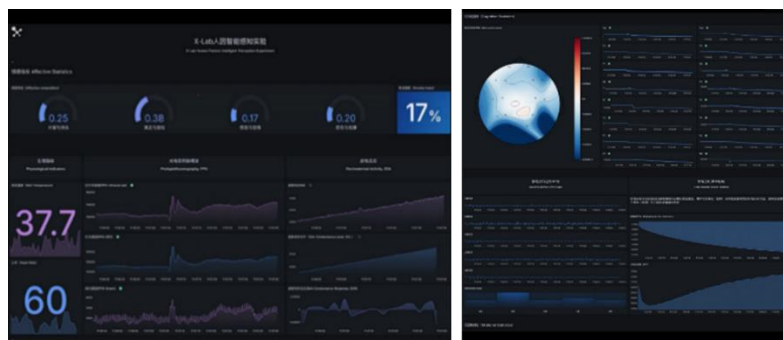


Figure 6. Panel for the display of human response data

## 4. APPLICATION: FIRE DRILL

### 4.1. Scenario building

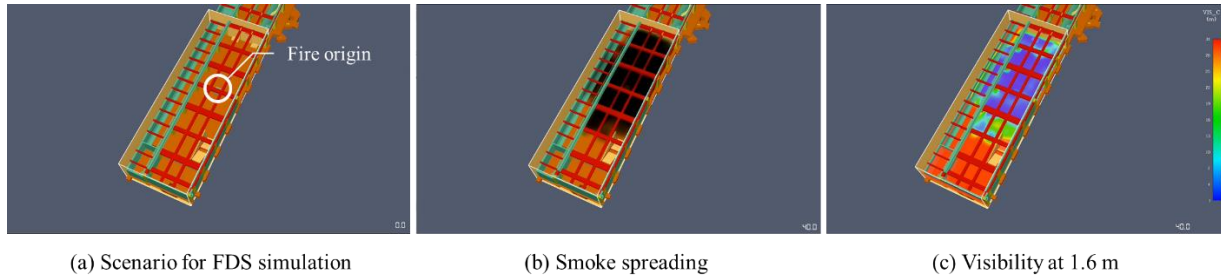
A MR enhanced fire drill is carried out in a 1:1 railway station section in November 2024, as a preliminary test of the validity of the proposed human perception system. The station section has an area of about 1500 m<sup>2</sup> and a height of 3 m, equipped with typical structural components of subway station such as tunnel and escape staircase(Figure 7(a)). A series of virtual elements, consisting of train, emergency guidance system, main service facilities and some decoration, are modeled by Unity and added to the physical space via MR technique to make the scenario more vivid(Figure 7(b)).



Figure 7. Scenario building based on the mixture of physical space and virtual elements

Fire and smoke modeled by particle system will be activated in MR format at a random time after the scenario is loaded, providing an escape scenario with low visibility. In order to endow scientific mechanism of smoke

spreading, the opacity of smoke particles at each time step is determined based on fire dynamics simulation(FDS). A full-scaled model of station is built and the fire is assumed to happen at the center of the site(Figure 8(a)).



**Figure 8.** FDS for determining the opacity of smoke particles in MR scenario

In order to quantify the influence of smoke spreading(Figure 8(b)), the dynamically changing visibility (m) is extracted at the height of 1.6 m, which is close to the eye level when bending over for evacuation(Figure 8(c)). Then the opacity of smoke particles is estimated using the formula below:

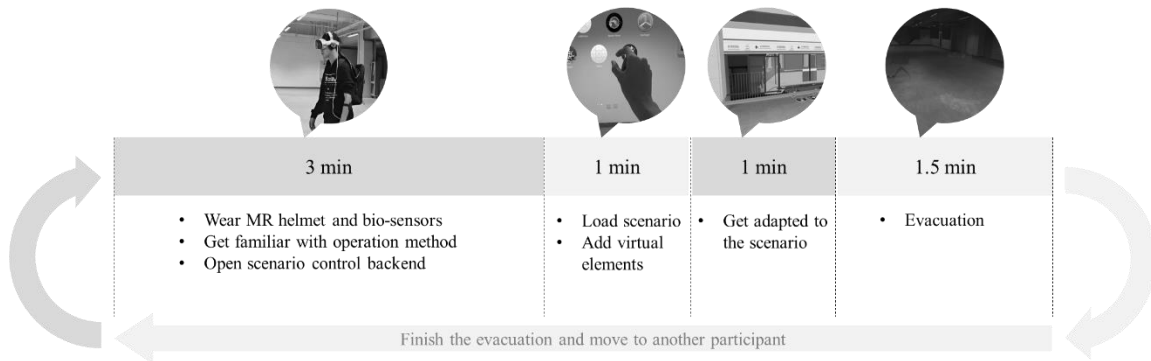
$$Opacity(x, y) = 1 - \frac{Vis(x, y)}{Vis_{max}} \quad (1)$$

where the  $Vis_{max}$  (m) is the initial visibility without any smoke, while  $Vis(x,y)$  (m) represents the real-time visibility at position (x,y).

A ring of smoke effect is deployed locally around the head of participant. For each frame advance in the scene, the participant's coordinates are transmitted back to the server, after which the corresponding smoke opacity value is calculated through 2D interpolation based on real-time positional data. This dynamically computed value is returned to the client-side and applied to the smoke assets, scientifically reproduces the movement through smoke-filled environment.

#### 4.2. Procedure design

The evacuation procedure is designed as the figure below. After wearing experiment equipment and receiving brief training, the participant opens the evacuation application and complete scenario loading. A short period of time is required to get adapted to the virtual-physical hybrid railway station, after which the formal evacuation begins. Participants will try to reach exit within a maximum of 90 seconds before their evacuation performance is evaluated.



**Figure 9.** Procedure of fire drill

#### 4.3. Performance evaluation

Time consumption is the main evaluation standard. The Chinese Code for Design of Metro (GB50157-2013) is referred where the permissible evacuation time is 6 min. However, the allowable time is adjusted to 90 s in this study, considering the limited spatial complexity and relatively low evacuation difficulty. If participants reach the exit within this timeframe, the system registers a successful evacuation and displays their escape time in a pop-up

window from the first-person perspective. Otherwise, the attempt is recorded as a failure. Physiological data collected during the evacuation process can also be analyzed to assess emotional and cognitive states, providing explanatory insights into the evacuation outcomes. But in this stage this part of data still wait for further analysis.

## 5. CONCLUSION

An equipment system for human perception experiment in underground space is developed and enhanced with mixed reality. Virtual elements are overlaid onto physical environments based on spatial computing to built a highly immersive experimental space, where scientific simulation result can be leveraged to scientize some key elements. The human-factor data can be collected and management in a platform for further analysis.

Fire drill design in a subway station is discussed as an application of this system. It is demonstrated that the equipment is able to build vivid experimental environment with modeling cost reduced. The human response is recorded and can be used as a powerful supplement for subjective evaluation in the further analysis.

In the future, it would be advisable to develop real-time interaction mechanisms between crowd simulation and MR experiments to enhance scenario realism. Additionally, an experimental framework capable of supporting multiple participants should be established to enable collaborative analysis of feedback from different test groups, thereby improving the reference value of the results.

## 6. BIBLIOGRAPHY

- [1] Cailing, W. (2018). Effects of Light and Signage on Evacuation Wayfinding Behavior in Underground Commercial Buildings. Chongqing University.
- [2] Chirag Deb, A. R. (2010). Evaluation of thermal comfort in a rail terminal location in India. *Building and Environment*, 45(11), 2571–2580.
- [3] Demirkan, D. C. (2020). An Evaluation of AR-Assisted Navigation for Search and Rescue in Underground Spaces. 2020 IEEE International Symposium on Mixed and Augmented Reality Adjunct (ISMAR-Adjunct), 3–4.
- [4] Mann, S., Furness, T., Yuan, Y., Iorio, J., & Wang, Z. (2018). All Reality: Virtual, Augmented, Mixed (X), Mediated(X, Y), and Multimediated Reality. Steve Mann, Tom Furness, Yu Yuan, Jay Iorio, and Zixin Wang. <https://arxiv.org/pdf/1804.08386>.
- [5] Milgram, P., & Kishino, F. (1994). A Taxonomy of Mixed Reality Visual Displays. *IEICE Trans. Information Systems*, E77-D(12), 1321–1329.
- [6] Mitsuhashi, H. (2024). Metaverse-Based Evacuation Training: Design, Implementation, and Experiment Focusing on Earthquake Evacuation. *IEEE Transactions on Systems, Man, and Cybernetics: Systems*, 53(4), 1–26.
- [7] Mossberg, A., Nilsson, D., & Wahlqvist, J. (2021). Evacuation elevators in an underground metro station: A Virtual Reality evacuation experiment. *Fire Safety Journal*, 120(April 2020), 1-9.
- [8] S. Lu, M. Rodriguez, Z. Feng, D. Paes, A. B. Daemei, R. Vancetti, S. Mander, T. Mandal, K. R. R. & R. L. (2025). A Virtual Reality Exit Choice Experiment to Assess the Impact of Social Influence and Fire Wardens in a Metro Station Evacuation. 1-24.
- [9] S, G. (2019). Evaluation of Smart Underground Mine Evacuation Efficiency through Virtual Reality Simulations. University of Nevada.
- [10] Sun, L., Ding, S., Ren, Y., Li, M., & Wang, B. (2022). Research on the Material and Spatial Psychological Perception Virtual Reality. *Buildings*, 12(9), 1–19.
- [11] Wang, C., Li, C., Zhou, T., Wang, D., An, X., Lv, J., & Wang, J. (2025). Immersive virtual reality experiments for emergency evacuation response in deep underground space. *Tunnelling and Underground Space Technology* incorporating Trenchless Technology, 163(April), 1–19.
- [12] Wang, S., Xu, J., Minping, L., & Ling, H. (2021). VR-based Data Acquisition and Evaluation of Pedestrian Traffic Behaviors in Buildings. *South Architecture*, 6, 32–37.
- [13] Yang, W., & Jun, H. (2018). Cross-modal effects of illuminance and room temperature on indoor environmental perception. *Building and Environment*, 146(May), 280–288.
- [14] Yang, W., & Jun, H. (2019). Combined effects of acoustic, thermal, and illumination conditions on the comfort of discrete senses and overall indoor environment. *Building and Environment*, 148(December 2018), 623–633.
- [15] Yang, W., & Moon, H. J. (2018). Combined effects of sound and illuminance on indoor environmental perception. *Applied Acoustics*, 141(July), 136–143.
- [16] Yao, G., Yusong, Z., Kaiyun, C., Yiyang, C., & Xianzhi, S. (2019). Solving Method of Effective Staying Activity Coefficient for Underground Commercial Streets Based on VR Experiment. *Research and Exploration in Laboratory*, 38(12), 10–13.
- [17] Zhuang, Y., Wang, F., Huang, Y., Song, X., & Rao, Y. (2025). Influence of guidance signs on platform evacuation in suburban railway tunnel under smoke and obstacle environment. *High-Speed Railway*, 3(1), 1–16.

## Road Tunnel Safety Evaluation and Crash Analysis: Experiences from Serbia

Dalibor Pešić<sup>1</sup>, Krsto Lipovac<sup>2</sup>, Boris Antić<sup>3</sup>, Emir Smailović<sup>4</sup>, Filip Filipović<sup>5</sup>,  
Nenad Marković<sup>6</sup>, Jelica Ščekić<sup>7</sup>

**Abstract:** Road tunnels represent critical sections of the transport infrastructure where the risk of traffic crashes and fire incidents is significantly increased due to confined space, specific geometry, and limited visibility and ventilation conditions. This paper presents an analysis of traffic crashes that occurred on the motorway network in the Republic of Serbia during the period 2020–2024, with a special focus on the Šarani and Lipak tunnels. Data from the national crash database and the internal records of the public enterprise “Roads of Serbia” were used to identify the most frequent crash types and related risk factors. Although crashes in tunnels account for less than 0.1% of all recorded crashes, they show a notably higher proportion of severe outcomes. The analysis includes factors such as lighting conditions, pavement surface, traffic signalization, and the functionality of safety equipment. Furthermore, the paper outlines the national methodology for conducting Road Safety Inspections (RSI) in tunnels, harmonized with the current PIARC recommendations and the Serbian Rulebook on tunnel safety requirements. The results highlight the need for systematic monitoring of tunnel safety equipment and the implementation of risk-management measures to enhance the safety of road users in closed traffic environments.

**Keywords:** road tunnels, traffic safety, road safety inspection, Serbia

### 1. INTRODUCTION

Road tunnels represent some of the most complex and safety-sensitive elements of modern road infrastructure. Their confined geometry, reduced visibility, and restricted space for maneuvering pose particular challenges to drivers and to those responsible for their safe operation. Although accident frequencies in tunnels are typically lower than on open roads, the consequences of incidents that occur are often much more severe due to limited escape routes, potential fire and smoke accumulation, and difficult access for rescue services (Lemke, 2000; Nussbaumer, 2007).

Numerous international studies have addressed various aspects of tunnel safety. Early research by Vashitz, Shinar, and Blum (2008) emphasized the role of in-vehicle information systems in enhancing driver awareness in tunnels. Ma, Shao, and Zhang (2009) analyzed accident data from Chinese freeway tunnels, highlighting distinct risk patterns compared to open-road environments. The impact of vehicle fires has also been the subject of numerical modeling by Caliendo et al. (2012), whose simulations of heavy-goods-vehicle (HGV) fire scenarios underscored the importance of tunnel geometry and ventilation design for user safety. Behavioral studies, such as

<sup>1</sup> PhD Dalibor Pešić, B.Sc. Traffic Engineer, Full Professor, University of Belgrade – Faculty of Transport and Traffic Engineering, Vojvode Stepe 305, 11000 Belgrade, Serbia. E-mail: [d.pesic@sf.bg.ac.rs](mailto:d.pesic@sf.bg.ac.rs). <https://orcid.org/0000-0001-8357-1746>

<sup>2</sup> PhD Krsto Lipovac, B.Sc. Traffic Engineer, Full Professor, University of Belgrade – Faculty of Transport and Traffic Engineering, Vojvode Stepe 305, 11000 Belgrade, Serbia. E-mail: [k.lipovac@sf.bg.ac.rs](mailto:k.lipovac@sf.bg.ac.rs). <https://orcid.org/0000-0002-6207-9629>

<sup>3</sup> PhD Boris Antić, B.Sc. Traffic Engineer, Full Professor, University of Belgrade – Faculty of Transport and Traffic Engineering, Vojvode Stepe 305, 11000 Belgrade, Serbia. E-mail: [b.antic@sf.bg.ac.rs](mailto:b.antic@sf.bg.ac.rs). <https://orcid.org/0000-0003-2504-9479>

<sup>4</sup> - PhD Emir Smailović, B.Sc. Traffic Engineer, Assistant Professor, University of Belgrade – Faculty of Transport and Traffic Engineering, Vojvode Stepe 305, 11000 Belgrade, Serbia. E-mail: [e.smailovic@sf.bg.ac.rs](mailto:e.smailovic@sf.bg.ac.rs). <https://orcid.org/0000-0001-9342-722X>

<sup>5</sup> MSc Filip Filipović, B.Sc. Traffic Engineer, Teaching Assistant, University of Belgrade – Faculty of Transport and Traffic Engineering, Vojvode Stepe 305, 11000 Belgrade, Serbia. E-mail: [f.filipovic@sf.bg.ac.rs](mailto:f.filipovic@sf.bg.ac.rs). <https://orcid.org/0000-0002-1930-9273>

<sup>6</sup> PhD Nenad Marković, B.Sc. Traffic Engineer, Associate Professor, University of Belgrade – Faculty of Transport and Traffic Engineering, Vojvode Stepe 305, 11000 Belgrade, Serbia. E-mail: [n.markovic@sf.bg.ac.rs](mailto:n.markovic@sf.bg.ac.rs). <https://orcid.org/0000-0003-0102-623X>

<sup>7</sup> PhD Jelica Ščekić, B.Sc. Traffic Engineer, Associate Professor, University of Belgrade – Faculty of Transport and Traffic Engineering, Vojvode Stepe 305, 11000 Belgrade, Serbia. E-mail: [j.davidovic@sf.bg.ac.rs](mailto:j.davidovic@sf.bg.ac.rs). <https://orcid.org/0000-0001-8402-8075>



Yeung and Wong (2014), explored car-following behavior in tunnels, revealing longer headways and lower speeds as typical adaptive responses to confined driving conditions.

Other authors have focused on the environmental and operational dimensions of tunnel safety. Li et al. (2015) investigated pollutant dispersion and its interaction with traffic flow, while Lu et al. (2015) identified key risk factors influencing the severity of crashes in Shanghai river-crossing tunnels. Bassan (2016) provided an overview of tunnel design principles and their influence on driver behavior and accident risk. Hou, Tarko, and Meng (2017) advanced this line of research through a correlated random-parameters model to explain crash-frequency variations across tunnel sections. More recent simulation-based studies, such as Król and Król (2021), have examined fire and evacuation dynamics in urban tunnels, confirming the need for integrated safety systems that combine engineering, operational, and behavioral perspectives.

Collectively, the literature shows that tunnel safety depends on the interaction between human behavior, infrastructure design, and traffic management measures. Following the EU Directive 2004/54/EC on minimum safety requirements for the Trans-European Road Network, many European countries have introduced systematic inspections and harmonized technical standards for tunnel safety.

### 1.1. Tunnel safety in Serbia

In Serbia, the expansion of motorway infrastructure in the past decade has introduced several long and complex tunnels, particularly along Corridors X and XI. Managing safety in these facilities has therefore become a strategic priority. In response, a national methodology for Road Safety Inspections (RSI) in tunnels was developed in 2022 (Lipovac et al., 2023; Smailović et al., 2023), based on PIARC and SEETO guidelines and harmonized with national regulations (Official Gazette RS 51/19, 52/19). The first complete RSI campaign was carried out in 2023, covering ten motorway tunnels on the state road network (Predajane, Manajle, Sarlah, Lipak, Šarani, and others).

Each inspection was conducted by a multidisciplinary team—comprising traffic, civil, mechanical, electrical, and fire-safety engineers—and included both video-based assessments under regular traffic and detailed pedestrian walkthroughs during scheduled closures. The inspection process evaluated over 15 categories, including geometric characteristics, lighting, ventilation, drainage, signage, ITS equipment, and passive safety features. Results were classified according to the risk level (low, medium, high) and accompanied by proposed countermeasures and cost categories (Antić et al., 2021; Smailović et al., 2021).

Parallel to the inspection activities, the Road Traffic Safety Agency of Serbia (ABS) provided data on traffic crashes in tunnels during the period 2020–2024. A total of 197 crashes were recorded, of which 6 were fatal and 81 involved injuries. The majority of crashes were single-vehicle loss-of-control events and rear-end collisions, indicating that driver behavior, inappropriate speed, and limited visibility are the main contributing factors. In more than 80% of cases, human factors were identified as the primary cause, while infrastructure and technical issues accounted for a smaller but still notable share—particularly near tunnel portals, where abrupt changes in luminance and speed adjustments occur.

### 1.2. Aim and scope of the study

This paper combines international research findings with national inspection and crash data to provide an integrated overview of tunnel safety and to identify practical directions for improvement. Specifically, it aims to:

- Present key insights from recent international studies on tunnel safety and human factors;
- Summarize the main findings from the 2023 RSI campaign in Serbian motorway tunnels;
- Analyze crash data from the ABS database (2020–2024) to identify prevailing accident types and causal factors; and
- Propose a set of targeted measures to enhance safety and operational resilience.

By linking engineering inspections, operational incident analysis, and real-world crash statistics, the study seeks to highlight the importance of a systematic, data-driven approach to tunnel safety. The ultimate goal is to contribute to the development of a comprehensive tunnel-safety framework applicable both to interurban motorways and to future urban underground corridors, in line with the ACUUS 2025 conference theme Safety, Security and Human Factors.

## 2. METHODOLOGY

### 2.1. Inspection scope

Inspections covered ten motorway tunnels on Class IA state roads and the corresponding influence zones extending up to 500 m from each portal, in both directions. This range was defined as the upper limit of the area potentially affected by tunnel systems or by changes in driving behavior when entering or exiting a tunnel.

The inspected tunnels included:

- **A1 corridor:** Predajane and Manajle (both tubes) and Železnik (right tube);
- **A2 corridor:** Veliki Kik, Savinac, and Brđani (both tubes);
- **A4 corridor:** Progon, Pržojna Padina, Sopot, and Sarlah (both tubes).

### 2.2. Field procedure

Inspections were conducted in two stages:

1. Drive-through surveys under regular traffic conditions, carried out during daylight hours with continuous video recording and commentary from the inspection team;
2. Detailed pedestrian walkthroughs, performed during planned closures of single tunnel tubes. These sessions included visual inspection, measurements, testing of installations, and documentation of observed problems.

All fieldwork was coordinated with tunnel operators and maintenance companies responsible for system testing and routine safety checks.

### 2.3. Elements and structure of assessment

Each tunnel was examined using a structured checklist covering all elements relevant to traffic safety and system operation.

The analysis included both the tunnel tubes and adjacent open sections, divided into thematic chapters corresponding to the standard RSI report format:

- |   |   |
|---|---|
| • Road function and classification;                               | • Ventilation and fire-detection systems;                   |
| • Cross-section and alignment;                                    | • Fire-suppression equipment and emergency facilities;      |
| • Pavement and drainage condition;                                | • Response systems for incident detection and notification. |
| • Intersections and service facilities within the influence area; | • For each observed issue, inspectors recorded:             |
| • Needs of vulnerable road users (where applicable);              | • the description of the deficiency;                        |
| • Traffic signs, markings, and ITS systems;                       | • potential risk to road users;                             |
| • Lighting and visibility conditions;                             | • recommended corrective or mitigating measure;             |
| • Roadside environment and passive-safety elements;               | • indicative cost category for implementation.              |
| • Electrical, telecommunication, and optical-cable installations; |   |

Risk levels were determined through expert evaluation, considering tunnel geometry, traffic characteristics, previous incident records, and possible accident consequences. Each issue was rated on a three-level scale: low, medium, or high risk. This classification provided a clear overview of priority problems and ensured systematic treatment of interrelated safety issues.

### 2.4. Incident database

Part of the analysis focused on operational data obtained from PE “Roads of Serbia”, covering extraordinary events and incident situations recorded in tunnel areas between 2016 and 2023. Each event was described by its type, duration, location, and brief circumstances. Two additional variables were added for analysis:

- Risk level, estimated by expert judgment based on event description and context;
- Cause category, defining whether the incident was related to driver behavior, technical malfunction, environmental influence, or maintenance activity.

A total of 5,411 incidents were included, comprising 3,997 traffic events and 1,414 equipment failures. The purpose of the analysis was not to assign responsibility but to identify groups of factors and recurring patterns that could influence safety performance and to provide supporting data for RSI interpretation.

## 2.5. Crash database

To complement field observations, crash data were collected from the Road Traffic Safety Agency (ABS) for the period 2020–2024. The dataset included all crashes that occurred inside tunnels and within their approach zones. Each record contained information on crash type, contributing factors, number of vehicles involved, injury severity, and location referenced to the national road network.

Crashes were categorized by mechanism (single-vehicle, rear-end, lane-change, pedestrian, and stationary-object collisions) and by primary contributing factor (human, road, technical, or environmental). Spatial coordinates and chainage data were used to align crash locations with RSI findings for subsequent analysis.

## 2.6. Data organization and integration

All collected information—inspection results, incident records, and crash data—was harmonized within a unified analytical framework. Data from different sources were standardized, coded, and georeferenced to ensure comparability. Descriptive statistics and qualitative coding were applied to prepare datasets for correlation analysis in the next phase of research. The integration of these datasets made it possible to link infrastructure conditions with real-world operational and safety performance, providing the basis for the results presented in the following section.

# 3. RESULTS

## 3.1. Overview of inspection findings

Road Safety Inspections conducted in 2023 confirmed that tunnel sections on Class IA state roads generally meet the required technical and safety standards. However, several recurring issues were identified, particularly in the zones of tunnel portals and emergency facilities.

The most common deficiencies included:

1. Insufficient or non-adaptive lighting at portal areas (Figure 1) – pronounced luminance contrast between external daylight and the interior of the tunnel, causing temporary glare and reduced visibility during entry or exit.
2. High curbs and unsafe edges of evacuation paths (Figure 2) – excessive curb height and abrupt transitions between the traffic lane and the pedestrian escape walkway, which can destabilize vehicles and hinder evacuation.
3. Unsafe positioning of electrical and control cabinets within the traffic zone (Figure 3) – cabinets and technical installations placed on tunnel walls inside the dynamic envelope, posing both passive-safety and operational-reliability risks in the event of impact.
4. Inadequate visibility and damaged or faded vertical signage (Figure 4) – reduced retroreflectivity and contrast of signs, combined with uneven lighting at portal areas.
5. Unprotected wall surfaces of emergency-stop niches (Figure 5) – lack of passive-safety elements or energy-absorbing protection, increasing the potential severity of collision impacts.
6. Limited space for emergency stops and lay-bys in longer tunnels (Figure 6) – insufficient width or depth of the stopping area preventing complete vehicle pull-off, especially for heavy goods vehicles.
7. Presence of passively unsafe obstacles (Figure 7) – rigid elements such as concrete edges, steel frames, or unprotected equipment located close to the traffic lane without deformable or shielding protection.



**Figure 1.** *Insufficient or non-adaptive lighting at portal areas,*



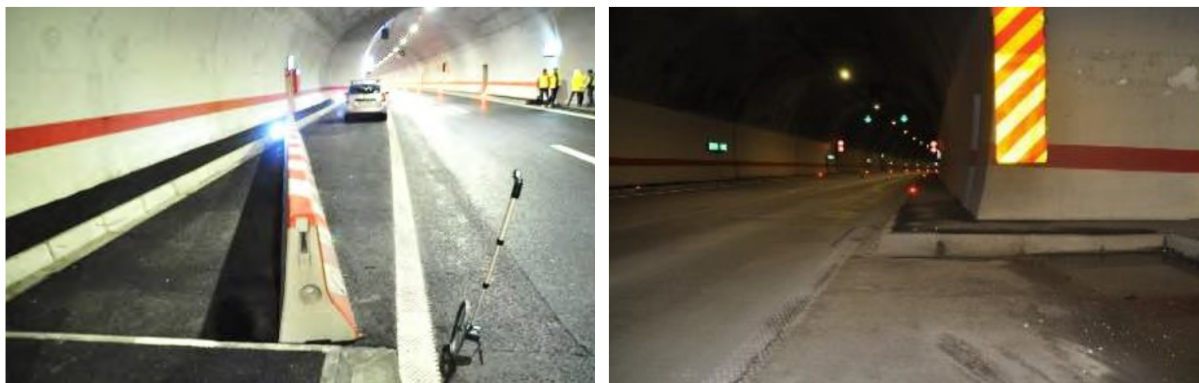
**Figure 2.** *High curbs and unsafe edge of the evacuation path*



**Figure 3.** *Unsafe positioning of electrical and control cabinets in the traffic zone*



**Figure 4.** *inadequate visibility and damaged or faded signage*



**Figure 5.** *limited space for emergency stops and lay-bys in longer tunnels*



**Figure 6.** *Unprotected wall of emergency stop niche*



**Figure 7.** *Passively unsafe obstacle*

### 3.2. Incident analysis

The database provided by PE “Roads of Serbia” contained 5,411 incident records for motorway tunnels between 2016 and 2023. Incidents were divided into four main categories: human-related, technical, environmental, and maintenance-related. Table 1 shows their distribution by cause and risk level, following the same format used in the 2024 national study.

**Table 1.** *Distribution of recorded incidents in motorway tunnels (2016–2023)*

Type of incident	Number of events	Share (%)	Dominant risk level	Typical examples
Driver-related	1,837	34.0	Medium	Stopped vehicles, pedestrians, wrong-way driving
Technical failures	1,414	26.1	High	Power supply interruption, lighting or ventilation failure
Environmental influences	1,051	19.4	Medium	Fog, ice, water leakage, low visibility
Maintenance and planned closures	1,109	20.5	Low	Cleaning, system testing, repair works
Total	5,411	100.0	—	—

About one third were driver-related, most often involving stopped vehicles (46%), pedestrians (18%), cyclists (4%), wrong-way or reverse driving (4%), and traffic crashes (15%). Such events typically occur in confined tunnel spaces where there is no shoulder or safe refuge. Among technical incidents, the most frequent problem was power supply interruption—present in 92% of recorded equipment failures—indicating the importance of reliable and redundant electrical systems.

Incidents caused by maintenance activities represented about one fifth of all cases and were generally low to medium in risk, while environmental influences were linked mainly to snow (43%), fog (32%), and ice (14%), usually in portal zones. Seasonal and daily variations were evident: most incidents occurred in summer (29%) and winter (32%), during morning (39%) and afternoon (28%) hours. Slightly higher frequencies were observed on Tuesdays (16%), Thursdays (14%), and Sundays (12%). About 60% of incidents lasted less than two hours; longer ones—often linked to adverse weather, power loss, or vehicle stoppage—had wider operational effects. Risk assessment showed that 45% of all events were rated as high-risk, mostly those involving pedestrians or wrong-way movements.

Roughly 35% of incidents could be attributed directly to user behavior, while others stemmed from environmental or system-related factors. Overall, the analysis confirms that tunnel safety depends equally on user discipline and system reliability. The clear seasonal and temporal peaks emphasize the need for adaptive management measures such as controlled lighting, variable speed limits, and automated incident detection to ensure stable safety performance year-round.



### 3.3. Crash analysis

Crash data from the Road Traffic Safety Agency (ABS) covered the period 2020–2024 and included all reported crashes that occurred within tunnel zones. A total of 197 crashes were recorded, of which 6 were fatal, 81 involved injuries, and 110 resulted only in material damage. The annual distribution of crashes is shown in Table 2.

Year	Fatal crashes (F)	Serious injuries (S)	Slight injuries (L)	Property damage only (PDO)	Total
2020	0	3	11	21	35
2021	4	9	13	28	54
2022	0	2	13	18	33
2023	1	4	5	14	24
2024	1	8	12	30	51
<b>Total</b>	<b>6</b>	<b>26</b>	<b>54</b>	<b>111</b>	<b>197</b>

The data show a fluctuation in annual crash frequency, with a clear peak in 2021 and a gradual stabilization in the following years. Fatal outcomes remain rare, but injury crashes represent more than 40% of all recorded cases, confirming that tunnel environments, although relatively safe in terms of frequency, can lead to severe consequences when crashes occur. When classified by type, single-vehicle crashes were most common (75 cases), followed by rear-end collisions (50), lane-change or overtaking conflicts (17), pedestrian crashes (6), and crashes with stationary vehicles or obstacles (4).

This pattern corresponds to the typical conditions of limited space, reduced visibility, and the absence of safe recovery zones inside tunnels.

## 4. DISCUSSION

The results of inspections, incident records, and crash analysis show that the safety level in Serbian motorway tunnels is generally satisfactory, but several recurring problems limit operational reliability and user safety. Most identified issues are linked to lighting quality, visibility, passive safety, and user behavior, rather than to major design or structural deficiencies.

Lighting and visibility stand out as a key factor. Non-adaptive lighting near portals creates sharp contrasts between external daylight and the tunnel interior, leading to temporary glare and reduced reaction time. This corresponds with the large share of single-vehicle crashes and driver-related incidents, confirming that visibility management directly affects driver performance.

Passive-safety elements such as high curbs, unprotected walls of stop niches, and rigid obstacles increase the consequences of errors rather than their frequency. Even when crash speeds are moderate, contact with these rigid structures can lead to severe damage. Improving edge profiles, adding protective barriers, and introducing energy-absorbing surfaces in lay-bys would significantly reduce impact severity.

Technical reliability also plays a major role. Nearly all equipment failures were caused by interruptions in power supply, emphasizing the need for redundant systems and better maintenance coordination. Although such failures are relatively rare, they can quickly escalate into safety-critical situations if lighting or ventilation is lost during heavy traffic.

Human behavior and operational control remain decisive. More than one third of all incidents were caused by drivers—mostly stopped vehicles, pedestrians, or wrong-way entries—showing that even well-designed tunnels require constant monitoring and rapid operator response. Automated Incident Detection (AID) and real-time surveillance are essential to shorten reaction times and prevent secondary collisions.

Seasonal and daily patterns of incidents suggest that tunnel safety management should adapt to changing conditions. High frequencies during summer and winter, and during morning and afternoon peaks, indicate that operational regimes—lighting, ventilation, and variable speed limits—should be dynamically adjusted according to traffic intensity and weather.

Comparing these findings with international studies confirms the same trend: tunnels generally record fewer crashes than open-road sections, but the severity of outcomes is higher due to confined space and lack of recovery areas. This pattern highlights the importance of risk mitigation measures, not only through infrastructure upgrades but also through operational management and user awareness.

In summary, the results emphasize three main priorities for improving tunnel safety in Serbia:

- Enhancing visibility and adaptive lighting, especially in transition zones at portals;
- Upgrading passive-safety elements and protecting technical installations within the traffic envelope;

- Strengthening operational reliability through redundant power systems, continuous monitoring, and automated incident detection.

Together, these measures form a practical basis for improving both user protection and the overall resilience of tunnel infrastructure on the national motorway network.

## 5. CONCLUSION

The conducted inspections and analyses show that the general technical condition of Serbian motorway tunnels is satisfactory, yet several recurring deficiencies continue to affect operational safety. Most of these problems are not structural but functional and behavioral, arising from limited visibility, insufficient passive protection, or inadequate user response in critical situations.

The findings highlight that tunnel safety cannot rely solely on design compliance—it depends equally on real-time monitoring, adaptive control, and user behavior management. Power-supply interruptions, non-adaptive lighting, and driver-related incidents remain the dominant risk factors, each requiring a tailored technical response.

In this context, smart technologies can play a decisive role. Automated Incident Detection (AID), variable speed management, adaptive lighting control, and integrated traffic supervision platforms represent key tools for timely response and prevention. These systems directly address the main causes identified in this study—human error, visibility changes, and delayed operator intervention—by providing early warnings and automatic countermeasures.

Future improvements should therefore focus on:

- Integrating AID and tunnel management systems to ensure rapid detection of stopped vehicles, pedestrians, or wrong-way movements;
- Introducing adaptive lighting and variable message signs that respond to external light, traffic density, and weather conditions;
- Enhancing redundancy of power and communication networks to maintain functionality during failures;
- Applying data-driven safety management, combining inspection reports, incident logs, and crash databases for continuous risk monitoring.

By linking traditional engineering measures with intelligent systems, tunnel safety management can evolve from reactive maintenance toward proactive, resilience-based operation.

## 6. BIBLIOGRAPHY

- [1] Agency for Traffic Safety. (2024). National road crash database (2020–2024). Belgrade, Serbia.
- [2] Antić, B., Pešić, D., Smailović, E., & Beronja, S. (2021). Specific characteristics of road safety inspections in tunnels. *Put i saobraćaj (Road and Traffic)*, 67(3), 33–38.
- [3] Bassan, S. (2016). Overview of traffic safety aspects and design in road tunnels. *IATSS Research*, 39(1), 3–9.
- [4] Caliendo, C., Ciambelli, P., De Guglielmo, M. L., Meo, M. G., & Russo, P. (2012). Numerical simulation of different HGV fire scenarios in curved bi-directional road tunnels and safety evaluation. *Tunnelling and Underground Space Technology*, 31, 33–43. <https://doi.org/10.1016/j.tust.2012.04.006>
- [5] European Commission. (2023). Revision of Directive 2004/54/EC on road tunnel safety – Impact assessment report. Brussels, Belgium.
- [6] Hou, Q., Tarko, A. P., & Meng, X. (2017). Analyzing crash frequency in freeway tunnels: A correlated random parameters approach. *Accident Analysis & Prevention*, 99(A), 72–80.
- [7] PE “Roads of Serbia”. (2023). Database of incidents and equipment failures in motorway tunnels (2016–2023). Internal report. Belgrade, Serbia.
- [8] Król, A., & Król, M. (2021). Numerical investigation on fire accident and evacuation in an urban tunnel for different traffic conditions. *Tunnelling and Underground Space Technology*, 108, 103730.
- [9] Li, Q., Chen, C., Deng, Y., Li, J., Xie, G., Li, Y., & Hu, Q. (2015). Influence of traffic force on pollutant dispersion of CO, NO and PM<sub>2.5</sub> measured in an urban tunnel in Changsha, China. *Tunnelling and Underground Space Technology*, 50, 116–122.
- [10] Lipovac, K., Antić, B., Davidović, J., Smailović, E., Petrović, J., & Maksimović, B. (2023). Methodology for conducting road safety inspections in tunnels. In *Proceedings of the 18th International Conference “Road Safety in Local Community – BSLZ 2023”* (pp. 15–25). Kopaonik.
- [11] Lu, J. J., Xing, Y., Wang, C., & Cai, X. (2015). Risk factors affecting the severity of traffic accidents at Shanghai river-crossing tunnels. *Traffic Injury Prevention*, 16(8), 814–819.
- [12] Ma, Z. L., Shao, C. F., & Zhang, S. R. (2009). Characteristics of traffic accidents in Chinese freeway tunnels. *Tunnelling and Underground Space Technology*, 24(3), 350–355.

- [13] Ministry of Construction, Transport and Infrastructure of the Republic of Serbia. (2019). Rulebook on safety requirements for road tunnels. Official Gazette of the Republic of Serbia, 51/19 and 52/19.
- [14] Pešić, D., Petrović, J., Smailović, E., Radulović, K., & Ilić, I. (2023). Specific traffic safety problems in the Šarani and Lipak tunnels. In Proceedings of the 18th International Conference “Road Safety in Local Community – BSLZ 2023” (pp. 401–416). Kopaonik.
- [15] Pešović, Z., Terzić, I., Lipovac, K., Pešić, D., Antić, B., Smailović, E., & Maksimović, B. (2024). Road safety inspections in highway tunnels in the Republic of Serbia. In Proceedings of the 19th International Conference “Road Safety in Local Community – BSLZ 2024” (pp. 70–81). Zlatibor.
- [16] PIARC – World Road Association. (2020). Road tunnels: Operational strategies for safety and efficiency (Technical Report No. 2020R19EN). Paris, France: PIARC.
- [17] Vashitz, G., Shinar, D., & Blum, Y. (2008). In-vehicle information systems to improve traffic safety in road tunnels. Transportation Research Part F: Traffic Psychology and Behaviour, 11(6), 395–406.
- [18] Yeung, J. S., & Wong, Y. D. (2014). The effect of road tunnel environment on car-following behaviour. Accident Analysis & Prevention, 62, 51–58.

## **DIGITALIZATION AND AI TOWARD UNDERGROUND SPACE SOLUTIONS**

## GEOLOGICAL ASPECTS OF URBAN PERSONAS: A COMPUTATIONAL AI PIPELINE FOR THE MULTIDIMENSIONAL CHARACTERIZATION OF CITY STREETS IN THE PROVINCE OF QUÉBEC

Michael R. Doyle<sup>1</sup>

**Abstract:** City streets tend to be conceptualized from a viewpoint of a particular or general observer. Smaller-scale studies and interventions focus on the perspectival and photographic views of particular streets, providing rich but highly nuanced information. On a larger scale, streets are elements within orthographic and axonometric views from a general observer placed at infinity, situating them in a standardized way within a single coordinate space. These representations require a selection of what will be shown. As research into the urban subsurface has observed, disciplines whose work is directly impacted by the geological conditions of a site are rarely confronted by geology in the early phases of the design process. The urban underground tends to remain hidden. Long-term holistic and multidimensional planning, which includes the subsurface as one among many characterizations of the location of a project, is complicated by the increasing number of dimensions that compete for priority in the politics of territorial transformation. Geographical information systems (GIS) have helped centralize and standardize heterogeneous data sources. These information management platforms have been accompanied by work conducted on how to synthesize that data and present it on a large scale. What has yet to be explored extensively is how geology can be looked at through a high-dimensional data model that harnesses the pattern-seeking capabilities of machine-learning techniques. From the standpoint of our contemporary information technology, artificial intelligence should be able to provide an impersonal viewpoint from which to look at all the available data for a street on a planetary scale.

The project presented as part of this communication will explore this computational potential, taking as a case the Canadian province of Quebec. It recognizes that working with the components of artificial intelligence challenges our inherited modes of thinking about the world. The underlying conceptual shift is one from a personal to an impersonal subjectivity. This can be summarized somewhat figuratively by saying that the streets 'know' without knowing what they know. In conceptual terms, it is a shift away from theory-driven modelling to data-driven modelling. The design of the research project becomes less about what a street 'is' in preparation for a statistical model than about how to invent the keys to revealing what the streets 'know' without knowing they know it. As such, a street is treated as an individual whose identity is simply the fact that it is not every other street. This conception preserves the aspects of identity that are not only rational or real, but also imaginary. Mathematically speaking, we could say identity is complex and, like the complex numbers, identity comprises both the real and the imaginary. Geological conditions become part of the street's character, along with other characteristics, such as the amount of vegetation in its vicinity, the moisture content, its topography and geometry, the degree of centrality of the street in the urban network in terms of different types of activities and land uses, the qualities and value of available property, as well as photos taken by people on and around the street.

This communication will focus mainly on the method for data acquisition and processing, conducted principally in Python from freely accessible sources. The street objects were scraped from OpenStreetMap at the level of the province of Quebec using the *osmnx* library. The satellite data was downloaded from the Sentinel-2 satellite data using the Google Earth engine API. The 2022 georeferenced geological maps of unconsolidated surface sediments and of the underlying geological formations of the province of Quebec (an area of 1.7 million km<sup>2</sup>) were downloaded from the web site of the *Ministère des ressources naturelles et des forêts*. In order to characterize each street according to its underlying geology, the algorithm takes 50 by 50-meter samples of the two geological maps at 50-meter intervals along each street object, recording the formations for each sample area and the percentage of coverage of each. Each street segment then has *n* samples with each formation and the percentage of the sample it occupies. Borrowing from natural language processing, the formations are treated as words and the percentages

<sup>1</sup> Michael R. Doyle, PhD, Associate professor, École d'architecture, Édifice du Vieux-Séminaire, Canada, email: michael.doyle@arc.ulaval.ca



as counts, producing a matrix where each row is a street and each column is a geological formation with the corresponding percentage of each.

In order to render the streets comparable to each other, the computational setup processes the matrices of formation proportions with a one-dimensional Self-Organizing Map (SOM). The algorithm is applied as a nonparametric encoder that fits an artificial neural network to the high-dimensional space, producing an ordered set of indexes whose relative distances preserve the topological structure of the original data. Each street is assigned two metrical values, one for each near subsurface and subsurface formations, which situates it on a line of positive real numbers. As such, the values are measures of relative geological similarity to all other streets. Although the SOM is not a new algorithm, this application is novel and takes advantage of the building blocks of contemporary AI, unsupervised machine learning and largely heterogeneous datasets. Mapping these values shows unsurprisingly that the characterizations strongly resemble the geological maps because we are basically visually summarizing trends that are already visible. Running the SOM on the geological formations from both unconsolidated near subsurface and subsurface bedrock conditions tells a more nuanced story, which will be presented in this communication.

An additional exercise was performed using ChatGPT and the resulting indexes of the one-dimensional SOM. A significant challenge for architects and urban planners provided with geological information is knowing how to interpret it. Although collaboration with geologists, hydrogeologists and geotechnical engineers cannot be replaced by AI, professionals outside those expert fields might not know where to begin when confronted with a list or map of geological formations. The premise of this exercise was that, with the right prompt, an initial assessment can be provided by ChatGPT (or another pretrained transformer) that can guide future discussions with geological specialists. The approach is inspired by recent attempts to use large language models as automated proxies for expert judgment. In the resulting SOM model, each neuron indexes streets having a similar but not necessarily identical proportional distribution of geological formations in its sampled vicinity. The SOM model stores, for each neuron, a prototype vector that represents the probable distribution of the streets indexed by that neuron. This provides a single 'typical' vector of values that can be used instead of providing each individual street to ChatGPT. This option was preferred as proof-of-concept. Using the OpenAI API, each neuron's characteristic vector was provided to ChatGPT-4o with a prompt asking it to provide a brief assessment for the combination of geological formations of the presence of groundwater or aquifers, for that installation of geothermal systems for heating or cooling, for shallow to deep foundation construction and for reuse of excavated geomaterials. The call to the API specifies that ChatGPT should respond as an expert speaking to architects and urban planners, providing justifications for its assessment if necessary. Although it cannot replace the expertise of local geologists and geotechnical engineers, working with LLMs can help architects and urbanists to formulate informed questions to ask of human experts.

The presentation will conclude with new questions and next steps in the ongoing research. Because of its exploratory nature, the author will not make any claims as to the utility of the approach in solving any pressing practical problems. Nor will it attempt to say how it is better or worse than existing approaches already being tested in planning departments or proposed by other researchers. This will need to be part of future work when the prototype has been tested further. The conclusions drawn will be limited to the overall pipeline, which, in its genericness, has the advantage but also the burden of a potentially general applicability.

**Keywords:** artificial intelligence, geospatial data, geology, urban streets, computational methodology

## LESSONS FROM BIM AND AI FOR INDOOR ENVIRONMENTAL QUALITY MANAGEMENT: APPLICATIONS TO UNDERGROUND SPACE ENVIRONMENTAL QUALITY RESEARCH

Samuel Twum-Ampofo<sup>1</sup>, Isabelle Y. S. Chan<sup>2</sup>, Hao Chen<sup>3</sup>

**Abstract:** Academic literature has well established the impact of indoor environmental quality on human wellbeing (health, comfort and productivity). In the case of underground spaces, increasing evidence suggests that the wellbeing of underground occupants may be compromised due to unique indoor environmental constraints. While Building Information Modelling (BIM) and artificial intelligence (AI) hold promise in addressing such risks, the potential these technologies to redefine the affordances of indoor environmental quality in underground spaces remains unknown. Through a bibliometric analysis of scholarly literature, a mapping of the evolution of BIM and AI technology usage in enhancing indoor environmental comfort is reported. The study identified seven thematic clusters of the use of BIM-AI in general IEQ research, with a surge in publications since 2019. However, a significant gap remains in applying BIM-AI technologies for underground space research. Among the technologies reviewed, supervised machine learning emerged as the predominant approach. Insight from the bibliographic themes suggests transformative opportunities to engineer underground spaces into adaptive environments that actively enhance human wellbeing. These include BIM-visualized early warning systems for occupant comfort management and AI-driven automated HVAC control. The results serve as a foundation for designers and policymakers to leverage BIM's data integration capabilities and AI's predictive insights to achieve both health-centric design and operation of underground spaces.

**Keywords:** Wellbeing, Indoor environmental quality, BIM, AI, Underground Space.

### 1. INTRODUCTION

Wellbeing is shaped by several factors, including external environmental stressors (e.g., climate), social determinants (e.g., lifestyle), and work-related factors (e.g., occupational stress) [1,2]. However, given the amount of time people stay indoors, significant attention has been directed toward the role of indoor parameters in shaping the psychophysiological wellbeing of building occupants [3,4,5]. A plethora of studies have demonstrated how indoor environmental variables (e.g., poor thermal conditions, inadequate lighting and noise) within suboptimal ranges act as stressors with cumulative effects on building occupants' psychophysiological wellbeing [4]. Hence there is the need to maintain optimal indoor environmental quality to safeguard building occupants' wellbeing. In addition, building use is dynamic, rarely remaining consistent over time. Shifts in occupancy patterns, functional changes and renovations can lead to deviations from initial design assumptions during the operational phase [6]. These changes necessitate proactive building management to address evolving occupant needs [6], while also considering locational constraints (e.g., aboveground vs. underground contexts) that may further complicate adaptations [7,8].

Emerging evidence suggests an increase in psychophysiological complaints of underground occupants [4]. Locating underground facilities within entrapped earth results in unconventional indoor environmental performance. This presents unique design challenges that differ significantly from those of aboveground considerations. Underground spaces are significantly impacted by site-specific geological conditions (e.g. soil composition, groundwater, thermal retention) [7,8]. In addition, the lack of comprehensive, context-sensitive

<sup>1</sup> Twum-Ampofo, Samuel, The University of Hong Kong, samtwum@connect.hku.hk

<sup>2</sup> Chan Y.S, Isabelle, The University of Hong Kong, iyschan@hku.hk.

<sup>3</sup> Chen Hao, The University of Hong Kong, haoc@connect.hku.hk

design guidelines further complicates the design process, as the functional needs of each space (e.g., commercial malls versus subways) and geological variations give rise to unique demands for indoor environmental quality [4].

Adopting digital technologies in the AEC industry has unlocked opportunities to enhance IEQ. Among these, artificial intelligence (AI) and Building Information Modeling (BIM) stand out as transformative technologies (e.g. [9,10,11]). BIM has gained prominence as a core technology, enabling parametric design optimization during the design stage of a project. Supported by AI, it could facilitate active control and monitoring of IEQ during operations through early hazard prediction analysis [12]. However, despite the extensive application of these technologies in aboveground building projects, a preliminary literature search revealed a significant gap in their deployment for analyzing and managing IEQ in underground facilities. A possible reason could be the prioritization of construction productivity and safety-centric issues of underground facilities [13,4]. Thus, it remains unclear which technologies are most applicable and how they might address the unique complexities of underground spaces. Notably, this contrasts with aboveground IEQ research, where BIM-AI technologies have been successfully implemented in field studies to address IEQ issues. Therefore, analyzing the empirically validated aboveground applications provides transferable frameworks for adapting BIM-AI technologies to underground contexts. Hence, this study employed bibliographic coupling analysis to map knowledge networks in digital indoor environmental quality research. The goal was to visualize themes from implementing BIM-AI technologies in aboveground IEQ research, towards identifying transferable knowledge for underground space research. By doing so, the study reveals actionable insights for adapting Industry 4.0 solutions to solve underground space IEQ management challenges.

### **1.1. Overview of IEQ and health conditions in underground spaces**

According to Chan et al. [4], post-occupancy IEQ evaluation studies show that actively controlled factors (e.g., lighting, air quality, thermal conditions, and noise) and design factors (e.g., building layout and ergonomics) significantly affect the health of underground occupants. The cumulative impact of these IEQ factors have also been confirmed in some studies. These studies span multiple scales, addressing not only the psychophysiological health effects, but also implications for comfort and work performance. In particular, indoor air quality is reported to have pronounced effects on health perceptions. Elevated pollutant levels have been found to increase stress, anxiety, and other negative psychological impacts. Likewise, sick building syndrome (SBS) is prevalent in various underground spaces, with affected individuals usually attributing it to perceived poor indoor air quality [4]. The evidence gathered to date spans various underground space types (e.g. shopping malls, subways, and offices) and suggests that the nature and intensity of indoor stressors may vary according to the functional use of the space [4]. Accordingly, there is a need for innovative approaches to address them.

### **1.2. The Concept of Healthy BIM**

BIM describes the process of creating a digital representation of a building's physical and functional characteristics. The embedded information about the facility forms a reliable basis for decision-making throughout its lifecycle [14]. The end product is a digitized model comprising building components represented by digital objects that carry computable graphic and data attributes, identifying them to software applications, as well as parametric rules that enable them to be manipulated intelligently. Recognizing BIM's capacity to address IEQ hazards, Rice [15] introduced the 'Healthy BIM' framework. The framework describes BIM's capacity to incorporate key IEQ health indicators (e.g., illuminance, acoustics, thermal comfort) during the design phase. This allows simulations to optimize IEQ and reduce health risks. Through Delphi technique, 14 feasible health indicators were identified [15]. However, current implementations remain limited by their reliance on static IEQ assumptions. Hence, data-driven intelligence, real-time pattern-driven simulation, and analysis for the control and management of building systems, particularly those in underground spaces, could be beneficial.

### **1.3. Overview of Artificial Intelligence**

Artificial intelligence describes the concept of developing intelligent machines and computer systems that exhibit humanlike intelligence. These systems can reason, learn, and solve problems similarly to humans by processing and learning from data as input. Given these capabilities, researchers are exploring their usefulness in tackling AEC industry problems [16]. Abioye et al. [16] described several key technologies as summarized in table 1. Their framework served as the analytical basis for this review, guiding the identification and classification of AI applications in the IEQ research domain.

**Table 1.** Types of AI technologies

Field	Description
<b>Machine learning</b>	Concerned with the design and use of computer programs to learn from experience or past data for modelling, control or prediction
<b>Computer Vision</b>	Focuses on artificial simulation of the human visual system
<b>Optimization</b>	Concerned with making decisions and choices that provides the best outcomes given a set of constraints
<b>Natural Language</b>	Creating models that mimic linguistic capabilities of human beings
<b>Robotics</b>	Automated devices that carry out physical activities n real world
<b>Knowledge-based systems</b>	Concerned with machine decision making based on existing knowledge

## 2. RESEARCH METHODOLOGY

The authors adopted a two-step approach for this study. First, the state-of-the-art research on the applications of BIM-AI in the context of IEQ is presented. Subsequently, studies specific to underground spaces were identified. This approach enabled a direct comparison of the maturity of underground space research relative to the broader domain of BIM-AI and IEQ research.

### 2.1. PRISMA approach

A systematic literature review on BIM-AI applications for IEQ management was conducted, adhering to PRISMA guidelines [17]. PRISMA is widely accepted in AEC review studies [18,19], as it ensures reproducibility and transparency of review studies. Accordingly, only studies demonstrating practical applications of BIM-AI to IEQ challenges, with empirical validation or real-world implementation, were selected. Conceptual studies were excluded unless substantiated by data, ensuring the synthesis reflected evidence-based advancements. The steps followed by this study are outlined below and in Fig. 1.

### 2.2. Step 1: Collection of publications

In sourcing studies, Scopus database was selected due to its broader coverage of scientific publications, faster indexing [20], and usefulness for science mapping [21]. Given the varying terminologies used for available artificial intelligence variants, and to ensure comprehensive coverage, the authors leveraged the capability of ChatGPT to generate an initial list of 40 potential keywords. Subject-matter experts then refined this list by removing off-topic terms (e.g., “AI in Education,” “AI in Finance”), retaining only keywords relevant to IEQ outcomes (i.e. health, comfort, or productivity). The final search string (ref. Table 2) combined these terms with Boolean operators, targeting titles, abstracts, and keywords.

The authors limited the search to research articles and conference papers in the engineering field published in English-language journals from 1993 to 20th June 2025. The initial search yielded 726 records. After applying the specified limitation criteria, the Scopus database yielded 349 records. Following the removal of 32 papers (comprising review articles and off-topic content identified through title, keyword, and abstract screening), 317 unique records remained for full-text evaluation. During the full-text assessment stage, each article was evaluated for eligibility to be included in the review. Out of this process, 21 other articles were omitted for several reasons (studies focusing on mathematical modelling rather than AI, outdoor transitional areas, etc.), leaving 296 studies deemed eligible for inclusion in the review.

**Table 2.** Keywords employed

Aim	Search strings
<b>Environmental Quality</b>	"Indoor environmental quality" OR "ieq" OR "thermal comfort" OR "air quality" OR "acoustic comfort" or "lighting comfort"
<b>Digital technologies</b>	"Building Information Modelling" OR "BIM" OR "Machine Learning" OR "Deep Learning" OR "Neural Networks" OR "Supervised Learning" OR "Unsupervised Learning" OR "Reinforcement Learning" OR "Artificial Neural Networks" OR "Recurrent Neural Networks" OR "Pattern Recognition" OR "Predictive Analytics" OR "Fuzzy Logic" OR "Support Vector Machine" OR "Decision Trees" OR "Random Forest" OR "Clustering" OR "K-means"
<b>Outcomes</b>	"physiological" OR "psychological" OR "productivity" OR "well-being"

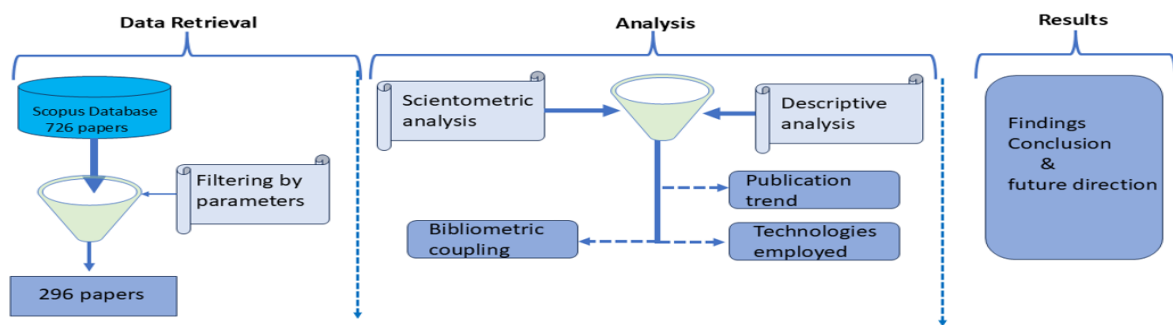


Figure 1. Overview of research methodology

### 2.3. Step 2: Quantitative analysis of studies

The selected papers were analyzed to map out publication trends, and BIM/AI employed for IEQ research. Following this, a Social Network Analysis was conducted using VOS viewer (v1.6.20) to examine intellectual structures and research networks [21]. Specifically, a bibliographic coupling network was generated. In this network, the size of the node reflects the influential nature of a study (i.e. Its citation frequency), line thickness indicates co-occurrence strength, and the proximity of nodes reveals thematic relationships.

## 3. RESULTS OF BIM-AI IN IEQ RESEARCH

### 3.1. Descriptive Analysis of Publications

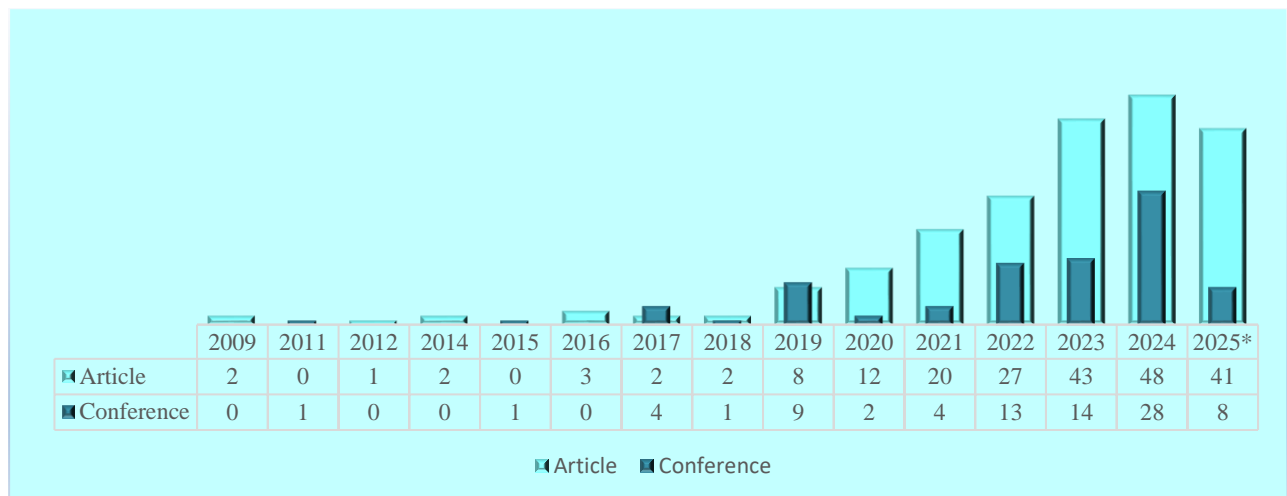


Figure 2. Trend of Publications

Figure 2 shows publication trends (from 1987 to 20th June 2025). Of the 296 studies reviewed, 211 (69%) were journal articles, while 85 others (31%) were conference papers. While the application of AI in AEC dates back to the 1980s [22], our dataset indicates AI as the first application for IEQ, and this emerged in 2009, demonstrating an adoption lag. Notably, 94% of publications (277 papers) appeared between 2019 and 2025, reflecting an accelerated research interest aligned with industry transformation trends [21]. This surge coincides with growing recognition of the value of data, from occupant behavior to indoor environmental metrics [23] for data-driven IEQ optimization.

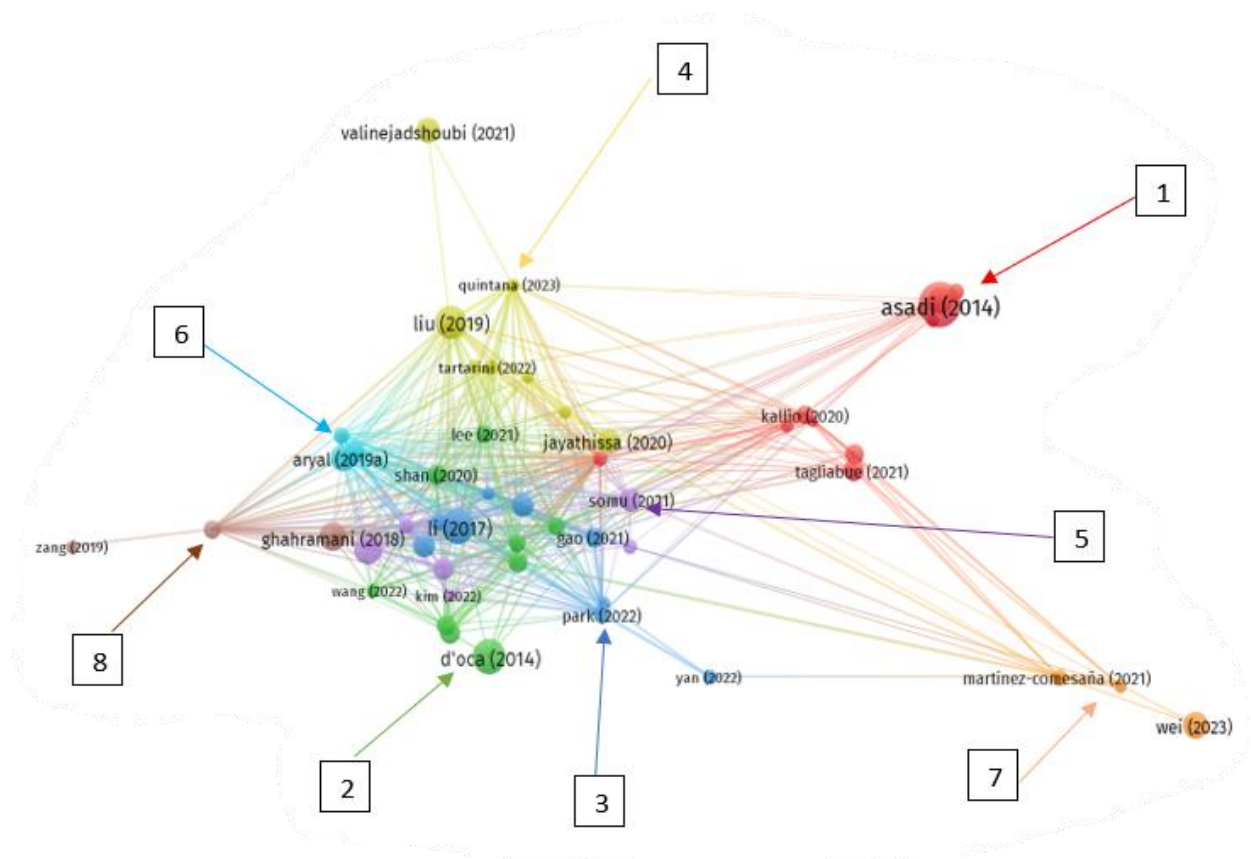
### 3.2. Bibliographic coupling analysis

As a preliminary investigation, bibliographic coupling was employed to map the intellectual structure of the BIM-AI IEQ research domain. This method offers an advantage over keyword co-occurrence, by minimizing



network noise from inconsistent terminology. Bibliographic coupling technique was particularly warranted given the wide and subtle application of BIM and AI technologies across the IEQ landscape, which often results in varied and fragmented keyword usage. Thus, instead of relying on frequently used terms, bibliographic coupling groups studies based on their shared citations [24, 25], allowing for a more stable and meaningful representation of thematic connections. A document is said to be bibliographically coupled when cited in two or more documents' references [25]. This technique helps discover clusters, similar to co-citation analysis, based on content similarity [24,25].

Using VOS viewer, a network threshold of 27 citations per document was set. Of the 296 articles selected for this study, a network was established across 46 interconnected papers (Fig. 3a). In this network, the proximity of nodes reflects the similarity of the reference lists of the studies, suggesting a relatedness of their content [25]. Bigger nodes signify articles with more robust bibliometric connections [24]. Seven clustered were identified and were numerically labelled 1 to 7. In addition, the timeline visualization (Fig. 3b) was generated to complement the bibliographic network by showing how the field has developed. It uses a color gradient where older publications appear in purple and more recent studies are highlighted in yellow. Hence, a visual cue of the discipline's development is presented [24]. After carefully evaluating the studies in each cluster, descriptive names were manually assigned to highlight the primary research focus of each cluster.



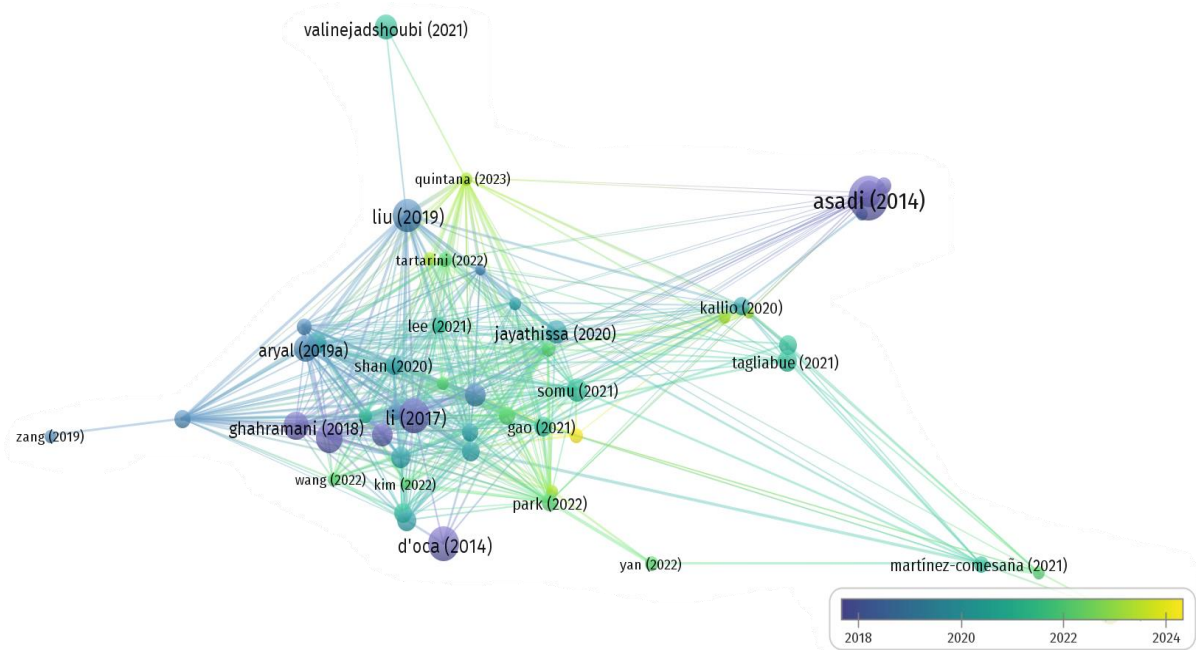


Figure 3. Bibliographic citation couplings and overlay timeline network clusters

### 3.2.1. Cluster 1: Towards non-intrusive personalized thermal comfort via physiological sensing

Cluster 1 encompasses a broad range of studies. The studies represent a shift from conventional thermal comfort modelling from traditional multi-input approaches (which combine environmental data, physiological signals, and subjective feedback) toward non-intrusive, physiology-driven personalized models.

Subjective perception of thermal conditions is a key input in comfort models, making user feedback essential [26]. Nevertheless, researchers have noted that obtaining longitudinal subjective input from building occupants can be disruptive and impractical, limiting its viability for continuous monitoring [26]. The studies in this cluster explore how accurate physiological sensing, such as bio signals from wearables, can autonomously infer thermal preferences, enabling real-time smart HVAC systems to operate dynamically without interrupting occupants. The studies also highlight the using machine learning to select between natural and mechanical ventilation based on current environmental conditions, balancing thermal comfort with energy efficiency. These approaches signal a shift toward adaptive, occupant-centered climate control that moves beyond traditional HVAC reliance [27].

### 3.2.2. Cluster 2: Occupant behavior and real-time automated HVAC control using physiological data from wearable devices

Buildings often use more energy than predicted, primarily due to unanticipated behaviors of building users at the design stage, particularly in HVAC (Heating, Ventilation, and Air Conditioning) systems [28]. This cluster explores how the actions and comfort perceptions of building occupants influence their control of building systems. Studies first collect data using sensors that track human actions and indoor conditions like temperature and humidity, subjective information on how warm or cold occupants feel, and physiological measurements like metabolic rate, heart rate or body temperature via wearing sensors to determine accurate thermal comfort models [28,29]. Such models lead to the development of real-time smart systems that adjust heating and cooling automatically, based on what indoor occupants actually need, using thermal sensor readings from smartwatch wearables. The goal is to make buildings more energy-efficient while keeping building occupants comfortable.

### 3.2.3. Cluster 3: Evaluating single sensor methods and scalable techniques for personalized thermal comfort modelling

Studies in this cluster evaluate the predictive accuracy of different sensing technologies, such as wearable devices, environmental sensors, and thermal imaging, for personalized thermal comfort assessment. Predicting human comfort in built environments is complex due to the input of several interacting variables (e.g. physiological, psychological, and environmental factors) [30]. Conventional data-driven personalized thermal comfort models rely on multi-sensor data, including environmental factors (e.g. humidity, temperature, air velocity), physiological inputs (e.g. skin temperature, variable heart rate, metabolic rate, blood pressure) and subjective feedback [e.g., 31]. However, these approaches can be impractical for real-world deployment since they

are laborious and often require multiple sensors, which are expensive [31]. The studies in this cluster explore whether single-sensor models (using only environmental or physiological data) can achieve comparable accuracy at a lower cost, e.g. 31]. The goal of these studies is to reduce costs and complexity while maintaining the predictive power of the models developed. In parallel, some studies apply transfer learning to improve model adaptability across different spaces.

#### 3.2.4. Cluster 4: Integrated multi-objective optimization approaches for high-performance indoor environments

Meeting the indoor environmental quality needs of building occupants is inextricably linked to a building's energy demands. Optimizing IEQ requires balancing multiple, often competing factors, including system types, their interaction with building materials, and the permeability of the building envelope [32]. Striking this balance is essential to ensuring a healthy and comfortable indoor environment while maintaining energy efficiency. By leveraging the capabilities of AI and BIM, complex trade-offs are optimized. For example, some studies focus on reducing energy consumption while maximizing comfort and health.

#### 3.2.5. Cluster 5: Methodological advances in personalized thermal comfort modelling

This group explores efforts to advance personalized thermal comfort models. Researchers in this cluster test a range of input features and algorithms to determine the most effective parameters that significantly shape people's perception of indoor thermal conditions. [33]. In a similar manner, some studies explore strategies to overcome the challenges of data scarcity and imbalance, employing strategies such as transfer learning and synthetic data augmentation to address these limitations [34]. The overlay timeline indicates that this cluster is emerging as a shift to more recent core research work.

#### 3.2.6. Cluster 6: Modeling and optimizing indoor environmental quality under data-constrained conditions

Machine learning techniques for modeling indoor environmental quality (IEQ) conditions and system diagnostics often depend heavily on the availability and quality of historical data. However, real-world datasets are frequently affected by gaps, noise, or imbalance, which can compromise model accuracy and reliability [35]. This research cluster focuses on developing optimized machine learning solutions that address data-related challenges [e.g. 36]. The studies leverage a range of strategies such as advanced optimization algorithms and cross-building knowledge transfer to enhance predictive accuracy in data-constrained settings.

#### 3.2.7. Cluster 7: Real-time spatial monitoring and cohort-based onboarding approaches for personalized thermal comfort modeling

This cluster brings together two complementary research directions that aim to enhance personalized thermal comfort in buildings through practical, data-efficient, and scalable solutions. The first group of studies focuses on the development of real-time early warning systems for thermal discomfort. Leveraging BIM-IoT integration, these frameworks continuously monitor building conditions to detect thermal risks and deliver timely alerts via smartphones or smartwatches to responsible parties [37]. The systems support proactive interventions and facilitate dynamic environmental adjustments across various building zones.

The second set of studies focuses on developing personalized comfort models based on group dynamics. It involves cohort-based modeling, where individual comfort predictions are created by matching new occupants to similar profiles using new occupants' basic personal profile data [e.g. 38]. Together, the studies demonstrate a shared goal of supporting scalable thermal comfort adaptation, enabling multi-zone management across entire buildings for different group dynamics, and efficiently adapting thermal comfort for new building occupants.

*Table 3. List of BIM-AI in IEQ influential Studies*

S/N	Label	Description	Cluster	Citations
1	Li (2017)	Personalized human comfort in indoor building environments under diverse conditioning modes	1	247
2	Ghahramani (2018)	Towards unsupervised learning of thermal comfort using infrared thermography	1	148
3	Farhan (2015)	Predicting individual thermal comfort using machine learning algorithms	1	95
4	Wang (2019)	Predicting Older People's Thermal Sensation in Building Environment Through a Machine Learning Approach: Modelling, Interpretation, And Application	1	93
5	Shan (2020)	Towards Non-Intrusive and High Accuracy Prediction of Personal Thermal Comfort Using A Few Sensitive Physiological Parameters	1	71

6	Cheng (2019)	Nidl: a pilot study of contactless measurement of skin temperature for intelligent building	1	53
7	Na (2019)	Development Of a Human Metabolic Rate Prediction Model Based on the Use of Kinect-Camera Generated Visual Data-Driven Approaches	1	49
8	Yeom (2021)	Local Body Skin Temperature-Driven Thermal Sensation Predictive Model for The Occupant's Optimum Productivity	1	39
9	Song (2022)	Using machine learning algorithms to multidimensional analysis of subjective thermal comfort in a library	1	27
10	D'oca (2014)	A data-mining approach to discover patterns of window opening and closing behavior in offices	2	238
11	Pigliautile (2020)	Assessing occupants' personal attributes in relation to human perception of environmental comfort: measurement procedure and data analysis	2	81
12	Deng (2020)	Development and validation of a smart HVAC control system for multi-occupant offices by using occupants' physiological signals from wristband	2	70
13	Morresi (2021)	Sensing physiological and environmental quantities to measure human thermal comfort through machine learning techniques	2	64
14	Wu (2020)	Using electroencephalogram to continuously discriminate feelings of personal thermal comfort between uncomfortably hot and comfortable environments	2	59
15	Yang (2022)	Comparison of models for predicting winter individual thermal comfort based on machine learning algorithms	2	55
16	Lee (2021)	Physiological sensing-driven personal thermal comfort modelling in consideration of human activity variations	2	46
17	Wang (2022)	Towards wearable thermal comfort assessment framework by analysis of heart rate variability	2	31
18	Aryal (2019a)	A comparative study of predicting individual thermal sensation and satisfaction using wrist-worn temperature sensor, thermal camera and ambient temperature sensor	3	126
19	Jayathissa (2020)	Humans-as-a-sensor for buildings—intensive longitudinal indoor comfort models	3	92
20	Aryal (2020)	Thermal comfort modeling when personalized comfort systems are in use: comparison of sensing and learning methods	3	85
21	Gao (2021)	Transfer learning for thermal comfort prediction in multiple cities	3	74
22	Aryal (2019b)	Skin temperature extraction using facial landmark detection and thermal imaging for comfort assessment	3	45
23	Bueno (2023)	Hierarchical and k-means clustering to assess thermal dissatisfaction and productivity in university classrooms	3	31
24	Quintana (2020)	Balancing thermal comfort datasets: we can, but should we?	3	31
25	Asadi (2014)	Multi-objective optimization for building retrofit: a model using genetic algorithm and artificial neural network and an application	4	427
26	Zhou (2009a)	Optimization of ventilation system design and operation in office environment, part i: methodology	4	134
27	Tagliabue (2021)	Data driven indoor air quality prediction in educational facilities based on iot network	4	87
28	Kallio (2021)	Forecasting office indoor co2 concentration using machine learning with a one-year dataset	4	73
29	Kallio (2020)	Assessment of perceived indoor environmental quality, stress and productivity based on environmental sensor data and personality categorization	4	54
30	Zhou (2009b)	Optimization of ventilation systems in office environment, part ii: results and discussions	4	46
31	Jalilzadehazhari (2019)	Achieving a trade-off construction solution using BIM, an optimization algorithm, and a multi-criteria decision-making method	4	31
32	Chaudhuri (2018)	Random forest based thermal comfort prediction from gender-specific physiological parameters using wearable sensing technology	5	165
33	Somu (2021)	A hybrid deep transfer learning strategy for thermal comfort prediction in buildings	5	91
34	Chaudhuri (2020)	Machine learning driven personal comfort prediction by wearable sensing of pulse rate and skin temperature	5	78
35	Nguyen (2024)	Modelling building HVAC control strategies using a deep reinforcement learning approach	5	36
36	Arakawa Martins (2022)	Performance evaluation of personal thermal comfort models for older people based on skin temperature, health perception, behavioral and environmental variables	5	34
37	Sulzer (2023)	Predicting indoor air temperature and thermal comfort in occupational settings using weather forecasts, indoor sensors, and artificial neural networks	5	29
39	Wei (2023)	Lstm-autoencoder-based anomaly detection for indoor air quality time-series data	6	132

40	Park (2022)	Prediction of individual thermal comfort based on ensemble transfer learning method using wearable and environmental sensors	6	53
42	Martínez-Comesaña (2021)	Use of optimized mlp neural networks for spatiotemporal estimation of indoor environmental conditions of existing buildings	6	47
38	Yan (2022)	Data-driven prediction and optimization of residential building performance in Singapore considering the impact of climate change	6	39
41	Martínez-Comesaña (2022)	Optimization of thermal comfort and indoor air quality estimations applied to in-use buildings combining nsga-iii and xgboost	6	30
44	Liu (2019)	Personal thermal comfort models with wearable sensors	7	231
45	Valinejadshoubi (2021)	Development of an IoT and BIM-based automated alert system for thermal comfort monitoring in buildings	7	108
46	Tartarini (2022)	Personal comfort models based on a 6-month experiment using environmental parameters and data from wearables	7	36
43	Quintana (2023)	Cohort comfort models using occupant's similarity to predict personal thermal preference with less data	7	27

#### 4. REVIEW OF BIM-AI IN IEQ RESEARCH FOR UNDERGROUND SPACES

Following the same search protocol outlined in Sections 2.1 and 2.2, the authors extended the search to include underground space-related terms (“underground” or “tunnelling” or “subway”). The search yielded four initial results, of which only two met the inclusion criteria defined in Section 2.

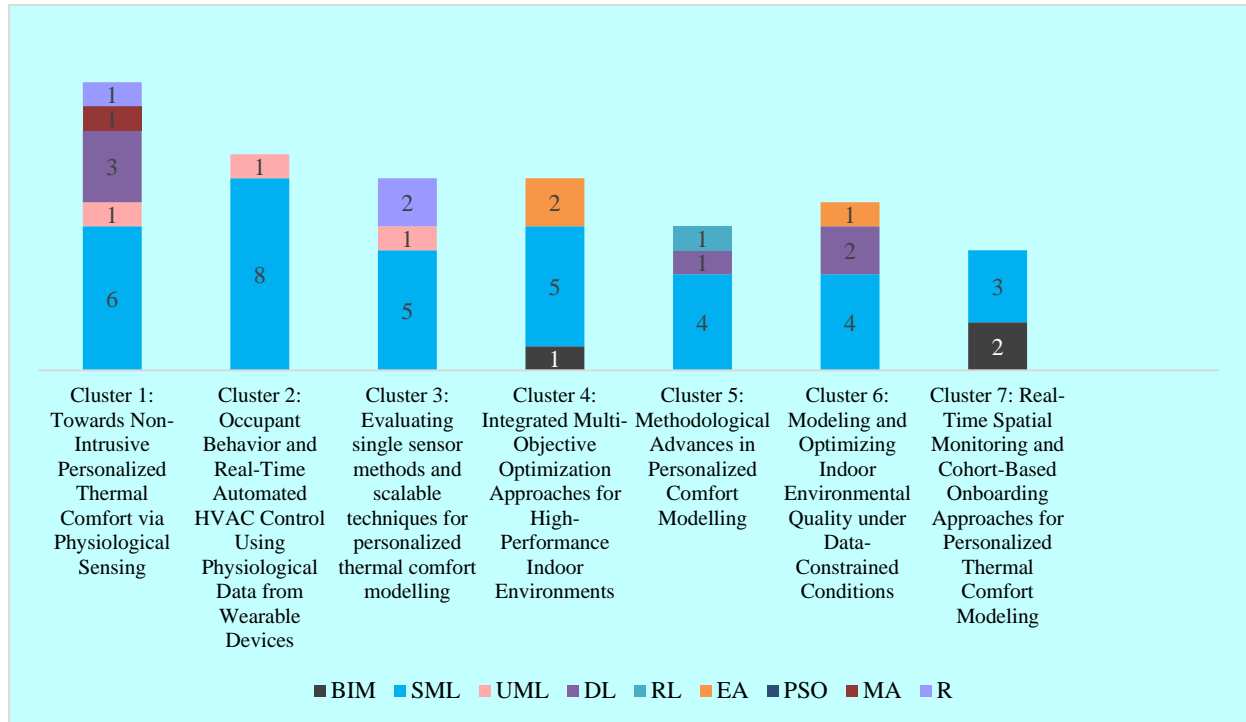
*Table 4. Results from Underground Specific BIM-AI in IEQ Studies*

S/N	Authors	Title	Document Type	Relevance	Technologies used
1	Shi et al., 2024	A review of applications of electroencephalogram in thermal environment: Comfort, performance, and sleep quality	Article	✗	✗
2	Chen et al., 2025	Study of Factors Influencing Thermal Comfort at Tram Stations in Guangzhou Based on Machine Learning	Article	✗	✗
3	Wang et al., 2025	An efficient thermal comfort prediction method for indoor airflow environment using a CFD-based deep learning model	Article	✓	Deep Learning (CNN, LSTM)
4	Marzouk et al., 2013	Evaluation of indoor environmental quality for subways in Egypt using BIM	Conference	✓	BIM

#### 5. BIM-AI TECHNOLOGIES IN IEQ RESEARCH

Fig.4 visually maps the spread of BIM-AI technologies across seven thematic clusters, indicating the methodological concentration within each. Analysis of the 46 bibliographic coupling studies reveals that supervised machine learning (SML) algorithms dominate the field, accounting for 64% of implementations (35 studies). The skew towards SML likely stems from the predominance of studies focusing on thermal comfort prediction, where labeled data (e.g., occupant feedback, sensor-derived variables) have conventionally served as inputs for regression models, which align conceptually with SML. All technologies were systematically classified using Abioye et al.’s [12] framework, which provides a comprehensive taxonomy of AI subtypes deployed in AEC research.





Key= BIM =Building information modelling, SML=Supervised machine learning, UML= Unsupervised machine learning, DL= Deep Learning, RL=Reinforcement Learning, Evolutionary algorithms, PSO= Particle Swarm Optimization, MA= Motion Analysis, R= Recognition

Figure 4. Distribution of BIM-AI Technologies employed across bibliographic clusters

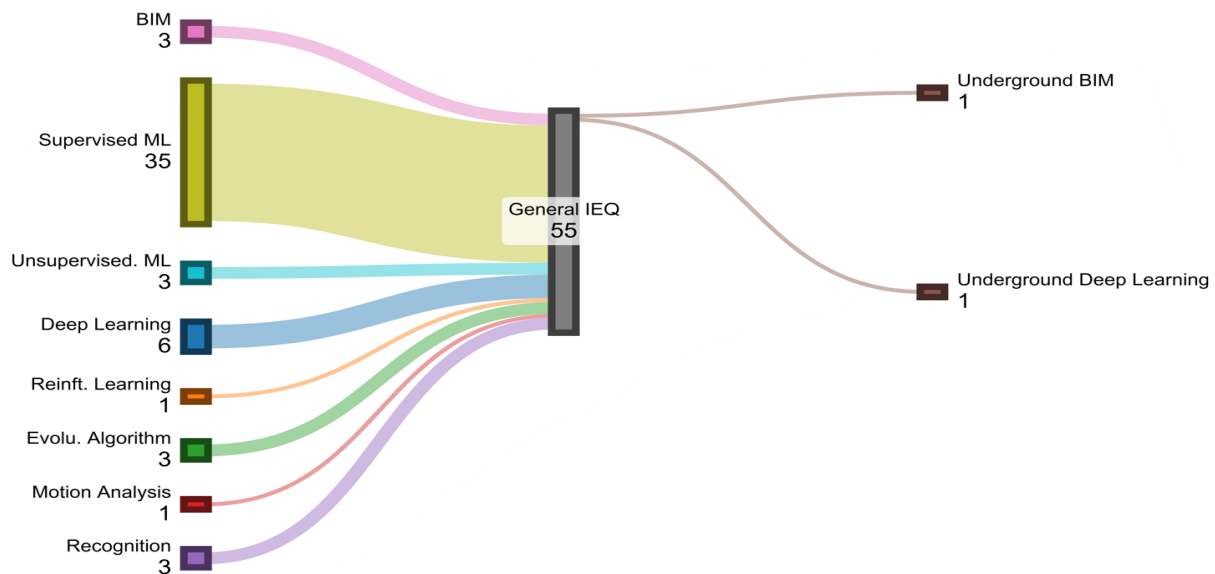


Figure 5. A Comparative Analysis of BIM-AI Technologies in General IEQ Research versus Underground Space Studies

## 6. CONCLUSION

This study presents a scientometric analysis of the evolution of BIM and AI applications in IEQ research. Bibliographic coupling analysis revealed 46 core influential studies, grouped under 7 themes. Whereas the analyzed themes revealed significant advancements in using BIM-AI technologies for above-ground IEQ management, a gap in applying such technologies in underground space IEQ optimization was noted. This is particularly concerning, given the heightened psychophysiological health risks associated with underground

environments, where factors such as perceived confinement and limited natural stimuli may amplify occupants' responses to IEQ conditions. The integration of AI technologies, leveraging multivariate data (e.g., environmental sensors, human physiological responses, and energy metrics), could bridge this gap by enabling real-time IEQ optimization and improving social acceptance of underground spaces. Current literature predominantly focuses on thermal comfort, yet opportunities exist to explore underrepresented variables such as acoustic quality (critical in subway stations) and lighting dynamics (vital in windowless environments). Furthermore, while supervised learning dominates existing research, future studies should expand into unsupervised learning (for pattern discovery in unlabeled data) and computer vision (to analyze human behavior interactions in underground spaces). Such advancements could reveal more profound insights into occupant adaptation mechanisms and context-specific IEQ thresholds, ultimately leading to healthier and more productive underground environments. In particular, given that humans are multimodal and experience IEQ holistically, AI techniques like unsupervised machine learning can help identify hidden patterns through multivariate analysis (e.g. interactions between lighting and thermal comfort or lighting and acoustics) [20], revealing new affordances for enhancing IEQ in underground spaces.

## 7. ACKNOWLEDGEMENT

This work was supported by the General Research Fund (Grant No.17203920) under the Research Grant Council, HKSAR.

## 8. BIBLIOGRAPHY

- [1] Intergovernmental Panel on Climate Change (IPCC). (2022). Climate change 2022: Impacts, adaptation and vulnerability. Contribution of Working Group II to the Sixth Assessment Report of the Intergovernmental Panel on Climate Change (H.-O. Pörtner, D. C. Roberts, M. Tignor, E. S. Poloczanska, K. Mintenbeck, A. Alegría, M. Craig, S. Langsdorf, S. Löschke, V. Möller, A. Okem, & B. Rama, Eds.). Cambridge University Press.
- [2] Burgard, S. A., & Lin, K. Y. (2013). Bad jobs, bad health? How work and working conditions contribute to health disparities. *American Behavioral Scientist*, 57(8), 1105-1127.
- [3] Mujan, I., Anđelković, A. S., Munčan, V., Kljajić, M., & Ružić, D. (2019). Influence of indoor environmental quality on human health and productivity - A review. *Building and Environment*, 144, 208-220.
- [4] Chan, I. Y., Twum-Ampofo, S., Ababio, B. K., Ghansah, F. A., & Li, S. (2025). Towards a whole process engineering approach for enhancing physical and psychological health in underground environments: A systematic review. *Tunnelling and Underground Space Technology*, 161, 106530.
- [5] Sadick, A. M., & Issa, M. H. (2018). Assessing physical conditions of indoor space enclosing elements in schools in relation to their indoor environmental quality. *Journal of Building Engineering*, 20, 520-530.
- [6] Langston, C., Wong, F. K., Hui, E. C., & Shen, L. Y. (2008). Strategic assessment of building adaptive reuse opportunities in Hong Kong. *Building and environment*, 43(10), 1709-1718.
- [7] Tan, Z., Roberts, A. C., Christopoulos, G. I., Kwok, K. W., Car, J., Li, X., & Soh, C. K. (2018). Working in underground spaces: Architectural parameters, perceptions and thermal comfort measurements. *Tunnelling and Underground Space Technology*, 71, 428-439.
- [8] Zhou, Y., & Zhao, J. (2016). Assessment and planning of underground space use in Singapore. *Tunnelling and Underground Space Technology*, 55, 249-256.
- [9] D'Amico, A., Bergonzoni, G., Pini, A., & Currà, E. (2020). BIM for healthy buildings: An integrated approach of architectural design based on IAQ prediction. *Sustainability*, 12(24), 10417.
- [10] Opoku, D. G. J., Perera, S., Osei-Kyei, R., Rashidi, M., Bamdad, K., & Famakinwa, T. (2024). Digital twin for indoor condition monitoring in living labs: University library case study. *Automation in Construction*, 157, 105188.
- [11] Aguilar, A. J., de la Hoz-Torres, M. L., Ruiz, D. P., & Martínez-Aires, M. D. (2022). Monitoring and assessment of indoor environmental conditions in educational building using building information modelling methodology. *International Journal of Environmental Research and Public Health*, 19(21), 13756.
- [12] Tang, S., Shelden, D. R., Eastman, C. M., Pishdad-Bozorgi, P., & Gao, X. (2019). A review of building information modeling (BIM) and the internet of things (IoT) devices integration: Present status and future trends. *Automation in Construction*, 101, 127-139.
- [13] Tender, M. L., & Couto, J. P. (2016). "Safety and health" as a criterion in the choice of tunnelling method.
- [14] Chen, K., Lu, W., Peng, Y., Rowlinson, S., & Huang, G. Q. (2015). Bridging BIM and building: From a literature review to an integrated conceptual framework. *International Journal of Project Management*, 33(6), 1405-1416.
- [15] Rice, L. (2021). Healthy BIM: the feasibility of integrating architecture health indicators using a building information model (BIM) computer system. *Archnet-IJAR: International Journal of Architectural Research*, 15(1), 252-265.
- [16] Abioye, S. O., Oyedele, L. O., Akanbi, L., Ajayi, A., Delgado, J. M. D., Bilal, M., ... & Ahmed, A. (2021). Artificial intelligence in the construction industry: A review of present status, opportunities and future challenges. *Journal of Building Engineering*, 44, 103299.

- [17] Petticrew, M., & Roberts, H. (2008). Systematic reviews in the social sciences: A practical guide. John Wiley & Sons.
- [18] Chen, H., Dong, Z., & Chan, I. Y. (2025). Biometric Evaluation and Immersive Construction Environments: A Research Overview of the Current Landscape, Challenges, and Future Prospects. *Journal of Construction Engineering and Management*, 151(7), 03125005.
- [19] Martin, M.L., Prince, A.A., Frimpong, S. and Thomas, N.S., 2025. Material Passports in Construction Waste Management: A Systematic Review of Contexts, Stakeholders, Requirements, and Challenges. *Buildings*, 15(11), p.1825.
- [20] Čulić, A., Nižetić, S., Gambiroža, J. Č., & Šolić, P. (2025). Progress in data-driven thermal comfort analysis and modeling. *Energy and Buildings*, 327, 115599.
- [21] Darko, A., Chan, A. P., Adabre, M. A., Edwards, D. J., Hosseini, M. R., & Ameyaw, E. E. (2020). Artificial intelligence in the AEC industry: Scientometric analysis and visualization of research activities. *Automation in Construction*, 112, 103081.
- [22] Gero, J. (Ed.). (2012). Design optimization. Elsevier.
- [23] Minassian, R., Mihăiță, A. S., & Shirazi, A. (2025). Optimizing indoor environmental prediction in smart buildings: A comparative analysis of deep learning models. *Energy and Buildings*, 327, 115086.
- [24] Zhang, Y., Chen, J., Liu, H., Chen, Y., Xiao, B., & Li, H. (2024). Recent advancements of human-centered design in building engineering: A comprehensive review. *Journal of Building Engineering*, 84, 108529.
- [25] Pandey, D. K., Hassan, M. K., Kumari, V., Zaied, Y. B., & Rai, V. K. (2024). Mapping the landscape of FinTech in banking and finance: A bibliometric review. *Research in International Business and Finance*, 67, 102116.
- [26] Ghahramani, A., Castro, G., Karvigh, S. A., & Becerik-Gerber, B. (2018). Towards unsupervised learning of thermal comfort using infrared thermography. *Applied Energy*, 211, 41-49.
- [27] Li, D., Menassa, C. C., & Kamat, V. R. (2017). Personalized human comfort in indoor building environments under diverse conditioning modes. *Building and Environment*, 126, 304-317.
- [28] D'Oca, S., & Hong, T. (2014). A data-mining approach to discover patterns of window opening and closing behavior in offices. *Building and Environment*, 82, 726-739.
- [29] Pigliautile, I., Casaccia, S., Morresi, N., Arnesano, M., Pisello, A. L., & Revel, G. M. (2020). Assessing occupants' personal attributes in relation to human perception of environmental comfort: Measurement procedure and data analysis. *Building and Environment*, 177, 106901.
- [30] Jayathissa, P., Quintana, M., Abdelrahman, M., & Miller, C. (2020). Humans-as-a-sensor for buildings—intensive longitudinal indoor comfort models. *Buildings*, 10(10), 174.
- [31] Aryal, A., & Becerik-Gerber, B. (2019). A comparative study of predicting individual thermal sensation and satisfaction using wrist-worn temperature sensor, thermal camera and ambient temperature sensor. *Building and Environment*, 160, 106223.
- [32] Asadi, E., Da Silva, M. G., Antunes, C. H., Dias, L., & Glicksman, L. (2014). Multi-objective optimization for building retrofit: A model using genetic algorithm and artificial neural network and an application. *Energy and buildings*, 81, 444-456.
- [33] Chaudhuri, T., Soh, Y. C., Li, H., & Xie, L. (2020). Machine learning driven personal comfort prediction by wearable sensing of pulse rate and skin temperature. *Building and Environment*, 170, 106615.
- [34] Somu, N., Sriram, A., Kowli, A., & Ramamritham, K. (2021). A hybrid deep transfer learning strategy for thermal comfort prediction in buildings. *Building and Environment*, 204, 108133.
- [35] Wei, Y., Jang-Jaccard, J., Xu, W., Sabrina, F., Camtepe, S., & Boulic, M. (2023). LSTM-autoencoder-based anomaly detection for indoor air quality time-series data. *IEEE Sensors Journal*, 23(4), 3787-3800.
- [36] Park, H., & Park, D. Y. (2022). Prediction of individual thermal comfort based on ensemble transfer learning method using wearable and environmental sensors. *Building and Environment*, 207, 108492.
- [37] Valinejadshoubi, M., Moselhi, O., Bagchi, A., & Salem, A. (2021). Development of an IoT and BIM-based automated alert system for thermal comfort monitoring in buildings. *Sustainable Cities and Society*, 66, 102602.
- [38] Quintana, M., Schiavon, S., Tartarini, F., Kim, J., & Miller, C. (2023). Cohort comfort models—Using occupant's similarity to predict personal thermal preference with less data. *Building and Environment*, 227, 109685.
- [39] Chinazzo, G., Andersen, R. K., Azar, E., Barthelmes, V. M., Becchio, C., Belussi, L., ... & Wei, S. (2022). Quality criteria for multi-domain studies in the indoor environment: Critical review towards research guidelines and recommendations. *Building and Environment*, 226, 109719.

## DIGITAL INTELLIGENCE EMPOWERS THE DEVELOPMENT AND UTILIZATION OF UNDERGROUND SPACE IN MEGACITIES

**Take the innovative practice of the refined management and control system of the National Exhibition and Convention Center (Shanghai) and the surrounding underground space as an example**

Yiqun Fan<sup>1</sup>, Li Zhang<sup>2</sup>

**Abstract:** This study focuses on the digital development of underground spaces in mega cities. Through the research of comprehensive risk management technology and multi subject collaborative governance system for large underground spaces with multiple and diverse functions, a comprehensive risk assessment model and emergency management capability assessment model for underground spaces based on the perspective of "human machine environment management" were constructed. A "scenario response" emergency decision-making model and an agile governance collaborative system were proposed. In terms of key technology research and development, we have broken through technical bottlenecks such as cloud based elastic architecture, multimodal data fusion, and BIM/CIM lightweighting, and developed a full lifecycle refined management platform that integrates intelligent travel guidance, accurate simulation of waterlogging risks, and multi-dimensional visualization analysis. The platform has achieved intelligent optimization of travel guidance, dynamic warning of waterlogging, and 3D visualization decision support in the demonstration application at the National Convention and Exhibition Center (Shanghai), significantly improving the efficiency of spatial management and emergency response capabilities during large-scale events, and providing innovative solutions for the sustainable development of underground spaces in mega cities.

**Keywords:** underground space, refined control, building information model, city information model

### 1. INTRODUCTION

With the acceleration of China's new urbanization process, the scale of urban underground space development continues to expand. By the end of 2023, a total of 3.276 billion square meters of urban underground space had been built across the country[1], with an additional 1.07 billion square meters added during the 13th Five-Year Plan period, and a development investment of 8 trillion yuan. Underground space has formed a multi-form infrastructure system including pipelines, transportation, civil defense, etc., and has become an important carrier for the safe operation of the city. However, the rapid expansion has led to the lack of resilience of underground space and the lack of multi-department collaborative management mechanism, and it is urgent to build a refined governance system for the whole life cycle.

Taking the National Exhibition and Convention Center (Shanghai) as a demonstration case, this study constructs a comprehensive risk assessment model of underground space from the four-dimensional perspective of "man-machine-environment-management" (personnel-facilities-equipment-environment-management), and integrates the risk matrix method, analytic hierarchy process-fuzzy comprehensive evaluation method to achieve quantitative analysis of multi-source risk factors. A multi-subject collaboration mechanism based on agile governance theory is innovatively proposed. Build a full-chain management system that includes emergency

<sup>1</sup> PhD, Fan Yiqun, Engineering Mechanics, Professor-level senior engineer, Shanghai Municipal Engineering Design Institute (Group) Co., Ltd., No. 901 Zhongshan North 2nd Road, Yangpu District, Shanghai, China, fanyiqun@smedi.com

<sup>2</sup> PhD, Zhang Li, Communication and Information Systems, senior engineer, Shanghai Municipal Engineering Design Institute (Group) Co., Ltd., No. 901 Zhongshan North 2nd Road, Yangpu District, Shanghai, China, zhangli3@smedi.com

capability assessment and scenario response decision-making model. At the level of technology research and development, breakthroughs have been made in the three core technology groups, including the research and development of an IoT (Internet of Things) sensing system that supports cloud-based elastic architecture and multi-protocol adaptation, the construction of an intelligent diagnosis platform for cross-temporal and spatial data fusion, and the development of a three-dimensional visual decision-making system based on Building Information Modeling (BIM)/City Information Model (CIM).

The smart platform built in the application demonstration stage integrates technologies such as the Internet of Things, GIS, and artificial intelligence, and significantly improves the efficiency of facility operation and maintenance and emergency response capabilities through data linkage and system integration, providing replicable solutions for the refined and intelligent management of urban underground space.

## **2. THE CURRENT SITUATION AND CHALLENGES OF THE DEVELOPMENT OF DIGITAL AND INTELLIGENT INTEGRATION OF UNDERGROUND SPACE**

### **2.1. Policy support and technical pathways**

At the national level, promote the digital transformation of urban underground space through multi-dimensional policies. The "13th Five-Year Plan for the Development and Utilization of Urban Underground Space" and the guidance of the Ministry of Housing and Urban-Rural Development clearly put forward the goal of achieving full coverage of the comprehensive management information platform by 2025. The CIM Basic Platform Technical Guidelines and the Outline of the Construction of Real 3D China construct a 3D digital space foundation and provide a unified technical framework for underground space development[2,3].

The digital application system of the whole life cycle includes three stages: planning and design, construction management, and monitoring and operation and maintenance [4]. In the planning and design stage, BIM+GIS technology realizes 3D visualization of geological information, and cross-section partition stitching modeling and multidimensional dynamic analysis technology significantly improve the design accuracy. In the construction management stage, the 3D digital disclosure system reduces the rework rate, and the intelligent equipment collects data in real time to ensure construction safety. In the monitoring and operation and maintenance stage, drones, optical fiber sensing and other technologies build a cloud data collection system.

At present, there are three major trends in technology convergence: 5G IoT enables real-time perception of underground space, digital twin technology builds a virtual mirror system, and intelligent algorithms improve the accuracy of risk prediction [5]. In the future, it is necessary to break through the bottlenecks of unified data standards, cross-departmental collaboration, and security assurance.

### **2.2. Application scenarios and bottlenecks**

The current core application scenarios of BIM technology include [6,7,8,9]:

1. Construction of scientific planning system: Through the integration of underground pipe network, existing buildings and geological data, a three-dimensional visual decision-making model is constructed to achieve pre-research and comparison of multiple schemes. With the help of parametric design and high-simulation simulation, the spatial layout and structural form are optimized, and the transformation of underground space planning from empirical decision-making to data-driven is promoted.

2. All-discipline collaborative design: Establish an interactive mechanism for multi-discipline BIM models such as buildings, structures, and equipment, and develop standardized design processes. Through data verification and model integration, the accurate transmission of design results at each stage is ensured, and the collaborative design efficiency of complex underground projects is significantly improved.

3. Construction life cycle management:

(1) Intelligent review system: realize digital delivery, intelligent verification and authority management

(2) 4D construction simulation: dynamic optimization of resource allocation and construction plan rehearsal

(3) Visual supervision: real-time monitoring of progress and three-dimensional layout of the construction site

(4) Completion management: Establish a digital file system through model comparison and analysis and correlation with acceptance data

4. Smart platform operation and maintenance:

(1) Space management: concealed engineering visualization and maintenance process simulation

(2) Monitoring and early warning: integrated sensors to achieve real-time monitoring of the environment and equipment status

(3) Emergency management: disaster scenario simulation and intelligent planning of evacuation paths

In terms of the bottlenecks and challenges of professional integration development, they mainly include[10,11]:



1. Deficiencies in the institutional system: the definition of underground space ownership and management rights is vague, there is a lack of unified management standards, and the legal subject of data ownership is not clear, which restricts the efficiency of resource integration and development.

2. Weak data foundation: there is a lack of systematic system for underground facilities and geological surveys, data is scattered and the update is lagging behind, and the cross-departmental coordination mechanism has not yet been established, forming an information island.

3. Limitations of technology application: the development of domestic core modeling software is lagging behind, the compatibility standard is missing, the digital twin technology has not yet achieved full life cycle coverage, and the maturity of special analysis tools for underground environment is insufficient.

In the future, with the in-depth development of the digital economy, BIM technology will be deeply integrated with digital twins, AI, IoT, etc., to build a complete industrial chain covering planning, design, construction, operation and maintenance. Promote the improvement of legislation and the unification of standards through policies, accelerate the digital transformation of underground space, and achieve efficient allocation and sustainable development of resources.

### 3. IN THE CONTEXT OF DIGITAL INTELLIGENCE, COMPREHENSIVE RISK MANAGEMENT AND CONTROL TECHNOLOGY FOR MULTI-COMPLEX AND LARGE-SCALE UNDERGROUND SPACE AND MULTI-SUBJECT COLLABORATIVE GOVERNANCE SYSTEM

The closed, systematic, and complex nature of underground space exposes it to multiple risks such as natural disasters, equipment failures, and human errors [12]. Based on the analysis framework of the "human-machine-environment-management" system, this paper provides innovative solutions for improving urban safety and resilience by constructing a theoretical system of underground space risk management and control [13]. The instructions are as follows:

#### 3.1. Construction and application of comprehensive risk assessment model for underground space

##### 3.1.1. Design of four-dimensional risk indicator system

In this study, the Delphi method and field investigation were used to construct a four-dimensional evaluation system including physical attributes, operating status, safety management, and environmental factors. The physical property dimension covers five indicators, such as structural durability (such as concrete carbonization depth) and seismic grade. The running status dimension includes three dynamic indicators, such as equipment failure rate and intelligent sensing device coverage. In the dimension of safety management, 6 system indicators such as the completeness of emergency plans and training coverage are set; Two natural indicators, such as groundwater level and land subsidence, were included in the dimension of environmental factors. The weight of each index was determined by analytic hierarchy process, in which the equipment failure rate and land subsidence degree were the key risk factors. Table 1 shows the indicators for assessing the comprehensive risk possibility of underground space.

**Table 1.** Comprehensive Risk Probability Assessment Indicators for Underground Space

First-level indicator ( $P_i$ )	Weight of first-level indicator ( $W_i$ )	Second-level indicator ( $P_{ij}$ )
physical property ( $P_1$ )	$W_1$	Construction time of facilities and equipment ( $P_{11}$ )
		Defects in facility and equipment design ( $P_{12}$ )
		Ground activity situation ( $P_{13}$ )
		Occupation of buildings ( $P_{14}$ )
		Facility and equipment setup ( $P_{15}$ )
running state ( $P_2$ )	$W_2$	Integrity level of facilities and equipment ( $P_{21}$ )
		Intelligent perception device ( $P_{22}$ )
		Daily operation and maintenance ( $P_{23}$ )

safety management ( $P_3$ )	$W_3$	Management system ( $P_{31}$ )
		Emergency plan ( $P_{32}$ )
		Professional competence of personnel ( $P_{33}$ )
		Guarantee funding situation ( $P_{34}$ )
		Suitable for teaching exercises ( $P_{35}$ )
		Information system ( $P_{36}$ )
environmental impact ( $P_4$ )	$W_4$	Degree of ground subsidence ( $P_{41}$ )
		Possible occurrence of severe weather conditions ( $P_{42}$ )

### 3.1.2. Risk matrix and AHP-FCE integrated assessment method

Innovative use of AHP-FCE method and risk matrix method to evaluate the comprehensive risk of underground space.

Through the analytic hierarchy process, the weight of the probability index is assigned, and the probability score  $P$  of the comprehensive risk of underground space is obtained. The formula for assessing the potential for comprehensive risk of underground space is as follows:

$$P = \sum_{i=1}^4 (W_i (\sum_{j=1}^n W_{ij} P_{ij})) \quad (1)$$

Among them,  $W_i$  is the weight of the first-level indicator,  $W_{ij}$  is the weight of the second-level indicator, and  $P_{ij}$  is the score of the second-level indicator.

Through the analytic hierarchy process, the weight of the consequence index is assigned to the consequence score of the comprehensive risk of underground space  $C$ . The formula for assessing the comprehensive risk and consequences of underground space is as follows:

$$C = \sum_{i=1}^4 W_i C_i \quad (2)$$

Among them,  $W_i$  is the weight of the first-level index, and  $C_i$  is the score of the first-level index.

According to the probability and consequences of the occurrence of risk factors in underground space, the risk level is determined by drawing a risk matrix map.

The formula for the risk value of risk factor  $i$  for underground space is:

$$R_i = f(P_i, C_i) = P_i * C_i \quad (3)$$

Taking a subway transfer station as an example, through 10 years of historical data statistics, the calculated risk value of facility aging is  $R=3.2$  ( $P=2.8$ ,  $C=1.1$ ), which is at the level II risk level. Combined with Monte Carlo simulation technology, the probability of high-risk events in the next five years is predicted to be 12.3%, which is 27% more accurate than the traditional method.

### 3.1.3. An empirical study on the risk assessment of rainstorm disasters

Taking an underground space in Shanghai as the research object, a spatial risk matrix containing 12 evaluation units was constructed. The results show that the risk level of the low-lying area reaches level I, and mobile drainage units need to be configured. The underground garage has a risk level of III, which can be reduced to level IV by optimizing the drainage system. This study provides accurate data support for urban flood control planning, and promotes the establishment of a "red, yellow and blue" three-color early warning mechanism.

## 3.2. Innovation of underground space emergency management capacity assessment system

### 3.2.1. Six-dimensional competency assessment framework

Based on the ISO 22301 standard, a six-dimensional evaluation system including organization and management, risk prevention and control, monitoring and early warning, emergency response, recovery and

reconstruction, and public participation is constructed. An evaluation scale containing 32 third-level indicators was developed, and the entropy weight method was used to determine the weights, in which monitoring and early warning ability and cross-departmental coordination were the core capability dimensions. Figure 1 shows the index system for the evaluation of underground space emergency management capacity.

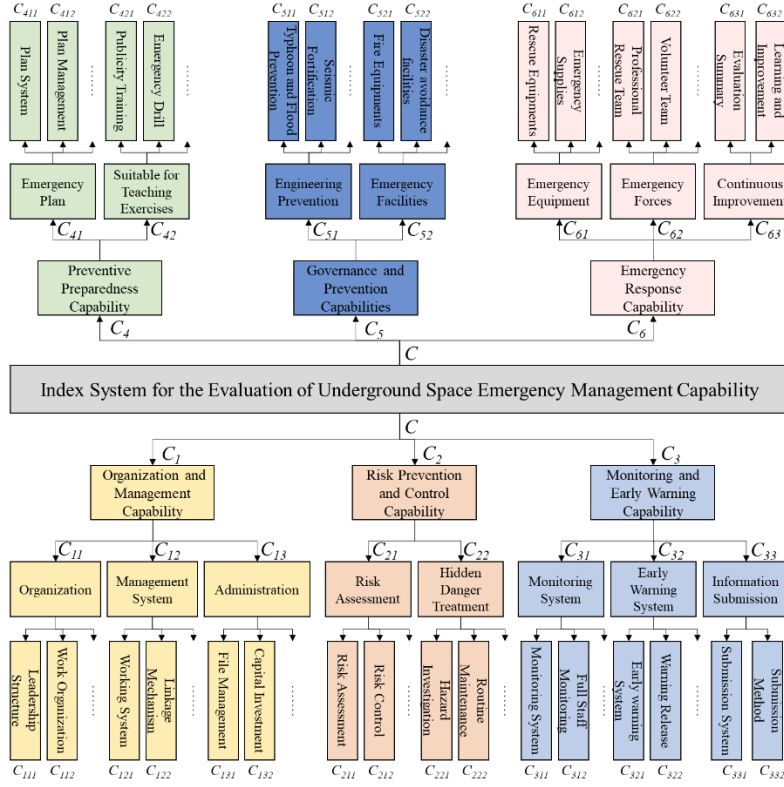


Figure 1. Evaluation index system of underground space emergency management capacity

### 3.2.2. Construction of underground space emergency management capacity assessment model

According to the evaluation index system, the evaluation formula for underground space emergency management capacity is as follows:

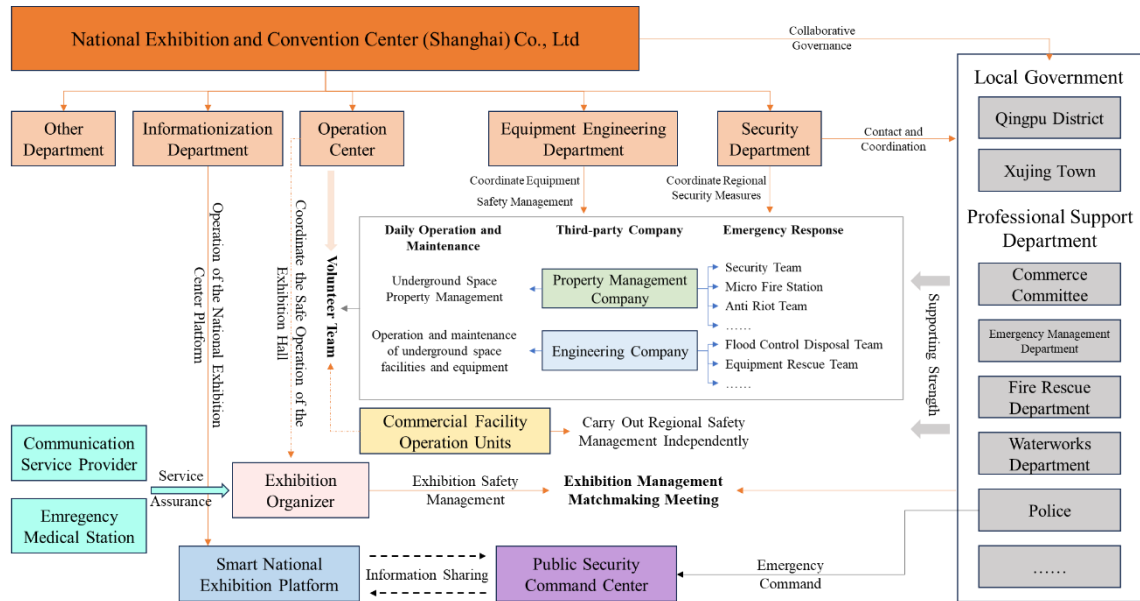
$$M = \sum_{i=1}^6 (\omega_i (\sum_{j=1}^n \omega_{ij} (\sum_{k=1}^m \omega_{ijk} M_{ijk}))) \quad (4)$$

Among them:  $\omega_i$  is the weight of the first-level index,  $\omega_{ij}$  is the weight of the second-level index, and  $\omega_{ijk}$  is the weight of the third-level index;  $M_{ijk}$  is a three-level indicator score.

### 3.3. Construction of a multi-subject collaborative governance system

#### 3.3.1. The multi-subject governance system of the International Exhibition Center

The multi-dimensional and complex system governance elements of the underground space of the International Exhibition Center from planning, construction, operation and service to emergency and disaster prevention are studied, and a multi-subject governance system of underground space is constructed [13], as shown in Figure 2.



**Figure 2.** The multi-subject governance structure of the National Exhibition and Convention Center

Design a data link with event governance as the core, and form a response plan for the collaborative governance of multiple subjects in underground space. It is planned to communicate with the International Exhibition Center to further improve the content of the plan.

### 3.3.2. Agile governance mechanism innovation

Establish a closed-loop management mechanism of "monitoring, research, judgment, disposal, and evaluation", and rely on the CIM platform to achieve cross-departmental data sharing. In the management of the underground space in the International Exhibition Center and the surrounding area, the data of 8 departments, including water affairs, emergency response, and transportation, were integrated, and the risk response time was reduced from 1 hour to 15 minutes.

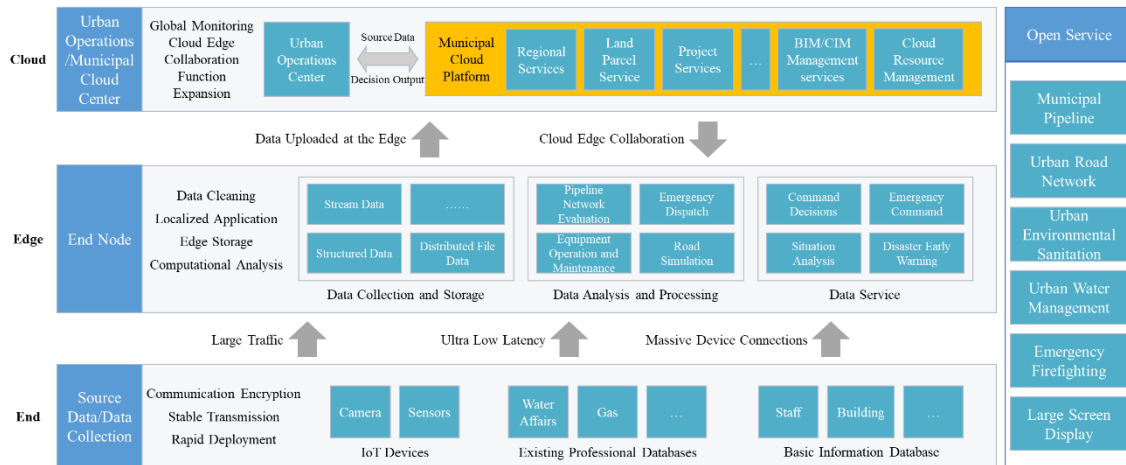
## 4. RESEARCH ON THE KEY TECHNOLOGIES OF THE WHOLE LIFE CYCLE FINE MANAGEMENT PLATFORM OF MULTI-COMPLEX FUNCTIONS AND LARGE-SCALE UNDERGROUND SPACE

Through the deep integration of IoT sensing, intelligent diagnosis and digital twin technology, a full-life cycle management platform for large-scale underground space with multiple complex functions is built, providing a new paradigm for urban safety and resilience construction.

### 4.1. Architectural innovation of IoT data ubiquitous access system

#### 4.1.1. Elastic cloud-edge collaboration architecture:

The refined management system of the whole life cycle of multiple complex functions and large-scale underground space adopts the "cloud-edge-end" architecture. This is shown in the figure below.



**Figure 3.** Overall system architecture

Through the "cloud-edge collaboration" mode, the tasks and interactions between the three levels are reasonably planned, and a large number of computing and processing work is placed at the edge, which reduces the pressure of data backhaul and data processing on the cloud platform, and at the same time reduces the coupling degree between various services, realizes resource deployment according to business needs, increases program running performance, and reduces the overall delay of data processing.

#### 4.1.2. Multimodal protocol adaptation technology

Develop protocol conversion middleware to realize real-time conversion of industrial protocols such as RS485 and OPC UA and MQTT IoT protocol. The device access module supports the hybrid access of 2G/3G/4G, NB-IoT, LoRa, WiFi and other networks according to different data communication connection modes of IoT terminal equipment, so as to realize large-scale access to various types of terminal devices in the IoT sensing layer.

### 4.2. Algorithm breakthrough of intelligent diagnosis system

#### 4.2.1. Martimodar beat him to Fucion Moder

The risk inference method and state intelligent diagnosis technology of municipal facilities based on multi-modal cross-spatiotemporal scale massive data include the following three aspects:

1. Improve the extraction of cross-temporal and spatial data information: The key features of historical time series data are analyzed by feature extraction technology, and the data sparsely distributed in geographic space is further supplemented based on expert knowledge. It is mainly used to solve the problems of incomplete raw data information and serious noise interference.

2. Multimodal data fusion analysis and utilization: The microservice analysis module with distributed characteristics is used to process multi-modal data in different scenarios. This process can be combined with some non-professional data, such as considering holidays, meteorological and other data, to assist in data prediction.

3. Iterative optimization based on massive data: Based on the machine learning model, the operation status analysis algorithm of municipal facilities is constructed, and the model is continuously trained and updated with massive data to realize its iterative optimization ability. It can realize trend prediction of massive data over a long period of time.

#### 4.2.2. Microservice-based intelligent applications

12 independent microservice modules are developed, and each module opens API interfaces for front-end access, which ensures the scalability of the system, and has the characteristics of low coupling and strong reusability.

#### 4.2.3. Predictive maintenance systems

An equipment health assessment model based on digital twins was constructed to improve the predictive maintenance coverage and reduce the equipment failure rate in the wind turbine monitoring of an underground parking lot in Shanghai. The system dynamically optimizes maintenance strategies through reinforcement learning, saving a lot of O&M costs every year.



### 4.3. BIM/CIM-driven emergency response platform construction

#### 4.3.1. BIM/CIM-driven spatiotemporal big data engine

Developed distributed 3D spatial index technology to support second-level loading of 100GB BIM models. In the underground space project in Qianhai, Shenzhen, the smooth browsing of 2 million square meters of models was realized. The rendering optimization algorithm developed based on the OpenSceneGraph engine stabilizes the frame rate of complex scenes at more than 60 fps.

#### 4.3.2. Digital twin emergency deduction

A digital twin of underground space containing hundreds of dynamic parameters was constructed to accurately predict the smoke diffusion path in the fire simulation of an underground transportation hub in Shanghai, and guide the optimization of the design of three evacuation channels. Monte Carlo simulations allow you to evaluate the effects of different contingency scenarios in less than 15 minutes.

#### 4.3.3. Linkage disposal of multi-source information

Establish an intelligent response mechanism of "risk early warning, plan matching, and resource scheduling". The hierarchical response system for emergency response includes functions such as incident scale assessment, response level determination, and emergency resource allocation, as shown in Figure 4.

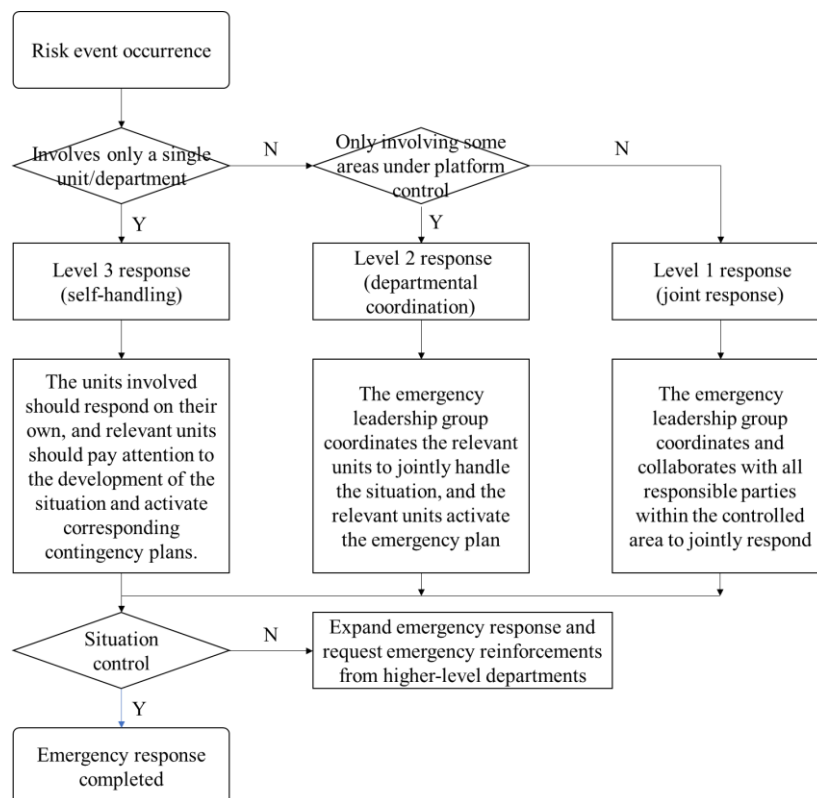


Figure 4. Hierarchical response process for emergency response

## 5. APPLICATION DEMONSTRATION: THE INNOVATIVE PRACTICE OF THE REFINED MANAGEMENT AND CONTROL SYSTEM OF THE NATIONAL EXHIBITION AND CONVENTION CENTER (SHANGHAI)

In today's accelerating urbanization, the underground space of super-large urban complexes has become the "lifeline" of urban operation. As the world's largest convention and exhibition complex, the underground space of the National Exhibition and Convention Center (Shanghai) carries the functions of traffic guidance, commercial operation and emergency support for tens of thousands of people per day. In 2023, the annual exhibition area will

exceed 7 million square meters, accounting for more than 40% of Shanghai's total operating data, posing unprecedented challenges to the management of underground space. In the face of complex crowd dynamics, extreme weather threats, and facility operation and maintenance pressures, the traditional management model has been difficult to adapt to demand. In this context, the "National Convention and Exhibition Center and the Surrounding Underground Space Refined Management and Control System" came into being, and through the integration of multi-source data and cutting-edge technology, an intelligent solution for underground space governance was built.

### 5.1. Technical Architecture: a multi-dimensional integrated intelligence hub

With the core concept of "data-driven and intelligent decision-making", the system has built a technical architecture system of "one core and three wings". Its core lies in building a standardized data platform, integrating multi-source heterogeneous data from transportation, meteorology, municipal, security and other fields, and realizing real-time data processing through edge computing. The dynamic enhanced knowledge graph technology endows the system with self-learning ability, which can automatically associate data from different fields to form a digital twin model of underground space operation. The containerized microservice architecture ensures the scalability and flexibility of the system and supports the rapid iterative upgrade of functional modules.

Three core modules constitute the "three wings of wisdom" of the system: Through the integration of 2.5D indoor maps and 3D outdoor models, the smart travel module realizes centimeter-level positioning and navigation; Based on the two-dimensional linkage simulation technology, the waterlogging risk module constructs a digital sand table of the urban drainage system. The Visual Analytics module uses a real-time rendering engine to transform complex data into intuitive and easy-to-understand 3D scenes. This architecture design not only meets the current management needs, but also reserves the technical interface for future expansion.

### 5.2. Functional innovation: intelligent upgrade of underground space management

#### 5.2.1. Smart Mobility: From Passive Guidance to Proactive Optimization

The system breaks through the limitations of the traditional static identification system and builds a dynamic navigation service system. Through real-time simulation analysis of the evacuation of large passenger flow of the exhibition, combined with dynamic guidance, seamless above-ground and underground navigation is realized. In the 2024 auto show test, the system predicts the exit pressure of the subway station through the passenger flow simulation model, and dynamically adjusts the channel opening strategy, so that the crowd density in key areas is greatly reduced.

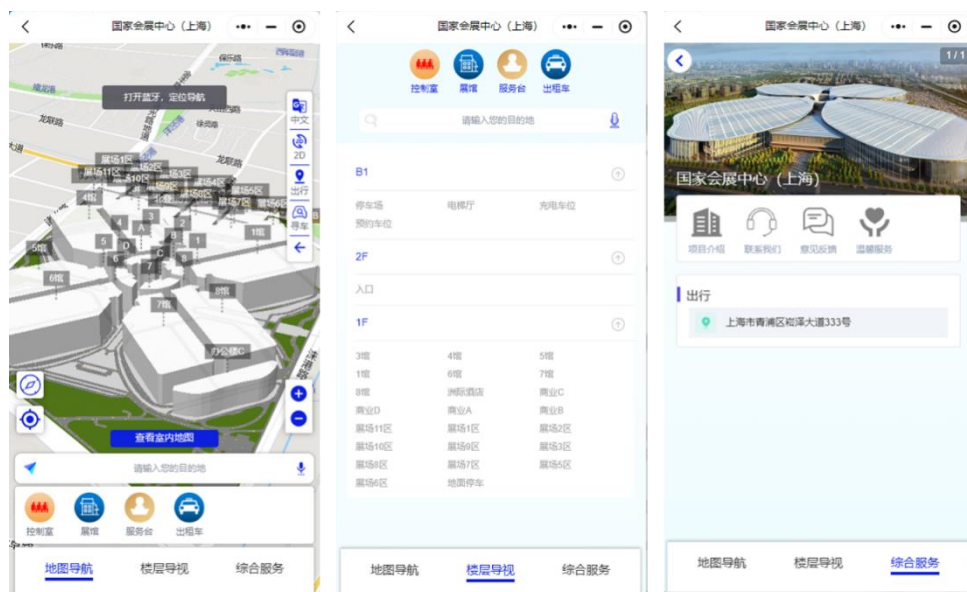


Figure 5. Smart mobility applet

### 5.2.2. Waterlogging prevention and control: from emergency response to risk pre-control

In view of the frequent extreme weather in the Yangtze River Delta region, a full-chain prevention and control system of "monitoring-simulation-early warning-disposal" has been systematically constructed. In the inversion of the "7 • 21" rainstorm in 2023, the error between the calculated water depth and the measured data was less than 5%, and 5 key water accumulation points were successfully located. Through the simulation of the 50-year rainstorm scenario, the system identifies three low-lying flood-prone areas, which provides a quantitative basis for the renovation of the pipe network. The intelligent scheduling algorithm can generate the optimal emergency plan within 10 minutes, which shortens the response time by 40% compared with the traditional mode.



Figure 6. Simulation of waterlogging risk in the waterlogging risk module

### 5.2.3. Visual decision-making: from data stacking to scenario insights

The 3D visualization platform integrates 12 types of dynamic data such as sunshine analysis, weather simulation, and human flow heat, and supports multi-dimensional scene switching. In foundation pit monitoring, the real-time linkage between BIM model and sensor data is used to achieve millimeter-level deformation early warning. The Flood Simulation Module dynamically demonstrates the process of water level rise and visualizes the difference in the effect of different flood control measures. This immersive, interactive experience enables managers to make scientific decisions quickly in extreme weather.

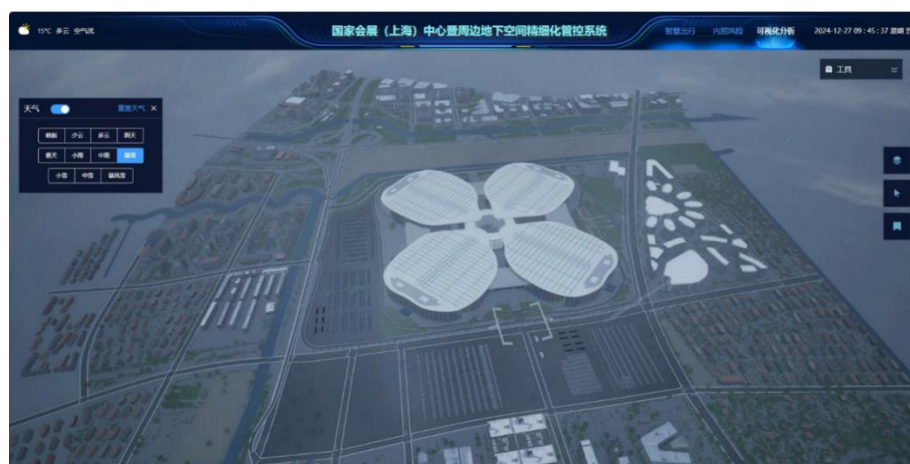


Figure 7. The weather system simulates rainstorm weather

### 5.3. Application results: from technological innovation to management change

Since its operation, the system has proven its value in multiple scenarios. In terms of safety and security, the early warning of waterlogging successfully predicted the process of heavy rainfall and avoided major economic losses. Significantly improved efficiency, smart travel shortens peak travel time, and parking lot turnover is accelerated; Optimized decision-making, assisted in the formulation of plans and reduced the duration of temporary traffic control; At the same time, it is green and low-carbon, and effectively saves energy consumption and reduces carbon emissions through intelligent linkage.

## 6. CONCLUSIONS

In this study, the National Exhibition and Convention Center (Shanghai) and the surrounding underground space are used as a pilot to carry out technical verification and form a replicable solution, including the establishment of technical standards for special scene monitoring, the realization of green and low-carbon operation management, and the verification of the applicability of the whole life cycle control technology in complex environments. The research value and innovation lie in constructing the theoretical system of underground space life cycle management, innovating the integration of multi-system collaborative governance and holographic perception technology, promoting the transformation of underground space management from passive response to active prevention and control, and providing standardized technical support for urban renewal. This study provides theoretical support and practical paradigm for the sustainable development of underground space in megacities, and the relevant results have been applied to the refined urban management of Shanghai, effectively improving the safety resilience and management efficiency of underground space.

In the future, we can further deepen the research on cross-regional data sharing mechanisms, explore the in-depth application of AI in complex scenarios, and promote the collaborative optimization of low-carbon technologies and intelligent management.

## 7. ACKNOWLEDGEMENTS

This research was supported by Shanghai 2022 "Science and Technology Innovation Action Plan" Social Development Science and Technology Key Project (22dz1203500).

## 8. BIBLIOGRAPHY

- [1] Strategic Consulting Center of Chinese Academy of Engineering, Underground Space Branch of Chinese Society of Rock Mechanics and Engineering, & Underground Space Planning Branch of China Urban Planning Society (2024). "2024 Blue Book of China's Urban Underground Space Development." Urban Planning Society of China. <https://www.planning.org.cn/news/view?id=16315>.
- [2] Ministry of Housing and Urban-Rural Development of the People's Republic of China (2021). "The Ministry of Housing and Urban-Rural Development issued the Technical Guidelines for City Information Modeling (CIM) Basic Platforms (Revised Edition)." Chinese government website. [https://www.gov.cn/xinwen/2021-06/14/content\\_5617553.htm](https://www.gov.cn/xinwen/2021-06/14/content_5617553.htm).
- [3] Ministry of Natural Resources of the People's Republic of China (2021). "Outline of Construction Technology of Real 3D China (2021 Edition)" The Paper. [https://www.thepaper.cn/newsDetail\\_forward\\_14093637](https://www.thepaper.cn/newsDetail_forward_14093637).
- [4] Li J. (2024). Research on the whole process management of highway construction based on BIM technology. Volkswagen Standardization, 22, 148-150.
- [5] Zeng S., Su D., & Gong H. (2025). Application and research progress of digital twin technology in the operation and maintenance stage of urban underground space. Tunnel Construction, 1, 57-76.
- [6] Ma Y., Yang J., & Cheng R. (2024). Application of BIM technology in construction of building engineering. Popular Science, 10, 44-46.
- [7] Cai M. (2022). Research on the Application of BIM Technology in Urban Underground Space Management. China Construction Informatization, 18, 73-75.
- [8] Guan X. (2016). Discussion on the Planning of Underground Space in Smart City Based on BIM Concept. Sichuan Building Materials, 42(8), 64-65.
- [9] Su X., Cai H., & Guo D. (2014). Application of BIM technology in urban underground space development. Journal of PLA University of Science and Technology (Natural Science Edition), 15(3), 219-224.
- [10] An W. (2022). Discussion and Reflection on the Digitization Path of Urban Underground Space Elements: A Case Study of Shanghai. Shanghai Land & Resources, 43(2), 107-112.

- [11] Yang H., Jiang Y., & Li Z. (2021). Research on the development strategy of comprehensive management of underground space development. *Strategic Study of Chinese Academy of Engineering*, 23(4), 126-136.
- [12] She L. (2017). Urban Comprehensive Disaster Prevention and Underground Space Risk Early Warning Management. *Urban and Rural Development*, 12, 59-61.
- [13] Shanghai Municipal Engineering Design & Research Institute (Group) Co., Ltd., & School of Social Development and Public Policy, Fudan University. (2024). "Digital Intelligence Empowers the Development and Utilization of Underground Space in Megacities". Scientific Research Project of Shanghai Municipal Commission of Housing and Urban-Rural Development.



## MODELING OF PUBLIC PERCEPTION IN METRO-LED UNDERGROUND PUBLIC SPACE FOR PLANNING OPTIMIZATION: A CASE STUDY OF HONG KONG

PAN Qi<sup>1</sup>, DONG Yunhao<sup>2</sup>, NG Shiu-Tong Thomas<sup>3</sup>, PENG Fangle<sup>4</sup>

**Abstract:** Metro-led underground public spaces (MUPS) have become integral components of modern urban environments, particularly in high-density cities. However, their enclosed nature and artificial characteristics present various challenges affecting user experience and well-being. While traditional surveys and questionnaires have provided valuable insights into public perception of these spaces, such methods are often resource-intensive and limited in scale. This study proposes an innovative framework for evaluating public perception in MUPS by leveraging social media data and Large Language Model (LLM) technology. We developed a six-dimensional perception indicator system termed “FEPICS” (Functionality, Engagement, Pleasurability, Inclusiveness, Comfort, and Safety), encompassing 37 distinct indicators. Using Google Maps review data from eight metro stations along Hong Kong’s Tsuen Wan Line, we employed LLM-based classification methods to extract and quantify public perception information, achieving a semantic recognition accuracy of 91.4%. Our analysis revealed that the “Functionality” dimension received the highest public attention, while “Inclusiveness” and “Comfort” garnered relatively less focus. The indicator “transfer” demonstrated the highest positive perception value, whereas “crowd congestion” exhibited the strongest negative sentiment. Through our perception evaluation index, we identified Jordan and Tsim Sha Tsui stations as best performers, attributable to their superior environmental design elements despite high crowding levels. These findings highlight the importance of balancing functional efficiency with environmental quality in MUPS design. The proposed FEPICS framework and LLM-based methodology offer a systematic approach for understanding and quantifying public perception in underground spaces, contributing to evidence-based planning practices. This study demonstrates the potential of integrating social media analytics with advanced language models for urban perception research, while providing practical insights for optimizing underground public space development.

**Keywords:** metro-led underground public space, social media data, public perception, large language model

### 1. INTRODUCTION

Metro-led underground public spaces, encompassing transportation hubs, pedestrian networks, retail areas, and other facilities within metro systems, have become integral to modern urban environments (Bobylyev, 2016, Dong et al, 2021). These spaces address land scarcity and growing transportation demands in high-density cities while serving as dynamic venues for shaping urban experiences (Ma et al, 2023, Liu et al, 2024, Shao et al, 2024). They play a crucial role in enhancing spatial vitality and improving regional livability (Dong et al, 2023). However, their enclosed nature and artificial environmental characteristics challenges such as crowding perception, insufficient spatial orientation, and thermal imbalances, directly impacting user experience and well-being

<sup>1</sup> PhD candidate, Qi PAN, Geotechnical Engineering, student, Department of Geotechnical Building and Engineering, Tongji University, 1239 Siping Road, P.R. China, Department of Architecture and Civil Engineering, City University of Hong Kong, 83 Tat Chee Avenue, Hong Kong SAR, P.R. China, [2211146@tongji.edu.cn](mailto:2211146@tongji.edu.cn).

<sup>2</sup> PhD, Yun-Hao DONG, Geotechnical Engineering, postdoc, Department of Geotechnical Building and Engineering, Tongji University, 1239 Siping Road, P.R. China, Department of Architecture and Civil Engineering, City University of Hong Kong, 83 Tat Chee Avenue, Hong Kong SAR, P.R. China, [yunhdong@cityu.edu.hk](mailto:yunhdong@cityu.edu.hk).

<sup>3</sup> PhD, Shiu-Tong Thomas NG, Smart and Sustainable Construction, professor, Department of Architecture and Civil Engineering, City University of Hong Kong, 83 Tat Chee Avenue, Hong Kong SAR, P.R. China, [thomasng@cityu.edu.hk](mailto:thomasng@cityu.edu.hk)

<sup>4</sup> PhD, Fang-Le PENG, Geotechnical Engineering, professor, Department of Geotechnical Building and Engineering, Tongji University, 1239 Siping Road, P.R. China, [pengfangle@tongji.edu.cn](mailto:pengfangle@tongji.edu.cn)

(Jasińska and Kłosek-Kozłowska, 2024). These challenges underscore the need for a comprehensive understanding of public perception.

Recent years have witnessed growing scholarly attention to public perception of underground spaces. Jalón et al. (2019) employed face-to-face surveys to collect multi-dimensional perception preference data regarding spatial quality, temperature, cleanliness, and seating facilities from diverse occupational groups using metro and bus systems. Liu et al. (2025) gathered safety perception dimensions of metro imagery through volunteer-based safety scoring. Zeng et al. (2025) utilized on-site questionnaires to collect public perception data on physical environment and satisfaction levels in underground complexes. While these studies provide valuable public perspective insights for optimizing multifunctional underground spaces, traditional data collection methods, though robust, are time and resource-intensive. The widespread application of social media data has introduced new possibilities for studying public perception. Su et al. (2025) proposed a machine learning-assisted text mining approach to transform unstructured social media reviews into structured urban behavioral insights. Guo et al. (2025) employed geo-tagged social media data to characterize public perception hotspots and their spatial distribution patterns. Yin et al. (2024) conducted sentiment analysis on COVID-19 vaccination-related tweets using OpenAI's large language models to explain the geographical distribution of emotional gradients. However, attempts to utilize social media data for underground space public perception mining remain limited. While Pan et al. (2025) proposed a method integrating social media and academic literature data to model public cognition knowledge graphs for underground public spaces, current research lacks a systematic quantitative evaluation framework that can directly guide planning practices.

To address these research gaps, this study aims to establish a perception evaluation framework tailored to metro-led underground public spaces and develop a quantitative modeling method for public perception using social media data and LLM technology. Specifically, this research addresses the following questions:

- (1) What are the key dimensions of perception in metro-led underground public spaces?
- (2) How can LLM technology extract and quantify perception information from social media data?
- (3) How can the quantitative model of public perception inform underground public space planning?

The remainder of this paper is structured as follows: **Section 2** outlines the methodology, including the development of the “FEPICS” perception indicator system and the LLM-based framework for public perception modeling. **Section 3** presents the results of quantitative analyses and evaluations of metro-led underground public spaces. **Section 4** discusses the implications of the findings for planning practices and identifies methodological limitations. Finally, **Section 5** summarizes the main contributions of this research.

## 2. MATERIAL AND METHODS

### 2.1. Research framework

Our study uses review data from the Google Maps platform as the data source. Google Maps is one of the most widely used digital mapping services, with a broad user base and a comprehensive geographical information database in Hong Kong, including location information for subway stations and a significant amount of user reviews. Additionally, Google Maps provides diverse data APIs, making it convenient to structure public comments using NLP techniques and Python.

We collected over 3,000 user reviews from eight subway stations in Hong Kong. From this initial dataset, we utilized NLP techniques to intelligently clean many meaningless or blank invalid comments. Building on previous research, we innovatively proposed a six-dimensional conceptual model, which includes “Functionality”, “Engagement”, “Pleasurability”, “Inclusiveness”, “Comfort”, and “Safety” (FEPICS). This model was expanded to include a perception indicator system for metro-led underground public spaces, comprising 37 indicators.

Based on the aforementioned data and theoretical foundation, we employed LLMs to structurally model public perception information for the eight subway stations. Subsequently, we defined and quantitatively analyzed the public perception heat and preferences, proposing a perception index value and an underground public space perception evaluation index based on this analysis. The framework of this method is illustrated in **Figure 1**.

### 2.2. Study area and data preparation

This study focuses on the Tsuen Wan Line in the Hong Kong Special Administrative Region, selecting eight representative subway stations for in-depth research (**Figure 2**). As a leading global metropolis with high density, Hong Kong has a subway system that has developed over more than 50 years, making its underground public spaces significant for research and reference. The Tsuen Wan Line, Hong Kong's first cross-sea railway, was completed in 1982 and serves as a crucial transportation artery connecting the Kowloon Peninsula and Hong Kong

Island. The line spans 16,9 kilometers and has 16 stations, with an average daily ridership of 944.100 (Hong Kong Legislative Council).

The selected representative stations along the Tsuen Wan Line are: Sham Shui Po, Prince Edward, Mong Kok, Yau Ma Tei, Jordan, Tsim Sha Tsui, Admiralty, and Central. These stations cover two core areas: Kowloon (from Sham Shui Po to Tsim Sha Tsui) and Hong Kong Island (Admiralty and Central), both of which experience extremely high passenger density. Additionally, the study sites encompass various urban typologies, including traditional retail areas (Mong Kok), modern business districts (Admiralty and Central), residential neighborhoods (Sham Shui Po and Prince Edward), tourist hotspots (Tsim Sha Tsui), and mixed-use areas (Yau Ma Tei and Jordan). These locations have been developed over different periods and exhibit significant variations in population density, commercial characteristics, and development patterns, adding substantial research value. These differences may impact the public's experience and perception of underground public spaces. Therefore, comparative research on these stations will help reveal the differing public perception characteristics of various types of underground public spaces, providing valuable insights for future planning and optimization.

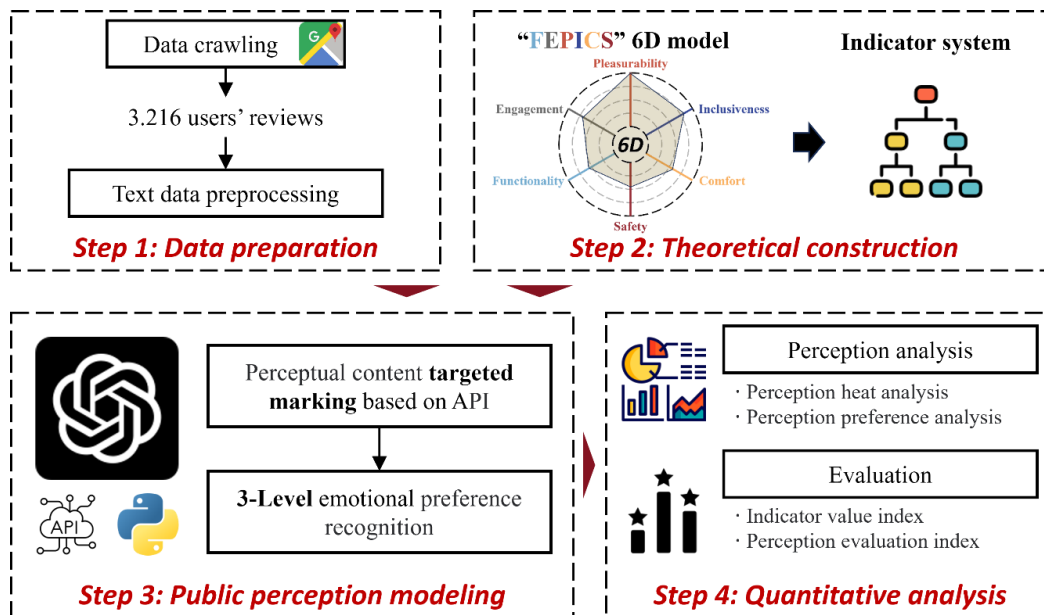


Figure 1. Methodological framework

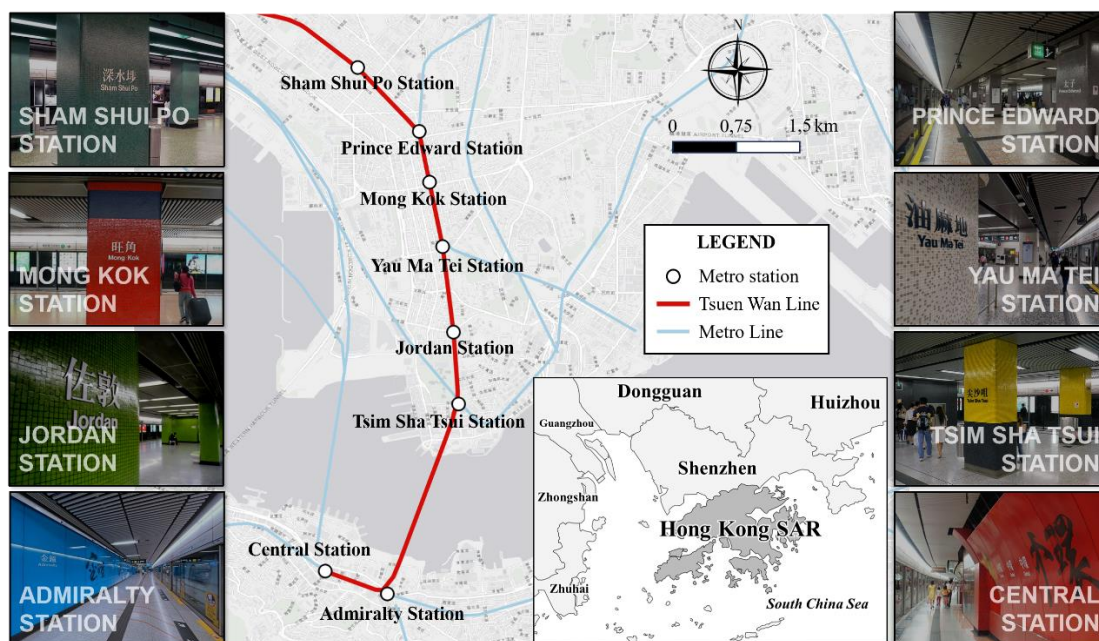


Figure 2. Methodological framework

We utilized the API provided by Google Maps (<https://www.google.com.hk/maps/>) to scrape all review data for the eight subway stations mentioned above, resulting in a total of 3,216 entries. Each review contains: [user ID, user rating star level, user review]. After applying NLP techniques to automatically filter out comments that were meaningless or blank, we obtained a total of 1,429 valid reviews. The number of valid reviews for each subway station is shown in **Table 1**.

*Table 1. The volume of valid reviews for each metro station*

Station	Sham Shui Po	Prince Edward	Mong Kok	Yau Ma Tei	Jordan	Tsim Sha Tsui	Admiralty	Central
num	216	62	267	127	114	218	209	216

## 2.3. Indicator system for public perception of MUPS

### 2.3.1. “FEPICS” perception model

Based on Mehta's (2014) five-dimensional model of public spaces (“Inclusiveness”, “Meaningful Activities”, “Safety”, “Comfort”, “Pleasurability”), this study develops a six-dimensional perception model termed “FEPICS,” which includes “Functionality”, “Engagement”, “Pleasurability”, “Inclusiveness”, “Comfort”, and “Safety”.

Firstly, the significance of spatial functionality in planning and design research necessitates the inclusion of the “Functionality” dimension, particularly given the transportation-centric nature of subway stations. Furthermore, this study reinterprets the “Meaningful Activities” dimension from Mehta's model as “Engagement” to more accurately capture the interaction between individuals and underground public spaces. The “FEPICS” model retains Mehta's dimensions of “Pleasurability”, “Inclusiveness”, “Comfort”, and “Safety”, while revising the elements within each dimension to better reflect the characteristics of underground public spaces in subway stations. This adaptation enhances the model's relevance and applicability, providing a comprehensive framework for evaluating public perception in these unique environments.

### 2.3.2. Indicator system for perception of MUPS

Building on previous research on public and underground spaces, we have innovatively developed a six-dimensional perception indicator system for underground public spaces, termed “FEPICS”. This comprehensive framework encompasses 37 distinct indicators, as illustrated in **Table 2**.

## 2.4. Quantitative modeling for public perception of MUPS

### 2.4.1. Public perception modeling

People's comments on different subway stations carry their perceived imagery and perceived conception. To better visualize and quantify public perception imagery, we refer to the public perception indicator system (see **Table 2**). Additionally, we categorize the perception context into three emotional tendencies, namely “positive”, “neutral”, and “negative”.

We designed a targeted classification extraction method for perceived imagery based on ChatGPT API technology (see **Figure 3**). Using Python to call the API, we carefully crafted prompts to input the review text data from various subway stations, allowing the LLM to automatically identify and extract perceived imagery corresponding to the indicators in **Table 2**. Furthermore, we determined emotional tendencies based on the user ratings associated with each comment (1-2 stars: negative; 3 stars: neutral; 4-5 stars: positive). We selected 100 reviews for manual classification and verification, finding that ChatGPT achieved a semantic recognition accuracy of 91.4% within the classification framework established for this study.

We stored the extracted perception content for the various subway stations using a multivalued dictionary data structure. In this structure, the 37 indicators serve as keys, while the extracted perceived imagery and perceived conception are stored in separate imagery and conception dictionaries, with perceived imagery and emotional scores as their respective values. We systematically processed the review data for the eight subway stations in Hong Kong, establishing quantitative models of public perception for each station. This approach allows for a structured analysis of the perceived attributes associated with each station, facilitating a deeper understanding of how different factors influence public sentiment and experience in metro-led underground public spaces.



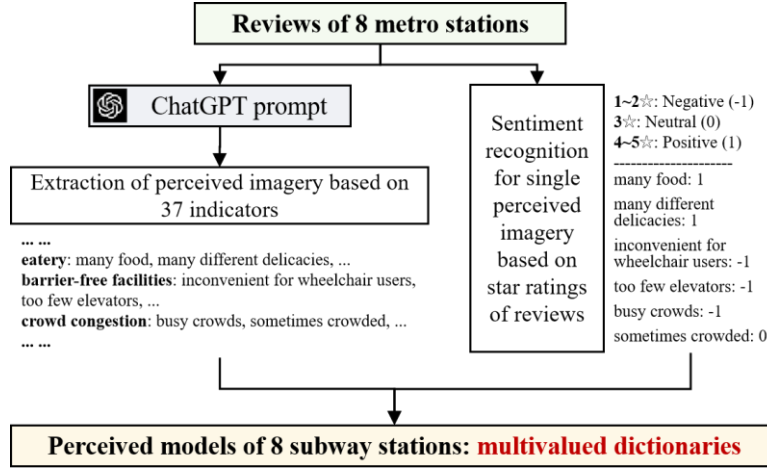


Figure 3. Public perception modeling workflow

#### 2.4.2. Quantitative analysis of perception

Firstly, to measure the public's perception heat for different dimensions and indicators, we define the perception frequency  $PF_{ij}$ . Here,  $i = 1, \dots, 37$ , represents the 37 perception indicators, and  $j = 1, \dots, 8$ , refers to the eight subway stations.  $PF_{ij}$  represents the count of perception content corresponding to the  $i$  indicator in the comment data for the  $j$  subway station. The weight calculation is shown in Equation (1):

$$w_i = \frac{\sum_{j=1}^8 PF_{ij}}{\sum_{i=1}^{37} \sum_{j=1}^8 PF_{ij}} \quad (1)$$

Secondly, based on the perception conception dictionary, we define the perception emotional preference index  $PP$ . Its calculation is presented in Equations (2) and (3):

$$PP_{ij} = \frac{1 \cdot n_{ij+} + 0 \cdot n_{ij0} + (-1) \cdot n_{ij-}}{n_{ij+} + n_{ij0} + n_{ij-}} \quad (2)$$

$$PP_i = \sum_{j=1}^8 \frac{N_j}{N} PP_{ij} \quad (3)$$

Here,  $n_{ij+}$  represents the count of positive perception content for the  $i$  indicator at the  $j$  subway station,  $n_{ij0}$  denotes the count of neutral perception content for the  $i$  indicator at the  $j$  subway station, and  $n_{ij-}$  indicates the count of negative perception content for the  $i$  indicator at the  $j$  subway station.  $N_j$  represents the total number of valid comments for the  $j$  subway station, with  $N$  set to 1.429, reflecting the total number of valid comments across these 8 subway stations.

#### 2.4.3. Quantitative evaluation of metro-led underground public spaces

To comprehensively evaluate the public perception of metro-led underground public spaces, we define the value index of perception indicators  $VP_i$ . Its calculation is presented in Equation (4):

$$VP_i = PP_i * w_i \quad (4)$$

Based on this, we further define the perception evaluation index of the subway station  $EP_j$ , with its calculation shown in Equation (5):

$$EP_j = \sum_{i=1}^{37} PP_{ij} * VP_i \quad (5)$$



### 3. RESULTS

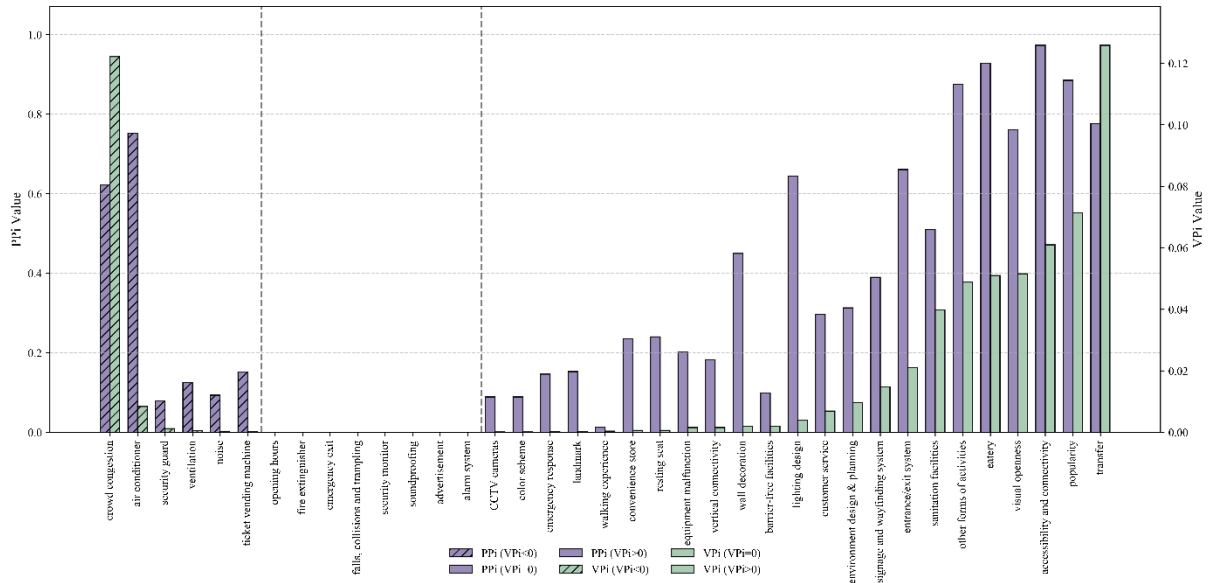
#### 3.1. Analysis of indicator system

We calculated the weights for each indicator according to Equation (1), and the results are presented in **Table 2**. It is evident that the public is most concerned about the “Functionality” dimension, while there is comparatively less attention given to “Inclusiveness” and “Comfort”.

*Table 2. “FEPICS” perception indicator system*

Dimensions	Perceptions	Indicators	weight_I	weight_D
Functionality	signage system clarity	signage and wayfinding system	0,038	0,325
	restroom needs	sanitation facilities	0,078	
	barrier-free design	barrier-free facilities	0,020	
	traffic efficiency	walking experience	0,027	
		transfer	0,162	
Engagement	social activity	popularity	0,081	0,218
	dining attraction	convenience store	0,003	
		eatery	0,055	
	other functions	customer service	0,023	
		ticket vending machine	0,001	
		other forms of activities	0,056	
Pleasurability	unique imagery design	wall decoration	0,004	0,182
		advertisement	0	
		landmark	0,001	
	visual appeal	lighting design	0,006	
		color scheme	0,001	
		environment design & planning	0,031	
	openness and connectivity	accessibility and connectivity	0,063	
		vertical connectivity	0,009	
		visual openness	0,068	
Inclusiveness	entrance and exit convenience	entrance/exit system	0,032	0,032
	opening hours	opening hours	0	
Comfort	sufficiency of rest seats	resting seat	0,003	0,021
	thermal comfort	air conditioner	0,011	
		ventilation	0,004	
	acoustic comfort	noise	0,003	
		soundproofing	0	
Safety	surveillance coverage	CCTV cameras	0,001	0,221
		security monitor	0	
	security trustworthiness	security guard	0,015	
		emergency response	0,001	
	traffic risks	equipment malfunction	0,008	
		crowd congestion	0,197	
		falls, collisions and trampling	0	
	disaster prevention and risk management	emergency exit	0	
		fire extinguisher	0	
		alarm system	0	

Subsequently, we computed the perception preference index  $PP_i$  and the perception value index  $VP_i$  for each indicator, with the results illustrated in **Figure 4**.



**Figure 4.** Perception preference index ( $PP_i$ ) and value index ( $VP_i$ ) of indicators

From **Figure 4**, we can observe that the indicator with the highest positive  $VP_i$  is “transfer”, while “crowd congestion” exhibits the greatest negative  $VP_i$ . Furthermore, indicators such as “opening hours” and “fire extinguisher” have a zero  $VP_i$ .

### 3.2. Modeling for public perception of metro-led underground public spaces

We further illustrated the perception distribution across the eight subway stations in Hong Kong. The perception heat is depicted in **Figure 5**, while the perception preferences are shown in **Figure 6**.



**Figure 5.** Perception frequency

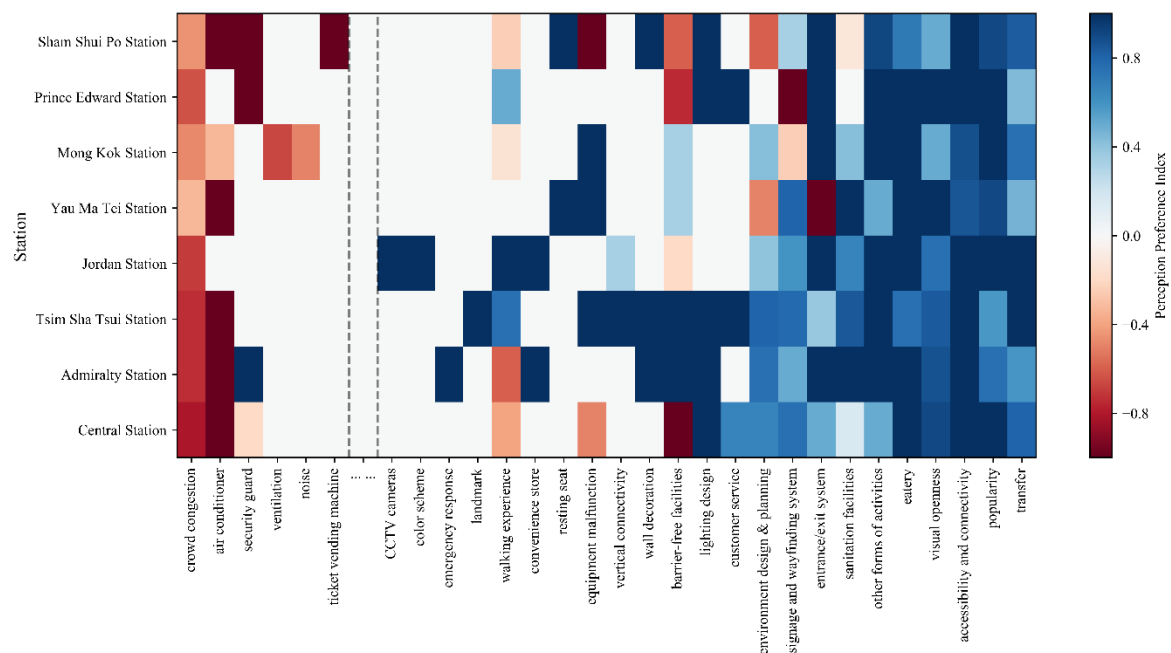


Figure 6. Perception preference

We omitted certain indicators with a zero  $VP_i$  to reduce blank spaces in the figures. It is evident that “crowd congestion” has the highest perception heat at Mong Kok Station, with a negative sentiment. In contrast, “transfer” has the highest perception heat at Admiralty Station, accompanied by a positive sentiment.

### 3.3. Evaluation of perceived metro-led underground public spaces

We evaluated the eight metro-led underground public spaces in Hong Kong using the perception evaluation index  $EP_j$ , with the results presented in Table 3:

Table 3. “FEPICS” perception indicator system

Station	Sham Shui Po	Prince Edward	Mong Kok	Yau Ma Tei	Jordan	Tsim Sha Tsui	Admiralty	Central
<b>EP</b>	0,420	0,434	0,448	0,381	0,544	0,536	0,514	0,504

Among them, Jordan Station and Tsim Sha Tsui Station received the highest  $EP_j$ , while Yau Ma Tei Station had the lowest.

## 4. DISCUSSION

### 4.1. Insights from perception quantification results for underground public space planning

Through the analysis of Google Maps review text data for eight popular metro-led underground public spaces along the Tsuen Wan Line in Hong Kong, we observed that the public exhibits notable enthusiasm for certain indicators, such as “transfer” and “crowd congestion”. However, the emotional attitudes towards these two indicators differ significantly. From Figure 6, it is evident that all subway stations have a positive sentiment towards “transfer”, while “crowd congestion” is associated with negative sentiment. This indicates that the public is relatively satisfied with the transfer functionality at these eight subway stations, aligning with the initial objectives of underground public space development. Conversely, the indicators with negative sentiment highlight existing issues in the utilization of metro-led underground public spaces. To further examine these issues, we



perception. Furthermore, this method's capacity for processing large-scale, real-time data could support more responsive and evidence-based urban planning practices, particularly in the context of smart city development.

## 5. CONCLUSION

This study developed an innovative framework for evaluating public perception of metro-led underground public spaces through the integration of social media analytics and LLM technology. By developing the six-dimensional "FEPICS" perception indicator system and constructing a corresponding quantitative modeling framework, we systematically analyzed Google Maps reviews from eight metro stations along Hong Kong's Tsuen Wan Line. This analysis identified key factors influencing public perception and their implications for urban planning, offering valuable insights into how different dimensions shape user experiences in underground spaces. Our methodology not only addresses the growing need for evidence-based underground space evaluation but also provides a replicable framework for understanding and quantifying public perception in complex urban environments. Specifically, our research demonstrates the following:

(1) The development of the FEPICS perception evaluation framework, which expands upon Mehta's five-dimensional model by incorporating "Functionality" and reinterpreting "Meaningful Activities" as "Engagement", provides a comprehensive system for evaluating public perception in metro-led underground spaces. This six-dimensional framework, encompassing 37 distinct indicators, offers a nuanced understanding of public perception across functional and experiential dimensions.

(2) Our LLM-based perception modeling approach, combining ChatGPT API technology with targeted classification extraction methods, achieved a semantic recognition accuracy of 91.4%, demonstrating the effectiveness of automated perception analysis from social media data. This methodological innovation enables efficient and scalable analysis of public sentiment in underground spaces.

(3) Quantitative analysis revealed significant variations in perception across different dimensions and stations. The "Functionality" dimension received the highest attention (weight = 0.325), with "transfer" emerging as the most positively perceived indicator. Conversely, "crowd congestion" exhibited the strongest negative perception, highlighting critical areas for improvement in underground space management.

(4) Station-specific evaluation identified Jordan and Tsim Sha Tsui stations as best performers, attributable to their superior environmental design elements despite high crowding levels. This finding underscores the importance of balanced development addressing both functional efficiency and environmental quality.

While our study provides valuable insights for underground space planning optimization, we acknowledge limitations in data source diversity and temporal coverage. Future research should explore multiple data sources and integrate temporal analysis to capture more comprehensive perception patterns. Additionally, investigating the interdependencies between perception indicators could enhance our understanding of how different aspects of underground spaces interact to shape overall public experience. Despite these limitations, our FEPICS framework and LLM-based methodology offer a robust foundation for evidence-based planning and design of metro-led underground public spaces, contributing to more user-centric urban development.

## 6. ACKNOWLEDGMENTS

This work was supported by the National Natural Science Foundation of China (NSFC) [grant number: 42301289] and [grant number: 42071251], and Hong Kong Scholars Program [grant number: XJ2023059].

## 7. REFERENCES

- [1] Bobylev, N. (2016). Underground space as an urban indicator: Measuring use of subsurface. *Tunnelling and Underground Space Technology*, 55, 40-51. <https://doi.org/https://doi.org/10.1016/j.tust.2015.10.024>
- [2] Delgado Jalón, M. L., Gómez Ortega, A., & De Esteban Curiel, J. (2019). The social perception of urban transport in the city of Madrid: the application of the Servicescape Model to the bus and underground services. *European Transport Research Review*, 11(1), 37. <https://doi.org/10.1186/s12544-019-0373-5>
- [3] Dong, Y.H., Peng, F.L., & Guo, T.F. (2021). Quantitative assessment method on urban vitality of metro-led underground space based on multi-source data: A case study of Shanghai Inner Ring area. *Tunnelling and Underground Space Technology*, 116, 104108. <https://doi.org/https://doi.org/10.1016/j.tust.2021.104108>
- [4] Dong, Y.H., Peng, F.L., Li, H., & Men, Y.Q. (2023). Spatiotemporal characteristics of Chinese metro-led underground space development: A multiscale analysis driven by big data. *Tunnelling and Underground Space Technology*, 139, 105209. <https://doi.org/https://doi.org/10.1016/j.tust.2023.105209>



- [5] Guo, C., & Yang, Y. (2025). A multi-modal social media data analysis framework: Exploring the complex relationships among urban environment, public activity, and public perception—A case study of Xi'an, China. *Ecological Indicators*, 171, 113118. <https://doi.org/https://doi.org/10.1016/j.ecolind.2025.113118>
- [6] Jasińska, K., & Kłosek-Kozłowska, D. (2024). Passengers' experience in underground non-transfer metro stations: The impact of spatial characteristics. *Tunnelling and Underground Space Technology*, 143, 105482. <https://doi.org/https://doi.org/10.1016/j.tust.2023.105482>
- [7] Liu, J., Yan, H., White, M., & Huang, X. (2025). A comparative analysis of perceptions of insecurity in Milan and Beijing metro stations. *Frontiers of Architectural Research*, 14(4), 863-884. <https://doi.org/https://doi.org/10.1016/j.foar.2024.12.003>
- [8] Liu, S.C., Peng, F.L., Qiao, Y.K., & Dong, Y.H. (2024). Quantitative evaluation of the contribution of underground space to urban resilience: A case study in China. *Underground Space*, 17, 1-24. <https://doi.org/https://doi.org/10.1016/j.undsp.2023.11.007>
- [9] Ma, C.X., Peng, F.L., Qiao, Y.K., & Li, H. (2023). Influential factors of spatial performance in metro-led urban underground public space: A case study in Shanghai. *Underground Space*, 8, 229-251. <https://doi.org/https://doi.org/10.1016/j.undsp.2022.03.001>
- [10] Mehta, V. (2014). Evaluating Public Space. *Journal of Urban Design*, 19(1), 53-88.
- [11] Pan, Q., Ng, S.T. T., Peng, F.L., & Dong, Y.H. (2025). A bottom-up approach of knowledge graph modelling for urban underground public spaces: Insights into public cognition. *Tunnelling and Underground Space Technology*, 163, 106710. <https://doi.org/https://doi.org/10.1016/j.tust.2025.106710>
- [12] Shao, Y., Ng, S. T., Xing, J., Zhang, Y., Kwok, C. Y., & Cheng, R. (2024). Dynamic station criticality assessment of urban metro networks considering predictive passenger flow. *Tunnelling and Underground Space Technology*, 154, 106088. <https://doi.org/https://doi.org/10.1016/j.tust.2024.106088>
- [13] Su, T., & Sun, M. (2025). Understanding park-based health-promoting behavior and emotion with large-scale social media data: The case of Tianjin, China. *Cities*, 162, 105987. <https://doi.org/https://doi.org/10.1016/j.cities.2025.105987>
- [14] Yin, L., Han, M., & Nie, X. (2024). Unlocking Blended Emotions and Underlying Drivers: A Deep Dive into COVID-19 Vaccination Insights on Twitter Across Digital and Physical Realms in New York, Using ChatGPT. *Urban Science*, 8(4). <https://doi.org/10.3390/urbansci8040222>
- [15] Zeng, R., Zhao, Z., Zhang, J., Shen, Z., & Luo, J. (2025). Indoor environmental quality and user satisfaction: Post-occupancy evaluation of urban underground complex. *Building and Environment*, 270, 112492. <https://doi.org/https://doi.org/10.1016/j.buildenv.2024.112492>

## INTEGRATION OF GEOGRAPHIC INFORMATION SYSTEMS (GIS) FOR UNDERGROUND SPACE MAPPING ON THE EXAMPLE OF BELGRADE

Staša Milošević<sup>1</sup>, Hristina Pićurić<sup>2</sup> and Luka Krznarić<sup>3</sup>

**Abstract:** The use of Geographic Information Systems (GIS) for underground space mapping is becoming essential in big cities where managing subterranean spaces is crucial for urban growth. Belgrade faces challenges due to its historical layers, complex infrastructure, and dense environment. GIS helps by mapping and managing underground areas such as public facilities, utility networks and transportation systems. GIS database creates detailed maps of various underground structures, helping city planners in visualizing the spatial relationships between different elements, which are essential for maintenance and new projects.

By integrating real-time data, authorities can monitor underground conditions, predict risks, and improve resilience to hazards.

Additionally, GIS enhances coordination between stakeholders, ensuring that underground infrastructure aligns with surface-level urban planning. This is particularly important for large projects like metro construction, where precise mapping is required to avoid conflicts with existing structures and ensure safety.

GIS also supports sustainable urban growth by optimizing underground space use for transportation, utilities, and infrastructure.

Therefore, Belgrade as a metropolitan city of 2 million inhabitants where important projects involving underground spaces are currently underway, represents a good case study and polygon for the implementation of a GIS system and database.

**Keywords:** underground, GIS, urban planning, innovation

### 1. INTRODUCTION

#### 1.1. Context and importance of underground spatial mapping

In the past few decades, cities have seen a drastic increase in urbanization, density and growth due to an increase in population. Cities are rapidly growing horizontally and vertically creating a strain on resources and damaging the quality of life of its inhabitants.

While underground space is not something new, it has been used traditionally for transportation and infrastructure tunnels but at large it remains an underutilized space.

Underground urban planning is the systematic development of subsurface space for urban use. Optimizing underground space relieves pressure on above ground infrastructure and opens spaces for much needed urban spaces: green and open spaces or other public facilities.

Our primary objective is to develop a comprehensive and interoperable spatial database of Belgrade's underground space

<sup>1</sup> MSc Urban planner, Milošević Staša, B.Sc Architecture, urban planner, Institute for urban planning of Belgrade, *Bulevar Despotina Stefana* 56, Belgrade, Serbia, [stasa.milosevic89@gmail.com](mailto:stasa.milosevic89@gmail.com)

<sup>2</sup> MSc Urban planner, Pićurić Hristina, B.Sc Architecture, urban planner, Institute for urban planning of Belgrade, *Bulevar Despotina Stefana* 56, Belgrade, Serbia, [hristinajovanovic26@gmail.com](mailto:hristinajovanovic26@gmail.com)

<sup>3</sup> MSc Urban planner, Krznarić Luka, B.Sc Architecture, urban planner, Institute for urban planning of Belgrade, *Bulevar Despotina Stefana* 56, Belgrade, Serbia, [lukakrznaric93@gmail.com](mailto:lukakrznaric93@gmail.com)

## 2. GIS AS A TOOL FOR URBAN PLANNING

The development of artificial intelligence and technology has greatly impacted our roles as urban planners, it has affected the speed, sorting, implementation and gathering of data that we use in planning. GIS is one tool that has become increasingly important in the process of gathering and analyzing data, it plays a transformative role in how cities are planned and managed.

With the use of data integration and visualization in spatial and urban planning we can better understand and optimize the space around us, it allows for a complete picture of our space and if used correctly can analyze and define potential problems as well as determine the value of proposed solutions.

## 3. METHODOLOGY FOR BUILDING SPATIAL DATABASE FOR UNDERGROUND SPACE IN BELGRADE

Creating a **spatial database for underground space in Belgrade** relied on a structured methodology that addresses data collection, integration, management, and application. The successful creation of a spatial database requires a multi-phase methodology that begins with identifying and engaging relevant stakeholders. These include the City of Belgrade Urban Planning Office, the Serbian Geodetic Authority, various utility providers (such as those responsible for water, gas, electricity, and telecommunications), academic institutions, and various literature. Their collaboration is essential for the integration and standardization of fragmented data sources.

The data inventory and collection phase involves both existing records and new field data acquisition. Existing data sources include utility cadastres, construction permits, geological and hydrogeological surveys and historical plans.

Once data is collected, it must be standardized and preprocessed. This involves converting diverse datasets into consistent GIS formats, georeferencing legacy and harmonizing data according to a unified coordinate reference system—typically EPSG: 32634 – WGS 84 / UTM zone 34N (used for Serbia including Belgrade in many projects with GPS coordinates in meters).

We started with basic literature analysis, the analysis of underground planning and global trends as well as detailed analysis of cities that have developed underground spaces

The analysis was carried out in multiple iterations and from various perspectives. First, a general and comprehensive analysis of a larger number of cities worldwide through their thematic frameworks: quality of life, development of underground infrastructure, integration of underground spaces into the urban landscape, preservation of green areas, sustainability of underground projects, water and waste management, technical execution, financial aspect, social acceptability and innovation.

Next, a targeted and more detailed analysis of ten cities was performed through a literature review based on a previously established matrix, which includes key characteristics of urban underground space development, such as: economic, sociological and environmental aspects, typology, use, realization mechanisms, legal framework, planning, the depth of object placement and the model of planning. Cities worldwide are using three models of urban underground space planning: incremental, independent and independent.

The most important motives for cities to develop underground have been identified based on previous research such as: climate extremes, lack of land as a resource and terrain configuration.

Specific conclusions and criteria were defined for the analysis and systematic presentation of the characteristics of existing underground spaces in Belgrade.

The database design phase focuses on developing a 3D spatial data model suitable for underground features as well as mapping existing underground spaces in Belgrade.

The data model is structured to include essential layers: utility networks (including sewage, water, electricity, and telecommunications), transportation structures (like subways and underpasses), geological strata, and underground cultural heritage sites. The database schema includes depth values, material types, construction dates, maintenance responsibility, legal constraints, and condition assessments.

Underground spaces such as basements of residential buildings, military structures and linear infrastructure at depths of up to 3 meters were not part of our study.

The implementation of the spatial database leverages GIS platforms such as PostGIS for open-source environments or ArcGIS Enterprise for advanced functionality and integration with other systems like AutoCAD Civil 3D and BIM tools.

The synthesis of the obtained data led to conclusions about the current development of underground space in Belgrade and suggested possible needs and realistic directions for future endeavors.

An analysis of planning and legal regulations, cadastral management of underground facilities, and the economic aspect of underground construction were performed, as key aspects necessary for the development of urban planning in this area.

A key step in the methodological process towards defining the areas of interest for planning and development of the underground space in Belgrade is the investigation of limitations and potentials from the aspect of natural and created characteristics, environmental conditions, regulatory framework and economic domain. The investigation of spatial limitations and potential also resulted in a graphical representation.

The synthesis of the results obtained in the previous research steps and their sublimation through a targeted set of criteria represents the final research step of our Study and results in a graphical representation of the areas of interest for planning and development of underground spaces in Belgrade.



Figure 1. Segments from the QGIS database

#### 4. IMPLEMENTATION IN THE CONTEXT OF BELGRADE

The implementation of a spatial database for underground space in Belgrade carries significant implications across multiple sectors of urban planning, infrastructure management, and disaster resilience. As a historic city with complex layers of development, Belgrade presents a compelling case for integrating Geographic Information Systems (GIS) into underground spatial planning.

One of the primary applications of such a database lies in the coordination of urban infrastructure systems. Belgrade's subsurface utility networks—including water supply, sewage, electricity, gas, and telecommunications—are often inadequately documented, especially in older and densely built neighborhoods. The development of a centralized spatial database enables planners and engineers to visualize the full extent of underground infrastructure, reducing the likelihood of spatial conflicts during excavation or maintenance activities. This approach supports safer and more efficient construction practices, mitigates service interruptions, and facilitates interdepartmental coordination by enabling all stakeholders to access a unified data environment.

Another major implementation concerns the streamlining of construction permitting processes. The current permitting system in Belgrade frequently relies on fragmented and outdated spatial data, which can lead to project delays, increased costs, and legal complications. By incorporating reliable underground data into the permitting workflow, municipal authorities can make more informed decisions. Developers and engineers can simulate construction impacts on nearby underground features and adjust designs proactively, reducing the likelihood of technical or regulatory setbacks. This shift toward data-driven permitting enhances transparency, compliance, and overall urban governance.

Transportation infrastructure development is another area where this technology can yield substantial benefits. Belgrade is currently undertaking major transportation projects, including the long-anticipated Belgrade Metro. In

such projects, accurate knowledge of the subsurface environment is essential to avoid conflicts with existing utilities, historic tunnels, or geological hazards. A GIS-based underground database allows for detailed 3D modeling, route optimization, and clash detection, thereby improving project feasibility and reducing risk during execution.

Environmental risk management is also enhanced through the application of underground spatial data. Belgrade faces several environmental challenges, including riverine flooding, soil instability, and aging infrastructure. An integrated spatial database allows for improved modeling of subsurface conditions, enabling authorities to assess the vulnerability of critical infrastructure and to develop more effective mitigation strategies. This supports the implementation of early warning systems and improves the city's capacity to respond to emergencies, particularly those involving underground assets.

Finally, this spatial database aligns with Belgrade's aspirations to evolve into a smart and sustainable city. By creating a digital twin of the underground environment, the city can support long-term urban planning, real-time asset monitoring, and predictive modeling for infrastructure maintenance and urban growth. The integration of spatial data into governance practices enables better collaboration among public institutions, private sector actors, and civil society stakeholders, fostering a more transparent, efficient, and resilient urban system.

## 5. CHALLENGES AND LIMITATIONS

Despite the substantial benefits of implementing a spatial database for underground infrastructure in Belgrade, several challenges and limitations must be acknowledged. These span technical, organizational, legal, and financial domains and can significantly affect the development, maintenance, and utility of such a system.

A primary technical challenge lies in the **incompleteness and inconsistency of existing data**. Much of Belgrade's underground infrastructure, particularly in the historical core, was developed in phases over decades with minimal documentation. Utility maps, if they exist, often vary in accuracy and may not reflect changes due to unregistered modifications or unauthorized constructions. The Republic Geodetic Authority has so far recorded underground structures only upon the request of investors. Some underground structures are represented merely as entry and exit points to the underground, without any information about their dimensions or other data that would allow determination of ownership, type of structure, purpose, area, or depth. Developing a 3D cadastre would help overcome the aforementioned obstacles. These inconsistencies present a risk of misinformation when attempting to visualize or simulate subsurface conditions (Aleksić et al., 2017). In some cases, the lack of precise depth (z-axis) data makes it difficult to construct reliable 3D models, which are essential for modern underground planning applications.

Data standardization is another significant obstacle. Institutions responsible for infrastructure—such as water, gas, telecommunications, and electricity—often use different formats, classification schemes, and coordinate systems. The absence of a legally enforced interoperability framework in Serbia complicates efforts to integrate datasets into a unified GIS platform. While national initiatives such as the Spatial Data Infrastructure of the Republic of Serbia (SDI-RS) provide some support, local implementation remains fragmented (Aleksić et al., 2017).

Institutional challenges are also considerable. Interagency cooperation in Belgrade is often hindered by **jurisdictional fragmentation**, lack of communication, and occasional competition between public and private stakeholders. This has been especially evident in large infrastructure projects such as the Belgrade Metro, where overlapping authorities and delayed decision-making have impeded progress (Suboticki & Sørensen, 2021). In the absence of formalized data-sharing agreements, many agencies remain reluctant to provide full access to their records, citing legal and security concerns.

From a legal perspective, there are **limited regulatory guidelines specifically addressing underground spatial planning** in Serbia. Existing urban planning laws primarily focus on above-ground development, and legislation governing data sharing, privacy, and security often lacks clarity or enforceability in the context of subsurface assets. This regulatory vacuum can lead to both administrative uncertainty and increased risk for developers. Also, there is also an **issue of defining ownership of underground spaces**. This Study aims to contribute to decision-making regarding the depths at which the owners of underground spaces are the same private individuals who own the above-ground spaces, while the ownership of all other underground levels belongs to the city or the state.

Financial limitations also constrain the feasibility of building and maintaining a high-quality spatial database. The technologies required—such as ground penetrating radar, 3D GIS software, and sensor-based monitoring systems—require significant upfront investment. Budgetary constraints at the municipal level can limit the continuity of data collection and hinder staff training, reducing the long-term viability of the system.

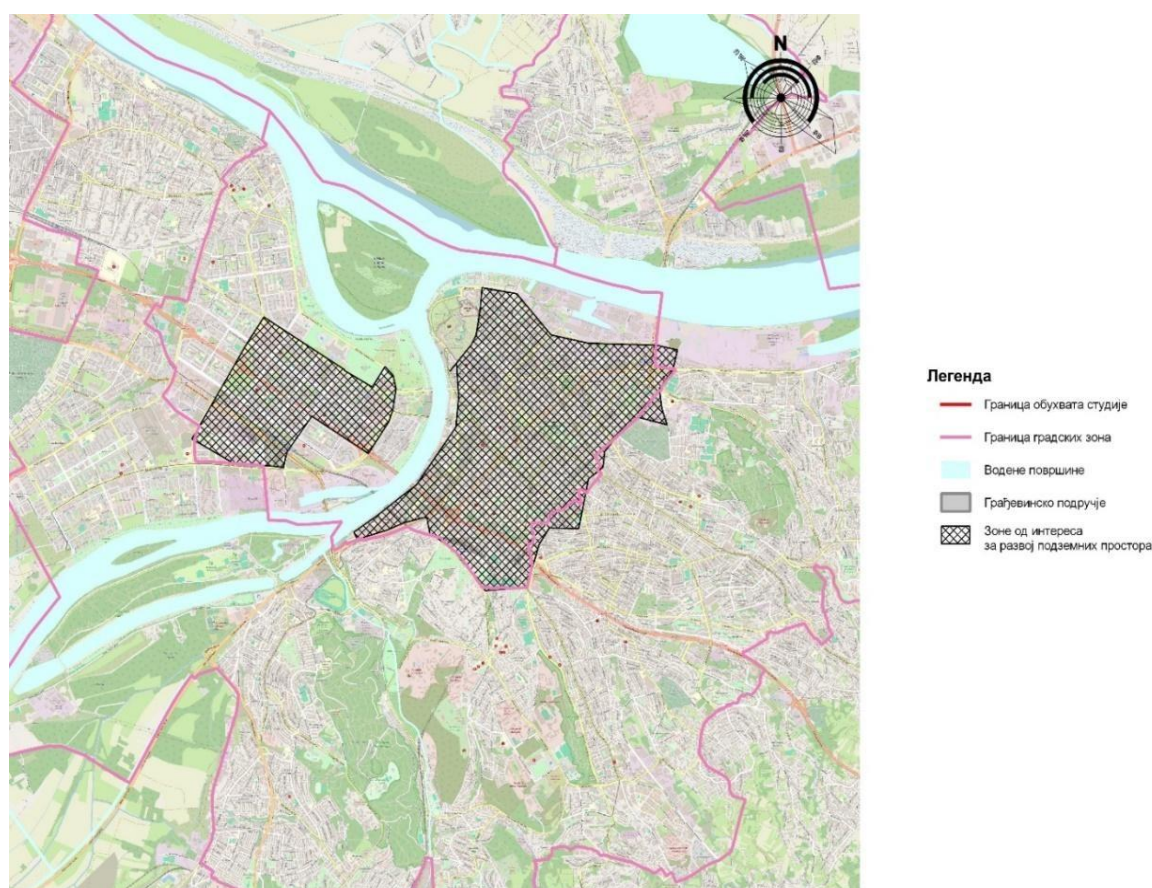


Finally, **public accessibility and digital literacy** represent potential social barriers. While the idea of a webbased GIS portal is appealing, its successful implementation depends on the availability of intuitive interfaces and ongoing public education. Without these, the system may be underutilized by planners, engineers, or citizens who could otherwise benefit from its insights.

## 6. RESULTS AND IMPLICATIONS FOR URBAN PLANNING PRACTICE

The establishment of a spatial database for underground space in Belgrade has yielded significant insights and practical benefits for urban planning and infrastructure management. The integration of historical, geotechnical, and utility datasets into a unified geospatial framework has revealed previously unknown or undocumented subsurface structures, clarified ownership boundaries, and allowed for the 3D visualization of complex underground networks. As a result, urban planners, engineers, and policymakers are now equipped with a more accurate and interactive representation of the city's subterranean environment.

One of the most impactful results has been the ability to perform **multi-layer spatial analysis**, which has greatly enhanced coordination between agencies during infrastructure planning and development. For instance, proposed projects such as the Belgrade Metro and flood-resilience upgrades in lower-lying areas have been optimized to avoid costly utility relocations and minimize excavation risks. The system has also enabled more effective **scenario modeling**, allowing planners to test the impact of different design alternatives in densely built urban cores, particularly in neighborhoods with narrow streets and overlapping underground systems. Also, one of the outcomes of the GIS database of existing underground spaces in Belgrade is the formation of a zone of interest for the further development of urban underground structures and facilities.



*Figure 2. Diagram of the zone of interest for underground planning development in Belgrade*

The availability of a dynamic underground database has improved the transparency and efficiency of the **construction permitting process**. Building permit applications can now be evaluated against a verified subsurface model, reducing the approval time and decreasing the incidence of planning errors. Developers benefit from early

warnings of spatial conflicts, such as proximity to gas pipelines or protected heritage structures, allowing them to adapt their designs at an early stage and avoid costly delays.

On a broader scale, the database has also contributed to **policy development and regulatory reform**. City authorities have begun incorporating underground space into urban master plans and land use strategies, treating the subsurface not merely as a constraint but as a functional layer of the urban environment. This shift has led to the delineation of underground development zones and the identification of areas suitable for underground parking, storage, and pedestrian passages. In turn, this has helped alleviate pressure on surface land use and facilitated more compact, vertically integrated urban growth.

Furthermore, the database has enabled Belgrade to adopt a **risk-based approach to underground infrastructure management**. By integrating geotechnical data and infrastructure condition assessments, authorities can now identify critical vulnerabilities in aging networks and prioritize maintenance interventions accordingly. This capability is particularly valuable in areas at risk of flooding, subsidence, or seismic activity, where the failure of underground systems could have cascading effects on above-ground infrastructure and public safety.

Perhaps most importantly, the successful implementation of this system has begun to foster a **culture of data sharing and interagency cooperation**. Institutions that previously operated in silos have begun to collaborate more actively, facilitated by clear data governance frameworks and shared digital tools. This institutional shift not only improves operational efficiency but also lays the groundwork for future smart city applications, including real-time monitoring, predictive maintenance, and integration with Building Information Modeling (BIM) systems.

The GIS database is an initial step in the further underground planning of the city of Belgrade and a means through which many benefits can be achieved. The maintenance of outdated infrastructure would be facilitated and improved, the construction and management of major infrastructure projects would be made easier, and an integrated approach to viewing both above-ground and underground layers would be introduced in the development of urban planning projects and documents. Public access to this data by all relevant institutions in Belgrade would also contribute to their interconnection and facilitate the assessment of the existing conditions before any interventions in the space are made.

The implications for urban planning in Belgrade are profound. With the underground environment now made legible and actionable through spatial data, planners are better equipped to manage the city's growth in a more sustainable, resilient, and spatially efficient manner. As Belgrade continues to densify and modernize its infrastructure, the underground space will increasingly serve as a strategic asset rather than a blind spot in urban policy. The experience also positions Belgrade as a regional leader in underground spatial data infrastructure, offering a transferable model for other Balkan and Eastern European cities facing similar urban challenges.

## 7. CONCLUSIONS

Belgrade is a city experiencing a growing population, increasing traffic congestion, decreasing amount of land available for the expansion of built structures and also densely built-up city center, where there is no room for new open public spaces and green areas. It is essential to guide the underground development of Belgrade in a way that allows the release of above-ground space for contemporary design solutions and planning of scarce land uses, which can integrate existing public, commercial, and residential functions without compromising the existing green infrastructure — instead, they further enhance it. Such solutions contribute to the creation of more humane and attractive spaces that ensure a healthier and higher-quality living environment.

The spatial database for Belgrade's underground space represents a critical step toward smarter and more sustainable urban development. Through the integration of GIS technology, systematic data collection, 3D modeling, and multi-agency collaboration, the city can unlock the potential of its subsurface environment. **This methodology provides a roadmap for the creation and implementation of a functional, accurate, and dynamic underground spatial data infrastructure.** With appropriate investment, policy support, and technical implementation, Belgrade can enhance urban resilience, reduce planning conflicts, and foster innovation in subsurface space management.

## 8. BIBLIOGRAPHY

- [1] Aleksić, M. M. (2017). *The significance of 3D cadastre for the development of urban underground space: A case study of Belgrade*. GeoJournal.

- [2] Baker, D. C. (2019). Integrating public utilities in urban planning: The importance of databases for effective management. *Journal of Urban Technology*, 15-29.
- [3] Bavič, J. &. (2018). *The role of GIS in urban underground space management: Challenges and prospects*.
- [4] Dale, P. F. (2017). *Spatial data infrastructures: A global perspective*. Springer.
- [5] Graham, S. &. (2020). Augmented cities and the underground: Mapping the urban future. *Environment and Planning B: Urban Analytics and City Science*, 95-117.
- [6] Suboticki, K. &. (2021). The role of interagency cooperation in infrastructure planning: Lessons from the Belgrade Metro project. *International Journal of Urban Sciences*, 191-209.

## BUILDING A NAVIGATION SYSTEM USING DIGITAL TWINS OF INFORMATION FROM ABOVE AND BELOW GROUND

Soichiro Takamine<sup>1</sup>, Suguru Miyazaki<sup>2</sup>

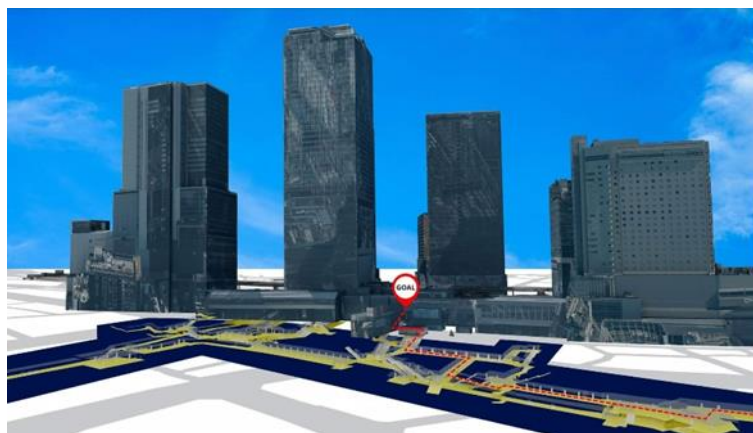
**Abstract:** In recent years, the advanced usage of underground spaces has progressed, and facilities such as underground shopping arcades, stations, and walkways, have combined to form networks covering wide areas. Furthermore, cities have developed by connecting the basement levels of buildings to underground spaces, creating urban areas where above-ground, underground, indoor, and outdoor spaces, have all become interconnected. While urban areas expect to see improvements in accessibility, complicated connections lead to issues such as maze.

In order to respond to these challenges, the Ministry of Land, Infrastructure, Transport and Tourism of Japan (MLIT) has created 3D foundation maps that combine information from above and below ground, through balancing 3D city models, BIM models, etc., and is developing and conducting proof-of-concept tests on navigation systems that use these maps, under the PLATEAU project creating digital twins of Japan cities promoted by MLIT. This paper introduces an overview of the project and the usefulness of digital twin technology for underground spaces.

**Keywords:** 3D City Model, Digital Twins, Navigation Systems, Project PLATEAU

### 1. INTRODUCTION

MLIT has been promoting “Project PLATEAU”, a project for the development, utilization, and open data of 3D city models since FY2020. The 3D city model data provided by PLATEAU has three major characteristics: “high quality (controlled accuracy as physical location and shape data of buildings, etc.)”, “structured (LOD definition as a 3D map and attribute information)”, and “open data (adoption of standardized open format)” [1].



*Figure 1. The 3D navigation system that combine information from above and below ground*

<sup>1</sup>Director, Soichiro Takamine, National Public Employee, MLIT, [takamine-s28z@mlit.go.jp](mailto:takamine-s28z@mlit.go.jp)

<sup>2</sup>Chief Official, Suguru Miyazaki, National Public Employee, MLIT, [miyazaki-s24a@mlit.go.jp](mailto:miyazaki-s24a@mlit.go.jp)

The 3D city models provided by PLATEAU are basically intended for “outdoor information” based on aerial surveys, so detailed models including “indoor information” are required depending on the intended use. In response, PLATEAU has defined architectural models (LOD4) that is compatible with IFC2 × 3, the international standard for BIM models, through verification studies conducted in previous years, and enables linkage (conversion and integration) with BIM data [2].

Regarding navigation systems utilizing 3D city models, Yan, Zlatanova et al. (2021) demonstrated that by constructing an integrated 3D space-based navigation model (U3DSNM) for a university campus, a navigation system can be realized across different spaces (facilities) such as indoor, semi-indoor, semi-outdoor, and outdoor environments [3]. However, a navigation system that constructs 3D foundation maps across the ground and underground for actual large urban spaces, and further incorporates indoor positioning technology, has yet to be demonstrated.

In this verification, we constructed 3D foundation maps that seamlessly integrates the existing 3D city models of the area and the converted 3D city models based on BIM data across the ground and underground. And we developed a 3D navigation system based on the infrastructure incorporating indoor positioning technology (Figure 1). This paper presents an overview of the system, its validation results, and the usefulness of digital twin technology in underground spaces.

## 2. SYSTEM OUTLINE

The 3D navigation system is based on the “Tokyo Station Navi” provided by JR East Consultants Company and has been modified to additionally implement (1) 3D navigation functions using 3D city models and (2) AR navigation functions using 3D city models. In addition, as the 3D city models to be used, an underground mall models (LOD4), which is formulated in the Standard Data Product Specification for 3D City Model, Version 5.0, was created. In addition, building models (LOD4) of representative buildings in the target area were converted from BIM models and generated. The building model (LOD4) is a model that represents the inner shape of buildings (indoor spaces) and is data that can be used for indoor navigation.

### 2.1. Ability to create map data using 3D city models

The 3D city models and the BIM models were combined by developing a converter that converts the IFC files of the BIM models to CityGML, which is the data format used by the 3D city models provided by PLATEAU [4]. Among the functions of the system, those related to the creation of map data are shown in Table 1.

*Table 1. List of Functions (Map Data Creation)*

ID	Function	Description
001	Editing BIM Models	Create and edit BIM models in Autodesk Revit, a BIM tool
002	IFC to CityGML conversion function	Using FME Desktop, convert the BIM models in IFC format into 3D city models in CityGML format.
003	CityGML to FBX conversion function	Using FME Desktop, convert the 3D city models in CityGML format to 3D model data in FBX format for use in each application.
004	Processing of GIS data	Using QGIS, process and output from the geometry and attribute data of the 3D city models to JSON format, which is the building master data, for advanced conversion of floors.
005	OBJ to USDZ conversion function	Using Reality Composer, combine OBJ generated from 3D city models and building master data and convert to USDZ format as map data for AR applications.

### 2.2. Navigation Functions

The 3D navigation system is a navigation application for pedestrians that seamlessly connects ground/underground and indoor/outdoor pedestrian spaces centered on stations. The system consists of 3D and AR navigation functions as its main features.

The route guidance, which is the basis of the 3D navigation function (Figure 2), uses POI (Point of Interest, data on representative points of buildings, facilities, stores, equipment, etc., which serve as destinations in route guidance) and network data (data related to travel routes consisting of node data indicating the starting and ending

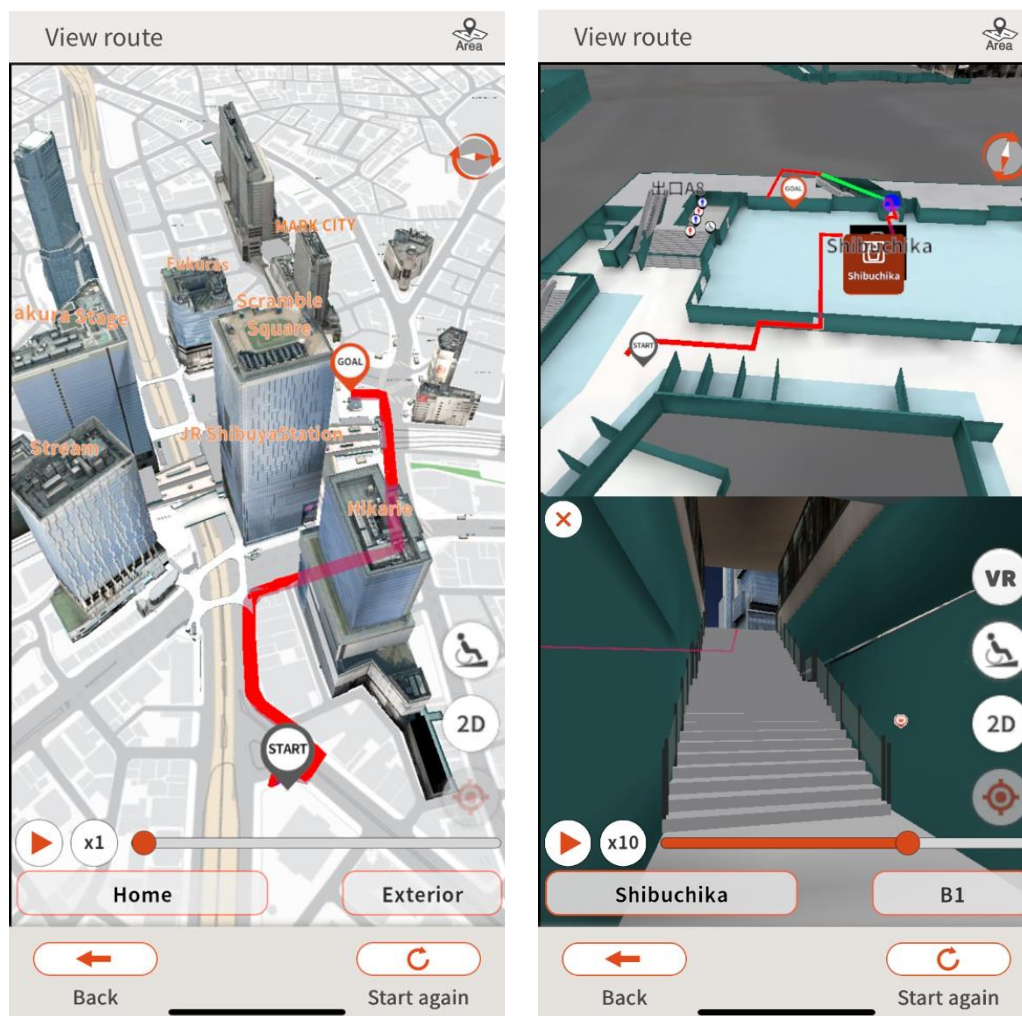


points of routes and points such as intersections, and link data indicating line segments connecting nodes and nodes) currently in operation in the existing “Tokyo Station Navi” system. The 3D route search results can be displayed on the 3D map by adding the height (elevation) information extracted from the building master data (JSON format), which compiles the floor height (elevation) information of each location.

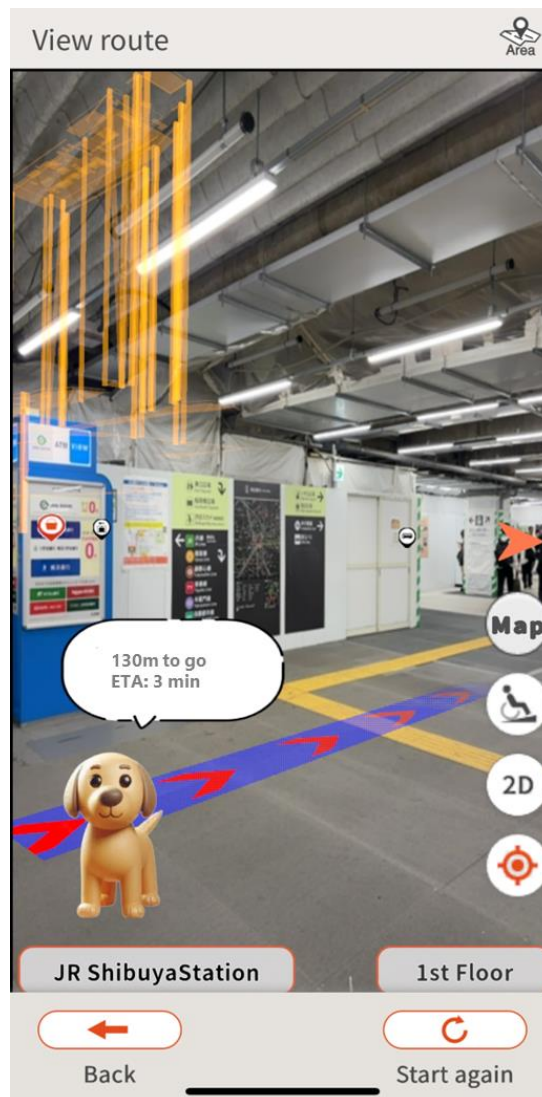
The route search function is based on the shortest route search logic based on the Dijkstra method, using network data, and is able to search for “barrier-free step-elimination routes” that pass through elevators, slopes, and other step-elimination facilities by applying its own weighting. This system is based on the existing “Tokyo Station Navi”. To estimate self-position for route search, the iOS version uses indoor positioning using Core Location, while the Android version uses the results of indoor positioning using the proprietary logic that combines Beacon and Fused Location Provider API. In the target area, map data creations and radio surveys are being conducted to enable indoor positioning of Core Location.

The AR navigation function allows users to intuitively understand which direction buildings and destinations on the ground are located while in underground spaces. When an app user in the underground space holds the smartphone up to the ceiling, wireframes of the destination building is displayed through the camera's reflection on the ceiling. This allows the user to see the 3D models of the above-ground building and the POI of the destination from the smartphone screen even while staying in the underground mall, and to confirm the direction to the destination. Also, the route from its own position to the destination and the surrounding facility POI can be displayed. (Figure-3)

Finally, we describe the software used in this development. Both the 3D navigation and AR navigation systems were developed using Unity, a widely used game development platform. This created WebGL data compatible with web browsers, which is visualized via a WebView within the Station Navigation App. Also, geospatial information—such as store and facility details, Points of Interest (POI), and route network data—was organized into a database using PostGIS and PostgreSQL. This data is acquired via Web APIs and utilized within the 3D navigation system.



**Figure 2.** 2D/3D navigation function



**Figure 3.** Screen image with AR navigation function

### 3. RESULTS, ISSUES, AND CONSIDERATIONS OBTAINED FROM THE VERIFICATION

#### 3.1. Verification Method

In the total of three areas (Shibuya Station, Sapporo Station, and Takamatsu Station), the functions developed in this verification were opened to the public from December 2, 2024 to January 31, 2025 for general users, and questionnaire surveys were conducted on the usefulness of the 3D navigation and AR navigation functions. The 3D navigation function was surveyed in terms of “ease of use of the search screen“, “clarity of route guidance“, “speed of display“, and “clarity of 2D maps“, while the AR navigation function was surveyed in terms of “convenience of AR navigation“ and “display speed“. The number of valid responses was 166 for the 3D navigation function and 153 for the AR navigation function, respectively.

#### 3.2. Verification results and issues

The 3D and AR navigation functions developed in this verification were generally highly evaluated by general users (Table 2). On the other hand, it was found that user satisfaction was relatively low in terms of some usefulness aspects, such as display speed, and that improvements are needed. In addition, there were many requests for

additional related information, such as store availability and train operation information, indicating the direction in which this development should be expanded.

### 3.3. Consideration

Through this demonstration, the superiority of the 3D city models provided by PLATEAU in terms of technology, business, and public policy was demonstrated. (Table 3)

**Table 2.** Summary of Questionnaire Results (excerpts)

Functions	Survey Items	Response Results
3D	Ease of use of the search screen	Positive responses were received from approximately 50% of users. Some users commented that it was easier to use than conventional 2D map applications.
	Clarity of route guidance	Nearly 60% of users answered that the system was easy to understand.
	Speed of display	More than 70% of users answered, “above average”. On the other hand, many users were able to use the system with a certain degree of comfort, but it was confirmed that there is room for improvement.
	Clarity of 2D maps	
AR	Convenience of AR navigation	While more than 60% of the users found the system convenient, there were many comments such as “it does not display correctly” and “I am not used to using it”, confirming that quality stability and improved positional accuracy are issues to be addressed.
	Speed of display	80% of users answered, “above average”.

Main result items	Result items	Superiority
Technology	Seamless switching between multiple viewpoints	<ul style="list-style-type: none"> <li>• In the case of use for navigation applications, the 2D map can be substituted by displaying the map vertically from directly above.</li> <li>• In the case of 3D city models provided by PLATEAU, correct height information is retained, allowing simple 3D display without artificially adding height information.</li> <li>• 3D view of land objects makes it easy to grasp vertical movement</li> </ul>
	Landscape restoration and understanding of current location	<ul style="list-style-type: none"> <li>• 3D city models make it easy to reproduce the landscape of a location through the use of textures, etc.</li> </ul>
	Select the type of land object	<ul style="list-style-type: none"> <li>• CityGML uses component tags to represent each type of building component, so the tags can be used to easily extract the necessary geographic features</li> </ul>
	Elevation	<ul style="list-style-type: none"> <li>• It is difficult to express in the 2D map when spatially connected facilities have different hierarchical names, but in the 3D city models, it is easy to create a seamless map without being bound by hierarchical names because of the use of elevation.</li> </ul>
Business	Reduction of development and operation costs through open data	<ul style="list-style-type: none"> <li>• The data is maintained as public open data, and operating costs can be reduced as the open data is updated in the future.</li> </ul>
	Scalability of business through wide scope of maintenance	<ul style="list-style-type: none"> <li>• In terms of business scale, the development of 3D city models nationwide will enable utilization that is not limited to specific regions.</li> </ul>
Public policy	Advancement of community development	<ul style="list-style-type: none"> <li>• By disseminating information on the navigation application for everyday use that utilizes 3D city models, it is possible to</li> </ul>

	and information dissemination	easily disseminate city planning and other related information.
--	-------------------------------	---

**Table 3.** *Superiority of 3D city models*

## 4. CONCLUSION

This paper presents the overview of navigation systems that utilize digital twins integrating above and below ground spaces and the usefulness of digital twins technology in the underground spaces. The verification results reaffirmed the high social demand for seamless three-dimensional navigation between the terminal station, indoor and outdoor, and above and below ground. In addition, it was also confirmed that the construction of a 3D foundation maps that can be commonly used by different facility managers (station and town) from BIM and its use in the navigation application can contribute to the advancement of information dissemination about the station and town. Furthermore, by utilizing the elevation information contained within the 3D city model data provided by PLATEAU, it is possible to offer barrier-free routes that account for steps and slopes. This contributes to realizing an urban environment where everyone can move comfortably, representing one of the core values of digital twin utilization within this service.

In addition, the capability to integrate CityGML-format GIS data — which handles urban spatial information — with BIM data — which handles design information in the architecture and civil engineering fields — enables the comprehensive utilization of an integrated information infrastructure for the entire city. This is also of significant importance for the future development of this project.

In order to develop this navigation system in the future, it is necessary to continue to improve the UI/UX required for the navigation application based on user requests, and to encourage the participation of facility managers in the existing area. It is also important to accelerate the incorporation of real-time information that is expected to expand in the future (e.g., information on vacancies in facilities, stores, coin lockers, etc., and the opening and acceptance status of evacuation centers and facilities for people having difficulty returning home).

Through this verification, the method of constructing 3D foundation maps utilizing 3D city models and BIM data owned by facility managers is considered to have been largely established.

In line with the development of 3D city models and the spread of open data in various regions, it is expected that the diffusion and expansion of 3D foundation maps that allows both city development businesses and visitors to share information will continue in various areas.

## 5. BIBLIOGRAPHY

- [1] Yuri Tsubaki (2024). Project PLATEAU-The Initiative of Digital Twin in Japan-, Intelligence. Informatics and Infrastructure, Volume 5, Issue 2, 1-12. [https://doi.org/10.11532/jsceiii.5.2\\_1](https://doi.org/10.11532/jsceiii.5.2_1).
- [2] Manual for the Integration of BIM Models in 3D City Models with CityGML Version 4.0. [https://www.mlit.go.jp/plateau/file/libraries/doc/plateau\\_doc\\_0003\\_ver04.pdf](https://www.mlit.go.jp/plateau/file/libraries/doc/plateau_doc_0003_ver04.pdf).
- [3] Yan, Zlatanova & Diakité (2021). A unified 3D space-based navigation model for seamless navigation in indoor and outdoor. International Journal of Digital Earth, Vol. 14, No. 8.
- [4] Conversion template from IFC to CityGML2.0 building models (LOD4) using FME. <https://github.com/Project-PLATEAU/PLATEAU-IFC-to-CityGML2.0-LOD4>.
- [5] Technical Report on Navigation System Utilizing Underground 3D City Models v2.0. [https://www.mlit.go.jp/plateau/file/libraries/doc/plateau\\_tech\\_doc\\_0108\\_ver01.pdf](https://www.mlit.go.jp/plateau/file/libraries/doc/plateau_tech_doc_0108_ver01.pdf).
- [6] Technical Report on Navigation System Utilizing Underground 3D City Models. [https://www.mlit.go.jp/plateau/file/libraries/doc/plateau\\_tech\\_doc\\_0075\\_ver01.pdf](https://www.mlit.go.jp/plateau/file/libraries/doc/plateau_tech_doc_0075_ver01.pdf).

## APPLICATION OF IMPROVED MACHINE LEARNING METHODS TOWARD BETTER ACCURACIES IN PREDICTING TBM PERFORMANCE

Dansheng Yao <sup>1</sup>, Mengqi Zhu <sup>2</sup>, Hehua Zhu <sup>3</sup>

**Abstract:** Tunnel Boring Machines (TBMs) play a pivotal role in modern underground construction, especially for tunneling through complex geological environments. Accurate real-time classification of surrounding rock masses is critical for optimizing TBM operation, yet conventional methods relying on engineering labels often suffer from subjectivity and label noise. To address these challenges, we propose a novel semi-supervised teacher-student framework that integrates engineering expertise, class prototype learning, and a Graph Neural Network (GNN)-based self-distillation mechanism. The model leverages soft labels, generated from domain-specific knowledge, to incorporate label uncertainty while improving feature cohesion. By employing self-supervised learning and iterative refinement of class prototypes, the framework effectively minimizes label noise, enhances classification boundaries, and adapts to unseen data. Experimental results on a real-world TBM tunneling dataset demonstrate that the proposed method significantly improves classification performance, offering more reliable and robust predictions in the presence of noisy labels. This work lays the foundation for future advancements in AI-driven geological inference, providing enhanced safety, efficiency, and reliability for TBM tunneling projects.

**Keywords:** Tunnel Boring Machine, Rock Mass Classification, Label Noise Correction, Self-Distillation, Prototype Learning.

### 1. INTRODUCTION

Tunnel Boring Machines (TBMs) are critical equipment widely used in modern underground engineering, particularly in tunnel construction. With their efficient and precise excavation capabilities, TBMs significantly enhance operational efficiency (Fu, Qiu, Xue, Shao, and Lan, 2024; Hansen, Erharter, and Marcher, 2024; M. Zhang, Ji, Zhou, Ding, and Wang, 2024, Gangrade et al., 2022). Ensuring the smooth operation of TBMs under complex geological conditions is essential, and this heavily relies on the accurate classification of surrounding rock masses. Accurate rock mass classification not only helps engineers assess the working environment of the TBM but also guides the adjustment of operational parameters, thereby optimizing excavation efficiency, reducing equipment failure, and mitigating risks during tunnel construction (Li, Tao, Du, and Wang, 2024; Qiu et al., 2022).

Traditional rock mass classification methods, such as the Rock Mass Rating (RMR), Barton's Quality Index (BQ), and the Q-system, are typically based on geological surveys and rely on expert experience and onsite measurements. While these methods have been widely adopted in practical engineering, they often suffer from a high degree of subjectivity (Ambah and Elmo, 2024; Azad et al., 2024; Rehman et al., 2018). Their applicability is limited in complex and unstable geological environments where traditional approaches may fail to accurately reflect the true characteristics of the rock mass, consequently affecting TBM excavation decisions and operational efficiency (Yang, Mitelman, Elmo, and Stead, 2021).

With the development of machine learning and artificial intelligence (AI) technologies, data-driven approaches have been increasingly introduced into rock mass classification, offering promising solutions to address the limitations of traditional methods. AI-based approaches leverage big data analytics and pattern recognition to

<sup>1</sup> MSc, Dansheng Yao, Intelligent Science and Technology, Shanghai Research Institute for Intelligent Autonomous Systems, Tongji University, Shanghai 200092, China, sorano@tongji.edu.cn

<sup>2</sup> PhD, Mengqi Zhu, Geotechnical and Underground Engineering, Department of Geotechnical Engineering, College of Civil Engineering, Tongji University, Shanghai 200092, China, mqzhu@tongji.edu.cn

<sup>3</sup> Prof., Hehua Zhu, Geotechnical and Underground Engineering, Department of Geotechnical Engineering, College of Civil Engineering, Tongji University, Shanghai 200092, China, zhuhehua@tongji.edu.cn



efficiently process large-scale geological data, overcoming some of the key challenges of conventional techniques (Mooney, M. A. et al., 2023). However, the application of AI methods in real-world scenarios still faces significant challenges, particularly the issue of label noise, which is especially pronounced when the labels are derived from TBM operational data.

Most current AI-based methods for rock mass classification rely on supervised learning, where models are trained on large quantities of labeled data to minimize the error between predicted and true labels, thereby improving classification accuracy (Adeli, 2001; Jiang and Zhang, 2020; C. Zhang, Tao, Wang, and Fan, 2024). While supervised learning methods have achieved impressive results on standardized datasets, their robustness diminishes when applied to real-world engineering data, particularly in the presence of noisy labels. In practice, rock mass grading labels are often based on geological survey results or subjective judgments made by engineers during TBM operations. These labels are prone to measurement errors, environmental changes, and inconsistencies in engineering expertise, resulting in label noise. Such noise can negatively impact the accuracy of model training, leading to overfitting or underfitting, and ultimately limiting the generalization ability of the model under complex geological conditions.

To address the challenge of label noise, researchers have explored unsupervised and semi-supervised learning approaches. Unsupervised learning methods, which rely on the intrinsic structure of the data for classification, completely eliminate dependence on labels, thus avoiding the negative effects of label noise. For example, several studies (Xue et al., 2023; Q. Zhang, Liu, and Tan, 2019) have demonstrated the potential of clustering algorithms and dimensionality reduction techniques in analyzing TBM data, offering valuable insights into overcoming the limitations of traditional supervised learning approaches. However, unsupervised methods often fail to leverage existing labeled data, which frequently contains substantial domain knowledge and geological guidelines that accurately reflect the fundamental properties of rock masses. As a result, while unsupervised learning excels at reducing label dependence, it cannot fully utilize the engineering value embedded in labeled data.

Semi-supervised learning, on the other hand, combines a small amount of labeled data with a large amount of unlabeled data to enhance model learning through techniques such as pseudo-labeling and consistency regularization. Significant progress has been made in this area. For instance, several studies (Honggan Yu et al., 2021; Hongjie Yu and Mooney, 2023) have successfully applied semi-supervised learning methods to classify complex geological data, achieving notable improvements in classification performance and laying a solid foundation for addressing the label noise problem. However, semi-supervised learning also has significant limitations in real-world engineering scenarios. TBM data often lacks a sufficient quantity of high-quality labeled data that can be considered “completely accurate,” as well as a large-scale unlabeled dataset. Consequently, traditional semi-supervised learning methods struggle to fully exploit the available data in such contexts. Furthermore, semi-supervised learning tends to be highly sensitive to noisy labels, which can result in an underestimation of the value of labeled data and limit classification performance.

To overcome these limitations, it is essential to design an approach that addresses the unique challenges of TBM data. Such an approach should integrate multiple strategies: leveraging domain knowledge to refine and improve label reliability, fully utilizing the information embedded in noisy labels without dismissing their engineering value, and extracting intrinsic data structures to reduce overreliance on imperfect labels. By combining these elements, we aim to maximize the utility of available labeled data, enabling more robust and accurate classification even in the presence of noisy labels.

This paper proposes an innovative approach to tackle these challenges, combining class prototype learning and self-supervised learning. The proposed model classifies data by computing class prototypes, refines label distributions using domain knowledge, and leverages self-supervised learning to extract the intrinsic structure of the data. This approach balances label knowledge with the inherent data distribution, providing a robust solution for noisy label correction and improved rock mass classification in TBM operations.

## 2. METHODOLOGY

In this section, we first define the problem and provide an overview of our approach. Then, we introduce the workflow of the proposed framework. Next, we describe each component of the framework, including the guidance generator, which incorporates domain-specific prior knowledge as guidance, the teacher-student structure, the feature iterators based on graph neural networks, along with the Semantic Level Graph (SLG) and Class Level Graph (CLG) modules, and finally, we detail our proposed loss function.

### 2.1. Problem Definition

In practical problems, it is often difficult to obtain samples from the true distribution  $D$  of a pair of random variables  $(X, Y) \in \mathcal{X} \times \{1, 2, \dots, K\}$ , where  $X$  is the feature space, and  $K$  is the number of classes. Specifically, we

are given a set of noisy labeled data, where the feature space  $\mathcal{X}$  consists of time-series samples, and the labels  $Y$  are corrupted due to noise.

For time series data, let:

(1)  $x_i \in \mathbb{R}^{n_{\text{feature}} \times L}$  represent the input feature vector of size  $n_{\text{feature}}$  and length  $L$ , where  $L$  is the time series length.

(2)  $\tilde{y}_i \in \mathbb{R}^K$  represent the noisy label vector for the  $i$ -th sample, where  $\tilde{y}_i[c]$  is the probability that the sample  $x_i$  belongs to class  $c$ .

The noisy data  $\{(x_i, \tilde{y}_i)\}_{i=1}^n$  are independently drawn from a noisy distribution  $\tilde{D}$  of samples  $(X, Y)$ , where the labels  $\tilde{y}_i$  are corrupted versions of the true labels  $y_i$ . The objective of this work is to learn a robust model  $f: \mathcal{X} \times \mathbb{R}^K \rightarrow \mathbb{R}^K$  that can both correct the label noise and make accurate predictions for the test samples. Rather than directly learning from noisy labels, we introduce class prototypes into the model's learning process. These class prototypes serve as the reference points in the feature space, which guide the model towards a more accurate understanding of the underlying class distributions. The model should ideally minimize the following objective, which now incorporates the learning of class prototypes  $p_c$  for each class  $c$ :

$$\min_f \mathbb{E}_{(x_i, \tilde{y}_i) \sim \tilde{D}} [\mathcal{L}(f(x_i), y_i)] \quad (1)$$

where  $\mathcal{L}(\cdot, \cdot)$  is a loss function that quantifies the difference between the predicted label  $f(x_i)$  and the true label  $y_i$ .

In this setting, we assume that the model learns to approximate the true class distribution via the class prototypes,  $p_c$ , which are learned iteratively through both supervised and self-supervised losses. The class prototype  $p_c$  represents the most typical feature vector for class  $c$ , helping the model to refine its understanding of each class by minimizing the distance between the predicted feature representation  $f(x_i)$  and the corresponding class prototype.

By learning these class prototypes through soft labels and optimizing the feature representations, we expect the model to improve its robustness to label noise. Furthermore, the iterative self-supervised updates allow the model to fine-tune these prototypes by minimizing the intra-class feature distances and maximizing the inter-class feature distances. This ultimately leads to a model that more accurately reflects the true distribution of the classes in the presence of noisy labels.

## 2.2. Framework Overview and Workflow

The proposed model addresses noisy labels and enhances generalization through a teacher-student framework, as illustrated in Fig. 1. The key idea is to learn robust class prototypes that guide the model toward accurate predictions, even under label noise.

During training, TBM operation data is fed into the backbone of both teacher and student models to extract feature embeddings and class probabilities. Simultaneously, hard labels from engineering records are input into the Guidance Generator to produce Leader Soft Labels (LSL)—a refined form of supervision that reflects label uncertainty and domain knowledge.

These soft labels help approximate true class distributions, guiding the learning of class prototypes. Feature representations are projected by the Feature Embedding Head, while the Classification Head produces class probabilities. These outputs, along with LSL, are used to iteratively refine class prototypes via a Self-Distillation Block, which aligns features within classes and separates those from different classes.

The teacher model further processes the LSL and feature embeddings to generate LSL Embeddings, serving as high-confidence targets to guide the student model. A composite loss function includes:

- **Leader Loss** for guiding the teacher via LSL,
- **CLG Loss** for supervising the student using teacher outputs,
- **SLG Loss** for encouraging better feature learning through semantic-level self-supervision.

Inspired by Xiao et al. (2024)(Xiao et al., 2024), this framework reduces the distance between features and their class prototypes, improving both robustness and accuracy.

We adopt the U-Time architecture (Perslev, Jensen, Darkner, Jennum, and Igel, 2019) as the backbone for feature extraction from multi-dimensional TBM time-series data. This fully convolutional network efficiently captures temporal patterns and outputs compact representations for downstream modeling.

At inference time, only the student model is used to make predictions based on the learned representations.



## 2.4. Graph-Based Representation Learning

To enhance feature learning under label noise and incorporate structural dependencies within the data, we construct two complementary graph structures: a Semantic-Level Graph (SLG) and a Class-Level Graph (CLG). The SLG captures local feature similarity between time steps, while the CLG models global consistency across predictions sharing the same class. Both graphs are constructed within each mini-batch and serve to propagate contextual information through neighborhood aggregation.

To further refine these representations, we introduce a mutual self-distillation mechanism between SLG and CLG. At each training iteration, the CLG is updated based on the semantically enriched features from the SLG, while the SLG is refined using class-level affinity derived from the CLG. This bidirectional interaction is modulated by dynamic confidence thresholds, which identify high- and low-confidence regions, allowing the model to balance reliance on confident predictions and contextual cues. After several iterations, we obtain enhanced feature embeddings from the SLG and refined class distributions from the CLG, which are used for pseudo-label generation and downstream supervision.

## 2.5. Loss Function

The overall training objective integrates three key components:

(1) Leader Loss, which aligns the teacher model's representations with soft labels provided by the Guidance Generator via prototype-level supervision.

(2) CLG Loss, which supervises the student model using confidence-weighted pseudo-labels derived from the CLG.

(3) SLG Loss, which enforces intra-class compactness and inter-class separability in the feature space, both at the batch level and across batches through global prototypes.

The combined loss encourages the model to learn discriminative, noise-resilient representations by jointly leveraging domain-informed soft supervision and structural consistency. This design facilitates robust training under uncertain labeling conditions and enhances generalization to unseen geological patterns.

# 3. EXPERIMENT

## 3.1. Project background

We evaluate our method using real-world operational data from the Yinchao water conveyance tunneling project in northeastern Inner Mongolia, China. The project employed an open-type gripper TBM (diameter: 5.2 m, thrust: 11,340 kN), which excavated a 55 km tunnel section over 509 days, with 4–10 cycles per day.

The dataset includes multi-dimensional time-series measurements (e.g., thrust, torque, penetration rate) recorded during excavation, along with corresponding geological labels derived from the Chinese Hydropower Classification (HC) system (Grades I–V). The distribution is dominated by Grade III rockmass (63%), followed by Grades II (19%), IV (14%), and V (4%).

## 3.2. Data preprocessing

To enhance training stability and label reliability, we applied a structured preprocessing pipeline following related studies (Xue et al., 2023; Zhu et al., 2022). TBM operational data were segmented into excavation cycles using thrust, torque, and net advance rate signals. Stable phases were then extracted from each cycle for subsequent analysis.

Geological records identified 74 rock mass transition points. Around each point, 2,294 samples were generated by symmetrically extracting 31 segments of 1,024 time steps from both sides. To balance the dataset, 2,287 additional samples were proportionally drawn from geologically stable segments across classes. Mixed-face conditions—where multiple lithologies coexisted at the excavation face—were not included, ensuring that each sample segment corresponds to a single dominant rock type.

The dataset was partitioned into training, validation, and testing subsets in a 60:20:20 ratio with consistent class distributions. While alternative splitting ratios were not exhaustively explored, the model design emphasizes robustness through confidence-weighted supervision and temporal context modeling. These properties reduce reliance on specific data partitions, and the theoretical formulation is not tightly coupled to a particular train/test ratio.

### 3.3. Results analysis

#### 3.3.1. Evaluation and Visualization of Model Performance

Our model is designed to correct label noise rather than mimic it. However, successful correction presupposes the model's ability to extract meaningful geological patterns from noisy data. Therefore, a moderate alignment between model predictions and the original engineering labels is expected: overly high agreement may indicate overfitting to noise, while overly low agreement suggests failure to learn from the data.

To evaluate this balance, we first assess model performance using the original hard labels provided by the engineering team. These labels, although imperfect, serve as a practical supervision source. The model is trained on them and further refined through the proposed self-distillation process. Evaluation metrics—including Intersection over Union(IoU), Dice score, and overall accuracy—are reported in Table 1. As anticipated, the model shows limited alignment for Grades II–IV due to label and data noise, but achieves significantly better agreement for Grade V, which is known to be more reliably labeled and geologically distinct.

To further test generalization, we conduct an extended evaluation across the entire 55 km excavation range. The full dataset is segmented into non-overlapping 1024-step sequences, and a majority-vote scheme is applied within each segment to assign a stable label. This helps reduce prediction variance and improves interpretability.

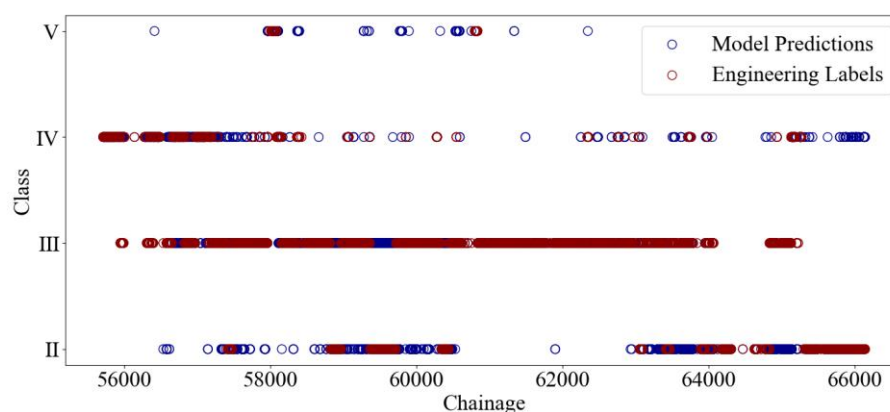
Figure 3 presents the model's predictions across the full tunnel length. Despite noisy supervision, the model exhibits strong alignment with geological trends, accurately capturing major transitions while maintaining robustness to local fluctuations. This confirms that the model not only avoids overfitting to noise but also effectively learns from weak labels. Class-wise precision, recall, and F1 scores from this extended evaluation are summarized in Table 2.

**Table 1.** Comparison between the proposed method and existing methods.

	Grade II	Grade III	Grade IV	Grade V	Mean
IoU	0.4807	0.4156	0.4401	0.8360	0.5431
Dice	0.6493	0.5871	0.6112	0.9107	0.6896
Accuracy			0.6640		

**Table 2.** Comparison between the proposed method and existing methods.

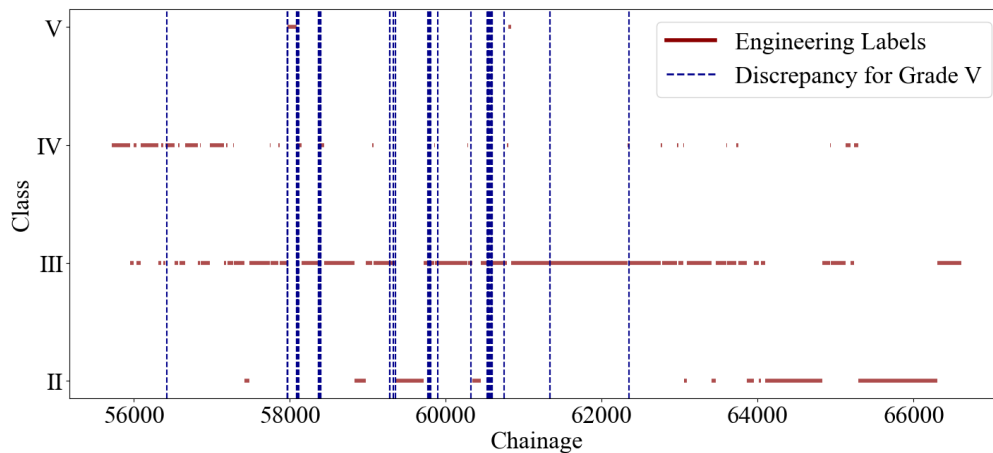
	Precision	Recall	F1 score
Grade II	0.59	0.72	0.65
Grade III	0.86	0.73	0.79
Grade IV	0.62	0.75	0.67
Grade V	0.54	0.99	0.70



**Figure 3.** Comprehensive Classification Evaluation Over Full Excavation Length



### 3.3.2. Evaluation of TBM Penetration in Soft Rock Zones and Labeling Discrepancies



**Figure 4.** Distribution of Label Discrepancies for Grade V across the Entire Chainage

Accurate geological surveys are crucial for the safety, efficiency, and cost management of TBM tunneling, especially in soft rock areas where incorrect rock mass classification can lead to accidents and delays. The significant discrepancies observed between the proposed model and the labels provided by field engineers for Grade V rock masses, as shown in Figure 3, indicate the need for further investigation of the data related to Grade V. This is particularly important because accident-prone areas are often found in soft rock regions, and the classification of weak strata (Grade V) is critical to ensuring safety. To this end, we visualized the spatial locations where the model's predictions differ from the noisy labels for Grade V, as illustrated in Figure 4. These discrepancies are primarily observed at the boundaries between Grade IV and Grade V excavation sections, where excavation markers from the engineering team are subject to changes. This suggests that the model may interpret the feedback from the engineers as either premature or insufficiently timely in reflecting changes in rock mass classification.

Our model, however, has successfully identified all sections that were considered vulnerable by the engineering units, which were previously classified as Grade V. In addition to recognizing the segments that the engineers deemed weak, our model also discovered hidden vulnerable sections—areas that were not immediately identified in the continuous engineering assessments. This ability to detect previously overlooked weak strata significantly contributes to improving overall safety by highlighting additional risks that might have otherwise remained undetected.

Compared to traditional methods, our model demonstrates a higher level of accuracy in processing noisy data, effectively extracting geological features, and minimizing the interference of noise on classification results. By optimizing the identification of weak strata (such as Grade V), the model provides more reliable decision support in real-world engineering applications. In doing so, it not only enhances the safety and efficiency of tunneling operations but also reduces engineering risks, construction delays, and costs.

## 4. CONCLUSIONS

Accurate classification of surrounding rock masses is critical for optimizing excavation efficiency, ensuring equipment stability, and maintaining construction safety in Tunnel Boring Machine (TBM) operations. Traditional classification methods primarily rely on labels provided by engineering teams, which are often subject to human bias and noise. These issues reduce the robustness and adaptability of such methods under complex geological conditions. Addressing these challenges is essential for enhancing TBM operational efficiency and mitigating risks in underground construction.

This study proposes an innovative framework to address the challenges posed by noisy engineering labels in real-time rock mass classification during TBM operations. By generating domain-knowledge-driven Leader Soft Labels (LSL) and incorporating a Graph Neural Network (GNN)-based self-distillation mechanism, the proposed method achieves significant improvements in both classification accuracy and feature representation. Experimental results demonstrate that, compared to baseline models, the framework exhibits notable advantages in feature clustering, intra-class cohesion, and inter-class separation. These improvements are further validated through t-SNE visualizations. The findings confirm that the proposed model effectively mitigates the impact of label noise and achieves stable and accurate classification under complex geological conditions.

Furthermore, a comparison between the model predictions and noisy engineering labels reveals a delay in updating the classification of the weakest rock masses (Grade V). This observation provides critical insights for real-time geological assessments, highlighting the need to focus on dynamic adjustments for weak rock mass classifications. Accurate classification of weak rock masses is particularly important for ensuring TBM safety and efficiency. To address this issue, it is recommended to adopt the proposed model or similar noise-reduction frameworks when performing geological assessments. Such models can reduce the interference of noisy engineering labels, especially in weak rock mass regions where geological conditions are highly complex and subject to frequent changes. Accurate classification of weak rock masses enables timely adjustment of excavation parameters, such as cutterhead rotational speed, thrust force, and torque, thereby reducing equipment wear and construction risks.

Despite the significant progress achieved in this study, there remain several areas for further improvement. The current framework relies on relatively simple prior knowledge assumptions. Future work could incorporate richer engineering insights and statistical expertise to further optimize the model. For instance, adaptive adjustments to soft labels could be applied to specific spatial regions, such as drill sites or areas where engineers have high confidence in the surrounding rock conditions. Additionally, integrating spatial-temporal characteristics of geological data could enhance the model's robustness and generalizability in practical applications.

## 5. REFERENCES

- [1] Adeli, H. (2001). Neural Networks in Civil Engineering: 1989–2000. *Computer-Aided Civil and Infrastructure Engineering*, 16(2), 126–142. <https://doi.org/10.1111/0885-9507.00219>
- [2] Ambah, E., and Elmo, D. (2024, June 23). Is there a Universal Rock Mass Classification System? Presented at the 58th U.S. Rock Mechanics/Geomechanics Symposium. OnePetro. <https://doi.org/10.56952/ARMA-2024-0784>
- [3] Azad, M. A., Najeh, T., Raina, A. K., Singh, N., Ansari, A., Ali, M., ... Singh, S. K. (2024). Development of correlations between various engineering rockmass classification systems using railway tunnel data in Garhwal Himalaya, India. *Scientific Reports*, 14(1), 10716. <https://doi.org/10.1038/s41598-024-60289-y>
- [4] Fu, K., Qiu, D., Xue, Y., Shao, T., and Lan, G. (2024). TBM tunneling strata automatic identification and working conditions decision support. *Automation in Construction*, 163, 105425. <https://doi.org/10.1016/j.autcon.2024.105425>
- [5] Gangrade, R., Grasmick, J., Trainor-Guitton, W., & Mooney, M. (2022). Risk-based methodology to optimize geotechnical site investigations in tunnel projects. *Tunnelling and Underground Space Technology*, 127, 104589.
- [6] Hansen, T. F., Erharter, G. H., and Marcher, T. (2024). Towards reinforcement learning—Driven TBM cutter changing policies. *Automation in Construction*, 165, 105505. <https://doi.org/10.1016/j.autcon.2024.105505>
- [7] Jiang, S., and Zhang, J. (2020). Real-time crack assessment using deep neural networks with wall-climbing unmanned aerial system. *Computer-Aided Civil and Infrastructure Engineering*, 35(6), 549–564. <https://doi.org/10.1111/mice.12519>
- [8] Li, Z., Tao, Y., Du, Y., and Wang, X. (2024). Classification and Prediction of Rock Mass Boreability Based on Daily Advancement during TBM Tunneling. *Buildings*, 14(7), 1893. <https://doi.org/10.3390/buildings14071893>
- [9] Mooney, M. A., Grasmick, J. G., & Gangrade, R. (2023). Methods for local big data integration to reduce geotechnical uncertainty and risk on subsurface infrastructure projects. In *Expanding Underground-Knowledge and Passion to Make a Positive Impact on the World* (pp. 2799-2806). CRC Press.
- [10] Perslev, M., Jensen, M. H., Darkner, S., Jennum, P. J., and Igel, C. (2019). U-Time: A fully convolutional network for time series segmentation applied to sleep staging. In *Proceedings of the 33rd International Conference on Neural Information Processing Systems* (pp. 4415–4426). Red Hook, NY, USA: Curran Associates Inc.
- [11] Qiu, D., Fu, K., Xue, Y., Tao, Y., Kong, F., and Bai, C. (2022). TBM Tunnel Surrounding Rock Classification Method and Real-Time Identification Model Based on Tunneling Performance. *International Journal of Geomechanics*, 22(6), 04022070. [https://doi.org/10.1061/\(ASCE\)GM.1943-5622.0002379](https://doi.org/10.1061/(ASCE)GM.1943-5622.0002379)
- [12] Rehman, H., Ali, W., Naji, A. M., Kim, J., Abdullah, R. A., and Yoo, H. (2018). Review of Rock-Mass Rating and Tunneling Quality Index Systems for Tunnel Design: Development, Refinement, Application and Limitation. *Applied Sciences*, 8(8), 1250. <https://doi.org/10.3390/app8081250>
- [13] Wang, X., Zhu, H., Zhu, M., Zhang, L., and Ju, J. W. (2021). An integrated parameter prediction framework for intelligent TBM excavation in hard rock. *Tunnelling and Underground Space Technology*, 118, 104196. <https://doi.org/10.1016/j.tust.2021.104196>
- [14] Xiao, H., Hong, Y., Dong, L., Yan, D., Zhuang, J., Xiong, J., ... Peng, C. (2024). Multi-Level Label Correction by Distilling Proximate Patterns for Semi-supervised Semantic Segmentation. *IEEE Transactions on Multimedia*, 26, 8077–8087. <https://doi.org/10.1109/TMM.2024.3374594>
- [15] Xue, Y.-D., Luo, W., Chen, L., Dong, H.-X., Shu, L.-S., and Zhao, L. (2023). An intelligent method for TBM surrounding rock classification based on time series segmentation of rock-machine interaction data. *Tunnelling and Underground Space Technology*, 140, 105317. <https://doi.org/10.1016/j.tust.2023.105317>
- [16] Yang, B., Mitelman, A., Elmo, D., and Stead, D. (2021). Why the future of rock mass classification systems requires revisiting their empirical past. *Quarterly Journal of Engineering Geology and Hydrogeology*, 55(1), qjgegh2021-039. <https://doi.org/10.1144/qjgegh2021-039>

- [17] Yu, Honggan, Tao, J., Qin, C., Xiao, D., Sun, H., and Liu, C. (2021). Rock mass type prediction for tunnel boring machine using a novel semi-supervised method. *Measurement*, 179, 109545. <https://doi.org/10.1016/j.measurement.2021.109545>
- [18] Yu, Hongjie, and Mooney, M. (2023). Characterizing the as-encountered ground condition with tunnel boring machine data using semi-supervised learning. *Computers and Geotechnics*, 154, 105159. <https://doi.org/10.1016/j.compgeo.2022.105159>
- [19] Zhang, C., Tao, M.-X., Wang, C., and Fan, J.-S. (2024). End-to-end generation of structural topology for complex architectural layouts with graph neural networks. *Computer-Aided Civil and Infrastructure Engineering*, 39(5), 756–775. <https://doi.org/10.1111/mice.13098>
- [20] Zhang, M., Ji, A., Zhou, C., Ding, Y., and Wang, L. (2024). Real-time prediction of TBM penetration rates using a transformer-based ensemble deep learning model. *Automation in Construction*, 168, 105793. <https://doi.org/10.1016/j.autcon.2024.105793>
- [21] Zhang, Q., Liu, Z., and Tan, J. (2019). Prediction of geological conditions for a tunnel boring machine using big operational data. *Automation in Construction*, 100, 73–83. <https://doi.org/10.1016/j.autcon.2018.12.022>
- [22] Zhu, M., Zhu, H., Gutierrez, M., Ju, J. W., Zhuang, X., and Wu, W. (2022). Predicting Tunneling-Induced Ground Collapse Based on TBM Operational Data and Geological Data. *International Journal of Computational Methods*, 19(08), 2142015. <https://doi.org/10.1142/S0219876221420159>

## RESEARCH ON DIGITAL MODELING PATH BASED ON IFC EXTENSION AND BIM LIGHTWEIGHT

Yang Zhaofeng<sup>1</sup>

**Abstract:** This paper focuses on the digital modeling of tunnels and underground engineering. Explore key technological breakthroughs from IFC to BIM. Firstly, the architecture of the IFC standard and its extension in the field of infrastructure (such as the IFC-Tunnel project) are introduced, and the IFC information model suitable for tunnel engineering is constructed by extending the component entities and establishing hierarchical associations. Secondly, the essence and implementation requirements of BIM are analyzed, and the idea of an online tunnel BIM platform based on WebGL is proposed, which is combined with GLTF format to solve the problems of inconsistent data format and difficult transmission of 3D model, so as to realize model lightweight and Web-side visualization. Finally, it is pointed out that the combination of IFC and BIM can promote the digitalization of tunnel construction, combine real-time simulation and advanced geological forecasting, improve decision-making efficiency and reduce construction risks, and provide a new path for tunnel engineering informatization.

**Keywords:** GLTF format, GIS Modeling, IFC Standard, BIM Technology, WebGL Visualization

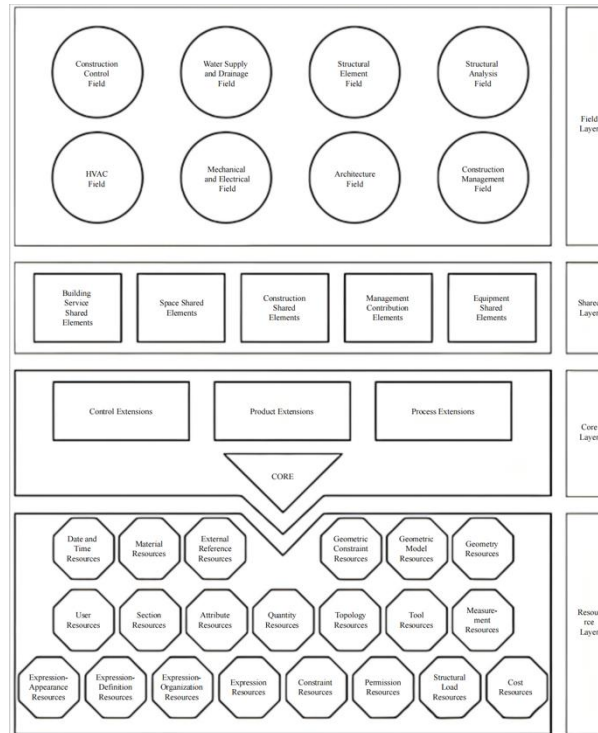
### 1. INTRODUCTION

The IFC standard is a standard for the description of building product data developed by the international buildingsmart organization for the AEC (ArchitectureEngineering andConstruction) field. The Industrial Foundation Class (IFC) is a comprehensive data model that allows for detailed geometric and semantic descriptions of buildings and is widely used as a standard for BIM data exchange independent of software vendors. It was developed by the international non-profit organization buildingsmart and published in 2013 as ISO Standard 16739. Prior to the IFC4 version, the IFC standard was mainly for buildings. However, due to increasing international demand, the standard is being significantly expanded to support the infrastructure.

The IFC-Tunnel extension project follows the official bSI Project Implementation Guidelines (buildingSMART International 2015) that came into effect in 2015. They define two basic components to be implemented for each project: the organizational structure, the development process. IFC uses the express language to define the Building Information model, borrowing from the step standard. After decades of development, the IFC standard has been widely used in the storage and interaction of Building Information Modeling (BIM). IFC provides an object-oriented model structure for construction engineering data, and its structure is shown in the figure[1].

---

<sup>1</sup> Department of Geotechnical Engineering, Wuhan China Geo University, Wuhan 430000, Hubei, China) E-mail: [y954689932@Outlook.com](mailto:y954689932@Outlook.com)



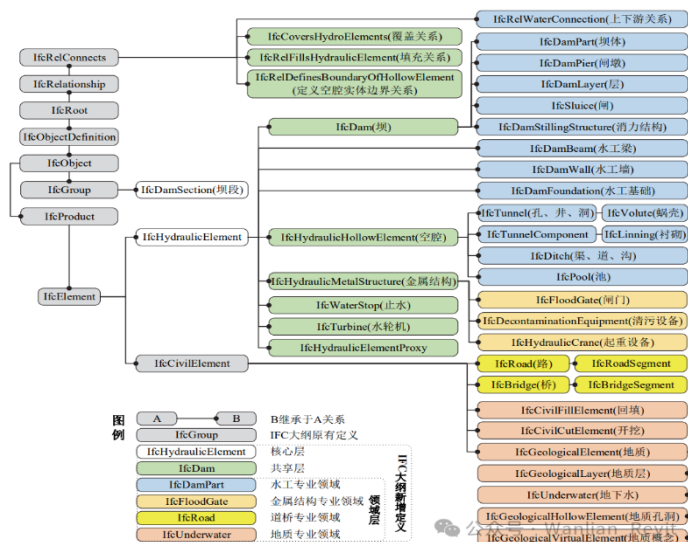
The IFC model structure consists of 4 levels. The first layer is the resource layer, which provides resource-related definitions that can be called at a high level. The second layer is the core layer, which provides the core data definition of the construction project, including a kernel module and three extension modules such as control, product and process. The third layer is the shared layer, which defines concepts and objects that are common to multiple areas of expertise. The fourth layer is the domain layer, which provides corresponding definitions for each professional field of architectural engineering.

#### 1. Define the structure of the engineering information model based on IFC

take IFC as the basis of the engineering information model structure, and expand the original IFC structure to form the engineering information model according to the special components and relationships of the project. As the carrier of Building Information Modeling, most of IFC's definitions can be applied to the engineering field, including:

- 1). a relatively complete definition of 3D geometric description, which supports the creation of 3D models;
- 2). Rich resource description, covering time, materials, engineering quantity, manpower and machine consumption, cost, participants, structural load and other aspects;
- 3). Various types of basic value types and units, supporting the expression of various physical quantities;

#### 4. Some of the entities of construction projects can be directly applied to the project.





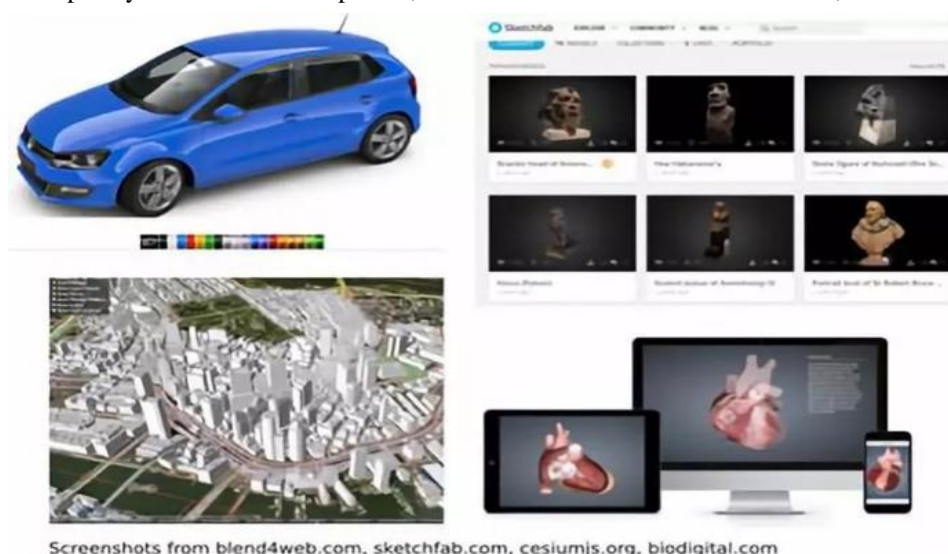
2. On this basis, the IFC development for the project mainly includes the following two aspects:

1) expanding the project component entity and its related definitions. According to the information characteristics and actual requirements of the project, the definitions of the corresponding component entity, component category entity, enumeration type, attribute set, quantity set and resource type of the project are added on the basis of the IFC model structure.

2) Establish hierarchical relationships and related relationships. The new entity should establish a hierarchical relationship based on object-oriented principles and integrate with the hierarchical relationship of the original IFC structure. On this basis, the association relationship between the new entities in the domain and the association between the new entities and the original IFC entities are established. The new definition hierarchical relationship of Engineering Information Model (IFC) is shown in the following figure:

Background: At present, digitalization is replicating the real world in the virtual world, digital cities, digital museums, online shopping malls in the three-dimensional display of goods, digital asset delivery and other scenarios, the use of three-dimensional models can provide a more realistic immersive experience, and the application of content display based on three-dimensional models is increasing. A large number of 3D graphic content to be transmitted and shared through the Web, there are many 3D modeling software at present, the 3D model data format between the various companies is not uniform, such as Maya, 3dMax, Blender, etc., there are more than 70 different 3D graphic file formats, applied to different scenes, and most of the models established by the existing 3D modeling software are not considered to be disseminated on the Internet, so the 3D model leaves the modeling software, and it often becomes very difficult to view. It is not conducive to the sharing and dissemination of models. The display of 3D models on browsers or mobile terminals is mainly realized through WebGL and OpenGL, but 3D models often have a large amount of data and a variety of 3D model data formats, which is not conducive to the development of applications, especially on the mobile side, limited by network speed, memory, computing power and other limitations, loading, browsing interaction, rendering effects, etc. are easily limited, affecting the user experience.

**1. About Three - Dimensional Models:** The essence of the 3D model is the combination of points, lines, surfaces, volumes, materials, and animations, so there is GLTF, JPEG in the 3D graphics industry, and everyone's models are converted into a unified data format for easy transmission on the Web. GLTF=GL Transmission Format, is a standard developed by the Khronos Group team, is a 3D scene data transmission format, Khronos Group is also



the developer of OpenGL, collada and other standards, 3D graphics field leader. Through this data format, it is easy to improve the rendering of the model, avoid a large number of import/export between various 3D processing programs when the texture binding, material rendering, animation effects and other problems, and the most important point is that the model can be lightweight, and can retain excellent rendering effects, including the famous 3D graphics sharing platform Sketchfab, Web3D GIS engine Cesiumjs.

At present, online 3D visualization engines such as Threejs, Cesiumjs, Babylonjs, and xeogljs all support gltf data.

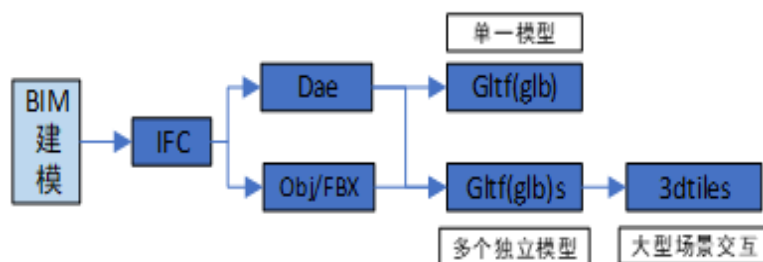
## 2. From IFC to BIM:

(1). BIM is Building Information Modeling, and the software that builds Building Information Modeling is known as BIM modeling software, such as Autodesk CAD, Revit, and many more. When many people talk about BIM,

they often have the most intuitive impression that 3D modeling is equivalent to architectural models, but they often ignore the information. Why use a BIM solution? In order to integrate the information of the entire life cycle of the project into a unified "model", all the engineeringAll participants complete their respective responsibilities in the "model" and leave information for other participants to apply the information to improve the efficiency of information flow and reuse, and the degree of "transparency" of information determines the efficiency of the process (efficiency is a comprehensive trade-off of time, quality, cost and other factors). What is the role of BIM software?

1) Engineering information integration - survey information, design information, construction information, operation and maintenance information integration (entry, integration, production)  
2) Information visualization - provide visual presentation of information  
3) Auxiliary decision-making - information reproduction based on existing model information and data, each participant is the producer of information and data, and information data are records of objective activities; Information is the description of the activity state of objective things, and it is the result of data processing Data = information + data redundancy BIM is the product of the development of 3C technology, but the essence is a collection of information organization, information production, and information presentation, but information organization involves data format issues, information production involves process problems, and information presentation involves three-dimensional modeling, visualization and other issues, so the implementation of BIM should not be confined to the form, but should be defined from the needs to define its presentation form. For example, it is not necessary to have large-scale localized modeling software, and all data is directly transferred to the cloud, referred to as cloud BIM. The parametric structure scheme of the online tunnel BIM platform defines the tunnel engineering structure form is relatively simple, parametric modeling can be realized, and the large-scale three-dimensional modeling software can be used to realize online modeling based on WebGL technology, and the data is directly stored in the cloud, at the same time, the more critical link of tunnel engineering construction is the construction stage, due to the unclear geology, involving frequent construction dynamic design, the application of information technology can play an important role, under the traditional way, there is a lack of unified information platform that all parties can participate in, It is difficult to dynamically change the model information according to the construction situation, and the parameterization method combined with the online information platform can be quickly implemented, that is, the cloud BIM platform for the construction of tunnel engineering, which is a hypothesis.

(2).Large-scale BIM models and 3D reality models can be shared and interacted with based on the Web. At present, there are many BIM modeling software, such as Autodesk, Bentley, CATIA, etc., but fortunately, BIM models also have a unified data exchange standard IFC (Industry Foundation Class).The IFC data format makes it easy to import and export models between BIM software. However, in order to realize the online display of the model, this involves the lightweight of the model, and the current BIM modeling software providers have their own model lightweight cloud platform. One is for data security, and the other is to show technical strength. How to develop an online BIM lightweight web platform based on open source programs? Solution: WebGL-based online 3D visualization for presentation and interaction.



1) The essence of BIM model data: description information + geometric information  
2) Existing unified data exchange standard: IFC data standard  
3) Basic technical route: through the analysis of IFC file content, separation of geometric information and corresponding description information, the presentation of geometric information is realized by the 3D engine, and the description information is obtained by querying the IFC file content according to the component, material, information, etc. BIM model visualization.

#### 4) Model conversion:

<1>IFC->obj+mtl+jpg (geometric mesh + material information + texture picture) -> gltf, (glb binary data format), discard the description information. Basic tools: The obj to gltf tool developed by the Cesium team enables lightweight and online loading of BIM models.

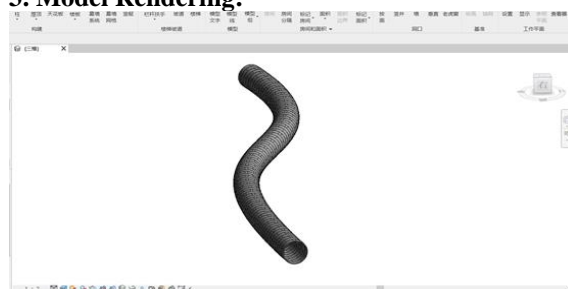
<2>IFC->Dae->gltf (glb binary data format), collada is an xml-based digital asset exchange scheme for interactive 3D applications, so that 3D authoring applications can freely exchange digital assets without loss of information, and gltf is a json format for data organization, and there is a lot in common between the two. Furthermore, Gltf->3dtile, organized into tile data, can be dynamically loaded by associating the spatial relationships of a large number of geometric models. This is the method used by the Cesiumjs library of the famous Web3D GIS engine to load the BIM model, and the traffic BIM is often said to be combined with GIS.

<3> XBIM (eXtensible Building Information Modelling), extensible, wexbrim binary format, only retains the Label-> ID and geometry and material information of the model components in IFC, and saves them in binary format, IFC->wexbim data compression is quite amazing, XBIM also provides WebGL-based js libraries, but there are several other 3D engine libraries that are so mature, Unable to load model in mobile browser.

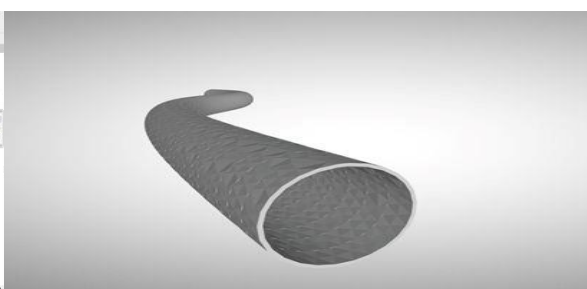
<4> BIMServer: BIM server developed based on Java combined with BIMsurfer provides a complete solution for online visualization and interaction of IFC data files. The core behind it is IFC openshell, which parses IFC data files and converts models.

<5>The shield tunnel model constructed by adaptive segments in revit has a file size of 10.4MB, and the exported IFC data file has 8.91MB, if the file size is stored in obj data format, the file size is 19.9MB when converted into a dae file by the method described in 2), and then converted into a gltf file is only 5.90MB, and converted into a glb file, that is, the binary gltf file has 3.92MB. And after being converted into a wexbim file by the XBIM tool, it is only 885KB, which is less than 1MB, which is more than 10 times compressed, which is quite amazing! The specific technical characteristics need to be studied.

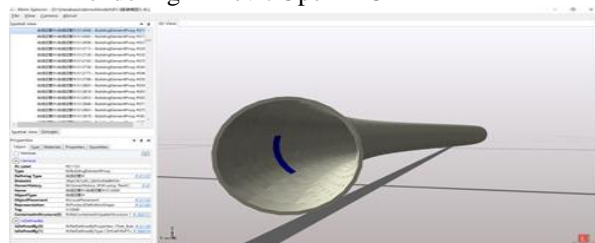
### 3. Model Rendering:



Rendering in Revit Open IFC



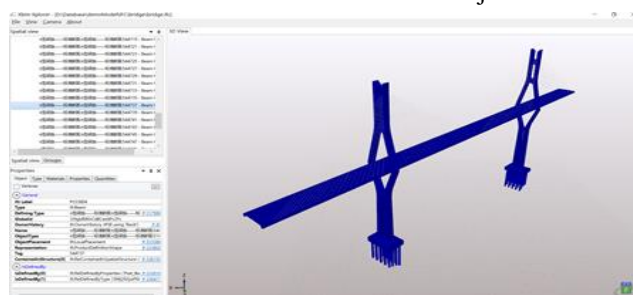
Model Residential Model



Directly in xBim Software:



obj Model .....



xBim opens IFC and turns blue....

**4..Summarize** It can be seen that GLTF as a 3D data transmission format can maintain the original rendering effect and geometric information of the model very well, and has a good effect in data compression, at present, most of the WebGL3D engines support the import and export of GLTF, the technology is mature, but for the loading of large, super-large models still need other technical solutions, such as 3dtile data organized into the form of tiles. However, there is no doubt that the application of GLTF as a unified 3D graphics conversion format can easily organize data and share models, and has a wide range of application scenarios, such as data sharing based on BIM models, online visual development and application of monitoring and inspection. BIM is moving towards the Web, and the combination of the Internet of Things and GIS is an inevitable trend, but the role of BIM in it is more important to visualize and provide description information of the 3D model.

In terms of tunnel excavation face information sharing, using three-dimensional reconstruction technology. there are mature technical solutions for image-based 3D reconstruction, but often the 3D reconstruction model file size is large, and if you want to share it on the Web, especially for movement the transmission and loading speed will be very slow.

if you want to completely save the image data of the excavation face after tunnel excavation, the number of pictures collected on site is very large, and the data volume will be very high, so it is not necessarily efficient to directly transmit images for viewing. For example, the following excavation face needs at least 78 images to be completely covered, with a total of about 241MB, but after 3D reconstruction and preservation in GLTF data format, the real information of the site can be completely preserved, and the file size is only one-tenth of the image data.

The generated model can be easily used for online browsing and sharing, and has a very realistic rendering effect, which can be viewed in the 3D viewer, which has a great effect on realizing the transparency of tunnel information and jointly constructing a "transparent tunnel".

**5.Outlook.:** IFC and BIM model transformation and advantages: IFC standard provides a structured framework for construction engineering data, By extending it to build information suitable for tunnels and other projects Converting the BIM model into GLTF format can effectively solve the problems of inconsistent data format and difficult transmission of 3D model, realize data compression while maintaining the rendering effect and geometric information, and facilitate the sharing and display of the model on the Web side, laying the foundation for BIM to go to the Web, and combine with the Internet of Things and GIS. Application prospect of tunnel information model:By integrating full-cycle data through IFC, achieving parametric visual planning with the WebGL platform, and merging BIM and GIS, the system breaks down information barriers, optimizes plans, and avoids spatial conflicts, thereby enhancing planning efficiency and systematization. Additionally, by combining advanced geological forecasting with real-time simulation for early warning of potential risks, the system converts the imagery of the excavation surface into a lightweight GLTF model for secure information sharing. Furthermore, the IFC model can synchronously update information on changes to components, thereby reducing the likelihood of accidents and safety hazards.

The unified format of IFC enables data reusability, GLTF compression reduces energy consumption, the model aids in the development of precise operation and maintenance plans, and it also supports mechanized construction, thereby conserving resources, lowering costs, and reducing carbon emissions.

## 2. REFERENCES

- [1] Meschke G. From advancet exploration to real time steering of TBMs: A review on pertinent research inthe Collaborative Research Center“Interaction Modeling in Mechanized Tunneling”[J]. Underground Space. 2018, 3(1): 1-20
- [2] Borrmann A, Kolbe T H,Donaubauer A, et al. Multi-Scale Geometric-Semantic Modeling of Shield Tunnels for GIS and BIM Applications[J].Computer-Aided Civil and Infrastructure Engineering. 2015, 30(4): 263-281.
- [3] Meschke G, Ninić J, Stascheit J, et al.Parallelized computational modeling of pile–soil interactions in mechanized tunneling[J]. Engineering Structures.2013, 47: 35-44.
- [4] Borrmann A, Flurl M, Jubierre J R, et al.Synchronous collaborative tunnel design based on consistency-preservingmulti-scale models[J]. Advanced Engineering Informatics. 2014, 28(4): 499-517.
- [5] [Alsahly A, Stascheit J, MeschkeG. Advanced finite element modeling of excavation and advancement processes inmechanized tunneling[J]. Advances in Engineering Software. 2016, 100: 198-214.
- [6] Ninić J, Meschke G. Simulation based evaluationof time-variant loadings acting on tunnel linings during mechanized tunnelconstruction[J]. Engineering Structures. 2017, 135: 21-40.

**LEGAL, ENTREPRENEURIAL, AND  
REAL ESTATE ASPECTS OF UNDERGROUND SPACE**



## CLASSIFICATION, CONFLICT MAPPING AND CRITICALITY ASSESSMENT OF UNDERGROUND ASSETS: A HOLISTIC APPROACH FOR INFORMED DECISION MAKERS

Mária Hámor-Vidó<sup>1</sup>, Tamás Hámor<sup>2</sup>, János Kovács<sup>3</sup>

**Abstract:** This study proposes a new classification of underground natural resources and provides pragmatic subclasses for consideration at spatial planning and asset management (e.g. in preparation for concessions). In case of urban underground space six major types are indicated: supply utilities, transport, housing & leisure, commerce & industry, public institutions, and civil protection. A quantitative, focused mapping of conflicts and interlinkages between these resources, regardless of the surface environmental compartments and the geological hazards, was carried out. It identified that groundwater, minerals and urban underground infrastructure have the most numerous conflicts, often resulting from the provisions of non-harmonized sectoral laws. Ownership of assets and permitting are the focal legal aspects to be resolved, especially in urban setting. For example, the collision of state vs. private ownership became obvious in case of inclined or horizontal wells for geothermal facilities and hydrocarbons. As well, the extension to depth of house- and landowners' rights shall be revised in national civil codes, construction laws and trespassing acts because of deep garages and cellars already entering the depth of others assets. Fine-tuning the legislation, the transformation of land use planning into spatial planning supported by publicly accessible online 3D(4D) geoinformation system, the comparative criticality assessment of underground assets, and the systematic use of strategic impact assessment for relevant national and regional programs are the set of potential tools that can improve the current malfunctioning silo-type sectoral governance.

**Keywords:** underground space, geological resources, criticality assessment, good governance

### 1. INTRODUCTION

In our rapidly changing world there is an intensifying competition for non-renewable or conditionally renewable underground resources and the new applications of underground space use which emerged during the last two decades. This demand appears both in urban and rural settings. These resources are either extractable (minerals, fossil fuels, groundwater, geothermal energy, geophysical forces) or imply the use of geological formations for infrastructure, energy storage, waste and carbon disposal and other novel applications (high voltage direct current underground electricity, Hyperlink, etc.). The facilities penetrate deep into the earth and their increasing density generate physical and legal conflicts with each other. Many of the underground innovations and classic utilizations (e.g. military and civil protection applications, research labs and archives, critical infrastructure, critical raw materials) are engaged by recent global challenges such as COVID, armed conflicts, disasters by weather extremes, and serious turbulences in the political and trade scene (Hámor-Vidó et al., 2021). In this regard, underground space and exploitable resources provide an extra buffer for enhancing strategic autonomy and socio-economic resilience. However, sustainability principles are endangered by the current segmented supervision of these resources, the numerous stakeholders with diverse socio-economic interest, and the dominantly first-come-

<sup>1</sup> PhD, geologist mining engineer, senior researcher, honorary associate professor, University of Pécs, Department of Geology and Meteorology, Vasvári P. u. 4., Pécs, Hungary, e-mail: vido.maria@pte.hu

<sup>2</sup> PhD, geologist mining engineer, honorary associate professor, University of Pécs, Department of Geology and Meteorology, Vasvári P. u. 4., Pécs, Hungary, e-mail: hamort4@gmail.com

<sup>3</sup> PhD, geologist, professor, head of department, University of Pécs, Department of Geology and Meteorology, Vasvári P. u. 4., Pécs, Hungary, e-mail: kovacs.janos2@pte.hu

first-served permitting practice. The business-as-usual attitude is not functioning, the issue calls for a paradigm change, for a systematic and pragmatic approach acceptable by all stakeholders.

The scientific literature is rather uneven across underground resources. Urban underground space planning is the most studied topic (Broere, 2016; Huanqing et al., 2016; Kaliampakos et al., 2016; Kishii, 2016) along with the traditional geoscientific fields on minerals, fossil energy fuels, renewables, and groundwater (Pearman, 2009; Christmann, 2021; Soltani et al., 2021; Dellapenna and Gupta, 2009), as well as the technical works on tunneling, mining engineering, and underground construction in general (e.g. Broch, 2016). In the most developed countries, such as the Netherlands, Japan, China and the UK, land use planning practices gradually turned into spatial planning during the last decade as reflected in the publications (Griffioen et al., 2014; Kishii, 2016; Chen et al., 2018; UK Government, 2024; European Commission, 2013). Numerous works deal with establishing a classification system on urban underground space, mineral reserves, waste disposal categories, infrastructure types but very few researchers proposed a holistic approach on most underground assets (Camody and Sterling, 1993; Admiraal and Cornaro, 2016; Kishii, 2016; Field et al., 2018; Volchko et al., 2020; Von der Tann et al., 2020; Hámor-Vidó et al., 2021).

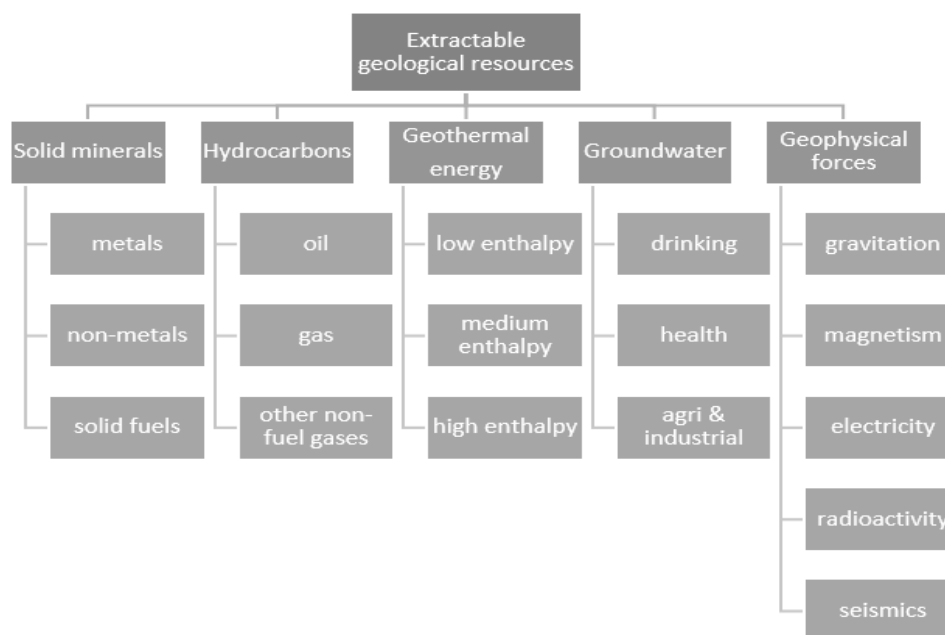
This paper is to further elaborate on the classification system of Hámor-Vidó et al. (2021) by providing detailed justification for its subclasses, the presentation of known conflicts and interlinkages, and on how this concept can be integrated into the current legislation and planning framework on the different scales of spatial governance. It is stressed that the surface environment nexus and the hazardous geological processes (“geohazards”, i.e. earthquakes) are out of the focus of this research.

## 2. METHODS

This paper reflects the outcome of four decades’ experience of the authors spent in geosciences and government administration both on regional, national, and EU level. It involves the thorough review of scientific literature and relevant press releases, the in-depth knowledge of the national (Hungarian, Dutch) and supranational (EU, OECD, UN) legislation, and the numerous international site visits to most of the facility types in focus. For the legislation reviews the European Union (EU) EUR-Lex, RMIS, and the Hungarian Jogtár services were used. This empirical knowledge was the basis both for the classification synthesis and the conflict mapping. This paper uses conventional terminology established internationally during the last two decades, such as underground space (a synonym for hosting subsoil, subsurface or geological formations), and underground natural resources (a synonym for geological resources or georesources). Earlier, “geospace” was also in use but recently it is commonly mentioned for the outer geospheres around the Earth. As indicated in the title, these resources are economic assets but the legal status and valuation of most them is rather inhomogeneous and subject to exploratory research. The proposed classification system tends to use the wording of the EU legal and political documents.

## 3. RESULTS

Hámor-Vidó et al. (2021) proposed a new classification with twelve categories in two distinct clusters, the extractable georesources and the underground space uses with the depth-range of the classes, and the typology of the resource (stock vs flow type, renewable vs non-renewable, role of natural vs. engineered barriers). Hereby, a further subdivision is provided for both clusters (Figs. 1-2).

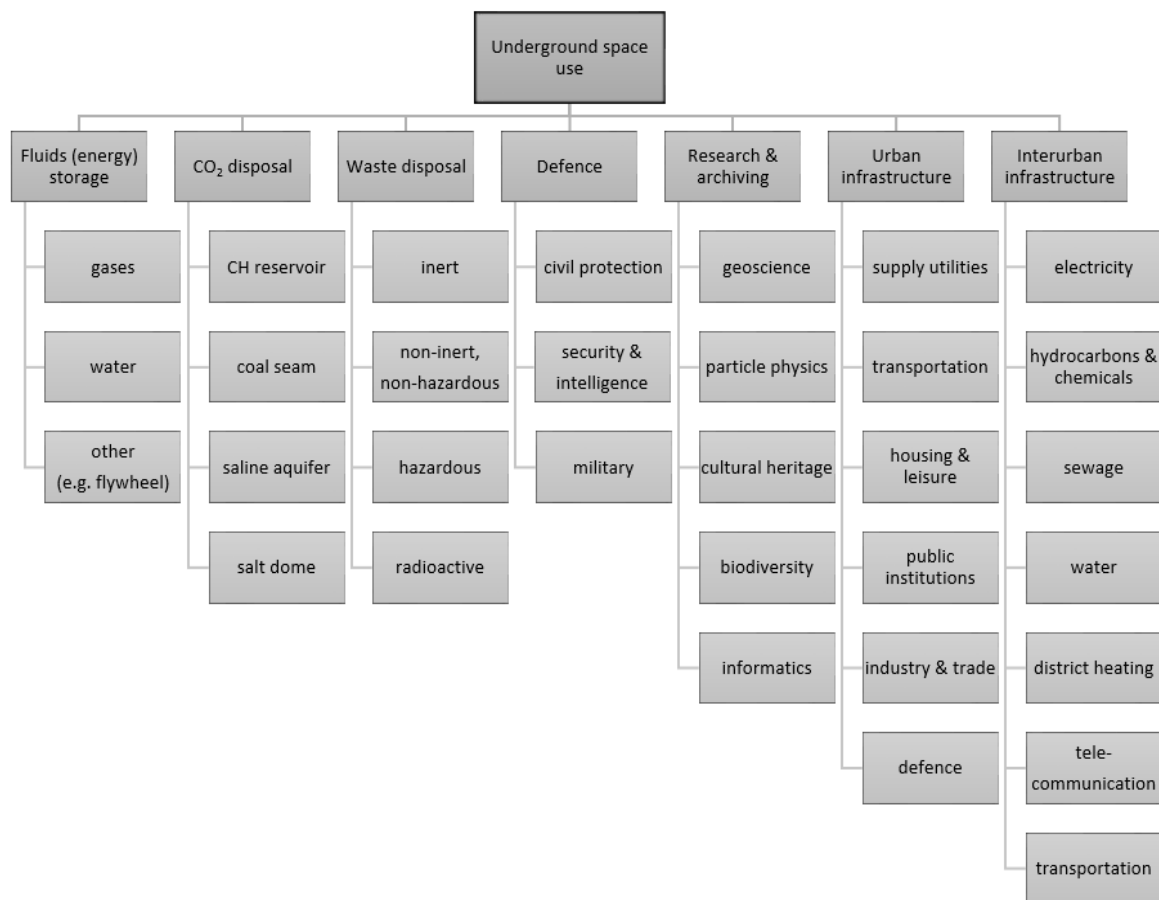


**Figure 1.** The classification of extractable resources

Most of the subclasses of extractable georesources reflect long standing industry consensus for minerals, hydrocarbons, and geothermal energy. These are manifested into international and EU legislation and have further subcategories, for example 80+ minerals by the United States Geological Survey and 170+ by the EU INSPIRE Directive Protocol which are not easily applicable for decision makers in land use planning. For example, non-metals consist of construction (sand, clay, ornamental stone) and industrial (potash, gypsum, magnesite) minerals.

Groundwater can be classified along its quality and chemistry (fresh vs. brackish vs. saline; carbonate vs. sulphate vs. chloride dominated; polluted vs. non-polluted), its aquifers (porous, karstic, fractured, confined vs. unconfined), vulnerability, and its eventual use (drinking, bathing, medical, industrial, energy, etc.). The proposed subclasses of groundwater indicate the major functions of its consumption. Drinking water has an absolute priority in all jurisdictions. The health category covers mineral waters, thermal waters for balneology, bathing, and swimming. The agricultural and industry use covers irrigation, animal breeding, and water use by all industries (mining, manufacturing, energy, etc.). Subclasses may overlap, for example, thermal groundwater is a geothermal energy source too, and minerals are extracted from saline groundwater, brines as well.

Geophysical forces occur all over and are widely used, for example magnetism and gravity for navigation, piezoelectricity for multiple use, radioactivity and tidal waves for energy generation, and all forces are applied in geoscientific research. There are a few overlaps with other categories, e.g. geothermal, metals (uranium, thorium), and research & archives. Geophysical fields are diffuse, dynamic, vectored forces changing in time but future applications can't be excluded, such as the energy generation from moving plates at locations with well exposed massive rocks (e.g. Iceland, Ethiopia).



**Figure 2.** The classification of underground space use

Utilization of underground space (Fig. 2) is the most rapidly growing segment and this is reflected in the lack of classification attempts, with exception of urban underground space and waste disposal. Waste disposal categories are defined in the EU Waste Framework Directive originating from international conventions (i.e. landfill, injection into wells, surface impoundment), its subclasses follow the waste quality groups and these define the preferred methodology of underground disposal. High level radioactive waste is the category for which deep geological disposal is the only viable option. On the contrary, for hazardous waste surface engineered structures are the eligible installations. Carbon dioxide disposal is a similar category, although a gaseous emission, not a waste in the strict legal sense. It emerged in frame of the de-carbonization efforts, and its categories are in accordance with the potential hosting geological formations, although, depleted hydrocarbon reservoirs are the only currently functioning ones.

The most recent cluster of underground space use is energy storage by applying different gases (compressed air, natural gases, synthetic gas, hydrogen), water (pumped water plants) or else (batteries, flywheels). Similarly new and growing field is the group “research & archives”. Geoscientific exploration is a traditional subgroup (mineral and groundwater exploration) and overlaps with many categories discussed in this paper. Particle physics applications have 70+ years’ history (nuclear tests, neutrino capture, accelerators). Archives conserve the biodiversity, cultural and information heritage (Seed Vault, GitHub). The defense sector is subdivided into the military, civil protection, and security & intelligence segments, all of them use underground facilities intensely.

The oldest and most studied category of underground space utilization is the urban infrastructure. Underground urbanization involves the allocation of most surface functions into the subsurface and all other extractable resources may occur beneath cities (Broere, 2016; Zhou and Zhao, 2016; Kishii, 2016; Besner, 2017; Mielby et al., 2017; Lee, 2018), its economic aspects (Kaliampakos et al., 2016; Qiao et al., 2017), and the sustainability context (Huanqing et al., 2016; Volchko et al., 2020). In spite of this long record, there is no one distinguished classification system that enjoys a wide consensus. Classifications are made as a function of depth vs. ownership (Kishii, 2016), depth vs. service type (Yu et al., 2022), and many more in accordance with the various functions allocated underground.

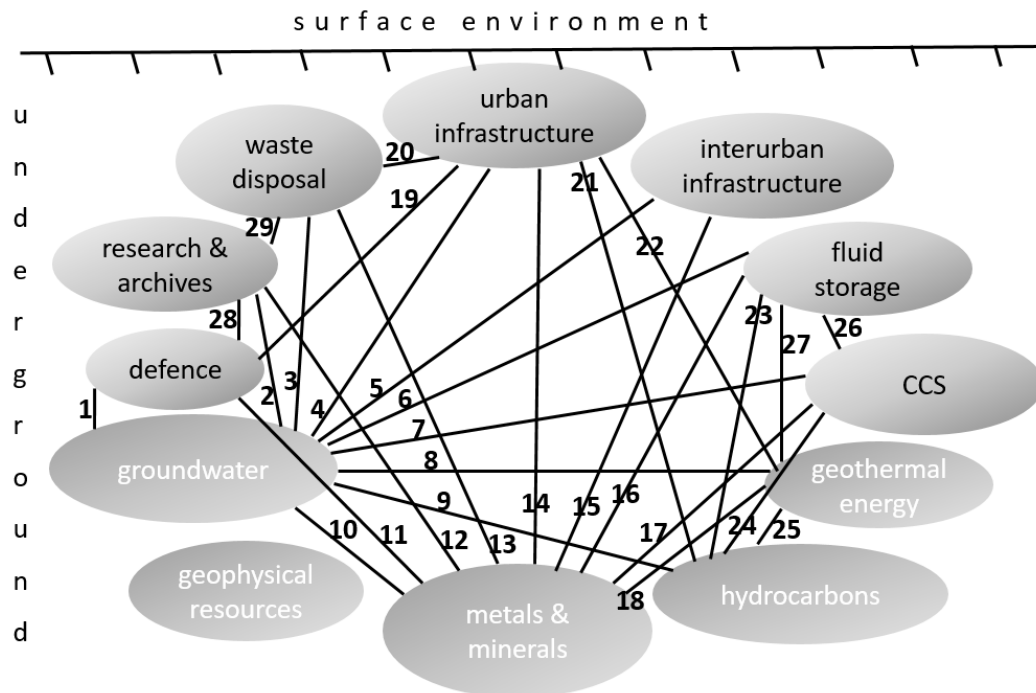
As a potential compromise, Fig. 2 indicates six major function groups commonly allocated into the subsurface which is an extension of the categories of Camody and Sterling (1993), i.e. residential/non-residential/infrastructure/defense. The first two categories (supply utilities and transportation) are the installations which extend beyond cities, and comprise interurban infrastructure, the so-called linear underground facilities running long distances (tunnels, pipelines, cable lines). As a legal justification, these categories are set in the EU INSPIRE Directive Protocol. Most works on interurban infrastructure deal with engineering aspects, and a few legal and social reviews are available (Broch, 2016; Takasaki et al., 2000; Zaini et al., 2017; Lee et al., 2016).

#### 4. DISCUSSION

The typology of Hámor-Vidó et al. (2021) extended by the current sub-classes is a complete and practical classification of underground resources based on a synthesis of the previous works and the EU legislation (Hámor et al., 2020). It reflects the technology development of the last two decades and a foresight of new functions. The previous efforts were too general (four classes by Admiraal and Cornaro, 2016), limited to extractables and energy storage (Field et al., 2018), restricted to urban setting (Kishii, 2016; Yu et al., 2022), or focused on the ecosystem services (Norrman et al., 2024). The number of classes and subclasses in our model allows to make the spatial planning by geoinformation tools, the conflict mapping and the comparative criticality assessment relatively easy. The outcome results can be interpreted by all stakeholders and the interested public. As an example, a proxy conflict map is shown on Figure 3., which is a potential input parameter of the criticality assessment (Fig. 4). Groundwater extraction and mining (incl. minerals and hydrocarbons) are clearly the most conflicted sectors. Issues occur with other resource uses and inside the sector, such as illegal or poorly designed wells connecting and polluting pristine aquifers, unsustainable extraction and many more (Dellapenna and Gupta, 2009). Urban underground infrastructure is similarly critical in respect of the risk of conflicts between subsurface installations and other natural resources. For example, hydrocarbons and geothermal fluids are produced by inclined and horizontal wells from beneath towns, metro lines are deviated because of these wells.

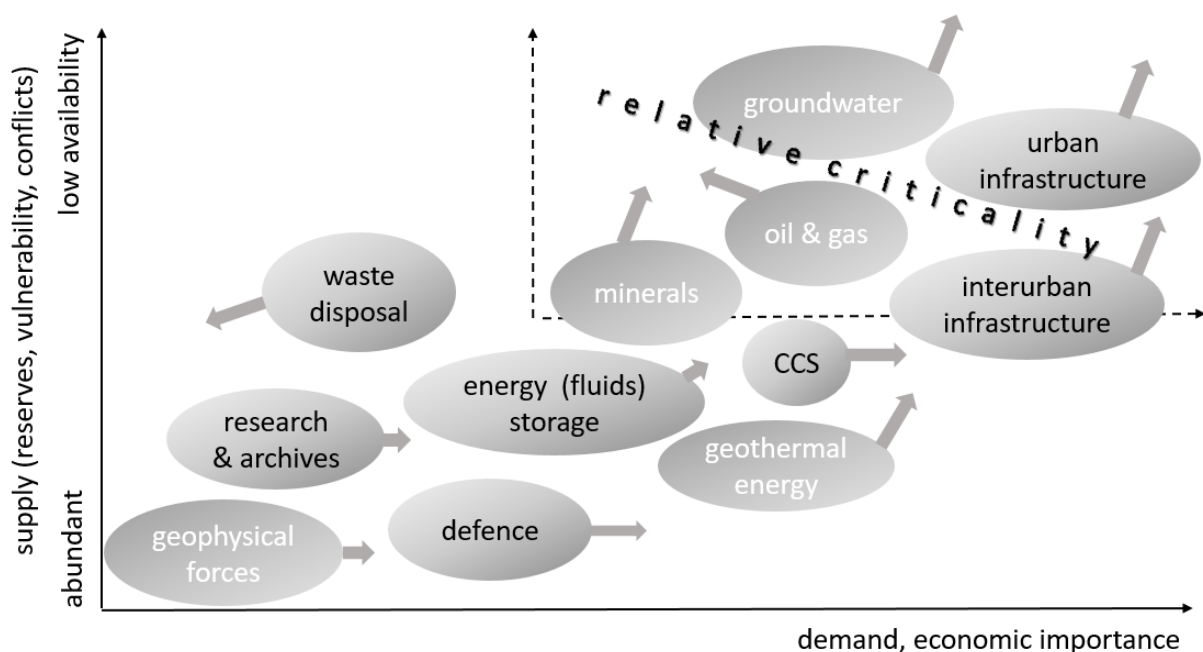
The assessment and evaluation of the value and importance of natural resources to an economy has been in focus for a long time. These include the valuation of ecosystem services and their protection (EU Natura 2000), the valorization of mineral and fuel reserves, the definition of criticality on basis of non-quantitative criteria (EU critical infrastructure and energy infrastructure of common interest) as function of supply security, market integration, open competition and sustainability. Monetary valuation of urban underground space was studied by Kaliampakos et al., 2016; and Qiao et al., 2017. Criticality can be also defined as a function of absolute scarcity (land in islands, water in arid settings). A traditional approach is to define criticality of a given resource as a function of supply and demand. This methodology is used for the assessment of strategic raw materials critical to the EU economy. It implies quantitative composite indicators for each axis, including geographic concentration of the production, country governance, import reliance on the supply risk side, and substitution potential and sectoral added value on the economic importance side.





**Figure 3.** Conflicts and synergies between underground resources. Each numbered nexus is described in the Appendice

Figure 4 is an empirical attempt to assess the criticality of the subsurface resources from a European perspective. This approach is a non-quantitative estimate of relative criticality as a function of demand (economic importance) and supply (availability and vulnerability (conflicts, environmental issues, service disruption)). The arrows indicate the current and near future trend of the resource clusters. Although the demand and supply may differ a lot across countries, regions and cities, groundwater and underground urban infrastructure are the two resources which are under increasing competition between different end-uses and stress in many regions of Europe. Hydrocarbons' importance is yet significant, EU reserves are limited, but decarbonization diminished its criticality. On the contrary, the number of strategic raw materials is on rise.



**Figure 4.** Figure 2 The relative criticality and trend of underground resources (modified after Hámor-Vidó et al., 2021)

For CCS, not storage space but capture, transmission, long term sealing and economics are the limiting factors. Energy storage share similarities to CCS. As well as geothermal energy, however, non-sustainable extraction led to local depletions and environmental conflicts. The interurban underground infrastructure has outstanding economic importance, part of it is *ex lege* classified as critical or „of common interest” but the space for future development projects is sufficient. Recent military and terrorist actions indicate that the protection of underground infrastructure is inefficient, its vulnerability has increased. Due to progressing circular economy in the EU, waste landfilling and deep disposal are not critical, their volume is rapidly decreasing. Defence applications, research and archival underground space use activities are likely not critical.

The evaluation of comparative criticality of subsurface assets should, in an ideal case, precede legislative and permitting actions and be integrated in land use planning. Parameters such as social and economic impacts of disruption of service of underground infrastructures, substitution options (e.g. relocation, replacing function), vulnerability to geohazards and unsuitable geo-environment must also be taken into account. Local and regional-scale assessments may change the outcome when interpreting local geoscientific, economic, and social data.

Good governance, the fourth pillar of sustainability, is a potential methodological tool to overcome the current situation. Legal governance is its important pillar, the conflicts in permitting originate from the unclear ownership of underground resources and spatial installations (Creutzig, 2017), as well as the non-harmonized, contradicting sectoral legislation and authority supervision. In the EU, a common legal tool is in force, the Directive on Strategic Impact Assessment which shall be applied prior to national, regional or local development programs. It implies that a complete inventory of underground resources integrated into a 3D(4D) knowledge base, a precautionary horizon scanning of future utilizations, and the comparative criticality assessment are preconditions for national, regional and local decision makers, legislators, land use planners, companies and the public. In an ideal case it is manifested in new regulations or the harmonized use of the legislation in force. These issues present in urban space, the rally for these resources does not stop at the perimeter of cities, and quasi all surface urban functions can be allocated to the underground. In this regard, the conventional urban land use planning must be transformed into spatial development. As an additional instrument for raising decision makers’ awareness, a SWOT analysis is shown on Fig. 5.



Figure 5. SWOT analysis on the enhanced use of underground space

## 5. CONCLUSIONS

A holistic multidisciplinary approach is needed when planning the use of underground space in urban environment. It implies the prudent management of extractable non-renewable natural resources in harmony with the accommodation space available in geological formations in order to avoid the sterilization of these resources. For developed societies this is the ultimate, invisible reserve, a natural buffer which can significantly contribute to social and economic resilience and strategic autonomy.

The proposed inventory of these assets is a pragmatic checklist for informed decision makers, not an academic classification scheme. Together with the collection of potential conflicts and synergies, it is the basis for establishing the input parameters of the spatial knowledge base of underground assets, an essential element of the good governance framework. Precautious local investment decisions shall take into account the broader national interests which involves a comparative economic analysis. In our view, the criticality assessment is the appropriate tool acceptable by all stakeholders. It shall be applied preferably in the course of strategic impact assessments, a precursor and legal precondition to major strategies and programs in the Member States of the European Union.

## 6. ACKNOWLEDGMENTS

This paper is a deliverable of Project No. K142550 financed by the Ministry of Innovation and Technology of Hungary, National Research, Development and Innovation Fund, K\_22 funding scheme. The comments of the anonymous reviewers improved the quality of this paper.

## 7. APPENDICE *Description of conflicts and synergies between underground resources*

No.	GROUNDWATER
1	<u>defense</u> : groundwater is a geotechnical and construction design issue, a potential threat on the long term integrity
2	<u>research &amp; archives</u> : groundwater is primarily a geotechnical and construction design issue, some facilities may require active dewatering, on the contrary, a few experiments are located in the saturated zone
3	<u>waste disposal</u> : favorable hydrogeological conditions and other geological barriers are preconditions, reinforced by engineered barriers. Requirements are more stringent at hazardous waste and radioactive waste disposal. For the latter, heat generation may mobilize liquids even in crystals. Injection into wells is a legal option but not a practice.
4	<u>urban infrastructure</u> : interactions and conflicts are numerous in both directions. Groundwater quality and reserve volumes are impacted by settlements both by point and diffuse pollutions sources and by intense extraction. Groundwater table depressions by production generate land subsidence and cracking on buildings. Pumping and deep installations (e.g. garages) deviate original flow patterns causing local flooding in nearby cellars and other facilities. Aggressive groundwater chemistry, either natural or polluted, is a threat to underground structures.
5	<u>interurban infrastructure</u> : relatively few conflicts, linear underground installations (pipelines, cables, tunnels) are well sealed, though corrosion by aggressive groundwater occur as well as seepage or flooding of tunnels and damages
6	<u>fluid (energy) storage</u> : favorable hydrogeological conditions and other geological barriers are preconditions for major facilities (compressed air, natural gas, and hydrogen; pumped water plants) reinforced by engineered barriers in order to prevent groundwater seepage into, and pumped fluid migration from the reservoir host rock
7	<u>carbon dioxide disposal</u> : favorable hydrogeological conditions and other geological barriers are preconditions in order to prevent groundwater seepage into, and pumped fluid migration from the reservoir host rock
8	<u>geothermal energy</u> : numerous conflicts known in the context of groundwater quality, quantity, temperature, hydrodynamics, and pore pressure regime especially at open geothermal systems which directly use shallow groundwater or deep aquifers of thermal water. Groundwater table depressions by production generate land subsidence. In open systems the re-injection of extracted groundwater into the same aquifer is usually required but with efficiency is uneven. Malfunctioning re-injection wells may endanger valuable reservoirs. Closed system shallow heat pumps can cool down the neighbors' soil and groundwater. Sustainable design and production plan, and stringent technology is a must. Hydraulic fracturing requires huge volume local groundwater supply, and proppants may involve dangerous chemicals posing a pollution risk. Potable groundwater reserves usually enjoy legal protection against geothermal use, and an absolute priority.
9	<u>hydrocarbons</u> : extraction of potable groundwater and hydrocarbons are very much interlinked, therefore conflicts are numerous. Although their reservoirs differ, the fluid dynamic units have impacts on each other on basin scale and on the long term. Groundwater hydraulic head depressions by production generate land subsidence. The oil, gas and water phases usually co-exist, oil and gas may appear in water wells, water is a by-product at hydrocarbon production, therefore separators are needed. Badly cemented wells may act as pollution pathways. Hydraulic fracturing requires huge volume local groundwater, enhanced efficiency hydrocarbons extraction involves dangerous chemicals posing a pollution risk. The ownership of orphan wells often means environmental legacy issues. Potable groundwater reserves usually enjoy legal protection against hydrocarbon extraction.

10	<u>solid minerals</u> : numerous conflicts and interlinkages known both at quarries and underground mines. Mining usually involves the active pumping of groundwater which generate local or regional depression causing desiccation of soil and vegetation, land subsidence and buildings' damages. Mineral processing requires voluminous water supply, and the used dangerous chemical pose a risk to groundwater quality. Pumped water can supply settlements and the formation of new wetlands.
<b>SOLID MINERALS</b>	
11	<u>defense</u> : nexus is synergetic, defense facilities frequently settle in abandoned underground mines, mining technology is the method for constructing new facilities. However, defense priorities may sterilize explored mineral reserves.
12	<u>research &amp; archives</u> : the linkage is synergetic, research facilities and archives frequently settle in abandoned underground mines, and if not, the advanced mining technology is the method for constructing new facilities.
13	<u>waste disposal</u> : multivalent and historically changing relationship. Abandoned mines were used for disposing all kinds of waste for centuries. The disposal of inert, and non-hazardous non-inert waste, typically construction and demolition waste, is a practice under controlled conditions. The deep geological disposal of high level radioactive waste is realized in structures analogue to mines and mining technology is applied for their construction. Prior to construction, underground laboratories are usually located into the candidate host rock formation of a nearby mine.
14	<u>urban infrastructure</u> : multivalent and historically changing relationship. Historically, quarry rock supplies engine urbanization, and abandoned mines were used for many surface urban functions (cemetery, storage, water reservoir, waste disposal) but old underground mines may pose a risk on buildings by land subsidence. Nowadays, only quarries for construction minerals operate in settlements due to public opposition. As well, spreading urbanization sterilize numerous explored mineral reserves.
15	<u>interurban infrastructure</u> : growing number of conflicts during planning and permitting. Priority is decided on case-by-case basis or on the first-come-first-serve principle. Legislation usually does not set an absolute or relative list of preference among them.
16	<u>fluid (energy) storage</u> : rare but positive synergy. Abandoned underground mines are used for pumped hydro-energy plants, and concepts also known for compressed air and gas storage with additional engineering.
17	<u>carbon dioxide disposal</u> : one-way positive synergy. Pilots are known in closed underground evaporate domes.
18	<u>geothermal energy</u> : positive synergies, mostly. Geothermal plants operate in abandoned underground mines (e.g. Heerlen, NL), deep-seated metalliferous ores and geothermal energy can be co-produced by leaching metals from the mineralized rock. In 2-4 km deep mines geothermal heat causes unfavorable working conditions.
<b>URBAN INFRASTRUCTURE</b>	
19	<u>defense</u> : numerous positive interlinkages and some conflicts. There are numerous underground civil protection facilities (also subway tunnels), military command centers, warfare storages, homeland security telecommunication installations beneath cities. The conflicts result from the confidential location of these facilities, although the competent authorities are standard participants in permitting. Defense facilities enjoy an absolute priority at permitting, these are "no-go-zones".
20	<u>waste disposal</u> : historical landfills still pollution sources and also pose a geotechnical issue for constructions. Nowadays it is quasi impossible to commission a waste disposal inside a settlement.
21	<u>hydrocarbons</u> : moderate number of conflicts and synergies, oil and gas is extracted from beneath cities through inclined or horizontal wells. As a by-product, it can supply thermal water to district heating. Hydraulic fracturing applied for unconventional hydrocarbons may induce moderate earthquakes, causing minor damages to buildings. Hydraulic depression may lead to local land subsidence.
22	<u>geothermal energy</u> : positive synergy with regard to carbon-neutral heating and cooling but numerous conflicts in the context of urban groundwater (see No. 8), buildings safety issues (see fracturing at No. 21) and physical conflicts of 10-400 m deep wells with other underground infrastructure (e.g. deviation of metro line in Amsterdam)
<b>HYDROCARBONS</b>	
23	<u>fluid (energy) storage</u> : positive synergies, a significant number of applications target at depleted hydrocarbon reservoirs. It also implies conflicts because of badly cemented communicating production wells, fractured sealing rocks, recovering hydraulic heads flooding the reservoir, remains of hydrocarbons, etc.
24	<u>carbon dioxide disposal</u> : positive synergies, a significant number of applications target at depleted hydrocarbon reservoirs. It also implies conflicts because of badly cemented communicating production wells, fractured sealing rocks, recovering hydraulic heads flooding the reservoir, remains of hydrocarbons, etc.
25	<u>geothermal energy</u> : emerging conflict by high enthalpy systems because both target at the same or overlapping depth interval and dynamic fluid system. A positive synergy that the exploration and extraction methodology is rather similar (deep drill holes, hydraulic fracturing, same permitting authority, concession tenders).
<b>FLUID (ENERGY) STORAGE</b>	
26	<u>carbon dioxide disposal</u> : a potential conflict is that the target formation can be the same for natural gas storage
27	<u>geothermal energy</u> : no known conflicts, though the targeted geological formation can be the same for both
<b>RESEARCH &amp; ARCHIVES</b>	
28	<u>defense</u> : positive synergy, both use closed mines frequently, or apply mining technology
29	<u>waste disposal</u> : positive synergy, e.g. neutrino capture in radioactive waste disposal site (WIPP, USA).

## 8. BIBLIOGRAPHY

- [1] Admiraal, H. and Cornaro, A. (2016). Why underground space should be included in urban planning policy – and how this will enhance an urban underground future. *Tunnelling and Underground Space Technology*, 55, 214-220.
- [2] Besner, J. (2017). Cities think underground–Underground space (also) for people. *Procedia engineering*, 209, 49-55.
- [3] Broch, E. (2016). Planning and utilisation of rock caverns and tunnels in Norway. *Tunnelling and Underground Space Technology*, 55, 329–338. <http://dx.doi.org/10.1016/j.tust.2015.08.010>
- [4] Broere, W. (2016). Urban underground space: Solving the problems of today's cities. *Tunnelling and Underground Space Technology*, 55, 245–248. <http://dx.doi.org/10.1016/j.tust.2015.11.012>
- [5] Carmody, J. and Sterling, R. (1993). *Underground Space Design: A Guide to Subsurface Utilization and Design for People in Underground Spaces*. Van Nostrand Reinhold, New York, ISBN10:0442013833
- [6] Chen, Z., Chen, J., Liu, H., Zhang, Z. (2018). Present status and development trends of underground space in Chinese cities: Evaluation and analysis, *Tunnelling and Underground Space Technology*, 71, 253-270. <https://doi.org/10.1016/j.tust.2017.08.027>.
- [7] Christmann, P. (2021). Mineral Resource Governance in the 21st Century and a sustainable European Union. *Mineral Economics*, 34, 187-208. <https://doi.org/10.1007/s13563-021-00265-4>
- [8] Creutzig, F. (2017). Govern land as a global commons. *Nature News*, 546(7656), 28.
- [9] Dellapenna, J. and Gupta, J. (eds.) (2009). *The Evolution of the Law and Politics of Water*. Springer, Dordrecht, 414.
- [10] EUR-Lex, <https://eur-lex.europa.eu/homepage.html>
- [11] EU INSPIRE Directive Protocol; [https://inspire-mif.github.io/technical-guidelines/data/mr/dataspecification\\_mr.pdf](https://inspire-mif.github.io/technical-guidelines/data/mr/dataspecification_mr.pdf)
- [12] European Commission, Raw Materials Information System, <https://rmis.jrc.ec.europa.eu/>
- [13] European Commission (2013). Strategic Implementation Plan of the European Innovation Partnership on Raw Materials. [https://ec.europa.eu/growth/sectors/raw-materials/eip/strategic-implementation-plan\\_en](https://ec.europa.eu/growth/sectors/raw-materials/eip/strategic-implementation-plan_en)
- [14] European Commission (2020a). Communication from the Commission to the European Parliament and the Council 2020 Strategic foresight report – Charting the course towards a more resilient Europe. COM/2020/493 final
- [15] European Commission (2020b). Circular Economy Action Plan, 28 p. [https://ec.europa.eu/environment/circular-economy/pdf/new\\_circular\\_economy\\_action\\_plan.pdf](https://ec.europa.eu/environment/circular-economy/pdf/new_circular_economy_action_plan.pdf)
- [16] Field, B., Barton, B., Funnell, R., Higgs, K., Nicol, A., Seebeck, H. (2018). Managing potential interactions of subsurface resources. *Proceedings of the Institution of Mechanical Engineers*, 232(1), 6-11.
- [17] Geologic Society of London (2019). 4D Subsurface Modelling: Predicting The Future. Burlington House, London <https://www.geolsoc.org.uk/~media/shared/documents/events/2019/4D%20subsurface%20modelling/4D%20Subsurface%20Modelling%20Programme.pdf>
- [18] Global CCS Institute, 2020. Global status of CCS 2020. 44 p. [https://www.globalccsinstitute.com/wpcontent/uploads/2020/12/Global-Status-of-CCS-Report-2020\\_FINAL\\_December11.pdf](https://www.globalccsinstitute.com/wpcontent/uploads/2020/12/Global-Status-of-CCS-Report-2020_FINAL_December11.pdf)
- [19] Griffioen, J., van Wensem, J., Oomes, J.L., Barends, F., Breunese, J., Bruining, H., van der Stoel, A.E. (2014). A technical investigation on tools and concepts for sustainable management of the subsurface in The Netherlands. *Science of the Total Environment*, 485, 810-819.
- [20] Hámor, T., Hámor-Vidó, M., Correia, V. (2020). Geology, the regulated discipline and profession in Europe. *Episodes*, 44(3), 219-226. <https://doi.org/10.18814/epiugs/2020/020075>
- [21] Hámorné Vidó, M., Hámor, T., Czirik, L. (2021). Underground Space, The Legal Governance of a Critical Resource in Circular Economy. *Resources Policy*, 73, DOI:10.1016/j.resourpol.2021.102171
- [22] Huanqing L., Xiaozhao, L., Kiong, S. C. (2016). An integrated strategy for sustainable development of the urban underground: From strategic, economic and societal aspects. *Tunnelling and Underground Space Technology*, 55, 67–82. <http://dx.doi.org/10.1016/j.tust.2015.12.011>
- [23] Hungarian Jogtár, <https://uj.jogtar.hu/#first/>
- [24] International Tunneling Association (2000). Planning and Mapping of Underground Space, an Overview. *Tunneling and Underground Space Technology*, 15(3), 271-286.
- [25] International Resource Panel (2020). Mineral Resource Governance in the 21st Century: Gearing extractive industries towards sustainable development. A Report by the International Resource Panel. United Nations Environment Programme, Nairobi, Kenya., 374, <https://resourcepanel.org/reports/mineral-resourcegovernance-21st-century>
- [26] Kaliampakos, D. (2016). Underground development: A springboard to make city life better in the 21st century. *Procedia Engineering*, 165, 205-213. <https://doi.org/10.1016/j.proeng.2016.11.792>.
- [27] Kaliampakos, D., Benardos, A., Mavrikos, A. (2016). A review on the economics of underground space utilization. *Tunnelling and Underground Space Technology* 55, 236–244. <http://dx.doi.org/10.1016/j.tust.2015.10.022>
- [28] Kishii, T. (2016). Utilization of underground space in Japan. *Tunnelling and Underground Space Technology* 55, 320–323. <http://dx.doi.org/10.1016/j.tust.2015.12.007>
- [29] Lee, J. (2018). *Urban Subterranean Space: A link between a ground level public space and underground infrastructure*. Thesis. Rochester Institute of Technology. 157 p., Accessed from <https://scholarworks.rit.edu/theses>
- [30] Lee, E.H., Christopoulos, G.I., Lu, M., Heo, M.Q., Soh, C.K. (2016). Social aspects of working in underground spaces. *Tunneling and Underground Space Technology* 55, 135–145. <http://dx.doi.org/10.1016/j.tust.2015.12.012>
- [31] Li, H.Q., Parriaux, A., Thalmann, P., Li, X.Z. (2013). An integrated planning concept for the emerging underground urbanism: Deep City Method, *Tunneling and Underground Space Technology* 38, 559–568.
- [32] Makana, L.O., Jefferson, I., Hunt, D.V.L., Rogers, C.V.F. (2016). Assessment of the future resilience of sustainable urban sub-surface environments. *Tunneling and Underground Space Technology*, 55, 21–31.



- [33] Mielby, S., Eriksson, I., Campbell, D.G., de Beer, J., Bonsor, H., Le Guern, C., van der Krogt, R., Lawrence, D., Ryżyński, G., Schokker, J., Watson, C. (2017). Opening up the subsurface for the cities of tomorrow. TU1206 COST Sub-Urban Report, 120. [www.sub-urban.eu](http://www.sub-urban.eu)
- [34] Norrman, J., Sandström, O. T., de Lourdes Melo Zurita, M., Mossmark, F., Frisk, L. E., Melgaço, L., Söderqvist, T., Lindgren, P., Volchko, Y., Svahn, V. (2024). Deep planning: improving underground developments through inter- and transdisciplinary collaboration on geosystem services. *European Geologist*, 57, pp. 58-62., <https://doi.org/10.5281/zenodo.12205943>
- [35] Qiao, Y.K., Penga, F.L., Wangb, Y. (2017). Monetary valuation of urban underground space: A critical issue for the decision-making of urban underground space development. *Land Use Policy*, 69, 12–24, <http://dx.doi.org/10.1016/j.landusepol.2017.08.037>
- [36] Pearman, G. (2009). 101 things to do with a hole in the ground. Post-mining Alliance, ISBN 978-0-9562213, 138.
- [37] Soltani, M., Kashkooli, F. M., Souri, M., Rafiei, B., Jabarifar, M., Gharali, K., Nathwani, J. S. (2021). Environmental, economic, and social impacts of geothermal energy systems. *Renewable and Sustainable Energy Reviews*, 140. <https://doi.org/10.1016/j.rser.2021.110750>
- [38] Takasaki, H., Chikahisa, H., Yuasa, Y. (2000). Planning and Mapping of Subsurface Space in Japan. *Tunnelling and Underground Space Technology*, 15(3), 287-301.
- [39] UK Government Office for Science (2024): Future of the subsurface: subsurface space management in the UK, 26 p. <https://www.gov.uk/government/publications/future-of-the-subsurface-report/future-of-the-subsurface-subsurface-space-management-in-the-uk-annex#references>
- [40] UN Economic and Social Commission for Asia and the Pacific (1998). What is good governance? UN, 3., <https://www.unescap.org/sites/default/files/good-governance.pdf>
- [41] United States Geological Survey, Mineral Resources Program, <https://www.usgs.gov/energy-and-minerals/mineral-resources-program>
- [42] Van der Meulen, M.J., Doornenbal, J.C., Gunnink, J.L., Stafleu, J., Schokker, J., Vernes, R.W., van Geer, F.C., van Gessel, S.F., van Heteren, S., van Leeuwen, R.J.W., Bakker, M.A., Bogaard, P.J.F., Busschers, F.S., Griffioen, J., Gruijters, S.H.L.L. Kiden, P., Schroot, B.M., Simmelink, H.J., van Berkel, W.O., van der Krogt, R.A.A., Westerhoff, W.E., van Daalen, T.M. (2013). 3D geology in a 2D country: perspectives for geological surveying in the Netherlands. *Netherlands Journal of Geosciences*, 92(4), 217-241.
- [43] Volchko, Y., Norrman, J., Ericsson, L.O., Nilsson, K.L., Markstedt, A., Oberg, M., Mossmark, F., Bobylev, N., Tengborg, P. (2020). Subsurface planning: Towards a common understanding of the subsurface as a multifunctional resource. *Land Use Policy* 90, 104316, <https://doi.org/10.1016/j.landusepol.2019.104316>
- [44] Von der Tann, L., Sterling, R., Zhou, Y., Metje, N. (2020). Systems approaches to urban underground space planning and management – a review. *Underground Space*, 5, 144-166. <https://www.sciencedirect.com/science/article/pii/S2467967418301119#s0025>
- [45] Xiea, H., Zhaoc, J.W., Zhoud, H.W., Renf, S.H., Zhangg, R.X. (2020). Secondary utilizations and perspectives of mined underground space. *Tunnelling and Underground Space Technology* 96 (2020) 103129, <https://doi.org/10.1016/j.tust.2019.103129>
- [46] Zaini, F., Hussin, K., Raid, M.M. (2017). Legal considerations for urban underground space development in Malaysia. *Underground Space* 2, 234–245, <https://doi.org/10.1016/j.undsp.2017.11.001>
- [47] Zhou, Y., Zhao, J. (2016). Assessment and planning of underground space use in Singapore. *Tunnelling and Underground Space Technology*, 55, 249–256. <http://dx.doi.org/10.1016/j.tust.2015.12.018>

## A CRITICAL REVIEW OF THE EXISTING METHODOLOGIES FOR THE ESTIMATION OF THE VALUE OF UNDERGROUND SPACE

Dimitrios Papadomarkakis<sup>1</sup>

**Abstract:** Ever since 2020, more than 50% of the world's population has been concentrated in large urban centers. Coupled with the rapidly growing global population, this shift has exacerbated major issues and challenges within modern cities. These problems span environmental, social, transportation, and energy-related concerns that must be addressed to ensure the sustainable development of emerging "mega-cities." One sustainable solution that has gained prominence over the past 30 years is the utilization of Urban Underground Space (UUS). Countries like Singapore and Japan, and cities such as Montreal and Paris, have consistently developed their underground spaces to create metro lines, underground parking lots, and roads to cope with these modern challenges. However, in many other parts of the world, underground projects remain unrealized, often stalled at the decision-making stage. The primary reason for this stagnation is the unfavorable comparison between underground structures and their above-ground counterparts, primarily due to the significantly higher capital costs associated with underground development. However, it is misleading to compare an underground project with an above-ground facility of the same utility and base the decision solely on construction cost estimates. UUS possesses a "hidden" value, often referred to as the indirect value, which represents the monetary value of the indirect benefits that arise from UUS development. This indirect value is frequently overlooked during the decision-making process because it is challenging to quantify in monetary terms. However, if systematically integrated into the decision-making process, the indirect value could allow underground facilities to compete directly with above-ground solutions, making them more attractive investments. Together, the indirect value and direct value constitute the real value of UUS. Consequently, the scope of the current study is to gather and critically evaluate all existing methodologies for estimating the real value, direct value, or indirect value, including losses that may arise from UUS development. To ensure comprehensive coverage of all available techniques, the study utilized the Preferred Reporting Items for Systematic Reviews and Meta-Analyses (PRISMA) method. The existing methodologies were thoroughly presented, highlighting their strengths and weaknesses, and proposing ways to improve them in the future.

**Keywords:** Urban Underground Space (UUS), Underground Space Value, Indirect Benefits of UUS, Valuation of Underground Space Benefits, Economics of Underground Space.

### 1. INTRODUCTION

Urbanization is a well-established worldwide trend that is continually increasing. According to data from the World Bank Group, in 1960, 34% of the world's population lived in urban centers (World Bank Group, Urban Development, 2024). By 2020, this percentage had risen by 22%, with 56% of the world's population residing in large urban areas (World Bank Group, Urban Development, 2024). Coupled with the fact that the global population has increased by more than 159% during this 60-year span, the overall result is a troubling increase in population density in modern cities. As urban areas continuously expand in size, population, and complexity, people, services, and industries compete for the decreasing available urban surface space (Mavrikos and Kaliampakos, 2021). Given the limited availability of surface space, the utilization of subsurface areas has become a necessity in modern urban planning (Papadomarkakis, 2025). The third dimension of a city has constantly proven that it can provide sustainable solutions to all the modern challenges urban centers face.

The primary criticism that most underground projects face, compared to their surface counterparts, is their increased construction cost. Ultimately, this factor often becomes the deciding one (Kaliampakos et al., 2016). Despite the numerous advantages of utilizing underground space, which have been highlighted by many

<sup>1</sup> Undergraduate Student, Laboratory of Tunnelling, School of Mining and Metallurgical Engineering, National Technical University of Athens, 9 Iroon Polytechniou Str., GR15780, Zografou Campus, Athens, Greece. E-mail address: [papadomarkakisdimitrios@gmail.com](mailto:papadomarkakisdimitrios@gmail.com)

researchers over the years (e.g. Barker and Jansson, 1982; Godard and Sterling, 1995; Tareau, 1995; ITA WG15, 1998; ITA WG13, 2004), underground projects are frequently avoided due to their higher capital costs relative to surface solutions. The main reason for this significant capital cost gap is that some of the benefits, particularly environmental ones, provided by underground projects cannot be easily quantified in monetary terms. Comparisons between surface and underground alternatives typically focus solely on construction costs, neglecting the substantial environmental contributions of underground projects. Consequently, the higher initial construction cost of underground structures often makes them a less favorable option (Mavrikos and Kaliampakos, 2021). To ensure the future growth of urban underground space utilization, two critical parameters must be secured (Kaliampakos and Benardos, 2008; Bobylev, 2009; Kaliampakos et al., 2016; Qiao et al., 2017; Mavrikos and Kaliampakos, 2021):

- The creation of a systematic methodology that can estimate the value of underground space, since nowadays it has a zero assigned value, and also
- Incorporate in the estimation process the major environmental benefits of underground projects, something that is often overlooked, because it is difficult to express in monetary terms.

It is imperative to consider the environmental benefits of underground projects during the decision-making process, a factor that can make these projects directly competitive with their surface counterparts. Consequently, the aim of this study is to critically review the existing methodologies proposed for estimating the value of underground space using the established Preferred Reporting Items for Systematic Reviews and Meta-Analyses (PRISMA) method. Methodologies will be collected from the Scopus search engine and previous conference proceedings, using specific keywords and phrases. This approach will allow the current literature on the subject to be gathered and organized, providing a comprehensive overview. The study will also discuss the strengths and weaknesses of each proposed method, paving the way for future researchers to develop better methodologies or improve existing ones. This critical collection can be of great significance to both future researchers and urban planners. Researchers can use this work as a foundation for future attempts to create new methodologies or improve existing ones. Urban planners, on the other hand, will benefit from a comprehensive database of existing methodologies for estimating the value of UUS, enabling them to choose the most appropriate technique based on the size and type of the underground project. This approach ensures that UUS is evaluated and utilized in a way that maximizes its potential for sustainable urban development.

## 2. METHODOLOGY

The Preferred Reporting Items for Systematic Reviews and Meta-Analyses (PRISMA) statement, published in 2009 (hereafter referred to as PRISMA 2009) (Moher et al., 2009; Page et al., 2021), is a reporting guideline created to improve the quality of systematic and critical review reporting (Moher et al., 2007; Page et al., 2021). The PRISMA 2009 statement consisted of a checklist with 27 items recommended for reporting in systematic reviews, accompanied by an "explanation and elaboration" paper (Liberati et al., 2009; Page et al., 2021) that offered further guidance for each item and included examples of proper reporting. A need for an updated version of the PRISMA 2009 statement became evident, as the terminology had greatly evolved since 2009 and the publishing landscape had significantly changed. Consequently, the newly proposed 2020 PRISMA statement replaced the 2009 version (Page et al., 2021). The 2020 PRISMA statement checklist includes seven sections with 27 items, some of which include sub-items (Page et al., 2021). The general steps of the PRISMA 2020 method are summarized as follows:

- The identification and gathering stage. In the initial stage, relevant articles are identified using specific keywords and phrases in an electronic search engine. The diverse keywords used include "underground space value," "economics of underground space," "estimation of the value of underground space," "economic evaluation of underground spaces," "economic benefits of underground development," "cost-benefit analysis of underground spaces," and "valuation methods for underground space," thereby ensuring comprehensive coverage. The primary database utilized was Scopus. Additionally, articles were sourced from previous conference proceedings of the World Tunnel Congress (WTC) and the Associated Research Centers for the Urban Underground Space (ACUUS), an organization that has been advocating for the utilization of urban underground space for over 30 years. Upon completion of the gathering process, duplicate articles are excluded from the review.
- The screening stage. In the second stage, the retrieved articles are closely evaluated to determine their relevance to the topic of underground space valuation methodologies. Articles that do not propose original methodologies and merely repeat existing ones are excluded to focus on innovative contributions.

- The eligibility stage. In the third stage, the articles deemed relevant from the screening stage are further assessed for eligibility. Articles that do not directly estimate the value of underground space in monetary terms are excluded. The reasons for exclusion are thoroughly documented, acknowledging that excluded articles might be relevant for other reviews but are omitted based on the authors' specific criteria for this study.
- The inclusion and presentation stage. In the final stage, the remaining articles are presented as the current existing methodologies for valuing underground space. Each methodology is analyzed, highlighting its strengths and weaknesses. This analysis provides a foundation for future research and helps urban planners choose the most suitable methods for their projects.

This structured approach ensures a thorough review and critical assessment of the methodologies used to estimate the value of underground space.

### **3. RESULTS**

#### **3.1. Identification and gathering stage**

As previously mentioned, the database of Scopus and conference proceedings from the World Tunnel Congress (WTC) and the Associated Research Centers for the Urban Underground Space (ACUUS) were utilized to gather the current literature on the methodologies for estimating the value of underground space. Using the following keywords in the Scopus search engine: "underground space value", "economics of underground space", "economic evaluation of underground spaces", "economic benefits of underground development", "cost-benefit analysis of underground spaces", and "valuation methods for underground space", a total of 81 articles were gathered. Additionally, 2 articles were obtained from previous WTC conference proceedings, and 58 articles were sourced from previous ACUUS conference proceedings. In total, 141 articles were collected. Of the 81 articles collected from Scopus, eight were excluded due to duplication, resulting in a total of 133 articles advancing to the screening stage.

#### **3.2. Screening stage**

In this stage, the 133 articles collected from the previous stage were meticulously examined to determine their relevance to the subject of estimating the value of underground space. At this juncture, it is essential to clarify the key concepts upon which the exclusion criteria were based. Generally, Urban Underground Space (UUS) encompasses both real and potential values. The real value comprises the direct and indirect values of UUS. The direct value refers to the economic benefits, such as the increase in surface land value following the construction of a metro station nearby. The indirect value, often overlooked in the decision-making process for underground projects, encompasses environmental and social benefits quantified in monetary terms. Examples include reductions in noise pollution, decreases in CO<sub>2</sub> emissions, and overall improvements in living standards. Conversely, the potential value represents the comprehensive benefits that could be derived from untapped underground resources, such as underground space, groundwater, geomaterials, and geothermal energy. At this stage, articles that estimate any of the aforementioned values of underground space were considered relevant and accepted. However, articles that did not propose new methodologies and merely reiterated existing ones were excluded for lacking original contributions. Overall, 110 articles were excluded for not being pertinent to the subject matter. The remaining 23 articles, 17 from Scopus and 6 from previous ACUUS conference proceedings, were forwarded to the eligibility stage.

#### **3.3. Eligibility stage**

In the eligibility stage, the 23 articles identified in the previous phase underwent a final examination process. During this stage, articles proposing new methodologies for estimating the potential value of Urban Underground Space (UUS) were excluded, as the primary focus of this study is to critically review existing methodologies for assessing the real value of UUS. Consequently, the final selection includes only those articles that present new and original methodologies for estimating the real value of UUS or the losses associated with its development. Additionally, in some instances, authors have published fragments of a larger methodology, later followed by a complete version of the method. In such cases, the final and complete work is retained, while the preliminary fragments are excluded. Overall, 13 articles were excluded at this stage, with the final 10 moving to the inclusion and presentation stage.

### 3.4. Inclusion and presentation stage

In this final stage, the remaining 10 articles are identified as the existing methodologies for estimating the real, direct, or indirect value and losses of Urban Underground Space (UUS). In Table 1 below, these 10 articles are presented, including their source of retrieval, reference, and the specific type of UUS value they estimate (whether real, direct, or indirect).

**Table 1.** A summary of the 10 articles that can estimate the real, direct, or indirect value and/or losses of UUS.

Title	UUS Value	Source	Reference
The Importance of Urban Underground Land Value in Project Evaluation: A Case Study of Barcelona's Utility Tunnel	Direct Value	Scopus	Riera and Pasqual (1992)
Underground Land Values	Real Value	Scopus	Pasqual and Riera (2005)
Urban Underground Space Value: Case Study of Kaisheng Square Planning in Lanzhou City	Direct Value	2009 ACUUS International Conference Proceedings	Zhu et al. (2009)
Monetary Valuation of Urban Underground Space: A Critical Issue for the Decision-Making of Urban Underground Space Development	Real Value	Scopus	Qiao et al. (2017)
Valuing External Benefits of Underground Rail Transit in Monetary Terms: A Practical Method Applied to Changzhou City	Indirect Value	Scopus	Qiao et al. (2019a)
Socio-Environmental Costs of Underground Space Use for Urban Sustainability	Indirect Losses	Scopus	Qiao et al. (2019b)
Monetary Evaluation Method of Comprehensive Benefits of Complex Underground Roads for Motor Vehicles Orienting Urban Sustainable Development	Real Value	Scopus	Ma and Peng (2021)
An Integrated Methodology for Estimating the Value of Underground Space	Real Value	Scopus	Mavrikos and Kaliampakos (2021)
Measuring the Monetary Value of Environmental Externalities Derived from Urban Underground Facilities: Towards a Better Understanding of Sustainable Underground Spaces	Indirect Value and Losses	Scopus	Dong et al. (2021)
Rethinking Underground Land Value and Pricing: A Sustainability Perspective	Real Value	Scopus	Qiao et al. (2022c)

## 4. DISCUSSION

### 4.1. Early attempts for estimating the value of UUS (early 1990s to late 2000s)

In their initial attempt to estimate the direct value of Urban Underground Space (UUS), Riera and Pasqual (1992) implemented a market-oriented approach. The authors proposed that when parameters such as the construction cost of the underground facility ( $c$ ), its selling price ( $p$ ), and the rate of return on this particular investment ( $b$ ) are known, the direct value of the underground space ( $u$ ) can be calculated using the following formula:

$$u = \left( \frac{p}{1+b} \right) - c \quad (1)$$

After presenting this straightforward equation, they applied it to estimate the direct value of an underground parking facility in central Barcelona. Their findings revealed that the value of the underground space in this particular case was \$6.518 per parking spot or \$113,3 per cubic meter (based on 1990 prices), assuming that a standard parking space occupies 57,5 cubic meters (Riera and Pasqual, 1992).

The two researchers enriched their previous work when they proposed a purely theoretical economic approach. Specifically, Pasqual and Riera (2005) introduced a simplified economic model that applied an



optimization algorithm using Lagrange multipliers to maximize a utility function. This approach generated a mathematical expression that quantifies the social value of underground space, and the associated externalities linked to its utilization. Finally, they concluded that the socially optimal price for using a certain amount of underground space has two components: the first represents the value of property rights, which includes the scarcity of underground land and the rising cost of access, and the second reflects the marginal productivity of the underground space and the externalities it produces (Pasqual and Riera, 2005). They also emphasized that the market typically overlooks these externalities, leading to suboptimal use of underground space for society unless some forms of corrective measures are implemented.

While these two efforts were significant first steps in evaluating the value of underground space, they do have some limitations. Firstly, the original method assumes the existence of a competitive market for buying and selling underground spaces, which is necessary to determine parameters like market prices and the rate of return, a market that does not exist in reality. Secondly, the first methodology overlooks the indirect benefits derived from utilizing underground space, failing to account for its indirect value. Although the later approach made a major advancement by incorporating social benefits into the estimation process, it is not easily applicable to real-world underground projects. The method demands a significant amount of input data, which is not always available, and the overall procedure can become somewhat complex, particularly when applied by individuals without a strong economic background.

Another important step forward was made by Zhu et al. (2009) when they utilized a cost-benefit analysis to calculate the direct value of UUS. In their study, they applied this method to compare three different development scenarios for UUS in Kaisheng Square. The first scenario proposed two underground floors, one for commercial use and one for parking. The second scenario added a third floor, one for commercial use, with the other two floors designated for parking. The third scenario suggested creating two floors solely for parking. The authors first estimated the construction costs for each scenario, including excavation and other related expenses. They also calculated the annual operating costs once the facility became operational, such as electricity, equipment depreciation, building depreciation, and rental income taxes. By summing the annual operating costs and construction costs, they derived the total cost of each scenario. As for the benefits, they estimated the commercial rental income and parking income, which, when combined, gave the total annual income for each scenario. To assess the financial feasibility, they calculated the annual net income by subtracting the total costs from the total annual income, and they determined the payback period by dividing the construction costs by the annual net income.

The results of the analysis indicated that the first scenario was the best development option, with a net annual income of  $153,704 \times 10^4$  RMB Yuan/year (based on 2009 prices) (Zhu et al., 2009), while the other two scenarios had negative net annual incomes. The payback period for the first scenario was 9 years (Zhu et al., 2009), shorter than the standard 12-year period typically expected in China. This methodology was a significant advancement, as it allowed for the estimation of the direct value of UUS through a straightforward cost-benefit analysis. It also enabled the comparison of different development scenarios, aiding in the creation of optimal facilities that maximize direct value. However, this method, like others before it, did not include the social and environmental benefits that come from the sustainable development of UUS. The analysis only considered commercial rental and parking income. If the social and environmental benefits had been included in the total annual income calculation, the annual net income would have been higher, further reducing the payback period for the project and making it an even more attractive investment.

#### **4.2. Attempts of the previous decade for estimating the value of UUS (late 2010s)**

Almost a decade later another attempt for estimating the real value of Urban Underground Space (UUS) was introduced by Qiao et al. (2017). Specifically, the authors proposed a modified Service Replacement Cost Method (SRCM), which values UUS by assessing the cost society would face if the urban services provided by UUS were to be replaced by alternative methods. Before conducting the monetary evaluation, it was noted by the authors how crucial it was to identify the urban services provided by UUS, allowing the replacement cost to be calculated based on each type of service. These services were initially categorized by their value, meaning internal or external, and further subdivided according to the type of benefit they offered, such as direct, social, or environmental benefits. Ultimately, UUS services were used as valuation indicators within the SRCM framework. The proposed SRCM can be divided into seven straightforward steps which are extensively analyzed in the original study of Qiao et al. (2017). When introducing the SRCM framework, the authors presented equations to estimate the monetary values of all UUS services. In order to demonstrate their method's effectiveness, they applied it in Changzhou, China, where the real value of UUS was calculated. The total value of UUS services was approximately 276.8 billion yuan, averaging 7.3 billion yuan annually (around 1.156 million USD based on 2012 prices) over a valuation period of 38 years, accounting for more than 1.8% of Changzhou's 2012 GDP (Qiao et al., 2017).

The latter methodology represents a significant advancement in estimating the real value of UUS and marks the second major attempt in this field. While the technique is well-structured and comprehensive, particularly in considering the often-overlooked indirect value, it does have some notable limitations, as acknowledged by the researchers themselves. Particularly, The SRCM relies on a comprehensive classification and identification process that covers all UUS services from underground facilities. Although the authors made considerable efforts to encompass a wide range of services, a systematic identification and classification process is necessary for the method's application across all types of UUS facilities. Additionally, the SRCM requires extensive input data, much of which may be unavailable or even nonexistent, raising concerns about the method's applicability in other regions, particularly in Europe, where such specialized data is challenging to obtain.

Qiao et al. (2019a) expanded upon their previous work on the Service Replacement Cost Method (SRCM) by refining it into a more concise three-step process, enhancing its ability to translate the indirect benefits of an underground rail transit system into monetary terms, by deepening its theoretical framework using marginal value theory for non-market goods. Specifically, they argued that the core economic principles of the SRCM framework were rooted in the concept of marginal value. Since the external benefits of underground rail transit reflect a use value rather than an exchange value, they cannot be directly expressed in monetary terms in the real-world market. However, by considering the marginal benefit, the impact of the external benefit provided by underground rail transit on a unit scale can be measured by assessing its influence on social welfare. In this context, the costs people incur or the monetary losses they suffer, known as replacement costs, can be viewed as the unit value (Qiao et al., 2019a). The updated SRCM framework was divided into three steps, that are thoroughly presented and consequently explained by Qiao et al. (2019a). Finally, the modified SRCM was applied to the Changzhou underground rail transit system in order to estimate its indirect value. The annual total indirect value of the transit services were approximately 11,5 billion yuan (about 1.769 million US dollars based on 2016 prices), accounting for nearly 2,0% of Changzhou's GDP in 2016 (Qiao et al., 2019a).

This modification marked a significant improvement over the original SRCM by better incorporating the indirect benefits of UUS, specifically those of underground rail transit systems, using the concept of marginal value. The framework was also made more robust by reducing the original seven steps to just three. Moreover, while the original methodology required a separate formula for calculating the replacement cost value of each listed service, the reformed approach allows the values of all services to be calculated using a single equation, again making the overall process more straightforward. However, some of the challenges present in the original method remain unaddressed. First, the SRCM still relies on a comprehensive classification and identification process for all services provided by UUS facilities. While the authors made considerable efforts to cover a broad range of services, a systematic approach for identifying and classifying is necessary for applying this method across various types of UUS facilities, and not just underground rail transit systems. Additionally, although the input data requirements were somewhat reduced due to the simplified formula, the method still demands a significant amount of input data, much of which may be unavailable or even nonexistent. This issue, as noted by the researchers themselves, raises concerns about the applicability of the SRCM in other regions and countries.

Less than a year later, Qiao et al. (2019b) expanded their research by assessing the socio-environmental losses caused by the development of UUS in monetary terms, from the perspective of urban sustainability. They used the service replacement cost method (SRCM), which they had introduced in their previous work. Initially, the authors identified and categorized these socio-environmental losses by examining the interactions between UUS and urban sustainability. To do this, they referenced the seventeen Sustainable Development Goals (SDGs) provided by the United Nations (UN). They also listed the main losses associated with UUS development, such as the reduction of physical underground space, loss of geomaterials, groundwater contamination, and the loss of geothermal energy. These compromised underground assets were then paired with their respective SDG contributions to urban sustainability (Qiao et al., 2019b). As for the SRCM, it was assumed that the costs would be at least equivalent to the amount of money required to restore the damaged underground assets to their original state, i.e., the condition of the underground environment before UUS development. The SRCM involved six steps, for a comprehensive explanation of these steps the author suggests reading the original manuscript of Qiao et al. (2019b).

Once again, the city of Changzhou, China, was chosen as a case study to apply the SRCM methodology to calculate the indirect losses from UUS development. The findings revealed that the total socio-environmental costs of UUS development in Changzhou amounted to approximately USD 719,76 million (Qiao et al., 2019b). When these costs were compared with the total external benefits, which were close to USD 36,16 billion, it was found that the socio-environmental costs could exceed 1,99% of the external benefits derived from UUS development (Qiao et al., 2019b). Overall, this study marks a significant milestone as it is the first to examine the indirect losses resulting from the development of Urban Underground Space (UUS), a previously unexplored area of research. By recognizing that the development of a city's third dimension can produce not only benefits but also losses, this research takes a major step forward in providing a more comprehensive estimation of UUS's real value. The methodology employed, a modified version of the Service Replacement Cost Method (SRCM) developed by the authors in their earlier work, was adapted to focus on capturing losses rather than advantages. However, the

approach has several critical limitations regarding its general applicability. The estimation of costs is heavily dependent on two key parameters: the magnitude of losses and the probability of their occurrence. These parameters are highly contingent on the local conditions of the case study and can be difficult, if not impossible, to predict accurately. As a result, their estimation is largely subjective, varying significantly depending on the user's judgment, which can lead to considerable differences in outcomes. This subjectivity means that the method may produce inconsistent results across different case studies, as each location would need to establish its own values for these parameters. Consequently, the method fails to provide a systematic approach for estimating indirect losses that are both easily applicable and highly efficient across various contexts. Moreover, the fact that underground space is a non-renewable resource further complicates the replacement cost approach. The underground environment can never be fully restored to its original state once altered by engineering structures and construction materials used for UUS development, raising questions about the accuracy of using replacement costs to assess socio-environmental losses. Finally, as highlighted in the authors' previous works, the SRCM's reliance on extensive input data, particularly for aspects like geothermal energy and groundwater, poses a significant challenge. This data is often difficult to obtain or even nonexistent, further restricting the method's applicability in different case studies.

#### **4.3. More recent attempts for estimating the value of UUS (early 2020s)**

Ma and Peng (2021) made a significant recent contribution by identifying nine sustainability-oriented benefits of complex underground roads and then estimated their monetary value. The researchers divided these benefits into two main categories. The first category, the intrinsic benefits (or direct benefits) that stemmed from the fundamental functions of the newly planned roads, primarily through increased traffic supply (Ma and Peng, 2021). The second category, the specific benefits (or indirect benefits) that were unique to complex underground roads and included the mitigation of adverse effects typically caused by aboveground arteries or expressways (Ma and Peng, 2021). In order to properly identify these nine sustainability-oriented benefits systematically, the authors employed a comparison-based approach. They used the "with-without comparison principle" to identify intrinsic benefits by assessing the differences between scenarios where the new transport infrastructure would be built versus scenarios where it would not. While for the specific benefits, they adopted the "aboveground-underground comparison principle," which focused on comparing the impacts on urban sustainability when a new road was built underground versus aboveground. This method considered scenarios with similar route selections, portal arrangements, and traffic volumes, allowing for a clear comparison of the sustainability impacts between underground and aboveground road placements.

Via the usage of the two aforementioned comparison principles, the researchers identified nine sustainability-oriented benefits associated with complex underground roads. These benefits included reducing carbon dioxide emissions, saving transportation time for passengers and cargo, lowering traffic accident risks, and reducing air and noise pollution, among others (Ma and Peng, 2021). To estimate the monetary value of these benefits, the General Substitute Cost Method (GSCM) was applied. This method is derived from substitute cost methods used in ecosystem valuations, which are based on the idea that environmental benefits provided by ecosystems can be monetarily assessed by calculating the costs of reproducing these benefits through alternative means. Each of the nine identified benefits was matched with a corresponding general substitute cost, allowing for a systematic valuation. The monetary value of each benefit was calculated using a specific equation tailored to that particular benefit. The authors applied their newly developed equations to the Bund Tunnel in Shanghai, estimating its total value at approximately 54,672 billion yuan (about 8,167 billion USD based on 2020 prices) over a 100-year period (Ma and Peng, 2021). Specifically, the intrinsic (direct) benefits accounted for 54,2% (or CNY 29,64 billion), while the specific (indirect) sustainability benefits unique to complex underground roads accounted for 45,8% (or CNY 25,03 billion) (Ma and Peng, 2021).

This study represents one of the most comprehensive efforts to estimate the real value of complex underground roads, introducing a systematic approach for identifying both direct and indirect benefits of underground facilities. However, the methodology has some significant drawbacks. First, the entire approach is tailored specifically for underground roads, limiting its applicability to other types of underground structures. Even if other facilities share similar benefits with underground roads, the equations used cannot be applied due to the specific data required, further narrowing the method's utility. Second, as with other methods that employ the replacement cost approach, obtaining the necessary input data can be challenging in many countries. Relevant studies are often scarce, and public documents containing the required information are not easily accessible.

Mavrikos and Kaliampakos (2021) made a significant and influential contribution by proposing a systematic methodology for estimating the real value of Urban Underground Space (UUS). The researchers emphasized the critical importance of including the monetary value of the indirect benefits of underground structures in the estimation process. To address this issue, the authors suggested employing environmental economics to quantify the indirect advantages of UUS, thereby enabling it to more effectively compete with above-

surface options. Their methodology can be summarized in 8 key steps, which involve estimating the direct value of an underground structure with the replacement cost method and the real estate income approach, while the indirect value is evaluated using the Benefit Transfer (BT) method, an environmental economics technique. Finally, by combining the direct and indirect values obtained through these methods, they were able to estimate the real value of UUS. The researchers applied their proposed methodology to an underground storage facility in the Attica region of Greece. The final estimated values are 1.022,49€ /m<sup>2</sup> for the replacement cost approach and 1.001,61€/m<sup>2</sup> for the income approach (Mavrikos and Kaliampakos, 2021). The two values differ by only 2,1%, confirming the correct implementation of the valuation approaches. It should be noted that the total cost for constructing an underground storage facility in the examined case was approximately 190€/m<sup>2</sup> (including excavation and improvements), while the value of the underground space was over five times greater (Mavrikos and Kaliampakos, 2021).

The proposed methodology stands out as one of the most comprehensive and systematic approaches for estimating the real value of Urban Underground Space (UUS). It employs the service replacement cost method and the income approach method, both well-established real estate valuation techniques, to calculate the direct value of underground structures. Notably, this methodology is among the few that fully incorporate the indirect value of underground facilities, an aspect often overlooked in other approaches. However, the authors themselves acknowledge a few limitations that could be addressed to further enhance the technique. First, the Benefit Transfer (BT) method, which is used to estimate the indirect value, requires a substantial amount of primary environmental studies. This reliance can limit the methodology's applicability, depending on the availability of such studies. Therefore, expanding the database on the monetization of benefits and advantages of underground structures compared to surface alternatives is crucial. This expansion would improve the accuracy of estimations and reduce uncertainties associated with the BT method, thereby strengthening the overall approach. Additionally, the methodology's results are highly land-use specific. When applied on a larger scale, with multiple potential land-use scenarios, the technique must be repeated for each scenario, making the process time-consuming and labor-intensive. Finally, while the methodology does account for the depth of the underground facility, this factor is not sufficiently emphasized in the final results. Given the increasing importance of three-dimensional urban planning, better integration of depth considerations into the final valuation would be a significant improvement.

A few months later Dong et al. (2021) made a significant advancement by substantially modifying the service replacement cost method (SRCM) to estimate the monetary value of environmental externalities resulting from the development of Urban Underground Space (UUS). This approach encompasses both the benefits and losses associated with underground facilities. The researchers began by identifying key environmental contributions and detriments linked to UUS, such as air and noise pollution reduction, greenhouse gas emission mitigation, groundwater disturbance, and waste from excavated geomaterials. They then introduced a new framework for applying the SRCM, which is structured into three primary steps, that are extensively showcased in their original work (read Dong et al., 2021). After introducing the general framework for the restoration cost method, the researchers presented formulas for calculating the monetary values of specific environmental externalities associated with the construction of various underground facilities. These included structures like underground buildings, transportation facilities, roads, and parking lots. The technique was then applied to several underground facilities in China, such as the Changzhou pedestrian underpass and Shanghai's Metro Line 10. The results demonstrated that the benefits of such facilities significantly outweigh the losses, and that the monetary value of the environmental externalities from underground structures are significantly higher in relation to their construction costs.

The newly proposed method represents a significant advancement in evaluating the indirect value of UUS, as it is the first to fully incorporate the losses resulting from UUS development, offering a comprehensive technique for estimating the indirect value of underground structures. However, a notable limitation of this method is that the formulas introduced are highly specific to the types of underground structures being evaluated, making it difficult to adapt them for a broader range of facilities. This specificity limits the method's applicability to other types of UUS, as the formulas are tailored to the structures mentioned by the authors. Additionally, the input data required for these equations is often difficult, if not impossible, to obtain in many countries, raising concerns about the method's general applicability. Moreover, the authors did not provide a systematic approach for determining and categorizing the environmental benefits and losses associated with different underground structures. While they covered a broad spectrum of indirect benefits and losses, their choices were limited to the facilities they evaluated.

One year later, Qiao et al. (2022c) presented their final and most recent work, building on their earlier research. In this study, they applied the service replacement cost method, previously detailed in their studies (Qiao et al., 2017; Qiao et al., 2019a; Qiao et al., 2019b), to estimate both the indirect value of UUS, encompassing both benefits and losses, as well as the direct value of UUS by using policy approaches employed by countries such as China, Germany, and Japan. By refining their earlier work and incorporating a new approach to estimate the direct value, they developed a comprehensive method for calculating the real value of UUS. The results of this method

were visualized using Geographic Information System (GIS) technology. A key distinction from their previous work is the researchers' acknowledgment that most existing techniques for monetarily evaluating the value of UUS are market-oriented and lack a sustainability perspective, which they integrated into their latest study. Furthermore, the authors pointed out that underground projects are generally undertaken by either private developers or the government, each with different objectives, private developers focus on profit, while the government emphasizes long-term sustainability for society. This difference in perspective underscores the importance of considering both external benefits and costs, along with business revenues from underground land development, in determining the sustainability-oriented underground land price (Qiao et al., 2022c). In order to monetize the indirect benefits and costs, the researchers relied on their service replacement cost method, which they had thoroughly developed and explained in their previous works (read Qiao et al., 2017; Qiao et al., 2019a; Qiao et al., 2019b). Finally, for valuing the land price (direct value) they employed policies from countries like China, Germany, and Japan as a basis for their calculations. The researchers applied their newly developed method to calculate the real value of UUS in Shinan District, Qingdao, China, as a case study. The results were then visualized using Geographic Information System (GIS) technology. The findings indicated that, in most of the underground spaces examined in the region, environmental benefits significantly outweighed environmental costs (Qiao et al., 2022c). Moreover, when the direct value of the underground structures was also considered, their overall value proved to be very high (Qiao et al., 2022c).

In this most recent work, the authors made a significant advancement in estimating the real value of UUS. They achieved this by refining their earlier efforts to calculate the indirect benefits and costs of underground facilities using the service replacement cost method, while also incorporating a more systematic and realistic approach to assessing their overall value. This shift from a primarily market-oriented perspective to a more sustainability-focused approach represents a major step forward. Additionally, it is noteworthy that this study was only the second time that the results of such estimations were visualized using GIS, providing a clearer spatial representation of UUS's real value. The first attempt at visualization occurred earlier that same year in studies by Qiao et al. (2022a) and Qiao et al. (2022b). However, several concerns previously raised about the applicability of the service replacement cost method remain unresolved. Firstly, the method heavily depends on a thorough classification and identification of all services provided by UUS facilities. While the authors made considerable efforts to cover a wide range of services, a more systematic approach to this classification is needed to make the method applicable across different types of UUS facilities. Furthermore, the method requires a substantial amount of input data, much of which may be unavailable or nonexistent in many regions. This limitation, acknowledged by the researchers themselves, casts doubt on the broader applicability of the service replacement cost method in other areas and countries. Despite these challenges, the researchers' integration of sustainability considerations and the use of GIS for visualization mark important progress in the field, even though further refinement and adaptation of the methodology are necessary for wider application.

## 5. CONCLUSIONS

The incorporation of underground space use has become a necessity in modern urban planning due to the increasing demands and challenges that 21st-century cities face. However, many underground projects are often stalled in the decision-making phase and never materialize. The primary reason is the significantly higher capital cost of underground facilities compared to above-surface alternatives, leading to their frequent neglect. It is crucial to integrate the indirect advantages of underground structures, particularly socio-environmental benefits, into the decision-making process. Doing so can enable underground options to compete directly with, or even surpass, their surface counterparts.

To systematically embed UUS into urban planning and make underground options more favorable, it is essential to estimate the real value of UUS. The real value encompasses both the direct and indirect value of UUS, with the latter often being more challenging to quantify in monetary terms, as it involves non-market goods. This study aimed to gather and review all existing methodologies that have been developed over the years to estimate either the real, direct value or indirect value, or losses from UUS development. To ensure comprehensive coverage, the study followed the guidelines of the Preferred Reporting Items for Systematic Reviews and Meta-Analyses (PRISMA). Most of the articles were sourced from the Scopus online database using specific keywords and phrases, with additional materials retrieved from conference proceedings of the Associated Research Centers for the Urban Underground Space (ACUUS) and the World Tunnel Congress (WTC).

The study's findings revealed that early attempts to create methodologies for estimating the value of UUS primarily focused on its direct value, neglecting the crucial indirect benefits and their corresponding values. However, over the past 15 years, researchers have increasingly recognized that excluding indirect advantages omits a significant portion of UUS's value. Consequently, methods like the service replacement cost have been carefully modified to account for the indirect benefits of UUS, with some approaches even estimating the indirect losses



resulting from inconsistent and reckless UUS development. The most recent methodologies have further advanced by visualizing their estimation results using Geographic Information System (GIS) technology, providing a more comprehensive spatial analysis of UUS's real value.

In summary, this critical review offers valuable insights for both future researchers and urban planners. Researchers can use this collection as a foundation for developing new methodologies or improving existing ones, serving as an organized and comprehensive database. Urban planners, on the other hand, can leverage this information in the decision-making process to identify the most suitable method for their specific projects. This approach promotes sustainable and cost-effective urban development, enabling planners to make informed choices based on thorough research. However, it is crucial that this collection be continuously updated to include the latest methodologies and improvements to existing ones, ensuring it remains a relevant and valuable resource.

## 6. APPENDIX

To ensure thorough documentation, the 141 articles initially retrieved by the author during the identification and gathering stage can be made available as supplementary material upon request.

## 7. BIBLIOGRAPHY

- [1] Barker, M.B., Jansson, B. (1982). Cities of the future and planning for subsurface utilization. *Underground Space*, Vol. 7, pp. 82-85.
- [2] Bobylev, N. (2009). Mainstreaming sustainable development into a city's Master plan: A case of Urban Underground Space use. *Land Use Policy*, Vol. 26, pp. 1128-1137. [10.1016/j.landusepol.2009.02.003](https://doi.org/10.1016/j.landusepol.2009.02.003)
- [3] Dong, Y.H., Peng, F.L., Qiao, Y.K., Zhang, J.B., Wu, X.L. (2021). Measuring the monetary value of environmental externalities derived from urban underground facilities: Towards a better understanding of sustainable underground spaces. *Energy & Buildings*, Vol. 250, 111313. <https://doi.org/10.1016/j.enbuild.2021.111313>
- [4] Godard, J.P., Sterling, R.L. (1995). General considerations in assessing the advantages of using underground space. *Tunnelling and Underground Space Technology*, Vol. 10, pp. 287-297. [https://doi.org/10.1016/0886-7798\(95\)00018-T](https://doi.org/10.1016/0886-7798(95)00018-T)
- [5] International Tunnelling Association (1998). Working Group 15, Final Report "Underground Works and the Environment", ITA-AITES.
- [6] International Tunnelling Association (2004). Working Group 13, Final Report "Underground or aboveground? Making the choice for urban mass transit systems". *Tunnelling and Underground Space Technology*, Vol. 19, pp. 3-28. [https://doi.org/10.1016/S0886-7798\(03\)00104-4](https://doi.org/10.1016/S0886-7798(03)00104-4)
- [7] Kaliampakos, D., Benardos, A. (2008). Underground space development: Setting modern strategies. *WIT Transactions on the Built Environment*, Vol. 102, pp. 1-10, 1<sup>st</sup> International Conference on Underground Spaces-Design, Engineering and Environmental Aspects, New Forest, United Kingdom, 8-10 September.
- [8] Kaliampakos, D., Benardos, A., Mavrikos, A. (2016). A review on the economics of underground space utilization. *Tunnelling and Underground Space Technology*, Vol. 55, pp. 236-244. <http://dx.doi.org/10.1016/j.tust.2015.10.022>
- [9] Liberati, A., Altman, D.A., Tetzlaff, J., Mulrow, C., Gotzsche, P.C., Ioannidis, J.P.A., Clarke, M., Devereaux, P.J., Kleijnen, J., Moher, D. (2009). The PRISMA statement for reporting systematic reviews and meta-analyses of studies that evaluate healthcare interventions: explanation and elaboration. *BMJ* 2009; 339:b2700. <https://doi.org/10.1136/bmj.b2700>
- [10] Ma, C.X., Peng, F.L. (2021). Monetary evaluation method of comprehensive benefits of complex underground roads for motor vehicles orienting urban sustainable development. *Sustainable Cities and Society*, Vol. 65, 102569. <https://doi.org/10.1016/j.scs.2020.102569>
- [11] Mavrikos, A., Kaliampakos, D. (2021). An integrated methodology for estimating the value of underground space. *Tunnelling and Underground Space Technology incorporating Trenchless Technology Research*, Vol. 109, 103770. <https://doi.org/10.1016/j.tust.2020.103770>
- [12] Moher, D., Liberati, A., Tetzlaff, J., Altman, D.G. (2009). Preferred reporting items for systematic reviews and meta-analyses: the PRISMA statement. *BMJ* 2009; 339:b2535. <https://doi.org/10.1136/bmj.b2535>
- [13] Moher, D., Tetzlaff, J., Tricco, A.C., Sampson, M., Altman, D.G. (2007). Epidemiology and Reporting Characteristics of Systematic Reviews. *PLoS Med* 4(3): e78. <https://doi.org/10.1371/journal.pmed.0040078>
- [14] Page, M.J., McKenzie, J.E., Bossuyt, P.M., Boutron, I., Hoffmann, T.C., Mulrow, C.D., Shamseer, L., Tetzlaff, J.M., Akl, T.C., Brennan, S.E., Chou, R., Glanville, J., Grimshaw, J.M., Hrobjartsson, A., Lalu, M.M., Li, T., Loder, E.W., Wilson, E.M., McDonald, S., McGuinness, L.A., Stewart, L.A., Thomas, J., Tricco, A.C., Welch, V.A., Whiting, P., Moher, D. (2021). The PRISMA 2020 statement: An updated guideline for reporting systematic reviews. *Journal of Clinical Epidemiology*, Vol. 134, pp. 178-189. [10.1016/j.jclinepi.2021.03.001](https://doi.org/10.1016/j.jclinepi.2021.03.001)
- [15] Papadomarkakis, D. (2025). Combatting Modern City Problems with the Usage of Underground Space: The Case Study of Greece. *Proceedings of the 19<sup>th</sup> ACUUS International Conference "Underground Mobility and Elevated Thinking: New Opportunities and Challenges in the Use of Underground Urban Space"*, November 4-7, Belgrade, Serbia (Submitted manuscript, under review).

- [16] Pasqual, J., Riera, P. (2005). Underground land values. *Land Use Policy*, Vol. 22, pp. 322-330. <https://doi.org/10.1016/j.landusepol.2004.03.005>
- [17] Qiao, Y.K., Peng, F.L., Wang, Y. (2017). Monetary valuation of urban underground space: A critical issue for the decision-making of urban underground space development. *Land Use Policy*, Vol. 69, pp. 12-24. <https://doi.org/10.1016/j.landusepol.2017.08.03>
- [18] Qiao, Y.K., Peng, F.L., Wang, Y. (2019a). Valuing external benefits of underground rail transit in monetary terms: A practical method applied to Changzhou City. *Tunnelling and Underground Space Technology*, Vol. 83, pp. 91-98. <https://doi.org/10.1016/j.tust.2018.09.039>
- [19] Qiao, Y.K., Peng, F.L., Sabri, S., Rajabifard, A. (2019b). Socio-environmental costs of underground space use for urban sustainability. *Sustainable Cities and Society*, Vol. 51, 101757. <https://doi.org/10.1016/j.scs.2019.101757>
- [20] Qiao, Y.K., Peng, F.L., Wu, X.L., Luan, Y.P. (2022a). Visualization and spatial analysis of socio-environmental externalities of urban underground space use: Part 1 positive externalities. *Tunnelling and Underground Space Technology incorporating Trenchless Technology Research*, Vol. 121, 104325. <https://doi.org/10.1016/j.tust.2021.104325>
- [21] Qiao, Y.K., Peng, F.L., Wu, X.L., Luan, Y.P. (2022b). Visualization and spatial analysis of socio-environmental externalities of urban underground space use: Part 2 negative externalities. *Tunnelling and Underground Space Technology incorporating Trenchless Technology Research*, Vol. 121, 104326. <https://doi.org/10.1016/j.tust.2021.104326>
- [22] Qiao, Y.K., Peng, F.L., Luan, Y.P., Wu, X.L. (2022c). Rethinking underground land value and pricing: A sustainability perspective. *Tunnelling and Underground Space Technology incorporating Trenchless Technology Research*, Vol. 127, 104573. <https://doi.org/10.1016/j.tust.2022.104573>
- Riera, P., Pasqual, J. (1992). The Importance of Urban Underground Land Value in Project Evaluation: a Case Study of Barcelona's Utility Tunnel. *Tunnelling and Underground Space Technology*, Vol. 7, pp. 243-250. [https://doi.org/10.1016/0886-7798\(92\)90005-3](https://doi.org/10.1016/0886-7798(92)90005-3)
- [23] Tareau, J.P. (1995). Underground Car Parks. *Tunnelling and Underground Space Technology*, Vol. 10, pp. 299-309. [https://doi.org/10.1016/0886-7798\(95\)00019-u](https://doi.org/10.1016/0886-7798(95)00019-u)
- [24] World Bank Group, Department of Urban Development, Urban Population Data (2024). <https://data.worldbank.org/indicator/SP.URB.TOTL>
- [25] Zhu, W., Fu, J., Yang, J., Tong, L. (2009). Urban Underground Space Value: Case Study of Keisheng Square Planning in Lanzhou City. *Proceedings of the 12<sup>th</sup> ACUUS International Conference "Using the Underground of Cities: for a Harmonious and Sustainable Urban Environment"*, November 18-19, China, pp. 151-157.

## RESEARCH ON COMPOSITION OF SHOPS IN UNDERGROUND MALL

Yuto NAKAMURA<sup>1</sup>, Masaharu OOSAWA<sup>2</sup>

**Abstract:** Underground mall located in central areas such as stations are made up of many stores. However, the actual situation is not clear. In addition, the store composition differs between underground malls located in metropolitan areas and other areas, and it is thought that there are regional characteristics. In recent years, renovation work due to the aging of underground malls has been completed. Therefore, in order to comprehensively understand the changes in store composition before and after the renovation, it is necessary to clarify the current store composition.

Therefore, this study targeted 60 underground malls with sites and collected data from April 2023 to September 2023. We will organize the types of stores that were identified based on the Ministry of Internal Affairs and Communications' standard industrial classification. We will compare the differences in store composition and among cities based on the total number of underground malls in each city. Finally, we will list the characteristic store usage.

As a result, the store composition in Tokyo Wards, Nagoya City, Osaka City, Sapporo City, Yokohama City, Fukuoka City, and underground malls across the country includes “textiles, clothing, and personal goods retailers”, “restaurants”, “other retail” and “food and beverage retails” are in the top four categories. The proportion of “textile, clothing, and personal goods retailers” is high in Tokyo Wards, Sapporo City, Yokohama City, and Fukuoka City, while the proportion of restaurants is high in Nagoya City and Osaka City. Within Tokyo 23 Wards, the proportion of “textile, clothing, and personal goods retailers” is high in Shinjuku Ward, Toshima Ward, and Shibuya Ward, while the proportion of “restaurants” is high in Chuo Ward and Minato Ward. As a characteristic store usage, is that stores allow vehicle delivery and stores where they can play table tennis.

**Keywords:** underground mall, shop, number of stores, city comparison

### 1. INTRODUCTION

In Japan, there is an underground mall that has been in operation for 70 years, and half of all underground malls have been open for over 50 years. Among them, some underground malls have retained their original interior appearance to the present day (*Figure 1.*), while others have been renovated resulting in changes to their interior landscapes. (*Figure 2.*) In metropolitan areas, government designated cities and regional cities, underground malls exist as a means of efficient land use near stations and are composed of a wide variety of stores. Underground networks of underground malls exist at Nagoya Station and Shinjuku Station. (*Figure 3.*) However, the composition of stores in underground malls is not clear. In addition, when comparing underground malls located in metropolitan areas and government designated cities with those located in other areas, it is possible that the composition of stores differs, and that there are regional characteristics in the composition of stores that make up underground malls. In addition, in recent years, there are several underground malls that have been renovated work due to aging. Therefore, it is important to clarify the current store composition in order to comprehensively understand the changes in the store composition before and after the renovation.

The purpose of this study is to investigate and discuss the actual situation of the composition of stores in underground malls throughout Japan, targeting underground malls with homepages.

<sup>1</sup> Master's Program, (Nakamura, Yuto), Civil Engineering, (Nihon University, 1-8-14 Kanda-Surugadai, Chiyoda-ku, Tokyo, Japan), [csyu24008@g.nihon-u.ac.jp](mailto:csyu24008@g.nihon-u.ac.jp)

<sup>2</sup> Professor, (Oosawa, Masaharu), Civil Engineering, (Nihon University, 1-8-14 Kanda-Surugadai, Chiyoda-ku, Tokyo, Japan), [oosawa.masaharu@nihon-u.ac.jp](mailto:oosawa.masaharu@nihon-u.ac.jp)

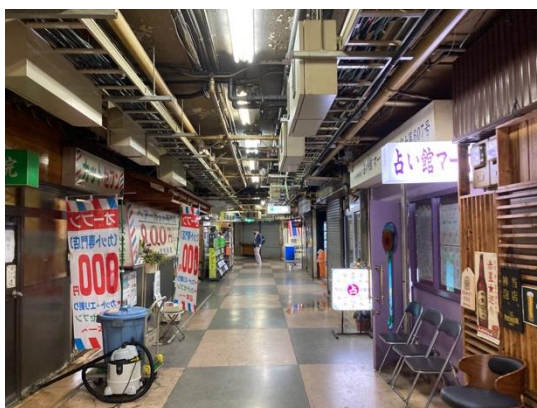
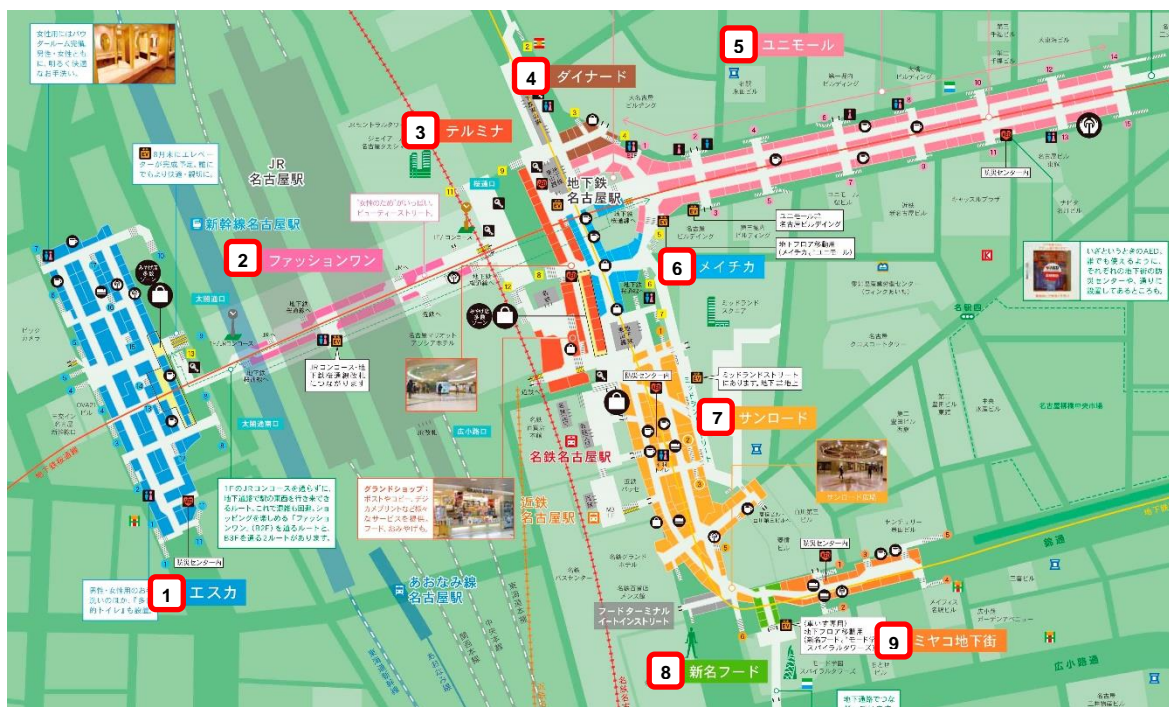


Figure 1. Photo of Asakusa Underground Mall



Figure 2. Photo of Tenjin Underground Mall



Underground Shopping Mall

1 ESCA	1 Gate Walk (TERMINA)	4 Unimall	7 SUNROAD	9 MIYAKO ave.
2 FASHION ONE	2 Dainard	5 MEICHIKA	8 Shinmei food	

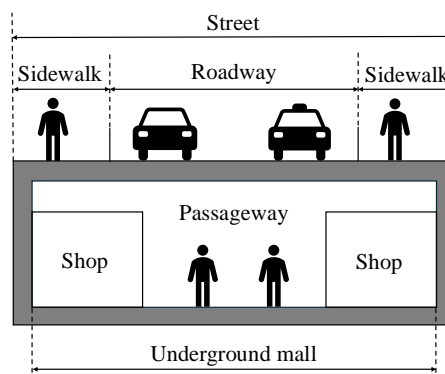
Figure 3. Underground mall network around Nagoya Station



## 2. MATERIAL AND METHODS

### 2.1. The underground mall examined in this study

The following two conditions are used to define the underground malls in this study. An underground mall is defined as an underground facility that integrates an underground walkway for public use and facilities such as stores facing the walkway, as specified in the “Outline of Underground Malls” by the Ministry of Land, Infrastructure, Transport and Tourism. (**Figure 4.**) The list of underground malls is based on the “List of Underground Malls” published by the Ministry of Land, Infrastructure, Transport and Tourism in March 2013, and 60 underground malls with homepages for underground malls are included from 78 underground malls.



*Figure 4. Overview plan of the underground mall*

### 2.2. Research methods

The data for underground malls were collected from April 2023 to September 2023, from “Aurora Town” to “Tenjin Underground Mall”. Based on these data, we will investigate what type of store use is most common according to the medium classification of the Standard Industrial Classification by the Ministry of Internal Affairs and Communications.

We will also investigate the characteristics of the composition of stores in underground malls throughout Japan using all the aggregated data. Based on the total number of underground malls in a city, we compare the differences in store composition among 6 metropolitan areas (Tokyo Wards, Yokohama, Nagoya, Osaka, Sapporo, and Fukuoka). Finally, we identify the characteristic uses of underground malls that were identified during the survey of underground malls.

## 3. RESULTS

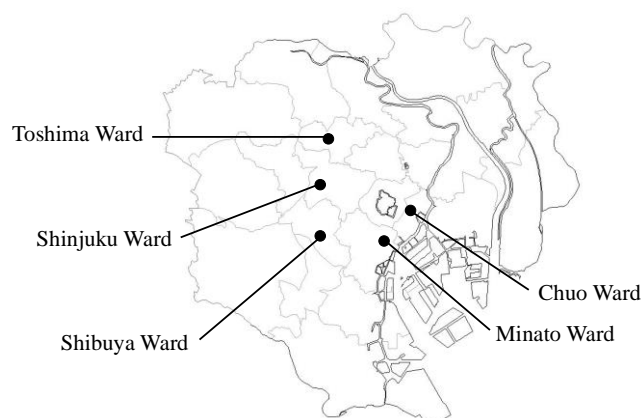
### 3.1. Japan-wide composition of store in underground malls

The total number of underground malls surveyed in this study was 60, and the total number of stores identified was 3,504. The number of cities with underground malls is 22, as shown in **Figure 5.** through **Figure 8.**

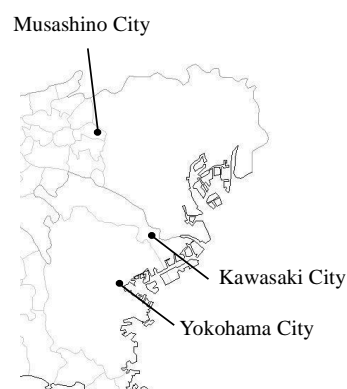




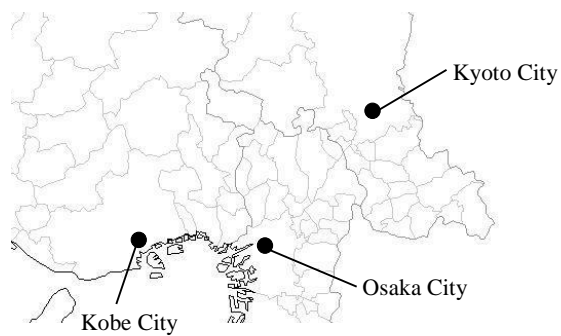
**Figure 5.** Cities with underground malls Japan-wide



**Figure 6.** Cities with underground malls in Tokyo wards



**Figure 7.** Cities with underground malls in Tokyo-Yokohama Area



**Figure 8.** Cities with underground malls in Kyoto-Osaka-Kobe Area

The mean number of stores in the underground malls was 58, and the median was 45. **Table 1** shows the composition of underground malls Japan-wide. Other retailers are engaged in the sale of products such as pharmaceuticals, cosmetics, and books. Other lifestyle-related services include businesses such as clothing repair and travel agencies. The data for the middle category below the banking industry is summarized in “Others” due to the large number of data items.

“Textile, clothing, and personal effects retailers” accounted for the largest share, followed by “restaurants”, “other retailers”, and “food and beverage retailers”. 26 underground malls had the highest percentage of “textile, clothing, and personal effects retailers”, and 23 underground malls had the highest percentage of “restaurants”. Three underground malls had the highest percentage of other retailers, and four underground malls had the highest percentage of “food and beverage retailers”. 15 underground malls had the second highest percentage of other retailers, and nine underground malls had the second highest percentage of “food and beverage retailers”.

**Table 1.** *The composition of underground malls Japan-wide*

<b>Standard Industrial Classification - Medium Classification</b>	<b>%</b>
<b>Textile, clothing, and personal effects retailers</b>	28
<b>Restaurants</b>	27
<b>Other retailers</b>	14
<b>Food and beverage retailers</b>	13
<b>Laundry, barber, beauty, bathhouse business</b>	4
<b>Other lifestyle-related services</b>	3
<b>Machinery and equipment retailers</b>	2
<b>Banking industry</b>	2
<b>Others</b>	7

### 3.2. Composition of stores in Tokyo Wards, Nagoya City, Osaka City, Sapporo City, Yokohama City, and Fukuoka City

**Table 2** shows a composition the number of underground malls and the total number of stores in Tokyo Wards, Nagoya, Osaka, Sapporo, Yokohama and Fukuoka cities. In Osaka City, the total number of underground malls is 8 and the total number of stores is 697, indicating that the average number of stores per underground mall is high. In Fukuoka City, the Tenjin Underground Mall is large in scale with 148 stores. **Table 3** shows the composition of underground malls in Tokyo Wards, Nagoya, Osaka, Sapporo, Yokohama and Fukuoka cities. The middle category, which has fewer stores than the number of stores in the machinery and equipment retailing industry, is summarized in the “Others” category due to the large number of industry categories.

Store use in Tokyo Wards and Yokohama City is led by textile and personal items retail, followed by restaurants. This is the same characteristic of underground malls Japan-wide. In Sapporo City, there are two more other retailers than restaurants, indicating that the percentage of other retailers is higher in Sapporo City than in the Japan-wide. Among Nagoya's underground malls, ESCA Underground Mall has 77 stores, with a high percentage of restaurants (43%). Fushimi Underground Mall have 39 stores, with a high percentage of “restaurants” (56%). In Osaka City, seven underground malls, excluding Diamor Osaka, have a high percentage of “restaurants”. In Fukuoka City, the Tenjin Underground Mall has the largest number of stores (148), with a high ratio of “textile, clothing and personal effects retailers” (50%), but a low ratio of “restaurants” (7%). On the other hand, the Hakata Station Underground Mall has fewer stores (35) than the Tenjin Underground Mall, and the percentages of textile, clothing and personal effects retailers” and “restaurants” are 31% and 26%, respectively.

**Table 2.** *Total number of underground malls and number of stores in Tokyo wards, Nagoya City, Osaka City, Sapporo City, Yokohama City, and Fukuoka City*

	<b>Tokyo Wards</b>	<b>Nagoya City</b>	<b>Osaka City</b>	<b>Sapporo City</b>	<b>Yokohama City</b>	<b>Fukuoka City</b>
<b>Total number of underground malls</b>	13	13	8	3	4	2
<b>Number of stores</b>	610	536	697	245	347	183

**Table 3.** The composition of underground malls in Tokyo Wards, Nagoya City, Osaka City, Sapporo City, Yokohama City, and Fukuoka City(%)

City	Tokyo Wards	Nagoya City	Osaka City	Sapporo City	Yokohama City	Fukuoka City
<b>Standard Industrial Classification - Medium Classification</b>						
Textile, clothing, and personal effects retailers	29	27	21	35	33	47
Restaurants	24	26	37	19	32	11
Other retailers	14	14	13	19	14	19
Food and beverage retailers	14	10	9	13	11	12
Laundry, barber, beauty, bathhouse business	5	5	4	4	2	3
Other lifestyle-related services	4	3	4	2	3	3
Machinery and equipment retailers	1	2	2	2	1	2
Others	9	13	10	6	4	3

### 3.3. Composition of stores in Tokyo wards (Chuo Ward, Minato Ward, Shibuya Ward, Shinjuku Ward, Toshima Ward)

**Table 4** shows the total number of underground malls and stores in Chuo, Minato, Shibuya, Shinjuku and Toshima wards.

**Table 4.** Total number of underground malls and number of stores in Chuo Ward, Minato Ward, Shibuya Ward, Shinjuku Ward, and Toshima Ward

	Chuo Ward	Minato Ward	Shibuya Ward	Shinjuku Ward	Toshima Ward
<b>Total number of underground malls</b>	2	2	1	5	3
<b>Number of stores</b>	175	51	21	233	130

In Chuo Ward, the Yaesu Underground Mall is the largest, with 171 stores. In Shinjuku and Toshima wards, the number of stores per underground mall is close to the Japan-wide median and average of underground malls. On the other hand, the number of stores per underground mall in Minato and Shibuya wards is small compared to the national median and average of underground malls, indicating that they are small underground malls. **Table 5** shows the store composition of underground malls in Chuo, Minato, Shibuya, Shinjuku, and Toshima wards. In Chuo Ward, the Yaesu Underground Mall has a large number of stores (171) and a high percentage of restaurants (39%) compared to the national average. On the other hand, the number of stores in the “Echika Ginza” is four, which is lower than that of the Yaesu Underground Mall. Therefore, the percentage of restaurants is high in the data for Chuo Ward. In Minato Ward, “Wing Shimbashi” has 25 stores and 32% of restaurants, which is slightly higher than the national data. In addition, the number of stores in Echika Omotesando is 26, and the ratio of restaurants is 34%, which is slightly higher than the national data, thus the ratio of restaurants is slightly higher in the Minato Ward data. In Shibuya Ward, the only underground mall is the Shibuya Underground Mall, which is characterized by the lack of restaurant stores. In Shinjuku Ward, “LUMINE EST SHINJUKU” has 79 stores, and the percentage of textile, clothing, and personal effects retailers is 67%, which is higher than the national value, suggesting a high percentage of textile, clothing, and personal effects retailers in the Shinjuku Ward data. The largest number of stores in Toshima Ward are textile, clothing, and personal effects retailers, followed by restaurants, which is similar to the composition of the number of stores in underground malls Japan-wide. The reason for the highest percentage of textile, clothing and personal effects retailers in the data for Tokyo wards may be due to the high percentage of textile, clothing and personal effects retailers in Shinjuku, Toshima and Shibuya wards, and the second highest percentage in Chuo and Minato wards.

**Table 5.** The composition of underground malls in Chuo Ward, Minato Ward, Shibuya Ward, Shinjuku Ward, and Toshima Ward (%)

City	Chuo Ward	Minato Ward	Shibuya Ward	Shinjuku Ward	Toshima Ward
<b>Standard Industrial Classification - Medium Classification</b>					
Textile, clothing, and personal effects retailers	18	29	33	38	29
Restaurants	39	33	0	19	25
Other retailers	11	8	19	16	16
Food and beverage retailers	6	16	14	14	15
Laundry, barber, beauty, bathhouse business	6	4	0	3	5
Other lifestyle-related services	4	4	14	3	5
Others	16	6	20	7	5

### 3.4. Characteristic store use

There are 20 characteristic store uses, which are shown in **Table 6**. Tesla Delivery Center Nagoya is located in the “Central Park Underground Mall. This is the only place in the underground mall where cars can be delivered. Metro Table Tennis is located in Metro Kobe, and table tennis can be played by paying a fee. This is the only place where table tennis is available in the underground mall.

**Table 6.** Characteristic store use

Underground Mall	Characteristic store use
Takaoka Station Underground Mall	Study Cafe Takaoka
ESCA Underground Mall	Tour Bus Counter
ESCA Underground Mall	H <sup>1</sup> T (Shared office)
Fushimi Underground Mall	Fushimi Underground Mall Cooperative Association
Fushimi Underground Mall	Chojamachi Satellite Studio
Fushimi Underground Mall	Small-scale workshop Dream
Central Park Underground Mall	Tesla Delivery Center Nagoya
Mori Underground Mall	Art Gallery Komori
Zest Oike	Kyoto City Certificate Issuance Corner
Dojima Underground Center	CAFÉ On the
NAMBA WALK	Minami Recruitment Office, Japan Self-Defense Forces, Ministry of Defense
AVETICA	Self-Defense Forces Recruitment Office
DIAMOR OSAKA	Osaka City Umeda Service Counter
DIAMOR OSAKA	cool MINT
DIAMOR OSAKA	Yamazawa Judicial Scrivener Corporation
DIAMOR OSAKA	DIAMOR LOBBY
Metro Kobe	Metro TT Studio
Metro Kobe	Metro Table Tennis
Shareo	Fureai Plaza
Shareo	Employment support counter IROHA

## 4. DISCUSSION

The store composition varied depending on the district, but since there are many restaurants in Osaka City, where has a relatively large number of stores, the store composition may differ depending on the number of stores.

In addition, since this study compared each district, no difference was found between before and after the renovation of the underground mall.

## 5. CONCLUSION

In this study, the composition of stores in underground malls Japan-wide was clarified, and the characteristics of the composition of underground malls were determined for the wards of Tokyo, Nagoya, Osaka, Sapporo, Yokohama, and Fukuoka cities. The top four categories in the composition of stores in underground malls are

textile, clothing and personal effects retailers, restaurants, other retailers, and food and beverage retailers. In the Sapporo City, Yokohama City, Fukuoka City, and Tokyo Wards, the majority of stores were textile, clothing, and personal effects retailers, while in the Nagoya and Osaka cities, the majority of stores were restaurants. In addition, the presence of stores that provide car delivery services and table tennis were identified as characteristic store uses.

In the future, we plan to compare the characteristics of the store composition in each underground mall, and at the same time, clarify the status of vacant stores and the transition of stores.

## 6. BIBLIOGRAPHY

- [1] Yuto NAKAMURA, Masaharu OOSAWA, "RESACH ON COMPOSITION OF SHOPS IN UNDERGROUND MALL- A CASE STUDY OF 60 UNDERGROUND MALLS IN JAPAN-", Proceedings of the Symposium on Underground Space Vol.30, JSCE, 2025.
- [2] Ministry of Land, Infrastructure, Transport and Tourism : Outline of Underground Mall , <https://www.mlit.go.jp/common/001005387.pdf>
- [3] Ministry of Land, Infrastructure, Transport and Tourism : About the Underground Mall , <https://www.mlit.go.jp/common/001005390.pdf>
- [4] Ministry of Internal Affairs and Communications: Japan Standard Industrial Classification (revised October 2013) (effective April 1, 2014) , [https://www.soumu.go.jp/toukei\\_toukatsu/index/seido/sangyo/02toukatsu01\\_03000023.html](https://www.soumu.go.jp/toukei_toukatsu/index/seido/sangyo/02toukatsu01_03000023.html)ampakos, D. (2016). Underground development: A springboard to make city life better in the 21st century. *Procedia Engineering*, 165, 205-213. <https://doi.org/10.1016/j.proeng.2016.11.792>.
- [5] Sapporo Underground Mall: Aurora Town | Floor Guide, <https://www.sapporo-chikagai.jp/floorguide/>,Homepage of 59 other underground malls
- [6] CraftMAP, <http://www.craftmap.box-i.net>
- [7] Tesla Support Japan: Delivery Method, [https://www.tesla.com/ja\\_jp/support/delivery-options](https://www.tesla.com/ja_jp/support/delivery-options)
- [8] Table Tennis Facility: Metro Table Tennis – Intermediate Passageway, Metro Kobe, <https://metrokobe.jp/table-tennis>



## ANALYZING CONTRACTUAL PRACTICES IN MAJOR UNDERGROUND INFRASTRUCTURE PROJECTS

Doris Skenderas<sup>1</sup>, Chrysothemis Paraskevopoulou<sup>2</sup>, Andreas Benardos<sup>3</sup>

**Abstract:** The underground space presents significant opportunities for infrastructure development. The infrastructure industry (architecture, engineering, construction, and operation) has historically struggled with poor project performance caused by complexity, fragmentation, and low digitalization. Underground projects face additional challenges due to the uncertainty of unknown subsurface conditions. The continued increase in materials and energy costs, inflation, and the COVID-19 pandemic are just a few of the unforeseen factors exacerbating this situation. Based on case studies, this analysis examines current contracting practices in major underground infrastructure projects, investigating their characteristics and their impact on conflicts, disputes, and claims. These factors in major projects often result in the use of multi-party contracts and complex contractual arrangements. Traditional contracting practices have primarily focused on risk allocation, commonly leading to disputes and inefficiencies that result in further delays and financial burdens in the project. Recent advances in contract management encourage integrated and collaborative approaches, while the adaptation of digital tools generates blockchain-based smart legal contracts to enhance automation, transparency, and sustainability. This shift in contractual practices influences performance optimization as well as dispute mitigation. Finally, key lessons are derived from their implementation.

**Keywords:** Underground infrastructure, smart contracts, claims, digitalization, sustainability

### 1. INTRODUCTION

The construction sector is a pillar of economic growth, making significant contributions to both the financial and infrastructure development of countries worldwide. It is mentioned that the share of this industry in terms of gross domestic product (GDP) is almost 10% for developed countries, and could be even higher in developing countries [1]. However, this sector faces significant challenges and is widely regarded as having one of the highest-risk profiles among industries worldwide, due to the inherent uncertainties and the unpredictable environmental factors that can disrupt successful project execution [2], [3]. The dynamic and complex environment, consisting of interactions and frictions among stakeholders and fragmented project delivery, adds to this characterization. These risks manifest as cost overruns, delays, and quality issues, which collectively undermine project success and its economic benefits. It has been observed that allocating these risks to project parties often results in claims being integrated into the contractual framework. Claims and disputes in construction projects and the cost associated with these adversarial relationships can reach up to €3,5-€10,5 billion per year [4], [5].

The excess urbanization and increasing demand for resilient infrastructure have driven the development of underground projects ranging from tunnels, subways, and underground utilities to subterranean corridors. Underground projects offer a solution to space constraints and environmental concerns, but introduce additional project management challenges [6]. The subsurface environment is characterized by incomplete geological data, unpredictable soil and groundwater conditions, and safety hazards, which increase technical complexity and risk.

<sup>1</sup> MSc. Skenderas Doris, Tunnelling/Mining Eng., School of Mining and Metallurgical Engineering, National Technical University of Athens, 15780 Athens, Greece, skenderasdoris@metal.ntua.gr.

<sup>2</sup> Professor Associate, Paraskevopoulou Chrysothemis, Tunnelling/Mining Eng, School of Earth and Environment, University of Leeds, Leeds, UK, c.paraskevopoulou@leeds.ac.uk; chrys.parask@gmail.com

<sup>3</sup> Professor Benardos Andreas, Tunnelling/Mining Eng., School of Mining and Metallurgical Engineering, National Technical University of Athens, 15780 Athens, Greece, abenardos@metal.ntua.gr

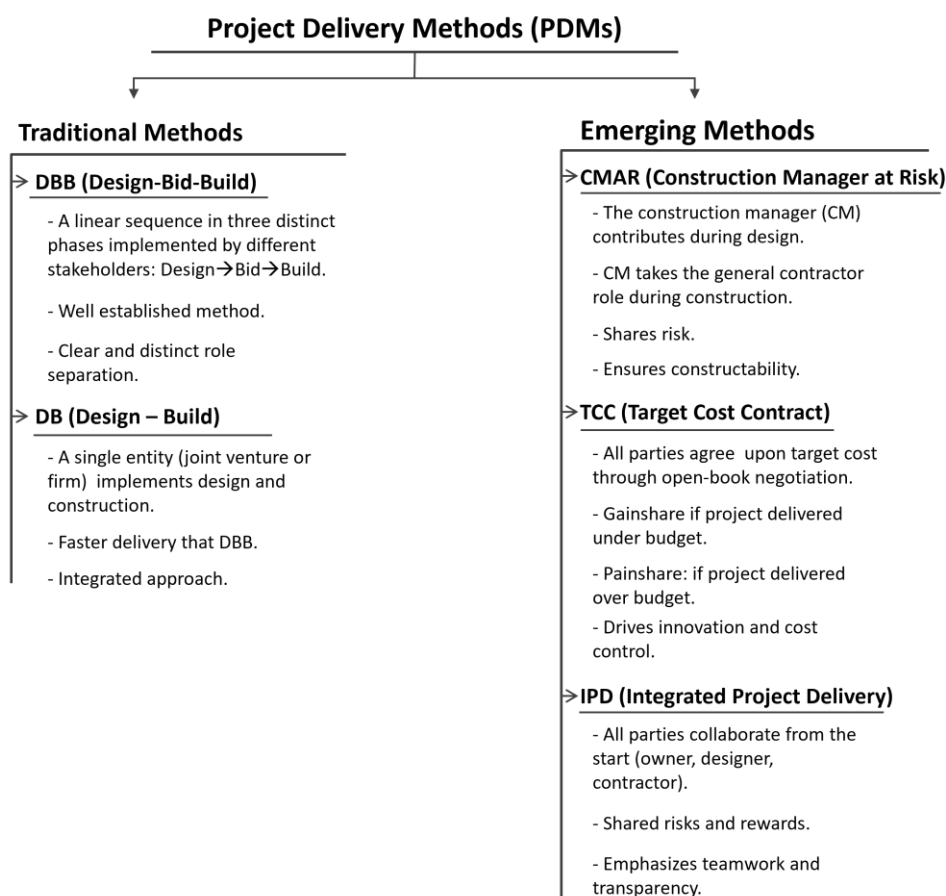
Choosing the appropriate project delivery method and contracting approach is critical to managing risks and achieving project objectives. The project delivery method (PDM) defines the overall process and relationships among the parties involved in a project [7]. Contracting methods (CM) focus on the legal and financial mechanisms that govern compensation and risk sharing. Meanwhile, technological advancements have influenced contracting methods as well, introducing smart contracts. Smart contracts are self-executing agreements where terms are encoded into blockchain-based code, automating enforcement and payments when predefined conditions are met [8], [9]. Project delivery methods and contracting methods are two distinct topics. However, the two are often discussed together, sometimes even interchangeably, because the chosen project delivery method typically dictates the types of contracts used and shapes the contractual relationships on a project. As a result, both are frequently grouped under the broader term contractual practices or contracts, reflecting their combined influence on project risk, collaboration, and performance [10].

Despite the critical role of contracts in underground infrastructure projects, comprehensive analyses of contractual practices remain limited. Most literature focuses on individual contract types or project delivery methods without integrating their combined impact on project performance, dispute resolution, and innovation adoption, particularly in the context of underground projects. Furthermore, emerging technologies such as blockchain-based smart contracts have not been extensively studied in this context. The evaluation of contractual practices used in an underground project is multifactorial. This paper makes a contribution to underground space knowledge by integrating an assessment of traditional and emerging project delivery methods with digital innovations such as blockchain-enabled smart contracts through assessing the contractual practices and their use in underground projects, evaluating and addressing their impact on project delivery success by analysing contractual practices in major underground projects through case studies, aiming to underscore the next steps required to improve their successful completion. The most used contractual practices in underground projects, along with alternative project delivery methods, were analysed using indicative use cases to showcase their efficiency. By evaluating the PDMs and the use cases, it was confirmed that major underground infrastructure projects face unique risks that traditional contracting methods struggle to manage effectively. Integrated and collaborative contractual practices offer improved performance in terms of dispute mitigation, cost control, and schedule adherence.

## **2. ANALYSIS OF CONTRACTUAL PRACTICES**

### **2.1. Background**

Selecting an appropriate project delivery method is an important decision that influences the relationships, risk allocation, and overall success of any construction project [10]. Over the years, the construction industry has relied on a variety of delivery methods and contracts, each offering distinct advantages and challenges. The most popular PDMs in underground construction are Design-Bid-Build (DBB) in which project development occurs through the sequential steps of design, procurement and construction and Design-Build (DB) in which a joint venture of a general contractor and an architectural/engineering firm will be in charge of the design and construction of the project. Emerging PDMs with potential in underground construction are Construction Manager at Risk (CMAR), in which the construction manager, in addition to offering preconstruction services during the design phase, serves as the general contractor overseeing the overall construction, and Integrated Project Delivery (IPD) [5], [11]. Additionally, some of the most frequently used CMs are also mentioned. The lump sum, in which the price for the whole work is proposed, cost-plus, guaranteed maximum price (GMP), in which the bidder is held accountable beyond the guaranteed price, and unit price contracts, which are a compensation method based on the actual amount of work performed [7], [12].



*Figure 1. Project Delivery Methods (PDMs) overview*

Gaining a solid understanding of the theoretical background behind these approaches is essential for making informed decisions and optimizing project outcomes. In the context of underground projects, where risks and uncertainties are often heightened, the most commonly utilized contractual practices include DBB, DB, CMAR, Target Cost Contracts (TCC), and IPD are analyzed.

### 2.1.1. Design-Bid-Build (DBB)

The **Design-Bid-Build** method has long been the most traditional and widely practiced project delivery method, especially throughout the late 20th century [6], [13], [14]. In DBB, the owner separately contracts with the designer and the contractor, with the designer preparing construction documents and bid packages for competitive bidding. While this structure provides clear separation of responsibilities, it often leads to poor communication and limited knowledge sharing between designers and contractors, as each party operates independently and tends to prioritize shifting risk and maximizing their profit [4], [15]. Managing changes is particularly challenging in DBB due to fragmented negotiations and a lack of collaboration, frequently resulting in claims and disputes [4]. The conflicts in DBB, compared to alternative delivery methods, have been well documented [16]. As projects grew in complexity and cost during the late 1970s, these disadvantages dictated the development and adoption of alternative project delivery methods that better address the limitations of the traditional DBB approach [6]. In DBB, the owner typically uses a lump sum contract type and contracts separately with designers and contractors, which is best suited for projects with a well-defined scope. This oldest and most common method that separates design and construction phases with fixed-price contracts while providing cost certainty for owners, often resulting in rival relationships and claims due to unforeseen subsurface conditions [12].

### 2.1.2. Design-Build (DB)

The **Design-Build** is one of the most widely adopted project delivery methods. Unlike Design-Bid-Build (DBB), where interaction between designers and contractors is limited to the beginning or end of construction, DB fosters continuous collaboration as design and construction services are consolidated under a single entity, either

a joint venture, an in-house team, or a partnership, providing the owner with a single point of communication [13]. This integration addresses many of the shortcomings of DBB, such as ineffective design, errors, change orders, and disputes, which often lead to increased costs and project delays. The popularity of DB surged in the late 1980s and early 1990s, and it currently accounts for over 40% of non-residential project deliveries [4].

In the DB process, owners typically issue a request for proposal outlining design parameters, after which DB teams develop conceptual designs and proposals, including schedules and cost estimates, for owner evaluation [4]. Construction often begins before design completion, enabling significant schedule reductions compared to DBB. Studies indicate that contractors, clients, and architects largely agree that DB offers schedule advantages and higher owner satisfaction with design quality. Common disputes in DB projects typically involve conflicting employer requirements, contractor obligations regarding designs and/or design changes, valuation of design variations, and additional work not specified in contracts. In literature, it is indicated that DB projects generally have better time performance than cost performance over the DBB, however, the cost benefits of DB over DBB remain debated among researchers, with some studies finding no significant advantage [6], [17], [18], [19]. In DB design and construction are integrated under a single contract, often leading to faster project delivery, but sometimes with a less clearly defined initial scope [17].

### **2.1.3. Construction Manager at Risk (CMAR)**

**Construction Manager at Risk (CMAR)**, also known as Construction Manager/General Contractor (CM/GC), is a project delivery method that integrates the contractor into the project team early in the design phase, allowing for essential input on constructability, cost, and scheduling before construction begins [20], [21]. In this approach, the owner holds separate contracts with the designer and the construction manager, who is selected based on qualifications or best value, not just lowest price. The process typically begins with a preconstruction services agreement, during which the CMAR collaborates with the designer and owner to review design documents, identify risks, and provide cost estimates. Once the design reaches a certain level of completion, CMAR and the owner negotiate a Guaranteed Maximum Price (GMP) for construction [20], [21]. The CMAR influences design decisions early, leading to improved constructability and quality, as well as enhanced cost and schedule certainty. The method enables fast-tracking, as construction can begin before design is fully complete, and allows for early bidding of work packages, which can mitigate price uncertainty and accelerate delivery. However, managing two separate contracts (designer and CMAR) can add complexity and requires careful coordination to avoid conflicting agendas and ensure collaboration [20], [21]. The actual project cost is not known until the GMP is set, and there can be ambiguity regarding the extent of the CMAR's responsibility for design errors or omissions. CMAR is most commonly used for complex, high-risk projects where early contractor involvement can add significant value [20], [21].

### **2.1.4. Target Cost Contract (TCC)**

A **Target Cost Contract (TCC)** is a collaborative construction contract where the client and contractor agree in advance on a target cost, an estimate of the expected project expenses, typically determined through open-book negotiation and joint risk assessment. Target cost contracts share both savings and overruns between the parties according to a pre-agreed formula. If the actual project cost comes in below the target, both parties split the savings (gainshare), on the other hand, if costs exceed the target, both share the overrun (pain share) [22]. This arrangement encourages the contractor to control costs as well as teamwork, as both sides benefit from efficiency and innovation, and both are motivated to avoid overruns. Target cost contracts are especially useful for complex or high-risk projects, such as underground infrastructure, where exact costs are difficult to predict, and collaboration is essential for managing uncertainty and achieving value for money. Challenges can include complexity in setting a realistic target cost, the need for robust contract administration, and potential disputes if the scope or risk allocation is unclear [23].

### **2.1.5. Integrated Project Delivery (IPD)**

**Integrated Project Delivery (IPD)** is a collaborative project delivery method that brings together the owner, designer, and contractor under a multiparty agreement, fostering open communication, joint risk/reward sharing, and early involvement of all key stakeholders [24]. Unlike traditional methods such as DBB, where roles are fragmented and adversarial relationships are common, IPD encourages a team-oriented approach, aligning all parties toward common project goals. Standard contract forms for IPD, such as the American Institute of Architects' (AIA) Integrated Form of Agreement (IFOA) and ConsensusDOCS, are designed to formalize these collaborative relationships and risk-sharing mechanisms. Survey results from industry practitioners indicate that while IPD is not yet widely adopted, it is more frequently used in large, complex projects, particularly in healthcare and technically challenging environments, where collaboration and flexibility are essential [25], [26].

### **2.1.6. FIDIC and Underground Project Contracts**

Internationally, several legal frameworks influence construction contract management. The FIDIC (Fédération Internationale des Ingénieurs-Conseils) contract conditions provide standardized contractual terms widely used in global construction projects to ensure consistency in contract administration. FIDIC has issued a suite of contracts through the books covering topics related to jobs and authority, work conditions, delays brought about by specialists, as well as methodology for dispute settlement, liability, and risk-related issues [27]. One of the most significant advancements in underground infrastructure contracting is the introduction of the ITA/FIDIC Emerald Book, a specialized standard contract designed to address the unique risks of subsurface construction. Unlike previous practices that unfairly placed all ground condition risks on contractors, often resulting in disputes, cost overruns, and bankruptcies, the Emerald Book establishes a more balanced framework for risk allocation. Central to this approach is the use of a Geotechnical Baseline Report (GBR), which clearly defines the allocation of ground risk between the employer and the contractor. This allows for contract adjustments if actual ground conditions differ from those anticipated, ensuring contractors are compensated for unforeseen conditions while still holding them accountable for performance under expected circumstances. The Emerald Book also introduces mechanisms for time and remuneration adjustments, prioritizes factual ground data over legal manoeuvring, and emphasizes the engineer's neutral and fair role in contract administration [28].

## **3. CONTRACTUAL PRACTICES CASE STUDIES**

Construction industry practices differ significantly across countries due to variations in culture, legal systems, and construction techniques. Despite these differences, certain challenges, such as effective project planning and control, are common worldwide, regardless of geographic location [2]. The case studies selected for this analysis represent a diverse range of underground infrastructure projects across different geographies and scales. They were chosen based on their relevance to tunnelling and underground construction, the variety of contractual and project delivery methods employed, and the availability of detailed information about their contractual frameworks and project outcomes. The cases demonstrate both traditional and innovative contractual practices.

### **3.1.1. Toronto-York Spadina Subway Extension (TYSSE)**

The Toronto-York Spadina Subway Extension (TYSSE) project is an expansion of Toronto's subway system, extending Line 1 by 8,6km and adding six new stations from Downsview to Vaughan. Delivered using the DBB method, the project was managed by the Toronto Transit Commission (TTC), which oversaw the design process and then awarded multiple construction contracts through competitive bidding to private contractors [29], [30], [31]. This approach allowed the TTC to maintain control over design standards and integration with the existing network, but also meant that contractors had no input into the design and were responsible for building exactly to the provided specifications [29], [30], [31].

The YYSSE project faced a series of significant challenges that affected its timeline, budget, and overall execution. From the outset, the project suffered an 18-month delay, with the opening date pushed back multiple times and completion not achieved until late 2017 [29], [32]. Additionally, cost overruns were significant, as the budget increased from an initial estimate of €2,27 billion to nearly €2.8 billion, driven by delays, scope changes, and unforeseen construction complexities. Contractor performance issues that led to safety issues were one of the factors of the project delays. Utility relocation also proved to be more complex and time-consuming than anticipated, causing up to 11 months of extra delay in some areas [30]. Additionally, frequent changes to station designs and project scope were not factored into the original schedule or budget, compounding both delays and cost increases. These factors were related to contractor claims. While some of these claims were acknowledged by the TTC as having merit and were billed for payment, others were expected to be contested through litigation. By early 2016, the TTC disclosed that up to €350 million would be required to address contractor claims. Persistent challenges ultimately led to a complete reset of the project, including the dismissal of two managers and the appointment of a new design team to restore control over costs and scheduling [29], [32], [33].

### **3.1.2. Doha Metro Gold Line project**

The Doha Metro Gold Line project in Qatar was delivered using a Design-Build project delivery method. Qatar Rail awarded a single, large-scale contract to a joint venture consortium, comprising Aktor, Larsen & Toubro, Yapi Merkezi, STFA, and Al Jaber Engineering, to both design and construct the underground Gold Line, including its tunnels and stations [34], [35]. Under this approach, the consortium was responsible for the full scope of design, engineering, and construction works, integrating all phases under one contract to streamline coordination, accelerate delivery, and manage risks more effectively. The contract covered the design and



construction of approximately 16 km of twin tunnels, 10 underground stations, and associated infrastructure, with the project running from 2014 to 2017 [35]. This method was chosen to meet tight timelines and complex technical requirements, enabling the contractor to optimize construction solutions and adapt to project challenges as they arose [34], [35], [36]. Nonetheless, the Doha Metro Gold Line project experienced significant time and cost overruns during its execution. Initially scheduled for completion between 2014 and 2017, phase I faced delays that pushed the opening to 2019 [37], [38]. These delays were attributed to design changes, the 2017 Gulf blockade, which disrupted material supply chains and labour logistics, and contractor disputes over scope adjustments and compensation claims [37]. In terms of cost, the broader Doha Metro project, initially estimated at €14,43 billion, saw substantial escalation, with the Gold Line contributing significantly to overruns [37], [39].

The project faced major arbitration and financial disputes alongside significant technical challenges. In 2017, a consortium including OHLA filed a €400 million arbitration claim against Qatar Rail following contract termination for work on key stations. The International Chamber of Commerce (ICC) ruled in 2025, awarding €315 million in compensation, with OHLA receiving €95 million [40]. This dispute centred on whether the contract should have been terminated or renegotiated, with the consortium arguing for negotiation or formal arbitration. Additionally, the project encountered unforeseen ground conditions, such as karstic limestone and aggressive groundwater, which required extra ground stabilization. Contractors claimed these were differing site conditions, leading to further claims for time extensions and cost adjustments [35], [41].

### **3.1.3. City of Atlanta Water Supply Program**

The City of Atlanta Water Supply Program is an infrastructure initiative designed to secure Atlanta's drinking water supply for the next century. The project included converting a 120m deep quarry into a 9 million cubic meter raw water storage facility, constructing 8km of 3.8m diameter tunnel through hard bedrock, and building new pump stations to connect the quarry to the Chattahoochee and Hemphill Water Treatment Plants. The project construction started in 2015 and was delivered as initially projected in 2020 [42]. The City of Atlanta selected the CMAR delivery method for this €280 million project due to its scale, complexity, and the need for cost and schedule certainty. Under CMAR, the construction manager, PC Construction and H.J. Russell JV, was engaged early to provide preconstruction services, value engineering, and risk management, and then assumed construction risk under a GMP. This approach fostered collaboration, expedited construction, and allowed for flexibility in addressing unforeseen challenges [42], [43].

The project faced significant technical and logistical challenges, including mining through hard gneiss bedrock, constructing eleven deep shafts, and managing complex connections to existing infrastructure while prioritizing safety and minimizing community disruption [43]. During construction, an unexpected zone of contaminated groundwater was encountered, necessitating slowed tunnel-boring operations and additional safety protocols. The final commissioning phase coincided with the COVID-19 pandemic, requiring adaptations such as masking, social distancing, and remote coordination for pump installations [43]. Despite these hurdles, the CMAR delivery method fostered collaboration and transparent risk-sharing, avoiding major disputes or litigation and enabling constructive resolution of issues. The project was completed on time and €4,37 million under budget, demonstrating resilience against pandemic-related and technical challenges [42].

### **3.1.4. Tsim Sha Tsui (TST) Underground Railway Station Modification and Extension Works**

The Tsim Sha Tsui (TST) Underground Railway Station Modification and Extension Works was a critical infrastructure project in Hong Kong aimed at enhancing connectivity between the Mass Transit Railway Corporation (MTRCL) Tsim Sha Tsui Station and the Kowloon-Canton Railway Corporation (KCRC) East Tsim Sha Tsui Station under a TCC framework. Key objectives included relieving passenger congestion, improving accessibility, and integrating pedestrian subways in one of Hong Kong's busiest districts. The project involved deep excavation beneath Nathan Road, construction of a 160m subway extension, and modifications to the existing station structure while maintaining uninterrupted railway operations. Completed in September 2005, the project was delivered seven months early and 5% under budget, achieving significant time and cost savings [23], [44], [45]. Management challenges included initial resistance to the TCC model and the need to modify existing contracts due to the lack of a standard TCC template, raising liability concerns [23].

The project encountered several key issues, disputes, and claims. Excavation close to operational tunnels required precise ground stabilization. The presence of contaminated groundwater and unstable geology led to delays and the need for additional safety protocols. These unforeseen ground conditions were addressed through joint risk assessments and contingency funds within the TCC framework, helping to mitigate disputes [46]. Disagreements also arose over whether certain design changes, such as station layout adjustments and utility relocations, constituted target cost variations or design developments. These were resolved through adjudication meetings involving the client, contractor, and a partnering facilitator, avoiding litigation.

#### 4. INSIGHTS FROM CASE STUDIES





To enable a critical assessment, the case studies were evaluated against four performance criteria: (i) cost performance, (ii) schedule performance, and (iii) dispute incidence.

The rigid separation of design and construction phases under DBB led to fragmented communication and inflexibility. Contractors had no input during design, resulting in impractical specifications and costly rework [30]. The TYSSE project underscores the challenges of using DBB for large, complex underground infrastructure. While DBB provided design control, its inflexibility in managing risks, scope changes, and contractor input led to significant delays, cost overruns, and disputes. The TTC bore most risks for unforeseen conditions leading to adversarial claims. DBB's fixed-price contracts urged contractors to submit claims rather than collaborate on solutions. On the other hand, the DB method utilisation in the Doha Metro Gold Line enabled integrated design-construction workflows and accelerated tunnelling rigid risk allocation for subsurface uncertainties, while design changes led to disputes, highlighting the need for adaptive contracting, robust geotechnical planning, and collaborative risk-sharing to balance efficiency with resilience.

The City of Atlanta Water Supply Program shows the effectiveness of CMAR in complex, high-risk infrastructure. By integrating the construction manager early, sharing risks transparently, and maintaining collaborative governance, the project achieved exceptional outcomes despite geological and external challenges. The GMP model led the CMAR to control costs while allowing flexibility for unforeseen conditions. Unlike traditional delivery methods, the collaborative CMAR approach avoided litigation and adversarial claims, resolving issues through joint decision-making.

Finally, the Tsim Sha Tsui case demonstrates that target cost contracting, when implemented with open-book transparency and equitable risk sharing, can deliver superior performance in underground infrastructure projects. This approach aligns stakeholder interests, fosters innovation, and provides measurable benefits in cost, time, and dispute reduction. The absence of a standard TCC contract template necessitated customization, highlighting the need for flexible contractual frameworks.

*Table 1. Case studies overview.*

Project	TYSSE (Toronto)	Doha Metro Gold Line	Atlanta Water Supply Program	TST Station (Hong Kong)
				
PDM	DBB	DB	CMAR	TCC
Key Characteristics	<ul style="list-style-type: none"> <li>- 8.6 km subway extension with 6 new stations.</li> <li>- Urban setting.</li> <li>- Utility relocation required.</li> <li>- Strict design</li> </ul>	<ul style="list-style-type: none"> <li>- 16 km twin tunnels &amp; 10 stations.</li> <li>- Major consortium.</li> <li>- Encountered karstic limestone, aggressive groundwater.</li> <li>- Impacted by regional political disruption.</li> </ul>	<ul style="list-style-type: none"> <li>- 120m deep quarry conversion.</li> <li>- 8 km tunnel through hard bedrock.</li> <li>- Critical municipal water infrastructure.</li> </ul>	<ul style="list-style-type: none"> <li>- Subway station modification under Nathan Road.</li> <li>- Deep excavation near operating tunnels and dense urban zone.</li> </ul>
Delays	18+ months	Approximately 2 years.	Completed on time.	Delivered 7 months early.
Cost Overruns	Overbudget	Overbudget	Underbudget	Underbudget
Claims/Disputes	Extensive contractor claims and legal disputes	Major arbitration and claims.	No major disputes, collaborative issue resolution.	Minor claims resolved via adjudication, no litigation required.

This multi-criteria assessment highlights that DBB and DB methods tend to score poorly on dispute incidence and collaboration, while CMAR and TCC demonstrate stronger performance in risk sharing and dispute avoidance.

## 5. RESULTS

The case studies analyzed indicate that CMAR and TCC perform better than the more traditional DBB and DB practices. However, the CMAR and TCC methods are mainly used in smaller and limited infrastructure projects. For instance, the implementation of TCC in bigger-scale projects, such as the Thames Tideway Tunnel in London, shows cost and time overruns as well [47]. Nonetheless, early contractor involvement in design can mitigate constructability issues, especially considering the disputes and claims that may arise. Future projects could benefit from hybrid models that integrate contractor expertise early and share risks equitably.

Additionally, the digitalization of construction contract management, driven by blockchain and automation technologies, is revolutionizing traditional processes. Blockchain-powered smart contracts enhance transparency, efficiency, and security by creating abiding, tamper-proof records that enable real-time verification of contract terms, payment tracking, and enforcement of compliance. Automation allows smart contracts to self-execute predefined actions, such as releasing payments upon milestone completion, without manual intervention, reducing delays and administrative overhead. These innovations lead to cost savings, faster dispute resolution, and reduced fraud risks. Linking the applicability of blockchain and smart contracts to the case studies, the TYSSE project, automated milestone payments encoded in smart contracts could have reduced prolonged disputes over contractor claims. For the Doha Metro, transparent recording of scope changes on a blockchain ledger would have provided auditable evidence to support renegotiation, reducing arbitration costs. In the Atlanta Water Supply Program, smart contracts could complement the GMP framework by automatically reconciling cost adjustments with real-time construction data. Finally, in the Tsim Sha Tsui project, joint risk registers and gain-share/pain-share mechanisms could be operationalized through blockchain to ensure transparent calculation and distribution of risk outcomes.

However, challenges remain, including the lack of legal recognition in many jurisdictions, potential coding errors in smart contracts, and the need to integrate these technologies within the existing regulatory frameworks [48], [49]. Even though smart contracts have promising benefits for construction projects, as they are capable of automating transaction protocols to achieve contractual conditions such as interim payments, liens, and confidentiality, while minimizing the need for trusted intermediaries, construction companies should modify the processes arising from smart contract implementation, which employees often resist. Except for employees, many companies believe that by utilizing smart contracts, they will lose their bargaining power, making the level of implementation of smart contracts not reach the desired level [50]. The inflexible nature of smart contracts, the shortage of professionals with both technical and legal expertise, and ongoing cybersecurity concerns are other factors that currently hinder companies from fully trusting and adopting smart contracts in construction, especially in underground projects [51], [52].

	Method	Advantages	Disadvantages	Challenges	Potential
Lower project delivery efficiency potential.	DBB	Clear design control, competitive bidding	Inflexible, adversarial claims, poor collaboration.	Scope changes, fragmented roles.	Suitable for simple projects; improved with early contractor input.
	DB	Fast delivery, single accountability	Limited owner control, rigid risk allocation.	Adapting to changes, underground uncertainties.	Works well with adaptive risk-sharing & geotech planning.
	Smart Contracts	Automated, transparent, tamper-proof.	Legal uncertainty, rigidity, resistance to change.	Cybersecurity, tech-legal integration.	Enables efficient, real-time project execution.
	IPD	Full team integration, shared rewards, low conflict	High coordination, limited familiarity.	Legal fit, stakeholder alignment.	High potential for complex, collaborative projects.
	TCC	Shared incentives, cost transparency, innovation-driven	Complex setup, non-standardized, cost disputes.	Realistic target setting, clear scope control.	Great for uncertain, high-risk projects.
Higher project delivery efficiency potential.	CMAR	Early contractor input, collaborative risk sharing, GMP control	Complex to scale, trust-dependent.	Managing GMP, governance setup.	High potential for complex, high-risk projects.

Figure 2. PDMs potential in project delivery efficiency in future projects.

## 6. DISCUSSION & CONCLUSION

The construction law is of great importance in governing contracts, trying to ensure that all involved parties will adhere to their obligations. However, the construction contracts are inherently complex due to the involvement of multiple stakeholders. In the case of underground constructions, the nature of such projects and the unpredictable conditions that may arise increase the difficulty of delivering such a project successfully, with delays and cost overruns becoming a universal phenomenon in such projects [48], [53]. The evolution of contractual practices in underground infrastructure projects reflects the sector's response to complexity and risk. Traditional risk-transfer contracts, while providing clarity, often foster adversarial relationships that worsen delays and cost overruns. Integrated and collaborative contracts, such as CMAR, TCC, and IPD, align stakeholder motives and promote transparency, which is essential for projects with high uncertainty like tunnelling, while simultaneously sharing the risks in a way that may improve the project delivery.

Additionally, digital innovations, particularly blockchain-enabled smart contracts, represent a promising option by automating contract execution of pre-defined actions and providing abiding records without manual intervention, reducing delays and administrative overhead. On the other hand, the limitations across jurisdictions, as underground projects are governed by diverse legal traditions, procurement laws, and regulatory frameworks, their inflexibility, the cybersecurity issues, and the lack of experts who can deal with both technical and law expertise are some of the most critical smart contract drawbacks. However, smart contracts are still developing, and there are several issues to be addressed. The input of construction companies in the process of refining these models and overcoming barriers to technology adoption would be beneficial for all parties, as smart contracts could better adapt to their requirements and needs. Owners and project managers must carefully select delivery and contracting methods that balance flexibility, risk sharing, and control, tailored to project complexity and stakeholder capabilities, taking into account that early engagement of contractors and designers is critical for optimizing outcomes in underground projects. Even though the use case analysis is critical, this paper aims to highlight the development of contractual practices required to improve underground projects' successful completion.

The conservative nature of construction companies and their hesitation and scepticism in adopting new methods in delivering infrastructure projects is one of the major factors of continued project failures, time delays, and financial loss that have characterised the sector. The impact of contractual practices extends beyond owners and contractors to a wider network of stakeholders, such as public authorities, consultants, regulators, and policy makers, considering that the project's cost and risk exposure are reshaped, and industry norms need to be re-evaluated and reformed accordingly. Future research must focus on how alternative contractual practices would affect the issues faced in underground projects. Specifically, how traditional methods could be combined with alternative methods, so that it could be more appealing for companies to adopt, combined with strategy analysis for overcoming resistance to new practices. Building on this study, further analysis may include developing hybrid models that combine traditional frameworks with collaborative features such as shared risk pools or early contractor involvement, promoting regulatory harmonization by updating national procurement guidelines and international standards to recognize digital contracting mechanisms, and institutionalizing dispute avoidance mechanisms supported by digital platforms to minimize litigation. However, the limitations in data availability and transparency, as well as detailed information on the projects' contract conditions, strongly determine the results of such analyses.

## 7. BIBLIOGRAPHY

- [1] W. Wang, I. Harsono, C.-J. Shieh, V. Samusenkov, and S. Shoar, "Identification of critical paths leading to cost claims for underground metro projects: a system dynamics approach," *Kybernetes*, vol. 52, no. 5, pp. 1861–1878, May 2023, doi: 10.1108/K-09-2021-0786.
- [2] E. Forcael, H. Morales, D. Agdas, C. Rodríguez, and C. León, "Risk Identification in the Chilean Tunneling Industry," *Engineering Management Journal*, vol. 30, no. 3, pp. 203–215, Jul. 2018, doi: 10.1080/10429247.2018.1484266.
- [3] A. S. Ahmed Marey Alhammadi and A. H. Memon, "Ranking of the Factors Causing Cost Overrun in Infrastructural Projects of UAE," *International Journal of Sustainable Construction Engineering and Technology*, vol. 11, no. 2, Sep. 2020, doi: 10.30880/ijscet.2020.11.02.025.
- [4] Hashem M. Mehany Mohammed S., G. Bashettiyavar, B. Esmaeili, and G. Gad, "Claims and Project Performance between Traditional and Alternative Project Delivery Methods," *Journal of Legal Affairs and Dispute Resolution in Engineering and Construction*, vol. 10, no. 3, Aug. 2018, doi: 10.1061/(ASCE)LA.1943-4170.0000266.
- [5] M. M. Niazmandi, R. Sedaeisoula, S. Lari, and M. Yousefi, "Integrated project delivery (IPD) capabilities on reducing claims in urban underground projects: A hybrid FAHP-FTOPSIS approach," *Sustainable Futures*, vol. 7, p. 100175, Jun. 2024, doi: 10.1016/j.sfr.2024.100175.

- [6] G. Bashettiyavar, "THESIS COMPARING CLAIMS AND DISPUTES PERFORMANCE BETWEEN TRADITIONAL PROJECT DELIVERY METHOD AND ALTERNATE PROJECT DELIVERY METHODS Submitted by," 2018.
- [7] A. Legesse, A. Nejat, and T. Ghebrab, "The coupling of project delivery methods and contract strategies for public building projects in Ethiopia," *Construction Innovation*, vol. 25, no. 2, pp. 400–418, Feb. 2025, doi: 10.1108/CI-02-2022-0043.
- [8] J. J. Hunhevicz, D. F. Bucher, K. Hong, D. M. Hall, and C. De Wolf, "Cheaper Smart Contracts for the Built Environment? Linking On-Chain and Off-Chain in a Blockchain-Governed Approach," Jul. 2024. doi: 10.35490/EC3.2024.269.
- [9] A. Ma, "Blockchain-Enabled Smart Legal Contracts," in *Blockchain Applications - Transforming Industries, Enhancing Security, and Addressing Ethical Considerations*, IntechOpen, 2023. doi: 10.5772/intechopen.109041.
- [10] CMAA, "AN OWNER'S GUIDE TO PROJECT DELIVERY METHODS Advancing Professional Construction and Program Management Worldwide ACKNOWLEDGMENTS," 2012.
- [11] T. Francom, M. El Asmar, and S. T. Ariaratnam, "Using Alternative Project Delivery Methods to Enhance the Cost Performance of Trenchless Construction Projects," in *Construction Research Congress 2014*, Reston, VA: American Society of Civil Engineers, May 2014, pp. 1219–1228. doi: 10.1061/9780784413517.125.
- [12] G. M. Winch, "Managing Construction Projects An Information Processing Approach," 2010. [Online]. Available: [www.ebook3000.com](http://www.ebook3000.com)
- [13] J. Cantirinio and S. S. Fodor, "Construction delivery systems in the United States," *Journal of Corporate Real Estate*, 1999.
- [14] G. M. Gad, A. K. Momoh, B. Esmacili, and D. G. Gransberg, "PRELIMINARY INVESTIGATION OF THE IMPACT OF PROJECT DELIVERY METHOD ON DISPUTE RESOLUTION METHOD CHOICE IN PUBLIC HIGHWAY PROJECTS," 2015.
- [15] J. Borowiec, N. Norboge, B. Huntsman, C. Schrank, and Beckerman. Wayne, "Design-Build Highway Projects: A Review of Practices and Experiences," 2016.
- [16] P. A. N. B. Senarath and M. Francis, "DISPUTE AVOIDANCE FROM THE PERSPECTIVE OF PROCUREMENT METHODS: A CONCEPTUAL FOCUS," in *Proceedings of the 9th World Construction Symposium 2021 on Reshaping construction: Strategic, Structural and Cultural Transformations towards the "Next Normal"*, The Ceylon Institute of Builders - Sri Lanka, Jul. 2021, pp. 256–267. doi: 10.31705/WCS.2021.22.
- [17] C. W. Ibbs, Y. H. Kwak, T. Ng, and A. M. Odabasi, "Project Delivery Systems and Project Change: Quantitative Analysis," *J Constr Eng Manag*, vol. 129, no. 4, pp. 382–387, Aug. 2003, doi: 10.1061/(ASCE)0733-9364(2003)129:4(382).
- [18] Q. Chen, Z. Jin, B. Xia, P. Wu, and M. Skitmore, "Time and Cost Performance of Design-Build Projects," *J Constr Eng Manag*, vol. 142, no. 2, Feb. 2016, doi: 10.1061/(ASCE)CO.1943-7862.0001056.
- [19] D. Rajaratnam, T. S. Jayawickrama, and B. A. K. S. Perera, "Use of total quality management to enhance the quality of design and build projects," *Intelligent Buildings International*, vol. 14, no. 5, pp. 527–543, Sep. 2022, doi: 10.1080/17508975.2021.1914536.
- [20] J. Shane, "Construction Manager-at-Risk Project Delivery for Highway Programs," 2008. [Online]. Available: <https://www.researchgate.net/publication/280610007>
- [21] J. S. Shane and D. D. Gransberg, "A Critical Analysis of Innovations in Construction Manager-at-Risk Project Delivery," in *Construction Research Congress 2010*, Reston, VA: American Society of Civil Engineers, May 2010, pp. 827–836. doi: 10.1061/41109(373)83.
- [22] CPPU, "Guidance on the operation of target cost contracts and pain share/gain share mechanisms," *Scottish Government Riaghaltas na h-Alba*, no. Construction Policy Note CPN 5/2017, 2017.
- [23] D. W. M. Chan, P. T. I. Lam, A. P. C. Chan, and J. M. W. Wong, "Achieving better performance through target cost contracts," *Facilities*, vol. 28, no. 5/6, pp. 261–277, Apr. 2010, doi: 10.1108/02632771011031501.
- [24] A. De Marco and A. Karzouna, "Assessing the Benefits of the Integrated Project Delivery Method: A Survey of Expert Opinions," *Procedia Comput Sci*, vol. 138, pp. 823–828, 2018, doi: 10.1016/j.procs.2018.10.107.
- [25] D. C. Kent and B. Becerik-Gerber, "Understanding Construction Industry Experience and Attitudes toward Integrated Project Delivery," *J Constr Eng Manag*, vol. 136, no. 8, pp. 815–825, Aug. 2010, doi: 10.1061/(ASCE)CO.1943-7862.0000188.
- [26] R. Ghassemi and B. Becerik-Gerber, "Transitioning to IPD: Potential Barriers & Lessons Learned," 2011. [Online]. Available: [www.leanconstructionjournal.org](http://www.leanconstructionjournal.org)
- [27] P. C. Nwogu and A. Emedosi, "FIDIC Form of Contract: A Study Review," *British Journal of Environmental Sciences*, vol. 12, no. 2, pp. 43–48, Feb. 2024, doi: 10.37745/bjes.2013/vol12n24348.
- [28] A. E. Dix, "THE RENAISSANCE OF FAIRNESS IN GROUND RISK ALLOCATION - THE NEW ITA/FIDIC EMERALD BOOK," *INTERNATIONAL JOURNAL OF CIVIL ENGINEERING AND TECHNOLOGY (IJCET)*, vol. 11, no. 1, Jan. 2020, doi: 10.34218/IJCET.11.1.2020.006.
- [29] TTC, "Toronto-York Spadina Subway Extension-Schedule and Budget Change (Staff Report Action Required)," 2015.
- [30] H. Bidhendi, D. Amm, and R. Staples, "The Toronto-York Spadina Subway Extension (TYSSE) Project-Introducing a Major Subway Project to the Tunnelling Fraternity," 2012.
- [31] A. Foley, "Holey breaks through on Spadina," *Tunnelling Journal*. Accessed: Jun. 09, 2025. [Online]. Available: <https://tunnellingjournal.com/holey-breaks-through-on-spadina/>



- [32] CityNews, "Toronto-York Spadina subway extension delayed until 2017," CityNews. Accessed: Jun. 03, 2025. [Online]. Available: <https://toronto.citynews.ca/2015/03/20/toronto-york-spadina-subway-extension-delayed-until-2017/>
- [33] York Region, "Toronto-York Spadina Subway Extension - Schedule and Cost Status Update," 2015.
- [34] C. Foreman, "Consortium signs Doha Metro Gold Line deal," Middle East Business Intelligence (MEED). Accessed: Jun. 05, 2025. [Online]. Available: <https://www.meed.com/consortium-signs-doha-metro-gold-line-deal/>
- [35] EncardioRite, "Gold Line - Doha Metro," 2017.
- [36] A. Senouci, A. A. Ismail, and N. Eldin, "Time and Cost Overrun in Public Construction Projects in Qatar," 2016.
- [37] TBH, "Doha Metro Gold Line Qatar," TBH Project Delivery Experts. Accessed: Jun. 05, 2025. [Online]. Available: <https://tbhconsultancy.com/experience/doha-metro-gold-line/>
- [38] STAF, "DOHA Gold Line Metro," STAF Yatirim Holding. Accessed: Jun. 04, 2025. [Online]. Available: <https://www.stfa.com/en/tag/gold-line-en/>
- [39] MEED, "Construction cost escalation to impact contractors in Doha," Middle East Business Intelligence. Accessed: Jun. 04, 2025. [Online]. Available: <https://www.meed.com/construction-cost-escalation-to-impact-contractors-in-doha/>
- [40] L. Hall, "Compensation for OHLA's derailed Doha project," EuroWeekly News. Accessed: Jun. 05, 2025. [Online]. Available: <https://euroweeklynnews.com/2025/03/06/compensation-for-ohlas-derailed-doha-project/>
- [41] Resol Services, "Doha Metro Project Dispute (Qatar)." Accessed: Jun. 05, 2025. [Online]. Available: <https://www.linkedin.com/pulse/doha-metro-project-dispute-qatar-resol-services-2yaqc/>
- [42] WCDA, "Atlanta Water Supply Program (GA)," Water Collaborative Delivery Association. Accessed: Jun. 02, 2025. [Online]. Available: <https://watercollaborativedelivery.org/project/atlanta-water-supply-program-ga/>
- [43] J. Parsons, "Southeast Project Of The Year: Collaboration Conquers Atlanta's Water Shortage," ENRTexas & Southeast. Accessed: Jun. 02, 2025. [Online]. Available: <https://www.enr.com/articles/52819-southeast-project-of-the-year-collaboration-conquers-atlantas-water-shortage>
- [44] Gammon, "MTR Tsim Sha Tsui Station & Subways." Accessed: Jun. 01, 2025. [Online]. Available: [https://www.gammonconstruction.com/en/project-details.php?project\\_id=113](https://www.gammonconstruction.com/en/project-details.php?project_id=113)
- [45] Arup Journal, "KCRC EAST RAIL EXTENSIONS SPECIAL ISSUE" 2007. Accessed: Jun. 01, 2025. [Online]. Available: <https://www.arup.com/globalassets/downloads/arup-journal/the-arup-journal-2007-issue-3.pdf>
- [46] A. Tam, "East Rail extension brings retail warren to Tsim Sha Tsui," The Hong Kong Institution of Engineers. Accessed: Jun. 01, 2025. [Online]. Available: [https://www.hkengineer.org.hk/issue/vol33-jan2005/cover\\_story/](https://www.hkengineer.org.hk/issue/vol33-jan2005/cover_story/)
- [47] S. Fullalove, "Construction of London's NEC-procured 'super sewer' now complete," nec.
- [48] E. O. Osifo, E. S. Omumu, and M. Alozie, "Contract Management in Construction Law: Mitigating Risks, Dispute Resolution, and Performance Enforcement," *International Journal of Research Publication and Reviews*, vol. 6, no. 3, pp. 5874–5890, Mar. 2025, doi: 10.55248/gengpi.6.0325.1279.
- [49] E. M. Alqodsi and L. Arenova, "Smart Contracts in Contract Law as an Auxiliary Tool or a Promising Substitute for Traditional Contracts," *Journal of Legal Affairs and Dispute Resolution in Engineering and Construction*, vol. 16, no. 3, Aug. 2024, doi: 10.1061/JLADAH.LADR-1132.
- [50] C. Budayan and O. Okudan, "Assessment of Barriers to the Implementation of Smart Contracts in Construction Projects—Evidence from Turkey," *Buildings*, vol. 13, no. 8, p. 2084, Aug. 2023, doi: 10.3390/buildings13082084.
- [51] A. A. Papantoniou, "Smart Contracts in the New Era of Contract Law," *Digital Law Journal*, vol. 1, no. 4, pp. 8–24, Dec. 2020, doi: 10.38044/2686-9136-2020-1-4-8-24.
- [52] F. Bassan and M. Rabitti, "From smart legal contracts to contracts on blockchain: An empirical investigation," *Computer Law & Security Review*, vol. 55, p. 106035, Nov. 2024, doi: 10.1016/j.clsr.2024.106035.
- [53] D. Zhang, H. Zhang, and T. Cheng, "Causes of Delay in the Construction Projects of Subway Tunnel," *Advances in Civil Engineering*, vol. 2020, no. 1, Jan. 2020, doi: 10.1155/2020/8883683.

## SUSTAINABLE URBAN REGENERATION THROUGH “BOUNDARYLESS” UNDERGROUND DEVELOPMENT: INTEGRATION OF UNDERGROUND AND ABOVEGROUND, PUBLIC-PRIVATE PARTNERSHIP, AND CONTINUITY FROM PLANNING TO OPERATION - A CASE STUDY OF SHIBUYA, TOKYO

Taro Fukuda<sup>1</sup>, Kento Yoshino<sup>2</sup>

**Abstract:** Tokyo has developed a rail-centered transport system above and below ground to support its vast population. Rapid development around railway stations in the late 20th century created complex urban structures and aging infrastructure. Today, Tokyo seeks regeneration strategies, with underground development key to improving livability and connectivity. As a solution to these problems, this study introduces strategies taken around Shibuya Station—one of Japan’s largest terminal stations—to discuss the benefits and challenges of “boundaryless” underground development led by NIKKEN SEKKEI. The strategies are integration of underground and aboveground, public-private partnerships, and continuity from planning to operation. The featured projects are as follows.

1. Planning and operation of vertical public plazas called “the Urban Core” by private entities located in private land. Following the concept of regional design developed under public-private partnership, these facilities ensure smooth pedestrian connections between underground and aboveground and designed to be the city’s new iconic landmark.
2. Planning and operation of underground public plaza by private entities located in public land. Revenue from contents such as cafes and advertisements within the plaza is reinvested into its maintenance and management, achieving both sustainable operation and area revitalization unique to underground spaces.
3. Planning and operation of underground parking network that transcends multiple property boundaries of both public and private lands. This allows us to establish an integrated parking service in the area and ensure smooth aboveground traffic.

“Boundaryless” underground development strategies play a key role in connecting people and driving urban regeneration in complex cities like Shibuya. However, since underground development is time and money consuming, creating a system such as BID will be effective to manage financial burden not only subjected to developers but shared among the entire area that benefits from it.

**Keywords:** Transit-Oriented Development (TOD), Boundaryless, Pedestrian Network, Parking Network, Shibuya Station Redevelopment

## 1. INTRODUCTION

### 1.1. Background

In Tokyo, a transportation system centered on railways has been systematically developed as a mass transit measure in both aboveground and underground to support the world's largest metropolitan population and complex urban structure. In tandem, areas especially around railway stations have quickly developed in late 20th century with numerous high-rise complexes, underground malls and underground networks. However, those rapid urban developments have been faced aging infrastructure and compounded complexities resulting from intermittent

<sup>1</sup> Fukuda Taro, General Manager, Urban Development Planning Group, Urban and Civil Project Department, NIKKEN SEKKEI LTD, 2-18-3 Iidabashi, Chiyoda-ku, Tokyo, 102-8117, Japan, [fukudat@nikken.jp](mailto:fukudat@nikken.jp)

<sup>2</sup> Yoshino Kento, Urban Planner, Urban Development Planning Group, Urban and Civil Project Department, NIKKEN SEKKEI LTD, 2-18-3 Iidabashi, Chiyoda-ku, Tokyo, 102-8117, Japan, [yoshino.kento@nikken.jp](mailto:yoshino.kento@nikken.jp)

planning. Therefore, the city of Tokyo is currently under the urgent consideration of efficient strategies to regenerate its urban environments, and underground development playing a crucial role in unraveling the complexities of urban structures and in contributing to the creation of more convenient and livable cities.

## 1.2. Research Objectives

While major cities worldwide also have been actively developing underground infrastructures centered on subway systems, utilizing underground spaces are facing challenges due to their unique spatial characteristics. As redevelopment or demolition of underground spaces after completion is hardly achievable, it is imperative to maximize its connectivity, sustainability and cost-effectiveness with a broad perspective that encompasses both spatial and temporal dimensions. This requires a comprehensive approach regardless of boundaries between underground and aboveground, public land and private land, and moreover, planning phase and operating phase.

In this paper, we define this approach as “Boundaryless” underground development that will fully harness the potential of underground spaces and enabling sustained use amid evolving urban environments. “Boundaryless” underground development is an integration of following 3 strategies: Integration of underground and aboveground, Public-private partnership, and Continuity from planning to operation.

In Japan, with the enactment of the act on special measures concerning urban renaissance in 2002, the Urban Renaissance Urgent Redevelopment Area were established to further accelerate urban regeneration. This initiative has facilitated integrated development of public spaces and architecture, including underground areas. This paper examines Shibuya, one of these priority areas, where large-scale development and regeneration, described as a “once-in-a-century” urban transformation, are taking place [1]. NIKKEN SEKKEI, leading urban development consulting and architectural design for decades in this area, plays a pivotal role in this urban transformation with “Boundaryless” underground development approach. Therefore, this paper examines the benefits and challenges of the 'boundaryless' underground development adopted in Shibuya, with the aim of envisioning a sustainable approach for underground development.

## 1.3. Research Structure

This paper is structured as follows; Chapter 2 organizes the characteristics of urban development and city regeneration in Tokyo, as well as the historical background and features of underground development that evolved in tandem with these efforts. Chapter 3 provides an overview of Shibuya's unique traits as the target area, followed



**Figure 1.** Projected Image of Shibuya Station Surrounding Area (Planned in 2013)

© 2013 Shibuya Ekimae Area Management All rights reserved.

by an analysis of three representative underground developments in Shibuya from three cross-field perspectives: Integration of underground and aboveground, Public-private partnership, and Continuity from planning to operation, to discuss the benefits and challenges of “boundaryless” underground development in Chapter 4. Finally, Chapter 5 concludes the paper with a summary and outlook.

## **2. OVERVIEW OF URBAN DEVELOPMENT AND REGENERATION IN TOKYO**

### **2.1. History and Features of Urban Development and Urban Regeneration**

#### **2.1.1. From Government to Private Sector: The Rise of “Privatization-Oriented Urban Development”**

The key characteristic of urban development in Tokyo is the “privatization-oriented urban development” introduced in the 1980s. This policy aims to delegate traditionally public sector tasks to private entities to leverage private sector capabilities to provide high-quality and efficient services. It comprises two main components: the distribution of publicly owned resources to the private sector, such as selling off public land and privatizing public projects, and the relaxation of legal restrictions, including easing floor-area ratio regulations. This system facilitated integrated urban development by enabling private enterprises to utilize previously public land, such as railway facilities and port areas, and to carry out large-scale developments in exchange for public contributions like infrastructure improvements and residential creation. Supported by ample private capital, it promoted richer architectural designs, infrastructure, and public spaces in a cohesive framework for urban progress.

#### **2.1.2. Transition to Private-Led Urban Regeneration: the Act on Special Measures Concerning Urban Renaissance and Special Urban Regeneration Districts**

Since the introduction of privatization-oriented urban development in the 1980s, development of former public land has progressed nationwide. Meanwhile, urban areas in city centers, which had undergone development since the rapid economic growth in the 1960s, faced challenges from increasingly complex urban structures.

Furthermore, entering the 2000s, the rapid growth of cities in Asia led to a continued decline in the relative international competitiveness of Japanese cities. In response to this, the Act on Special Measures Concerning Urban Renaissance was enacted in 2002 to leverage private capital once again and “regenerate” complex city centers into internationally competitive urban hubs. Under this legislation, the government designated Urban Renaissance Urgent Redevelopment Area in major cities nationwide, aiming to create international urban hubs through public-private collaboration. These areas became subject to special measures such as deregulation, financial support, and tax incentives for private projects. Within these designated areas, private enterprises propose urban plans, and government establishes a designated areas called Special Urban Regeneration Districts based on these proposals. Using these designated areas and mutual agreements, urban regeneration projects are promoted through public-private cooperation.

Shibuya Station area, targeted in this paper, is one of the Urban Renaissance Urgent Redevelopment Areas where unprecedented large-scale urban development is underway.

#### **2.1.3. Promotion of Transit-Oriented Development (TOD) through Private Railway Businesses**

One of the driving forces behind the acceleration of privatization-oriented urban development is the role played by private railway companies. Most railways in Japan are operated by private enterprises, and in the Tokyo metropolitan area, multiple private companies manage railway networks that efficiently connect central business districts (CBDs) with suburban residential areas. Moreover, to maximize revenue, these companies have ventured into land development and real estate businesses around railway stations, promoting Transit-Oriented Development (TOD) that integrates stations with surrounding neighborhoods to enhance user convenience. The competition among these companies has expanded beyond building construction to encompass large-scale projects linked with public spaces, including roads, plazas, and underground spaces. Shibuya, the subject of this paper, represents one of Tokyo's most notable and largest TOD projects.

### **2.2. Underground Development Supporting Tokyo's Urban Transformation**

#### **2.2.1. Underground Development in Tokyo Beginning with Subway Operations**

The history of underground development and utilization in Tokyo began in 1927 with the opening of the Asakusa–Ueno section of the Tokyo Underground Railway Company (currently Tokyo Metro), marking the first subway project in East Asia. As modernization progressed and the demand for transportation among citizens



rapidly increased, urban planning in Tokyo evolved around railway transport, capable of efficiently handling mass transit. By 1939, the Ginza Line extended to its present-day route between Asakusa and Shibuya, becoming a vital means of transportation that traverses Tokyo from east to west and connects major areas.

### 2.2.2. Crossing Boundaries between Public and Private Land: Formation of an Integrated Underground Network Between Subways and Surrounding Buildings

The development of subway networks has significantly enhanced the convenience for citizens while incurring substantial construction costs. For this reason, the Ginza Line incorporated contributions from major department stores near stations alongside Tokyo Underground Railway Company, in exchange for underground connections between subway stations and their facilities. This initiative broke the boundaries between public and private lands, creating an integrated pedestrian network that connects subways and department stores underground.

### 2.2.3. Integration of Underground and Aboveground: The Rise of Underground Spaces through Parking Facilities and Underground Malls

Following the rapid economic growth of the 1960s, the development of underground railways in Tokyo has progressed, leading to the formation of the current metropolitan subway network. Similarly, the expansion of underground parking facilities and commercial spaces also gained momentum. In response to rapid urban development projects and the increasing demand for automobile transportation, the government promoted the establishment of underground parking facilities. These facilities were categorized into two types: those managed by public authorities and those developed by private entities through licensed projects. Particularly in the latter case, private developers utilized underground malls, to generate the necessary revenue for constructing and maintaining parking facilities. By relocating parking lots and commercial facilities underground, traffic congestion on the surface was alleviated, while encouraging the public to make greater use of underground spaces.

### 2.2.4. Continuity from Planning to Operation: Shifting from the “Era of Construction” to the “Era of Continued Use”

With more than half a century having passed since the period of rapid economic growth, Tokyo has undergone multiple phases of redevelopment, including secondary redevelopment efforts aimed at revitalizing previously

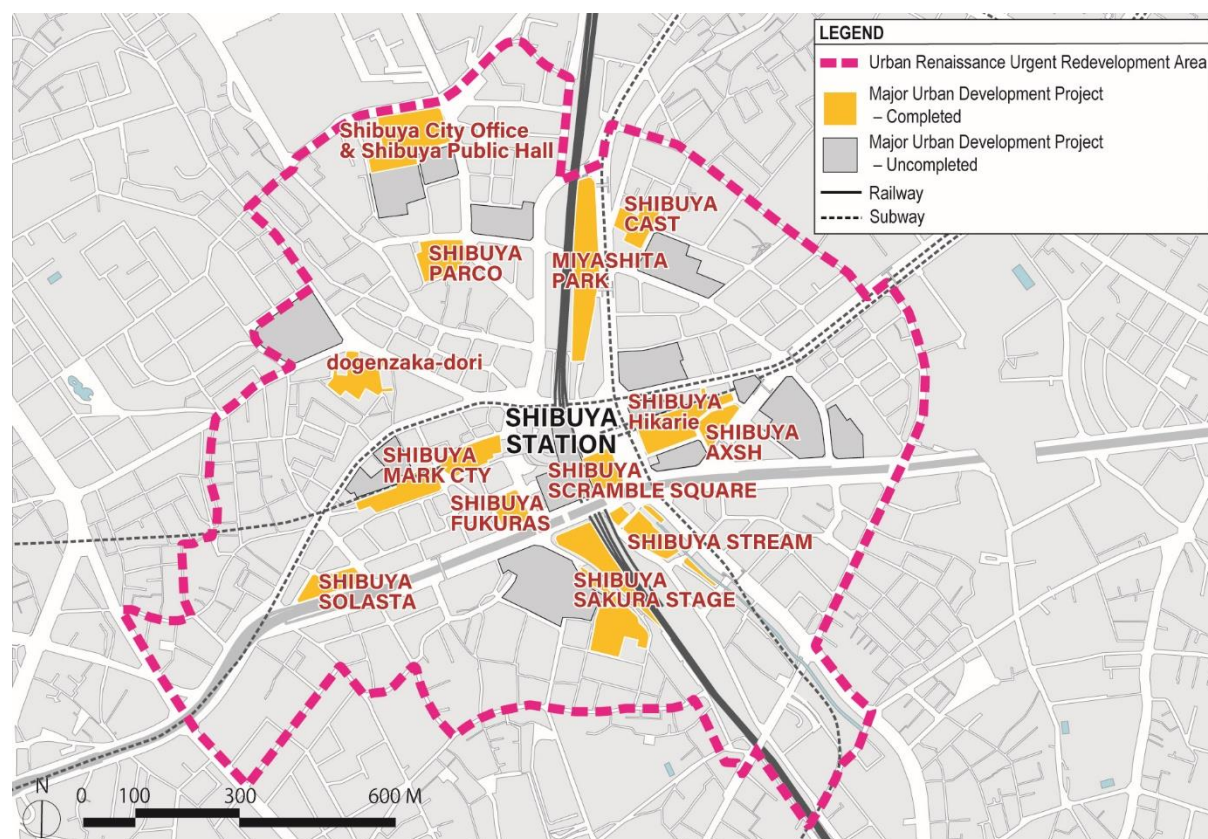


Figure 2. Major Urban Development Projects in Shibuya



redeveloped areas. In major districts, these second-round redevelopment projects are nearing completion. On the other hand, aiming to reduce the costs associated with new urban development and to lower environmental impact, sustainable development projects have recently been in demand. Accordingly, future urban development, including underground spaces requires a paradigm shift from “scrap and build” toward prolonged use and management. This approach encompasses the entire lifecycle of development, fostering a continuation from planning to operation with the aim of sustaining usability over the long term.

### 3. METHODOLOGY + RESULTS

#### 3.1. Target Site Overview

##### 3.1.1. Positioning of Shibuya in Tokyo

Shibuya has long developed as Tokyo's “hub of the content industry”. During the 1970s, Shibuya emerged as a cultural beacon for youth, broadcasting diverse trends in fashion, music, art, and dance across the nation. Subsequently, spurred by the IT bubble of the 1990s, Shibuya attracted headquarters of companies involved in cutting-edge IT, video, music, and gaming industries. Today, it stands as a significant content hub, hosting numerous global tech corporations' offices and branches.

At the same time, one of the longstanding challenges for Shibuya's further development lies in its unique “bowl-shaped” valley terrain. Shibuya forms an enormous valley centered on Shibuya Station, spanning a diameter of approximately 1 kilometer with a height difference of around 20 meters, surrounded by various slopes connecting the valley bottom to its outer edges. In comparison to other major cities with grid-like urban layouts—such as Marunouchi which is a core CBD in Tokyo, or Manhattan in New York—Shibuya's distinctive valley terrain and intricate road patterns are both a hallmark of its regional character and a significant barrier to improving accessibility in the area.

##### 3.1.2. Urban Development Trends in Shibuya

Figure 2 illustrates the trends in urban development within Shibuya. Designated as the Urban Renaissance Urgent Redevelopment Area in 2005, Shibuya represents one of Japan's major Transit-Oriented Development (TOD) projects, with significant involvement from NIKKEN SEKKEI. Addressing the challenges posed by Shibuya's valley terrain, the development has adopted a comprehensive approach encompassing “point” (stations and mixed-use facilities), “line” (underground passages and elevated decks), and “area” (multi-block development spanning 30 years, connecting points and lines). Dubbed a “once-in-a-century” large-scale project, the initiative not only revitalizes the central district but also stimulates the development and investment momentum in surrounding areas connected via ground and underground routes. The surroundings of Shibuya Station, which are major mixed-use facilities and the infrastructure connecting them, including underground passages and elevated decks, have already been operated for several years. The remaining projects include Shibuya Station updating repairs and plaza developments, as well as the completion of SHIBUYA SCRAMBLE west and central wing, scheduled for completion by 2034.

#### 3.2. Methodology

The study focused on representative examples of “boundaryless” underground development in Shibuya, including:

- (1) **The Urban Core:** A multi-level public plaza planned and operated by private entities on private lands.
- (2) **Shibuya Station East Entrance Underground Plaza:** A public space operated by private entities on public lands.
- (3) **The Parking Network:** A network of parking facilities traversing both public and private lands in both underground and aboveground and operated by private entities.

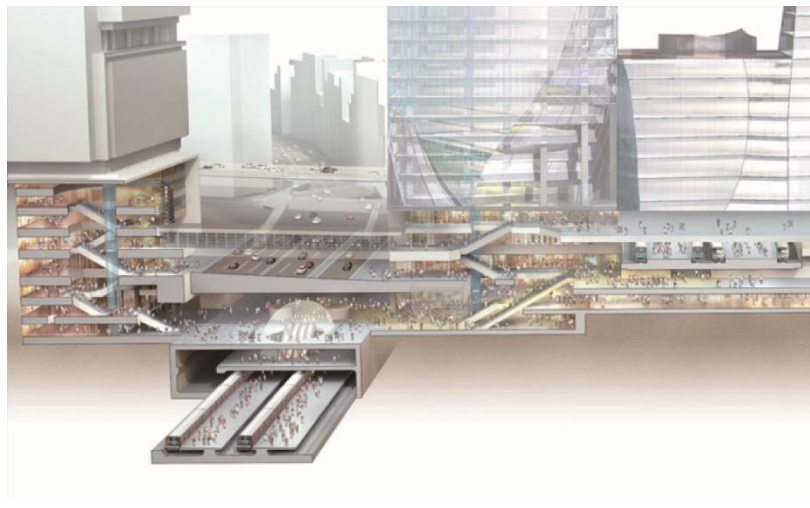
These cases were analyzed through three perspectives:

- A) **Integration of Underground and Aboveground:** Examining the integration of underground and aboveground spaces.
- B) **Public-Private Partnership:** Investigating the collaboration and utilization of both public and private lands.
- C) **Continuity from Planning to Operation:** Evaluating seamless management and future utilization of spaces.

Based on this analysis, Chapter 4 discusses the benefits and challenges of “boundaryless” underground development for sustainable urban development and regeneration.



**Figure 3.** The Urban Core of SHIBUYA Hikarie



**Figure 4.** Projected Image of the East Exit Urban Cores

© 2013 TOKYU CORPORATION, East Japan Railway Company, Tokyo Metro Co., Ltd.  
All rights reserved

### 3.3. Results

#### 3.3.1. The Urban Core

##### A) Integration of Underground and Aboveground

The Urban Core aims to overcome the valley terrain of Shibuya, highlight the presence of underground spaces to visitors, and establish distinct identities for the east, west, south, and north areas of the city. As Figure 3 shows the Urban Core of SHIBUYA Hikarie, this interconnected vertical circulation space between the surface and underground is designed to enhance accessibility while simultaneously serving as a visual icon within the urban landscape.

##### B) Public-Private Partnership

Space creation and utilization are centered around private land owned by developers but also include integrated use of public land such as roads and rivers, planned without dividing zones. As illustrated in Figure 4, which is a projected image of the East Entrance Urban Core district, This kind of such cross-sectoral space creation and utilization is refined and decided through “Design Conferences”, a platform composed of municipalities, residents, and academics, including developers, working collaboratively.

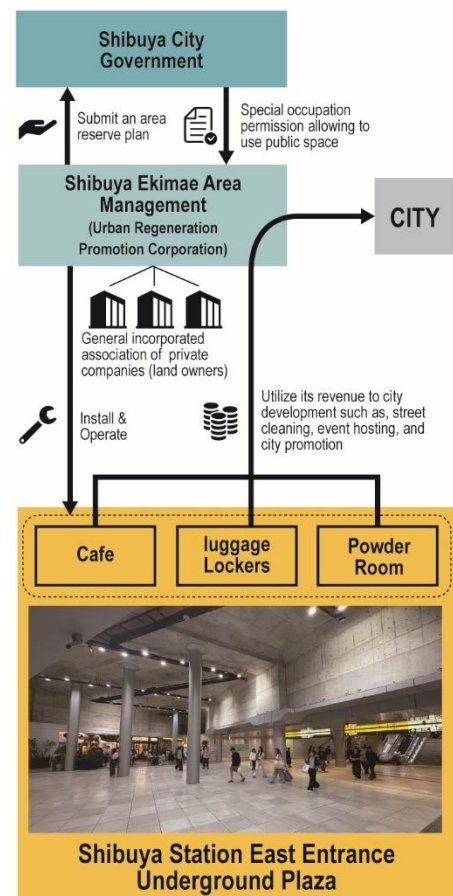
##### C) Continuity from Planning to Operation

Design, development, and operation are consistently carried out under the leadership of the development entities. Future utilization is anticipated, enabling efficient investment by determining plans, designs, and specifications for development. Furthermore, the “public nature” of the space is ensured by designating it as a Privately Owned Public Space (POPS) within urban planning.

#### 3.3.2. Shibuya Station East Entrance Underground Plaza

##### A) Integration of Underground and Aboveground

Through the construction of new subway stations, redevelopment of ground-level station plazas, redirection of existing river courses, and the installation of underground water storage tanks, new niche spaces have been created underground. Vehicle and pedestrian flow functions are assigned to the ground-level plazas, while the underground plazas are designed with a focus on pedestrian retention and all-weather activity hubs.



**Figure 5.** Development and Management Scheme of Shibuya Station East Entrance Plaza

B) Public-Private Partnership

The planning and development are carried out as public facilities (underground plaza designated as “public road”) under the jurisdiction of the municipality. At the same time, as the space directly connects to private railway facilities and private development buildings, close coordination with each private entity has been undertaken since the planning stage. Furthermore, the management and operation are planned to be handled by the local community development organization, which is called Area Management Organization).

C) Continuity from Planning to Operation

Figure 5 illustrates the development and management scheme of the plaza. From planning to operation, the process is consistently carried out under the leadership of municipalities. Regarding specific management and operational responsibilities, the municipality conducts public recruitment and selects Area Management Organizations. In the plaza facility plan, future utilization and operational projects are anticipated, including various revenue-generating facilities such as dining establishments, coin lockers, powder rooms, event spaces, and advertisement facilities. The income generated is reinvested into community-building activities for regional benefit.

### 3.3.3. The Parking Network

A) Integration of Underground and Aboveground

To ensure smooth vehicle and pedestrian traffic on the surface and achieve a well-formed landscape, parking spaces across the entire area are consolidated underground. The parking plan aims to facilitate mutual utilization, centralize and appropriately allocate entrances and exits across the area, and network both public and private Public to Private.

B) Public-Private Partnership

As illustrated in Figure 6, to ensure integrated parking functionality across public and private spaces, specific sections of parking spaces and entrances/exits are developed within the boundaries of private development sites, while parts of the networked vehicle pathways and entrances/exits are established within public roads. Furthermore, comprehensive management of parking operations extends to utilizing existing parking facilities in

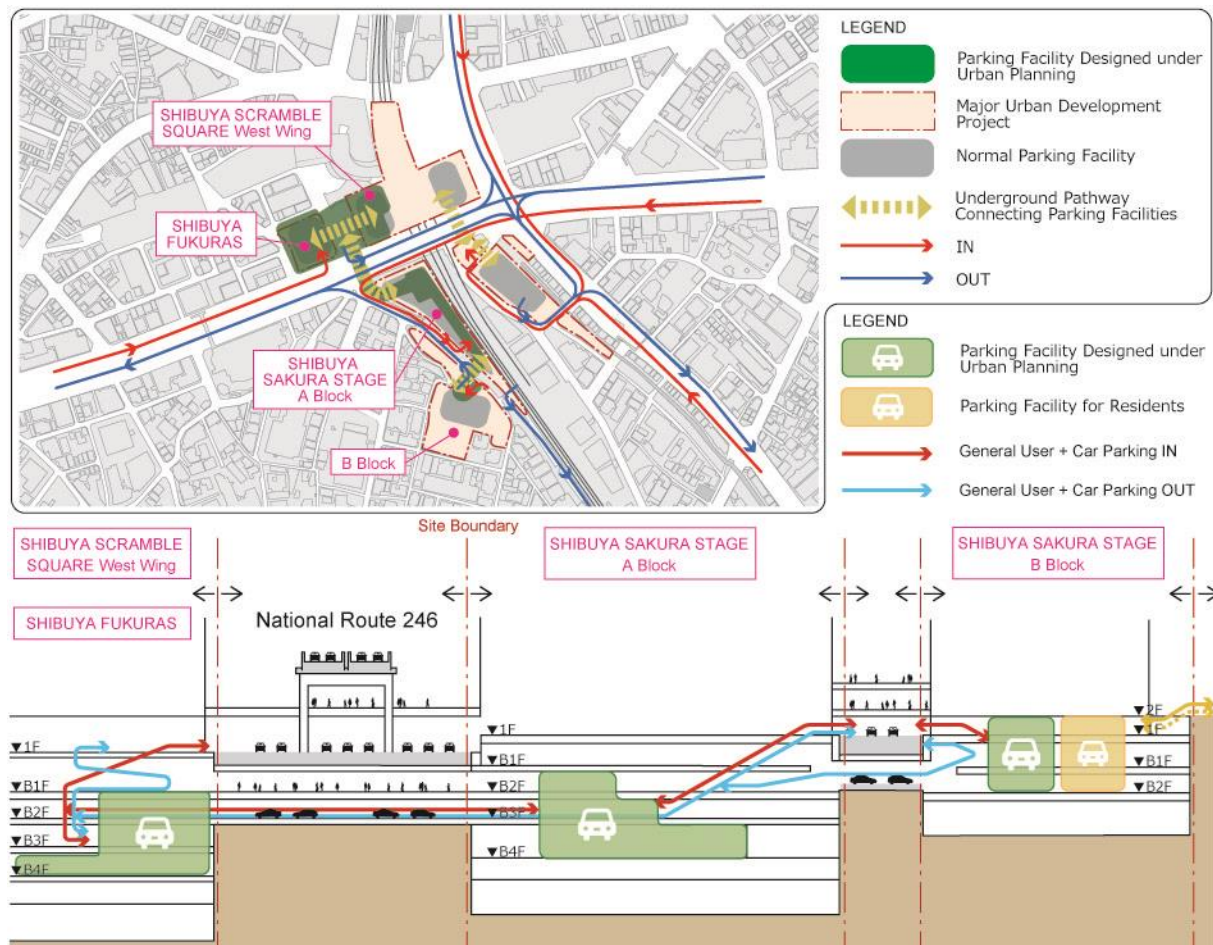


Figure 6. The Parking Network Developed in Shibuya



surrounding areas. These operations are controlled by municipal authorities through guidelines such as the “Regional Parking Rules” and the “Parking Countermeasure Council”.

#### C) Continuity from Planning to Operation

The planning stage envisioned an integrated management approach through the underground network system, with operational methodologies specifically coordinated by the local community development organization (area management organization). Currently, unified management and operational systems for each networked parking facility have been established, achieving integrated operations across the network.

## 4. DISCUSSION

### 4.1. Benefits of “Boundaryless” Underground Development

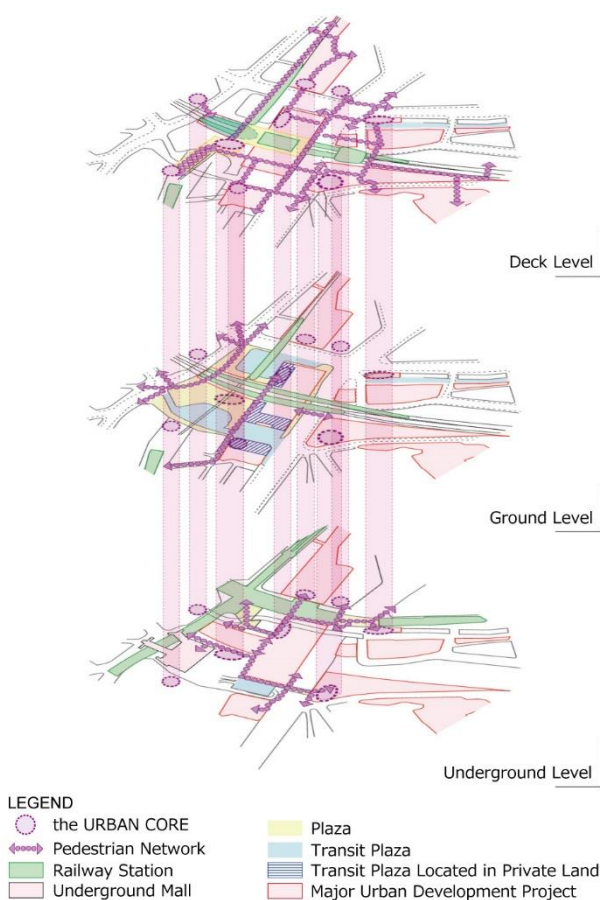
Shibuya's series of underground developments aims to revitalize the city by connecting stations and hub complex facilities through underground pathways. As illustrated in Figure 4, the expansive underground space created by linking the East Exit underground plaza, the ticket gates area of the Shibuya Subway Station, and the adjacent hub complex facility's urban core demonstrates this concept. This space accommodates both transit passengers, who move continuously throughout the day, and stationary visitors who remain within the station area.

Over the past 20 years, Shibuya has expanded such point-and-line-structured spaces through successive developments. As illustrated in Figure 7, integrated underground pedestrian network connecting the station to surrounding buildings supported by the Urban Cores linking underground and aboveground areas, Shibuya provides a comfortable environment for pedestrians unaffected by automobile traffic or weather conditions.

### 4.2. Challenges of “Boundaryless” Underground Development

While the benefits of “boundaryless” underground development have been highlighted, several challenges have been discovered. The first issue is the extension of construction timelines due to the scale of such large-scale projects. Specifically, the Shibuya Station district project, which serves as the core of the Shibuya Station central area has seen its completion delayed significantly—from the initial plan of 2027 to a projected completion in 2034 [2]. The complex vertical and horizontal interferences between infrastructure and buildings necessitate detailed and extensive construction planning, with the outlook for the project only taking shape this year. During the extended construction period, efforts are required to ensure safe and comfortable usage, such as enhancing the temporary transit spaces and disseminating information on future development visions and current construction progress.

The second issue is the heavy reliance on private developers and landowners in large-scale urban development projects, such as those in Shibuya. Within the existing urban development system in Japan, undertaking the development of public spaces, including underground ones, through private projects requires planning high-density buildings capable of generating sufficient revenue to cover construction costs. However, these large-scale projects demand substantial resources -people, money, and time- and are further burdened by challenges such as severe labor shortages in Japan's construction industry, rising material costs, increasing wages, and the costly complexity of infrastructure-linked development projects that extend construction timelines. These adverse conditions have led to numerous cases of redevelopment plans being canceled due to unprofitability. Given the significant public



**Figure 7.** The Pedestrian Network Supported by the Urban Cores in Shibuya

contributions included in private urban development, it might be essential to gather all stakeholders benefiting from the development to advance urban development initiatives collectively at a community-wide level.

## 5. CONCLUSIONS

“Boundaryless” underground development serves as an essential element in efficiently connecting people and advancing urban development and regeneration in cities with complex structures like Shibuya. This approach expands the possibilities of underground utilization by demonstrating how effectively integrating underground spaces can promote urban development and regeneration in other global cities.

However, to ensure sustainable urban development and regeneration, it is necessary to consider a system where the financial burden of utilizing underground spaces is shared not only by private developers responsible for building projects directly above the underground spaces but across the entire area benefiting from these underground developments. A framework such as BID (Business Improvement District), which involves the broader area, could contribute toward achieving a more enduring development model.

NIKKEN SEKKEI will continue to promote the realization of “Boundaryless” underground development to achieve sustainable urban regeneration.

## 6. ACKNOWLEDGEMENT

Special thanks to TOKYU CORPORATION, East Japan Railway Company, Tokyo Metro Co., Ltd., and Shibuya Ekimae Area Management for providing specific images (Figure 1 and Figure 4).

## 7. BIBLIOGRAPHY

- [1] “Hyakunenn ni Ichido” no Daikibo-saikaihatsu, Shibuya-ekigaiku-keikaku, Saishusho he. TOKYU CORPORATION, East Japan Railway Company, Tokyo Metro Co., Ltd. 2025.05.09.  
<https://www.tokyu.co.jp/company/news/detail/56376.html> (2025.06.23)
- [2] Shibuya Saikaihatsu, Kansei 7-nenn Okure -SCRAMBLE SQUARE 2-to no Kouji Hajimaru. The Asahi Shimbun, 2025.05.19.
- [3] Shin, A. (2021). Heisei Toshikeikaku-shi. Kaden-sha, 44-70
- [4] Ministry of Land, Infrastructure, Transport and Tourism. (n.d.). Various Policy Measures in Urgently Implemented Urban Renaissance Districts. [https://www.mlit.go.jp/toshi/crd\\_machi\\_tk\\_000008.html](https://www.mlit.go.jp/toshi/crd_machi_tk_000008.html) (2025.06.14).
- [5] Tokyo Metropolitan Government. (2020). The Changing Face of Tokyo: From Edo to Today, and into the Future, 54-55.
- [6] Takayuki, K. (2022). Urban Development Centered Around Stations. Public Relations Office, Government of Japan. [https://www.gov-online.go.jp/eng/publicity/book/hlj/html/202202/202202\\_01\\_en.html](https://www.gov-online.go.jp/eng/publicity/book/hlj/html/202202/202202_01_en.html) (2025.06.14)
- [7] Shinkenchiku Editorial Department. (2025). Doboku to Kenchiku ga Mukau Saki: Kyokai wo Tsunagu Chika Kukan. Shinkenchiku, Vol 100 (4), 170-177.
- [8] Junji, N, Kiyoshi, T, Keiichi, S, Mitsuyuki, A. (1995). Analysis of Motives of Opening in Urban Underground Shopping Malls. Historical Studies in Civil Engineering, Vol. 15, 45-60.
- [9] Shibuya City Office. (2022). Basic Philosophy of Community Development around Shibuya Station, 3-6.
- [10] Future Design Shibuya. (2021). Kawaritsudukeru! Shibuya-kei Machidukuri. Kosakusha, 22-33.



## ENHANCING THE DEVELOPMENT OF UNDERGROUND LAND: ISSUES ON LEGAL, SOCIAL AND ECONOMIC ASPECTS

Ahmad Hamidi Mohamed<sup>1</sup>, Noorfajri Ismail<sup>2</sup>, Kamilah Wati Mohd<sup>3</sup>, Saiful Aman Hj Sulaiman<sup>4</sup>,  
Noorasiah Sulaiman<sup>5</sup>

**Abstract:** Underground development has been the way forward in the current development approach, especially in Malaysia. However, underground development has legal, social, and economic impacts on the nation's growth. This study examined the importance and issues involving current legal provisions, social concerns and cost or compensation for land acquisition. The study embarks on the qualitative methodology of doctrinal study and thematic content analysis from legal documents and legislation. Interviews and focus group discussions have been conducted with two (2) subject matter experts recognised by the Government of Malaysia in land acquisitions and land legislation, and engaged with land administrators for every state. The study also analyses the current legal provision and practice for compensation payment in underground land acquisition through case law. The study finds that the current ownership and rights are provided in the National Land Code of Malaysia, but the issue is on the implementation and decision of the State Authority in alienating the underground land. In addition, it is found that underground development needs to be readily accepted by the nation, in all aspects such as planning, legal provision and compensation for the underground space. Hence, the use of the physical underground land and the legal aspect must be in parallel with the development approach to provide a balance of needs.

**Keywords:** acquisition, development, land, legal, underground

### 1. INTRODUCTION

Development in current trends is to be vertical in nature. This development approach has been in the market to cater for the development in urban areas (bt Zaini et al., 2012). Thus, urban development is more towards vertical development, especially in developed countries (Zaini et al., 2021; Z. Zhang et al., 2020). Developments such as underground tunnels for train tracks are very much attached to the development in urban areas in developed countries (M. Zhang et al., 2022). Other development purposes, such as residential and commercial, are also alongside this development in such countries (Zaini et al., 2013).

However, developing countries are still looking into the implementation of the vertical development approach. In Malaysia, for example, underground developments are gaining its token as the preferred approach for urban development. Urban developments are vertical developments in addition to at-grade developments or horizontal developments. The scenario in Malaysia for vertical developments is fairly equal to other developed countries' approaches, but mainly on the public purpose development – public roads, rail tracks, and a combination of several uses, such as roads and flood mitigation.

<sup>1</sup> LL.M (IUM), M.LARM (UPM), Mohamed, Ahmad Hamidi, Land Administrator, PhD Candidate, Malaysia, [midi.trg@gmail.com](mailto:midi.trg@gmail.com).

<sup>2</sup> Dr, Ismail, Noorfajri, Legal Advisor, Islamic Science University of Malaysia (USIM), Bandar Baru Nilai, 71800 Nilai, Negeri Sembilan, Malaysia, [noorfajri@usim.edu.my](mailto:noorfajri@usim.edu.my).

<sup>3</sup> Dr, Mohd, Kamilah Wati, Senior Lecturer, Faculty of Syariah and Law, Islamic Science University of Malaysia (USIM), Bandar Baru Nilai, 71800 Nilai, Negeri Sembilan, Malaysia, [kamilah@usim.edu.my](mailto:kamilah@usim.edu.my).

<sup>4</sup> Ts. Sr. Dr., Saiful Aman Hj Sulaiman, Associate Professor, Faculty of Built Environment, Universiti Teknologi MARA (UiTM), 40450 Shah Alam, Selangor, Malaysia, [saifulaman@uitm.edu.my](mailto:saifulaman@uitm.edu.my).

<sup>5</sup> Dr. Noorasiah Sulaiman, Associate Professor, Faculty of Economics and Management, National University of Malaysia (UKM), 43600 Bangi, Selangor, Malaysia, [rasiahs@ukm.edu.my](mailto:rasiahs@ukm.edu.my).

Vertical developments in a conventional method or approach connote the developments upward. The infrastructure is built from the surface of the land upwards, such as stratified buildings. References to the stratified buildings may differ for their purposes. In Malaysia, it is reported that the current stratified scheme amounts to 24,611 schemes throughout Peninsular Malaysia (Bakri, 2025). The buildings may be built for residential purposes, like condominiums and apartments. On the other hand, the buildings may be for commercial purposes, such as office spaces and shop lots. Moreover, there are also infrastructures with multi-purpose and combinations of different purposes. These developments introduced terms such as Small Office Home Office (SOHO), Services Apartments, commercial complexes, as well as hotels and residences. These instances are covered by legal frameworks such as the Strata Titles Act 1985 in Malaysia, the Land Titles (Strata) Act 1967 in Singapore and the Strata Scheme Development Act 2015 in New South Wales, Australia.

Conversely, the vertical development is also going downwards. The downward developments in the vertical approach may be initially for the basement parking, storage spaces or bunkers (Perperidou et al., 2021). Not to mention, the downward development is also for military purposes as safety vaults or weapon storage. At least, the use of underground land is linked to utilities such as electricity, sewerage and water supply (Land Acquisition Plan Tuz Gölü Underground Gas Storage Project, 2005; Yan et al., 2019).

However, the main concern of the research is on the civil and public infrastructure of daily activities. Several works of literature show that downward developments have evolved from rail tracks as for public amenities, to further advanced use of the underground land, such as to provide a city or a neighbourhood underground (Konykhov & Kolybin, 2021). Thus, this development of vertical downwards approaches is gaining extension to other purposes (Bobylov, 2009; Zhou & Zhao, 2016).

Defining underground development, some scholars refer to the term underground as the subsoil, sub-terrain and subsurface (Volchko et al., 2020). In Malaysia, the definition of underground land is found in the National Land Code [Act 828] (NLC). Section 92A was inserted in the NLC in 1990 to define underground land and matters connected to it. It is a move to provide the legal framework for underground land ownership for development. Besides, there are also vertical land use regulations that need to be adhered to (Zaini et al., 2021). Land use is governed by specific legislation for land development. It is suggested by scholars that the development of underground land needs to have a master plan (Jamalludin et al., 2016). Additionally, the Malaysian framework in NLC also introduces another term, such as stratum. Under NLC, stratum is defined as “*a cubic layer of underground land*”, whereas underground land means “*land which lies below the surface of the earth*”.

Further, in Malaysia, the underground land is rarely involved in the alienation of land as the first option of disposal of land by the State Authority. Most of the underground land use in Malaysia is prepared through mutual agreement and compulsory land acquisitions. The theory of land ownership in Malaysia, which confers ownership and rights to the proprietor for the surface, above and underground land, should also be read together with the obligations to the public for the support of the land. Similarly, as the land is among the main factors in economic and infrastructure development, valuation of the land and compensation should be adequate, fair and just to the land owner in the case of compulsory land acquisition.

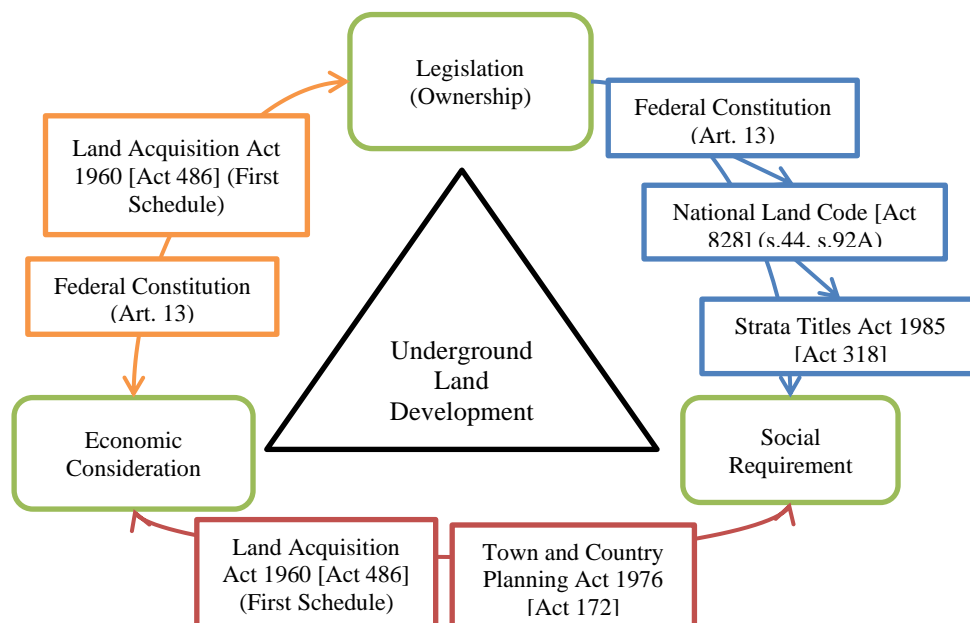


Figure 1. Conceptual Legal Framework on theory and principles in underground land development

In such a case, this paper seeks to explore the connectivity and nexus of legal, social and economic aspects in considering how to enhance the underground land development framework as in Figure 1. This discussion will be further elaborated in a subsequent section on the legal position of underground land development. Nevertheless, the research is narrowed down to the implementation of compulsory land acquisition in Malaysia. The findings from the content analysis will be discussed in the subsequent paragraph. This paper will complete with a conceptualisation and policy reform recommendation before the formal conclusions on the findings of the research.

## 2. MATERIAL AND METHODS

The researcher embarks on the use of qualitative methods. The qualitative method in the current study is the preferred option to answer the question of how the connection between several elements can impact the development of underground spaces. As the study is based on the doctrinal study, as to the legal position of the development, content analysis is done on the data available to the study. The data are from the provision of the law of a selected country, which is Malaysia. Several lists of legislation used are as Table 1 below.

*Table 1. List of Considered Legislation*

Short title	Act	Status and date of enforcement	Year
<b>National Land Code</b>	Act 828	In force	Revised 2020
<b>Strata Titles Act 1985</b>	Act 318	In force	Updated 2021
<b>Land Acquisition Act 1960</b>	Act 486	In force	Updated 2022

Apart from the legislation, this research also approaches subject matter experts in land administration, who is in the land administration organisation. These subject matter experts are recognised by the Public Service Department of Malaysia (*Jabatan Perkhidmatan Awam – JPA*) in their field of land administration. They are now attached to the Department of Director General of Lands and Mines, Malaysia (*Jabatan Ketua Pengarah Tanah dan Galian Persekutuan – JKPTG*).

Besides, the information and awareness of underground development in Malaysia are still new, so a non-probability sampling is chosen. Participants are from specific players in underground development, especially the land administrators and underground developers. Small group discussions are also organised to gain inputs from well-known scholars in land acquisition, such as a Professor in Land Law, as well as the President of the Association of Land Professionals of Malaysia (*Pertubuhan Professional Tanah Malaysia – PERTAMA*).

## 3. RESULTS

### 3.1. Legal provision

The provision of law in the underground legal framework has been in place under the National Land Code of Malaysia. The initial introduction of the underground legal framework is based on the development and construction of underground parking at Dataran Merdeka. It is debated in the House of Representatives in the Parliament of Malaysia as to the development of the underground land and the need to have an underground legal framework. Thus, in 1990, the National Land Code [Act 828] (NLC) was amended to introduce underground ownership. It is introduced under Part Five (A), which is a portion of the NLC on the Disposal of Underground Land (National Land Code [Act 828], 2020). Section 92A of the NLC provides 3 important terms, which is as follows –

#### **“92A Interpretation**

*In this Part, unless the context otherwise requires—*

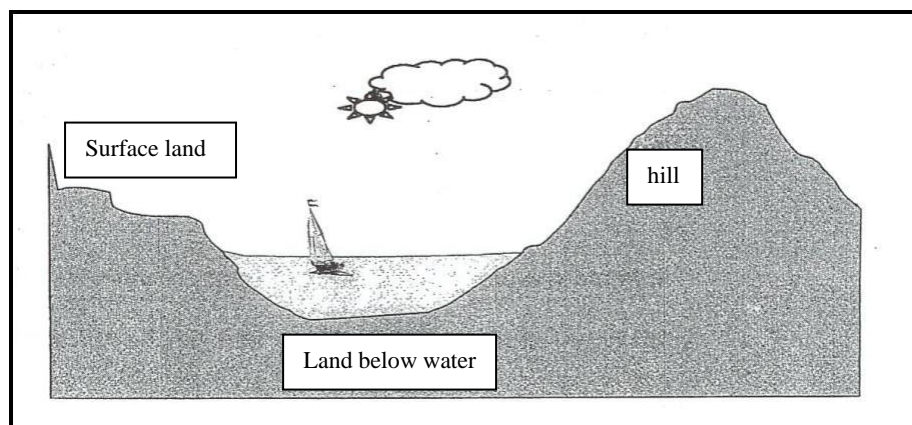
*"adjoining underground land" means underground land adjoining a stratum above, below, and on the sides of, the stratum;*

*"stratum" means a cubic layer of underground land; and*

*"underground land" means land which lies below the surface of the earth."*

These definitions mentioned in the NLC will be used in any development of underground lands. The development refers to the development of below the surface of the earth, which is below the surface of the land.

As such, it includes the land at the same level, but may differ as to the height of the land. It is further explained in the circular published by the JKPTG on underground land disposal, as in Figure 2, including the land below water, and underground in a hill. The circular was in force in 2018 before being revised due to the development of the law. The current circular published by JKPTG further advises in relation to the amendment to the NLC and the consequences of the land acquisition (Panduan Pelaksanaan Pelupusan Tanah Bawah Tanah Di Bawah Kanun Tanah Negara (Disemak-2020) [Akta 828], 2021).



*Figure 2. The underground land (label amended from the source)*

Besides, the development of underground land is guided by the planning authority. In Malaysia, the Department of Town and Country Planning (*Jabatan Perancangan Bandar dan Desa – JPBD/PLANMalaysia*)<sup>6</sup> is the planning authority and provides the guidelines for development. In this particular case, PLANMalaysia published several planning guidelines to cater for the needs of development as well as to govern the planning activities. One of the planning guidelines is the planning guidelines for underground development (PLANMalaysia, 2022). It was published in 2022, echoing the amendments to the law on the underground legal framework.

In addition, the preparation of land for underground development is also provided by the Land Acquisition Act 1960 [Act 486]. The previous legal framework on land acquisition did not provide for underground land acquisition. This scenario created hiccups in the development of the project, at that time, the Mass Rapid Transit (MRT). It establishes the need for various research gaps and contributes to various research findings by scholars, particularly on the underground legal framework in Malaysia<sup>7</sup>. Several records of the findings are to amend the current law, and others suggested enacting another law (Hassan, 2016; Zaini, 2016). This particular finding seems consistent with the initiative taken by the government.

As such, in 2016, Act 486 was amended to include the land acquisition for underground land, together with the provisions of various situations and scenarios of acquisition under strata title (Mohamed, 2017; Senawi et al., 2018). This legal framework came into force in 2017 after being assented to by the King on 31<sup>st</sup> August 2016. Thus, it will support the needs of development, such as the Mass Rapid Transit (MRT) development, and other development needs for the use of underground land.

For the purpose of clarification, further guidelines were published by the JKTPG. The circular of the JKPTG provides detailed explanations of the process and procedure for implementing the land acquisition (Panduan Pelaksanaan Pengambilan Tanah Bawah Tanah, 2020). It is mentioned that the acquisition of underground land is a land acquisition of part of the land, which can be acquired through Act 486. Section 7 of Act 486 says –

***“Preparation of plan and list of lands***

*7. (1) Whenever any lands are needed for any of the purposes referred to in section 3 the Land Administrator shall prepare and submit to the State Authority—*

*(a) a plan of the whole area of such lands, showing the particular lands, or parts thereof, which it will be necessary to acquire; and*

*(b) a list of such lands, in Form C.*

*(2) Where the acquisition of part of the land refers to underground land, the plan referred to in paragraph (1)(a) shall also describe the extent and area of the underground land to be acquired.”(emphasis added)*

<sup>6</sup> PLANMalaysia is the rebranding name referring to the Department to provide clear picture of its functions.

<sup>7</sup> Various publications and research done by Farah Zaini, scholars from Malaysia, focusing on the development of the underground legal framework in Malaysia.

By virtue of this section, compulsory land acquisition can be invoked for the preparation of underground land development. It is worth noting that compulsory land acquisition is applicable only to individual land titles. It refers to the alienated land which has been disposed of by the government, in particular, the State Authority, for the purposes as per the application.

Thus, the invocation of compulsory land acquisition will come together with the requirement to provide and payment of compensation. It is a general rule that the land acquired, which is the property of a person, is to be compensated because of the acquisition. The principle of Article 13 of the Federal Constitution of Malaysia needs to be adhered to. In addition, Act 486 also requires payment of compensation as formulated in the First Schedule of Act 486. This legal proposition illustrates the need to focus on the economic and social aspects of the aggrieved parties involved in the compulsory land acquisition, as well as the development of the underground land.

### 3.2. Economic valuation method

Therefore, the payment of compensation must be at the heart of the compulsory land acquisition process and proceedings. The payment of compensation is basically guided by the economic principle of the market value of the land. It is the first principle of payment of compensation. The land needs to be valued according to the market value. As per the discussion with the participants in the research, the market value for the underground land is not yet ready in a solid way. According to Jaiya (2025), one of the subject matter experts says that the valuation of land is subject to the respected authority, and the land administrator has no authority to decide deliberately. As in Malaysia, the valuation is done by a valuer who is guided by an institutional authority known as the Valuation and Property Services Department (*Jabatan Penilaian dan Perkhidmatan Harta - JPPH*). The JPPH will provide guidelines through their circular, which will be used by not only government valuers, but also private valuers.

The research finds that there are several methods of underground valuation as proposed by scholars. The valuation methods are suggested to differ on a case-by-case basis, depending on their purpose. In general, the literature and scholars suggest several methods. The methods of valuation that are currently discussed by scholars can be summarised as in Table 2 below.

Based on Malaysian cases and jurisdiction, one of the scholars suggested that the underground valuation should use the extended version of the Residual Method and the Comparison Method with a mixture of other principles (Abd Rashid, 2016). The findings show that several methods can be used for the valuation of underground land. The initial possible approaches are the comparison method, the residual method, the cost method and the shadow method. However, it is maintained that the legal aspects must be in place for the best solution as to the rights and ownership of the land.

*Table 2. Valuation Methods for Underground Land*

Type	Description	Scholars and Sources
<b>Residual Value Analysis</b>	This method quantifies the economic benefit and subsurface land value by <b>comparing the economic returns</b> of the underground space development with the original land use. It is particularly useful in urban planning to ensure the economic feasibility of underground projects.	Zhu, W., Fu, J., Yang, J., Tong, L. Urban underground space value: Case study of Kaisheng Square Planning in Lanzhou city Proceedings of 12th International Conference of the Associated Research Centers for Urban Underground Space, ACUUS 2009, 2009
<b>Integrated Valuation Models</b>	Combining the <b>cost method, income reduction method, and floor utility ratio method</b> can provide a comprehensive value assessment model for underground space use. Factors such as location, traffic, and business type significantly influence the value of underground commercial space.	Shi, Y., Zhou, L. Land value assessment and spatial variation in underground commercial space in Shanghai Dili Xuebao/Acta Geographica Sinica, 2017
<b>Direct Evaluation Method</b>	This method is increasingly used due to its ability to directly assess the value of underground space use rights, considering <b>market data and policy impacts</b> . It involves selecting appropriate evaluation methods, determining parameters, and accounting for policy subsidies.	Zhang, J. Appraisal Methods and Case Analysis of the Land-use Right's Price of Urban Underground Space Chinese Journal of Underground Space and Engineering, 2020



Type	Description	Scholars and Sources
<b>Space Distribution Theory</b>	Establishing a land-use price evaluation model based on space distribution theory helps in quickly determining the land-use prices for underground spaces. This model supports <b>orderly land transactions</b> and legal compliance.	Lin, G.-B., Cai, W.-M., Hao, S., Liu, H.-W. Evaluation of land-use right price of urban underground space Journal of Tianjin Polytechnic University, 2012
<b>Real and Potential Value</b>	Underground space resources can generate economic value, and the methods used to evaluate this vary depending on the type of <b>resource used directly and indirectly</b> . Some considerations factors such as the <b>carrying capacity</b> , geological suitability, and overall quality to ensure the optimal utilisation of underground spaces.	Wu, Y., Wen, H., & Fu, M. (2024). A Review of Research on the Value Evaluation of Urban Underground Space. <i>Land</i> , 13(4), 474.

Meanwhile, in order to give value to the underground land, the legal and administrative aspects need to be considered as well (Hussin et al., 2017). This finding concurs with the previous finding that involves the consideration of legal and administrative aspects. It is also important to differentiate the approach of valuation methods as to the disposal of land by alienation and the payment of compensation, as discussed above.

### 3.3. Social impacts

The element of social value is also discussed for the underground development. The rights of access, for example, must be clearly mentioned in securing the ownership and rights (Abdul Jalil & Mohd Arshad, 2019, 2020). The rights of access have been provided to allow the owner to have full use of his land rights. Similarly, the NLC also provides that the adjacent land needs to provide support to the land. As such, the underground land must also be in consideration of the principle of accessibility.

According to Ismail (2024), social impact is one of the principles in the discussion of the valuation of the land. It is important to note that the development, including underground developments, should always consider the social status of the affected parties<sup>8</sup>. An example is the development at Kampung Bharu, Kuala Lumpur, which is an area of totally Malay residents. They must consider the impact on its social value, as the development may involve the influx of other members of society to stay and dwell in the area after the development. The development of an underground station for light rail transit (LRT) has also been an example of the loss of *in situ* social value, and affects the compensation of compulsory land acquisition at the site (Omar, 2024).

This proposal is agreed upon by another participant, and according to Saiful Azman (2024), as the social impact assessment plays an important role in development, the social value must be considered<sup>9</sup>. Additionally, the Social Impact Assessment has been a requirement for any development which falls within the ambit of its guidelines. The guidelines known as Social Impact Assessment Implementation Guidelines (Panduan Pelaksanaan SIA - PPSIA) provide that projects which fall under the purview of Federal PLANMalaysia and State PLANMalaysia must adhere to the guidelines, especially on understanding the land use.

In a case study on underground development involving compulsory land acquisition, the plot of land has the sentimental value of becoming the earliest shopping mall in Kuala Lumpur. According to one land administrator<sup>10</sup>. The advice given to them by the respective government valuer is that the sentimental value of the land or property is not calculated and cannot be considered to be included in the compensation value of the land. Thus, an issue such as goodwill is not considered to be an element of compensation, although it has social value for the property or land.

<sup>8</sup> Discussion and interview with the participant acting as the President of the Association of Land Professionals of Malaysia on 5<sup>th</sup> September 2024.

<sup>9</sup> Presentation on 5<sup>th</sup> September 2024 in *Seminar Pembangunan Semula Bandar 2025*, at Kuala Lumpur.

<sup>10</sup> An online consultation and interview held on 10<sup>th</sup> December 2024 between all the land administrator for compulsory land acquisition in Peninsular Malaysia under JKPTG.

## 4. DISCUSSION

### 4.1. Evolution In Underground Development

#### 4.1.1. Whole land ownership

Taking into consideration the underground land development, there is significant and emerging development of underground development in Malaysia (Mohamed et al., 2023). Since the introduction of the alienation of underground land in Malaysia, there is still no single title that has been alienated and registered to the proprietor throughout the country, particularly in Peninsular Malaysia<sup>11</sup>. According to the record of the interview session, most of the underground development in Malaysia is arranged under the State land and involves State or Federal projects. This is shown by several projects, as mentioned by JPPH, and several studies, as in Table 3 below (Abd Rashid, 2016; Abu, 2023; bt Zaini et al., 2012; Zaini et al., 2013).

*Table 3. Development of underground land in Malaysia (Abu, 2023)*

Purpose	Development Projects	Completed
Commercial and Parking area	Plaza Dataran Merdeka (Merdeka Square)	1990
Commercial and Parking area	Petronas Twin Tower	1997
Rail Track Tunnel/Station	Light Rail Transit (LRT)(Kelana Jaya Line)	1998
Dam	Pergau Dam	2000
Road / Flood Tunnel	SMART Tunnel	2007
Rail Track Tunnel/Station	Mass Rapid Transit (MRT) 1	2016

On the contrary, underground developments in urban areas are very much intense. As such, it is said that the land in urban areas is very scarce, which invites vertical development, whether it be stratified buildings upwards, or be it vertical development underground downwards. In the case where the development of an alienated land vertically upwards, the Strata Titles Act 1985 [Act 318] is ready and enables the development in its legal framework. This stratified development also used the underground land for its development, but it falls under the purview and ambit of Act 318.

The silo development of underground land is rarely be developed, other than several developments as in Table 3. The commercial area of underground land is also not meant to be an individual title which transfers the right and ownership to another person, but only on the tenancy or lease transaction. This situation mirrors the earlier development of underground land or strata title in New South Wales, Australia (Strata Community Association, 2025).

#### 4.1.2. Mutual Agreement

Furthermore, the development of the underground in Malaysia is still in its infancy stage. This emerging development is not fully explored, while the development is mostly on the public amenities and infrastructure, such as rail tracks and train stations. These developments can initially only be done by using State lands or acquiring the whole land, not only the underground land. This happens as the legal framework is not up-to-date to cope with the current emerging development approach (Mohamed et al., 2023; Mohamed & Musa, 2019). Thus, the part of the land which is underground land cannot be prepared for development, although the development needs the underground land only.

Thus, the only solution to the underground development at that time was to resort to an agreement known as a Mutual Agreement (MA) to co-exist on the plot of the land. Several MAs have been signed by the project proponents or the project implementation of Mass Rapid Transit (MRT) with the proprietor of the surface land. This resulted in the cost of underground development being borne by the proprietor of the land and the MRT, as agreed for the co-existence.

In order to secure the land ownership and the rights of the co-existence parties, it must be registered in the land title, as the principle of “registration is everything” is still applicable (Syed Abdul Kader et al., 2023; *Teh Bee v K. Maruthamuthu*, 1977). The registration took place under the “express condition” of the title, which will define the depth and rights of the parties, expressly and impliedly, if any.

<sup>11</sup> Records from interview and small group discussion between the participants on the compulsory land acquisition of the underground land through 2023 until 2025.

## 4.2. Challenges of Developing Underground Land

### 4.2.1. Underground land ownership

There are challenges in providing ownership of the underground land (Saeidian et al., 2021; Zaini et al., 2014, 2015). Ownership is very important as it carries rights to the land (Zaini & Mohsin, 2021). As per the principles of Malaysian land legislation, registration is everything; the title to the underground land, to this extent, is very important (Alias et al., 2000). As such, it is agreed that similar legal considerations need to be clearly mentioned (Itagaki, 2020).

This research finds that there is still no stratum title issued just yet. While the underground use has been emerging, the State Authorities in Peninsular Malaysia seem not ready to embrace the stratum title. From a legal perspective, the NLC only provides and enables the ownership of the underground land. Similarly, Act 486 provides that the underground land can be compulsorily acquired. This enabling provision was in force in 1990 and 2017, respectively.

However, the underground land acquisition is subject to the readiness of the State Authority. It is based on the requirement that the State Authority need to come out with the rules and regulations on the implementation matter of the underground development. These include the issuance of titles in continuation as a result of the partial underground land acquisition. On the other hand, the premium of the land, which is referred to as a fee in some countries, needs to be determined. The calculation of the premium as well as the quit rent, must be in accordance with the new area, more accurately, the cubic volume, and must consider the volume that has been taken and left to the surface land proprietor.

Hence, the underground land should be regulated from the early stage of alienation or disposal policy as provided under the NLC, until the implementation of the disposal. The State should be ready with the provision detailing the implementation of the underground land development, with the calculation of the premium and rent under the State land rules, to accommodate the successful and timely process of the development.

### 4.2.2. 3D element

In order to proceed with the stratum or underground land title, the plan of the land is now evolving from two-dimensional (2D) into three-dimensional (3D). Fortunately, the NLC has provided the plan to the title in continuation of the partial underground land acquisition as amended under section 396 of the NLC. It provides that the element of 3D, which confers the cubic volume of the land, must be stated through the plan of the land. In such a case, the respective authority, namely the Department of Survey and Mapping Malaysia (*Jabatan Ukur dan Pemetaan Malaysia – JUPEM*), has issued the guidelines under its power to issue circulars for the purpose of cadastre and plan preparation.

According to JUPEM, the plan in a 3D element is practically ready, and they are able to produce the plan of the land for the purpose of issuance of the underground title or title with specific depth. However, a holistic approach to the implementation of a 3D survey is yet to be finalised. Meanwhile, several plans which involve the element of 3D for the title in continuation and the title with specific depth have been prepared by JUPEM. For instance, the plan for the underground land acquisition has been prepared pending registration of the land. Yet, JUPEM is still improving the procedure and standard operating procedures to guide the surveyor in preparing the plans.

The proprietor of the land, which consists of a natural person or body or corporation, needs to be aware of the limitations of their rights and ownership (Bahagian Dasar dan Konsultasi, 2021). Under this 3D environment, the extent of enjoyment of the land might be reduced accordingly. The surface land will have to be the land with limited to a certain depth, though originally the title of the land might confer full rights of enjoyment to the land. As such, this situation must be advocated to the public for their acceptance and readiness in this change of ownership throughout the nation.

In addition, vertical development extends to the underground land; space above the surface of the land also exists within the current development. A tunnel within a building or a tunnel passing through the hill requires the same attention as underground development. It involves the need for a future 3D framework in the development of infrastructure above the surface of the land (Mohamed et al., 2024). Hence, the development of underground land or above the surface of the land involves multi-layer development, which involves different rights and ownership that should be addressed and compensated in a new land legislation framework.

### **4.3. Compensation rights**

#### **4.3.1. Economic value**

As regards the economic impact and social impact, they can be combined under the compensation rights. It is also worth to note also that the legal spaces or ownership need to be in 3D perspective for underground land (Ramlakhan et al., 2023). This element will define the actual rights as regards to the border or boundaries of the land and its surface land. By virtue of guidelines prepared by the JPPH, the valuation of the underground land is still vague and might be open to challenges. This issue is recognised by JPPH, according to the presentation by the JPPH officers in 2024.

The underground land is the rights of the surface landowner or proprietor as long as the title does not specifically mention the depth of the land. Similarly, the ownership of the land also provides full rights to the underground land use by the proprietor. Subject to other laws, the enjoyment rights of the underground land are protected by the NLC, as mentioned under section 44 of the NLC. Thus, the surface landowner or proprietor can develop the land upwards to the sky and downwards to the underground lands.

Any attempt to use the underground land should come with the application of a different use from the proprietor or application of compulsory land acquisition from the other parties regarding the land of another. Here is the main issue that comes to consider the compensation payable to the current surface land proprietor. According to all the participants and respondents, the underground land still falls under the right of the proprietor, which requires payment of compensation if there is compulsory underground land acquisition.

#### **4.3.2. Best practices**

However, the effective and reasonable use of the underground land is not specifically mentioned. According to Anesh (2025)<sup>12</sup>, the reasonable use and underground enjoyment of the land must be set or tied to the category of land. He gives an example of the application of underground development in Singapore, where the element of underground compensation is limited to 30 meters downwards only.

This finding seems similar to the suggestion of the respondent in one of the research studies done on the valuation of underground land (Abd Rashid, 2016). In addition, he further reiterated that the Constitution of Singapore did not mention the rights of property in the same way as the Malaysian Federal Constitution. As such, the payment of compensation to the aggrieved parties is not solely a legal obligation. As compared to Malaysia, the payment of compensation must be paid and must be adequate, as mentioned in the Federal Constitution and Act 486.

Moreover, in most cases of payment of compensation in compulsory land acquisition, the aggrieved parties will object to the award by the land administrator and appeal to the court for a better payment of compensation. The issue of adequacy of compensation deals with the social impact of the use of the compulsory land acquisition provision. It will be a similar case with the underground land acquisition, where the land which belongs to the company or corporation has more potential for development, especially in urban areas. Thus, the depth of the rights and reasonable use play an important role in determining the adequacy of payment of compensation. The valuation of the land might be best to considering the real and potential value of the land.

### **4.4. Contextualisation and policy reform**

The findings of this study can be summarised that there are interdependencies between legal, social and economic aspects of underground land development. The underground land development should be provided and guided by the legal framework, clearly and substantively. In Malaysia, there should be a solid legal framework on underground land ownership and defining the rights and obligations of the landowner as well as the authorities involved, the Federal and State Authorities. As State Authorities in Malaysia are the direct and authoritative jurisdiction on land matters, the provisions of the land ownership together with its rights and obligations should be ready for the implementation of underground land development.

This can be replicated and modified by the international cases where the legal framework of land administration needs to be reviewed in order to implement underground land development. Especially, countries which adopt the Torrens system of land tenure should also embark on the revision of the framework and strengthen it for the success of underground land development. In addition, in compulsory land acquisition practices, the compensation needs to be addressed for adequate, fair and just compensation. The Constitution of a country plays a vital role in addressing these issues, as mentioned in previous discussions.

---

<sup>12</sup> Interview and discussion conducted on 22<sup>nd</sup> January 2025.

Policy reform in Malaysia may focus on amending the NLC and the Land Acquisition Act 1960 [Act 486]. The policymakers should incorporate the three-dimensional (3D) elements in land ownership to cater the preparation for a plan to be attached to the land, especially the surface land with a particular depth, as a result of the compulsory land acquisition of the underground land for underground land development. Particularly, the preparation for a plan as provided under section 396 of NLC should be revisited. Moreover, the depth which can be lawfully enjoyed by the landowners should also be specific, in the NLC as well as in Act 486, to accommodate the fair and just payment of compensation in the case of underground land acquisition.

Furthermore, the other legislation related to the development, such as the Town and Country Planning Act 1976 [Act 172], should also guide the developer for the obligations and rights of the landowner so as, no further challenge brought to the court because of being affected by the underground development. Current guidelines can be further incorporated into the Act 172 to further enhance the underground development.

## 5. CONCLUSION

The study finds that the current ownership and rights are provided in the National Land Code of Malaysia, but the issue is in the implementation and decision of the State Authority in alienating the underground land. The State Authority need to be more responsive to the development, especially the emerging development of stratified and underground land. Rules and regulations need to be amended in support of the enabling provision as amended by the NLC or related land legislation.

In addition, it is found that underground development needs to be ready and accepted by the nation in all aspects as discussed in the above sections, such as planning, legal provision and compensation for the underground space. The planning of the underground land must be and should be feasible to the economic values of the land development. As to the urban development, the underground seems imminent and should be well-advised by the respective parties on the social, environmental and economic perspectives.

Hence, the use of the physical underground land and the legal aspect must be in parallel with the development approach to provide a balance of needs. The nation could receive a return on investment, while the people may obtain the benefit of the development. Further study may look into the involvement of the technological aspects, such as GIS and BIM, as well as the cadastre aspects, because this study is limited and did not cover these aspects.

## ACKNOWLEDGEMENTS

The researcher would like to thank all the parties involved in data collection, as well as the guide who provided to the researcher.

## BIBLIOGRAPHY

- [1] Abd Rashid, F. (2016). *The Legal And Valuation Aspect Of Underground And Stratum Title*. Universiti Teknologi Malaysia (UTM).
- [2] Abdul Jalil, N. I., & Mohd Arshad, A. H. (2019). Reconciliation of right to easement between surface and stratum owner in underground development in Malaysia. *Journal of Legal, Ethical and Regulatory Issues*, 22(3).
- [3] Abdul Jalil, N. I., & Mohd Arshad, 'Ain Husna. (2020). Right Of Access On Underground Land Development: Guidance From Singapore And Australia. *International Journal of Law, Government and Communication*, 5(21). <https://doi.org/10.35631/ijlgc.5210022>
- [4] Abu, M. Z. Z. (2023). *Penilaian Harta Tanah Strata Dan Tanah Bawah Tanah*.
- [5] Alias, B., Ghazali, M. M., & Abd Rasid, K. (2000). The Development and Administrative Issues of Stratum Title for Underground Land Resources in Malaysia. In *Pacific Rim Real Estate Society (PRRES) Conference 2000*. <https://www.researchgate.net/publication/240611119>
- [6] Bahagian Dasar dan Konsultasi, , JKPTG. (2021). *Laporan Soal Selidik Pengenalan 4 Konsep Pindaan Kanun Tanah Negara*.
- [7] Bakri, I. (2025). Keterjaminan Hakmilik Strata Kepada Tuan Punya Bagi Unit Yang Dibeli / Security Of Ownership For The Strata Parcel Of A Purchased Unit.
- [8] Bobylev, N. (2009). Mainstreaming sustainable development into a city's Master plan: A case of Urban Underground Space use. *Land Use Policy*, 26(4), 1128–1137. <https://doi.org/10.1016/j.landusepol.2009.02.003>
- [9] bt Zaini, F., bt Hussin, K., bt Arrifin, A., & bt Ali, N. (2012). The Future Use of Underground Space in Malaysia: A Literature Review. *International Journal of Real Estate Studies*, 7(2).



- [10] Hassan, M. H. (2016). Potensi Keperluan Perundangan Khas Yang Berkaitan Hak Pemilikan Tanah Bagi Pembangunan Projek Mrt. UTM.
- [11] Hussin, K., Megat Mohamed Ghazali Megat Abd Rahman, Mohammad Tahir Sabit Mohamad En Kamaruzaman Abdul Rasid, S., Zaini, F., & Nor Aisyah Jamalludin. (2017). Legal And Administrative Consideration In Underground Land Development. 13TH NAPREC Conference.
- [12] Itagaki, K. (2020). Legal Consideration on Public Use of Underground Space. The Japanese Journal of Real Estate Sciences, 34(2). [https://doi.org/10.5736/jares.34.2\\_43](https://doi.org/10.5736/jares.34.2_43)
- [13] Jamalludin, N. A., Zaini, F., & Hussin, K. (2016). Development of Underground Land in Malaysia: The Need for Master Plan of Urban Underground Land Development. Procedia - Social and Behavioral Sciences, 219. <https://doi.org/10.1016/j.sbspro.2016.05.061>
- [14] Konykhov, D. S., & Kolybin, I. V. (2021). Principles of the integrated development of Moscow City underground space. IOP Conference Series: Earth and Environmental Science, 703(1). <https://doi.org/10.1088/1755-1315/703/1/012005>
- [15] Land Acquisition Plan Tuz Gölü Underground Gas Storage Project. (2005).
- [16] Mohamed, A. H. (2017). Akta Pengambilan Tanah (Pindaan) 2016 [A1517].
- [17] Mohamed, A. H., Ismail, N., & Mohd, K. W. (2023). Conflict of Law and Policy in Land Development. Malaysian Journal of Syariah and Law, 11(2), 180–186. <https://doi.org/10.33102/mjssl.vol11no2.433>
- [18] Mohamed, A. H., & Musa, Y. (2019). Pertikaian Cadangan Pembangunan Tanah dan Syarat Nyata Tanah: Satu Kupasan. Jurnal Pentadbiran Tanah LAND, 3(1), 149–156.
- [19] Mohamed, A. H., Razai, M. H., Sulaiman, S. A., & Ab Latip, A. S. (2024). Land Administration in Malaysia: An Insight of the 3D-Based Future Development Framework. In A. Abdul-Rahman, I. A. musliman, I. Hassan, & A. Zamzuri (Eds.), Lecture Notes in Geoinformation and Cartography (GeoWeek 2024). Springer.
- [20] National Land Code [Act 828], Pub. L. No. Act 828, Laws of Malaysia (2020).
- [21] Omar, I. (2024). Land Acquisition Act 486 (Amended): Critical Issues and The ROle of SIA. In M. S. Mohd Ihsan & H. O. Mohd Shahwahid (Eds.), MSIA Reading Series (Vol. 17, Issue 2). Malaysian Association of Social Impact Assessment (MSIA).
- [22] Panduan Pelaksanaan Pelupusan Tanah Bawah Tanah Di Bawah Kanun Tanah Negara (Disemak-2020) [Akta 828], Pub. L. No. 2/2021, Pekeliling Ketua Pengarah Tanah dan Galian Persekutuan Bilangan 2/2021 (2021).
- [23] Panduan Pelaksanaan Pengambilan Tanah Bawah Tanah, Pub. L. No. PKPTG 5/2020, Pekeliling Ketua Pengarah Tanah dan Galian Persekutuan Bilangan 5/2020 (2020).
- [24] Perperidou, D. G., Sigizis, K., & Chotza, A. (2021). 3d underground property rights of transportation infrastructures: Case study of piraus metro station, greece. Sustainability (Switzerland), 13(23). <https://doi.org/10.3390/su132313162>
- [25] PLANMalaysia. (2022). Garis Panduan Perancangan Pembangunan Tanah Bawah Tanah. Jabatan Perancangan Bandar Dan Desa.
- [26] Ramlakhan, R., Kalogianni, E., van Oosterom, P., & Atazadeh, B. (2023). Modelling the legal spaces of 3D underground objects in 3D land administration systems. Land Use Policy, 127. <https://doi.org/10.1016/j.landusepol.2023.106537>
- [27] Saeidian, B., Rajabifard, A., Atazadeh, B., & Kalantari, M. (2021). Underground land administration from 2d to 3d: Critical challenges and future research directions. Land, 10(10). <https://doi.org/10.3390/land10101101>
- [28] Senawi, A., Ahmad@Mohamed, N., & Mat Zan, R. (2018). Improving The Compulsory Land Acquisition Procedure: Interpreting The Land Acquisition (Amendment) Act 2016 (Act A1517). Voice of Academia, 13(2), 98–107.
- [29] Strata Community Association. (2025, February 12). What is Strata? <https://nsw.strata.community/>
- [30] Syed Abdul Kader, S. Z., Mohamad, N. A., & Hj Ali, Z. (2023). This Land Of Ours-Protecting Ownership, Interest And Dealings In Land. IIUM Law Journal, 31(1), 69–94.
- [31] Teh Bee v K. Maruthamuthu (January 1977).
- [32] Volchko, Y., Norrman, J., Ericsson, L. O., Nilsson, K. L., Markstedt, A., Öberg, M., Mossmark, F., Bobylev, N., & Tengborg, P. (2020). Subsurface planning: Towards a common understanding of the subsurface as a multifunctional resource. Land Use Policy, 90. <https://doi.org/10.1016/j.landusepol.2019.104316>
- [33] Yan, J., Jaw, S. W., Soon, K. H., Wieser, A., & Schrotter, G. (2019). Towards an underground utilities 3D data model for land administration. Remote Sensing, 11(17). <https://doi.org/10.3390/rs11171957>
- [34] Zaini, F. (2016). The Legal Framework For Determining The Land Tenure And Development Of Underground Land In Malaysia [Thesis]. Univeriti Teknologi Malaysia.
- [35] Zaini, F., Hussin, K., Suratman, R., & Rasid, K. A. (2013). Underground Land Ownership In Malaysia: A Review.
- [36] Zaini, F., Hussin, K., & Zakaria, S. R. A. (2014, April 29). Legal And Administrative Issue For Underground Land Development In Malaysia. International Real Estate Research Symposium.
- [37] Zaini, F., Hussin, K., & Zakaria, S. R. A. (2015). Legal and administrative issue for underground land development in Malaysia. Proceedings of the 25th International Business Information Management Association Conference - Innovation Vision 2020: From Regional Development Sustainability to Global Economic Growth, IBIMA 2015, 3674–3683.
- [38] Zaini, F., & Mohsin, A. (2021). Underground Space Ownership in Malaysia: Defining the Rights. International Journal of Academic Research in Business and Social Sciences, 11(14). <https://doi.org/10.6007/ijarbss/v11-i14/8565>

- [39] Zaini, F., Suratman, R., & Kassim, A. C. (2021). The Vertical Land Use Zoning For Underground Space Development In Malaysia. *Planning Malaysia*, 19(4), 36–47. <https://doi.org/10.21837/pm.v19i18.1031>
- [40] Zhang, M., Xie, Z., & He, L. (2022). Does the scarcity of urban space resources make the quality of underground space planning more sustainable? A case study of 40 urban underground space master plans in China. *Frontiers in Environmental Science*, 10. <https://doi.org/10.3389/fenvs.2022.966157>
- [41] Zhang, Z., Paulsson, J., Gong, J., & Huan, J. (2020). Legal framework of urban underground space in China. *Sustainability (Switzerland)*, 12(20). <https://doi.org/10.3390/su12208297>
- [42] Zhou, Y., & Zhao, J. (2016). Assessment and planning of underground space use in Singapore. *Tunnelling and Underground Space Technology*, 55, 249–256. <https://doi.org/10.1016/j.tust.2015.12.018>

## **ADVANCED TECHNOLOGIES AND INNOVATIVE SOLUTIONS**

## FORECASTING THE TBM PERFORMANCE USING GREY-STOCHASTIC SIMULATIONS

Krivošić Vladimir<sup>1</sup>, Crnogorac Luka<sup>2</sup>, Tokalić Rade<sup>3</sup>, Gligorić Zoran<sup>4</sup>, Gluščević Branko<sup>5</sup>

**Abstract:** Tunnel boring machines (TBMs) are widely used in urban spaces tunneling projects because they provide safer working environment with higher efficiency compared to other underground construction methods. As for any project, good time management and cost control are of high importance. Tunneling in urban areas is challenging because of diverse geological conditions and other factors which affect the performance of TBM. From a mining engineer's point of view, prediction of performance of TBM is of vital role for good organization of the work on tunnel construction. Good time management of all operations that are connected to the penetration rate of the machine (timely delivery and installation of support segments, installation of additional transport segments and all other auxiliary work) opens a possibility to plan construction costs and deadlines more appropriately. Penetration rate is the principal measure of TBM performance. For that reason, in this paper the focus was on developing a precise model based on grey-stochastic theory for TBM penetration rate prediction. Grey simulations models are widely used in forecasting in engineering and are scientifically proven. The stochastic grey model (GM 1,1) where stochastic parameter is described with Brownian motion is conceptualized to forecast five future data values based on the previously known twenty-five data values of penetration rate. Input data, penetration rate, can be expressed in millimeters per minute or any other unit considering the time resolution coefficient. Forecasted data accuracy of developed model is placed in a group of highly accurate models. Proposed model can successfully be used by mining and civil engineers on different underground construction projects in terms of better planning of the performance of tunneling machines, optimization of work organization, cost balancing as well as defining the deadlines more accurately.

**Keywords:** TBM, performance, forecasting, penetration rate, grey-stochastic simulations

### 1. INTRODUCTION

The development of cities must be followed by infrastructure development in urban areas to ensure a sustainable lifestyle. Construction of tunnels, underground structures, used for transportation of people and vehicles, canalization, communication and other purposes are increasingly present in development of infrastructure (He & Lai, 2022; Abdullah, 2016). Tunnel construction methods can in general be classified in three groups: construction with explosives (drill and blast), construction with tunnel machines and cut and cover construction (Karoly, 1980; Jovanović, 1984). Each type of construction technology has its positive and negative sides and there are some limitations for each group (such as depth, geological conditions, advancement rates, automatization...).

<sup>1</sup> PhD candidate, Krivošić Vladimir, M.Sc. in Mining Eng., University of Belgrade – Faculty of Mining and Geology, Dušina 7, 11000, Belgrade, Serbia, [R713-23@dok.rgf.bg.ac.rs](mailto:R713-23@dok.rgf.bg.ac.rs)

<sup>2</sup> Assistant professor, Crnogorac Luka, PhD in Mining Eng., University of Belgrade – Faculty of Mining and Geology, Dušina 7, 11000, Belgrade, Serbia, [luka.crnogorac@rgf.bg.ac.rs](mailto:luka.crnogorac@rgf.bg.ac.rs), <https://orcid.org/0000-0002-9897-270X>

<sup>3</sup> Full professor, Head of Chair for Underground construction, Tokalić Rade, PhD in Mining Eng., University of Belgrade – Faculty of Mining and Geology, Dušina 7, 11000, Belgrade, Serbia, [rade.tokalic@rgf.bg.ac.rs](mailto:rade.tokalic@rgf.bg.ac.rs), <https://orcid.org/0000-0001-9360-2892>

<sup>4</sup> Full professor, Head of Chair for Underground mining, Gligorić Zoran, PhD in Mining Eng., University of Belgrade – Faculty of Mining and Geology, Dušina 7, 11000, Belgrade, Serbia, [zoran.gligoric@rgf.bg.ac.rs](mailto:zoran.gligoric@rgf.bg.ac.rs), <https://orcid.org/0000-0003-4532-8694>

<sup>5</sup> Full professor, Vice-dean, Gluščević Branko, PhD in Mining Eng., University of Belgrade – Faculty of Mining and Geology, Dušina 7, 11000, Belgrade, Serbia, [branko.gluscevic@rgf.bg.ac.rs](mailto:branko.gluscevic@rgf.bg.ac.rs), <https://orcid.org/0000-0003-0707-9797>

Table 1 shows some advantages and disadvantages of mentioned tunnelling methods.

**Table 1.** *Advantages and disadvantages of tunnelling methods (Abdullah, 2016; Jovanović, 1984; Girmscheid & Schexnayder, 2002; Abdallah, & Marzouk, 2013; Sharma, 2016)*

Method	Advantages	Disadvantages
Drill and blast	<ul style="list-style-type: none"> <li>Highly adaptable and flexible in application</li> <li>Requires minimal mobilization time</li> <li>Capable of accommodating tunnel cross-sections of any required shape</li> <li>Allows for the installation of primary rock support</li> <li>Involves relatively lower total investment costs</li> <li>Enables modification of tunnel geometry along the excavation alignment</li> </ul>	<ul style="list-style-type: none"> <li>Worker safety presents a significant concern</li> <li>The rate of excavation progress is relatively low</li> <li>Overall labour costs are comparatively high</li> <li>Operations involve intensive and physically demanding manual labour</li> <li>Tasks exhibit a low degree of automation and mechanization</li> </ul>
Tunnel boring machines	<ul style="list-style-type: none"> <li>Demonstrates high operational efficiency with significantly reduced labour costs</li> <li>Achieves a high rate of progress, particularly in soft ground conditions</li> <li>Offers excellent cost-effectiveness combined with a high level of automation</li> <li>Supports continuous excavation and construction processes</li> <li>Generates minimal noise and disturbance to adjacent structures</li> <li>Represents the most effective method for constructing deep and long tunnels</li> </ul>	<ul style="list-style-type: none"> <li>Limited adaptability to extreme or highly variable geological conditions</li> <li>Requires substantial initial investment and complex support systems</li> <li>TBM mobilization entails significant time and logistical effort</li> <li>Restricts tunnel design to a fixed circular cross-section and diameter</li> <li>Characterized by extended mobilization periods and elevated capital expenditure</li> <li>Requires highly qualified and trained personnel</li> </ul>
Cut and cover	<ul style="list-style-type: none"> <li>Promotes environmental preservation throughout the construction process</li> <li>Ensures safe initiation and completion of highway tunnel projects</li> <li>Facilitates secure excavation in unstable or weak ground conditions</li> <li>Can be implemented as a sequential construction method under highly adverse geotechnical circumstances</li> <li>Generally more cost-effective and practical compared to alternative underground tunnelling methods</li> <li>Involves relatively lower risk compared to other tunnelling techniques</li> </ul>	<ul style="list-style-type: none"> <li>Not well-suited for applications involving very deep excavations</li> <li>May generate increased levels of dust and noise during construction</li> <li>Can lead to disruptions in traffic flow and interference with other urban activities</li> </ul>

As seen from the table above, each method has its pros and cons. When tunnelling in urban areas is required, construction with tunnel boring machines represents the best option due to its high advancement rates, minimal environmental impact and high automation and mechanization state.

One of the problems with TBM construction is limited adaptability to extreme or highly variable geological conditions. This can cause downtimes, slower advancement rates and project delays. Delays in tunnel construction represent serious concern, sometimes tunnelling projects have 45% longer schedule than original one (Shelake et al., 2022).

As monitoring of different parameters during tunnelling projects has become a standard approach, we now have a large set of data that can be scientifically addressed to set best practice examples.

In this paper focus will be on analysis of the time series of TBM performance data to develop an accurate model for prediction of advancement rate of TBM. With accurate prediction model of advancement rate engineers on tunnelling projects can timely define deadlines more accurately and improve work organization.



## 2. MATERIALS AND METHODS

Prediction of TBM performance is mostly connected to parameters such as rate of penetration rate, utilization rate, advancement rate and these parameters are regarded as the key factors of TBM performance (Latif et al., 2023)]. These parameters mainly depend on TBM construction, cutting elements type and geometry, rotation rate, pressure on the work face etc.

In literature performance prediction is based on different models such as artificial neural network models (Armaghani et al., 2019; Armaghani et al., 2017; Benardos & Kaliampakos, 2004), fuzzy logic and neuro-fuzzy inference systems (Armaghani et al., 2019; Yagiz & Karahan, 2015; Alvarez Grima et al., 2000; Ghasemi et al., 2014). In this paper a model based on grey system theory with implementation of Brownian motion as stochastic parameter to describe uncertainties that are present in process of tunnel boring. Model is based on (Crnogorac et al., 2023) which was used to describe steel support deformations in underground mine roadways. Grey models are proven as accurate and applicable models for forecasting land subsidence caused by mining operations (Xu et al., 2014), roof pressure prediction (Wang et al., 2020), energy consumption (Hamzacebi & Es, 2014), natural gas demand (Zeng & Li, 2016), manpower demand in construction industry (Ho, 2010), mining method selection (Dehghani et al., 2017) etc. Grey systems were first introduced by Deng (1985; 1989).

Time series of performance of TBM that was used for developing a model was taken from Yalei et al. (2024). The TBM penetration rate was recorded in different surrounding rocks.

Grey system model for a time series of penetration rate  $R_{(t)} = \{r(t)\}$ ,  $t = 1, 2, \dots, T$  was formed based on actual values of TBM penetration rates on Xinjiang project presented in paper by Yalei et al. (2024). Elements of a cumulative series are calculated by Accumulated Generation Operation (AGO) as follows:

$$r_t^{(1)} = \sum_{i=1}^t r_i, t = 1, 2, \dots, T \quad (1)$$

Where  $r_1^{(1)} = r_1, r_2^{(1)} = r_1 + r_2, r_3^{(1)} = r_1 + r_2 + r_3$ , etc.

Average (mean) values of adjacent values of AGO series is calculated as:

$$m_t^{(1)} = \frac{1}{2} \cdot (m_t^{(1)} - m_{t-1}^{(1)}), t = 2, 3, \dots, T \quad (2)$$

A grey model differential equation for sequence modelling of mean value is:

$$\frac{dr_t^{(1)}}{dt} + a \cdot dr_t^{(1)} = b \quad (3)$$

Parameters  $a$  and  $b$  are calculated according by least square method:

$$[a, b]^T = (B^T B)^{-1} B^T Y \quad (4)$$

Where  $B$  and  $Y$  are:

$$B = \begin{bmatrix} -m_1^{(1)} & 1 \\ -m_2^{(1)} & 1 \\ \vdots & \vdots \\ -m_T^{(1)} & 1 \end{bmatrix}, Y = \begin{bmatrix} r_2 \\ r_3 \\ \vdots \\ r_T \end{bmatrix} \quad (5)$$

Equation (3) presents an ordinary differential equation of the form:

$$dr_t^{(1)} = f(t, r_t^{(1)}) dt \quad (6)$$

Where are the initial condition  $dr_{t=1}^{(1)} = r_1$ . Penetration rate is subject to random variations of rotation speed of TBM, different geological conditions, varying cutting force and other influencing factors of tunnel development. These factors contribute to the presence of uncertainty, and they influence the AGO series making it a stochastic process. Because of this equation (6) cannot simply be defined as deterministic, so stochastic differential equation with additive noise is developed as following:

$$dr_t^{(1)} = f(t, r_t^{(1)}) dt + dW_t, t = 1, 2, \dots, T \quad (7)$$

Where  $dW_t$  is an increment to a standard Brownian motion,  $dW_t \sim N(0, Var)$ .

Now grey system has been transformed into a stochastic system (Gligorić et al. 2020; Crnogorac et al., 2023) making equation of following form:

$$dr_t^{(1)} = (b - ar_t^{(1)}) dt + dW_t, r_t^{(1)} = r_1 \quad (8)$$

Following algorithm presented by Crnogorac et al. (2023) using Euler-Maruyama discretization (Maruyama, 1955) we get numerical approximation of  $r_t^{(1)}$ :

$$r_t^{(1)} = r_{t-1}^{(1)} + (b - ar_{t-1}^{(1)})\Delta t + \Delta W_t, t = 1, 2, 3 \dots, T \quad (9)$$

Where  $\Delta W_t$  represents an increment to a standard Brownian motion, with fixed initial value of  $r_{t=1}^{(1)} = r_1$ . Setting  $\Delta t = \frac{T}{\varphi}$ ,  $\varphi \leq T$  and  $\Delta W_t = W_t - W_{t-1} \sim N(0, \frac{\sigma^2}{\omega})$  where  $\varphi$  is number of timesteps in time  $T$  and  $N(0, \frac{\sigma^2}{\omega})$  is normal distribution with expected value of 0 and variance  $\frac{\sigma^2}{\omega}$ . Variance in AGO series is  $\sigma^2$  and  $\omega$  is the time resolution coefficient, which is defined as follows:

$$\omega = \begin{cases} 1; \text{annual time resolution} \\ \frac{1}{\sqrt{12}} \approx 0.2887, \text{monthly time resolution} \\ \frac{1}{\sqrt{365}} \approx 0.0523, \text{daily time resolution} \\ \frac{1}{\sqrt{8760}} \approx 0.0107, \text{hourly time resolution} \\ \frac{1}{\sqrt{525600}} \approx 0.0014, \text{minute time resolution} \end{cases} \quad (10)$$

As results we have for penetration rate of the TBM that are used for model validation are expressed in mm per minute  $\omega$  that will be used has value of approximately 0.0014.

Simulation of previous equation gives us expected values of AGO stochastic process:

$$E_t^{AGO} = \frac{1}{S} \sum_{s=1}^S r_{t,s}^{(1)}, t = 2, 3 \dots, T, E_1^{AGO} = r_1 \quad (11)$$

Where  $S$  is the number of simulations. In this paper a total of 500 simulations of equation (9) were conducted. For every point in time there is an adequate probability density function of AGO. Next step is reconstruction of the series  $R_{(t)}$  using Inverse Accumulated Generation Operation (IAGO) as follows:

$$E_{t+1}^{IAGO} = E_{t+1}^{AGO} - E_t^{AGO}, t = 1, 2, \dots, T-1$$

$$E_1^{IAGO} = r_1 \quad (12)$$

Making a reconstructed series of  $R_{(t)}$  with following form:

$$\widehat{R}_{(t)} = (r_1, \widehat{r}_2, \dots, \widehat{r}_t), t = 1, 2, \dots, T \quad (13)$$

Input information for developing a model consists of 30 values in total. In this paper 25 values were used for reconstruction of time series (as calibration of model) to validate this approach for forecasting future values of penetration rate of TBM. Accuracy of the fitting of every value in monitoring time is estimated according to absolute percentage error (APE):

$$APE_t = 100 \cdot \left| \frac{\Delta r_t - \Delta \widehat{r}_t}{\Delta r_t} \right|, t = 1, 2, \dots, T \quad (14)$$

Where  $\Delta r_t$  are monitored values and  $\Delta \widehat{r}_t$  are predicted (reconstructed) values of penetration rate of TBM. Mean Average Percentage Value (MAPE) is used for evaluation of model accuracy. Linguistic descriptions of model accuracy can be found in literature (Montaño Moreno et al., 2013; Lewis, 1982) and is presented in table 2.

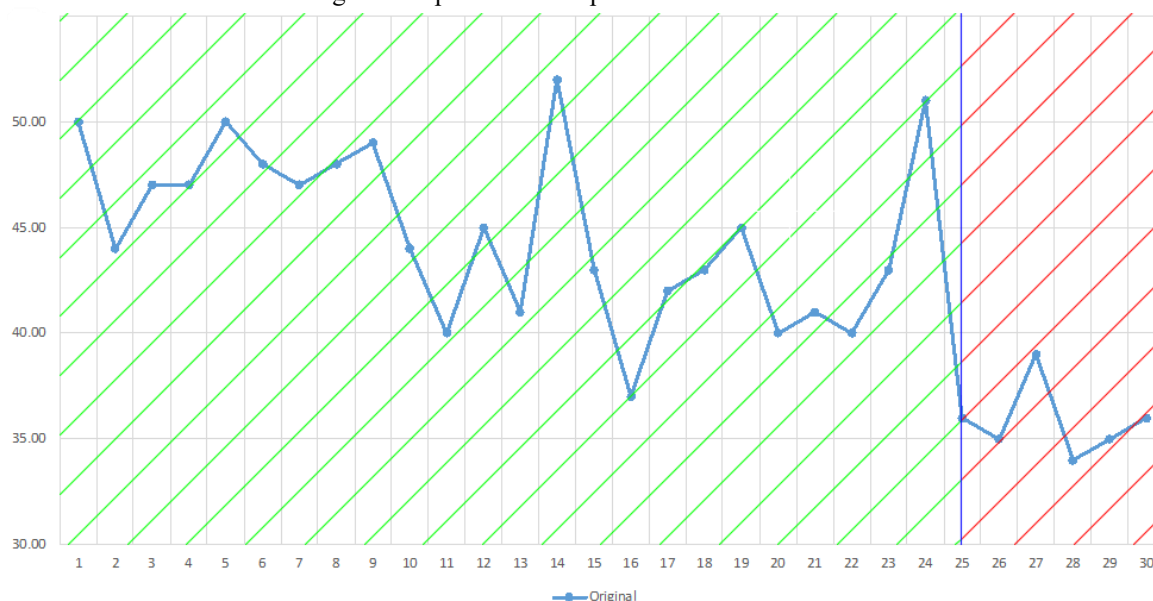
**Table 2.** Linguistic description of model accuracy (Montaño Moreno et al., 2013; Lewis, 1982; Crnogorac et al., 2023)

Linguistic description of accuracy	Value of Mean Average Percentage Error
<ul style="list-style-type: none"> <li>High</li> <li>Good</li> <li>Reasonable</li> <li>Inaccurate</li> </ul>	<ul style="list-style-type: none"> <li>Bellow 10 %</li> <li>10 to 20 %</li> <li>20 to 50 %</li> <li>Over 50 %</li> </ul>

For forecasting phase same equation (9) as for reconstruction is used just for values  $T$  to  $T + h$ , where  $h$  present number of points in time that is to be forecasted. The whole process for forecasting is analog to the process of reconstruction phase previously described.

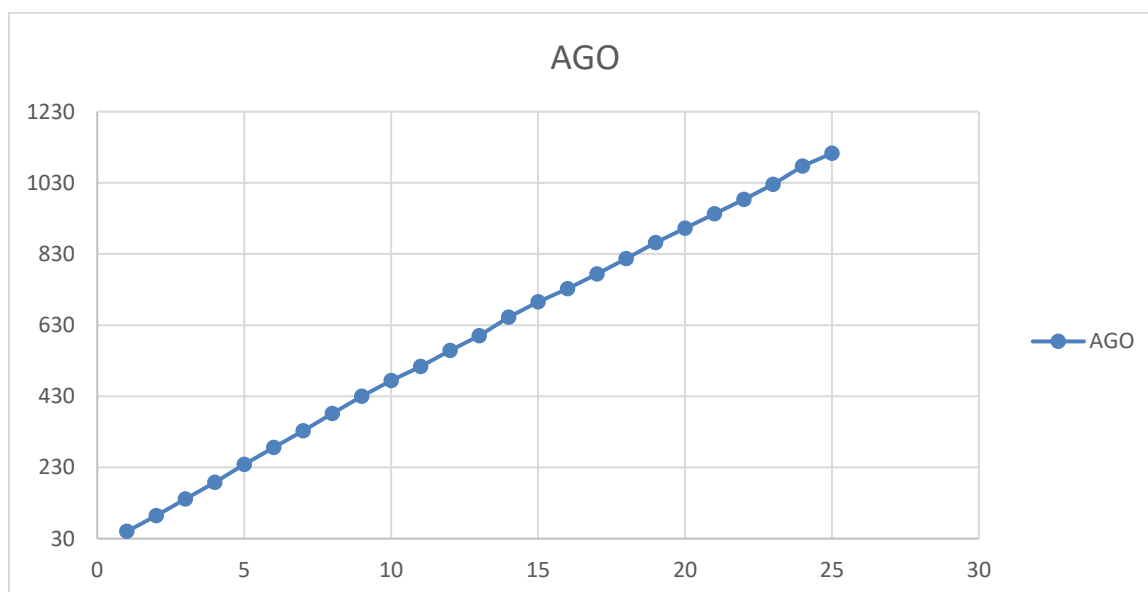
### 3. RESULTS AND DISCUSSION

Data used for developing a model in this paper represents the values of TBM penetration rate expressed in millimetres per minute. The set of data is divided into two groups, the first one consisting of 25 values (1 to 25) and the second one consisting of 5 values. The first group of data was used for reconstruction of TBM penetration rate values and validation of model was calculated in this phase with comparing reconstructed and actual values of the TBM penetration rate. The group of 5 values (26 to 30) was used for forecasting period evaluation comparing forecasted and actual values. In Figure 1. Input values are presented.



**Figure 1.** Original time series of data (hatched green - group 1, hatched red – group 2)

First step was making AGO series for values for reconstruction period  $t = 2$  to  $t = 25$  as presented on figure 2.



**Figure 2.** Values of AGO series

In table 3 values of original series and AGO series are presented.

**Table 3.** Values of original and AGO series

<b>t</b>	<b>R<sub>(t)</sub></b>	<b>r<sub>t</sub><sup>(1)</sup></b>	<b>t</b>	<b>R<sub>(t)</sub></b>	<b>r<sub>t</sub><sup>(1)</sup></b>
<b>1</b>	50	50	<b>14</b>	52	652
<b>2</b>	44	94	<b>15</b>	43	695
<b>3</b>	47	141	<b>16</b>	37	732
<b>4</b>	47	188	<b>17</b>	42	774
<b>5</b>	50	238	<b>18</b>	43	817
<b>6</b>	48	286	<b>19</b>	45	862
<b>7</b>	47	333	<b>20</b>	40	902
<b>8</b>	48	381	<b>21</b>	41	943
<b>9</b>	49	430	<b>22</b>	40	983
<b>10</b>	44	474	<b>23</b>	43	1026
<b>11</b>	40	514	<b>24</b>	51	1077
<b>12</b>	45	559	<b>25</b>	36	1113
<b>13</b>	41	600			

Following matrices were used to calculate parameters  $a$  and  $b$  of grey modelling:

$$B = \begin{bmatrix} -72 \\ -117.5 \\ -164.5 \\ -213 \\ -262 \\ -309.5 \\ -357 \\ -405.5 \\ -452 \\ -494 \\ -536.5 \\ -579.5 \\ -626 \\ -673.5 \\ -713.5 \\ -753 \\ -795.5 \\ -839.5 \\ -882 \\ -922.5 \\ -963 \\ -1004.5 \\ -1051.5 \\ -1095 \end{bmatrix} \quad \text{and} \quad Y = \begin{bmatrix} 50 \\ 44 \\ 47 \\ 47 \\ 50 \\ 48 \\ 47 \\ 48 \\ 49 \\ 44 \\ 40 \\ 45 \\ 41 \\ 52 \\ 43 \\ 37 \\ 42 \\ 43 \\ 45 \\ 40 \\ 41 \\ 40 \\ 43 \\ 51 \end{bmatrix}$$

And according to the equation (4) calculated values are  $a = 0.009467699$  and  $b = 49.4539963$ . Other parameters of grey stochastic process are presented in table 4.

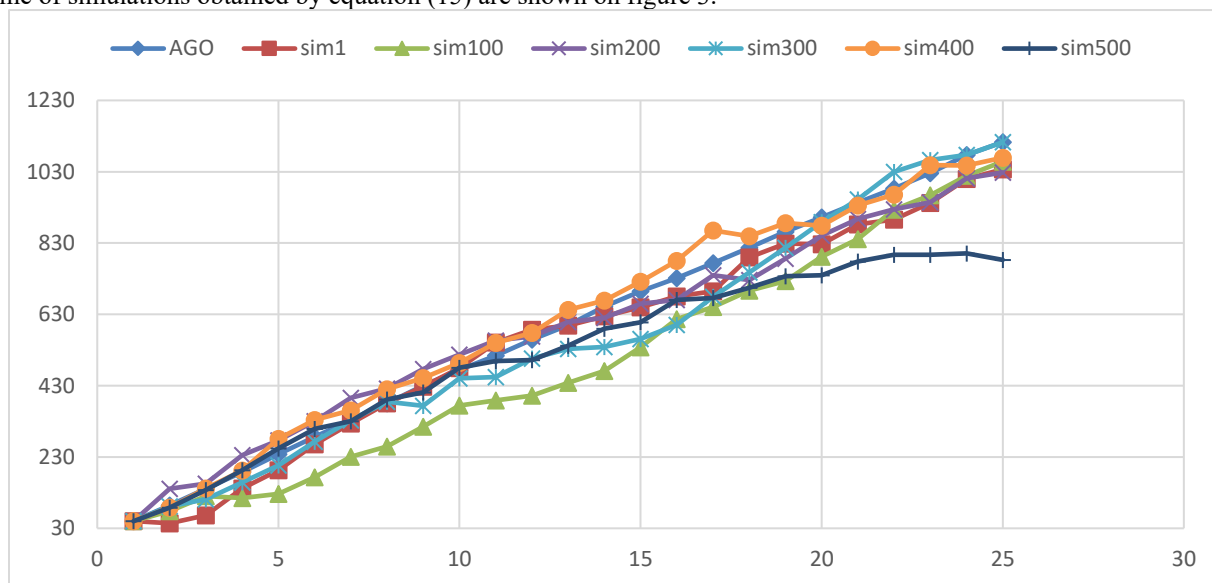
**Table 4.** Grey stochastic process parameters for TBM performance forecasting

<b>Parameter</b>	<b>Value</b>
Variance of AGO Series, $\sigma$	325.56
Time ( $T$ )	30 minutes
Number of steps ( $\varphi$ )	30
Timestep of $\Delta t$	1 minute
Minute time resolution coefficient ( $\omega$ )	$\approx 0.0014$
Brownian increment, $\Delta W_t = W_t - W_{t-1} \sim N\left(0, \frac{\sigma^2}{\omega}\right)$	$\sim N\left(0, \frac{325.56}{0.0014}\right)$

Numerical approximation of  $r_t^{(1)}$  is based on following Euler-Maruyama discretization:

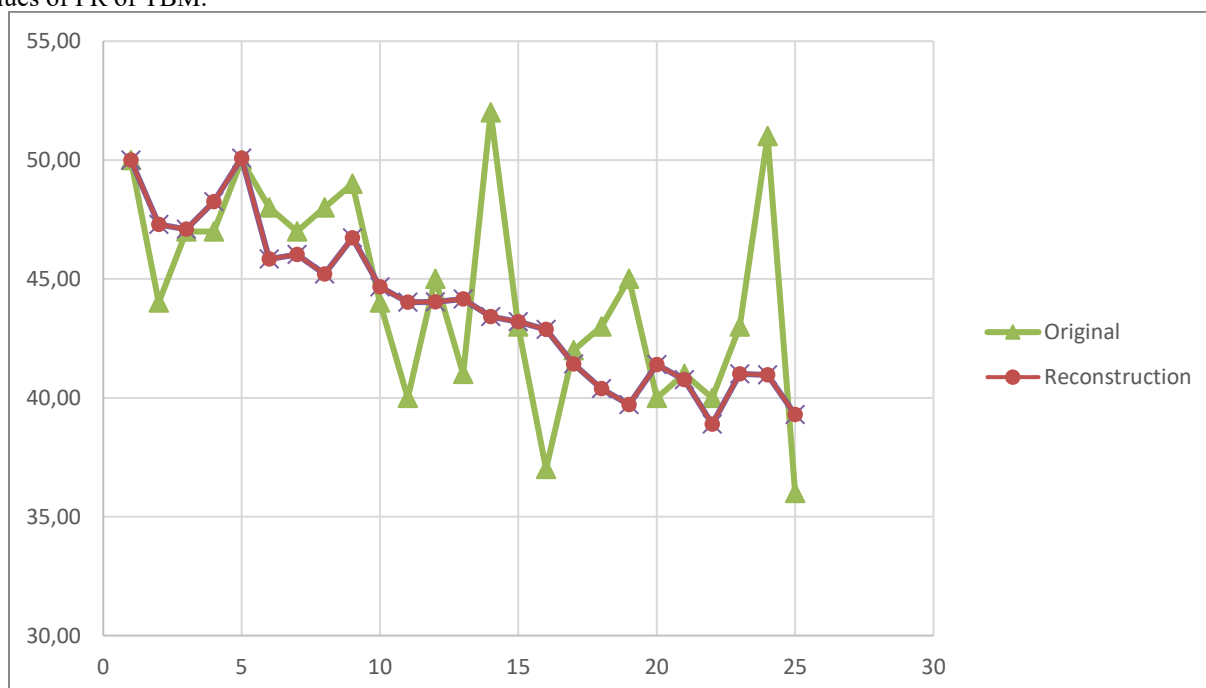
$$r_t^{(1)} = r_{t-1}^{(1)} + \left(49.4539963 - 0.009467699 \cdot r_{t-1}^{(1)}\right) \cdot 1 + N\left(0, \frac{325.56}{0.0014}\right), t = 2, 3 \dots 25 \quad (15)$$

After 500 simulations of equation (5) following AGO and IAGO values are generated (shown in table 5.). Some of simulations obtained by equation (15) are shown on figure 3.



**Figure 3.** Some simulated values of AGO series

From 500 simulation we get an average value of expected AGO and IAGO values, and according to equation (14) we can calculate the APE of reconstruction phase of the model. Figure 4. Shows reconstructed and original values of PR of TBM.

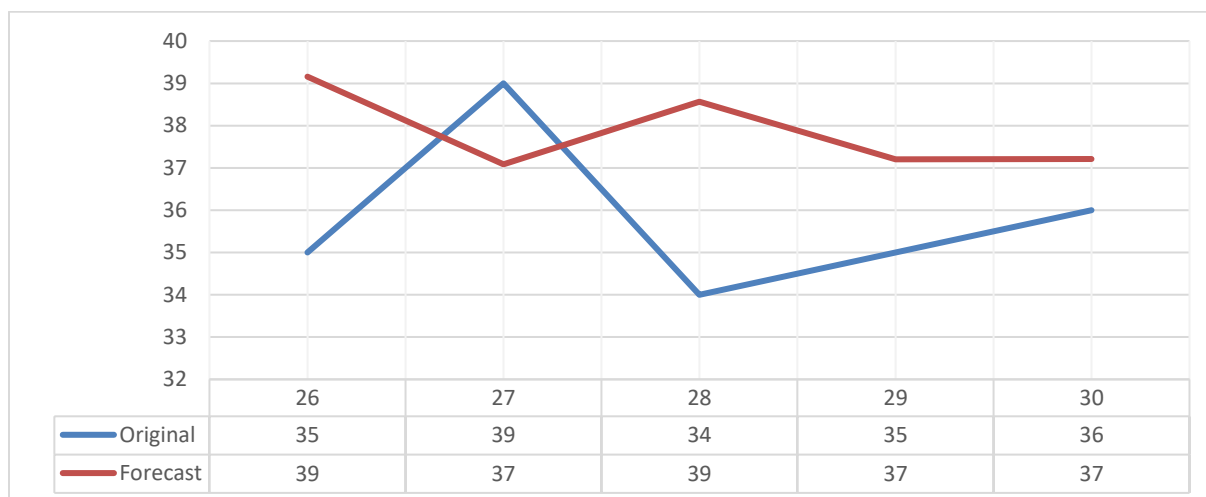


**Figure 4.** Original and reconstructed values of penetration rate of TBM

Mean Average Percentage Error of the reconstructed series is 5.75%, putting a reconstruction accuracy into group of highly accurate models with MAPE below 10%.

As we see that this model is applicable to the TBM performance (penetration rate) prediction, we will now forecast 5 values based on the same simulation equation used in the reconstruction phase, just for values  $T$  to  $T + h$ , where  $h$  present number of points in time that is to be forecasted, as previously described.

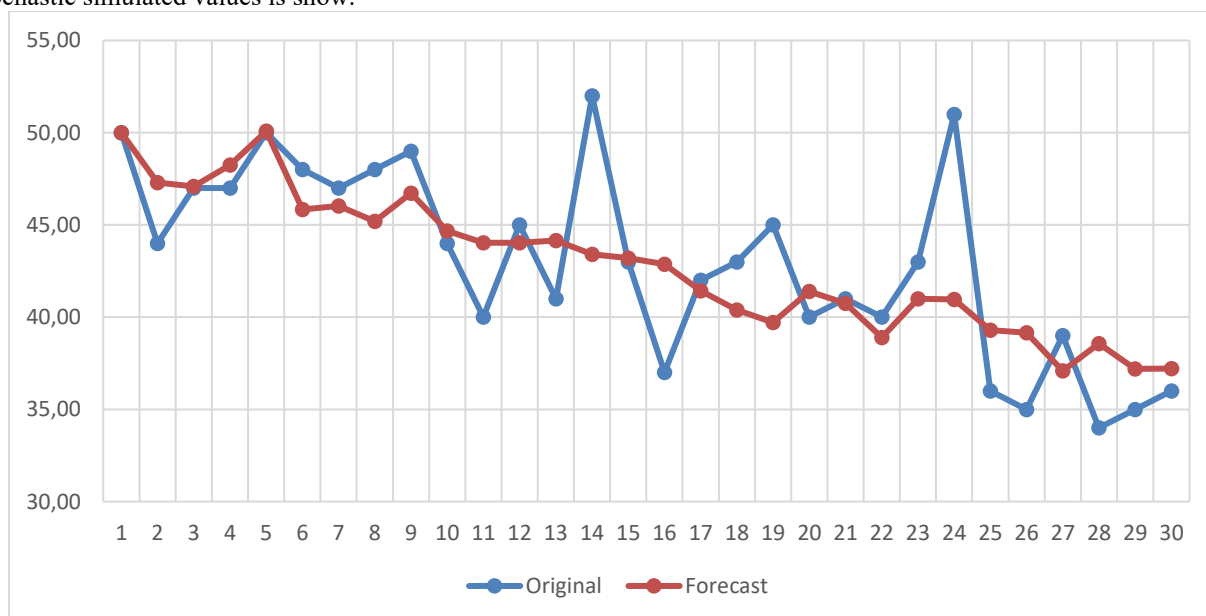
Results of the forecasting phase can be seen on figure 5.



**Figure 5.** Original recorded and forecasted values of TBM penetration rate

As in previous steps for reconstruction phase, APE and MAPE were calculated and the MAPE of forecasting phase is 7.98% also putting this forecast model into group of highly accurate models.

On next figure a graph of original values of TBM penetration rate time series as well as the time series of grey stochastic simulated values is show.



**Figure 6.** Time series of original and grey stochastic simulated (forecasted) values of TBM penetration rates

Calculated Mean Average Percentage Error of a model (both reconstruction and forecast phase) is 6.135%.

#### 4. CONCLUSION

Knowing TBM performance rates is one of the most important factors during tunnelling operations. Forecasting models are constantly developed to optimize planning of the working operations on tunnelling projects. This model gives a new approach to forecasting of TBM performance based on grey stochastic simulation equation. First 25 values out of 30 were taken for testing the model accuracy. When it was calculated that the model gives a high accuracy results next 5 values were forecasted. Forecasted values were compared to the values from original time series and mean average percentage error of 7.98% was calculated, proving that a forecasting model can be usefully applied for forecasting TBM performance on tunnelling projects. Model can be used on ongoing tunnelling projects by mining and civil engineers to evaluate deadlines of tunnel construction process and optimize projects efficiency. This model should be reevaluated as well with more case studies. As tunnelling projects are done in various rock



conditions that can affect the penetration rate it may be needed to implement fuzzy logic for solving penetration rate performance of TBM in complex environments in further research.

The forecasting model presented in this paper has a mean average percentage error of 7.98%, compared to the 15.15% model for prediction of penetration rate presented in paper by Yelei et al. (2024) from which data was used. This model presents a totally different approach for forecasting TBM performance rating using only historical data of penetration rating in time dependent series for forecasting future values instead of numerous geological input parameters that are usually used for forecasting models making it more applicable for widespread used on different projects. Application of this model on different sites can help building a database of performance forecasting in different ground conditions and help to develop clusters for developing a combined fuzzy grey stochastic model.

## 5. ACKNOWLEDGMENTS

This research has been financially supported by the Ministry of Science, Technological Development and Innovation of the Republic of Serbia (Contract No: 451-03-136/2025-03/200126).

## 6. REFERENCES

- [1] He, B., Armaghani, D. J., & Lai, S. H. (2022). A short overview of soft computing techniques in tunnel construction. *The Open Construction & Building Technology Journal*, 16 (1).
- [2] Abdullah, R. A. (2016). A review on selection of tunnelling method and parameters effecting ground settlements. *Electronic Journal of Geotechnical Engineering*, 21 (14), 4459-75.
- [3] Karoly, S. (1970). *The Art of Tunnelling. Budapest printed in Hungari. 891p.*
- [4] Jovanović, P. (1984). Izrada podzemnih prostorija velikog profila. *Grđevinska knjiga*, Belgrade.
- [5] Girmscheid, G., & Schexnayder, C. (2002). Drill and blast tunnelling practices. *Practice periodical on structural design and construction*, 7(3), 125-133.
- [6] Abdallah, M., & Marzouk, M. (2013). Planning of tunnelling projects using computer simulation and fuzzy decision making. *Journal of Civil Engineering and Management*, 19 (4), 591-607.
- [7] Sharma, P. D. (2016). Tunnel Construction Methods and their comparison.
- [8] Shelake, A. G., Gogate, N. G., & Rajhans, N. R. (2022). An integrated approach for identification and prioritization of risk factors in tunnel construction. *Materials Today: Proceedings*, 65, 1805-1812.
- [9] Latif, K., Sharafat, A., & Seo, J. (2023). Digital twin-driven framework for TBM performance prediction, visualization, and monitoring through machine learning. *Applied Sciences*, 13 (20), 11435.
- [10] Armaghani, D.J.; Koopialipoor, M.; Marto, A.; Yagiz, S. (2019) Application of Several Optimization Techniques for Estimating TBM Advance Rate in Granitic Rocks. *J. Rock Mech. Geotech. Eng.* 2019, 11, 779–789.
- [11] Armaghani, D.J.; Mohamad, E.T.; Narayanasamy, M.S.; Narita, N.; Yagiz, S. (2017) Development of Hybrid Intelligent Models for Predicting TBM Penetration Rate in Hard Rock Condition. *Tunn. Undergr. Sp. Technol.* 2017, 63, 29–43.
- [12] Benardos, A.G.; Kaliampakos, D.C. (2004) Modelling TBM Performance with Artificial Neural Networks. *Tunn. Undergr. Sp. Technol.* 2004, 19, 597–605.
- [13] Yagiz, S.; Karahan, H. (2015) Application of Various Optimization Techniques and Comparison of Their Performances for Predicting TBM Penetration Rate in Rock Mass. *Int. J. Rock Mech. Min. Sci.* 2015, 80, 308–315.
- [14] Alvarez Grima, M.; Bruines, P.A.; Verhoef, P.N.W. (2000) Modeling Tunnel Boring Machine Performance by Neuro-Fuzzy Methods. *Tunn. Undergr. Sp. Technol.* 2000, 15, 259–269.
- [15] Ghasemi, E.; Yagiz, S.; Ataei, M. (2014) Predicting Penetration Rate of Hard Rock Tunnel Boring Machine Using Fuzzy Logic. *Bull. Eng. Geol. Environ.* 2014, 73, 23–35.
- [16] Crnogorac, L., Lutovac, S., Tokalić, R., Gligorić, M., & Gligorić, Z. (2023). Steel Arch Support Deformations Forecast Model Based on Grey–Stochastic Simulation and Autoregressive Process. *Applied Sciences*, 13(7), 4559. <https://doi.org/10.3390/app13074559>
- [17] Xu, H., Liu, B., & Fang, Z. (2014). New grey prediction model and its application in forecasting land subsidence in coal mine. *Natural Hazards*, 71, 1181-1194.
- [18] Wang, K., Zhuang, X., Zhao, X., Wu, W., & Liu, B. (2020). Roof pressure prediction in coal mine based on grey neural network. *IEEE access*, 8, 117051-117061.
- [19] Hamzacebi, C., & Es, H. A. (2014). Forecasting the annual electricity consumption of Turkey using an optimized grey model. *Energy*, 70, 165-171.
- [20] Zeng, B., & Li, C. (2016). Forecasting the natural gas demand in China using a self-adapting intelligent grey model. *Energy*, 112, 810-825.
- [21] Ho, P. H. (2010). Forecasting construction manpower demand by gray model. *Journal of Construction Engineering and Management*, 136(12), 1299-1305.
- [22] Dehghani, H., Siami, A., & Haghi, P. (2017). A new model for mining method selection based on grey and TODIM methods. *Journal of Mining and Environment*, 8 (1), 49-60.

- [23] Deng, J. (1985) Grey Control Systems; Press of Huazhong University of Science and Technology: Wuhan, China.
- [24] Deng, J. (1989) Introduction to Grey system theory. *J. Grey Syst.* 1, 1–24.
- [25] Yalei, Y., Lijie, D., Rong, T., Fei, W., & Huilan, Z. (2024). Prediction of TBM penetration rate for different surrounding rocks and cutter head diameters. *Heliyon*, 10 (12).
- [26] Gligorić, Z.; Gligorić, M.; Halilović, D.; Beljić, Č.; Urošević, K. (2020) Hybrid Stochastic-Grey Model to Forecast the Behavior of Metal Price in the Mining Industry. *Sustainability* **2020**, 12, 6533.
- [27] Maruyama, G. (1955). Continuous Markov processes and stochastic equations. *Rendiconti del Circolo Matematico di Palermo*, 4, 48-90.
- [28] Moreno, J. J. M., Pol, A. P., Abad, A. S., & Blasco, B. C. (2013). Using the R-MAPE index as a resistant measure of forecast accuracy. *Psicothema*, 25 (4), 500-506.
- [29] Lewis, C. D. (1982). Industrial and business forecasting methods: A practical guide to exponential smoothing and curve fitting. (*No Title*).

## MULTI-RISK MANAGEMENT FOR UNDERSEA TUNNEL CONSTRUCTION BASED ON NSGA-III ALGORITHM

Sihan Liu<sup>1</sup>, Hongwei Huang<sup>2</sup>

**Abstract:** Due to the complexity of construction techniques, long construction periods, high investment costs, numerous safety-related factors, and stringent quality requirements, managing multi-source information in subsea tunnel projects often lacks coordination, making it difficult to achieve unified multi-objective goals. This poses a common challenge for construction decision-makers during on-site management. To address these gaps, this study focuses on safety, schedule, and cost risks in undersea tunnel construction, designing a multi-object model to address these challenges. By integrating the relationships among safety levels, schedule and cost across various construction processes, a multi-objective optimization model tailored to the management of complex undersea tunnel construction projects is proposed. The model is solved by the NSGA-III algorithm to obtain the Pareto solution set. This approach is applied to a subsea tunnel project, and the results show that when the number of generations is set to 600, the population size to 140, and the number of reference points per dimension to 14, a total of 170 solutions are obtained. Among them, the construction duration can be optimized by up to 132 days, and the cost by up to 110.58 million CNY, while both quality and safety levels remain within acceptable project limits. These results can assist decision-makers in selecting the optimal construction plan from multiple perspectives.

**Keywords:** Tunnel construction; Construction management; Multi-object optimization; NSGA-III algorithm

### 1. INTRODUCTION

The current scale of tunnel construction in China is enormous, but due to complex procedures, poor processes, and long construction duration, safety accidents frequently occur during tunnel construction. Compared to other underground engineering projects, tunnel projects are more prone to frequent safety accidents due to complex uncertainties (Zhao et al., 2007). These accidents not only cause delays in construction schedules, resulting in economic losses and quality defects but also lead to adverse societal impacts. How to comprehensively consider various types of losses derived from core safety risks to achieve optimal decision-sharing among multiple stakeholders is a challenge in the process of undersea tunnel construction.

The ideal scenario for undersea tunnel construction is to achieve the shortest construction period, the lowest cost, and the highest quality while maintaining safety risks at a low level - an outcome that is challenging to achieve in practical construction processes. Safety risks, construction period, cost, and quality are not independent factors; rather, they form an interrelated and contradictory unified system. Any change in one of these objectives inevitably impacts the levels of the others. As large-scale, high-risk engineering projects, undersea tunnels face the critical challenge of addressing and controlling safety risks during the construction process. However, there is a critical balance point between contractors' safety investment and cost control. When confronted with high safety risk levels, determining how to enhance risk detection and monitoring equipment to reduce safety risks to an acceptable level for contractors is a topic worthy of discussion (Bachar et al., 2025). In the field of multi-objective optimization for engineering projects, the relationship between cost and construction period has garnered the most attention from scholars and contractors. Metrics such as labor, labor utilization, and profit can serve as

<sup>1</sup> Ph.D Candidate, Civil Engineering, Department of Geotechnical Engineering, College of Civil Engineering, Tongji University, 1239 Siping Road, Shanghai, 200092, China, 2210345@tongji.edu.cn

<sup>2</sup> Professor, Hongwei Huang, Civil Engineering, Department of Geotechnical Engineering, College of Civil Engineering, Tongji University, 1239 Siping Road, Shanghai, 200092, China, huanghw@tongji.edu.cn

indicators for quantifying cost risks (Jun et al., 2010; Agrama et al., 2014), thereby enabling the establishment of relationships between project duration fluctuations and total cost demands (Parente et al., 2015; El-Abbasy et al., 2016). Compared to other risks, the relationship between safety and quality is often overlooked. However, in 2013, Wanberg, J. et al. (2013) demonstrated a correlation between quality performance and safety performance, developing a safety-quality correlation model. P. E. D. Love et al. (2023) also emphasized that balancing the competing demands of quality and safety in construction processes enables managers to minimize rework and improve project safety in an optimal manner. Nevertheless, the aforementioned studies generally focus only on the interactions between two risks. With the evolving societal demands, many scholars have begun to examine the interrelationships among multiple risks. Wang, T. (2023) developed a multi-parameter grey GERT model to discuss the functional relationships among time, cost, and quality in scenarios of both normal execution and rework, proposing a multi-objective joint optimization model based on schedule-oriented and quality-oriented approaches. Meng, F. (2024) introduced environmental impact into the analysis, constructing a multi-objective optimization model encompassing time, cost, safety, and environmental factors. However, most existing studies on multi-objective optimization models focus on general projects with fixed timelines and single-line engineering. Tunnel projects, characterized by their linear nature, complex procedures, and repetitive tasks, pose unique challenges to multi-objective optimization management.

In recent years, scholars have explored various challenges in solving algorithms for multi-objective optimization models. Currently, most research focuses on low-dimensional multi-objective optimization models with up to three objectives, utilizing algorithms such as Ant Colony Optimization, Genetic Algorithms, and NSGA-II (Xiong et al., 2007; Li et al., 2024). Among these, NSGA-II is widely regarded for its high computational efficiency and convergence performance, making it a popular choice in fields like project scheduling and construction period optimization (Zhang et al., 2021; Wu et al., 2022). However, despite the ability of NSGA-II to generate well-converged and evenly distributed solution sets, its original algorithmic capacity becomes insufficient as the number of objectives increases. The NSGA-III algorithm builds upon NSGA-II by introducing a reference point mechanism that retains non-dominated individuals close to the reference points. This makes NSGA-III better suited for solving high-dimensional multi-objective optimization models with more than three objectives (Dehghani et al., 2019; Liu et al. 2022; Razmi et al., 2022; Zhao et al., 2024).

In summary, research on balanced optimization models targeting safety-cost-schedule-quality in undersea tunnel construction projects is scarce, and studies addressing optimization algorithms for models with more than three objectives are also limited. To address these gaps, this study focuses on safety risk control in undersea tunnel construction to establish an inter-objective constraint model. By integrating the relationships among safety levels, schedule, cost, and quality across various construction processes, this study proposes a multi-objective optimization model tailored to the management of complex undersea tunnel construction projects. The model is solved using the NSGA-III algorithm. The proposed optimization model and NSGA-III algorithm are validated through a case study of an undersea tunnel project in China. This research offers a novel approach to addressing multi-objective optimization problems in undersea tunnel construction, providing a more effective framework for achieving optimal construction management outcomes.

## 2. MULTI-OBJECTIVE OPTIMIZATION MODEL FOR TUNNEL CONSTRUCTION

### 2.1 Safety Function

According to the national standard (GB50652-2011) *Code for Risk Management in the Construction of Urban Rail Transit Underground Works* (hereinafter referred to as the "National Standard"), safety risks are classified into five levels. Safety risks of different levels may lead to varying impacts on construction schedule and cost. For ease of coding, the safety risk level function is simplified as follows:

$$S = g(R_i) = \begin{cases} 1, & R_i = V \\ 2, & R_i = IV \\ 3, & R_i = III \\ 4, & R_i = II \\ 5, & R_i = I \end{cases} \quad (1)$$

Where  $R_i$  is derived from the risk level of safety incidents.

### 2.2 Schedule Function

By analyzing the relationship between all construction procedures during the tunnel construction process, the construction sequence is divided into multiple cycles, each consisting of several procedures with finish-to-start

dependencies. Each procedure affects the others. Tunnel construction mainly includes two types of operations: excavation and pre-excavation grouting. During excavation, the time spent on excavation per cycle typically depends on the rock grade. The total grouting time depends on the required grouting length and the effectiveness of the grouting. Assuming each procedure in the construction process has a maximum acceptable operation time and a minimum achievable time, the objective function of the work is:

$$T_N = \sum_1^{N_P} \sum_{k=1}^{n_P} p_{P,k} * t_{P,k} + \sum_1^{N_E} \sum_1^{n_E} p_{E,k} * t_{E,k} \quad (2)$$

s.t.  $t_{min,i} \leq t_i \leq t_{max,i}$

Where:  $T_N$  is the total duration of normal construction;  $p_{P,k}$  is the proportion of grouting length in the total project;  $t_{P,k}$  is the time required for grouting procedure  $k$ ;  $n_P$  is the number of grouting operations;  $N_P$  is the total number of grouting operations in the entire project;  $p_{E,k}$  is the proportion of different surrounding rock grades;  $n_E$  is the number of excavation operations;  $N_E$  is the total number of excavation cycles in the entire project;  $t_{E,k}$  is the time required for excavation procedure;  $t_{min,i}$  is the minimum time for procedure  $i$ ;  $t_{max,i}$  is the maximum time for procedure  $i$ .

In addition to the normal fluctuations in construction schedule, this study also considers the impact of safety risks on the schedule. The delay caused by safety risks typically depends on the risk level  $R_i$ . It is assumed that the impact on the schedule is represented by a random number falling within the corresponding interval, as shown in Equation (3) and (4).

$$T_{ES,i} = f(R_i) = \begin{cases} [0, 1), R_i = V \\ [1, 3), R_i = IV \\ [3, 10), R_i = III \\ [10, 90), R_i = II \\ [90, +\infty), R_i = I \end{cases} \quad (3)$$

$$T_E = \sum_{i=1}^n T_{E,i} \quad (4)$$

Where  $R_i$  is derived from the risk level of safety incidents, and  $T_{ES,i}$  is a random number falling within the corresponding interval.

Then, the total construction duration is:

$$T = T_N + T_E \approx \sum_1^{N_P} \sum_{k=1}^{n_P} p_{P,k} * t_{P,k} + \sum_1^{N_E} \sum_1^{n_E} p_{E,k} * t_{E,k} + \sum_{i=1}^n T_{E,i} \quad (5)$$

### 2.3 Cost Function

In general, the total construction cost of a project consists of the sum of direct and indirect costs. However, for tunnel projects with long construction durations and complex construction processes, various safety incidents may arise during construction. The potential consequences of these incidents—such as casualties, schedule delays, and direct economic losses—cannot be ignored. Therefore, this study incorporates safety risk factors into the cost function.

Direct costs mainly consist of labor, material, and equipment costs associated with each construction procedure and are directly related to specific construction activities. There is a direct relationship between the duration of a procedure and its cost: when the procedure time increases, the cost inevitably rises; conversely, shortening the duration (i.e., fast-tracking) often requires a substantial increase in resource input, which also raises costs. Thus, the relationship between direct cost and time is illustrated in Figure 1 and Equation (6) and (7).

$$C_{m,i} = C_{n,i} + \varphi_i(t_i - t_{n,i})^2 \quad (6)$$

$$C_M = C_N + \sum_{l=1}^L \varphi_l(t_i - t_{n,i})^2 \quad (7)$$

Where:  $C_{m,i}$  is the adjusted direct cost of procedure  $i$  after marginal cost correction;  $C_{n,i}$  is the direct cost of procedure  $i$  under normal conditions;  $\varphi_i$  is the marginal cost growth coefficient of procedure  $i$ ;  $t_{n,i}$  is the normal duration of procedure  $i$ ;  $C_N$  is the originally planned direct cost.

During the construction process, indirect costs are incurred for construction management, contract administration, quality control, and other activities. These costs cannot be directly attributed to a specific construction task but are closely related to the overall project duration. Therefore, this study distributes the total

indirect cost evenly across the entire construction process and approximates the total indirect cost as a linear function of the project duration, as shown in Equation (8).

$$C_j = \gamma T \quad (8)$$

Where,  $C_j$  represents the total indirect cost;  $\gamma$  is the indirect cost coefficient.

For tunnel projects with long construction durations and complex construction processes, numerous safety incidents may arise during construction. The occurrence of such incidents can lead to casualties, schedule delays, and direct economic losses, which cannot be ignored. Therefore, this study incorporates the unit cost under the influence of safety risks  $C_S$  into the cost function., as shown in Equation (9).

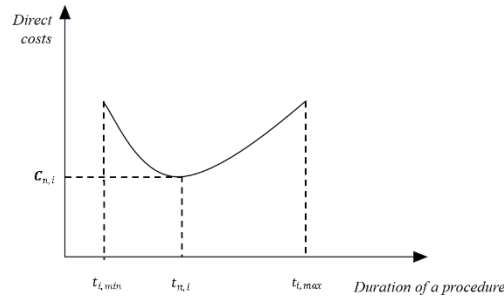
$$C_S = \varphi(R_i) \cdot \left[ \sum C_{Sg,i} + \sum C_{Sf,i} \right] \quad (9)$$

Where:  $\varphi(R_i)$  is the safety risk impact coefficient;  $C_{Sg,i}$  represents the direct loss caused by each safety risk level;  $C_{Sf,i}$  represents the indirect loss caused by each safety risk level.

In summary, the total cost function can be expressed as:

$$C = C_N + \sum_{i=1}^L \varphi_i(t_i - t_{n,i})^2 + \gamma T + \varphi(R_i) \cdot \left[ \sum C_{Sg,i} + \sum C_{Sf,i} \right] \quad (10)$$

**Figure 1.** Function of direct costs and duration of procedure  $i$



## 2.4 Quality Function

When the duration of an individual task is either too short or too long, it cannot achieve optimal quality. Only within a certain range of duration can the task maintain a high level of quality with minimal variation. This pattern of quality fluctuation better reflects the actual conditions in engineering projects. This study assumes that the relationship between quality and excavation time follows a bell-shaped function, as illustrated in Figure 2 and Equation (11) and (12).

$$Q_i = \exp\left(-\frac{(t_i - t_{i,mean})^2}{m \cdot (t_{i,max} - t_{i,min})^2}\right) \quad (11)$$

$$Q = \text{avg } Q_i \quad (12)$$

Where:  $m$  is the coefficient representing the relationship between quality and schedule, determined by the frequency of quality nonconformities and construction time on site;  $t_{i,mean}$  is the ideal construction duration for procedure  $i$ ;  $Q_{i,max}$  is the optimal construction quality level, defined as the quality achieved when construction is completed within the ideal time and unaffected by factors such as geological conditions. When the duration is shorter than  $t_{i,min}$ , fast-tracking may lead to quality risks; when it exceeds  $t_{i,max}$ , repeated rework may occur on site, resulting in suboptimal quality.



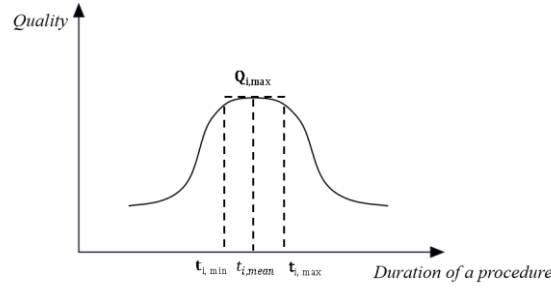


Figure 2. Function of quality and duration of procedure  $i$

## 2.5 Tunnel Construction Safety-Schedule-Cost-Quality Correlation Model

In summary, this study focuses on safety management and establishes analytical models for safety, schedule, cost, and quality. Based on the concept of multi-objective optimization, the integrated model is formulated as follows.

$$\begin{cases}
 T = T_N + T_E \approx \sum_1^{N_P} \sum_{k=1}^{n_P} p_{P,k} * t_{P,k} + \sum_1^{N_E} \sum_{k=1}^{n_E} p_{E,k} * t_{E,k} + \sum_{i=1}^n T_{E,i} \\
 T_{ES,i} = f(R_i) = \begin{cases} [0, 1), R_i = V \\ [1, 3), R_i = IV \\ [3, 10), R_i = III \\ [10, 90), R_i = II \\ [90, +\infty), R_i = I \end{cases} \\
 C = C_N + \sum_{i=1}^L \varphi_i(t_i - t_{n,i})^2 + \gamma T + \varphi(R_i) \cdot (\sum C_{Sg,i} + \sum C_{Sf,i}) \\
 Q = avg \left( exp \left( - \frac{(t_i - t_{i,mean})^2}{m * (t_{i,max} - t_{i,min})^2} \right) \right) \\
 S = g(R_i) = \begin{cases} 1, R_i = V \\ 2, R_i = IV \\ 3, R_i = III \\ 4, R_i = II \\ 5, R_i = I \end{cases} \\
 \text{s.t.} \begin{cases} t_{min,i} \leq t_i \leq t_{max,i} \\ T \leq T_{max} \\ C \leq C_{max} \\ S \leq S_{max} \\ Q > Q_{min} \end{cases}
 \end{cases} \quad (13)$$

$$\begin{cases}
 t_{min,i} \leq t_i \leq t_{max,i} \\
 T \leq T_{max} \\
 C \leq C_{max} \\
 S \leq S_{max} \\
 Q > Q_{min}
 \end{cases} \quad (14)$$

The Non-Dominated Sorting Genetic Algorithm III (NSGA-III) is a reference-point-based non-dominated sorting algorithm capable of generating a more uniformly distributed Pareto solution set using reference-point-based decision criteria. It is particularly suitable for solving high-dimensional optimization problems with more than three objectives, making it more useful for decision-makers in comparative analyses.

In the model developed in this study, there are a total of 29 decision variables: 10 excavation procedure durations  $t_i$  for Grade III/IV surrounding rock, 10 excavation procedure durations  $t_i$  for Grade V surrounding rock, 8 grouting procedure durations  $t_i$ , and 1 safety risk index  $R_i$ .

There are 4 constraints:

- (1) total construction duration must not exceed the upper limit of acceptable delay;
- (2) total cost must not exceed the upper limit of investment;
- (3) overall quality must not fall below 0.9;
- (4) safety risk level must not exceed Grade II.

Considering the large number of variables, integer encoding is adopted in this study to reduce computational complexity and solving time.

## 3. CASE STUDY

The case project in this study is a subsea tunnel with a total length of 3768 meters. Due to the complex geological conditions of the tunnel project, both progress and various auxiliary measures—such as advanced geological forecasting, water exploration, and grouting for water sealing—must be carefully considered in this

challenging construction environment. Achieving the above progress targets is therefore quite difficult. The relevant data and parameters regarding the construction processes of this project are presented in Table 1 and 2, wherein the estimated completion time for each process is derived from the construction organization design document.

**Table 1.** Time Consumption of Excavation Processes

Serial Number	Process Name	Planned Time per Cycle Advance (min)					
		Class III–IV			Class V		
		Most Probable	Min	Max	Most Probable	Min	Max
1	Scaling the tunnel face, moving to the working platform	40	30	50	40	30	50
2	Surveying and setting out, connecting air and water pipelines	30	25	35	30	25	35
3	Drilling	135	110	165	90	80	100
4	Charging and blasting	30	25	40	20	15	25
5	Ventilation and blast inspection	10	8	20	10	8	20
6	Mucking	165	140	195	150	120	170
7	Scaling	30	25	35	30	25	35
8	Installing steel frames and mesh	60	55	65	60	55	65
9	Installing rock bolts, foot locking bolts, and welding	30	25	38	30	25	38
10	Shotcreting	135	115	162.5	100	85	123
11	Cycle Time	665	558	805.5	560	468	661
12	In Total (h)	11.5	9.3	13.5	9	7.8	10.2

**Table 2.** Time Consumption of Grouting Processes

Serial Number	Process Name		Time Required (days)		
			Most Probable	Min	Max
1	5m Advance Grouting for Rock Consolidation	Drilling	2	1.8	2.5
2		Pipe Installation	0.5	0.4	0.6
3		Grouting	2	1.5	3
4	First Round Grouting	Drilling	2	1.8	2.5
5		Grouting	2.5	2	3
6	Second Round Grouting	Drilling	2	1.8	2.5
7		Grouting	2.5	2	3
8	Verification Drilling		1	0.5	1.3
9	In Total		14.5	11.8	18.4

The estimated completion times for the construction procedures are derived from the construction organization design documents. The functional relationships between construction duration and cost were obtained by reviewing relevant literature and integrating on-site project data.

In this study, the NSGA-III algorithm is implemented using the PYMOO library. PYMOO is a Python library specifically designed for multi-objective optimization and supports various evolutionary algorithms, including NSGA-II and NSGA-III.

Based on the model developed in this study, the number of reference points per dimension is preliminarily set between 10 and 18, the population size between 100 and 160, and the number of generations at 600. To determine the optimal reference point setting and population size, the hypervolume (HV) of the Pareto solution set obtained in the final iteration of each run is calculated. HV represents the volume enclosed by the Pareto front and the reference point; a larger hypervolume indicates a higher quality Pareto solution set.

After performing iterative computations with different combinations of reference points and population sizes, the results are shown in Table 3 and Table 4. The results indicate that for the characteristics of the model established in this study, setting the population size to 140, the number of reference points per dimension to 14, and the number of generations to 600 yields the optimal Pareto solution set.

**Table 3. Optimal Number of Reference Points**

<b>Reference Points</b>	10	14	18
<b>Population Size</b>	120	120	120
<b>Number of Generations</b>	600	600	600
<b>HV</b>	0.3840	0.4499	0.3883

**Table 4. Optimal Population Size**

<b>Reference Points</b>	14	14	14	14
<b>Population Size</b>	100	120	140	160
<b>Number of Generations</b>	600	600	600	600
<b>HV</b>	0.4317	0.4499	0.5033	0.4436

After computation, a total of 175 Pareto solutions were obtained and visualized, and Table 3 presents a subset of the optimal Pareto solutions. Among all the solutions:

(1) The maximum construction duration is 1695 days and the minimum is 1563 days. The required construction period is 57 months (i.e., 1720 days), achieving a maximum possible reduction of 132 days.

(2) The total cost ranges from a minimum of 597.17 million CNY to a maximum of 707.75 million CNY. Given that the project can accept a maximum cost of 800 million CNY, the model achieves an optimal cost reduction of 110.58 million CNY.

(3) The quality level ranges from a minimum of 0.9754 to a maximum of 0.9824, all above the minimum acceptable level of 0.9, thus meeting project requirements.

The safety risk level ranges from Grade V to a maximum of Grade II. Since the project does not accept Grade I risks, all solutions meet the safety requirements.

Table 5 presents a subset of the optimal Pareto solutions. In a Pareto solution set containing multiple non-dominated solutions, different stakeholders and decision-makers may prioritize the objectives differently.

When the current site condition is at Risk Level III and is about to escalate to Risk Level II, Solution 8 offers a construction duration of 1578.65 days, a total cost of 599.39 million CNY, and an overall quality level of 0.9810. If the goal is to downgrade the risk level with minimal additional time, Solution 1 may be selected, requiring 1608.22 days—an additional 29.57 days—while the cost rises to 620.80 million CNY, an increase of 22.41 million CNY.

Based on the procedure durations in each solution, decision-makers can reasonably prioritize objectives, adjust the model's decision variables accordingly, and formulate practical emergency plans and safeguard measures—ultimately achieving optimal decision-making among safety, schedule, cost, and quality in tunnel construction.

**Table 5. Selected Pareto Solutions**

<b>Solution ID</b>	<b>Duration / d</b>	<b>Cost (million CNY)</b>	<b>Quality Level</b>	<b>Safety Risk Level</b>
1	1608.22	620.8	0.9796	II
2	1632.38	605.7	0.9815	II
3	1641.48	643.42	0.9784	II
4	1648.82	643.15	0.9783	II
5	1658.04	633.37	0.9791	II
6	1665.93	655.8	0.9779	II
7	1695.51	651.65	0.9780	II
8	1578.65	599.39	0.9810	III
9	1589.82	621.49	0.9790	III
10	1593.62	623.38	0.9789	III

#### 4. CONCLUSION

This study proposes a multi-objective optimization model for safety, schedule, cost, and quality in subsea tunnel construction. The model is based on the actual duration ranges of various construction procedures and potential on-site safety risk levels, incorporating a total of 29 decision variables. It can be adapted to different projects by adjusting the variation ranges of these variables according to specific construction conditions. The model is solved using the NSGA-III algorithm.

Using a subsea tunnel project as a case study, site data were used to refine the variable ranges and define the upper limits for each objective. The optimized Pareto solution set was obtained through model computation. The results show that the construction schedule can be optimized by up to 132 days, and the cost by up to 110.58 million CNY, while both quality and safety levels remain within acceptable limits. These findings provide valuable support for decision-makers to develop effective construction strategies under varying project demands.

This study provides long-term and effective risk decision-making references for construction sites at the overall project level; however, the impact of safety risks on other risks is treated as a random variable within a fixed interval. In practical engineering, different types of safety risks lead to significantly varying losses in other risk categories. Therefore, it is necessary to refine risk classifications, investigate the correlations between individual risks and other risks during tunnel construction, translate safety risks into specific risk cases, and analyze the diverse consequences caused by different types of safety risks. Such an approach will provide construction stakeholders with more detailed and targeted risk decision-making sets.

## 5. ACKNOWLEDGMENTS

The work described in this paper is supported by the Qingdao Conson Second Jiaozhou Bay Subsea Tunnel Co., Ltd, National Natural Science Foundation of China (Grant Nos. 52130805, 52408434) and the Shanghai Pujiang Talent Program (2022PJD077).

## 6. REFERENCES

- [1] Agrama, F. A. (2014). Multi-objective genetic optimization for scheduling a multi-storey building. *Automation in Construction*, 44, 119–128. <https://doi.org/10.1016/j.autcon.2014.04.005>
- [2] Bachar, R., Urlainis, A., Wang, K. C., & Shohet, I. M. (2025). Optimal allocation of safety resources in small and medium construction enterprises. *Safety Science*, 181, 106680. <https://doi.org/10.1016/j.ssci.2024.106680>
- [3] Dehghani, M., Vahdat, V., Amiri, M., Rabiei, E., & Salehi, S. (2019). A multi-objective optimization model for a reliable generalized flow network design. *Computers & Industrial Engineering*, 138, 106074. <https://doi.org/10.1016/j.cie.2019.106074>
- [4] El-Abbasy, M. S., Elazouni, A., & Zayed, T. (2016). MOSCOPEA: Multi-objective construction scheduling optimization using elitist non-dominated sorting genetic algorithm. *Automation in Construction*, 71, 153–170. <https://doi.org/10.1016/j.autcon.2016.08.038>
- [5] Jun, D. H., & El-Rayes, K. (2010). Optimizing the utilization of multiple labor shifts in construction projects. *Automation in Construction*, 19(2), 109–119. <https://doi.org/10.1016/j.autcon.2009.12.015>
- [6] Liu R.N., Feng X., Yao Y.P., Zhang X.M. & Zhang J.(2024). Multi-objective optimization of airport runway construction schemes based on improved genetic algorithm. *Journal of Beijing University of Aeronautics and Astronautics*, 50(12): 3720-3728 (in Chinese). doi:10.13700/j.bh.1001-5965.2022.0893
- [7] Liu, Y., You, K., Jiang, Y., Wu, Z., Liu, Z., Peng, G., & Zhou, C. (2022). Multi-objective optimal scheduling of automated construction equipment using non-dominated sorting genetic algorithm (NSGA-III). *Automation in Construction*, 143, 104587. <https://doi.org/10.1016/j.autcon.2022.104587>
- [8] Love, P. E. D., Ika, L. A., Matthews, J., Fang, W., & Carey, B. (2023). The duality and paradoxical tensions of quality and safety: Managing error in construction projects. *IEEE Transactions on Engineering Management*, 70(2), 791–798. <https://hdl.handle.net/10536/DRO/DU:30154786>
- [9] Meng, F., Xu, J., Xia, C., Chen, W., Zhu, M., Fu, C., & Chen, X. (2024). Optimization of deep excavation construction using an improved multi-objective particle swarm algorithm. *Automation in Construction*, 166, 105613. <https://doi.org/10.1016/j.autcon.2024.105613>
- [10] Parente, M., Cortez, P., & Gomes Correia, A. (2015). An evolutionary multi-objective optimization system for earthworks. *Expert Systems with Applications*, 42(19), 6674–6685. <https://doi.org/10.1016/j.eswa.2015.04.051>
- [11] Razmi, A., Rahbar, M., & Bemanian, M. (2022). PCA-ANN integrated NSGA-III framework for dormitory building design optimization: Energy efficiency, daylight, and thermal comfort. *Applied Energy*, 305. <https://doi.org/10.1016/j.apenergy.2021.117828>
- [12] Wanberg, J., Harper, C., Hallowell, M. R., & Rajendran, S. (2013). Relationship between construction safety and quality performance. *Journal of Construction Engineering and Management*, 139(10). [https://doi.org/10.1061/\(ASCE\)CO.1943-7862.0000732](https://doi.org/10.1061/(ASCE)CO.1943-7862.0000732)
- [13] Wang, T., & Feng, J. (2023). Multi-objective joint optimization for concurrent execution of design-construction tasks in design-build mode. *Automation in Construction*, 156. <https://doi.org/10.1016/j.autcon.2023.105078>
- [14] Wu, X., Wang, L., Chen, B., Feng, Z., & Qin, Y. W. (2022). Multi-objective optimization of shield construction parameters based on random forests and NSGA-II. *Advanced Engineering Informatics*, 54. <https://doi.org/10.1016/j.aei.2022.101751>
- [15] Xiong, Y., & Kuang, Y. (2007). Construction project schedule-cost optimization based on ant colony algorithm. *Systems Engineering Theory and Practice*, (3), 105–111.
- [16] Xu, Q., Chong, H., & Liao, P. (2019). Collaborative information integration for construction safety monitoring. *Automation in Construction*, 102. <https://doi.org/10.1016/j.autcon.2019.02.004>

- [17] Yang, Z. (2019). Research on Deep Integration of Construction Management and Computer BIM Technology. *Journal of Advanced Computational Intelligence and Intelligent Informatics*, 23(3). [tps://doi.org/10.20965/jaciii.2019.p0379](https://doi.org/10.20965/jaciii.2019.p0379)
- [18] Zhang, Y., & Cui, N. (2021). Project scheduling and material ordering problem with storage space constraints. *Automation in Construction*, 129. <https://doi.org/10.1016/j.autcon.2021.103796>
- [19] Zhao, C., Tang, J., Gao, W., Zeng, Y., & Li, Z. (2024). Many-objective optimization of multi-mode public transportation under carbon emission reduction. *Energy*, 286. <https://doi.org/10.1016/j.energy.2023.129627>.

## FLOOD RISK ASSESSMENT USING A LITERATURE-BASED APPROACH

Wei-Wei Zhao<sup>1</sup>, Shui-Long Shen<sup>2</sup>, Annan Zhou<sup>3</sup>, Yan-Ning Wang<sup>4</sup>

**Abstract:** Urban flood risk is intensifying under the dual pressures of rapid urbanization and climate change, highlighting the need for robust, transparent, and scalable assessment frameworks. This study presents a fully data-driven framework for urban flood risk assessment that integrates region-specific risk factors and minimizes subjective bias. A bibliometric-informed weighting method is employed to objectively assign importance to each factor based on its prominence in peer-reviewed literature. The framework was applied to a case study in Guilin, China, where twenty localized indicators were synthesized through spatial analysis to produce a composite flood risk map. Model validation against the major flood event of June 2024 demonstrated strong spatial agreement between predicted high-risk areas and actual flood-affected zones. These results confirm the framework's predictive validity and practical applicability. By enhancing transparency, reproducibility, and adaptability, this approach offers valuable support for urban flood resilience planning and disaster mitigation.

**Keywords:** Urban flood risk, Data-driven framework, Region-specific indicators, Literature-based weighting, Flood risk mapping

### 1. INTRODUCTION

Urban flood risk is increasingly critical due to rapid urbanization and climate change, which intensify both the frequency and severity of flooding (Zhou et al., 2019). Beyond infrastructure damage, floods disrupt transportation, public services, health systems, and local economies (Allaire., 2018; Hammond et al., 2015), necessitating robust and scalable assessment frameworks for resilience planning. Traditionally, flood risk is conceptualized as a function of hazard, exposure, and vulnerability (Maranzoni et al., 2023), typically assessed using proxy indicators and models. Physically based hydrodynamic models like HEC-RAS (Joyce et al., 2009) simulate flood dynamics but depend on high-resolution data, often unavailable in urban settings.

Considering these limitations, there is a pressing need to explore alternative, objective, and scalable frameworks for flood risk assessment. A conventional flood risk assessment framework typically conceptualizes risk as the intersection of hazard, exposure, and vulnerability (Maranzoni et al., 2023). These components are typically assessed using proxy variables supported by numerical simulations and geospatial analysis techniques. Physically based hydrodynamic models, such as HEC-RAS (Joyce et al., 2009), are commonly used to simulate flood propagation and estimate hazard intensity. While effective, these models rely on high-resolution data that are often scarce or costly in urban areas.

An alternative approach employs multi-criteria decision analysis to construct composite risk indices (Lin et al., 2019). Popular weighting methods include AHP (Lyu et al., 2020; Wu et al., 2022), entropy (Liu et al., 2019; Wu et al., 2022) and Principal Component Analysis (PCA) (Liu et al., 2021). However, these techniques often suffer from subjectivity, particularly in expert-driven weighting schemes, which can affect reproducibility and policy relevance (Munier et al., 2021). To mitigate this, literature analysis offers a data-informed means of determining indicator weights by examining keyword frequencies, co-occurrence, and research trends (Lieber et al., 2022).

This study proposes a novel urban flood risk assessment framework that combines literature insights with data-driven modeling to reduce bias and enhance objectivity. A case study in Guilin, China, demonstrates its practical applicability.

<sup>1</sup> Ph.D. Candidate, Zhao, Wei-Wei, M.Sc. Computer Science, Shantou University, Shantou, China; [14wwzhao@stu.edu.cn](mailto:14wwzhao@stu.edu.cn).

<sup>2</sup> Professor, Shen, Shui-Long, Ph.D. Civil Engineering, Dean College of Engineering, Shantou University, Shantou, China, [shensl@stu.edu.cn](mailto:shensl@stu.edu.cn).

<sup>3</sup> Professor, Zhou, Annan, Ph.D. Civil Engineering, School of Engineering, RMIT University, Melbourne, Australia, [annan.zhou@rmit.edu.au](mailto:annan.zhou@rmit.edu.au).

<sup>4</sup> Professor, Wang, Yan-Ning, Ph.D. Civil Engineering, College of Engineering, Shantou University, Shantou, China, [wangyn@stu.edu.cn](mailto:wangyn@stu.edu.cn).



## 2. METHODOLOGY

### 2.1. Risk Assessment Framework

The flood risk assessment framework adopted in this study consists of five main stages: risk factor identification, data preprocessing, Flood Risk Index (FRI) construction, comparison analysis, and validation.

In the first stage, six major categories of flood-related factors were identified through an integrated approach combining literature review and expert knowledge: topography, hydrology, natural buffering, anthropogenic activities, socioeconomic resilience, and infrastructure. This factor selection process ensures a comprehensive and context-specific representation of flood risk drivers. The selected factors were then standardized and spatially aligned during data preprocessing to maintain consistency across datasets.

The FRI construction stage incorporates two key innovations: the comprehensive factor selection mentioned above, and the use of bibliometric-based weighting methods to assign relative importance to each factor. Specifically, **three** weighting approaches were employed: entropy method, PCA, and **literature** frequency. For index classification, two methods were applied: the normal distribution method, which segments the FRI based on standard deviations from the mean, and the Natural Breaks method, which optimizes classification for skewed or non-normal distributions.

To assess the consistency and robustness of the FRI outputs generated by these different approaches, comparison analyses were conducted using metrics such as consistency level, Kappa coefficient, and Gi\* statistic. Finally, the model's validity was evaluated by comparing the spatial distribution of flood risk against historical flood records, providing empirical evidence of the FRI's predictive accuracy.

### 2.2. Risk Factor Identification with Urban Characteristics

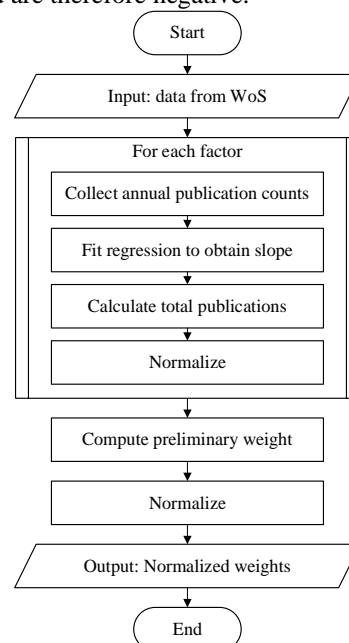
Accurate flood risk assessment requires selecting factors that reflect local geographic and socioeconomic conditions. In Guilin, the dense river network, rapid urbanization, and economic reliance on tourism and transport necessitate a context-specific approach. Key factors such as tourism density, river proximity, transport hubs, and flood control structures capture the city's unique risk profile, ensuring that both hazard and mitigation elements are appropriately represented in the evaluation framework.

*Table 1. Flood risk assessment factors*

Factor	Category	Direction
Digital evaluation model (DEM)	Topography	Negative
Slope	Topography	Negative
River density	Hydrology	Positive
River proximity	Hydrology	Positive
Precipitation	Hydrology	Positive
Natural landscape features	Natural Buffering	Negative
Land cover - risk	Natural Buffering	Positive
Land cover - mitigation	Natural Buffering	Negative
Population density	Anthropogenic	Positive
Tourism density	Anthropogenic	Positive
Land use - risk	Anthropogenic	Positive
Land use - mitigation	Anthropogenic	Negative
Per capita income	Socioeconomic Resilience	Negative
Public fiscal expenditure	Socioeconomic Resilience	Negative
Transport hubs	Infrastructure	Positive
Railways	Infrastructure	Positive
Roads	Infrastructure	Positive
Building density	Infrastructure	Positive
Flood control structures	Infrastructure	Negative
Reservoir influence	Infrastructure	Positive

Table 1 summarizes twenty flood risk factors grouped into six categories: Topography, Hydrology, Natural Buffering, Anthropogenic Activity, Socioeconomic Resilience, and Infrastructure. The factors were chosen for their roles in hazard, exposure, or mitigation, with the six categories collectively representing the different aspects that contribute to flood risk. The table also includes a “Direction” column indicates whether a factor increases

(positive) or decreases (negative) flood risk. Topography includes the Digital Elevation Model (DEM) and slope, both of which influence how water moves across the landscape; higher elevation and steeper slopes generally reduce flood accumulation, so these factors are marked as negative contributors to flood risk. Hydrology captures the direct drivers of flooding, including river density, river proximity, and precipitation. Areas with dense river networks, closer proximity to rivers, or higher rainfall are more prone to flooding, and these factors are therefore considered positive. Natural Buffering reflects the protective capacity of the environment. Features such as natural landscapes and land cover designed for mitigation help absorb or slow floodwaters and are marked negative, whereas land cover that increases vulnerability (e.g., impervious surfaces or risk-prone land use) is marked positive. Anthropogenic Activity represents human-driven factors that influence exposure. Higher population density, tourism activity, and land use that increases flood exposure all contribute positively to flood risk. Conversely, land use designed for mitigation, such as parks or green spaces that reduce runoff, is treated as negative. Socioeconomic Resilience captures a community's capacity to withstand floods. Higher per capita income and greater public fiscal expenditure provide resources for adaptation and recovery, and thus are considered negative contributors to risk. Finally, Infrastructure encompasses built structures that can either increase or decrease risk. Transport hubs, railways, roads, building density, and reservoirs can amplify exposure and are marked positive, while flood control structures are designed to reduce risk and are therefore negative.



**Figure 1.** Flowchart of Literature Frequency Analysis

### 2.3. Literature-Based Weighting Method

To reduce subjectivity in assigning weights to flood risk factors, this study proposes a literature-based weighting approach that draws on academic literature as an objective source of evidence. Literature analysis quantifies the extent and attention each factor has received in flood-related research, thereby reflecting its relative importance in the scientific community. The core idea of the literature frequency analysis is to use the volume of relevant publications as a proxy for the significance of each risk factor. To operationalize this, we carried out keyword-based searches in the Web of Science database, carefully defining search terms for each risk factor category (e.g., “slope AND flood,” “infrastructure AND flood”). The number of retrieved publications serves as an indicator of how extensively each factor has been studied. Factors with higher publication counts are thus assigned greater weights, while those with fewer references were down-weighted. This approach offers a data-driven and reproducible method for weighting, grounded in the collective focus of flood research. By relying on publication volume, it avoids potential biases inherent in expert opinion-based methods while reflecting research community consensus.

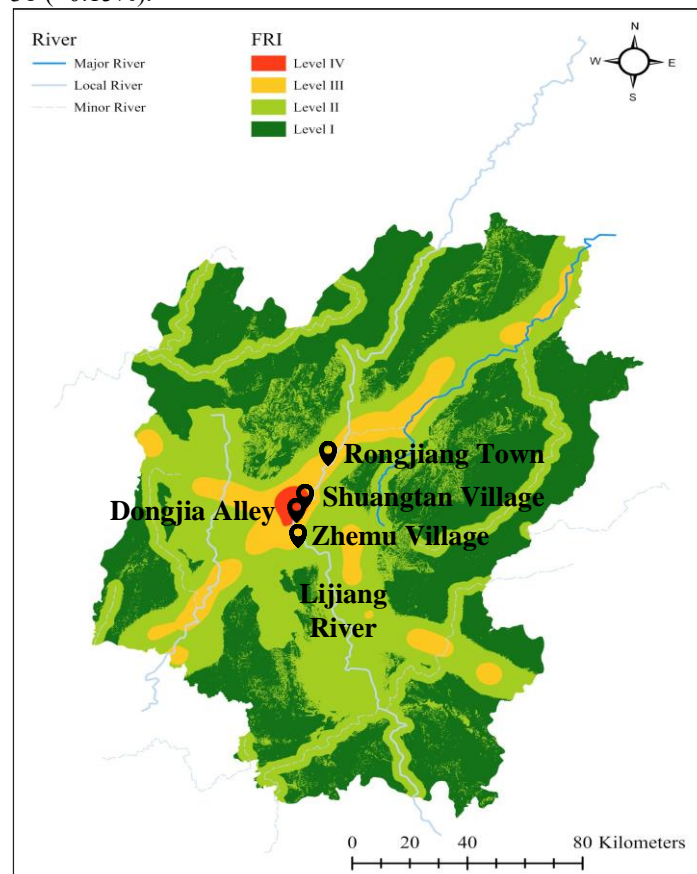
Figure 1 presents the Literature Frequency Analysis, which derives factor weights from both publication volume and observed research trends. The flowchart breaks down the procedure into a series of systematic steps. The process begins with collecting raw bibliometric data from the Web of Science database. For each flood risk factor, annual publication counts are compiled over the study period, providing a temporal profile of research attention. A regression analysis is then calculated to estimate the trend, represented by the slope, which captures whether interest in a particular factor is increasing, decreasing, or stable over time. Next, the total number of

publications for each factor is provided to measure overall academic focus. These values are subsequently normalized to bring all factors onto a common scale, facilitating direct comparison. From this, preliminary weights are computed by combining the normalized total publication counts and the trend information. A final normalization step converts these preliminary weights into standardized bibliometric weights, which are assigned to each factor for integration into the Flood Risk Index.

### 3. RESULTS

This study conducts a case study in Guilin, China. Located in the Guangxi Zhuang Autonomous Region of southern China, Guilin lies within the upper reaches of the Pearl River basin and is characterized by a complex karst landscape with steep limestone hills and an extensive river network. This unique geographic and hydrological setting makes Guilin particularly vulnerable to flooding, as rapid runoff from the steep terrain and concentrated river flows increase flood risk in the urban area.

Flood Risk Index (FRI) maps were generated using the literature frequency analysis Frequency weighting method, which assigns factor weights based on publication volume in relevant literature. To enhance comparability across the three weighting methods, the continuous FRI values were reclassified using the Normal Distribution Rule. According to this rule, the FRI values are stratified into four ordinal levels based on their positive deviation from the mean ( $\mu$ ): (i) Level I (Low Risk):  $FRI \leq \mu + 1\sigma$  (~68%); (ii) Level II (Moderate-Low Risk):  $\mu + 1\sigma < FRI \leq \mu + 2\sigma$  (~13.5%); (iii) Level III (Moderate-High Risk):  $\mu + 2\sigma < FRI \leq \mu + 3\sigma$  (~2.35%); (iv) Level IV (High Risk):  $FRI > \mu + 3\sigma$  (~0.15%).

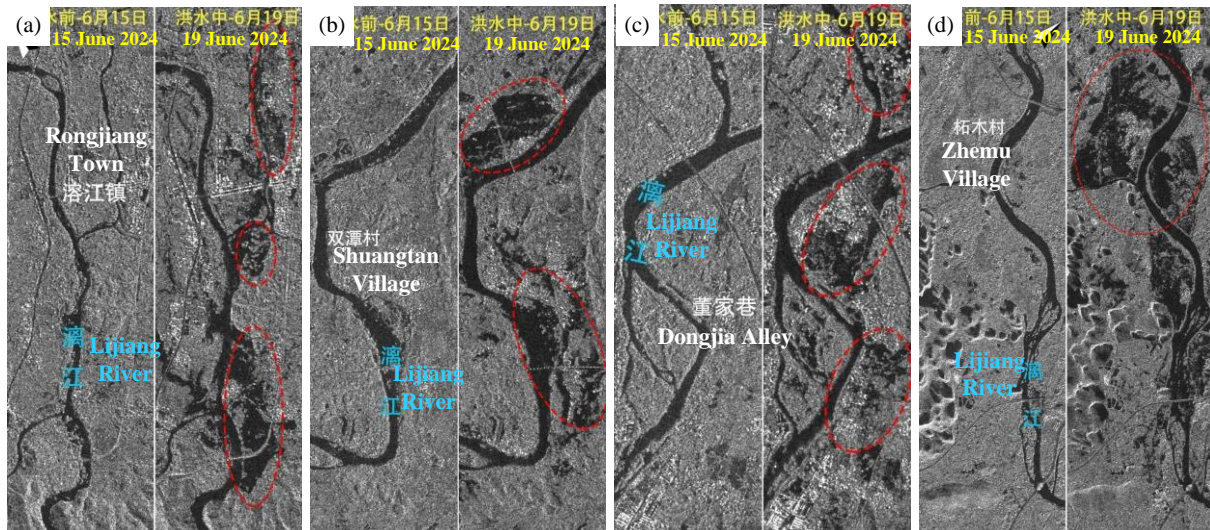


**Figure 2.** FRI Map Classified by the Normal Distribution Rule

### 4. DISCUSSIONS

The Flood Risk Index (FRI) map shown in Figure 2 was generated solely using the literature frequency weighting method. Its practical validity was assessed by comparing the spatial distribution of flood risk with a significant flood event in Guilin in June 2024, which exceeded a 30-year recurrence interval. Figure 3 presents the FRI map alongside satellite images from before (June 15) and during (June 19) the flood event. Four representative

sites—Rongjiang Town, Shuangtan Village, Dongjia Alley, and Zhemu Village—highlighted in Figure 3, were selected for detailed spatial comparison. At each site, satellite imagery reveals substantial water expansion consistent with inundation, which aligns well with the high-risk areas identified in the FRI map. This strong spatial agreement confirms the robustness of the literature-based FRI model and underscores its applicability for urban flood risk assessment in Guilin.



*Figure 3. Validation Using Satellite Imagery, recreated based on News (2025)*

Future developments should prioritize the integration of dynamic and real-time data sources to improve model responsiveness. Although this study used June 2024 rainfall data and validated with June 2025 flood events, the lack of real-time inputs constrains adaptability to fast-changing flood conditions. Incorporating satellite rainfall estimates, real-time hydrological data, and IoT-based monitoring would enable more accurate assessments, particularly in rapidly urbanizing or climate-sensitive regions. Additionally, the model can support flood governance by simulating human interventions such as reservoir releases or pumping station operations. These improvements would allow the framework to evolve from a static risk map into a dynamic, data-driven tool for adaptive urban flood management.

## 5. CONCLUSIONS

This study introduces a fully data-driven framework for urban flood risk assessment, demonstrated through a case study in Guilin, China. By integrating region-specific risk factors, objective weighting, and robust validation, the framework produces reliable and actionable flood risk maps to support informed decision-making.

The main contributions are summarized as follows:

- (1) A comprehensive data-driven framework was developed to assess urban flood risk. The framework integrates region-specific flood risk factors tailored to Guilin's geographic and socio-economic conditions. This localized approach improves model sensitivity and accuracy in capturing spatial flood risk patterns.
- (2) A novel **literature**-based weighting method was introduced to quantify the relative importance of risk factors. This technique reduces subjectivity by aligning indicator weights with their empirical prominence in peer-reviewed literature.
- (3) The framework was validated using the major flood event of June 2024 in Guilin. The results demonstrate strong predictive performance and practical value, confirming its effectiveness in supporting targeted flood mitigation and urban resilience planning.

## 6. ACKNOWLEDGMENTS

The research work was funded by Guangdong Provincial Basic and Applied Basic Research Fund Committee (2022A1515240073).

## 7. BIBLIOGRAPHY

- [1] Allaire, M. J. W. S. (2018). Socio-economic impacts of flooding: A review of the empirical literature. *3*, 18-26.
- [2] Hammond, M. J., Chen, A. S., Djordjević, S., Butler, D., & Mark, O. J. U. W. J. (2015). Urban flood impact assessment: A state-of-the-art review. *12*(1), 14-29.
- [3] Lieber, M., Chin-Hong, P., Kelly, K., Dandu, M., & Weiser, S. D. J. G. P. H. (2022). A systematic review and meta-analysis assessing the impact of droughts, flooding, and climate variability on malnutrition. *17*(1), 68-82.
- [4] Lin, L., Wu, Z., & Liang, Q. J. N. H. (2019). Urban flood susceptibility analysis using a GIS-based multi-criteria analysis framework. *97*, 455-475.
- [5] Liu, Y., You, M., Zhu, J., Wang, F., & Ran, R. J. I. J. o. D. R. R. (2019). Integrated risk assessment for agricultural drought and flood disasters based on entropy information diffusion theory in the middle and lower reaches of the Yangtze River, China. *38*, 101194.
- [6] Liu, Z., Jiang, Z., Xu, C., Cai, G., & Zhan, J. J. N. H. (2021). Assessment of provincial waterlogging risk based on entropy weight TOPSIS-PCA method. *108*, 1545-1567.
- [7] Lyu, H.-M., Sun, W.-J., Shen, S.-L., Zhou, A.-N. J. J. o. C. E., & Management. (2020). Risk assessment using a new consulting process in fuzzy AHP. *146*(3), 04019112.
- [8] Lyu, H.-M., Zhou, W.-H., Shen, S.-L., & Zhou, A.-N. (2020). Inundation risk assessment of metro system using AHP and TFN-AHP in Shenzhen. *Sustainable Cities and Society*, *56*, 102103. doi:<https://doi.org/10.1016/j.scs.2020.102103>
- [9] Maranzoni, A., D'Oria, M., & Rizzo, C. J. J. o. F. R. M. (2023). Quantitative flood hazard assessment methods: A review. *16*(1), e12855.
- [10] Munier, N., & Hontoria, E. (2021). *Uses and Limitations of the AHP Method*: Springer.
- [11] News, S. (2025). Gaofen-3 satellite assists in flood disaster relief in Guilin. Sohu.com. [https://www.sohu.com/a/789788556\\_120502346](https://www.sohu.com/a/789788556_120502346) (in Chinese: accessed June 25, 2025)
- [12] Wu, J., Chen, X., & Lu, J. J. I. J. o. D. R. R. (2022). Assessment of long and short-term flood risk using the multi-criteria analysis model with the AHP-Entropy method in Poyang Lake basin. *75*, 102968.
- [13] Zhou, Q., Leng, G., Su, J., & Ren, Y. (2019). Comparison of urbanization and climate change impacts on urban flood volumes: Importance of urban planning and drainage adaptation. *658*, 24-33.



## A MULTI-FIDELITY DEEP OPERATOR FRAMEWORK WITH GENERATIVE ADVERSARIAL NETWORK FOR LOAD PREDICTION AND DISPLACEMENT RECONSTRUCTION OF TUNNEL STRUCTURES

Chen Xu<sup>1</sup>, Zhen Liu<sup>2\*</sup>, Ba Trung Cao<sup>3</sup>, Günther Meschke<sup>4</sup>, Yong Yuan<sup>5</sup>, Xian Liu<sup>6</sup>

**Abstract:** Accurately predicting external loads and evaluating the health condition of tunnel structures are fundamental for ensuring the safety and resilience of underground infrastructure. This study presents an advanced multi-fidelity Deep Operator Network (MF-DeepONet) framework that incorporates a generative adversarial network (GAN) to address these challenges by integrating simulation-based low-fidelity data and sparse high-fidelity real-world measurements. Within this framework, the GAN is employed for inverse prediction of external loads from measured displacements, ensuring that the resulting load distributions remain consistent with simulation-informed patterns. The predicted loads are then fed into the MF-DeepONet to reconstruct the full displacement field through data fusion. The MF-DeepONet framework consists of two subnetworks: a low-fidelity network trained on data generated by a validated macro-scale numerical model to capture general deformation patterns of tunnel linings, and a high-fidelity network trained on limited real-world monitoring data to learn the correlations between field observations and simulations. A full-scale test on a quasi-rectangular shield tunnel (QRST) lining structure is conducted for validation. The results demonstrate that the proposed framework enables both reliable estimation of external loads and accurate reconstruction of displacement fields, showing strong agreement with experimental observations. This data-driven approach significantly reduces reliance on dense sensing networks and offers a robust, interpretable solution for tunnel health diagnosis and predictive maintenance in real-world engineering applications.

**Keywords:** Tunnel lining, Multi-fidelity DeepONet framework, Generative adversarial network (GAN), Limited measurements, Inverse load determination, Health evaluation

### 1. INTRODUCTION

In tunnel engineering, accurately understanding the external loading conditions and their impact on the structural integrity of tunnel linings is of paramount importance (X. Huang et al., 2020; Xu et al., 2023). Tunnels, as critical components of urban infrastructure, are often subjected to complex and variable loading scenarios during both construction and service stages, including overburden pressure and groundwater variations (Colombo et al., 2018; Guo et al., 2018; J.-L. Zhang et al., 2023; W. Zhang et al., 2022). These loads, if not properly identified and evaluated, may induce progressive deformation, joint failures, or even catastrophic collapse (W. Lu et al., 2023; Qiu et al., 2021). Therefore, precise estimation of external loads and timely evaluation of the structural health condition are essential for ensuring the safety, durability, and operational continuity of tunnel systems (H. Huang et al., 2024; Soga et al., 2025).

<sup>1</sup> MSc, Chen Xu, PhD student, Institute for Structural Mechanics, Ruhr University Bochum, Universitätsstraße 150, Bochum 44801, Germany, chen.xu@rub.de

<sup>2</sup> PhD, Zhen Liu, Postdoc, College of Civil Engineering, Tongji University, 1239 Siping Road, Shanghai 200092, China, lhugospace@tongji.edu.cn

<sup>3</sup> PhD, Ba Trung Cao, Postdoc, Institute for Structural Mechanics, Ruhr University Bochum, Universitätsstraße 150, Bochum 44801, Germany, ba.cao@rub.de

<sup>4</sup> PhD, Günther Meschke, Professor, Institute for Structural Mechanics, Ruhr University Bochum, Universitätsstraße 150, Bochum 44801, Germany, Guenther.Meschke@ruhr-uni-bochum.de

<sup>5</sup> PhD, Yong Yuan, Professor, College of Civil Engineering, Tongji University, 1239 Siping Road, Shanghai 200092, China, yuany@tongji.edu.cn

<sup>6</sup> PhD, Xian Liu, Professor, College of Civil Engineering, Tongji University, 1239 Siping Road, Shanghai 200092, China, xian.liu@tongji.edu.cn



Conventional methods for tunnel health assessment typically rely on numerical simulations calibrated against a limited set of field measurements. While finite element (FE) modeling provides a powerful tool for analyzing tunnel responses under prescribed loads, the inverse identification of unknown external loads based on observed displacements remains a major challenge (Gao et al., 2025; Yuan et al., 2021). This is particularly true in complex tunnel geometries or segmental linings with discontinuities and nonlinear joint behaviors, where the system's response may be highly sensitive to localized loading (X. Liu et al., 2025; Z. Liu, B. T. Cao, et al., 2025; Z. Liu, X. Liu, et al., 2025). Furthermore, such inverse analyses often suffer from ill-posedness and high computational cost, limiting their practicality in real-time monitoring and decision-making scenarios. In parallel, dense deployment of sensors across the tunnel lining to directly capture external loads or reconstruct full displacement fields is rarely feasible in practice due to prohibitive installation and maintenance costs (Latif et al., 2023; Lin et al., 2023; X. Zhang et al., 2024). As a result, there is a growing need for data-driven frameworks that can effectively leverage sparse measurements, integrate prior knowledge from simulations, and provide reliable predictions of both loading conditions and structural states.

With the rapid development of physics-informed machine learning, especially the operator learning technology (Koric et al., 2024; L. Lu et al., 2021), new opportunities have emerged to overcome these challenges. By treating external loads and structural responses as functional inputs and outputs, operator learning-based models such as DeepONet enable direct mappings between them, bypassing traditional physics-based formulations and offering significant advantages in terms of flexibility, efficiency, and generalizability (Koric et al., 2024; L. Lu et al., 2021).

Several recent studies have demonstrated the effectiveness of Deep Operator Networks (DeepONet) in solving complex forward and inverse problems in engineering mechanics. He et al. (2023) introduced a ResUNet-based DeepONet for elastoplastic stress field prediction, significantly reducing computational cost. Garg et al. (2022) employed DeepONet for time-dependent reliability analysis under stochastic loads, showcasing its capability in uncertainty quantification and zero-shot learning. Ahmed et al. (2025) proposed a physics-informed DeepONet with stiffness-based loss terms to improve accuracy in displacement prediction under static loads. Koric et al. (2024) further extended DeepONet to small-strain plasticity problems involving variable material properties and loading conditions. These advances demonstrate DeepONet's promise as a flexible and efficient surrogate model for both forward simulation and inverse estimation tasks.

Building on these developments, Chen Xu et al. (2024) proposed a multi-fidelity DeepONet (MF-DeepONet) framework that integrates simulations with sparse real-world measurements to reconstruct displacement fields induced by tunnel boring machine (TBM) excavation in real-time. In a follow-up study (C Xu et al., 2024), we extend the MF-DeepONet framework to capture the structural response of tunnel linings subjected to external loads, aiming to achieve effective fusion between numerical simulations and monitoring data. However, a major limitation in real-world tunnel operations is that external loads are typically unknown, which greatly restricts the applicability of the approach.

To address this challenge, this study proposes an advanced Multi-Fidelity Deep Operator Network (MF-DeepONet) framework augmented with a generative adversarial network (GAN) to simultaneously identify external loads and reconstruct structural responses during tunnel service. Specifically, we introduce a GAN module in which the generator takes displacement measurements at limited points as input and predicts the corresponding external loads. The discriminator is designed to distinguish between two types of predicted loads: (1) those generated from simulated displacements, and (2) those generated from real displacement measurements. The generator is trained on simulation data and further refined through adversarial training, enabling it to produce load predictions from real measurements that closely follow the distribution patterns learned from simulations.

The predicted external loads obtained via the GAN module are then fed into the MF-DeepONet framework developed in Chen Xu et al. (2024) for subsequent reconstruction of the full displacement field. A full-scale test on a quasi-rectangular shield tunnel (QRST) lining structure is used to validate the proposed framework. The results demonstrate that the enhanced MF-DeepONet not only successfully identifies the unknown external loads but also reconstructs displacement fields with high accuracy. The proposed method offers a promising solution for efficient tunnel diagnosis, with the potential to significantly reduce monitoring costs while enhancing safety and resilience.

## 2. METHODOLOGY

To achieve accurate identification of external loads and reliable structural response prediction of tunnel linings, we propose a multi-fidelity Deep Operator Network (MF-DeepONet) framework enhanced with a Generative Adversarial Network (GAN). As illustrated in Figure 1, the overall workflow consists of the following key steps:

### (1) Data Preparation and Pre-processing

A large low-fidelity dataset  $\mathcal{J}_L = \{u_L, y_L, s_L(u)(y)\}$  is generated from a validated finite element model under a wide range of external loading combinations. In parallel, a high-fidelity dataset  $\mathcal{J}_H = \{u_H, y_H, s_H(u)(y)\}$  is obtained

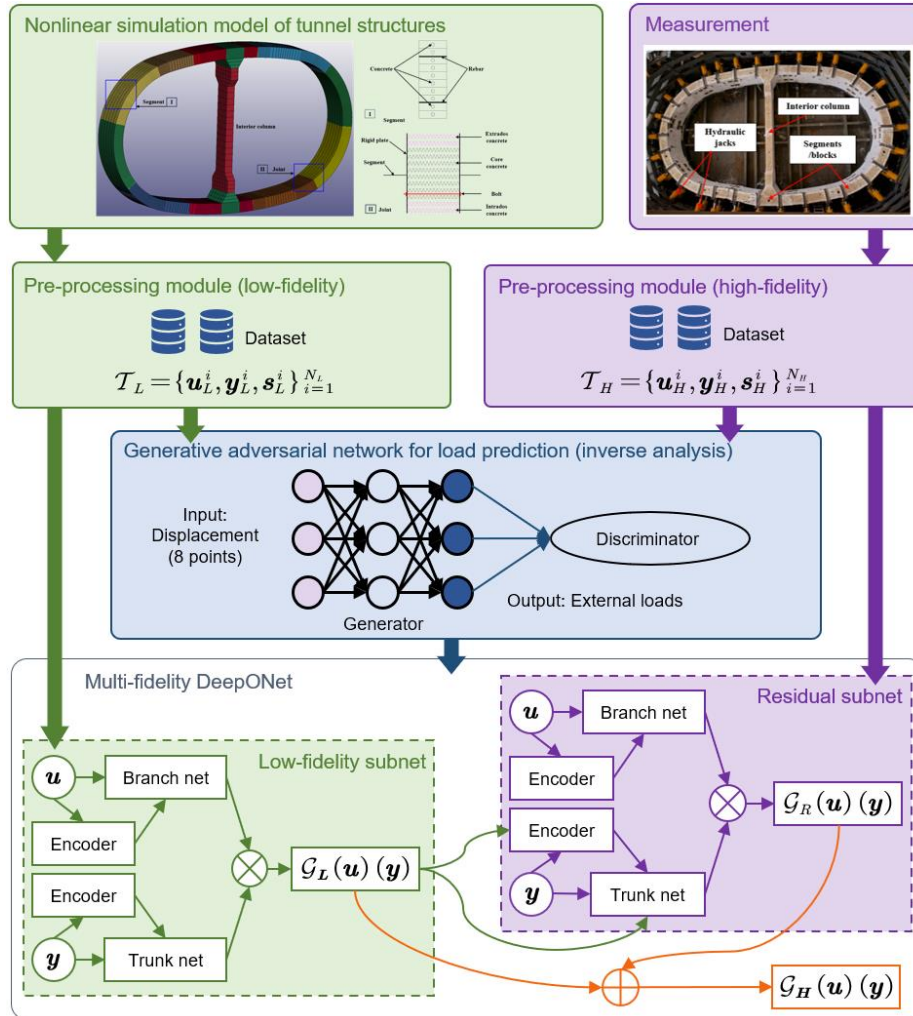
from laboratory tests, representing real-world measurements. The data structure and preprocessing procedures follow the triplet form in [Chen Xu et al. \(2024\)](#). In this context,  $u$  denotes the external load,  $y$  is the spatial coordinate, and  $s(u)(y)$  represents the displacement response at location  $y$  under the load scenario  $u$ .

### (2) GAN for Load Prediction

A GAN is employed as the core tool for inverse analysis, i.e., external load prediction. The generator, implemented as a fully connected neural network, takes sparse displacement measurements as input and outputs the corresponding external load. The discriminator, which is also a fully connected neural network, evaluates loads from two sources: the predicted load generated by the generator and the load obtained from laboratory measurements. Its objective is to distinguish between these two types of loads. The generator is trained not only through supervised learning on simulation data, but also through adversarial feedback from the discriminator. This dual training strategy enables the generator to produce load distributions from real displacement inputs that exhibit similar patterns to those from simulation. It is important to note that the true external loads corresponding to real measurement data are unknown during training process and thus cannot be used directly for supervised training. In contrast, training a neural network solely on simulated data without incorporating the discriminator typically results in poor generalization to experimental data and often yields unrealistic and highly noisy load predictions.

### (3) MF-DeepONet Training for Full-Field Displacement Prediction

The multi-fidelity DeepONet architecture follows the approach introduced in [C Xu et al. \(2024\)](#). The low-fidelity subnet learns the general physical behavior embedded in numerical simulations, while the residual subnet captures the nonlinear correlation between simulation and real-world observations. Supported by abundant simulated data, the trained MF-DeepONet can reconstruct the full displacement field based on only limited real displacement measurements. A key distinction from the previous framework lies in the treatment of high-fidelity loads  $u_H$ : in this study, they are not directly measured but inferred through GAN-based inverse analysis. The true experimental loads are used only for validation and are not involved in training.



**Figure 1.** Illustration of the proposed multi-fidelity DeepONet framework with an integrated generative adversarial network for external load and displacement field prediction, which is an extension of the work in [C Xu et al. \(2024\)](#).

### 3. IMPLEMENTATION OF THE PRESENTED APPROACH

#### 3.1. Generation of the high-fidelity dataset: Quasi-rectangular segmental tunnel (QRST) tests

To validate the proposed approach, we use a quasi-rectangular shield tunnel (QRST) project as a representative case. The QRST features a non-circular cross-section designed to optimize underground space utilization in urban environments. The lining structure has an outer dimension of 11.5 m (width)  $\times$  6.937 m (height) and consists of ten precast concrete segments and an interior column. Each segment is 1.2 m wide and 0.45 m thick, while the interior column is 0.7 m wide and 0.35 m thick (Liu, Liu, Yuan, et al., 2018; Liu, Ye, et al., 2018).

A full-scale experimental test, as shown in Figure 2, was previously conducted to examine the mechanical performance and failure process of the QRST lining under overburden loading conditions (Liu, Liu, Ye, et al., 2018). Thirty load points were applied across the ring, divided into three groups (P1, P2, and P3) to simulate diverse loading combinations. Displacements at 20 locations around the structure were recorded during 23 load-bearing states, covering the transition from elastic deformation to ultimate failure. This test provides a valuable high-fidelity dataset  $\mathcal{T}_H$  for training and validating the proposed framework.

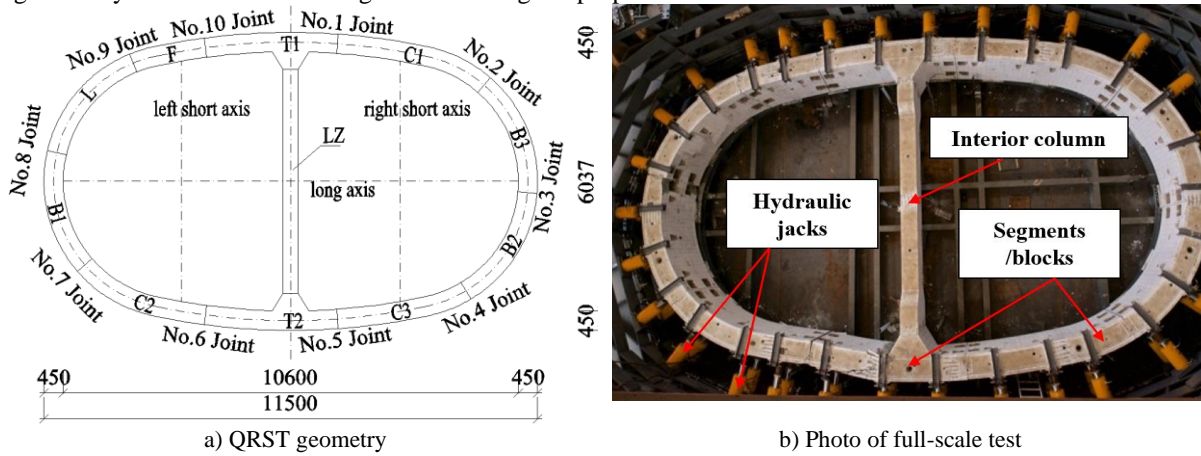


Figure 2. Full-scale test of QRST.

#### 3.2. Generation of low-fidelity dataset: Numerical modeling

As shown in Figure 3, a validated macro-scale finite element model of the QRST lining was developed using LS-DYNA to simulate the full range of structural responses under varying external loads (Liu et al., 2022; Wu et al., 2012; Zhao et al., 2017). The model incorporates both geometric and material nonlinearities. Segments are modeled using layered thick shell elements, with concrete and reinforcement layers explicitly represented based on material test data and the Chinese code GB 50010-2010 (Chinese Standard, 2002). Longitudinal joints are modeled using a rigid-plate-spring system, consisting of nonlinear zero-length springs to simulate concrete compression and bolt tension behavior.

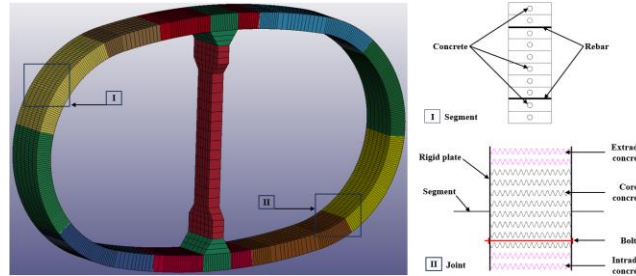


Figure 3. Illustration of macro-level nonlinear structural model.

To generate the low-fidelity dataset  $\mathcal{T}_L$  for the MF-DeepONet model, a parametric study was conducted by varying the load magnitudes of P1, P2, and P3 from 150 kN to 750 kN in 100 kN increments, resulting in 343 loading scenarios. After filtering out unstable cases, a total of 302 valid simulations were retained. The resulting displacement fields were extracted at multiple locations (totally 519 points) and used as inputs for the low-fidelity training process. This numerical model effectively captures the multi-stage deformation of the QRST structure, including the transition from elastic to plastic behavior and the formation of plastic hinges, as verified by comparisons with full-scale test results.

### 3.3. Inverse analysis of the tunnel lining: predicting the unknown external loads

Figure 4 shows the spatial distribution of 20 displacement measurement points used in the experiment. Among them, data from 8 orange points are used as inputs to the GAN generator for predicting the corresponding external loads.

The generator is composed of four hidden layers, each with 20 neurons. The discriminator consists of two hidden layers, also with 20 neurons each. Both networks use the LeakyReLU activation function and are optimized using the Adam optimizer with a learning rate of 0.001 and a batch size of 80. After 500 epochs, the training converges. The predicted loads generated by the GAN are then compared to the experimentally measured loads. The resulting coefficient of determination  $R^2$  reaches 0.7378, which is considered acceptable given the limited amount of experimental data.

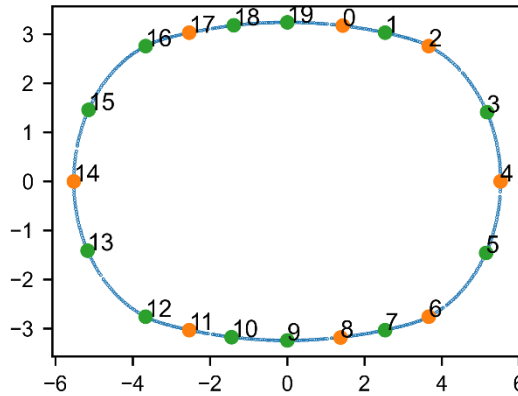


Figure 4. Layout of displacement measurement points (orange: used for training; green: used for validation).

### 3.4. Displacement field reconstruction

Displacement field reconstruction was achieved through training the MF-DeepONet framework. To more clearly illustrate the data used for training each part of the neural network, Table 1 is provided. Notably, the external loads used to train the residual subnet were not the  $u_H$  directly measured in the experiment, but rather the  $u_{pred}$  inferred via the GAN model described in Subsection 3.3.

Table 1 Input, Output, and Training Data for Each Network Component

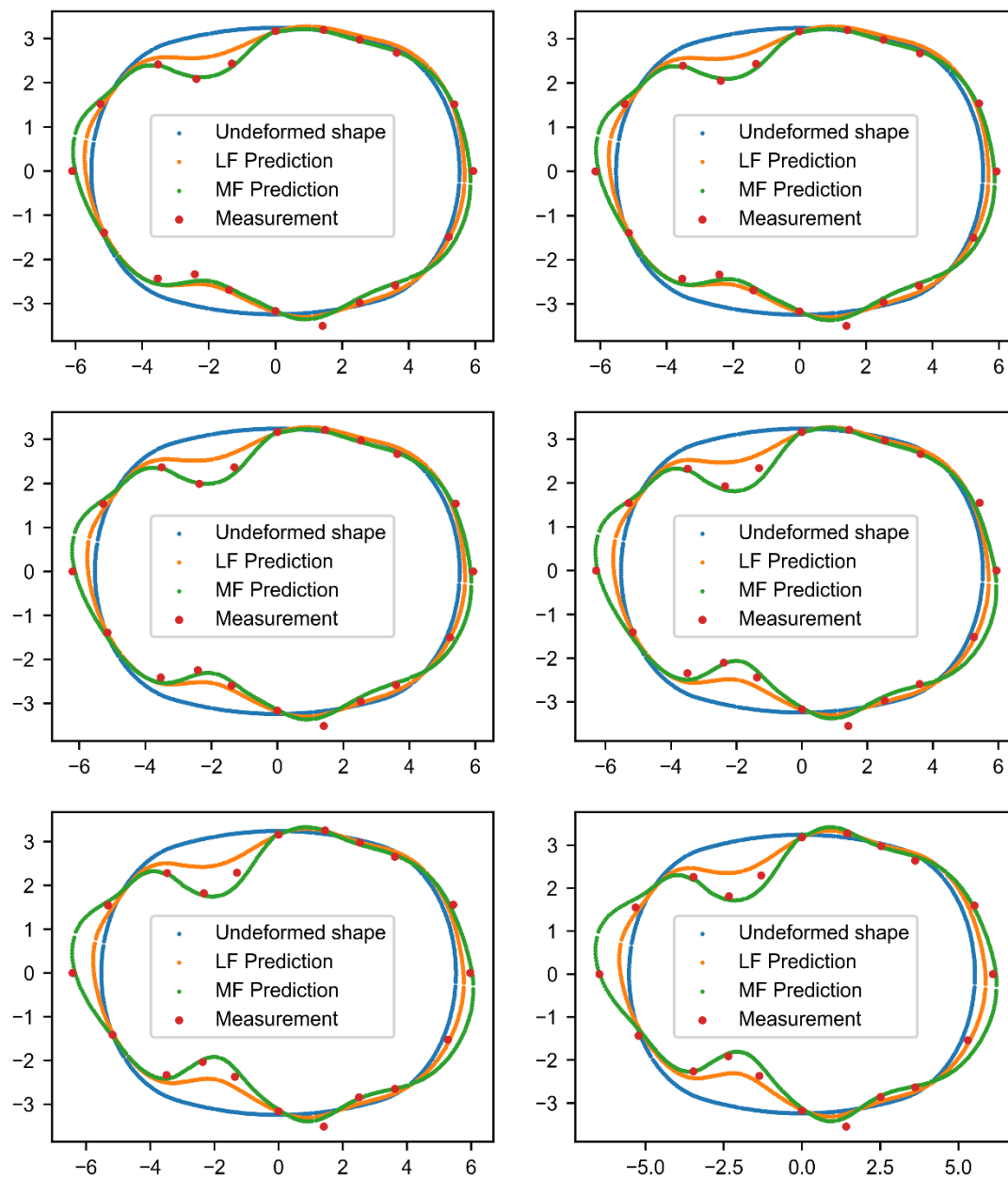
Network Component	Input	Output	Training Data
GAN Generator	Displacement at 8 orange points (shown in Figure 4)	Predicted loads (P1, P2, P3)	$\mathcal{T}_L: u_L, s_L$ (at 8 points) $\mathcal{T}_H: u_L, s_H$ (at 8 points)
Low-fidelity Subnet	$u_L, y_L$	$\mathcal{G}_L(u_L)(y_L)$	$\mathcal{T}_L: u_L, y_L$ (totally 519 points), $s_L(u_L)(y_L)$
Residual Subnet	$u_{pred}, y_H$	$\mathcal{G}_R(u_{pred})(y_H)$	$\mathcal{T}_H: u_{pred}, y_H$ (totally 8 points), $s_H(u_H)(y_H)$

To reconstruct the displacement field at a given load-bearing state  $t$ , displacement measurements from load states 1 to  $t$  were required at the 8 sensor locations. The training process was efficient, requiring only 200 epochs. More detailed training settings can be referred to in Chen Xu et al. (2024).

Figure 5 presents the reconstruction results for selected load scenarios. Compared to predictions from the LF subnet, the MF predictions show significantly improved agreement with the experimental results. For the 12 points used to validate the framework's accuracy, the predicted displacements from the MF-DeepONet achieved an  $R^2$  score above 0.8, which is sufficient for practical engineering applications.

Due to the support of extensive numerical simulations, the framework can reconstruct the full displacement field (519 points in total) using measurements from only 8 locations. This demonstrates the strong generalization capability and data efficiency of the proposed approach. Remarkably, despite the GAN-inferred loads not being perfectly accurate, the displacement reconstructions remain highly consistent with the experimental observations.





**Figure 5.** Predicted displacement fields under different external load scenarios using the proposed framework. The subplots from top-left to bottom-right correspond to load scenarios 14 to 19, respectively.

#### 4. CONCLUSION

This study presents a multi-fidelity Deep Operator Network (MF-DeepONet) framework enhanced with a Generative Adversarial Network (GAN) for external load prediction and displacement field reconstruction of tunnel structures. By combining simulation-generated low-fidelity data and sparse experimental measurements, the framework enables accurate forward prediction of structural responses and inverse identification of external loads, even in the absence of direct load labels. The GAN component improves load inference by learning realistic distributions aligned with simulation physics.

Validation on a full-scale quasi-rectangular shield tunnel test confirms the framework's effectiveness in reconstructing displacement fields with high accuracy and robustness. The predicted displacements show strong agreement with experimental measurements, achieving an average  $R^2$  value above 0.8 across multiple load states. Additionally, the GAN-inferred load distributions remain physically consistent with simulation patterns, enabling reliable inverse identification.

While these results are promising, the transferability of the proposed approach to different tunnel geometries, lining types, or load scenarios remains an open question. Moreover, the GAN module may need retraining or fine-tuning when applied to significantly different structural or loading conditions, depending on the degree of deviation from the original training domain. Future work will explore these aspects and evaluate the framework's adaptability across various tunnel types and operational environments.

Overall, this approach offers a promising direction for integrating physics-based modeling and operator learning in underground infrastructure monitoring, supporting real-time evaluation and maintenance decision-making with reduced dependence on dense sensor networks.

## 5. REFERENCES

- [1] Ahmed, B., Qiu, Y., Abueidda, D. W., El-Sekelly, W., de Soto, B. G., Abdoun, T., & Mobasher, M. E. (2025). Physics-informed deep operator networks with stiffness-based loss functions for structural response prediction. *Engineering Applications of Artificial Intelligence*, 144, 110097. doi:<https://doi.org/10.1016/j.engappai.2025.110097>
- [2] Chinese Standard, G. (2002). 50010-2010, "Code for Design of Concrete Structures,". In: Chinese Building Press, Beijing, China.
- [3] Colombo, L., Gattinoni, P., & Scesi, L. (2018). Stochastic modelling of groundwater flow for hazard assessment along the underground infrastructures in Milan (northern Italy). *Tunnelling and Underground Space Technology*, 79, 110-120. doi:<https://doi.org/10.1016/j.tust.2018.05.007>
- [4] Gao, B.-Y., Chen, R.-P., Wu, H.-N., Chen, T., & Zhang, Y. (2025). Enhancement mechanism of UHPC secondary lining on the mechanical performance at joints of shield tunnels: Full-scale experiment and simulation. *Tunnelling and Underground Space Technology*, 157, 106282. doi:<https://doi.org/10.1016/j.tust.2024.106282>
- [5] Garg, S., Gupta, H., & Chakraborty, S. (2022). Assessment of DeepONet for time dependent reliability analysis of dynamical systems subjected to stochastic loading. *Engineering Structures*, 270, 114811. doi:<https://doi.org/10.1016/j.engstruct.2022.114811>
- [6] Guo, C., Qi, J., Shi, L., & Fang, Q. (2018). Reasonable overburden thickness for underwater shield tunnel. *Tunnelling and Underground Space Technology*, 81, 35-40. doi:<https://doi.org/10.1016/j.tust.2018.06.016>
- [7] He, J., Koric, S., Kushwaha, S., Park, J., Abueidda, D., & Jasiuk, I. (2023). Novel DeepONet architecture to predict stresses in elastoplastic structures with variable complex geometries and loads. *Computer Methods in Applied Mechanics and Engineering*, 415, 116277. doi:<https://doi.org/10.1016/j.cma.2023.116277>
- [8] Huang, H., Ruan, B., Wu, X., & Qin, Y. (2024). Parameterized modeling and safety simulation of shield tunnel based on BIM-FEM automation framework. *Automation in Construction*, 162, 105362. doi:<https://doi.org/10.1016/j.autcon.2024.105362>
- [9] Huang, X., Liu, W., Zhang, Z., Zhuang, Q., Zhu, Y., Wang, Q., Kwok, C. y., & Wang, S. (2020). Structural behavior of segmental tunnel linings for a large stormwater storage tunnel: insight from full-scale loading tests. *Tunnelling and Underground Space Technology*, 99, 103376. doi:<https://doi.org/10.1016/j.tust.2020.103376>
- [10] Koric, S., Viswantah, A., Abueidda, D. W., Sobh, N. A., & Khan, K. (2024). Deep learning operator network for plastic deformation with variable loads and material properties. *Engineering with Computers*, 40(2), 917-929. doi:<https://doi.org/10.1007/s00366-023-01822-x>
- [11] Latif, K., Sharafat, A., & Seo, J. (2023). Digital twin-driven framework for TBM performance prediction, visualization, and monitoring through machine learning. *Applied Sciences*, 13(20), 11435. doi:<https://doi.org/10.3390/app132011435>
- [12] Lin, F., & Yang, X. (2023). Mechanical properties analysis of joints for prefabricated metro station structure based on Whole-process in-situ monitoring. *Tunnelling and Underground Space Technology*, 138, 105202. doi:<https://doi.org/10.1016/j.tust.2023.105202>
- [13] Liu, X., Hong, J., & Liu, Z. (2025). Investigations on mechanical behavior of longitudinal joints in segmental tunnel linings reinforced with epoxy bonded-bolted steel plates. *Tunnelling and Underground Space Technology*, 163, 106724. doi:<https://doi.org/10.1016/j.tust.2025.106724>
- [14] Liu, X., Liu, Z., Ye, Y., Bai, Y., & Zhu, Y. (2018). Mechanical behavior of quasi-rectangular segmental tunnel linings: Further insights from full-scale ring tests. *Tunnelling and Underground Space Technology*, 79, 304-318. doi:<https://doi.org/10.1016/j.tust.2018.05.016>
- [15] Liu, X., Liu, Z., Yuan, Y., & Zhu, Y. (2018). Quasi-Rectangular Shield Tunneling Technology in the Ningbo Rail Transit Project. In *High Tech Concrete: Where Technology and Engineering Meet* (pp. 2765-2773): Springer.
- [16] Liu, X., Ye, Y., Liu, Z., & Huang, D. (2018). Mechanical behavior of Quasi-rectangular segmental tunnel linings: First results from full-scale ring tests. *Tunnelling and Underground Space Technology*, 71, 440-453. doi:<https://doi.org/10.1016/j.tust.2017.09.019>
- [17] Liu, X., Zhang, Y., Bao, Y., & Song, W. (2022). Investigation of the structural effect induced by stagger joints in segmental tunnel linings: Numerical explanation via macro-level structural modeling. *Tunnelling and Underground Space Technology*, 120, 104284. doi:<https://doi.org/10.1016/j.tust.2021.104284>
- [18] Liu, Z., Cao, B. T., Xu, C., Liu, X., Yuan, Y., & Meschke, G. (2025). Mechanics of longitudinal joints in segmental tunnel linings: Role of connecting bolts. *Tunnelling and Underground Space Technology*, 161, 106601. doi:<https://doi.org/10.1016/j.tust.2025.106601>



- [19] Liu, Z., Liu, X., Alsahly, A., Yuan, Y., & Meschke, G. (2025). Mechanics of longitudinal joints in segmental tunnel linings: A semi-analytical approach. *Tunnelling and Underground Space Technology*, 163, 106696. doi:<https://doi.org/10.1016/j.tust.2025.106696>
- [20] Lu, L., Jin, P., Pang, G., Zhang, Z., & Karniadakis, G. E. (2021). Learning nonlinear operators via DeepONet based on the universal approximation theorem of operators. *Nature machine intelligence*, 3(3), 218-229. doi:<https://doi.org/10.1038/s42256-021-00302-5>
- [21] Lu, W., Meng, L., Li, S., Xu, Y., Wang, L., Zhang, P., Dou, S., & Sun, H. (2023). Study on progressive failure behavior and mechanical properties of tunnel arch support structures. *Tunnelling and Underground Space Technology*, 140, 105285. doi:<https://doi.org/10.1016/j.tust.2023.105285>
- [22] Qiu, Y., Hu, X., Walton, G., He, C., He, C., & Ju, J. W. (2021). Full scale tests and a progressive failure model to simulate full mechanical behavior of concrete tunnel segmental lining joints. *Tunnelling and Underground Space Technology*, 110, 103834. doi:<https://doi.org/10.1016/j.tust.2021.103834>
- [23] Soga, K., Chen, Z., Hubbard, P. G., Ford, C., Taha, M. R., Heras Murcia, D., Tang, P., Glisic, B., Ozbulut, O., & Lu, N. (2025). Evaluating Contributions of Emerging Technologies to Civil Infrastructure System Resilience. II: Case Studies. *ASCE-ASME Journal of Risk and Uncertainty in Engineering Systems, Part A: Civil Engineering*, 11(3), 04025032. doi:<https://doi.org/10.1061/ajrua6.rueng-1495>
- [24] Wu, Y., Crawford, J. E., & Magallanes, J. M. (2012). *Performance of LS-DYNA concrete constitutive models*. Paper presented at the 12th International LS-DYNA users conference.
- [25] Xu, C., Cao, B. T., Yuan, Y., & Meschke, G. (2023). Transfer learning based physics-informed neural networks for solving inverse problems in engineering structures under different loading scenarios. *Computer Methods in Applied Mechanics and Engineering*, 405, 115852. doi:<https://doi.org/10.1016/j.cma.2022.115852>
- [26] Xu, C., Cao, B. T., Yuan, Y., & Meschke, G. (2024). A multi-fidelity deep operator network (DeepONet) for fusing simulation and monitoring data: Application to real-time settlement prediction during tunnel construction. *Engineering Applications of Artificial Intelligence*, 133, 108156. doi:<https://doi.org/10.1016/j.engappai.2024.108156>
- [27] Xu, C., Liu, Z., Cao, B., Meschke, G., & Liu, X. (2024). *Multifidelity operator learning for predicting displacement fields of tunnel linings under external loads*. Paper presented at the IOP Conference Series: Earth and Environmental Science.
- [28] Yuan, Q., Liang, F., & Fang, Y. (2021). Numerical simulation and simplified analytical model for the longitudinal joint bending stiffness of a tunnel considering axial force. *Structural Concrete*, 22(6), 3368-3384. doi:<https://doi.org/10.1002/suco.202000796>
- [29] Zhang, J.-L., Yuan, Y., Liu, X., Mang, H. A., & Pichler, B. L. (2023). Quantification of the safety against groundwater ingress through longitudinal joints of segmental tunnel linings by means of convergences. *Tunnelling and Underground Space Technology*, 136, 105102. doi:<https://doi.org/10.1016/j.tust.2023.105102>
- [30] Zhang, W., Liu, X., Liu, Z., Zhu, Y., Huang, Y., Taerwe, L., & De Corte, W. (2022). Investigation of the pressure distributions around quasi-rectangular shield tunnels in soft soils with a shallow overburden: A field study. *Tunnelling and Underground Space Technology*, 130, 104742. doi:<https://doi.org/10.1016/j.tust.2022.104742>
- [31] Zhang, X., Zhu, H., Jiang, X., & Broere, W. (2024). Distributed fiber optic sensors for tunnel monitoring: A state-of-the-art review. *Journal of Rock Mechanics and Geotechnical Engineering*. doi:<https://doi.org/10.1016/j.jrmge.2024.01.008>
- [32] Zhao, H., Liu, X., Bao, Y., & Yuan, Y. (2017). Nonlinear simulation of tunnel linings with a simplified numerical modelling. *Structural Engineering and Mechanics*, 61(5), 593-603. doi:<https://doi.org/10.12989/sem.2017.61.5.593>

## COMPRESSED AIR ENERGY STORAGE (CAES) SYSTEM IN ARTIFICIAL UNDERGROUND CAVERNS WITHIN ROCK SALT FORMATION OF MONOLITHI, IOANNINA, GREECE.

Konstantinos Bampousis<sup>1,2</sup>, Ioannis Vlachogiannis<sup>1,2</sup>, Andreas Benardos<sup>1</sup>

**Abstract:** Compressed Air Energy Storage (CAES) is emerging as a strategic solution to address the increasing need for scalable, long-duration energy storage in systems with high renewable penetration. As Greece transitions toward decarbonized electricity networks, the Monolithi site in Ioannina offers a unique opportunity to develop the country's first underground CAES system using naturally sealed salt formations. This study evaluates the feasibility, design optimization, and long-term geomechanical stability of artificial spherical storage caverns within the halite deposit, which lies at a depth of approximately 150 m and exhibits high cohesion and low permeability.

The geological and geotechnical assessment was conducted using historical data from Hellenic Survey of Geology & Mineral Exploration (HSGME), followed by 2D and 3D numerical analyses to assess the optimal design of the complex and to evaluate its performance in the construction and operation phase, in terms of stability. This optimization in the design started from a simplistic layout of 2 main caverns and finally progressed in the suggestion of a 3-cavern layout that allowed for an increased capacity, ensuring the feasibility of the project. At the same time the analysis verified the stability of the cavern structures at all construction and operating conditions, with limited plastic zone development and displacements. More particularly, the 3D numerical analyses confirmed the optimal caverns' spatial configuration and insights were attained for all important effects, such as surface uplift and stress redistribution near cavern boundaries, validating the benefits of internal pressurization. The system remained structurally stable with all strength factors exceeding safety thresholds - even under a full cyclic pressure range (0-6-0 MPa).

Thermodynamic calculations estimate an energy potential of 150 MWh per cycle, translating to up to 30 GWh/year under modern round-trip efficiency assumptions (70%) and 300 annual cycles. The initial CAPEX is estimated between 19,5–29,3 million EUR, indicating that the Monolithi CAES system could represent a cost-effective, spatially flexible alternative to pumped hydro storage. This research demonstrates the critical role of 3D numerical modeling in design validation and highlights the strategic importance of such infrastructure in supporting Greece's renewable integration and compliance with EU decarbonization objectives.

**Keywords:** CAES, Salt Caverns, 3D Numerical Modeling, Energy Storage, Greece Energy Transition

### 1. INTRODUCTION

The global shift toward renewable energy has accelerated the need for robust, long-duration energy storage systems capable of balancing intermittent generation and ensuring grid stability. Technologies such as Compressed Air Energy Storage (CAES) are gaining renewed attention due to their scalability, longevity, and compatibility with underground geological formations. In contrast to lithium-ion batteries or pumped hydroelectric storage, CAES systems offer a cost-effective solution particularly well-suited for regions with suitable subsurface conditions, such as halite (rock salt) formations.

<sup>1</sup> National Technical University of Athens, School of Mining & Metallurgical Engineering, Athens, GR15780, Greece

<sup>2</sup> Geomine J&K, Athens, GR14451, Greece

In the European Union, and particularly in Greece, the integration of wind and solar power has led to increasing instances of overgeneration and curtailment. These developments highlight an urgent need for storage technologies capable of absorbing excess energy during off-peak periods and releasing it when demand surges. Recognizing this, the European Commission has identified underground storage—including CAES—as a key enabler of the EU’s climate-neutral energy system objective by 2050 [European Parliament, 2020].

Salt formations, with their high sealing capacity, low permeability, and favorable ductile behavior under stress, offer ideal conditions for CAES cavern development. In northwestern Greece, the Monolithi area presents a notable geological opportunity: a thick halite dome, previously studied by the Hellenic Survey of Geology & Mineral Exploration (HSGME) [21] [14], that may support the development of the country’s first underground energy storage system of this type.

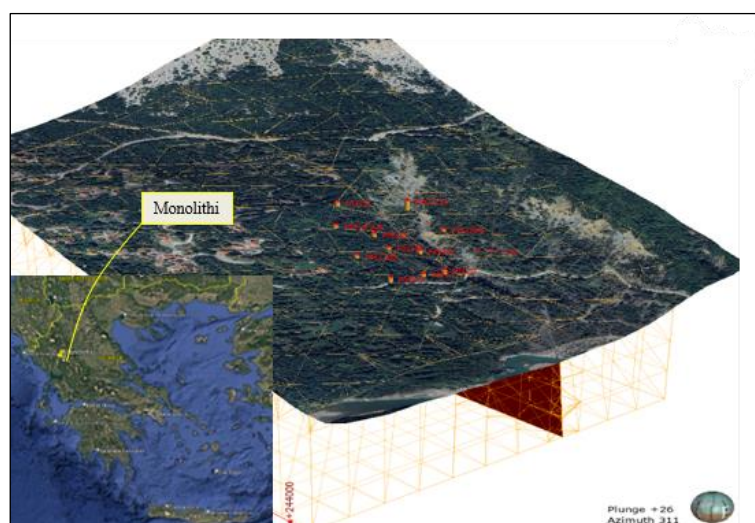
This paper investigates the design and feasibility of an underground CAES system that can be developed in salt caverns at the Monolithi salt deposit. Emphasis is given on the design with the use of advanced 3D finite element modeling (FEM), which enables a more comprehensive assessment of stress interactions, deformation behavior, and operational safety than conventional two-dimensional approaches. The objective is to evaluate whether the proposed cavern design can meet the structural and functional criteria required for safe and efficient operation, while also establishing a replicable model for Greece’s energy transition aligned with European Union directives on renewable integration and energy resilience. Finally, an assessment of its feasibility is given, to bear in mind the required CAPEX expenditure as well as the benefits of the energy storage that can be offered by the underground CAES project.

## 2. THEORY AND NUMERICAL METHODS USED

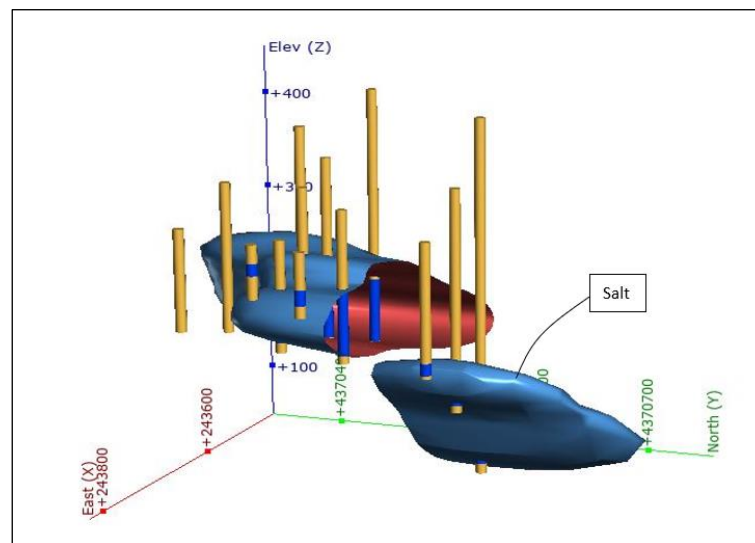
This study assesses the feasibility and geomechanical stability of a Compressed Air Energy Storage (CAES) system in artificial underground salt caverns at the Monolithi site, Ioannina, Greece. The methodological approach combines geological modeling, empirical assumptions, and numerical analyses to evaluate the performance of the system under various operational pressures.

### 2.1. Geological and Geotechnical Data Collection

The geological characterization of the study area was based on historical data from the HSGME [15], including borehole logs, geological investigations, stratigraphy, and geophysical investigations conducted in the 1970s as shown in Figure 1. The predominant geological formation in the area is flysch, a low-permeability, mechanically heterogeneous sedimentary sequence that serves as the host rock. Within this formation, a dome-shaped halite body has intruded, forming a structurally confined salt deposit with an estimated thickness of approximately 90 m, suitable for underground storage applications. The salt deposit was modeled in 3D using Leapfrog Geo as illustrated in Figure 2, with inferred geometry calibrated through interpretation of available borehole information and structural data. Due to the lack of georeferenced borehole coordinates, spatial uncertainty was acknowledged and addressed through conservative modeling assumptions.



**Figure 1.** Location of the Monolithi area and presentation of boreholes investigation layout (HSGME, 1996).



**Figure 2.** Three-dimensional geological mapping of the rock salt deposit in the Monolithi area based on existing boreholes.

## 2.2. Material Properties and Assumptions

Mechanical and physical properties of halite and surrounding flysch were derived from international literature and similar geological settings. For halite, typical values from the Klodawa, Poland [9] formation were adopted. Flysch properties were referenced from the Driskos tunnel study [22], as it closely resembles the local formation characteristics. In Table 1, these data are given as range values along with the finally selected design values for the project.

**Table 1.** Characteristic Mechanical and Physical Properties of Rock Salt (Source: Kolano et al., 2024).

Properties	Range	Design value
Poisson ratio, $\nu$	0,04 – 0,49	0,35
Unit weight, $\gamma$ (kN/m <sup>3</sup> )	28,4-22,5	21
Geological Strength Index, GSI	-	80*
Uniaxial compressive strength, $\sigma_{ci}$ (MPa)	2,80 – 34,20	20
Young Modulus, $E_i$ (GPa)	10 - 30	20
$m_i$	-	11
$m_b$	-	5.3
$s$	-	0,108
$a$	-	0,50
Deformation Modulus, $E_{rm}$ (GPa)	0,4 – 4,9	3,5

\*Intact rock salt formation with very good to good joint surface conditions.

**Table 2.** Characteristic Mechanical and Physical Properties of Flysch (Source: Vlachopoulos et al., 2013).

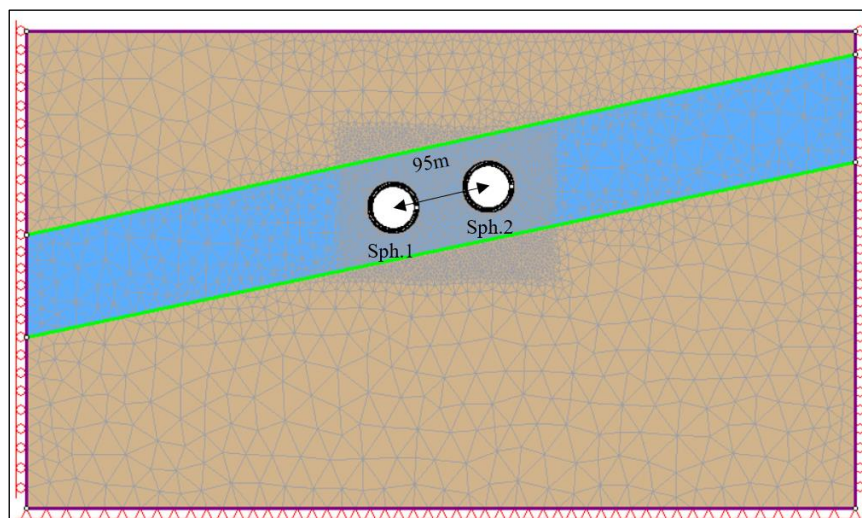
Properties	Design Value
Poisson ratio ( $\nu$ )	0,25
Unit weight, $\gamma$ (kN/m <sup>3</sup> )	27 kN/m <sup>3</sup>
Geological Strength Index, GSI	31–40 (mean value: 35)
Uniaxial compressive strength, $\sigma_{ci}$ (MPa)	26,25
Young modulus, $E_i$ (GPa)	13,453
$m_i$	8
$m_b$	0,76
$s$	0,00073
$a$	0,52
Deformation Modulus, $E_{rm}$ (GPa)	1,5

### 2.3. Geometry and model setup

The geometric layout of the underground compressed air energy storage (CAES) system evolved through successive 2D & 3D numerical analyses. In the initial phase, a 2D plane strain model was developed using Rocscience RS2 software. The authors acknowledge the inherent limitation of 2D FEA in accurately representing a pair of ideally spherical caverns, as it simulates the behavior of infinitely long tunnels. Nevertheless, this approach was intentionally selected as a starting point for the present investigation.

Moreover, spherical cavern geometry was selected due to its effectiveness attaining a favorable pressure distribution in the salt formation. Furthermore, this achieves a robust buffer zoning between the caverns and the boundaries of the salt formation. Several sizing and spacing scenarios were examined to prevent interaction between the caverns and ensure stable conditions. The 2D analysis results indicated the setup of two spherical caverns with a diameter of 45 m and 95 m distance center-to-center, satisfying the criteria for acceptable strength factor, limited displacements and plastic zone as shown in Figure 3.

To improve spatial setup and account for a much more realistic approach, a 3D finite element model (Figure 4) was developed using Rocscience RS3 software, validating the two cavern-configuration derived from the 2D analysis. Building on the results, a third spherical cavern with a diameter of 45 m was introduced to further optimize the use of the available salt volume and increase the capacity of the complex. The three caverns were arranged in an equilateral triangular pattern with 60° angular spacing and center-to-center distances reduced to 80 m. This arrangement was specifically chosen to evaluate the structural integrity and performance of the underground project, checking and evaluating potential interactions between the cavern structures.



**Figure 3.** 2D model setup and generated mesh for FEA.



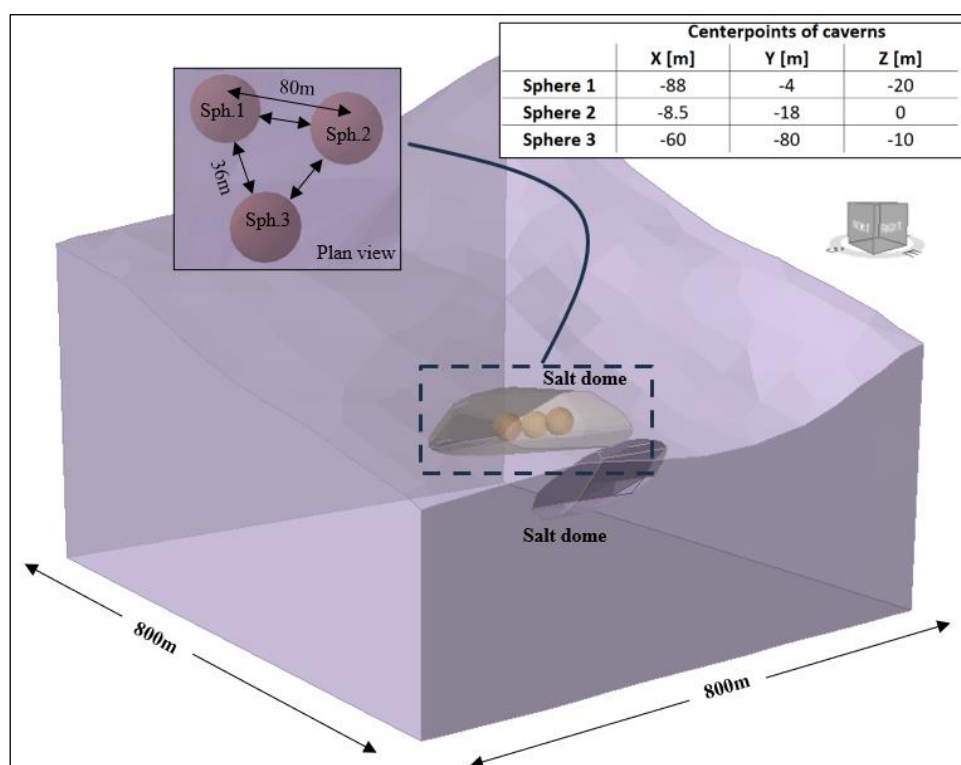


Figure 4. 3D model setup for FEA.

In both 2D and 3D analysis, the gravity type stress condition was selected to simulate the in-situ field stress, with a horizontal to vertical stress ratio,  $k$  ( $\sigma_h/\sigma_v$ ) set to 1. The material behavior was modeled as a least – perfect plastic, using the Generalized Hoek–Brown constitutive criterion.

The boundary conditions were defined such as that the base of the model was fully constrained in all directions, while the lateral boundaries were restricted only in the horizontal direction, allowing free vertical movement. In the 2D analysis a graded mesh composed of 3-noded triangular elements was employed, resulting in approximately 10.000 elements for accurate resolution of stress and displacement fields around the cavern boundaries, while a refinement area (200m x 150m) with a uniform 5m element length was applied to achieve more accurate and detailed results around the caverns. In the 3D analysis a graded mesh of 4-noded tetrahedral elements was applied, resulting in the generation of more than 400.000 elements (Figure 5).

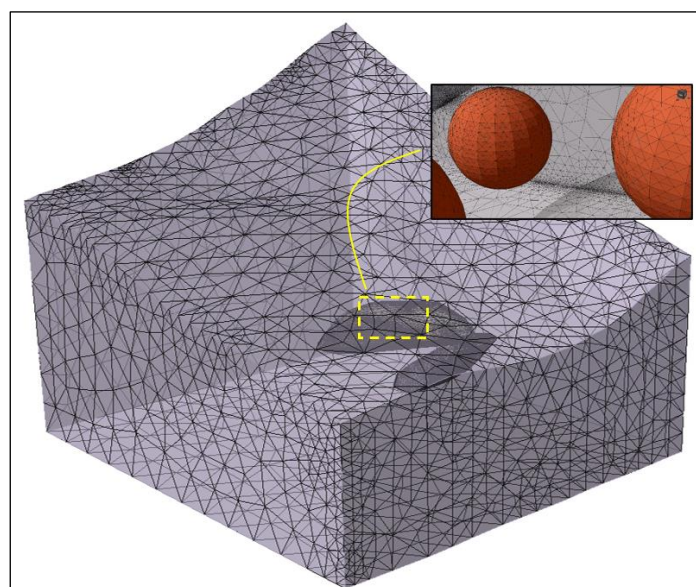


Figure 5. Generated mesh for 3D FEA.



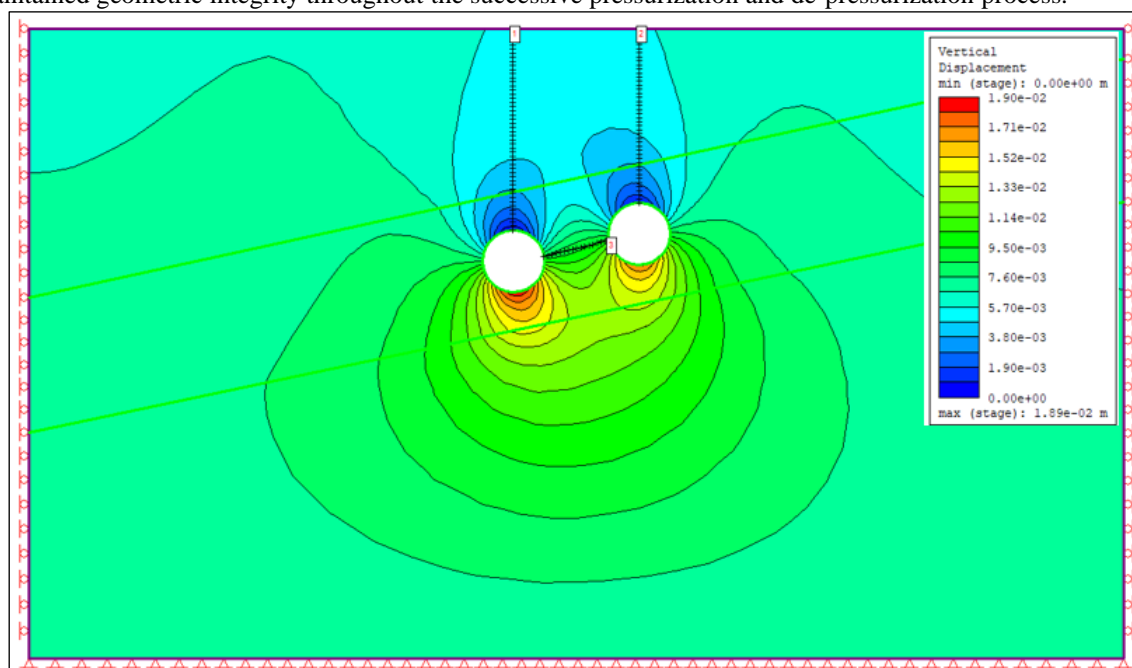
The loading sequence applied in both 2D, and 3D numerical models was modelled to replicate a full operational cycle of a CAES system, including both charging (pressurization) and discharging (depressurization) phases. Initially, the caverns were simulated in an unpressurized state immediately following excavation, representing zero internal pressure. Subsequently, internal pressure was incrementally increased in steps of 0,8 MPa, up to a maximum operational pressure of 6,0 MPa. After reaching the peak pressure, the system was gradually unloaded following the same stepwise pattern—decreasing the internal pressure by 0,8 MPa per stage until it returned to 0 MPa. This symmetric pressure path allowed for the evaluation of the geomechanical response of the surrounding rock mass under cyclic loading-unloading, including stress redistribution, development of plastic zones, and potential residual deformations induced by the pressure reversals.

### 3. RESULTS

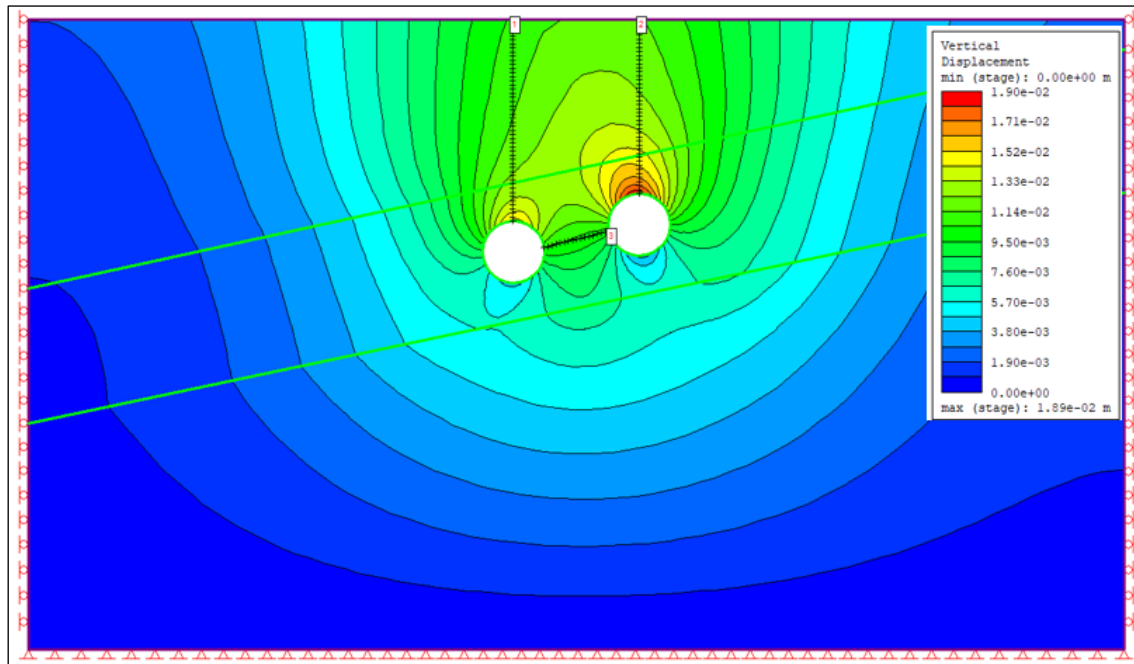
The results of the analysis are given hereinafter. The primary objective is to assess the geomechanical stability and performance of the proposed CAES cavern configurations under internal pressure and geostatic stress conditions. Key metrics evaluated include vertical displacements, strength factor (SF) distributions, and plastic zone development, with special emphasis on comparing the behavior observed in 2D versus 3D analyses. The following figures provide a detailed summary of the model geometries, material parameters, and results from each scenario, enabling a direct comparison of performance and recorded deformation specifics between the two modeling approaches.

#### 3.1. 2D Results

The numerical analyses conducted in RS2 revealed limited vertical displacements. During the excavation phase ( $P = 0$  MPa), the maximum surface settlement was recorded at -2 mm, while the vertical displacement at the crown of the cavity reached -10 mm (Figure 6). In the subsequent pressurization phase, 60 bar ( $P = 6,0$  MPa), the displacements increased, as expected: surface rose to +11 mm, and vertical displacement at the crown reached +18 mm (Figure 7). Despite the increase, these values remain within stability thresholds and do not indicate any structural compromise. Overall, the 45 m diameter configuration exhibited predictable deformation behavior and maintained geometric integrity throughout the successive pressurization and de-pressurization process.

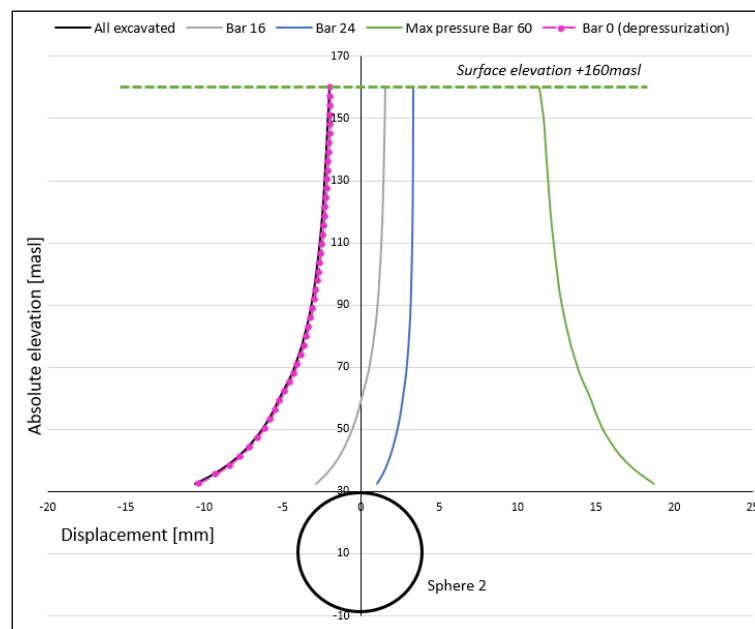


*Figure 6. Vertical displacement after the excavation in the 2D analysis.*



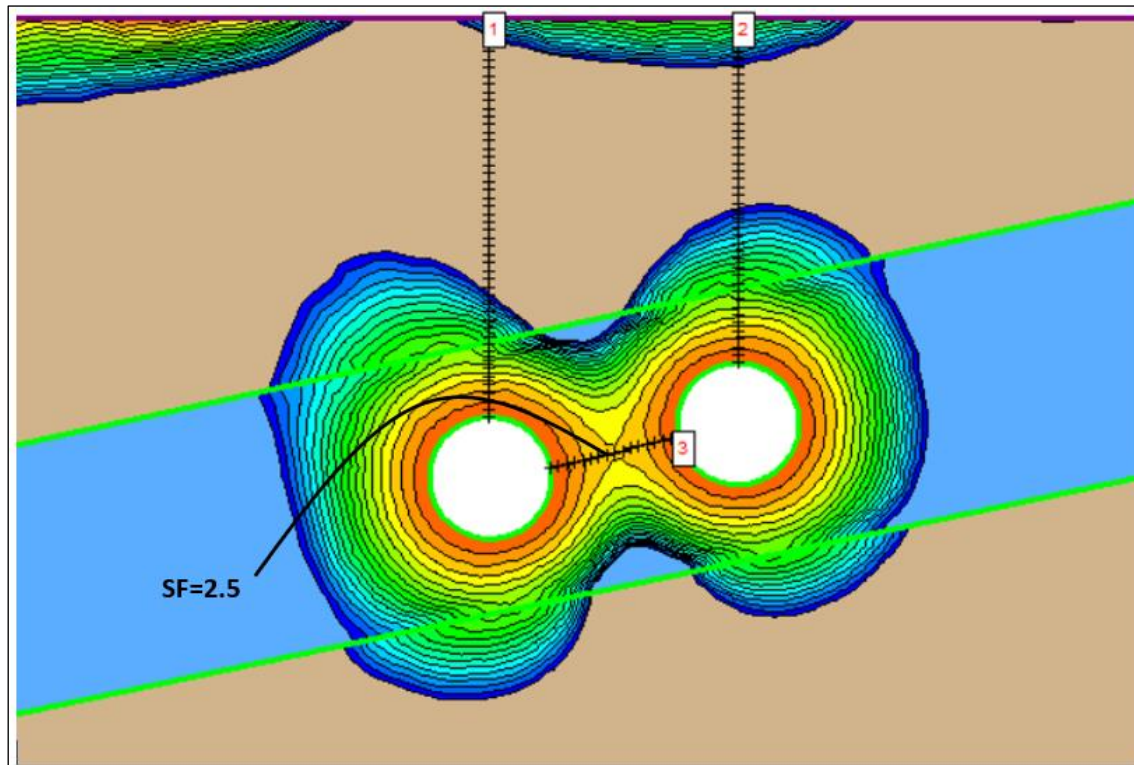
**Figure 7.** Vertical displacement after applying 6Mpa internal pressure in the 2D analysis.

As shown in the corresponding displacement graph (Figure 8), the transition from excavation to maximum pressurization results in a clear uplift pattern above the storage sphere. The plot highlights a reversal in the displacement field from negative (subsidence) to positive (heave) - with the maximum vertical uplift concentrated directly above the crown of sphere 2.

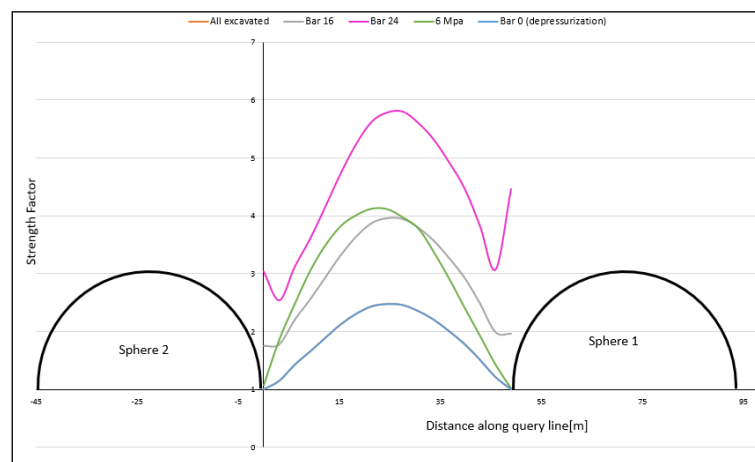


**Figure 8.** Vertical displacement distribution above Sphere 2.

The Strength Factor (SF) between the caverns remains above 1.0 (Figure 9) across all along pillar formed between the two caverns right after the excavation with a narrow plastic zone of 3,0m around the caverns. In Figure 10, the formed pillar consistently remains above stable limits, with the SF above 2.0 in low pressurized state and reaching approximately 4.1 under an internal pressure of 60 bar (6,0Mpa).



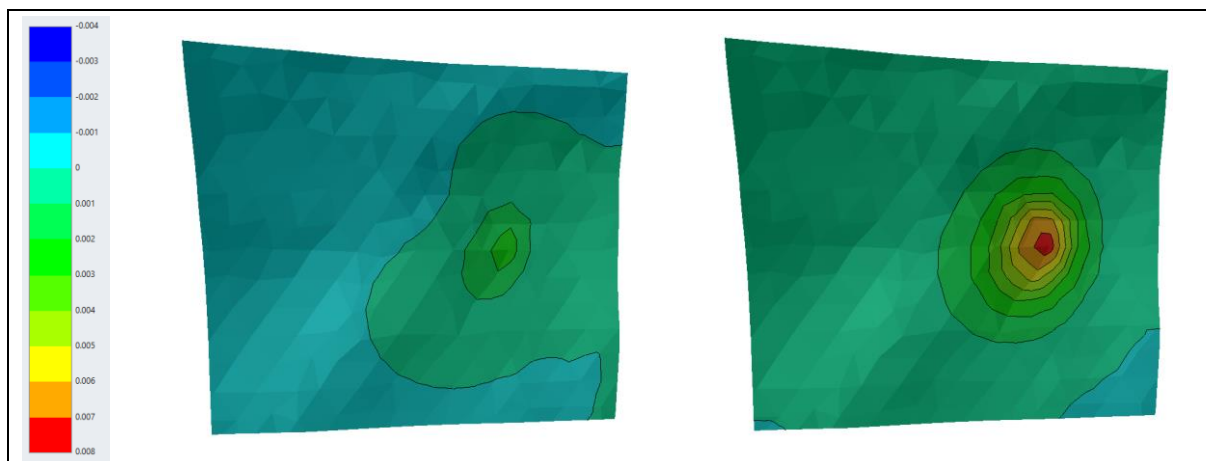
**Figure 9.** Strength factor between caverns (stage: all caverns excavated).



**Figure 10.** Strength factor along the query line between the caverns.

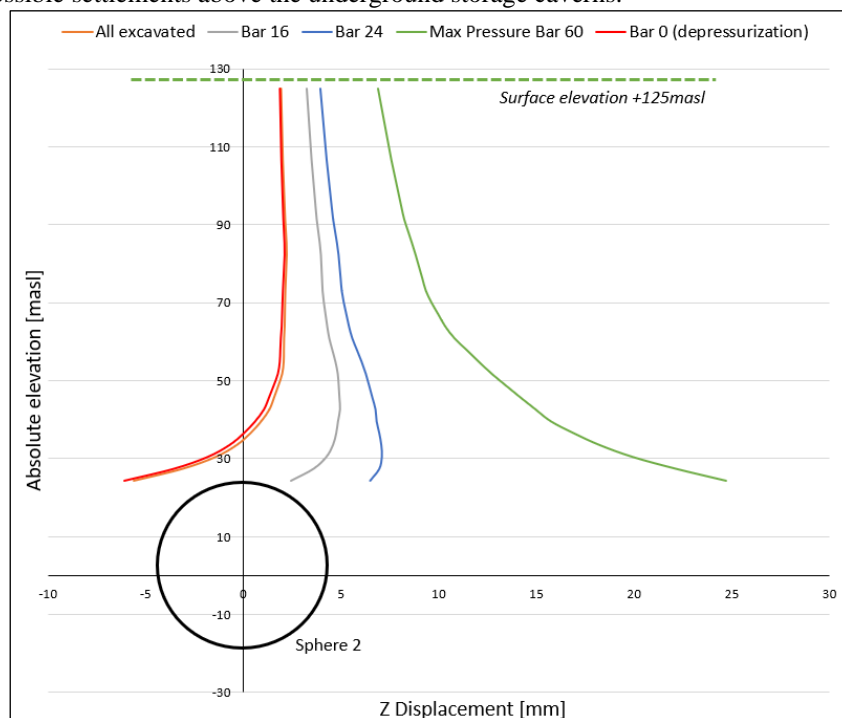
### 3.2. 3D Results

The vertical displacement as imposed on the surface area is given in Figure 11, with a contour interval of 1 mm. On the left, the surface deformation is shown after the full excavation of all caverns, where a localized settlement zone is observed directly above the caverns, with maximum vertical displacements reaching approximately  $-2$  mm. In contrast, on the right, it highlights the effect of internal pressurization at 60 bars. The ground surface directly above the cavern experiences a small uplift, with peak vertical displacements reaching up to 7-8 mm. This behavior illustrates the interplay between excavation-induced subsidence and pressure-induced uplift phenomena. The analysis confirms that internal pressurization substantially mitigates surface settlement and can even result in net uplift—an effect that is crucial for maintaining the stability of surface infrastructure in CAES operations.

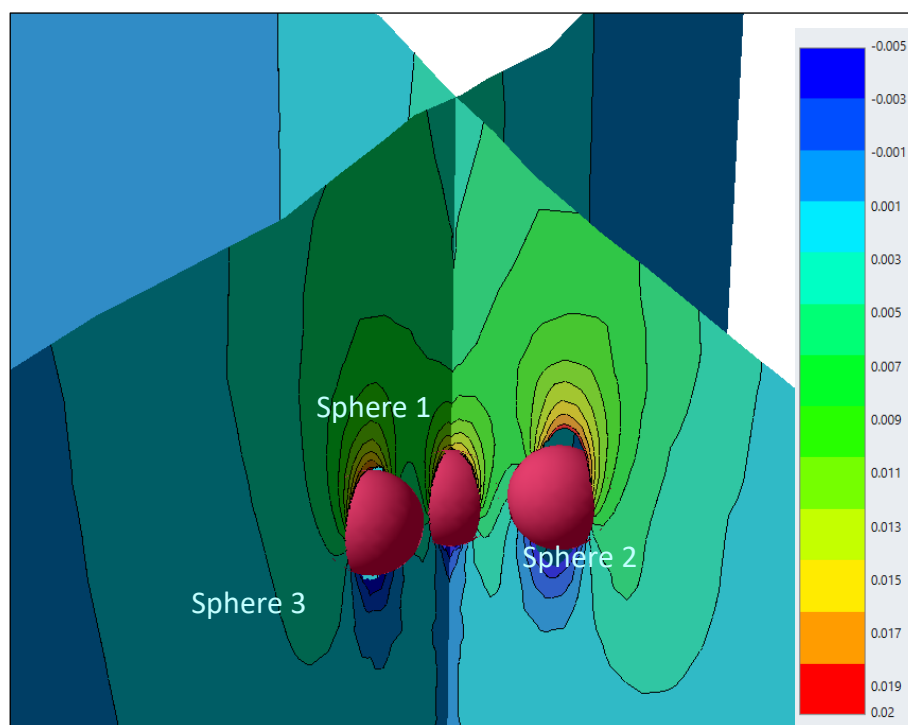


**Figure 11.** Vertical displacement contours on surface with 1mm interval (left: after excavation; right: at operational phase with a max pressure of 60 bar (6 MPa)).

Vertical displacements occurring directly above Sphere 2, from the cavern crest up to the ground surface at +125 masl, are presented in Figure 12 and Figure 13. The profile illustrates how the rock mass responds to excavation and internal pressurization. Following full excavation, the zone above the cavern undergoes measurable subsidence, with downward displacements reaching approximately 6mm near the cavern roof and gradually decreasing toward the surface. As internal pressure increases, this trend is reversed. At the maximum internal pressure of 60 bars, a distinct uplift develops in the same zone (green curve), with vertical displacements exceeding +24 mm at the cavern roof and remaining noticeable up, approximately +7 mm at the ground surface. This behavior highlights the sensitivity of the overburden to internal pressure changes and emphasizes the role of pressurization in controlling possible settlements above the underground storage caverns.



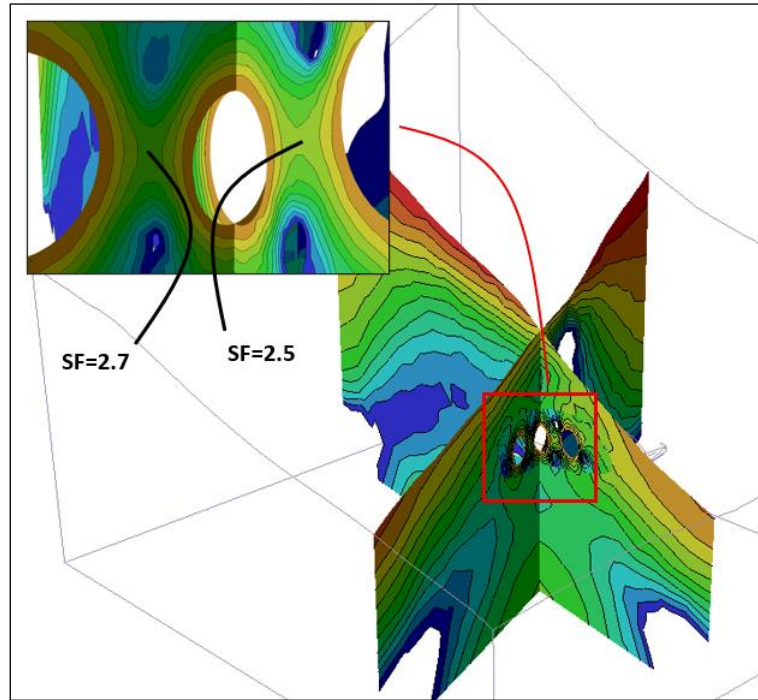
**Figure 12.** Vertical displacement distribution above Sphere 1.



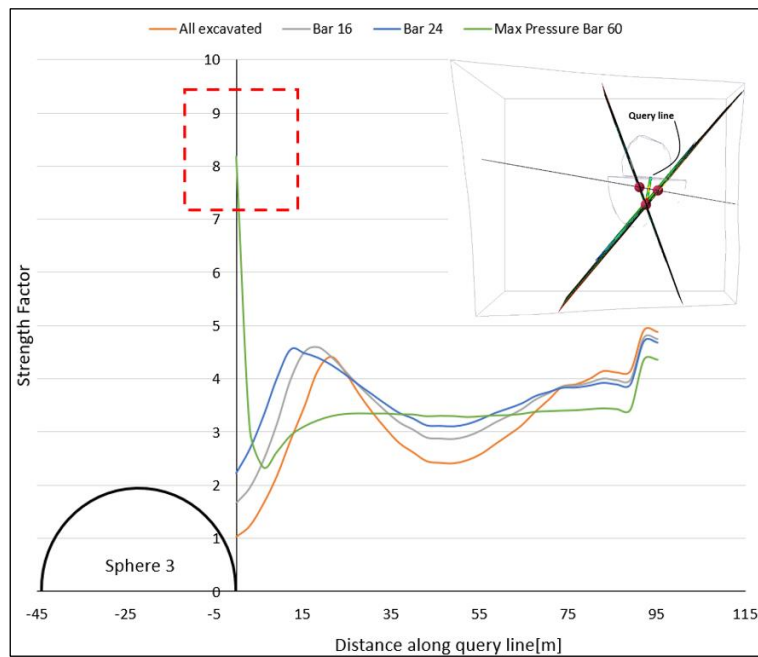
**Figure 13.** Vertical displacements at the underground cavern complex (stage: max pressure, 60bar).

The strength factor (SF) distribution in the region between the caverns after the full excavation stage is presented in Figure 16. The 3D contour plot reveals that the maximum SF values range from 2,5 to 2,7 (Figure 14).

An accompanying graph shown in Figure 15 illustrates how the strength factor (SF) varies along a horizontal line that passes through the rock pillar between caverns, starting at Sphere 3 and moving toward and between Spheres 1 and 2. It shows how excavation and different internal pressure levels affect the stability of the surrounding rock. Specifically, when all caverns are excavated without any internal pressure, the SF drops to a minimum of just above 1,0 immediately adjacent to Sphere 3, indicating the plastic zone formed around the underground opening. As the distance from the cavern increases and the line approaches the central region between the three spheres, i.e. within the core of the inter-cavern pillar, the SF rises reaching a maximum of approximately 4,5 (for stage: 24 bars). However, under the maximum internal pressure of 60 bars (6 MPa), a markedly different trend emerges: the SF elevates to values above 8 right next to the cavern wall because of internal pressure, and then gradually settles to uniform values of 3,3 along the central part of the pillar. This reversal of the typical SF gradient highlights the strong influence of high internal pressure in improving local stability around the openings. The mechanism behind the increase of the SF lies in the lateral forces imposed through the air pressure in the cavern that provides a significant  $\sigma_3$  stress regime that increases the ultimate strength of the pillar between caverns.



**Figure 14.** Strength factor contours and values at regions between caverns (stage: all caverns excavated).



**Figure 15.** Strength factor along query line extending through the enclosed pillar (surrounded by the three caverns).

### 3.3. Thermodynamic Estimation of Recoverable Energy

The thermodynamic assessment of the theoretical energy output that can be recovered from the CAES scheme is crucial for the assessment of the overall feasibility of the storage project. The preliminary approach presented in this section is based on principal thermodynamic equations that describe the adiabatic expansion of an ideal gas:

$$W = \frac{nRT}{\gamma - 1} \left[ 1 - \left( \frac{P_i}{P_f} \right)^{\frac{\gamma-1}{\gamma}} \right] \quad (1)$$



Where:

- W: Total mechanical energy recovered (Joules)
- n: Number of moles of air in the reservoir
- R: Specific gas constant for air (287 J/kg·K)
- T: Absolute temperature (Kelvin)
- $\gamma$ : Adiabatic expansion coefficient ( $\gamma = 1,4$  for air)
- $P_1, P_2$ : Initial and final pressure (Pa)

Each storage unit (cavern) is a sphere with a diameter of 45 m, resulting in an individual volume of:

$$V = \frac{4}{3}\pi R^3 = 47,713 \text{ m}^3$$

Other assumptions of the project are:

- Temperature:  $T = 300 \text{ K}$
- Initial pressure:  $P_1 = 6,0 \cdot 10^6 \text{ Pa}$
- Final pressure:  $P_2 = 1,5 \cdot 10^6 \text{ Pa}$
- Number of spheres: 3

The number of moles stored in each cavern is given by:

$$n = \frac{P_i \cdot V}{R \cdot T} \quad (2)$$

where V is the volume of the storage cavern. Finally, the conversion of the energy result from Joules to megawatt-hours is performed using:

$$E_{\text{MWh}} = \frac{W}{3,6 \cdot 10^9} \quad (3)$$

Using Equation (2), the number of moles of air per cavern is:

$$n = \frac{6 \times 10^6 \cdot 47,713}{287 \cdot 300} \approx 3.324.943 \text{ mol}$$

$$W = \frac{3.324.943 \cdot 287 \cdot 300}{0,4} \left[ 1 - \left( \frac{1,5 \times 10^6}{6,0 \times 10^6} \right)^{0,286} \right]$$

$$W \approx 715,693 \cdot 10^9 \cdot (1 - 0,673) \approx 234 \cdot 10^9 \text{ J}$$

Applying Equation (3) the storage of energy (E) can be estimated as:

$$E = \frac{234 \cdot 10^9}{3,6 \cdot 10^9} \approx 65 \text{ MWh per cavern}$$

Thus, the theoretical maximum energy recoverable per full discharge cycle of the entire CAES project (three caverns) it can be estimated that as  $E_{\text{project}} = 195 \text{ MWh}$ . Under a more conservative assumption the CAES project could provide an energy storage capacity of approximately 150MWh.

To assess the practical usability of the system, the theoretical energy output is adjusted based on typical round-trip efficiencies. Two representative scenarios are considered. In the first case, assuming a conservative efficiency of 50%, which is typical for an older CAES installation, the usable energy is calculated as approximately 75 MWh. In the second scenario, assuming a modern CAES system with thermal integration and an efficiency of 70%, the usable energy becomes 100 MWh. With respect to this data assuming 300 full charge–discharge cycles annually, the corresponding annual energy output of the Monolith CAES is approximately between 22 GWh (50% efficiency) and 30 GWh (70% efficiency).

Finally, the installed capacity of the Monolithi CAES can be estimated at 20-35MW given a discharge duration of 3-4 hours and the usable storage capacity of the project ranging between 75 and 100MWh.

#### 4. ECONOMIC ASSESSMENT AND TECHNOLOGY COMPARISON

For the investment cost estimation of the CAES system in Monolithi, Ioannina, the basis is the cost range found in the international literature, which indicates that the capital expenditure (CAPEX) for compressed air energy storage projects ranges from €100 to €150 per kWh. Given that the total storage capacity of the proposed project is 150 MWh, the total CAPEX ranges between €19,5 million and €29,3 million, depending on the compressor technology, the geological configuration of the underground space, and the system's energy efficiency. In contrast, for the pumped hydro storage project that is under construction in Amfilochia a major energy storage project in Greece—the total investment cost amounts, to €650 million for a storage capacity of 8.000 MWh according to Terna Energy [20]. This translates to approximately €81,25 per stored kWh. The OPEX of the Monolithi CAES project, based data from [12] can be estimated at approximately €20/MWh, indicating a promising investment opportunity.

The installation of a small or medium-scale CAES energy storage system, such as the one proposed for Monolithi in Ioannina, is particularly advantageous in cases where there is a need for local energy autonomy and improved power quality in peripheral or isolated grids. Such units are ideal for supporting local industrial loads, agricultural grids, or small residential communities, with the capability to provide power during peak demand periods or supply interruptions.

The proposed installation aims to meet local energy demands, especially in areas with increasing penetration of renewable energy sources (RES). The geological suitability of the area, along with the absence of a need for elevation differences or water resources, makes CAES an attractive alternative to pumped hydro storage.

#### 5. DISCUSSION

The results of this study confirm the technical feasibility of implementing a Compressed Air Energy Storage (CAES) system in artificial underground salt caverns at the Monolithi site. While 2D simulations provided a solid initial assessment, the implementation of 3D modeling proved essential in capturing complex spatial interactions between adjacent caverns, more realistic deformation patterns, and surface uplift due to internal pressurization. These phenomena underline the dual role of internal pressure—not only for energy storage but also for mitigating excavation-related deformations—reinforcing the importance of pressurization control in system design and operation.

Importantly, this study builds upon international experience (e.g., Huntorf and McIntosh plants) while adapting the CAES concept to the Greek geological context. To date, halite formations in Greece have not been utilized for subsurface energy storage. The Monolithi salt dome thus emerges as a promising candidate for pilot implementation, potentially setting a precedent for similar projects across Southern Europe.

Nevertheless, it must be emphasized that several simplifications were made in the current design (creep behavior, seasonal thermal fluctuations, etc.). The uncertainty associated with the above should be efficiently addressed by an investigation campaign that will provide all the required information.

#### 6. CONCLUSION

The implementation of three-dimensional (3D) numerical modeling proved essential in accurately evaluating the structural integrity and performance of the proposed CAES system in the Monolithi salt dome. While 2D simulations offered a useful preliminary assessment, the 3D finite element analysis could fully capture the spatial interactions between caverns, the redistribution of stress fields, and the resulting displacements at the ground surface, offering a significant advantage in the overall spatial optimization of the designated caverns. The 3D results highlighted critical phenomena such as uplift due to internal pressurization and stress relief near cavern wall, features that are key to long-term operational safety that cannot be assessed in 2D-models in a sufficient manner.

This study represents a pioneering step for Greece in exploring the application of underground energy storage technologies that are already proven in Central and Northern Europe. The Monolithi site offers a geological opportunity to align national infrastructure development with European Union priorities for clean, decentralized energy systems. As Greece works to meet its commitments under the EU Green Deal and Fit-for-55 targets, modular CAES installations such as the one proposed here could play a vital role in increasing grid resilience, reducing curtailment of renewable sources, and ensuring energy autonomy for peripheral and rural regions.

In this context, the Monolithi CAES project is more than a technical proof of concept; it is a strategic initiative that embodies the transition toward a decarbonized, flexible, and future-ready energy system anchored not only in sound engineering, but also in alignment with European environmental and energy policies.

## 7. BIBLIOGRAPHY

- [1] Adiabatic Compressed Air Energy Storage. (n.d.). [www.ease-storage.eu](http://www.ease-storage.eu).
- [2] Bauer, S. J., Song, B., & Sanborn, B. (2019). Dynamic compressive strength of rock salts. *International Journal of Rock Mechanics and Mining Sciences*, 113, 112–120. <https://doi.org/10.1016/j.ijrmms.2018.11.004>.
- [3] Caglayan, D. G., Weber, N., Heinrichs, H. U., Linßen, J., Robinius, M., Kukla, P. A., & Stolten, D. (2020). Technical potential of salt caverns for hydrogen storage in Europe. *International Journal of Hydrogen Energy*, 45(11), 6793–6805. <https://doi.org/10.1016/j.ijhydene.2019.12.161>.
- [4] Chen, H., Cong, T. N., Yang, W., Tan, C., Li, Y., & Ding, Y. (2009). Progress in electrical energy storage system: A critical review. In *Progress in Natural Science* (Vol. 19, Issue 3, pp. 291–312). Science Press. <https://doi.org/10.1016/j.pnsc.2008.07.014>.
- [5] Davidson, B., Glendenning, I., Harman, R., & Hart, A. (1980). Large-scale electrical energy storage.
- [6] Diabatic Compressed Air Energy Storage. (n.d.). [www.ease-storage.eu](http://www.ease-storage.eu).
- [7] European Parliament, C. 371/08. (2020). A comprehensive European approach to energy storage (2019/2189(INI)) (2021/C 371/08).
- [8] Kendall Mongird, Vilayanur Viswanathan, Patrick Balducci, Jan Alam, Vanshika Fotedar, Vladimir Koritarov, Boualem Hadjerioua (2020). An Evaluation of Energy Storage Cost and Performance Characteristics. *Energies*. 13. 3307. doi:10.3390/en13133307.
- [9] Kolano, M., Cała, M., & Stopkiewicz, A. (2024). Mechanical Properties of Rock Salt from the Kłodawa Salt Dome—A Statistical Analysis of Geomechanical Data. *Materials*, 17(14). <https://doi.org/10.3390/ma17143564>.
- [10] Kuczyński, S., Skokowski, D., Włodek, T., & Polański, K. (2015). Compressed air energy storage as backup generation capacity combined with wind energy sector in Poland - implementation possibilities. *AGH Drilling, Oil, Gas*, 32(1), 23. <https://doi.org/10.7494/drill.2015.32.1.23>.
- [11] Marcus N. (2006). Compressed Air Energy Storage (CAES) 10\_2006.
- [12] Mountrakis, Dimosthenis. (2010). *Geology and Geotectonic Evolution of Greece*. University Studio Press.
- [13] Nikolaou, Evangelos (2010, IGME). Update of Groundwater Data in Epirus.
- [14] Papanikolaou, Nikolaos. (1978, IGME). Geophysical Reconnaissance Survey for Rock Salt Exploration in the Areas: (a) Monolithi, Ioannina and (b) Karydea, Arta.
- [15] Papastavrou, St. (1978, IGME). Report on the 1977 Investigation Activities for the “Rock Salt of Monolithi” Project.
- [16] Safaei, H., Keith, D. W., & Hugo, R. J. (2013). Compressed air energy storage (CAES) with compressors distributed at heat loads to enable waste heat utilization. *Applied Energy*, 103, 165–179. <https://doi.org/10.1016/j.apenergy.2012.09.027>.
- [17] Shabbir Ahmed A, Patrick J. Balducci, A. & Daniel L. Flowers, L. (2023). Technology Strategy Assessment - Compressed Air Energy Storage. <https://www.energy.gov/oe/storage-innovations-2030>.
- [18] Sofianos, Alexandros, & Nomikos, Pavlos. (2008). *Rock Mechanics*. National Technical University of Athens (NTUA).
- [19] Succar, S., & Williams, R. H. (2008). Compressed Air Energy Storage: Theory, Resources, And Applications for Wind Power.
- [20] Terna-Energy (2025) Amfilochia Pumped Storage. Source: <https://www.terna-energy.com/acivities/erga-antlisotamieysis/antlisotamiefsi-amfilochias/> [accessed June 2025].
- [21] Vekios, Pavlos. (1979, IGME). *The Rock Salt of Monolithi, Ioannina*.
- [22] Vlachopoulos, N., Diederichs, M. S., Marinos, V., & Marinos, P. (2013). Tunnel behavior is associated with the weak Alpine rock masses of the Driskos Twin Tunnel system, Egnatia Odos Highway. *Canadian Geotechnical Journal*, 50(1), 91–120. <https://doi.org/10.1139/cgj-2012-0025>.
- [23] Wang, T., Yang, C., Wang, H., Ding, S., & Daemen, J. J. K. (2018). Debrining prediction of a salt cavern used for compressed air energy storage. *Energy*, 147, 464–476. <https://doi.org/10.1016/j.energy.2018.01.071>.

## **TECHNICAL TRACK (TECHNICAL SESSION)**

## APPLICATION OF EMBEDDED FIBER OPTIC IN THE WHOLE PROCESS MONITORING OF CAVERN DEVELOPMENT PROJECT

Yifeng LI<sup>1</sup>, Zhikai WEI<sup>2</sup>, Joseph Z. HONG<sup>3</sup> and Xuefeng LI<sup>4</sup>

**Abstract:** To provide new land supply, the Hong Kong Government issued the Long-term Strategy for Cavern Development, creating space inside mountains for utilizations. To conduct full process rock mass monitoring during the construction and operation stages of super large cavern projects, fiber optic detection was piloted in a certain cavern project in Hong Kong for the first time. The project team designed and installed 17 optical fibers with 2660 sensors around one of the main caverns with a cross-sectional area of nearly 900 square meters. After completion, real-time and continuous rock condition monitoring can be carried out. The installed fibers have a maximum depth of 67 meters, while the on-site conditions are limited with no similar project for reference. To achieve the required monitoring effect without affecting normal construction conditions, optimized design and a series of auxiliary construction methods were implemented. At present, the installed fibers are well protected, operating normally, the data transmission is timely and stable, and provide real-time monitoring and early warning. The fiber optic monitoring method summarized in this article has strong innovation, which has not been studied and applied in the past. practical project verifies that can meet the existing monitoring needs, and has good application in the whole process of cavern development monitoring. Methods summarized in this paper can provide design and construction references for future projects.

**Keywords:** Fiber optic monitoring; Cavern construction; wFBG fiber; Rock mass monitoring; Drill-in fiber design

### 1. INTRODUCTION

Due to the proximity to residential and urban areas, strict safety, environmental, and quality controls are mandated. The use of explosives, stringent blast design standards, and environmental monitoring requirements necessitate advanced instrumentation for stability assessment. Among the monitoring methods deployed, fiber optic detection was implemented for the first time in a main cavern. Existing cases primarily involve surface-mounted fibers on tunnel linings or embedded fibers in concrete, with no prior examples of pre-drilled fiber installation in rock masses for full-process monitoring. Thus, this project represents the first attempt at such an application, with the team developing tailored designs and construction methods.

### 2. SITE CONDITIONS AND FIBER DESIGN

The main cavern monitored measures 91 m long, 32 m wide, and 28 m high. Geological surveys revealed heterogeneous rock masses (Grade II–IV), with localized weathering necessitating robust monitoring. 10 vertical and 7 horizontal fibers were designed to envelop the cavern.

The optical fiber used in the project is a Weak Fiber Bragg Grating (wFBG), with each borehole equipped with four strain-sensing fiber sets and one temperature-sensing fiber set. The wFBG is a specialized fiber grating with extremely low reflectivity (typically < -30dB). Its ultra-low reflection characteristic allows gratings of the same period to penetrate each other, enabling the multiplexing of numerous grating points on a single fiber.

<sup>1</sup> China State Construction Engineering (Hong Kong) Limited, Hong Kong China, E-mail: li\_yf@cohl.com.

<sup>2</sup> China State Construction Engineering (Hong Kong) Limited, Hong Kong China, E-mail: weizhikai@cohl.com

<sup>3</sup> China State Construction Engineering (Hong Kong) Limited, Hong Kong China, E-mail: zhengqiang.hong@cohl.com.

<sup>4</sup> China State Construction Engineering (Hong Kong) Limited, Hong Kong China, E-mail: xuefeng.li@cohl.com.

By arranging multiple conventional Fiber Bragg Grating (FBG) sensors at predefined spatial locations and adopting a serial or other networking topology combined with time-division multiplexing (TDM) technology, a distributed monitoring network system can be established. The strain and temperature sensing performance of wFBG is consistent with that of FBG, offering equivalent measurement accuracy. Multiple gratings with identical periods can be multiplexed on the same fiber, allowing thousands of grating sensing points to be densely inscribed on a single fiber to achieve quasi-distributed intensive monitoring. Additionally, the system features high-speed demodulation capability, supporting real-time testing.

This technology combines the sensing advantages of fiber Bragg gratings with the localization benefits of optical time-domain reflectometry (OTDR), meeting the real-time monitoring requirements of long-distance engineering projects. The wFBG used has a 9.9 mm diameter, 20000  $\mu\epsilon$  measuring range and 5 mm allowable bending radius. The allowable tension exceeds 100 N, elastic modulus below 0.8 GPa and has a strain parameter of 1,183 pm/ $\mu\epsilon$ . The working temperature is between -20 – 80 °C, which can be maintained.

### **3. CONSTRUCTION AND PROTECTION**

The drilling rigs will be deployed on existing berms or relatively flat rock slopes for vertical core drilling. Each platform requires five vertical boreholes, necessitating sequential rig repositioning. A 101 mm diameter borehole design is adopted, utilizing rotary drilling with water jet flushing for cuttings removal. Upon completing vertical drilling, the rig will be hoisted from the berm platforms to the steel scaffolding in front of the cavern for subsequent horizontal drilling and fiber installation. For horizontal drilling operations, it is necessary to construct anti-seismic scaffolding and drilling platforms exceeding 30 meters in height to facilitate the setup of drilling equipment and personnel access. After installation, grouting is performed. A cement slurry with a water-cement ratio of 0.36 is mixed with an appropriate water-reducing admixture. As grouting nears completion, overflow is monitored to ensure complete filling. Sufficient curing time is allowed to achieve full grout consolidation and borehole stabilization.

This project primarily employs the drill-and-blast method for tunnel excavation. During blasting excavation, overbreak must be managed and controlled based on nearby fiber positions to ensure it remains below 300 mm. Given the original 2 m safety distance between fibers and the designed excavation face, the actual excavation face during blasting should maintain at least 1.7 m clearance from the fibers. For temporary support using shotcrete and permanent rock bolts, rock bolt installation risks damaging fibers during drilling into the rock mass. Drilling must avoid areas close to fiber cables, maintaining at least 350 mm offset from fiber positions. Rock bolt drilling angles can be adjusted by 6° to 10° as needed to prevent fiber damage. During forepoling (pipe roof support), no pipe roof drilling should be conducted near fiber locations. During advance probing, probe holes must maintain at least 2 m clearance from fibers. Moreover, no additional drilling or blasting is permitted in non-excavation zones.

### **4. DATA TESTING AND MONITORING**

The fiber optic signal testing procedure consists of the following steps: connecting the optical fiber to the DAU; executing the DAU test program which transmits optical signals and subsequently receives corresponding optical responses. Through this process, the response of each fiber optic sensor can be determined, and its operational status (such as monitoring frequency, signal strength, etc.) can be verified. If all parameters are confirmed to be within normal ranges, the fiber optic signal testing process is considered successful.

During actual monitoring, the sampling frequency can be set as required. Different deformation control standards can be established for various locations, with each fiber optic cable configured with three warning levels: "Alert", "Alarm", and "Action". The project team, referencing relevant standards and through consultation with the owner, determines the three warning threshold values for different fiber optic cables and the specific actions to be taken. Any triggered warning will immediately notify the responsible personnel via the platform or SMS to initiate corresponding actions. The fiber optic monitoring data will be permanently stored in the data collection platform, with weekly and monthly analysis reports generated.

### **5. ACKNOWLEDGMENTS**

This paper is sponsored by the Technology Research and Development Project of China State Construction International Holdings Limited (CSCI-2023-Z-17).



## RESEARCH ON CARBON ACCOUNTING AND LOW-CARBON CONSTRUCTION PATH FOR A SUPER LARGE CAVERN PROJECT IN HONG KONG

Li Yifeng<sup>1</sup>, Yuan Juntao<sup>2</sup>, Hong Zhengqiang<sup>3</sup>, Li Wei<sup>4</sup>

**Abstract:** This paper adopts a quantitative methodology based on the Greenhouse Gas (GHG) Emission Factor methodology and refers to the latest version of the ISO 14064 Carbon Emission Standard Evaluation System to conduct a comprehensive carbon accounting about a mega cavern project located in Hong Kong. Based on the characteristics of the project, four categories of carbon emission sources and carbon emission data in the project are analyzed, including direct GHG emissions and removals, indirect GHG emissions from input energy, indirect GHG emissions from transportation and indirect GHG emissions from products used. Finally, the feasibility of low-carbon construction is analyzed for the subsequent construction phase of the project. Using the results of the project's subsequent carbon emissions analysis as a baseline, the design of low-carbon construction proposals is carried out in four aspects: concrete, steel, owned vehicles and construction machinery. Then the low-carbon construction proposals for three cases are discussed. And the final proposal is determined taking into account costs and carbon reduction benefits.

**Keywords:** Mega cavern project; Carbon accounting; Quantitative methodology; Low-carbon construction

### 1. INTRODUCTION

According to the United Nations Environment Programme (UNEP), the construction industry accounts for 30% to 40% of global energy consumption (Ramesh et al., 2010). Additionally, data from the International Energy Agency indicates that the construction sector contributes 30% to 50% of total greenhouse gas emissions. Therefore, the construction industry plays a crucial role in energy conservation and emission reduction. In the context of global efforts to promote energy conservation, emission reduction, and green, low-carbon development, the construction industry, being a high-energy-consuming and high-emission sector, has the responsibility and obligation to actively explore sustainable development paths and seek effective solutions for energy conservation, emission reduction, and green, low-carbon practices.

The lifecycle of a building typically consists of four stages: design, construction, operation, and demolition and recycling. During the construction phase, which involves the consumption of building materials, carbon emissions account for 10% to 20% of the building's lifecycle, second only to the operational phase. Therefore, conducting systematic qualitative analysis and reasonable quantitative calculations of carbon emissions during the construction phase is crucial for promoting green buildings and implementing green construction in China, providing both theoretical foundations and practical methods. Additionally, various organizations have established numerous norms and standards to guide enterprises, governments, and the public in achieving the goal of a low-carbon economy through emission reduction and energy conservation. These standards include the Greenhouse

<sup>1</sup> Li Yifeng, M.Sc., B.Eng., Assistant General Manager, Civil Department, China State Construction Engineering (Hong Kong) Limited, 27/F, China Overseas Building, 139 Hennessey Road, Hong Kong China, e-mail address: li\_yf@cohl.com.

<sup>2</sup> Yuan Juntao, M.Eng., B.Eng., Engineer, Civil Department, China State Construction Engineering (Hong Kong) Limited, 27/F, China Overseas Building, 139 Hennessey Road, Hong Kong China, e-mail address: juntao.yuan@cohl.com.

<sup>3</sup> Hong Zhengqiang, M.Eng., B.Eng., Assistant Site Manager, Civil Department, China State Construction Engineering (Hong Kong) Limited, 27/F, China Overseas Building, 139 Hennessey Road, Hong Kong China, e-mail address: zhengqiang.hong@cohl.com.

<sup>4</sup> Li Wei, M.Eng., B.Eng., Deputy Site Manager, Civil Department, China State Construction Engineering (Hong Kong) Limited, 27/F, China Overseas Building, 139 Hennessey Road, Hong Kong China, e-mail address: gzliwei@cohl.com.

Gas Protocol, PAS 2050, ISO 14064, and the 2006 IPCC Guidelines for National Greenhouse Gas Inventories, all of which serve as important references for carbon emission assessments.

As research deepens, the construction industry is becoming more professional in calculating carbon emissions and carbon footprint, advancing qualitative analysis to higher levels of quantitative calculation (Wackemagel et al., 1997, Jessica A, 2008, Thomas et al., 2007, Andrew, 2008). Nicolas H (Nicolas et al., 2012). Researchers consider key variables in the design and construction phases, gather data from material suppliers, and develop tools to estimate the total carbon footprint of construction projects, covering various stages. A. Thomas A (Thomas et al., 2009) proposed a decision-making framework that can analyze the carbon emissions of aggregates used in construction, providing a basis for grading and mixing aggregates. Monahan J (Monahan et al., 2011) uses a lifecycle approach to calculate the consumption of materials and fossil fuels during the building's use phase, comparing the implicit carbon emissions of traditional and modern construction methods. He found that concrete, a key material, accounts for nearly 36% of the total implicit carbon (Hammond et al., 2008). G.P. Hammond created a database of embodied energy and carbon emission factors for building materials, primarily targeting the UK market but widely used in multiple fields and by developers of various carbon and environmental footprint calculation tools.

To address the impact of construction on greenhouse gas emissions, governments and research institutions in several countries have conducted foundational studies. These studies aim to support the auditing of greenhouse gas emissions and promote the evaluation of sustainable buildings. Through these efforts, research teams have compiled a list of building materials and developed a database of carbon emission coefficients, forming a set of tools for assessing the environmental impact of construction. These tools provide crucial support and reference for evaluating the environmental impact of construction projects. Notable examples include the Build Carbon Neutral program in the United States and the UK's Construction Carbon Footprint Calculator, both of which are known for their high data integrity and consistency.

This article, based on a super-large cavern project in Hong Kong, uses the ISO 14064-1:2018 carbon emission evaluation standard system to conduct a carbon inventory during the construction phase and provides a feasibility analysis of low-carbon construction. As the largest cavern project in Hong Kong and even in Asia, the results of this carbon inventory analysis will serve as a reference for the design of low-carbon construction plans for future cavern projects, offering significant engineering guidance.

## **2. PROJECT OVERVIEW**

In December 2017, the Hong Kong Development Bureau issued policy guidelines for the development of caverns to increase land supply. These guidelines included the issuance of the Cavern Master Plan and related planning and technical guidelines. This large-scale cavern project is the first initiative by the Development Bureau to relocate government facilities into caverns, freeing up 28 hectares of land for other public welfare purposes. The project involves site development, main cavern construction, ventilation systems, and ancillary buildings. Construction methods include drilling and blasting, permanent anchor support, OHVD, and other techniques. Additionally, the project includes stone crushing and recycling measures to reduce carbon emissions.

The Hong Kong government has launched the 2035 Resource Recycling Blueprint, with the slogan : Reduce Waste for All, Recycle Resources, and Achieve Zero Landfill. This was followed by the 2025 Hong Kong Climate Blueprint, which aims to achieve an absolute emission reduction of 26%-36%. This project is the largest cave engineering development project currently underway in Hong Kong and Asia. To understand the current greenhouse gas emissions, identify, quantify, and analyze potential emission reduction directions and measures, and to develop relevant management strategies for the construction team in this cave engineering project, the project team has planned this greenhouse gas quantification report.

This GHG quantification report is prepared in accordance with ISO 14064-1:2018, which is established by the International Organization for Standardization (ISO) to provide international uniform specifications and guidelines for quantification of GHG emissions and removals and for this report.

## **3. PRINCIPLE OF DRILLING AND BLASTING METHOD**

### **3.1. Purpose and process of carbon inventory**

To actively respond to local policies and the group's sustainable development plan, this paper analyzes the carbon emissions during the current construction phase of the project, based on its characteristics. It also examines the carbon emissions from different methods of gravel processing and evaluates the effectiveness of current

emission reduction measures. Through a carbon inventory, an internal carbon management process is established, and the feasibility of low-carbon construction practices in this project is studied, laying the groundwork for future implementation.

The technical route of carbon inventory and low-carbon construction feasibility analysis in this paper is shown in Figure 1:

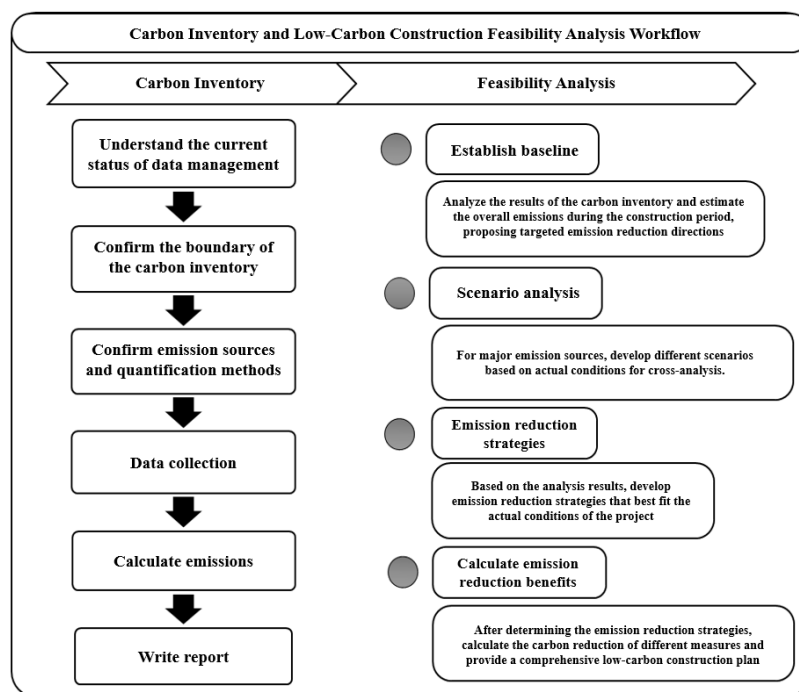


Figure 1. Carbon Inventory and Low-Carbon Construction Feasibility Analysis Technology Roadmap.

### 3.2. Organizational boundaries and reporting period

#### 3.2.1. Organization boundary setting

This report defines the organizational boundaries according to the operational control rights law, identifies direct and indirect emission sources of facilities managed or controlled by the construction team in terms of operations, and quantifies the identified greenhouse gas emissions. The greenhouse gas accounting for this construction period will cover the works undertaken by the construction team in the cave project, including site survey and leveling, main cave engineering, earthwork and pile foundation engineering, road channel engineering, interstone engineering, office building construction, public utility engineering, and the daily operation of the site office. The defined organizational boundaries include the tunnels and peripheral works of this cave project, as well as the stone quarry and new and old office buildings.

#### 3.2.2. Reporting period and report description

The time frame of this report covers the construction period from July 1, 2021 to March 31, 2023 (hereinafter referred to as "reporting period"). This report takes all greenhouse gases generated or involved by the project within the organizational boundary during the reporting period as the accounting scope and quantifies the expected emission reduction measures.

In order to ensure the accuracy of data quality, the project working group will keep the original data files, such as purchase records, transportation records, measurement records, etc., through internal electronic platforms or reports for future verification and tracking.

### 3.3. Report boundaries

#### 3.3.1. Report boundary definition

Within the established organizational boundaries, the scope of direct and indirect GHG emissions from the project construction process is referred to as the reporting boundary. Based on the characteristics of the emission activities, the reporting boundary is divided into categories 1 through 6:

Category 1: Direct greenhouse gas emissions and removals, i.e. direct emissions and removals owned or controlled by reporting organizations within the organizational boundary;

Category 2: Indirect greenhouse gas emissions from energy inputs, which include only indirect greenhouse gas emissions from fuel combustion associated with the production of final energy and utilities (excluding upstream emissions associated with fuels);

Category 3: Indirect greenhouse gas emissions from transport, that is, indirect greenhouse gas emissions related to transport outside the organizational boundary, such as material and building materials transportation, waste transportation and business travel;

Category 4: Indirect greenhouse gas emissions from the products used, that is, indirect emissions from the products or services used by the project from outside the organizational boundary, such as the implied carbon of outsourced products and capital goods, waste and water treatment processes;

Category 5: Greenhouse gas emissions related to the use of products, that is, greenhouse gas emissions or removals involved in the life cycle of products produced and sold by the project, such as emissions or removals during the use phase of the product, emissions at the end of the life of the product, emissions associated with investment, etc.;

Category 6: Greenhouse gas emissions from other sources, that is, emissions involved in any project but not included in the above categories, as defined by the reporting agency.

#### 3.3.2. Report boundary setting

This report identifies emission sources across various categories by carefully defining the reporting boundaries, identifying all potential emission sources. Based on interviews with personnel, feedback from data collection lists, data collection, and field visits, the report primarily assesses whether these emission activities are quantified based on the reporting organization's control over these activities within its organizational boundaries and the sources of activity data.

After a thorough investigation of the emission sources of the project during the reporting period, the boundaries for this greenhouse gas accounting report are set from Category 1 to Category 6. However, emissions in Categories 3, 5, and 6 are not currently relevant or applicable to this project. In accordance with the ISO 14064-1:2018 reporting standards and requirements, the emission sources of this super-large cavern project during the reporting period are detailed in Table 1.

*Table 1. List of Emission Sources in the Reporting Period of the Mega Cavern Project*

Emission categories	Emissions activities	Emission source
Category 1: Direct greenhouse gas emissions and removals	1.1 Fixed source combustion	Mechanical equipment
	1.2 Combustion of mobile sources	Personal vehicles, machinery and equipment
	1.3 Process	Welding process
	1.4 Emissary discharge	Fire extinguishers, refrigerants
	1.5 Explosive blasting discharge	Explosive
Category 2: Indirect greenhouse gas emissions from energy inputs	2.1 Input power	External power purchase
Category 3: Indirect greenhouse gas emissions from transport	3.1 Transportation of building materials, materials and mechanical equipment	Conveyance
	3.2 Waste transportation	Conveyance
	3.3 Commuting	Not applicable
	3.4 Travel of customers and visitors	Not applicable
	3.5 Business travel	Uninvolved
Category 4: Indirect greenhouse gas emissions from products	4.1 Outsourced goods and services	Municipal water (including sewage treatment), crushed stone crushing and screening, paper, steel bars, concrete

used	4.2 Capital goods	ED
Category 5: Greenhouse gas emissions associated with product use		Uninvolved
Category 6: Other indirect greenhouse gas emissions		Uninvolved
Direct greenhouse gas emissions from biomass combustion	B5 biodiesel	Mechanical equipment

The criteria for judging the significance of indirect GHG emissions include: quantification methods, availability of emission factors, significance of emissions, availability and accuracy of data, and quantification costs. The exclusion items and explanations of the boundaries of this report are as follows:

(1) For category 3.3 employee commuting and 3.4 customer and visitor travel, considering the complexity of employee or customer travel patterns during the reporting period, the difficulty of systematic data collection and collation, and the quantified costs, such emissions activities cannot collect accurate data and are relatively insignificant, so they are excluded from the boundary of this report.

(2) For category 3.5 Business travel, the reporting institution is not involved in such emissions as it does not involve any business travel related activities during the reporting period.

(3) For category V, the reporting institution is not involved in such emissions as it did not produce or sell any related products or services during the reporting period.

For category VI, the reporting institution is not involved in any other project-related emissions activities during the reporting period, and therefore the reporting institution is not involved in such emissions.

### 3.4. Quantification of greenhouse gases

#### 3.4.1. Quantitative criteria

According to the Kyoto Protocol, six greenhouse gases are included: carbon dioxide (CO<sub>2</sub>), methane (CH<sub>4</sub>), nitrous oxide (N<sub>2</sub>O), hydrofluorocarbons (HFCs), perfluorocarbons (PFCs), and sulfur hexafluoride (SF<sub>6</sub>). This report also references ISO 14064-1:2018, which includes nitrogen trifluoride (NF<sub>3</sub>) as one of the categories for calculating direct greenhouse gas emissions. When original data is sufficient, the most suitable quantification standard at the project site is prioritized for calculation. If original data collection is limited, the actual situation will be considered, and a feasible method will be chosen for calculation. The final result of this greenhouse gas quantification is expressed in carbon dioxide equivalent (CO<sub>2</sub>e).

The specific information involved in the accounting process, such as quantitative methods, activity data and emission factors, is shown in Table 2.

*Table 2. Quantitative methodology and emission factors for GHG*

<b>Quantitative approach</b>	The main method is emission coefficient method, and the calculation formula is: Greenhouse gas emissions = activity data x emission coefficient x global warming potential (GWP); Some emissions sources obtain data from other publicly available databases.
<b>Activity data</b>	It is mainly collected by two methods: actual measurement and estimation; Priority is given to actual measurements. Where actual measurement data are not available, the report makes an estimate of emissions from activities based on reasonable assumptions or applicable reference materials.
<b>Emission factor</b>	The emission factors calculated in this carbon inventory are selected according to the following priorities to ensure the accuracy of the calculation results: Existing greenhouse gas quantification standards of national or regional governments; Industry emission factors in specific industry literature; General emission factors issued by international authoritative organizations and government agencies; Enterprises themselves publish greenhouse gas quantification standards to

	select emission factors; Complete the quantification work.
--	---

For category five, which pertains to indirect greenhouse gas emissions related to product use, this project does not currently address such emissions. Similarly, for category six, which involves indirect greenhouse gas emissions from other sources, this project also does not address these emissions. Therefore, this article will focus on greenhouse gas emissions related to categories one through four.

### 3.4.2. Category 1: Direct GHG emissions and removals

#### (1) Fixed source combustion

According to the statistical records from the reporting period, the fixed-source machinery and equipment used by the reporting institution include generators, fans, and vibration clamps. Given the significant difficulty and labor intensity of record segmentation, the project's equipment, including both owned and leased by contractors, is combined for calculation. The machinery and equipment used in the project were utilized from July 2021 to March 2022, during the first and second phases of the project. The usage frequency and power consumption of the machinery and equipment were nearly equal between the two phases, so the fixed-source greenhouse gas emissions from the use of machinery and equipment are allocated equally between the first and second phases. The fuel used for the machinery and equipment includes B5 biodiesel, and the greenhouse gas emission coefficient for fuel combustion is detailed in Appendix I. The CO<sub>2</sub> emissions from the combustion of the biomass portion of B5 biodiesel will be separately calculated and reported under the category 'Direct greenhouse gas emissions from biomass combustion' in Section 3.4.6, and will not be included in the total emissions.

Direct emissions from mechanical equipment (fixed sources):

$$\text{Emissions}(CO_2) = \sum \text{Fuel consumption} \times CO_2 \text{Emission coefficient} \quad (1)$$

$$\text{Emission} \left( \frac{CH_4}{N_2O} \right) = \sum \text{Fuel consumption} \times \text{Emission coefficient} \left( \frac{CH_4}{N_2O} \right) \times GWP \quad (2)$$

In formulas (1) and (2), the calculation is based on the emission coefficient of different fuels; fuel consumption is measured in litres (L).

#### (2) Mobile source combustion

During the reporting period, a total of 24 private cars, 9 light trucks, 4 medium and heavy trucks, 2 minibuses, and 1 traffic signal vehicle were held. The private cars, light trucks, medium and heavy trucks, and minibuses were used for personnel transportation, while the traffic signal vehicle was used for site traffic management. The non-road mobile sources used in the project included excavators, pile foundations, large cranes, concrete spraying trucks, dump trucks, loaders, aerial work platforms, tunnel drilling machines, earth compactors, concrete tankers, sand-carrying barges, tugboats, and flat barges. The transportation vehicles used in the project participated in the first and second phases of the project from July 2021 to March 2022. The usage frequency and power consumption ratio of the vehicles in both phases were nearly 1:1, so the greenhouse gas emissions from the use of transportation vehicles were allocated equally between the first and second phases. Private cars run on gasoline, light trucks, medium and heavy trucks, and traffic signal vehicles run on diesel, and minibuses run on liquefied petroleum gas. The fuel for non-road mobile source equipment is B5 biodiesel and fuel oil (ship use). The emission factors for the fuels used in the selected own vehicles and non-road mobile sources are detailed in Appendix I.

Direct emission reference formula (1) and (2) for self-owned vehicles and mechanical equipment (non-road mobile sources). Emission is based on the corresponding emission coefficient of vehicle type and fuel used by mechanical equipment; fuel consumption L count.

#### (3) Welding process

During the construction process, this project uses acetylene to protect the carbon dioxide shielding gas, which is directly released into the air. To address the greenhouse gas emissions from the combustion of acetylene during welding, this project quantified the emissions using Hong et al. (Hong et al., 2015) academic paper, selecting a value of 3.39 kgCO<sub>2</sub>e/kg for the greenhouse gas emissions from acetylene welding.

The direct emission of the welding process (process) by the institution is referenced to formula (1), and the consumption of acetylene is measured in kg.

#### (4) Escape discharge

During the reporting period, institutions purchased and used fire extinguishers and air conditioners, leading to greenhouse gas emissions during storage and use. To quantify these emissions, this study references the IPC (Agarwal et al., 2005) report on refrigerants, which provides annual emission rates for different types of air conditioners. Based on the institutional data on the purchase quantities of fire extinguishers and air conditioners,



their pre-filling amounts, and their global warming potential (GWP) coefficients, the study calculates the greenhouse gas emissions from these emissions. The annual emission rate for window and split-type air conditioners is assumed to be 1%, while for ceiling-mounted air conditioners, it is assumed to be 3%. For some air conditioners, the pre-filling amount of refrigerant was not provided, so the report estimates it based on the specifications of the air conditioners. The fire extinguishing system used in the project was shared between the first and second phases of the project from July 2021 to March 2022, so the emissions from the fire extinguishing system are allocated equally between the two phases.

Direct emission of fire extinguishers and refrigerants:

$$\text{Emission}(CO_2e) = \sum \frac{\text{Fire extinguishers}}{\text{Refrigerant purchase amount}} \times \text{Annual emission rate} \times \text{Global warming potential coefficient} \quad (3)$$

In formula (3), the pre-filled amount of greenhouse gas in the fire extinguisher/refrigerant is measured in kg.

(5) Ejection of explosives

During the project's reporting period, blasting operations were conducted using explosives, and the carbon dioxide produced during the blasting process was directly released into the air. To quantify the greenhouse gas emissions from the combustion of explosives during blasting, the emission factors were calculated using the chemical metering method based on the components that would produce greenhouse gases when burned. The emission factors for various types of explosives are detailed in Appendix I.

The direct discharge reference formula for explosives is (1), and the consumption of explosives is measured in kg, nos. (nos.) and m according to different types.

### 3.4.3. Category 2: Indirect greenhouse gas emissions from purchased energy

During the reporting period, the project's power system operated normally, and the power usage of both the new and old office buildings and the site was combined for calculation. The project is located in the New Territories and is supplied by CLP Power Limited. This project quantified the greenhouse gas emissions from purchased electricity using the emission factors published in CLP Power Limited's 2021-2022 Sustainability Report. The electricity purchased by the project was used jointly by the first and second phases from July 2021 to March 2022, so the indirect greenhouse gas emissions from the purchased electricity were allocated equally between the first and second phases. For more details on the greenhouse gas emission factors for the purchased electricity, see Appendix I.

Indirect emissions from purchased electricity:

$$\text{Emissions}(CO_2e) = \text{Electricity purchased} \times \text{Emission coefficient} \quad (4)$$

In formula (4), the purchased electricity is measured in kilowatt-hours (kWh).

### 3.4.4. Category 3: Indirect greenhouse gas emissions from transport

This report calculates the greenhouse gas emissions from the transportation of building materials, supplies, and machinery to construction sites, as well as the transportation of waste generated at these sites to landfills. Due to the lack of information on transportation distances and types of transport for building materials, supplies, machinery, and general waste, only the manufacturer/supplier, warehouse location, and waste disposal points are provided. Therefore, this report estimates and assumes the transportation distances from the starting point of building materials, supplies, and machinery to the construction site, and from the construction site to the disposal points (including overseas, cross-border, and domestic transportation if applicable) using Google Maps' general transportation distances. The transport vehicles are assumed based on the weight of the transported items. For the greenhouse gas emission factors for these transportation processes, please refer to Appendix I.

Indirect emissions from transport:

$$\text{Emissions}(CO_2e) = \frac{\text{Transport weight} \times \text{Distance}}{\text{Emission coefficient}} \quad (5)$$

In formula (5), the transport weight and transport distance are measured in tons (t) and kilometers (km) respectively.

### 3.4.5. Category 4: Indirect greenhouse gas emissions from products used

(1) Outsourced goods and services

Municipal water (including sewage treatment) is supplied to the office building and site by the Water Supplies Department. The municipal water and sewage treatment used in the project were shared between the first and

second phases of the project from July 2021 to March 2022. Therefore, the indirect greenhouse gas emissions from municipal water and sewage treatment are allocated in a 1:1 ratio to the first and second phases of the project for calculation purposes. As of the date of this report's release, the Water Supplies Department has not published the 2021/2022 annual report. Thus, this quantification reference is based on the greenhouse gas emission factor for electricity use in water treatment published in the 2020/2021 annual report. For more details on the greenhouse gas emission factor, see Appendix I.

Indirect emissions from the use of electricity by the Water Supplies Department to treat drinking water:

$$\text{Emissions}(CO_2e) = \text{Fresh water consumption} \times \text{Emission coefficient} \quad (6)$$

In formula (6), water consumption is measured in cubic meters (m<sup>3</sup>).

Wastewater discharge from office buildings. This item combines the domestic wastewater from office buildings and mobile toilets with the wastewater from mobile toilets on the site for calculation. It quantifies the average greenhouse gas emissions per unit volume of domestic wastewater treated by the Drainage Department. All wastewater from office buildings is discharged through sewage pipes into the Drainage Department's sewage wells, while the wastewater from mobile toilets on the site is collected by a contracted company and sent to the Drainage Department's wastewater treatment facilities. The volume of domestic wastewater from office buildings is estimated based on the specifications of mobile toilets and the collection records of the contracted company's suction trucks. The collection frequency of the contracted company is recorded by the institution, with mobile toilets having a capacity of 0.5m<sup>3</sup> and suction trucks having a capacity of 12m<sup>3</sup>. This item references the greenhouse gas emission factors for electricity used in wastewater treatment, as published in the Drainage Department's 2020/2021 and 2021/2022 Sustainability Reports, with detailed reference information provided in Appendix I.

Indirect discharge from the treatment of sewage by the Water Supplies Department

$$\text{Emissions}(CO_2e) = \text{Sewage discharge} \times \text{Emission coefficient} \quad (7)$$

In formula (7), the sewage discharge is measured in m<sup>3</sup>.

Crushed stone crushing and screening. Within the organizational boundary, the project purchased crushed stone crushing and screening services from sub-contractors during the reporting period. The machinery and equipment used for crushing and screening involved B5 biodiesel, which indirectly generated greenhouse gas emissions. Refer to Table 5 for the emission factors of B5 biodiesel.

The indirect emission of machinery and equipment (fixed source) in outsourcing services is referenced to formula (1) and (2).

Paper, steel bars, and concrete. Within the project's organizational boundaries, the project mainly purchased and used materials such as paper, I-beams, angle irons, and concrete during the reporting period. Since the recycling ratio of all materials used could not be provided, they were all assumed to be produced from pig iron. The paper purchased was used jointly by the first and second phases of the project from July 2021 to March 2022. Therefore, the greenhouse gas emissions from the paper used during this period were allocated equally between the first and second phases. For more details on the carbon emission coefficients of the main materials and building materials used during the reporting period, see Appendix One.

Indirect emissions from the use of materials and building materials (material implied carbon)

$$\text{Emissions}(CO_2e) = \sum \text{Material purchase} \times \text{Emission coefficient} \quad (8)$$

In formula (8), different material types are calculated according to the corresponding weight or volume units, including t, kg and m<sup>3</sup>; the emission coefficient of some building materials such as concrete and steel is estimated by referring to academic articles, databases and combining the actual production mode and ratio of materials.

## (2) Capital goods

During the reporting period, the project purchased copiers, computer hosts, etc.

The indirect emissions caused by capital goods such as laptops and printers are calculated as follows, and the corresponding emission factors are recorded in the table below.

The indirect emission reference formula (8) for capital goods is based on different material types according to the corresponding units; it involves the integration of emission coefficients and unit conversion.

The emission coefficient of concrete will vary depending on the proportion of fly ash (PFA) regenerated components contained in it. The emission coefficient of concrete used in this project is calculated according to the proportion of fly ash regenerated components used. For example, the emission coefficient of concrete 20/20D+PFA with 3% regenerated components can be calculated as:

$$262 \times (1-3\%)+3\% \times 12 = 254.50 \text{ kgCO}_2\text{e/kg}$$

### 3.4.6. Direct greenhouse gas emissions from biomass combustion

The direct greenhouse gas emissions from biomass combustion include the carbon dioxide released by the combustion of biomass components in B100 biodiesel and B5 biodiesel, that is, the amount of carbon dioxide absorbed by the fuel source itself during its growth stage. See Table 12 for the emission coefficient used in the calculation.

The reference for direct emission of biomass combustion is formula (1), and the fuel consumption is measured in L.

### 3.5. Summary of greenhouse gas emission quantification results

From July 1, 2021, to March 31, 2023, the total greenhouse gas emissions from this super-large cavern project were 18,383.46 tCO<sub>2</sub>e, with Category I emissions at 4,007.39 tCO<sub>2</sub>e, Category II emissions at 2,025.73 tCO<sub>2</sub>e, Category III emissions at 3,157.57 tCO<sub>2</sub>e, and Category IV emissions at 9,192.77 tCO<sub>2</sub>e. There were no emissions from Category V or Category VI. The total direct greenhouse gas emissions and indirect greenhouse gas emissions were 4,007.39 tCO<sub>2</sub>e and 14,376.06 tCO<sub>2</sub>e, respectively. Appendix II: The quantified results of greenhouse gas emissions summarize the various sources and data of greenhouse gas emissions from this super-large cavern project.

The percentages of greenhouse gas emissions by each emission category are as follows: Category One accounts for 21.80%, Category Two for 11.02%, Category Three for 17.18%, Category Four for 50.01%, and Categories Five and Six together account for 0% (no sources or data for these emissions). Ranked by the source of emissions, the use of concrete is the primary source of greenhouse gas emissions, with a total of 5,604.80 tCO<sub>2</sub>e, accounting for 30.49% of the project's total emissions. The second largest contributor is the embodied carbon from purchased steel, at 3,185.38 tCO<sub>2</sub>e (17.33%), followed by waste transportation, at 3,101.11 tCO<sub>2</sub>e (16.87%). The remaining emissions account for 35.32% of the project's total.

### 3.6. Greenhouse gas strategy

Unlike the carbon reduction during the operation phase, which primarily focuses on direct greenhouse gas emissions from fixed and mobile sources, as well as indirect emissions from purchased electricity, the carbon footprint of building materials accounts for over 80% of construction period emissions. Therefore, emission reduction measures downstream in the value chain are essential for reducing construction period emissions. However, achieving this requires the collaborative efforts of the construction industry value chain, meeting the design requirements of developers and architects while working with suppliers to find suitable low-carbon building materials. The specific carbon reduction measures implemented on the site are listed in Table 3.

*Table 3. Carbon reduction measures*

Carbon reduction measures	Domain	Office
Direct greenhouse gas emissions	Use biodiesel to operate site machinery and equipment.	Low-carbon travel, promote electric vehicles.
Other indirect greenhouse gas emissions	Supply chain management, using low carbon building materials such as PFA concrete.	Increase the application rate of smart construction sites on new sites.

By March 31, 2023, the project had implemented various carbon reduction measures, including replacing conventional diesel with B5 biodiesel and substituting ordinary concrete with PFA (fly ash) concrete that contains recycled materials. The effectiveness of these measures has been documented. During the reporting period, these measures collectively reduced carbon emissions by 412.60 tCO<sub>2</sub>e. For details on the effectiveness of each measure, see Table 4.

*Table 4. Effectiveness of carbon reduction measures*

Carbon reduction measures	Carbon footprint reduction (tCO <sub>2</sub> e)	Office carbon reduction (tCO <sub>2</sub> e)	Overall carbon reduction (tCO <sub>2</sub> e)
<b>Scope 1 carbon reduction measures</b>			
1.1 Use of B5 biodiesel (as opposed to regular diesel)	179.16	-	179.16

Scope 3 carbon reduction measures			
3.1 PFA concrete (as compared to concrete without recycled components)	233.44	-	233.44
<b>Total (tCO<sub>2</sub>e)</b>	<b>412.60</b>		

## 4. FEASIBILITY ANALYSIS OF LOW-CARBON CONSTRUCTION

### 4.1. Baseline and scenario setting

This article analyzes the carbon emissions of the project over a 46-month period from April 2023 to February 2027, based on the construction plan. The analysis results are used as a baseline to design low-carbon construction solutions for four areas: concrete, steel, company-owned vehicles, and construction machinery. Three scenarios are established. In each scenario, the selection of low-carbon building materials is guided by local and international standards, the product catalogs of local suppliers, and recommendations from relevant institutions. The number of electric vehicle replacements is determined based on the data and types planned by the procurement department. Construction machinery replacements prioritize the types needed for future projects. The implementation scenarios combine emission reduction measures under different conditions, considering factors such as feasibility, practicality, economic costs, and carbon reduction benefits.

*Table 5. Low-carbon construction proposals for a baseline and three cases*

Emission reduction measures	Baseline scenario setting	Scenario 1 is set	Scenario 2 is set	Scenario 3 is set	Implement scenario setting
<b>Concrete</b>	Based on the actual concrete mix ratio provided	All replaced with 35% PFA (fly ash)	All replaced with 45% GGBS (fly ash)	All replaced with 75% GGBS	All replaced with 45% GGBS
<b>Steel Products</b>	0% RC BF-BOF (Oxygen furnace smelting)	50% RC EAF (Arc furnace smelting)	75% RC EAF	100% RC EAF	100% RC EAF
<b>Private vehicles</b>	Eight fuel private cars Two natural gas minibuses Nine fuel-powered pickup trucks	Eight electric private cars Two natural gas minibuses Nine fuel-powered pickup trucks	Eight electric private cars Two electric minibuses	Eight electric private cars Two electric minibuses Nine electric pickup trucks	Eight electric private cars Two natural gas minibuses Nine fuel-powered pickup trucks
<b>Construction machinery</b>	Diesel machinery and equipment	Replacement of electrical and mechanical equipment, including: Other mechanical equipment: air compressor, dump truck, forklift, aerial work platform, concrete tank truck, crane	Replacement of electrical and mechanical equipment, including: Other mechanical equipment: air compressor, dump truck, forklift, aerial work platform, concrete tank truck, crane excavator	Replacement of electrical and mechanical equipment, including: Other mechanical equipment: air compressor, dump truck, forklift, aerial work platform, concrete tank truck, crane Excavators,	Replacement of electrical and mechanical equipment, including: Other mechanical equipment: air compressor, dump truck, forklift, aerial work platform, concrete tank truck, crane

				loaders	

## 4.2. Quantitative methodology--prediction method and prediction results

The carbon emission analysis of section 4.1 baseline and three scenarios is carried out by using the quantitative methodology in Section 3.4. The greenhouse gas emission sources and emissions of the project are based on past carbon emission data per unit time and future construction period or related unit estimates.

The emission results under the baseline scenario are shown in Figure 2. It is evident that the primary sources of emissions during the project's 46-month construction period are concrete, steel embodied carbon, the use of machinery and equipment, and waste transportation. Under the baseline scenario, the total greenhouse gas emissions for the project over the 46-month construction period are 155,018.93 tCO<sub>2</sub>e. The largest source of greenhouse gas emissions is concrete, with an emission of 105,844.38 tCO<sub>2</sub>e; followed by steel embodied carbon, with an emission of 27,500.57 tCO<sub>2</sub>e; machinery and equipment emissions amount to 7,337.87 tCO<sub>2</sub>e, and waste transportation emissions amount to 5,536.75 tCO<sub>2</sub>e.

The percentages of future construction period emissions and reductions under each scenario are shown in Table 6. Compared to the baseline scenario, the total greenhouse gas emissions for Scenarios 1, 2, and 3 are 119,375.50 tCO<sub>2</sub>e, 105,019.55 tCO<sub>2</sub>e, and 67,794.73 tCO<sub>2</sub>e, respectively, with carbon reduction percentages of 22.99%, 32.25%, and 56.27%. The total greenhouse gas emissions for the implementation scenarios are 105,025.49 tCO<sub>2</sub>e, with a total carbon reduction of 9,993.44 tCO<sub>2</sub>e, representing a carbon reduction percentage of 32.25%.

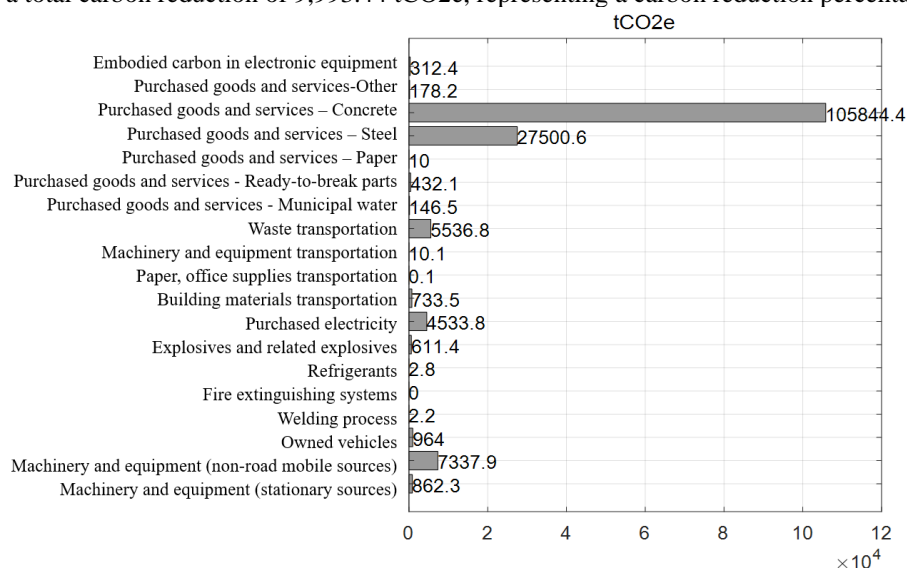


Figure 2. GHG emission results for the baseline during the next 46 months of the construction period

Table 6. Results of GHG emissions of three cases for the future construction period

Emission categories	Emission source	Scenario 1 Future emissions (tCO <sub>2</sub> e)	Scenario 2 Future emissions (tCO <sub>2</sub> e)	Scenario 3 Future emissions (tCO <sub>2</sub> e)	Implement scenario future emissions (tCO <sub>2</sub> e)
Category 1: Direct	MECHANICAL EQUIPMENT	858.07	858.07	858.07	858.07

greenhouse gas emissions and removals	(FIXED SOURCES)				
	Mechanical equipment (non-road mobile sources)	5,964.73	2,015.52	1,495.68	2,015.52
	Personal vehicles	824.01	818.07	698.40	824.01
	Process engineering	2.16	2.16	2.16	2.16
	Fire-extinguishing system	0.00	0.00	0.00	0.00
	Cryogen	2.76	2.76	2.76	2.76
	Explosives and related blasting supplies	611.39	611.39	611.39	611.39
	Direct greenhouse gas emissions	8,263.13	4,307.97	3,668.46	4,313.91
Category 2: Indirect greenhouse gas emissions from energy inputs	External power purchase	5,560.42	8,504.07	8,891.54	8,504.07
Category 3: Indirect greenhouse gas emissions from transport	Building materials transportation	733.51	733.51	733.51	733.51
	Paper and office supplies transportation	0.11	0.11	0.11	0.11
	Mechanical and electrical equipment transportation	10.14	10.14	10.14	10.14
	Waste transport	5,536.75	5,536.75	5,536.75	5,536.75
Category 4: Indirect greenhouse gas emissions from products used	Outsourced goods and services-municipal water	146.48	146.48	146.48	146.48
	Sourced goods and services-crushed stone crushing and screening	432.13	432.13	432.13	432.13
	Sourcing of goods and services-paper	10.01	10.01	10.01	10.01
	External goods and services-steel	13,764.11	10,253.68	6,743.25	10,253.68
	Outsourced goods and services-concrete	84,428.14	74,594.13	41,131.78	74,594.13



		178.17	178.17	178.17	178.17
	Electronic devices have hidden carbon	312.40	312.40	312.40	312.40
	Indirect greenhouse gas emissions	111,112.37	100,711.58	64,126.27	100,711.58
	Total greenhouse gas emissions	119,375.50	105,019.55	67,794.73	105,025.49
	Total carbon reduction	35,643.43	49,999.38	87,224.20	49,993.44
	Percentage of carbon reduction	22.99%	32.25%	56.27%	32.25%

#### 4.2.1. Replace ordinary concrete with low carbon concrete

In order to facilitate the analysis, the following assumptions are made: The implied carbon emission of concrete in the baseline scenario is estimated according to the actual concrete type and mix ratio. It is assumed that the concrete purchased in the future construction period can be replaced by low-carbon concrete, and the total amount of concrete purchased in the future construction period is estimated by subtracting the measured amount at the time of bidding from the already ordered amount.

When analyzing, it is important to consider the impact of concrete with different recycled components on the construction period, contract restrictions, and the testing required for using higher recycled component content. Moreover, the actual availability of concrete (with varying recycled component levels) largely depends on the supplier, and further communication with the supplier is necessary to determine the availability of low-carbon concrete. The changes in the implied carbon emissions of concrete under three scenarios are shown in Figure 3. When 35% PFA (fly ash), 45% GGBS (gypsum blast furnace slag), and 75% GGBS are used, the implied carbon emissions of concrete in future construction projects are reduced by 20.23%, 29.52%, and 61.14% compared to the baseline scenario, respectively. Adding fly ash negatively affects the strength of concrete, particularly its early strength[29,30]. Considering that a high proportion of GGBS replacement may not meet the engineering requirements for concrete strength, the implementation scenario selects a GGBS replacement ratio of 45%.

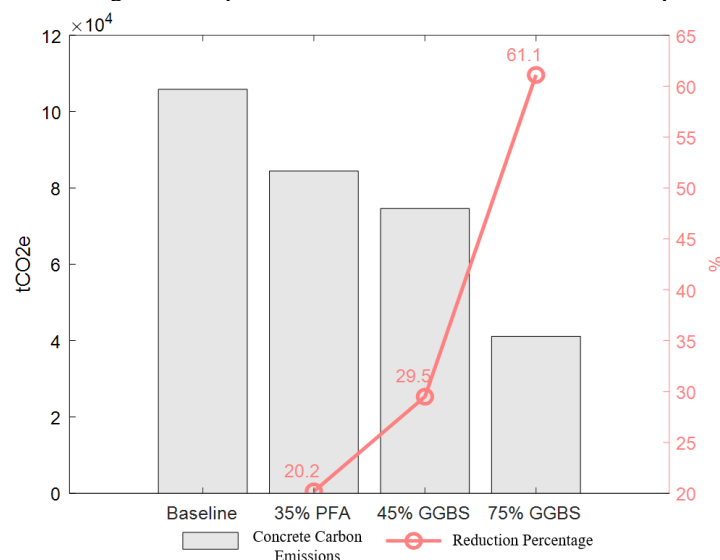


Figure 3. Variations of implied carbon emissions from concrete for three cases

#### 4.2.2. Replace ordinary steel with low carbon steel

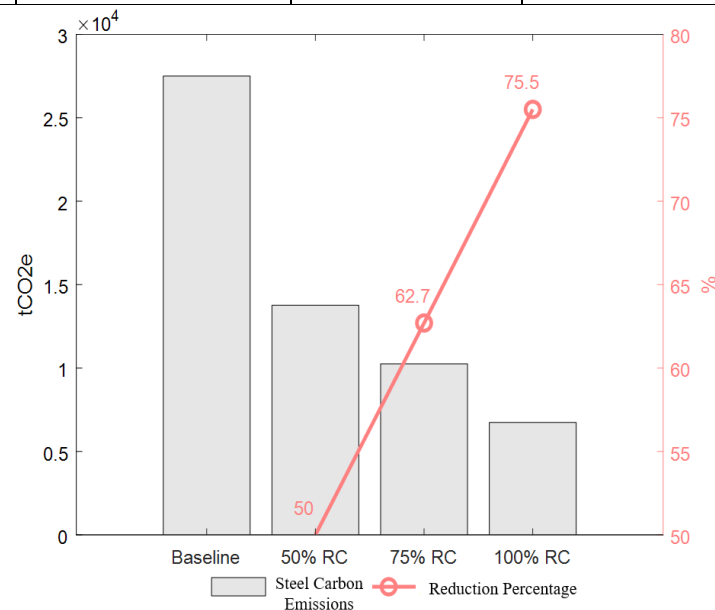
Under the baseline scenario, the types and quantities of steel for future construction periods are detailed in Table 17. For ease of analysis, this paper makes the following assumptions: the implicit carbon emissions from steel in the baseline scenario are estimated based on future actual procurement types. It is assumed that all steel

purchased during the future construction period can be replaced with low-carbon steel. Additionally, it is assumed that all steel purchased under the baseline scenario is produced using the BF-BOF (blast furnace) method (without any recycled components). The total amount of steel expected to be purchased during the future construction period will be updated at any time. Currently, the latest measurement (as of the end of July) is used, minus the data received by the end of March 2023.

When conducting actual analysis, it is important to note that the availability of low-carbon steel (with varying degrees of recycled content) largely depends on the supplier. Further communication with the supplier is necessary to ensure the availability of low-carbon steel. The three scenarios involve replacing 50%, 75%, and 100% of the recycled content in the steel. The changes in the implicit carbon emissions of the steel are shown in Figure 4. Compared to the baseline scenario, the implicit carbon emissions of the steel used in future construction projects are reduced by 49.95%, 62.71%, and 75.48%, respectively. In the implementation scenario, the steel is replaced with 100% recycled content steel.

**Table 7.** Types and amount of steel for the baseline case in the future construction period

Order number	Type of steel	Unit	The total amount of work to be purchased is estimated
1	Steel	/t	121.16
2	Steel pipe	/t	215.56
3	Other section steel	/t	43.70
4	Concrete iron Rebar	/t	9090.77
Total		/t	9471.19



**Figure 4.** Variations of implied carbon emissions from steel for three case

#### 4.2.3. Replace the self-owned fuel vehicle with electric vehicle

Under the baseline scenario, fuel consumption is calculated based on the average monthly fuel consumption of existing vehicles and their future operational duration, and the carbon emissions from gasoline and diesel combustion are estimated. To facilitate the calculations, the following assumptions are made: 8 private cars, 2 small buses, and 9 pickup trucks will be replaced; some existing vehicles have been scrapped, and electric vehicles will be replaced 12 months after the start of the project; the energy consumption per kilometer for electric vehicles is estimated based on the battery capacity and maximum range provided by the supplier.

The carbon emissions of electric and fuel vehicles are calculated under three scenarios, as shown in Figure 5. Compared to the baseline, the carbon emission reduction ratios for future construction period vehicles are 14.52%, 15.14%, and 27.55%, respectively. To ensure the project's vehicle needs while considering both costs and carbon reduction benefits, all eight fuel-powered private cars will be replaced with electric private cars.

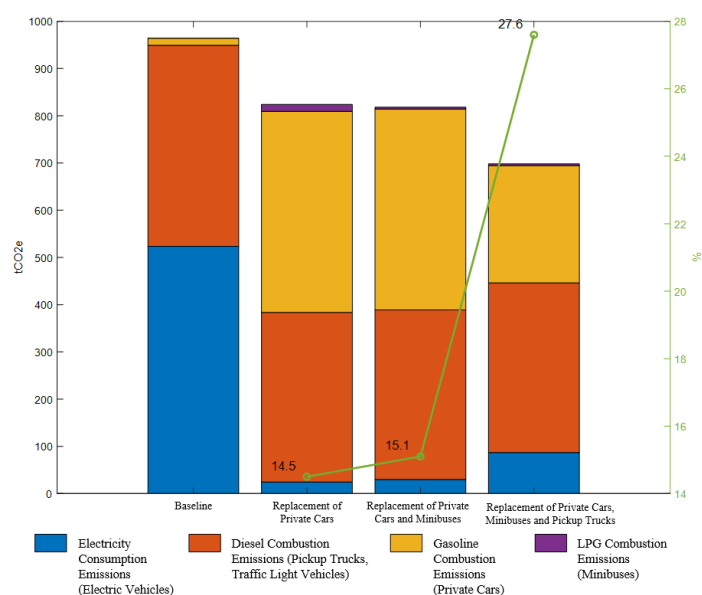
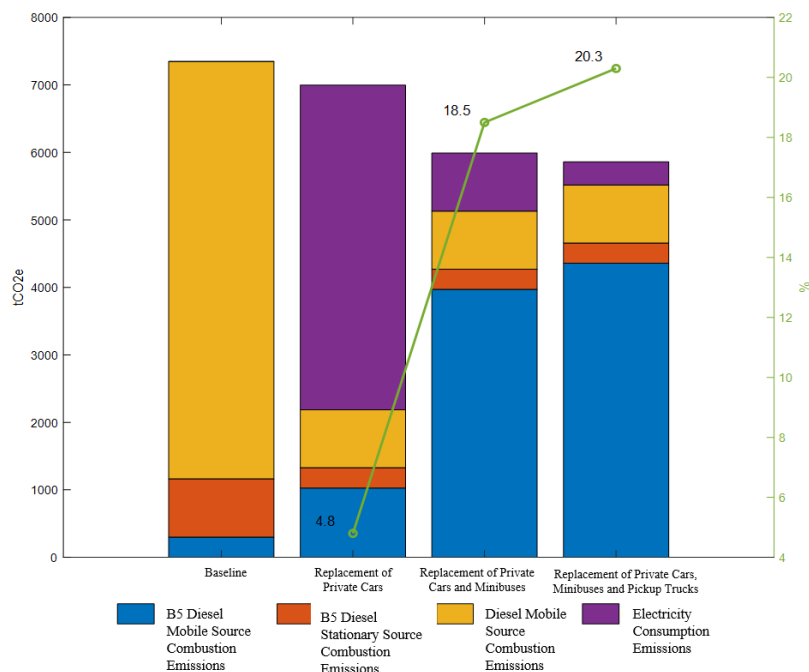


Figure 5. GHG emission results for electric and fuel vehicles for three cases

#### 4.2.4. Replace diesel machinery with pure electric machinery

Under the baseline scenario, diesel consumption is calculated based on the average monthly fuel consumption of diesel machinery and the expected operating duration in the future, to estimate the carbon emissions from diesel combustion. For ease of calculation, the following assumptions are made: only replacement of newly added or currently rented machinery (purchased or existing machinery is not considered for replacement) is taken into account; it is assumed that electric equipment will replace diesel equipment on a 1-for-1 basis (based on working weight), starting from the beginning of the future construction period; according to research findings, the typical engine conversion efficiency is approximately 46%; the charging and discharging efficiency of the power battery is approximately 95%.

In the three scenarios, the calculation results of carbon reduction benefits of replacing diesel machinery with pure electric machinery are shown in Figure 6. The percentage of carbon reduction is 4.77%, 18.46% and 20.26% respectively. The diesel machinery mainly replaced in the implementation scenario is air compressor, dump truck, forklift, aerial work platform, concrete tank truck, crane truck, etc.



*Figure 6. Results of carbon reduction benefits of pure electric machinery for three cases*

## 5. CONCLUSION

This article focuses on the construction phase of a super-large cavern project in Hong Kong, from July 1, 2021, to March 31, 2023. It employs a quantification method based on greenhouse gas emission factors to calculate the project's greenhouse gas emissions during this period. Based on the sources of greenhouse gas emissions, the project's emissions can be categorized into four main types: direct greenhouse gas emissions and removals, indirect emissions from energy inputs, indirect emissions from transportation, and indirect emissions from the products used. The article then forecasts the carbon emissions for the remaining construction phase of the project, sets three scenarios for carbon reduction measures, and selects the final implementation plan by considering the feasibility, economic cost, and carbon reduction benefits of each option. The main conclusions of this article are as follows:

(1) During the reporting period from July 1, 2021 to March 31, 2023, the total greenhouse gas emissions of this super large cavern project were 18,383.46 tCO<sub>2</sub>e. The percentage of greenhouse gas emissions in four categories accounted for 21.80%, 11.02%, 17.18% and 50.01% of the total, respectively.

(2) The primary sources of greenhouse gas emissions are the carbon footprint of concrete and steel, as well as waste transportation. Concrete use is the main source of greenhouse gas emissions for the project, accounting for 5,604.80 tCO<sub>2</sub>e, or 30.49% of the total emissions. Steel has a carbon footprint of 3,185.38 tCO<sub>2</sub>e, or 17.33%, waste transportation contributes 3,101.11 tCO<sub>2</sub>e, or 16.87%, and other factors account for 35.32% of the total emissions.

(3) Under the baseline scenario, the total greenhouse gas emissions of the project in the next 46 months are 155,018.93 tCO<sub>2</sub>e, among which the largest source of greenhouse gas emissions is concrete, followed by steel implied carbon, machinery and equipment and waste transportation.

Compared to the baseline scenario, the future greenhouse gas emission reductions for scenarios 1, 2, and 3 are 22.99%, 32.25%, and 56.27%, respectively. The total greenhouse gas emissions from the final implementation scenario are 105,025.49 tCO<sub>2</sub>e, with a total reduction of 49,993.44 tCO<sub>2</sub>e, representing a 32.25% reduction. The implementation scenario involves replacing all concrete with 45% GGBS (fly ash), switching to 100% RC EAF (electric arc furnace) for steel, and using 8 electric private cars, 2 natural gas minibuses, and 9 fuel-powered pickup trucks for mechanical vehicles. Additionally, electric machinery and equipment, including air compressors, dump trucks, forklifts, aerial work platforms, concrete mixer trucks, and cranes, will be replaced.

(5) Implementation of carbon management and emission reduction measures. During the process of carbon inventory and feasibility analysis, the granularity of data significantly impacts the accuracy of the results. For instance, breaking down the fuel consumption of vehicles or machinery can provide insights into the emission status of individual vehicles or machines. Currently, the feasibility analysis is based on numerous assumptions. In the future, it is necessary to monitor the implementation of each measure and collect actual data for more accurate comparisons. For example, the carbon reduction performance of a single machine can be assessed by monitoring emissions over a period and comparing them with the historical emissions of the replaced model.

This article, set against the backdrop of a super-large cavern project in Hong Kong, conducts a comprehensive carbon footprint assessment for certain construction phases and completes a feasibility analysis for low-carbon construction in subsequent stages. It serves as a comprehensive reference for carbon footprint assessments during other construction phases and provides valuable guidance for future low-carbon construction feasibility analyses and carbon reduction plan designs.

## 6. ACKNOWLEDGMENTS

This paper is sponsored by the Technology Research and Development Project of China State Construction International Holdings Limited (CSCI-2023-Z-17).

## 7. BIBLIOGRAPHY

- [1] Ramesh, T., Prakash, R., Shukla, K.K., 2010. Life cycle energy analysis of buildings: An Overview. *Energy and buildings*, 42(10), 1592-1600.
- [2] BS ISO14064-1:2018. Greenhouse gases. Specification of a level-of-organisation guideline for quantifying and reporting greenhouse gas emissions and removals.
- [3] Intergovernmental Panel on Climate Change 2006 IPCC Guidelines for National Greenhouse Gas Inventories ,2006. Japan: Institute for Global Environmental Strategies, Japan.

- [4] Wackemagel, M., Rees, W.E., 1997. Our ecological footprint reducing human impact on the earth. *Population and Environment*, 19(2): 185-189.
- [5] Jessica, A., 2008. What is a Carbon Footprint?. UK: The Edinburgh Centre for Carbon Management.
- [6] Thomas, W., Jan, M., 2007. A Definition of Carbon Footprint, UK: Research and Consulting.
- [7] Andrew, J.E., 2008. What is a Carbon Footprint? An overview of definitions and methodologies.
- [8] Nicolas, H., Ali, A., Issam, S., 2012. Developing a Carbon Footprint Calculator for Construction Buildings. *Construction Research Congress*, United States: American Society of Civil Engineers(ASCE), 1689-1699.
- [9] Thomas, A., Mice, 2009. Estimating carbon dioxide emissions for aggregate use. *Proceedings of the Institution of Civil Engineers*, 162(3): 135-144.
- [10] Monahan, J., Powell, J. C., 2011. An embodied carbon and energy analysis of modern methods of construction in housing: A case study using a lifecycle assessment framework. *Energy and Buildings*, 43: 179-188.
- [11] Hammond, G.P., Jones, C.I., 2008. Embodied energy and carbon in construction materials. *Proceedings of the Institution of Civil Engineers-Energy*, 161(2):87-98.
- [12] Environmental Protection Department and Electrical and Mechanical Services Department, 2010. Guidelines for Accounting and Reporting of Greenhouse Gas Emissions and Removals for Buildings (Commercial, Residential or Public) in Hong Kong.
- [13] United State Environmental Protection Agency (US EPA), Center for Corporate Climate leadership, 2020-2023, GHG Emission Factors Hub.
- [14] Hong, J.K., Shen, G.Q.P., Feng, Y., 2015. Greenhouse Gas Emissions during the Construction Phase of a Building: A Case Study in China. *Journal of Cleaner Production*, Vol 103, 249–259.
- [15] Agarwal, R., 2005. IPCC/TEAP Special Report: Safeguarding the Ozone Layer and the Global Climate System. IPCC.
- [16] China Power Sustainability Report, 2022. CLP Group.
- [17] GBT 51366-2019. Ministry of Housing and Urban-Rural Development of China, Standard for Calculating Carbon Emissions from Buildings.
- [18] Water Supplies Department, Hong Kong, 2020/21.
- [19] Drainage Services Department Sustainability Report 2020-2021.
- [20] Drainage Services Department Sustainability Report 2020-2021.
- [21] UK Business Reporting Conversion Factors, 2023. Department for Energy Security & Net Zero and Department for Environment, Food & Rural Affairs.
- [22] Apple Product Environmental Report, 2021-2022. Apple. iPhone 13,14, iPad Pro.
- [23] Samsung Product Environmental Report, 2023. Samsung. GALAXY S21 ULTRA, SAMSUNG GALAXY TabS7.
- [24] CFP Quantification Tool - Ready-mixed Concrete, 2018. Hong Kong Construction Industry Council.
- [25] Gan, V.J., Cheng, J.C., Lo, I.M., 2017. Developing a CO<sub>2</sub>-e accounting method for quantification and analysis of embodied carbon in high-rise buildings, *Journal of Cleaner Production*, 141, 825-836.
- [26] Gan, V.J., Chan, C.M., Tse, K.T., 2019. Sustainability analyses of embodied carbon and construction cost in high-rise buildings using different materials and structural forms. *HKIE Transactions*, 24(4), 216-227.
- [27] Better Utilization of Ultimate Strength Gain of Concrete with Pozzolanic Materials for Sustainable Development of Construction Works in Hong Kong, 2018. Hong Kong Construction Industry Council.
- [28] Gao, L., Chen, M. Z., Gao, B., 2015. Research on large dosage of mineral powder to formulate C30 concrete. *New Building Materials*, 47-49, 53.

8. Appendix I: Carbon emission coefficient

Table 1. Emission factor table for machinery and vehicle fuel combustion

type	Fuel category	CO2 Emission factor (kg/L)	CH4 Emission factor (g/L)	N2O Emission factor (g/L)	Reference sources
MECHANICAL EQUIPMENT (FIXED SOURCES)	Diesel oil	2.614	0.024	0.007	Environmental protection agency And the Electrical and Mechanical Engineering Department, 2010
	B100 biodiesel	2.496	0.037	0.003	U.S. Environmental Protection Agency, 2020- 2023
	B5 biodiesel	2.483	0.025	0.007	The calculation is based on the mixing ratio and the above emission coefficient
Private car	Clear gasoline	2.360	0.253	1.105	Environmental protection agency And the Electrical and Mechanical Engineering Department, 2010
Light trucks, medium and heavy trucks, traffic signal vehicles	Diesel oil	2.614	0.145	0.072	Environmental protection agency And the Electrical and Mechanical Engineering Department, 2010
Microbus	Liquefied petroleum gas	1.679	1.679	1.679	Environmental protection agency And the Electrical and Mechanical Engineering Department, 2010
Mechanical equipment (non-road mobile sources)	Fuel oil (shipboard)	2.645	0.146	1.095	Environmental protection agency And the Electrical and Mechanical Engineering Department, 2010
biomass fuel	B100 biodiesel	2.496	0.037	0.003	U.S. Environmental Protection Agency, 2020- 2023
	B5 Biodiesel (excluded from the statistical scope)	0.125	-	-	The calculation is based on the mixing ratio and the above emission coefficient

Table 2. Emission coefficients for various types of explosives

Type of explosive	CO2 Emission factor	unit	Component reference product
Bulk emulsion explosive ( Cartridge )	0.013	kgCO2e/kg	EMULSION HIGH EXPLOSIVE (CARTRIDGED)
Emulsion explosive ( Bulk Emulsion )	0.164	kgCO2e/kg	No.1 Rock Emulsion Explosive-Aoxin Technology
Initiator (Booster)	0.887	kgCO2e/kg	Relay detonator-Aoxin Technology
In-hole delay detonator (IHD)	0.000300	kgCO2e/nos.	Austin SHOCK*STAR MS
Electronic detonators ( Electric Detonator )	0.000476	kgCO2e/nos.	Electric detonator-Xi 'an Qinghua Civil explosive Equipment Co., LTD
Bundle connectors ( Bunch Connector )	0.0000501	kgCO2e/nos.	Austin SHOCK*STAR Surface
Detonating cord ( CordtexTM 5G )	0.002	kgCO2e/m	CordtexTM5G
Detonating cord ( CordtexTM 40G )	0.017	kgCO2e/m	CordtexTM40G

Table 3. Greenhouse gas emission factor table for outsourced electricity

Year	Emission factor	Unit	Reference sources
2021	0.39	kgCO2e/kWh	China Power Limited 2021,2022 Sustainability Report
2022	0.39		

Table 4. Greenhouse gas emission factors for modes of transport involved

Type of shipping	Emission factor	Unit	Reference sources
Light petrol truck transport (2t load)	0.334	kgCO2e/t • km	Ministry of Housing and Urban-Rural Development, China, 2019
Medium diesel truck transport (8t load)	0.179		
Heavy duty diesel truck transport (18t)	0.129		
Heavy duty diesel truck transport (30t)	0.078		
Heavy duty diesel truck transport (46t)	0.057		
Dry bulk ship transportation (2500t deadweight)	0.015		
Container ship transport (200TEU deadweight)	0.012		

Table 5. Greenhouse gas emission factor table for municipal water use

Year	Emission factor	Unit	Reference sources
2020/2021	0.428	kgCO2e/m3	Hong Kong Government Water Supplies Department 2020/2021



			Annual Report
--	--	--	---------------

Table 6. Greenhouse gas emission factor of sewage treatment

Year	Emission factor	Unit	Reference sources
2020-2021	0.21	kgCO2e/m3	Hong Kong Government Water Supplies Department 2020-2021 Sustainable Development Report
2021-2022	0.22	kgCO2e/m3	Hong Kong Government Water Supplies Department 2021-2022 Sustainability Report

Table 7. Carbon emission factors for the use of capital goods and materials involved

Product name	Emission factor	Unit	Reference sources
Paper			
Paper, 2021	919.40	kgCO2e/t	Department of Energy Security and Net Zero, Department for Environment, Food and Rural Affairs
Paper, 2022	919.40		
Paper, 2023	910.48		
Capital goods			
Computer mainframe	24865.48	kgCO2e/t	Department of Energy Security and Net Zero, Department for Environment, Food and Rural Affairs
Display screen			
Computer interface equipment			
Storage system			
Printer			
Network switches			
Server			
Camera	5647.95	kgCO2e/t	Department of Energy Security and Net Zero, Department for Environment, Food and Rural Affairs
Gas testing machine			
Scanner			
Measuring apparatus			
Electric vehicle charging equipment			
Noise monitoring station	3267.00	kgCO2e/t	Department of Energy Security and Net Zero, Department for Environment, Food and Rural Affairs
Electronic scale bridge			
Source	6308.00	kgCO2e/t	Department of Energy Security and Net Zero, Department for Environment, Food and Rural Affairs
iPhone 13 128GB	64.00	kgCO2e per unit	Apple, US, 2021
iPhone14 128GB	61.00	kgCO2e per unit	Apple, US, 2021
iPad Pro 128GB	118.00	kgCO2e per unit	Apple, US, 2021
iPad Pro 256GB	129.00	kgCO2e per unit	Apple, US, 2021
GALAXY S21 ULTRA	22.90	kgCO2e per unit	Samsung, 2023
SAMSUNG GALAXY TabS7 + (5G)(8GB RAM +256GB) (Mystic Navy)	48.20	kgCO2e per unit	Samsung, 2023
Concrete			
Portland cement	2,315.25	kgCO2e/m3	Emission factors are referenced to GBT 51366-2019
Ordinary Portland Cement			
Fly ash	12.00	kgCO2e/m3	CICGPC CFP Quantification Tool - Ready-mixed Concrete
Concrete C20*	262.00	kgCO2e/m3	* Since there is a linear relationship between the minimum cement-based binder content and strength grade, the emission coefficient of C20 can be inferred from the emission coefficient of C30 and C40
Concrete C30	295.00	kgCO2e/m3	Refer to Gan et al. (Gan et al., 2017)
Concrete C40	335.00	kgCO2e/m3	Refer to Gan et al. (Gan et al., 2017)
Concrete C45*	349.00	kgCO2e/m3	* Since there is a linear relationship between the minimum cement-based binder content and strength grade, the emission coefficient of C45 can be inferred from the emission coefficient of C30 and C40
Concrete 20/20D + PFA	254.50	kgCO2e/m3	Concrete containing recycled components is calculated by the method below this table
Concrete 30/10 FV600MM PFACSF plain shotcrete	283.68	kgCO2e/m3	
Concrete 30/20D+PFA	283.68	kgCO2e/m3	
Concrete 40/20D+PFA	318.85	kgCO2e/m3	
Concrete 45/20D+PFA	332.15	kgCO2e/m3	
Concrete 45/10 FV600MM PFA	335.52	kgCO2e/m3	
Concrete iron			
Steel plate	2.25	kgCO2e/kg	The emission coefficient is estimated based on the research data in Gan et al. (Gan et al., 2019) and the actual situation, assuming that the steel is produced by blast furnace-converter method and does not contain scrap steel recycling components.
Merchant steel	2.30		
Steel pipe	2.34		
Concrete iron	2.25		

## DEVELOPING A STANDARD FOR GEOLOGICAL SUITABILITY EVALUATION OF URBAN UNDERGROUND SPACE: A CASE STUDY IN BEIJING

Hanhan He<sup>1,2</sup>, Jing He<sup>2</sup>, Tongming Fang<sup>2</sup>, Fangzhen Li<sup>2</sup>, Yiting Zhao<sup>3</sup>

**Abstract:** The development of urban underground space (UUS) makes a significant contribution to urban sustainability (Bobylev, 2016; Broere, 2016; Hunt et al., 2016; Wang et al., 2016). The subsurface, however, constitutes a sensitive geological environment where disturbances can result in long-lasting or irreversible impacts (Sterling et al., 2012; Li et al., 2016; Zhu et al., 2016). Therefore, a scientific geological evaluation of UUS resources prior to development is essential for informing strategic planning and ensuring sustainable use (Peng and Peng, 2018). This process involves a comprehensive analysis of geological data to assess the suitability of subsurface conditions, within a given depth, for development (Liu et al., 2011). As a densely populated megacity, Beijing increasingly relies on subsurface space to address urban pressure and enhance resilience. Despite numerous geological assessments of UUS (Huang et al., 1995; Wang and Zhu, 2006; Jiang et al., 2007; Cai et al., 2010; He et al., 2020; Sun et al., 2024), challenges such as a lack of consistent criteria and insufficient integration with urban planning remain. The former issue leads to fragmented evaluations based on varying frameworks, compromising the comparability of results. The latter is evident in a reactive, rather than proactive, application of geological assessments within the planning process. This reveals a vital research gap, the absence of evaluation criteria aligned with distinct planning stages (e.g., master and detailed planning). Developing a local standard may provide an effective way to address these issues.

**Keywords:** geological suitability evaluation, urban underground space, evaluation standard, urban planning

### 1. SOLUTION AND RESULTS

To address this gap, we develop a standard for the geological suitability evaluation of UUS in the Beijing plain. This standard establishes a comprehensive framework comprising four principal components:

- (1) pre-evaluation analysis;
- (2) an index system encompassing both basic geological conditions and major constraints;
- (3) index quantification; and
- (4) the classification of overall suitability grades.

A key feature of this standard is the integration with urban planning, which is achieved by both aligning required precision of geological evaluation with different planning levels, and scaling the size of evaluation units for various planning stages. Specifically, at the master planning level, it is recommended that assessments range from city-wide evaluations using a 1 km grid (1:50,000 horizontal / 1:2,000 vertical precision) to district-level evaluations requiring a 500 m grid (1:25,000 / 1:1,000). For the detailed planning stage, the use of a 200 m grid (1:10,000 / 1:500) is suggested for general areas, advancing to a high-resolution 20–50 m grid (1:5,000 / 1:200) for specific regions.

<sup>1</sup> Hanhan He, China University of Geosciences (Beijing), China; Beijing Institute of Geological Survey, China, email: [he.hanhan@163.com](mailto:he.hanhan@163.com)

<sup>2</sup> Jing He, Beijing Institute of Geological Survey, China, e-mail: [48406199@qq.com](mailto:48406199@qq.com)

<sup>2</sup> Tongming Fang, Beijing Institute of Geological Survey, China, email: [fangtongming@163.com](mailto:fangtongming@163.com)

<sup>2</sup> Fangzhen Li, Beijing Institute of Geological Survey, China, email: [184692298@qq.com](mailto:184692298@qq.com)

<sup>3</sup> Yiting Zhao, Beijing Municipal Institute of City Planning & Design, email: [zhaoyt\\_07@163.com](mailto:zhaoyt_07@163.com)

## 2. CONCLUSIONS

The standard establishes a systematic procedure for UUS geological suitability evaluation in Beijing plain and tailors the evaluation scale and precision to specific planning stages. The primary aim of this work is to enhance the consistency and comparability of evaluation results, thereby supporting their effective application.

## ACKNOWLEDGEMENTS

This work was conducted in collaboration with the Standardization Center of the Beijing Municipal Commission of Planning and Natural Resources, Beijing Municipal Institute of City Planning & Design, and BGI Engineering Consultants LTD.

## 3. REFERENCES:

- [1] Bobylev, N. (2016). Underground space as an urban indicator: Measuring use of subsurface. *Tunnelling and Underground Space Technology*, 55, 40–51. <https://doi.org/10.1016/j.tust.2015.10.024>
- [2] Broere, W. (2016). Urban underground space: Solving the problems of today's cities. *Tunnelling and Underground Space Technology*, 55, 245–248. <https://doi.org/10.1016/j.tust.2015.11.012>
- [3] Hunt, D. V. L., Makana, L. O., Jefferson, I., & Rogers, C. D. F. (2016). Liveable cities and urban underground space. *Tunnelling and Underground Space Technology*, 55, 8–20. <https://doi.org/10.1016/j.tust.2015.11.015>
- [4] Wang, C. S., Zhou, C. H., Peng, J. B., Fan, J., Zhu, H. H., Li, X. Z., Cheng, G. H., Dai, C. S., & Xu, N. X. (2019). A discussion on high-quality development and sustainable utilization of China's urban underground space in the new era. *Earth Science Frontiers*, 26(3), 1–8. <https://doi.org/10.13745/j.esf.sf.2018.9.2>
- [5] Sterling, R., Admiraal, H., Bobylev, N., Parker, H., Godard, J.-P., Vahaaho, I., Rogers, C., Shi, X. D., & Hanamura, T. (2012). Sustainability issues for underground space in urban areas. *Proceedings of the ICE – Urban Design and Planning*, 165, 241–254. <https://doi.org/10.1680/udap.10.00020>
- [6] Li, X. Z., Li, C. C., Parriaux, A., Wu, W. B., Li, H. Q., Sun, L. P., & Liu, C. (2016). Multiple resources and their sustainable development in Urban Underground Space. *Tunnelling and Underground Space Technology*, 55, 59–66. <https://doi.org/10.1016/j.tust.2016.02.003>
- [7] Zhu, H., Huang, X., Li, X., Zhang, L., & Liu, X. (2016). Evaluation of urban underground space resources using digitalization technologies. *Underground Space*, 1, 124–136. <https://doi.org/10.1016/j.undsp.2016.08.002>
- [8] Peng, J., & Peng, F. L. (2018a). A GIS-based evaluation method of underground space resources for urban spatial planning: Part 1 methodology. *Tunnelling and Underground Space Technology*, 74, 82–95. <https://doi.org/10.1016/j.tust.2018.01.002>
- [9] Liu, K., Peng, J., & Peng, F. L. (2011). Evaluation model for the suitability of underground space resources exploitation and utilization. *Chinese Journal of Underground Space and Engineering*, 7(2), 219–231. <https://doi.org/10.3969/j.issn.1673-0836.2011.02.003>
- [10] Huang, Y. T., Zhang, Q. X., & Sun, J. L. (1995). The evaluation of the resource of the underground space of DOWNTOWN Beijing. *Journal of Beijing Polytechnic University*, 21(2), 93–99.
- [11] Wang, H., & Zhu, W. J. (2006). GIS-based investigation and evaluation of urban underground space resources. *Chinese Journal of Underground Space and Engineering*, 2, 1308–1312. <https://doi.org/10.3969/j.issn.1673-0836.2006.z2.006>
- [12] Jiang, Y., Wu, L. X., Che, D. F., & Xu, L. (2007). On cell cube for quality evaluation of urban underground space resource. *Geomatics and Information Science of Wuhan University*, 32, 275–278.
- [13] Cai, X. M., He, J., Bai, L. Y., & Liu, H. (2010). The geology problem in the development and utilization programming of underground space resources in Beijing. *Chinese Journal of Underground Space and Engineering*, 6, 1105–1111. <https://doi.org/10.3969/j.issn.1673-0836.2010.06.001>
- [14] He, J., Zhou, Y. X., Zheng, G. S., Wang, J. M., & Liu, Y. (2020). Research on the geological suitability evaluation system of underground space resource utilization in Beijing. *Chinese Journal of Underground Space and Engineering*, 16(4), 955–966.
- [15] Sun, W. J., Yang, W. K., Deng, Y. F., & Li, W. J. (2024). Geological suitability evaluation of underground space in Beijing urban area based on fuzzy mathematics. *Acta Geoscientica Sinica*, 45(1), 73–79. <https://doi.org/10.3975/cagsb.2023.051001>

## INTEGRATING “SCAN TO BIM” TECHNOLOGY INTO THE CONSTRUCTION OF A CAVERN PROJECT

Yifeng. Li <sup>1</sup>, Zhikai, Wei <sup>2</sup>, Joseph Z. Hong<sup>3</sup>, H.S. Lok<sup>4</sup>

### Abstract:

#### 1. INTRODUCTION: ADDRESSING UNDERGROUND CONSTRUCTION CHALLENGES

A large-scale cavern project involving the construction of underground facilities for government use faced significant challenges in spatial accuracy, documentation, and coordination. Traditional surveying methods lack real-time updates and precision in complex subsurface conditions.

To overcome these limitations, “Scan to BIM” technology was implemented, combining high-resolution laser scanning with Building Information Modeling (BIM) workflows. This integration enabled accurate documentation, progress tracking, clash detection, and digital twin generation, enhancing both efficiency and safety in underground construction [Autodesk, n.d.].

#### 2.SOLUTION: PRACTICAL APPLICATION OF SCAN TO BIM

##### 2.1 EQUIPMENT AND WORKFLOW

The project team used the Leica RTC360 laser scanner for rapid and accurate point cloud capture and the Leica TS16 total station to establish spatial control. Point cloud registration and post-processing were completed using Cyclone software, achieving millimeter-level accuracy [Leica Geosystems, n.d.-a]. The data was then integrated into BIM environments to support design validation and decision-making.

##### 2.2 3D VISUALIZATION AND MONITORING

Post-blast conditions were scanned regularly to generate a visual record of excavation progress. When integrated with 4D BIM software, these scans enabled timeline visualization and improved schedule forecasting.

##### 2.3 CLASH DETECTION AND SPATIAL VALIDATION

The point cloud data enabled early detection of geometric conflicts, such as overbreak and underbreak areas. This was particularly beneficial in ensuring alignment with design tolerances, especially through complex rock formations.

<sup>1</sup> Mr. Yifeng LI, M.Sc., B.Eng., Assistant General Manager of Civil Department, China State Construction Engineering (Hong Kong) Limited, 27/F, China Overseas Building, 139 Hennessey Road, Hong Kong China, e-mail address: li\_yf@cohl.com.

<sup>2</sup> Mr. Zhikai WEI, M.Sc., B.Eng., Deputy Site Manager, Civil Department, China State Construction Engineering (Hong Kong) Limited, 27/F, China Overseas Building, 139 Hennessey Road, Hong Kong China, e-mail address: weizhikai@cohl.com

<sup>3</sup> Mr. Joseph Z. HONG, M.Eng., B.Eng., Assistant Site Manager, Civil Department, China State Construction Engineering (Hong Kong) Limited, 27/F, China Overseas Building, 139 Hennessey Road, Hong Kong China, e-mail address: zhengqiang.hong@cohl.com.

<sup>4</sup> Mr. H. S. LOK, B.Sc., Surveyor, Civil Department, China State Construction Engineering (Hong Kong) Limited, 27/F, China Overseas Building, 139 Hennessey Road, Hong Kong China, e-mail address: hingshing.lok@cohl.com.

## 2.4 AS-BUILT DOCUMENTATION AND QUANTITY ESTIMATION

“Scan to BIM” also allowed for precise verification of shotcrete thickness and captured the conditions of rock faces. These digital records supported quality assurance and facilitated future inspections. Accurate volume estimation between blasts improved budgeting and resource planning through integration with 5D BIM.

## 3.RESULTS: IMPACT AND BENEFITS

### 3.1 EFFICIENCY AND SCHEDULING GAINS

Laser scanning reduced site documentation time to under 10 minutes per blast cycle. The improved data flow advanced the blasting schedule by 13 working days and enhanced coordination across multiple disciplines.

### 3.2 RISK AND SAFETY IMPROVEMENTS

Remote data acquisition minimized worker exposure to hazardous environments, reducing risks related to rockfalls and airborne dust. Digital verification of shotcrete application also contributed to improved structural safety.

### 3.3 COST OPTIMIZATION

By integrating point cloud data with 5D BIM tools, the project team achieved more accurate cost forecasting and reduced rework through early detection of spatial deviations, leading to significant cost savings and improved budget control.

## 4.CONCLUSION

The integration of “Scan to BIM” technology in this cavern construction project significantly improved accuracy, safety, and cost-effectiveness. The approach offered a scalable, real-time solution for decision-making and spatial analysis in complex underground environments. Future directions may include exploring mobile scanning tools such as the BLK2GO and evaluating the role of photogrammetry in complementing underground data acquisition workflows.

## 5.REFERENCES

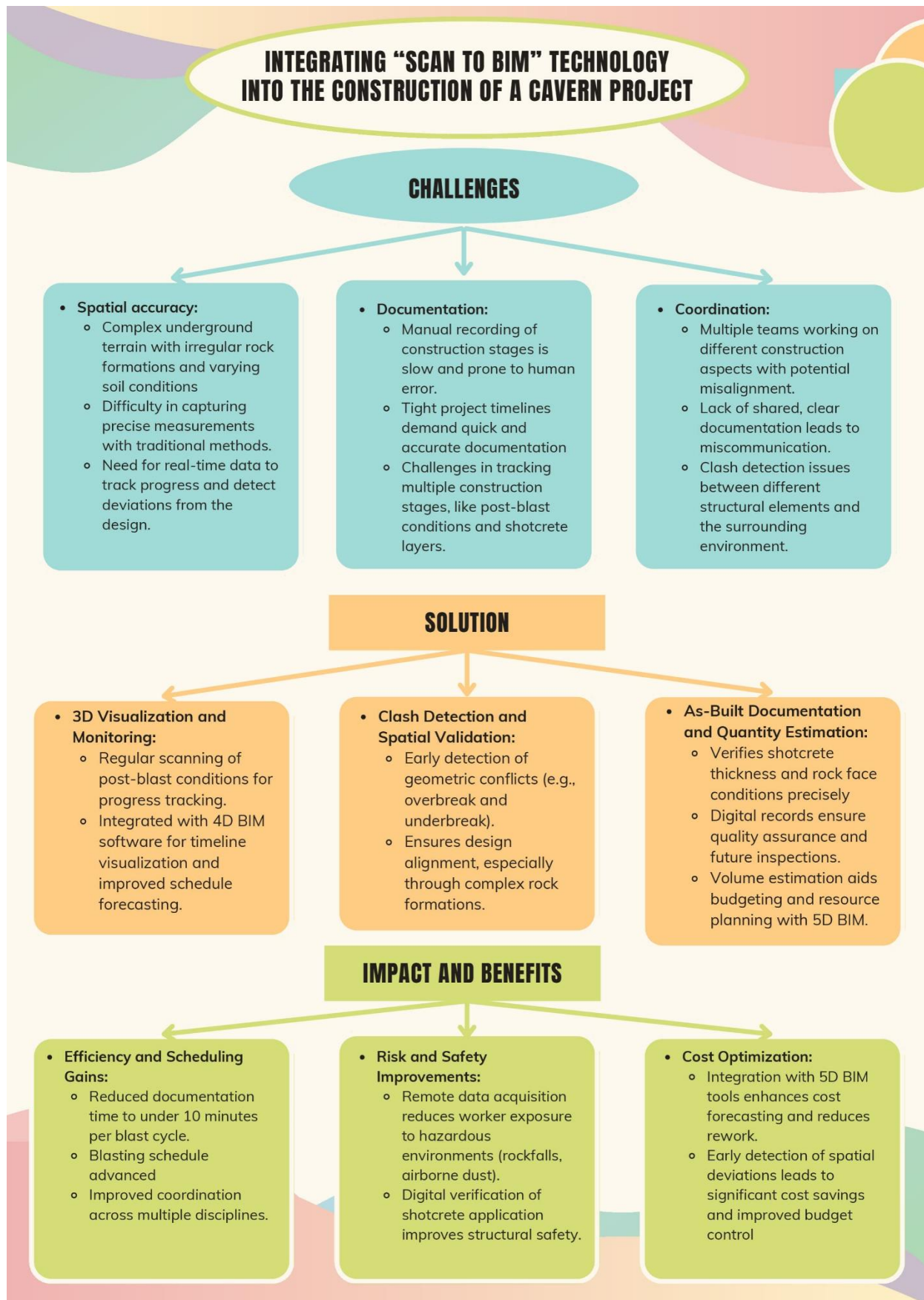
Autodesk. (n.d.). What is Scan to BIM? Retrieved April 25, 2025, from <https://www.autodesk.com/industry/land-development/scan-to-bim>

Leica Geosystems. (n.d.-a). Leica RTC360 3D laser scanner. Retrieved April 25, 2025, from <https://leica-geosystems.com/products/laser-scanners/scanners/leica-rtc360>

Leica Geosystems. (n.d.-b). Leica TS16 total station specifications. Retrieved April 25, 2025, from <https://leica-geosystems.com/products/total-stations/robotic-total-stations/leica-ts16>

**Keywords:** Scan to BIM; Laser Scanning; Point Cloud Data; Underground Construction; Digitalization

**Conceptual framework:**





## TRI-DIMENSIONAL SUSTAINABILITY IN URBAN UNDERGROUND TRANSPORT (INTEGRATING ENVIRONMENT, GOVERNANCE, AND RESILIENCE IMPERATIVES)

Ghada A. Alssadah<sup>1</sup>, Mohammed M. Ali<sup>2</sup>, Yuan Hong<sup>3</sup>, Zoran Đukanović<sup>4</sup>

**Abstract:** Urban underground transport (UUT) systems are increasingly critical for sustainable urban development, yet their purported benefits require systematic reassessment through integrated analytical frameworks. This study introduces a novel tri-dimensional analytical framework that moves beyond these constraints by integrating environmental efficiency, adaptive governance, and contextual resilience. We demonstrate that geographical bias in case studies (75% focused on Global North), fragmented sustainability dimensions, and absent standardized metrics—via a systematic literature review (2010–2023) of 135 peer-reviewed sources. Employing a novel tri-dimensional framework (environmental efficiency, governance coherence, spatial resilience), we demonstrate that net carbon savings from UUT are offset by 35–70% due to energy-intensive ventilation, with stark disparities between contexts (e.g., Stockholm’s 25% carbon surplus vs. Cairo’s 15% deficit). Resilience analyses reveal seismic robustness but acute hydraulic vulnerability, where 70% of failures stem from institutional-environmental-structural fragmentation (e.g., Kuala Lumpur’s 2022 inundation). Crucially, sustainability hinges on simultaneous optimization of: (1) environmental net gains (renewable energy integration), (2) adaptive governance (subnational policy capacity), and (3) contextual resilience (risk-sensitive design). We propose context-sensitive pathways: AI-driven retrofitting for Global North systems and phased modular financing (e.g., Mumbai’s sovereign bonds) for Global South cities. Future research must prioritize underground-renewable symbiosis, social recovery metrics, and computational modeling of tri-dimensional interactions.

**Keywords:** Tri-dimensional framework, contextual resilience, adaptive governance, Global North/South divide, sociotechnical ecosystems.

### 1. INTRODUCTION

Urban underground spaces (UUS) have emerged as a critical solution to the escalating challenges of urban density, environmental degradation, and infrastructure resilience. While existing literature extensively documents the benefits of underground transport systems—from decongesting surface traffic (Bilbao-Ubillos, 2008) to reducing carbon emissions three fundamental limitations persist in current research paradigms (Ali et al., 2025; Bian et al., 2024).

First, the geographical bias in studies has created significant knowledge gaps. Over 75% of published research focuses on European and North American cities (Deng et al., 2024; Skopec et al., 2020), while rapidly urbanizing regions in the Global South remain underrepresented despite facing unique geological and socioeconomic constraints (Edwards Jr et al., 2024; Owusu-Peprah, 2024). This imbalance obscures critical insights about system adaptability across different development contexts (Wang et al., 2025).

Second, the artificial segregation of sustainability dimensions in academic discourse has hindered holistic understanding. Environmental analyses of air quality improvements rarely intersect with governance studies of policy implementation or disaster resilience research (Buck et al., 2021; Haque, 2000; Kallianiotis & Batjakas, 2023). Such fragmentation prevents the development of integrated solutions that address underground systems’ complex interdependencies (He et al., 2024).

1 PhD Candidate, Ghada Abdulbaqi Alssadah, MSc, Architecture Eng, Southwest Jiaotong University, Zhixing Road, Pidu District, Chengdu, China, ghada123@my.swjtu.edu.cn

2 MSc, Mohammed Mokhtar Ali, MSc, Architecture Eng, Southwest Jiaotong University, Zhixing Road, Pidu District, Chengdu, China, mo95mokhtar@my.swjtu.edu.cn

3 Prof, Hong Yuan, Prof, Architecture Eng, professor, Southwest Jiaotong University, Zhixing Road, Pidu District, Chengdu, China, arcyan@home.swjtu.edu.cn

4 prof, Zoran Đukanović, prof, Architecture Eng, professor, University of Belgrade, Bulevar kralja Aleksandra 75, 11000 Belgrade, Belgrade, Serbia, duke@arh.bg.ac.rs

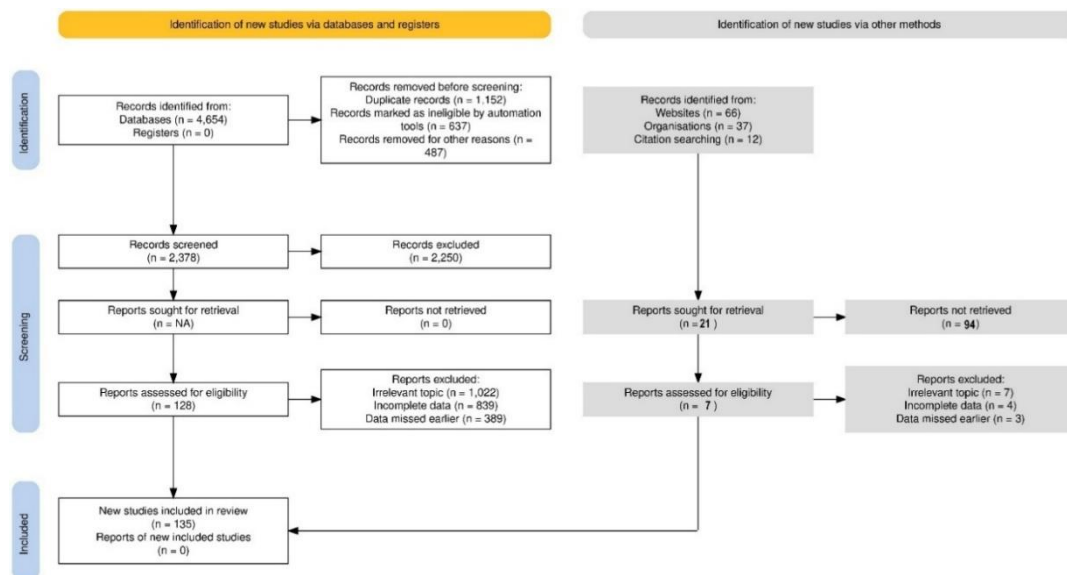
Third, the absence of standardized metrics for comparative assessment limits evidence-based decision making. Claims about emission reductions or cost efficiency vary dramatically across studies due to inconsistent methodologies (Minx et al., 2017), while long-term operational data particularly regarding climate change adaptation remains scarce for most systems (Allan et al., 2023; Qihu, 2016).

While the benefits of urban underground transport (UUT) systems are widely acknowledged in extant literature, this study argues that their purported sustainability remains critically overstated and conceptually fragmented. Prevailing research suffers from three systemic limitations: a pronounced geographical bias favoring Global North cities, a disciplinary siloing of sustainability dimensions, and a lack of standardized metrics for cross-contextual comparison. This paper moves beyond these constraints by introducing a novel tri-dimensional analytical framework that integrates environmental efficiency, adaptive governance, and contextual resilience into a unified assessment model. Unlike prior studies that examine these dimensions in isolation, our integrated approach reveals the complex interdependencies and trade-offs that ultimately determine a system's net sustainability impact. Through a systematic review of 135 peer-reviewed sources (2010–2023), this research not only quantifies the hidden environmental costs of UUT operations but also establishes the critical role of subnational governance and context-sensitive risk management—thereby providing a more holistic, evidence-based paradigm for evaluating and planning underground transport infrastructure globally.

Our analysis reveals that the true potential of underground transport systems lies not in isolated technical solutions, but in their capacity to function as adaptive urban organs—simultaneously mitigating surface-level environmental pressures while requiring carefully balanced subsurface management strategies. The paper concludes by proposing actionable pathways for context-sensitive implementation, with particular emphasis on bridging the knowledge divide between developed and developing urban contexts.

## 2. METHODOLOGY

This study conducts a comprehensive literature review to investigate the effects of underground transportation systems, focusing on both the Critical Reassessment the Tri-Dimensional Mitigation associated with their implementation. To ensure a high-quality and inclusive selection of articles, relevant publications were sourced from well-established academic databases, including Scopus, Web of Science Core Collection, and Google Scholar. These databases index a wide range of scholarly literature across disciplines such as engineering, social sciences, urban studies, medicine, and the arts and humanities, providing a broad scope for review (**Figure 1**).



**Figure 1:** Methodology Flowchart for Systematic Literature Review

The search strategy involved the identification of key search terms, which were derived from a combination of prior literature and the expertise of the research team. To capture a comprehensive range of relevant studies, the search terms encompassed various terms related to underground transportation systems, such as underground railway systems, (metro, subway), underground car parks, urban underground roads and expressways, underground freight transport systems, and underground pedestrian systems. In addition, the search also included terms related to potential hazards associated with these systems, such as hazards underground transport systems.

The focus of the review was primarily on articles within the fields of urban planning, urban studies, and transportation engineering. To maintain a rigorous selection process, only empirical studies published in English were included. The review sought to balance the selection of publications by considering a wide array of topics, ensuring that both developed and developing countries were represented in the analysis (**Figure 2**).

The following sections present the findings from the reviewed literature, discussing the effects of underground transport systems, their associated hazards, and the impact of these systems on urban sustainability (

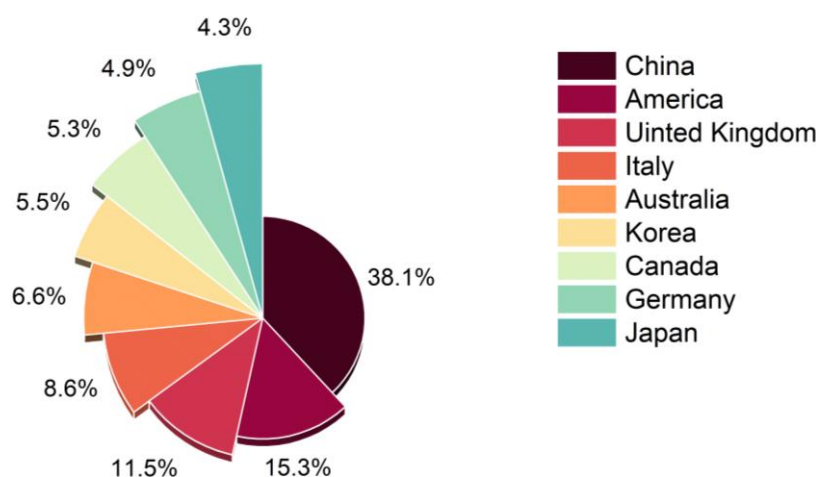
Table 1).

### 3. INTEGRATED FINDINGS

#### 3.1. Integrated Sustainability Assessment of Underground Transport Systems: A Critical Tri-Dimensional Analysis

The purported sustainability benefits of underground transport systems require rigorous re-examination through an integrated analytical lens. While consensus exists regarding their capacity to alleviate traffic congestion and reduce carbon emissions, comprehensive assessment reveals these advantages are fundamentally contingent upon neutralizing hidden operational expenditures and governance-mediated tradeoffs. Empirical studies across forty global systems demonstrate that mechanical ventilation infrastructure consumes 35-50% of achieved carbon savings (Cui et al., 2019; Cui & Nelson, 2019), with this proportion escalating to 70% in tropical climates where cooling demands impose exceptional energy burdens (Bobylev, 2009; Hata et al., 2014). Stark geographical disparities in net environmental efficiency emerge: Stockholm achieves a 25% net carbon surplus through strategic hydropower integration (Azevedo dos Santos Silva, 2023), whereas Cairo and Jakarta exhibit 15% carbon deficits attributable to fossil fuel-dependent ventilation systems (Edwards Jr et al., 2024). This divergence conclusively establishes that environmental efficacy is inextricably linked to subnational governance capacities for renewable energy adoption and infrastructure integration.

Regarding spatial efficiency—frequently cited as a principal advantage methodical scrutiny exposes significant paradoxes (Petchey, 2009). Excavation activities chronically disrupt local ecosystems throughout 3-5 year construction phases (Kauffman, 2022), with toxic drilling compounds including acrylamide monomers infiltrating aquifers at concentrations reaching 8,5 mg/L (Al-Mukhtar, 2019; Wang et al., 2025).



**Figure 2:** Distribution of Studies by Region

Financial viability metrics reveal extreme contextual variance, with return-on-investment ratios fluctuating from marginal 1,2: in low-density suburban developments to robust 5:1 in high-density urban cores (Goldstein et al., 2016). Furthermore, post-project land utilization patterns frequently undermine theoretical benefits, as merely 60% of reclaimed surface areas are allocated to environmental enhancements such as green corridors, while 40% accommodate traffic-generating commercial developments that exacerbate urban congestion (Valdenebro & Gimena, 2018).

*Table 1: Global Case Studies of Underground Transport Systems*

Reference	Form of underground transport systems exploitation	City, Country	Goals of Using Underground Transport Systems Underground Street
(Leach et al., 2019)	Metro	London, UK	Improve the local transport network and extend the surrounding East London area
(Hanamura, 2017)	Underground Infrastructure	Tokyo, Japan	Develop efficient urban systems to maintain daily operations and ensure functional resilience during emergencies
(Cui et al., 2021)	UUTS	Qingdao, China	Tackle urban challenges and improve urban space functionality for sustainable development
(Liang et al., 2016)	UUTS	Chongqing, China	Enhance the social benefits derived from urban infrastructure
(Qiao et al., 2018)	Metro; Underground Road; Underground Parking Space	Qingdao, China	Revitalize the energy and vibrancy of the local area
(Zhang et al., 2021)	UUTS	Shanghai, China	Create transportation infrastructure that integrates smoothly with existing networks
(Carteni et al., 2018)	Metro	Naples, Italy	Revitalize areas above subway stations
(Dong et al., 2023)	Underground Parking Space	Basilicata, Italy	Improve city environments through underground parking
(Besner, 2017)	Underground Street	Tokyo, Japan	Revitalize deteriorating central areas through underground streets
(Suhr & Jung, 2016)	Underground Parking Space	Beijing, China	Tackle urban growth challenges by establishing a central hub for high-tech industries
(Forero-Ortiz & Martinez-Gomariz, 2020)	Underground Transport System	Shanghai, China	Build transportation infrastructure that complements the existing transport system
(Huang et al., 2023)	Underground Road	Qingdao, China	Improve road systems to optimize traffic flow
(Q. Li et al., 2017)	Metro	Chongqing, China	Propose a broad conceptual framework for enhancing transportation safety and network resilience
(Odlyzko, 1999)	Metro	London, UK	Introduce a resilience metric to assess system recovery after disruptions, using a mean-reverting stochastic model applied to the London Underground
(Guan et al., 2021)	Metro	Shanghai, China	Evaluate metro network vulnerability by analyzing operational disruptions and offering improvement recommendations

(Fanourakis et al., 2020)	Metro	Singapore, USA	Research factors influencing model to assess the impact of disruptions using
(Li et al., 2019)	Metro	Shanghai, China	Design passenger flow simulations to
(Bragado et al., 2023)	Metro	Madrid	Provide smoke-free escape routes
(Bragado et al., 2023)	Railway	Tainan, Taiwan	Investigate how public transport systems, focusing on the Madrid Metro
(Kim et al., 2017)	Metro	Seoul, Korea	Station challenges in monitoring and forecasting levels at subway stations
(Bleil-Filho et al., 2024)	Automatic Underground	Hanoi, Germany	Investigate physical infrastructure to study the effect of platform on underground traffic systems
(Wei et al., 2022)	Traffic congestion	Multiple cities, China	Analyze traffic congestion through real-time data from China's top digital mapping service provider
(Zhao et al., 2016)	UUS utilization	Shanghai, China	Utilize metro line data and space syntax indices to assess underground utilization.
(L. Li et al., 2017)	Metro	Xi'an, China	Survey data collected via questionnaires
(Park, 2023)	Traffic congestion	Busan, Daegu, Daejeon and Gwangju, Korea	Analyze housing transaction data and traffic congestion patterns

**Table 1 (Continued)**

Resilience performance manifests equally contradictory duality. These systems demonstrate exceptional seismic resistance, empirically validated during the 2023 Komatsu seismic event (M7.1) where Shinkansen tunnel networks maintained structural integrity despite catastrophic failure of twelve surface bridges (Fanourakis, 2024; Zhang et al., 2025). Conversely, profound hydraulic vulnerability materializes during pluvial events, evidenced by Kuala Lumpur's 2022 catastrophe

where sedimentary bedding planes facilitated complete tunnel inundation within forty minutes (ASEAN, 2023; Hong et al., 2025). Forensic engineering analyses attribute over 70% of such failures to tri-dimensional systemic fragmentation: hydrogeological infiltration pathways (environmental oversight), neglected pump maintenance regimes (governance deficit), and critically insufficient vertical emergency egress (resilience planning failure) (Liu et al., 2022; Zaki & Jaafar, 2025).

These findings collectively affirm that substantive sustainability derives not from isolated technical interventions but from conscientiously balanced integration of net environmental efficiency, context-responsive resilience, and governance equity. Copenhagen's Metropolitan Expansion (2023) exemplifies this synthesis: 40% net carbon reduction through geothermal-ventilation symbiosis, deployment of twenty-eight oxygen-supplemented evacuation shafts at 200-meter intervals, and innovative financing through citizen-participated green bonds securing 65% local capital (CSO, 2023). This paradigm validates urban subsurface development as a complex sociotechnical ecosystem requiring meticulous orchestration between ecological, institutional, and structural components (Broere, 2016).

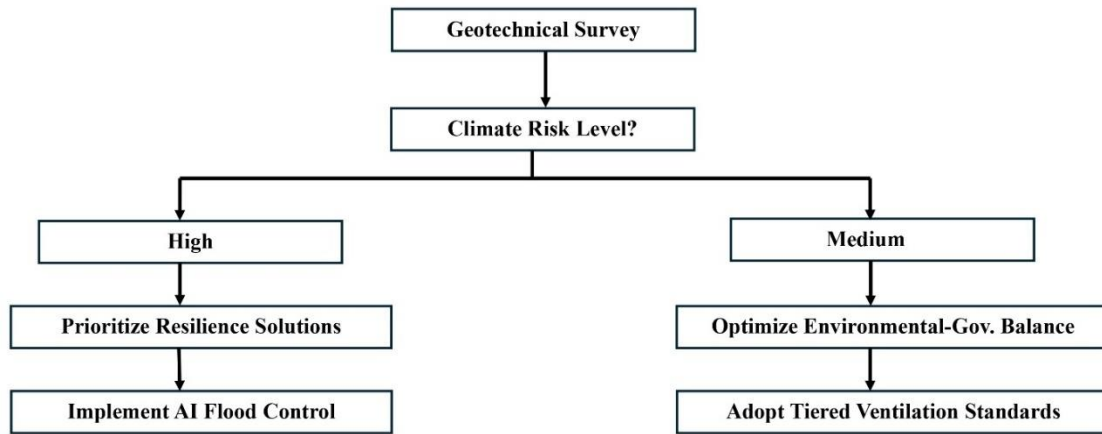
The evidence necessitates reconceptualization of underground transport not as isolated infrastructure but as embedded urban service systems where ventilation energy portfolios determine carbon balance, governance coherence dictates disaster preparedness, and spatial reclamation strategies dictate net livability gains. Future sustainability assessments must therefore adopt mandatory tri-dimensional accounting frameworks that quantify interactions between atmospheric emissions, hydrological impacts, and institutional performance (Broere-Brown et al., 2016). Such integrated methodologies will enable evidence-based prioritization of geothermal energy integration in volcanic regions, sedimentological reinforcement in alluvial basins, and community-funded resilience infrastructure in fiscally constrained municipalities. Only through such contextualized, multidimensional optimization can subsurface transportation fulfill its theoretical potential as an urban sustainability accelerator rather than an energy-intensive enclave solution.

The frontier of subterranean innovation lies not in novel engineering but in reconnecting fragmented knowledge domains across environmental science, institutional economics, and risk governance (Broere, 2016).

### 3.2. Tri-Dimensional Mitigation Pathway: Advanced Integration of Finance, Design & Risk Management

In (Figure 3) show the Hybrid financing embodies a transformative approach integrating public funding (60-70%), green infrastructure bonds (20-30%), and private capital through risk-adjusted return mechanisms (10-20%). In Mumbai's Coastal Road Tunnel, this model achieved a 28,5% cost reduction by linking investor repayments to stringent performance benchmarks: 15% energy reduction over five years and radon levels maintained below 50 Bq/m<sup>3</sup>. The mechanism leverages Certified Emission Reductions (CERs) from the Clean Development Mechanism, converting each ton of CO<sub>2</sub> saved into tradable financial assets, thus monetizing environmental gains (Rahman & Kirkman, 2015). In design engineering, standardization of precast concrete segments (2,5×10m dimensions with ±3mm tolerance per ISO 21650:2023) revolutionizes construction efficiency. Implementation at London's Stansted Tunnel demonstrated a reduction in construction time from 14 to 8,2 months per kilometer, coupled with a decrease in embodied carbon emissions to 8,5 kg/m<sup>3</sup> versus 14,2 kg/m<sup>3</sup> in conventional methods.

This precision relies on 3D LiDAR scanning at 2mm resolution and integrated Building Information Modeling (BIM) simulating geotechnical stresses with a maximum 6,7% error margin (Zhang & Huisinigh, 2017).



**Figure 3:** Schematic Design of Triple-Layer Hybrid Ventilation System

Hybrid ventilation systems comprise three functional layers: thermosiphon-driven natural ventilation exploits atmospheric pressure gradients through  $22,5^{\circ} \pm 0,5^{\circ}$  axial shafts, generating convective currents fulfilling 55-68% of baseline requirements (Gomis et al., 2021), while Variable Frequency Drive (VFD) fans operating at 0,4 bar during peak demand provide smart mechanical support powered by high-efficiency PV panels (23,5% conversion) (Wilberforce et al., 2019). The system is completed with 0,3nm porosity activated carbon filters capturing 94,2% of PM<sub>2.5</sub>, complemented by laser-based radon sensors triggering air recycling above 30 Bq/m<sup>3</sup>. Singapore's MRT implementation achieved a 43,7% energy reduction while exceeding WHO Air Quality Guidelines (Maroto-Valer, 2010).

Triple-defense flood management integrates smart hydraulic gates activated within 8 seconds upon detecting 25cm water depth via LiDAR/radar hybrid sensors (OKSANYCH & GRECHANINOV, 2024), with advanced 4.5m-diameter evacuation shafts featuring  $30^{\circ} \pm 2^{\circ}$  helical staircases coated in Nomex-XT (fire-resistant to 1200°C) and 200-bar compressed oxygen reservoirs sustaining 120-minute life support. Intelligent pumping systems employ Kaplan turbines handling 550 L/sec, powered by hydrodynamic energy from water flow at 92% efficiency. Tokyo Institute of Technology simulations demonstrated evacuation of 2,000 passengers in 8,5 minutes under 3 m<sup>3</sup>/sec flow conditions (Sommerfeldt, 2020).

**Table 2:** Comparative Risk Management Models

City Profile	Reference	Priority Dimension	Protocol
<i>Mature (e.g., Stockholm)</i>	(Ólafsson & Steingrímssdóttir, 2024)	Environmental efficiency	Phase-out diesel ventilation by 2030
<i>Rapid-growth (e.g., Mumbai)</i>	(Bendale & Thakur)	Governance financing	Sovereign infrastructure bonds
<i>Coastal (e.g., Miami)</i>	(Eldwib, 2024)	Resilience	Compulsory floodgates every 50m



The Copenhagen City Circle Line exemplifies holistic integration: modular design reduced construction costs by 28% through 85% component standardization, hybrid ventilation saved 2,7 GWh annually, and smart gates prevented 6,500 m<sup>3</sup> water intrusion during 2023 floods (Monterumisi & S  berg, 2025). Advanced computational modeling (Finite Element Method + BIM) projects an operational lifespan extension from 50 to 80 years with 33% life-cycle cost reduction per ISO 15686-1:2022, establishing a new paradigm in subsurface infrastructure sustainability (Ritts & Rutt, 2024). In (Error! Reference source not found.) show the Comparative Risk Management Models (Contrasts geological, cost, and operational challenges across regions with solutions).

This integration transforms tunnels from static entities into living systems adapting to subsurface complexities (Monoi et al., 2025).

To translate these technical and financial innovations into actionable strategies, (Table 3) synthesizes context-specific mitigation pathways that align the tri-dimensional framework (environmental, governance, resilience) with the practical needs of diverse urban settings. Proposed tri-dimensional mitigation pathways tailored to different urban contexts, demonstrating the application of the framework for practical policy and planning interventions.

**Table 3:** Context-Specific Mitigation Pathways for UUT Sustainability

City Context	Priority Dimension	Technical Solution	Financing Mechanism	Governance Tool
Mature (Global North)	Environmental Efficiency	AI-driven retrofitting, Hybrid ventilation	Green Bonds, Public budget	Performance-based regulations
Rapid-Growth (Global South)	Governance and Financing	Phased modular construction	Sovereign Infrastructure Bonds	International capacity building
Coastal/Flood-Prone	Contextual Resilience	Smart floodgates, Advanced pumping systems	Resilience-focused PPPs	Mandatory risk-sensitive zoning

### 3.3. Research Contributions and Novel Insights

This study makes several distinct contributions to the field of urban underground space and sustainable transportation:

It proposes and validates a tri-dimensional framework that challenges the traditionally siloed approach to UUT sustainability. By simultaneously analyzing environmental, governance, and resilience imperatives, the framework offers a more robust and realistic assessment model that captures the complex synergies and trade-offs between these dimensions.

It provides groundbreaking quantitative insights that recalibrate the sustainability narrative of UUTs. Specifically, it reveals that net carbon savings are offset by 35–70% due to energy-intensive ventilation—a critical correction to the prevailing literature. Furthermore, it identifies that 70% of system failures stem from institutional-environmental-structural fragmentation, a linkage previously underexplored.

The study actively addresses the Global North-South knowledge divide. By comparing disparate cases like Stockholm, Cairo, and Kuala Lumpur, it moves beyond Eurocentric models to offer context-sensitive pathways for implementation, such as AI-driven retrofitting for mature systems and phased modular financing for rapid-growth cities.

Beyond analysis, the research proposes tangible, context-driven solutions—such as hybrid financing models, standardized precast designs, and triple-layer ventilation systems—thereby bridging the gap between theoretical assessment and practical implementation for policymakers and engineers.

## 4. CONCLUSION

In conclusion, this research demonstrates that the sustainable development of urban underground transport is not merely an engineering challenge but a complex sociotechnical endeavor requiring integrated optimization across environmental, governance, and resilience domains. The tri-dimensional framework advanced here provides a transformative lens for reassessing UUT sustainability, revealing significant offsets in carbon savings and exposing systemic vulnerabilities overlooked in conventional analyses. (Table 4)

The novel contributions of this work lie not in reinventing individual components but in re-synthesizing fragmented knowledge across disciplines to create a more coherent and actionable understanding. Our findings

necessitate a paradigm shift—from viewing UUTs as isolated infrastructure to treating them as embedded urban service systems whose sustainability is dictated by energy portfolios, governance coherence, and spatial reclamation strategies.

practical Implications for Policymakers and Planners: The findings of this study offer clear, actionable insights for urban stakeholders:

- For Policymakers: Mandate integrated tri-dimensional impact assessments for all future UUT projects, moving beyond cost-benefit analysis to include carbon life-cycle accounting linked to energy sources and mandatory resilience stress-testing against contextual hazards.
- For Urban Planners & Engineers: Adopt the context-sensitive pathways outlined, prioritizing AI-driven energy efficiency in mature systems and phased, modular construction financed by innovative instruments in developing cities.
- For City Governments: Foster stronger subnational governance capacity by creating specialized agencies for underground space management that bridge the gaps between environmental, transportation, and emergency response departments.

Future research must build upon this integrated foundation, prioritizing underground-renewable energy symbiosis, social recovery metrics, and computational modeling of the tri-dimensional interactions we have identified. True innovation will be achieved not by further technological isolation but by fostering deeper transdisciplinary collaboration, ensuring that the underground spaces of tomorrow are not just built, but are built wisely, resiliently, and equitably for all urban contexts.

**Table 4:** Context-Driven Implementation Protocol (Prioritizes dimensions by city type: environmental, governance, resilience).

Challenge	The Chinese model	The European model	The Nordic model	Proposed solutions for your research
Geological Challenges	Soft soil rich in groundwater (Yangtze Delta). • Water seepage during excavation. • Risk of soil collapse.	• Heterogeneous rock layers. • Presence of historical monuments underground. • Vibrations that damage heritage buildings.	• Hard granite rocks that hinder excavation. • Frostbite in winter. • Limited layers suitable for construction.	• 3D geophysical surveys prior to implementation. • Thermal freezing techniques for fragile soils. • Tunnel path modifications to protect monuments.
Construction costs	• Very high (up to \$300 million/km <sup>2</sup> ). • High cost of groundwater control technologies.	• Moderate to high (\$250 million/km <sup>2</sup> ). • Additional costs for heritage protection.	• Highest globally (\$500 million/km <sup>2</sup> ). • Investment in sustainable building materials.	• Long-term cost-benefit modeling. • Public-private partnerships (PPPs) to reduce burdens. • Use of recycled materials in structures.
Operational Risks	• Flash floods (such as the 2021 Zhengzhou disaster). • Inadequate ventilation. • Difficulty evacuating in disasters.	• Fires due to outdated electrical systems. • Poor underground communications signals.	• Radon gas buildup in enclosed spaces. • Snowstorms disrupting entrances.	• Flood and fire early warning systems. • Hybrid (natural + mechanical) ventilation. • Storm-proof emergency entrances.
Risk Management	• Rapid response after disasters. • Focus on repair rather than prevention.	• A preventative approach: Continuous monitoring of structures. • Periodic evacuation drills.	• Integrating safety into design: backup tunnels. • Using artificial intelligence to detect cracks.	• An integrated digital platform for 24/7 structural monitoring. • Real-life disaster simulations for training. • Resilient design that adapts to climate change.

Strengths	<ul style="list-style-type: none"> <li>• Speed of implementation.</li> <li>• Advanced excavation techniques.</li> </ul>	<ul style="list-style-type: none"> <li>• Heritage protection.</li> <li>• Community engagement.</li> </ul>	<ul style="list-style-type: none"> <li>• High sustainability.</li> <li>• Integration with nature.</li> </ul>	<ul style="list-style-type: none"> <li>• Leveraging strengths</li> <li>• Combining Chinese expertise with European prevention and Nordic sustainability.</li> </ul>
-----------	---	---	--	---

## 5. FUNDING

This study was funded by the following funding projects:

(1) Research on Green Construction and Resilient Technology of Urban Underground Transportation Facilities (No. 2022YFE0104300, a joint research project between the Ministry of Science and Technology of China and the Japan International Cooperation Agency (JICA);

(2) Research on Design and Control Mechanism of Intensive and Compact Urban Areas under the “Dual Carbon” Strategy (No. 22YJCZH226, a general project of humanities and social sciences of the Ministry of Education);

(3) Digital Technology and Application of Compact and Low-Carbon Urban Areas in the Rail Transit Influence Areas of Chengdu-Chongqing Economic Circle (No. 2024YFHZ0220, a project of Sichuan International Science and Technology Innovation Cooperation/Hong Kong, Macao and Taiwan Science and Technology Innovation Cooperation)

## 6. REFERENCE

- [1] Al-Mukhtar, M. (2019). Random forest, support vector machine, and neural networks to modelling suspended sediment in Tigris River-Baghdad. *Environmental monitoring and assessment*, 191(11), 673.
- [2] Ali, M. M., Alssadah, G. M., Yu, Y., Althahir, M. M., Damos, M. A., Zhou, R., & Abdrhman, H. (2025). Evaluating transit-oriented development (TOD) in Khartoum: A spatial analysis of bus terminals. *Journal of Urban Management*.
- [3] Allan, R. P., Arias, P. A., Berger, S., Canadell, J. G., Cassou, C., Chen, D., Cherchi, A., Connors, S. L., Coppola, E., & Cruz, F. A. (2023). Intergovernmental panel on climate change (IPCC). Summary for policymakers. In *Climate change 2021: The physical science basis. Contribution of working group I to the sixth assessment report of the intergovernmental panel on climate change* (pp. 3-32). Cambridge University Press.
- [4] ASEAN. (2023). The ASEAN – 20th Year of The ASEAN Committee on Disaster Management. asean. Retrieved 2025/6/10 from <https://asean.org/serial/building-community-resilience/>
- [5] Azevedo dos Santos Silva, F. (2023). Energy Transition in Norway, Sweden, and Portugal: Reconciling Conflicts Between Climate and Environmental Objectives in the context of Hydropower Production UiT Norges arktiske universitet].
- [6] Besner, J. (2017). Cities think underground–Underground space (also) for people. *Procedia Engineering*, 209, 49-55.
- [7] Bian, X., Gao, Z., Zhao, P., & Li, X. (2024). Quantitative analysis of low carbon effect of urban underground space in Xinjiekou district of Nanjing city, China. *Tunnelling and Underground Space Technology*, 143, 105502.
- [8] Bienenzeisler, L., Lelke, T., & Friedrich, B. (2024). Autonomous Underground Freight Transport Systems--The Future of Urban Logistics? arXiv preprint arXiv:2403.08841.
- [9] Bilbao-Ubillos, J. (2008). The costs of urban congestion: Estimation of welfare losses arising from congestion on cross-town link roads. *Transportation Research Part A: Policy and Practice*, 42(8), 1098-1108.
- [10] Bobylev, N. (2009). Mainstreaming sustainable development into a city's Master plan: A case of Urban Underground Space use. *Land use policy*, 26(4), 1128-1137.
- [11] Bragado Fernández, N. (2023). Movilidad sostenible en Madrid: evolución del uso de metro y autobuses.
- [12] Broere-Brown, Z. A., Baan, E., Schalekamp-Timmermans, S., Verburg, B. O., Jaddoe, V. W., & Steegers, E. A. (2016). Sex-specific differences in fetal and infant growth patterns: a prospective population-based cohort study. *Biology of sex differences*, 7, 1-9.
- [13] Broere, W. (2016). Urban underground space: Solving the problems of today's cities. *Tunnelling and Underground Space Technology*, 55, 245-248.
- [14] Buck, K. D., Summers, J. K., & Smith, L. M. (2021). Investigating the relationship between environmental quality, socio-spatial segregation and the social dimension of sustainability in US urban areas. *Sustainable cities and society*, 67, 102732.
- [15] Bureau, T. (2024). Tourism Bureau, Republic of China (Taiwan)-The 2024 Taiwan Lantern Festival will light up Tainan from February 24th to March 10th. Two areas will display lanterns, the " High Speed Rail Lantern Area" a. In: Tourism Bureau, Republic of China (Taiwan).
- [16] Carteni, A., Henke, I., & Moliterno, C. (2018). A cost-benefit analysis of the metro line 1 in Naples, Italy. *WSEAS Transactions on Business and Economics*, 15, 529-538.

- [17] CSO. (2023). Copenhagen Sustainability Office, 2023. sustainability. Retrieved 2025/6/10 from <https://sustainability.ku.dk/>
- [18] Cui, J., Broere, W., & Lin, D. (2021). Underground space utilisation for urban renewal. *Tunnelling and Underground Space Technology*, 108, 103726.
- [19] Cui, J., Huang, T.-Y., Luo, Z., Testa, P., Gu, H., Chen, X.-Z., Nelson, B. J., & Heyderman, L. J. (2019). Nanomagnetic encoding of shape-morphing micromachines. *Nature*, 575(7781), 164-168.
- [20] Cui, J., & Nelson, J. D. (2019). Underground transport: An overview. *Tunnelling and underground space technology*, 87, 122-126.
- [21] Del Fabbro, M. (2018). The institutional history of Milan metropolitan area. *Territory, Politics, Governance*, 6(3), 342-361.
- [22] Deng, F., Cheng, T., Huang, Y., Chen, Z., & Han, Q. (2024). Evaluation of urban underground space via automated constraint identification and hybrid analysis. *Tunnelling and Underground Space Technology*, 153, 106005.
- [23] Dong, Y.-H., Peng, F.-L., Li, H., & Men, Y.-Q. (2023). Spatial autocorrelation and spatial heterogeneity of underground parking space development in Chinese megacities based on multisource open data. *Applied Geography*, 153, 102897.
- [24] Edwards Jr, D. B., Caravaca, A., Rapoport, A., & Sperduti, V. R. (2024). World Bank influence on policy formation in education: a systematic review of the literature. *Review of Educational Research*, 94(4), 584-622.
- [25] Fanourakis, G. C. (2024). A Comparative Assessment of the Accuracy of the Hong Kong (HKBD) and Japanese (JSCE) Code Concrete Shrinkage Prediction Models. 20th fib Symposium on ReConStruct: Resilient Concrete Structures, 2024,
- [26] Forero-Ortiz, E., & Martinez-Gomariz, E. (2020). Hazards threatening underground transport systems. *Natural Hazards*, 100(3), 1243-1261.
- [27] Fraszczyk, A., Weerawat, W., & Kirawanich, P. (2020). Metro station naming strategies in selected megacities and lessons for new metro systems. *Transportation Research Procedia*, 48, 2608-2620.
- [28] Goldstein, D., Moskowitz, A. J., Gelijns, A. C., Ailawadi, G., Parides, M. K., Perrault, L. P., Hung, J. W., Voisine, P., Dagenais, F., & Gillinov, A. M. (2016). Two-year outcomes of surgical treatment of severe ischemic mitral regurgitation. *New England Journal of Medicine*, 374(4), 344-353.
- [29] Gomis, L. L., Fiorentini, M., & Daly, D. (2021). Potential and practical management of hybrid ventilation in buildings. *Energy and Buildings*, 231, 110597.
- [30] Guan, M., Nada, O. A., Wu, J.-j., Sun, J.-l., Li, N., Chen, L.-m., & Dai, T.-m. (2021). Dental caries and associated factors in 3–5-year-old children in Guizhou province, China: an epidemiological survey (2015–2016). *Frontiers in public health*, 9, 747371.
- [31] Hanamura, T. (2017). Underground Space Networks in the 21st Century: New Infrastructure with Modal Shift Technology and Geotechnology. In *Modern Tunneling Science And Technology* (pp. 55-65). Routledge.
- [32] Haque, M. S. (2000). Environmental discourse and sustainable development: Linkages and limitations. *Ethics and the Environment*, 5(1), 3-21.
- [33] Hata, T. R., Audish, D., Kotol, P., Coda, A., Kabigting, F., Miller, J., Alexandrescu, D., Boguniewicz, M., Taylor, P., & Aertker, L. (2014). A randomized controlled double-blind investigation of the effects of vitamin D dietary supplementation in subjects with atopic dermatitis. *Journal of the European Academy of Dermatology and Venereology*, 28(6), 781-789.
- [34] He, R., Tiong, R. L., Yuan, Y., & Zhang, L. (2024). Enhancing resilience of urban underground space under floods: Current status and future directions. *Tunnelling and Underground Space Technology*, 147, 105674.
- [35] Hong, X., Li, S., Chen, T., Ji, X., & Song, X. (2025). Spatial performance evaluation and optimization of integrated aboveground and underground spaces in urban commercial complexes. *Journal of Asian Architecture and Building Engineering*, 24(2), 623-649.
- [36] Huang, Y., Chen, F., Song, M., Pan, X., & You, K. (2023). Effect evaluation of traffic guidance in urban underground road diverging and merging areas: A simulator study. *Accident Analysis & Prevention*, 186, 107036.
- [37] Kallianiotis, A., & Batjakas, I. (2023). Temporal and Environmental Dynamics of Fish Stocks in the Marine Protected Area of the Artificial Reef of Kitros, Pieria (Northern Greece, Mediterranean Sea). *Journal of Marine Science and Engineering*, 11(9), 1773.
- [38] Kauffman, N. (2022). *The Material and Industrial Ecologies of Excavated Sediment: Insights for Climate Change Adaptation Planning*. University of California, Berkeley.
- [39] Kim, T., Sohn, D.-W., & Choo, S. (2017). An analysis of the relationship between pedestrian traffic volumes and built environment around metro stations in Seoul. *KSCE Journal of Civil Engineering*, 21, 1443-1452.
- [40] Leach, J. M., Rogers, C. D., Ortegón-Sánchez, A., & Tyler, N. (2019). The liveable cities method: Establishing the case for transformative change for a UK metro. *Proceedings of the Institution of Civil Engineers-Engineering Sustainability*,
- [41] Li, L., Ren, H., Zhao, S., Duan, Z., Zhang, Y., & Zhang, A. (2017). Two dimensional accessibility analysis of metro stations in Xi'an, China. *Transportation Research Part A: Policy and Practice*, 106, 414-426.
- [42] Li, Q., Song, L., List, G. F., Deng, Y., Zhou, Z., & Liu, P. (2017). A new approach to understand metro operation safety by exploring metro operation hazard network (MOHN). *Safety science*, 93, 50-61.
- [43] Li, Z., Han, Z., Xin, J., Luo, X., Su, S., & Weng, M. (2019). Transit oriented development among metro station areas in Shanghai, China: Variations, typology, optimization and implications for land use planning. *Land use policy*, 82, 269-282.

- [44] Liang, Q., Li, J., Wu, X., & Zhou, A. (2016). Anisotropy of Q 2 loess in the Baijiapo Tunnel on the Lanyu Railway, China. *Bulletin of Engineering Geology and the Environment*, 75, 109-124.
- [45] Liu, B., Zheng, D., Zhou, S., Chen, L., & Yang, J. (2022). VFDB 2022: a general classification scheme for bacterial virulence factors. *Nucleic acids research*, 50(D1), D912-D917.
- [46] Maroto-Valer, M. M. (2010). Developments and innovation in carbon dioxide (CO<sub>2</sub>) capture and storage technology: carbon dioxide (CO<sub>2</sub>) storage and utilisation. Elsevier.
- [47] Minx, J. C., Callaghan, M., Lamb, W. F., Garard, J., & Edenhofer, O. (2017). Learning about climate change solutions in the IPCC and beyond. *Environmental Science & Policy*, 77, 252-259.
- [48] Monoi, A., Kamio, R., Tamura, H., Kibi, Y., & Yasuoka Jensen, M. (2025). The Design Pattern of Participatory Urban Design for the “-Able City”-Applying Copenhagen’s Pattern to Japanese Case. *International Conference on Human-Computer Interaction*.
- [49] Monterumisi, C., & Sørberg, M. (2025). Reformistic approaches to mass housing in the metropolis: 1920s Copenhagen and Stockholm perimeter blocks. *Planning Perspectives*, 1-45.
- [50] Odlyzko, A. (1999). Paris metro pricing for the internet. *Proceedings of the 1st ACM Conference on Electronic Commerce*.
- [51] OKSANYCH, I., & GRECHANINOV, V. (2024). *Intellectual Informational Technologies and Systems*.
- [52] Owusu-Peprah, N. T. (2024). *World Development Report 2022: Finance for an Equitable Recovery*: by World Bank, Washington, DC, World Bank Publications, 2022, 267 pp., \$0.00 (E-book), ISBN 9781464817311. In: Taylor & Francis.
- [53] Park, J.-s. (2023). Efficiency Analysis of Tramways in the Metropolitan Areas in South Korea: Focusing on the Daejeon Metropolitan Area. *Future Transportation*, 3(4), 1223-1239.
- [54] Petchey, J. (2009). Theoretical analysis of equalization and spatial location efficiency. *Regional Studies*, 43(7), 899-914.
- [55] Qiao, Y.-K., Peng, F.-L., Wu, X.-L., & Ding, S.-F. (2018). Underground space planning in urban built-up areas: a case study of Qingdao, China. *Proceedings of 16th ACUUS International Conference*. Hong Kong, China: 16th ACUUS Conference Organizing Committee.
- [56] Qihu, Q. (2016). Present state, problems and development trends of urban underground space in China. *Tunnelling and Underground Space Technology*, 55, 280-289.
- [57] Rahman, S. M., & Kirkman, G. A. (2015). Costs of certified emission reductions under the Clean Development Mechanism of the Kyoto Protocol. *Energy Economics*, 47, 129-141.
- [58] Ritts, M., & Rutt, R. (2024). Growing up sustainable? Politics of race and youth in Urbanplan, Copenhagen. *Urban Geography*, 45(4), 631-651.
- [59] Skopec, M., Issa, H., Reed, J., & Harris, M. (2020). The role of geographic bias in knowledge diffusion: a systematic review and narrative synthesis. *Research integrity and peer review*, 5, 1-14.
- [60] Sommerfeldt, K. D. (2020). Predictive Integrated Stratigraphic Modeling (PRISM®) Work Plan Center Wide Per-and Polyfluoroalkyl Substances (PFAS) Potential Release Location (PRL) 237 Kennedy Space Center, Florida.
- [61] Suhr, J. K., & Jung, H. G. (2016). Automatic parking space detection and tracking for underground and indoor environments. *IEEE Transactions on Industrial Electronics*, 63(9), 5687-5698.
- [62] Tan, S. T., Mohamed, N., Ng, L. C., & Aik, J. (2022). Air quality in underground metro station commuter platforms in Singapore: A cross-sectional analysis of factors influencing commuter exposure levels. *Atmospheric Environment*, 273, 118962.
- [63] Valdenebro, J.-V., & Gimena, F. N. (2018). Urban utility tunnels as a long-term solution for the sustainable revitalization of historic centres: The case study of Pamplona-Spain. *Tunnelling and Underground Space Technology*, 81, 228-236.
- [64] Wang, J., Duan, H., Chen, K., Chan, I. Y., Xue, F., Zhang, N., Chen, X., & Zuo, J. (2025). Role of urban underground-space development in achieving carbon neutrality: a national-level analysis in China. *Engineering*, 45, 212-221.
- [65] Wei, X., Ren, Y., Shen, L., & Shu, T. (2022). Exploring the spatiotemporal pattern of traffic congestion performance of large cities in China: A real-time data based investigation. *Environmental Impact Assessment Review*, 95, 106808.
- [66] Wilberforce, T., Baroutaji, A., Soudan, B., Al-Alami, A. H., & Olabi, A. G. (2019). Outlook of carbon capture technology and challenges. *Science of the total environment*, 657, 56-72.
- [67] Zaki, N. A., & Jaafar, A. M. (2025). Uncovering the potential of underground architecture: A comprehensive study on its benefits, applications, and impacts on urban landscapes. *AIP Conference Proceedings*.
- [68] Zhang, P., Jin, T., Wang, M., Zhou, N., & Jia, X. (2025). Evaluation of the Suitability of Urban Underground Space Development Based on Multi-Criteria Decision-Making and Geographic Information Systems. *Applied Sciences*, 15(2), 543.
- [69] Zhang, Z.-Y., Peng, F.-L., Ma, C.-X., Zhang, H., & Fu, S.-J. (2021). External benefit assessment of urban utility tunnels based on sustainable development. *Sustainability*, 13(2), 900.
- [70] Zhang, Z., & Huisingsh, D. (2017). Carbon dioxide storage schemes: technology, assessment and deployment. *Journal of Cleaner Production*, 142, 1055-1064.
- [71] Zhao, J.-W., Peng, F.-L., Wang, T.-Q., Zhang, X.-Y., & Jiang, B.-N. (2016). Advances in master planning of urban underground space (UUS) in China. *Tunnelling and Underground Space Technology*, 55, 290-307.

## RESEARCH ON THE PERFORMANCE-DRIVEN SPATIAL INTERFACE DESIGN FOR CLIMATE-ADAPTIVE URBAN UNDERGROUND SPACE

Kai ZHOU<sup>1</sup>, Jia-Wei LENG<sup>2</sup>

**Abstract:** Rapid urbanisation is placing immense pressure on modern cities, with escalating issues such as increasing population density, scarcity of land resources, traffic congestion, challenging parking, massive energy usage, and severe environmental pollution<sup>[1-3]</sup>. In 1950, only 30% of the world's population lived in cities, but this number has grown to 56% in 2021 and is predicted to exceed 68 % by 2050<sup>[4]</sup>. Traditional vertical expansion, such as skyscrapers, while effective, is increasingly insufficient to addressing these challenges. Urban underground space (UUS) offers a viable alternative. By accommodating one-third of the urban functions - including traffic, commerce or office, and municipal facilities – below ground<sup>[5]</sup>, UUS not only enhances urban capacity, but also contributes to restoring the natural landscape, improving ecological conditions and protecting cultural and historical values above ground.

Despite its recognition as a potential contributor to low-carbon cities by academics, UUS still faces significant sustainability challenges<sup>[6]</sup>. Unlike ground-level buildings, UUS is surrounded by soil and rocks, creating semi-sealed environment that hinders natural ventilation and lighting. This necessitates reliance on energy-intensive mechanical systems to maintain a pleasant environment. Lighting and ventilation in an underground street in Xuzhou, China, consume 45% and 44% of energy, respectively, accounting for nearly 90% of total energy consumption<sup>[7,8]</sup>. This underscores a substantial need for energy-efficient solutions, particularly in terms of reducing the energy required for ventilation and lighting.

To address these challenges, the pursuit of maximising the prospects for the sustainable development of UUS is increasingly rooted in theoretical science and architectural practice, sparking discourse on the relationship between architecture and climate. The introduction and adoption of air-conditioning in the early 1910s marked a significant shift from passive climate adaptation to active environmental control, gradually isolating buildings from their external environments. During the energy and environmental challenges of the 1970s, interest in the integration of active and passive control technologies intensified, aligning with the growing emphasis on green and ecological development. This integrated approach became a defining paradigm in the architecture-climate relationship.

Within this context, spatial interface, a key element in sustainable design, assumes a crucial function in facilitating climate adaptation mechanisms through enabling buildings to regulate the exchange of material, energy and information between buildings and the natural environment. By guiding natural ventilation and optimising lighting conditions, spatial interfaces directly influence both microclimate and indoor comfort, as well as reduce energy consumption. Natural light not only fulfils visual requirements but also positively influences psychological well-being, circadian rhythms, productivity, and emotional health. It reduces the reliance on artificial lighting, lowers heating demand in winter, and mitigates the psychological discomfort commonly associated with underground environments. Likewise, natural ventilation enhances indoor air quality, regulates temperature and humidity, and improves occupant comfort. It enables higher thermal tolerance, reducing dependence on mechanical cooling and contributing to energy conservation. Besides, spatial interfaces, due to their close interaction with natural systems, enable the incorporation of renewable energy sources to provide power, substantially reducing environmental footprint. This approach fosters a balance between the performance of natural lighting, natural ventilation, and energy usage. Considering this increased interest in UUS, as well as the importance of sustainable UUS development and the pertinent role of spatial boundary, the focus should be expanded to the spatial interface design.

Based on this premise, this study adopts a “Identification of building performance metrics - Investigation of spatial interface typologies - Implementation through empirical validation (3I)” framework to conduct a quantitative analysis of spatial interfaces from a performance-oriented perspective. This framework facilitates a more precise and holistic understanding of the influence of spatial interfaces on environmental performance.

<sup>1</sup> MArch. Zhou Kai, PhD candidate in Architecture, Southeast University, No.2 Sipailou, Nanjing, 210096, PR China, [masonchow@seu.edu.cn](mailto:masonchow@seu.edu.cn)

<sup>2</sup> Prof. Leng Jia-Wei, DEng, Southeast University, No.2 Sipailou, Nanjing, 210096, PR China, [jw\\_leng@seu.edu.cn](mailto:jw_leng@seu.edu.cn)



Key performance evaluation metrics—including daylight autonomy (DA), daylight glare probability (DGP), ventilation rate, air changes per hour (ACH), and annual energy load—are utilised to construct mathematical models that theoretically explore the intrinsic connection between the design variables, such as window-to-wall ratio, and building performance. The analysis reveals the existence of optimal thresholds or selection ranges that balance natural lighting, ventilation efficiency, and energy consumption, underscoring the need for performance-based decision-making in UUS design. Furthermore, by analysing 30 relevant cases in subtropical monsoon climate zones with hot and humid summers, and cool to mild winters, the form of spatial interface was identified from the perspective of performance, and matched with the natural element such as sun, wind, soil, water and vegetation to complete the identification. This performance-oriented spatial interfaces are visualised as a spatial interface design atlas tailored to UUS in subtropical monsoon climates, offering a comprehensive framework for performance-oriented UUS design in these climatic conditions. To validate the effectiveness of the proposed design strategies, physical environmental monitoring of the Suzhou Bay underground space was conducted. This empirical data provides a practical basis for assessing the impact of the proposed design solutions on building performance. Ultimately, this research aims to shift underground space environmental regulation from “passive adaptation” to “active response”. By offering systematic and practical design guidelines for low-carbon, comfortable underground environments, it provides both theoretical insights and actionable solutions for advancing sustainable UUS development.

Looking ahead, future research efforts should focus on the development of climate-specific low-carbon design guidelines that identify strategies with the greatest impact on energy conservation across diverse climatic zones. In addition, an integrated design platform capable of integrated modelling, simulating, evaluating, optimising, and generating should be further developed and incorporated into the design workflow to enable rapid and accurate performance analysis, making performance-based architectural design possible. Finally, a standardised, scientific evaluation system for UUS sustainability is essential to guide industry adoption and fully realise the energy-saving potential of underground development.

**Keywords:** Urban underground space, Spatial interface, Building performance, Sustainable development

## Reference

- [1] Broere, W. (2016). Urban underground space: Solving the problems of today's cities. *Tunnelling and Underground Space Technology*, 55, 245–248. <https://doi.org/10.1016/j.tust.2015.11.012>
- [2] Zhou, K., & Leng, J.-W. (2023). State-of-the-art research of performance-driven architectural design for low-carbon urban underground space: Systematic review and proposed design strategies. *Renewable and Sustainable Energy Reviews*, 182, 113411. <https://doi.org/10.1016/j.rser.2023.113411>
- [3] von der Tann, L., Sterling, R., Zhou, Y., & Metje, N. (2020). Systems approaches to urban underground space planning and management – A review. *Underground Space*, 5(2), 144–166. <https://doi.org/10.1016/j.undsp.2019.03.003>
- [4] UN-Habitat. (2022). *World Cities Report 2024: Cities and Climate Action*.
- [5] Xia, H., Lin, C., Liu, X., & Liu, Z. (2022). Urban underground space capacity demand forecasting based on sustainable concept: A review. *Energy and Buildings*, 255, 111656. <https://doi.org/10.1016/j.enbuild.2021.111656>
- [6] Qiao, Y.-K., Peng, F.-L., Sabri, S., & Rajabifard, A. (2019). Low carbon effects of urban underground space. *Sustainable Cities and Society*, 45, 451–459. <https://doi.org/10.1016/j.scs.2018.12.015>
- [7] Wu L, Ji X. (2009). Research on energy conservation strategies of underground buildings. *Chin Oversea Archit*, 69 – 70.
- [8] Cao, S.-J., Leng, J., Qi, D., Kumar, P., & Chen, T. (2022). Sustainable underground spaces: Design, environmental control and energy conservation. *Energy and Buildings*, 257, 111779. <https://doi.org/10.1016/j.enbuild.2021.111779>

## RESEARCH OF DRILLING AND BLASTING METHOD BASED ON A SUPER-LARGE CROSS-SECTION CAVERN IN HONG KONG

Li Yifeng<sup>1</sup>, Yuan Juntao<sup>2</sup>, Hong Zhengqiang<sup>3</sup>, Li Wei<sup>4</sup>

**Abstract:** With the increasing demand for urban underground space, the construction of oversized caverns has become an important issue in the field of underground engineering. The traditional drilling and blasting methods face challenges such as difficult design, large charge and large blasting volume when applied to the construction of oversized caverns. In this paper, a large cavern project in Hong Kong is used as an example to systematically study the drilling and blasting method applicable to super-large cross-section caverns. The method adopts large-diameter holes (51mm), micro-differential blasting technology, combined with high-precision rock drilling cart for fully automatic drilling, which significantly improves the blasting efficiency, reduces the rate of duds, and effectively controls the problem of over-under-excavation. By optimizing the arrangement of the holes and the selection of explosives, the average amount of explosives per cubic meter of rock was reduced to 1.2kg, which significantly saves the construction cost. In addition, the method is excellent in safety, environmental protection and flexibility, and the vibration monitoring points are provided at the construction site. So, the vibration generated by blasting has minimal impact on the surrounding environment. The research results of this paper provide an important reference for the construction of similar super-large cross-section caverns by drilling and blasting method, which has a high popularization value.

**Keywords:** super-large cross-section cavern; drilling and blasting method; differential blasting; rock drilling cart; blasting efficiency

### 1. INTRODUCTION

With the growing demand for underground space in urban development, the construction scale of tunnels and caverns projects is constantly expanding. Such projects usually face challenges such as complex surrounding environment, variable geological conditions, high construction costs, and technical difficulties, among which the excavation construction is particularly critical (Wang et al., 2010, Yan, 2019). In recent years, the development of mega-section tunnels and caverns construction technology is closely related to the rapid growth of transportation demand. Many early construction tunnels have been unable to meet the current transportation needs, prompting the development of larger span engineering construction. From the beginning of the 21st century, single tunnel 2 lanes gradually developed to single tunnel 3 lanes, 4 lanes, construction technology has made great progress. However, there are still few super-large cross-section caverns in the world, and the related technology system has yet to be perfected (Tan et al., 2019, Zhang et al., 2010, Chen et al., 2018, Zhang et al., 2020, Bi et al., 2011 & 2021).

<sup>1</sup> Li Yifeng, M.Sc., B.Eng., Assistant General Manager, Civil Department, China State Construction Engineering (Hong Kong) Limited, 27/F, China Overseas Building, 139 Hennessey Road, Hong Kong China, e-mail address: li\_yf@cohl.com.

<sup>2</sup> Yuan Juntao, M.Eng., B.Eng., Engineer, Civil Department, China State Construction Engineering (Hong Kong) Limited, 27/F, China Overseas Building, 139 Hennessey Road, Hong Kong China, e-mail address: juntao.yuan@cohl.com.

<sup>3</sup> Hong Zhengqiang, M.Eng., B.Eng., Assistant Site Manager, Civil Department, China State Construction Engineering (Hong Kong) Limited, 27/F, China Overseas Building, 139 Hennessey Road, Hong Kong China, e-mail address: zhengqiang.hong@cohl.com.

<sup>4</sup> Li Wei, M.Eng., B.Eng., Deputy Site Manager, Civil Department, China State Construction Engineering (Hong Kong) Limited, 27/F, China Overseas Building, 139 Hennessey Road, Hong Kong China, e-mail address: gzliwei@cohl.com.

As the traditional construction method of tunnels and caverns, the drilling and blasting method plays an important role in infrastructure construction. With the continuous expansion of tunnel construction scale, drilling and blasting construction technology has experienced a leapfrog development from manual operation to mechanization and intelligence. According to the International Tunneling Association statistics, the global tunnel construction to the use of drilling and blasting method of construction is dominated by the proportion of China is as high as more than 70% (Guo et al., 2007). However, for the application of drilling and blasting method for large section tunnels and caverns there are still major difficulties. From the perspective of engineering mechanics, the distribution of surrounding rock loads and mechanical properties of support in mega-span tunnels have significant special characteristics. As the section size increases, the problem of surrounding rock stability becomes increasingly prominent, and engineering problems such as surrounding rock instability and lining structure cracking are prone to occur (Zhao et al., 2018, Huang et al., 2017, Zhang et al., 2001).

In recent years, China has made a series of breakthroughs in the field of super-large cross-section underground engineering (Zhu et al., 2002). The Liantang Tunnel of the Shenzhen Eastern Transit Highway, which was opened in 2018, created a record for the world's largest section highway tunnel at the time, with an excavated section of 428.5m<sup>2</sup>. The project included a variety of complex section forms. The New Badaling Tunnel of Beijing-Zhangzhou Highway is a typical representative of large-section tunnels constructed by drilling and blasting method, and its underground station project contains 78 large and small chambers, with the largest single-arch span of 32.7 m, and the construction process adopts the advanced technologies of mechanized construction and information management, which provides valuable experience for similar projects.

Currently, the section area of the world's largest span underground cavern has reached 1000 square meters, and China has made significant progress in this field, such as Chongqing Railway Hongqihegou Station, which has achieved 760 square meters of large section excavation. However, for this kind of large cross-section project, there are still many technical challenges in the selection of construction methods, parameter optimization, equipment development. The solution of these problems will be directly related to economy and safety of oversized section underground projects (Wang et al., 2010).

With the continuous growth of the demand for underground space development, the following development trends will be faced in the mega-section underground engineering: 1) construction technology will develop in the direction of intelligence and refinement, and new technologies such as digital twin and artificial intelligence will be more widely used; 2) the concept of green construction will be deeply rooted in the engineering, and environmentally friendly blasting technology and low-carbon support materials will be gradually promoted; 3) the research and development of standardized and modular construction equipment will enhance the engineering efficiency; 4) the cross-integration of disciplines will promote the innovative development of design theory. These technological advances will provide new ideas and methods for solving the technical difficulties currently faced (Tan et al., 2023, Yang et al., 2023, Tan et al., 2018, Wang et al., 2018, Hong et al. 2018). This paper describes the research and application of drilling and blasting construction method for oversized caverns in Hong Kong as an example, aiming to provide some engineering reference and theoretical guidance for similar oversized cavern projects in the future.

## 2. PROJECT OVERVIEW

In May 2011, Development Bureau (DEVB) in Hong Kong briefed the Legislative Council Panel on Development on its plan to identify feasible reclamation sites, identify suitable existing government facilities that could be relocated to rock caverns, and conduct relevant technical assessments. In December 2017, DEVB issued a policy guideline on rock cavern development to increase land supply, which included the promulgation of the Rock Cavern Master Plans and related planning and technical guidelines. This mega cavern project is the first of its kind in the DEVB's plan to relocate government facilities into rock caverns, freeing up 28 hectares of land for other uses beneficial to people's livelihoods. The project mainly comprises site development, main cavern construction, cavern ventilation system and ancillary buildings, etc. Construction methods such as drilling and blasting, permanent anchor support, OHVD, etc., as well as carbon-reduction measures such as rubble disposal and rock recycling, etc., have been adopted.

This project is a complex urban environment of oversized section drilling and blasting method construction cavern group, most of the palisade in more than 200m<sup>2</sup>, the largest cavern palisade width of up to 32m, the height of up to 32m, need to be split into the upper, middle, and lower levels of blasting operations, the average size of palisade up to 300m<sup>2</sup>, a rare Hong Kong and even the world's oversized section. This paper combines the actual construction situation, introduces the drilling and blasting method applied to this type of section construction method, in the hope of providing reference for similar projects.

### 3. PRINCIPLE OF DRILLING AND BLASTING METHOD

Drilling and blasting method is the traditional rock excavation method. For general highway or municipal road tunnels, the palm face size is generally below 100m<sup>2</sup>, and will not change the design with the increase in depth. It is only necessary to understand the geological conditions in order to carry out a relative simple blasting design. However, for cavern projects, since the excavated space will be used for construction facilities, the size of the face is mostly over 100m<sup>2</sup>. The drilling and blasting method has the characteristics of high design difficulty, large amount of explosives, and large amount of blasting engineering. At the same time, cavern groups with different vertical and horizontal combinations also have faces of different sizes. How to design the blasting form at the junction is also a difficulty in the drilling and blasting construction of cavern projects compared to tunnel projects.

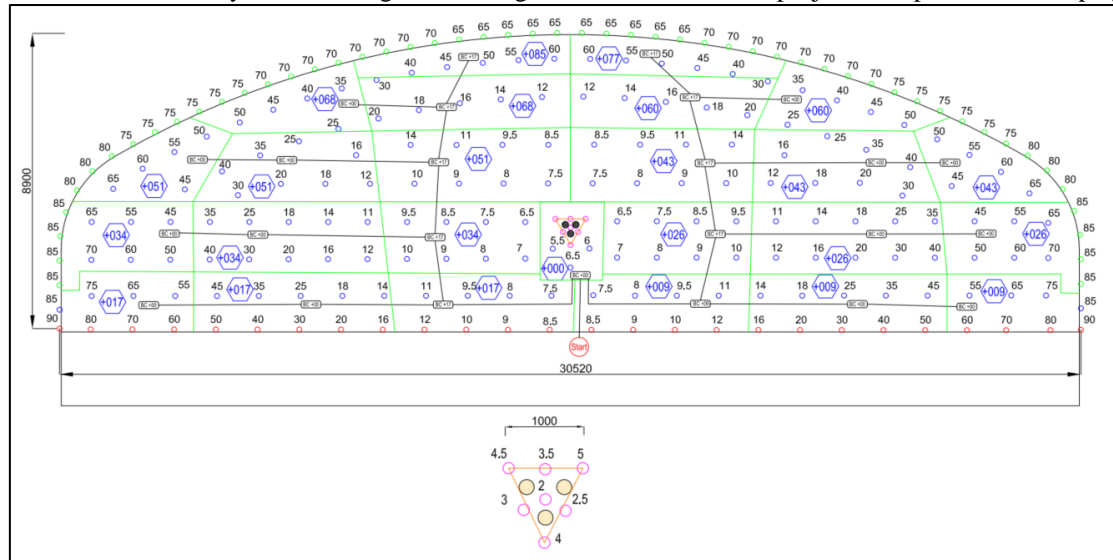


Figure 1. Typical blasting design.

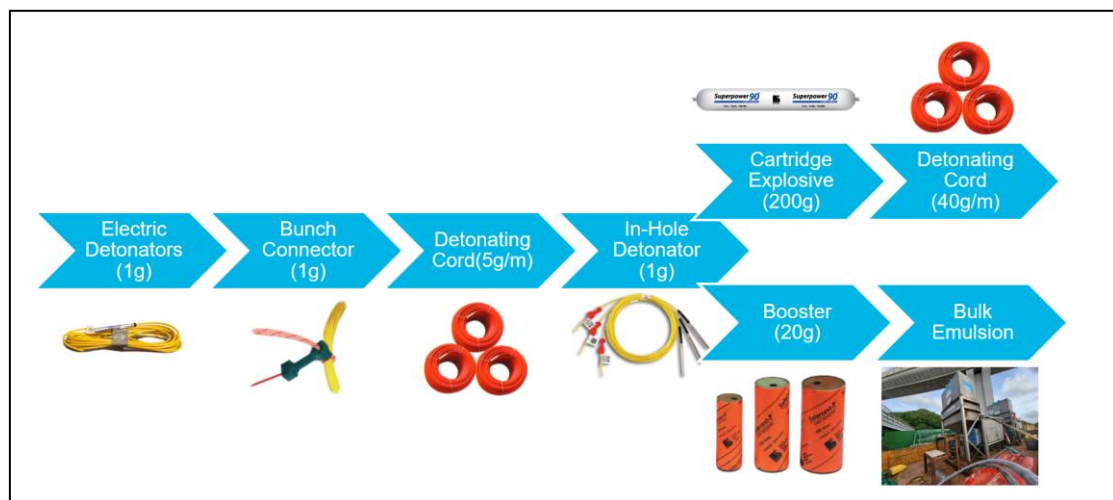


Figure 2. Charging scheme.

This method utilizes micro-difference blasting to construct tunnels with extremely large cross-sections, featuring rapid and simple construction, high flexibility, low cost, and high efficiency. After geological surveys are completed, the excavation face is first automatically drilled using a CNC drilling rig, into which emulsion explosives and electric detonators, as well as detonating cords, are placed according to the designed mix ratio; subsequent blasting operations follow, followed by quality inspection and evaluation of the blasting. The entire process centers on blasting design, combined with automatic drilling rig technology, significantly simplifying the tunnel support structure construction process, making it convenient and efficient. The following case study will focus on this rock cavern project.

It is suitable for tunnel projects with good geological conditions and super large sections. It is mainly used for rock caverns or tunnels with short distance and large blasting surface that are not suitable for shield machine

construction, but it needs to ensure the excavation depth and efficiency of underground space projects. It has the following construction advantages:

(1) High blasting efficiency: Traditional blasting construction follows the approach of "short advance, dense holes, weak blasting," and due to limitations in operating machinery, the diameter of each blasting hole generally does not exceed 40mm, with no more than 1.5kg of explosives per meter, and the penetration depth does not exceed 4m. Using this method, under conditions of large-span full-face blasting, each blasting hole can reach 51mm, the explosive charge can reach 2kg/m, and the penetration depth is maintained at around 5m. Additionally, all blasting uses micro-difference blasting, allowing all explosives to be detonated within 10 seconds on a blasting face of about 300m<sup>2</sup>, significantly improving the efficiency of cave group construction.

(2) High Flexibility: This method designs different blasting sequences and charge ratios for rock faces of varying sizes. After each blasting, geologists and supervisors evaluate the quality to determine the effectiveness of this blasting. Practical engineering has shown that this method offers high flexibility in blasting, with good blasting effects tailored to different blasting faces, free from template constraints, demonstrating significant versatility.

(3) High safety and environmental protection: This method has a high degree of mechanization, eliminating the need for manual operation by workers, ensuring construction safety. At the same time, over ten vibration monitoring points are installed around the project site. Based on data from each blasting and on-site experience, the vibrations generated by blasting can be negligible, with almost no impact on the surrounding environment, and people at the site do not feel the blasting process.

(4) High construction quality: This method uses high-precision rock drilling cart instead of air gun to ensure the quality of hole formation. Through the arrangement of precision micro-difference blasting, the blasting efficiency is significantly improved, the rate of silent blasting is reduced, and the over-excavation control of the blasting surface after blasting is good, and the amount of work that needs to be adjusted is less.

(5) High economic efficiency: This method has a high degree of mechanization, reducing labor costs and shortening construction periods, thus significantly lowering construction costs. At the same time, for the layout of blasting holes, under the premise of meeting the requirements for full-face blasting and depth in super-large sections, the spacing between bottom cut-off holes and auxiliary holes can be increased to over 1m, and the spacing between peripheral holes can be increased to over 0.6m. On average, each blasting hole can cover an area of 1.03m<sup>2</sup>, with an average of only 1.2kg of explosives used per cubic meter of rock, greatly reducing the amount of explosives used and improving management efficiency.

## 4. CONSTRUCTION METHODOLOGY

### 4.1. Process flow

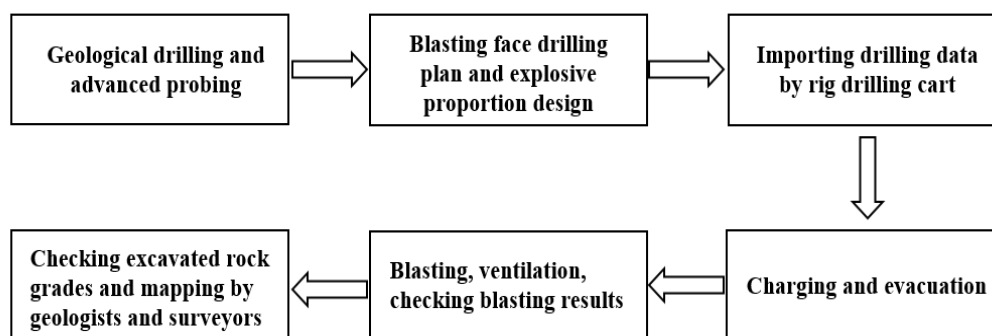


Figure 3. Process flow diagram.

### 4.2. Construction technology operation points

#### 4.2.1. Pre-processing

For tunnel excavation using the drilling and blasting method, the preparatory procedures mainly include advanced drilling and pre-grouting of advance small pipes. The rock encountered in the project is generally classified as Grade I to Grade III grade, with sufficient strength and ideal weathering conditions, providing certain

convenience for construction and support. After the tunnel geologist confirms which method should be used for the preparatory procedures, the blasting engineer designs the blasting based on actual conditions.

The selection and arrangement of explosive types, as well as the design of blasting holes, are related to the value of maximum charge quantity (MIC). The MIC value should be determined by selecting the minimum MIC value at all positions on the blasting face. Specifically, for a typical blasting face, only the MIC values at key locations need to be calculated, and the minimum among them is taken. The calculation formula is:  $PPV = 644(R/W^{1/2})^{-1.22}$ , where PPV is generally taken as 25mm/s. In this project, R represents the distance between the blasting hole position and THEES (Tolo Harbour Effluent Export Scheme) Tunnel, and W is the MIC value.

#### 4.2.2. Blasting design

##### 4.2.2.1 Borehole design

This method employs a three-arm drilling cart, using unidirectional slotting for hole excavation, which includes both air holes and blasting holes (slotting holes, auxiliary holes, and surrounding holes). The diameter of the air holes ranges from 89 to 127 mm (commonly 102 mm), while the diameter of the blasting holes is uniformly designed between 42 and 51 mm (commonly 51 mm), as shown in Figure 4. The selection of blasting hole diameters is also closely related to the MIC value. If the MIC exceeds 3 kg, the hole diameter is typically chosen to be  $\Phi 51$  mm; if it is less than 3 kg, a diameter of 45 mm is generally selected. In this method, the MIC for all blasting faces reaches 10 kg, so most hole diameters are designed to be 51 mm.

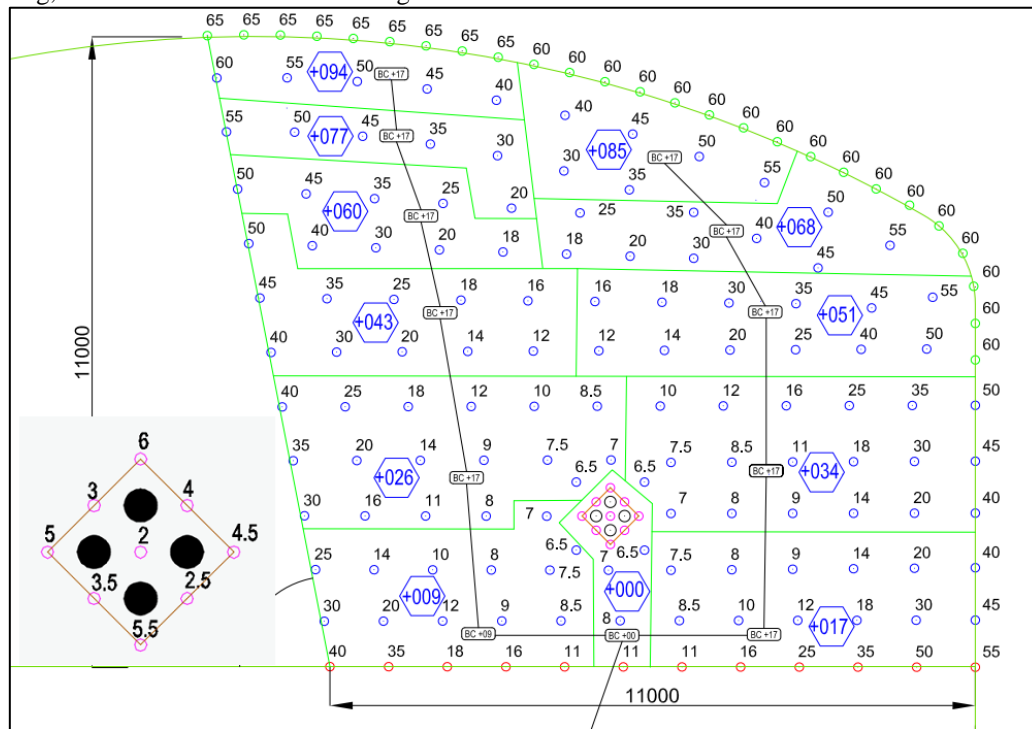


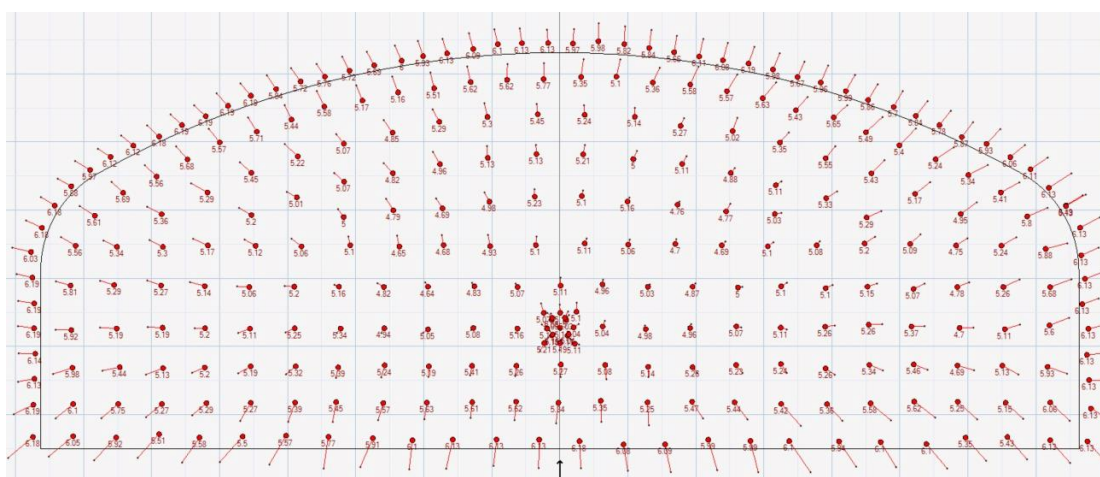
Figure 4. Design of the borehole.

The spacing between boreholes is larger due to the larger diameter of the drilled holes, which results in a greater amount of explosives being loaded into each hole. Therefore, the spacing between blasting holes is also greater than that of traditional drilling methods. The distance between auxiliary holes generally exceeds 1m, and the distance between peripheral holes generally exceeds 0.5m. On average, only one blasting hole is needed for every 1.03m<sup>2</sup> area of blasting face.

In terms of drilling depth, the filling length (Stemming)  $L_s$  should generally not be less than the hole spacing, the loading length (Emulsion Charge)  $L_c = MIC/1.59$ , and the drilling depth  $L = L_s + L_c$ . In this project, the hole depth is generally 5.0m to 6.0m.

The typical borehole drilling records are shown in Figure 5. In the case of using a three-arm automatic rock drilling car, the hole quality can be controlled very ideally.





**Figure 5.** Typical borehole records for the blasting face.

#### 4.2.2.2 MIC value

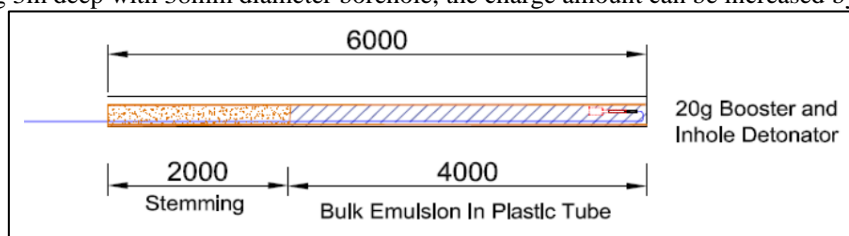
According to the requirements of relevant legal provisions and project characteristics, bagged emulsion explosive, bulk emulsion explosive, non-electric detonator, electric detonator (only used for initiation), detonating cord, igniter and other blasting materials are selected.

For the selection of explosives, generally, when  $MIC \leq 1.0\text{kg}$ , packaged emulsion explosive (cartridges) is selected; when  $MIC > 1.0\text{kg}$ , bulk emulsion explosive (emulsion) is selected. This method involves achieving a MIC of 10kg at blasting face, so bulk emulsion explosive is mainly chosen for the main blasting holes except for the surrounding holes.

#### 4.2.2.3 Arrangement of explosives

In order to enhance the blasting efficiency, save cost and control the rate of silent shots, this method only uses non-electric detonators and electric detonators in the selection of detonators. For a single blasting, electric detonators are only used at the initiation point, and all other holes are filled with non-electric detonators.

After calculation, the maximum charge amount per meter of 51mm diameter borehole designed for the project can reach 2kg/m under the premise of ensuring the environmental impact requirements (Section 4.2.5). If the depth of the borehole is calculated as 5m, then the MIC of each borehole can reach 10kg. Compared with the traditional method of drilling 3m deep with 38mm diameter borehole, the charge amount can be increased by about 3 times.



**Figure 6.** Borehole charging diagrams.

#### 4.2.2.4 Design of differential blasting parameters

Due to production limitations, the delay time of the detonator will have an inherent error of about 2% during product design. At the same time, explosive manufacturers will not customize blasting materials with ideal delay times for projects. Therefore, when designing the delay time for micro-differential blasting, the time interval between holes should be larger as they move outward to ensure that the blasting progresses from the core to the periphery. In the design of the maximum blasting face, the maximum delay time for the outermost peripheral holes is 9000ms (i.e., 9s, as shown in Figure 1). All blasting faces can be completed within 10s. All of the blasting faces can be guaranteed to be completed within 10s.

#### 4.2.2.5 Comparison with traditional methods

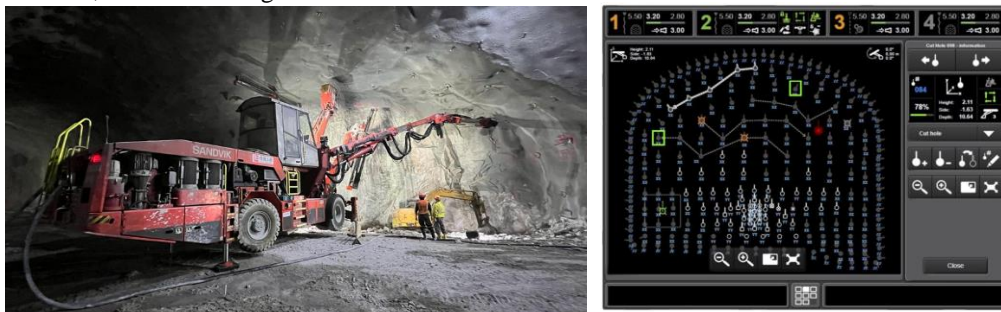
A detailed comparison with traditional method is shown in Table 1:

**Table 1.** Comparison between traditional methods.

Item	unit (of measure)	Traditional methods	Method in this paper
Bore size	mm	32~50	51
Auxiliary hole spacing	m	0.7~0.8	$\geq 1$
Number of holes required per square meter of surface	Nos.	1.8	0.97
Blasting depth	m	$\leq 4$	5
Maximum charge (per borehole)	kg	$\leq 5$	10
Unit consumption of explosives	kg/m <sup>3</sup>	1.2~2.4	1.2
Operational staffing requirements	/	At least 1 person is required for each wind drill	3-arm automatic drilling
Construction environment and noise	/	Poor environment and high noise level	Good environment, moderate noise
Forms of grooving	/	Wedge, Straight	Straightness

#### 4.2.3. Rock drilling cart

Three-arm rock drilling cart is used for hole construction. The blasting design diagram is input into the machine, and the automatic positioning and automatic drilling functions of the machine are used to realize automatic drilling construction, and the hole marking points made by the surveyor on the blasting surface are double confirmed, as shown in Figure 7.



**Figure 7.** Automatic construction of rock drilling dolly.

#### 4.2.4. Charging and evacuation

The explosives are charged by the registered blasting workers.

(1) The loading inspection should be completed 30 minutes before the detonation, the blasting worker and the foreman worker start the clearance procedure, the blasting worker notifies the blasting engineer that the blasting will be carried out within 30 minutes, and the foreman worker notifies all the workers to start evacuating to the designated area;

(2) Fifteen minutes before the detonation, the foreman worker needs to make sure that he is the last person to evacuate, and the blasting worker will check again that everyone has evacuated;

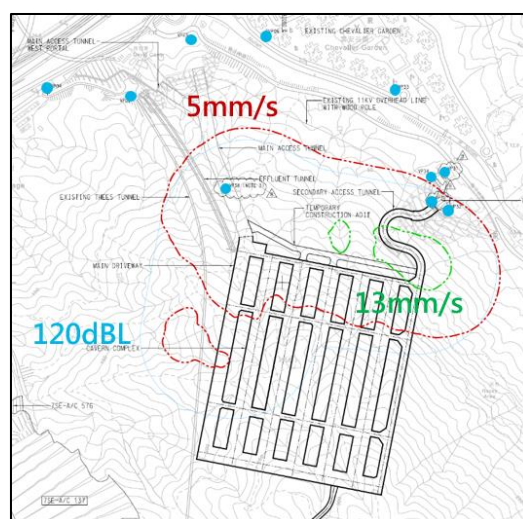
(3) Two minutes before detonation, the gun king and the blasting engineer will confirm with the supervisor that all personnel have been evacuated and sign the confirmation form;

(4) One minute before detonation, the blasting engineer gives the order to the master gunner to detonate.

(5) After receiving the order, the total blasting worker carried out the detonation operation at the designated position.

#### 4.2.5. Blasting monitoring and ventilation detection

During the blasting process, two indexes, namely peak vibration velocity of mass point (PPV) and overpressure of air shock wave (AOP), are mainly detected. The value of PPV and AOP is used to guide the design of the next blasting every time. The monitoring points and indexes of the two indexes are shown in Figure 8 and Figure 9 respectively.



**Figure 8.** Monitoring locations and vibration predictions.

PPV		AOP	
Alert	90% of the PPV limit	Alert	118 dBL
Action	95% of the PPV limit	Action	119 dBL
Alarm	100% of the PPV limit	Alarm	120 dBL

**Figure 9.** PPV and AOP related limit requirements.

After the blasting is completed, continuous ventilation should be carried out to ensure the air quality in the cavern. The five gases in the air, including oxygen, methane, hydrogen sulfide, carbon monoxide and radon gas, should be monitored and controlled, and the wind speed in the cavern should meet at least 0.5m/s.

#### 4.2.6. Blasting check

When the gas detection is basically qualified, the registered blasting worker will enter the tunnel to inspect the blasting face. After confirming safety, the blasting engineer and explosives supervisor will enter the tunnel to check the blasting face and ensure that all explosives have detonated. If any duds are found, they should be reported immediately and handled promptly; if immediate handling is not possible, clear signs should be set up nearby, and appropriate safety measures taken.

When handling a dud, no irrelevant personnel shall be present, and the boundary of the danger zone shall be guarded. Other operations shall be prohibited within the danger zone; when the blasting circuit of the borehole is confirmed to be intact after inspection, it can be reblasting. When blasting a dud, the power supply shall be cut off immediately and the blasting network shall be short-circuited in time.

#### 4.2.7. Geological inspection and blasting surface mapping

After the spoil is removed, a geologist conducts geological surveys on the tunnel excavation face to check if the exposed rock mass is stable and can specify reinforcement measures or require further clearance of hazardous rocks. The geologist calculates the NGI-Q value based on parameters such as the size of the exposed rock mass, interblock shear strength, and degree of joint development, to assess the stability of the rock mass. This determines the design support grade for the excavation face at that location. All geological survey records, Q-value calculations, and support structure designs should be documented and submitted for approval by the supervising engineer.

Before and after temporary and permanent shotcrete construction, the contour line of the excavation face must be surveyed, and the measurement data should be submitted for supervision and acceptance. For under-excavation, the excavation section should be surveyed at intervals of 1m, with the under-excavated areas marked and the over-excavated rock removed using a hydraulic hammer. After completion, re-surveying should be conducted; for over-excavated sections, if the over-excavation depth exceeds 200mm, permanent shotcrete backfilling should be used; if the over-excavation is at the bottom, Grade 200 graded fill material should be used for backfilling.

### 4.3. Explosives and equipment

The explosives and equipment involved in this method are shown in Table 2 and Table 3.

**Table 2.** *Materials required for construction of super-large cross-sections by drilling and blasting method.*

Serial number	Name of material	unit (of measure)	Quantities
1	Cartridge Explosives	Ton	10
2	Underground Bulk Emulsion Matrix	Ton	2900
3	Booster	Nos.	340000
4	Detonating Cord 5g	m	72000
5	Detonating Cord 40g	m	10000
6	In-hole delay Non-electric Detonators with around 9m signal tube	Nos.	336000
7	Surface/Bunch Detonators	Nos.	20000
8	Electric Detonators around 1.5m leg wire	m	4100
9	Electric Detonators w/ around 6m wire	m	3000
10	Electric Detonators Branch Wire / Bus Line 400m or 200m per coil	m	600
11	Lead in Line shock tube w/ detonator (STARLINE) 300m/roll	Nos.	100

**Table 3.** *Permanent spray anchor rapid support construction main mechanical equipment configuration.*

Serial number	Equipment Name	Specification	Unit (of measure)	quantities
1	Rock drilling cart	Epiroc X3E	Nos.	2
2	Lifting platform	AICHI SR182	Nos.	4

#### 4.4. Quality control

When inputting the corresponding point data into rock drilling cart, the surveying department should conduct re-measurement at the face and mark the drill hole positions on the face to ensure that the automatic drilling is performed at the marked points without deviation. If any deviation is found, immediately stop the automatic drilling, confirm the issue, and continue drilling or switch to manual operation for mechanical drilling.

After the filling of explosives and wires is completed, a second inspection should be carried out to ensure that the type and quantity of filling materials are correct.

After the blasting is completed, ventilation should be carried out for a certain period to ensure that the environment inside the cavern meets the operational requirements. Then the registered blasting worker shall enter the work face first to inspect the quality of the blasting. If any dud shots are found, immediate action should be taken to handle them with a second detonation; if the explosives are buried under debris and cannot be processed, relevant departments should be notified immediately for handling.

After ensuring safety, geologists and surveyors enter the site to control and check the quality of blasting. This includes whether the depth of blasting meets the requirements, whether the over-excavation is within the allowable range, whether there is a lack of excavation, and whether there are suspended stones.

#### 4.5. Security measures

Tunnel workers must obtain the closed space work certificate and other approved certificates, and have undergone project safety training. Strict safety briefing is required before each process, and workers are not allowed to work alone.

Tunnel workers should wear the correct personal protective equipment, including safety helmet, reflective clothing, safety shoes, dust-proof masks, goggles and sound insulation earphones in designated areas.

There should be safety management personnel or traffic commanders in the tunnel working face to avoid workers from entering the operation range of large machinery or operating the machinery without authorization.

Welding or cutting work shall not be carried out in the tunnel. If relevant procedures are required, the regulations and safety management requirements shall be complied with, and the hot operation permit system shall be activated.

In case of emergency, the staff in the tunnel should evacuate to the outside of the tunnel in an orderly manner to the guard room, which is not only the passage for entering and exiting the tunnel, but also the temporary assembly point and work coordination center.

The area below the exposed rock surface and the area where shotcrete is sprayed is a restricted area, and it is forbidden to pass through within 1 hour after the completion of shotcrete spraying. All restricted areas should be enclosed by guardrails until the early strength of shotcrete is reached.

## 5. BENEFIT ANALYSIS OF ENGINEERING CASES

The drilling and blasting construction method described in this paper is a summary and improvement of traditional drilling and blasting techniques. Applying this construction method to the excavation of super-large cross-section caverns has several advantages, including simple construction procedures, high mechanization, high construction efficiency, and lower costs. It also demonstrates considerable flexibility in response to varying geological conditions at the excavation face. Taking the example of this super-large cross-section cavern project, preliminary economic benefits are estimated as follows: a cost savings of HKD 45 million, a time-saving of 6 months, with a total cost benefit of approximately HKD 65 million.

To optimize the utilization of urban land resources and address the aging facilities and odor issues at existing wastewater treatment plants, the Hong Kong government implemented the relocation plan for the Wastewater Treatment Plant in 2014. The project is divided into five main phases, which involve constructing the new cavern within the mountain near the original plant, relocating the existing plant into this new cavern, and updating the related facilities to free up approximately 28 hectares of land for other civilian uses. This project represents the second phase of the relocation plan, focusing on the construction of a 14-hectare main cavern cluster. The first phase, completed earlier, included the construction of a 340-meter-long main tunnel and its surrounding site leveling, retaining structures, road and drainage works, temporary traffic bridges, and community liaison centers. The main tunnel and the main cavern cluster were constructed using the drilling and blasting method, which is a large-section tunneling technique with a cross-sectional area exceeding 200m<sup>2</sup>.

This project is a rare super-large cross-section cavern engineering in Hong Kong and even the world. It represents an optimized construction plan proposed after comprehensively considering factors such as laws and regulations, surrounding environment, geological conditions, cost, and schedule. The engineering team studied and compared various blasting hole layout schemes and explosive choices, overcoming challenges like dud explosions. They successfully applied and summarized the drilling and blasting method for super-large cross-section cavern, significantly improving construction efficiency, reducing costs and duration, with evident overall economic benefits.

## 6. CONCLUSION

This study proposes an innovative drilling and blasting construction method for the technical problems of super-large cross-section cavern construction in Hong Kong granite strata, and verifies its technical feasibility and economic benefits through engineering practice. The main conclusions are as follows:

(1) The three-arm rock drilling cart precision positioning system developed can realize high-precision drilling, and the design of large diameter  $\Phi 51$ mm blasting hole makes the single hole charge amount increase to 10kg, and the maximum single cycle advance reaches 5m, which greatly improves the blasting efficiency compared with traditional methods.

(2) The proposed graded micro-differential blasting system adopts a 9-second delay control structure, which successfully reduces the blasting vibration velocity of 300m<sup>2</sup> section and reduces the single consumption of explosives to 1.2kg/m<sup>3</sup>.

(3) The established mechanized construction system has realized the whole process of "drilling-loading-support" mechanized operation, reducing the demand for manpower by 33%, with small over-excavation rate and good overall contour surface flatness.

(4) Engineering applications have shown that this construction method can shorten the project duration by 6 months and reduce overall costs, forming a standardized construction system suitable for hard rock strata. The research findings provide important references for similar urban underground space development projects, with subsequent efforts focusing on the integrated application of intelligent propelling technology and digital twin systems.

## 7. ACKNOWLEDGMENTS

This paper is sponsored by the Technology Research and Development Project of China State Construction International Holdings Limited (CSCI-2023-Z-17).

## 8. BIBLIOGRAPHY

- [1] WANG, M.S., TAN, Z.S., 2010. The construct technology of tunnel and underground engineering in China. *Engineering Sciences*, 12(12): 4.
- [2] YAN, J.X., 2019. Achievements and challenges of tunnelling technology in China over past 40 years. *Tunnel Construction*, 39(4): 537.
- [3] TAN, Z.S., 2019. Construction concepts and key technologies for tunnel and underground engineering: A celebration of main academic thoughts and achievements of Academician WANG Mengshu. *Hazard Control in Tunnelling and Underground Engineering*, 1(2): 1.
- [4] ZHANG, N., MAO, J., TAN, Z.S., et al, 2010. Research on the problem of emergency station safe evacuation in super-long tunnel. *Journal of Beijing Jiaotong University*, 34(1): 20.
- [5] CHEN, J.X., LUO, Y.B., 2018. WAN Li, et al. Research status and challenges of highway tunnel with super long span. *Road Machinery & Construction Mechanization*, 35(6): 36.
- [6] ZHANG, J.R., WU, J., YAN, C.W., et al, 2020. Construction technology of super-large section of highway tunnels with four or more lanes in China. *China Journal of Highway and Transport*, 33(1): 14.
- [7] BI Q., WU J.G., 2011. Study on key technologies for structural design of large-span forked tunnel. *Tunnel Construction*, 31(6): 668.
- [8] BI Q., WU J.G., 2012. Secondary lining design of four lane long-span highway tunnel. *Railway Engineering*, (3): 54.
- [9] GUO S.Y., 2007. Progresses and developments of tunnel construction technology with bored blasting method. *Journal of Railway Engineering Society*, (9): 67.
- [10] ZHAO Q.C., 2018. Study on mechanical characteristics and waterproof and drainage technology of lining structure of large section highway tunnel in high pressure and rich water area. Southwest Jiaotong University, Chengdu, China.
- [11] HUANG M.L., NING R., QU X.W., et al, 2017. Research on the construction technology of large cross section of Chongqing north railway station. *Journal of Railway Engineering Society*, (1): 108.
- [12] ZHANG C.D., 2001. Treatment on large-scale landslide for long-span highway tunnel. *Journal of Railway Engineering Society*, 18(4): 100.
- [13] ZHU L.L., 2002. Construction technology of shallow burying big span tunnel in soft and weak surrounding rock. *Journal of Henan Polytechnic University (Natural Science)*, 21(3): 235.
- [14] TAN Z.S., WU J.G., 2023. Review and prospects of drilling and blasting tunnel construction technology in China. *Tunnel Construction*, 43(6): 899.
- [15] YANG N.H., 2021. Reflection on the mechanized development of tunnel excavation operation by drilling and blasting method. *Tunnel Construction*, 41 (12):2023.
- [16] TAN Z.S., HE W.G., WANG M.S., 2018. Study of engineering geological conditions and railway tunnel scheme across Qiongzhou Strait. *Tunnel Construction*, 38(1): 1.
- [17] WANG Z.J., 2018. Research on key technology of large crosssectional mechanized construction of Zhengzhou-Wanzhou high-speed railway tunnel. *Tunnel Construction*, 38(8): 1257.
- [18] HONG K.R., 2018. Challenging problems facing the extralong tunnel and some food for thought. *Science & Technology Review*, 36(10): 93.



## INNOVATIVE PRACTICES AND SUSTAINABLE DEVELOPMENT FOR CAVERN DESIGN AND CONSTRUCTION BASED ON THE Q-SYSTEM AND ROCK REINFORCED APPROACH

Joseph Z. Hong<sup>1</sup>, Yifeng Li<sup>2</sup>, Zhikai Wei<sup>3</sup> Xuefeng Li<sup>4</sup>

**Abstract:** The Guangdong-Hong Kong-Macao Greater Bay Area (GBA) is advancing decisively towards high-quality development goals. The Cavern Master Plan (CMP) launched by the Hong Kong Government exemplifies innovative underground space development emerging from this strategic context. This paper focuses on a cavern project, one of the largest in Hong Kong, featuring a maximum excavation face span of 36.2 meters. Using this project as a case study, it systematically investigates the application of the Q-system, Rock Reinforcement Approach (RRA), and construction optimization under complex geological conditions. The Q-system quantifies the engineering characteristics and stability of rockmasses through multi-parameter coupling analysis, providing a scientific basis for decision-making in underground engineering. Addressing Hong Kong's mountainous terrain and competent rock geology, the project employed the Rock Reinforcement Approach (RRA), integrating rock bolts and shotcrete to form a synergistic support system. Support design was optimized during construction through dynamic Q-value verification and 3D numerical modeling. This approach successfully enabled the excavation of the 36.2-meter super-large span cavern, demonstrating the applicability of the Q-system in composite hard-rock/fractured-rock strata.

**Keywords:** Q-system; Rock Reinforcement Approach; Cavern engineering; Construction design; Construction management

### 1. COMMENTS: BACKGROUND:

In land-scarce Hong Kong, the future of development lies underground. Picture a city where every inch of land is precious, yet beneath its hilly terrain and robust rock formations lies untapped potential. Over the years, cavern engineering has evolved from hosting nuisance facilities to becoming a cornerstone of sustainable development. The Hong Kong Government has embraced this vision, introducing a territory-wide Cavern Master Plan and expanding land-use guidelines to unlock the full potential of these hidden spaces. By relocating facilities like sewage treatment plants into caverns, surface land is freed for vital uses such as housing and commerce. This approach not only mitigates community nuisances but also transforms underutilized spaces into opportunities for growth. Innovations in construction, such as vibration-resistant concrete and digital rock analysis, are fast-tracking these projects while ensuring cost-effectiveness. Cavern development also addresses the city's acute land shortage by providing cost-effective, land-intensive spaces for public and private uses without further land encroachment. This underground approach represents a paradigm shift from traditional two-dimensional planning to a forward-looking, multi-dimensional strategy. Through strategic studies and implementation of enabling measures, Hong Kong is leveraging its geological strengths to deliver innovative, sustainable solutions for urban expansion.

<sup>1</sup> CSCHK, Hong Kong, Email: zhengqiang.hong@cohl.com

<sup>2</sup> CSCHK, Hong Kong, Email: li\_yf@cohl.com

<sup>3</sup> CSCHK, Hong Kong, Email: weizhikai@cohl.com

<sup>4</sup> CSCHK, Hong Kong, Email: xuefeng.li@cohl.com

## **2. HIGHLIGHT CAVERN INFORMATION:**

The project includes the Relocation of public works to caverns. North cavern is drained structure, with excavation span 36.20m x excavation height 28.29m. The cross-section dimension is constant along its entire 79.6m length. South cavern is drained structure, with varying excavation span 33.20m x excavation height 27.89m. The excavation span is 34.2m wide for first 20m length of cavern and 33.2m wide for the remaining length of cavern. Adit is drained structure, with excavation span 12.20m x excavation height 9.94m. The cross-section dimension of Adit is constant along its entire 30.8m length.

## **3. INNOVATION POINS:**

### **1. Construction Challenges and Information:**

- a. Probing: Utilize advanced probing to assess rock cover, quality, and groundwater inflow, ensuring accurate geological evaluations.
- b. Grouting: Implement pre-excavation grouting if water inflow exceeds contract limits to maintain structural integrity.
- c. Excavation: Use drill-and-blast methods for top-heading excavation, prioritizing safety and efficiency.
- d. Surface Assessment: After mucking and scaling, map the exposed surface; a qualified geologist will categorize rock support class and integrate permanent spot bolting for stabilization.
- e. Support Systems: Employ permanent rock bolts and temporary shotcrete tailored to rock class to ensure stability during excavation.
- f. Sequential Excavation: Follow up with middle and bottom bench excavations consistently.
- g. Drainage and Waterproofing: Install drainage strips and apply a high-performance waterproofing membrane to manage water ingress effectively.
- h. Structural Layers: Finish with permanent sprayed concrete and construct internal structures such as drainage layers and DfMA RC walls.

### **2. Design Challenges and Information:**

Long-lasting Rockbolts: Permanent rockbolts are designed for a lifespan of 100 years, incorporating double corrosion protection for durability in all permanent structures.

- a. Temporary Support Strategy: Permanent sprayed concrete is not used for temporary rock support due to integrity concerns after nearby blasting. Instead, separate temporary sprayed concrete stabilizes excavations.
- b. Rock Quality Assessment: Utilizes the Generalized Hoek-Brown Strength Criterion to derive Q-values. Two assessment systems are employed. The Q-System is for rock mass quality. The RMR is for advance length and stand-up time evaluations.
- c. Kinematic Analysis for Stability: Main caverns and adits are excavated in competent rock, focusing on rock discontinuities. Kinematic analysis estimates potential rock wedges, informed by Borehole Televiewer Data and slope face mapping.
- d. Rock Reinforcement Approach (RRA): In deep rock cover zones, a RRA is implemented, using permanent rockbolts to enable the rock to support the excavated ground efficiently.

### **3. Geotechnical Challenges:**

Adverse geological structures, such as faults and joints, present significant challenges for deep underground projects under high in situ stresses, as they directly impact rock mass stability. While site selection typically aims to avoid large faults due to their fractured, loose, and poorly self-stabilizing nature, functional and layout constraints of underground caverns often make it unavoidable to encounter faults. In this project, two NW-SE trending faults have been identified, potentially causing adverse effects on the surrounding rock mass, including higher degrees of fracturing and weathering within the fault zone. Additionally, a NE-SW trending basaltic andesite/andesite dyke has been mapped, further complicating geological conditions. These factors highlight the importance of detailed geological assessments and mitigation strategies to ensure stability and safety in cavern development.

## **4. ACKNOWLEDGMENT**

This paper is sponsored by the Technology Research and Development Project of China State Construction International Holdings Limited (CSCI-2023-Z-17).

Image de wirestock sur Freepik

